



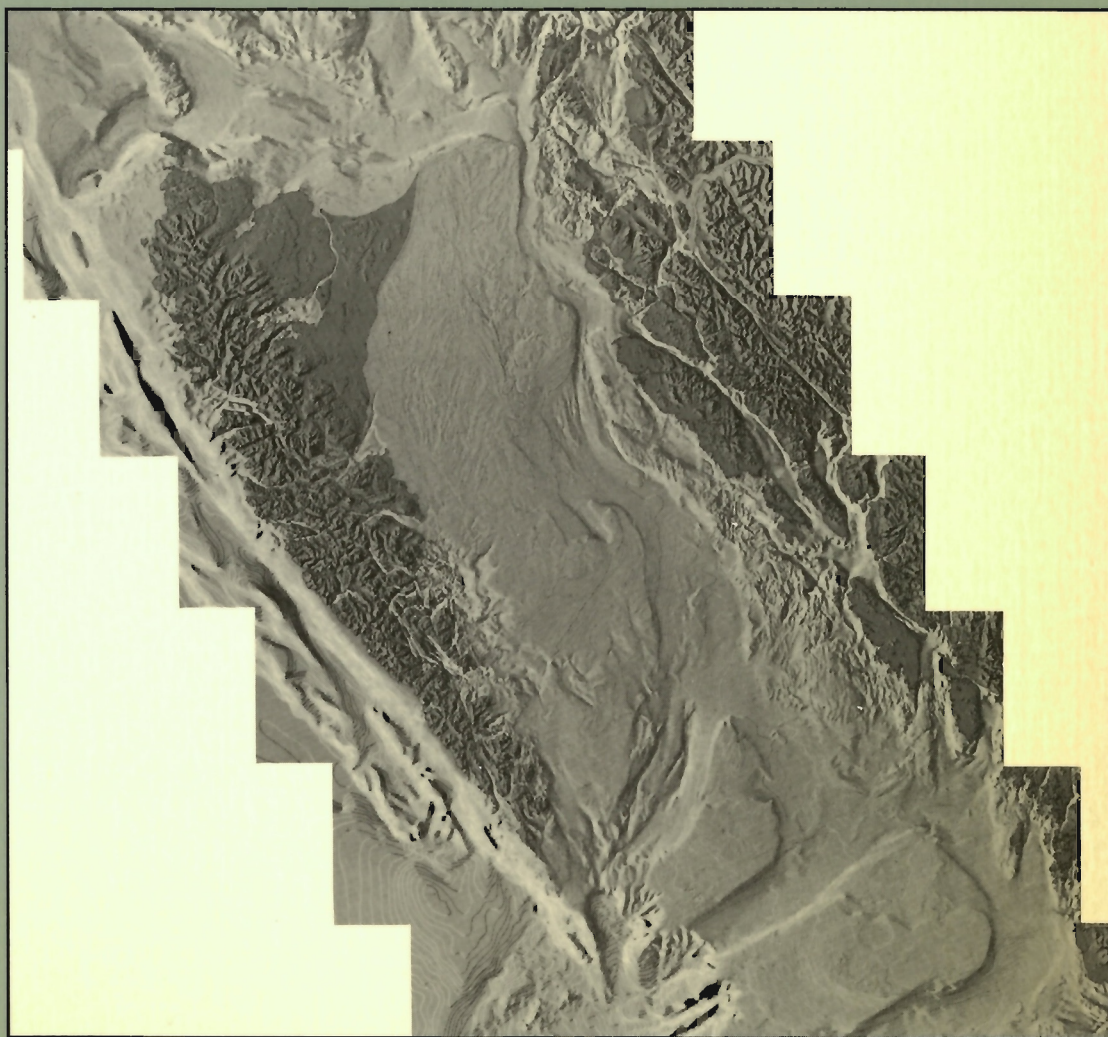
This document was produced  
by scanning the original publication.

Ce document est le produit d'une  
numérisation par balayage  
de la publication originale.

GEOLOGICAL SURVEY OF CANADA  
PAPER 90-10

# EVOLUTION AND HYDROCARBON POTENTIAL OF THE QUEEN CHARLOTTE BASIN, BRITISH COLUMBIA

edited by G.J. Woodsworth



Energy, Mines and  
Resources Canada

Énergie, Mines et  
Ressources Canada

Canada

**THE ENERGY OF OUR RESOURCES**

**THE POWER OF OUR IDEAS**



GEOLOGICAL SURVEY OF CANADA  
PAPER 90-10

**EVOLUTION AND HYDROCARBON POTENTIAL  
OF THE QUEEN CHARLOTTE BASIN,  
BRITISH COLUMBIA**

edited by G.J. Woodsworth

1991



Minister of Supply and Services Canada 1991

Available in Canada through authorized  
bookstore agents and other bookstores

or by mail from

Canadian Government Publishing Centre  
Supply and Services Canada  
Ottawa, Canada K1A 0S9

and from

Geological Survey of Canada offices:

601 Booth Street  
Ottawa, Canada K1A 0E8

3303-33rd Street N.W.  
Calgary, Alberta T2L 2A7

100 West Pender Street  
Vancouver, B.C. V6B 1R8

A deposit copy of this publication is also available  
for reference in public libraries across Canada

Cat. No. M44-90/10E  
ISBN 0-660-13563-9

Price subject to change without notice

### **Cover description**

Bathymetry and topography of the Queen Charlotte Basin.  
Compilation and cartography by Brian Sawyer.

Final version approved for publication: 08-08-90



# CONTENTS

## INTRODUCTION

- 1 D.J. TEMPELMAN-KLUIT

## BASIN STRUCTURE AND EVOLUTION

- 3 R.I. THOMPSON, J.W. HAGGART and P.D. LEWIS  
Late Triassic through early Tertiary evolution of the Queen Charlotte Basin, British Columbia, with a perspective on hydrocarbon potential
- 31 P.D. LEWIS and J.V. ROSS  
Mesozoic and Cenozoic structural history of the central Queen Charlotte Islands, British Columbia
- 51 J. INDRELID, J. HESTHAMMER and J.V. ROSS  
Structural geology and stratigraphy of Mesozoic rocks of central Graham Island, Queen Charlotte Islands, British Columbia
- 59 R.G. ANDERSON and I. REICHENBACH  
U-Pb and K-Ar framework for Middle to Late Jurassic (172- $\geq$ 158 Ma) and Tertiary (46-27 Ma) plutons in Queen Charlotte Islands, British Columbia
- 89 J.F. SWEENEY and D.A. SEEMANN  
Crustal density structure of Queen Charlotte Islands and Hecate Strait, British Columbia
- 97 H.V. LYATSKY  
Regional geophysical constraints on crustal structure and geologic evolution of the Insular Belt, British Columbia
- 107 R.D. HYNDMAN and T.S. HAMILTON  
Cenozoic relative plate motions along the northeastern Pacific margin and their association with Queen Charlotte area tectonics and volcanism
- 127 K. ROHR and J.R. DIETRICH  
Deep seismic reflection survey of the Queen Charlotte Basin, British Columbia
- 135 G.D. SPENCE, J.A. HOLE, I. ASUDEH, R.M. ELLIS, R.M. CLOWES, T. YUAN and K.M.M. ROHR  
A seismic refraction study in the Queen Charlotte Basin, British Columbia

## BASIN (BIO)STRATIGRAPHY

- 151 G.J. WOODSWORTH and P.E. TERCIER  
Evolution of the stratigraphic nomenclature of the Queen Charlotte Islands, British Columbia
- 163 A. DESROCHERS and M.J. ORCHARD  
Stratigraphic revisions and carbonate sedimentology of the Kunga Group (Upper Triassic-Lower Jurassic), Queen Charlotte Islands, British Columbia
- 173 M.J. ORCHARD  
Late Triassic conodont biochronology and biostratigraphy of the Kunga Group, Queen Charlotte Islands, British Columbia
- 195 E.S. CARTER  
Late Triassic radiolarian biostratigraphy of the Kunga Group, Queen Charlotte Islands, British Columbia
- 203 H.W. TIPPER, P.L. SMITH, B.E.B. CAMERON, E.S. CARTER, G.K. JAKOBS and M.J. JOHNS  
Biostratigraphy of the Lower Jurassic formations of the Queen Charlotte Islands, British Columbia
- 237 T.P. POULTON, R.L. HALL, H.W. TIPPER, B.E.B. CAMERON and E.S. CARTER  
Current status of Middle Jurassic biostratigraphy of the Queen Charlotte Islands, British Columbia
- 253 J.W. HAGGART  
A synthesis of Cretaceous stratigraphy, Queen Charlotte Islands, British Columbia



- 279 J.A.S. FOGARASSY and W.C. BARNES  
Stratigraphy and diagenesis of the middle to Upper Cretaceous Queen Charlotte Group, Queen Charlotte Islands, British Columbia
- 295 R. HIGGS  
Sedimentology and implications for petroleum exploration of the Honna Formation, northern Queen Charlotte Islands, British Columbia
- 305 C.J. HICKSON  
The Masset Formation on Graham Island, Queen Charlotte Islands, British Columbia
- 325 G.J. WOODSWORTH  
Neogene to Recent volcanism along the east side of Hecate Strait, British Columbia
- 337 R. HIGGS  
Sedimentology, basin-fill architecture and petroleum geology of the Tertiary Queen Charlotte Basin, British Columbia
- 373 J.M. WHITE  
Palynostratigraphy of Tow Hill No. 1 Well in the Skonun Formation, Queen Charlotte Basin, British Columbia

#### **BASIN MATURATION AND THERMAL HISTORY**

- 381 D. VELLUTINI and R.M. BUSTIN  
Source rock potential of Mesozoic and Tertiary strata of the Queen Charlotte Islands
- 411 D. VELLUTINI and R.M. BUSTIN  
Organic maturation and source rock potential of Mesozoic and Tertiary strata, Queen Charlotte Islands, British Columbia
- 453 M.J. ORCHARD and P.J.L. FORSTER  
Conodont colour and thermal maturity of the Late Triassic Kunga Group, Queen Charlotte Islands, British Columbia
- 465 J.G. SOUTHER and A.M. JESSOP  
Dyke swarms in the Queen Charlotte Islands, British Columbia, and implications for hydrocarbon exploration
- 489 T.J. LEWIS, W.H. BENTKOWSKI and J.A. WRIGHT  
Thermal state of the Queen Charlotte Basin, British Columbia: warm

#### **HAZARDS AND ENVIRONMENTAL STUDIES**

- 507 J.V. BARRIE, J.L. LUTERNAUER and K.W. CONWAY  
Surficial geology and geohazards of Queen Charlotte Basin, northwestern Canadian continental shelf, British Columbia
- 513 B.J. BURD and G.S. JAMIESON  
Survey of larval stages of commercial species in the area and time of the 1988 seismic survey in Queen Charlotte Sound and Hecate Strait

#### **DATABASES**

- 545 M.L. WESTON, G.J. WOODSWORTH, M.J. ORCHARD and M. JOHNS  
Design of an electronic database for biostratigraphic data
- 555 G.J. WOODSWORTH  
Annotated bibliography of geoscience studies of the Queen Charlotte Islands and Queen Charlotte Basin, British Columbia



## **LIST OF OVERSIZE FIGURES THAT ACCOMPANY THIS VOLUME**

- Structural geology of selected areas of northwest Graham Island, Figure 4. (To accompany P.D. Lewis and J.V. Ross, Mesozoic and Cenozoic structural history of the central Queen Charlotte Islands)
- Structural geology of southeastern Rennell Sound, Figure 6. (To accompany P.D. Lewis and J.V. Ross, Mesozoic and Cenozoic structural history of the central Queen Charlotte Islands)
- Structural geology of Long Inlet/Kagan Bay area, Figure 9. (To accompany P.D. Lewis and J.V. Ross, Mesozoic and Cenozoic structural history of the central Queen Charlotte Islands)
- Structural geology of southeastern Louise Island, Figure 10. (To accompany P.D. Lewis and J.V. Ross, Mesozoic and Cenozoic structural history of the central Queen Charlotte Islands)
- Potential-field maps for the Queen Charlotte Basin, Figure 2. (To accompany H.V. Lyatsky, Regional geophysical constraints on crustal structure of the Insular Belt)
- Tow Hill No. 1 well, palynomorph percentages by last occurrence, Figure 2. (To accompany J.M. White, Palynostratigraphy of Tow Hill No. 1 Well)
- Structural cross-section, Queen Charlotte Basin, Figure 3. (To accompany R. Higgs, Sedimentology, basin-fill architecture and petroleum geology of the Tertiary Queen Charlotte Basin)
- Distribution, orientation and lithology of dyke swarms in the southern Queen Charlotte Islands, Figure 2. (To accompany J.G. Souther and A.M. Jessop, Dyke swarms in the Queen Charlotte Islands)

---

# Evolution and Hydrocarbon potential of the Queen Charlotte Basin, British Columbia

---

## INTRODUCTION

The Queen Charlotte Basin is one of Canada's hydrocarbon exploration frontiers. In 1987, the Geological Survey of Canada began a multidisciplinary basin analysis project for the basin under the auspices of the Frontier Geoscience Program (FGP). The purpose of this Frontier Geoscience Program is to provide policy makers and the Canadian public with the best possible assessment of hydrocarbon potential in the Basin. The FGP mandate specifies four primary areas of scientific investigation: 1) deep crustal structure; 2) internal basin geology, 3) source rock potential and thermal evolution, and 4) hazards to development. A team of 49 scientists was assembled from the Geological Survey of Canada, the University of British Columbia, the University of Ottawa, and the private sector. Disciplines brought to the program include: biostratigraphy, sedimentology, seabed mapping, potential field mapping, seismic reflection and refraction surveying, geological mapping, volcanology, thermal and geochemical analysis, and isotopic dating. Preliminary reports of many of the studies have been published by the Geological Survey of Canada in its annual publication *Current Research* for the past three years. The 31 papers in the present volume range from final products to interim reports; certain investigations are still in progress. Nonetheless this volume and the accompanying maps provide a significant contribution to our understanding of the evolution and hydrocarbon potential of the Queen Charlotte Basin.

The Queen Charlotte Basin includes all Middle Jurassic and younger stratigraphic units. During Tertiary, Cretaceous and Middle Jurassic time the Queen Charlotte Islands probably formed part of a larger basin that extended west of today's continental margin. Today, the basin is restricted to Hecate Strait, Queen Charlotte Sound, and Dixon Entrance.

Commercial quantities of petroleum, if present in the basin, will likely be found in the offshore regions of Hecate Strait and Queen Charlotte Sound. However, lack of offshore seismic reflection data displaying stratigraphic and structural relationships beneath the cover of Tertiary clastic and volcanic rocks leaves onshore geology as the only means of inferring pre-Tertiary offshore relationships. Fortunately, this is not true for the Tertiary: the complex structural and stratigraphic relationships between volcanic and sedimentary rocks mapped onshore are well imaged on reflection profiles offshore. Together with potential field, heat flow and refraction data, an increasingly comprehensive database is becoming available for the interpretation of Tertiary geologic history.

Seeps of "live" oil on-land fuel speculation that hydrocarbon accumulations are geologically possible. The on-land distribution and character of thermally mature, Lower Jurassic organic-rich shales are now known in detail. Very recently a geochemical link was established between hydrocarbons in these potential source rocks and oil stains in Tertiary strata drilled offshore. These discoveries imply that some Lower Jurassic source rocks must exist offshore and that mature hydrocarbons migrated into the younger Tertiary succession. On land, Cretaceous sandstones having some reservoir potential locally overlie source strata directly. The structural and stratigraphic history deciphered to date suggests that Tertiary strata may also directly overlie source rocks.

## INTRODUCTION

Le bassin de la Reine-Charlotte est l'une des régions pionnières au Canada où l'on effectue des travaux d'exploration des hydrocarbures. En 1987, la Commission géologique du Canada a entrepris un projet d'analyse pluridisciplinaire du bassin sous les auspices du Programme géoscientifique des régions pionnières (PGP). Ce programme a pour objectif de fournir aux décideurs et au grand public canadien la meilleure évaluation possible du potentiel en hydrocarbures de ce bassin. Il est précisé dans le mandat du PGP quatre principaux domaines d'analyse scientifique : 1) la structure profonde de la croûte; 2) la géologie interne du bassin, 3) le potentiel et l'évolution thermique de la roche mère et 4) les obstacles à la mise en valeur. Une équipe de 49 scientifiques de la Commission géologique du Canada, de l'Université de la Colombie-Britannique, de l'Université d'Ottawa et du secteur privé a été formée. Les disciplines dont bénéficie le programme sont les suivantes : la biostratigraphie, la sédimentologie, la cartographie du fond océanique, la cartographie du champ potentiel, la sismique réflexion et la sismique réfraction, la cartographie géologique, la volcanologie, l'analyse de données thermiques et géochimiques et la datation isotopique. Les rapports préliminaires de plusieurs de ces études ont été publiés par la Commission géologique dans ses publications annuelles sur les Recherches en cours au cours des trois dernières années. Les 31 documents contenus dans le présent volume sont des rapports finaux ou provisoires; de nombreuses études ne sont pas encore terminées. Toutefois, le présent volume et les cartes jointes constituent une contribution importante à la reconstitution de l'évolution du bassin de la Reine-Charlotte et à la détermination de son potentiel en hydrocarbures.

Le bassin de la Reine-Charlotte comprend toutes les unités stratigraphiques depuis le Jurassique moyen jusqu'à plus récent. Au cours du Tertiaire, du Crétacé et du Jurassique moyen, les îles de la Reine-Charlotte faisaient probablement partie d'un plus grand bassin qui s'étendait à l'ouest de la marge continentale actuelle. Aujourd'hui, le bassin se limite au détroit d'Hécate, au détroit de la Reine-Charlotte et à l'entrée Dixon.

Si le bassin contient des quantités commerciales de pétrole, on devrait également en trouver dans les régions au large du détroit d'Hécate et du détroit de la Reine-Charlotte. Cependant, comme les données de sismique réflexion recueillies au large des côtes indiquant les liens stratigraphiques et structuraux au-dessous de la couverture de roches clastiques et volcaniques tertiaires sont insuffisantes, le seul moyen d'inférer les liens extracôtiers pré-tertiaires est d'analyser la géologie littorale. Heureusement, cela ne s'applique pas aux roches tertiaires : les liens structuraux et stratigraphiques complexes qui existent entre les roches volcaniques et sédimentaires cartographiées sur le littoral sont bien représentés sur les profils de sismique réflexion recueillis au large. En ajoutant les données sur le champ potentiel, l'écoulement thermique et la sismique réfraction, on obtient une base de données de plus en plus complète pour l'interprétation de la géologie tertiaire. La présence d'indices de pétrole sur les îles de la Reine-Charlotte laisse supposer qu'il est géologiquement possible que des hydrocarbures s'y soient accumulés. La distribution sur terre et les caractéristiques des schistes argileux riches en matière organique et thermiquement mature du Jurassique inférieur n'ont pas été déter-



Although this program focuses on hydrocarbon potential, it also recognizes the need to understand the natural hazards that could affect exploration and/or development. Traditionally, hazard assessment has involved engineering tests on sediment cores combined with high resolution, single-channel seismic surveys and seabed mapping—methods designed to determine the relative stability of the sea bottom and the physical forces that might disrupt it. However, other environmental issues have arisen. There are fears within the fishing industry and among other concerned Canadians that exploration techniques, such as multichannel seismic surveys employing large airgun arrays, have a negative impact on sea life, especially fish stocks. To examine this issue, resources were allocated to a baseline study of plankton and fish larvae density and distribution in Queen Charlotte Sound and Hecate Strait. Understanding the diversity and quantity of marine life is a crucial first step in the preparation of an environmental impact assessment. We acknowledge the advice and willing participation of the Federal Department of Fisheries and Oceans.

An indefinite moratorium on hydrocarbon exploration along Canada's west coast was imposed by the Federal Government in 1972; its purpose is to prevent crude oil tankers from travelling through Dixon Entrance, Hecate Strait and Queen Charlotte Sound en route from the Trans-Alaska pipeline terminal in Valdez, Alaska. Subsequently, a federal Order-in-Council indefinitely relieved existing offshore exploration permit holders of their obligations to conduct exploratory drilling in these waters and prohibited any further drilling. In 1981, the Province of British Columbia reinforced the moratorium by declaring these waters to be part of an Inland Marine Zone. The moratorium on exploration remains indefinite pending an agreement between the Federal and British Columbia governments on terms and conditions for the resumption of hydrocarbon exploration. Contributions of the Queen Charlotte Islands Frontier Geoscience Program represent a scientific framework essential to policy formulation and to negotiations between different levels of government.

D.J. Tempelman-Kluit,  
Director, Cordilleran Division,  
Geological Survey of Canada

minées en détail; on a établi très récemment un lien géochimique entre les hydrocarbures et ses roches mères potentielles et les taches de pétrole observées dans les couches tertiaires forées au large des côtes. Ces découvertes indiquent qu'il doit exister au large des roches mères du Jurassique inférieur et que des hydrocarbures matures ont migré vers la succession tertiaire plus récente. Sur terre, les grès crétacés présentant un certain potentiel de roches réservoirs reposent directement par endroits sur des couches mères. Selon l'histoire structurale et stratigraphique reconstituée à ce jour, les couches tertiaires pourraient également reposer directement sur des roches mères.

Même si ce programme est axé sur la détermination du potentiel en hydrocarbures du bassin, il est nécessaire de connaître les dangers naturels qui pourraient contrecarrer l'exploration ou la mise en valeur de ces ressources. Traditionnellement, l'évaluation des dangers consistaient à réaliser des essais techniques sur des carottes de sédiments combinés à des levés sismiques monocanaux à haute résolution et à cartographier le fond océanique — méthodes conçues pour déterminer la stabilité relative du fond océanique et les forces physiques qui pourraient le perturber. Or, d'autres questions environnementales ont émergé. Il s'agit des craintes exprimées par l'industrie de la pêche et par d'autres Canadiens qui croient que les techniques d'exploration, comme les levés sismiques multicanaux mettant en oeuvre de grands dispositifs de canons à air, auront des répercussions négatives sur la vie marine, en particulier sur les stocks de poissons. Pour analyser cette question, des ressources ont été affectées à une étude de base sur la densité et la distribution des planctons et des larves de poisson dans les détroits de la Reine-Charlotte et d'Hécaté. À la première étape de la préparation d'une évaluation des répercussions sur l'environnement, il est crucial de connaître la diversité et la quantité des organismes marins. Nous remercions donc le ministère fédéral de Pêches et Océans pour leurs conseils et leur participation spontanée.

En 1972, un moratoire indéfini sur l'exploration des hydrocarbures le long de la côte Ouest du Canada a été imposé par le gouvernement fédéral; il visait à empêcher les pétroliers en provenance du terminal du pipeline trans-alaskien à Valdez (Alaska) de traverser l'entrée Dixon et les détroits d'Hécaté et de la Reine-Charlotte. Par la suite, un ordre en conseil du gouvernement fédéral a relevé, pour une période indéfinie, les détenteurs de permis d'exploration extracôtière de leurs obligations de réaliser des forages d'exploration dans ces eaux et a interdit tout forage supplémentaire. En 1981, la province de la Colombie-Britannique a remis en vigueur le moratoire en déclarant que ces eaux faisaient partie d'une zone marine intérieure. Le moratoire sur l'exploration est maintenu jusqu'à ce qu'un accord intervienne entre le gouvernement fédéral et celui de la Colombie-Britannique sur les modalités de la reprise de l'exploration des hydrocarbures. Les contributions faites par le Programme géoscientifique des régions pionnières dans les îles de la Reine-Charlotte représentent un cadre scientifique essentiel à la formulation de politiques et à la tenue de négociations entre les différents niveaux de gouvernement.

D.J. Tempelman-Kluit,  
Directeur, Division de la géologie de la Cordillère,  
Commission géologique du Canada

# Late Triassic through early Tertiary evolution of the Queen Charlotte Basin, British Columbia, with a perspective on hydrocarbon potential

R.I. Thompson<sup>1</sup>, J.W. Haggart<sup>1</sup> and P.D. Lewis<sup>2</sup>

Thompson, R.I., Haggart, J.W., and Lewis, P.D., Late Triassic through early Tertiary evolution of the Queen Charlotte Basin, British Columbia, with a perspective on hydrocarbon potential; in *Evolution and Hydrocarbon Potential of the Queen Charlotte Basin, British Columbia*, Geological Survey of Canada, Paper 90-10, p. 3-29, 1991.

## Abstract

*The stratigraphic succession of the Queen Charlotte Islands is composed of two, lithologically distinct, tectonostratigraphic packages. The older package comprises the classic Wrangellian succession: a thick sequence of Upper Triassic volcanic rocks (Karmutsen Formation) overlain by Upper Triassic and Lower Jurassic carbonates, siliciclastics, and minor tuffs (Kunga and Maude groups), all deposited in a stable shelf setting. The extensive distribution of very similar Wrangellian rocks across the Insular Belt reflects deposition in a continuous and widespread Late Triassic-Early Jurassic basin.*

*A regional Middle Jurassic (Bajocian) unconformity marks the end of Wrangellian deposition in the Queen Charlotte Islands and the initiation of a volcanic arc (Yakoun Group). Rocks beneath the unconformity experienced south-west-directed folding and contractional faulting, and this is not reflected in the overlying strata. This deformation event may have resulted from the accretion of the Wrangell Terrane with North America.*

*A distinct change in sedimentation style is reflected in the composition and facies of the overlying stratigraphic succession, the second tectonostratigraphic package present in the Queen Charlotte Islands. The sedimentary strata of this package are composed dominantly of coarse clastics rather than carbonates. The thickness, facies, and distribution of many of these strata appear to have been controlled by Late Jurassic, Cretaceous, and early Tertiary syn-depositional block faulting. This package includes the Yakoun and Moresby groups (Middle Jurassic), the Longarm Formation and Queen Charlotte Group (uppermost Jurassic? to Upper Cretaceous), and Tertiary rocks. Although strata of similar age to the second package are found on Vancouver Island and in the southern Coast Mountains, continuity of map units between the Queen Charlotte Islands and these regions can not be demonstrated.*

*A second episode of folding and thrust faulting occurred in the Late Cretaceous and/or early Tertiary. Newly recognized nonmarine clastic rocks of Eocene and/or Oligocene age (unnamed) constrain the age of this deformation. Widespread volcanism (Masset Formation) postdates this second shortening event, accompanied by deposition of a thick succession of marine and nonmarine Miocene and Pliocene sedimentary rocks (Skonun Formation).*

*Parts of the Kunga and Maude groups have good source-rock potential. Possible reservoir rocks include the basal transgressive phase of the Cretaceous succession (Longarm and Haida formations) and Tertiary sandstones (Skonun Formation). Juxtaposition of reservoir rocks over source strata has been documented on-land; a similar relationship is likely for local regions offshore.*

## Résumé

*Les îles de la Reine-Charlotte sont composées de deux successions tectonostratigraphiques : 1) des roches volcaniques, des calcaires et des roches silicoclastiques du Trias supérieur et du Jurassique inférieur de la formation de Karmutsen et des groupes de Kunga et de Maude respectivement; et 2) des roches volcaniques, du grès, du schiste argileux et du conglomérat du Jurassique moyen, du Crétacé et du Tertiaire faisant partie des groupes de Yakoun et de Moresby (Jurassique moyen), de la formation de Longarm (Crétacé inférieur), du groupe de Queen Charlotte (Crétacé), des formations de Masset et de Skonun (Tertiaire) et de plusieurs unités cartographiques non désignées.*

*La succession tectonostratigraphique la plus ancienne s'est accumulée sur le fragment continental de la Wrangellia. L'activité volcanique mafique du Trias supérieur a été suivie d'une subsidence synchrone lente accompagnée d'un dépôt de roches carbonatées et clastiques de plate-forme. Selon les données fossiles et paléomagnétiques recueillies, la Wrangellia se trouvait à des latitudes plus basses pendant le Trias et le début du Jurassique. Le déplacement vers le nord, accompagné d'une segmentation et d'une accréation éventuelle de la Wrangellia à la marge continentale du Canada et de l'Alaska, a eu lieu entre le Jurassique moyen et le Crétacé supérieur.*

<sup>1</sup> Cordilleran Division, Geological Survey of Canada, 100 West Pender Street, Vancouver, B.C. V6B 1R8

<sup>2</sup> Department of Geological Sciences, University of British Columbia, 6339 Stores Road, Vancouver, B.C. V6T 2B4

Un plissement et un chevauchement à direction nord-est a accompagné la déformation et le plutonisme du Jurassique moyen dans les îles de la Reine-Charlotte. Après le Jurassique moyen, il y a eu un changement de style de sédimentation mis en évidence par la composition et le faciès de l'assemblage tectono-stratigraphique le plus récent. Les zones d'origine étaient proximales et les bassins étaient de taille relativement petite. Même si les caractéristiques de ces roches sont typiques de couches d'âge semblable dans l'île de Vancouver et dans le sud de la chaîne Côtière, il n'a pas été possible d'établir une corrélation des unités cartographiques entre ces régions. Durant le Jurassique supérieur et le Crétacé, un morcèlement par failles synsédimentaire a eu des répercussions sur l'épaisseur, le faciès et la distribution des unités au sein de séquences de grès-schiste argileux transgressives. Ce style de sédimentation s'est poursuivi jusqu'au Tertiaire. Des roches clastiques marines et non marines (non désignées) récemment découvertes de l'Éocène et de l'Oligocène se sont accumulées à la même époque par débordement de roches pyroclastiques et de coulées mafiques (non désignées). Un deuxième épisode de plissements et de chevauchements à direction nord-est a eu lieu pendant la fin de l'Oligocène et/ou au début du Miocène. La réactivation de l'activité volcanique (formation de Masset) a été accompagnée de la sédimentation de dépôts épais de roches clastiques miocènes et pliocènes (formation de Skonun).

Des parties des groupes de Kunga et de Maude offrent de bonnes possibilités de contenir des roches mères. Les roches réservoirs possibles sont notamment les formations de Longarm et de Honna et les grès tertiaires. La juxtaposition de roches réservoirs au-dessus de roches mères a été reconnue sur terre; les mêmes liens pourraient exister au large. Pour identifier les cibles crétacées au large des côtes, il faudra acquérir des données de sismique réflexion de meilleure résolution dans les roches sous-jacentes aux roches clastiques et volcaniques tertiaires.

Le bassin de la Reine-Charlotte possède plusieurs caractéristiques géologiques semblables à celles de l'inlet Cook (Alaska) : 1) ils ont tous les deux évolués dans des milieux d'avant-arc, 2) des suintements de pétrole brut ont été observés, 3) ils sont surtout composés (après le Jurassique inférieur) de grès feldspatholithe, 4) ils sont caractérisés par une histoire tectonique complexe qui s'est traduite par la juxtaposition de couches réservoirs au-dessus de couches mères, 5) la maturation et la migration des hydrocarbures n'a pas eu lieu avant le Tertiaire et 6) ils ont subi au Tertiaire inférieure une déformation qui a pu créer des pièges d'hydrocarbures.

## INTRODUCTION

Cumulative production from the Cook Inlet Basin, southern Alaska (Fig. 1), to December 31, 1984 is 1.5 billion barrels of oil; recoverable reserves exceed 1.1 billion barrels. The largest gas field has estimated recoverable reserves of 235 billion cubic metres of dry gas. Undiscovered reserves are estimated at 0.3-1.4 billion barrels of oil and 17-76 billion cubic metres of gas.

Fifteen hundred kilometres southeast of Cook Inlet, the Queen Charlotte Basin on Canada's west coast (Fig. 1) has never produced oil or gas and, to date, has no proven hydrocarbon reserves. It does, however, have a stratigraphic and tectonic history comparable in several respects to that for Cook Inlet. Does this suggest it has the potential to equal Cook Inlet as a hydrocarbon producer? In an attempt to address this question, this paper describes the Late Triassic through early Tertiary geologic history of the Queen Charlotte Basin and how it may relate to hydrocarbon potential.

In Cook Inlet, oil fields occur near the basin margin, where Tertiary reservoir rocks unconformably overlie Middle Jurassic source strata. Exploration is based on a two-part geological model (Magoon and Claypool, 1981): 1) burial and maturation of Jurassic source rocks during the Cretaceous and early Tertiary was followed by updip migration of hydrocarbons into conglomerate and sandstone reservoirs of Oligocene age; 2) hydrocarbons were remobilized during Pliocene and Pleistocene deformation, filling new traps created in faulted anticlines and upturned stratigraphic pinchouts. The model is constrained by detailed geological mapping around the basin margins; interpretation of thousands of kilometres of industry seismic reflection data; and stratigraphic, biostratigraphic, and geochemical examination of more than 1200 exploration wells.

The Queen Charlotte Basin, in contrast, is an exploration frontier. Between 1958 and 1961 Richfield Oil Corporation drilled 6 wildcat wells on northeastern Graham Island and Shell Oil drilled 8 more wells offshore between 1967 and 1969 (Fig. 2; Shouldice,

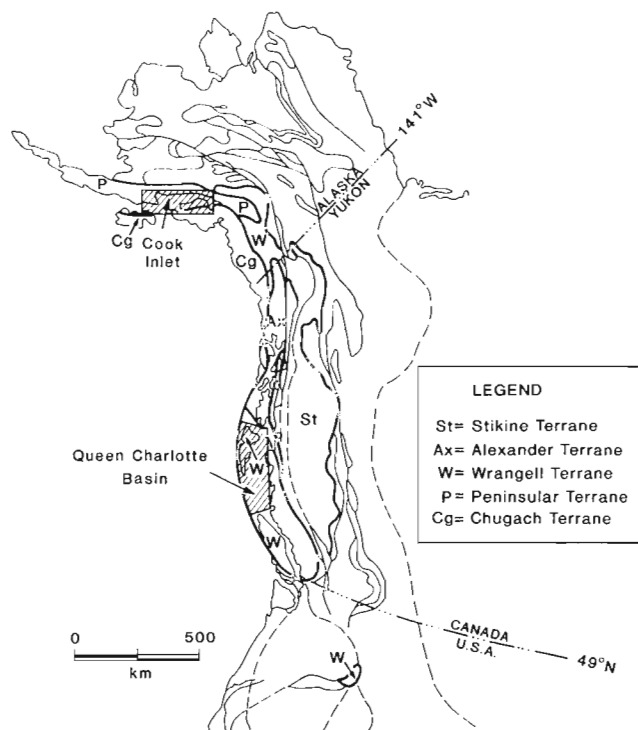


**Figure 1:** Terrane map of the western part of the Cordillera showing the locations of Queen Charlotte Basin, British Columbia, and Cook Inlet Basin, Alaska.



1971). Marine seismic reflection coverage is sparse and of poor quality. In 1972 the Federal Government imposed an indefinite moratorium on offshore hydrocarbon exploration (West Coast Offshore Exploration Environmental Assessment Panel, 1986).

Does the geologic history that led to hydrocarbon maturation, migration, and accumulation in Cook Inlet apply to the Queen Charlotte Basin as well? There are important geologic parallels between the two regions. In Cook Inlet, source rocks are Jurassic sandstones (Magoon and Claypool, 1979); in the Queen Charlotte Basin the most likely source rocks are organic-rich Upper Triassic to Lower Jurassic carbonate and shale (Macauley, 1983; Macauley et al., 1985; Vellutini, 1988; Vellutini and Bustin, 1988; Bustin and Macauley, 1988). Oil-seeps occur in both regions, proof that maturation and migration of hydrocarbons has occurred (Snowdon et al., 1988; Hamilton and Cameron, 1990).

In Cook Inlet, reservoir strata overlie source strata unconformably; in the Queen Charlotte Basin, source and potential reservoir rocks are also found in unconformable relationship. In Cook Inlet, hydrocarbon maturation did not occur until the late Tertiary, after burial of Jurassic source rocks beneath a thick Tertiary cover; in large parts of the Queen Charlotte Basin hydrocarbon maturation was also dependant upon burial beneath Tertiary strata. In Cook Inlet, hydrocarbon traps consist of faulted anticlines formed during Pliocene deformation; in offshore areas of the Queen Charlotte Basin, faulted anticlines formed during an episode of Pliocene compression.

Comparisons at a more regional scale are also encouraging. Like Cook Inlet, the Queen Charlotte Basin evolved in intra-arc and forearc settings, beginning (probably) in the Middle Jurassic when terrane accretion was accompanied by subduction of oceanic crust and

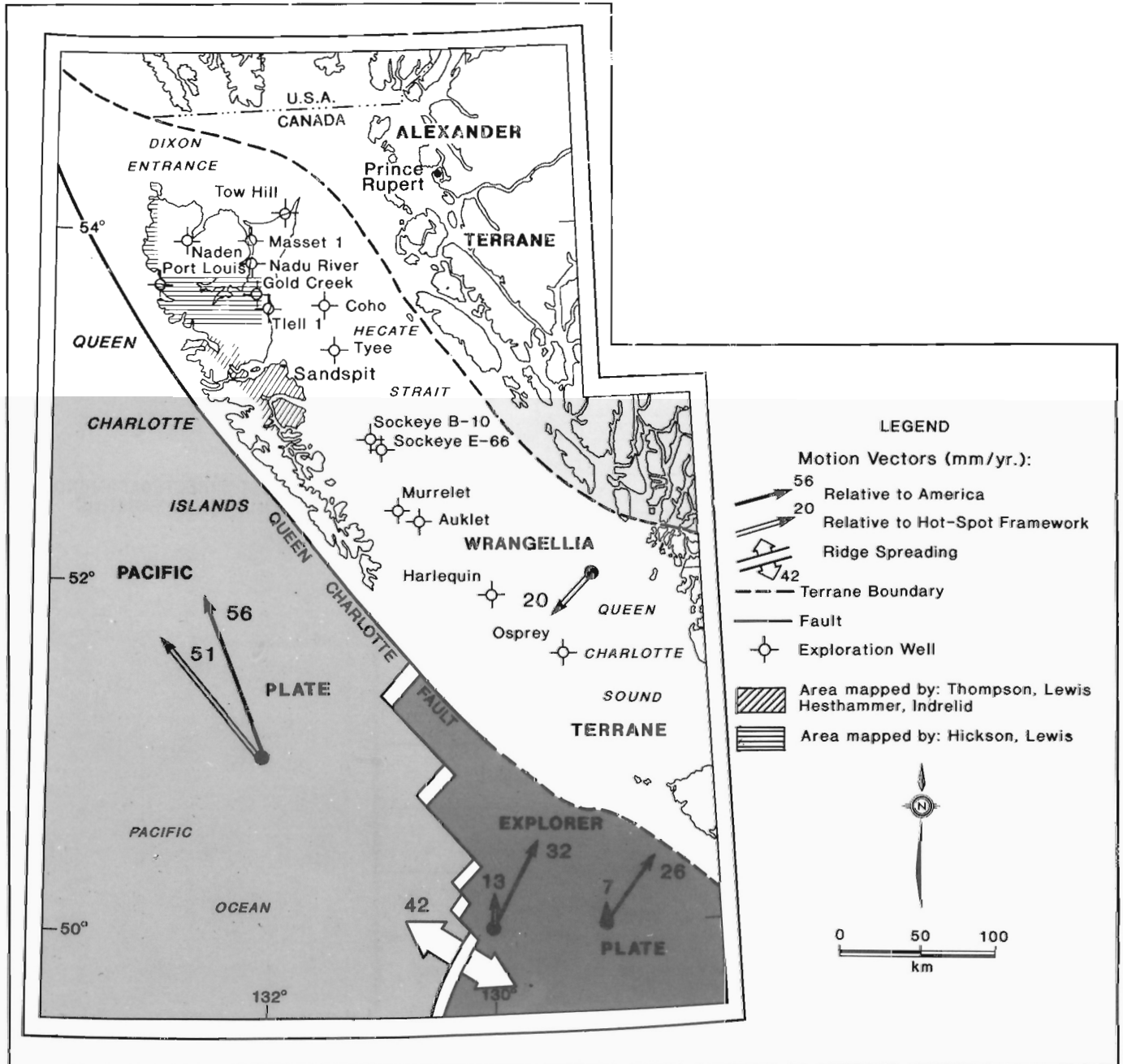


**Figure 2:** Map of the principal crustal elements of the west-central Canadian Cordillera and contiguous oceanic plates. Limits of the Queen Charlotte Basin shown in white. Compiled from Wheeler et al. (1988) and Riddihough (1983).



inception of the Coast Plutonic Complex magmatic arc (van der Heyden, 1989).

Some events and relationships specific to the Queen Charlotte Basin, however, weaken this positive comparison with Cook Inlet. Heating associated with Middle Jurassic plutonism (Anderson and Reichenbach, 1989, 1991) ruined source potential over large areas of the southern Queen Charlotte Islands and an unknown but potentially large part of the offshore region (Vellutini and Bustin, 1988, 1991; Orchard and Forster, 1991). Uplift associated with Late Jurassic and Cretaceous block faulting may have stripped much of the offshore region of source strata (Thompson and Thorkelson, 1989). An important change in plate dynamics during the Eocene also affected the Queen Charlotte Basin. A regime of convergence accompanied by subduction gave way to northward transcurrent motion of oceanic plates along the continental margin (Stock and Molnar, 1988; Engebretson et al.,

1985; Yorath and Hyndman, 1983; Hyndman and Hamilton, 1991), replacing the forearc setting that had previously existed with a strike-slip margin having limited potential for subduction.

Comparison of geological details between Cook Inlet and the Queen Charlotte Basin are hampered by a critical difference in the quality of seismic data collected: reflection records from Cook Inlet show Cretaceous and Jurassic events beneath the thick Tertiary cover, allowing interpretation of pre-Tertiary basin configurations in offshore areas. Records from the Queen Charlotte Basin, however, show few events below the presumed base of the Tertiary sedimentary succession — the data are insufficient to assess the thickness, distribution, and structure of pre-Tertiary source and reservoir strata.

Fortunately, there is sufficient onshore exposure in the Queen Charlotte Islands to assemble a geologic history from Late Triassic until early Tertiary time (Figs. 3 and 4). Analysis and interpretation

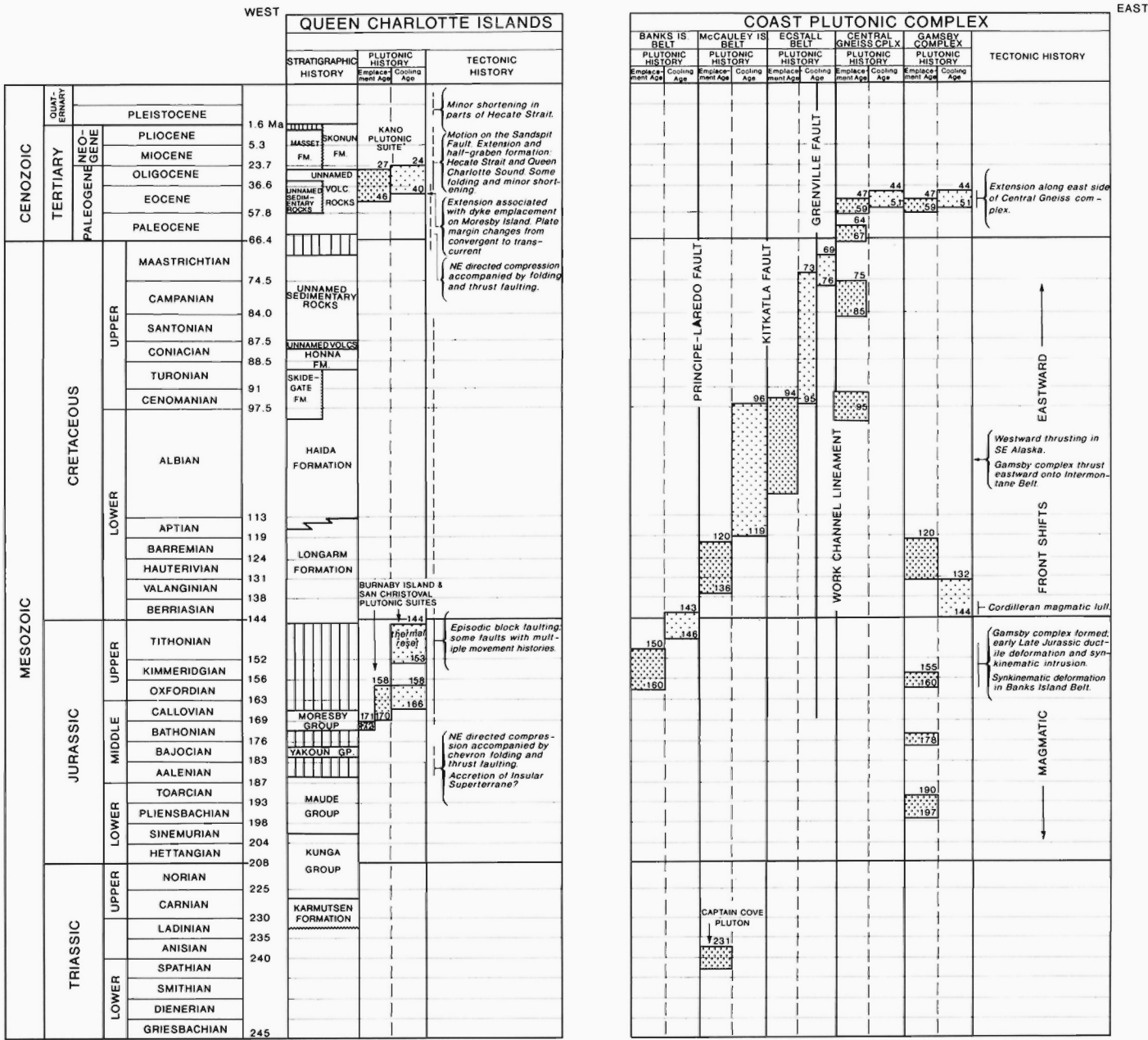
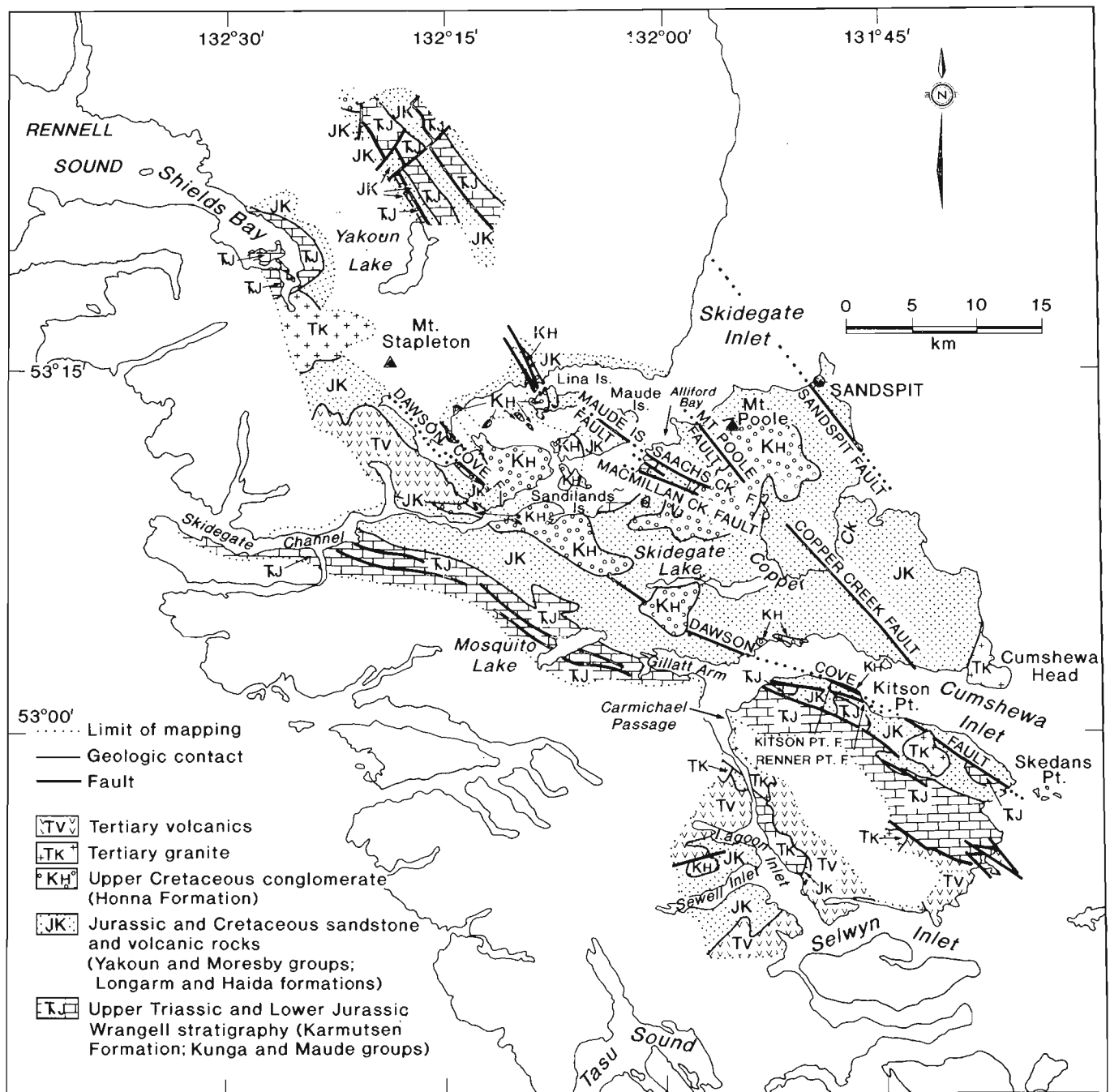


Figure 4: Comparative stratigraphic, plutonic, and tectonic histories for the Queen Charlotte Islands and the Coast Plutonic Complex along a cross section at 53°N.



**Figure 5:** Generalized geological map of northern Moresby Island and southern Graham Island that encompasses mapping by Thompson (1990), Thompson and Lewis (1990a,b) and P. Lewis et al. (1990).

of on-land geology provide analogues and constraints that can assist in the interpretation of structures, stratigraphic relations, and levels of maturation in the offshore part of the basin — especially for Cretaceous and older strata. This is critical because if commercial quantities of hydrocarbons exist in the Queen Charlotte Basin, they are likely to be found in the offshore, beneath Hecate Strait, Dixon Entrance, and Queen Charlotte Sound.

Many of the ideas expressed in this paper evolved from new geological mapping (Fig. 5; Thompson, 1990; Thompson and Lewis, 1990a,b; P. Lewis et al., 1990) and stratigraphic studies undertaken during the 1987-1989 field seasons. This paper is best read with the

maps at hand. Thompson did the bulk of the regional mapping (scale 1:50 000); Lewis prepared detailed maps (scale 1:25 000) and carried out structural analyses of Long Inlet, Rennell Sound, and southeastern Louise Island (Lewis and Ross, 1988, 1989, 1991); Haggart provided stratigraphic analysis as well as biostratigraphic control on Cretaceous strata (Haggart, 1991). Our data support four main conclusions:

- 1) Regional folding and faulting occurred in Middle Jurassic time.
- 2) Block faulting influenced Mesozoic and Tertiary sedimentary patterns.



- 3) Folding and faulting occurred late in the Cretaceous or early in the Tertiary, or both.
- 4) Basin development was not controlled by strike-slip faulting.

## REGIONAL TECTONIC SETTING

The Queen Charlotte Islands, Hecate Strait, and Queen Charlotte Sound are all parts of Wrangell Terrane, an exotic crustal block that now consists of four crustal segments distributed along more than 2000 km of the western Cordillera (Jones et al., 1977; Fig. 1). A distinctive Middle Triassic to Lower Jurassic stratigraphic signature sets Wrangell Terrane apart from adjoining terranes. Middle and Upper Triassic tholeiitic basalt several kilometres thick is overlain disconformably by Upper Triassic and Lower Jurassic shelf limestone and fine-grained calcareous clastic and siliciclastic strata (Fig. 3). The volcanic succession, called the Karmutsen Formation on the Queen Charlotte Islands and Vancouver Island, is evidence of a prodigious outpouring of tholeiitic basalt: thicknesses range from 2-5 km over a vast area. Shelf carbonate deposition followed the volcanism and was synchronous everywhere, commencing in the Late Carnian with shallow water limestones and succeeded, in the latest Norian and the Early Jurassic, by deeper water fine-grained detrital successions. This time-stratigraphic succession, present from the Hells Canyon area of western Idaho and eastern Oregon to the Wrangell Mountains of eastern Alaska (Jones et al., 1977), is absent from areas now contiguous with Wrangell Terrane (Fig. 1).

Both paleomagnetic (Monger and Irving, 1980; Irving et al., 1985) and paleontologic (Tozer, 1982; Smith and Tipper, 1986) evidence have been cited to suggest that Wrangell Terrane originated at low latitudes, possibly near present-day Baja Peninsula, that it moved northward, became segmented, and was subsequently accreted to the continental margin. However, debate exists as to when this northward movement occurred and the nature and timing of accretion. Paleontologic and stratigraphic data suggest that Wrangell Terrane was likely in place as early as the Middle Jurassic, and certainly so by the Late Cretaceous (Smith and Tipper, 1986). An alternative view is that of Monger and Irving (1980) and Irving et al. (1985) who interpreted the paleomagnetic data as indicating that Wrangell Terrane was still at low latitudes in Cretaceous time; its subsequent northward journey must therefore have been swift, with accretion occurring by the Late Cretaceous. Butler et al. (1989) cautioned, however, that the apparent latitudinal displacement suggested by the paleomagnetic data may be an artifact of regional tilt and that paleomagnetic results from the Coast Plutonic Complex do not necessarily constrain the timing of terrane accretion.

Independent geological results from the Coast Plutonic Complex led van der Heyden (1989) to conclude that Wrangell Terrane was joined with North America by the Middle Jurassic, as part of a much larger superterrane that also included the Stikine and Alexander terranes (Fig. 1). This latter assertion is supported by the recent dating of a Late Paleozoic pluton that crosscuts the boundary between Wrangell and Alexander terranes in southeastern Alaska (MacKevett et al., 1986; Gardner et al., 1988) and by a Late Jurassic to Early Cretaceous magmatic arc (Gravina-Gambier) that strikes obliquely across the Coast Plutonic Complex from Wrangell Terrane on the west to Stikine Terrane on the east.

Van der Heyden (1989) thus interpreted the evolution of the Queen Charlotte Islands region and the adjacent part of the Coast Plutonic Complex within the framework of a long-lived east-dipping subduction complex. In this interpretation, the Queen Charlotte Islands were part of a mid-Jurassic arc that gradually shifted eastward, leaving the Queen Charlotte Basin in a forearc setting in Cretaceous time (Fig. 4), similar to Cook Inlet. The alternative model, that Wrangell

Terrane was accreted during the late Early or early Late Cretaceous, and separate from Stikine Terrane, interprets the Coast Plutonic Complex as a metamorphic-plutonic welt representing the suture between Wrangell Terrane and the Cretaceous continental margin (Monger et al., 1982; Monger, 1984).

Today, as for the past 6 million years (Yorath and Hyndman, 1983), the Queen Charlotte Islands segment of Wrangell Terrane has been separated from the Pacific Plate by the Queen Charlotte Fault (Fig. 2). The southern 150 km of this fault is oriented slightly oblique to Pacific Plate motion, resulting in oblique subduction along the western margin of Moresby Island (Yorath and Hyndman, 1983; Fig. 2). Other crustal boundaries of the Queen Charlotte Basin are more difficult to characterize. Dixon Entrance separates Wrangell Terrane from Alexander Terrane to the north, but the nature of the boundary is not known. Wrangellian stratigraphy (Karmutsen Formation) crops out at one locality on the east side of Hecate Strait (Woodsworth, 1988), but steeply dipping faults and early Late Jurassic plutons obscure the character of any crustal boundary that might be present to the east. To the south, Wrangell Terrane rocks are presumed to extend beneath Queen Charlotte Sound, linking with equivalents on Vancouver Island.

## A DEFINITION OF THE QUEEN CHARLOTTE BASIN

Shouldice (1971, p. 407) used the term Queen Charlotte Basin in referring to the area: "...lying mainly between the Queen Charlotte Islands and the mainland...". In his Figure 2 the basin encompasses Hecate Strait, Queen Charlotte Sound, and the narrow continental terrace outboard of the Queen Charlotte Islands. Yorath (1988) adopted this usage with slight modification: he excluded the continental terrace but included Dixon Entrance. Both authors imply that Mesozoic and older strata are basement to the basin.

In our definition, the Queen Charlotte Basin embraces the suite of Middle Jurassic and younger strata found on the Queen Charlotte Islands and offshore beneath Dixon Entrance, Hecate Strait, and Queen Charlotte Sound. By expanding the time-stratigraphic limits for the basin, we are able to include all stratigraphic successions dominated by feldspatholithic sandstone, acknowledging that deposition in the basin has been essentially continuous since the Early Cretaceous. The Middle Jurassic Yakoun and Moresby groups are included because they contain the first significant deposits of feldspatholithic sandstone and, as such, herald the beginning of arc- and forearc-related basin development. The significant hiatus in Late Jurassic time (Fig. 3) resulted from uplift and unroofing of Middle Jurassic plutons (Anderson and Reichenbach, 1989).

Our definition emphasizes the overall consistency of depositional processes and products since the Middle Jurassic, and obviates any requirement to define additional basins or sub-basins, such as the Cretaceous Skidegate Basin of Yorath (1988).

In practice, the boundaries of the Queen Charlotte Basin are little changed from those used by earlier workers except for the addition of the Queen Charlotte Islands. The new basin boundaries are: the Queen Charlotte Fault on the west; the northern margin of Dixon Entrance on the north; the eastern margin of Hecate Strait and Queen Charlotte Sound on the east; and the southern margin of Queen Charlotte Sound on the south (Figs. 1 and 2).

## A SYNOPSIS OF QUEEN CHARLOTTE BASIN GEOLOGIC HISTORY

Figure 3 is a synopsis of the stratigraphic, igneous, and tectonic events that fashioned Queen Charlotte Islands geology from the Late Triassic through the Tertiary; we assume this history applies to the

Queen Charlotte Basin as a whole. The stratigraphic column can be divided into two parts: Upper Triassic through Lower Jurassic Wrangellia stratigraphy and Middle Jurassic through Tertiary Queen Charlotte Basin stratigraphy.

### Wrangell Terrane succession

The Upper Triassic Karmutsen Formation is a succession of pillow lava, breccia, hyaloclastite, and flows and sills, all composed almost entirely of basalt. The aggregate thickness of the formation on the islands is estimated at 4200 m (Sutherland Brown, 1968) but its base is not exposed. For mapping purposes, the Karmutsen Formation is structural basement. It is fractured, jointed, and sliced by a host of steeply-dipping faults (Lewis and Ross, 1991) and is deformed by broad warps but not folded.

Karmutsen volcanism ceased late in the Carnian with the onset of shallow-water shelf carbonate deposition, as seen in the massive grey limestone of the Kunga Group (Sadler Limestone of Desrochers and Orchard, 1991). This limestone overlies Karmutsen volcanic rocks with apparent conformity; beds of Upper Carnian limestone within the upper few metres of Karmutsen volcanic rocks suggest a gradation with no interruption in sedimentation (Orchard, 1991). The massive limestone passes upward into medium- to thick-bedded, organic-rich limestone (Peril Formation of Desrochers and Orchard, 1991) succeeded by variegated, thin- to medium-bedded calcareous siltstone and tuff (Sandilands Formation). These three sedimentary units form the Kunga Group, having an aggregate thickness of approximately 1000 m (Desrochers and Orchard, 1991). Thicknesses of individual formations are variable, however, and it is rare to encounter more than 500 m of unfaulted section at any one locality.

The remainder of the Lower Jurassic succession, called the Maude Group, is dominated by well-bedded, fine-grained detrital rocks (Ghost Creek, Fannin, Whiteaves, and Phantom Creek formations). The succession is internally conformable, up to 175 m thick, and consistent with a stable-shelf depositional environment (Cameron and Tipper, 1985). The presence of time-stratigraphic correlatives on northern Vancouver Island (Quatsino Formation; Jeletzky, 1976; Desrochers, 1989) suggests that the Upper Triassic-Lower Jurassic shelf was of regional extent.

### Queen Charlotte Basin succession

A regionally important fold and fault event affected Karmutsen, Kunga, and Maude rocks early in the Middle Jurassic (Late Aalenian-earliest Bajocian) time (Fig. 3). This event marked the end of Wrangell Terrane-type deposition. Deformation and erosion was followed by Middle Jurassic (Bajocian) volcanism (Yakoun Group) and the first influx of locally derived conglomerate and feldspatholithic wackes (Yakoun and Moresby groups). Figure 4 suggests that the Yakoun arc and the San Christoval and Burnaby Island plutonic suites may have been the initial manifestations of a diachronous, subduction-related magmatic arc that evolved into the Coast Plutonic Complex during Late Jurassic through Tertiary time (van der Heyden, 1989).

Little Upper Jurassic strata has been identified in the Queen Charlotte Islands (Fig. 3). Cooling dates (Fig. 4) reported from the Burnaby Island and San Christoval plutonic suites (Anderson, 1988; Anderson and Greig, 1989; Anderson and Reichenbach, 1989, 1991) suggest that the islands experienced extensive uplift and erosion during this time. By the Early Cretaceous, uplift was sufficient to expose some of the plutons on southern Moresby Island, which are overlain nonconformably by a granitic-rich transgressive lag of the Longarm Formation (Yorath and Chase, 1981; Anderson and Greig, 1989; Haggart and Gamba, 1990; Haggart, 1991). Because the nonconformity has not been observed on the northern part of Moresby Island

or on Graham Island, we speculate uplift was greater in the southern islands.

Map patterns suggest that uplift was associated with block faulting. Stratigraphic omissions, especially of the Yakoun Group, suggest initial vertical offsets on the order of one kilometre. These faults and their influence on Queen Charlotte Islands geology are discussed in a later section.

The Cretaceous succession in the basin consists of two fining upward sequences of conglomerate, sandstone, and shale. The lower sequence includes the Longarm, Haida, and Skidegate formations, whereas the upper includes the Honna Formation and an overlying unnamed shale succession (Haggart, 1991). Cretaceous sandstones of the Queen Charlotte Islands are dominated by feldspatholithic wackes which are compositionally similar to Yakoun Group volcanic flows; conglomerates also contain an abundance of clasts derived from the Yakoun Group. Together, these compositions suggest that the source of clastic material for Cretaceous strata was local and centred on the Middle Jurassic Yakoun Group, or cannibalized products thereof.

Volcanic activity was dormant throughout most of Cretaceous time in the islands region. A succession of subaqueous volcanic debris flows, volcanic breccias, and subaerial volcanic flows locally overlying the Upper Cretaceous Honna Formation in Skidegate Inlet represents the first definite evidence of volcanism since Middle Jurassic time (Haggart et al., 1989).

Cretaceous sedimentation was terminated by an episode of regional uplift and erosion. An unconformity between uppermost Cretaceous and Paleogene rocks was identified by Lewis (1990), predating the onset of Tertiary sedimentation and volcanism. Lewis (1990) showed that this period was characterized by northeast-directed folding and thrust faulting.

Two recent discoveries of Paleogene strata, one in the Union Port Louis well (Fig. 2) and the other in Long Inlet on southern Graham Island (White, 1990; Haggart, 1991), are evidence that both marine and nonmarine sedimentation occurred in the region during Paleogene time. On Moresby Island, volcanic flows and breccias erupted during the Eocene, marking the onset of a protracted period of Tertiary volcanism (Hickson, 1988, 1989, 1991). These volcanic rocks have the same age and composition as dyke swarms cutting the eastern and northern parts of Moresby Island which appear to be comagmatic, in part, with the Kano plutonic suite (46-27 Ma; Anderson and Reichenbach, 1989, 1991). Souther and Jessop (1991) have proposed a model of Eocene crustal extension to account for local dyke emplacement in the islands.

The Eocene was a time of widespread crustal extension in the Canadian Cordillera (van der Heyden, 1989; Parrish et al., 1988; Tempelman-Kluit and Parkinson, 1986; Friedman and Armstrong, 1988), including the eastern margin of the Coast Plutonic Complex. With new evidence for Eocene extension from the Queen Charlotte Islands, it seems reasonable to speculate that the Queen Charlotte Basin, encompassing large portions of Hecate Strait, Queen Charlotte Sound, Dixon Entrance, and the Queen Charlotte Islands, was revitalized during the Eocene and Oligocene — a time when much of the southern Cordillera was undergoing regional crustal attenuation.

Volcanism and sedimentation continued through the Neogene with great volumes of Masset Formation basalt and rhyolite accumulating on northern and western Graham Island; the volcanic rocks are intercalated with, and overlain by, marine and nonmarine detrital sediments belonging to the Skonun Formation (Hickson, 1988, 1989, 1991; Higgs, 1991; Haggart et al., 1990).

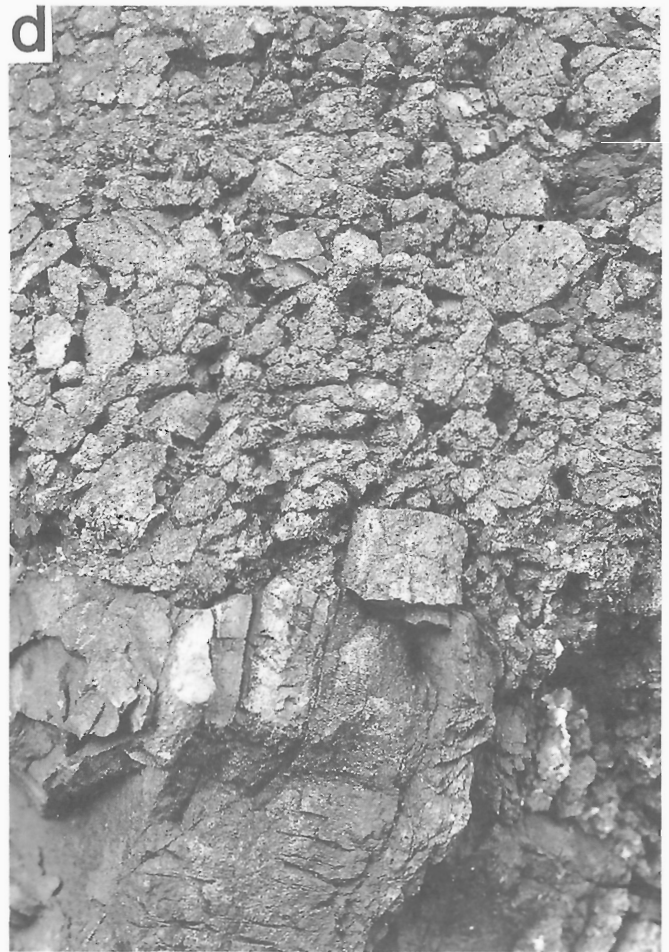
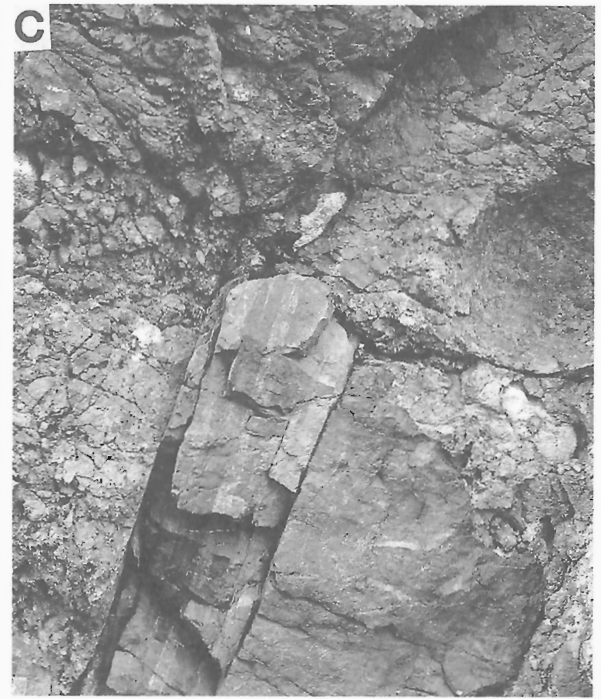
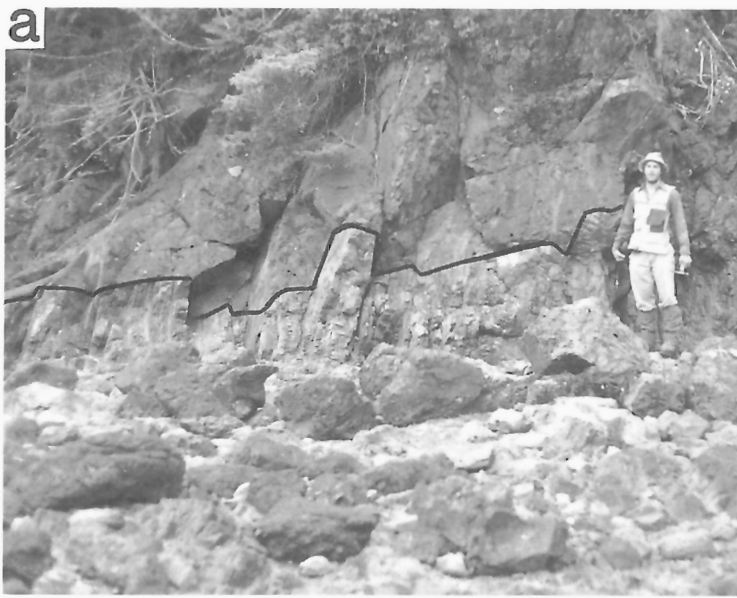


**Figure 6:** (a) Angular unconformity separating Yakoun Group volcanic breccias (above) from Sandilands Formation siltstone (below); (b) upright beds of Sandilands Formation having erosional relief exceeding 0.5 m; (c) infillings of Yakoun Formation clasts showing no clast rotation or interclast shear, and no slip along the unconformity; (d) undeformed interclasts in Yakoun volcanic breccia immediately overlying unconformity.



## MIDDLE JURASSIC DEFORMATION

Southwest-directed compression, beginning just prior to the onset of Middle Jurassic volcanism, produced contraction faults and chevron folds within the Kunga and Maude groups. Evidence of this Middle Jurassic deformation is displayed throughout northern Moresby and southern Graham islands (Thompson and Thorkelson, 1989; Lewis and Ross, 1989; Taite, 1990), as well as on southern Moresby Island (R. Anderson, pers. comm., 1989); we interpret this as a regional deformation event that probably extended well beyond the Queen Charlotte Islands.

Three lines of evidence support Middle Jurassic (pre-Yakoun Group) deformation: 1) an angular unconformity separates Maude Group and older strata from Middle Jurassic Yakoun Group and younger strata; 2) a pluton of Middle Jurassic age intrudes folded Lower Jurassic strata; and 3) the total amount of shortening is greater in the older strata.

On the north shore of Cumshewa Inlet, 2 km west of Dawson Cove (Fig. 5; Thompson and Lewis, 1990a), a sharp angular unconformity separating the Yakoun Group and the Sandilands Formation is exposed (Fig. 6a). Bedding in the Sandilands Formation dips 70° southwest, whereas the overlying breccias of the Yakoun Group dip 30° to the northeast. The unconformity has been stripped clean of any Kunga (and Maude) Group detritus, leaving more than one metre of erosional relief (Fig. 6a). Interpretation of this unconformity as a detachment surface can be ruled out for four reasons: 1) it abruptly and irregularly truncates steeply dipping fold limbs in the Sandilands Formation (Fig. 6b); 2) it has substantial erosional relief; 3) there is no evidence of deformation or slip along the unconformity (Fig. 6c); and 4) the infill of volcanic breccia clasts shows no evidence of interclast deformation or preferred clast orientation (Fig. 6d). The structural disharmony evident across the unconformity must have resulted from deformation prior to deposition of the Yakoun Group, as seen in the complex geometry of faulted chevron folds present just beneath the unconformity (Fig. 7). The stratigraphic relationships at this locality place close time limits on the onset of folding — late in the Early Jurassic or early in the Middle Jurassic.

Time of onset of deformation is further constrained on the south slope of Maude Island (Fig. 5; Thompson, 1990) in Skidegate Inlet where the unconformity separates the Toarcian Whiteaves Formation from the overlying Lower Bajocian Yakoun Group (Jakobs, 1989). Because the youngest map unit of the Maude Group, the Phantom Creek Formation, ranges in age from Toarcian to Aalenian, and because deformation postdated Maude Group deposition, we conclude that folding first occurred during the latest Aalenian and earliest Bajocian. The unconformity is also exposed at other localities (Fig. 5), including the northern and southern shores of Cumshewa Inlet (Thompson and Lewis, 1990a), the south slope of Skidegate Inlet (Thompson, 1990), on Louise Island (Thompson and Lewis, 1990a), and northwest of Mosquito Lake on Moresby Island (Thompson and Lewis, 1990b). At all localities the unconformity separates Kunga or Maude group strata from either the Yakoun Group, the Longarm Formation (Lower Cretaceous), the Haida Formation (upper Lower Cretaceous), or the Honna Formation (Upper Cretaceous); an exception occurs on southwestern Louise Island where Tertiary volcanic rocks lie directly on Kunga Group strata (Fig. 5; Thompson and Lewis, 1990a). Large time-stratigraphic omissions above the unconformity apparently resulted from uplift and erosion during the Late Jurassic, and during the Late Cretaceous or the early Tertiary, or both (described below).

In central Graham Island, Indrelid et al. (1991) mapped northwest-trending contractional faults which emplace Lower Jurassic strata (Sandilands Formation) over Yakoun Group strata. They speculate that these faults were active prior to Cretaceous deposition in

the area. If so, Middle Jurassic shortening extended into, and possibly through, the time of Yakoun Group deposition.

Further evidence for Middle Jurassic deformation comes from Clapp Basin in Shields Bay (at the head of Rennell Sound; Fig. 5) where Anderson and Reichenbach (1991) have mapped a  $168 \pm 2$  Ma pluton crosscutting southwest-vergent folds involving the Pliensbachian Sandilands Formation; this restricts deformation to post-Pliensbachian/pre-Callovian time, consistent with other constraints on the timing of deformation discussed above.

Middle Jurassic deformation is also recognizable in map scale patterns. On northern Louise Island and north of Mosquito Lake (Fig. 5; Thompson and Lewis, 1990a,b) outcrop belts of Yakoun Group volcanic rocks are exposed above structurally thickened successions of the Peril and Sandilands formations. The relatively flat lying unconformity truncates steeply dipping beds.

Map patterns also provide constraints on the size and geometry of individual structures. For example, on northern Louise Island, 1 km southwest of Kitson Point (Fig. 5; Thompson and Lewis, 1990a), steeply dipping to vertical beds of the Peril Formation were traced more than 250 m vertically, to a gently dipping contact with overlying Yakoun Group volcanic rocks. Sandilands Formation siltstone with equally steep dips crops out on either side of the Peril Formation here. This relationship suggests a chevron fold structure having an amplitude exceeding 200 m and a narrow hinge zone formed of Peril Formation beds. Because Sadler Limestone does not occur in the fold hinge, one can speculate that there is a detachment between the Sadler and Peril formations (Lewis and Ross, 1991). A similar geometric relationship occurs on northwestern Louise Island and on the northern and south-



**Figure 7:** Faulted chevron folds in the Lower Jurassic Sandilands Formation.

ern slopes above Mosquito Lake on Moresby Island (Fig. 5; Thompson and Lewis, 1990a,b). Bedding in the Peril and Sandilands formations generally dips steeply, and it is common for beds in both formations to follow steep gullies for hundreds of metres. A chevron fold style satisfies this outcrop pattern. Unfortunately, limited exposure often makes tracing out individual folds difficult.

In Figure 8a-c, equal-area plots of poles-to-bedding support the interpretation of Middle Jurassic folding. Maxima for units older than Middle Jurassic (Fig. 8b) indicate folds in Kunga and Maude group strata have more steeply dipping limbs; maxima for units Middle Jurassic and younger (Fig. 8c) suggest folds in these strata have limbs with

gentle to moderate dips. In both cases, the dominant fold trend is north-northwest.

Total bed-length shortening caused by Middle Jurassic folding is difficult to estimate. Ideal chevron folds with average limb dips of  $60^\circ$  can account for 50% bed length shortening. Lewis and Ross (1991) have measured total finite strain in ammonite impressions found in the Maude and Kunga groups and their analysis suggests up to 20% shortening along a southwest-northeast axis.

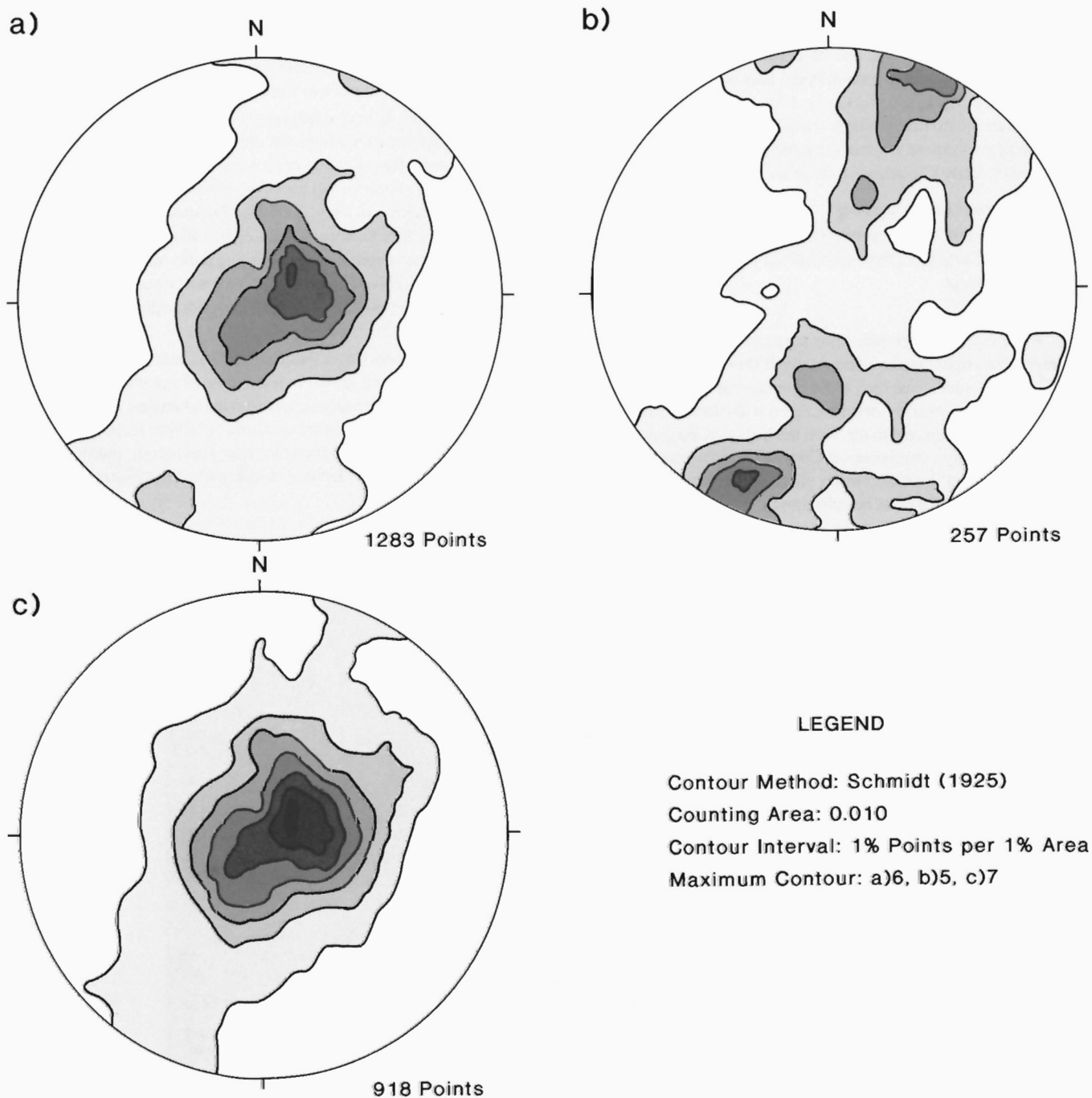


**Figure 8:** (a) Equal-area plot of poles-to-bedding for all stratigraphic units mapped, (b) for Yakoun Group and younger strata, and (c) for the Kunga and Maude groups.



Other manifestations of compression are outcrop-scale thrust faults within the Sandilands Formation (Fig. 9). There are, however, no constraints on when they moved or on how much total shortening they accommodate.

## UPPER JURASSIC AND YOUNGER BLOCK FAULTING AND SEDIMENTATION RESPONSE

Most of Late Jurassic time is represented as a distinct hiatus in the stratigraphic record of the Queen Charlotte Islands. Following the accumulation of Moresby Group strata in the Late Bathonian and Early Callovian no further marine sedimentation occurred in the islands region until the Tithonian (latest Jurassic) when basal strata of the Cretaceous succession were deposited in the northern islands (Haggart, 1989). K-Ar dates from the San Christoval and Burnaby Islands plutonic suites (Anderson and Reichenbach, 1991) show that Late Jurassic time in the islands was one of uplift (Fig. 4). By Early Cretaceous time, at least one pluton in Poole Inlet on Burnaby Island had been unroofed (Anderson and Greig, 1989). Early Cretaceous (Hauterivian/Barremian) marine strata unconformably overlie Late Jurassic plutonic rocks there, evidence that the plutons were emplaced and exhumed by Early Cretaceous time in the southern islands.

### Pre-Cretaceous block faulting

Block faulting accompanied the uplift of Late Jurassic plutons. Exposures in Cumshewa Inlet and Skidegate Inlet readily display this important concept.

#### *Cumshewa Inlet*

A variety of stratigraphic units are exposed in Cumshewa Inlet, more-or-less continuously along its north shore (Fig. 5; Thompson, 1990). At the inlet's east end, extensive outcrops of Yakoun Group volcanic and sedimentary strata occupy a wide area east of the Copper Creek Fault. Adjacent to this fault the Yakoun Group outcrops are locally overlain by a thin veneer of Cretaceous sedimentary strata. The total thickness of Yakoun Group strata east of the Copper Creek Fault is unknown but must be substantial.

Similarly, on the south side of the inlet, especially on the northern side of Louise Island, Yakoun Group strata are also extensive, form-

ing a very thick accumulation similar to that seen on the north shore east of the Copper Creek Fault. On the inlet's south side, however, Yakoun Group strata are overlain by a relatively thick succession of Cretaceous rocks. The important point is that similar, thick accumulations of Yakoun Group strata are found in both areas, on the south shore of the inlet as well as on the north shore east of the Copper Creek Fault.

Along the north shore of the inlet west of the Copper Creek Fault, however, Cretaceous strata, locally variable in thickness, are seen resting unconformably on Jurassic and Triassic rocks, including the Sandilands Formation and older Kunga Group rocks. The thick accumulations of Yakoun Group which characterize the successions east of the Copper Creek Fault and along the south shore of the inlet are missing. Only minor, thin sections of Yakoun Group strata are found locally beneath the Cretaceous strata here, indicating that the Yakoun Group, once much more extensive, was reduced to minor outliers in this part of the inlet prior to Cretaceous deposition.

Thus, two distinct stratigraphic successions characterize different areas of Cumshewa Inlet. On the east and south sides of the inlet, Yakoun strata are present in great thickness, but in the block between these areas Yakoun Group rocks are absent or very thin. Therefore, a second, more westerly fault, the Dawson Cove Fault (Fig. 5, Thompson, 1990; Thompson and Lewis, 1990a,b), is required. Movement along the central block's bounding faults must have elevated the block after it received its blanket of Yakoun Group strata to allow for the subsequent removal of Yakoun rocks prior to deposition of the Cretaceous succession.

The Dawson Cove Fault (Fig. 5) is inferred for most of its length and has been drawn in most areas along the zone separating thick Yakoun Group volcanic rocks on the southwest from thin to non-existent Yakoun strata on the northeast. In a later section we describe how this zone became a focus for Late Cretaceous and/or early Tertiary folding and thrust faulting, due, in part, to reactivation of old basement weaknesses.

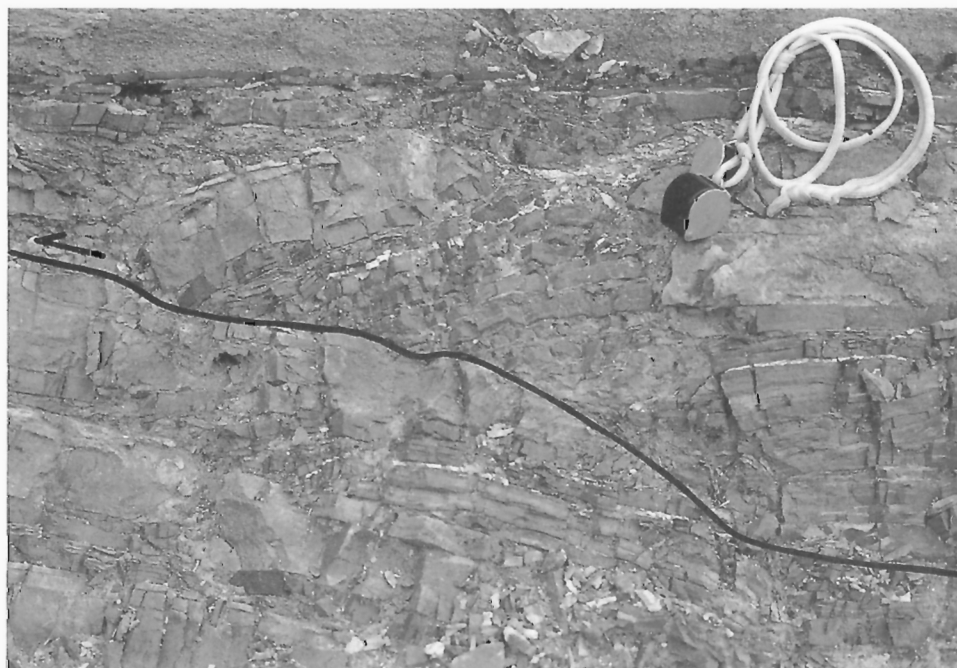


**Figure 9:** Small-scale thrust faults within the Sandilands Formation.

## Skidegate Inlet

Another locality showing evidence of pre-Cretaceous block faulting is in the Skidegate Inlet region (Fig. 5; Thompson, 1990; Thompson and Lewis, 1990b). On the inlet's south shore, near Alliford Bay, the Macmillan Creek and Saachs Creek faults define a narrow block exhibiting a thick Yakoun Group succession overlying strata of the Maude Group. Overlying the Yakoun Group is a thin veneer of Cretaceous strata. East of the Saachs Creek Fault, Cretaceous rocks overlie a thick succession of Yakoun and Moresby groups (Fig. 10a-e).

In contrast, the area west of the Macmillan Creek Fault is composed of a thick succession of Cretaceous sandstone overlying Kunga Group strata; no Moresby or Yakoun group strata have been identified here. The Yakoun and Moresby sequences which were originally present west of the Macmillan Creek Fault must have been removed prior to the onset of Cretaceous deposition. Similarly, the succession of Moresby Group strata originally present between the Saachs Creek and Macmillan Creek faults must also have been eroded. Substantial (more than 1 km of offset) Late Jurassic movement along the Macmillan Creek Fault resulted in the stripping of the entire Middle Jurassic sequence from the region just to the west, and lesser movement on the Saachs Creek Fault resulted in the stripping of only the Moresby Group from the narrow block bounded by the two faults (Fig. 10e).

Thus, the pre-Cretaceous surface topography was strongly influenced by Late Jurassic block faulting. Local deposition of Cretaceous strata must have been controlled in part by this underlying block-fault topography.

### Cretaceous sedimentation

Cretaceous time saw the accumulation of one of the more important components of the Queen Charlotte Islands stratigraphic succession, for Cretaceous strata have been identified as potential reservoir strata in the basin and locally are known to directly overlie the older Mesozoic source rocks. Details of the nature of the Cretaceous depositional system are discussed in another paper in this volume (Haggart, 1991).

### Cretaceous transgression

Cretaceous strata in the Queen Charlotte Islands are readily divided

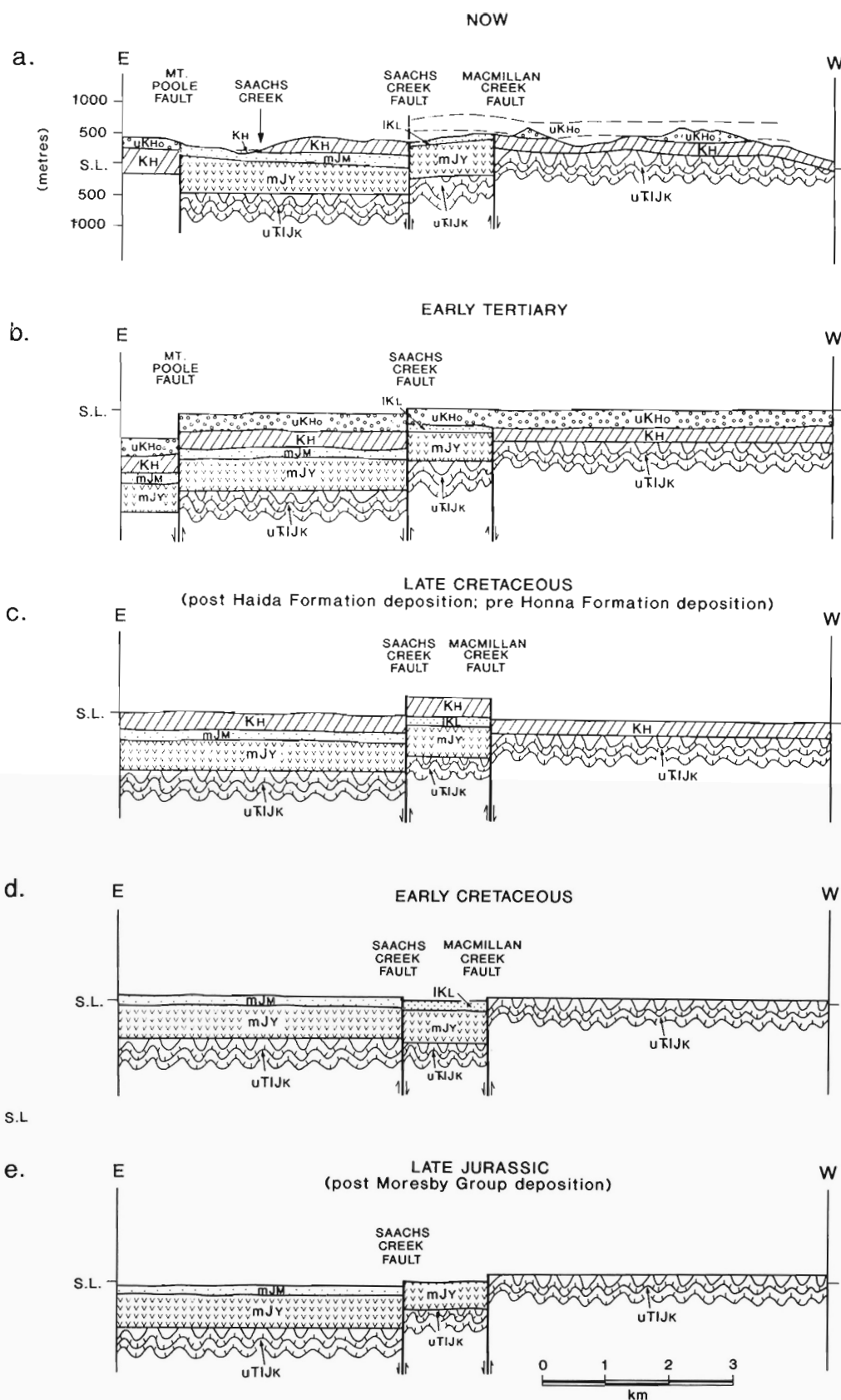


**Figure 10:** Cross-sections, south slope of Skidegate Inlet (see Fig. 5 for location). (a) Present geological relationships; (b) during the Tertiary after deposition of the Honna Formation; (c) during the Late Cretaceous just before deposition of the Honna Formation; (d) during the Early Cretaceous just after deposition of the Longarm Formation; and (e) during the Late Jurassic after deposition of the Moresby Group.

into conglomerate and sandstone of shallow-marine origin (inner shelf environments), deeper water shale (outer shelf and slope settings), and turbiditic sandstone and shale and conglomerate which accumulated in sediment distribution networks and submarine fan settings (Haggart, 1991). Most of the Cretaceous succession reflects shelf deposition in a relatively stable tectonic setting.

The basal strata found in complete sections of Cretaceous rocks unconformably onlap older Jurassic and Triassic strata and plutonic rocks. These Cretaceous strata, typically sandstone and pebble-cobble-boulder conglomerate, reflect deposition in shallow-water environments as the initial response to local sealevel rise (Haggart, 1991). Sections fine upward into siltstone and shale, locally with turbidites, reflecting a gradual deepening of marine waters in response to continued inundation. The general fining-upward sequence of lithofacies which is present in all the Cretaceous sections constitutes a transgressive sequence.

The stratigraphic record in the islands indicates that transgression and consequent sedimentation proceeded without interruption through the Cretaceous until the Turonian or Coniacian. At this time extensive fan deposits (conglomerate and sandstone) of the Honna Formation rapidly prograded into the basin from the east. Several hypotheses have been proposed to explain this progradational event, including Late Cretaceous thrust faulting and eustatic sealevel fall. A combination of tectonic factors and sealevel effects is probably the most likely explanation (see Haggart, 1991 for summary and discussion).

Plots of the position of the shoreline at successive time intervals show that the direction of Cretaceous transgression was generally eastward (Haggart, 1991). The earliest record of this transgression in the northern part of the islands is latest Jurassic (Tithonian) while in the southern islands region the oldest strata yet identified are of Hauterivian/Barremian age.

On a regional scale deposition of the Cretaceous sediments appears to have been essentially continuous over a large area. The widespread distribution of Cretaceous rocks reflects subsidence in an extensive and continuous basin during a period of general tectonic stability and quiescence, at least relative to the Late Jurassic.

However, local variability in sediment thicknesses, disconformities within the Cretaceous succession, and irregularities in paleogeographic interpretation all point to additional, local, controls on sedimentation type and rate. The geology of several localities on the islands indicates that the localized block faulting which was prominent during Late Jurassic time apparently continued through the Cretaceous as well, although likely of lesser magnitude and extent. We present evidence below of block faulting activity which occurred during deposition of the Cretaceous succession; such activity must have significantly influenced sedimentation on the local scale.

#### *Late Jurassic structural controls*

The underlying topography established by Late Jurassic block faulting influenced the distribution of Cretaceous sedimentation and the thickness of sediment that accumulated in local areas. Some areas must have been elevated significantly above Cretaceous shorelines; today they support little or no Cretaceous strata but are surrounded by Cretaceous sandstone. In other areas condensed sequences are found, suggesting these locales were submarine topographic highs which most Cretaceous sediment bypassed in favour of deeper and quieter water environments nearby.

Such a pattern is displayed in the western Skidegate Inlet area. On the north side of the peninsula forming the southeast corner of Sandilands Island (Fig. 5; Thompson and Lewis, 1990b) a thin succession of Haida Formation sandstone unconformably overlies Upper Triassic Peril Formation. A short distance to the north (presumably rep-

resenting a thin section of Haida strata) a thick accumulation of Honna Formation conglomerates crop out. The conglomerates can be traced to the south and west where they are apparently in unconformable relationship with the Upper Triassic Sadler Limestone.

Several kilometres to the north, on the south shore of Maude Island (Fig. 5; Thompson, 1990) a considerably greater thickness of Haida Formation sandstone is associated with a thin section of Haida Formation shale. The same pattern is seen on Lina Island (Fig. 5) and along the shore of Bearskin Bay, where the sections of both Haida Formation sandstone and shale reach great thicknesses. The Cretaceous section in Skidegate Inlet thus thickens to northward, as one moves away from the topographic high which must have been present at Sandilands Island.

An additional example of block fault control on Cretaceous sedimentation is seen on Moresby Island north of Cumshewa Inlet (Fig. 5; Thompson, 1990). The Copper Creek Fault can be traced from the shore of the inlet, just east of McLellan Island, for a long distance across the Island to the northwest. The fault appears to mark the general eastward limit of Cretaceous deposits. The block to the east of the fault is composed completely of Yakoun Group strata with only a thin veneer of possible Cretaceous strata preserved at one locality.

Based on the model of eastward-directed transgression, Haggart (1991) suggested that Cretaceous deposits older than Middle Albian will not be found east of the region of the fault. Cretaceous rocks of very shallow marine character are found essentially onlapping the Yakoun Group in the immediate vicinity of the fault. It thus appears likely that Cretaceous deposition east of the fault, if it occurred, was nonmarine. The block east of the Copper Creek Fault appears to have acted as a topographic high limiting further Cretaceous deposition to the northeast.

#### *Cretaceous block faulting*

Although Cretaceous deposition was widespread and continuous on a regional scale, at local levels disruptions apparently occurred in this regime. Evidence for such disruptions is preserved in the geological map patterns; they indicate that the block faulting which characterized the Late Jurassic apparently continued through the Cretaceous. Because of the lithological similarity of most of the Cretaceous rocks and the typically poor fossil control for many outcrops, stratigraphic evidence for local discontinuities within most sections of the Cretaceous rocks is generally not available.

The significant lithologic contrast between the conglomerates of the Honna Formation and the rest of the Cretaceous, and indeed the Mesozoic, succession in the islands, however, does provide a readily recognizable horizon that can be studied at many localities. Stratigraphic and sedimentologic evidence indicate that the Honna Formation conglomerates are generally conformable within the Cretaceous succession (Haggart, 1991). There are several localities, however, where the relationship of the Honna conglomerates on underlying rock units strongly supports an interpretation of intra-Cretaceous disconformity.

The origin of these apparent disconformities is problematic. Some of the observed map patterns showing Honna Formation conglomerates overlying older Cretaceous units, such as the broad belt from Skidegate Channel southeast to Cumshewa Inlet where the Honna Formation is mapped overlying Longarm Formation, likely result from poor faunal control and inability to precisely differentiate the ages of the Cretaceous outcrops.

The evidence seen at some other localities, though, is more compelling. The evidence for Late Jurassic block faulting in the area south and southeast of Alliford Bay (Thompson, 1990; Thompson and Lewis, 1990b) is described above. Further study of outcrop relationships in the region bounded by the Saachs Creek and Macmillan

Creek faults (Fig. 5) shows that in this area the Cretaceous succession as well has been modified by apparently syndepositional block faulting (Fig. 10d). The block defined by the two faults supports a thin succession of Cretaceous sandstone on its top, of Barremian/Aptian age; these sandstones crop out at the 375 m (1200 ft.) level. Both west and east of the block's bounding faults, however, a thick succession of Cretaceous sandstone and shale of Albian and younger age crops out at the 200 m (600 ft.) elevation. The entire region is blanketed by conglomerate of the Honna Formation, which is not offset by the Macmillan Creek Fault (Fig. 10b). Thus, the block, with its older Cretaceous stratigraphy, must have been elevated relative to the adjoining terrain, after deposition of the Barremian/Aptian sequence but prior to deposition of the Honna conglomerates (Fig. 10c).

A second problem area is on the east facing slopes approximately 8 km southwest of Sandspit. Here, Honna Formation conglomerates directly overlie Yakoun Group volcanic rocks. If the Honna Formation were conformable within the Cretaceous succession at this locality what has happened to the older Cretaceous sequence?

Map relationships in Cumsheewa Inlet show that the Honna Formation there locally overlies pre-Yakoun and even Triassic rocks. On the inlet's north shore, 0.5 km north of Duval Rock, the Honna Formation conglomerates unconformably overlie steeply dipping *Monotis*-bearing beds of the Peril Formation (Fig. 11). On the south side of the inlet, 2 km west of Kitson Point, the Honna Formation overlies strata of the Sandilands Formation unconformably.

While the Skidegate Inlet example (Fig. 10c) clearly indicates some component of Cretaceous block fault activity, evidence for block faulting at the other localities is not so distinct. It is possible that observed map relationships at these localities may reflect underlying sedimentological controls. For example, the Honna conglomerates are considered to have rapidly prograded into the Cretaceous depositional basin during the Turonian to Coniacian and this event appears correlative with a worldwide sealevel drop of several hundred metres (Haggart, 1991). Such a drop would have significantly lowered erosional base level, potentially resulting in extensive local reworking of previously deposited Cretaceous sections. The effects of such re-

working would have been concentrated in the shallow areas of the basin, where the interaction between marine and nonmarine deposition was greatest. Conformable deposition would have continued in the deeper reaches of the basin, to westward. It is interesting to note that most of the localities with Honna Formation resting on older Cretaceous or sub-Cretaceous units occur in the eastern part of the outcrop area, presumably closer to the eastern edge of the basin and thus more responsive to base level changes.

### Tertiary block faulting

Evidence for Tertiary block faulting occurs on the peninsula separating Lagoon Inlet from Sewell Inlet (Fig. 5; Thompson and Lewis, 1990a). There, Honna Formation conglomerate is juxtaposed against early Tertiary volcanic rocks along an east-west trending fault. Both the conglomerate and the volcanic rocks overlie the same substrata — Cretaceous shale of the Skidegate Formation. This implies that the block on the north side of the fault was high prior to volcanism and its cover of Honna Formation conglomerate was removed. This event must have been followed by subsequent uplift of the southern block *after* volcanism to juxtapose the volcanic rocks against the Honna Formation conglomerates and at the same time remove the volcanic rocks from the southern side. Alternatively, the uplifted southern block may have been the southern flank of a structural graben within which the volcanic rocks accumulated.

Another example of probable Tertiary block faulting, although timing constraints are poor, is found south of Alliford Bay where the Mount Poole Fault cuts the conglomerates of the Honna Formation (Thompson, 1990). Interestingly, this east-side-down fault is parallel to the Sandspit Fault, a Tertiary growth fault bordering the eastern limit of northern Moresby Island (Sutherland Brown, 1968). We speculate that the Mount Poole Fault may be a small, on-land analogue of the Sandspit Fault. Other faults having similar north-northwest trends include the Maude Island Fault, and two north-northwest-trending extensional faults at Lina Narrows (Fig. 5; Thompson, 1990; P. Lewis et al., 1990). In all cases, these are east-side-down faults that may be small scale analogues of the Sandspit Fault.

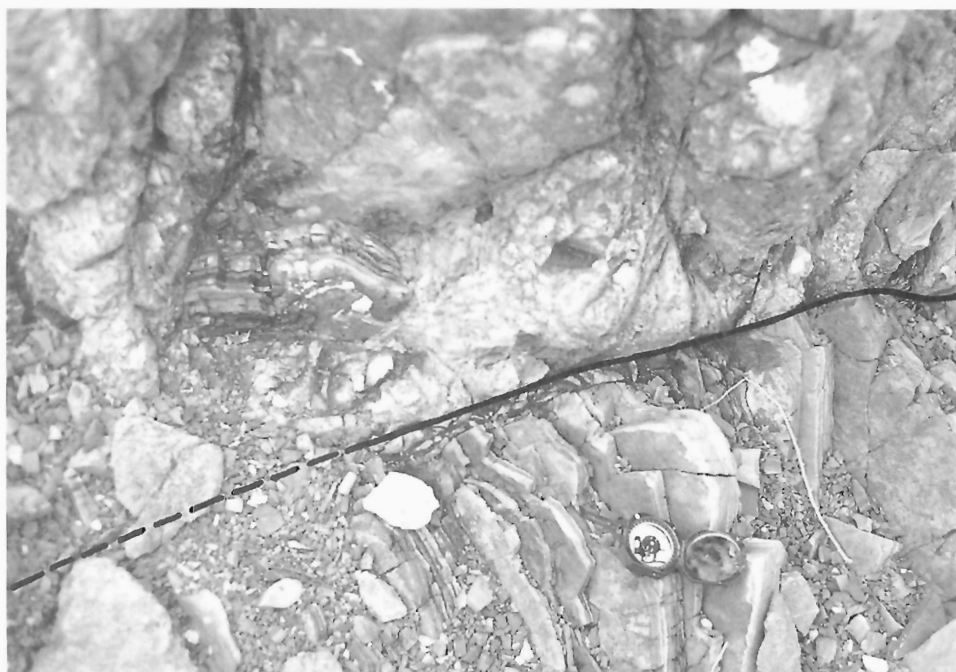


**Figure 11:** Unconformity between vertically-dipping *Monotis*-bearing Peril Formation limestone and Honna Formation conglomerate.

## LATE CRETACEOUS/EARLY TERTIARY FOLDING AND THRUSTING

Until the 1989 field season, the time of folding and thrusting of Cretaceous rocks was loosely constrained as Late Cretaceous or Paleocene. It now appears that there were four distinct episodes of deformation within this time period (Lewis, 1990): 1) northeast-directed shortening, in Late Cretaceous to early Tertiary time; 2) extensional block faulting, postdating the above shortening but pre-dating deposition of Eocene/Oligocene sediments; 3) northeast-directed shortening, in Oligocene time; and 4) post-Oligocene block faulting, possibly synchronous with extensional structures which cut Neogene strata in Hecate Strait. This sequence of structural events is based on contact relationships exposed east of Long Inlet adjacent to Mount Seymour (Fig. 5; Lewis, 1990).

Folds and thrust faults affecting strata as young as Paleogene can be traced from Louise Island across northern Moresby Island into central and western Graham Island. Deformation is most intense in a 5-10 km-wide belt extending from Louise Island to Long Inlet and from there to Rennell Sound. Farther east, on northern Moresby Island, the region is broadly folded. Thrust faults verge northeast on Louise Island, and southwest on northern Moresby Island, between Mosquito Lake and Skidegate Narrows, and on southern Graham Island. In some instances, thrust faults are spatially associated with tight folds. For example, at Kitson Point in Cumshewa Inlet, Longarm Formation beds are thrust northeast over steeply dipping to overturned Honna Formation strata (Fig. 12a).

In earlier publications (Thompson, 1988; Thompson and Thorkelson, 1989) we referred to the belt of most intense folding and faulting as the Rennell Sound Fold Belt. We have abandoned this usage as misleading because it suggests Tertiary deformation is restricted to that narrow zone. Results from Sewell Inlet (Taite, 1990) and central Graham Island (Hesthammer et al., 1989; Indrelid et al., 1991; P. Lewis et al., 1990) show that Tertiary deformation was also important in areas distant from the belt.

From northeastern Louise Island to near Skidegate Narrows, Late Cretaceous and/or Tertiary folds are coaxial with Middle Jurassic folds; at Skidegate Narrows they diverge, the older structures bending west-northwest and the younger ones continuing northwest to Rennell Sound (Fig. 5; Thompson and Lewis, 1990b; P. Lewis et al., 1990). We speculate that the divergence was controlled by a zone of basement weakness coincident with the Dawson Cove Fault. Because the Dawson Cove Fault postdates Middle Jurassic deformation, it would have had no effect on those structures.

An example of this possible interrelation between pre-existing faults and younger structures occurs at Kitson Point (Figs. 5 and 12; Thompson and Lewis, 1990a), where the hanging wall block, consisting of a thick succession of Longarm and Yakoun strata is thrust over a footwall block consisting of Honna Formation conglomerate, Longarm Formation, and Kunga Group. There is an obvious stratigraphic omission within the footwall block. In our interpretation (Fig. 12), pre-Honna Formation movement on the Dawson Cove Fault accounts for the stratigraphic omission (Fig. 12c), and Late Cretaceous and/or Tertiary reactivation of the Dawson Cove Fault produced the fold(s) (Fig. 12b) that were precursory to the Renner Point and Kitson Point thrust faults (Fig. 12c).

The trend of Late Cretaceous and/or early Tertiary contractional structures is consistently north-northwest on both Graham Island and northeastern Moresby Island (Fig. 5; Hesthammer et al., 1989; Indrelid et al., 1991; P. Lewis et al., 1990). However, in the Sewell Inlet area west of Louise Island, trends are east-west and north-south (Fig. 5; Thompson and Lewis, 1990a; Thompson and Thorkelson, 1989; Taite, 1990). On the south side of Sewell Inlet, north of Trotter Bay,

two pre-Tertiary thrust faults are interpreted to cause south to north repetition of the Honna and Skidegate formations. We do not know how or if this pattern relates to northwest-trending structures. Taite (1990) was not able to map these thrusts farther to the west. Stratigraphic repetition of conglomerate units within the Honna Formation is an alternative interpretation requiring further investigation.

## BASIN EVOLUTION: STYLES AND CONSTRAINTS

### Mesozoic history

Basin evolution underwent a profound change in the Middle Jurassic with the onset of regional deformation. Upper Triassic and Lower Jurassic Wrangell Terrane strata were deposited on a stable, slowly subsiding shelf that extended well beyond the areal limits of the Queen Charlotte Basin. Near continuous deposition is reflected in the remarkable time-stratigraphic completeness of the Upper Triassic

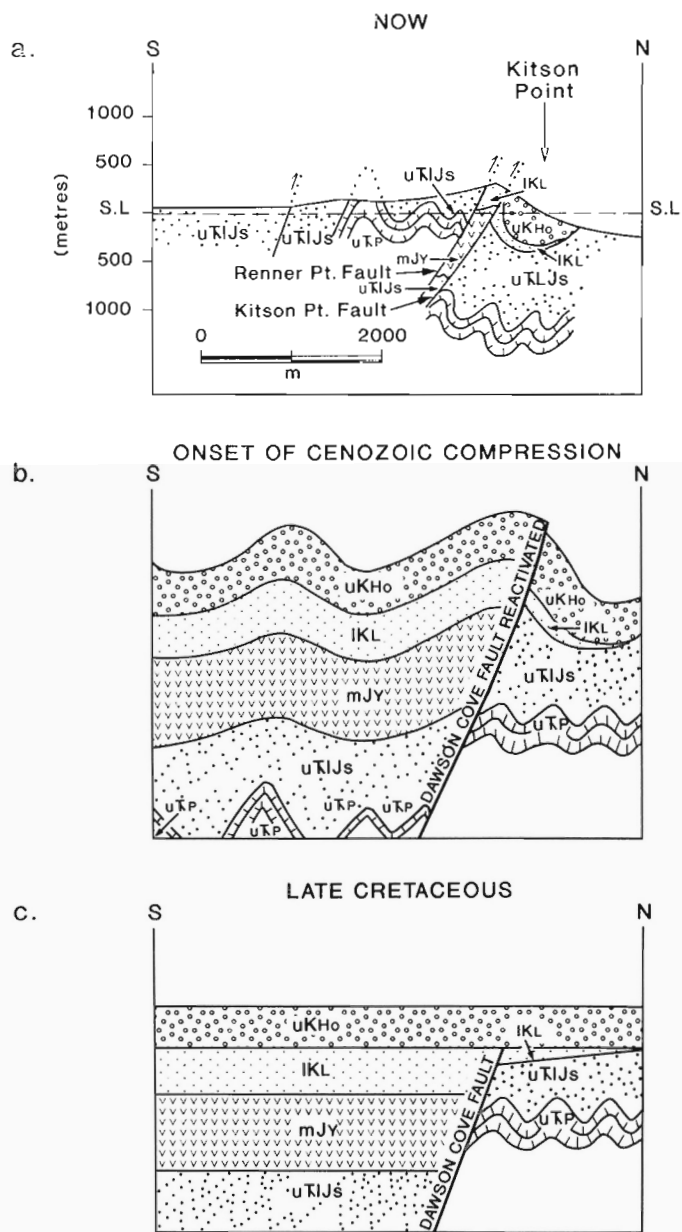


**Figure 12:** Cross-sections showing structural relationships at Kitson Point (see Fig. 5 for location). (a) Present; (b) during the Late Cretaceous or early Tertiary; and (c) during the Late Cretaceous just after deposition of the Honna Formation.



and Lower Jurassic succession (Tipper et al., 1991). The regional continuity of rock units attests to the widespread nature of this deposition. A slow, uniform subsidence rate in combination with gradually increasing water depth is reflected in the change through time of stratigraphic facies, from inner-shelf carbonates to outer-shelf carbonaceous limestones to fine-grained clastics.

This stable basin was replaced by widespread folding, thrust faulting, uplift, and erosion in the Late Aalenian and Early Bajocian. When deposition recommenced, the Wrangellian shelf formed part of a new tectonic setting within a volcanic arc: the Queen Charlotte Basin. Early in the Late Jurassic, eastward migration of the magmatic front left the Queen Charlotte Basin within a forearc setting, where it thus remained until early in the Tertiary. The thick succession of Middle Jurassic Yakoun Group volcanic breccias, flows, and sandstones formed an extensive intrabasinal source for succeeding clastic successions; feldspatholithic sandstones would dominate the stratigraphic record. Late Jurassic uplift, which led to the unroofing of some plutons on southern Moresby Island, was accompanied by block faulting on northern Moresby Island and southern Graham Island. Renewed deposition in latest Jurassic and Cretaceous time produced two fining-upward clastic successions, reflecting two cycles of marine transgression (Haggart, 1991). Some block fault activity continued into the Cretaceous and influenced the thickness and facies of those strata on a local scale.

### Paleogene history

The recent discovery of Eocene and Oligocene strata on the Queen Charlotte Islands, near Long Inlet and in the Union Port Louis well (Fig. 2; Haggart et al., 1990; White, 1990; Haggart, 1991), is significant because it demonstrates that deposition was largely continuous from the Cretaceous into the Tertiary. But the Tertiary did bring one important change, the renewal of volcanism and plutonism. Volcanism was episodic, beginning late in the Cretaceous with a local event found interstratified with the top of the Honna Formation (Haggart et al., 1989), and becoming widespread and voluminous during the Paleogene and the Neogene (Hickson, 1988, 1989, 1991).

During the Tertiary, the Queen Charlotte Basin must have been physiographically complex. Areas of localized nonmarine sedimentation and volcanic activity were transitional, both geographically and through time, with marine environments. Eocene/Oligocene deposits, principally nonmarine and locally including coals, have been identified at several localities (Haggart et al., 1990; White, 1990). Marine molluscs of Miocene age occur locally in the Skonun Formation (Addicott, 1978; Higgs, 1991) on eastern and northern Graham Island and Higgs (1989) has demonstrated local interfingering of nonmarine and shallow-marine deposits in this formation. Nonmarine deposits of likely mid-Miocene age have also been identified from south-central Graham Island (Haggart et al., 1990), where they are interstratified with volcanics.

There is no particular reason to suspect that the present margin of the Queen Charlotte Islands was also the Paleogene (or earlier) margin. The presence of thick Paleogene shales, sandstones, and volcanic rocks, of shallow-marine(?) and nonmarine aspect in the Union Port Louis well (White, 1990), and nonmarine shales with coal in the Long Inlet area (Haggart, 1991), suggest that the Paleogene margin was likely farther west.

We speculate that basin evolution during the Tertiary may have been strongly influenced by Eocene extension. On the Queen Charlotte Islands, Eocene extension is manifest as dyke swarms (Souther, 1988, 1989; Souther and Bakker, 1988; Souther and Jessop, 1991) and this extension appears to have been contemporaneous with an episode of regional extension which affected a large part of south-central British

Columbia (Tempelman-Kluit and Parkinson, 1986; Parrish et al., 1988) and the eastern Coast Plutonic Complex (van der Heyden, 1989; Friedman and Armstrong, 1988). This is also the time when plate interactions at the continental margin changed from convergent to transcurrent regimes (Stock and Molnar, 1988; Engebretson et al., 1985; Hyndman and Hamilton, 1991).

The accumulations of Eocene-Oligocene strata found in the islands are sufficiently thick that they probably once were far more widespread than they are today. Time-stratigraphic equivalents may have underlain all, or parts of, Hecate Strait and Queen Charlotte Sound. Many of the half-graben structures imaged by a recent seismic reflection experiment in the offshore (Rohr et al., 1989; Rohr and Dietrich, 1991) may have been initiated during Eocene and Oligocene time. There is no biostratigraphic evidence available to test this notion, but the paucity of palynomorphs from the Union Port Louis well suggests that a lack of data may be the problem. A complicating factor — Late Cretaceous and/or early Tertiary folding and thrusting — may also have influenced early Tertiary depositional patterns. For instance, uplift associated with Late Oligocene deformation could have resulted in erosion of Eocene and Oligocene strata but we have no data to assess this hypothesis. Clearly a thorough paleontologic re-examination of existing well cuttings for evidence of Paleogene or older strata is required.

### Constraints on basin evolution

Our interpretation of basin evolution in the Queen Charlotte region differs from that of Yorath and Chase (1981) and Yorath and Hyndman (1983) in several important ways. First, we do not view the Sandspit-Rennell Sound faults as the boundary separating the Wrangell and Alexander terranes. Second, we do not interpret Cretaceous and Tertiary stratigraphy in terms of a three-part suture, post-suture and rift succession. Third, we find no support for the notion that Queen Charlotte Sound formed separate of, and much earlier than, Hecate Strait. And fourth, our data do not support crustal flexure as the mechanism controlling formation of Hecate Strait.

There are three reasons for suggesting there is no Late Jurassic-Early Cretaceous suture between the Wrangell and Alexander terranes along the Rennell Sound-Sandspit fault systems: 1) Wrangell Terrane rocks are present on the eastern side of Hecate Strait on Bonilla Island (Woodsworth, 1988); 2) sedimentological and structural evidence is lacking (Haggart, 1991); and 3) a pluton of late Paleozoic age in southeastern Alaska crosscuts both the Wrangell and Alexander terranes (MacKevett et al., 1986; Gardner et al., 1988), evidence that the terranes had been amalgamated by Late Paleozoic time.

Yorath and Chase (1981) interpreted the Longarm Formation as a suture assemblage. But within the proposed suture zone on the Queen Charlotte Islands, Longarm strata onlap toward the northeast across a basement topography locally controlled by syndepositional block faulting. The Longarm is not restricted to a narrow "graben-like trough" as previously interpreted (Sutherland Brown, 1968; Yorath and Chase, 1981), and the postulated belt of deep water turbiditic facies extending from Cumsheewa Inlet northwestward through Long Inlet (Yorath and Chase, 1981) is, in reality, shallow water in nature (Haggart, 1989, 1991). A suture assemblage would presumably contain elements of both the Wrangell and Alexander terranes. We have recognized clasts from the Kunga, Maude, and Yakoun groups, and granitics derived from Middle Jurassic plutons, but nothing to suggest that the Alexander Terrane was a source (this fact was also noted by Yorath and Chase, 1981). Other elements one might expect along a suture, such as a regressive succession characterized by a flysch to molasse sequence produced from rapid basin infilling, a tectonic melange, remnants of oceanic crust, high pressure metamorphic



assemblages, and folds and thrusts of Late Jurassic or Early Cretaceous age, are lacking. Potential field data do not image a crustal suture (Lyatsky, 1991; Sweeney and Seemann, 1991), and new seismic reflection data have failed, as yet, to show definite evidence for one (Rohr and Dietrich, 1991).

Because the remainder of Cretaceous deposition did not differ significantly in style or facies from the Longarm Formation deposits, we do not characterize it as a post-suture assemblage. Rather, later Cretaceous deposition essentially mirrored the stable-shelf setting of earlier Cretaceous time. The subsequent initiation of Paleogene sedimentation may have been related to Cordillera-wide Eocene extension as discussed above; we see this as an important event in the ongoing evolution of the Queen Charlotte Basin.

The Harlequin well, drilled near the centre of Queen Charlotte Sound (Fig. 2), is the only offshore well in which Tertiary strata of Early Miocene age have been confirmed; the remainder of the wells intersect Late Miocene and younger strata (Patterson, 1988a,b; Shouldice, 1971). On the strength of this fact, and the assumption that no Tertiary sediments older than Late Miocene were known from the Queen Charlotte Islands or Hecate Strait, Yorath and Hyndman (1983) proposed that Queen Charlotte Sound formed earlier than Hecate Strait, through crustal attenuation during the Late Oligocene and Early Miocene (22–17 Ma). This was followed by thermal subsidence during the Miocene (17–9 Ma), when the basin filled with sediment. The amount of crustal attenuation — over 300%, or approximately 70 km in a north-south direction — was based on estimates of right lateral strike-slip offset on the Louscoone Inlet Fault system.

Our mapping suggests that there is no discernible offset along the northern part of this fault system. Paleogene volcanic rocks can be projected across one of the strands of this fault system in Selwyn Inlet, with no evidence of offset. Farther north, Triassic and Jurassic strata project from Louise Island west onto Moresby Island, across the trace of the fault strand, again without offset. Other strands of the Louscoone Inlet Fault system shown by Sutherland Brown (1968) along the east side of Louise Island have not been found. A myriad of steeply-dipping faults do cut the Karmutsen Formation, but they are not strike-slip faults and they do not have an appropriate orientation. Stratigraphic and structural contacts which trend northwest across central and northern Louise Island are also not offset. Thus, our mapping does not support the notion that rifting in Queen Charlotte Sound is linked, mechanically, to strike-slip faults on the Queen Charlotte Islands. Yorath and Hyndman (1983) based their estimate of crustal attenuation beneath Queen Charlotte Sound ( $\beta = 3.3$ ) on the 70 km of strike-slip they interpreted along the Louscoone Inlet Fault; our data suggest that an alternative approach to estimating crustal attenuation is required.

We also find it difficult to accept the suggestion that the Sandspit Fault is the offset continuation of the Louscoone Inlet Fault. This interpretation is based on the notion that the so-called Rennell Sound Fault system is a right-lateral strike-slip fault system, linked to crustal rifting in southern Hecate Strait during the Middle Miocene (Sutherland Brown, 1968; Yorath and Chase, 1981; Yorath and Hyndman, 1983). The Honna Formation conglomerate overlaps all postulated strands of the fault system (Thompson, 1990; Thompson and Lewis, 1990b), and kinematic indicators on faults in Rennell Sound suggest down-dip displacement, rather than strike-slip (Lewis and Ross, 1991). The main strand of the Rennell Sound system proposed by Sutherland Brown (1968) is the Dawson Cove Fault, which we interpreted above as a Late Jurassic and Cretaceous block fault. There is no evidence in the area of Cumsheewa Inlet, Skidegate Narrows, Long Inlet, or Rennell Sound to suggest that strike-slip faulting was an important deformation mechanism during the Late Tertiary or earlier.

Higgs (1989, 1990b, pers. comm.) suggested that horizontal slickensides seen on brittle fractures in the Cumsheewa Inlet area are evidence supporting strike-slip. We raise several objections to his interpretation of this field observation. First, slickenside lineations relate to only the latest offset along a fracture, and tell nothing of the cumulative offset along that surface. Second, mesoscopic faulting with subhorizontal slip directions is not limited to areas adjacent to regional strike-slip faults. The orientation and slip direction of mesoscopic faults is related primarily to the local orientations of the principal stress directions and rock anisotropies. Steeply-dipping fractures with subhorizontal slip would be expected where the maximum and minimum principal stress directions are horizontal, and the intermediate principal stress direction is vertical — a condition common to both regional strike-slip fault zones and compressional regimes. Indeed, mesoscopic fractures with subhorizontal offset are well-documented features in the Rocky Mountain Fold and Thrust Belt where strike-slip faulting is essentially absent (Price, 1967; Bielenstein, 1969).

Finally, Hecate Strait was interpreted by Yorath and Hyndman (1983) to have formed as a result of crustal flexure associated with underthrusting along the western margin of the Queen Charlotte Islands: upward deflection of the plate margin caused downward deflection of the plate interior (i.e., Hecate Strait). They proposed that underthrusting of the Pacific Plate beneath the Queen Charlotte Islands began about 6 Ma ago resulting in an uplifted continental edge. The flexure model predicts that 5–7 km of covering rocks have been stripped from the western margin of the islands, and that the null point (the point where deposition would begin) is 15 km east of the present trace of the Sandspit Fault.

Our mapping suggests that none of these points is valid. Structure contours drawn at the level of the Kunga Group (Fig. 13) indicate that the level of exposure is the same across northern Moresby and southern Graham Island; this suggests there is no west-to-east dip of the Kunga Group across the islands. This conclusion is also supported by burial history studies by Vellutini (1988). For example, the thickness of eroded section calculated for the Union Port Louis well, located on the western margin of Graham Island (Fig. 2), is 1685 m; that eroded from the Nadu River No. 1 well, located 65 km farther east, is 1160 m. The difference in amount of eroded section between these wells is only 600 m — a thickness equal to the difference in topographic relief between the two areas. This supports Hickson's (1991) interpretation that the topography on the west side of Graham Island is constructional, formed by accumulation of the subaerial Masset Formation volcanic pile, rather than resulting from crustal flexure. Vitrinite reflectance results from the Tow Hill No. 1 well, located 95 km northeast of the Union Port Louis well (Fig. 2), support this interpretation as well: there, 985 m of section were eroded, 700 m less than from the Union Port Louis well. Farther south, in Rennell Sound, eastern Skidegate Inlet (Onward Point), and in Cumsheewa Inlet, 1725 m, 1500 m, and 1985 m of section were eroded, respectively — values near those calculated for the Union Port Louis well. The most significant difference in amount of eroded section — up to 800 m — occurs between the Nadu River No. 1 well, and the Cape Ball, Gold Creek No. 1, and Tlell No. 1 wells on east central Graham Island (Fig. 2).

The structure contour data (Fig. 13), when combined with the burial history data of Vellutini (1988), and the regional mapping of Hickson (1991) suggest that Graham Island and northern Moresby Island experienced little or no eastward tilt during the Pliocene.

The outcrop evidence of Eocene, Oligocene, and Miocene strata, the lack of geological evidence for west to east regional tilt, and the burial history analysis derived from vitrinite reflectance measurements (Vellutini, 1988) leave little room for the interpretation that

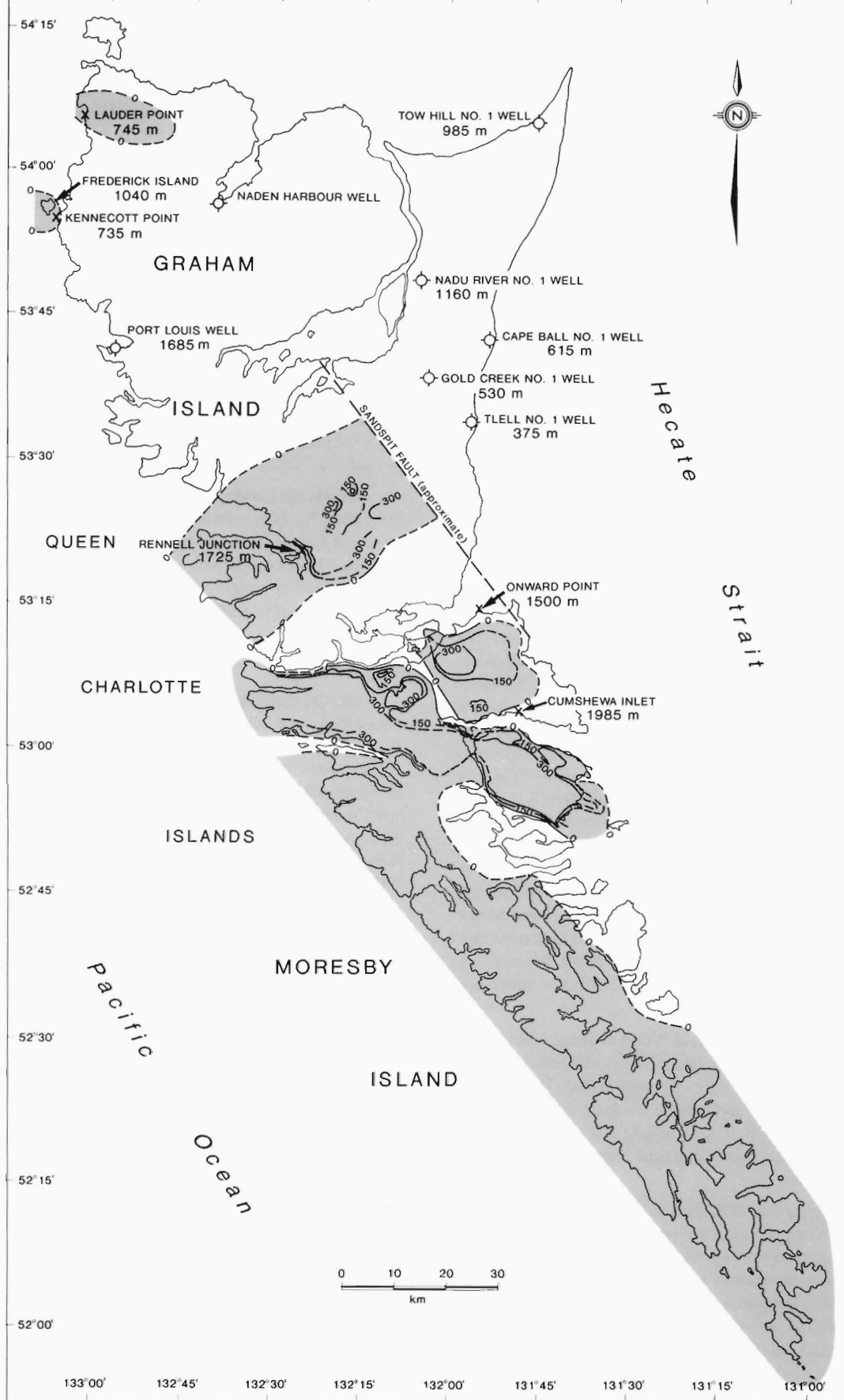


**Figure 13:** Generalized structure contour map drawn on the top of the Kunga Group (150 m contour interval; compiled from Thompson and Lewis, 1990a,b; Thompson, 1990; P. Lewis et al., 1990; and Sutherland Brown, 1968); area below sea level is shaded. Bold numbers represent the thickness of eroded section (calculated by extrapolating the measured maturation gradient to the zero maturation level of  $0.15\%R_{o_{rand}}$  and assuming a constant paleogeothermal gradient; compiled from Vellutini, 1988, p. 88).

sedimentation beneath Hecate Strait was initiated only 6 Ma ago, as a consequence of crustal flexure.

## HYDROCARBON POTENTIAL

If commercial quantities of hydrocarbons are recovered from the Queen Charlotte Basin, it will probably be from the offshore, beneath Hecate Strait and Queen Charlotte Sound. An estimate of hydrocarbon potential must address three parameters: the areal extent of potential source strata, thermal history, and areal distribution and geometry of potential reservoir strata.

It is known that some rocks on the Queen Charlotte Islands locally exhibit good hydrocarbon-source potential (Macauley, 1983; Macauley et al., 1985; Snowdon et al., 1988). It has also been established that some potential source strata on the Queen Charlotte Islands are in the oil window (Vellutini, 1988; Vellutini and Bustin, 1988, 1991). A critical piece of the puzzle, establishing a link between source and reservoir (in this case the Tertiary Skonun Formation), has recently been demonstrated geochemically by L.R. Snowdon and M.G. Fowler (pers. comm., 1989) for the Sockeye B-10 well (Fig. 2): oil stains in sandstone in the well have geochemical characteristics suggesting that some of the oil was derived from organic material in Lower Jurassic strata.

### Distribution of source rocks

Portions of the Kunga and Maude groups have good source-rock characteristics. Did Middle Jurassic deformation affect their source rock potential? Lewis and Ross (1989) analyzed cleavage formation within the Maude Group and concluded that deformation occurred at elevated pore fluid pressures, while the rocks were still poorly lithified. It is unlikely that temperatures and pressures were sufficiently high during deformation to permit overmaturation and loss of organic material. Regional analysis of maturation levels (Vellutini and Bustin, 1988, 1991; Vellutini, 1988) shows a close correspondence between the spatial distribution of Middle Jurassic plutons and increasing level of organic maturation. Because deformation preceded plutonism, it is unlikely that deformation played a significant part in the maturation process. Burial of the source-rocks beneath a pile of post-Maude Group/pre-Yakoun Group strata thick enough (2-4 km) to promote thermal maturation of organic material is also not feasible. We conclude that Middle Jurassic deformation had little or no effect on maturation levels.

Kunga and Maude strata are part of Wrangell Terrane stratigraphy and therefore, likely to have been once widely distributed. There is every reason to conclude they once extended beneath Hecate Strait and Queen Charlotte Sound, and may do so today; the geochemical analyses from the Sockeye B-10 well support this notion. Yet, some caution must be exercised in predicting the regional extent of these potential source rocks.

On-land mapping has demonstrated, for instance, that local crustal blocks were stripped of their Kunga Group and Maude Group stratigraphies prior to deposition of potential reservoir strata. As well, basal Longarm Formation strata on Burnaby Island contain cobbles and boulders derived *in situ* or from nearby unroofed Middle Jurassic plutons; higher in the Longarm section, clasts of Yakoun Group volcanic rocks are abundant. This implies that significant uplift occurred during the Late Jurassic, exposing both the plutons and Yakoun Group volcanic rocks to erosion. Additionally, local paleocurrent data (Yorath and Chase, 1981; Yagishita, 1985a,b; Higgs, 1988; Gamba et al., 1990) indicate an eastern source for Cretaceous sediment, suggesting that parts of Hecate Strait may have been uplifted and eroded.

Clast compositions in the Upper Cretaceous Honna Formation provide additional evidence for uplift and erosion in the east. It is probable that some of the granitic clasts in the Honna Formation were eroded from the Coast Plutonic Complex or Alexander Terrane of south-east Alaska (G.J. Woodsworth, pers. comm., 1990). However, large angular clasts of Kunga Group limestone indicate a proximal source for some components of the Honna conglomerate. We suggest that some Upper Triassic and Lower Jurassic source strata were likely eroded from offshore regions due to episodic Late Jurassic through Tertiary block faulting.

If Late Jurassic through Tertiary block faulting occurred in the offshore, as it did on-land, erosion could potentially have removed likely source strata from some areas. We have no way of predicting where, or how large, those areas might be, and Kunga Group and Maude Group source rocks would presumably not have been immune. If the sediment source was proximal, it would suggest that little potential exists for preservation of Kunga Group and Maude Group strata adjacent to the eastern side of southern Moresby Island.

Jurassic and Cretaceous uplift along the Coast Plutonic Complex to the east (Fig. 4) may also have affected offshore areas, but we have no way of knowing how broad an area was affected or how much material may have been removed. Unfortunately, results from a recent seismic reflection experiment provide no clue as to the distribution and thickness of pre-Tertiary strata offshore (Rohr and Dietrich, 1991).

### Thermal history

The thermal history of Queen Charlotte Basins rocks is discussed by several authors in this volume (Vellutini and Bustin, 1991; T. Lewis et al., 1991; Anderson and Reichenbach, 1991; Souther and Jessop, 1991). Yorath and Hyndman (1983) used vitrinite reflectance data from the offshore wells as the basis for a model in which high heat flow was generated by rifting prior to 17 Ma, followed by cooling associated with the underthrusting of oceanic lithosphere. New vitrinite reflectance determinations are in progress (M. Bustin, pers. comm., 1990) and interpretations are pending.

### Reservoir rocks

Cretaceous strata are dominantly feldspatholithic sandstones and, as such, do not exhibit good reservoir characteristics from a petrographic standpoint. Fogarassy and Barnes (1988, 1989, 1991) and Fogarassy (1989) showed that shallow-water sandstones adjacent to the trend of the Dawson Cove Fault are most mature, contain the greatest primary pore space, and represent the best reservoir facies among the Cretaceous strata. This suggests that the upside of any block fault margin, where sediment reworking is likely, may produce facies with good primary reservoir characteristics. This is especially true if the block was stripped of strata down to the Kunga and Maude source rocks. Identification of such fault blocks in the subsurface offshore remains a problem. Until better geophysical constraints are provided for details of pre-Tertiary offshore geology, there is little hope of estimating the extent to which Cretaceous sandstones have reservoir potential.

The distribution and geometry of Tertiary strata beneath Hecate Strait and Queen Charlotte Sound has been discussed extensively by other workers, including Shouldice (1971), Rohr and Dietrich (1991), and Higgs (1990, 1991).

## A COMPARISON WITH THE COOK INLET BASIN

The rocks of Cook Inlet are part of a belt of Mesozoic and Cenozoic strata that extends from the Matanuska Valley at the head of the Inlet, southwest along the Alaska Peninsula and Shelikof Strait

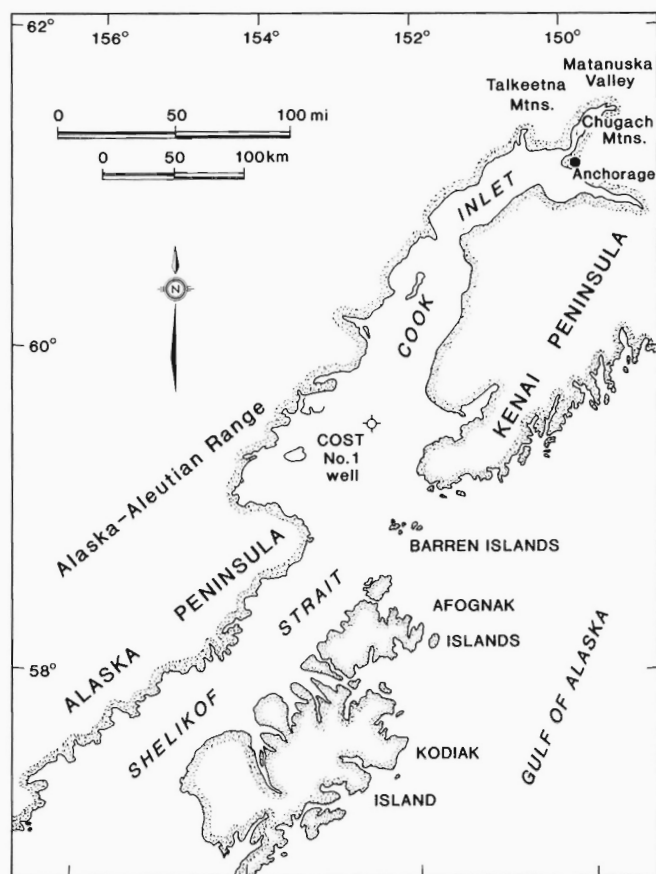


**Figure 14:** Geography of the Cook Inlet region, Alaska (modified from Magoon and Egbert, 1986, Fig. 32).

(Fig. 14). To the northwest is the Alaska-Aleutian Range Batholith, and the Bruin Bay and Castle Mountain faults; on the southeast is the Border Ranges Fault and several accreted terranes (Fig. 15). Hydrocarbon production is from six oil fields and three gas fields in upper Cook Inlet (Fig. 15). A generalized time-stratigraphic chart for Cook Inlet is presented in Figure 16 along with a companion chart for the Queen Charlotte Islands. Our discussion of Cook Inlet geology and the hydrocarbon exploration model used there is taken from Magoon and Egbert (1986) and Magoon and Claypool (1981).

Cook Inlet has been a focus of plate convergence and subduction throughout the Mesozoic and Cenozoic. It is a forearc basin bordering a magmatic arc on the northwest called the Alaska-Aleutian Range Batholith — together they form the Peninsular Terrane (Fig. 1). To the southeast, beyond the Border Ranges Fault are three accreted terranes, Kachemak, Chugach, and Prince William (Fig. 15; Jones et al., 1977).

Mesozoic strata in Cook Inlet are principally marine and more than 10 750 m thick, whereas Cenozoic strata are continental in nature and exceed 7000 m in thickness. Sandstone is the dominant rock type and was derived from two main sources: the magmatic arc and recycled intrabasinal strata.

Any comparison of the Queen Charlotte Islands with Cook Inlet must accommodate the probability that each evolved in entirely different Late Triassic and Early Jurassic settings. There are scattered occurrences of Late Triassic strata on either side of Cook Inlet, in the northeastern part of the Alaska Peninsula and on the Kenai Peninsula (Fig. 15). On the Alaska Peninsula, thick Norian limestones occur, not unlike those on the Queen Charlotte Islands, overlying (at one lo-

cality) 300-600 m of mafic volcanic flows and tuffs. To the east, on the Kenai Peninsula, there are two successions: 1) basalt capped by radiolarian chert; and 2) limestone, chert, and tuff, all underlying Jurassic volcanoclastic rocks. Because rocks older than Late Carnian appear to be absent, and because volcanic activity appears restricted to the Norian, Jones et al. (1977) did not include the region as part of the Wrangell Terrane. They pointed out, however, that paleomagnetic data (Packer and Stone, 1974) did not exclude the possibility that presumed allochthonous rocks of the Alaska and Kenai peninsulas are part of Wrangell Terrane.

From Early Jurassic to Early Cretaceous time, the Aleutian Range-Talkeetna Mountain magmatic arc was active; it produced primary volcanic flows and volcanoclastics in Cook Inlet Basin, as well as sand, silt, and gravel, all rich in feldspar and lithic fragments. Some of these rocks, the Middle Jurassic Tuxedni Group and Chinitna Formation (Fig. 16), are moderately rich in organic carbon (0.5-1.5%; Magoon and Claypool, 1979, 1981) and are the hydrocarbon source rocks for Cook Inlet.

The interaction between arc and forearc basin continued from Early Cretaceous time onward. Four sequential tectonic episodes — Early/Late Cretaceous, Late Cretaceous, early Cenozoic, late Cenozoic — are defined by the ages of unconformities separating the clastic successions (Fig. 16) and by radiometric dates on plutonic rocks (Hudson, 1986). Lower Cretaceous, Upper Cretaceous, and lower Tertiary successions accumulated during brief time intervals, but the younger Tertiary is represented by near-continuous deposition. Cretaceous strata are mostly marine whereas Tertiary strata are nonmarine.

Late Tertiary deposition was crucial to hydrocarbon maturation and migration. The Tertiary succession is thickest in the basin centre, thinning toward the basin margins (Fig. 17a). The Paleocene West Foreland Formation, the Oligocene Hemlock Conglomerate, and the Oligocene part of the Tyonek Formation comprise reservoir strata (Fig. 16).

Producing oil fields — Trading Bay, McArthur River, Middle Ground, Granite Point, Swanson River, Beaver Creek — are located on the basin flanks where Tertiary reservoir rocks truncate (stratigraphically) Middle Jurassic source rocks (Fig. 17). In the first part of their two-stage hydrocarbon exploration model, Magoon and Claypool (1981) suggest that burial and maturation of source rocks during the late Tertiary was followed by migration of hydrocarbons upward, through the source strata and into the Tertiary reservoir strata (Fig. 17c). In the second stage of the model, folding and contractional faulting of Plio-Pleistocene age was accompanied by remobilization of oil and gas into these structures (Fig. 17b).

Unlike Cook Inlet, Early Cretaceous through early Tertiary sedimentation in the Queen Charlotte Basin was more continuous and has not (as yet) been tied to discrete pulses of arc magmatism and unroofing; however a tie with events in the adjacent Coast Plutonic Complex, where magmatic activity occurred during the Early Cretaceous, Late Cretaceous, and early Tertiary (van der Heyden, 1989), may eventually prove possible.

A model similar to that for Cook Inlet may also apply for the Queen Charlotte Basin. Surface mapping shows that some fault-bounded blocks have been stripped of Middle Jurassic strata, and in places, Lower Cretaceous strata, placing Triassic/Jurassic source rocks adjacent to potential Cretaceous reservoir strata. We suspect this applies to offshore areas as well. One might expect up-dip migration of hydrocarbons into overlying sandstones and even secondary migration along the youngest set of Tertiary extension faults. Pliocene deformation in the Queen Charlotte Basin has produced faulted anticlines (Rohr and Dietrich, 1991)

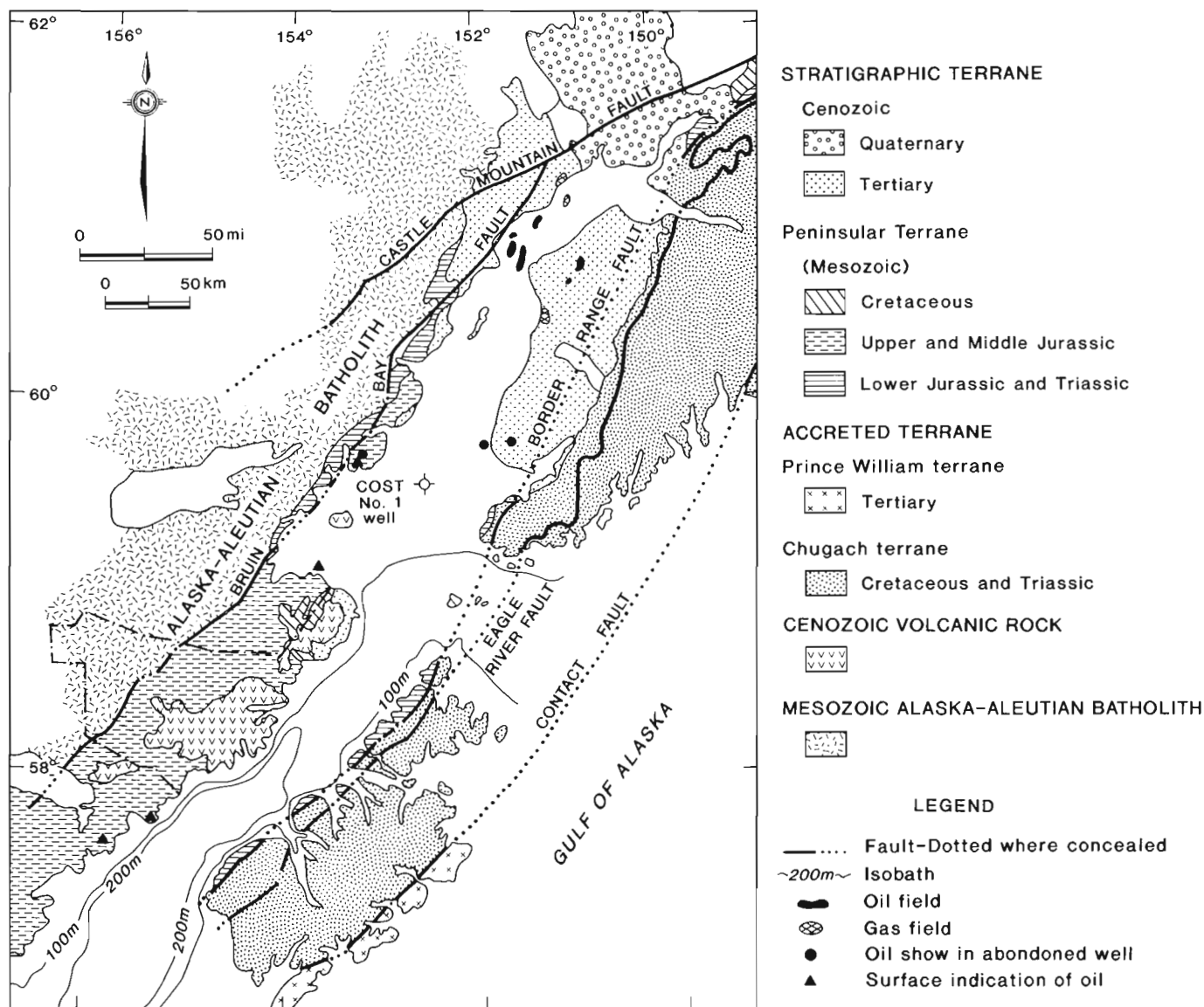


Figure 15: Regional geology of the Cook Inlet area (modified from Magoon and Egbert, 1986, Fig. 34).

similar in some respects to those seen in Cook Inlet; like Cook Inlet, these anticlines may constitute traps for remobilized oil and gas.

## SUMMARY

Middle Jurassic events recorded in the geological history of the Queen Charlotte Basin may reflect accretionary processes. These include: 1) southwest-northeast compression; 2) the initiation of volcanism; 3) intrusion of plutons; and 4) a significant change in the style and character of sedimentation. It is possible that this mid-Jurassic history of the Queen Charlotte Basin may be related to accretion of a superterrane, composed of the Wrangell, Stikine, and Alexander terranes, with North America.

From Middle Jurassic until early Tertiary time, the Queen Charlotte Basin was in an arc, and later, a forearc, setting, adjacent to the Coast Plutonic Complex magmatic arc. Late Jurassic uplift and erosion accompanied by block faulting, was followed by the deposition of two transgressive clastic sequences during the Cretaceous. Deposition was largely continuous throughout Cretaceous time. Thicknesses and facies vary on a local scale, reflecting continued minor adjustment

along faults that had been active during the Late Jurassic. The uppermost Jurassic-Lower Cretaceous Longarm Formation is not viewed as a suture assemblage between Wrangell and Alexander terranes. Rather, it is interpreted as the basal part of an essentially continuous Cretaceous succession that also includes the Haida and Skidegate formations.

The recent discovery of on-land nonmarine and marine detrital rocks of Eocene and Oligocene age is evidence that at least parts of the Queen Charlotte Basin were receiving sediment early in the Tertiary. The onset of Eocene and Oligocene deposition appears to coincide with two events of regional importance occurring at this time: crustal extension in south-central British Columbia and along parts (and perhaps all) of the eastern margin of the Coast Plutonic Complex (Parrish et al., 1988; Tempelman-Kluit and Parkinson, 1986; van der Heyden, 1989; Friedman and Armstrong, 1988), and a significant change in plate dynamics along the Queen Charlotte Basin margin, from convergent to transcurrent motion (Engelbreton et al., 1985; Stock and Molnar, 1988; Yorath and Hyndman, 1983; Hyndman and Hamilton, 1991). We believe that Tertiary evolution of the Queen Charlotte



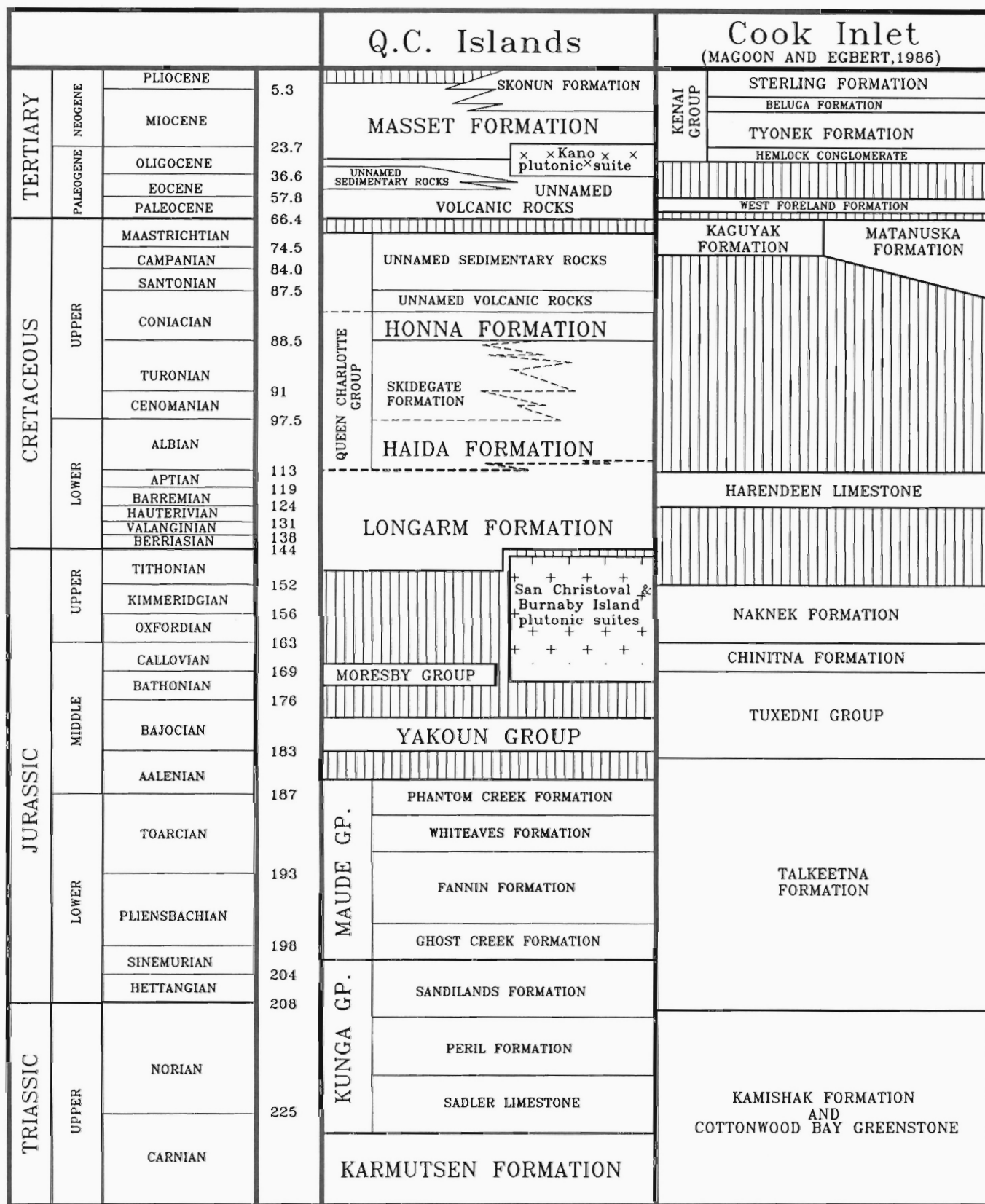


**Figure 16:** Comparative stratigraphic columns for the Queen Charlotte Basin and the Cook Inlet COST No. 1 well. Data for the COST No. 1 well from Magoon and Claypool (1981, Fig. 2) and Magoon and Egbert (1986, Fig. 37).



Basin was likely tied to crustal attenuation which affected large parts of the Canadian Cordillera.

It is premature to propose a hydrocarbon exploration model for the Queen Charlotte Basin; however, similarities with the exploration model for Cook Inlet do exist. Like Cook Inlet, hydrocarbon maturation within much of the Queen Charlotte Basin occurred as a consequence of burial beneath thick sedimentary and volcanic deposits

of Tertiary age. Similarly, the migration of oil into stratigraphic traps might have occurred in those areas where source rocks are overlain unconformably by Lower Cretaceous transgressive sandstones or Tertiary sandstones. Finally, as for Cook Inlet, Pliocene deformation in the Queen Charlotte Basin may have resulted in remobilization of oil and gas into anticlinal traps.

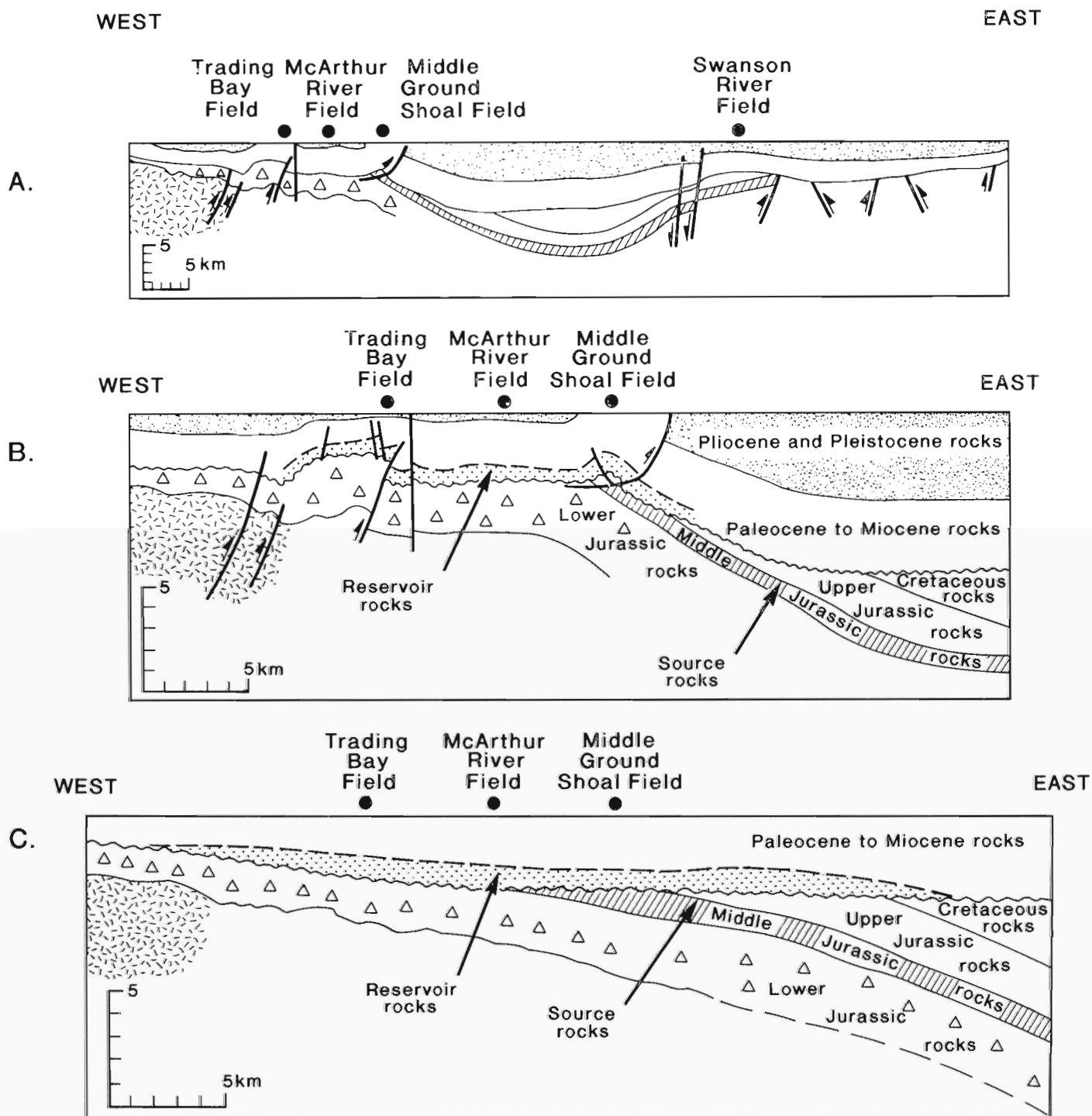


**Figure 17:** Diagrammatic cross-sections of upper Cook Inlet Basin (modified from Magoon and Claypool 1981, Figs. 19 and 20). (a) Regional cross-section; (b) detailed interpretation of the west flank of upper Cook Inlet showing the relationship between Middle Jurassic oil source beds and Tertiary reservoir rocks within faulted anticlines; (c) diagrammatic cross-section showing unconformable relationships prior to Pliocene folding and faulting.

## ACKNOWLEDGMENTS

The Queen Charlotte Frontier Geoscience Project has involved a large number of scientists and support personnel, all of whom have contributed generously of their energy, time, ideas, and goodwill. In particular, we appreciate the willingness, humour and positive outlook of those who assisted us in the field. Camp morale was ensured, thanks to the culinary delights provided by two outstanding cooks — Mary Anne Annable and Dianna April. Our expeditors, Ella Ferland and Audrey Putterill, provided expert, and at times innovative support, ensuring efficiency and a minimum of unanticipated emergencies. Those working with the Ministry of Transport in Sandspit kindly allowed us access to temporary housing. The people of Sandspit accepted their transient neighbours with warmth and good will.

Our work builds on that of our predecessors, especially the excellent regional mapping of Athol Sutherland Brown. Howard Tipper kindly (and patiently) introduced us to the stratigraphy and geological problems of the Queen Charlotte Islands.

Finally, we thank Christine Davis for drafting the line diagrams and Bev Vanlier for typing and checking.

## REFERENCES

- Addicott, W.O.  
1978: Late Miocene mollusks from the Queen Charlotte Islands, British Columbia, Canada; United States Geological Survey, Journal of Research, v. 6, p. 677-690.
- Anderson, R.G.  
1988: Jurassic and Cretaceous-Tertiary plutonic rocks on the Queen Charlotte Islands, British Columbia; *in* Current Research, Part E, Geological Survey of Canada, Paper 88-1E, p. 213-216.
- Anderson, R.G. and Greig, C.J.  
1989: Jurassic and Tertiary plutonism in the Queen Charlotte Islands, British Columbia; *in* Current Research, Part H, Geological Survey of Canada, Paper 89-1H, p. 95-104.
- Anderson, R.G. and Reichenbach, I.  
1989: A note on the geochronometry of Late Jurassic and Tertiary plutonism in the Queen Charlotte Islands, British Columbia; *in* Current Research, Part H, Geological Survey of Canada, Paper 89-1H, p. 105-112.
- 1991: U-Pb and K-Ar framework for Middle to Late Jurassic (172-2158 Ma) and Tertiary (46-27 Ma) plutons in Queen Charlotte Islands, British Columbia; *in* Evolution and Hydrocarbon Potential of the Queen Charlotte Basin, British Columbia, Geological Survey of Canada, Paper 90-10.
- Bielenstein, H.U.  
1969: The Rundle thrust sheet, Banff, Alberta: a structural analysis; Ph.D. thesis, Queens University, Kingston, Ontario, 148 p.
- Bustin, R.M. and Macauley, G.  
1988: Organic petrology and Rock-Eval pyrolysis of the Jurassic Sandilands and Ghost Creek formations, Queen Charlotte Islands; Bulletin of Canadian Petroleum Geology, v. 36, p. 168-176.
- Butler, R.F., Gehrels, G.E., McClelland, W.C., May, S.R., and Klepacki, D.  
1989: Discordant paleomagnetic poles from the Canadian Coast Plutonic Complex: regional tilt rather than large-scale displacement?; *Geology*, v. 17, p. 691-694.
- Cameron, B.E.B. and Tipper, H.W.  
1985: Jurassic stratigraphy of the Queen Charlotte Islands, British Columbia; Geological Survey of Canada, Bulletin 365, 49 p.
- Desrochers, A.  
1989: Depositional history of Upper Triassic carbonate platforms on Wrangellia Terrane, western British Columbia; American Association of Petroleum Geologists, Bulletin 73, p. 349-350 (abs.).
- Desrochers, A. and Orchard, M.J.  
1991: Stratigraphic revisions and carbonate sedimentology of the Kunga Group (Upper Triassic-Lower Jurassic), Queen Charlotte Islands, British Columbia; *in* Evolution and Hydrocarbon Potential of the Queen Charlotte Basin, British Columbia, Geological Survey of Canada, Paper 90-10.
- Engelbreton, D.C., Cox, A., and Gordon, R.R.  
1985: Relative motion between oceanic and continental plates in the Pacific basin; Geological Society of America Special Paper 206, p. 59.
- Fogarassy, J.A.S.  
1989: Stratigraphy, diagenesis and petroleum reservoir potential of the Cretaceous Haida, Skidegate and Honna formations, Queen Charlotte Islands, British Columbia; M.Sc. thesis, University of British Columbia, Vancouver, 177 p.
- Fogarassy, J.A.S. and Barnes, W.C.  
1988: Stratigraphy, diagenesis and petroleum reservoir potential of the mid- to Upper Cretaceous Haida and Honna formations of the Queen Charlotte Islands, British Columbia; *in* Current Research, Part E, Geological Survey of Canada, Paper 88-1E, p. 265-268.
- 1989: The middle Cretaceous Haida Formation: a potential hydrocarbon reservoir in the Queen Charlotte Islands, British Columbia; *in* Current Research, Part H, Geological Survey of Canada, Paper 89-1H, p. 47-52.
- 1991: Stratigraphy and diagenesis of the mid- to Upper Cretaceous Queen Charlotte Group, Queen Charlotte Islands, British Columbia; *in* Evolution and Hydrocarbon Potential of the Queen Charlotte Basin, British Columbia, Geological Survey of Canada, Paper 90-10.
- Friedman, R.M. and Armstrong, R.L.  
1988: The Tatla Lake Metamorphic Complex: an Eocene metamorphic core complex on the southwest edge of the Intermontane Belt, British Columbia; *Tectonics*, v. 7, p. 1141-1166.
- Gamba, C.A., Indrelid, J., and Taite, S.  
1990: Sedimentology of the Upper Cretaceous Queen Charlotte Group, with special reference to the Honna Formation, Queen Charlotte Islands, British Columbia; *in* Current Research, Part F, Geological Survey of Canada, Paper 90-1F, p. 67-73.
- Gardner, M.C., Bergman, S.C., Cushing, G.W., MacKevett, E.M., Jr., Plafker, G., Campbell, R.B., Dodds, C.J., McClelland, W.C., and Mueller, P.A.  
1988: Pennsylvanian pluton stitching of Wrangellia and the Alexander Terrane, Wrangell Mountains, Alaska; *Geology*, v. 16, p. 967-971.
- Haggart, J.W.  
1989: Reconnaissance lithostratigraphy and biochronology of the Lower Cretaceous Longarm Formation, Queen Charlotte Islands, British Columbia; *in* Current Research, Part H, Geological Survey of Canada, Paper 89-1H, p. 39-46.
- 1991: A synthesis of Cretaceous stratigraphy, Queen Charlotte Islands, British Columbia; *in* Evolution and Hydrocarbon Potential of the Queen Charlotte Basin, British Columbia, Geological Survey of Canada, Paper 90-10.
- Haggart, J.W. and Gamba, C.A.  
1990: Stratigraphy and sedimentology of the Longarm Formation, southern Queen Charlotte Islands, British Columbia; *in* Current Research, Part F, Geological Survey of Canada, Paper 90-1F, p. 61-66.
- Haggart, J.W., Indrelid, J., Hesthammer, J., Gamba, C.A., and White, J.M.  
1990: A geological reconnaissance of the Mount Stapleton-Yakoun Lake region, central Queen Charlotte Islands, British Columbia; *in* Current Research, Part F, Geological Survey of Canada, Paper 90-1F, p. 29-36.
- Haggart, J.W., Lewis, P.D., and Hickson, C.J.  
1989: Stratigraphy and structure of Cretaceous strata, Long Inlet, Queen Charlotte Islands, British Columbia; *in* Current Research, Part H, Geological Survey of Canada, Paper 89-1H, p. 65-72.
- Hamilton, T.S. and Cameron, B.E.B.  
1990: Hydrocarbon occurrences on the western margin of the Queen Charlotte Basin; Bulletin of Canadian Petroleum Geology, v. 37, p. 443-466.
- Hesthammer, J., Indrelid, J., and Ross, J.V.  
1989: Preliminary structural studies of the Mesozoic rocks of central Graham Island, Queen Charlotte Islands, British Columbia; *in* Current Research, Part H, Geological Survey of Canada, Paper 89-1H, p. 19-22.
- Hickson, C.J.  
1988: Structure and stratigraphy of the Masset Formation, Queen Charlotte Islands, British Columbia; *in* Current Research, Part E, Geological Survey of Canada, Paper 88-1E, p. 269-274.
- 1989: An update on structure and stratigraphy of the Masset Formation, Queen Charlotte Islands, British Columbia; *in* Current Research, Part H, Geological Survey of Canada, Paper 89-1H, p. 73-79.
- 1991: The Masset Formation on Graham Island, Queen Charlotte Islands, British Columbia; *in* Evolution and Hydrocarbon Potential of the Queen Charlotte Basin, British Columbia, Geological Survey of Canada, Paper 90-10.
- Higgs, R.  
1988: Sedimentology and tectonic implications of Cretaceous fan-delta conglomerates, Queen Charlotte Islands; *in* Sequences, Stratigraphy, Sedimentology: Surface and Subsurface, D.P. James and D.A. Leckie (ed.), Canadian Society of Petroleum Geologists, Memoir 15, p. 307-308.
- 1989: Sedimentological aspects of the Skonun Formation, Queen Charlotte Islands, British Columbia; *in* Current Research, Part H, Geological Survey of Canada, Paper 89-1H, p. 87-94.
- 1990: Sedimentology and tectonic implications of Cretaceous fan-delta conglomerates, Queen Charlotte Islands, Canada; *Sedimentology*, v. 37, p. 83-103.
- 1991: Sedimentology, basin-fill architecture and petroleum geology of the Tertiary Queen Charlotte Basin, British Columbia; *in* Evolution and Hydrocarbon Potential of the Queen Charlotte Basin, British Columbia, Geological Survey of Canada, Paper 90-10.
- Hudson, T.  
1986: Plutonism and provenance: implications for sandstone compositions; *in* Geologic Studies of the Lower Cook Inlet COST No. 1 Well, Alaska Outer Continental Shelf, L.B. Magoon (ed.), United States Geological Survey, Bulletin 1596, p. 55-60.
- Hyndman, R.D. and Hamilton, T.S.  
1991: Cenozoic relative plate motions along the northeastern Pacific margin and their association with Queen Charlotte arc tectonics and volcanism; *in* Evolution

and Hydrocarbon Potential of the Queen Charlotte Basin, British Columbia, Geological Survey of Canada, Paper 90-10.

**Indrelid, J., Hesthammer, J., and Ross, J.V.**

**1991:** Structural geology and stratigraphy of Mesozoic rocks of central Graham Island, Queen Charlotte Islands, British Columbia; *in* Evolution and Hydrocarbon Potential of the Queen Charlotte Basin, British Columbia, Geological Survey of Canada, Paper 90-10.

**Irving, E., Woodsworth, G.J., Wynne, P.J., and Morrison, A.**

**1985:** Paleomagnetic evidence for displacement from the south of the Coast Plutonic Complex, British Columbia; *Canadian Journal of Earth Sciences*, v. 22, p. 584-598.

**Jakobs, G.K.**

**1989:** Toarcian (Lower Jurassic) biostratigraphy of the Queen Charlotte Islands, British Columbia; *in* Current Research, Part H, Geological Survey of Canada, Paper 89-1H, p. 35-37.

**Jeletzky, J.A.**

**1976:** Mesozoic and Tertiary rocks of Quatsino Sound, Vancouver Island, British Columbia; Geological Survey of Canada, Bulletin 242, 243 p.

**Jones, D.L., Silberling, N.J., and Hillhouse, J.**

**1977:** Wrangellia — A displaced terrane in northwestern North America; *Canadian Journal of Earth Sciences*, v. 14, p. 2565-2577.

**Lewis, P.D.**

**1990:** New timing constraints on Cenozoic deformation in the Queen Charlotte Islands, British Columbia; *in* Current Research, Part F, Geological Survey of Canada, Paper 90-1F, p. 23-28.

**Lewis, P.D. and Ross, J.V.**

**1988:** Preliminary investigations of structural styles in Mesozoic strata of the Queen Charlotte Islands, British Columbia; *in* Current Research, Part E, Geological Survey of Canada, Paper 88-1E, p. 275-279.

**1989:** Evidence for Late Triassic-Early Jurassic deformation in the Queen Charlotte Islands, British Columbia; *in* Current Research, Part H, Geological Survey of Canada, Paper 89-1H, p. 13-18.

**1991:** Mesozoic and Cenozoic structural history of the central Queen Charlotte Islands, British Columbia; *in* Evolution and Hydrocarbon Potential of the Queen Charlotte Basin, British Columbia, Geological Survey of Canada, Paper 90-10.

**Lewis, P.D., Hesthammer, H., Indrelid, J., and Hickson, C.J.**

**1990:** Geology, Yakoun Lake, British Columbia; Geological Survey of Canada, Map 5-1990, scale 1:50 000.

**Lewis, T.J., Bentkowski, W.H., and Wright, J.A.**

**1991:** Thermal state of the Queen Charlotte Basin, British Columbia: warm; *in* Evolution and Hydrocarbon Potential of the Queen Charlotte Basin, British Columbia, Geological Survey of Canada, Paper 90-10.

**Lyatsky, H.V.**

**1991:** Regional geophysical constraints on crustal structure and geologic evolution of the Insular Belt, British Columbia; *in* Evolution and Hydrocarbon Potential of the Queen Charlotte Basin, British Columbia, Geological Survey of Canada, Paper 90-10.

**Macauley, G.**

**1983:** Source rock — oil shale potential of the Jurassic Kunga Formation, Queen Charlotte Islands; Geological Survey of Canada, Open File 921.

**Macauley, G., Snowden, L.R., and Ball, F.D.**

**1985:** Geochemistry and geological factors governing exploitation of selected Canadian oil shale deposits; Geological Survey of Canada, Paper 85-13, p. 65.

**MacKevett, E.M., Gardner, M.C., Bergman, S.C., Cushing, G.W., and McLeland, W.D.**

**1986:** Geological evidence for Late Pennsylvanian juxtaposition of Wrangellia and the Alexander Terrane, Alaska; Geological Society of America, Abstracts with Programs, v. 18, no. 2, p. 128.

**Magoon, L.B. and Claypool, G.E.**

**1979:** Origin of Cook Inlet oil; *in* The Relationship of Plate Tectonics to Alaskan Geology and Resources, A. Sisson, (ed.), Proceedings, Alaska Geological Society Symposium, Anchorage, Alaska, p. G1-G17.

**1981:** Petroleum geology of Cook Inlet Basin: an exploration model; American Association of Petroleum Geologists, Bulletin, v. 65-6, p. 1043-1061.

**Magoon, L.B. and Egbert, R.M.**

**1986:** Framework geology and sandstone composition; *in* Geologic Studies of the Lower Cook Inlet COST No. 1 Well, Alaska Outer Continental Shelf, L.B. Magoon (ed.), United States Geological Survey, Bulletin 1596, p. 65-99.

**Monger, J.W.H.**

**1984:** Cordilleran tectonics: a Canadian perspective; *Bulletin de la Société Géologique de France*, v. 26, no. 2, p. 255-278.

**Monger, J.W.H. and Irving, E.**

**1980:** Northward displacement of north-central British Columbia; *Nature*, v. 285, p. 289-294.

**Monger, J.W.H., Price, R.A., and Tempelman-Kluit, D.J.**

**1982:** Tectonic accretion and the origin of the two major metamorphic and plutonic belts in the Canadian Cordillera; *Geology*, v. 10, p. 70-75.

**Orchard, M.J.**

**1991:** Late Triassic conodont biochronology and biostratigraphy of the Kunga Group, Queen Charlotte Islands, British Columbia; *in* Evolution and Hydrocarbon Potential of the Queen Charlotte Basin, British Columbia, Geological Survey of Canada, Paper 90-10.

**Orchard, M.J. and Forster, P.J.**

**1991:** Conodont colour and thermal maturity of the Late Triassic Kunga Group, Queen Charlotte Islands, British Columbia; *in* Evolution and Hydrocarbon Potential of the Queen Charlotte Basin, British Columbia, Geological Survey of Canada, Paper 90-10.

**Packer, D.R. and Stone, D.B.**

**1974:** Paleomagnetism of Jurassic rocks from southern Alaska and the tectonic implications; *Canadian Journal of Earth Sciences*, v. 11, p. 976-997.

**Parrish, R.R., Carr, S.D., and Parkinson, D.L.**

**1988:** Eocene extensional tectonics and geochronology of the southern Omineca Belt, British Columbia and Washington; *Tectonics*, v. 7, no. 2, p. 181-212.

**Patterson, R.T.**

**1988a:** Early Miocene to Quaternary foraminifera from three wells in the southern Queen Charlotte Basin; Geological Survey of Canada, Open File 1985.

**1988b:** Early Miocene to Quaternary foraminifera from three wells in the Queen Charlotte Basin off the coast of British Columbia; *in* Sequences, Stratigraphy, Sedimentology: Surface and Subsurface, D.P. James and D.A. Leckie (ed.), Canadian Society of Petroleum Geologists, Memoir 15, p. 497.

**Price, R.A.**

**1967:** The tectonic significance of mesoscopic subfabrics in the southern Rocky Mountains of Alberta and British Columbia; *Canadian Journal of Earth Sciences*, v. 4, p. 39-70.

**Riddiough, R.P.**

**1983:** Recent plate motions; Geological Survey of Canada, Open File 83-6.

**Rohr, K. and Dietrich, J.R.**

**1991:** Deep seismic reflection survey of the Queen Charlotte Basin, British Columbia; *in* Evolution and Hydrocarbon Potential of the Queen Charlotte Basin, British Columbia, Geological Survey of Canada, Paper 90-10.

**Rohr, K.M., Spence, G., Asudeh, I., Ellis, R., and Clowes, R.**

**1989:** Seismic reflection and refraction experiment in the Queen Charlotte Basin, British Columbia; *in* Current Research, Part H, Geological Survey of Canada, Paper 89-1H, p. 3-5.

**Shouldice, D.H.**

**1971:** Geology of the western Canadian continental shelf; *Bulletin of Canadian Petroleum Geology*, v. 19, p. 405-436.

**Smith, P.L. and Tipper, H.W.**

**1986:** Plate tectonics and paleobiogeography: Early Jurassic (Pliensbachian) endemism and diversity; *Palaeo*, v. 1, p. 399-412.

**Snowdon, L.R., Fowler, M.G., and Hamilton, T.S.**

**1988:** Progress report on organic geochemistry, Queen Charlotte Islands, British Columbia; *in* Current Research, Part E, Geological Survey of Canada, Paper 88-1E, p. 251-253.

**Souther, J.G.**

**1988:** Implications for hydrocarbon exploration of dyke emplacement in the Queen Charlotte Islands, British Columbia; *in* Current Research, Part E, Geological Survey of Canada, Paper 88-1E, p. 241-245.

**1989:** Dyke swarms in the Queen Charlotte Islands, British Columbia; *in* Current Research, Part H, Geological Survey of Canada, Paper 89-1H, p. 117-120.

**Souther, J.G. and Bakker, E.**

**1988:** Petrography and chemistry of dykes in the Queen Charlotte Islands, British Columbia; Geological Survey of Canada, Open File 1833.

**Souther, J.G. and Jessop, A.M.**

**1991:** Dyke swarms in the Queen Charlotte Islands, British Columbia, and implications for hydrocarbon exploration; *in* Evolution and Hydrocarbon Potential of the Queen Charlotte Basin, British Columbia, Geological Survey of Canada, Paper 90-10.

**Stock, J. and Molnar, P.**

**1988:** Uncertainties and implications of the Late Cretaceous and Tertiary position of North America relative to the Farallon, Kula and Pacific plates; *Tectonics*, v. 7, p. 1339-1384.

**Sutherland Brown, A.**

**1968:** Geology of the Queen Charlotte Islands, British Columbia; British Columbia Department of Mines and Petroleum Resources, Bulletin 54, 226 p. Contains Figure 5, sheets A, B, and C, Geology of the Queen Charlotte Islands (1:125 000).

**Sweeney, J.F. and Seemann, D.A.**

**1991:** Crustal density structure of Queen Charlotte Islands and Hecate Strait, British Columbia; *in* Evolution and Hydrocarbon Potential of the Queen Charlotte Basin, British Columbia, Geological Survey of Canada, Paper 90-10.

**Taite, S.**

**1990:** Observations on structure and stratigraphy of the Sewell Inlet-Tasu Sound, area, Queen Charlotte Islands, British Columbia; *in* Current Research, Part F, Geological Survey of Canada, Paper 90-1F, p. 19-22.

**Tempelman-Kluit, D. and Parkinson, D.**

**1986:** Extension across the Eocene Okanagan crustal shear in southern British Columbia; *Geology*, v. 14, p. 318-321.

**Thompson, R.I.**

**1988:** Late Triassic through Cretaceous geological evolution, Queen Charlotte Islands, British Columbia; in *Current Research, Part E, Geological Survey of Canada, Paper 88-1E*, p. 217-219.

**1990:** *Geology, Cumsheewa Inlet, British Columbia; Geological Survey of Canada, Map 3-1990, scale 1:50 000.*

**Thompson, R.I. and Lewis, P.D.**

**1990a:** *Geology, Louise Island, British Columbia; Geological Survey of Canada, Map 2-1990, scale 1:50 000.*

**1990b:** *Geology, Skidegate Channel, British Columbia; Geological Survey of Canada, Map 4-1990, scale 1:50 000.*

**Thompson, R.I. and Thorkelson, D.**

**1989:** Regional mapping update, central Queen Charlotte Islands, British Columbia; in *Current Research, Part H, Geological Survey of Canada, Paper 89-1H*, p. 7-11.

**Tipper, H.W., Smith, P.L., Cameron, B.E.B., Carter, E.S., Jakobs, G.K., and Johns, M.J.**

**1991:** Biostratigraphy of the Lower Jurassic formations of the Queen Charlotte Islands, British Columbia; in *Evolution and Hydrocarbon Potential of the Queen Charlotte Basin, British Columbia, Geological Survey of Canada, Paper 90-10.*

**Tozer, E.T.**

**1982:** Marine Triassic faunas of North America: their significance in assessing plate and terrane movements; *Geologische Rundschau*, v. 71, p. 1077-1104.

**van der Heyden, P.V.**

**1989:** U-Pb and K-Ar geochronometry of the Coast Plutonic Complex, 53° to 54°N, British Columbia, and implications for the Insular-Intermontane Superterrane boundary; Ph.D. thesis, University of British Columbia, Vancouver, 392 p.

**Vellutini, D.**

**1988:** Organic maturation and source rock potential of Mesozoic and Tertiary strata, Queen Charlotte Islands, British Columbia; M.Sc. thesis, University of British Columbia, British Columbia, 262 p.

**Vellutini, D. and Bustin, R.M.**

**1988:** Preliminary results on organic maturation of the Tertiary Skonun Formation, Queen Charlotte Islands, British Columbia; in *Current Research, Part E, Geological Survey of Canada, Paper 88-1E*, p. 255-258.

**1991:** Organic maturation of Mesozoic and Tertiary strata of the Queen Charlotte Islands, British Columbia; in *Evolution and Hydrocarbon Potential of the Queen Charlotte Basin, British Columbia, Geological Survey of Canada, Paper 90-10.*

**West Coast Offshore Exploration Environmental Assessment Panel [Vancouver and Victoria]**

**1986:** Offshore hydrocarbon exploration: report and recommendations of the West Coast Exploration Environmental Assessment Panel, April 1986; Prepared for Environment Canada: Energy, Mines and Resources; British Columbia Ministry of the Environment; British Columbia Ministry of Energy, Mines and Petroleum Resources (Supply and Services Canada Catalogue No. En 105-37/1986E).

**Wheeler, J.O., Brookfield, A.J., Gabrielse, H., Monger, J.W.H., and Woodsworth, G.J.**

**1988:** Terrane Map of the Canadian Cordillera; Geological Survey of Canada, Open File 1894.

**White, J.M.**

**1990:** Evidence of Paleogene sedimentation on Graham Island, Queen Charlotte Islands, west coast, Canada; *Canadian Journal of Earth Sciences*, v. 27, p. 533-538.

**Woodsworth, G.J.**

**1988:** Karmutsen Formation and the east boundary of Wrangellia, Queen Charlotte Basin, British Columbia; in *Current Research, Part E, Geological Survey of Canada, Paper 88-1E*, p. 209-212.

**Yagishita, K.**

**1985a:** Mid- to Late Cretaceous sedimentation in the Queen Charlotte Islands, British Columbia: lithofacies, paleocurrent and petrographic analyses of sediments; Ph.D. thesis, University of Toronto, Ontario.

**1985b:** Evolution of a provenance as revealed by petrographic analyses of Cretaceous formations in the Queen Charlotte Islands, British Columbia, Canada; *Sedimentology*, v. 32, p. 671-684.

**Yorath, C.J.**

**1988:** Petroleum geology of the Canadian Pacific continental margin; in *Geology and Resource Potential of the Continental Margin of Western North America and adjacent Ocean Basins -- Beaufort Sea to Baja California*, D.W. Scholl, A. Grantz, and J.G. Vedder (ed.), Circum-Pacific Council for Energy and Mineral Resources Earth Science Series, v. 6, p. 283-304.

**Yorath, C.J. and Chase, R.L.**

**1981:** Tectonic history of the Queen Charlotte Islands and adjacent areas -- a model; *Canadian Journal of Earth Sciences*, v. 18, p. 1717-1739.

**Yorath, C.J. and Hyndman, R.D.**

**1983:** Subsidence and thermal history of Queen Charlotte Basin; *Canadian Journal of Earth Sciences*, v. 20, p. 135-159.



# Mesozoic and Cenozoic structural history of the central Queen Charlotte Islands, British Columbia

P.D. Lewis<sup>1</sup> and J.V. Ross<sup>1</sup>

Lewis, P.D. and Ross, J.V., Mesozoic and Cenozoic structural history of the central Queen Charlotte Islands, British Columbia; in *Evolution and Hydrocarbon Potential of the Queen Charlotte Basin, British Columbia*, Geological Survey of Canada, Paper 90-10, p. 31-50, 1991.

## Abstract

*Regional and detailed structural studies on the central and northern Queen Charlotte Islands delineate four episodes of deformation spanning Mesozoic and Cenozoic time: 1) Middle Jurassic shortening, 2) Late Jurassic through mid-Cretaceous block faulting, 3) Late Cretaceous/Early Tertiary contractional folding and faulting, and 4) Neogene extensional block faulting. During all deformation, structural styles reflect mechanical rock properties, which vary with structural level. In deepest crustal rocks, strain is accommodated along steeply dipping faults and shear zones during both extension and contraction. In overlying well-bedded rocks, shortening is manifested in open to tight folds and shallowly dipping detachment surfaces, and extension occurs along steeply dipping normal faults. At highest structural levels, in thick homogeneous sedimentary and volcanic strata, dominant structures are broad map-scale folds or steeply-dipping fault surfaces. Northwest-trending structural features are common to all deformation events, and regional strain analyses record northwest elongation directions. Kinematic analyses of fault fabrics indicate that dominant movement directions along steeply-dipping fault surfaces are east-side-up, or southwest directed. No evidence is seen for large transverse offsets along major faults through the Queen Charlotte Islands. Throughout deformation, strains were accommodated by a combination of brittle and ductile processes, facilitated by elevated pore fluid pressures and fluid circulation.*

## Résumé

*Des études structurales, régionales et détaillées, sur le centre et le nord des îles de la Reine-Charlotte ont permis de délimiter quatre épisodes de déformation couvrant le Mésozoïque et le Cénozoïque : 1) un raccourcissement au Jurassique moyen, 2) un morcellement par failles du Jurassique supérieur jusqu'au Crétacé moyen, 3) la formation de plis et de failles par contraction au Crétacé supérieur et au Tertiaire inférieur, et 4) un morcellement par failles de distension au Néogène. Durant toute la déformation, les styles structuraux reflètent les propriétés mécaniques des roches lesquels varient selon le niveau structural. Dans les roches de la croûte inférieure, la déformation a longé des failles à pendage abrupt et des zones de cisaillement durant la distension et la contraction. Dans les roches bien stratifiées sus-jacentes, le raccourcissement se manifeste dans des plis ouverts à serrés et dans des surfaces de détachement à pendage peu profond, et la distension s'observe le long de failles normales à pendage abrupt. Aux niveaux structuraux les plus élevés dans les épaisses couches sédimentaires et volcaniques homogènes, les principales structures sont des plis d'échelle cartographique ou des surfaces de faille à pendage abrupt. Les formes structurales à direction nord-ouest sont fréquentes dans tous les événements de déformation, et des analyses de la déformation régionale indiquent des directions d'allongement nord-ouest. Des analyses cinématiques de la fabrique des failles révèlent que les directions de déplacement dominantes le long des surfaces de faille à pendage abrupt sont l'est, indiqué par le côté relevé, ou le sud-ouest. Il n'existe aucun indice de décalages transversaux importants le long des failles principales dans les îles de la Reine-Charlotte. Les déformations, tout au long de leur processus, ont été accompagnées de phénomènes cassants et ductiles, facilités par des pressions de fluide interstitiel élevées et par une circulation de fluides.*

<sup>1</sup> Department of Geological Sciences, University of British Columbia, 6339 Stores Road, Vancouver, B.C. V6T 2B4



## INTRODUCTION

The Queen Charlotte Basin Frontier Geoscience Program (FGP) has utilized a multidisciplinary approach to sedimentary basin analysis and hydrocarbon resource evaluation, incorporating contributions from numerous geological and geophysical studies. Regional mapping and structural geology studies have been integral parts of the on-land portion of this program, and have followed two closely linked approaches: 1:50 000 scale regional geologic maps were completed for a large part of the central and northern Queen Charlotte Islands (see Thompson et al., 1991), while this study concentrated on detailed mapping and structural analysis of rocks at specific locations. The regional maps help to establish stratigraphic and structural relations between map units and to outline a regional structural history. The types of information provided by the maps are critical for predicting the distribution of lithologic units in the offshore basin areas and for interpreting geophysical data, and will be instrumental to developing models for the evolution of the Queen Charlotte Basin. The detailed map studies and structural analysis reported here are designed to complement the regional geologic mapping. Structural data and oriented rock samples were collected at key locations to provide a basis for local and regional strain analysis, kinematic analysis of structural fabrics, and evaluation of processes of deformation. The results, presented below, provide more rigid constraints on the timing, style, and kinematics of deformation events than could be achieved from the regional studies alone.

In addition to the mapping and structural studies outlined above, other workers involved in the Queen Charlotte Basin FGP have addressed specific structural problems which bear on the present study and contribute to our knowledge of the structural history of the region. Hickson (1989, 1991) has recorded structures within the Tertiary (Masset Formation) volcanic succession on Graham Island. Anderson (1988), Anderson and Reichenbach (1991), and Anderson and Greig (1989) have analyzed fracture patterns and penetrative fabrics within plutonic rocks throughout the Queen Charlotte Islands, to evaluate the relative roles of emplacement and tectonic generation of structures. Souther (1988) and Souther and Jessop (1991) have completed a comprehensive survey of igneous dyke orientation, distribution, and chemistry, to determine the amounts and directions of extension associated with different episodes of dyke emplacement.

### Previous Structural Work

Previous structural interpretations for the Queen Charlotte Islands region have relied heavily on wrench-fault tectonic styles, and have incorporated large transverse offsets along faults through the Queen Charlotte Islands. Sutherland Brown (1968) was the first worker to describe the structural geology of the Queen Charlotte region in detail. He completed regional mapping of all of the Queen Charlotte Islands and described the dominant structures as several major north-west-trending fault systems: the Rennell Sound/Louscoone Inlet Fault Zone (RSFZ), the Sandspit Fault (SF), and the Queen Charlotte Fault (QCF) (Fig. 1). Sutherland Brown proposed that the RSFZ represents a crustal-scale, strike-slip fault zone with up to tens of kilometres of offset dating from late Jurassic to Cretaceous time. The Sandspit Fault is less well constrained and is not exposed in surficial outcrops, but he suggested dominantly dip-slip movement with a possible horizontal component. Sutherland Brown also suggested that many folds mapped on the islands could be related to movements along the major faults.

Drawing heavily on the existing geologic map and limited new geophysical data, Yorath and Chase (1981) and Yorath and Hyndman (1983) expanded Sutherland Brown's interpretations and proposed tectonic models for the evolution of the Queen Charlotte Basin. Their

models require significant right-lateral offset along the Rennell Sound and Sandspit Fault systems, and they interpreted the Louscoone Fault as the offset southern extension of the Sandspit Fault. In addition, they suggested that the Alexander/Wrangell terrane boundary coincides with the Sandspit Fault and the offshore extension of the RSFZ.

Young (1981) reviewed available geological data for the Queen Charlotte Islands and demonstrated that nearly all structural features mapped by Sutherland Brown could be interpreted as elements of a wrench fault system. He also presented geophysical data (high resolution seismic reflection and aeromagnetic surveys) that indicate a structural anomaly in Hecate Strait southeast of and along trend with the Sandspit Fault.

### Outline of present study

Detailed structural mapping was completed on the northern and central Queen Charlotte Islands during the 1987 and 1988 field seasons. Four areas were examined; from north to south these are northwest Graham Island, Rennell Sound, Long Inlet/Kagan Bay, and southeast Louise Island (Fig. 1; Figs. 4, 6, 9, 10, in pocket). These locations provide exposures of a variety of structural and stratigraphic levels in the Mesozoic and Cenozoic section. All represent well-exposed, structurally complex areas which are identified on existing maps as being critical to evaluating the structural history of the region. The Rennell Sound and Long Inlet/Kagan Bay areas both span the Rennell Sound Fault Zone of Sutherland Brown (1968), and the Louise Island area is located where the Louscoone Inlet Fault Zone and Rennell Sound Fault Zone join. The northwest Graham Island exposures were examined to assess the regional continuity of structures and to provide further constraints to the overall structural history.

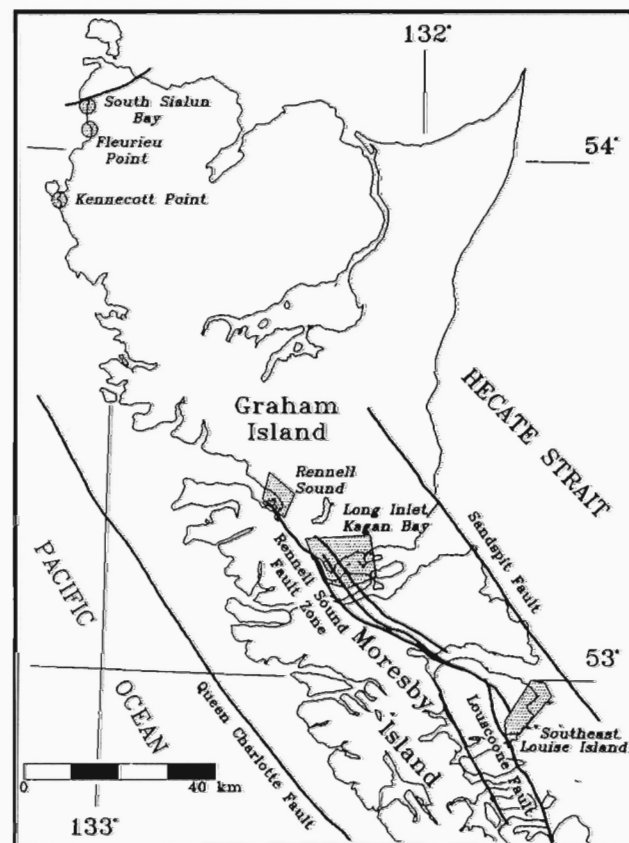
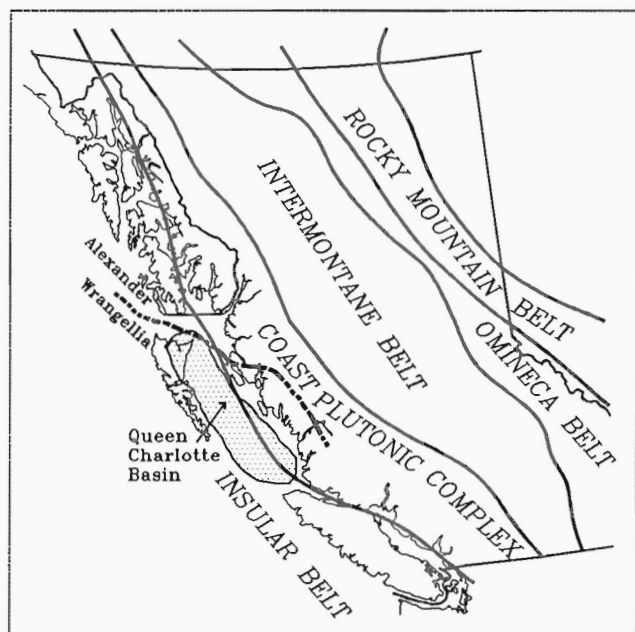


Figure 1: Locations of areas mapped in this study, and approximate traces of major structural features described by Sutherland Brown (1968).



**Figure 2:** Position of the Queen Charlotte Basin with respect to the five major tectonic belts of the Canadian Cordillera and approximate boundary between rocks of Wrangellia and Alexander terrane affinity, as proposed by van der Heyden (1989).

To complement the mapping studies, a regional strain analysis was completed using deformed ammonites and belemnites as strain markers. Samples were collected from locations on Moresby, Louise, and central and southern Graham islands. In addition, oriented rock samples were collected from all levels of the stratigraphic section to examine microstructural development and analyze mechanisms of deformation on the microscopic scale.

### Geologic framework

The Queen Charlotte Islands region lies within the Insular Belt of the Canadian Cordillera on the westernmost edge of the North American continental plate (Fig. 2). The Queen Charlotte Basin is defined as the Neogene basin occupying the depression bounded by the Coast Mountains on the east and by the uplifted ranges of the Queen Charlotte Islands to the west. The basin is superimposed on older Mesozoic sedimentary basins, and much of it lies under Hecate Strait and the Queen Charlotte Sound. Most strata exposed on the Queen Charlotte Islands are Mesozoic and Paleogene, and form the basement to the Queen Charlotte Basin. Exposures of Neogene rocks are limited to volcanic strata covering much of Graham Island and possibly areas to the south, and small outcrops of Pliocene sedimentary rocks. Mesozoic strata in the Queen Charlotte Islands comprise Upper Triassic and Lower Jurassic rocks of the Wrangell Terrane (Jones et al., 1977), and overlying Jurassic and Cretaceous sedimentary and volcanic strata. The Wrangellia Terrane at the latitude of the Queen Charlotte Islands is bounded to the west by the Queen Charlotte Fault, the major transform fault forming the boundary between Pacific and North American plates. Wrangellian strata may extend to the east of the islands under Hecate Strait, and Triassic volcanic rocks correlated with Wrangellia have been identified east of Hecate Strait on Bonilla Island (Roddick, 1970; Woodsworth, 1988). The Wrangell Terrane is juxtaposed against the Alexander Terrane to the east. Radiometric data indicate that the Alexander Terrane and Wrangellia have been amalgamated since at least Middle Pennsylvanian time (Gardner et al., 1988). van der Heyden (1989) suggests, on the basis of field mapping and geochronologic studies in the Coast Mountains, that both

terrane are elements of a single Alexander/Wrangell/Stikine megaterrene, which represents a single coherent crustal block with no internal sutures.

Rocks of the Queen Charlotte Islands range in metamorphic grade from unmetamorphosed to amphibolite grade. The highest metamorphic grades occur in basic volcanic rocks of the Karmutsen Formation, which commonly display penetrative metamorphic foliations outlined by chlorite and/or amphibolite. Metamorphic mineralogy, conodont colour alteration indices (Orchard, 1988), and thermal maturation trends (Vellutini, 1988) all reflect a general increase in metamorphic grade to the south and west. In addition, strongly hornfelsed volcanic and sedimentary rocks form aureoles around many of the plutons. This contact metamorphism is pronounced enough to completely overprint primary textures, and may extend for several hundreds of metres from intrusive contacts.

### Stratigraphy

Strata of the Queen Charlotte Islands can be viewed simplistically as defining three distinct tectonostratigraphic sequences. Each sequence is bounded by unconformities, may contain internal unconformities, and is subdivided into several map units (Fig. 3). In ascending order, these sequences are: 1) an Upper Triassic to lower Middle Jurassic succession comprising Wrangellian strata, 2) Middle

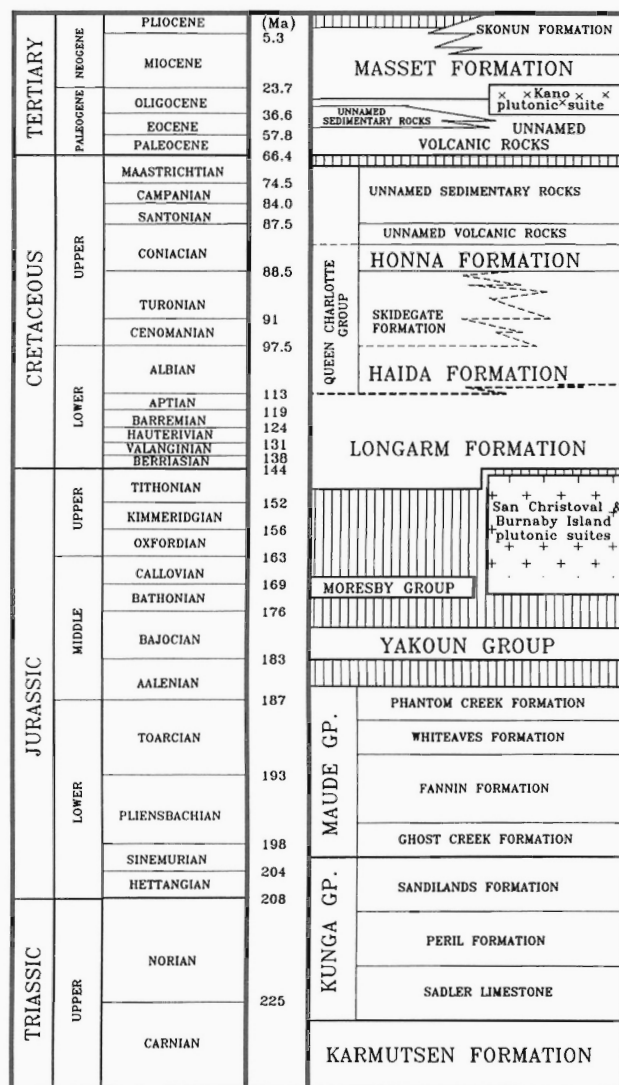


**Figure 3:** Simplified stratigraphic column showing ages of major lithologic units in the Queen Charlotte Islands.

Jurassic and Cretaceous volcanic, volcanoclastic, and siliciclastic units, the distribution and facies of which are largely structurally controlled, and 3) Tertiary volcanic and sedimentary rocks. Intrusions related to two periods of plutonism are exposed throughout the islands. For detailed stratigraphic descriptions, the reader is referred to Cameron and Tipper (1985), Desrochers (1988), Fogarassy (1989), Haggart (1986, 1987, 1989, 1991), Haggart and Higgs (1989), Higgs (1989), and Hickson (1989, 1991).

#### *Triassic to lower Middle Jurassic*

The oldest rocks found in the Queen Charlotte Islands comprise the Wrangellian assemblage of Karmutsen Formation, Kunga Group, and Maude Group. The Kunga Group is divided into the Sadler Limestone and the Peril and Sandilands formations, while the Maude Group comprises the Ghost Creek, Fannin, Phantom Creek, and Whiteaves formations. This sequence is a continuous succession of Late Triassic to lower Middle Jurassic age, and contains no significant unconformities. Paleozoic rocks have not been identified in the Queen Charlotte Islands, and for the purposes of discussion the Karmutsen Formation/Kunga Group/Maude Group succession will be referred to as structural and stratigraphic basement in this report.

Organic-rich shales occurring within the Sandilands and Ghost Creek formations are considered to have the greatest petroleum source rock potential of the Queen Charlotte region (Vellutini, 1988; Vellutini and Bustin, 1991).

#### *Middle Jurassic and Cretaceous*

A regional angular unconformity separates the Triassic to lower Middle Jurassic succession from all overlying rocks. Some previous workers considered the Middle Jurassic and Cretaceous section above this unconformity to represent two tectonostratigraphic packages (e.g., Yorath and Chase, 1981; Yorath, 1988). However, present studies suggest most Middle Jurassic and Cretaceous rocks share a common depositional style, and therefore they are not subdivided in the present discussion. Middle Jurassic through Cretaceous rocks in the Queen Charlotte Islands include the dominantly volcanic Yakoun Group and siliciclastic sedimentary rocks of the Moresby Group, the Longarm Formation, and the Queen Charlotte Group. The Queen Charlotte Group is further divided into the Haida, Skidegate, and Honna formations, and unnamed volcanic and sedimentary rocks. The Haida and Skidegate formations, together with the underlying Longarm Formation, are interpreted as a Lower to mid-Cretaceous transgressive shelf sequence younging eastwards across the islands (Haggart, 1991). The overlying Honna Formation is a widespread conglomerate/sandstone unit with uncertain stratigraphic relationships to the older rocks.

A distinctive sandy, locally fossiliferous lithofacies of Lower to mid-Cretaceous age contains the highest porosity values measured in any of the stratigraphic succession preserved in the Queen Charlotte Islands, and is considered a primary hydrocarbon reservoir target (Fogarassy and Barnes, 1988). This unit was originally considered to represent a basal member of the Haida Formation, but macrofossil collections from several outcrops have been identified as having equivalent age to parts of the Longarm Formation (Haggart, 1991).

The distribution of Middle Jurassic and Cretaceous strata in the Queen Charlotte Islands is controlled in part by block faults which were active prior to and possibly during deposition. Thompson and Thorkelson (1989) have identified three northwest-trending fault blocks on Louise, Graham, and northern Moresby islands, each of which has a different Middle Jurassic and Lower to mid-Cretaceous stratigraphic succession preserved. The Upper Cretaceous Honna Formation overlaps all fault blocks.

#### *Tertiary volcanic and sedimentary rocks*

Tertiary strata crop out over much of the Queen Charlotte Islands and form thick accumulations in the offshore portion of the Queen Charlotte Basin. The oldest documented Tertiary sedimentary rocks occur at Long Inlet and Hippa Island and are intersected by the Port Louise well, and have yielded Eocene/Oligocene palynomorphs (White, 1990). The regional extent of Eocene/Oligocene sedimentary rocks is uncertain, but several hundreds of metres of section are recognized in both locations.

Tertiary volcanic rocks in the Queen Charlotte Islands have historically all been assigned to the Masset Formation, but Hickson (1991) now recognizes two petrologically distinct suites within these rocks. Oligocene and Miocene volcanic rocks covering much of Graham Island and interdigitating with Miocene and younger sedimentary strata of the Skonun Formation (Cameron and Hamilton, 1988) are assigned to the Masset Formation. Eocene and Lower Oligocene volcanic rocks making up many of the exposures previously mapped as Masset Formation south of central Graham Island are an unnamed petrologically distinct suite (Hickson, 1991).

The Skonun Formation is extensive under Hecate Strait, but surficial exposures are limited to a few outcrops on eastern and central Graham Island. Up to 5 km of Miocene and Pliocene sandstone and shale of the Skonun Formation are encountered in oil-company boreholes in Hecate Strait (Shouldice, 1971). The Skonun Formation includes both organic-rich sediments and porous sandstones and conglomerates, and may have potential as both a hydrocarbon source and a hydrocarbon reservoir beneath Hecate Strait.

#### **Intrusive rocks**

Anderson and Greig (1989) assign most intrusive rocks in the Queen Charlotte Islands to either a Tertiary (Oligocene) plutonic suite or one of two Late Jurassic plutonic suites. These suites all represent calc-alkaline, I-type plutonism and define northwest-trending magmatic belts. Intrusive rocks are volumetrically most abundant in the southern portion of the islands.

## **STRUCTURAL GEOLOGY**

Mesozoic and Cenozoic deformation in the Queen Charlotte Islands has resulted in complex faults, folds, and structural fabrics in rocks of all ages. Structures were analyzed in the four map areas at northwest Graham Island, Rennell Sound, Long Inlet/Kagan Bay, and Louise Island (see also Fig. 25). Mapping in these areas, a regional strain analysis study, and regional mapping by Thompson et al. (1991) all combine to outline a structural model involving at least four separate pulses of deformation.

#### **Map descriptions**

The four map areas examined in this study provide glimpses of deformation styles at a number of structural and stratigraphic levels at separate locations across the Queen Charlotte Islands. Regional mapping programs have helped establish continuity between these areas, and have added timing constraints to some of the structures described.

#### *Northwest Graham Island map area*

On Graham Island north of Kennecott Point, strata of Late Triassic to Cretaceous age are continuously exposed along wave-cut benches. Detailed structural maps were completed at Kennecott Point, along the south shore of Sialun Bay, and just north of Fleurieu Point. At these locations, well bedded limestone, sandstone, and siltstone of the Peril Formation are complexly deformed by several generations of folds and faults.

**Kennecott Point.** 1:1000 scale structural mapping was completed at Kennecott Point for an area measuring roughly 500 m by 200 m

(Fig. 4a, in pocket). Mapping was aided by a 1:660 scale aerial photograph of the outcrop, prepared as a base for biostratigraphic studies in the area.

Bedding at Kennecott Point strikes approximately east-west, and dips moderately to the south. Dominant structural features comprise two nearly orthogonal sets of subvertical faults, striking 030-040° and 130-140°. The northeast-trending faults consistently cut and offset northwest-trending faults. Fault surfaces for both sets are either discrete surfaces or narrow (<2 m) brittle shear zones. Northeast-trending faults span the width of exposed outcrop, whereas northwest-trending faults can be traced with certainty for only tens of metres. Offset amount and direction were determined through examination of slickensides, fault-drag folds, and offsets of marker beds. Both sets of faults record subhorizontal, left-lateral offset. The older, northwest-trending faults commonly have metres to tens of metres of offset, whereas younger, northeast-trending faults have separations greater than their exposed strike length, at least 200 m.

Within fault-bounded blocks, bedding is buckled into broad, open, northwest-trending warps. Tight folds are rare and limited to strata immediately adjacent to fault surfaces. Both types of folds are likely minor local features related to fault movement.

The most elongate fault blocks, which are bounded by closely spaced northeast-trending faults, have bedding attitudes striking 050-080°. This is slightly more northerly than regional bedding trends, and may be related to anticlockwise rotation of the strata within the block during faulting. This rotation was accompanied by slip along bedding surfaces, and the sense of rotation displayed is consistent with the left-lateral offsets along the bounding faults.

**South Sialun Bay.** 1:1000 scale maps were completed for wave-cut benches of Triassic bedded limestone (Peril Formation) along the south shore of Sialun Bay (Fig 4b, in pocket). In this area, bedding strikes northwest and dips moderately to the southwest. Three major sets of faults were mapped; all dip subvertically. The oldest faults trend 055-065° and have apparent left-lateral offset. Younger faults form two sets: a northwest-trending (150-160°) set with apparent right-lateral offset, and an east-west (090-095°) set with apparent left-lateral offset. Variable crosscutting relations suggest the two younger sets formed synchronously as conjugate faults. Slickensides are rarely preserved, leaving the vertical component of offset uncertain. All faults display metres to tens of metres apparent offset.

Throughout the south Sialun Bay map area intermediate composition feldspar-hornblende-phyric dykes intrude the stratified rocks. These intrusions measure metres to tens of metres in width and up to 200 m in length, and are cut by all faults. Hickson (1989) suggests intrusions in this region are petrologically distinct from Masset Formation volcanic rocks and associated feeders, and may be of similar age to either Honna Formation or Haida Formation sedimentary strata (mid- to Late Cretaceous). Alternatively, the dykes may be related to Middle Jurassic volcanism or Late Jurassic plutonism.

Mesoscopic folds are common within the fault-bounded blocks. These folds have wavelengths of 10-30 m, and outline open to tight buckle forms. Fold hinges are subangular to subrounded, and the tighter folds have faulted cores. Axial surfaces are subvertical and approximately parallel to the younger, east-west trending faults. Fold axes plunge gently to the east or west.

**Fleurieu Point.** The structural geology of the shoreline area just north of Fleurieu Point was described previously by Lewis and Ross (1989). This area differs from others mapped on northwest Graham Island in that the dominant features present are northwest-trending, moderately southwest-dipping thrust faults (Fig. 4c, in pocket). These faults are parallel to bedding or cut across bedding at small angles.



**Figure 5:** Fault duplex structures between adjacent bedding-parallel slip surfaces in bedded Triassic limestone at Fleurieu Point. View looking west demonstrates north-directed sense of transport.

The faults bound 5-10 m thick tabular blocks of Peril Formation bedded limestone, and can be traced for over 100 m along strike. In one location, a three-fold thickening of strata is documented across successive faults. Duplex structures are commonly associated with minor ramps across bedding (Fig. 5).

Tight to isoclinal recumbent folds occur in strata immediately adjacent to fault surfaces. These folds commonly contain axial-planar cleavage parallel to regional compositional layering. Fold axis orientations lie within the fault plane, and are approximately parallel to fault ramp/flat intersection lines. This orientation and the spatial association between folds and faults suggest that the folds formed during faulting as drag features. Fold asymmetry and fault ramp and duplex geometry indicate north to northeast transport directions.

Steeply-dipping faults striking 055-065° and 115-125° offset folds and southwest-dipping faults. Both sets of steeply-dipping faults have subhorizontal slickensides. Drag folds and offset of stratigraphic markers document several metres of left-lateral offset along northeast-trending faults, and uncertain amounts of right-lateral offset along northwest-trending faults.

Faults and folds at all three map locations on northwest Graham Island record a similar structural history. At all locations, at least two generations of crosscutting structures are delineated. Thrust faults at Fleurieu Point and early left-lateral strike-slip faults at south Sialun Bay both record an early episode of north-south directed shortening. Younger left-lateral strike-slip faults at Fleurieu Point and a conjugate set of strike-slip faults at south Sialun Bay indicate a slight clockwise rotation in shortening direction to north-northwest. At Kennecott Point, earliest structures are northeast-striking sinistral strike-slip faults, more compatible with initial east-west directed shortening. These faults have only minor offsets, and the dominant northwest-trending strike-slip faults in the area accommodate north-south shortening, similar to that inferred for the other map areas.

The absolute ages of structures on northwest Graham Island are uncertain. Gently-dipping Cretaceous strata (Haida and Honna formations) overlie the Triassic rocks with pronounced angular unconformity, and are deformed only by broad, map-scale warps and minor faults. It seems likely, therefore, that most of the faulting described is related to Middle to Late Jurassic deformation. Fabric studies of folded strata at Fleurieu Point support this inference (see following section).

#### *Rennell Sound map area*

At the southeastern end of Rennell Sound (Shields Bay), complexly deformed Upper Triassic to Lower Cretaceous strata crop out



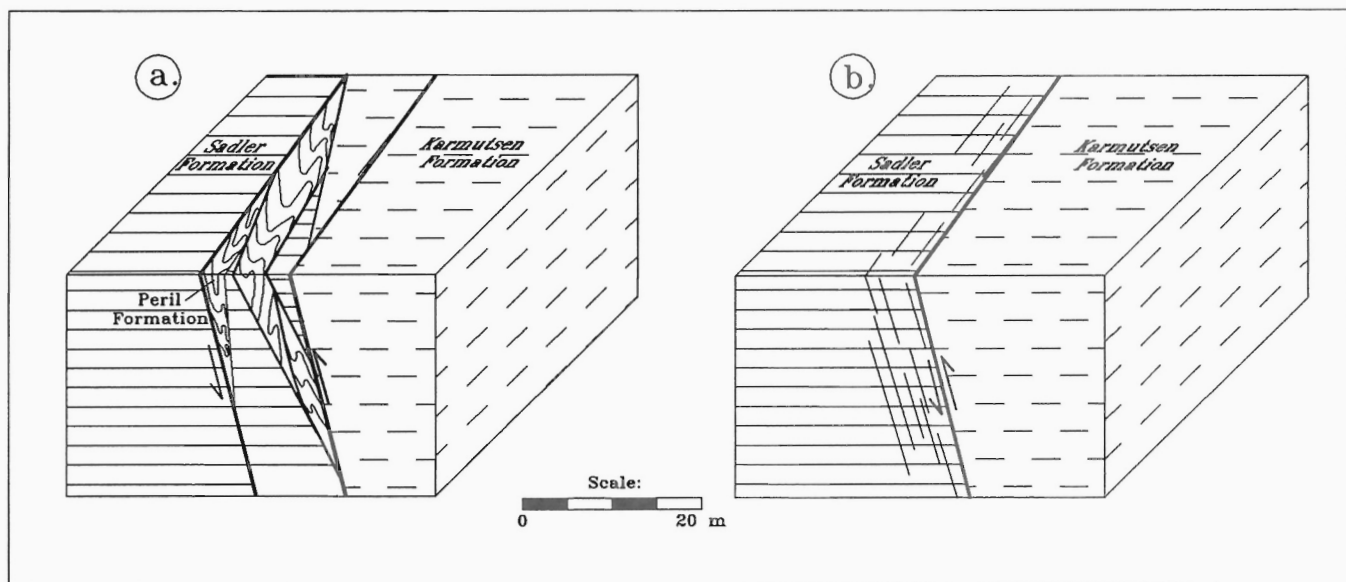


**Figure 7:** Sketches showing contrasting fault styles in Triassic strata at Rennell Sound: a) anastomosing fault surfaces bound fault slivers of intensely folded, bedded limestone and fractured massive limestone and volcanics, b) discrete fault surfaces accompanied by well developed foliations in adjacent massive limestones.

along shorelines and on surrounding hillsides. Shoreline exposures in this area were mapped at 1:20 000 and greater scales, and the hills surrounding Rennell Sound were mapped at 1:25 000 scale (Fig. 6, in pocket).

The Upper Triassic-Lower Jurassic stratigraphic section is particularly well exposed along rocky shorelines of closely spaced islands in Shields Bay. Throughout this area, the structure is characterized by tabular blocks of northeast-dipping strata separated by and repeated across steeply-dipping, northwest-striking ( $135\text{--}160^\circ$ ) faults. Younger subvertical faults strike  $080\text{--}090^\circ$  and have minor offset.

Faults of both orientations occur as either discrete fault surfaces, or as complex brittle fault zones up to 20 m wide (Fig. 7). Within brittle fault zones, anastomosing fault surfaces juxtapose slivers of well-bedded strata (Peril and Sandilands formations) between blocks of older, more massive volcanic or sedimentary rocks (Karmutsen Formation and Sadler Limestone). These slivers of bedded rocks are themselves internally faulted and strongly folded. Folds are disharmonic, tight, and have subhorizontal axes which trend parallel to fault zone boundaries.

Discrete fault surfaces commonly are accompanied by pervasive foliations in adjacent rocks. These foliations are best developed in massive rocks of the Sadler Limestone and are limited to rocks within 5–15 m of the fault surface. Recrystallized calcite veins cut across the foliation at small to moderate angles. Many are tightly to isoclinally folded, with axial planes parallel to the foliation and fold axes parallel to the mineral lineation.

In addition to those folds occurring within fault zones and clearly related to faulting, recumbent isoclinal folds occur rarely within bedded limestones and siltstones of the Peril Formation (Fig. 8). These folds are typified by northwest-trending axes and layer thickening in hinges, and the amount of regional structural thickening they represent is uncertain. The relationship between these folds and the faults described above is unclear, but they probably represent an earlier phase of deformation.

#### *Long Inlet/Kagan Bay map area*

Regional mapping was completed at 1:25 000 scale for the Long Inlet and Kagan Bay map areas, extending as far south as Skidegate Channel (Fig. 9, in pocket). Reconnaissance mapping of shoreline exposures as far east as Sandspit and as far west as Chaatl Island was conducted. Within the Long Inlet/Kagan Bay map area strata of Middle Jurassic to Paleogene age are represented. A discussion of the structure and stratigraphy of the area at the south end of Long Inlet alone is included in Haggart et al. (1989).

Structures throughout the map area are dominated by northwest-trending faults and megascopic folds, and are reflected in consistent northwest bedding strikes. Megascopic folds have upright axial surfaces, subhorizontal axes, and wavelengths of 1–3 km. Fold styles range from tight, locally overturned structures to broad, open warps. The tightest structures occur in an easterly overturned anticline-syncline pair which transects Long Inlet and coincides with Sutherland Brown's (1968) Rennell Sound Fault Zone. This structure involves strata as young as Upper Cretaceous and has been traced over 40 km



**Figure 8:** Recumbent, northwest-trending isoclinal fold of Triassic Peril Formation limestone exposed along Rennell Sound road. These folds are the oldest recognized structures in the areas mapped.



to the southeast on Moresby Island (Thompson and Thorkelson, 1989). For convenience, Thompson (1988) informally designated these folds the "Rennell Sound Fold Belt", although continuity into Rennell Sound has not been demonstrated. Furthermore, the structural feature contains only a single anticline-syncline pair, and the use of the term "fold belt" is misleading. Therefore, we here designate these major structures the Long Inlet Anticline and Long Inlet Syncline and discourage further use of the terms "fault zone" and "fold belt". The timing of folding is constrained to Late Cretaceous or Early Tertiary by newly described Paleogene strata which unconformably overlie the folds north of Gosset Bay (Lewis, 1990). Total regional shortening associated with Late Cretaceous/Early Tertiary folding is less than 15%, as estimated from fold geometry. This is considerably less than the amounts of shortening observed in Jurassic rocks at the Rennell Sound and Louise Island map areas.

Thompson and Thorkelson (1989) note that the Long Inlet Syncline and Long Inlet Anticline spatially coincide with a major fault (Dawson Cove Fault) which separates two northwest-trending tectonic blocks. In the southwest block, the Longarm Formation directly overlies Kunga Group or Yakoun Group rocks, and in the northeast block, the Haida/Skidegate succession overlies this same Triassic-Jurassic succession. The continuation of the Dawson Cove Fault into Long Inlet is implied by thick successions of Longarm and Skidegate formation strata juxtaposed across the inlet, but the fault has not been observed in outcrop. The fault is overlapped by Upper Cretaceous Honna Formation conglomerate along much of its length, and by volcanic rocks of probable Tertiary age north of Skidegate Channel. We postulate that this major pre/syn-Cretaceous fault may have been reactivated during Late Cretaceous/Early Tertiary folding, and helped localize strain along the Long Inlet Anticline/Syncline fold set.

Steeply-dipping, northwest-trending faults cut all Jurassic and Cretaceous strata and the folds described above. Some of these faults were originally mapped by Sutherland Brown (1968) as components of the Rennell Sound Fault Zone. Although unequivocal offset direction indicators are lacking, the simplest offsets which adequately account for present outcrop patterns involve only hundreds of metres of dip-slip movement.

Youngest structures in the Long Inlet/Kagan Bay area comprise steeply-dipping faults striking 055-070°. Slip direction indicators are lacking, but simplest reconstructions indicate a few hundreds of metres of left-lateral offset. These faults are similar in orientation and sense of offset to faults described at Rennell Sound and in central Graham Island (Indrelid et al., 1991).

Mesoscopic structures related to folding and faulting are ubiquitous in shale sequences of the Skidegate and Haida formations. Low-angle detachments produce minor stratal repetition in cores of major folds and are likely space-accommodating features. Well-defined pencil lineations are parallel to fold axes, and locally a weak cleavage is parallel to axial planes. Mesoscopic structures in coarse clastic and volcanic lithologies are limited to fracture surfaces with minor offset and ubiquitous calcite- and quartz-filled veins, and cannot be conclusively related to specific megascopic structures.

#### *Southeast Louise Island map area*

Shoreline exposures and adjacent hillsides and offshore islands were mapped at 1:25 000 scale along southeast Louise Island from Dass Point to Skedans Point (Fig. 10, in pocket). Most exposures in this area are of Triassic and Jurassic strata. Exceptions occur at Skedans Point where Cretaceous rocks of the Longarm and Haida formations crop out. Structures in Triassic and Jurassic rocks on southeast Louise Island are similar in style and orientation to those described in similar age strata at Rennell Sound. Bedding dips in the area are

generally to the northeast, especially in the Karmutsen Formation and Sadler Limestone, but strike directions are overall more westerly than those recorded at Rennell Sound.

Most map-scale faults in the area are steeply dipping and strike between 090° and 140°. Distinct sets with consistent crosscutting age relationships cannot be delineated. In the massive rocks of the Karmutsen Formation and Sadler Limestone, faults dip steeply to the north-northeast and occur both as discrete surfaces and as 10-30 m wide anastomosing brittle fault zones. In the Sadler Limestone, many discrete fault surfaces have an associated foliation which is parallel to the fault surface. Brittle fault zones are characterized by a complex internal geometry and strongly folded slivers of well-bedded limestone (Peril Formation). Folds in the limestone are disharmonic, bedding dips are subvertical, and internal faults are closely spaced. These bedded limestones occur bounded by blocks of massive Karmutsen Formation or Sadler Limestone strata, and therefore must be displaced from higher levels in the stratigraphic succession.

In the well-bedded Peril and Sandilands formations, fault attitudes are much shallower, and measurable displacements across single surfaces are smaller. Folds occur as map-scale features and, more commonly, as mesoscopic structures. Mesoscopic folds have wavelengths of metres and are characterized by subvertical axial surfaces and tight chevron forms. Bed-length shortening across fold sets typically measures 10-20%, but may locally exceed 40%. Most folds are asymmetric and record a southeast-directed sense of vergence.

Estimates of direction and amount of net slip along faults are made by measurement of observed offsets in stratigraphic markers and kinematic analyses of fault fabrics. Kinematic indicators (discussed in following section) all indicate a dominant down-dip component of slip. Down-dip separation of stratigraphic markers is commonly only hundreds of metres in a north-side-up sense. With the northwesterly bedding dips common to this area, this displacement represents a net shortening and structural thickening. Although the total shortening across any one fault is relatively minor, the close spacing of faults allows larger regional strains to be accommodated.

Between Skedans Point and Skedans Bay, the Jurassic Yakoun Group and Cretaceous Longarm Formation unconformably overlie the Triassic-Lower Jurassic succession. These younger strata are broadly folded about northwest-trending axes; it is unclear if they are affected by the faults mapped at deeper structural levels.

Strata of the Peril and Sandilands formations between Dass Point and Vertical Point are intruded by numerous, closely spaced dykes and sills. These intrusions locally comprise up to 80% of exposed rocks, and in places pass into poorly stratified or unstratified brecciated volcanic lithologies which may represent subaerial volcanic flows. Dykes of similar character on western Louise Island have been shown to be related to Tertiary volcanism (R.I. Thompson, pers. comm., 1989).

#### **Discussion**

The map studies described above, when combined with the regional mapping described by Thompson et al. (1991), delineate four episodes of deformation which affected the Queen Charlotte region in Mesozoic and Cenozoic time. From earliest to most recent, these are: a) Middle Jurassic shortening, b) Late Jurassic to mid-Cretaceous block faulting, c) Late Cretaceous or Early Tertiary folding, and d) Neogene block faulting. An additional Tertiary shortening event is inferred from structures in Paleogene strata north of Long Inlet and is discussed by Lewis (1990). The regional significance of this event is uncertain, and it is not addressed here. Northwest-trending structures are common to all episodes of deformation. As a result individual structures observed in the field, especially in older rocks, are difficult to ascribe to specific episodes of deformation. Multiple offset histo-

ries are likely for many faults, and folds formed during early deformation may have been subsequently modified. The geometry of each of these episodes and the geologic evidence which constrains the timing of deformation are summarized below.

#### *Middle Jurassic shortening*

Earliest structures recognized in the Queen Charlotte Islands comprise northwest-trending folds and contractional faults in Triassic-Middle Jurassic strata. Several lines of evidence constrain the onset of compression to Aalenian time:

- The Late Triassic (Carnian) to Middle Jurassic (Aalenian) sedimentary section represents a continuous succession unbroken by internal unconformities (Tipper, 1989).
- Bajocian Yakoun Group strata unconformably overlie all older rocks. In places, the unconformity surface represents a sharp, angular discordance where gently dipping undeformed strata overlie subvertically dipping, strongly folded rocks (see Thompson et al., 1991).
- Amounts of shortening across contractional structures are much greater in the Triassic to Middle Jurassic section than at higher stratigraphic levels.
- Structural fabrics in folds of Kunga Group rocks indicate that deformation occurred in poorly lithified sediments, at relatively shallow levels (see following section).
- Dykes of Tithonian age crosscut folds within the Sandilands Formation (Anderson and Reichenbach, 1991).

Northwest-trending reverse faults at Rennell Sound and Louise Island are probably manifestations of this early shortening. Strike-slip faults mapped on northwest Graham Island would have accommodated similar orientations of shortening.

#### *Middle Jurassic/Cretaceous block faulting*

The present distribution of Middle Jurassic through mid-Cretaceous strata suggests a strong control on sedimentation pattern by episodic block faulting. Thompson and Thorkelson (1989) and Thompson et al. (1991) describe three northwest-trending stratigraphic belts which transect northern Moresby and Louise islands. Each stratigraphic belt is bounded by steep faults, which in turn are overlapped by Upper Cretaceous Honna Formation conglomerates. Within each belt, the Middle Jurassic to mid-Cretaceous stratigraphic section preserved differs from that in neighbouring blocks: the central block lacks Yakoun Group and Longarm Formation strata, the northeast block has no Longarm Formation strata and only a thin section of Haida Formation strata, and the southwest block completely lacks Haida Formation strata (Thompson and Thorkelson, 1989). The thicknesses and facies preserved in these belts vary with position relative to the bounding faults (Fogarassy, 1989; Thompson et al., 1991). These stratigraphic relations require several periods and senses of offset on the bounding faults, controlling the erosion and sedimentation of the Middle Jurassic through Cretaceous units. This theme is developed more fully by Thompson et al. (1991) in their discussion of regional stratigraphic distribution.

#### *Late Cretaceous/Early Tertiary folding*

A northwest-trending belt of tightly folded Cretaceous strata has been mapped through Long Inlet (Lewis and Ross, 1988) and southwest across northern Moresby Island to Louise Island (Thompson and Thorkelson, 1989). Volcanic strata which conformably overlie Honna Formation conglomerates in Long Inlet are involved in this folding (Haggart et al., 1989). However, Miocene (Masset Formation) volcanic rocks throughout Graham Island are generally flat-lying (Hickson, 1989), and gently-dipping Eocene/Oligocene sedimentary strata unconformably overlie the upturned edge of steeply dipping

Honna strata both north and south of Long Inlet (Lewis, 1990). These field relations restrict the timing of folding of Upper Cretaceous strata to Late Cretaceous and/or Early Tertiary.

#### *Tertiary Block Faulting*

Evidence of Tertiary block faulting occurs both in surficial exposures and in offshore regions. Steeply-dipping, northwest-trending faults cut all Mesozoic strata exposed on the Queen Charlotte Islands. Both northwest-trending and east-northeast-trending faults cut Late Cretaceous/Early Tertiary folds in the Long Inlet area. The Sandspit Fault bounds a thick accumulation of Neogene strata on its east side and displays evidence of recent movements (Sutherland Brown, 1968). Reflection seismic data from Hecate Strait indicate numerous steeply-dipping faults of uncertain strike orientation cutting the Tertiary basin fill (Rohr and Dietrich, 1991).

Seismic data from Hecate Strait and onshore exposures show folding of Neogene Skonun Formation strata (Rohr and Dietrich, 1991; Lewis et al., 1990). The regional significance of this folding is uncertain, and it may be related to pencontemporaneous block faulting.

Styles of mesoscopic structures vary regularly throughout the stratigraphic section, reflecting the mechanical response of the different lithologic layers to deformation. At deepest levels, in massive strata of the Karmutsen Formation and Sadler Limestone, regional strain is accommodated by displacements along steeply-dipping faults or is distributed across shear zones during both contractional and extensional deformation. Less competent, bedded strata occurring at higher stratigraphic levels are strung out along anastomosing fault zones, reflecting multiple periods of faulting. As faults pass upward into bedded rocks, both mesoscopic and map-scale folds accommodate increasing amounts of strain. A transition from block faulting to broad folding is particularly well displayed on southeast Louise Island, where a map-scale warp of the Sadler Limestone is cored by a faulted block of the Karmutsen Formation (Fig. 11). This style transition is related to strong lithologic layering (bedding) playing an increasing role in controlling structural development at higher levels. One exception to this progression of structural styles occurs on northwest Graham Island, where north-northwest-directed shortening in bedded limestones (Peril Formation) occurs by strike-slip movement along subvertical faults. This change in style may reflect a local change in stress configuration, to one in which minimum stresses are in a horizontal rather than vertical orientation.



**Figure 11:** Faulted anticline on southeast Louise Island. Massive block of Karmutsen Formation volcanic rock (dark colour) is faulted into core of structure outlined by basal Kunga limestone.

Most of the Mesozoic rocks above the Maude Group behaved as thick, competent structural units during deformation. Although bedding is well-defined in many of these units, it does not represent the strong mechanical layering characteristic of the Maude Group and upper parts of the Kunga Groups. Consequently, bedding-parallel detachments and folding are less common. Mechanical layering instead is defined by major lithologic boundaries, which occur with a spacing of hundreds of metres. As a result, structural styles are dominated by broad folds with wavelengths of hundreds of metres to kilometres, and by steeply-dipping faults. Within hinges of these megascopic folds, especially in thinly- to medium-bedded siltstones and shales of the Queen Charlotte Group, greater strains are manifested in detachment surfaces at low angles to bedding, in mesoscopic folding, and in the development of weak penetrative fabrics.

## Strain analysis

### Introduction

Invertebrate fossils can often be used as markers to determine the magnitude and direction of finite strain in deformed rocks. In the Queen Charlotte Islands, deformed ammonites from the Kunga, Maude, and Yakoun groups and belemnites from the Yakoun Group were used to characterize the strain patterns associated with regional deformation.

Many ammonites have keel lines which outline logarithmic spirals when undeformed. The deformation of a logarithmic spiral can be quantified using one of several methods; the method described by Blake (1878) was used in this study. Blake's method requires visual estimation of elongation direction and, therefore, is less accurate for low values of strain. Strains determined by this method are two-dimensional and reflect only the deformation in the plane containing the keel spiral. In all samples measured, the ammonites were preserved as prints on bedding surfaces (Fig. 12), and consequently the values obtained are a measure of bedding plane finite strain. Ammonites within concretions were not measured, as the competency contrast between concretions and surrounding rocks effectively shields the fossils from regional deformation.

Belemnites are preserved as either empty casts or as calcite shells within sandstone and siltstone lithologies. The calcite shells are a more competent material than surrounding rocks, and underwent brittle failure during deformation. Strain magnitudes and directions were determined by measuring the amount of elongation of belemnites in different orientations, and applying a Mohr circle solution (Ramsay and Huber, 1983). Ideally, a randomly oriented distribution of fossils will allow three-dimensional strains to be analyzed; in this case, belemnites are preserved along bedding planes, and only bedding plane strains were quantified.

Ammonites were collected and/or photographed at 19 locations on Graham, Louise, Moresby, Maude, and Sandilands islands, and belemnites were collected at one location near Rennell Sound. A total of 96 ammonites were measured at these locations. Intervals within the Sandilands, Ghost Creek, and Phantom Creek formations and the Yakoun Group are represented. None of the fossils observed in Cretaceous strata in the course of the mapping studies displayed measurable distortion. Measured strains were restored to horizontal by a single rotation about bedding strike. Procedures and calculations are tabulated in Appendix 1.

### Results and discussion

All samples showed restored elongation directions in the northwest quadrant (Fig. 13). This elongation direction is approximately parallel to regional structural trends and perpendicular to the shortening direction inferred from mapping studies. In central Graham Island, the two most northerly locations sampled show an abrupt change

towards a more east-west elongation direction. Structures mapped in this area do not display a similar change in orientation (Indrelid et al., 1991). Strata at these locations may have undergone a structural history which makes restoring bedding by a simple rotation about strike invalid. Belemnites from the Yakoun Group sandstones above Rennell Sound have elongation directions and magnitudes similar to those obtained using ammonites as strain markers.

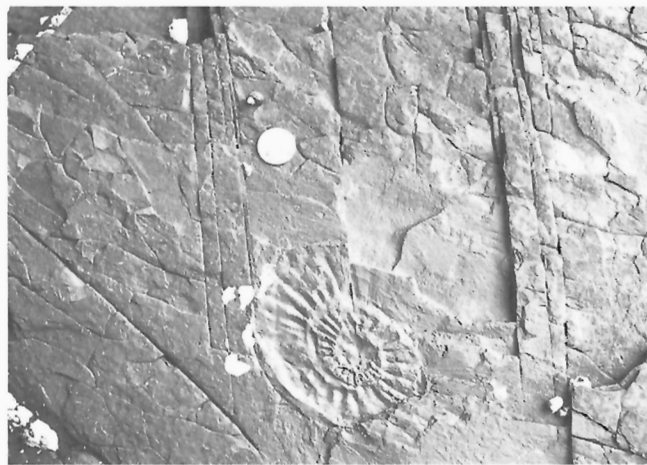


**Figure 12:** Example of deformed ammonite print used to characterize regional bedding-plane finite strain.

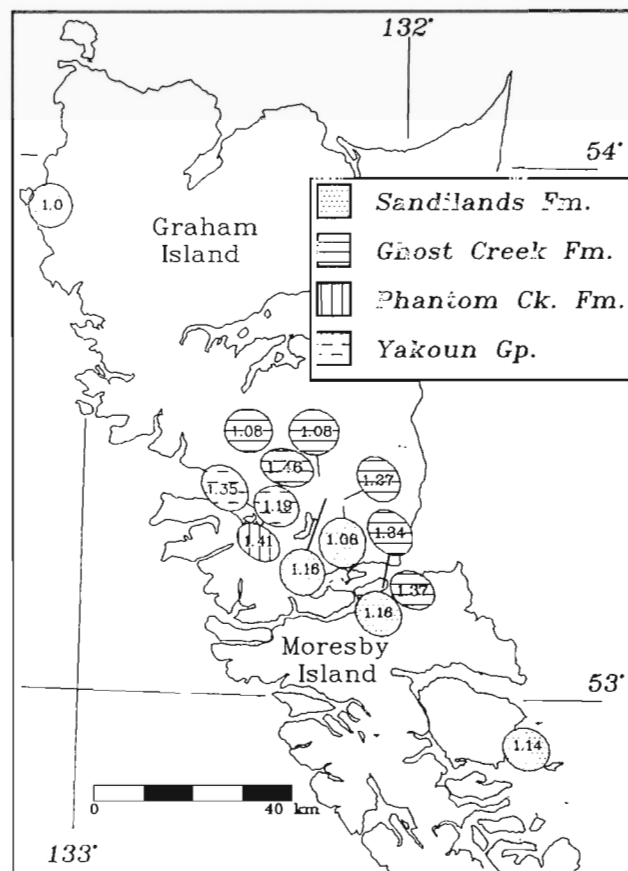


**Figure 13:** Map showing variation in bedding-plane finite strain with geographic position and stratigraphic level, as determined from deformed ammonites and belemnites. At all locations studied, northwest elongation directions are observed, with highest strain values occurring in massive or thickly bedded Ghost Creek Formation siltstones.

Magnitudes of strain ratios ( $1+e_1/1+e_3$ ) measured range from 1.0 (unstrained) to 1.51. The strain ratios can be directly correlated with lithologic characteristics: lower strain values were obtained from strongly bedded rocks with well defined mechanical stratification (Sandlands Formation), while uniform, massive siltstones and sandstones (Phantom Creek and Ghost Creek formations) contained more highly strained fossils.

Several limitations to the regional significance of these results must be recognized:

1. Measured strains may be cumulative from several deformation events, and may thus represent both Jurassic and Late Cretaceous/Tertiary shortening. However, fossils in Cretaceous rocks are rarely preserved as bedding plane prints, and are not observed in deformed states. This makes the effect of younger deformation in the older rocks difficult to quantify. Shortening related to the Late Cretaceous/Early Tertiary folding can be estimated by measuring bed-length shortening in cross sections drawn perpendicular to structure. Total shortening in a section through the Long Inlet/Kagan Bay area (Fig. 9, in pocket) measures only 7-10%. This shortening is considerably less than values determined from ammonites in Jurassic rocks, which range up to 20%, assuming constant volume deformation and plane strain (volume loss yields greater values of shortening). The strains calculated, therefore, reflect to a large extent shortening prior to folding of Cretaceous strata, i.e., deformation during the Middle Jurassic compression. Deformed belemnites from Yakoun Group rocks indicate that the regional penetrative strain associated with Middle Jurassic shortening may locally affect rocks above the basal Yakoun Group unconformity.
2. Measured strains reflect the bulk internal strain of the layers in which the fossils occur. In addition to this bulk strain, shortening is accommodated by displacement along mesoscopic and megascopic faults and by folding. Therefore, calculated strains reflect only a minimum value for regional shortening.

## Structural fabrics

### Introduction

Structural fabrics preserved in Mesozoic strata of the Queen Charlotte Islands include fissility and spaced cleavage in shales, foliation in the Sadler Limestone, and mylonitic fabrics in metavolcanic rocks of the Karmutsen Formation. In addition, folded Peril Formation bedded limestones at Fleurieu Point have locally well-developed axial-planar cleavages. Nearly all lithologies contain abundant quartz or calcite veins. Thin section analyses have helped to describe the microscopic elements defining these fabrics, and helped to identify weak fabrics not visible mesoscopically.

### Mesoscopic description

**Shale fabrics.** Shales and siltstones of the Haida, Skidegate, and Ghost Creek formations contain two morphologically distinct types of cleavage. The most common is a strong fissility (cleavage) inclined to bedding at small to moderate angles ( $<30^\circ$ ) (Fig. 14). This fabric is defined by planar parting surfaces, which occur penetratively or with a spacing of up to 5 mm. The cleavage generally strikes northwesterly, but dip amount and direction are variable. Conclusive geometric relations between cleavage orientation and local folds could not be established in field exposures, except in parts of the Long Inlet map area where cleavage is locally parallel to megascopic fold axial planes. In some locations, a second, bedding-parallel fissility results in pencil intersection lineations; these structures are prismatic or bladed in form, depending on the angle between parting surfaces (Fig. 15).

A separate subclass of spaced cleavage occurs only in concretionary shales of the upper part of the Haida Formation. This cleav-

age cuts bedding at high angles, but, unlike the fabrics described above, the cleavage surfaces are not planar, and refract sharply across lithologic layering (Fig. 16). The resultant form is one in which cleavage surfaces approximate angular fold forms with axial planes following lithologic boundaries. Cleavage spacing is variable from 2-10 mm; the more closely spaced examples are limited to finer-grained lithologies. Cleavage surfaces are continuous for at least tens of centimetres, and in some locations anastomose slightly. Rocks fracture readily along cleavage surfaces, revealing shiny surfaces with striations oriented perpendicular to bedding traces. Rarely, bedding is offset by up to 20 cm across cleavage traces.

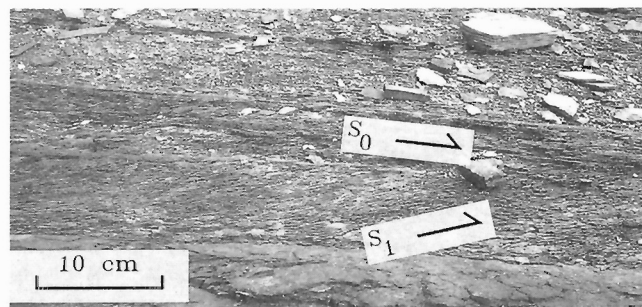


**Figure 14:** Bedding ( $S_0$ ) at small angles to cleavage ( $S_1$ ) in Skidegate Formation siltstone at Kagan Bay, Graham Island.



**Figure 15:** Pencil lineation structures in Skidegate Formation siltstone from East Skidegate Narrows. Lineation directions are consistently parallel to regional fold axial trends.



**Figure 16:** Spaced, refracted cleavage in Haida Formation mudstone near Onword Point, Moresby Island. Cleavage surfaces refract sharply across bedding surfaces.



Several relationships exist between concretions and the refracted cleavage. Rarely, cleavage is preserved intact within concretions with no change in orientation or style from that in the enclosing shales. More commonly, cleavage is only preserved in the outermost few centimetres of concretions. In a few examples, cleavage is sharply refracted around massive, unclesaved concretions.

**Foliation (Sadler Limestone).** Foliations occur spatially associated with fault surfaces in massive rocks of the Sadler Limestone in the Louise Island and Rennell Sound map areas. A well-developed foliation is limited to a zone up to 15 m wide adjacent to fault surfaces. This fabric is most common along west-northwest-trending, steeply-dipping faults, and is usually absent along east-west-trending faults. The foliation is approximately parallel to fault surfaces, and usually contains a pronounced down-dip lineation. The foliation forms a strong parting surface in outcrop, which is heightened by preferential weathering and fracture. In the few examples where bedding is measurable, bedding traces are folded about open to tight structures with axial surfaces parallel to the foliation, and, in the most extreme cases is transposed parallel to the foliation.

These fault-associated fabrics are unique to the Sadler Limestone. At other stratigraphic levels, faults are represented by discrete surfaces or cataclastic zones and lack associated penetrative fabrics. However, planar fabrics occur along apparently conformable contacts between the Karmutsen Formation and the overlying Sadler Limestone. Along these contacts, the uppermost 0.5-1.0 m of Karmutsen Formation strata is highly altered and weakly foliated parallel to the contact. This altered zone contains abundant sulfide minerals and zeolite amygdules partially or completely replaced by calcite.

**Mylonitic fabrics.** Zones of strongly foliated and banded metavolcanic rocks of the Karmutsen Formation were observed in reconnaissance studies on Shuttle Island in Darwin Sound, and on Chaatl Island. Both exposures are characterized by strong planar fabrics occurring over a zone several hundred meters wide. These fabrics grade from weakly foliated actinolite-chlorite schist along the margins to banded, very fine grained, mylonitic fabrics in the centres. In places, compositional layering forms small angles (10-20°) to foliation, and small offsets of layering are visible (Fig. 17). Discontinuous carbonate layers occur within the foliated zone at both locations and vary in thickness from 0.1-2.0 m. The foliation strikes between 100° and 130° on Chaatl Island and between 140° and 155° on Shuttle Island, and is subvertical in both locations. On Shuttle Island, the most strongly developed fabrics have weak subhorizontal elongation lineations. In addition, both Sutherland Brown (1968) and Woodsworth (1988) reported schistosity within Karmutsen Formation strata at locations not covered by this study.

**Veins.** All rocks in the Mesozoic section contain a high density of veins. Veins vary from planar forms to highly irregular folded surfaces and occur as multiple sets in most locations. In some cases, veins occur in axial-planar orientations along the crests of buckle folds, and as enechelon extension gashes on fold limbs, but most cannot be easily related to mesoscopic structures. Both quartz- and calcite-filled veins are common, and most are between 1 mm and 5 cm in width.

#### *Microscopic description*

All of the mesoscopic fabrics described above are observed on the microscopic scale, as are some weak fabrics not visible on the mesoscopic scale. Thin sections were prepared from samples of Karmutsen Formation, Kunga and Maude groups, and Queen Charlotte Group. In samples containing mylonitic foliation and fault fabrics, sections were cut normal to foliation, both parallel and perpendicular to lineation, to assess kinematic indicators.

In undeformed sections, the Karmutsen Formation is characterized by an igneous fabric with fine- to medium-grained plagioclase (0.5-3 mm) altered to calcite and sericite, set in a patchy matrix of very fine-grained (<0.1 mm) chlorite and sericite. Abundant vesicles are filled with radiating, clear albite, spherulitic chalcedony, chlorite, or cryptocrystalline quartz. This igneous fabric is usually overprinted by a metamorphic/tectonic fabric. In samples collected from margins of mylonitic zones, this fabric is a weak foliation outlined by small (0.5 mm) blades of actinolite set in a matrix of weakly aligned chlorite, sericite, and quartz. Granular epidote, clinozoisite, and calcite outline feldspar remnants. This fabric commonly has thin (1-5 mm) quartz-epidote veins aligned parallel to the foliation. In moderately deformed rocks a strong foliation is defined by elongate grains or clusters of grains of calcite, epidote, clinozoisite, and actinolite. These minerals outline a grain elongation fabric which is crosscut at a small angle (15-30°) by a secondary fabric defined by fine-grained chlorite and sericite (Fig. 18). Agglomerates of epidote and quartz behave as resistant masses and frequently have asymmetric pressure shadows with quartz tails parallel to the secondary fabric. The intersection of these two fabrics is subhorizontal and west-northwest trending, and defines a weak subhorizontal intersection lineation. Small offsets of the primary fabric across the secondary fabric occur in a northeast-side-up sense. In the cores of mylonite zones, the included angle be-



**Figure 17:** Well-developed foliation in Karmutsen Formation on Chaatl Island. Compositional layering is inclined to foliation at small angles and is offset along foliation.

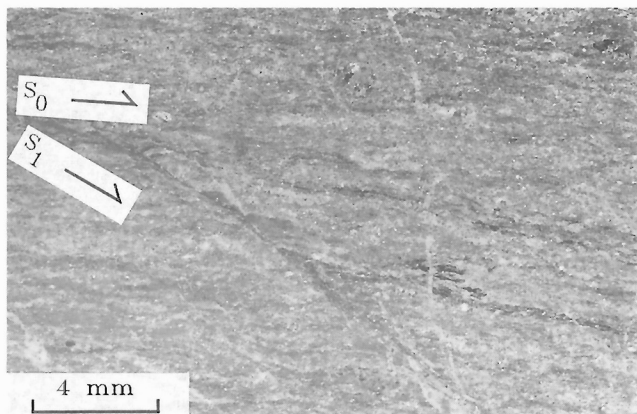


**Figure 18:** Photomicrograph of asymmetric composite fabrics in Karmutsen Formation schist along margins of mylonite zone, Chaatl Island.  $S_0$  is grain elongation foliation,  $S_1$  is secondary shear surface, recording north-side-up shear. These two fabrics intersect in a subhorizontal mesoscopic lineation.



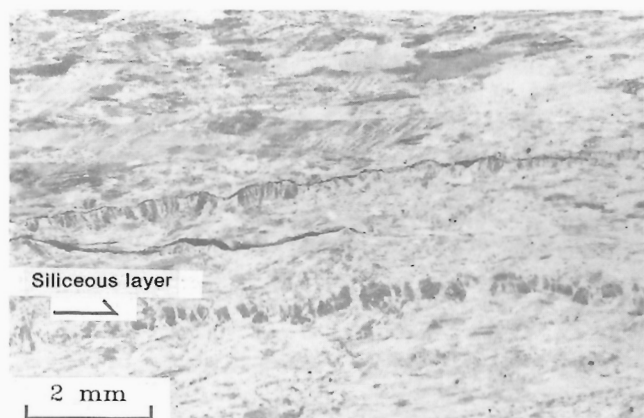


**Figure 19:** Photomicrograph of strongly twinned elongate calcite grains defining foliation in basal Kunga Group limestone adjacent to fault surface. Note brittle pull-apart of more competent siliceous layer (pointed to by arrow) and fibrous calcite infilling fractures.

tween fabrics is only 5–10°, and a concomitant decrease in grain size occurs. Thin marble layers within the highly strained zones have an extremely well-developed foliation. This foliation is defined by elongate calcite grains exhibiting strong twin lamellae that are commonly kinked (Fig. 19). These calcite porphyroblasts are themselves set in a fine-grained groundmass of calcite grains and up to 5% strain-free quartz grains. These finer grains define sutured margins on the larger grains.

Textures in the Sadler Limestone vary from coarsely crystalline to very fine-grained, and are composed almost exclusively of calcite. Calcite grains are strongly twinned, with the greatest twin densities observed in the coarser grains. Abundant stylolites are present, and are filled with organic material and rare, fine quartz grains. Several generations of stylolites are apparent, and many occur nearly perpendicular to planar syntaxial calcite veins. In samples of well-foliated limestone, calcite grains have elliptical or ribbon shapes. In the most strongly foliated samples, grains are highly elongate (up to 8:1) parallel to the down-dip mesoscopic lineation, and moderately elongate (up to 5:1) in strike orientations. In one sample, deformed fecal pellets allow strains to be quantified more accurately (Fig. 20). Axial ratios of 6.1:1 and 3.3:1 were obtained by centre-to-centre strain analysis (see Appendix 2). In some down-dip sections, a weak secondary fabric defined by discrete slip surfaces cuts and offsets the elongation fabric at small angles (10–20°). The sense of offset recorded along this fabric is consistently northeast-side-up.

The bedded limestone of the Peril Formation contains well-developed microscopic fabrics associated with axial planar foliations at Fleurieu Point on northwest Graham Island (Lewis and Ross, 1989). At this location, the limestone is an extremely fine-grained, organic-rich micrite, with abundant calcified radiolaria and scattered, fine-grained andesine feldspar crystals. Bedding is defined by bands of unaltered, fine-grained, euhedral andesine which are closely packed with little intergranular matrix. In cores of mesoscopic folds, these feldspar layers are bent about small-scale buckle folds parasitic to the larger structures. On the outer hinges of these buckles, veins filled with feldspar grains and small amounts of matrix are injected into the adjacent micritic layers, and are parallel to the axial planes of the buckles. A penetrative foliation commonly occurs within the micritic layers parallel to fold axial planes. This foliation is defined by a preferred orientation of elongate calcified radiolaria and particulate organic matter. At one location, shell fragments of the bivalve *Monotis subcir-*

*cularis* outline the foliation. In samples collected near hinge zones of mesoscopic folds, where bedding is at high angles to cleavage, large shell segments are broken and folded into accordion-like forms, with enveloping surfaces parallel to bedding (Fig. 21).

Rocks of the Sandilands Formation are nearly devoid of internal deformation structures, except for those interpreted to be related to sediment loading. In a few samples, a weakly-developed planar zoning of organic concentrations occurs at high angles (45°) to stratification. This weak secondary fabric is not clearly related to any larger scale structures.

Microscopic examinations of Maude Group strata were limited to shales of the Ghost Creek Formation. In these rocks, planar, organic-rich zones similar to those described in the Sandilands Formation occur at high angles to bedding. This zoning is poorly developed even when deformed fossils record up to 20% shortening.

Shales and siltstones of the Haida and Skidegate formations containing fissility or spaced cleavages were examined. Both fissility and spaced cleavages are barely visible on the microscopic scale. In thin sections containing spaced cleavages, phyllosilicate grains are weakly aligned parallel to cleavage traces. Cleavages occur as narrow planar domains (0.1–0.2 mm wide); within these domains, multiple cleavage surfaces anastomose, and the coarser clastic grains may be slightly aligned parallel to domain boundaries (Fig. 22). Bedding traces show small apparent offsets (0.2–1.0 mm) across cleavage surfaces.

#### Discussion

**Fissility, spaced cleavage.** Most cleavages observed in shales could not be related geometrically to any local mesoscopic or megascopic structures. Fissility is most common in rocks with abundant soft-sediment deformation structures, and occurs often as an axial-planar fabric in slump folds. One can therefore speculate that the fissile, bedding-subparallel fabrics formed early in the compaction history of the sediments and may be related to local strains induced by downslope sediment creep and dewatering.

Pencil intersection lineations form as a result of a secondary fabric superimposed on the early bedding subparallel fissility. These features are typical of the early stages of formation of tectonic cleavages (Ramsay and Huber, 1983) and commonly form in an orientation parallel to the Y tectonic direction. West-northwest trends of pencil structures throughout the map area are parallel to mesoscopic and megascopic fold axes, consistent with their formation being related to tectonic strains.

Fabrics similar to the spaced, refracted cleavage of the Haida Formation shale are not well documented in the literature. Spaced cleavage is usually interpreted as a shortening feature associated with larger tectonic structures, formed as a consequence of pressure solution paired with crystalline plasticity and oriented growth of minerals (Williams, 1972). Spaced cleavage has also been demonstrated to represent extensional fractures, or closely spaced joints (Siddans, 1977; Foster and Hudleston, 1986). The spaced cleavage of the Haida Formation lacks any of the characteristic features of pressure solution surfaces, and shows no microscopically visible evidence of oriented mineral growth. Varying relationships with carbonate concretions suggest early formation. We therefore interpret the cleavage surfaces to have originated as extensional microfractures, coincident with dewatering and compaction. The refraction of fracture surfaces observed may be either a primary feature or, more likely, a result of deformation of existing planar fractures. If the refracted form is a primary feature, it likely reflects changes in principal stress directions across lithologic layering as a result of competency contrast. Alternatively, the degree of refraction may have been intensified by post-fracture compaction, or

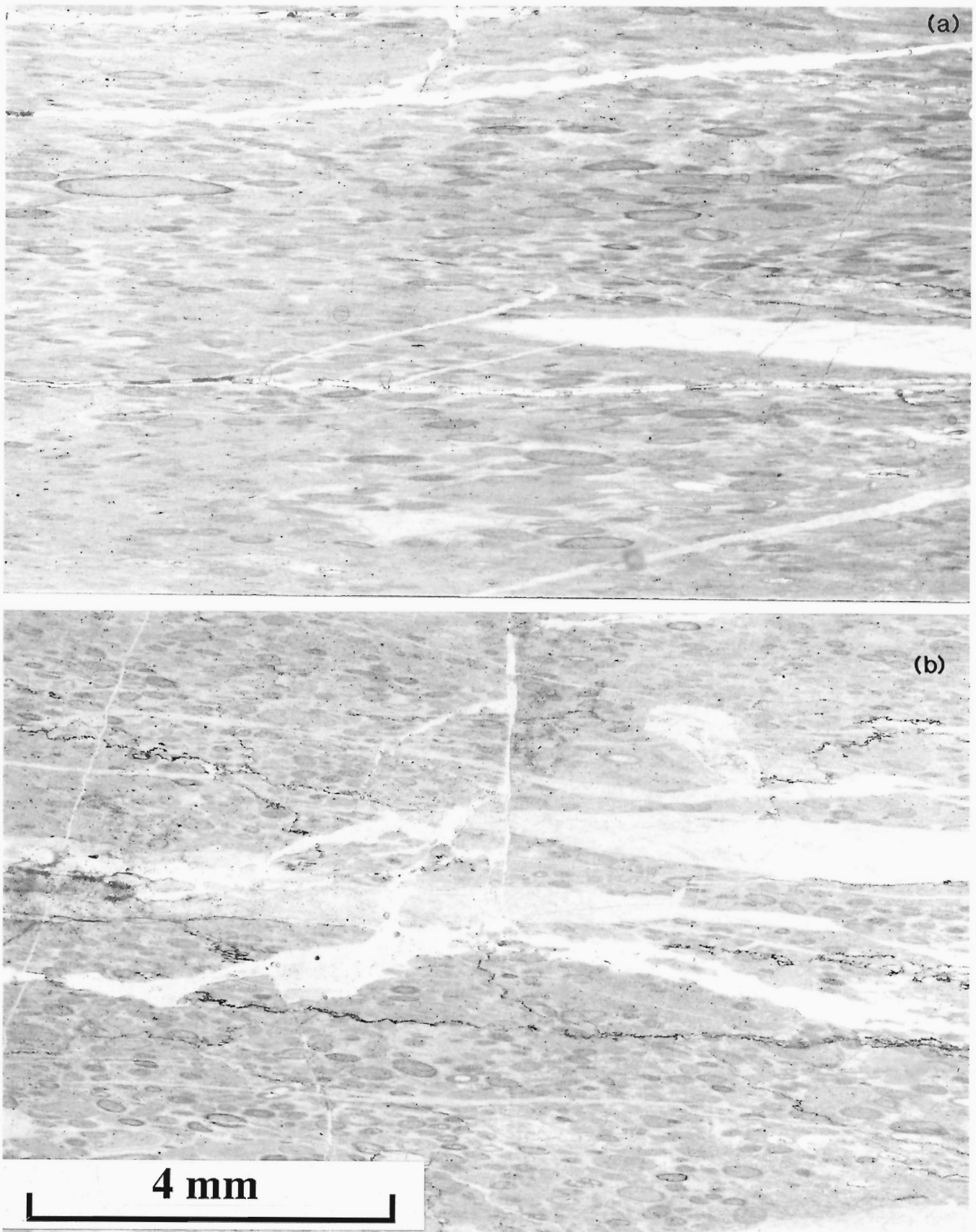


**Figure 20:** Photomicrograph of foliated limestone containing deformed fecal pellets used in centre-to-centre strain analysis: a) thin section cut in down-dip orientation, parallel to mesoscopic lineation, b) section cut perpendicular to lineation and foliation.

by simple-shear of sediment layers during later regional buckle folding. The down-dip striations commonly marking cleavage surfaces and minor offsets of bedding across cleavage may be related to shear movements along fracture surfaces during this folding or compaction.

Possible analogues to the refracted cleavage of the Haida Formation are "vein structures" or spaced foliations found in partially consolidated muds from Deep Seas Drilling Project (DSDP) cores (Cowan, 1982; Lundberg and Moore, 1986). These structures are interpreted to have formed through dewatering as either extensional or passive features (Arthur et al., 1980; Cowan, 1982; Knipe, 1986a; Lundberg and Moore, 1986).

**Fault fabrics.** The use of fault and shear zone fabrics as kinematic indicators is discussed in numerous papers (e.g. Simpson and Schmid, 1983; Cobbold and Gapais, 1987). Composite fabrics and asymmetric porphyroblast strain shadows both occur in sufficient abundance in sheared Triassic rocks of the Sadler Limestone to infer offset sense during deformation. In all samples studied, shear fabrics and flattening foliations intersect in a subhorizontal line, indicating down-dip slip directions. The sense of inclination of shear bands to the flattening foliation indicates northeast-side-up shear associated with fabric development. The specific timing of deformation related to these fabrics is not conclusively determined. The faults associated with these fabrics originated as reverse faults during the earliest (Middle Jurassic) deformation, but a multiple movement history is likely.

**Mylonitic foliations.** Mylonitic zones in the Karmutsen Formation have well developed asymmetric fabrics which in some cases record similar senses of offset (northeast-side-up) to the fault fabrics observed in the Kunga Group limestone. The mylonitic zones are probably a deeper-level manifestation of discrete fault surfaces or brittle fault zones in the Kunga Group, and reflect a transition to distributed strains over

a wider area. Again, the offset direction recorded by mylonitic fabrics cannot be related conclusively to specific episodes of deformation.

**Mechanisms of deformation.** In the Mesozoic section, strains were accommodated throughout deformation by a combination of localized slip on fault surfaces and distributed deformation (folding, microstructure development). Microfabric analyses show that for both localized and distributed deformation, strains have been accommodated through a combination of brittle failure and processes of pressure solution, mechanical twinning, and dislocation creep. The partitioning of strain between these mechanisms through time is largely a function of composition and structural level.

Brittle features include both extensional fractures (veins, extension joints, microcracks) and brittle faults and cataclastic zones. These occur at all structural levels throughout deformation. Veins with blocky or fibrous calcite or quartz filling occur as both planar and folded surfaces, attesting to formation at various stages of structural development. Both syntaxial and antitaxial forms are observed; antitaxial veins formed by the crack-seal mechanism (Ramsay, 1980) are the most common.

The widespread occurrence of stylolites and microscopic pressure solution surfaces provides evidence for strains accommodated through dissolution processes. Stylolites are most common in the calcareous Kunga Group rocks, where they occur at varying angles to bedding. In siliciclastic rocks, sutured quartz grain contacts provide

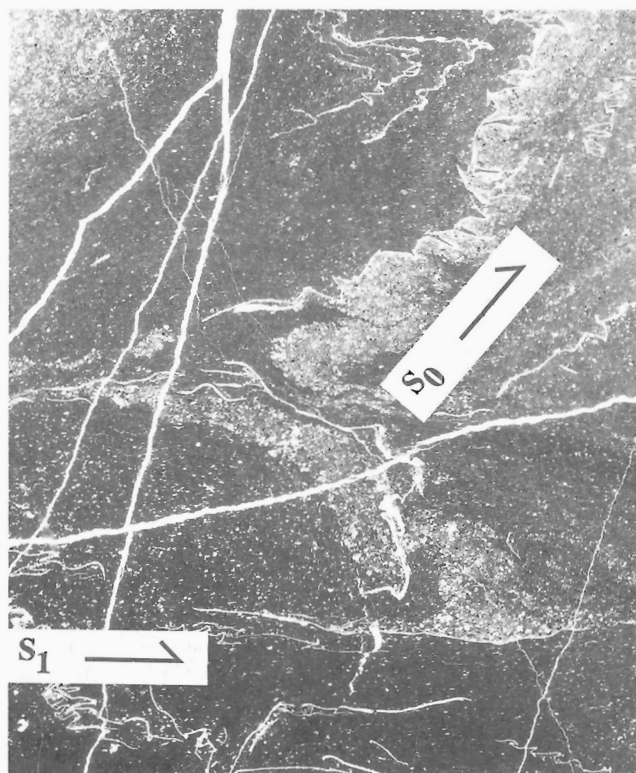


**Figure 21:** Photomicrograph of cleavage ( $S_1$ ) in micritic fossiliferous limestone defined by preferred orientation of elongate calcified radiolaria and parallel arrangement of broken *Monotis subcircularis* shell fragments. The approximate orientation of bedding is shown by the line  $S_0$ .

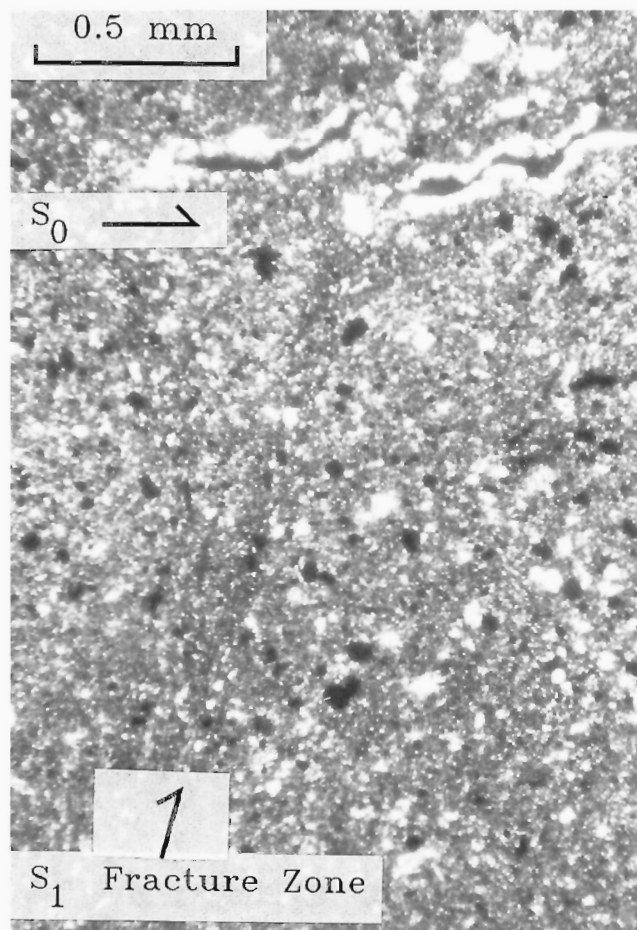


**Figure 22:** Photomicrograph of spaced cleavage ( $S_1$ ) in Skidegate Formation siltstone. Weak cleavage is defined by narrow zones of anastomosing fractures. Note offset of bedding fabric ( $S_0$ ) across fracture.



evidence for pressure solution. Dissolution is likely associated both temporally and spatially with the opening of extensional veins at high angles to dissolution surfaces. These veins may have provided sinks for material which entered the pore fluids at sites of dissolution. This combination of veins and dissolution surfaces leads to cyclic pore-fluid pressure fluctuations, which aid in the transport of fluids through the deforming rocks (Etheridge et al., 1984).

Crystal-plastic processes of deformation included both mechanical twinning and dislocation glide and creep. Calcite grains in limestones have abundant twin lamellae, which are most strongly developed in ribbon grains associated with fault fabrics. The most highly strained carbonate rocks contain recrystallized, strain-free grains concentrated along boundaries between larger, internally strained grains of equal composition. This association is a typical feature of dynamic recrystallization, which occurs through dislocation creep processes.

Rocks at several stratigraphic levels show evidence of fabric development by grain-boundary sliding and intergranular flow at elevated pore-fluid pressures. The most notable features of this type are those observed in *Monotis Subcircularis*-bearing Peril Formation limestone at Fleurieu Point. Shell fragments in these rocks are broken and rotated into cleavage planes, a process which could occur only if the surrounding matrix lacked internal cohesion. In these rocks, elongate calcite grains (calcified radiolaria?) have attained their present shapes through pressure solution. This combination of disaggregation, grain boundary sliding, and pressure solution is compatible with low temperature deformation of partially-consolidated sediments under elevated pore pressures (Knipe, 1986b; Groshong, 1988), and suggests that deformation occurred soon after deposition of the sediments.

## SUMMARY AND IMPLICATIONS FOR HYDROCARBON RESOURCE POTENTIAL

Surficial structural geology studies on regional, mesoscopic, and microscopic scales have led to a more complete understanding of the structural evolution of the Queen Charlotte region than could be gained through studies restricted to a single scale. The present study, paired with the regional mapping of Thompson (see Thompson et al., 1991), has helped constrain a tectonic model for the region involving alternating periods of contraction and extension through Mesozoic and Cenozoic time.

Earliest structures are contractional faults and folds which record south-southeast directed compression in Middle Jurassic time. Middle Jurassic to mid-Cretaceous extension is manifested in northwest-trending block faults. A second episode of compressional deformation in Late Cretaceous and/or Early Tertiary time modified older contractional structures and deformed the Cretaceous section into broad, northwest-trending folds. Latest deformation involved further extension along steeply-dipping northwest-trending and north-south-trending faults. Movement along the Sandspit Fault and along steeply dipping faults imaged by seismic data from Hecate Strait is associated with this last event.

Structural styles during all phases of deformation were controlled by a combination of mechanical rock properties and pre-existing structures. Regional strain is accommodated either by slip along discrete detachment surfaces, by folding, or, at deeper levels, by semi-brittle shear distributed across narrow zones. Shortening of thick, mechanically homogeneous layers was accommodated by offset along steeply-dipping reverse faults and shear zones and by formation of broad folds. Strata with well-developed internal stratification were shortened by slip along contractional faults subparallel to bedding and by formation of tight, mesoscopic folds. Basement faults, formed during the early shortening, controlled at least in part

the location and orientation of later block faults. The present distribution of Middle Jurassic through Cretaceous strata is closely linked to episodic movement along these faults (Thompson et al., 1991).

Throughout deformation, the Mesozoic succession was buried at shallow to moderate crustal depths. Outcrop of greenschist and amphibolite grade metamorphic rocks is restricted to the southern and western portions of the islands, coincident with the greatest occurrence of intrusive rocks. Many of the structures described in the Mesozoic section are compatible with deformation at shallow levels, sometimes in poorly lithified rocks. Regional penetrative fabrics are rare in the areas examined.

Kinematic analyses of fault and shear zone fabrics in Triassic and Jurassic strata corroborate field interpretations based on regional and mesoscopic structural geometry. All asymmetric or composite structural fabrics preserved indicate a dominant dip-slip displacement direction along northwest-trending faults and shear zones, in a southwest-directed or northeast-side-up sense. Megascopic folds in Cretaceous strata at Long Inlet are overturned to the northeast, indicating a reversal in vergence direction during later deformation. This change in vergence may be a local phenomena related to the configuration of reactivated pre-existing structures.

The regional continuity of structural trends throughout the central Queen Charlotte Islands suggests that structural styles observed on land may be successfully extrapolated into offshore areas of the Queen Charlotte Basin. Preliminary results from the offshore seismic reflection survey indicate a strong, north-dipping event on-trend with the Rennell Sound Fold Belt and the Dawson Cove Fault. This event may represent the offshore extension of a major block-bounding fault.

Neither regional mapping nor mesoscopic and microscopic structural analyses supports significant strike-slip offsets along any faults through the Queen Charlotte Islands, and models for the formation of the Queen Charlotte Basin must recognize these constraints. The Rennell Sound Fault Zone, originally mapped as a large transform fault zone, represents a structurally complex zone which has been active throughout the Mesozoic and Cenozoic. It records both contractional and extensional deformation. Several structural features characterize this complex zone of folding and faulting:

- 1) It coincides with the trace of Dawson Cove Fault, a major block fault separating stratigraphically dissimilar outcrop belts (Thompson et al. 1991),
- 2) It coincides with the zone of most intense folding of Cretaceous strata (Long Inlet Anticline and Syncline),
- 3) On northern Moresby Island, it separates a domain to the southwest where the Middle Jurassic unconformity is elevated several thousand metres above sea-level from a domain to the north where the unconformity occurs at near sea-level, and
- 4) At Long Inlet, it forms the locus of deposition for two previously unrecognized stratigraphic units, Upper Cretaceous volcanic rocks and Eocene/Oligocene shales, and as such, may be the location of limited basins during periods of emergence.

Neither "fault zone" nor "fold belt" unambiguously describes this structurally complex region, and the future use of these terms is discouraged.

These conclusions have important implications for the hydrocarbon potential of the Queen Charlotte region:

### 1. Structural controls on distribution of source and reservoir strata:

In many areas mapped, Yakoun Group strata unconformably overlie Kunga Group rocks, and intervening Maude Group strata are

missing. This implies that potential Lower Jurassic source rocks were exposed subaerially and eroded from some areas during Middle Jurassic deformation. In some locations, these potential source strata were structurally thickened during this same deformation event, and are preserved intact. The role of Upper Jurassic/Cretaceous block faulting on preservation of source and reservoir strata is even more pronounced, as discussed by Thompson et al. (1991). Areas where Cretaceous reservoir strata directly overlie Triassic/Jurassic source strata are well documented in the mapping studies, and should be expected to occur in both onshore and offshore regions. Continued surficial geologic mapping on central Graham Island and in the southern Queen Charlotte Islands is necessary to predict the location and extent of these areas.

## 2. Timing of hydrocarbon migration

Middle Jurassic contractional deformation occurred when potential source rocks were at shallow structural levels under low pressure and temperature conditions. Kunga and Maude Group strata did not reach the oil window until after this early deformation event. Maturation associated with local heat sources would not have been significant until Late Jurassic plutonism. The presence of Jurassic biomarkers in Skonun Formation well cuttings from the Sockeye B-10 well (L.R. Snowden, pers. comm., 1989) implies that hydrocarbon migration continued well into the Tertiary, when structural and stratigraphic traps were well established.

## 3. Structures observed in reflection seismic data

Most structures mapped in the Triassic and Lower Jurassic section comprise mesoscopic folds and closely spaced faults, and would not be discernible in seismic sections. Many of the larger-scale structures are steeply-dipping and laterally discontinuous, and would also present problems. The major lithologic and structural break at the base of the Yakoun Group is expected to be a good reflector, as may be the major lithologic transitions within the Cretaceous section. Folds in Cretaceous strata are generally broad, open structures with long wavelengths, and may be recognizable.

## 4. Structural hydrocarbon traps

The episodic deformation described above has resulted in many structures which may prove to be suitable hydrocarbon traps. Broad antiformal folds are common within the Cretaceous sequence, and involve potential hydrocarbon reservoir strata. Unconformities occur throughout the Middle Jurassic to Tertiary section, and, in some places, are associated with strata with high porosity values. Steeply-dipping faults may serve as either up-dip reservoir seals or as migration pathways. The strong northwest structural trends observed on land will probably be retained in the geometry of any subsurface reservoirs.

## ACKNOWLEDGMENTS

We thank R.I. Thompson and the Queen Charlotte Basin Frontier Geoscience Program for logistic and technical support. B.E.B. Cameron, E.S. Carter, J. Haggart, M.J. Orchard, and H.W. Tipper provided macrofossil and microfossil identifications which kept us from straying too far in the stratigraphic column. This study benefited greatly from discussions with many others involved in the Queen Charlotte Basin project; W. Barnes, J. Haggart, C.J. Hickson, J. Hesthammer, J. Indrelid, S. Taite, and R.I. Thompson are thanked in particular. H. Lyatsky and M. Journeay provided useful critical reviews of a preliminary manuscript. We thank S. Dennison, A. Huntley, T. Hale, D. Mercer, and J. Miller for enthusiastic assistance in field work.

## REFERENCES

- Anderson, R.G.  
1988: Jurassic and Cretaceous-Tertiary plutonic rocks on the Queen Charlotte Islands, British Columbia; *in* Current Research, Part E, Geological Survey of Canada, Paper 88-1E, p. 213-216.

- Anderson, R.G. and Greig, C.J.  
1989: Jurassic and Tertiary plutonism in the Queen Charlotte Islands, British Columbia; *in* Current Research, Part H, Geological Survey of Canada, Paper 89-1H, p. 95-104.
- Anderson, R.G. and Reichenbach, I.  
1991: U-Pb and K-Ar framework for Middle to Late Jurassic (172-158 Ma) and Tertiary (46-27 Ma) plutons in Queen Charlotte Islands, British Columbia; *in* Evolution and Hydrocarbon Potential of the Queen Charlotte Basin, British Columbia, Geological Survey of Canada, Paper 90-10.
- Arthur, M.A., Carson, B., and von Huene, R.  
1980: Initial tectonic deformation of hemipelagic sediment at the leading edge of the Japan convergent margin; *in* Initial Reports of the Deep Seas Drilling Project, M. Lee, L. Stout, and others (ed.), Washington, D.C., U.S. Government Printing Office, v. 56, 57, p. 568-615.
- Blake, J.F.  
1878: On the measurements of the curves formed by cephalopods and other mollusks; *Philosophical Magazine*, v. 5, p. 241-262.
- Cameron, B.E.B. and Hamilton, T.S.  
1988: Contributions to the stratigraphy and tectonics of the Queen Charlotte Basin, British Columbia; *in* Current Research, Part E, Geological Survey of Canada, Paper 88-1E, p. 221-227.
- Cameron, B.E.B. and Tipper, H.W.  
1985: Jurassic stratigraphy of the Queen Charlotte Islands, British Columbia; *Geological Survey of Canada, Bulletin* 365, 49 p.
- Cobbold, P.R. and Gapais, D.  
1987: Shear criteria in rocks: an introductory review; *Journal of Structural Geology*, v. 9, p. 521-524.
- Cowan, D.S.  
1982: Origin of "vein structure" in slope sediments on the inner slope of the Middle America Trench off Guatemala; *in* Initial Reports of the Deep Seas Drilling Project, J. Aubouin, R. von Huene and others (ed.), Washington, D.C., U.S. Government Printing Office, v. 67, p. 645-650.
- Crespi, J.M.  
1986: Some guidelines for the practical application of Fry's method of strain analysis; *Journal of Structural Geology*, v. 8, p. 799-808.
- Desrochers, A.  
1988: Sedimentology of the Kunga Group, Queen Charlotte Islands; *in* Some Aspects of the Petroleum Geology of the Queen Charlotte Islands, R. Higgs (compiler), Canadian Society of Petroleum Geologists, Field Trip Guide to Sequences, Stratigraphy, and Sedimentology: Surface and Subsurface, p. 32-36.
- Etheridge, M.A., Wall, V.J., and Vernon, R.H.  
1984: The role of the fluid phase during regional metamorphism and deformation; *Journal of Metamorphic Geology*, v. 1, p. 205-226.
- Fogarassy, J.A.S.  
1989: Stratigraphy, sedimentology, and diagenesis of the Cretaceous Queen Charlotte Group, Queen Charlotte Islands, British Columbia; M.Sc. thesis, University of British Columbia, Vancouver.
- Fogarassy, J.A.S. and Barnes, W.C.  
1988: Stratigraphy, diagenesis, and petroleum reservoir potential of the mid- to Upper Cretaceous Haida and Honna formations of the Queen Charlotte Islands, British Columbia; *in* Current Research, Part E, Geological Survey of Canada, Paper 88-1E, p. 265-268.
- Foster, M.E. and Hudleston, P.J.  
1986: "Fracture cleavage" in the Duluth complex, northeastern Minnesota; *Geological Society of America Bulletin*, v. 7, p. 86-96.
- Gardner, M.C., Bergman, S.C., Cushing, G.W., MacKevett, E.M., Jr., Plafker, G., Campbell, R.B., Dodds, C.J., McClelland, W.C., and Mueller, P.A.  
1988: Pennsylvanian pluton stitching of Wrangellia and the Alexander Terrane, Wrangell Mountains, Alaska; *Geology*, v. 16, p. 967-971.
- Groshong, R.H.  
1988: Low temperature deformation mechanisms and their interpretation; *Geological Society of America Bulletin*, v. 100, p. 1329-1360.
- Haggart, J.W.  
1986: Stratigraphic investigations of the Cretaceous Queen Charlotte Group, Queen Charlotte Islands, British Columbia; Geological Survey of Canada, Paper 86-20, 24 p.
- 1987: On the age of the Queen Charlotte Group of British Columbia; *Canadian Journal of Earth Sciences*, v. 24, p. 2470-2476.
- 1989: Reconnaissance lithostratigraphy and biochronology of the Lower Cretaceous Longarm Formation, Queen Charlotte Islands, British Columbia; *in* Current Research, Part H, Geological Survey of Canada, Paper 89-1H, p. 39-46.
- 1991: A synthesis of Cretaceous stratigraphy, Queen Charlotte Islands, British Columbia; *in* Evolution and Hydrocarbon Potential of the Queen Charlotte Basin, British Columbia, Geological Survey of Canada, Paper 90-10.
- Haggart, J.W. and Higgs, R.  
1989: A new Late Cretaceous mollusc fauna from the Queen Charlotte Islands, British Columbia; *in* Current Research, Part H, Geological Survey of Canada, Paper 89-1H, p. 59-64.



- Haggart, J.W., Lewis, P.D., and Hickson, C.J.**  
**1989:** Stratigraphy and structure of Cretaceous strata, Long Inlet, Queen Charlotte Islands, British Columbia; *in* Current Research, Part H, Geological Survey of Canada, Paper 89-1H, p. 65-72.
- Hickson, C.J.**  
**1988:** Structure and stratigraphy of the Masset Formation, Queen Charlotte Islands, British Columbia; *in* Current Research, Part E, Geological Survey of Canada, Paper 88-1E, p. 269-274.  
**1989:** An update on structure and stratigraphy of the Masset Formation, Queen Charlotte Islands, British Columbia; *in* Current Research, Part H, Geological Survey of Canada, Paper 89-1H, p. 73-80.  
**1991:** The Masset Formation on Graham Island, Queen Charlotte Islands, British Columbia; *in* Evolution and Hydrocarbon Potential of the Queen Charlotte Basin, British Columbia, Geological Survey of Canada, Paper 90-10.
- Higgs, R.**  
**1989:** Sedimentological aspects of the Skonun Formation, Queen Charlotte Islands, British Columbia; *in* Current Research, Part H, Geological Survey of Canada, Paper 89-1H, p. 87-94.
- Indrelid, J., Hesthammer, J., and Ross, J.V.**  
**1991:** Structural geology and stratigraphy of Mesozoic rocks of central Graham Island, Queen Charlotte Islands, British Columbia; *in* Evolution and Hydrocarbon Potential of the Queen Charlotte Basin, British Columbia, Geological Survey of Canada, Paper 90-10.
- Jones, D.L., Silberling, N.J., and Hillhouse, J.**  
**1977:** Wrangellia – a displaced terrane in northwestern North America; *Canadian Journal of Earth Sciences*, v. 14, p. 2565-2577.
- Knipe, R.J.**  
**1986a:** Microstructural evolution of vein arrays preserved in Deep Seas Drilling Project cores from the Japan Trench, Leg 57; *Geological Society of America Memoir*, 166, p. 75-87.  
**1986b:** Deformation mechanism path diagrams for sediments undergoing lithification; *Geological Society of America Memoir* 166, p. 151-160.
- Lewis, P.D.**  
**1990:** New timing constraints on Cenozoic deformation, Queen Charlotte Islands, British Columbia; *in* Current Research, Part F, Geological Survey of Canada, Paper 90-1F, p. 23-28.
- Lewis, P.D., Haggart, J.W., Rohr, K.M., Dietrich, J.R., and Thompson, R.I.**  
**1990:** Mesozoic and Cenozoic evolution of the Queen Charlotte Islands and Queen Charlotte Basin; *in* Program with Abstracts, Geological Association of Canada-Mineralogical Association of Canada Joint Annual Meeting, Vancouver, B.C.
- Lewis, P.D. and Ross, J.V.**  
**1988:** Preliminary investigations of structural styles in Mesozoic strata of the Queen Charlotte Islands, British Columbia; *in* Current Research, Part E, Geological Survey of Canada, Paper 88-1E, p. 275-279.  
**1989:** Evidence for Late Triassic-Early Jurassic deformation in the Queen Charlotte Islands, British Columbia; *in* Current Research, Part H, Geological Survey of Canada, Paper 89-1H, p. 13-18.
- Lundberg, N. and Moore, J.C.**  
**1986:** Macroscopic structural features in Deep Seas Drilling Project cores from forearc regions; *Geological Society of America Memoir* 166, p. 13-44.
- Orchard, M.J.**  
**1988:** Studies of the Triassic Kunga Group, Queen Charlotte Islands, British Columbia; *in* Current Research, Part E, Geological Survey of Canada, Paper 88-1E, p. 229.
- Ramsay, J.G.**  
**1980:** The Crack-Seal mechanism of rock deformation; *Nature*, v. 284, p. 135-139.
- Ramsay, J.G. and Huber, M.I.**  
**1983:** The techniques of modern structural geology. Volume 1: strain analysis; Academic Press, London, 307 p.
- Roddick, J.A.**  
**1970:** Douglas Channel-Hecate Strait map-area, British Columbia; Geological Survey of Canada, Paper 70-41, 56 p.
- Rohr, K. and Dietrich, J.R.**  
**1991:** Deep seismic reflection survey of the Queen Charlotte Basin, British Columbia; *in* Evolution and Hydrocarbon Potential of the Queen Charlotte Basin, British Columbia, Geological Survey of Canada, Paper 90-10.
- Shouldice, D.H.**  
**1971:** Geology of the western Canadian continental shelf; *Bulletin of Canadian Petroleum Geology*, v. 19, p. 405-436.
- Siddans, A.W.B.**  
**1977:** The development of slaty cleavage in part of the French Alps; *Tectonophysics*, v. 39, p. 533-557.
- Simpson, C. and Schmid, S.M.**  
**1983:** An evaluation of criteria to deduce the sense of movement in sheared rocks; *Geological Society of America Bulletin*, v. 94, p. 1281-1288.
- Souther, J.G.**  
**1988:** Implications for hydrocarbon exploration of dyke emplacement in the Queen Charlotte Islands, British Columbia; *in* Current Research, Part E, Geological Survey of Canada, Paper 88-1E, p. 241-245.
- Souther, J.G. and Jessop, A.M.**  
**1991:** Dyke swarms in the Queen Charlotte Islands, and implications for hydrocarbon exploration; *in* Evolution and Hydrocarbon Potential of the Queen Charlotte Basin, British Columbia, Geological Survey of Canada, Paper 90-10.
- Sutherland Brown, A.**  
**1968:** Geology of the Queen Charlotte Islands, British Columbia; British Columbia Department of Mines and Petroleum Resources, Bulletin 54, 226 p.
- Thompson, R.I.**  
**1988:** Late Triassic through Cretaceous geological evolution, Queen Charlotte Islands, British Columbia; *in* Current Research, Part E, Geological Survey of Canada, Paper 88-1E, p. 217-219.
- Thompson, R.I. and Thorkelson, D.**  
**1989:** Regional mapping update, central Queen Charlotte Islands, British Columbia; *in* Current Research, Part H, Geological Survey of Canada, Paper 89-1H, p. 7-12.
- Thompson, R.I., Haggart, J.W., and Lewis, P.D.**  
**1991:** Late Triassic through early Tertiary evolution of the Queen Charlotte Basin, British Columbia, with a perspective on hydrocarbon potential; *in* Evolution and Hydrocarbon Potential of the Queen Charlotte Basin, British Columbia, Geological Survey of Canada, Paper 90-10.
- Tipper, H.W.**  
**1989:** Lower Jurassic (Hettangian and Sinemurian) biostratigraphy, Queen Charlotte Islands, British Columbia; *in* Current Research, Part H, Geological Survey of Canada, Paper 89-1H, p. 31-33.
- Van der Heyden, P.**  
**1989:** U-Pb and K-Ar geochronology of the Coast Plutonic Complex, 53° to 54°N, British Columbia, and implications for the Insular-Intermontane superterrane boundary; Ph.D. thesis, University of British Columbia, Vancouver, 392 p.
- Vellutini, D.**  
**1988:** Organic maturation and source rock potentials of Mesozoic and Tertiary strata, Queen Charlotte Islands, British Columbia; M.Sc. thesis, University of British Columbia, Vancouver.
- Vellutini, D. and Bustin, R.M.**  
**1991:** Organic maturation of Mesozoic and Tertiary strata of the Queen Charlotte Islands, British Columbia; *in* Evolution and Hydrocarbon Potential of the Queen Charlotte Basin, British Columbia, Geological Survey of Canada, Paper 90-10.
- White, J.M.**  
**1990:** Evidence of Paleogene sedimentation on Graham Island, Queen Charlotte Islands, west coast, Canada; *Canadian Journal of Earth Sciences*, v. 27, p. 533-538.
- Williams, P.F.**  
**1972:** Development of metamorphic layering and cleavage in low grade metamorphic rocks at Bermagui, Australia; *American Journal of Science*, v. 272, p. 1-47.
- Woodsworth, G.J.**  
**1988:** Karmutsen Formation and the east boundary of Wrangellia, Queen Charlotte Basin, British Columbia; *in* Current Research, Part E, Geological Survey of Canada, Paper 88-1E, p. 209-212.
- Yorath, C.J.**  
**1988:** Petroleum geology of the Canadian Pacific continental margin; *in* Geology and Resource Potential of the Continental Margin of Western North America and Ocean Basins-Beaufort Sea to Baja California, D.W. Scholl, A. Grantz and J.G. Vedder (ed.), United States Geological Survey, Menlo Park, p. 283-304.
- Yorath, C.J. and Chase, R.L.**  
**1981:** Tectonic history of the Queen Charlotte Islands and adjacent areas-a model; *Canadian Journal of Earth Sciences*, v. 18, p. 1717-1739.
- Yorath, C.J. and Hyndman, R.D.**  
**1983:** Subsidence and thermal history of Queen Charlotte Basin; *Canadian Journal of Earth Sciences*, v. 20, p. 135-159.
- Young, I.F.**  
**1981:** Structure of the western margin of the Queen Charlotte Basin, British Columbia; M.Sc. thesis, University of British Columbia, Vancouver.

## APPENDIX 1: STRAIN ANALYSIS ON FOSSILS

Bedding plane finite strain was analyzed at 18 locations using deformed prints of ammonites, and at one location using elongated belemnite moulds. Strains were determined from ammonite prints using the method of Blake (1878) (see also Ramsay and Huber, 1983). Most Jurassic ammonites define a logarithmic spiral when undeformed. Blake's method allows the distortion of a this spiral to be determined using three successive radial measurements at increments of 90°. A logarithmic spiral is described by the equation:

$$r = k e^{n \cot(a)}$$

where r is the spiral radius measured from the origin, k is a constant, n is the angle through which the spiral has passed, and a is the angle between the tangent to the spiral and the radius at the point of

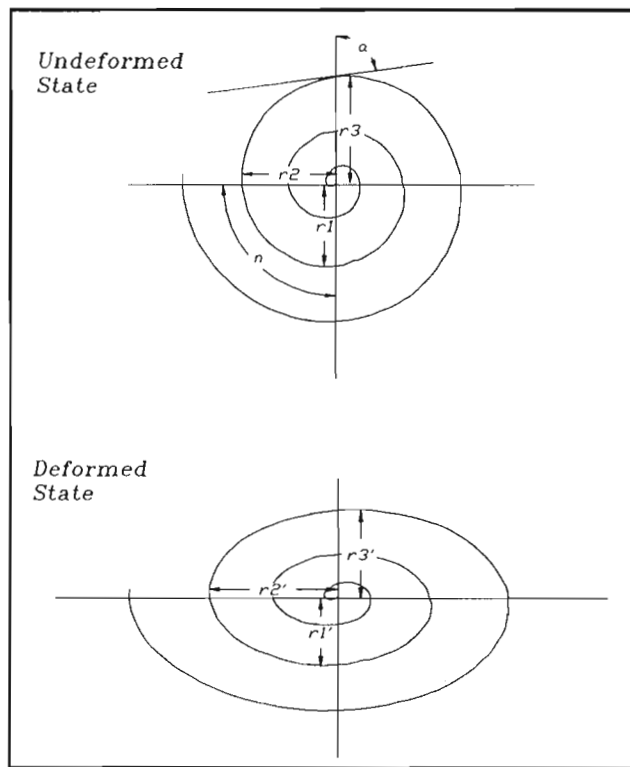


**Figure 23:** Logarithmic spiral in undeformed and deformed states, showing measurements required for strain analysis.

tangency (Fig. 23). For three successive radial measurements at intervals of  $90^\circ$ , radii calculated would therefore be:

$$r_1 = ke^0$$

$$r_2 = ke^\pi$$

$$r_3 = ke^{\pi \cot(a)}$$

and

$$r_2 = (r_1 \cdot r_3)^{1/2}$$

When the spiral is homogeneously deformed with principal strain axes parallel to these radii, the strain ratio,  $R$ , becomes:

$$R = (r_1' \cdot r_3')^{1/2} / r_2'$$

where  $r_1'$ ,  $r_2'$ , and  $r_3'$  are the lengths of the deformed radii. This ratio can be determined by three measurements along visually estimated principal strain axes.

Using the strain ratios obtained with the above method, percent shortening values were calculated assuming 1) constant volume deformation, and 2) volume reduction, where  $e_3 = 0$ . The values obtained provide limits for actual shortening values.

Measured strain axes were rotated to horizontal by a single rotation about bedding strike direction; this simple rotation was considered reasonable given regional subhorizontal fold axial trends.

Strain values for each ammonite were given a weight of 1-5, reflecting the spiral preservation and confidence of measurement. The arithmetic mean of the weighted strain values was taken to determine the representative strain magnitude for each location, and a vector mean of weighted orientations was used as the representative strain orientation (Table 1).

Belemnite moulds at one location were extended along micro-extensional faults. A Mohr circle construction (Ramsay and Huber, 1983) was used to determine the strain orientation and magnitude from three moulds with different orientations and amounts of extension.

## APPENDIX 2: STRAIN ANALYSIS FOR PELLOIDAL LIMESTONES

The distribution of fecal pellets in a sample of deformed Sadler Limestone was used to quantify strains. Several methods were considered in making these measurements: if strain markers were originally spherical, simple measurements of the ellipsoidal shapes are sufficient to characterize strain. A deformed aggregate of originally randomly oriented elliptical markers can be analyzed using the  $R/\phi$  technique. The Fry centre-to-centre method can be used if the deformed aggregate of originally had a statistically uniform (anticlustered) distribution, and is independent of original shape. The centre-to-centre method was chosen as providing the most accurate solution, because, 1) the uncertainty of initial shape makes simple ellipsoid shape measurements suspect, and 2) only small amounts of elongation axis dispersion were observed in sections, making the  $R/\phi$  method inac-

**Table 1:** Results of Strain Analysis of Deformed Fossils

Latitude	Longitude	Map Unit	N	Elongation Direction	Strain Ratio	Percent Shortening <sup>1</sup>	Percent Shortening <sup>2</sup>
53°18'40"	132°26'00"	Phantom Ck.	2	123°	1.41	18.7	29.1
53°21'20"	132°25'52"	Yakoun Gp.	2	115°	1.19	9.1	16.0
53°21'13"	132°26'05"	Yakoun Gp.	6	090°	1.35	15.6	26.0
53°10'20"	132°05'16"	Sandilands	14	128°	1.16	7.7	13.8
53°11'50"	132°03'28"	Ghost Ck.	7	136°	1.34	15.4	25.4
53°11'16"	132°01'25"	Ghost Ck.	15	119°	1.32	14.9	24.2
53°21'52"	132°13'19"	Sandilands	9	165°	1.08	3.9	7.4
53°22'11"	132°15'28"	Ghost Ck.	14	155°	1.08	3.9	7.4
53°23'00"	132°16'18"	Ghost Ck.	2	102°	1.46	20.8	31.5
53°22'20"	132°13'30"	Ghost Ck.	1	139°	1.27	12.7	21.3
53°24'50"	132°18'05"	Ghost Ck.	2	100°	1.08	3.9	7.4
52°53'39"	131°39'27"	Sandilands	2	123°	1.16	7.7	13.8
52°53'27"	131°39'30"	Sandilands	2	185°	1.10	4.9	9.1
52°26'00"	132°19'18"	Ghost Ck.	9	98.5°	1.08	3.9	7.4

N = number of samples  
<sup>1</sup> Calculated assuming constant volume, plane strain.  
<sup>2</sup> Calculated assuming volume reduction with  $e_1 = e_2 = 0$ .

curate. The centre-to-centre method provides a graphical solution based on a difference in nearest-neighbour spacing with direction in the deformed aggregate. The accuracy of Fry's method is independent of the original shape of the objects and the competency contrast between markers and matrix, and is directly related to the degree of anticlustering and number of objects used (Crespi, 1986). Two perpendicular sections of the same sample were analyzed. One section was oriented perpendicular to foliation and parallel to mineral lineation, the other was oriented perpendicular to foliation and lineation. Centres of 224 fecal pellets were digitized in the lineation-parallel section, and 381 were digitized in the lineation-perpendicular section to produce the graphical solutions in Figure 24. Finite strain ratios of 6.1:1 parallel to lineation and 3.3:1 perpendicular to lineation were measured.

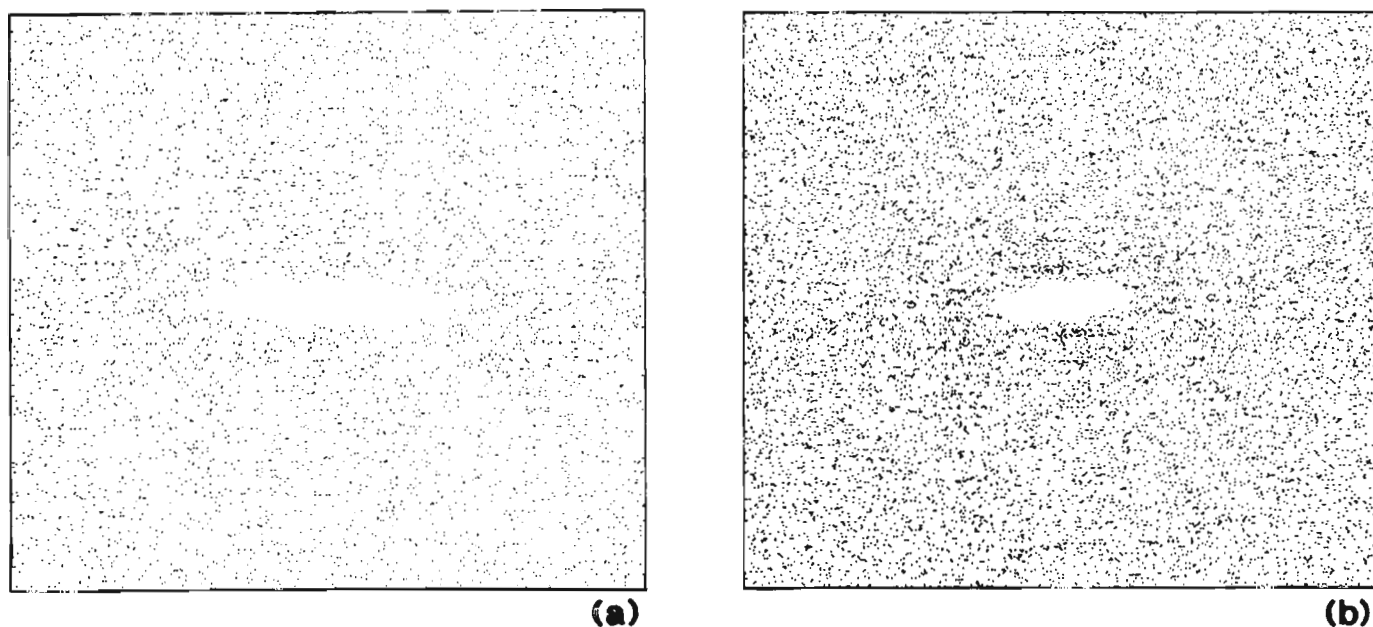


**Figure 24:** Fry strain analysis plots constructed using thin sections with deformed fecal pellets: a) XZ section oriented parallel to lineation, perpendicular to foliation, constructed from 228 points, b) XY section oriented perpendicular to lineation and foliation, constructed from 385 points.

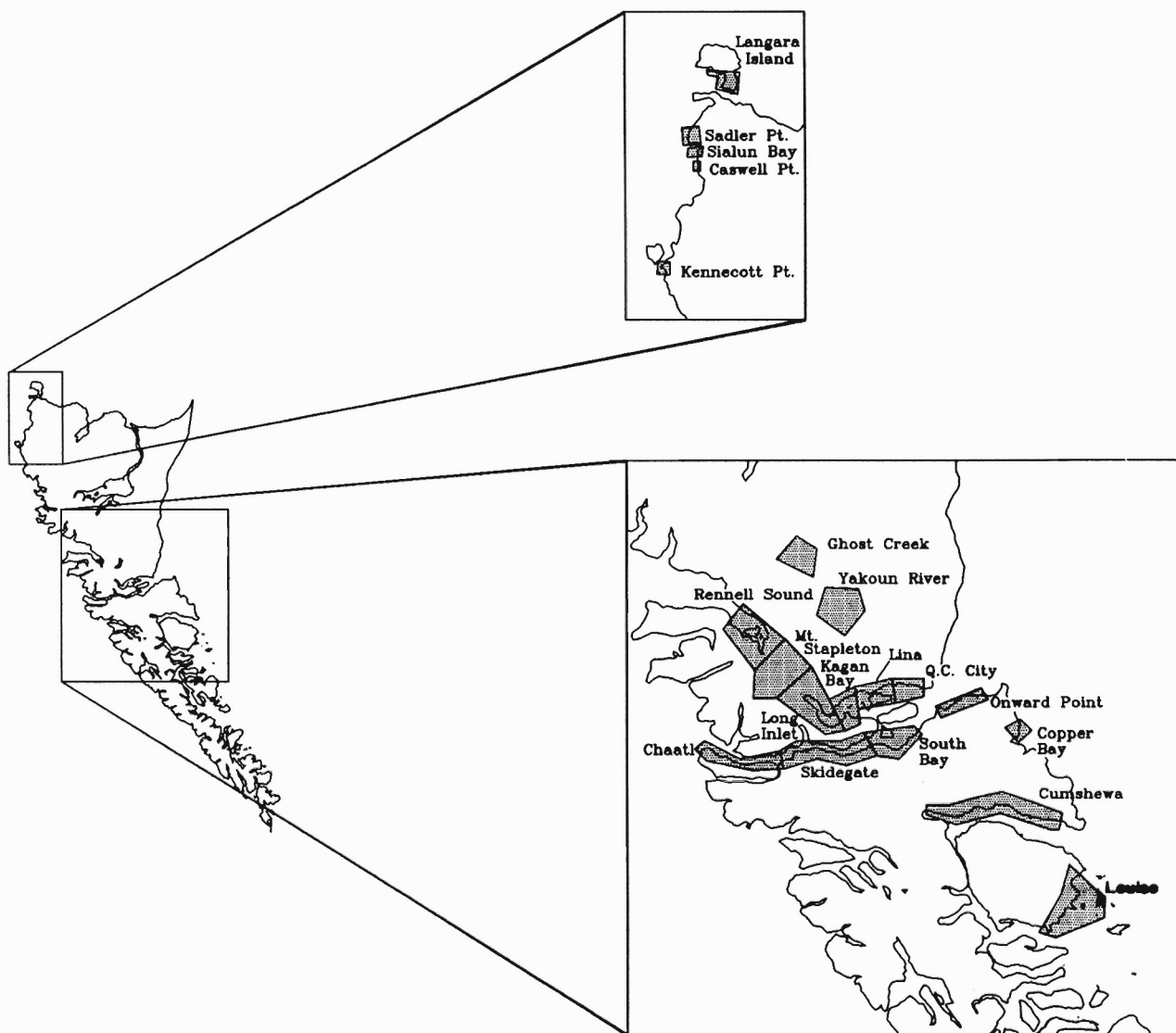


**Figure 25:** Location map of the Queen Charlotte Islands showing geographical region.

# Structural geology and stratigraphy of Mesozoic rocks of central Graham Island, Queen Charlotte Islands, British Columbia

J. Indrelid<sup>1</sup>, J. Hesthammer<sup>1</sup>, and J.V. Ross<sup>1</sup>

Indrelid, J., Hesthammer, J., and Ross, J.V., Structural geology and stratigraphy of Mesozoic rocks of central Graham Island, Queen Charlotte Islands, British Columbia; in *Evolution and Hydrocarbon Potential of the Queen Charlotte Basin, British Columbia*, Geological Survey of Canada, Paper 90-10, p. 51-58, 1991.

## **Abstract**

*Mesozoic rocks of central Graham Island comprise a basal limestone unit conformably overlain by interbedded shales, silts, and sandstones with ages ranging from Late Triassic (Norian) to Middle Jurassic (Aalenian). Unconformably overlying these are Middle Jurassic (Bajocian) volcanic and volcanic derived sedimentary rocks. Cretaceous rocks are represented by limited exposures of sandstones and conglomerates. Major folds are subhorizontal, tight to open with a trend towards northwest. Major normal and thrust faults have a northwestward trend. Minor faults trend north-east and might be related to strike-slip motion.*

## **Résumé**

*Les roches mésozoïques du centre de l'île Graham sont composées d'une unité calcaire basale sur laquelle reposent en discordance des schistes argileux, des silts et des grès interstratifiés dont l'âge varie du Trias supérieur (Norien) au Jurassique moyen (Aalénien). Sur ces derniers reposent en discordance des roches volcaniques et des roches sédimentaires d'origine volcanique du Jurassique moyen (Bajocien). Les roches crétacées sont représentées par des affleurements de grès et de conglomérats. Les principaux plis sont subhorizontaux, de serrés à ouverts, à direction nord-ouest. Les principales failles normales et chevauchantes sont orientées vers le nord-ouest. Les failles secondaires sont orientées vers le nord-est et pourraient être liées à un rejet horizontal.*

---

<sup>1</sup> Department of Geological Sciences, University of British Columbia, 6339 Stores Road, Vancouver, B.C. V6T 2B4



## INTRODUCTION

This paper summarizes the sedimentology and structural geology in the area north of Yakoun Lake, central Graham Island (Fig. 1). Sutherland Brown's (1968) geological map of the Queen Charlotte Islands indicated complex structural geology in several areas, including the Yakoun River valley. The area has previously been mapped by Cameron and Tipper (1985). Additional mapping in the surrounding areas has been done by geologists involved in detailed studies (e.g. Lewis and Ross, 1988; Thompson, 1988; Thompson and Thorkelson, 1989; Haggart et al., 1989).

Mesozoic sedimentary and volcanic rocks in the area show folding and faulting related to periods of compression and extension.

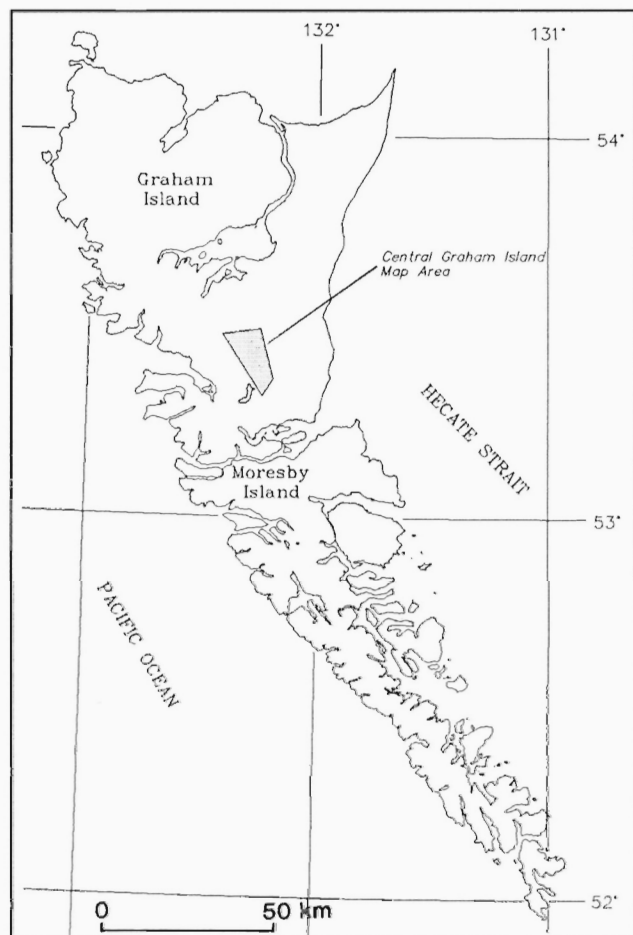


Figure 1: Regional map showing studied area in central Graham Island, Queen Charlotte Islands.

## STRATIGRAPHY

Figure 2 shows the stratigraphy found on the Queen Charlotte Islands according to Cameron and Hamilton (1988). Rocks exposed in the map area consist mainly of Upper Triassic to Middle Jurassic volcanic and sedimentary strata. Middle to Upper Cretaceous sedimentary rocks occur in the northwestern portion of the mapped area.

The oldest rocks observed in the area belong to the Peril Formation of the Kunga Group, a deep water pelagic fallout (Desrochers, 1988). Outcrops of this unit are characterized by an abundance of the bivalve *Monotis subcircularis*. This fauna is known to occur in the upper part of the unit and constrains the age to Late Norian (Carter et al., 1989). The limestone is overlain by the Sandilands Formation of the Kunga Group, which is an uninterrupted sedimentary sequence from Upper Norian to Sinemurian age (Tipper, 1989). The most common litholo-

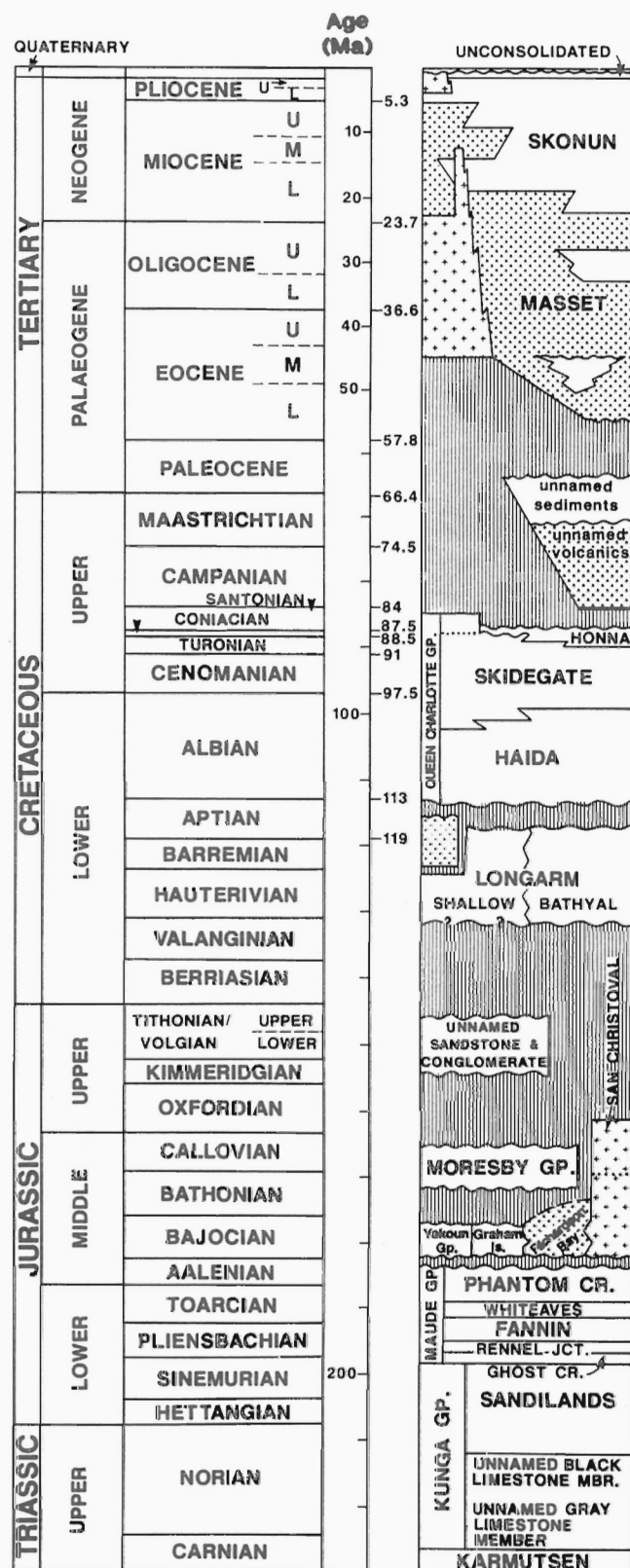
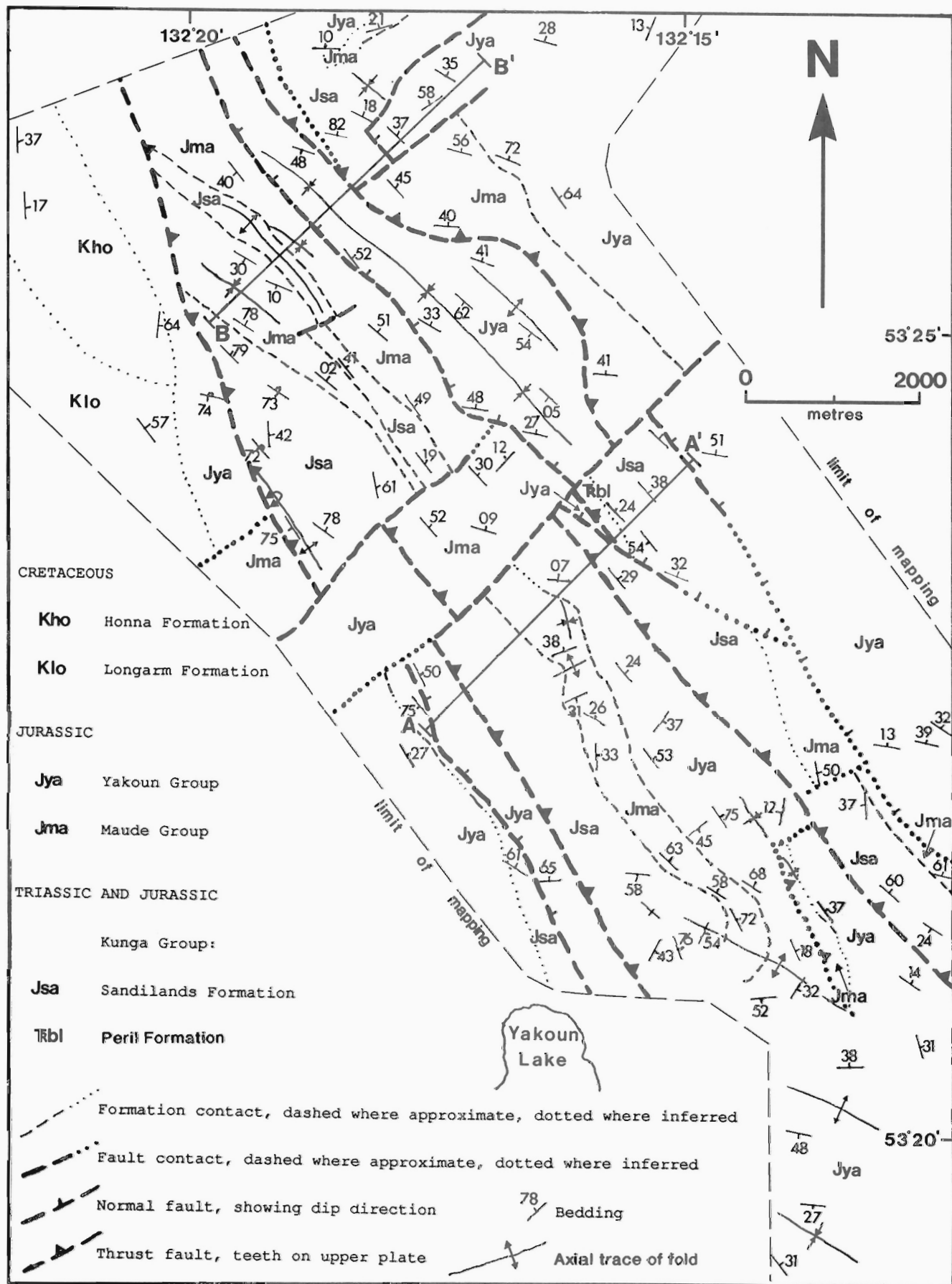


Figure 2: Stratigraphic column for Queen Charlotte Islands (after Cameron and Hamilton, 1988).



**Figure 3:** Structural map of the central Graham Island area. For location see Figure 1. A-A' and B-B' are locations of the structural sections shown in Figure 7.

gies of the formation are interbedded 2-12 cm thick black-grey siliceous sandstone and argillite, thin laminations of black siltstone, shale, and grey siliceous tuff. Rare sandstone beds with thicknesses of more than a metre have been observed in a few outcrops but are not abundant. Load structures and coarsening upward grading are common sedimentary structures. Synsedimentary folds are also present.

The Sandilands Formation grades conformably into the Sinemurian to Aalenian Maude Group. The Maude Group represents two marine regressive cycles and, using the stratigraphic nomenclature of Cameron and Tipper (1985), consist of five formations.

The Ghost Creek Formation (lowest Pliensbachian) is silty shale and a dark grey to black massive shale. The formation is very homogeneous. Higher shale content and less volcanic material distinguish this formation from the underlying Sandilands Formation.

The Lower Pliensbachian Rennell Junction Formation of Cameron and Tipper (1985) overlies the Ghost Creek Formation. The gradational contact is marked by an upward increase in the amount of turbiditic siltstone and sandstone and a decrease in shale content. The main lithologies in the Rennell Junction Formation are 5-15 cm thick greenish grey sandstone layers interbedded with siltstone and shale. Calcareous concretions and glauconitic sandstone layers are common.

Fannin Formation (Upper Pliensbachian to Lower Toarcian) lies paraconformably on the Rennell Junction Formation. The contact is marked by a hiatus (Cameron and Tipper, 1985). The formation consists of coarser and thicker calcareous sandstone layers and less shale than the underlying strata. The sandstone beds are calcareous, hard, and contain abundant fossiliferous calcareous concretions. Some limestone beds are also present. Iron-rich minerals such as siderite, glauconite and chamosite exist. The chamosite is cryptocrystalline and occurs as oolites, commonly with a nucleus of a volcanic fragment.

Whiteaves Formation (Lower and Middle Toarcian) is a concretionary pale grey weathering shale, with a few sandy and silty shale layers. Grey ash beds are also common. The boundary between this formation and the Fannin Formation is abrupt and marked by a hiatus (Cameron and Tipper, 1985).

Phantom Creek Formation (Upper Toarcian to Lower Aalenian) lies conformably on the Whiteaves Formation. It consists of brownish weathering, interbedded, fine to coarse grained shallow marine sandstone and silty shale. The sandstone is locally calcareous and may contain concretions. Belemnites and bivalves are common. Some sandstone layers are rich in chamosite oolites.

Unconformably overlying the Upper Triassic and Lower Jurassic Kunga and Maude groups is the Middle Jurassic (Bajocian) Yakoun Group. An angular unconformity separates the less deformed Yakoun Group from the more deformed older units (Hesthammer et al., 1989). In the mapped area this unconformity is observed to cut down section to the Sandilands Formation. The lithology of the Yakoun Group is diverse and contains an abundance of primary and reworked volcanic material deposited in marine or subaerial environments. The volcanic rocks comprise tuff, lapilli, volcanic breccia, and andesitic flows. The main lithologies of the sedimentary reworked sections are: i) relatively deep water, interbedded tuff and red-weathering shale; ii) shallower marine, interbedded 2-20 cm thick tuffaceous shale, siltstone and fine to coarse sandstone, locally with thicker (1-5 m) sandstone layers; iii) conglomerate, ranging from matrix supported gravel conglomerate to clast supported pebble and cobble conglomerate. Boulders are locally present. Clasts are generally rounded and poorly sorted. The clast material is polymict, comprising mainly sandstone from underlying Yakoun layers, andesite and lesser plutonic rocks. Coal and wood fragments are common constituents of the group. The succession of these lithologies is not well understood. The only trace-

able unit we have found to date is a volcanic cobble conglomerate. Despite the many different lithologies, the Yakoun Group is often recognized in the field by its brown weathering colour, and spherical weathering nodules within the sandstone layers.

Cretaceous rocks crop out in the northwestern corner of the mapped area. Structural relationships between the Cretaceous and Jurassic rock units are uncertain. The oldest Cretaceous unit present is the Longarm Formation, which in this area is represented by a hard, massive, dark green, medium to coarse grained sandstone.

Overlying this unit is sandy gravel and pebble conglomerate of the Honna Formation. The Haida and Skidegate formations are not observed in the area (but might be present in unexposed areas). Clasts in the conglomerate include rounded plutonic and quartzite clasts, fewer rounded clasts derived from the Yakoun Formation, angular mud clasts, and clasts derived from the Sandilands Formation. The conglomerate varies from clast to matrix supported and is locally well sorted. Lenses of coarse grained green volcanic sandstone are common.

## STRUCTURES

Figure 3 shows a structural map of the area north of Yakoun Lake, central Graham Island. Major structures in the Triassic and Jurassic rocks in this area are northwest trending faults and folds. Folds plunge gently northwest and southeast. A second fault set strikes northeast, and minor folds with different trends are recorded. Consistent north-striking bedding with moderate eastward dip was observed in the Cretaceous Honna Formation. The underlying Longarm Formation has a more northwesterly strike, similar to the older units.

### Faults

Few regional large scale faults are observed in the area, due to lack of exposures. Interpretation of the regional map pattern requires the presence of several large scale faults with offsets of several hundreds of metres.

Outcrop-scale faults observed in the field do not show any preferred orientation and have offsets of generally a few metres or less. Both normal and reverse offsets are present. The most intensely faulted units in the central Graham Island area are volcanic rocks of the Yakoun Group.

### Folds

#### *Regional scale*

For the description of the regional fold pattern it is useful to divide the studied area into two domains separated by the large fault striking northeast just north of structural section A-A', the northern area being domain 1.

Most folds in domain 1 have subhorizontal fold axes plunging less than 5° towards the northwest. Folds in the Sandilands Formation vary from tight and overturned to open (Fig. 4). In the Maude Group the folds are close to open and in the Yakoun Group they are generally open. In the northernmost part of the map area, the Jurassic sequence strikes east-west, oblique to the northwest-southeast trend found elsewhere.

In domain 2 there are no continuous northwest trending folds, and the bedding generally dips towards the northeast. Some more locally developed folds are parallel with those folds recorded in domain 1, others differ notably from this orientation. Folds with northeast trending axes are recorded in the Lower Jurassic Kunga and Maude Group. In the southernmost area, folds in the Yakoun Group trend west-northwest.

#### *Outcrop scale*

The intensity of folding varies in the different rock units. Sandilands Formation strata are generally more intensely folded than the overlying units (Fig. 4). The folds in Sandilands Formation are open to tight buckle folds. Chevron folds are commonly observed. Folds in the Maude



**Figure 4:** Typical chevron folds in the Sandilands Formation.



**Figure 5:** Gently folded Rennell Junction Formation.

Group are more gentle (Fig. 5), and anticline-syncline pairs are rarely seen in outcrop. Outcrop scale folds are uncommon in the Yakoun Group, but a few gentle to open folds have been observed in large outcrops. Small scale folds in the Yakoun Group generally exist adjacent to faults or shear zones.

Cleavage was not observed or was poorly developed throughout the whole sequence from the Sandilands Formation to the Cretaceous units, except for the well developed bedding-planar cleavage present in the Ghost Creek Formation.

## DISCUSSION

Intense folding in the Sandilands Formation and the somewhat weaker folding in the Maude Group probably resulted from the first compressional event in the area. The Sandilands Formation deforms by layer parallel flexural slip into concentric and chevron folds. This fold style is caused by high viscosity contrast across the layering in the unit. The fairly uniform thicknesses of both competent and less competent layers in the Sandilands Formation gave rise to the chevron folds. The space problem created in the core of the buckle folds due

to compression is accommodated by thrust faulting (Fig. 6). A detachment surface in the underlying Kunga limestones probably provided a decollement accommodating the major buckle folds in the Sandilands Formation. Figure 7 shows two structural sections drawn through the area. The angular unconformity at the base of the much less deformed Yakoun Group restricts the timing of a compressional deformation of the Kunga and Maude groups to early Bajocian, possibly continuing into the early period of deposition of the Yakoun Group (Thompson, 1988). Northeast and west-northwest trending structures might have developed as a result of a differential stress regime under the main deformational event, or they may represent other periods in the tectonic history of the area.

Both normal and reverse relative displacement on faults are observed in outcrops, indicating a complex tectonic history with both extensional and compressional periods. Compressional faults in the Triassic and Jurassic rocks are commonly contraction faults related to folding. Fold styles, shown in the two structural sections with an alignment of large scale folds and thrust faults, support the theory of northeast-southwest oriented compression with development of thrust faults. The thrust faults are probably listric in origin and have their detachment within the Kunga Group. This explains the very few exposures of the limestone units in the central Graham Island. The

northeast-southwest striking faults can be interpreted as strike-slip faults on the lateral edges of thrust sheets. The thrusting has affected the Middle Jurassic Yakoun Group and is related to a later compressional event than the initial folding of the Upper Triassic and Lower Jurassic rock units. This later compression can be related to a Late Cretaceous to Tertiary event (Thompson, 1988).

Just north of Yakoun Lake a northwest striking, steeply dipping normal fault juxtaposes the Sandilands Formation and the Yakoun Group. This is one of the few large scale faults observed in the field, and it is compatible with the theory of an extensional event in the tectonic history. This extensional period postdates the mid-Jurassic compression (Thompson, 1988). The parallelism of the normal faults with the thrust faults might have been caused by reactivation of earlier structures.

The uniform eastward dip of the Cretaceous Honna Formation suggests post depositional tilting. This tilting may be related to the Late Cretaceous and/or early Tertiary compression suggested by Thompson (1988).

**Note added in proof:** Recent field work by the authors and others has resulted in revision to several of the ideas in this paper. For an updated discussion, see the papers in "Current Research, Part F", Geological Survey of Canada, Paper 90-1F.



**Figure 6:** Folding in the Sandilands Formation accommodated by a thrust fault (marked by a black line) running in to the core of the fold. Offset across the fault decreases towards the core of the fold.



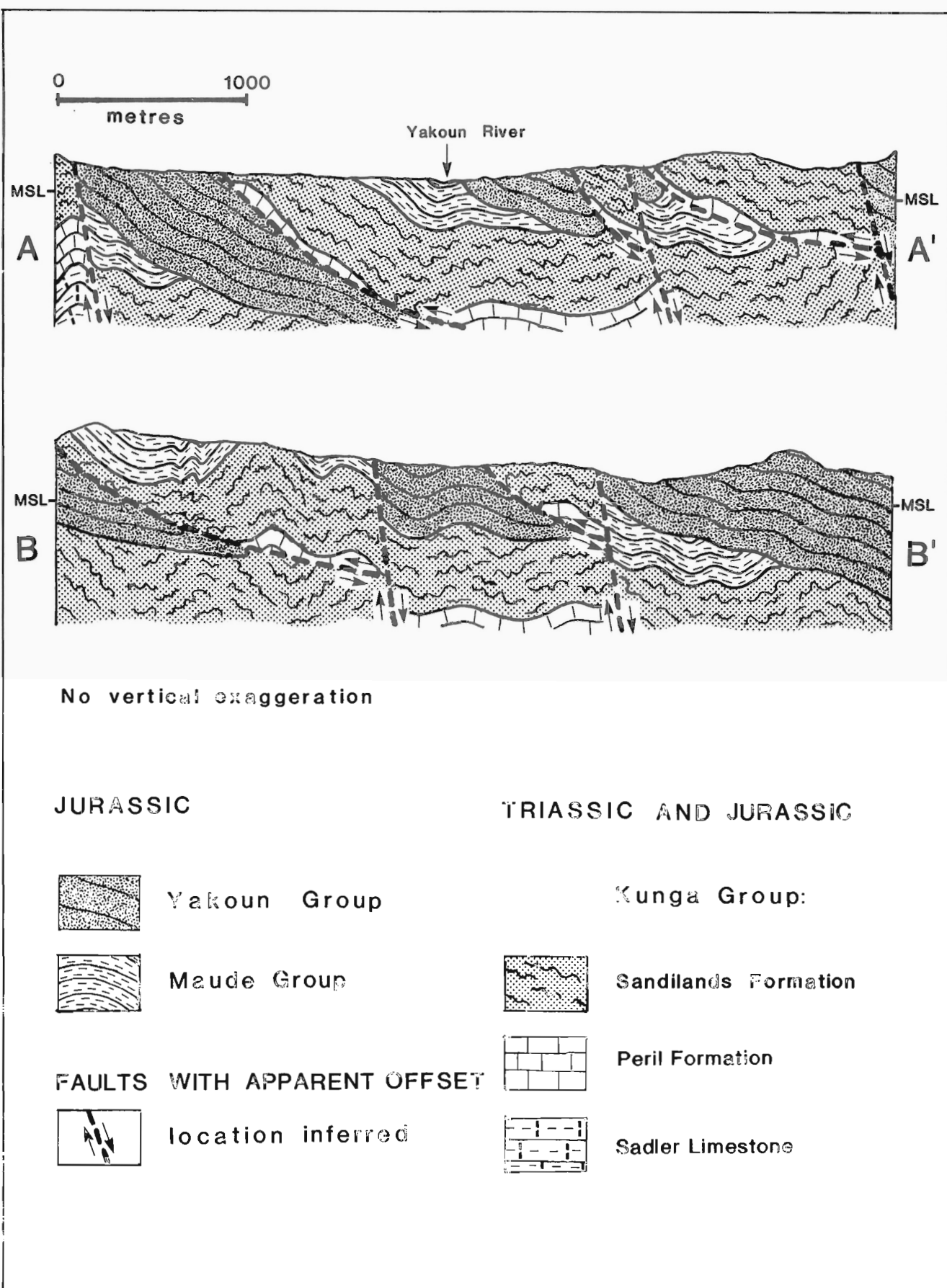


Figure 7: Northeast trending structural sections in the central Graham Island area. For location see Figure 3.

## REFERENCES

**Cameron, B.E.B. and Tipper, H.W.**

**1985:** Jurassic stratigraphy of the Queen Charlotte Islands, British Columbia; Geological Survey of Canada, Bulletin 365.

**Cameron, B.E.B. and Hamilton, T.S.**

**1988:** Contributions to the stratigraphy and tectonics of the Queen Charlotte Basin, British Columbia; *in* Current Research, Part E, Geological Survey of Canada, Paper 88-1E, p. 221-227.

**Carter, E.S., Orchard, M.J., and Tozer, E.T.**

**1989:** Integrated ammonoid-conodont-radiolarian biostratigraphy, Late Triassic Kunga Group, Queen Charlotte Islands, British Columbia; *in* Current Research, Part H, Geological Survey of Canada, Paper 89-1H, p. 23-30.

**Desrochers, A.**

**1988:** Sedimentology of the Kunga Group, Queen Charlotte Islands; *in* Some Aspects of the Petroleum Geology of the Queen Charlotte Islands, R. Higgs (compiler), Canadian Society of Petroleum Geologists Field Guide to Sequences, Stratigraphy, Sedimentology: Surface and Subsurface Technical Meeting, September 14-16, 1988, Calgary, Alberta, p. 32-37.

**Haggart, J.W., Lewis, P.D., and Hickson, C.J.**

**1989:** Stratigraphy and structure of Cretaceous strata, Long Inlet, Queen Charlotte Islands, British Columbia; *in* Current Research, Part H, Geological Survey of Canada, Paper 89-1H, p. 65-72.

**Hesthammer, J., Indrelid, J., and Ross, J.V.**

**1989:** Preliminary structural studies of the Mesozoic rocks of central Graham Island, Queen Charlotte Islands, British Columbia; *in* Current Research, Part H, Geological Survey of Canada, Paper 89-1H, p. 19-22.

**Lewis, P.D. and Ross, J.V.**

**1988:** Preliminary investigations of structural styles in Mesozoic strata of the Queen Charlotte Islands, British Columbia; *in* Current Research, Part E, Geological Survey of Canada, Paper 88-1E, p. 275-279.

**Sutherland Brown, A.**

**1968:** Geology of the Queen Charlotte Islands, British Columbia; British Columbia Department of Mines and Petroleum Resources, Bulletin 54, 226 p.

**Thompson, R.I.**

**1988:** Late Triassic through Cretaceous geological evolution, Queen Charlotte Islands, British Columbia; *in* Current Research, Part E, Geological Survey of Canada, Paper 88-1E, p. 217-219.

**Thompson, R.I. and Thorkelson, D.**

**1989:** Regional mapping update, central Queen Charlotte Islands, British Columbia; *in* Current Research, Part H, Geological Survey of Canada, Paper 89-1H, p. 7-11.

**Tipper, H.W.**

**1989:** Lower Jurassic (Hettangian and Sinemurian) biostratigraphy, Queen Charlotte Islands, British Columbia; *in* Current Research, Part H, Geological Survey of Canada, Paper 89-1H, p. 31-33.

# U-Pb and K-Ar framework for Middle to Late Jurassic (172– $\geq$ 158 Ma) and Tertiary (46–27 Ma) plutons in Queen Charlotte Islands, British Columbia

R.G. Anderson<sup>1</sup> and I. Reichenbach<sup>2</sup>

Anderson, R.G. and Reichenbach, I., U-Pb and K-Ar framework for Middle to Late Jurassic (172–158 Ma) and Tertiary (46–27 Ma) plutons in Queen Charlotte Islands, British Columbia; in *Evolution and Hydrocarbon Potential of the Queen Charlotte Basin*, British Columbia, Geological Survey of Canada, Paper 90-10, p. 59–87, 1991.

## Abstract

*We present 46 new U-Pb isotopic determinations for zircon and eight new K-Ar hornblende and muscovite dates for plutons in Queen Charlotte Islands. Two eastward younging suites of Middle to Late Jurassic (172– $\geq$ 158 Ma) plutons include: San Christoval plutonic suite (SCPS; 172–171 Ma); and Burnaby Island plutonic suite (BIPS; 168– $\geq$ 158 Ma). Northward younging of the Tertiary Kano plutonic suite (KPS; 46–27 Ma), identified in previous work, resolves into 3 distinct episodes recording passage of a northwesterly accelerating magmatic front.*

*Two of the three segments of the linear, northwest-trending SCPS plutonic belt are coeval: 171  $\pm$  6 Ma (U-Pb; all errors 2 $\sigma$ ) for the Woodruff Bay segment and 172  $\pm$  5 Ma and 172  $\pm$  3 Ma (U-Pb) for the San Christoval Range segment. The Rennell-Kano-Van inlets segment of SCPS is no younger than 164  $\pm$  4/–2 Ma (U-Pb date for BIPS apophysis within SCPS). Mineral foliation developed during waning stages of mainly Early Jurassic contraction characterizes SCPS. The deformation involved the Upper Triassic Karmutsen Formation and Upper Triassic and Lower Jurassic Kunga Group host rocks but had ceased by at least 168  $\pm$  4 Ma (U-Pb date for a pluton that crosscuts folded Sine-murian strata).*

*The younger (168– $\geq$ 158 Ma) Burnaby Island plutonic suite comprises discrete plutons scattered along the east coasts of Moresby and Graham islands and small intrusions within SCPS. Bajocian Yakoun Formation volcanic rocks are the youngest country rock; Lower Cretaceous (Hauterivian age) Longarm Formation sedimentary rocks non-conformably overlie BIPS. Zircon from the youngest, leucocratic trondhjemite phase, is at least 158  $\pm$  4 Ma old and contains inherited Pb of at least Pennsylvanian age (309  $\pm$  14/–13 Ma upper concordia intercept). This is the first indication of pre-Triassic basement in the Queen Charlotte Islands.*

*K-Ar dates for the Middle to Late Jurassic plutonic suites range from 192–145 Ma. Most are concordant with U-Pb dates and indicate coeval rapid uplift and cooling. Late Jurassic (147–145 Ma) K-Ar dates for plutons and for plutonic debris in the Longarm Formation may represent resetting during the widespread Late Jurassic–Early Cretaceous vein formation common within BIPS and less common within SCPS. The veins are likely part of the formation of co-spatial copper-iron skarn metallic mineral deposits. Advective circulation of hydrothermal fluids was partly responsible for thermal overmaturation of organic material in the Kunga Group. Overmaturation of potential source rocks by this process would have occurred before deposition of Cretaceous potential reservoir beds.*

*Tertiary Kano plutonic suite plutons on eastern and western Moresby Island and along western Graham Island intruded co-spatial and broadly coeval Tertiary volcanic rocks. The southern group of extension-related, partly bimodal Eocene (46–39 Ma) plutons and coeval dykes may herald inception of the Tertiary Queen Charlotte Basin. The steady 2.6 cm/yr northwesterly migration of the magmatic front, represented by the medial group of Early Oligocene (36–32 Ma) intrusions, records the change from mainly orthogonal to mainly oblique convergence of the Pacific plate relative to North America. An extensive, coeval northern group of Late Oligocene (28–27 Ma) plutons is co-extensive with (but slightly predates) the nearby Miocene Masset Formation volcanic rocks.*

## Résumé

*Quatorze-six nouvelles datations selon la méthode U-Pb sur zircons et huit selon la méthode K-Ar sur hornblende et muscovite de plutons dans les îles de la Reine-Charlotte ont permis de définir : un rajeunissement vers l'est des suites plutoniques du Jurassique moyen à tardif (158–172 Ma), soit la suite plutonique San Christoval (171–172 Ma) et la suite plutonique de l'île Burnaby (158–168 Ma) et un rajeunissement vers le nord de la suite plutonique Kano du Tertiaire (Éocène et Oligocène; 27–46 Ma).*

*Les trois segments de la suite plutonique de Burnaby (du sud vers le nord : segment de Woodruff, du chaînon San Christoval et des inlets Rennell-Kano-Van) longeant la côte ouest de l'île Moresby et la côte sud-ouest de l'île Graham recoupent des roches du Trias supérieur et du Jurassique inférieur. Neuf fractions sur zircons de trois*

<sup>1</sup> Cordilleran Division, Geological Survey of Canada, 100 West Pender Street, Vancouver, B.C. V6B 1R8

<sup>2</sup> Continental Geoscience Division, Ottawa. Present address: Department of Earth Sciences, University of Waterloo, Waterloo, Ontario N2L 3G1.

*échantillons de la suite San Christoval donnent des âges de  $172 \pm 10$  Ma (toutes les erreurs correspondent à deux fois l'écart-type) pour le segment de Woodruff et  $172 \pm 5$  Ma et  $171 \pm 12$  Ma pour le segment du chaînon San Christoval. Le segment des inlets Rennell-Kano-Van de la suite San Christoval ne dépasse pas  $164 \pm 4$ -2 Ma (âge U-Pb pour l'apophyse de la suite Burnaby dans celle de San Christoval).*

*La suite plutonique de l'île Burnaby du Jurassique moyen et supérieur est composée de plutons distincts, disséminés le long de la côte est des îles Moresby et Graham, et de petites intrusions dans la suite San Christoval. Les roches encaissantes les plus récentes recoupées par la suite sont les roches volcaniques de la formation de Yakoun du Bajocien. Les roches sédimentaires de la formation de Longarm du Crétacé inférieur reposent en discordance sur la suite Barnaby. Le zircon d'un échantillon de la suite Barnaby recueilli près de la discordance a donné un âge isotopique de  $165 \pm 4$  Ma. Les intrusions de la suite Barnaby dans celle de San Christoval comportent l'intrusion de monzonite quartzique du détroit de Rennell datée à  $164 \pm 4$ -2 Ma et la trondhjémite de l'inlet Beresford (typique d'une phase leucocratique de la suite Barnaby dont la datation de l'intrusion selon la méthode U-Pb sur zircons donne  $158 \pm 4$  Ma. La systématique uranium-plomb de la trondhjémite indique la présence de Pb héritée du Pennsylvanien ou d'âge antérieur ( $309 \pm 14$ -13 Ma, intercept supérieur du diagramme de Concordia), ce qui correspond à la première indication de la présence d'un socle pré-triasique dans les îles de la Reine-Charlotte. Une datation U-Pb à  $168 \pm 2$  Ma d'une intrusion porphyrique à hornblende-plagioclase près du bassin Clapp dans la baie Shields traversant des plis à vergence sud dans la formation de Sandilands du Pliensbachien limite l'âge de la déformation à une période située entre le Pliensbachien et le Callovien.*

*Les datations K-Ar des suites plutoniques du Jurassique moyen à tardif varient de 145 à 192 Ma. La datation au Jurassique moyen par la méthode K-Ar concorde avec les estimations obtenues par la méthode U-Pb et indique un soulèvement et un refroidissement rapides contemporains des deux suites. La datation des plutons et des débris plutoniques de la formation de Long Arm au Jurassique tardif est jusqu'à 25 millions d'années plus récente que leur datation U-Pb. Cela pourrait refléter une remise en place par la formation de vastes filons au Jurassique supérieur-Crétacé inférieur, filons qui caractérisent la suite Barnaby et que l'on trouve dans la suite San Christoval. Ces filons ont donné naissance à des gisements skarnifères de fer-cuivre et sont en partie à l'origine de l'hyper maturation des roches mères du groupe de Kunga.*

*Les plutons de la suite plutonique Kano du Tertiaire recoupent toutes les unités plus anciennes. Dix datations U-Pb de 32 fractions délimitent trois épisodes plutoniques diachrones distincts vers le nord de périodicité décroissante : un groupe méridional de plutons éocènes en partie bimodaux liés à une distension (39-46 Ma); un groupe médian d'intrusions de l'Oligocène inférieur (32-36 Ma); et un groupe septentrional de massifs de l'Oligocène supérieur de même étendue (et vraisemblablement contemporains) que les roches volcaniques voisines de la formation de Mas-set du Miocène inférieur. En ce qui concerne tous les plutons de la suite Kano, les datations K-Ar sur hornblende et biotite concordent avec celles établies selon la méthode U-Pb. Une datation K-Ar ( $43.7 \pm 1.1$  Ma) sur hornblende de l'Éocène d'un membre de dykes d'andésite porphyritique de l'essaim de dykes de la baie Carpenter à direction nord est conforme à la datation U-Pb des plutons de la baie Carpenter qui renferment une partie de l'essaim. Le plutonisme bimodal éocène contemporain et la formation de dykes indiquent un important épisode de distension pendant l'Éocène supérieur pouvant annoncer l'ouverture du bassin de la Reine-Charlotte.*

## INTRODUCTION

Granitic rocks underlie about one-tenth of the area of Queen Charlotte Islands and span about 140 million years of its more than 230 million year evolution. Thermal overmaturation of potential hydrocarbon source rocks of the Kunga Group is cospatial with some plutons on southeastern Moresby Island (Orchard, 1988; Vellutini, 1988; Orchard and Forster, 1991). Distribution, nature, age, thermal regime and tectonic setting of granitic plutons are important in understanding their genesis and ultimately in assessment of prospective ground for hydrocarbon plays in the Queen Charlotte Basin.

A program of U-Pb and K-Ar dating sought to enhance knowledge of the timing and extent of different plutonic suites gained from a complementary mapping program (Anderson, 1988a; Anderson and Greig, 1989) and to assess the influence of plutonism on the thermal maturation of potential hydrocarbon source rocks. The Middle Jurassic (172-171 Ma) San Christoval plutonic suite (SCPS) outcrops on the western margin of the islands. The younger ( $168 \geq 158$  Ma) Burnaby Island plutonic suite (BIPS), which outcrops mainly along the eastern margin of the islands, intrudes SCPS. Small BIPS intrusions within SCPS provide a minimum age for SCPS. Tertiary plu-

tons of the Kano plutonic suite (KPS) occur as two northwest-trending belts along the archipelago's margins. They represent three discrete, geographically restricted, Eocene (46-39 Ma), Early Oligocene (36-32 Ma), and Late Oligocene (28-27 Ma) plutonic episodes marking passage of a northwardly-accelerating magmatic front.

The study greatly extends mineral and whole rock K-Ar isotopic data from other workers (e.g. Wanless et al., 1968, 1970, 1972; Young, 1981; Yorath and Chase, 1981). That work established the existing geochronometric framework for Queen Charlotte Islands plutonism and pointed out contradictions among the isotopic dates and Sutherland Brown's (1968) age assignments for plutons and plutonic classifications. Jurassic syntectonic plutons were shown to be coeval with post-tectonic plutons, formerly thought to be Cretaceous-Tertiary (Sutherland Brown, 1968; Young, 1981). The objective of the U-Pb dating was to confirm and extend the K-Ar reconnaissance data compiled by Young (1981) for plutons along the margins of the Queen Charlotte Islands. New and existing geochronometry have refined dates for: 1) emplacement of two Middle to Late Jurassic plutonic suites; 2) Middle Jurassic contraction; 3) possible timing of Jura-

Cretaceous advective heating of country rocks cospacial with BIPS; and 4) intrusion of a Tertiary plutonic suite (Figs. 1-3).

## GEOLOGICAL SETTING AND PLUTONIC STYLES

Middle Jurassic and Tertiary plutons on Queen Charlotte Islands account for 1000 km<sup>2</sup> of the land area and about 140 million years of geological history. Each plutonic episode produced granitoid rocks distinguished by distribution, geophysical signature, composition, mineralogy, intrusive and geological relations, fabric, and age.

Middle to Late Jurassic (172–158 Ma) plutons consist of the San Christoval plutonic suite (SCPS), which occurs on the west coasts of Queen Charlotte Islands (Fig. 1), and the Burnaby Island plutonic suite (BIPS), distributed along the islands' east coasts (Fig. 2). BIPS also occurs as small intrusions within SCPS. SCPS outcrops in three segments: southernmost Woodruff Bay segment; medial San Christoval Range segment; and northernmost Rennell-Kano-Van inlets segment along southwestern Graham Island. The suite comprises homogeneous, medium grained, foliated diorite and quartz diorite that contain common 10–30 cm long mafic inclusions but few dykes. The mineral and inclusion fabric led Sutherland Brown (1968) to classify the suite as "syntectonic." The fabric occurs within 1–2 km of the eastern margin of SCPS and parallels the trend of the contact with Upper Triassic Karmutsen Formation in the Woodruff and San Christoval Range segments. In the northern segment, foliation is widespread but uncommon and everywhere north- or northwest-trending. Hornblende is distinctly prismatic; biotite is rare, texturally late, and commonly chloritized. Upper Triassic and Lower Jurassic Kunga Group strata are the youngest strata intruded by SCPS (Sutherland Brown, 1968).

BIPS is more heterogeneous than SCPS. In order of intrusion, gabbro or diorite, quartz monzodiorite, quartz monzonite and trondhjemite (leucodiorite) make up the main phases. They are typically unfoliated and pervasively brittle fractured and veined; Sutherland Brown (1968) considered these plutons "post-tectonic." Hornblende is subhedral and as abundant as biotite except in felsic phases, where biotite is the main mafic mineral. The trondhjemite phase is devoid of hornblende but contains muscovite and rare biotite.

BIPS plutons crosscut Middle Jurassic (Bajocian) and older strata. Locally, Lower Cretaceous (Hauterivian) Longarm Formation rocks (Haggart and Gamba, 1990) nonconformably overlie the highly altered and veined granitic rocks (Anderson and Greig, 1989). The nonconformity observed at Rebecca Point (Fig. 8a) differs from intrusive contacts involving the Burnaby pluton and Longarm Formation reported by Sutherland Brown (1968, p. 139). The nonconformable relations explain the apparent discrepancy between his suggested Cretaceous-Tertiary age for these "post-tectonic" plutons and the pluton's Late Jurassic K-Ar date determined by Wanless et al. (1968). Hydrothermal alteration and veining of the plutons, which are cospacial with copper-iron skarns (Anderson, 1988b), are much more intense and regular in the granitic rocks than in the overlying Longarm Formation.

Late Eocene to Oligocene (46–27 Ma) Kano plutonic suite (KPS) comprises two northwest-trending, subparallel belts of (quartz) monzodiorite and lesser diorite and granite stocks along the west coast of Graham Island and west and east coasts of Moresby Island. The suite includes: a southern group of Eocene plutons (Carpenter Bay and Lyell Island complexes); a medial group of Early Oligocene plutons (Sedgwick Bay, Atli-Dog Island, Talunkwan-Porter Head, Sewell, southern Louise Island, northwest Louise Island, Sandspit, Deena River, and Kano plutons); and a northern group of Late Oligocene plutons (Sheila Lake, Pivot Mountain, Sialun Creek and Langara Island plutons). Finer grain size, unfoliated and homogeneous character of individual plutons, small size (commonly <20 km<sup>2</sup>), orthopyroxene, com-

mon miarolitic cavities, seriate texture and intrusive relations distinguish KPS from Middle Jurassic plutons. Tertiary, felsic volcanic rocks (probable pre-Miocene Masset Formation) are the youngest strata intruded by KPS. The oldest (southern) plutons within KPS are bimodal or contain coeval, consistently north-trending, intraplutonic porphyritic dykes and stocks. The porphyritic intrusions may have been feeders for Eocene volcanism. These features suggest an extensional tectonic regime during Eocene plutonism (Anderson and Reichenbach, 1989). K-Ar dates from the western plutons decrease from south to north (Young, 1981).

Aphanitic and porphyritic dykes are an important part of magmatism associated with the plutonic suites (Souther, 1988, 1989; Souther and Bakker, 1988). All suites except the Jurassic San Christoval suite have common (hornblende-) plagioclase-phyric and aphanitic green andesite dykes. Concordance of the subvertical, north-trending Carpenter Bay dykes (Souther, 1988, 1989; Souther and Jessop, 1991) with intraphase plutonic contacts within the coeval Eocene Carpenter Bay plutonic host is strong evidence of contemporaneity of plutonism and dyking.

## GEOCHRONOMETRY

### Previous work

Wanless et al. (1968, 1970, 1972), Yorath and Chase (1981) and Young (1981) contributed to the existing K-Ar isotopic age database (Table 3). They showed that "syntectonic" and some "post-tectonic" plutons were coeval and Late Jurassic (159–145 Ma), as were hornblende-bearing quartz diorite (BIPS-equivalent?) clasts common in Cretaceous coarse clastic sedimentary rocks (Yorath and Chase, 1981).

K-Ar dates for the western belt of known Tertiary "post-tectonic" plutons (Pocket Inlet, Kano, and Langara plutons) decrease from south (39–40 Ma) to north (about 24 Ma; Young, 1981; Table 3). Whole rock and alkali-feldspar K-Ar dates are younger than coexisting hornblende-biotite mineral pairs (e.g. 26 and 31 Ma for Pocket Inlet pluton alkali-feldspar and whole rock compared with 38 and 40 Ma for hornblende and biotite). Some are difficult to interpret (e.g. <5 Ma whole rock date for Pivot Mountain).

### Sampling and analytical methods

Samples were collected in 1987 and 1988 for zircon U-Pb dating from the Jurassic and Tertiary plutonic suites (Figures 1–3 and Tables 1–3). New K-Ar dates for hornblende were determined from only the freshest, representative samples of central SCPS, central BIPS, and two Carpenter Bay hornblende-phyric andesite dykes (Table 2) because alteration of the rocks is so common (pervasive within BIPS). Petrographic criteria for sample selection for hornblende and muscovite K-Ar dating included minimal alteration and, for hornblende, minimal clinopyroxene cores. Thus, samples dated by U-Pb were not suitable for K-Ar dating, but in some cases, K-Ar dates are available for nearby samples for comparison.

Zircon was dated by U-Pb methods using analytical procedures summarized by Parrish et al. (1987). Zircons selected for analysis were the clearest and devoid of visible inclusions or features resembling inherited zircon cores. Abrasion of most zircon fractions decreased the effect of alteration and recent Pb loss (e.g. Krogh, 1982). Pb and U blanks during the course of this study were 7–20 pg and 1–5 pg respectively. Analytical techniques for K-Ar dating follow Roddick and Souther (1987). All dates are consistent with decay constants of Steiger and Jäger (1977) and uncertainties are at 2 standard deviations (2σ).

Tertiary and most of the Jurassic samples yielded at least one concordant fraction (asterisks highlight fractions in Table 1 used in the age calculation). Age estimates for the Jurassic samples (Table 3 and Figs. 4 and 5) derive from <sup>207</sup>Pb/<sup>206</sup>Pb dates (and uncertainties de-



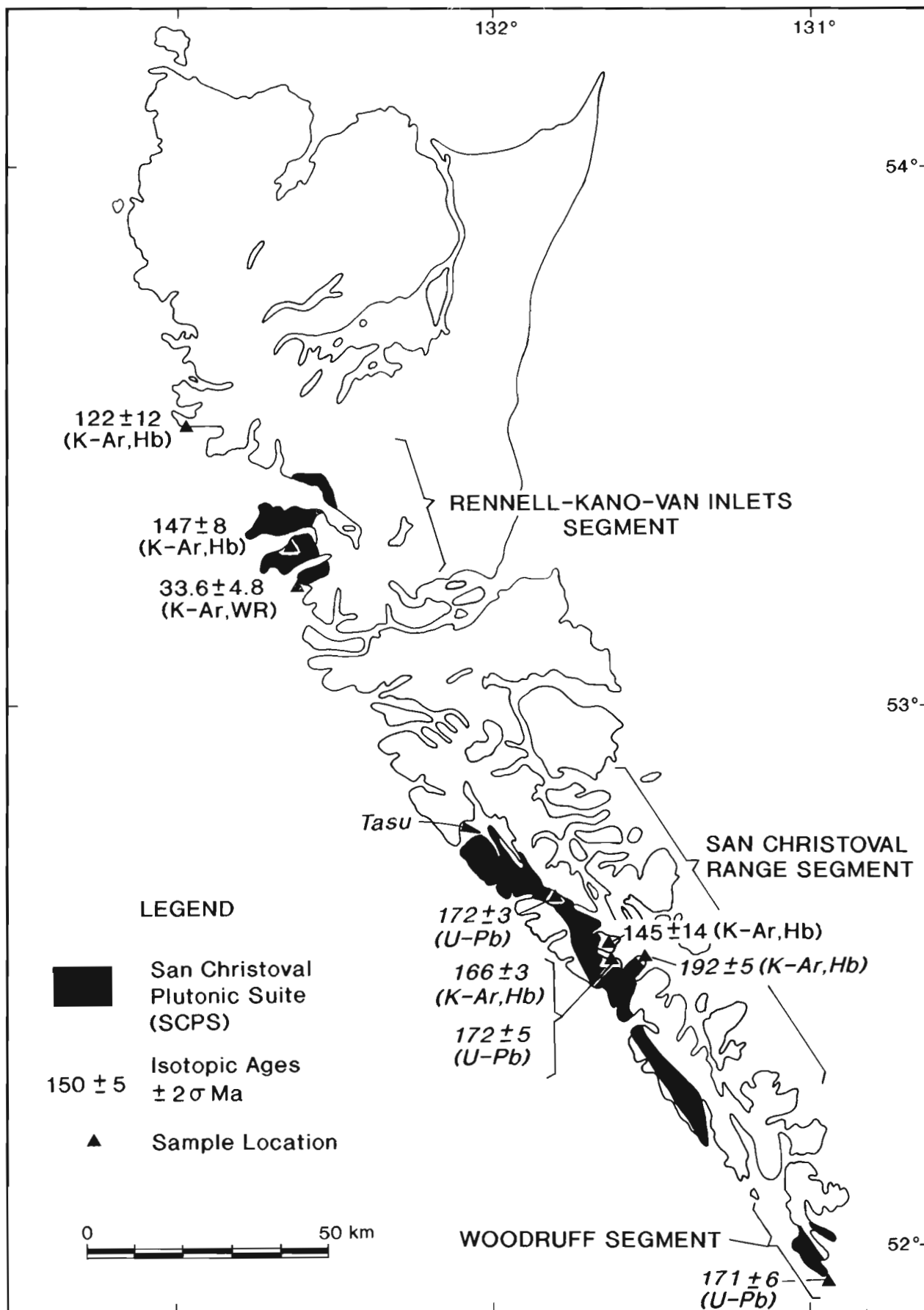


**Figure 1:** Distribution of K-Ar and U-Pb geochronometry for Middle Jurassic San Christoval plutonic suite (SCPS). New dates presented in this report are in *italics*.

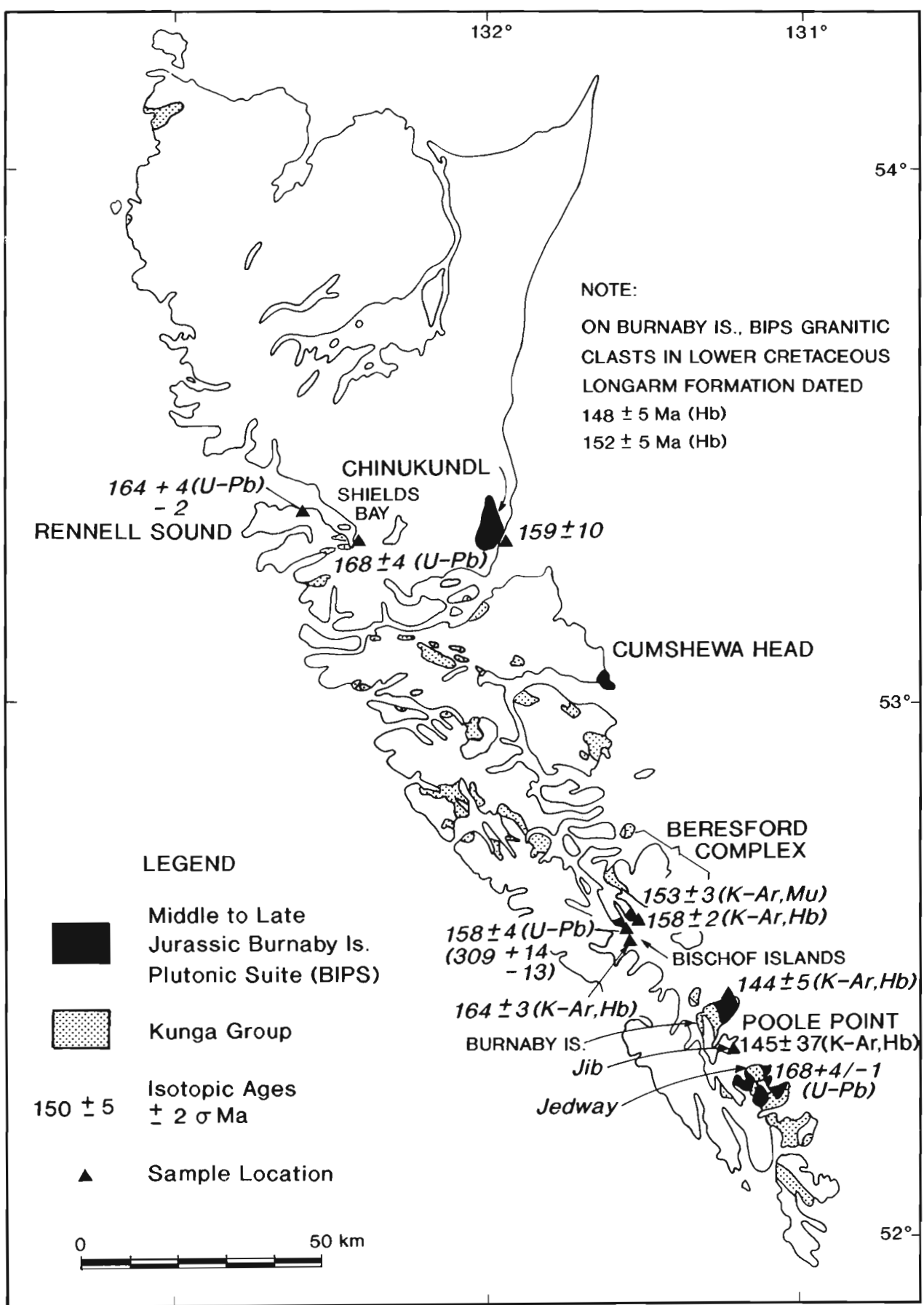


**Figure 2:** Distribution of K-Ar and U-Pb geochronometry for Middle to Late Jurassic Burnaby Island plutonic suite (BIPS). New dates presented in this report are in italics.

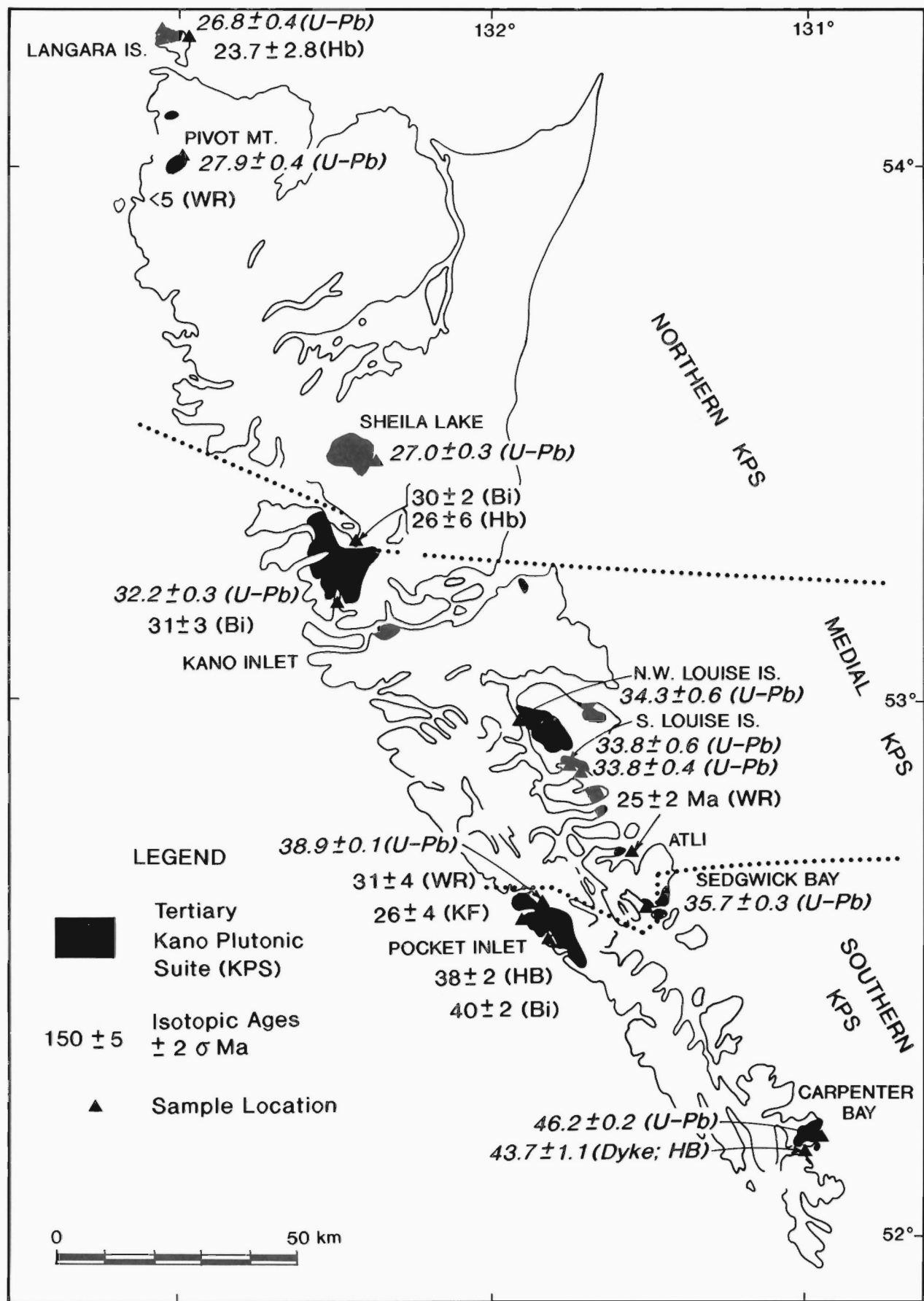


**Figure 3:** Distribution of K-Ar and U-Pb geochronometry for Tertiary Kano plutonic suite (KPS) and associated Carpenter Bay-Lyell Island dykes. New dates presented in this report are in *italics*.

terminated from the  $^{207}\text{Pb}/^{206}\text{Pb}$  experimental errors) for the most concordant fraction with the smallest analytical errors. Discordance in Jurassic zircons is assumed to result from Pb loss.

Zircon from Tertiary plutons was characteristically devoid of visible cores and produced excellent U-Pb analyses. Most samples yielded concordant Pb/U dates (Fig. 3 and 6; Table 1). Slight discordance is mainly attributable to the common Pb correction. The internal agreement of dates from the concordant fractions from a particular pluton and concordance with available K-Ar data (e.g. Langara, Kano and Pocket Inlet plutons; Table 3) suggests that further work would not change the results appreciably. Tertiary U-Pb dates and uncertainties were calculated from the mean  $^{206}\text{Pb}/^{238}\text{U}$  and  $^{207}\text{Pb}/^{235}\text{U}$  dates and standard deviations of concordant data for 2 (or more) fractions with the least analytical error (Table 3 and Fig. 3).

Large errors in  $^{207}\text{Pb}/^{235}\text{U}$  ratio (and relatively large errors in  $^{206}\text{Pb}/^{238}\text{U}$  ratio) relate to fractions containing a predominance of inclusion-rich zircons or to fractions containing few zircons, analyses having large common Pb blank values, and/or low radiogenic Pb amounts. We omitted some of these data in making the final age estimates. Quoted uncertainties reflect full error propagation (Roddick, 1987). The geological context of the samples and Palmer's (1983) time-scale provide the framework for discussion of the dates below.

## U-Pb results

### *Jurassic plutons*

U-Pb data for three SCPS and four BIPS samples indicate mainly Middle Jurassic dates (Figs. 1, 2, 4, and 5; Tables 1 and 3). Middle Jurassic  $^{207}\text{Pb}/^{206}\text{Pb}$  dates for the most concordant zircon fractions from SCPS samples (Fig. 4) are nearly identical and include:  $172 \pm 5$  Ma (Haswell Bay part of the San Christoval Range segment);  $172 \pm 3$  Ma (Pocket Inlet area of the San Christoval Range segment); and  $171 \pm 6$  Ma (Woodruff Bay segment). The Rennell-Kano-Van inlets segment of SCPS is no younger than  $164 +4/-2$  Ma based on the U-Pb date for a BIPS apophysis crosscutting SCPS).

BIPS samples include those from discrete intrusions and satellite intrusions in SCPS or country rock. The Poole Point sample represents one discrete pluton of BIPS. The near concordant zircon fraction having the smallest Pb/U error yielded a late Middle Jurassic date,  $168 +4/-1$  Ma, from concordia overlap (Fig. 5; error encompasses maximum range of ages from Pb/U and Pb/Pb estimates and uncertainties). The sample comes from the Burnaby Island pluton near the non-conformity with overlying, fossiliferous Lower Cretaceous Longarm Formation of Hauterivian age (Anderson and Greig, 1989; Haggart and Gamba, 1990; Fig. 8a). The fossil age and isotopic dates suggest the nonconformity represents a minimum hiatus of 37 million years.

The hornblende-plagioclase porphyry sample from Clapp Basin, Shields Bay area, yielded a  $^{207}\text{Pb}/^{206}\text{Pb}$  date of  $168 \pm 4$  Ma from a nearly concordant fraction with the smallest Pb/U errors (Table 1; Fig. 5). The Jurassic date was a surprise because the porphyry was expected to be coeval with texturally similar and nearby Tertiary Masset Formation volcanic rocks and an Early Oligocene quartz monzodiorite of the Kano pluton (see sample AT-87-80-1, Table 3). These geological relations led Sutherland Brown (1968) to include the porphyry as the porphyritic facies of the Cretaceous-Tertiary central Kano pluton. However, the lack of visible cores and little evidence for inherited lead in the U-Pb data support a late Middle Jurassic date. The Shields Bay pluton crosscuts southerly-vergent chevron folds developed in the Lower Jurassic Sandilands Formation (Fig. 8b). The intrusion's age and geological relations constrain deformation to post-Sinemurian and pre-168 Ma.

Fine grained quartz monzonite, thought to be a Tertiary KPS felsic phase, intruded SCPS along the southern shore of Rennell Sound. The U-Pb data for a sample of it suggest Pb loss occurred in the four discordant fractions and a late Middle Jurassic  $^{207}\text{Pb}/^{206}\text{Pb}$  date of  $164 +4/-2$  derives from concordia intercept (Fig. 5c). Again, there is nothing to support a Tertiary date for an intrusion that texturally resembles KPS.

Perhaps the most interesting of the BIPS samples yielding discordant U-Pb data for zircon is ATG-88-299-1 from a moderately deformed leucocratic biotite trondhjemite. The trondhjemite is part of the leucocratic phase of BIPS that includes muscovite-bearing, peraluminous variants (see also K-Ar sample AT-87-124-4). The phase crosscuts intensely foliated SCPS diorite of the Beresford complex at Beresford Inlet. The U-Pb data for the sample's 3 fractions define a chord with a lower concordia intercept of  $\geq 158 \pm 4$  Ma and an upper intercept date of  $309 +14/-13$  (Fig. 5; Table 3). The lower intercept is a minimum date for the trondhjemite phase. The discordance suggests inheritance of older radiogenic Pb by the Jurassic zircon, although the zircons contain no visible cores. The upper concordia intercept date is the first indication of an older, pre-Late Triassic, basement for the Queen Charlotte Islands and is a minimum age (Pennsylvanian). About 4 km southwest of the trondhjemite locality, near Darwin Point, undated felsic volcanic rocks occur structurally if not stratigraphically below Upper Triassic Karmutsen Formation basalt (Woodsworth, 1988). These may represent part of the inferred Paleozoic basement.

One zircon fraction from the felsic phase biotite quartz monzonite phase of the BIPS Cumshewa Head pluton, was analyzed. We sought to resolve a mapping problem arising from the Early Oligocene ( $34.3 \pm 0.3$  Ma) U-Pb date from a lithologically similar sample of the nearby northwest Louise Island pluton (Fig. 3; Tables 1 and 3). The pervasive veining in Cumshewa Head pluton distinguished it as part of BIPS despite similarities in grain size and composition. The U-Pb data, although discordant and of little use by themselves in determining a precise date, suggest a Middle to Late Jurassic date for the Cumshewa Head body.

### *Tertiary plutons*

U-Pb dates for 10 samples of KPS define three temporally distinct groups of KPS plutons that mark the passage of a northwesterly-accelerating magmatic front: southern Eocene ( $46-39$  Ma); medial Early Oligocene ( $36-32$  Ma); and northern Late Oligocene ( $28-27$  Ma) plutons (Figs. 3 and 7; Table 3). The data corroborate and refine the Tertiary K-Ar data reported by Young (1981). Southern belt plutons dated are Pocket Inlet ( $38.9 \pm 0.1$  Ma) and Carpenter Bay pluton at Point Langford ( $46.2 \pm 0.2$ ). Medial belt plutons sampled are Kano pluton ( $32.2 \pm 0.7$  Ma), northwest Louise Island pluton ( $34.3 \pm 0.6$  Ma), southern Louise Island pluton (younger quartz monzonite felsic phase,  $33.8 \pm 0.6$  Ma and older quartz monzodiorite intermediate phase,  $33.8 \pm 0.4$  Ma), and Sedgwick Bay pluton ( $35.7 \pm 0.3$  Ma). Northern belt plutons include Langara pluton ( $26.8 \pm 0.4$  Ma), Pivot Mountain pluton ( $27.9 \pm 0.4$  Ma), and Sheila Lake pluton ( $27.0 \pm 0.3$  Ma).

Previously determined K-Ar hornblende and biotite dates (Young, 1981) agree closely with U-Pb dates for nearby samples of Langara Island pluton (K-Ar:  $23.7 \pm 2.8$  Ma, U-Pb:  $26.8 \pm 0.4$  Ma), Kano pluton (K-Ar:  $31 \pm 3$  Ma; U-Pb:  $32.2 \pm 0.7$  Ma), and Pocket Inlet pluton (K-Ar:  $38-40 \pm 2$  Ma; U-Pb:  $38.9 \pm 0.1$  Ma; Table 3). The rapid, post-emplacement uplift and cooling of the plutons indicated by the geochronometry and the fine- to medium-grain size, seriate texture and miarolitic cavities characteristic of the suite (Anderson and Greig, 1989) all suggest high-level intrusion.

**TABLE 1.** U-Pb data for zircon in Jurassic and Tertiary plutons in Queen Charlotte Islands. Data with \* were used to calculate isotopic ages in Table 3.

Mineral Fraction <sup>1</sup> size, appearance	Wt. (mg)	U (ppm)	Pb <sup>2</sup> (ppm)	$\frac{206\text{Pb}^3}{204\text{Pb}}$	Pb <sub>c</sub> <sup>4</sup> (pg)	$208\text{Pb}^2$ (%)	$\frac{206\text{Pb}}{238\text{U}}$ ( $\pm 1\sigma$ (%)) <sup>5</sup>	$\frac{207\text{Pb}}{235\text{U}}$ ( $\pm 1\sigma$ (%)) <sup>5</sup>	$\frac{207\text{Pb}}{206\text{Pb}}$ ( $\pm 1\sigma$ (%)) <sup>5</sup>	$\frac{206\text{Pb}}{238\text{U}}$ ( $\pm 2\sigma$ Ma)	$\frac{207\text{Pb}}{235\text{U}}$ ( $\pm 2\sigma$ Ma)	$\frac{207\text{Pb}}{206\text{Pb}}$ ( $\pm 2\sigma$ Ma) <sup>6</sup>
<b>KANO PLUTONIC SUITE (KPS)</b>												
<b>Langara Island pluton – Sample CH-87-56-6<sup>7a</sup></b>												
*-105+74, abr., clear, prisms	0.0538	354.8	1.504	324	16	11.8	0.004153 (0.14)	0.02656 (0.43)	0.04638 (0.39)	26.7 ± 0.1	26.6 ± 0.2	17.5 ± 18.9
*-105+74, abr., clear, equant	0.0364	241.1	1.071	169	15	15.9	0.004148 (0.19)	0.02709 (0.80)	0.04737 (0.72)	26.7 ± 0.1	27.1 ± 0.4	67.9 ± 34.4
<b>Pivot Mountain pluton – Sample CH-87-56-10<sup>7b</sup></b>												
*abr., equant to stubby, clear	0.0042	2322	12.24	150	20	25.5	0.004360 (0.33)	0.02792 (1.6)	0.04645 (1.4)	28.0 ± 0.2	28.0 ± 0.9	20.9 ± 67.1
*abr., prisms, clear	0.0044	2230	11.49	251	11	24.2	0.004332 (0.14)	0.02758 (0.37)	0.04617 (0.29)	27.9 ± 0.1	27.6 ± 0.2	6.6 ± 14.1
<b>Sheila Lake pluton – Sample CH-87-30-09<sup>7c</sup></b>												
*-149+105, abr. clear, equant	0.0271	762.2	3.541	393	15	18.9	0.004182 (0.25)	0.02685 (0.51)	0.04656 (0.44)	26.9 ± 0.1	26.9 ± 0.3	26.6 ± 21.0
*-149+105, abr. clear, prisms	0.0191	605.0	2.760	292	11	17.3	0.004189 (0.12)	0.02717 (0.62)	0.04705 (0.56)	26.9 ± 0.1	27.2 ± 0.3	51.6 ± 26.8
<b>Kano pluton (Dawson Inlet) – Sample AT-87-80-1<sup>7d</sup></b>												
*+105, equant	0.124	174.8	0.8902	345	21	11.6	0.004999 (0.12)	0.03223 (0.30)	0.04675 (0.24)	32.1 ± 0.1	32.2 ± 0.2	36.7 ± 11.6
*-105+74, equant	0.155	374.0	1.921	865	22	12.2	0.005008 (0.11)	0.03238 (0.15)	0.04689 (0.082)	32.2 ± 0.1	32.4 ± 0.1	43.4 ± 3.9
<b>Northwest Louise Island pluton – Sample ATG-88-333-1<sup>7e</sup></b>												
*-105+74, clear, euhed., equant/ stubby	0.1867	399.4	2.132	2043	12	10.2	0.005324 (0.12)	0.03452 (0.14)	0.04703 (0.062)	34.2 ± 0.1	34.5 ± 0.1	50.5 ± 3.0
*-149+105, abr., clear, euhed., equant/stubby	0.0122	296.5	1.616	156	8	11.5	0.005365 (0.19)	0.03394 (0.59)	0.04588 (0.48)	34.5 ± 0.1	33.9 ± 0.4	-8.7 ± 23.1
+149, abr. clear, frags.	0.0086	327.8	1.807	142	8	12.0	0.005390 (0.42)	0.03445 (1.0)	0.04636 (0.77)	34.7 ± 0.3	34.4 ± 0.7	16.2 ± 36.6
<b>Southern Louise Island pluton (felsic (quartz monzonite) phase) – Sample ATG-88-260-1<sup>7f</sup></b>												
*-149+105, abr., frags.	0.1012	159.3	0.9095	238	25	16.5	0.005297 (0.19)	0.03379 (0.45)	0.04626 (0.36)	34.1 ± 0.1	33.7 ± 0.3	11.3 ± 17.4
*-105+74 incl., frags.	0.081	209.8	1.195	238	25	17.6	0.005212 (0.16)	0.03337 (0.42)	0.04644 (0.34)	33.5 ± 0.2	33.3 ± 0.4	20.5 ± 16.5
*+105, abr., incl., frags.	0.055	241.5	1.403	201	24	18.1	0.005282 (0.16)	0.03409 (0.50)	0.04681 (0.42)	34.0 ± 0.1	34.0 ± 0.1	39.3 ± 20.2



**TABLE 1.** U-Pb data for zircon in Jurassic and Tertiary plutons in Queen Charlotte Islands. Data with \* were used to calculate isotopic ages in Table 3.

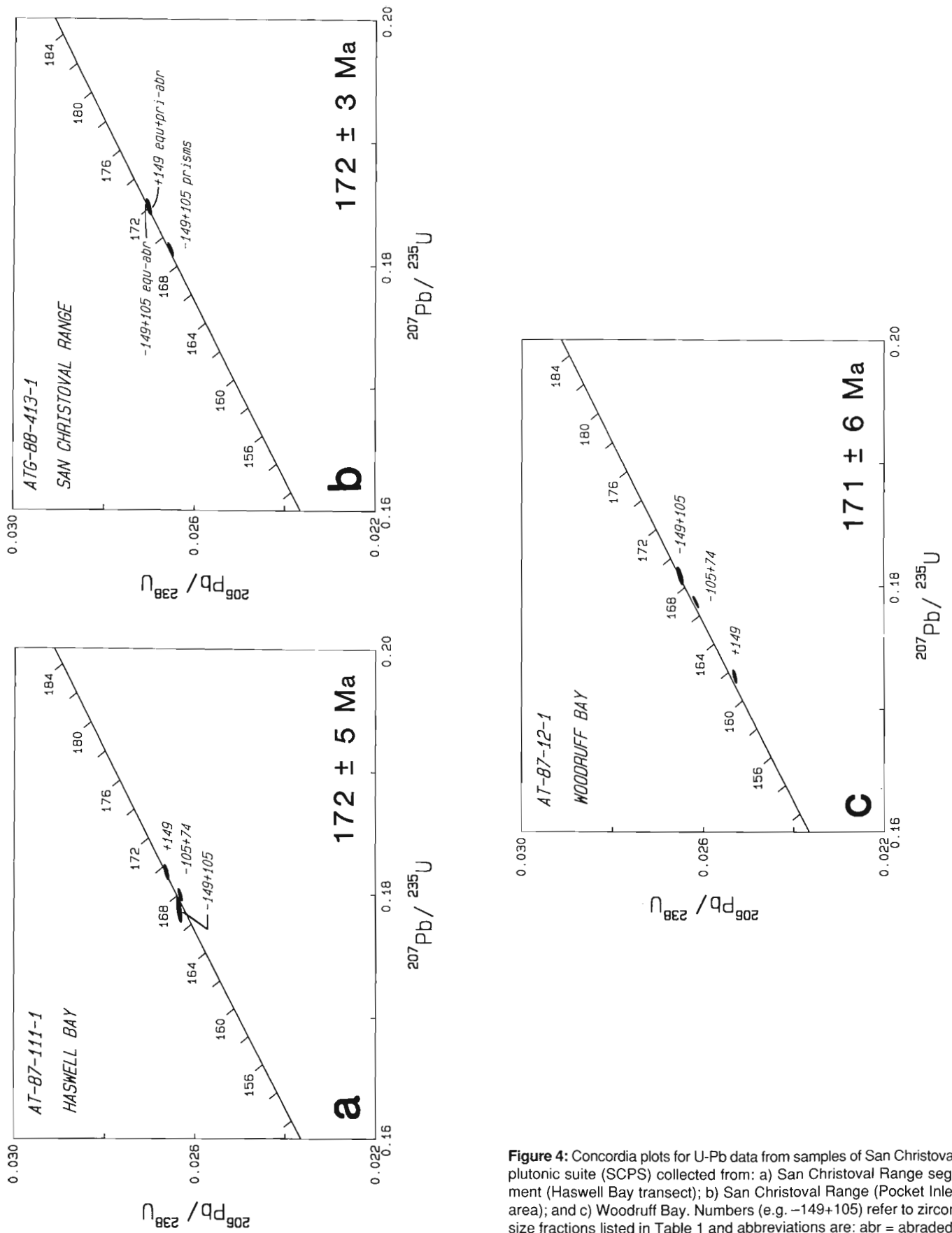
Mineral Fraction <sup>1</sup> size, appearance	Wt. (mg)	U (ppm)	Pb <sup>2</sup> (ppm)	$\frac{206\text{Pb}^3}{204\text{Pb}}$	Pb <sub>c</sub> <sup>4</sup> (pg)	$^{208}\text{Pb}^2$ (%)	$\frac{^{206}\text{Pb}}{^{238}\text{U}}$ ( $\pm 1\sigma$ (%)) <sup>5</sup>	$\frac{^{207}\text{Pb}}{^{235}\text{U}}$ ( $\pm 1\sigma$ (%)) <sup>5</sup>	$\frac{^{207}\text{Pb}}{^{206}\text{Pb}}$ ( $\pm 1\sigma$ (%)) <sup>5</sup>	$\frac{^{206}\text{Pb}}{^{238}\text{U}}$ ( $\pm 2\sigma$ Ma)	$\frac{^{207}\text{Pb}}{^{235}\text{U}}$ ( $\pm 2\sigma$ Ma)	$\frac{^{207}\text{Pb}}{^{206}\text{Pb}}$ Age ( $\pm 2\sigma$ Ma) <sup>6</sup>
<b>KANO PLUTONIC SUITE (cont'd)</b>												
<b>Southern Louise Island pluton (intermediate (quartz monzodiorite) phase) – Sample ATG-88-263-1<sup>7g</sup></b>												
*+149 (large), abr. clear, irregular frags.	0.477	262.3	1.536	793	53	19.5	0.005233 (0.16)	0.03371 (0.24)	0.04672 (0.15)	33.6 $\pm$ 0.1	33.7 $\pm$ 0.2	34.8 $\pm$ 7.3
*+149 (small), abr. clear, irregular frags.	0.300	272.9	1.612	401	71	19.6	0.005269 (0.17)	0.03424 (0.39)	0.04713 (0.31)	33.9 $\pm$ 0.1	34.2 $\pm$ 0.3	55.7 $\pm$ 14.7
*-149+105, abr. clear, irregular frags.	0.120	278.7	1.686	491	23	21.8	0.005243 (0.12)	0.03385 (0.22)	0.04682 (0.17)	33.7 $\pm$ 0.1	33.8 $\pm$ 0.1	39.8 $\pm$ 8.2
<b>Sedgwick Bay pluton – Sample AT-88-288-1<sup>7h</sup></b>												
*+105 (A) incl., equant to stubby	0.2085	204.4	1.248	642	24	18.0	0.005556 (0.12)	0.03589 (0.19)	0.04685 (0.13)	35.7 $\pm$ 0.1	35.8 $\pm$ 0.1	41.3 $\pm$ 6.2
*+105 (B) incl., equant to stubby	0.1305	158.6	0.9173	354	22	13.8	0.005539 (0.18)	0.03563 (0.34)	0.04665 (0.26)	35.6 $\pm$ 0.1	35.5 $\pm$ 0.2	31.5 $\pm$ 12.6
<b>Pocket Inlet pluton – Sample ATG-88-415-2<sup>7i</sup></b>												
*-105+74 incl., prisms	0.1765	1224	7.436	2009	41	10.4	0.006048 (0.16)	0.03910 (0.18)	0.04689 (0.075)	38.9 $\pm$ 0.1	38.9 $\pm$ 0.1	43.8 $\pm$ 3.6
*+105 incl., euhed., prisms and equant	0.136	1034	6.227	1500	36	9.6	0.006044 (0.16)	0.03909 (0.19)	0.04691 (0.10)	38.8 $\pm$ 0.1	38.9 $\pm$ 0.1	44.5 $\pm$ 4.8
<b>Carpenter Bay pluton, Point Langford – Sample AT-87-27-3<sup>7j</sup></b>												
*-149+105 clear, prisms	0.1574	401.6	3.090	1125	26	15.7	0.007194 (0.39)	0.04670 (0.47)	0.04708 (0.33)	46.2 $\pm$ 0.4	46.3 $\pm$ 0.4	53.4 $\pm$ 15.9
*-149+105 clear, equant	0.2153	362.1	2.674	1625	22	12.5	0.007177 (0.28)	0.04661 (0.33)	0.04710 (0.23)	46.1 $\pm$ 0.3	46.3 $\pm$ 0.3	54.4 $\pm$ 11.0
*-105+74 clear, prisms and equant	0.0530	486.2	3.779	630	19	16.8	0.007174 (0.71)	0.04655 (0.84)	0.04706 (0.61)	46.1 $\pm$ 0.7	46.2 $\pm$ 0.8	52.2 $\pm$ 29.1
<b>BURNABY ISLAND PLUTONIC SUITE (BIPS)</b>												
<b>Cumshewa Point pluton – Sample AT-87-61-2<sup>7k</sup></b>												
-149+105 clear, incl., prisms	0.1653	191.5	4.478	1259	37	10.2	0.02328 (0.10)	0.1586 (0.15)	0.04942 (0.093)	148.3 $\pm$ 0.3	149.5 $\pm$ 0.4	167.9 $\pm$ 4.3
<b>Poole Point Pluton – Sample ATG-88-291-4<sup>7l</sup></b>												
*+149, abr. clear, frags.	0.1683	419.6	11.45	6999	17	13.3	0.02621 (0.11)	0.1788 (0.12)	0.04947 (0.037)	166.8 $\pm$ 0.4	167.0 $\pm$ 0.4	170.3 $\pm$ 1.7
-149+105, abr. clear, frags.	0.0351	368.0	9.724	484	45	11.3	0.02596 (0.13)	0.1761 (0.33)	0.04920 (0.26)	165.2 $\pm$ 0.4	164.7 $\pm$ 1.0	157.3 $\pm$ 12.2
-105+74 clear, euhed.	0.2278	687.7	17.89	14,060	18	11.3	0.02556 (0.13)	0.1743 (0.14)	0.04947 (0.031)	162.7 $\pm$ 0.4	163.2 $\pm$ 0.4	170.0 $\pm$ 1.4

TABLE 1. U-Pb data for zircon in Jurassic and Tertiary plutons in Queen Charlotte Islands. Data with \* were used to calculate isotopic ages in Table 3.

Mineral Fraction <sup>1</sup> size, appearance	Wt. (mg)	U (ppm)	Pb <sup>2</sup> (ppm)	$\frac{^{206}\text{Pb}}{^{204}\text{Pb}}$ <sup>3</sup>	Pb <sub>c</sub> <sup>4</sup> (pg)	$\frac{^{206}\text{Pb}}{^{238}\text{U}}$ ( $\pm 1\sigma$ (%)) <sup>5</sup>	$\frac{^{207}\text{Pb}}{^{235}\text{U}}$ ( $\pm 1\sigma$ (%)) <sup>5</sup>	$\frac{^{207}\text{Pb}}{^{206}\text{Pb}}$ ( $\pm 1\sigma$ (%)) <sup>5</sup>	$\frac{^{206}\text{Pb}}{^{238}\text{U}}$ Age ( $\pm 2\sigma$ Ma)	$\frac{^{207}\text{Pb}}{^{235}\text{U}}$ Age ( $\pm 2\sigma$ Ma)	$\frac{^{207}\text{Pb}}{^{206}\text{Pb}}$ Age ( $\pm 2\sigma$ Ma) <sup>6</sup>
<b>BURNABY ISLAND PLUTONIC SUITE (cont'd)</b>											
<b>Shields Bay porphyry phase, Kano Inlet – Sample AT-88-345-1<sup>7m</sup></b>											
+149 incl., equant/prisms	0.3001	136.2	3.630	1425	48	0.02622 (0.12)	0.1787 (0.16)	0.04945 (0.079)	166.8 $\pm$ 0.4	167.0 $\pm$ 0.5	169.0 $\pm$ 3.7
*-149+105 incl., equant	0.2004	111.6	2.933	1310	28	0.02601 (0.094)	0.1773 (0.13)	0.04943 (0.074)	165.5 $\pm$ 0.3	165.7 $\pm$ 0.4	168.2 $\pm$ 3.5
<b>Rennell Sound intrusion – Sample ATG-88-362-2<sup>7n</sup></b>											
*+149 clear > incl., equant	0.232	176.3	3.735	485	121	0.02180 (0.13)	0.1484 (0.34)	0.04939 (0.26)	139.0 $\pm$ 0.4	140.5 $\pm$ 0.9	166.4 $\pm$ 12.3
*-149+105 clear > incl., prisms	0.185	166.1	4.058	943	52	0.02459 (0.10)	0.1673 (0.17)	0.04936 (0.12)	156.6 $\pm$ 0.3	157.1 $\pm$ 0.5	165.1 $\pm$ 5.5
*-149+105 clear > incl., equant	0.350	241.5	5.221	507	241	0.02206 (0.16)	0.1504 (0.37)	0.04946 (0.29)	140.6 $\pm$ 0.4	142.3 $\pm$ 1.0	169.8 $\pm$ 13.5
*-149+74, abr. prisms	0.187	121.3	3.139	1343	28	0.02558 (0.10)	0.1742 (0.13)	0.04938 (0.067)	162.8 $\pm$ 0.3	163.0 $\pm$ 0.4	165.9 $\pm$ 3.1
<b>Beresford complex trondhjemite – Sample ATG-88-299-1<sup>7o</sup></b>											
*+149 abr., clear, equant	0.1128	162.2	5.795	1469	29	0.03589 (0.099)	0.2537 (0.14)	0.05128 (0.083)	227.3 $\pm$ 0.4	229.6 $\pm$ 0.6	253.2 $\pm$ 3.8
*+149, abr. clear, prisms	0.0385	196.2	6.516	1143	14	0.03206 (0.11)	0.2244 (0.15)	0.05077 (0.099)	203.4 $\pm$ 0.5	205.6 $\pm$ 0.6	230.5 $\pm$ 4.6
*-149+105 clear, euhed., equant to stubby prisms	0.226	277.3	7.834	3072	37	0.02830 (0.092)	0.1952 (0.11)	0.05004 (0.043)	179.9 $\pm$ 0.3	181.1 $\pm$ 0.4	196.9 $\pm$ 2.0
<b>SAN CHRISTOVAL PLUTONIC SUITE (SCPS)</b>											
<b>San Christoval Range segment (Haswell Inlet area) – Sample AT-87-111-1<sup>7p</sup></b>											
*+149, incl., euhed., stubby/prisms	0.1051	176.7	4.612	899	35	0.02664 (0.11)	0.1818 (0.17)	0.04950 (0.12)	169.5 $\pm$ 0.4	169.6 $\pm$ 0.5	171.6 $\pm$ 5.4
-149+105, incl., euhed., stubby/prisms	0.0978	185.4	4.786	229	143	0.02635 (0.12)	0.1788 (0.30)	0.04910 (0.24)	167.7 $\pm$ 0.4	167.0 $\pm$ 0.9	156.8 $\pm$ 11.2
-105+74 clear, euhed., equant	0.0858	159.1	4.128	954	24	0.02634 (0.094)	0.1800 (0.14)	0.04967 (0.089)	167.6 $\pm$ 0.3	168.1 $\pm$ 0.4	175.1 $\pm$ 4.1
*+149, abr. incl., euhed., equant/stubby	0.1548	117.5	3.240	2504	12	0.02703 (0.094)	0.1845 (0.11)	0.04951 (0.054)	171.9 $\pm$ 0.3	171.9 $\pm$ 0.4	171.9 $\pm$ 2.5

TABLE 1. U-Pb data for zircon in Jurassic and Tertiary plutons in Queen Charlotte Islands. Data with \* were used to calculate isotopic ages in Table 3.

Mineral Fraction <sup>1</sup> size, appearance	Wt. (mg)	U (ppm)	Pb <sup>2</sup> (ppm)	$\frac{206\text{Pb}}{204\text{Pb}}$ <sup>3</sup> (ppm)	Pb <sub>c</sub> <sup>4</sup> (pg)	$\frac{206\text{Pb}}{238\text{U}}$ ( $\pm 1\sigma$ (%)) <sup>5</sup>	$\frac{207\text{Pb}}{235\text{U}}$ ( $\pm 1\sigma$ (%)) <sup>5</sup>	$\frac{207\text{Pb}}{206\text{Pb}}$ ( $\pm 1\sigma$ (%)) <sup>5</sup>	$\frac{206\text{Pb}}{238\text{U}}$ ( $\pm 2\sigma$ Ma)	$\frac{207\text{Pb}}{235\text{U}}$ ( $\pm 2\sigma$ Ma)	$\frac{207\text{Pb}}{206\text{Pb}}$ Age ( $\pm 2\sigma$ Ma) <sup>6</sup>
<b>SAN CHRISTOVAL PLUTONIC SUITE (cont'd)</b>											
<b>San Christoval Range segment (Pocket Inlet) – Sample ATG-88-413-1<sup>7q</sup> (cont'd)</b>											
-149+105 clear, euhed., prisms	0.1354	204.0	5.496	1889	25	10.9	0.02655 (0.12)	0.1813 (0.15)	0.04954 (0.068)	169.2 $\pm$ 0.5	173.5 $\pm$ 3.1
-149+105, abr. clear, euhed., equant	0.0913	101.9	2.797	924	18	11.1	0.02704 (0.12)	0.1847 (0.18)	0.04955 (0.13)	172.1 $\pm$ 0.6	174.1 $\pm$ 5.9
<b>Woodruff Bay segment – Sample AT-87-12-1<sup>7r</sup></b>											
*-149+105 clear/incl., euhed., stubby/prisms	0.0783	182.1	4.744	774	32	8.2	0.02651 (0.14)	0.1809 (0.20)	0.04948 (0.13)	168.7 $\pm$ 0.5	170.6 $\pm$ 6.2
+149 clear/minor incl., euhed. stubby/prisms	0.0447	308.2	7.618	836	27	7.6	0.02531 (0.096)	0.1727 (0.16)	0.04948 (0.11)	161.1 $\pm$ 0.3	170.7 $\pm$ 5.1
-105+74 clear/incl., euhed., stubby/prisms	0.2168	189.9	4.887	2951	23	8.2	0.02617 (0.12)	0.1787 (0.14)	0.04954 (0.054)	166.5 $\pm$ 0.4	173.7 $\pm$ 2.5
<ol style="list-style-type: none"> <li>1. Sizes (e.g., 105+74) refer to range of zircon length aspect in microns. Abbreviations are: abr. = abraded; clear = very few inclusions or inclusions-free; equant = stubby, equant grains; euhed. = euhedral crystals; frags. = crystal fragments; incl. = inclusions present in grains; prisms = euhedral prismatic crystals. Symbol "****" indicates fractions used to determine age.</li> <li>2. radiogenic Pb in parts per million (ppm); corrected for blank and common Pb.</li> <li>3. measured ratio, corrected for spike and fractionation.</li> <li>4. total picograms (pg) common Pb in analysis corrected for spike and fractionation.</li> <li>5. corrected for blank Pb and U. common Pb, errors quoted are 1 standard deviation (<math>\sigma</math>) in per cent.</li> <li>6. corrected for blank and common Pb, errors are 2 standard deviations (<math>\sigma</math>) in Ma.</li> <li>7. Sample information: <ol style="list-style-type: none"> <li>a. Langara Island pluton (KPS), sample CH-87-56-6: hornblende-biotite quartz monzonite; UTM (zone 8) 6013750 N, 627250 E; 54°15'28" N, 133°02'48" W (NTS 103 K3E-K6E); northwest corner of Langara Island, near lighthouse, 0.75 km east-northeast from Langara Point, 4.5 km north of Rhodes Point, at sea level; collected by C. Hickson.</li> <li>b. Pivot Mountain pluton (KPS), sample CH-87-36-10: clinopyroxene-orthopyroxene diorite; UTM (zone 8) 5986900 N, 630860 E; 54°00'57" N, 133°00'10" W (NTS 103 K3E-K6E); west flank of Pivot Mountain (1650 feet elevation), 3.2 km southeast of mouth of Beresford Creek, 5.4 km east-northeast of mouth of Hanakoot Creek; collected by C. Hickson.</li> <li>c. Sheila Lake pluton (KPS), sample CH-87-30-09: clinopyroxene-orthopyroxene diorite; UTM (zone 8) 5929875 N, 667550 E; 53°29'35" N, 132°28'28" W (NTS 103 F8); from quarry outcrop 1 km northwest of north end of Sheila Lake, 0.5 km south-southwest of south end of Pam Lake, 2 km southwest of island in Marie Lake, 1050 feet elevation; collected by C. Hickson.</li> <li>d. Kano Inlet pluton (KPS), sample AT-87-40-1: hornblende (clinopyroxene)-biotite quartz monzonite; UTM (zone 8) 598850 N, 666550 E; 53°12'51" N, 132°28'30" W (NTS 103 F1); northeast side of Dawson Inlet, 1 km from north end of inlet, 4 km north-northwest of Meadow Mountain, at sea level.</li> <li>e. Northwest Louise Island pluton (KPS), sample ATG-88-333-1: biotite quartz monzonite; UTM (zone 9) 5874375 N, 303950 E; 52°59'06" N, 131°55'13" W (NTS 103 B13); east side of Carmichael Passage, northwest coast of Louise Island, 5.25 km north-west of Mount Kermode, 6.5 km north-northeast of mouth of Dass Creek, at sea level; collected by C.J. Greig.</li> <li>f. Southern Louise Island pluton (KPS), sample ATG-88-260-1: younger, biotite quartz monzonite phase; UTM (zone 9) 5862575 N, 313800 E; 52°52'57" N, 131°46'02" W (NTS 103 B13); southern Louise Island, 1 km east of Alfred Point, 2.5 km north-north-west of Procter Rocks, at sea level; collected by C.J. Greig.</li> <li>g. Southern Louise Island pluton (KPS), sample ATG-88-263-1: older, hornblende monzonite phase; UTM (zone 9) 5861750 N, 317025 E; 52°52'35" N, 131°43'08" W (NTS 103 B13); southern Louise Island, 2.25 km northwest of Dass Point, 2.5 km north-east of Harbidge Point, at sea level; collected by C.J. Greig.</li> <li>h. Sedgwick Bay pluton (KPS), sample AT-88-288-1: biotite monzogranite; UTM (zone 9) 5832425 N, 329475 E; 52°37'01" N, 131°31'08" W (NTS 103 B12); Lyell Island coast, southeastern Sedgwick Bay, 0.75 km north-northwest of Kogangas Rock, 3 km northeast of Sedgwick Point, at sea level.</li> <li>i. Pocket Inlet pluton (KPS), sample ATG-88-415-2: equigranular biotite granite; UTM (zone 9) 5834100 N, 308000 E; 52°37'29" N, 131°50'12" W (NTS 103 B12); San Christoval Range, 2 km northeast of east end of Pocket Inlet, 6.5 km south of Mount Laysen, 1680 feet elevation; collected by C.J. Greig.</li> <li>j. Carpenter Bay pluton (KPS), sample AT-87-27-3: biotite-hornblende quartz monzonite; UTM (zone 9) 5781000 N, 360000 E; 52°03'49" N, 131°02'49" W (NTS 103 B3); small headland, 0.25 km north-northwest of Point Langford, at sea level.</li> <li>k. Cumshewa Head pluton (BIPS), sample AT-87-61-2: hornblende-biotite quartz monzonite; UTM (zone 9) 5883730 N, 323430 E; 53°04'33" N, 131°38'09" W (NTS 103 G4); north of Cumshewa Head, 5.25 km south of Gray Point, 4.5 km north-northwest of Cumshewa Island, at sea level.</li> <li>l. Burnaby Island pluton (BIPS), Poole Point locality, sample ATG-88-291-4: biotite-hornblende quartz monzonite; UTM (zone 9) 5804025 N, 345175 E; 52°22'00" N, 131°16'26" W (NTS 103 B6); 2.25 km west-southwest of Poole Point in Francis Bay, 1.75 km south-southeast of Rebecca Point, at sea level; collected by C.J. Greig.</li> <li>m. Shields Bay porphyry (BIPS), sample AT-88-345-1: hornblende-plagioclase andesite porphyry; UTM (zone 8) 5909275 N, 671950 E; 53°19'24" N, 132°25'10" W (NTS 103 F8); large cliff exposure at intersection of Rennell Sound road and disused Mountain Creek road, 1.5 km south of mouth of Rockkoon Creek, 4 km east-southeast of Twin Creek, 100 feet elevation.</li> <li>n. Rennell Sound intrusion (BIPS), sample ATG-88-362-2: hornblende quartz monzonite; UTM (zone 8) 5915300 N, 560925 E; 53°21'51" N, 132°34'54" W (NTS 103 F7E); 3.0 km south of Gossel Island, 4.5 km west-northwest of Richardson Head, at sea level; collected by C.J. Greig.</li> <li>o. Beresford Inlet leucocratic phase (BIPS), sample ATG-88-299-1: weakly foliated biotite trondhjemite; UTM (zone 9) 5829550 N, 325500 E; 52°35'04" N, 131°34'32" W (NTS 103 B12); 0.5 km north-northeast of Richardson Point, 2.5 km southwest of Sedgwick Point, at sea level; collected by C.J. Greig.</li> <li>p. San Christoval segment of SCPS, Haswell Bay transect, sample AT-87-111-1: biotite-hornblende quartz monzonite; UTM (zone 9) 5825150 N, 318025 E; 52°32'52" N, 131°41'02" W (NTS 103 B12E); near northwest end of De La Beche Inlet, 2 km north-northwest of south end of Sac Bay and 5 km west-southwest of Darwin Point, at sea level.</li> <li>q. San Christoval segment of SCPS, Pocket Inlet locality, sample ATG-88-413-1: biotite-hornblende quartz diorite; UTM (zone 9) 5833900 N, 308425 E; 52°37'23" N, 131°49'49" W (NTS 103 B12); on spur ridge at about 2750 feet elevation, 2.23 km north-east of east end of Pocket Inlet, 6.5 km south-southeast of Mount Laysen; collected by C.J. Greig.</li> <li>r. Woodruff Bay segment of SCPS, sample AT-87-12-1: biotite-hornblende quartz diorite; UTM (zone 9) 5755875 N, 361400 E; 51°56'18" N, 131°00'56" W (NTS 102 U14 and 15); at boat harbour just north of meteorological station and lighthouse, St. James Island, at sea level.</li> </ol> </li> </ol>											



**Figure 4:** Concordia plots for U-Pb data from samples of San Christoval plutonic suite (SCPS) collected from: a) San Christoval Range segment (Haswell Bay transect); b) San Christoval Range (Pocket Inlet area); and c) Woodruff Bay. Numbers (e.g. -149+105) refer to zircon size fractions listed in Table 1 and abbreviations are: abr = abraded; clr = clear; equ = equant; frag = fragments; and pris or pri = prisms. Dates from Table 3.

**Table 2.** New K-Ar data for hornblende and muscovite from Middle to Late Jurassic and Tertiary plutons, Queen Charlotte Islands.

Sample Number	G.S.C. No. or (Lab Number)	Locality	K (wt. %)	Rad. <sup>40</sup> Ar ((10 <sup>-7</sup> ) cc/g STP)	% atmos. <sup>40</sup> Ar	Age (± 2σ <sup>1</sup> Ma) (Hb = hornblende) (Mu = muscovite)
<b>KANO PLUTONIC SUITE (KPS)</b>						
<b>BURNABY ISLAND-CARPENTER BAY DYKE SWARM</b>						
AT-87-7-3	GSC 89-20 <sup>2</sup> (3980)	Benjamin Point <sup>3</sup>	0.511	8.783	34.0	43.7 ± 1.1 (Hb)
AT-87-19-1	GSC 90-24 (3976)	Benjamin Point <sup>4</sup>	0.157	14.94	49.0	230 ± 13 (Hb)
<b>BURNABY ISLAND PLUTONIC SUITE (BIPS)</b>						
<b>BERESFORD COMPLEX, BIPS TRONDHJEMITE</b>						
AT-87-124-4	GSC 90-27 (3982)	Beresford Inlet <sup>5</sup>	8.37	517.7	3.8	153 ± 3 (Mu)
<b>BERESFORD COMPLEX, BIPS INTERMEDIATE PHASE</b>						
AT-87-122-1	GSC 89-18 <sup>2</sup> (3977)	Bischof Islands <sup>6</sup>	0.262	17.44	22.0	164 ± 3 (Hb)
<b>BERESFORD COMPLEX, BIPS MAFIC PHASE (HORNBLLENDE DIORITE)</b>						
AT-87-124-6	GSC 90-25 (3978)	Beresford Inlet <sup>7</sup>	0.521	33.37	24.0	158 ± 4 (Hb)
<b>BURNABY ISLAND PLUTON, INTERMEDIATE PHASE</b>						
AT-87-83-1	GSC 90-26 (3981)	Burnaby Island <sup>8</sup>	0.353	20.56	20.0	144 ± 5 (Hb)
<b>SAN CHRISTOVAL PLUTONIC SUITE (SCPS)</b>						
<b>HASWELL TRANSECT, SAN CHRISTOVAL SEGMENT</b>						
AT-87-105-1	GSC 90-28 (3983)	Haswell Bay <sup>9</sup>	0.636	50.2	8.8	192 ± 5 (Hb)
AT-87-115-1	GSC 89-19 <sup>2</sup> (3979)	Sac Bay <sup>10</sup>	0.521	35.23	38.0	166 ± 3 (Hb)

1. σ = standard deviation.

2. revised from Anderson and Reichenbach (1989) and Anderson (in Hunt and Roddick, 1990).

3. hornblende-plagioclase andesite porphyry dyke; UTM (zone 9) 5786550 N, 363100 E; 52°12'51" N, 131°00'14" W (NTS 103 B/3); peninsula south of Carpenter Bay, north of Benjamin Point, 2 km south of Langtry Island at sea level.

4. hornblende (clinopyroxene)-plagioclase andesite porphyry dyke; UTM (zone 9) 5787050 N, 363200 E; 52°09'36" N, 131°00'00" W (NTS 103 B/3); peninsula south of Carpenter Bay, 1 km north of Benjamin Point, 1.5 km south of Langtry Island, at sea level. Clinopyroxene accounts for less than 10 percent of hornblende grains but in some grains makes up one-third to one-half of grain.

5. muscovite trondhjemite; UTM (zone 9) 5830125 N, 326850 E; 52°35'44" N, 131°33'23" W (NTS 103 B/12E); southwestern tip of Lyell Island between Beresford and Sedgwick bays, 0.75 km west of Sedgwick Point at sea level.

6. biotite-hornblende quartz monzodiorite; UTM (zone 9) 5828400 N, 325925 E; 52°34'47" N, 131°34'09" W (NTS 103 B/12E); western coast of northernmost island of Bischof Islands, 1 km east of Richardson Point, 2.6 km southwest of Sedgwick Point, at sea level.

7. hornblende diorite; UTM (zone 9) 5830125 N, 326850 E; 52°35'44" N, 131°33'23" W (NTS 103 B/12E); southwestern tip of Lyell Island between Beresford and Sedgwick bays, 0.75 km west of Sedgwick Point, at sea level.

8. biotite-hornblende quartz diorite; UTM (zone 9) 5813000 N, 344200 E; 52°26'49" N, 131°17'33" W (NTS 103 B/6); north shore of Burnaby Island, 0.5 km southwest of Saw Reef, 1.5 km east-northeast of southeastern tip of Alder Island, at sea level.

9. biotite-hornblende quartz diorite; UTM (zone 9) 5821650 N, 323050 E; 52°31'05" N, 131°36'29" W (NTS 103 B/12E); in small cove off Haswell Bay, 3.25 km southwest of Hoskins Point, 2.75 km south-southeast of De La Beche Island, at sea level.

10. biotite-hornblende diorite; UTM (zone 9) 5823375 N, 318650 E; 52°31'56" N, 131°40'25" W (NTS 103 B/12E); southeast end of Sac Bay, off de la Beche Inlet, 3.5 km west-southwest of de la Beche Island, 5.6 km southwest of Darwin Point, at sea level.



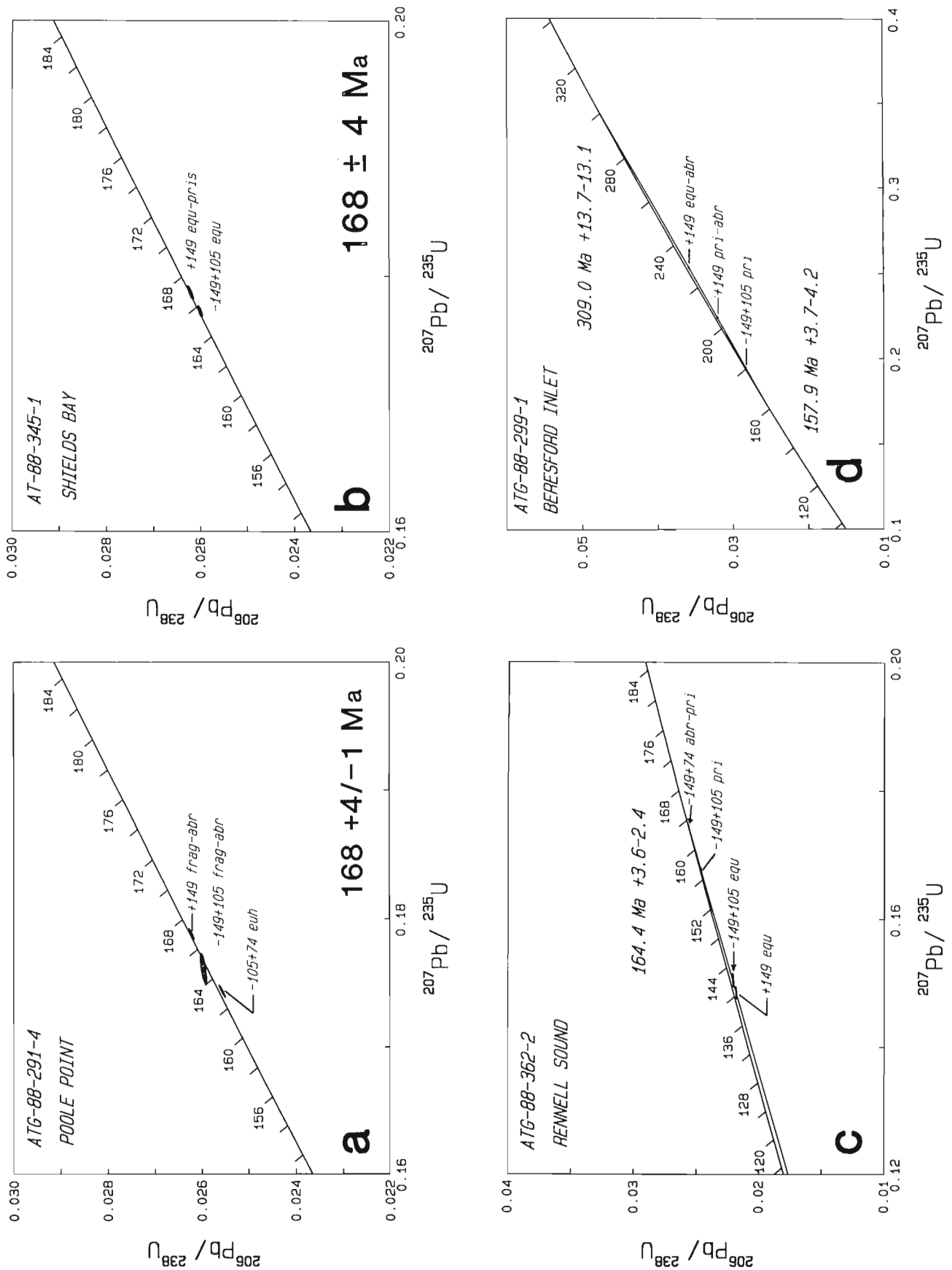


**Figure 5:** Concordia plots for U-Pb data from samples of Burnaby Island plutonic suite (BIPS) collected from discrete BIPS intrusions at: a) Burnaby Island (Poole Point); and from BIPS intrusions within SCPS at: b) Shields Bay (Clapp Basin); c) Rennell Sound; and d) Beresford Inlet. Abbreviations as for Figure 4 and dates from Table 3.

**Table 3.** Compilation of U-Pb and K-Ar geochronometry for Middle to Late Jurassic and Tertiary plutons, Queen Charlotte Islands.

Pluton/Locale (lithology <sup>2</sup> )	G.S.C. No.	Sample Number	U-Pb Date (Zircon) ( $\pm 2\sigma$ , in Ma)	K-Ar Date <sup>1</sup> $\pm 2\sigma$ , in Ma (mineral <sup>2</sup> )	Reference <sup>3</sup> and Comments
<b>TERTIARY GEOCHRONOMETRY</b>					
<b>CARPENTER BAY DYKES</b>					
<b>CARPENTER BAY DYKE</b> (hornblende-plagioclase porphyry andesite)	GSC 89-20	AT-87-7-3		43.7 $\pm$ 1.1 (Hb)	<b>a and e</b> ; north-trending dykes crosscut 46.2 $\pm$ 0.5 Ma Carpenter Bay plutons (see below)
<b>CARPENTER BAY DYKE</b> (hornblende-plagioclase porphyry andesite)	GSC 90-24	AT-87-19-1		230 $\pm$ 13 (Hb)	<b>this report</b> ; north-trending dykes crosscut 46.2 $\pm$ 0.5 Ma Carpenter Bay plutons (see below) and Lower Jurassic Sandilands Formation; <i>date unreliable</i> because of clinopyroxene cores in hornblende.
<b>KANO PLUTONIC SUITE (KPS)</b>					
<b>LANGARA ISLAND</b> (Bi-Hb quartz monzodiorite)		CH-87-56-6	26.8 $\pm$ 0.4		<b>a</b> (average U-Pb date and $2\sigma$ error for best 2 fractions)
		GS-50-66		23.7 $\pm$ 2.8 (Hb)	<b>b</b> ; Pan American Petroleum Corp. (unpublished data noted in Steen, 1967); McPherson Point, north west shore of Langara Island, 54°15.02' N, 132°58.83' W
<b>PIVOT MOUNTAIN</b> (clinopyroxene-orthopyroxene diorite)		CH-87-56-10	27.9 $\pm$ 0.4		<b>a</b> (average U-Pb date and $2\sigma$ error for best 2 fractions)
		SD-257-63		<5 (WR)	<b>b</b> ; Shell Canada Resources, Ltd. (unpublished data); 4 km southeast of Beresford Bay, southwest Graham Island, 54°00.63' N, 133°00.57' W
<b>SHEILA LAKE</b> (clinopyroxene-orthopyroxene diorite)		CH-87-30-09	27.0 $\pm$ 0.3		<b>a</b> (average U-Pb date and $2\sigma$ error for best 2 fractions)
<b>KANO INLET (Dawson Inlet)</b> (Bi-Hb quartz monzodiorite)		AT-87-80-1	32.2 $\pm$ 0.3		<b>a and this report</b> (average U-Pb date and $2\sigma$ error for best 2 fractions)
	GSC 67-16 GSC 67-17	65 AB-21 "		26 $\pm$ 6 (Hb) 30 $\pm$ 2 (Bi)	<b>c</b> ; southern head of Shields Bay, southwest Graham Island, 53°17' N, 132°26' W
	GSC 70-2	65-AB-19		31 $\pm$ 3 (Bi)	<b>d</b> ; head of Dawson Inlet, southwest Graham Island, 53°13' N, 132°29' W
<b>NORTHWEST LOUISE ISLAND</b> (Bi quartz monzonite)		ATG-88-333-1	34.3 $\pm$ 0.6		<b>this report</b> (average U-Pb date and $2\sigma$ error for best 2 fractions)
<b>SOUTHERN LOUISE ISLAND</b> (younger, Bi quartz monzonite phase)		ATG-88-260-1	33.8 $\pm$ 0.6		<b>this report</b> (average U-Pb date and $2\sigma$ error for best 2 fractions)
<b>SOUTHERN LOUISE ISLAND</b> (older, Hb monzodiorite phase)		ATG-88-263-1	33.8 $\pm$ 0.4		<b>this report</b> (average U-Pb date and $2\sigma$ error for best 2 fractions)
<b>SEDGWICK BAY</b> (Bi monzogranite)		AT-88-288-1	35.7 $\pm$ 0.3		<b>this report</b> (average U-Pb date and $2\sigma$ error for best 2 fractions)

**Table 3.** Compilation of U-Pb and K-Ar geochronometry for Middle to Late Jurassic and Tertiary plutons, Queen Charlotte Islands. (cont'd)

Pluton/Locale (lithology <sup>2</sup> )	G.S.C. No.	Sample Number	U-Pb Date (Zircon) ( $\pm 2\sigma$ , in Ma)	K-Ar Date <sup>1</sup> $\pm 2\sigma$ , in Ma (mineral <sup>2</sup> )	Reference <sup>3</sup> and Comments
<b>ATLI INLET</b>		SD-265-63		25 $\pm$ 4 (WR)	<b>b</b> ; single date considered minimum date and of unknown reliability by Young (1981); Shell Canada Resources, Ltd. (unpublished data); southeastern shore of Richardson Inlet, southeast of Dog Island, 52°43.67' N, 131°35.95' W
<b>POCKET INLET</b> (Bi granite)		ATG-88-415-2	38.9 $\pm$ 0.1		<b>this report</b> (average U-Pb date and 2 $\sigma$ error for best 2 fractions)
		SD-262-63		26 $\pm$ 4 (Kf)	<b>b</b> ; date considered unreliable by Young (1981); Shell Canada Resources, Ltd. (unpublished data); western margin of Pocket Inlet batholith, south shore, head of Pocket Inlet, 52°36.35' N, 131°54.43' W
		SD-263-63		31 $\pm$ 4 (WR)	<b>b</b> ; date considered minimum age by Young (1981); Shell Canada Resources, Ltd. (unpublished data); western margin of Pocket Inlet batholith, north shore, head of Pocket Inlet, 52°36.91' N, 131°52.08' W
	GSC 67-18 GSC 67-19	65-AB 10 "		38 $\pm$ 2 (Hb) 40 $\pm$ 2 (Bi)	<b>c</b> ; central Pocket Inlet batholith, south shore of Barry Inlet, 52°34' N, 131°48' W
<b>POINT LANGFORD</b> <b>(CARPENTER BAY</b> <b>pluton)</b> (Bi-Hb quartz monzodiorite)		AT-87-27-3	46.2 $\pm$ 0.2		<b>this report</b> (average U-Pb date and 2 $\sigma$ error for best 3 fractions north-trending dykes dated at 43.7 $\pm$ 1.1 Ma (see above) crosscut Carpenter Bay plutons.
<b>MISCELLANEOUS TERTIARY DATES</b>					
<b>SCPS(?),</b> <b>RENNELL-KANO-</b> <b>VAN INLET</b> <b>SEGMENT</b> (Bi quartz diorite)		GS 31-66		33.6 $\pm$ 4.8 (WR)	<b>b</b> ; date considered unreliable by Young (1981); Pan American Petroleum Corp. (unpublished data noted in Steen, 1967); south shore, mouth of Van Inlet, 53°14.87' N, 132°37.0' W
<b>KPS (?)</b> (Bi quartz diorite)		SD-261-63		33 $\pm$ 4 (Bi)	<b>b</b> ; Shell Canada Resources, Ltd. (unpublished data); near contact with Masset Formation, 4 km southeast of Mount De La Touche, west coast Moresby Island, 52°40.53' N, 131°59.70' W
<b>CRETACEOUS GEOCHRONOMETRY</b>					
<b>HIPPA ISLAND</b> (Hb quartz diorite)		GS 33-66		122 $\pm$ 12 (Hb)	<b>b</b> ; single, unconfirmed date considered minimum date by Young (1981); Pan American Petroleum Corp. (unpublished data noted in Steen, 1967); northwest tip Hippa Island, 53°32.17' N, 132°57.17' W
<b>JURASSIC GEOCHRONOMETRY</b>					
<b>BURNABY ISLAND PLUTONIC SUITE (BIPS)</b>					
<b>DISCRETE BIPS INTRUSIONS</b>					
<b>CHINUKUNDL</b> (Hb quartz diorite)	GSC 70-3	65-AB-22		159 $\pm$ 10 (Hb)	<b>d</b> ; considered a minimum date by Young (1981) and of uncertain interpretation by J.E. Reesor ( <i>in</i> Wanless et al., 1972, p. 7) because of alteration state of sample and uncertain geological relations; Chinukundl Creek, 53°19' N, 131°58' W

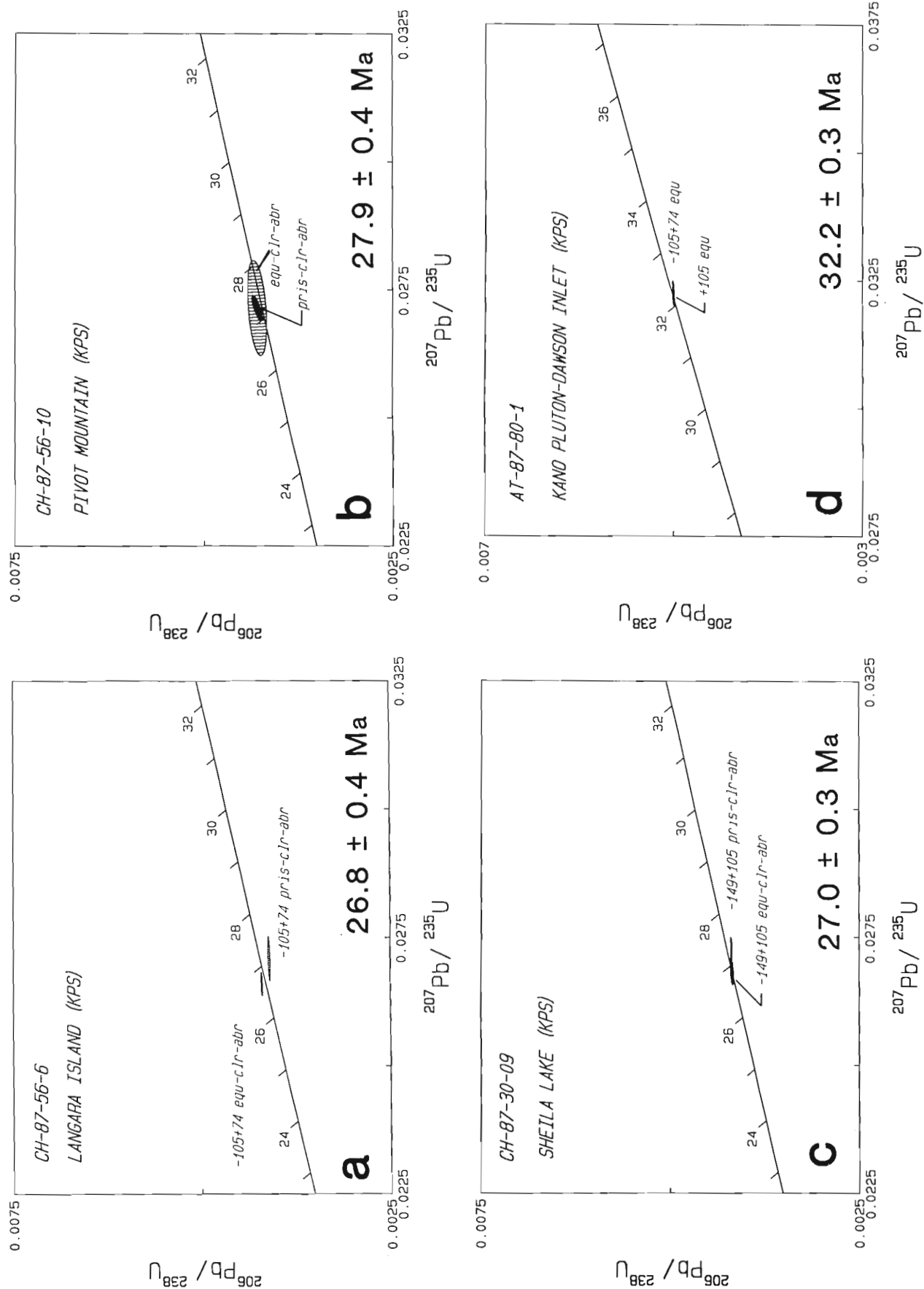
**Table 3.** Compilation of U-Pb and K-Ar geochronometry for Middle to Late Jurassic and Tertiary plutons, Queen Charlotte Islands. (cont'd)

Pluton/Locale (lithology <sup>2</sup> )	G.S.C. No.	Sample Number	U-Pb Date (Zircon) ( $\pm 2\sigma$ , in Ma)	K-Ar Date <sup>1</sup> $\pm 2\sigma$ , in Ma (mineral <sup>2</sup> )	Reference <sup>3</sup> and Comments
<b>CUMSHEWA HEAD</b> (Hb-Bi quartz date monzonite)		AT-87-61-2	Middle to Late Jurassic (148 to >168? Ma)		<b>this report</b> (one discordant fraction indicates $^{206}\text{Pb}/^{238}\text{U}$ of 148.3 Ma; $^{207}\text{Pb}/^{235}\text{U}$ date of 149.5 Ma and $^{207}\text{Pb}/^{206}\text{Pb}$ date of $167.9 \pm 4.3$ Ma; see Table 1)
<b>BURNABY ISLAND</b> (Bi-Hb quartz monzodiorite)	GSC 90-26	AT-87-83-1		$144 \pm 5$ (Hb)	<b>this report</b>
<b>BURNABY ISLAND (POOLE POINT)</b> (Bi-Hb quartz monzodiorite)		ATG-88-291-4	$168 \pm 4/-1$		<b>this report</b> (Pb-Pb date and $2\sigma$ error for most concordant fraction); cf. K-Ar date below
(Hb-Bi granodiorite)	GSC 66-14	65-AB4		$145 \pm 37$ (Hb)	<b>f</b> ; considered a minimum date by Young (1981); cf. U-Pb date above; Poole Point, Burnaby Island, $52^{\circ}22' \text{ N}$ , $131^{\circ}15' \text{ W}$
<b>BIPS INTRUSIONS IN SCPS</b>					
<b>SHIELDS BAY</b> (Hb-plagioclase porphyry)		AT-88-345-1	$168 \pm 4$		<b>this report</b> (Pb-Pb date and $2\sigma$ for most concordant fraction); porphyry intrusion crosscuts east-verging chevron folds in Lower Jurassic Sandilands Formation of Kunga Group
<b>RENNELL SOUND</b> (fine grained Hb quartz monzonite)		ATG-88-362-2	$164 \pm 4/-2$		<b>this report</b> (upper concordia intercept date and $2\sigma$ error determined for 4 discordant fractions); intrusion crosscuts Rennell- Kano-Van inlets segment of SCPS
<b>BERESFORD INLET</b> (Mu-Bi trondh- jemite)		ATG-88-299-1	$158 \pm 4$ ( $309 \pm 14/-13$ )		<b>this report</b> (3 discordant fractions which show evidence for inherited Pb); younger date (and $2\sigma$ error) interpreted as minimum date for emplacement of massive to moderately foliated BIPS leucocratic phase into well foliated SCPS Beresford complex diorite
	GSC 90-27	AT-87-124-4		$153 \pm 3$ (Mu)	<b>this report</b> ; muscovite trondhjemite is part of BIPS leucocratic phase which is faintly foliated but intrudes massive Hb diorite of BIPS mafic phase in Beresford complex (see sample AT-87-124-6 below); cf. U-Pb date above for same trondhjemite phase
(hornblende diorite)	GSC 90-25	AT-87-124-6		$158 \pm 4$ (Hb)	<b>this report</b> ; hornblende diorite is part of BIPS mafic phase which is mas- sive and likely intruded intensely foliated agmatite of Beresford complex (SCPS?); massive Hb diorite intruded by muscovite trondhjemite (sample AT-87-124-4 (above)) of BIPS leucocratic phase; cf. K- Ar date with leucocratic phase U-Pb and K- Ar dates above
<b>BISCHOF ISLANDS</b> (Bi-Hb quartz monzodiorite)	GSC 89-18	AT-87-122-1		$164 \pm 3$ (Hb)	<b>a and e</b>

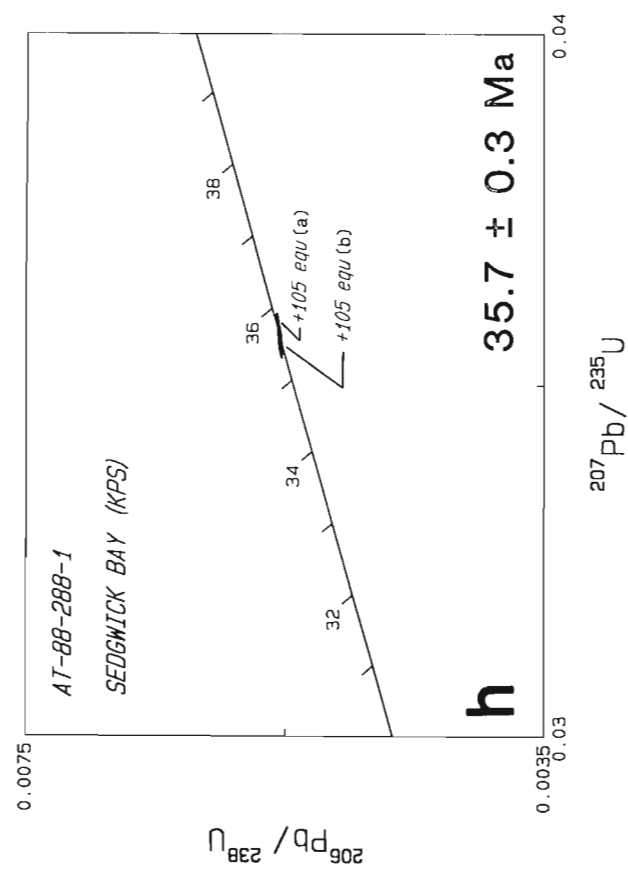
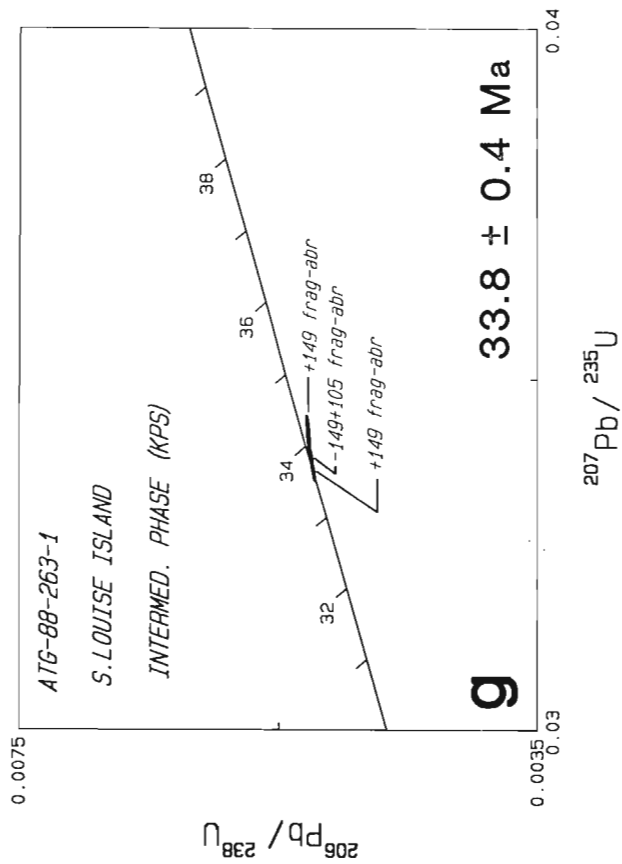
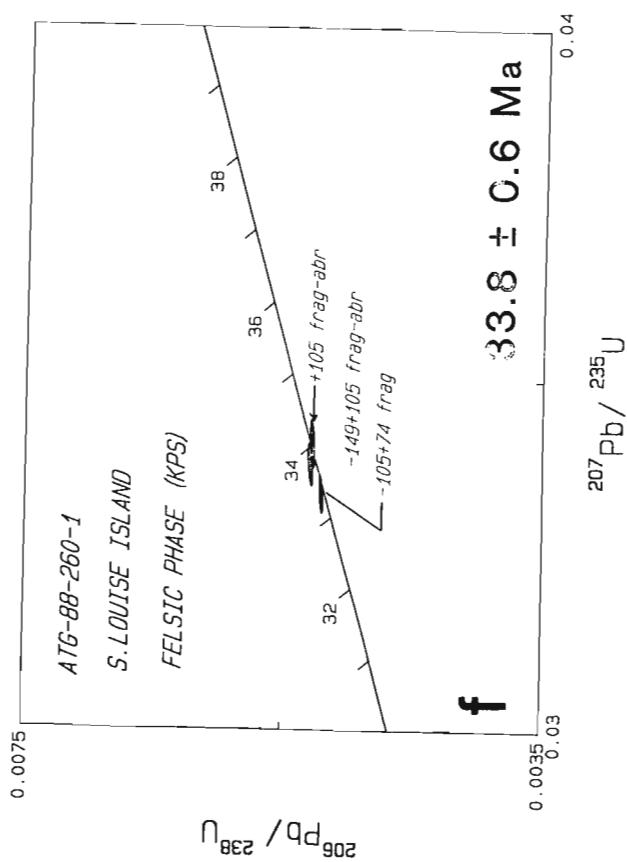
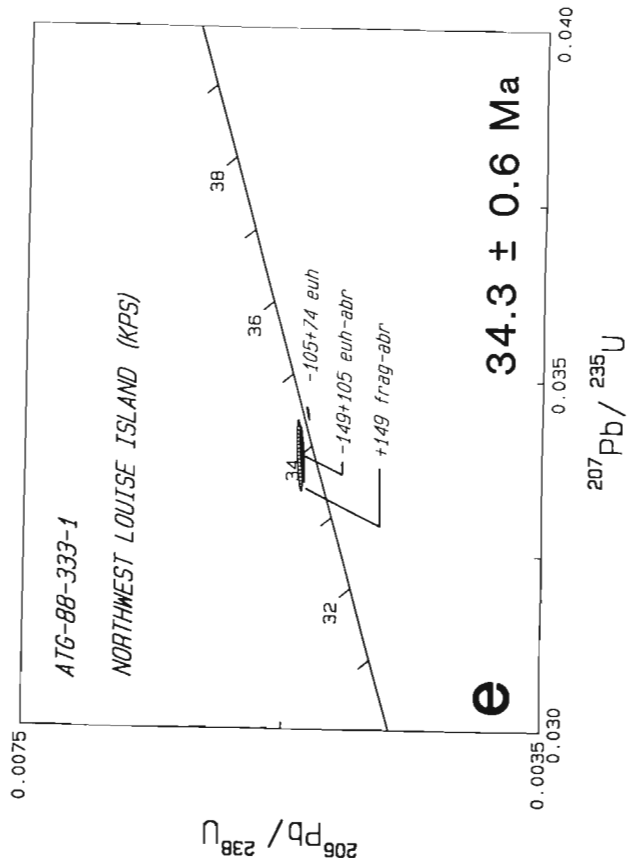
**Table 3.** Compilation of U-Pb and K-Ar geochronometry for Middle to Late Jurassic and Tertiary plutons, Queen Charlotte Islands. (cont'd)

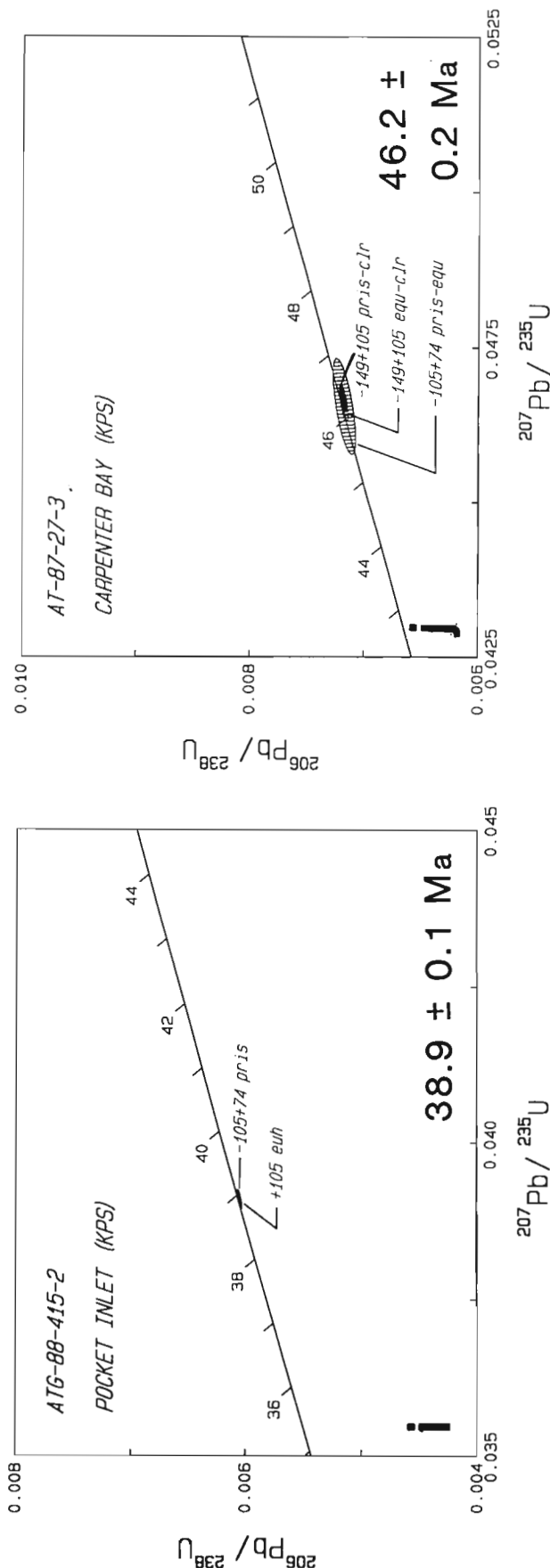
Pluton/Locale (lithology <sup>2</sup> )	G.S.C. No.	Sample Number	U-Pb Date (Zircon) ( $\pm 2\sigma$ , in Ma)	K-Ar Date <sup>1</sup> $\pm 2\sigma$ , in Ma (mineral <sup>2</sup> )	Reference <sup>3</sup> and Comments
<b>SAN CHRISTOVAL PLUTONIC SUITE (SCPS)</b>					
<b>RENNELL-KANO-VAN INLETS SEGMENT</b> (gneissic Hb granodiorite)	GSC 70-1	65-AB-20		147 $\pm$ 8 (Hb)	<b>d</b> ; single date considered reliable minimum date estimate by Young (1981); southeast tip of Cadman Island in Kano Inlet, Graham Island, 53°17.5' N, 132°38.5' W
<b>SAN CHRISTOVAL RANGE SEGMENT (Darwin Sound)</b> (foliated Bi-Hb quartz diorite)	GSC 67-20	65-AB 9		145 $\pm$ 14(Hb)	<b>c</b> ; single date considered reliable minimum date estimate by Young (1981); eastern Darwin Sound, 3.2 km (2 miles) south of Bigsby Inlet, 52°34'30" N, 131°40' W
<b>SAN CHRISTOVAL RANGE SEGMENT (Haswell Bay transect)</b> (Bi-Hb monzodiorite)		AT-87-111-1	172 $\pm$ 5		<b>this report</b> (Pb-Pb date and 2 $\sigma$ error for most concordant fraction); cf. K-Ar date below
(Bi-Hb diorite)	GSC 89-19	AT-87-115-1		166 $\pm$ 3 (Hb)	<b>a and e</b> ; K-Ar date for older mafic phase of SCPS; cf. with U-Pb date above and K-Ar date for AT-87-105-1 below
(Bi-Hb quartz diorite)	GSC 90-28	AT-87-105-1		192 $\pm$ 5 (Hb)	<b>this report</b> ; cf. U-Pb date above from similar lithology and with K-Ar date above for earlier intruded phase; <i>date uninterpretable</i>
<b>SAN CHRISTOVAL RANGE SEGMENT (Pocket Inlet)</b> (Bi-Hb quartz diorite)		ATG-88-413-1	172 $\pm$ 3		<b>this report</b> (Pb-Pb date and 2 $\sigma$ error for most concordant fraction)
<b>WOODRUFF BAY SEGMENT</b> (Bi-Hb quartz diorite)		AT-87-12-1	171 $\pm$ 6		<b>this report</b> (Pb-Pb date and 2 $\sigma$ error for most concordant fraction)
<ol style="list-style-type: none"> <li>1. Dates consistent with decay constants of Steiger and Jäger (1977); old determinations (Young, 1981) recalculated by R.L. Armstrong (U.B.C. Geochronology File, unpublished data)</li> <li>2. Abbreviations are Bi = biotite; Hb = hornblende; Kf = alkali feldspar; Mu = muscovite; WR = whole rock</li> <li>3. References are: a) Anderson and Reichenbach (1989); b) Young, (1981; see Table III, p. 51 for original sources of data); c) Wanless et al., 1970; d) Wanless et al., 1972; e) Hunt and Roddick, 1989; f) Wanless et al., 1968</li> </ol> <p>Abbreviation <math>\sigma</math> = standard deviation</p>					





**Figure 6:** Concordia plots for U-Pb data from samples of Kano plutonic suite (KPS) collected from Late Oligocene northern plutons at: a) Langara Island; b) Pivot Mountain; c) Sheila Lake; from Early Oligocene medial belt plutons at: d) Dawson Inlet (Kano pluton); e) northwest Louise Island; f) southern Louise Island (younger quartz monzonite felsic phase); g) southern Louise Island (older quartz monzodiorite intermediate phase); h) Sedgwick Bay; and from Eocene northern belt plutons at: i) Pocket Inlet; and j) Carpenter Bay (Point Langford). Abbreviations as for Figure 4 and dates from Table 3.





## K-Ar results

K-Ar dates for hornblende and muscovite were determined for central SCPS, Burnaby Island pluton of central BIPS, BIPS intrusions within SCPS, and two north-trending, Carpenter Bay hornblende-phyric andesite dykes (Figs. 1-3; Table 2). Almost all the K-Ar samples are from the same phase as samples collected for U-Pb dating or are nearby (see Table 3). The dykes sampled crosscut the Lower Jurassic Sandilands Formation; they are cospatial, concordant, and compositionally similar to dykes in a dated Eocene pluton at Langford Point. Table 2 includes data given in Anderson and Reichenbach (1989) and Hunt and Roddick (1990).

## Jurassic plutons

One of the two new K-Ar hornblende dates for San Christoval Ranges segment of SCPS ( $166 \pm 3$  Ma) is younger than but concordant with an U-Pb date of  $172 \pm 5$  Ma from a nearby sample. The other K-Ar date (Haswell Bay area) is anomalously old and discordant at  $192 \pm 5$  Ma. The sample is the same petrographically, geochemically and structurally as any other sample of this segment of SCPS. The date is not meaningful. The hornblende separate contains anomalously low atmospheric Ar content; the old date suggests excess Ar in the hornblende.

Two of the three new K-Ar dates for hornblende and one K-Ar muscovite date from BIPS phases compare closely with U-Pb determinations (Tables 2 and 3). Hornblende from intermediate phase rocks on Bischof Islands gave a  $164 \pm 3$  Ma date that is concordant with the U-Pb date ( $168 \pm 4/-1$  Ma) for intermediate phase rocks farther south at Poole Point on Burnaby Island. Intermediate phase rocks on the north shore of Burnaby Island yielded an anomalously young Late Jurassic K-Ar hornblende date of  $144 \pm 5$  Ma that compares closely with a less precise, previous K-Ar determination for hornblende from Poole Point (Wanless et al., 1968; Table 3). The similarity between the oldest hornblende K-Ar dates for SCPS and BIPS ( $166 \pm 3$  Ma and  $164 \pm 3$  Ma, respectively) and concordance with respective U-Pb dates suggest contemporaneity of rapid post-emplacement uplift and cooling for the two suites.

Hornblende from unfoliated BIPS mafic phase diorite yielded an anomalously young Late Jurassic K-Ar date of  $158 \pm 4$  Ma. The date conflicts with intrusive relations involving the mafic phase diorite. The mafic phase probably intrudes the foliated SCPS Beresford complex and is intruded by BIPS intermediate phase (about 168 Ma, U-Pb) elsewhere. Faintly foliated leucocratic muscovite trondhjemite (BIPS leucocratic phase) crosscuts the mafic phase diorite at the sample locality. The diorite's K-Ar hornblende date is concordant with a Late Jurassic K-Ar muscovite date ( $153 \pm 3$  Ma) determined for the trondhjemite at the sample locality (Table 2). The date from the diorite is also identical with a minimum U-Pb date for zircon ( $\geq 158 \pm 4$  Ma) from trondhjemite that intruded the Beresford complex northwest of sample locality AT-87-124. The younger date for the diorite likely reflects resetting by the younger leucocratic phase of BIPS.

The leucocratic muscovite-biotite trondhjemite phase is unique to BIPS. Together with mafic and intermediate phases, it intruded foliated, heterogeneous diorite of the Hunter-Kindakun points complex and the Beresford complex that flank SCPS (Anderson and Greig, 1989). Concordant Late Jurassic K-Ar and U-Pb dates for two samples of the leucocratic phase suggest a short interval for intrusion, uplift and cooling of the trondhjemite and supports geological evidence that it is the latest intruded phase of BIPS.

## Tertiary dykes

The latest Middle Eocene hornblende date for one of the Carpenter Bay porphyritic dykes ( $43.7 \pm 1.1$  Ma; Table 2) is slightly younger than but compares closely with the U-Pb date for the Carpenter Bay plu-

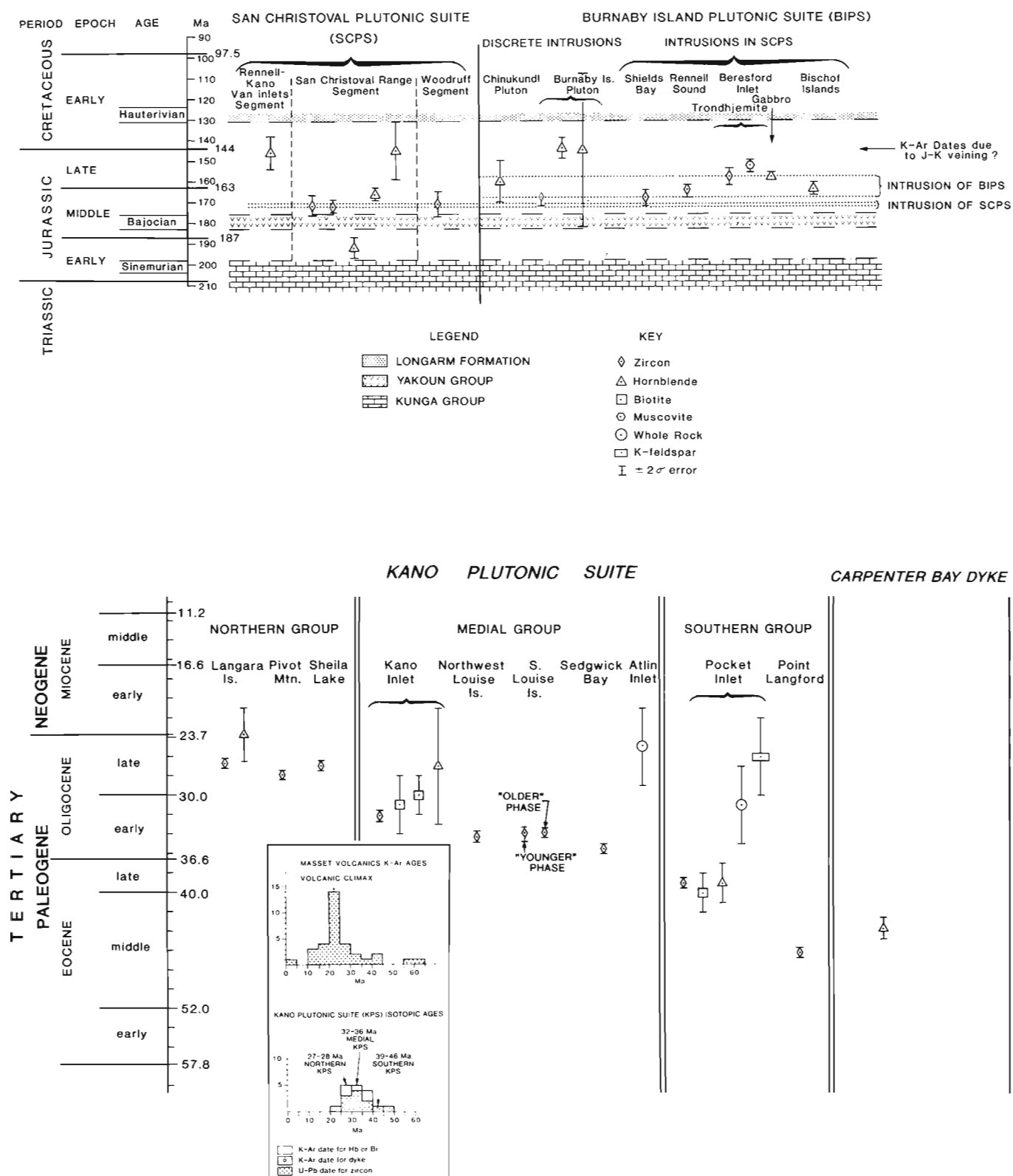


**Figure 7:** Compilation of Jurassic and Tertiary geochronometry from Table 3 and the time scale of Palmer (1983). Inset diagram for Tertiary geochronometry permits comparison of histogram of Tertiary K-Ar dates for Masset Formation volcanics and Kano plutonic suite.

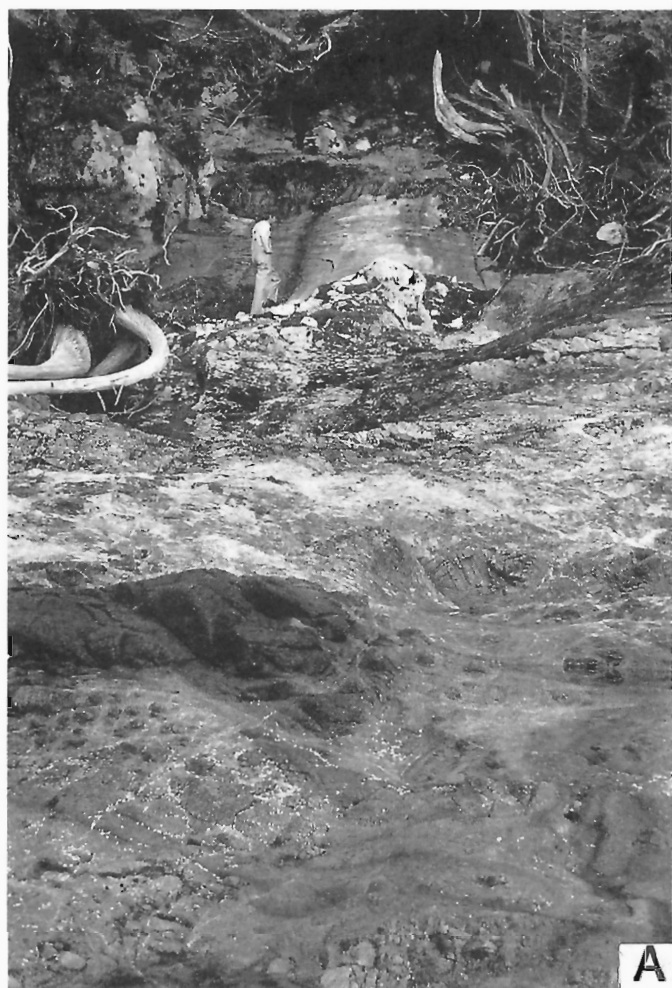


**Figure 8:** Geological relations involving Middle to Late Jurassic plutons or phases of Burnaby Island plutonic suite: a) View west-northwest to nonconformity at Rebecca Point between intensely veined Middle Jurassic BIPS monzodiorite and massive, rarely-veined Lower Cretaceous Longarm Formation (sta. AT-278). A sample (ATG-88-291-4) collected from fresher monzodiorite from Poole Point nearby yielded a  $168 \pm 4/-1$  Ma date (U-Pb, zircon). Hornblende from Jurassic (likely BIPS) granitic debris within Lower Cretaceous Longarm Formation on Burnaby Island yielded dates of  $148 \pm 5$  Ma and  $152 \pm 5$  Ma (Yorath and Chase, 1981). b) Plagioclase porphyry variety of BIPS at Clapp Basin, Shields Bay crosscuts southerly-vergent folds involving Lower Jurassic Sandilands Formation (sta. AT-342). A sample of the plagioclase porphyry nearby was dated at  $168 \pm 4$  Ma (U-Pb, zircon).

ton at Point Langford ( $46.2 \pm 0.2$  Ma). The K-Ar and U-Pb dates are consistent with the intrusive relations between the dykes and host Lower Jurassic Sandilands Formation argillite and middle Eocene plutons.

The Carnian K-Ar date ( $230 \pm 13$  Ma) for hornblende from another Carpenter Bay porphyritic dyke is anomalous because the dyke occurs in the identical geological setting as sample AT-87-7-3. The date likely indicates excess argon, possibly contained in clinopyroxene cores within less than 10% of the hornblende grains. The date is unreliable.

## DISCUSSION

The Jurassic and Tertiary U-Pb and K-Ar geochronometry contributes to the understanding of Queen Charlotte Islands' geologic history in 3 ways. First, it refines distribution and recurrence of plutonism in the Queen Charlotte Islands. Second, timing of possible overmaturation of potential source rocks of the Upper Triassic and Lower Jurassic Kunga Group by advective circulation of hydrothermal fluids may be estimated. And third, it constrains timing for regional synplutonic tectonic processes including the Early Jurassic contraction, Jurassic terrane interactions, Tertiary plate motions in the Pacific basin, Tertiary Masset volcanism, and inception of the Tertiary Queen Charlotte Basin.

### Jurassic plutonism

#### *Distribution, recurrence and terrane interactions*

The geochronometry corroborates division of Middle and Late Jurassic plutons into two northwest-trending suites, an older, Middle Jurassic (172-171 Ma) San Christoval plutonic suite (SCPS) on the west (Fig. 1) and a younger, Middle to Late Jurassic ( $168 \geq 158$  Ma) Burnaby Island plutonic suite (BIPS) on the east (Fig. 2; e.g. Anderson and Greig, 1989). U-Pb and K-Ar dates from both suites overlap within  $2\sigma$  uncertainty. However, SCPS yielded older dates than the discrete plutons and satellitic intrusions of BIPS.

Other Island Intrusions farther south on Vancouver Island share characteristics distinctive of Jurassic plutons in Queen Charlotte Islands (Woodsworth et al., 1989a,b, in press). The Vancouver Island plutons are somewhat older (200-185 Ma compared to  $172 \geq 158$  Ma; Armstrong, 1988; Isachsen, 1987; Isachsen et al., 1985).

Mapping and U-Pb geochronometry of Jurassic to Tertiary intrusions across the northwest trend of the Insular and Coast belts between  $52-54^\circ\text{N}$  shows eastward younging and geochemical evolution of magmatism (Anderson and Greig, 1989; van der Heyden, 1989; and this report). Five Jura-Cretaceous suites are recognized: Middle Jurassic SCPS (172-171 Ma) and Middle to Late Jurassic BIPS ( $168 \geq 158$  Ma) in Queen Charlotte Islands; and Late Jurassic Banks Island belt (160-155 Ma), Early Cretaceous McCauley Island belt (131-123 Ma), and mid-Cretaceous Ecstall belt (110-94 Ma) on the mainland (van der Heyden, 1989). Our new data support van der Heyden's hypothesis that subduction-related Middle to Late Jurassic plutonism records the monotonic eastward advance of the Mesozoic magmatic front across the Wrangellia-Alexander terrane boundary (east of Bonilla Island; Woodsworth, 1988).

West to east modal and geochemical changes across trend are also consistent with proposed east-dipping subduction: felsic (even peraluminous) compositions become more abundant to the east. Middle Jurassic SCPS on western Queen Charlotte Islands includes minor mafic rocks (Hunter-Kindakun and Beresford diorite complexes) and extensive rocks of intermediate composition. Middle to Late Jurassic BIPS farther east is more variable. The greater compositional range is dominated by intermediate compositions but includes subordinate mafic and felsic phases. For example, the leucocratic, locally peraluminous, Late Jurassic trondhjemite phase of BIPS is important

but local in Queen Charlotte Islands. Farther east, Late Jurassic Banks Island belt comprises abundant and extensive monazite-, garnet-, muscovite-, and biotite-bearing felsic rocks and minor mafic phases (van der Heyden, 1989). At this latitude the advance and evolution of Middle to Late Jurassic magmatic front across Wrangellia and Alexander Terrane is consistent with magmatism above an east-dipping subduction zone west of SCPS.

#### *Early Jurassic contraction and late synkinematic intrusions*

The Middle Jurassic ( $168 \pm 4$  Ma) date for hornblende-plagioclase porphyry at Shields Bay that crosscuts southerly-vergent folds in Sandilands Formation rocks (Fig. 8a) constrains timing for the tectonic regime within which Middle and Late Jurassic plutonism developed. Stratigraphic and structural studies by Thompson and Thorkelson (1989), Thompson et al. (1991) and Lewis and Ross (1989, 1991) indicate late Early Jurassic to early Middle Jurassic north-south- to northeast-southwest-directed contraction. The south-vergent folds intruded by the porphyry phase are geometrically similar to fold styles described by Lewis and Ross (1989). The intrusive relations and geochronometry constrain the timing of deformation to post-Sinemurian, pre-168 Ma (198–168 Ma) and support the more restrictive regional stratigraphic constraints (post-Sinemurian to pre-Bajocian, ca. 193–183 Ma; Thompson et al., 1991).

Mineral and mafic xenolith foliation in Middle Jurassic (172–171 Ma) SCPS plutons led Sutherland Brown to term them “syn-kinematic.” Intensely foliated rocks restricted to the suite’s eastern margin and foliation trends commonly concordant with the northwest elongation of SCPS suggest external tectonic control. However, in the southern segments of SCPS, foliation is most intense along and oriented parallel to plutonic margins (Anderson, 1988a; Anderson and Greig, 1989). This suggests that much of the fabric formed during emplacement and was not superimposed. In the northern segment of SCPS (Rennell-Kanovan inlets area), subvertical mineral foliation is widespread but not pervasive and is consistently north-trending. It is unlikely that the foliation solely resulted from flattening associated with a radially expanding diapir. Foliation in Middle Jurassic SCPS may record the waning stages of a mainly Early to Middle Jurassic contractional event that was most pronounced, extensively developed and best preserved in the Upper Triassic and Lower Jurassic strata in the Cumshewa Inlet and Skidegate Inlet areas (Thompson et al., 1991; Lewis and Ross, 1991). The younger, Middle to Late Jurassic BIPS, intruded at about the same crustal level, contains few ductile fabrics but abundant brittle faults and veins.

#### *Timing of possible overmaturation of Kunga Group rocks*

The nine Middle to Late Jurassic K-Ar dates for SCPS and BIPS plutons show a bimodal distribution attributable to two cooling events (Table 3 and Fig. 7). The older age range (5 dates: 166–153 Ma) compares closely with U-Pb dates for samples nearby or with U-Pb dates from samples of the same phase. These K-Ar dates suggest rapid (and coeval) uplift and cooling of both Jurassic plutonic suites.

The other four Late Jurassic K-Ar dates (147–145 Ma) likely record a later thermal event. Dates from earlier studies (Wanless et al., 1968, 1970) dominate the data set and have correspondingly larger  $2\sigma$  errors than more recent determinations. However, the dates are widespread and highly discordant to U-Pb dates for SCPS and BIPS intrusions (e.g. Burnaby Island samples AT-87-83-1 (K-Ar:  $144 \pm 5$ ) and ATG-88-291-4 (U-Pb:  $168 \pm 4/-1$  Ma)). Similar hornblende dates characterize Jurassic (BIPS-equivalent?) granitic clasts within Lower Cretaceous Longarm Formation conglomerate in Burnaby Island ( $148 \pm 5$  Ma and  $152 \text{ Ma} \pm 5$  Ma; Yorath and Chase, 1981).

The younger dates likely record when advective circulation of hydrothermal fluids reset the K-Ar systems in brittle fractured and veined

BIPS and SCPS. A latest Jurassic age for fracture and vein formation is consistent with field relations that indicate a Late Jurassic to Early Cretaceous age for the veins (Anderson and Greig, 1989). The veins may be cogenetic with cospatial Cu-Fe skarn deposits (Anderson, 1988b) and the Late Jurassic age provides an indirect estimate for the age of the skarn deposits.

High conodont colour alteration indices (C.A.I.) and vitrinite reflectance values in Kunga Group rocks are characteristic of southeastern Moresby Island (Orchard, 1988; Orchard and Forster, 1991; Vellutini, 1988) and cospatial with BIPS. Narrow (0.5 km or less) contact metamorphic aureoles and concordant U-Pb and K-Ar dates, suggestive of high level emplacement accompanied by rapid uplift and cooling, rule out widespread and protracted conductive heating of Kunga Group host. Advective transfer of heat by hydrothermal solutions that produced the skarn deposits may be a more effective mechanism for heating potential hydrocarbon source rocks and for local resetting of K-Ar systematics. If so, overmaturation of Kunga Group potential source rocks occurred before deposition of Cretaceous potential reservoir beds.

#### *Cretaceous and Tertiary K-Ar dates for plutons mapped as Jurassic*

Cretaceous and Tertiary K-Ar dates for samples apparently collected from SCPS (Sutherland Brown, 1968) are more difficult to interpret because none of the three localities reported by Young (1981) were visited (see “Miscellaneous Tertiary Dates” and “Cretaceous Geochronometry” in Table 3). Young considered the whole rock Tertiary K-Ar date unreliable. The Tertiary K-Ar biotite date and the meager geological relations reported by Shell Canada Resources (in Young, 1981) suggest that it might represent a small unmapped KPS monzogranite intrusion (perhaps an extension of KPS Pocket Inlet pluton to the northwest?). The date likely represents a minimum age.

The mid-Cretaceous K-Ar date from Hippa Island is the most baffling because it does not correspond with any other known magmatic or thermal event recognized on the islands. Most likely it indicates partial resetting of K-Ar systematics in SCPS rocks by Tertiary magmatism.

#### **Tertiary plutonism**

Dates for the Tertiary plutons and dykes in Queen Charlotte Islands bear on interpretations of: relations of an accelerating northwesterly-migrating Tertiary magmatic front in the Queen Charlotte Islands to the relative plate motions in the northeastern Pacific basin; the age of Tertiary Masset volcanism; and the inception of the Tertiary Queen Charlotte Basin.

#### *Tertiary Queen Charlotte Islands plutonism and plate motions*

The more precise U-Pb dates permit greater resolution in tracking the progress of the Tertiary magmatic front first identified by Young (1981). The more extensive sampling of plutons within KPS resolves the plutonism into three groups (Figs. 3 and 7): a southern group of Eocene plutons (46–39 Ma); a medial group of Early Oligocene (36–32 Ma) intrusions; and a northern group of Late Oligocene (28–27 Ma) bodies. The transition between southern belt plutons (Fig. 3) and medial belt plutons includes part of the west-northwest-trending boundary between compositionally and structurally distinct Group 1 and Group 2 Tertiary dykes (Souther and Bakker, 1988; Souther, 1989). Medial group plutons extend only as far northwest as southwestern Graham Island coincident with the southwestern edge of the Miocene Masset volcanic field. The northern group occurs farther north where it is co-extensive (and nearly coeval) with the Lower Miocene Masset Formation volcanic rocks.

Nine million years elapsed between the mean age of plutonism of the southern and medial groups and about 7 million years between medial and northern groups. Accelerated northwesterly advance



of the magmatic front in three discrete episodes is apparent in a longitudinal time-space profile (Fig. 9). Sharp discontinuities mark the transitions between relatively slow advance of the Eocene front (about 1 cm/yr for two samples), the faster advance of Early Oligocene plutonism (2.6 cm/yr for four samples) and the widespread but nearly contemporaneous Late Oligocene plutonism. This south to north progression is a marked change from the monotonic west to east migration of the Mesozoic and early Tertiary magmatic front attributable to a simple Andean model of eastward-dipping subduction (van der Heyden, 1989).

There is no consistent modal or geochemical evolution with intrusive age (Fig. 9; Anderson and Greig, 1989; Anderson et al., 1989a, b). Mafic plutons are more common in the northern group. Bimodal compositions or northerly-trending pluton-dyke complexes characterize the southern group and suggest an extensional regime during Eocene plutonism.

Although the focusing process remains poorly understood, migration of the Tertiary magmatic front on the Queen Charlotte Islands must be linked somehow to plate interactions within the northeastern Pacific basin. Eocene (46–39 Ma) extension-related plutonism and dyking of southern KPS and pre-Oligocene normal faulting at Long Inlet involving Cretaceous rocks (Lewis, 1990) just precede or accompany an abrupt change in the interactions among Kula-Farallon (Vancouver), Pacific and North American plates about 43 Ma (Engebretson et al., 1985; Engebretson, 1989; Stock and Molnar, 1988). Moderate right-lateral oblique convergence of Kula and Farallon plates (with respect to the North American plate) decreased about 43 Ma. The formerly mainly orthogonally-convergent Pacific plate fused with the Kula plate, decelerated by 45 km/Ma (from 75–30 km/Ma) and its azimuth rotated 65° counterclockwise from N45E–N20W.

Medial group (32–36 Ma) KPS plutonism occurred as relative plate motions began to stabilize. From 35–5 Ma, relative plate motion data suggests that the Pacific plate's velocity relative to North America was 50 km/Ma at N30W azimuth (Engebretson, 1989). Significant acceleration of the Early Oligocene KPS magmatic front compared with the Eocene front, at half the velocity of predicted relative plate motions, resulted. The change from more orthogonal to mainly oblique convergence of the Pacific plate around 35 Ma (Engebretson, 1989; Stock and Molnar, 1988) is preserved in the trace of medial group KPS plutonism.

Widespread, coeval northern group 27–28 Ma plutons in western Graham Island define a westerly convex arc from Sheila Lake to Langara Island. Steady northwestern advance of the magmatic front had apparently stalled; the age and widespread distribution of the plutonism suggests that a change from oblique to more orthogonal (east-northeastward) convergence of the Pacific plate west of Graham Island might account for production of the northern KPS plutons. Coeval northeast-directed shortening that involved Oligocene rocks at Long Inlet (Lewis, 1990) predates uplift, erosion, and mid-Miocene sedimentation and Masset volcanism (Haggart et al., 1990; Hickson, 1991).

#### *Eocene and Oligocene plutonism and relation to Tertiary volcanism*

If the dykes studied by Souther (1988, 1989), Souther and Bakker (1988), Souther and Jessop (1991) were feeders to eroded Tertiary volcanoes and coeval with their host plutons, the northerly time-transgressive Eocene to Oligocene plutonism may provide the best age estimate for the duration of the volcanism. For example, on Graham Island, the northern KPS is co-extensive with (and only slightly older than) the greatest areal extent of Miocene Masset Formation volcanic rocks (Fig. 7; Anderson and Reichenbach, 1989;

Hickson, 1988, 1991; Haggart et al., 1990). That plutonism probably marks the onset of late Tertiary Masset volcanism (Hickson, 1989, 1991).

The distribution of Tertiary volcanic centres in time and space may be more complicated than that for the plutons. For example, suspected Eocene (but possibly Upper Cretaceous?) pre-Masset Formation volcanic flows (e.g. at Cape Knox, K-Ar date  $45.7 \pm 3$  Ma; Young, 1981; Hickson, 1989) are not cospatial with known Eocene plutons.

#### *Inception of Tertiary Queen Charlotte Basin*

Reconstructing the inception of the Queen Charlotte Basin must consider the inventory of coeval tectonostratigraphic elements. Implicit is the definition of the basin. Thompson et al. (1991) expanded the basin's definition to include Middle Jurassic and younger sedimentary strata. The Tertiary basin of Yorath (1988; following Shouldice, 1971) included the Miocene and Pliocene marine and nonmarine sedimentary rocks underlying northeastern Graham Island, Hecate Strait and Queen Charlotte Sound. Higgs (1989) and Dietrich et al. (1989) included the largely subaerial Masset Formation volcanics and, in the Port Louis well and Skidegate Inlet region, the underlying, well-dated Eocene to upper Oligocene unnamed terrestrial shale and coal unit (e.g., White, 1991) as basin fill rather than basement.

That broadened definition led to a two-fold Tertiary basin subdivision and proposed evolution: an Eocene rift phase (Yorath and Chase, 1981) shown in Masset Formation volcanic rocks by rift-type geochemical affinities (Hamilton, 1985, 1989; Dostal and Hamilton, 1988); and the cyclic, coarsening-upward clastic basin fill represented by sedimentary rocks of the Miocene-Pliocene Skonun Formation.

Eocene tectonics in Queen Charlotte Islands are dominated by extensional features manifest in: 46–39 Ma plutonism (Anderson and Greig, 1989; Anderson et al., 1989a); circa 44 Ma north-trending dyking around Carpenter Bay and southeastern Lyell Island (Souther, 1988, 1989; Souther and Bakker, 1988; Anderson and Reichenbach, 1989; Souther and Jessop, 1991); and post-Cretaceous, pre-Eocene or –Oligocene, northwest-trending, down-to-the-northeast normal faulting at Long Inlet on Graham Island (Lewis, 1990). On Moresby Island, the western limit of Carpenter Bay–Lyell Island dykes and the southeastern extent of the medial belt of Early Oligocene plutons (Fig. 3) may define the western limit of Eocene extension and the edge of a developing western margin for part of the Tertiary Queen Charlotte Basin.

If Eocene extension-related magmatism in southern Moresby Island is related to inception of the mainly Miocene-Pliocene part of the Queen Charlotte Basin, little stratigraphic or sedimentological evidence was preserved as a record. No marine Eocene sedimentary rocks are recognized in southern Moresby Island or from the nearby offshore wells. Eocene strata, if present on the islands (Hickson, 1989, 1991; Hyndman and Hamilton, 1991), and the Eocene-Oligocene sedimentary rocks at Skidegate Inlet and in the Port Louis well, suggest a terrestrial, locally swampy, sedimentary environment and associated subaerial volcanism. These would be unlikely components of an evolving Eocene Queen Charlotte marine basin but probably indicate construction of a largely subaerial volcanic highland along the basin's western margin.

Eocene extension within the Coast Belt on the mainland provides insight into evolution of the presumed eastern margin of the late Tertiary Queen Charlotte Basin. Rapid Eocene cooling and uplift at rates of as much as 1 mm/yr between 51–44 Ma in the Coast Plutonic Complex are recorded in well-behaved fission track, K-Ar and Rb-Sr systems (Armstrong and Runkle, 1979; Harrison et al., 1979; Woodsworth et al., 1983; Crawford et al., 1987; van der Heyden, 1989). Uplift, which exhumed the Quottoon pluton and high grade

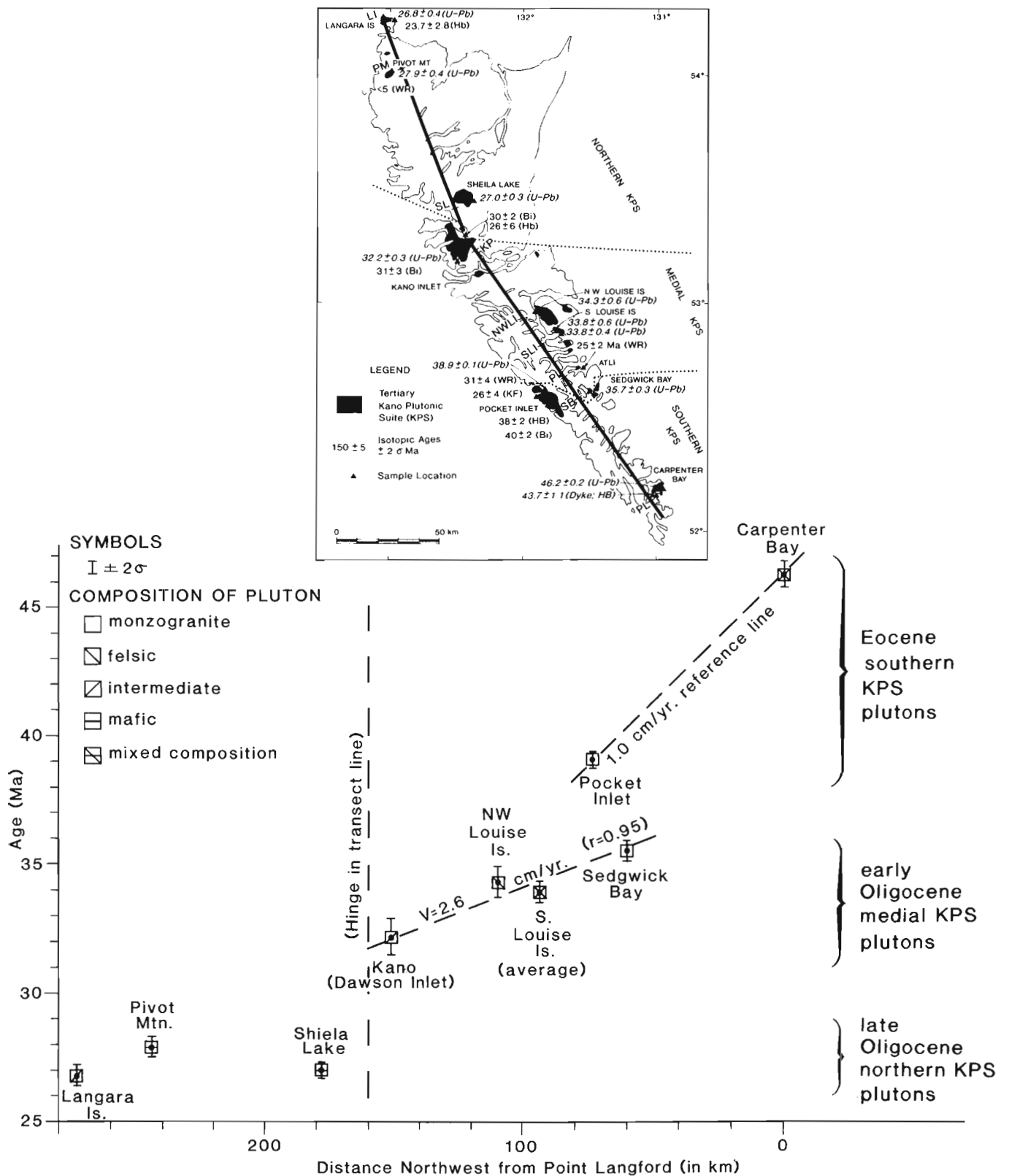


**Figure 9:** Longitudinal time-space profile of northerly time-transgressive Tertiary plutonism in the Queen Charlotte Islands. Section line (shown on inset) extends from Woodruff Bay to Langara Point and bends at Shields Island. It bisects distribution of KPS and the U-Pb sample sites are projected onto it. Abbreviations are: KP = Kano pluton; LI = Langara Island pluton; NWLI = northwest Louise Island pluton; PI = Pocket Inlet pluton; PL = Point Langford pluton; PM = Pivot Mountain pluton; SB = Sedgwick Bay; SL = Shiela Lake pluton; and SLI = southern Louise Island pluton (average of two U-Pb dates). Slopes of best-fit or reference lines for the data give average advance of magmatic front for Eocene southern plutons and Early Oligocene medial plutons (correlation coefficient  $r = 0.95$ ). There is poor correlation between distance and age for the nearly contemporaneous Late Oligocene northern group of KPS plutons.

Central Gneiss Complex some 10-15 km between 51 and 46 Ma (Harrison et al., 1979; Crawford et al., 1987), may have occurred along steep to vertical ductile shear zones at depth and by possible high level brittle extensional faulting farther east (Crawford et al., 1987). Alternatively, Eocene uplift and unroofing of the Central Gneiss Complex records an intra-arc metamorphic core complex (van der Heyden, 1989) along gently to moderately northeast-dipping Eocene extensional shear zones on the east side of the Coast Belt.

Structures and the direction along which Eocene extension might have propagated are poorly known for the western margin of the Coast Plutonic Complex (van der Heyden, 1989) and for southern Moresby Island. Contemporaneous, extension-related metamorphic or volcanic highlands in these areas are indicated by the existing geology and geochronometry and argue for an intervening lowland, the Tertiary Queen Charlotte Basin.

## SUMMARY

Widespread granite plutons that characterize the east and west coasts of the Queen Charlotte Islands intruded sequentially in Middle to Late Jurassic and again in mid-Tertiary times.

Middle Jurassic (172-171 Ma) San Christoval plutonic suite (SCPS) plutons, intruded as a northwest-trending linear belt in a waning contractional regime, were followed by intrusion of discrete plutons of the Burnaby Island plutonic suite (BIPS) to the east 168- $\geq$ 158 Ma ago. The oldest hornblende K-Ar dates for SCPS and BIPS correspond closely to nearby zircon U-Pb dates and confirm a contemporaneous and rapid uplift and cooling for both suites. Contraction, which produced the characteristic fabric of SCPS, ceased by at least 168 Ma (the date for a post-kinematic pluton) and did not involve Bajocian strata (Thompson et al., 1991). The youngest zircons for BIPS ( $\geq$ 158 Ma), from a peraluminous trondhjemite, indicate involvement of Paleozoic (>309 Ma) basement in generation of the last granitic phase within BIPS.

These Middle and Late Jurassic plutons are part of a general eastward younging and petrological evolution. Mesozoic plutonism, which migrated east from the Queen Charlotte Islands onto the mainland from Late Jurassic (165-160 Ma) to early Tertiary (van der Heyden, 1989), probably developed above an east-dipping subduction zone west of SCPS.

Latest Jurassic (ca. 147-145 Ma) hornblende K-Ar dates common to both suites probably reflect a regional re-heating of the plutons and country rock by advective circulation of hydrothermal fluids. The record of this circulation is preserved as the widespread veining pervasive within BIPS and less common within SCPS. The veining postdates intrusion of the  $\geq$ 158 Ma trondhjemite phase and predates deposition of Lower Cretaceous Longarm Formation. BIPS plutons and veining are associated with the co-spatial Cu-Fe skarn deposits and high conodont C.A.I. and vitrinite reflection values in Upper Triassic and Lower Jurassic Kunga Group. Kunga Group rocks probably became overmature as hydrocarbon source rocks before deposition of Cretaceous potential reservoir rocks.

Eocene and Oligocene Kano plutonic suites and dykes comprise 3 discrete intrusive episodes and record the passage of a remarkable, northwesterly-accelerating, time-transgressive magmatic front. K-Ar mineral dates for the Tertiary plutons are concordant with U-Pb dates, indicate rapid uplift and cooling, and corroborate the fine grain size, seriate texture, and miarolitic cavities suggestive of high level emplacement.

Extension-related Eocene (46-39 Ma) plutonism in southeastern Moresby Island involved intermediate and felsic plutons and co-spatial, slightly younger (44 Ma) uniformly north-trending dykes (Souther, 1988, 1989; Souther and Bakker, 1988; Souther and Jessop, 1991) and bimodal (predominantly felsic), Pocket Inlet pluton on the west.

Mafic to felsic plutonism in the medial portion of the islands dominated the Early Oligocene (36-32 Ma) episode characterized by uniform 2.6 cm/yr northwesterly migration of the magmatic front. Northern Late Oligocene plutonism produced a westwardly convex curvilinear array of coeval plutons. The plutons are co-spatial with but just predated the widespread Miocene Masset Formation volcanism.

Evolution of Tertiary plutonism, associated volcanism and Eocene extension-related inception of the late Tertiary Queen Charlotte Basin are linked to Eocene plate reorganization in the northeast Pacific basin. They record the change from mainly orthogonal to mainly oblique convergence of the Pacific plate in the Oligocene.

## ACKNOWLEDGMENTS

Charlie Greig and Cathie Hickson collected samples of some of the plutons as part of the regional mapping of the plutonic rocks and Masset Formation in 1987 and 1988. Members of the "Rogue crew," Kathleen Dixon, Steve Hedberg, Kevin May and Dave Rhys provided cheerful assistance during the field mapping as well as a firm hand on the tiller. Doug Hartley (skipper) and Paddy Herman (mate and cook) of the *M.V. "Beatrice"* and Rob Pettigrew (and the *M.V. "Tomram"*) provided secure bases of operations and wonderful movable feasts. Ella Ferland conscientiously kept us provisioned and in touch with the outside world.

We owe a debt of thanks to Dianne Bellerive (K-Ar) and Dale Loveridge, Klaus Santowski, and Bob Sullivan (U-Pb) for their meticulous analytical work on the mineral fractions; they really gave us something to write home about.

We thank R.L. Armstrong, C.J. Greig, R.R. Parrish, and R.I. Thompson for constructive reviews of earlier versions of the manuscript that led to many improvements in the present one. Careful drafting of the figures by Christine Davis and Helen Vyv Dahl and final checking of the text by Bev Vanlier are appreciated.

## REFERENCES

- Anderson, R.G.  
1988a: Jurassic and Cretaceous Tertiary plutonic rocks on the Queen Charlotte Islands, British Columbia; in *Current Research, Part E*, Geological Survey of Canada, Paper 88-1E, p. 213-216.  
1988b: Plutonic rocks and skarn deposits on the Queen Charlotte Islands; *Mining Review*, v. 8, no. 2, March/April, p. 19-24.
- Anderson, R.G. and Greig, C.J.  
1989: Jurassic and Tertiary plutonism in the Queen Charlotte Islands, British Columbia; in *Current Research, Part H*, Geological Survey of Canada, Paper 89-1H, p. 95-104.
- Anderson, R.G. and Reichenbach, I.  
1989: A note on the geochronometry of Late Jurassic and Tertiary plutonism in the Queen Charlotte Islands, British Columbia; in *Current Research, Part H*, Geological Survey of Canada, Paper 89-1H, p. 105-112.
- Anderson, R.G., Greig, C.J., and Reichenbach, I.  
1989a: Oligocene Plutonism in the Queen Charlotte Islands; (abstract). EOS, Transactions of the American Geophysical Union, v. 70, no. 9, p. 137.
- Anderson, R.G., Reichenbach, I., and Greig, C.J.  
1989b: Jurassic and Tertiary plutonic evolution in the Queen Charlotte Islands, British Columbia; (abstract), Geological Association of Canada-Mineralogical Association of Canada, Program with Abstracts, v. 14, p. A4.
- Armstrong, R.L.  
1988: Mesozoic and early Cenozoic magmatic evolution of the Canadian Cordillera; Geological Society of America, Special Paper 218, p. 55-91.
- Armstrong, R.L. and Runkle, D.  
1979: Rb-Sr geochronometry of the Ecstall, Kitkiata, and Quottoon plutons and their country rocks, Prince Rupert region, Coast Plutonic Complex, British Columbia; *Canadian Journal of Earth Sciences*, v. 16, p. 387-399.
- Crawford, M.L., Hollister, L.S., and Woodsworth, G.J.  
1987: Crustal deformation and regional metamorphism across a terrane boundary, Coast Plutonic Complex, British Columbia; *Tectonics*, v. 6, no. 3, p. 343-361.
- Dietrich, J.R., Higgs, R., and White, J.M.  
1989: Seismic, sedimentological and palynological investigations in the Tertiary Queen Charlotte Basin; (abstract), Canadian Society of Exploration Geophysicists-Canadian Society of Petroleum Geologists, "Exploration Update '89", Program and Abstracts, p. 163.

- Dostal, J. and Hamilton, T.S.**  
**1988:** Oceanic volcanism on the western Canadian continental margin: Masset Formation (U. Eocene to U. Miocene); (abstract), Geological Association of Canada, Program with Abstracts, v. 13, p. A33.
- Engebretson, D.C.**  
**1989:** Northeast Pacific-North America plate kinematics since 70 Ma; (abstract), Geological Association of Canada, Pacific Section, Annual Symposium Programme and Abstracts, April 14, 1989.
- Engebretson, D.C., Cox, A., and Gordon, R.G.**  
**1985:** Relative motions between oceanic and continental plates in the Pacific basin; Geological Society of America, Special Paper 206, 59 p.
- Haggart, J.W. and Gamba, C.A.**  
**1990:** Stratigraphy and sedimentology of the Longarm Formation, southern Queen Charlotte Islands, British Columbia; *in* Current Research, Part F, Geological Survey of Canada, Paper 90-1F, p. 61-66.
- Haggart, J.W., Indrelid, J., Hesthammer, J., Gamba, C.A., and White, J.M.**  
**1990:** A geological reconnaissance of the Mount Stapleton-Yakoun Lake area, central Queen Charlotte Islands, British Columbia; *in* Current Research, Part F, Geological Survey of Canada, Paper 90-1F, p. 29-36.
- Hamilton, T.S.**  
**1985:** Volcanics of the Cenozoic Masset Formation: implications for geological and tectonic evolution of the Queen Charlotte Islands, British Columbia, Canada; Geological Society of America, Cordilleran Section Annual Meeting, Program with Abstracts, v. 17, no. 6, p. 359.  
**1989:** Tertiary extensional volcanism and volcanotectonic interactions along the Queen Charlotte portion of the western Canadian continental margin; (abstract), Geological Association of Canada, Pacific Section Symposium, Northeast Pacific-North America Plate Interactions Throughout the Cenozoic, April 14, 1989, Victoria, B.C., Programme and Abstracts.
- Harrison, T.M., Armstrong, R.L., Naeser, C.W., and Harakal, J.**  
**1979:** Geochronology and thermal history of the Coast Plutonic Complex near Prince Rupert, British Columbia; Canadian Journal of Earth Sciences, v. 16, p. 400-410.
- Hickson, C.J.**  
**1988:** Structure and stratigraphy of the Masset Formation, Queen Charlotte Islands, British Columbia; *in* Current Research, Part E, Geological Survey of Canada, Paper 88-1E, p. 269-274.  
**1989:** An update on structure and stratigraphy of the Masset Formation, Queen Charlotte Islands, British Columbia; *in* Current Research, Part H, Geological Survey of Canada, Paper 89-1H, p. 73-79.  
**1990:** The Masset Formation on Graham Island, Queen Charlotte Islands, British Columbia; *in* Evolution and Hydrocarbon Potential of the Queen Charlotte Basin, British Columbia, Geological Survey of Canada, Paper 90-10.
- Higgs, R.**  
**1989:** Sedimentological studies in Queen Charlotte Basin: implications for basin origin and for petroleum exploration; (abstract), Geological Association of Canada, Pacific Section Symposium, Northeast Pacific-North America Plate Interactions Throughout the Cenozoic, April 14, 1989, Victoria, B.C., Programme and Abstracts.
- Hunt, P.A. and Roddick, J.C.**  
**1990:** A compilation of K-Ar ages, Report 19; *in* Radiogenic Age and Isotopic Studies: Report 3, Geological Survey of Canada, Paper 89-2, in press.
- Hyndman, R. and Hamilton, T.S.**  
**1991:** Cenozoic relative plate motions along the northeastern Pacific margin and their association with Queen Charlotte area tectonics and volcanism; *in* Evolution and Hydrocarbon Potential of the Queen Charlotte Basin, British Columbia, Geological Survey of Canada, Paper 90-10.
- Isachsen, C.E.**  
**1987:** Geology, geochemistry, and cooling history of the Westcoast Crystalline complex and related rocks, Meares Island and vicinity, Vancouver Island, British Columbia; Canadian Journal of Earth Sciences, v. 24, p. 2047-2064.
- Isachsen, C., Armstrong, R.L., and Parrish, R.R.**  
**1985:** U-Pb, Rb-Sr, and K-Ar geochronometry of Vancouver Island igneous rocks (abstract); Geological Association of Canada, Victoria Section Symposium, April 19, 1985, Sidney, B.C., Abstracts, p. 21-22.
- Krogh, T.E.**  
**1982:** Improved accuracy of U-Pb ages by the creation of more concordant systems using an air abrasion technique; *Geochimica et Cosmochimica Acta*, v. 46, p. 637-649.
- Lewis, P.D.**  
**1990:** New timing constraints on Cenozoic deformation in the Queen Charlotte Islands, British Columbia; *in* Current Research, Part F, Geological Survey of Canada, Paper 90-1F, p. 23-28.
- Lewis, P.D. and Ross, J.V.**  
**1989:** Evidence for Late Triassic-Early Jurassic deformation in the Queen Charlotte Islands, British Columbia; *in* Current Research, Part H, Geological Survey of Canada, Paper 89-1H, p. 13-18.  
**1991:** Mesozoic and Cenozoic structural history of the central Queen Charlotte Islands, British Columbia; *in* Evolution and Hydrocarbon Potential of the Queen Charlotte Basin, British Columbia, Geological Survey of Canada, Paper 90-10.
- Orchard, M.J.**  
**1988:** Maturation of Triassic strata: conodont colour alteration index; *in* Some Aspects of the Petroleum Geology of the Queen Charlotte Islands, R. Higgs (compiler), Canadian Society of Petroleum Geologists' Field Guide to Sequences, Stratigraphy, Sedimentology, September 14-16, 1988, p. 44.
- Orchard, M.J. and Forster, P.J.L.**  
**1991:** Conodont colour and thermal maturity of the Late Triassic Kunga Group, Queen Charlotte Islands, British Columbia; *in* Evolution and Hydrocarbon Potential of the Queen Charlotte Basin, British Columbia, Geological Survey of Canada, Paper 90-10.
- Palmer, A.R.**  
**1983:** The Decade of North American Geology 1983 Geologic time scale; *Geology*, v. 11, p. 503-504.
- Parrish, R.R., Roddick, J.C., Loveridge, W.D., and Sullivan, R.W.**  
**1987:** Uranium-lead analytical techniques at the geochronology laboratory, Geological Survey of Canada; *in* Radiogenic Age and Isotopic Studies: Report 1, Geological Survey of Canada, Paper 87-2, p. 3-8.
- Roddick, J.C.**  
**1987:** Generalized numerical error analysis with applications to geochronology and thermodynamics; *Geochimica et Cosmochimica Acta*, v. 51, p. 2129-2135.
- Roddick, J.C. and Souther, J.G.**  
**1987:** Geochronology of Neogene volcanic rocks in the northern Garibaldi Belt, British Columbia; *in* Radiogenic Age and Isotopic Studies: Report 1, Geological Survey of Canada, Paper 87-2, p. 21-24.
- Shouldice, D.H.**  
**1971:** Geology of the western Canadian continental shelf; Canadian Society for Petroleum Geology, Bulletin, v. 19, no. 2, p. 405-436.
- Souther, J.G.**  
**1988:** Implications for hydrocarbon exploration of dyke emplacement in the Queen Charlotte Islands, British Columbia; *in* Current Research, Part E, Geological Survey of Canada, Paper 88-1E, p. 241-245.  
**1989:** Dyke swarms in the Queen Charlotte Islands, British Columbia; *in* Current Research, Part H, Geological Survey of Canada, Paper 88-1H, p. 117-120.
- Souther, J.G. and Bakker, E.**  
**1988:** Petrography and chemistry of dykes in the Queen Charlotte Islands, British Columbia; Geological Survey of Canada, Open File 1833.
- Souther, J.G. and Jessop, A.**  
**1991:** Dyke swarms in the Queen Charlotte Islands, British Columbia, and implications for hydrocarbon exploration; *in* Evolution and Hydrocarbon Potential of the Queen Charlotte Basin, British Columbia, Geological Survey of Canada, Paper 90-10.
- Steen, G.E.**  
**1967:** Report on surface geologic examinations by Pan American Petroleum Corporation of the stratigraphy of the west coast of British Columbia; Petroleum Resources Branch, British Columbia Department of Mines, and Petroleum Resources, Open File 1289.
- Steiger, R.H.J. and Jäger, E.**  
**1977:** Subcommission on Geochronology: Convention on the use of decay constants in geo- and cosmochronology; *Earth and Planetary Science Letters*, v. 36, p. 359-362.
- Stock, J. and Molnar, P.**  
**1988:** Uncertainties and implications of the Late Cretaceous and Tertiary position of the North America relative to the Farallon, Kula and Pacific plates; *Tectonics*, v. 7, p. 1339-1384.
- Sutherland Brown, A.**  
**1968:** Geology of the Queen Charlotte Islands, British Columbia; British Columbia Department of Mines and Petroleum Resources, Bulletin 54, 226 p.
- Thompson, R.I. and Thorkelson, D.**  
**1989:** Regional mapping update, central Queen Charlotte Islands, British Columbia; *in* Current Research, Part H, Geological Survey of Canada, Paper 89-1H, p. 7-11.
- Thompson, R.I., Haggart, J.W., and Lewis, P.D.**  
**1991:** Jurassic through Late Cretaceous evolution of the Queen Charlotte Islands, British Columbia, and implications for hydrocarbon potential; *in* Evolution and Hydrocarbon Potential of the Queen Charlotte Basin, British Columbia, Geological Survey of Canada, Paper 90-10.
- van der Heyden, P.**  
**1989:** U-Pb and K-Ar geochronometry of the Coast Plutonic Complex, 53°N to 54°N, British Columbia and implications for the Insular-Intermontane Superterrane boundary; Ph.D. thesis, University of British Columbia, Vancouver, 253 p.
- Vellutini, D.**  
**1988:** Organic maturation and source rock potential of Mesozoic and Tertiary strata, Queen Charlotte Islands, British Columbia; M.Sc. thesis, University of British Columbia, Vancouver, 262 p.
- Wanless, R.K., Stevens, R.D., Lachance, G.R., and Delabio, R.N.**  
**1970:** Age determinations and geological studies, K-Ar isotopic ages, Report 9; Geological Survey of Canada, Paper 69-2A, p. 11-13.

- 1972:** Age determinations and geological studies. K-Ar isotopic ages. Report 10; Geological Survey of Canada, Paper 71-2, p. 6-7.
- Wanless, R.K., Stevens, R.D., Lachance, G.R., and Edmonds, C.M.**
- 1968:** Age determinations and geological studies. K-Ar isotopic ages. Report 8; Geological Survey of Canada, Paper 67-2, Part A, p. 19.
- White, J.M.**
- 1991:** Palynostratigraphy of Tow Hill No. 1 Well in the Skonun Formation, Queen Charlotte Basin, British Columbia; *in* Evolution and Hydrocarbon Potential of the Queen Charlotte Basin, British Columbia, Geological Survey of Canada, Paper 90-10.
- Woodsworth, G.J.**
- 1988:** Karmutsen Formation and the east boundary of Wrangellia, Queen Charlotte Basin, British Columbia; *in* Current Research, Part E, Geological Survey of Canada, Paper 88-1E, p. 209-212.
- Woodsworth, G.J., Anderson, R.G., and Armstrong, R.L.**
- 1989a:** Plutonic regimes in the Canadian Cordillera; Geological Survey of Canada, Open File 1983.
- Woodsworth, G.J., Anderson, R.G., Brookfield, A., and Tercier, P.**
- 1989b:** Distribution of Proterozoic to Miocene plutonic suites in the Canadian Cordillera; Geological Survey of Canada, Open File 1982.
- Woodsworth, G.J., Anderson, R.G., and Armstrong, R.L.**
- in press:** Plutonic Regimes; *in* Chapter 15, Plutonic Regimes; *in* The Cordilleran Orogen: Canada, H. Gabrielse and C.J. Yorath (ed.), Geological Survey of Canada, Geology of Canada, no. 4. (also Geological Society of America, The Geology of North America, no. G-2).
- Woodsworth, G.J., Loveridge, W.D., Parrish, R.R., and Sullivan, R.W.**
- 1983:** Uranium-lead dates from the Central Gneiss Complex and Ecstall pluton, Prince Rupert map area, British Columbia; Canadian Journal of Earth Sciences, v. 20, p. 1475-1483.
- Yorath, C.J.**
- 1988:** Petroleum geology of the Canadian Pacific continental margin; *in* Geology and Resource Potential of the Continental Margin of Western North America and Adjacent Ocean Basins - Beaufort Sea to Baja California, D.W. Scholl, A. Grantz and J.G. Vedder (ed.), Circum-Pacific Council for Energy and Mineral Resources, Earth Science Series, v. 6, p. 283-304.
- Yorath, C.J. and Chase, R.L.**
- 1981:** Tectonic history of the Queen Charlotte Islands and adjacent areas - a model; Canadian Journal of Earth Sciences, v. 18, p. 1717-1739.
- Young, I.F.**
- 1981:** Structure of the western margin of the Queen Charlotte Basin, British Columbia; M.Sc. thesis, University of British Columbia, Vancouver, 380 p.





# Crustal density structure of Queen Charlotte Islands and Hecate Strait, British Columbia

J.F. Sweeney<sup>1</sup> and D.A. Seemann<sup>2</sup>

Sweeney, J.F. and Seemann, D.A., Crustal density structure of Queen Charlotte Islands and Hecate Strait, British Columbia; in *Evolution and Hydrocarbon Potential of the Queen Charlotte Basin, British Columbia*, Geological Survey of Canada, Paper 90-10, p. 89-96, 1991.

## Abstract

*The westward rise in regional gravity anomaly values over a 400 km-long zone extending from the Coast Belt to the Queen Charlotte Islands is caused mainly by thinning of continental crust by about 8 km toward the Pacific Ocean. Low gravity over Hecate Strait is produced by thick sediments within the Queen Charlotte Basin. Local gravity highs over Hecate Strait are related to sources within the upper crust near the basement-sediment interface. Density structure models infer an extensional origin for these features, before much sediment had accumulated in the Queen Charlotte Basin. High gravity over the Queen Charlotte Islands reflects in part the thick accumulation of dense Karmutsen mafic volcanic rocks within the shallow crust. The Sandspit Fault appears to be normal and eastward-dipping with little requirement for a strike-slip component. It may be listric. Gravity models indicate that oceanic crust may be present east of the Queen Charlotte Fault below western Graham Island.*

## Résumé

*L'augmentation vers l'ouest des valeurs gravimétriques régionales au-dessus d'une zone de 400 km de longueur, de la zone côtière aux îles de la Reine-Charlotte, est causée principalement par un amincissement de la croûte continentale d'environ 8 km vers l'océan Pacifique. Les valeurs gravimétriques négatives au-dessus du détroit d'Hécate sont dues à la présence de sédiments épais au sein du bassin de la Reine-Charlotte. Des valeurs gravimétriques positives locales au-dessus du détroit d'Hécate sont liées à la présence de sources dans la croûte supérieure près de l'interface socle-sédiment. Les modèles de la structure de la densité laissent présumer une origine d'extension de ces formes, avant l'accumulation d'une grande partie de ces sédiments dans le bassin de la Reine-Charlotte. Des valeurs gravimétriques positives enregistrées au-dessus des îles de la Reine-Charlotte reflètent en partie l'épaisse accumulation de roches volcaniques mafiques denses de Karmutsen au sein de la croûte peu profonde. La faille Sandspit semble normale et plonge vers l'est sans comporter nécessairement un rejet horizontal. Elle pourrait être listrique. Les modèles gravimétriques indiquent que la croûte océanique pourrait être présente à l'est de la faille de la Reine-Charlotte, au-dessous de l'ouest de l'île Graham.*

<sup>1</sup> Cordilleran Division, Geological Survey of Canada, 100 West Pender Street, Vancouver, B.C. V6B 1R8

<sup>2</sup> Pacific Geoscience Centre, P.O. Box 6000, Sidney, B.C. V8L 4B2

## INTRODUCTION

In the summers of 1987 and 1988, a total of 197 gravity measurements were made in the Queen Charlotte Islands and added to the national gravity data base as part of a concerted GSC effort to assess the geological setting and structure of the region (Fig. 1). The new data improve the regional gravity coverage on Graham Island and provide detailed profiles over selected surface features.

The intent of this preliminary report is to describe the gravity anomaly field in the Queen Charlotte region and to present initial density structure models of the crust below the area.

## GRAVITY SURVEY

Gravity measurements were made with Lacoste-Romberg gravity meters G009 and G444. Instrument readings were reduced to simple Bouguer anomalies using the International Gravity Standardization Net (IGSN71) and the Geodetic Reference System (GRS67). A standard density of  $2.67 \text{ g/cm}^3$  was used in the Bouguer correction.

For each gravity station, the horizontal position was plotted on 1:50 000 NTS maps and the vertical position was determined with digital altimeters. Location accuracies are estimated as  $\pm 25 \text{ m}$  and  $\pm 3 \text{ m}$  respectively. Terrain effects were removed from simple Bouguer values using a one-kilometre digital elevation grid and, within a few kilometres of stations near steep topography, elevation data gridded at 125–500 m. The resulting complete Bouguer anomalies are considered accurate to within  $\pm 2 \text{ mGal}$  (Fig. 2). See Seemann et al. (1988) and Sweeney and Seemann (1989) for details of the gravity surveys.

## GRAVITY FIELD

The gravity field is characterized by strong negative anomalies, locally exceeding  $-100 \text{ mGal}$ , over the high elevations of the mainland Coast Mountains (Fig. 2). Except for a major anomaly low over Hecate Strait, the regional anomaly level rises gradually toward the Pacific and culminates in a linear high of up to  $80 \text{ mGal}$  along the western edge of the Queen Charlotte archipelago. The high closely parallels a pronounced offshore gravity low, below  $-90 \text{ mGal}$  in places. The exceptionally steep anomaly gradient ( $>6 \text{ mGal/km}$ ) between the high-low pair lies over the Queen Charlotte Fault, the seismically active boundary between the Pacific and North America plates.

Low anomalies over the mainland are attributed to thickened continental crust beneath the Coast Mountains (Stacey and Stephens, 1969; Forsyth et al., 1974). The low over Hecate Strait appears to be associated with low-density sedimentary rocks of the Queen Charlotte Basin (Figs. 2 and 3).

The paired high-low anomaly belt over the plate boundary is partly an edge effect produced by the abrupt change in crustal thickness (Stacey and Stephens, 1969). The low anomaly is enhanced by the presence of seawater, a low-density accretionary wedge and deformed low-density basement rocks as inferred from low P-wave crustal velocities on the Pacific side of the Queen Charlotte Fault (Hyndman et al., 1982; Horn et al., 1984). The high anomaly on the North American side is produced by thinned crust below Graham Island (Forsyth et al., 1974; Mackie et al., 1989), and may be enhanced by flexural uplift produced over the last 5–6 Ma by oblique convergence and underthrusting of the Pacific Plate beneath North America in the Queen Charlotte region (Yorath and Hyndman, 1983). However, Mesozoic and Tertiary rocks within 50 km of the plate boundary on Moresby and Graham islands show little evidence of recent eastward regional tilting (Thompson and Thorkelson, 1989; Hickson, 1989).

A northwest-trending anomaly gradient (up to  $2.5 \text{ mGal/km}$ ) extends along much of the east side of the archipelago (Fig. 2) and dissipates north of Masset Inlet. Between Masset and Skidegate inlets the anomaly gradient lies over the Sandspit Fault which, on Graham

Island, separates Tertiary sediments of the Skonun Formation from Mesozoic sedimentary and igneous units to the west (Sutherland Brown, 1968).

## INITIAL DENSITY STRUCTURE MODELS

We assess subsurface density structure by comparing observed gravity anomaly values with those generated by crustal models, constrained at the surface by mapping and rock density measurements and at depth by bathymetry, borehole logs and by seismic reflection and refraction horizons (Table 1; Figs. 3 and 4).

Mapping and rock density data are taken from Sutherland Brown (1968), Stacey (1974), Hickson (1988, 1989), Roddick (1970), G.J. Woodsworth and J.G. Souther (pers. comm., 1989) and Thompson and Thorkelson (1989). Bathymetry is from Seemann (1982). Compaction within Skonun rocks below Hecate Strait is calibrated with borehole density logs (Shell Canada Ltd., 1968; Table 1). Sediment thickness below Hecate Strait is taken from a preliminary analysis of seismic reflection data collected in 1988 along Line 6 in Rohr et al. (1989a). Moho depths are based on seismic refraction determinations by Johnson et al. (1972), Forsyth et al. (1974), Horn et al. (1984), Dehler and Clowes (1988), G. Spence (pers. comm., 1988) and Mackie et al. (1989).

The density model in Figures 3 and 4 was calculated with the program GRAMA (Seemann et al., 1990). Local (Airy) isostatic balance is assumed. The mantle, deep continental crust and deep oceanic crust are assigned nominal densities of  $3.30$ ,  $2.92$  and  $2.80 \text{ g/cm}^3$ , respectively.

### Regional features

Thinning of the crust by about 8 km, as determined by the seismic refraction experiments, accounts for much of the westward rise in the regional gravity field over the mainland and the Queen Charlotte Islands (Figs. 2 and 3). This regional trend is interrupted over Hecate Strait by a major gravity low that appears to vary with the thickness of the Skonun Formation. The Coast Plutonic Complex appears broadly trough-shaped and can be no more than about 5 km thick, assuming that its mean surface density ( $2.73 \text{ g/cm}^3$ , Table 1) persists with depth.

The calculated gravity field over the Pacific is generated using the available depth constraints and a density for oceanic crust that is about four percent less than that used for continental crust below the mainland. The change in crustal density occurs below Graham Island (Fig. 3). The low densities assigned to the seabed sediments (unit U, Fig. 3) and to the crust immediately west of the Queen Charlotte Fault (F1) are based on reduced P-wave velocities within these units (Horn et al., 1984; Dehler and Clowes, 1988).

### Specific features

On southern Graham Island, surface mapping and stratigraphic relations suggest that Tertiary volcanics and post-Karmutsen Mesozoic strata are less than a few kilometres thick (Hickson, 1989; Thompson and Thorkelson, 1989; Sutherland Brown, 1968). In the crustal density model, these rocks are portrayed as a surface veneer (Fig. 3), with the Rennell Sound Fold Belt (F2) shown as a monoclinical step at the base of the Mesozoic stratigraphy (R.I. Thompson, pers. comm., 1988).

Granitic rocks appear to be at most 2–3 km thick (Fig. 3). Dips of pluton contacts, shown as near-vertical, are poorly constrained by the present gravity data.

Underlying these surface rocks are thick mafic volcanics of the Karmutsen Formation (unit K, Fig. 3). Their presence is inferred by the fact that Karmutsen volcanics underlie Mesozoic strata south of Skidegate Inlet and are exposed locally along the west coast of Graham Island (Sutherland Brown, 1968). Furthermore, significant Bouguer anomaly peaks over exposed Karmutsen volcanics suggest that the high

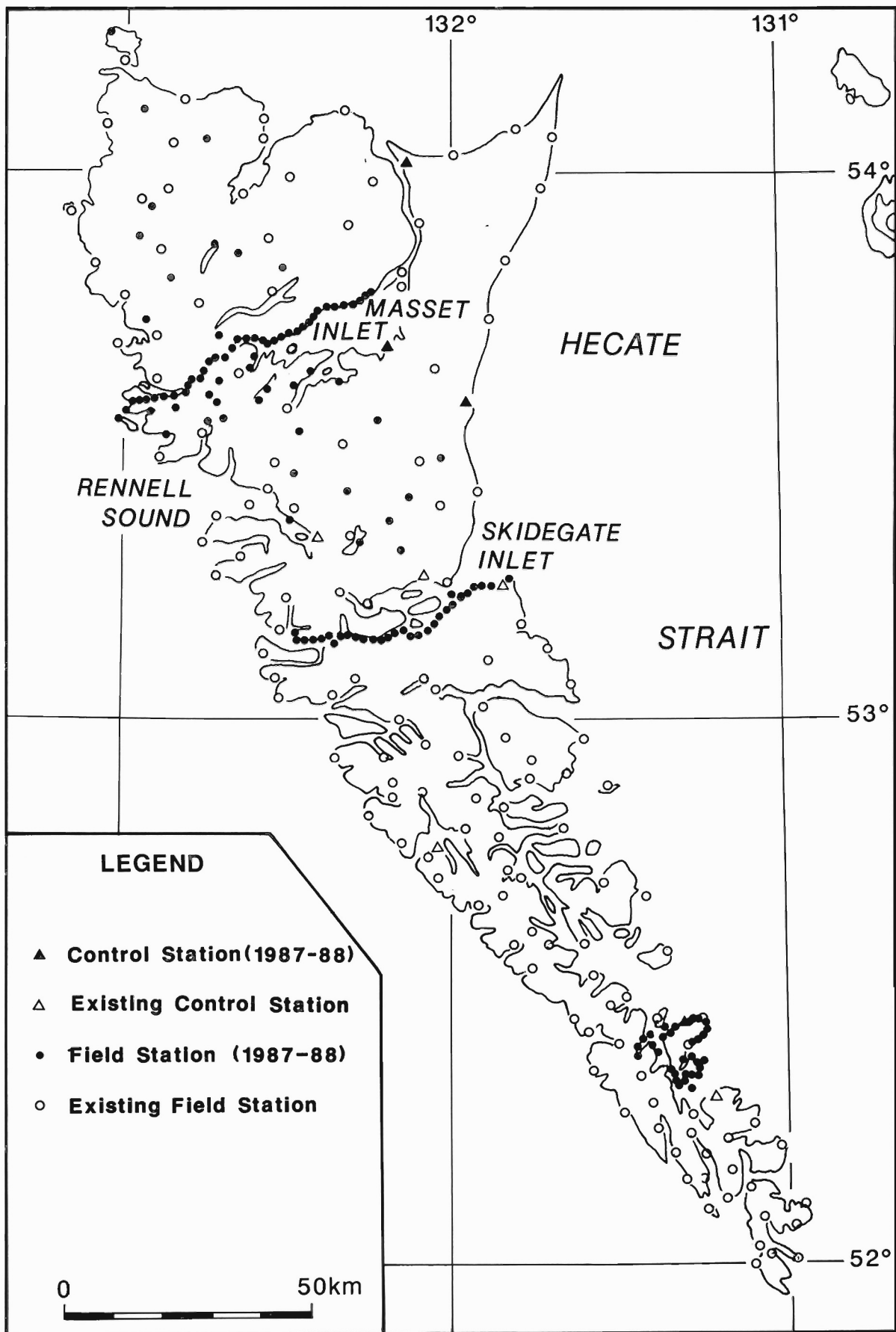


Figure 1: Gravity station locations, Queen Charlotte Islands.

regional gravity field observed throughout the Queen Charlotte Islands may be generated partly by large volumes of dense Karmutsen rocks within the upper crust (Figs. 2 and 3; Seemann et al., 1988).

Just south of the line of section, the thickness of Karmutsen rocks is thought to be at least 4.2 km (Sutherland Brown, 1968). On Figure 3 unit K is shown to be 5-6 km thick. This estimate is imprecise because, in the gravity model, Karmutsen thickness depends upon the density of

underlying crustal rocks, and this is loosely constrained by available P-wave velocity data (Horn et al., 1984; Mackie et al., 1989; Barton, 1986). Karmutsen rocks could be much thicker than 5-6 km, in which case the underlying deep crustal rocks would be less dense.

The Skonun Formation is modeled using densities and thicknesses based on well logs and seismic reflection horizons from Hecate Strait. Skonun densities from Graham Island (Table 1) are excluded

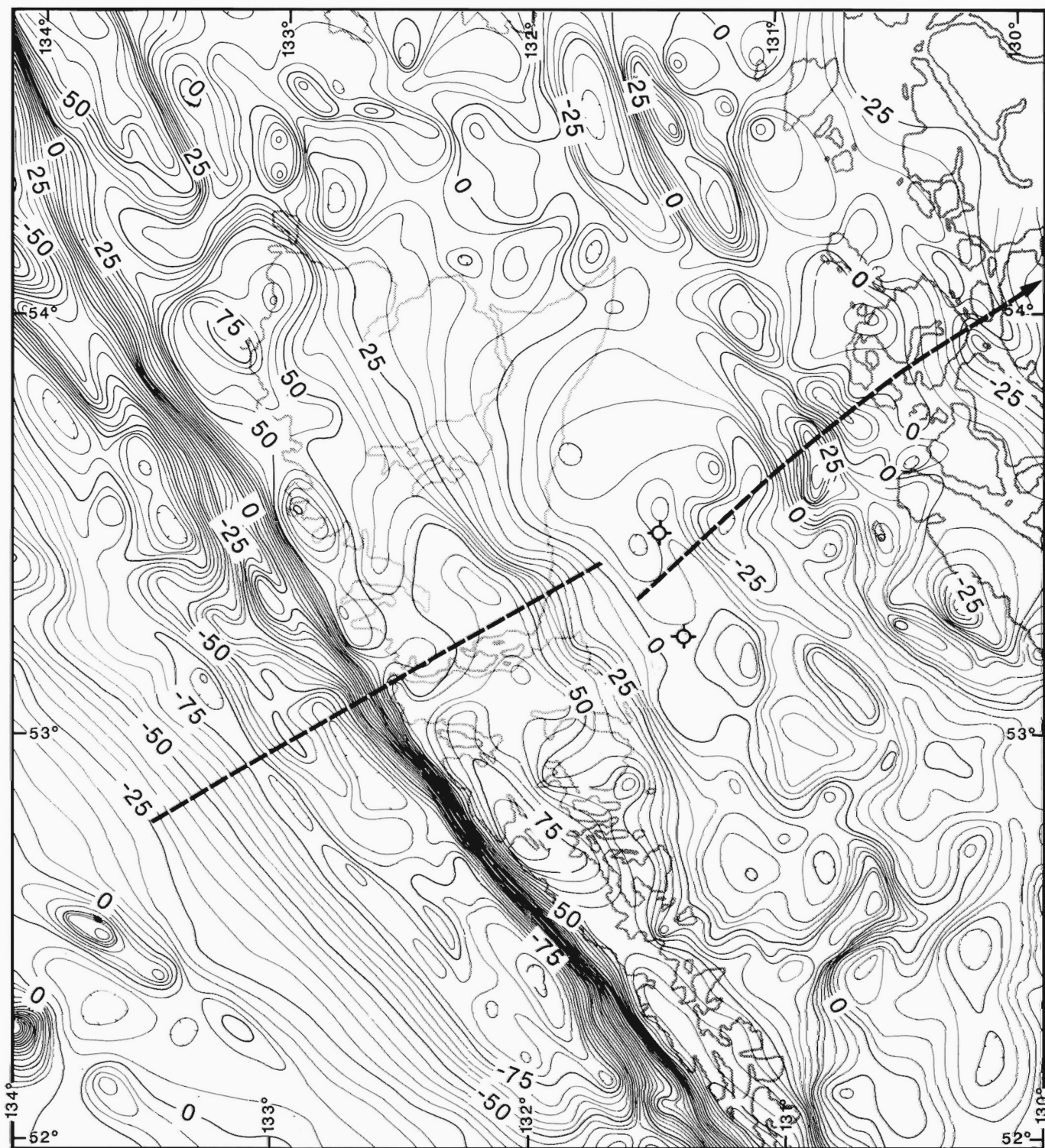


**Figure 2:** Gravity anomaly field, Bouguer on land, free air offshore (Earth Physics Branch, 1982). Contour interval 5 mGal. Profile location for gravity model (Fig. 3) shown. Boreholes near the profile also shown, South Coho to the northwest, Tye to the southeast.

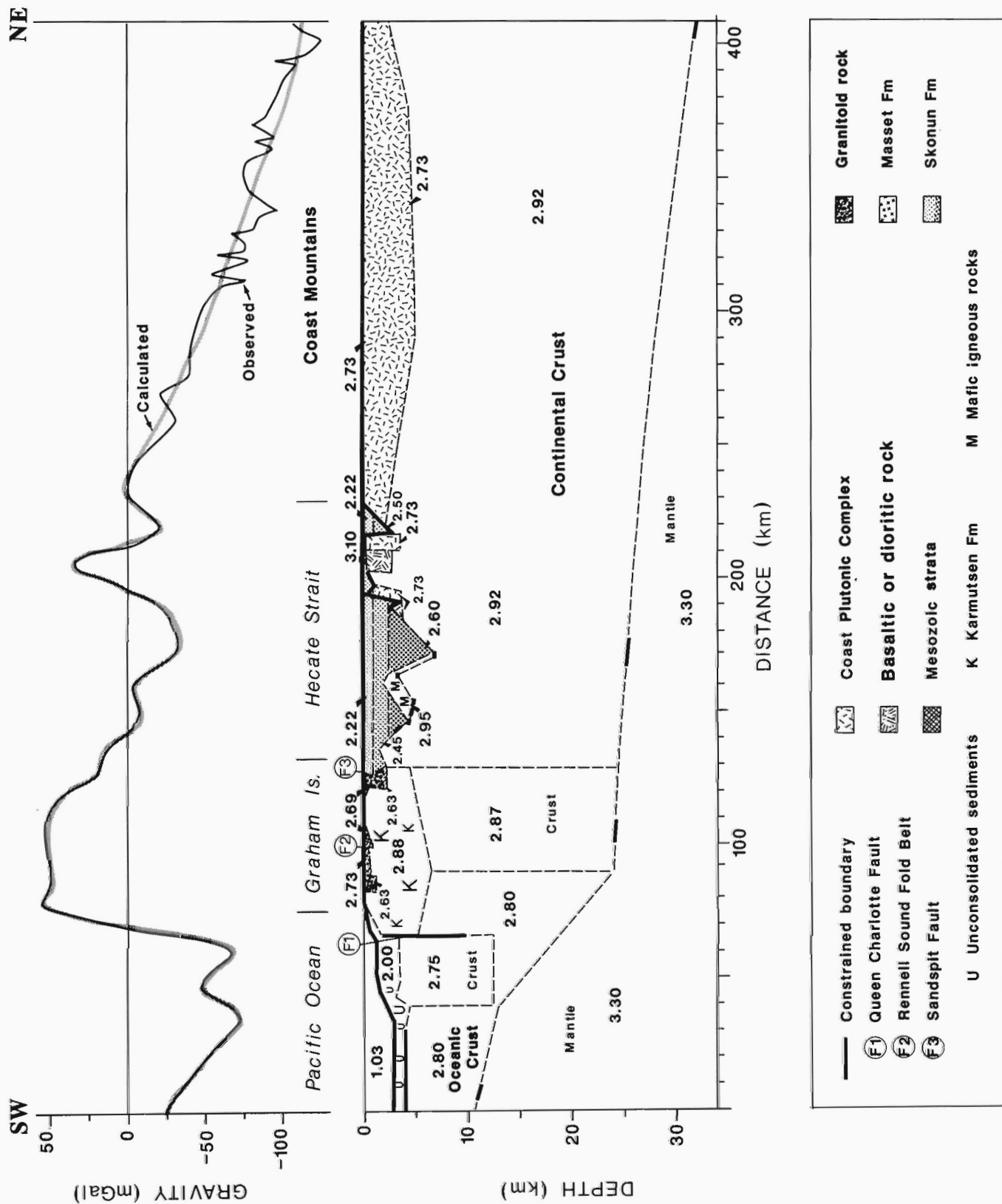


**Figure 3:** A 2.5-dimensional density structure model of the crust along profile shown on Figure 2. Solid (dashed) lines indicate constrained (unconstrained) boundaries. Densities in  $\text{g/cm}^3$ .

because lithified outcrop samples are uncharacteristic of this dominantly friable formation (Sutherland Brown, 1968; R. Higgs, pers. comm., 1989). The resulting model of the Skonun Formation in Queen Charlotte Basin yields a substantial mismatch between the calculated and observed gravity profiles. An initial fit was achieved with density shifts in basement blocks below Hecate Strait.

This approach is warranted for the mismatch over a horst-like basement edifice near the Coast Mountains because the overlying sediments are too thin to make the necessary contribution to the calculated gravity field (Figs. 3 and 4). The density ( $2.73 \text{ g/cm}^3$ ) used for two of the basement units is intended to suggest equivalence with rocks of the nearby Coast Plutonic Complex. The proposed  $3.10 \text{ g/cm}^3$  block may related to basalt flows exposed on small islands just southeast of the profile, or the block could represent magnetite-rich dioritic rock exposed nearby (Roddick, 1970). If the density of the latter unit ( $2.90$

$\text{g/cm}^3$ , Table 1) were used instead of  $3.10 \text{ g/cm}^3$ , the model block would need to be about twice as thick to generate a calculated gravity field similar to the one shown over the block in Figures 3 and 4.

A dense block is also required below central Hecate Strait to account for the northwest-trending gravity high observed over the area (Fig. 2). Calculations using the Bancroft (1960) inequality indicate that the top of the block must be within 4 km of the surface. A dense mass would therefore lie close to its maximum depth if it was part of the basement.

To generate a fit to the observed gravity field, a basement model block must be quite dense ( $>3.20 \text{ g/cm}^3$ ) and very thick ( $>5 \text{ km}$ ). These requirements strain credibility. A smaller, lighter mass closer to the surface is therefore needed to produce the desired gravity effect (Figs. 3 and 4).

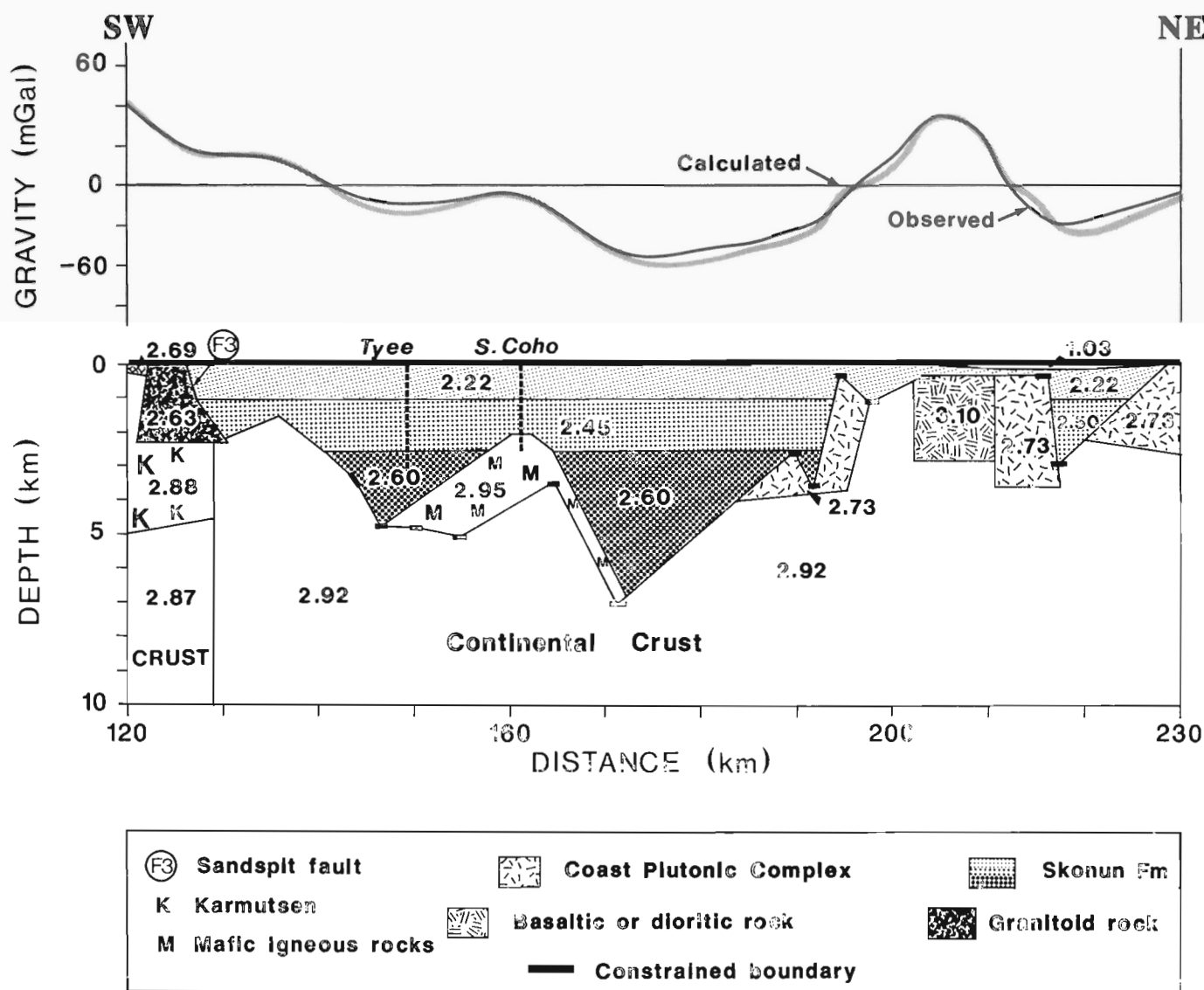


Figure 4: Detail of Figure 3 showing density structure below Hecate Strait.



TABLE 1: Density Data				
UNIT	g/cm3 MEAN	# SAMPLES	g/cm3 STANDARD DEVIATION/RANGE	SOURCE
Coast Plutonic Complex	2.73	3021	—/2.55-2.99	1
Granitoid rocks	2.63	7	0.01/—	2
		136	—/2.40-3.70	3
Magnetite-rich dioritic rock	2.90	83	—/—	4
Dyke rocks	2.76	81	0.11/2.51-3.00	5
Karmutsen Fm.	2.88	52	0.10/2.73-2.99	1,2
Masset Fm.-volcanics	2.73	10	0.11/—	1,2
Skonun Fm., Graham I.	2.48	12	0.10/2.40-2.71	1,2
Skonun Fm., Hecate St.	2.22-2.60	none	—/2.15-2.60	6
Unconsolidated seafloor sediments	2.00	none	—/1.95-2.05	7,8
Post-Karmutsen Mesozoic strata	2.69	131	0.06/2.42-2.78	1,2

1. Stacey (1974)
2. Sutherland Brown (1968)
3. Anderson and Greig (1989)
4. Roddick (1970)
5. Souther and Bakker (1988)
6. Shell Canada Ltd. (1968)
7. Horn et al. (1984)
8. Mackie et al. (1989)

The Tyee and South Coho boreholes, projected onto the profile in Figure 4, penetrate Skonun Formation sediments in Hecate Strait (Fig. 2; Shell Canada Ltd., 1968). The former well, projected from the southeast, intersects basaltic rock about 2 km above the reflection-defined basement (K.M.M. Rohr, pers. comm., 1989). A 2 km-thick model block placed upon the basement-sediment interface generates a good fit to the observed gravity field using a block density of  $2.95 \text{ g/cm}^3$ , reasonable for basalt. It is unclear that the basalt is massive as shown in Figures 3 and 4; a series of volcanic interbeds could produce the same gravitational effect.

The South Coho well does not penetrate basaltic rock while the Tyee well does, the reverse of what is indicated by projecting their positions onto the profile in Figure 4. It seems likely that this dense zone within the Skonun Formation thins or deepens to the northwest below central Hecate Strait in concert with the decline in amplitude of the positive gravity anomaly trend (Fig. 2). It may also be that the dense source lies partly within the basement. This notion is supported by the Rohr et al. (1989a) seismic reflection data that show a highly contorted horizon near the top of basement below the gravity high in question. The disturbed zone is interpreted by K.M.M. Rohr et al. (pers. comm., 1989) as a concentration of high-angle offsets or dykes, perhaps a conduit for dense magma that was either extruded on the basement surface before the onset of sedimentation or subsequently intruded into the overlying strata. If the former, then the disturbed zone with its linear trend in the gravity field (Fig. 2) may have genetic links with pre-Skonun-age dyke swarms mapped on the Queen Charlotte Islands by Souther (1989). Surface samples of these dykes have a mean density of  $2.76 \text{ g/cm}^3$  (Table 1). To satisfy the gravity and depth constraints, basaltic material of this density would need to be about 8 km thick and extend about 6 km below the basement-sediment interface below central Hecate Strait.

On southeastern Graham Island the Sandspit Fault (F3, Fig. 3) forms the western boundary of the Queen Charlotte Basin. The gravity model, constrained by density differences between the Skonun For-

mation and surface rocks to the west, shows that the Sandspit Fault may be normal with its east side downdropped about 3 km near Skidegate Inlet (Fig. 3). Fault offset may become insignificant north of Masset Inlet where the gravity anomaly associated with the fault disappears (Fig. 2). Model results indicate a near-surface dip on the fault of  $30\text{-}50^\circ$  east with some indication, illustrated in Figure 3, of gentler dips at depth.

## SUMMARY

The low regional gravity anomaly field over Hecate Strait is generated by thick sediments within the Queen Charlotte Basin. These sediments are assumed to be the Neogene Skonun Formation. Older sedimentary units could be present at deep levels within the basin but, if present, they must have relatively high density.

Local linear positive gravity trends over the strait appear to be produced by anomaly sources near the basement-sediment interface as defined by seismic reflection (Figs. 2, 3 and 4). Sources near the mainland are contained within basement rocks; the source near the basin centre probably lies mostly above the basement surface.

Shallow basement structure below Hecate Strait has been modeled to suggest the effects of regional extension that thinned the crust and presumably facilitated the early development of the Queen Charlotte Basin (Figs. 3 and 4; Rohr et al., 1989b). In the east, basement units may have been detached from equivalent rocks exposed within the Coast Mountains. In the centre, mafic magma may have penetrated to the earth's surface through a swarm of dyke feeders. In the west, the Sandspit Fault dips basinward with a large apparent normal offset near Skidegate Inlet. Within the deep crust, extension appears to have affected a much broader region, as suggested by the gradual westward shallowing of the Moho over several hundred kilometres (Fig. 3).

The high gravity anomaly field over the Queen Charlotte Islands is generated partly by thick mafic volcanics of the Karmutsen Formation. The change in deep crustal density modeled below Graham Island could

be related to the transition from continental to oceanic crust. This would imply that oceanic crust (density =  $2.80 \text{ g/cm}^3$ , Fig. 3) is present east of the Queen Charlotte Fault (F1), as might be expected along a plate boundary with a component of convergence (e.g., Rogers, 1983). The gravity model does not suggest, as do Yorath and Hyndman (1983) and Mackie et al. (1989), that a slab of oceanic crust extends below the continent as far east as the mainland.

## ACKNOWLEDGMENTS

We thank R.I. Thompson for logistic support in the field, K.M.M. Rohr, R. Higgs, J.G. Souther for kindly providing unpublished information, and R.G. Currie, R.D. Hyndman and G.J. Woodsworth for helpful comments and suggestions. Special thanks to Chevron Resources Canada Ltd. for permitting gravity data acquired in 1987 to be included in Figure 2.

## REFERENCES

- Anderson, R.G. and Greig, C.J.**  
**1989:** Jurassic and Tertiary plutons in the Queen Charlotte Islands, British Columbia; *in* Current Research, Part H, Geological Survey of Canada, Paper 89-1H, p. 95-104.
- Bancroft, A.M.**  
**1960:** Gravity anomalies over a buried step; *Journal of Geophysical Research*, v. 65, p. 1630-1631.
- Barton, P.J.**  
**1986:** The relationship between seismic velocity and density in the continental crust—a useful constraint?; *Geophysical Journal of the Royal Astronomical Society*, v. 87, p. 195-208.
- Dehler, S.A. and Clowes, R.M.**  
**1988:** The Queen Charlotte Islands refraction project. Part I. The Queen Charlotte Fault Zone; *Canadian Journal of Earth Sciences*, v. 25, p. 1857-1870.
- Earth Physics Branch**  
**1982:** Gravity maps; Open File Map 82-15, 2 sheets.
- Forsyth, D.A., Berry, M.J., and Ellis, R.M.**  
**1974:** A refraction survey across the Canadian Cordillera at  $54^\circ$ ; *Canadian Journal of Earth Sciences*, v. 11, p. 533-548.
- Hickson, C.J.**  
**1988:** Structure and stratigraphy of the Masset Formation, Queen Charlotte Islands, British Columbia; *in* Current Research, Part E, Geological Survey of Canada, Paper 88-1E, p. 269-274.  
**1989:** An update on structure and stratigraphy of the Masset Formation, Queen Charlotte Islands, British Columbia; *in* Current Research, Part H, Geological Survey of Canada, Paper 89-1H, p. 73-79.
- Horn, J.R., Clowes, R.M., Ellis, R.M., and Bird, D.N.**  
**1984:** The seismic structure across an active oceanic/continental transform fault zone; *Journal of Geophysical Research*, v. 89, p. 3107-3120.
- Hyndman, R.D., Lewis, T.J., Wright, J.A., Burgess, M., Chapman, D.S., and Yamano, M.**  
**1982:** Queen Charlotte fault zone: heat flow measurements; *Canadian Journal of Earth Sciences*, v. 19, p. 1657-1669.
- Johnson, S.H., Couch, R.W., Gemperle, M., and Banks, E.R.**  
**1972:** Seismic refraction measurements in southwest Alaska and western British Columbia; *Canadian Journal of Earth Sciences*, v. 9, p. 1756-1765.
- Mackie, D.J., Clowes, R.M., Dehler, S.A., Ellis, R.M., and Morel-à-Huissier, P.**  
**1989:** The Queen Charlotte Islands refraction project. Part II. Structural model for transition from Pacific plate to North American plate; *Canadian Journal of Earth Sciences*, v. 26, 1713-1725.
- Roddick, J.A.**  
**1970:** Douglas Channel-Hecate Strait map-area, British Columbia; Geological Survey of Canada, Paper 70-41, 56 p.
- Rogers, G.C.**  
**1983:** Seismotectonics of British Columbia; Ph.D. thesis, University of British Columbia, Vancouver, 247 p.
- Rohr, K.M.M., Spence, G., Asudeh, I., Ellis, R., and Clowes, R.**  
**1989a:** Seismic reflection and refraction experiment in the Queen Charlotte Basin, British Columbia; *in* Current Research, Part H, Geological Survey of Canada, Paper 89-1H, p. 3-5.
- Rohr, K., Spence, G., and Sweeney, J.**  
**1989b:** Evidence for crustal thinning in the Queen Charlotte Basin; *EOS, Transactions of the American Geophysical Union*, 70, p. 1318.
- Seemann, D.A.**  
**1982:** Bathymetry off the coast of British Columbia; Earth Physics Branch, Open File Map 82-25.
- Seemann, D.A., Brandys, M., Perks, D., Reid, D., MacDonald, D., and Sweeney, J.F.**  
**1990:** GRAMA, an interactive 2.5-dimensional gravity and magnetics modeling program; Geological Survey of Canada, Open File 2290, diskette with manual, 20 p.
- Seemann, D.A., Collins, A., and Sweeney, J.F.**  
**1988:** Gravity measurements on the Queen Charlotte Islands, British Columbia; *in* Current Research, Part E, Geological Survey of Canada, Paper 88-1E, p. 283-286.
- Shell Canada Ltd.**  
**1968:** Well history reports; Released to open file in 1970 by Department of Energy Mines and Resources, Ottawa.
- Souther, J.G.**  
**1989:** Dyke swarms in the Queen Charlotte Islands, British Columbia; *in* Current Research, Part H, Geological Survey of Canada, Paper 89-1H, p. 117-120.
- Souther, J.G. and Bakker, E.**  
**1988:** Petrography and chemistry of dykes in the Queen Charlotte Islands, British Columbia; Geological Survey of Canada, Open File 1833.
- Stacey, R.A.**  
**1974:** Structure of the Queen Charlotte Basin; *in* Canada's Continental Margins, C.J. Yorath, E.R. Parker and D.J. Glass (ed.), Canadian Society of Petroleum Geologists, Memoir 4, p. 723-741.
- Stacey, R.A. and Stephens, L.E.**  
**1969:** An interpretation of gravity measurements on the west coast of Canada; *Canadian Journal of Earth Sciences*, v. 6, p. 463-474.
- Sutherland Brown, A.**  
**1968:** Geology of the Queen Charlotte Islands, British Columbia; British Columbia Department of Mines and Petroleum Resources, Bulletin 54, 226 p.
- Sweeney, J.F. and Seemann, D.A.**  
**1989:** Gravity measurements over the Burnaby Island pluton, Queen Charlotte Islands, British Columbia; *in* Current Research, Part H, Geological Survey of Canada, Paper 89-1H, p. 113-115.
- Thompson, R.I. and Thorkelson, D.J.**  
**1989:** Regional mapping update, central Queen Charlotte Islands, British Columbia; *in* Current Research, Part H, Geological Survey of Canada, Paper 89-1H, p. 7-11.
- Yorath, C.J. and Hyndman, R.D.**  
**1983:** Subsidence and thermal history of Queen Charlotte Basin; *Canadian Journal of Earth Sciences*, v. 20, p. 135-159.

# Regional geophysical constraints on crustal structure and geologic evolution of the Insular Belt, British Columbia

Henry V. Lyatsky<sup>1</sup>

Lyatsky, H.V., Regional geophysical constraints on crustal structure and geologic evolution of the Insular Belt, British Columbia; in *Evolution and Hydrocarbon Potential of the Queen Charlotte Basin, British Columbia*. Geological Survey of Canada, Paper 90-10, p. 97-106, 1991.

## Absiract

*A multidisciplinary geoscience study of large-scale structural fabrics was undertaken off the west coast of British Columbia. The objective was to elucidate the crustal structure of this part of the Insular Belt and to study its Mesozoic and Cenozoic tectonics, to constrain evolution of its sedimentary basins and to provide a framework for detailed interpretation of seismic data.*

*Regional magnetic, gravity and physiographic lineaments were examined. Geological calibration was provided by mappable structure onshore. Geological, geophysical and physiographic trends suggest the existence of several regional structural fabrics of Paleozoic and Mesozoic age. The Principe Laredo, Kitkatla and Sandspit fault systems apparently continue from land areas into Dixon Entrance. No compelling evidence has been uncovered to substantiate significant horizontal displacements, whether rotational or translational, of large crustal blocks east of the Queen Charlotte Fault in the Mesozoic and Cenozoic. The lateral crustal movements that accompanied the formation of the Tertiary Queen Charlotte Basin were probably small, and no rift-related structural or geophysical fabrics have been identified. A fault-block tectonic pattern likely dominated, both onshore and offshore, in the Mesozoic and Cenozoic. Such an interpretation avoids conflict with geological data onshore while remaining compatible with geophysical information. Regional block faulting and limited influence of nearby orogenies on the structural evolution of the Insular Belt suggests the existence of a pre-middle Paleozoic(?) crystalline basement complex.*

## Résumé

*Une étude géoscientifique multidisciplinaire des grandes fabriques structurales a été entreprise au large de la côte Ouest de la Colombie-Britannique. L'objectif était d'élucider la structure crustale de cette partie de la zone Insulaire et d'étudier sa tectonique mésozoïque et cénozoïque, pour préciser l'évolution de ses bassins sédimentaires et définir un cadre d'interprétation détaillée des données sismiques.*

*Des linéaments magnétiques, gravimétriques et physiographiques ont été examinés. L'étalonnage géologique a été réalisé à partir d'une structure littorale cartographiable. Les tendances géologiques, géophysiques et physiographiques indiquent l'existence de plusieurs fabriques structurales régionales datant du Paléozoïque et du Mésozoïque. Les systèmes de failles Principe Laredo, Kitkatla et Sandspit semblent se prolonger depuis la terre dans l'entrée Dixon. Aucune preuve irréfutable n'a été établie pour confirmer d'importants déplacements horizontaux, de rotation ou de translation, de la faille de la Reine-Charlotte dans le Mésozoïque et le Cénozoïque. Les mouvements latéraux de la croûte qui ont accompagné la formation du bassin tertiaire de la Reine-Charlotte ont probablement été faibles, et aucune fabrique structurale ou géophysique liée à des rifts n'a été identifiée. Une structure tectonique de blocs faillés a probablement dominé, sur terre et dans la mer, durant le Mésozoïque et le Cénozoïque. Une telle interprétation ne contredit pas les données géologiques continentales tout en demeurant compatibles avec les données géophysiques. Les réseaux régionaux de blocs faillés et l'influence limitée d'orogénèses environnantes sur l'évolution structurale de la zone Insulaire indiquent qu'il existerait un socle cristallin antérieur au Paléozoïque moyen.*

<sup>1</sup> Department of Geological Sciences, University of British Columbia, 6339 Stores Rd., Vancouver, B.C. V6T 2B4

## INTRODUCTION

The study area is located within the Insular Belt along the west coast of Canada, between southeast Alaska, Queen Charlotte Islands, Vancouver Island and the mainland. Most of the region is covered by the waters of Dixon Entrance, Hecate Strait and Queen Charlotte Sound (Fig. 1). These areas are part of Hecate Depression (Holland, 1964) which contains most of the Tertiary Queen Charlotte Basin. Although outcrop mapping in surrounding land areas defines lithologies and structural patterns which may continue offshore, the limited data base results in speculative tectonic interpretations and challenges the interpreter to take into account all the geological and geophysical constraints available.

The objective was to provide general constraints on crustal structure and tectonic evolution of the area and to test Young's (1981) wrench-fault structural model. This would lead to a greater understanding of the processes which caused the formation of sedimentary basins in the Insular Belt, as well as shedding new light on the Phanerozoic history of the area. A framework for detailed interpretation of seismic data would also be provided. Examination of regional magnetic, gravity, geologic and physiographic lineament fabrics was undertaken. Elsewhere, various authors (Wellman, 1985; Maughan and Perry, 1986; Anfiloff, 1988; Murray et al., 1989) have related linear-anomaly domains in potential-field data, topography and geologic structure to crustal blocks and/or structural fabrics.

Linear-fabric analysis of potential-field data is a more powerful tool than matching of different areas with similar geophysical signatures for generating tectonic reconstructions. The weakness of the latter approach lies in its reliance on an arbitrary and frequently unjustified assumption that similar geophysical patterns in different areas result from separation of a once continuous geologic feature. Moreover, lithology-anomaly relationships are often obscure, especially offshore. A conservative approach was taken in this study, requiring specific, compelling evidence before large crustal movements are postulated. This work was aimed at producing a structural model for the Insular Belt which would be compatible with both geological and geophysical observations, thus limiting the problem of non-uniqueness inherent in geophysical interpretation.

The stratigraphic nomenclature of Cameron and Hamilton (1988) is used in this report. Where other nomenclatures are utilized, specific references are made.

## POTENTIAL-FIELD DATA

Magnetic and gravity data were utilized to examine regional structural patterns in the study area. Although such data do not always yield the resolution obtainable with reflection-seismic techniques, they are useful where preliminary interpretations over large areas are required, whereas seismic reflection data provide images of the subsurface which are largely two-dimensional. Trends observed on magnetic and gravity maps were correlated with geologic structure and geomorphologic lineament patterns. In this section, only the Insular-Belt portion of the study area is considered as most of the Coast Plutonic Complex was excluded due to lack of data.

## AEROMAGNETIC DATA

### Data processing

The magnetic data were flown 305 m and 610 m above sea level or ground level, and gridded at an 813 m interval. Side-lighting of total-field magnetic anomaly data was used to enhance linear anomalies, and three maps were produced using the numerical technique described by Broome et al. (1985). The declination of the "light source" was 45° (Fig. 2a in pocket), 90° (Fig. 2b) and 135° (Fig. 2c), with an inclination of 30°.

To investigate large-scale and possibly deep-seated geologic features, the magnetic data were upward continued to 5 km (Fig. 2d in pocket) and 20 km (Fig. 2e). The general theory behind upward continuation has been outlined by Briusov (1980). The procedure is numerical and amounts to filtering the data on the basis of anomaly wavelength, with long-wavelength anomalies passed preferentially. The cut-off wavelength is proportional to the nominal elevation of the recording level, and local, short-wavelength anomalies are suppressed. Broad anomalies of shallow origin are not excluded, so most features in upward-continued data are caused by relatively large-scale sources at various depths in the crust.

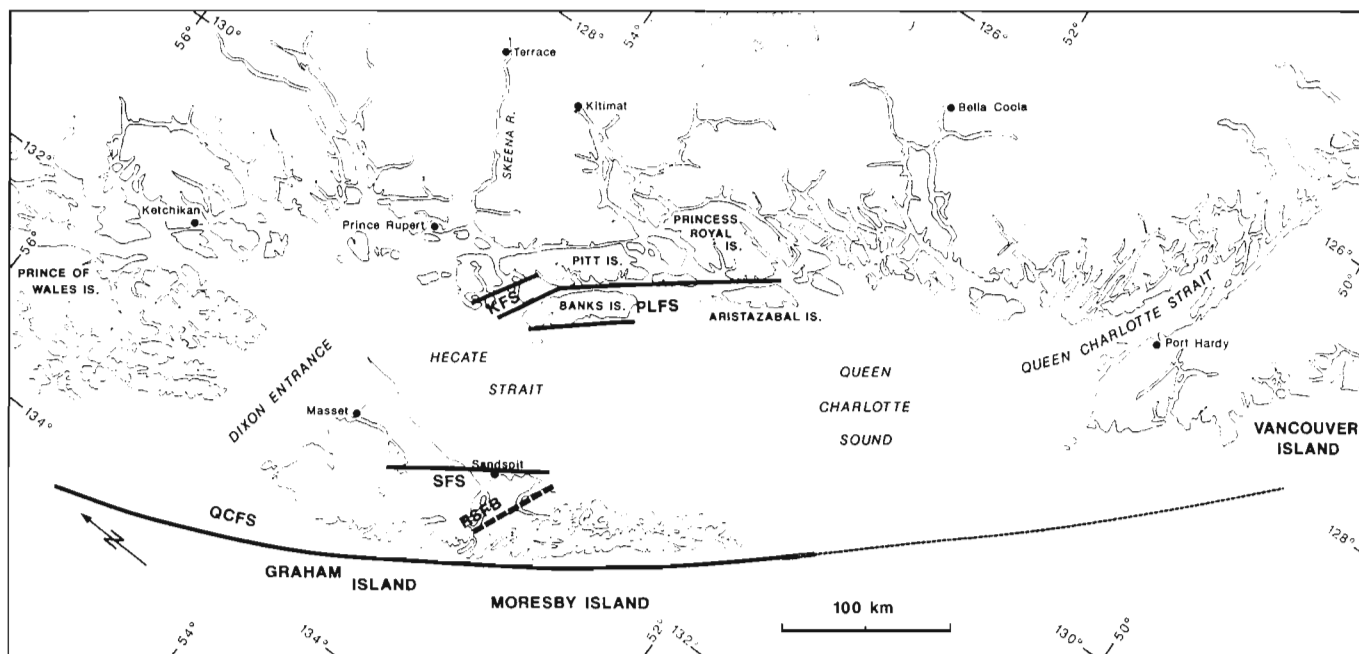


**Figure 1:** Study area location map and the major structural zones as recognized from geological field mapping. QCFS – Queen Charlotte fault system, SFS – Sandspit fault system, PLFS – Principe Laredo fault system, KFS – Kitkatla fault system, RSFB – Rennell Sound fold belt.

## Side-lit data

Many of the magnetic anomalies in Queen Charlotte Sound and Hecate Strait appear to be correlative with structures within the Queen Charlotte Basin interpreted from reflection seismic data (J.R. Dietrich, pers. comm., 1989). This confirms that the magnetic-anomaly pattern in the study area is controlled largely by structural deformation of the volcano-sedimentary supracrustal assemblage.

Various magnetic lineaments can be correlated with known geologic structures onshore and with physiographic lineaments in Figure 3. The strongest linear anomaly occurs in the northeastern corner of the map area (Figs. 2a and 2b in pocket). It has a west-northwesterly orientation and extends across the northern part of Hecate Strait and into Dixon Entrance. It cuts across magnetic anomalies which run in a north-northwesterly direction, with one intersection occurring at 54°10'N, 131°30'W, north of Banks Island. The north-northwesterly trend probably represents an extension of the Principe Laredo fault system, and the west-northwesterly magnetic lineament likely reflects a northwestward continuation of the Kitkatla fault zone (Fig. 1). Elements of the Kitkatla fault system are currently active, as evidenced by earthquake-seismicity data (Rogers et al., 1988; R.B. Homer, pers. comm., 1989). The character of the Kitkatla and Principe Laredo magnetic anomalies indicates that both these fault systems are broad and internally complex.

Queen Charlotte Islands contain numerous, but weaker, magnetic lineaments with various orientations. Easterly trends occur mostly on northern Graham Island. North-northwesterly trends may be associated locally with the Sandspit Fault, which is shown in Figure 1. The magnetic lineament related to this fault is lost over northern Graham Island but reappears in Dixon Entrance. The west-northwesterly lineament seen in Figure 2a, at about 53°N, 132°W, likely corresponds to the early Middle Jurassic Rennell Sound fold belt (Thompson, 1988). This anomaly is restricted largely to Queen Charlotte Islands and has no significant extension offshore. The Rennell Sound fold belt magnetic anomaly is intersected without offset by a north-south lineament at 131°40'W. Faint west-northwest-oriented magnetic lineaments (Fig. 2a) also occur on Graham Island and near the eastern margin of the map area, north of 52°N, and the subparallel lineaments in the two areas may line up. Since the absence of such anomalies in the intervening parts of Hecate Depression could be due to increased depth to source, continuity of causative geologic structures is suspected but not proved. The persistence, especially on Graham Island, of west-northwesterly magnetic lineaments suggests that the Rennell Sound fold belt could be part of a more pervasive fabric.

In general, the magnetic field is more subdued offshore than over land areas. This probably reflects variations in depth to source, although variations in rock composition may contribute. In Hecate Strait, a north-east-trending magnetic lineament is observed (Figs. 2b and 2c) between 53°N and 54°N, roughly on trend with some of the physiographic lineaments on the mainland (Fig. 3). This magnetic anomaly may cross-cut the west-northwesterly (Kitkatla) and north-northwesterly (Principe Laredo) lineaments at about 54°N.

Another northeast-trending anomaly can be observed in Figures 2b and 2c, at 52°30'N, 131°W. This lineament, which may have a faint extension on Moresby Island, coincides spatially with a similarly oriented bathymetric feature (Fig. 3) and is likely associated with the structurally uplifted Moresby Ridge. The strong magnetic signature of the ridge indicates that it is composed at least partly of igneous rocks (Young, 1981). East of the Moresby Ridge, a north-south magnetic lineament can be observed at 53°N, 131°W.

In Queen Charlotte Sound, the north-northeasterly fabric is the same as physiographic trends onshore (Fig. 3), and it may reflect ge-

ologic structures within the Queen Charlotte Basin. The same is true of the north-south and west-northwesterly trends, which are concentrated largely in southern Queen Charlotte Sound.

## Upward-continued data

Magnetic data were upward continued to 5 km (Fig. 2d) and 20 km (Fig. 2e) to investigate large-scale crustal structure. Examination of these maps reveals that the numerous, small anomalies north of 52°N, in eastern Queen Charlotte Sound (Figs. 2a-c) merge into a few large highs. Several explanations are possible.

1. The shape of these anomalies results from a loss of lateral resolution of the data due to filtering, and their source is shallow. However, shallow-seated volcanics elsewhere in the study area fail to produce such prominent magnetic highs.
2. An uplifted crustal block is the cause of the anomalies. However, this interpretation is weakened by the absence of an associated gravity high in Figures 2f-h (in pocket).
3. The sources merge at depth to form a larger geologic feature. Anomalies may then be produced by a large, deep-seated pluton with multiple apophyses and structures at shallower depths. This interpretation is preferred but cannot be proved at this time.

Two localized magnetic highs are observable over Queen Charlotte Islands (Figs. 2d and 2e), where they coincide approximately with outcrops of Late Jurassic and Tertiary intrusive rocks, as mapped by Anderson and Greig (1989). It is possible, therefore, that these anomalies are caused by plutons. Young (1981) suggested an association of the anomalies in observed total-field data with Masset eruption centres. I prefer the first interpretation due to the large size of the highs and the lack of exact coincidence with the outcrops of Masset volcanics.

The character of the upward-continued magnetic field (Figs. 2d and 2e) over eastern Graham Island is generally similar to the one over Hecate Strait. The localized positive anomaly at the northern edge of the map area may be related to the igneous and metamorphic rocks on southern Prince of Wales Island, which were noted by Buddington and Chapin (1929), Brew et al. (1966) and Gehrels and Saleeby (1987).

The "Cordilleran" north-northwesterly trends were largely removed by upward continuation of magnetic data to 20 km. In Figure 2e, such trends are restricted almost entirely to the vicinity of the Queen Charlotte Fault. Their absence elsewhere suggests that these magnetic lineaments are caused by comparatively shallow and small geologic features which may represent a relatively young structural overprint.

Most west-northwesterly trends were also removed by upward continuation. The lineaments representing northwestward extensions of the Principe Laredo and Kitkatla fault systems (Figs. 2a-c) become fragmented in 5-km magnetic data (Fig. 2d) and are lost on the 20-km map (Fig. 2e). The only feature preserved is a localized, positive anomaly north of Banks Island. The magnetic lineament associated with the Rennell Sound fold belt is absent in Figures 2d and 2e. In Figures 2a-c, this anomaly is intersected by other trends. All this suggests that both the scale and the regional tectonic significance of the Rennell Sound feature may have been overestimated by some of the previous workers (e.g. Yorath and Chase, 1981; Young, 1981; Yorath and Hyndman, 1983).

Only in the southern part of the map area (Figs. 2d and 2e) is a west-northwesterly trend preserved in upward-continued data, a local lineament being observable at 51°N.

The filtering used to produce the maps in Figures 2d and 2e passed three of the major trends discussed earlier: northerly, easterly and north-easterly. North-south trends are common in the southern part of the map area but can also be observed in its northeastern part, especially at longitude 131°30'W (Fig. 2e). No strong north-south lineament

at that location appears in Figures 2a-c and 3. East-west trends occur in most parts of the map area in Figure 2e.

Northeasterly trends are prominent in upward-continued magnetic data at various locations. The most prominent occurs east of the southern tip of Moresby Island. This lineament is expressed only weakly in the low-level data in Figures 2a-c, where it is crosscut by northerly and north-northwesterly trends. This may point to partial overprinting of the northeasterly trend by the other two. All these orientations are expressed bathymetrically (Fig. 3). In Figure 2e, the northeast-trending magnetic-gradient (fault?) zone separates a domain of positive anomalies to the south, where plutons are suspected, from a negative-anomaly area to the north. Both the gradient zone and the positive anomalies are weakened over eastern Queen Charlotte Sound, where elevated heat-flow values were reported by Hyndman et al. (1982). Other northeast-trending lineaments occur mostly to the north of the gradient zone.

From the analysis of seismic refraction data (Yuan et al., 1989), a change in crustal thickness and composition may be inferred under southern Hecate Strait. This, and the magnetic-anomaly pattern discussed, suggests that a large, northeast-trending structure may exist in northern Queen Charlotte Sound. The effect of this zone on the geologic evolution of the area is uncertain and warrants further study.

## GRAVITY DATA

### General statement

Gravity data were examined to investigate the nature of density contrasts in the study area. Due to the regional nature of the data over much of the Coast Mountains, the study has been restricted to the Insular Belt and western Coast Plutonic Complex. The data were gridded at a 2-km interval, and the reduction was Bouguer on land and free-air offshore. The results are shown in Figure 2f (in pocket). Side-lit images were generated but proved unsuccessful at revealing new linear-anomaly patterns. The data were upward continued to 5 km (Fig. 2g) and 20 km (Fig. 2h) to investigate large-scale structure.

## Interpretation

Much of the early gravity work in the study area was carried out by Stacey and Stephens (1969) and Stacey (1975), who examined the character of the gravity field along the west coast of Canada. Stacey and Stephens (1969) noted that the large positive anomalies, such as the one over Queen Charlotte Islands, were associated with uplifted parts of the Insular Belt. The positive-gravity zone is missing over the mouth of Queen Charlotte Sound, as illustrated in the low-level data in Figure 2f, but reappears farther south. Stacey and Stephens (1969) noted this gap and associated it with a discontinuity in the uplifted portion of the Insular Belt. The Queen Charlotte Fault is expressed as a gravity-gradient zone along the western edge of the map area.

The western boundary of Hecate Depression was shown by Stacey and Stephens (1969) as being locally coincident with the Sandspit Fault (Fig. 1). In this report, it was suggested that the magnetic lineament associated with this fault is relatively faint and discontinuous (Figs. 2a-c). However, the correlative gravity-gradient zone extends across much of the study area (Figs. 2f-h). Sweeney and Seemann (1991) have shown that this zone is likely produced by the Sandspit Fault. If this fault were associated with significant, recent strike-slip displacements, the supracrustal section would be disrupted. However, continuity of magnetic fabrics is observed on northern Graham Island (Figs. 2a-c). It is thus likely that the Sandspit Fault is part of a larger, north-northwest-trending fault system, which was designated by Sutherland Brown (1968) as the Sandspit fault system. Displacements across it are interpreted to have been largely dip-slip, accommodated differently by various elements of the system. On Queen Charlotte Islands, the lack of strike-slip displacements across the Sandspit Fault was also noted by Thompson (1988) on the basis of geologic field mapping.

North-northwest-trending linear anomalies occur throughout the map area. They are associated with known large-scale fault systems including the Queen Charlotte Fault. These trends appear also in Hecate Depression, especially in its northern part. Over northern Vancouver Island and southern Queen Charlotte Sound, several east-west-trending and west-northwest-trending anomalies are apparent. Stacey and Stephens (1969) and Stacey (1974) related the former to

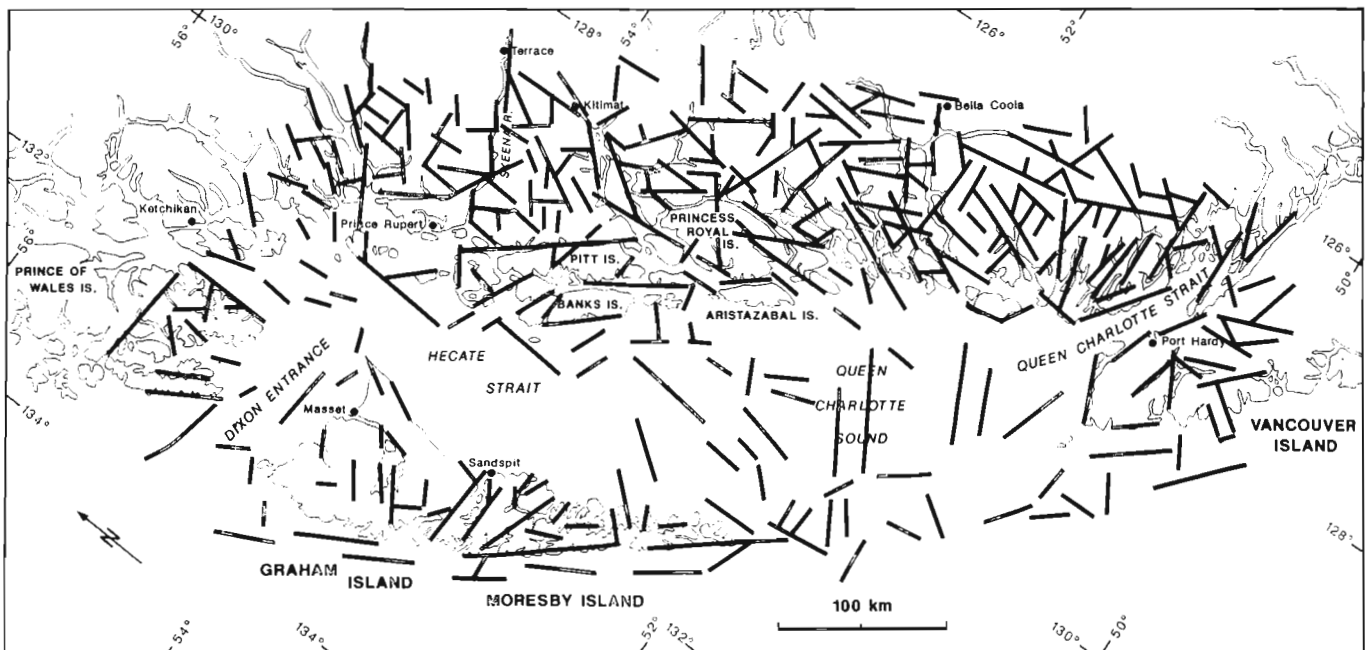


Figure 3: Major physiographic lineaments in the study area.



east-west physiographic lineaments on the mainland (see Fig. 3, latitude 51°N). The southern Queen Charlotte Sound gravity high is rectangular in shape, with a west-northwest elongation but an east-west-trending core.

Easterly trends occur throughout the study area but are more common in the south. Hecate Depression contains both north- and northeast-trending anomalies. Northerly trends are more prominent in the south and centre, and northeasterly trends in the north and centre of the depression, especially near Moresby Ridge and other ridges in the Queen Charlotte Basin. Thus, a north-south/east-west anomaly network dominates in Queen Charlotte Sound, and a northeast/northwest one is prominent in Hecate Strait. However, no sharp boundary between these two domains can be defined as a substantial overlap is observed.

Some gravity lineaments may be associated with the Principe Laredo fault system, but the Kitkatla system is expressed less clearly.

The upward-continued gravity data shown in Figures 2g and 2h were used to investigate large-scale structures in the study area. In Figure 2g, positive anomalies persist over Queen Charlotte Islands and southern Queen Charlotte Sound. The anomalies at the latter location have a westerly/west-northwesterly main trend. Over Hecate Depression, the gravity field is generally subdued. North-northwest-trending anomalies are faint but become stronger again over the mainland. The lineament associated with the Principe Laredo fault zone in Dixon Entrance persists. A few north- and northeast-trending anomalies also remain in Figure 2g, but they are weakened substantially.

The gravity field upward continued to 20 km (Fig. 2h) is dominated by regional north-northwesterly trends. A positive-anomaly belt is maintained over Queen Charlotte Islands, and it extends across Dixon Entrance. This could be a result of the large size of the causative uplifted block, which is bounded by the Queen Charlotte Fault on the west and by the Sandspit fault system on the east. However, the anomaly is fragmented, and individual highs do not always coincide with the magnetic highs in Figure 2e. North-northwesterly gravity trends are also strong over the Coast Mountains, where anomalies are negative (Fig. 2h) due to thicker crust (Stacey and Stephens, 1969). The positive anomaly over northern Vancouver Island and southern Queen Charlotte Sound maintains a west-northwesterly orientation; east-west trends are no longer apparent. The existence of an uplifted block in that area is confirmed by interpretation of reflection seismic data (J.R. Dietrich, pers. comm., 1989). A north-south trend can be seen along 130°W, and hints of northeasterly orientations occur at 52°N, 53°N and 54°N. However, these anomalies are too small to be interpretable unambiguously.

The gravity-field pattern discussed shows correlations with large uplifted blocks in the Insular Belt. Such blocks may produce shallow density contrasts, but even a relatively shallow feature exceeding in size the entire Queen Charlotte Islands may cause a gravity anomaly which is not removed by upward continuation. Thus, large gravity highs in Figure 2h likely correspond to uplifted blocks. Admittedly, such an interpretation is complicated north of Queen Charlotte Islands, where the correlation between the positive-gravity belt and the uplifted land areas is lost, but geologic structure imaged in reflection seismic data in Dixon Entrance (Snively et al., 1980) may explain the northward continuation of the gravity high.

## GEOLOGIC TRENDS

### Vancouver Island

Vancouver Island contains a northwest-trending core of the Paleozoic Sicker Group (Muller, 1977, 1980). According to Sutherland Brown (1966), fold axes in the Sicker Group are more northerly than those in younger rocks and were formed earlier than large, northwest-

trending open folds in Mesozoic rocks. Muller et al. (1981) reported north-striking faults that cut rocks as young as Early Jurassic, suggesting that the north-trending structures were reactivated in post-Early Jurassic time.

Muller et al. (1974) showed that both north- and northwest-striking faults affected Cretaceous rocks on Vancouver Island. Northeastern faults cut Eocene and younger rocks. North-northwesterly and east-northeasterly faults also cut elements of the Upper Triassic Karmutsen Formation, but the age of initiation of these structures is unknown.

Jeletzky (1976) proposed that a west-northwesterly trend controlled the distribution of Late Triassic to Middle Jurassic sedimentary facies on northern Vancouver Island. This trend may be a product of a latest Triassic deformation pulse. Throughout the Cretaceous, the northeasterly trend may have been prominent in the form of the Brooks Peninsula uplift, although the exact orientation and shape of this feature are ambiguous.

### Queen Charlotte Islands

Sutherland Brown (1966, 1968) noted, in addition to the regional, north-northwesterly orientation, three others: northerly, northeasterly and easterly, but did not provide well-constrained ages for these trends.

Souther (1989) and Souther and Jessop (1991) undertook a detailed study of age, orientation and distribution of dykes on Queen Charlotte Islands, many of which are concentrated in distinct swarms separated by areas with randomly oriented dykes. A number of north-trending swarms were defined on southern Moresby Island. To the north, other swarms were encountered, their orientations varying between east-northeasterly and north-northeasterly. The age of most dykes is Middle Eocene to Early Miocene. Souther (1989) associated ordered dyke swarms with crustal weakness zones separating relatively rigid blocks, but no independent confirmation of this hypothesis has so far been obtained from field mapping in the area.

Structures with a northeasterly orientation are common on Graham Island (Sutherland Brown, 1968), but the timing of their origin is not known regionally. On northwestern Graham Island, small faults with a N60°E strike may have been active in the Late Triassic or Early Jurassic, as a part of a larger structural pattern (Lewis and Ross, 1989). However, the small scale of these structures complicates correlations with regional fabrics. In central Graham Island, similar trends were encountered by Hesthammer (1990) and Indrelid (1990). Northeast-trending structures in younger rocks (Sutherland Brown, 1968; Sutherland Brown et al., 1983) may be products of reactivation of older features.

Steep, north-striking faults are also known on Queen Charlotte Islands (Sutherland Brown, 1968). Hickson (1989) showed that, on Graham Island, such faults cut the Tertiary Masset Formation. On Moresby Island, however, north-striking faults reported by Taite (1990) may have been active in both Jurassic and Tertiary time. The early Middle Jurassic Rennell Sound fold belt has a west-northwesterly orientation, oblique to the general north-northwest trend of the Queen Charlotte Islands.

In Hecate Depression, some structural information is available from the interpretation of reflection seismic data (J.R. Dietrich, pers. comm., 1989). Although the elongation of the basin is north-northwest, some of the intrabasinal trends are northerly, north-northeasterly, northeasterly and easterly.

### British Columbia mainland

As in the Insular Belt, the dominant geologic trend in the Coast Plutonic Complex is north-northwest, but other trends are also present. Woodsworth et al. (1983) and Crawford et al. (1987) provided

a geologic summary of the Coast Plutonic Complex east of Hecate Strait. Rocks in southeast Alaska and islands east of Hecate Strait are generally considered to belong to the Alexander Terrane (Woodsworth and Orchard, 1985), and their relationship to Wrangellia is uncertain.

Of particular interest is the area of the Skeena River, where Roddick and Hutchison (1972) reported northeast-trending ductile structures in rocks they thought are late Paleozoic. More recent work (e.g. Crawford et al., 1987) has cast doubt on the age of the protolith of the Central Gneiss Complex, nonetheless, northeast-southwest-trending minor ductile structures are common in the core of the Coast Plutonic Complex between 53° and 55°N (e.g. Roddick, 1970; Hutchison, 1982; Woodsworth et al., 1985; Heah, 1990). Douglas (1986) suggested that the Skeena River structural feature may have influenced rock deformation in the Late Cretaceous. He speculated that structural variations possibly reflect heterogeneities caused in part by pre-existing fabrics, although Clague (1984) found no obvious structural control of the orientation of the Skeena valley.

The northeast-trending Skeena Arch in the Intermontane Belt, whose northern flank coincides roughly with the Skeena River lineament, was active throughout the Jurassic (Tipper and Richards, 1976; Tipper, 1984). In Middle and Late Jurassic time, the Skeena Arch was the shoreline along the southern margin of the Bowser Basin. This northeast-trending strandline probably continued westward into what is now the core of the Coast Plutonic Complex. Although the western extent of the Skeena Arch is uncertain (Tipper and Richards, 1976), it may have in some fashion controlled east-northeast-trending deformation in the Central Gneiss Complex (Hutchison, 1982). In Early to mid-Cretaceous time, the arch was inactive. The alignment between the Skeena Arch in the Intermontane Belt and the Skeena River lineament in the Coast Plutonic Complex may suggest an early geologic relationship between Wrangellia and Stikinia. In fact, Brew and Ford (1983) and van der Heyden (1989) proposed that the Coast Plutonic Complex was not formed by mid-Cretaceous superterrane collision as suggested by Monger et al. (1982), and that no crustal sutures are present there.

An east-northeasterly volcanic trend at about 52°N (the Anahim belt) was interpreted by Bevier et al. (1979) as a product of the passage of North America over a mantle hot spot, or as a rift zone. The hot-spot hypothesis is consistent with the general eastward-younging age of volcanic centres in the belt, but the same trend appears also in many other parts of the Coast Plutonic Complex.

Northeast-trending lamprophyre dykes of Miocene age were reported by Smith (1973) north of Prince Rupert, where their emplacement may have been controlled by older structure (Hutchison, 1982). Baer (1973) noted north-striking dykes of presumed Miocene to Pleistocene age between 52° and 53°N. Tertiary(?) dykes in the Prince Rupert area have northerly, northeasterly and easterly orientations (Hutchison, 1982). On Porcher Island, Woodsworth (1991) described northeast-trending basaltic dykes of Early Miocene age that crosscut all fabrics on the northwest-trending Kitkatla Fault.

## PHYSIOGRAPHIC LINEAMENTS

### Construction of map

Figure 3 shows some of the prominent physiographic lineaments in the study area. The data base consisted of topographic and bathymetric maps as well as airphotos, with scales varying from 1:2 000 000 to 1:50 000. Although correlation between physiography and geologic structure is commonly tenuous, it can be inferred with greater confidence where linear features are relatively long or persistent over a large area. The origin of relationships between topography and underlying structure was discussed by Press and Siever (1978) and Smythe et al. (1978). In southeast Alaska, examples of structural con-

trol on existing physiography were presented by Buddington and Chapin (1929). In Hecate Strait and Queen Charlotte Sound, recent sedimentary bedforms and glacial scouring of the seafloor (Barrie and Bornhold, 1989) are a complicating factor as they are probably unrelated to the underlying structure. However, the amplitude of such, recent physiographic features is often small on the submerged shelf and on the onshore plains, and the use of low-amplitude features was generally avoided in the construction of the map in Figure 3. In the Coast Mountains, Quaternary glaciation resulted largely in the sculpting of pre-existing topography (Baer, 1973; Clague, 1984) and thus had a limited influence on the distribution of major lineaments.

The map in Figure 3 is based on observation of linears in topography, seafloor morphology, rivers, lakes and coast lines. Initially, all suspect lineaments were expressed as straight lines on a base map. To emphasize large-scale, regional fabrics and to eliminate local effects, features having uncommon orientations were subsequently removed. Relatively long lineaments, or those which appeared to be widespread, were preserved. This amounted to manual filtering of the data on the basis of coherency and repeatability. Quantitative filtering was considered but rejected because even where digital computing is used, filtering parameters are still selected by the user, making human biases unavoidable.

### Description of data

Three paired sets of mutually perpendicular physiographic orientations can be seen in Figure 3:

- 1) northerly and easterly,
- 2) west-northwesterly and north-northeasterly, and
- 3) north-northwesterly and east-northeasterly to northeasterly.

North-northwesterly trends are common in most parts of the study area (Fig. 3). However, there are a number of other prominent orientations, including the regionally persistent northeasterly trend, which may correspond to geologic structures which predate the north-northwesterly fabric. Northeasterly trends are especially prominent south and east of Prince Rupert, where they are associated with the Skeena valley. Similar trends can also be found north of Prince Rupert and on northeastern and central Graham Island, as well as on the mainland between 52° and 53°N. Fraser glaciation lineations on northeastern Graham Island are oriented to the north and north-northwest (Sutherland Brown, 1968; Clague et al., 1982) and are too small to appear in Figure 3.

North-south physiographic trends are generally widespread, except on Queen Charlotte Islands. These trends are more apparent east of Prince Rupert, and they extend into Hecate Strait and Queen Charlotte Sound. East-west trends occur throughout the study area, but they are more prominent at about 51°N, where Stacey (1974) related them to fairly recent, localized tectonic activity. However, this interpretation is weakened by the wide regional distribution of east-west trends and by the probable old age of some of the causative structures. At 53°N, east-west lineaments appear on Queen Charlotte Islands and on the mainland.

A less common physiographic trend is west-northwest, particularly east and south of Prince Rupert. At the latter location, it is associated spatially with the Kitkatla Fault and with the northern segment of the Principe Laredo fault system (Fig. 1), whose southern part has a different, north-northwesterly orientation. The Kitkatla topographic lineament may continue across the Coast Mountains and merge with the Yalakom Fault, but the geologic causes of this configuration are unknown. A parallel trend occurs on Queen Charlotte Islands (Fig. 3), near the Rennell Sound fold belt. Another set of physiographic lineaments in the region has a north-northeasterly orientation, and these trends are the most apparent on the mainland.

## DISCUSSION

### Regional structural style

Correlation between gravity- and magnetic-field patterns (Figs. 2a-h) is predictably imperfect. The magnetic field is controlled largely by the distribution of magnetite and hence of igneous rocks at relatively shallow levels, whereas deep-seated rocks may be demagnetized by heating above their Curie temperature. Thus, magnetic data largely reflect structure in the supracrustal assemblage. In contrast, gravity data reflect the entire crustal section.

On the basis of geophysical data alone, it is impossible to interpret definitively the history of deformation across the Principe Laredo and Kitkatla fault systems. The Kitkatla Fault appears to be one of a series of large faults that, in the Cretaceous and Tertiary, accommodated differential vertical uplift of various blocks in western Coast Plutonic Complex (Hutchison, 1982; van der Heyden, 1989). Evidence for significant strike-slip displacements across the Kitkatla Fault is lacking. Based on interpretation of magnetic data, the Kitkatla and Principe Laredo faults appear to intersect and extend into Dixon Entrance.

Another important observation concerns the continuity and wide areal distribution of various geological, geophysical and physiographic lineaments. These fabrics are regionally penetrative, and their domains overlap considerably. Many of the causative geologic structures were likely emplaced in the Paleozoic and Mesozoic and repeatedly reactivated since.

Geologic mapping onshore (Thompson, 1988; Thompson and Thorkelson, 1989; Muller et al., 1974, 1981; Jeletzky, 1976; Baer, 1973; Hutchison, 1982) has so far revealed no evidence for the existence of faults accommodating considerable translational or rotational movements of large parts of the Canadian Insular Belt. Block faulting appears to be the dominant structural style on Queen Charlotte Islands and northern Vancouver Island, and it may be prominent on the mainland. Where strike-slip movements were documented by geologic mapping in western Coast Plutonic Complex (Baer, 1973; Hutchison, 1982), they were probably small and appear to have been both dextral and sinistral. Thus, if large horizontal tectonic displacements did occur in the study area, the accommodating faults must be located in Hecate Strait or Queen Charlotte Sound. However, the data discussed above provide no evidence to suppose that the general structural style in the marine parts of the Insular Belt is significantly different from the style observed onshore.

Continuity and overlap of crustal fabrics indicates that even the largest fault systems east of the Queen Charlotte Fault may not have considerable lateral displacements associated with them. No convincing evidence has been found to support major strike-slip movements across the other large faults surrounding Hecate Depression. This suggests that the depression was formed largely by vertical movements across the bounding fault systems, and the associated horizontal displacements were small. Thus, the wrench-faulting model of Young (1981) is not supported.

Significant horizontal rotations of large crustal blocks are also thought to be lacking. This contradicts the early conclusions reached by Hicken and Irving (1977) on the basis of paleomagnetic investigations on Queen Charlotte Islands, but their results were not confirmed in a subsequent paleomagnetic study (Wynne and Hamilton, 1989).

### Formation of the Queen Charlotte Basin

The data examined in this report are compatible with a regional fault-block structural pattern in the study area. The fault network was reactivated repeatedly. Cumulative lateral displacements across the whole area in the Mesozoic and Cenozoic were likely small. The horizontal crustal movements which may have accompanied the for-

mation of the Tertiary Queen Charlotte Basin (Yorath and Hyndman, 1983) are thus constrained. None of the structural or geophysical fabrics observed can be related unambiguously to Cenozoic rifting in the Queen Charlotte Sound or Hecate Strait. The results of this study also complicate any interpretation of the Queen Charlotte Basin as a pull-apart tectonic feature bounded by master faults.

A decision between conflicting models of basin formation cannot, of course, be made solely on the basis of the geophysical information presented. With sufficient imagination, many hypotheses can be reconciled with the observed potential-field data. However, my structural model has a significant advantage of avoiding conflict with the current understanding of geology onshore while meeting the geophysical constraints.

### Tectonic style in the Canadian Insular Belt

The lack of compelling evidence for large horizontal crustal movements calls for a new interpretation of the tectonic style that dominated in this part of the Insular Belt in the Mesozoic and Cenozoic. The model proposed below is an attempt to account for the fault-block structure in the study area.

Jeletzky (1976) suggested that the fault-block structural pattern on northern Vancouver Island is caused by the presence of a rigid shield of Upper Triassic Karmutsen volcanics underneath the younger section, which provided control on deformation. I speculate that the actual basement core of the Insular Belt in Canada is substantially deeper and older.

A large orogenic belt, the Coast Plutonic Complex, is located to the east of the study area. Haines et al. (1971) noted that the Insular Belt has a subdued magnetic field compared to that in the Coast Mountains. Coles and Currie (1977, p. 1768) explained this by suggesting that "the deep crust in Vancouver Island is much less magnetic than in the western Coast Plutonic Complex, perhaps due to compositional differences". The relatively quiet magnetic field over the Canadian Insular Belt, both onshore and offshore, is also consistent with a comparatively low degree of structural deformation of rocks. Marine sediment deposition continued on present-day Queen Charlotte Islands until at least the Late Santonian (Haggart and Higgs, 1989; Haggart, 1991), long after the initiation of orogeny in the Coast Plutonic Complex. If the Cretaceous orogeny were not related to superterrane accretion, as was suggested by Brew and Ford (1983) and van der Heyden (1989), a sharp contrast in tectonic styles existed in the Late Cretaceous between adjacent areas of the Insular Belt and the Coast Plutonic Complex. The numerous orogenies in southeast Alaska (Brew et al., 1966) also seem to have left the Canadian portion of the Insular Belt relatively undisturbed.

In general, it appears that the Insular Belt in the study area behaved as a single, stable, massif-type crustal block at least in the Cretaceous and Tertiary. This block felt distal effects of various orogenies but was not involved in them directly; many of the crustal movements in the Canadian Insular Belt were likely epeirogenic (the terms "massif" and "epeirogeny" are used as defined by King, 1969). During quiescent periods, sediments were deposited and basins were formed. Such a geologic history is compatible with the rigid-shield hypothesis.

The nature of the basement shield is not known. The volcanic Karmutsen Formation is widespread and is thought to underlie all or most of the study area. However, its original thickness may vary from one part of the area to another (Muller et al., 1974, 1981), and its regional metamorphism, where it is observed at all, appears to be only slight. It is unlikely, therefore, that the Karmutsen Formation by itself was strong enough to act as a structural basement except locally.

The underlying Sicker Group contains both volcanic and sedimentary units. Its lower levels are regionally metamorphosed to a low grade, whereas the upper levels are commonly unmetamorphosed (Muller et al., 1974, 1981). The areal extent of the Sicker Group is uncertain. Thus, these rocks are also unlikely to have played the role of a rigid shield. The base of the Sicker Group is not known (Muller, 1977, 1980), and the oldest reliable dates are Late Devonian (C.J. Yorath, pers. comm., 1990).

This leads to the hypothesis that the Insular Belt in the study area may contain an unexposed, rigid, crystalline core that predates most of the middle to late Paleozoic Sicker Group, although it might have been strengthened in Middle Jurassic time (Jeletzky, 1976). These rocks could form the true basement of the Insular Belt in Canada; unqualified application of the term "basement" to other geologic units is misleading and should be avoided.

The existence of a crystalline crustal complex in the core of the Insular Belt is consistent with the seismic refraction data studied by Clowes and Gens-Lenartowicz (1985), Mackie et al. (1989) and Yuan et al. (1989). Muller (1977) proposed that parts of Vancouver Island may be underlain by crystalline rocks of Devonian(?) age. The nature of the basement in the Insular Belt could be investigated further by petrologic studies of xenoliths and composition of igneous rocks whose parent magmas may have passed through deep crustal levels. Contamination of Sicker and Karmutsen volcanics and other igneous rocks on Vancouver Island with continental-derived isotopes (Andrew and Godwin, 1989a,b,c) could be viewed in this light. The structural relationship of the "Wrangellia basement" to the Alexander Terrane could be studied by means of detailed analysis of geological and potential-field data over Dixon Entrance and adjacent land areas.

The relative tectonic stability of the Insular Belt in the past allows for better preservation of pre-Tertiary sedimentary basins and of any petroleum-source and -reservoir rocks contained within them.

## CONCLUSIONS

1. Several penetrative structural fabrics of pre-Cenozoic age are present in the crust of the Insular Belt. Areal domains occupied by these fabrics overlap greatly.
2. The Kitkatla, Principe Laredo and Sandspit faults are probably parts of regional, block-bounding fault systems which extend into Dixon Entrance.
3. A northeast-trending crustal structural feature (fault?) is suspected in southern Hecate Strait, and deep-seated plutons may be present in Queen Charlotte Sound.
4. No clear evidence for substantial horizontal displacements across any of the fault systems east of the Queen Charlotte Fault has been found.
5. Crustal extension that accompanied the formation of the Tertiary Queen Charlotte Basin was likely small, and none of the geological or geophysical-lineament fabrics can be correlated unambiguously with Cenozoic rifting. Epeirogenic crustal movements may have been partly responsible for the formation of Hecate Depression.
6. The overall structural style in the study area is the one of crustal-scale block faulting, possibly controlled by an ancient crystalline complex in the basement.
7. Regional structural constraints imposed herein may serve as a framework for interpretation of seismic data.
8. Integrated studies of geological- and geophysical-lineament fabrics can be used to test various Cordilleran "suspect terranes" for allochthoneity with respect to each other and to North America.

## ACKNOWLEDGMENTS

The author is grateful to Glenn Woodsworth (GSC, Vancouver), Roy Hyndman (GSC, Sidney), Ralph Currie (GSC, Sidney) and George Spence (University of Victoria), whose comments on early versions of this paper helped improve its quality considerably. Jim Dietrich (GSC, Calgary) kindly granted me access to his unpublished structural map of the Queen Charlotte Basin based on his interpretation of reflection seismic data offshore. Dave Seemann (GSC, Sidney) helped obtain the gravity data. Some of the airphotos used in this study were provided by Tark Hamilton (GSC, Sidney). Many useful discussions took place with Ralph Currie (GSC, Sidney), who also helped obtain the magnetic data. Special thanks go to Bob Thompson, Jim Haggart, Glenn Woodsworth, Cathie Hickson and Dirk Tempelman-Kluit (GSC, Vancouver) for their generous advice, encouragement and support.

The potential-field data were provided and their processing was carried out by the Geophysics Division of the GSC. The diagrams were prepared by Brian Sawyer (GSC, Sidney). This work constitutes a part of the author's doctoral-thesis research.

## REFERENCES

- Anderson, R.G. and Greig, C.J.  
**1989:** Jurassic and Tertiary plutonism in the Queen Charlotte Islands, British Columbia; in *Current Research, Part H*, Geological Survey of Canada, Paper 89-1H, p. 95-104.
- Andrew, A. and Godwin, C.I.  
**1989a:** Lead- and strontium-isotope geochemistry of Paleozoic Sicker Group and Jurassic Bonanza Group volcanic rocks and Island Intrusions, Vancouver Island, British Columbia; *Canadian Journal of Earth Sciences*, v. 26, p. 894-907.  
**1989b:** Lead- and strontium-isotope geochemistry of the Karmutsen Formation, Vancouver Island, British Columbia; *Canadian Journal of Earth Sciences*, v. 26, p. 908-919.  
**1989c:** Lead- and strontium-isotope geochemistry of the Tertiary Catface intrusions and related mineralization, Vancouver Island, British Columbia; *Canadian Journal of Earth Sciences*, v. 26, p. 920-926.
- Anfiloff, V.  
**1988:** Polycyclic rifting – an interpretation of gravity and magnetics in the North West Shelf; in *The North West Shelf, Australia*, P.G. and R.R. Purcell (ed.), *Proceedings of the North West Shelf Symposium*, Perth, Western Australia, p. 443-455.
- Baer, A.J.  
**1973:** Bella Coola – Laredo Sound map-areas, British Columbia; Geological Survey of Canada, Memoir 372, 122 p.
- Barrie, J.V. and Bornhold, B.D.  
**1989:** Surficial geology of Hecate Strait, British Columbia continental shelf; *Canadian Journal of Earth Sciences*, v. 26, p. 1241-1254.
- Bevier, M.L., Armstrong, R.L., and Souther, J.G.  
**1979:** Miocene peralkaline volcanism in west-central British Columbia – its temporal and plate-tectonics setting; *Geology*, v. 7, p. 389-392.
- Brew, D.A. and Ford, A.B.  
**1983:** Comment on "Tectonic accretion and the origin of the two major metamorphic and plutonic belts in the Canadian Cordillera"; *Geology*, v. 11, p. 427-428.
- Brew, D.A., Loney, R.A., and Muffler, L.J.P.  
**1966:** Tectonic history of Southeastern Alaska; in *Tectonic History and Mineral Deposits of the Western Cordillera*, Canadian Institute of Mining and Metallurgy, Special Volume No. 8, p. 149-170.
- Briusov, B.A.  
**1980:** Discrimination of anomalies by means of frequency selection; in *Magnitotrazvedka (Magnetic Exploration)*, V.E. Nikitinsky and Yu.S. Glebovsky (ed.), Nedra Publishers, p. 231-240 (in Russian).
- Broome, J., Simard, R., and Teskey, D.  
**1985:** Presentation of magnetic anomaly map data by stereo projection of magnetic shadowgrams; *Canadian Journal of Earth Sciences*, v. 22, p. 311-314.
- Buddington, A.F. and Chapin, T.  
**1929:** Geology and mineral deposits of southeastern Alaska; United States Geological Survey, Bulletin 800, 398 p.
- Cameron, B.E.B. and Hamilton, T.S.  
**1988:** Contributions to the stratigraphy and tectonics of the Queen Charlotte Basin, British Columbia; in *Current Research, Part E*, Geological Survey of Canada, Paper 88-1E, p. 221-227.
- Clague, J.J.  
**1984:** Quaternary geology and geomorphology, Smithers-Terrace-Prince Rupert area, British Columbia; Geological Survey of Canada, Memoir 413, 71 p.

- Clague, J.J., Mathewes, R.W., and Warner, B.G.  
1982: Late Quaternary geology of eastern Graham Island, Queen Charlotte Islands, British Columbia; *Canadian Journal of Earth Sciences*, v. 19, p. 1786-1795.
- Clowes, R.M. and Gens-Lenartowicz, E.  
1985: Upper crustal structure of southern Queen Charlotte Basin from sonobuoy refraction studies; *Canadian Journal of Earth Sciences*, v. 22, p. 1696-1710.
- Coles, R.L. and Currie, R.G.  
1977: Magnetic anomalies and rock magnetizations in the southern Coast Mountains, British Columbia: possible relation to subduction; *Canadian Journal of Earth Sciences*, v. 14, p. 1753-1770.
- Crawford, M.L., Hollister, L.S., and Woodsworth, G.J.  
1987: Crustal deformation and regional metamorphism across a terrane boundary, Coast Plutonic Complex, British Columbia; *Tectonics*, v. 6, p. 343-361.
- Douglas, B.J.  
1986: Deformation history of an outlier of metasedimentary rocks, Coast Plutonic Complex, British Columbia, Canada; *Canadian Journal of Earth Sciences*, v. 23, p. 813-826.
- Gehrels, G.E. and Saleeby, J.B.  
1987: Geology of southern Prince of Wales Island, Southeastern Alaska; *Geological Society of America Bulletin*, v. 98, p. 123-137.
- Haggart, J.W.  
1991: A synthesis of Cretaceous stratigraphy, Queen Charlotte Islands, British Columbia; in *Evolution and Hydrocarbon Potential of the Queen Charlotte Basin*, British Columbia, Geological Survey of Canada, Paper 90-10.
- Haggart, J.W. and Higgs, R.  
1989: A new Late Cretaceous mollusc fauna from the Queen Charlotte Islands, British Columbia; in *Current Research, Part H*, Geological Survey of Canada, Paper 89-1H, p. 59-64.
- Haines, G.V., Hannaford, W., and Riddihough, R.P.  
1971: Magnetic anomalies over British Columbia and the adjacent Pacific Ocean; *Canadian Journal of Earth Sciences*, v. 8, p. 387-391.
- Heah, T.S.T.  
1990: Eastern margin of the Central Gneiss Complex in the Shames River area, Terrace, British Columbia; in *Current Research, Part E*, Geological Survey of Canada, Paper 90-1E, p. 159-169.
- Hesthammer, J.  
1990: Structural interpretation of Upper Triassic and Jurassic units exposed on central Graham Island, Queen Charlotte Islands, British Columbia; in *Current Research, Part F*, Geological Survey of Canada, Paper 90-1F, p. 11-18.
- Hicken, A. and Irving, E.  
1977: Tectonic rotation in Western Canada; *Nature*, v. 268, p. 219-220.
- Hickson, C.J.  
1989: An update on structure and stratigraphy of the Masset Formation, Queen Charlotte Islands, British Columbia; in *Current Research, Part H*, Geological Survey of Canada, Paper 89-1H, p. 73-79.
- Holland, S.S.  
1964: Landforms of British Columbia -- a physiographic outline; British Columbia Department of Mines and Petroleum Resources, Bulletin 48, 138 p.
- Hutchison, W.W.  
1982: Geology of the Prince Rupert-Skeena map area, British Columbia; Geological Survey of Canada, Memoir 394, 116 p.
- Hyndman, R.D., Lewis, T.J., Wright, J.A., Burgess, M., Chapman, D.S., and Yamano, M.  
1982: Queen Charlotte fault zone: heat flow measurements; *Canadian Journal of Earth Sciences*, v. 19, p. 1657-1669.
- Indrelid, J.  
1990: Stratigraphy and structures of Cretaceous units, central Graham Island, Queen Charlotte Islands, British Columbia; in *Current Research, Part F*, Geological Survey of Canada, Paper 90-1F, p. 5-10.
- Jeletzky, J.A.  
1976: Mesozoic and Tertiary rocks of Quatsino Sound, Vancouver Island, British Columbia; Geological Survey of Canada, Bulletin 242, 243 p.
- King, P.B.  
1969: The tectonics of North America -- a discussion to accompany the Tectonic Map of North America, scale 1:5,000,000; United States Geological Survey, Professional Paper 628, 95 p.
- Lewis, P.D. and Ross, J.V.  
1989: Evidence for Late Triassic-Early Jurassic deformation in the Queen Charlotte Islands, British Columbia; in *Current Research, Part H*, Geological Survey of Canada, Paper 89-1H, p. 13-18.
- Mackie, D.J., Clowes, R.M., Dehler, S.A., Ellis, R.M., and Morel-à-Huissier, P.  
1989: The Queen Charlotte Islands refraction project. Part II. Structural model for transition from Pacific plate to North American plate; *Canadian Journal of Earth Sciences*, v. 26, p. 1713-1725.
- Maughan, E.K. and Perry, Jr., W.J.  
1986: Lineaments and their tectonic implications in the Rocky Mountains and adjacent Plains regions; in *Paleotectonics and Sedimentation in the Rocky Mountain Region*, J.A. Peterson (ed.), American Association of Petroleum Geologists, Memoir 41, p. 41-53.
- Monger, J.W.H., Price, R.A., and Tempelman-Kluit, D.J.  
1982: Tectonic accretion and the origin of the two major metamorphic and plutonic belts in the Canadian Cordillera; *Geology*, v. 10, p. 70-75.
- Muller, J.E.  
1977: Evolution of the Pacific margin, Vancouver Island, and adjacent regions; *Canadian Journal of Earth Sciences*, v. 14, p. 2062-2085.  
1980: The Paleozoic Sicker Group of Vancouver Island, British Columbia; Geological Survey of Canada, Paper 79-30, 23 p.
- Muller, J.E., Cameron, B.E.B., and Northcote, K.E.  
1981: Geology and mineral deposits of Nootka Sound map-area (92E) Vancouver Island, British Columbia; Geological Survey of Canada, Paper 80-16, 53 p.
- Muller, J.E., Northcote, K.E., and Carlisle, D.  
1974: Geology and mineral deposits of Alert-Cape Scott map-area (92L-102I) Vancouver Island, British Columbia; Geological Survey of Canada, Paper 74-8, 77 p.
- Murray, C.G., Scheibner, E., and Walker, R.N.  
1989: Regional geological interpretation of a digital coloured residual Bouguer gravity image of eastern Australia with a wavelength cut-off of 250 km; *Australian Journal of Earth Sciences*, v. 36, p. 423-449.
- Press, F. and Siever, R.  
1978: Earth; 2nd Edition, W.H. Freeman & Company, 649 p.
- Roddick, J.A.  
1970: Douglas Channel-Hecate Strait map-area, British Columbia; Geological Survey of Canada, Paper 70-41, 56 p.
- Roddick, J.A. and Hutchison, W.W.  
1972: Plutonic and associated rocks of the Coast Mountains of British Columbia; Twenty-Fourth International Geological Congress, Guidebook for Excursion AC04, 71 p.
- Rogers, G., Horner, B., and Weichert, D.  
1988: Lithospheric structure from earthquake depth, Queen Charlotte Islands, British Columbia; in *Current Research, Part E*, Geological Survey of Canada, Paper 88-1E, p. 289-290.
- Smith, J.G.  
1973: A Tertiary lamprophyre dike province in Southeastern Alaska; *Canadian Journal of Earth Sciences*, v. 10, p. 408-420.
- Smythe, J.M., Brown, C.G., Fors, E.H., and Lord, R.C.  
1978: Physical geography; MacMillan of Canada, 342 p.
- Snively, P.D., Tiffin, D.L., and Tompkins, D.H.  
1980: Seismic reflection profile across the Queen Charlotte fault zone, Dixon Entrance, Canada-U.S.; United States Geological Survey, Open-File Report 80-1063.
- Souther, J.G.  
1989: Dyke swarms in the Queen Charlotte Islands, British Columbia; in *Current Research, Part H*, Geological Survey of Canada, Paper 89-1H, p. 117-120.
- Souther, J.G. and Jessop, A.M.  
1991: Dyke swarms in the Queen Charlotte Islands, and implications for hydrocarbon exploration; in *Evolution and Hydrocarbon Potential of the Queen Charlotte Basin*, British Columbia, Geological Survey of Canada, Paper 90-10.
- Stacey, R.A.  
1974: Plate tectonics, volcanism and the lithosphere in British Columbia; *Nature*, v. 250, p. 133-134.  
1975: Structure of the Queen Charlotte Basin; in *Canada's Continental Margins and Offshore Petroleum Exploration*, C.J. Yorath, E.R. Parker and D.J. Glass (ed.), Canadian Society of Petroleum Geologists, Memoir 4, p. 723-741.
- Stacey, R.A. and Stephens, L.E.  
1969: An interpretation of gravity measurements on the West Coast of Canada; *Canadian Journal of Earth Sciences*, v. 6, p. 463-474.
- Sutherland Brown, A.  
1966: Tectonic history of the Insular Belt of British Columbia; in *Tectonic History and Mineral Deposits of the Western Cordillera*; Canadian Institute of Mining and Metallurgy, Special Volume No. 8, p. 83-100.  
1968: Geology of the Queen Charlotte Islands, British Columbia; British Columbia Department of Mines and Petroleum Resources, Bulletin 54, 226 p.
- Sutherland Brown, A., Yorath, C.J., and Tipper, H.W.  
1983: Geology and tectonic history of the Queen Charlotte Islands; Geological Association of Canada, Mineralogical Association of Canada, Canadian Geophysical Union, Joint Annual Meeting, Victoria, B.C., Field Trip 8, 21 p.
- Sweeney, J.F. and Seemann, D.A.  
1991: Crustal density structure, Queen Charlotte Islands and Hecate Strait, British Columbia; in *Evolution and Hydrocarbon Potential of the Queen Charlotte Basin*, British Columbia, Geological Survey of Canada, Paper 90-10.
- Taite, S.  
1990: Observations on structure and stratigraphy of the Sewell Inlet-Tasu Sound area, Queen Charlotte Islands, British Columbia; in *Current Research, Part F*, Geological Survey of Canada, Paper 90-1F, p. 19-22.



- Thompson, R.I.**  
**1988:** Late Triassic through Cretaceous geological evolution, Queen Charlotte Islands, British Columbia; *in* Current Research, Part E, Geological Survey of Canada, Paper 88-1E, p. 217-219.
- Thompson, R.I. and Thorkelson, D.**  
**1989:** Regional mapping update, central Queen Charlotte Islands, British Columbia; *in* Current Research, Part H, Geological Survey of Canada, Paper 89-1H, p. 7-11.
- Tipper, H.W.**  
**1984:** The allochthonous Jurassic-Lower Cretaceous terranes of the Canadian Cordillera and their relation to correlative strata of the North American craton; *in* Jurassic-Cretaceous Biochronology and Paleogeography of North America, G.E.G. Westermann (ed.), Geological Association of Canada, Special Paper 27, p. 113-120.
- Tipper, H.W. and Richards, T.A.**  
**1976:** Jurassic stratigraphy and history of north-central British Columbia; Geological Survey of Canada, Bulletin 270, 73 p.
- van der Heyden, P.**  
**1989:** U-Pb and K-Ar geochronometry of the Coast Plutonic Complex, 53°N to 54°N, British Columbia; Ph.D. thesis, Department of Geological Sciences, University of British Columbia, Vancouver, 253 p.
- Wellman, P.**  
**1985:** Block structure of continental crust derived from gravity and magnetic maps, with Australian examples; *in* The Utility of Regional Gravity and Magnetic Anomaly Maps, W.J. Hinze (ed.), Society of Exploration Geophysicists, p. 102-108.
- Woodsworth, G.J.**  
**1991:** Neogene to Recent volcanism along the east side of Hecate Strait, British Columbia; *in* Evolution and Hydrocarbon Potential of the Queen Charlotte Basin, British Columbia, Geological Survey of Canada, Paper 90-10.
- Woodsworth, G.J., Crawford, M.L., and Hollister, L.S.**  
**1983:** Metamorphism and structure of the Coast Plutonic Complex and adjacent belts, Prince Rupert and Terrace areas, British Columbia; Geological Association of Canada, Mineralogical Association of Canada, Canadian Geophysical Union, Joint Annual Meeting, Victoria, B.C., Field Trip No. 14, 62 p.
- Woodsworth, G.J. and Orchard, M.J.**  
**1985:** Upper Paleozoic to lower Mesozoic strata and their conodonts, western Coast Plutonic Complex, British Columbia; Canadian Journal of Earth Sciences, v. 22, p. 1329-1344.
- Woodsworth, G.J., van der Heyden, P., and Hill, M.L.**  
**1985:** Regional tectonic styles in the Coast Mountains between 52 and 55°N, B.C.; Geological Society of America, Abstracts with Programs, v. 17, p. 418 (abstr.).
- Wynne, P.J. and Hamilton, T.S.**  
**1989:** Polarity and inclination of magnetization of the Masset Formation from a deep drillhole on Graham Island, Queen Charlotte Islands, British Columbia; *in* Current Research, Part H, Geological Survey of Canada, Paper 89-1H, p. 81-86.
- Yorath, C.J. and Chase, R.L.**  
**1981:** Tectonic history of the Queen Charlotte Islands and adjacent areas – a model; Canadian Journal of Earth Sciences, v. 18, p. 1717-1739.
- Yorath, C.J. and Hyndman, R.D.**  
**1983:** Subsidence and thermal history of Queen Charlotte Basin; Canadian Journal of Earth Sciences, v. 20, p. 135-159.
- Young, I.F.**  
**1981:** Structure of the western margin of the Queen Charlotte Basin, British Columbia; M.Sc. thesis, Department of Geological Sciences, University of British Columbia, 380 p.
- Yuan, T., Spence, G.D., and Queen Charlotte Seismic Group.**  
**1989:** Interpretation of seismic refraction data in the Queen Charlotte Basin; EOS, Transactions of the American Geophysical Union, v. 70, p. 1204 (abstr.).



# Cenozoic relative plate motions along the northeastern Pacific margin and their association with Queen Charlotte area tectonics and volcanism

R.D. Hyndman<sup>1</sup> and T.S. Hamilton<sup>1</sup>

Hyndman, R.D. and Hamilton, T.S., Cenozoic relative plate motions along the northeastern Pacific margin and their association with Queen Charlotte area tectonics and volcanism; in *Evolution and Hydrocarbon Potential of the Queen Charlotte Basin, British Columbia*, Geological Survey of Canada, Paper 90-10, p. 107-126, 1991.

## Abstract

*The Cenozoic relative plate interactions along the Queen Charlotte margin, based on published models for the North America and northeast Pacific plates, are related to the tectonic and igneous history of the region. Plate motion models indicate convergence and subduction prior to the Eocene. We model subsequent transcurrent motion with varying amounts of oblique extension and compression, assuming that the Pacific-America-Farallon triple junction was south of the region. A Late Miocene or Early Pliocene (3.4-5.5 Ma) to present period of oblique convergence is clear. The present Queen Charlotte fault zone along the west coast of the islands may have been initiated more recently.*

*A number of tentative correlations are made between this plate interaction history and volcanism and tectonics in the Queen Charlotte area. The onset of Masset volcanism corresponds, within a few Ma, to the time of major plate reorganization at about 43 Ma that has tectonic expression around the entire Pacific basin. Within the Cenozoic transcurrent regime, times of extensive Masset volcanism and plutonism also may correlate with periods of oblique extension. Syntectonic deposition within an extensional regime in Queen Charlotte Basin appears to coincide with oblique extension between 36 and 20 Ma. Post-tectonic subsidence and deposition may correlate with the model time interval of general transcurrent or oblique convergence motion from 20-5 Ma. More recent compressive deformation seen in outcrop and seismic sections of the northern parts of the basin may reflect oblique convergence from 5 Ma to the present. This convergence is associated with underthrusting that formed an accretionary wedge along the west coast of the Queen Charlotte Islands and with inferred uplift and erosion of the western part of the islands.*

*We show that the geochemistry and physical volcanology of the Masset volcanics indicate an extensional regime. A variety of data have been used to estimate crustal extension ranging from about 10-40% in the Queen Charlotte Basin.*

*There appears to be a close analogy between the Queen Charlotte Basin and the Gulf of California extensional province, both in Late Tertiary plate margin interactions and in magmatic and tectonic expression. Tectonics of parts of the Pacific margin of North America where plate models have nearly orthogonal convergence through the Cenozoic are very different from those of the Queen Charlotte area.*

## Résumé

*Les interactions relatives des plaques le long de la marge de la Reine-Charlotte au Cénozoïque, suivant des modèles publiés pour les plaques nord-américaine et nord-est pacifique, sont alliées à l'histoire tectonique et magmatique de la région. Les modèles cinématiques indiquent une convergence et une subduction antérieures à l'Eocène. Le mouvement décrochant postérieur est modélisé en appliquant des quantités variables d'extension oblique et de compression, présumant que le point triple des plaques Pacifique-Américaine-Farallon se situait au sud de la région. Une période de convergence oblique depuis le Miocène supérieur ou le Pliocène inférieur (3.4-5.5 Ma) jusqu'à l'actuel est très probable. La zone de faille actuelle de la Reine-Charlotte le long de la côte occidentale de ces îles pourrait avoir été initialisée plus récemment.*

*De possibles corrélations sont faites entre l'histoire de ces mouvements de plaques et les manifestations volcaniques et tectoniques dans la région de la Reine-Charlotte. Le début du volcanisme de Masset correspond, à quelques Ma près, à une période de réorganisation majeure des plaques il y a environ 43 Ma, et qui s'est produit tout autour du bassin pacifique. Durant le régime décrochant cénozoïque, les périodes d'importants volcanisme et plutonisme de Masset pourraient correspondre aux périodes de distension oblique. La sédimentation syntectonique qui a accompagné le régime d'extension dans le bassin de la Reine-Charlotte semble coïncider avec une période d'extension oblique de 36 à 20 Ma. La subsidence et la sédimentation post-tectoniques peuvent être corrélées à la période de mouvement général décrochant ou convergent oblique du modèle, de 20 à 5 Ma. La déformation compressive plus récente observée dans les affleurements et profils sismiques des parties nord du bassin pourrait refléter la convergence oblique de 5 Ma jusqu'à l'actuel. Cette convergence est associée à des sous-charriages qui ont formé un prisme d'accrétion le long de la côte occidentale des îles de la Reine-Charlotte ainsi qu'au soulèvement et à l'érosion de la partie occidentale des îles.*

*Nous montrons ici que la géochimie et la pétrographie des roches volcaniques de Masset indiquent un régime d'extension. Les données disponibles nous ont permis d'estimer l'extension crustale de 10 à 40% dans le bassin de la Reine-Charlotte.*

*Une étroite analogie paraît exister entre le bassin de la Reine-Charlotte et la zone d'extension du Golfe de Californie, en ce qui concerne à la fois les mouvements aux marges des plaques au Néogène et l'activité magmatique et tectonique. La géodynamique des parties de la marge pacifique de l'Amérique du Nord pour lesquelles les modèles cinématiques indiquent une convergence presque orthogonale durant le Cénozoïque, est très différente de celle de la région de la Reine-Charlotte.*

<sup>1</sup> Pacific Geoscience Centre, Geological Survey of Canada, P.O. Box 6000, Sidney, B.C. V8L 4B2

## INTRODUCTION

The Tertiary Queen Charlotte Basin lies beneath the continental shelf and northeastern Queen Charlotte Islands of western Canada, and extends from Vancouver Island to Dixon Entrance (Fig. 1). This article reviews the data available on the Cenozoic history of relative motions between North America and the plates of the northeast Pacific as expressed across the Queen Charlotte margin, and associates the plate interactions with the tectonic and igneous history of the Queen Charlotte Basin, Queen Charlotte Islands and adjacent areas. Responses to changing plate regimes across the margin have been sought in volcanism, sedimentation, uplift and subsidence history, and styles of deformation. For example, prolonged convergence should result in arc volcanism, while oblique extensional or transcurrent regimes should result in extensional volcanism. A convergent regime should result in formation of a trench and an accretionary sedimentary wedge, in margin uplift, and in tectonic shortening through folding and thrusting. Extension should result in crustal thinning, normal faulting and basin subsidence. Convergence and extension are also expressed in characteristic heat flow and gravity patterns that persist for several tens of Ma after relative motion has changed or ceased. Some of the correlations are as yet very tentative; they will be improved as the recent work in the region is more completely analyzed and interpreted.

The absence of a spreading ridge between the Pacific and America plates through most of the Cenozoic requires an indirect solution to the problem of relative plate motions across the northeast Pacific margin. Also, most of the magnetic anomalies produced on one side of the northeast Pacific spreading ridges have been subducted and are not available for reconstruction. However, there has been intensive recent effort on this problem using both global plate circuits and the "fixed hot-spot" reference frame, and results are now available for the Cenozoic of sufficient accuracy to allow useful associations with margin tectonics.

The article finishes with a brief discussion of other areas of the North America margin where associations of plate regimes with

local tectonics and igneous activity have been made. While there is no exact analogue to the Queen Charlotte margin, useful insight is possible from the comparisons, particularly with the Gulf of California.

## MARGIN PLATE INTERACTIONS

### Relative plate motion models for the northeast Pacific margin

It was recognized in earlier northeast Pacific plate reconstructions that the complex pattern of offshore plates resulted in North America margin interactions that were highly variable in time and space, ranging from nearly orthogonal subduction to transcurrent motion (Atwater, 1970; Riddihough, 1982). In this article, we concentrate on the recent studies of northeast Pacific-North America plate interactions by Stock and Molnar (1988) and by Engebretson et al. (1984, 1985) (Fig. 2). The former authors employed global plate circuits to obtain the plate interactions across the western margin of North America. The results of Engebretson et al. (1984) are based on the assumption that the hot-spots in the Pacific and Atlantic regions have remained fixed with respect to one another. While the hot-spot reference frame is a robust control in that major errors are not expected, the probable small relative motions among the hot-spots limits the resolution. The global plate circuit approach allows greater resolution, but because of the large number of plate steps involved, it has a greater chance of large error, for

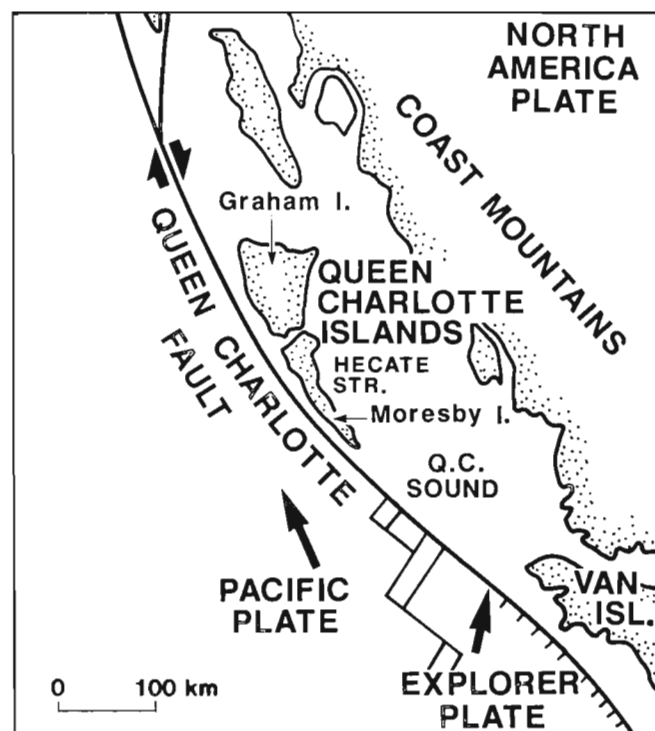


**Figure 1:** Location map showing the current plate tectonic regime in the Queen Charlotte area.

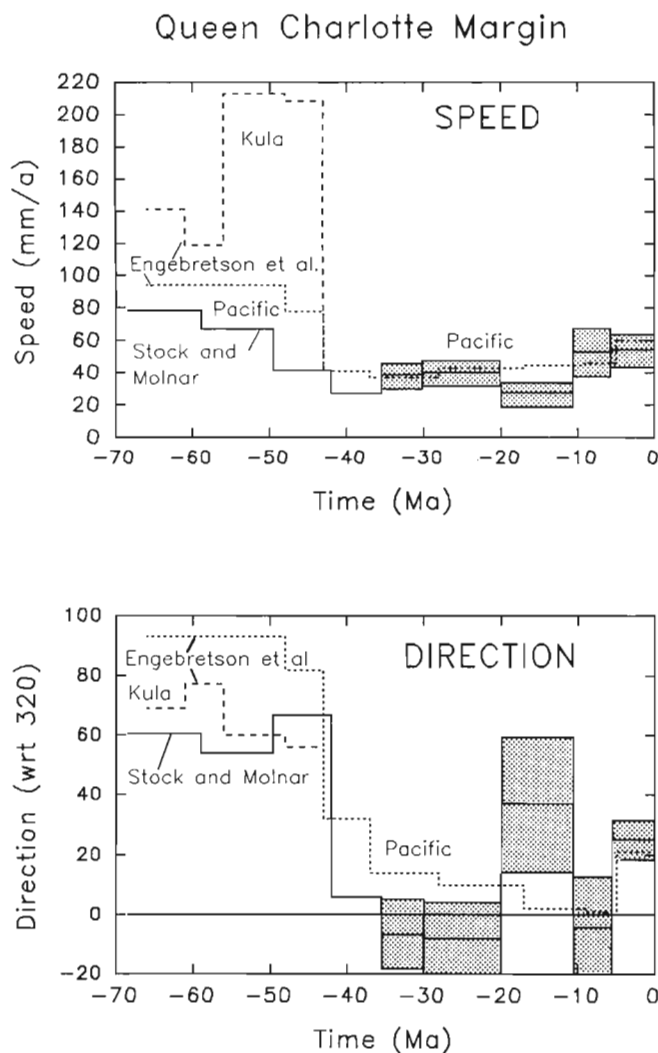


**Figure 2:** The model directions and speeds of relative plate motion across the Queen Charlotte margin through the Tertiary, assuming a plate boundary strike of 320° (after Stock and Molnar, 1988; and Engebretson et al., 1985). The error limits are estimates of 95% confidence.

example, from magnetic anomaly mis-identification or omission of short lived plate boundaries. As seen below, while the two approaches give different results in detail, the most important tectonic changes are well resolved and agree in both studies. Atwater (1989) provides a general review, and Engebretson (1989) and Kelley and Engebretson (1989) provide recent discussions. For the period prior to the Late Eocene, important constraints have also been provided by Lonsdale (1988); for example the conclusion that there was Kula-America plate interaction across the Queen Charlotte margin for some time prior to about 43 Ma. Yorath and Hyndman (1983), Cox and Engebretson (1985), Pollitz (1986) and Harbert and Cox (1989) discussed the Late Miocene to Pliocene (estimates range between about 3.6 and 5.5 Ma) change in absolute Pacific plate motion that resulted in increased Pacific-America convergence (also see DeMets et al., 1987 for recent Pacific-America relative motion). A secondary effect on margin tectonics may result from changes in absolute motion of North America. For example, Pollitz (1988) presented evidence for a change at about 9 Ma from a nearly westward motion to a more southwestward motion.

The plate interaction chronology used is based on the magnetic anomaly time scale; for the results used in this study, the DINAG scale of Berggren et al. (1985) or scales not greatly different have been used. It should be noted that the time intervals are chosen to correspond to the times of sea floor magnetic anomalies. Thus, the times of plate motion changes are only resolved to about  $\pm 3$  Ma, except the change to oblique convergence at about 5 Ma which is resolved to about  $\pm 1$  Ma.

An important uncertainty in modelling plate margin interactions is identification of which plate has been offshore from the Queen Charlotte Islands through the period of study. Earlier studies (e.g. Riddihough, 1982) allowed the possibility that the Farallon (Juan de Fuca) plate was offshore, which could give convergence such as inferred off Vancouver Island through much of the Cenozoic. However, in recent analyses (Atwater, 1989; Lonsdale, 1988; Stock and Molnar, 1988; Engebretson et al., 1985) it has been concluded that the Pacific plate probably has been offshore of the Queen Charlotte Islands since the major mid-Eocene (43 Ma) plate motion change, with the Pacific-Farallon-America triple junction located to the south of the Queen Charlotte Islands approximately at its present position. This position of the triple junction is well constrained for the past 10 Ma (e.g. Riddihough, 1984) and, based on the magnetic anomaly reconstructions presented by Stock and Molnar (1988), it almost certainly has been to the south of the Queen Charlotte Islands since about 20 Ma, and probably since 30 Ma. Reconstruction of the magnetic anomaly pattern gives a ridge trending northward towards northern Vancouver Island or southern Queen Charlotte Sound (Stock and Molnar, 1988). For the triple junction to have been north of the Islands, the offshore ridge system must have had a large northwestward transform offset which was subsequently subducted. Prior to 43 Ma, the Kula plate was probably offshore (e.g. Lonsdale, 1988) but the presence of the Pacific plate cannot be excluded. Fortunately, the resulting plate interactions are not fundamentally different; a strongly convergent regime is implied prior to 43 Ma with either plate offshore (Fig. 2).

The other important uncertainty that affects the estimated relative plate motions along the Queen Charlotte margin is the location and orientation of the plate boundary. Two processes could change the margin location and orientation: tectonic rotation and margin truncation. The Queen Charlotte Islands probably have been moved seaward as a consequence of Tertiary extension in Queen Charlotte Sound and Hecate Strait, and may have been rotated (Yorath and Chase, 1981). Wynne and Hamilton (1988) found a consistent clockwise rotation in a palaeomagnetic study of a number of suites of Masset rocks, but the result was not statistically significant at the 95% confidence level. Rotation

of small scale blocks may have occurred (Higgs, 1990, 1991). However, these data suggest that, if there has been large scale Tertiary rotation of the Queen Charlotte islands during or subsequent to Masset volcanism, the earlier margin was probably more east-west at an orientation such as to give a greater component of convergence.

If the margin of the Queen Charlotte Islands has been tectonically truncated, the earlier plate boundary may have had a different orientation. We have assumed that if there were terranes offshore, they were attached to the Pacific plate and that the plate boundary along the Queen Charlotte margin has had its present orientation through the Cenozoic. The margin's plate regime is particularly uncertain prior to the Eocene. For younger times, the Yakutat block now impinging on the southern Alaska margin (Plafker, 1989; Davis and Plafker, 1986) could have been off the Queen Charlotte Islands as recently as 20 Ma if it moved attached to the Pacific plate. In the analysis given here, it has been assumed that the orientation of the plate boundary at the margin has remained that of the Queen Charlotte Fault along the southern two thirds of the Queen Charlotte Islands, i.e.,  $320^\circ$ . If there was clockwise block rotation of the Queen Charlotte Islands such that the Early Tertiary margin trend was at say  $300^\circ$ , there would have been greater convergence; if the earlier trend was similar to that of the long nearly linear margin to the north, i.e., an azimuth of about  $340^\circ$ , there would have been greater oblique extension. Prior to about 55 Ma there were large strike-slip motions within the western Canadian Cordillera (summary in Irving and Thorkelson, 1990) that make relative motions in the region of the present margin difficult to determine from plate models.

#### Application to the Queen Charlotte margin

The relative plate motions from Engebretson et al. (1985) and Stock and Molnar (1988) are shown in Table 1, and Figures 2 and 3. They have been expressed as the component orthogonal to the Queen Charlotte margin (azimuth  $320^\circ$ ) at about  $52.5^\circ\text{N}$   $132^\circ\text{W}$  in Figure 4a. The relative motion vectors have been computed using the shortest great circle between two successive positions of a point on the seafloor just seaward of the Queen Charlotte Islands (starting at the

**TABLE 1. RELATIVE PLATE MOTION PARAMETERS USED IN THIS STUDY**

#### **Stock and Molnar, (1988), Pacific-America:**

Time Interval (Ma)	Distance (km)	Rate (km/Ma)	Direction (Deg. Azimuth)
68.5-58.9	744	78.1	20.5
58.9-49.6	633	67.4	14.0
49.6-42.0	313	41.5	26.6
42.0-35.6	176	27.3	325.9
35.6-30.0	216	38.6	313.0
30.0-25.8	169	40.2	311.9
25.8-19.9	238	40.3	311.9
19.9-10.6	256	27.5	357.1
10.6-5.5	270	53.0	315.6
5.5-0.0	300	54.5	345.2

#### **Engebretson et al. (1985):**

Pacific-America and Kula-America motions at "Queen Charlotte Islands" and "Juan de Fuca Strait" are given in their Table 5, p. 39.

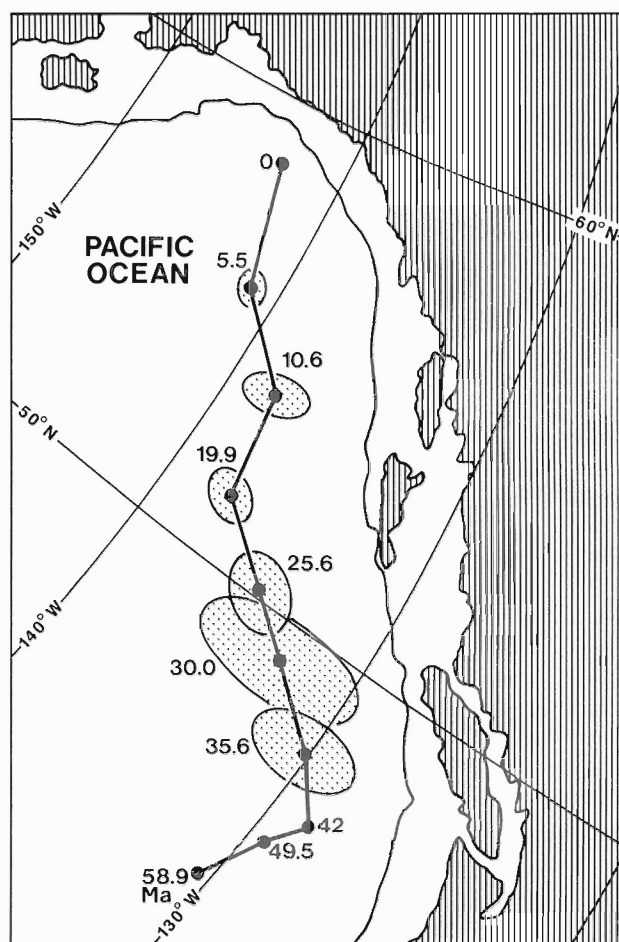


**Figure 3:** The progression of a point on the deep seafloor off the Queen Charlotte Islands as a function of time through the Tertiary (after Stock and Molnar, 1988). The ellipses are 95% confidence limits.

above position). This is an adequate approximation to the actual path of relative plate motion, since the poles of relative motion do not change rapidly and are distant from the study area. The changes in the orthogonal component of motion in Figure 4a are mainly a consequence of direction changes. Relative motion directions were approximately orthogonal to the margin prior to about 43 Ma (between 49 and 42 Ma), and approximately transcurrent after that time, although the relative rates have changed significantly through the Cenozoic. As discussed by Stock and Molnar (1988), the errors in the plate models are difficult to determine quantitatively. The 95% confidence error limits for the Stock and Molnar (1988) model are illustrated in Figures 2 and 3 (see also Atwater, 1989 and Kelley and Engebretson, 1989); they should be treated as qualitative estimates as discussed by Stock and Molnar (1988). Figure 4 gives the 95% and 67% (taken as 1/2 the 95%) confidence intervals for the orthogonal component of relative motion.

With these error estimates and the assumptions given above, three important features of the Queen Charlotte margin plate interaction are significant. First, there was fairly rapid convergence approximately orthogonal to the margin prior to the mid-Eocene (43 Ma) comparable to that elsewhere along the Pacific margin of North America. Second, from 43 Ma to the present, the regime has been primarily transcurrent, with small changes in plate directions resulting in either transpression or transtension (if the Farallon plate was offshore, there would have been convergence very similar to that shown below for the Cascadia margin). Third, at approximately 5 Ma, there was a small

but well resolved change in plate motion (significant at 95% confidence) that resulted in a component of compression across the Queen Charlotte margin that continues until the present. The components of extension and compression in the models between 43 and 5 Ma are not well resolved within the estimated errors, but the periods with greater oblique extension from about 36-20 Ma and oblique convergence from 20-10 Ma in the Stock and Molnar model may be important. The inferred oblique extension is not significantly different from zero at 95%, but is significant at 67% confidence.

The main differences between the two models is that Stock and Molnar (1988) argued that pre-Eocene Kula-America convergence rates were lower than those estimated by Engebretson et al. (1985), and that the change from a convergent to transcurrent regime was more gradual and perhaps somewhat earlier. There is a period of slightly oblique extension from 10-5.5 Ma in the model of Stock and Molnar (1988) that is not in the models of Engebretson et al. (1985) or Harbert and Cox (1989), but the model for this time interval has a large uncertainty so the result is not significantly different from zero.

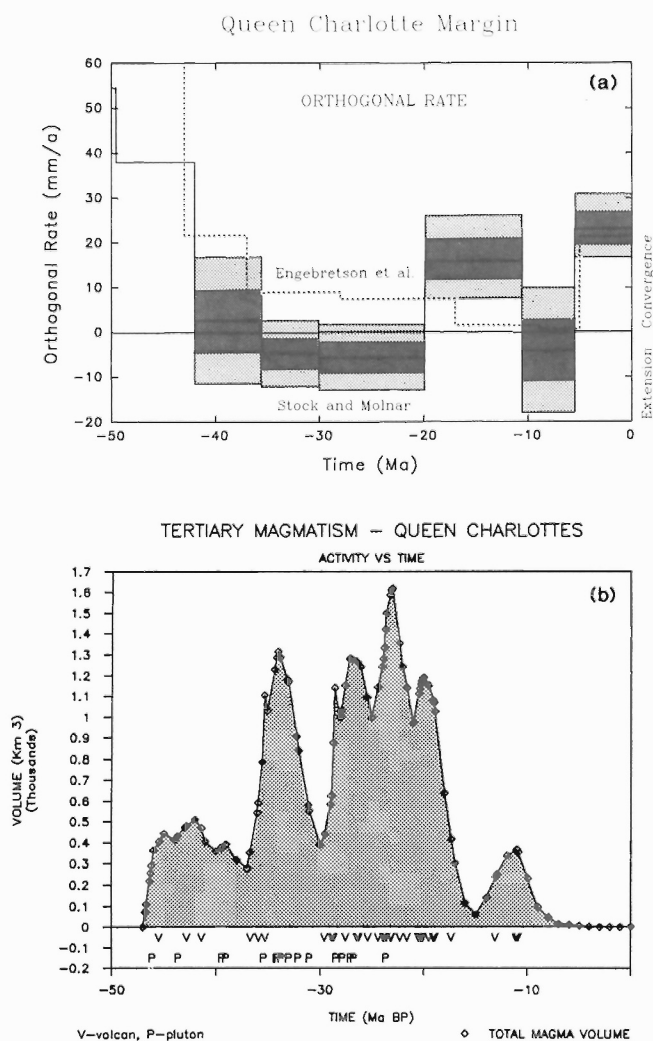


**Figure 4:** (a) Plate model components of orthogonal convergence across the Queen Charlotte margin through the Tertiary assuming a boundary strike of  $320^\circ$ . Uncertainty bounds are 67% and 95% confidence estimates. (b) Estimated volume of Tertiary igneous activity on the Queen Charlotte Islands as a function of age. "V" represents a volcanic date, "P" a pluton. Note the temporal correspondence between the time of inferred oblique extension and the main period of Masset volcanism.

The mid-Tertiary oblique extension period from 36-20 Ma in the Stock and Molnar model provides a rough estimate of 80 km of total extension (with an uncertainty of about  $\pm 60$  km at 67% confidence), that may have been expressed as extension in the Queen Charlotte Basin. This estimate assumes a  $320^\circ$  plate boundary. The motion for the period from 20-10 Ma has a large uncertainty but a total convergence of about 300 km is inferred. If the current azimuth of the Queen Charlotte margin is a recent development and the earlier transform trend was that of the margin to the north, i.e.,  $340^\circ$ , a much larger component of extension is inferred since the Eocene. The orthogonal component of motion given in Figure 4a offset by  $20 \text{ mm a}^{-1}$  gives an approximate estimate

of the motion for this latter plate boundary azimuth, i.e., a component of extension of about  $20 \text{ mm a}^{-1}$  for much of the middle Tertiary.

The change of Pacific – America motion to a more convergent direction across the Queen Charlotte margin in the Late Miocene to Early Pliocene is well resolved in all models, and the current motion clearly is oblique convergence (e.g. DeMets et al., 1987). The exact time of this change to oblique convergence is not well resolved; Cox and Engebretson (1985), Engebretson et al. (1985) and Stock and Molnar (1988) have suggested 5.5 Ma, but Harbert and Cox (1989) suggested between magnetic anomalies 2A and 3, i.e., between 3.4 and

**TABLE 2: COMPILATION OF ISOTOPIC AGES FOR TERTIARY VOLCANIC AND PLUTONIC ROCKS**

No.	SAMPLE	REF	ELEV	LONG	LAT	AGE	THICK	PRE?	POST?	METH	MAT	FORM	COMP	LOCALITY
1	TMV33(7/7-108)	1	2	132.368	54.108	$19.0 \pm 0.7$	1500	Y	Y	K/Ar	WR	LAVA	BASIC	WIAH POINT
2	BVI203	1	-44.2	132.702	53.935	$23.0 \pm 0.8$	1500	Y	Y	K/Ar	WR	LAVA	BASIC	NADEN WELL
3	BVI3684	1	-1105	132.702	53.935	$23.6 \pm 0.8$	1500	Y	Y	K/Ar	WR	LAVA	BASIC	NADEN WELL
4	6/8-70/2130	1	649	132.767	53.580	$11.0 \pm 0.7$	910	Y	Y	K/Ar	WR	LAVA	FELSIC	QC.RNG/SEAL IN.
5	6/29-163/225	1	69	132.697	53.643	$13.1 \pm 0.7$	400	Y	Y	K/Ar	WR	LAVA	FELSIC	DINAN CREEK
6	6/30-193/1815	1	553	132.515	53.718	$18.9 \pm 0.7$	550	N	Y	K/Ar	WR	DYKE	INTER.	MCKAY RANGE
7	6/4-18/44	1	13	132.722	53.443	$20.0 \pm 0.7$	910	Y	N	K/Ar	WR	LAVA	BASIC	TARTU POINT
8	TMV61.5	1	11	131.917	53.410	$20.4 \pm 0.7$	150	N	Y	K/Ar	WR	LAVA	BASIC	LAWN HILL
9	7/3-300/495	1	151	132.513	53.743	$22.3 \pm 0.8$	550	N	Y	K/Ar	WR	DYKE	FELSIC	IAN LAKE
10	7/11-342/1020	1	311	132.293	53.547	$23.9 \pm 0.8$	310	N	Y	K/Ar	WR	LAVA	FELSIC	FLORENCE CREEK
11	6/28-137/410	1	125	132.495	53.710	$24.4 \pm 0.8$	550	Y	Y	K/Ar	WR	LAVA	BASIC	MCKAY RANGE
12	6/29-161/790	1	241	132.687	53.638	$26.4 \pm 0.9$	400	Y	Y	K/Ar	WR	LAVA	BASIC	DINAN BAY
13	6/7-38/2310	1	704	132.202	52.827	$23.2 \pm 0.8$	760	Y	Y	K/Ar	MIN	LAVA	FELSIC	MT.RUSS
14	TMV21	1	116	132.162	52.805	$28.9 \pm 1.1$	760	Y	Y	K/Ar	WR	LAVA	BASIC	PORTLAND CK.
15	TMV50	1	3	131.350	52.553	$35.9 \pm 1.4$	1350	Y	Y	K/Ar	WR	LAVA	BASIC	RAMSAY ISLAND
16	TMV10	1	6	131.357	52.550	$41.1 \pm 1.4$	1350	Y	Y	K/Ar	WR	LAVA	BASIC	RAMSAY ISLAND
17	SD-261-63	2,3	0	131.995	52.676	$33.0 \pm 4.0$	1368	Y	N	K/Ar	MIN	PLUT	INTER.	MT.DE LA TOUCHE
18	CH-87-56-6	2	5	133.047	54.258	$26.8 \pm 0.4$	4407	N	N	U/Pb	MIN	PLUT	INTER.	LANGARA ISLAND
19	GS-50-66	2,3	0	132.981	54.250	$23.7 \pm 2.8$	4407	N	N	K/Ar	MIN	PLUT	INTER.	LANGARA ISLAND
20	CH-87-56-10	2	503	133.003	54.133	$27.9 \pm 0.4$	2763	N	N	U/Pb	MIN	PLUT	INTER.	PIVOT MOUNTAIN
21	CH-87-30-09	2	150	132.475	53.493	$27.0 \pm 0.3$	4000	N	N	U/Pb	MIN	PLUT	INTER.	SHEILA LAKE
22	AT-87-80-1	2	0	132.475	53.214	$32.2 \pm 0.7$	11987	N	N	U/Pb	MIN	PLUT	INTER.	KANO INLET
23	65 AB-21	2,3	0	132.433	53.283	$28.5 \pm 4.0$	11987	N	N	K/Ar	MIN	PLUT	INTER.	KANO INLET
24	65 AB-19	2,3	0	132.483	53.217	$31.0 \pm 3.0$	11987	N	N	K/Ar	MIN	PLUT	INTER.	KANO INLET
25	ATG-88-333-1	2	200	131.890	53.020	$34.3 \pm 0.4$	8795	Y	N	U/Pb	MIN	PLUT	INTER.	LOUISE ISLAND
26	ATG-88-260-1	2	150	131.830	52.870	$34.0 \pm 0.4$	8795	N	Y	U/Pb	MIN	PLUT	INTER.	LOUISE ISLAND
27	ATG-88-263-1	2	100	131.840	52.880	$33.8 \pm 0.4$	8795	Y	N	U/Pb	MIN	PLUT	INTER.	LOUISE ISLAND
28	ATG-88-288-1	2	0	131.530	52.600	$35.5 \pm 0.4$	4003	N	N	U/Pb	MIN	PLUT	INTER.	LYELL ISLAND
29	ATG-88-415-2	2	10	131.890	53.020	$39.0 \pm 0.3$	8911	N	N	U/Pb	MIN	PLUT	INTER.	POCKET INLET
30	65-AB-10	2	0	131.480	52.570	$39.5 \pm 2.0$	8911	N	N	K/Ar	MIN	PLUT	INTER.	POCKET INLET
31	AT-87-27-3	2	0	131.000	52.214	$46.2 \pm 0.5$	3715	N	N	U/Pb	MIN	PLUT	INTER.	CARPENTER BAY
32	AT-87-7-3	2	0	131.004	52.214	$43.7 \pm 1.1$	3715	N	Y	K/Ar	MIN	DYKE	INTER.	CARPENTER BAY
33	GS-54-66	3	0	132.238	54.070	$28.7 \pm 2.0$	500	Y	Y	K/Ar	WR	LAVA	BASIC	WESTACOTT POINT
34	GS-51-66	3	0	132.650	54.156	$23.8 \pm 1.3$	1600	Y	N	K/Ar	WR	LAVA	BASIC	SHAG POINT
35	SD-256-N63	3	0	132.239	54.059	$11.0 \pm 3.0$	400	Y	Y	K/Ar	WR	LAVA	BASIC	MASSET
36	MR8	3	0	131.004	53.214	$20.2 \pm 1.4$	150	N	N	K/Ar	WR	LAVA	BASIC	LAWN HILL
37	SD-544-N63	3	15	132.353	53.528	$20.4 \pm 4.0$	200	Y	Y	K/Ar	WR	LAVA	BASIC	MAMIN RIVER
38	MR9&2	3	100	132.333	53.510	$26.3 \pm 1.6$	200	Y	Y	K/Ar	WR	LAVA	BASIC	MAMIN RIVER
39	GS-39-66	3	0	132.988	53.700	$21.6 \pm 8.0$	750	Y	Y	K/Ar	WR	LAVA	BASIC	PORT LOUIS
40	GS-49-66	3	0	132.967	54.167	$45.5 \pm 6.0$	150	Y	N	K/Ar	WR	LAVA	BASIC	PARRY PASSAGE
41	SD-250-N63	3	0	131.637	53.113	$17.3 \pm 2.0$	50	N	N	K/Ar	WR	LAVA	BASIC	POINT GREY
42	SD-252-N63	3	5	131.388	52.690	$20.4 \pm 2.0$	650	N	Y	K/Ar	WR	LAVA	BASIC	GOGIT PASSAGE
43	SD-253-N63	3	2	131.413	52.673	$27.5 \pm 2.0$	650	Y	N	K/Ar	WR	LAVA	BASIC	GOGIT PASSAGE
44	4136D	3	-2152	129.347	51.602	$29.6 \pm 8.0$	3500	Y	Y	K/Ar	WR	LAVA	BASIC	OSPNEY WELL
45	4143	3	-3228	129.970	51.918	$42.8 \pm 4.0$	3500	N	Y	K/Ar	WR	LAVA	BASIC	HARLEQUIN WELL
46	4135J	3	-2370	130.609	52.338	$36.7 \pm 8.0$	3500	Y	Y	K/Ar	WR	LAVA	BASIC	AUKLET WELL
47	85V-12	4	0	130.500	53.850	$19.5 \pm 0.7$	50	N	Y	K/Ar	WR	DYKE	BASIC	PORCHER ISLAND
48	GW.AVG.	4	5	130.500	53.850	$25.4 \pm 0.9$	50	Y	N	K/Ar	WR	LAVA	BASIC	PORCHER ISLAND

Column labels are: Number of date or average (No.); original sample number (SAMPLE); source (REF); elevation in metres (ELEV); longitude (LONG); latitude (LAT); date or weighted average  $\pm$  standard deviation (AGE); estimated thickness in metres (THICK); indication of whether the rock rests on older Tertiary volcanic or plutonic rock (PRE?) or is cut or overlain by magmatic rock (POST?); dating method (METH) and material dated (MAT); and the sample geology (FORM), general composition (COMP), and LOCALITY.

Sources for dates:

1. Collected by T.S. Hamilton and analyzed at University of British Columbia (K. Scott and J. Harakal. See Table 3).
2. Dates reported in Anderson and Reichenbach (1990); some dates recalculated from Young (1981).
3. Dates compiled by Young (1981) from GSC and industry sources; recalculated using new decay constants.
4. Dates reported by van der Heyden (1989) and Woodsworth (1991).



3.9 Ma. We have used 5 Ma in the discussions below. The magnitude of the present convergence component resolved perpendicular to the margin is close to  $20 \text{ mm a}^{-1}$  in all of the models, with estimated errors (67% confidence) of less than about  $5 \text{ mm a}^{-1}$ .

The initial oblique convergence following the 5 Ma plate motion change was probably accommodated by oblique underthrusting. However, based on the development of the Dellwood and Tuzo Wilson spreading centres outlined by Riddihough et al. (1980) and Davis and Riddihough (1982), Yorath and Hyndman (1983) suggested that the modern Queen Charlotte fault zone formed in the Pacific plate between 0.5 and 1.0 Ma. In more recent work, Carbotte et al. (1989) have concluded that the inception of Dellwood spreading was between 1.8 and 2.5 Ma so the modern fault may have formed at that somewhat earlier time. In any case, this fault is thought to have cut off the underthrust lithosphere from the Pacific plate. Since that time, the continuing oblique convergence has been resolved into margin-parallel motion on the Queen Charlotte transform fault and approximately orthogonal underthrusting of a separate piece of lithosphere beneath the Queen Charlotte Islands.

## RELATION TO QUEEN CHARLOTTE TECTONICS

This section contains a discussion of associations between the geological record in the Queen Charlotte area and the plate interaction history of the margin. The main associations are with volcanism and inferred tectonics on the Queen Charlotte Islands, and with subsidence and deformation in the Queen Charlotte Basin. In addition to the continuing tectonic responses during intervals of different margin interaction, the transitions may be important, particularly the change from convergence to largely transcurrent motion at about 43 Ma. Such a transition may have resulted in a "slab window" if the portion of the Pacific plate already beneath the margin continued to sink, separating from the offshore part of the plate which then had begun to move parallel to the margin. When such separation occurs, hot asthenosphere must rise to fill the gap. Relaxation of compressive structures and re-establishment of isostatic equilibrium are also to be expected. Thorkelson and Taylor (1989) have discussed possible slab windows in this area.

### Plate models and Tertiary Masset volcanism and plutonism

Tertiary volcanics of the Masset formation cover large areas of the Queen Charlotte Islands from  $52\text{--}54^\circ\text{N}$ , particularly on northern Graham Island (Sutherland Brown, 1968). In this discussion we will include all Cenozoic volcanics of the region in the Masset Formation after the manner of Sutherland Brown (1968), Cameron and Hamilton (1988) and Hamilton and Cameron (1989). The composite Tertiary stratigraphic column in Cameron and Hamilton (1988) includes references to dated and analyzed samples in Tables 2 and 4 (e.g. Naden, Lawn Hill, Mt. Russ, and Ramsay Island). In places these volcanics are seen to underlie and to be interbedded with sediments of the Tertiary Skonun Formation. Tertiary volcanics penetrated by several wells in southern Hecate Strait and Queen Charlotte Sound may be their equivalents (Sutherland Brown, 1968; Shouldice, 1971; Hickson, 1989, 1991; Hamilton, 1989; Dostal and Hamilton, 1988). Woodsworth (1991) has described flows on the eastern margin of Hecate Strait that have similar ages and geochemistry to the largest pulse of Masset volcanism on the Queen Charlotte Islands. Thus, the inferred total width for Masset volcanism is about 150 km. There are numerous dyke swarms on the Queen Charlotte Islands associated with the Masset volcanics (Sutherland Brown, 1968; Souther, 1988; Souther and Jessop, 1991), and several small plutonic stocks with a similar or slightly older age range are aligned in a northwesterly direction through the Queen Charlotte Islands (Young, 1981; Anderson and Greig, 1989; Anderson and Reichenbach, 1991).

The Masset volcanics have a complex petrology and geochemistry and their origin is a subject of debate. The presence of calc-alkaline compositions may be taken to imply a volcanic arc origin. However, Hamilton (1989) and Hamilton and Dostal (1988) interpret the trace element signatures and physical volcanology to reflect volcanism through an extended continental margin. They conclude that the calc-alkaline derivatives reflect tholeiitic to calc-alkaline lines of descent, as has been observed in the Yellowknife volcanic series (Baragar, 1966) and crustal contamination. The geochemical arguments for an origin of the Masset volcanism in an extensional regime are given in a later section.

The preferred margin plate models discussed above, first, do not indicate an arc association for these Tertiary volcanics, since a largely transcurrent regime is indicated since about 43 Ma. However, as discussed above, convergence is possible if the Farallon plate rather than the Pacific plate was offshore, but this required a major offshore transform of the Pacific-Farallon ridge and a margin subduction zone to have existed, for which no evidence remains in the ocean basin. Second, if the volcanics are associated with an extensional regime, a correlation of greater volume of volcanism with periods having an extensional component of motion is to be expected.

### Tertiary magmatic volume versus time and location

Figures 4b and 5, and Tables 2 and 3 give age and volume relationships for Tertiary magmatism on the Queen Charlotte Islands based on available age data and a simple volume calculation as described below. The volume versus age curves offer a convenient visual comparison of magmatic activity with plate motion. The sample locations and ages, and the stratigraphic thickness estimates are given in Tables 2 and 3. The volume estimates are compared to the orthogonal component of relative plate motion from Stock and Molnar (1988) and Engebretson et al. (1985) in Figure 4b. The radioactive age data are from Anderson and Reichenbach (1991), Hickson (1988, 1991), Young (1981), and some unpublished data referred to in Cameron and Hamilton (1988) and Wynne and Hamilton (1989); ages have been

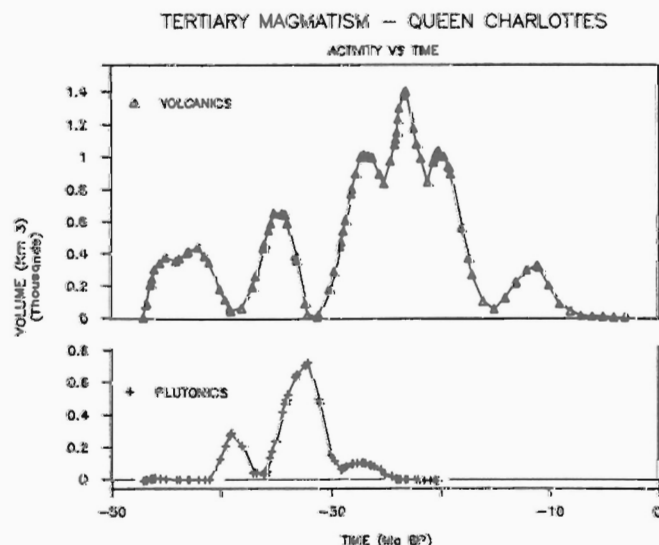


Figure 5: Estimated volumes of Tertiary volcanic and plutonic rocks on the Queen Charlotte Islands as a function of age. The total volume is  $17\,000 \text{ km}^3$  of volcanics and  $4000 \text{ km}^3$  of plutons.



recalculated using the latest decay constants where necessary (Steiger and Jager, 1977) (Table 2). The corrections for K-Ar dates from the middle Tertiary are about 2%.

Previous representation of magmatism versus time (Young, 1981; Yorath and Chase, 1981; Yorath and Hyndman, 1983; Hickson, 1988; Anderson and Reichenbach, 1989) were simple age histograms. In this study we have attempted semi-quantitative volume estimates, firstly dealing with multiple dates on the same stratigraphic section or pluton, and secondly trying to relate dates to specific volcanic volumes. For multiple dates on a volcanic section or pluton, averages have been formed with weighting inversely proportional to the analytical errors given. This heavily weights the higher precision U-Pb dates for the plutons. The volume estimate for each section or pluton was then apportioned over a time window assuming a normal distribution with width given by the date precision or standard deviation of multiple dates. Thus, points with well constrained dates are assigned to shorter time intervals than those with a larger uncertainty.

The thicknesses (and inferred volumes) represented by individual sections of volcanic stratigraphy and plutons (Table 3) have been estimated, based on field or other data. The volcanic thicknesses are minima since unknown amounts have been removed by erosion, and commonly the base is not exposed. For dates from wells where only the top of the volcanic interval was sampled, for example in Queen Charlotte Sound, very approximate thickness estimates have been obtained from seismic data (Rohr et al., 1989; Clowes and Gens-Lenartowicz, 1985). The approach used emphasizes the thicker sections, which in general are the best constrained (usually to about  $\pm 30\%$ ). Pluton thicknesses have been estimated assuming thickness equal to the square root of the surface area, i.e., based on the crude assumption that the bodies are approximately equidimensional and do not have deep roots. Most thicknesses are a few kilometres to a few tens of kilometres and are thought generally to be accurate to about  $\pm 50\%$ . There is a disproportionate amount of older plutonic and younger volcanic components represented because younger deep seated plutons will not yet have been exposed by erosion, and many older volcanics will have been eroded. The volume estimates might be improved by adding the eroded volcanic component now in the Queen Charlotte Basin and offshore sediments, and by gravity modelling of buried pluton components, but these have not been attempted. However, the total volumes including both volcanic and plutonic components as a function of time are thought to be reasonably well represented in the plots.

To obtain the total volumes as a function of time, the thickness contribution of each section or pluton was integrated, taking the simple assumption that each dated volcanic section or pluton represents the same surface area. Thus, the thickest sections contribute the most to the volume time curves. The smoothed thickness versus time curves were then scaled to represent a reasonable total volume of Tertiary magmatism for the Queen Charlotte region, estimated to be  $17\,000\text{ km}^3$ , i.e.  $370\text{ km}$  by  $185\text{ km}$  by an average thickness of  $250\text{ m}$ . It must be emphasized that this estimate of volume versus time has an uncertainty of perhaps a factor of 5-10, but it should be an improvement over simple date histograms. Over the time span of substantial volcanism, the estimated volumes represent a rate of about  $0.06\text{ km}^3$  (one or two lava flows) per 100 years. This rate is typical of within-plate volcanism in the Cordillera and elsewhere, and substantially less than for major hot-spot volcanic sources, for ridge volcanic production, or for the Cascade volcanic arc (e.g. Sherrod and Smith, 1989).

While correspondence between magmatism and modelled plate interactions may be accidental bearing in mind the uncertainties associated with the dates, with the magma volumes because of the non-uniform sampling and representation, and the uncertainties in the plate models, the agreement is surprisingly good. Substantial magma volume first

appears in the period 45-40 Ma, in agreement with the change from a convergent to a strike-slip margin regime. The largest peaks in the inferred igneous activity occur in the 36-20 Ma period, comprising widespread volcanism and intrusion of the Kano and Louise plutonic suites (Anderson and Reichenbach, 1989, 1991), corresponding well with the period of oblique extension in the Stock and Molnar (1988) model. The average of all dates weighted according to volume is  $28 \pm 9\text{ Ma}$ , i.e., 37-19 Ma which corresponds well to the model extension period. We note also that the termination of the major period of Masset volcanism ( $\sim 20\text{ Ma}$ ) could correspond to the truncation of the margin by the northward displacement of the Yakutat terrane.

The small peak in igneous activity near 12 Ma may be associated with the initiation of oblique extension modelled as starting at 10 Ma in the model of Stock and Molnar (1988) and with the youngest growth faulting (Rohr and Dietrich, 1990). The absence of Late Miocene to Recent volcanism corresponds to the 5 Ma to present period of oblique convergence in the plate models. There is inadequate resolution in the plate models to infer whether the generally transcurrent motion had a component of oblique extension or oblique compression at the time corresponding to the smaller pulse of Masset volcanism in the Eocene at the onset of Tertiary magmatism (Fig. 4b). However, even without an extensional component of plate motion, upwelling into a slab window and the crustal relaxation associated with a change from pronounced to convergence to generally transcurrent motion may have resulted in extensional processes.

There is no clear trend of location of volcanism with time, but Figure 6 shows that an important trend does exist in the plutonic rocks. There is a decrease in plutonic age northward as noted by Young (1981)

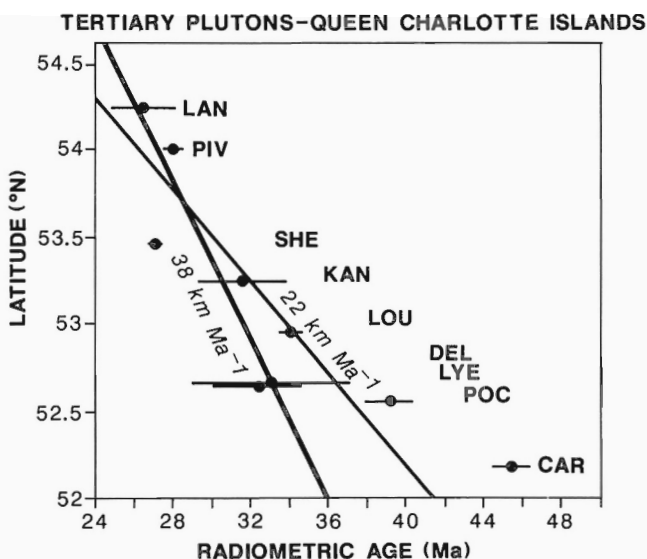


**Figure 6:** Age of Tertiary plutons as a function of position on the Queen Charlotte Islands, illustrating the decrease in age northward. The error bars are 2 sigma analytical uncertainty on single dates or date averages. The pluton identifications are as in Table 2: LAN – Langara Is. pluton; PIV – Pivot Mtn. stock; SHE – Sheila Lake stock; KAN – Kano batholith; LOU – Louise Is. batholith; DEL – Mt. de la Touche; LYE – Lyell pluton; POC – Pocket Inlet batholith; CAR – Carpenter Bay pluton. The fitted lines are referred to a margin plate boundary orientation of  $320^\circ$ . The  $22\text{ km Ma}^{-1}$  line is a fit to all of the data; the  $38\text{ km Ma}^{-1}$  line is a fit to the pluton data for the modelled extensional period, i.e. excluding CAR and POC.

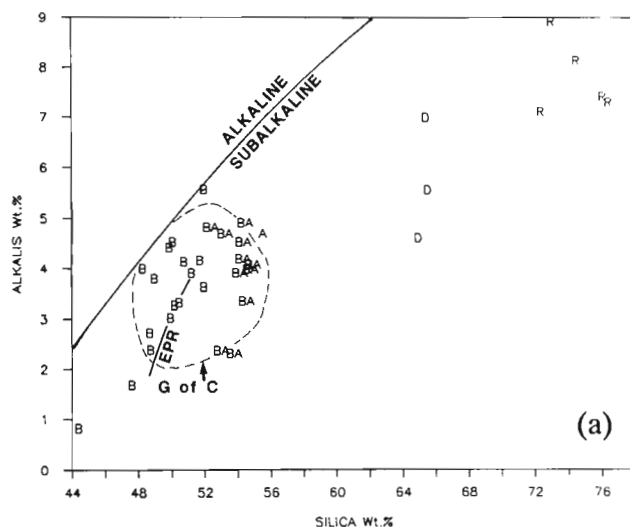
**Table 4: Major and trace element chemistry of the Masset Formation**

LOC.	Northern Graham Island												Central Graham Island												GOSPEL CK. ELLS PT.																																																																																																																																																																																																																																																																																																																																																																																																																																																																																																																																																																																																																																																																																																																																																																																																																																																																																																																																																																																																																																																																																																																																																																																																																																																																																																																																																																																																																																																																																																													
	TOW HILL						EDEN LAKE						BVI et al MADEN						TIAN						LAWN HILL						CINOLA						SEAL-TARTU RIDGE						CLONARD POINT						GOSPEL CK. ELLS PT.																																																																																																																																																																																																																																																																																																																																																																																																																																																																																																																																																																																																																																																																																																																																																																																																																																																																																																																																																																																																																																																																																																																																																																																																																																																																																																																																																																																																																																																																																					
	1	2	3	4	5	6	7	8	9	10	11	12	13	14	15	16	17	18	19	20	21	22	23	24	25	26	27	28	29	30	31	32	33	34	35	36	37	38	39	40	41	42	43	44	45	46	47	48	49	50	51	52	53	54	55	56	57	58	59	60	61	62	63	64	65	66	67	68	69	70	71	72	73	74	75	76	77	78	79	80	81	82	83	84	85	86	87	88	89	90	91	92	93	94	95	96	97	98	99	100	101	102	103	104	105	106	107	108	109	110	111	112	113	114	115	116	117	118	119	120	121	122	123	124	125	126	127	128	129	130	131	132	133	134	135	136	137	138	139	140	141	142	143	144	145	146	147	148	149	150	151	152	153	154	155	156	157	158	159	160	161	162	163	164	165	166	167	168	169	170	171	172	173	174	175	176	177	178	179	180	181	182	183	184	185	186	187	188	189	190	191	192	193	194	195	196	197	198	199	200	201	202	203	204	205	206	207	208	209	210	211	212	213	214	215	216	217	218	219	220	221	222	223	224	225	226	227	228	229	230	231	232	233	234	235	236	237	238	239	240	241	242	243	244	245	246	247	248	249	250	251	252	253	254	255	256	257	258	259	260	261	262	263	264	265	266	267	268	269	270	271	272	273	274	275	276	277	278	279	280	281	282	283	284	285	286	287	288	289	290	291	292	293	294	295	296	297	298	299	300	301	302	303	304	305	306	307	308	309	310	311	312	313	314	315	316	317	318	319	320	321	322	323	324	325	326	327	328	329	330	331	332	333	334	335	336	337	338	339	340	341	342	343	344	345	346	347	348	349	350	351	352	353	354	355	356	357	358	359	360	361	362	363	364	365	366	367	368	369	370	371	372	373	374	375	376	377	378	379	380	381	382	383	384	385	386	387	388	389	390	391	392	393	394	395	396	397	398	399	400	401	402	403	404	405	406	407	408	409	410	411	412	413	414	415	416	417	418	419	420	421	422	423	424	425	426	427	428	429	430	431	432	433	434	435	436	437	438	439	440	441	442	443	444	445	446	447	448	449	450	451	452	453	454	455	456	457	458	459	460	461	462	463	464	465	466	467	468	469	470	471	472	473	474	475	476	477	478	479	480	481	482	483	484	485	486	487	488	489	490	491	492	493	494	495	496	497	498	499	500	501	502	503	504	505	506	507	508	509	510	511	512	513	514	515	516	517	518	519	520	521	522	523	524	525	526	527	528	529	530	531	532	533	534	535	536	537	538	539	540	541	542	543	544	545	546	547	548	549	550	551	552	553	554	555	556	557	558	559	560	561	562	563	564	565	566	567	568	569	570	571	572	573	574	575	576	577	578	579	580	581	582	583	584	585	586	587	588	589	590	591	592	593	594	595	596	597	598	599	600	601	602	603	604	605	606	607	608	609	610	611	612	613	614	615	616	617	618	619	620	621	622	623	624	625	626	627	628	629	630	631	632	633	634	635	636	637	638	639	640	641	642	643	644	645	646	647	648	649	650	651	652	653	654	655	656	657	658	659	660	661	662	663	664	665	666	667	668	669	670	671	672	673	674	675	676	677	678	679	680	681	682	683	684	685	686	687	688	689	690	691	692	693	694	695	696	697	698	699	700	701	702	703	704	705	706	707	708	709	710	711	712	713	714	715	716	717	718	719	720	721	722	723	724	725	726	727	728	729	730	731	732	733	734	735	736	737	738	739	740	741	742	743	744	745	746	747	748	749	750	751	752	753	754	755	756	757	758	759	760	761	762	763	764	765	766	767	768	769	770	771	772	773	774	775	776	777	778	779	780	781	782	783	784	785	786	787	788	789	790	791	792	793	794	795	796	797	798	799	800	801	802	803	804	805	806	807	808	809	810	811	812	813	814	815	816	817	818	819	820	821	822	823	824	825	826	827	828	829	830	831	832	833	834	835	836	837	838	839	840	841	842	843	844	845	846	847	848	849	850	851	852	853	854	855	856	857	858	859	860	861	862	863	864	865	866	867	868	869	870	871	872	873	874	875	876	877	878	879	880	881	882	883	884	885	886	887	888	889	890	891	892	893	894	895	896	897	898	899	900	901	902	903	904	905	906	907	908	909	910	911	912	913	914	915	916	917	918	919	920	921	922	923	924	925	926	927	928	929	930	931	932	933	934	935	936	937	938	939	940	941	942	943	944	945	946	947	948	949	950	951	952	953	954	955	956	957	958	959	960	961	962	963	964	965	966	967	968	969	970	971	972	973	974	975	976	977	978	979	980	981	982	983	984	985	986	987	988	989	990	991	992	993	994	995	996	997	998	999	1000	1001	1002	1003	1004	1005	1006	1007	1008	1009	1010	1011	1012	1013	1014	1015	1016	1017	1018	1019	1020	1021	1022	1023	1024	1025	1026	1027	1028	1029	1030	1031	1032	1033	1034	1035	1036	1037	1038	1039	1040	1041	1042	1043	1044	1045	1046	1047	1048	1049	1050	1051	1052	1053	1054	1055	1056	1057	1058	1059	1060	1061	1062	1063	1064	1065	1066	1067	1068	1069	1070	1071	1072	1073	1074	1075	1076	1077	1078	1079	1080	1081	1082	1083	1084	1085	1086	1087	1088	1089	1090	1091	1092	1093	1094	1095	1096	1097	1098	1099	1100	1101	1102	1103	1104	1105	1106	1107	1108	1109	1110	1111	1112	1113	1114	1115	1116	1117	1118	1119	1120	1121	1122	1123	1124	1125	1126	1127	1128	1129	1130	1131	1132	1133	1134	1135	1136	1137	1138	1139	1140	1141	1142	1143	1144	1145	1146	1147	1148	1149	1150	1151	1152	1153	1154	1155	1156	1157	1158	1159	1160	1161	1162	1163	1164	1165	1166	1167	1168	1169	1170	1171	1172	1173	1174	1175	1176	1177	1178	1179	1180	1181	1182	1183	1184	1185	1186	1187	1188	1189	1190	1191	1192	1193	1194	1195	1196	1197	1198	1199	1200	1201	1202	1203	1204	1205	1206	1207	1208	1209	1210	1211	1212	1213	1214	1215	1216	1217	1218	1219	1220	1221	1222	1223	1224	1225	1226	1227	1228	1229	1230	1231	1232	1233	1234	1235	1236	1237	1238	1239	1240	1241	1242	1243	1244	1245	1246	1247	1248	1249	1250	1251	1252	1253	1254	1255	1256	1257	1258	1259	1260	1261	1262	1263	1264	1265	1266	1267	1268	1269	1270	1271	1272	1273	1274	1275	1276	1277	1278	1279	1280	1281	1282	1283	1284	1285	1286	1287	1288	1289	1290	1291	1292	1293	1294	1295	1296	1297	1298	1299	1300	1301	1302	1303	1304	1305	1306	1307	1308	1309	1310	1311	1312	1313	1314	1315	1316	1317	1318	1319	1320	1321	1322	1323	1324	1325	1326	1327	1328	1329	1330	1331	1332	1333	1334	1335	1336	1337	1338	1339	1340	1341	1342	1343	1344	1345	1346	1347	1348	1349	1350	1351	1352	1353	1354	1355	1356	1357	1358	1359	1360	1361	1362	1363	1364	1365	1366	1367	1368	1369	1370	1371	1372	1373	1374	1375	1376	1377	1378	1379	1380	1381	1382	1383	1384	1385	1386	1387	1388	1389	1390	1391	1392	1393	1394	1395	1396	1397	1398	1399	1400	1401	1402	1403	1404	1405	1406	1407	1408	1409	1410	1411	1412	1413	1414	1415	1416	1417	1418	1419	1420	1421	1422	1423	1424	1425	1426	1427	1428	1429	1430	1431	1432	1433	1434	1435	1436	1437	1438	1439	1440	1441	1442	1443	1444	1445	1446	1447	1448	1449	1450	1451	1452	1453	1454	1455	1456	1457	1458	1459	1460	1461	1462	1463	1464	1465	1466	1467	1468	1469	1470	1471	1472	1473	1474	1475	1476	1477	1478



and Anderson and Reichenbach (1989, 1991). Processes that could produce this trend are: (1) a northward migration of the change from convergent to transcurrent margin interaction. This change is not indicated in the plate models. (2) The migration of a triple junction northward along the margin. This mechanism also does not fit plate model data well. (3) The movement to the north of the Yakutat block or other offshore terrane from off the west coast of the Queen Charlotte Islands. This latter mechanism generally agrees with the time required for the block to reach its present position in collision with Alaska. Two lines are given in Figure 6. The first is an unweighted least squares fit to all of the data, giving an average rate along the margin of  $22 \text{ km Ma}^{-1}$ . The trend extrapolates to zero age at a point off the Alaska panhandle near latitude  $57.5^\circ\text{N}$ . The second line is the fit to the data during the modelled period of extension and the period of major volcanism, i.e., excluding the older POC and CAR plutons. The rate along the margin is  $38 \text{ km Ma}^{-1}$ , not significantly different from the average Pacific-America rate for this period of about  $40 \text{ km Ma}^{-1}$  (see Fig. 3). The extrapolation of this trend to zero age is near the location of the Yakutat block at about  $60^\circ\text{N}$ . Thus, the former transform margin may have been between the Queen Charlotte Islands and the Yakutat block riding on the Pacific plate with the Queen Charlotte plutonic activity being in some way related to the presence of the Yakutat block offshore.

**Figure 7:** Major element geochemistry for Masset volcanics. (a) Alkali elements versus silica, weight percent anhydrous. In this and subsequent petrochemical diagrams, points are labelled by rock type to coincide with Table 4: B – basalt; BA – basaltic andesite; A – andesite; D – dacite; R – rhyolite. The alkaline/subalkaline dividing line is from Irvine and Baragar (1971). The enclosed field in this and the following diagrams is for tholeiites and transitional basalts from the Gulf of California (Sawlan, 1990). The trend (EPR) for basalts drilled from the Guaymas Basin and the East Pacific Rise is also given, based on data in Batiza (1978), Batiza et al. (1979), Bender et al. (1984) and Saunders et al. (1982, 1983, 1987). (b) Silica versus the ratio of total iron oxide (as ferrous) to magnesia for basaltic lavas. The calc-alkaline – tholeiite discriminant line and the trends are from Miyashiro (1974) and Miyashiro and Shido (1975). (c)  $\text{FeO}^*$  versus  $\text{FeO}^*/\text{MgO}$  for basaltic lavas. The calc-alkaline – tholeiite discriminant line and the trends are from Miyashiro (1974).

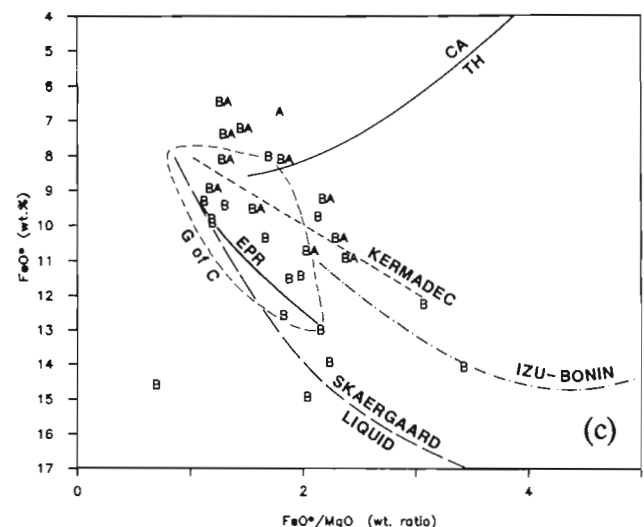
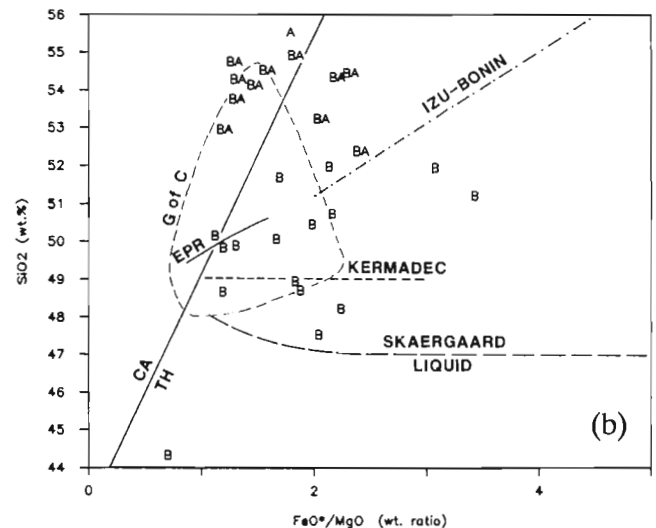


## Masset volcanism and crustal extension

Support for an origin of the Masset volcanics by progressive crustal extension is provided by a variety of physical volcanology and geochemistry data. These include the observation that large volcanic volumes accumulated in depressions rather than in stratacones, and that flows dominate over pyroclastics. An extensional environment is also suggested by several widespread sequences that culminate in thick dacite and rhyolite ignimbrites as at Mt. Russ and on western Graham Island, and by coeval dyke swarms of various orientations (Souther, 1988; Souther and Jessop, 1991).

If the Masset volcanism is arc in origin, the normal arc-trench gap of about 200 km (rarely outside 100-300 km) requires that the trench was located well seaward of the present margin. The only way that such a configuration could have existed is for the trench to have been seaward of the Yakutat terrane then located seaward of the Queen Charlotte Islands. The 150 km width of Tertiary volcanism is also unusually large for a volcanic arc.

The petrological and geochemical evidence includes the change from high to low pressure fractionates, and the increased melt fraction inferred from trace element inversion of cogenetic packages (Dostal and Hamilton, 1988). The most persistent and primitive lavas in the Masset volcanics are transitional tholeiites whose geochemistry resembles lavas of the adjacent Juan de Fuca ridge system (Cousens et al., 1984; Eaby and Clague, 1984) and continental tholeiites (Dupuy



and Dostal, 1984). A summary of major and trace element chemistry is given below.

It is useful to compare and contrast the Masset lavas to volcanics from a number of other areas; the three noted here are the Cascade arc, Mt. Edgecumbe and the Gulf of California. In contrast to the Cascades arc (Smith and Leeman, 1987), the Masset lavas of any composition (i.e.,  $\text{SiO}_2$  fraction) have higher trace element concentrations and flatter, more chondritic patterns (see below). From this data, it may be inferred that the Masset source is enriched, chondritic upper mantle without the meta-basalt (subducted, altered oceanic crust?) source component and its depleted signature characteristic of the Cascades arc. The Quaternary volcanism of Mt. Edgecumbe (Kosco, 1981) on Revillagigedo Island, approximately 250 km to the north of the Queen Charlotte Islands, is very similar to small centres within the Masset such as Lawn Hill. The similarity includes the combination of volcanic products and style of a small composite basaltic, tholeiitic and calc-alkaline, shield volcano. Mt. Edgecumbe is located just inboard of the Queen Charlotte fault zone, clearly in a transcurrent plate tectonic regime. A tholeiitic primary melt having some degree of within-plate crustal contamination is inferred for this volcano and for the

Masset volcanism. Sawlan (1990) provides a detailed discussion of the complex volcanic expression in the Gulf of California area where there was a Late Miocene change from subduction to transcurrent motion along the margin. As seen below, this volcanism has many similarities to the Masset, including emplacement of calc-alkaline lavas through an extended continental lithosphere.

Table 4 provides a selection of major and trace element chemistry analyses for Tertiary igneous rocks from the Queen Charlotte area. Analyses were selected to describe the variation of volcanic chemistry in space and time. The dominant lava types have been represented at each location and analyses from dated specimens or sections and correlative strata have been included where available (Table 2). The table is organized geographically and stratigraphically, rather than by rock type, to allow recognition of bimodal sections. A number of important discriminants are illustrated in Figures 7 and 8. The bimodal character of this suite is clearly evident in the alkali versus silica plot (Fig. 7a). All samples were fresh; the basaltic lavas were hypocrys- talline with some groundmass glass. Rhyolites and dacite analyses were limited to the interiors of glassy flows to avoid the alteration present in the devitrified and crystalline flows.

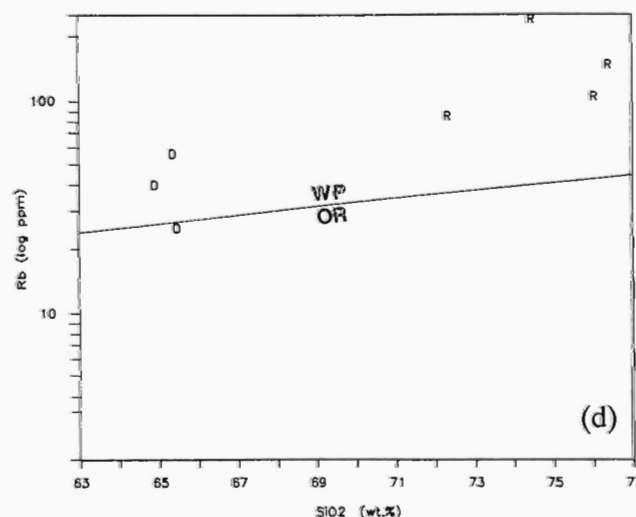
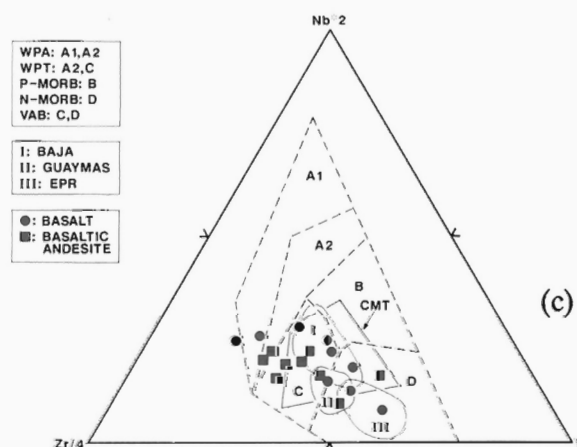
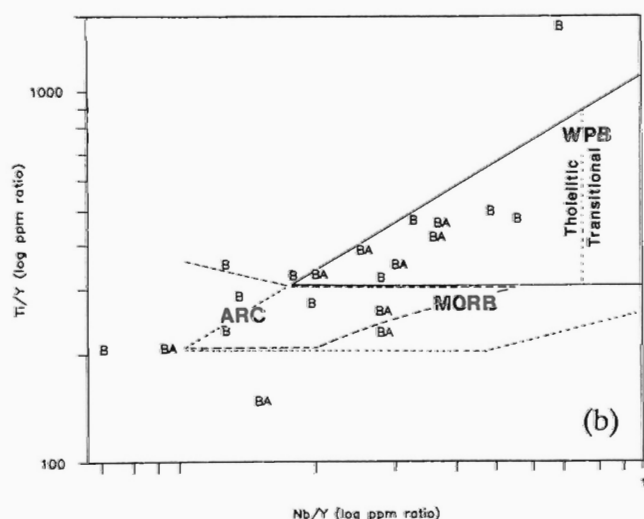
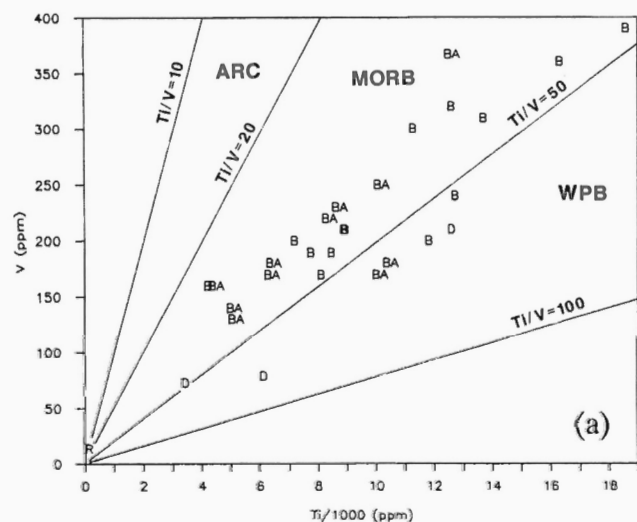


**Figure 8:** Trace element geochemistry for Masset volcanics. (a) V versus Ti plot, points labelled as in Figure 7. The V/Ti discriminants are from Shervais (1982). (b) Ti/Y versus Nb/Y weight ratio for Masset basaltic lavas. Discriminant fields are after Pearce (1983). (c) Zr/4 - Nb\*2 - Y trace element discriminant plot for Masset lavas. The fields are after Meschede (1986). (d) Rb versus  $\text{SiO}_2$  for Masset dacites and rhyolites. Rb and other LILE are enriched for Masset silic lavas like granites from within-plate settings. The discriminant boundary after Pearce et al. (1984); WP - within-plate; OR - orogenic settings.

The basaltic andesites are distinguished here from basalts, in the lack of modal olivine, in the higher contents of silica and in the incompatible elements. Porphyritic flows dominate with plagioclase and one or two pyroxene types, and with occasional amphibole and oxide primocrysts or xenocrysts. However, since these basaltic andesite analyses pass most of the basaltic compositional screens for discriminant diagrams, they are plotted along with the basalts. In the Western Woodlark Basin (Binns and Whitford, 1987; Johnson et al., 1987; Perfit et al., 1987), lavas similar to these form the spreading ridge.

Subalkaline basalts, the dominant lava type (Fig. 7a), are aphyric to sparsely porphyritic with textures ranging from glomeroporphyritic to ophitic and with phenocrysts of olivine, clinopyroxene, plagioclase and sometimes an oxide phase. Basalts occur alone, in bimodal association as at Eden Lake, and stratigraphically admixed with basaltic andesites to andesites as at Naden, Lawn Hill and Ramsay Island. Chemically the Masset basalts are tholeiites with affinities to ocean floor basalts, marginal basin basalts and continental margin tholeiites. As well as plotting within and adjacent to the fields of the Gulf of California and East Pacific Rise, the Masset basalts scatter about Miyashiro's general trend for abyssal tholeiites (i.e. EPR and Izu-Bonin on Figs. 7b and 7c). Based on their high Ni and Cr contents and low incompatible elements, these lavas are thought to be mantle derived and parental to the other lavas shown.

Collectively the basaltic lavas plot in the MORB (mid-ocean ridge basalts) and within-plate fields of most trace element discriminant diagrams (Fig. 8a,b,c); Ti/V is notably more enriched than in arcs (Fig. 8a). On Meschede's (1986) plot  $Zr/4 - Nb \cdot 2 - Y$  (Fig. 8c), the Masset basalts span the fields for N-MORB, within-plate tholeiites and within-plate alkali basalts; with chondritic values near  $Zr/Nb = 16$  like transitional MORBs (Erlank and Kable, 1976). To show the genetic comparison of the Masset to the Gulf of California area, the fields are shown in Figure 7c for Baja California, Guaymas basin and the East Pacific Rise tholeiites. The Masset basalts follow the trend for the Gulf

of California and extend to higher Zr values like alkaline lavas from within-plate settings. Also for comparison, the CMT field for Mesozoic rifted continental margin tholeiites (Meschede, 1986) encompasses most of the Masset basaltic lavas.

Rhyolites and dacites occur in sparsely porphyritic pitchstone flows with phenocrysts of: oxide, alkali feldspar and/or plagioclase (andesine to oligoclase), with occasional quartz, soda-iron pyroxene, amphibole, and biotite. The unusual trace element chemistry of the Ells Point sample resembles depleted rhyolites derived from MORB (Carmichael, 1964) and is expressed petrographically as an anomalous green Cr-rich biotite. The elevated levels of Rb (Fig. 8d) and rare earths (Hamilton and Dostal, unpub. data) compared to the trace element chemistry for granitic rocks of Pearce et al. (1984), suggest within-plate origin and preclude a volcanic arc origin. Overall, the trace element patterns for these evolved Masset lavas exhibit the same range of depletion to enrichment as the coeval basalts. The Zr/Nb ratios of the rhyolites and dacites range from chondritic to more enriched values comparable to ocean islands (Table 4 and Erlank and Kable, 1976). Note that there is little fractionation in Ti/V from basalt to rhyolite (Fig. 8a).

While flows from the same stratigraphic section may plot in different discriminant fields, the overall groupings are diagnostic. The conclusion from all of the discriminants discussed above is that the Tertiary basaltic lavas from the Queen Charlotte area reflect extension; they range from depleted oceanic tholeiites to variably enriched tholeiites characteristic of rifted continental margins and within-plate settings. The evolved dacites and rhyolites exhibit the same range of trace element variation as the basalts and are thought to be derived from them by extensive fractional crystallization.

In overview, the Tertiary Masset volcanism is subalkaline and silica saturated with abundant mantle derived basalts and both tholeiitic and calc-alkaline lines of descent commonly in a single succession. All lavas are Fe and Ti rich, representing either a source signa-

**Table 3:** K-Ar analytical data for Masset volcanic rocks of this study

Geographic Area	Material	Sample # Dated	Elev (m)	K %	% Ar40	1.00E-10	Date (Ma) mol/g $\pm$ 1 s.d.	Sample Description
<b>Northern Graham Island</b>								
1. N.CST. GRAHAM, W.WIAH PT.	WR	TMV33(7/7-108)	1.5	0.518 $\pm$ .002	41.0	1.712	19.0 $\pm$ 0.7	bas, dk grey, fine grn
2. BVI NADEN b-A27-J/103-F-15	WR	BVI203	-44.2	0.235 $\pm$ .001	42.4	0.941	23.0 $\pm$ 0.8	bas, black subophitic
3. BVI NADEN b-A27-J/103-F-15	WR	BVI3684	-1105.2	0.371 $\pm$ .004	66.8	1.531	23.6 $\pm$ 0.8	bas, grey, chl. veins
<b>Central Graham Island</b>								
4. QC RANGE, N. SEAL IN.	WR	6/18-70/2130	649	2.52 $\pm$ 0.01	21.5	4.84	11.0 $\pm$ 0.7	rhy, black pitchstone
5. S. SLOPE TO DINAN CK.	WR	6/29-163/225	69	1.54 $\pm$ 0.01	20.5	3.52	13.1 $\pm$ 0.7	rhy, grey porphyritic
6. SUMMIT, MCKAY RANGE	WR	6/30-193/1815	553	0.605 $\pm$ .001	27.4	1.994	18.9 $\pm$ 0.7	dacite, dk grey porph.
7. TARTU POINT	WR	6/4-18/44	13.4	1.38 $\pm$ .002	68.3	4.8	20.0 $\pm$ 0.7	oliv. basalt, black amygd.
8. LAWN HILL, E. CST. GRAHAM	WR	TMV61.5	11.1	0.291 $\pm$ .002	47.2	1.034	20.4 $\pm$ 0.7	oliv. basalt, black columnar
9. MCKAY RING. - IAN LK.	WR	7/3-300/495	151	3.25 $\pm$ 0.01	60.4	1.266	22.3 $\pm$ 0.8	rhy pitchst, b&w cryst
10. CINOLA/FLORENCE CREEK	WR	7/11-342/1020	311	2.17 $\pm$ 0.01	65.3	9.06	23.9 $\pm$ 0.8	dacite, black porphyritic
11. MCKAY RING. - MASSET IN.	WR	6/28-137/410	125	1.29 $\pm$ 0.01	85.2	5.49	24.4 $\pm$ 0.8	bas, black cpx-phyric
12. MTN. S. OF DINAN BAY	WR	6/29-161/790	241	0.74 $\pm$ .003	87.7	3.44	26.4 $\pm$ 0.9	oliv. basalt, subophitic
<b>Southern Moresby Island</b>								
13. SADDLE, MT. RUSS	FELDSPAR	6/7-38/2310	704	4.04 $\pm$ 0.04	80.3	16.33	23.2 $\pm$ 0.8	rhy, white silicified
14. E. OF PORTLAND BAY	WR	TMV21	116	0.184 $\pm$ .008	29.3	0.929	28.9 $\pm$ 1.1	bas, cut by rhy dyke
15. E. RAMSAY IS.	WR	TMV50	3.1	0.388 $\pm$ .003	38.1	2.439	35.9 $\pm$ 1.4	bas, lt grey 5m flow
16. S. RAMSAY IS.	WR	TMV10	6.1	0.504 $\pm$ .003	90.2	3.636	41.1 $\pm$ 1.4	bas, dk grey chlorite clots
<b>Notes:</b>								
1. Analyses performed at University of British Columbia Geochronometry Laboratory by J.E. Harakal and K. Scott								
2. Constants are those of Steiger and Jager (1977)								
3. WR = whole-rock								



ture or a primary fractionation at depth. The range in trace element chemistry for basalts of similar evolution reflects a range from depleted (like N-MORB) to enriched chondritic sources. In that much of this variation is stratigraphically controlled, it must arise from the melting process and source heterogeneity below this extensional basin, rather than from a range of tectonic environments. Comparisons to other continental margin settings that were formerly forearc such as the Gulf of California (Sawlan, 1990) and the Western Woodlark Basin (Binns and Whitford, 1987; Johnson et al., 1987), seem most appropriate both geochemically and tectonically.

### Queen Charlotte Basin subsidence and tectonics

The Queen Charlotte Basin sedimentary succession is seen in new multichannel seismic data (Rohr and Spence, 1989; Rohr et al., 1989; Rohr and Dietrich, 1989, 1991), and in exploration wells drilled by Shell Canada (Shouldice, 1971; Yorath and Hyndman, 1983; Higgs, 1990, 1991). The sediments are associated with the Tertiary Skonun sequences of northeastern Graham Island (Sutherland Brown, 1968; Higgs, 1989a, 1991). Figures 4 and 5 of Rohr and Dietrich (1991) show multichannel lines across central Hecate Strait crossing the location of exploration well Tyee N-39 and across Queen Charlotte Sound parallel to the margin. Two distinct intervals are evident in the seismic profiles (Rohr and Dietrich, 1991) and from the Tertiary of the Queen Charlotte Basin (Higgs, 1991). The lower sequence is interpreted as syntectonic sediments with intercalated volcanics that accumulated in grabens and half grabens (Higgs, 1989b, 1990, 1991). Rotated normal fault blocks are evident and of the type associated with crustal extension, for example in the North Sea (White et al., 1986). Overlying this unit is a (Pliocene) sequence that appeared to have little disturbance during deposition. The sediments of this upper sequence drape deeper structures and exhibit greater lateral stratigraphic continuity. This sequence may be associated with a post-tectonic cooling subsidence phase. In Hecate Strait there is also clear evidence for relatively recent compression and shortening (Rohr and Dietrich, 1991). Several of the block faults appear to have been reactivated and the sediments deformed as a result of the shortening. There is some erosional truncation of folds at the seafloor which suggests very recent or continuing deformation. Steeply dipping Late Miocene strata on northern Graham Island (Sutherland Brown, 1968) also indicate young compressive deformation. Some anticlines are cut by fault arrays that are similar to positive "flower structures" of the type that characterize compressive strike-slip deformation (Rohr and Dietrich, 1991). In Queen Charlotte Sound, the seismic sections exhibit normal faulting as in Hecate Strait but unlike Hecate Strait show little evidence for late Cenozoic compressive folding.

The Tertiary sequences drilled in Hecate Strait are largely unfossiliferous (nonmarine and sandy marine; Higgs, 1990, 1991) with very poor biostratigraphic controls on subsidence and depositional history. The well reports provide data for only the upper 50-60% of the seismic sections, and indicate Middle and Upper Miocene ages in most wells. Lower Miocene ages were inferred from the Harlequin well in Queen Charlotte Sound which penetrated marine sediments in its lower section. A re-analysis of samples from the Queen Charlotte Sound wells (Patterson, 1988, 1989) has allowed limited additional constraints, i.e., Lower to Middle Miocene in the Murrelet and Harlequin wells and Lower Miocene toward the base of the Osprey well. A thick sequence of submarine lavas from Ramsay Island give Eocene to Oligocene ages (Table 2). Recently acquired palynology data suggests the presence of older Tertiary sediments near the base of one Hecate Strait well and in at least one Queen Charlotte Islands exposure (J.M. White, pers. comm., 1989). In any case, most of the basin section penetrated by wells appears to be Early Miocene to Recent. Thus, the syntectonic phase may be Early Miocene or older (older than about 17

Ma). The combination of present heat flow, about  $70 \text{ mW m}^{-2}$  (Lewis et al., 1991) and vitrinite reflectance data (reported in Yorath and Hyndman, 1983) indicating a higher heat flow ( $>100 \text{ mW m}^{-2}$ ) in the past but subsequent to most sediment deposition, suggests that extension ended at approximately 20 Ma (see extension models in Yorath and Hyndman, 1983; and Lewis et al., 1991).

Based on the limited constraints discussed above, the data on the sedimentary succession are consistent with a model having most crustal extension during the main phase of Masset volcanism and of plate model extension from 36-20 Ma, reduced extension and the onset of thermal cooling from 20-5 Ma, and convergence and shortening with continued cooling from 5 Ma to the present (Higgs, 1991). Some oblique convergence and shortening could have occurred in the period from 20-10 Ma. The role of flexural subsidence associated with oblique underthrusting and margin uplift as postulated by Yorath and Hyndman (1983) cannot be resolved with current basin subsidence and deposition age constraints. More confident associations with the volcanic history and with plate models are also dependent on better biostratigraphic and other age control of the Queen Charlotte Basin section.

The seismic coverage of the basin and the land data are inadequate to map the orientations of the normal faulting. Based on the limited data, the modelled oblique extension between the Pacific and North America plates was probably resolved into orthogonal extension in the basin landward of the margin and transcurrent motion along the west coast (see model for early Gulf of California referenced below). However, there could have been en-echelon pull apart basins as are forming in the present Gulf of California. The inferred compressive transcurrent motion in the Hecate Strait part of the basin may be associated with the post-5 Ma period of oblique compression in the plate models. A recent earthquake in Hecate Strait ( $m_b$  5.3, January 12, 1990) gave a mechanism that was predominantly strike slip (R.B. Horner, pers. comm.). The young deformation of northern Graham Island and northwestern Hecate Strait and persistent microseismic activity suggest the focus of strain and ongoing deformation.

### Amount of Queen Charlotte area extension

Recent geophysical and geological data allow new estimates of the amount of crustal extension in the Queen Charlotte area. A previous estimate was made for Queen Charlotte Sound of about 70 km over an original width of 100 km (Yorath and Hyndman, 1983). A detailed analysis of crustal extension is beyond the scope of this article, but a brief discussion of extension indicators is given here. Crustal extension indicators include: (1) margin plate model extension, (2) extension expressed as dykes, (3) extension expressed in normal or block faults, (4) extension indicated by crustal thinning revealed by seismic data, (5) crustal thinning and extension required to accommodate basin subsidence and sediment deposition, (6) extension required to produce the present surface heat flow and paleo-heat flow indicators.

As described above, the mid-Tertiary oblique extension period from 36-20 Ma in the Stock and Molnar model provides a rough estimate of extension in the Queen Charlotte Basin, i.e. 80 km of total extension with an uncertainty of about  $\pm 60$  km.

Crustal extension may be expressed by two main mechanisms, dyke intrusion and normal faulting (Royden et al., 1980). The former is more readily observed in outcrop on land, while the latter is more readily seen in marine seismic reflection data. On the Queen Charlotte Islands, a minimum extension during Masset volcanism may be obtained from the fraction of dyke widths that make up outcrop sections. Tertiary dykes have been observed in many areas of the Queen Charlotte Islands (Sutherland Brown, 1968; Souther, 1988; Souther and Jessop, 1991). One of the authors (T.H.) has estimated the frac-

tion of dykes in outcrop at widely separated coastal exposures from Ikeda Cove on South Moresby Island to Wiah Point on North Graham Island and found generally north-south orientations implying east-west extension of between 2 and 15%. Examples are: (1) Nelson Point on southeast Louise Island where dykes 1-4 m in width, 20-40 m apart and oriented at N 15° W-N 10° E are related to normal faults. The dilation is estimated to be 2-10%; (2) Ikeda Cove on South Moresby where 15-20% extension occurs over 1.5 km; (3) Wiah Point to Shag Rock on Northern Graham Island where 15% extension is estimated. Extension in these areas may be concentrated adjacent to vents such that the total regional extension in dykes is smaller, but a regional average extension of at least 5% is expressed in dykes over much of the islands. In addition, as noted above, a substantial extension has probably occurred on normal faults such as are well resolved in the seismic sections for Queen Charlotte Sound and Hecate Strait.

Offshore, the extension in normal or block faulting is more easily observed, as recognized for other extensional basins (i.e. the North Sea; see White et al., 1986). In the seismic sections for Queen Charlotte Sound and Hecate Strait (Rohr and Dietrich, 1991), extension has been qualitatively estimated to be at least 10% by restoring the major block faults. To this must be added extension accommodated by dyke intrusion which is expected to be at least as great as that estimated on the Islands.

Crustal extension may also be estimated from apparent crustal thinning. Present crustal thicknesses from seismic refraction and reflection are 18-21 km beneath central Hecate Strait and Queen Charlotte Sound (see Spence et al., 1991; Rohr and Dietrich, 1991) compared to 30 km on the eastern margin of Hecate Strait and approximately 40 km in the adjacent Coast Plutonic Complex and Vancouver Island (McMechan and Spence, 1983). This inferred crustal thinning to 75% or 50% of the original thickness gives an extensional parameter Beta (McKenzie, 1978) of 1.5-2.0.

The extension required to give a (sediment filled) syntectonic basin subsidence of 1-2 km followed by post-tectonic subsidence of an additional 1-2 km, inferred from the well and seismic data, after 20 Ma, is approximately 25% (Beta = 1.5) (Royden et al., 1980). A similar order of extension is required to explain both the present heat flow 20 Ma after estimated termination of extension, and paleo-heat flow indicators. The observed average heat flow for the Queen Charlotte area is about 70 mW m<sup>-2</sup> (Lewis et al., 1991) compared to a reasonable equilibrium value of 40-50 mW m<sup>-2</sup>. Vitrinite reflectance data from Hecate Strait and Queen Charlotte Sound wells (e.g. Yorath and Hyndman, 1983) require that the heat flow was much higher than at present at some time in the past, but subsequent to deposition of most of the sediment section in the Queen Charlotte Basin.

The general conclusion from the above constraints is that considerable extension has occurred in the Queen Charlotte area, primarily in the mid-Tertiary. The amount of extension is at least 10-15% and may be as high as 40% and perhaps 50% in parts of Hecate Strait and Queen Charlotte Sound.

#### **Uplift of the western Queen Charlotte Islands and development of the accretionary wedge**

Current convergence and underthrusting beneath the margin of the Queen Charlotte Islands is indicated by a wide range of offshore and margin data (Chase and Tiffin, 1972; Hyndman and Ellis, 1981; Hyndman et al., 1982; Yorath and Hyndman, 1983; Dehler and Clowes, 1988). These include existence of the Queen Charlotte Trench (Fig. 9) which appears to be an accretionary sedimentary wedge with high amplitude folds, a marginal deep-sea depression or shallow trench seaward of the terrace into which offshore sedimentary horizons dip, a characteristic offshore bathymetric bulge and gravity

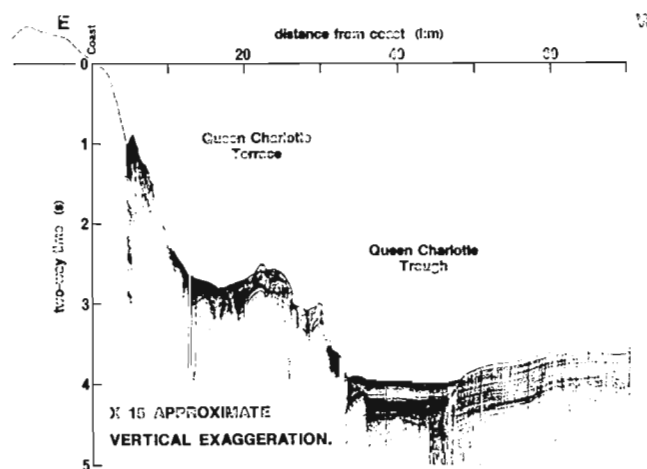


**Figure 9:** Single channel seismic section of the Queen Charlotte Trough and Queen Charlotte Terrace accretionary wedge.

high about 100 km seaward of the depression, and the characteristic parallel bands of very low and high gravity over the trough and the west coast of the islands respectively. The heat flow pattern across the margin corresponds to that predicted for subducting young oceanic crust i.e. high offshore and low on the margin. The high heat flow observed farther inland was probably caused by the main episode of extension. Relatively recent initiation of underthrusting is suggested by the lack of arc volcanics which are normally about 200 km inland of the trench. The total orthogonal convergence since 5 Ma predicted by the plate models is about 100 km.

An estimate of the duration of present underthrusting can be obtained from a comparison of the volume rate of sediment coming in on the oceanic plate and the volume contained in the accreted wedge. The thickness of incoming sediments increases from a few hundred metres near the southern tip of the islands where the crust is very young, to about 1.5 km off central Graham Island (Davis and Seemann, 1981; Dehler and Clowes, 1988; and unpublished seismic reflection profiles). The component of convergence is estimated to be about 20 mm a<sup>-1</sup> (see above). The mass balance has been computed offshore from central Moresby Island where the deep sea sediment section is about 1.0 km thick and the accreted wedge has an average thickness of about 4 km over a 30 km width (the layer of velocity 3.8 km s<sup>-1</sup> in Dehler and Clowes (1988) is assumed to be consolidated sediments). Changes in sedimentation rate during the Pleistocene and the decrease in sediment porosity from offshore to incorporation in the prism have been neglected in this rough calculation. Assuming that all of the incoming sediment is scraped off at the margin, these parameters give a volume balance for a convergence duration of 5 Ma. This result has an uncertainty of at least a factor of two, i.e. 2.5-10 Ma, but it is in agreement with the plate model duration of oblique convergence, i.e. approximately 5 Ma.

Late Tertiary uplift and partial erosion of the western Queen Charlotte Islands has been postulated by Yorath and Hyndman (1983). Based on structural cross-sections for units of the Masset Formation given by Sutherland Brown (1968) and a variety of other data they estimated uplift of 3-4 km. However, it has been argued that the high elevation zone along the west coast of Graham Island is a constructional volcanic plateau and could have been the volcanic source area such that the regional dip of the volcanics reflects primary slopes rather than subsequent tilting (Hickson, 1989, 1990). A lack of consistent strati-

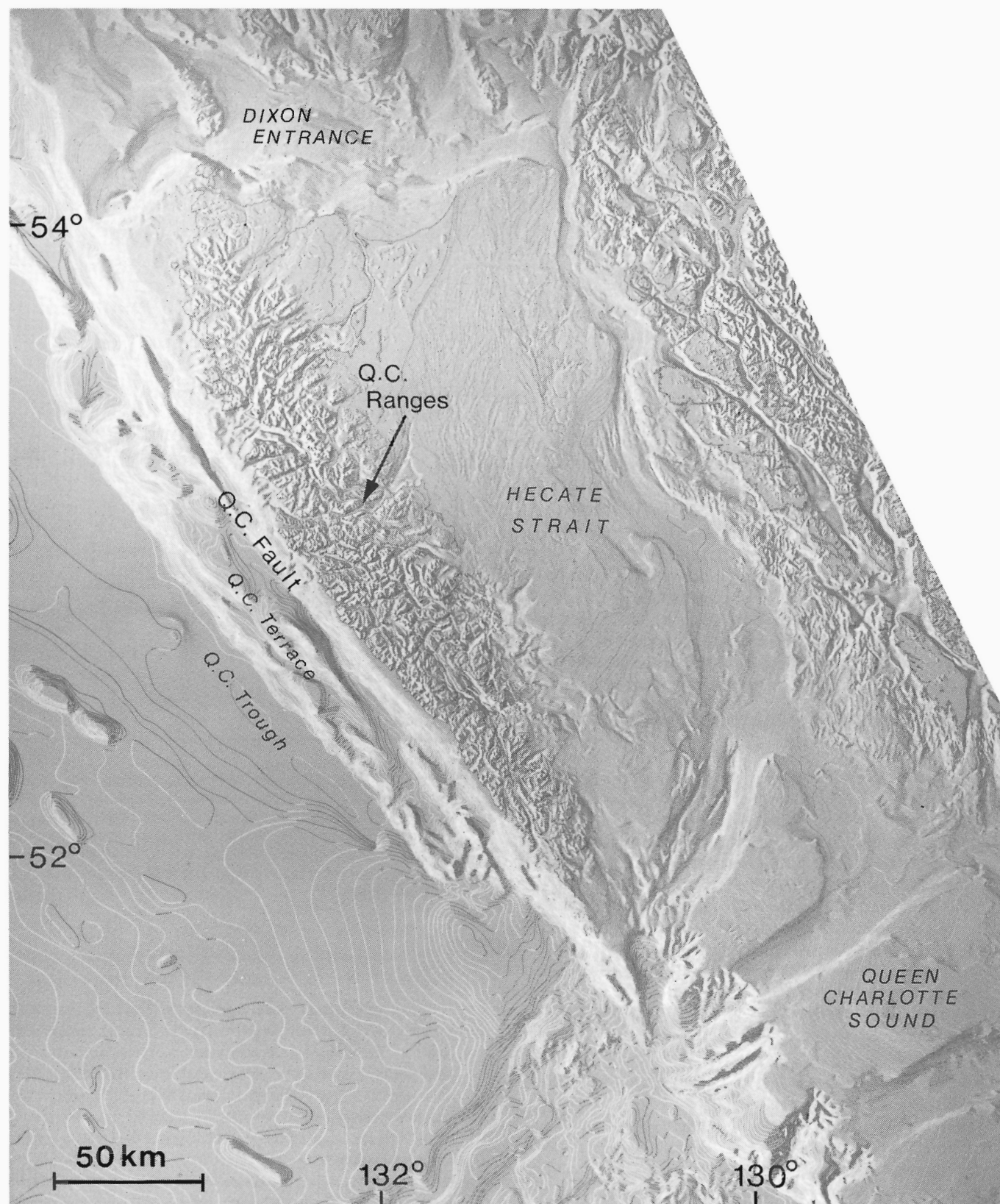


**Figure 10:** Artificially side-lit topography-bathymetry for the Queen Charlotte area after Sawyer (1989). The Queen Charlotte Ranges are postulated to have been uplifted by oblique underthrusting of the Pacific plate in the Late Tertiary.

graphic tilting in older rocks has also been cited by Thompson et al. (1990).

Geomorphic evidence for uplift is given by the linear physiographic height of land about 50 km wide parallel to and near the west coast of the islands, identified as the Queen Charlotte Ranges by Mathews (1986). The topographic ridge seen clearly in the artificially side-lit physiography maps of Sawyer (1989) (Fig. 10), appears to be tectonically controlled, in that it is continuous across a wide range of bedrock geology (Sutherland Brown, 1968). Wynne and Hamilton (1989) have examined paleomagnetic inclinations in the Naden well into the Masset (dated at 23 Ma) and found no resolvable dip, but the resolution of 3 degrees is comparable to the expected average regional tilting. Post-Masset uplift is supported by the erosional exposure of epizonal plutonic rocks primarily along the seaward part of the islands (Anderson and Greig, 1989), and by the regional outcrop pattern of older rocks exposed to the southwest and younger rocks exposed to the northeast (Sutherland Brown, 1968). Uplift is also suggested by the presence of subaqueous Masset volcanics above sealevel (e.g. Hamilton and Cameron, 1989), particularly if one allows for thermal subsidence following Masset volcanism which could have carried sub-aerial volcanics to as much as 1 or 2 km below sealevel. Higgs (1991) also discussed late Tertiary uplift and erosion which removed almost all of the Skonun sediments and some of the Masset volcanics from the western part of the Queen Charlotte Islands.

Quite recent (<1 Ma) breaking of the obliquely underthrusting oceanic lithosphere to form the modern Queen Charlotte Fault within the Pacific plate has been suggested by Yorath and Hyndman (1983) (see their Fig. 20). New interpretation by Carbotte et al. (1989) for the Dellwood and Tuzo Wilson knolls spreading centres indicates a somewhat earlier date. In any case, this break may have relieved the shear stress inland, the underthrusting beneath the Queen Charlotte area becoming more orthogonal to the margin.

## OTHER WESTERN NORTH AMERICA MARGINS

### Gulf of California

The Gulf of California provides a useful analogue to the Queen Charlotte region. The Gulf region has had both extensive geological study (Sawlan, 1990 and references therein; Moore, 1973) and detailed plate modelling (Stock and Hodges, 1989). The area has been interpreted to have had a phase of opening in the Late Tertiary associated with very oblique extension on the Pacific-America plate boundary (Fig. 11). Opening of the Gulf of California is attributed to two extensional phases, a Middle to Late Miocene (11-5 Ma) protogulf (Gulf Extensional Province) extension approximately orthogonal to the margin (Fig. 11), and a Pliocene to Recent development of the modern Gulf of California through en-echelon spreading centres and transform faults. The latter phase is associated with the development of and motion on the San Andreas fault system.

Initiation of the first phase of extension has been associated by Stock and Hodges (1989) with triple junction migration southward along the Baja California margin, i.e., transit of the Pacific-Rivera spreading centre. The triple junction migration progressively replaced Rivera plate convergence with Pacific plate transcurrent motion. The Pacific-America motion may have initially been purely transcurrent (between about 20 and 11 Ma), but by about 11 Ma motion became oblique extension (angle of about 25°) on the Gulf of California margin (Fig. 11). The total extension from 11-5 Ma from the Stock and Hodges (1989) plate model is about  $160 \pm 80$  km or about 70% extension in the Gulf Extensional Province. Within the Gulf Extensional Province, there are normal faults parallel to the margin suggesting orthogonal extension, but the actual direction of extension is not well constrained. Reconstruction of normal faults gives 5-50% extension,

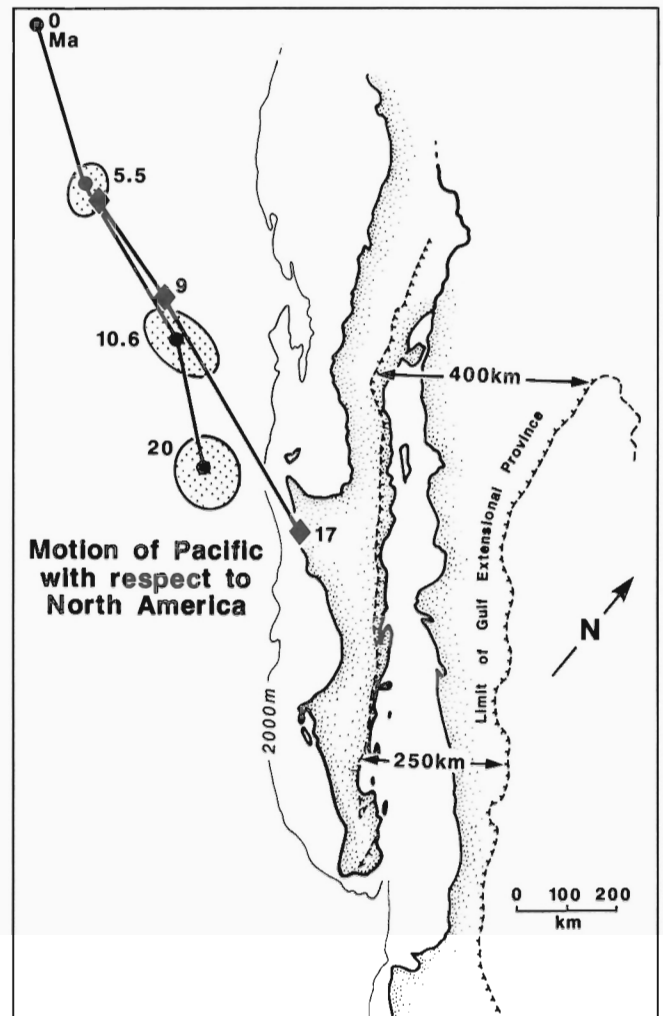


**Figure 11:** The Gulf Extensional Province at about 5 Ma, prior to the opening of the modern Gulf of California (after Stock and Hodges, 1989). Note the similar scale to Hecate Strait and the Queen Charlotte Islands. The progression of points on the deep seafloor as a function of time are from Stock and Molnar (1988) (with 95% confidence ellipses) and from Engebretson et al. (1985). The oblique extension prior to 5.5 Ma is well resolved.

while other geological data give 20-200% extension (Stock and Hodges, 1989), in general agreement with the plate estimate.

The plate tectonic model postulated by Stock and Hodges (1989) for the Gulf of California area has Pacific-America motion resolved into pure strike-slip on a margin fault and orthogonal extension inland during the phase of oblique extension. Baja California may have acted as a nearly rigid microplate. The extension appears to have occurred at the axis of the previous arc where the lithosphere was thermally weakened and thinned. If the margin of the Queen Charlotte Islands behaved in a similar manner to the Gulf of California, during the periods of modelled oblique extension there may have been a transform fault along the west coast, with approximately orthogonal extension on an inland zone. However, there is no evidence of comparable pre-Masset arc volcanism in the Hecate Strait region (or further inland for nearly 400 km, Armstrong, 1988).

Stock and Hodges (1989) associated the initiation of extension in the Gulf Extensional Province with the change to oblique extension in the Pacific-America model of Stock and Molnar (1988) at about



10 Ma. However, Sawlan (1990) reports somewhat older dates of extensional type volcanic rocks, and extension in the Gulf of California area may have been initiated by the southward triple junction migration rather than by the modelled 10 Ma relative plate motion change.

The Gulf of California-Baja area was formerly a volcanic arc with extensive outcrop of older pyroclastics and epiclastics, and which retains a calc-alkaline series from andesites to rhyolites throughout the period of extensional tectonics to the present (Sawlan, 1990). In addition to these calc-alkaline lavas and the MORBs and transitional basalts of the Gulf that are characteristic of extensional volcanism, there is a strongly potassic arc-alkaline series. Sawlan (1990) explains the derivations of these rocks from an arc-modified upper mantle source. By contrast, the Queen Charlotte area contains only the tholeiitic and calc-alkaline series. Evidence for volcanism between Middle Jurassic (Cameron and Hamilton, 1988; Sutherland Brown, 1968) and Eocene is scant. Haggart et al. (1989) described an isolated occurrence of volcanics with conglomerate mapped as Cretaceous. The lava however yielded a whole rock K-Ar age of  $35.3 \pm 1$  Ma (C.J. Hickson, unpub. data). Lacking precursory arc volcanics, the region appears to have formerly been in a forearc setting. The paired tholeiitic and calc-alkaline assemblage of the Queen Charlotte area also occurs in other marginal basins which were formerly in a forearc position. Examples are the Western Woodlark Basin (Perfit et al., 1987; Johnson et al., 1987), and the southern California borderland basins, including Santa Cruz Island (Crowe et al., 1976) and the Los Angeles Basin (Higgins, 1976).

### Cascadia and the Aleutian Islands margins

It is useful to contrast the tectonic and volcanic histories of margins that have had mainly strike-slip margin plate motion for the Middle to Late Tertiary with those that have had nearly orthogonal convergence. The Cascadia margin has had nearly orthogonal convergence at about  $50 \text{ mm a}^{-1}$  since the Eocene (Fig. 12). The result is a margin structure and tectonic history (Finn, 1989; Wells et al., 1984; Hyndman et al., 1990) and volcanic history (Priest, 1989) and composition (Leeman et al., 1989; Sherrod and Smith, 1989; Smith and Leeman, 1987) that is very different from the Queen Charlotte Islands and Gulf of California transcurrent margins. Similarly, the Aleutian Island margin (Wallace and Engebretson, 1984) exhibits the strikingly different tectonic and volcanic history characteristic of an arc.

For example, there are major accretionary sedimentary wedges 100-200 km wide along both subduction zone margins. The Cascadia accretionary wedge is approximately equal in sediment volume to the estimated amount of material that has been carried in on the subducting Juan de Fuca plate since the start of the current phase of convergence in the Eocene. As described above, the volcanic expressions of these subduction zone margins are also very different from the expressions of transcurrent margins. In both the Cascades and Aleutian arcs, separated central constructional volcanoes dominate, with pyroclastics and andesites to dacites being the most common volcanic products. Thus, there is a strong correlation between the nature of the volcanism and tectonics and the relative plate motions between North America and the adjacent plates of the northeast Pacific.

### CONCLUSIONS

The data available for the chronology of plate interactions along the margin, for igneous activity, for basin subsidence and for tectonics have been reviewed. Although there are substantial uncertainties in all of these processes, some tentative correlations are suggested. Recent northeast Pacific plate models for the Cenozoic indicate the following Queen Charlotte margin interactions:

1. Convergence and subduction are modelled for the Early Tertiary until approximately the time of major Pacific-wide plate reorganization in the Eocene (43 Ma).
2. General transcurrent motion with varying amounts of very oblique extension or compression has occurred since that time, assuming that the Pacific plate rather than the Farallon was offshore. A total of  $80 \pm 60$  km of extension resolved orthogonal to the margin is predicted for the middle Tertiary.
3. There is a well resolved latest Miocene or earliest Pliocene change from transcurrent motion or oblique extension to oblique convergence, the latter continuing from about 5 Ma to the present. Since approximately 1-2 Ma, the oblique convergence may have been divided into transcurrent motion along the margin on the Queen Charlotte fault and roughly orthogonal underthrusting beneath the Queen Charlotte Islands. The predicted component of convergence orthogonal to the margin since 5 Ma is about 100 km.

The onset of Masset volcanism corresponds approximately to the major plate reorganization at about 43 Ma. There also appears to be a correlation between the period of maximum magmatic activity and the time during the general Tertiary transcurrent regime when one plate interaction model shows oblique extension (36-20 Ma).

Syntectonic deposition in the Queen Charlotte Basin may be temporally correlated with the interval from 36-20 Ma of oblique extension in one plate model, continued deposition with reduced extension

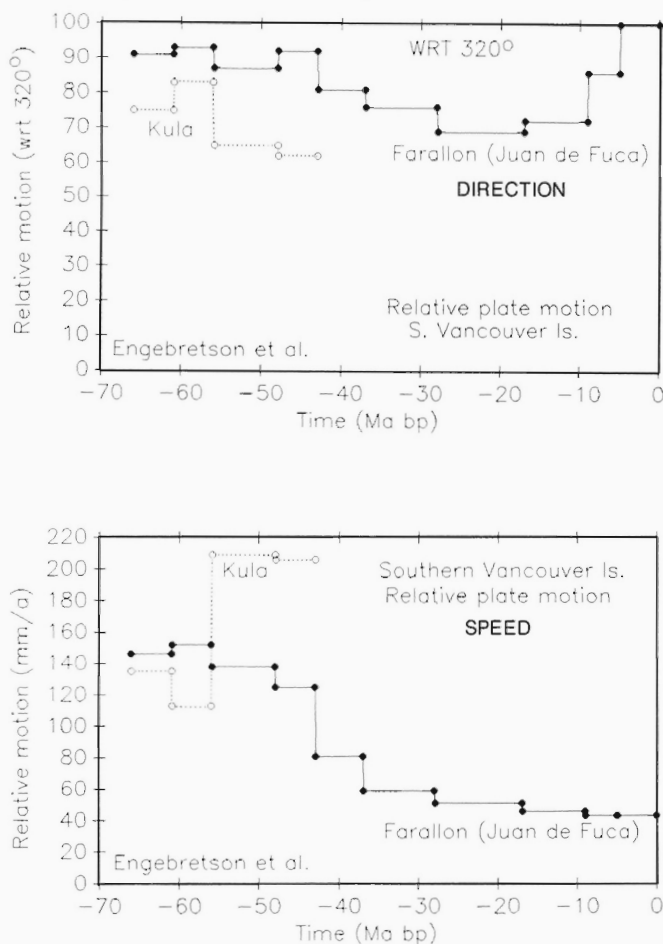


**Figure 12:** (a) The model angle of relative plate motion across the Cascadia margin at Vancouver Island through the Tertiary assuming a plate boundary strike of  $320^\circ$  (after Engebretson et al., 1985). (b) The model speed of plate relative motion.

and post-tectonic subsidence with the period from 20-5 Ma and the youngest deposition and latest deformation with the 5-0 Ma period of oblique convergence. Some of the shortening seen in the seismic sections may be the result of the oblique convergence modelled from 20-10 Ma.

The modelled convergence for 5 Ma to the present is probably associated with the formation of an accretionary wedge along the west coast, with uplift and deformation of the Queen Charlotte Islands, and possibly with the compression that locally deforms the complete Tertiary succession as observed in seismic sections of Hecate Strait.

The extensive Masset volcanism is inferred to arise in an extensional environment from numerous physical volcanic and geochemical indicators. Locally, estimates of extension within the Queen Charlotte Basin from a variety of data range from about 10% to as much as 40%.

There is a pronounced difference in the magmatic and tectonic activity between the Pacific margin areas with modelled Cenozoic transcurrent (e.g. Queen Charlottes, California borderlands, Gulf of California) versus convergent (e.g. Cascadia and Aleutians) relative motions. There may be a close analogy in the plate margin interactions and their tectonic expression between the Queen Charlotte Basin and the Gulf of California extensional province, i.e. oblique plate extension resolved into margin transcurrent motion and inland orthogonal extension. However, en-echelon rift-transform (pull-apart) extension such as that evident in the modern Gulf of California and along the margin of California may also have occurred.

## ACKNOWLEDGMENTS

The authors thank C.J. Yorath, B.D. Bornhold, G.J. Woodsworth, R.I. Thompson, C.J. Hickson, R.P. Riddihough, R. Higgs and H. Lyatsky for reviews and constructive comments. R.G. Anderson and K.M.M. Rohr are thanked for providing access to unpublished data and J. Stock for providing plate model error estimates.

## REFERENCES

- Anderson, R.G. and Greig, C.J.  
**1989:** Jurassic and Tertiary plutonism in the Queen Charlotte Islands, British Columbia; *in* Current Research, Part H, Geological Survey of Canada, Paper 89-1H, p. 95-104.
- Anderson, R.G. and Reichenbach, I.  
**1989:** A note on the geochronometry of Late Jurassic and Tertiary plutons in Queen Charlotte Islands, British Columbia; *in* Current Research, Part H, Geological Survey of Canada, Paper 89-1H, p. 105-112.
- 1991:** Geochronometric (U-Pb and K-Ar) framework for Middle to Late Jurassic (172-158 Ma) and Tertiary (46-27 Ma; Eocene and Oligocene) plutons in Queen Charlotte Islands, British Columbia; *in* Evolution and Hydrocarbon Potential of the Queen Charlotte Basin, British Columbia, Geological Survey of Canada, Paper 90-10.
- Armstrong, R.L.  
**1988:** Mesozoic and early Cenozoic magmatic evolution of the Canadian Cordillera; Geological Society of America, Special Paper 218 (Rogers Volume), p. 55-91.
- Atwater, T.  
**1970:** Implications of plate tectonics for the Cenozoic tectonic evolution of western North America; Geological Society of America Bulletin, v. 81, p. 3513-3536.
- 1989:** Plate tectonic history of the northeast Pacific and western North America; *in* The Eastern Pacific Ocean and Hawaii, E.L. Winterer, D.M. Hussong and R.W. Decker (ed.), Geological Society of America, Boulder, Colorado, U.S.A., p. 21-72.
- Baragar, W.R.A.  
**1966:** Geochemistry of the Yellowknife volcanic rocks; Canadian Journal of Earth Sciences, v. 3, p. 9-30.
- Batiza, R.  
**1978:** Geology, petrology, and geochemistry of Isla Tortuga, a recently formed tholeiitic island in the Gulf of California; Geological Society of America Bulletin, v. 89, p. 1309-1324.
- Batiza, R., Futa, K., and Hedge, C.E.  
**1979:** Trace element and strontium isotope characteristics of volcanic rocks from Isla Tortuga: a young seamount in the Gulf of California; Earth and Planetary Science Letters, v. 43, p. 269-278.
- Bender, J.F., Langmuir, C.H., and Hanson, G.N.  
**1984:** Petrogenesis of basalt glasses from the Tamayo region, East Pacific Rise; Journal of Petrology, v. 25, p. 213-254.
- Berggren, W.A., Kent, D.V., Flynn, J.J., and van Couvering, J.A.  
**1985:** Cenozoic geochronology; Geological Society of America Bulletin, v. 96, p. 1407-1418.
- Binns, R.A. and Whitford, D.L.  
**1987:** Petrology of the Western Woodlark Basin; *in* Proceedings of the Pacific Rim Conference, Brisbane, 1987, p. 525-529.
- Cameron, B.E.B. and Hamilton, T.S.  
**1988:** Contributions to the stratigraphy and tectonics of the Queen Charlotte Basin, British Columbia; *in* Current Research, Part E, Geological Survey of Canada, Paper 88-1E, p. 221-227.
- Carbotte, S.M., Dixon, J.M., Farrar, E., Davis, E.E., and Riddihough, R.P.  
**1989:** Geological and geophysical characteristics of the Tuzo Wilson Seamounts: implications for plate geometry in the vicinity of the Pacific - North America - Explorer triple junction; Canadian Journal of Earth Sciences, v. 26, p. 2365-2384.
- Carmichael, I.S.E.  
**1964:** The petrology of Thingmuli, a Tertiary volcano in eastern Iceland; Journal of Petrology, v. 5, p. 435-460.
- Chase, R.L. and Tiffin, D.L.  
**1972:** Queen Charlotte fault zone, British Columbia; 24th International Geological Congress, Vancouver, British Columbia, Marine Geology and Geophysics Section, v. 8, p. 17-28.
- Clowes, R.M. and Gens-Lenartowicz, E.  
**1985:** Upper crustal structure of southern Queen Charlotte Basin from sonobuoy refraction studies; Canadian Journal of Earth Sciences, v. 22, p. 1696-1710.
- Cousens, B.L., Chase, R.L., and Schilling, J.-G.  
**1984:** Basalt geochemistry of the Explorer Ridge area, northeast Pacific Ocean; Canadian Journal of Earth Sciences, v. 21, p. 157-170.
- Cox, A. and Engebretson, D.C.  
**1985:** Change in motion of Pacific plate at 5 m.y. B.P.; Nature, v. 313, p. 472-474.
- Crowe, B.M., McLean, H., Howell, D.G., and Higgins, R.E.  
**1976:** Petrography and major-element chemistry of the Santa Cruz Island volcanics; *in* Aspects of the Geologic History of the California Continental Borderland, D.G. Howell (ed.), Pacific Section, American Association of Petroleum Geologists, Miscellaneous Publication 24, p. 196-215.
- Davis, A.S. and Plafker, G.  
**1986:** Eocene basalts from the Yakutat terrane: evidence for the origin of an accreting terrane in southern Alaska; Geology, v. 14, p. 963-966.
- Davis, E.E. and Seemann, D.A.  
**1981:** A compilation of seismic reflection profiles across the continental margin of western Canada; Geological Survey of Canada, Open File 751.
- Davis, E.E. and Riddihough, R.P.  
**1982:** The Winona Basin: structure and tectonics; Canadian Journal of Earth Sciences, v. 19, p. 767-788.
- Dehler, S. and Clowes, R.M.  
**1988:** The Queen Charlotte Islands refraction project. Part I. The Queen Charlotte Fault Zone; Canadian Journal of Earth Sciences, v. 25, p. 1857-1870.
- DeMets, C., Gordon, R.G., Stein, S., and Argus, D.F.  
**1987:** A revised estimate of Pacific-North America motion and implications for western North America plate boundary zone tectonics; Geophysical Research Letters, v. 14, p. 911-914.
- Dostal, J. and Hamilton, T.S.  
**1988:** Oceanic volcanism on the western Canadian continental margin: Masset Formation (U. Eocene-U. Miocene); Geological Association of Canada, Annual Meeting, Program with Abstracts, v. 13, p. A33.
- Dupuy, C. and Dostal, J.  
**1984:** Trace element geochemistry of some continental tholeiites; Canadian Journal of Earth Sciences, v. 67, p. 61-69.
- Eaby, J. and Clague, D.A.  
**1984:** Sr isotopic variations along the Juan de Fuca ridge; Journal of Geophysical Research, v. 89, p. 7883-7890.
- Engelbreton, D.C.  
**1989:** Northeast Pacific-North America plate kinematics since 70 Ma; *in* Northeast Pacific-North America Plate Interactions throughout the Cenozoic, Program with Abstracts, Pacific Section of the Geological Association of Canada, Victoria, Canada, April 14, 1989, p. 9-11.
- Engelbreton, D.C., Cox, A., and Thompson, G.A.  
**1984:** Correlation of plate motions with continental tectonics: Laramide to Basin-Range; Tectonics, v. 3, p. 115-120.
- Engelbreton, D.C., Cox, A., and Gordon, R.G.  
**1985:** Relative motions between oceanic and continental plates in the Pacific Basin; Geological Society of America, Special Paper 206, 59 p.



- Erlank, A.J. and Kable, Z.J.D.**  
**1976:** The significance of incompatible elements in mid-Atlantic ridge basalts from 45°N with particular reference to Zr/Nb; *Contributions to Mineralogy and Petrology*, v. 54, p. 281-291.
- Finn, C.**  
**1989:** Structure of the convergent Washington margin; in *Geological, Geophysical and Tectonic Setting of the Cascade Range*, United States Geological Survey Open File Report 89-178, p. 291-317.
- Haggart, J., Lewis, P.D., and Hickson, C.J.**  
**1989:** Stratigraphy and structure of Cretaceous strata, Long Inlet, Queen Charlotte Islands, British Columbia; in *Current Research, Part H*, Geological Survey of Canada, Paper 89-1H, p. 65-72.
- Hamilton, T.S.**  
**1989:** Tertiary extensional volcanism and volcanotectonic interactions along the Queen Charlotte portion of the western Canadian continental margin; in *North-east Pacific-North America Plate Interactions Throughout the Cenozoic*, Programme and Abstracts, Geological Association of Canada, Pacific Section Symposium, 14 April, 1989, p. 8-9.
- Hamilton, T.S. and Cameron, J.E.B.**  
**1989:** Hydrocarbon occurrences on the western margin of the Queen Charlotte Basin; *Canadian Bulletin of Petroleum Geology*, v. 37, p. 443-466.
- Harbert, W. and Cox, A.**  
**1989:** Late Neogene motion of the Pacific plate; *Journal of Geophysical Research*, v. 94, p. 3052-3064.
- Hickson, C.J.**  
**1988:** Structure and stratigraphy of the Massett Formation, Queen Charlotte Islands, British Columbia; in *Current Research, Part E*, Geological Survey of Canada, Paper 88-1E, p. 269-274.  
**1989:** An update on structure and stratigraphy of the Massett Formation, Queen Charlotte Islands, British Columbia; in *Current Research, Part H*, Geological Survey of Canada, Paper 89-1H, p. 73-79.  
**1991:** The Massett Formation on Graham Island, Queen Charlotte Islands, British Columbia; in *Evolution and Hydrocarbon Potential of the Queen Charlotte Basin*, British Columbia, Geological Survey of Canada, Paper 90-10.
- Higgins, R.E.**  
**1976:** Major-element chemistry of the Cenozoic volcanic rocks in the Los Angeles Basin and vicinity; in *Aspects of the Geological History of the California Continental Borderland*, D.G. Howell (ed.), Pacific Section, American Association of Petroleum Geologists, Miscellaneous Publication 24, p. 216-240.
- Higgs, R.**  
**1989a:** Sedimentological aspects of the Skonun Formation, Queen Charlotte Islands, British Columbia; in *Current Research, Part H*, Geological Survey of Canada, Paper 89-1H, p. 87-94.  
**1989b:** Architecture of the Queen Charlotte Basin fill and implications for tectonic history and petroleum exploration; in *Contributions to the Geological Survey of Canada, Cordilleran Geology and Exploration Roundup*, Feb. 7-10, Program and Abstracts.  
**1990:** Sedimentology and tectonic implications of Cretaceous fan-delta conglomerates, Queen Charlotte Islands, Canada; *Sedimentology*, v. 37.  
**1991:** Sedimentology, basin-fill architecture and petroleum geology of the Tertiary Queen Charlotte Basin, British Columbia; in *Evolution and Hydrocarbon Potential of the Queen Charlotte Basin*, British Columbia, Geological Survey of Canada, Paper 90-10.
- Hyndman, R.D., Yorath, C.J., Clowes, R.M., and Davis, E.E.**  
**1990:** The northern Cascadia subduction zone at Vancouver Island: seismic structure and tectonic history; *Canadian Journal of Earth Sciences*, v. 27, p. 313-329.
- Hyndman, R.D., Lewis, T.J., Wright, J.A., Burgess, M., Chapman, D.S., and Yamano, M.**  
**1982:** Queen Charlotte fault zone: heat flow measurements; *Canadian Journal of Earth Sciences*, v. 19, p. 1657-1669.
- Hyndman, R.D. and Ellis, R.M.**  
**1981:** Queen Charlotte fault zone: microearthquakes from a temporary array of land stations and ocean bottom seismographs; *Canadian Journal of Earth Sciences*, v. 18, p. 776-788.
- Irvine, T.N. and Baragar, W.R.A.**  
**1971:** A guide to the chemical classification of the common volcanic rocks; *Canadian Journal of Earth Sciences*, v. 8, p. 513-548.
- Irving, E. and Thorkelson, D.J.**  
**1990:** Paleomagnetism of Spences Bridge Group: evidence for northward displacement of the Intermontane Belt of British Columbia; *Journal of Geophysical Research*, in press.
- Johnson, R.W., Langmuir, C.H., Perfit, M.R., Staudigel, H., Dunkley, P.N., Chappell, B.W., Taylor, S.R., and Baekispa, M.**  
**1987:** Ridge subduction and forearc volcanism: petrology and geochemistry of rocks dredged from the Western Woodlark Basin; in *Marine Geology, Geophysics, and Geochemistry of the Woodlark Basin-Solomon Islands*, B. Taylor and N.F. Exon (ed.), Circum-Pacific Council for Energy and Mineral Resources Earth Science Series, v. 7, p. 155-226.
- Kelley, K. and Engebretson, D.C.**  
**1989:** Comparison of the relative motion between North America and oceanic plates of the Pacific basin as determined by fixed-hotspot and global plate circuit approaches; *Transactions of the American Geophysical Union, EOS*, p. 1341.
- Kosco, D.G.**  
**1981:** The Mt. Edgecumbe volcanic field, Alaska: an example of tholeiitic and calc-alkaline volcanism; *Journal of Geology*, v. 89, p. 459-477.
- Leeman, W.P., Smith, D.R., Hildreth, W., Palacz, Z., and Rogers, N.**  
**1989:** Compositional diversity of late Cenozoic basalts in a transect across the southern Washington Cascades: implications for subduction zone magmatism; in *Geological, Geophysical and Tectonic Setting of the Cascade Range*, United States Geological Survey, Open-File Report 89-178, p. 318-350.
- Lewis, T.J., Bentkowski, W.H., and Wright, J.A.**  
**1991:** Thermal state of the Queen Charlotte Basin: warm; in *Evolution and Hydrocarbon Potential of the Queen Charlotte Basin*, British Columbia, Geological Survey of Canada, Paper 90-10.
- Lonsdale, P.**  
**1988:** Palaeogene history of the Kula Plate: offshore evidence and onshore implications; *Geological Society of America Bulletin*, v. 100, p. 733-754.
- MacKenzie, D.P.**  
**1978:** Some remarks on the development of sedimentary basins; *Earth and Planetary Science Letters*, v. 40, p. 25-32.
- McMechan, G.A. and Spence, G.D.**  
**1983:** P-wave velocity structure of the Earth's crust beneath Vancouver Island; *Canadian Journal of Earth Sciences*, v. 20, p. 742-752.
- Mathews, W.H.**  
**1986:** Physiographic Map of the Canadian Cordillera; Geological Survey of Canada, Map 1701A.
- Meschede, M.**  
**1986:** A method of discriminating between different types of mid-ocean ridge basalts and continental tholeiites with the Nb-Zr-Y diagram; *Chemical Geology*, v. 56, p. 207-218.
- Miyashiro, A.**  
**1974:** Classification, characteristics, and origin of ophiolites; *Journal of Geology*, v. 83, p. 249-281.
- Miyashiro, A. and Shido, F.**  
**1975:** Tholeiitic and calc-alkalic series in relation to the behaviours of titanium, vanadium, chromium and nickel; *American Journal of Science*, v. 275, p. 265-277.
- Moore, D.G.**  
**1973:** Plate-edge deformation and crustal growth, Gulf of California structural province; *Geological Society of America Bulletin*, v. 84, p. 1883-1906.
- Patterson, R.T.**  
**1988:** Early Miocene to Quaternary foraminifera from three wells in the Queen Charlotte Basin off the coast of British Columbia; in *Sequences, Stratigraphy, Sedimentology: Surface and Subsurface*, D.P. James and D.A. Leckie (ed.), Canadian Society of Petroleum Geologists, Memoir 15, p. 497.  
**1989:** Neogene foraminiferal biostratigraphy of the southern Queen Charlotte Basin; in *Contributions to Canadian Paleontology*, Geological Survey of Canada, Bulletin 396, p. 229-265.
- Pearce, J.A.**  
**1983:** Role of the subcontinental lithosphere in magma genesis at continental margins; in *Continental Basalts and Mantle Xenoliths*, C.J. Hawkesworth and M.J. Norry (ed.), Shiva Press, Nantwich, p. 230-249.
- Pearce, J.A., Harris, N.B.W., and Tindle, A.G.**  
**1984:** Trace element discrimination diagrams for tectonic interpretation of granitic rocks; *Journal of Petrology*, v. 25, p. 965-983.
- Perfit, M.R., Langmuir, C.H., Baekispa, M., Chappell, B., Johnson, R.W., Staudigel, H., and Taylor, S.R.**  
**1987:** Geochemistry and petrology of volcanic rocks from the Woodlark Basin: addressing questions of ridge subduction; in *Marine Geology, Geophysics, and Geochemistry of the Woodlark Basin-Solomon Islands*, B. Taylor and N.F. Exon (ed.), Circum-Pacific Council for Energy and Mineral Resources Earth Science Series, v. 7, p. 113-154.
- Plafker, G.**  
**1989:** Tectonic evolution of the Yakutat Terrane: an actively accreting terrane in southern Alaska; in *Northeast Pacific-North America Plate Interactions Throughout the Cenozoic*, Program with Abstracts, Geological Association of Canada, Pacific Section, Victoria, April, 1989, p. 21-23.
- Pollitz, F.F.**  
**1986:** Pliocene change in Pacific-plate motion; *Nature*, v. 320, p. 738-741.  
**1988:** Episodic North America and Pacific plate motions; *Tectonics*, v. 7, p. 711-726.
- Priest, G.R.**  
**1989:** Volcanic and tectonic evolution of the Cascade volcanic arc, 44°00' to 44°52'30"N; in *Geological, Geophysical and Tectonic Setting of the Cascade Range*, United States Geological Survey Open-File Report 89-178, p. 430-489.
- Riddihough, R.P.**  
**1982:** One hundred million years of plate tectonics in western Canada; *Geoscience Canada*, v. 9, p. 28-34.

- 1984:** Recent movements of the Juan de Fuca plate system; *Journal of Geophysical Research*, v. 89, p. 6980-6994.
- Riddihough, R.P., Currie, R.G., and Hyndman, R.D.**
- 1980:** The Dellwood Knolls: an active triple junction off western Canada; *Canadian Journal of Earth Sciences*, v. 17, p. 577-593.
- Rohr, K.M.M. and Dietrich, J.R.**
- 1989:** Seismic reflection survey of the Queen Charlotte region of the west coast offshore; *in* Northeast Pacific-North America Plate Interactions Throughout the Cenozoic, Programme and Abstracts, Geological Association of Canada, Pacific Section Symposium, Victoria, B.C., 1989, p. 20.
- 1991:** Deep seismic reflection survey of the Queen Charlotte Basin; *in* Evolution and Hydrocarbon Potential of the Queen Charlotte Basin, British Columbia, Geological Survey of Canada, Paper 90-10.
- Rohr, K.M.M. and Spence, G.D.**
- 1989:** Evidence for crustal thinning in the Queen Charlotte Basin; *Transactions of the American Geophysical Union, EOS*, p. 1318.
- Rohr, K.M.M., Spence, G.D., Asudeh, I., Ellis, R.M., and Clowes, R.M.**
- 1989:** Seismic reflection and refraction experiment in the Queen Charlotte Basin, British Columbia; *in* Current Research, Part H, Geological Survey of Canada, Paper 89-1H, p. 3-5.
- Royden, L., Sclater, J.G., and Von Herzen, R.P.**
- 1980:** Continental margin subsidence and heat flow: important parameters in formation of petroleum hydrocarbons; *American Association of Petroleum Geologists Bulletin*, v. 64, p. 173-187.
- Saunders, A.D., Fornari, D.J., and Morrisson, M.A.**
- 1982:** The composition and emplacement of basaltic magmas produced during the development of continental-margin basins: the Gulf of California, Mexico; *Journal of the Geological Society of London*, v. 139, p. 335-346.
- Saunders, A.D., Fornari, D.J., Joron, J.-L., Tarney, J., and Treuil, M.**
- 1983:** Geochemistry of basic igneous rocks, Gulf of California, Deep Sea Drilling Project, Leg 64; *in* Initial Reports of the Deep Sea Drilling Project, v. 64, J.R. Curran and D.G. Moore (ed.), Washington (U.S. Government Printing Office), p. 595-641.
- Saunders, A.D., Rogers, G., Marriner, G.F., Terrell, D.J., and Verma, S.P.**
- 1987:** Geochemistry of Cenozoic volcanic rocks, Baja California, Mexico: implications for the petrogenesis of post-subduction magmas; *Journal of Volcanology and Geothermal Research*, v. 32, p. 223-245.
- Sawlan, M.G.**
- 1990:** Magmatic evolution of the Gulf of California rift; *in* Gulf of California, J.P. Dauphin (ed.), American Association of Petroleum Geology, Memoir, in press.
- Sawyer, B.**
- 1989:** Physiography, Queen Charlotte area, Geological Survey of Canada, Maps 1,2,3-1989.
- Sherrod, D.R. and Smith, J.G.**
- 1989:** Quaternary extrusion rates from the Cascade Range, northwestern United States and British Columbia; *in* Geological, Geophysical and Tectonic Setting of the Cascade Range, United States Geological Survey Open File Report 89-178, p. 94-103.
- Shervais, J.W.**
- 1982:** Ti-V plots and the petrogenesis of modern and ophiolitic lavas; *Earth and Planetary Science Letters*, v. 59, p. 101-118.
- Shouldice, D.H.**
- 1971:** Geology of the western Canadian continental shelf; *Bulletin of Canadian Petroleum Geology*, v. 19, p. 405-436.
- Smith, D.R. and Leeman, W.P.**
- 1987:** Petrogenesis of Mount St. Helens dacite magmas; *Journal of Geophysical Research*, v. 92, p. 10,313-10,334.
- Souther, J.G.**
- 1988:** Implications for hydrocarbon exploration of dyke emplacement in the Queen Charlotte Islands, British Columbia; *in* Current Research, Part E, Geological Survey of Canada, Paper 88-1E, p. 241-245.
- Souther, J.G. and Jessop, A.M.**
- 1991:** Dyke swarms in the Queen Charlotte Islands, implications for hydrocarbon exploration; *in* Evolution and Hydrocarbon Potential of the Queen Charlotte Basin, British Columbia, Geological Survey of Canada, Paper 90-10.
- Spence, G.D., Hole, J.A., Asudeh, I., Ellis, R., Clowes, R.M., Yuan, T., and Rohr, K.**
- 1991:** A seismic refraction study in the Queen Charlotte Basin; *in* Evolution and Hydrocarbon Potential of the Queen Charlotte Basin, British Columbia, Geological Survey of Canada, Paper 90-10.
- Steiger, R.H.J. and Jager, E.**
- 1977:** Subcommittee on geochronology: convention on the use of decay constants in geo- and cosmochronology; *Earth and Planetary Science Letters*, v. 36, p. 359-362.
- Stock, J.M. and Hodges, K.V.**
- 1989:** Pre-Pliocene extension around the Gulf of California and the transfer of Baja California to the Pacific Plate; *Tectonics*, v. 8, p. 99-115.
- Stock, J.M. and Molnar, P.**
- 1988:** Uncertainties and implications of the Late Cretaceous and Tertiary position of North America relative to the Farallon, Kula, and Pacific plates; *Tectonics*, v. 6, p. 1339-1384.
- Sutherland Brown, A.**
- 1968:** Geology of the Queen Charlotte Islands; British Columbia Department of Mines and Petroleum Resources, Bulletin 54, 226 p.
- Thompson, R.L., Haggart, J.W., and Lewis, P.D.**
- 1991:** Late Triassic through early Tertiary evolution of the Queen Charlotte Basin, British Columbia, with a perspective on hydrocarbon potential; *in* Evolution and Hydrocarbon Potential of the Queen Charlotte Basin, British Columbia, Geological Survey of Canada, Paper 90-10.
- Thorkelson, D.J. and Taylor, R.P.**
- 1989:** Cordilleran slab windows; *Geology*, v. 17, p. 833-836.
- Wells, R.E., Engebretson, D.C., Snively, P.D., Jr., and Coe, R.S.**
- 1984:** Cenozoic plate motions and the volcano-tectonic evolution of western Oregon and Washington; *Tectonics*, v. 3, p. 275-294.
- Wallace, W.K. and Engebretson, D.C.**
- 1984:** Relationships between plate motions and Late Cretaceous to Paleogene magmatism in southwestern Alaska; *Tectonics*, v. 3, p. 295-315.
- White, N.J., Jackson, J.A., and McKenzie, D.P.**
- 1986:** The relationship between the geometry of normal faults and that of the sedimentary layers in their hanging walls; *Journal of Structural Geology*, v. 8, p. 879-909.
- Woodsworth, G.J.**
- 1991:** Neogene to Recent volcanism along the east side of Hecate Strait, British Columbia; *in* Evolution and Hydrocarbon Potential of the Queen Charlotte Basin, British Columbia, Geological Survey of Canada, Paper 90-10.
- Wynne, P.J. and Hamilton T.S.**
- 1988:** Paleomagnetism of the Masset Formation (U. Eocene-Upper Miocene): a composite magnetostratigraphy and evidence for Neogene deformational style of the Queen Charlotte Islands; Pacific Northwest Region American Geophysical Union, Proceedings of the Thirty-fifth Annual Meeting, Victoria, British Columbia, September 28-30, p. 20.
- 1989:** Polarity and inclination of magnetization of the Masset Formation from a deep drillhole on Graham Island, Queen Charlotte Islands, British Columbia; *in* Current Research, Part H, Geological Survey of Canada, Paper 89-1H, p. 81-86.
- Yorath, C.J. and Chase, R.L.**
- 1981:** Tectonic history of the Queen Charlotte Islands and adjacent areas – a model; *Canadian Journal of Earth Sciences*, v. 18, p. 1717-1739.
- Yorath, C.J. and Hyndman, R.D.**
- 1983:** Subsidence and thermal history of Queen Charlotte Basin; *Canadian Journal of Earth Sciences*, v. 20, p. 135-159.
- Young, I.F.**
- 1981:** Structure of the western margin of the Queen Charlotte Basin, British Columbia; M.Sc. thesis, University of British Columbia, Vancouver, 380 p.

# Deep seismic reflection survey of the Queen Charlotte Basin, British Columbia

K. Rohr<sup>1</sup> and J.R. Dietrich<sup>2</sup>

Rohr, K. and Dietrich, J.R., Deep seismic reflection survey of the Queen Charlotte Basin, British Columbia; in *Evolution and Hydrocarbon Potential of the Queen Charlotte Basin, British Columbia*, Geological Survey of Canada, Paper 90-10, p.127-133, 1991.

## Abstract

*One thousand kilometres of 14 second marine reflection seismic data collected in the Queen Charlotte Basin region in 1988 provide excellent images of Tertiary sedimentary basin fill as well as deep crustal structure. This paper presents preliminary interpretations of two seismic lines: one in Hecate Strait and one in Queen Charlotte Sound. The Tertiary section is highly variable in thickness, with up to 6500 m of strata occurring in the deepest depocentres in a complex array of sub-basins and half-grabens. Widespread extensional deformation including normal faulting during basin development was followed later by compressional deformation in the northern half of the basin. Sediments have been compressed into open folds and flower structures. Seismic interpretations of structural features suggest that Tertiary extension and compression have developed in response to strike-slip tectonics.*

*Crust under Hecate Strait is more reflective than under Queen Charlotte Sound; geological interpretation of these discontinuous and structurally variable crustal reflections requires further analysis. In some areas of the basin (e.g. near the Sockeye wells, Hecate Strait) coherent reflections occur directly beneath the Tertiary section and may be images of Mesozoic strata. Deep reflections imaged at times of 7.0-10.0 s on many profiles, provide for the seismic differentiation between reflective lower crust and non-reflective upper mantle. Estimated crustal thicknesses of 18-21 km beneath Hecate Strait and Queen Charlotte Sound indicate significant crustal thinning beneath the Queen Charlotte Basin.*

## Résumé

*Mille kilomètres de données de sismique réflexion marine aux 14 secondes, recueillies dans la région du bassin de la Reine-Charlotte en 1988, ont fourni d'excellentes images des matériaux de remplissage du bassin sédimentaire du Tertiaire ainsi que de la structure profonde de la croûte. Cette communication présente les interprétations préliminaires de deux lignes sismiques: une dans le détroit d'Hécate et l'autre dans le détroit de la Reine-Charlotte. La section du Tertiaire a une épaisseur très variable, atteignant 6500 m de couches situées dans les points de sédimentation maximum les plus profonds dans un réseau complexes de sous-bassins et de demi-grabens. Une déformation d'extension générale avec formation de failles normales pendant le développement du bassin a été suivie plus tard d'une déformation de compression dans la moitié nord du bassin. Des sédiments ont été tassés dans des plis ouverts et des structures en fleur. Les interprétations sismiques des caractéristiques structurales indiquent que l'extension et la déformation du Tertiaire résultent de mouvements tectoniques de décrochement.*

*La croûte réfléchit davantage sous le détroit d'Hécate que sous le détroit de la Reine-Charlotte; l'interprétation géologique de ces réflexions crustales discontinues et structurellement variables nécessite une analyse plus poussée. Dans certaines parties du bassin (p. ex. près des puits Sockeye dans le détroit d'Hécate), des réflexions cohérentes se produisent directement sous la section du Tertiaire; il pourrait s'agir d'images des couches mésozoïques. Des réflexions profondes enregistrées à des temps de 7,0-10,0 s sur de nombreux profils permettent la différenciation sismique entre la croûte inférieure réfléchissante et le manteau supérieur non réfléchissant. L'épaisseur de la croûte, estimée à de 18 à 21 km sous le détroit d'Hécate et le détroit de la Reine-Charlotte, indique que la croûte est beaucoup plus mince sous le bassin de la Reine-Charlotte.*

<sup>1</sup> Pacific Geoscience Centre, Geological Survey of Canada, P.O. Box 6000, Sidney, B.C. V8L 4B2

<sup>2</sup> Institute of Sedimentary and Petroleum Geology, 3303 – 33rd Street N.W., Calgary, Alberta T2L 2A7

## INTRODUCTION

The Tertiary Queen Charlotte Basin in the Hecate Strait and Queen Charlotte Sound region of Canada's western continental shelf was the site of petroleum exploration in the 1960s and early 1970s, prior to establishment of an exploration moratorium in 1971. Exploration by the petroleum industry (principally Shell Canada Ltd. and Chevron Canada Resources Ltd.) included acquisition of a regional grid of multi-

channel reflection seismic data and drilling of eight offshore wells. The seismic and well data provided the basis for initial descriptions of the regional geology of the offshore Queen Charlotte Basin (Shouldice, 1971; Yorath and Chase, 1981). The industry seismic data was acquired with seismic sources and record lengths which provided only limited and often poor quality images of the deeper portions of the basin fill and underlying basement. To provide new informa-

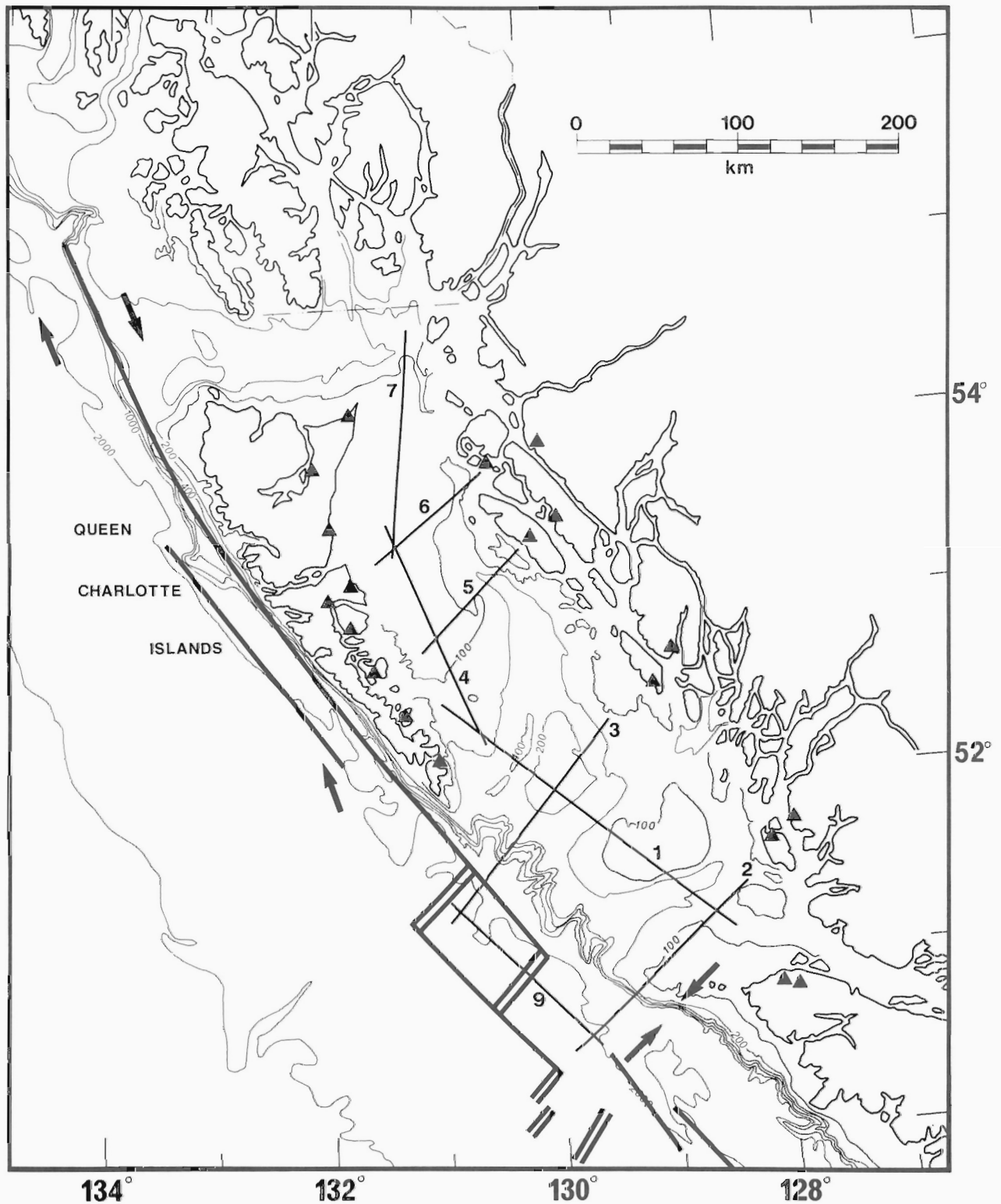


Figure 1: Map of multi-channel seismic reflection data collected in 1988.

tion on the structure and stratigraphy of the basin fill and crustal structure down to Moho, a regional deep reflection seismic survey was carried out in July, 1988 (Rohr and Dietrich, 1990). This report describes the acquisition and processing of the deep reflection data and presents preliminary interpretations of 2 of the 8 lines collected. Detailed interpretations of the complete data set are continuing and more comprehensive accounts of the regional geology and tectonic history of the basin will be incorporated into future publications.

## ACQUISITION

One thousand kilometres of 40-fold marine reflection data were collected under contract by Geophoto Services Ltd. using the seismic vessel M/V E.O. VETTER. The seismic source consisted of a 6358 in<sup>3</sup> (106L) tuned airgun array towed at 12 m depth. Shotpoints were spaced at 45 m intervals and 14 seconds of data were recorded at a sample rate of 4 milliseconds. The streamer was 3600 m long and contained 240 groups of hydrophones with a group length of 15 m. Field data were recorded with a 8-90 Hz filter. Data were acquired along 8 lines crossing Hecate Strait and Queen Charlotte Sound (Fig. 1). The lines were oriented to run across and parallel to the main northwest-southeast trend of the basin, with direct ties to the locations of 5 of the 8 offshore wells; the southern lines QC88-02 and -03 cross the present day plate boundary adjacent to Queen Charlotte Sound. In Hecate Strait data were collected on lines QC88-05 and QC88-06 within 3 km of the eastern shoreline of the strait but the western extent of data collection was limited to about 20 km offshore from the Queen Char-

lotte Islands due to shallow water depths for line QC88-06 and an excluded marine park area for line QC88-05. The lack of data collected closer to the Queen Charlotte Islands hinders correlation between the exposed geology onshore and the reflection data offshore.

## PROCESSING

The reflection data were processed under contract by Geophoto Services Ltd., Calgary. True amplitude recovery was applied to the first 3.5 s of data at 6 db/s with a constant gain of 21 db for the remaining 10.5 s. First breaks were muted and an f-k filter (-3 to 7 ms/trace) was applied to the shot records. The effect of the f-k filter on the stacked data is illustrated in Figure 2. The stacked data without the filter are dominated by seafloor-generated diffractions and linear noise which are effectively removed by the filter. The shot records were then deconvolved using both a source signature deconvolution and gap deconvolution. Mean amplitudes of the traces were equalized and the shot records were decimated from 240 to 120 traces per shot. This eliminates every other common-depth-point (CDP) gather so our CDP spacing is 15 m. Velocity analyses of the CDP gathers were carried out every 3 km. Below 6 s little difference in the CDP stacks were observed for a wide range of velocities (Fig. 3); stacking velocities of 6000-7000 m/s were used to stack data below 6 s. Note reflection events at 4, 6.5 and 7.2 s. Following normal move out and 40-fold stack, another deconvolution filter was applied to the data to further attenuate water bottom multiples. A filter was applied to remove random noise in the f-x domain, followed by time variant filtering and scal-

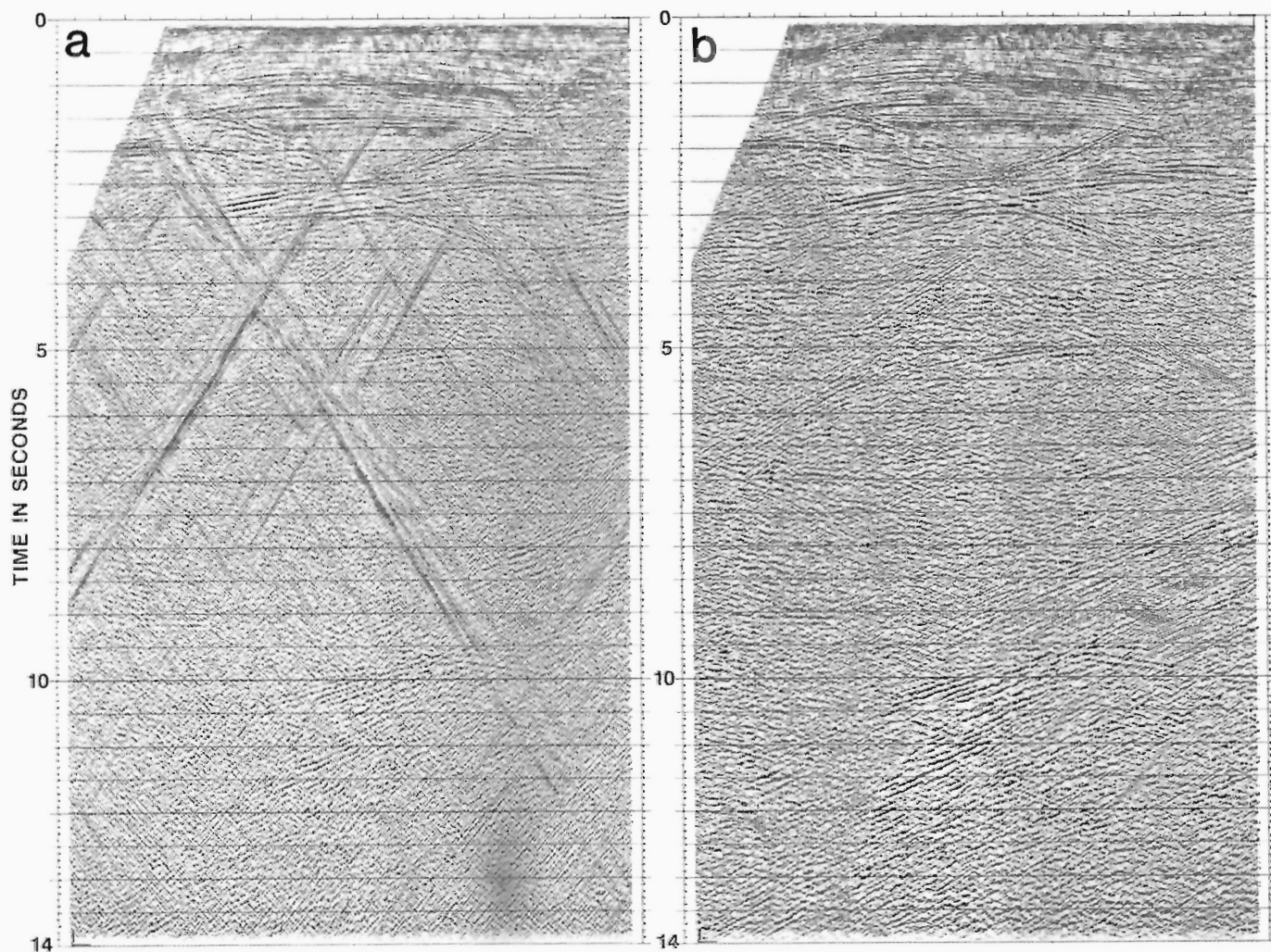


**Figure 2:** Brute stack of data: a) before and b) after f-k filter. Note that the steeply dipping diffractions in a) have been eliminated by the filter.



ing. The data were filtered 10-45 Hz from 0-4.0 s and the filter below 8 s was reduced to 10-15 Hz. The frequency filter was not varied laterally and some high frequency noise remains in areas where high velocity basement rocks occur at shallow depths. The final step in the data processing involved f-k migration using smoothed stacking velocities. Migration improved the imaging of structures within the sedimentary basin, but did little to resolve the structurally complex reflections sub-basement. Improved imaging of specific areas and features may result from advanced or specialized processing techniques, such reprocessing is currently planned or in progress for portions of the data set.

## INTERPRETATION

### Line QC88-06 – Hecate Strait

Line QC88-06 is a 90 km long southwest-northeast oriented profile crossing northern Hecate Strait (Fig. 1). The southwest end of the line crossed the location of the Tyee N-39 well which was drilled in

1969 to a depth of 3469 m and bottomed in microgabbro. The Queen Charlotte Basin sedimentary strata penetrated by the Tyee well are mostly Miocene and Pliocene in age (Shouldice, 1971), but parts of the basin may contain Tertiary strata as old as Eocene (Dietrich et al., 1989; Higgs, 1989). Seismically the Tertiary basin fill is characterized by relatively continuous, coherent reflections of variable amplitude (Fig. 4). The Tertiary clastic section contains intervals with interbedded coal and locally, interbedded volcanics; both sequences can produce high amplitude reflections. The Tertiary section displays considerable variability in thickness along line QC88-06, with the thickest deposits occurring in fault-bounded half-grabens; they can exceed 3.0 s or 5000 m in thickness. Basement along QC88-06 is interpreted to be at or near the base of the coherent, continuous reflections (#3 in Fig. 4). Depth estimates to seismically identified basement were derived from sonic well log data and seismic stacking velocities. Within the basin fill an unconformity at approx. 0.6 s at the Tyee well divides the Tertiary section into two units (labelled #1 and #2 in Fig. 4), with the lower unit

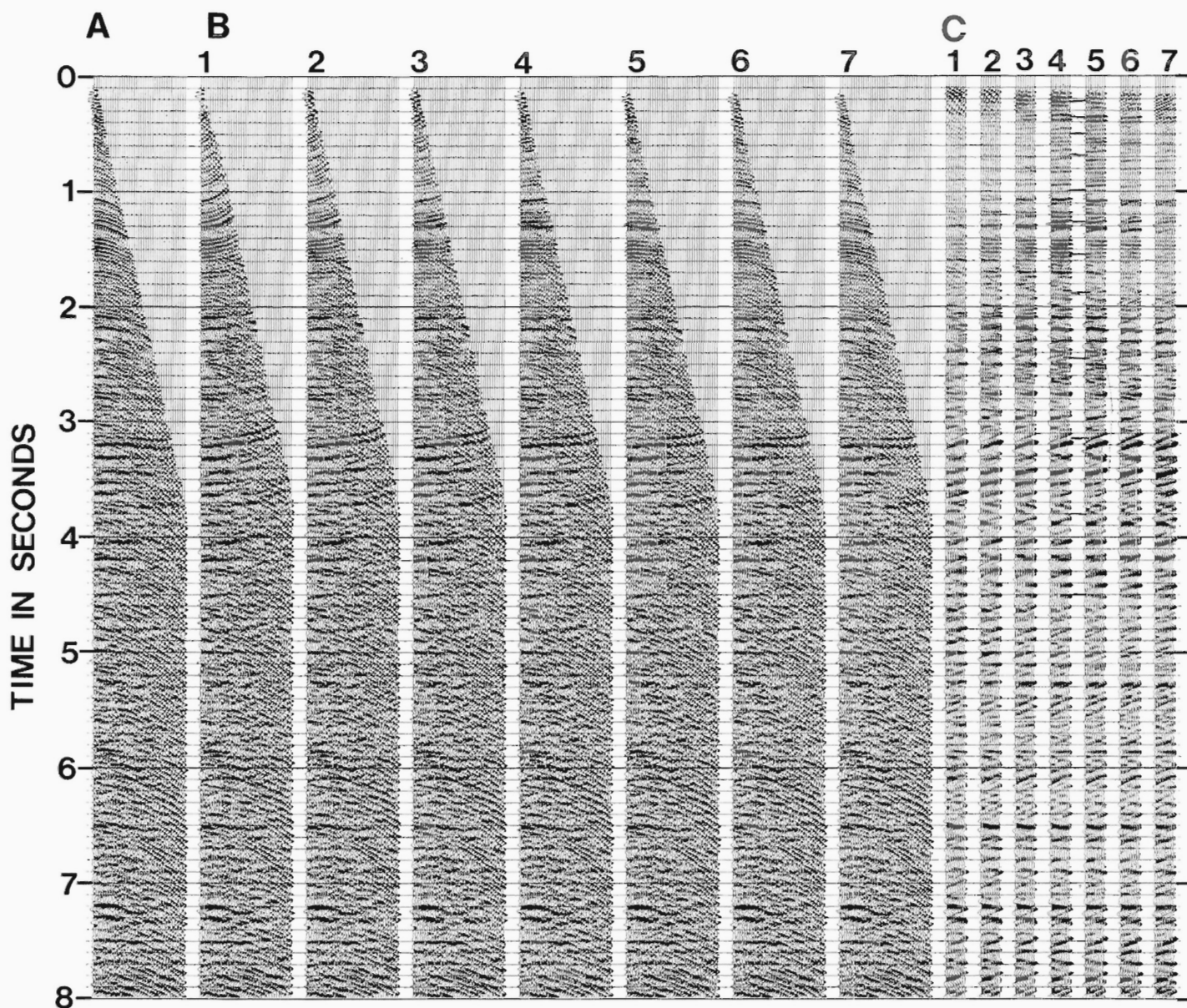


**Figure 3:** a) Gather #364 from line QC88-06; b) moved-out gather at velocity functions 1-7 on Figure d. Note that below 6 s there is little difference between the different velocities used. c) Stacks of gather plus 5 adjacent gathers using velocity functions in d.



displaying more variability in structural attitude and thickness than the upper unit. The unconformity has yet to be precisely dated from the well data, but is probably Early to mid-Pliocene in age. The basal portions of the lower unit locally contain high amplitude reflections, interpreted to be interbedded clastics and volcanic flows.

Along QC88-06 and throughout Hecate Strait the Tertiary section is extensively faulted and locally folded. The folds involve strata in both upper and lower units and clearly represent a young phase of deformation. The folds are isolated features eg. the anticline beneath the Tyee well and are usually cut by both normal and reverse faults; seismically they appear similar to positive flower structures,

faulted anticlines which form through convergent strike-slip deformation (Harding et al., 1983). The crest of the Tyee anticline has been truncated by erosion. Most of the faults disrupting the Tertiary section along QC88-06 and elsewhere in the basin are basement-involved normal faults with variable geometries and dips. The east end of QC88-06 crosses the Principe Laredo Fault which is imaged as a steeply dipping, down to northeast, normal fault; the fault bounds a half-graben containing up to 2.0 s (3000 m) of Tertiary sediments. The half-graben (informally named here the Feeney basin) appears similar in cross-section to some of the strike-slip basins in southern California (e.g. Crowell, 1984). The basin-bounding Principe Laredo Fault

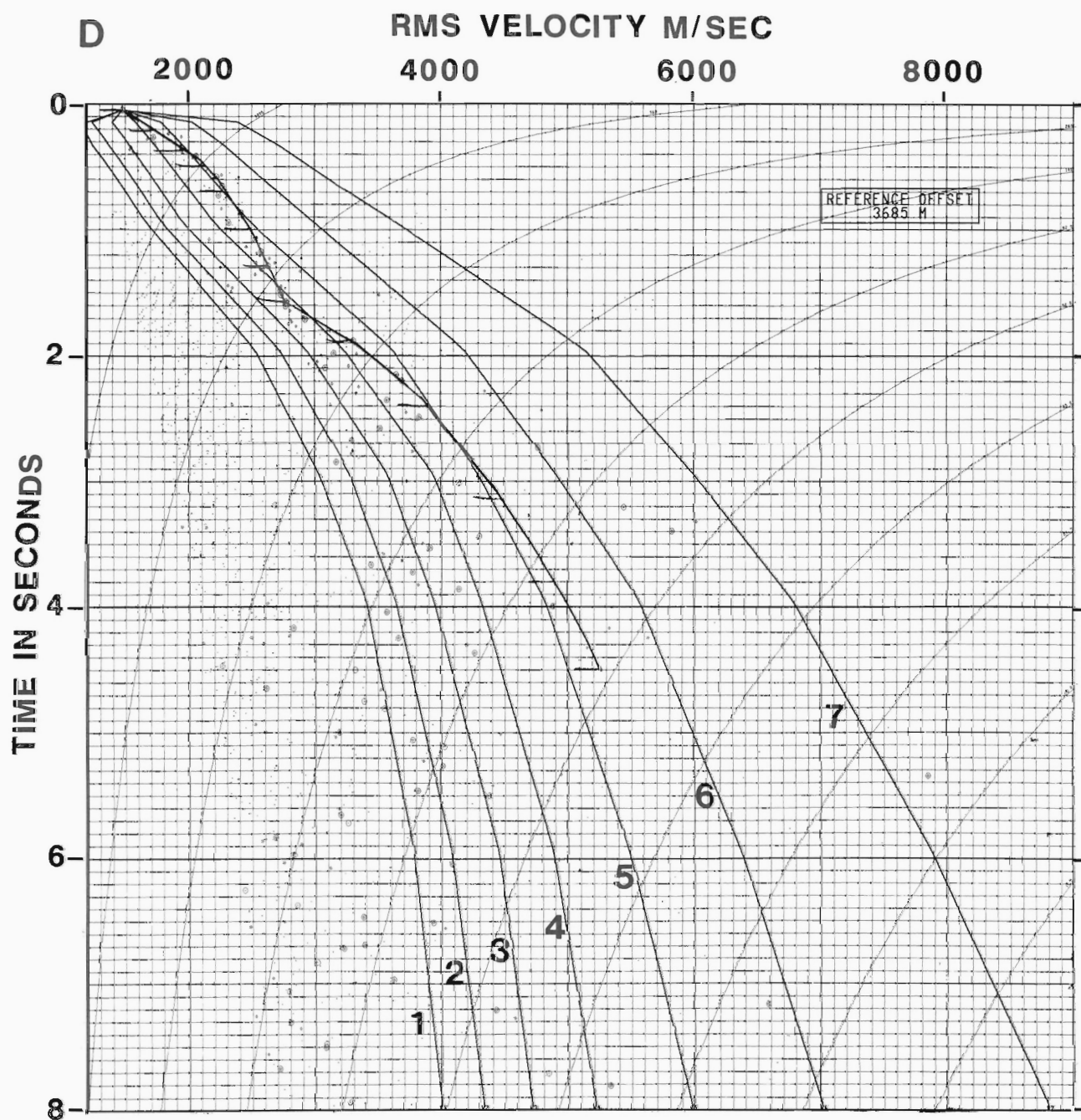


Figure 3: d) Velocity functions used to move-out and stack data.

appears to extend to considerable depths into the crust as evidenced by the truncation and apparent offset of crustal reflections below 6 s (#6 in Fig. 4).

Reflections within basement are variably dipping (#4 in Fig. 4) and display complex structural geometries, e.g. wedge-shaped structure at #5 in Figure 4. They can be observed from the sediment-basement interface down to 8-10 s. Below this depth no reflections are observed and we interpret the deepest of these events to be from reflection Moho (Klemperer et al., 1986). In western Hecate Strait high amplitude reflections and bright events cut each other between 5 and 7 s; they are underlain by weaker events down to 10.0 s. At the location of the velocity analysis discussed above note reflections at 4.0, 6.5 and 7.2 s. Under the Tyee well a discontinuous series of reflections dip from 3.0 s at the sediment-basement interface (near #3 on Fig. 4) to 8 s. East of this reflector bands of subhorizontal reflections lie between 6 and 9.5 s; these events fade under the crustal block uplifted west of the Principe Laredo Fault.

Interpretations of lithology, age and internal structure of the basement are still preliminary. The basement rocks penetrated by the Tyee well at 2.2-2.24 s (3364-3469 m) consist of microgabbro of possible Paleozoic age (Yorath and Chase, 1981). Igneous rocks of the Coast Plutonic complex exposed east of Hecate Strait probably comprise much of the non-reflective basement section at the east end of QC88-06. East of the Principe Laredo Fault crust is 10 s or 30 km thick whereas in the basin crystalline crust is 18-21 km thick, using an interval velocity of 6.0 km/s. The estimated 20 km depth to the Moho based on reflection times is in general agreement with crustal thickness interpreted from seismic refraction data on this line (Spence et al., 1991).

#### Line QC88-01 – Queen Charlotte Sound

The southeastern portion of QC88-01, crossing southern Queen Charlotte Sound (Fig. 1), is illustrated in Figure 5. This segment of QC88-01 crosses the location of the Osprey D-36 well, drilled to a depth of 2531 m and bottomed in basalt. Along QC88-01 the seismic differentiation between Tertiary strata (#1 in Fig. 5) and underlying

basement (#2 in Fig. 5) is more distinct than that observed on QC88-06. Coherent, moderate to high amplitude reflections within the Tertiary section are in marked contrast to the weakly reflective to non-reflective character of the underlying crust. Very high amplitude reflections in the lower part of the basin fill at the Osprey location are generated from interbedded clastics and volcanics. Unlike the Hecate Strait area, the Tertiary section beneath Queen Charlotte Sound is rarely folded and shows little effects of the late Tertiary-Quaternary compression observed further north. Seafloor canyons within Queen Charlotte Sound cut upper parts of the basin fill and do not appear to be controlled by basement structure; they have eroded into the sediments over basement highs and lows and are not coincident with basement faults. Tertiary strata and underlying basement along QC88-01 are cut by several large offset normal faults that bound tilted basement blocks and adjacent sediment and volcanic filled half-grabens; some faults can be followed for a few seconds into basement (#3 in Fig. 5). They appear to flatten in basement but this is mostly a velocity effect (Peddy et al., 1986). Fewer crustal reflections are imaged here than on the QC88-06. Weak discontinuous events between 6 and 8 s (#4 in Fig. 5) are interpreted to be lower crustal reflections with the deepest events marking Moho. Using an interval velocity of 6 km/s crystalline crust is then 18 km thick under the deepest portion of the basin shown.

#### SUMMARY

One thousand kilometres of 14 second marine reflection seismic data collected in the Queen Charlotte Basin region in 1988 have been processed to final stack and migrated sections. Detailed interpretations of the data are continuing but a number of observations can presently be summarized. All of the seismic profiles provide excellent images of the Tertiary sedimentary basin fill. The Tertiary section is highly variable in thickness, with up to 6500 m of strata occurring in the deepest depocentres beneath Hecate Strait. The basin fill and underlying basement are extensively faulted and, in a regional sense, form a complex array of sub-basins and half-grabens. Widespread extensional deformation including normal faulting during the early

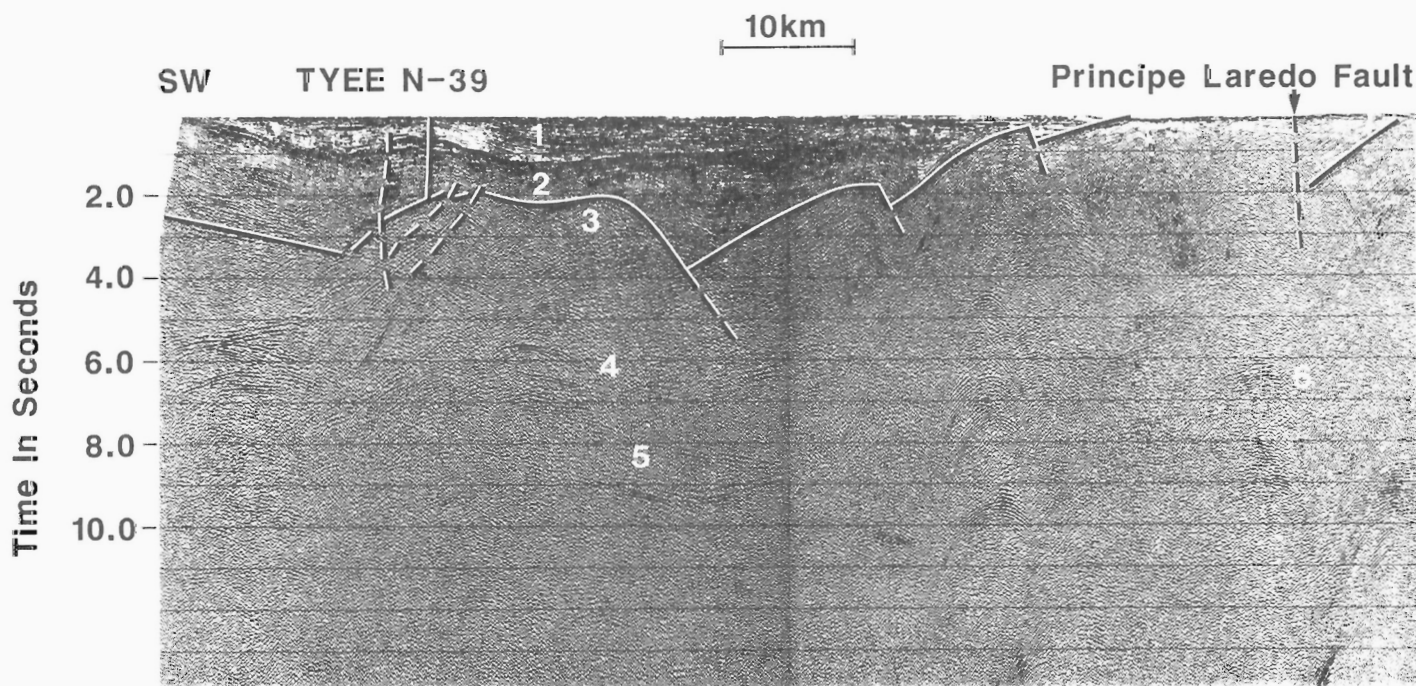


Figure 4: Stack of the QC88-06. See text for discussion.

phases of basin development was followed by compressional deformation in the northern half of the basin. Seismic interpretations of structural features suggest that the Tertiary extension and compression may have developed in response to strike-slip tectonics.

Crust under Hecate Strait is more reflective than under Queen Charlotte Sound; geological interpretation of these discontinuous and structurally variable crustal reflections requires further analysis. Beneath the Tertiary section in the Queen Charlotte Basin the seismic identification of Mesozoic sedimentary strata remains equivocal on some of the seismic sections, including lines QC88-01 and QC88-06, discussed here. In some areas of the basin (e.g. near the Sockeye wells, Hecate Strait) coherent reflections occur directly beneath the Tertiary section and may be images of Cretaceous strata. Deep reflections imaged at times of 7.0-10.0 s on many profiles, provide for the seismic differentiation between reflective lower crust and non-reflective upper mantle. Estimated crustal thicknesses of 18-21 km beneath Hecate Strait and Queen Charlotte Sound indicate significant crustal thinning beneath the Queen Charlotte Basin.

## ACKNOWLEDGMENTS

We would like to thank C.E. Keen and C.A. Spencer for their reviews.

## REFERENCES

- Crowell, J.C.  
1984: The tectonics of Ridge Basin, Southern California; in *Guidebook for Ridge Basin Field Trip*, J.C. Crowell (ed.), Rubey Conference Field Trip, Oct. 7, 1984, p. 25-42.
- Dietrich, J.R., Higgs, R., and White, J.M.  
1989: Seismic, sedimentological and palynological investigations in the Tertiary Queen Charlotte Basin; Abstract, Exploration Update 89, Canadian Society of Exploration Geophysicists, Canadian Society of Petroleum Geologists.
- Harding, T.P., Gregory, R.F., and Stephens, L.H.  
1983: Convergent wrench fault and positive flower structure, Ardmore Basin, Oklahoma; in *Seismic Expression of Structural Styles*, Vol. III, A.W. Bally (ed.), American Association of Petroleum Geologists.
- Higgs, R.  
1989: Sedimentological studies in Queen Charlotte Basin: implications for basin origin and petroleum exploration; Abstract, Northeast Pacific-North America Plate Interactions Throughout the Cenozoic, Geological Association of Canada.
- Klemperer, S.L., Hauge, T.A., Hauser, E.C., Oliver, J.E., and Potter, C.J.  
1986: The Moho in the northern Basin and Range province, Nevada, along the CO-CORP 40°N seismic-reflection transect; *Geological Society of America Bulletin*, v. 97, p. 603-618.
- Peddy, C.P., Brown, L.D., and Klemperer, S.L.  
1986: Interpreting the deep structure of rifts with synthetic seismic sections; in *Reflection Seismology: A Global Perspective*, M. Barazangi and L. Brown (ed.), Washington, D.C., American Geophysical Union Geodynamics Series, v. 13, p. 301-311.
- Rohr, K. and Dietrich, J.R.  
1990: Deep Seismic Survey of Queen Charlotte Basin; Geological Survey of Canada, Open File 2258.
- Shouldice, D.L.  
1971: Western Canadian continental shelf; in *The Future Petroleum Provinces of Canada - Their Geology and Potential*, R.G. McCrossan (ed.), Canadian Society of Petroleum Geologists, Memoir 1.
- Spence, G.D., Hole, J.A., Asudeh, E., Ellis, R.M., Clowes, R.M., Yuan, T., and Rehr, R.M.M.  
1991: A seismic refraction study in the Queen Charlotte Basin, British Columbia; in *Evolution and Hydrocarbon Potential of the Queen Charlotte Basin*, British Columbia, Geological Survey of Canada, Paper 90-10.
- Torath, C.J. and Chase, R.L.  
1981: Tectonic history of the Queen Charlotte Islands and adjacent areas; *Canadian Journal of Earth Sciences*, v. 18, p. 1717-1739.

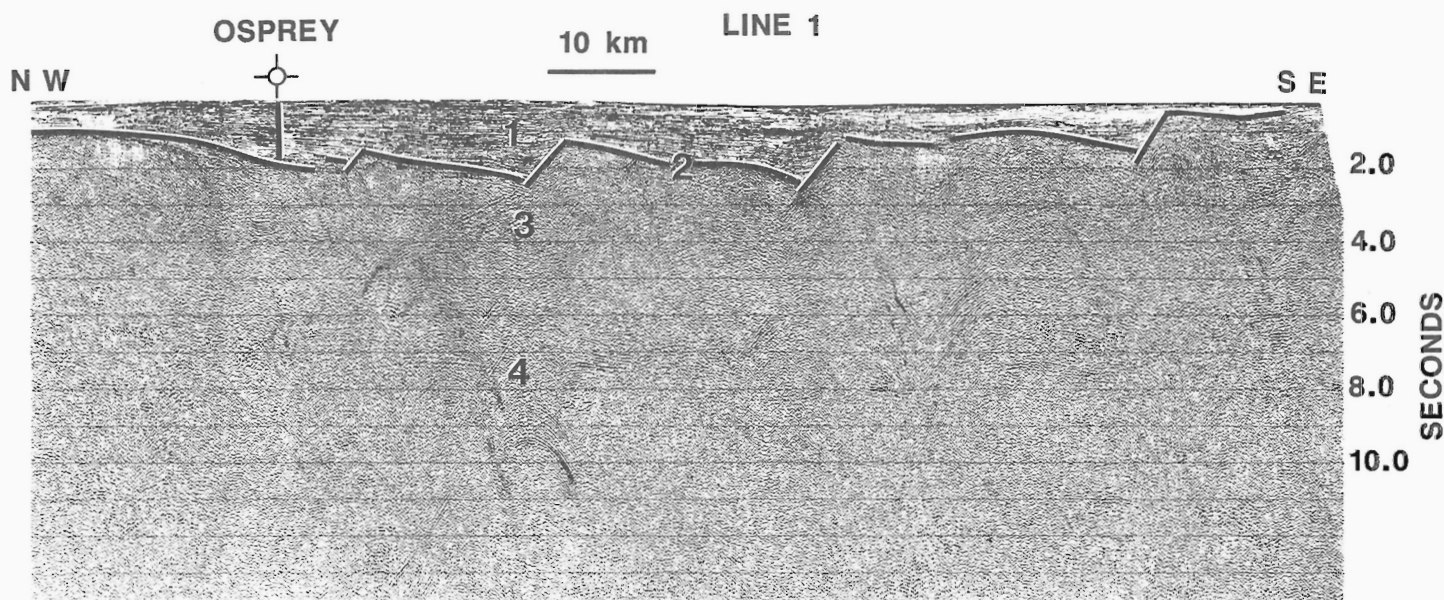


Figure 5: Stack of the QC88-01. See text for discussion.



# A seismic refraction study in the Queen Charlotte Basin, British Columbia

G.D. Spence<sup>1</sup>, J.A. Hole<sup>2</sup>, I. Asudeh<sup>3</sup>,  
R.M. Ellis<sup>2</sup>, R.M. Clowes<sup>2</sup>, T. Yuan<sup>1</sup>, and K.M.M. Rohr<sup>4</sup>

Spence, G.D., Hole, J.A., Asudeh, I., Ellis, R.M., Clowes, R.M., Yuan, T., and Rohr, K.M.M., A seismic refraction study in the Queen Charlotte Basin, British Columbia; in *Evolution and Hydrocarbon Potential of the Queen Charlotte Basin, British Columbia*, Geological Survey of Canada, Paper 90-10, p. 135-149, 1991.

## Abstract

*Refractions and wide-angle reflections from a 102L (6300 cu. in.) marine airgun array were recorded on single channel land stations during a combined seismic reflection and refraction survey in the Queen Charlotte Basin. The objective of the survey was to obtain a better understanding of the basin architecture and evolution. In this report, we describe the seismic refraction/wide angle reflection survey and present 13 representative sections out of the total of 47 recorded. The major characteristics of the sections are described, including the following observations: (1) a prominent mid-crustal reflection was often recorded at stations near the coast but was absent from stations 20-40 km farther inland; a traveltime delay in the first arrivals at about 60 km range was commonly associated with the reflection; (2) a prominent Moho reflection typically over the 60-100 km range; (3) mantle refraction arrivals with apparent velocities near 8.0-8.1 km/s observed out to 280 km range.*

*Preliminary traveltime models were determined for three record sections. The models should be considered as only generally representative of the velocity structure; further details will be confirmed in later synthetic seismogram interpretations. Across central Hecate Strait, the upper crust can be divided into two regions. Below the sediments, velocities in the first layer increase from 6.2-6.3 to 6.4-6.5 km/s over a thickness of 3-5 km. In the second layer, from about 8-17 km subsurface depth, the velocity gradient is small and may even become negative. At 15-17 km depth, velocities increase abruptly to at least 6.8-6.9 km/s. A sliver of 1-3 km thickness with velocity 7.2 km/s or more may be present below the interface in both Hecate Strait and southern Queen Charlotte Sound; the sliver may be a piece of ocean crust or mantle stranded in a past subduction episode. Crustal thickness beneath Hecate Strait is no more than 23 km, implying significant thinning relative to the crust outside the basin.*

## Résumé

*Durant un levé combinant la sismique réflexion et la sismique réfraction dans le bassin des îles de la Reine-Charlotte, les réfractons et les réflexions grand angle d'un dispositif de canons à air sous-marins de 102L (6300 po. cu.) ont été enregistrées à des stations terrestres monocéaniques. Le présent rapport contient une description du levé de sismique réflexion et réfraction grand angle et présente 13 coupes représentatives des 47 qui ont été enregistrées au total. Les principales caractéristiques des coupes sont les suivantes : 1) une importante réflexion a souvent été enregistrée dans la croûte intermédiaire à partir des stations situées près de la côte mais pas à partir de stations situées entre 20 à 40 km à l'intérieur des terres; un retard enregistré dans les premières arrivées à une distance d'environ 60 km a été en général associé à la réflexion; 2) une importante réflexion de Moho sur une distance typique de 60 à 100 km; 3) des temps d'arrivée de la réfraction dans le manteau caractérisées par des vitesses apparentes de près de 8,0 et 8,1 km/s jusqu'à une distance de 280 km.*

*On a déterminé pour trois coupes d'enregistrement, des modèles préliminaires de durée de trajet. Ces modèles ne devraient être considérés que pour une représentation générale de la structure de la vitesse; d'autres données détaillées seront confirmées par des interprétations ultérieures de sismogrammes synthétiques. À travers le centre du détroit d'Hécaté, la croûte supérieure peut se subdiviser en deux régions. Au-dessous des sédiments, les vitesses dans la première couche passent de 6,2 et 6,3 km/s à 6,4 et 6,5 km/s au-dessus d'une épaisseur de 3 à 5 km. Dans la deuxième couche, à partir d'environ 8 à 17 km sous la surface, le gradient de vitesse est faible et peut même être négatif. À la profondeur de 15 à 17 km, les vitesses augmentent subitement à au moins 6,8 et 6,9 km/s. Un fragment de 1 à 3 km d'épaisseur donnant une vitesse d'au moins 7,2 km/s pourrait être présent au-dessus de l'interface dans le détroit d'Hécaté et dans le sud du détroit de la Reine-Charlotte; ce fragment pourrait être un morceau de croûte océanique ou de manteau échoué au cours d'un épisode de subduction antérieur. L'épaisseur de la croûte au-dessous du détroit d'Hécaté ne dépasse pas 23 km, indiquant un amincissement important de la croûte à l'extérieur du bassin.*

<sup>1</sup> Department of Physics and Astronomy, University of Victoria, Victoria, B.C. V8W 3P6

<sup>2</sup> Department of Geophysics and Astronomy, University of British Columbia, Vancouver, B.C. V6T 1W5

<sup>3</sup> Continental Geoscience Division, Geological Survey of Canada, 1 Observatory Crescent, Ottawa, Ontario K1A 0Y3

<sup>4</sup> Pacific Geoscience Centre, Geological Survey of Canada, P.O. Box 6000, Sidney, B.C. V8L 4B2



## INTRODUCTION

The Queen Charlotte Islands are located on the western Canadian margin near the triple junction between the Juan de Fuca ridge system, the subduction zone of the Juan de Fuca plate system, and the Queen Charlotte transform fault (Fig. 1). The Queen Charlotte Basin includes the area underlying Hecate Strait and Queen Charlotte Sound, and extends under eastern Graham Island. Exploration in the 1960's included extensive reflection seismic surveying and the drilling of 8 offshore wells. These established that the maximum thickness of sediments in the basin was at least 4.5 km (Shouldice, 1971). Most of the basin sediments were dated as late Miocene or Pliocene (about 6 Ma). Based on more recent studies of marine microfaunas by B.E.B. Cameron (*in* Yorath and Hyndman, 1983), subsidence and basin formation were initiated at about 17 Ma in the region of the Harlequin well in Queen Charlotte Sound (Fig. 1).

Many problems exist in our understanding of the Queen Charlotte Basin. Yorath and Hyndman (1983) proposed that extension in Queen Charlotte Sound was taken up by strike-slip motion along the then-continuous Louscoone Inlet-Sandspit fault system, which was subsequently offset by the Rennell Sound Fault zone (Fig. 1). However, Thompson and Thorkelson (1989) found no evidence of Tertiary strike-slip motion in detailed mapping of northern Moresby Island. They observed block faulting from late Jurassic to early Tertiary, and suggested that reactivation of the block faults may have caused subsidence in the late Tertiary as well. Yorath and Hyndman (1983) also discussed geophysical evidence for oblique convergence and underthrusting of the oceanic plate beneath southern Moresby Island. They argued that the associated lithospheric flexure produced subsidence in Queen Charlotte Basin and uplift along western Graham Island, where up to 5 km of uplift were inferred from the geological observations

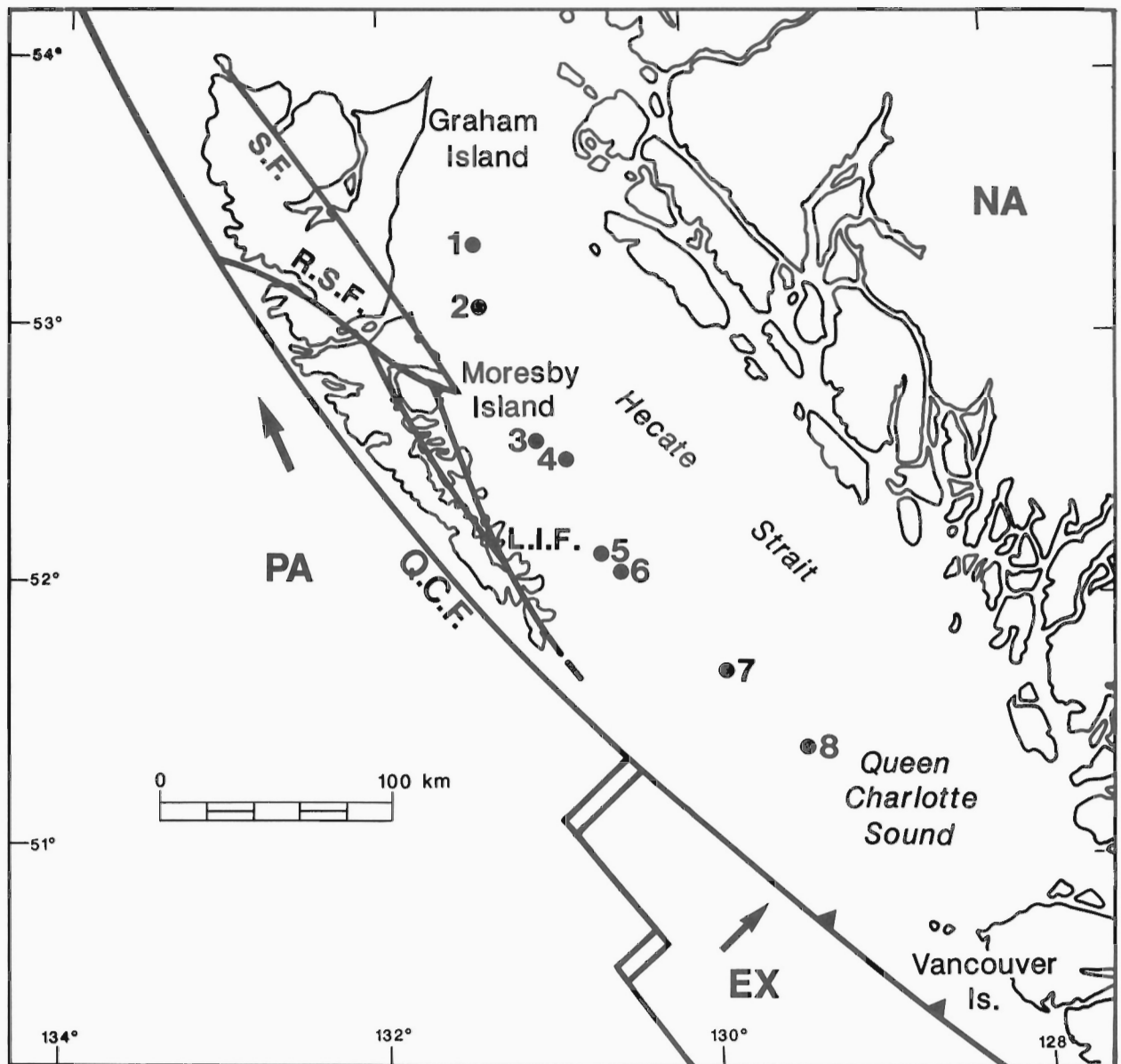


**Figure 1:** General location and tectonic map. Solid arrows show direction of plate motions with respect to North America (NA). PA = Pacific plate; EX = Explorer plate of the Juan de Fuca plate system; S.F. = Sandspit fault; R.S.F. = Rennell Sound fold zone; L.I.F. = Louscoone Inlet fault; Q.C.F. = Queen Charlotte Fault. Exploratory wells: 1-South Coho; 2-Tyee; 3-Sockeye B-10; 4-Sockeye E-66; 5-Murrelet; 6-Auklet; 7-Harlequin; 8-Osprey.



of Sutherland Brown (1968). However, Thompson and Thorkelson (1989) found no preferred eastward dip in their detailed mapping, and so question the inference of uplift. Thus, there appears to be a conflict between general tectonic and geophysical considerations and some current geological interpretations, regarding the origin of the Queen Charlotte Basin.

As part of the Frontier Geoscience Program, a combined seismic reflection and refraction survey was carried out in July 1988 to study the structure of the sediments and underlying basement of the Queen Charlotte Basin. The main objective of the program was to obtain a better understanding of the basin architecture and evolution, and to study plate structure and plate interactions in the region. Specifically, the program hoped to test various aspects of the rift and flexure model of Yorath and Hyndman (1983). The Queen Charlotte area is one of Canada's most seismically active regions, including the largest earthquake recorded in Canada – the 1949 magnitude 8.1

event described by Rogers (1983). Thus, an additional objective of the program was to provide structural and velocity information useful for earthquake analysis. This information could improve the accuracy of earthquake locations, identify potentially active faults, and suggest models and mechanisms for improved understanding of the origin of the earthquakes.

The seismic refraction survey is described in this report; the seismic reflection study is presented in a companion paper (Rohr and Dietrich, 1991). The major benefit of recording wide-angle reflections and refractions is that the large source-receiver offsets allow both structure and velocities to be obtained within and below the crust. This is particularly important for the lower crust and upper mantle, where velocity resolution determined by the reflection method is poor. Refraction velocities may then be used to convert traveltimes on reflection sections to depth. Onshore recording of offshore shots also enables major crustal features interpreted from the marine reflection lines to

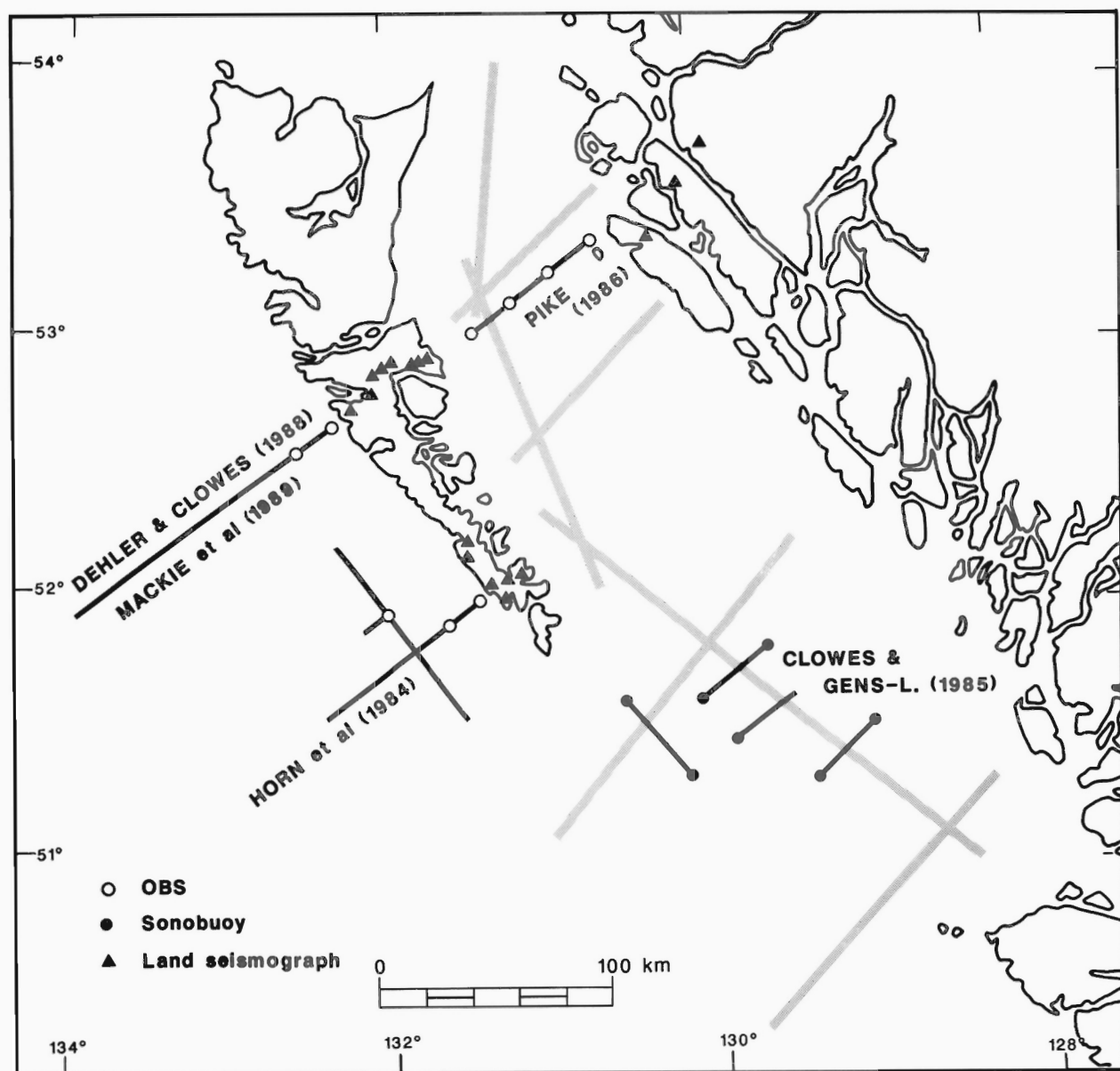


**Figure 2:** Location of recent seismic refraction profiles. Representative velocity models for some of the profiles are shown in Figure 3.

be extrapolated to the land where they may be correlated with geological studies.

This report describes the refraction experiment and provides a compilation of the refraction data. The dataset is very extensive, consisting of 47 record sections. In this report we present 13 representative sections, describe the major features of the reflected and refracted arrivals, and present preliminary interpretations of portions of the dataset. The preliminary nature of the refraction interpretation must be stressed. A final refraction model awaits a more careful analysis of the data and integration with geological and other geophysical interpretations, in particular that of the seismic reflection data.

## PREVIOUS SEISMIC REFRACTION STUDIES

Velocity models from several recent seismic refraction studies in the Queen Charlotte Island region are given in Figure 3, with corresponding profile locations shown in Figure 2.

Results from a 1983 refraction experiment are shown in Figures 3a and 3b. Figure 3a presents a velocity model deduced from airguns and 34 explosive shots sited west of Moresby Island (Dehler and Clowes, 1988; Mackie et al., 1989). The main features include: (1) anomalously low velocities below the Queen Charlotte terrace, supporting the interpretation of the terrace as a sedimentary accretionary wedge; (2) a thin crust (21-27 km) beneath the Queen Charlotte Islands; and (3) the Moho beneath Hecate Strait deepening eastward from 27-32 km. The velocity model converted to density also is consistent with models of the gravity anomaly field along the profile (Mackie et al., 1989).

The upper crustal velocity structure beneath Hecate Strait is shown in Figure 3b (Pike, 1986). Sediment thicknesses are estimated only from the refracted arrivals since no multichannel reflection profile was then available. Velocities near 6 km/s are reached by 5 km depth, and velocities near 6.5 km/s are interpreted at 7 km depth. The model also includes a low velocity zone at 3 km depth at the east end of the profile, plus high velocities of 7 km/s and greater at the base of the model, although this characteristic was poorly constrained. By comparison with the high-quality dataset along a nearly-coincident line presented later in this report, we feel that these latter two features are not justified due to the low signal-to-noise ratios in the 1983 data.

Horn et al. (1984) interpreted a refraction profile across the Queen Charlotte Fault off southern Moresby Island; the profile used explosive sources recorded on OBS's and land-based stations. Their results, shown in Figure 3c, are consistent with the model off northern Moresby Island (Fig. 3a). Beneath the terrace, the crustal velocities are anomalously low and the thickness of the crust rapidly increases eastwards from 12-18 km.

In Queen Charlotte Sound, Clowes and Gens-Lenartowicz (1985) obtained a crustal velocity model (Fig. 3d) from a series of sonobuoy profiles using a 32 L airgun source. Below a cover of about 2 km of sediments, they found basement velocities of 5.1-5.5 km/s which they associated with Masset extrusives. They also observed an elongated wave train and a possible 200 ms delay in the 5.5 km/s arrival, and interpreted this as due to a low-velocity zone beneath the volcanics. Clowes and Gens-Lenartowicz (1985) proposed that the low velocity material represented sediments which were subsequently cov-

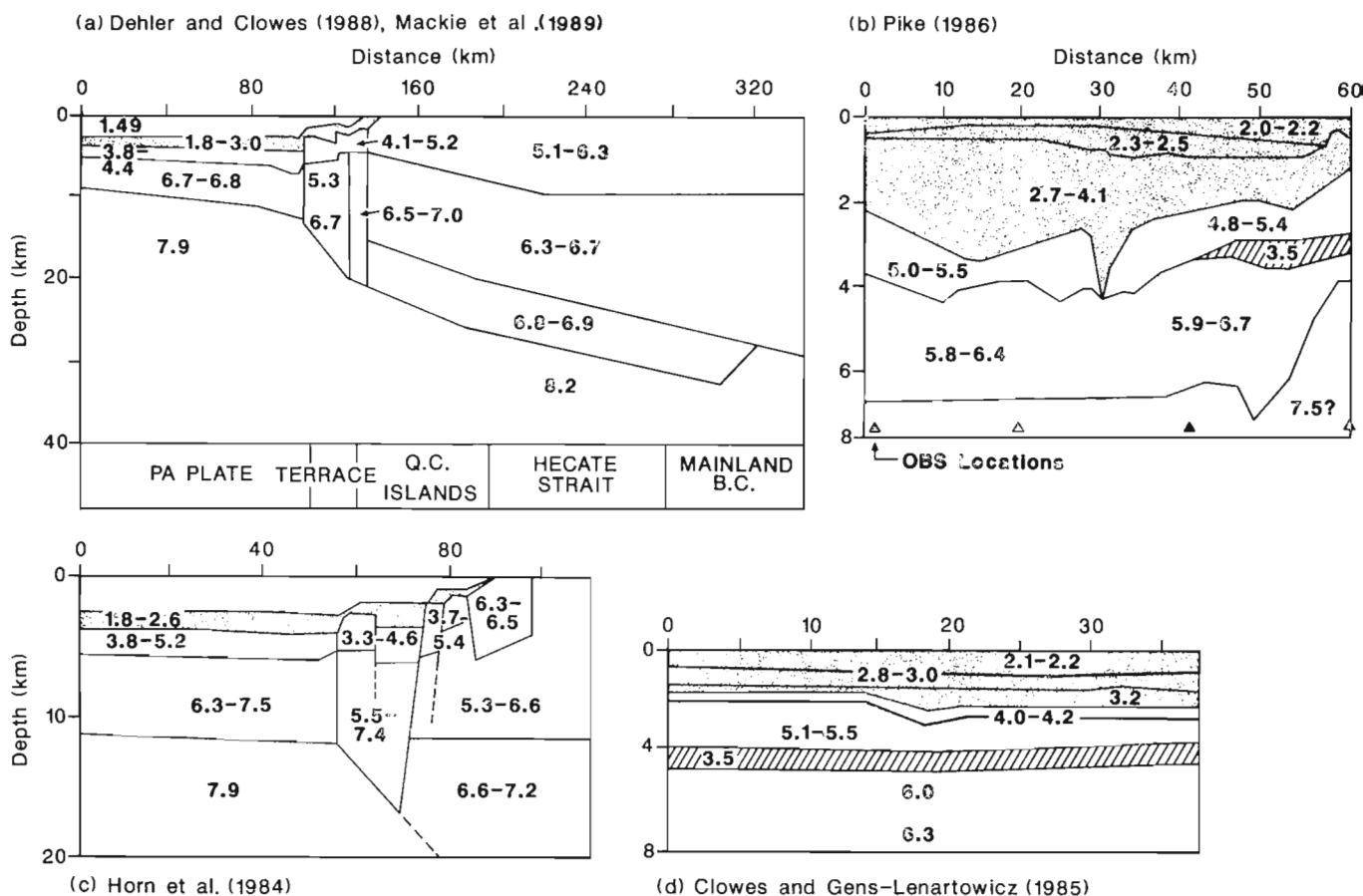


**Figure 3:** Velocity models in the Queen Charlotte Island region based on recent seismic refraction interpretations. The lightly shaded regions just below the surface represent sediments. The hatched regions in (b) and (c) have been interpreted as low velocity zones. See Figure 2 for profile locations.

ered by the extrusives. They noted that this is consistent with the gravity interpretation of Stacey (1975), who proposed that the low gravity values in Queen Charlotte Sound could also be explained by low-density sediments occurring below the volcanics.

## ACQUISITION OF THE SEISMIC REFRACTION DATA

A coincident seismic reflection and refraction experiment was carried out utilizing a 102 L airgun array. A total of 1135 km of 14s marine reflection data were collected. Simultaneously, refractions and wide-angle reflections from the airgun shots were recorded on land seismographs distributed around Hecate Strait and Queen Charlotte Sound (Fig. 4). Single channel digital seismographs, maintained by the Geological Survey of Canada, were deployed at 11 sites, and FM analog systems from the University of British Columbia recorded arrivals at 9 sites.

Each airgun line was recorded at one digital and one analog site at the landward ends of the lines, as well as at nearby offshore or broadside sites. Receiver site locations were determined from 1:50 000 topographic maps to accuracies of approximately 75 m. The airgun shots were fired every 45 m by the ship's navigation system, which was controlled by Loran C and supplementary satellite fixes; the relative accuracy from shot-to-shot was 1-2 m, whereas the absolute shot location error was 100-300 m. The shot firing system, which was tied into a GOES satellite receiver clock, gave shot times to an accuracy of about 2 ms.

Unfortunately, for the last three lines of the survey, a significant number of shot times were not recorded due to equipment problems.

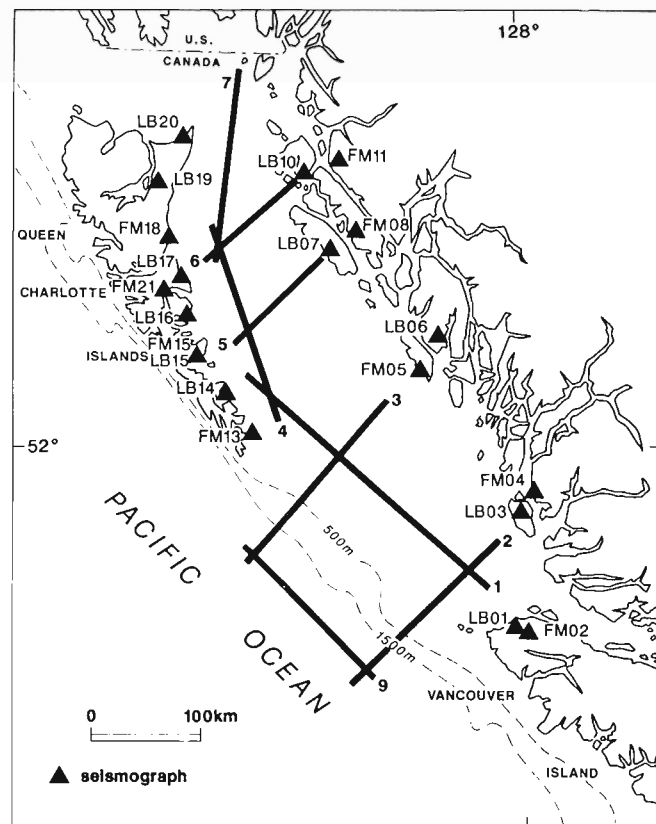


**Figure 4:** Location of marine airgun profiles and land-based seismograph sites during the Queen Charlotte seismic experiment. The 102 L airgun array fired shots every 45 m. At sites starting with LB, digital Lunchbox recorders were deployed, while those beginning with FM recorded arrivals on 5-day analog FM seismographs.

The percentage of shots missed was 35%, 15% and 45% for lines 5, 6 and 7 respectively. Missing shot times were objectively interpolated from the existing ones based on the repetitive nature of the shooting supplemented by the alignment of refracted arrivals. This process is complete for lines 5 and 6, and nearly finished for line 7.

A total of 51 digital seismographs were deployed. The output of vertical 2 Hz geophones was recorded at a rate of 120 samples per second, with a total of 1 Mbyte or 1.2 hours of data stored in the solid state memory of each instrument. Only line 6 at its western end was recorded continuously. For all remaining sites, the instruments recorded 40 s windows separated by 40 s gaps, effectively doubling the elapsed time covered. The internal clock of each instrument was rated against a GOES satellite clock, and the clock drift for each trace automatically calculated. Total drifts were commonly less than 15 ms for deployments of 1-2 days, with an estimated drift error of ~3 ms.

The FM analog instruments recorded the output from vertical 1 Hz seismometers at three amplitude levels. A WWVB radio time code, 1 Hz and 15 Hz internal clocks, and a short circuit were recorded on the remaining tape channels. The data were digitized at 120 samples per second using the 15 Hz clock to trigger the digitizer in order to compensate for tape speed variations. Changes in tape speed also produced amplitude variations because of the FM recording. These were corrected by subtracting the short circuit channel signal from the data channels. At three sites (FM05, FM15 and FM18), additional large, high frequency tape speed variations occurred. Special hardware and software were designed to correct this problem, but its severity nevertheless resulted in increased noise levels at these sites.

Arrivals out to about 10 km range were recorded using an anchored, telemetered sonobuoy at the western end of line 6. The signal received on the shooting ship was digitized and recorded on a DFS-V recording system.

## DATA PROCESSING

All data were converted to the extended SEG-Y format adopted by Lithoprobe for refraction data storage (Spencer et al., 1989). Field records for the digital seismograph data were initially 40 s in length and usually separated by 40 s gaps. The shot interval was nominally 20 s, and so SEG-Y records were written with a record length of 20 s. Because of the 40 s recording gaps, not all shots were recorded for the full 20 s, and either the beginning or end of many records had to be padded with zeroes.

Subsequent processing included filtering and trace binning. The dominant signal frequency is 8-10 Hz, and so bandpass filtering from 5-20 Hz was applied. All traces within non-overlapping bins of 135 m width were summed, using a summing velocity of 8 km/s. This bin width was chosen in order to span the traces missed during the 40 s time gap (i.e. a minimum gap in offset of 90 m), and also to compress the data to a more easily displayed trace interval.

On lines for which a preliminary interpretation was done, water layer and sediment statics corrections were calculated for each trace, and plots were generated both with and without this correction. The statics correction usually smoothed out traveltimes undulations due to rapid variations in sediment thickness. Water depths were obtained from the shipboard echo sounder. Two-way times through the sediments were determined from the multichannel seismic lines and then converted from time to depth by simple ray tracing through a velocity model based on well velocity logs. The statics correction applies traveltimes delays to strip off the water and sediment layers and replace them with a uniform sediment layer above a constant velocity basement. By "filling in" material to a horizontal datum level, this correction assumes that the immediate sub-basement velocity structure is effectively horizontal. The alternate correction is not to replace the stripped

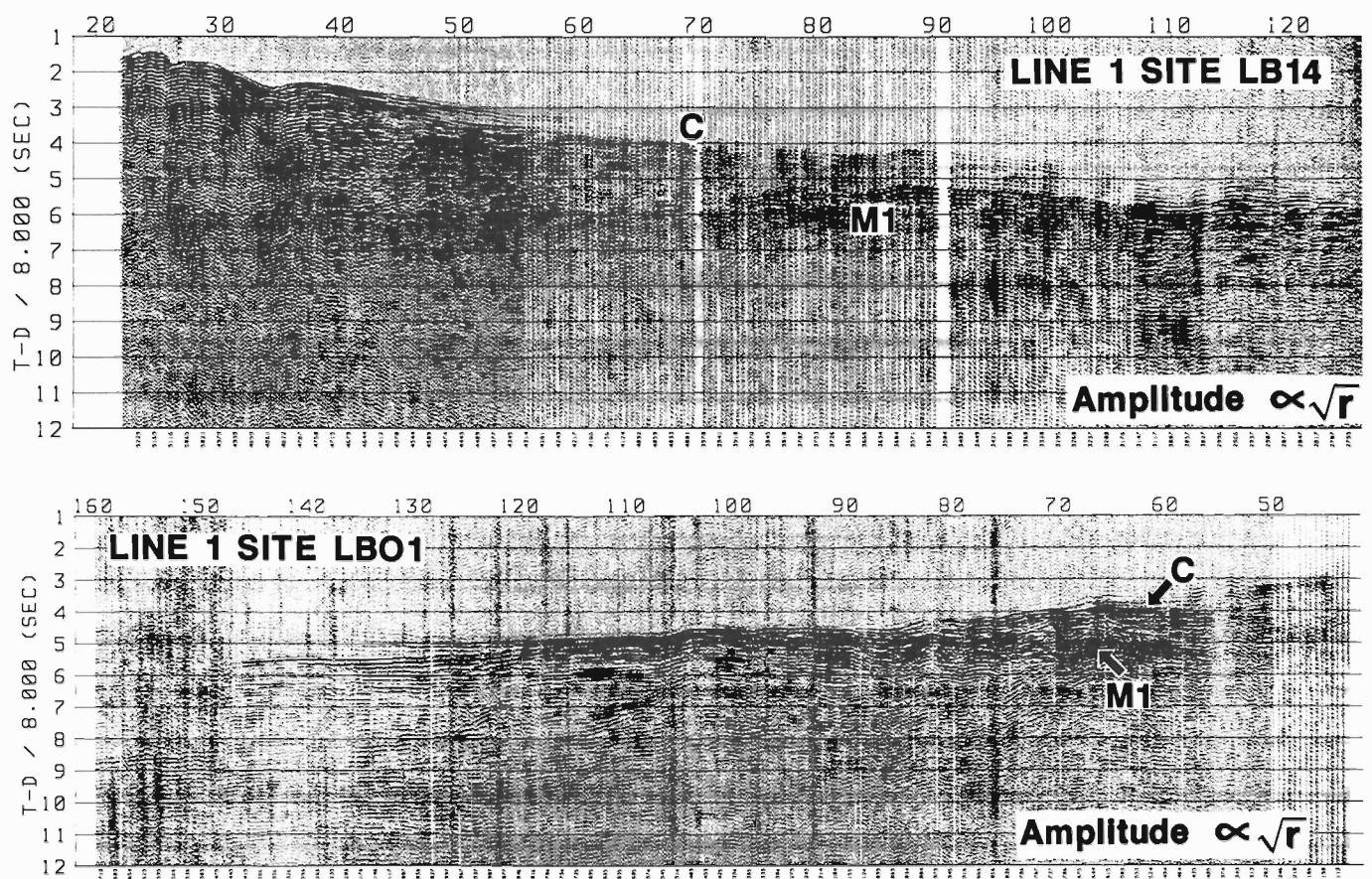


**Figure 5:** Near-offset portion of record sections for sites LB01 and LB14 on Line 1. Arrivals labelled C originate from a mid-crustal interface. Moho reflections are labelled M1. Amplitudes are multiplied by a factor proportional to the square root of the trace range.

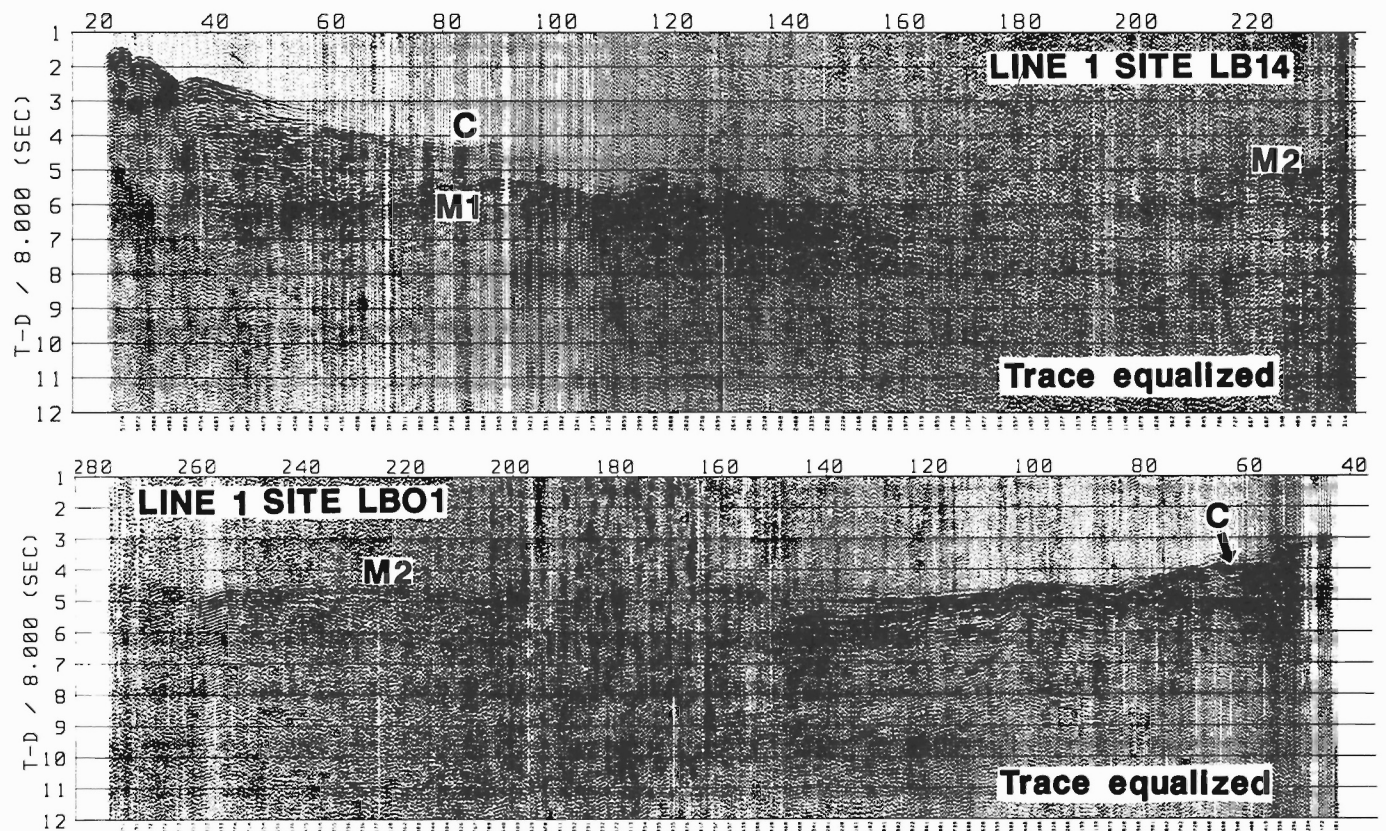


**Figure 6:** Record sections out to maximum recorded offsets for sites LB01 and LB14 on Line 1. Arrivals labelled C originate from a mid-crustal interface. Moho reflections are labelled M1. Mantle arrivals, labelled M2, have velocity 8.0-8.1 km/s. Record sections are plotted trace normalized, and no sediment statics corrections are applied.



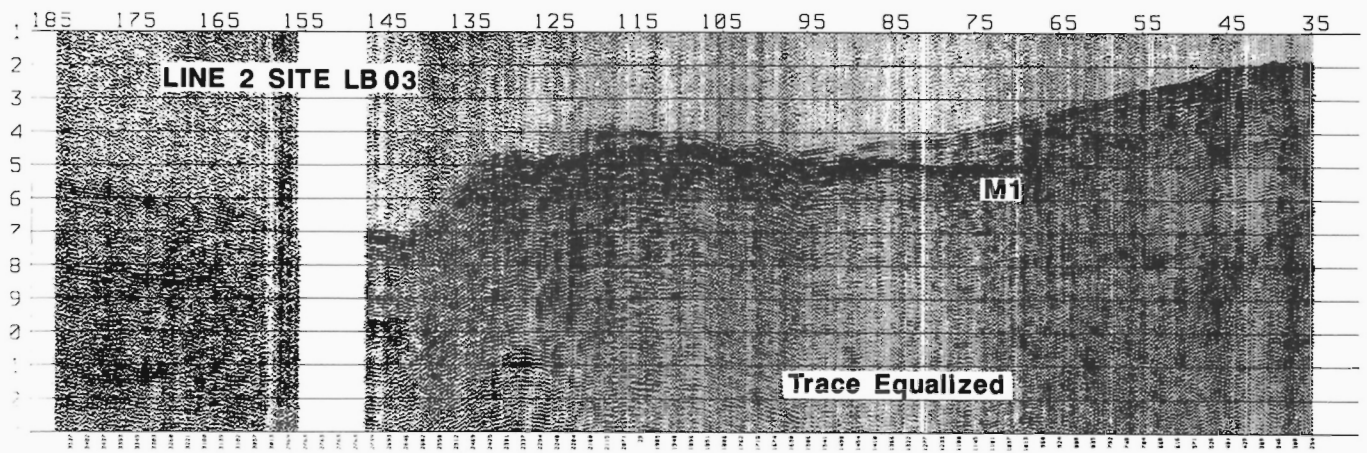


Figure 7: Trace equalized section for Lunchbox site LB03 on Line 2. See caption for Figure 6.

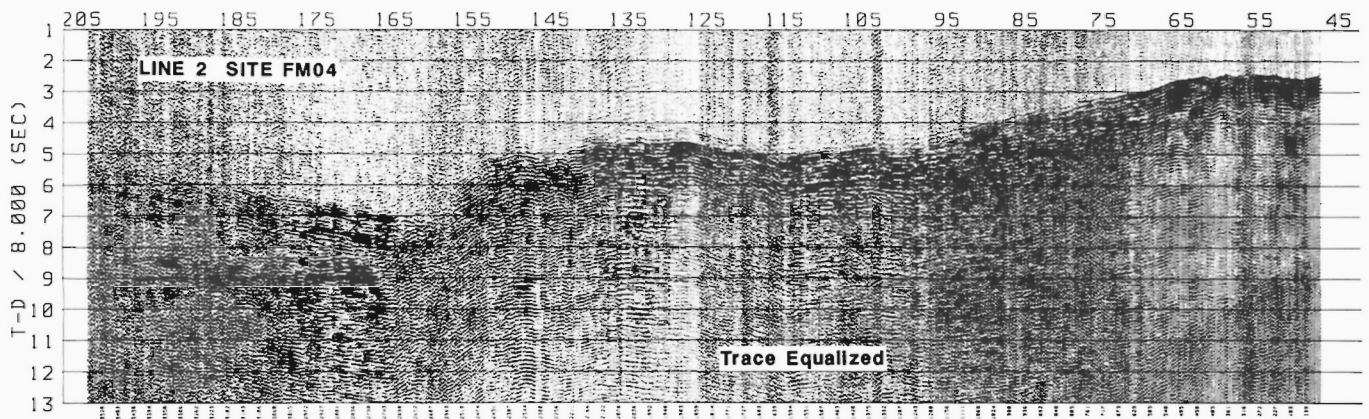


Figure 8: Trace equalized section for analog site FM04 on line 2. See caption for Figure 6.

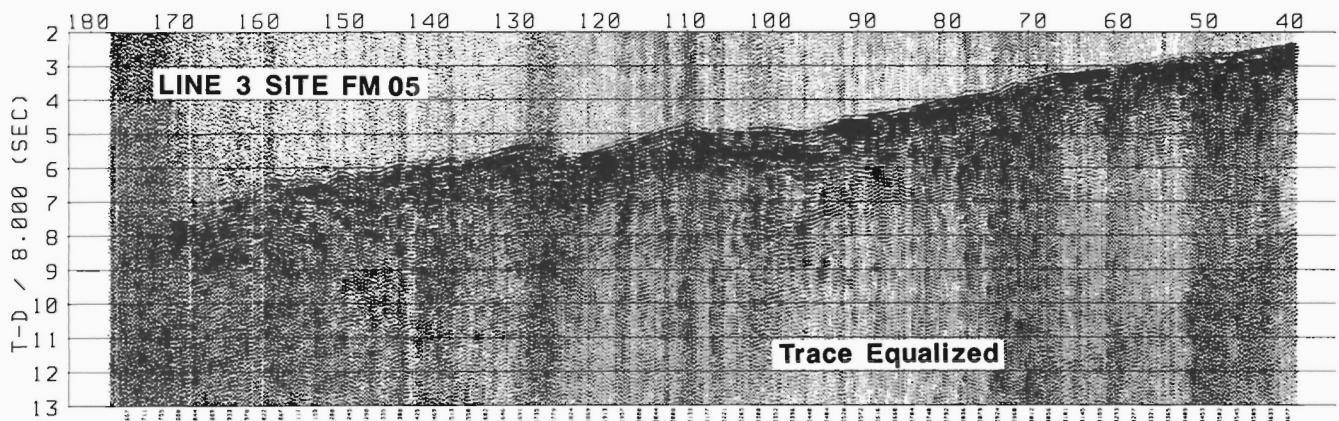


Figure 9: Trace equalized section for analog site FM05 on Line 3. See caption for Figure 6.

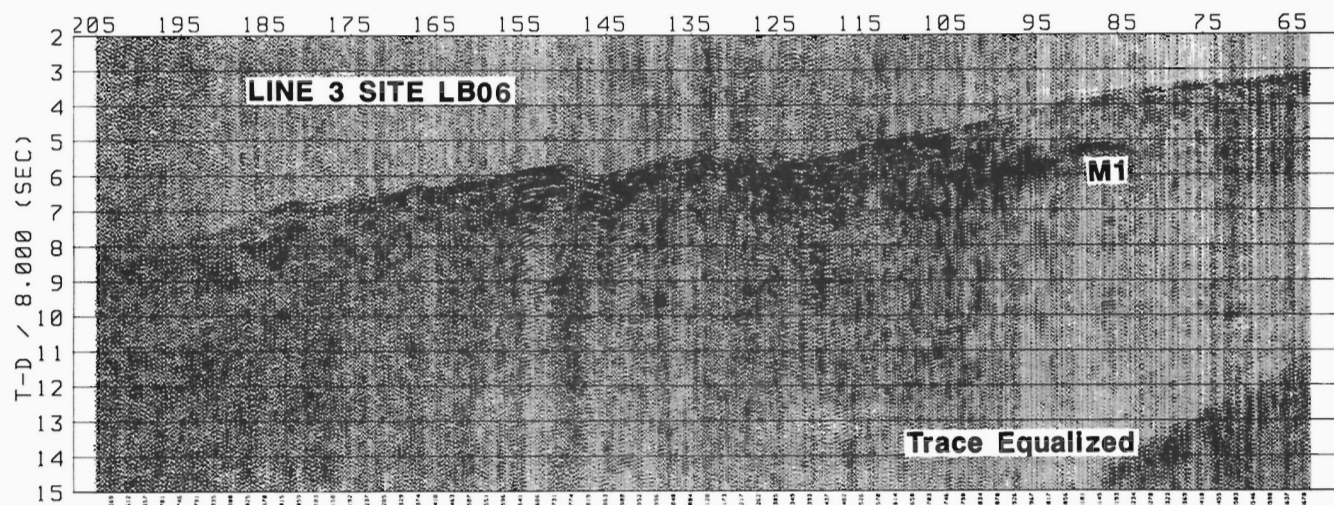


Figure 10: Trace equalized section for Lunchbox site LB06 on Line 3. See caption for Figure 6.

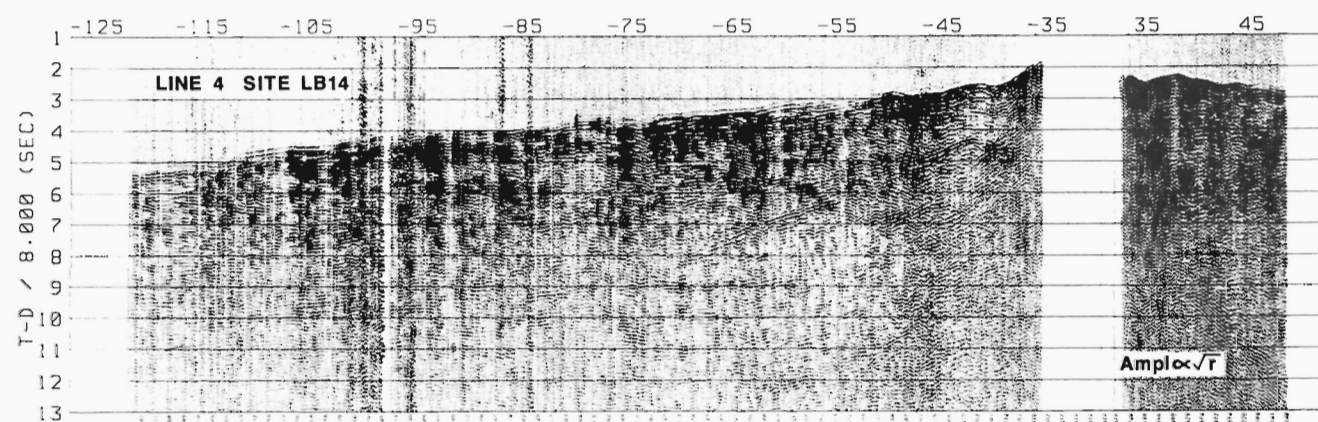


Figure 11: True amplitude section for Lunchbox site LB14 on Line 4. See caption for Figure 6.

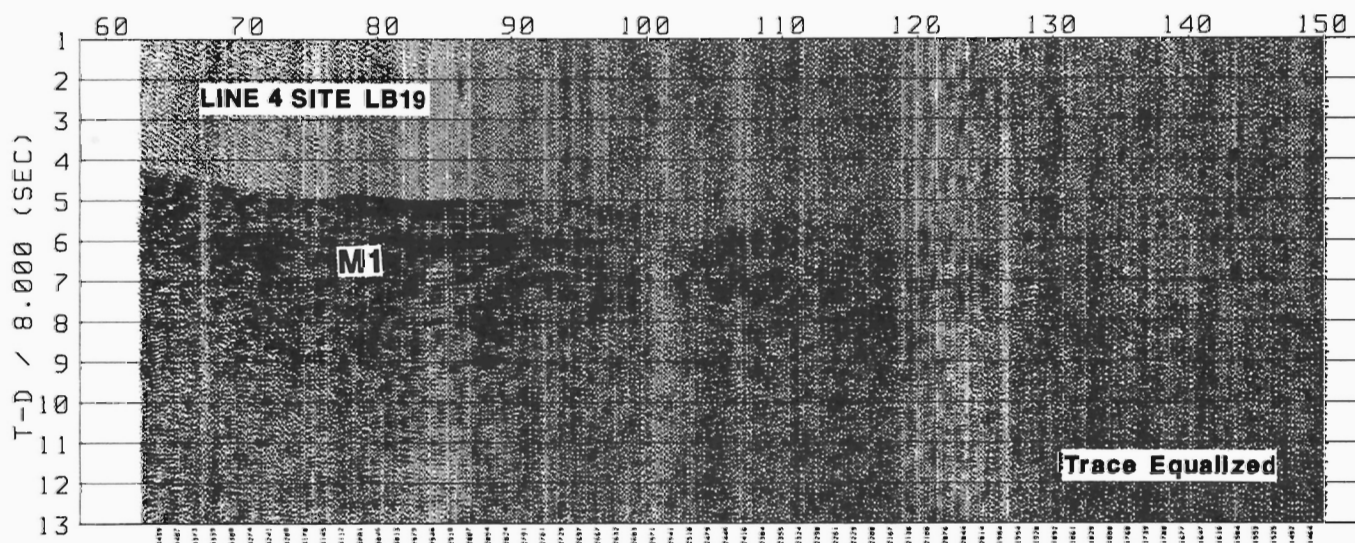


Figure 12: Trace equalized section for Lunchbox site LB19 on Line 4. See caption for Figure 6.



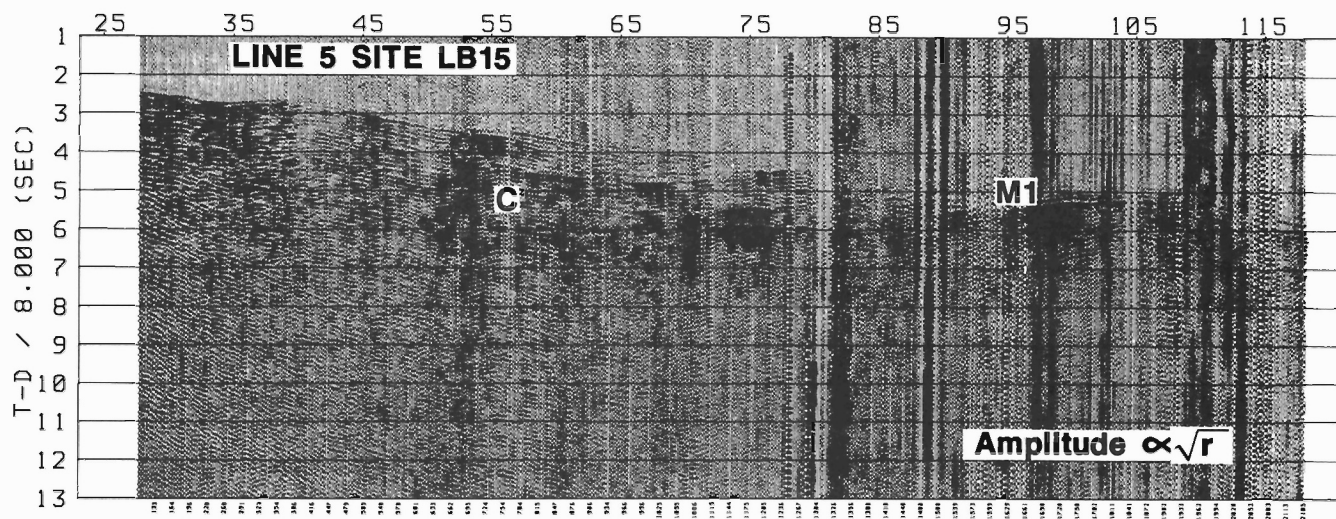


Figure 13: True amplitude section for Lunchbox site LB15 on Line 5. See caption for Figure 6.

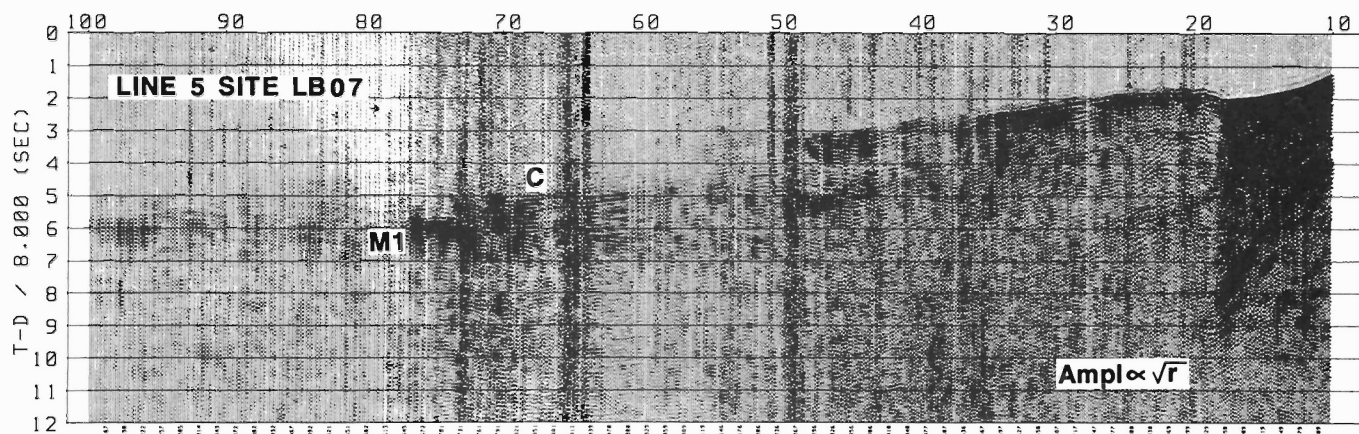


Figure 14: True amplitude section for Lunchbox site LB07 on Line 5. See caption for Figure 6.

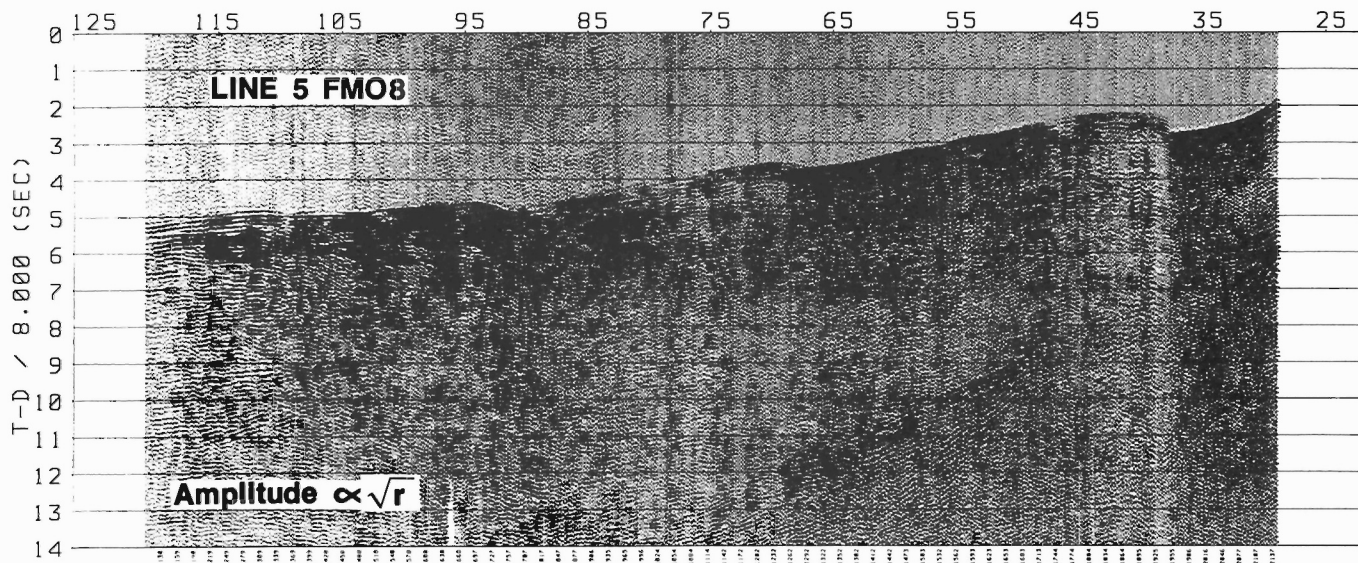


Figure 15: True amplitude section for analog site FM08 on Line 5. See caption for Figure 6.

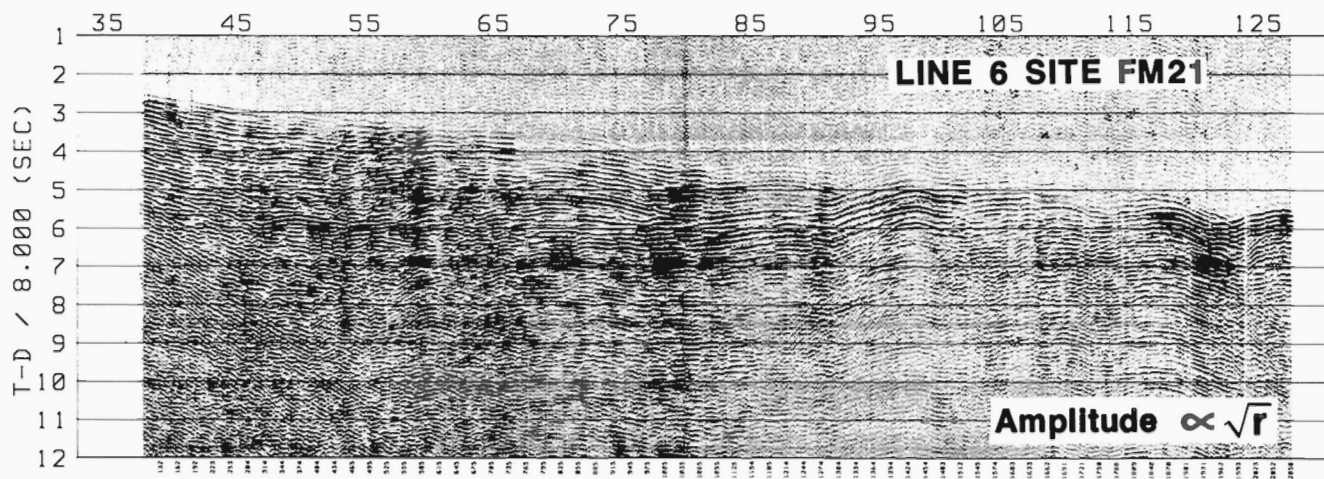


Figure 16: True amplitude section for analog site FM21 on Line 6. See caption for Figure 6.

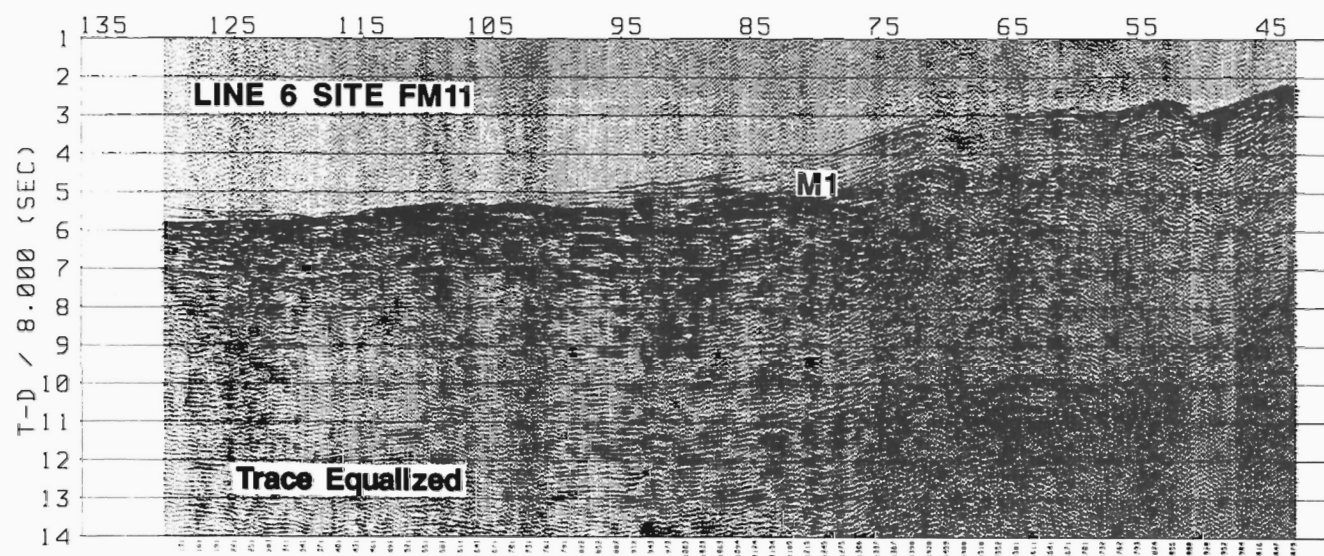


Figure 17: Trace equalized section for analog site FM11 on Line 6. See caption for Figure 6.

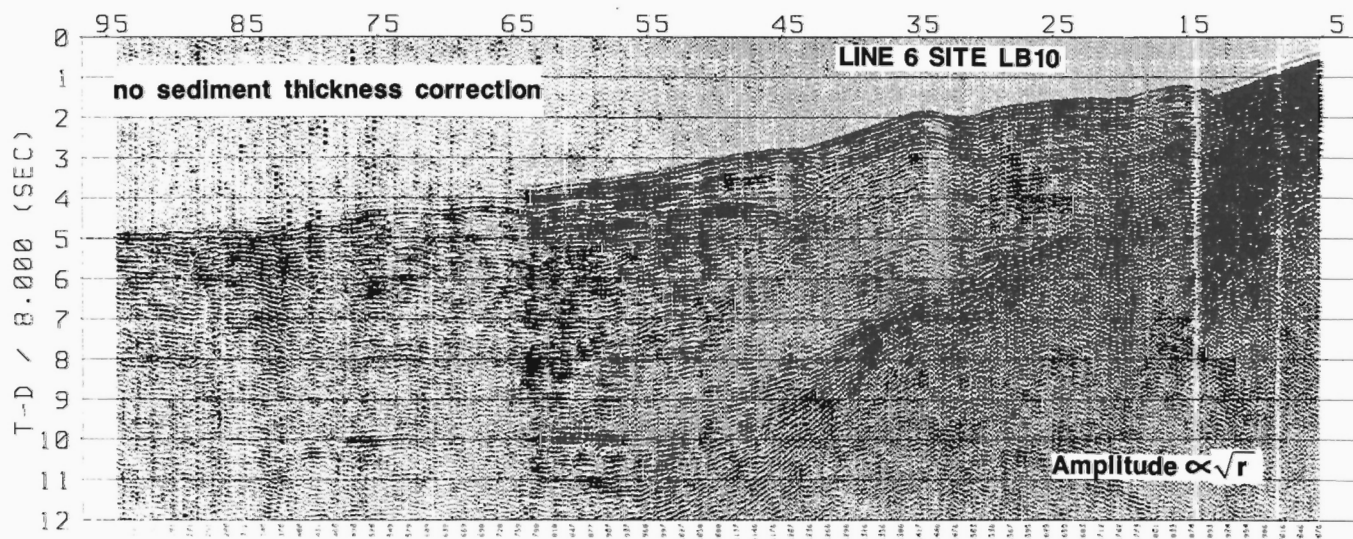


Figure 18: True amplitude section for Lunchbox site LB10 on Line 6.



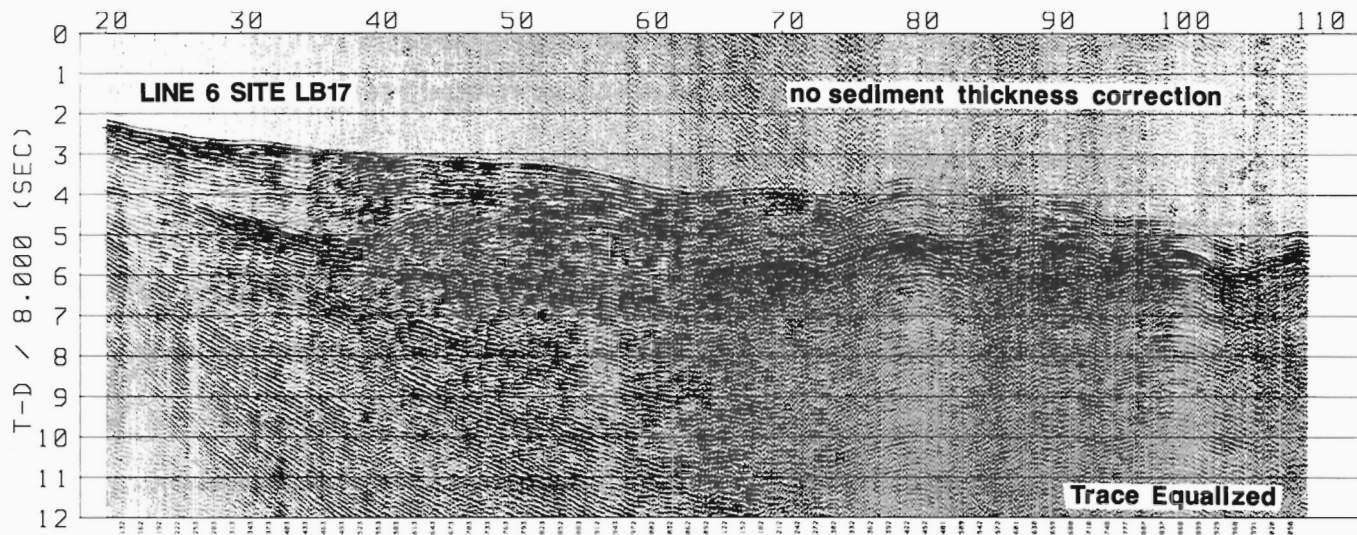


Figure 19: Trace equalized section for Lunchbox site LB17 on Line 6.

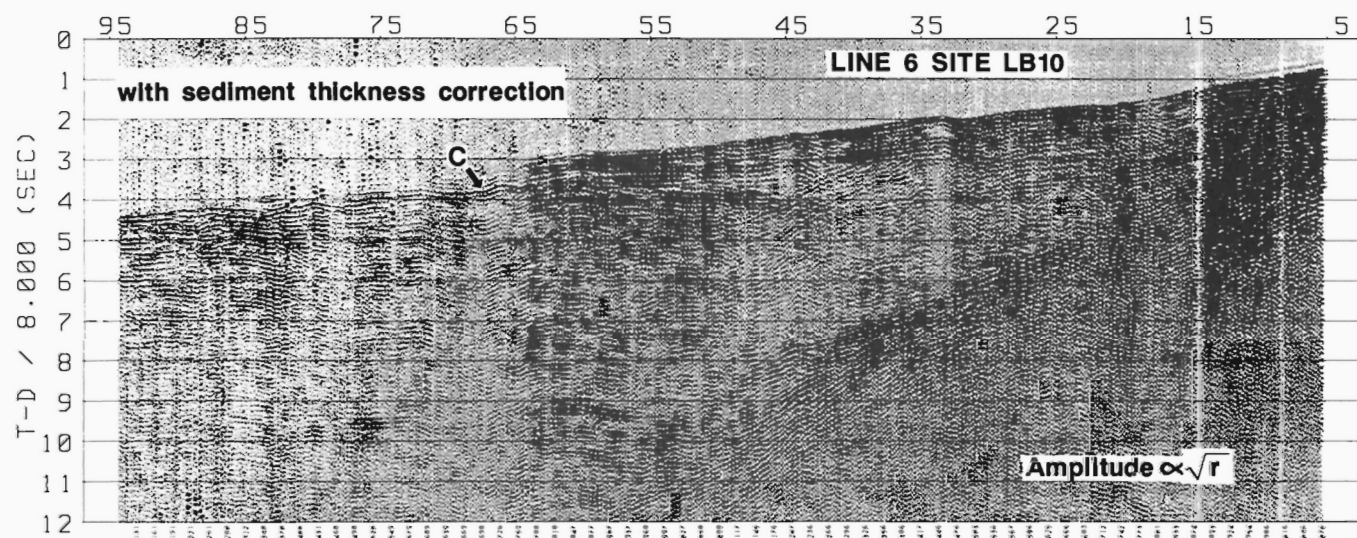


Figure 20: Same as Figure 18, but with sediment thickness statics correction applied. Note that most of the rapid travelt ime undulations have been smoothed out.

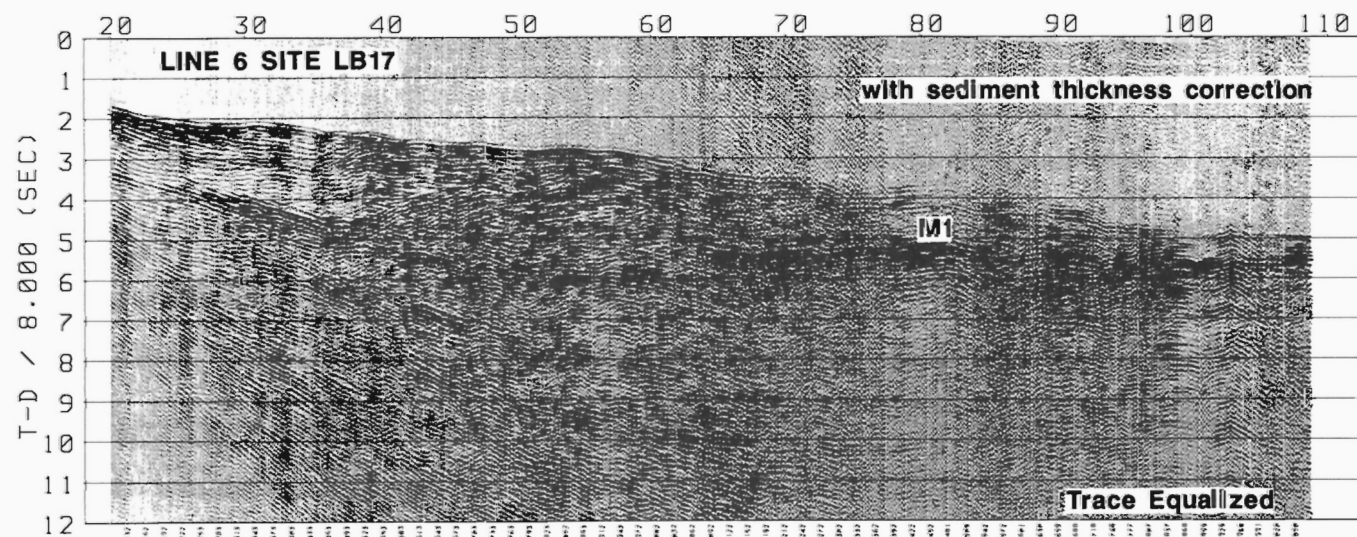


Figure 21: Same as Figure 19, but with sediment thickness statics correction applied.

water and sediment with anything, which assumes that all deeper structures are effectively parallel to the basement.

## DATA DESCRIPTION

The digital systems recorded a total of 21 seismic refraction sections and 96000 traces. The FM analog seismographs recorded 26 seismic sections and 72379 traces. Figures 5-21 show representative record sections for Lines 1-6. Line 7 is not yet complete. All sections are plotted with a reducing velocity of 8.0 km/s, so that arrivals which are horizontal on the section have an apparent velocity of 8.0 km/s. Most sections do not include a correction for variations in water depth or sediment thickness. However, in Figures 20 and 21 the data from site LB17 and LB10 on Line 6 are displayed after correction for these effects. A comparison with the uncorrected sections in Figures 18 and 19 shows that most of the rapid traveltimes undulations have been smoothed out.

The first arrivals on all sections are continuous from the nearest offsets out to distances of 50-60 km, where the apparent velocities are typically 6.5-7.0 km/s. On many sections, a delay of ~600 ms occurs at this range, and a secondary event (labelled as C in the diagrams), which is seen at near offsets of 40-50 km, then becomes the first arrival. This feature is generally more prominent for sites nearest to the end of the lines (e.g. LB01 and LB14 for Line 1; LB07 and LB15 for Line 5; LB10 for Line 6). That is, it appears to be more confined to the basin itself (Spence et al., 1989).

Moho reflections (labelled as M1 in the figures) are observed on nearly all sections. As an example, Figure 5 shows a true amplitude record section for the near ranges of LB01 and LB14 on Line 1. On most lines, significant amplitudes for the Moho reflection generally

occur over the 60-100 km range, although large amplitudes sometimes extend out to 120 km, as seen on Line 1.

The mantle refraction (labelled as M2) generally becomes the first arrival beyond the 100 km range, although the critical distance where the refraction is tangent to the Moho reflection occurs at ranges as small as 70 km. The entire offset range for Line 1 is shown in Figure 6. In order to display the weak amplitudes of the far arrivals, the sections in Figure 6 are plotted with all traces normalized to the same maximum amplitude; this results in an apparent increase in the background noise level at the far distances. Mantle refractions are seen as weak but clearly identifiable arrivals out to the maximum shot-receiver range of 280 km. The velocities of mantle arrivals for Line 1 are near 8.0 km/s, although they are slightly larger for site LB14 than for site LB01. As well, the intercept times are about 0.5 s larger for LB14, indicating a somewhat thicker crust in the northern portion of Queen Charlotte Sound than in the south.

Figures 7-10 show refraction sites at the mainland end of Lines 2 and 3 across Queen Charlotte Sound. Water depths increased from 100-300 m in Queen Charlotte Sound to over 2.5 km seaward of the continental slope. The transition to deep water is more rapid along Line 2, as evidenced by the sudden increase in first arrival times seen at 135 km for site LB03 (Fig. 7) and 155 km for site FM04 (Fig. 8). Moho reflections (labelled M1) are seen as strong secondary arrivals, and the mantle refractions probably become first arrivals beyond 110-120 km. Although these lines are unreversed, additional constraints will come from refraction results along the intersecting Line 1, and from Moho depths observed on the corresponding reflection lines.

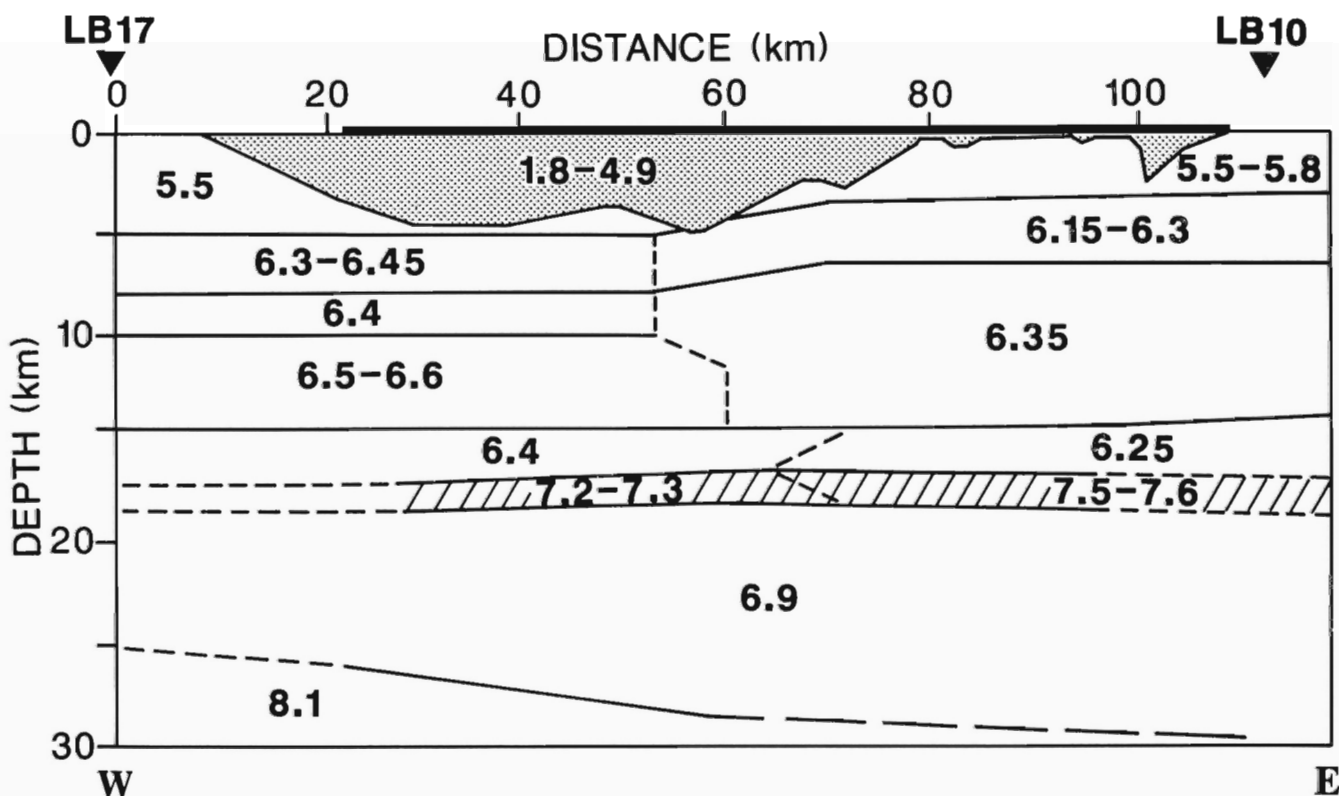


**Figure 22:** Preliminary velocity model representative of the structure beneath Line 6 in Hecate Strait. Velocities are based on ray trace modelling of refraction traveltimes data from sites LB10 and LB17. The shaded region corresponds to the sediments; the base of the sediments has been picked from the coincident multichannel reflection line, with sediment velocities consistent with Tye well velocity logs and with the OBS interpretation of Pike (1986). The hatched region is a high-velocity mid-crustal sliver. The thickened line at zero depth shows the distance range where airgun shots were fired along Line 6.

In Figures 11-12 the record sections for sites LB14 and LB19 on Line 4 are displayed. Line 4 was recorded at many sites, such as LB14, for which the travel paths were broadside to the line direction (Fig. 4). The data for LB14 are plotted at the appropriate shot-receiver offset for each trace, so at the nearest offsets the difference in ranges for neighbouring traces is quite small and the line is effectively compressed; an alternative display would be to plot each trace at its shot-receiver azimuth angle. In any case, the first-arrival character of the sections for LB14 and LB19 is similar to that on other lines, and on LB19 (Fig. 12) a Moho reflection occurs as a secondary arrival starting at ranges of 70-80 km.

Figures 13-21 are for Lines 5 and 6 across Hecate Strait. The mid-crustal reflector C and associated traveltime delay are prominent at sites LB07 and LB15 on Line 5 and at site LB10 on Line 6, while sites FM21 and LB17 on the west end of Line 6 show indications of successive delays in the first arrivals as the offsets are increased. No evidence for a strong mid-crustal reflector can easily be found in the data for site FM08 on Line 5 or FM11 on Line 6. Prominent Moho reflections M1 are seen at sites LB07 and LB15 on Line 5 and at LB17 and FM11 on Line 6. The identification of the Moho reflection is more difficult at site FM08 on Line 5 and FM21 on Line 6, and the shot-receiver offsets at site LB10 on Line 6 do not reach large enough values for a confident identification of this event.

## PRELIMINARY INTERPRETATION AND DISCUSSION

Preliminary traveltime interpretations have been carried out for sites LB10 and LB17 at either end of Line 6, and for site LB01 at the south end of Line 1. Figure 22 shows a velocity model below Line 6 which approximately fits the traveltimes for both receivers; the fit between the observed traveltimes and the model traveltimes is shown in Figure 23. Model traveltimes were obtained using the two-dimensional ray tracing algorithm of Spence et al. (1984). The model

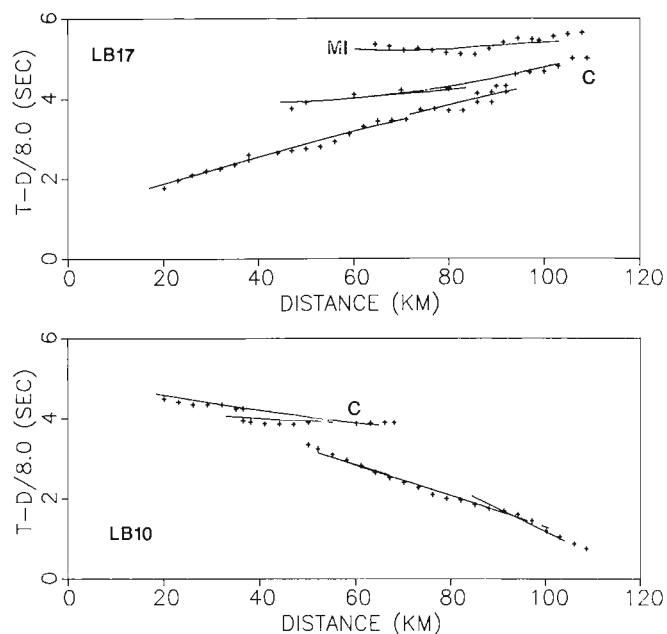


**Figure 23:** Traveltimes fit for receivers LB10 and LB17 on Line 6. Model traveltimes calculated for the velocity model of Figure 22 are shown by the solid lines. Observed traveltimes, indicated by the '+' symbols, were picked from the sediment-corrected sections of Figures 20 and 21. The event labelled C corresponds to reflections/refractions from a high-velocity mid-crustal sliver. The event M1 on LB17 is the Moho reflection.

in Figure 22 should be considered as only generally representative of the structure beneath Line 6. Only crude first-pass modelling of the data has been completed, and details of the model are not well-determined because of the problems of non-uniqueness in any travel-time interpretation. A more careful and tightly constrained interpretation will be derived in future synthetic seismogram modelling.

### (a) Sediments

The velocity model in Figure 22 includes a horizon to volcanic basement as picked from the corresponding seismic reflection section. The velocity profile in the sediments was a three-layer model based on velocities from the Tyee well logs, which incorporated check shot information (J.R. Dietrich, pers. comm., 1989). The velocity logs were also consistent with the results of Pike (1986), who interpreted data from ocean bottom seismographs along a line a few kilometres to the south of Line 6 (Fig. 2). Sediment velocities in the well reached ~4.9 km/s at 4-5 km depth. The velocity gradient in the lower part of the well was then used to extrapolate velocities at depths below the base of the well. A similar procedure was used in the preliminary interpretation of site LB01 on Line 1, where velocity logs were available from the Harlequin and Osprey wells (Fig. 1).

Rapid variations in sediment thickness produced traveltime undulations in the seismic refraction data. Statics corrections usually smoothed out these undulations (e.g. Figs. 20 and 21 compared to Figs. 18 and 19). In some cases the statics correction overcorrected the data, which indicated that the deep velocities at those locations should be higher than normal sediment velocity. This can be explained as interbedded clastics and volcanic flows, as was seen at the base of some wells (e.g. Osprey). The concept is also supported by the recent interpretation of Sweeney and Seemann (1990), in which positive gravity anomalies indicated high densities deep in the basin. As well, the explanation is generally consistent with the seismic reflection data where the lower part of the basin fill locally contained high amplitude reflections generated by the flows (Rohr and Dietrich, 1991).

### (b) Upper crustal velocity structure

For determining the structure below the sediments, observed traveltimes (Fig. 23) were picked from sections with the sediment statics correction applied (Figs. 20 and 21). Corrected sections were modelled because: (1) with the effect of sediments removed, the traveltime trends of the arrivals show only the sub-basement velocity structure, and (2) the ray tracing was both faster and easier to run.

The results for Line 6 displayed in Figure 22 and Figure 23 indicate that the velocity below the sediments rapidly reaches 6.2-6.3 km/s by 5 km subsurface depth, increasing to 6.4-6.5 km/s by 8 km depth. This gradient region probably contains volcanic material corresponding to the Masset Formation on the Queen Charlotte Islands. The refracted arrivals are continuous out to 50-60 km range, indicating that for Line 6, at least the upper 3-5 km beneath the sediments contain no velocity reversal. This contrasts with the interpretation of Clowes and Gens-Lenartowicz (1985) in Queen Charlotte Sound (see Fig. 3d), where a 200 ms traveltime delay at 15 km range indicated a 1 km thick low velocity zone beneath 1-3 km of volcanics. The zone was interpreted as a layer of Cretaceous sediments at 4-5 km subsurface depth. An equivalent low velocity zone does not appear to be present below Line 6 in Hecate Strait. However, the data below Line 6 would not indicate localized lenses of low velocity material or a low velocity zone with a thickness much less than 1 km.

Between 8 km and about 17 km depth in the model of Figure 22, the velocity stays nearly constant or possibly even decreases. On the Queen Charlotte reflection lines, normal faults are found which are near-vertical at the basement but may sole out at 3-4 s or ~10 km depth (Rohr and Dietrich, 1991). This depth is close to the top of the con-



stant velocity block found in the refraction interpretation, indicating that the block may be acting as a decollement zone for the extensional faulting. At least the upper portion of this block is likely Wrangellia terrane (Woodsworth, 1988). In the lower portion, velocities are lower than those interpreted for Wrangellia terrane beneath Vancouver Island, where a velocity gradient region continued to 16 km depth and velocities reached 6.8 km/s (Spence et al., 1985; Drew and Clowes, 1990).

### (c) Mid-crustal interface

Below the constant velocity region from ~8-17 km depth, a 1-3 km thick sliver of high-velocity material is present. For site LB10 (Fig. 20 and Fig. 23), the apparent velocity of the event labelled C implies that the velocity of the sliver is perhaps as high as 7.5 km/s. The significant velocity contrast at the interface produces the large amplitudes associated with event C, and the large thickness of the low- or constant-velocity region causes the traveltime delay in this arrival (e.g. the 600 ms delay at 65 km range in Fig. 20). An alternative feature which can explain a traveltime delay is a two-dimensional structure such as fault or step. However, this is rejected for Line 6 because for a fault a traveltime advance would be expected on the reverse profile, and this is not seen for site LB17 (Fig. 21).

As described in the previous section, equivalent mid-crustal arrivals and traveltime delays are observed on refraction sections throughout the Queen Charlotte Basin, generally at those sites on the edge of the basin. Visual inspection indicates that other lines will include similar constant or low velocity zones above a significant velocity interface. For example, a preliminary interpretation of the data from site LB01 on Line 1 shows a mid-crustal reflector at about 15 km depth (T. Yuan, pers. comm., 1989).

Only a speculative explanation can be given for the high-velocity layer. Perhaps it is related to past subduction events, in which pieces of ocean crust or mantle become stranded as the locus of the subduction zone shifts due to regional tectonic adjustments. A stranded high-velocity sliver was also interpreted for the Vancouver Island margin (Spence et al., 1985).

### (d) Lower crust and Moho

Moho depths were determined mainly from wide-angle reflections from the Moho (labelled M1 in Fig. 21 and Fig. 23). Preliminary traveltime interpretations yielded a Moho depth of about 26-28 km beneath Line 6 (Fig. 22) and 24 km beneath the southern portion of Line 1. The thinner crust on line 1 in Queen Charlotte Sound compared to line 6 in Hecate Strait is significant in that it may indicate greater extension in the more southerly region. On Line 6, the Moho depths correspond to the portion of the basin where sediment thicknesses are 5 km and greater, and so a crustal thickness of 23 km or less is implied. Converted to vertical traveltime, the refraction Moho occurs at a two-way time of 9.9 s, which generally agrees with the seismic reflection Moho for this line (Rohr and Dietrich, 1991). On the eastern portion of the line where sediment is thin, the reflection data indicate a crustal thickness of 30 km. Thus, significant crustal thinning due to extension is implied beneath the Queen Charlotte Basin.

Crustal velocities for the lower crust are poorly-determined, but appear to be 6.9(±0.2) km/s. Tighter constraints are expected in later synthetic seismogram interpretations. If lower crustal velocities are found to be greater than 7.0 km/s, then this would be an indicator of an extensional rift origin of the basin. High-velocity "rift pillows" have been found in the lower crust beneath extensional margins (White et al., 1988; LASE, 1986) and beneath rift and graben features such as the Rhinegraben and the Mississippi embayment (Mooney et al., 1983). If deep velocities are less than 7.0 km/s, then a rift or thermal origin should perhaps be questioned. Extension oc-

curing in a strike-slip environment, for which there are indicators in the seismic reflection data, would remain a favourable explanation.

## SUMMARY

Refractions and wide-angle reflections from a 102L (6300 cu. in.) airgun array were recorded on single channel land stations during a combined seismic reflection and refraction survey in Queen Charlotte Basin. A velocity model has been obtained from preliminary traveltime interpretations for two receivers on Line 6 in Hecate Strait and one receiver at the south end of Line 1 in Queen Charlotte Sound. Beneath the sediment package of up to 5 km thickness, the upper crust for Line 6 can be divided into two regions. The first layer, which probably contains volcanic flows equivalent to the Masset Formation, is approximately 3-5 km thick in which velocities increase from 6.2-6.3 to 6.4-6.5 km/s. The second layer likely corresponds to Wrangellia terrane, at least over its top portion. The layer extends from about 8-17 km below the surface, and velocities remain nearly constant or perhaps even decrease. At 15-17 km depth a major velocity interface is present. Below the interface a high-velocity sliver may exist with a thickness of 1-3 km and velocity of 7.2 km/s or more; such high-velocity slivers may be pieces of ocean crust or mantle stranded in past subduction episodes. The lower crustal velocity below the sliver is 6.8-6.9 km/s, but this is not yet well-constrained. Estimates of Moho depth are 26-28 km for Line 6 and 24 km for the south end of Line 1. Crustal thickness beneath the deepest basin on Line 6 may then be 21-23 km, and with an estimated thickness of 30 km at the east end of Line 6, significant crustal thinning is implied.

## ACKNOWLEDGMENTS

The authors gratefully acknowledge that the refraction field program could not have been undertaken without the participation and enormous help of many colleagues, technical support staff, and graduate students. In addition to the authors, the field participants included: Tim Côté and Marcel Gervais from the GSC, Ottawa, plus Andy Calvert, John Cassidy, Ben Ciamaichella, Connie Cudrak, Sonya Dehler, Stan Dosso, Janet Freeth, Elizabeth Hasselgren, Yaoguo Li, Bob Meldrum, and Colin Zelt from the University of British Columbia.

We are also grateful to Bob Thompson of the GSC, Vancouver for arranging accommodation for most participants in the Queen Charlotte Islands at the GSC field camp in Sandspit.

Funding to the University of British Columbia was through DSS contract 23445-8-0070/02-5B and NSERC operating grants. JAH is the recipient of NSERC and UBC Killam pre-doctoral fellowships. The Frontier Geoscience Program (Queen Charlotte Project) provided funding for the data acquisition and support for GDS through an NSERC Government Laboratory Postdoctoral Fellowship.

## REFERENCES

- Clowes, R.M. and Gens-Lenartowicz, E.  
1985: Upper crustal structure of southern Queen Charlotte Basin from sonobuoy refraction studies; *Canadian Journal of Earth Sciences*, v. 22, p. 1696-1710.
- Dehler, S.A. and Clowes, R.M.  
1988: The Queen Charlotte Islands refraction project: Part I – the Queen Charlotte fault zone; *Canadian Journal of Earth Sciences*, v. 25, p. 1857-1890.
- Drew, J.J. and Clowes, R.M.  
1990: A re-interpretation of the seismic structure across the active subduction zone of western Canada; in *Studies of Laterally Heterogeneous Structures Using Seismic Refraction and Reflection Data*, Proceedings of the 1987 Commission on Controlled Source Seismology Workshop, A.G. Green (ed.), Geological Survey of Canada, Paper 89-13, p. 115-132.
- Horn, J.R., Clowes, R.M., Ellis, R.M., and Bird, D.N.  
1984: The seismic structure across an active oceanic/continental transform fault zone; *Journal of Geophysical Research*, v. 89, p. 3107-3120.
- LASE Study Group  
1986: Deep structure of the US east coast passive margin from large aperture seismic experiments (LASE); *Marine and Petroleum Geology*, v. 3, p. 234-242.

- Mackie, D.J., Clowes, R.M., Dehler, S.A., Ellis, R.M., and Morel-à-l'Huissier, P.**  
**1989:** The Queen Charlotte Island Refraction Project: Part II -- structural model for transition from Pacific plate to North American plate; *Canadian Journal of Earth Sciences*, v. 26, p. 1713-1725.
- Mooney, W.D., Andrews, M.C., Ginzburg, A., Peters, D.A., and Hamilton, R.M.**  
**1983:** Crustal structure of northern Mississippi embayment and a comparison with other continental rift zones; *Tectonophysics*, v. 94, p. 327-348.
- Pike, C.J.**  
**1986:** A seismic refraction study of the Hecate sub-basin, British Columbia; M.Sc. thesis, University of British Columbia, Vancouver, 133 p.
- Rogers, G.C.**  
**1983:** Seismotectonics of British Columbia; Ph.D. thesis, University of British Columbia, Vancouver, 247 p.
- Rohr, K. and Dietrich, J.R.**  
**1991:** Deep seismic reflection survey of the Queen Charlotte Basin, British Columbia; *in* Evolution and Hydrocarbon Potential of the Queen Charlotte Basin, British Columbia, Geological Survey of Canada, Paper 90-10.
- Shouldice, D.H.**  
**1971:** Geology of the western Canadian continental shelf; *Bulletin of Canadian Petroleum Geology*, v. 19, p. 405-436.
- Spence, G.D., Whittall, K.P., and Clowes, R.M.**  
**1984:** Practical synthetic seismograms for laterally varying media calculated by asymptotic ray theory; *Bulletin, Seismological Society of America*, v. 74, p. 1209-1223.
- Spence, G.D., Clowes, R.M., and Ellis, R.M.**  
**1985:** Seismic structure across the active subduction zone of western Canada; *Journal of Geophysical Research*, v. 90, p. 6754-6772.
- Spence, G.D. and the Queen Charlotte Seismic Group**  
**1989:** Deep structure beneath the Queen Charlotte Basin from seismic refraction data (abstract); *Seismology Research Letters*, v. 60, p. 17.
- Spencer, C.A., Asudeh, I., and Cote, T.**  
**1989:** SEG-Y-LDS Version 2.0 Format Reference Document; Geological Survey of Canada, 17 p.
- Stacey, R.A.**  
**1975:** Structure of the Queen Charlotte Basin; *in* Canada's Continental Margins and Offshore Petroleum Exploration, C.J. Yorath, E.R. Parker and D.J. Glass (ed.), Canadian Society of Petroleum Geologists, Memoir 4, p. 723-741.
- Sutherland Brown, A.**  
**1968:** Geology of the Queen Charlotte Islands, British Columbia; British Columbia Department of Mines and Petroleum Resources, Bulletin 54, 226 p.
- Sweeney, J.F. and Seemann, D.A.**  
**1990:** Crustal density structure of Queen Charlotte Islands and Hecate Strait, British Columbia; *in* Evolution and Hydrocarbon Potential of the Queen Charlotte Basin, British Columbia, Geological Survey of Canada, Paper 90-10.
- Thompson, R.I. and Thorkelson, D.J.**  
**1989:** Regional mapping update, central Queen Charlotte Islands, British Columbia; *in* Current Research, Part H, Geological Survey of Canada, Paper 89-1H, p. 7-11.
- White, R.S., Spence, G.D., Fowler, S.R., McKenzie, D.P., Westbrook, G.K., and Bowen, A.N.**  
**1987:** Magmatism at rifted continental margins; *Nature*, v. 330, p. 439-444.
- Woodsworth, G.J.**  
**1988:** Karmutsen Formation and the east boundary of Wrangellia, Queen Charlotte Islands, British Columbia; *in* Current Research, Part E, Geological Survey of Canada, Paper 88-1E, p. 209-212.
- Yorath, C.J. and Hyndman, R.D.**  
**1983:** Subsidence and thermal history of the Queen Charlotte Basin; *Canadian Journal of Earth Sciences*, v. 20, p. 135-158.



# Evolution of the stratigraphic nomenclature of the Queen Charlotte Islands, British Columbia

G.J. Woodsworth<sup>1</sup> and P.E. Tercier<sup>1,2</sup>

Woodsworth, G.J. and Tercier, P.E., Evolution of the stratigraphic nomenclature of the Queen Charlotte Islands, British Columbia; in *Evolution and Hydrocarbon Potential of the Queen Charlotte Basin*, British Columbia, Geological Survey of Canada, Paper 90-10, p. 151-162, 1991.

## *Abstract*

*We review the history of geological exploration of the Queen Charlotte Islands and show how the stratigraphic nomenclature has developed over the last century. The Triassic and Jurassic stratigraphy of the islands is now reasonably well understood, and much progress has been made with Cretaceous strata. Our understanding of the stratigraphy of latest Cretaceous and early Tertiary rocks is fragmentary.*

## *Résumé*

*Les auteurs examinent l'histoire de l'exploration géologique des îles de la Reine-Charlotte et montrent comment la nomenclature stratigraphique a évolué au cours du siècle dernier. La stratigraphie du Trias et du Jurassique des îles est maintenant assez bien établie, et l'étude des couches du Crétacé progresse bien. L'état des connaissances de la stratigraphie des roches du Crétacé supérieur et du Tertiaire inférieur est fragmentaire.*

---

<sup>1</sup> Cordilleran Division, Geological Survey of Canada, 100 West Pender Street, Vancouver, B.C. V6B 1R8

<sup>2</sup> Present address: Department of Geological Sciences, University of British Columbia, Vancouver, B.C. V6T 2B4

## INTRODUCTION

The recent work in the Queen Charlotte Basin described in the papers in this volume builds on and extends the framework erected by previous studies, particularly past stratigraphic and structural studies on the Queen Charlotte Islands themselves.

In this note we review the history of geological exploration of the Queen Charlotte Islands, with emphasis on the development of stratigraphic nomenclature. Our object is to give an introduction to the state of knowledge of the pre-Pleistocene stratigraphy prior to the beginning of the Frontier Geoscience Program, to give an entry to the stratigraphic and structural literature of the islands, and to illustrate the high degree to which geological understanding depends on regional mapping and biostratigraphic studies. We treat the material historically rather than by stratigraphic unit or time slices to highlight the controversies that have taken place over the years. Our paper builds on previous historical compilations, particularly those by McLearn (1949), Cameron and Tipper (1985), and Haggart (1987). The areas studied by some of the workers discussed below are shown in Figure 1, and comparative stratigraphic columns are given in Figure 2.

## THE EARLIEST STUDIES: RICHARDSON AND BILLINGS

Geological interest in the Queen Charlotte Islands dates back to 1852 when Captain Mitchell of the Hudson's Bay Company directed a short mining operation on Mitchell Inlet, then known as Port Kuper or Gold Harbour. The mining operation is reputed to have yielded some \$75,000 in gold but, as the carrier was shipwrecked on route to Cape Flattery, the actual amount remains uncertain (Dalzell, 1968). This, the first lode mining operation in British Columbia, was shortly to spark more exploration interest in the Queen Charlotte Islands.

In 1859 Major William Downie spent three months in the Queen Charlotte Islands in search of gold at the request of Governor James Douglas. Downie, a veteran of the California gold rush, prospected the old gold site on Mitchell Inlet without success. He did, however, find coal near Skidegate Inlet, and in 1865 the Queen Charlotte Coal Company was formed to exploit these deposits. Exploration and preparation for mining the coal at Cowgitz (now Kagan Bay) began in 1865, despite lack of preliminary geological studies. By 1872 the mine had closed: much capital had been wasted and only 435 tons on coal had been mined (Dalzell, 1968).

However, the project did result in the first visit to the islands by the Geological Survey of Canada. At the request of those interested in the coal, James Richardson spent twelve days in the region in 1872. Most of this time was spent working with the Queen Charlotte Mining Company evaluating the coal potential in the workings at Kagan Bay, but he did find time for brief examinations of the shoreline along Skidegate Inlet and Skidegate Channel. Richardson (1873) divided the "coal bearing rocks of the Queen Charlotte Islands" into three Jura-Cretaceous sedimentary units (Fig. 2, column 1) which together lie in a north-south trough bounded to the west by a "high range of volcanic rocks" of unstated age.

Richardson's fossils were examined by E. Billings and J.W. Dawson; their reports were published as appendices to his. Dawson (1873) assigned the plant fossils to the Lower Jurassic or Lower Cretaceous. Billings (1873) studied the invertebrate fossils and reported, "...the *Ammonites* and *Belemnites* tend to prove that the Queen Charlotte Islands rocks are Jurassic, while the *Nautilus* would place them in the Cretaceous". Billings correctly recognized the mixed nature of Richardson's collections and presence of two faunas (one Jurassic and one Cretaceous). But despite his report, studies for the next thirty years failed to make this crucial separation of Jurassic and Cretaceous strata.

In 1876 the Geological Survey of Canada published the first section of J.F. Whiteaves' five-part treatise on Mesozoic fossils, three parts of which deal with the Queen Charlotte Islands. In part 1, Whiteaves (1876) re-described Richardson's fossil collections from the Queen Charlotte Islands. Although Whiteaves realized that some of the fossils had Jurassic affinities, he failed to recognize the mixed faunal nature of Richardson's collections. Whiteaves wrote, "It is sufficiently obvious that they exhibit a blending of life of the Cretaceous period with that of the Jurassic..." (p. 91). He concluded, "At present it would be premature to express any very decided opinion on the exact age of these Coal-bearing rocks. All that the fossils show with any degree of probability is that the series can scarcely be much newer than the Middle Cretaceous, or older than the Upper Jurassic." (p. 92).

## THE FIRST THOROUGH RECONNAISSANCE: G.M. DAWSON

In 1878 the remarkable natural scientist G.M. Dawson set sail from Victoria in the small schooner "*Wanderer*" to explore the Queen Charlotte Islands. In two and one half months of stormy weather Dawson explored the eastern shoreline of most of the islands and mapped in detail along Skidegate Inlet. Because of the unfavourable weather conditions and the large amount of shoreline exposed on the many islands on the east side of the archipelago, time did not permit exploration of the west coast. The resulting comprehensive report (Dawson, 1880) included studies of the geology, physiography, flora and fauna, and a monograph on the Haida people. The report contains the first geological map of the islands, the first workable stratigraphy, a thoughtful discussion of the Quaternary deposits, and the first attempt at a tectonic history of the islands. These contributions remained invaluable for the next eighty years.

Dawson (1880, 1889) divided the strata into four broad units ranging in age from Triassic (possibly Carboniferous) to post-Pliocene (Fig. 2, column 2). The oldest of these has four subdivisions, three of which remain today as the Karmutsen Formation and the lower two divisions of the Kunga Group (Sadler Limestone and Peril Formation). After his season on Vancouver Island, Dawson (1887, 1889) correlated these units with the Vancouver Group, recognizing the similarities between lower Mesozoic strata on Vancouver and Queen Charlotte islands.

Dawson (1880) subdivided the "Cretaceous coal-bearing rocks" unconformably overlying the Triassic strata into five units, from youngest to oldest called A-E. In 1889, following Whiteaves (1883), he named the lower three units (C-E) the "Queen Charlotte Island formation" (Dawson, 1889; Fig. 2, column 2). He believed the lithologically similar sandstones in units C and E were the same age and that the volcanic agglomerates (D, now the Yakoun Group) separating them represented contemporaneous volcanism. Although Dawson remarked on the irregular surface between units C and D he concluded, "This partial unconformity is, however, believed to be essentially unimportant, and only such as might be anticipated at the junction of two classes of deposits so dissimilar." (Dawson, 1880, p. 67B).

Probably influenced by Whiteaves' reports on Richardson's fossil collections indicating that units C and E are the same age, Dawson failed to recognize the unconformity separating his unit C (correctly recognized by Dawson as Cretaceous) from unit D (incorrectly thought to be Cretaceous and found later to be Jurassic). This failure to separate Jurassic from Cretaceous strata was Dawson's main error in interpretation and was to persist for the next twenty-five years.

Dawson's interpretation of the tectonic history of the islands contains the seeds of many later ideas and is worth quoting at some length:

*After the deposition of the rocks coloured as Triassic, and before the newer series with which the coal is associated began to be formed, a period of some disturbance must have*



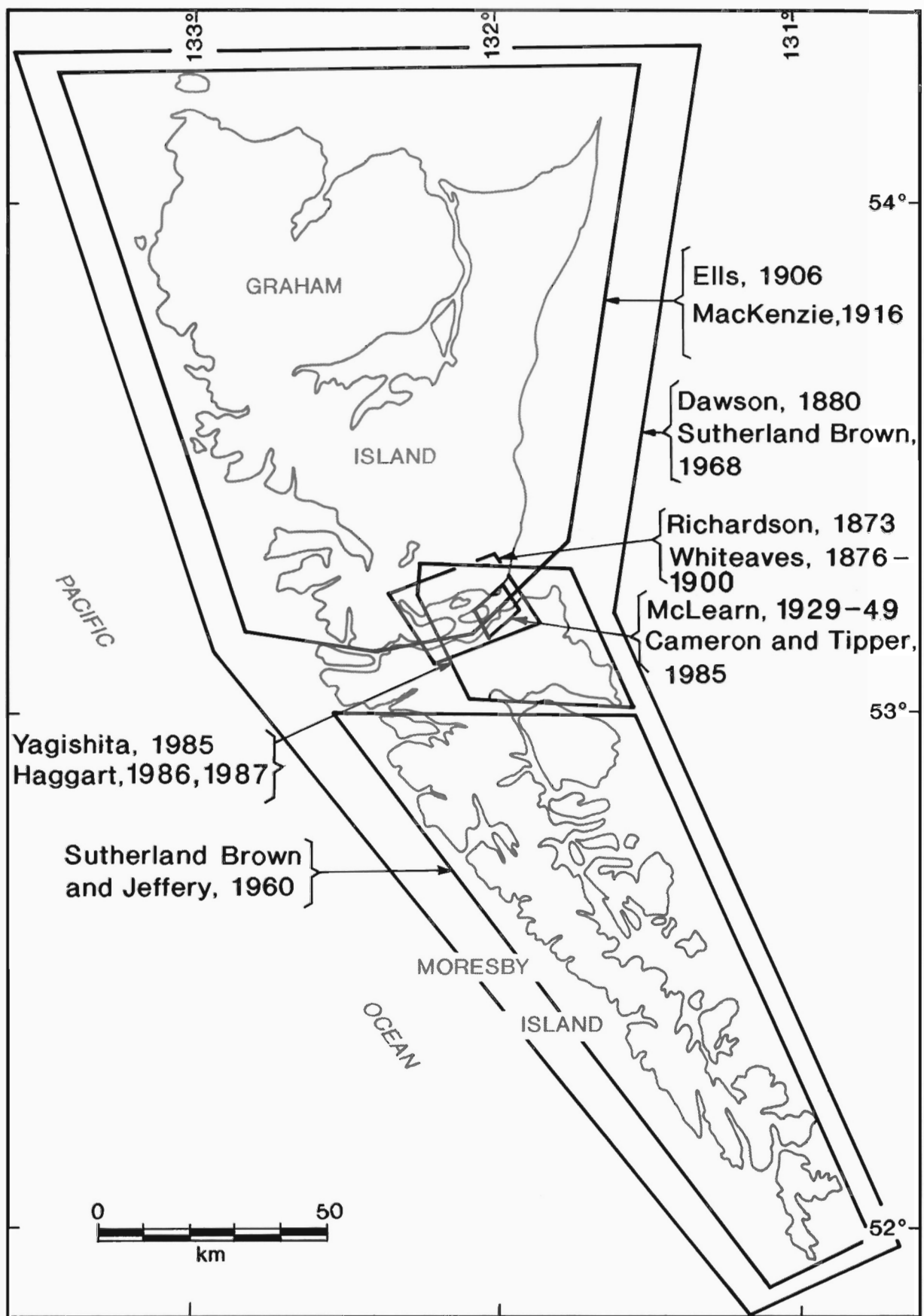


**Figure 1:** Areas studied by some previous workers on the Queen Charlotte Islands.

*intervened, to which a great part of the granitoid intrusive rocks of the region are possibly referable. Portions of these older rocks were raised above the sea level at this time, and the deposition of the Cretaceous coal-bearing rocks was inaugurated. This did not proceed uninterruptedly, however, for we have evidence of the occurrence of a period of great volcanic activity, which led to the intercalation of several thousand feet of almost unmixed volcanic products. Following this, without any marked unconformity was a tranquil period, during which a great thickness of shales and shaly sandstones was deposited, and in connection with the earliest beds of which the Skidegate coal was formed. The overlying conglomerates probably evidence a period of depression, after which, and closing as far as we know the record of the Cretaceous period in this region, an upper series of shales and sandstones was produced in a shallow and quiet sea. The great period of disturbance and mountain formation for the region now supervened, and the only record we have of the time elapsing between the Cretaceous and later Tertiary is in the flexure, crumpling and fracture of the beds.* (Dawson, 1880, p. 46B-47B).

In some ways, this is a thoroughly modern synthesis, particularly coming after just one season of field work. Dawson noted the similarity of the Triassic rocks with those on Vancouver Island and clearly recognized two "periods of disturbance". The older occurred in post-Triassic time (now known to be Middle Jurassic) and was associated with extensive plutonism (San Christoval and Burnaby Island plutonic suites of Anderson and Reichenbach, 1991). Uplift and erosion were followed by renewed sedimentation and volcanism that ended with deposition of conglomerates (Honna Formation in today's nomenclature) and shales (Skidegate Formation). The second main "period of disturbance" was in the Cretaceous or early Tertiary. Dawson thought that, following this deformation, sea level in late Tertiary time was probably much as it is today. Slight changes in sea level resulted in the deposition of sediments (Skonun Formation); volcanic rocks (Masset Formation) were probably erupted from a number different eruptive centres.

Dawson's fossil collections were described by J.F. Whiteaves (1884) in the third part of "Mesozoic Fossils." This report further enforced the idea that the "coal-bearing" rocks were a conformable sequence of Cretaceous age. "By far the largest number of fossils collected by Dr. Dawson, however, consisting of upwards of one thousand specimens, are from the Newer Mesozoic strata of Skidegate and Cumshewa Inlets, which can now be shown to be of Cretaceous rather than of Jurassic age." (Whiteaves, 1884, p. 192).

In 1895 and 1897 the anthropologist Dr. C.F. Newcombe of Victoria collected fossils from Skidegate and Cumshewa inlets. These were the subject of Part 4 of "Mesozoic Fossils" (Whiteaves, 1900). Whiteaves stuck to his conviction that the fossils were Cretaceous in age. He also revised his identifications of Richardson's and Dawson's collections from Jurassic forms to Cretaceous forms based on the better material supplied by Newcombe.

Not until the first years of the twentieth century were Whiteaves' conclusions seriously questioned and a resolution to the problem found. Two American paleontologists, T.W. Stanton and G.C. Martin (1905), working on the Mesozoic strata of Cook Inlet, Alaska, noted that some of the Cook Inlet ammonites were clearly Jurassic in age yet were strikingly similar to specimens figured by Whiteaves and assigned by him to the Cretaceous. The following year, D.B. Dowling (1906), working on the Jurassic of southwestern Alberta, also noted the Jurassic aspect of some of Whiteaves' "Cretaceous" forms from the Queen Charlottes. He concluded that the fossils from Dawson's unit C were in fact from two units and suggested that the problems

could be resolved if the Queen Charlotte series were divided into two formations, one Jurassic and the other Cretaceous.

## BEGINNINGS OF MODERN NOMENCLATURE: CLAPP AND MACKENZIE

In the 1880s, the "Wilson" coal seam had been found on Graham Island by Mr. W.A. Robertson, while evaluating timber resources for the provincial government. In 1905, R.W. Ells of the Geological Survey of Canada spent the summer on Graham Island, under instructions to examine the coal field represented by the Wilson seam. Ells made the first geological reconnaissance of the west coast of Graham Island and completed a traverse of the island from Masset Inlet via the Yakoun River to Skidegate Inlet, but he spent most of his time on the "Cretaceous coal-bearing rocks" that were then of economic interest. Ells' (1906) map and report added little new to the understanding of the area, but he did recognize that some of the igneous rocks in Dawson's Queen Charlotte Island formation were pre-Cretaceous in age (Fig. 2, column 3).

In 1912, C.H. Clapp of the Geological Survey of Canada spent seventeen days on Graham Island at the request of a company working on the coal deposits. Clapp examined parts of Masset and Skidegate inlets and traversed the island from the mouth of the Honna River to the mouth of the Yakoun River. Clapp was also actively working on Vancouver Island and his familiarity with stratigraphy there no doubt aided him on the Charlottes.

Clapp (1914) divided the strata into several main units ranging in age from Triassic to Recent (Fig. 2, column 4). Following Dawson (1889) he recognized that the Triassic-Jurassic strata are similar to those on Vancouver Island and referred to these units as the Vancouver Group. He abandoned Dawson's Queen Charlotte Island formation (Dawson's units C-E) and proposed instead the Queen Charlotte series for Dawson's units A to D; this is essentially the Queen Charlotte Group of modern usage. Within the Queen Charlotte series he recognized four members: the Image (now Yakoun Group, in part), Haida, Honna, and Skidegate. Clapp recognized an unconformity between his Image and Haida members and also recognized that Middle to Late Jurassic plutons cut what is now called the Yakoun Group. He thought the Skidegate was younger than the Honna conglomerate, a mistake that was perpetuated by succeeding geologists until corrected by Haggart (1987).

Clapp's comments on the geological history and tectonic setting of the Queen Charlotte series and younger rocks are interesting and show that he recognized the pre-Yakoun uplift and erosion emphasized by Thompson et al. (1991) and the constructional nature of Masset volcanism described by Hickson (1991). According to Clapp (1914, p. 14-15):

*The [Queen Charlotte] series is of sedimentary origin, and was apparently deposited in a wide valley between highlands of the metamorphic and granitic rocks. In the valley itself, there appear to have been three or four large monadnocks, which remained above the depositional level during the formation of, at least, the lower members of the series, including the coal seams. The date of deposition is generally considered to be Lower to Upper Cretaceous.... Breaking through the Queen Charlotte series and forming sills, dykes, and probably laccoliths, and also flows, are igneous rocks, ranging from dacites to basalts. They are doubtless largely of Tertiary age, although possibly erupted at widely separated intervals.... In the central part of Graham island the basalts apparently form intrusive masses, presumably laccoliths, and possibly flows, and now occur*

*capping the large monadnocks which surmount the basin underlain by the Queen Charlotte series.*

Clapp's short visit was highly productive and prompted a more detailed study by J.D. MacKenzie. He spent a total of five months during the summers of 1913 and 1914 on reconnaissance and detailed mapping on Graham Island. His final report (MacKenzie, 1916) was the most comprehensive since Dawson's and included a geological map of Graham Island at 1 inch to 4 miles.

MacKenzie proposed a number of new stratigraphic names (Maude, Yakoun, Masset, and Skonun) that continue in use today, although some have changed rank (Fig. 2, column 5). He divided the Vancouver Group on Graham Island into two formations: the Lower Jurassic and possibly Triassic Maude Formation (sedimentary) and the Middle Jurassic Yakoun Formation (largely volcanic and volcanoclastic). The rocks of Clapp's Image member became part of the newly defined Yakoun Formation. The Cretaceous members of Clapp's Queen Charlotte series (Haida, Honna, and Skidegate) were raised to the formational status that they enjoy today.

MacKenzie divided the Tertiary rocks of Graham Island into two main units: the Skonun Formation (dated as Miocene or Pliocene by Whiteaves on the basis of MacKenzie's fossils) and the Pliocene Masset Formation (which he thought overlay the Skonun). However, he noted that some Tertiary volcanic rocks predate the Masset. In the preliminary report on his first summer of field work (MacKenzie, 1914), he suggested the name Etheline Formation for basalt flows found on Mt. Etheline in central Graham Island. Field work the following year convinced him that these flows were part of the Pliocene Masset Formation, but he kept the name Etheline Formation for subvolcanic intrusions that he presumed were Eocene in age. The Etheline Formation has not been accepted by later workers, and the rocks they represent are included in the Masset Formation and Kano plutonic suite and various dyke swarms.

MacKenzie's interpretation of the tectonic history of the region extended Clapp's ideas. Sedimentary rocks of the Maude Formation were deposited under widespread, quiet and stable conditions during Late Triassic and Early Jurassic time. Towards the end of Early Jurassic time, minor uplift resulted in deposition of slightly coarser sediments; these were followed by a great period of explosive volcanic activity (Yakoun Group) in Middle Jurassic time. Following Yakoun volcanism there was a period of uplift, erosion, and plutonism:

*The length of this stage of vulcanism is unknown as the volcanics are everywhere removed or truncated by the surface of pre-Cretaceous erosion. That there was considerable covering over the formations now exposed at the surface is evident from the fact that they are intruded by batholithic rocks, requiring at least several hundred feet of cover.... the lower and middle Jurassic rocks were folded to a considerable degree, and intruded by masses of igneous rocks in the form of batholiths...[that] may be correlated with the intrusion of the Coast Range batholith, generally supposed to be upper Jurassic in age. (MacKenzie, 1916, p. 115).*

At the beginning of Cretaceous sedimentation, the region was one of moderate relief. Renewed marine sedimentation began, first in local basins, then more widespread as subsidence continued (compare Haggart, 1991 for a modern treatment of Cretaceous sedimentation patterns).

At the close of the Cretaceous, the region was uplifted and folded, though much less strongly than in the Jurassic. Cretaceous sediments were largely removed by erosion, remaining only in synclinalia. The Eocene was marked by the intrusion of dacite and andesite dykes, sills, and hypabyssal intrusions. In the Miocene and Pliocene(?),

marine and nonmarine sediments of the Skonun Formation were deposited on northeastern Graham Island prior to eruption of the Miocene(?) and Pliocene Masset Formation. MacKenzie recognized that both the Masset and Skonun formations were folded into broad open warps and cut by faults.

Finally, MacKenzie devoted 13 pages to a discussion of the petroleum potential of Graham Island. He recognized the source-rock potential of the Maude Group, described the Lawn Hill and other bitumen occurrences, but concluded that it was extremely remote that significant hydrocarbon reserves existed on the island.

## **THE FIRST DETAILED BIOSTRATIGRAPHY: F.H. MCLEARN**

The publications of Whiteaves and the ensuing controversy had brought the remarkable Jurassic and Cretaceous fossils from Skidegate Inlet to world-wide attention. In 1921, the Geological Survey of Canada paleontologist Frank McLearn made the first of many trips to Skidegate Inlet. Unlike previous geologists to visit the islands, he was not motivated by economic concerns or interest in the regional geology. He systematically and carefully collected from the relatively narrow span of time represented by sections in the small area (Fig. 1) centred on Maude Island and Alliford Bay. He published several interim papers (e.g. McLearn, 1929, 1930, 1932) on Jurassic paleontology and stratigraphy in which he concluded that the Maude Formation was Toarcian in age.

In 1949 he summarized his information on the Jurassic of Skidegate Inlet in a bulletin (McLearn, 1949). In his revision of the Jurassic stratigraphy he retained MacKenzie's Maude and Yakoun formations and further divided the Maude into two unnamed lithologic units and the Yakoun into three (Fig. 2, column 6).

McLearn's work on the Cretaceous molluscs remained unpublished at his death in 1964. His rough manuscript, edited and completed by George Jeletzky, was finally published more than 50 years after his first visit to the islands (McLearn, 1972). McLearn was predominantly a Triassic specialist and his Jurassic work has undergone severe revision by later workers. His Cretaceous work has stood up well, though, and his careful collections remain of value to present-day biostratigraphers.

## **THE FIRST COMPLETE MAP AND SYNTHESIS: A. SUTHERLAND BROWN**

Apart from McLearn's detailed biostratigraphy, little regional work was done in the 40 years after publication of MacKenzie's report. Although there had been extensive mineral exploration between about 1906 and 1915, there was little between 1915 and the late 1940s. The 1950s were a time of intense exploration. Moresby Island saw active exploration for Fe-Cu skarn deposits, and on Graham Island Richfield Oil Corporation drilled five exploratory wells in 1958 to assess the hydrocarbon potential of the region. In 1958 Atholl Sutherland Brown of the British Columbia Department of Mines and Petroleum Resources began systematic mapping of the region as an aid to mineral exploration. His original intent was to map Moresby and adjacent islands (which had not been systematically examined since Dawson) but in 1961 work was extended to include Graham Island. He spent the summers of 1958-62, and several weeks in each of the following years in the field. The final publication (Sutherland Brown, 1968) contains detailed and elegant descriptions and syntheses of the bedrock geology, mineral and surficial deposits, and glacial history. The first geophysical survey of the area, an aeromagnetic survey of central Moresby Island intended to aid mineral exploration, was done as part of the overall project. The excellent geological map of the archipelago (at 1:125 000 scale) that accompanies the report re-

**Figure 2:** Stratigraphic columns for the Queen Charlotte region, based on previous work. Column 11 includes offshore data; all other columns are for the Queen Charlotte Islands only.

7. Sutherland Brown (1968)  
Queen Charlotte Islands

[illegible]

8. Cameron and Tipper (1985)  
Graham, Moresby, and Maude Islands

KIMMERIDGIAN TO TITHONIAN	united	sandstone, grtl. fine conglomerate, woody fragments
L. CALLOVAN TO U. BATHONIAN	WORESBY GROUP	ALLIFORD FM. allatone, shale, sandstone NEWCOMBE FM. sandstone, pebble conglomerate ROBER POINT FM. shale, allatone, pebble conglomerate
L. BAJOCIAN	YAKOLIN GROUP	RICHARDSON BAY FM. volcanic breccia, sandstone, tuff GRAHAM ISLAND FM. conglomerate, allatone, shale, tuff
ALENIAN TO U. TORCIAN		
U. TORCIAN TO M. TORCIAN		
M. TORCIAN	MAUDE GROUP	PHANTOM CREEK FM. Eelernite sandstone, coquilmold sandstone
L. TORCIAN TO U. PUERSBACHIAN		
L. PUERSBACHIAN		
UPPER & LOWER SINEMURIAN	KUNGA (in part)	WHITEVES FM. shale FANNIN FM. luffaceous sandstone, limestone, tuff REINELL shale, allatone, limestone GHOST CK. FM. shale, allatone, limestone SANDLANDS FM. shale, tuff, sandstone, allatone

9. Yagishita (1985)  
Skidegate Inlet

[illegible]

10. Haggart (1987)  
Cumshewa Inlet, western  
Skidegate Inlet, Beresford Bay

CRETACEOUS		SANTONIAN CONIACIAN TURONIAN L. CRETACEAN CENOMANIAN  ALBIAN		QUEEN CHARLOTTE gp.     HONNA FM. SHIDEGATE FM. HADA FM. shale member sandstone member
------------	--	--------------------------------------------------------------------------------	--	-------------------------------------------------------------------------------------------------------------------

11. Cameron and Hamilton (1988) Queen Charlotte Islands, Hecate Strait

[illegible]



mains highly useful, although large parts have been superseded by more recent work.

In his treatment of the stratigraphy, Sutherland Brown introduced several new names and subdivided some older ones (Fig. 2, column 7). He called the basal basaltic unit of the Vancouver Group the Karmutsen Formation, thus formally recognizing what had been known since Dawson's time: the Upper Triassic volcanic rocks on Vancouver and Queen Charlotte islands are identical. In a preliminary report (Sutherland Brown and Jeffrey, 1960) he introduced the name Kunga Formation for the Upper Triassic and Lower Jurassic sedimentary sequence characterized and generally dominated by limestone. In the final report (Sutherland Brown, 1968) he subdivided the Kunga into three members (now called the Sadler, Peril, and Sandilands formations).

Sutherland Brown gave the name Longarm Formation to Lower Cretaceous, mainly sedimentary rocks that unconformably overlie the Yakoun Formation. MacKenzie (1916) had included these rocks in his Triassic-Jurassic Maude Formation; all other workers had placed them the Queen Charlotte series. For the mid-Cretaceous rocks, Sutherland Brown used the term Queen Charlotte Group and retained MacKenzie's Haida, Honna and Skidegate formations. The Haida Formation he further subdivided into two members.

Sutherland Brown kept MacKenzie's Skonun and Masset formations but, in opposition to MacKenzie, he placed the Skonun Formation unconformably above the Masset Formation. He subdivided the Masset into three facies based on areal distribution: the Tartu, Kootenay and Dana facies. He concluded that the olivine basalts at Tow Hill are sills within the Skonun Formation and are distinct both temporally and petrographically from the Masset Formation.

The plutonic rocks received their first systematic study by Sutherland Brown. He recognized two suites, an older (possibly Late Jurassic) syntectonic category, and a younger (perhaps Eocene) post-tectonic suite.

Sutherland Brown's summary of the structural and tectonic history of the region, although conceived before the widespread acceptance of plate tectonics, gave an integrated and coherent picture that had a strong influence on later workers, particularly Yorath and Chase (1981) and Yorath and Hyndman (1983). Sutherland Brown was the first to study seriously the pattern of faulting on the islands. He believed that the distribution and nature of volcanic, sedimentary, and plutonic rocks was controlled by motion along three subparallel, northwest-trending fault zones: the Rennell Sound-Louscoone Inlet fault zone in the centre, the Sandspit fault zone on the east, and the Queen Charlotte fault offshore to the west. Movement along these faults occurred from Triassic time to the present. The history of the fault systems is complicated, but Sutherland Brown suggested that the net movement on the Rennell Sound-Louscoone and Sandspit systems combined large right-lateral displacement with significant east-side-down motion.

In his reconstruction of the tectonic history, the mantle-derived Karmutsen Formation erupted from a series of vents controlled by northwest trending faults. The Kunga Group was deposited in a basin that was initially shallow but deepened by Early Jurassic time; the Maude Group represents turbidite deposits in a deep basin. Marine and non-marine Yakoun volcanic rocks erupted from a series of vents parallel to and west of the Sandspit fault. Volcanism was followed by intense deformation and the emplacement of syntectonic plutons.

The earliest sediments of Cretaceous age, the Longarm Formation, were deposited in a graben-like basin controlled by the Rennell Sound-Louscoone Inlet fault and lapped onto the eroded margins of Yakoun deposits to the east. During Haida deposition, a land mass existed in what is now the western part of the archipelago; exposed units

included the Karmutsen and Kunga formations and the syntectonic plutons. The strand line roughly followed the trace of the Rennell-Louscoone fault. To the east there may have been a chain of islands underlain by Yakoun volcanics; Haida sediments may have been deposited beneath what is now Hecate Strait. The change in sedimentary style shown by the Honna Formation resulted from extensive fault motion along the margins of the Haida basin during Honna time.

Like many later workers, Sutherland Brown worried about the mode of origin of the Masset Formation. He suggested that the basalts represented remelting of Karmutsen basalts or a new tap of mantle materials. The Masset rhyolites, on the other hand, may represent remelting of early Paleozoic plutons such as those now exposed in southeastern Alaska. He recognized that the Tow Hill basalts are petrogenetically different than the Masset volcanics, and suggested that they may be correlative with alkaline basalts east of Hecate Strait (see Woodsworth, 1991 for a discussion of this point).

The marine and nonmarine Skonun Formation was deposited into an extensive, rapidly sinking basin, possibly fault-controlled on its margins, with sediment derived from both the Queen Charlotte Islands and from the mainland.

## POST-SUTHERLAND BROWN, PRE-FGP SYNTHESSES AND BIOSTRATIGRAPHY

Little regional mapping was done on the Queen Charlotte Islands in the two decades following the completion of Sutherland Brown's field work. Several syntheses were published based on his mapping, on geophysical surveys, new concepts of plate tectonics, new K-Ar dating, and the data gleaned from the active petroleum exploration program in Queen Charlotte Basin in the 1960s. Of these syntheses, only Shouldice (1971) added significantly to the stratigraphic database for the Queen Charlotte region. However, the models of Yorath and Chase (1981) and Yorath and Hyndman (1983) have been sufficiently influential that we outline them briefly without critical comment.

D.H. Shouldice (1971) interpreted the Tertiary part of the Queen Charlotte Basin from a petroleum exploration viewpoint, using largely proprietary geophysical and well data from Hecate Strait collected by Richmond Oil Corporation and Shell Canada. In his interpretation, volcanism began in Early to Middle Eocene time and continued sporadically into Miocene time. Tertiary sedimentation in the Queen Charlotte basin began in Miocene time and continued, interrupted by periods of uplift and erosion, through Pliocene time into the Pleistocene. The seismic data indicate large topographic relief on the top of the pre-Tertiary sediments; Tertiary sediments onlap onto this surface and thicken basinwards.

In his M.Sc. thesis, Ian Young (1981) presented the first comprehensive set of K-Ar dates for plutons and volcanic rocks of the Queen Charlotte Islands and interpreted the Mesozoic and Cenozoic history of the region in terms of a wrench-fault model. However, the most influential and controversial paper was that by Chris Yorath and Dick Chase. Using the geological framework developed by Sutherland Brown (1968), radiometric data obtained by Young (1981), gravity and magnetic data, and multichannel seismic data supplied by Chevron Standard Ltd. and Shell Canada Resources Ltd., Yorath and Chase (1981) interpreted the stratigraphic succession in terms of four tectonic assemblages: allochthonous, suture, post-suture, and rift. In their model, the Paleozoic through Jurassic strata of Alexander terrane and Wrangellia comprise allochthonous assemblages. Longarm Formation and Late Jurassic plutons on Queen Charlotte Islands represent suturing of Wrangellia to Alexander terrane along a proposed Rennell Sound-Sandspit fault system. Sedimentary rocks of the post-suture Queen Charlotte Group may have had an easterly source and may represent the final accretion of the amalgamated terranes to the

continent in mid-Cretaceous time. Masset Formation volcanic rocks and Tertiary plutons may represent middle to late Tertiary rifting in Queen Charlotte Sound above a mantle plume. Rifting resulted in strike-slip motion and subsidence in Queen Charlotte Sound and Hecate Strait.

In a related paper, Yorath and Roy Hyndman (1983) gave a model for the Tertiary evolution of the Queen Charlotte region. In their interpretation, rifting and crustal extension occurred in Queen Charlotte Sound until about 17 Ma ago. The Queen Charlotte Islands were displaced northwards by strike-slip motion. Rifting and crustal thinning resulted in a large thermal anomaly, Masset volcanism, and a restricted deep basin. Beginning about 6 Ma ago, oblique subduction along the continental margin caused flexural uplift of the western part of the Queen Charlotte Islands coupled with subsidence and widespread sedimentation in Hecate Strait and Queen Charlotte Sound.

Beginning in 1974, there was a renewed interest in the Jura-Cretaceous biostratigraphy of the Queen Charlotte Islands. Howard Tipper, later joined by Bruce Cameron, Beth Carter and Paul Smith, began systematic study of the Jurassic sections on Maude, Moresby and central Graham islands, integrating studies of macrofossils, radiolarians, and foraminifera. The first formal, substantial publication resulting from this work, Cameron and Tipper (1985), thoroughly revised the Jurassic nomenclature of the islands based on their new and detailed biostratigraphic work (Fig. 2, column 8). Cameron and Tipper (1985) abandoned the Vancouver Group, raised the Kunga Formation to group status, and gave the formal name Sandilands Formation to Sutherland Brown's (1968) black argillite member of the Kunga Group. Cameron and Tipper (1985) elevated the Lower to Middle Jurassic Maude Formation to group status and divided it into five new formations: Ghost Creek, Rennell Junction, Fannin, Whiteaves (named for J.F. Whiteaves), and Phantom Creek formation.

In treating the Yakoun Formation as it was described by Sutherland Brown (1968), they recognized that there was a hiatus between his lower, volcanogenic members and the upper, entirely sedimentary member. Cameron and Tipper (1985) restricted the term "Yakoun" to the lower, volcanogenic strata and raised the term to group status, consistent with their treatment of the Maude and Kunga groups. They subdivided the Yakoun Group into two formations: the lower shale and tuff-dominated Graham Island Formation and the conformably overlying, volcanic-dominated Richardson Bay Formation (indirectly named for James Richardson). The new term Moresby Group was given by Cameron and Tipper (1985) to the sedimentary beds that previously formed the upper part of the Yakoun Formation. Three new formations were formally defined within the Moresby Group: the Alliford, Newcombe, and Robber Point formations.

The mid-Cretaceous Queen Charlotte Group was also a focus of renewed interest in the 1980s. K. Yagishita (1985a,b), in his sedimentological study, placed the Honna Formation below the Skidegate Formation, in common with most earlier workers (Fig. 2, column 9). Yagishita concluded that the Haida and Honna formations are fore-arc basin deposits and were derived from the east.

James Haggart (1986, 1987) took a biostratigraphic and lithostratigraphic approach to the first significant revision of the Queen Charlotte Group in over a century. He identified early Turonian fossils from both the Skidegate and Haida formations, indicating that the two units are at least in part facies equivalents (Fig. 2, column 10). The greater part of the Honna Formation is Coniacian in age and thus caps the stratigraphic sequence (Haggart, 1987). Interestingly, Haggart showed that T.W. Stanton (paraphrased in MacKenzie, 1916) recognized the Turonian age of at least part of the Skidegate Member and the shale member of the Haida, but the stratigraphic implications were overlooked at the time.

Cameron and Hamilton (1988) published a stratigraphic column for the Queen Charlotte Islands and Hecate Strait (Fig. 2, column 11) that attempted to summarize the state of stratigraphic knowledge to date. The main changes from earlier workers were in the Tertiary, where the Masset and Skonun formations were recognized as being in part correlative.

## PRESENT STATE OF KNOWLEDGE

Work done under the Geological Survey of Canada's Frontier Geoscience Program has resulted in revisions to most parts of the stratigraphic column. These revisions are based on detailed biostratigraphy, geochronology, and regional mapping. The present state of stratigraphic nomenclature for the Queen Charlotte Islands is shown in Figure 3.

Upper Triassic and Lower to Middle Jurassic Kunga and Maude groups have seen intense study in the last several years. Desrochers and Orchard (1991), as part of an integrated biostratigraphic and sedimentological study of the Kunga Group, proposed the names Sadler Limestone and Peril Formation for the "grey limestone" and "black limestone" members of the Kunga Group. Tipper et al. (1991) continued their work on Lower and Middle Jurassic biostratigraphy. They abandoned the Rennell Junction Formation and included its beds within a revised Fannin Formation. Further major revisions to the Kunga and Maude groups seem unlikely in the near future, although refinement of the ages will continue and the Maude Group is ripe for a modern sedimentological study.

The Yakoun and Moresby groups have seen relatively little study in the last three years, thus the stratigraphic nomenclature of Cameron and Tipper (1985) has not been thoroughly tested. Both units need more study.

Haggart (1991), continuing his work on Cretaceous biostratigraphy, suggested that the Longarm Formation may extend down into the Jurassic. He interpreted the Longarm Formation and much of the younger Cretaceous Queen Charlotte Group as transgressive sequences deposited primarily in response to rising sea level. Haggart (1991) concluded that the previously inferred unconformity separating the two units does not exist: a continuous stratigraphic succession indicates that deposition in the basin was continuous through Early Cretaceous and into Late Cretaceous time. These results are preliminary; Upper Jurassic and Lower Cretaceous strata remain poorly understood relative to the Kunga and Maude groups.

Haggart's (1987) revisions to the Queen Charlotte Group remain essentially unchanged, but it is clear that there are several poorly exposed, poorly dated, and unnamed units on the northern half of the Queen Charlotte Islands. The age ranges and stratigraphic relations of these units (Fig. 3) are largely speculative; the Late Cretaceous to early Tertiary time span needs much more work.

The informally named "Gust Island volcanics" (Haggart et al., 1989) are intermediate volcanogenic rocks intercalated with the Honna conglomerate and sandstone. Haggart and Higgs (1989) reported a previously unrecognized shale unit containing Late Santonian to Early Campanian fossils. The coal deposits at the old Cowgitz site in Kagan Bay, which sparked much of the early geological work on the islands, are now known to be Early Eocene to Early Oligocene in age (White, 1990; Haggart, 1991), not Cretaceous as was long thought. This is the first identification of Paleogene strata in the Queen Charlotte Islands (White, 1990).

The definition of the Masset Formation remains controversial. Cameron and Hamilton (1988), based largely on unpublished work by Hamilton, used the term Masset for all Eocene through Miocene volcanic rocks on Queen Charlotte Islands and in Hecate Strait. Hickson (1991), based on detailed mapping on Graham Island, chem-

# 12. Frontier Geoscience Program (1990) Queen Charlotte Islands

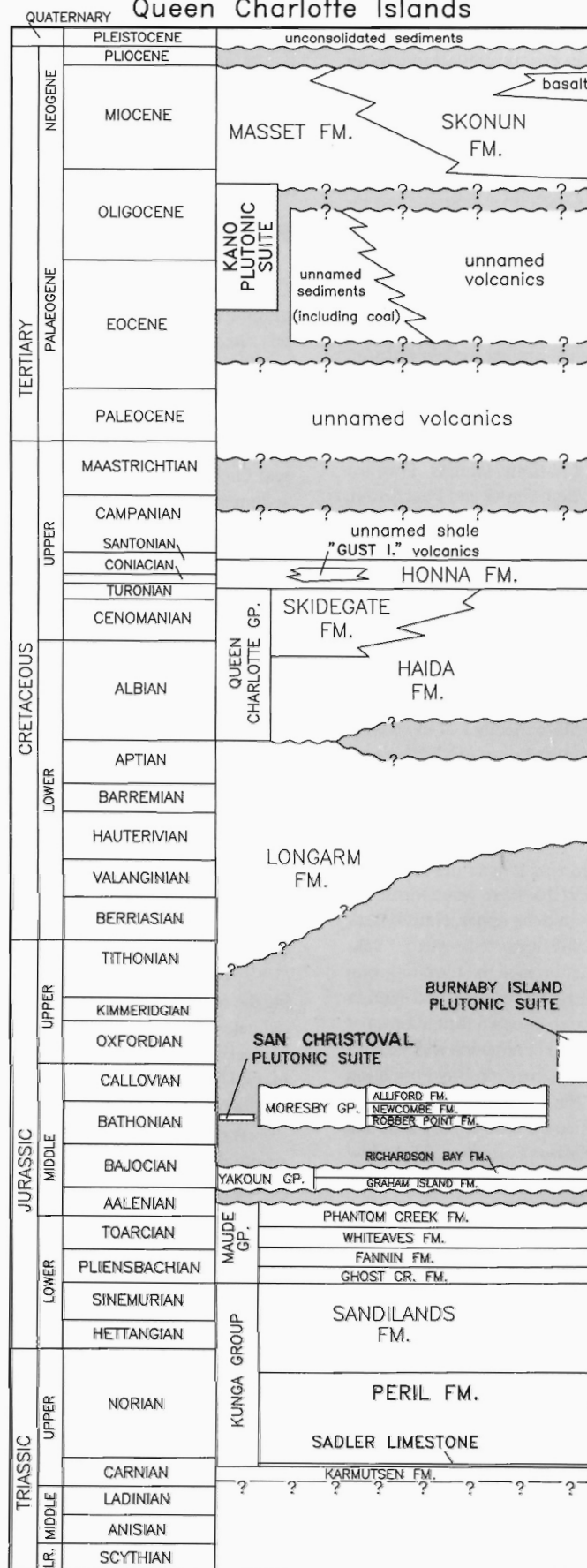


**Figure 3:** Stratigraphic column for the Queen Charlotte Islands. This synthesis incorporates work between 1987 and 1989 under the Frontier Geoscience Program.

istry, and petrography, restricted the Masset Formation to Late Oligocene to earliest Pliocene, aphyric to sparsely phytic, calc-alkalic volcanic rocks and associated epiclastic sediments. Under this definition, rocks of Sutherland Brown's (1968) Kootenay facies are included in the Masset Formation, but breccias of his Dana facies are excluded. In contrast to Cameron and Hamilton (1988), the Miocene basalts along the east side of Graham Island, beneath and along the east side of Hecate Strait are also excluded from the Masset Formation (Woodsworth, 1991). All active workers, however, agree that the Skonun Formation is in large part correlative with the Masset Formation (Fig. 3).

Although Young (1981) had done some K-Ar dating on some plutons on the Queen Charlotte Islands, plutonic rocks had been largely ignored since Sutherland Brown (1968). In the last few years, Bob Anderson and others have made a systematic study of plutons on the islands (Anderson, 1988; Anderson and Greig, 1989; Anderson and Reichenbach, 1991). This work has shown that Sutherland Brown's (1968) inferred Cretaceous age for his syntectonic and post-tectonic batholiths is incorrect. Instead, they showed that there are two suites of Middle Jurassic plutons on the islands. They named these the San Christoval suite (on the east) and the Burnaby Island suite (younger, and on the east) (Fig. 3). They showed that Tertiary plutonic rocks, which they named the Kano plutonic suite, are Middle Eocene and Miocene in age and are roughly coeval and cospatial with the Masset volcanic rocks.

## CONCLUSION

The stratigraphic nomenclature of the Queen Charlotte Islands has developed over the last century in a piecemeal fashion. The stratigraphic column used by any individual worker is an interpretation reflecting the scientific paradigms of the day, his/her geological training and prejudices, the stratigraphic record preserved in the area studied, and the cumulative knowledge gained from the literature. Thus different workers may use different (and often contradictory) stratigraphic nomenclature, and not all studies that have been published represent significant progress.

## ACKNOWLEDGMENTS

This paper could not have been written without discussions with many colleagues in the Frontier Geoscience Program, particularly Jim Haggart, Cathie Hickson, Peter Lewis, Mike Orchard, Howard Tipper, and Bob Thompson.

## REFERENCES

- Anderson, R.G.  
**1988:** Jurassic and Cretaceous-Tertiary plutonic rocks on the Queen Charlotte Islands, British Columbia; *in* Current Research, Part E, Geological Survey of Canada, Paper 88-1E, p. 213-216.
- Anderson, R.G. and Greig, C.J.  
**1989:** Jurassic and Tertiary plutonism in the Queen Charlotte Islands, British Columbia; *in* Current Research, Part H, Geological Survey of Canada, Paper 89-1H, p. 95-104.
- Anderson, R.G. and Reichenbach, I.  
**1991:** U-Pb and K-Ar framework for Middle to Late Jurassic (172±158 Ma) and Tertiary (46-27 Ma) plutons in Queen Charlotte Islands, British Columbia; *in* Evolution and Hydrocarbon Potential of the Queen Charlotte Basin, British Columbia, Geological Survey of Canada, Paper 90-10.
- Billings, E.  
**1873:** On the Mesozoic Fossils from British Columbia, collected by Mr. James Richardson in 1872; Geological Survey of Canada, Report of Progress for 1872-1873, p. 71-75.
- Cameron, B.E.B. and Hamilton, T.S.  
**1988:** Contributions to the stratigraphy and tectonics of the Queen Charlotte Basin, British Columbia; *in* Current Research, Part E, Geological Survey of Canada, Paper 88-1E, p. 221-227.
- Cameron, B.E.B. and Tipper, H.W.  
**1985:** Jurassic stratigraphy of the Queen Charlotte Islands, British Columbia; Geological Survey of Canada, Bulletin 365, 49 p.
- Clapp, C.H.  
**1914:** A geological reconnaissance on Graham Island, Queen Charlotte Group, B.C.; Geological Survey of Canada, Summary Report for 1912, p. 12-40.
- Dalzell, K.E.  
**1968:** The Queen Charlotte Islands, 1774-1966; C.M. Adam, Terrace, British Columbia, 340 p.
- Dawson, G.M.  
**1880:** Report on the Queen Charlotte Islands, 1878; Geological Survey of Canada, Report of Progress for 1878-1879, p. 1B-239B.  
**1887:** Report on a geological examination of the northern part of Vancouver Island and adjacent coasts; Geological Survey of Canada, Annual Report (new series), v. 2, 1886, Report B, 129 p.  
**1889:** On the earlier Cretaceous rocks of the northwest portion of the Dominion of Canada; American Journal of Science, 3rd Series, v. 38, p. 120-127.
- Dawson, J.W.  
**1873:** Note on the fossil plants from British Columbia, collected by Mr. James Richardson in 1872; Geological Survey of Canada, Report of Progress for 1872-1873, p. 66-71.
- Desrochers A. and Orchard, M.J.  
**1991:** Stratigraphic revisions and carbonate sedimentology of the Kunga Group (Upper Triassic-Lower Jurassic), Queen Charlotte Islands, British Columbia; *in* Evolution and Hydrocarbon Potential of the Queen Charlotte Basin, British Columbia, Geological Survey of Canada, Paper 90-10.
- Dowling, D.B.  
**1906:** Cretaceous section in the Moose Mountain district, southern Alberta; Bulletin of the Geological Society of America, v. 17, p. 295-302.
- Ells, R.W.  
**1906:** Report on Graham Island, B.C.; Geological Survey of Canada, Annual Report, New Series, v. 16, 1904, Part B, p. 1-46.
- Haggart, J.W.  
**1986:** Stratigraphic investigations of the Cretaceous Queen Charlotte Group, Queen Charlotte Islands, British Columbia; Geological Survey of Canada, Paper 86-20, 24 p.  
**1987:** On the age of the Queen Charlotte Group of British Columbia; Canadian Journal of Earth Sciences, v. 24, p. 2470-2476.  
**1991:** A synthesis of Cretaceous stratigraphy, Queen Charlotte Islands, British Columbia; *in* Evolution and Hydrocarbon Potential of the Queen Charlotte Basin, British Columbia, Geological Survey of Canada, Paper 90-10.
- Haggart, J.W. and Higgs, R.  
**1989:** A new Late Cretaceous mollusc fauna from the Queen Charlotte Islands, British Columbia; *in* Current Research, Part H, Geological Survey of Canada, Paper 89-1H, p. 59-64.
- Haggart, J.W., Lewis, P.D., and Hickson, C.J.  
**1989:** Stratigraphy and structure of Cretaceous strata, Long Inlet, Queen Charlotte Islands, British Columbia; *in* Current Research, Part H, Geological Survey of Canada, Paper 89-1H, p. 65-72.
- Hickson, C.J.  
**1991:** The Masset Formation on Graham Island, Queen Charlotte Islands, British Columbia; *in* Evolution and Hydrocarbon Potential of the Queen Charlotte Basin, British Columbia, Geological Survey of Canada, Paper 90-10.
- MacKenzie, J.D.  
**1914:** South-central Graham island, B.C.; Geological Survey of Canada, Summary Report for 1913, p. 34-54.  
**1916:** Geology of Graham Island, British Columbia; Geological Survey of Canada, Memoir 88, 221 p.
- McLearn, F.H.  
**1929:** Contributions to the stratigraphy and palaeontology of Skidegate Inlet, Queen Charlotte Islands, B.C.; Geological Survey of Canada, Museum Bulletin 54, p. 1-27.  
**1930:** Notes on some Canadian Mesozoic faunas; Transactions of the Royal Society of Canada, 3rd Series, v. 24, sect. 4, p. 1-7.  
**1932:** Contributions to the stratigraphy and palaeontology of Skidegate Inlet, Queen Charlotte Islands, B.C. (continued); Royal Society of Canada, Transactions, 3rd Series, v. 26, sec. IV, p. 51-80.  
**1949:** Jurassic formations of Maude Island and Alliford Bay, Skidegate Inlet, Queen Charlotte Islands, British Columbia; Geological Survey of Canada, Bulletin 12, 19 p.  
**1972:** Ammonoids of the Lower Cretaceous Sandstone Member of the Haida Formation, Skidegate Inlet, Queen Charlotte Islands, western British Columbia; Geological Survey of Canada, Bulletin 188, 78 p.
- Richardson, J.  
**1873:** Report on the coal-fields of Vancouver and Queen Charlotte Islands; Geological Survey of Canada, Report of Progress for 1872-73, p. 32-65.
- Shouldice, D.H.  
**1971:** Geology of the western Canadian continental shelf; Bulletin of Canadian Petroleum Geology, v. 19, p. 405-436.
- Stanton, T.W. and Martin, G.C.  
**1905:** Mesozoic section on Cook Inlet and Alaska Peninsula; Bulletin of the Geological Society of America, v. 16, p. 391-410.

- Sutherland Brown, A.**  
**1968:** Geology of the Queen Charlotte Islands, British Columbia; British Columbia Department of Mines and Petroleum Resources, Bulletin 54, 226 p.
- Sutherland Brown, A. and Jeffrey, W.G.**  
**1960:** Preliminary geological map, southern Queen Charlotte Islands; British Columbia Department of Mines.
- Thompson, R.I., Haggart, J.W., and Lewis, P.D.**  
**1991:** Late Triassic through early Tertiary evolution of the Queen Charlotte Basin, British Columbia, with a perspective on hydrocarbon potential; *in* Evolution and Hydrocarbon Potential of the Queen Charlotte Basin, British Columbia, Geological Survey of Canada, Paper 90-10.
- Tipper, H.W., Smith, P.L., Cameron, B.E.B., Carter, E.S., Jakobs, G.K., and Johns, M.J.**  
**1991:** Biostratigraphy of the Lower Jurassic formations of the Queen Charlotte Islands, British Columbia; *in* Evolution and Hydrocarbon Potential of the Queen Charlotte Basin, British Columbia, Geological Survey of Canada, Paper 90-10.
- White, J.M.**  
**1990:** Evidence of Paleogene sedimentation on Graham Island, Queen Charlotte Islands, west coast, Canada; Canadian Journal of Earth Sciences, v. 27, p. 533-538.
- Whiteaves, J.F.**  
**1876:** On some invertebrates from the coal-bearing rocks of the Queen Charlotte Islands, collected by Mr. James Richardson in 1872; Geological Survey of Canada, Mesozoic Fossils, v. 1, Part 1, 92 p.  
**1883:** On the Lower Cretaceous rocks of British Columbia; Proceedings and Transactions of the Royal Society of Canada, Transactions, v. 1, section 4, p. 81-86.
- 1884:** On the fossils of the coal-bearing deposits of the Queen Charlotte Islands collected by Dr. G.M. Dawson in 1878; Geological Survey of Canada, Mesozoic Fossils, v. 1, Part 3, p. 191-262.
- 1900:** On some additional or imperfectly understood fossils from the Cretaceous rocks of the Queen Charlotte Islands, with a revised list of the species from these rocks; Mesozoic Fossils, v. 1, Part 4, p. 263-307.
- Woodsworth, G.J.**  
**1991:** Neogene to Recent volcanism along the east side of Hecate Strait, British Columbia; *in* Evolution and Hydrocarbon Potential of the Queen Charlotte Basin, British Columbia, Geological Survey of Canada, Paper 90-10.
- Yagishita, K.**  
**1985a:** Mid- to Late Cretaceous sedimentation in the Queen Charlotte Islands, British Columbia; lithofacies, paleocurrent and petrographic analyses of sediments; Ph.D. thesis, University of Toronto, Ontario.  
**1985b:** Evolution of a provenance as revealed by petrographic analyses of Cretaceous formations in the Queen Charlotte Islands, British Columbia, Canada; Sedimentology, v. 32, p. 671-684.
- Yorath, C.J. and Chase, R.L.**  
**1981:** Tectonic history of the Queen Charlotte Islands and adjacent areas-a model; Canadian Journal of Earth Sciences, v. 18, p. 1717-1739.
- Yorath, C.J. and Hyndman, R.D.**  
**1983:** Subsidence and thermal history of Queen Charlotte Basin; Canadian Journal of Earth Sciences, v. 20, p. 135-159.
- Young, I.F.**  
**1981:** Structure of the western margin of the Queen Charlotte Basin, British Columbia; M.Sc. thesis, University of British Columbia, Vancouver, B.C., 380 p.



# Stratigraphic revisions and carbonate sedimentology of the Kunga Group (Upper Triassic-Lower Jurassic), Queen Charlotte Islands, British Columbia

A. Desrochers<sup>1</sup> and M.J. Orchard<sup>2</sup>

Desrochers, A. and Orchard, M.J., Stratigraphic revisions and carbonate sedimentology of the Kunga Group (Upper Triassic-Lower Jurassic), Queen Charlotte Islands, British Columbia; in *Evolution and Hydrocarbon Potential of the Queen Charlotte Basin*, British Columbia, Geological Survey of Canada, Paper 90-10, p. 163-172, 1991.

## Abstract

*In the Queen Charlotte Islands (QCI), three lithostratigraphic subdivisions of the Late Triassic-Early Jurassic Kunga Group are recognized. These are the Sadler Limestone at the base (new formation, 42-200 m in thickness, Late Carnian in age), the Peril Formation (new formation, ~350 m, Late Carnian-early Late Norian), and the Sandilands Formation at the top (~500 m, middle Late Norian-Sinemurian). Three informal subdivisions of the Peril Formation are recognized on the basis of predominant limestone lithofacies: a lower concretionary calcilutite member (Upper Carnian-Lower Norian), a middle laminated calcarenite member (Lower-Middle Norian), and an upper pelecypod coquina member (lower Upper Norian).*

*The geologic history of the Kunga Group involves three distinct depositional stages corresponding to the three lithostratigraphic units. The Sadler Limestone represents deposition on a widespread carbonate platform that was established on a relatively flat volcanic basement after the termination of volcanic activity in the Carnian. An open platform facies, and on-shelf sand shoal facies developed during the Upper Carnian polygnathiformis Zone time.*

*The Peril Formation records a relatively rapid sea level rise beginning in Upper Carnian nodosus Zone time. This resulted first in the formation of hardgrounds over the drowned platform, and then in the deposition of deeper water sediments representative of a slope to basin setting throughout the remainder of the Late Carnian and through early Late Norian time. Depositional facies include pelagic/hemipelagic sediments, proximal to distal calciturbidites, and platform-to-slope-derived debris flows. No carbonate source for these is known in QCI.*

*With the advent of middle Late Norian time, within the bidentata Zone, carbonate sedimentation ended abruptly in QCI. This event is coincident with the drowning of isolated carbonate platforms in other parts of Wrangellia. Thereafter, predominantly terrigenous sediments of the Sandilands Formation were deposited in the basin.*

## Résumé

*Dans les îles de la Reine-Charlotte, on a déterminé trois subdivisions lithostratigraphiques du groupe de Kunga du Trias supérieur au Jurassique inférieur. Ce sont le calcaire de Sadler à la base (nouvelle formation, de 42 à 200 m d'épaisseur, datant du Carnien supérieur, la formation de Peril (nouvelle formation, ~350 m, du Carnien tardif-début du Norien supérieur et la formation de Sandilands au sommet (~500 m, du milieu du Norien supérieur au Sinémurien). En se fondant sur le lithofaciès calcaire prédominant, on a déterminé trois subdivisions informelles de la formation de Peril : un membre inférieur de calcilutite concrétionnée daté du Carnien supérieur au Norien inférieur, un membre intermédiaire de calcarenite laminée du Norien inférieur à moyen et un membre supérieur calcaire à pélecypodes appartenant à la partie inférieure du Norien supérieur.*

*L'histoire géologique du groupe de Kunga comporte trois étapes sédimentaires distinctes correspondant aux trois unités lithostratigraphiques. Le calcaire de Sadler correspond à la sédimentation d'une vaste plate-forme carbonatée sur un socle volcanique relativement plat après la fin de l'activité volcanique du Carnien. Un faciès de plate-forme ouverte et un faciès de haut fond sableux de plate-forme continentale se sont formés durant la mise en place de la zone à polygnathiformis du Carnien supérieur.*

*La formation de Peril contient des indices d'une augmentation relativement rapide du niveau de la mer commençant à l'époque de la formation de la zone à nodosus du Carnien supérieur. Il s'ensuivit la formation d'un fond marin induré au-dessus de la plate-forme inondée, suivie du dépôt de sédiments d'eau plus profonde correspondant à une sédimentation de talus à celle de bassin pendant tout le reste du Carnien supérieur et pendant le début du Norien supérieur. Le faciès de sédimentation comprend des sédiments pélagiques et hémipélagiques, des calciturbidites de proximales à distales et des coulées de débris provenant d'une zone variant de la plate-forme au talus. On n'a repéré aucune source de carbonates dans les îles de la Reine-Charlotte.*

*Au milieu du Norien supérieur durant la zone à bidentata, la sédimentation des carbonates a cessé brusquement dans les îles. Ce phénomène coïncide avec l'inondation de plates-formes carbonatées isolées dans d'autres parties de la Wrangellia. Par la suite, des sédiments principalement terrigènes de la formation de Sandilands se sont déposés dans le bassin.*

<sup>1</sup> Ottawa-Carleton Geoscience Centre, Department of Geology, University of Ottawa, Ottawa, Ontario K1N 6N5

<sup>2</sup> Cordilleran Division, Geological Survey of Canada, 100 West Pender St., Vancouver, B.C. V6B 1R8

## INTRODUCTION

The Kunga Group (Upper Triassic-Lower Jurassic) is the oldest sedimentary sequence recognized in the Queen Charlotte Islands, off the west coast of British Columbia (Fig. 1). During the field seasons 1987 and 1988, the principal Triassic outcrops of the group delineated by Sutherland Brown (1968) were visited and sampled. The resulting integration of lithostratigraphy and conodont biostratigraphy provide a basis for formal comprehensive subdivision of the Kunga Group presented here.

In this paper, new formational names are introduced for the lower and middle parts of the Kunga Group, the lithostratigraphic relationships and internal structure of the carbonate units are described, and biostratigraphic constraints are summarized. The second part of this paper documents the variety of carbonate lithofacies and gives a brief overview of the sedimentary history of the Kunga Group.

## STRATIGRAPHY OF THE KUNGA GROUP

### Previous nomenclature

Kunga Group strata were first recognized as a distinct unit by Dawson (1880), but Sutherland Brown and Jeffrey (1960) introduced the name Kunga Formation for a sedimentary sequence of limestone and argillite of Carnian to Sinemurian age (early Late Triassic-mid-Early Jurassic). Sutherland Brown (1968) subdivided the formation into three informal members, from base to top: 1) massive, grey limestone; 2) thinly bedded, black limestone; and 3) thinly bedded, black argillite.

In addition, Sutherland Brown (1968) defined more precisely the Vancouver Group, a term originally proposed by Clapp (1914) for Triassic and Jurassic volcanic and sedimentary rocks on Vancouver Island. The Vancouver Group comprises four formations, in ascending order: 1) the Karmutsen Formation composed of basalt pillow lava and breccia, and minor sediments of Triassic age; 2) the Kunga Formation comprising Upper Triassic to Lower Jurassic limestone and argillite; 3) the Maude Formation composed of Lower Jurassic argillite, shale, limestone, and sandstone; and 4) the Yakoun Formation comprising Middle Jurassic tuff, agglomerate, volcanic sandstone, shale, sandstone, and conglomerate.

### Existing nomenclature

Cameron and Tipper (1985) proposed a profound revision of the Jurassic stratigraphy of the Queen Charlotte Island, by elevating old formational names to group status, introducing new formational names, and subdividing formations into informal members (Fig. 2). In their new nomenclature, they abandoned the term Vancouver Group arguing that it could not be applied to the Queen Charlotte Islands because of lithological dissimilarities between the two regions. They also elevated the Kunga Formation to a group level and redefined the upper member as the Sandilands Formation. The two lower, wholly Triassic members have remained un-named until now.

### Proposed nomenclature

The Kunga Group is characterized by distinctive lithologies and laterally persistent members as defined by Sutherland Brown (1968). In addition, these members can be mapped regionally at a scale of 1:50,000. For these reasons, the members should be redefined and elevated to a formational status according to the spirit of the Code of Stratigraphic Nomenclature.

The new names Sadler Limestone and Peril Formation are here proposed for, respectively, the massive, grey limestone member and the thinly bedded, black limestone member (Fig. 3,4). The Peril Formation is divided into three informal members: 1) a lower concretionary-

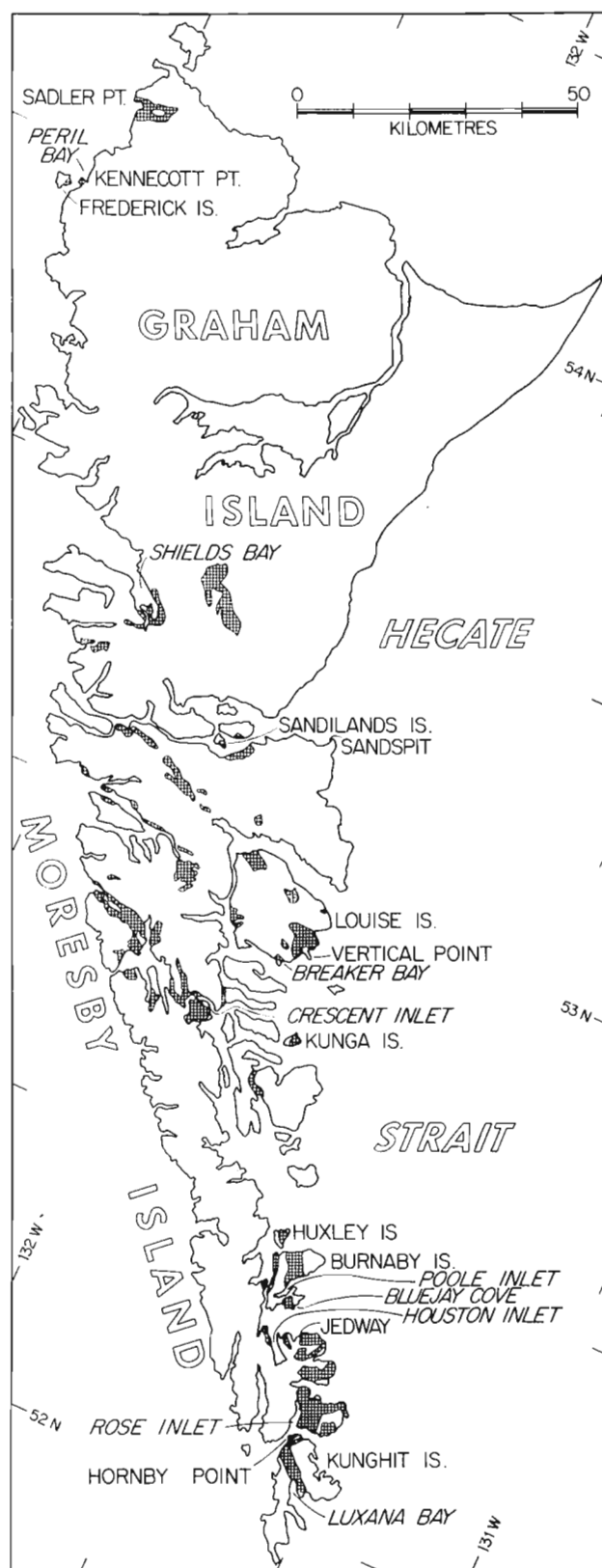


**Figure 1:** Map of the Queen Charlotte Islands showing Triassic outcrop, and key localities cited in the text (compiled from Sutherland Brown, 1968).

limestone member, 2) a middle calcarenite member, and 3) an upper coquinoid-limestone member.

The Triassic part of the Kunga Group including the two newly defined formations are described below. The reader is referred to Cameron and Tipper (1985) for details on the Jurassic part of the Kunga Group.

LITHOSTRATIGRAPHIC UNITS

Sadler Limestone (new formation)

Reference section

The type section is located at Sadler Point (Grid Reference Zone 8, 624300E, 5997680N) on the northwest tip of Graham Island (Fig. 1). The section consists of superb coastal exposure comprising accessible cliffs with good bedding plane view of the lower and upper contacts of the formation.

Lithology

The sequence was originally defined as massive, thick-bedded grey limestones that are more or less recrystallized near intrusive bodies (Sutherland Brown, 1968). When unaffected by thermal metamorphism, these massive limestones comprise three distinct lithofacies (Fig. 5): 1) lime mudstone to peloidal wackestone, 2) bioclastic wackestone to packstone, and 3) oolitic calcarenite.

Distribution

This formation has been found throughout the entire length of the Queen Charlotte Islands but is best exposed on northwest Kunghit

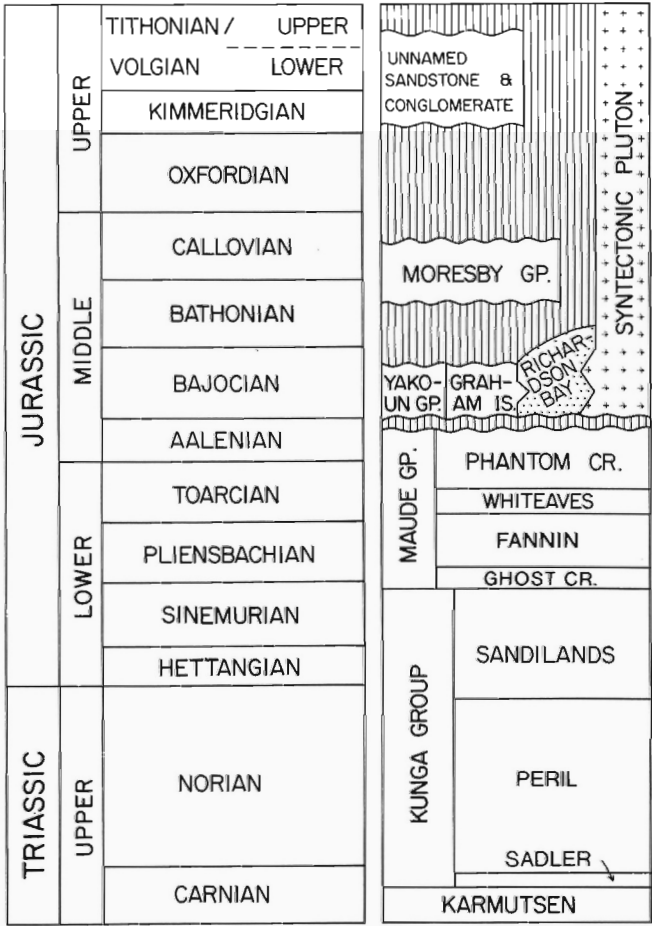


Figure 2: General stratigraphic column for the revised Triassic-Jurassic units of the Queen Charlotte Basin (modified from Cameron and Hamilton, 1988).

Island (Hornby Point), Huston Inlet, northern Kunga Island (including Titul Island), and at Sadler Point (Fig. 1). Other sections are also present in most outcrop areas but occur in small fault blocks.

Thickness

The thickness of the formation calculated from well exposed sections in simple structural situations is variable and ranges from 42-200 m. The minimum thickness is seen at the type section at Sadler Point, where no structural or stratigraphic breaks are evident. Sections up to 150 m thick were measured at Huston Point and western Kunghit Island (Hornby Point) but the formation is only partially exposed, and probably repeated by faulting. Sutherland Brown (1968) reported a 200 m thick section of grey limestone on the north shore of the Kunga Island, and a similar thickness is also exposed a few kilometres north of Kunga Island on Titul Island; both sections are faulted.

Definition of boundary

The formation is in sharp but apparently conformable contact with the underlying Karmutsen Volcanics (Fig. 3,5A). The upper contact with the Peril Formation is also conformable and is placed at the top of the last massive grey limestone. The upper contact is furthermore characterized by a thin (0.5-1.0 m) transition zone composed of distinctive thin-bedded, nodular echinoderm calcarenites that are interpreted as hardgrounds (see below).

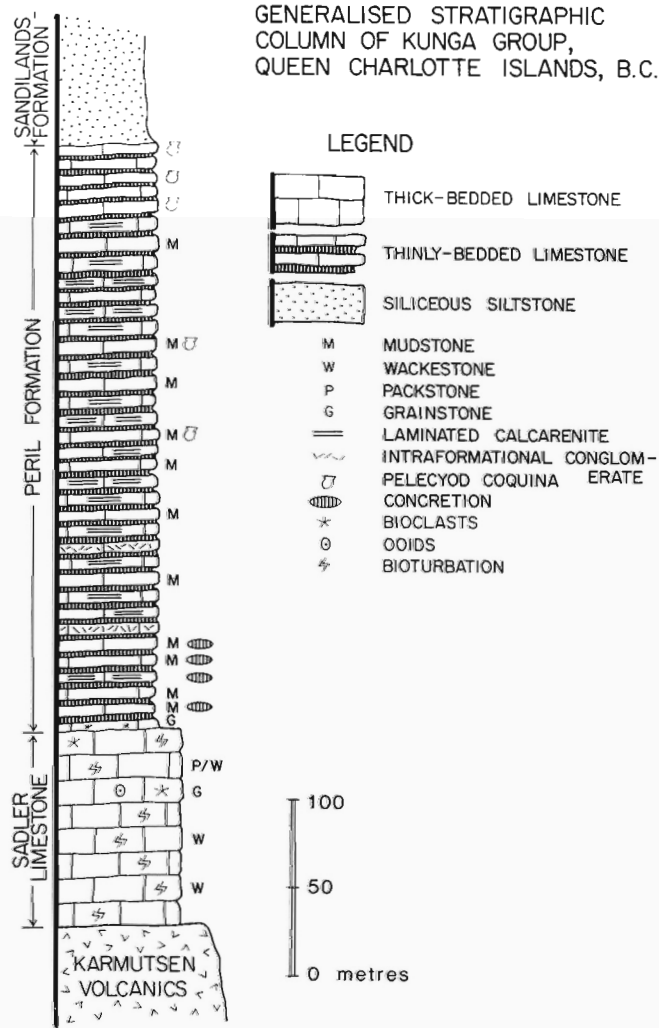
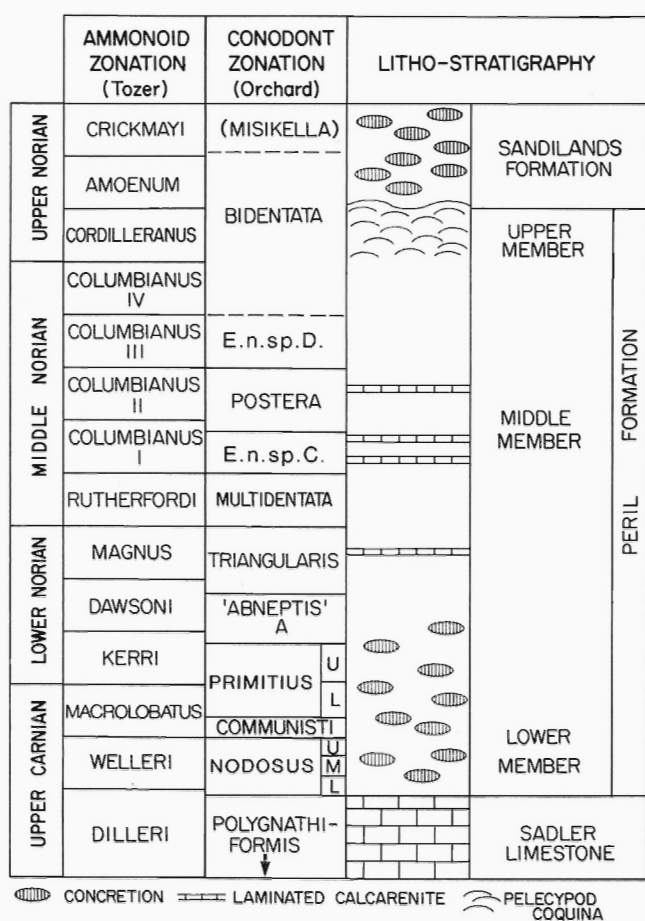


Figure 3: Generalized stratigraphic column of major carbonate lithofacies in the Upper Triassic portion of the Kunga Group.



**Figure 4:** Schematic diagram showing ammonoid and conodont zonation of the Upper Triassic in relation to lithostratigraphy of the Kunga Group (modified from Carter et al., 1989).

#### Fauna

Although the fauna is not abundant, the formation has yielded a great variety of fossils representing mainly benthic organisms. These fossils are best observed in thin-section and include gastropods, thick-shelled pelecypods, echinoderms, ostracodes, oncolites, brachiopods, dasycladacean algae, and foraminiferids. Rare ammonites are also present, and according to Sutherland Brown (1968, p. 60), unidentifiable corals occur. Conodonts were found in about half of the samples taken. Silicified holothurian sclerites and ichthyoliths also occur in the acid residues. *Thalassinoides* is a common trace fossil in the limestones.

#### Age

Prior to the present investigation, age control on the Sadler Limestone was minimal. Sutherland Brown (1968, p. 60-61, Table IV) records an atypical ammonoid-belemnoid-pelecypod fauna from the Sadler Limestone at Kaisun that was determined as Carnian by E.T. Tozer, but no more direct age was available. It should be noted that this association is more typical of the overlying Peril Formation. New ammonoid collections from within the Sadler Formation at Huston Inlet are now referred to the Upper Carnian Dilleri Zone (Tozer, in Orchard et al., 1990). Two further collections from the transition beds of the Sadler Limestone and Peril Formation at Breaker Bay and Sadler Point are also referred to the Dilleri Zone (op. cit.), but are included in the Peril Formation. Conodont collections from the Sadler Limestone are referred to the *polygnathiformis* Assemblage Zone, which is typical of, but not exclusive to the Upper Carnian (Orchard, 1991). Rare conodont faunules from carbonate pods with-

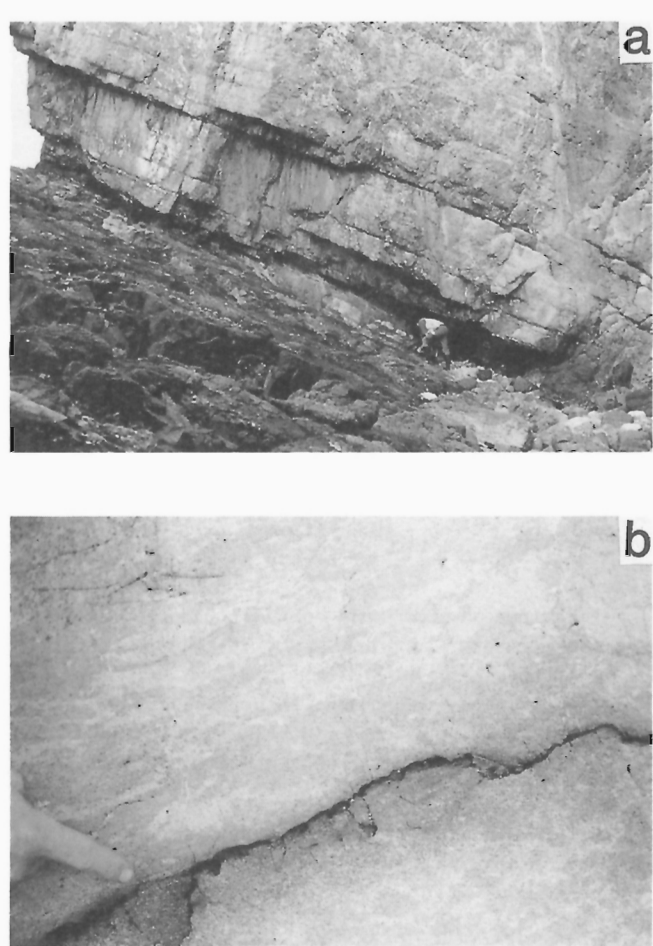


**Figure 5:** Sadler Limestone. A) Field exposure of the contact between the Karmutsen Volcanics and the thick-bedded, grey limestones of the Sadler Limestone. Sadler Point. B) Field exposure (cross-section view) of typical bioturbated lime mudstone and peloidal wackestone. Note the burrow-mottled fabric and bedding plane contact outlined by centimetre-wide stylolite. Sadler Point.

in the underlying Karmutsen Formation are essentially the same as those from the Sadler Limestone and this argues for a close temporal relationship between the two units (Fig. 4).

#### Remarks

The type section of the Kunga "Formation" (*sensu* Sutherland Brown, 1968) is located on the north shore of Kunga Island. This section is unsuitable for defining new subdivisions of the group because: 1) the internal and external stratigraphic relations of the grey limestones are obscured by faulting; 2) primary depositional fabrics are poorly preserved in the limestones; and 3) the thermal effects of Middle to Upper Jurassic plutons in eastern South Moresby is evident from CAI values (i.e. conodont colour alteration index) of 4.5-5 (Orchard, 1988; Orchard and Forster, 1991). In contrast, the newly proposed type sections are characterized by well defined internal and external stratigraphic relations, by well preserved limestone lithofacies, and by lower CAI values (i.e. 1.5-2.5).

#### Peril Formation (new formation)

##### Reference section

The Peril Formation outcrops as fault-bounded sections of thinly-bedded, black limestones. No single locality exposes the complete sequence but a composite stratigraphic section (Fig. 3) has been compiled through ammonoid, bivalve, radiolarian, and particularly conodont based correlations (Fig. 4; Carter et al., 1989; Orchard, 1991). The sections exposed on the south and west shores of Peril Bay (Fig. 1) on northwest Graham Island are selected as the primary ref-

erence sections. On the south, Kennecott Point (Grid Reference: Zone 8, 621170E, 5975500N) represents the only locality where the contact with the overlying Sandilands Formation is well exposed and not obscured by faulting. To the west, much of the Peril Formation is exposed in a series of fault blocks (see Orchard and Forster, 1991) on Frederick Island (Grid Reference: Zone 8, 620960E, 5977500N). However, neither the top nor the base of the Peril Formation occur on Frederick Island, and recovered conodont fauna from throughout QCI indicates that a total composite section for the formation may only be derived from several sections (see below).

### *Lithology*

The Peril Formation consists mainly of thinly bedded, siliceous dark-grey to black limestone. Three major limestone lithofacies are recognized: 1) radiolarian-rich calcilitite, 2) laminated calcarenite, and 3) pelecypod coquina. The formation is subdivided into three informal members on the basis of predominant limestone lithofacies (Fig. 3,4): 1) a lower member dominated by radiolarian-rich calcilitite in which dense micritic concretions are present (Fig. 6); 2) a middle member dominated by laminated calcarenite (Fig. 7); and 3) an upper member dominated by pelecypod coquina (Fig. 8). In addition, intraformational conglomerate and echinoderm calcarenite occur as minor lithofacies.

The primary depositional textures and structures of these limestone lithofacies are commonly difficult to recognize in the field because silicification is locally pervasive. Silicification is usually concentrated at the lower and upper boundaries of limestone beds but only relict fabrics of the original limestone bed remain where it is more widespread.

### *Distribution*

The formation has been found over the whole length of the Queen Charlotte Islands, but the most important sections are those on northwestern Kunghit Island, the north side of Poole Inlet, Burnaby Island at Section Cove, southeastern Kunga Island, northern and eastern Huxley Island, on Frederick Island, and north of Sadler Point (Fig. 1): these collectively embrace the complete faunal sequence (Orchard, 1991). Other sections are structurally complex and consist of many faulted-bounded exposures.

### *Thickness*

Sutherland Brown (1968) reported variable thickness for the thinly-bedded black limestones but faulting may be responsible for making this more apparent than real. He reported thicknesses of 278 m and (905 ft) and 188 m (610 ft) at sections on Kunga Island and Burnaby Island respectively. Conodont based compilation of a composite section provides a thickness of about 350 m for the Peril Formation. Approximate thicknesses of 90 m, 210 m, and 40+ m are determined for, respectively, the lower, middle, and upper members.

### *Definition of boundaries*

The lower contact is sharp but conformable (Fig. 6A). At its base, a thin transitional zone, 0.5-1.0 m thick, comprises thin- to medium-bedded, nodular echinoderm calcarenite quite distinct from the un-

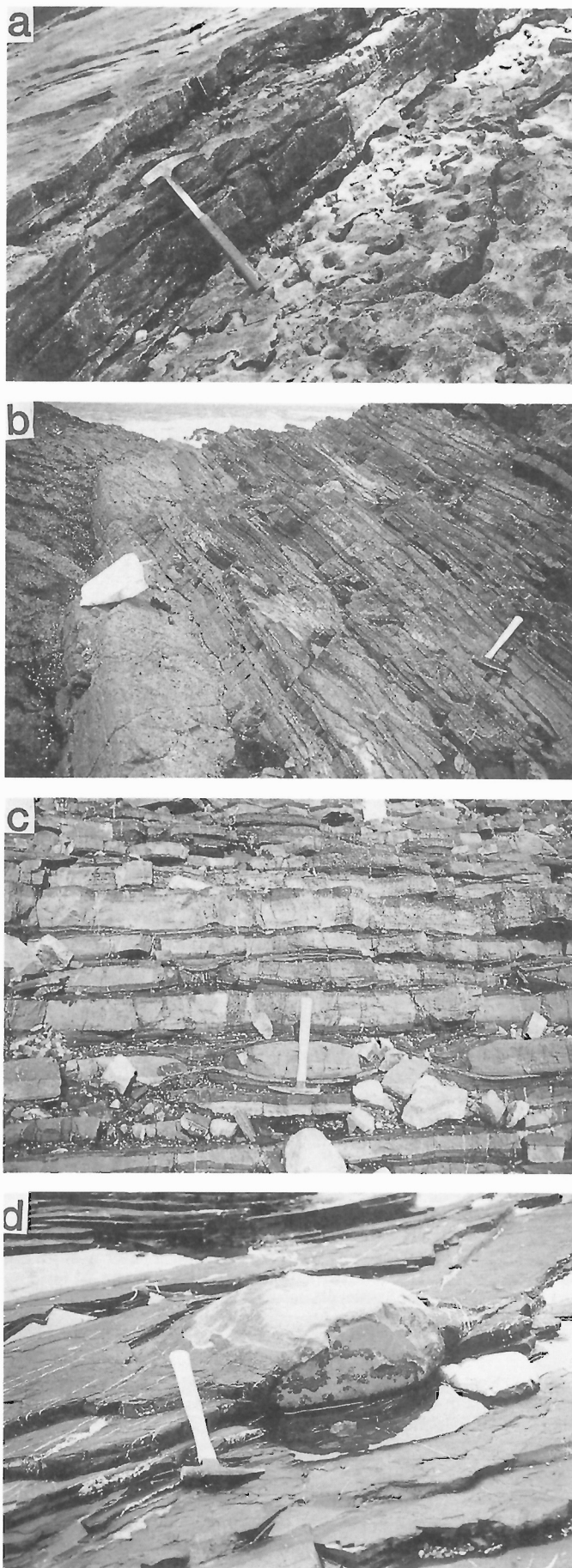


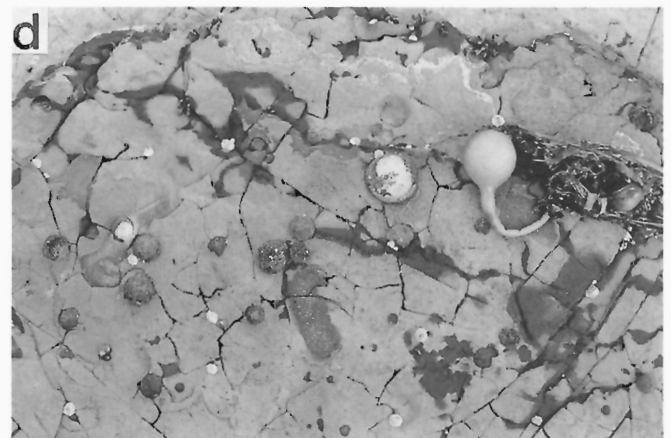
**Figure 6:** Peril Formation, lower member. A) Field exposure of the transition zone at the base of the Peril Formation comprising pelmatozoan calcarenite conformably overlying the burrowed hardground surface of the Sadler Limestone. Kunghit Island. B) Field exposure of well bedded grainstones at the base of the Peril Formation. Sadler Point. C) Field exposure of thinly bedded, dark-grey calcilitite with silicified black margins and a layer of micritic nodules. Kunghit Island. D) Field exposure of a large micritic nodule in thinly bedded calcilitite separated by more recessive argillaceous interbeds; these nodules often yield rich fossil faunas. Sadler Point.





**Figure 7:** Peril Formation, middle member. A) Field exposure (cross-section view) of laminated calcarenite showing Tb-d subdivisions of Bouma sequence and grading up into darker-grey argillaceous limestone. Section Cove, Burnaby Island. B) Field exposure (bedding plane view) of intraformational conglomerate characterized by an apparent clast-supported fabric. Section Cove, Burnaby Island. C) Field exposure (bedding plane view) of intensively bioturbated calcilitute with several different ichnofossils preserved. Frederick Island.

**Figure 8:** Peril Formation, upper member. A) Field exposure (bedding plane view) with abundant *Monotis* pelecypods in coquinaoid limestone. Frederick Island. B) Photomicrograph of thin-shelled pelecypods in *Monotis* coquina; note the abundance of spherical radiolarian tests in the micritic matrix. C) Field exposure (bedding plane view) of the silicified *Thalassinoides* burrow networks that are commonly interbedded with *Monotis*. Huxley Island. D) Field exposure (bedding plane view) of numerous specimens of the hydrozoan *Heterastridium*. The seaweed bladder may be a modern analogue in terms of habitat. Kennecott Point.



derlying thick-bedded, grey limestones and from the overlying thinly-bedded, black limestones. The upper contact of the Peril Formation is conformable and transitional with the Sandilands Formation and arbitrarily placed at top of the last *Monotis* coquina bed, as originally suggested by Sutherland Brown (1968) for the contact between the middle and upper "members" of the Kunga "Formation".

#### Fauna

In contrast with the underlying Sadler Limestone, the fauna of the Peril Formation is mainly pelagic but echinoderms are present in the thin transition zone between the formations and in rare beds elsewhere. The macrofauna is dominated by the thin-shelled pelecypods *Halobia*, in the lower and middle members, and *Monotis*, in the upper member. Ammonoids occur throughout, but are most common in the lower member where they are locally associated with belemnoids. The spherical hydrozoan *Heterastridium* is commonly found in association with *Monotis* in the upper member. The Peril Formation contains a rich microfauna. This is particularly true of the lower member where conodonts (Orchard, 1991) and radiolarians (Carter, 1991), together with fewer foraminiferids and ichthyoliths, occur with ammonoids and thereby provide good potential for an integrated zonation (Carter et al., 1989). All of these microfossils also occur in the middle and upper members, but they are generally fewer in number.

#### Age

Macrofossil determinations have previously established that the Peril Formation is Upper Carnian to Upper Norian (Sutherland Brown, 1968). However, within this time frame, only two zones were confidently determined: those of the Upper Carnian Welleri Zone and monotids indicating the lower Upper Norian (Sutherland Brown, 1968, p. 61). New discoveries of ammonoids during this study (Fig. 4), in addition to Upper Carnian Dilleri Zone ammonoids at or near the base of the formation (see above), include fauna of the Upper Carnian Welleri and Macrolobatus zones from western Kunghit Island, Burnaby Island (Bluejay and Section coves), Huxley Island, and Sadler Point (Tozer, in Orchard et al., 1990). Lower Norian collections of the pelecypod *Perihalobia* were also collected from Huxley Island, Shields Island, and on Frederick Island. A single Middle Norian ammonoid was found in Poole Inlet (op. cit.). Upper Norian *Monotis* beds occur throughout the islands, but the best sections are to be seen at Rose Inlet, Huxley Island-Arichika Island, Shields Bay, Frederick Island, and Kennecott Point.

The Peril Formation extends from the Late Carnian Dilleri zone at its base to Late Norian at its top (Fig. 4). The lower nodular member of this formation is mostly Late Carnian in age (Welleri and Macrolobatus ammonoid zones; *nodosa*, *communisti*, *primitia* conodont zones). The middle calcarenite member is poor in megafossils but dated mainly on conodonts as Lower and Middle Norian (chiefly *triangularis* to *postera* conodont zones). Coquinas of the upper member are characterized by the Upper Norian pelecypod *Monotis* (Cordilleranus ammonoid Zone; *bidentata* conodont Zone).

#### The Sandilands Formation

##### Reference section

The type area for the Sandilands Formation was designated as Sandilands Island in Skidegate Inlet (Cameron and Tipper, 1985, p. 12), where the formation is dated as Sinemurian. Older parts of the formation are not well displayed on the island, and more complete reference sections are found at Kennecott Point and on Kunga Island.

##### Lithology

The Sandilands Formation consists predominantly of thin-bedded, dark siliceous siltstone, with minor tuffaceous sandstone, shale, and conspicuous carbonate concretions.

##### Distribution

In addition to the sections described by Sutherland Brown (1968) from Kunga and Burnaby islands, and by Cameron and Tipper (1985) on Graham Island and around Cumshewa Inlet, additional significant sections are to be found at Kennecott Point (Tipper, 1989), on southern Kunghit Island (southeast Luxana Bay), on northern Huxley Island, and on eastern Louise Island, south of Vertical Point (Fig. 1). On Kunghit and Huxley islands the formation forms high cliffs and is not easily accessible.

##### Thickness

Estimations of a cumulative thickness of about 500 m have been given by Sutherland Brown (1968), Cameron and Tipper (1985), and E.S. Carter (pers. comm., 1989).

##### Definition of boundaries

The base of the Sandilands Formation is drawn at the top of the last monotid coquina, which coincides with a lithological change from carbonate-rich to carbonate poor strata. At Kennecott Point, the highest Peril Formation strata form a resistant bluff and the overlying Sandilands Formation is relatively recessive. The top of the formation lies within the Lower Jurassic and has not been considered here.

##### Fauna

Ammonoids occur sporadically in the Triassic part of the Sandilands Formation but they are rare. Rare pelecypods also occur, but the microfauna is the most persistent element. Radiolarians, foraminiferids, and ichthyoliths are present in many collections from the Triassic part of the formation. Conodonts are common in the lower part but become uncommon upward and are rare in the highest Triassic strata.

##### Age

Cameron and Tipper (1985) reviewed the age control on the Sandilands Formation from which no data was previously available for most of the Upper Norian and Hettangian time. The basal strata of this formation lying above *Monotis* beds but below the first appearance of Sinemurian aretoid ammonites was originally thought to be unfossiliferous, but is now known to include Late Triassic ammonoids (Crickmayi Zone; Tozer in Orchard et al., 1990), and conodonts (*bidentata* Zone et seq.; Orchard, 1990), and diverse radiolarian faunas (Carter, 1990), as well as Hettangian macrofauna (Tipper, 1989).

## CARBONATE SEDIMENTOLOGY OF THE KUNGA GROUP

Although silicification and/or thermal metamorphism are locally important, a wide variety of carbonate lithofacies can be recognized in the Triassic portion of the Kunga Group. The lithofacies can be grouped into two principal environmental associations: shallow water carbonate shelf, and slope and basinal sediments. These two associations correspond to the Sadler Limestone and Peril Formation respectively.

#### Sadler Limestone

##### *Bioturbated lime mudstone to peloidal wackestone – deep open shelf facies*

Lime mudstone to peloidal wackestone is the most common lithofacies representing 60-70% of the formation (Fig. 5B). These subtidal carbonates are rather uniform, comprising only burrowed lime mudstone to peloidal wackestone with small amounts of mollusc debris, foraminifers, and ostracodes. Ammonoids and radiolarians are also present. *Thalassinoides* is the most common trace fossil producing a densely packed burrow system and giving a typical burrow-mottled fabric to these limestones (Fig. 5B). The burrows contain large amounts of faecal pellets, and some show longitudinal canals characteristic of many groups of deposit-feeding crustaceans (Ekdale et

al., 1984). Black chert "nodules" are ubiquitous and represent partially silicified horizontal networks of *Thalassinoides* burrows.

This lithofacies represents typical open shelf carbonate sediments deposited in a low energy setting below wave base (Wilson and Jordan, 1983). This is in agreement with the common occurrence of *Thalassinoides* in quiet water carbonate sediments deposited near or below the wave base (Sheehan and Schiefelbein, 1984).

#### *Bioturbated bioclastic wackestone to packstone – shallow open shelf facies*

This lithofacies occurs commonly in the upper half of the formation interbedded with bioturbated lime mudstone to peloidal wackestone. Generally it consists of a burrowed micritic matrix with variable amounts of bioclasts that are whole to fragmented, but generally unabraded. The diverse biota is dominated by gastropods, thick-shelled pelecypods, and echinoderms, with ostracodes, brachiopods, and dasycladacean algae being much less common. Locally, slightly asymmetrical oncolites up to 5.0 mm in size occur mixed with small amounts of ooids. Peloids and micritic intraclasts are abundant where bioturbation is pervasive. *Thalassinoides* is the most conspicuous trace fossil in this lithofacies too.

This lithofacies represents low-energy subtidal sediments deposited under open marine conditions. However, the local development of irregular, poorly laminated oncolites indicates intermittent turbulence (Wright, 1983) and suggests a shallower position with respect to the wave base than the previous lithofacies. In addition, the common association of ooids with oncolites may represent either a transitional facies with active ooid sand shoals, or inactive portions of ooid sand shoals reworked by pervasive bioturbation (Hine, 1983). Similar sediments are present in modern, open shelf deposits which are generally muddy with burrowed wackestone and packstone dominating the shelf environments (Wilson and Jordan, 1983).

#### *Oolitic calcarenite – on-shelf sand shoal facies*

Oolitic calcarenite is a minor lithofacies which is commonly present in the upper half of the formation. Although primarily composed of ooids, the calcarenites also contain mollusc fragments, brachiopods, and some peloids and intraclasts. The calcarenites usually form massive, lenticular units up to 3.0 m thick, but poorly developed cross-bedding may be present locally. The usually massive appearance of these units may be due to the extremely well sorted ooids and insufficient grain-size variation to produce prominent crossbedding.

This lithofacies represents well winnowed oolitic sand accumulating in high-energy shoal environments. Active sand shoals characterized by open marine fauna have been reported from several Holocene platforms (Wilson and Jordan, 1983). Most of these shoals formed only a few metres below sea level. The lateral extent of these on-shelf shoals in the Peril Formation is more restricted than in modern counterparts of the Bahamas where extensive ooid sand shoals occur at the margin of the platform (Hine, 1983).

### **Peril Formation**

#### *Radiolarian-rich calcilutites – peri-platform oozes*

This lithofacies consists of 3–10 cm thick beds of dark grey calcilutite (mainly lime mudstone to wackestone) separated by thin argillaceous interbeds (Fig. 6C,D). The calcilutites display gradational contacts over a few centimetres with siliceous black beds (3–10 cm thick) which represent silicified calcilutites that have been more severely affected by physical compaction, as indicated by flattened burrows and radiolarian tests.

The calcilutites are poor in megafossils but contain common microfossils including conodonts, radiolarians and sparse sponge spicules. Thin-shelled pelecypods and ammonoids are also present. The cal-

cilutites are locally laminated but are commonly massive where bioturbation is more pervasive. A restricted assemblage of small trace fossils (mainly horizontal) is well preserved and typically dominated by the deposit-feeding burrows, mainly *Planolites* and *Chondrites* (Fig. 7C).

The calcilutites are fine-grained limestones that were deposited in deep waters as indicated by their pelagic faunal assemblage. Locally abundant horizontal trace fossils suggest a low-energy environment with slow to moderate sedimentation rates (Ekdale et al., 1984). The lack of any megafossils *in situ* also suggests low-oxygen conditions, and the presence of restricted benthic infaunal activities may further indicate dysaerobic bottom-water conditions (Bromley and Ekdale, 1984).

In the absence of major sources of pelagic carbonate sediments (i.e. coccoliths, foraminifers) during Triassic time (Scholle et al., 1983), these fine-grained carbonates were probably derived from adjacent shallow-water carbonate platforms. The platform-derived lime mud in modern settings, also termed peri-platform ooze (Schlager and James, 1978), are usually placed into suspension during storm events and transported and redeposited into deep-marine environments.

#### *Laminated calcarenites – calciturbidites*

Laminated calcarenite occurs in 3–20 cm thick beds interbedded with calcilutites and pelecypod coquinas. It is a major lithofacies of the middle member of the formation but is also present in the other members. The calcarenites range in composition from micropelletoid packstone/grainstone to bioclastic grainstone. The former are composed of well-sorted, silt- to fine sand-sized micritic particles within a micritic or spar matrix. The fauna is sparse and consists of fragmented thin-shelled pelecypods and radiolarians. In addition, a significant amount (10–20%) of fine-grained terrigenous sediment (mainly silt) is present. The bioclastic grainstone comprise coarser-grained limestones with clastic textured fabrics containing sand- to pebble-sized particles composed mainly of echinoderm grains. Mollusc debris, intraclasts, and ooids are less common.

Classic Ta-e Bouma sequence are locally present in the calcarenites, but graded Ta-b in bioclastic grainstones, and Tc-e in micropelletoid packstone/grainstone are more common (Fig. 7A). Flutes and other sole markings are rare and difficult to recognize because bed contacts are commonly obscured by pervasive silicification.

The calcarenites represent carbonate equivalent of siliciclastic turbidites deposited from currents moving downslope that formed by the sudden surge-type release of dense fluids generated at the shelf edge (McIlreath and James, 1984). Although a sediment source for these calciturbidites is not known in the Lower and Middle Norian portion of the Kunga Group, small isolated shallow-water carbonate platforms have been recognized in the other parts of Wrangellia (Desrochers, 1988, 1989), and their margins produced skeletal material, especially pelmatozoans that can be easily remobilized and transported downslope. The micropelletoid packstone/grainstone may represent more distal turbidites generated further down the slope and mixed with fine-grained clastic terrigenous or volcanoclastic sediment.

#### *Pelecypod coquinas – pelagic limestones*

The coquinas form 3–15 cm thick beds characterized by abundant, thin-shelled pelecypods within a dark-grey micritic matrix. The pelecypods are compacted and flattened parallel to the bedding plane reducing to a minimum the micritic matrix and giving a distinctive fissile fabric to these coquinas (Fig. 8A,B). Two distinct genera of pelecypods are recognized: *Halobia* present in the lower and middle members of the formation, and *Monotis* restricted to the upper member. Calcified radiolarians are also common (Fig. 8B). *Thalassi-*

*noides* burrow networks are locally interbedded with *Monotis coquinas* (Fig. 8C).

The coquinas represent deep basinal environments similar to those in which radiolarian-rich calcilutites were deposited. In this case, the influx of peri-platform components (mainly lime mud) was overridden by that of pelagic components (mainly thin-shelled pelecypods). *Halobia* and *Monotis* pelecypods are regarded as having an epiplanktic mode of life, and represent a deep neritic ecological group that is known only from Upper Triassic basinal limestones (Hallam, 1981). Their accumulation was related to periods of high productivity in surface waters due to favourable ecological factors such as nutrient supply, temperature, light, and salinity (Scholle et al., 1983).

#### *Intraformational conglomerate – debris flow deposits*

Conglomerate beds up to 2.0 m thick are a minor but conspicuous lithofacies of the lower and basal middle members of the Peril Formation (Fig. 7B). Conglomerates range from matrix-supported fabric with 10–20% of clasts floating in a calcarenite matrix, to clast-supported fabric comprising different pebble-to cobble-sized clasts within a calcarenite matrix. Most of the clasts are platy and represent reworked fragments of calcilutite and to a lesser extent of pelecypod coquina. In addition, a few conglomerates at the base of this formation comprise mainly Karmutsen-like volcanic fragments mixed with some calcilutite clasts. The matrix is commonly poorly-sorted and composed of pelmatozoan-rich packstone to grainstone.

Conglomerates are submarine debris flows composed almost entirely of intraformational clasts derived from the surrounding slope sediments. The association of pelmatozoan-rich calcarenite with conglomerate suggests that turbidity currents moving downslope from coeval sand shoals may have been important agents of erosion of intraformational clasts. The presence of platy clasts, commonly derived by separation along bedding planes, clearly indicates that they were lithified very early, probably by submarine cementation (Coniglio, 1986).

Evidence of synsedimentary deformation are reported in the Kunga Group (Lewis and Ross, 1989). Active faulting may have locally affected the underlying Karmutsen basement and provided volcanic fragments that were incorporated in associated debris flows.

#### *Pelmatozoan calcarenite – hardgrounds recording the drowning of the carbonate platform*

Distinctive, nodular calcarenite beds (5–15 cm thick) occur at the base of the Peril Formation and form a transitional zone up to 1.0 m thick with the underlying grey limestones of the Sadler Limestone (Fig. 6A,B). The calcarenites consist of well winnowed pelmatozoan-rich grainstone containing various amounts of thin-shelled pelecypods. Ammonoids are locally abundant and concentrated along bedding plane surfaces. The sediment is moderately bioturbated and silicified *Thalassinoides* burrows are present. In thin-section, the sediment displays minor effects of physical compaction and retains its high original porosity (30–40%) that is filled by a thick isopachous layer of prismatic or fibrous calcite cement.

These calcarenites represent hardgrounds formed during the rapid drowning of large portions of an extensive carbonate platform. Hardgrounds result from penecontemporaneous sea floor lithification (James and Choquette, 1983), but the absence of borings or encrusting organisms indicates that those at the base of the Peril Formation may have formed at shallow depths below the sediment-water interface. Although early diagenetic, sea floor lithification has been described from a number of deep water settings (Scholle et al., 1983), the formation of hardground is favoured by long contact between sediment and seawater, such as in areas of slow sedimentation where fine grained material is removed by bottom currents.

## SUMMARY AND CONCLUSIONS

The geologic history of the Kunga outcrops exposed in the Queen Charlotte Islands can be summarized as three distinct depositional stages corresponding to the three lithostratigraphic subdivisions of the Kunga Group (i.e. Sadler Limestone, Peril, and Sandilands formations).

- 1) A widespread carbonate platform was established on relatively flat volcanic basement after the termination of major volcanic activity in the Carnian. During this initial phase, open-marine conditions were maintained and two sub-environments developed: open platform facies (bioturbated lime mudstone to peloidal wackestone, and bioclastic muddy limestones), and on-shelf sand shoals (oolitic calcarenite).
- 2) Relatively rapid sea level rise in the Upper Carnian (*nodosus* Zone) resulted first in the formation of hardgrounds over the drowned platform, and then in the deposition of deeper water sediments beyond carbonate platforms in a slope to basin setting during the Carnian through early Upper Norian. Carbonate platforms did not develop in the Queen Charlotte Islands during the Early and Middle Norian but they were present in other parts of Wrangellia (Desrochers, 1988, 1989). Depositional facies are: 1) pelagic/hemipelagic sediment (calcilutite, pelecypod coquina), 2) proximal to distal calciturbidite (laminated calcarenite), and 3) platform- to slope-derived debris flow (intraformation conglomerate).
- 3) Following the drowning of isolated carbonate platforms in other parts of Wrangellia during the Late Norian, carbonate sedimentation ended abruptly in QCI. Thereafter, terrigenous sediments were deposited in a relatively deep water basin that was remote from the volcanic centres and which received only fine detritus (Cameron and Tipper, 1985).

## ACKNOWLEDGMENTS

The authors thank R.I. Thompson and the Queen Charlotte Islands Frontier Geoscience Program for logistical support and research funding. The crew of the vessel “Beatrice”, skipper Doug Hartley assisted by Paddy Herman, are thanked for skilfully ploughing the seas off South Moresby during June 1987. In June 1988, the “Mayor of Kennecott Point”, Howard Tipper provided shelter whilst expeditor Ella Ferland provided support from Sandspit. Special thanks are extended to colleagues E.S. Carter and E.T. Tozer for stimulating discussions in the field. B. Jones kindly read an earlier version of this manuscript and contributed towards its improvement.

## REFERENCES

- Bromley, R.G. and Ekdale, A.A.  
1984: *Chondrites*: a trace fossil indicator of anoxia in sediments; *Science*, v. 224, p. 872–874.
- Cameron, B.E.B. and Tipper, H.W.  
1985: Jurassic stratigraphy of the Queen Charlotte Islands, British Columbia; *Geological Survey of Canada, Bulletin* 365, 49 p.
- Cameron, B.E.B. and Hamilton, T.S.  
1988: Contributions to the stratigraphy and tectonics of the Queen Charlotte Basin, British Columbia; in *Current Research, Part E, Geological Survey of Canada, Paper* 88-1E, p. 221–227.
- Carter, E.S.  
1990: New biostratigraphic elements for dating the Upper Norian Sandilands Formation, Queen Charlotte Islands, British Columbia, Canada; *Marine Micropalaeontology*, v. 15, p. 313–328.
- 1991: Late Triassic radiolarian biostratigraphy of the Kunga Group, Queen Charlotte Islands, British Columbia; in *Evolution and Hydrocarbon Potential of the Queen Charlotte Basin, British Columbia, Geological Survey of Canada, Paper* 90-10.
- Carter, E.S., Orchard, M.J., and Tozer, E.T.  
1989: Integrated ammonoid-conodont-radiolarian biostratigraphy, Late Triassic Kunga Group, Queen Charlotte Islands, British Columbia; in *Current Research, Part H, Geological Survey of Canada, Paper* 89-1H, p. 23–30.

- Clapp, C.H.**  
**1914:** A geological reconnaissance on Graham Island; Geological Survey of Canada, Summary Report 1912, p. 12-40.
- Coniglio, M.**  
**1986:** Synsedimentary submarine slope failure and tectonic deformation in deep-water carbonates, Cow Head Group, western Newfoundland; Canadian Journal of Earth Sciences, v. 23, p. 476-490.
- Dawson, G.M.**  
**1880:** Queen Charlotte Islands; Geological Survey of Canada, Report of Progress, 1878, 1879.
- Desrochers, A.**  
**1988:** Sedimentology of the Kunga Group, Queen Charlotte Islands; in Some Aspects of the Petroleum Geology of the Queen Charlotte Islands (R. Higgs, compiler). Canadian Society of Petroleum Geologists Field Trip Guide to: Sequences Stratigraphy, Sedimentology: Surface and Subsurface, p. 32-36.  
**1989:** Depositional history of Upper Triassic carbonate platforms on Wrangellia Terrane, western B.C.; American Association of Petroleum Geologists, Bulletin 73, p. 349-350.
- Ekdale, A.A., Bromley, R.G., and Pemberton, S.G.**  
**1984:** Ichnology: trace fossils in sedimentology and stratigraphy; Society of Economic Paleontologists and Mineralogists Short Course #15, 317 p.
- Hallam, A.**  
**1981:** The end-Triassic bivalve extinction event; Paleogeography, Paleoclimatology, Paleocology, v. 35, p. 1-44.
- Hine, A.C.**  
**1983:** Relict sand bodies and bedforms of the Northern Bahamas: evidence of extensive Early Holocene transport; in Coated Grains, T.M. Peryt (ed.), Springer Verlag, p. 116-131.
- James, N.P. and Choquette, P.W.**  
**1983:** Diagenesis of limestones – the sea floor diagenetic environment; Geoscience Canada, v. 10, p. 162-180.
- Lewis, P.D. and Ross, J.V.**  
**1989:** Evidence of Late Triassic-Early Jurassic deformation in the Queen Charlotte Islands, British Columbia; in Current Research, Part H, Geological Survey of Canada, Paper 89-1H, p. 13-18.
- McIlreath, I.A. and James, N.P.**  
**1984:** Carbonate slopes; in Facies Models, R.G. Walker, (ed.), Geoscience Canada, Reprint Series #1, p. 245-258.
- Orchard, M.J.**  
**1988:** Maturation of Triassic strata: conodont colour alteration index; in Some Aspects of the Petroleum Geology of the Queen Charlotte Islands (R. Higgs, compiler). Canadian Society of Petroleum Geologists Field Trip Guide to: Sequences, Stratigraphy, Sedimentology: Surface and Subsurface, p. 44.
- 1991:** Late Triassic conodont biochronology and biostratigraphy of the Kunga Group, Queen Charlotte Islands, British Columbia; in Evolution and Hydrocarbon Potential of the Queen Charlotte Basin, British Columbia, Geological Survey of Canada, Paper 90-10.
- Orchard, M.J. and Forster, P.J.L.**  
**1991:** Conodont colour and thermal maturity of the Late Triassic Kunga Group, Queen Charlotte Islands, British Columbia; in Evolution and Hydrocarbon Potential of the Queen Charlotte Basin, British Columbia, Geological Survey of Canada, Paper 90-10.
- Orchard, M.J., Carter E.S., Tozer, E.T. (paleontological data); Forster, P.J.L., Lesack, K., McKay, K. (compilers); Weston, M., Woodsworth, G.J., Orchard, M.J., Johns, M. (database design)**  
**1990:** Electronic database of Kunga Group biostratigraphic data; Geological Survey of Canada, Open File.
- Schlager, W. and James, N.P.**  
**1978:** Low-magnesian calcite limestones forming at the deep-sea floor, Tongue of the Ocean, Bahamas; Sedimentology, v. 25, p. 675-702.
- Scholle, P.A., Arthur, M.A., and Ekdale, A.A.**  
**1983:** Pelagic environment; in Carbonate Depositional Environments, P.A. Scholle and others (ed.), American Association of Petroleum Geologists, Memoir 33, p. 620-692.
- Sheehan, P.M. and Schiefelbein, D.R.**  
**1984:** The trace fossil *Thalassinoides* from the Upper Ordovician of the eastern Great Basin: deep burrowing in the early Paleozoic; Journal of Paleontology, v. 59, p. 440-447.
- Sutherland Brown, A.**  
**1968:** Geology of the Queen Charlotte Islands, British Columbia; British Columbia Department of Mines and Petroleum Resources, Bulletin 54, 226 p.
- Sutherland Brown, A. and Jeffrey, W.G.**  
**1960:** Preliminary geological map, southern Queen Charlotte Islands; British Columbia Department of Mines.
- Tipper, H.W.**  
**1989:** Lower Jurassic (Hettangian and Sinemurian) biostratigraphy, Queen Charlotte Islands, British Columbia; in Current Research, Part H, Geological Survey of Canada, Paper 89-1H, p. 31-34.
- Wilson, J.E. and Jordan, C.**  
**1983:** Middle shelf; in Carbonate Depositional Environments, P.A. Scholle and others (ed.), American Association of Petroleum Geologists, Memoir 33, p. 297-343.
- Wright, V.P.**  
**1983:** Morphogenesis of oncoids in the Lower Carboniferous Llanelly Formation of South Wales; in Coated Grains, T.M. Peryt (ed.), Springer Verlag, p. 424-434.



# Late Triassic conodont biochronology and biostratigraphy of the Kunga Group, Queen Charlotte Islands, British Columbia

M.J. Orchard<sup>1</sup>

Orchard, M.J., Late Triassic conodont biochronology and biostratigraphy of the Kunga Group, Queen Charlotte Islands, British Columbia; in *Evolution and Hydrocarbon Potential of the Queen Charlotte Basin, British Columbia*, Geological Survey of Canada, Paper 90-10, p. 173-193, 1991.

## Abstract

*Conodont faunas from the Upper Triassic Kunga Group represent a relatively complete conodont record from the Late Carnian to the Late Norian. Important conodont genera are Metapolygnathus, redefined to include all Upper Carnian and one Lower Norian species, and Epigondolella, which is restricted to the Norian. On the basis of nine conodont species of Metapolygnathus (four new, five redefined), six new Upper Carnian conodont zones are introduced for the Kunga Group (Sadler and Peril formations). Five of these zones are also recognized in northeast British Columbia. In ascending order, the zones are: polygnathiformis; Lower, Middle, and Upper nodosus; communisti; Lower primitius. These zones are correlated with the Dilleri, Welleri, and Macrolobatus ammonoid zones.*

*The base of the Norian is marked by the incoming of 'Neogondolella' navicula, which I suggest developed from advanced morphotypes of M. communisti at the beginning of the Upper primitius Zone. Epigondolella developed from Metapolygnathus primitius within the Lower Norian, and thereafter provided most of the zonal indices for the remainder of the Triassic. Six, possibly seven, of the eight Norian Epigondolella conodont zones established in the Norian Pardonnet Formation (Kerri-Cordilleranus ammonoid zones) of northeastern B.C. are recognized in the Kunga Group (Peril and Sandilands formations). In addition, post-Epigondolella faunas occur in which first 'Neogondolella' and then Misikella occur alone, the latter within the latest Triassic Crickmayi ammonoid Zone.*

*The Karmutsen Volcanics and Sadler Limestone ("grey limestone") were deposited, at least in part, within the Upper Carnian polygnathiformis Zone. The Peril Formation ("black limestone") ranges in age from the Lower nodosus Zone of the Upper Carnian through bidentata Zone of the Upper Norian; a conodont-based composite section shows this unit is about 350 m thick. The Sandilands Formation includes the bidentata Zone at its base and embraces the remainder of the Triassic conodont record in its lower part.*

## Résumé

*Les faunes de conodontes du groupe de Kunga du Trias supérieur donnent un compte rendu relativement complet des conodontes du Carnien supérieur au Norien supérieur. Les principaux genres sont Metapolygnathus, redéfini pour inclure toutes les espèces du Carnien supérieur et une espèce du Norien inférieur, et Epigondolella, qui est limitée au Norien. En se fondant sur neuf espèces de conodontes de Metapolygnathus (quatre nouvelles, cinq redéfinies), on a introduit six nouvelles zones à conodontes du Carnien supérieur dans le groupe de Kunga (formations de Sadler et de Peril). Cinq de ces zones se retrouvent également dans le nord-est de la Colombie-Britannique. Dans l'ordre ascendant, ce sont : la zone à polygnathiformis; les zones inférieure, moyenne et supérieure à nodosus; la zone à communisti; la zone inférieure à primitius. Ces zones englobent les zones à ammonoïdes Dilleri, Welleri et Macrolobatus.*

*La base du Norien est marquée par l'apparition de 'Neogondolella' navicula qui découlerait, selon l'auteur, de morphotypes avancés de M. communisti au début de la zone supérieure à primitius. Epigondolella s'est développé à partir de Metapolygnathus primitius au sein du Norien inférieur et a par la suite fourni presque tous les indices des zones du reste du Trias. Six, peut-être sept, des huit zones à conodontes Epigondolella du Norien établies dans la formation de Pardonnet du Norien (zones à ammonoïdes Kerri-Cordilleranus) dans le nord-est de la Colombie-Britannique ont été identifiées dans le groupe de Kunga (formations de Peril et de Sandilands). De plus, les faunes post-Epigondolella sont présentes là où 'Neogondolella' et ensuite Misikella sont apparues seules, cette dernière au sein de la zone à ammonoïdes Crickmayi de la toute fin du Trias.*

*La formation de Karmutsen et le calcaire de Sadler ("calcaire gris") se sont déposés, du moins en partie, au sein de la zone à polygnathiformis du Carnien supérieur. L'âge de la formation de Peril ("calcaire noir") varie de la zone inférieure à nodosus du Carnien supérieur jusqu'à la zone à bidentata du Norien supérieur; une coupe composite à base de conodontes montre que cette unité mesure environ 350 m d'épaisseur. La formation de Sandilands comprend à sa base la zone à bidentata et englobe le reste des conodontes triasiques dans sa partie inférieure.*

<sup>1</sup> Cordilleran Division, Geological Survey of Canada, 100 West Pender Street, Vancouver, B.C. V6B 1R8

## INTRODUCTION

Systematic investigation of conodonts in the Late Triassic Kunga Group of the Queen Charlotte Islands (Fig. 1) began after reconnaissance

sampling demonstrated a potential for valuable conodont biostratigraphical and biochronological data. Macrofossils collected by Sutherland Brown (1968) ranged in age from Late Carnian to Late

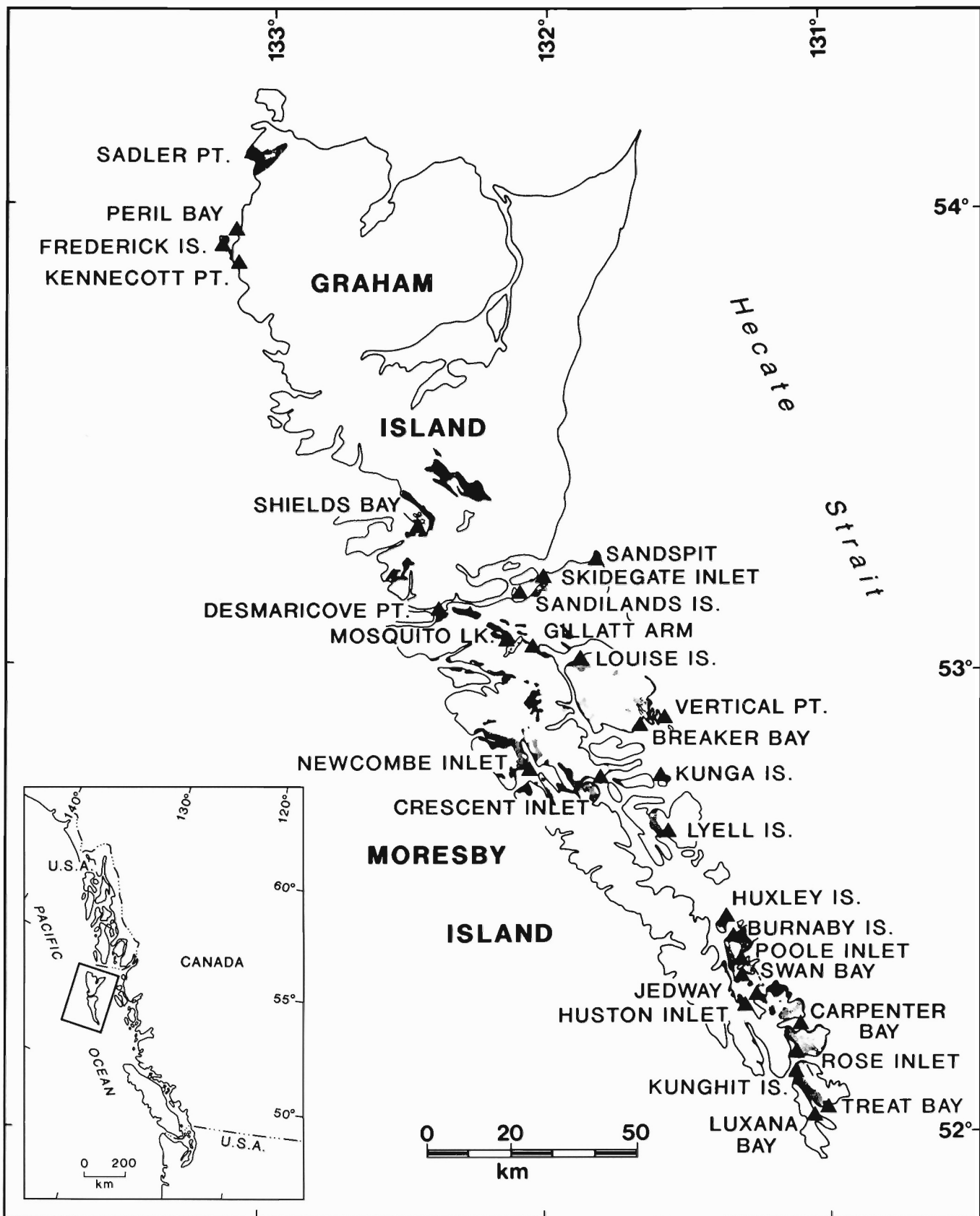


**Figure 1:** Map of the Queen Charlotte Islands showing the principal conodont bearing sections of the Kunga Group. Inset shows position of QCI off the west coast of Canada.

Norian, but provided little information in between. A total of 375 conodont faunas now recovered provide both a critical test of the Norian conodont zonation developed in the Norian Pardonnet Formation in northeast British Columbia (Orchard, 1983), and provide an important Upper Carnian supplement to that zonation. The resulting biochronological scale provides excellent resolution of the stratigraphy and evolution of the Kunga Group (Fig. 2).

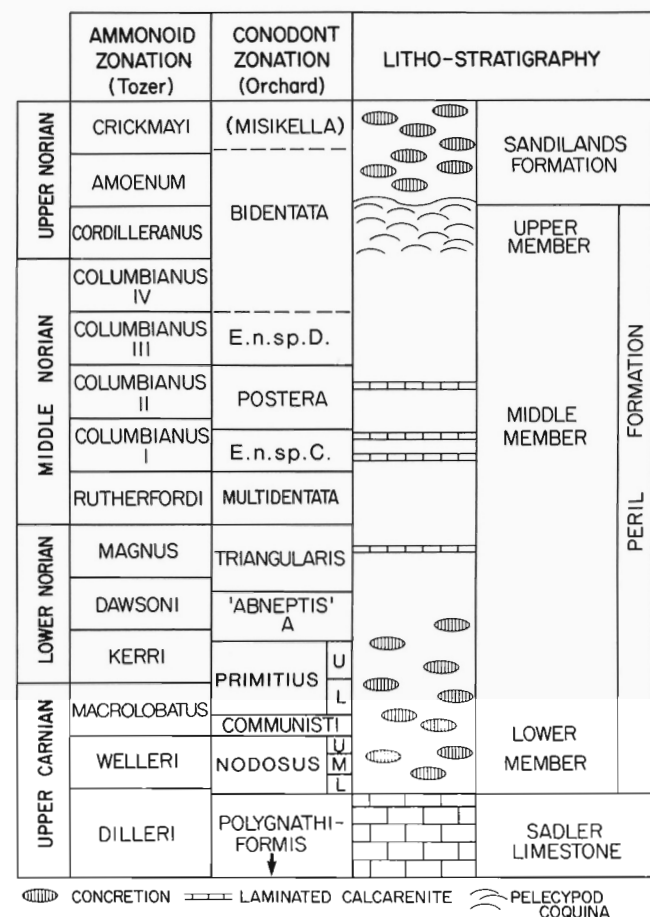


**Figure 2:** Schematic diagram showing ammonoid and conodont zonation of the Upper Triassic in relation to lithostratigraphy of the Kunga Group (from Desrochers and Orchard, 1990).

Suspected differences between Tethyan (low latitude) and Canadian autochthonous (mid- to high latitude) conodont faunal sequences, and the wish to determine biogeographical relationships of the Kunga Group 'Wrangellian' faunas, also provided a background for this study.

In this paper, I:

1. describe the extent of the conodont record in the Kunga Group,
2. define new Upper Carnian conodont zones and their calibration with ammonoid zones,
3. present the phylogenetic basis for the Upper Carnian conodont zonation,
4. outline taxonomic concepts that provide definition for the new Upper Carnian zonation,
5. show the general application of existing Norian conodont zonation to the Kunga succession,
6. present a preliminary conodont-based time-stratigraphic framework for correlation of Kunga Group section.

Complete geographic, stratigraphic, taxonomic, and numeric data covering the conodont samples from the Kunga Group may be found in the database accompanying this volume (Orchard et al., 1990). New lithostratigraphy of the Kunga Group (Desrochers and Orchard, 1991; Fig. 2), and a study of conodont Colour Alteration Indices (CAI) (Orchard and Forster, 1991), may also be found elsewhere in this volume. Formal new taxonomy and thorough description of the conodont fauna will be presented in a future paper.

## TAXONOMIC DEFINITIONS

Below I outline taxonomic differentiations employed in this paper. Most of the species concepts differ fundamentally from previous usage. In my classification, the intraspecific variability of species forms an integral part of the species definition, as it does for Norian *Epigondolella* populations (Orchard, 1983).

Genus *Epigondolella* Mosher 1968: gondolelloid species that have a distinctly free blade, large and discrete anterior platform denticles that are at least as high as the depth of the platform base, and a subdued, irregular and open style of platform microreticulation (Fig. 9 of Orchard, 1983). Growth is isometric about a single platform expansion. A basal pit is generally developed beneath the central or anterior part of the platform. *Epigondolella* is here regarded as a wholly Norian genus.

'*E. primitia*' is removed from this genus, otherwise the species described by Orchard (1983) are retained within *Epigondolella*. The type species, *E. abneptis*, is here restricted to the type material because the original description and illustration is inadequate to distinguish between several similar species, and the holotype is broken and partly lost. *E. abneptis* subsp. A Orchard is retained pending future nomenclatural revision; *E. abneptis* subsp. B Orchard is now referred to *E. triangularis* (Budurov) (Orchard in Carter et al., 1989, p. 28).

Genus *Metapolygnathus* Hayashi 1968: gondolelloid species that are characterized by a reduced platform anterior of variably pronounced geniculation points, and relatively robust, regular and compact platform microreticulation in most species (Fig. 8. of Orchard, 1983). Species may be unornamented or show varying degrees of node formation that is subdued in some species, well developed in others. In sharp noded species (mostly lacking microreticulae), the nodes are small relative to those in *Epigondolella*: node height is less than the depth of the platform base. Growth often proceeds through 'dual' outgrowth of the anterior and, later, posterior portions of the platforms so as to commonly produce a marked posterior constriction in early to median growth stages. A basal pit is generally developed beneath the posterior half of the platform. As here conceived, *Metapolygnathus* ranges throughout the Carnian and into the basal Norian.

Several new species of *Metapolygnathus* are introduced informally in this paper. Some other species recognized in the Kunga Group have previously been referred to the genera *Gondolella*, which I regard as a wholly Late Carboniferous gondolelloid genus, and/or *Paragondolella*, which might be valid for Middle Triassic species (*P. excelsa*). All Carnian species are brought here to *Metapolygnathus*. Specific criteria for the Upper Carnian species are:

*Metapolygnathus communisti* Hayashi 1968: a weakly- to unornamented species characterized by elements with longitudinally and/or laterally reduced platforms, particularly in early growth stages; in some small specimens the platform is vestigial. Broader morphotypes commonly have a high parapet or geniculation point. In many specimens, the basal pit is more anteriorly located than in other metapolygnathids. This species probably also includes *Metapolygnathus parvus* Kozur (cf. Krystyn, 1980, p. 76).

*Metapolygnathus echinatus* (Hayashi 1968): herein regarded as a derivative of *M. n. sp. G*, this species is characterized by a long blade, and a short quadrate platform that bears small, usually sharp marginal

denticles, particularly on the anterior part. The basal edge is characteristically straight when viewed laterally. The holotype of *M. echinatus* was poorly illustrated and its characteristics need to be clarified.

*Metapolygnathus nodosus* (Hayashi 1968): a broad species concept in which elements are characterized by a platform with marginal nodes that may be low and weak (particularly in larger specimens), but are often distinctly developed as a result of irregular incision of the anterior and/or lateral platform margins. Advanced specimens show a trend toward elevating discrete, often irregular nodes above the platform surface, but the posterior platform margins remain relatively high compared with *M. primitius*. Strong posterior platform constriction occurs in early growth stages of this species. In large specimens, the nodes commonly coalesce and become indistinct (as in ‘*Gondolella noah*’ (Hayashi, 1968)). The populations of *Metapolygnathus nodosus* include a wide range of both platform shape and node formation. I concur with Krystyn (1980, p. 76) that the anteriorly nodose ‘*Gondolella carpathica*’ Mock 1979 cannot be maintained as a separate species.

*Metapolygnathus ex gr. polygnathiformis* (Budurov and Stefanov 1965): a group characterized by elements with unornamented platform margins of uniform height. The platform is generally broadest at midlength or anterior of that point. Relatively broad adcarinal troughs, and round, discrete carinal nodes are typical. Incipient anterior nodes are rarely developed in large specimens. During early growth, platforms generally develop more uniformly compared with *Metapolygnathus nodosus*, and less commonly have a posterior constriction.

*Metapolygnathus primitius* (Mosher 1970): a species with uniformly developed, discrete, roundly terminated, anterior platform nodes of moderate size that project above the level of the platform, which is relatively flattened and low-lying posterior of the anterior nodes. The platform nodes tend to coalesce in large specimens.

*Metapolygnathus n. sp. E* Orchard: an elongate derivative of the *nodosus* stock characterized by a strong posterior platform constriction, and variable, absent to subdued platform nodes. The platform posteri-

or of the constriction is often developed asymmetrically with respect to the anterior part. Narrow morphotypes mimic *Neogondolella*.

*Metapolygnathus n. sp. F* Orchard: a derivative of *M. n. sp. E* characterized by large, well defined but low, rounded nodes on the anterior platform. In advanced specimens, the anteriormost nodes may become sharp. In some specimens a slight anterior shift of basal pit is seen.

*Metapolygnathus n. sp. G* Orchard: a derivative of *M. n. sp. F* characterized by relatively small, sharply terminated nodes, which usually occur on all platform margins, although they are often smaller in the posterior part.

*Metapolygnathus n. sp. K* Orchard: a small species with a short blade and a bowl-like platform with variable marginal sculpture on the upturned platform margins.

UPPER CARNIAN ZONATION

Conodont zonation of the Upper Carnian has not been particularly refined to date, particularly for North American sequences. In the compilation of Sweet et al. (1971), a single zone, the *Paragondolella polygnathiformis* Assemblage-Zone was shown to embrace the whole interval. Subsequently, European workers have proposed several zones for the Upper Carnian based on taxonomic distinctions that have not been attempted in North America prior to the present work. The European zonations were presented in a series of papers culminating in syntheses by Kovacs and Kozur (1980), Kozur (1980), and Krystyn (1980). Kozur (1980) recognized the uniformity of conodont succession through the interval and proposed a standard zonation consisting of (in ascending order) the *noah* (~*polygnathiformis*), *carpathica* (early *nodosus*), and *nodosus(us)* assemblage-zones; these three zones were shown as corresponding to, respectively, the Dilleri, Subbullatus (~Welleri), and Macrolobatus ammonoid zones (Kozur, 1980, Fig. 8).

The zonation proposed by Krystyn (1980) differs from the former in both the taxonomic concepts employed and the ammonoid correlation presented. Within the Carnian Krystyn (1980) recognized *polygnathiformis*, Lower and Upper *nodosus(us)* assemblage-zones, and a

CONODONT ZONES AMMONOID ZONES		MOSHER 1968	KOVACS & KOZUR 1980	KRYSTYN 1980		ORCHARD this paper	
UPPER CARNIAN	MACROLOBATUS	POLYGNATHIFORMIS	NODOSA	COMMUNISTI A U	PRIMITIA	L	PRIMITIUS
	WELLERI		L	NODOSA		COMMUNISTI	
	DILLERI		CARPATICA	POLYGNATHIFORMIS	POLYGNATHIFORMIS	M	NODOSUS
			NOAH			L	POLYGNATHIFORMIS

Figure 3: New conodont zonation of the Upper Carnian (on the right) and its calibration with the ammonoid zones (on the left); previous schemes are shown for comparison.

*communisti* morphotype A Zone. According to Krystyn (1980, Figs. 7,8), correlation with the ammonoid zones are, respectively, Dilleri-lower Subbullatus (~Welleri), upper Subbullatus (~Welleri)-lower Anatroites (~Macrolobatus), lower upper Anatroites (~Macrolobatus), and upper upper Anatroites (~Macrolobatus) Zone.

In this paper, both my proposed zonation and its taxonomic basis, as outlined under species concepts, differ from those of previous authors. In so far as a comparison between these zonations is possible, it is shown on Figure 3. In western Canada, several taxa appear to have differing ranges, and some appear earlier in relation to the ammonoid chronology than proposed on the basis of eurasian records. To some extent these differences are attributed to differing species concepts, but they may also result from differing provinciality, or from faunal mixing within the Hallstatt Limestone.

In the Kunga Group, continuous sequences of Upper Carnian conodonts has facilitated the subdivision of the interval into six rather than one (Mosher, 1968), three (Krystyn, 1980), or four (Kozur, 1980) conodont zones. These are presented below in stratigraphic order.

### The *Metapolygnathus polygnathiformis* Assemblage Zone

A *polygnathiformis* Assemblage Zone was originally proposed by Mosher (Mosher, 1968, p. 911) on the basis of fauna from Upper Carnian *Tropites* beds in both Europe and North America. Somer-auekogel, Austria was designated as type locality for the zone, which ranges from 43 m (141 ft.) through 91 m (299 ft.) in the Hallstatt Limestone.

The *polygnathiformis* A-Zone of Mosher (1968) is characterized by an abundance of the zonal index. However, the concept of the species employed by Mosher (1968, p. 939-940) includes the variably ornate *Metapolygnathus nodosus* of this paper whereas the holotype of the nominal species (Budurov and Stepanov, 1965), from the Lower Carnian *Trahycceras aon* Zone, has no platform nodes and is regarded here as a separate entity. This situation has produced nomenclatural confusion.

Originally, Sweet et al., (1971, p. 458) noted that '*Paragondolella*' *polygnathiformis* or a similar form occurred first in the Upper Ladinian. Mosher (1973, p. 164) recorded the species from the Macleari Zone in Canada, and Krystyn (1980, p. 78, Figs. 7, 8) also showed the range extending from near top of the late Ladinian Sutherlandi Zone (~Longobard 3) in Europe. Later, taxonomic revision of the Ladinian-Carnian boundary taxa led Krystyn (1983, p. 240,254) to conclude that '*Gondolella*' *polygnathiformis* first appeared in strata with trachyceratids of the *T. aon* group (which provided the original definition for the base of the Carnian); similar elements in the Ladinian were referred to '*G.*' *inclinata* Kovacs 1983. Krystyn (1983, p. 253) suggested that the appearance of '*G.*' *polygnathiformis* should be used to define the Ladinian-Carnian boundary, although he named the basal Carnian zone defined by its appearance as the *tudpole* A-Zone (= *foliata foliata* of Kovacs 1983) in order to avoid conflict with the established, but apparently mis-named, *polygnathiformis* Zone of the Upper Carnian.

The Upper Carnian *polygnathiformis* A-Zone of Krystyn (1980, p. 77-79) differs from that of Mosher (1968) in both its lower and upper boundaries. Krystyn characterized the zone as "the exclusive presence of..." the species, and proposed its base be drawn at the disappearance of *Gladigondolella tethydis* (Huckriede 1958). According to Krystyn (1983, p. 249), this latter event "...can easily be traced throughout the "pelagic" conodont region." Recent data (op. cit.) indicates that the base of the zone, thus defined, can be drawn at the base of the Tuvalian (Dilleri Zone) in the Tethyan Realm. However, *Gladigondolella* does not occur in western Canada. Recognition of the *polygnathiformis* A-Zone in non-Tethyan sections must therefore rest on an abun-

dance of the zonal index, and may be older than the *polygnathiformis* Assemblage Zone of Krystyn (1980).

The upper limit of the *polygnathiformis* Assemblage Zone of Krystyn (1980) is defined by the appearance of *Metapolygnathus nodosus* which occurs at the base of the upper part of the Subbullatus (~Welleri) Zone in Europe (Krystyn, 1980, p. 79). This position is well within the *polygnathiformis* A-Zone of Mosher (1968).

In the present paper, the *polygnathiformis* Assemblage Zone is defined as embracing the range of *Metapolygnathus* ex gr. *polygnathiformis* prior to the appearance and conspicuous radiation of *Metapolygnathus nodosus*, as defined above. The base of the zone is not seen in QCI, but clearly the European definition (Krystyn, 1980, 1983) is not tenable in North American sections known to date.

Additional elements regarded as representative of the *polygnathiformis* Zone in QCI comprise the septimembrate apparatus referred to *Cornudina?* sp. by Orchard (in Carter et al., 1989). At present, this multi-element taxon does not provide diagnostic age criteria, but it is locally common (e.g. Huston Inlet) in the lower part of the Sadler Limestone, where it presumably represents a particular environmental niche. The taxon provides faunal identity in the absence of metapolygnathids.

Although the present collections from the Queen Charlotte Islands lack conodonts indicative of the Lower Carnian, their exact position within the Carnian Stage cannot be determined with complete confidence. However, co-occurrence with Dilleri Zone ammonoids in Huston Inlet, and immediately beneath the same zone at Sadler Point support an early Late Carnian age.

Reference sections: Sadler Point (SP-1A - 3), Kunghit Island, west (KT-A1 - 12), Huston Inlet (HU-2 - 11).

Other QCI occurrences: Treat Bay (TB-A3A), Rose Inlet (WV-52), Rose Harbour (RH3), Huston Point (HP2), Bush Rock (BR-1 - 4), Blue Jay Cove (BJ-5), Burnaby Island (BI-86/2, 87/2), Vertical Point (TWL-403), Newcombe Inlet (NI-1), Cumshewa Inlet (TWT-69, EC86-4), Mosquito Lake (TW-494), Shields Island (TWL-246), Frederick Island (TWL-81B).

### The *Metapolygnathus nodosus* Zone

This zone has not previously been differentiated within the North American Upper Triassic. The base of the zone is herein defined by the appearance of the index species, and its top is marked by the appearance of *M. communisti*. *M. nodosus* is the most common and widespread of Upper Carnian conodonts ranging through most of the Upper Carnian and into the basal part of the Norian. The *nodosus* Zone of Krystyn (1980, p. 79), established in the Tethyan region, is a range zone and is separated into lower and upper parts based on the appearance of *Metapolygnathus primitius* in the upper part. According to Krystyn (1980), the conodont zone, in his sense, corresponds to the upper Subbullatus (~Welleri) through lower upper Anatroites (~Macrolobatus) zones. In this paper, the *Metapolygnathus nodosus* Zone (revised) is shown to include the whole of the Welleri Zone, as well as the uppermost part of the Dilleri Zone. Informal subdivision of the North American Welleri Zone into lower and upper parts by E.T. Tozer (pers. comm., 1989) has not been fully assimilated in this paper, but provisional calibration of the ammonoid and conodont zonations are given below under the three proposed subdivisions of the *nodosus* Zone.

Weakly ornamented to apparently unornamented quadrate forms similar to *Metapolygnathus* ex gr. *polygnathiformis* occur in the *nodosus* Zone. These probably correspond to '*Gondolella*' *noah* (Hayashi) but I have not differentiated such forms because I regard them as intraspecific variants of the *nodosus* population (cf. Krystyn, 1980, p.



76). The morphology often develops in larger specimens of *M. nodosus* because the nodes coalesce.

### Lower *Metapolygnathus nodosus* Zone

This zone is characterized by the occurrence of *Metapolygnathus nodosus* and/or *Metapolygnathus* n. sp. E prior to the appearance of *Metapolygnathus* n. sp. F. This fauna arose during the initial radiation of the *nodosus* stock and in addition to the elongate *Metapolygnathus* n. sp. E also includes similar morphological end members that resemble '*Neogondolella*'. For the present, these extreme forms are retained within *Metapolygnathus* n. sp. E; '*N. reversa*' Mosher 1973, from the Welleri Zone of Arctic Canada, is thought to be an example of a similar derivative form. Conodonts indicative of this zone apparently occur in association with ammonoids indicative of both lower and upper parts of the Welleri Zone (Tozer, in Orchard et al., 1990).

Reference section: Kunghit Island, west (KT-A13-18).

Other QCI occurrences: Kunghit Island, southwest (KT-B2-5), Huston Point (HP-5.7), Blue Jay Cove (BJ-8-13), Poole Inlet (HO-3), Burnaby Island (BI-3A.4), Huxley Island (HUX-A4), Crescent Inlet (CRE-2.3), Cumsheewa Inlet (TW-92), Sadler Point (SP-4-?10).

### Middle *Metapolygnathus nodosus* Zone

The Middle *nodosus* zone is defined by the concurrent range of *Metapolygnathus* n. sp. F and *Metapolygnathus nodosus* prior to the appearance of *Metapolygnathus* n. sp. G. In addition to these species, *Metapolygnathus* n. sp. E and its '*Neogondolella*'-like derivatives may occur but they are less common in the present collections. In the reference section, this conodont zone is associated with ammonoids indicative of the upper part of the Welleri Zone (Tozer, in Orchard et al., 1990).

Reference Section: Kunghit Island, west (KT-A19-21).

Other QCI occurrences: Huston Inlet, south (SHU-4-5), Huston Point (HP-8), Jedway Bay (JED-9), Sandilands Island (SI-84/20-11).

### Upper *Metapolygnathus nodosus* Zone

This zone is defined by the co-occurrence of *Metapolygnathus* n. sp. G and *Metapolygnathus nodosus* prior to the appearance of *Metapolygnathus communisti*. In good examples of fauna representative of this zone, the sharp-noded *Metapolygnathus* n. sp. G is relatively common, although conservative *Metapolygnathus nodosus* is usually dominant. Older members of the *Metapolygnathus* n. spp. E-F-G lineage may also occur. This zone is not associated with ammonoids in QCI, so its exact equivalence to upper Welleri or lower *Macrolobatus* ammonoid levels is unresolved. It occurs at the top of the Baltonnel Formation in northeast B.C.

Reference Section: Kunghit Island, west (KT-A24).

Other QCI occurrences: Huston Inlet, south (SHU-2.6,7), Sandilands Island (SI-84/20-10, 87-5).

### The *Metapolygnathus communisti* Zone

The index for this zone was first recorded as a constituent of the mixed fauna described from the Adoyama Formation in Japan by Hayashi (1968). Its stratigraphic significance, not recognized at first, has continued to be hindered through variable taxonomic interpretation. Krystyn (1980) recognized two morphotypes with mutually exclusive ranges about the Carnian-Norian boundary interval. In this paper, my definition of *M. communisti* excludes morphotype B of Krystyn (1980).

The range of *Metapolygnathus communisti* can be shown to span part of the *Macrolobatus* (~*Anatropites*) and superadjacent Kerri (~*Jandianus*) ammonoid zones both in Western Canada (herein) and in Europe (Krystyn, 1980). In contrast to the European range shown by Krystyn (1980, Fig. 8), in western Canada the species appears before *Metapolygnathus primitius* and therefore provides the basis for

a new zone of wholly Upper Carnian age. The *communisti* Zone is well represented in both northeast B.C. and in QCI, where it includes within it the *Macrolobatus* ammonoid level (with '*Juvavites*' *carlottensis* (Whiteaves)) originally collected by G.M. Dawson (Tozer, in Orchard et al., 1990).

The base of the zone is defined by the appearance of *Metapolygnathus communisti*, and the top by the appearance of *Metapolygnathus primitius*, which represents a widespread faunal turnover. A further important index species that occurs in this zone is the ornate *Metapolygnathus echinatus*, which I interpret as the end member in the lineage *Metapolygnathus* n. spp. E-F-G, isolated specimens of which also occur. These ornate species have often been identified previously (e.g. Krystyn, 1980, p. 79) as *Epigondolella abneptis* (Huckriede 1958), which has contributed to the long range attributed to that species. In my view, the lineage represents an unrelated Upper Carnian experiment within the *metapolygnathid* stock that resulted in a homeomorphic *epigondolellid*-like morphology: the Middle Triassic *mungoensis* group is an earlier example of a similar phenomenon. For the present, I have chosen not to refer the Upper Carnian lineage to a new genus.

A few collections are known from northeast B.C. and QCI in which *Metapolygnathus echinatus* occurs without *M. communisti*. This raises the possibility that there may be an older *echinatus* faunal unit prior to the *communisti* Zone, a proposition currently under review.

*Metapolygnathus nodosus* continues as an important, and often dominant constituent of the *communisti* zone, but some elements begin to display a morphology that approaches that of the descendant *M. primitius*. At about the same time, *Metapolygnathus* n. sp. K developed as a further offshoot of *Metapolygnathus nodosus*.

Reference Section: Kunghit Island, west (KT-A26A,27).

Other QCI occurrences: Huxley Island (HUX-B8A), Kunga Island, south (86/7SKU-A10-8B), Sandilands Island (86/79)SI-2; 85-6), Shields Island (SHI-6), Frederick Island (FI-A6.7), Sadler Point (SP-12).

### The *Metapolygnathus primitius* Zone

When Mosher (1970) first introduced '*Epigondolella*' *primitia*, the species was regarded as an intermediate between *Metapolygnathus polygnathiformis*, in which Mosher included *nodosus* forms, and *Epigondolella abneptis*. The selection of morphological criteria to separate *polygnathiformis* from *primitius* was stated to be arbitrary (Mosher, 1970, p. 741) and does not hold up well in comparing the species *nodosus* and *primitius*, which Mosher did not do at the time. Later, Mosher (1973, p. 161) stated that the two latter species differed in length to breadth ratio as well as in the lateral platform constriction of *primitius*. In my view, none of these published criteria are sufficient to separate the two species consistently, and this has led to some earlier authors synonymizing them (e.g. Krystyn, 1973; Kovacs and Kozur, 1980, p. 53). On the contrary, the two are clearly different when viewed in lateral profile (see taxonomic definitions). In fact, the development of *Metapolygnathus primitius* from *Metapolygnathus nodosus* is the major conodont faunal event of the Upper Carnian.

As found by Krystyn (1980), the appearance of *Metapolygnathus primitius* occurs within the *Macrolobatus* (~*Anatropites*) ammonoid Zone of the Upper Carnian. The species crosses the Carnian-Norian boundary, as originally shown by Mosher (1970), and extends to near the top of the Lower Norian Kerri Zone (Orchard, 1983), or a little beyond in the Tethyan region (Krystyn, 1980, Fig. 8).

The oldest fauna of the Norian described by Orchard (1983) was characterized by both *Metapolygnathus primitius* and '*Neogondolella*' *navicula*, which represents an upper subdivision of the *primitius* Zone. Collections from the Kunga Group and others newly recovered from northeast British Columbia include both lower and upper zones

in sequence and are key to understanding their relationship. The *primitia* Assemblage Zone of Krystyn (1980, p. 79) is rather different in scope from the present one and is not adopted in this paper.

### The Lower *Metapolygnathus primitius* Zone

This zone is recognized by the occurrence of the name giver prior to the appearance of '*Neogondolella*' *navicula*, which defines the base of the succeeding Upper *primitius* Zone. The base of the zone is characterized by the development of *Metapolygnathus primitius* from its immediate precursor *Metapolygnathus nodosus*, which may continue to occur, although usually in subordinate numbers. Associated species include most of the species known in the subjacent *communisti* Zone, although platformless variants of *Metapolygnathus communisti* may appear first in this zone. On QCI, ammonoids of the Macrolobatus Zone are associated with this fauna in the reference section on Huxley Island (Tozer, in Orchard et al., 1990).

Reference Section: Huxley Island (HUX-B8,9 – 10A).

Other QCI occurrences: Kunga Island, south (86/7SKU-A8A,8), Shields Island (SHI-5), Huston Inlet, south (SHU-8), Sadler Point (SP-13).

## NORIAN ZONATION

New conodont zonation of the Norian Series was proposed in a preliminary way several years ago (Orchard, 1983). Eight zones were recognized in the Pardonnet Formation in northeast British Columbia as a result of collaborative research with E.T. Tozer (GSC, Vancouver). The zonal succession, from near the base of the Lower Norian through the early Upper Norian, was developed in conjunction with ammonoid collections that provided a framework for calibration. Subsequently, this zonation has been supplemented by studies of youngest Norian (Amoenum and Crickmayi zones) strata in the Tyaughton Creek area of south-central British Columbia and, in cooperation with D. Taylor (Portland), in the Upper Norian of Nevada. As a consequence of this work, intercalibration of Norian ammonoid and conodont biochronologies has found a firm foundation that had not been entirely possible in the condensed Hallstatt (Tethyan) facies of the Eurasian Triassic.

In North America, the base of the Norian is drawn at the base of the Kerri ammonoid Zone, which is well developed near the base of the Pardonnet Formation in northeast British Columbia. In terms of superimposition of key ammonoid faunas, the Carnian-Norian boundary is less well displayed than intra-Norian zones in this area. However, a continuous succession of conodonts are known across the Baldonnel-Pardonnet formational contact at one locality (Black Bear Ridge, BBR in Fig. 8), and the succession compares favourably with that in several sections of the Kunga Group where, unfortunately, Lower Norian ammonoids are not known. In both regions, the appearance of '*Neogondolella*' *navicula* in association with *Metapolygnathus primitius* is regarded as definitive of the basal Norian.

The Norian conodonts of the Pardonnet Formation, and formal description of the Norian conodont zonation will be described in a later paper. In the following, I briefly discuss the key zonal species, note their occurrence within the Kunga Group, and focus on differences between the Queen Charlotte Islands and northeastern British Columbia.

### The Upper *Metapolygnathus primitius* Zone

This zone is defined by the co-occurrence of '*Neogondolella*' *navicula* (Huckriede 1958) and *Metapolygnathus primitius*. The base of the zone is drawn at the appearance of the neogondolellid and the top at the appearance of common *Epigondolella abneptis* subsp. A Orchard, a relatively sudden event near the top of the Kerri Zone in northeast B.C. (Orchard, 1983). In northeast B.C., '*N.*' *navicula* occurs first in association with Kerri Zone ammonoids (E.T. Tozer, pers.

comm., in Orchard, 1983). In the Kunga Group, the pelecypod *Perithalobia* commonly occurs at this level (Tozer, in Orchard et al., 1990).

Recognition of the Upper *primitius* Zone poses some problems because of both the uncertainty about the origin of '*Neogondolella*' *navicula*, and the erratic appearance of this species in Lower Norian faunules. The species has been regarded as confined to Norian strata (Krystyn, 1980, p. 76), but its ancestor is not obvious in Carnian collections. The species almost certainly has its roots in *Metapolygnathus* rather than directly from true *Neogondolella* of the Middle Triassic; Krystyn (1980) regarded '*Gondolella*' *polygnathiformis* as its ancestor. A further alternative is derivation from a platformless xanognathiform-like conodont, although such candidates are extremely rare in the authors collections, and none occur in subjacent (Macrolobatus Zone) strata. In this paper, I suggest platformless specimens allied to *Metapolygnathus communisti* may represent the source for '*Neogondolella*' *navicula*. If this phylogeny (see below) is correct, it puts the index species in context with Upper Carnian progenitors and produces a more reliable zonation.

Reference Section: Sadler Point (SP-14 – 18).

Other QCI occurrences: Huxley Island (HUX-B13), Kunga Island, south (SKU-A7), Crescent Inlet (CRE-4), Shields Island (SHI-3), Frederick Island (FI-1,2,A9 – 14,B15).

### The *Epigondolella abneptis* subsp. A Zone

This zone is recognized by the common occurrence of the name giver, which resembles *Metapolygnathus primitius* but has much more prominent anterior platform nodes, a consistently different platform length to breadth ratio (Orchard, 1983, Fig. 5), and ontogenetic development and microreticulation typical of *Epigondolella*.

The index species, which appears to be a cosmopolitan form, will need a new name. *Epigondolella abneptis* (Huckriede 1958) could be a specimen of either a Lower or Middle Norian epigondolellid (e.g. *Epigondolella* n. sp. C Orchard) but both the original illustration and present condition of the holotype precludes positive identification.

The base of this zone is drawn near the top of the Kerri ammonoid Zone in northeast B.C., where it extends to a position within the Dawsoni Zone (Orchard, 1983).

Reference Section: northeast B.C. (in prep.).

QCI occurrences: Treat Bay (TB-A4 – 5), ?Huston Inlet, south (SHU-9 – 10), Huxley Island (HUX-B15), Kunga Island, south (SKU-A6 – 1), Desmariscove Point (DEM-2), Frederick Island (FI-3 – 4,B16 – 20), Sadler Point (SP-19).

### The *Epigondolella triangularis* Zone

This is a new name applied to the zone of *Epigondolella abneptis* subsp. B Orchard, which is synonymous with the older name of Budurov (1972). The index species is characterized by an ornate, generally symmetrical platform that in later growth stages commonly becomes laterally broadened posteriorly to produce the distinctive shape described by Budurov (1972) under *Ancyrogondolella*. I do not regard the species as the same as *Epigondolella spatulata* (Hayashi 1968) of authors although it is similar (Orchard, in prep.). Typical representatives of this latter species may be restricted to Tethyan faunas.

Early growth stages of *Epigondolella triangularis* resemble *Epigondolella postera* (Kozur and Mostler 1971) and the two have often been confused. This probably explains the range attributed to the latter by some authors (e.g. Krystyn, 1980, Fig. 8), who record it within the Lower Norian. Retention of this juvenile morphology appears to have led to the development of some Middle Norian epigondolellids, but *Epigondolella postera* is strictly a Middle Norian Columbianus Zone index (Orchard, 1983).

In a few collections (e.g. EPO-1, HO-5, FI-25) from the Peril Formation, '*Neogondolella*' *hallstattensis* (Mosher 1968) occurs in the *triangularis* zone. This is the first record of the neogondolellid species in North America. The species is more common in the Tethyan succession, where it is confined to the *Epigondolella spatulata*-Assemblage Zone of Krystyn (1980), equivalent to the latest Paulcke and Magnus ammonoid zones. In western Canada, the *triangularis* Zone similarly embraces part of the Dawsoni Zone through the Magnus Zone (Orchard, 1983).

Reference Section: northeast B.C. (in prep.).

QCI occurrences: Swan Bay (SB-1,24), Deluge Point (DP-1), Poole Inlet (NPO-5, EPO-1, HO-A5 – 9), Burnaby Island (86/87BI-11 – 13a), Sandilands Island (SI-86/1), Desmariscove Point (DEM-6), Frederick Island (FI-21,22,25,33-36).

### **The *Epigondolella multidentata* Zone**

This base of this zone is defined by the appearance of *Epigondolella multidentata* Mosher, which coincides with the base of the Rutherfordi ammonoid Zone in northeast B.C. (Orchard, 1983). In rich collections from this zone in autochthonous western Canada, several different morphotypes occur, of which the most distinctive is characterized by a long, narrow platform with several strong anterior denticles on each platform margin, and a remarkably high posterior carina. This morphotype is not presently known to occur in the Kunga Group, elsewhere in allochthonous western Canada, or in the Tethyan region. However, in several collections from the Peril Formation, an association of elements similar to the other components of the *multidentata* Zone in northeast B.C. do occur along with elements of the older *triangularis* Zone. These are tentatively referred to the *multidentata* Zone, although they may be slightly older than examples from the Pardonnet Formation, where the faunal turnover between the Lower (*triangularis* Zone) and Middle (*multidentata* Zone) Norian is abrupt.

Reference Section: northeast B.C. (in prep.).

QCI occurrences: Swan Bay (SB-5), ?Poole Inlet (HO-A11), ?Burnaby Island (86BI-15), Huxley Island (HUX-1).

### **The *Epigondolella* n. sp. C Zone**

This zone is dominated by strongly serrate, typically asymmetric epigondolellids (Orchard, 1983). In northeast B.C., the zone occurs in the Columbianus I ammonoid Zone, postdating the *multidentata* Zone which intervenes between the present zone and the Lower Norian *triangularis* Zone. The index species for the latter zone and that for the *Epigondolella* n. sp. C Zone are similar and both have been referred to *Epigondolella abneptis* (Huckriede) in the past, giving that species an alleged range through most of the Norian (as well as the Upper Carnian – see *communisti* Zone).

In the Peril Formation, *Epigondolella* n. sp. C is known from several localities, the best examples being Poole Inlet, where it overlies older faunas of the *triangularis* and ?*multidentata* zones, and on Burnaby Island where it is overlain by the *postera* Zone. Its occurrence in the QCI is thus comparable to its established position in other parts of western Canada.

Reference Section: northeast B.C. (in prep.).

QCI occurrences: Poole Inlet (HO-A13), Burnaby Island (86/87BI19 – 19B), Frederick Island (FI-30 – 32).

### **The *Epigondolella postera* Zone**

The type material of this species originated from Middle Norian strata of Sommeraukogel, Austria (Kozur and Mostler, 1971). The zone is well represented in the Pardonnet Formation in association with ammonoids of the Middle Norian Columbianus II Zone

(Orchard, 1983), and reports of it from deeper levels are suspect (see *triangularis* Zone). Faunules representative of this zone are easily identified and show a consistent range of variation.

The zone occurs in several collections from the Peril Formation, in which it commonly occurs in association with '*Neogondolella*' *steinbergensis* (Mosher). This is also the case in northeast B.C. where neogondolellids become very common at this level. The significance of this 'acme' is not known, but it was certainly widespread.

Reference section: northeast B.C. (in prep.).

QCI occurrences: Burnaby Island (86BI-24,25, 87BI-A2 – 6), Huxley Island (HUX-C19 – 20), Desmariscove Point (DEM-8), Frederick Island (FR-A12,13).

### **The *Epigondolella* n. sp. D Zone**

The *Epigondolella* n. sp. D Orchard fauna is known from several localities in autochthonous western Canada where it co-occurs with Middle Norian Columbianus III ammonoids and the pelecypod *Eomonotis*.

No good examples of this fauna have been recovered from the Kunga Group. In fact, very few conodonts have been recovered from between *postera* Zone levels and *Monotis* beds, partly due to the lack of suitable lithologies. Rare elements that resemble the nominal species do occur in younger beds, but they are associated with *Monotis* and other conodonts referred to the *bidentata* Zone. The zonal fauna may be endemic to autochthonous western Canada.

Reference section: northeast B.C. (in prep.).

QCI occurrences: ?Kunga Island, north (KU-3).

### **The *Epigondolella bidentata* Zone**

As stressed by Orchard (1983, p. 188-9), the 'bidentate morphology' is common to most early growth stages of *Epigondolella* species and therefore bidentate elements need to be assessed very carefully in differentiating the age of Norian collections. Small specimens of most Norian species may be difficult to separate from *Epigondolella bidentata* Mosher, which is itself a small species. Krystyn (1980, p. 80) recognized this problem but his *bidentata* Zone began well down in the Middle Norian Columbianus Zone whereas I consider the zone is typically Late Norian, as was the type material from Austria.

The best collections of *Epigondolella* ex gr. *bidentata* in the Pardonnet Formation of northeast B.C. come from ammonoid bearing beds of the lower Upper Norian Cordilleranus ammonoid Zone interbedded with *Monotis coquina* (Orchard, 1983). These populations represent my standard for the *bidentata* Zone. However, several species of Upper Norian epigondolellids have been proposed since Mosher (1968) described *Epigondolella bidentata*. These include *E. mosheri* (Kozur and Mostler 1971), *E. slovakensis* (Kozur 1972), and *E. humboldtensis* Meek 1987. For the moment, all these species (the separation of which is far from clearcut) and possibly others undescribed, are included under *Epigondolella* ex gr. *bidentata*. These Upper Norian epigondolellids range throughout the Cordilleranus and Amoenum zones in British Columbia and Nevada. Bidentate species occur in latest Middle Norian strata in western Canada but none of the present collections are large enough to fully evaluate the intraspecific variability.

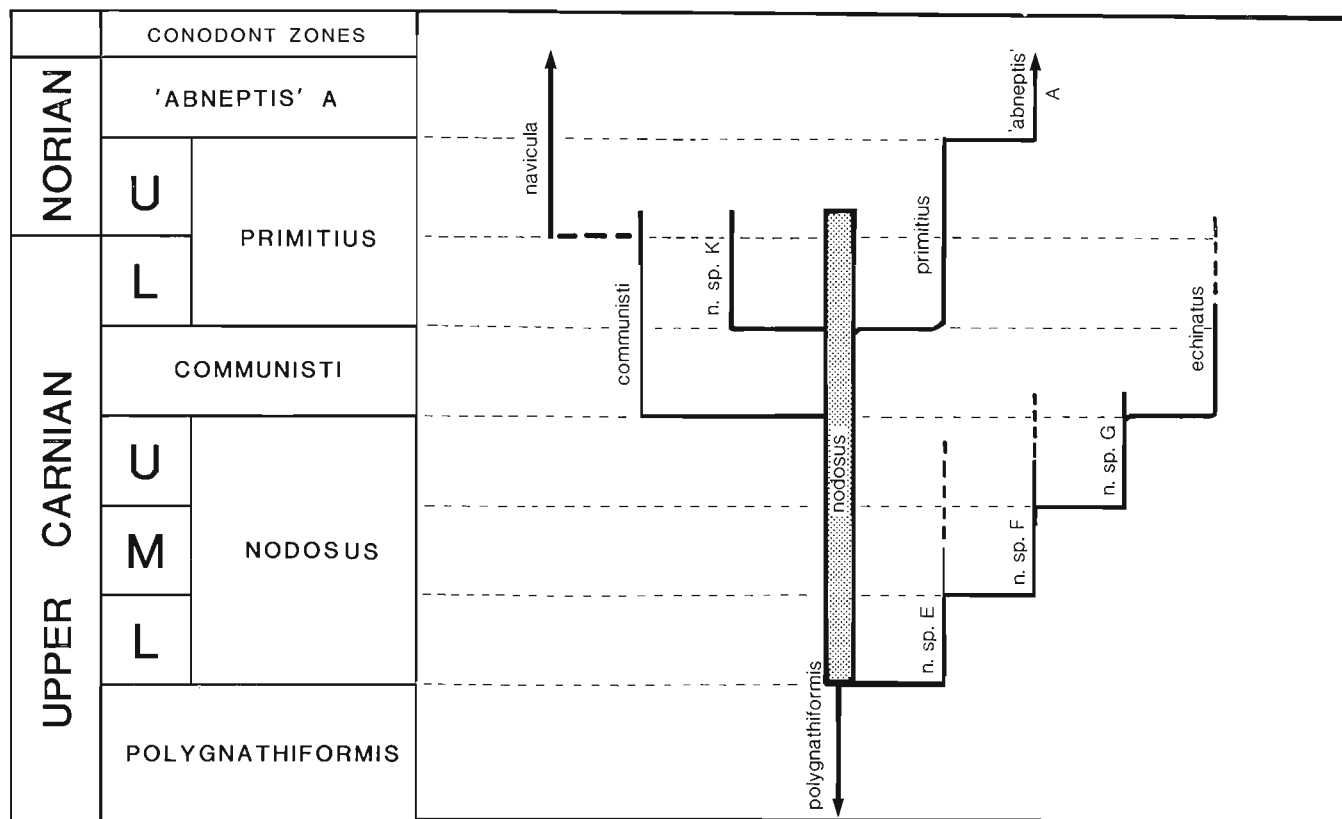
In the QCI, this zone, characterized by the common occurrence of *Epigondolella* ex gr. *bidentata*, occurs in the upper member (*Monotis* beds) of the Peril Formation and in overlying post-*Monotis* strata of the Sandilands Formation. The age of the *bidentata* bearing part of the latter in terms of ammonoid chronology is uncertain, but an Amoenum Zone age seems probable. Ammonoids of the Crickmayi Zone occur higher in the Sandilands Formation, but no epigondolellids have been found in association.

Other QCI occurrences: South Cove (SC-3), Swan Bay (SB-6), Poole Inlet (HO-A18, SPO-2), Burnaby Island (86BI-32; 87BI-A10 – 16), Huxley Island (HUX-5), Arichika Island (AI-1), Kunga Island, south (SKU-D1,2), Kunga Island, north (KU-E4,6; F2 – 7), Newcombe Inlet (NI-5), Sandilands Island (88SI-4,11A,12), Skidegate Channel (EC85-12; SKID-5), ?Desmariscove Point (DEM-9), Frederick Island (86FR-A1-6).

Upper Norian conodonts are uncommon in strata above the disappearance of *Epigondolella* in western Canada. None are known in the autochthonous sections of the Pardonnet Formation and overlying units, and they are rare in the suspect terranes. This contrasts with the record of conodonts in Tethyan regions where several species of *Misikella* provide useful indices through the remaining part of the Triassic. In North America, *Misikella* (including *Axiothea* Fahraeus and Ryley) has never been well documented, although *M. hernsteini* is noted to occur, with *Epigondolella bidentata*, in the Glenn Shale of east-central Alaska (Robinson and Carr, 1985). My own collections from Canada include a single specimen of *M. posthernsteini* from presumed Crickmayi Zone strata in the Tyauhton Creek area (Cadwallader Terrane) of southern B.C., and a second collection of the same species from chert of the Cache Creek Group in southern Yukon where there is no independent age constraint.

clude at first neogondolellids, and then a single fauna of *Misikella posthernsteini*; undifferentiated ramiform elements occur throughout. Pending further study of this key interval, no attempt has been made to formally differentiate these post-*bidentata* conodont faunas. They do, however, have parallels with the European sections where Krystyn (1980, 1988) recognized a '*Gondolella*' *steinbergensis* Zone within the transitional beds from the Hallstatt Limestone to the marls of the Zlambach Formation; this zone embraces the range of '*Neogondolella*' above the last epigondolellid. In a more recent paper (Krystyn, 1988), the *steinbergensis* Zone is shown as equivalent to, in the ammonoid chronology, the lower subzone (Choristoceras "haueri") of the Vandaite stuerzenbaumi Zone based on sections of the Zlambach marls.

QCI occurrences: Huxley Island (HUX-18), Sandilands Island (88SI-13), Shields Bay (SHB-21), Kennecott Point (KPA-7A – 18A, C3.5, D1AA).



181

## PHYLOGENY OF UPPER TRIASSIC CONODONTS

Considerable uncertainty has surrounded the relationship between Upper Carnian conodonts and their Norian offspring. This has resulted in varying phylogenetic schemes, strongly differing nomenclature, and zonations that have lacked precision and resolution. My initial study of the relationships between Norian epigondolellid conodonts (Orchard, 1983) has yet to be fully documented, and has been delayed to some extent by the need to clarify the origins of the group in Carnian strata. The Kunga Group has provided both the impetus and the key.

The following account starts with *Metapolygnathus* ex gr. *polygnathiformis*, which has been regarded as the root stock for all Upper Carnian platform conodonts (Fig. 4). This fauna is the oldest in the QCI although, as discussed above, the relationship with the Lower Carnian type material is uncertain. Typical populations of *Metapolygnathus nodosus* appear at about the base of the Peril Formation, a position close to the highest occurrence of Dilleri Zone ammonoids. The faunules from successively higher beds show diverse development of platform nodes and an ontogenetic series in which early growth stages have a strongly constricted platform. Specimens with a relatively elongate platform and relatively low blade denticles also appear, and are separated as *Metapolygnathus* n. sp. E. This trend culminated in a neogondolellid morphology, similar to '*N.* reversa'.

A further trend begins somewhat later and is characterized by a steepening of the anterior platform margins in elements that otherwise resemble *M.* n. sp. E. At the beginning of Middle *nodosus* Zone times, strong but low rounded nodes appeared for the first time in this latter stock to produce *Metapolygnathus* n. sp. F. This trend continued and reached an extreme in *Metapolygnathus* n. sp. G of the Upper *nodosus* Zone. Thereafter, *M. echinatus* developed through reduction of the anterior platform (see below).

Whilst the ornamental elaboration in the E-F-G lineage was underway, the conservative stock of *M. nodosus* went through relatively little change. Elements of *M. nodosus* continued as strongly to weakly noded forms in which platform margins maintained a uniform height regardless of the degree of node development. Beginning in the *communisti* Zone, the conservative stock of *M. nodosus* diversified (Fig. 4). One descendant species, *Metapolygnathus communisti*, arose through suppression of both nodes and platform, whereas in a second trend nodes were emphasized and some ornate specimens began to resemble *Metapolygnathus primitivus* (Mosher). Initially, both trends involved a relative lowering of the posterior platform to produce a relatively high geniculation point in the former, and more discrete upstanding nodes in the latter; anterior migration of the pit occurred in both. Particularly in the case of *M. communisti*, there was also a trend to reduce the platform both longitudinally and/or laterally, and large populations of this species show a lot of variation in platform shape.

Concurrent with (or possibly a little earlier than) the appearance of *M. communisti* and advanced species of *M. nodosus*, there was a similar longitudinal retardation in platform development in the *Metapolygnathus* n. spp. E-F-G lineage to produce what is herein called *Metapolygnathus echinatus*. Specimens of *M. communisti* and *M. echinatus* may have a similar platform shape but the former usually have longer free blades and no platform sculpture.

The *communisti* Zone appears to have been a time when the platform conodonts began to undergo some fundamental changes in platform growth, with the development of both *M. communisti* and *M. echinatus* involving platform reduction. A similar trend is also evident in the diminutive *Metapolygnathus* n. sp. K Orchard which appeared in this zone. In the younger *primitivus* Zone, this trend continued and the proportion of abbreviated morphotypes increased. The most sig-

nificant event at this time was the metamorphosis of *M. nodosus* (Hayashi) into *M. primitivus* through the development of relatively high anterior nodes clearly projecting above the platform; the advantages were clearly great and *M. primitivus* quickly became the dominant and then exclusive metapolygnathid.

The ultimate event in the evolution of Carnian conodonts was the development of '*Neogondolella*' *navicula* (Huckriede), which appeared at, and marks the base of the Norian. In my opinion, a clue to the origin of this species may be seen in the extraordinary plasticity of *M. communisti*. This species is extremely variable and even early growth stages show variation from a small quadrate platform to one that is sagittate, or extremely narrow and sinuous. In some specimens, the platform is vestigial at the posterior extremity of the element, or completely absent. These manifestations are not merely a result of differing growth stages but are, I summarize, the beginning of a trend that culminated in a neogondolellid morphology. In some samples from the Kunga Group, rare elements occur that are quite large but still lack a platform (comparable with *Parvigondolella* of the Upper Norian). These platform variations are also accompanied by a shifting in the position of the basal pit, which commonly lies far anterior of the posterior end of the element in 'typical' *M. communisti*, but which is posteriorly located in some small elements. '*N.*' *navicula* may have developed as a result of the stabilization of this platformless condition, followed by rapid development of uniform platform growth along most of the length of the carina.

As discussed under the Upper *primitivus* Zone, alternative candidates for the *navicula* ancestor in subjacent strata are unknown, and I discount a direct relationship between '*Neogondolella*' *reversa*, or similar *nodosus* Zone morphotypes, and '*N.*' *navicula*.

The innovations shown by the platform conodonts close to the Carnian-Norian boundary set the stage for one more development. The advantage of discrete anterior nodes exerted strong selective pressure and toward the top of the Lower Norian Kerri ammonoid Zone, true *Epigondolella* was born. Now nodes became universally developed rather than variable as in many metapolygnathids, and they grew to effectively double the 'height' of the conodont platform. In order to accommodate this change in morphology, or in response to it, the microreticulation of the platforms changed. Whereas in *Metapolygnathus* microreticulae had been uniformly developed, close-packed, and with some relief, in *Epigondolella* they became more dispersed, irregular and subdued. A further change, here regarded as generically significant, is manifest in the growth of the two genera. The posterior constriction and common dual platform growth that characterizes early growth stages of all species of *Metapolygnathus* is not a feature of *Epigondolella*.

The phylogenetic development of later Norian conodonts was briefly outlined by Orchard (1983, p. 191). The transition from *Epigondolella abneptis* subsp. A Orchard to *Epigondolella triangularis* (Budurov) is reaffirmed in the Kunga Group. '*Neogondolella*' *hallstattensis* (Mosher) developed from '*N.*' *navicula* at this time according to Krystyn (1980, Fig. 6); it is noteworthy that the former species in particular shows attributes of its proposed *Metapolygnathus* roots.

New data from the Kunga Group and further work on abundant collections from northeast B.C., as well as observations on the global distribution of species, has shown that it may be possible to recognize a more complex history amongst the Middle Norian epigondolellids beginning with retention of early growth morphology in *E. triangularis*. By the *multidentata* Zone, diverse morphology was present in the epigondolellid populations (Orchard, 1983). Further work is required on the relationships of the Middle and Upper Norian conodonts, including *Misikella*, the origin of which remains an enigma.



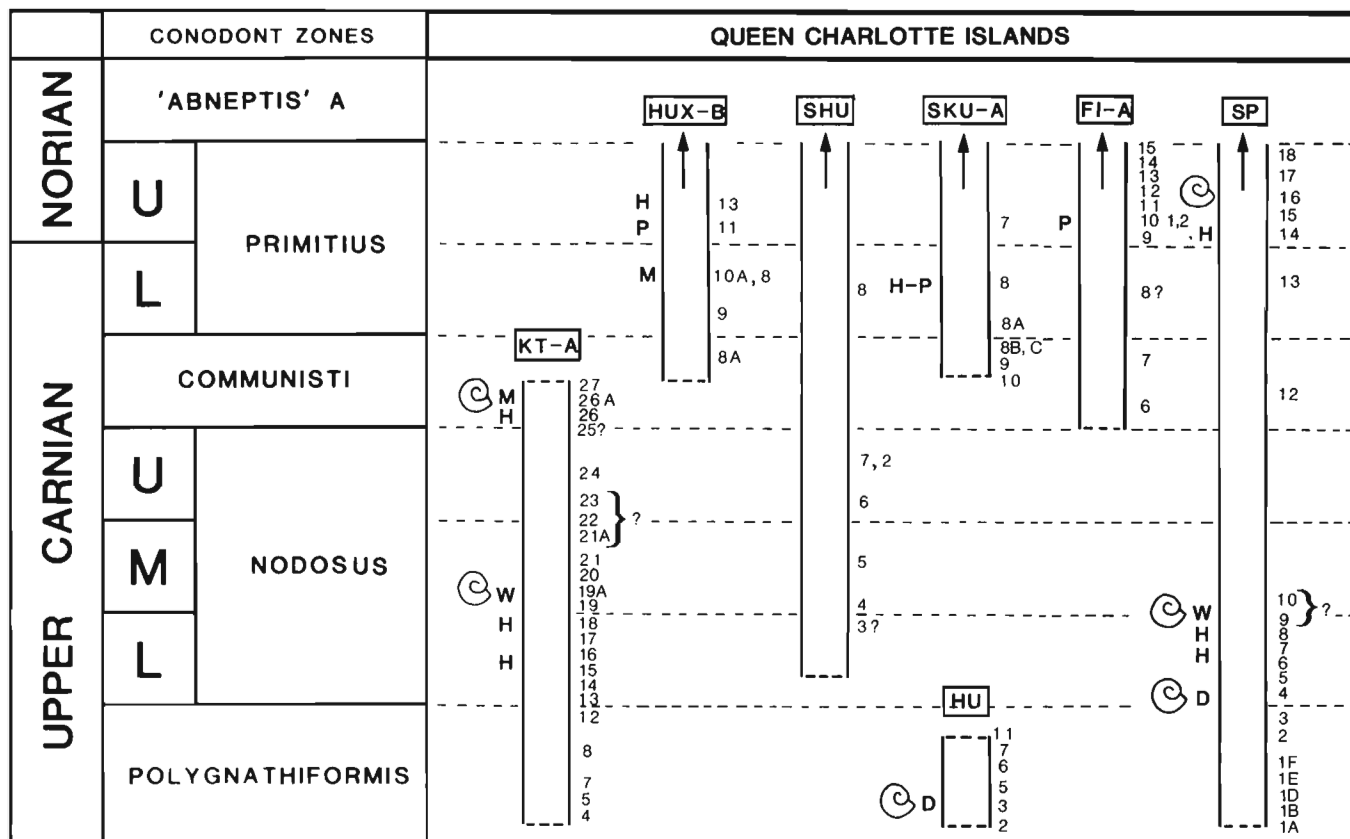


**Figure 5:** Time stratigraphic correlation of Kunga Group sections on Queen Charlotte Islands. These seven sections have been the most important for the development of the Upper Carnian conodont zonation. Section locations are listed under the description of each zone. No vertical scale is intended. Conodont sample numbers are shown on the right of the columns; ammonoid zonal assignments (D = Dilleri, W = Welleri, M = Macrolobatus, K = Kerri, C = Columbianus) and pelecypod occurrences (H = *Halobia*, P = *Perihalobia*, M = *Monotis*) are shown on the left.

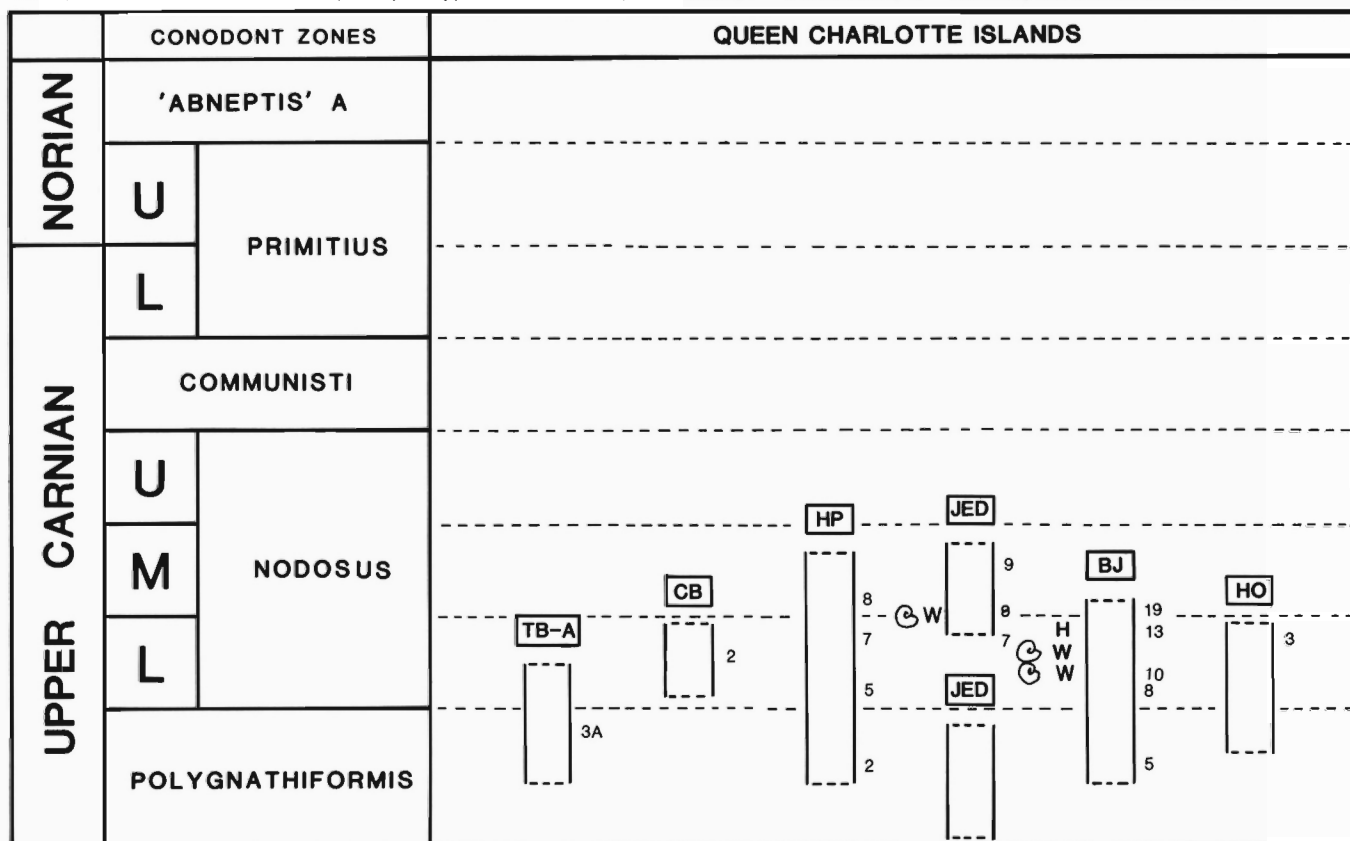


**Figure 6:** Time stratigraphic correlation of Kunga Group sections on Queen Charlotte Islands: Upper Carnian sections. See Figure 5 for explanation of abbreviations.

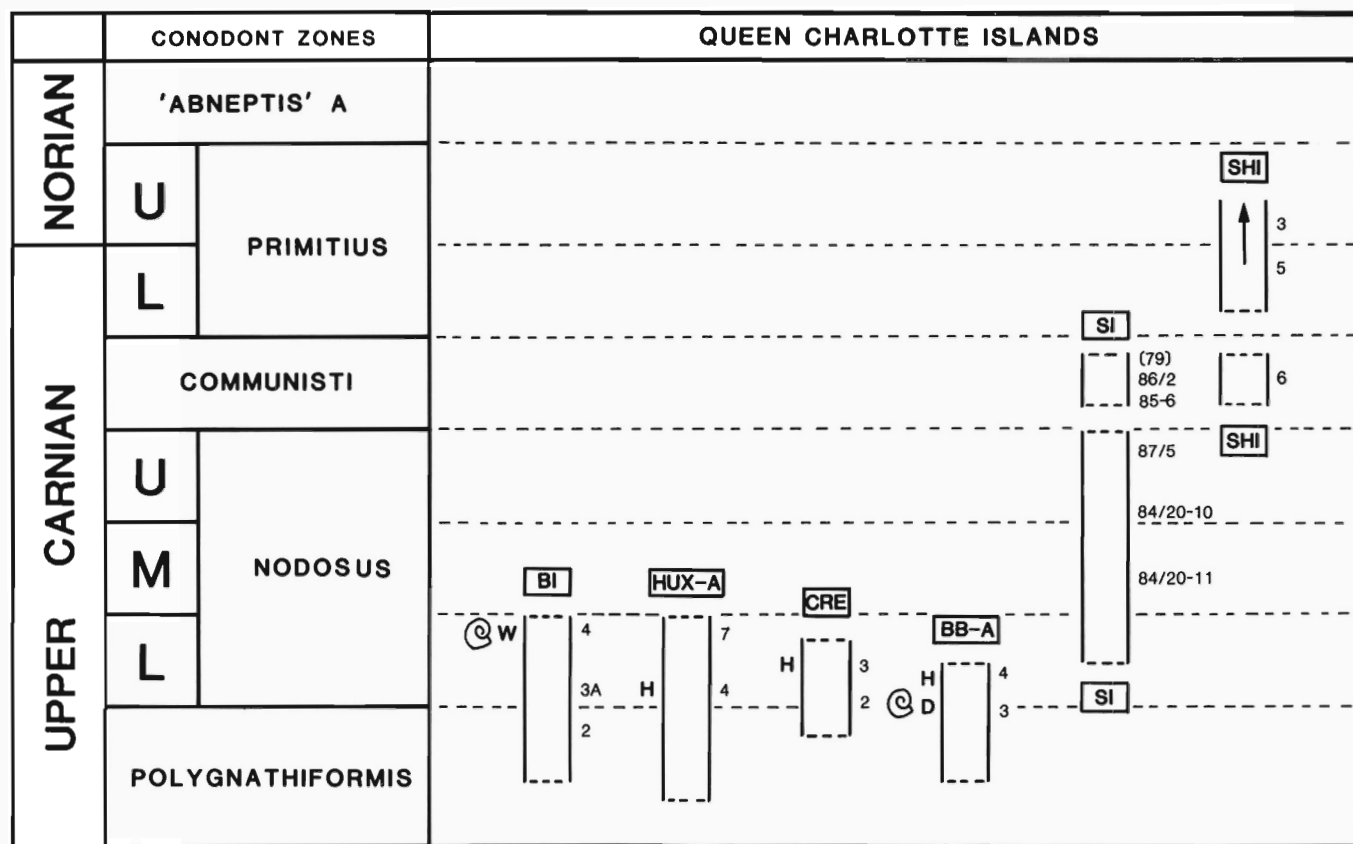


**Figure 7:** Time stratigraphic correlation of Kunga Group sections on Queen Charlotte Islands: Upper Carnian-Lower Norian sections. See Figure 5 for explanation of abbreviations.

## BIOSTRATIGRAPHIC CORRELATION OF KUNGA GROUP

Figures 5-12 show time-correlation of the Kunga Group sections based on conodont collections from samples indicated to the right of each column. The sections represent time duration only – lithological characteristics and vertical scale are omitted in this paper. By way of supporting data, correlation of some Upper Carnian sections in northeast B.C. utilizing the new zonation is also presented (Fig. 8). Sample occurrences of each of the conodont zones within the Kunga Group are also listed under the appropriate zone above. Most of the zones are widespread and can be confidently employed as a biochronological framework for Kunga Group correlation. Preliminary work suggests that many can also be recognized throughout western Canada, and perhaps beyond.

For the QCI, the results show that both the Karmutsen Volcanics and the Sadler Limestone were deposited within a single faunal unit, the *polygnathiformis* Zone, and no great time separation is evident. Rare carbonates interbedded with the volcanics attest to contemporaneous volcanism and carbonate deposition in QCI, but to what extent the Sadler Limestone and Karmutsen Volcanics are co-eval is not known. It has not been possible to recognize structural repetition in the commonly faulted Sadler Limestone on the basis of conodont fauna, so absolute thicknesses for the unit remain speculative: 42 m at Sadler Point is a minimum, whereas at Kunghit Island west (KT-A) and on Huston Inlet west (HU) about 150 m was measured (Desrochers and Orchard, 1991).

The Peril Formation is now known to embrace the whole of the Lower and Middle Norian, as well as most of the Upper Carnian, and

the lowest part of the Upper Norian. Structural repetition is not always obvious, but can often be demonstrated on the basis of conodont fauna. This constitutes one valuable application of the conodont study for it has allowed a reasonable estimate of the total thickness of the formation to be made. These figures are best developed from variously summing sections on Kunghit Island west (KT-A), Burnaby Island (BI), Huxley Island (HUX-C), Frederick Island (FI-FR), and Kennecott Point (KP-M). Some small intervals of time that cannot be demonstrated on these long sections (e.g. Carnian-Norian boundary beds as on Huxley Island (HUX-B)) apparently do not represent very much strata. The total thickness for the Peril Formation is determined at about 350 m.

The thickness of strata represented by an individual conodont zone varies considerably and some are very thin. Nevertheless, I believe that close-spaced sampling within the lower nodule member of the Peril Formation (Desrochers and Orchard, 1991) has yielded a relatively complete conodont record for the Upper Carnian and Carnian-Norian boundary beds. The higher strata of the middle grainstone member is less productive and it is not possible to demonstrate the presence of all zones in all sections that span the Lower to Middle Norian. Intraformational conglomerates are developed within the late Lower Norian (Swan Bay, SB-1) and/or early Middle Norian (Burnaby Island, BI-15). It is possible that these mark a sedimentary break close to the Lower-Middle Norian boundary because typical *multidentata* Zone conodonts, as found in northeast B.C., have not been recovered. However, this absence might reflect biogeographic differences between the two regions.

Further minor stratigraphic breaks may also be developed locally in post-Peril Formation strata. For example, on Kunga Island a dis-

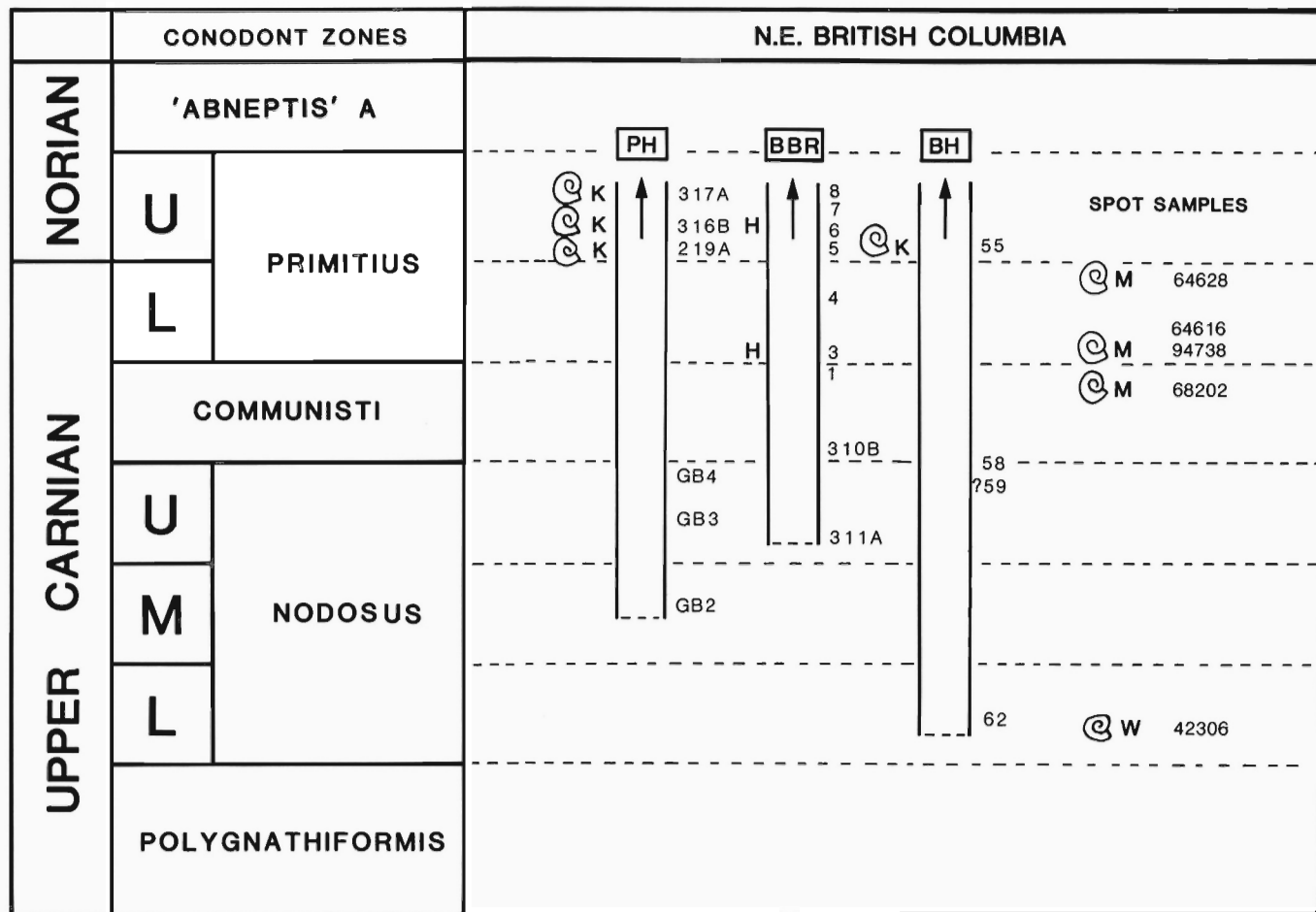


**Figure 8:** Time stratigraphic correlation of sections of the Baldonnel and Pardonnet formations in northeast B.C.: Upper Carnian-Lower Norian sections. PH = Pardonnet Hill, BBR = Black Bear Ridge, BH = Brown Hill. GSC locality numbers are given for spot samples. See Figure 5 for explanation of other abbreviations.

continuity occurs in the lower part of the Sandilands Formation, and in the Skidegate Channel area there are coarse clastic beds within the same formation that include reworked monotids from the Peril Formation (SI-11A, SKID-5). However, faunal continuity at Kennecott Point suggests there is no significant break in that section.

## SUMMARY

On the basis of nine conodont species of *Metapolygnathus* (four of them new, five redefined), six Upper Carnian conodont zones are introduced for the Kunga Group and correlative strata in northeast British Columbia. These are, in ascending order, the *polygnathiformis*, Lower, Middle, and Upper *nodosus*, *communisti*, and Lower *primitius* zones.

The conservative *polygnathiformis* stock is present in the Karmutsen Volcanics and in the Sadler Limestone, where it is associated with Dilleri Zone ammonoids. The development of *M. nodosus* began close to the boundary between the Sadler and Peril formations, near the upper limit of the Dilleri Zone. Further calibration of the conodont and ammonoid zones is summarized in Figures 2 and 3.

Four (three new) Upper Carnian conodont species, which form the basis for subdivision of the *nodosus* Zone, are related in a phylogenetic lineage that results in forms homeomorphic with Norian *Epigondolella*.

Radiation of the conservative *nodosus* stock in the Macrolobatus Zone led first to the development of the index for the *communisti* Zone and later to that for the *primitius* Zone. Metamorphosis of ad-

vanced *communisti* morphotypes is thought to have given rise to '*Neogondolella*' *navicula*, the index for the base of the Norian (Upper *primitius* Zone).

*Epigondolella* developed from *Metapolygnathus primitius* within the Lower Norian, and thereafter provided most of the zonal indices for the remainder of the Triassic. Nomenclatural changes will be necessary as a result of the proposed taxonomic isolation of *E. abneptis*.

Six of the eight Norian conodont zones recognized in the Norian Pardonnet Formation (Orchard, 1983) are recognized in the Kunga Group. The equivalent of a seventh, the Middle Norian *multidentata* Zone, is probably present, but it differs in some important respects. Compositional differences between several of the zones are possibly due to paleoenvironmental and/or paleogeographic differences.

Several conodont taxa appear to have differing ranges, and some appear earlier in respect to the ammonoid chronology compared with Eurasian records. To some extent, these differences are attributed to differing species concepts, but they may also result from differing provinciality, or from the vagaries of the condensed and reworked Hallstatt Limestone facies.

The Karmutsen Volcanics and Sadler Limestone (42-200 m) were deposited within a single Carnian conodont zone. The Peril Formation ranges in age from low in the Upper Carnian through lower Upper Norian, and is about 350 m thick. There may be minor local stratigraphic breaks within the middle part of the Peril Formation, and in the lower part of the overlying Sandilands Formation.

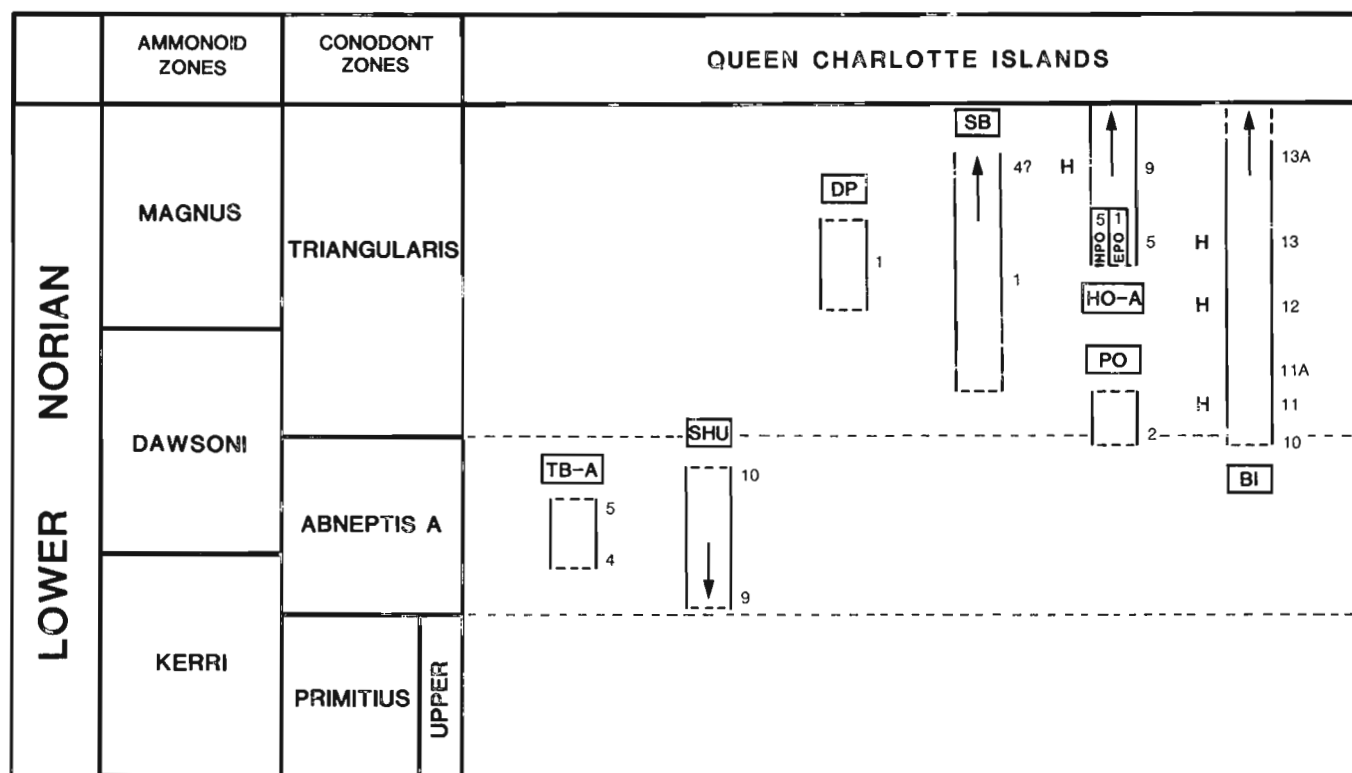


**Figure 9:** Time stratigraphic correlation of Kunga Group sections on Queen Charlotte Islands: Lower Norian sections. See Figure 5 for explanation of abbreviations.

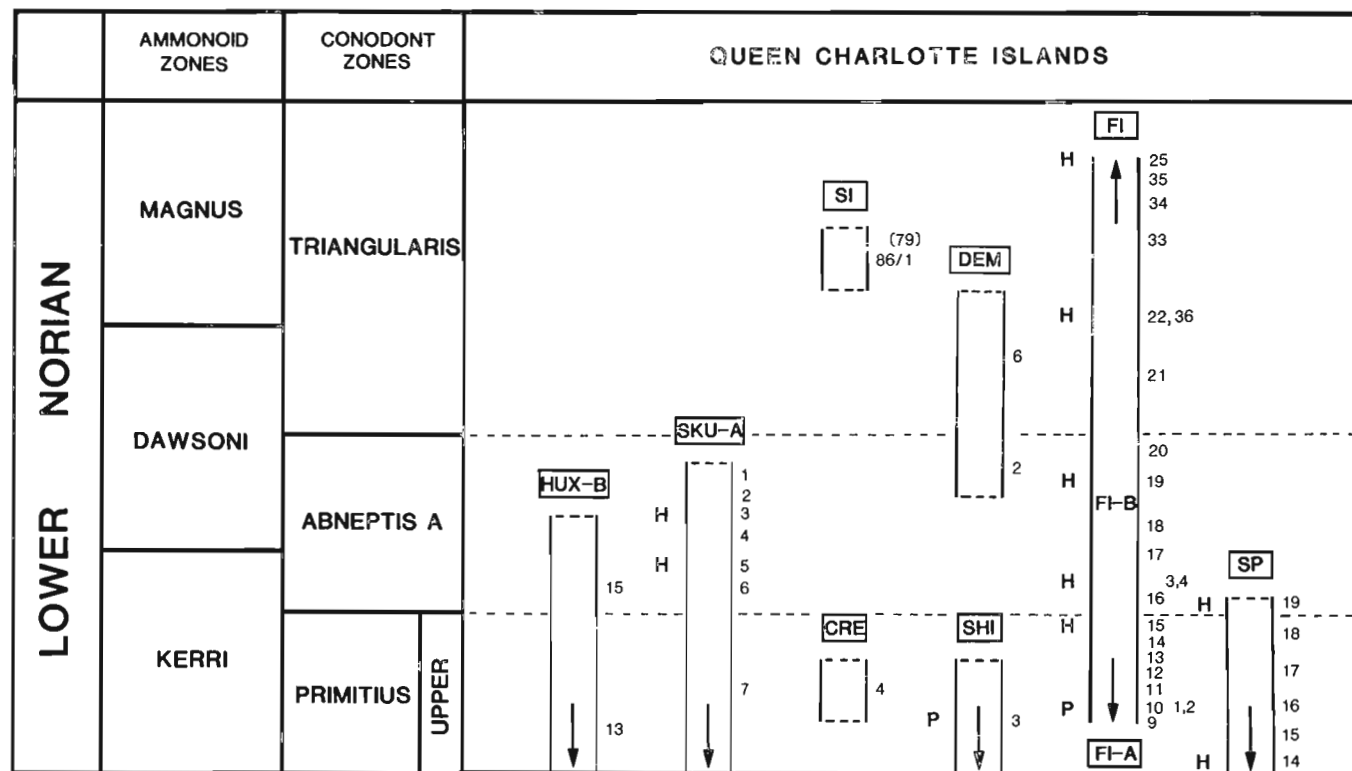


**Figure 10:** Time stratigraphic correlation of Kunga Group sections on Queen Charlotte Islands: Lower Norian sections. See Figure 5 for explanation of abbreviations.

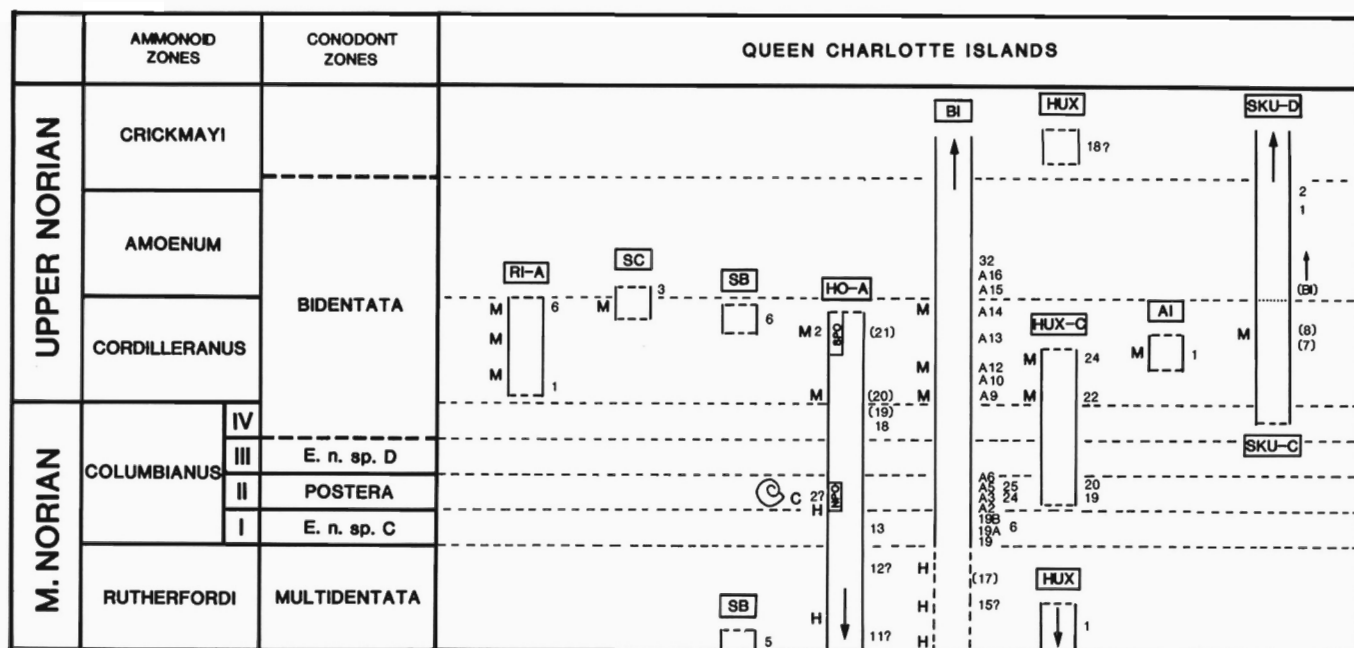


Figure 11: Time stratigraphic correlation of Kunga Group sections on Queen Charlotte Islands: Middle-Upper Norian sections. See Figure 5 for explanation of abbreviations.

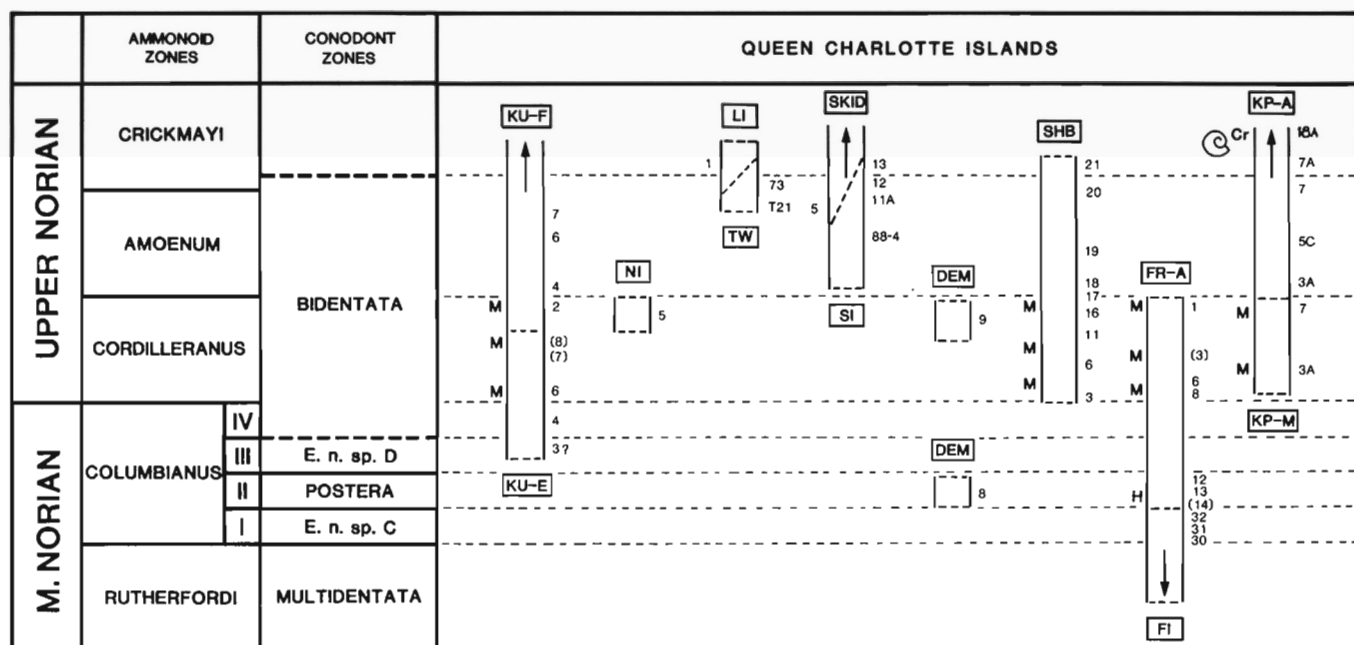


Figure 12: Time stratigraphic correlation of Kunga Group sections on Queen Charlotte Islands: Middle-Upper Norian sections. See Figure 5 for explanation of abbreviations.

## ACKNOWLEDGMENTS

Special thanks are due to E.T. Tozer who provided essential macrofossil calibration during all stages of both this work and earlier work on which much of it hinges. I thank the folk of the former Beban logging camp on Lyell Island who showed us great hospitality during the summer of 1986. The crew of the vessel "Beatrice", skipper Doug Hartley assisted by Paddy Herman, are thanked for skillfully ploughing the seas off South Moresby during June 1987. In June 1988, the "Mayor of Kennecott Point", Howard Tipper provided shelter whilst

expediter Ella Ferland provided support from Sandspit. During these years, the following people helped make collections in the field: P. Benham, E.S. Carter, A. Desrochers, A. McCracken, P. Forster, and E.T. Tozer. In addition, further samples were collected independently by B.E.B. Cameron, P.D. Lewis, R.I. Thompson, D.J. Thorkelson, and G.J. Woodsworth. Laboratory help was provided by P. Krauss, P. Forster, K. Lesack, H. Bourgeois, and K. McKay. P. Krauss is thanked for the photography. C. Davies and S. Irwin for the drafting. Finally, thanks to L. Krystyn for commenting on the manuscript.



## REFERENCES

**Budurov, K.**

- 1972: *Ancyrogondolella triangularis* genus and new species (Conodonten); Mitteilungen Gesellschaft Geologisch Bergbaustud., v. 21, p. 853-860.

**Budurov, K. and Stefanov, S.**

- 1965: Gattung *Gondolella* aus der Trias Bulgariens; Academie Bulgarian Sciences, Travaux Geologiques de Bulgare, serie Paleontologie, v. 7, p. 115-127.

**Carter, E.S., Orchard, M.J., and Tozer, E.T.**

- 1989: Integrated ammonoid-conodont-radiolarian biostratigraphy. Late Triassic Kunga Group, Queen Charlotte Islands, British Columbia; in Current Research, Part H, Geological Survey of Canada, Paper 89-1H, p. 23-30.

**Desrochers, A. and Orchard, M.J.**

- 1991: Stratigraphic revisions and carbonate sedimentology of the Kunga Group (Upper Triassic-Lower Jurassic), Queen Charlotte Islands, British Columbia; in Evolution and Hydrocarbon Potential of the Queen Charlotte Basin, British Columbia, Geological Survey of Canada, Paper 90-10.

**Golebiowski, R.**

- 1986: Neue Misikellen-Funde (Conodonta) und ihre Bedeutung für die Abgrenzung des Rhäts. str in den Kössener Schichten, Sitzungsberichten der Österr. Akademie der Wissenschaften in Wien, Mathematisch- Naturwissenschaftliche Klasse, 196/1-4, p. 21-33.

**Hayashi, S.**

- 1968: The Permian conodonts in chert of the Adoyama Formation, Ashio Mountains, central Japan; Earth Science, v. 22, no. 2, p. 63-77.

**Huckriede, R.**

- 1958: Die Conodonten der mediterranen Trias und ihr stratigraphischer Wert; Paläontologische Zeitschrift, v. 32, p. 141-151.

**Kovacs, S.**

- 1983: On the evolution of the *excelsa*-stock in the Upper Ladinian-Carnian (Conodonta, genus *Gondolella*, Triassic); in Schriftenreihe der Erdwissenschaftlichen Kommissionen, H. Zapfe (ed.), v. 5, p. 107-120.

**Kovacs, S. and Kozur, H.**

- 1980: Stratigraphische Reichweite der wichtigsten Conodonten (ohne Zahnreihen-conodonten) der Mittel- und Obertrias; Geologisch Paläontologische Mitteilungen Innsbruck, v. 10, p. 47-78.

**Kozur, H.**

- 1972: Die Conodontengattung *Metapolygnathus* Hayashi, 1968 und ihr stratigraphischer Wert; Geologisch Paläontologische Mitteilungen Innsbruck, v. 2, no. 11, p. 1-37.  
1980: Revision der Conodontenzonierung der Mittel- und Obertrias des tethyalen Faunenreichs; Geologisch Paläontologische Mitteilungen Innsbruck, v. 10, p. 79-172.

**Kozur, H. and Mostler, H.**

- 1971: Probleme der Conodontenforschung in der Trias; Geologisch Paläontologische Mitteilungen Innsbruck, v. 1, no. 4, p. 1-19.

**Krystyn, L.**

- 1973: Zur Ammoniten- und Conodonten-Stratigraphie der Hallstätter Obertrias (Salzkammergut, Österreich); Geologisches Bundesanstalt Verhandlungen, Austria, p. 113-153.

- 1980: Triassic conodont localities of the Salzkammergut region (northern Calcareous Alps); in Second European Conodont Symposium, Guidebook and Abstracts, H.P. Schonlaub (ed.), Abhandlungen des Geologischen Bundesanstalt, Austria, p. 61-98.

- 1983: The Epidaurus Section (Greece) – a contribution to the conodont standard zonation of the Ladinian and Lower Carnian of the Tethys Realm (English translation); Schriftenreihe der Erdwissenschaftlichen Kommissionen, v. 5, p. 231-258.

- 1988: Zur RHAT-Stratigraphie in den Zlambach-Schichten (vorläufiger Bericht); Sitzungsberichten der Österr. Akademie der Wissenschaften in Wien, Mathematisch-Naturwissenschaftliche Klasse, 196/1-4, p. 21-33.

**Meek, R.H.**

- 1987: A new Late Triassic (Norian) conodont species; Journal of Paleontology, v. 61, no. 1, p. 196-197.

**Mosher, L.C.**

- 1968: Triassic conodonts from western North America and Europe and their correlation; Journal of Paleontology, v. 42, no. 4, p. 895-946.  
1970: New conodont species as Triassic guide fossils; Journal of Paleontology, v. 44, no. 4, p. 737-742.  
1973: Triassic conodonts from British Columbia and the northern Arctic Islands; Geological Society of Canada, Bulletin 222, p. 141-193.

**Orchard, M.J.**

- 1983: *Epigondolella* populations and their phylogeny and zonation in the Upper Triassic; Fossils and Strata, no. 15, Oslo, p. 177-192.

**Orchard, M.J. and Forster, P.J.L.**

- 1991: Conodont colour and thermal maturity of the Late Triassic Kunga Group, Queen Charlotte Islands, British Columbia; in Evolution and Hydrocarbon Potential of the Queen Charlotte Basin, British Columbia, Geological Survey of Canada, Paper 90-10.

**Orchard, M.J., Carter, E.S., Tozer, E.T. (paleontological data); Forster, P.J.L., Lesack, K., McKay, K. (compilers); Weston, M., Woodsworth, G.J., Orchard, M.J., Johns, M. (database design)**

- 1990: Electronic database of Kunga Group biostratigraphic data; Geological Survey of Canada, Open File.

**Robinson, B.E. and Carr, T.R.**

- 1985: Upper Triassic (Karnian-Norian) conodonts from the Glenn Shale, east-central Alaska; Geological Society of America, Abstracts with Programs, v. 17, no. 2, p. 132.

**Sutherland-Brown, A.**

- 1968: Geology of the Queen Charlotte Islands, British Columbia; British Columbia Department of Mines and Petroleum Resources, Bulletin 54, 226 p.

**Sweet, W.C., Mosher, L.C., Clark, D.L., Collinson, J.W., and Hansenmueller, W.A.**

- 1971: Conodont biostratigraphy of the Triassic; in Conodont Biostratigraphy, W.C. Sweet and S.M. Bergstrom (ed.), Geological Society of America, Memoir 127, 499 p.

## Plate 1

All specimens from Peril Formation, Kunga Group. x80, unless stated otherwise. Numbers shown in parentheses are field numbers.

**Figures 1-6:** *Metapolygnathus* n. sp. E Orchard. 1,2,6. GSC 95193 – 5, from GSC loc. no. 0-42306 (un-named unit, Alaska Highway, hill south of Mile Post 427). 3,5. GSC 95196, -7, from GSC loc. no. C-157374 (KT-A19A). 4. GSC 95198, from GSC loc. no. C-157373 (KT-A19); specimen is transitional to *M.* n. sp. F.

**Figures 7-11:** *Metapolygnathus* n. sp. F Orchard. 7-10. GSC 95199 – 202, from GSC loc. no. C-157379 (KT-A24); figs. 9,10, x90. 11. GSC 95203, from GSC loc. no. C-157037 (SHU-2).

**Figures 12-18:** *Metapolygnathus* n. sp. G Orchard. 12,18. GSC 95204, -5, from GSC loc. no. C-157042 (SHU-7); 18 is transitional from *M.* n. sp. F. 13,17. GSC 95206, -7, from GSC loc. no. 0-23419 (Lewes River Group, Yukon Territory). 14. GSC 95208, from GSC loc. no. C-157379 (KT-A24). 15. GSC 81244, from GSC loc. no. C-157037 (SHU-2). 16. GSC 95209, from GSC loc. no. C-87955 (BBR-310B, Baldonnel Formation, Black Bear Ridge, Peace River).

**Figures 19, 21-26:** *Metapolygnathus echinatus* (Hayashi). 19,21, 23-26. GSC 95210 – 15, from GSC loc. no. C-87955 (BBR-310B, Baldonnel Formation, Black Bear Ridge, Peace River). 22. GSC 95216, from GSC loc. no. C-150169 (86SKU-A10).

**Figure 20:** *Epigondolella abneptis* subsp. A Orchard. GSC 95217, from GSC loc. no. C-879090 (BH-48, Pardonnet Formation, Brown Hill, Peace River).

## Plate 2

All specimens from Peril Formation, Kunga Group. x80, unless stated otherwise. Numbers shown in parentheses are field numbers.

**Figures 1-7:** *Metapolygnathus primitus* (Mosher). 1,4-7. GSC 95218 – 22, from GSC loc. no. O-64628 (Pardonnet Formation, head of Western Gully on Pardonnet Hill, Peace River). 2,3. GSC 95223, -4, from GSC loc. no. C-150167 (86SKU-A8); Fig. 2 x100.

**Figures 8-13:** *Metapolygnathus nodosus* (Hayashi). 8. GSC 95225, from GSC loc. no. C-157378 (KT-A23). 9. GSC 81242, from GSC loc. no. C-157381 (KT-A26). 10. GSC 95226, from GSC loc. no. C-157383 (KT-A27). 11,13. GSC 95227, -28, from GSC loc. no. C-87903 (BH-59, Baldonnel Formation, Brown Hill, Peace River). 12. GSC 95229, from GSC loc. no. C-87955 (BBR-310B, Baldonnel Formation, Black Bear Ridge, Peace River).

**Figures 14-24:** *Metapolygnathus communisti* Hayashi. 14,15,21,24. GSC 95230 – 33, from O-64628 (Pardonnet Formation, head of Western Gully on Pardonnet Hill, Peace River); Figs. 21,24 x100. 16,17. Two views of GSC 95234, from O-94738 (Ludington Formation, Mount Laurier). 18,19. Two views of GSC 81245, from GSC loc. no. C-157275 (87SKU-A10). 20. GSC 95235, from GSC loc. no. C-87955 (BBR-310B, Baldonnel Formation, Black Bear Ridge, Peace River). 22,23. GSC 95236, -37, x90, from GSC loc. no. C-157121 (HUX-B9). Figures 21-24 are extreme morphotypes with vestigial or completely reduced platform. Compare profiles of Figures 21 and 27.

**Figures 25-27:** *'Neogondolella' navicula* (Huckriede). 25,27. GSC 95238, -39, from GSC loc. no. C-87941 (PH-316B, Pardonnet Formation, Pardonnet Hill, Peace River). 26. GSC 95240, from GSC loc. no. C-87910 (BH-47/48, Pardonnet Formation, Brown Hill, Peace River).

## Plate 3

Lateral views of specimens from Peril Formation of the Kunga Group (A-F), and from the Pardonnet Formation (G-I), x160. Numbers shown in parentheses are field numbers. Denticle profile outlined in black ink. Arrows show proposed phyletic relationships. Bar scale is about 200 microns long.

**Figure A:** *Metapolygnathus nodosus* (Hayashi). GSC 81242, from GSC loc. no. C-157381 (KT-A26); also illustrated on Plate 2, Fig. 9.

**Figure B:** *Metapolygnathus* n. sp. F Orchard. GSC 95203, from GSC loc. no. C-157037 (SHU-2); also illustrated on Plate 1, Fig. 11.

**Figure C:** *Metapolygnathus* n. sp. G Orchard. GSC 95205, from GSC loc. no. C-157042 (SHU-7); also illustrated on Plate 1, Fig. 18. Specimen is transitional from *M.* n. sp. F.

**Figure D:** *Metapolygnathus* n. sp. G Orchard. GSC 81244, from GSC loc. no. C-157037 (SHU-2); also illustrated on Plate 1, Fig. 15.

**Figure E:** *Metapolygnathus echinatus* (Hayashi). GSC 95216, from C-150169 (86SKU-A10); also illustrated on Plate 1, Fig. 22.

**Figure F:** *Metapolygnathus primitus* (Mosher). GSC 95241, from GSC loc. no. C-87941 (PH-316B, Pardonnet Formation, Pardonnet Hill, Peace River).

**Figure G:** *Epigondolella abneptis* subsp. A Orchard. GSC 95242, from GSC loc. no. C-87909 (BH-48, Pardonnet Formation, Brown Hill, Peace River).

**Figure H:** *Epigondolella triangularis* (Budorov). GSC 95243, from GSC loc. no. C-87981 (MS82-1, Pardonnet Formation, McLay Spur, Peace River).

**Figure I:** *Epigondolella* n. sp. C Orchard. GSC 95244, from GSC loc. no. C-87988 (MS82-8, Pardonnet Formation, McLay Spur, Peace River).

## Plate 4

Figure 1 from the Kamutsen Volcanics, 2-4 from the Sadler Limestone, 17,19 from the Pardonnet Formation, and the remainder from the Peril Formation. Numbers shown in parentheses are field numbers. All specimens x80, unless stated otherwise.

**Figures 1,3,4:** *Metapolygnathus* ex gr. *polygnathiformis* (Budorov and Stefanov). 1. GSC 95245, from GSC loc. no. C-157413 (WV-52). 3,4. GSC 95246, -7, from GSC loc. no. C-157361 (KT-A7).

**Figure 2:** *Cornudina?* n. sp. A. GSC 81241, x100, from GSC loc. no. C-157008 (HU-5).

**Figures 5,11:** *'Neogondolella' hallstattiensis* (Mosher). GSC 81246, 95249, x100, from GSC loc. no. C-157110 (EPO-1).

**Figures 6,7:** *Metapolygnathus* n. sp. K Orchard. GSC 95249, -50, x90, from respectively, GSC loc. no. C-157123 (HUX-B10A), and GSC loc. no. C-157122 (HUX-B10).

**Figures 8-10:** *Epigondolella abneptis* subsp. A Orchard. 8,10. GSC 95251, -2, from GSC loc. no. C-156547 (FI-B18). 9. GSC 95253, from GSC loc. no. C-150163 (SKU-A5).

**Figure 12:** *Epigondolella triangularis* (Budorov). GSC 81247, from GSC loc. no. C-157325 (BI-13).

**Figure 13:** *'Neogondolella' navicula* (Huckriede). GSC 95254, x70, from GSC loc. no. C-157126 (HUX-B13).

**Figure 14:** *'Neogondolella' steinbergensis* (Mosher). GSC 95255, from GSC loc. no. C-157133 (HUX-C19).

**Figures 15,16:** *Epigondolella* ex gr. *multidentata* Mosher. GSC 95256, -7, from GSC loc. no. C-157112 (HUX-1).

**Figure 17:** *Epigondolella multidentata* Mosher. GSC 95258, from GSC loc. no. C-87984 (MS82-4, Pardonnet Formation, McLay Spur, Peace River).

**Figure 18-20:** *Epigondolella* n. sp. C Orchard. 18,20. GSC 95259, -60, from GSC loc. no. C-157300 (BI-19A). 19. GSC 95261, from GSC loc. no. C-87988 (MS82-4, Pardonnet Formation, McLay Spur, Peace River).

**Figure 21:** *Epigondolella postera* (Kozur and Mostler). GSC 95262, from GSC loc. no. C-157133 (HUX-C19).

**Figure 22:** *Epigondolella* ex gr. *bidentata* Mosher. GSC 95263, from GSC loc. no. C-156793 (KPA-E).

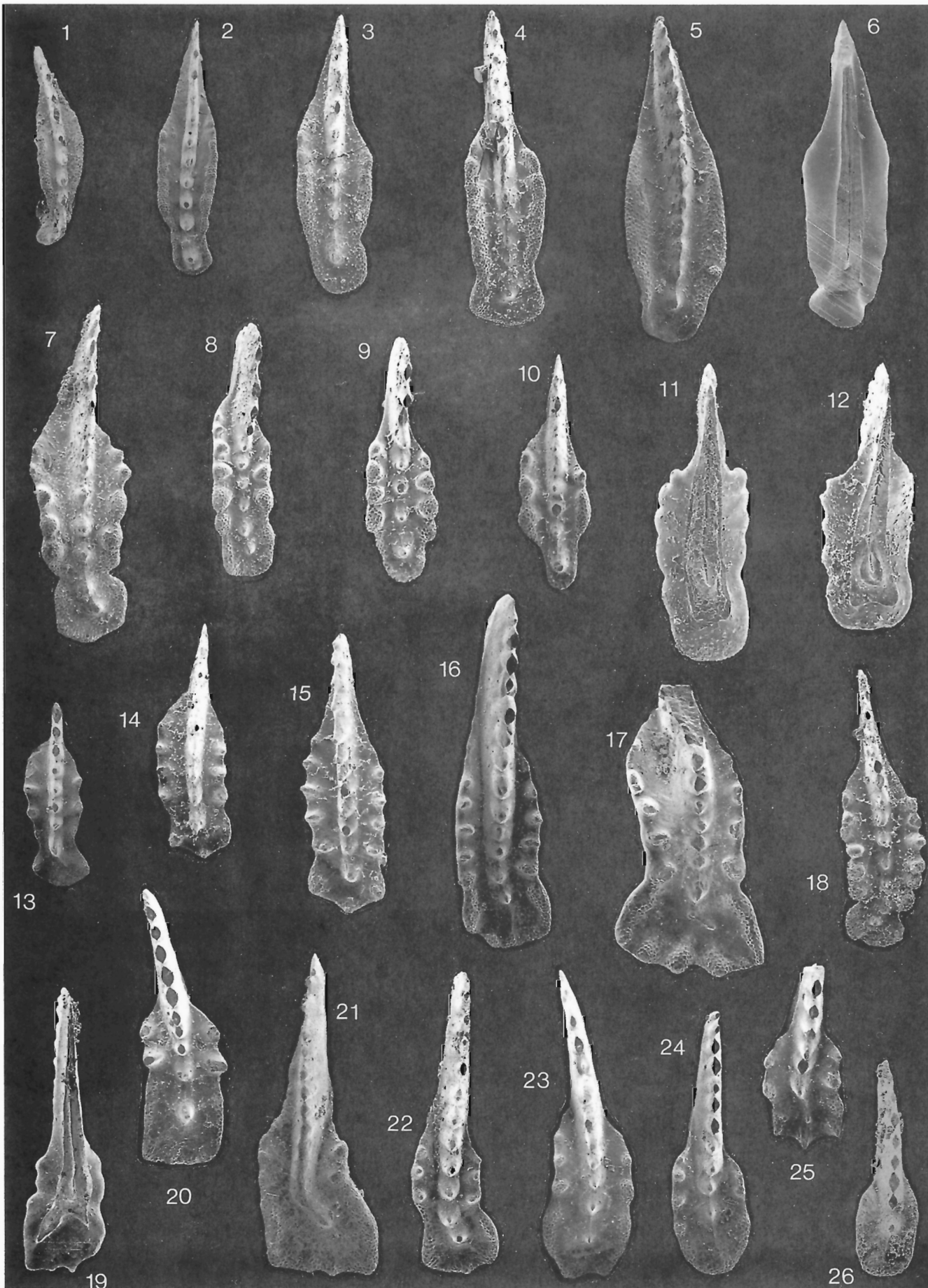


Plate 1

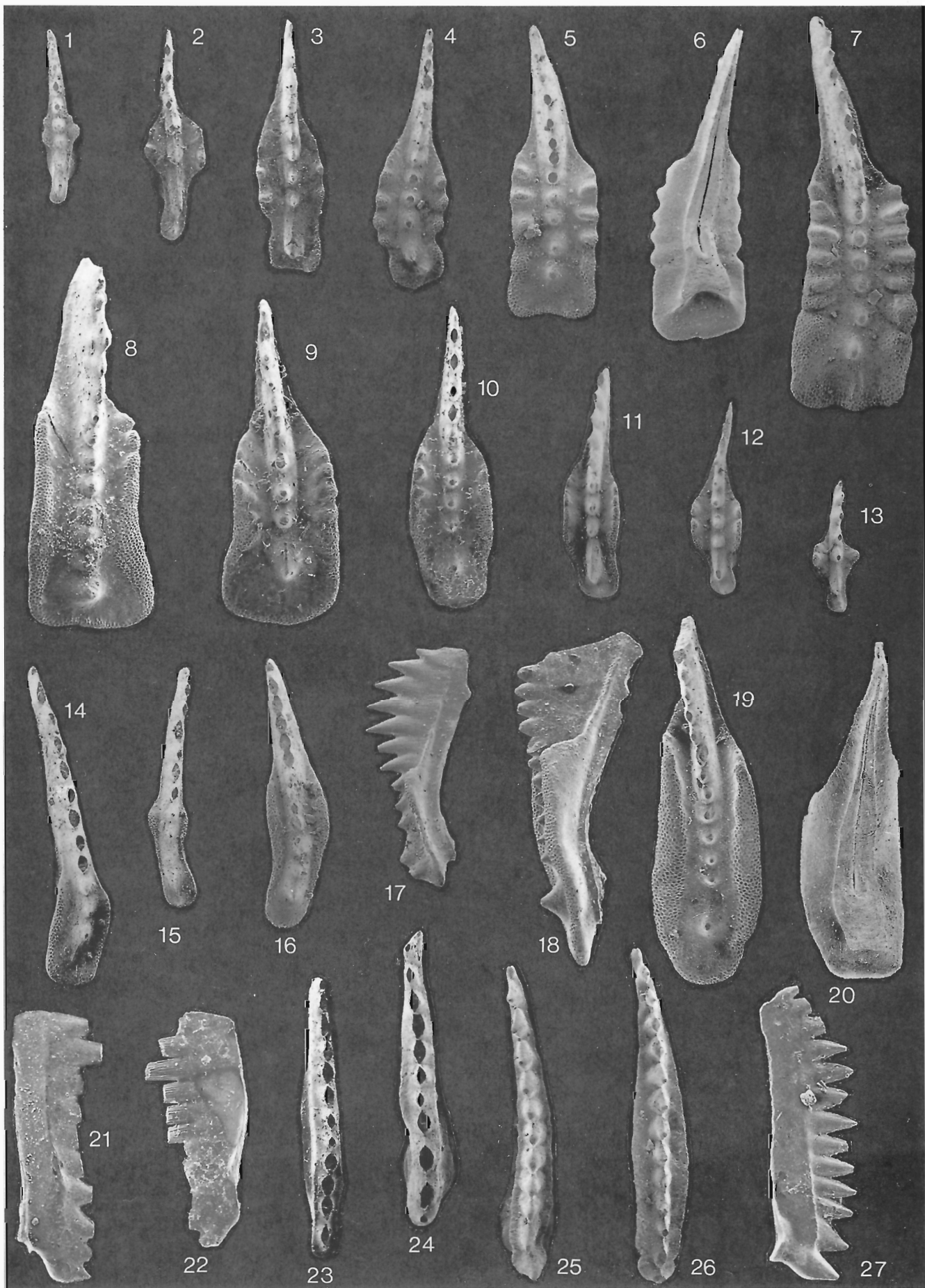


Plate 2



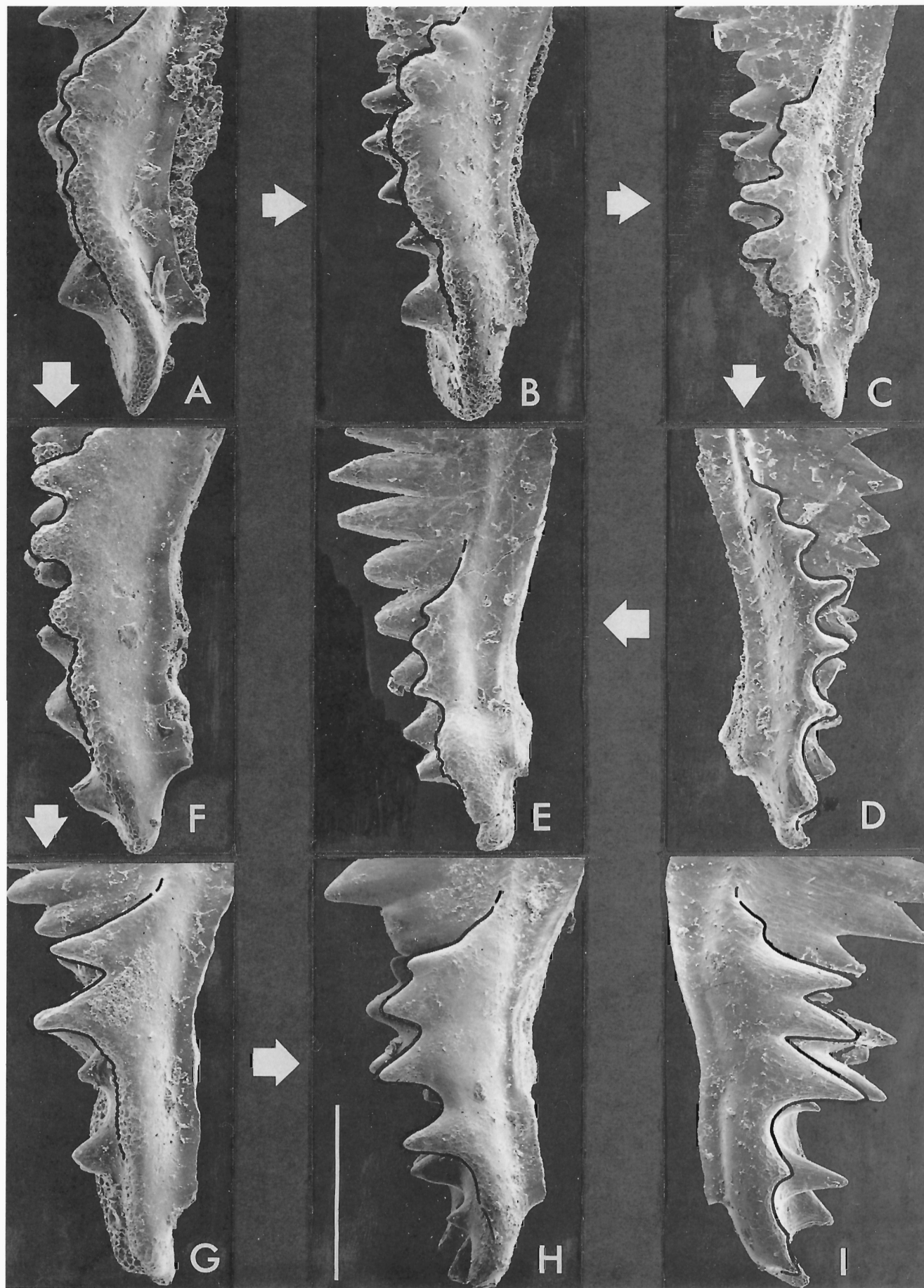


Plate 3

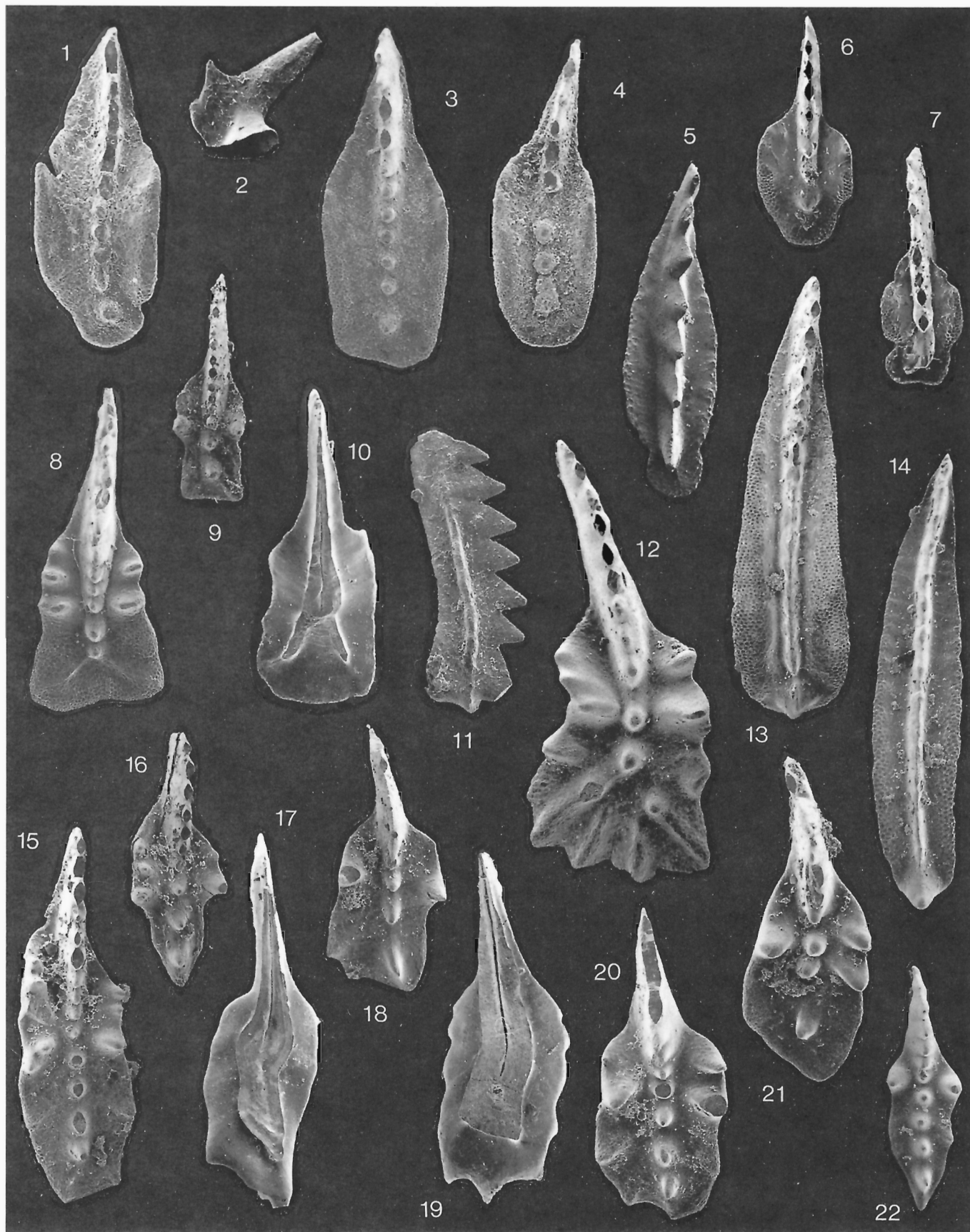


Plate 4





# Late Triassic radiolarian biostratigraphy of the Kunga Group, Queen Charlotte Islands, British Columbia

Elizabeth S. Carter<sup>1</sup>

Carter, E.S., Late Triassic radiolarian biostratigraphy of the Kunga Group, Queen Charlotte Islands, British Columbia; in *Evolution and Hydrocarbon Potential of the Queen Charlotte Basin, British Columbia*, Geological Survey of Canada, Paper 90-10, p. 195-201, 1991.

## Abstract

*Diverse, well preserved Upper Carnian and Norian radiolarians are present in the Peril and Sandilands formations of the Kunga Group, Queen Charlotte Islands. Ammonoids, bivalves, and conodonts are associated with most radiolarian assemblages. The oldest faunas are Late Carnian and occur with ammonoids from the Lower Welleri Zone. Capnodoce De Wever is rare in these assemblages but becomes more abundant and diverse in uppermost Carnian ones. Described radiolarian species from eastern Oregon, western Europe, and the Mediterranean area are present in all samples, but the majority of taxa (particularly Upper Carnian) are new.*

*Capnodoce fragilis Blome, Harsa siscwaiensis n. gen. n. sp., and Xiphosphaera fistulata n. sp. are abundant in upper Lower Norian to lower Middle Norian strata of the Queen Charlotte Islands. This three-fold radiolarian association is a useful marker for this interval of time; it has not been found in older or younger assemblages. Two new species and one new genus are described in this report.*

*Upper Norian radiolarians of the Betraccium deweveri Subzone are present in the Monotis beds of the uppermost Peril Formation. Three informal Upper Norian radiolarian assemblages have been proposed for post-Monotis strata of the overlying Sandilands Formation.*

## Résumé

*Les formations de Peril et de Sandilands du groupe de Kunga, dans les îles de la Reine-Charlotte renferment divers radiolaires bien conservés du Carnien et du Norien supérieurs. Des ammonotidés, des bivalves et des conodontes sont associés à la plupart des assemblages de radiolaires. Les faunes les plus anciennes sont du Carnien supérieur et se retrouvent avec des ammonotidés de la zone inférieure de Welleri. Capnodoce De Wever est rare dans ces assemblages, mais devient plus abondant et plus varié dans les assemblages supérieurs du Carnien. Des espèces décrites de radiolaires de l'est de l'Orégon, d'Europe occidentale et de la région méditerranéenne sont présentes dans tous les échantillons, mais la majorité des taxons (notamment du Carnien supérieur) sont nouveaux.*

*Capnodoce fragilis Blome, Harsa siscwaiensis n. gen. n. sp. et Xiphosphaera fistulata n. sp. abondent dans les couches supérieures du Norien inférieur et les couches inférieures du Norien moyen des îles de la Reine-Charlotte. Cette triple association de radiolaires est un repère utile pour cet intervalle de temps; on ne la retrouve pas dans les assemblages plus anciens ou plus jeunes. Deux nouvelles espèces et un nouveau genre sont décrits dans ce rapport.*

*Des radiolaires du Norien supérieur de la sous-zone de Betraccium deweveri sont présents dans les couches de Monotis de la formation sommitale de Peril. Trois assemblages informels de radiolaires du Norien supérieur ont été proposés pour les couches post-Monotis de la formation sus-jacente de Sandilands.*

---

<sup>1</sup> 58335 Timber Road, Vernonia, Oregon, 97064 U.S.A.

## INTRODUCTION

Progress continues in the study of Upper Triassic radiolarians from the Queen Charlotte Islands. Intensive biostratigraphic investigations of the Kunga Group by the Geological Survey of Canada began in 1987 (Orchard, 1988). Since then most outcrops of Upper Triassic Kunga Group have been visited and systematically sampled for conodonts, radiolarians, and microfossils. Unfortunately the rocks proved too hard for the recovery of calcareous microfauna (B.E.B. Cameron, pers. comm., 1989) but a variety of other microfaunas, including holothurians, ichthyoliths, and sponge spicules, have been found.

The Lower Mesozoic Kunga Group in the Queen Charlotte Islands consists of the Sadler Limestone (Desrochers and Orchard, 1991; equivalent to the grey limestone member of Sutherland Brown, 1968), the Peril Formation (Desrochers and Orchard, 1991; equivalent to the black limestone member of Sutherland Brown, 1968), and the Sandilands Formation. Kunga Group strata in general are strongly deformed; consequently, in many areas only short uninterrupted sections can be measured. Using biostratigraphic control provided by ammonoids, bivalves, conodonts, and radiolarians, these sections have been combined to give an almost complete succession of Upper Carnian and Norian strata.

Diverse, well preserved radiolarians have been recovered from micrite concretions and lenses in the Peril and Sandilands formations. The faunas contain Upper Triassic taxa described by Kozur and Mostler (1972, 1979, 1981), De Wever et al. (1979), Pessagno et al. (1979), and Blome (1983, 1984), among others. New genera and species have been recognized in both lower and uppermost Norian successions, but a greater number of new taxa are found in the thick Upper Carnian succession.

Over 1500 microfossil samples were collected during this study. Of these, over 230 collections of well preserved and well dated Upper Triassic radiolarians have been examined. Data pertaining to all collections is available in the Upper Triassic database for the Queen Charlotte Islands (Orchard et al., 1991).

This report summarizes initial Triassic radiolarian studies of Carter (1988, 1990; Carter et al., 1989) and furnishes some new information on taxa related to specific stratigraphic intervals. Two new species and one new genus are described.

## BIOSTRATIGRAPHY

### Upper Carnian

The Sadler Limestone is a massive, bioclastic unit recording the widespread development of a shallow subtidal platform (Desrochers, 1988). It contains Upper Carnian ammonoids (Dilleri Zone), conodonts, and locally common holothurians, but no radiolarians have been found.

The lower part of the overlying Peril Formation contains an excellent Upper Carnian radiolarian succession. This strata also contains ammonoids from the Welleri and Macrolobatus zones (mid- to upper Upper Carnian) and conodonts from the Lower, Middle, and Upper *nodosus* Zone, the *communisti* Zone, and the Lower *primitius* Zone (Fig. 1). Upper Carnian radiolarian faunas are characterized by diverse and abundant *Capnuchosphaera* De Wever, *Kahlerosphaera* Kozur and Mostler, and *Sarla* Pessagno; common *Poulpus* De Wever, *Xenorum* Blome, and *Xiphotheca* De Wever; and a vast number of undescribed saturniid and nassellarian taxa.

The oldest radiolarian faunas are associated with ammonoids from the Lower Welleri Zone and conodonts from the Lower *nodosus* Zone. These rich faunas contain a few Lower Carnian species from Austria described by Kozur and Mostler (1979, 1981) and other

species having affinities to Lower Carnian forms, but the majority of taxa are undescribed. Two undescribed species of *Capnodoce* De Wever have been observed, but specimens are generally rare.

Slightly younger faunas, associated with conodonts from the Middle and Upper *nodosus* Zone and *communisti* Zone, contain the same species of *Capnodoce* and rare specimens of *Justium novum* Blome. In other genera, however, there are considerable differences between the species in this fauna and their counterparts in the older fauna previously discussed. For example, long-spined forms of *Kahlerosphaera* Kozur and Mostler are dominant in the older fauna, whereas in the younger faunas some species have shorter spines with large bladed tips and are generally smaller. Several distinctive kahlerosphaerid species in the younger faunas were recognized previously in a suite of samples from Sandilands island (Carter, unpub. data). Originally these samples were thought to be from the Carnian-Norian boundary interval (Carter, 1988), but the associated conodonts are now known to be Upper Carnian from the Middle to Upper *nodosus* Zone and the *communisti* Zone (M.J. Orchard, pers. comm., 1989). This and other evidence suggest the possibility of a zonal break in the radiolarian succession during the mid- to lower upper Upper Carnian. The position of this break and how extensive it may be is not known. Other species present at this level include *Capnuchosphaera concava* De Wever, *C. colemani* Blome, *C. deweveri* Kozur and Mostler, *C. aff. puncta* De Wever, *C. theloides* De Wever, and *Paleosaturnalis latiamulatus* Kozur and Mostler.

Upper Carnian faunas that occur with conodonts from the Lower *primitius* Zone are characterized by increasingly diverse *Capnodoce* De Wever, common *Justium novum* Blome, and further differing species of *Kahlerosphaera* Kozur and Mostler and *Sarla* Pessagno. *Icrioma tetrancistrum* De Wever is first observed in the uppermost

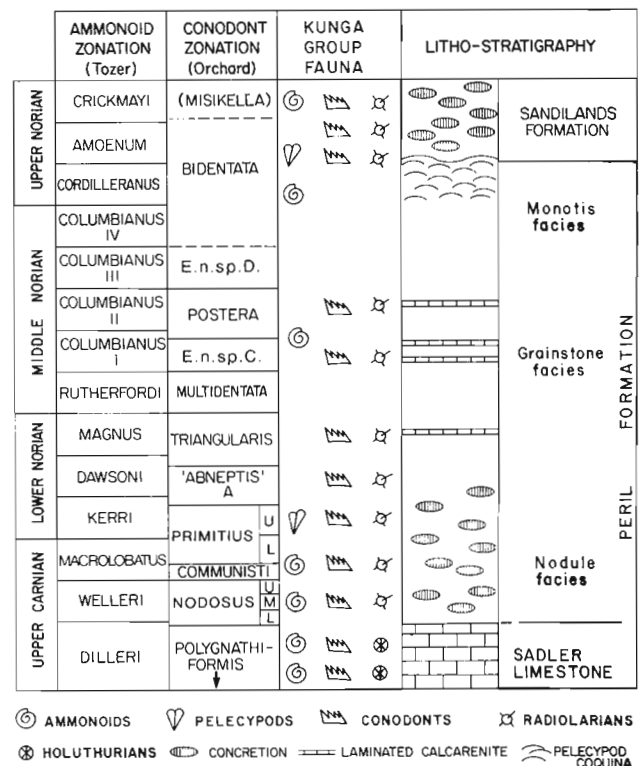


**Figure 1:** Triassic fauna from the Kunga Group. Position of recovered fossil collections shown against the ammonoid and conodont zonation of the Upper Triassic. Modified from Carter et al., 1989.

Carnian although rare specimens with affinity to this species have been found in older strata containing conodonts of the *communisti* Zone. Significant faunal change takes place within the Radiolaria in the Carnian-Norian transitional beds. This fauna must be studied much more carefully in order to understand the morphological development within key genera and the range of index species.

### Lower Norian

Well preserved, diverse radiolarian assemblages are known from Lower Norian strata dated by conodonts from the Upper *primitus* Zone, the *abneptis* A Zone, and the *triangularis* Zone. In these assemblages, *Capnuchosphaera* De Wever, *Kahlerosphaera* Kozur and Mostler, and *Sarla* Pessagno are common and *Capnodoce* De Wever becomes much more abundant and diverse. *Capnuchosphaera deweveri* Kozur and Mostler, *C. theloides* De Wever, *C. triassica* De Wever, *Icrioma tetrancistrum* De Wever, *Kahlerosphaera norica* Kozur and Mostler, *Paleosaturnalis mocki* Kozur and Mostler, *Pseudosaturniforma minuta* Blome, and *Syringocapsa batodes* De Wever have been observed at many levels throughout the Lower Norian.

Radiolarians found in association with lower Lower Norian conodonts of the Upper *primitus* Zone include *Capnuchosphaera colemani* Blome, *C. smithorum* Blome, *Catoma concinna* Blome, *Catoma geometrica* Blome, *Pseudosaturniforma carnica* Kozur and Mostler, *Spongostylus tortilis* Kozur and Mostler, *Syringocapsa turgida* Blome, *Xenorum largum* Blome, and *Xiphotheca karpenissionensis* De Wever.

In younger assemblages that are parallel but not equivalent to the *abneptis* A conodont zone, abundant radiolarian species include *Capnodoce* aff. *anapetes* De Wever, *C. crystallina* Pessagno, *C. insueta* Blome, *Icrioma traversa* Blome, *Latium longulum* Blome, *Triassocampe proprium* Blome, and *Vinassaspongius transitus* Kozur and Mostler.

In still younger assemblages associated with conodonts of the *triangularis* Zone, *Capnodoce fragilis* Blome, *Capnuchosphaera* aff. *theloides* De Wever, *Paleosaturnalis lupheri* (Blome), *P. macoyensis* (Blome), *P. rotundus* (Blome), *P. silverensis* (Blome), *P. vibrassii* (Blome), *Renzium adversum* Blome, *Spongostylus trispinosus* Kozur and Mostler, *Quasipetatus disertus* Blome, *Q. insolitus* Blome, *Veghha sulovensis* Kozur and Mostler, and a new genus, herein named *Harsa*, are common.

*Capnodoce fragilis* Blome ranges through Lower and Middle Norian strata that contains conodonts from the *abneptis* A, *triangularis*, and n. sp. C zones (conodonts from the *multidentata* Zone have not been found in the Queen Charlotte Islands). From data presently available, the peak abundance of *Capnodoce fragilis* Blome occurs in upper Lower Norian strata that contains conodonts from the *triangularis* Zone. *Capnodoce fragilis* Blome is distinctive and relatively easy to identify even when poorly preserved. It appears to be a significant marker for the upper Lower Norian. *Harsa siscwaiensis* n. gen. n. sp. and *Xiphosphaera fistulata* n. sp. are also important indicators for this interval in the Queen Charlotte Islands. This informal association of radiolarians, (figured on Plate 1) is subsequently referred to in this report as the "*Capnodoce fragilis* – *Harsa siscwaiensis* – *Xiphosphaera fistulata*" association.

### Middle Norian

Middle Norian radiolarians from the Kunga Group were reported as "rare and not well preserved" in Carter et al. (1989). Since then new collections from Frederick Island have yielded better preserved faunas that are associated with conodonts from the *Epigondolella* n. sp. C Zone (Fig. 1). The "*Capnodoce fragilis* – *Harsa siscwaiensis* – *Xiphosphaera fistulata*" association is moderately abundant in this

strata but has not been found higher in the sequence. This absence may be due to preservation but, as all component species are quite sturdy and generally can be recognized even if poorly preserved, it is possible these forms may be very rare or absent by mid-Middle Norian time.

Radiolarians equivalent in age to the *postera* conodont zone are rare in the Queen Charlotte Islands presumably because grainstone beds, rather than micrite concretions, are the prevailing form of limestone in the Middle Norian part of the Peril Formation. *Pentactinocarpus sevaticus* Kozur and Mostler is present in these assemblages along with species of *Capnuchosphaera* De Wever and *Sarla* Pessagno that have affinities to the species described from upper Middle Norian strata of Baja California Sur by Pessagno, in Pessagno et al. (1979). Rare specimens of *Livarella* Kozur and Mostler, *Mesosaturnalis* Kozur and Mostler, *Natraglia* Pessagno, and gen. nov. E (Carter, 1990) are first recorded at this level. Species of *Paratriassoastrum* Kozur and Mostler, *Pseudoheliodiscus* Kozur and Mostler, *Tetraporobrachia* Kozur and Mostler, *Veghicyclia* Kozur and Mostler, and other saturnalid taxa constitute an important part of this Middle Norian fauna.

A well preserved, convincing example of the upper Middle Norian radiolarian fauna from Baja California Sur described by Pessagno et al. (1979) has not been found in the Queen Charlotte Islands.

### Upper Norian

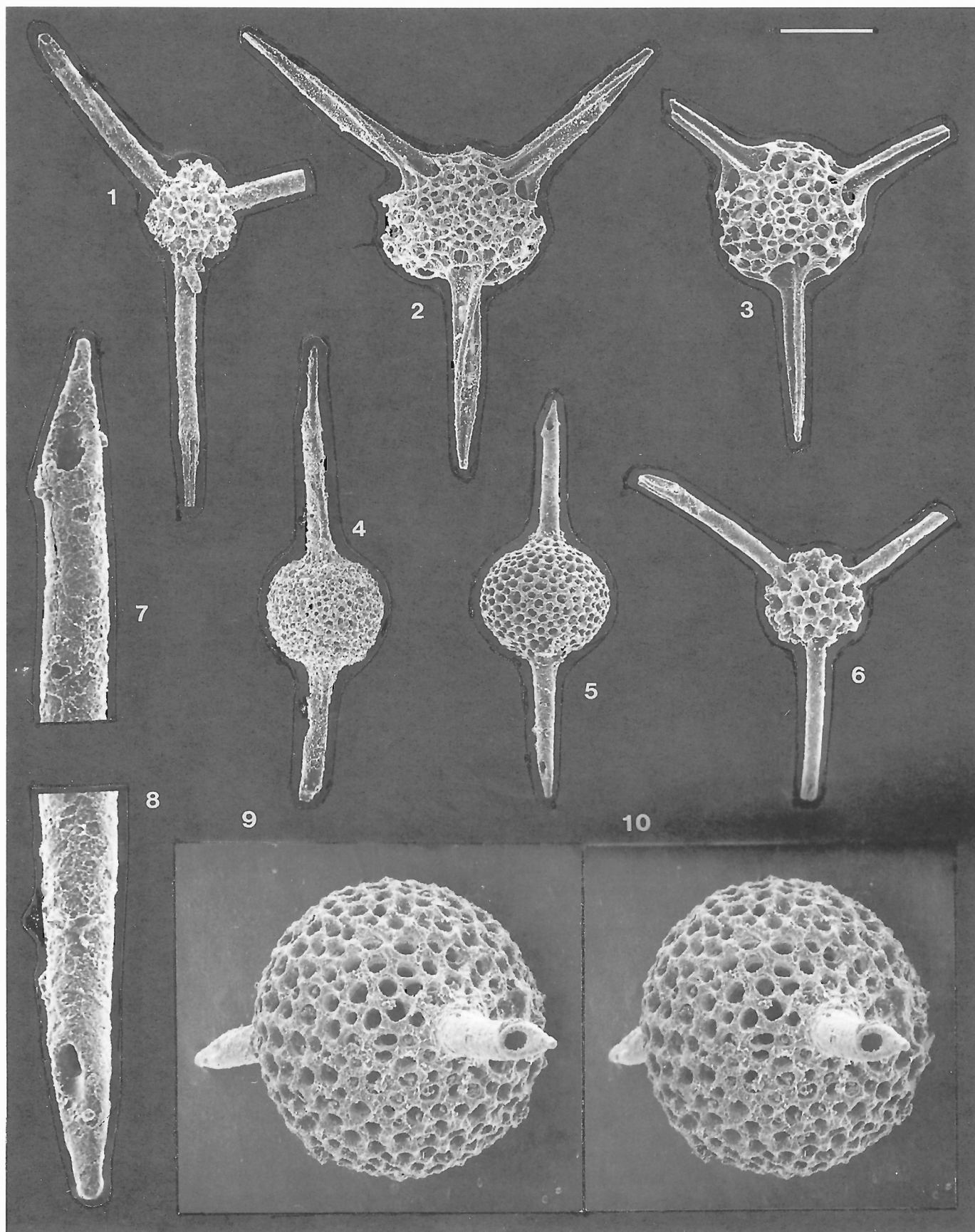
#### Peril Formation

Well preserved radiolarians have been recovered from limestone concretions in the upper part of the Peril Formation at Shields Bay and Kennecott Point. These faunas are associated with the pelagic bivalve *Monotis* in strata generally equated with the Cordilleran ammonoid zone. Conodonts from the *Epigondolella bidentata* Mosher group are associated with these radiolarians in most collections. *Betraccium deweveri* Pessagno and Blome, *B. maclearni* Pessagno and Blome, *Gorgansium richardsoni* Pessagno and Blome, *Livarella densiporata* Kozur and Mostler, *Norispongius poetschenensis* Kozur and Mostler, *Pentactinocarpus sevaticus* Kozur and Mostler, *Pseudohagiasstrum* cf. *monstruosum* Pessagno, *Spongosaturnalis bifidus* Kozur and Mostler, and *S.* aff. *kahleri* Kozur and Mostler have been observed in these collections along with other Upper Norian taxa described by Blome (1984). Undescribed species of *Pseudohagiasstrum* Pessagno and *Tetraporobrachia* Kozur and Mostler are abundant, and a few specimens of gen nov. A and gen. nov. E (Carter, 1990) are present. Very rare specimens of *Poulpus* De Wever have been observed only in the stratigraphically lowest collections. The entire fauna is characteristic of the Upper Norian *Betraccium deweveri* Subzone of Blome (1984).

#### Sandilands Formation

The Sandilands Formation is best exposed at Kennecott Point and Kunga Island where it conformably overlies the *Monotis* beds of the Peril Formation. The Sandilands Formation is Late Norian to Sinemurian in age (Carter, 1990; Tipper, 1989). Late Triassic ammonoids indicating the Crickmayi Zone, namely *Choristoceras* cf. *C. rhaeticum* (Gümbel), are known from basal strata at Kennecott Point. No Amoenum Zone indicators have been found at this locality, but the sequence is probably complete. Rare conodonts of the *Epigondolella bidentata* Mosher group are associated with radiolarians in post-*Monotis* strata at Kennecott Point, Louise Island, and Kunga Island, and at one locality *Misikella* has been found (Orchard, 1991). At Kunga Island, no Upper Norian macrofossils have been found above the level of *Monotis*. The upper part of the Sandilands Formation contains Hettangian and Sinemurian ammonites and radiolarians (Tipper et al., 1991).

The focus of the most recent radiolarian studies of the Upper Triassic has been the uppermost Norian fauna of the Sandilands Formation





(Carter, 1990). Abundant, diverse, and well preserved radiolarians have been recovered from micrite concretions in the basal part of the formation at Kennecott Point and Kunga Island (south side). The potential for zoning the uppermost Triassic and identifying the Triassic-Jurassic boundary beds is excellent as the sequence appears to be continuous.

Some characteristic Upper Norian and/or Rhaetian radiolarian species found in these assemblages include *Canoptum rhaeticum* Kozur and Mostler, *Cantalum alium* Blome, *Livarella densiporata* Kozur and Mostler, *L. validus* Yoshida, *Norispongia poetschenensis* Kozur and Mostler, *Pantanellium skidegatisensis* Pessagno and Blome, *Pentactinocarpus sevaticus* Kozur and Mostler, *Pseudohagiastrium monstrosus* Pessagno, *Pseudoheliodiscus sandspitensis* Blome, *Praecitriduma mostleri* Kozur, and *Squinabolella?* sp. C (in Yao, 1982). Other forms have affinities to Lower Jurassic species such as *Canoptum dixonii* Pessagno and Whalen, *C. unicum* Pessagno and Whalen, and *Pantanellium browni* Pessagno and Blome. The overall fauna is dominated by species of *Betracium* Pessagno, *Pantanellium* Pessagno, *Canoptum* Pessagno and Poisson, *Ferresium* Blome, *Haecelicyrtium* Kozur and Mostler, *Praecitriduma* Kozur, *Squinabolella* Pessagno; forms with affinities to *Canutus* Pessagno and Whalen, *Lactorum* Blome, *Podocapsa* Rüst; and several new genera. *Betracium deweveri* Pessagno and Blome, and *B. maclearni* Pessagno and Blome occur in samples 7.5 and 8 m above the base of the section at Kennecott Point, but have not been found higher.

Three preliminary radiolarian assemblages are recognized in Upper Norian strata lying above the *Monotis* beds (Carter, 1990). Assemblage 1, the lower one, is tentatively correlated with the Upper part of the Cordilleranus Zone; Assemblage 2 is thought to approximate the Amoenum Zone; and Assemblage 3 is correlated with the Crickmayi Zone.

## SYSTEMATIC PALEONTOLOGY

Holotypes and all illustrated material have been deposited with the Geological Survey of Canada. These specimens remain attached to SEM stubs. Other specimens are in E.S. Carter's collections.

Phylum PROTOZA  
Subclass RADIOLARIA Müller, 1858  
Order POLYCYSTINA Ehrenberg, 1838  
emend. Riedel, 1967  
Suborder SPUMELLARIA Ehrenberg, 1875  
Genus *Capnodoce* De Wever, 1979  
emend. Pessagno, 1979; emend. Blome, 1983

**Type species.** *Capnodoce anupetes* De Wever, 1979

*Capnodoce fragilis* Blome, 1983  
Plate 1, figures 1 and 6

## PLATE 1

Scanning electron micrographs of Lower to Middle Norian Radiolaria from the Peril Formation, Kunga Group, Queen Charlotte Islands, British Columbia. Bar scale – number of  $\mu\text{m}$  cited for each specimen illustrated.

**Figure 1.** *Capnodoce fragilis* Blome. GSC 85958 from GSC Loc. No. C-140407 (sample 86 CAA (EC) SP-1) Sandilands Island. Scale = 150  $\mu\text{m}$ .

**Figure 2.** *Harsa siscwaiensis* n. sp. Holotype, GSC 85959 from GSC Loc. No. C-156585 (sample 88 FI 25) Frederick Island. Scale = 163  $\mu\text{m}$ .

**Figure 3.** *Harsa* sp. cf. *H. siscwaiensis* n. sp. GSC 85960 from GSC Loc. C-150118 (sample 86 BI 13) Burnaby Island. Scale = 150  $\mu\text{m}$ .

**Figure 4.** *Xiphosphaera fistulata* n. sp. Paratype, GSC 85962 from GSC Loc. No. C-156585 (sample 88 FI 25) Frederick Island. Scale = 150  $\mu\text{m}$ .

**Figures 5, 7, 8, 9, 10.** *Xiphosphaera fistulata* n. sp. Holotype, GSC 85962 from GSC Loc. No. C-15325 (sample 87 BI 13) Burnaby Island; (7-8) detail of bipolar spines; (9-10) stereoscopic pair showing single pore at end of hollow spine. Scales = 150, 37 and 61  $\mu\text{m}$ , respectively.

**Figure 6.** *Capnodoce fragilis* Blome. GSC 85963 from GSC Loc. C-150118 (sample 86 BI 13), Burnaby Island. Scale = 150  $\mu\text{m}$ .

*Capnodoce fragilis* Blome, 1983, p. 26-27, pl. 6, figs. 4, 10, 18; pl. 11, fig. 5. Blome, 1984, p. 34, pl. 4, fig. 11. Carter et al., 1989, pl. 1, fig. 10.

**Measurements** ( $\mu\text{m}$ ). Based on 9 specimens; diameter of cortical shell 133-150; length of primary spines 225-313.

**Remarks.** These forms are slightly larger than the species described by Blome, but in all other respects they are very similar.

**Range.** Upper Triassic; Lower to upper Middle Norian.

**Occurrence.** Illustrated specimens GSC 85958 from GSC Loc. C-140407, Sandilands Island, and GSC 85963 from GSC Loc. C-150118, Burnaby Island. Peril Formation, Queen Charlotte Islands. Hurley Formation, near Bralorne, British Columbia. Rail Cabin Argillite, Suplee-Izee area, east-central Oregon: see Blome (1983).

Genus *Harsa* n. gen.

**Type species.** *Harsa siscwaiensis* n. sp.

**Description.** Cortical shell large, subcircular in outline and flattened in plane of spines; three radially arranged primary spines of approximately equal length lie in the same plane. Upper and lower surfaces of cortical shell horizontal to slightly convex; sides convex. Meshwork of cortical shell consists of three layers: the two inner layers are composed of coarse polygonal pore frames; the outer one consists of coarse polygonal pore frames with nodes at pore frame vertices. Nodes superimposed on vertices of underlying layer of pore frames. Cortical shell has three-six large subcircular to subtriangular pores situated at the base of each spine: one pore at base of each spine groove, others (usually of lesser size) may or may not lie at base of spine ridges. Test lacking medullary shell. Central cavity contains a simple internal spicule; spicule connected to outer shell by primary radial beams. Primary spines equal to unequal in length; symmetrically to asymmetrically arranged. Spines solid, bladed, triradial in axial section; composed of ridges and grooves.

**Remarks.** *Harsa* n. gen. differs from *Sarla* Pessagno by having a three-layered cortical shell that is strongly compressed in the plane of the spines; an internal spicule rather than a medullary shell; and large pores that are situated at base of each primary spine. It differs from *Ferresium* Blome by its much larger size, and by having flattened upper and lower surfaces on the cortical shell, and large pores at the base of each spine.

**Etymology.** *Harsa* is a name formed by an arbitrary combination of letters (International Code of Zoological Nomenclature, 1985, Appendix D, Recommendation 40).

**Range.** Upper Triassic; Lower to Middle Norian.

**Occurrence.** Peril Formation, Kunga Group, Queen Charlotte Islands; Hurley Formation, near Bralorne, British Columbia.

*Harsa siscwaiensis* n. sp.

Plate 1, figure 2

**Description.** Test as for genus. Cortical shell large, subcircular in outline; upper and lower surfaces very slightly convex, sides convex. Pore

frames and nodes are small in center of test becoming larger towards the periphery. Nodes have moderate to high relief. Primary spines long (about one and one-fourth times diameter of cortical shell) and triradiate. Configuration of ridges and grooves is variable: ridges may be narrow to wide, grooves shallow to deep. Spines are nearly equal in length and exhibit slight torsion throughout although sometimes torsion is more prominent in distal portion of spine. One large subcircular pore situated at base of each spine groove.

**Remarks.** *Harsa siscwaiensis* n. sp. has a larger cortical shell and longer, stouter spines than other undescribed forms of this genus.

**Etiology.** This species is named for Frederick Island (type locality), known as SISCWAI to the ancient Haida.

Measurements (µm).	Holotype	Avg. of 10 spec.	Max.	Min.
Diameter, cortical shell	240	238	263	225
Length, primary spines	342	307	375	244

**Type locality.** GSC Loc. C-156585. See Appendix.

**Range.** Upper Triassic; Lower to Middle Norian.

**Occurrence.** Illustrated specimen GSC 85959 (holotype) from locality on Frederick Island. Peril Formation, Kunga Group, Queen Charlotte Islands. Hurley Formation, near Bralorne, British Columbia.

*Harsa* sp. cf. *H. siscwaiensis* n. sp.

Plate 1, figure 3

**Remarks.** This form is very similar to *Harsa siscwaiensis* n. sp. but the cortical shell has a smoother surface with larger pores, and primary spines are straight.

**Range.** Upper Triassic; Lower to Middle Norian.

**Occurrence.** Illustrated specimen GSC 85960 from GSC Loc. C-150118, Burnaby Island. Peril Formation, Kunga Group, Queen Charlotte Islands.

Genus *Xiphosphaera* Haeckel, 1882

**Type species.** *Xiphosphaera tredecimporata* Rüst, 1885.

**Description.** *Xiphosphaera* Haeckel has a single lattice shell with two similar polar spines (from Campbell, 1954, p. D54).

*Xiphosphaera fistulata* n. sp.

Plate 1, figures 4, 5, 7, 8, 9, 10

**Description.** Cortical shell large and spherical in outline. Meshwork of wall thick, composed of small, irregularly arranged pore frames (mostly hexagonal and pentagonal). Nodes at vertices of pore frames are low in relief. Shell has long, smooth, tubular, bipolar primary spines; spines approximately equal in length, slightly tapering distally. One long tapering pore visible at the tip of each spine.

**Remarks.** The cortical shell of *Xiphosphaera globosa* Rüst, 1885 (pl. 27, fig. 16) appears similar to *X. fistulata* n. sp. However, from Rüst's line drawing it is difficult to determine the exact morphology of the spines i.e. whether they are solid or hollow. *X. fistulata* n. sp. differs from other undescribed forms of this genus by having hollow rather than solid spines.

**Etiology.** *Fistulatus-a-um* (Latin) = with pipes.

Measurements (µm).	Holotype	Avg. of 10 spec.	Max.	Min.
Diameter, cortical shell	206	199	225	169
Length, primary spines	281	277	345	225

**Type locality.** GSC locality C-150325. See Appendix.

**Range.** Upper Triassic; Lower to Middle Norian.

**Occurrence.** Illustrated specimen GSC 85962 (holotype) and GSC 85961 (paratype) from GSC Loc. C-150325 and C-156585, respectively. Peril Formation, Kunga Group, Queen Charlotte Islands.

## ACKNOWLEDGMENTS

This work is part of a joint biostratigraphic study of Upper Triassic faunas of the Queen Charlotte islands; discussions with M.J.

Orchard and E.T. Tozer (other members of this group) have been stimulating, informative, and absolutely essential to the overall understanding of the faunas.

I thank the Queen Charlotte Frontier Geoscience Program and R.I. Thompson who provided logistic support. Peter Krauss is thanked for the SEM photography. Critical review of the manuscript by Fabrice Cordey was most appreciated.

## REFERENCES

- Blome, C.D.**  
**1983:** Upper Triassic Capnuosphaeridae and Capnodocinae (Radiolaria) from east-central Oregon: Micropaleontology, v. 29, no. 1, p. 11-49.  
**1984:** Upper Triassic Radiolaria and radiolarian zonation from western North America: Bulletins of American Paleontology, v. 85, no. 318, 88 p.
- Campbell, A.S.**  
**1954:** Treatise of Invertebrate Paleontology, Part D. Protista 3. Protozoa (chiefly Radiolaria and Tintinnina), R.C. Moore (ed.): Geological Society of America, 195 p.
- Carter, E.S.**  
**1988:** Radiolarian studies in the Queen Charlotte Islands, British Columbia; in Current Research, Part E. Geological Survey of Canada, Paper 88-1E, p. 235-237.  
**1990:** New biostratigraphic elements for dating Upper Norian strata from the Sandilands Formation, Queen Charlotte Islands, British Columbia, Canada: Marine Micropaleontology, v. 15, p. 313-328.
- Carter, E.S., Orchard, M.J., and Tozer, E.T.**  
**1989:** Integrated ammonoid - conodont - radiolarian biostratigraphy. Late Triassic Kunga Group, Queen Charlotte Islands, British Columbia; in Current Research, Part H, Geological Survey of Canada, Paper 89-1H, p. 33-30.
- Desrochers, A.**  
**1988:** Sedimentology of the Kunga Group, Queen Charlotte Islands; in Some Aspects of Petroleum Geology of the Queen Charlotte Islands, R. Higgs (compiler), Canadian Society of Petroleum Geologists' Field Trip Guide to: Sequences, Stratigraphy, Sedimentology, September 14-16, 1988, p. 33-37.
- Desrochers, A. and Orchard, M.J.**  
**1991:** Stratigraphic revisions and carbonate sedimentology of the Kunga Group (Upper Triassic-Lower Jurassic), Queen Charlotte Islands, British Columbia; in Evolution and Hydrocarbon Potential of the Queen Charlotte Basin, British Columbia, Geological Survey of Canada, Paper 90-10.
- De Wever, P., Sanfilippo, A., Riedel, W.R., and Gruber, B.**  
**1979:** Triassic radiolarians from Greece, Sicily and Turkey; Micropaleontology, v. 25, no. 1, p. 75-110.
- Ehrenberg, C.G.**  
**1838:** Über die Bildung der Kreidefelsen und des Kreidemergels durch unsichtbar Organismen: Königlich Preussischen Akademie der Wissenschaften zu Berlin, Abhandlungen, Jahre 1838, p. 59-147.  
**1875:** Fortsetzung der mikrogeologischen Studien als Gesamtübersicht der mikroskopischen Paläontologie gleichartig analysierter Gebirgsarten der Erde, mit spezieller Rücksicht auf den Polycystinen-Mergel von Barbados; Königlich Preussischen Akademie der Wissenschaften zu Berlin, Abhandlungen, Jahre 1875, p. 1-225.
- International Code of Zoological Nomenclature**  
**1985:** Adopted by the 20th General Assembly of the International Union of Biological Sciences, London, 338 p.
- Kozur, H. and Mostler, H.**  
**1972:** Beiträge zur Erforschung der mesozoischen Radiolarien. Teil I: Revision der Oberfamilie Coccodiscacea Haeckel 1862, emend. und Beschreibung ihrer triassischen Vertreter; Geologisch - Paläontologische Mitteilungen, Innsbruck, v. 2, (nos. 8/9), p. 1-60.  
**1979:** Beiträge zur Erforschung der mesozoischen Radiolarien. Teil 2: Oberfamilie Trematodiscacea Haeckel 1862, emend. und Beschreibung ihrer triassischen Vertreter; Geologisch - Paläontologische Mitteilungen, Innsbruck, v. 8, p. 123-182.  
**1981:** Beiträge zur Erforschung der mesozoischen Radiolarien. Teil 4: Thalassosphaeracea HAECKEL, 1862, Hexastylacea HAECKEL, 1882, emend. Petrushevskaja, 1979, Sponguracea HAECKEL, 1862 emend. und weitere triassische Lithocyliacea, Trematodiscacea, Actinommacaea und Nassellaria; Geologisch - Paläontologische Mitteilungen, Innsbruck, Sonderband 1, 208 p.
- Müller, J.**  
**1858:** Über die Thalassicolle, Polycystinen und Acanthometren der Mittelmeeres; Abhandlungen der Preussischen Akademie der Wissenschaften zu Berlin, Jahrgang, 1858, p. 1-62.
- Orchard, M.J.**  
**1983:** *Epigondolella* populations and their phylogeny and zonation in the Upper Triassic; Fossils and Strata, no. 15, p. 177-192.  
**1988:** Studies of the Triassic Kunga Group, Queen Charlotte Islands, British Columbia; in Current Research, Part E, Geological Survey of Canada, Paper 88-1E, p. 229.

- 1991:** Late Triassic conodont biochronology and biostratigraphy of the Kunga Group, Queen Charlotte Islands, British Columbia; *in* Evolution and Hydrocarbon Potential of the Queen Charlotte Basin, British Columbia, Geological Survey of Canada, Paper 90-10.
- Orchard, M.J., Carter, E.S., Tozer, E.T. (paleontological data); Weston, M., Woodsworth, G.J., Orchard, M.J., Johns, M. (database design); Forster, P.J.L., Lesack, K., and McKay, K. (compilers)**
- 1991:** Electronic database of Kunga Group biostratigraphic data; *in* Evolution and Hydrocarbon Potential of the Queen Charlotte Basin, British Columbia, Geological Survey of Canada, Paper 90-10.
- Pessagno, E.A. Jr., Finch, W., and Abbott, P.L.**
- 1979:** Upper Triassic Radiolaria from the San Hipólito Formation, Baja California; *Micropaleontology*, v. 25, no. 2, p. 160-197.
- Riedel, W.R.**
- 1967:** Subclass Radiolaria; *in* The Fossil Record, W.R. Harland (ed.), Geological Society of London, p. 291-298.
- Sutherland Brown, A.**
- 1968:** Geology of the Queen Charlotte Islands, British Columbia; British Columbia Department of Mines and Petroleum Resources, Bulletin 54, 226 p.
- Tipper, H.W.**
- 1989:** Lower Jurassic (Hettangian and Sinemurian) biostratigraphy, Queen Charlotte Islands, British Columbia; *in* Current Research, Part H, Geological Survey of Canada, Paper 89-1H, p. 31-33.
- Tipper, H.W., Smith, P.L., Cameron, B.E.B., Carter, E.S., Jacobs, G.K., and Johns, M.**
- 1991:** Biostratigraphy of the Lower Jurassic formations of the Queen Charlotte Islands, British Columbia; *in* Evolution and Hydrocarbon Potential of the Queen Charlotte Basin, British Columbia, Geological Survey of Canada, Paper 90-10.
- Tozer, E.T.**
- 1967:** A standard for Triassic time; Geological Survey of Canada, Bulletin 156, 103 p.
- 1979:** Latest Triassic ammonoid faunas and biochronology, Western Canada; *in* Current Research, Part B, Geological Survey of Canada, Paper 79-1B, p. 127-135.
- Yao, A.**
- 1982:** Middle Triassic to Early Jurassic Radiolarians from the Inuyama area, Central Japan; *Journal of Geoscience, Osaka City University*, v. 25, p. 53-70.

## APPENDIX: LOCALITY REGISTER

Information is provided below for illustrated material.

**GSC Loc. C-140407.** Sandilands Island (86 CAA (EC) SP 1); 53°10'44.1"N, 132°07'19.7"W. Kunga Group, Peril Formation. Spot sample of black limestone. Occurs with *Halobia* and with conodonts of the *triangularis* Zone (M.J. Orchard, pers. comm., 1989).

**GSC Loc. C-150118.** Burnaby Island, N side, E of Section Cove (86 OF BI 13); 52°25'54.1"N, 131°19'56.1"W. Kunga Group, Peril Formation. Section BI; from a 5 x 50 cm medium grey micrite nodule with finely disseminated pyrite and shell fragments, at 195.5 m above datum. Occurs with conodonts of the *triangularis* Zone (M.J. Orchard, pers. comm., 1989).

**GSC Loc. C-150325.** Burnaby Island, N side, E of Section Cove (87 OF BI 13); 52°25'54.1"N, 131°19'56.1"W. Kunga Group, Peril Formation. Section BI; from a 5 x 50 cm limestone nodule at 194 m above datum. Occurs with conodonts of the *triangularis* Zone (M.J. Orchard, pers. comm., 1989).

**GSC Loc. C-156585.** Frederick Island (88 OF FI 25); 53°55'33.2"N, 133°09'33.2"W. Kunga Group, Peril Formation. Section FI-D; from a 20-50 cm shell bed 3 m above disturbed zone (datum). Occurs with conodonts of the *triangularis* Zone (M.J. Orchard, pers. comm., 1989).



# Biostratigraphy of the Lower Jurassic formations of the Queen Charlotte Islands, British Columbia

H.W. Tipper<sup>1</sup>, P.L. Smith<sup>2</sup>, B.E.B. Cameron<sup>3</sup>,  
E.S. Carter<sup>4</sup>, G.K. Jakobs<sup>2</sup>, and M.J. Johns<sup>3</sup>

Tipper, H.W., Smith, P.L., Cameron, B.E.B., Carter, E.S., Jakobs, G.K., and Johns, M.J., Biostratigraphy of the Lower Jurassic formations of the Queen Charlotte Islands, British Columbia; in *Evolution and Hydrocarbon Potential of the Queen Charlotte Basin, British Columbia*. Geological Survey of Canada, Paper 90-10, p. 203-235, 1991.

## Abstract

*The Lower Jurassic strata of Queen Charlotte Islands have been divided into five lithologically distinct formations, namely: the Sandilands Formation of the Kunga Group and the Ghost Creek, Fannin, Whiteaves, and Phantom Creek formations of the Maude Group. The Rennell Junction unit is abandoned as a formation and the beds included within a redefined Fannin Formation.*

*Macrofossils, particularly ammonites, and microfossils, notably Radiolaria, Foraminifera, Ostracoda, and ichthyoliths, are abundant, generally well-preserved, reasonably diverse, and are found, to a degree, in all formations. The record suggests a complete Lower Jurassic sequence with few, if any, hiatuses of consequence. The Pliensbachian ammonite zonation for North America is defined by stratotype and reference sections in Skidegate Inlet. Toarcian Radiolaria likewise have been zoned. The biostratigraphic studies of all faunas has as a goal, zonations based on many faunas and a satisfactory correlation of these schemes.*

*Important macrofossils and microfossils are illustrated and zones and faunal assemblages have been described. The importance of fossils to mappers and stratigraphers and the application of these data to an understanding of paleogeography and tectonics is emphasized.*

## Résumé

*Les couches du Jurassique inférieur des îles de la Reine-Charlotte ont été divisées en cinq formations lithologiquement distinctes : la formation de Sandilands du groupe de Kunga et les formations de Ghost Creek, de Fannin, de Whiteaves et de Phantom du groupe de Maude. L'unité de Rennell Junction n'est plus considérée comme une formation et les couches ont été incluses dans une formation de Fannin redéfinie.*

*Les macrofossiles, en particulier les ammonites, et les microfossiles, notamment les radiolaires, foraminifères, ostracodes et ichthyolithes, sont abondants, généralement bien conservés, raisonnablement diversifiés et présents, dans une certaine mesure, dans toutes les formations. La colonne indique une séquence du Jurassique inférieur complète avec quelques lacunes s'il y a lieu. La zonation des ammonites du Pliensbachien en Amérique du Nord est définie par le stratotype et les coupes de référence contenues dans l'inlet Skidegate. Les radiolaires toarciens ont été zonés de la même façon. Les études biostratigraphiques de toutes les faunes ont pour objectif des zonations basées sur de nombreuses faunes et une corrélation satisfaisante de ces schémas.*

*Les macrofossiles et microfossiles importants sont illustrés et les zones et assemblages fauniques ont été décrits. L'importance des fossiles pour les cartographes et les stratigraphes et l'application de ces données à la paléogéographie et à la tectonique sont mis en relief.*

---

<sup>1</sup> Cordilleran Division, Geological Survey of Canada, 100 West Pender Street, Vancouver, B.C. V6B 1R8  
<sup>2</sup> Department of Geological Sciences, University of British Columbia, 6339 Stores Road, Vancouver, B.C. V6T 2B4  
<sup>3</sup> Pacific Geoscience Centre, Geological Survey of Canada, 9860 West Saanich Road, Sidney, B.C. V8L 4B2  
<sup>4</sup> 58335 Timber Road, Vernonia, Oregon, U.S.A. 97064



## INTRODUCTION

Paleontology and biostratigraphy are essential to a full geological understanding of any area and the Queen Charlotte Islands are no exception. Previous work in these fields was largely preliminary, particularly for the Lower Jurassic faunas. The opportunity to begin a detailed study in a region that is poorly known and yet so geologically and economically important was both rare and exciting. It is particularly intriguing as both macrofossils and microfossils are available in abundance with a high diversity of genera and species.

The macrofossils, particularly the ammonites, provide constraints for surface mappers to effect local and regional correlations. In Queen Charlotte Islands the complex structure and the relatively poor exposure dictate the need for such a tool in correlation. The macrofossils when fully understood biostratigraphically provide a standard reference for microfossil correlation both locally and worldwide. In this way correlation on the surface and in the subsurface is possible and provides a service to the surface mapping and subsurface stratigraphic work of mining and oil companies.

The ammonites found in Queen Charlotte Islands display good to excellent preservation and are a diverse and abundant fauna. A few genera and many species are endemic to this area or to western North America. Several species show affinities to species in South America, Siberia and Japan and to the faunas of northwest Europe. From studies to date, there is no reason to believe there is any large gap in the faunal sequence; frequently collection failure in one section is amply compensated for in other sections. Thus the ammonite fauna is ideal in most aspects for taxonomy, correlation, and paleobiogeography.

Foraminifera are abundant throughout the Lower Jurassic strata of the Queen Charlotte Islands and the succession is essentially complete. The recovery of Foraminifera by conventional laboratory means from some of the more indurated rocks has proven to be a problem in some cases. Nevertheless, through more sophisticated laboratory techniques, it is hoped to fully document the foraminiferal and ostracodal succession in these rocks. Ostracods occur much less frequently in the Lower Jurassic possibly due to the interpreted relatively deep water paleoenvironments of at least the lower part of the succession. A few species, occurring in the Pliensbachian and Toarcian, appear to have important stratigraphic significance.

The distribution and frequency of occurrence of these microfaunas is currently being documented in detail. Some of the more significant microfossils are discussed and illustrated herein for purposes of the present preliminary treatment. Since no formal zonation has yet been proposed for these rocks based on the foraminiferal succession, the occurrences of the microfossils are discussed in terms of lithostratigraphic units.

Well preserved, diverse radiolarians have been recovered from micrite concretions and lenses throughout most Lower Jurassic formations in the Queen Charlotte Islands. Many new taxa are recognized. In most cases the faunas are closely associated with the Lower Jurassic ammonites currently under study. As with the ammonites, collection failure of radiolarians in one section (commonly the lack of suitable concretions) can usually be compensated for in other sections. Given the completeness of section, the abundance of well preserved radiolarian faunas and the precise megafossil dating becoming available, the potential for refining the existing zonation of Pessagno et al. (1987), is excellent. Such zonation will provide an essential tool for correlating between the allochthonous terranes of western North America and will contribute to widespread correlation around the Pacific Rim and perhaps globally.

Lower Jurassic radiolarian faunas of the Queen Charlotte Islands are diverse and when well preserved contain many pantanelliid

species. The faunas demonstrate affinities to Tethyan assemblages from British Columbia, eastern Oregon, the Mediterranean area, Japan and New Zealand.

## PREVIOUS WORK

The earliest paleontological studies in Queen Charlotte Islands were carried out in conjunction with exploration and reconnaissance mapping by James Richardson in 1872 (1873, p. 56-63), G.M. Dawson in 1878 (1880), R.W. Ellis in 1906 (1906), C.H. Clapp in 1912 (1914) and J.D. MacKenzie in 1913-14 (1916, p. 40). These men investigated the Cretaceous rocks and became involved in the controversy of defining what was Cretaceous and what was Middle Jurassic. Although they never recognized them as such, some Lower Jurassic beds were included inadvertently in the Cretaceous or Middle Jurassic. For example, Dawson collected some Early Jurassic faunas believing them to be Cretaceous; two of these species later were used as Jurassic holotypes. Various paleontologists were involved in identifying the Cretaceous to Middle Jurassic faunas namely E. Billings (1873), J.F. Whiteaves (1876, 1883, 1884, 1900) and Stanton and Martin (1905) but none recognized Lower Jurassic faunas.

In 1921 F.H. McLearn carried out the first detailed biostratigraphic and paleontologic study in the Queen Charlotte Islands when he studied and published on the Cretaceous (Albian) faunas (McLearn, 1972) and the Jurassic faunas (McLearn, 1927, 1929, 1932, 1949). In his publications he recognized a *Fanninoceras* fauna (now known to be Pliensbachian in age) and a *Dactylioceras* and *Harpoceras* fauna (now identified as *Tiltoniceras* and others known to be of Toarcian and Pliensbachian age). This initiated Lower Jurassic faunal studies.

A. Sutherland Brown mapped the islands from 1958 to 1965 and published a bulletin for the B.C. Department of Mines (1968). This was the last major mapping project in the Queen Charlotte Islands prior to the present investigations.

Hans Frebold (1967b) discussed the stratigraphic position of the genus *Fanninoceras* and later (Frebold, 1970) described some new species from the Pliensbachian beds. This was the last paleontological report published prior to the current studies.

The first reference to radiolarians in the strata of the Queen Charlotte Islands was by Sutherland Brown (1968, p. 59), who suggested that abundant spherules in the Kunga Formation were pelagic microfossils, "probably Radiolaria and Foraminifera". In the late 1970's, Cameron found radiolarians in samples previously collected by Tipper and later he collected additional samples on Maude Island and in central Graham Island. Initial study of faunas from the Queen Charlotte Islands was begun soon after by E.A. Pessagno, C.D. Blome, and P.A. Whalen on material from Kunga Island, Whiteaves Bay and Maude Island. The resulting works were primarily taxonomic but some biostratigraphic data for Lower Jurassic (Hettangian?, Sinemurian and Pliensbachian) forms were included (Pessagno and Blome, 1980; Pessagno and Whalen, 1982; Pessagno et al., 1986; Whalen, 1985). This information together with biostratigraphic data derived from E.S. Carter's study of Upper Pliensbachian and Toarcian faunas (1985), was incorporated in a preliminary radiolarian zonation for the Jurassic of North America (Pessagno et al., 1987).

## PRESENT WORK

The present research was begun in 1974 when Tipper began an examination of the occurrences of *Fanninoceras* and work has continued intermittently to the present. Cameron joined the investigations in 1978 after he discovered Foraminifera and Radiolaria in samples collected previously by Tipper. In 1982 Carter began a graduate thesis on the Radiolaria and in the same year Smith began a detailed analysis of the Pliensbachian ammonites. In 1987 Jakobs began a comprehensive

biostratigraphic and paleontologic consideration of the Toarcian ammonites and continued the study in 1988. Tipper recognized an Hettangian section in 1987 at Kennecott Point and collected ammonites in both 1987 and 1988. As a result, the authors have been involved in studies in all stages of the Lower Jurassic, Tipper, Smith, and Jakobs with the ammonites and Cameron and Carter with Foraminifera and Radiolaria respectively. Ichthyolith studies by Johns are a recent venture. Many short papers and two bulletins have resulted from our work and the reader is referred to the bibliography for details.

THE LOWER JURASSIC FORMATIONS

The Lower Jurassic rocks of the Queen Charlotte Islands (Table 1) are soft shale, crumbly sandstone, or brittle, closely fractured siltstone, tuff, and sandstone. As a result, exposures are recessive, occurring as intertidal outcrops and exposures in creeks, and less commonly, on low, rounded hills. The complex structure further disrupts the exposure and thick, unfaulted sections are the exception rather than the rule. As a result the work dictated that as many sections as possible, however short, be searched out, measured carefully, collected bed by bed and pieced together into a reasonable stratigraphic sequence. The abundance and great diversity of faunas facilitated this task. Where the microfauna and macrofauna are considered together good control, zonation, and correlation results.

The following summary reviews the lithostratigraphy and biostratigraphy of the Lower Jurassic formations of the Queen Charlotte Islands and discusses some aspects of facies, sedimentology, volcanology and tectonics that have manifested themselves during the faunal studies. This is not intended as a final, comprehensive report, particularly with regard to the biostratigraphy and paleontology. It is meant to be a presentation of our present understanding of several topics and problems, some of which will be dealt with in separate reports by the individual authors.

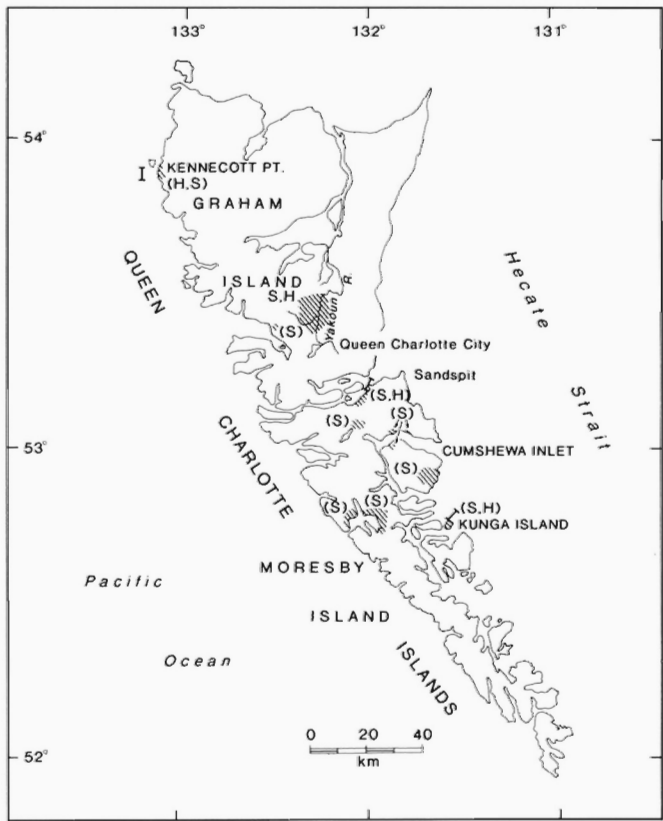


Figure 1: Distribution of main Sandilands Formation outcrops of Sinemurian (S) and Hettangian (H) age.

SANDILANDS FORMATION

Lithostratigraphy

The Sandilands Formation (Fig. 1) was named (Cameron and Tipper, 1985) for

"a thinly bedded, hard dense, black to dark grey siliceous siltstone or argillite in beds 2.5 to 10 cm thick (Fig. 2). It is interbedded with minor beds of grey siliceous tuff, lithic sandstone derived mainly from tuffs, green to grey-green shale (possibly tuffaceous), fine volcanic breccia with clasts to 2.5 cm in diameter and thin laminations of black shale or siltstone"

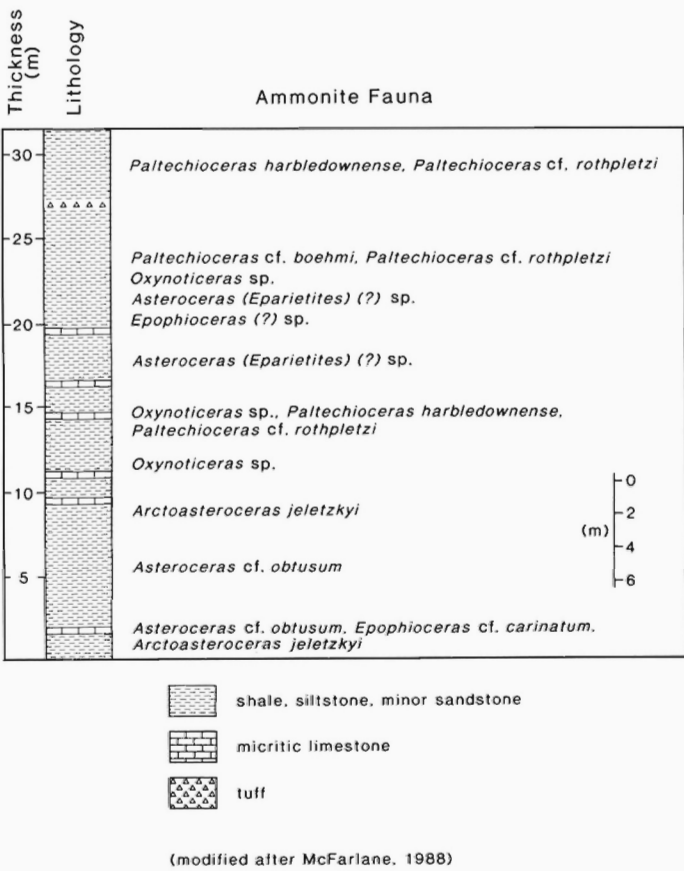


Figure 2: Typical Upper Sinemurian measured section of Sandilands Formation from a quarry in central Graham Island.



Figure 3: Upper Sinemurian Sandilands Formation on north side of Cumshewa Inlet. The thickest bed is about 15 cm thick. Interbedded siliceous tuff, siltstone and shale.

		STAGES		FORMATION	LITHOLOGY	AMMONITE ZONES	AMMONITE FAUNA	RADIOLARIA ZONES	RADIOLARIA FAUNA	FORAMINIFERA FAUNA	OTHER SIGNIFICANT FAUNAS			
Middle Jurassic	LOWER AALENIAN	T O A R C I A N	Phantom Creek		-fine to coarse grained, greenish sandstone with common buff-weathering concretionary beds.		<i>Tmetoceras</i> sp.	ZONE 6	<i>Transhsuum optimus</i> <i>Elodium cameroni</i> <i>Mesosaturnalis hexagonus</i>					
					-commonly glauconitic.		<i>Bredya</i> sp.							
				Whiteaves	Upper	<i>Hammatoceras speciosum</i> <i>Phlyseogrammoceras</i> ? sp.	ZONE 5			<i>Trilpocylla rosespitense</i> <i>Tympaneides charlottensis</i> <i>Sponglostoma saccideon</i>	<i>Falsopalmula jurensis</i>	pectinid bivalves ostreoid bivalves dicoelittid belemnites gastropods		
						<i>Sphaerocoeloceras brochiforme</i>							ZONE 4	<i>Homeoparonella raciproca</i> <i>Rolimbus klustaense</i> <i>Mesosaturnalis hexagonus</i>
						<i>Grammoceras thouarsense</i>							ZONE 3	<i>Elodium cameroni</i>
													ZONE 2	<i>Protounuma paulsmithi</i> <i>Transhsuum optimus</i> <i>Jacus magnificus</i>
				Middle	<i>Phymatoceras copiapense</i> <i>Paroniceras sternale</i>					<i>Lenticullna d'orbigny</i> var.	nautiloids			
					Lower	<i>Hildaites</i> cf. <i>chrysanthemum</i> <i>Harpoceras exaratum</i>					<i>Lenticulina</i> sp.	trigonal bivalves		
				F a n n i n		Ghost Creek	-coarsening upwards sequence passing from alternating shales, sandstones and diagenetic limestones into coarser, more tuffaceous, partly calcareous sandstones.			Carlottense	<i>Tiltoniceras propinquum</i> <i>Fanninoceras carlottense</i> <i>Protogrammoceras pectinatum</i>	ZONE 1	<i>Katroma ninstintsi</i> <i>Bipedis fannini</i> <i>Praeconocaryomma whiteavesi</i> <i>Parahsuum edenshawii</i> <i>Crucella angulosa</i>	paracuprils
					Kunae						<i>Reynoceras ragazzoni</i> <i>Leptaleoceras</i> aff. <i>accuratum</i> <i>Fanninoceras crassum</i> <i>Fanninoceras fannini</i> <i>Aveyroniceras colubriforme</i> <i>Phricodoceras</i> cf. <i>taylori</i> <i>Metaderoceras mouterdei</i>			
Freboldi	<i>Gemmellaroceras</i> aff. <i>aegniaticum</i> <i>Dubariceras freboldi</i> <i>Acanthopleuroceras whiteavesi</i> <i>Tropidoceras masseanum</i> <i>Metaderoceras evolutum</i>													
Whiteavesi	<i>Phricodoceras</i> cf. <i>taylori</i> <i>Tropidoceras flandrini</i> <i>Pseudoskiloceras imlayi</i>				<i>Ichthyolaria piqmaea</i> <i>Paralingulina</i> ? <i>tenera tenuistriata</i> <i>Ichthyolaria bicostata</i>			pectinid bivalves						
	S a n d i a n	S a n d i a n	-thinly bedded black to dark grey siliceous siltstone interbedded with siliceous tuff, green to grey shale, thin sandy limestone, and thin beds of fine sandstone.	Upper	<i>Paltechloceras harbledownense</i> <i>Asteroceras</i> sp.		<i>Canoptum unicum</i> <i>Pantanellum browni</i> <i>Crucella</i> sp. <i>Gorgansium</i> sp. <i>Relanus</i> ? sp. <i>Ecyrtis</i> ? <i>Canoptum</i> ?	pyritized nodosarids and polymorphinids	fish ichthyosaur leaves fish coleoids					
Lower					<i>Arnloceras arnouldi</i> <i>Badouxia canadensis</i> <i>Vermiceras</i> sp.									
Canadensis														
?														
H E T T A N G I A N	S a n d i a n	-siltstone, coarse sandstone, shale, concretionary siltstone, green tuff, interbedded ilmei beds.	Upper	<i>Paradiscamphiceras</i> sp. <i>Sunrisites</i> cf. <i>sunrisensis</i>		<i>Relanus reelfensis</i> <i>Pseudohellodiscus</i> sp. 2 <i>Pseudohellodiscus</i> sp. 1 <i>Pantanellum tanuense</i> <i>Paleosaturnalis</i> sp.	<i>Glomospira</i> <i>Amodiscus</i>	crustaceans  fish						
				Middle					<i>Schlothelmia</i> cf. <i>angulata</i>  <i>Paradasyceras</i> sp.  <i>Franziceras</i> aff. <i>ruldm</i>					
			Lower		<i>Fergusonites striatus</i> <i>Kammerkarites</i> sp.  <i>Discamphiceras silberlingi</i>									
									-coarse sandstone, siltstone; minor concretionary beds.		<i>Choristoceras</i> sp.			
Triassic	UPPER NORIAN													

**Table 1:** Summary of the present status of the Early Jurassic lithostratigraphy and biostratigraphy in the Queen Charlotte Islands.



**Figure 4:** Upper Sinemurian Sandilands beds on the south side of Maude Island, Skidegate Inlet, Queen Charlotte Islands. The white bands are well-bedded tuffs and the light grey are tuffaceous siltstone. Dark grey beds are argillite or siliceous siltstone.



**Figure 5:** Typical Hettangian-Lower Sinemurian beds exposed at Kennecott Point, northwest Graham Island, Queen Charlotte Islands. Even, well-defined bedding is characteristic. The light grey bed in the foreground is about 15 cm thick.

(Figs. 3 and 4). They concluded that it was an uninterrupted sequence of all or most of Sinemurian time. Recent work has changed this interpretation somewhat.

The Kunga Formation of Sutherland Brown (1968, p. 50-61) was raised to group status by Cameron and Tipper (1985, p. 11-16) and the youngest member of the formation, the black argillite member of Sutherland Brown raised to formation status, as the Sandilands Formation (Cameron and Tipper, 1985, p. 11). The other two members, which are of Triassic age, were similarly considered to be formations but were not named or redefined.

Sutherland Brown's black argillite member was stratigraphically above the *Monotis subcircularis*-bearing beds but the only known fossils in the member were of Sinemurian age. Because of apparent continuous sedimentation between the Triassic Norian beds with *Monotis* and the Sinemurian beds, the presence of uppermost Norian beds (=Amoenum and Crickmayi zones) and of Hettangian beds was expected (Sutherland Brown, 1968, p. 60) but was not proven. In 1987 Sutherland Brown's suggestion was proven correct in a fossiliferous section (Figs. 5 and 6) found at Kennecott Point (Tipper, 1989). Subsequently other sections of this age have been identified by ammonites and radiolarians (Carter, 1988). As a result the Sandilands Formation is now considered to be of the same age as Sutherland Brown's black argillite member, namely from the top of the *Monotis*-bearing beds (above the Cordilleranus Zone) to the top of Sinemurian with one slight modification, a diachronous contact with the mainly Lower Pliensbachian Ghost Creek Formation.

The Sandilands Formation is easily recognized by its characteristic well-bedded nature, by its hardness, in places verging on a chert-like consistency, and by its tuffaceous layers that commonly weather white or green. In a few places, fine volcanic breccia has been noted but nowhere has conglomerate been seen. Very thin limestone bands, up to 10 cm thick, limestone lenses, and concretions have been observed and many of the siltstone beds are calcareous.

The source of the volcanic detritus in the formation has not been clearly demonstrated. On Maude Island in Skidegate Inlet, beds of white-weathering tuff are conspicuous in an upper Sinemurian section reaching thicknesses of 10-15 cm for individual beds, more commonly 5 cm. Other sections on Moresby Island and Louise Island to the south similarly have prominent tuff beds. However, Upper Sinemurian sec-

# KENNECOTT POINT, QCI

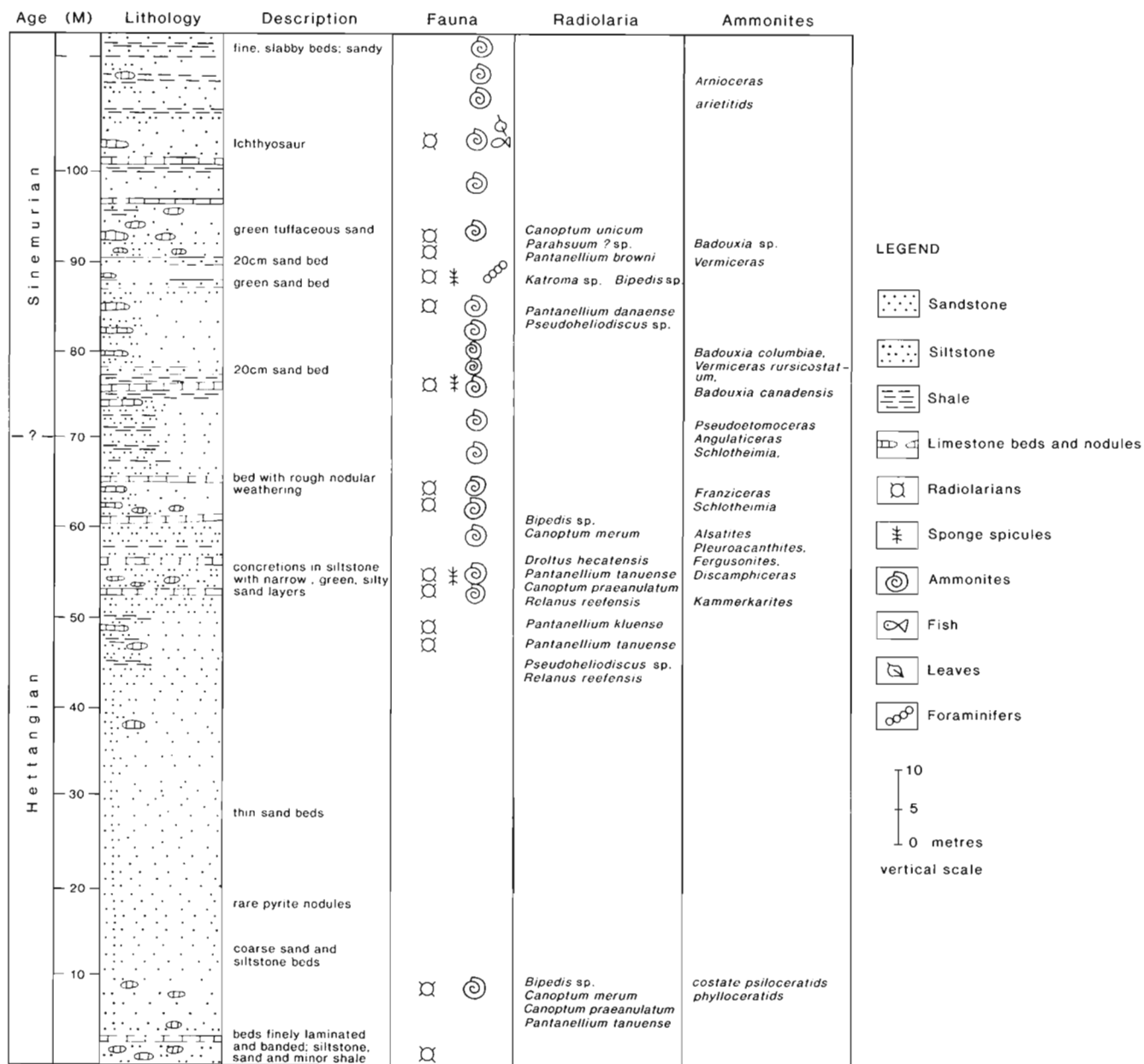


Figure 6: Restored Hettangian and earliest Sinemurian measured section of Sandilands Formation exposed at Kennebec Point.

tions in central Graham Island some 30 or more kilometres to the north have noticeably thinner bands of tuff, one centimetre or less is common, or the tuff is mixed with fine rock detritus to form a tuffaceous siltstone. Clearly there is a volcanic source nearby as many of the tuff beds are suggestive of air-fall deposits. Evidence of water transport of the volcanic detritus is generally lacking and the apparent thinning of the tuff beds of the same age, Late Sinemurian, suggests a source to the south or southwest. A similar situation exists on Vancouver Island where the Sinemurian Bonanza volcanics are exposed as massive primary volcanic piles. To the east, on Harbledown Island, Sinemurian shale and siltstone with interbedded tuff beds of the Harbledown Formation are similar or identical in lithology and fossil faunas to the upper part of the Sandilands Formation. It would appear that the tuff of the

Harbledown Formation was derived as an air-fall deposit from the Bonanza volcanics, a few kilometres to the west. Thus the tuffs of the Sandilands Formation may have been derived from a volcanic source to the south or southwest, a volcanic source not presently seen within the Queen Charlotte Islands.

As mentioned above, the contact with the Pliensbachian Ghost Creek Formation is diachronous. The Ghost Creek Formation is largely a soft shale or siltstone. In central Graham Island the Ghost Creek Formation extends downward into the Late Sinemurian as *Paltechioceras* is found in its basal beds, clearly of Late Sinemurian age as a result. In Skidegate Inlet the lowest beds of the Ghost Creek Formation contain earliest Pliensbachian faunas and the subjacent Sandilands Formation in its topmost beds has latest Sinemurian ammonites.

The stage boundary there coincides with the formation boundary. However, in the southern part of Queen Charlotte Islands, on Huxley Island, the Sandilands Formation contains ammonites which, from photographs, suggest *Pseudoskirroceras* of earliest Pliensbachian age (E.T. Tozer, pers. comm., 1988). Thus the top of the Sandilands Formation varies in age from Early Pliensbachian in the south to Late Sinemurian in the north, probably reflecting the diminishing volcanic activity near the close of Sinemurian time.

### Biostratigraphy

The ammonite fauna of the Sandilands Formation is in places, diverse and abundant as at Kennecott Point and a few rare places near Skidegate Inlet and in central Graham Island but in most exposures the sequences are devoid of fossils or nearly so and diversity is limited to one or two species. Commonly the specimens are secondarily compressed and only in undeformed concretions.

The study of the ammonite fauna of the Sandilands has just begun. Sutherland Brown collected material from many isolated localities, both ammonites and bivalves, but in most instances identification to generic level was all that was attempted; no sequence from an extended section was established. In 1987 R.B. McFarlane studied a section (Fig. 2) of Upper Sinemurian strata in detail and established a preliminary sequence of faunas (1988). From 1974 to the present numerous scattered collections from isolated Sinemurian localities were made by Tipper and by Cameron but few were in sequence. In 1987 and 1988 Tipper and Carter measured a section and collected ammonites and samples for Radiolaria at Kennecott Point (Fig. 6); Hettangian and earliest Sinemurian ages were determined. Future study of the Sandilands fauna will be carried out by Tipper and Smith (Hettangian ammonites) and by J. Pálfi, a graduate student of Smith (Sinemurian ammonites). Carter will be continuing her study of both Hettangian and Sinemurian radiolarians, mainly from Kennecott Point and Kunga Island. Although Foraminifera are known to be present as pyritized forms or steinkerns, few taxa have been recovered yet that are suitable for a detailed study (see below).

Preliminary study of the Hettangian faunas suggests a strong similarity to the Hettangian faunas of Nevada (Guex, 1980). Guex has established eight Hettangian zones in Nevada (as yet unpublished) and seven are apparently represented at Kennecott Point (Jean Guex, pers. comm., 1989). The eighth zone, the lowest is possibly represented by an interval, so far barren of any fossils. Those illustrated (Plate 1) are only a few of the common forms; the fauna at Kennecott Point is diverse and abundant although poorly preserved.

The Lower Hettangian is characterized by *Discamphiceras*, *Kammerkarites*, and phylloceratids. The Middle Hettangian has several species of *Schlotheimia*, *Alsatites*, phylloceratids and several other genera. The Upper Hettangian has several genera that are forerunners of Sinemurian forms. First appearances of *Vermiceras*, *Pseudetomoceras* and others are noted.

The Lower Jurassic section at Kennecott Point is underlain by beds containing faunas that are believed to be the uppermost Triassic. As there is no obvious structural or stratigraphic break in evidence, there is ample reason to believe that the Triassic and Jurassic rocks represent continuous deposition and it is reasonable to assume that the faunal gap is a result of collection failure. There are a few other localities on Moresby Island and Kunga Island that are probably Hettangian as indicated by radiolarians but ammonites are few. The section at Kennecott Point that contains both Norian and Hettangian faunas probably is an uninterrupted sequence fully exposed across the Triassic-Jurassic boundary and as such is the first known in Canada. It is also the most complete Hettangian section in Canada. This fauna was collected in greater detail in 1989.

The Sinemurian fauna on the other hand is widespread but is exposed only in short, faulted sections except at Kennecott Point. There the Sinemurian overlies the Hettangian in a continuous sedimentary section and contains faunas of Frebold's Canadensis Zone (Frebold, 1967a) and overlying beds containing arietitids such as *Coroniceras* sp. and in the highest beds the first occurrence of *Arnioceras*. Below the Canadensis Zone and above the Hettangian faunas is a 10 m section that has not yielded any determinable ammonites and these beds could be either Sinemurian or Hettangian.

In central Graham Island, on Maude Island and at a few localities on Moresby Island sections have yielded a few species of *Arnioceras* that tentatively are thought to represent sections of mid-Early Sinemurian time. No other Lower Sinemurian ammonite faunas are yet known but many unfossiliferous sections several tens of metres thick may overlie the *Arnioceras* beds and underlie the next higher fauna, the Upper Sinemurian *Asteroceras*.

In central Graham Island, Bruce McFarlane studied a section of Upper Sinemurian Sandilands Formation for a Bachelor's degree thesis (McFarlane, 1988). He found a succession with *Asteroceras* and *Epophioceras* at the base followed by oxynoticeratids in the middle part and *Paltechioceras* at the top (Plate 2). The sequence was not particularly diverse. *Paltechioceras* was relatively abundant and is one of the more commonly found genera in the Sandilands on Graham Island and southward.

Foraminifera and ostracoda of Sandilands Formation have not been recovered in abundance. Disintegration of the thoroughly hard indurated rocks of the formation has proven to be very difficult by conventional laboratory techniques, however it is hoped that through new procedures more recognizable calcareous taxa will be recovered. Acidization of some of the calcareous beds has yielded a great variety of small pyritized forms as well as a few agglutinating taxa. The pyritized forms are characteristically steinkerns and thus do not provide much surface detail. This microfauna consists of a very highly diversified nodosarid and polymorphinid fauna with less frequently occurring agglutinating taxa such as *Ammodiscus*, *Ammobaculites* and *Glomospira*. A few of the latter agglutinating taxa appear to be distinctive.

Since 1986 Jurassic radiolarian studies by Carter have focused on Hettangian and Sinemurian faunas from the Sandilands Formation. The present North American radiolarian zonation for this interval (Pessagno et al., 1987) was based on well preserved but imprecisely dated faunas from the Sandilands Formation on Kunga Island. When this zonation was established, Hettangian strata in the Queen Charlotte Islands were not recognized and the extent of Sinemurian, other than upper, was poorly known. The purpose of current studies is to understand the basal Jurassic radiolarian succession, to define precisely existing zonal boundaries by integrating them with North American ammonite zones, and to determine if subdivision of these radiolarian zones is feasible.

Recent studies of ammonites and radiolarians confirm the Sandilands Formation is upper Norian (Carter, 1988, 1990; Carter et al., 1989) and Hettangian (Tipper, 1989), as well as Sinemurian. Ammonite collections from Kennecott Point suggest all Hettangian and earliest Sinemurian time is represented in an essentially continuous sequence. Limestone concretions yielding well preserved radiolarians are in close association with ammonites at many levels. Hettangian and Sinemurian radiolarians have also been collected from measured sections on Kunga Island, and from localities on the Yakoun River (central Graham Island), Maude Island, Sandilands Island, and Tasu Sound (Lomgong Bay and Wilson Bay) (Fig. 7).



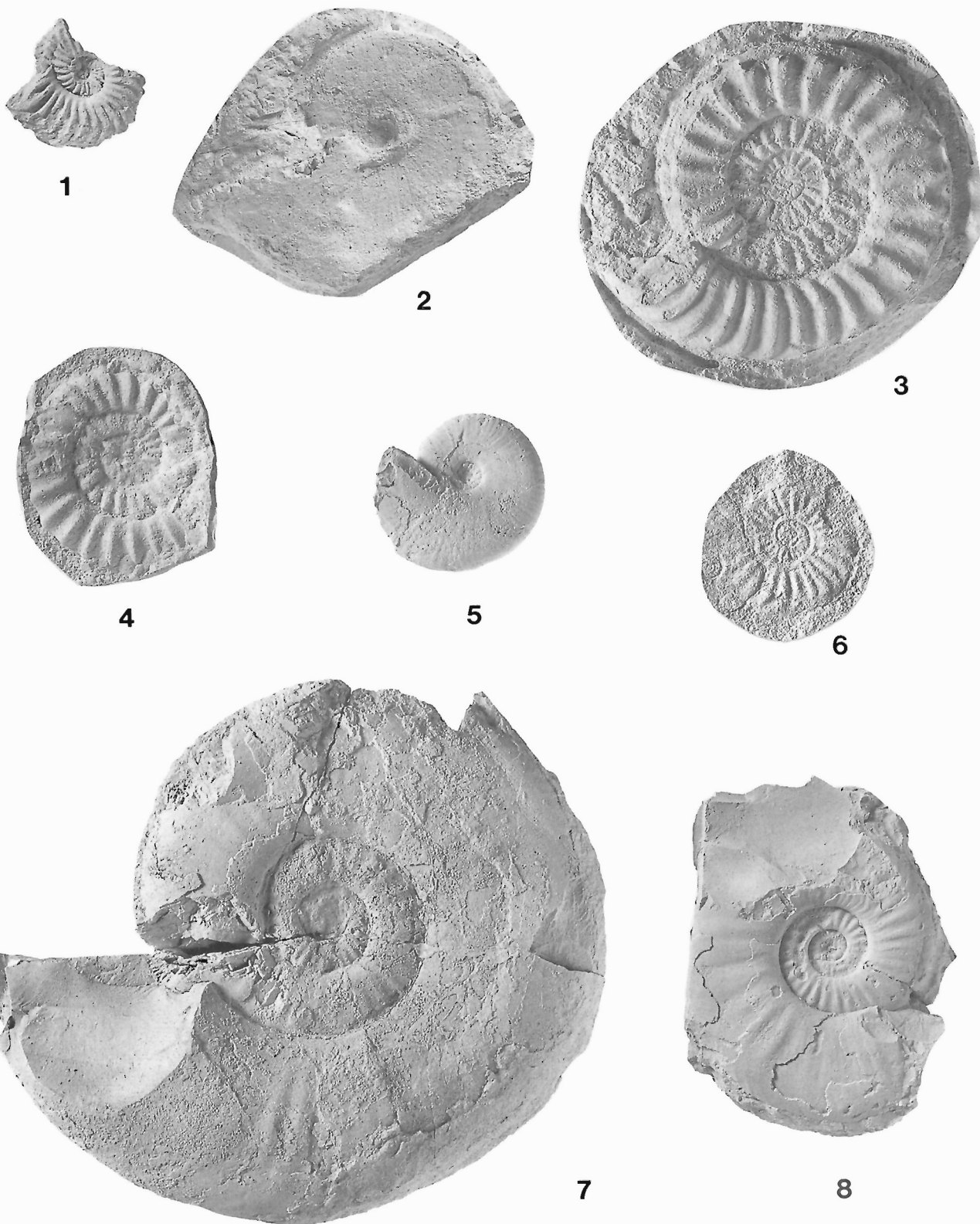


# **PLATE 1**

Hettangian ammonites from the Sandilands Formation. All figures are natural size.

**Figure 1:** *Schlotheimia* sp.; GSC 95560; GSC Loc. No. C-156915; Middle Hettangian.

**Figure 2:** *Phylloceratid*; GSC 95561; GSC Loc. No. C-156915; Middle Hettangian.

**Figure 3:** *Franziceras* sp.; GSC 95562; GSC Loc. No. C-156915; Middle Hettangian.

**Figure 4:** *Franziceras* sp.; GSC 95563; GSC Loc. No. C-156915; Middle Hettangian.

**Figure 5:** *Fergusonites striatus* Guex, 1980; GSC 95564; GSC Loc. No. C-156906; Lower Hettangian.

**Figure 6:** *Kammerkarites*? sp.; GSC 95565; GSC Loc. No. C-156907; Lower Hettangian.

**Figure 7:** *Discamphiceras* sp.; GSC 95566; GSC Loc. No. C-156906; Lower Hettangian.

**Figure 8:** *Discamphiceras* sp.; GSC 95567; GSC Loc. No. C-156906; Lower Hettangian.

At Kennecott Point radiolarians are associated with ammonites at two levels: the lower level, lower Lower Hettangian, occurs 55 m above the base of Section D (=12.5 m above base of the Jurassic); the upper level, Lower Hettangian, occurs 10 m above base of Section B (Plate 8). On Figure 6 these samples occur at 12.5 and 53 m, respectively. The lower assemblage contains *Bipedis* sp., *Canoptum merum* Pessagno and Whalen, *C. praeannulatum* Pessagno and Whalen, and *Pantanellium tanuense* Pessagno and Blome. The upper assemblage contains the above species plus *Droetus hecatensis* Pessagno and Whalen, *Relanus reefensis* Pessagno and Whalen, some forms documented by Whalen (1985), and many other new taxa.

On Kunga Island, well preserved Lower Jurassic radiolarian collections were made by Carter and Orchard in 1986, and by Carter in 1987. Because the Sandilands Formation is frequently disrupted and the beds difficult to trace on the north side of Kunga Island, the formation was measured in discrete uninterrupted sections rather than as a whole (see Fig. 7 for approximate location of sections A-D). Precise megafossil dating is not yet available for Kunga Island faunas but detailed comparison of the radiolarian faunas with well dated faunas from Kennecott Point provides a fairly close correlation. Based on this comparison, a rich sample (KU-D2; C-164676) collected 22.5 m above the base of Section D (Kunga Island), is probably Early to Mid-

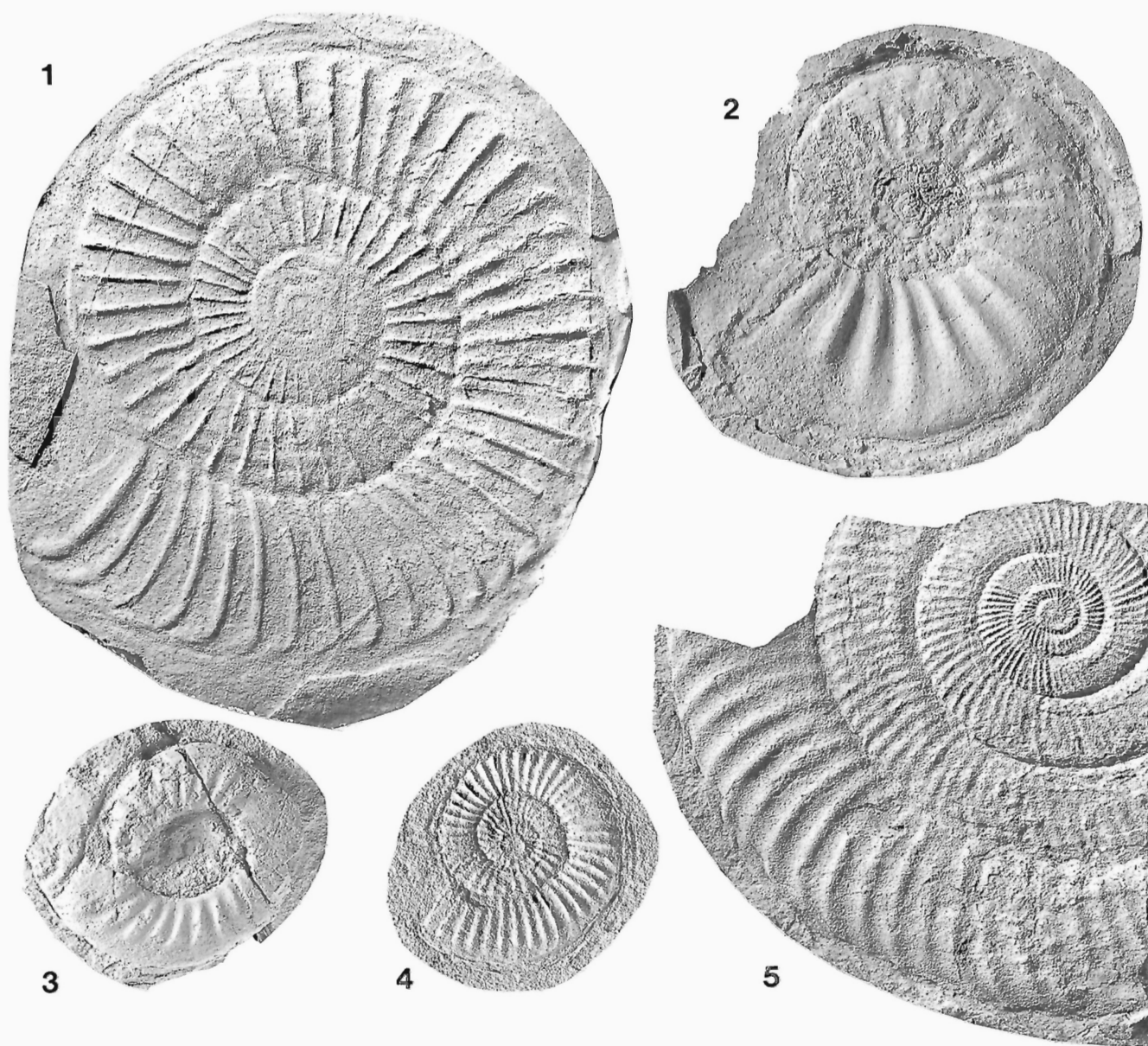


## PLATE 2

Sinemurian ammonites from the Sandilands Formation. All figures are natural size.

**Figure 1:** *Arnioceras arnouldi* (Dumortier, 1867); UBC 08; south shore of Maude Island; Lower Sinemurian.

**Figure 2:** *Asteroceras* sp.; GSC 95568; GSC Loc. No. C-157501; Upper Sinemurian.

**Figure 3:** *Badouxia canadensis* (Frebold, 1951); GSC 95569; GSC Loc. No. C-157629; Canadensis Zone.

**Figure 4:** *Vermiceras* sp.; GSC 95570; GSC Loc. No. C-157623; Lower Sinemurian.

**Figure 5:** *Paltechioceras harbledownense* (Crickmay, 1928); GSC 95571; GSC Loc. No. C-157517; Upper Sinemurian.

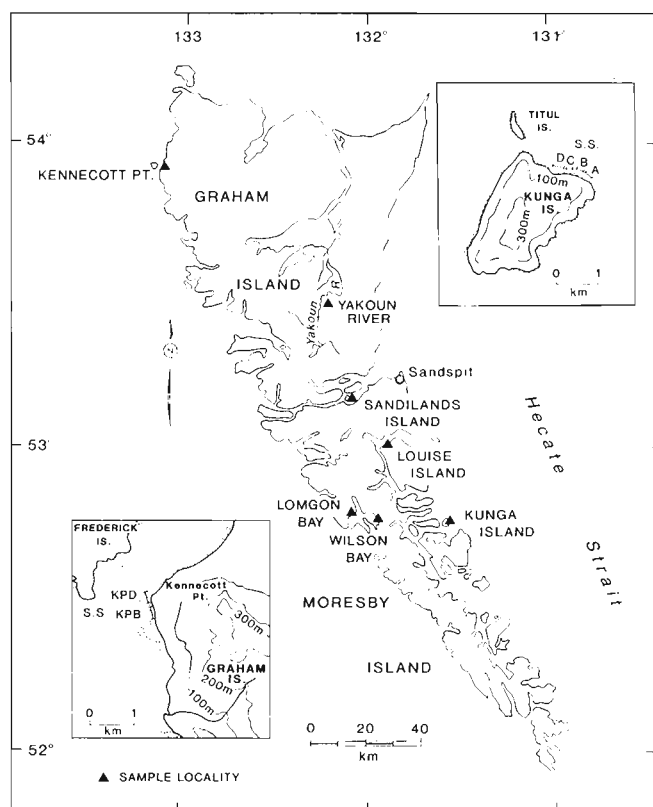


**Figure 7:** Location of radiolarian samples and sections in the Queen Charlotte Islands referred to in this report.

dle Hettangian. All Hettangian taxa previously mentioned are present in this sample plus *Pantanellium kluense* Pessagno and Blome, *P. browni* Pessagno and Blome, and *P. talunkwanense* Pessagno and Blome. Another sample, collected 4.5 m higher, contains abundant *P. browni* and *P. talunkwanense*, but lacks *P. kluense* and *P. tanuense*. This shift in species abundance suggests the latter assemblage may be slightly younger.

A sample from Wilson Bay (Tasu Sound) has yielded *Canoptum unicum* Pessagno and Whalen, *Drotius hecatensis* Pessagno and Whalen, *Pantanellium browni* Pessagno and Blome, *P. talunkwanense* Pessagno and Blome, and other Hettangian taxa documented by Whalen (1985). The fauna is probably Hettangian, but not Early Hettangian in age.

Radiolarians associated with ammonites from the basal Sinemurian Canadensis Zone (North American equivalent of the lower part of the Northwest European Bucklandi Zone) have been recovered from limestone concretions 44.5, 47 and 50 m above the base of Section B, Kennecott Point (shown at 85, 87.5 and 90.5 m, respectively, on Fig. 6). The faunas are similar and contain *Canoptum unicum* Pessagno and Whalen, *Pantanellium browni* Pessagno and Blome, *P. danaense* Pessagno and Blome, *P. talunkwanense* Pessagno and Blome, and *Parahsuum?* sp. (Plate 8). They are further characterized by new taxa belonging to the genera *Bipedis*, *Crucella*, *Katroma*, and by many nodose spumellarian forms commonly having three radial spines in one plane (see Whalen, 1985). At Kunga Island, limestone concretions collected 68, 70 and 75 m above the base of Section D, contain well preserved radiolarians that compare closely with the lowest Sinemurian faunas listed above from Kennecott Point. Higher in Section D (above beds slightly disrupted by faulting and folding), assemblages contain *Pantanellium kungaense* Pessagno and Blome, *Crucella* sp. and common *Drotius*; these collections are younger, but still probably Early Sinemurian.

Many other excellent radiolarian collections have been obtained from limestone concretions in sections C, B and A on Kunga Island. These sections young towards the east (Section C, the older; Section A, the younger) but until more precise macrofossil dating is available, it is uncertain if the sequence is complete or if there is repetition. Within these sections the occurrence of some significant taxa are listed below:

1. *Canutus rockfishensis* Pessagno and Whalen is first observed in the upper part of Section C, associated with *Pantanellium kungaense* Pessagno and Blome, *P. skedansense* Pessagno and Blome, and *P. danaense* Pessagno and Blome. These taxa co-occur with several ammonites believed to be Sinemurian. 12.5 m higher, the genus *Wrangellium* is first observed in association with an ammonite regarded as Sinemurian, possibly upper.
2. *Bagotum erraticum* Pessagno and Whalen, *B.(?) helmetense* Pessagno and Whalen, *Canoptum dixonii* Pessagno and Whalen, *Drotius lassekensis* Pessagno and Whalen, and *Napora graybayensis* Pessagno, Whalen and Yeh, occur together near the base of Section B. An ammonite imprint collected 16.5 m higher in the section resembles *Asteroceras* sp.; possibly very early Late Sinemurian.
3. *Drotius lyellensis* Pessagno and Whalen is first observed near the base of Section A; approximately midway through this section *Pantanellium haidaense* Pessagno and Blome and *Wrangellium thurstonense* Pessagno and Whalen are present. Rare specimens strongly resembling *Parahsuum* s.s. are found in the upper part of this section (sample KU-A6; C-150151).

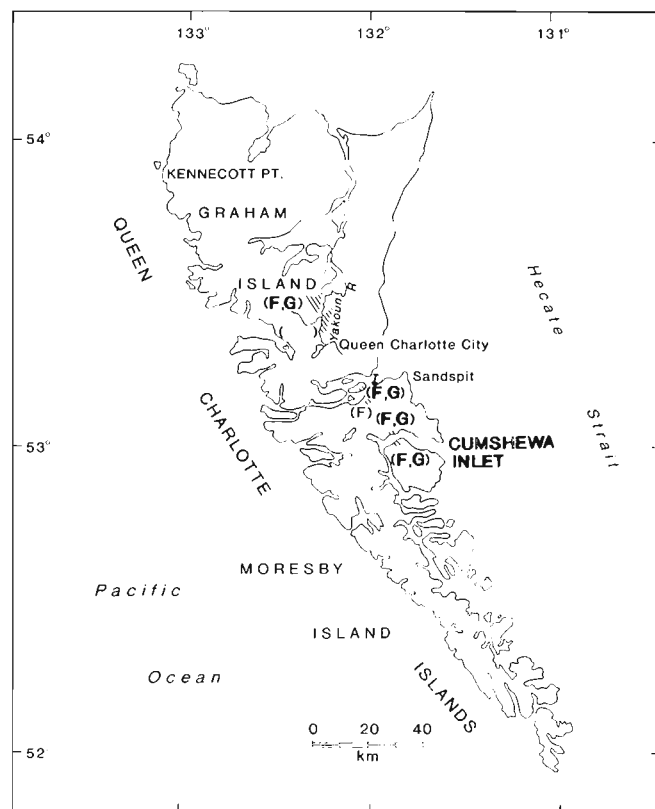


**Figure 8:** Distribution of main Ghost Creek (G) and Fannin (F) Formation outcrops of Pliensbachian age.

Radiolarian collections from the Yakoun River and Sandilands Island are Late Sinemurian, associated with the ammonite *Paltechioceras*. Collections from Maude Island and Lomgon Bay, by comparison, are also Late Sinemurian. No radiolarian collections from the latest Sinemurian have yet been found.

Some Hettangian and Sinemurian radiolarians from Kunga Island and Kennecott Point are illustrated on Plate 9.

## THE GHOST CREEK FORMATION

### Lithostratigraphy

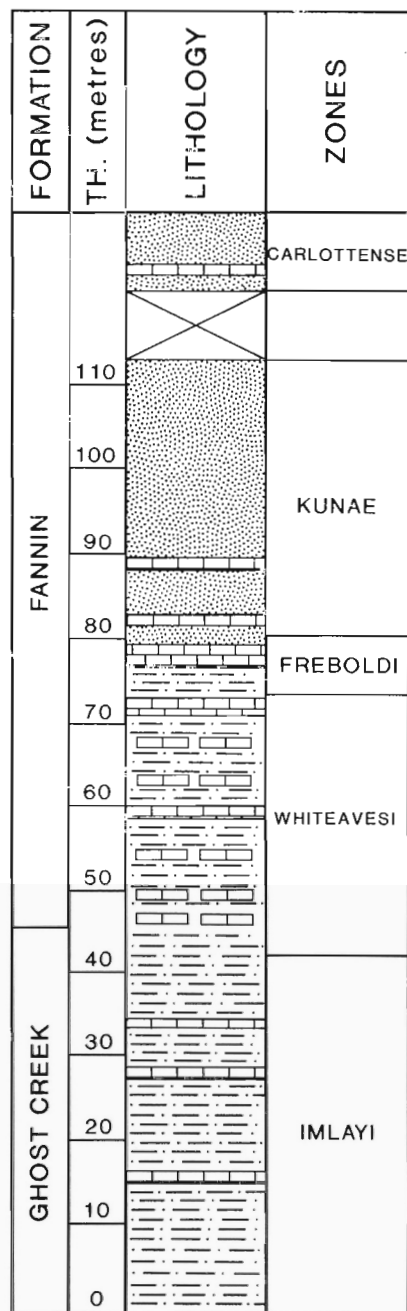
The Ghost Creek Formation, named by Cameron and Tipper (1985), is the basal unit of the Maude Group. It consists of fetid shales, siltstones and mudstones with rare sandstones and thin beds or nodules of limestone. Outcrops of this characteristically recessive unit have been recognized from Cumshewa Inlet to central Graham Island where the type section was designated (Fig. 8). Because of its incompetence, it has not been possible to measure a complete section through the Ghost Creek Formation but the unit reaches thicknesses in excess of 60 m in both its northern and southernmost outcrops (Figs. 9 and 10).

The diachronous relationship between the Ghost Creek and Sandilands formations is discussed above. The Ghost Creek Formation itself shows only subtle lateral variations in lithology from slightly tuffaceous and more resistant in the south to darker, more regularly bedded and locally glauconitic in the north. Sedimentation seems to have been uniform in a relatively deep water setting. The high total organic carbon content, particularly compared to the overlying Fannin Formation (Vellutini, 1988), and the high pyrite content of the sediments suggest a euxinic environment of deposition and this is supported by the dearth of benthonic organisms, trace fossils and bioturbation. Benthonic and trace fossils are slightly more common in both the upper part of the unit generally, and throughout the entire unit in more southerly exposures.

### Biostratigraphy

The bulk of the Ghost Creek Formation is assignable to the Imlayi Zone, the lowest North American Zone of the Pliensbachian Stage (Smith et al., 1988). Ammonites that are particularly common at this level include species of *Pseudoskirroceras*, *Metaderoceras* and *Tropidoceras* (Fig. 11; Plate 3). Less common are species of *Phricodoceras*, *Polymorphites* and *Gemmellaroceras*.

At all localities where the contact between the Ghost Creek and Fannin formations is exposed, up to 10 m or so of the upper Ghost Creek Formation yields ammonites of the superjacent Whiteavesi Zone (Smith et al., 1988), par-



### LEGEND

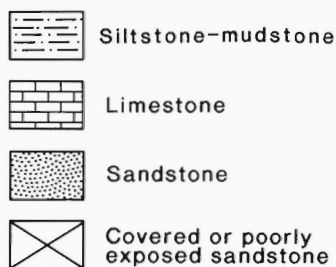
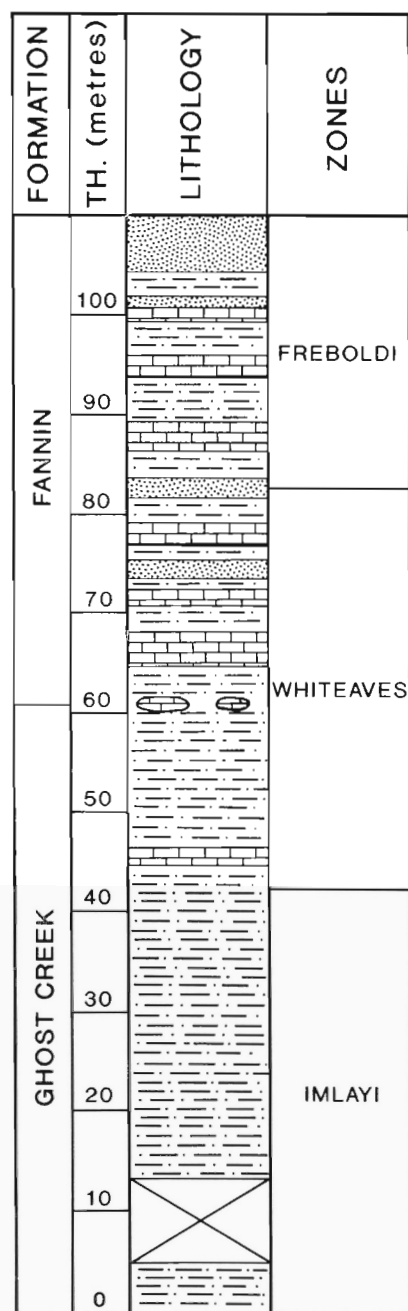


Figure 9: Measured Lower and Upper Pliensbachian stratigraphic section on the west side of Fannin Bay, Maude Island.



### LEGEND

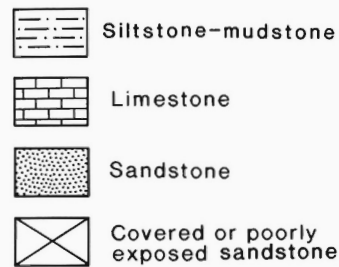


Figure 10: Measured Lower Pliensbachian stratigraphic section at Rennell Junction, Central Graham Island.



**Figure 11:** A sandstone bedding surface within the Ghost Creek Formation exposed on the north shore of Cumshewa Inlet. Poorly preserved ammonites are *Pseudoskirroceras* sp. and *Tropidoceras* sp. of the Imlayi Zone. Field of view approximately 25 cm across.

ticularly species of *Acanthopleuroceras*, *Metaderoceras*, *Tropidoceras* and *Dubariceras* (Plate 4). At one locality in the Whiteaves Bay section, the presence of *Dubariceras freboldi* indicates the Freboldi Zone, the uppermost zone of the Lower Pliensbachian. Ammonites of the Imlayi and Whiteavesi zones have been retrieved from the sub-surface in Intercoast Resources core DDH 179, which penetrated the Ghost Creek Formation in central Graham Island (section 3 of Cameron and Tipper, 1985).

The first common, well preserved calcareous foraminiferal faunas occur in the dark shales of the Ghost Creek Formation (base of

### PLATE 3

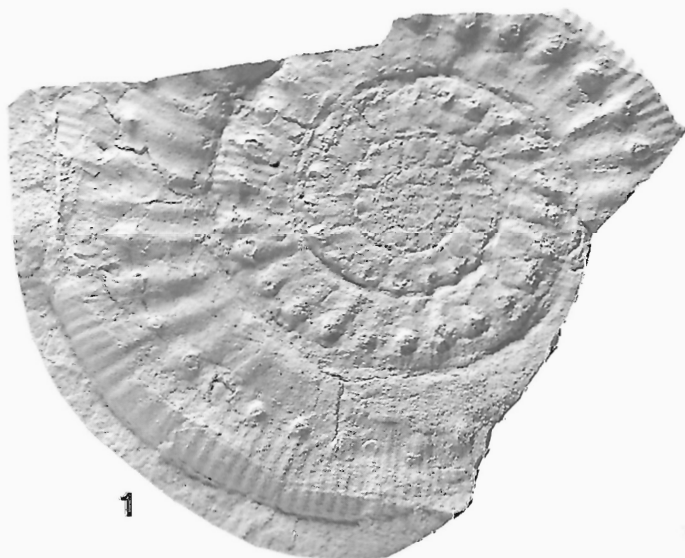
Lower Pliensbachian ammonites from the Ghost Creek Formation. All figures are natural size.

**Figure 1:** *Pseudoskirroceras imlayi* Smith and Tipper, 1988; GSC 95572; GSC Loc. No. C-157551; Imlayi Zone.

**Figure 2:** *Tropidoceras masseanum* (D'Orbigny, 1844); GSC 95573; GSC Loc. No. C-093575; Whiteavesi Zone.

**Figure 3:** *Tropidoceras flandrini* (Dumortier, 1869); GSC 95574; GSC Loc. No. C-090977; Imlayi and Whiteavesi Zone.

**Figure 4:** *Phricodoceras* cf. *taylori* (J. de C. Sowerby, 1826); GSC 87789; GSC Loc. No. C-090974; Imlayi to Freboldi Zone.



1



2



3



4



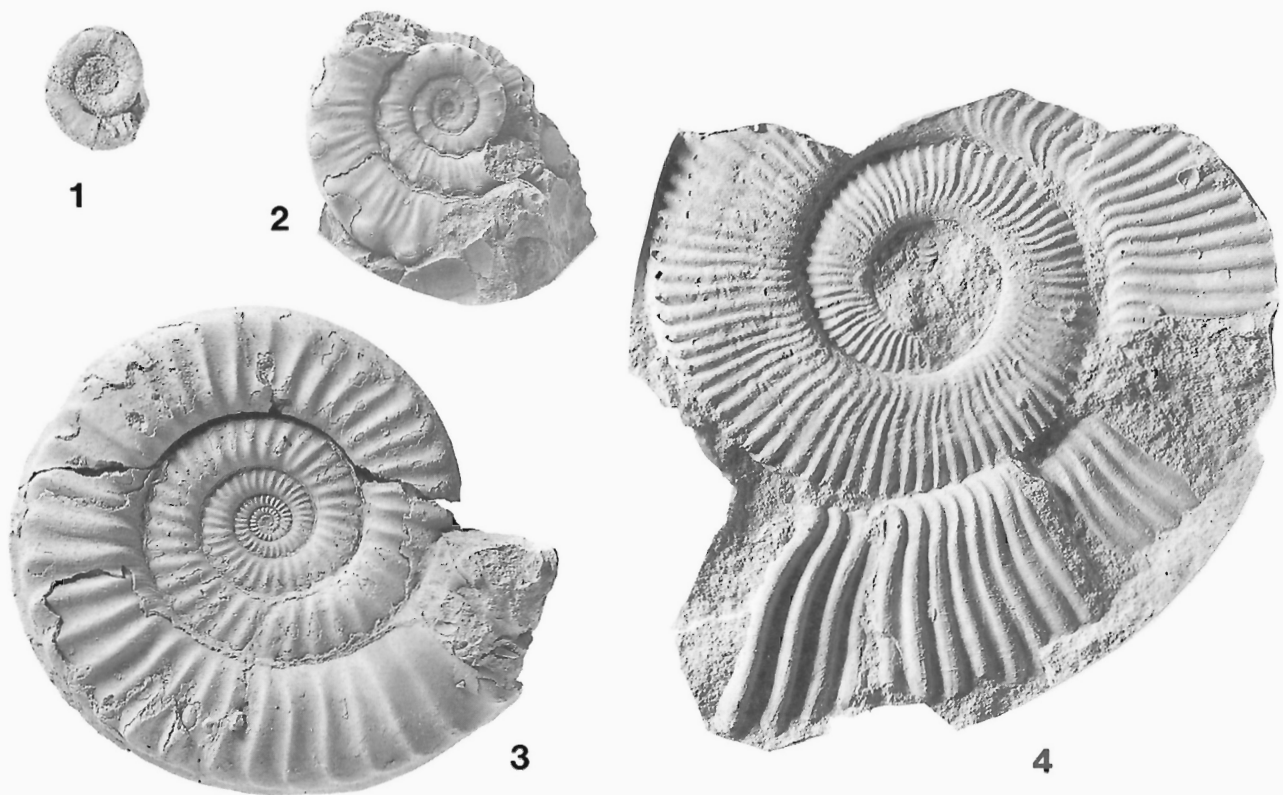


## PLATE 4

Lower Pliensbachian ammonites from the Fannin Formation (beds transitional to the Ghost Creek Formation). All figures are natural size.

**Figure 1:** *Gemmellaroceras aenigmaticum* (Gemmellaro, 1884); GSC 95575; GSC Loc. No. C-117019; Whiteavesi and lowermost Freboldi Zone.

**Figure 2:** *Metaderoceras evolutum* (Fucini, 1921); GSC 95576; GSC Loc. No. 091794; Imlayi to lowermost Freboldi Zone.

**Figure 3:** *Acanthopleuroceras whiteavesi* Smith and Tipper, 1988; GSC 87790; GSC Loc. No. 091794.

**Figure 4:** *Dubariceras freboldi* Dommergues, Mouterde and Rivas, 1985; GSC 87794; GSC Loc. No. C-090587; Freboldi Zone.

Lower Pliensbachian). This distinctive microfauna was recovered from a road-side exposure near the Yakoun River (GSC Loc. Nos. C-127868, C-127899 and C-127933) and consists of predominantly small nodosarids including: *Ichthyolaria bicostata bicostata* (d'Orbigny, 1850), *I. bicostata mesoliassica* (Brand), *Paralingulina tenera pupa* (Terquem), *P. sp.*, *Mesodentalina tenuistriata* (Terquem), *M. hausleri* (Schick), *Nodosaria simplex* Terquem.

The upper part of the Ghost Creek Formation continues the important *P. tenera* lineage with occurrences of *P. tenera tenuistriata* (Norvang). This assemblage is low in diversity and specimens are very small in size. Representatives of the following also occur here: *Mesodentalina* spp., *Nodosaria* spp., *Marginulina prima* d'Orbigny var., *Vaginulina* spp., *Ramulina* sp., *Citharina* sp., *Lenticulina* spp.

## THE FANNIN FORMATION

### Lithostratigraphy

The lower part of the Maude Group is characterized by a conformable transition from a basal argillaceous unit (the Ghost Creek

Formation) into a sequence dominated by calcareous sandstone (the Fannin Formation as defined by Cameron and Tipper, 1985). The gradational interval of alternating sandstones and argillaceous rocks with some irregularly bedded, diagenetic limestones was named the Rennell Junction Formation by Cameron and Tipper (1985) but it is here recommended that this unit be abandoned as a formation for the following reasons: 1) although the Rennell Junction Formation is easily recognizable in the Skidegate Inlet area, it has not always been possible to separate it from the Fannin Formation during the course of regional mapping elsewhere in the islands, particularly when isolated outcrops of either unit occur; 2) the channelling at the contact between the Rennell Junction and Fannin formations reported by Cameron and Tipper (1985) was a misinterpretation of diagenetically produced, irregularly bedded limestones; and 3) continued collecting has shown that there is no biostratigraphic gap at the Rennell Junction-Fannin formation contact as previously reported (Cameron and Tipper, 1985).

The beds that were previously included within the Rennell Junction Formation should be included in the Fannin Formation whose basal contact is now defined by the incoming of sandstones and irregularly bedded limestones which are more resistant than the underlying Ghost Creek Formation. The type section for the redefined Fannin Formation is Fannin Bay on Maude Island (Figs. 9 and 10; section 8 and part of section 6 of Cameron and Tipper, 1985) where the basal contact is easily recognizable and a complete sequence of the lithologies that characterize the Fannin Formation is developed. The section exposed at Rennell Junction is retained as an auxiliary reference section (Fig. 14; section 10 of Cameron and Tipper, 1985). The unit reaches a thickness of at least 75 m.

The Fannin Formation represents a regressive, coarsening-upward sequence passing from alternating shales, sandstones and limestones into coarser, more tuffaceous, partly calcareous sandstones





**Figure 12:** Exposures of the Fannin Formation at Fannin Bay on Maude Island (section 8 of Cameron and Tipper, 1985) showing alternating sandstones, siltstones and limestones in the foreground and more resistant sandstones in the background. The white strip in the foreground marks the boundary between the Whiteavesi and Freboldi zones, the strip in the background, the boundary between the Freboldi and Kunae zones. Hammer for scale.



**Figure 13:** Close up of the boundary between the Freboldi and Kunae zones (at the level of the hammer heads) with transitional beds of the Fannin Formation in the foreground beneath darker sandstones of the upper Fannin Formation.

(Fig. 12). Lenses with rhynchonellid brachiopods and pectinoid bivalves are frequent in the upper part of the unit. The uppermost part of the unit is characterized by sandstones and some shales with chamosite oolites the ramifications of which are discussed by Cameron and Tipper (1985). Bioturbation is common in the lower part of the Fannin Formation and the sandstones of the upper part of the unit contain trace fossils of the near-shore *Skolithos* ichnofacies such as *Thalassinoides* and *Diplocraterion*.

The Fannin Formation was thought to be present in Sialun Bay in northwestern Graham Island (Cameron and Tipper, 1985) but this has not been verified by subsequent work. The only sandstones present in Sialun Bay are Cretaceous in age and it can only be assumed that the *Tiltoniceras propinquum* reportedly collected from this area by T. Potter Chamney of Petro-Canada was mislabelled. The Fannin Formation has been conclusively recognized from exposures in central Graham Island southwards to the north shore of Louise Island in Cumshewa Inlet. In the southern exposures rocks are generally coarsely grained with breccias present in the upper part of the unit.

### Biostratigraphy

The Fannin Formation as a whole ranges from the Whiteavesi Zone of the Lower Pliensbachian to the basal Toarcian. The transitional alternating shales and sandstones (formerly the Rennell Junction Formation) range from the Whiteavesi to the Freboldi zones of the Lower Pliensbachian. Typical ammonites include species of *Tropidoceras*, *Acanthopleuroceras*, *Dubariceras*, *Gemmellaroceras* and *Metaderoceras* (Plate 4). Rare examples of species of *Reynesocoeloceras*, *Liparoceras* (*Becheiceras*), and *Phylloceras* are also known.

The passage from the transitional beds of the Fannin Formation to the upper sandstones seems to have occurred in all areas near the top of the Freboldi Zone (Fig. 13) with deposition of the Fannin sandstones occurring throughout the Kunae and Carlottense zones and even into the earliest Toarcian in the Skidegate Inlet area. The chamosite oolite beds are restricted to the Carlottense Zone.

The upper Fannin sandstones of the Kunae and Carlottense zones have yielded a diverse suite of ammonites including species of *Fanninoceras*, *Aveyroniceras*, *Reynesoceras*, *Reynesocoeloceras*, *Cymbites*, *Arietoceras*, *Leptaleoceras*, *Fontanelliceras*, *Protogrammoceras*, *Fucinoceras*, *Tiltoniceras* and *Lioceratoides* (Plate 5). Rare examples of species of *Amaltheus*, *Liparoceras* (*Becheiceras*) and *Phylloceras* also occur. The basal Toarcian is marked by the occurrence

### PLATE 5

Pliensbachian and Toarcian ammonites from the Fannin Formation. All figures are natural size.

**Figure 1:** *Metaderoceras mouterdei* (Frebold, 1970); GSC 87797; GSC Loc. No. C-080610; upper Whiteavesi to lowermost Kunae Zone (Pliensbachian).

**Figure 2:** *Aveyroniceras colubriforme* (Bettoni, 1900); GSC 87796; GSC Loc. No. C-090614; uppermost Freboldi and lower Kunae Zone (Pliensbachian).

**Figure 3:** *Reynesoceras ragazzoni* (Hauer, 1861); GSC 87800; GSC Loc. No. 048564; Kunae Zone (Pliensbachian).

**Figure 4:** *Dactyloceras kanense* McLearn, 1930; GSC 9051; GSC Loc. No. C-080778; Lower Toarcian.

**Figure 5:** *Fanninoceras carlottense* McLearn, 1930; GSC 4878; GSC Loc. No. C-117003; Carlottense Zone (Pliensbachian).

**Figure 6:** *Fanninoceras fannini* McLearn, 1930; GSC 9054; GSC Loc. No. C-117032; Kunae Zone (Pliensbachian).

**Figure 7:** *Fanninoceras crassum* McLearn, 1932; GSC 6517; GSC Loc. No. C-117032; Kunae Zone (Pliensbachian).

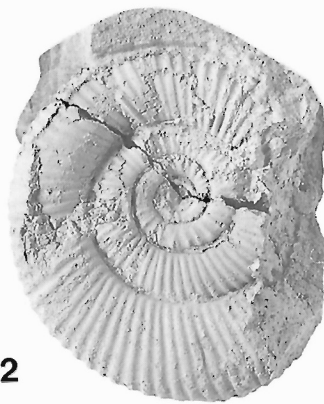
**Figure 8:** *Tiltoniceras propinquum* (Whiteaves, 1884); GSC 87804; GSC Loc. No. C-117003; Carlottense Zone (Pliensbachian and lower Toarcian).

**Figure 9:** *Leptaleoceras* aff. *accuratum* (Fucini, 1931); GSC 95577; GSC Loc. No. C-081703; Kunae Zone (Pliensbachian).

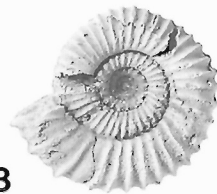
**Figure 10:** *Protogrammoceras pectinatum* (Meneghini, 1881); GSC 87808; GSC Loc. No. C-080786; Kunae to Carlottense Zone (Pliensbachian).



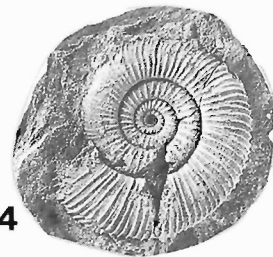
1



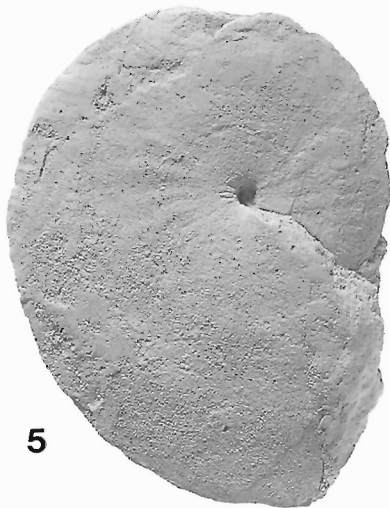
2



3



4



5



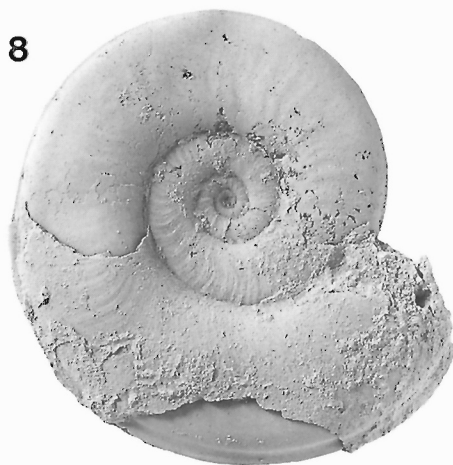
6



7



9



8



10

of *Dactylioceras kanense* (Plate 5). The beds immediately below the Fannin-Whiteaves formational contact, contain *Dactylioceras kanense*, *Tiltoniceras propinquum* and *Taffertia* sp.

The occurrence of Pliensbachian and lowest Toarcian zones in the lower Maude Group of the Queen Charlotte Islands is illustrated schematically in Figure 14 which also demonstrates the extent of diachronism. A comprehensive report on the Pliensbachian ammonite biostratigraphy and systematic paleontology is in preparation by Smith and Tipper.

The foraminiferal faunas within the Lower Pliensbachian part of the Fannin Formation are not highly diversified and are relatively small in size (Plate 10). The *Paralingulina tenera* lineage is represented in the basal part by *P. tenera subprismatica* (Franke). Among the less frequently occurring taxa are *Ichthyolaria? pygamaea* Franke, *Bigennerina? sp.*, *Reinholdella* sp., *Ophalmidium* sp., *Astacolus* spp., *Nodosaria* spp., and the earliest occurrence of a form referred to by various authors as *Brizalina* or *Bolivina*.

The overlying strata of the Frobaldi zone have yielded a relatively meagre microfauna which is due in part to the shallowing water and the coarsening of the clastic sediments (presumably a higher energy regime). In these coarser clastics, large agglutinating genera such as *Reophax* and *Ammobaculites* are common. In the shales and calcareous beds an abundant and diverse assemblage of tiny, completely pyritized foraminifers is found. This includes a form referred to here-in as *Neobulimina? sp.* This form, as well as some of the other small pyritized species, extend into the Kunae zone.

The remaining part of the Upper Pliensbachian Fannin Formation represents a relatively shallow water clastic environment. A good part of this section is tuffaceous thus making the recovery of microfauna rather difficult. Nevertheless, robust agglutinating Foraminifera are fairly well represented by *Reophax*, *Ammobaculites* and *Ammodiscus*. The small pyritized fauna is well represented in the base. Other significant foraminifers recovered from this interval include *Marginulina prima prima* d'Orbigny, *M. burgundiae* Terquem, *Paralingulina tenera tenera* (Bornemann), *Reinholdella* sp., *Lingulodosaria* sp., *Nodosaria* spp., *Mesodentalina* spp., "*Brizalina*" sp.

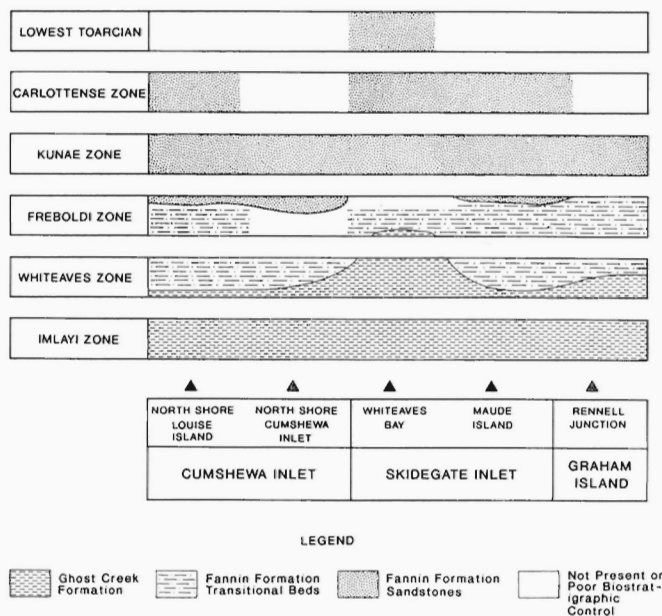


**Figure 14:** Schematic representation of the distribution of Pliensbachian and Lower Toarcian zones in the Queen Charlotte Islands.

An abundant microfauna was found associated with the ammonite *Tiltoniceras propinquum* in the tuffaceous beds of the uppermost part of the Fannin Formation on Maude Island. This included an abundance of siliceous sponge spicules and silicified paracyprid ostracods. Although these ostracods are not specifically identifiable, they mark the first common occurrence of ostracods in the Lower Jurassic of the Queen Charlotte Islands.

## WHITEAVES FORMATION

### Lithostratigraphy

The Whiteaves Formation (Figs. 15 and 18) consists, primarily, of a greenish-grey silty shale which weathers to a rusty-grey colour. It is a recessive unit (Fig. 16) best exposed in creek and river beds. The shale is very fragmented and lacks well-defined bedding planes. Interbedded with the shale are a number of glauconitic, greenish sandy layers; limy layers and concretionary horizons are also common. The concretions are of two types: septarian and non-septarian. The septarian concretions are usually the larger and can reach diameters of approximately 30 cm. Due to their septarian nature, they are generally unfossiliferous and any ammonites that are preserved in their interiors are highly fragmented. In many cases, the septarian concretions have hollow interiors which can contain bituminous material. The non-septarian concretions, ranging in diameter from 1-25 cm, are more prevalent in the upper part of the formation, usually concentrated in bands. The concretions range in shape from nearly spherical to discoidal and commonly contain well-preserved ammonites. Ammonites are found in either variety and are usually parallel to bedding. Thin (1-5 cm), bentonitic ash beds are common in the shales. Two members were recognized by Cameron and Tipper (1985, p. 25), a lower one characterized by the septarian concretions and an upper one characterized by the non-septarian concretions.

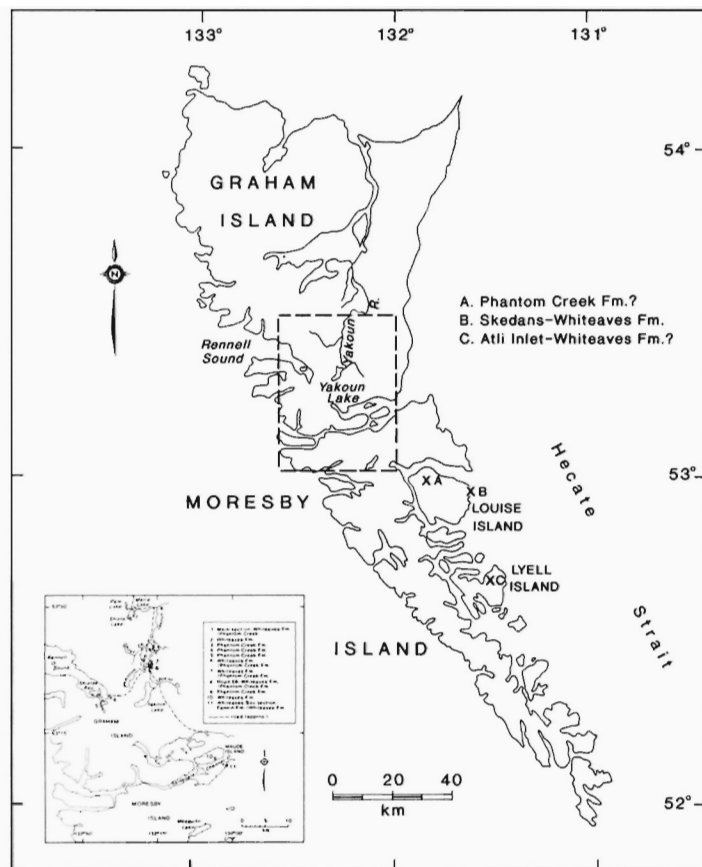


**Figure 15:** Locality map of Toarcian lithostratigraphic units.



**Figure 16:** Soft shale and siltstone of the Whiteaves Formation on the Yakoun River. A few small concretions can be seen scattered randomly through the section. Stick at the right is about 60 cm long.

No significant lateral changes were observed in the formation between its exposures throughout the Charlottes from Louise Island to Yakoun River. Ash beds are too thin and of too uniform an appearance to serve as correlative tools. The sandy and limy beds except for the concretionary beds, appear to be of restricted geographical extent.

The Whiteaves Formation is underlain by the Fannin Formation but there is only one exposure where the contact is seen, namely at Whiteaves Bay where it appears to be conformable (Cameron and Tipper, 1985).

The Whiteaves Formation was deposited in a fairly continuous deep basinal setting. Portions were probably deposited under anoxic conditions as indicated by the general lack of a benthonic fauna. The sandier layers contain some benthonic bivalves and probably represent a partially oxygenated environment. It was deposited during an interval of time characterized by the deposition of black shale coincident with a world wide rise in sea level in Early and Middle Toarcian time.

#### Biostratigraphy

The Whiteaves Formation ranges in age from the Late Early Toarcian to the Early Late Toarcian.

The lowermost part of the formation occurs only at Whiteaves Bay and due to the poor outcrop exposure, ammonites collected here are generally talus samples only. The uppermost part of the Lower Toarcian beds is exposed along the Yakoun River in several places. It is represented by *Hildaïtes* cf. *chrysanthemum* (Yokoyama, 1904), *Harpoceras exaratum* (Young and Bird, 1822), *Dactylioceras* sp. and *Peronoceras* sp. (Plate 6).

The Middle Toarcian is marked by the appearance of *Phymatoceras*; *Hildaïtes* cf. *chrysanthemum* (Yokoyama, 1904) is absent. It is represented by *Phymatoceras narbonense* (Buckman, 1898), *Phymatoceras erbaense*(?) (Hauer, 1856), *Paroniceras sternale* (von Buch, 1832), *Peronoceras* cf. *desplacei* (D'Orbigny, 1844) and *Leukadiella* sp.

The uppermost part of the Formation represents the lower part of the Upper Toarcian. The Upper Toarcian is marked by the appearance of *Grammoceras*; *Peronoceras* is not present. The Whiteaves portion of the Upper Toarcian is represented by *Grammoceras* cf. *striatulum* (Sowerby, 1823), *Grammoceras thouarsense* (D'Orbigny, 1843), *Phymatoceras* cf. *robustum* (Hyatt, 1867), *Phymatoceras copiapense* (Moricke, 1894), *Phymatoceras* spp. and *Podagrosites* sp.

The foraminifers of the Whiteaves Formation, are among the most abundant and diverse of the Lower Jurassic of the Queen Charlotte Islands. Nodosarid genera are characteristic and dominate the faunas with rotaloid and agglutinating forms somewhat less common. The

ostracods *Kinkelinella*, *Cytherella*, *Cytherelloidea* and *Monoceratina* are a conspicuous and common element of the microfaunas.

Foraminifers characteristic of the lower part of the Whiteaves Formation (Plate 11) include *Reinholdella* sp. cf. *R. macfadyeni* (Ten Dam), *Falsopalmula varians* (Bornemann), *Lenticulina gottingensis* (Bornemann), *Lenticulina d'orbignyi* (Roemer), *Pseudonodosaria pygmaea* (Terquem), *Citharina sagquittiformis* (Terquem), and *Lenticulina* sp. T1 – a form restricted to the lower Whiteaves Formation and characterized by its large size, partly evolute test in the adult stage and truncate peripheral margin when observed in side view.

The upper part of the Whiteaves Formation has yielded an equally diverse foraminiferal fauna. Agglutinating forms are more abundant however, perhaps suggesting a gradual shallowing of the seas. *Lenticulina d'orbignyi* is one of the main constituents of this fauna and consistently appears to be much more reticulate than other representatives of this species in the lower part of the formation (compare figs. 6 and 10 in Plate 11). Other important species of the upper Whiteaves Formation include *Lenticulina prima* (d'Orbigny), *Lenticulina* spp., *Vaginulina listi* (Bornemann).

## PHANTOM CREEK FORMATION

### Lithostratigraphy

The Phantom Creek (Figs. 17 and 18) Formation is a fine- to coarse-grained greenish-grey sandstone with thin shale interbeds.



**Figure 17:** Sandy, irregularly bedded Phantom Creek Formation on the Yakoun River. A few concretionary, limy masses are scattered through the section.



The sandstone may be glauconitic in its upper layers and is a bright green, sometimes blue-green colour. Buff-weathering concretion beds are common in the lower part of the formation. Some of the concretions which reach diameters of 1.3 m are exceedingly fossiliferous. The lower part of the formation is richly fossiliferous and coquinoid in nature. The sandstone is generally quite friable and thinly bedded. The upper part of the formation is generally thickly bedded, well indurated and contains few ammonites.

The contact of the Phantom Creek Formation with the overlying Graham Island Formation is quite distinguishable as an abrupt change from thickly bedded greenish sandstones to thinly bedded black siltstones of Late Bajocian age. A paraconformable hiatus is present as

evidenced by the absence of Upper Aalenian and earliest Lower Bajocian beds (Cameron and Tipper, 1985).

The contact of the Phantom Creek Formation with the underlying Whiteaves Formation is also distinct. There is an abrupt change from the greenish-grey shales of the Whiteaves Formation to the sandstone of the Phantom Creek Formation with no transitional beds. A hiatus of variable duration is represented here. Along the Yakoun River, the Phantom Creek Formation is approximately 15 m thick, at Road 59 it is 3 m thick and on Maude Island it is less than 3 m thick and probably Aalenian in age. The fauna at Road 59 indicates that the lower part of the formation is absent and suggests that the effect of the hiatus increases with increasing distance southwards.

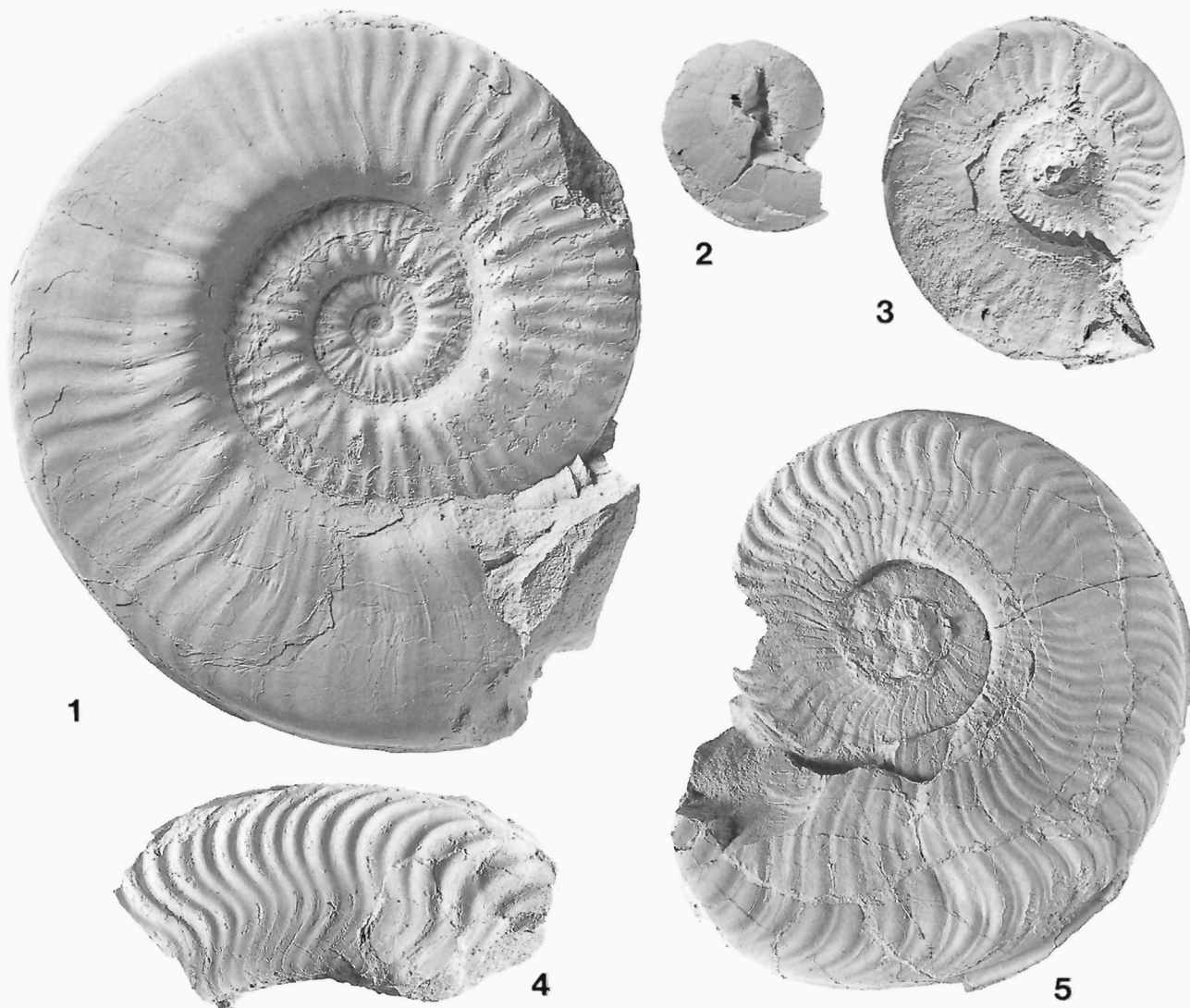


## PLATE 6

Toarcian ammonites from the Whiteaves Formation. All figures are natural size.

**Figure 1:** *Phymatoceras copiapense* (Moricke, 1894); GSC 95578; GSC Loc. No. C-157728; Middle Toarcian.

**Figure 2:** *Paroniceras sternale* (von Buch, 1832); GSC 95579; GSC Loc. No.

C-087105; Middle Toarcian.

**Figure 3:** *Grammoceras thouarsense* (D'Orbigny, 1843); GSC 95580; GSC Loc. No. C-087122; Upper Toarcian.

**Figure 4:** *Hildaites* cf. *chrysanthemum* (Yokoyama, 1904); GSC 95581; GSC Loc. No. C-158008; Lower Toarcian.

**Figure 5:** *Harpoceras* cf. *exaratum* (Young and Bird, 1828); GSC 95582; GSC Loc. No. C-158027; Lower Toarcian.



QUEEN CHARLOTTE ISLANDS  
Toarcian Sections

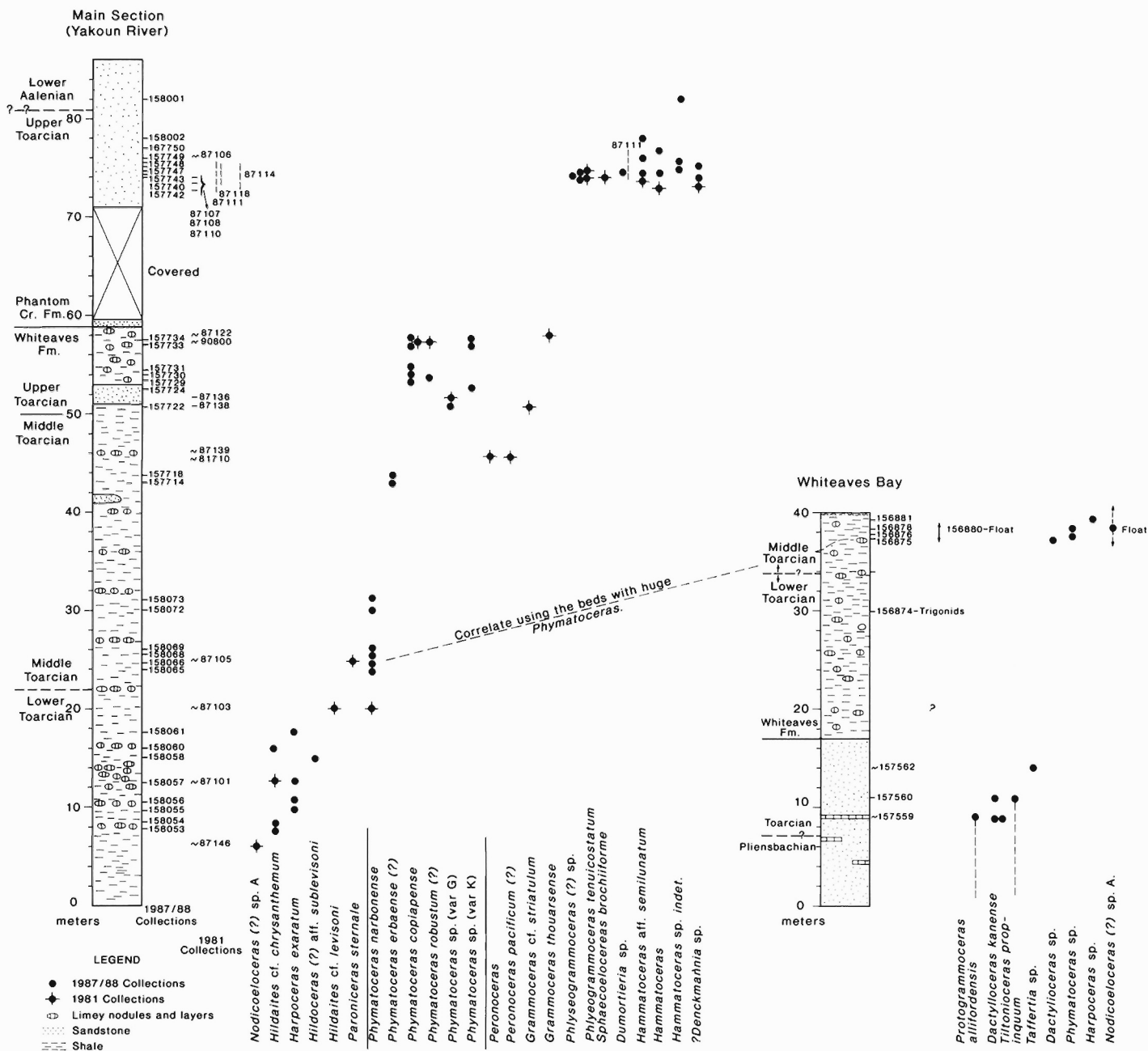


Figure 18: Measured sections of Whiteaves, Phantom Creek and Fannin (in part) formations and ammonite faunas.

The Phantom Creek Formation probably represents deposition in a fairly shallow basin. Benthonic bivalves are common and suggest oxygenated conditions. Plant fragments such as fern leaves and wood pieces are common suggesting a relatively close sediment source. The upper part of the formation probably represents a deepening trend as evidenced by the paucity of bivalves and the predominance of pelagic fauna such as ammonites and belemnites.

#### Biostratigraphy

The Phantom Creek Formation ranges in age from the Middle Late Toarcian to the Early Aalenian.

The main section on the Yakoun River has a covered interval of approximately 10 m just above the Whiteaves/Phantom Creek boundary. Above the covered interval is a "coquinoid" part of the formation which is represented (Plate 7) by *Hammatoceras speciosum* (Janensch, 1902), *Sphaercoeloceras brochiiforme* (Jaworski, 1926), *Phlyseogrammoceras tenuicostatum* (Jaworski, 1926), and *Dumortieria* sp. The upper part of the formation consists of hard, massive sands and has yielded *Hammatoceras* sp., *Pleydellia* and the large, involute ammonite that Frebold (internal report) referred to as "*Esericeras*" but is probably another *Hammatoceras*. In addition, the lower part of the formation is represented by a number of species which Fre-

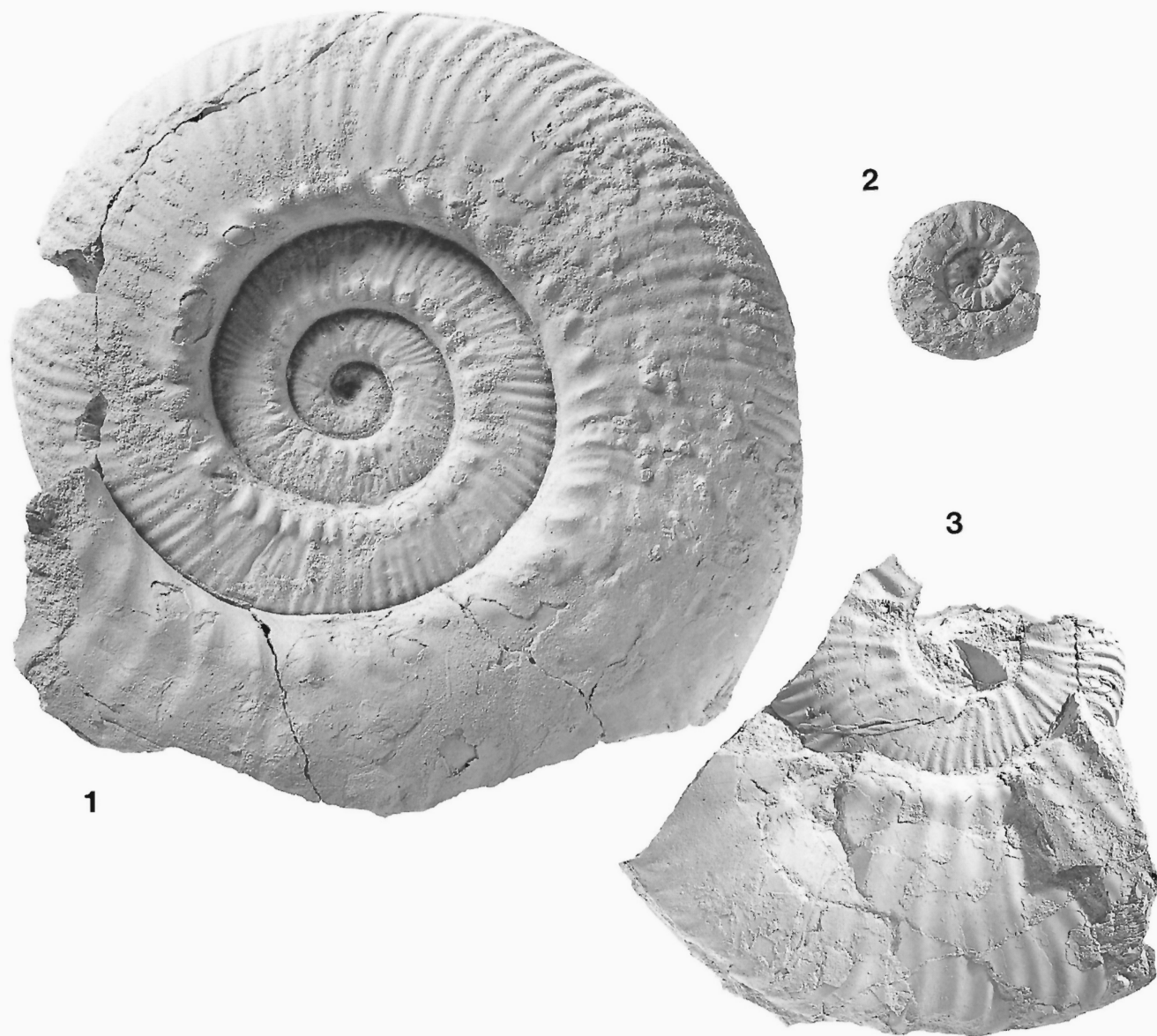


#### PLATE 7

Toarcian ammonites from the Phantom Creek Formation. All figures are natural size.

**Figure 1:** *Hammatoceras speciosum* (Janensch, 1902); GSC 95583; GSC Loc. No. C-087215; Upper Toarcian.

**Figure 2:** *Sphaercoeloceras brochiiforme* (Jaworski, 1926); GSC 95584; GSC Loc. No. C-087118; Upper Toarcian.

**Figure 3:** *Phlyseogrammoceras*(?) sp.; GSC 95585; GSC Loc. No. C-087114; Upper Toarcian.

bold assigned to *Denckmannia*. They are similar to some *Phymatoceras* but display very prominent nodes at the base of the whorl flanks. They have been tentatively identified as ?*Denckmannia*. The uppermost part of the formation is Early Aalenian in age and is represented by *Tmetoceras* sp. and *Bredya* sp. (see Poulton et al., 1991).

The foraminiferal faunas of the lower part of the Phantom Creek Formation (Upper Toarcian) are similar to those of the underlying Whiteaves Formation. Their diversity is much reduced and their recovery much more difficult due to the dominance of sandstone in the formation. A few species that appear to be restricted to the lower Phantom Creek include *Falsopalmula jurensis* (Franke), *Lenticulina* sp., *Citharina* sp. cf. *C. lonquemari* (Terquem), *Pseudonodosaria pygmaea* (Terquem).

## UPPER PLIENSCHACHIAN-TOARCIAN RADIOLARIA

The radiolarian studies begun in 1982, resulted in preliminary zonation for Lower and Middle Jurassic faunas of late Pliensbachian, Toarcian, Aalenian and early Bajocian age from the Fannin, Whiteaves and Phantom Creek formations of the Maude Group, and the Graham Island Formation of the Yakoun Group (Carter et al., 1988). For discussion of Middle Jurassic (Aalenian and lower Bajocian) radiolarians see Poulton et al. (1991). Toarcian radiolarians were emphasized because little was known previously of their morphology and distribution. Rich, well preserved faunas were recovered from limestones of the Whiteaves and Phantom Creek formations at localities on Maude Island and in the Yakoun River area of Graham Island. Assemblages were dated by closely associated suites of ammonites (Table 1) and five informal radiolarian zones (1-5) were distinguished within the late Pliensbachian to Toarcian interval (see Carter et al., 1988, p. 20, Fig. 1). Zone 1 is late Pliensbachian (Carlottense Zone). Corresponding ammonite zones for Toarcian radiolarian zones 2-5 have not yet been worked out for North America; thus Zone 2 is early Middle Toarcian (approximately equivalent to the Bifrons Zone), Zones 3 and 4 are late middle to early Late Toarcian, and Zone 5 is Late Toarcian. A synopsis of zonal indicators for these zones is as follows:

Zone 1: Base undetermined (no subjacent fauna to provide basis for definition). Top of zone marked by final appearance of *Katroma ninstintsi* Carter, *Bipedis fannini* Carter and *Canutus* s.s.

Zone 2: Base recognized by first appearance of *Protoperispyridium*, *Parvingula* s.l., and *Emiluvia*. Abundant species characteristic of this zone are *Hsuum optimus* Carter, *Protounuma paulsmithi* Carter *Protoperispyridium*(?) *hippaensis* Carter, *Emiluvia*(?) *moresbyensis* Carter and *Hsuum* cf. *rosebudense* Pessagno and Whalen. Top of zone marked by final appearance of *Jacus magnificus* Carter and *Parvingula*(?) sp A.

Zone 3: Base recognized by first appearance of *Turanta marinae* Pessagno and Blome, and the genus *Elodium*. This zone is defined on first appearances of species only; no significant extinctions are observed.

Zone 4: Base recognized by first appearance of *Tripocyclia* s.s. and the genus *Maudia*. Other genera abundant in this zone are *Emiluvia*, *Staurolonche*, *Hsuum*, *Elodium* and spongy forms such as *Paronaella*, *Crucella*, *Spongostaurus*, *Spongotrochus* and *Spongotropis*. Top of zone marked by final appearance of *Crucella angulosa* Carter and *Rolubus kiustaense* Carter.

Zone 5: Base recognized by first appearance of *Higumastra*. Abundant genera making up the bulk of this zone are *Emiluvia*, *Hagias-trum*, *Praeconocaryomma*, *Hsuum*, *Elodium* and many of the spongy forms mentioned above in Zone 4. Top of zone marked by final appearance of *Canoptum* s.s. and *Spongostoma saccideon* Carter. This zone is approximately equivalent to the top of Subzone 1A<sub>2</sub> of Pessagno et al. (1987).

Details of this zonation and description of many new taxa are found in Carter et al. (1988). Some data on Toarcian faunas was incorporated in a preliminary radiolarian zonation for the Jurassic of North America by Pessagno et al. (1987).

Toarcian assemblages are characterized by abundant hagiastroid and patulibracchiid forms, e.g. *Paronaella*, *Crucella*, *Homeoparonaella*, *Hagias-trum* etc. These forms are particularly abundant in the Middle to Upper Toarcian Phantom Creek Formation. Lithological and faunal evidence suggests at least the lower part of this formation was deposited in a high energy, shallow water environment. The exceptional abundance of spumellarian radiolarians (particularly spongy forms) in a Jurassic nearshore setting may suggest future possibilities for comparing Mesozoic faunas with recent ones in the modern ocean.

Some index taxa for the late Pliensbachian and Toarcian are illustrated in Plate 9.

## OTHER SIGNIFICANT FOSSILS OF THE LOWER JURASSIC OF QUEEN CHARLOTTE ISLANDS

Ammonites, Radiolaria, and Foraminifera are the fossil faunas that have been studied in detail and will continue to receive most of our attention. There are, however, other faunas, probably not as abundant, that may be worthy of attention in the future. Some preliminary work has in some cases already begun. The following brief comments will outline the potential for study that exists.

### Vertebrates

**Fish Remains.** In the Sinemurian beds of the Sandilands Formation a few partial skeletons of small fish have been noted. In particular in the upper part of the Upper Sinemurian beds, at about the level of *Paltechioceras*, several specimens have been noted at two localities in central Graham Island. In the Lower Sinemurian beds of Kennecott Point fish skeletons were noted in the Canadensis Zone and slightly higher. Also fish scales and small bones are commonly seen on shale bedding surfaces throughout the Hettangian section. As yet no study of this material has been attempted.

**Ichthyoliths.** Fish debris has been noted at several stratigraphic levels throughout the Lower Jurassic beds in several formations as well as in Upper Triassic beds of the Sandilands Formation. Ichthyolith studies have been initiated by Johns to determine their potential usefulness to ongoing biostratigraphical work in B.C. The initial objectives have been to recognize morphological differences in specimens, develop and apply a taxonomic system and to obtain specimens from dated sections to determine ichthyolith zonation. Once ichthyolith zones have been determined, these can be applied to dating and correlating sediments. The Lower Jurassic of Queen Charlotte Islands was thought to be a good starting area. As conodonts became extinct at the Jurassic-Triassic boundary, a new fossil group, insoluble in acid, could prove to be a useful additional biostratigraphic tool.

Ichthyoliths are microscopic skeletal remains of fishes composed of calcium phosphates – mainly the mineral apatite. Fish teeth and dermal denticles (scales of sharks, skates and rays) are the most commonly recognized forms. Ichthyoliths are particularly resistant to dissolution and have been recovered from deep water, otherwise unfossiliferous, pelagic clays (Helms and Riedel, 1971) to marginal marine environments. Ichthyolith recovery techniques are compatible with those used to recover other microfossils (Foraminifera, ostracods, radiolarians, conodonts, etc.) where specimens can be obtained from a variety of lithologies.

To date, the ichthyolith collection contains specimens removed from various microfossil slides from samples collected in the Queen Charlotte Islands by Cameron and others. Much potential still exists

## PLATE 8

Scanning electron micrographs of Hettangian and Sinemurian Radiolaria from the Sandilands Formation, Queen Charlotte Islands, British Columbia. Bar scale = number of  $\mu\text{m}$  cited for each illustration.

- Figure 1:** *Paleosaturnalis* sp. 1; GSC 85940; GSC Loc. No. C-164676; Kunga Island; Hettangian; scale = 267  $\mu\text{m}$ .
- Figure 2:** *Pseudoheliodiscus* sp. 1; GSC 85941; GSC Loc. No. C-164676; Kunga Island; Hettangian; scale = 267  $\mu\text{m}$ .
- Figure 3:** *Pseudoheliodiscus* sp. 2; GSC 85942; GSC Loc. No. C-164676; Kunga Island; Hettangian; scale = 267  $\mu\text{m}$ .
- Figure 4:** *Relanus reelfensis* Pessagno and Whalen, 1982; GSC 85943; GSC Loc. No. C-164676; Kunga Island; Hettangian; scale = 200  $\mu\text{m}$ .
- Figure 5:** *Pantanellium* sp. aff. *P. tanuense* Pessagno and Blome, 1980; GSC 85944; GSC Loc. No. C-164676; Kunga Island; Hettangian; scale = 200  $\mu\text{m}$ .
- Figure 6:** Gen. indet. I. sp. 1; GSC 85945; GSC Loc. No. C-164676; Kunga Island, north; Hettangian; scale = 200  $\mu\text{m}$ .
- Figure 7:** Gen. indet. J. sp. 1; GSC 85946; GSC Loc. No. C-164676; Kunga Island; Hettangian; scale = 200  $\mu\text{m}$ .
- Figure 8:** Gen. indet. Z. sp. A (in Cordey, 1988, pl. 24, fig. 9); GSC 85947; GSC Loc. No. C-164659; Kennecott Point, Graham Island; Lower Sinemurian; scale = 200  $\mu\text{m}$ .
- Figure 9:** *Gorgansium* sp. 1; GSC 85948; GSC Loc. No. C-164659; Kennecott Point, Graham Island; Lower Sinemurian; scale = 200  $\mu\text{m}$ .
- Figure 10:** *Crucella* sp. 1; GSC 85949; GSC Loc. No. C-164659; Kennecott Point, Graham Island; Lower Sinemurian; scale = 200  $\mu\text{m}$ .
- Figure 11:** Gen. indet. K. sp. 1; GSC 85950; GSC Loc. No. C-164676; Kunga Island; Hettangian; scale = 200  $\mu\text{m}$ .
- Figure 12:** *Relanus?* sp. 1; GSC 85951; GSC Loc. No. C-164676; Kunga Island; Hettangian; scale = 200  $\mu\text{m}$ .
- Figure 13:** *Pantanellium browni* Pessagno and Blome, 1980; GSC 85952; GSC Loc. No. C-164659; Kennecott Point, Graham Island; Lower Sinemurian; scale = 200  $\mu\text{m}$ .
- Figure 14:** *Pantanellium* sp. 1; GSC 85953; GSC Loc. No. C-164661; Kennecott Point, Graham Island; Lower Sinemurian; scale = 200  $\mu\text{m}$ .
- Figure 15:** Gen. indet. L. sp. 1; GSC 85954; GSC Loc. No. C-164676; Kunga Island; Hettangian; scale = 200  $\mu\text{m}$ .
- Figure 16:** *Canoptum unicum* Pessagno and Whalen, 1982; GSC 85955; GSC Loc. No. C-164659; Kennecott Point, Graham Island; Lower Sinemurian; scale = 200  $\mu\text{m}$ .
- Figure 17:** *Eucyrtis?* sp. 1; GSC 85956; GSC Loc. No. C-164661; Kennecott Point, Graham Island; Lower Sinemurian; scale = 200  $\mu\text{m}$ .
- Figure 18:** Gen. indet. M. sp. 1; GSC 85957; GSC Loc. No. C-164659; Kennecott Point, Graham Island; Lower Sinemurian; scale = 200  $\mu\text{m}$ .

## PLATE 9

Scanning electron micrographs of Pliensbachian and Toarcian Radiolaria from the Queen Charlotte Islands, British Columbia. Bar scale = number of  $\mu\text{m}$  cited for each illustration.

- Figure 1:** *Praeconocaryomma whiteavesi* Carter, 1988; GSC 80528; GSC Loc. No. C-080577; Fannin Formation, Maude Island; Upper Pliensbachian; scale = 128  $\mu\text{m}$ .
- Figure 2:** *Katroma ninstintsi* Carter, 1988; GSC 80694; GSC Loc. No. C-080577; Fannin Formation, Maude Island, Upper Pliensbachian; scale = 200  $\mu\text{m}$ .
- Figure 3:** *Bipedis fannini* Carter, 1988; GSC 80702; GSC Loc. No. C-080577; Fannin Formation, Maude Island; Upper Pliensbachian; scale = 144  $\mu\text{m}$ .
- Figure 4:** *Parahsuum edenshawii* (Carter, 1988); GSC 80653; GSC Loc. No. C-080577; Fannin Formation, Maude Island; Upper Pliensbachian; scale = 200  $\mu\text{m}$ .
- Figure 5:** *Crucella angulosa* Carter, 1988; GSC 80591; GSC Loc. No. C-080577; Fannin Formation, Maude Island; Upper Pliensbachian; scale = 216  $\mu\text{m}$ .
- Figure 6:** *Jacus magnificus* Carter, 1988; GSC 80676; GSC Loc. No. C-080579; Whiteaves Formation, Maude Island; Middle Toarcian; scale = 191  $\mu\text{m}$ .
- Figure 7:** *Hsuum optimum* (Carter, 1988); GSC 80674; GSC Loc. No. C-080579; Whiteaves Formation, Maude Island; Middle Toarcian; scale = 217  $\mu\text{m}$ .
- Figure 8:** *Protounuma paulsmithi* Carter, 1988; GSC 80657; GSC Loc. No. C-080579; Whiteaves Formation, Maude Island; Middle Toarcian; scale = 137  $\mu\text{m}$ .
- Figure 9:** *Homeoparonaella reciproca* Carter, 1988; GSC 80505; GSC Loc. No. C-080584; Phantom Creek Formation, Yakoun River, Graham Island; Upper middle/lower upper Toarcian; scale = 224  $\mu\text{m}$ .
- Figure 10:** *Tympaneides charlottensis* Carter, 1988; GSC 80555; GSC Loc. No. C-080583; Phantom Creek Formation, Yakoun River, Graham Island; Upper middle/lower upper Toarcian; scale = 170  $\mu\text{m}$ .
- Figure 11:** *Triopocyclia rosespitense* Carter, 1988; GSC 80502; GSC Loc. No. C-080597; Phantom Creek Formation, Yakoun River, Graham Island; Upper Toarcian; scale = 170  $\mu\text{m}$ .
- Figure 12:** *Elodium cameroni* Carter, 1988; GSC 80631; GSC Loc. No. C-080597; Phantom Creek Formation, Yakoun River, Graham Island; Upper Toarcian; scale = 217  $\mu\text{m}$ .
- Figure 13:** *Mesosaturnalis hexagonus* (Yao, 1972); GSC 80615; GSC Loc. No. C-080583; Phantom Creek Formation, Yakoun River, Graham Island; Upper middle/lower upper Toarcian; scale = 236  $\mu\text{m}$ .
- Figure 14:** *Spongiostoma saccideon* Carter, 1988; GSC 80611; GSC Loc. No. C-080583; Phantom Creek Formation, Yakoun River, Graham Island; Upper middle/lower upper Toarcian; scale = 191  $\mu\text{m}$ .
- Figure 15:** *Rolubus kiustaense* Carter, 1988; GSC 80681; GSC Loc. No. C-080583; Phantom Creek Formation, Yakoun River, Graham Island; Upper middle/lower upper Toarcian; scale = 200  $\mu\text{m}$ .

**Figure 16:** *Parahsuum* sp. B; GSC 80758; GSC Loc. No. C-080583; Phantom Creek Formation, Yakoun River, Graham Island; Upper middle/lower upper Toarcian; scale = 188  $\mu\text{m}$ .

## PLATE 10

Scanning electron micrographs of Pliensbachian Foraminifera from the Queen Charlotte Islands, British Columbia. Bar scale = number of  $\mu\text{m}$  cited for each specimen illustrated.

- Figure 1:** *Paralingulina tenera tenuistriata* (Norvang); GSC 95659; GSC Loc. No. C-172558; Ghost Creek Formation; Early Pliensbachian; scale = 150  $\mu\text{m}$ .
- Figure 2:** *Paralingulina tenera subprismatica* (Franke); GSC 95660; GSC Loc. No. C-127851; Ghost Creek Formation; Early Pliensbachian; scale = 150  $\mu\text{m}$ .
- Figure 3:** *Paralingulina tenera pupa* (Terquem); GSC 95661; GSC Loc. No. C-127933; Ghost Creek Formation; Early Pliensbachian; scale = 150  $\mu\text{m}$ .
- Figure 4:** *Paralingulina tenera* subsp. A; GSC 95662; GSC Loc. No. C-127851; Ghost Creek Formation; Early Pliensbachian; scale = 150  $\mu\text{m}$ .
- Figure 5:** *Paralingulina* sp.; GSC 95663; GSC Loc. No. C-127868; Ghost Creek Formation; Early Pliensbachian; scale = 150  $\mu\text{m}$ .
- Figure 6:** *Marginulina prima* d'Orbigny var.; GSC 95664; GSC Loc. No. C-172565; Ghost Creek Formation; Early Pliensbachian; scale = 150  $\mu\text{m}$ .
- Figure 7:** *Ichthyolaria bicostata bicostata* (d'Orbigny); GSC 95665; GSC Loc. No. C-127899; Ghost Creek Formation; Early Pliensbachian; scale = 190  $\mu\text{m}$ .
- Figure 8:** *Ichthyolaria bicostata mesoliasica* (Brand); GSC 95666; GSC Loc. No. C-127868; Ghost Creek Formation; Early Pliensbachian; scale = 190  $\mu\text{m}$ .
- Figure 9:** *Mesodentalina hausieri* (Schick); GSC 95667; GSC Loc. No. C-127868; Ghost Creek Formation; Early Pliensbachian; scale = 190  $\mu\text{m}$ .
- Figure 10:** *Mesodentalina tenuistriata* (Terquem); GSC 95668; GSC Loc. No. C-127899; Ghost Creek Formation; Early Pliensbachian; scale = 190  $\mu\text{m}$ .
- Figure 11:** *Marginulina burgundiae* Terquem; GSC 95669; GSC Loc. No. C-172715; upper part of the Fannin Formation; Late Pliensbachian; scale = 514  $\mu\text{m}$ .
- Figure 12:** *Bigennerina?* sp.; GSC 95670; GSC Loc. No. C-172595; lower part of the Fannin Formation; Early Pliensbachian; scale = 514  $\mu\text{m}$ .
- Figure 13:** *Ichthyolaria? pygmaea* (Franke); GSC 95671; GSC Loc. No. C-127840; lower part of the Fannin Formation; Early Pliensbachian; scale = 514  $\mu\text{m}$ .
- Figure 14:** *Lingulonodosaria* sp.; GSC 95672; GSC Loc. No. C-172607; upper part of the Fannin Formation; Late Pliensbachian; scale = 150  $\mu\text{m}$ .
- Figure 15:** *Neobulimina?* sp.; GSC 95673; GSC Loc. No. C-172607; upper part of the Fannin Formation; Late Pliensbachian; scale = 112  $\mu\text{m}$ .

## PLATE 11

Scanning electron micrographs of Toarcian Foraminifera and ostracoda from the Queen Charlotte Islands, British Columbia. Bar scale = number of  $\mu\text{m}$  cited for each specimen illustrated.

- Figure 1:** *Reinholdella cf. macfadyeni* (Ten Dam); GSC 95644; GSC Loc. No. C-127824; Whiteaves Formation, Septarian Shale Member; Middle Toarcian; scale = 312  $\mu\text{m}$ .
- Figure 2:** *Falsopalmula jurensis* (Franke); GSC 95645; GSC Loc. No. C-172619; Phantom Creek Formation, Coquinoid Sandstone Member; Upper Toarcian; scale = 312  $\mu\text{m}$ .
- Figure 3:** *Kinkelina* sp.; GSC 95646; GSC Loc. No. C-127824; Whiteaves Formation, Septarian Shale Member; Middle Toarcian; scale = 500  $\mu\text{m}$ .
- Figure 4:** *Lenticulina* sp. T1; GSC 95647; GSC Loc. No. C-172423; Whiteaves Formation, Septarian Shale Member; Middle Toarcian; scale = 500  $\mu\text{m}$ .
- Figure 5:** *Falsopalmula varians* (Bornemann); GSC 95648; GSC Loc. No. C-127824; Whiteaves Formation, Septarian Shale Member; Middle Toarcian; scale = 500  $\mu\text{m}$ .
- Figure 6:** *Lenticulina d'orbignyi* (Roemer) var.; GSC 95649; GSC Loc. No. C-172372; Whiteaves Formation, Concretionary Shale Member; Middle Toarcian; scale = 500  $\mu\text{m}$ .
- Figure 7:** *Lenticulina prima* (d'Orbigny); GSC 95650; GSC Loc. No. C-172378; Whiteaves Formation, Concretionary Shale Member; Middle Toarcian; scale = 500  $\mu\text{m}$ .
- Figure 8:** *Lenticulina* sp. T2; GSC 95651; GSC Loc. No. C-172621; Phantom Creek Formation, Coquinoid Sandstone Member; Upper Toarcian; scale = 714  $\mu\text{m}$ .
- Figure 9:** *Lenticulina* sp.; GSC 95652; GSC Loc. No. C-172378; Whiteaves Formation, Concretionary Shale Member; Middle Toarcian; scale = 714  $\mu\text{m}$ .
- Figure 10:** *Lenticulina d'orbignyi* (Roemer); GSC 95653; GSC Loc. No. C-172706; Whiteaves Formation, Septarian Shale Member; Middle Toarcian; scale = 714  $\mu\text{m}$ .
- Figure 11:** *Lenticulina gottingensis* (Bornemann); GSC 95654; GSC Loc. No. C-172390; Whiteaves Formation, Septarian Shale Member; Middle Toarcian; scale = 714  $\mu\text{m}$ .
- Figure 12:** *Pseudonodosaria pygmaea* (Terquem); GSC 95655; GSC Loc. No. C-172706; Whiteaves Formation, Septarian Shale Member; Middle Toarcian; scale = 714  $\mu\text{m}$ .
- Figure 13:** *Citharina cf. longuemari* (Terquem); GSC 95656; GSC Loc. No. C-172619; Phantom Creek Formation, Coquinoid Sandstone Member; Upper Toarcian; scale = 714  $\mu\text{m}$ .
- Figure 14:** *Citharina saggittiformis* (Terquem); GSC 95657; GSC Loc. No. C-172424; Whiteaves Formation, Septarian Shale Member; Middle Toarcian; scale = 714  $\mu\text{m}$ .
- Figure 15:** *Vaginulina listi* (Bornemann); GSC 95658; GSC Loc. No. C-172378; Whiteaves Formation, Concretionary Shale Member; Middle Toarcian; scale = 714  $\mu\text{m}$ .

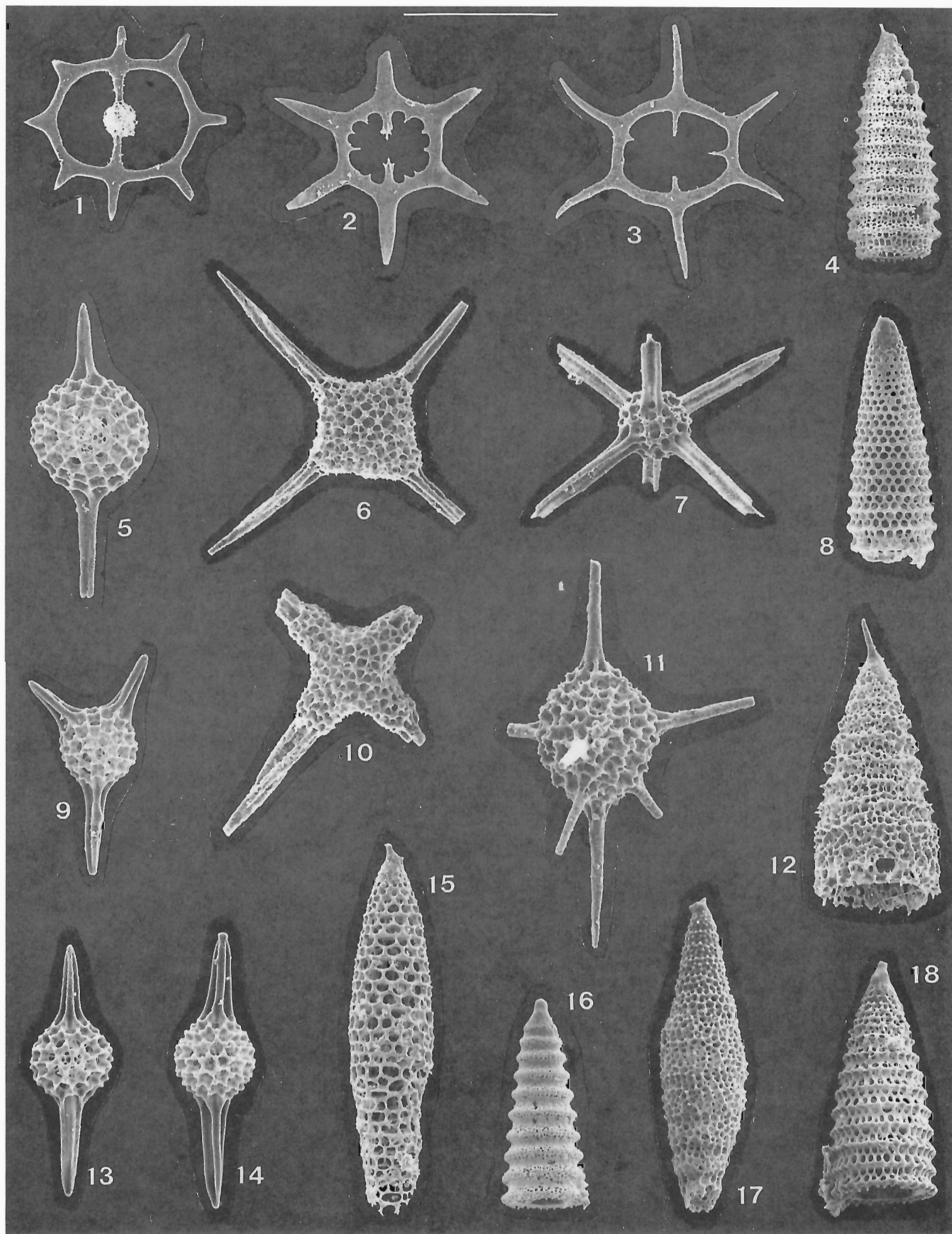
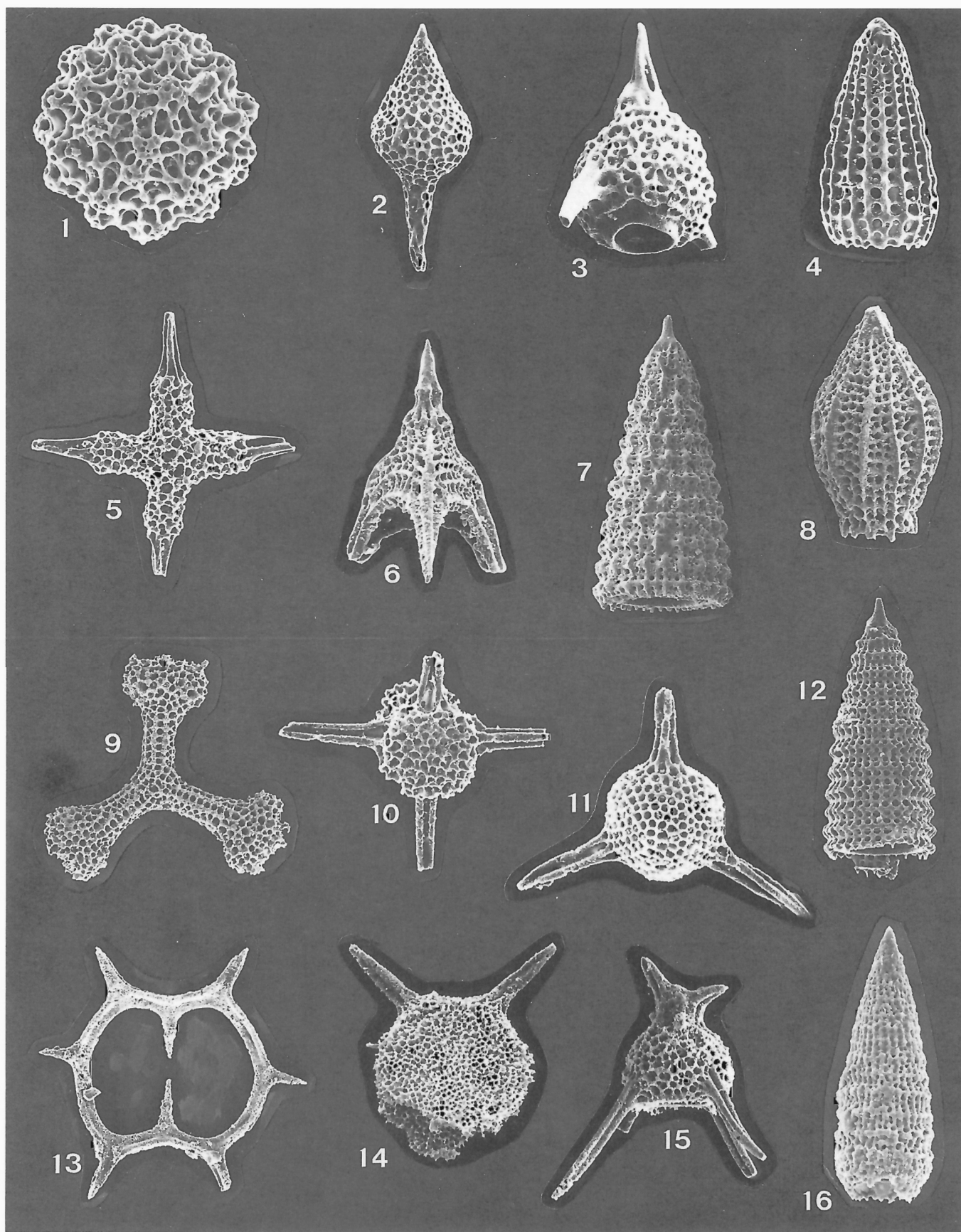
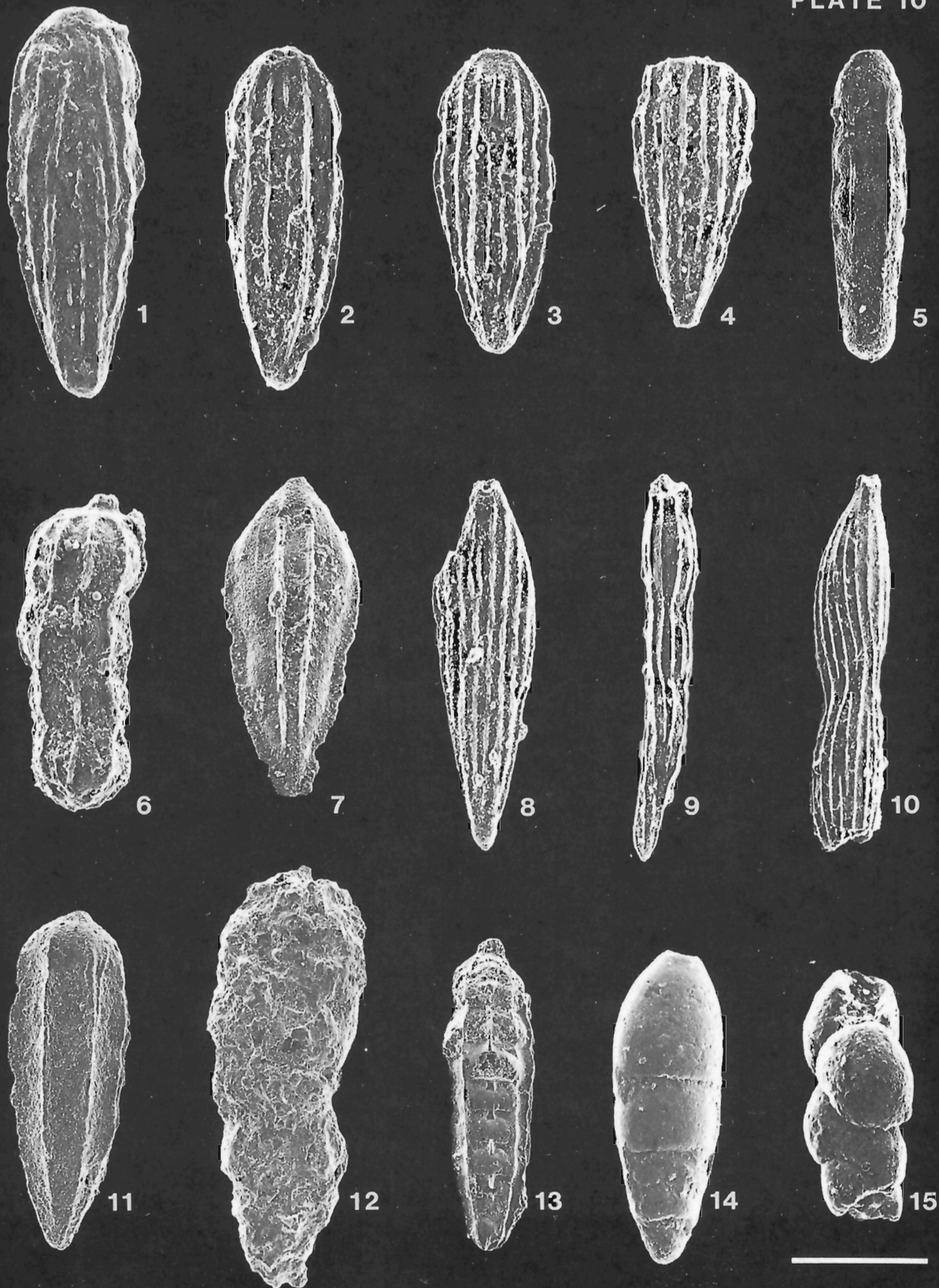
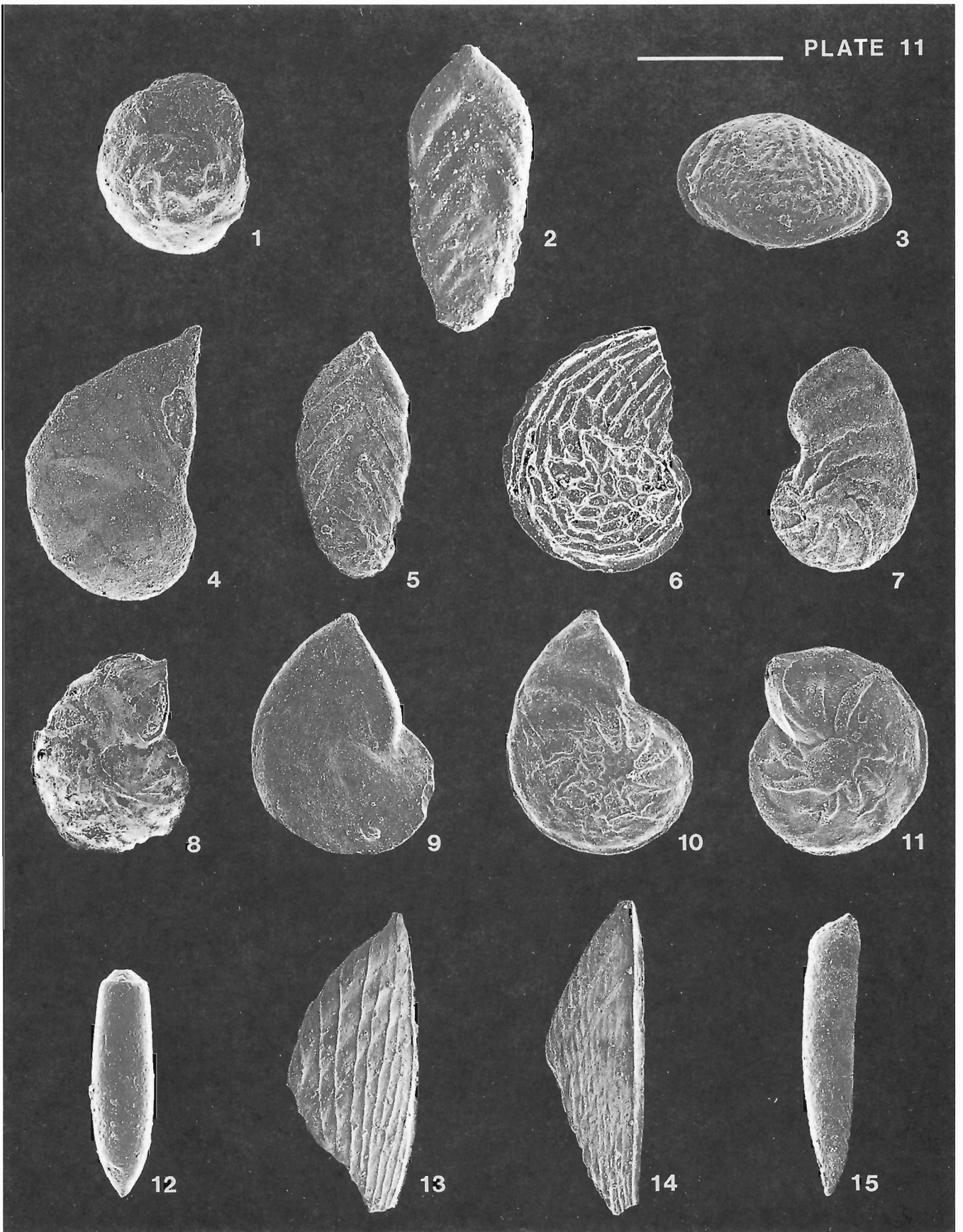


PLATE 8











for locating additional specimens in other microfossil residues and slide collections and by processing samples obtained from previous field work.

Most ichthyoliths have been recovered from the Lower Jurassic shale samples of the Toarcian Whiteaves Formation. Other ichthyolith occurrences have been found in the Fannin and Ghost Creek formations of the Pliensbachian.

Ichthyoliths from the Whiteaves Formation have a variety of distinct forms, with one common type (Plate 12, figs. 9 and 10). Other forms illustrated in this plate show some of their diversity. Figures 1-12 illustrate teeth and 13-18 dermal denticles. An interesting feature of ichthyoliths is that they appear to show colour changes in specimens from different sections (Plate 12, figures 4 and 5) Fannin Formation types are very dark brown-black whereas other types show varying grades of transparent amber; the potential for colour/thermal alteration indices needs to be explored.

Ichthyolith zonation would be premature at this stage. The number of specimens needs to be increased through additional sampling. A new taxonomic system (initiated by Doyle et al., 1974 for Cenozoic ichthyoliths) will need to be expanded to include new Jurassic forms. Johns is confident that in samples collected from the Queen Charlotte Islands and other localities, distinctive ichthyolith types will be recognized with specific age/zone ranges.

There is clearly a growing interest in ichthyolith biostratigraphical studies at other institutions. Since 1971 to the present, Doyle, Riedel, Tway and many others from Scripps Institute of Oceanography have contributed many papers describing new ichthyolith forms and utilized them to date Cenozoic and Upper Mesozoic sediments from D.S.D.P. cores. Doyle and Riedel (1985) give an excellent summary of current ichthyolith taxonomy and stratigraphic ranges. Ichthyoliths have been particularly useful for dating pelagic sediments which are often lacking calcareous and siliceous microfossils (Helms and Riedel, 1971; Doyle et al., 1974; other references within). Ichthyoliths have been used to recognize reworking in sediments and low biological productive areas and in addition, distinguish hiatuses from slowly accumulating sediments (Doyle et al., 1977; Edger-ton et al., 1977; Doyle and Riedel, 1979, 1980; Kaneps et al., 1981; Gottfried et al., 1984a,b).

As ichthyoliths are found in most sediments they could be particularly useful for dating those rocks that are apparently otherwise unfossiliferous.

**Ichthyosaurs.** At Kennecott Point, particularly in the Lower Sinemurian beds of the Sandilands Formation, fragments of bone, including parts of two skulls, from several ichthyosaurs have been recovered. The occurrences suggest a stratigraphic position slightly higher than Canadianis Zone ammonites. The fossils have been studied by Shane Dennison, a student of P.L. Smith, and a report on his findings will be published soon. Preservation is poor but the rarity of such finds in the Canadian Lower Jurassic makes this occurrence important. One specimen has been identified as *Ichthyosaurus* sp. showing some similarities to *I. tenuirostris* and *I. conybeari* (S. Dennison, pers. comm., 1989).

## Invertebrates

**Coleoids.** The Lower Jurassic strata commonly but not abundantly yield representatives of coleoidea. Material collected was sent to the late J.A. Jeletzky who, from time to time reported on the submitted material. However, the material has not formed the basis of any comprehensive investigation.

Species of *Atractites* have been collected infrequently in Hettangian through Pliensbachian rocks but no specimens were well-preserved. Probably the Sandilands Formation has yielded the greater number.

In the upper part of the Whiteaves Formation and the lower half of the Phantom Creek Formation dicoelid belemnites are common

and in a few places relatively abundant. The only part of the geological column in Queen Charlotte Islands that yields dicoelid belemnites is the Middle Toarcian and the lower part of the Upper Toarcian. As such they are easily recognized index fossils. They also are the earliest belemnite recorded, as coleoids of the Early Toarcian are extremely rare and believed to be *Atractites*. Other belemnites have been found in the highest Toarcian beds, commonly above the highest *Hammato-ceras* species, but these are not dicoelids. The stratigraphic position of these coleoids in Queen Charlotte Islands seems to be reflected in other areas of British Columbia.

**Nautiloids.** In the Fannin Formation (Carlottense Zone, Late Pliensbachian) a few large but poorly preserved nautiloids have been found. A few were also found in the Whiteaves and Phantom Creek formations of the Toarcian. None has as yet been found in the Hettangian or Sinemurian of Sandilands Formation.

**Bivalves.** Bivalves are common throughout the Lower Jurassic strata but seldom are they the more prevalent taxa in any collection. Seldom, are beds encountered that are coquinoid in character. There seems however, to be a fairly great diversity in genera. Thin-shelled specimens that might characterize moderate to deep water depth are associated with ammonite species in shale or siltstone sequences. Pectinid species are common in the Fannin Formation and in the Phantom Creek Formation and usually small in size. *Weyla* has been found in the Upper Pliensbachian Fannin Formation, possibly the Sandilands Formation and possibly the Toarcian part of the Fannin Formation. *Weyla* is most abundant in shallow water settings and the general lack of this fauna may point to a moderate to deep water depth.

**Brachiopods.** Rhynchonellid brachiopods are present in the Fannin Formation, particularly in the upper parts. Elsewhere the Lower Jurassic beds are devoid of brachiopods or rare single specimens may be encountered.

**Other.** Faunas such as gastropods and crustaceans are rare, distributed without any particular stratigraphic reason. In general most beds of the Early Jurassic show evidence of organic remains. Trace fossils are common and bioturbation is characteristic of many beds.

## Flora

Leaves are found occasionally as single, fortuitously preserved specimens. Nowhere are they abundant or suggest extensive nonmarine deposition. Wood is a common constituent of the beds throughout the Lower Jurassic but seldom are pieces larger than 15 cm seen. For some unknown reason leaves appear more common in the Upper Pliensbachian Fannin Formation but this may be more apparent than real.

## FUTURE BIOSTRATIGRAPHIC WORK IN QUEEN CHARLOTTE ISLANDS

The biostratigraphic work on the Early Jurassic faunas is well advanced. The lithostratigraphy has been described and published (Cameron and Tipper, 1985) and will be modified as work continues. Smith and Tipper have completed the study of Pliensbachian ammonites and a monograph will be forthcoming. Jakobs and Jozsef Pálffy are currently investigating the Toarcian and Sinemurian respectively as thesis topics. Tipper will be publishing on Hettangian ammonites after field work and study are completed. Carter has published one bulletin on Radiolaria (Carter et al., 1988) and further publications on the Hettangian, Sinemurian, and Early Pliensbachian forms are planned as soon as possible. The field work on Toarcian-Pliensbachian Foraminifera is complete and Cameron plans reports in the future. The study of ichthyoliths is still in its infancy but Johns hopes to pursue this further. Studies on other faunas will be encouraged when interest in them is forthcoming.

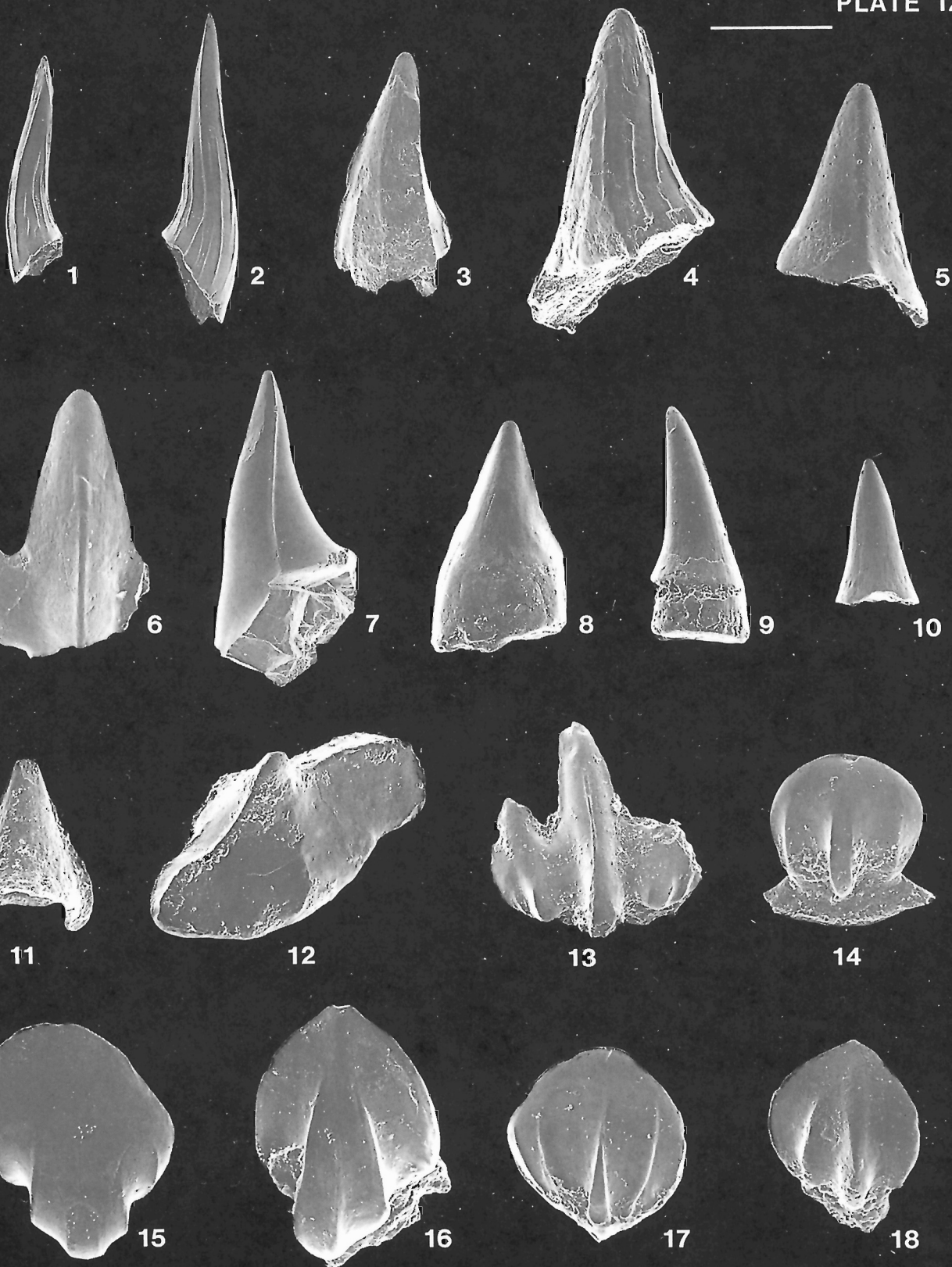




## PLATE 12

Scanning electron micrographs of Lower Jurassic ichthyoliths from the Queen Charlotte Islands, British Columbia. Specimens are from samples described in stratigraphic sections from Cameron and Tipper (1985). Temporary type numbers have been assigned to each specimen, since identification has yet to be completed. Bar scale = number of  $\mu\text{m}$  cited for each specimen illustrated.

**Figure 1:** Type Jur-01; GSC 95626; GSC Loc. No. C-127928; Strat. Sect. No. 10; Rennell Junction, Graham Island, Maude Group, Ghost Creek Formation; Early Pliensbachian; scale = 500  $\mu\text{m}$ .

**Figure 2:** Type Jur-02; GSC 95627; GSC Loc. No. C-127895; Strat. Sect. No. 10; Rennell Junction, Graham Island, Maude Group, Fannin Formation; Early Pliensbachian; scale = 500  $\mu\text{m}$ .

**Figure 3:** Type Jur-03; GSC 95628; GSC Loc. No. C-127837; Strat. Sect. No. 10; Rennell Junction, Graham Island, Maude Group, Fannin Formation; Early Pliensbachian; scale = 500  $\mu\text{m}$ .

**Figure 4:** Type Jur-04; GSC 95629; GSC Loc. No. C-172522; Strat. Sect. No. 9; Maude Island, Maude Group, Fannin Formation; Late Pliensbachian to Early Toarcian; scale = 500  $\mu\text{m}$ .

**Figure 5:** Type Jur-05; GSC 95630; GSC Loc. No. C-172523; Strat. Sect. No. 9; Maude Island, Maude Group, Fannin Formation; Late Pliensbachian to Early Toarcian; scale = 300  $\mu\text{m}$ .

**Figure 6:** Type Jur-06; GSC 95631; GSC Loc. No. C-172440; Strat. Sect. No. 15; Yakoun River, Graham Island, Maude Group, Whiteaves Formation; Middle Toarcian; scale = 500  $\mu\text{m}$ .

**Figure 7:** Type Jur-07; GSC 95632; GSC Loc. No. C-172390; Strat. Sect. No. 14; Branch Road 57, Graham Island, Maude Group, Whiteaves Formation; Middle Toarcian; scale = 700  $\mu\text{m}$ .

**Figure 8:** Type Jur-08; GSC 95633; GSC Loc. No. C-127817; Strat. Sect. No. 10; Graham Island, Maude Group, Whiteaves Formation; Middle Toarcian; scale = 300  $\mu\text{m}$ .

**Figure 9:** Type Jur-09; GSC 95634; GSC Loc. No. C-172307; Strat. Sect. No. 11; Yakoun River, Graham Island, Maude Group, Whiteaves Formation; Middle Toarcian; scale = 300  $\mu\text{m}$ .

**Figure 10:** Type Jur-10; GSC 95635; GSC Loc. No. C-127818; Strat. Sect. No. 10; Graham Island, Maude Group, Whiteaves Formation; Middle Toarcian; scale = 300  $\mu\text{m}$ .

**Figure 11:** Type Jur-11; GSC 95636; GSC Loc. No. C-172477; Strat. Sect. No. 15; Yakoun River, Graham Island, Maude Group, Whiteaves Formation; Middle Toarcian; scale = 300  $\mu\text{m}$ .

**Figure 12:** Type Jur-12; GSC 95637; GSC Loc. No. C-172438; Strat. Sect. No. 15; Yakoun River, Graham Island, Maude Group, Whiteaves Formation; Middle Toarcian; scale = 300  $\mu\text{m}$ .

**Figure 13:** Type Jur-13; GSC 95638; GSC Loc. No. C-127824; Strat. Sect. No. 10; Graham Island, Maude Group, Whiteaves Formation; Middle Toarcian; scale = 500  $\mu\text{m}$ .

**Figure 14:** Type Jur-14; GSC 95639; GSC Loc. No. C-127824; Strat. Sect. No. 10; Graham Island, Maude Group, Whiteaves Formation; Middle Toarcian; scale = 190  $\mu\text{m}$ .

**Figure 15:** Type Jur-15; GSC 95640; GSC Loc. No. C-172390; Strat. Sect. No. 14; Branch Road 57, Graham Island, Maude Group, Whiteaves Formation; Middle Toarcian; scale = 190  $\mu\text{m}$ .

**Figure 16:** Type Jur-16; GSC 95641; GSC Loc. No. C-127824; Strat. Sect. No. 10; Graham Island, Maude Group, Whiteaves Formation; Middle Toarcian; scale = 190  $\mu\text{m}$ .

**Figure 17:** Type Jur-17; GSC 95642; GSC Loc. No. C-127824; Strat. Sect. No. 10; Graham Island, Maude Group, Whiteaves Formation; Middle Toarcian; scale = 190  $\mu\text{m}$ .

**Figure 18:** Type Jur-18; GSC 95643; GSC Loc. No. C-172519; Strat. Sect. No. 5; Maude Island, Maude Group, Whiteaves Formation; Middle Toarcian; scale = 190  $\mu\text{m}$ .

The Queen Charlotte Islands will act as a type area for much of the standard North American zonation whether based on ammonites, radiolarians, or foraminifers and are therefore pivotal to precise correlations between the allochthonous terranes and between the terranes and the craton. This is a critical region because here Tethyan, east Pacific and some Boreal faunas occur together, a unique situation. The preservation of faunas is good to excellent, there is an abundant supply of specimens, there is a high diversity in the faunas, and the stratigraphic sequence, although in numerous short sections can be worked out and checked in several sections. As an example the Pliensbachian section has been painstakingly reconstructed so that we are confident we have a complete Pliensbachian sequence that is continuous with the Sinemurian below and the Toarcian above. We have been able to establish an ammonite zonation that readily falls into five zones (Smith et al., 1988) which, with further work may be subdivided into subzones. This zonation is the first of four for ammonites in each stage and in time zonations based on Foraminifera and Radiolaria are possible and will be closely tied to the ammonite zonation. This is already under way for the Radiolaria (Carter et al., 1988).

In addition to their stratigraphic utility, fossils can be used as powerful tools in biogeography and the study of allochthonous terranes (Smith and Tipper, 1986). High diversity faunas and high endemism in the faunas suggest a low latitude position of the area in Pliensbachian time. The presence of *Fanninoceras* and other faunas indicate an east Pacific position in Pliensbachian time and the presence of *amalteids* indicates an origin in the northern hemisphere resolving the hemisphere ambiguity inherent in paleomagnetic data. Studies such as these place constraints on paleogeographic models independent of geological or geophysical data (Smith, 1988).

Macrofossils and microfossils are a means of providing fast, accurate, and precise dating of rock units, unconformities, and structural events. Macrofossils such as ammonites can provide a standard zonation that can be correlated world wide with great precision. Microfossils of several classes or orders can together offer even greater detail and precision of zonation and when correlated with an ammonite standard, offer a high resolution method of precise world wide correlation. The Queen Charlotte Islands have fossil faunas that are admirably suited to achieving this result.

## REFERENCES

- Billings, E.**  
**1873:** On the Mesozoic fossils from British Columbia collected by Mr. James Richardson in 1872; in Report of Progress, 1872-1873, Geological Survey of Canada, p. 71-75.
- Cameron, B.E.B. and Tipper, H.W.**  
**1985:** Jurassic stratigraphy of the Queen Charlotte Islands, British Columbia; Geological Survey of Canada, Bulletin 365.
- Carter, E.S.**  
**1985:** Early and Middle Jurassic radiolarian biostratigraphy, Queen Charlotte Islands, British Columbia; M.Sc. thesis, University of British Columbia, Vancouver, 291 p.  
**1988:** Uppermost Norian (Triassic) radiolaria from the Sandilands Formation, Queen Charlotte Islands, British Columbia; Program with Abstracts, The Canadian Paleontology and Biostratigraphy Seminar, Winnipeg, Manitoba, September, 1988.  
**1990:** New biostratigraphic elements for dating Upper Norian strata from the Sandilands Formation, Queen Charlotte Islands, British Columbia, Canada; Marine Micropaleontology, v. 15, p. 313-328.
- Carter, E.S., Cameron, B.E.B., and Smith, P.L.**  
**1988:** Lower and Middle Jurassic radiolarian biostratigraphy and systematic paleontology, Queen Charlotte Islands, British Columbia; Geological Survey of Canada, Bulletin 386, 109 p.
- Carter, E.S., Orchard, M.J., and Tozer, E.T.**  
**1989:** Integrated ammonoid-conodont-radiolarian biostratigraphy, Late Triassic Kunga Group, Queen Charlotte Islands, British Columbia; in Current Research, Part H, Geological Survey of Canada, Paper 89-111, p. 23-30.

- Clapp, C.H.**  
**1914:** A geological reconnaissance on Graham Island; in Summary Report, 1912. Geological Survey of Canada, p. 12-40.
- Cordey, F.**  
**1988:** Étude des radiolaires permien, triasiques et jurassiques des complexes ophiolitiques de Cache Creek, Bridge River et Hozomeen (Colombie Britannique, Canada); implications paléogéographiques et structurales; Académie de Paris, Université Pierre et Marie Curie, Mémoires des Sciences de la Terre, no. 88-17, 374 p.
- Dawson, G.M.**  
**1880:** Queen Charlotte Islands; in Report of Progress, 1878-1879, Geological Survey of Canada.
- Doyle, P.S., Dunsworth, M.J., and Riedel, W.R.**  
**1977:** Reworking of ichthyoliths in eastern tropical Pacific sediments; Deep-Sea Research, v. 24, p. 181-198.
- Doyle, P.S., Kennedy, G.G., and Riedel, W.R.**  
**1974:** Stratigraphy; in Initial Reports of the Deep Sea Drilling Project, T.A. Davies, B.P. Luyendyk et al. (ed.), (U.S. Government Printing Office), Washington, D.C. v. 26, p. 825-906.
- Doyle, P.S. and Riedel, W.R.**  
**1979:** Cretaceous to Neogene ichthyoliths in a giant piston core from the central North Pacific; Micropaleontology, v. 25, no. 4, p. 337-364.  
**1980:** Ichthyoliths from Site 436, Northwest Pacific, Leg 56, Deep Sea Drilling Project; in Scientific Party, Initial Reports of the Deep Sea Drilling Project, v. 56, Washington, D.C., (U.S. Government Printing Office), p. 887-893.  
**1985:** Cenozoic and Late Cretaceous ichthyoliths; in Plankton Stratigraphy, H.M. Bolli, J.B. Saunders, and K. Perch-Nielsen (ed.), Cambridge, (Cambridge University Press), p. 965-995.
- Edgerton, C.C., Doyle, P.S., and Riedel, W.R.**  
**1977:** Ichthyolith age determinations of otherwise unfossiliferous deep sea drilling project cores; Micropaleontology, v. 23, no. 2, p. 194-205.
- Ells, R.W.**  
**1906:** Report on the geology of Graham Island; in Annual Report, 1904, New Series, Geological Survey of Canada, v. 16, Part B, p. 1-46.
- Frebold, H.**  
**1967a:** Hettangian ammonite faunas of the Taseko Lakes area; Geological Survey of Canada, Bulletin 158.  
**1967b:** Position of the Lower Jurassic genus *Fanninoceras* McLearn and the age of the Maude Formation on Queen Charlotte Islands; Canadian Journal of Earth Sciences, v. 4, p. 1145-1149.  
**1970:** Pliensbachian ammonoids from British Columbia and southern Yukon; Canadian Journal of Earth Sciences, v. 7, p. 435-452.
- Gottfried, M.D., Doyle, P.S., and Riedel, W.R.**  
**1984a:** Advances in ichthyolith stratigraphy of the Pacific Neogene and Oligocene; Micropaleontology, v. 30, no. 1, p. 71-85.  
**1984b:** Stratigraphic interpretations of pelagic sequences revised on the basis of ichthyoliths; Micropaleontology, v. 30, no. 4, p. 426-444.
- Guex, J.**  
**1980:** Remarques préliminaires sur la distribution stratigraphique des ammonites hettangiennes du New York Canyon (Gabbs Valley Range, Nevada); Bulletin de Géologie Lausanne, no. 250, p. 127-140.
- Helms, P.B. and Riedel, W.R.**  
**1971:** Skeletal debris of fishes; in Initial Reports of the Deep Sea Drilling Project, E.L. Winterer et al. (ed.), v. 7, Washington, D.C., (U.S. Government Printing Office), p. 1709-1720.
- Hillebrandt, A. von.**  
**1987:** Liassic ammonite zones of South America and correlations with other provinces, with descriptions of new genera and species of ammonites; in Biostratigrafía de los sistemas regionales del Jurásico y Cretácico en América del Sur. Mendoza, Argentina, p. 111-157.
- Kaneps, A.G., Doyle, P.S., and Riedel, W.R.**  
**1981:** Further ichthyolith age determinations of otherwise unfossiliferous deep sea cores; Micropaleontology, v. 27, no. 3, p. 317-331.
- McFarlane, R.B.**  
**1988:** Lower Jurassic biostratigraphy of central Graham Island, Queen Charlotte Islands, British Columbia; the Upper Sinemurian of the Sandilands Formation; B.Sc. thesis, University of British Columbia, Vancouver, 70 p.
- MacKenzie, J.D.**  
**1916:** Geology of Graham Island, British Columbia; Geological Survey of Canada, Memoir 88.
- McLearn, F.H.**  
**1927:** Some Canadian Jurassic faunas; in Transactions, Royal Society of Canada, 3rd Series, v. 21, sec. IV, p. 61-73.  
**1929:** Contributions to the stratigraphy and paleontology of Skidegate Inlet, Queen Charlotte Islands, B.C.; Geological Survey of Canada, Museum Bulletin 54, p. 1-27.
- 1932:** Some Canadian Jurassic faunas (continued); in Transactions, Royal Society of Canada, 3rd Series, v. 26, sec. IV, p. 51-80.
- 1949:** Jurassic formations of Maude Island and Alliford Bay, Queen Charlotte Islands, B.C.; Geological Survey of Canada, Bulletin 12.
- 1972:** Ammonoids of the Lower Cretaceous sandstone member of the Haida Formation, Skidegate Inlet, Queen Charlotte Islands, Western British Columbia; Geological Survey of Canada, Bulletin 188.
- Pessagno, E.A., Jr. and Blome, C.D.**  
**1980:** Upper Triassic and Jurassic Pantanellinae from California, Oregon and British Columbia; Micropaleontology, v. 26, no. 3, p. 225-273.
- Pessagno, E.A., Jr. and Whalen, P.A.**  
**1982:** Lower and Middle Jurassic radiolaria (multicystid Nassellariina) from California, east-central Oregon and the Queen Charlotte Islands, B.C.; Micropaleontology, v. 28(2), p. 111-169.
- Pessagno, E.A., Jr., Whalen, P.A., and Yeh, K.-Y.**  
**1986:** Jurassic Nassellariina (radiolaria) from North American geologic terranes; Bulletins of American Paleontology, v. 91(326), 68 p.
- Pessagno, E.A., Jr., Blome, C.D., Carter, E.S., MacLeod, N., Whalen, P.A., and Yeh, K.-Y.**  
**1987:** Preliminary radiolarian zonation for the Jurassic of North America; in Studies of North American Jurassic Radiolaria, Part 2, Cushman Foundation for Foraminiferal Research, Special Publication no. 23, p. 1-18.
- Poulton, T.P., Hall, R.L., Tipper, H.W., Cameron, B.E.B., and Carter, E.S.**  
**1991:** Current status of Middle Jurassic biostratigraphy of the Queen Charlotte Islands, British Columbia; in Evolution and Hydrocarbon Potential of the Queen Charlotte Basin, British Columbia, Geological Survey of Canada, Paper 90-10.
- Richardson, J.**  
**1873:** Coal-fields of Vancouver and Queen Charlotte Islands; in Report of Progress, 1872-1873, Geological Survey of Canada.
- Smith, P.L.**  
**1988:** Paleobiogeography and plate tectonics; Geoscience Canada, v. 15, p. 261-279.
- Smith, P.L. and Tipper, H.W.**  
**1986:** Plate tectonics and paleobiogeography: Early Jurassic (Pliensbachian) endemism and diversity; Palaeos, 1, p. 399-412.
- Smith, P.L., Tipper, H.W., Taylor, D.G., and Guex, J.**  
**1988:** An ammonite zonation for the Lower Jurassic of Canada and the United States; the Pliensbachian; Canadian Journal of Earth Sciences, v. 25, no. 9, p. 1503-1523.
- Stanton, T.W. and Martin, G.C.**  
**1905:** Mesozoic section on Cook Inlet and Alaska Peninsula; Geological Society of America, Bulletin, v. 16, p. 39-410.
- Sutherland Brown, A.**  
**1968:** Geology of the Queen Charlotte Islands, British Columbia; British Columbia Department of Mines and Petroleum Resources, Bulletin 54, 226 p., 17 pls.
- Tipper, H.W.**  
**1989:** Lower Jurassic (Hettangian and Sinemurian) biostratigraphy, Queen Charlotte Islands, British Columbia; in Current Research, Part H, Geological Survey of Canada, Paper 89-1H, p. 31-33.
- Vellutini, D.**  
**1988:** Organic maturation and source rock potential of Mesozoic and Tertiary strata, Queen Charlotte Islands, British Columbia; M.Sc. thesis, University of British Columbia, Vancouver.
- Whalen, P.A.**  
**1985:** Lower Jurassic radiolarian biostratigraphy of the Kunga Formation, Queen Charlotte Islands, British Columbia, and the San Hipolito Formation, Baja California Sur; Ph.D. thesis, University of Texas at Dallas, 440 p.
- Whiteaves, J.F.**  
**1876:** On some invertebrates from the coal-bearing rocks of the Queen Charlotte Islands; Geological Survey of Canada, Mesozoic Fossils, v. 1, Part 1, p. 1-92.  
**1883:** On the Lower Cretaceous rocks of British Columbia; in Transactions, Royal Society of Canada, v. 1, sec. IV, p. 81-86.  
**1884:** On the fossils of the coal-bearing deposits of the Queen Charlotte Islands collected by Dr. G.M. Dawson in 1878; Geological Survey of Canada, Mesozoic Fossils, v. 1, Part 3, p. 191-262.  
**1900:** On some additional or imperfectly understood fossils from the Cretaceous rocks of the Queen Charlotte Islands with a revised list of the species from these rocks; Geological Survey of Canada, Mesozoic Fossils, v. 1, Part 4, p. 263-308.

## APPENDIX 1

### Hettangian ammonite locality register

Information is provided here for illustrated Hettangian ammonite material.

GSC Loc. No. C-156906. 88-3-3-G, 103F/14E, Frederick Island, 621300E, 5975200N. Graham Island, Kennecott Point, Kunga Group, Sandilands Formation; Lower Hettangian.

GSC Loc. No. C-156907. 88-3-4-G, 103F/14E, Frederick Island, 621300E, 5975200N. Graham Island, Kennecott Point, Kunga Group, Sandilands Formation; Lower Hettangian.

GSC Loc. No. C-156915. 88-5-2-TD, 103F/14E, Frederick Island, 621300E, 5975200N. Graham Island, Kennecott Point, Kunga Group, Sandilands Formation; Middle Hettangian.

## APPENDIX 2

### Sinemurian ammonite locality register

Information is provided here for illustrated Sinemurian ammonite material.

GSC Loc. No. C-157501. 103F/8, Yakoun Lake, 679050E, 5921200N. central Graham Island, Kunga Group, Sandilands Formation; Upper Sinemurian.

GSC Loc. No. C-157517. 103F/8, Yakoun Lake, 679050E, 5921200N. central Graham Island, Kunga Group, Sandilands Formation; Upper Sinemurian.

GSC Loc. No. C-157623. 87TD-21T, 103F/14E, Frederick Island, 621300E, 5975200N. Graham Island, Kennecott Point, Kunga Group, Sandilands Formation; Lower Sinemurian.

GSC Loc. No. C-157629. 87TD-210, 103F/14E, Frederick Island, 621300E, 5975200N. Graham Island, Kennecott Point, Kunga Group, Sandilands Formation; Lower Sinemurian.

UBC 08 103F/1, Skidegate Channel, 697200E, 5998400N. south shore of Maude Island, Kunga Group, Sandilands Formation; Lower Sinemurian.

## APPENDIX 3

### Pliensbachian ammonite locality register

Information is provided here for illustrated Pliensbachian ammonite material.

GSC Loc. No. 048564. 103F/1, Skidegate Channel, 698800E, 5897300N. Whiteaves Bay, north shore of Moresby Island, Maude Group, Fannin Formation; Kunae Zone.

GSC Loc. No. C-080610. 103G/4, Cumshewa Inlet, 302500E, 5881500N. Cumshewa Inlet, northeast of Barge Point, Maude Group, Fannin Formation (lower part); Whiteavesi to Freboldi Zone.

GSC Loc. No. C-080786. 103F/1, Skidegate Channel, 697200E, 5898300N. Fannin Bay, south shore of Maude Island, Maude Group, Fannin Formation; 1 m below the top of the section in Figure 9; Carlottense Zone.

GSC Loc. No. C-081703. 103F/8, Yakoun Lake, central Graham Island; Maude Group, Fannin Formation; Kunae Zone.

GSC Loc. No. C-090587. 103F/8, Yakoun Lake, 681700E, 5917700N. central Graham Island (Strat. Sect. No. 10 of Cameron and Tipper, 1985); Maude Group, Fannin Formation (lower part); 12.5-16.5 m above the base of the "Rennell Junction Formation" of Strat. Sect. No. 10 of Cameron and Tipper, 1985; Whiteavesi Zone.

GSC Loc. No. C-090614. 103F/1, Skidegate Channel, 697200E, 5898300N. Fannin Bay, south shore of Maude Island, Maude Group, Fannin Formation; 4 m above the base of the Fannin Formation of Strat. Sect. No. 8 of Cameron and Tipper, 1985; Kunae Zone.

GSC Loc. No. C-090974. 103F/8, Yakoun Lake, 679800E, 5921000N. central Graham Island, Maude Group, Ghost Creek Formation; Imlayi Zone.

GSC Loc. No. C-090977. 103F/8, Yakoun Lake, 679800E, 5921000N. central Graham Island, Maude Group, Ghost Creek Formation; Imlayi Zone.

GSC Loc. No. C-091794. 103F/1, Skidegate Channel, 697200E, 5898300N. Fannin Bay on south shore of Maude Island, Maude Group, Fannin Formation (lower part); 14 m above the base of the "Rennell Junction Formation" of Strat. Sect. No. 8 of Cameron and Tipper, 1985; Whiteavesi Zone.

GSC Loc. No. C-093575. 103F/1, Skidegate Channel, 698000E, 5897300N. Whiteaves Bay, north shore of Moresby Island, Maude Group, Ghost Creek Formation; Whiteavesi Zone.

GSC Loc. No. C-117003. 103F/1, Skidegate Channel, 697200E, 5898300N. Fannin Bay on south shore of Maude Island, Maude Group, Fannin Formation; 1 m below the top of the section in Figure 9; Carlottense Zone.

GSC Loc. No. C-117019. 103G/4, Cumshewa Inlet, 302500E, 5881500N. Cumshewa Inlet, northeast of Barge Point, Maude Group, Fannin Formation (lower part); Whiteavesi and lowest Freboldi Zone.

GSC Loc. No. C-117032. 103F/1, Skidegate Channel, 697200E, 5898500N. Fannin Bay on south shore of Maude Island, Maude Group, Fannin Formation; loose 1.5 m above the base of the Fannin Formation of Strat. Sect. No. 8 of Cameron and Tipper, 1985; Kunae Zone.

GSC Loc. No. C-157551. 103F/8, Yakoun Lake, 679800E, 5921000N. central Graham Island, Maude Group, Ghost Creek Formation; Imlayi Zone.

## APPENDIX 4

### Toarcian ammonite locality register

Information is provided here for illustrated Toarcian ammonite material.

GSC Loc. No. C-080778. 103F/1, Skidegate Channel, 698800E, 5897300N. Moresby Island, Whiteaves Bay, Fannin Formation; 9.0 m above the base of the Whiteaves Bay section. Lower Toarcian.

GSC Loc. No. C-087105. 80TD-63FA, 103F/8, Yakoun Lake, 681500E, 5922000N. Graham Island, Yakoun River, Whiteaves Formation; 25 m above the base of the Yakoun River section. Middle Toarcian.

GSC Loc. No. C-087114. 80TD-84FA, 103F/8, Yakoun Lake, 681500E, 5922000N. Graham Island, Yakoun River, Phantom Creek Formation; 74 m above the base of the Yakoun River section. Upper Toarcian.

GSC Loc. No. C-087118. 80TD-80FA, 103F/8, Yakoun Lake, 681500E, 5922000N. Graham Island, Yakoun River, Phantom Creek Formation; 75 m above the base of the Yakoun River section. Toarcian.

GSC Loc. No. C-087122. 80TD-76FA-1, 103F/8, Yakoun Lake, 681500E, 5922000N. Graham Island, Yakoun River, Whiteaves Formation; 58 m above the base of the Yakoun River section. Upper Toarcian.

GSC Loc. No. C-087215. 80TD-50FA, 103F/8, Yakoun Lake, 682000E, 5922500N. Graham Island, Yakoun River, Phantom Creek Formation; 20 m below the top of Strat. Sect. No. 12 (Cameron and Tipper, 1985). Upper Toarcian.

GSC Loc. No. C-157728. 87TDJ, 103F/8, Yakoun Lake, 681500E, 5922000N. Graham Island, Yakoun River, Whiteaves Formation; Talus from the section on the Yakoun River. Upper Toarcian.

GSC Loc. No. C-158008. 87TDJ, 103F/8, Yakoun Lake, 6821500E, 5922100N. Graham Island, Yakoun River, Whiteaves Formation; Talus from the Yakoun River on the shore opposite Strat. Sect. No. 15 (Cameron and Tipper, 1985). Lower Toarcian.

GSC Loc. No. C-158027. 87TDJ, 103F/8, Yakoun Lake, 6821500E, 5922100N. Graham Island, Yakoun River, Whiteaves Formation; 79.0 m above the base of the section opposite Strat. Sect. No. 15 (Cameron and Tipper, 1985). Lower Toarcian.

## APPENDIX 5

### Radiolaria locality register

Information is provided here for illustrated radiolarian material.

GSC Loc. No. C-080577. Maude Island; 53°11.82'N, 132°3.63'W. Maude Group, Fannin Formation; fine calcarenite collected 54.3 m below top of Fannin Formation (Strat. Sect. 4 of Cameron and Tipper, 1985).

GSC Loc. No. C-080579. Maude Island, 53°11.94'N, 132°3.25'W. Maude Group, Whiteaves Formation; limestone nodule collected 20.5 m below top of Whiteaves Formation (Strat. Sect. 6 of Cameron and Tipper, 1985). Occurs with one poorly preserved specimen of *Phymatoceras* sp.; middle Toarcian (H.W. Tipper, pers. comm., 1983).

GSC Loc. No. C-080583, C-080584. Yakoun River, Graham Island, 53°25.19'N, 132°15.64'W. Maude Group, Phantom Creek Formation; fine calcarenite samples collected 10.5 and 14.5 m, respectively, above top of Whiteaves Formation (Strat. Sect. 12 of Cameron and Tipper, 1985). Based on co-occurring ammonites, samples are late middle or early late Toarcian (H.W. Tipper, pers. comm., 1984).

GSC Loc. No. C-080597. Yakoun River, Graham Island, 53°25.22'N, 132°15.73'W. Maude Group, Phantom Creek Formation; sample is fine calcarenite, collected with ammonites referred to the late Toarcian (H.W. Tipper, pers. comm., 1983).

GSC Loc. No. C-164676. Kunga Island, north (87CAA(EC)KUD-2); 52°46.33'N, 131°33.58'W. Kunga Group, Sandilands Formation; 22.5 m above exposed base of section D; micrite concretion.

GSC Loc. No. C-164659. Kennecott Point, Graham Island (87CAA(EC)KPB10); 53°54.73'N, 133°9.15'W. Kunga Group, Sandilands Formation; 44.5 m above exposed base of section B; limestone lense. Occurs with *Badouxia canadensis*, basal Sinemurian (H.W. Tipper, pers. comm., 1988).

GSC Loc. No. C-164661. Kennecott Point, Graham Island (87CAA(EC)KPB12); 53°54.73'N, 133°9.15'W. Kunga Group, Sandilands Formation; 50 m above exposed base of section B; limestone concretion (20 x 40 cm). Occurs with *Badouxia canadensis*, basal Sinemurian (H.W. Tipper, pers. comm., 1988).

## APPENDIX 6

### Foraminifera locality register

Information is provided here for illustrated foraminifera material. Stratigraphic sections are described in Cameron and Tipper, 1985.

GSC Loc. No. C-127824. 80-CAA-T-01, Stn. 22B, Sh 01B; 103F/8W, Yakoun Lake; 681800E, 5917750N. Graham Island, Rennell Junction, Whiteaves Formation, Septarian Shale Member; 258.0-258.9 m below the top of Strat. Sect. No. 10; Middle Toarcian.

GSC Loc. No. C-127840. 80-CAA-T-07, Stn. 05, Sh 01; 103F/8W, Yakoun Lake; 681600E, 5917750N. Graham Island, Rennell Junction, lower part of the Fannin Formation; 327.9 m below the top of Strat. Sect. No. 10; Early Pliensbachian.

GSC Loc. No. C-127851. 80-CAA-T-07, Stn. 11, Sh 01; 103F/8W, Yakoun Lake; 681600E, 5917750N. Graham Island, Ren-

nell Junction, Ghost Creek Formation; 356.7 m below the top of Strat. Sect. No. 10; Early Pliensbachian.

GSC Loc. No. C-127868. 80-CAA-T-07, Stn. 14, Sh 13B; 103F/8W, Yakoun Lake; 681500E, 5917750N. Graham Island, Rennell Junction, Ghost Creek Formation; 414.9 m below the top of Strat. Sect. No. 10; Early Pliensbachian.

GSC Loc. No. C-127899. 82-CAA-01, Sh 16; 103F/8W, Yakoun Lake; 681500E, 5917750N. Graham Island, Rennell Junction, Ghost Creek Formation; 415.5-416.1 m below the top of Strat. Sect. No. 10; Early Pliensbachian.

GSC Loc. No. C-127933. 79-CAA-RP-01, Sh 08; 103F/8W, Yakoun Lake; 681500E, 5917750N. Graham Island, Rennell Junction, Ghost Creek Formation; 417.0 m below the top of Strat. Sect. No. 10; Early Pliensbachian.

GSC Loc. No. C-172372. 80-CAA-T-06, Stn. 10, Sh 06B; 103F/8W, Yakoun Lake; 681400E, 5919100N. Graham Island, Branch Road 57, Whiteaves Formation, Concretionary Shale Member; 276.0 m below the top of Strat. Sect. No. 14; Middle Toarcian.

GSC Loc. No. C-172378. 80-CAA-T-06, Stn. 10, Sh 11; 103F/8W, Yakoun Lake; 681400E, 5919100N. Graham Island, Branch Road 57, Whiteaves Formation, Concretionary Shale Member; 289.5-291.0 m below the top of Strat. Sect. No. 14; Middle Toarcian.

GSC Loc. No. C-172390. 80/82-CAA-TT-06, Sh 08; 103F/8W, Yakoun Lake; 681300E, 5919100N. Graham Island, Branch Road 57, Whiteaves Formation, Septarian Shale Member; 308.1-309.0 m below the top of Strat. Sect. No. 14; Middle Toarcian.

GSC Loc. No. C-172423. 80-CAA-T-08, Sh 01; 103F/8W, Yakoun Lake; 682100E, 5922000N. Graham Island, Yakoun River, Whiteaves Formation, Septarian Shale Member; 96.0 m below the top of Strat. Sect. No. 15; Middle Toarcian.

GSC Loc. No. C-172424. 80-CAA-T-08, Sh 02; 103F/8W, Yakoun Lake; 682100E, 5922000N. Graham Island, Yakoun River, Whiteaves Formation, Septarian Shale Member; 93.9 m below the top of Strat. Sect. No. 15; Middle Toarcian.

GSC Loc. No. C-172558. 78-CAA-02, Sh 08; 103F/1E, Skidegate Channel; 696100E, 5897700N. Maude Island, Type Maude, Ghost Creek Formation; 9.0-10.5 m above the base of the Ghost Creek Formation, Strat. Sect. No. 8; Early Pliensbachian.

GSC Loc. No. C-172565. 78-CAA-02, Sh 15; 103F/1E, Skidegate Channel; 696200E, 5897700N. Maude Island, Type Maude, Ghost Creek Formation; 19.5-21.0 m above the base of the Ghost Creek Formation, Strat. Sect. No. 8; Early Pliensbachian.

GSC Loc. No. C-172595. 78-CAA-02, Sh 45; 103F/1E, Skidegate Channel; 696400E, 5897800N. Maude Island, Type Maude, lower part of the Fannin Formation; 61.5-63.0 m above the base of the Ghost Creek Formation, Strat. Sect. No. 8; Early Pliensbachian.

GSC Loc. No. C-172607. 78-CAA-02, Sh 57; 103F/1E, Skidegate Channel; 696400E, 5897900N. Maude Island, Type Maude, upper part of the Fannin Formation; 81.0-84.0 m above the base of the Ghost Creek Formation, Strat. Sect. No. 8; Late Pliensbachian.

GSC Loc. No. C-172619. 80-CAA-T-03, Sh 03; 103F/8W, Yakoun Lake; 682000E, 5922550N. Graham Island, Yakoun River, Phantom Creek Formation, Coquinoid Sandstone Member; 12.6-13.5 m below the top of Strat. Sect. No. 12; Upper Toarcian.

GSC Loc. No. C-172621. 80-CAA-T-03, Sh 05; 103F/8W, Yakoun Lake; 682000E, 5922550N. Graham Island, Yakoun River, Phantom Creek Formation, Coquinoid Sandstone Member; 23.1-24.0 m below the top of Strat. Sect. No. 12; Upper Toarcian.

GSC Loc. No. C-172706. 78/79-CAA-T-06, Sh 06; 103F/1E, Skidegate Channel; 696700E, 5898300N. Maude Island, Fannin Bay, Whiteaves Formation, Septarian Shale Member; 37.5-39.0 m below the top of Strat. Sect. No. 6; Middle Toarcian.

GSC Loc. No. C-172715. 78-CAA-T-03, Stn. 01, Sh 05; 103F/1E, Skidegate Channel; 697050E, 5898300N. Maude Island, Fannin Bay, upper part of the Fannin Formation; Late Pliensbachian.

## APPENDIX 7

### Ichthyolith locality register

Information is provided here for illustrated ichthyolith material. Stratigraphic sections are described in Cameron and Tipper, 1985.

GSC Loc. No. C-127817. 80-CAA-T-01, Stn. 16, Sh 01; 103F/8W, Yakoun Lake; 681800E, 5917750N. Graham Island, Rennell Junction, Whiteaves Formation, Concretionary Shale Member; 231.0-232.5 m below the top of Strat. Sect. No. 10; Middle Toarcian.

GSC Loc. No. C-127818. 80-CAA-T-01, Stn. 17, Sh 01; 103F/8W, Yakoun Lake; 681800E, 5917750N. Graham Island, Rennell Junction, Whiteaves Formation, Concretionary Shale Member; 234.0-235.2 m below the top of Strat. Sect. No. 10; Middle Toarcian.

GSC Loc. No. C-127824. 80-CAA-T-01, Stn. 22B, Sh 01B; 103F/8W, Yakoun Lake; 681800E, 5917750N. Graham Island, Rennell Junction, Whiteaves Formation, Septarian Shale Member; 258.0-258.9 m below the top of Strat. Sect. No. 10; Middle Toarcian.

GSC Loc. No. C-127837. 80-CAA-T-07, Stn. 02, Sh 01; 103F/8W, Yakoun Lake; 681600E, 5917750N. Graham Island, Rennell Junction, lower part of the Fannin Formation; 318.0 m below the top of Strat. Sect. No. 10; Early Pliensbachian.

GSC Loc. No. C-127895. 82-CAA-01, Sh 13; 103F/8W, Yakoun Lake; 681600E, 5917750N. Graham Island, Rennell Junction, lower part of the Fannin Formation; 336.3-337.2 m below the top of Strat. Sect. No. 10; Early Pliensbachian.

GSC Loc. No. C-127928. 79-CAA-RP-01, Sh 03A; 103F/8W, Yakoun Lake; 681600E, 5917750N. Graham Island, Rennell Junction, Ghost Creek Formation; 360.0 m below the top of Strat. Sect. No. 10; Early Pliensbachian.

GSC Loc. No. C-172307. 80-CAA-T-05, Stn. 07, Sh 01; 103F/8W, Yakoun Lake; 681500E, 5921900N. Graham Island, Yakoun River, Whiteaves Formation, Septarian Shale Member; 51.0 m, at the base of Septarian Shale Member, Strat. Sect. No. 11; Middle Toarcian.

GSC Loc. No. C-172390. 80/82-CAA-TT-06, Sh 08; 103F/8W, Yakoun Lake; 681300E, 5919100N. Graham Island, Branch Road 57, Whiteaves Formation, Septarian Shale Member; 308.1-309.0 m below the top of Strat. Sect. No. 14; Middle Toarcian.

GSC Loc. No. C-172438. 80-CAA-T-08, Sh 16; 103F/8W, Yakoun Lake; 682100E, 5922100N. Graham Island, Yakoun River, Whiteaves Formation, Septarian Shale Member; 67.5 m below the top of Strat. Sect. No. 15; Middle Toarcian.

GSC Loc. No. C-172440. 80-CAA-T-08, Sh 18; 103F/8W, Yakoun Lake; 682100E, 5922100N. Graham Island, Yakoun River, Whiteaves Formation, Septarian Shale Member; 64.5 m below the top of Strat. Sect. No. 15; Middle Toarcian.

GSC Loc. No. C-172447. 82-CAA-04, Sh 04; 103F/8W, Yakoun Lake; 682100E, 5922000N. Graham Island, Yakoun Lake, Whiteaves Formation, Septarian Shale Member; 82.8-84.0 m below the top of Strat. Sect. No. 15; Middle Toarcian.

GSC Loc. No. C-172519. 78/82-CAA-T-01, Sh 01; 103F/1E, Skidegate Channel; 697300E, 5898600N. Maude Island, Whiteaves Formation, Concretionary Shale Member; 61.5-63.0 m below the top of Strat. Sect. No. 5; Middle Toarcian.

GSC Loc. No. C-172522. 79-CAA-02, Sh 01; 103F/1E, Skidegate Channel; 696400E, 5898400N. Maude Island, Fannin Bay, upper part of the Fannin Formation; 0.9-2.4 m below the top of Strat. Sect. No. 9; Late Pliensbachian.

GSC Loc. No. C-172523. 79-CAA-02, Sh 02; 103F/1E, Skidegate Channel; 696400E, 5898400N. Maude Island, Fannin Bay, upper part of the Fannin Formation; 4.5-5.4 m below the top of Strat. Sect. No. 9; Late Pliensbachian.





# Current status of Middle Jurassic biostratigraphy of the Queen Charlotte Islands, British Columbia

T.P. Poulton<sup>1</sup>, R.L. Hall<sup>2</sup>, H.W. Tipper<sup>3</sup>,  
B.E.B. Cameron<sup>4</sup> and E.S. Carter<sup>5</sup>

Poulton, T.P., Hall, R.L., Tipper, H.W., Cameron, B.E.B., and Carter, E.S., Current status of Middle Jurassic biostratigraphy of the Queen Charlotte Islands, British Columbia; in *Evolution and Hydrocarbon Potential of the Queen Charlotte Basin, British Columbia*, Geological Survey of Canada, Paper 90-10, p. 237-252, 1991.

## Abstract

*Ammonites from the upper Maude Yakoun and Moresby groups of the Queen Charlotte Islands indicate the presence of at least 10 zones, representing small parts of each of the four Middle Jurassic stages. The radiolarians, Foraminifera, bivalves and other fossils associated with the ammonites are summarized. Previously reported Upper Jurassic faunas and rocks are poorly substantiated and may be absent.*

*With few exceptions, the ammonite localities are isolated occurrences, thus the sequence is pieced together by inference and relies on international correlations to a large degree. Because of the discontinuous exposure and faulting between the scattered outcrops, such correlations have proven to be essential for understanding the stratigraphy and structure of the Queen Charlotte Islands.*

*Major faunal gaps support the lithologic and tectonic evidence for major tectonic events before the Late Bathonian (following deposition of the thick pile of Yakoun volcanics) and prior to the Early Cretaceous. A major hiatus suggests a further event prior to the Early Bajocian. Zemistephanus and Iniskinites of Early Bajocian and Late Bathonian age respectively have essentially northern North American affinities, perhaps suggesting relatively little northward transport of the Queen Charlotte Islands since Early Bajocian.*

## Résumé

*Des ammonites des groupes de Yakoun de Maude supérieur et de Moresby dans les îles de la Reine-Charlotte indiquent la présence d'au moins 10 zones représentant de petites parties de chacun des quatre stades du Jurassique moyen. Les radiolaires, les foraminifères, les bivalves et les autres fossiles associés aux ammonites sont passés en revue. Les mentions antérieures de faunes et de roches du Jurassique supérieur sont mal documentées, de sorte qu'il est difficile de conclure à leur existence.*

*À quelques exceptions près, les populations d'ammonites sont isolées, de sorte que la séquence est reconstituée par inférence et repose surtout sur des corrélations internationales. À cause d'une exposition discontinue et des failles entre les affleurements dispersés, ces corrélations se sont avérées essentielles pour comprendre la stratigraphie et la structure des îles de la Reine-Charlotte.*

*D'importantes lacunes fauniques renforcent la preuve lithologique et tectonique de grands événements tectoniques avant le Bathonien supérieur (après le dépôt des épaisses couches de roches volcaniques de Yakoun) et avant le Crétacé inférieur. Un important hiatus laisse croire à un autre événement avant le Bajocien inférieur. Zemistephanus du Bajocien inférieur et Iniskinites du Bathonien supérieur ont des affinités nord-américaines essentiellement boréales, ce qui pourrait indiquer qu'il y a eu relativement peu de déplacement vers le nord des îles de la Reine-Charlotte depuis le Bajocien inférieur.*

<sup>1</sup> Institute of Sedimentary and Petroleum Geology, 3303-33rd Street, N.W., Calgary, Alberta T2L 2A7

<sup>2</sup> Department of Geology and Geophysics, University of Calgary, Calgary, Alberta T2N 1N4

<sup>3</sup> Cordilleran Division, Geological Survey of Canada, 100 West Pender Street, Vancouver, B.C. V6B 1R8

<sup>4</sup> Pacific Geoscience Centre, Geological Survey of Canada, P.O. Box 6000, Sidney, B.C. V8L 4B2

<sup>5</sup> 58335 Timber Road, Vernonia, Oregon, U.S.A. 97064

## INTRODUCTION

The lithostratigraphy of the Middle Jurassic of the Queen Charlotte Islands (Fig. 1) was described by Cameron and Tipper (1985) and is summarized in Figure 2. The biostratigraphy and much of the paleontology are described in other reports (e.g. Cameron and Tipper, 1985) and only a summary, with new data, is provided here. The recent mapping, structural and biostratigraphic work has resulted in a new understanding of geological relationships on the Queen Charlottes. To a large degree the more detailed biostratigraphy available (Cameron

and Tipper, 1985) has aided this understanding. The unravelling of the stratigraphy has had a long and checkered history because of the lithological similarity of many of the units and their structural complexity and because of early confusion of a great variety of Early Jurassic through Cretaceous fossils. The first major strides toward a modern biostratigraphy, based on detailed taxonomic studies combined with field work, were made by McLearn (1929, 1949) and similar studies continue toward the same goals.

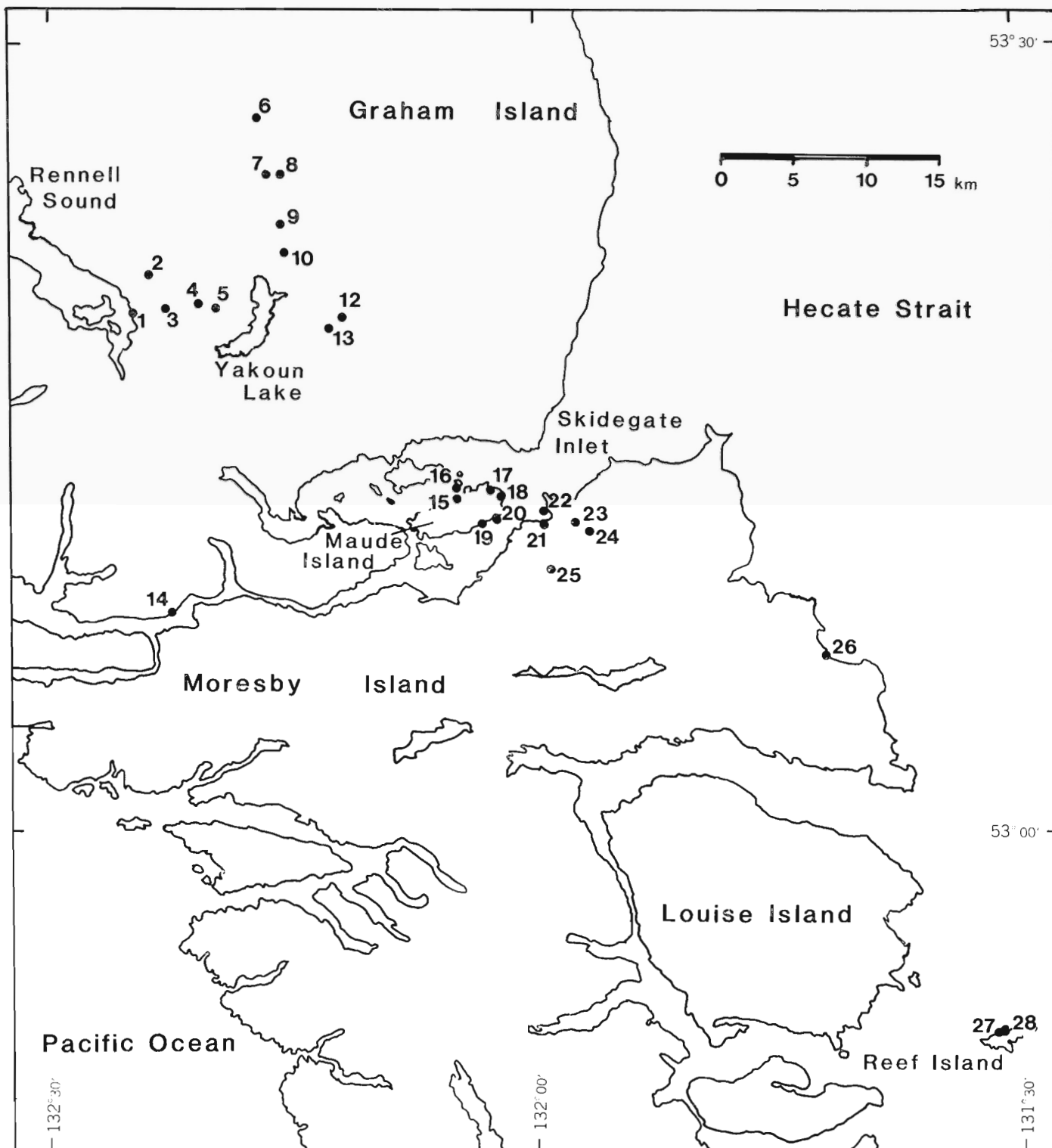


Figure 1: Index map showing significant Middle Jurassic fossil localities, Queen Charlotte Islands.

The sequence as presently known (Cameron and Tipper, 1985) is an elaboration of what was earlier called the Maude and Yakoun formations (McLearn, 1949). The Maude, with incomparably better fossil control than was available previously, was elevated to group status by Cameron and Tipper (1985) and subdivided into five formations, some of them separated by disconformities. Only the uppermost 3-5 m are Middle Jurassic. These Aalenian beds appear to overlie gradationally Upper Toarcian beds.

The Yakoun was also elevated to group rank by Cameron and Tipper (1985), has had the upper part separated from it, and the remaining major part subdivided into two formations. The lower, thicker part consists of a thick pile of monotonous flow and pyroclastic volcanic rocks with lesser amounts of volcanoclastic sedimentary rocks, mainly in the lower part. These lower beds, the 'lower Yakoun sediments' of previous authors, are Bajocian in age. Several ammonite assemblages are present in the Lower Bajocian (Plate 1, Figs. 1-4; Plate 2), but no continuous sequence has been observed because of the lack of exposure between discontinuous outcrops (Hall and Westermann, 1980). Therefore the assignment to zones is based on correlation with ammonites outside the area and not on an observed succession, so that it is possible that future discoveries will require that the sequence be revised. At least two significant new faunas, still not studied in detail, have been found since Hall and Westermann (1980) described two of the assemblages, and all available early collections have been re-examined. Because of the unfossiliferous nature of much of the Yakoun Group and the discontinuous outcrop of the fossiliferous parts, knowledge of its succession and characteristics remain unsatisfactory. The Yakoun volcanic and volcanoclastic package apparently overlies a regional unconformity (Thompson et al., 1991) which, with the volcanic nature of the unit itself, indicates the occurrence of significant tectonic events in the early Middle Jurassic. The 'upper Yakoun sediments' of previous authors have been reassigned to the Moresby Group and subdivided into three formations (Cameron and Tipper, 1985) which span the Bathonian-Callovian boundary. The fossil zones (Plate 1, Fig. 5; Plate 3) suggest a substantial hiatus between this sedimentary package and the underlying volcanics. The thick volcanic pile, regional structural relationships (Thompson et al., 1991), and a possible angular discordance at the contact (Cameron and Tipper, 1985), indicate further tectonic activity within the Middle Jurassic.

Upper Jurassic sedimentary rocks, and supposedly Upper Jurassic *Buchia* collections, have been reported in the literature on the Queen Charlotte Islands (Jeletzky, 1984; Jeletzky, in Cameron and Tipper,

1985). The identification and age of the fossils are not firmly established, and stratigraphic relations suggest that a Late Jurassic age may be doubtful, but cannot be ruled out entirely at some localities. The relationship between the Lower Callovian beds and the structurally discordant Lower Cretaceous Longarm Formation remains poorly understood. The long hiatus separating these two units regionally is one of the major breaks in the Mesozoic succession of the Queen Charlotte Islands and coincides with a widespread plutonic event (Anderson and Reichenbach, 1991).

In the locality descriptions that follow, the locations and stratigraphic context are taken directly from the field "pink slips" supplied by the collector, thus there is considerable variation in the format and quality of this information.

## AALENIAN

The lower Aalenian is represented in Queen Charlotte Islands by a belemnite-rich, calcareous sandstone at the top of the Phantom Creek Formation, conformably overlying beds with latest Toarcian fossils. The Aalenian beds are almost certainly Lower Aalenian (*Leioceras opalinum* or *Tmetoceras scissum* Standard zones) based on the presence of *Tmetoceras scissum* Benecke and *Bredya* cf. *manflasensis* Westermann ("Hammatoceras" of previous reports) (Poulton and Tipper, in press). The Aalenian ammonites have been found on Yakoun River and on logging road 59 (section 13, Cameron and Tipper, 1985), both on Graham Island.

Carter et al. (1988) described a distinctive association of radiolaria from the Aalenian sandstone on road 59. It comprises a mixture of species, some of which range upward from older beds into the Aalenian. Others which are characteristic of the Middle Jurassic first appear in this zone. Both the base and top of this zone (Zone 6, Figure 8, Carter et al., 1988) are notable for being either the lower or upper limit of a number of species. *Turanta morinae* Pessagno and Blome, *Hsuum optimum* Carter, and *Elodium* sp. make their final appearance in this zone. No microfossils other than radiolaria have been recovered.

North of Yakoun Lake, logging road 59 (Fig. 1, loc. 10)

**C-39516.** (Formerly miscatalogued as C-90974) H.W. Tipper, 1983. Road 59, Graham Island, Lat. 53°23'N, Long. 132°16'W (NTS 103F). Phantom Creek Formation, at top. This specimen occurs within inches above *Tmetoceras* (C-90567) and is in place in the same bed (see Section 13 of Cameron and Tipper, 1985).

*Bredya* aff. *manflasensis* Westermann

SERIES	GROUP	FORMATION	MEMBER	LITHOLOGY	THICKNESS	AMMONITE ASSEMBLAGES	RAD. ZONES
unconformity							
E. CALLOVIAN	MORESBY	ALLIFORD		Siltstone, shale, minor sandstone	60 m	<i>Kepplerites spinosum</i>	
		NEWCOMBE		Sandstone, minor pebble conglomerate	30 - 45 m	<i>Cadoceras doroschlini</i> <i>Oxycerites</i> <i>Kepplerites (Seymourites) spp.</i>	
ROBBER POINT				Shale, siltstone, pebble conglomerate	15 - 90 m	<i>Iniskinites cepoides</i>	
L. BATHONIAN							
erosional interval, possible slight angular discordance							
E. BAJOCIAN	YAKOUN	RICHARDSON BAY	VOLCANIC BRECCIA	Volcanic breccia	60 - 530 m		7
			DARK SANDSTONE	Sandstone	30 - 110 m		
		GRAHAM ISLAND	LAPILLI	Lapilli tuff, agglomerate	200 m	<i>Chondroceras oblatum</i>	
			VOLCANIC SANDSTONE	Sandstone, congl., minor shale	140 - 170 m	<i>Stephanoceras kirschneri</i>	
			MOTTLED SANDSTONE	Siltstone	30 m	<i>Kumatostephanus</i> , sonniniids	
			SHALE-TUFF	Shale, tuff	75 - 85 m	sonniniids, <i>Fontannesia(?)</i>	
hiatus, paraconformity							
E. AALENIAN	MAUDE	PHANTOM CREEK (part)	BELEMNITE SANDSTONE (part)	Belemnite-rich sandstone	3 - 5 m	<i>Tmetoceras scissum</i> , <i>Bredya</i>	6

Figure 2: Chart showing Middle Jurassic formations and fossil assemblage zones, Queen Charlotte Islands.

**C-90567.** H.W. Tipper, 1980. Road 59, Graham Island. Lat. 53°23'N, Long. 132°16'W (NTS 103F). Top of Phantom Creek Formation, within centimetres of C-39516, below it in the same bed (Section 13 of Cameron and Tipper, 1985).

*Tmetoceras scissum* (Benecke)

**C-157552.** H.W. Tipper, 1987. Road 59 at waterfall. Lat. 53°23'00"N, Long. 132°16'00"W (NTS 103F/8). Phantom Creek Formation. Same as earlier *Bredya* and *Tmetoceras* locality on road 59 (see Poulton and Tipper, in press).

*Bredya* sp.

*Yakoun River north of Yakoun Lake (Fig. 1, loc. 8)*

**C-117482.** H.W. Tipper, 1984. Yakoun River. Graham Island (NTS 103F). Phantom Creek Formation, Maude Group. 53°25'N, Long. 132°16'W.

*Bredya* sp.

*Oxytoma* sp.

## EARLY BAJOCIAN

### *Docidoceras widebayense* Zone

The lowest Bajocian zone in the Queen Charlotte Islands has been correlated with the *D. widebayense* Assemblage Zone by Cameron and Tipper (1985). It characterizes the Graham Island Formation which comprises a mixture of volcanic and sedimentary lithologies. This zone was originally designated by Hall and Westermann (1980) who designated a type area at Wide Bay, southern Alaska, where the succession was described by Westermann (1969). It comprises much of the lower part of the Lower Bajocian, approximately equivalent to the *Hyperlioceras discites* and *Sonninia ovalis* (lower *Witchellia laeviuscula*) zones of Northwest Europe. In addition to *Docidoceras*, the assemblages in southern Alaska contain late *Pseudolioceras*, and early *Witchellia*, *Sonninia* (*Euhoploceras*) and *S. (Alaskinia)* as well as other genera. *Docidoceras* itself is rare in British Columbia, and the earlier parts of the Bajocian are dominantly represented by sonniniids.

Frebold (in Cameron and Tipper, 1985) identified species of *Docidoceras* and *Sonninia* from the south shore of Maude Island, and several forms were reported by Cameron and Tipper from Graham Island, including *Witchellia*, *Dorsetensia*, *Sonninia*, *Guhnsania*, *Bradfordia* and other sonniniids. Detailed taxonomic study still has not been undertaken, but a preliminary review suggests that *Docidoceras* is probably not present in the collections and that *Fontannesia* may be represented.

Foraminifera are rare and comprise two assemblages, listed by Cameron and Tipper (1985) and Carter et al. (1988). The lower fauna contains distinctive species of *Lenticulina*, *Astacolus* and *Marginulina* and *Marginulopsis* and the upper fauna contains species of *Bigenerrina*, *Ammobaculites*, *Reophax*, *Trochammina* and *Trochamminoides*(?).

Radiolarians from two sections (sections 13 and 14 of Cameron and Tipper, 1985) were described in Carter et al. (1988). They are abundant, generally distinct from those of older rocks and were included in Zone 7 of Carter et al. The base of this zone is recognized by the earliest appearance of *Parvicingula matura* Pessagno and Whalen. *Gorgansium silviesensis* Pessagno and Blome and *Zartus thayeri* Pessagno and Blome appear near the base of the zone as well as forms similar to *Trillus seidersi* Pessagno and Blome and *Hsuum mirabundum* Pessagno and Whalen. The association of these forms, together with *Emiluvia* Foreman, *Tricolocapsa* Haeckel and *Stichocapsa* Haeckel, is characteristic. *Perispyridium* and *Parvicingula*, which occur rarely in Toarcian rocks, are abundant in the Lower Bajocian.

Chlorophyte algal cysts (Rouse, in Carter et al., 1988) similar to *Lophodictyotidium sarjeanti* Pocock occur in this unit.

Significant ammonite-bearing localities and their faunas are listed below (\* indicates identifications by H. Frebold):

*Fannin Bay area, south shore of Maude Island (Fig. 1, loc. 19)*

**91826.** H.W. Tipper, 1974. Southeast side of Maude Island, between McLearn's M4 and M5. 137 m east of fault which separates these beds from Toarcian rocks.

\**Docidoceras* sp. aff. *warmspringsense* Imray

\**Sonninia* sp.

\**Witchellia*(?) sp.

**91831.** H.W. Tipper, 1974. South side of Maude Island, between McLearn's M4 and M5 localities. Just east of Toarcian-Bajocian fault. Between McLearn's localities M4 and M5.

\**Sonninia* spp.

\**Docidoceras* sp.

*Dorsetensia*(?) sp.

sonniniid ammonites, indet.

**C-80787.** H.W. Tipper and B.E.B. Cameron, 1978. South shore of Maude Island. Lat. 53°12'N, Long. 132°03'W.

sonniniid ammonites, indet.

**C-81714.** H.W. Tipper, 1982. East end of Fannin Bay. Maude Island. Lat. 53°12'N, Long. 132°03'W.

*Sonninia* sp.

*Fontannesia*(?) sp.

*Witchellia*(?) sp.

belemnite, indet.

*Ghost Creek area west of Yakoun River (Fig. 1, loc. 7)*

**C-81715.** H.W. Tipper, 1982. Camp by quarry 1.6 km west of junction of Ghost Creek road and Queen Charlotte Island road. Lat. 53°25'35"N, Long. 132°16'W. Graham Island Formation, possibly the highest part.

*Sonninia (Papilliceras)* sp.

*North of Yakoun Lake, logging road 59 (Fig. 1, loc. 10)*

**C-81732.** H.W. Tipper, 1982. Road 59, quarry at first bend north of waterfall. Graham Island, Lat. 53°22'15"N, Long. 132°16'40"W. Same as GSC locality C-90570.

*Fontannesia*(?) sp.

*Sonninia*(?) sp.

belemnite, indet.

**C-81748.** H.W. Tipper, 1982. Creek north of road 59, Rennell Junction. Same locality as C-87201.

*Fontannesia* sp.

**C-81910.** H.W. Tipper, 1979. Logging road north of Rennell Junction to coast. Graham Island, Lat. 53°22'35"N, Long. 132°16'W. Lower part, Yakoun Group.

sonniniid ammonites, indet.

**C-87201.** B.E.B. Cameron, 1980. Creek north of road 59, Rennell Junction. Same as GSC locality C-81748.

*Fontannesia* sp.

ammonites, indet.

**C-90562.** H.W. Tipper, 1980. Road 59, Graham Island, Lat. 53°22'15"N, Long. 132°16'40"W. Shale-tuff member, Graham Island Formation, first quarry (Section 13 of Cameron and Tipper, 1985).

*Fontannesia* sp.

*Brent Creek east of Yakoun Lake (Fig. 1, loc. 12)*

**C-90563.** H.W. Tipper, 1980. Brent Creek. Graham Island.

*Sonninia* sp.



belemnite, indet.

North of Yakoun Lake, logging road 57 (Fig. 1, loc. 9)

**C-81705.** H.W. Tipper, 1982. Section 14 of Cameron and Tipper (1985). Road 57. Graham Island, Lat. 53°23'36"N, Long. 132°16'W. Shale-tuff member, Graham Island Formation.

*Sonninia* sp.

*Docidoceras*(?) sp.

*Fontannesia*(?) sp.

bivalves, indet.

**C-90585.** B.E.B. Cameron and H.W. Tipper. Road 57, Graham Island, Lat. 53°23'36"N, Long. 132°16'W (Section 14 of Cameron and Tipper, 1985).

*Fontannesia*(?) sp.

*Sonninia*(?) sp.

belemnites, indet.

**C-90586.** B.E.B. Cameron and H.W. Tipper, 1980. Road 57, Graham Island, Lat. 53°23'36"N, Long. 132°16'W. Graham Island Formation (Section 14 of Cameron and Tipper, 1985).

*Fontannesia* sp.

#### ***Parabigotites crassicosatus* Zone**

The ammonite assemblages from three localities that include *Kumatostephanus* are correlated with the *P. crassicosatus* Assemblage Zone, based on southern Alaska assemblages (Hall and Westermann, 1980) and the *Otoites sauzei* Standard Zone of northwest Europe. A new ammonite fauna, containing an evolute ammonite listed below as *Parabigotites*(?) sp. was discovered in 1988 in black sandstones of the Yakoun Group. However the ammonites are small and not well preserved, so that the age and the identifications given below are tentative. Another locality, containing oppeliid(?) ammonites is also thought to be of this age.

King Creek area (Fig. 1, loc. 6)

**C-163798.** H.W. Tipper, R.L. Hall, and T.P. Poulton, 1988. Quarry on King Creek road, UTM Zone 8U 67924E, 59249N, Graham Island.

*Parabigotites*(?) sp.

oppleiid(?) ammonites

other ammonites, indet.

North of Yakoun Lake, logging road 59 (Fig. 1, loc. 10)

**C-81740.** H.W. Tipper, 1982. Second quarry on road 59 above waterfall. Graham Island, Lat. 53°20'N, Long. 132°15'28"W. Shale-tuff member, Graham Island Formation. Recollection of 1980 localities C-90564, C-90565.

oppleiid(?) ammonites

*Astarte* sp.

bivalves, indet.

gastropods, indet.

terebratulid brachiopods, indet.

**C-90565.** H.W. Tipper, 1980. Same as GSC locality C-81740.

oppleiid(?) ammonite

Fannin Bay area, southern Maude Island (Fig. 1, loc. 19).

**C-168504.** T.P. Poulton and R.L. Hall, 1988. East side of Fannin Bay, south coast of Maude Island. In large boulders; no equivalent exposure up the hill. UTM Zone 8U 6971E 58983N.

*Sonninia* sp.

*Stephanoceras* sp.

*Kumatostephanus*(?) sp.

*Docidoceras*(?) sp.

belemnites, indet.

**C-142948.** R.I. Thompson, 1987. UTM 973990, Lat. 53°12'20"N, Long. 132°02'45"W.

*Docidoceras*(?) sp.

*Kumatostephanus*(?) sp.

*Fontannesia*(?) sp.

**C-171157.** R.L. Hall, 1985. Quarry above Richardson Bay, up hill from coastline exposures, southern Maude Island. UTM 977 989.

*Kumatostephanus* sp.

*Sonninia* sp.

#### ***Stephanoceras kirschneri* Zone**

The lowest beds with *Stephanoceras* are assigned to the *S. kirschneri* Assemblage Zone, erected by Hall and Westermann (1980) based on a type area in Cook Inlet, southern Alaska. Hall and Westermann (1980) recognized an upper subzone, that of *Zemistephanus richardsoni*, but did not designate characteristic species for lower parts of the zone in southern Alaska or western Canada. In Queen Charlotte Islands the two are, at present, essentially synonymous and contain the lower faunas of the Richardson Bay Formation. Upper beds of the underlying and partially equivalent Graham Island Formation may also contain stephanoceratid ammonites of these zones. They are considered to be equivalent with upper parts of the *Otoites sauzei* and lower parts of the *Stephanoceras humphriesianum* Standard Zone (Hall and Westermann, 1980).

The fauna in Queen Charlotte Islands, present at MacKenzie Bay on the north shore of Maude Island, contains *Zemistephanus richardsoni* (Whiteaves), *Z. carlottensis* (Whiteaves), *Z. alaskensis* Hall, *Z. crickmayi* (McLearn), *Stephanoceras* aff. *acuticostatum* Weisert and *Chondroceras* sp. (Hall and Westermann, 1980; Cameron and Tipper, 1985). The taxonomic assignments follow Hall and Westermann (1980), who revised many of the earlier identifications (McLearn, 1929, 1932) in light of modern procedures which take into account sexual dimorphism. As a result, many of the original species are placed into synonymy with others (see Hall and Westermann, 1980) and the following genera are no longer recognized: *Itinsaites* (microconch of *Stephanoceras itinsae*), *Kanastephanus* (= *Zemistephanus*), *Normannites* (= *Zemistephanus*), *Defonticeras* (= *Chondroceras*). Additionally, the record (Arkell and Playford, 1954) of *Pseudotoites* in the Queen Charlottes refers to a species of *Zemistephanus* and of *Frogdenites* (McLearn, 1929) to *Chondroceras*.

Significant fossil localities and their faunas are listed below (\* indicates identifications by H. Frebold):

MacKenzie Bay area, northern Maude Island (Fig. 1, loc. 15)

**13635.** F.H. McLearn, 1921. Between MacKenzie and Maude Bay, Skidegate Inlet.

*Zemistephanus* sp.

*Oxytoma* sp.

**48593.** A. Sutherland Brown, 1961. Lat. 53°12'45"N, Long. 132°05'W.

*Zemistephanus richardsoni* (Whiteaves)

**48598.** A. Sutherland Brown, 1961. Lat. 53°12'45"N, Long. 132°05'W.

*Zemistephanus*(?) sp.

**93738.** H.W. Tipper, 1976. North shore of Maude Island, 4 km west-southwest of Robber Island. Lat. 53°12'45"N, Long. 132°05'W.

*Zemistephanus* sp.

**C-81909.** H.W. Tipper, 1979. MacKenzie Bay, north side of Maude Island. Lat. 53°12'32"N, Long. 132°05'W. Lower part of Yakoun Group.

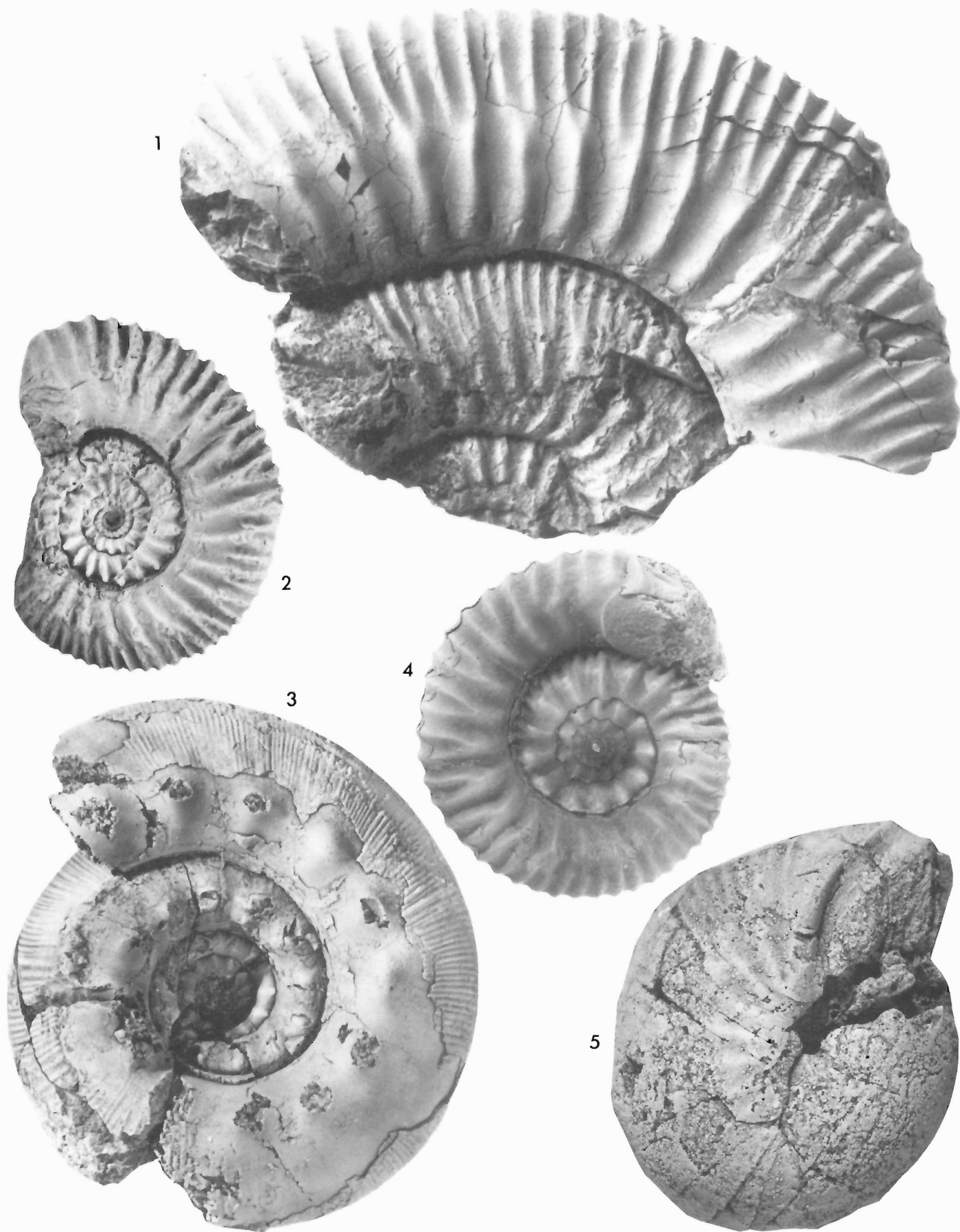
*Stephanoceras* sp.

*Lissoceras*(?) sp.

*Zemistephanus* sp.

**C-168505.** T.P. Poulton and R.L. Hall, 1988. MacKenzie Bay, north side of Maude Island, UTM Zone 8U 69474E 589976N.

*Zemistephanus* sp.



**C-168506.** T.P. Poulton and R.L. Hall, 1988. MacKenzie Bay, north side of Maude Island, UTM Zone 8U 69478E 589976N. Stratigraphically above C-168505.

*Chondroceras* sp.

**C-168507.** T.P. Poulton and R.L. Hall, 1988. MacKenzie Bay, north side of Maude Island, UTM Zone 8U 6948E 58998N. Stratigraphically above C-168506.

*Zemistephanus* sp.  
belemnites

*Fannin Bay area, southern Maude Island (Fig. 1, loc. 19)*

**C-80816.** H.W. Tipper, 1978. Fannin Bay, south side of Maude Island, Lat. 53°12'N, Long. 132°03'W.

*Stephanoceras* sp.  
sonniniid ammonite, indet.

**C-80828.** H.W. Tipper, 1978. In creek at east end of Fannin Bay, south side of Maude Island, Lat. 53°12'00"N, Long. 132°03'10"W.

*Stephanoceras* sp.  
*Fontannesia*(?) sp.

*Richardson Bay, southern Maude Island (Fig. 1, loc. 20)*

**13636.** F.H. McLearn, 1921. South shore of Richardson Bay.  
*Stephanoceras skidegatensis* (Whiteaves)

*Yakoun River near Ghost Creek (Fig. 1, loc. 8)*

**52331.** A. Sutherland Brown, 1962. Yakoun River near Ghost Creek, station 52, Graham Island.  
stephanoceratid(?) ammonite, indet.

*King Creek area (Fig. 1, loc. 6)*

**52344.** A. Sutherland Brown, 1962. Hill west of King Creek, station 259, Graham Island.

*Zemistephanus* sp.

## PLATE 1

All figures natural size.

"McM" indicates specimens stored in the paleontological collection at the Department of Geology, McMaster University, Hamilton, Ontario.

"GSC" indicates specimens stored in the Type Collection, Geological Survey of Canada, Ottawa, Ontario.

"RBCM" indicates specimens stored in the Biological Collections of the Royal British Columbia Museum, Victoria, British Columbia.

**Figures 1 and 2.** *Stephanoceras (Stephanoceras) skidegatense* Whiteaves. 1. macroconch with part of body chamber, McM J1878, from Dark Sandstone Member, Richardson Bay Formation (Yakoun Group) at Richardson Bay, south shore of Maude Island, Skidegate Inlet; grid reference 978989, Skidegate Channel 1:50 000 topographic sheet, 103F/1E. 2. microconch, complete with lappets, allotype McM J1802b, from same bed as Figure 1. Early Bajocian *Chondroceras oblatum* Zone, loc. 20 of Figure 1.

**Figures 3 and 4.** *Zemistephanus richardsoni* (Whiteaves). 3. macroconch, holotype GSC 5013, collected from Skidegate Inlet by J. Richardson in 1872. 4. microconch, complete with lappets, allotype McM J1796a, from Dark Sandstone Member, Richardson Bay Formation (Yakoun Group), at MacKenzie Bay, north shore of Maude Island, Skidegate Inlet; grid reference 946997, Skidegate Channel 1:50 000 topographic sheet, 103F/1E. Early Bajocian *Stephanoceras kirschneri* Zone, loc. 15 of Figure 1.

**Figure 5.** *Iniskinites cepoides* (Whiteaves). Probably macroconch with apertural constriction. RBCM figured specimen EH89.1.1 from collection No. 990. Alliford Bay (?), collected by C.F. Newcombe in 1897. Probably Late Bathonian from loc. 20 of Figure 1.

**C-163799.** T.P. Poulton and R.L. Hall, 1988. Loose in road material, King Creek road, central Graham Island. UTM Zone 8U 67924E 59249N.

*Stephanoceras yakounense* McLearn

*North of Yakoun Lake, logging road 59 (Fig. 1, loc. 10)*

**C-90571.** H.W. Tipper, 1980. Road 59, top quarry, Graham Island; clasts in conglomerate of the Albion Haida Formation.

*Stephanoceras* sp.  
*Myophorella* sp.  
*Astarte* sp.  
*Oxytoma* sp.  
belemnite, indet.

**C-171158.** R.L. Hall, 1985. Same as loc. C-90571. UTM 821 171. Pebble in Haida conglomerate.

*Stephanoceras* sp.

*Brent Creek area east of Yakoun Lake (Fig. 1, loc. 12)*

**52351.** A. Sutherland Brown, 1962. Near Brent Creek, station 75x, Graham Island (see Sutherland Brown, 1968, p. 74, loc. 15).

\**Chondroceras* sp.  
*Zemistephanus richardsoni* (Whiteaves)

**52354.** A. Sutherland Brown, 1962. Near Brent Creek, station 75.

*Zemistephanus* sp.

**C-168502.** T.P. Poulton and R.L. Hall, 1988. Quarry west of Brent Creek, central Graham Island. UTM Zone 8U 6872E 591225N; fossils in clasts within Cretaceous conglomerate.

*Stephanoceras* sp.  
*Zemistephanus* sp.  
*Chondroceras*(?) sp.  
*Inoceramus* sp.

*Between Yakoun Lake and Rennell Sound (Fig. 1, loc. 4)*

**C-90957.** H.W. Tipper, 1980. Rennell road. Lat. 53°20'24"N, Long. 132°21'48"W.

*Stephanoceras* sp.

**C-90965.** H.W. Tipper, 1980. Rennell road, .5 km west of 7 km milepost, Lat. 53°20'36"N, Long. 132°21'W.

*Zemistephanus*(?) sp.  
*Pinna* sp.  
bivalves, indet.  
belemnites, indet.

*Rennell Sound (Fig. 1, loc. 1)*

**C-171154.** R.L. Hall and G. Jakobs, 1988. Rennell Sound. Graham Island Formation.

*Stephanoceras (Stemmatoceras) ex gr. S. acuticostatum* (Weisert)

*East of Rennell Sound (Fig. 1, loc. 2)*

**C-90969.** Q.C. Timber Ltd., H.W. Tipper, 1979. Riley Creek near Rennell road. Lat. 53°21'30"N, Long. 132°24'18"W.

*Stephanoceras itinsae* (McLearn)

*East of Rennell Sound (Fig. 1, loc. 3)*

**C-90972.** H.W. Tipper, 1980. Rennell road, Lat. 53°20'30"N, Long. 132°23'30"W.

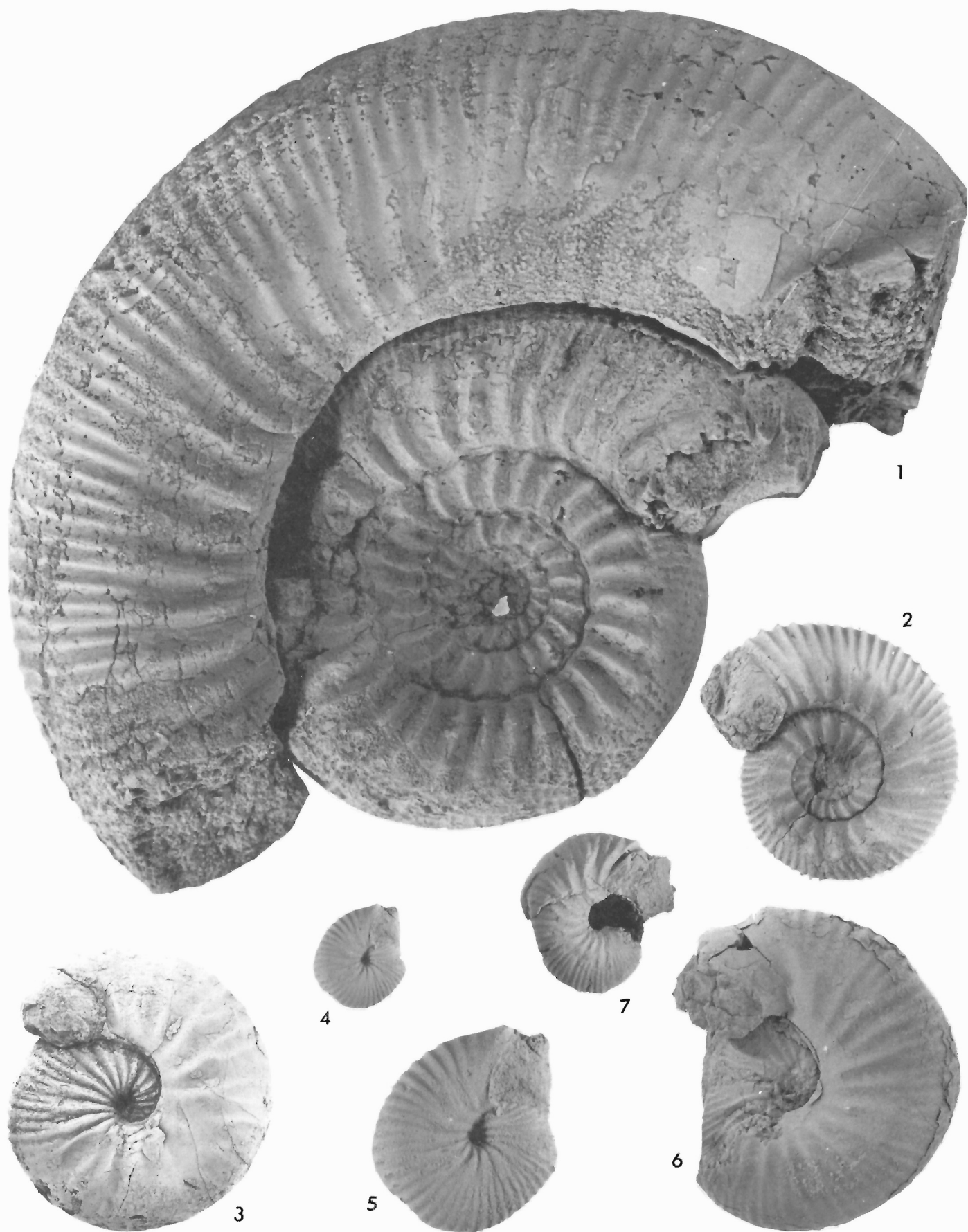
*Zemistephanus* sp.  
stephanoceratid ammonite, indet.

*Western Skidegate Channel (Fig. 1, loc. 14)*

**C-101704.** R. Higgs, 1987. Skidegate Channel, UTM 076906.

*Stephanoceras* sp.

*South of Alliford Bay (Fig. 1, loc. 25)*



C-140272. J.W. Haggart, 1988. Cumshewa area, Lat. 53°10'14"N, Long. 131°59'30"W, UTM 000952.

*Stephanoceras* sp.

### *Chondroceras oblatum* Zone

The younger ammonite fauna recognized by Hall and Westermann (1980) in the Richardson Bay Formation was assigned to the *C. oblatum* Zone, which was based on a type area designated at Ribbon Creek, southwestern Alberta. It is characterized by the association of *C. oblatum* (Whiteaves) with *Stephanoceras itinsae* (McLearn), *Teloceras crickmayi* (Frebold) and other ammonites. The association, characterizing the "Dark Sandstone Member" of the Richardson Bay Formation, has been correlated with the middle and upper parts of the *Stephanoceras humphriesianum* Standard Zone (Hall and Westermann, 1980).

*Stephanoceras itinsae* (McLearn) and *Chondroceras oblatum* (Whiteaves) occur on South Balch Island within a rich and varied shallow marine fauna including bivalves, belemnites and plants, as does *S. skidegatensis* (Whiteaves), *Chondroceras defontii* (McLearn) and *C. maudense* (McLearn) at Richardson Bay (McLearn, 1929; Hall and Westermann, 1980; Cameron and Tipper, 1985).

A few distinctive microfossils, mostly foraminifera, have been recovered from this zone at Richardson Bay. They include *Marginulina turgida* (Schwäger), *Marginulinopsis* sp., *Lenticulina* sp. aff. *L. munsteri* (Roemer), *Pseudonodosaria pupoides* (Bornemann), *Citharina* sp. aff. *C. inconstans* (Terquem) and several unidentified ostracod species (Cameron and Tipper, 1985).

The *C. oblatum* fauna occurs at many localities in the Queen Charlotte Islands. The lithological and paleontological characteristics of this zone are remarkably uniform over a broad band from Maude Island in Skidegate Inlet as far south as Reef Island off the east coast of Moresby Island. This perhaps indicates a northwest-southeast depositional trend, consistent with proposed structural trends, and suggests stability of the fault block on which they were deposited during Early Bajocian time. Significant fossil localities and their faunas are listed below (\* indicates identifications by H. Frebold, which have not been revised):

## PLATE 2

All figures natural size except 5.  
Abbreviations as on Plate 1.

**Figures 1 and 2.** *Stephanoceras (Stephanoceras) itinsae* (McLearn). 1. macroconch, with ultimate half-whorl of body chamber and aperture. Figured specimen GSC 56691, from Dark Sandstone Member, Richardson Bay Formation (Yakoun Group), south shore of South Balch Island, Skidegate Inlet; grid reference 951008, Skidegate Channel 1:50 000 topographic sheet, 103F/1E. 2. microconch, complete with lappets, McM J1799a, from same member and locality as Figure 1. Early Bajocian *Chondroceras oblatum* Zone, loc. 16 of Figure 1.

**Figures 3-5.** *Chondroceras oblatum* (Whiteaves). 3. macroconch, complete specimen with aperture, holotype GSC 4964. From unknown locality in Skidegate Inlet. 4. microconch, allotype McM J1794a, from Dark Sandstone Member, Richardson Bay Formation (Yakoun Group), on south shore of Balch Island, Skidegate Inlet; grid reference 951008, Skidegate Channel 1:50,000 topographic sheet 103F/1E. 5. Same specimen as Figure 4, X2. Early Bajocian *Chondroceras oblatum* Zone, loc. 16 of Figure 1.

**Figures 6 and 7.** *Chondroceras defontii* (McLearn). 6. macroconch, complete with aperture, GSC 56696, from Dark Sandstone Member, Richardson Bay Formation (Yakoun Group), Richardson Bay on south shore of Maude Island, Skidegate Inlet; grid reference 978989, Skidegate Channel 1:50,000 topographic sheet 103F/1E. 7. microconch, complete with aperture, allotype McM J1793a, from same locality as Figure 6. Early Bajocian *Chondroceras oblatum* Zone, loc. 20 of Figure 1.

*Between Yakoun Lake and Rennell Sound (Fig. 1, loc. 5)*

C-96964. H.W. Tipper, 1980. 7 km milepost, Rennell road. Lat. 53°20'30"N, Long. 132°20'48"W.

*Stephanoceras* sp.

*Chondroceras* sp.

*Pinna* sp.

crustacean fragment

*South Balch Island, north of Maude Island (Fig. 12, loc. 16)*

!3634. F.H. McLearn, 1921. "Logan Island" (south Balch Island probably), south shore. Collection apparently mixed, and includes *Zemistephanus* from McLearn's Loc. 11 (Fig. 1, loc. 15), north side of Maude Island, so that actual associations are unknown.

*Chondroceras oblatum* (Whiteaves)

*Stephanoceras itinsae* (McLearn)

*Zemistephanus* sp.

*Oppelia* sp.

*Corbula* sp.

*Myophorella* sp.

bivalve, indet.

13638. F.H. McLearn, 1921. Station 414, Skidegate Inlet. Probably south Balch Island.

*Chondroceras* sp.

44711. A. Sutherland Brown, 1960. Station 82xd, south Balch Island.

*Stephanoceras itinsae* (McLearn)

*Pleuromya* sp.

C-81908. H.W. Tipper, 1979. South Balch Island. Lat. 53°13'N, Long. 132°05'W. Lower part, Yakoun Formation.

*Stephanoceras itinsae* (McLearn)

*Chondroceras* sp.

*Nautilus* sp.

bivalves, indet.

fossil fruits, indet.

*Richardson Bay, southern Maude Island (Fig. 1, loc. 20)*

13637. F.H. McLearn, 1921. Richardson Bay.

*Stephanoceras* sp.

*Chondroceras defontii* (McLearn)

*Pleuromya* sp.

*Entolium* sp.

*Inoceramus(?)* sp.

ostreid bivalves, indet.

belemnites, indet.

21129. Shell Oil Co., 1951. South side of Maude Island.

*Stephanoceras* sp.

48594. A. Sutherland Brown, 1961. Richardson Bay, south side of Maude Island. Lat. 53°12'15"N, Long. 132°02'30"W.

*Chondroceras* sp.

*Stephanoceras* sp.

*Myophorella* sp.

*Pholadomya* sp.

*Pleuromya* sp.

bivalves, indet.

belemnites, indet.

gastropods, indet.

93739. H.W. Tipper, 1976. Southeast shore of Maude Island, slightly southwest of Richardson Bay. Lat. 53°12'15"N, Long. 132°02'20"W.

*Stephanoceras* sp.

*Chondroceras defontii* (McLearn)

*Pleuromya* sp.

gastropods



**93740.** H.W. Tipper, 1976. Southeast shore of Maude Island, Lat. 53°12'15"N, Long. 132°02'20"W.

*Chondroceras* sp.  
*Stephanoceras* sp.  
*Pinna* sp.  
*Entolium* sp.  
*Camptonectes* sp.  
*Astarte* sp.  
belemnites

**C-80822.** H.W. Tipper, 1978. South side of Maude Island, on beach near volcanic breccia. Richardson Bay. Lat. 53°12'15"N, Long. 132°02'30"W.

*Stephanoceras* sp.  
*Stephanoceras skidegatensis* (Whiteaves)  
*Chondroceras defontii* (McLearn)  
*Calliphylloceras*(?) sp.  
*Corbula* sp.  
*Pleuromya* sp.  
*Astarte* sp.  
belemnites

**C-80823.** B.E.B. Cameron, 1978. Richardson Bay, south side of Maude Island, Lat. 53°12'10"N, Long. 132°02'20"W. 2.5 m below GSC locality C-80822.

*Stephanoceras* sp. cf. *skidegatensis* (Whiteaves)  
*Chondroceras*(?) sp.  
*Inoceramus* sp.  
*Pinna* sp.  
*Plagiostoma* sp.  
*Astarte* sp.  
*Pleuromya* sp.  
belemnites, indet.

*MacKenzie Bay area, northern Maude Island (Fig. 1, loc. 15)*

**48601.** A. Sutherland Brown, 1961. Lat. 53°13'30"N, Long. 132°04'30"W (see Sutherland Brown, 1968).

*Stephanoceras* sp.  
*Chondroceras* sp.  
*Nautilus* sp.  
*Myophorella* sp.  
bivalves, indet.

**52356.** A. Sutherland Brown, 1962. Rockrun Creek, station 96xc (see Sutherland Brown, 1968, p. 78, loc. 14).

*Chondroceras* sp.

*Gray Bay, east side of Moresby Island (Fig. 1, loc. 26)*

**C-168511.** T.P. Poulton and R.L. Hall, 1988. Middle part of shore of Gray Bay. UTM Zone 9U 3195E 58885N.

*Stephanoceras* sp.

*Reef Island, east side of northern point (Fig. 1, loc. 28)*

**40946.** A. Sutherland Brown, 1959. Reef Island.

*Chondroceras* sp. cf. *oblatum* (Whiteaves)  
bivalves, indet.

**40985.** A. Smith, 1959. Reef Island. Lower member, Yakoun Formation.

*Stephanoceras itinsae* (McLearn)  
bivalves, indet.  
belemnites, indet.

**C-168508.** T.P. Poulton and R.L. Hall, 1988. North side of Reef Island. UTM Zone 9U 33058E 586132N.

*Stephanoceras* sp.

**C-168510.** T.P. Poulton and R.L. Hall, 1988. North side of Reef Island, UTM Zone 9U 33132E 586145N. East of C-168508.

*Stephanoceras itinsae* (McLearn)  
*Chondroceras* sp.

*Pleuromya* sp.  
bivalves, indet.

*Reef Island, west side of northern point (Fig. 1, loc. 27)*

**C-168509.** T.P. Poulton and R.L. Hall, 1988. North side of Reef Island. UTM Zone 9U 33026E 586122N. West of C-168508.

*Stephanoceras* sp.

## BATHONIAN

The Robber Point Formation, exposed at Cairnes Bay near Robber Point on eastern Maude Island, overlies the thick volcanic pile of the Yakoun Group which contains Bajocian fossils in its lower parts. It is gradationally overlain by the Newcombe Formation which contains Late Bathonian and Early Callovian ammonite faunas discussed below. The Robber Point Formation, a shallow, marine siltstone-mudstone unit, has not yielded ammonites. The abundant and varied bivalves from these "*Gryphaea* beds", revised and listed by Poulton (1981), are characterized principally by *Gryphaea persimilis* Whiteaves, *Parallelodon simillima* (Whiteaves), and *Trigonia* sp.. Microfaunas include abundant Foraminifera and common Ostracoda. They were listed by Tipper and Cameron (1980) and Cameron and Tipper (1985).

Significant fossil localities and their faunas from the Robber Point Formation are listed below:

*Robber Point at east end of Maude Island (Fig. 1, loc. 18)*

**C-86362.** T.P. Poulton, 1979. Cairnes Bay, Robber Point. Maude Island. Upper member, Yakoun Formation. "*Gryphaea*" shale. See Poulton, 1981.

*Astarte carlottensis* Whiteaves  
*Entolium* sp.  
*Gryphaea persimilis* Whiteaves  
*Homomya*(?) sp.  
*Isognomon* sp.  
*Modiolus* sp.  
*Parallelodon simillima* (Whiteaves)  
*Prionoella*(?) sp.  
*Protocardia subsimile* Whiteaves  
*Protocardia* sp.

## PLATE 3

All specimens natural size.

All abbreviations as in Plate 1.

**Figures 1-4.** *Iniskinites cepoides* (Whiteaves). 1. intermediate sized specimen, complete with apertural constriction; figured specimen EH89.1.2 from RBCM Collection No. 936, collected by C.F. Newcombe in 1897 at Alliford Bay, northern Moresby Island (loc. 21 of Figure 1). 2. probable microconch, with apertural modifications; figured specimen EH89.1.3 from RBCM Collection No. 860, collected by C.F. Newcombe in 1897, detailed locality unknown. 3. incomplete figured specimen EH89.1.4 from RBCM Collection No. 856, collected by C.F. Newcombe in 1897, probably from Robber Point, east end of Maude Island. Skidegate Inlet (loc. 18 of Figure 1). 4. probable microconch with apertural modifications; figured specimen from same locality as Figure 1. Late Bathonian.

**Figures 5-7.** *Cadoceras* sp. aff. *catostoma* Pompeckj. 5. intermediate sized specimen, complete with umbilical constriction, figured specimen EH89.1.5 from RBCM Collection No. 881, collected by C.F. Newcombe in 1897 at Alliford Bay, northern Moresby Island. 6. incomplete macroconch, figured specimen EH89.1.6 from RBCM Collection No. 987, collected by C.F. Newcombe in 1897 from Alliford Bay. 7. inner whorls, from same collection as Figure 6. Early Callovian(?), loc. 21 of Figure 1.

**Figures 8 and 9.** *Kepplerites gitinsi* McLearn. Intermediate sized specimens with apertural smoothing and lappet (on Fig. 9). Figured specimens EH89.1.7 and 8 from RBCM Collection No. 882, collected by C.F. Newcombe in 1897 at Alliford Bay, northern Moresby Island. Latest Bathonian or earliest Callovian, loc. 21 of Figure 1.



1



2



4

3



5



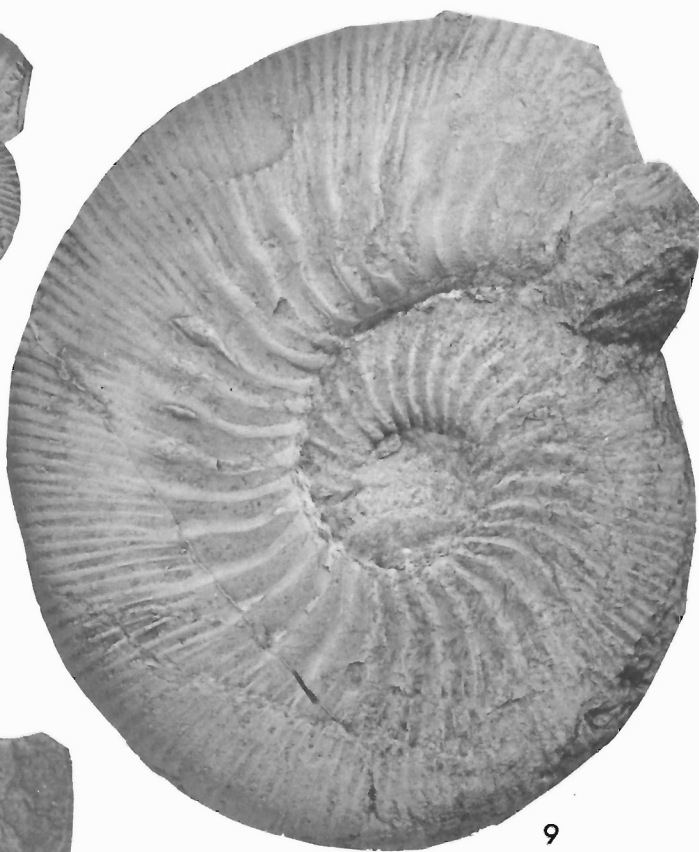
6



7



7



9



8

**C-86372.** H.W. Tipper, 1978. Robber Point, east end of Maude Island, Lat. 53°13'N, Long. 132°01'48"W. "*Gryphaea*" beds, upper part of Yakoun Formation. See Poulton, 1981.

*Ostrea*(?) sp.  
*Anomia* sp.  
*Astarte carlottensis* Whiteaves  
*Camptonectes* sp.  
*Corbula* sp.  
*Cyprina*(?) sp.  
*Grammatodon* sp.  
*Gryphaea persimilis* Whiteaves  
*Isognomon* sp.  
*Modiolus* sp.  
*Palaeonucula*? sp.  
*Parallelodon simillima* (Whiteaves)  
*Pleuromya* sp.  
*Pleuromya* sp. aff. *laevigata* Whiteaves  
*Protocardia subsimile* Whiteaves  
*Thracia* sp.  
bivalves, indet.  
gastropods, indet.

## LATE BATHONIAN AND EARLY CALLOVIAN

Ammonites of Late Bathonian and Early Callovian age are known in the Queen Charlotte Islands from Newcombe Bay and Robber Point on eastern Maude Island and from Alliford Bay and adjacent areas inland on northern Moresby Island. Five faunas have been recognized, probably spanning the Bathonian-Callovian boundary (Tipper and Cameron, 1980; Cameron and Tipper, 1981, 1985). It is not entirely clear that they represent a succession of assemblage zones having the same level of confidence as assemblage zones in other areas or intervals. Furthermore, the status of Bathonian zones and correlation of the basal Callovian boundary are unsatisfactory worldwide and are poorly known in western Canada. Therefore the biostratigraphy of this interval remains tentative; the previously suggested succession and dating are applicable locally and are maintained for present purposes.

The following upward sequence of faunas, the lower of which is almost certainly Late Bathonian in age, has been found in the Newcombe Formation sandstone (Cameron and Tipper, 1985): *Iniskinites cepoides*, *Keplerites* spp., and *Oxycerites* sp. The overlying faunas in the same formation, characterized by species reported as *Cadoceras doroschini* (Eichwald) and *Keplerites* sp. respectively are probably Early Callovian in age. These correlations are based on similarity of the faunas with successions in southern Alaska and elsewhere in western North America, which remain poorly understood with respect to the standard zones of East Greenland and western Europe. The ammonite taxonomy is still poorly known as well so that no rigor is implied in the various specific identifications of the ammonites used in this report. Some are identified with the abundantly illustrated, but biostratigraphically and taxonomically poorly known collections from southern Alaska (Imlay, 1953) and others with the equally prolifically illustrated *Keplerites* specimens of McLearn (1929). Although no formal revision has yet been undertaken, the following old Queen Charlottes genera are no longer recognized; all are synonyms of *Keplerites*: *Yakounoceras*, *Seymourites*, *Yakounites*, *Galilaieites* (eg. Callomon, 1984). A distinctive bivalve characterizing the *Iniskinites* beds is *Vaugonia flexicostata* (Burwash) (Poulton, 1981). The *Iniskinites* were described by Frebold (1979). Callomon (1984) has suggested correlations of some of the species with those of southern Alaska and Europe.

The succession of faunas listed above is based on eastern Maude Island, and the presence of *Cadoceras* sp. at Alliford Bay on north-

ern Moresby Island as well as the presence of *Keplerites* at MacKenzie Bay on northeastern Maude Island and at Alliford Bay (McLearn, 1929) serve as ties between the various outcrop areas. The faunas listed below from individual fossil collections suggest that further data might be available to correlate from one locality to another in Skidegate Inlet, but they have not yet been studied in detail. The shales of the Alliford Formation at Alliford Bay, containing *Keplerites* sp., are distinguished particularly by the bivalve *Myophorella packardii* (Crickmay) (Poulton, 1981) and belemnites. They also carry a suite of biostratigraphically significant Foraminifera and ostracods (Tipper and Cameron, 1980; Cameron and Tipper, 1985).

Following is a list of the significant macrofossil localities and faunas within the Late Bathonian (and earliest Callovian?) Newcombe sandstone and the probably Early Callovian Alliford shale (\* indicates identifications by H. Frebold which have not been revised):

*Newcombe Bay, northeastern Maude Island (Fig. 1, loc. 17)*

**13616.** F.H. McLearn, 1921. Newcombe Bay, Skidegate Inlet, Maude Island. See Poulton, 1979, 1981.

*Keplerites* sp.  
*Myophorella devexa* (Eichwald)  
*Astarte carlottensis* Whiteaves  
*Camptonectes* (*Camptonectes*) sp.  
*Myophorella packardii* (Crickmay)(?)

**13620.** F.H. McLearn, 1921. Newcombe Bay, Maude Island.

*Keplerites* sp.  
*Pleuromya* sp.  
*Grammatodon*(?) sp.

**13621.** F.H. McLearn, 1921. Maude Island, Newcombe Bay, float from probable Callovian beds (see Poulton, 1979).

*Keplerites* sp.  
*Oxycerites* sp.  
*Partschiceras* sp.  
*Pleuromya* sp.  
*Myophorella packardii* (Crickmay)  
*Myophorella charlottensis* (Packard)  
*Myophorella*(?) *devexa* (Eichwald)  
*Perna* sp.  
*Entolium* sp.  
*Cyprina*(?) sp.  
*Protocardia subsimile* Whiteaves  
ostreiid bivalves, indet.  
gastropods, indet.  
rhynchonellid brachiopods, indet.  
terebratulid brachiopods, indet.  
*Lingula* sp.

**13625.** F.H. McLearn, 1921. Newcombe Bay, Maude Island (see Poulton, 1981).

*Goniomya* sp.  
*Pleuromya* sp.  
*Homomya*(?) sp.  
*Pseudomonotis*(?) sp.  
*Plagiostoma*(?) sp.  
*Tancredia*(?) sp.  
*Corbula*(?) sp.  
*Astarte*(?) sp.  
*Entolium* sp.  
*Cercomya* sp.  
*Astarte carlottensis* Whiteaves  
*Protocardia subsimile* Whiteaves  
ostreiid bivalves, indet.

**13633.** F.H. McLearn, 1921. Loose at Newcombe Bay (see Frebold, 1979).

*Iniskinites* sp. cf. *mclearnii* Frebold.

**C-81904.** H.W. Tipper, 1979. Newcombe Bay, McLearn's main "Callovian" locality. Maude Island, Lat. 53°13'20"N, Long. 132°02'40"W. Highest part of short section.

*Phylloceras* (*Partschiceras*) *grantzi* (Imlay)

*Keplerites* (*Seymourites*) *abruptus* (McLearn)

**C-81905.** H.W. Tipper, 1979. Newcombe Bay, McLearn's main "Callovian" locality. Maude Island, Lat. 53°13'20"N, Long. 132°02'40"W. Few feet below GSC locality C-81904 in green sand.

*Iniskinites* sp. cf. *cepoides* (Whiteaves)

*Robber Point at east end of Maude Island (Fig. 1, loc. 18)*

**4959.** J. Richardson, 1872. Robber Point, Skidegate Inlet.

*Cadoceras* sp. cf. *catostoma* Pompeckj

**4967.** J. Richardson, 1872. Robber Point, Skidegate Inlet.

*Iniskinites* sp.

**7595.** F.H. McLearn, 1921. At point at the east end of Maude Island on shore in front of Indian village, in float.

\**Iniskinites* sp. cf. *cepoides* (Whiteaves)

*Myophorella*(?) sp.

*Pleuromya* sp.

*Entolium* sp.

*Isognomon* sp.

*Thracia* sp.

*Lingula* sp.

rhynchonellid brachiopods, indet.

**13617.** F.H. McLearn, 1921. Robber Point, Maude Island (see McLearn, 1929; Poulton, 1979, 1981).

*Keplerites* sp.

*Entolium* sp.

*Thracia* sp.

*Pleuromya* sp.

*Myophorella devexa* (Eichwald)

*Myophorella packardi* (Crickmay)(?)

*Camptonectes* (*Mclearnia*) sp.

*Perna*(?) sp.

*Gryphaea* sp.

*Ceromya*(?) sp.

*Protocardia subsimile* Whiteaves

*Camptonectes* (*Camptonectes*)(?) sp.

*Astarte carlottensis* Whiteaves

ostreiid bivalves, indet.

**48602.** A. Sutherland Brown, 1961. Lat. 53°13'15"N, Long. 132°02'30"W. Above *Cadoceras doroschini* and below *Keplerites spinosum* (see Cameron and Tipper, 1985).

*Keplerites* sp.

*Cadoceras* sp.

*Iniskinites* sp.

*Myophorella* sp.

*Anditrigonia* sp. cf. *plumasensis* (Hyatt)

*Camptonectes* (*Mclearnia*) sp.

*Isognomon* sp.

belemnites, indet.

pelecypods, indet.

gastropods, indet.

corals, indet.

gastropods, indet.

terebratulid brachiopods, indet.

**48605.** A. Sutherland Brown, 1961. Same as GSC locality 93737. Lat. 53°13'N, Long. 132°01'45"W. Original identification of *Chondro-*

*ceras* by H. Frebold (*in* Sutherland Brown, 1968) indicates the presence of *Iniskinites* (see Sutherland Brown 1968, p. 74; Frebold, 1979; Poulton, 1981).

*Iniskinites* sp. cf. *cepoides* (Whiteaves)

*Pleuromya* sp.

*Myophorella* sp.

**93736.** H.W. Tipper, 1976. East shore of Maude Island on point southwest of Robber Island. Lat. 53°13'N, Long. 132°01'40"W (see Frebold, 1979).

*Iniskinites cepoides* (Whiteaves)

*Keplerites* sp.

*Astarte carlottensis* Whiteaves

*Entolium* sp.

*Corbula*(?) sp.

*Thracia* sp.

*Protocardia subsimile* Whiteaves

*Pleuromya laevigata* Whiteaves

*Myophorella devexa* (Eichwald)(?)

*Myophorella packardi* (Crickmay)(?)

*Isognomon*(?) sp.

*Pronoella*(?) sp.

**93737.** H.W. Tipper, 1976. East shore of Maude Island on point southwest of Robber Island. Lat. 53°12'55"N, Long. 132°01'40"W. Same as GSC locality 48605.

*Trigonia* sp.

*Gryphaea* sp.

*Parallelodon simillima* (Whiteaves)

gastropods, indet.

**C-81906.** H.W. Tipper, 1979. Robber Point. Maude Island, Lat. 53°12'40"N, Long. 132°02'10"W. Top of section with abundant large pelecypods.

*Keplerites* sp.

**C-81907.** H.W. Tipper, 1979. Robber Point. Maude Island, Lat. 53°12'40"N, Long. 132°02'10"W. About 1.5 m below *Keplerites* in green sandstone.

*Iniskinites* sp. cf. *cepoides* (Whiteaves)

*Myophorella montanaensis* (Meek)

bivalves, indet.

**C-86356.** T.P. Poulton, 1979. Cairnes Bay, Robber Point, at or near McLearn's locality 45. Maude Island, Bathonian sandstone bluff (see Poulton, 1981).

*Entolium* sp.

*Gervillia* sp.

*Pleuromya* sp.

*Vaugonia*(?) *doroschini* (Eichwald)

*Vaugonia flexicostata* (Burwash)

**C-86369.** T.P. Poulton and H.W. Tipper, 1978. Robber Point, east end of Maude Island. Lat. 53°13'N, Long. 132°01'48"W. *Keplerites* beds (see Poulton, 1981).

*Keplerites* sp.

*Cucullaea ponderosa* Whiteaves

*Isognomon skidegatensis* (Whiteaves)

*Ostrea* sp.

*Pleuromya laevigata* Whiteaves

belemnites, indet.

**C-86370.** H.W. Tipper, 1978. Robber Point, east end of Maude Island. Lat. 53°13'N, Long. 132°01'48"W. *Iniskinites* bed (see Poulton, 1981).

*Entolium* sp.

*Isognomon skidegatensis* (Whiteaves)

*Myophorella* sp.

- Ostrea* sp.  
*Pleuromya laevigata* Whiteaves(?)  
*Pleuromya* sp.  
*Pronoella*(?) sp.  
*Protocardia subsimile* Whiteaves  
*Vaugonia doroschini* (Eichwald)
- C-86371.** H.W. Tipper, 1978. Robber Point, east end of Maude Island, Lat. 53°13'N, Long. 132°01'48"W. *Iniskinites* bed.
- Anatina*(?) sp.  
*Anomia*(?) sp.  
*Camptonectes (Camptochlamys)*(?) sp.  
*Camptonectes (Camptonectes?)* sp.  
*Cucullaea? (Idonearca?) tumida* (Whiteaves)  
*Entolium* sp.  
*Gervillia newcombii* Whiteaves  
*Goniomya*(?) sp.  
*Gryphaea* sp.  
*Myophorella* sp.  
*Myophorella charlottensis* (Packard)  
*Myophorella*(?) sp. aff. *yellowstonensis* Imlay  
*Ostrea skidegatensis* Whiteaves  
*Pinna* sp.  
*Pleuromya* sp.  
*Thracia*(?) sp.  
*Vaugonia flexicostata* (Burwash)  
*Vaugonia doroschini* (Eichwald)(?)  
*Cercomya*(?) sp.  
*Placunopsis*(?) sp.  
bivalves, indet.  
belemnites, indet.  
rhynchonellid brachiopods, indet.  
corals, indet.
- East of Yakoun Lake (Fig. 1, loc. 13)*
- C-101719.** R. Higgs, 1987. East of Yakoun Lake, UTM 880114.  
*Iniskinites cepoides* (Whiteaves)  
ammonite, indet.
- C-101720.** R. Higgs, 1987. East of Yakoun Lake, UTM 875109.  
*Iniskinites* sp. cf. *cepoides* (Whiteaves)  
belemnite, indet.
- C-101721.** R. Higgs, 1987. East of Yakoun Lake, UTM 875108.  
*Keplerites* sp.
- Alliford Bay, east side (Fig. 1, loc. 22)*
- 13618.** F.H. McLearn, 1921. On island, northeast shore of Alliford Bay, Skidegate Inlet (see Poulton, 1979, 1981).  
*Pleuromya*(?) sp.  
*Myophorella packardi* (Crickmay)  
*Thracia* sp.  
*Gryphaea* sp.  
*Astarte carlottensis* Whiteaves
- 13624.** F.H. McLearn, 1921. Talus on island northeast side of Alliford Bay (see Poulton, 1979, 1981).  
*Keplerites* sp.  
*Myophorella devexa* (Eichwald)  
*Myophorella packardi* (Crickmay)(?)  
*Corbula*(?) sp.  
*Astarte* sp.  
*Entolium*(?) sp.  
*Pleuromya* sp.  
*Cyprina*(?) sp.  
*Myophorella devexa* (Eichwald)  
*Astarte carlottensis* Whiteaves
- Pronoella*(?) sp.  
*Lingula* sp.
- 14923.** G.M. Dawson, 1878. East coast of Alliford Bay (see Poulton, 1979).  
*Myophorella devexa* (Eichwald)
- C-80808.** H.W. Tipper, 1978. Island with beacon northwest of ferry terminal at Alliford Bay. Lat. 53°12'45"N, Long. 131°59'24"W. Top of section (see Poulton, 1981).  
*Cadoceras* sp.  
*Iniskinites* sp.  
*Keplerites* sp.  
*Grammatodon*(?) sp.  
*Homomya* sp.  
*Myophorella devexa* (Eichwald)  
*Myophorella*(?) sp.  
*Neocrassina (Coelastarte)*(?) sp.  
*Pholadomya* sp.  
*Pleuromya*(?) sp.  
*Pronoella* sp.  
*Thracia*(?) sp.  
*Palaeonucula* sp.  
*Plagiostoma* sp.  
belemnites, indet.
- C-80809.** H.W. Tipper, 1978. Island with beacon northwest of ferry terminal at Alliford Bay, Lat. 53°12'45"N, Long. 131°59'24"W. Upper member, Yakoun Formation.  
*Oxycerites* sp.
- C-80810.** H.W. Tipper, 1978. Island northwest of ferry terminal with beacon. Alliford Bay, Lat. 53°12'45"N, Long. 131°59'24"W (see Poulton, 1981).  
*Corbula*(?) sp.  
*Grammatodon*(?) sp.  
*Myophorella devexa* (Eichwald)  
*Myophorella packardi* (Crickmay)(?)  
*Ostrea*(?) sp.  
*Plagiostoma*(?) sp.  
*Pleuromya laevigata* Whiteaves  
*Pleuromya*(?) sp.  
*Thracia* sp.  
*Goniomya* sp.
- Alliford Bay, south side (Fig. 1, loc. 21)*
- 13619.** F.H. McLearn, 1921. South side of Alliford Bay (see Poulton, 1979, 1981).  
*Keplerites* sp. cf. *loganianus* (Whiteaves)  
*Oxycerites* sp.  
*Iniskinites* sp.  
*Vaugonia* sp.  
*Thracia*(?) sp.  
*Pleuromya*(?) sp.  
*Goniomya* sp.  
*Entolium* sp.  
*Corbula* sp.  
*Myophorella devexa* (Eichwald)  
*Myophorella packardi* (Crickmay)  
*Ostrea* sp.  
*Astarte carlottensis* Whiteaves(?)  
*Protocardia subsimile* Whiteaves  
*Vaugonia flexicostata* (Burwash)  
*Pleuromya laevigata* Whiteaves(?)  
*Myophorella charlottensis* (Packard)  
*Ostrea skidegatensis* Whiteaves



**13626.** F.H. McLearn, 1921. South side of Alliford Bay, Skidegate Inlet. Talus from probable Callovian beds (see Poulton, 1979, 1981).

*Astarte* sp.

*Myophorella packardi* (Crickmay)

*Astarte carlottensis* Whiteaves

*Pronoella*(?) sp.

*Thracia* sp.

**21124.** Shell Oil Co., 1951. Skidegate Inlet, Alliford Bay.

*Iniskinites* sp.

**44707.** A. Sutherland Brown, 1960. South shore of Alliford Bay (see Poulton, 1979).

*Cadoceras*(?) sp. aff. *nordenskjoldi* Callomon

*Iniskinites*(?) sp.

ammonite, indet.

pelecypods, indet.

*Myophorella packardi* (Crickmay)

**44708.** A. Sutherland Brown, 1960. Fossil Point, Alliford Bay (see Poulton, 1981).

*Myophorella packardi* (Crickmay)(?)

**93734.** H.W. Tipper, 1976. Alliford Bay on north shore of Moresby Island. Lat. 53°12'N, Long. 132°W.

\**Keplerites* sp. aff. *spinosum* (Imlay)

*Cadoceras* sp. aff. *nordenskjoldi* Callomon

*Myophorella packardi* (Crickmay)

*Ostrea*(?) sp.

**93735.** H.W. Tipper, 1976. Alliford Bay on north shore of Moresby Island, Fossil Point. Lat. 53°12'N, Long. 132°00'10"W.

*Keplerites* sp.

*Iniskinites* sp.

*Ostrea*(?) sp.

*Myophorella packardi* (Crickmay)(?)

*Astarte carlottensis* Whiteaves

*Pleuromya carlottensis* Whiteaves

*Pleuromya laevigata* Whiteaves(?)

*Thracia* sp.

*Thracia depressa* (Sowerby)

*Modiolus* sp.

*Pronoella* sp.

*Isognomon*(?) sp.

**C-80803.** H.W. Tipper, 1978. Fossil Point, west side of Alliford Bay. Lat. 53°12'06"N, Long. 131°59'25"W. Upper member, Yakoun Formation.

*Keplerites* sp.

*Myophorella packardi* (Crickmay)(?)

*Thracia semiplanata* Whiteaves

*Cercomya* (*Capillimya*) *semiradiata* (Whiteaves)

*Isognomon* sp.

*Plagiostoma*(?) sp.

*Pleuromya carlottensis* Whiteaves

*Pleuromya* sp.

*Vaugonia doroschini* (Eichwald)(?)

gastropods, indet.

**C-80804.** H.W. Tipper, 1978. Fossil Point, west side of Alliford Bay. Lat. 53°12'06"N, Long. 131°59'25"W. Upper member, Yakoun Formation.

*Lytoceras* sp.

*Oxycerites* sp.

**C-80805.** H.W. Tipper, 1978. Fossil Point, west side of Alliford Bay. Lat. 53°12'06"N, Long. 131°59'25"W. Upper member, Yakoun Formation.

*Keplerites* sp.

**C-80807.** H.W. Tipper and B.E.B. Cameron, 1978. South end of Alliford Bay in centre of syncline. Lat. 53°12'06"N, Long. 131°59'W.

\**Keplerites* sp. cf. *spinosum* (Imlay)

*Cadoceras* sp. aff. *nordenskjoldi* Callomon

*Cadoceras* sp.

*Myophorella packardi* (Crickmay)

*Myophorella* sp.

*Palaeonucula* sp.

*Plagiostoma* sp.

*Pleuromya* sp.

*Ostrea* sp.

**C-171156.** R.L. Hall, 1985. Fossil Point, west side of Alliford Bay. UTM 004 986.

*Iniskinites* sp.

*East of Alliford Bay, northern Moresby Island (Fig. 1, loc. 23)*

**C-101728.** R.I. Thompson, 1987. UTM 028989, Lat. 53°12'15"N, Long. 131°57'15"W.

*Iniskinites* sp.

*East of Alliford Bay (Fig. 1, loc. 24)*

**C-142919.** R.I. Thompson, 1987. UTM 035972, Lat. 53°11'20"N, Long. 131°56'30"W.

*Keplerites* sp.

## CONCLUDING PALEOGEOGRAPHIC REMARKS

The Queen Charlotte Islands form part of Wrangellia, a tectonostratigraphic terrane that also includes Vancouver Island, and some westernmost parts of mainland British Columbia. The origin and timing and nature of the amalgamation of the western allochthonous terranes to North America remain controversial. The Jurassic rocks appear to form part of an overlap assemblage, deposited with relative uniformity over a wide area on a variety of older units: Triassic Wrangellia in the Queen Charlottes and Vancouver Island, the Triassic Cadwallader Terrane near Yakalom Fault, southwestern mainland B.C., and on a Triassic terrane between the two that may be part of Stikinia.

The Middle Jurassic ammonite faunas of the Queen Charlotte Islands contain a few species with a distinctly western North American affinity, but most are pandemic. The distinctive North American genera include *Zemistephanus* of the Early Bajocian and *Iniskinites* of the Late Bathonian. Their distribution, on and adjacent to the western North American cratonic platform was taken to characterize the 'Athabaskan Province' of the East Pacific Realm (Taylor et al., 1984). Because the southern limit of these ammonites in the autochthonous western interior Jurassic succession seems to be in southern Alberta, they may be considered as evidence that the plate carrying the Queen Charlotte Islands Jurassic was not located farther south than about 49°N latitude in Middle Jurassic time. Equivalent rocks of western interior U.S.A. are apparently not in favourable facies for similar ammonite faunas to be preserved, however, so that no definitive statement regarding the degree of northerly transport can be made.

The thin Aalenian succession, gradational from the relatively complete Lower Jurassic sequence, appears to be earliest Aalenian in age and to be truncated at its top by an unconformity above which are Lower Bajocian beds. The Aalenian in the Queen Charlottes must represent tiny remnants of what was a much thicker, more complete and more widespread Aalenian sedimentary and volcanic sequence such as is found elsewhere in western British Columbia, in other parts of Wrangellia and Stikinia terranes (Poulton and Tipper, in press).

Bajocian beds are similarly widely distributed in western British Columbia. They are highly variable from one place to another, and include volcanic units as on Queen Charlotte Islands. Tectonic/volcanic activity and deposition in small, isolated basins is clearly indicated.

Late Bathonian and Callovian rocks over much of western British Columbia, as on Queen Charlotte Islands, are shales, siltstones and mudstones with little evidence for influx of coarse sediment from local source areas or tectonic activity. Tipper (1984) suggested that they may be an overlap assemblage indicating amalgamation of western Cordillera, allochthonous terranes with others to the east. In this case, the hiatus between the Moresby and Yakoun groups on Queen Charlotte Islands has supra-regional significance.

## REFERENCES

- Anderson, R.G. and Reichenbach, I.**  
**1991:** U-Pb and K-Ar framework for Middle to Late Jurassic (172-2158 Ma) and Tertiary (46-27 Ma) plutons in Queen Charlotte Islands, British Columbia; *in* Evolution and Hydrocarbon Potential of the Queen Charlotte Basin, British Columbia, Geological Survey of Canada, Paper 90-10.
- Arkell, W.J. and Playford, P.E.**  
**1954:** The Bajocian ammonites of western Australia; Royal Society of London Philosophical Transactions, Series B, v. 237, p. 547-601.
- Callomon, J.H.**  
**1984:** A review of the biostratigraphy of the post-Lower Bajocian Jurassic ammonites of western and northern North America; *in* Jurassic-Cretaceous Biochronology and Paleogeography of North America, G.E.G. Westermann (ed.), Geological Association of Canada, Special Paper 27, p. 143-174.
- Cameron, B.E.B. and Tipper, H.W.**  
**1981:** Jurassic biostratigraphy, stratigraphy, and related hydrocarbon occurrences of Queen Charlotte Islands, British Columbia; *in* Current Research, Part A, Geological Survey of Canada, Paper 81-1A, p. 209-212.  
**1985:** Jurassic stratigraphy of the Queen Charlotte Islands, British Columbia; Geological Survey of Canada, Bulletin 365.
- Carter, E.S., Cameron, B.E.B., and Smith, P.L.**  
**1988:** Lower and Middle Jurassic radiolarian biostratigraphy and systematic paleontology, Queen Charlotte Islands, British Columbia; Geological Survey of Canada, Bulletin 386, p. 1-109.
- Frebold, H.**  
**1979:** Occurrence of the Upper Bathonian ammonite genus *Iniskinites* in the Queen Charlotte Islands, British Columbia; *in* Current Research, Part C, Geological Survey of Canada, Paper 79-1C, p. 63-66.
- Hall, R.L. and Westermann, G.E.G.**  
**1980:** Lower Bajocian (Jurassic) cephalopod faunas from western Canada and proposed assemblage zones for the Lower Bajocian of North America; *Palaontographica Americana*, v. 9, no. 52, p. 1-87.
- Imlay, R.W.**  
**1953:** Callovian (Jurassic) ammonites from the United States and Alaska, Part 2, Alaska Peninsula and Cook Inlet Regions; United States Geological Survey, Professional Paper 249-B, p. 41-108, pl. 25-55.
- Jeletzky, J.A.**  
**1984:** Jurassic-Cretaceous boundary beds of Western and Arctic Canada and the problem of the Tithonian-Berriasian stages in the boreal realm; *in* Jurassic-Cretaceous Biochronology and Paleogeography of North America, G.E.G. Westermann (ed.), Geological Association of Canada, Special Paper 27, p. 175-256.
- McLearn, F.H.**  
**1929:** Contributions to the stratigraphy and paleontology of Skidegate Inlet, Queen Charlotte Islands, B.C.; Geological Survey of Canada, Museum Bulletin 54, p. 1-27.  
**1932:** Contributions to the stratigraphy and paleontology of Skidegate Inlet, Queen Charlotte Islands, B.C. (cont'd); Royal Society of Canada Transactions, 3rd ser., v. 26, sec. 4, p. 51-84.  
**1949:** Jurassic formations of Maude Island and Alliford Bay, Queen Charlotte Islands, B.C.; Geological Survey of Canada, Bulletin 12.
- Poulton, T.P.**  
**1979:** Jurassic trigonitid bivalves from Canada and western United States of America; Geological Survey of Canada, Bulletin 282, 82 p.  
**1981:** Stratigraphic distribution and taxonomic notes on bivalves of the Bathonian and Callovian (Middle Jurassic) Upper Yakoun Formation, Queen Charlotte Islands, British Columbia; *in* Current Research, Part B, Geological Survey of Canada, Paper 81-1B, p. 63-72.
- Poulton, T.P. and Tipper, H.W.**  
**in press:** Aalenian ammonites and strata of western Canada; Geological Survey of Canada, Bulletin.
- Sutherland Brown, A.**  
**1968:** Geology of the Queen Charlotte Islands, British Columbia; British Columbia Department of Mines and Petroleum Resources, Bulletin 54.
- Taylor, D.C., Callomon, J.H., Hall, R., Smith, P.L., Tipper, H.W., and Westermann, G.E.G.**  
**1984:** Jurassic ammonite biogeography of western North America: the tectonic implications; *in* Jurassic-Cretaceous Biochronology and Paleogeography of North America, G.E.G. Westermann (ed.), Geological Society of Canada, Special Paper 27, p. 121-142.
- Thompson, R.L., Haggart, J.W., and Lewis, P.D.**  
**1991:** Late Triassic through early Tertiary evolution of the Queen Charlotte Basin, British Columbia, with a perspective on hydrocarbon potential; *in* Evolution and Hydrocarbon Potential of the Queen Charlotte Basin, British Columbia, Geological Survey of Canada, Paper 90-10.
- Tipper, H.W.**  
**1984:** The allochthonous Jurassic-Cretaceous terranes of the Canadian Cordillera and their relation to correlative strata of the North American craton; *in* Jurassic-Cretaceous Biochronology and Paleogeography of North America, G.E.G. Westermann (ed.), Geological Association of Canada, Special Paper 27, p. 113-120.
- Tipper, H.W. and Cameron, B.E.B.**  
**1980:** Stratigraphy and paleontology of the Upper Yakoun Formation (Jurassic) in Alliford Bay Syncline, Queen Charlotte Islands, British Columbia; *in* Current Research, Part C, Geological Survey of Canada, Paper 80-1C, p. 37-44.
- Westermann, G.E.G.**  
**1969:** The ammonite fauna of the Kialagvik Formation at Wide Bay, Alaska Peninsula, Part II: Sonninia Sowerbyi Zone (Bajocian); *Bulletins of American Paleontology*, v. 57, no. 255.

# A synthesis of Cretaceous stratigraphy, Queen Charlotte Islands, British Columbia

James W. Haggart<sup>1</sup>

Haggart, J.W., A synthesis of Cretaceous stratigraphy, Queen Charlotte Islands, British Columbia; in *Evolution and Hydrocarbon Potential of the Queen Charlotte Basin, British Columbia*, Geological Survey of Canada, Paper 90-10, p. 253-277, 1991.

## Abstract

*A new model of Cretaceous deposition in the Queen Charlotte Islands region is proposed. This interpretation is based on field study of stratigraphic sections and on correlation by megafossils, primarily ammonites and bivalves.*

*The latest Jurassic and Early Cretaceous Longarm Formation and much of the younger Cretaceous Queen Charlotte Group are transgressive sequences, both deposited primarily in response to rising sea level. Most strata of these units accumulated in shallow-marine environments on the shelf. The previously inferred hiatus or unconformity separating the two units is now known to be non-existent; a continuous stratigraphic succession spanning the interval of the supposed hiatus indicates that deposition in the basin was continuous through the Early Cretaceous and into the Late Cretaceous.*

*The development of the Cretaceous stratigraphic succession in the Queen Charlotte Islands can be readily explained by relative sea level rise and fall. The correlation of the local sea level curve for the islands with independently-produced eustatic curves is striking. Earlier models invoking large-scale tectonic processes for the development of the Cretaceous sequence in the islands appear unnecessary.*

*The model can be used to predict the occurrence of Cretaceous strata in the subsurface of Hecate Strait. The potential of the Cretaceous sequence as a hydrocarbon source and reservoir rock in the subsurface is discussed.*

## Résumé

*Un nouveau modèle de sédimentation crétacée dans la région des îles de la Reine-Charlotte est proposé. Cette nouvelle interprétation se fonde sur une étude sur place de coupes stratigraphiques et leur corrélation par des macro-fossiles, principalement les ammonites et les bivalves.*

*La formation de Longarm de la toute fin du Jurassique supérieur et du Crétacé inférieur et une grande partie du groupe de Queen Charlotte du Crétacé sont des séquences transgressives, qui se sont déposées principalement par suite d'une hausse du niveau de la mer. La plupart des couches de ces unités se sont accumulées dans des milieux marins peu profonds sur la plate-forme continentale. On sait maintenant que la lacune stratigraphique ou discordance précédemment inférée séparant les deux unités n'existe pas; une succession stratigraphique continue reliant l'intervalle de la lacune présumée révèle que la sédimentation du bassin a été continue du Crétacé inférieur et jusqu'au Crétacé supérieur.*

*On peut facilement expliquer la formation de la succession stratigraphique crétacée dans les îles par l'oscillation du niveau de la mer. La corrélation entre la courbe locale du niveau de la mer dans les îles et les courbes eustatiques produites indépendamment ressort nettement. Les anciens modèles faisant intervenir des processus tectoniques à grande échelle pour reconstituer la formation de la séquence crétacée dans les îles ne sont pas nécessaires.*

*On peut utiliser le modèle pour prévoir la présence de couches crétacées dans le sous-sol du détroit d'Hécaté. La possibilité de trouver des roches mères et des roches réservoirs dans le Crétacé en subsurface est étudiée.*

<sup>1</sup> Cordilleran Division, Geological Survey of Canada, 100 West Pender Street, Vancouver, B.C. V6B 1R8

## INTRODUCTION

The Queen Charlotte Islands serve as an important cornerstone for interpreting the tectonic history of the Cordilleran region of Canada (Fig. 1). The Cretaceous succession in the Queen Charlotte Islands represents a significant portion of the total stratigraphic package and thus must be considered as an integral part of any tectonostratigraphic model for Canada's Pacific coast.

Recent structural investigations in the Queen Charlotte Islands have led to the recognition of the Cretaceous strata as an important constraining factor in interpreting the geological evolution of the islands themselves (Thompson and Thorkelson, 1989; Thompson et al., 1991). A comprehensive understanding of Cretaceous stratigraphy is therefore of vital concern in conceptualizing the structural history of the region.

Finally, a detailed model of Cretaceous stratigraphy and sedimentation is of paramount importance for oil exploration, because Cretaceous rocks in the Queen Charlotte Islands (and possibly in the offshore, Hecate Strait, region as well) overlie Jurassic source rocks (Cameron and Tipper, 1981; Macauley, 1983; Hamilton and Cameron, 1989) and have been identified as a potential secondary hydrocarbon target (Fogarassy, 1989; Fogarassy and Barnes, 1989).

The author's field program in the Queen Charlotte Islands was initiated to improve the biostratigraphic framework for correlation of Cretaceous strata within the islands, as well as with other areas of west-

ern North America. In addition to enhancing the biostratigraphic control, fieldwork supported by the Queen Charlotte Islands Frontier Geoscience Program (QCI FGP) in 1988 and 1989 has shown that the Cretaceous system in the islands is much more extensive than previously believed, both geographically and temporally. Additionally, the environments in which many of the Cretaceous rocks accumulated are now recognized to be distinctly different than previously hypothesized.

Linking all the stratigraphic and sedimentological studies, the correlations provided by molluscan biostratigraphy have allowed for the formulation of an integrated model of the Cretaceous depositional systems of the Queen Charlotte Islands region. This model unites the stratigraphy of the islands into a simple model of sedimentation which is also predictive of the subsurface distribution of strata under Hecate Strait to the east.

This paper describes this new, integrated model of the Cretaceous system in the Queen Charlotte Islands. First, I will review and summarize data regarding the major stratigraphic units recognized in the islands. This will be followed by a presentation of the new model of Cretaceous deposition and its implications for Cretaceous paleogeography, tectonic interpretations, and hydrocarbon potential.

Some of the major stratigraphic relationships discussed in this paper were first recognized in 1989. Several of the papers in this volume were prepared before that time and consequently may not reflect the updated stratigraphic interpretation.

## STRATIGRAPHY

For more than a century, the study and correlation of Mesozoic strata in the Queen Charlotte Islands has relied almost exclusively on molluscs, chiefly ammonites and bivalves. Molluscan remains occur in great profusion at some levels in the succession, and these fossils were initially described by Whiteaves (1876, 1884, 1900). The utility of ammonites for correlation resulted in the early development of a stratigraphic scheme based in large measure on this fossil group.

Recent efforts to incorporate microfossils into the study and correlation of the Cretaceous system have not proved greatly successful. In contrast, in older levels of the Mesozoic succession in the Queen Charlotte Islands, integrated ammonoid, conodont, and radiolarian biostratigraphic schemes have been developed (e.g. Carter et al., 1989). Compared to the Triassic and Jurassic sequences, the coarse-grained lithologies which characterize much of the Cretaceous system are relatively barren in these microfossil groups.

Whatever the fossil groups used for correlation, a precise geographic location for each fossil collection is mandatory if a reliable stratigraphic scheme is to be developed. Unfortunately, some of the early fossil collections made by Richardson (1873) and other geologists visiting the Queen Charlotte Islands were mixed, resulting in confused interpretations. It was not until this century that McLearn (1949) unravelled the succession of faunas present in several key sections visited by the early geologists, and established the basic framework within which successive stratigraphic studies in the Queen Charlotte Islands have been undertaken.

The development of stratigraphic nomenclature for the Jurassic and Cretaceous systems of the islands was detailed by McLearn (1949). Subsequent informative discussion is provided by Sutherland Brown (1968), Cameron and Tipper (1985), Haggart (1987), and Woodsworth and Tercier (1991). A summary of the Cretaceous nomenclatorial evolution of the Queen Charlotte Islands, gleaned from these sources, is presented by Woodsworth and Tercier (1991). The references cited above should also be consulted for background detail regarding the origin of stratigraphic names. This paper utilizes the established Cretaceous stratigraphic nomenclature for purposes of

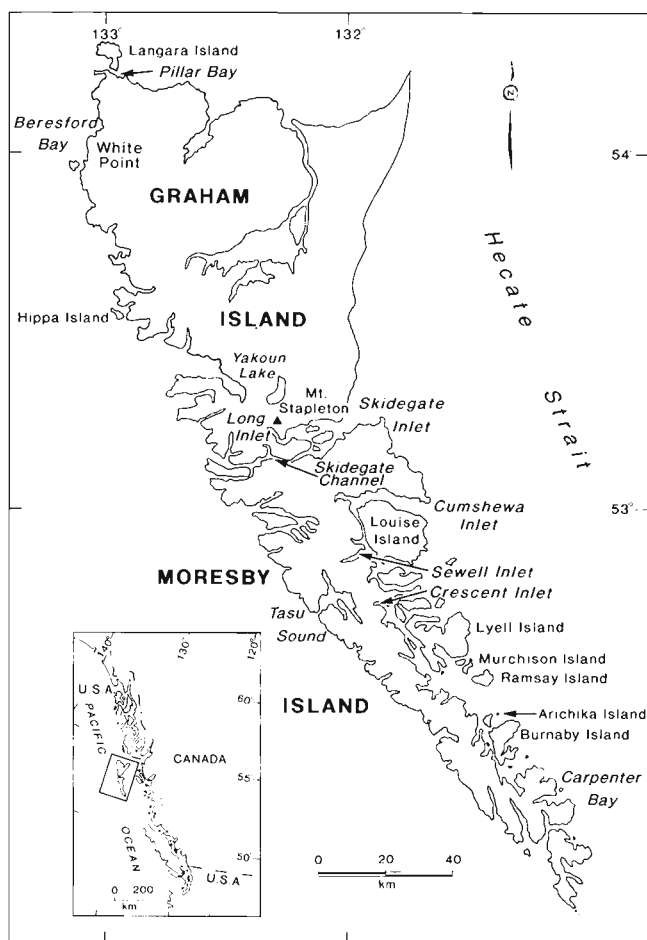


**Figure 1:** Location map of Queen Charlotte Islands showing main localities discussed in text.

discussion, while recognizing that a revision of Cretaceous stratigraphy is now timely.

To date, four major Cretaceous stratigraphic units have been recognized in the Queen Charlotte Islands on the basis of paleontological studies (Fig. 2). In chronological order of their recognition, these are:

- 1) the Queen Charlotte Group;
- 2) the Longarm Formation;
- 3) an unnamed succession of Late Cretaceous sedimentary rocks, principally shales; and
- 4) a succession of Late Cretaceous volcanic rocks, also presently unnamed.

Prior to the Geological Survey of Canada's QCI FGP, only the first two of these four stratigraphic units were recognized (see Sutherland Brown, 1968; Haggart, 1986c). The Queen Charlotte Group and the Longarm Formation were interpreted as distinct stratigraphic packages representing discrete episodes of Cretaceous sedimentation in the islands (Sutherland Brown, 1968; Yorath and Chase, 1981; Cameron and Hamilton, 1988; Hamilton and Cameron, 1989) (summarized in Fig. 2).

A brief summary of these four stratigraphic units is presented below, in order of their dates of description. This order, rather than stratigraphic sequence, is preferred because it allows the Cretaceous depositional framework to be simply described in terms of its basic components, sandstone and shale lithologic units.

#### Queen Charlotte Group – general statement

The Queen Charlotte Group was originally defined as the Queen Charlotte Series by Clapp (1914), for the younger Jurassic and Cretaceous strata found in the Skidegate Inlet region of the Queen Charlotte Islands. Clapp (1914) subdivided his Queen Charlotte Series into three units, the Haida Member, the Honna Member, and the Skidegate Member, and considered them a stratigraphically-successional package. Faunal differentiation allowed MacKenzie (1916) to restrict the group to the Cretaceous portion of the section. MacKenzie (1916) also raised Clapp's (1914) members to formation status, rec-

ognizing the Haida, Honna, and Skidegate formations, in ascending stratigraphic order.

#### Haida Formation

Clapp's (1914) definition of the Haida Member was based on exposures in the Skidegate Inlet region (Fig. 1). The strata which are found on both sides of the presently recognized Cretaceous outcrop belt in the central Queen Charlotte Islands were placed by Clapp within this unit. Thus, he included rocks which are now assigned to the Longarm Formation within the Haida stratigraphic unit. Clapp (1914) recognized a basal fine-grained sandstone lithofacies within the Haida member, which grades upward into shale. Sutherland Brown (1968) subsequently defined the Sandstone member and the Shale member of the Haida Formation for these two distinct lithologies, which characterize the lower and upper portions of the formation, respectively. The distribution of Haida Formation outcrops in the Queen Charlotte Islands is shown in Figure 3.

#### Sandstone member

**Lithology.** Details of the lithological composition of the Sandstone member of the lower Haida Formation were discussed by Sutherland Brown (1968) and Yagishita (1985), who measured and described sections for the type locality in Bearskin Bay, and by Haggart (1986c), Fogarassy and Barnes (1988, 1991), and Higgs and Bornhold (1988). The Sandstone member contains a number of distinct lithofacies which, when present, consistently succeed each other through an outcrop section; these have been described under various names by the workers cited above.

In general, the Sandstone member consists of medium- to fine-grained, greenish, cross-stratified sandstone, locally exhibiting extensive bioturbation. A discontinuous basal pebble conglomerate lithofacies, no more than a few tens of metres in thickness, occurs in the lowermost part of the member. The composition of the conglomerate clasts at many localities indicates the Jurassic Yakoun Group volcanics as the dominant source. The matrix of the sandstones has a volcanic-fragment component, also likely derived from the Yakoun Group rocks (Sutherland Brown, 1968; Yagishita, 1985). The member is rich in plant debris and other fossils, including ammonites, bivalves, other molluscs, and decapod crustaceans.

**Thickness.** The Sandstone member of the Haida Formation is separated by a considerable unconformity from all underlying units except the Longarm Formation. The total thickness of the member is difficult to ascertain because of intermittent exposure and local disruptions due to faulting. Sutherland Brown (1968) gave a thickness of 823 m at the type locality in Bearskin Bay. It is suggested here that this number is exaggerated due to the mapping difficulties noted above. Based on composite measured sections of Sandstone member strata in Cumsheewa Inlet, I estimate the actual thickness to be approximately half that of Sutherland Brown (1968).

**Depositional environment.** The lower part of the Sandstone member includes a rich and diverse mollusc fauna and a variety of sedimentary structures which are indicative of shallow-marine deposition. Haggart (1986c) recognized that the sequence of lithofacies making up the member represents an inner-shelf succession which accumulated in a regime of gradually rising sea level, *i.e.*, a marine transgression. Higgs and Bornhold (1988) further ascertained that much of the member was deposited as a result of storm events. It appears that the Sandstone member of the Haida Formation represents the basal transgressive phase of deposition in the eastern part of the Cretaceous basin.

Fogarassy and Barnes (1989) have suggested that the Sandstone member may locally contain nonmarine beds. Some of the beds they identified as possibly nonmarine have yielded shallow-marine bivalves (trigoniids and oysters), however, indicating that at

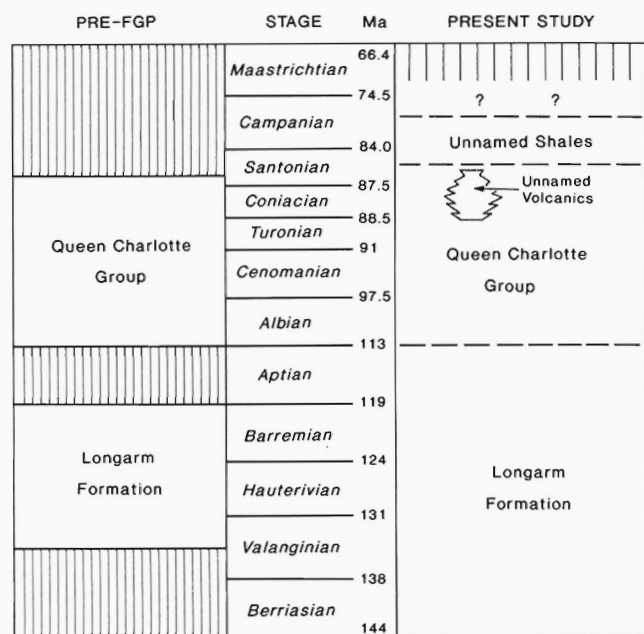


**Figure 2:** Interpretations of Cretaceous stratigraphy of the Queen Charlotte Islands prior to, and resultant from, the FGP study. Absolute ages after Palmer (1983).



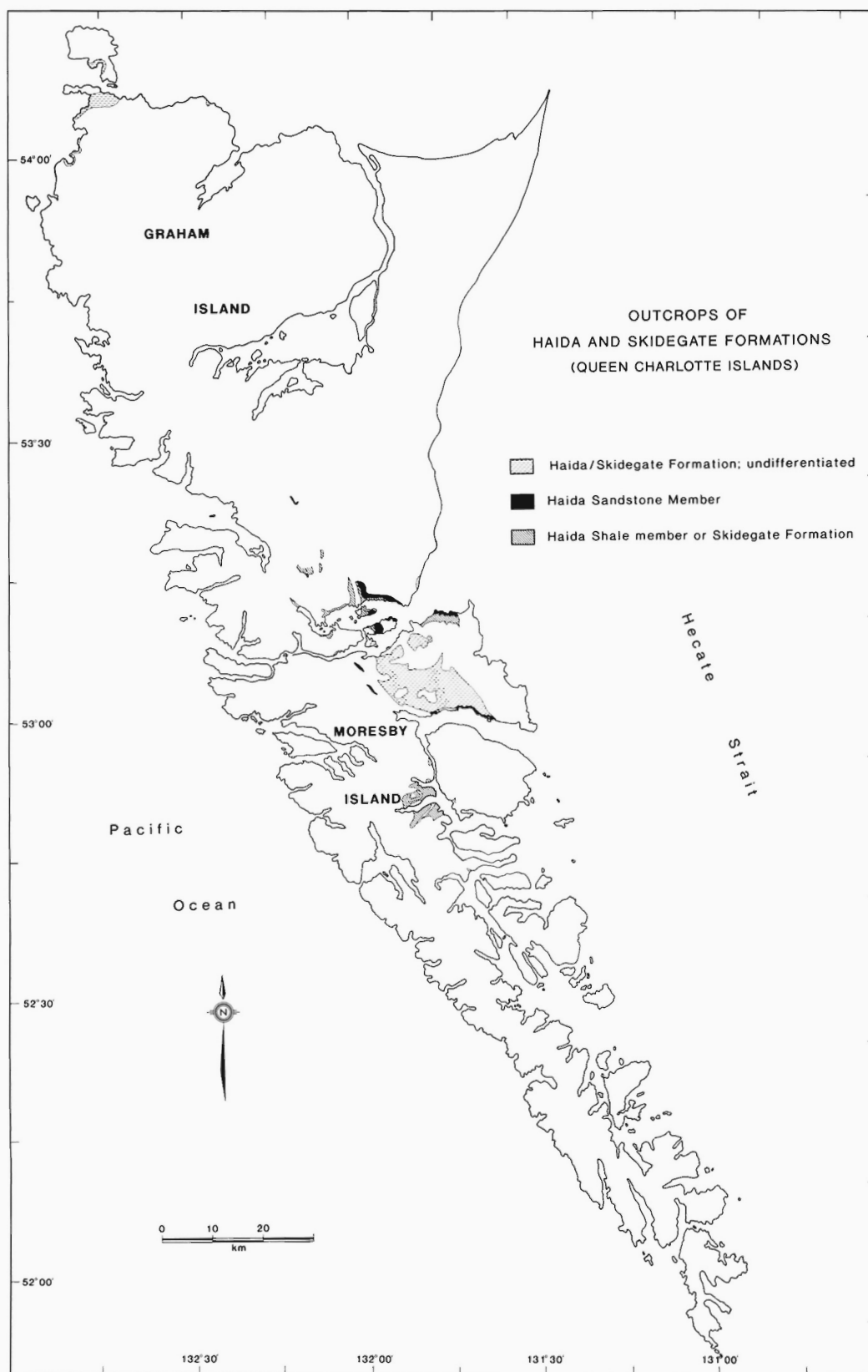


**Figure 3:** Distribution of known outcrops of the Haida Formation and the Skidegate Formation in the Queen Charlotte Islands. Data from Sutherland Brown (1968), Thompson (1990), Lewis et al. (1990), and writer's observations.

least these localities are of marginal-marine origin. On the other hand, some support for a nonmarine interpretation for some parts of the member comes from the Beresford Bay area, where thin (less than 4 cm), laterally discontinuous coal seams occur at the base of the section (Haggart, 1986c).

**Distribution.** The Sandstone member of the Haida Formation has been identified at many localities in the Queen Charlotte Islands. In the central islands area, these outcrops form a belt approximately 3 km in width which trends across the region in a general northwest to southeast direction (see Sutherland Brown, 1968, his Fig. 13; Thompson, 1990; Lewis et al., 1990). The Sandstone member outcrop belt forms the easternmost Cretaceous outcrop recognized in the islands.

Exposures of this unit also occur extensively along the northwest coast of Graham Island north of Beresford Bay, and on Langara Island at the northern tip of the Queen Charlotte Islands (Sutherland Brown, 1968; Haggart, 1986c). No exposures of the Sandstone member have so far been recognized south of Cumshewa Inlet, in the southern two-thirds of the archipelago.

**Age.** The age of the Sandstone member is well constrained by rich assemblages of ammonites. Many of these fossils have come from the type section in Skidegate Inlet. These and other collections from nearby locales were described by McLearn (1972), who recognized that the Sandstone member in the Skidegate Inlet region includes strata representing most of the Albian stage. McLearn (1972) proposed a sequence of ammonite zones for the Albian of the Queen Charlotte Islands, based on the Skidegate Inlet collections. He compared this succession with other areas of the Pacific coast of North America, noting that the basal Albian did not appear to be represented in Skidegate Inlet.

Jones et al. (1965) suggested the possibility that the Skidegate Inlet area might contain the lowest Albian, and they definitely identified basal Albian strata from the Sandstone member in the Beresford Bay area of the islands (Fig. 1). Thus, as summarized by Jeletzky (1977), the Sandstone member of the Haida Formation in the Queen Charlotte Islands is firmly identified as including strata spanning the entire Albian stage.

#### *Shale member*

Sutherland Brown (1968) defined the Shale member of the upper Haida Formation on the basis of exposures in western Bearskin Bay, Skidegate Inlet (Fig. 1), where shale and silty shale predominate. The Shale member conformably overlies the Sandstone member at its type section and at all other localities where its base has been studied. Transitional strata are sometimes encountered, and the assignment of these rocks to either member is somewhat arbitrary (see Haggart, 1986c in regards to exposures in eastern Cumshewa Inlet). Nonetheless, the well-exposed sequences of distinctive lithology seen at the type locality and in many other sections indicate that the unit is a viable stratigraphic entity.

Cameron and Hamilton (1988) suppressed the use of the name Shale member, preferring to include this unit within a greatly expanded Skidegate Formation. For reasons discussed below this assignment is considered inappropriate.

**Lithology.** Sutherland Brown (1968) described a measured section and lithologies for the Shale member at its type locality. Other discussions were provided by Haggart (1986c) and Fogarassy and Barnes (1988).

The Shale member consists primarily of a monotonous succession of black, silty shale with abundant calcareous concretions. Lenticular bedding, with sand dispersed throughout the mud matrix, is noted throughout the member, but distinct sandstone beds are rare. Those that are noted consist of fine- to medium-grained sandstone and

sometimes include a basal granule or grit lithology with associated shell debris. The proportion of mud to sand in the member is quite high, generally greater than 10:1. The early diagenetic concretions are spherical or potato-shaped and range from several centimetres to more than 50 cm in diameter. It is within the concretions that the best-preserved, three-dimensional fossils are found, generally in aggregations; flattened impressions of some forms, especially bivalves, often occur singly in the mud matrix.

At one locality in Cumshewa Inlet, near McLellan Island (Fig. 8), the member includes abundant conglomeratic debris, primarily granitic cobbles and small boulders, intraformational clasts, and transported fossils, all found in a chaotic melange.

Yagishita (1985), Haggart (1986c), and Fogarassy and Barnes (1988) described the uppermost strata of the Shale member as commonly containing thinly-interbedded siltstone and fine-grained sandstone, commonly bioturbated. As discussed below, these strata are locally transitional to the Skidegate Formation.

**Thickness.** The Shale member conformably overlies the Sandstone member of the Haida Formation at the type locality at Bearskin Bay, as well as at Cumshewa Inlet. Sutherland Brown (1968) measured the unit to be approximately 325 m thick at its type locality, whereas Haggart (1986c) gave a composite thickness of approximately 100 m for the Shale member at Cumshewa Inlet.

**Depositional environment.** The conformable nature of the contact of the Shale member with the underlying Sandstone member indicates that a gradual change in depositional environment must have occurred. The rocks of the Shale member accumulated as a result of the same transgression which produced the underlying Sandstone member. The mudstones of the Shale member reflect a deeper-water, generally more offshore facies, interfingering with, and laterally equivalent to, the Sandstone member deposits. The storm deposits which characterize the nearshore Sandstone member (Higgs and Bornhold, 1988) are also found in the Shale member and are represented by the infrequent fine sandstones with basal grit and shell lags.

Haggart (1986c) suggested that sedimentological and faunal evidence pointed to an outer-shelf setting for most of the Shale member. The presence of the chaotic conglomerates described above, as well as local slump features, indicates that at least locally the member may represent slope environments (Gamba et al., 1990).

**Distribution.** The utility of the Shale member as a mapping unit in field studies further underscores its value as a stratigraphic unit. Outcrops of the member have been identified at numerous localities across the Queen Charlotte Islands. In general, the outcrop of the member forms a belt about 3–4 km in width, situated parallel to the outcrop of the more easterly occurring Sandstone member (see Sutherland Brown, 1968, his Fig. 13 and geologic maps by Thompson, 1990 and Lewis et al., 1990). In addition to the type locality, the Shale member is displayed well along the north shore of Cumshewa Inlet. The outcrop belt can be traced into central Graham Island (Haggart et al., 1990; Indrelid, 1990) where, again, it is typically found parallel to, and west of, the Sandstone member outcrops.

Shale member strata also occur on the northwest coast of Graham Island, as well as on nearby Langara Island. The rocks at these locales are very gently dipping and typically show a greater component of lenticular bedding. Fossils in these strata are somewhat sparse, found principally in the thin, coarse grit and pebble conglomerates which occur locally.

**Age.** In its type section at Bearskin Bay, as well as at several other localities in Skidegate Inlet, the Shale member contains rocks of Cenomanian and Early Turonian age (McLearn, 1972). The same age range characterizes most other known outcrops of the Shale member.

At several localities on the north coast of Graham Island, just south of Langara Island, the member contains Cenomanian fossils immediately beneath the overlying Honna Formation. No fossil evidence of Turonian-age strata has been found anywhere on the northwest coast of Graham Island to date. Some sections, such as the ones at Beresford Bay and Hanna Koot Creek, could conceivably include Turonian rocks, however, as they are undated or contain significant amounts of section overlying known Albian horizons.

At Cumshewa Inlet, rocks of the Shale member just beneath the overlying Honna Formation are of Early Turonian age (Haggart, 1986c). Farther south, several exposures of Early Turonian age are found on the northeast shore of Sewell Inlet.

### Skidegate Formation

Much of the Cretaceous strata found at shoreline level in Long Inlet and Skidegate Channel (Fig. 1) was recognized by the early geologists as lithologically distinct from typical Haida Formation strata farther east, in Bearskin Bay. These rocks were thus described as a separate stratigraphic unit, to which Clapp (1914) gave the name Skidegate Member. Apparent field relationships of various rock units suggested to the early geologists that the Skidegate Formation rocks exposed along the north shore of Kagan Bay formed the uppermost part of the Cretaceous stratigraphic succession in the Skidegate Inlet region (e.g., Richardson, 1873; Dawson, 1880).

**Lithology.** Rocks of the Skidegate Formation are perhaps the most lithologically distinct Cretaceous strata in the Queen Charlotte Islands. The lithology was described in detail by Sutherland Brown (1968), Haggart (1986c), and Fogarassy and Barnes (1988). These rocks are composed of strongly indurated, silty shale and interbedded turbidite sandstone, often forming spectacular and jagged exposures at shoreline level. The fine- to coarse-grained sandstone beds are often channelized into the underlying strata, are graded and show partial Bouma sequences, and range in thickness from 5 cm to more than a metre. Sole marks are sometimes seen on the undersides of individual sandstone beds, while the upper surfaces are extensively bioturbated. Mollusc remains are quite rare, and are found principally in the sandstones, and a limited amount of small-size plant debris is observed locally.

Various outcrops of the Skidegate Formation exhibit a lesser or greater development of turbidite sandstone beds. On outcrop scale, the proportion of sandstone to shale ranges from about 10:1 to 1:1. Those outcrops where the ratio approaches 1:1 appear somewhat similar to the Shale member of the Haida Formation. For mapping purposes, the two units can usually be differentiated on the basis of presence or absence of the turbiditic sandstone beds, and of stratigraphic context; sandstone-free shale successions in the Skidegate Formation rarely persist for more than a few metres stratigraphically. Outcrops of the Shale member frequently contain common calcareous concretions, which do not appear to be present in the Skidegate Formation.

The exposures of siltstone and fine-grained sandstone interbedded with shale at Cumshewa Inlet, described by Yagishita (1985), Haggart (1986c), and Fogarassy and Barnes (1988) and correlated by these authors with the upper part of the Shale member of the Haida Formation, probably represent transitional strata between the Haida Shale member and Skidegate Formation.

**Thickness.** The Skidegate Formation is gradational with the Haida Shale member (see discussion below). The total thickness of shale and sandstone forming the unit is unknown because its base is undefined. Sutherland Brown (1968) estimated an approximate thickness of 630 m for the formation at its type section in Kagan Bay.

**Depositional environment.** Sutherland Brown et al. (1983) interpreted the Skidegate Formation at the type locality as a unit deposited in a

lacustrine or shallow-marine environment. Haggart (1986c) reported marine fossils from the formation, and Cameron (unpublished GSC fossil report BEBC-1989-1) has subsequently identified foraminifers from outcrops in Long Inlet which indicate that those localities represent outer-shelf to upper-slope marine environments. The abundance of turbidite deposits interbedded with shales, the paucity of mollusc fossils, and the intergradational nature and age equivalence of the formation with the Shale member of the Haida Formation (see below), all point to a submarine-fan setting for much of the formation.

Haggart et al. (1989) suggested that Skidegate exposures in Long Inlet represent distal-turbidite deposits of a submarine fan complex. Gamba et al. (1990) interpreted the Skidegate Formation more specifically, as levee deposits adjacent to fan-channel complexes of the Honna Formation. This interpretation holds on a local scale, especially at Yakoun Lake or Sewell Inlet, where the conglomerates of the Honna Formation are thin and interstratified with shales and weakly-developed turbidite sandstones of the Skidegate Formation. However, the oldest Skidegate Formation deposits appear to predate those of the Honna Formation (see below), and the Skidegate Formation depositional system had apparently existed for a substantial period of time prior to progradation of Honna deposits into the basin.

In general, the thick accumulations of Skidegate Formation rocks which are found on the western flank of the outcrop belt are considered to reflect a submarine fan setting. Minor occurrences of Skidegate-type rocks within shale sequences of the Haida Formation, such as occur in the Sewell Inlet area, indicate that the Skidegate Formation also accumulated locally in non-fan settings. Interpreting the formation strictly as of submarine fan origin overlooks the possibility that minor turbiditic deposition may have occurred at sites on the outer shelf or slope where gradient and sediment supply were sufficient, perhaps in localized subbasins.

**Distribution.** The Skidegate Formation is much more restricted in its areal distribution than is the Haida Formation (Fig. 3). Outcrops of the Skidegate Formation are oriented subparallel to the general trend of the Haida Formation outcrop belt but are generally located west of that belt. Local exposures of the Skidegate Formation occur on southeastern Langara Island and northwestern Graham Island, in western Skidegate Inlet, and in the Sewell Inlet region. The most southerly exposures yet identified are in the Crescent Inlet area of Logan Inlet (Fig. 1).

**Age.** Until recently, the age of the Skidegate Formation was considered problematic. Based on confusing field relationships, early geologists maintained that the Skidegate Formation was the youngest Cretaceous stratigraphic unit in the Skidegate Inlet area, supposedly overlying the Honna Formation conglomerates at Kagan Bay (Richardson, 1873; Dawson, 1880; Clapp, 1914; MacKenzie, 1916). However, Whiteaves (1884) had recognized that the Skidegate rocks included fossils of Turonian age and that the same fossils occurred in the Haida Formation. This connection was lost on the field geologists, however, who continued to maintain a stratigraphic segregation of the two lithologic units. Haggart (1987) summarized the geological and paleontological investigations which ultimately led to the recognition that the Skidegate Formation is essentially the same age as the Haida Sandstone and Shale members.

The scarcity of mollusc remains in the Skidegate Formation complicates dating of individual outcrops and even sections. However, a number of collections from several areas have shown that the formation includes strata of at least Cenomanian and Early Turonian, and probably Albian, age (Haggart, 1986c, 1987). When fossils are found in the highest Skidegate Formation and Haida Shale member beds immediately beneath the overlying Honna Formation conglomerates, at most localities in the Queen Charlotte Islands (including western

Skidegate Inlet, Cumshewa Inlet, and Sewell Inlet), they are consistently of Early Turonian age. Fossils of likely Early Turonian age have also been collected by the writer from Skidegate Formation outcrops just beneath Honna Formation strata on central Graham Island (Ghost Creek area).

Cameron and Hamilton (1988) expanded the definition of the Skidegate Formation to include all the finer clastics of similar age occurring throughout the archipelago, including many rocks previously assigned to the Shale member of the Haida Formation. This fails to recognize the lithologic differences between the Skidegate Formation and the Shale member rocks. In addition, the areal extent of true Skidegate-lithology strata in the Queen Charlotte Islands is much more restricted than that of Shale member deposits. Most of the outcrop belt on northern Graham Island, for instance, is lacking in turbidites and is conspicuously distinct from the typical beds of the Skidegate Formation type section. As discussed below, the distribution of Haida Shale member and Skidegate Formation lithologies can be readily interpreted in an integrated lithogenetic and sedimentological context. For these reasons, it is preferable to retain the Shale member of the Haida Formation as a practical stratigraphic term and mapping unit.

### Honna Formation

The Honna Formation is the third of Clapp's (1914) members comprising the Queen Charlotte Group. No other Cretaceous stratigraphic unit in the islands has attracted the attention given to this formation. Sutherland Brown (1968), Yagishita (1985), Haggart (1986c), Fogarassy and Barnes (1988), and Higgs (1990) provided extensive descriptions of the Honna Formation outcrops in the central part of the Queen Charlotte Islands, and Higgs (1991a) gave a lithological description for the formation on the north coast of Graham Island. Higgs (1988, 1990, 1991a) has proposed a regional depositional model for the Honna Formation that relates it to tectonic activity east of the Queen Charlotte Islands.

**Lithology.** The Honna Formation consists predominantly of cobble conglomerate and medium- to coarse-grained sandstone rich in volcanic rock fragments, with minor fine-grained sandstone and shale occurring locally. The formation is notoriously lacking in fossil remains. The composition of clasts in the conglomerates suggests that most of the material was derived from proximal sources.

Haggart (1986c) noted that the Honna Formation forms an overall fining-upward sequence, but this is not readily discernible on outcrop scale. In general, the base of the formation is characterized by thickly-bedded, coarse conglomerates that gradually thin and fine upsection into sandstone. In the highest parts of the formation, turbiditic sandstone occurs, interbedded with bioturbated shale. Haggart (1986c) described such a succession through the Honna Formation at Cumshewa Inlet, and a similar sequence is seen on the south coast of Langara Island.

Higgs (1988) and Fogarassy and Barnes (1988) have noted a basal scour of the Honna into underlying strata of the Shale member of the Haida Formation and the Skidegate Formation. The uppermost beds of these sub-Honna units at the type section in western Skidegate Inlet (Sutherland Brown, 1968; Yagishita, 1985), as well as in Cumshewa Inlet (Haggart, 1986c), often exhibit an influx of intraformational clasts several metres below the formation contact.

Locally, the lower part of the Honna Formation lacks abundant conglomerate but is rather characterized by thickly bedded, massive to cross-stratified feldspathic sandstone interbedded with thin shale and siltstone intervals. This sandstone facies of the Honna Formation is extensively developed in the Long Inlet area, where it has been described by Haggart et al. (1989).

**Thickness.** Sutherland Brown measured the thickness of the Honna Formation at its type locality in Lina Narrows, giving an approximate number of 415 m. Haggart (1986c) suggested that the total thickness of the Honna Formation at Cumshewa Inlet was significantly less, about 200 m.

**Depositional environment.** A variety of lithofacies have locally been identified in the Honna Formation by several workers (Yagishita, 1985; Haggart, 1986c; Fogarassy and Barnes, 1988). Interpreting this assemblage of lithofacies, Yagishita (1985) proposed a canyon-fed submarine fan model for the origin of the formation. He further suggested that the source of the volcanic-derived Honna sandstones may have been a deeply-dissected volcanic arc lying somewhere to the east of the islands.

Higgs (1988) maintained that Yagishita's (1985) submarine fan model could not account for the granitoid megaclasts noted locally within the formation. Higgs (1988, 1990, 1991a) thus proposed another model for the origin of the Honna Formation deposits. In his model on-land deposits of the Honna Formation reflect a complex of coalescing fan-deltas which extended across a very narrow shelf from an alluvial fan system in the east into a deep-water basin in the west. The various lithofacies in the Honna Formation have been related by Higgs (1988, 1990) to specific environments in the fan-delta complex, and imbrication studies of the conglomerates indicate that paleoflow was generally to the west (Yagishita, 1985; Higgs, 1990; Gamba et al., 1990).

The source of material for the fans was suggested by Higgs (1988) to have been uplifted mountain blocks a few tens of kilometres to the east, likely fronting the Sandspit Fault or related fault systems. The alluvial fan equivalents of the deep water fan deposits preserved on the Queen Charlotte Islands are inferred by Higgs (1990) to have been located to the east of the Honna Formation outcrop belt before they were eroded.

**Distribution.** The Honna Formation is presently known from a wide area of the northern half of the archipelago (Fig. 4), and most of its outcrops were recognized by Sutherland Brown (1968). The thickness of the unit is highly variable. Outcrops in the Mount Stapleton area, previously identified by Sutherland Brown (1968), are now known to be of a Tertiary sedimentary and volcanic succession partly correlative with the Skonun and Masset formations (Haggart et al., 1990). Some outcrops north of Tasu Sound, also identified by Sutherland Brown (1968) as the Honna Formation, have subsequently been described by Higgs (1991b). Higgs' description of these rocks suggests that they may be of similar composition to the Tertiary strata in the Mount Stapleton area.

Higgs (1989) also indicated that the conglomerate and sandstone found on the west coast of the Queen Charlotte Islands, at Hippa Island (the so-called "Hippa beds"), might be of Cretaceous or Tertiary age, and hence are possibly correlative with the Honna Formation. Poorly-preserved palynomorphs showing high thermal maturity and probably of Cenozoic age have subsequently been identified in these strata (J. White, pers. comm., 1989). Given the occurrence of thermally mature Paleogene deposits found at depth in the Union Port Louis well 6 km to the north (White, 1990a), it is thus likely that the "Hippa beds" are of Paleogene, rather than Cretaceous, age.

**Age.** The age of the Honna Formation is problematic. Most outcrop evidence studied by the author indicates that the formation is largely conformable within the Cretaceous succession and resulted from the rapid progradation of several fan complexes into the shale basin.

Several lines of evidence support this interpretation. First, conglomerates of the Honna Formation can be seen to interfinger directly with shales of the Skidegate and Haida formations at several locali-

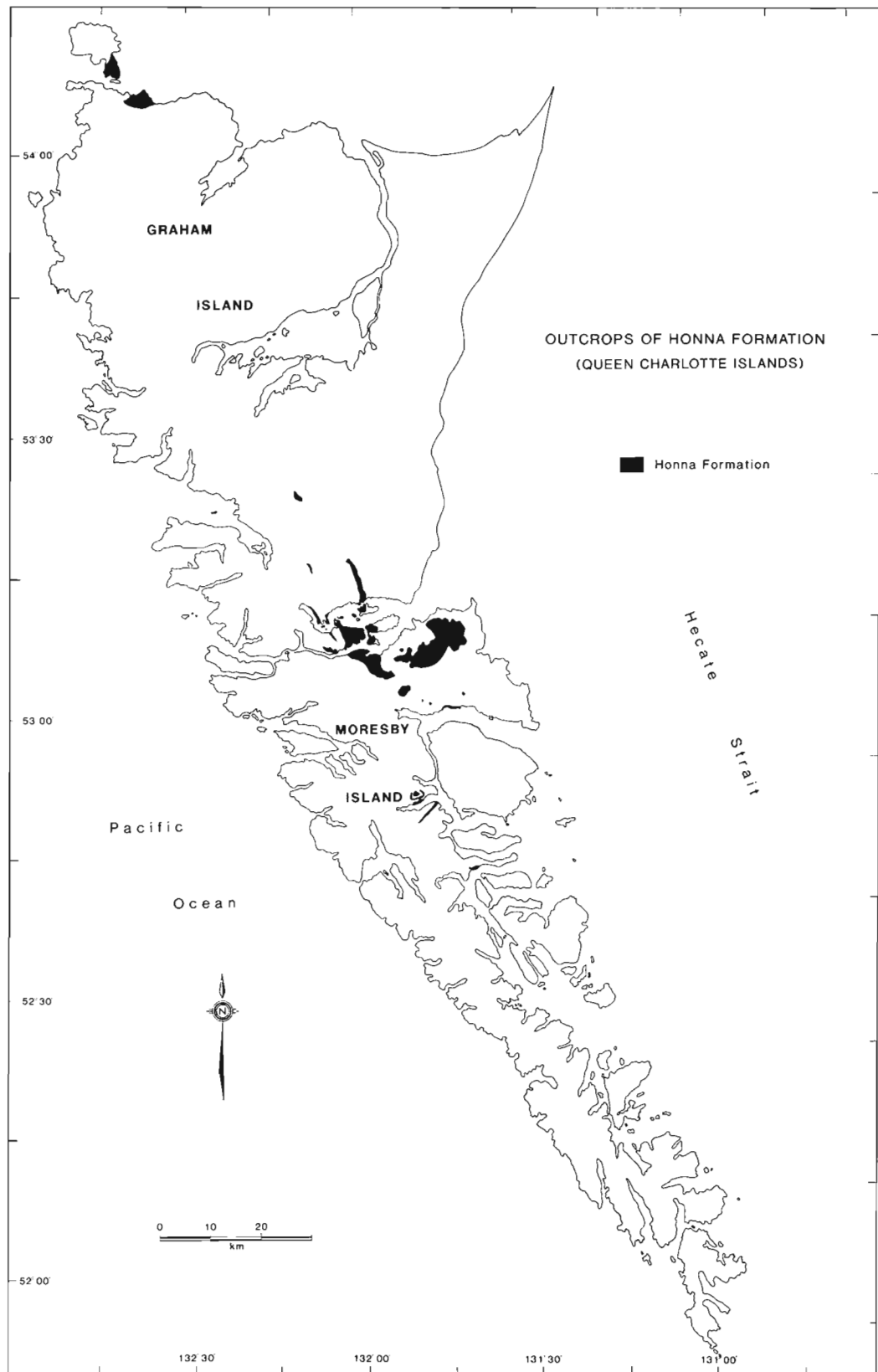


**Figure 4:** Distribution of outcrop of Honna Formation in the Queen Charlotte Islands. Data sources as for Figure 3.

ties, including Langara Island, Yakoun Lake, and Sewell Inlet. Second, an apparently conformable contact of the Honna Formation with the Haida and Skidegate formations has been noted in several other areas (Haggart, 1986c; Fogarassy and Barnes, 1988).

Finally, wherever fossil control is available, it supports a generally conformable age relationship between the Honna Formation and the underlying Haida and Skidegate formations. A few ammonite and bivalve collections have been made from higher parts of the Honna Formation in western Skidegate Inlet, and these bracket an age range of Early Coniacian to Early Santonian (Riccardi, 1981; Haggart, 1986c). Thus, the base of the formation may include older, Turonian, strata. Bivalves of Early Turonian age (*Mytiloides labiatus*) have consistently been collected from shales of the Skidegate Formation and the Shale member of the Haida Formation, which underlie Honna Formation conglomerates at several localities in the central Queen Charlotte Islands. On the northwest coast of Graham Island and on Langara Island, the Honna Formation also overlies deposits of the Skidegate Formation and the Shale member of the Haida Formation. In this region, however, only Cenomanian fossils have been identified from the sub-Honna beds.

This circumstantial evidence supports the hypothesis that the Honna Formation conglomerates conformably overlie the Skidegate and Haida formations and that the earliest phase of Honna deposition in the central Queen Charlotte Islands region may be of later Turonian age. In the northern Queen Charlotte Islands, deposition may have commenced in Cenomanian time.

However, geologic mapping has identified several localities where the Honna Formation is apparently resting in unconformable relationship on top of older Cretaceous units, Middle Jurassic Yakoun Group strata, and even Late Triassic Kunga Group rocks (Thompson, 1990; Lewis et al., 1990; summarized in Thompson et al., 1991). Some of these examples (e.g., the area from Skidegate Channel southeast to Cumshewa Inlet, where Honna conglomerates are shown on the maps overlying Longarm Formation rocks) may be resultant from inadequate fossil control and hence, incorrect identification of map units. Other examples, however, such as south of Sandspit where the Honna rests on Middle Jurassic Yakoun Group, are more problematic.

Thompson et al. (1991) proposed two hypotheses to explain these anomalous relationships. First, syndepositional block faulting appears to have occurred, at least locally, during part of later Cretaceous time. Block faulting was extensive and of large-scale in the Late Jurassic (Thompson et al., 1991) and Cretaceous activity, apparently of smaller-scale and less widely distributed, may have occurred locally as a reactivation of the older, Late Jurassic fault system. Thus, adjoining local areas separated by bounding faults sometimes exhibit different Cretaceous stratigraphic successions, as is seen southeast of Alliford Bay.

Second, some of the Cretaceous unconformities may be related to lowered erosional base level associated with sea level drop. The rapid progradation of Honna Formation fan complexes into the basin may have locally resulted in erosion and reworking of some of the earlier Cretaceous and older Mesozoic section. Such stripping would be expected to be most pronounced in the more nearshore, or eastern, parts of the basin and this is roughly supported by the age distribution of the sub-Honna rocks as shown on the geological maps.

### Longarm Formation

Sutherland Brown (1968) was the first to recognize that some of the strata previously assigned to the Queen Charlotte Group included beds substantially older than the typical Queen Charlotte Group sections in eastern Skidegate Inlet. Fossil identifications revealed that these

older beds included strata of Valanginian through Barremian age (Jeletzky in Sutherland Brown, 1968). Sutherland Brown (1968) reported that these strata consist of conglomerate, lithic wacke, shale, and minor volcanic rocks. Because of the apparently dissimilar lithological character of these strata from typical Queen Charlotte Group rocks, as well as their significantly greater age, Sutherland Brown (1968) proposed that they be placed within a new stratigraphic unit, which he informally named the Longarm Formation.

A type section for the Longarm Formation was not proposed by Sutherland Brown (1968) although he indicated that strata in Long Inlet (rocks originally included by Clapp [1914] in his Haida member) are typical of the unit. No upper or lower limits to the formation can be defined at that location. The Long Inlet section includes most of the lithologies recognized in the Longarm Formation (see Haggart, 1989; Haggart and Gamba, 1990), though most are better displayed at other localities.

**Lithology.** Sutherland Brown (1968) described the spectacular exposures of the basal conglomerate of the Longarm Formation, which unconformably overlies Triassic Peril Formation rocks on Arichika Island (Fig. 1). Haggart and Gamba (1990) described this basal conglomerate in detail and interpreted it as a transgressive lag deposit. The basal conglomerate facies is well developed in the southern Queen Charlotte Islands but is only poorly developed north of Cumshewa Inlet. Haggart and Gamba (1990) pointed out that the basal beds of the Longarm conglomerates are rich in clasts derived from the locally underlying stratigraphic units. Upsection in the conglomerates, however, clasts of Jurassic Yakoun Group volcanics become predominant, reflecting the apparently ubiquitous presence of these source rocks throughout the Longarm depositional basin.

The formation grades upward into sandstone and shale (Haggart, 1989; Haggart and Gamba, 1990). The composition of the Longarm sandstone is similar to that of the Haida Sandstone member, although a greater proportion of volcanic detritus is present. Fossils, especially ammonites, bivalves, and wood fragments, are locally abundant.

One of the lithological characteristics traditionally used to distinguish Longarm Formation rocks from those of the Haida Sandstone member is the greater degree of lithification and induration which characterizes the former. This is not a function of compositional variation, however. Rather, it appears to be related to the greater degree of diagenetic alteration associated with structural deformation and intrusive activity which characterizes many of the Longarm Formation outcrops. Much of the formation in central Cumshewa Inlet is soft and friable, similar to the Haida Sandstone member; where it is intruded by dyke complexes, however, it becomes strongly indurated and dense. Longarm Formation outcrops are concentrated in the zone of intense deformation which trends across the central islands region (Thompson, 1988; formerly Rennell Sound fault system of Sutherland Brown, 1968) and the formation has thus experienced a greater degree of alteration than Haida Formation rocks, which crop out generally east of this deformation zone.

Fogarassy (1989) and Fogarassy and Barnes (1989) have described a mylonitic quartz texture in rocks they correlated with the base of the Haida Sandstone member. They suggested that this mineralogy is unique to the basal Haida Formation deposits. Several localities of this lithofacies have since been shown to be of Longarm age (J. Haggart, unpublished GSC fossil reports). Thus, this mineralogical texture is not unique to the basal Haida Sandstone member and might be expected in other basal Cretaceous sections. Indeed, Jurassic plutonic rocks of Lyell Island exhibit the mylonitic texture (Fogarassy and Barnes, 1989); thus, any post-Late Jurassic strata could conceivably include detritus exhibiting this texture.



**Thickness.** The Longarm Formation rests unconformably upon a variety of sub-Cretaceous units, including the Karmutsen Formation (Sea Pigeon Island), the Sadler Formation (Bolkus Island), the Peril Formation (Arichika Island), the Sandilands Formation (Cumshewa Inlet), probable Yakoun Group (western Skidegate Inlet), and Late Jurassic plutons (Poole Inlet, Burnaby Island; see Anderson and Greig, 1989). Haggart (1989) gave an interpolated thickness of 450 m for the formation in the Long Inlet area, based on composite measured sections. The continuously exposed section on Arichika Island includes 175 m of Longarm strata (Sutherland Brown, 1968), but it represents only the lower part of the formation.

**Depositional environment.** Haggart (1989) noted that most of the Longarm rocks on Graham Island and northern Moresby Island are of shallow-marine origin. A similar interpretation of the formation in the southern Queen Charlotte Islands was proposed by Haggart and Gamba (1990). The diverse and abundant mollusc fauna, the associated sedimentary structures, and the succession of lithofacies, all indicate that the Longarm Formation accumulated in a variety of shelf and, perhaps locally, upper-slope environments (Haggart and Gamba, 1990). The fining-upward trend exhibited through the formation, from the basal conglomeratic lag deposit through the shales, indicates that the formation accumulated in a regime of rising sea level, much like the one that existed in Haida time.

**Distribution.** Sutherland Brown (1968: Fig. 11) suggested that the Longarm Formation occupied a narrow north-northwest-trending belt in the central and southeastern part of the Queen Charlotte Islands. Improved access to previously inaccessible exposures in central Graham Island has resulted in the recognition that the Longarm Formation is actually much more widespread in that area than previously mapped (Fig. 5). As well, new fossil collections from outcrops in Skidegate and Cumshewa inlets, which were previously mapped as Haida Formation (Sutherland Brown, 1968: Fig. 5), have produced molluscs of Longarm age. The distribution of Longarm outcrops in the southern Queen Charlotte Islands remains essentially as indicated in the maps of Sutherland Brown (1968), with minor additions.

**Age.** Jeletzky (*in* Sutherland Brown, 1968) determined that the rocks of the Longarm Formation in the Long Inlet and Cumshewa Inlet exposures include beds of Hauterivian and Barremian age. Jeletzky also noted that Late Valanginian fossils occur at several localities in the northern half of the Queen Charlotte Islands. A more detailed study of exposures in Cumshewa Inlet enabled Haggart (1989) to recognize that the formation includes beds of probable Early Aptian age.

Field work in 1989 led to the identification of a continuous Cretaceous stratigraphic section in Cumshewa Inlet (adjacent to Section A of Haggart, 1986c: Fig. 2) which includes additional, younger Aptian, strata. Fossils identified from this section include *Shastoceras* sp., *Lytoceras* (*Gabbioceras*) sp., *Shasticioceras* sp., and *Tropaeum* sp. This new Cretaceous section contains the same shallow-water facies which characterize much of the Longarm Formation in the Cumshewa Inlet area, and grades upward into similar, shallow-water deposits of the Haida Formation containing *Breweriaceras hulenense*, of Albian age (see Haggart, 1986c).

The rocks preserved in a section on a small island off the northwest coast of Graham Island, 2.5 km southwest of White Point (Fig. 1), were dated as Tithonian by Jeletzky (1984). Cameron and Tipper (1985) referred these strata to an unnamed Upper Jurassic sedimentary unit. Haggart (1989) gave details of the lithologies and facies present in these beds, and in Valanginian-Hauterivian Longarm Formation outcrops situated nearby, on the coast of Graham Island. Based on stratigraphic evidence, Haggart (1989) tentatively correlated the Tithonian strata with the Longarm Formation rather than with an independent cycle of deposition. Both sections contain markedly sim-

ilar rocks: abundant conglomerate interbedded with coarse- to medium-grained sandstone. Haggart (1989) suggested that the Tithonian section might represent the earliest phase of deposition in the area, equivalent to the unfossiliferous lower part of the onshore section. However, no exposures of Berriasian strata have yet been identified in the area, and none are known anywhere in the Queen Charlotte Islands, and it is questionable whether a correlation of the Tithonian section with the Longarm Formation purely on lithological grounds is fully appropriate. Still, the marked similarity of this section to the Graham Island exposures likely indicates that the former represents the earliest phase of Longarm deposition in the Queen Charlotte Islands. For this reason, the Longarm Formation in the Queen Charlotte Islands is tentatively considered to include rocks as old as Tithonian.

**Longarm volcanics?** Much of the Longarm Formation is intruded by extensive dykes and sills, and Sutherland Brown (1968) suggested that minor amounts of volcanic rocks occur in the formation. However, no Longarm volcanic rocks have yet been identified, except for possible occurrences in Sewell Inlet and on northern Lyell Island. The Sewell Inlet exposure consists of boulder and cobble conglomerate grading upwards into cross-stratified sandstone and siltstone. Although no definite volcanic interbeds occur, the sandstones have a highly tuffaceous aspect, suggesting close proximity to a volcanic source. Improved fossil control is needed to ascertain whether these rocks belong to the Longarm Formation or Yakoun Group.

The outcrops on northern Lyell Island were previously mapped as Longarm Formation by Sutherland Brown (1968), but this assignment was questioned by Cameron and Hamilton (1988). They submitted that the lithologic composition of these rocks suggests they are locally derived from the Middle Jurassic Richardson Bay Formation and, in the absence of fossil control, a correlation with the Middle Jurassic strata was preferred.

The beds which crop out on northern Lyell Island are found in two closely associated stratigraphic sections. At the top of one of these sections, extensive andesites and andesite flow breccias occur. No volcanic rocks are noted in stratigraphic continuity with the sedimentary rocks in the second section. Ammonites found there are of Middle Jurassic age (H.W. Tipper, pers. comm., 1989) and, as this section includes strata of similar but not identical lithology to the section lacking ammonite control, the correlation of both sections with the Middle Jurassic, as made by Cameron and Hamilton (1988), is highly suggestive. In any event, should any of these sections ultimately prove assignable to the Longarm Formation, the total occurrence of Lower Cretaceous volcanic rocks present in the Queen Charlotte Islands will still be of relatively minor extent. The evidence for the existence of Longarm volcanics is considered unreliable and very circumstantial at this time.

### Unnamed Upper Cretaceous shales

A new Upper Cretaceous shale unit was recently recognized by Haggart and Higgs (1989) in the vicinity of western Skidegate Inlet.

**Lithology.** The unit is composed of bioturbated, brittle, dark grey shale with abundant calcareous concretions up to 30 cm in diameter. Rare, very thin (less than 3 cm), fine-grained sandstone beds are found at some localities and sandstone dykes intrude the shales. Fossils are preserved both singly in the matrix, in which case they disaggregate and are preserved poorly, or in the calcareous concretions, where they are preserved well.

**Thickness.** As the unnamed shale unit is known only from isolated exposures, with no top or base yet identified, its total thickness is unknown. At least 30 m of continuously exposed strata were noted at one locality (Haggart and Higgs, 1989), but it is quite likely that this is only a fraction of the total thickness.

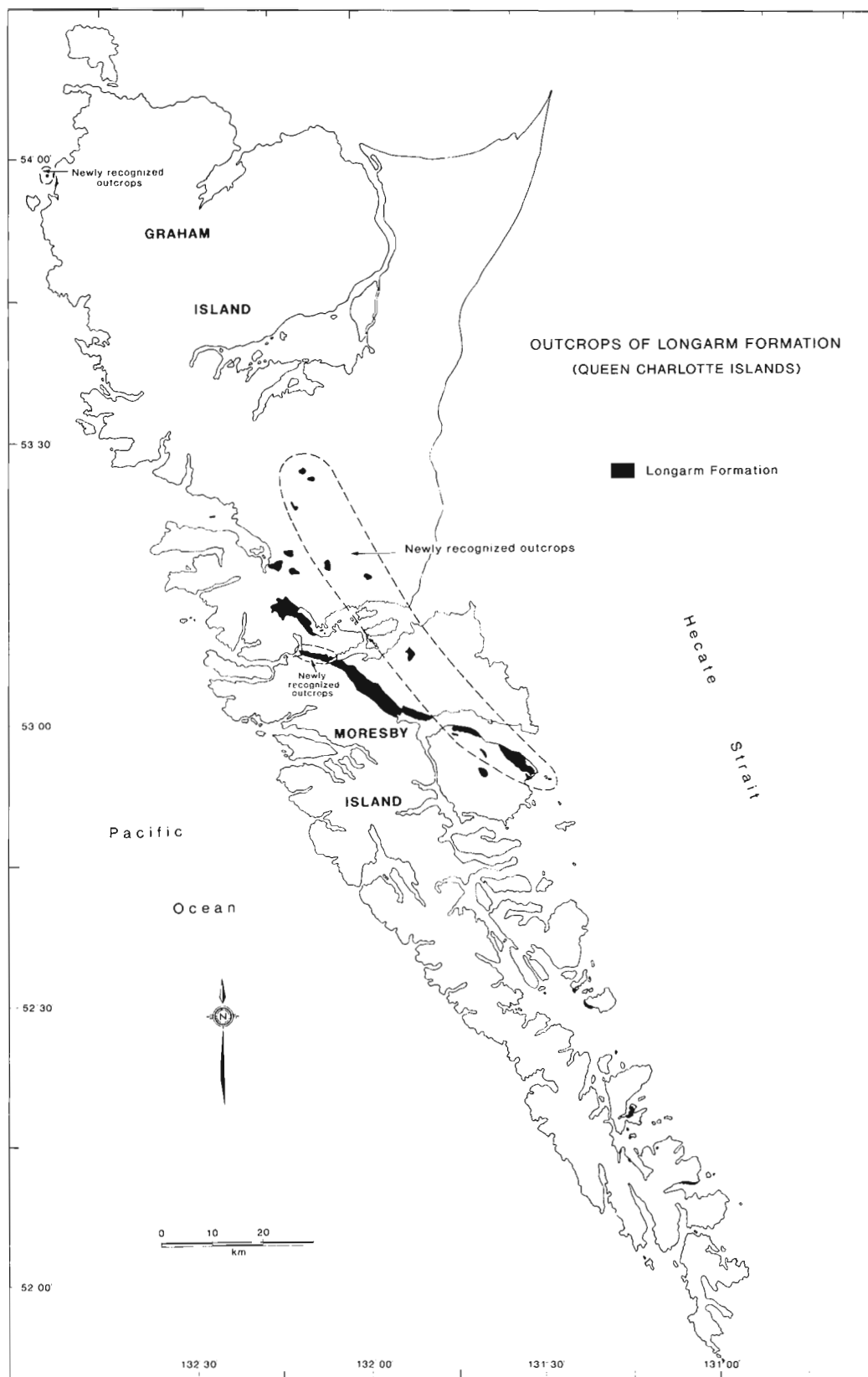


**Figure 5:** Distribution of Longarm Formation outcrop in the Queen Charlotte Islands. Data sources as for Figure 3.

**Depositional environment.** The diverse molluscan assemblages present in the unnamed shale unit, the undamaged nature of the fossils in the concretions, and the lack of a sand component in most outcrops, led Haggart and Higgs (1989) to suggest that this shale unit was deposited in an outer-shelf setting.

**Distribution.** To date, the unnamed shale unit has been recognized only in the Slatechuck Mountain area of western Skidegate Inlet (Fig. 6). However, the shales overlying, apparently conformably, the Honna Formation conglomerates on Langara Island and in Pillar Bay, on the north coast of Graham Island, may be correlative with this unit. Isolated outcrops of shale in the valley bottoms east of Yakoun Lake contain foraminifers of possible Campanian-Maastrichtian age (unpublished Bujak Davies Group fossil report, 1989), and may also be correlative.

**Age.** Ammonites and bivalves collected from the shale unit indicate a Late Santonian to Early Campanian age for several localities (Haggart and Higgs, 1989). Microfossils recovered from the topographically highest exposed shales in the area of these mollusc collections indicate that those beds are of Late Cretaceous age, possibly Campanian to Maastrichtian (unpublished Bujak Davies Group fossil report, 1989). Thus, the unit includes rocks of Santonian, Campanian, and possibly Maastrichtian age, spanning much of the latest Cretaceous.

### Cretaceous volcanics

Prior to the 1988 field season, evidence for onshore volcanic deposits of Late Cretaceous age was lacking in the Queen Charlotte Islands. Haggart et al. (1989) reported a volcanic succession found in the western Skidegate Inlet area, which is interstratified with the Honna Formation. A detailed description of the age, composition, and stratigraphic setting of this volcanic succession is presently being prepared.

**Lithology.** The description of the volcanic rocks was provided by Haggart et al. (1989). The succession consists of intermediate volcanic debris flows, massive flows, and scoria. Euhedral plagioclase and lesser pyroxene phenocrysts are common. The base of the volcanic succession at Gust Island in Long Inlet consists of a series of poorly sorted debris flows interstratified with sandstone and conglomerate of the upper Honna Formation. Within the volcanic unit these interstratified deposits are quickly succeeded by flows, which are in turn overlain by scoriaceous deposits and, near the top of the section, by massive subaerial flows.

**Thickness and distribution.** The volcanic unit reaches a maximum thickness of 700-800 m in the vicinity of Josette Point, just north of Gust Island. Laterally, however, the unit appears to thin dramatically; the extremely limited areal distribution of the volcanic rocks in the Skidegate Inlet area (Fig. 6) implies a rapid pinching-out of the unit.

**Depositional environment.** The base of the volcanic succession is interstratified with Honna Formation clastics. The Honna deposits are interpreted as having accumulated in a relatively deep-water basin which rapidly shallowed due to progradation of fan complexes into the basin (Haggart et al., 1989). Further shallowing is indicated by the accumulation, at the top of the volcanic succession, of subaerial flows and scoria.

**Age.** The age of the volcanics is poorly constrained. The only definite evidence is their interstratification with the Honna Formation rocks on Gust Island. Unfortunately, the numerous foraminiferal and palynological collections made from these Honna rocks have proved barren. Fossil data from other localities, however, indicate that the Honna Formation ranges in age from possible Turonian through Coniacian (Haggart, 1986c, 1987). As the volcanic rocks in Long Inlet occur near the top of the Honna Formation, a Coniacian to Santonian age is suspected.

## STRATIGRAPHIC SYNTHESIS

### Depositional model

The numerous recent investigations of the Cretaceous sequence of the Queen Charlotte Islands, conducted as a part of the Geological Survey of Canada's QCI FGP, coupled with improved biostratigraphic control for important parts of the section, have now allowed for the compilation of an integrated model of Cretaceous deposition in the islands. The model is based on the interpretation that the Cretaceous stratigraphic units of the islands were deposited in response to marine transgression. Two units, the Haida and Skidegate formations, with their relatively well-described outcrop sedimentology and good biostratigraphic control, provide a readily studied system. It is appropriate to examine this depositional system first; extrapolation to the rest of the Cretaceous sequence then naturally follows.

#### *The Haida/Skidegate depositional system*

The age relationships and facies associations of the Haida and Skidegate formations indicate that they are temporally equivalent (Haggart, 1986c, 1987). Their component parts represent different environments within a single depositional system which existed during late Early Cretaceous to early Late Cretaceous time. If a time line representing the late Albian-early Cenomanian is drawn through the stratigraphic sections in the central part of the islands, it is readily seen that the three major components of the system, the Haida Sandstone member, the Haida Shale member, and the Skidegate Formation, form a continuum of coexisting depositional environments. Shallow-marine littoral deposits of the Haida Sandstone member on the east are transitional westward to deeper-shelf deposits of the Haida Shale member. The Shale member is transitional, in turn, to the outer-shelf and slope deposits of the Skidegate Formation (Haggart, 1986c, 1987; Haggart et al., 1989). These relationships are summarized schematically in Figure 7.

Of course, the complex topography of the shelf, presumably established by block faulting, would dictate that a simple gradational continuum between all three units, one perpendicular to the shoreline, was the exception rather than the rule. Locally, the Haida Shale member and the Skidegate Formation may reflect laterally equivalent deposits that accumulated parallel to the shoreline.

On a regional scale, however, the interpretation of an east-west continuum of depositional environments is generally supported by the position and orientation of regionally mappable outcrop belts. The Haida Sandstone belt is the most easterly one observed. The Haida Shale outcrop belt occurs in the central portion of the basin, indicating that the basin deepened to the west. In general, the Skidegate Formation occurs even farther westward, possibly reflecting a shelf/slope break in the deepest part of the basin. As well, the interpretation of the basin as deepening to the west is consistent with the easterly provenance determined for Queen Charlotte Group sediments (Yagishita, 1985; Higgs, 1988; Gamba et al., 1990).

#### *What is the Longarm Formation?*

At first glance, the interpretation of the Longarm depositional system is less straightforward than that for the overlying Haida and Skidegate formations. Because of the structural disruption of many Longarm outcrops, the relatively poor biostratigraphic control, and the *a priori* belief that the formation accumulated in a narrow, restricted trough related to terrane accretion (Yorath and Chase, 1981), the true nature and extent of the formation was interpreted incorrectly in earlier models. In spite of the lesser quality of the faunal control, however, it is now clear that the Longarm Formation, like the overlying Haida Formation, represents a fining-upward succession which accumulated in response to a relative sea level rise. The basal part of the Longarm Formation, the conglomerate and sandstone sequence,

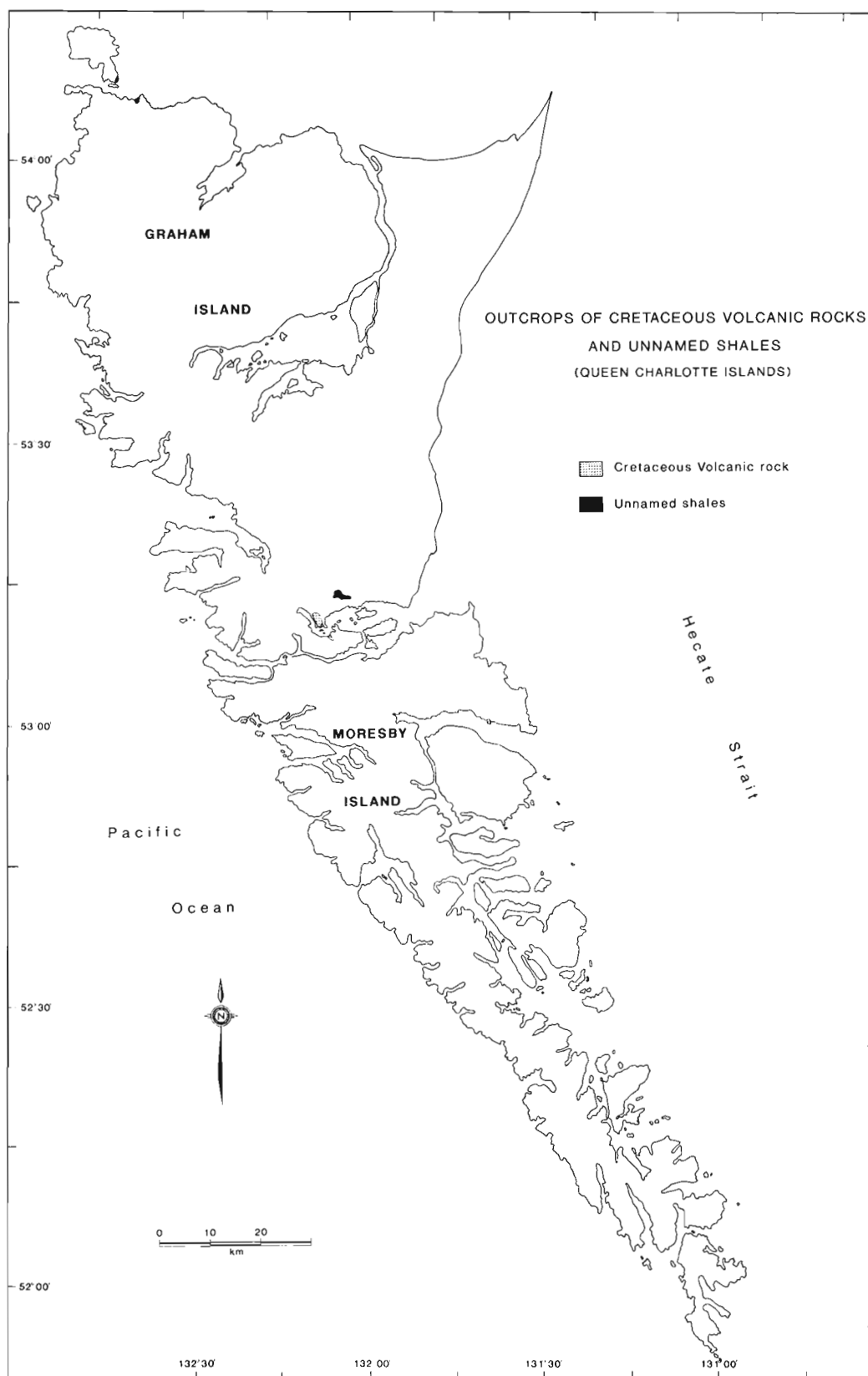


**Figure 6:** Distribution of outcrop of Santonian-Campanian shale succession and Late Cretaceous volcanic rocks in the Queen Charlotte Islands. Data from Haggart and Higgs (1989) and Haggart et al. (1989).

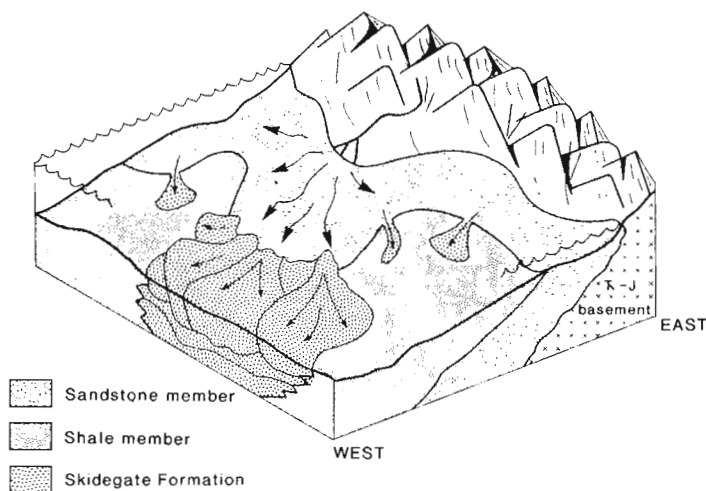


**Figure 7:** Paleoenvironmental relationship of Sandstone and Shale members of the Haida Formation and the Skidegate Formation. The Sandstone member reflects nearshore deposition strongly influenced by storm events. The Shale member is a more offshore, deeper-water equivalent of the Sandstone member. The Skidegate Formation is a deep-water facies associated with sediment distributary systems. Locally, the Skidegate Formation occurs westward of the Shale member deposits and may represent the deepest waters in the basin.

grades upward into shales. Thus, the deepest-water environments represented in the formation occur at its top.

Although a time line cannot yet be drawn through various sections of the Longarm Formation to show equivalence of the component facies belts, eastward-stepping onlap can be demonstrated (see below). As with Haida/Skidegate deposition, the deeper part of the Longarm basin was also located to the west. Also like the Haida Formation, an easterly, shallow-marine sandstone belt in the east coexisted with a deeper-marine shale belt in the west.

#### *A continuous Cretaceous depositional system*

The identification of Aptian beds in Cumshewa Inlet, linking the Longarm Formation below with the Haida Formation above, is of considerable significance. This discovery indicates that no regional hiatus exists between the two formations, and deposition in the basin was continuous through the Early Cretaceous and the early part of the Late Cretaceous. The transgressive event which produced the Haida Formation, with its Sandstone and Shale members, had also produced the Longarm Formation, with its basal sandstone and conglomerate and upper shale beds. Accumulation of the Longarm and Haida portions of the Cretaceous succession resulted from a continuous transgressive episode and the Longarm Formation exposures, located on the west side of the outcrop belt, represent the earliest deposition (Tithonian-Valanginian). By Albian time, shallow-marine deposition had migrated eastward, to the vicinity of the Haida Sandstone member outcrop belt.

Study of stratigraphic sections in the Cumshewa Inlet area helps interpret the nature of the Cretaceous transgression (Fig. 8). The western end of the inlet is characterized by outcrops of the shales of the Longarm Formation, which are deeper-water deposits containing only poorly-preserved belemnites. The first exposure of basal Longarm Formation rocks occurs about 2.2 km east of Aero townsite, where the formation unconformably overlies the Lower Jurassic Sandilands Formation. The age of the oldest Cretaceous rocks identified in this section is Hauterivian, and the section continues into the Aptian (sections B and A of Haggart, 1989; Fig. 7). At the west end of Dawson Cove, basal Longarm strata are in fault contact with another exposure of the Sandilands Formation, and the age of oldest Cretaceous fossils is Barremian. The overlying section is semi-continuous along the north shore of Dawson Cove into the lower Albian strata of the Haida Formation (Section A of Haggart, 1986; Fig. 2).

Moving east, the next exposure with a basal Cretaceous contact is on the triangular peninsula 1 km west of Conglomerate Point (Fig. 8). At this locality, beds with the bivalve *Quoiechia* are noted, of probable Barremian to Aptian age. The easternmost locality where a basal Cretaceous contact is preserved occurs east of McLellan Island, where basal Haida strata apparently onlap Yakoun Group rocks. No fossils have been found in this exposure, but beds nearby, just north-east of McLellan Island (Section G of Haggart, 1986; Fig. 2), are of Middle Albian age. The age of onlap of Cretaceous strata in Cumshewa Inlet thus young eastward. The total thickness of Cretaceous sandstones present at various localities is approximately constant, regardless of their age. The resultant Cretaceous outcrop pattern preserved from this eastward-directed transgressive system is a series of time-transgressive facies belts. Moving west from the easternmost exposures seen today (the youngest Cretaceous, Haida beds), one encounters progressively older basal sandstones.

The same relationship appears to exist for the accompanying shale belt, although faunal control is much more sparse. For example, no good shale sections with Albian fossils have yet been identified, although pre-Albian shales are known from western Cumshewa Inlet and the west end of Yakoun Lake. This relative scarcity of older shale sections is attributed to three factors: 1) the shales are not as well exposed as the sandstones; 2) the shales are more sparsely fossiliferous and many exposures have not yet been precisely identified as to their age; and 3) the shales are predicted to reach their greatest extent in the western part of the basin, and this is the region which has experienced a high degree of structural deformation (Thompson, 1988; Thompson and Thorkelson, 1989).

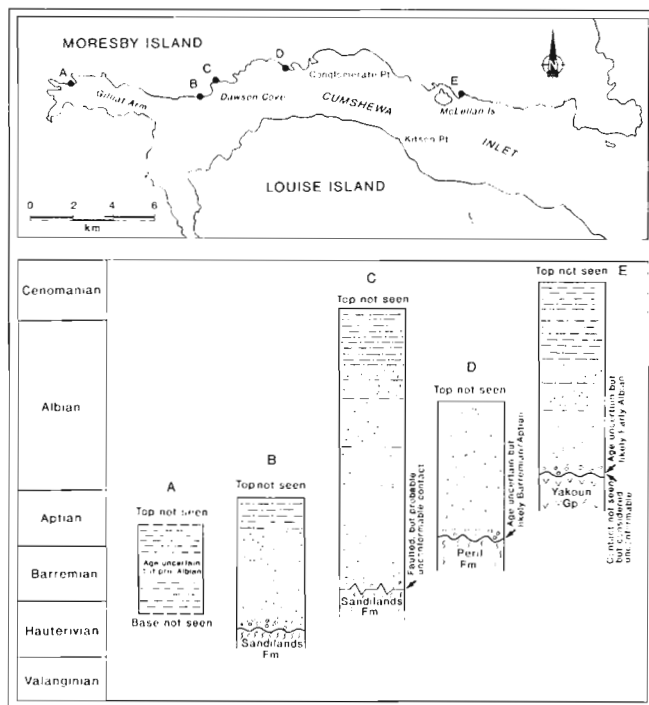


**Figure 8:** Cretaceous stratigraphic sections in Cumshewa Inlet. Section thicknesses not to scale. Note eastward younging of base of Cretaceous section.

### Basin history

Several syntheses of Cretaceous depositional history in the Queen Charlotte Islands have been undertaken, and other studies have served to detail events during specific periods of Cretaceous time. The most comprehensive effort to elucidate the geological history of the islands and the adjacent offshore basin has been that of Yorath and Chase (1981); aspects of their model have been utilized and expanded upon by other workers (Yorath and Hyndman, 1983; Yorath, 1987). Concomitant with the overall basin-evolution studies has been a series of shorter contributions dealing with specific aspects of Cretaceous deposition in the islands. Some of this work has already been discussed.

Central to the model proposed by Yorath and Chase (1981) is the concept that the Cretaceous succession in the Queen Charlotte Islands is fundamentally related to terrane accretion, specifically to the amalgamation of Wrangellia and the Alexander Terrane. In this model, the Lower Cretaceous Longarm Formation is interpreted as a "suture assemblage", derived directly from the suturing of the two terranes and deposited in a deep trough (Sutherland Brown, 1968) which supposedly traversed the area approximately parallel to the trend of the suture.

Overlying the "suture assemblage", according to Yorath and Chase (1981), is the "post-suture assemblage", represented by the mid- to Upper Cretaceous Queen Charlotte Group. Yorath and Chase (1981) inferred that the Queen Charlotte Group rests with a pronounced angular unconformity upon all older units, including the Longarm Formation, even though a direct contact of the Longarm Formation with the younger rocks had not been observed by these authors. The post-suture assemblage was subsequently deposited over the terrane suture and represents stable, low-energy deposition during a time of tectonic quiescence (Yorath and Chase, 1981).

Based on new geological observations, I believe that fundamental flaws exist in this model of Cretaceous basin history. In the following sections, I will attempt to explain why the earlier model must be revised. The first step will be an assessment of Cretaceous basinal history as it is now understood.

#### *Tithonian to Early Turonian*

Deposition in the basin was initiated in the latest Jurassic (Tithonian), when transgression in the northwest coast of Graham Island region resulted in accumulation of the oldest deposits of the Longarm Formation (Fig. 9). Cretaceous rocks are preserved in several sections in the area, although actual Tithonian rocks are known only at one locality (Haggart, 1989). Deposition continued through the earliest Cretaceous and, by the Late Valanginian, a deeper-marine environment was well established (Haggart, 1989).

Late Valanginian transgressive deposits are known also from the western Skidegate Inlet region (Jeletzky in Sutherland Brown, 1968), forming the most westerly Cretaceous deposits in this part of the Queen Charlotte Islands. The continual eastward transgression resulted in the gradual onlap of basin fill on basement rocks. In Cumsheewa Inlet, the onlap appears to have initiated in Hauterivian time; in the Carpenter Bay region, onlap may have initiated as late as Barremian, although the base of this section is not exposed.

The transgression continued into the Turonian, producing an eastward-onlapping strandline and resulting in a gradual deepening of marine environments in the western part of the basin, until that area was receiving mostly fine-grained detritus, probably at outer-shelf depths. The deeper marine shale subbasin which thus developed in the western part of the basin persisted for much of Early and early Late Cretaceous time. The earliest phase of this, deeper-water de-

position, is represented by the accumulation of the fine clastics at the top of the Longarm Formation, of approximately Barremian to Aptian age. Shale accumulation continued into the Late Cretaceous, with the deposition of the Shale member of the Haida Formation. In the westernmost parts of the shale subbasin, the Skidegate Formation developed at the time of maximum flooding, in the Cenomanian-Turonian.

This stable shale subbasin is one of the major components of the Cretaceous depositional system and it appears to have been mostly open to the ocean on the west during its existence. The Tithonian to Early Turonian stratigraphic succession of the Queen Charlotte Islands, deposited in a tectonically quiescent regime in response to gradually rising sea level, forms the first major stratigraphic package of the Cretaceous sequence.

#### *Early Turonian to Maastrichtian*

Deposition of the stratigraphic package just described was terminated abruptly sometime after the Early Turonian with the progradation of the fan complexes of the Honna Formation. The fans were sourced in the east (Yagishita, 1985; Higgs, 1988; Gamba et al., 1990). Coincident with fan progradation in the western Skidegate Inlet area, localized igneous activity produced a thick sequence of volcanic strata (the Late Cretaceous unnamed volcanics described above) which rapidly built up to subaerial exposure. This centre of volcanism may have developed along a zone of prior structural deformation (Haggart et al., 1989).

The fan complexes must have traversed the basin rapidly, because, by Santonian time, they were beginning to fine upward into the subsequent shale succession. This return to shale deposition following the Honna event is evidenced by the thick accumulation of shales overlying the Honna Formation in Pillar Bay and on Langara Island, at the northern end of the Queen Charlotte Islands, as well as by the thick, unnamed shale succession seen in the Skidegate Inlet area. Little data exists to help interpret the paleogeography associated with the Late Cretaceous volcanic accumulation. However, as evidenced by its proximity to the outcrop of the unnamed shales on Slatechuck Mountain, the region appears likely to have also been inundated by marine transgression by the late Santonian to early Campanian.

The cycle of deposition represented by the Honna Formation and the overlying shales is the second major Cretaceous stratigraphic package of the Queen Charlotte Islands. The age of termination of shale deposition is poorly constrained. The youngest shales found to date are of possible Campanian-Maastrichtian age (unpublished Bujak Davies Group fossil report, 1989) and show no evidence of shoaling. Certainly, an end to deposition must have occurred shortly after this time, because Lewis (1990) has documented an unconformity separating Cretaceous strata from Paleogene nonmarine rocks in western Skidegate Inlet.

The depositional model detailed above differs significantly from previously formulated hypotheses, in that it now appears that tectonic quiescence persisted through most of Cretaceous time. Volcanic activity was at a low, with only one local event recorded, in the Late Cretaceous. Fault activity appears to have been of small-scale and of localized extent. On a regional scale, Cretaceous deposition was continuous and essentially homogeneous throughout the Queen Charlotte Islands, with an eastward-migrating shoreline and a deeper shale basin probably open to the west. There is no reason to interpret the various parts of the succession as "suture" and "post-suture" assemblages, and stratigraphic evidence for the existence of a terrane boundary in the islands is lacking.



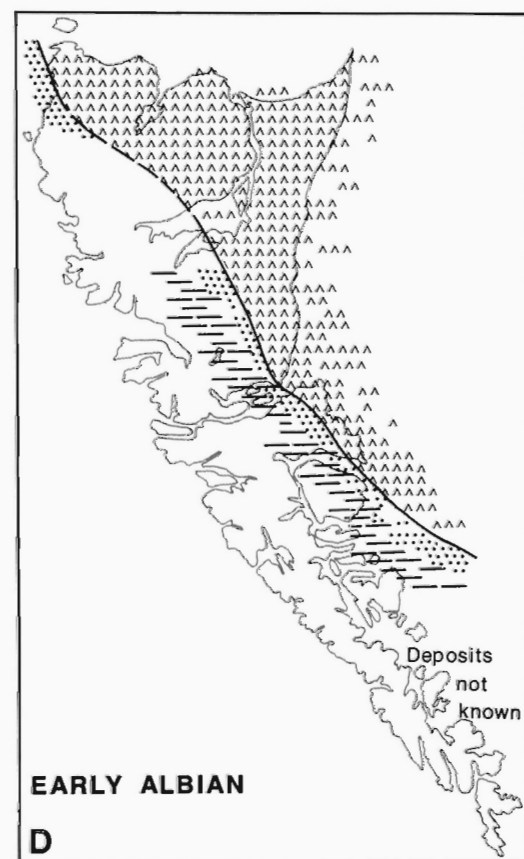
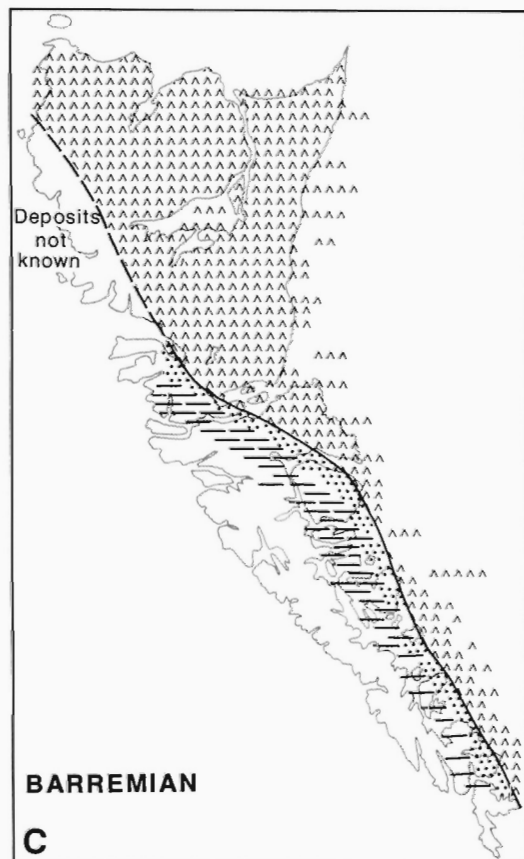
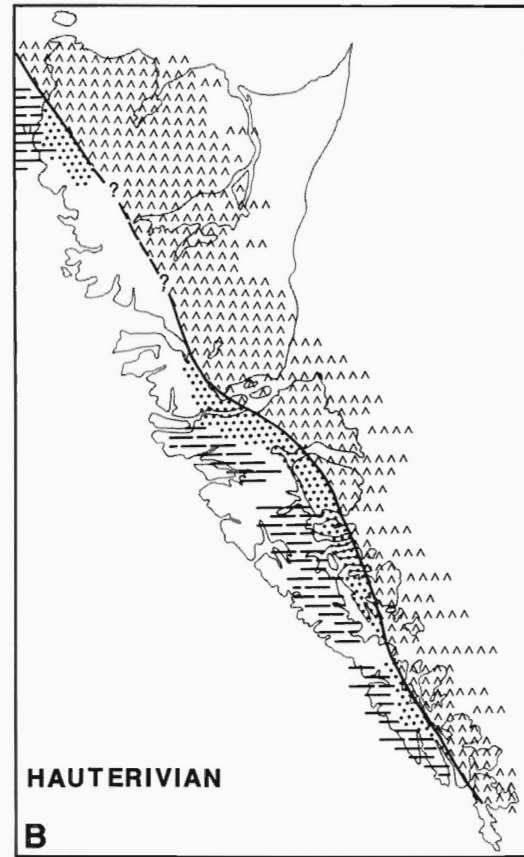
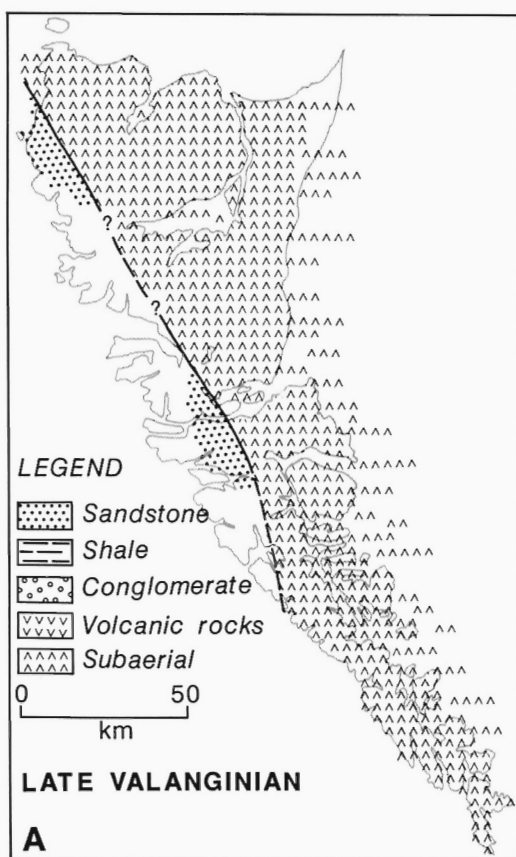
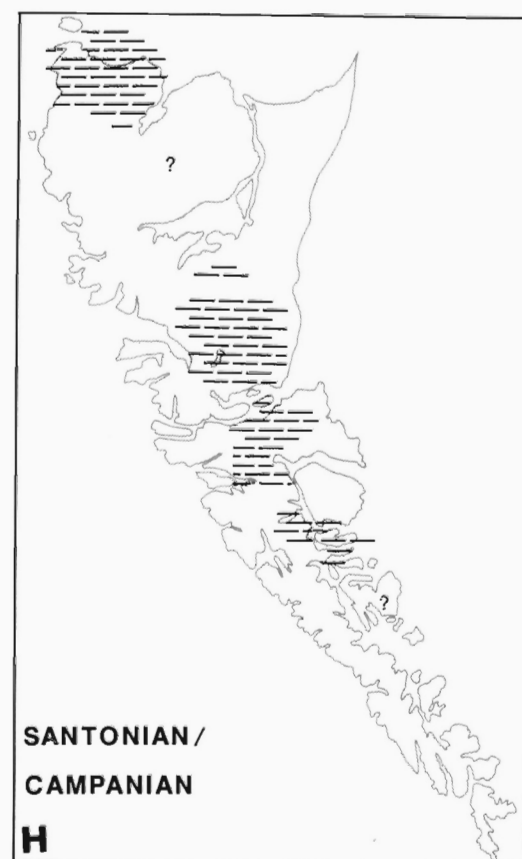
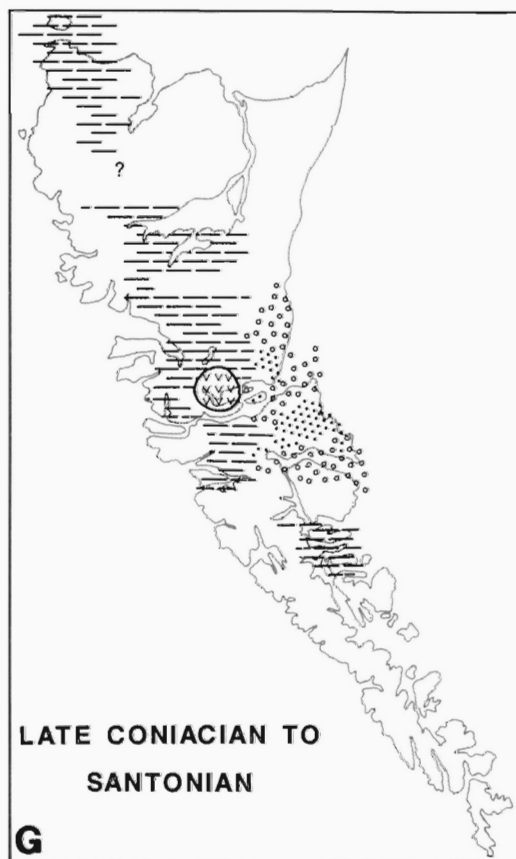
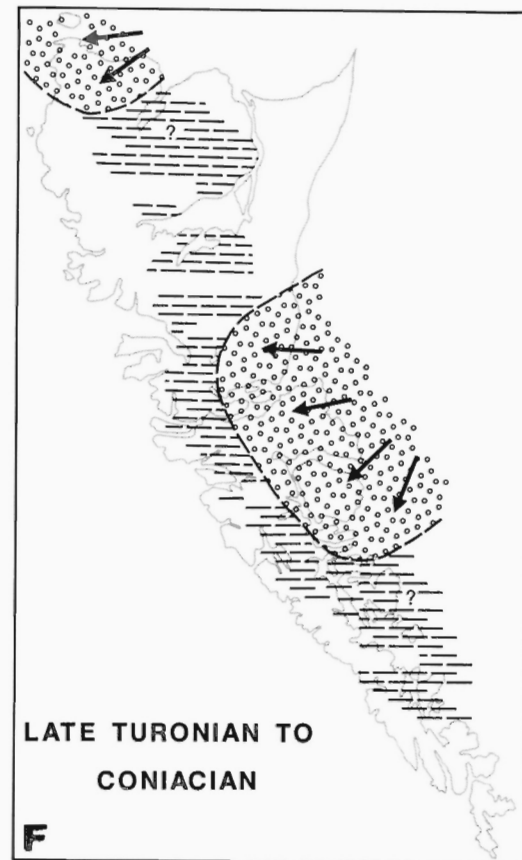
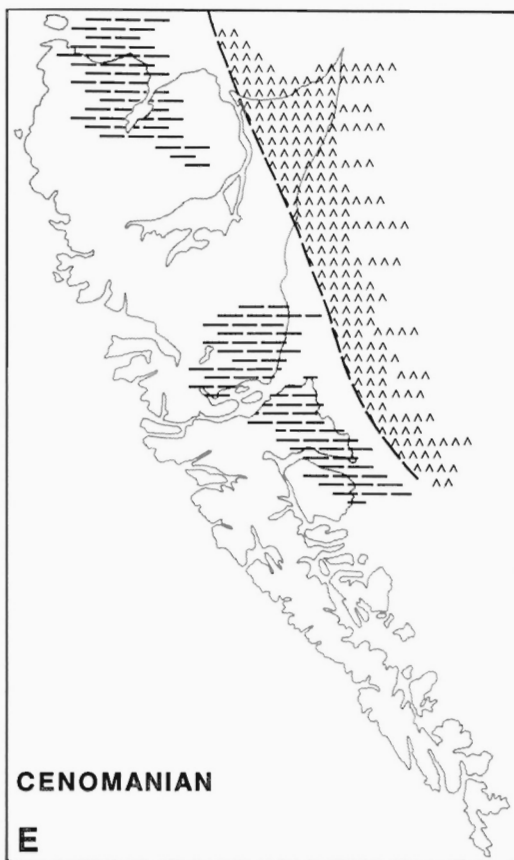


**Figure 9:** Valanginian through Early Campanian depositional history, Queen Charlotte Islands.



## CRETACEOUS PALEOGEOGRAPHY

### Migrating Cretaceous strandlines

Examination of Figure 8 shows that shallow marine facies of the basal Cretaceous transgressive sequence can be traced across Cumshewa Inlet, stepping eastward at progressively younger times. Thus, the strandline must have been migrating eastward as well. One can approximately locate the strand on a map for a particular instant of geologic time, and it is possible to locate the approximate position of the Hauterivian, Barremian, Aptian, and Middle Albian strands in Cumshewa Inlet. Similarly, basal transgressive outcrops can be recognized in the Skidegate Inlet region, and Late Valanginian, probable Aptian, and Early Albian strands have been identified there as well.

Using this technique, a series of strandlines, migrating eastward across the central Queen Charlotte Islands, can be established (Fig. 10). The strandline is an important paleogeographic feature as it delimits the land/sea interface at a particular time. Areas landward of the strand were topographic landmasses, shedding detritus, while areas basinward from the strand were receiving the sediments.

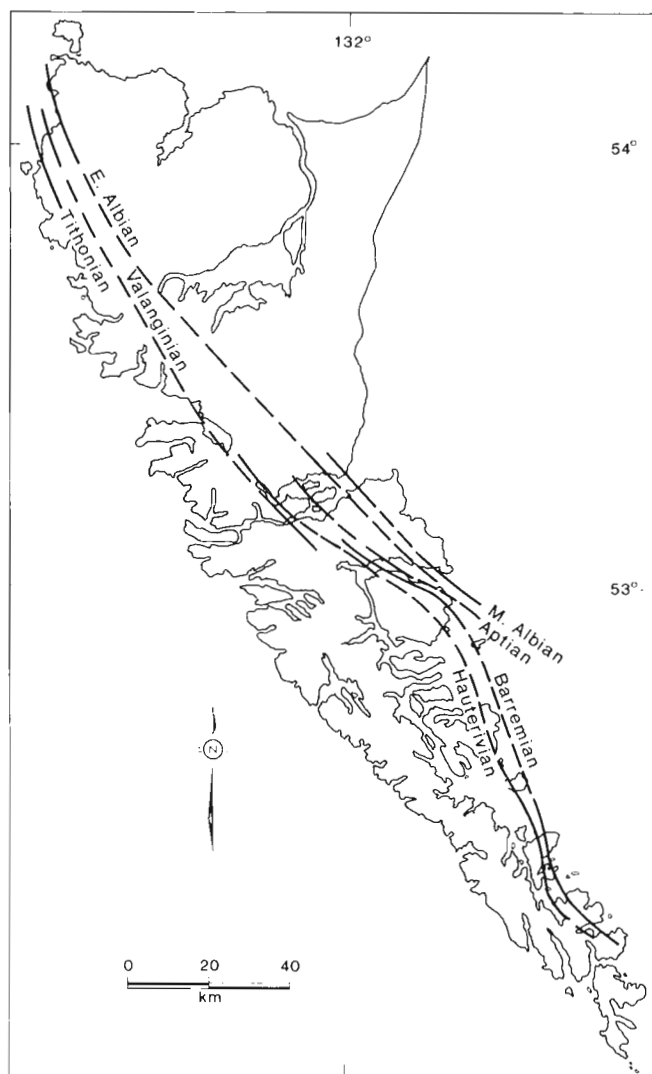


**Figure 10:** Approximate position of the strandline at various times during the Cretaceous, Queen Charlotte Islands. Solid lines indicate good faunal control, dashed lines reflect no faunal control, thus inferred trend.

Referring to the geologic map of the Cumshewa Inlet region prepared for the QC'1 FGP report (Thompson, 1990), one can see that the outcrop belt of sandstone of Hauterivian/Barremian age passes down the length of the inlet, from the vicinity of Dawson Cove across to, and along the north shore of, Louise Island. Albian-age sandstone does not crop out south of this line. This suggests that transgression was likely directed to the northeast in this region, toward Cumshewa Inlet's north shore. Thus, one would not expect any Albian or younger sandstone south of Cumshewa Inlet.

It is interesting to note that the Cretaceous shoreline trends are approximately parallel to the regional structural trends noted by other workers (i.e., Rennell Sound fault zone, Sandspit Fault, and Louscoone Inlet Fault of Sutherland Brown, 1968). Thompson et al. (1991) have shown that some of these structural trends are related to older Mesozoic structures. Thus, prior block fault topography may have influenced the location of Cretaceous deposition. It is tempting to suggest that the eastward limit of Albian deposition in the Cumshewa Inlet region may have been an active scarp formed along the Copper Creek Fault of Thompson (1990).

Eastward-directed transgression in the Queen Charlotte Islands appears to mirror the Cretaceous transgressive history of northern California/southern Oregon. In that region, deposition resultant from transgression commenced in Valanginian time and continued through the Turonian (Jones and Irwin, 1971; Ingersoll, 1979; Sliter et al., 1984). A progradational event in Turonian/Coniacian time marks an interruption of transgression, but inundation was subsequently renewed in the Santonian (Haggart, 1986a). It is tempting to suggest that analogous transgressive depositional regimes may have been in place at what are today, widely separated locations on the Pacific margin.

### The shelf

Most of the Cretaceous strata in the Queen Charlotte Islands were deposited at shelf depths. The maximum width of the shelf was probably achieved at the time of maximum flooding, in the Early Turonian, prior to Honna fan progradation. At this time, the shelf was at least 18 km wide. The actual width may have been much greater because the Early Turonian strand was evidently located some distance east of the islands: the only Early Turonian age-strata known from the eastern outcrop belt are the Haida Shale member.

The estimation of shelf width is dependent on the interpreted location of the shelf/slope boundary. In contrast to locating strandlines, the identification of this boundary is more subjective. For the purposes of this paper, the shelf/slope break is arbitrarily assumed to be approximately coincident with the transition of the Haida Shale member into the Skidegate Formation. Locally, as at Sewell Inlet, this transition zone occurs over a wide area and is poorly constrained by fossil control.

### Honna Channel complexes

The Honna Formation is not a widespread, blanket unit. Rather, it thickens and thins dramatically in its outcrop belt trending across the northern half of the Queen Charlotte Islands. Regional thickness variations of the formation may reflect the location of Honna fan complexes. Presumably, the greatest thickness of fan deposits will occur in the vicinity of the fan channel, with areas lateral to the channel system receiving a lesser amount of sediment. Examination of an outcrop-thickness map (Fig. 11) shows two areas with thick Honna accumulations: on the north coast of Graham Island at Pillar Bay and the adjacent Langara Island; and in the central islands between Skidegate and Cumshewa inlets.

In the latter of these two centres, on northern Moresby Island and southernmost Graham Island, considerable thicknesses of Honna

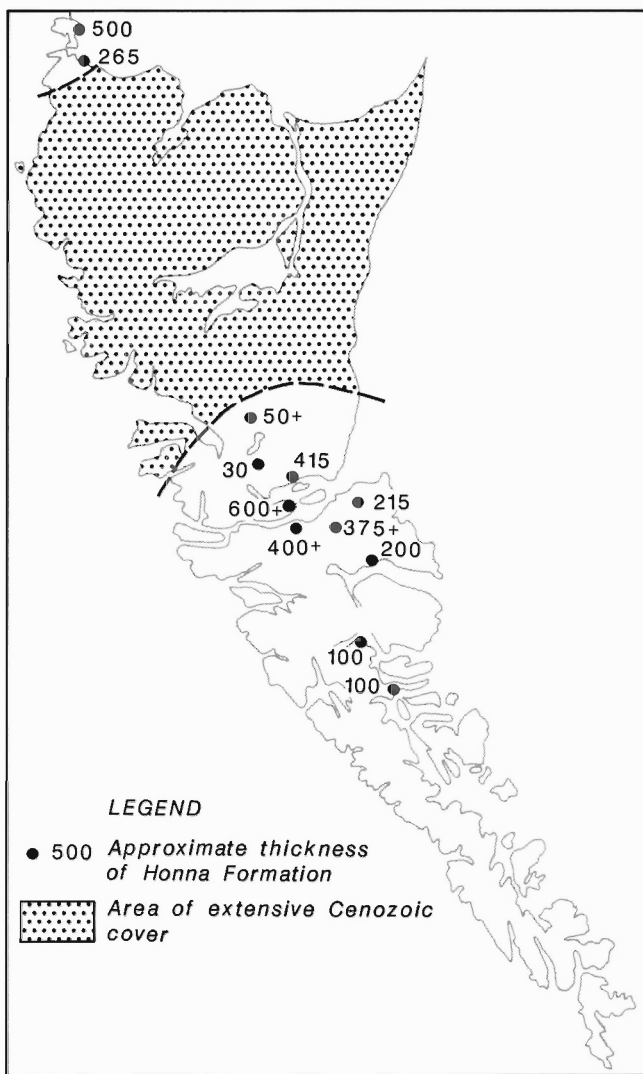


**Figure 11:** Map showing approximate thickness of Honna Formation outcrops (in metres). Two main depocentres are defined: the central islands region, in the vicinity of Skidegate and Cumshewa inlets; and northwestern Graham Island and nearby Langara Island. Paleocurrent data for these regions (Higgs, 1988, 1990, 1991a; Gamba et al., 1990) indicate a general westerly direction of transport. Lateral to these depocentres, the Honna Formation thins dramatically. Depocentres are considered to represent two major fan complexes which prograded into the islands region during Turonian-Coniacian time.

rocks are present, significantly greater than at localities to the north and south, at Yakoun Lake and Sewell Inlet, respectively. The thicker sections of Honna Formation strata are composed, in great part, of massive conglomerate and sandstone. The thinner Honna sections to the north and south, in contrast, consist of conglomerate horizons, 3-30 m in thickness, interstratified with shale. The thick accumulations of conglomerate and sandstone may represent the main channel system of the Honna fans, and the thinner packages of conglomerate interbedded with shale to the north and south may reflect lateral interfingering of channel overbank or avulsion deposits with basin shales. Although many different individual channels, and perhaps several fan complexes, are probably represented in the single outcrop region centred on Skidegate Inlet, the total north-south distance from Yakoun Lake to Sewell Inlet suggests that this particular Honna fan complex had an approximate cross-fan width of 50 km.

The Skidegate Formation, also, is irregularly distributed across the islands. The most extensive development of the formation occurs in the western Skidegate Inlet region, and it is closely associated with the thick and extensive Honna Formation deposits described above. Where the Honna Formation is thin, as at Yakoun Lake and Sewell Inlet, the Skidegate Formation lithology is not extensively developed either. These relationships indicate that the same distribution network that transported materials across the shelf to the Skidegate Formation submarine fan complexes was utilized in subsequent deposition of the Honna Formation clastics.

### Cretaceous coal?

Over the last 100 years, considerable interest was directed to the search for exploitable coal deposits in the Queen Charlotte Islands. Sutherland Brown (1968) discussed the stratigraphic occurrences of coal in the islands and chronicled some of the mining ventures. According to Sutherland Brown (1968), Jurassic and Tertiary, and likely Cretaceous, coals are to be found in the islands. This record of Cretaceous coals in the islands has been incorporated in subsequent large-scale compilations of Cretaceous paleogeographic data for North America (e.g. Beeson, 1984).

One of the most interesting coal localities is the Cowgitz site in western Skidegate Inlet. This mine was one of the earliest areas to be surveyed and mined for coal in the Queen Charlotte Islands and was the focus of much of the early geological interest. The early geologists (Richardson, 1873; Dawson, 1880) considered the strata hosting the coals to be Cretaceous because of their geographic proximity to outcrops containing Cretaceous fossils. Thus, the coals were believed to be of Cretaceous age, located at approximately the same stratigraphic level as the Haida Formation of the Queen Charlotte Group.

Occurrence of Cretaceous coals in this part of the basin is of considerable paleogeographic interest. Although occurrences of minor amounts of coal are known from marginal marine facies of basal Cretaceous strata on northern Graham Island (Haggart, 1986c), it is difficult to reconcile the presence of a relatively thick coal deposit with the essentially marine Cretaceous depositional model for the central Queen Charlotte Islands. Thus, Haggart et al. (1989) tentatively proposed that the coal in Skidegate Inlet might represent still another cycle of Late Cretaceous deposition, this one with a substantial nonmarine phase.

An unsuccessful attempt was made to locate the old mine site in 1988. However, coal float obtained from the vicinity was analyzed for pollen content. The age of the flora present in the associated matrix indicates an Early Eocene to Early Oligocene age (J. White, unpublished GSC fossil report JMW-89-2). According to White (1990a), this is the first identification of Paleogene strata in the Queen Charlotte Islands. A second, successful, attempt was made to locate the mine site in 1989. The Paleogene shale unit which hosts the coals can be followed northward, into Slatechuck Creek, where it hosts the Slatechuck Creek argillite quarry, source of the famed Haida carving argillite, also previously considered to be a Cretaceous deposit (Sutherland Brown, 1968). The unit has also been identified in the Yakoun Lake area (Haggart et al., 1990).

Thus, no substantial coal deposits are known in the Cretaceous system of the Queen Charlotte Islands.

### SEDIMENTATION CONTROLS – TECTONICS OR EUSTASY?

The preceding discussion has served to illustrate the importance of relative sea level rise in interpreting the history of Cretaceous deposition in the Queen Charlotte Islands. However, Cretaceous de-

position was not likely related solely to relative sea level fluctuations, and the contributions of other factors should be considered.

## Structural controls

Detailed geological field mapping by members of the QCI FGP has provided a tremendous amount of local data relevant to the analysis of Cretaceous stratigraphy in the Queen Charlotte Islands. Perhaps the most important contribution is the recognition of basement structural control on Cretaceous deposition (Thompson et al., 1991). As discussed earlier in this paper, Thompson et al. (1991) have determined that syndepositional block faulting appears to have played a role in defining local Cretaceous depositional trends.

Other workers have invoked even larger-scale tectonic processes to explain gross aspects of the Cretaceous stratigraphic succession. As noted above, Yorath and Chase (1981) proposed that the Longarm Formation represented a "suture assemblage" resultant from the amalgamation of Wrangellia with the Alexander Terrane. Higgs (1988, 1990, 1991a) has invoked extensive thrust faulting to the east of the islands in Cretaceous time to form a highland which provided the detritus for the locally thick Honna fan sequences. How necessary are these large-scale tectonic factors in explaining the observed Cretaceous succession? I feel the most parsimonious explanation to the question of the major control on Cretaceous sedimentation in the Queen Charlotte Islands lies in sea level rise and fall.

## Sea level rise

I have shown that much of the stratigraphic succession in the Queen Charlotte Islands represents a fining-upward trend caused by a relative sea level rise. Figure 12 shows the relative sea level trends preserved in the Cretaceous section in the islands, as deduced from outcrop stratigraphy.

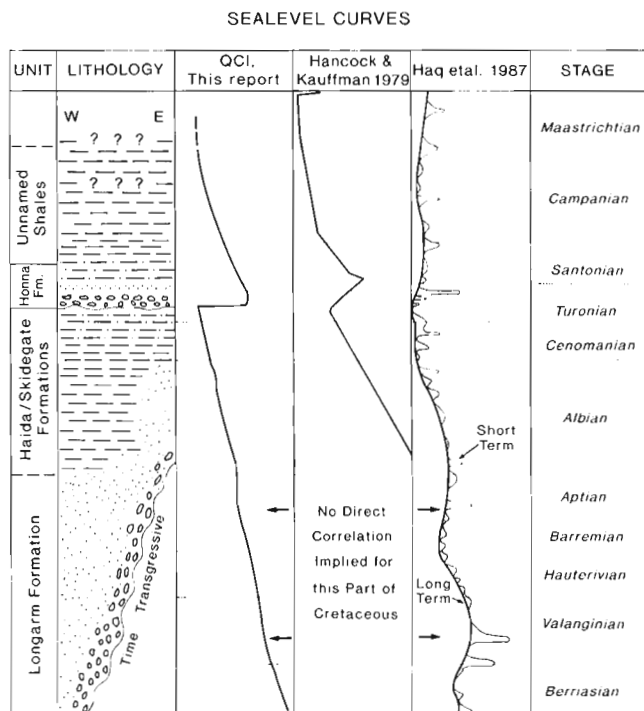


**Figure 12:** Local sea level history for Cretaceous of Queen Charlotte Islands and the Cretaceous eustatic curves of Hancock and Kauffman (1979) and Haq et al. (1987). Stage boundary dates of Hancock and Kauffman equilibrated to those of Haq et al. Base of Hancock and Kauffman curve is set at Early Albian sea level.

## Early to Early Late Cretaceous sea level rise

As shown above, there is no evidence to support the interpretation that the Longarm Formation and overlying Haida Formation were deposited in response to the amalgamation of two tectonostratigraphic terranes. Rather, both units are parts of a continuous stratigraphic sequence, deposited in response to a relative sea level rise during a period of tectonic quiescence. Interestingly, the local sea level trends reflected for the Queen Charlotte Islands in the Longarm/Haida succession (Fig. 12) closely parallel eustatic sea level trends determined by other workers (Hancock and Kauffman, 1979; Haq et al., 1987).

## Turonian-Coniacian sea level drop

Continued transgression through most of the Early Cretaceous and early part of the Late Cretaceous in the Queen Charlotte Basin was disrupted in the later Turonian to Coniacian with the progradation of the coarse Honna clastics. This event has been previously been attributed to the "final assembly of Superterrane II (Wrangellia, Alexander and Taku)" by Cameron and Hamilton (1988: p. 227) or to west-verging thrusting associated with a "west-migrating foreland basin upon the accreting terrane" of Wrangellia-Alexander by Higgs (1988: p. 21-22). Both of these explanations rely heavily on large-scale tectonic processes as the ultimate determinant of Honna deposition.

However, on land evidence for Late Cretaceous tectonism in the Queen Charlotte Islands is sparse. The localized occurrence of intraformational clasts in the uppermost parts of the Haida shale, just beneath the overlying Honna conglomerates, might perhaps be suggested as evidence for the initiation of a tectonic episode. A local change in depositional environments is a more simple and likely explanation, however: intraformational clasts occur within the Shale member at other localities (i.e., McLellan Island, Cumshewa Inlet), well below this stratigraphic level.

The unconformity which has been locally mapped at the base of the Honna Formation might also be equated with a tectonic episode but, as discussed above, the unconformity is only local in extent and can be explained by local erosion of section resultant from lowered base level and, in some cases, reactivation of Late Jurassic block faults. No widespread and unequivocal evidence for Late Cretaceous tectonism presently exists in the islands.

The initiation of Honna fan progradation into the basin corresponds almost exactly, however, with the major eustatic sea level drop in the Turonian and Coniacian which is recognized by numerous workers (Hancock and Kauffman, 1979; Harris et al., 1984; Seiglie and Baker, 1984; Flexer et al., 1986; Haq et al., 1987). A similar progradation event at this time has also been documented for northern California (Haggart, 1986a, b). Most of the Early Cretaceous in the Queen Charlotte Islands, and the earlier part of the Late Cretaceous, some 45 million years of geologic time, was characterized by relative tectonic quiescence and a regime of gradual sediment accumulation in response to a rising sea level. Why should the period beginning in the Turonian be necessarily different? A sea level drop would likely have resulted in an abundance of detrital material prograding into the Queen Charlotte Basin from highlands to the east.

A further complication in Higgs' (1988) tectonic interpretation for the origin of the Honna fan complexes is his assessment of the geometry of the fans themselves. According to Higgs' analysis of lithofacies belts in the Honna Formation, some of the proximal-fan-facies belts span the entire east-west width of the Honna outcrop zone, which exceeds 20 km, and for which no modern analogues exist. Higgs' explanation for this geometry is based on a static model of Honna fan development, with a fan banked against a sediment-shedding scarp to the east. This model seems to ignore Walther's Law, which implies that a significant width of a facies' outcrop belt reflects geographic

migration of the causative environment in time. The wide distribution of the same lithofacies across the region can be explained by a relatively rapid and time-transgressive progradational event, exactly as would be expected in a period of rapid sea level drop.

#### *Santonian-Campanian sea level rise*

Further evidence for sea level control on Cretaceous sedimentation is found in the post-Honna stratigraphic record. Relative sea level rise from the later Coniacian through Campanian in the Queen Charlotte Islands produced the fining-upward sequence in the middle and upper parts of the Honna, with the unnamed shale sequence at the top of the succession marking a return to the higher levels of earlier time. Again, this pattern is mirrored in the eustatic sea level curves (Fig. 12).

Clearly, tectonic factors must have influenced deposition in the Queen Charlotte Islands on a local scale: I have previously noted several examples of small-scale Cretaceous block faulting. However, the dramatic correlation of the Cretaceous sea level curve for the Queen Charlotte Islands with the eustatic curves deduced independently by other workers supports possible eustatic control on regional sedimentation. Certainly, one can argue that tectonic factors may be one driving force, for what produces the eustatic trends? However, complicated large-scale tectonic models do not seem necessary to explain the origin of the relatively simple Cretaceous sequences found on the islands.

### CRETACEOUS IN THE OFFSHORE

Woodsworth (1988) showed that Wrangellian strata likely underlie most, or all, of Hecate Strait. Thus, continuity of Cretaceous strata might be considered likely beneath much of the strait and adjacent Queen Charlotte Sound. Recent seismic surveys have to date failed to define sub-Tertiary stratigraphy and structure in the offshore region, and the sole source of hard data bearing on the presence or absence of Cretaceous strata offshore is the series of exploration boreholes drilled by Shell in the late 1960s (Fig. 13).

#### Offshore well data

##### *Cretaceous sedimentary rocks*

Unfortunately, the extent and distribution of Cretaceous rocks in the subsurface offshore cannot be established because most of the wells were abandoned before reaching the base of the Tertiary section. Numerous workers, including Shouldice (1971, 1973), Stacey (1975), Young (1981), and Leslie (1989), have discussed the well data. Unfortunately, the data are not concisely summarized in a single publication, and there are conflicting interpretations of the stratigraphy encountered.

Cretaceous strata were originally identified in the Tyee N-39 and the Sockeye B-10 and E-66 wells (Shouldice, 1971, 1973). All three of these wells lie north of the Moresby Ridge, which divides the Queen Charlotte Basin into the northern Hecate Subbasin and the southern Charlotte Subbasin (Young, 1981). Audretsch (*in* Higgs, 1991b, p. 341) indicated that some of the original Cretaceous ages were based on very poorly constrained pollen analyses and could perhaps represent reworked assemblages. White (1990b) has re-examined the floral assemblages and concluded that in-place Cretaceous palynomorphs are present in coaly intervals in the Sockeye E-66 and Tyee wells, thus confirming the presence of probable nonmarine strata of Cretaceous age.

Leslie (1989) described the supposed Late Cretaceous-Paleocene sedimentary rocks encountered in the Tyee and Sockeye wells. Leslie also identified the same units in the South Coho I-74 well, from which earlier workers had only reported Miocene strata (*i.e.*, Shouldice, 1973; Stacey, 1975). No new data were provided by Leslie (1989) to

constrain the ages of these units. The sedimentary rocks are sandstone and siltstone of lithic-wacke composition, and they overlie volcanic conglomerates of predominantly basaltic composition (Leslie, 1989). Leslie invoked a Triassic Karmutsen Formation source for the basalt clasts in the conglomerates and suggested that the provenance of all the strata in the wells was the west side of the basin, *i.e.* the Queen Charlotte Islands region. Petrographic data suggest a shallow-marine origin for the sedimentary strata, possibly a fan-delta (Leslie, 1989). Unfortunately, without better constrained age data, correlation of this supposed Late Cretaceous-Paleocene sequence from well to well or with onshore exposures is unlikely to be reliable.

Thus, the only confirmed Cretaceous strata in the offshore are found in the Sockeye E-66 and Tyee wells, and these include probable nonmarine deposits.

##### *Cretaceous volcanic rocks?*

Reported radiometric dates from volcanic rocks in the wells are considered unreliable because of possible contamination and alteration (Young, 1981; C.J. Hickson, pers. comm., 1988). However, Cameron and Hamilton (1988) have suggested that two episodes of Cretaceous volcanic activity may be represented in the drilled successions, an Early Cretaceous event and a latest Cretaceous-Paleocene event.

Young (1981) reported a radiometric age date of  $118 \pm 7$  Ma for volcanics in the Shell Anglo Sockeye E-66 well in Hecate Strait (Fig. 13). These volcanics lie beneath sediments that were originally dated as Paleocene based on palynomorphs but which are now known to include Cretaceous forms (White, 1990b). Cameron and Hamilton (1988) embraced the radiometric date, suggesting that it reflects a period of Early Cretaceous (Barremian-Aptian) volcanism, approximately contemporaneous with the Longarm Formation. Hickson (*in* Haggart et al., 1989) cautioned, however, that this date can only be considered

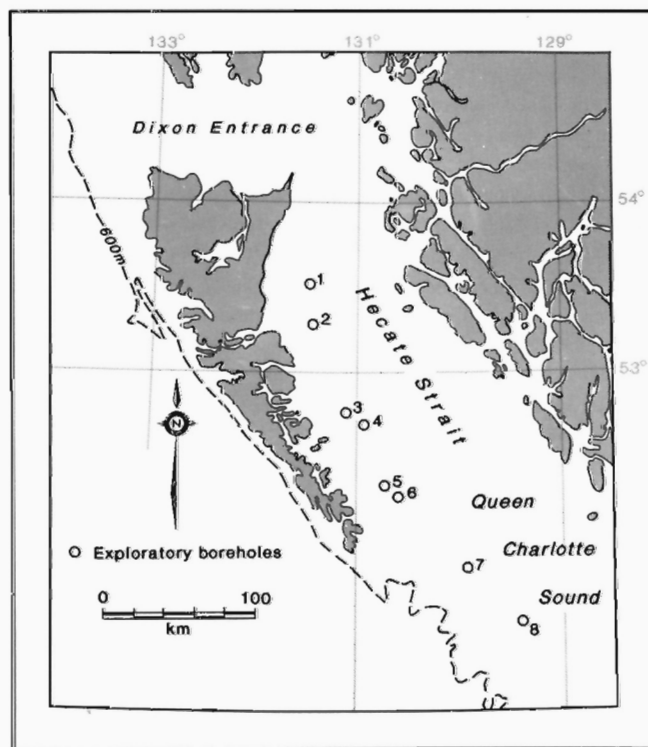


**Figure 13:** Distribution of wells in offshore areas of Queen Charlotte Basin. 1= South Coho; 2= Tyee; 3= Sockeye B-10; 4= Sockeye E-66; 5= Murrelet; 6= Auklet; 7= Harlequin; 8= Osprey.



as tentative because of possible sidewall contamination in the original well cuttings. In any event, no volcanic rocks of this age have been definitely identified onshore.

Young (1981) reported other radiometric dates, of  $72 \pm 6$  and  $84 \pm 10$  Ma, from volcanic rocks in the Sockeye B-10 well (Fig. 13). Because of the potential of contamination, these dates, too, must also be treated as tentative. They are, however, generally Late Cretaceous in age and may thus be correlative with the Coniacian-Santonian unnamed volcanic rocks found in Long Inlet (Haggart et al., 1989; this paper).

Given the rarity of volcanic rocks in the Cretaceous section on land, it is worth reiterating that identifications of any volcanic rocks in the offshore must be considered highly speculative at present.

### Onshore-offshore trends

It has been suggested above that Cretaceous deposition in the Queen Charlotte Islands region proceeded roughly from west to east with the earliest sediments, the Longarm Formation, accumulating in the western part of the basin. The outcrop belts defined by geologic mapping reflect the gradual eastward migration of the Cretaceous shoreline. Knowing the position of the strandline at any particular time, as well as the direction of basin deepening, one can predict the approximate depocentre location and the local lithology of deposits: either shallow-marine sandstones or deeper-water shales.

For example, the lack of Albian-age sandstone of the Queen Charlotte Group in the southern part of the archipelago is not a function of subsequent erosion of those strata, but likely of nondeposition. The Cretaceous succession in the southern islands consists of older, Longarm Formation sandstone and shale, a transgressive sequence deposited during Hauterivian and Barremian time on a variety of underlying strata. The model predicts that younger deposits in the southern islands would be shales, deposited in response to continued deepening of deposition. No younger strata have been firmly identified in the southern islands although shales of possible Campanian age crop out on Burnaby Island (unpublished Bujak Davies Group fossil report, 1989).

Sandstones of Haida-age (Albian) would have been deposited to the northeast of the Longarm outcrop belt in the southern islands, when the strandline, migrating in response to the transgression, eventually shifted to that part of the islands (Fig. 10). Northeast of the Longarm outcrop belt, one should not expect to find an additional section of Longarm Formation preserved in the subsurface. The only Cretaceous strata which should be encountered in drilling in this area will be the younger Queen Charlotte Group deposits.

Similarly, the lack of Longarm strata in the eastern Cumshewa Inlet area is not a function of their subsequent erosion from that region, but rather, because they were never deposited there: transgression had not advanced that far east. Moving offshore north and east from the Cumshewa Inlet area, one should not expect to encounter any Cretaceous strata older than Middle Albian, as these are the youngest Cretaceous rocks deposited in the eastern outcrop belt. Rocks offshore to the northeast can be predicted to be Middle Albian or younger. One must keep in mind, though, that the transgression which reestablished itself after Honna fan progradation in the Turonian-Coniacian may not have reached this far east, and younger Cretaceous marine deposits were likely never deposited in this area.

As a final example, I cite the distribution of Cretaceous deposits on the northwest coast of Graham Island. Longarm deposits in the vicinity of White Point represent the earliest phase of transgression and deposition in that area. According to the transgression model, Longarm deposits should not be found northeast of the present outcrops; instead younger Cretaceous deposits of the Queen Charlotte Group are expected. This relationship is seen in the geology of this area. A corollary to this argument is that basal transgres-

sive strata of Albian age, the Haida Sandstone member, will not be found to the west of its present outcrop distribution, for the same reason: the transgression had progressed farther eastward by Albian time.

The interpretation of Cretaceous deposition proposed in this paper suggests that a significant section of marine Cretaceous rocks will not be found in the Hecate Strait area. Study of the shoreline trends displayed in Figure 10 indicates that the Cretaceous strandline likely projected to the southeast from the vicinity of Cumshewa Inlet. Thus, the only Cretaceous rocks which might be expected in Hecate Strait would likely be nonmarine in nature. The presence of coaly intervals with Cretaceous palynomorphs in the Sockeye E-66 and Tyee wells (White, 1990b) supports this interpretation. If sea level drop occurred in Turonian-Coniacian time in the islands region, as suggested earlier, then the possibility exists that substantial parts of Hecate Strait may have been subaerially exposed at the time, resulting in loss of earlier section in that part of the offshore.

Based on projection of the shoreline trend, the occurrence of marine Cretaceous rocks would appear to be more likely in Queen Charlotte Sound. Significantly, Stacey (1975) suggested that an appreciable section of latest Mesozoic-Cenozoic deposits may be present in this region, his analysis based on gravity and other geophysical data.

One additional point should be made regarding the prediction of occurrences of Cretaceous strata. The total thickness of the Cretaceous system in the Queen Charlotte Islands is not a composite based on Longarm Formation plus Queen Charlotte Group thicknesses (as followed by Hamilton and Cameron [1989]), because the various elements of the Cretaceous system are distributed unevenly. The total thickness at any particular locality is rather a function of geographic position. The total Cretaceous section in the eastern part of the islands, and presumably offshore, will be the local thickness of the Albian transgressive sequence plus the overlying Honna Formation. The Longarm Formation thickness is zero at that location and is not included. Similarly, in the southern and western parts of the Queen Charlotte Islands, the total thickness of Cretaceous rocks should include the Hauterivian/Barremian basal transgressive sequence (the Longarm Formation) and any younger shales, but should not include a component for the Albian-age Haida Sandstone member because that unit was never deposited in the western part of the islands.

## HYDROCARBON POTENTIAL OF THE CRETACEOUS SYSTEM

Exploratory drilling for hydrocarbons on the Queen Charlotte Islands dates back to the early part of this century (see Sutherland Brown, 1968; Haimila and Proctor, 1982), and the offshore wells in Hecate Strait and Queen Charlotte Sound were drilled in the late 1960s (Fig. 13). The results of these investigations were not promising. The identification of potential Triassic/Jurassic source-rock strata onshore (Cameron and Tipper, 1981; Macauley, 1983) reestablished the interest in the hydrocarbon potential of the islands and of the West Coast region in general.

One aspect of the QCI FGP has been to assess the geochemistry of potential source rocks on the islands and offshore, and to identify potential reservoir rocks in the Phanerozoic succession.

### Source rocks

The study of source-rock potential and organic maturation of Cretaceous strata on the Queen Charlotte Islands has not been promising. Spot samples collected from the Longarm, Haida, Skidegate, and Honna formations at various localities have shown that the total-organic-carbon (TOC) content is generally low, composed principally of Type III organic matter (Vellutini and Bustin, 1991; R.M. Bustin, pers. comm., 1990). The degree of organic maturation of Cretaceous strata in-

creases from north to south across the islands and this appears to be correlated with the heating caused by local plutonism (Vellutini and Bustin, 1991). Cretaceous strata on Graham Island are immature to overmature and have fair to moderate gas-source potential. Cretaceous strata on Moresby Island are generally overmature and exhibit poor source potential.

Samples collected from the unnamed Upper Cretaceous shale unit in the vicinity of Slatechuck Mountain were also found to be overmature. However, TOC values indicate that this unit, when it was mature, was a good source rock, capable of producing hydrocarbons (L. McCulloch-Smith, pers. comm., 1989). The type of hydrocarbons, either gas or oil, is not identifiable.

### Reservoir rocks

The best hydrocarbon-reservoir rocks yet identified in the Cretaceous sequence are the strata described as the "basal Haida lithofacies" by Fogarassy and Barnes (1989). This lithofacies, cropping out in Cumshewa Inlet, was described by Haggart (1986c) under the name pebbly sandstone lithofacies. These rocks are not stratigraphically extensive (a 24 m-thick succession was described from central Cumshewa Inlet by Haggart, 1986c), but they are widespread and, according to Yagishita (1985) and Fogarassy and Barnes (1989), exhibit high visual porosity.

The "basal Haida lithofacies" of Fogarassy and Barnes (1989) is a misnomer as this lithofacies actually characterizes the base of the diachronous Cretaceous transgressive succession at multiple stratigraphic horizons, including the base of the Longarm Formation. Thus, this unit is better referred to as the Cretaceous basal transgressive lithofacies. In addition to the exposures in the Cumshewa Inlet region, this lithofacies has also been identified at Skidegate Inlet (Fogarassy and Barnes, 1989) and at Beresford Bay and Caswell Point, on the north-west coast of Graham Island (Haggart, 1986c; Fogarassy, 1989).

### Offshore hydrocarbon potential

The prospect for significant reserves of hydrocarbons offshore (i.e. Hecate Strait and Queen Charlotte Sound) has been enhanced since the discovery of Jurassic-derived bitumen in cuttings in the Sockeye B-10 well (L. Snowdon, pers. comm., 1989). If Jurassic source rocks occur in the vicinity of this well, then it is possible that Cretaceous strata may also occur, acting as a source for Tertiary horizons, or capping the Jurassic and forming a potential reservoir.

The source potential of Cretaceous strata offshore is considered marginal (Snowdon et al., 1989). However, generally low maturation and quality of organic matter levels for Cretaceous exposures onshore are attributed to heating associated with local plutonism (Vellutini and Bustin, 1991). If plutons are absent in the offshore region, the present geochemical characteristics of Cretaceous strata could be more favourable for hydrocarbon generation. However, a caution must be raised: Lyatsky (1991) suggests that plutons may be present in the eastern Queen Charlotte Sound region.

As described above, the possible reservoir-rock lithofacies at the base of the Cretaceous transgressive succession can be expected to continue, for some distance at least, offshore into Hecate Strait. Unfortunately, Leslie (1989), who studied the supposed Upper Cretaceous to Lower Paleocene strata in the Tyee and Sockeye wells, found these rocks to have low visual porosity with no evidence of secondary porosity; the rocks thus have a very poor hydrocarbon-reservoir potential. It should be reiterated here, though, that the age control on the strata studied by Leslie (1989) is inadequate. It is quite possible that rocks older or younger than Cretaceous may have inadvertently been the subject of Leslie's study.

## CONCLUSIONS

- 1) The previously inferred Barremian-Aptian hiatus between the Lower Cretaceous Longarm Formation and the younger Cretaceous Queen Charlotte Group does not exist. Deposition was continuous through most of Cretaceous time in the Queen Charlotte Islands region.
- 2) Cretaceous strata in the islands consist principally of shallow-marine sandstones and deeper-water shales. The strata were deposited over a wide area, accumulating mainly in shelf environments.
- 3) Previous models suggesting that the Cretaceous deposits represent "suture" and "post-suture" assemblages which evolved in response to the amalgamation of Wrangellia and the Alexander Terrane, are not supported. There is no stratigraphic or sedimentologic evidence for the existence of a Cretaceous terrane suture in the Queen Charlotte Islands.
- 4) The Cretaceous stratigraphic succession forms two large-scale transgressive sequences which appear to have developed primarily in response to a regional sea level rise. Small-scale block faulting reactivated along Late Jurassic bounding faults may have influenced sedimentation on the local scale.

## ACKNOWLEDGMENTS

The author was ably assisted in the field by Tonia Hale, Mike Neyland, and Greg Gillstrom, and each are thanked for their efforts in collecting fossils. Bob Thompson, Peter Lewis, Roger Higgs, Susan Taite, Jarend Indrelid, and Jonny Hesthammer all provided fossil material which contributed to the evolution of the ideas expressed herein. Clarence Schuchman provided invaluable help, as always, in locating and collecting many ammonite specimens and his interest and enthusiasm are keenly appreciated. Bob Thompson provided generous field logistical support in 1988 through his Frontier Geoscience Program project. Finally, Bob Thompson, Peter Lewis, and Charle Gamba engaged the author in many hours of fruitful discussion regarding the interpretation of Cretaceous stratigraphy in the Queen Charlotte Islands and for this they are warmly thanked.

For the final product, Christine Davis and Tonia Oliveric turned my scribbles into organized figures. Charle Gamba, Peter Lewis, and Henry Lyatsky are all thanked for their thoughtful and penetrating reviews.

## REFERENCES

- Anderson, R.G. and Greig, C.J.  
 1989: Jurassic and Tertiary plutonism in the Queen Charlotte Islands, British Columbia; in *Current Research, Part H, Geological Survey of Canada, Paper 89-1H*, p. 95-104.
- Beeson, D.C.  
 1984: The relative significance of tectonics, sea level fluctuations, and paleoclimate to Cretaceous coal distribution; M.Sc. thesis, University of Colorado, Boulder, 202 p., 13 pls.
- Cameron, B.E.B. and Hamilton, T.S.  
 1988: Contributions to the stratigraphy and tectonics of the Queen Charlotte Basin, British Columbia; in *Current Research, Part E, Geological Survey of Canada, Paper 88-1E*, p. 221-227.
- Cameron, B.E.B. and Tipper, H.W.  
 1981: Jurassic biostratigraphy, stratigraphy, and related hydrocarbon occurrences of Queen Charlotte Islands, British Columbia; in *Current Research, Part A, Geological Survey of Canada, Paper 81-1A*, p. 209-212.
- 1985: Jurassic stratigraphy of the Queen Charlotte Islands, British Columbia; *Geological Survey of Canada, Bulletin 365*, p. 1-49.
- Carter, E.S., Orchard, M.J., and Tozer, E.T.  
 1989: Integrated ammonoid-conodont-radiolarian biostratigraphy, Late Triassic Kunga Group, Queen Charlotte Islands, British Columbia; in *Current Research, Part H, Geological Survey of Canada, Paper 89-1H*, p. 23-30.
- Clapp, C.H.  
 1914: A geological reconnaissance on Graham Island, Queen Charlotte Group, British Columbia; *Geological Survey of Canada, Summary Report for 1912*, p. 12-40.

- Dawson, G.M.**  
**1880:** Report on the Queen Charlotte Islands, 1878; Geological Survey of Canada, Report of Progress for 1878-79, Part B, p. 1-239.
- Flexer, A., Rosenfeld, A., Lipson-Benitah, S., and Honigstein, A.**  
**1986:** Relative sea level changes during the Cretaceous in Israel; American Association of Petroleum Geologists Bulletin, v. 70, no. 11, p. 1685-1699.
- Fogarassy, J.A.S.**  
**1989:** Stratigraphy, diagenesis and petroleum reservoir potential of the Cretaceous Haida, Skidegate and Honna formations, Queen Charlotte Islands, British Columbia; M.Sc. thesis, University of British Columbia, Vancouver, 177 p.
- Fogarassy, J.A.S. and Barnes, W.C.**  
**1988:** Stratigraphy, diagenesis and petroleum reservoir potential of the mid- to Upper Cretaceous Haida and Honna formations of the Queen Charlotte Islands, British Columbia; *in* Current Research, Part E, Geological Survey of Canada, Paper 88-1E, p. 265-268.  
**1989:** The middle Cretaceous Haida Formation: a potential hydrocarbon reservoir in the Queen Charlotte Islands, British Columbia; *in* Current Research, Part H, Geological Survey of Canada, Paper 89-1H, p. 47-52.  
**1991:** Stratigraphy and diagenesis of the mid- to Upper Cretaceous Queen Charlotte Group, Queen Charlotte Islands, British Columbia; *in* Evolution and Hydrocarbon Potential of the Queen Charlotte Basin, British Columbia, Geological Survey of Canada, Paper 90-10.
- Gamba, C.A., Indrelid, J., and Taite, S.**  
**1990:** Sedimentology of the Upper Cretaceous Queen Charlotte Group, with special reference to the Honna Formation, Queen Charlotte Islands, British Columbia; *in* Current Research, Part F, Geological Survey of Canada, Paper 90-1F, p. 67-73.
- Haggart, J.W.**  
**1986a:** Stratigraphy of the Redding Formation of north-central California and its bearing on Late Cretaceous paleogeography; *in* Cretaceous Stratigraphy, Western North America, P.L. Abbott (ed.), Society of Economic Paleontologists and Mineralogists, Pacific Section, Special Volume 46, p. 161-178.  
**1986b:** Cretaceous stratigraphic sequences of north-central California suggest a discontinuity in the Late Cretaceous forearc basin; *Geology*, v. 14, p. 860-863.  
**1986c:** Stratigraphic investigations of the Cretaceous Queen Charlotte Group, Queen Charlotte Islands, British Columbia; Geological Survey of Canada, Paper 86-20, p. 1-24, 1 pl.  
**1987:** On the age of the Queen Charlotte Group of British Columbia; *Canadian Journal of Earth Sciences*, v. 24, p. 2470-2476.  
**1989:** Reconnaissance lithostratigraphy and biochronology of the Lower Cretaceous Longarm Formation, Queen Charlotte Islands, British Columbia; *in* Current Research, Part H, Geological Survey of Canada, Paper 89-1H, p. 39-46.
- Haggart, J.W. and Gamba, C.A.**  
**1990:** Stratigraphy and sedimentology of the Longarm Formation, southern Queen Charlotte Islands, British Columbia; *in* Current Research, Part F, Geological Survey of Canada, Paper 90-1F, p. 61-66.
- Haggart, J.W. and Higgs, R.**  
**1989:** A new Late Cretaceous mollusc fauna from the Queen Charlotte Islands, British Columbia; *in* Current Research, Part H, Geological Survey of Canada, Paper 89-1H, p. 59-64, 1 pl.
- Haggart, J.W., Lewis, P.D., and Hickson, C.J.**  
**1989:** Stratigraphy and structure of Cretaceous strata, Long Inlet, Queen Charlotte Islands, British Columbia; *in* Current Research, Part H, Geological Survey of Canada, Paper 89-1H, p. 65-72.
- Haggart, J.W., Indrelid, J., Hesthammer, J., Gamba, C.A., and White, J.M.**  
**1990:** A geological reconnaissance of the Mount Stapleton-Yakoun Lake region, central Queen Charlotte Islands, British Columbia; *in* Current Research, Part F, Geological Survey of Canada, Paper 90-1F, p. 29-36.
- Haimila, N.E. and Proctor, R.M.**  
**1982:** Hydrocarbon potential of offshore British Columbia; Geological Survey of Canada, Open File 824, 28 p.
- Hamilton, T.S. and Cameron, B.E.B.**  
**1989:** Hydrocarbon occurrences on the western margin of the Queen Charlotte Basin; *Bulletin of Canadian Petroleum Geology*, v. 37, p. 443-466.
- Hancock, J.M. and Kauffman, E.G.**  
**1979:** The great transgressions of the Late Cretaceous; *Journal of the Geological Society*, v. 136, pt. 2, p. 175-186.
- Haq, B.U., Hardenbol, J., and Vail, P.R.**  
**1987:** Chronology of fluctuating sea levels since the Triassic; *Science*, v. 235, p. 1156-1167.
- Harris, P.M., Frost, S.H., Seiglie, G.A., and Schneidermann, N.**  
**1984:** Regional unconformities and depositional cycles, Cretaceous of the Arabian Peninsula; *in* Interregional Unconformities and Hydrocarbon Accumulation, J.S. Schlee (ed.), American Association of Petroleum Geologists, Memoir 36, p. 67-80.
- Higgs, R.**  
**1988:** Sedimentology of the Honna Formation, Upper Cretaceous fan-delta conglomerates; *in* Some Aspects of the Petroleum Geology of the Queen Charlotte Islands, R. Higgs (compiler), Canadian Society of Petroleum Geologists' Field Guide to Sequences, Stratigraphy, Sedimentology: Surface and Subsurface Technical Meeting, September, 1988, Calgary, p. 14-22.
- 1989:** Sedimentology and implications for hydrocarbon exploration of the "Hippa beds", Queen Charlotte Islands, British Columbia; *in* Current Research, Part H, Geological Survey of Canada, Paper 89-1H, p. 53-58.
- 1990:** Sedimentology and tectonic implications of Cretaceous fan-delta conglomerates, Queen Charlotte Islands, Canada; *Sedimentology*, v. 37, p. 83-103.
- 1991a:** Sedimentology and implications for petroleum exploration of the Honna Formation, northern Queen Charlotte Islands, British Columbia; *in* Evolution and Hydrocarbon Potential of the Queen Charlotte Basin, British Columbia, Geological Survey of Canada, Paper 90-10.
- 1991b:** Sedimentology, basin-fill architecture and petroleum geology of the Tertiary Queen Charlotte Basin, British Columbia; *in* Evolution and Hydrocarbon Potential of the Queen Charlotte Basin, British Columbia, Geological Survey of Canada, Paper 90-10.
- Higgs, R. and Bornhold, B.D.**  
**1988:** Stop 7. Haida Formation, Onward Point; *in* Some Aspects of the Petroleum Geology of the Queen Charlotte Islands, R. Higgs (compiler), Canadian Society of Petroleum Geologists' Field Guide to Sequences, Stratigraphy, Sedimentology: Surface and Subsurface Technical Meeting, September, 1988, Calgary, p. 69-72.
- Indrelid, J.**  
**1990:** Stratigraphy and structures of Cretaceous units, central Graham Island, Queen Charlotte Islands, British Columbia; *in* Current Research, Part F, Geological Survey of Canada, Paper 90-1F, p. 5-10.
- Ingersoll, R.V.**  
**1979:** Evolution of the Late Cretaceous forearc basin, northern and central California; *Geological Society of America Bulletin*, v. 90, Part 1, p. 813-826.
- Jeletzky, J.A.**  
**1977:** Mid-Cretaceous (Aptian to Coniacian) history of Pacific slope of Canada; *Palaeontological Society of Japan, Special Papers*, no. 21, p. 97-126, pl. 3.  
**1984:** Jurassic-Cretaceous boundary beds of western and arctic Canada and the problem of the Tithonian-Berriasian stages in the Boreal Realm; *in* Jurassic-Cretaceous Biochronology and Paleogeography of North America, G.E.G. Westermann (ed.), Geological Association of Canada, Special Paper 27, p. 175-255.
- Jones, D.L. and Irwin, W.P.**  
**1971:** Structural implications of an offset Early Cretaceous shoreline in northern California; *Geological Society of America Bulletin*, v. 82, p. 815-822.
- Jones, D.L., Murphy, M.A., and Packard, E.L.**  
**1965:** The Lower Cretaceous (Albian) ammonite genera *Leconteites* and *Breweriaceras*; *United States Geological Survey, Professional Paper 503-F*, p. 1-21, pls. 1-11.
- Leslie, D.R.**  
**1989:** Petrography and sedimentology of an unnamed Upper Cretaceous to Lower Paleocene sedimentary unit, Queen Charlotte Basin, British Columbia; B.A.Sc. thesis, University of British Columbia, Vancouver, 88 p.
- Lewis, P.D.**  
**1990:** New timing constraints on Cenozoic deformation in the Queen Charlotte Islands, British Columbia; *in* Current Research, Part F, Geological Survey of Canada, Paper 90-1F, p. 23-28.
- Lewis, P.D., Hesthammer, J., Indrelid, J., and Hickson, C.J.**  
**1990:** Geology, Yakoun Lake, British Columbia; Geological Survey of Canada, Map 5-1990, scale 1:50 000.
- Lyatsky, H.V.**  
**1991:** Regional geophysical constraints on crustal structure and geologic evolution of the Insular Belt, British Columbia; *in* Evolution and Hydrocarbon Potential of the Queen Charlotte Basin, British Columbia, Geological Survey of Canada, Paper 90-10.
- Macauley, G.**  
**1983:** Source rock - oil shale potential of the Jurassic Kunga Formation, Queen Charlotte Islands; Geological Survey of Canada, Open File 921, p. 1-52.
- MacKenzie, J.D.**  
**1916:** Geology of Graham Island, British Columbia; Geological Survey of Canada, Memoir 88, 221 p., 16 pls.
- McLearn, F.L.**  
**1949:** Jurassic formations of Maude Island and Alliford Bay, Skidegate Inlet, Queen Charlotte Islands, British Columbia; Geological Survey of Canada, Bulletin 12, p. 1-19.  
**1972:** Ammonoids of the Lower Cretaceous Sandstone member of the Haida Formation, Skidegate Inlet, Queen Charlotte Islands, western British Columbia; *Geological Survey of Canada, Bulletin 188*, 78 p., 45 pls.
- Palmer, A.R. (compiler)**  
**1983:** The Decade of North American Geology 1983 Geologic Time Scale; *Geology*, v. 11, p. 503-504.
- Riccardi, A.C.**  
**1981:** An Upper Cretaceous ammonite and inoceramids from the Honna Formation, Queen Charlotte Islands, British Columbia; *in* Current Research, Part C, Geological Survey of Canada, Paper 81-1C, p. 1-8, pl. 1.1.

- Richardson, J.**  
**1873:** Report on the coal-fields of Vancouver and Queen Charlotte islands, with a map of the distribution of the former; Geological Survey of Canada, Report of Progress for 1872-73, p. 32-65.
- Seiglie, G.A. and Baker, M.B.**  
**1984:** Relative sea-level changes during the middle and Late Cretaceous from Zaire to Cameroon (central west Africa); *in* Interregional Unconformities and Hydrocarbon Accumulation, J.S. Schlee (ed.), American Association of Petroleum Geologists, Memoir 36, p. 81-88.
- Shouldice, D.H.**  
**1971:** Geology of the western Canadian continental shelf; Bulletin of Canadian Petroleum Geology, v. 19, p. 405-436.  
**1973:** Western Canadian continental shelf; *in* The Future Petroleum Provinces of Canada – Their Geology and Potential, R.G. McCrossan (ed.), Canadian Society of Petroleum Geologists, Memoir 1, p. 7-35.
- Sliter, W.V., Jones, D.L., and Throckmorton, C.K.**  
**1984:** Age and correlation of the Cretaceous Hornbrook Formation, California and Oregon; *in* Geology of the Upper Cretaceous Hornbrook Formation, Oregon and California, T.H. Nilsen (ed.), Society of Economic Paleontologists and Mineralogists, Pacific Section, v. 42, p. 89-98.
- Snowdon, L.R., Fowler, M.G., and Hamilton, T.S.**  
**1989:** Oil in the Queen Charlotte Basin; Canadian Society of Exploration Geophysicists, Canadian Society of Petroleum Geologists, Exploration Update '89, Calgary, Programs and Abstracts, p. 167.
- Stacey, R.A.**  
**1975:** Structure of the Queen Charlotte Basin; *in* Canada's Continental Margins and Offshore Petroleum Exploration, C.J. Yorath, E.R. Parker, and D.J. Glass (ed.), Canadian Society of Petroleum Geologists, p. 723-741.
- Sutherland Brown, A.**  
**1968:** Geology of the Queen Charlotte Islands, British Columbia; British Columbia Department of Mines and Petroleum Resources, Bulletin 54, p. 1-226, pls. 1-18.
- Sutherland Brown, A., Yorath, C.J., and Tipper, H.W.**  
**1983:** Geology and tectonic history of the Queen Charlotte Islands; Geological Association of Canada, Mineralogical Association of Canada, Canadian Geophysical Union, Joint Annual Meeting, Victoria, B.C., Fieldtrip 8 Guidebook, 21 p.
- Thompson, R.I.**  
**1988:** Late Triassic through Cretaceous geological evolution, Queen Charlotte Islands, British Columbia; *in* Current Research, Part E, Geological Survey of Canada, Paper 88-1E, p. 217-219.  
**1990:** Geology, Cumsheewa Inlet, British Columbia; Geological Survey of Canada, Map 3-1990, scale 1:50 000.
- Thompson, R.I. and Thorkelson, D.J.**  
**1989:** Regional mapping update, central Queen Charlotte Islands, British Columbia; *in* Current Research, Part H, Geological Survey of Canada, Paper 89-1H, p. 7-11.
- Thompson, R.I., Haggart, J.W., and Lewis, P.D.**  
**1991:** Late Triassic through early Tertiary evolution of the Queen Charlotte Basin, British Columbia, with a perspective on hydrocarbon potential; *in* Evolution and Hydrocarbon Potential of the Queen Charlotte Basin, British Columbia, Geological Survey of Canada, Paper 90-10.
- Vellutini, D. and Bustin, R.M.**  
**1991:** Organic maturation and source rock potential of Mesozoic and Tertiary strata, Queen Charlotte Islands, British Columbia; *in* Evolution and Hydrocarbon Potential of the Queen Charlotte Basin, British Columbia, Geological Survey of Canada, Paper 90-10.
- White, J.M.**  
**1990a:** Evidence of Paleogene sedimentation on Graham Island, Queen Charlotte Islands, west coast, Canada; Canadian Journal of Earth Sciences, v. 27, p. 533-538.  
**1990b:** Palynological correlation of Cenozoic and latest Mesozoic strata from sections and boreholes in the Queen Charlotte Basin and Islands; Geological Association of Canada – Mineralogical Association of Canada, Joint Annual Meeting, Vancouver, 1990, Program with Abstracts, v. 15, p. A139.
- Whiteaves, J.F.**  
**1876:** On some invertebrates from the coal-bearing rocks of the Queen Charlotte Islands; Geological Survey of Canada, Mesozoic Fossils, v. 1, pt. 1, p. 1-92, pls. 1-10.  
**1884:** On the fossils of the coal-bearing deposits of the Queen Charlotte Islands collected by Dr. G.M. Dawson in 1878; Geological Survey of Canada, Mesozoic Fossils, v. 1, pt. 3, p. 191-262, pls. 21-32.  
**1900:** On some additional or imperfectly understood fossils from the Cretaceous rocks of the Queen Charlotte Islands, with a revised list of the species from these rocks; Geological Survey of Canada, Mesozoic Fossils, v. 1, pt. 4, p. 263-308, pls. 33-39.
- Woodsworth, G.J.**  
**1988:** Karmutsen Formation and the east boundary of Wrangellia, Queen Charlotte Basin, British Columbia; *in* Current Research, Part E, Geological Survey of Canada, Paper 88-1E, p. 209-212.
- Woodsworth, G.J. and Tercier, P.E.**  
**1991:** Evolution of the stratigraphic nomenclature of the Queen Charlotte Islands, British Columbia; *in* Evolution and Hydrocarbon Potential of the Queen Charlotte Basin, British Columbia, Geological Survey of Canada, Paper 90-10.
- Yagishita, K.**  
**1985:** Evolution of a provenance as revealed by petrographic analyses of Cretaceous formations in the Queen Charlotte Islands, British Columbia, Canada; Sedimentology, v. 32, p. 671-684.
- Yorath, C.J.**  
**1987:** Petroleum geology of the Canadian Pacific continental margin; *in* Geology and Resource Potential of the Continental Margin of Western North America and Adjacent Ocean Basins – Beaufort Sea to Baja California, D.W. Scholl, A. Grantz, and J.G. Vedder (ed.), Circum-Pacific Council for Energy and Mineral Resources, Earth Science Series, v. 6, p. 283-304.
- Yorath, C.J. and Chase, R.L.**  
**1981:** Tectonic history of the Queen Charlotte Islands and adjacent areas – a model; Canadian Journal of Earth Sciences, v. 18, p. 1717-1739.
- Yorath, C.J. and Hyndman, R.D.**  
**1983:** Subsidence and thermal history of Queen Charlotte Basin; Canadian Journal of Earth Sciences, v. 20, p. 135-159.
- Young, I.F.**  
**1981:** Structure of the western margin of the Queen Charlotte Basin, British Columbia; M.Sc. thesis, University of British Columbia, Vancouver, 380 p.



# Stratigraphy and diagenesis of the middle to Upper Cretaceous Queen Charlotte Group, Queen Charlotte Islands, British Columbia

J.A.S. Fogarassy<sup>1</sup> and W.C. Barnes<sup>1</sup>

Fogarassy, J.A.S. and Barnes, W.C., Stratigraphy and diagenesis of the mid- to Upper Cretaceous Queen Charlotte Group, Queen Charlotte Islands, British Columbia; in *Evolution and Hydrocarbon Potential of the Queen Charlotte Basin, British Columbia*, Geological Survey of Canada, Paper 90-10, p. 279-294, 1991.

## Abstract

*The Queen Charlotte Group is composed of mainly marine shales, sandstones and conglomerates of the Haida, Skidegate and Honna formations. Total stratigraphic thickness of the Queen Charlotte Group is up to 1700 m. Sandstone and conglomerate dominate the succession and offer some petroleum reservoir potential.*

*The Haida Formation (Albian) is a fining upwards, transgressive succession which rests unconformably on older rocks. It consists of a basal pebbly sandstone to granule conglomerate unit up to 190 m thick interpreted as fluvial deposits, overlain by 700 m or more of fine to very fine sandstone beds exhibiting bioturbation and hummocky cross-stratification. The Haida Formation grades upward into at least 200 m of concretionary shale of the Skidegate Formation (Cenomanian-Santonian). The Honna Formation (Coniacian-Santonian), which succeeds unconformably and probably also interfingers with the Skidegate Formation, is locally thicker than 800 m and is dominated by clast-supported pebble to cobble and rare boulder conglomerate. The depositional environment of the Honna Formation was a marine fan-delta or submarine canyon and fan system passing upward to Cretaceous mudstones and rare subaerial volcanics.*

*Primary grain composition, together with diagenesis, determine the reservoir potential of the Queen Charlotte Group. The pebbly basal part of the Haida Formation has the best reservoir potential, due to high quartz framework grain content which restricts precipitation of authigenic phases. Diagenesis of Queen Charlotte Group sandstones involved carbonate precipitation and dissolution, and the growth of authigenic minerals, creating a complex paragenetic sequence. Appreciable secondary porosity development, combined with preservation of intergranular primary porosity, results in visual porosity locally exceeding 15% in the basal Haida. Younger sandstones and conglomerates of the Queen Charlotte Group exhibit uniform diagenetic trends throughout all major outcrops on the islands, and are generally poor reservoir prospects.*

## Résumé

*Le groupe de Queen Charlotte est surtout composé de schistes argileux, de grès et de conglomérats marins des formations Haida, Skidegate et Honna. L'épaisseur stratigraphique totale du groupe de Queen Charlotte atteint 1700 m. Le grès et le conglomérat qui sont les roches dominantes de la succession pourraient contenir du pétrole.*

*La formation de Haida de l'Albien est une succession transgressive à granulométrie positive reposant en discordance sur des roches plus anciennes. Elle est formée d'une unité basale de grès caillouteux à conglomérat graveleux, mesurant jusqu'à 190 m d'épaisseur, qui s'apparente à des dépôts fluviaux. Elle est surmontée de plus de 700 m de couches de grès fin à très fin, bioturbées et à stratification oblique bosselée. La formation de Haida se transforme vers le haut en un schiste argileux de concrétion d'au moins 200 m d'épaisseur faisant partie de la formation de Skidegate (Cénomanien et Santonien). La formation de Honna (Coniacien et Santonien) qui suit la formation de Skidegate de façon discordante, en s'y interdigitant peut-être, mesure par endroits plus de 800 m et est surtout composée d'un conglomérat constitué d'éléments allant de galets à de gros cailloux entremêlés de clastes, et d'une petite quantité de blocs. Le milieu sédimentaire de la formation de Honna était un delta sous-marin ou un réseau de canyons et de cônes sous-marins se transformant vers le haut en mudstones crétacés et en roches volcaniques subaériennes rares.*

*Le potentiel de trouver des roches réservoirs dans le groupe de Queen Charlotte est fondé sur la composition du grain primaire et les caractéristiques diagénétiques. La partie basale caillouteuse de la formation de Haida offre le meilleur potentiel de constituer des roches réservoirs étant donné sa forte teneur en grains structuraux de quartz qui ont restreint la précipitation des phases authigènes. La diagénèse des grès du groupe de Queen Charlotte a impliqué la précipitation et la dissolution des carbonates ainsi que la croissance de minéraux authigènes, créant une séquence paragenétique complexe. La formation d'une porosité secondaire appréciable et la conservation d'une porosité primaire intergranulaire ont créé une porosité visuelle dépassant par endroits 15 % dans la base de la formation de Haida. Les grès et conglomérats plus récents du groupe de Queen Charlotte présentent des directions diagénétiques uniformes dans tous les principaux affleurements de la région et ils sont en général peu susceptibles de constituer des roches réservoirs.*

<sup>1</sup> Department of Geological Sciences, University of British Columbia, 6339 Stores Road, Vancouver, B.C., V6T 2B4



## INTRODUCTION

Geologic study of the Queen Charlotte Islands, and more particularly the Queen Charlotte Group, has been sporadic. Richardson (1873), Dawson (1880), Ellis (1906), Clapp (1914) and MacKenzie (1916) made early lithostratigraphic studies. Sutherland Brown (1968) produced the first comprehensive maps and report on the geology of the islands, including the Queen Charlotte Group.

The middle to Upper Cretaceous sequence (Fig. 1) has received recent study. McLearn (1972) and Riccardi (1981) described the ammonoid and inoceramid faunas of the Haida and Honna formations. Yagishita (1985) studied sedimentation patterns in relation to plate tectonic theory as formulated by Yorath and Chase (1981) and Yorath and Hyndman (1983). Haggart (1986, 1987), using ammonoid faunas, and Cameron and Hamilton (1988), employing foraminiferal biostratigraphy, refined the stratigraphy of the Queen Charlotte Group. Fogarassy and Barnes (1988a) divided the sequence into eight lithostratigraphic units which correlate well with these biostratigraphic divisions.

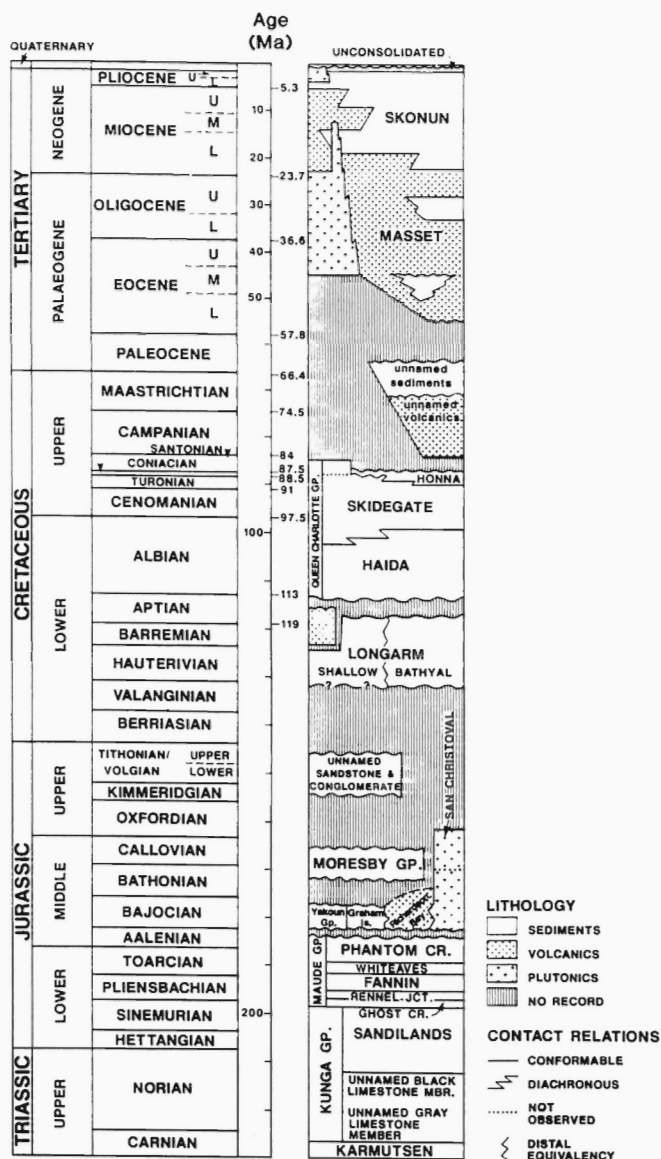


**Figure 1:** Stratigraphic column for the Queen Charlotte Islands (modified from Cameron and Hamilton, 1988).

Yagishita (1985) conducted a preliminary diagenetic study of the Haida-Skidegate-Honna sequence. Fogarassy and Barnes (1988a,b; 1989) examined all important sections of Queen Charlotte Group on the islands and documented diagenetic controls on petroleum reservoir development in sandstones and conglomerates. Using porosity development, they rated the Haida Formation as a secondary reservoir objective after the Tertiary Skonun Formation in the Queen Charlotte Basin.

## Methods

Stratigraphic sections of middle to Upper Cretaceous strata were measured in four separate areas of exposure (Fig. 2). Helicopter supported camps were used in the Beresford Bay-Langara Island region, whereas a four wheel drive vehicle and inflatable boat were employed for reaching southerly outcrops in Skidegate, Cumsheewa, Sewell and Logan inlets. Study of stratigraphic sections was generally limited to shoreline outcrops. Inland outcrops are discontinuous and found only in isolated quarries and logging roadcuts and thus were not extensively sampled.

Two hundred and fifteen thin sections of conglomerates and sandstones were cut from selected hand samples. All thin sections were stained with sodium cobaltinitrite, using the technique of Houghton (1980), for K-feldspar and clay determination. Sixty-two thin sections were vacuum impregnated with blue dyed epoxy resin to aid in visual porosity estimates (Yanguas and Paxton, 1986). Selected sections were stained with alizarin red S (sodium alizarin sulphonate) and potas-

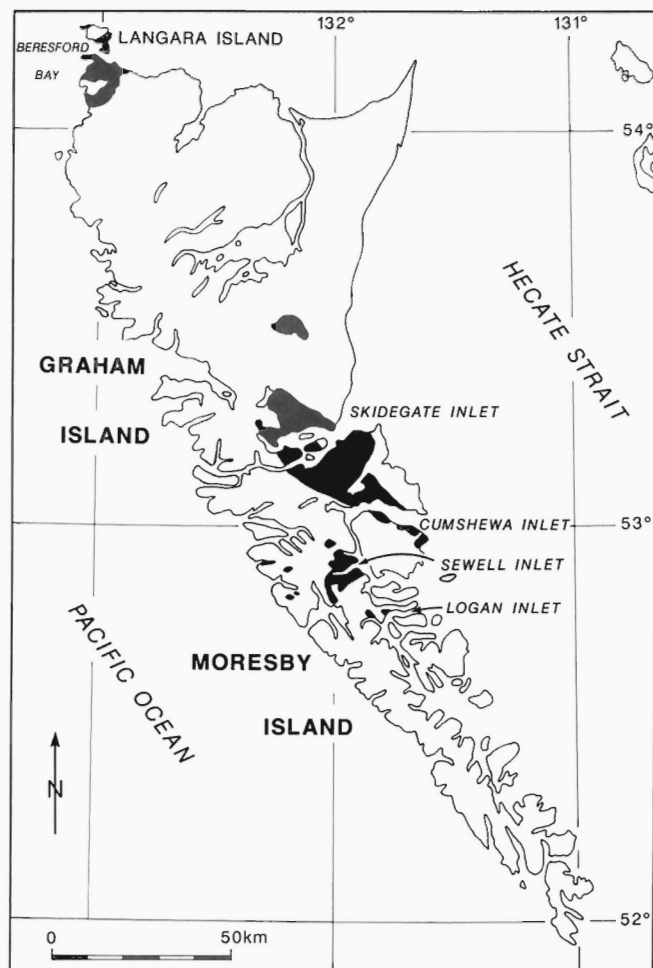


**Figure 2:** Middle to Upper Cretaceous outcrops (modified from Sutherland Brown, 1968).

sium ferricyanide for identification of calcite and ferroan carbonates respectively (Dickson, 1965).

Thin section analysis identified lithofacies of petrographic and diagenetic interest. These units were examined with a Nanolab 7 Scanning Electron Microscope (S.E.M.) and a Kevex Energy Dispersive Spectrometer (E.D.S.). Rough and polished sections were coated with 50 nm and 25 nm of carbon respectively and analyzed with 30 keV accelerating voltage using 50 nm and 100 nm beam diameters.

Clay mineralogy was studied with a Philips X-ray diffractometer (X.R.D.) equipped with a Cu K $\alpha$  tube and Ni filter. Three separate X-ray diffractograms were obtained for each sample. Upon gathering an initial pattern, from 3-65° 2 $\theta$ , the slide was heated in a furnace for 12 hours at 550°C, then transferred to a desiccator to avoid rehydration of expandable clays before loading into the diffractometer for a second run from 3-35° 2 $\theta$ . A third diffractogram, to aid in the identification of mixed-layer clay assemblages, was run from 3-35° 2 $\theta$  on a duplicate oriented clay slide which was treated for 48 hours with ethylene glycol vapour to determine the presence or absence of swelling clays and mixed-layer assemblages containing swelling clays.

Stable carbon and oxygen isotope ratios on carbonate cements were determined by a VG Isogas Ltd. isotope ratio mass spectrometer. Sample preparation involved heating a minimum of 2 mg of sample at 430°C for half an hour to volatilize organic components. Samples were reacted with 100% H<sub>3</sub>PO<sub>4</sub> at 90°C, to generate CO<sub>2</sub> gas. All isotope values presented are referenced to *Belemnitella americana* from the Peedee Formation (PDB).

STRATIGRAPHY

The middle to Upper Cretaceous sequence of the Queen Charlotte Islands is composed of a tripartite sedimentary package of conglomerates, sandstones and mudstones. The Albian Haida Formation, the Cenomanian-Santonian Skidegate Formation and the Coniacian-Santonian Honna Formation collectively form the Queen Charlotte Group. Cameron and Hamilton (1988) restructured the original stratigraphic nomenclature suggested by Sutherland Brown (1968) for the middle to Upper Cretaceous (Fig. 3). Employing foraminiferal evidence, they equated Sutherland Brown's Upper Haida shale member to the Skidegate Formation. These coeval units were recognized

as older than the Honna Formation. Haggart (1986) had previously demonstrated equivalence of the upper Haida shale member and the Skidegate Formation with ammonoid faunas.

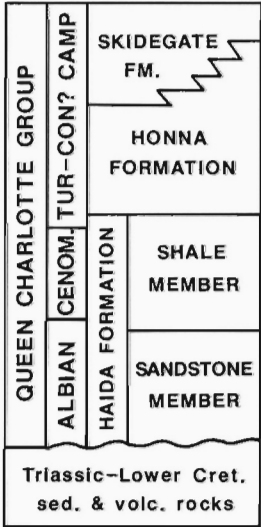
The Queen Charlotte Group lies with marked unconformity on Lower Cretaceous, Jurassic and Upper Triassic strata and may be overlain unconformably by volcanics of the Tertiary Masset Formation. The Haida-Skidegate-Honna sequence represents an overall fining upwards package deposited during a marine transgression (Yagishita, 1985). The Haida Formation is a nonmarine, probably fluvial deposit at its base and quickly grades upward into nearshore, shallow marine deposits. Gradual deepening of waters is seen in the deposition of mudstones of the Skidegate Formation. Abruptly overlying the Haida and Skidegate formations is the Honna Formation. These coarse grained clastics may represent submarine channel and turbidite deposition (Yagishita, 1985) or a fan-delta deposit (Higgs, 1988).

The Haida, Skidegate and Honna formations are divided into eight regionally mappable lithofacies (Fig. 4). The Haida Formation is

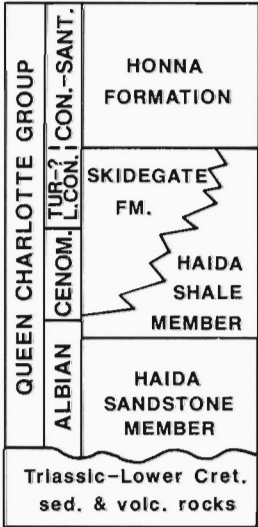
	UPPER HONNA	Clast supported pebble to cobble conglomerate interbedded with lenticular coarse grained sandstone.	HONNA FM
	MIDDLE HONNA	Turbiditic sandstones, siltstones and shales with occasional conglomerate interbeds and massive coarse grained sandstones.	
	BASAL HONNA	Clast supported pebble to cobble conglomerate interbedded with lenticular coarse grained sandstone.	
	SKIDEGATE SANDSTONE-SILTSTONE	Well bedded fine grained sandstone, siltstone and shale.	SKIDEGATE FM.
	SKIDEGATE SHALE	Silty, concretionary shale.	
	UPPER HAIDA	Interbedded sandstones, siltstones and silty shales.	HAIDA FM.
	LOWER HAIDA SANDSTONE	Fine to medium grained carbonaceous sandstones.	
	BASAL HAIDA	Granule conglomerate interbedded with medium to coarse grained pebbly sandstones.	

Figure 4: Middle to Upper Cretaceous lithofacies chart (adapted from Yagishita, 1985 and Haggart, 1986).

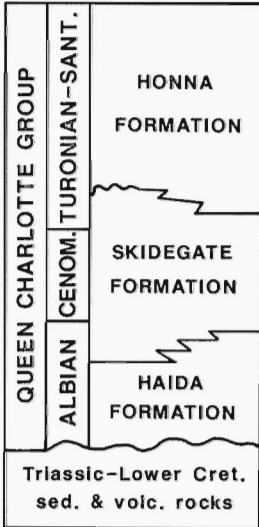
SUTHERLAND BROWN (1968)



HAGGART (1987)



CAMERON & HAMILTON (1988)



THIS STUDY

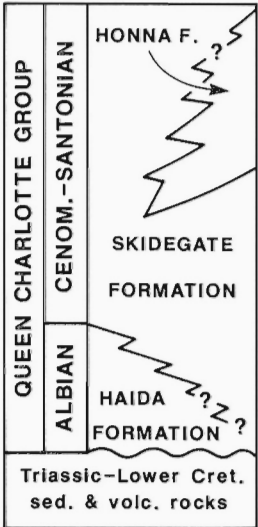


Figure 3: Stratigraphic nomenclature for the Queen Charlotte Group (modified from Haggart, 1987).

composed of medium to coarse grained sandstone with granule to pebble conglomerate at its base. The Skidegate Formation is a concretionary mudstone unit and the Honna Formation is a variably thick sequence of pebble to boulder conglomerate and turbiditic sandstone. The source for all middle to Upper Cretaceous sediments appears to be the same local underlying sedimentary, volcanic and plutonic units now exposed on the Queen Charlotte Islands. Fault repetition complicates measurement of the true stratigraphic thicknesses of the units, but the middle to Upper Cretaceous section is inferred to thin southward from the Beresford Bay-Langara Island region to Cumsheewa and Sewell inlets (Fig. 5).

### Haida Formation

The lowermost unit of the Queen Charlotte Group, the Haida Formation, is subdivided into three lithofacies: 1) basal Haida; 2) lower Haida sandstone; and 3) upper Haida. Each lithofacies progressively fines and increases in argillaceous content upwards.

#### Basal Haida lithofacies

The basal Haida is the coarsest of the Haida Formation lithofacies and has a variable thickness throughout the islands. It has a measured outcrop thickness ranging from a postulated pinchout on Louise Island in the south to 190 m in the Beresford Bay-Langara Is-

land region of northwestern Graham Island. The unit is typified by well developed low and high angle planar and trough cross-lamination. Coalified wood and plant fragments and fine grained terrigenous carbonaceous organic debris are locally abundant. A paucity of ichnofossils characterizes this lithofacies, indicating freshwater conditions or rapid deposition rates. The basal Haida lithofacies is suggested to be a fluvial deposit. It grades vertically over a few metres into the lower Haida sandstone lithofacies.

The basal Haida lithofacies is the most petrographically distinct of the eight lithofacies present in the Queen Charlotte Group. The lithofacies is composed of granule to pebble, matrix to clast supported conglomerate and medium to coarse grained arkosic and feldspathic arenite. The unit has a bimodal grain size distribution with very well rounded, polycrystalline and strained quartz (Fig. 6) and plutonic rock fragments and medium grained, subangular to subrounded feldspars, monocrystalline quartz and sedimentary rock fragments. Polycrystalline and highly strained quartz dominates the framework with an average grain size of greater than 2 mm that comprises up to 30% of total framework. Subordinate monocrystalline quartz, feldspar and rock fragments account for the remaining 70% and have an average grain size of 500  $\mu\text{m}$ . Matrix is negligible, but a pseudomatrix of deformed sedimentary and volcanic rock fragments occurs (Dickinson, 1970). Detrital muscovite was found only in the basal Haida lithofacies. Cement is restricted to patchy, infrequently poikilitic, calcite and minor amounts of interstratified clays forming at the expense of orthoclase and plagioclase.

The basal Haida lithofacies is petrographically unique; we suggest that it be recognized as a separate formation in the Queen Charlotte Group or as a formal member of the Haida Formation.

The source of the coarser fractions of the basal Haida lithofacies appears to be Late Jurassic plutons. Thin sections from samples from the margins of Late Jurassic intrusions on Lyell Island (R.G. Anderson, pers. comm., 1989; Anderson and Greig, 1989) display strain textures identical to those present in basal Haida sandstones. Moderate to highly strained "ribbon" grains characterize polycrystalline quartz. Mineralogy of strained grains is predominantly quartz (60-100%) but includes albite twinned plagioclase, orthoclase and fine grained sericite parallel to foliation. Although a plutonic source is postulated, a ductilely deformed quartz-rich siltstone and sandstone is a possibility. The high degree of rounding and sphericity seen in the majority of coars-

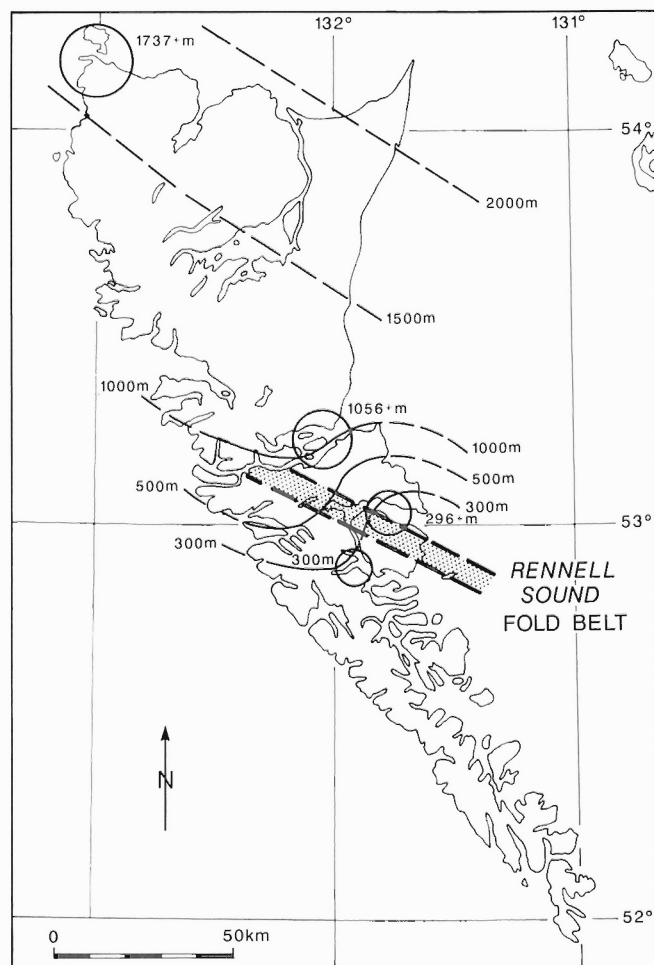


**Figure 5:** Isopach: Haida, Skidegate and Honna formations. Note southeasterly thinning. Circles represent studied regions; as outcrops are generally shallow dipping ( $<25^\circ$ ) their exposure covers long stretches of coastline. Dashed contours represent possible isopach extrapolations.



**Figure 6:** Basal Haida: polycrystalline quartz. These large grains readily distinguish the basal Haida lithofacies from the rest of the Queen Charlotte Group. Highly strained "ribbon" quartz, increases in abundance in southerly outcrops. Thin section photomicrograph, crossed nicols, width of photomicrograph is 4 mm.

er framework grains suggests sediment recycling, possibly from the Moresby Group or the Longarm Formation. Initial denudation of Late Jurassic plutons may have caused the deposition of quartz-rich Jura-Cretaceous sedimentary strata which in turn were the source of the basal Haida lithofacies. The areal distribution of the strained quartz grains is generally restricted mainly to Skidegate and Cumshe-wa inlets, but small percentages are present in the Beresford Bay-Langara Island region. The origin of basal Haida sediments in the Beresford Bay-Langara Island region appears mainly to be nearby Triassic and Jurassic cherty radiolarian mudstones and volcanoclastics.

#### Lower Haida sandstone lithofacies

The sandstones of the Lower Haida are generally texturally and compositionally immature. They are locally stained with dead oil and contain carbonized wood fragments, including logs exceeding 2 m in length. The unit is characterized by abundant ammonites, the mollusc *Trigonia* and locally intense bioturbation. It ranges from 200-700 m in thickness. Argillaceous content and buff-brown weathering calcite concretions increase upsection. In some places, concretions coalesce to form "beds" up to 1 m thick, preserving original sedimentary textures and structures. Yagishita (1985) described desiccation crack casts in many outcrops, but these were not recognized during the present study. Cameron and Hamilton (1988) also indicated the absence of desiccation structures.

Discrete offshore bar build-ups occur in this transgressive sandstone. Low and high angle planar cross-stratification and distinctive coarsening upward sequences, 2-6 m thick, punctuate the section. Recognized trace fossils include *Ophiomorpha* and *Planolites*. *Ophiomorpha* is a common, shallow water, nearshore marine ichnofossil characteristic of the *Skolithos* ichnofacies (Chamberlain, 1978; Frey and Pemberton, 1985).

An overall upward fining trend, however, and increased clay content may represent deposition in a transgressive marine environment (Yagishita, 1985). In the upper part of the unit, hummocky and swaley cross-stratification suggests reworking below fair weather wave-base (Walker, 1979a). The lower Haida sandstone grades, over tens of metres, into the upper Haida lithofacies.

The sandstones of the lower Haida lithofacies are poorly to moderately sorted, subangular to subrounded, fine to medium grained, arkosic to lithic wackes and arenites. The offshore bar build-ups which punctuate the sequence are characteristically more mature and in places exhibit visible porosity. Abundant coalified, woody organic matter may contribute to porosity development. Abundant orthoclase, plagioclase, quartz, fragments of Triassic-Jurassic carbonaceous shales, and minor biotite, glauconite, sphene, epidote, and pyrite typify mineral assemblages.

Although Yagishita (1985) described plagioclase to K-feldspar ratios in excess of 50:1 for this lithofacies, point counting of stained thin sections in the present study indicates ratios of 3:2 to be the norm. These ratios are more consistent with the approximately 4:1 ratios described by Sutherland Brown (1968). E.D.S. analysis of a series of polished sections confirmed subequal amounts of alkali and sodic/calcic feldspars. The more alkali-rich sandstones suggest major contributions from Jurassic plutons rather than, for example, the more plagioclase-rich Karmutsen Formation.

#### Upper Haida lithofacies

The upper Haida lithofacies is an interbedded, very fine grained sandstone, siltstone and mudstone unit. The unit represents a thick transition between the sandstones of the underlying Lower Haida lithofacies to the shales and mudstones of the overlying Skidegate Formation.

The upper Haida is typified by abundant ammonoid faunas, pyritized in places, and a suite of other molluscs including the bivalve *Trigonia*. Calcareous concretions exceeding one metre in diameter locally form resistant marker "beds". Coalified and silicified wood fragments decrease in abundance near the Skidegate Formation contact. The unit ranges from 0-200 m thick, and is found chiefly in the area of Skidegate and Cumshe-wa inlets. It grades, over tens of metres, into the Skidegate Formation.

The sandstones of the upper Haida lithofacies are similar petrographically to the lower Haida sandstone lithofacies but are generally finer grained, more angular and poorly sorted, and more argillaceous than the remainder of the Haida sandstones. The upper Haida lithofacies is classified as lithic wacke.

#### Skidegate Formation

The Skidegate Formation is a dark grey marine mudstone (Haggart, 1986). It is subdivided into two lithofacies: 1) Skidegate shale; and 2) Skidegate sandstone-siltstone.

#### Skidegate shale lithofacies

The Skidegate shale lithofacies is 100-300 m thick, consisting of illitic and iron-rich chloritic mudstone and shale with rare calcareous sandstone and siltstone interbeds less than 30 cm thick.

Ammonites and calcitic concretions are common in the mudstones. Complex septarian concretions occur in the upper portion of the lithofacies in the Beresford Bay-Langara Island region where they may be used as a stratigraphic marker. Slump structures (Fig. 7) increase in abundance to the northwest and may be related to growth faulting. Thickness of section, slump and shallow water sedimentary structures may indicate syn-sedimentary faulting. Load, ball and pillow, and flame structures and syn-sedimentary microfaults are abundant in coarser sandstone interbeds. This unit grades rapidly over a few tens of metres into the overlying Skidegate sandstone-siltstone lithofacies.

Sandstones layers, 1-10 cm thick, punctuate the Skidegate shale lithofacies. They are argillaceous, very poorly sorted, have angular grains, and generally grade upward from very fine grained sandstone to siltstone. They are classified as lithic wackes.

#### Skidegate sandstone-siltstone lithofacies

The Skidegate sandstone-siltstone lithofacies is a fine grained sandstone with thin pebble conglomerate lenses at its top and intercalat-



**Figure 7:** Skidegate shale: slump structures. The lithofacies is characterized by syn-sedimentary deformation structures. Slump and convolute lamination is pronounced in the Beresford Bay-Langara Island region. Northerly shallowing of waters is interpreted on the basis of increased sandstone and siltstone content and slump structures.



ed mudstones and siltstones near its base. Yagishita (1985) informally designated the Skidegate sandstone-siltstone unit as a member in the Queen Charlotte Group. The sandstones show poorly developed A and B divisions of the Bouma sequence, with accompanying basal scour and normal grading. Turbidite sedimentation appears to presage deposition of the Honna Formation (Yagishita, 1985; Haggart, 1986). Although usually less than 30 m thick, the lithofacies was recognized at scattered localities throughout the islands underlying conglomerates of the Honna Formation.

Petrologically the Skidegate sandstone-siltstone lithofacies is similar to the overlying Honna Formation. Plagioclase, volcanic rock fragments, biotite, and detrital and authigenic clays such as chlorite, occur in greater abundance than in the underlying Haida Formation sandstones and conglomerates. The unit is moderately sorted, subrounded to subangular, fine grained sandstone and siltstone and is classified as a lithic and arkosic wacke or arenite.

### Honna Formation

The Honna Formation is a thick sequence of conglomerate and sandstone that erosionally overlies the Skidegate and Haida formations as well as Jurassic and Triassic strata. The formation is informally subdivided into three lithofacies: 1) basal Honna; 2) middle Honna; and 3) upper Honna.

#### Basal Honna lithofacies

The basal Honna lithofacies is a clast supported pebble to boulder conglomerate containing plutonic, volcanic and sedimentary clasts derived from underlying Cretaceous and older strata (Sutherland Brown, 1968) with a matrix of medium to very coarse grained argillaceous arkosic to lithic sandstone. Conglomerate beds are sharp based, variably graded, and up to 5 m thick. Massive medium to very coarse grained sandstone lenses, usually less than 30 m long and 3 m thick, are present throughout the lithofacies (Fig. 8). Yagishita (1985) interpreted source directions within the conglomerate based on clast imbrication. However, imbrication of basal Honna clasts is extremely scarce except on northwest Graham Island.

The occurrence of massive sandstone lenses and interfingering with the overlying middle Honna turbiditic sandstones suggests the basal Honna lithofacies is a submarine channel deposit. Deposition of the lithofacies appears to be controlled by channeling processes which typify gravelly submarine fans.



**Figure 8:** Basal Honna: lenticular sandstone and pebble-cobble clast supported conglomerate. Massive, medium to very coarse grained sandstones are devoid of visible sedimentary structures. Paucity of structures may indicate the sandstone was deposited from a mass flow. Height of outcrop approximately 10 m.

Sandstones of the basal Honna lithofacies are characterized by plagioclase, trachytic volcanic rock fragments and a suite of heavy minerals that includes biotite, hornblende, epidote, sphene, ilmenite and garnet, in order of decreasing abundance. Angular and poorly sorted, the Honna sandstones are classified, with the rest of the Honna Formation, as lithic wackes.

Increased abundance of volcanic rock fragments and plagioclase, the presence of hornblende and the lower proportions of quartz serve to distinguish the Honna sandstones from those in the Haida and Skidegate formations. Decreased compositional maturity is accompanied by decreased textural maturity. Sphericity and roundness are much lower than in the Skidegate and Haida formations.

#### Middle Honna lithofacies

The middle Honna lithofacies is a sequence of interbedded conglomerates and sandstones. The unit is divisible into two parts: 1) lower conglomerate and sandstone; and 2) upper turbiditic sandstones and shales.

The lower part is a clast supported pebble to cobble conglomerate intercalated with massive, well sorted fine to medium grained sandstones. The sandstones are 0.5-2 m thick and may represent grain flow deposition within the confines of submarine channels.

The upper part of the middle Honna lithofacies is composed of turbiditic sandstones and mudstones. Well developed B-C and B-C-D divisions of the Bouma sequence may represent deposition on the margins of a submarine fan (Walker, 1979b). Trace fossils are abundant in more argillaceous portions of this sub-unit but have not been found to be diagnostic in terms of water depth.

Conglomerate and sandstone of the middle Honna are overlain abruptly by conglomerates of the upper Honna lithofacies.

The sandstones are petrographically similar to underlying lenticular sandstones of the basal Honna lithofacies. They are composed of plagioclase, volcanic rock fragments, orthoclase, monocrystalline quartz, and a variety of ferromagnesian constituents including biotite and hornblende. The unit is classified as a lithic wacke or a lithic arenite. Middle Honna sandstones are distinctive in that hornblende abundance can locally reach 10% of the framework grain assemblage. The hornblende is generally very fresh and is commonly the largest framework grain in thin section.

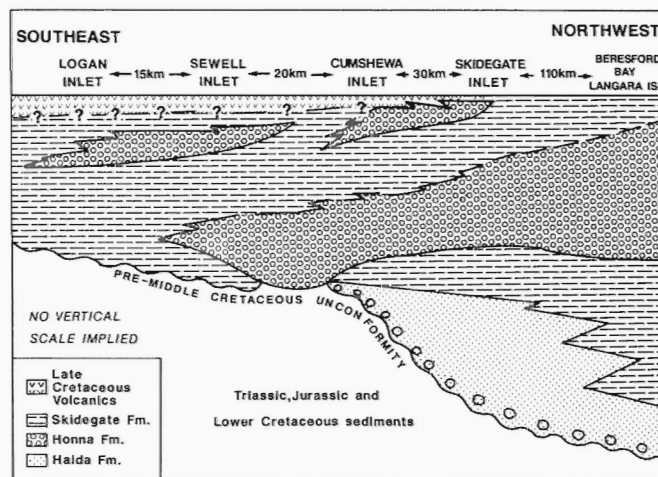


**Figure 9:** Schematic stratigraphic cross-section, Queen Charlotte Group. Modified from Yagishita (1985); Haggart and Higgs (1989); and B.E.B. Cameron, J.W. Haggart and R. Higgs (pers. comm., 1988). Dashed lines indicate inferred contacts.

The upper Honna lithofacies is a clast supported pebble to cobble conglomerate containing an angular, poorly sorted medium to coarse grained lithic sandstone matrix. The unit is similar petrologically and sedimentologically to the basal Honna lithofacies. It contains a variety of clast types and has massive, lenticular sandstones scattered throughout the section. Differences include locally well developed bedding and clast imbrication. The unit averages 40 m thick, about one-fifth the thickness of the basal Honna conglomerates.

### Discussion: Stratigraphy

Deposition of the Queen Charlotte Group can be subdivided into two separate periods: Haida-Skidegate deposition with a south-south-west provenance; and Honna and continued Skidegate deposition with a north-northeast provenance (Fig. 9). Deposition is postulated to have been the greatest in two sub-basins. One, in the Beresford Bay-Langara Island region, has pronounced petrographic and diagenetic characteristics which distinguish it from the areally larger southern sub-basin extending from Logan Inlet to north of Skidegate Inlet. Yagishita (1985) proposed four contemporaneous sedimentary basins for the Queen Charlotte Group based on a tectonic interpretation heavily reliant upon postulated large scale strike-slip fault offsets. Lewis and Ross (1988) and Thompson and Thorkelson (1989) suggested that little or no right-lateral strike-slip offset exists along presumed regional faults such as the Rennell Sound fault system (Sutherland Brown, 1968). In Skidegate and Cumshewa inlets, Cretaceous sedimentation may be related to episodic block faulting (Thompson and Thorkelson, 1989).

Haida-Skidegate deposition represents a major marine transgression (Yagishita, 1985). Haida sandstones and conglomerates are presently found only northeast of the Rennell Sound fold belt; a southerly depositional edge appears to occur in the area of Cumshewa Inlet. A structural cross-section by Lewis and Ross (1988) also infers a southerly pinchout of the Haida Formation. Regional variations in thickness of all units of the Queen Charlotte Group suggests stratigraphic thinning in a southerly direction. Increased abundance of high density detrital components, including zircon and epidote, in south Cumshewa Inlet outcrops may indicate a southerly provenance. All our data contradict Yagishita's (1985) suggestion of an easterly source for Haida sediments.

The Skidegate Formation may be a correlative facies of the Haida and Honna formations and may be younger in places than the other formations of the Queen Charlotte Group (B.E.B. Cameron, J.W. Haggart and R. Higgs, pers. comm., 1988; Haggart and Higgs, 1989; see Fig. 9). Intercalations of Skidegate mudstone and shale in the Haida and especially the Honna formations may indicate sporadic transgressive pulses.

The Honna Formation has received concentrated study recently, particularly in the Skidegate Inlet area. Yagishita (1985) and Higgs (1988) both infer an eastern provenance based on poor imbrication and regional tectonic interpretations. The depositional environment appears to be either a submarine channel and fan system (Yagishita, 1985) or a fan-delta (Higgs, 1988). Stratigraphic observations of Haggart et al. (1989) indicate subaerial volcanic debris flows conformably overlying and interfingering with a conglomeratic facies thought to be part of the Honna Formation in northwestern Skidegate Inlet (Long Inlet). Friable, green silty shale beds, 10-15 cm thick, locally occur in the Skidegate shale and the upper Haida lithofacies. X-ray diffractograms indicate a distinctive clay mineralogy dominated by interstratified illite/smectite and iron-rich chlorite. These beds may be aquagene tuffs, possibly related to Late Cretaceous subaerial volcanism described by Haggart et al. (1989).

The basal Haida lithofacies is unique petrologically in the Queen Charlotte Group. It is composed of a distinctive suite of framework

and cementing minerals. Sutherland Brown (1968) described the basal deposits of the Haida as "...exceptional in being relatively mature..." (p. 87). Fogarassy and Barnes (1989) related petroleum reservoir potential in the basal Haida lithofacies to increased mineralogical and textural maturity.

The amount and composition of matrix is variable throughout the Queen Charlotte Group. "Matrix" in many sandstones is a pseudomatrix (Dickinson, 1970) of deformed micas, sedimentary rock fragments and, to a lesser extent, volcanic rock fragments which have been forced during compaction into the interstices between more rigid framework grains. Variation of matrix amount creates a broad spectrum of rock types ranging from "clean" arenites to "dirty" immature wackes. As a result the classification of individual samples does not exhibit discernible trends. An exception is the basal Haida lithofacies, which almost uniformly contains less than 10% matrix. Identification of matrix and pseudomatrix constituents other than micas, glauconite and organic material is difficult in thin section. Unidentified clays may be authigenic and thus classified as cement. Differentiating clay matrix from clay cement can only be done reliably in a few thin sections.

The Queen Charlotte Group is petrologically similar to other siliciclastic units in the northeastern Pacific margin area (Dickinson and Suczek, 1979) and the Queen Charlotte Islands (Yagishita, 1985; Sutherland Brown, 1968). Framework grain compositions for the Queen Charlotte Group, except for the basal Haida lithofacies and the Honna Formation, are composed of variable amounts of quartz, K-feldspar, plagioclase and lithic fragments. The basal Haida lithofacies is a feldspathic/arkosic arenite, whereas the Honna Formation contains abundant plagioclase, volcanic rock fragments and mafic components, including epidote and hornblende.

Using the framework grain ternary plots of Dickinson and Suczek (1979), sediments of the Haida Formation are derived in part from a recycled orogen whereas the Honna and Skidegate formations were derived from a magmatic arc (Fig. 10). These sandstone composition data are similar to those of Sutherland Brown (1968) except for the increased maturity observed in the Haida Formation. The

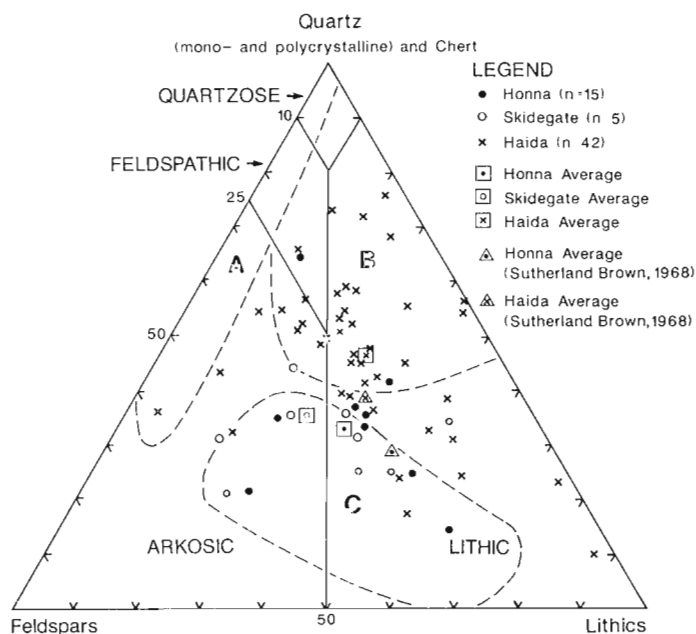


**Figure 10:** Sandstone classification; Haida, Skidegate and Honna formations. Ternary diagram; framework grain compositions. Classification scheme modified from Williams et al. (1954). A = sediments sourced from a continental block provenance, B = sediments sourced from a recycled orogen provenance, and C = sediments sourced from a magmatic arc provenance (Dickinson and Suczek, 1979).



distinctive petrologic and diagenetic make-up of the Haida Formation, particularly the basal Haida lithofacies, indicates potential sediment sources from deformed and subduction zone sequences; and/or along collision orogens; and/or within foreland fold-thrust belts (Dickinson and Suczek, 1979). The coarse grained and varied petrologic character of the Haida Formation supports a collision orogen provenance, particularly for the basal Haida lithofacies. The Honna-Skidegate formations, with their high percentage of volcanic and ferromagnesian framework grains, and association with intercalated volcanics and aquagene tuffs, are interpreted as being derived from an active island arc or active continental margin.

## DIAGENESIS

The diagenetic history of the Queen Charlotte Group and the rest of the geologic section is extremely complex due to the labile and reactive composition of the strata (Galloway, 1974; Fogarassy and Barnes, 1988a,b). Of the eight lithofacies studied, the basal Haida exhibits the greatest diagenetic variability, involving precipitation and dissolution of carbonate and aluminosilicate components. The remainder of the Queen Charlotte Group, although compositionally immature, exhibits generally uniform diagenetic trends throughout the islands.

Chlorite, smectite and interstratified chlorite/smectite (corrensite) and interstratified chlorite/smectite/illite group minerals dominate clay assemblages in the sandstone and conglomerate petrofacies of the Queen Charlotte Group. Authigenic laumontite and glauconite, and allogenic biotite and muscovite occur in lesser but locally significant

amounts. The clay mineralogy of shale units, primarily the Skidegate shale lithofacies, varies significantly from sandstone and conglomerate units in that iron-rich chlorite and illite are the main phyllosilicate phases. Smectite and illite/smectite occur locally in minor amounts.

## Chlorite

Chlorite is the most abundant phyllosilicate in the Queen Charlotte Group. It is easily recognized in virtually all thin sections by its distinctive green hue, pore-lining and pore-filling habit and its characteristic basal reflections in X-ray diffractograms. Ripidolite, an iron-rich member of the chlorite group, is the dominant species. Diffractograms (Fig. 11) show strong (002) and (004) reflections and correspondingly weak (001), (003) and (005) peaks indicating iron-rich chlorite.

Iron-rich chlorites deduced from X.R.D. patterns were confirmed with S.E.M./E.D.S. (Figs. 12, 13). Wilson and Pittman (1977) described four authigenic chlorite S.E.M. morphologies: plate, rosette, honeycomb and cabbagehead, corresponding to decreasing iron concentrations. Plate-type chlorite is the dominant form seen in the Queen Charlotte Group. Where chlorite occurs in a monomineralic form and not as part of a mixed-layer clay assemblage, it is invariably iron-rich. Where found interstratified with smectite, chlorite tends to be iron-poor. Chlorite of the Honna Formation is generally more iron-rich and tends to form thicker platelets than chlorite of the Haida and Skidegate formations. This probably reflects the more mafic composition of the Honna Formation protolith, shown also by an abundance of mafic volcanic rock fragments.

Chlorite in the sandstone and conglomerate is entirely diagenetic. Textural observations indicate chlorite formation occurred at an in-

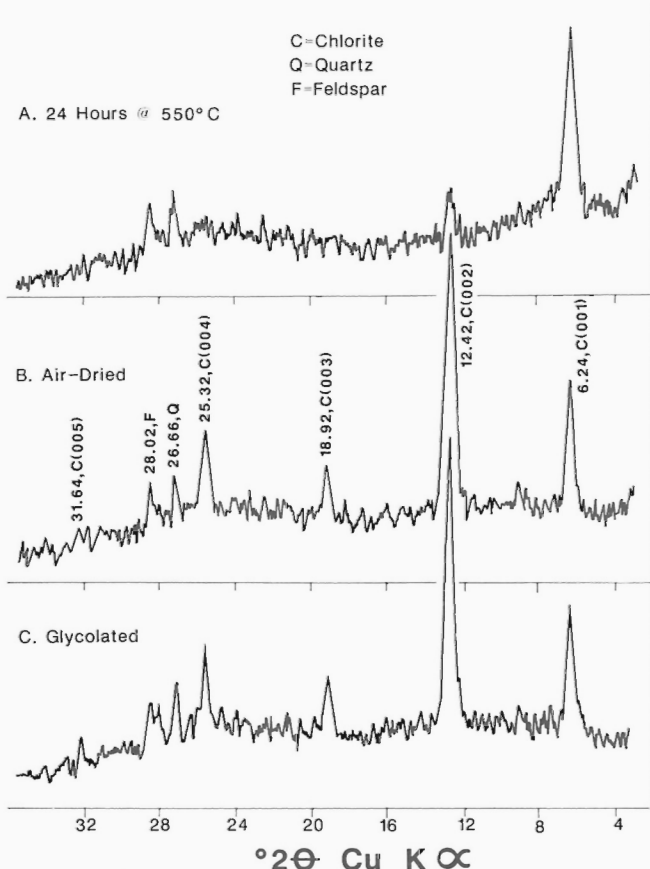


**Figure 11:** Chamosite, X-ray diffractograms. Characteristic patterns for iron-rich chlorite (B). Note partial to complete loss of (002), (003), (004) and (005) peaks after heat treatment (A); (001) peak is sharpened and intensified with a small decrease in the c unit cell length. Glycolation of chamosite has no effect on basal spacings (C).

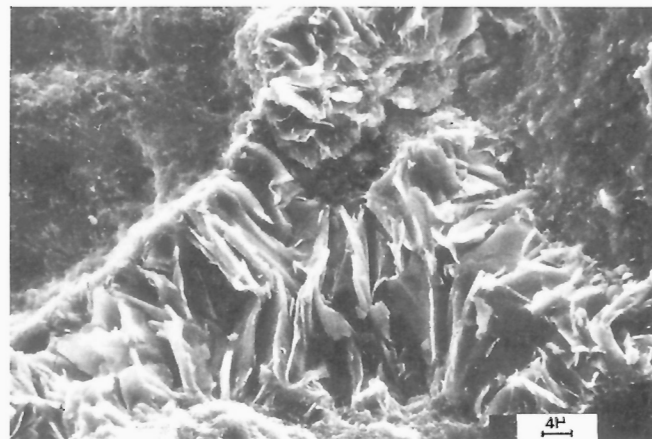


**Figure 12:** Pore-fill chlorite. Thick, large authigenic platelets of iron-rich chlorite. Scanning electron microscope photomicrograph.

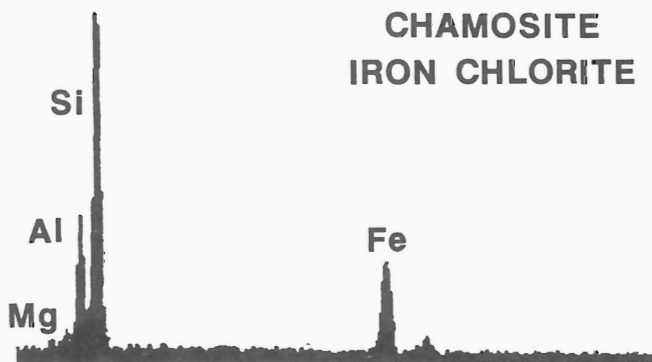
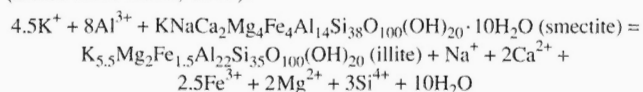


**Figure 13:** Chamosite (iron-rich chlorite), energy dispersive spectrometer elemental spectra.

intermediate stage of diagenesis at temperatures 75-150°C (Hoffman and Hower, 1979), after concretionary calcite and ferroan calcite cementation episodes. Iron-rich chlorite formed at temperatures less than 100°C, probably at the expense of mafic framework grain components such as iron bearing volcanic lithic fragments. Occurrence of iron-poor chlorites indicates a later stage of formation. The highly varied and complex nature of isomorphous substitution in chlorites may reflect illitization of smectites in mixed-layer groups. Burial and concomitant illitization of smectite may have mobilized octahedral magnesium from smectite at temperatures of 100-150°C (Boles and Franks, 1979) to octahedral positions in the talc and brucite layers of chlorite, formerly occupied by iron.

Release of iron and calcium during smectite illitization according to the equation below may also have resulted in the precipitation of the later stage ferroan calcite cement, at temperatures greater than 120°C, filling secondary porosity produced by the leaching of feldspars and other aluminosilicates (Fig. 14). Such a diagenetic sequence (Boles and Franks, 1979):



is seen in the Beresford Bay-Langara Island region where smectite abundance is much higher than elsewhere in the Queen Charlotte Islands. Potassium and aluminum ions for the smectite to illite conversion are supplied, in part, from the partial to complete leaching of K-feldspars (Boles and Franks, 1979) and potassium bearing volcanic rock fragments, possibly during secondary porosity enhancement. Figure 15 is a diagenetic sequence of mineral precipitation and dissolution constructed for the middle to Upper Cretaceous sequence.

Textural and mineralogical data indicate the Beresford Bay-Langara Island region to be much more complex diagenetically than other areas of outcropping Cretaceous sandstones and conglomerates. The abundance of iron-poor chlorite and interstratified clay assemblages in the Beresford Bay-Langara Island area may be associated with the abundance of smectite, which in turn may be related to a volcanic-rich sedimentary or igneous source. Lack of appreciable amounts of smectite elsewhere in the islands appears to correlate with an abundance of iron-rich chlorites.

Chlorites of the Queen Charlotte Group indicate growth in a diagenetic environment. Euhedral crystals and pore-lining or pore-filling habit rule out a detrital or metamorphic origin. Brown and Bailey (1962) identified four polytypes, based on a study of 303 chlorites of diverse origin, Ia, Ib( $\beta=97^\circ$ ), Ib( $\beta=90^\circ$ ) and IIa. Types Ia, Ib( $97^\circ$ )

and Ib( $90^\circ$ ) are indicative of diagenetic environments whereas type IIa is formed at low metamorphic temperatures, about 150-200°C (Hayes, 1970). Chlorites of the Queen Charlotte Group fall into the type Ia or Ib (diagenetic) categories based on textures derived from the S.E.M. and from thin section observations.

## Smectite

Authigenic smectite is ubiquitous throughout the sandstone and conglomerate units of the Queen Charlotte Group. Abundant amounts of this 2:1 layer silicate occur in the Honna Formation and the Skidegate sandstone-siltstone lithofacies of the Beresford Bay-Langara Island region. Smectite was confirmed to be trioctahedral by the lattice spacing of the (060) reflection which places it in the saponite subgroup. Saponite forms in magnesium-rich environments associated with mafic volcanics at temperatures generally less than 70°C (Hoffman and Hower, 1979; Chang et al., 1986). The analyses of Post (1984), Suquet et al. (1975) and Faust and Murata (1953) suggest observed first order basal spacings of smectite in the Queen Charlotte Group are indicative of calcium saponite.

In the majority of samples, saponite is partly illitized. Discrete saponite illitization is easily identified by morphological transformation of honeycomb, web-like crystals to fine, ribbon fibres (Keller et al., 1986) (Fig. 16). Neoformation of quartz, observed rarely in the Queen

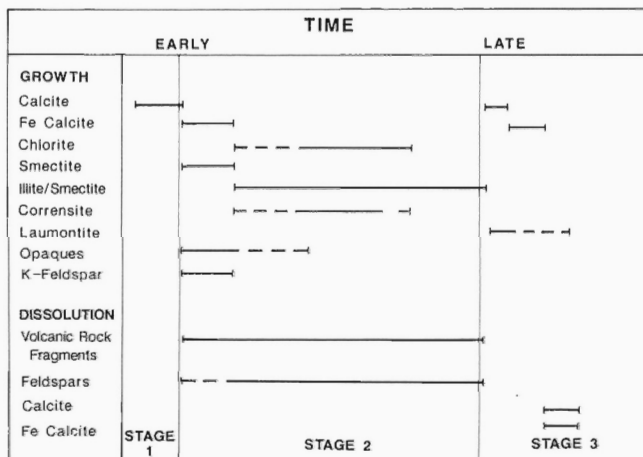


**Figure 15:** Composite diagenetic sequence of Queen Charlotte Group sandstones as determined by S.E.M./E.D.S., X.R.D., thin section inspection and oxygen/carbon stable isotope ratios.

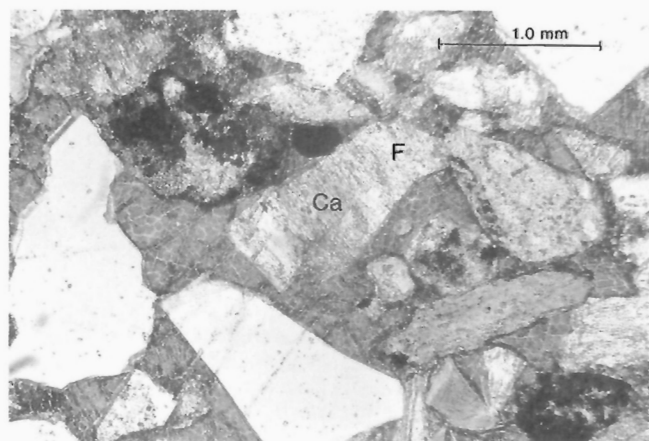


**Figure 14:** Ferroan calcite cement (Ca) infilling secondary fabric selective porosity in feldspar (F). Thin section photomicrograph, plane polarized light, width of photomicrograph is 4 mm.

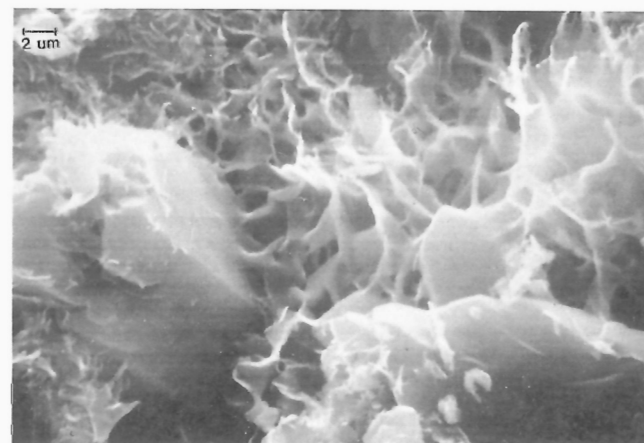


**Figure 16:** Illitization of smectite. Note delicate fibres forming atop webby smectite. Scanning electron microscope photomicrograph.

Charlotte Group, may be related to the illitization process (Boles and Franks, 1979).

## Illite

Illite is found mainly in mudstone and shale units. X.R.D. patterns indicate that illite forms mixed-layer assemblages with smectite. The presence of interstratified illite/smectite indicates an authigenic, rather than allogenic origin for illite as this mixed-layer clay is observed growing on framework grains in sandstones.

## Interstratified clays

Minor amounts of mixed-layer chlorite/smectite (corrensite), illite/smectite, and perhaps chlorite/smectite/illite occur throughout the middle to Upper Cretaceous sequence in all outcrops.

Interstratified assemblages containing chlorite and smectite are recognized on X-ray diffractograms by high background at low 2 angles and by small, but observable, shifts in peak position. Superlattice peaks at 25-30 Å (3.53-2.94° 2θ) are strong evidence of chlorite/smectite interstratification. The best examples of corrensite were found in samples of the Haida Formation from Cumshewa Inlet and in the Honna Formation from the Beresford Bay-Langara Island region.

Corrensite may be a transformation product from magnesium saturated chlorite (Brigatti and Poppi, 1984), with the smectite to illite conversion providing magnesium ions for incorporation into the chlorite structure. Formation of trioctahedral smectite (saponite) may in part be related to iron oxidation of chlorite (Brigatti and Poppi, 1984). Conversely, the transformation of saponite to chlorite via corrensite, due to the formation of intermicellar hydroxide sheets resulting from aluminum substitution of silicon in tetrahedral layers, may explain the authigenic clay make-up observed in the Beresford Bay-Langara Island strata. The volcanic-rich nature of siliciclastic framework grains in this region favours the formation of corrensite (Eslinger and Pevear, 1988). Corrensite forms at diagenetic temperatures of 85-95°C in argillaceous Cretaceous siliciclastics of the Cassipore Basin, Brazil (Chang et al., 1986).

Recognition of mixed-layer illite/smectite was based upon a comparison of X-ray diffractograms to computer-generated illite/smectite X-ray patterns of Reynolds and Hower (1970) and S.E.M. observations. Illite/smectite of Queen Charlotte Group sandstones is irregularly interstratified with non-expandable illite comprising up to about 30% of the illite/smectite assemblage. Similar mixed-layer illite/smectite percentages were deduced from valley-to-peak ratios of the (001) smectite reflection, which are empirically related to the percentage of illite in a mixed-layer illite/smectite assemblage (Hoffman, 1976; Schoonmaker, 1986). Illite/smectite ratio estimates were confirmed with complementary examination of crystal morphology with the S.E.M. in the manner of Keller et al. (1986).

Other mixed-layer clay minerals probably exist in the Queen Charlotte Group. Heterogeneous, mafic framework grain and matrix assemblages may give rise to the growth of three component mixed-layer minerals. The complex nature of fine fraction (<2 μm) X-ray diffractograms where numerous reflections remain unidentified suggests such interstratification. Chlorite/smectite/illite may be one such assemblage as the dual occurrence of corrensite and illite/smectite in samples is not unusual, particularly in the Beresford Bay-Langara Island region.

## Other minerals

Biotite, laumontite, muscovite and glauconite make up the remainder of the clay-size (<2 μm) fraction of Queen Charlotte Group sediments. Biotite is the major detrital phyllosilicate constituent in the sequence. It is strongly pleochroic, is partly to completely chloritized, and contains displacive intergrowths of pyrite and other unidentified

iron sulphides. Samples rich in biotite commonly exhibit discrete partings associated with the mica.

Laumontite is irregularly distributed in the Haida-Skidegate-Honna package, and is difficult to identify in the S.E.M. and in thin section. Confirmation of laumontite was made by X-ray diffractometry. Heat treatment of laumontite produces a characteristic peak shift from 9.31 to 10.4° 2θ (Fig. 17). This peak shift may be the dehydration phenomenon commonly observed in other zeolites (Coombs, 1952; Boles, 1972). Yagishita (1985) suggested that mordenite occurs in the Queen Charlotte Group, but is rare and was not found in this study. Traces of an unidentified calcium aluminosilicate, possibly wairakite, occur throughout the section and may be related to thermal effects of nearby intrusions (P.B. Read, pers. comm., 1989).

Although occurring in trace amounts to 2%, detrital muscovite is an important provenance indicator. It is most abundant in the basal Haida lithofacies where it generally is fresh and unaltered and occurs mainly in association with schistose and plutonic rock fragments containing K-feldspar and quartz. The presence of muscovite indicates an alkalic source, possibly related to that of the strained quartz grains.

Glauconite is apple green in plane- and cross-polarized light. It is well rounded and is often seen filling microfossils, primarily foraminifera and radiolaria. Although scattered throughout the Queen Charlotte Group, glauconite is concentrated in the lower Haida sandstone and upper Haida lithofacies. Glauconite comprises more than 40% of some sandstones in Cumshewa Inlet.

Opaque minerals account for a small fraction of cement observed in the Queen Charlotte Group. Pyrite is the dominant phase but other iron sulphides and oxides make up a significant proportion of the diagenetic fraction. Yagishita (1985) discussed the diagenetic aspects

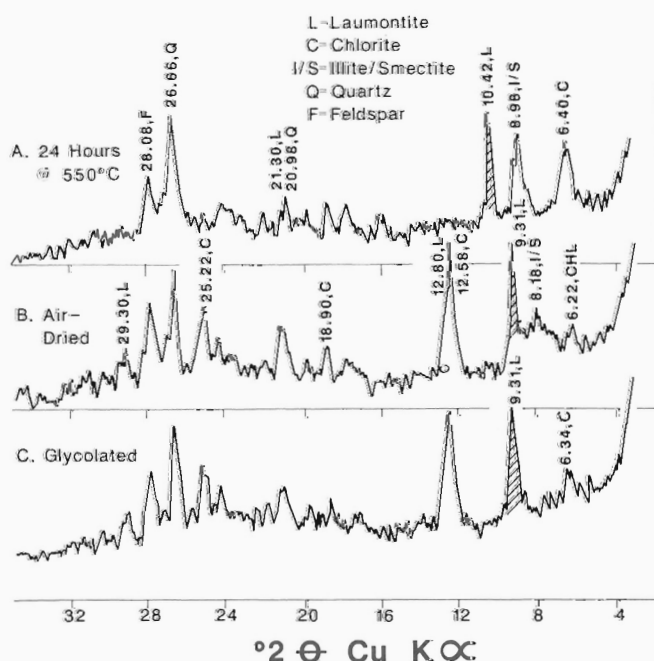


**Figure 17:** Laumontite peak shift, X-ray diffractograms. Peak shifts due to dehydration have been documented in the zeolite group, particularly heulandite (Boles, 1972) and the transformation of laumontite to leonhardite (Coombs, 1952). Untreated (B) and glycolated (C) samples reveal an intense peak at 9.31° 2θ with minor peaks at 12.80°, 21.30° and 29.30° 2θ confirming the presence of laumontite. Heat treatment (A) shifts the 9.31° peak to 10.42° 2θ, possibly due to dehydration. The other minor peaks are not affected. This sample also displays irregularly interstratified I/S and chlorite (variety chamosite).

of pyrite formation, noted its occurrence with plant fragments and inferred an early diagenetic origin. Textural evidence indicates pyrite formed during early diagenesis.

Trace amounts of other diagenetic phases, identified with S.E.M. back scattered electron imaging and the E.D.S., include barite and leucocene.

### Diagenetic history

#### Basal Haida lithofacies

The diagenesis of the basal Haida lithofacies in Skidegate and Cumshewa inlets involved the precipitation of carbonate cements with subsequent dissolution followed by aluminosilicate framework grain dissolution. Calcite is the dominant carbonate observed, but ferroan calcite is present in subordinate amounts and may be abundant locally. The content of detrital and authigenic clays is low for an arc-derived greywacke assemblage. Dissolution textures observed in carbonates contribute to the majority of secondary porosity development. Although proportionately less, aluminosilicate dissolution involving the leaching of orthoclase, plagioclase and lithic rock fragments created appreciable secondary porosity.

In the basal Haida sandstones of the Beresford Bay-Langara Island region, early diagenetic cements include complexly zoned calcite and ferroan calcite, indicating a variable diagenetic environment. Fer-

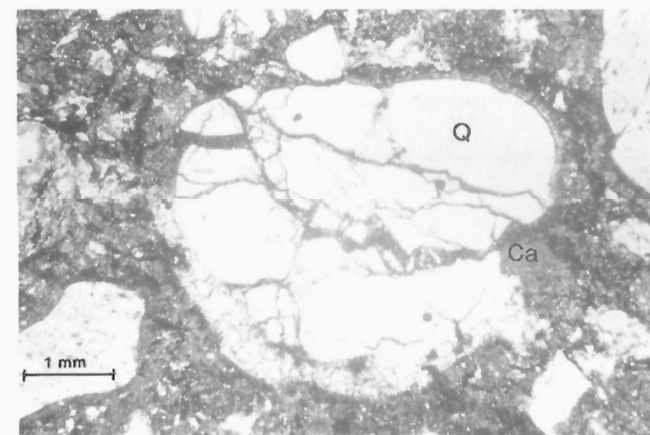


**Figure 18:** Displacive exfoliation texture of calcite and ferroan calcite (Ca) in quartz (Q). Thin section photomicrograph, plane polarized light, width of photomicrograph is 4 mm.

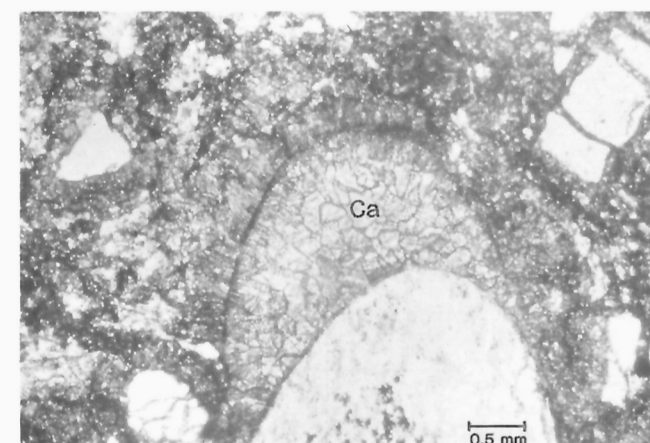


**Figure 19:** Carbonate microstalactitic cement (Ca) indicating precipitation under vadose conditions. Thin section photomicrograph, plane polarized light, basal Haida lithofacies, width of photomicrograph is 4 mm.

roan calcite is the most abundant carbonate cement observed. "Floating" framework grains are common in calcareous beds and concretions, indicating early diagenesis. Growth of fibrous carbonate cements creates exfoliation textures in outcrop (Fig. 18), and growth has fractured and separated framework grains. Typical of the Beresford Bay-Langara Island region, this displacive texture indicates an initial cementation episode under vadose conditions (Buczynski and Chafetz, 1987). Well developed calcite and ferroan calcite microstalactitic cement confirm formation in the vadose zone (Fig. 19). Iron-free calcite frequently rims framework grains and thus predates ferroan calcite cementation, an observation consistent with cementation in the vadose zone, an oxidizing environment (James, 1984).

Stable carbon and oxygen isotopes ratios are variable in the basal Haida lithofacies, particularly in the Cumshewa Inlet region. Carbon isotope ratios are lighter on the north shore of Cumshewa Inlet than on the south shore. An analogous but more subdued trend exists for oxygen isotope ratios (Fig. 20). Large carbon isotope data variations observed in the rocks of Cumshewa Inlet may be related to  $C_3$  higher plants which commonly have  $-25$  to  $-30\text{‰}$   $\delta^{13}C$  values (DeNiro, 1983; Schidlowski, 1986). Sedimentological indicators from outcrops of sandstones with anomalously light carbon isotope values suggest fluvial deposition. Light carbon isotope values documented from strata of the north shore of Cumshewa Inlet coincide with the best visual porosity development.

Aluminosilicate framework grains of the basal Haida lithofacies were partly or completely dissolved during diagenesis. Textures such as fabric selective dissolution are abundant, particularly in the Cumshewa Inlet region. Orthoclase, plagioclase and volcanic rock fragments are highly leached in sandstones with little carbonate cement. Thin section and S.E.M. studies indicate the former presence of interstitial carbonates (Schmidt and McDonald, 1979a,b; Burley and Kantorowicz, 1986). Angular pores, corroded and embayed framework grains and enlarged pore throats occur throughout the basal Haida lithofacies.

A diagenetic similarity exists between outcrops of basal Haida lithofacies in the Queen Charlotte Islands, but framework grain compositions are different. The basal Haida lithofacies of the Beresford Bay-Langara Island region had a similar diagenetic history despite having a volcanic provenance, whereas the southerly sections were dominated by plutonic and sedimentary sources. All areas have coarse framework grain sizes, in places reaching cobble dimensions, a high degree of rounding and sphericity, and a bimodal grain size distribution.

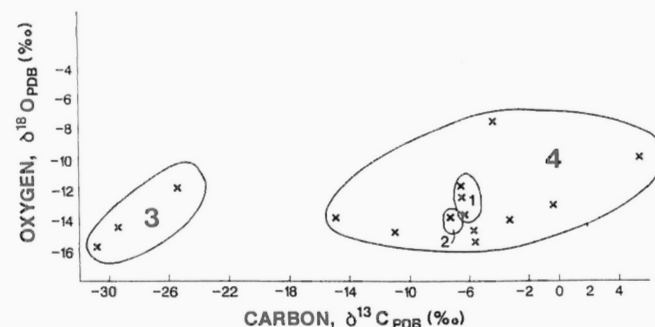


**Figure 20:** Graph of  $^{13}C_{PDB}$  versus  $^{18}O_{PDB}$  of carbonate cements, basal Haida lithofacies. 1 = Beresford Bay-Langara Island; 2 = Skidegate Inlet; 3 = Cumshewa Inlet-north shore; 4 = Cumshewa Inlet-south shore. Anomalous light isotopic ratio compositions of Cumshewa Inlet-north shore may be related to higher plant ( $C_3$ ) matter. Presence of higher plants agrees well with fluvial sedimentological indicators seen in outcrop such as herringbone crossbedding, absence of trace fossils and coarse grain size. Outcrops with light  $^{13}C$  values exhibit the best visual porosity and reservoir characteristics. Contouring of carbon isotope data may be useful in delineating prospective, potentially porous fluvial sedimentary environments.



#### *Lower Haida sandstone and upper Haida lithofacies*

Feldspars and volcanic rock fragments are preferentially dissolved in specific facies of the stratigraphic sequence. Aluminosilicates leached in the lower Haida sandstone lithofacies are observed mainly in units interpreted as offshore bars. Minor amounts of primary porosity apparently remained after burial and compaction due to the good sorting in bar deposits. Subsequent maturation of in situ organic matter released acids which migrated through the primary pores, chelating and dissolving early cements and detrital grains. Thus, to create porosity a formation must first have porosity (Surdam et al., 1984).

#### *Skidegate Formation*

Chlorite is the dominant diagenetic mineral in the Skidegate Formation. Chloritization of biotite and the precipitation of authigenic pore-filling and pore-lining chlorite is similar to that in the overlying Honna Formation. Numerous chloritized biotite flakes contain displacive opaque minerals, including pyrite and possibly magnetite and hematite.

Plagioclase grains are generally very fresh with little or no effects of weathering or diagenetic alteration; orthoclase, on the other hand, is generally weathered. The susceptibility of orthoclase to dissolution and alteration has created sporadic zones of secondary porosity development. Fabric selective dissolution creating oversized pores is a strong indicator of secondary porosity (Schmidt and McDonald, 1979b). Detrital and authigenic calcite remnants in porous samples may indicate large-scale carbonate dissolution. Organic matter is very abundant in the lithofacies and may have contributed to minor porosity enhancement in the same manner postulated for the basal Haida and lower Haida sandstone lithofacies. The paucity of pore-filling carbonate in porous samples may indicate significant leaching. Although textural evidence to explain the zones of porosity development is lacking, an important prerequisite for porosity enhancement, the existence of primary porosity (Siebert et al., 1984) appears to be fulfilled. A qualitative correlation between initial porosity development and subsequent secondary porosity formation is observed in the lithofacies.

#### *Honna Formation*

The diagenetic mineralogy of the Honna Formation is dominated by the chlorite group. Pore-lining and pore-filling authigenic chlorite and smectite impart green hues on outcrops. Chloritization of ferromagnesian grains, primarily biotite, is pervasive.

Dissolution of hornblende and orthoclase creates substantial porosity locally exceeding 12%. Good secondary porosity enhancement is confined to the Cumshewa Inlet area and may be related to a combination of a hornblende-rich source and structural effects which result in deposition of middle Honna sandstones on Kunga Group paleotopographic highs (Thompson and Thorkelson, 1989).

#### *Diagenetic indications of block faulting*

A diagenetic fingerprint of Late Jurassic through Tertiary block faulting (Thompson and Thorkelson, 1989) and implied multiple episodes of concomitant uplift and subsidence is documented in terms of carbonate cementation/deccementation episodes (Fig. 15).

The preservation of carbonate at increased burial depths decreases substantially, particularly in argillaceous sediments (Hower et al., 1976). Stages 1 and 2 of the composite Queen Charlotte Group diagenetic sequence (Fig. 15) depict an expected pattern of progressively greater burial with the early precipitation and later dissolution of carbonate cements. However, a repeat of carbonate growth and dissolution (Fig. 15, stage 3) may reflect rapid tectonic uplift and repeated burial. Petrologic evidence indicates that a carbonate precipitation/dissolution cycle may have occurred twice in some areas, principally in the Beresford Bay-Langara Island and Cumshewa Inlet regions. Such diagenetic observations may corroborate the suggestion

of Thompson and Thorkelson (1989) that steeply dipping (extension?) faults were active throughout Cretaceous time, creating block uplift and subsidence in the area of Cumshewa Inlet.

#### **PETROLEUM RESERVOIR POTENTIAL**

The middle to Upper Cretaceous sequence of the Queen Charlotte Basin was first suggested as a potential hydrocarbon target by Yorath and Cameron (1982). Lying below Upper Cretaceous and Tertiary Masset volcanics and resting upon Mesozoic basalts, limestones and immature siliciclastics, these volcanoclastic sandstones and conglomerates hold good reservoir potential if the underlying probable source beds, organic-rich Jurassic shales of the Kunga and Maude groups, are not overmature as a result of burial or Jurassic igneous activity (Thompson, 1988). Haimila and Procter (1982) infer the middle to Upper Cretaceous rocks in Dixon Entrance, Hecate Strait and Queen Charlotte Sound to have reservoir potential. Souther (1988) indicates Yakoun volcanism may have created overmaturation in Jurassic Kunga Group source rocks, particularly in southerly areas of the Queen Charlotte Islands; Masset volcanics appear to be localized and have little thermal effect on hydrocarbon source and reservoir rocks. Vellutini (1988) concludes Mesozoic strata on Moresby Island hold poor hydrocarbon source potential due to high heat flows associated with plutonism, whereas Mesozoic strata of Graham Island are immature to mature and hold fair to good oil and gas source potential.

Stacey (1975) suggests sediments of pre-Tertiary age may be found beneath Masset volcanics in Hecate Strait and Queen Charlotte Sound. Clowes and Gens-Lenartowicz (1985) inferred the Masset to be widely deposited in Queen Charlotte Sound; they traced a Mesozoic sedimentary package up to 1 km thick in a sonobuooy refraction

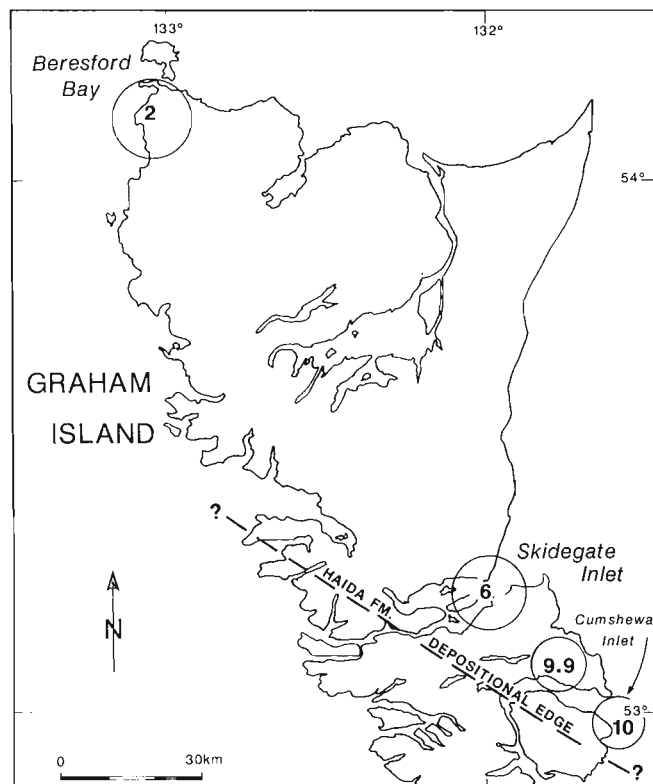


**Figure 21:** Outcrop porosity, basal Haida lithofacies. Average porosity values expressed as percent, estimated from visual inspection of blue dyed epoxy impregnated thin sections. Although data are limited a porosity increase is seen as the Haida Formation depositional edge is approached.

study. Fogarassy and Barnes (1988a, 1988b; 1989) and McWhae et al. (1988) have upgraded the potential of the Cretaceous strata to the level of a secondary objective, following the primary hydrocarbon objective in the Queen Charlotte Basin, the Miocene-Pliocene Skonun Formation (Shouldice, 1971).

### Basal Haida and lower Haida sandstone lithofacies

Porosity in the basal Haida lithofacies increases in a southeasterly direction (Fig. 21). Maximum porosity development is preserved in outcrops on the north and south shores of Cumshewa Inlet where values may exceed 15%. The majority of porosity is regarded as effective, because the presence of well rounded framework grains and the lack of clay minerals contribute to fair observed permeabilities which would significantly increase recoverable reserves of oil and gas. The thickness of the basal Haida is about 40 m in southern sections and approaches 190 m on northwest Graham Island. Porosity is variable; approximately 30% of the basal Haida lithofacies in Skidegate and Cumshewa inlets exceeds a 10% effective porosity cut-off, the minimum believed required to generate economic recoveries of hydrocarbons. Attractiveness of the basal Haida lithofacies may in part may related to high energy fluvial sedimentation processes, which have probably winnowed labile fractions.

The sandstones of the lower Haida lithofacies may hold marginal potential, despite exhibiting low porosity values (less than 5%) and composed chiefly of feldspars, lithic fragments and clays. The thickness of the lower Haida sandstone averages 500 m. Porosity development is limited, with a 10% porosity cut-off applicable to 10% of the lithofacies. Porosity occurrences, however, correlate well with observed offshore bar build-ups which developed during the middle to Upper Cretaceous marine transgression in the Queen Charlotte Islands.

### Prospects

Analogies which may be of use in hydrocarbon exploration of the Queen Charlotte Basin include developed plays in Cook Inlet, Alaska (Magoon and Claypool, 1981) and western Washington and Oregon (Armentrout and Suck, 1985). These two areas have established production in strata initially considered non-prospective. Cook Inlet, for example, is similar, both structurally and stratigraphically, to the Queen Charlotte Basin. Trapping of hydrocarbons there appears to be related, at least in part, to secondary porosity development in Tertiary strata which unconformably overlie marine Middle Jurassic source rocks. Reservoir quality sandstones may also exist in Cretaceous strata.

Thompson (1988) and Lewis and Ross (1988) have documented a prominent fold belt trending through Cumshewa Inlet and possibly southeastward into Hecate Strait. Active Late Jurassic through Tertiary extensional block faulting in the vicinity of the Rennell Sound fold belt appears to have influenced sedimentation patterns in the middle to Upper Cretaceous sequence (Thompson, 1988; Thompson and Thorkelson, 1989). Porous zones observed in the basal Haida lithofacies may be related to specific depositional environments localized near the fold belt. Extensional structural events may have also influenced sedimentation patterns in the lower Haida sandstone where observed marginal porosity development is confined to probable offshore bar build-ups. Folding and faulting of pre-Cretaceous strata may also have occurred in the Beresford Bay-Langara Island region. As at Cumshewa Inlet, basal Haida conglomerates and coarse grained sandstones rest on Late Triassic *Monotis* beds of the black limestone member (Peril Formation) of the Kunga Group. Investigations indicate a northwesterly structural trend (Lewis and Ross, 1988).

The organic maturation data of Vellutini (1988) outline broad areas of interest with respect to secondary porosity development in the Queen Charlotte Group. Areas in which aluminosilicate dissolution textures were observed are coincident with areas of mature and overmature Juras-

sic strata (Fig. 22). Thus, a positive correlation exists on a regional scale between the organic and inorganic diagenetic histories of Cretaceous rocks of the Queen Charlotte Islands.

### Areas of interest

Cumshewa Inlet has many positive geological factors in terms of reservoir development including: 1) primary and secondary porosity development; 2) proximity to the Rennell Sound fold belt which, during extensional block faulting episodes has influenced sedimentation and reservoir development patterns; 3) organic maturation data indicate in situ organic material (kerogen) has undergone sufficient diagenesis in terms of CO<sub>2</sub> and organic acid production; and 4) potential for conduction of aluminosilicate and carbonate leaching fluids along multiple unconformity surfaces that exist at the base of the Queen Charlotte Group and potentially elsewhere throughout the sequence due to reactivation of bounding extensional block faults. This greatly enhances porosity of all units, particularly the basal Haida lithofacies.

The Beresford Bay-Langara Island region is less prospective. A structural trend similar to the Rennell Sound fold belt exists; however organic maturation data indicate insufficient heat for CO<sub>2</sub> and organic acid production. Tertiary intrusions, by creating maturation anomalies, may have contributed to local secondary porosity development. Intrusions or thermal solution effects of regional faults cutting Honna Formation sandstones at Pillar Bay (near Langara Island) may have produced anomalous visual porosity values approaching 30% (T.S. Hamilton, pers. comm., 1987).

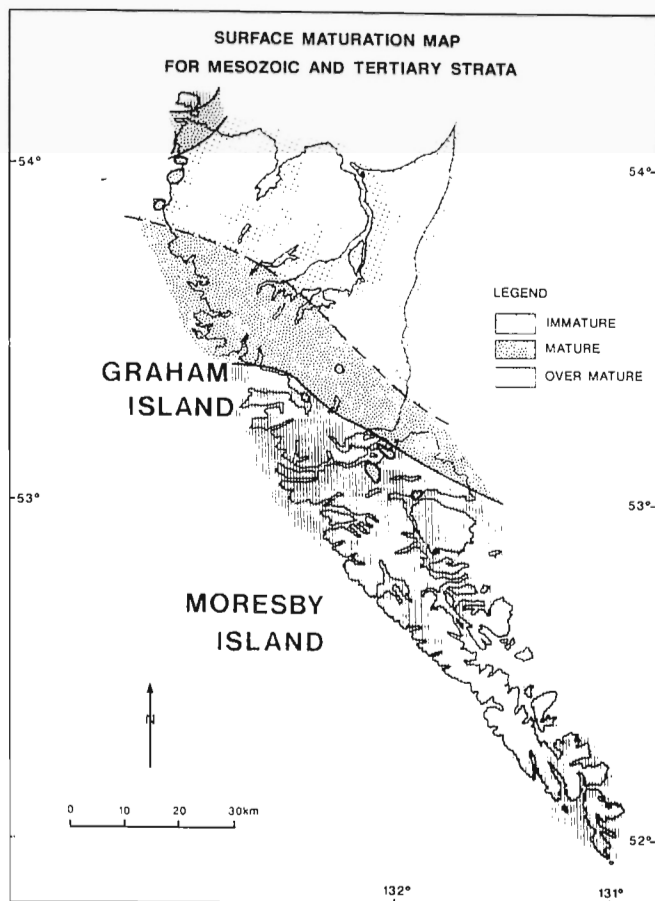


**Figure 22:** Surface maturation trends for Mesozoic and Tertiary strata derived from vitrinite reflectance data. Immature = 0.00-0.50 %Ro<sub>rand</sub>, mature = 0.50-1.35 %Ro<sub>rand</sub> and overmature = greater than 1.35 %Ro<sub>rand</sub> (adapted from Vellutini, 1988).



## Discussion: petroleum reservoir potential

Structural highs may provide the best areas of interest for secondary porosity development. Subaerial exposure and development of an unconformity surface overlain by porous fluvial conglomerates and sandstones, which may eventually conduct groundwaters capable of leaching secondary porosity, are seen at Cumshewa Inlet, near the Rennell Sound fold belt. This area of interest may be extrapolated to adjacent offshore regions. Results of seismic surveys done under the Frontier Geoscience Program may show the continuation of onshore structural features to the offshore (Thompson and Thorkelson, 1989).

The basal Haida sandstones and conglomerates can be regarded as a potential secondary hydrocarbon exploration objective in the Queen Charlotte Basin. Outcrop assessment of this siliciclastic sequence indicates the presence of potential reservoir strata. *Inoceramus* assemblages collected in Cumshewa Inlet indicate correlation with the basal Haida lithofacies and the Longarm Formation (J.W. Haggart and R.I. Thompson, pers. comm., 1989). If these units are coeval then the Longarm Formation (or basal Haida lithofacies) may hold reservoir potential in southerly areas of the Queen Charlotte Islands. Petrologic examination of southerly Longarm outcrops may confirm the Lower Cretaceous strata as a hydrocarbon objective.

With the exception of isolated porous zones in outcrop, the remainder of the Haida Formation and the Skidegate and Honna formations hold minor reservoir potential. Poor reservoir quality in the Honna Formation may, in part, be related to mode of deposition. Fan-delta deposits generally have little or no porosity development due to poor sorting, matrix abundance and polymictic and heterolithic composition (McPherson et al., 1987).

## CONCLUSIONS

1. The basal Haida lithofacies is a separate and distinct unit from the rest of the Queen Charlotte Group. High quartz framework grain percentages and lack of abundant phyllosilicate cement combined with nonmarine sedimentological indicators provide a strong basis for formalizing this lithofacies as a separate member or formation in the Queen Charlotte Group.
2. The Haida Formation has a southwesterly source area with a probable pinchout occurring south of Cumshewa Inlet; Honna Formation sediments are derived from the northeast and probably interfinger with the Skidegate Formation. The Skidegate Formation is also likely to be a basinward, deeper water equivalent of some parts of the Haida and Honna formations.
3. Clay mineralogy is much more complex than previously documented. Mixed-layer clays, illite/smectite, corrensite, and illite/smectite/chlorite, along with iron-rich chlorite, dominate sandstone phyllosilicate assemblages.
4. A composite tripartite paragenetic sequence, involving the growth and dissolution of clays, carbonates and aluminosilicates best describes the diagenetic history.
5. Petroleum reservoir potential exists in the basal Haida lithofacies. The lower Haida sandstone lithofacies may have minor potential; the remainder of the Queen Charlotte Group has little or no potential.

## ACKNOWLEDGMENTS

Thanks are given for technical assistance to Ms. Stanya Horsky, Mr. John Knight, Ms. Bente Nielsen, all from the Department of Geological Sciences, University of British Columbia, and Dr. Les Lavkulich of the Department of Soil Science, University of British Columbia. Thanks are extended to Mr. David Mercer, Mr. David Rhys, Mr. Jason Miller and Mr. Ken Hoffman for assistance in the field.

This work was funded by the Frontier Geoscience Program of the Geological Survey of Canada; Dr. Bob Thompson, Party Chief, is thanked expressly. Research grants from Texaco Canada Resources Ltd., Chevron Canada Resources Ltd. and the American Association of Petroleum Geologists are gratefully acknowledged. Financial support for J.A.S.F. was provided by a University of British Columbia Graduate Teaching Assistantship and a Natural Sciences and Engineering Research Council Postgraduate Scholarship.

## REFERENCES

- Anderson, R.G. and Greig, C.J.  
1989: Jurassic and Tertiary plutonism in the Queen Charlotte Islands, British Columbia; in *Current Research, Part H*, Geological Survey of Canada, Paper 89-111, p. 95-104.
- Armentrout, J.M. and Suek, D.H.  
1985: Hydrocarbon exploration in western Oregon and Washington; *American Association of Petroleum Geologists Bulletin*, v. 69, p. 627-643.
- Boles, J.R.  
1972: Composition, optical properties, cell dimensions, and thermal stability of some heulandite group zeolites; *American Mineralogist*, v. 57, p. 1463-1493.
- Boles, J.R. and Franks, S.G.  
1979: Clay diagenesis in Wilcox sandstones of southwest Texas: implications of smectite diagenesis on sandstone cementation; *Journal of Sedimentary Petrology*, v. 49, p. 55-70.
- Brigatti, M.F. and Poppi, L.  
1984: Crystal chemistry of corrensite: a review; *Clays and Clay Minerals*, v. 32, p. 391-399.
- Brown, B.E. and Bailey, S.W.  
1962: Chlorite polytypism: I. Regular and semi-random one-layer structures; *American Mineralogist*, v. 47, p. 819-850.
- Buczynski, C. and Chafetz, H.S.  
1987: Siliciclastic grain breakage and displacement due to carbonate crystal growth: an example from the Leuders Formation (Permian) of north-central Texas, U.S.A.; *Sedimentology*, v. 34, p. 837-843.
- Burley, S.D. and Kantorowicz, J.D.  
1986: Thin section and S.E.M. textural criteria for the recognition of cement-dissolution porosity in sandstones; *Sedimentology*, v. 33, p. 587-604.
- Cameron, B.E.B. and Hamilton, T.S.  
1988: Contributions to the stratigraphy and tectonics of the Queen Charlotte Basin, British Columbia; in *Current Research, Part E*, Geological Survey of Canada, Paper 88-1E, p. 221-227.
- Chamberlain, C.K.  
1978: Recognition of trace fossils in cores; in *Trace Fossil Concepts*, P.A. Basan (ed.), Society of Economic Paleontologists and Mineralogists Short Course No. 5, p. 133-183.
- Chang, H.K., MacKenzie, F.T., and Schoonmaker, J.  
1986: Comparisons between the diagenesis of dioctahedral and trioctahedral smectite, Brazilian offshore basins; *Clays and Clay Minerals*, v. 34, p. 407-423.
- Clapp, C.H.  
1914: A geological reconnaissance on Graham Island, Queen Charlotte Group, B.C.; Geological Survey of Canada, Summary Report, 1912, p. 12-40.
- Clowes, R.M. and Gens-Lenartowicz, E.  
1985: Upper crustal structure of southern Queen Charlotte Basin from sonobuoy refraction studies; *Canadian Journal of Earth Sciences*, v. 22, p. 1696-1710.
- Coombs, D.S.  
1952: Cell size, optical properties and chemical composition of laumontite and leonhardtite; *American Mineralogist*, v. 37, p. 812-830.
- Dawson, G.M.  
1880: Report on the Queen Charlotte Islands, 1878; Geological Survey of Canada, Report of Progress for 1878-1879, p. 1B-239B.
- DeNiro, M.J.  
1983: Distribution of the stable isotopes of carbon, nitrogen, oxygen, and hydrogen among plants; in *Organic Geochemistry of Contemporary and Ancient Sediments*, W.G. Meinschein and J.M. Hayes (ed.), Society of Economic Paleontologists and Mineralogists Short Course, Great Lakes Section, p. 4-1 - 4-27.
- Dickinson, W.R.  
1970: Interpreting detrital modes of greywacke and arkose; *Journal of Sedimentary Petrology*, v. 40, p. 695-707.
- Dickinson, W.R. and Suczek, C.A.  
1979: Plate tectonics and sandstone compositions; *American Association of Petroleum Geologists Bulletin*, v. 63, p. 2164-2182.
- Dickson, J.A.D.  
1965: A modified staining technique for carbonates in thin section; *Nature*, v. 205, p. 587.

- Ells, R.W.  
1906: Report on Graham Island, B.C.; Geological Survey of Canada Annual Report, New Series, v. 16, Part B, p. 1-46.
- Eslinger, E. and Pevear, D.  
1988: Clay minerals for petroleum geologists and engineers; Society of Economic Paleontologists and Mineralogists Short Course No. 22, 413 p.
- Faust, G.T. and Murata, K.J.  
1953: Stevensite, redefined as a member of the montmorillonite group; *American Mineralogist*, v. 38, p. 973-987.
- Fogarassy, J.A.S. and Barnes, W.C.  
1988a: Stratigraphy, diagenesis and petroleum reservoir potential of the mid- to Upper Cretaceous Haida and Honna formations of the Queen Charlotte Islands, British Columbia; *in* Current Research, Part E, Geological Survey of Canada, Paper 88-1E, p. 265-268.  
1988b: Petroleum reservoir aspects of middle to Upper Cretaceous and Tertiary strata of the Queen Charlotte Islands; *in* Some Aspects of the Petroleum Geology of the Queen Charlotte Islands, R. Higgs (compiler), Canadian Society of Petroleum Geologists Field Trip Guidebook, p. 22-25.  
1989: The middle Cretaceous Haida Formation: a potential hydrocarbon reservoir in the Queen Charlotte Islands, British Columbia; *in* Current Research, Part H, Geological Survey of Canada, Paper 89-1H, p. 47-52.
- Frey, R.W. and Pemberton, S.G.  
1985: Biogenic structures in outcrops and cores. I. Approaches to ichnology; *Bulletin of Canadian Petroleum Geology*, v. 33, p. 72-115.
- Galloway, W.E.  
1974: Deposition and diagenetic alteration of sandstone in northeast Pacific arc-related basins: implications for greywacke genesis; *Geological Society of America Bulletin*, v. 85, p. 379-390.
- Haggart, J.W.  
1986: Stratigraphic investigations of the Cretaceous Queen Charlotte Group, Queen Charlotte Islands, British Columbia; Geological Survey of Canada, Paper 86-20, 24 p.  
1987: On the age of the Queen Charlotte Group of British Columbia; *Canadian Journal of Earth Sciences*, v. 24, p. 2470-2476.
- Haggart, J.W. and Higgs, R.  
1989: A new Late Cretaceous mollusc fauna from the Queen Charlotte Islands, British Columbia; *in* Current Research, Part H, Geological Survey of Canada, Paper 89-1H, p. 59-64.
- Haggart, J.W., Lewis, P.D., and Hickson, C.J.  
1989: Stratigraphy and structure of Cretaceous strata, Long Inlet, Queen Charlotte Islands, British Columbia; *in* Current Research, Part H, Geological Survey of Canada, Paper 89-1H, p. 65-72.
- Haimila, N.E. and Procter, R.M.  
1982: Hydrocarbon potential of offshore British Columbia; Geological Survey of Canada, Open File 824, 28 p.
- Hayes, J.B.  
1970: Polyttypism of chlorite in sedimentary rocks; *Clays and Clay Minerals*, v. 18, p. 285-306.
- Higgs, R.  
1988: Sedimentology of the Honna Formation, Upper Cretaceous fan-delta conglomerates; *in* Some Aspects of the Petroleum Geology of the Queen Charlotte Islands, R. Higgs (compiler), Canadian Society of Petroleum Geologists Field Trip Guidebook, p. 14-22.
- Hoffman, J.  
1976: Regional metamorphism and K-Ar dating of clay minerals in Cretaceous sediments of the disturbed belt of Montana; Ph.D. thesis, Case Western Reserve University, 266 p.
- Hoffman, J. and Hower, J.  
1979: Clay mineral assemblages as low grade metamorphic geothermometers: application to the thrust faulted disturbed belt of Montana, U.S.A.; *in* Aspects of Diagenesis, P.A. Scholle and P.R. Schluger (ed.), Society of Economic Paleontologists and Mineralogists Special Publication 26, p. 55-79.
- Houghton, H.F.  
1980: Refined techniques for staining plagioclase and alkali feldspar in thin section; *Journal of Sedimentary Petrology*, v. 50, p. 629-631.
- Hower, J., Eslinger, E.V., Hower, M.E., and Perry, E.A.  
1976: Mechanism of burial metamorphism of argillaceous sediment: 1. Mineralogical and chemical evidence; *Geological Society of America Bulletin*, v. 87, p. 725-737.
- James, N.P.  
1984: Diagenesis 9. Limestones – the meteoric diagenetic environment; *Geoscience Canada*, v. 11, p. 161-194.
- Keller, W.D., Reynolds, R.C., and Inoue, A.  
1986: Morphology of clay minerals in the smectite-to-illite conversion series by scanning electron microscopy; *Clays and Clay Minerals*, v. 34, p. 187-197.
- Lewis, P.D. and Ross, J.V.  
1988: Preliminary investigations of structural styles in Mesozoic strata of the Queen Charlotte Islands, British Columbia; *in* Current Research, Part E, Geological Survey of Canada, Paper 88-1E, p. 275-279.
- MacKenzie, J.D.  
1916: Geology of Graham Island, British Columbia; Geological Survey of Canada Memoir 88, 221 p.
- Magoon, L.B. and Claypool, G.E.  
1981: Petroleum geology of Cook Inlet Basin – an exploration model; *American Association of Petroleum Geologists Bulletin*, v. 65, p. 1043-1061.
- McLearn, F.H.  
1972: Ammonoids of the Lower Cretaceous sandstone member of the Haida Formation, Skidegate Inlet, Queen Charlotte Islands, western British Columbia; *Geological Survey of Canada, Bulletin* 188, 78 p.
- McPherson, J.G., Shanmugam, G., and Moiola, R.J.  
1987: Fan-deltas and braid deltas: varieties of coarse grained deltas; *Geological Society of America Bulletin*, v. 99, p. 331-340.
- McWhae, J.R., Ross, R., and Ross, K.  
1988: Evolution and hydrocarbon potential of Queen Charlotte Basin, Canada; *American Association of Petroleum Geologists Bulletin*, v. 72, p. 222.
- Post, J.L.  
1984: Saponite from near Ballarat, California; *Clays and Clay Minerals*, v. 32, p. 147-153.
- Reynolds, Jr., R.C. and Hower, J.  
1970: The nature of interlayering in mixed-layer illite-montmorillonites; *Clays and Clay Minerals*, v. 18, p. 25-36.
- Riccardi, A.C.  
1981: An Upper Cretaceous ammonite and inoceramids from the Honna Formation, Queen Charlotte Islands, British Columbia; *in* Current Research, Part C, Geological Survey of Canada, Paper 81-1C, p. 1-8.
- Richardson, J.  
1873: Report on the coal-fields of Vancouver and Queen Charlotte Islands, with a map of the distribution of the former; Geological Survey of Canada, Report of Progress for 1872-73, p. 32-86.
- Schidlowski, M.  
1986:  $^{13}\text{C}/^{12}\text{C}$  ratios as indicators of biogenicity; *in* Biological Markers in the Sedimentary Record, R.B. Johns (ed.), Elsevier, Amsterdam, p. 347-361.
- Schmidt, V. and McDonald, D.A.  
1979a: The role of secondary porosity in the course of sandstone diagenesis; *in* Aspects of Diagenesis, P.A. Scholle and P.R. Schluger (ed.), Society of Economic Paleontologists and Mineralogists Special Publication 26, p. 175-207.  
1979b: Texture and recognition of secondary porosity in sandstones; *in* Aspects of Diagenesis, P.A. Scholle and P.R. Schluger (ed.), Society of Economic Paleontologists and Mineralogists Special Publication 26, p. 209-225.
- Schoonmaker, J.  
1986: Clay mineralogy and diagenesis of sediments from deformation zones in the Barbados accretionary wedge (Deep Sea Drilling Project Leg 78A); *Geological Society of America Memoir* 166, p. 105-116.
- Shouldice, D.H.  
1971: Geology of the western Canadian continental shelf; *Bulletin of Canadian Petroleum Geology*, v. 19, p. 405-436.
- Siebert, R.M., Moncure, G.K., and Lahann, R.W.  
1984: A theory of framework grain dissolution in sandstones; *in* Clastic Diagenesis, D.A. McDonald and R.C. Surdam (ed.), American Association of Petroleum Geologists Memoir 37, p. 163-175.
- Souther, J.G.  
1988: Implications for hydrocarbon exploration of dyke emplacement in the Queen Charlotte Islands, British Columbia; *in* Current Research, Part E, Geological Survey of Canada, Paper 88-1E, p. 241-245.
- Stacey, R.A.  
1975: Structure of the Queen Charlotte Basin; *in* Canada's Continental Margins and Offshore Petroleum Exploration, C.J. Yorath, E.R. Parker, and D.J. Glass (ed.), Canadian Society of Petroleum Geologists Memoir 4, p. 723-741.
- Suquet, H., de la Calle, C., and Pezerat, H.  
1975: Swelling and structural organization of saponite; *Clays and Clay Minerals*, v. 23, p. 1-9.
- Surdam, R.C., Boese, S.W., and Crossey, L.J.  
1984: The chemistry of secondary porosity; *in* Clastic Diagenesis, D.A. McDonald and R.C. Surdam (ed.), American Association of Petroleum Geologists Memoir 37, p. 127-149.
- Sutherland Brown, A.  
1968: Geology of the Queen Charlotte Islands, British Columbia; British Columbia Department of Mines and Petroleum Resources Bulletin 54, 226 p.
- Thompson, R.I.  
1988: Late Triassic through Cretaceous geological evolution, Queen Charlotte Islands, British Columbia; *in* Current Research, Part E, Geological Survey of Canada, Paper 88-1E, p. 217-219.
- Thompson, R.I. and Thorkelson, D.  
1989: Regional mapping update, central Queen Charlotte Islands, British Columbia; *in* Current Research, Part H, Geological Survey of Canada, Paper 89-1H, p. 7-11.

- Vellutini, D.**  
**1988:** Organic maturation and source rock potential of Mesozoic and Tertiary strata, Queen Charlotte Islands, British Columbia; M.Sc. thesis, University of British Columbia, Vancouver.
- Walker, R.G.**  
**1979a:** Facies models 7. Shallow marine sands; *in* Facies Models, R.G. Walker (ed.), Geoscience Canada Reprint Series 1, p. 75-89.  
**1979b:** Facies models 8. Turbidites and associated coarse clastic deposits; *in* Facies Models, R.G. Walker (ed.), Geoscience Canada Reprint Series 1, p. 91-102.
- Wheeler, J.O. and Gabrielse, H.**  
**1972:** The cordilleran structural province; Geological Association of Canada Special Paper 11, 81 p.
- Williams, H., Turner, F.J., and Gilbert, C.M.**  
**1954:** Petrography. An Introduction to the Study of Rocks in Thin Sections; W.H. Freeman and Company, San Francisco, 406 p.
- Wilson, M.D. and Pittman, E.D.**  
**1977:** Authigenic clays in sandstones: recognition and influence on reservoir properties and paleo-environmental analysis; *Journal of Sedimentary Petrology*, v. 47, p. 3-31.
- Yagishita, K.**  
**1985:** Mid- to Late Cretaceous sedimentation in the Queen Charlotte Islands, British Columbia: lithofacies, paleocurrent and petrographic analyses of sediments; Ph.D. thesis, University of Toronto.
- Yanguas, J.E. and Paxton, S.T.**  
**1986:** A new technique for preparation of petrographic thin sections using ultraviolet-curing adhesive; *Journal of Sedimentary Petrology*, v. 56, p. 539-540.
- Yorath, C.J. and Cameron, B.E.B.**  
**1982:** Oil off the west coast?; *Geos*, v. 11, no. 2, p. 13-15.
- Yorath, C.J. and Chase, R.L.**  
**1981:** Tectonic history of the Queen Charlotte Islands and adjacent areas – a model; *Canadian Journal of Earth Sciences*, v. 18, p. 1717-1739.
- Yorath, C.J. and Hyndman, R.D.**  
**1983:** Subsidence and thermal history of the Queen Charlotte Basin; *Canadian Journal of Earth Sciences*, v. 20, p. 135-159.

# Sedimentology and implications for petroleum exploration of the Honna Formation, northern Queen Charlotte Islands, British Columbia

Roger Higgs<sup>1</sup>

Higgs, R., Sedimentology and implications for petroleum exploration of the Honna Formation, northern Queen Charlotte Islands, British Columbia; in *Evolution and Hydrocarbon Potential of the Queen Charlotte Basin*, British Columbia, Geological Survey of Canada, Paper 90-10, p. 295-304, 1991.

## Abstract

*The Honna Formation, consisting of Coniacian conglomerates, sandstones and subordinate mudstones, has two main outcrops, one in the central Queen Charlotte Islands, the subject of an earlier sedimentological study by the author, and the other in the north, the subject of this study. Facies in the northern outcrop, dominated by clast-supported pebble-cobble conglomerate, are very similar to those of the central outcrop. Conglomerates occur as beds 1-5 m thick, graded in some cases, stratified in others, and commonly imbricated; cross-stratification is exceedingly rare. The conglomerates are interpreted as being of submarine mass-flow origin, deposited on a deep-water fan which draped a fault-controlled basin-margin slope. Imbrication studies indicate that the paleoslope was northward, hence the basin-margin (active) fault lay to the south (Beresford Bay Fault?).*

*It is possible, given the dextral-transform character of the present-day continental margin, that discrete crustal blocks within the Queen Charlotte Islands have rotated clockwise. If the northern Honna outcrop belongs to one such rotated block, the sediments may actually be easterly derived, like the strata of the central outcrop. If so, uplift along just one fault (Sandspit Fault), rather than two orthogonal faults, may be responsible for both the northern and central Honna conglomerates. This raises the possibility of additional Honna conglomerates occurring along the Sandspit Fault in the intervening region, beneath Tertiary overburden, offering petroleum-reservoir potential.*

## Résumé

*La formation de Honna, composée de conglomérats, de grès et de mudstones accessoires du Coniacien, affleure principalement dans deux régions : dans le centre des îles de la Reine-Charlotte, qui a été le sujet d'une étude sédimentologique antérieure par l'auteur, et dans le nord de la même région, zone qui fait l'objet de la présente étude. Les faciès dans l'affleurement septentrional, surtout composés de conglomérats de cailloux-petits blocs mélangés de clastes sont très semblables à ceux de l'affleurement du centre. Les conglomérats se présentent sous forme de couches de 1 à 5 m d'épaisseur, granoclassées dans certains cas, stratifiées dans d'autres, et souvent imbriquées; la stratification oblique est très rare. Les conglomérats seraient le résultat d'un écoulement de masse sous-marin déposé sur un cône d'e ou au profonde drapant un talus de limite de bassin contrôlé par failles. L'analyse de l'imbrication indique que le paléotalus est orienté vers le nord; par conséquent, la faille de limite de bassin (active) se dirige vers le sud (faille Beresford Bay?).*

*Il est possible, compte tenu du caractère dextre des failles transformantes de la marge continentale actuelle, que des blocs crustaux distincts au sein des îles de la Reine-Charlotte se soient déplacés dans le sens horaire des aiguilles d'une montre. Si l'affleurement septentrional de la formation de Honna appartient à l'un des blocs ayant subi une telle rotation, les sédiments ont pu en réalité dériver vers l'est, comme les couches de l'affleurement du centre. Si c'est le cas, le soulèvement le long d'une seule faille (faille Sandspit) plutôt que de deux failles orthogonales, peut être à l'origine des deux conglomérats de la formation de Honna, celui du nord et celui du centre. Il ressort de ce qui précède qu'il est possible que d'autres conglomérats de la formation de Honna reposent le long de la faille Sandspit dans la région intermédiaire, au-dessous des roches de couverture tertiaires, et qu'elles constituent des roches réservoirs de pétrole.*

<sup>1</sup> Pacific Geoscience Centre, Geological Survey of Canada, P.O. Box 6000, Sidney, B.C. V8L 4B2  
Present address: Higgs Petroleum Consulting Ltd., 743 Oliver Street, Victoria, B.C. V8S 4W5

## INTRODUCTION

The Honna Formation, which crops out in central and northern Queen Charlotte Islands (Figs. 1, 2), is thick and coarse grained, and therefore has petroleum-reservoir potential in the subsurface. However, the subsurface extent of the Honna Formation is unknown: none of the oil-exploration boreholes in the region (Fig. 1) penetrated the Honna Formation, most holes bottoming in younger (Tertiary) deposits. Whereas an earlier study (Higgs, 1988a,b, 1990) described the sedimentology of the **central** outcrop (Fig. 1), the present study deals with the **northern** outcrop.

Meagre paleontological collections from the central outcrop indicate that the Honna Formation is Coniacian, at least in part (Haggart, 1986; Higgs, 1990). Microfossils collected in the present study

(below) suggest the same age for the northern outcrop. The Honna conglomerates and sandstones of the central outcrop were interpreted as mass-flow deposits of a deep-water fan delta (Fig. 3; Higgs, 1988a,b, 1990). Development of a fan delta, as for an alluvial fan, implies adjacent mountains. The inferred tectonic setting was a west-verging foreland basin, with the Honna conglomerates accumulating ahead of an active thrust sheet which was supported by an ancestral Sandspit thrust fault (Figs. 2, 3; Higgs, 1988a,b, 1990). The foreland-basin model is supported by seismic profiles acquired subsequently in Hecate Strait to the east (Rohr and Dietrich, 1991), which show low-angle (thrust?) faults with an eastward component of dip. Thompson and Thorkelson (1989) criticized the foreland-basin model, arguing that deformation more likely progressed eastward, "judging by the greater

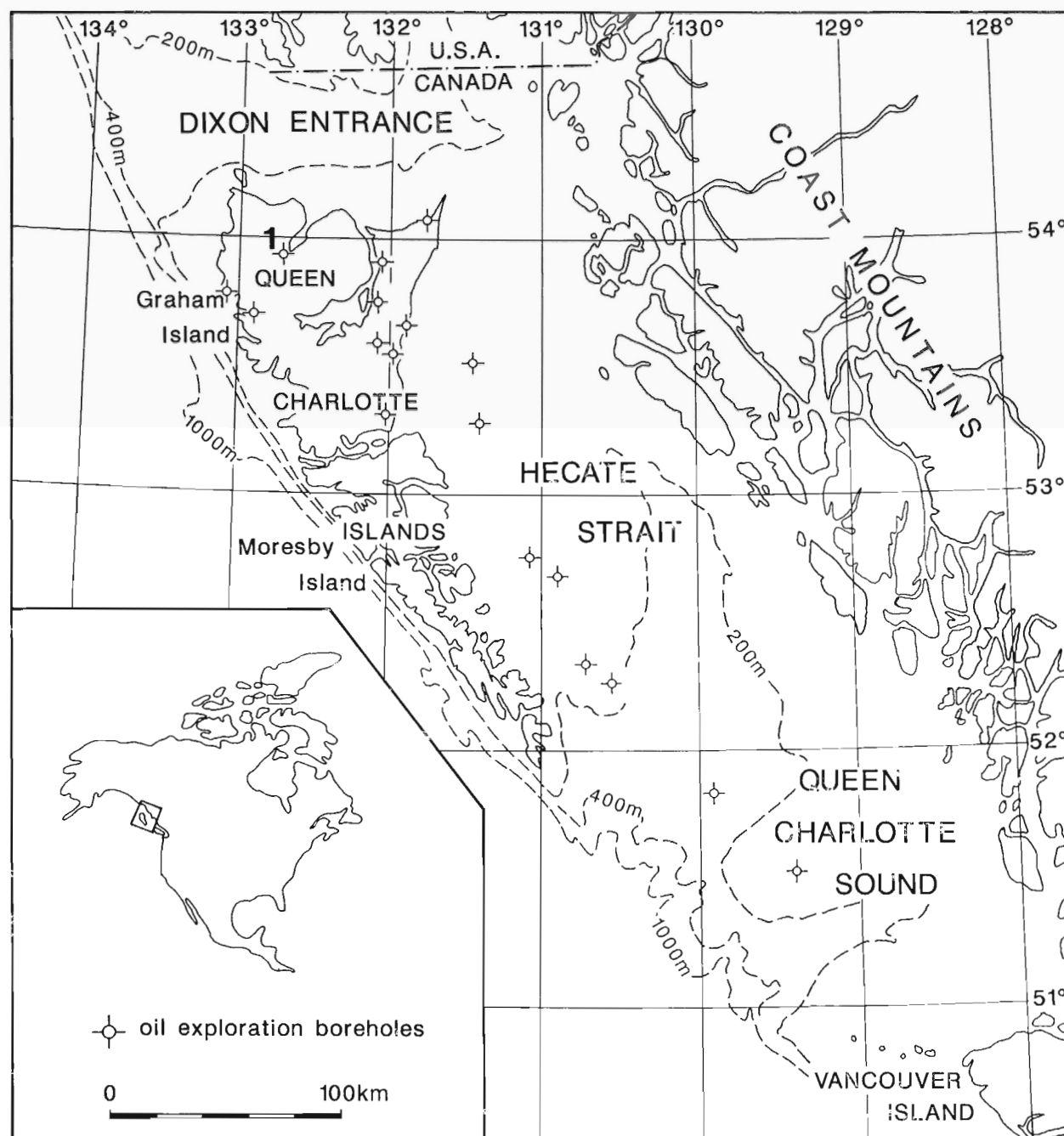


**Figure 1:** Map showing location of the Queen Charlotte Islands. Borehole marked "1" is the Naden borehole (see text).

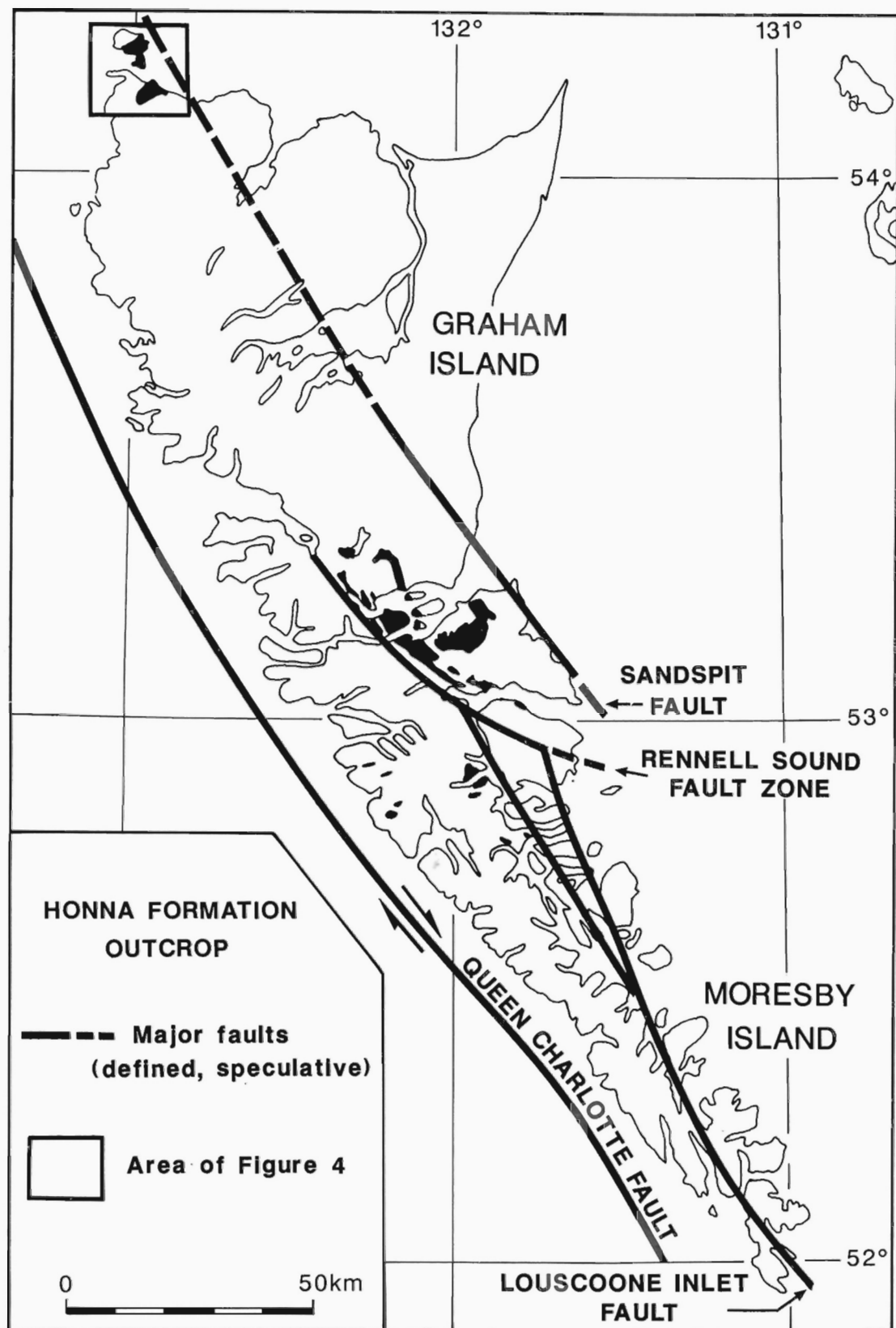


**Figure 2:** Outcrops of the Honna Formation and principal faults of the Queen Charlotte Islands (after Sutherland Brown, 1968; Yorath and Chase, 1981).



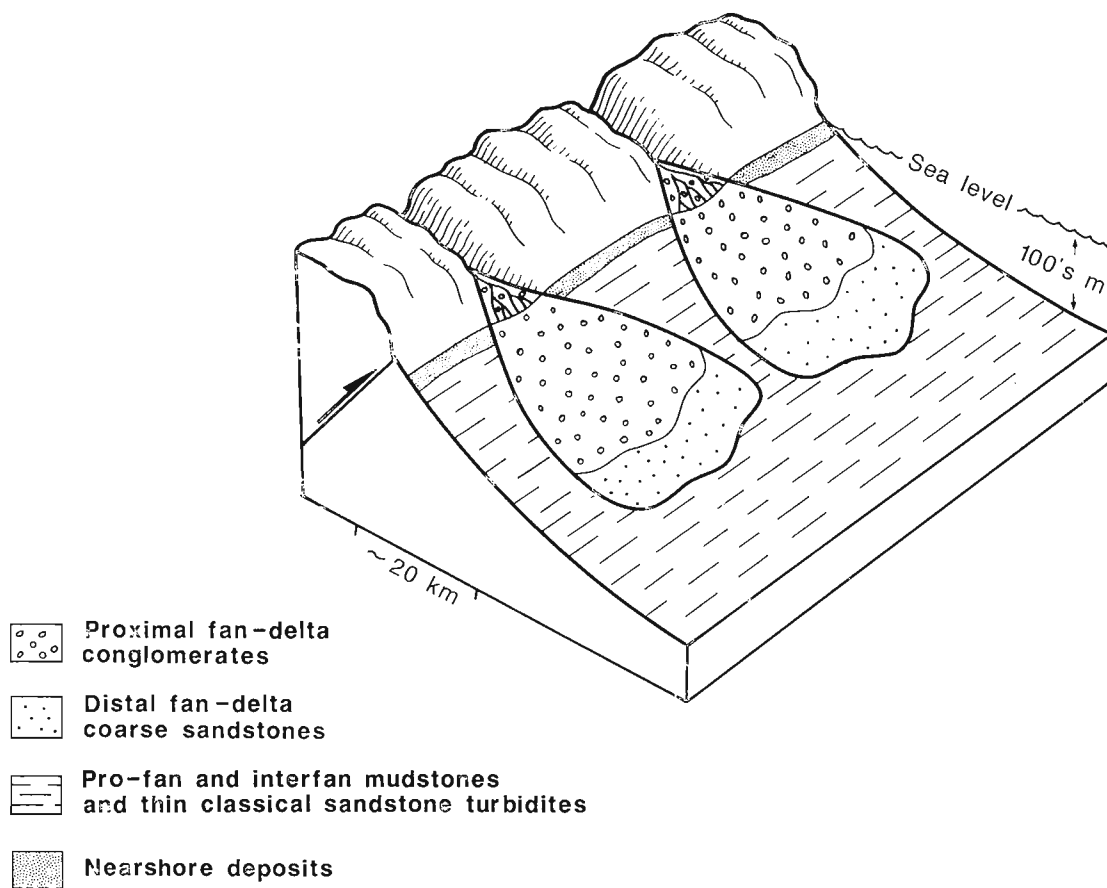


**Figure 3:** Sedimentary environment model for the Honna Formation (after Higgs, 1990). Deposition took place on a gravelly, deep-water fan delta. Additional fan deltas may have developed along strike, as shown here, and may even have coalesced. For illustrative purposes, the source area is depicted as a thrust sheet, but may instead have been a horst block.

amount and complexity of shortening" within the Rennell Sound fault zone (RSF), lying west of the Honna outcrop (Fig. 2). However, this argument overlooks the fact that much of the deformation within the RSF may relate to a younger, Tertiary tectonic episode, possibly involving strike-slip (Sutherland Brown, 1968; Yorath and Chase, 1981); indeed, the RSF resembles a strike-slip flower structure (Young, 1981, p. 242), and a seismic profile across the offshore extension of the RSF (Rohr and Dietrich, 1991) shows flower-type deformation of Tertiary strata.

The northern Honna outcrop (Fig. 4) was visited by the author in June, 1988, and three sections were measured (Fig. 5). Due to forest and muskeg cover, exposures are confined to the coast, where short stratigraphic sections (max. 30 m) are exposed in wave-cut platforms and low cliffs.

In addition to the northern and central Honna outcrops, small outcrops mapped as Honna Formation by Sutherland Brown (1968) occur further south (Fig. 2). However, these strata may instead be Tertiary, based on their intimate association with the Tertiary Masset Formation (Higgs, 1991).

## GEOLOGICAL SETTING

The thickness of the Honna Formation in the northern outcrop is unknown, due to structural complications and discontinuous exposure; however, a thickness of several hundred metres seems likely. In the central outcrop, the Honna Formation rests conformably or paraconformably on Skidegate Formation deep-marine shales and turbidite sandstones (Higgs, 1990). In the northern outcrop, Honna conglomerates can be seen resting on Skidegate Formation shales, with apparent

conformity, at UTM Grid References PR302091 and 302085, on Langara Island. At the first locality, the contact is a low-angle scour, incising a few decimetres over a few metres laterally. At the second locality, the contact is exposed for about 20 m laterally, with no obvious scouring; stratigraphic conformity seems likely, but awaits paleontological confirmation. The Skidegate Formation on Langara Island consists of laminated shale with thin (cm), graded sandstone beds, low to moderate bioturbation (including *Muensteria*), and slump beds; the interpreted depositional environment is a deep-water slope, based on the slump beds and the absence of wave-formed structures (cf. Higgs, 1990).

The top of the Honna Formation is an unconformity, according to Cameron and Hamilton (1988). However, newly discovered Santonian and Campanian marine shales near the central outcrop area (Cameron, 1989; Haggart and Higgs, 1989) may rest conformably on the Honna Formation, or they may be laterally equivalent to the Honna. In the present study area, the Honna Formation appears to be unconformably overlain by Tertiary volcanics (Sutherland Brown, 1968, his Fig. 5).

Unfortunately, no megafossils were discovered during the present study. However, two composite mudstone samples, one from Section B (Fig. 5b, 19.35–21.45 m) and the other from Section C (Fig. 5c, 0.0–3.6 m), yielded upper Cretaceous, post-Turonian foraminifera (Cameron, 1989).

## FACIES

### Description

Like the central outcrop, the dominant lithology in the north is clast-supported, pebble-cobble conglomerate. Beds are mostly 1–5 m

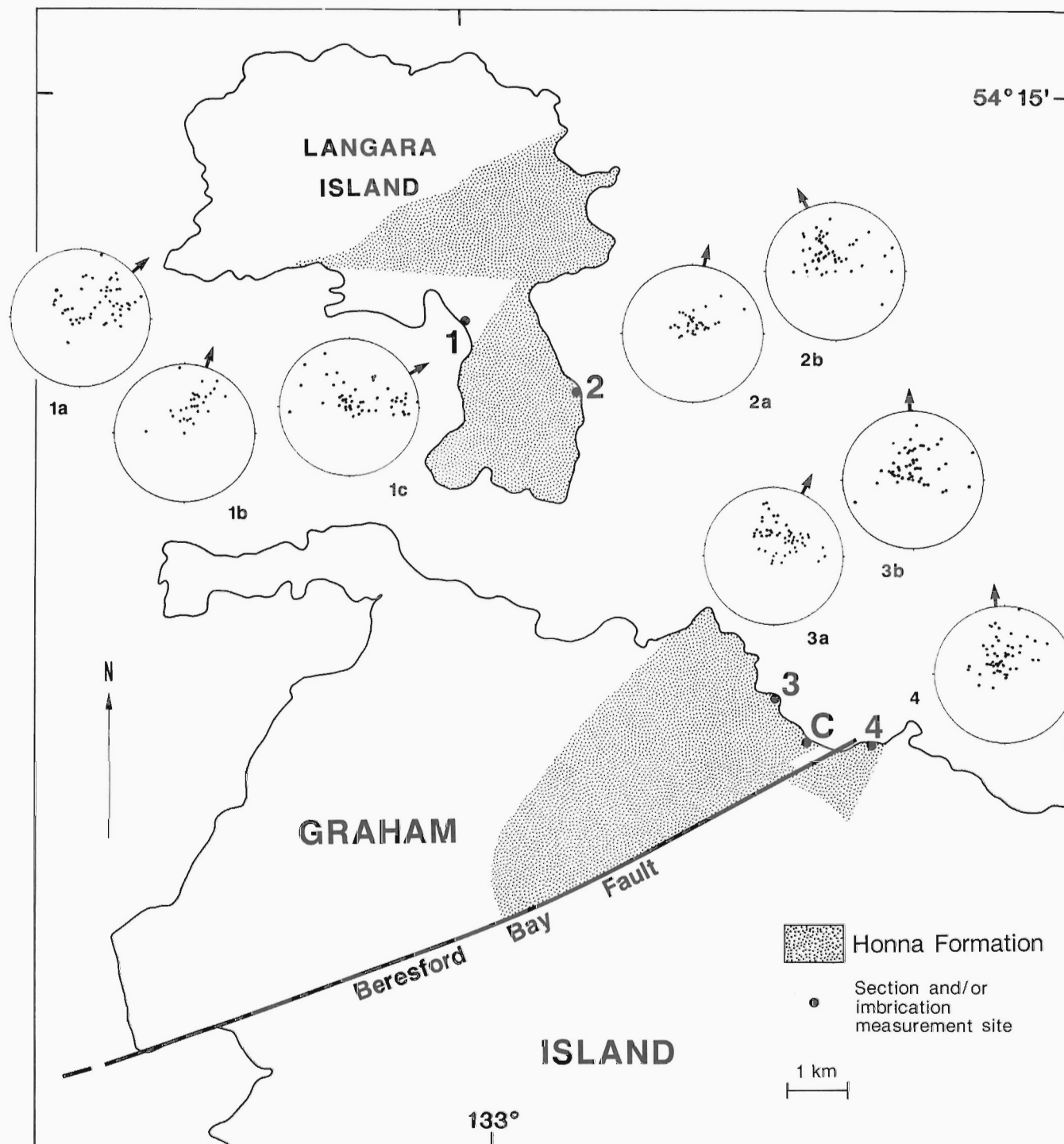


**Figure 4:** Northern outcrop of the Honna Formation (from Sutherland Brown, 1968, his Fig. 5). For map location, see Figure 2. The eight stereonets show clast fabric in eight conglomerate beds at localities 1 to 4 (e.g. stereonets 1a, 1b and 1c correspond to three different beds at Locality 1). An arrow representing the direction of maximum clustering (eigenvector V1) is plotted on each stereonet; this is a measure of the mean paleoflow direction (see text). Locality 1 is a small outcrop of Honna Formation separated from the main outcrop area (stippled) by faulting. Also shown is location of Measured Section C (Fig. 5); the other measured sections, A and B, are at localities 2 and 3 respectively. Beresford Bay Fault (Yorath and Chase, 1981) is plotted from Sutherland Brown (1968, his Fig. 5).

thick and are picked out by abrupt changes in clast size and/or fabric (Figs. 5, 6a). The matrix is fine to coarse sandstone, and sorting is poor, both among the clasts and within the matrix. There are rare examples of openwork (matrix-free) conglomerate, cemented by calcite (Fig. 6b). Most clasts are volcanic rock fragments, with subordinate granitoid and minor sedimentary rock fragments; this contrasts with the central out-

crop, where volcanic and granitoid clasts are equally abundant (Higgs, 1990). Pale grey clasts of aphanitic, aphyric volcanic rock are prominent in the north but uncommon in the central area. Sedimentary clasts include intraformational pebble conglomerate and sandstone (Fig. 6c). A few clasts of mylonite and presumed Kamutsen Formation greenstone were observed. Some granitoid clasts are foliated, and may

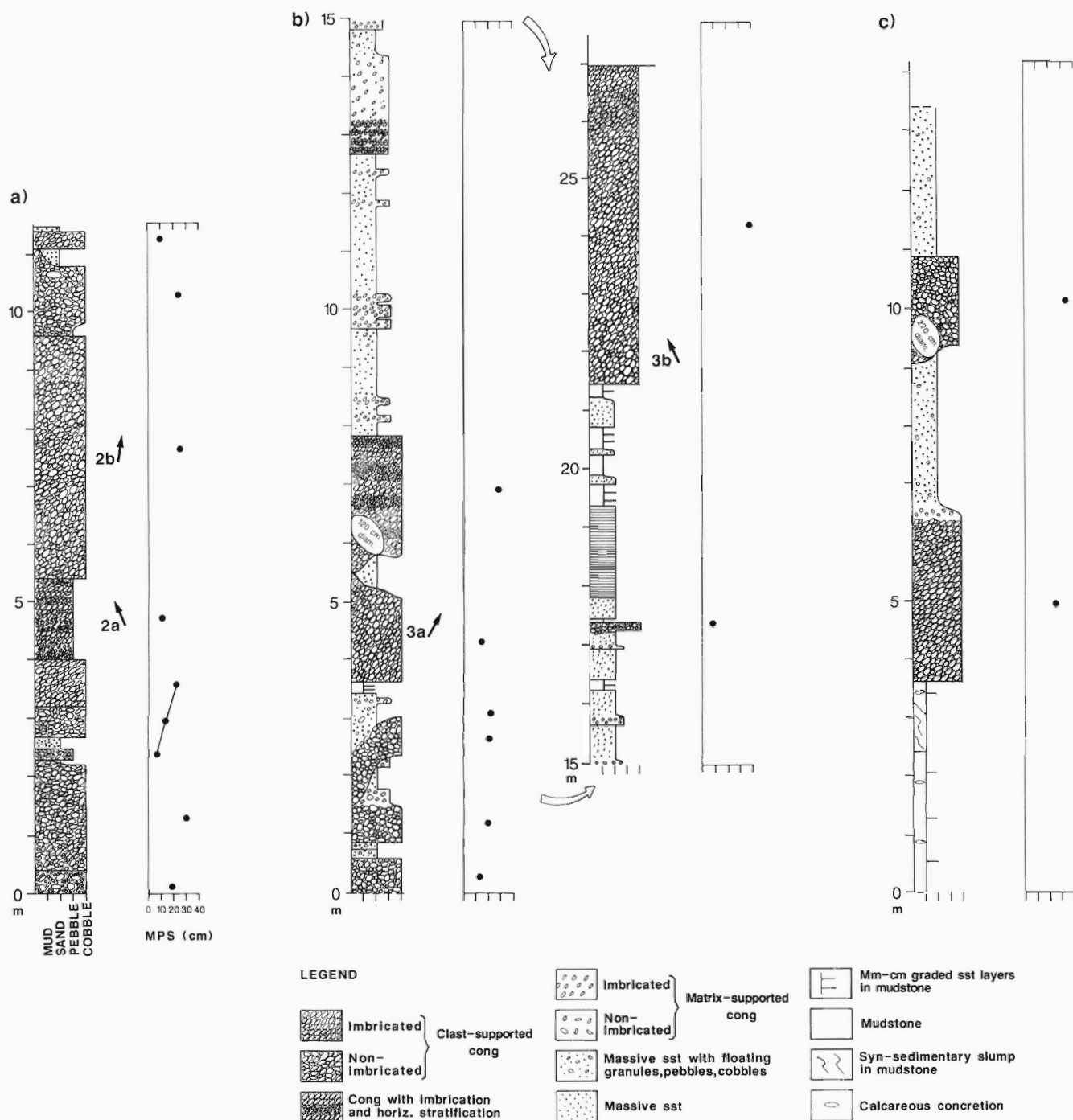


**Figure 5:** Measured sections in the northern outcrop of the Honna Formation. Numbers beside paleocurrent arrows (2a etc.) are keyed to the corresponding imbrication site (see Fig. 4 and Table 1). Section A is in shoreline bluffs at Locality 2 (Fig. 4; see Table 1 for grid reference). Section B is on a wave-cut platform at Locality 3 (Fig. 4). Section C is a foreshore platform at PR360020 (Fig. 4). MPS is maximum particle size, calculated as the average of the ten largest accessible clasts (area generally about 2 m<sup>2</sup>), excluding megaclasts. The continuous line in the MPS column of Section A indicates a possible coarsening-upward sequence (see text).

therefore be derived from the “syntectonic plutons” of Sutherland Brown (1968; see also Anderson and Reichenbach, 1991). Granitoid rocks also occur as isolated “megaclasts” up to 2.7 m across (Fig. 5c, 9-10 m). Clasts of Yakoun Formation feldspar porphyry and Kunga Formation mudstone, both common in the central outcrop (Sutherland Brown, 1968), are absent in the north.

Conglomerate facies are similar to those of the central outcrop (Higgs, 1988a,b, 1990). They include ungraded beds (e.g. Fig. 5a, 3.2-4.0 m), inverse-graded beds (9.6-11.1 m) and parallel-stratified beds (4.0-5.4 m), the first two being the most common. Many beds show imbrication. Most beds appear tabular within the limited extent of individual exposures, but some beds are lenticular due to scouring at

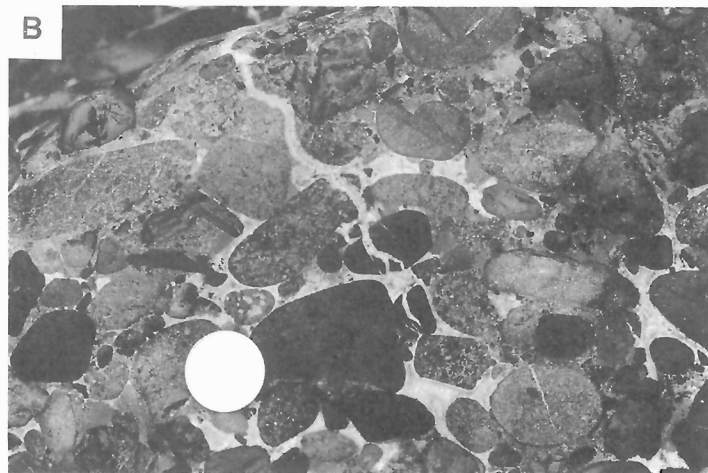


**Figure 6:** Honna Formation conglomerate, northern outcrop. **A.** General view of Measured Section A (Fig. 5). The section was measured on the right-hand (west) side of the fault crevice. Note sharp-based conglomerate beds, and "sandstone cappings" (see text). Staff 1.5 m long. **B.** Open-work conglomerate cemented by zoned calcite. Note that locally the conglomerate has a matrix (coarse sand). Note also the zoned calcite vein, filling a fracture which cuts across cement and clasts alike; this relationship indicates that fracturing postdated cementation. Grid reference PR350033, western extremity of extensive rock platform. Coin 2.4 cm in diameter. **C.** Conglomerate containing a clast of intraformational pebble conglomerate (Fig. 5b, 25.0-26.0 m). Hammer 30 cm long. **D.** Conglomerate (and two sandstone) cross-strata, dipping to the left (north). The inclination of the cross-strata decreases toward the left, the strata eventually becoming subhorizontal and concordant with the bed beneath. Base of staff rests on a (recessive) bedding plane which, traced toward the left, coincides with the base of a sandstone layer. Current flowed from right to left. Staff 1.5 m long. Grid reference PR372019, west face of sea stack about 100 m east of Pillar Rock.

the base. Scour walls are seldom steeper than 30°, and few scours are deeper than 1 m; one scour shows about 1 m of relief over 2 m laterally (Fig. 5b, 1.5–2.3 m). Many conglomerate beds have a thin (cm–dm) “sandstone capping” (Nemec et al., 1980), whose lower and upper surfaces are smooth or undulatory (e.g. Fig. 5b, 5–6 m; Fig. 6a; cf. Higgs, 1990).

Conglomerates of the northern outcrop differ from those of the central outcrop in some respects. For example, matrix-supported conglomerate beds are more common in the north, generally consisting of granules and/or pebbles floating in structureless medium sandstone, and commonly grading abruptly upward into clast-free medium sandstone (e.g. two beds in Fig. 5b, 14.9–16.2 m). Many of these beds show imbrication. One rare facies, not recorded in the central outcrop, consists of clast-supported granule conglomerate with a sandstone matrix and with floating pebbles and cobbles; the grain-size distribution is thus trimodal (e.g. Fig. 5a, 0.0–0.4 m). Another facies found in the north, of which only one bed is known, is cross-stratified conglomerate (Fig. 6d).

Two sandstone facies and a heterolithic (mudstone-sandstone) facies also occur, identical to those of the central outcrop (Higgs, 1990). The **massive-sandstone facies** occurs as intervals of medium sandstone up to at least 2.5 m thick (e.g. Fig. 5c, 10.9–13.4 m); some of these intervals comprise amalgamated beds up to 1 m thick, as shown by subtle breaks in grain size. The **parallel-laminated sandstone facies** occurs in units up to at least 1.5 m thick (e.g. Fig. 5b, 17.9–19.4 m). The **heterolithic facies** occurs as units up to at least 3.5 m thick (e.g. Fig. 5c, 0.0–3.6 m), and consists of mudstone with sharp-based, graded interbeds of sandstone. The sandstone beds vary in thickness (mm–dm) and grain size (silt to medium sand), and show TA, TAB and TC turbidite sequences. The mudstone ranges from massive (thoroughly bioturbated?) to millimetre-laminated with sparse burrows; one ichnogenus is a horizontal, branching, bed-interface burrow, possibly *Thalassinoides*. Some of the thicker (m) mudstone intervals contain bedding-parallel strings of calcareous concretions; individual concretions are lensoidal (bedding-parallel), up to 30 cm long, and connected or unconnected. Some mudstone intervals contain disturbed units in which the stratification is folded and concretions are randomly oriented. One such contorted bed has an irregular upper surface (Fig. 5c, 2.4–3.3 m).

## Interpretation

The clast-supported conglomerate beds, like their counterparts in the central outcrop, are interpreted as the deposits of cohesionless debris flows and/or high-density turbidity currents (Higgs, 1990). A subaqueous setting was deduced by Higgs (1990), based on sedimentary characteristics of the conglomerate beds; this is supported in the present study by the discovery of foraminifera in intervening mudstone layers. The sandstone cappings between these beds are interpreted as TA turbidites (Higgs, 1990). Matrix-supported conglomerate beds are attributed to sandy, high-density turbidity currents ( $S_3$  division of Lowe, 1982), based on the lack of stratification and the common presence of grading. The cross-stratified conglomerate bed could be either: (1) lateral-accretion deposits of a submarine channel or intra-channel bar (cf. Hein and Walker, 1982); or (2) foresets of a bedform produced by traction at the base of a gravelly turbidity current (cf. Winn and Dott, 1979; Lowe, 1982). The latter explanation is preferred, because: (a) deep (1–10 m) channels have not been observed in the Honna Formation, unlike the laterally accreted conglomerates described by Hein and Walker (1982); (b) the lateral-accretion surfaces illustrated by Hein and Walker (1982, their Fig. 9) show less than 10° of dip, whereas the Honna cross-strata have steeper dips (Fig. 6d); and (c) the Honna cross-strata dip northward, which is the down-paleoslope

direction based on imbrication in other beds (see below). The variation in clast size from one foreset stratum to the next (Fig. 6d) may reflect a surging flow.

The massive sandstone facies and parallel-stratified sandstone facies are inferred to represent Bouma A and B turbidite divisions, respectively (Higgs, 1990). In the heterolithic facies, the mudstone represents low-energy suspension deposition, with the graded sandstones deposited from low-density turbidity currents (Higgs, 1990). The contorted mudstone units are interpreted as slump beds.

## PALEOCURRENTS

### Method

Imbrication provides the only measurable paleocurrent indicator in the study area (sole marks and ripples do not weather out). Imbrication was measured at four localities (Fig. 4). At each locality, one, or two, or three separate beds were measured, for a total of eight imbrication sites (Fig. 4; Table 1). At each site, the dip and strike of at least 30 flat (i.e. bladed or discoid) clasts in a single bed were measured, starting with an arbitrarily selected clast and then measuring adjacent clasts until the required total was reached. Clast orientations were then plotted, as poles to the plane of flattening, on a Schmidt equal area lower hemisphere net (Fig. 4), after correcting for tectonic tilt. Finally, eigenvalue analysis (e.g. Davis, 1973) was performed by computer to determine the direction of preferred clustering of poles (eigenvector  $V_1$ ; Table 1), a measure of the mean paleoflow direction. The observed clustering is highly significant statistically: for all sites, the probability that the clasts are indeed preferentially oriented exceeds 99%, as determined by the eigenvalue-ratio ( $S_1/S_3$  in Table 1) test of Woodcock and Naylor (1983).

**Table 1.** Eigenvector and eigenvalue statistics for imbricated conglomerates, northern outcrop, Honna Formation.

Site	Grid ref.	$V_1$	Dip	$S_1$	$S_1/S_3$	N	P
1a	PR302091	48.9	57.3	0.701	7.563	50	>99
1b	"	17.5	53.3	0.820	22.877	30	>99
1c	"	59.3	69.7	0.661	10.482	50	>99
2a	PR322079	11.7	77.4	0.897	34.672	35	>99
2b	"	334.8	62.9	0.756	10.063	50	>99
3a	PR356026	24.5	63.9	0.806	12.837	50	>99
3b	"	357.4	71.5	0.773	9.076	50	>99
4	PR371019	352.8	66.2	0.808	12.136	50	>99

Successive columns give: site number; grid reference; eigenvector  $V_1$ ; dip of  $V_1$ ; normalized eigenvalue  $S_1$ ; ratio of eigenvalues  $S_1$  and  $S_3$ ; number of clasts measured, N; and probability, P, that the clast orientations are non-random. Three beds were measured at Locality 1 (hence, Sites 1a, 1b and 1c), two beds each at Localities 2 and 3, and one bed at Locality 4.

### Interpretation

The overall paleoflow direction was northward (Fig. 4). As flows are inferred to have been gravity-driven, northward flow implies a north-dipping paleoslope. Locally, paleoflow was northeastward (e.g. Fig. 4, Locality 1).

## DEPOSITIONAL ENVIRONMENT AND TECTONIC SETTING

The facies and inferred depositional processes in the study area are very similar to those of the central outcrop (Higgs, 1990); hence, the same depositional environment is invoked, namely a deep-water

fan delta alongside an active fault scarp (Fig. 3). This interpretation is consistent with the inferred deep-water slope setting of the underlying Skidegate Formation (see above). The evidence for northward paleoflow implies that the fan delta faced north, and that the active fault lay to the south. The presence of slump beds, not seen in the central outcrop, is consistent with the fan-delta interpretation. The inferred subaerial component of the fan delta, an alluvial fan (Fig. 3), has not been observed, and is assumed to be either concealed or eroded. The proximal subaqueous part of the fan is envisaged as an essentially unchanneled gravel belt (Fig. 3), because the Honna Formation lacks real channels. The downslope length of the gravel belt was at least 10 km, as shown by the north-south (downslope) length of the outcrop (Fig. 4). There is no obvious south-to-north (i.e. proximal-to-distal) decrease in clast size (Fig. 5), except very large (>1 m) megaclasts were only observed in the more proximal region, on Graham Island (e.g. Fig. 5). This lack of downslope fining suggests that flows originated on all parts of the fan surface due to an inherent instability; this is typical for relatively steep subaqueous slopes, where gravel is emplaced unstably and becomes subject to episodic remobilization, moving downslope in step-wise fashion (W. Nemec, written comm., 1988). Flows may have started spontaneously due to depositional oversteepening, or may have been triggered by earthquakes. Supply of gravel to the fan slope may have been by river floods which transformed into sediment gravity flows upon entering the sea (Porebski, 1984).

The active fault was probably oriented approximately east-west, in view of the northward paleoslope. The active fault may have been the Beresford Bay Fault (Fig. 4), in which case part of the fan delta accumulated south of the fault (Fig. 4; cf. Fig. 3). Alternatively, the active fault may have been one of the (approximately) east-west faults exposed on the west coast, a few kilometres south of the Beresford Bay Fault (Sutherland Brown, 1968, his Fig. 5). A third possibility is that the active fault was a north-south fault lying to the east, as in the case of the central Honna outcrop (Higgs, 1988a,b, 1990), and that the entire northern outcrop has undergone clockwise rotation of about 90° (cf. rotations of this magnitude in California (Luyendyk and Hornafius (1987)). Such a rotation is certainly not unreasonable, given that rotations are common in strike-slip regimes (Freund, 1974), and that the Queen Charlotte continental margin has been a transform plate boundary for at least the last 10 m.y. (Riddihough, 1982), and possibly for as long as 43 m.y. (Hyndman and Hamilton, 1991). If the strata of the northern outcrop are indeed easterly derived, then just one active fault may have been responsible for deposition of both the central and northern Honna strata (Sandspit Fault in Fig. 2). In support of the rotation hypothesis, Yorath and Chase (1981) argued for post-Honna strike-slip (6 km) on the Beresford Bay Fault, in a sinistral sense, which is consistent with clockwise rotation of a crustal block embracing the study area. In addition, on Langara Island the author observed other east-northeast-trending post-Honna faults with sinistral offsets (1-5 m), as well as a fault with subhorizontal slickensides. Furthermore, a similar clockwise rotation has been postulated for part of the central outcrop (Higgs, 1990).

## FACIES SEQUENCES

Large-scale (>100 m) coarsening (C-U) or fining-upward (F-U) sequences are undetectable in the Honna Formation due to the lack of long, exposed stratigraphic sections (Higgs, 1990). However, small-scale (10-30 m) F-U sequences occur in the northern outcrop. Each sequence comprises an upwards transition from conglomerate, through sandstone, into mudstone with thin turbidites (e.g. Fig. 5b, 0.0-21.4 m). The basal conglomerate commonly rests, with sharp contact, on mudstone with turbidites. Similar sequences occur in the central outcrop (Higgs, 1990). The F-U sequences may reflect grad-

ual abandonment of gravelly depositional lobes (Higgs, 1990), or they may be tectonically controlled. A possible C-U sequence only 1.7 m thick was observed, but is tenuous because it involves only three conglomerate beds (Fig. 5a, 2.3-4.0 m).

## RELEVANCE TO PETROLEUM EXPLORATION

The present study has the following implications for petroleum exploration in the Queen Charlotte Islands:

- 1) If the Sandspit Fault (Fig. 2) was responsible for both the central and northern Honna fan deltas, additional fan deltas may fringe the fault beneath the extensive Tertiary (Masset Formation) deposits of Graham Island, offering exploration targets. This may have been the rationale of the Naden well (Fig. 1).
- 2) The porosity and permeability of Honna Formation conglomerates and sandstones are poor due to occlusion of porosity by alteration products of volcanic rock fragments (Fogarassy and Barnes, 1988a,b). However, undiscovered Honna fan deltas beneath Graham Island (see "1" above) may be entirely of granitic provenance, resulting in better reservoir properties. In addition, secondary porosity could be present (Fogarassy and Barnes, 1988a,b). Intervals of openwork conglomerate (Fig. 6b) would have excellent porosity and permeability if they lacked cement.
- 3) Deep-water fan deltas appear to be characterized by gravel belts which extend many kilometres downslope (Higgs, 1990). The northern Honna fan delta was no exception, with a gravel belt longer than 10 km (above). Such a long gravel belt, bordered by a sandy fringe (e.g. Fig. 3), has obvious petroleum reservoir potential.

## ACKNOWLEDGMENTS

I thank Ken Hoffman for dependable field assistance, Bob Thompson for supervising field logistics, Peter Fraser for skilful helicoptering, Brian Sawyer and his team for expert drafting, Brian Bornhold for discussions on fan deltas, Peter Lewis for help with tilt correction of clast-orientation data, and Peter Bobrowsky for instruction on eigenvalue analysis.

## REFERENCES

- Anderson, R.G. and Reichenbach, I.  
**1991:** Geochronometric (U-Pb and K-Ar) framework for Middle to Late Jurassic and Tertiary (Eocene and Oligocene) plutons in Queen Charlotte Islands, British Columbia; in *Evolution and Hydrocarbon Potential of the Queen Charlotte Basin*, British Columbia, Geological Survey of Canada, Paper 90-10.
- Cameron, B.E.B.  
**1989:** Internal paleontological report; Geological Survey of Canada, BEBC-1989-2, 14 p.
- Cameron, B.E.B. and Hamilton, T.S.  
**1988:** Contributions to the stratigraphy and tectonics of the Queen Charlotte Basin, British Columbia; in *Current Research, Part E*, Geological Survey of Canada, Paper 88-1E, p. 221-227.
- Davis, J.C.  
**1973:** *Statistics and Data Analysis in Geology*; John Wiley and Sons, New York.
- Fogarassy, J.A.S. and Barnes, W.C.  
**1988a:** Petroleum reservoir aspects of middle to Upper Cretaceous and Tertiary strata of the Queen Charlotte Islands; in *Some Aspects of the Petroleum Geology of the Queen Charlotte Islands*, R. Higgs (compiler), Canadian Society of Petroleum Geologists Field Guide to Sequences, Stratigraphy, Sedimentology; Surface and Subsurface, Technical Meeting, September 14-16, 1988, Calgary, Alberta, p. 22-25.
- 1988b:** Stratigraphy, diagenesis and petroleum reservoir potential of the mid- to Upper Cretaceous Haida and Honna formations of the Queen Charlotte Islands, British Columbia; in *Current Research, Part E*, Geological Survey of Canada, Paper 88-1E, p. 265-268.
- Freund, R.  
**1974:** Kinematics of transform and transcurrent faults; *Tectonophysics*, v. 21, p. 93-134.



- Haggart, J.W.**  
**1985:** Stratigraphic investigations of the Cretaceous Queen Charlotte Group, Queen Charlotte Islands, British Columbia; Geological Survey of Canada, Paper 86-20, 24 p.
- Haggart, J.W. and Higgs, Z.**  
**1989:** A new Late Cretaceous mollusc fauna from the Queen Charlotte Islands, British Columbia; *in* Current Research, Part H, Geological Survey of Canada, Paper 89-1H, p. 59-64.
- Hein, F.J. and Walker, R.G.**  
**1982:** The Cambro-Ordovician Cap Enragé Formation, Québec, Canada: conglomeratic deposits of a braided submarine channel with terraces; *Sedimentology*, v. 29, p. 309-329.
- Higgs, Z.**  
**1988a:** Sedimentology and tectonic implications of Cretaceous fan delta conglomerates, Queen Charlotte Islands (extended abstract); *in* Sequences, Stratigraphy, Sedimentology: Surface and Subsurface, D.P. James and D.A. Leckie (ed.), Canadian Society of Petroleum Geologists, Memoir 15, p. 307-308.  
**1988b:** Sedimentology of the Honna Formation, Upper Cretaceous fan-delta conglomerates; *in* Some Aspects of the Petroleum Geology of the Queen Charlotte Islands, R. Higgs (compiler), Canadian Society of Petroleum Geologists Field Guide to Sequences, Stratigraphy, Sedimentology: Surface and Subsurface, Technical Meeting, September 14-16, 1988, Calgary, Alberta, p. 1-122.  
**1990:** Sedimentology and tectonic implications of Cretaceous fan-delta conglomerates, Queen Charlotte Islands, Canada; *Sedimentology*, v. 37, p. 83-103.  
**1991:** Sedimentology, basin-fill architecture and petroleum geology of the Tertiary Queen Charlotte Basin; *in* Evolution and Hydrocarbon Potential of the Queen Charlotte Basin, British Columbia, Geological Survey of Canada, Paper 90-10.
- Hyndman, R.D. and Hamilton, C.J.**  
**1991:** Cenozoic relative plate motions along the northeastern Pacific margin and their association with Queen Charlotte area tectonics and volcanism; *in* Evolution and Hydrocarbon Potential of the Queen Charlotte Basin, British Columbia, Geological Survey of Canada, Paper 90-10.
- Lowe, D.C.**  
**1982:** Sediment gravity flows: II. Depositional models with special reference to the deposits of high-density turbidity currents; *Journal of Sedimentary Petrology*, v. 52, p. 279-297.
- Luyendyk, B.P. and Hornafius, J.S.**  
**1987:** Neogene crustal rotations, fault slip, and basin development in southern California; *in* Cenozoic Basin Development of Coastal California, R.V. Ingersoll and W.G. Ernst (ed.), Prentice-Hall, Englewood Cliffs, p. 259-283.
- Nemec, W., Porebski, S.J., and Steel, R.J.**  
**1980:** Texture and structure of resedimented conglomerates: example from Ksiaz Formation (Famennian-Tournaisian), southwestern Poland; *Sedimentology*, v. 27, p. 519-538.
- Porebski, S.J.**  
**1984:** Clast size and bed thickness trends in resedimented conglomerates: example from a Devonian fan-delta succession, southwest Poland; *in* Sedimentology of Gravels and Conglomerates, E.H. Koster and R.J. Steel (ed.), Canadian Society of Petroleum Geologists, Memoir 10, p. 399-411.
- Riddihough, Z.P.**  
**1982:** One hundred million years of plate tectonics in western Canada; *Geoscience Canada*, v. 9, p. 28-34.
- Rohr, K. and Dietrich, J.Z.**  
**1991:** Deep seismic reflection survey of the Queen Charlotte Basin; *in* Evolution and Hydrocarbon Potential of the Queen Charlotte Basin, British Columbia, Geological Survey of Canada, Paper 90-10.
- Sutherland Brown, A.**  
**1968:** Geology of the Queen Charlotte Islands, British Columbia; British Columbia Department of Mines and Petroleum Resources, Bulletin 54, 226 p.
- Thompson, E.L. and Fjorkelson, D.**  
**1989:** Regional mapping update, central Queen Charlotte Islands, British Columbia; *in* Current Research, Part H, Geological Survey of Canada, Paper 89-1H, p. 7-11.
- Winn, R.D., Jr. and Dott, R.H., Jr.**  
**1979:** Deep-water fan channel conglomerates of Late Cretaceous age, southern Chile; *Sedimentology*, v. 26, p. 203-228.
- Woodcock, W.H. and Naylor, M.A.**  
**1983:** Randomness testing in three-dimensional orientation data; *Journal of Structural Geology*, v. 5, p. 539-548.
- Worath, C. and Chase, R.L.**  
**1981:** Tectonic history of the Queen Charlotte Islands and adjacent areas—a model; *Canadian Journal of Earth Sciences*, v. 18, p. 1717-1739.
- Young, M.**  
**1981:** Structure of the western margin of the Queen Charlotte Basin, British Columbia; M.Sc. thesis, University of British Columbia, 380 p.

# The Masset Formation on Graham Island, Queen Charlotte Islands, British Columbia

Catherine J. Hickson<sup>1</sup>

Hickson, C.J., The Masset Formation on Graham Island, Queen Charlotte Islands, British Columbia; in *Evolution and Hydrocarbon Potential of the Queen Charlotte Basin, British Columbia*. Geological Survey of Canada, Paper 90-10, p. 305-324, 1991.

## Abstract

*The Masset Formation (as studied on Graham Island) is a Late Oligocene to Early Pliocene tholeiitic to calc-alkaline suite of volcanic rocks that underlies much of Graham Island. These lavas, with minor intercalated felsic pyroclastic flows, underlie eastern Graham Island but probably do not extend any great distance beneath Hecate Strait. The Formation comprises intercalated, aphyric to feldsparphyric, mafic to felsic lava flows and pyroclastics. Thick rhyolite flows core inland hills along the west coast and may represent vent areas from which volcanic products and sediments were shed east and west. K-Ar dates suggest eruptions climaxed from 20-25 Ma; there was contemporaneous extrusion of felsic and mafic magmas; mafic magmas dominate volumetrically and travelled farthest from vent areas. The extrusion of these rocks was rapid, leaving little time for sedimentation or weathering between eruptions. Epiclastic sediments consist mostly of debris flow deposits.*

*The Masset Formation is undeformed except for steep north-trending faults. Bedding attitudes represent primary slopes of constructional volcanic landforms.*

*Basaltic lavas found in offshore drilling in Queen Charlotte Sound and Hecate Strait are older and lithologically distinct from the bulk of Masset rocks and it is proposed that they represent one or more volcanic episodes distinct from the Masset eruptions. Older volcanic rocks were also found intercalated within the Honna and Haida formations. These volcanic rocks are distinct in that they contain hornblende phenocrysts which were not found in the Masset Formation of Graham Island.*

## Résumé

*La formation de Masset (telle qu'étudiée dans l'île Graham) est une suite de roches volcaniques de tholéitiques à calco-alkalines de l'Oligocène supérieur au Pliocène inférieur qui s'étend dans le sous-sol de presque toute l'île Graham. Ces laves, ainsi que quelques coulées pyroclastiques felsiques intercalées, s'étendent sous l'est de l'île Graham mais ne se prolongent probablement pas sur une grande distance au-dessous du détroit d'Hécate. La formation comprend quelques coulées de lave et des roches pyroclastiques intercalées, d'aphyriques à porphyriques feldspathiques et de mafiques à felsiques. D'épaisses coulées de rhyolite occupent le centre des collines de l'île le long de la côte ouest et pourraient représenter des zones de cheminées à travers lesquelles des produits volcaniques et des sédiments auraient été expulsés vers l'est et l'ouest. Des datations K-Ar indiquent que les éruptions ont atteint leur activité maximale entre 20 et 25 Ma; il y a eu une extrusion contemporaine de magmas felsiques et mafiques; les magmas mafiques dominant par leur volume et ont parcouru une plus grande distance à partir des cheminées d'expulsion. L'extrusion de ces roches a été rapide, laissant peu de temps pour une sédimentation ou une érosion entre les éruptions. Les sédiments épicaustiques sont surtout composés de dépôts de coulées de débris.*

*La formation de Masset n'est pas déformée, à l'exception de failles abruptes orientées vers le nord. L'attitude des couches correspond à des pentes primaires de reliefs volcaniques de construction.*

*Les laves de basalte découvertes par des forages en mer dans les détroits de la Reine-Charlotte et d'Hécate sont plus anciennes et leur lithologie diffère de l'ensemble des roches de Masset. Il est par conséquent proposé qu'elles pourraient représenter un ou plusieurs épisodes volcaniques différents des éruptions de Masset. On a également trouvé des intercalations de roches volcaniques plus anciennes dans les formations de Honna et d'Haida. Ces roches volcaniques diffèrent par leur teneur en phénocristaux de hornblende qui sont absents de la formation de Masset dans l'île Graham.*

<sup>1</sup> Cordilleran Division, Geological Survey of Canada, 100 West Pender Street, Vancouver, B.C. V6B 1R8

## INTRODUCTION

The Queen Charlotte Islands contain a thick succession of Tertiary volcanic rocks named the Masset Formation by MacKenzie (1916). Sutherland Brown (1968) provided the first detailed descriptions of the succession as part of a geological reconnaissance of the islands. The Masset Formation underlies much of west-central Graham Island and, indeed, is the dominant formation found on Graham Island. More limited exposures are found on Moresby and adjacent islands (Fig. 1). The present study focuses on the internal character of the volcanic complex as preserved on Graham Island. Here, despite less than 5% overall exposure, good sections can be found along the west coast. The internal relationships exposed in these sections allow a reinterpretation of the tectonic setting and mode of emplacement. Preliminary results were given in Hickson (1988, 1989) but this paper integrates and refines the previous findings.

Tertiary volcanism represents an important stage in the geologic evolution of the Queen Charlotte Islands, especially with regard to the potential for maturation, migration and trapping of hydrocarbons. Epithermal activity associated with Tertiary volcanism is thought to be responsible for the Cinola gold deposit. The distribution and relative

volumes of volcanic rocks are important in the interpretation of seismic and gravity data. In addition, the flows themselves pose technical difficulties for any drilling program, be it for hydrocarbons or mineral deposits.

Sutherland Brown (1968, p. 104) described the Masset Formation as comprising "thin flows of columnar basalt, basalt breccia, thick sodic rhyolite ash flow tuffs, and welded tuff breccias and breccias of mixed basalt and rhyolite clasts." He recognized three volcanic facies and named them Tartu, Kootenay and Dana (Fig. 1). This was partly for ease of reference but was also based on lithostratigraphy. It was noted that the "Kootenay facies is typified by welded rhyolite tuff breccias and spherulitic rhyolites....The Dana facies is formed principally of pyroclastic breccias of mixed basalt and rhyolite clasts" (Sutherland Brown, 1968; p. 106). The Tartu facies was noted to be more of a mixed succession, an observation amplified by the present study.

Sutherland Brown (1968) indicated that the Masset Formation consists of alkalic basalts and sodic rhyolites. Petrochemical work by Hamilton (1985) and Dostal and Hamilton (1988) showed a range in chemical composition from T-MORB to metaluminous rhyolite. Dostal and Hamilton (1988) suggested that the Masset volcanics reflect pronounced fractional crystallization and some degree of magma mixing.

Sutherland Brown (1968) noted that the Masset Formation overlies all older strata with angular unconformity. However, in the east, it is conformably overlain by, or interfingers with, the Miocene-Pliocene Skonun Formation (Cameron and Hamilton, 1988; Sutherland Brown, 1968). On this basis Sutherland Brown (1968) assigned an age of Paleocene to Miocene for the Masset Formation. On the basis of K-Ar dates, Young (1981) suggested the Masset may in part be as old as Late Cretaceous. Using further K-Ar dating, Hamilton (1985) and Cameron and Hamilton (1988) determined a more restricted, Early Eocene to Late Miocene, age for Masset volcanism.

Of the eight exploratory wells drilled in Hecate Strait and Queen Charlotte Sound in the early 1960s by Shell Canada Ltd., several intersected basaltic flows. These were correlated with the Masset Formation by Shouldice (1973) and Young (1981), possibly implying that the Masset Formation may extend beneath Hecate Strait and Queen Charlotte Sound.

In 1987, field work was concentrated in the area between Masset Inlet and the west coast (excluding the coastal exposures); in 1988 exposures along the west coast were studied in detail (Fig. 1). Reconnaissance of areas to the south and north of these two areas was also undertaken. Data were recorded at a 1:50 000 scale using vehicle, boat and helicopter support. The geology of much of the Masset Formation is shown on four 1:50 000 map sheets (Hickson, 1990a,b; Hickson and Lewis, 1990; Lewis and Hickson, 1990).

## STRATIGRAPHY AND FIELD RELATIONS

In this paper, for the reasons outlined in sections on chemistry, petrology, K-Ar dating and field relations, the Masset Formation is restricted to Late Oligocene to earliest Pliocene, aphyric to sparsely phyrlic, calc-alkalic volcanic rocks and associated epiclastic sediments (Fig. 2). Excluded from this definition are the alkalic, olivine-phyric basalts of Tow Hill, Lawn Hill (Fig. 1) and those along the east side of Hecate Strait (Woodsworth, 1991). Rocks of Sutherland Brown's (1968) Kootenay Facies fit the definition of Masset Formation, but breccias of the Dana Facies (Fig. 1) and spatially associated basalts on Tar Islets and Ramsay Island represent phases of volcanism distinct from the Masset. Volcanic rocks on southern Graham Island (Fig. 1) are older, representing early Tertiary (Eocene?) and Cretaceous volcanism (Lewis et al., 1989; Hickson, 1989).

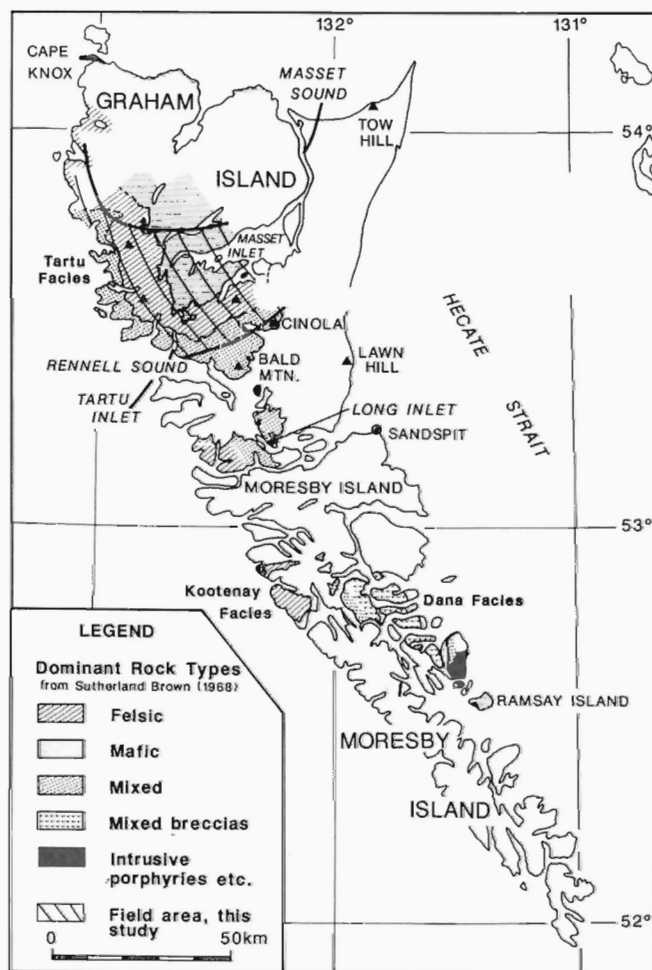
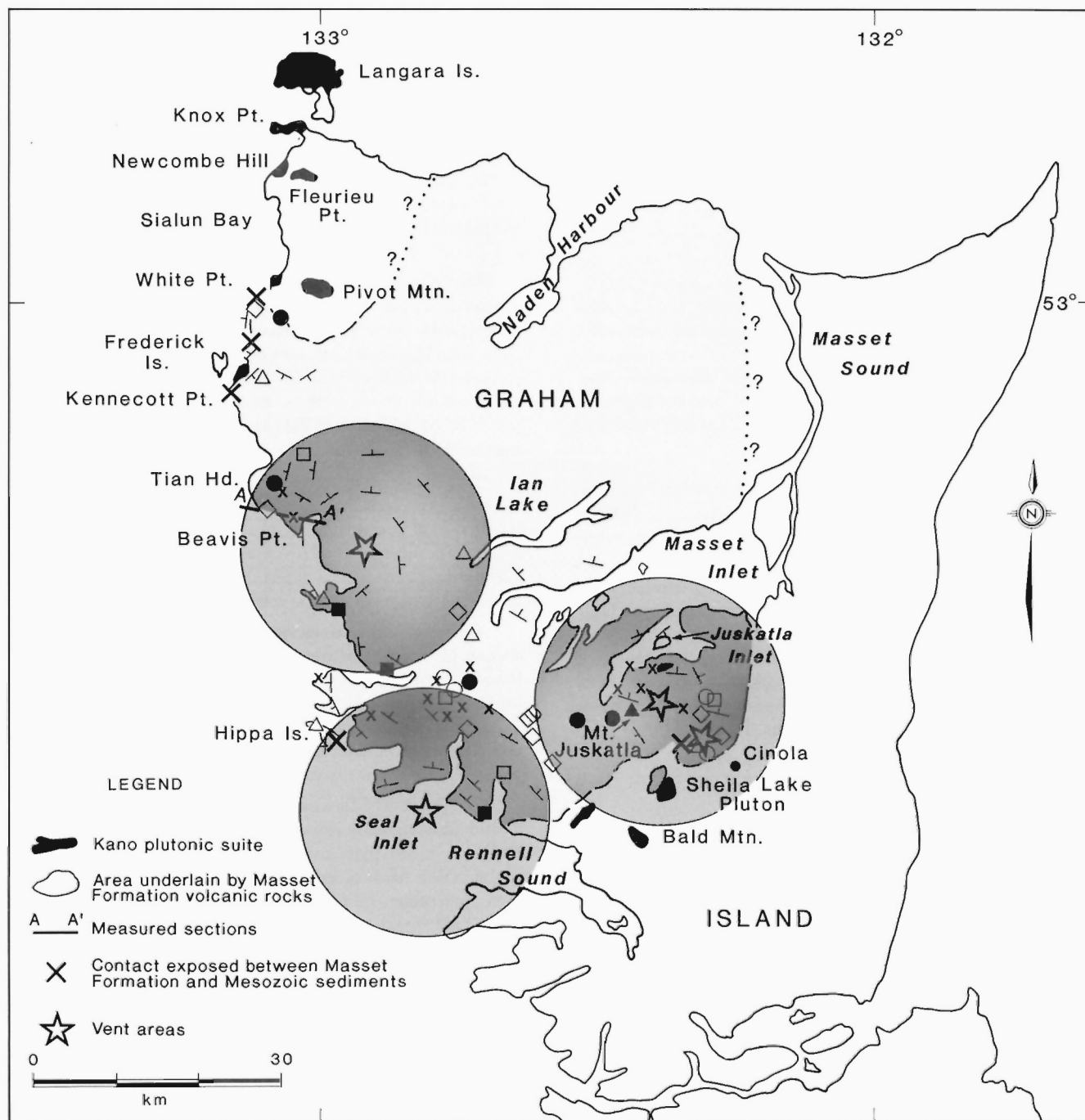


**Figure 1:** Distribution of Tertiary volcanic rocks studied by Sutherland Brown (1968; his Fig. 17) in relation to the region studied in detail during this work. The Tartu Facies comprises most of the rocks belonging to the Masset Formation as defined in this paper (western Graham Island); the Kootenay Facies occurs on Western Moresby Island, and the Dana Facies on eastern Moresby and offshore islands as far south as Ramsay Island.



#### Whole Rock Chemical Classification

△ Basalt	● Andesite	■ Dacite	x Rhyolite
◇ Basaltic Andesite	○ Trachy-Andesite	□ Trachy-Dacite	

**Figure 2:** Distribution of the Masset Formation, exposed plutons of the Kano Plutonic suite and locations where the contact between the Masset Formation and older strata is exposed. Also noted are the location and compositions of whole rock chemical samples (results listed in Table 1 and Hickson 1990b). Symbols are based on classification shown in Figure 3. Details of the measured section can be found in Figure 7.

The Masset Formation consists of mafic through felsic flows and pyroclastics with minor intercalated sediments. Regions several kilometres in size are predominantly mafic or felsic, but over several hundred metres of section both rock types occur. Mafic volcanic map units (Hickson, 1990a,b; Hickson and Lewis, 1990; Lewis and Hickson, 1990) are composed of multiple flows with minor interflow breccias. Felsic map units (Hickson, 1990a,b; Hickson and Lewis, 1990; Lewis and Hickson, 1990) represent combinations of lava flows, densely welded pyroclastics and unwelded pumiceous lapilli deposits. The thickness of the entire stratigraphic section does not exceed 3000 m and there is little evidence that the section has been reduced through erosion.

The phenocryst assemblage, rock weathering characteristics, and colour on weathered and unweathered surfaces were the field criteria used to estimate rock composition and distinguish between map units. Whether felsic or mafic, Masset Formation rocks are aphyric to feldsparphyric. Pyroxene and quartz occur only rarely as phenocryst phases. The rocks are commonly aphanitic and are grey to black in colour. Eutaxitic textures, flow banding, or general weathering characteristics are often the only indication of rock composition. Because of these attributes it was often not possible, based on hand samples and field exposures, to determine the presence and/or volumes of intermediate rock types.

Felsic rocks, all of which have an aphanitic groundmass, are subdivided into four units on the 1:50 000 maps (Hickson 1990a,b; Hickson and Lewis, 1990; Lewis and Hickson, 1990): aphyric to less than 5% (T<sub>mfa</sub>) feldspar phenocrysts; 15-40% feldspar phenocrysts (T<sub>mfc</sub>); quartz-feldsparphyric (T<sub>mfe</sub>); and pyroxene-feldsparphyric (T<sub>mfg</sub>). Felsic units were subdivided into lava flows and pyroclastic rocks. The mafic rocks are subdivided into two units: 1) aphanitic-aphyric lavas (T<sub>mmb</sub>), and 2) aphanitic lavas with plagioclase phenocrysts (T<sub>mmb</sub>). Sedimentary units are also subdivided into two units: 1) reworked primary volcanic rock (T<sub>msa</sub>), and primary volcanic deposits emplaced by sedimentary processes (lahars, T<sub>msb</sub>).

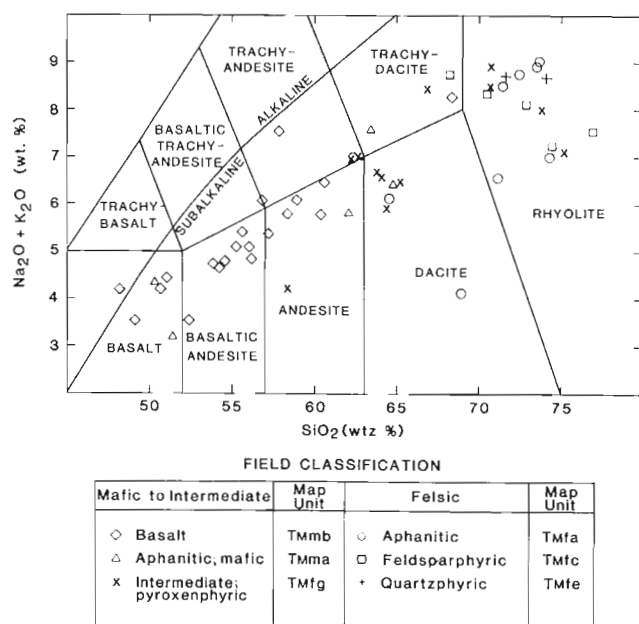


**Figure 3:** Plot of total alkali versus silica for samples from the Masset Formation. Sample symbols are based on the field classification. All other diagram classify the rock chemically, based on the fields shown here. Fields are from LeBas et al. (1986). Map units are from Hickson (1990a,b; Hickson and Lewis, 1990; Lewis and Hickson, 1990).

The volcanic map units were classified chemically (Fig. 3) using the scheme of LeBas et al. (1986). Aphyric aphanitic rock types posed the greatest difficulties in field classification. For example, based on field observations rocks of unit T<sub>mmb</sub> were thought to be andesites. However, chemically these rocks span the basalt to dacite fields. Similarly, unit T<sub>mfg</sub> contains both dacites and rhyolites.

Sedimentary rocks that are non-volcanic in origin are rare and have limited lateral extent. They are nonmarine, presumably fluvial deposits that range from coarse conglomerates to fine-grained sand- and siltstones. These sediments commonly contain layers of silicified and carbonized wood debris (flattened logs) up to 30 cm thick. Primary volcanic lahars and secondary debris flows consist of hetero- and monolithological diamictos that accumulated along the flanks of the volcano.

The Masset Formation accumulated at or above sea level: neither volcanics nor sedimentary intercalations contain evidence of a marine environment. Hamilton and Cameron (1989) report that some rocks in the Masset, in the vicinity of King Creek, Graham Island, were deposited in a marine setting. Re-examination of this locality indicates that these rocks do not belong to the Masset Formation, but rather are part of the Middle Jurassic Yakoun and Lower Cretaceous Longarm Formation (Indrelid et al., 1991; Lewis et al., 1990).

Regoliths were observed at two stratigraphic levels. One, west of Cinola (Fig. 2), occurs at the base of the volcanic succession and is composed of weathered porphyritic rocks of the Yakoun(?) Formation (Fig. 4). The other, north of Juskatla Mountain, within the Masset sequence, represents an area (kipuka) that escaped inundation by lava flows for a longer period than surrounding areas.

Felsic volcanic rocks are dominantly pyroclastic in origin; flows are rare. In the field, due to extreme welding of some of the pyroclastic flows they can be mistaken for lava flows. However, the pyroclastic origin is evident in thin section. Because only a fraction of the collected samples were sectioned, no attempt was made to change the field identification. Thus the map does not accurately reflect the proportions of lava flow to pyroclastic material.

The pyroclastic flows are dominantly welded lapilli tuffs (Fig. 5) and are commonly associated with pumiceous airfall material. The bases of both pyroclastic and lava flows are generally vitreous, though perlitic fractures and associated devitrification features are common. Spherulites, up to 3 cm in diameter, are abundant in many flows. Lithophysae, up to 10 cm in diameter (Fig. 6), have destroyed primary textures in the upper parts of many flows. Felsic lava and pyroclastic flows are much thicker (10-200 m) than mafic lava flows which are commonly only a few metres to 30 m thick. Felsic rocks dominate around Ironside Mountain and the Mount Hobbs area (Fig. 2).

Coastal exposures provide better outcrop continuity than inland exposures. A felsic pyroclastic unit exposed along 1.5 km of wave-cut terrace at White Point (Fig. 2) can be traced for a further 5 km along the beach south of Kennebec Point. Below the pyroclastic flow is a 1 m thick airfall layer composed of pumiceous clasts up to 2 cm across and lithic fragments reaching 1 cm in diameter. Carbonized and silicified tree stumps up to 1.5 m in diameter (Fig. 7) are preserved in the growth position in this layer, which has in turn been scoured and overlain by a 30 m thick pyroclastic flow. Three kilometres inland, similar breccia material outcrops as a thick (150 m) flow at the base of the hills. This unit unconformably overlies conglomerates of the Longarm and Honna formations (J.W. Haggart, pers. comm., 1989; H.W. Tipper, pers. comm., 1988; Hickson and Lewis, 1990; Lewis and Hickson, 1990).

Mafic map units consist of multiple flows. Individual flows range from 2-30 m thick and are associated with thin (a few tens of



**Figure 4:** Exposed paleosol below the Masset Formation composed of feldsparphyric volcanic rocks of the Yakoun Formation. Exposure is between Juskatla Mountain and Cinola (Fig. 2).



**Figure 5:** Eutaxitic texture in Masset Formation rhyolite. Exposure is along the north shore of Port Chanal.





**Figure 6:** Lithophysae which have formed in the top section of a rhyolite flow within the Masset Formation, Cameron Range, Graham Island.



**Figure 7:** Carbonized and silicified tree stump eroded out of lithified pyroclastic rock, Masset Formation, White Point, Graham Island.

centimetres or less) interflow breccias. Mafic dykes are common and in some areas appear to have been feeders for localized eruptions. Agglutinate, found at several localities between Juskatla Inlet and Cino-la (Fig. 2), probably represents eroded cinder cones fed by the dykes.

The succession from Tian Head to Beavis Point perhaps best illustrates the mixed mafic and felsic nature of the Masset Formation as well as the sedimentary layers intercalated with the volcanic units (Fig. 8). The section includes cumulate(?) nodule-bearing mafic

flows, debris flows, felsic pyroclastics and flows, and coarse- to fine-grained, well-bedded sandstones.

The division into felsic, mafic and mixed 'members' (Fig. 1) described by Sutherland Brown (1968) only crudely approximates the distribution of felsic and mafic rocks on Graham Island. The west coast is dominated by mafic flows that are stratigraphically below the thick felsic flows and domes that dominate the west-central area. Mafic flows are prevalent in eastern Graham Island but many may have orig-

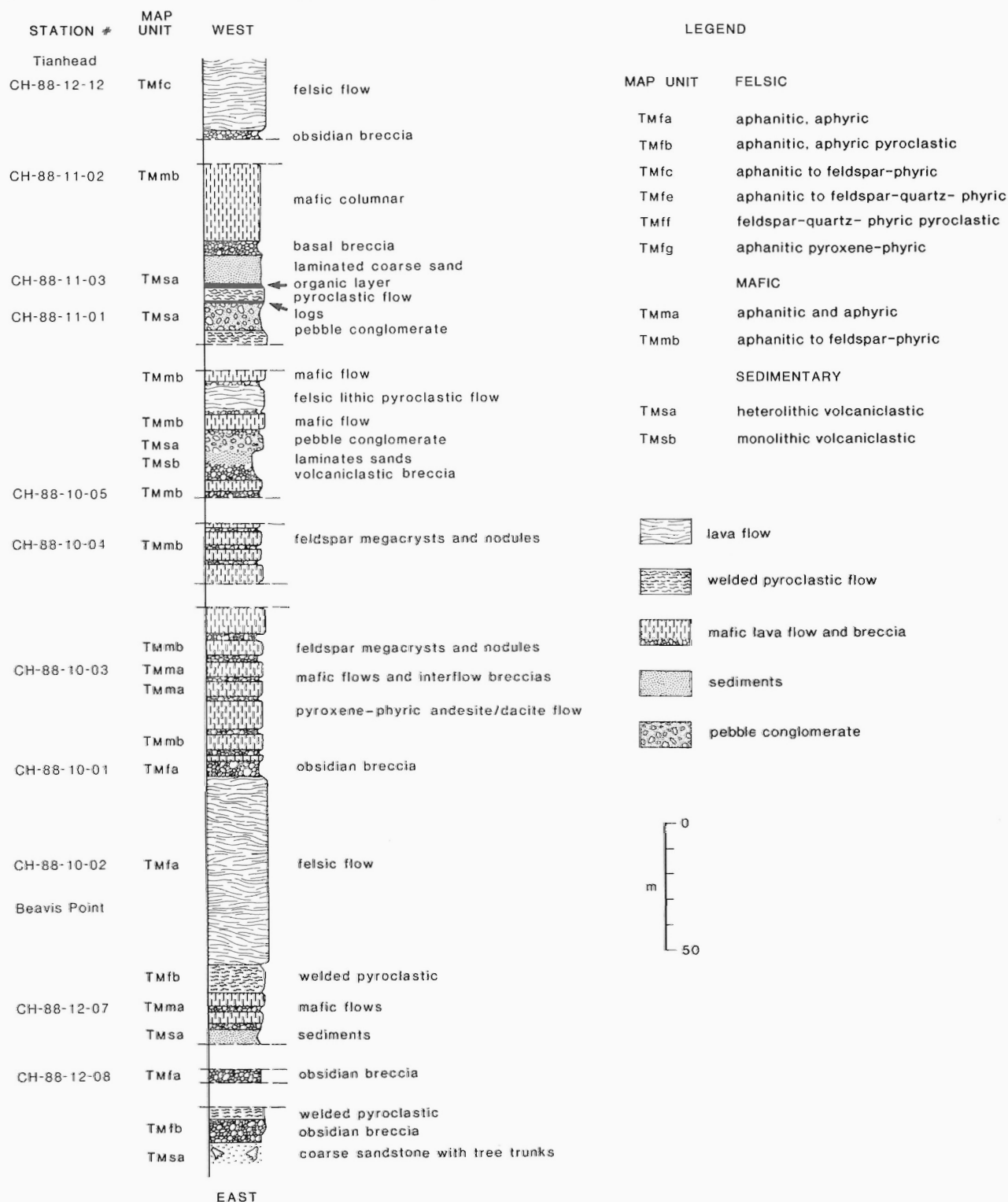


Figure 8: Stratigraphic section exposed along the coastline between Tian Head and Beavis Point; location is shown in Figure 2. Map units are from Hickson (1990a,b; Hickson and Lewis, 1990; Lewis and Hickson, 1990).

inated in the central region where remnants of mafic flows cap many of the ridges (Fig. 9; Hickson, 1990a,b).

## STRUCTURE

Layering attitudes within the Masset Formation are uniform at the kilometre scale (Figs. 2, 9), suggesting present morphology may be strongly influenced by primary depositional patterns. There are abundant breccias but most appear to be primary flow top and flow bottom breccias resulting from deposition. Intense folding associated with flow emplacement was noted in many outcrops, but tectonically related folding was noted only in the vicinity of Juskatla Mountain (see below) and south of Port Louis (Hickson, 1990b).

Along the west coast of Graham Island flows and pyroclastics dip from 10-30° toward the west and flatten inland (Fig. 2), where thick rhyolite flows, up to 200 m thick, predominate (Fig. 9; Hickson 1990b). These flows (possibly domes), up to 200 m thick, underlie a range of hills just inland of the coast. East of this line of hills, flows dip consistently east to northeast. North of Rennell Sound the flows dip northward and in the vicinity of Ironside Mountain the dips are concentric about the peak (Fig. 2; Hickson, 1990a,b; Hickson and Lewis, 1990). Based on the presence of alteration zones, thick areally restricted flows, and dip directions, three major sources for much of the felsic volcanic rocks are suggested. These are in the vicinity of Ironside and Juskatla mountains and Seal Inlet (Fig. 2).

It is proposed that volcanic outpourings produced several large, low profile, shield volcanoes that are on the order of 20-30 km in diameter. These volcanoes may never have attained typical stratomorphology because they were built of multiple layers of densely welded, far travelled, pyroclastic flows and fluid andesitic flows. They were, however, at least 1500 m in height, based on present day topography and well data from the Port Louis well. Thick accumulations of Masset volcanics along the west side of Graham Island suggest that the westernmost parts of the Masset Formation and much of western Graham Island are missing and have been transported northward along

the Queen Charlotte transform fault. This would explain the apparent truncation of the formation along the west coast.

Sutherland Brown suggested that the dips of bedding may represent sagging into an evacuated magma chamber (Sutherland Brown, 1968: p. 159). Yorath and Chase (1981), and Yorath and Hyndman (1983) have interpreted dips within the Masset Formation as structural, the result of uplift along the west coast.

If dips were a result of eastward tilting, all dip data would be skewed in an easterly direction. Such is not the case; see for instance Sutherland Brown's (1968: Fig. 30, p. 157) summary diagram for folds in Tertiary and older rocks, Figure 2, and Hickson (1990a,b; Hickson and Lewis, 1990; Lewis and Hickson, 1990). Eastward dipping beds would be oversteepened and beds dipping westward would have shallower dips than those dipping to the east. The eastward dipping beds should also show higher dip angles than is common in constructional volcanic edifices, where dips can range up to 30°. No evidence of either phenomena was found.

Yorath and Hyndman (1983) also suggested that wave-cut terraces along the west coast are the result of differential uplift. However, these terraces are not unique to the west coast (Sutherland Brown, 1968) and are present along the east coast of Moresby Island and elsewhere.

Near Juskatla Mountain, steep north-trending normal faults with an east-side-down sense of motion are exposed and inferred from map patterns and bedding orientation. Inferred displacements from offsets are on the order of a 100 m; the actual displacements seen in the field are much smaller, only a few metres at most. Three closely spaced en echelon faults have a cumulative displacement of 10 m, east-side down. Along Blackwater Creek and the north slope of Juskatla Mountain, units have been tilted to vertical over distances of only a few tens of metres, suggesting drag on steep fault(s) (P.D. Lewis, pers. comm., 1988). Preliminary paleomagnetic results (Wynne and Hamilton, 1989) from the vicinity of Naden Harbour (Fig. 2) suggest a small amount of tilting (less than 5°) but indicate no consistent orientation.



**Figure 9:** Southward view of the locally northeast dipping Masset Formation, Port Chanal area, Graham Island.

On Graham Island, there is an apparent spatial relationship between the Masset Formation, pre-Masset stratigraphy and rocks of the Kano Plutonic suite (Fig. 2). The plutons give U-Pb dates of 26-28 Ma (Anderson and Reichenbach, 1989), contemporaneous with early phases of Masset volcanism. The limits of exposure of the Masset Formation parallel major topographic features such as Naden Harbour to the north, Ian Lake, and Juskatla Inlet in the central region, and dykes near Rennell Sound (Souther, 1988) in the south.

Whether (or how) these relationships relate to the structural history of Graham Island is not clear. One interpretation is that the Masset Formation on Graham Island is preserved in a large east-west trending, down faulted block similar to that proposed for the preservation of some of the Mesozoic strata further south (Thompson et al., 1991). This has uplifted and exposed the plutons and basement rocks along the northern and southern margins and preserved Eocene sediments and older volcanics (White, 1991) in more central areas.

The west side of this block probably coincides with the Queen Charlotte transform fault and the east margin with Masset Sound rather than the proposed projection of the Sandspit Fault.

At Cinola the Spegonia Fault, a normal fault dipping 45° east, is thought to be a splay of the Sandspit Fault. The Spegonia Fault trend changes from northwest trending to north trending in the vicinity of

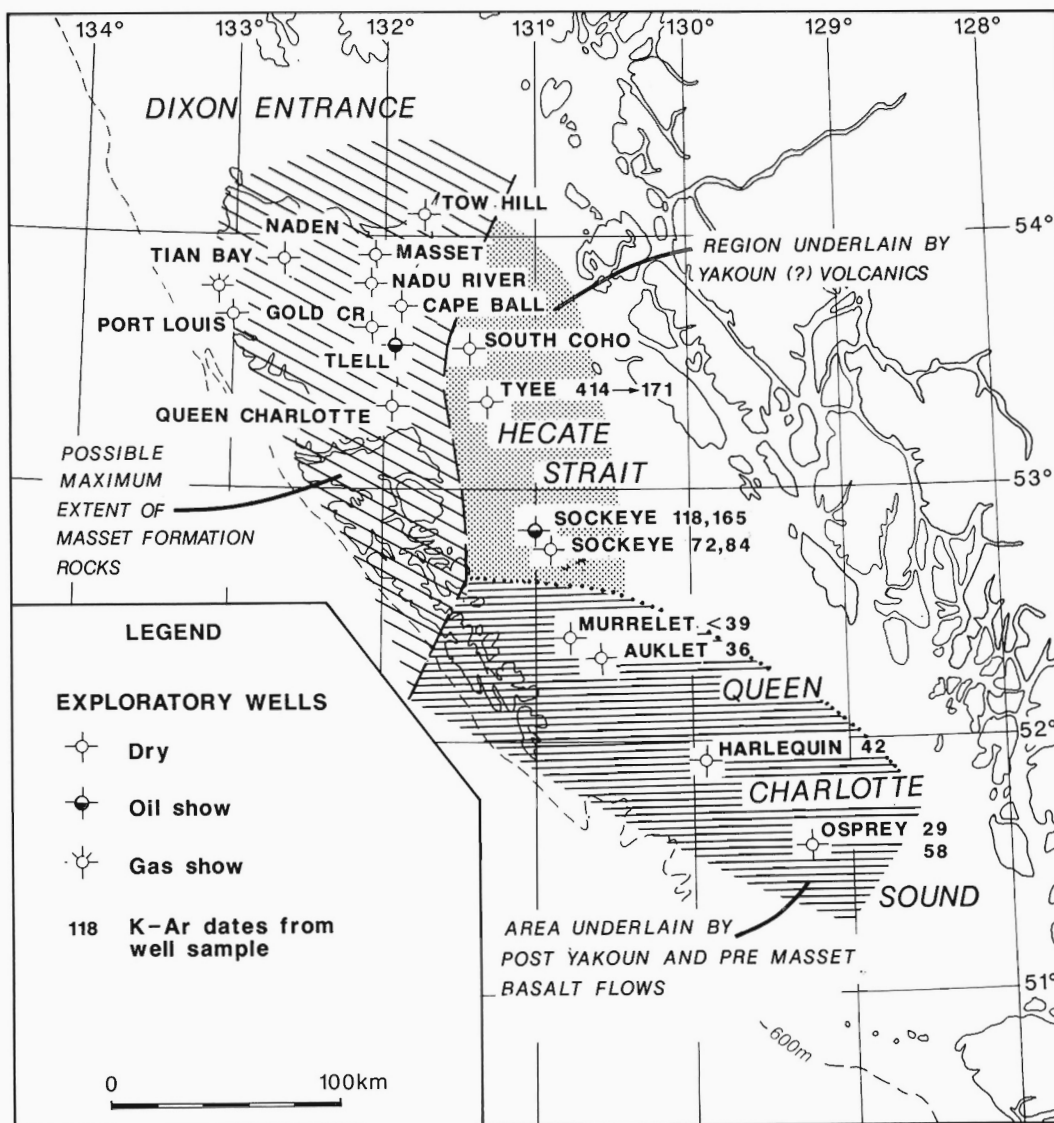
the mine. This northerly trend is parallel to Masset Sound and fault trends near Juskatla Mountain.

There is no evidence to continue the Sandspit Fault northeast from Cinola. Many northeasterly trending linear features cut across the northerly projection of the fault (Sutherland Brown, 1968: Fig. 26, p. 148) and no evidence of offset or alteration was seen at the northwest end of Ian Lake. However, stratigraphic levels exposed at surface on either side of Masset Sound are different. On the west side Early Miocene Masset volcanic rocks outcrop; on the east Miocene-Pliocene sediments of the Skonun Formation are exposed.

Drill data also supports an east-side-down fault. Volcanic rocks correlated with the Masset Formation have been intersected in drill holes east of the sound at depths of 200-2000 m (Masset well and Cape Ball well respectively, Fig. 18). The flows appear to be subaerial with little intercalated sediments; they are overlain by Skonun Formation rocks deposited in a shallow marine to fluvial environment. Therefore, the east side of Masset Sound must have subsided during and after Masset Formation volcanism.

Of note for development in areas underlain by Masset Formation rocks is the instability of the slopes. The "flaggy" weathering texture of the pyroclastic flows leaves them vulnerable to surface failure. In addition to numerous surface slips two large landslides have

**Figure 18:** Location of off-shore and onshore wells and inferred original extent of the Masset Formation before block faulting and erosion.



been noted. A two kilometre-long, postglacial landslide deposit on the northwest side of Juskatla Mountain (Hickson, 1990a) parallels the trace of a steep north-trending fault. The headwall is at 490 m and debris was carried to the base of Towustansin Hill at 200 m elevation. A second landslide north of Masset Inlet (Hickson, 1990b) carried debris from the top of the ridge at 600 m to the shore of the inlet.

## WHOLE ROCK CHEMISTRY

Volcanic rock chemistry can be used to recognize distinct petrogenetic rock suites. These chemical rock suites suggest genetic relationships with specific tectonic regimes. The tectonic regime may dictate the depth of melting, the source material, and petrogenetic processes within the melt and may hence affect magmatic composition. The stress state of the crust is thought to control the location and size of magma chambers, thus influencing the final magmatic products.

Whole rock chemistry can help choose one tectonic regime over another. In general “rift” generated magmas are tholeiitic to alkaline; peralkaline magmas are associated with continental rifting. Subduction zones are characterized by calc-alkaline to tholeiitic magmas with rare alkaline rocks.

Fifty-three samples were analyzed by X-ray fluorescence (XRF) methods for major, minor and trace elements. Trace elements were analyzed by means of pressed powder pellets on a Phillips Model 1400 at the Department of Oceanography, University of British Columbia; M. Soon, analyst. Major and minor elements were analyzed using glass powder discs. The samples were fused with a light absorber (lithium tetraborate) then crushed, formed into a pellet and analyzed on a Phillips Model 1410 at the Department of Geological Sciences, University of British Columbia; S. Horsky, analyst. Table 1 gives results for selected samples for which petrographic descriptions are also available (Table 2). Complete chemical analyses can be found in Hickson (1990b). Sample locations are plotted schematically in Figure 2 and by reference

number on the maps of Hickson (1990a,b; Hickson and Lewis, 1990; Lewis and Hickson, 1990).

All volcanic rocks are subalkaline (Irvine and Baragar, 1971; Fig. 3) save one. The subalkaline chemistry of these rocks is further supported by the presence of normative quartz and orthopyroxene (Fig. 10; Table 1). When plotted on a  $K_2O$  versus  $SiO_2$  diagram (Fig. 11) the samples extend from the field of low-K tholeiites to high-K rhyolites (Ewart, 1982). This trend crosses that of several established calc-alkaline suites; including the Andean, Japanese and Cascade trends (Ewart, 1979, 1982). On an AFM diagram (Fig. 12) most of the samples fall below the iron enrichment trend typical of tholeiites. However, when plotted as  $FeO^*/MgO$  versus  $SiO_2$  (Fig. 13) they straddle the calc-alkaline tholeiitic boundary (Ewart, 1982).

It has been suggested (Hamilton, 1985; Dostal and Hamilton, 1988) that the basalts of the Masset Formation have T-MORB characteristics. However, their sample set includes analyses of rocks from localities, such as Lawn Hill, which have been specifically excluded from the Masset Formation. Of those samples analyzed from Graham Island in this study, all are higher in  $P_2O_5$ ,  $TiO_2$  (Fig. 14),  $K_2O$  (Fig. 11), Rb, Ba (Fig. 15) and lower in Ni, V (Fig. 15) than typical T-type MORBs (Basaltic Volcanism Study Project, 1981). Additionally, they do not contain normative olivine (Fig. 10), though a few samples contain modal groundmass olivine with reaction rims (see petrology section).

A more alkalic to MORB type chemistry has been recognized by Souther and Jessop (1991) for dyke swarms on the Queen Charlotte Islands, and by Timms (1989) for the Tertiary flows and sills at Tow Hill. These suites are not spatially associated with the samples analyzed from Graham Island and Tow Hill is specifically excluded from the Masset Formation. These suites contain groundmass and olivine phenocrysts and are olivine to nepheline normative. It is noteworthy that these sequences (Tow Hill, Lawn Hill and Tar Islets) overlap in age with the Masset Formation and form a linear band along the eastern margin of

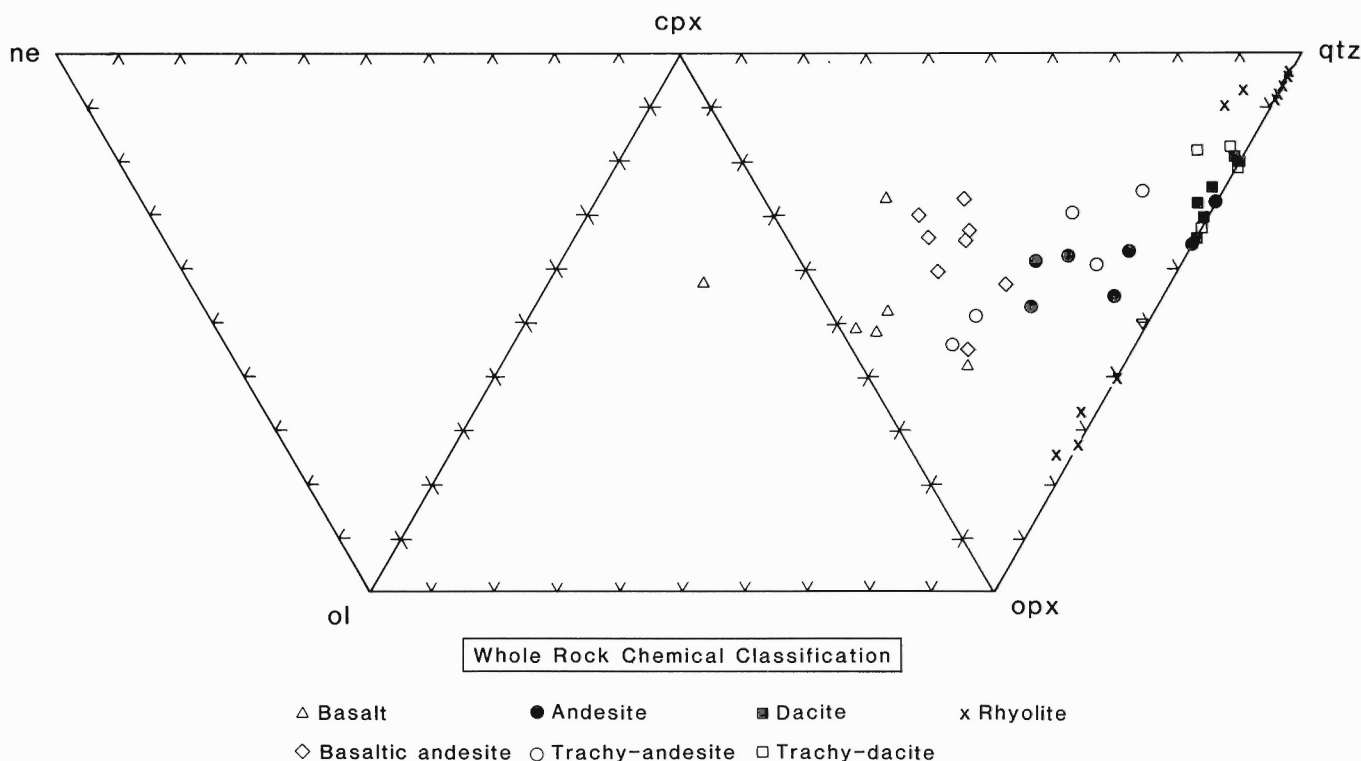
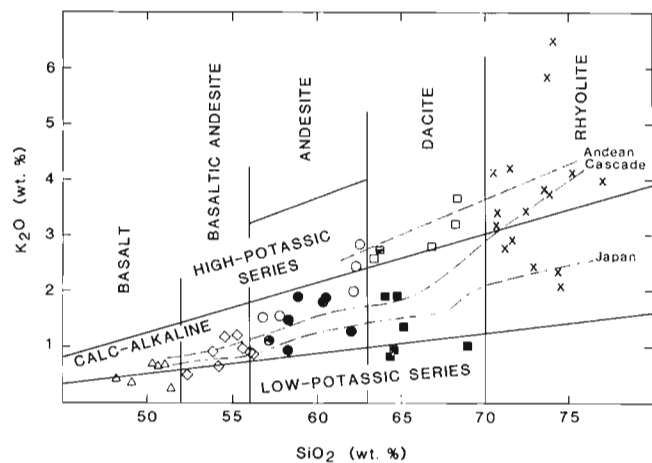


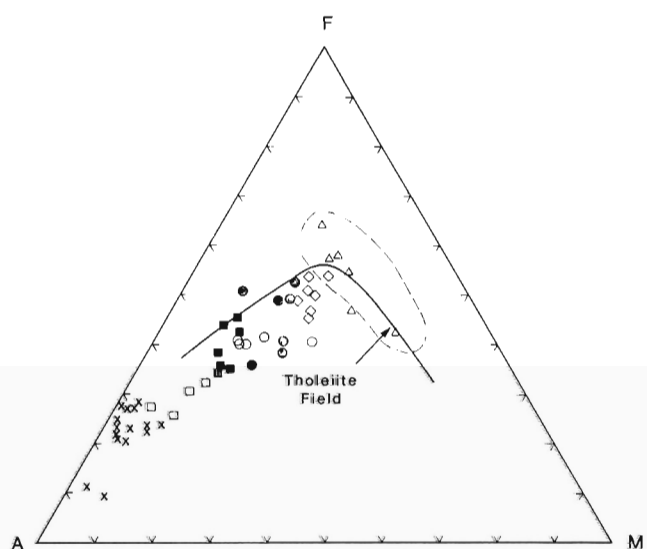
**Figure 10:** Normative nepheline (ne), olivine (ol), orthopyroxene (opx), clinopyroxenes (cpx) and quartz (qtz) plot of the Masset Formation. Symbols are based on classification shown in Figure 3.





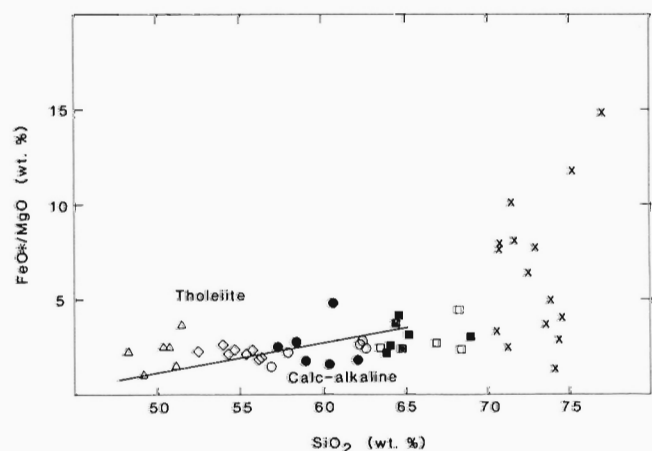
Whole Rock Chemical Classification

△ Basalt ● Andesite ■ Dacite x Rhyolite  
◇ Basaltic andesite ○ Trachy-andesite □ Trachy-dacite



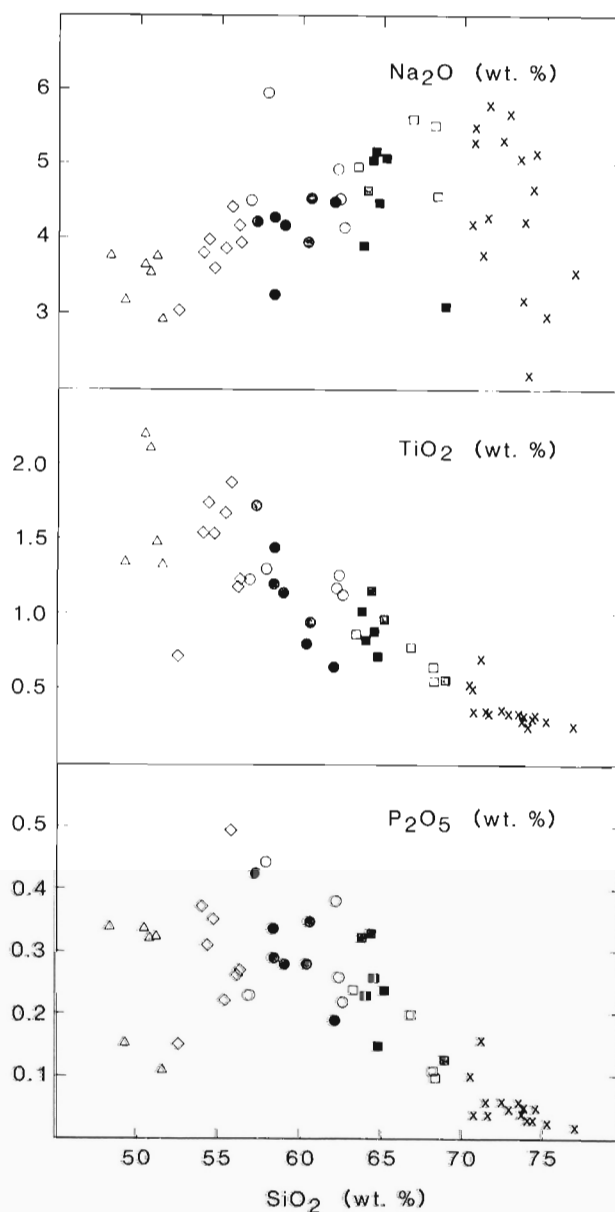
Whole Rock Chemical Classification

△ Basalt ● Andesite ■ Dacite x Rhyolite  
◇ Basaltic andesite ○ Trachy-andesite □ Trachy-dacite



Whole Rock Chemical Classification

△ Basalt ● Andesite ■ Dacite x Rhyolite  
◇ Basaltic andesite ○ Trachy-andesite □ Trachy-dacite



Whole Rock Chemical Classification

△ Basalt ● Andesite ■ Dacite x Rhyolite  
◇ Basaltic andesite ○ Trachy-andesite □ Trachy-dacite

Figure 14:  $P_2O_5$ ,  $TiO_2$ ,  $Na_2O$  versus  $SiO_2$ . Symbols are based on classification shown in Figure 3.

Figure 11:  $K_2O$  versus  $SiO_2$ . Fields after Ewart (1982). Symbols are based on classification shown in Figure 3.

Figure 12: AFM diagram of whole-rock chemical analyses of samples from the Masset Formation. Symbols are based on classification shown in Figure 3.

Figure 13:  $FeO^*/MgO$  versus  $SiO_2$ . Calc-alkaline versus tholeiite plot after Ewart (1982). Symbols are based on classification shown in Figure 3.



TABLE 1: Selected whole rock chemical analyses

Sample # <sup>1</sup>	CH-87-47-02	CH-87-07-08b	CH-88-02-05	CH-87-40-02	CH-87-07-12	CH-87-33-03	CH-88-10-05	CH-87-1	CH-88-07-02	CH-88-22-03A	CH-88-06-08	CH-87-45-07	CH-87-35-06	CH-88-30-07A	Detection limit
Chem. Class <sup>2</sup>	BAS	BAS	BAS	BAS	BAS	AND	AND	TAND	DAC	DAC	TDAC	RHY	RHY	RHY	
Petrography <sup>3</sup>	Olv.Bas.	Tho.	T.Bas	BAS	BAS	AND	AND	T.Bas.	Basan.	Basan.	Basan.	RHY	Rhydac.		
UTM North	5956950	5933225	5982825	5937020	5934425	5939500	5959475	5937725	5960575	5924450	5965400	5936300	5933950	5942225	
UTM East	649900	678575	623475	637950	678725	649700	626950	677175	655725	653525	629250	651700	656750	669575	
SiO <sub>2</sub>	48.33	50.55	51.93	54.36	55.18	58.52	60.73	61.77	63.86	64.60	68.27	69.90	72.81	73.81	0.201
Al <sub>2</sub> O <sub>3</sub>	16.45	17.16	20.22	16.92	16.03	16.42	16.53	15.74	17.09	16.99	15.58	15.20	13.53	14.72	0.180
Fe <sub>2</sub> O <sub>3</sub> T	9.98	10.40	9.31	9.77	9.59	7.45	9.47	6.92	5.17	4.74	3.72	3.15	2.78	1.30	0.008
Fe <sub>2</sub> O <sub>3</sub>	1.33	5.49	2.94	4.73	2.67	2.96	5.18	1.60	2.97	1.93	1.47	2.07	2.58	.65	
FeO	7.78	4.42	5.73	4.54	6.22	4.04	3.86	4.78	1.98	2.53	2.03	.97	.18	.58	
CaO	10.59	8.71	9.89	8.42	7.43	6.01	4.22	4.38	4.23	4.47	2.10	1.20	.73	.94	0.015
MgO	8.78	6.28	3.72	3.78	3.70	3.71	1.76	2.35	1.82	1.78	1.43	.87	.51	.32	0.050
Na <sub>2</sub> O	3.12	3.72	3.01	3.59	4.39	4.16	4.57	4.91	4.64	4.48	4.58	4.17	4.19	5.11	0.106
K <sub>2</sub> O	.35	.67	.49	1.17	.96	1.88	1.89	1.98	1.89	1.90	3.66	4.09	3.69	3.83	0.015
TiO <sub>2</sub>	1.32	1.46	.71	1.53	1.86	1.14	.95	1.17	.83	.72	.56	.53	.32	.34	0.006
P <sub>2</sub> O <sub>5</sub>	.15	.32	.15	.35	.49	.28	.35	.38	.23	.15	.10	.10	.05	.06	0.010
MnO	.18	.18	.25	.16	.20	.17	.17	.20	.11	.15	.07	.04	.05	.02	0.007
TOTAL	98.38	98.98	99.04	99.54	99.14	99.31	100.20	99.26	99.66	99.71	99.85	99.13	98.64	100.38	
LOI	2.38	1.67	1.58	2.61	2.31	1.69	2.44	2.02	1.43	1.93	1.18	1.87	1.36	3.81	
PPM															
Ba	101	243	310	374	488	444	1010	889	646	752	781	787	765	779	8
Cr	275	114	127	82	59	107	2	69	4	13	164	84	89	143	4
Cu	79	59	80	47	53	38	28	33	28	34	27	6	<det	<det	7
Nb	5	8	4	9	12	12	20	23	9	11	31	31	41	11	2
Ni	191	90	<det	19	22	35	13	28	<det	12	26	40	30	<det	3
Rb	6	8	14	15	39	42	40	121	47	48	89	100	86	137	4
Sr	301	558	488	535	580	368	342	424	405	413	143	72	23	30	3
V	204	229	279	258	242	155	<det	100	94	92	21	29	16	4	1
Y	19	22	21	25	28	32	61	47	22	25	65	93	77	24	3
Zn	79	106	91	112	115	84	130	132	71	57	58	59	107	46	4
Zr	102	140	69	169	201	265	334	393	183	225	480	601	659	258	2
Co	46	36	30	27	22	21	36	16	46	41	6	5	3	<det	
q	.00	1.36	4.62	8.13	5.69	9.63	15.53	12.13	18.57	18.67	20.53	26.64	32.58	27.01	
c	.00	.00	.00	.00	.00	.00	.13	.00	.27	.00	.51	1.99	1.46	.60	
or	2.10	4.00	2.92	6.95	5.72	11.19	11.15	11.79	11.21	11.26	21.66	24.38	22.11	22.55	
ab	26.38	31.81	25.72	30.51	37.47	35.45	38.59	41.85	39.40	38.02	38.81	35.59	35.94	43.07	
an	30.33	28.43	40.59	26.71	21.38	20.72	18.60	15.17	19.54	20.69	9.78	5.34	3.34	4.25	
ne	.25	.00	.00	.00	.00	.00	.00	.00	.00	.00	.00	.00	.00	.00	
wo	.00	.00	.00	.00	.00	.00	.00	.00	.00	.00	.00	.00	.00	.00	
cpx	17.88	10.31	6.53	10.30	10.28	5.99	.00	3.49	.00	.45	.00	.00	.00	.00	
opx	.00	12.49	13.60	6.77	10.83	9.86	5.93	10.11	4.56	6.38	5.29	2.19	1.29	.80	
fo	11.58	.00	.00	.00	.00	.00	.00	.00	.00	.00	.00	.00	.00	.00	
fa	6.62	.00	.00	.00	.00	.00	.00	.00	.00	.00	.00	.00	.00	.00	
mt	1.96	8.04	4.30	6.89	3.90	4.32	7.49	2.34	4.32	2.81	2.13	1.74	.00	.94	
hm	.00	.00	.00	.00	.00	.00	.00	.00	.00	.00	.00	.89	2.62	.00	
il	2.55	2.80	1.36	2.92	3.56	2.18	1.80	2.24	1.58	1.37	1.07	1.02	.49	.64	
ru	.00	.00	.00	.00	.00	.00	.00	.00	.00	.00	.00	.00	.00	.00	
ap	.36	.75	.35	.82	1.15	.66	.81	.89	.54	.35	.23	.24	.66	.14	

<sup>1</sup> numbers below sample numbers refer to complete listing of data (Hickson, 1990b).

<sup>2</sup> BAS = basalt, BASAN = basaltic andesite, AND = andesite, TAND = trachy-andesite, TDAC = trachy-dacite, DAC = dacite, RHY = rhyolite. Refer to Figure 3 for compositional boundaries.

<sup>3</sup> petrographic classification, for details see Table 2.

<sup>4</sup> FeO was determined by wet chemistry. FeO used in norm calculations was as measured.

**TABLE 2: Selected petrographic descriptions and phenocryst assemblage**

# <sup>1</sup>	Petrographic classification	Chem class <sup>2</sup>	Qtz	K-fsp	Plag	An content <sup>3</sup>	Ol	En	Hy	Aug	Bio	Hb	Other: minor and secondary phases
<b>Olivine Basalt</b>													
3	CH-87-07-08b	BAS			12%	60	8%						
<b>Trachybasalt</b>													
10	CH-87-40-02	BASAND			9%	66	0.5%			0.5%			
29	CH-88-07-02	DAC			13%	70	2%			3%			2% (op)
<b>Olivine Tholeiite</b>													
6	CH-88-05-07	BAS					10.5%	12%		12%			
33	CH-88-19-03	DAC			10%	51	2%	1%		7.5%			1% (gl), 1% (op)
<b>Tholeiite</b>													
7	CH-88-02-05	BASAND			28%	40			6%	6%			
23	CH-87-11-05a	TAND			18%	33-46			1.5%	10%			3.6% (gl), 0.9% (op)
32	CH-88-23-06a	DAC			18%	44-23			4.5%	7.5%			
<b>Basaltic Andesite</b>													
4	CH-87-51-17	BAS			8%	70-53	6%			1%			2% (op), 3% (gl)
5	CH-88-14-01b	BAS			6%	53					3%		6% (cl)
22	CH-88-10-05	AND			14%	19	1%						1% (cl), 4% (gl)
31	CH-88-22-03a	DAC			10%	37	4%			6%	8%		4% (tm), 2% (gl), 4% (op), 25 (ca)
36	CH-88-06-08	TDAC			34%	40	2%						4% (op)
<b>Andesite</b>													
2	CH-88-21-11b	BAS	NO PHENOCRYSTS										
8	CH-87-40-04a	BASAND		0.5%	8.5%	55				1%			
12	CH-87-07-12	BASAND			9%	64		1%					
13	CH-87-35-07	BASAND			19%	62				1%			
14	CH-87-53-07	BASAND			24%	43				6%			4.5% (cl)
22	CH-87-10-03	AND			18%	70				9%			
28	CH-88-22-10	TDAC			26%	46				6%			2% (gl), 2% (op), 4% (qu+cl)
39	CH-88-12-02	RHY			16%	29							2% (gl), 1% (op), 1% (cl)
51	CH-88-20-01b	RHY			14%	33			6%				
<b>Dacite</b>													
9	CH-87-52-05b	BASAND			15%	30							
49	CH-88-28-09	RHY			20%	21							
<b>Rhyodacite</b>													
30	CH-88-16-04b	DAC			10.5%	40				4.5%			
34	CH-87-57-18	TDAC	9%		21%	33							
44	CH-87-47-17a	RHY	2%		2.5%	22							0.25% (op), 0.5% (cl)
47	CH-88-30-07a	RHY	10%										
48	CH-87-46-23b	RHY	3.5%		1%	14				0.5%			
<b>Rhyolite</b>													
25	CH-87-46-10a	TAND	NO PHENOCRYSTS										
38	CH-87-45-07	RHY			19.5%	31	1.5%						7.5% (qu+chl), 1.5% (gl)

Minerals listed are all those that could be determined optically. Qu=quartz; K-fsp=K-feldspar; Plag=plagioclase; Ol=olivine; En=enstatite; Hy=hypersthene; Aug=augite; Bio=biotite; Hb=hornblende; op=opaques; gl=glass; cl=chlorite; tm=tourmaline; ca=calcite

<sup>1</sup> Numbers in this column refer to Table 1 and Hickson (1990b), where the complete chemical analyses can be found.

<sup>2</sup> BAS = basalt, BASAND = basaltic andesite, AND = andesite, TAND = trachy-andesite, TDAC = trachy-dacite, DAC = dacite, RHY = rhyolite, see Figure 3 for compositional boundaries.

<sup>3</sup> An content determined by optical means. Petrography was completed by S. Higman. Percentages (%) given are fractions of total modal composition.

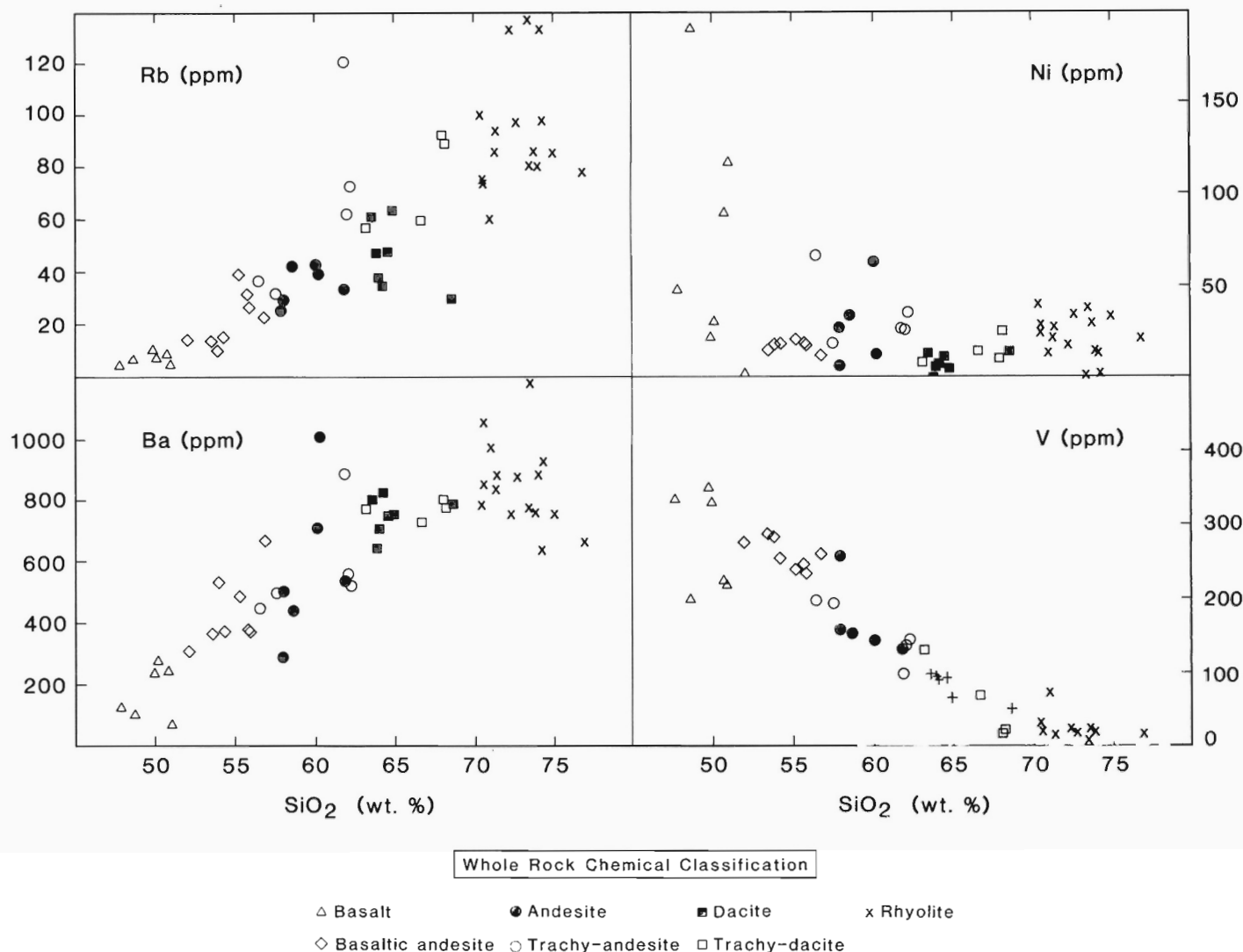


Figure 15: Rb, Ba, Ni, V versus SiO<sub>2</sub>. Symbols are based on classification shown in Figure 3.

the islands (western side of Hecate Strait). The alkalic basaltic rocks described by Woodsworth (1991) form a linear trend along the eastern side of Hecate Strait. It is suggested that these more "alkalic" rocks may be tapping a deeper magma source or have shorter crustal residence times than that associated with the Masset Formation on Graham Island. This source may be related to deep normal faults associated with the development of the Queen Charlotte Basin and Hecate Strait.

At about 42 Ma Pacific Plate motion with respect to North America changed from dominantly convergent to transform (Engelbreton et al., 1986). During convergent motion a subduction zone must have existed somewhere along the western margin of the Queen Charlotte Islands. This would have resulted in calc-alkaline, arc type, volcanism. After the change in plate motion, volcanism may have become more alkalic in affinity. This, however, does not seem to be reflected in the whole rock chemistry of the bulk of the Masset Formation. Instead, both calc-alkaline and alkalic volcanism appear to have occurred simultaneously, but spatially separated, and climaxed some ten million years after the change in plate motion.

## PETROGRAPHY

Some mafic flows along the west coast contain cumulate (mantle-derived?) nodules. Near Tian Head, anorthosite nodules (up to 8

cm) and plagioclase megacrysts (up to 3 cm) were found (Hickson, 1989). Pyroxenite nodules and pyroxene megacrysts occur in flows and breccias exposed along the coast between White and Kennecott points. Other mafic flows are dominated by plagioclase phenocrysts; pyroxene occurs infrequently and olivine is rare, everywhere occurring with a reaction rim.

Aside from megacrysts and nodules, mafic and felsic flows of the Masset Formation contain a limited variety of phenocrysts, all 3 mm or less in diameter. They are unlike most calc-alkaline felsic flows which generally contain varied, large (0.5-1 cm) phenocrysts (Ewart, 1979, 1982). In the felsic rock of the Masset, plagioclase is the only phenocryst phase that is consistently present; quartz, pyroxene, K-feldspar and opaques are rare (Table 2). Pyroxene phenocrysts, found in a small percentage of rocks classified in the field as both felsic and mafic, are characteristic of rocks whose silica content straddles the andesite-dacite compositional boundary (Fig. 2). Biotite was found in two samples and hornblende phenocrysts were not seen.

Petrologically volcanic rocks of the Masset Formation are typical neither of arc volcanics nor of rocks which have undergone any amount of fractionation. Their aphyric character may reflect eutectic melts with low (<5%) water content but it should be noted that the presence of arc

related aphyric tholeiitic rocks worldwide has been underestimated (Ewart, 1982; C. Wood, pers. comm., 1989). This appears to be because research has focused on the phenocryst-rich stratovolcanoes in the arcs. The complete answer to the origin of the Masset volcanics is the focus of ongoing detailed chemical studies.

## AGE RELATIONSHIPS AND DISTRIBUTION

### Pre-Masset volcanics

Some volcanics on Graham Island mapped as Masset by Sutherland Brown (1968) are now thought to be part of an older suite. The evidence outlined below suggests that parts of Graham Island are underlain by an extensive Late Cretaceous-early Tertiary volcanic assemblage that has been largely unrecognized until now. This assemblage is excluded on lithological and geochronological grounds from the Masset Formation as used in this paper. The lithology of rocks of the Masset Formation as studied on Graham Island make them distinguishable in the field from Paleogene and older volcanic rocks. The lack of large feldspar and hornblende phenocrysts in felsic lavas and the absence of olivine phenocrysts (and normative olivine) in mafic lavas are distinctive characteristics. K-Ar dating confirms that lithologically distinct rocks are, in general, older than the Masset Formation.

### Masset Formation

Thirty-two K-Ar ages are available from rocks assigned to the Masset Formation (Table 3; Fig. 16). A histogram (Fig. 17) showing the

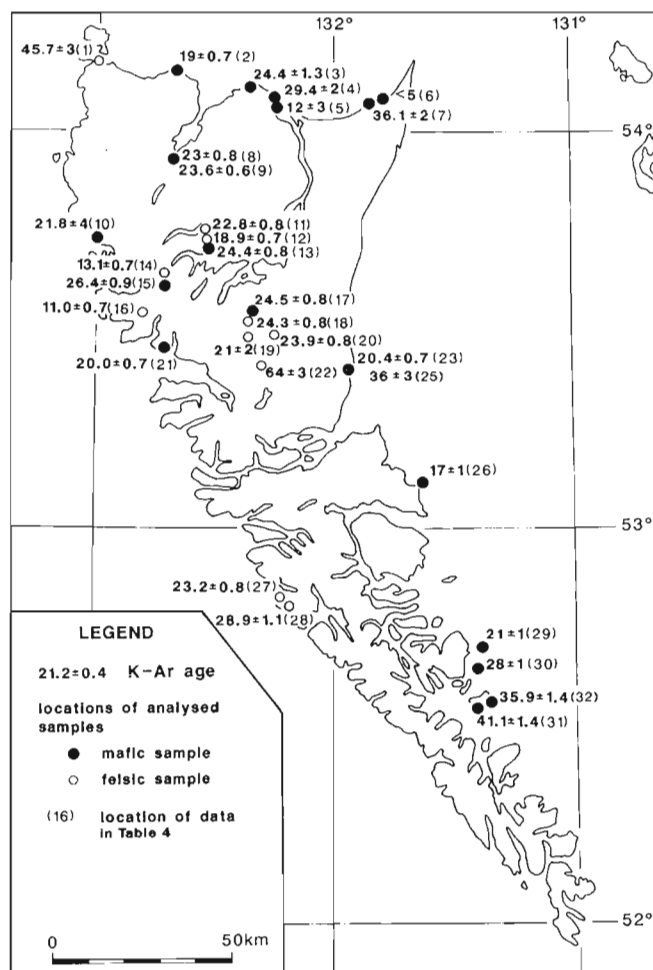


**Figure 16:** Location map of onshore K-Ar dates (for analytical details and references see Table 3).

spread of ages, suggests that eruption of the Masset Formation was restricted in time, and climaxed during a five million year period between 20 and 25 Ma. Palynological ages for intercalated sedimentary rocks (Table 4) are not conclusive, but also suggest Neogene volcanism.

Dates from Bald Mountain (64 Ma, #22, Table 3) and Cape Knox (46 Ma, #1, Table 3) are older than most dates for the Masset Formation on Graham Island. The strata were previously correlated with the Masset Formation (Sutherland Brown, 1968; Young, 1981) but lithologically these rocks are unlike Masset rocks. They are strongly porphyritic, with feldspar, biotite and minor hornblende phenocrysts. They may represent older (Cretaceous, Eocene-Oligocene?) volcanic episodes correlative with volcanism represented by samples from wells in Queen Charlotte Sound.

Sutherland Brown (1968) indicated outcrops of Masset Formation north of White Point. These rocks, examined in 1988, are lithologically unlike Masset rocks farther south. At Fleurieu Point and Sialun Bay dykes and sills contain hornblende phenocrysts, whereas Newcombe Hill is a high-level plutonic body (Fig. 9) (Lewis and Hickson, 1990). Field evidence suggests a much deeper erosion level north of Pivot Mountain. Erosion has stripped any rocks of the Masset Formation that may have existed, exposing plutonic rocks and older stratigraphic sequences.

Further evidence that the northern part of Graham Island is underlain by subaerial, pre-Masset flows is a feldspar-biotite-phyric flow on Lucy Island (between Langara and Graham islands). This flow is overlain by finely laminated siltstone of the Honna(?) Formation and lithologically resembles that at Cape Knox where a  $45.7 \pm 3$  Ma K-Ar date (Young, 1981; recalculated with new constant) was obtained from a rhyolite ash flow tuff. On Langara Island feldsparphyric mafic and felsic flows are interbedded with the Haida Formation. R.G. Anderson (pers. comm., 1988) noted that these volcanics are cut by the Langara Island pluton which gives a 27 Ma U-Pb date (Anderson and Reichenbach, 1989).

Farther south, in the vicinity of Rennell Sound, volcanics previously mapped as Masset (Sutherland Brown, 1968) were found to be hom-

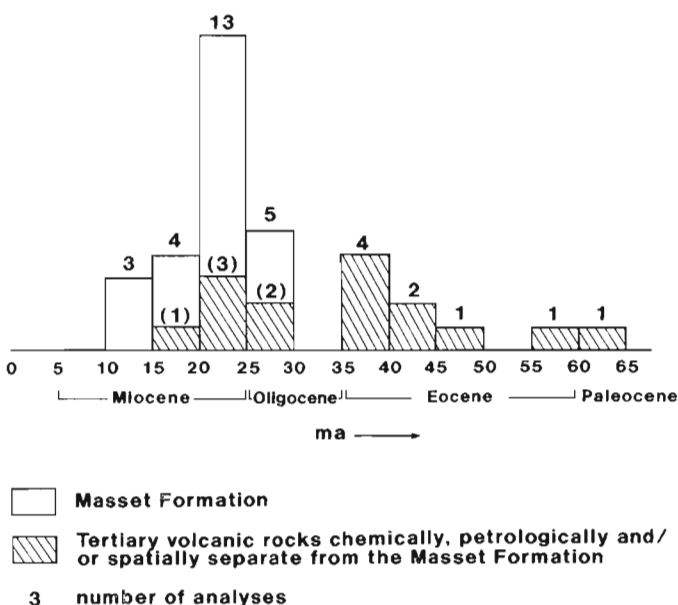


**Figure 17:** Histogram showing the distribution of dates from the Masset Formation and older volcanic units. Dates used are those given in Table 3 excluding the <5 Ma date from Tow Hill and the duplicate dates from Lawn Hill (#24 and 25 in Table 3). Included are 5 dates listed in Figure 18 from wells in Queen Charlotte Sound.

**TABLE 3:** Compilation of K-Ar dates for the Masset Formation and other Tertiary volcanic units

No. <sup>1</sup>	Rock type	Age <sup>2</sup> (Ma $\pm$ 1 $\sigma$ )	Lat.	Long.	Sample # <sup>3</sup>	Data source <sup>4</sup>
1	*felsic ash flow	45.7 $\pm$ 3	54°10.17'	132°58.0'	GS-49-66	b
2	basalt	19.0 $\pm$ 0.7	54°06.5'	132°22.1'	TMV33	d
3	basalt	24.4 $\pm$ 1.3	54°09.33'	132°39.0'	GS-51-66	b
4	basalt	29.4 $\pm$ 2	54°04.17'	132°14.25'	GS-54-66	b
5	basalt	12 $\pm$ 3	54°03.53'	132°14.33'	SD-256-N63	b
6	*ol. basalt	36.1 $\pm$ 2	54°04.4'	131°47.7'	GS-29-66	b
7	*ol. basalt	<5	54°04.73'	131°47.65'	SD-546-M63	b
8	basalt	23.0 $\pm$ 0.8	53°56.1'	132°42.1'	BVI203	d
9	basalt	23.6 $\pm$ 0.8	53°56.1'	132°42.1'	BVI3684	d
10	basalt	21.8 $\pm$ 4	53°42.08'	132°59.17'	GS-39-66	b
11	rhyolite	22.3 $\pm$ 0.8	53°44.6'	132°30.8'	300/495	d
12	dacite	18.9 $\pm$ 0.7	53°43.1'	132°30.9'	193/1815	d
13	basalt	24.4 $\pm$ 0.8	53°42.6'	132°29.7'	137/410	d
14	rhyolite	13.1 $\pm$ 0.7	53°38.6'	132°41.8'	163/225	d
15	basalt	26.4 $\pm$ 0.9	53°38.3'	132°41.2'	161/790	d
16	rhyolite	11.0 $\pm$ 0.7	53°34.8'	132°46.0'	70/2130	d
17	andesite	24.5 $\pm$ 0.8	53°30.6'	132°20.0'	MR 9	c
18	felsic ash flow	24.3 $\pm$ 0.8	53°30.6'	132°20.0'	MR 2	c
19	felsic ash flow	21 $\pm$ 2	53°31.68'	132°21.2'	SD-544-N63	b
20	dacite	23.9 $\pm$ 0.8	53°32.8'	132°17.6'	342/1020	d
21	basalt	20.0 $\pm$ 0.7	53°26.6'	132°43.3'	18/44	d
22	bio.fdspr.porp.	64 $\pm$ 3	53°24.2'	132°23.1'	AK 378	a
23	*basalt	20.4 $\pm$ 0.7	53°24.6'	131°55.0'	TMV61.5	d
24	*basalt	20.3 $\pm$ 0.7	53°24.6'	131°55.5'	MR 8	c
25	*ol. basalt	36 $\pm$ 3	53°25.1'	131°54.8'	SD-278-N63	b
26	*andesite	17 $\pm$ 1	53°06.8'	131°38.23'	SD-250-N63	b
27	*rhyolite	23.2 $\pm$ 0.8	52°49.6'	132°12.1'	38/2310	d
28	*basalt	28.9 $\pm$ 1.1	52°48.3'	132°09.7'	TMV21	d
29	*basalt	21 $\pm$ 1	52°41.4'	131°23.27'	SD-252-N63	b
30	*basalt	28 $\pm$ 1	52°40.4'	131°24.75'	SD-253-N63	b
31	*basalt	41.1 $\pm$ 1.4	52°33.0'	131°21.4'	TMV10	d
32	*basalt	35.9 $\pm$ 1.4	52°33.2'	131°21.0'	TMV50	d

1. Number refers to plotted locations on Figure 16.

2. Refer to original source for details of analyses; dates have been recalculated using new constants, where applicable (R.L. Armstrong, pers. comm.).

3. Original sample number quoted by source.

4. Source of dates:

a: Mathews, 1964;

b: Young, 1981; unpublished data from Shell Development Corp. (Houston, Texas) and Pan-America Petroleum Corporation;

c: Young, 1981; run at Geochron Laboratory, University of British Columbia;

d: U.B.C. Geochron File. Samples collected by T. Hamilton and dated by J. Harakal under contract to the G.S.C.;

\*: Samples prefaced with a '\*' are excluded from the Masset Formation on chemical, petrological and/or spatial grounds.

**TABLE 4:** Palynological for samples from the Masset Formation

Sample #	Lat.	Long.	Probable age	GSC Loc. #
CH-87-61-01c	53°43'11"	132°36'38"	Eocene-Pliocene	C-158301
CH-87-61-01a	53°43'11"	132°36'38"	L. Miocene-E. Pliocene	C-158302
CH-87-23-11e	53°33'18"	132°22'29"	L. Miocene-E. Pliocene	C-158303
CH-87-25-15c	53°33'20"	132°22'22"	Eocene-Pliocene	C-158304
CH-87-27-11b	53°34'50"	132°23'37"	undeterminable	C-158305
CH-87-28-09e	53°32'30"	132°26'44"	pre-Quaternary	C-158306
CH-87-33-02a	53°35'02"	132°44'18"	undeterminable	C-158308
CH-87-33-02b	53°35'02"	132°44'18"	pre-Quaternary	C-158307
CH-87-02-18a	53°38'19"	132°21'31"	undeterminable	C-158310
CH-87-02-18c	53°38'19"	132°21'31"	undeterminable	C-158309
CH-88-02-08b	53°58'02"	133°06'45"	undeterminable	C-158317
CH-88-30-09a	53°53'31"	132°26'44"	undeterminable	C-158315
CH-88-30-09b	53°35'31"	132°26'44"	undeterminable	C-158316
CH-88-03-04c	53°57'65"	133°06'46"	undeterminable	C-158314
CH-88-22-01c	53°26'48"	132°41'57"	Cenozoic	C-158313

Data from GSC Paleontology Reports JMW-89-5 and JMW-88-1, J. White pers. comm. (1988, 1989).

blende-biotite-quartzphyric rocks which are not in stratigraphic continuity with Masset rocks. Nearby, on Bald Mountain, a lithologically similar biotite-feldspar porphyritic intrusive body ( $64 \pm 3$  Ma K-Ar date; recalculated with new constants) was dated by Mathews (1964). A few kilometres north of Bald Mountain, is a southeasterly-trending ridge capped by a pebble-cobble conglomerate unit lithologically similar to the Upper Cretaceous Honna Formation (Indrelid et al., 1991; Lewis et al., 1990). This conglomerate contains plutonic clasts resembling the Bald Mountain intrusion and volcanic clasts resembling rocks seen closer to Rennell Sound. The evidence, though circumstantial, suggests that the rocks in Rennell Sound represent an older (Late Cretaceous-Paleocene?) phase of volcanism.

In the vicinity of Long Inlet mafic (basaltic andesite) flows interfinger with conglomerates of the Honna Formation as described by Haggart et al. (1989). These flows are unconformably overlain by freshwater shale of Eocene age. In the Port Louis well a thick sedimentary package has been dated as Eocene (White, 1991). The sediments overlie a volcanic unit that may be correlative with the Long Inlet volcanics.

In the area near Cinola, distinctive quartz-eye porphyry dykes cut rocks of the Yakoun and Haida formations. Detailed mapping has revealed a quartzphyric flow within fine grained shales of the shale member of the Haida Formation (J. Deighton, pers. comm., 1988). Isolated exposures of hornblende-phyric rocks were found in an area mapped as Yakoun Formation by Sutherland Brown (1968) south of the proposed mine site (M.A. Hepp, pers. comm., 1988).

K-Ar dates on older volcanic rocks from boreholes in Hecate Strait are of dubious analytical quality (Young, 1981). However, the youngest date from the Hecate Strait wells (Sockeye; Fig. 16) is 72 Ma (Young, 1981), suggesting that these volcanics are older than the Masset. Detailed petrological work by Leslie (1989) suggest that all the reported volcanic rocks are reworked volcanoclastic sandstones and conglomerates. The Jurassic Yakoun Formation was suggested by Leslie (1989) as a possible source for much of the volcanic detritus.

The evidence from the Hecate Strait and Port Louis wells and on-land exposures implies that porphyritic mafic and felsic rocks represent volcanic activity prior to the Masset eruptions. This corroborates field evidence that the Masset Formation may be more areally and temporally restricted than previously thought (Fig. 18). There is no compelling evidence to suggest that Masset flows formed a continuous sheet south of Graham Island. Based on work to the south, Souther (1988) noted that there is an increase in dyke density around areas of "Masset" outcrop; he suggested that the present distribution of volcanic rocks may correspond closely to an original accumulation around localized centres.

Dating and mapping suggest that over time there have been many phases of Tertiary volcanism on the Queen Charlotte Islands. The late Eocene-Oligocene pulse may be related to change in plate motions around 42 Ma (Engelbreton et al., 1986). However, the chemistry and areal distribution of these older units and how they differ from Masset volcanism (as defined in this paper) on Graham Island must await further study.

## DISCUSSION

The Masset Formation is interpreted as a product of orogenic volcanism during Late Oligocene to Early Pliocene time. Assuming the Kula-Farallon triple junction was north of the Queen Charlotte Islands during the Miocene, oblique subduction would have triggered magma production in a region of thinned crust and high heat flow as the triple junction migrated southward to its present position. The eruptive episode climaxed 20-25 Ma ago with voluminous outpourings of a range of magma types.

It is noteworthy that the Masset Formation is chemically, petrologically and morphologically similar to Miocene volcanics in the Cascade mountains of Washington (D.A. Swanson, pers. comm., 1989;

Schultz, 1988). Swanson and Schultz have interpreted the Cascade volcanics to be the product of subduction off the west coast. Souther and Yorath (in press) have suggested that the Masset volcanics may be part of the "Pemberton arc" system based on the coeval ages of volcanics and plutons in the Pemberton belt (35-16 Ma).

Other postulated origins for the Masset volcanics include rifting (Yorath and Hyndman, 1983), possibly initiated by a mantle hotspot (Yorath and Chase, 1981); an "edge effect" of the subducted margin of the Farallon plate (Stacey, 1974), and wrench tectonics along the Sandspit and Rennell-Louscoone fault systems (Young, 1981).

The Masset Formation appears to have had little effect on the regional thermal maturation of the country rocks, possibly reflecting the apparent lack of high level magma chambers and the short duration of eruptive activity. In addition, volcanism was marginal to the sedimentary basin, affecting only localized areas. The easterly thinning and interfingering of Masset flows with sediments of the Skonun Formation is relevant to offshore drilling in Hecate Strait. Wells there, intersect clastic rocks derived from a volcanic event older than the Masset and, at depth may intersect flows from an event that may be as old as Jurassic.

Volcanic rocks have not previously been noted in outcrops of the Albion and Late Cretaceous Queen Charlotte Group, although volcanics have been intersected in drill holes (Young, 1981). Previously, volcanic rocks were assigned to either the Masset Formation, Yakoun Group or Karmutsen Formation, but the occurrences near Langara Island, Rennell Sound, Cinola and Long Inlet cannot be correlated with any of the above units. Volcanic rocks that are post-Yakoun Group and pre-Masset Formation (as used in this paper) should be considered separately, either as distinct formations or as members of existing formations.

## ACKNOWLEDGMENTS

Field assistance was ably provided by A. Huntley (1987) and C. Timms (1988). The hospitality of City Resources (Canada) Limited at Cinola was very much appreciated. Discussions with M.P. Twyman (Consultant, United Pacific Gold Ltd.), J. Deighton (City Resources (Canada) Limited), and M.A. Hepp (Fairbanks Engineering Ltd.) were stimulating and informative. Cooperative large-scale mapping with M.P. Twyman helped illuminate aspects of the structure and stratigraphy not noted before. Employees of MacMillan Bloedel Limited (Queen Charlotte Division) were most helpful in providing information on active logging in the study area. Adroit helicopter piloting by P. Fraser (Vancouver Island Helicopters Ltd.) increased the efficiency and enjoyment of the work. Petrographic work and help with manuscript preparation by S. Hignman was most appreciated. Critical reading by R.I. Thompson, J.K. Russell and G.J. Woodsworth helped improve the manuscript.

Discussions with A. Sutherland Brown were most helpful. Access to his original maps and notebooks provided insight which helped in the final interpretations. Many members of the Queen Charlotte FGP team helped and contributed to this work with ideas and encouragement and for this I thank them. However, particular thanks go to R.I. Thompson for initiating the project and keeping it humming through thick and thin.

## REFERENCES

- Anderson, R.G. and Reichenbach, I.  
1989: A note on the geochronometry of Late Jurassic and Tertiary plutonism in the Queen Charlotte Islands, British Columbia; in Current Research, Part H, Geological Survey of Canada, Paper 89-1H, p. 105-112.
- Basaltic Volcanism Study Project  
1981: Basaltic volcanism on the terrestrial planets; Pergamon Press, Inc., New York, 1286 p.
- Cameron, B.E.B. and Hamilton, T.S.  
1988: Contributions to the stratigraphy and tectonics of the Queen Charlotte Basin, British Columbia; in Current Research, Part E, Geological Survey of Canada, Paper 88-1E, p. 221-227.
- Dostal, J. and Hamilton, T.S.  
1988: Oceanic volcanism on the western Canadian continental margin: Masset Formation (U. Eocene-U. Miocene); Geological Association of Canada, Annual Meeting, St. John's, Newfoundland, Program with Abstracts, v. 13, p. A33.



- Engelbreton, D.C., Cox, A., and Gordon, R.G.**  
**1986:** Relative motions between oceanic and continental plates in the Pacific Basin: Geological Society of America, Special Paper 206, 56 p.
- Ewart, A.**  
**1979:** A review of the mineralogy and chemistry of Tertiary-Recent dacitic, latitic, rhyolitic, and related silic volcanic rocks; *in* Trondhjemites, Dacites and Related Rocks, F. Barker (ed.), Elsevier, New York, p. 13-121.
- 1982:** The mineralogy and petrology of Tertiary-Recent orogenic volcanic rocks: with special reference to the andesite-basaltic compositional range; *in* Andesites, R.S. Thorpe (ed.), John Wiley and Sons, New York, p. 25-95.
- Gordon, R.G. and Jurdy, D.M.**  
**1986:** Cenozoic global plate motions; *Journal of Geophysical Research*, v. 91, B12, p. 12389-12406.
- Haggart, J.W., Lewis, P.D., and Hickson, C.J.**  
**1989:** Stratigraphy and structure of Cretaceous strata, Long Inlet, Queen Charlotte Islands, British Columbia; *in* Current Research, Part H, Geological Survey of Canada, Paper 89-1H, p. 65-72.
- Hamilton, T.S.**  
**1985:** Volcanics of the Cenozoic Masset Formation: implications for geological and tectonic evolution of the Queen Charlotte Islands, British Columbia, Canada; Geological Society of America, Cordilleran Section Annual Meeting, Program with Abstracts, Vancouver, British Columbia, May 8-10, p. 359.
- Hamilton, T.S. and Cameron, B.E.B.**  
**1989:** Hydrocarbon occurrences on the western margin of the Queen Charlotte Basin; *Bulletin of Canadian Petroleum Geology*, v. 37, p. 443-466.
- Hickson, C.J.**  
**1988:** Structure and stratigraphy of the Masset Formation, Queen Charlotte Islands, British Columbia; *in* Current Research, Part E, Geological Survey of Canada, Paper 88-1E, p. 269-274.
- 1989:** An update on structure and stratigraphy of the Masset Formation, Queen Charlotte Islands, British Columbia; *in* Current Research, Part II, Geological Survey of Canada, Paper 89-1H, p. 73-79.
- 1990a:** Geology, Port Clements, British Columbia; Geological Survey of Canada, Map 6-1990, scale 1:50 000.
- 1990b:** Geology, Awun Lake, British Columbia; Geological Survey of Canada, Map 7-1990, scale 1:50 000.
- Hickson, C.J. and Lewis, P.D.**  
**1990:** Geology, Frederick Island (west half), British Columbia; Geological Survey of Canada, Map 8-1990, scale 1:50 000.
- Indrelid, J., Hesthammer, J., and Ross, J.V.**  
**1991:** Structural geology and stratigraphy of Mesozoic rocks of central Graham Island, Queen Charlotte Islands, British Columbia; *in* Evolution and Hydrocarbon Potential of the Queen Charlotte Basin, British Columbia, Geological Survey of Canada, Paper 90-10.
- Irvine, T.N. and Baragar, W.R.**  
**1971:** A guide to the chemical classification of the common volcanic rocks; *Canadian Journal of Earth Sciences*, v. 8, p. 523-548.
- LeBas, M.J., LeMaitre, R.W., Streckeisen, A., and Zanettin, B.**  
**1986:** Chemical classification of volcanic rocks; *Journal of Petrology*, v. 27, p. 746-750.
- Leslie, D.R.**  
**1989:** Petrography and sedimentology of an unnamed Upper Cretaceous to Lower Paleocene sedimentary unit, Queen Charlotte Basin, British Columbia; B.A.Sc. thesis, University of British Columbia, Vancouver, 57 p.
- Lewis, P.D. and Hickson, C.J.**  
**1990:** Geology, Langara Island (west half), British Columbia; Geological Survey of Canada, Map 9-1990, scale 1:50 000.
- Lewis, P.D., Hesthammer, H., Indrelid, J., and Hickson, C.J.**  
**1990:** Geology, Yakoun Lake, British Columbia; Geological Survey of Canada, Map 5-1990, scale 1:50 000.
- MacKenzie, J.D.**  
**1916:** Geology of Graham Island, British Columbia; Geological Survey of Canada, Memoir 88, 221 p.
- Mathews, W.H.**  
**1964:** Potassium-argon age determinations of Cenozoic volcanic rocks from British Columbia; Geological Society of America Bulletin, v. 75, p. 465-468.
- Schultz, J.M.**  
**1988:** Mid-Tertiary volcanic rocks of the Timberwolf Mountain area, south-central Cascades, Washington; M.Sc. thesis, Western Washington University, Bellingham, 145 p.
- Shouldice, D.H.**  
**1971:** Geology of the western Canadian continental shelf; *Bulletin of Canadian Petroleum Geology*, v. 19, p. 405-436.
- Souther, J.G.**  
**1988:** Implications for hydrocarbon exploration of dyke emplacement in the Queen Charlotte Islands, British Columbia; *in* Current Research, Part E, Geological Survey of Canada, Paper 88-1E, p. 241-245.
- Souther, J.G. and Jessop, A.M.**  
**1991:** Dyke swarms in the Queen Charlotte Islands, British Columbia, and implications for hydrocarbon exploration; *in* Evolution and Hydrocarbon Potential of the Queen Charlotte Basin, British Columbia, Geological Survey of Canada, Paper 90-10.
- Souther J.G. and Yorath, C.J.**  
**in press:** Neogene assemblages; *in* The Cordilleran Orogen: Canada, Geology of Canada, No. 4, H. Gabrielse, and C.J. Yorath (ed.), Geological Survey of Canada (also Geological Society of America, The Geology of North America, v. G-2).
- Stacey, R.A.**  
**1974:** Plate tectonics, volcanism and the lithosphere in British Columbia; *Nature*, v. 250, p. 133-134.
- Sutherland Brown, A.**  
**1968:** Geology of the Queen Charlotte Islands, British Columbia; British Columbia Department of Mines and Petroleum Resources, Bulletin 54, 226 p.
- Thompson, R.L., Haggart, J.W., and Lewis, P.D.**  
**1991:** Late Triassic through Early Tertiary evolution of the Queen Charlotte Basin, British Columbia, with a perspective on hydrocarbon potential; *in* Evolution and Hydrocarbon Potential of the Queen Charlotte Basin, British Columbia, Geological Survey of Canada, Paper 90-10.
- Timms C.E.**  
**1989:** The origin and tectonic setting of Tow Hill, Queen Charlotte Islands; B.Sc. thesis, McMaster University, Hamilton, Ontario, 79 p.
- White, J.M.**  
**1991:** Palynostratigraphy of Tow Hill No. 1 Well in the Skonun Formation, Queen Charlotte Basin, British Columbia; *in* Evolution and Hydrocarbon Potential of the Queen Charlotte Basin, British Columbia, Geological Survey of Canada, Paper 90-10.
- Woodsworth, G.J.**  
**1991:** Neogene to Recent volcanism along the east side of Hecate Strait, British Columbia; *in* Evolution and Hydrocarbon Potential of the Queen Charlotte Basin, British Columbia, Geological Survey of Canada, Paper 90-10.
- Wynne, P.J. and Hamilton T.S.**  
**1989:** Polarity and inclination of magnetization of the Masset Formation from a deep drillhole on Graham Island, Queen Charlotte Islands, British Columbia; *in* Current Research, Part H, Geological Survey of Canada, Paper 89-1H, p. 81-86.
- Yorath, C.J. and Chase, R.L.**  
**1981:** Tectonic history of the Queen Charlotte Islands and adjacent areas - a model; *Canadian Journal of Earth Sciences*, v. 18, p. 1717-1739.
- Yorath, C.J. and Hyndman, R.D.**  
**1983:** Subsidence and thermal history of Queen Charlotte Basin; *Canadian Journal of Earth Sciences*, v. 20, p. 135-159.
- Young, I.F.**  
**1981:** Structure of the western margin of the Queen Charlotte Basin, British Columbia; M.Sc. thesis, University of British Columbia, Vancouver.

## APPENDIX: XRF ANALYSES LIMITATIONS AND ERRORS

Chemical analysis by X-ray fluorescence has become routine in laboratories around the world. However, as with any analytical tool there are limitations to the method. As greater emphasis is placed on detailed petrogenesis and comparison of rock suites on regional and global scales, more concern must be placed on the accuracy and reproducibility of the analytical results.

Error analysis is a time consuming process that must take into account many factors. The counting error is the single most crucial source of error. It depends only on the total accumulated counts, but represents the maximum possible precision that can be obtained. Increasing counting time will increase the total counts (thereby reducing the detection limit) but must be balanced with other sources of error such as device or instrumental error, operational errors, specimen preparation errors and other miscellaneous errors, many of which are not completely quantifiable.

For analytical results that are greater than three times the detection limit, the errors are relatively low (less than 1% of the value). At these concentrations, factors such as the calibration and reproducibility of analytical results become important but are difficult to assess. Counts for major elements are generally very high, thus the errors are small. Because of this, the focus of this study has been on the minor and trace elements which may have low total counts and therefore be subject to large errors.

The accuracy of the result, i.e., how well it compares to results achieved in other labs, was checked by running external laboratory standards as unknowns and excluding them from the calibration. The results (Table A1) include runs completed in three different years using the same instrument, analytical techniques and machine conditions (i.e. count times, and peak and background positions).

The precision of the analytical value was assessed by running a homogenized, internal laboratory standard multiple times. The purpose of this exercise was to try to evaluate differences that might exist between the three sets of data and how accurate the results are. The work also points out the problem in reproducibility of analytical values. The errors, though not necessarily large in themselves, should be

carefully weighed. These errors can become significant when the user compares this data set to that of another laboratory for purposes such as producing tectonic discriminant diagrams or goes about detailed petrogenetic calculations. When the errors within and between the data sets are taken into account the results may not be valid. Results are shown in Table A2.

**TABLE A1:** Standard data: comparisons

Name Date <sup>2</sup>	Element	Stand. comp. <sup>1</sup>	Det. Comp.	Diff.	Det. comp.	Diff.	Det. comp.	Diff.
			1987		02-89		03-89	
AGV-1	Ba	1200.	1151.	+49	1229.9	+30	1296.4	+96
	Co	16.	20.	+4	12.1	-4	16.8	+1
	Cr	10.	-25.	-15	8.6	-1	9.7	0
	Cu	59.	65.	+6	87.1	+28	86.8	+27
	Mn	???	825.	-	806.4	-	838.7	-
	Nb	16?	14.	+2?	13.5	-3?	15.7	0?
	Ni	15.	12.	+3	10.6	-4	16.0	+1
	Pb	33.	44.	+11	37.	+4	40.7	-8
	Rb	67.	66.	+1	68.6	+2	70.0	+3
	Sr	660.	711.	+51	666.8	+7	673.0	+13
	V	125.	124.	+1	123.8	-1	132.0	+7
	Y	19.	22.	+3	17.0	-2	18.6	0
	Zn	86.	89.	+3	80.6	-5	89.9	+4
	Zr	230.	243.	+13	239.3	+9	243.1	+13
GSP-1	Ba	1300.	1300.	0	1315.5	+15	1368.7	+69
	Co	8.	9.	+1	1.0	-7	4.3	-4
	Cr	12.	-14.	-2	7.7	-4	9.5	-3
	Cu	33.	31.	+2	46.0	+13	45.6	+13
	Mn	???	327.	-	286.7	-	290.3	-
	Nb	23?	23.	23?	21.8	-1?	22.5	-1?
	Ni	9.	10.	+1	16.2	+7	16.3	+7
	Pb	54.	52.	-2	55.0	+1	56.3	+2
	Rb	250.	257.	+7	255.7	+6	251.7	+2
	Sr	240.	245.	+5	243.6	+4	240.1	0
	V	54.	69.	+15	52.3	-2	55.1	+1
	Y	29.	27.	+2	31.4	+2	30.2	+1
	Zn	105.	107.	+2	112.2	+7	106.3	+1
	Zr	500.	502.	+2	481.3	-19	494.3	-6
GA	Ba	850.	892.	+42	880.7	+31	897.5	+47
	Co	5.	8.	+3	6.7	+2	9.1	+4
	Cr	12.	1.	+11	9.0	-3	8.3	-4
	Cu	16.	21.	+5	29.3	+13	33.1	+17
	Mn	???	823.	-	769.0	-	777.0	-
	Nb	10?	14.	+4	11.5	+1?	13.1	+3?
	Ni	7.	4.	-3	3.0	-4	6.7	0
	Pb	30.	34.	+4	31.0	+1	33.2	+3
	Rb	175.	169.	+6	173.3	-2	174.3	-1
	Sr	310.	315.	+5	306.1	-4	304.2	-6
	V	38.	33.	+5	36.1	-2	39.7	+2
	Y	21.	21.	0	20.5	-1	21.6	+1
	Zn	80.	71.	+9	71.6	-8	71.4	-8
	Zr	150.	153.	+3	145.1	-5	147.2	-3
SY-2	Ba	460.	498.	+38	462.7	+3	463.0	+3
	Co	11.	6.	+5	7.8	-3	4.6	-5
	Cr	12.	2.	+10	3.5	-9	3.2	-9
	Cu	5.	2.	+3	22.3	+17	15.7	+16
	Mn	???	2619.	-	2639.0	-	2533.5	-
	Nb	23?	26.	+3?	11.2	-12?	11.2	-12?
	Ni	10.	23.	+13	69.5	+59	68.9	+59
	Pb	80.	39.	+41	76.7	-3	79.4	-1
	Rb	220.	233.	+13	182.9	-38	176.4	-44
	Sr	275.	297.	+22	262.3	-13	256.2	-19
	V	52.	-1.	+51	61.2	+9	61.0	+9
	Y	130.	137.	+7	172.5	+42	177.0	+47
	Zn	250.	278.	+28	269.5	+19	263.2	+13
	Zr	280.	275.	+5	269.2	-11	272.1	-8
G-2	Ba	1900.			2003.3	+103	2092.6	+193
	Co	5.			2.2	-3	-0.4	-5
	Cr	8.			4.6	-3	3.9	-4
	Cu	10.			31.4	+21	27.1	+17
	Mn	???			247.4	-	267.7	-
	Nb	13.?			11.3	-2?	13.4	0?
	Ni	3.			-3.4	-6	-1.4	-4
	Pb	30.			33.2	+3	33.4	+3
	Rb	170.			173.8	+4	171.7	+2
	Sr	480.			498.6	+19	489.2	+9
	V	36.			42.8	+7	50.1	+14
	Y	11.			8.9	-2	8.3	-3
	Zn	84.			91.0	+7	91.9	+8
	Zr	300.			308.9	+9	315.5	+15

<sup>1</sup> All analyses in ppm

<sup>2</sup> Year or month-year analyses were completed

TABLE A2: Replicate analyses of standards

Std name Date <sup>1</sup> :	Ba 88	Ba 89	Ba Mar-89	Co 88	Co 89	Co Mar-89	Cr 88	Cr 89	Cr Mar-89	Cu 88	Cu 89	Cu Mar-89	Mn 88	Mn 89	Mn Mar-89	Nb 88	Nb 89	Nb Mar-89	Ni 88	Ni 89	Ni Mar-89
MONCH-A	283	232.8	247.6	56	43.2	50.1	455	375.5	366.4	27	44.2	42.7	1251	1233.2	1196.7	15	18	18.6	124	124.3	121.8
MONCH-N	282	262	248.3	63	51.4	52.1	434	400.4		31	46.4		1203	1349.8		15	17.7		125	122.2	
MONCH-F	280	248.3	254.1	66	45.5	52.1	463	379.6	404.1	26	52.4	48.6	1256	1269	1338.2	17	17.9	20.3	132	130.3	130.9
MONCH-L	275	232.6		57	55.9		466	388.5		22	45.5		1249	1265.8		17	19.2		132	132.6	
MONCH-H	278	248.2	256	58	56.6	53	456	399.7	391.5	33	47.4	59.8	1248	1288.2	1277.1	17	19.2	18.6	130	132.6	125.9
MONCH-O	297	250		66	54		473	367.9		30	53.4		1288	1235.8		14	17.9		127	125.3	
MONCH-E	287	244.3	249.4	57	48.2	54.5	481	387.3	391.8	37	51.8	63.2	1275	1248	1273.9	14	17.7	20.5	132	128.2	135.3
MONCH-M	279	223.3		63	49.4		488	379.3		31	53.1		1319	1239.9		17	18.3		123	125.6	
MONCH-D	272	258.7	281.3	65	48.7	56.5	454	373.6	390.2	32	53.5	55.3	1251	1230.7	1301.2	13	17.9	18.9	134	118.1	131.9
MONCH-C	291	243.7	257.6	59	55.5	64.4	485	368.4	375.1	29	44.9	56.4	1238.4	1238.4	1238.4	16	19.1	19.9	121	122.2	130.7
MONCH-B	274	248.7	238.2	66	50.8	45.1	478	381.5	389.5	32	50.7	48.9	1270	1261.1	1262.7	15	18.9	20.2	129	121.1	126.6
MONCH-K	287	253.6		61	52.3		456	380.8		25	45.9		1234	1251.5		14	19.9		132	131.8	
MONCH-J	263	273.9		65	46.2		476	388.4		36	44.3		1272	1268.4		15	17.1		138	124.3	
MONCH-G	278	247.6	254.8	60	60.1	59.4	456	378.4	374	34	48.7	48.9	1251	1271.6	1229.2	14	18.7	20.2	136	124.8	128.8
MONCH-I	302	228.9		59	53.2		476	376.4		29	40.9		1317	1277		16	19.4		131	119.3	
MONCH-J2	294	245.4		62	50.6		490	390.7		31	49.5		1324	1284.2		14	19.3		130	129.9	
Mean	283	246.4	254.9	61	51.4	54.4	468	381.6	385.3	30	48.3	53.6	1270	1263.3	1264.7	15	18.5	19.7	130	125.8	129
S.D.	10.5	12.8	12.4	3.54	4.5	5.9	15.4	48.7	12.3	3.96	3.91	7.2	34.8	29.59	44	1.33	0.8	0.8	4.71	4.66	4.2
%	3.6	5.2	4.9	5.8	8.8	10.8	3.3	2.3	3.2	13.2	8.1	13.4	2.7	2.3	3.5	8.9	4.3	4.1	3.6	3.7	3.2
Std name Date <sup>1</sup> :	Pb 88	Pb 89	Pb Mar-89	Rb 88	Rb 89	Rb Mar-89	Sr 88	Sr 89	Sr Mar-89	V 88	V 89	V Mar-89	Y 88	Y 89	Y Mar-89	Zn 88	Zn 89	Zn Mar-89	Zr 88	Zr 89	Zr Mar-89
MONCH-A	0.49	10.6	11.9	14	15.5	13.2	482	462.3	447.6	167	129.6	145.6	19	15.5	15.8	99	101.7	101.2	124	121.5	126.4
MONCH-N	5.4	4.2		13	13.9		480	455.4		162	146.9		18	13.3		106	104.6		129	124.8	
MONCH-F	6.87	7.3	6.8	16	14.8	15.2	486	464.3	463.8	167	159.9	151.3	18	13.1	14.3	109	110.6	105.3	123	123	125.4
MONCH-L	0.9	9.3		17	16.8		485	471.8		167	141.2		18	16.1		104	109.1		127	125.4	
MONCH-H	3.51	6.2	5.1	13	15.2	15.6	465	471	461.7	169	163.1	148.8	20	17.3	13.5	105	109	100.2	123	125.2	123.5
MONCH-O	-3.12	3.6		15	15.4		481	466.3		173	139.2		18	16.1		106	103.7		125	124.2	
MONCH-E	-2.54	4.7	6.4	19	14	14.1	479	453.8	466	172	141.4	156.3	21	14.7	16.1	109	101.9	107.5	122	121.3	124.3
MONCH-M	2.32	8.4		16	13.9		475	464.9		178	139.8		16	15.1		108	99.2		123	123.7	
MONCH-D	-7.19	9	9.3	16	15.2	14.2	467	455	461.4	169	159.9	181.6	17	14.9	15.6	106	102.5	105.3	121	120.9	126.3
MONCH-C	4.13	7.8	12.9	15	15.3	14.8	461	456.6	466.3	181	172.6	145.6	20	14.6	14.7	100	100.7	103	125	123.4	127.5
MONCH-B	-0.14	3.8	7.7	16	15.1	14.5	481	455.9	457.8	174	162.4	119.2	18	13.8	15.6	110	96.9	108.7	125	121.5	124.5
MONCH-K	3.4	3		13	13.5		483	466.8		168	145		21	15		109	107.2		125	125.2	
MONCH-J	5.58	5.3		18	13.8		484	460.8		171	164.3		18	16.5		113	103.3		127	121.6	
MONCH-G	0.09	10	4.5	16	15.1	13.3	488	462.1	458.7	168	152.9	122.2	16	14.5	12.9	110	103	101.2	124	121.6	124.7
MONCH-I	5.32	6.7		14	13.1		479	456.6		181	168.9		18	14.9		110	97.2		122	120.2	
MONCH-J2	-3.64	10.5		12	15.7		478	463.7		182	150.8		11	15.8		108	105.1		125	123.9	
Mean	1.34	6.9	8.08	15	14.77	14.36	478	461.7	460.4	172	152.4	146.3	18	15.8	14.81	107	103.5	104	124	122.9	125.3
S.D.	3.96	2.59	3.06	1.94	0.97	0.85	7.74	5.72	6.02	5.93	12.48	19.62	2.38	1.13	1.17	3.71	4.05	3.14	2.09	1.82	1.33
%	37.5	37.9		6.6	6.6	5.9	1.2	1.3	1.3	3.45	8.2	13.41	7.2	7.2	7.9	3.01	3.9	3.01	1.5	1.5	1.06

<sup>1</sup> Year or month-year analyses were completed.  
All analyses in ppm.

# Neogene to Recent volcanism along the east side of Hecate Strait, British Columbia

G.J. Woodsworth<sup>1</sup>

Woodsworth, G.J., Neogene to Recent volcanism along the east side of Hecate Strait, British Columbia: in *Evolution and Hydrocarbon Potential of the Queen Charlotte Basin, British Columbia*, Geological Survey of Canada, Paper 90-10, p. 325-335, 1991.

## Abstract

*Mafic volcanic rocks are preserved in several small areas on islands east of Hecate Strait; much of southeast Hecate Strait may be underlain by similar rocks. K-Ar dates show that the volcanics are 19-26 Ma in age and are contemporaneous with the main phase of Masset volcanism on Queen Charlotte Islands. Petrographic, chemical and isotopic data suggest that the rocks are nonmarine olivine basalt and andesite, are transitional to slightly alkaline in chemistry, have a mantle origin, and were erupted in a back-arc or incipient rift setting.*

*The volcanic rocks probably formed in localized extensional basins. Episodic extensional reactivation of older structures appears to have been the dominant structural style along the west side of the Coast Mountains from Late Oligocene to Recent time.*

## Résumé

*Des roches volcaniques mafiques ont été conservées dans plusieurs petites zones des îles situées à l'est du détroit d'Hécate, et une grande partie du sous-sol du sud-est du détroit d'Hécate pourrait contenir des roches semblables. Des datations K-Ar indiquent que les roches volcaniques remontent de 19 à 26 Ma et qu'elles sont contemporaines à la principale phase du volcanisme de Masset dans les îles de la Reine-Charlotte. Les données pétrographiques, chimiques et isotopiques recueillies révèlent que les roches sont des basaltes et des andésites à olivines non marines, que leur composition chimique varie d'intermédiaire à légèrement alcaline, qu'elles proviennent du manteau et que leur éruption a eu lieu dans un milieu de rift embryonnaire ou d'arrière-arc.*

*Les roches volcaniques ont dû se former dans des bassins d'extension localisée; la réactivation épisodique par distension de structures plus anciennes semble être le principal style tectonique caractérisant le versant occidental de la chaîne Côtière, de l'Oligocène supérieur au Quaternaire.*

---

<sup>1</sup> Cordilleran Division, Geological Survey of Canada, 100 West Pender Street, Vancouver, B.C. V6B 1R8

## INTRODUCTION

Most islands east of Hecate Strait are underlain entirely by Cretaceous and older plutonic and metamorphic rocks of the Coast Plutonic Complex. However, Neogene to Recent volcanic rocks are exposed in several small areas (Fig. 1).

The best studied of these volcanics are those in the western part of the Anahim Volcanic Belt, exposed near Bella Bella. There, a bimodal suite of alkaline to peralkaline eruptive rocks and dyke swarms comprises the Bella Bella Formation. Most dykes appear to form a conjugate set with  $345^\circ$  and  $020^\circ$  trends and may have been controlled by older structures (Souther, 1986). K-Ar dates from the Bella Bella Formation and cogenetic King Island syenite and soda granite range from 12.5 to 14.5 Ma. The peralkaline chemistry of the Anahim Volcanic Belt, the general east-west trend, and the systematic eastward decrease in age of initial volcanism suggests that the belt may reflect the westward movement of North America relative to a mantle hot spot (Bevier et al., 1979; Souther, 1986).

The other volcanic rocks collectively consist of a northwest-trending series of Oligocene-Miocene and postglacial basalt and andesite centres. The two main postglacial volcanic centres are at Kitasu Hill and Lake Island (Fig. 1). Smaller exposures of probable Pleistocene to Recent volcanics are present on Price and Lady Douglas islands. Most of these rocks are strongly alkaline olivine basalt flows and pyroclastic cones that were included in the Lake Island Formation by Dolmage (1922). Brief descriptions of Kitasu Hill and Lake Island were given by Baer (1973) and Souther (1966, in press). Two chemical analyses, one each from Kitasu and Lake Island, were given by Erdman (1985) and confirm the strongly alkaline nature of the rocks.

The older, northern volcanic centres are the subject of the present paper. These consist of remnants of basalt along the west side of Aristazabal Island northwest of Bella Bella and along Kitkatla Inlet south of Prince Rupert, and poorly exposed but substantial areas of southeastern Hecate Strait (Fig. 1). These rocks were noted by Souther (1966), Roddick (1970) and Baer (1973) during reconnaissance mapping. A chemical analysis of one of Souther's samples from Aristazabal Island was given by Erdman (1985). The present study was undertaken to examine these rocks, obtain petrographic, chemical, and isotopic data, compare the rocks with the Miocene Masset Formation on Queen Charlotte Islands, and discuss their bearing on the evolution of the Queen Charlotte Basin.

## FIELD ASPECTS

### Aristazabal Island

Volcanic rocks are exposed in a 5 km by 1 km area southwest of Kettle Inlet on the west side of Aristazabal Island. The volcanics form rocky spines and islets, many of which have a pronounced northwest to north-northwest elongation (Fig. 2). No Tertiary volcanics were found on Aristazabal Island itself. The small area mapped as such by Baer (1973) about 1.5 km southeast of Trenaman Island is underlain instead by greenschist to amphibolite facies volcanics and plutonic rocks that are probably pre-Tertiary in age.

The volcanic rocks are entirely black, fresh basalt flows with few vesicles. No ultramafic nodules were found here, or in any of the volcanic rocks east of Hecate Strait. Each islet consists of one or two flows. Most islets show well developed columnar jointing that appears to extend the full height of the outcrops. Columns plunge  $60-70^\circ$  northeast. This plunge is uniform over the entire area of exposure, suggesting that the volcanics are flows rather than necks and have been tilted about  $20-30^\circ$  to the southwest during subsidence of the Queen Charlotte Basin, if the columns were originally vertical.

The base of the volcanics is exposed on an islet at the mouth of Kettle Inlet. A poorly consolidated conglomerate about 10 m thick containing cobbles and boulders of granitoid material in a vesicular basaltic matrix lies unconformably on granitoid rocks of the Coast Plutonic Complex. The conglomerate is overlain by columnar-jointed basalt flows. Both the basement surface and the flows dip about  $20-30^\circ$  to the southwest. The number of flows and total preserved thickness of the pile is uncertain but the minimum thickness on the largest of the islets exceeds 30 m. Assuming a  $20^\circ$  dip and no repetition by faulting, the total structural thickness exposed in the area probably does not exceed 250 m.

### Kitkatla Inlet

Tertiary volcanic rocks in the Kitkatla Inlet area underlie two areas, one centred on the Ness Islands and the other on Serpentine Inlet about 11 km to the northwest (Fig. 3). These rocks were originally mapped and briefly described by Roddick (1970), who suggested they were Late Miocene(?) in age.

The Ness Islands area is the better exposed of the two volcanic centres. The islands and surrounding rocks are underlain by brown-weathering, black to dark green-grey basalt flows. Most outcrops show well developed columnar jointing. Bedding, where present, and col-

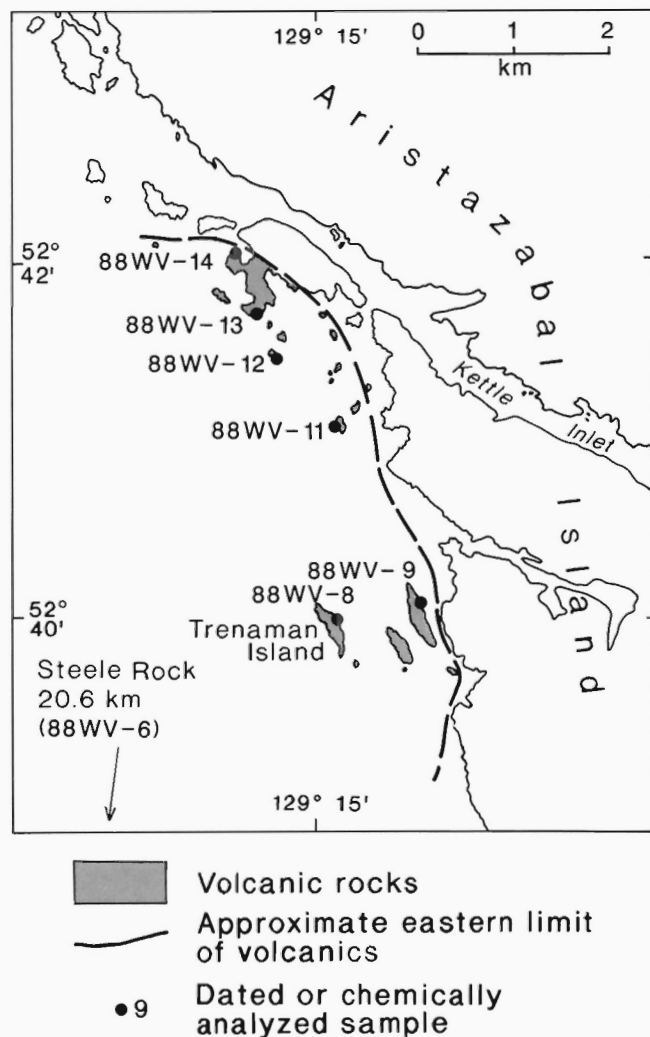


**Figure 2:** Distribution of Oligocene-Miocene volcanic rocks exposed along west coast of Aristazabal Island, with locations of samples analyzed during this study.

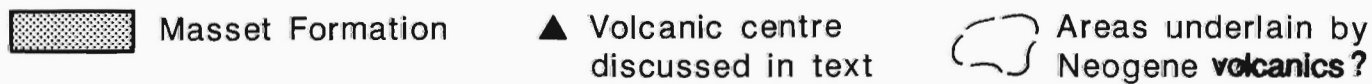
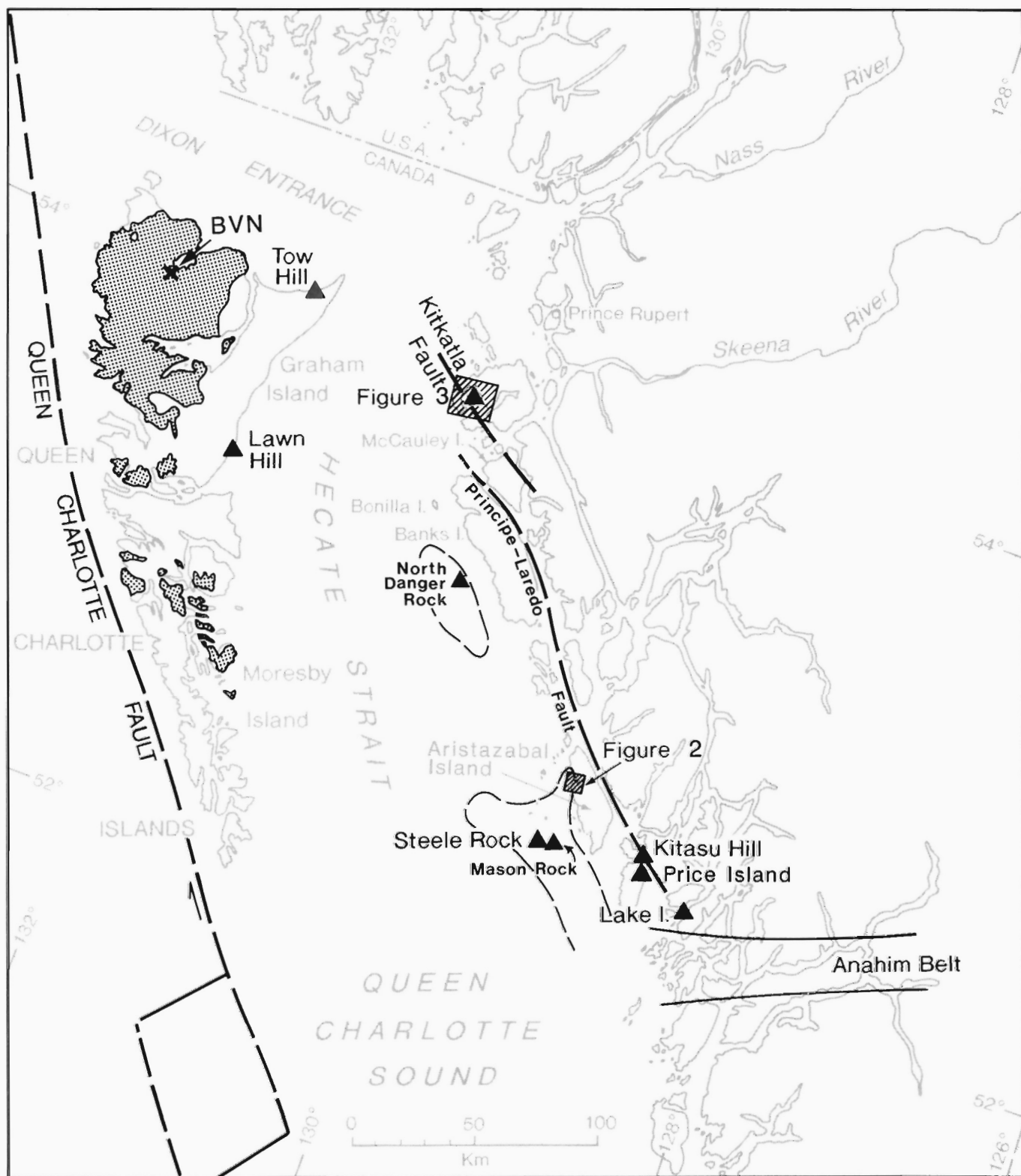


**Figure 1:** Inferred distribution of Neogene volcanic rocks on the east and west sides of Queen Charlotte Basin. Small rectangles indicate Aristazabal (Fig. 2) and Kitkatla (Fig. 3) areas. Lady Douglas Island is immediately west of Lake Island and cannot be shown separately on this scale. The X marks the location of the BV Naden Harbour well (BVN).



umn attitudes suggest that the flows dip about 20-30° southwest to southeast. On the east side of the main island, two flows are exposed. These are separated by highly amygdaloidal and scoriaceous basalt. On the northeast side of the main island, an isolated outcrop of agglomerate is exposed. This rock contains rounded pebble- and cobble-sized clasts of amygdaloidal basalt in a basaltic matrix. Total exposed thickness of the Ness Islands volcanics is estimated to exceed 50-100 m. A small patch of fresh, vesicular basalt is exposed on the shore of Porcher Island northeast of Ness Islands (A.J. Baer, unpub. field notes, 1963). Hand specimens of basalt from the Ness Islands area contain conspicuous olivine and pyroxene phenocrysts. Amygdules of calcite and zeolites (chabazite?) form up to 10% of the rock.

There are few exposures of the volcanic rocks in the Serpentine Inlet area, thus the areal extent of the volcanics farther northwest is unknown, but it is not likely to be great. The thickness of the unit is unknown but is probably less than 200 m.

The volcanic rocks are dark brown-weathering, fresh, black olivine basalt flows. Columnar jointing is generally present. Vesicles and amygdules are less abundant than on Ness Islands. Vesicle sheets, pipe vesicles, and column attitudes suggest that initial dips are gentle to moderate to the south or southeast.

On the shoreline of Porcher Island about 1 km east of the entrance to Serpentine Inlet, the flows are underlain by a poorly consolidated

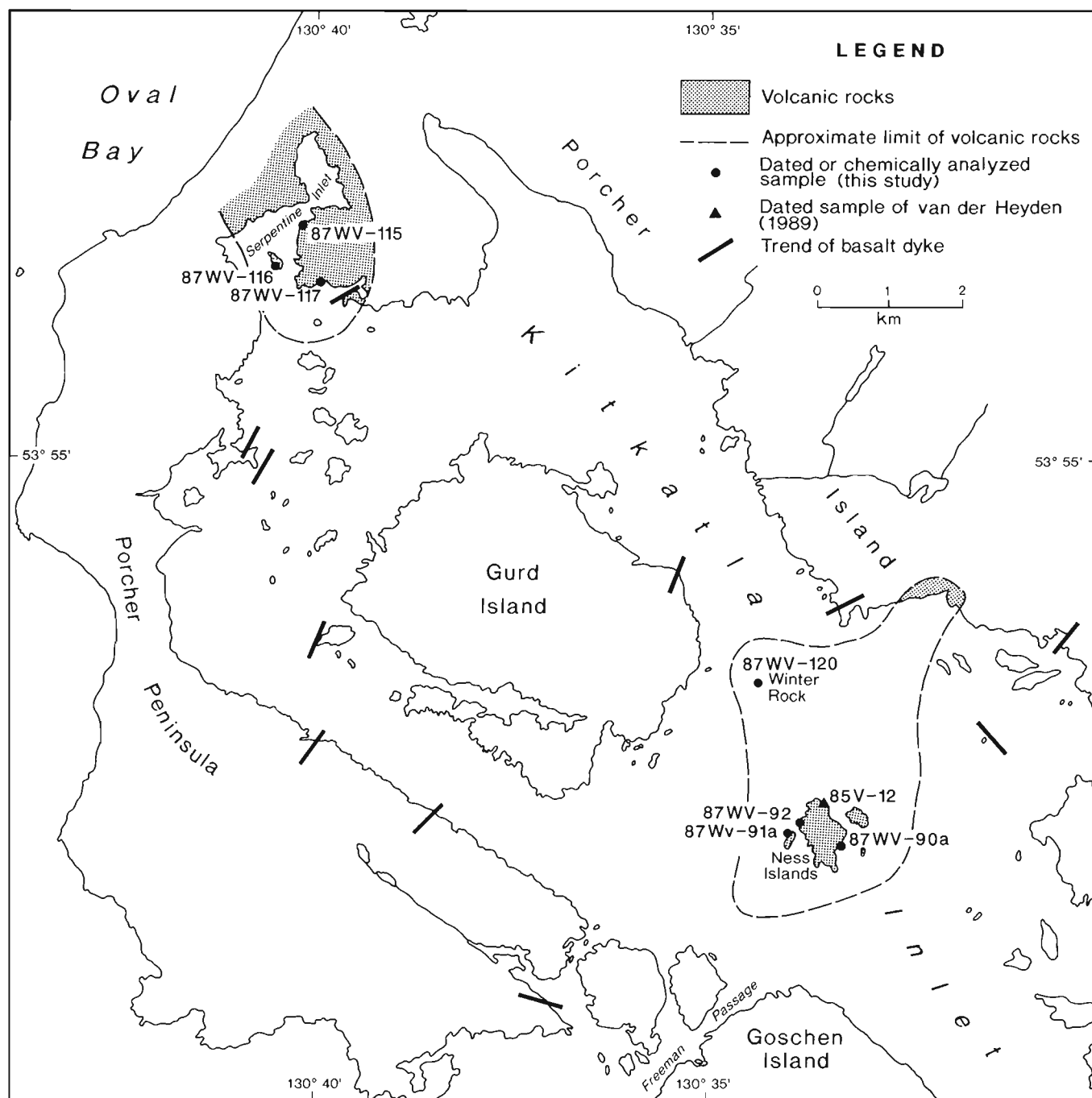


Figure 3: Kitkatla Inlet volcanic centres, showing sample locations and trends of basalt dykes.

pyroclastic deposit. Most clasts are round but some are angular. Clasts average about 10-30 cm in diameter; the largest is about 2 m across. Although most clasts are olivine basalt, a few are vesicular, white in colour, contain conspicuous quartz eyes, and are probably rhyolites. These are the only known felsic to intermediate volcanics in the Kitkatla Inlet area. The pyroclastic deposit is cut by two north-east-striking olivine basalt dykes; the relation of the dykes to the overlying basalt flows is obscured by overburden.

### Steele Rock

This isolated islet about 18 km southwest of Aristazabal Island (Figs. 1, 2) is composed entirely of fresh, black andesite that appears to represent a single flow or sill. Strong sheeting and poorly developed columns are the only structures seen; these suggest that the volcanics dip moderately to the south. Mason Rock, 2.5 km east of Steele Rock, was not examined during the present study but was described as consisting entirely of dark greenish-black basalt with strong primary sheeting dipping about 40° south (J.G. Souther, unpub. field notes, 1963).

## PETROGRAPHY

Almost all the samples from Aristazabal Island and Kitkatla Inlet are fairly fresh, porphyritic, olivine basalt. Phenocrysts of olivine, plagioclase, and clinopyroxene constitute about 1-35% of the rock volume. In most samples, olivine forms up to 7% of the rock as phenocrysts up to 4 mm in diameter. These are commonly glomeroporphyritic and slightly to entirely replaced by iddingsite and other alteration products. Plagioclase phenocrysts, some with partly resorbed cores, comprise up to 35% of the Aristazabal samples but are rare in the Kitkatla rocks. About half the Aristazabal samples contain up to 15% strongly zoned augite phenocrysts about 1 mm across.

The groundmass of most samples is intergranular, pilotaxitic, and composed largely of plagioclase, clinopyroxene, and opaques. About half the samples contain patches of chlorite, calcite and cryptocrystalline material that may represent devitrified and altered glass. One sample (88WV-8) from Aristazabal Island contains traces of reddish brown biotite. Amygdules are rare and consist of calcite, zeolites, chlorite, and pumpellyite.

The one sample examined from Steele Rock consists of about 10% plagioclase phenocrysts about 2 mm in diameter in a fine-grained, trachytic groundmass. Plagioclase phenocrysts are euhedral to subhedral; many grains have sodic overgrowths on strongly resorbed cores. Roughly equant patches of chlorite and calcite may be pseudomorphs after primary pyroxene. The groundmass consists of tiny plagioclase laths, a few percent granular opaques, and minor chlorite and calcite.

## AGE

K-Ar dates and field relationships indicate that volcanic rocks east of Hecate Strait were extruded in latest Oligocene to earliest Miocene (26-23 Ma), Late Miocene (19.5 Ma), and Quaternary to Recent times.

Whole-rock K-Ar dates were obtained from three of the freshest samples from Kitkatla Inlet and Aristazabal Island and the sole sample available from Steele Rock. The four dates and one from van der Heyden (1989) are given in Table 1; sample locations are shown on Figures 2 and 3. Except for the one from van der Heyden, the dates cluster fairly tightly between 22.9 and 26.2 Ma and indicate a latest Oligocene to earliest Miocene age for most of the volcanism. The two dates from Kitkatla Inlet, one each from Serpentine Inlet and Ness Islets, are the same within analytical error and average 25.4 Ma. These dates are somewhat older than the 19.5 ± 0.5 Ma date reported by van der Heyden (1989) for a sample of fresh olivine basalt from Ness Is-

TABLE 1: Whole-rock K-Ar data

Area Sample No.	K (%)	<sup>40</sup> Ar <sup>1</sup>	% <sup>40</sup> Ar <sup>2</sup>	Date (Ma) ± 1σ
<b>Aristazabal Island</b>				
88WV-11	0.533	0.4770	24.7	22.9 ± 1.0
<b>Steele Rock</b>				
88WV-6	1.19	1.190	58.6	25.5 ± 0.9
<b>Kitkatla Inlet</b>				
87WV-115	0.511	0.524	67.8	26.2 ± 0.9
87WV-120	0.338	0.325	63.2	24.6 ± 0.9
85V-12	0.498	0.379	52.9	19.5 ± 0.7

<sup>1</sup> Radiogenic <sup>40</sup>Ar (x 10<sup>-6</sup> cm<sup>3</sup>/g STP).

<sup>2</sup> Radiogenic Ar as percentage of total Ar.

Sample sources:

87WV and 88WV series: this study.

85V-12: van der Heyden (1989).

Analyses were done at the University of British Columbia by D. Runkle (K) and J.E. Harakal (Ar). K was determined in duplicate by atomic absorption using a Techtron AA4 spectrophotometer on dilute sulphate solutions buffered by Na and Li nitrates. Ar was determined by isotope dilution using an AEI MS-10 mass spectrometer with Carey Model 10 vibrating read electrometer, high purity <sup>39</sup>Ar spike, and conventional gas extraction and purification procedures as described by White et al. (1967). The errors reported are for range of multiple analyses for K and for estimated 1σ for the calculated date. Decay constants are those recommended by Steiger and Jäger (1977).

lands. All three dates appear to be analytically sound, and suggest that volcanism in the Kitkatla Inlet area may have persisted until well into Miocene time.

No K-Ar dates are available for the Kitasu Hill and Lake Island centres. However, they have long been known to be Quaternary to Recent in age; volcanic rocks unconformably overlie Pleistocene glacial deposits (Souther, 1966, in press).

## STRUCTURAL CONTROL AND AREAL EXTENT OF THE VOLCANICS

There is evidence for both a northwest- and northeast-trending structural control to Neogene and Quaternary volcanism east of Hecate Strait. In the Kitkatla Inlet area, pre-Tertiary basement consists of highly deformed, greenschist facies metavolcanic and metasedimentary rocks and Early Cretaceous plutons. The rocks have a pronounced northwest grain, reflecting mylonitization along northwest-trending faults and shears, the largest of which was named the Kitkatla Fault by Roddick (1970). These northwest-trending structures are shown topographically in the remarkably straight north-east shorelines of Porcher Peninsula and Goschen Island (Figs. 1, 3) and are also conspicuous on the bathymetry map of Sawyer (1989). Further, Kitkatla Inlet forms the northeastern edge of a very strong, positive, linear magnetic anomaly (Geological Survey of Canada, 1987b) that trends N50°W.

Northeast-striking linear features are prominent in the Kitkatla Inlet region. One marks the northwest side of McCauley Island; another marks the northwest side of Porcher Island. Yet another extends along the northwest side of Goschen Island and may continue to the northeast on Porcher Island. Still others are conspicuous on air photos of western Porcher Island as straight, northeast-southwest drainage patterns and on the bathymetry map (Sawyer, 1989). Trends of fresh, columnar-jointed olivine basalt dykes in the Kitkatla Inlet region support the idea of a northeast-striking system of structures. Al-

though such dykes are not abundant, they generally trend north-northeast to northeast and have moderate to vertical dips (Fig. 3). No isotopic dates are available from these dykes, but petrographically they are similar to the Kitkatla volcanics and it seems reasonable to assume that they are feeders to the subaerial volcanic rocks nearby.

The Kitkatla volcanics are localized at the intersections of the northwest-striking faults of the Kitkatla fault system (perhaps reactivated in Neogene time) and the northeast-striking lineaments that mark the northwest sides of Goschen and Porcher islands. On Ness Islands, the volcanics are cut by steep, irregularly-striking fractures and brittle faults, and the generally southerly dips in both the Ness and Serpentine areas suggest a moderate amount of post-eruptive tilting to the south.

Although he was unaware of the time span represented by the rocks, Souther (1966) noted that the Lake Island, Kitasu Hill and Aristazabal Island centres form a northwest-trending, linear chain that follows conspicuous northwest-trending topographic features. The trend of this chain is about N55°W, oblique to the dominantly N40°W trend of the east margin of Queen Charlotte Basin and the exposed west margin of the Coast Plutonic Complex in this area. Many of the rocks and spines of the Aristazabal Island volcanic centre have a pronounced north to northwest trend, and northwest trends are common in brittle and ductile structures in the basement rocks on nearby Aristazabal Island (A.J. Baer, unpub. field maps). Basalt on the easternmost islet is cut by fractures and narrow, northwest-trending, brittle fracture zones. These reach 2 cm in width, are filled with calcite and basaltic fault breccia. On the shore of Aristazabal Island, much of the plutonic rock shows intense brittle fracturing and shearing.

Although the evidence is not conclusive, it appears probable that the Aristazabal Island, Kitasu Hill, and Lake Island volcanics are controlled by pre-existing, northwest-trending structural features. The 20–30° southwest dip of the Aristazabal volcanics and the brittle faults that cut them suggest that these structures were reactivated after eruption, and that the volcanics are preserved in west-dipping blocks that may have formed in half-grabens or east-side-down normal faults.

## GEOPHYSICAL EXPRESSION

Magnetic anomaly maps (Geological Survey of Canada, 1987b) show extensive, irregular areas southwest of Aristazabal Island with positive magnetic anomalies, commonly exceeding 200 nanoteslas. The irregular, high frequency nature of the magnetic topography suggests a near-surface origin for the anomalies. Near-surface reflectors appropriate for mafic volcanic rocks are conspicuous in seismic reflection lines in eastern Hecate Strait (K.M. Rohr, pers. comm., 1989).

Heavy seas and sea lions prevented a landing on North Danger Rocks (Fig. 1) some 120 km northwest of Steele Rock and 15 km offshore, but binocular study indicates that they are underlain by volcanic rocks. In appearance these closely resemble the Neogene volcanics of Steele Rock and Aristazabal Island rather than the Late Triassic Karmutsen Formation on Bonilla Island (Woodsworth, 1988). All other rocks and islets between North Danger Rocks and Steele Rock are composed of granitoid rocks of the Coast Plutonic Complex.

Volcanics in Kitkatla Inlet have no clear expression on the magnetic anomaly map (Geological Survey of Canada, 1987a). This corroborates the field evidence that the volcanics are a thin, locally preserved veneer on an older basement. Unlike the Aristazabal Island and Steele Rock areas, there is no compelling evidence from the magnetics or bathymetry to suggest that the Kitkatla volcanics are much more extensive than their present surface exposures.

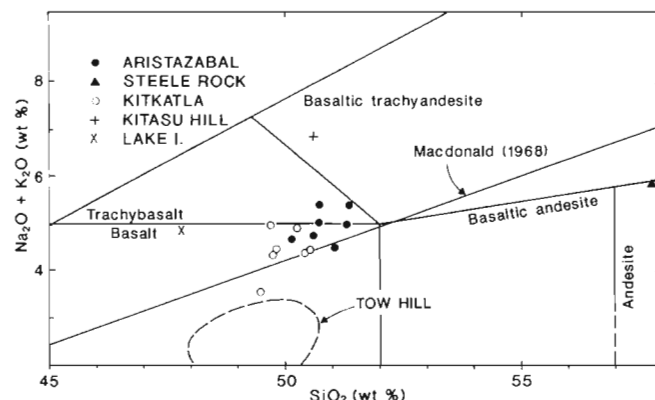


**Figure 4:** Alkali-silica diagram for Hecate Strait volcanic rocks using data in Table 2. Classification fields are from Le Bas et al. (1986). Data for Tow Hill basalts are from Timms (1989).

## CHEMISTRY AND TECTONIC SETTING

Major and trace element analyses for 6 basalts from Kitkatla Inlet, 7 basalts from Aristazabal Island, and one andesite from Steele Rock are given in Table 2, along with an analyses for Aristazabal basalt given by Erdman (1985). Locations of samples collected during this study are shown on Figures 2 and 3. The results confirm both the limited compositional range suggested by the petrography and the much more siliceous nature of Steele Rock compared to basalts on Aristazabal Island. In general, the Aristazabal and Kitkatla rocks overlap in compositional range, but the Kitkatla basalts shows more internal variability. For example, CaO ranges from 8.5–10.9% in Kitkatla rocks, compared with 9.1–10.1% for Aristazabal samples. Contrary to the general pattern, Kitkatla samples show less variation in  $Mg$  values ( $100 \times Mg/(Mg + Fe^{2+})$ , cation per cent) than Aristazabal rocks (62–71 versus 49–72). Basalts from Kitkatla Inlet have higher MgO than the Aristazabal samples (6.8–8.3% versus 5.1–7.0%), higher Ni (78–241 versus 23–63 ppm), higher Co (36–60 to 26–35 ppm), and lower  $P_2O_5$  (0.23–0.38 against 0.41–0.65%).

$SiO_2$  values of the basalts lie between 49.0 and 51.8 weight percent. None of the samples are quartz normative; five of the samples contain small amounts of normative nepheline. On a total alkali-silica diagram (Fig. 4) the basalts straddle the basalt and trachybasalt fields of Le Bas et al. (1986); Steele Rock plots in the andesite field. The basalts fall near or above the line used by Macdonald (1968) to separate alkaline and subalkaline fields. On an AFM diagram (not shown) most samples plot within the tholeiitic field.

Petrographically, the basalts are alkali olivine basalt in that calcic clinopyroxene is the only pyroxene present. Chemically, the rocks are transitional basalt in the sense of Bevier (1983a) in that they are olivine-normative with either normative hypersthene or nepheline (Fig. 5).

Initial  $^{87}Sr/^{86}Sr$  ratios (Table 3) mostly of 0.7035–0.7037 for the Kitkatla and Aristazabal basalts are consistent with a mantle origin with little crustal contamination. However, Pearce element ratio diagrams (Russell and Nichols, 1988) using conserved constituents suggest that neither the Kitkatla nor Aristazabal basalts can be derived from a single magma and cannot be derived from each other by crystal fractionation. Although the data are few, the variation in  $^{87}Sr/^{86}Sr$  initial ratios for each suite supports this view and suggests a heterogeneous mantle beneath Hecate Strait or contamination with small amounts of radiogenic Sr. The  $Mg$  values of 62–72 suggest that the basalts do not represent primary magmas in equilibrium with the mantle, unless the mantle beneath the western side of Hecate Strait is anomalously Fe-rich. The low Ni values (23–241 ppm) compared with pri-

**TABLE 2: Chemical analyses and sample locations**

Sample no.	87WV-90a	87WV-91a	87WV-92	87WV-115	87WV-116	87WV-117	87WV-120	88WV-6	88WV-8
Area	Kitkatla	Kitkatla	Kitkatla	Kitkatla	Kitkatla	Kitkatla	Kitkatla	Steele Rk.	Aristazabal
Latitude	53 52.10	53 52.18	53 52.28	53 56.77	53 56.49	53 56.34	53 53.33	52 28.94	52 40.05
Longitude	130 33.25	130 33.99	130 32.94	130 40.19	130 40.50	130 39.97	130 34.35	129 18.95	129 14.83
<b>Major elements (weight percent)</b>									
SiO <sub>2</sub>	50.06	50.05	49.25	49.51	49.21	49.95	49.25	57.72	51.69
TiO <sub>2</sub>	1.53	1.11	1.60	1.54	1.27	1.64	0.97	1.24	1.16
Al <sub>2</sub> O <sub>3</sub>	15.85	17.25	17.00	16.29	16.77	16.42	17.31	17.80	17.63
Fe <sub>2</sub> O <sub>3</sub>	2.47	3.92	0.89	3.54	3.76	2.24	2.70	3.74	2.91
FeO	7.59	5.50	8.52	5.82	6.17	7.33	6.70	4.08	5.01
MnO	0.17	0.17	0.16	0.16	0.17	0.16	0.16	0.19	0.19
MgO	8.26	7.40	7.72	7.23	6.81	7.57	7.74	2.69	7.04
CaO	8.49	10.61	9.28	9.18	9.89	9.05	10.94	6.16	9.57
Na <sub>2</sub> O	3.94	4.01	3.77	3.75	3.94	3.79	3.11	4.39	3.94
K <sub>2</sub> O	0.98	0.50	0.54	0.62	0.49	0.58	0.44	1.49	1.13
P <sub>2</sub> O <sub>5</sub>	0.38	0.24	0.34	0.38	0.33	0.36	0.23	0.44	0.49
Total	99.72	100.76	99.07	98.02	98.81	99.09	99.55	99.94	100.76
LOI	1.25	3.28	1.77	1.05	0.67	1.08	0.68	2.72	1.60
CO <sub>2</sub>								1.12	1.10
<b>Trace elements (ppm)</b>									
Ba	300.2	195.1	139.1	180.4	193.6	179.8	165.6	730.14	430.21
Co	60.1	47.1	52.9	56.8	36.1	50.2	45.2	16.05	28.06
Cr	281.7	169.0	217.0	228.7	87.8	245.6	196.7	102.84	244.23
Cu	78.9	85.1	62.9	69.8	64.0	60.5	72.1	39.26	65.29
Mn	1239.3	1290.1	1229.0	1241.6	1282.9	1286.5	1262.1	1101.20	1086.80
Nb	11.7	5.5	7.9	9.9	6.3	7.9	4.7	14.07	10.44
Ni	241.1	112.5	170.9	162.9	77.5	191.4	114.8	6.38	62.95
Pb	9.0	9.3	3.7	5.4	10.6	11.9	9.7	12.75	8.07
Rb	14.1	4.5	5.7	9.1	7.1	8.8	5.9	25.60	15.40
Sr	1142.4	489.4	632.9	599.8	676.9	571.7	473.2	523.39	901.11
V	210.2	230.4	183.8	231.9	248.3	217.8	204.8	110.51	266.27
Y	22.0	23.0	22.5	23.0	20.1	21.4	20.3	26.64	14.92
Zn	107.6	85.8	84.3	90.3	100.6	91.0	82.3	98.76	92.24
Zr	195.8	104.8	209.7	176.5	131.9	188.6	104.4	192.20	126.71
Sample no.	88WV-9	88WV-11	88WV-12	88WV-13	88WV-14	SE-090265	SE-050365	SE-030865	
Area	Aristazabal	Aristazabal	Aristazabal	Aristazabal	Aristazabal	Aristazabal	Kitasu Hill	Lake Island	
Latitude	52 40.06	52 41.08	52 41.60	52 41.75	52 42.01	52 40.0	52 29.5	52 21.3	
Longitude	129 14.02	129 14.81	129 15.27	129 15.49	129 15.73	129 15.5	128 43.5	128 21.0	
<b>Major elements (weight percent)</b>									
SiO <sub>2</sub>	49.02	51.40	51.45	50.84	51.80	50.38	50.15	47.24	
TiO <sub>2</sub>	1.38	2.24	2.14	2.58	1.77	1.85	2.35	2.51	
Al <sub>2</sub> O <sub>3</sub>	17.39	15.70	17.05	15.51	18.70	16.53	15.18	13.91	
Fe <sub>2</sub> O <sub>3</sub>	2.51	2.35	2.27	2.66	3.40	9.90	13.07	16.20	
FeO	5.42	8.99	7.57	8.61	5.19	0.00	0.00	0.00	
MnO	0.19	0.20	0.19	0.20	0.16	0.15	0.19	0.20	
MgO	6.18	5.05	4.66	4.59	4.60	6.46	3.66	6.31	
CaO	9.28	9.76	10.14	10.09	9.14	8.64	7.62	8.00	
Na <sub>2</sub> O	4.11	3.90	4.03	4.09	4.46	4.33	5.27	3.86	
K <sub>2</sub> O	0.76	0.65	0.71	0.73	1.01	1.07	1.55	0.96	
P <sub>2</sub> O <sub>5</sub>	4.11	0.41	0.52	0.62	0.65	0.69	0.96	0.81	
Total	100.35	100.65	100.73	100.52	100.88	100.00	100.00	100.00	
LOI	1.48	1.16	1.27	1.25	1.55				
CO <sub>2</sub>	1.17	0.97	1.01	1.09	0.48				
<b>Trace elements (ppm)</b>									
Ba	293.68	279.33	288.09	245.97	349.77	579.0	404.0	457.0	
Co	25.78	33.49	28.36	35.43	25.63	21.0	28.0	25.0	
Cr	95.64	147.88	14.54	142.44	175.76	84.0	63.4	60.3	
Cu	70.38	99.85	75.45	86.99	110.67	86.0	43.0	46.0	
Mn	1095.50	1509.70	1527.90	1486.70	1151.20				
Nb	12.54	17.03	16.07	17.36	16.34	17.0	54.0	23.0	
Ni	40.79	22.66	30.44	25.77	42.09	44.0	42.0	29.0	
Pb	8.00	10.01	8.94	9.00	13.39				
Rb	13.22	14.03	8.17	11.80	16.71	12.0	28.0	18.0	
Sr	881.57	574.21	541.60	538.13	871.82	898.0	420.0	449.0	
V	253.35	332.40	194.76	224.66	235.32	242.0	174.0	266.0	
Y	14.86	27.94	33.01	33.84	27.52	29.0	39.0	41.0	
Zn	91.01	115.60	101.05	118.72	98.97				
Zr	119.04	169.30	174.46	164.05	174.03	161.0	246.0	188.0	

Sample sources:

87WV and 88WV series: this study, collected and analyzed in 1987 and 1988.

SE series: Collected in 1965 by J.G. Souther. Analyses reported by Erdman (1985).

All analyses were done at the University of British Columbia. For this study, major and minor elements were analyzed by S. Horsky in the Department of Geological Sciences.

Powdered samples were fused with lithium tetraborate and then ground to form a pressed glass powder disc. Analyses were done using a Phillips 1410 XRF. FeO was determined by titration. LOI: loss on ignition. Trace elements were analyzed by M. Soon in the Department of Oceanography using a fully automated Phillips PW1400 XRF with autosampler.

See Hickson (1991) for estimate of analytical errors.

TABLE 3: Rb-Sr data

Area	Rb (ppm)	Sr (ppm)	$^{87}\text{Rb}/^{86}\text{Sr}$	$^{87}\text{Sr}/^{86}\text{Sr}$ (measured)	$^{87}\text{Sr}/^{86}\text{Sr}$ (initial)
Sample No.					
<b>OLIGOCENE and MIOCENE VOLCANICS</b>					
Aristazabal Island					
88WV-11	11.4	559	0.059	0.70372	0.70370
SE-090265	12.5	921	0.039	0.7042	0.7042
Steele Rock					
88WV-6	24.8	503	0.142	0.70424	0.70419
Kitkatla Inlet					
87WV-115	9.4	574	0.047	0.70352	0.70350
87WV-120	7.2	452	0.046	0.70378	0.70376
<b>QUATERNARY TO RECENT VOLCANICS</b>					
Kitasu Hill					
SE-050365d	29.0	457	0.184	0.7026	0.7026
SE-022465	16.5	446	0.107	0.7027	0.7027
Lake Island					
SE-030865	16.0	425	0.108	0.7035	0.7035
Lady Douglas Island (52° 20.7'N, 128° 23.5'W)					
SE-040165	20.5	422	0.141	0.7037	0.7037
Price Island (52° 27.0'N, 128° 37.3'W)					
SE-040665	21.5	557	0.112	0.7026	0.7026
Sample sources:					
87WV and 88WV series: this study.					
SE series: collected in 1965 by J.G. Souther; data from Erdman (1985).					
Analyses were done at the University of British Columbia by D.E. Runkle and K. Scott. Rb and Sr were determined by replicate analyses of pressed powder pellets using XRF. U.S. Geological Survey rock standards were used for calibration. Mass absorption coefficients were obtained from Mo K $\alpha$ Compton scattering measurements. Concentrations have a precision of 5% or 1 ppm, whichever is greater. Blanks for Rb and Sr are about 0.8 and 6 nanograms, respectively. Sr isotopic composition was measured on unspiked samples prepared with standard ion exchange methods using a Vacuum-Generator Isomass 54R mass spectrometer automated with a Hewlett-Packard HP-85 computer. Measured ratios were normalized to a $^{86}\text{Sr}/^{88}\text{Sr}$ ratio of 0.1194 and adjusted so that the NBS standard $\text{SrCO}_3$ (SRM 987) gave a $^{87}\text{Sr}/^{86}\text{Sr}$ ratio of $0.7109 \pm 0.00002$ and the Eimer and Amend Sr standard a ratio of $0.70800 \pm 0.00002$ . The precision of a single $^{87}\text{Sr}/^{86}\text{Sr}$ ratio is normally $\pm 0.0001$ (1 $\sigma$ ).					

mary magmas (200-450 ppm; Basaltic Volcanism Study Project, 1981) suggest that the Kitkatla and Aristazabal magmas were derived at least in part by fractionation of olivine from a more primitive magma. This suggestion is supported by the presence of olivine phenocrysts in all but one of the Kitkatla and Aristazabal samples. Clinopyroxene and plagioclase (commonly resorbed) are additional phenocryst phases in some samples from Aristazabal Island, suggesting that these minerals were additional liquidus phases during partial melting or ascent of the magmas.

On tectonic discriminant diagrams appropriate for basalts or alkali basalts, analyses from Aristazabal Island and Kitkatla Inlet plot mainly in the within-plate field (e.g. Fig. 6) or scatter across the within-plate and MORB fields (e.g. Fig. 7). An 'island arc' setting appears to be ruled out. None of the commonly used discriminant diagrams is consistently able to separate the various within-plate environments such as mantle plume, incipient rift, or back-arc. Transitional olivine basalts with low  $^{87}\text{Sr}/^{86}\text{Sr}$  ratios are characteristic of back-arc and incipient rift settings (Basaltic Volcanism Study Project, 1981). Similar basalts are indeed found in island arc settings, but there they are volumetrically minor compared with the differentiated, calc-alkaline rocks characteristic of arcs and tend to occur at kinks, breaks, and ends of arcs (e.g. Lawrence et al., 1984; Green et al., 1988). In contrast, felsic volcanic rocks are unknown east of Hecate Strait, except for a few clasts in basaltic agglomerate in Kitkatla Inlet. All available chemical, isotopic and petrographic data indicate that the mafic volcanics of the Aristazabal and Kitkatla suites are modified mantle melts that were generated in a within-plate setting, possibly a back-arc or (more likely) an incipient rift setting.

The Quaternary to Recent volcanic rocks of Kitasu Hill and Lake, Lady Douglas and Price islands have generally higher Rb/Sr ratios and lower (0.7026-0.7037)  $^{87}\text{Sr}/^{86}\text{Sr}$  initial ratios than the Oligocene-Miocene volcanic rocks. These ratios and the two available chemical analyses (Table 2, Fig. 4) suggests that they are more alkaline and reflect a more limited amount of partial melting or a deeper mantle source than the older basalts.

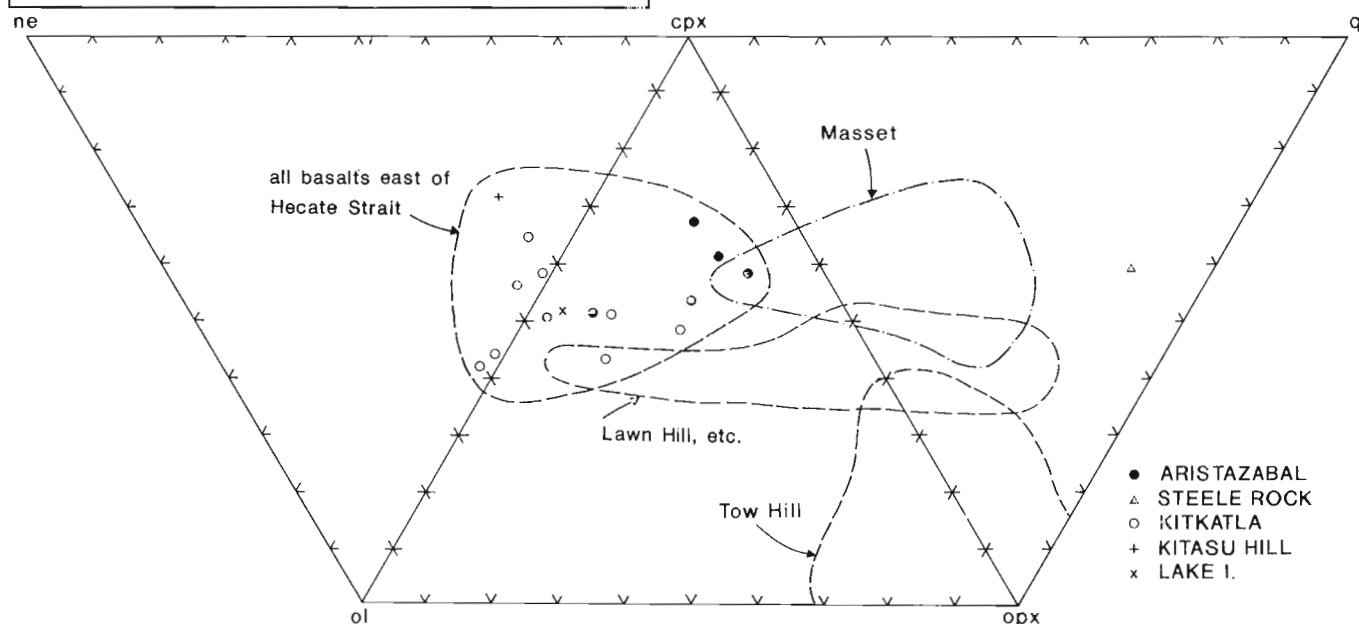
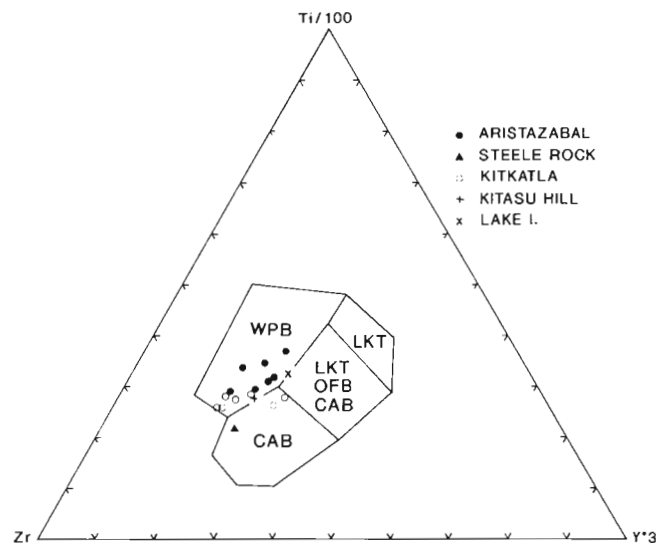


Figure 5: Plots of molecular-normative quartz (q), orthopyroxene (opx), clinopyroxene (cpx), olivine (ol) and nepheline (ne) for volcanics east of Hecate Strait suite. The field for Masset basalts and basaltic andesite is based on data in Hickson (1991) and her definition of the Masset Formation. The field for Lawn Hill includes analyses from the BV Naden Harbour well and Ramsay Island and is derived from data in Hyndman and Hamilton (1991). The field for Tow Hill basalts was calculated from data in Timms (1989).



**Figure 6:** Ti-Zr-Y discriminant diagram for rocks of the Hecate Strait suite. Field boundaries from Pearce and Cann (1973). WPB, within-plate basalt; LKT, low-K tholeiite; OFB, ocean-floor basalt; CAB, calc-alkaline basalt.

## DISCUSSION

### Regional comparisons

Chemically and petrographically, the Hecate Strait volcanics have many similarities with the transitional flood basalts of the Chilcotin Group in west-central British Columbia (Bevier, 1983a). Most K-Ar dates from the Chilcotin Group are between 2 and 15 Ma (Bevier, 1983b), making them younger than the Hecate Strait suite. Bevier (1983a) suggested that the Chilcotin basalts erupted in a back-arc environment, behind the calc-alkaline Pemberton volcanic arc.

Erdman (1985) tentatively correlated the basalts east of Hecate Strait with the Anahim Volcanic Belt on chemical grounds. Volcanic rocks of the western Anahim Volcanic Belt (Souther, 1986) differ from Aristazabal and Kitkatla basalts in being peralkaline in chemistry and younger (12.5-14.5 Ma compared with 20-26 Ma). Further, Aristazabal Island and Kitkatla Inlet do not lie on the well defined east-northeast trend of the Anahim belt, suggesting that they are not directly related to the Anahim Belt.

Van der Heyden (1989) suggested that the volcanics east of Hecate Strait are an eastern extension of the Masset Formation on Queen Charlotte Islands. The Masset Formation (Fig. 1) is controversial in definition, age, chemistry, and tectonic setting. In most papers, the term "Masset Formation" has been used for all Tertiary volcanics on the Queen Charlotte Islands and in Queen Charlotte Basin. K-Ar dates on these Tertiary volcanics range from <5 to 62 Ma; most fall between 20 and 25 Ma (data summarized in Hickson, 1991 and Hyndman and Hamilton, 1991). Based on detailed field work, Hickson (1991) suggested that the Masset Formation be restricted to Late Oligocene to earliest Pliocene, aphyric to sparsely phytic, calc-alkaline volcanics and associated epiclastic sediments. The basalts at Tow Hill, Lawn Hill, in the BV Naden Harbour drill hole, and volcanics encountered in wells in Hecate Strait were specifically excluded from the Masset Formation by Hickson (1991). Her definition of the Masset Formation is used in the following discussion.

Reliable K-Ar dates from the Masset Formation indicate that volcanism is 20-25 Ma in age (Hickson, 1991; Hyndman and Hamilton, 1991) and was thus clearly contemporaneous with eruptions at Steele Rock, Aristazabal Island, and Kitkatla Inlet. Petrographically, how-

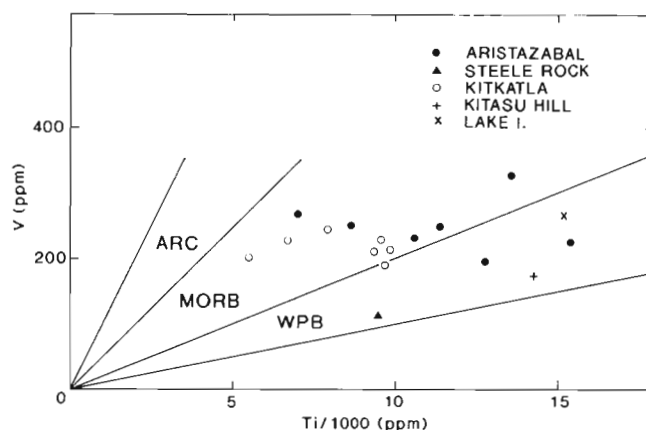


**Figure 7:** V-Ti discriminant diagram for the Hecate Strait suite; field boundaries from Shervais (1982).

ever, these rocks are very different from the Masset Formation. In contrast with Aristazabal, Kitkatla, and Steele volcanics, the Masset is composed of intercalated, mostly aphyric, felsic to mafic flows and pyroclastic rocks. Feldspar is the common phenocryst phase; olivine is conspicuously absent. The chemistry of the Masset also differs markedly from that of basalts east of Hecate Strait. For example, on the normative q-opx-cpx-ol plot (Fig. 5), the field for Masset basalts and basaltic andesites barely overlaps that for the Hecate Strait basalts. The Masset has a calc-alkaline signature (e.g. Fig. 2 of Hickson, 1991) rather than the transitional to alkaline chemistry of the basalts east of Hecate Strait.

The tectonic setting of the Masset Formation is controversial. But whatever setting eventually proves correct, the chemical contrasts between the Masset Formation and the Hecate Strait volcanics are sufficiently marked to suggest that the two contemporaneous assemblages may have formed in appreciably different tectonic settings. Although they are the same age, volcanic rocks east of Hecate Strait should not be treated as part of the Masset Formation.

The volcanic rocks at Tow Hill, Lawn Hill and in the BV Naden Harbour well (Fig. 1) were excluded by Hickson (1991) from the Masset Formation on field, petrographic, and chemical evidence. Tow Hill consists of basalt sills or flows within the Miocene to Pliocene Skonun Formation (Sutherland Brown, 1968). Petrographically, the rocks are similar to the volcanics east of Hecate Strait in that olivine is the common phenocryst phase. Chemically, Tow Hill basalts are quartz- and hypersthene-normative and tholeiitic (e.g. Fig. 5; Timms, 1989), unlike the transitional nature of the Hecate Strait basalts. Timms (1989) concluded that the Tow Hill basalts formed in an extensional setting similar to that inferred for the Hecate Strait volcanics. There are no reliable K-Ar dates for Tow Hill, owing in part to the highly altered nature of the basalts, and thus correlation with the Hecate Strait suite remains speculative.

Volcanic rocks intersected in the Naden Harbour well and exposed at Lawn Hill (Fig. 1) may be the closest relatives on the Queen Charlotte Islands to the volcanic rocks east of Hecate Strait. Reliable K-Ar dates indicate that they are about 20-24 Ma old, contemporaneous with rocks at Steele Rock, Aristazabal Island, and Kitkatla Inlet.



Unlike the Masset Formation, the Lawn Hill and Naden Harbour volcanics are basalt and basaltic andesite, commonly containing olivine phenocrysts. Chemical analyses (Hyndman and Hamilton, 1991; T.S. Hamilton, pers. comm., 1990) suggest that the rocks are transitional between the Masset Formation and basalts east of Hecate Strait (e.g. Fig. 5). On most tectonic discriminant diagrams, analyses for Lawn Hill and BV Naden Harbour well plot in the same fields as the Hecate Strait rocks, suggesting a common tectonic setting.

### Neogene tectonic history east of Hecate Strait

During early Tertiary time, convergence of the Kula Plate with North America produced widespread subduction-related magmatism in west-central B.C. Eocene magmatism ceased abruptly about 45 Ma (e.g. van der Heyden, 1989), at about the time convergent motion gave way to dominantly transcurrent motion along the Kula-North America boundary (e.g. Stock and Molnar, 1988). No magmatic activity is known from the Coast Plutonic Complex in central and northern British Columbia from about 42 Ma until the beginning of Kitkatla and Aristazabal volcanism at about 26 Ma.

Based on fission track dates, Parrish (1983) suggested that since 40 Ma the maximum total uplift east of Hecate Strait ranged from nil near the coast to several kilometres inland and from 0.2 km since 10 Ma. However, the data are very sparse in the region between Prince Rupert and Bella Bella. In both the Aristazabal and Kitkatla volcanic centres, features such as pillows, interbedded marine sediments, and hyaloclastic texture that would indicate a marine depositional environment for the volcanics are absent. The scoriaceous basal conglomerate on Aristazabal Island and the abundant columnar jointing suggest that the volcanics were erupted subaerially. If so, then there has been at least a small net amount of subsidence, not uplift, in these areas since Early Miocene time, because the volcanics are now close to sea level.

The 20–30° dips, generally to the southwest, for the volcanics in both areas suggest that the region was tilted to the southwest in post-Early Miocene time. The brittle faults that cut the Aristazabal volcanics may indicate that listric normal faulting accompanied tilting. Such a style of deformation is consistent with the abundant half-grabens seen on seismic reflection profiles from Hecate Strait (Rohr and Dietrich, 1991) and could explain the absence of Neogene volcanics from the low areas farther east on Aristazabal Island and their preservation beneath eastern Hecate Strait. On the other hand, the Kitkatla Inlet volcanics occur in a northwest-trending depression flanked on either side by high-relief islands. Speculatively, Kitkatla Inlet represents a half-graben that is controlled on the southwest by Neogene movement along the northwest-trending, Early Cretaceous or younger (van der Heyden, 1989) Kitkatla Fault. The volcanics may have been erupted into this fault-bounded basin and owe their preservation to renewed post-Early Miocene normal faulting along the graben-bounding fault. At least some of the deformation observed in the seismic records is thus post-Early Miocene.

This conclusion implies at least a small amount of extension along the eastern margin of Queen Charlotte Basin during early Neogene time. Such extension is consistent with a back-arc tectonic setting and is required for an incipient rift origin. The chemistry of the volcanic rocks can be used to support either tectonic setting. The amount of extension along the east margin of Hecate Strait was probably less than a few percent, because the percent of dykes associated with the volcanic rocks is very small (probably <0.1% using the dyke distribution in Kitkatla Inlet). Reactivation of older, northwest-trending faults in Oligocene-Miocene time could have provided conduits for mantle-derived magma with only a very small amount of extension. Episodic extensional reactivation of older structures appears to have

been the dominant structural style along the west side of the Coast Mountains since Late Oligocene time.

Extension-related magmatism in the western Coast Mountains did not cease with the Early Miocene end of Kitkatla volcanism. Numerous northeast-trending basalt and lamprophyre dykes are known in an area extending north from Prince Rupert into southeastern Alaska (Smith, 1973; Hutchison, 1982). One of these dykes from north of Prince Rupert gave a K-Ar whole-rock date of  $7.3 \pm 0.8$  Ma (Table 1; Erdman, 1985). Chemical analyses (Smith, 1973) indicate that the dykes are alkaline in composition, suggesting that they formed in an extensional regime.

Farther south, conventional chemical discriminant diagrams suggest that the Quaternary-Recent alkali basalts of Lake Island and Kitasu Hill probably formed in an extensional setting. However, the plate tectonic regime for the last 5 Ma has been one of oblique convergence of the Pacific Plate with North America (Hyndman and Hamilton, 1991). Such local and sporadic alkalic extensional magmatism within a regionally convergent setting indicates that caution is required when interpreting volcanic chemistry in terms of plate tectonic settings.

### ACKNOWLEDGMENTS

I thank Kathleen Dixon for cheerful assistance during field work in Kitkatla Inlet. The Aristazabal Island outcrops were examined during a cruise of *CFAV Endeavour* led by Trevor Lewis. Discussions with Cathie Hickson, Jack Souther, Tark Hamilton, and Peter van der Heyden were extremely helpful. Critical reviews by Dick Armstrong and Cathie Hickson and a final polish by Jack Souther greatly improved the paper.

### REFERENCES

- Baer, A.J.  
**1973:** Bella Coola–Laredo Sound map-areas, British Columbia: Geological Survey of Canada, Memoir 372, 122 p.
- Basaltic Volcanism Study Project**  
**1981:** Basaltic Volcanism on the Terrestrial Planets: Pergamon Press, New York, 1286 p.
- Bevier, M.L.  
**1983a:** Implications of chemical and isotopic compositions for petrogenesis of Chilcotin Group basalts, British Columbia: *Journal of Petrology*, v. 24, p. 207–226.  
**1983b:** Regional stratigraphy and age of the Chilcotin Group basalts, south-central British Columbia: *Canadian Journal of Earth Sciences*, v. 20, p. 515–524.
- Bevier, M.L., Armstrong, R.L., and Souther, J.G.  
**1979:** Miocene peralkaline volcanism in west-central British Columbia—its temporal and plate tectonic setting: *Geology*, v. 7, p. 389–392.
- Dolmage, V.  
**1922:** Coast and islands of British Columbia between Burke and Douglas channels: Geological Survey of Canada, Summary Report, 1921, Part A, p. 22–49.
- Erdman, L.R.  
**1985:** Chemistry of Neogene basalts of British Columbia and the adjacent Pacific Ocean floor: a test of tectonic discriminant diagrams: M.Sc. thesis, University of British Columbia, Vancouver, 294 p.
- Geological Survey of Canada**  
**1987a:** Hecate Strait, British Columbia: Geological Survey of Canada, Geophysical (Aeromagnetic) Map 7752G.  
**1987b:** Magnetic anomaly map, Prince Rupert, British Columbia: Geological Survey of Canada, Map NN-8-9-M.
- Green, N.L., Armstrong, R.L., Harakal, J.E., and Souther, J.G.  
**1988:** Eruptive history and K-Ar geochronology of the late Cenozoic Garibaldi volcanic belt, southwestern British Columbia: *Geological Society of America Bulletin*, v. 100, p. 563–579.
- Hickson, C.J.  
**1991:** The Masset Formation on Graham Island, Queen Charlotte Islands, British Columbia: in *Evolution and Hydrocarbon Potential of the Queen Charlotte Basin*, British Columbia, Geological Survey of Canada, Paper 90-10.
- Hutchison, W.W.  
**1982:** Geology of the Prince Rupert-Skeena map-area: Geological Survey of Canada, Memoir 394, 116 p.

**Hyndman, R.D. and Hamilton, T.S.**

**1991:** Cenozoic relative plate motions along the northeastern Pacific margin and their association with Queen Charlotte area tectonics and volcanism; *in* Evolution and Hydrocarbon Potential of the Queen Charlotte Basin, British Columbia, Geological Survey of Canada, Paper 90-10.

**Lawrence, R.B., Armstrong, R.L., and Berman, R.G.**

**1984:** Garibaldi Group volcanic rocks of the Salal Creek area, southwestern British Columbia: alkaline lavas on the fringe of the predominantly calc-alkaline Garibaldi (Cascade) volcanic arc; *Journal of Volcanology and Geothermal Research*, v. 21, p. 255-276.

**Le Bas, M.J., Le Maitre, R.W., Streckeisen, A., and Zanettin, B.**

**1986:** Chemical classification of volcanic rocks; *Journal of Petrology*, v. 27, p. 746-750.

**Macdonald, G.A.**

**1968:** Composition and origin of Hawaiian lavas; *in* Studies in Volcanology, R.R. Coats, R.L. Hay, and C.A. Anderson (ed.), Geological Society of America, Memoir 116, p. 477-522.

**Parrish, R.R.**

**1983:** Cenozoic thermal evolution and tectonics of the Coast Mountains of British Columbia: 1. Fission track dating, apparent uplift rates, and patterns of uplift; *Tectonics*, v. 2, p. 601-631.

**Pearce, J.A. and Cann, J.R.**

**1973:** Tectonic setting of basic volcanic rocks determined using trace element analyses; *Earth and Planetary Science Letters*, v. 19, p. 290-300.

**Roddick, J.A.**

**1970:** Douglas Channel-Hecate Strait map area, British Columbia; Geological Survey of Canada, Paper 70-41, 56 p.

**Rohr, K. and Dietrich, J.R.**

**1991:** Deep seismic reflection survey of the Queen Charlotte Basin, British Columbia; *in* Evolution and Hydrocarbon Potential of the Queen Charlotte Basin, British Columbia, Geological Survey of Canada, Paper 90-10.

**Russell, J.K. and Nichols, J.**

**1988:** Analysis of petrologic hypotheses with Pearce element ratios; *Contributions to Mineralogy and Petrology*, v. 99, p. 25-35.

**Sawyer, B.**

**1989:** Physiography/Physiographie, Dixon Entrance-Hecate Strait; Geological Survey of Canada, Map F-1989.

**Servais, J.W.**

**1982:** Ti-V plots and the petrogenesis of modern and ophiolitic lavas; *Earth and Planetary Science Letters*, v. 59, p. 101-118.

**Smith, J.G.**

**1973:** A Tertiary lamprophyre dike province in southeastern Alaska; *Canadian Journal of Earth Sciences*, v. 10, p. 408-420.

**Souther, J.G.**

**1966:** Cordillera volcanic study; *in* Report of Activities, May to October, 1965, Geological Survey of Canada, Paper 66-1, p. 87-89.

**1986:** The western Anahim Belt: root zone of a peralkaline magma system; *Canadian Journal of Earth Sciences*, v. 23, p. 895-908.

**in press:** Milbanke Sound cones; *in* Volcanoes of North America, C.A. Wood (ed.), Cambridge University Press.

**Steiger, R.H. and Jäger, E.**

**1977:** Subcommittee on geochronology: convention on the use of decay constants in geo- and cosmochemistry; *Earth and Planetary Science Letters*, v. 36, p. 359-362.

**Stock, J. and Molnar, P.**

**1988:** Uncertainties and implications of the Late Cretaceous and Tertiary position of North America relative to the Farallon, Kula, and Pacific plates; *Tectonics*, v. 7, p. 1339-1384.

**Sutherland Brown, A.**

**1968:** Geology of the Queen Charlotte Islands, British Columbia; British Columbia Department of Mines and Petroleum Resources, Bulletin 54, 226 p.

**Timms, C.E.**

**1989:** The origin and tectonic setting of Tow Hill, Queen Charlotte Islands; B.Sc. thesis, McMaster University, Hamilton, Ontario, 78 p.

**van der Heyden, P.V.**

**1989:** U-Pb and K-Ar geochronometry of the Coast Plutonic Complex, 53° to 54°N, British Columbia, and implications for the Insular-Intermontane superterrane boundary; Ph.D. thesis, University of British Columbia, Vancouver, 392 p.

**White, W.H., Erickson, G.P., Nothcote, K.E., Dixon, G.E., and Harakal, J.E.**

**1967:** Isotope dating of the Guichen batholith, B.C.; *Canadian Journal of Earth Sciences*, v. 4, p. 677-699.

**Woodsworth, G.J.**

**1988:** Karmutsen Formation and the east boundary of Wrangellia, Queen Charlotte Basin, British Columbia; *in* Current Research, Part E, Geological Survey of Canada, Paper 88-1E, p. 209-212.



# Sedimentology, basin-fill architecture and petroleum geology of the Tertiary Queen Charlotte Basin, British Columbia

Roger Higgs<sup>1</sup>

Higgs, R., Sedimentology, basin-fill architecture and petroleum geology of the Tertiary Queen Charlotte Basin, British Columbia; in *Evolution and Hydrocarbon Potential of the Queen Charlotte Basin, British Columbia*, Geological Survey of Canada, Paper 90-10, p. 337-371, 1991.

## Abstract

*The onshore-offshore Queen Charlotte Basin (QCB), conventionally viewed as entirely sedimentary (Skonun Formation) on a volcanic basement (Masset Formation), is here redefined to include the Masset in the lower basin fill, based on partial Skonun-Masset age-equivalence, and on probable interfingering. The redefined basin covers a greater area than before, the on-land portion comprising the entire Queen Charlotte Islands, instead of only northeastern Graham Island. Delimiting the western edge of both the QCB and the Queen Charlotte Islands is the convergent-transform Queen Charlotte Fault, representing the Pacific-North America plate boundary.*

*Well-log correlations reveal a bipartite basin fill. The upper unit, Unit II, is a Miocene-Recent sedimentary blanket covering the offshore area, but absent onshore except for northeast Graham Island. Characterizing Unit II on well logs are coarsening-up shale-sand sequences of regional extent, 10-30 m thick, interpreted as allogenic regressive cycles. Underlying Unit II, Unit I lacks basinwide correlations and comprises Eocene to Miocene volcanics (including the Masset Formation) and intercalated sediments.*

*Facies analysis of cores and small exposures shows that Unit I includes alluvial fan, fan delta and fluvial facies. Unit II strata exposed in northeast Graham Island are of Miocene age and include three facies associations: (1) delta-plain mudstone, sandstone and coal; (2) tidal-shelf cross-stratified sandstone; and (3) amalgamated shelf storm beds. The outcrop data suggest that the regressive cycles recognized on well logs comprise shelf deposits shallowing up into delta-plain deposits.*

*The bipartite basin fill is interpreted in terms of an extensional basin with a McKenzie-type, two-stage subsidence history. Unit I is interpreted as a "rift" succession, based on the volcanics, local conglomerates, and lack of correlations; deposition was in half-grabens in an extensional, block-faulting regime. Subsequently, Unit II was deposited under "post-rift" regional (thermal?) subsidence. Seismic profiles support the proposed two-stage evolution.*

*Iceberg dropstones occur in exposures on northeast Graham Island of late Miocene shelf sediments (Skonun Formation, Unit II), suggesting that mountains with valley glaciers were nearby. Some of the dropstones are of intraformational composition, implying that the mountains were a formerly submerged part of the QCB undergoing syn-depositional uplift. In addition, these shelf deposits show tidal sedimentary structures, indicating that a land barrier existed to the west, to provide the semi-enclosed shelf conditions necessary for large tides (cf. modern Hecate Strait). Taken together, the dropstones and the evidence for tides suggest uplift of a (previously submerged) proto-Queen Charlotte landmass before or during the late Miocene. Uplift is postulated to have started at 20 Ma when, based on a published plate-kinematic model, plate interaction along the Moresby Island sector of the Queen Charlotte margin (oriented 320°) changed from transcurrent to transpressive. The result was oblique subduction, causing emergence and uplift of proto-Moresby Island. Meanwhile Graham Island remained submerged until 5 Ma, when a further shift in relative plate motion initiated oblique subduction along the adjacent sector of the plate margin (340°). As a result of uplift, erosion stripped Skonun sediments from much of the Queen Charlotte Islands, exposing Masset volcanics and Mesozoic basement. Moresby Island, having emerged earlier than Graham Island, is eroded to a deeper structural level.*

*Some implications for oil exploration are: (1) extensional basins are hydrocarbon-prone worldwide, and the QCB may be no exception; (2) intra-Masset QCB sediments offer exploration targets in west Graham Island and elsewhere; (3) ongoing uplift of the western part of the basin means that the present-day oil window there may contain (uplifted) overmature strata; (4) potential reservoirs include fan deltas in Unit I and, in Unit II, delta-front sand bodies, offshore tidal sand bodies, and amalgamated storm sands; and (5) tidal sands may be mineralogically mature due to long-distance transportation, resulting in improved porosity and permeability.*

<sup>1</sup> Geological Survey of Canada, Pacific Geoscience Centre, P.O. Box 6000, Sidney, B.C. V8L 4B2  
Present address: Higgs Petroleum Consulting Ltd., 743 Oliver Street, Victoria, B.C., V8S 4W5

## Résumé

*Le bassin de la Reine-Charlotte, que ce soit sur le littoral ou au large, était conventionnellement considéré comme entièrement composé de sédiments (formation de Skonun) reposant sur un socle volcanique (formation de Masset). Il est redéfini pour inclure la formation de Masset dans sa partie inférieure des sédiments de remplissage, en se fondant sur une équivalence chronologique partielle Skonun-Masset et sur une interdigitation probable. Le bassin redéfini couvre l'ensemble des îles de la Reine-Charlotte plutôt que seulement le nord-est de l'île Graham. La faille convergente et transformante de la Reine-Charlotte délimite la marge occidentale du bassin et des îles de la Reine-Charlotte. Elle marque la limite entre les plaques pacifique et nord-américaine.*

*Des corrélations de diagraphies de puits révèlent un remplissage de bassin en deux parties. L'unité supérieure ou unité II, est une nappe de sédiments miocènes-pliocènes couvrant la zone extracôtière et le nord-est de l'île Graham. Selon les diagraphies de puits, l'unité II est caractérisée par des séquences de schiste argileux-sable à granulométrie négative d'extension régionale que l'on considère être des cycles de régression allogène. L'unité I sous-jacente ne peut pas être corrélée; elle comprend des roches volcaniques de l'Éocène au Miocène (incluant la Formation de Masset) et des intercalations de sédiments.*

*L'unité I contient des faciès de cônes alluviaux et deltaïques et des faciès fluviaux. L'unité II comporte trois associations de faciès : mudstone, grès et charbon de plaine deltaïques; grès à stratification oblique de plate-forme tidale; et couches de tempête de plate-forme amalgamées. Les affleurements indiquent que les cycles de régression décelés sur les diagraphies de puits ont eu pour effet de transformer les sédiments de plate-forme en sédiments de plaine deltaïque.*

*Le remplissage en deux parties du bassin est interprété en fonction d'un bassin de distension de type Mckenzie dont la subsidence aurait eu lieu en deux étapes. L'unité I est interprétée comme une succession de "rifts", si l'on se base sur les roches volcaniques, les conglomérats locaux et le manque de corrélations possibles; elle s'est déposée dans des demi-grabens dans un régime de morcellement par failles de distension. L'unité II s'est déposée dans des conditions de subsidence flexurale (thermale?) "post-rift". Les profils sismiques appuient l'idée d'une évolution en deux étapes.*

*Des icebergs ont largué des cailloux dans les sédiments de plate-forme de l'unité II de la formation Skonun dans le nord-est de l'île Graham, suggérant que des monts entaillés de vallées glaciaires se trouvaient à proximité. La composition intraformationnelle de certaines de ces roches implique que ces montagnes étaient une partie auparavant immergée du bassin subissant un soulèvement syn-dépositionnel. La présence de sédiments de plate-forme tidale dans les roches miocènes du nord-est de l'île Graham n'est possible que si une barrière de terre a existé à l'ouest, fournissant les conditions de plate-forme semi-fermée nécessaires aux grandes marées (voir l'actuel détroit d'Hécate). La présence de ces roches et l'existence de marées suggèrent le soulèvement d'une proto-masse continentale Reine-Charlotte avant ou pendant le Miocène supérieur. Le soulèvement a dû commencer postérieurement à 20Ma lorsque, suivant un modèle publié de cinématique de plaques, le décrochement transversal est devenu transpressif au niveau du secteur de l'île Moresby le long de la marge de la Reine-Charlotte (direction 320°). La subduction résultante a entraîné l'émergence et le soulèvement de la proto-île Moresby. Cependant, l'île Graham est restée immergée jusqu'à 5Ma lorsqu'un changement dans le mouvement relatif des plaques a initialisé une subduction oblique le long du secteur adjacent de la marge (direction 340°). Les sédiments de Skonun ont donc été décapés de la partie ouest de l'île Graham, mettant à jour les roches volcaniques de Masset et le socle mésozoïque. Puisque l'île Moresby a émergé plus tôt que l'île Graham, l'érosion a affecté un niveau structural plus profond.*

*Voici quelques conclusions à tirer en ce qui concerne l'exploration pétrolière : 1) dans le monde entier, les bassins d'extension ont tendance à contenir des hydrocarbures et le bassin de la Reine-Charlotte pourrait ne pas faire exception à la règle; 2) les sédiments qui se trouvent dans la formation de Masset constituent des cibles d'exploration, notamment dans l'ouest de l'île Graham; 3) le soulèvement en cours de la partie occidentale du bassin signifie que la fenêtre à huile qui s'y trouve pourrait contenir des couches hypermatures (soulevées); 4) les roches réservoirs potentielles sont les cônes deltaïques dans l'unité I et les massifs de sable de front deltaïque, les massifs de haute mer de sable de marée et les sables de tempête amalgamés de l'unité II; et 5) les sables de marée pourraient avoir atteint une certaine maturité de composition ayant été transportés sur de longues distances, ce qui aurait eu pour effet d'en améliorer la porosité et la perméabilité.*

## INTRODUCTION

The Tertiary Queen Charlotte Basin (QCB), on Canada's western continental margin, embraces the Queen Charlotte Islands, Dixon Entrance, Hecate Strait and Queen Charlotte Sound (Fig. 1). The continental edge is delimited by the Queen Charlotte Fault (Fig. 1), which accommodates mainly (dextral) transform motion between the Pacific and North America plates, although a small component of

convergence causes oblique underthrusting (Yorath and Hyndman, 1983). The QCB has significant petroleum potential (Yorath and Cameron, 1982; Yorath, 1987), but has been scarcely explored, only 17 wells (all dry) having been drilled. Exploration is currently minimal due to a government moratorium on offshore drilling. Encouraging for exploration are: thick porous sandstones; oil-stained sand in the Sockeye B-10 offshore well (Shell Canada Ltd., 1968b;

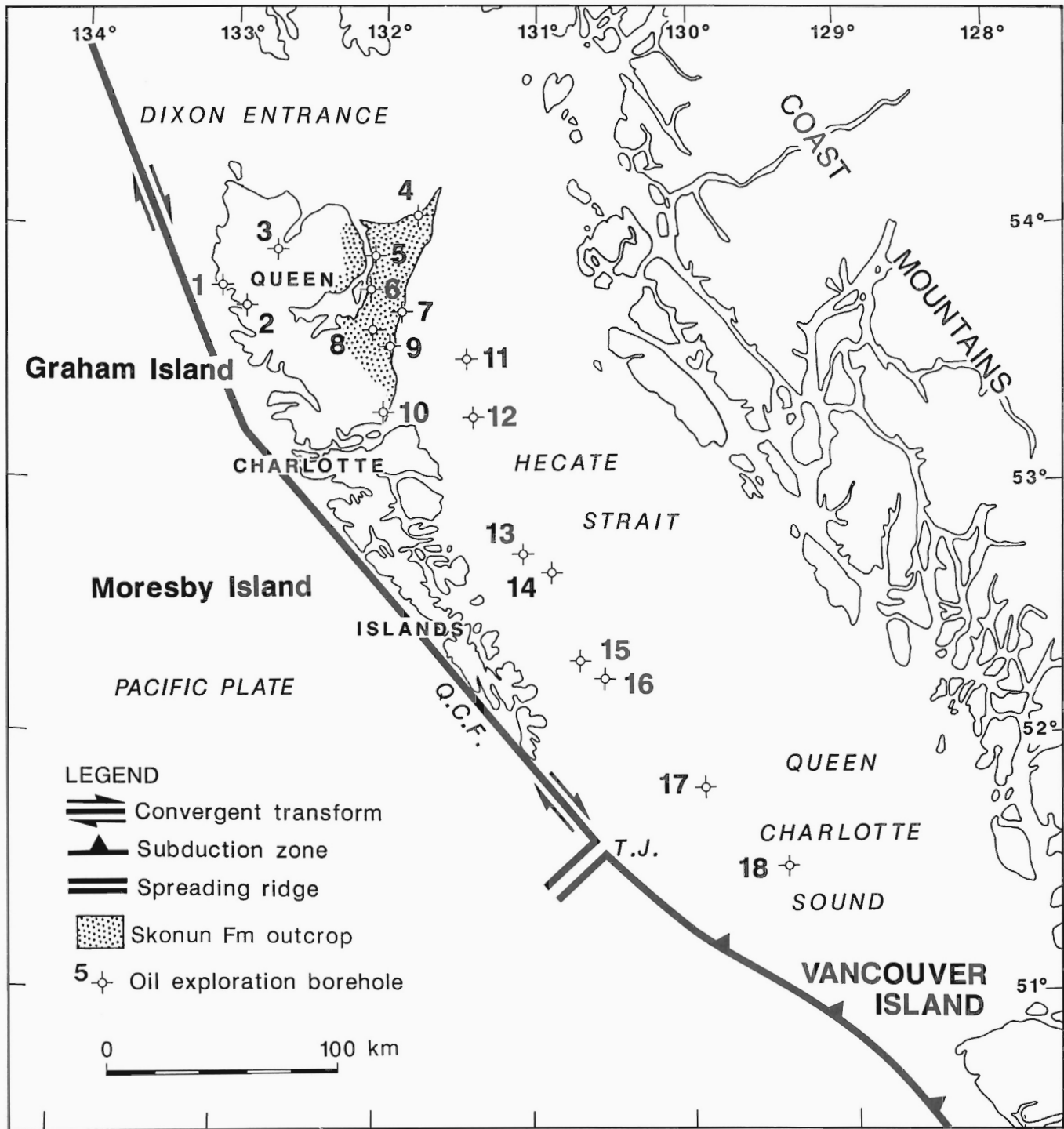


**Figure 1:** Location map of the Queen Charlotte Islands region. QCF = Queen Charlotte Fault (after Hutchison et al., 1979); TJ = triple junction. Oil exploration wells: 1 Tian Bay; 2 Port Louis; 3 Naden (twin wells; see text); 4 Tow Hill; 5 Masset; 6 Nadu River; 7 Cape Ball; 8 Gold Creek; 9 Tlell; 10 Queen Charlotte (spudded in Mesozoic basement); 11 South Coho; 12 Tyee; 13 Sockeye B-10; 14 Sockeye E-66; 15 Murrelet; 16 Auklet; 17 Harlequin; 18 Osprey.



Shouldice, 1971); abundant onshore oil seeps in Tertiary Masset Formation volcanics (Hamilton and Cameron, 1989; lack of known onshore seeps in the Skonun Formation may simply reflect poor exposure); and rich Jurassic source rocks in onshore strata of the pre-Tertiary basement (Bustin and Macaulay, 1988). Exploratory drilling began with the Tian Bay well (Fig. 1), abandoned in 1915. Multi-well drilling programs were conducted onshore by Richfield in the 1950s and offshore by Shell in the 1960s. The most recent well was drilled at Naden in 1984.

Exploration to date has been conducted with minimal knowledge of the sedimentology and basin-fill configuration of the QCB, and two critical questions remain unanswered: What is the geometry of potential reservoir bodies? What type of basin is the QCB, hence what is its intrinsic petroleum potential? This paper addresses these questions. The paper is in five sections. The first section discusses well-log correlations and the architecture of the basin fill. This is followed by two sections comprising a facies analysis of all known Skonun Formation exposures and cores, respectively; these were examined by the author in 1987 and 1988. In accordance with standard practice, the facies are first described, and are then interpreted in terms of depositional process and environment. The fourth section is a heavy-mineral analysis of sandstone samples taken from cores. The final section discusses

basin origin, summarizes depositional environments, and considers implications for petroleum exploration and production.

As defined by Shouldice (1971, 1973), the QCB contains up to 5 km of Tertiary marine and nonmarine siliciclastic sediments. These sediments, known as the Skonun Formation, consist of sandstone, mudstone, conglomerate and coal (Sutherland Brown, 1968); they occur throughout northeast Graham Island, Hecate Strait and Queen Charlotte Sound (Figs. 1 and 2; Fig. 3, in pocket), beneath a cover of Quaternary sediment (Sutherland Brown, 1968; Shouldice, 1971). The Quaternary deposits were excluded from the Skonun Formation by Sutherland Brown (1968), but it may be more practical to include them, because the boundary between the Skonun Formation and the Quaternary both onshore and offshore does not appear to be a distinct lithological break (Sutherland Brown, 1968, p. 33, 123). Confusion may also have arisen from previous assumptions that all glacial deposits on Graham Island are Quaternary, when in fact several exposures of known Miocene-age Skonun strata include glaciomarine (ice-rafted) deposits, as described below. Hence, some exposures previously assumed to be Quaternary may actually be older. For example, exposures of crossbedded sand and dropstone-bearing mud in sea cliffs near Cape Ball, eastern Graham Island (Sutherland Brown, 1968, Plate 10C; Clague et al., 1982), previously assumed to be Quaternary and not visited by the author, are possibly Miocene or Pliocene, in view of: 1) the lack of dates from these exposures; and 2) the occurrence of similar facies with the same (subhorizontal) attitude at several exposures of Miocene-age Skonun Formation. The only true Quaternary deposits in northeast Graham Island may be the "postglacial" deposits, including fluvial sands in channels, described by Clague et al. (1982), and the "channels of late glacial to Recent age" of Sutherland Brown (1968, p. 32). Similar channels containing pebbly sand and gravel of inferred Quaternary outwash origin are exposed at the top of the Yakoun River sand pit (see below and Figs. 5D, 10). Hence, it is recommended that the Skonun Formation be redefined to include the Quaternary deposits of the region. Furthermore, like the Skonun, the Quaternary strata should be regarded as part of the QCB fill because, in the offshore area at least, subsidence and deposition appear to have been continuous from at least the Miocene to the present, as discussed below.

The Skonun Formation includes Miocene and Pliocene strata, based on foraminifera, palynomorphs and molluscs (Sutherland Brown, 1968; Shouldice, 1971; Addicott, 1978; Champigny et al., 1981; Patterson, 1988, 1989; White, 1990, 1991). However, parts of the succession are nonmarine (Sutherland Brown, 1968; Shouldice, 1971) and therefore poorly dated, and could include pre-Miocene sediments (White, 1990, 1991).

The Skonun Formation was considered by Sutherland Brown (1968) to overlie the volcanic Masset Formation. However, recent work has shown that the two formations are instead time-equivalent, at least in part, as shown by the presence of early and middle Miocene strata in both the Skonun (Shouldice, 1971; Champigny et al., 1981; Patterson, 1988, 1989) and the Masset (Cameron and Hamilton, 1988; Hickson, 1988, her Fig. 5). An interfingering relationship between the Skonun and Masset is likely (Hamilton and Cameron, 1988, their Fig. 2), because Masset volcanics are intercalated with sediments both at outcrop (Hickson, 1988, Fig. 2; 1989, Fig. 4, and 1991) and in offshore and onshore wells (Fig. 3, in pocket; Shouldice, 1971). An interfingering relationship implies that the Masset accumulated, like the Skonun, in a subsiding basin. Hence, the Masset should be viewed as part of the QCB fill, along with the Skonun Formation. (In contrast, earlier workers have regarded the Masset as basement.) Thus, the QCB is redefined here to include the Masset Formation, thereby extending the basin westward, beyond the western zero isopach depicted by

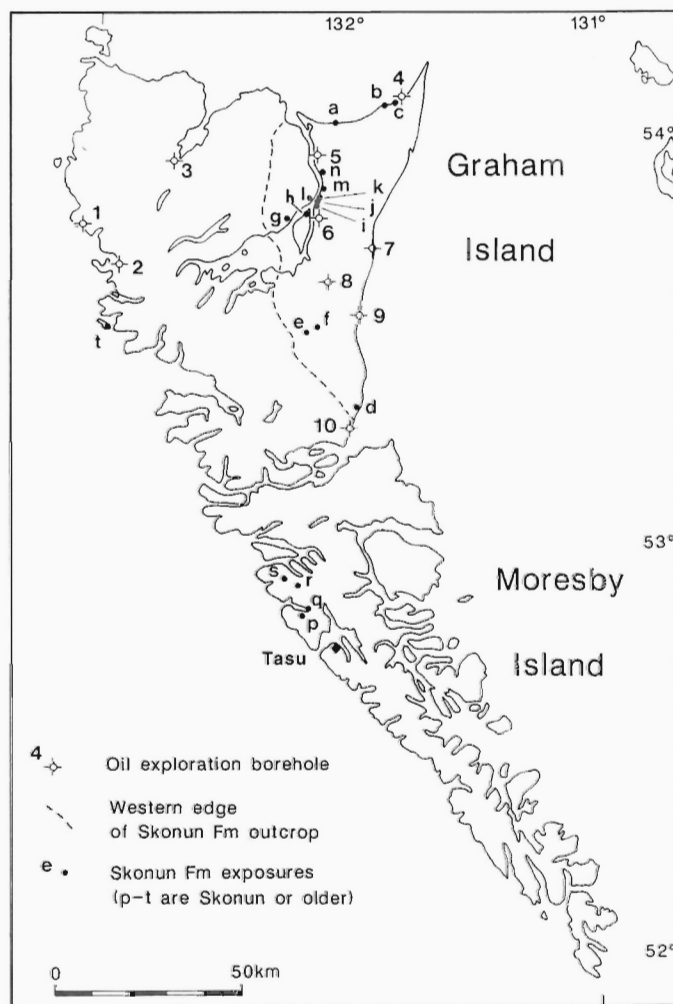


**Figure 2:** Oil exploration wells and Skonun Formation exposures on the Queen Charlotte Islands. See Figure 1 caption for borehole listing. Exposures: a Skonun Point; b Yakoun Point; c Tow Hill; d Miller Creek; e Cinola; f Yakoun River; g Collision Point; h Kumdis Island; i Nadu River mouth; j Grid reference PQ892688; k PQ898695; l Allan Point; m PQ907720; n Watun River mouth; p, q, r, s Tasu; t Hippa Island.

Shouldice (1973, his Fig. 32; see Fig. 3. inset), to the western edge of the Queen Charlotte Islands.

Access to the Skonun Formation is limited to: (1) a few small exposures on Graham Island; (2) drill core, a quarry, and an adit at the Cinola gold property (Fig. 2); and (3) fifteen onshore and offshore oil-exploration wells (Fig. 1). Outcrop sections are seldom longer than 15 m, while no core is longer than 8 m; hence, interpretation of depositional environments is hampered by a lack of continuous facies sequences (cf. Walker, 1984). Another constraint on sedimentological interpretation is the difficulty of determining lateral facies changes, hence paleogeography, due to the poor biostratigraphic control arising from the abundance of nonmarine strata and foram-free marine sandstones. In view of these shortcomings, it is essential that the maximum amount of sedimentological information be extracted from the limited material (core and exposures) available.

The Skonun Formation will be important in any future petroleum-exploration program in the QCB, because it includes abundant sandstone with high porosity (Shouldice, 1971; McWhae, 1986), and because it has the highest mineralogical maturity (hence least susceptibility to diagenetic reduction of porosity and permeability) of all the formations exposed on the islands (Sutherland Brown, 1968). However, effective oil exploration is hindered by a lack of knowledge about the depositional environments of the Skonun Formation and about the origin of the QCB. It is critical to know what type of basin is the QCB, because some basins are inherently more hydrocarbon-prone than others (e.g. Dickinson, 1978). Similarly, a thorough understanding of depositional environment is essential for predicting the subsurface distribution and geometry of (potential reservoir) sandstone bodies.

Field measurements made by the author are given in SI units, whereas core and sample depths are given in the original English or metric units, for ease of cross-reference to the well logs and well history reports.

## PREVIOUS INTERPRETATIONS

There have been no previous purely sedimentological studies of the Skonun Formation. Based partly on palynomorphs, Martin and Rouse (1966, p. 178) concluded that Skonun strata exposed on Graham Island are "interbedded marine and nonmarine beds" deposited in an environment that was "low, relatively flat, close to the sea, swampy or marshy". According to Sutherland Brown (1968, p. 125), the Skonun was deposited under alternating marine and nonmarine conditions: the "marine environment is all shallow water, near shore, and the nonmarine is all near sea-level and may include swamp, lagoon, lacustrine, and delta". In a report summarizing the results of offshore seismic surveys and drilling by Shell, Shouldice (1971, 1973) stated that the QCB deposits are nonmarine and marine (inner neritic to upper bathyal). Conglomerates at Cinola were interpreted as braided-stream deposits by Champigny and Sinclair (1982).

## WELL-LOG CORRELATIONS AND BASIN-FILL ARCHITECTURE

A wireline log cross-section through the QCB has been constructed, using the fifteen wells for which logs are available (Fig. 3; Richfield Oil Corporation, 1958a-c, 1961; Shell Canada Ltd., 1968a-f, 1969a,b; Union Oil Company of Canada Ltd., 1971). Logs can be correlated from one well to another, but only in the upper part of the succession. The correlatable entities are 10-30 m packets of upward-decreasing gamma, SP and sonic velocity, commonly forming continuous "saw-tooth" successions (Fig. 3). Individual packets probably represent coarsening-upward (shale-sand) sequences, because these are virtually ubiquitous in the stratigraphic record (e.g. Goodwin and Anderson, 1985). However, coarsening-up sequences are hard to verify in this

case, because well cuttings from the QCB are generally of poor quality due to the poorly lithified nature of the sediments and the rapid drill penetration rate (see well history reports). Nevertheless, in the Harlequin well, three successive sequences between 3800 and 4100 ft (Fig. 3, beside "MR") correspond closely to coarsening-up sequences defined by cuttings, as illustrated on the Canadian Stratigraphic Service Ltd. ("CanStrat", Calgary) lithological log. Additional coarsening-up sequences may be masked, because the Skonun Formation sandstones are feldspathic (Galloway, 1974) and therefore have a "shaly" gamma response (e.g. Cant, 1984).

The coarsening-up(?) sequences, either singly or in groups, can be correlated laterally for at least 175 km (from Sockeye to Osprey; Fig. 3). Their regional extent implies that sequences are transgressive-regressive cycles of allogenic (eustatic or tectonic) origin, rather than local, autogenic cycles. The probable coarsening-up nature of the sequences suggests that they are regressive (i.e. shallowing-up), separated by surfaces of abrupt regional transgression representing time lines (Goodwin and Anderson, 1985).

The cross-section (Fig. 3) suggests that the QCB fill is divisible into two stratigraphic units. The lower unit, here named Unit I, lacks correlations and comprises intercalated sediments and volcanics. In contrast, Unit II lacks volcanics and contains laterally correlatable sequences. Unit I is buried beneath Unit II in Queen Charlotte Sound, Hecate Strait and northeast Graham Island (Fig. 3), but Unit I shallows toward the north and west, ultimately occurring at surface in the Tow Hill and Port Louis wells, which are entirely Unit I (Fig. 3); between these wells, Unit I crops out extensively in western Graham Island as the Masset Formation (volcanics with subordinate sediments; Hickson, 1991). Graham Island thus consists essentially of Unit I Masset volcanics in the west and, in the east, Unit II (Skonun) sediments overlying Unit I sediments and volcanics (Fig. 3). This east-younging outcrop pattern is attributed to (ongoing) uplift of Graham Island being faster in the west than in the east (see below), causing exhumation of Unit I in the west.

The twin Naden wells (Fig. 1) were drilled entirely in Unit I volcanics. The Tow Hill exposure (Fig. 2, locality c) is attributed to Unit I because it includes the volcanic Tow Hill sills (see below; Sutherland Brown, 1968), which also occur in the Tow Hill well (Fig. 3). Borehole cuttings, described in the well history reports, indicate that sediments in Unit I include sandstone, shale and coal. In addition, there are conglomerate-dominated intervals more than 500 m thick, for example in the Tow Hill well (Fig. 3). Thick conglomerates also occur at Cinola, which is therefore assigned to Unit I. Intervals of intercalated sediments and volcanics attributed to Unit I can exceed 1 km (Fig. 3). Some wells penetrated more than 1 km of Unit I sediments before (or without) penetrating volcanics. The thickness of Unit I is uncertain, because few wells reach pre-Tertiary basement. However, Cretaceous palynomorphs were reported in the basal sediments of Tyee and Sockeye E-66 (Shell Canada Ltd., 1968a,c), but these could be reworked specimens (A.P. Audretsch, pers. comm., 1989). From the bottom of Sockeye B-10, unreliable late Cretaceous radiometric ages were obtained on basalt cuttings and on altered basalt from a sidewall core (Fig. 3; Young, 1981). Only the Tyee well, which bottomed in pre-Tertiary intrusives, reached unequivocal basement rocks underlying the QCB. This well penetrated 2.7 km of Unit I, more than any other well, providing a minimum thickness for the unit. Tyee penetrated no volcanics, proving that the Masset Formation is not a basin-wide blanket.

Deposition of Unit I sediments and volcanics began at 45-40 Ma (middle Eocene; time scale of Palmer (1983)) and continued until 15-10 Ma (middle to late Miocene), based on K-Ar ages of Masset Formation volcanics (summarized by Hickson, 1988, her Fig. 5). (The

Tow Hill sills, chemically equivalent to the Masset volcanics (Cameron and Hamilton, 1988), are of equivocal age, having yielded two unreliable K-Ar dates of 35 and <5 Ma (Young, 1981). Fossils in Unit I sediments at Cinola are Lower to Middle Miocene (Champigny et al., 1981). Palynomorphs indicate that Unit I sediments in the Port Louis well are within the range early Eocene to early Oligocene (White, 1990), and in the Tow Hill well are Miocene to possibly as old as late Oligocene (White, 1991).

Unit II, the upper stratigraphic unit, is characterized by correlatable sequences and absence of volcanics. The maximum thickness of Unit II in the offshore wells is 2 km (Fig. 3). The age of Unit II, based on forams in the Murrelet, Harlequin and Osprey wells (Patterson, 1988, 1989), is early Miocene through Quaternary (Fig. 3). Skonun Formation strata along Masset Sound (g through n in Fig. 2) are here assigned to Unit II, because they are near wells in which Unit II occurs at surface (Figs. 2, 3). Rocks at Skonun Point (a), Yakan Point (b) and Yakoun River (f) are likewise assigned to Unit II, because fossils indicate that they are the same age (late Miocene) as Masset Sound localities g and h (below and Addicott, 1978). The Miller Creek section (d) is also assigned to Unit II, based on facies similarities with Yakan Point and Yakoun River, as described below. Addicott's (1978) late Miocene (Wishkahan) age for the beds at Yakan Point and Skonun Point was estimated as 13-11 Ma by Champigny et al. (1981); hence, deposition of Unit II began no later than 11 Ma on Graham Island. However, eruption of underlying Unit I volcanics persisted until 15-10 Ma (Hickson, 1988, Fig. 5 and Table 1). Thus, deposition of Unit II on Graham Island began at some time in the interval 15-11 Ma, or middle to late Miocene. Further south, deposition of Unit II began earlier, in early Miocene time, in Queen Charlotte Sound (Fig. 3, Osprey and possibly Harlequin wells). This suggests that Unit II is diachronous, with its base younging northward.

An important lateral facies change occurs in Unit II. In the southernmost two wells (Harlequin and Osprey), cuttings suggest that Unit II is entirely marine, since it lacks coal and contains foraminifera (Shouldice, 1971). In contrast, correlative strata to the north include both marine intervals and coal-bearing continental intervals, as shown by well cuttings (Sutherland Brown, 1968; Shouldice, 1971) and exposures (see descriptions below). This facies change was documented by Shouldice (1971), but he implied that the Skonun Formation in the north is *entirely* continental, whereas in fact the onshore exposures are dominantly marine (see below), and the onshore wells contain shelly marine intervals (Sutherland Brown, 1968, p. 123 and Fig. 20). In the north, on Graham Island, Unit II facies include delta-plain muds, sands and coals, and tidal-shelf sands, as described below. Offshore in the south, the three available cores indicate a storm-dominated shelf environment. The absence of continental facies in Unit II in the southern two wells, indicated by the presence of forams and the absence of coal in cuttings (Shouldice, 1971), suggests that during each regressive episode (corresponding to a single coarsening-up sequence), the shoreline failed to prograde as far as the southern area (Fig. 4).

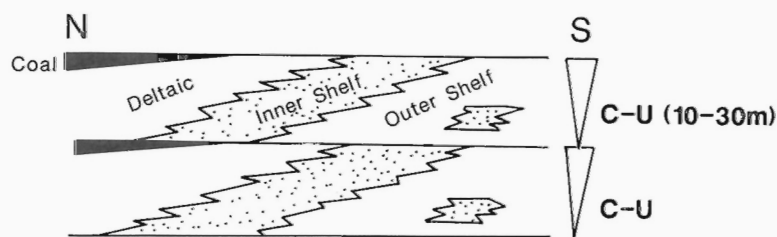


**Figure 4:** Two schematic coarsening-upward sequences, showing a possible explanation for the lateral facies change from marine in the south to marine and continental in the north (see text).

The base of Unit II is picked in Figure 3 to underlie the lowest correlatable sequence and to coincide with a distinct change in log character, below which the logs of most wells are more "spiky" due to a higher frequency of coal beds in Unit I (Fig. 3; see also Sutherland Brown, 1968, Fig. 20, and the CanStrat logs for Sockeye E-66, Nadu River, Gold Creek and Cape Ball). The Unit II-Unit I contact may or may not be an (intra-Miocene) unconformity, possibly corresponding to the regional unconformity recognized by McWhae (1986) on offshore seismic profiles. This unconformity was dated as Pliocene rather than Miocene by McWhae (1986), but this date is based on 1960s palynological data (well history reports and Shouldice, 1971), of doubtful reliability in view of their vintage. The unconformity, if it exists, has presumably been exhumed in those parts of the Queen Charlotte Islands where uplift and erosion have breached Unit II. The unconformity may be manifested as the Skidegate Plateau, a gently north-east-dipping surface dominating western Graham Island and truncating (slightly steeper-dipping) Masset strata by a few degrees (Sutherland Brown, 1968).

The bipartite basin fill is interpreted in terms of a "rift" and "post-rift" evolution, as discussed below under "Basin origin".

## EXPOSURES: DESCRIPTION AND INTERPRETATION

### Summary

All known exposures in the Skonun Formation are described and interpreted in this section. As mentioned above, exposures which belong to Unit I are Tow Hill and Cinola (c and e in Fig. 2). The exposures at Tasu (p through s) and Hippa Island (t) may also belong to Unit I, based on their conglomeratic nature and their intimate association with volcanics. All other exposures belong to Unit II.

Unit I strata at Cinola and Tasu are conglomeratic, interpreted respectively as fan delta and braided stream deposits. Unit II facies are entirely different. Exposed Miocene strata comprise three facies associations: (1) delta-plain muds with coal beds (Skonun Point and Miller Creek); (2) tidal-shelf cross-stratified sand with ice-rafted dropstones (Skonun Point, Yakan Point, Miller Creek, Yakoun River and Collison Point); and (3) storm-dominated shelf deposits with dropstones (Skonun Point). Minor conglomerates are associated with the tidal sands; these are interpreted as dropstone "condensation layers" formed by slow accumulation of ice-rafted dropstones under high tidal-current velocities (Skonun Point, Miller Creek, Masset Sound). These are thought to be the first known tidal deposits in the Tertiary of Canada south of latitude 60°N. Furthermore, the dropstones are possibly the first known evidence for pre-Quaternary (Miocene) glaciers in western Canada.

The nature and geometry of sand and conglomerate bodies in Units I and II are important for petroleum exploration and are discussed below.

### Skonun Point

This locality (a in Fig. 2), the type section and largest exposure of the Skonun Formation, was described in some detail by Sutherland Brown (1968), who pointed out its inadequacy as a type section due to the small amount of rock exposed; he recommended instead using the onshore boreholes as the standard. Two types of exposure occur at Skonun Point: 1) the point itself, consisting of two sea stacks; and 2) the intertidal beach stretching for up to 1 km eastward and exposing low ribs of lignite and sandstone which are submerged at high tide and which are separated by covered intervals.

#### Eastern sea stack

**Description.** The largest sea stack, at UTM grid reference PQ928909, exposes about 15 m of fine to medium sandstone dipping north at about 20°. The sandstone consists of amalgamated beds which are individually

5-50 cm thick (Fig. 5A). Bed sutures are marked by concentrations of bivalve shells, by discontinuous mudstone partings up to 2 cm thick, and by abrupt changes in grain size or sedimentary structures. Individual sandstone beds are massive to hummocky cross-stratified. Lamination in many beds is faint and discontinuous, suggestive of post-depositional liquefaction. Some beds comprise a massive basal division overlain by hummocky cross-stratification (HCS) (Fig. 6A). Locally, the HCS is transitional to low-angle trough cross-stratification (cf. Nottvedt and Kreisa, 1987), in which the troughs are open to the north, indicating northward paleoflow. Ripple cross-lamination was not seen, but one bedding plane shows poorly preserved ripples. Disarticulated bivalve shells, seldom abraded, are dispersed throughout some beds (Fig. 6A); they also occur as a coquina up to 40 cm thick at the base of some beds (Fig. 6B), similar to the coquinas described by Kreisa (1981). In some coquinas the shells are all convex-up, while other coquinas comprise mixed convex-up and convex-down shells, with subordinate vertical shells (Fig. 6B). Rare articulated valves also occur, some with a mud fill (Fig. 6B). The bivalves are of late Miocene age according to Addicott (1978). Vertical *Ophiomorpha* burrows occur locally, similar to those at other Skonun Formation exposures described by Higgs (1989c). Also present are chevron structures, caused by collapse of vertical *Ophiomorpha* burrows (Frey et al., 1978), as well as possible bivalve escape shafts. Angular to rounded pebbles, cobbles, and boulders occur as isolated clasts "floating" in sandstone; they include sedimentary, volcanic and granitoid rock types (Fig.

6C; Sutherland Brown, 1968, Plate 10B). One mudstone clast carries a fossil claw, which was not recovered for fear of breakage (Fig. 6D).

The sandstone is well-indurated by calcite cement, possibly derived locally from the abundant bivalve shells. Subvertical sandstone dykes up to 1 cm wide, laminated parallel to their length, are locally visible; some can be traced downward into a "donor" bed. Calcite veins up to 2 mm thick are also common.

**Interpretation.** The environment was marine, as shown by the bivalves; this is consistent with the presence of *Ophiomorpha* (Frey et al., 1978). The floating clasts are interpreted as ice-rafted dropstones, deposited from icebergs or shore-connected floating ice. An alternative possibility, that the clasts are dropstones rafted in the roots of drifting trees, is rejected because: 1) a few of the inferred dropstones at the nearby western sea stack (see below) have possible facets, diagnostic of glacial transport; and 2) one of the inferred dropstones in the western sea stack is at least 5 m across. Probable dropstones have also been reported in the Skonun Formation at Collison Point and Miller Creek (Higgs, 1989c). At Collison Point, floating clasts are accompanied by dispersed wood fragments. The wood implies that the coast was at least partially ice-free, suggesting that the glaciers were tidewater valley glaciers rather than ice sheets. The dropstones were probably supplied by icebergs, rather than by shore-connected ice tongues, because at Miller Creek (Higgs, 1989c) and Yakoun River (below), dropstones occur in tidal-shelf sandstones but not in interbedded shallow-marine mudstones, suggesting that the ice was in

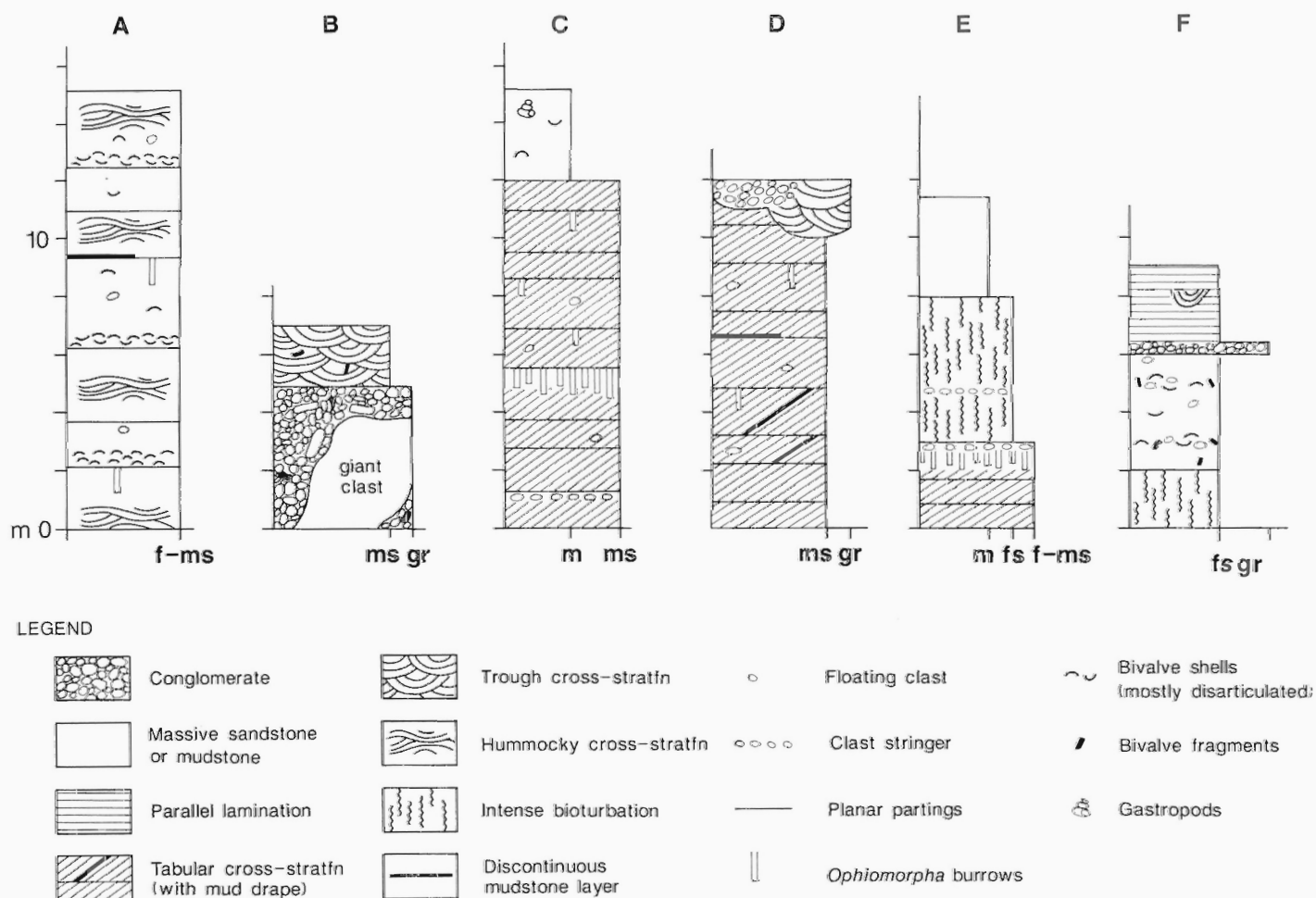
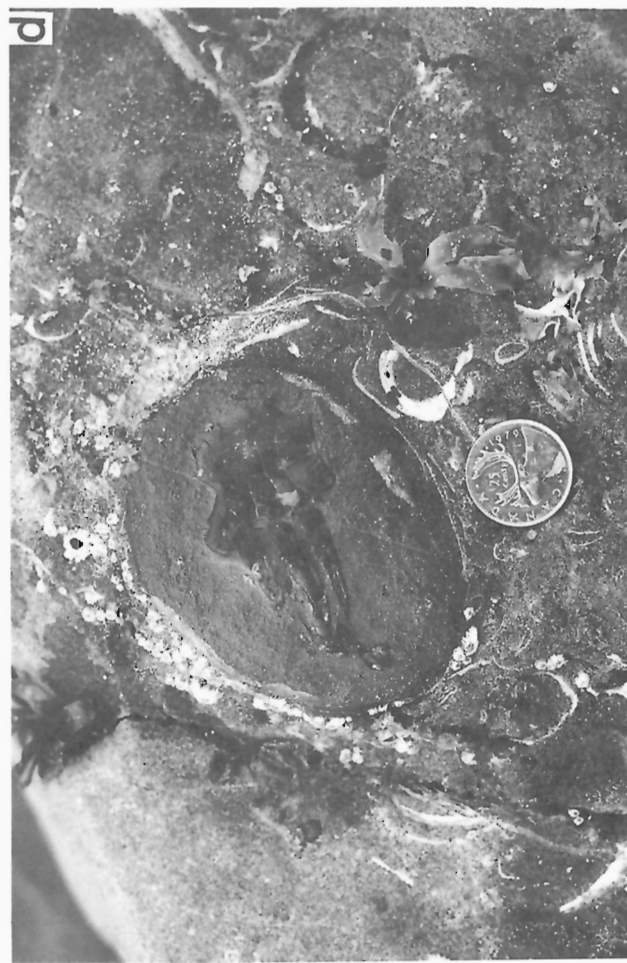
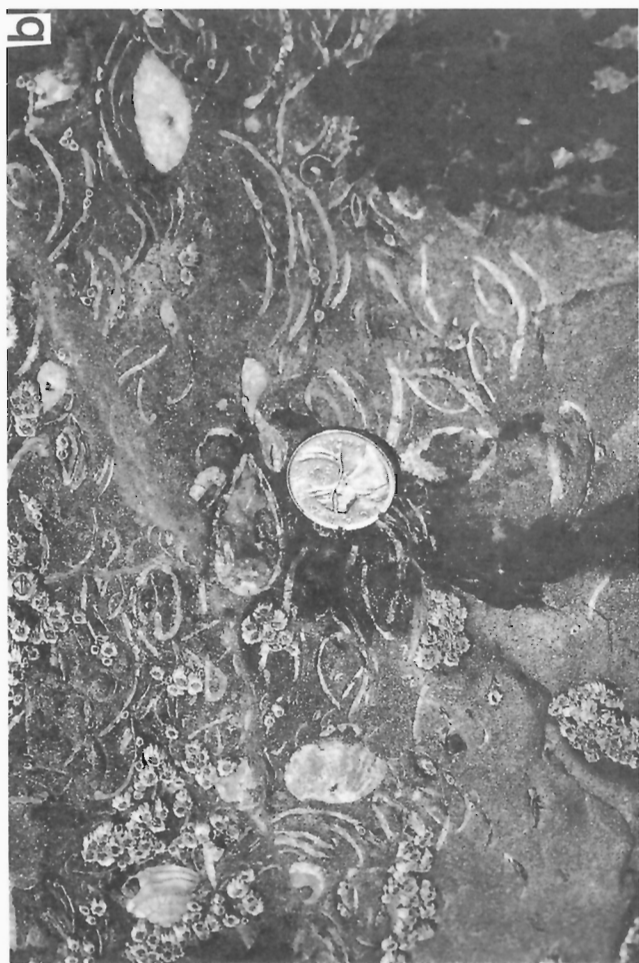


**Figure 5:** Graphic sedimentological logs of: **A** Skonun Point, eastern sea stack; **B** Skonun Point, western sea stack; **C** Yakoun River cliff at PQ 888375; **D** Yakoun River sand pit; **E** Yakoun River road cut at PQ881380; **F** Masset Sound bank at PQ898695. Key: **m** mud; **fs** fine sand; **ms** medium sand; **gr** gravel.





the form of icebergs entrained along tidal-current pathways. The dropstones imply an offshore environment, rather than an estuary or lagoon. The inferred icebergs may have been calving from glaciers of the ancestral (Miocene) mountains of Moresby Island, as discussed below, or from the mainland Coast Ranges (Higgs, 1989c).

The sandstone beds at the eastern stack are interpreted as shallow-marine storm beds, deposited under the influence of waves, as shown by the presence of HCS (Dott and Bourgeois, 1982). Each bed was rapidly deposited during a short-lived event, as indicated by sharp bed bases and by the possible bivalve escape shafts. Similar sequences of internal structures, involving basal coquinas overlain by a massive division and/or HCS, are well known in ancient (Kreisa, 1981; Dott and Bourgeois, 1982; Walker et al., 1983) and modern (Aigner and Reineck, 1982) storm beds. The transitional HCS/trough cross-stratification suggests that strong unidirectional currents supplemented the storm-wave oscillatory currents (Nottvedt and Kreisa, 1987); the supplementary current may have been tidal in this case, given the evidence for tidal currents at other Skonun Formation exposures (see below and Higgs, 1989c). Instances of faint, discontinuous lamination are suggestive of post-depositional disruption by liquefaction. This suggests that the massive appearance of some beds may be secondary. Liquefaction was possibly triggered by earthquakes, as inferred for the sandstone dykes (below). The coquinas are interpreted as winnowed lag deposits, consisting of burrowing bivalves exhumed from a layer (thickness unknown) of host sediment which was winnowed away by strong currents early in the storm, prior to sand-bed deposition. The host sediment in some cases was probably mud, as shown by those bivalves with a mud fill and by the presence of discontinuous mud layers. The winnowed bivalves underwent limited transportation, as shown by their unbroken, non-abraded state, and by the presence of articulated specimens. In coquinas whose constituent shells are all convex-up, the shells were probably thrown into suspension by storm currents, and then, after sinking concave-up (Allen, 1984), they were flipped over, upon striking the bed, by a one-way current whose velocity exceeded the "overturning threshold ... for settling particles" (Allen, 1984). In contrast, mixed convex-up and convex-down coquinas suggest one of three possibilities: (1) the current velocity exceeded the overturning threshold for some species but not for others; (2) the suspension contained a high concentration of sand, which was commonly trapped on the (concave) upper side of settling shells due to the separation vortex above each shell (Allen, 1984), thereby causing the effective mass (hence, overturning threshold) of settling shells to increase (Allen, 1984); or (3) the shell suspension was so dense that interference effects prevented some shells from overturning, an explanation that is consistent with the presence of vertical valves.

Hence, the strata of the eastern sea stack are interpreted as amalgamated storm beds, deposited on a storm-dominated shallow sea floor. The sandstone dykes suggest that the strata underwent early lithification, and were then intruded by sand injected from an underlying donor bed, liquefied possibly by an earthquake.

## Western sea stack

**Description.** About 150 m farther west along the sand beach is another sea stack, exposing about 5 m of clast-supported conglomerate overlain by 2 m of pebbly sandstone (Fig. 5B). These strata are probably of late Miocene age, because they are along strike from, and of similar attitude to, the (late Miocene) strata of the eastern stack. The conglomerate is extremely poorly sorted: clasts range in size from granules to boulders. The conglomerate grades laterally at one place into a patch of trough cross-stratified pebbly sandstone. Clast roundness is highly variable, from subangular to well rounded. A few rounded clasts are truncated by flat faces, possibly representing glacial facets. Lithology is also very variable, including volcanic, plutonic, metamorphic and sedimentary rock types. Sedimentary clasts include subangular boulders of massive shelly sandstone, and of hummocky(?) cross-stratified sandstone, similar to lithologies exposed at the eastern sea stack. A body of fine sandstone at least 5 m across dominates the western sea stack and extends below beach level. This sandstone body is interpreted as a giant clast, because subvertical contacts with the enveloping conglomerate can be seen on its north, east and south flanks. (However, on the south and east flanks, the conglomerate envelope has been reduced to a patchy veneer by ongoing erosion.) In an alternative interpretation, Sutherland Brown (1968, p. 122) viewed the sandstone body as *in situ* sandstone "irregularly cut and filled by and intercalated with ... conglomerate". The inferred megaclast is lithologically similar to the massive sandstone of the eastern sea stack. Gravel-size fragments of thick-shelled bivalves comprise about 5% of the conglomerate. The conglomerate matrix is medium to coarse sand.

The overlying pebbly sandstone is trough cross-stratified, in sets 20–40 cm thick. Foreset attitudes indicate paleoflow to the north-west. The sandstone is medium grained and contains about 5% gravel-size fragments of thick-shelled bivalves.

**Interpretation.** Both the conglomerate and the overlying pebbly sandstone are probably marine, based on the shell fragments. The conglomerate is thought to be an accumulation of dropstones, rather than a mass-flow deposit, based on: (1) the possible faceted clasts; (2) the extreme diversity of clast size, roundness and composition; and (3) the presence of probable dropstones at other Skonun Formation localities, occurring both as dispersed clasts in sandstone and as clast accumulations (see above and below, and Higgs, 1989c). The conglomerate is not a dropstone *lag* deposit, left behind by winnowing of an enclosing sediment layer (sand or mud), because winnowing would produce only a one-clast-thick surface layer, sufficient to "armour" the bed against further erosion. Instead, the conglomerate is thought to be a condensation layer, formed by slow accumulation of dropstones under a high ambient current velocity, such that sand and mud were swept past, except for sand and shell fragments entrapped in the "current shadow" behind individual dropstones on the sea floor. The ambient current was probably tidal, rather than wind- or wave-induced, based on the abundant evidence for tidal-shelf deposition at other Skonun Formation exposures (see below and Higgs, 1989c). The patch of cross-stratification within the conglomerate may have been formed

**Figure 6:** Sandstone facies at Skonun Point, eastern sea stack. Hammer 30 cm long; coin 24 mm across. **A** Two amalgamated sandstone beds, each consisting of a basal, massive shelly interval passing up into hummocky cross-stratification. Note that the shells are disarticulated, unbroken, and almost invariably convex-up. Beach sand at top left and bottom. **B** Coquina of bivalve shells at base of a sandstone bed. Stratigraphic top is up. Shells are mostly disarticulated, and are oriented convex-up, convex-down, or vertical. A few shells are articulated; the one at top right has a calcite cement fill; the one at centre has a mud fill (see text). **C** Bedding-plane view of a sandstone bed containing a "floating" boulder of granitoid rock. The sandstone bed, which is dipping to the left (north), has a basal coquina (visible at top, bottom and right) overlain by faint hummocky cross-stratification (visible below boulder). **D** Sandstone bed containing a floating 10 cm mudstone clast bearing a fossil claw. Bedding plane view. The sandstone is massive and contains sparse, disarticulated bivalve shells. Circular structure on right-hand side is a modern limpet attachment mark.



by tidal bedforms in a sandy depression on an otherwise gravelly sea floor. The bivalve detritus underwent considerable transportation, as shown by the degree of fragmentation. The thick-walled nature of the shells suggests that the bivalves were epifaunal, inhabiting a high-energy environment; they may have been attached to nearby boulders or rock outcrops, comparable to bivalves in the modern English Channel and Scottish shelf, in areas of strongest tidal current (Wilson, 1982).

With regard to the source area of the inferred dropstones, many of the clasts lithologically resemble bedrock units of the Queen Charlotte Islands, particularly the sandstone clasts (including the megaclast), which are thought to be intraformational Skonun Formation material. This implies contemporaneous uplift of a former "Skonun-depositing" area, to form mountains in which uplifted Skonun material was eroded and entrained by glaciers. Hence, the mainland Coast Mountains are excluded as a possible source: they appear to have existed throughout the Eocene to Recent span of the QCB (Parrish, 1983) and would therefore never have been the site of Skonun deposition. Instead, it is proposed that a mountainous, proto-Queen Charlotte Islands landmass lay to the west. These mountains must have existed by late Miocene time if they were the source of the dropstones in the (upper Miocene) strata of the western sea stack. Hence, it is argued (see "Discussion" below) that proto-Moresby Island was uplifted at about 20 Ma, due to a change in relative motion of the Pacific plate which initiated oblique subduction at the previously transform Queen Charlotte margin. In addition to the proto-Moresby mountains, some of the dropstones may have been derived from the mainland Coast Mountains (Higgs, 1989c). Indeed, Sutherland Brown (1968, p. 124) noted that while most of the "coarse clasts" in the Skonun Formation "can or must have been derived from the Queen Charlotte Islands", the metamorphic clasts "must have originated from the mainland or southeastern Alaska".

The cross-stratified pebbly sandstone capping the western sea stack is thought to reflect gravelly bedforms migrating under a strong tidal current in a shallow-marine setting (cf. Belderson et al., 1982).

#### *Intertidal beach*

**Description.** On the beach to the east of the sea stacks is an intermittently exposed succession estimated to be 98 m thick by Sutherland Brown (1968). Unfortunately, the stratigraphic relationship between these south-dipping beds and the (north-dipping) strata of the sea stacks is unknown, because the contact is covered by beach sand. The facies are entirely different. Forming resistant ribs in the beach are lignite beds ranging from 5 cm to 1 m thick. Up to ten lignite ribs are present, separated by covered intervals up to a few metres thick. Individual ribs can be traced laterally for at least 50 m. Tree stumps are discernible in the lignite beds, as well as fallen tree trunks at least 1 m long and 30 cm wide. Intermittently exposed between the lignite ribs, largely covered by beach sand, is semi-consolidated mudstone. Where the base of a lignite bed is visible, the contact with the underlying mudstone is sharp, and vertical to subhorizontal roots are locally visible, extending downward into the mudstone for up to 1 m (Fig. 7A). The mudstone is generally massive, but locally shows traces of disturbed (by rooting?), millimetre-scale lamination. The mudstone is mostly grey to brown; some exposures show colour mottling, with various shades of grey, brown and pink. Some mottled intervals contain irregular, centimetre-size patches of muddy sand with diffuse boundaries and a different colour from the enclosing mudstone. Strings of lensoidal calcareous concretions occur in the mudstone, forming resistant ribs. Concretions are individually up to 60 cm thick and 3 m across; they are connected laterally to one another in some cases, and are disconnected in others. The most southerly (i.e. shoreward) rib is a layer of fine to medium sandstone 1 m thick, comprising a single planar-tabular cross-set in which the foresets dip approximately north.

Tracing the rib laterally to the east and west, it thins to about 30 cm, and the cross-stratification passes into ripple cross-lamination.

**Interpretation.** The presence of roots demonstrates that the vegetation comprising the lignite beds grew *in situ*. The rooted, colour-mottled mudstones are interpreted as paleosols (Collinson, 1986). The association of paleosols and *in situ* coal suggests an overbank setting on a fluvial or deltaic plain. The single rib of sandstone is interpreted as a fluvial or distributary channel: the large-scale cross-set represents a downstream-migrating sand bar in the channel proper, while the flanking cross-lamination represents the channel levees.

### **Yakan Point**

#### *Description*

The main section at Yakan Point has been described and interpreted by Higgs (1989c). Molluscs and an echinoid at this locality indicate a late Miocene age (Addicott, 1978). Tidal sedimentary structures at this section include herringbone cross-stratification, first reported by McWhae (1986). These are probably the first tidal deposits reported from the Tertiary in Canada, south of latitude 60°N. An additional exposure at UK147948 near high-water mark on the eastern side of the point, separated from the main section by a zone of no exposure, reveals about 1 m of subhorizontally bedded fine sandstone. The sandstone consists of alternating units, up to 10 cm thick, of ripple cross-laminated sandstone and parallel-laminated carbonaceous sandstone (Fig. 7B). Each of the cross-laminated units comprises several sets of erosional-stoss, tabular cross-lamination with north-dipping foresets. Asymmetrical, north-facing ripples are exposed on the upper surfaces of the cross-laminated units; ripple crests strike N85°E in one case. The intervening parallel-laminated units comprise millimetre-thick alternating quartzose laminae and carbonaceous laminae; the latter consist of sand-size plant detritus. About 20-30 quartzose laminae occur in each unit, although counts are unreliable because the lamination is commonly faint.

#### *Interpretation*

The laminated sandstone at UK147948 is interpreted as a "tidal rhythmite" (Reineck and Singh, 1980), based on: (1) regularly alternating units; (2) regularly alternating laminae; and (3) approximately consistent number of laminae in each laminated unit. Evidence for emergence or wave action is lacking, suggesting deposition below wave base. Each cross-laminated unit may represent a single (peak) spring tide, either ebb or flood, while the succeeding plane-laminated unit represents the remainder of the (two-week) spring-neap cycle. The implication is that the carbonaceous laminae represent material which settled from suspension during slack-water episodes, whereas quartzose laminae represent traction deposition during the ebb and/or flood. The fact that 20-30 quartzose laminae occur in each (inferred two-week) cycle is consistent with either: (1) deposition of one quartzose lamina during every flood and every ebb, in a diurnal tidal regime ("ideal" total of 28 quartzose laminae); or (2) deposition of one quartzose lamina during every flood or every ebb (but not both) in a regime which was semi-diurnal and in which only the ebb or flood was strong enough to transport sand. The consistent orientation of ripple crests suggests a consistently oriented (flood- or ebb-) current. Tidal rhythmites have been described by Reineck and Singh (1980),

**Figure 7:** Hammer 30 cm long. **A** Seaweed-covered lignite rib (top), with two roots penetrating downward into underlying recessive mudstone (one root at each end of hammer). Intertidal beach at Skonun Point. **B** Tidal rhythmite facies at Yakan Point. See text for explanation. Right way up.



but in their examples the sand is interlaminated with mud rather than carbonaceous litter.

## Tow Hill

### Description

Immediately beneath the sill which forms Tow Hill (Sutherland Brown, 1968), an interval of mudstone 1.5 m thick is exposed, at UK171955. The contact between the sill and the mudstone is sharp, and the base of the mudstone is covered by beach shingle. The mudstone shows millimetre-scale lamination, which is variably disturbed by burrowing, producing a mottled texture. The uppermost 10 cm of the mudstone, adjacent to the sill, is better indurated than the rest, possibly due to baking (Sutherland Brown, 1968).

Thirty metres along the beach to the southwest, a second sill protrudes above the beach gravel, forming a rib 40 cm thick. Beneath this sill 75 cm of mudstone is exposed. The mudstone is similar to that beneath the main sill, except that the basal 30 cm is contorted.

### Interpretation

The presence of burrows suggests a subaqueous depositional environment, but the data are insufficient to judge whether the water was fresh or marine. The contorted mudstone may be a slump deposit, or may have been disturbed *in situ*, possibly by an earthquake. A slump interpretation is consistent with the interpretation (see discussion below) that Unit I was deposited in high-gradient environments (alluvial fans and fan deltas) during active tectonism.

## Miller Creek

The exposure at Miller Creek was discussed by Higgs (1989c).

## Cinola

At the Cinola gold property, disseminated microscopic gold occurs in silicified Skonun Formation deposits (Champigny and Sinclair, 1982). Exposure of the Skonun Formation in 1987 comprised an adit, a small quarry for extraction of road material, and several kilometres of diamond drill core taken from numerous shallow boreholes (up to 300 m deep; see Champigny and Sinclair, 1982). The Skonun strata at Cinola are dominated by conglomerate, and are dated as early Miocene based on palynomorphs, bivalves and K-Ar ages of a rhyolite intrusion (Champigny et al., 1981).

### Core

**Description.** Much of the core material is unsuitable for sedimentological description because extensive alteration (Champigny and Sinclair, 1982) has obliterated sedimentary structures. One of the least altered cores was examined in detail (Corehole 84-1; Fig. 8). The dominant facies is clast-supported conglomerate in beds up to 7 m thick. Clasts include felsic and mafic volcanics, granite, and sedimentary rock types (Champigny and Sinclair, 1982). Neither grading nor imbrication is conspicuous. Subordinate matrix-supported conglomerate beds also occur; the matrix consists of mud in some cases and sand in others. In addition to conglomerates, there are sharp-based beds of massive sandstone up to 1 m thick, some of which are

## CINOLA COREHOLE 84-1

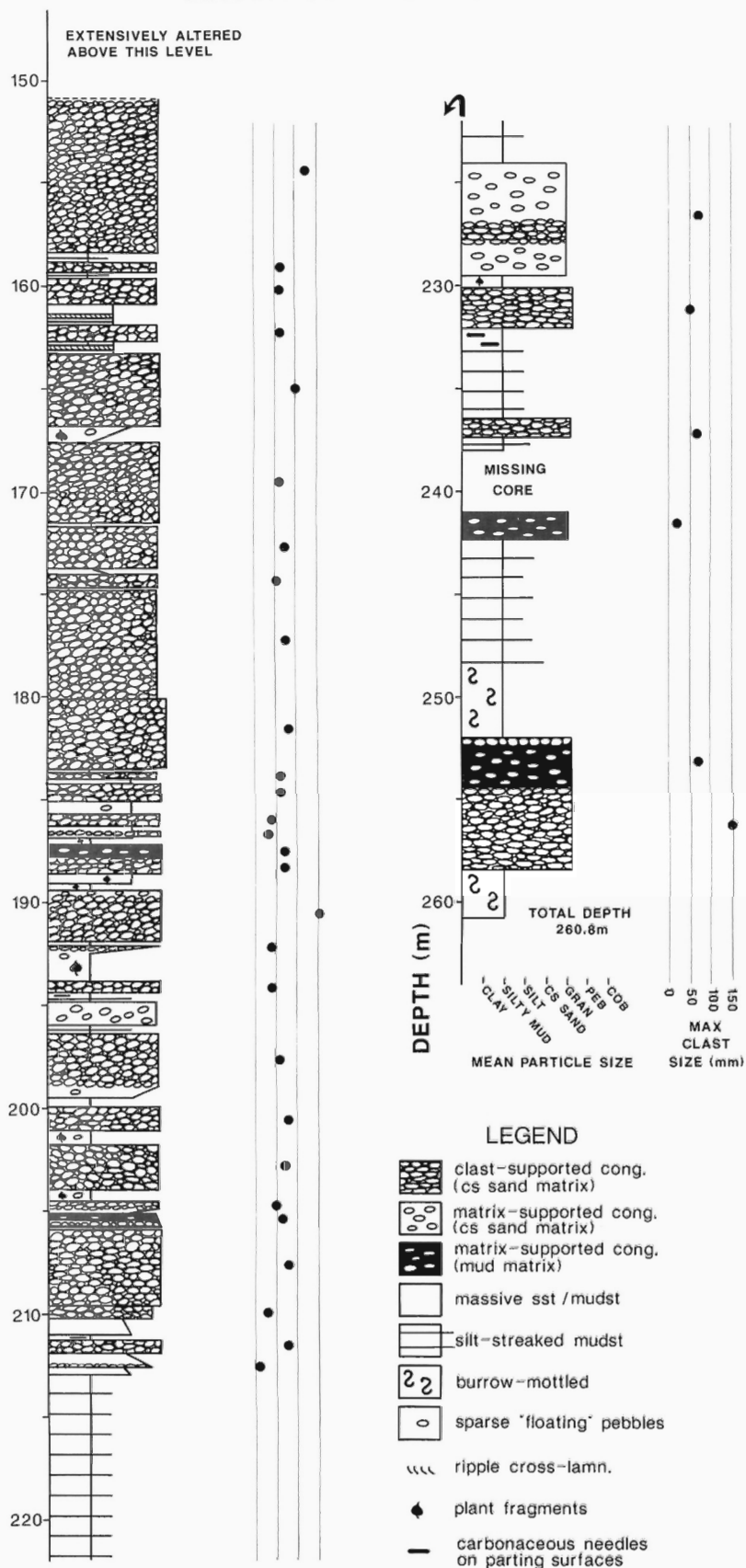


Figure 8: Graphic sedimentological log of Cinola Corehole 84-1.

graded. Interbedded with the conglomerates and sandstones are mudstone intervals up to 11 m thick; these range from mudstone in which silt streaks define a millimetre-scale lamination, to thoroughly bioturbated mudstone with a mottled appearance.

**Interpretation.** The conglomerate beds are interpreted as mass-flow deposits, based on their sharp upper and lower contacts, and their lack of stratification. Deposition in or beside a high-gradient terrain is implied, to enable gravel transportation. The clast-supported conglomerates were probably deposited by high-density turbidity currents or by cohesionless debris flows (Lowe, 1982; Nemec and Steel, 1984), while the mud-supported conglomerates were deposited by cohesive debris flows. The sandstone beds are interpreted as turbidites. Thus, the conglomerate and sandstone beds represent catastrophic depositional "events", possibly floods, while the mudstone represents normal "background" deposition. The depositional environment was probably subaqueous, since there is no evidence for emergence, such as coal, paleosols, roots or desiccation cracks. A subaqueous environment is consistent with the presence of burrows in the mudstone. The water was probably marine because marine bivalves were collected from a trench at Cinola by Champigny et al. (1981); the author also found bivalves in a Cinola quarry (below). Wave-formed sedimentary structures are absent, suggesting deposition in relatively deep water, below storm wave base. There are two possible depositional environments for submarine mass-flow gravels: (1) a deep-water subaqueous valley, such as a submarine canyon or fan valley; and (2) an unchanneled fan-delta slope extending from shallow water into deep water ("deep-water fan delta" of Higgs, 1990). The fan-delta interpretation is the more likely in this case, based on the association with "beach to nearshore marine" bivalves (Champigny et al., 1981, p. 1902).

#### Quarry

**Description.** The quarry face was inaccessible due to active quarrying at the time of the author's visit. However, loose quarried blocks up to 2 m across were examined at the quarry mouth. The dominant lithology was silicified, matrix-supported conglomerate, referred to informally as the "Upper Debris Flow" by personnel of City Resources (Canada) Limited, the minesite operator. This unit has also been recognized in core at Cinola and is 20-25 m thick (R. Tolbert, pers. comm., 1987). The conglomerate matrix is unstratified and consists of poorly sorted, muddy, very fine sand. Clasts include volcanic, plutonic and sedimentary rock types, ranging from angular to rounded, and from granule to cobble grade. Another quarried block, about 1 m across, consisted of massive very fine sandstone containing a 5 cm layer of coquina, comprising whole bivalve shells, including some articulated specimens. Yet another block, about 50 cm across, was composed of cross-stratified very fine sandstone.

**Interpretation.** The "Upper Debris Flow" is interpreted as the deposit of a cohesive debris flow, based on its massive texture, poor sorting and muddy matrix (Middleton and Hampton, 1976). The association of this mass-flow conglomerate with bivalves is consistent with deposition on a deep-water fan delta, as inferred above for the Cinola core.

#### Adit

**Description.** An adit, driven into the hillside for assay tests, enabled the author to view the Skonun Formation underground. In 1987, the adit comprised a main drift about 400 m long, and a crosscut of similar length. The dominant exposed facies were conglomerate and mudstone. A matrix-supported conglomerate unit about 25 m thick is informally termed the "Lower Debris Flow" by City Resources staff. This unit stratigraphically underlies the "Upper Debris Flow" (R. Tolbert, pers. comm., 1987). The matrix is structureless mudstone, and more than 90% of the clasts are light-grey rhyolite. Most clasts are

angular, but some are rounded. Clasts are poorly sorted, and seldom exceed 20 cm in diameter; however, one megaclast composed of conglomerate is more than 2 m long, and another of volcanic breccia is at least 1 m long. One 20 cm bed of graded, clast-supported conglomerate appears to occupy a channel, although only one channel wall was exposed, inclined at about 45° to bedding. The graded conglomerate is underlain by mottled mudstone, and overlain by mottled mudstone containing subvertical roots. Exposed in the adit roof was a carbonized tree trunk at least 40 cm across and 2 m long, oriented parallel to bedding.

**Interpretation.** The "Lower Debris Flow" is interpreted as the deposit of a cohesive debris flow, based on the massive muddy matrix, lack of grading and poor sorting. The rooted, mottled mudstone is interpreted as a paleosol, implying that part of the adit succession was deposited in a subaerial environment. The association of paleosols and debris-flow conglomerates suggests deposition on an alluvial fan. The graded conglomerate bed, in view of the grading, channeling and inferred subaerial setting, is interpreted as the deposit of a turbulent, fluvial sediment flow (Nemec and Steel, 1984).

An alluvial-fan interpretation is consistent with the fan-delta-slope environment proposed above for the core and quarry strata. Hence, the overall depositional system inferred for Cinola is a fan delta, comprising an alluvial fan building directly into deep water (cf. Higgs, 1990).

#### Yakoun River

Several Skonun Formation exposures occur in cliffs along the Yakoun River and in a nearby sand pit and roadcuts. Horizontal or near-horizontal strata occur in three cliff exposures along a 1.5 km stretch of the river.

#### Cliff at PQ888375

**Description.** The bare cliff is about 150 m long and exposes about 12 m of tabular-crossbedded medium sandstone overlain by about 3 m of pale grey, massive mudstone containing whole, disarticulated bivalves and gastropods (Fig. 5C). Sandstone cross-sets are 30-100 cm thick, and foresets dip north. Only in one set was the true (three-dimensional) attitude of the foresets visible, yielding a dip direction of 335°. The top few decimetres of each set contain vertical *Ophiomorpha* burrows, sufficiently crowded in some cases to obliterate the cross-stratification. Dispersed within the sets are "floating" pebbles up to 3 cm across. (The same crossbedded facies with *Ophiomorpha* burrows and floating clasts is exposed at Collision Point (see below and Higgs, 1989c)). About 1 m above river level, the sandstone contains a layer of angular to rounded pebbles and cobbles, one clast thick; a few clasts are in contact with their neighbours. One angular volcanic clast is 50 cm long.

The mudstone is inaccessible at the cliff top, but talus at the base of the cliff can be examined. Molluscs recovered from the talus are upper Miocene (L. Marincovich, Jr., pers. comm., 1989; Higgs et al., in prep.), and include the bivalve *Acila empirensis*, which has not previously been described from the Skonun Formation.

**Interpretation.** The presence of *Ophiomorpha* suggests that a marine environment is most likely for the sandstone (Frey et al., 1978). Similarly, the mudstone mollusc fauna is marine, and indicates an inner or middle shelf setting (L. Marincovich, Jr., pers. comm., 1989). The floating clasts are interpreted as ice-rafted dropstones, while the discrete layer of clasts is interpreted as either a dropstone condensation layer or a winnowed lag (see Skonun Point above). The presence of dropstones supports the mollusc evidence for an offshore shelf environment, rather than an estuary or lagoon. The cross-stratification was produced by bedforms migrating across the sea floor under the influence of a strong current. The current was probably tidal, based



on the evidence for tidal currents at other Skonun Formation exposures (especially Yakan Point above and Yakoun sand pit below). The thickness and tabular geometry of the cross-sets suggest that the parent bedforms were straight-crested sandwaves (*sensu* Collinson and Thompson, 1982) up to at least 1 m high. The consistent northward dip of the foresets indicates that the dominant tidal flow (ebb or flood) at this locality was northward (see discussion below). The apparent lack of clay laminae draping the foresets (cf. Visser, 1980) suggests that slack water never occurred, presumably due to a supplementary (wind-driven?) current.

The upward transition from shallow-marine sandstone into shallow-marine mudstone presumably reflects a sudden decrease of tidal current velocity, possibly due to a tectonically or glacially induced change in basin configuration, causing tidal currents to diminish, or tidal flow paths to shift laterally. The absence of dropstones in the mudstone suggests that icebergs were kept away, possibly by entrainment in tidal-current pathways. Nevertheless, glaciers may have continued to influence deposition: the lack of structure in the mudstone is typical of glaciomarine muds (e.g. Eyles and Miall, 1984), and may reflect continuous rainout from sediment-rich overflows fed by glacial meltwater.

#### Cliff at PQ894374

**Description.** The cliff exposes about 2 m of apparently massive (burrowed?) sandstone, overlain by about 2 m of tabular-cross-stratified sandstone. The two units are separated by a string, one clast thick, of pebbles and cobbles. The crossbedded sandstone comprises two sets, each about 1 m thick, with opposed foreset dips (southward in the lower set and northward in the upper set), forming a herringbone pattern.

**Interpretation.** The herringbone cross-stratification is strongly suggestive of tidal currents, and the pebble-cobble layer may represent dropstones (see above). The inferred depositional environment is a glacially influenced tidal shelf, as for the previous cliff exposure.

#### Cliff at PQ898365

**Description.** The cliff consists of about 30 m of tabular-cross-stratified sandstone, massive sandstone and massive mudstone, interbedded in units 2–5 m thick (Fig. 9). Individual cross-sets are up to about 1 m thick, and all foresets dip northward. The massive sandstone interval contains a bedding-parallel stringer of pebbles and/or cobbles (Fig. 9).

**Interpretation.** The facies resemble those at other Skonun Formation exposures and are likewise interpreted in terms of a glacially influenced, tide-dominated shallow-marine environment (see above and Higgs, 1989c).

#### Sand pit

A sand pit at PQ882380, about 600 m west of the Yakoun River, exposes friable Skonun Formation sandstone extracted to pave logging roads. About 10 m of subhorizontal, tabular-cross-stratified sandstone are exposed (Figs. 5D, 10). This is capped by 1–3 m of gravel and cross-stratified pebbly sand, with an irregular, compound-channelled base with up to 2 m of relief and with locally subvertical channel walls (Figs. 5D, 10). No fossils were found in the sand-pit deposits, so their age is unknown. However, the gravelly capping is tentatively interpreted as Quaternary fluvio-glacial outwash (see above). The underlying sandstone is very similar to late Miocene facies which occur less than 1 km away along the Yakoun River (PQ888375; see above), in strata which are likewise subhorizontal; hence, the quarry sediments are probably also upper Miocene.

**Description.** The cross-stratified sandstone is fine to medium grained, and contains sparse, floating pebbles up to 3.5 cm across. Sets are essentially tabular and are 30–150 cm thick. Set boundaries are planar, but successive pairs of set boundaries are commonly not quite par-

allel, diverging by up to 20° (Fig. 10). The foresets in every cross-set dip northward. Foresets are arranged such that groups of concave foresets (with contiguous bottomsets) alternate, on a decimetre scale, with groups of planar foresets (Fig. 11). Bottomsets are moderately to strongly burrowed in places, forming burrowed intervals 5–15 cm thick (Fig. 12A). The burrows are 1–2 mm in diameter, vertical to horizontal, and include a branching ichnogenus (*Chondrites?*) and possible U-tubes. Foresets contain sparse *Ophiomorpha* burrows, measuring 1–3 cm in diameter and up to 50 cm long, which descend vertically from upper set boundaries.

Locally, two sets are separated by a thin (1–2 cm) layer of massive, pale grey mudstone. There are also rare mud drapes within cross-sets, intercalated in the foreset lamination (Fig. 12B). The mud drapes occur as doublets enclosing a millimetre-thick sand lamina; the thickness of this “sandwich” is up to 3.5 cm.

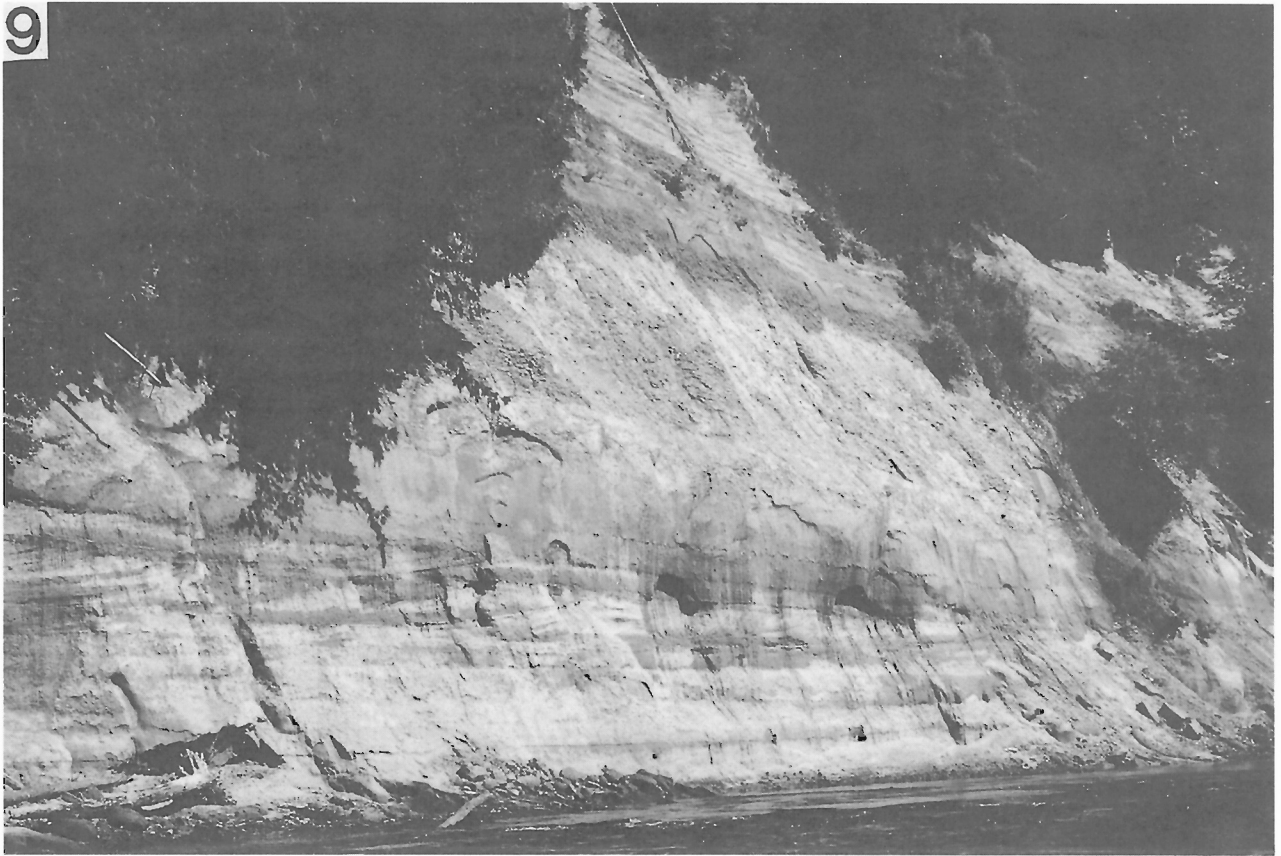
In some cross-sets, a bundle of foresets is deformed into decimetre-scale folds (Figs. 11, 12B,C). The deformed bundle is up to about 1 m thick, measured perpendicular to the foresets. The bundle is bounded laterally by undeformed foresets, and is either truncated at the top by the overlying cross-set (Fig. 11) or else the deformation affects the overlying set as well (Fig. 12C). The folds consist of sharp anticlines separated by broad, rounded synclines (Fig. 11); it is not known how far the anticlines extend in the third dimension, or indeed if they are domal. Anticlines become sharper upward within a deformed bundle, culminating in a diapir-like fold. Anticline axes are vertical, and the axial zone is commonly a structureless pillar a few centimetres across (Fig. 12C). In one folded foreset bundle, the foresets are offset by a downward verging thrust (Fig. 12C).

**Interpretation.** The floating clasts are interpreted, like those at other Skonun Formation localities, as iceberg dropstones, implying an offshore environment. The double mud drapes are proof of a subaqueous tidal environment (Visser, 1980), lending support to the tidal interpretation already inferred for similar facies at other Skonun Formation exposures (above). The cross-sets were produced by migration of relatively straight-crested sandwaves up to at least 1.5 m high, as shown by the relatively tabular set geometry and by the thickness of sets: in the terminology of Allen (1980), the bedforms were Class IIIB sand waves. The double mud drapes represent deposition between two dominant tides, with the mud laminae reflecting slack water and the intervening sand lamina the subordinate tide (Visser, 1980). The scarcity of mud drapes (cf. Visser, 1980) suggests that slack water seldom occurred, presumably due to a supplementary (wind-driven?) current. The alternating groups of concave and planar foresets lend further support to a subaqueous tidal environment. Similar groupings in Belgian Eocene deposits were interpreted as neap-spring cycles by Houthuys and Gullentops (1988). If this interpretation is correct, the horizontal spacing between two consecutive concave groups (or two planar groups), generally in the order of 50 cm, represents the distance that the bedform advanced in two weeks (spring-neap-spring). According to Houthuys and Gullentops (1988), the concave groups were deposited around neap tide. However, con-

**Figure 9:** Yakoun River cliff at PQ898365, comprising massive sandstone, massive mudstone, and cross-stratified sandstone. Height of section in this view is about 15 m. Two superimposed tabular cross-sets are visible at bottom left, immediately below the foliage. Foresets dip to the left (north) in both cases. Traced toward the right, the upper set becomes massive.

**Figure 10:** Sand pit near Yakoun River, showing tabular cross-stratified sandstone. Paleoflow to left (north). Note that the sandstone is incised by an irregular, composite scour, which is overlain by gravel and pebbly sand of probable glacial-outwash origin (see text).

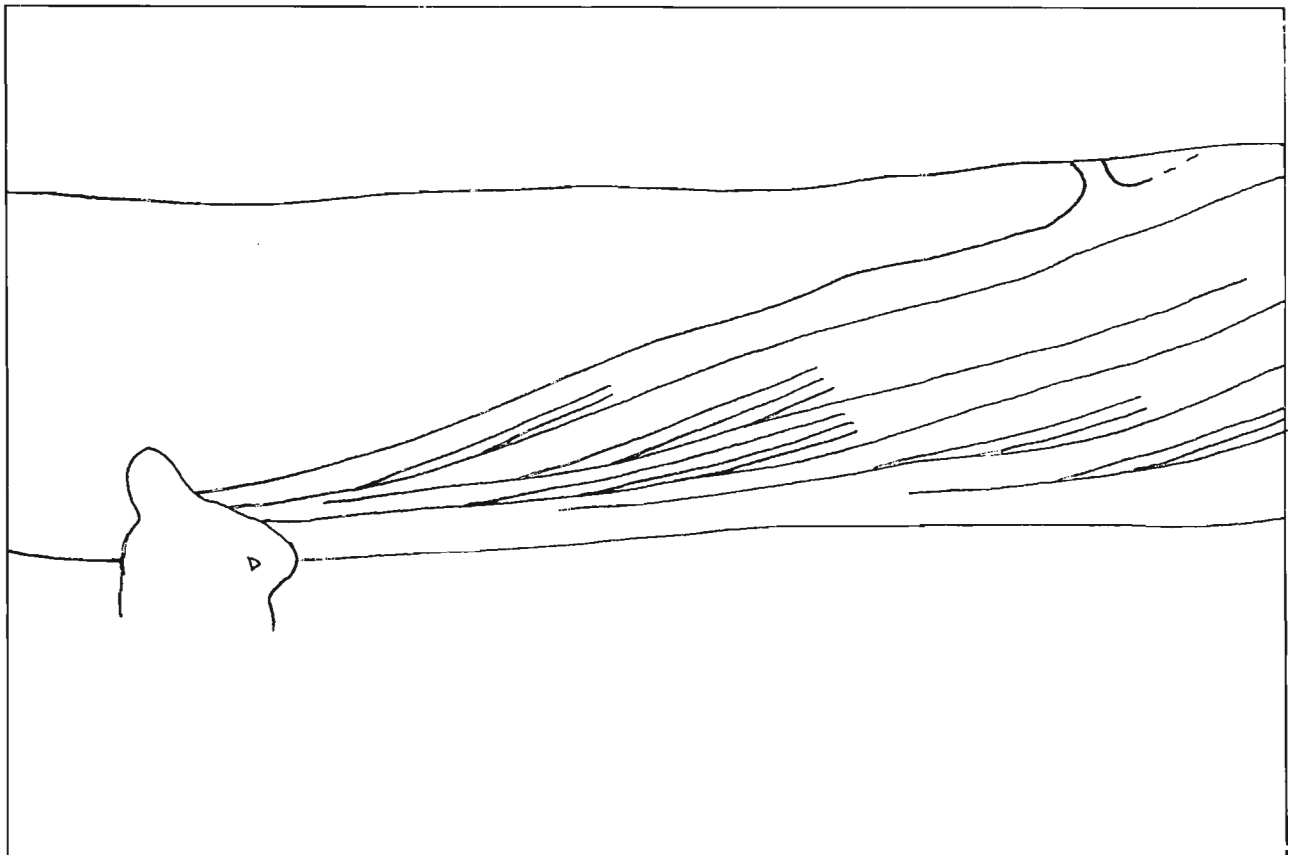
9



10







cave foresets (and their contiguous bottomsets) usually reflect stronger currents than angular foresets (Jopling, 1965), hence the concave groups may instead represent *spring* tide; during the ensuing neap phase, the bottomsets were non-depositional and underwent burrowing.

The *Ophiomorpha* burrows reflect burrowing on the stoss sides of the sandwaves. The observed sparse burrow density may not reflect the actual population density because stoss sides may have been deeply eroded by current-scour ahead of the next (advancing) sandwave.

The cross-strata are of fair-weather, not storm-tidal origin (cf. Anderton, 1976), based on the presence of mud drapes and neap-spring foreset groups. Where a 1-2 cm mud layer separates two sets, this may reflect a temporary decrease in the tidal current velocity, perhaps due to a temporary diversion of the tidal current flow path.

The folded foreset bundles are thought to reflect dewatering, the anticlines forming by upward expulsion of pore water along discrete channels corresponding to anticline axes; this would explain why axes are vertical and why the axial sediment is commonly structureless. Individual anticlines sharpen upward because positions progressively higher up the axis are flushed by increasing amounts of escaping water. The inferred dewatering implies that the deformed bundle underwent liquefaction, possibly triggered by an earthquake. Liquefaction was contemporaneous with deposition, and took place at or near the sea floor, as shown by one set in which the deformed bundle is truncated by the overlying (undeformed) cross-set (Fig. 11). The fact that fold axes are vertical rather than inclined implies that dewatering was not accompanied by downslope sliding of the deforming bundle. In the one definite instance where such sliding took place, deformation was accommodated by thrusting (Fig. 12C).

#### Roadcuts

**Description.** Several roadcuts occur along logging roads within 1 km of the quarry, exposing Skonun Formation strata. At PQ 880383, a roadcut about 100 m long exposes horizontal strata, dominated by a 4-5 m unit of massive, pale grey mudstone. There is also an interval of millimetre-scale interlaminated mudstone and very fine sandstone, containing vertical, sand-filled *Ophiomorpha* burrows. Another roadcut at PQ881380, some 300 m further south and about 100 m west of the quarry, exposes what is possibly the same 4-5 m massive mudstone unit, underlain by about 5 m of fine sandstone which is thoroughly bioturbated by *Ophiomorpha* and therefore has a mud matrix (cf. Higgs, 1989c; Fig. 5E). Beneath the muddy sandstone is about 3 m of tabular cross-stratified, fine to medium sandstone, with foresets dipping approximately northward. The top few decimetres of the upper cross-set contain closely spaced, vertical *Ophiomorpha* burrows up to 1 cm in diameter; burrow density decreases downward due to “fallout” of the shallower burrows. A stringer of disconnected pebbles, one clast thick, follows the upper contact of the crossbedded sandstone, and another occurs within the overlying muddy sandstone unit. The clasts include an angular volcanic clast about 15 cm across, and an angular granitoid clast about 8 cm across.

**Interpretation.** All except the interlaminated sand-mud facies have been described and interpreted at other Skonun Formation localities (see above and Higgs, 1989c), and are indicative of a shallow, glacially-influenced, tidal sea floor. The interlaminated sand-mud facies may reflect either daily tidal-current fluctuations, or seasonal fluctuations in the velocity (hence competence) of meltwater plumes.

**Figure 11A,B:** Photograph and corresponding line drawing of three tabular cross-sets at Yakoun River sand pit. The central cross-set shows alternating groups of concave and planar foresets, highlighted in the line diagram. The central set also shows vertical, diapir-like anticlines formed by dewatering, and truncated by the overlying set boundary (e.g. top right).

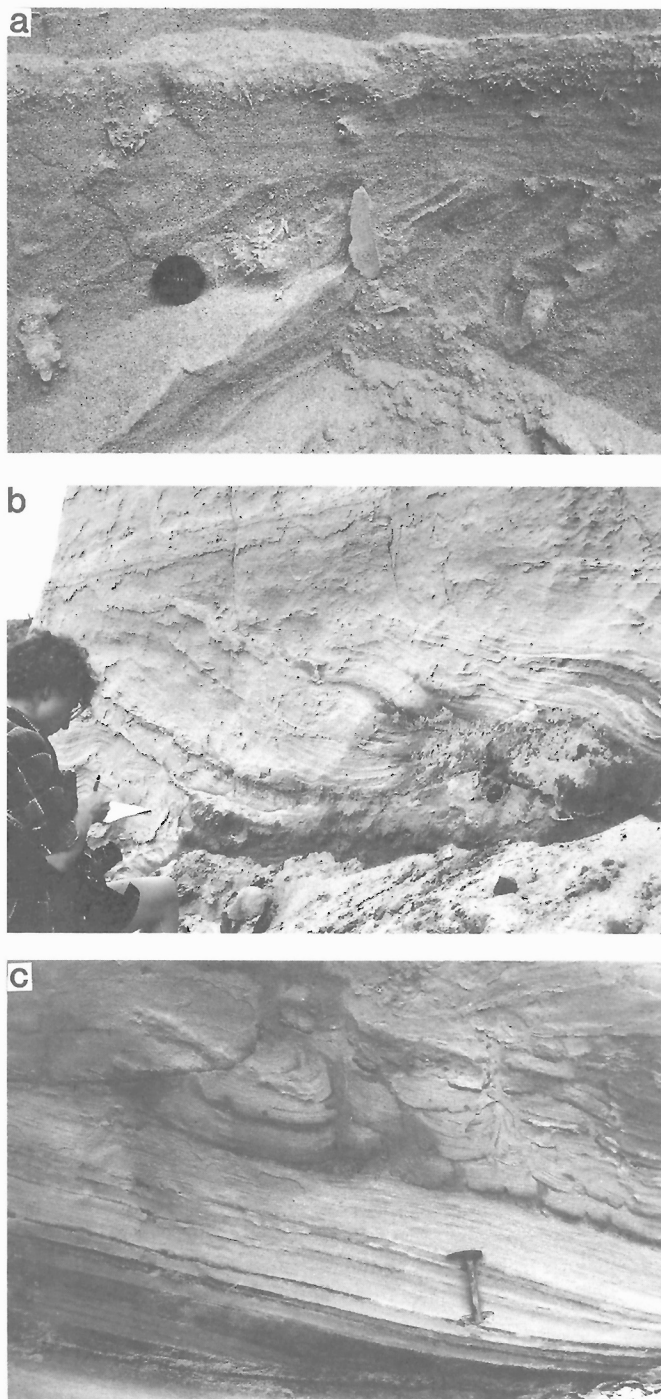


**Figure 12:** Yakoun River sand pit. **A** Subhorizontal toeset lamination (upper third) overlying steeply dipping foresets. A 5 cm toeset interval shows densely packed, filamentous burrows. Sparse burrows are also visible in the foresets. Lens cap 5.3 cm across. **B** Tabular cross-set, showing low to moderate deformation due to dewatering (see text). Two resistant foreset laminae “emanate” from the person’s forehead and trend toward the bottom right. The upper, darker lamina is a double mud drape (see text) which has been thickened to about 4 cm near its right-hand end (above lens cap) due to soft-sediment deformation. **C** Tabular cross-set showing two kinds of soft-sediment deformation: 1) diapir-like anticlines, formed by dewatering, punching upward through the overlying set boundary (horizontal line at top right); and 2) a downward-verging thrust (upper left), which soles out along a foreset lamina, and which involves both the upper and lower cross-sets. The thrust is listric, curves upward abruptly toward the right, and terminates in a thrust tip. Dark foresets are *not* mud drapes; the dark colour is due to preferential algal(?) growth along relatively permeable foreset laminae. Hammer 30 cm long.

## Masset Sound

Several small exposures of subhorizontal Skonun Formation strata occur along the shores of Masset Sound (Fig. 2, g to n). Most of these localities appear on the map of Sutherland Brown (1968, Fig. 5). The exposures are discussed individually below, from south to north.

### Collision Point

The Collision Point section was described and interpreted by Higgs (1989c). The facies include the familiar tabular cross-stratified sandstone with *Ophiomorpha* burrows and dropstones. The inferred depositional environment was a glacially influenced, tide-dominated shallow sea floor (Higgs, 1989c). The Collision Point strata were tentatively dated as late Miocene to early Pliocene by Martin and Rouse (1966), based on palynomorphs. Higgs (1989c) pointed out that a late Miocene age is likely, because bivalves of this age were found 7 km to the north, on Kumdis Island (Addicott, 1978; see below), in strata which are likewise subhorizontal and close to sea level. A late Miocene age has now been confirmed (L. Marincovich, Jr., pers. comm., 1989), based on bivalves collected at Collision Point in 1988 by the author and by Dr. James White (Higgs et al., unpub. data).

### Kumdis Island

**Description.** A rock ledge on the foreshore at PQ878670, on the west side of Kumdis Island, exposes about 1 m of well indurated, poorly sorted sandstone containing dispersed granules and small pebbles. The sandstone is partially coated by seaweed and mud, but appears massive. There is possibly a northward dip of a few degrees at this locality.

At PQ882675, 500 m to the northeast, on the northern tip of Kumdis Island (Hogan Point), a few decimetres of rock are poorly exposed in foreshore ledges. Facies include silt-laminated mudstone, fine to medium sandstone, and coarse pebbly sandstone.

Addicott (1978) recovered and identified a late Miocene bivalve, and an undetermined gastropod, from northern Kumdis Island, although his precise sampling locality was not specified.

**Interpretation.** Exposure is too poor for detailed interpretation. The dispersed pebbles may be ice-rafted dropstones, as inferred for other Skonun Formation exposures (above and Higgs, 1989c).

### Nadu River mouth

**Description.** A slime-veneered rock platform is intermittently exposed on the foreshore for a distance of about 400 m south of the Nadu River mouth (PQ890682), on the east bank of Masset Sound. Structural dip is less than 5°. Exposed at PQ888679 is a lignite bed 10 cm thick. The lignite is underlain by colour-mottled sandstone, of which only 2 cm are visible, and overlain by silty mudstone, of which some 10 cm are exposed. A covered interval of about 20 m separates this exposure from the next one to the south, which consists of a few decimetres of massive, mottled-green, fine to coarse sandstone, containing dispersed, angular to rounded pebbles.

**Interpretation.** The mottled sandstone underlying the lignite bed is interpreted as a paleosol. The association of lignite and paleosol suggests an overbank setting on an alluvial or delta plain. The dispersed pebbles at the southern exposure are possibly ice-rafted dropstones, as inferred for similar pebbles in sandstone at other Skonun Formation localities (above; Higgs, 1989c).

### Grid reference PQ892688

The foreshore at this locality (j in Fig. 2) is a rock ledge whose seaward edge is a vertical cliff at least 1 m high. The upper part of the cliff is emergent at low tide. The ledge extends more than 100 m north of a subdued promontory and 200 m south. At least the top 70 cm of the ledge consists of well cemented conglomerate. The ledge is essentially horizontal, suggesting that the conglomerate bed has negligible dip; this is supported by the occurrence of a similar con-

glomerate ledge on the foreshore at Allan Point, 1 km to the north, and at Watun River mouth, 7 km to the north.

**Description.** The conglomerate is mostly matrix-supported, but locally clast-supported. The matrix consists of poorly sorted, fine to coarse sandstone. Clasts are likewise poorly sorted, ranging from granule to boulder grade (maximum 60 cm across). Clasts include shell fragments, volcanic and granitoid rock types, and siltstone. Pale grey rhyolite(?) clasts are possibly derived from the Masset Formation. The clasts are rounded to subangular. The conglomerate lacks grading and imbrication. At least locally, the conglomerate contains a 10 cm layer of shell gravel composed of broken bivalves. About 100 m south of the promontory, the sandy matrix between clasts is crowded with whole, articulated bivalves in probable life position (Fig. 13A).

A slump scar on the tree-covered slope behind the conglomerate ledge exposes 10–20 m of horizontally bedded sandstone and mudstone. These strata are separated from the conglomerate bed below by a covered interval several metres thick.

**Interpretation.** The shells indicate that the conglomerate is not fluvial, but probably marine. Deposition by subaqueous gravelly mass flow is unlikely, based on the poor sorting and the lack of grading and imbrication (Lowe, 1982; Nemec and Steel, 1984). The most likely interpretation is that the conglomerate is a dropstone condensation layer (see Skonun Point above). A strong ambient current is implied, hindering deposition of sand and mud; the current was probably tidal, in view of the evidence for tidal-current deposition at other Skonun Formation exposures (above). Hence, the inferred environment is a glacially influenced, tide-dominated shallow sea. The sandy-gravelly sea floor was colonized by burrowing bivalves, analogous to modern burrowing bivalves in high-energy gravelly areas in the tidal English Channel (Wilson, 1982). The shell gravel reflects transportation and accumulation of shell detritus, analogous to the shell accumulations found in gravelly areas of the English Channel (Wilson, 1982).

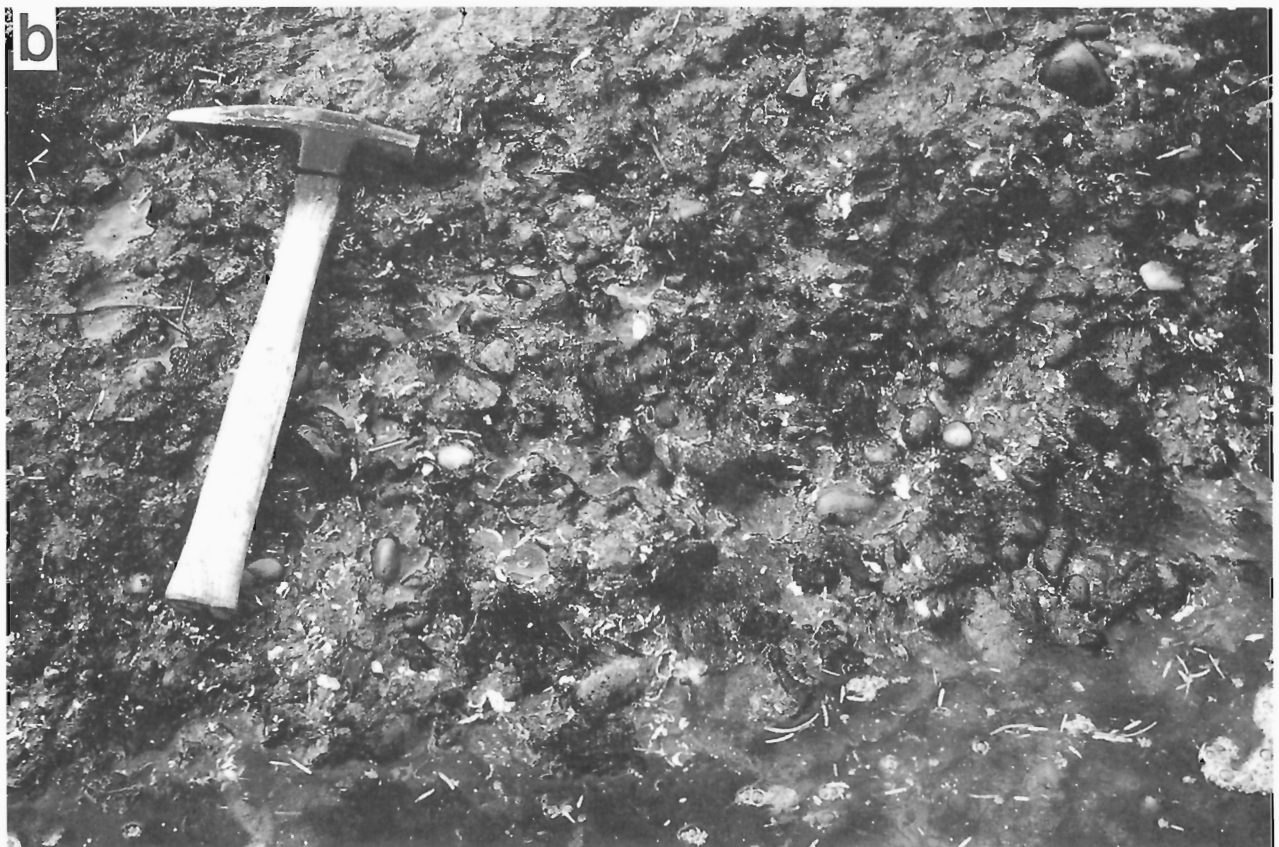
Similar conglomerate beds containing shells were described from the Pleistocene of southern Alaska and from the Permian of Australia by Eyles and Lagoe (1989), their “planar muddy Coquinas” and their Figs. 5C, 6D (lower half) and 14A). These authors inferred slow accumulation of ice-rafted dropstones on current-swept (sediment-starved) areas of the continental shelf.

The age of the conglomerate is unknown; the bivalves are difficult to extract and identify because they are tightly cemented in the rock. Sutherland Brown (1968, p. 126, his Locality 3) collected molluscs from “fossiliferous sands” in this vicinity, and quoted F.J.E. Wagner and also S. Davidson as saying that a Pleistocene age was likely. These sands are probably those exposed in the cliff behind (and above) the conglomerate. A late Miocene age is probable for the conglomerate, since late Miocene fossils occur nearby at Collision Point and Kumdis Island (above), in strata which are likewise close to sea level and essentially horizontal.

### Grid reference PQ894690

At this locality, just 200 m north of the last one, the base of the tree-covered slope exposes about 2 m of horizontal beds, comprising mudstone interbedded on a millimetre-centimetre scale with sandstone containing shell fragments.

**Figure 13:** Bedding-plane view of a horizontal Skonun Formation conglomerate bed forming an intertidal rock platform intermittently exposed along Masset Sound. Hammer 30 cm long. **A** Matrix-supported conglomerate, partly obscured by seaweed, at PQ892688. All visible clasts are *in situ* and firmly cemented. Numerous articulated bivalves are visible in the sand matrix, in probable life position (hinges vertical). **B** Clast-supported conglomerate at Watun River mouth. Bivalve fragments and disarticulated shells are conspicuous in the sand matrix.





**Description.** The base of the steep forested bank of Masset Sound is bare at this locality (k in Fig. 2), exposing about 9 m of horizontal strata, comprising three units (Fig. 5F). Thoroughly bioturbated fine sandstone (2 m) is overlain by faintly stratified fine sandstone (4 m) which contains dispersed clasts up to 10 cm across and also dispersed bivalve fragments and valves, some articulated. A faint horizontal stratification in this middle unit is defined by centimetre-thick bands, with diffuse margins, in which shell material is more concentrated. Some of the clasts are rounded and some are encrusted by barnacles. The top unit consists of parallel-laminated fine sandstone with interspersed trough cross-sets and with a 10–20 cm matrix-supported conglomerate layer at the base. The top unit lacks shells, burrows and dispersed clasts.

**Interpretation.** The lower two units are probably marine, based on the burrowing and fossils. The floating clasts are interpreted as dropstones, as at other localities (above), implying that the middle unit was deposited in an offshore environment. The presence of parallel lamination rather than cross-stratification suggests “upper plane bed” deposition (e.g. Harms et al., 1982, Fig. 2-5); the sand may have been too fine to form dunes or sandwaves. Sedimentation of the middle unit was relatively slow, allowing barnacles to colonize dropstones on the sea floor. The bands of greater shell concentration may reflect episodes of stronger current and therefore increased sediment by-passing. The current was probably tidal, as inferred for the majority of Skonun Formation exposures (above). The top unit is probably a deltaic distributary channel, with a basal conglomeratic lag; this interpretation is consistent with the absence of fossils, burrows and dropstones. Hence, the succession appears to be regressive, with tidal-shelf deposits passing up into delta-plain sediments. Delta-front and/or nearshore sediments would normally be expected to separate the marine from the delta-plain sediments, according to Walther’s Law; their absence may reflect channel erosion.

#### Allan Point (PQ890698)

**Description.** The foreshore at Allan Point is a subhorizontal ledge comprising about 50 cm of well cemented conglomerate. The ledge is undercut below low-water level, so that the underlying strata are unknown. The conglomerate is matrix- (fine sand) to clast-supported, and contains sparse shell fragments. Clasts are poorly sorted, ranging from granules to boulders (max. 40 cm across), and from rounded to angular. Clasts include volcanic and granitoid rocks.

**Interpretation.** The conglomerate is thought to be the same as that at PQ892688 (above), which similarly forms an essentially horizontal ledge at sea level, only 1 km away. Hence, the Allan Point conglomerate is likewise interpreted as a dropstone condensation layer deposited on a shallow sea floor where strong tidal currents caused by-passing of mud and most sand.

#### PQ907720

**Description.** The foreshore at this locality (m in Fig. 2) is a rock ledge capped by about 30 cm of the same conglomerate as at Allan Point (above), underlain by at least 50 cm of fine sandstone with faint parallel lamination and sparse, millimetre-size burrows. The base of the sandstone is underwater.

**Interpretation.** The conglomerate is thought to be a dropstone condensation layer, as previously argued, while the fine sandstone could have been deposited by strong tidal currents under upper-plane-bed conditions (see PQ898695 above).

#### Watun River mouth

**Description.** A foreshore ledge at PQ912762, immediately south of Watun River mouth, is formed by a horizontal conglomerate bed, at

least 50 cm thick, lithologically identical to the conglomerate bed at the previous two localities (Fig. 13B). Whole and broken bivalve shells are conspicuous (Fig. 13B). Fossils were collected in this vicinity by Sutherland Brown (1968), to which he tentatively assigned a Pleistocene age, but the exact sampling locality was not stated.

**Interpretation.** The conglomerate is interpreted as a dropstone condensation layer, as above.

#### “Tasu beds”

The geological map of Sutherland Brown (1968, Fig. 5) shows four small outcrops of Cretaceous Honna Formation in northwest Moresby Island, situated 10–25 km northwest of the Tasu mine (p through s in Fig. 2). These strata are here informally named the Tasu beds. Sutherland Brown (1968) probably assigned these beds to the Honna Formation based on: (1) their conglomeratic nature, like the Honna type section; and (2) the perception that the Tasu beds underlie the Masset Formation (although this is equivocal because no contacts have been seen and because the strata are undated). However, an alternative possibility is that the Tasu beds are a tongue of Skonun Formation intercalated with Masset volcanics. Indeed, the strata at Cinola (above) were likewise mapped as Honna Formation by Sutherland Brown (1968, Fig. 5), but were subsequently recognized as Skonun Formation (Champigny et al., 1981; Champigny and Sinclair, 1982).

The author spent one day examining the Tasu beds with Dr. Brian Bornhold in 1988. Only outcrop p was found. Helicopter reconnaissance of the other three localities (q, r and s) showed numerous crags exposing Masset volcanics, but no sign of sediments. Beach and creek traverses of locality s likewise revealed only volcanics at outcrop and in float, apart from two decimetre-size sandstone boulders on the beach (PP834652) and in a creek bed (PP837652).

#### Description

Locality p is a stepped plateau, largely bare rock, measuring approximately 500 m by 150 m (Fig. 14A). Exposed here are 30–40 m of sandstone and conglomerate, dipping northwest at about 20°; no folds or faults were observed. Strata are well exposed on dip slopes corresponding to the flat steps of the plateau, and in low scarps separating the steps (Figs. 14A,B). The Tasu beds are surrounded by Masset volcanics (Fig. 14A; Sutherland Brown, 1968, Fig. 5), but no contacts were seen, so the stratigraphic relationship with the Masset is unknown.

The Tasu beds comprise cross-stratified sandstone intercalated with pebble-conglomerate layers up to 50 cm thick (Figs. 14B,C). Contacts between sandstone and conglomerate vary from sharp to diffuse. The proportion of conglomerate in any 5 m interval ranges from 0–50%. The sandstone is poorly sorted; modal grain size ranges from medium to coarse. Cross-sets are 5–50 cm thick and include both tabular and trough sets. Foreset dips show that paleoflow was toward the northwest quadrant, with a considerable spread in direction, between westward and northward. The conglomerate is clast-supported, with

**Figure 14:** Tasu beds. Hammer 30 cm long. **A** Helicopter view, looking southwest, of the stepped-plateau outcrop of the Tasu beds (left-hand side). Strata dip to the right (northwest), and the total thickness exposed is about 30–40 m. The light-coloured ridge on the right-hand side consists of Masset Formation volcanics. The contact between the Masset and the Tasu beds, which is not exposed, could be either: (1) stratigraphic, with the Masset overlying the Tasu beds; or (2) a fault running along the wooded valley immediately left of the volcanic ridge. **B** Scarp showing cross-stratified sandstone with conglomerate layers (visible near base). Both trough and tabular cross-sets are present, and foresets in every set dip to the right (north). **C** Intercalated conglomerate and cross-stratified sandstone. **D** Conglomerate bed, overlain by cross-stratified sandstone.





a sand matrix (Fig. 14D). Clasts are subangular to rounded and mainly volcanic; 10-20% of the clasts are white, finely crystalline vein(?) quartz. The conglomerate locally shows imbrication, whereas grading and internal stratification are lacking.

#### *Interpretation*

A fluvial-channel environment is likely, based on the coarse grain size, cross-stratification and lack of fossils. The presence of conglomerate and the absence of overbank mud suggest a braided rather than meandering stream. This is consistent with the wide (90°) spread in cross-bedding orientation, reflecting the variable orientation of bedform slip faces in braided streams (e.g. Cant and Walker, 1978). The trough and tabular cross-stratification was produced by migrating dunes and transverse bars, respectively (Cant and Walker, 1978). In view of the evidence for alluvial fan and fan-delta deposition at Cinola (above), the Tasu braided streams may have been part of an alluvial fan, which itself may have been part of a deep-water fan-delta system. The stepped nature of the outcrop may reflect cyclicity, each step representing a single cycle (cf. Steel and Aasheim, 1978).

#### **Hippa beds**

A small outcrop of conglomerate, sandstone and mudstone occurs on Hippa Island, unconformably beneath Masset volcanics (t in Fig. 2; Higgs, 1989b). These braided-stream and lacustrine deposits are either pre- or intra-Masset (Higgs, 1989b) and could belong to Unit II.

### **BOREHOLE CORES: DESCRIPTION AND INTERPRETATION**

Cores were cut in the Skonun and/or Masset Formations in the Harlequin and Osprey offshore wells, and in all of the onshore wells except Tian Bay and Cape Ball (Fig. 1). The onshore and offshore cores are stored, respectively, at the B.C. government core storage facility at Charlie Lake and at the federal government Institute of Sedimentary and Petroleum Geology in Calgary. The author examined all of the cores. Due to the repetitive nature of the data (96 cores), this section contains only a summary discussion of the depositional environments interpreted from the cores. Individual core descriptions and interpretations are given in Appendix 1.

Interpretation of cores is seldom as detailed as for exposures, because cores may fail to expose small, dispersed features (e.g. dropstones), or may only partially expose large-scale features, hindering their recognition (e.g. hummocky cross-stratification).

The cores have been previously described, with emphasis on lithology, mineralogy and porosity rather than sedimentary structures, in the respective well history reports (Richfield Oil Corporation, 1958a,b,c,e; Shell Canada Ltd., 1968e,f; Union Oil Company of Canada Ltd., 1971; Bow Valley Industries, 1984a,b), and in CanStrat lithological logs (Tow Hill, Nadu River, Cape Ball, Gold Creek, Harlequin and Sockeye E-66 wells).

As explained above under "Well-log correlations and basin-fill architecture", the Port Louis, Naden and Tow Hill wells were drilled entirely in Unit I; consequently, all cores from these two wells belong to Unit I. Also assigned to Unit I are Cores 2 through 10 in the Masset well, 13 through 23 in Nadu River, 7 through 18 in Gold Creek, and 5 and 6 in Tlell (Fig. 3, in pocket; note that all cores are marked on Fig. 3 using a bar symbol and a code for lithology). The remaining cores, including all three cores in Harlequin and Osprey, are from Unit II.

#### **Union Port Louis c-28-L 103-F-10, Bow Valley et al. Naden b-27-J 103-F-15 and Bow Valley et al. Naden b-A27-J 103-F-15**

Cores in these three wells are entirely volcanics, belonging to Unit I or possibly, in the Port Louis well, to the Middle Jurassic Yakoun Group.

#### **Richfield et al. Tow Hill d-93-C 103-J-4**

All cores belong to Unit I as discussed above. A pronounced facies change occurs between cores 15 and 16. Cores 1 through 15 are

dominantly mudstone and sandstone interpreted as fluvial deposits. In contrast, Cores 16 through 33 are mostly conglomerate and sandstone interpreted as turbidites and allied gravity-flow deposits.

#### **Richfield et al. Masset c-10-I 103-F-16**

Core 1 is loose fine sand, unfit for interpretation due to absence of sedimentary structures. The remaining cores are (Unit II) volcanics.

#### **Richfield et al. Nadu River b-69-A 103-F-16**

Cores 1 through 12 belong to Unit II and consist mostly of sandstone, interpreted as cross-stratified tidal-shelf deposits, with or without dropstones. In contrast, cores 13 through 23 are from Unit I and are mostly volcanics and/or epiclastic mudflow deposits.

#### **Richfield et al. Gold Creek c-56-H 103-F-9**

Cores 1 through 6 belong to Unit II; recovery was insufficient for interpretation. Cores 7 through 18 are assigned to Unit I (Fig. 3), but cores 7 and 8 may instead belong to Unit II because Core 8 contains possible dropstones, typical of Unit II. This implies that the base of Unit II in the Gold Creek well may be slightly lower than shown in Figure 3. Cores 9 through 15 are mostly sandstone and mudstone, undiagnostic in most cases, but probably fluvial or delta-plain in cores 13 and 15. The three deepest cores (16 through 18) are volcanic.

#### **Richfield et al. Tlell c-56-D 103-G-12**

Cores 1 through 4 are from Unit II and comprise pebbly mud of probable glaciomarine origin, and mud of fluvial or delta-plain origin. Cores 5 and 6, from Unit I, include probable turbidites and fluvial overbank mud.

#### **Shell Anglo Harlequin D-86**

Both cores are in Unit II sandstone and are interpreted as amalgamated shelf storm beds.

#### **Shell Anglo Osprey D-36**

One core was cut in Unit II sandstone and is interpreted as amalgamated shelf storm beds.

### **HEAVY-MINERAL ANALYSIS**

Heavy-mineral analysis of 50 sandstone samples taken from cores from 6 wells (5 onshore and 1 offshore) was conducted in order to elucidate provenance, as an aid to determining the tectonic setting of the basin.

When comparing the heavy-mineral suites of different sand samples, it is desirable to restrict the analysis to a standard, narrow grain-size fraction (Carver, 1971). Carver (1971) suggests that the 2-3 phi fraction is an excellent compromise for most studies. However, many of the QCB sandstone samples are finer than this, so the 3-4 phi fraction was used instead.

#### **Method**

Samples were first disaggregated, either by crushing between the fingers or by treatment with 10% or 20% HCl, followed, if necessary, by light grinding with a mortar and pestle. Samples were then washed with distilled water, and oven-dried. Next, samples were dry-sieved and the heavy minerals extracted from the 3-4 phi sieve fraction using sodium polytungstate. Grain mounts were then prepared on microscope slides using Canada balsam.

Heavy-mineral compositions were determined by conducting a grain count of each grain mount. Only the non-opaque heavy-mineral grains (i.e. those most diagnostic of provenance) were counted. At least 100, and in most cases 200 non-opaque grains were counted per grain mount (cf. Hubert, 1971), depending on the number of grains present.

#### **Results and interpretation**

The main non-opaque heavy minerals present, in approximate order of decreasing abundance, are hornblende, epidote group (clinozoisite and epidote), zircon, garnet, biotite and tourmaline (Table 1; Fig. 15). This heavy-mineral association is clearly diagnostic of a

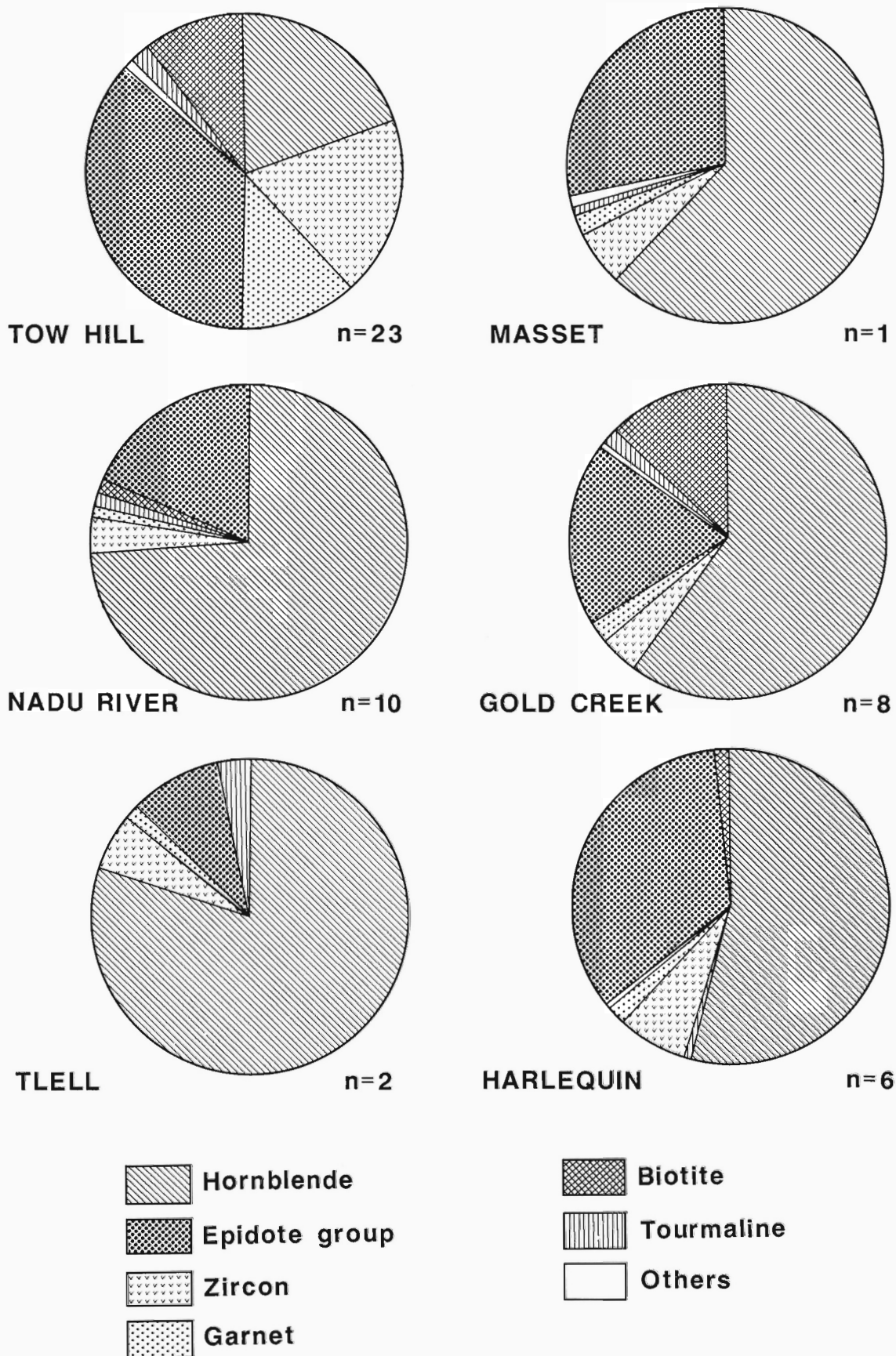


Figure 15: Pie diagrams showing heavy-mineral compositions of the studied wells. n = number of samples.

high-rank metamorphic provenance (Hubert, 1971, his Table 2). Hornblende grains are mostly green and are commonly etched, reflecting intrastratal solution. Epidote is marginally more abundant than clinzoisite in most samples. Garnet grains are almost invariably colourless, with rare pink grains. Minerals occurring in trace amounts (usually 0-1%) in just a few samples are augite, corundum, diopside, muscovite, rutile and staurolite; these minerals are fully consistent with derivation from a metamorphic source. Riebeckite is present in small amounts (up to 5%) in many samples, indicating a subordinate granite or syenite provenance. There is no obvious difference between the samples of Unit I and those of Unit II in terms of heavy-mineral composition.

With regard to the location of the source area, high-grade metamorphic rocks are rare in the Queen Charlotte Islands (Sutherland Brown, 1968), as indeed they are throughout Wrangellia, the terrane to which most of the Queen Charlottes landmass belongs (Monger and Berg, 1984). Hence, Wrangellia is discounted as the source of the studied Skonun samples. In contrast, high-grade metamorphic rocks are common in the Coast Mountains (Fig. 1); these rocks belong to the Alexander Terrane (Monger and Berg, 1984) and were probably even more widespread prior to unroofing of the plutons which now dominate the Coast Mountains (Coast Plutonic Complex). Hence, the Skonun samples were probably derived from the Alexander Terrane. According to Yorath and Chase (1981), the Alexander Terrane includes northeast Graham Island and much of Hecate Strait. In contrast, Woodsworth (1988) suggested that these areas have a Wrangellian foundation and that the Wrangellia-Alexander boundary is further east, along the eastern shore of Hecate Strait. Of these two models, the Yorath and Chase (1981) model is the more likely, because heavy-mineral samples from northeast Graham Island belonging to "syn-rift" Unit I (i.e. most samples in the Tow Hill, Gold Creek and Tlell wells) were presumably derived locally, from active fault scarps (see "Basin origin" below), implying that northeast Graham Island is underlain by high-grade metamorphic rocks (i.e. Alexander Terrane). In contrast, the source regions for "post-rift" Unit II sediments were presumably located farther afield: sediment was probably transported from an Alexander Terrane provenance in the area of the present-day Coast Mountains by rivers and shallow-marine (tidal and storm) currents.

All wells show broadly similar heavy-mineral compositions (Fig. 15). However, the Tow Hill well shows considerably more zircon and garnet than the other wells, at the expense of amphibole. Two wells show pronounced uphole changes in heavy-mineral composition. Firstly, in the Tow Hill well, there are two distinct "floods" of hornblende, at about 4500 ft and above 1500 ft (Table 1); in the rest of the well hornblende is negligible, and is compensated by a proportional increase in the epidote-group minerals. The fluctuating hornblende concentration suggests either that the source area switched with time, or that there are uphole variations in intrastratal solution, possibly due to permeability variations. In the Nadu River well, there is a weak trend of uphole-decreasing hornblende (Table 1).

## DISCUSSION AND IMPLICATIONS FOR PETROLEUM EXPLORATION

### Basin origin

Two stages of basin subsidence are inferred, corresponding to Units I and II, defined above. Unit I, the lower stratigraphic unit, resulted from extensional block faulting, with sedimentation and volcanism (including the Masset Formation) taking place in grabens and half-grabens. Block faulting is suggested by three attributes of Unit I: the volcanics, the presence of local conglomerates (presumably banked against active fault scarps), and the lack of correlations. Further-

more, grabens and half-grabens are visible on published seismic-reflection profiles (Snively et al., 1981; Yorath and Chase, 1981; McWhae, 1986), and on new profiles acquired by the Geological Survey of Canada in 1988 (Dietrich et al., 1989; Rohr and Dietrich, 1991). A modelled structural profile of Dixon Entrance, based on a seismic *refraction* line (Shor, 1962, Fig. 3, east end), likewise shows half-grabens. The volcanics in Unit I were presumably erupted via active faults. Block faulting lasted from Eocene to Miocene time, as shown by the radiometric age-span of Unit I (see above).

Block faulting and deposition of Unit I gave way to deposition of Unit II. Subsidence changed from block faulting to regional sagging, as shown by the fact that sequences in Unit II can be correlated laterally for at least 100 km, with little thickness change (Fig. 3). Fossils in Unit II indicate that regional subsidence began in the Miocene and continued into the Plio-Quaternary. The northward younging of the base of Unit II mentioned previously may indicate that the transition from block faulting to regional subsidence is diachronous, younging to the north. The *onset* of block faulting may also have been diachronous; this is supported by a distinct northward-younging trend among Tertiary plutons in the Queen Charlotte Islands (Anderson and Reichenbach, 1989, 1991); a similar but less distinct trend is shown by offshore and onshore Tertiary volcanics (Hickson, 1988).

Hence, the internal architecture of the QCB reveals a two-stage development, whereby a block-faulting or "rift" stage (Eocene to Miocene) gave way to ongoing "post-rift" regional subsidence (Miocene to Quaternary). The inferred two-stage subsidence history is supported by seismic profiles (Yorath and Chase, 1981; McWhae, 1986; Dietrich et al., 1989; Rohr and Dietrich, 1991). An extensional origin of the QCB is also indicated by: the composition of Masset Formation volcanics (Hamilton, 1989; Hyndman and Hamilton, 1991); the probable fissure style of volcanic eruptions (Sutherland Brown, 1968; Hickson, 1988); the abundance of Tertiary dykes (Souther, 1989; Souther and Jessop, 1991); and the bimodality of Tertiary plutons (Anderson and Greig, 1989). A two-stage evolution of extension confined to Queen Charlotte Sound followed by basinwide regional subsidence related to oblique subduction was postulated by Yorath and Hyndman (1983). Higgs (1989a) pointed out that extension followed by regional (thermal) subsidence is typical of rift basins (McKenzie, 1978) and of large strike-slip pull-apart basins (Christie-Blick and Biddle, 1985). A pull-apart model is implicit in a paleogeographic sketch of the Canadian Cordillera by Eisbacher (1985, Fig. 8).

The *cause* of extension in the QCB is germane to the question of what *type* of basin is the QCB. Yorath and Chase (1981) postulated extension ("rifting") in Queen Charlotte Sound which they attributed to a mantle plume, whereas Yorath and Hyndman (1983) suggested that underthrusting of an oceanic spreading ridge may have been responsible. Higgs (1988) speculated that the basin may be due to strike-slip extension, based on the dominantly transform present-day character of the margin.

A model explaining the underlying cause of extension in the QCB is presented by Hyndman and Hamilton (1991), founded on the plate-motion models of Engebretson et al. (1985) and Stock and Molnar (1988). Hyndman and Hamilton argue that since a major plate reorganization at 43 Ma, the Queen Charlotte margin has been characterized by transcurent interaction between the Pacific and North America plates, with varying amounts of oblique extension or compression. They correlate an interval of oblique extension between 36 and 20 Ma (their Figs. 2 and 3) with syntectonic deposition (cf. Unit I) and maximum magmatic activity in the QCB (their Fig. 4). This oblique extension, they argue, was probably resolved into orthogonal extension in the

QCB landward of the plate margin and transcurrent motion along the west coast. A period of "general transcurrent motion" from 20–5 Ma is inferred to correlate with post-tectonic regional subsidence (cf. Unit II). Finally, oblique convergence from 5–0 Ma is responsible, they suggest, for uplift and erosion of the western part of the Queen Charlotte Islands. However, as discussed below, uplift of the islands may in fact have begun earlier, at 20 Ma, when plate interaction at the Queen Charlotte margin may have changed from oblique extension to oblique convergence (see plot labelled "Stock and Molnar" in Figs. 2 and 3 of Hyndman and Hamilton, 1991).

The cause of the post-extension, regional subsidence (Unit II) is contentious. The subsidence is possibly due to thermal cooling, such subsidence being a typical post-extension response in both rift basins (McKenzie, 1978) and in large strike-slip pull-apart basins (Christie-Blick and Biddle, 1985). An alternative possibility is simple downflexing of an elastic plate due to uplift at the western edge (Yorath and Hyndman, 1983). However, evidence that the islands were uplifted as discrete fault blocks (see below) raises doubts about the plate's ability to transmit flexure. A third possibility is that underplating of the QCB since 20 Ma by oceanic lithosphere (see below) has caused subsidence by downdrag.

As well as causing uplift, oblique convergence at the Queen Charlotte margin may have the following structural manifestations: (1) possible (clockwise) rotations of discrete crustal blocks in the Queen Charlotte Islands (Souter, 1988; Higgs, 1990, 1991); (2) narrow, faulted antiforms affecting the entire QCB succession on offshore seismic profiles (Yorath and Chase, 1981, Fig. 12, left side; McWhae, 1986, Fig. 57, left side, and Plate 5; Rohr and Dietrich, 1991); these antiforms are probably wrench-related (McWhae, 1986); they resemble Harding et al.'s (1983) "positive flower structures", of convergent-wrench origin; some of the antiforms are truncated by erosion at the seafloor (Higgs, 1989a), suggesting that they are still growing; erosion of the (poorly consolidated) Skonun deposits may be due to Pleistocene glaciers or present-day tidal currents; (3) a possible exhumed flower structure, the Rennell Sound Fault system, in central Queen Charlotte Islands (Young, 1981, p. 237–248); slickensides on this fault system are sub-horizontal (Sutherland Brown, 1968); deformation is younger than the (Eocene to Miocene) Masset Formation, as shown by a fault slice containing Masset volcanics (Sutherland Brown, Fig. 5).

The inference that the QCB is extensional is important to petroleum exploration because extensional basins are hydrocarbon-prone worldwide (e.g. North Sea, Southern California). Such basins typically provide ideal conditions for the genesis of source rocks, reservoir rocks and traps, as well as providing enhanced organic maturation due to deep burial and high heat flow (Dickinson, 1978). Recognition that the Masset Formation is part of the basin fill (i.e. not basement) means that wells should not necessarily be terminated upon reaching volcanics. On the contrary, QCB sediments intercalated with the volcanics are a viable exploration play both onshore and offshore, and may have been the objective of some of the wells which spudded in volcanics (Tian Bay, Port Louis, Naden; Fig. 1).

### Uplift of the western part of the basin

Of the fourteen known exposures of the Skonun Formation in northeast Graham Island, six have been dated using fossils: all six are Miocene (a, b, e, f, g and h in Fig. 2; see descriptions above). The apparent absence of younger strata onshore (glacial outwash excepted), in contrast to the offshore area where Plio-Quaternary sediments occur (Fig. 3), suggests that northeast Graham Island has undergone tectonic uplift and erosion, beginning in or after the late Miocene (youngest fossils). Uplift and erosion are confirmed by vitrinite-reflectance measurements in the onshore wells (Vellutini and Bustin,

1988). However, some of the *offshore* wells also reveal uplift (Vellutini and Bustin, 1988), but this might simply reflect *local* uplift in an otherwise subsiding region (e.g. growth of positive flower structures in a subsiding basin). At Cinola, at least 1 km of erosion has occurred since the early Miocene, based on fluid-inclusion evidence (Shen et al., 1982). Uplift is also indicated by the occurrence of erosionally truncated, steeply dipping Skonun strata exposed at Skonun and Yakan points and Tow Hill (Sutherland Brown, 1968, Fig. 5). Erosion due to uplift is inferred to have stripped Unit II from large areas of the Queen Charlotte Islands, exposing Unit I Masset volcanics. The volcanics are themselves missing in places, either due to erosion or non-deposition, exposing Mesozoic basement.

Uplift is continuing at the present day, as indicated by ubiquitous raised shoreline features (Sutherland Brown, 1968, p. 27; Clague et al., 1982). The present-day uplift is probably other than glacial rebound, because there was only a "thin localized ice cover" in the Queen Charlotte Islands in the last glacial (Clague et al., 1982, p. 1793). Instead, the uplift is attributed to oblique underthrusting of the Queen Charlotte Islands by the Pacific plate (Hyndman and Ellis, 1981; Yorath and Hyndman, 1983). According to Yorath and Hyndman (1983), uplift commenced at about 6 Ma, in the latest Miocene (see also Hyndman and Hamilton, 1991). However, uplift may have commenced sooner than this, as shown by the presence of intraformational Skonun clasts among iceberg dropstones in upper Miocene strata at Skonun Point (see above), indicating that a former Skonun-depositing area had been uplifted to form glacier-bearing mountains by late Miocene time. Hence, it is postulated that part of the QCB was uplifted in or before late Miocene time, forming mountainous proto-Queen Charlotte Islands. In these mountains, newly uplifted Skonun strata (entirely eroded today) underwent erosion, entrainment by glaciers, and finally deposition from icebergs in neighbouring, still-submerged areas of the QCB. It is likely that the uplift started at 20 Ma (early Miocene), triggered by a northward shift in the relative motion of the Pacific plate at that time (Stock and Molnar, 1988; see Hyndman and Hamilton, 1991, Table 1 and Figs. 1 and 2). The shift would have caused plate interaction along the southern 2/3 of the Queen Charlotte margin (i.e. Moresby Island sector) to change from transtension to transpression, assuming that: 1) this stretch of coastline had an orientation of about 320°, as it has today (see Fig. 2 of Hyndman and Hamilton, 1991); and that 2) the Pacific plate, rather than the Farallon plate, was offshore the QCB (Hyndman and Hamilton, 1991). It is proposed, therefore, that transpression along the Moresby Island sector caused uplift of the western edge of the QCB and emergence of proto-Moresby Island from 20 Ma onward. In contrast, along the northern 1/3 of the margin, oriented more northerly (340°), the plate-motion change at 20 Ma would have caused plate interaction to become less transtensional but not transpressive. However, transpression and uplift of Graham Island eventually did begin at about 5 Ma (Yorath and Hyndman, 1983), when a further plate reorganisation caused Pacific relative motion to become even more northerly (see Fig. 2 of Hyndman and Hamilton, 1991).

The inferred 20 Ma uplift of Moresby Island also explains the tidal sedimentary structures in Unit II shelf deposits, in that the ancestral Moresby mountains would have partially barred the shelf areas of the QCB from the ocean, thereby ensuring large tides. Furthermore, the proposal that Moresby Island has been undergoing uplift for much longer than Graham Island explains why the former has a far higher proportion of (exhumed) pre-Tertiary basement rocks at outcrop than Graham Island (Sutherland Brown, 1968, Fig. 5). In other words, erosion has proceeded to a deeper structural level on Moresby Island. Erosion of more than 5 km of material in western Graham Island was estimated by Yorath and Hyndman (1983), based on



structural cross-sections. Since 8000 years B.P., uplift of Graham Island has amounted to 15 m (Clague et al., 1982).

Oblique subduction beneath the Queen Charlotte Islands is supported by a recent seismic-refraction study which indicates a probable underplated oceanic slab beneath Hecate Strait (Mackie et al., 1989). These authors pointed out (their Fig. 1) that if oblique subduction has occurred, the subducted slab would appear in plan as a southward-tapering sliver, terminating at the triple junction south of the Queen Charlotte Islands (see also Yorath and Hyndman, 1983, Fig. 20). The north-south length of the slab can be calculated approximately. Neglecting slab dip and assuming that subduction commenced at 20 Ma, and that the relative velocity of the subducting plate has been constant at 40 km/m.y. (cf. Fig. 2 of Hyndman and Hamilton, 1991), a length of 800 km is obtained. Assuming also that the triple junction has lain between Vancouver Island and the Queen Charlotte Islands since 20 Ma, an 800 km-long subducted slab would reach northward about 200 km beyond the Kupreanof volcanic field of southeastern Alaska (e.g. Brew, 1989). Hence, these volcanics are possibly arc volcanics derived by melting of the subducting oceanic sliver; their 5-0 Ma age (Brew, 1989) implies that the slab-front reached here about 5 m.y. ago, in accordance with the calculation above. However, the inferred 600 km "arc-trench gap" is anomalous; widths exceeding 400 km are exceptional (Mitchell and Reading, 1986). A possible explanation is that the sliver is subducting at a very shallow angle. This is consistent with subduction of young oceanic crust and with the high relative velocity of the overriding plate toward the "trench" (see discussion and references in Mackie et al., 1989).

The regional outcrop pattern of the Queen Charlotte Islands, with older rocks to the southwest and younger rocks to the northeast (Sutherland Brown, 1968, Fig. 5), can be explained either by 1) northeastward tilting accompanying uplift; or 2) by differential uplift of the southwest and northeast parts of the islands as independent fault blocks, with the southwestern block having the greatest uplift. The first hypothesis is unlikely, because Thompson and Thorkelson (1989) found a lack of preferred eastward tilting in the pre-Tertiary basement stratigraphy. The second hypothesis is therefore favoured, and is supported by the pronounced linearity of the eastern edge of the mountains of western Graham Island. This edge is considered to be tectonically controlled by Hyndman and Hamilton (1991; see their Fig. 10).

With the onset of oblique subduction, the western edge of the QCB was uplifted, causing the Queen Charlotte Islands to emerge and the area of Unit II deposition to shrink eastward. Deposition of Unit II continued in Hecate Strait and Queen Charlotte Sound, as shown by the presence of Pliocene and Quaternary strata in the offshore wells (Fig. 3; Shouldice, 1971; Patterson, 1988, 1989). Locally in the offshore areas, antiformal uplifts (flower structures) were formed along convergent wrench faults, in an overall regime of (thermal?) subsidence. Flower structures might also be present onshore. For example, the Skonun Point and Yakan Point exposures show steep dips and abrupt changes in dip across (non-exposed) faults, characteristic of flower structures. Furthermore, flower structures are generally interspersed with areas of essentially flat-lying strata (e.g. Harding et al., 1983), and this is comparable to the situation on Graham Island, where areas of steeply dipping Skonun or Masset beds (e.g. Skonun Point; Yakan Point; Tow Hill; Rennell Sound Fault system) contrast markedly with undisturbed Skonun and Masset beds nearby (e.g. Yakoun River; Masset Sound; see also Sutherland Brown, 1968, Fig. 5). Exposures of Unit I volcanics at Tow Hill and Lawnhill (Sutherland Brown, 1968, Fig. 5) possibly represent the uplifted cores of positive flower structures.

The proposal, discussed above, that Unit II has been stripped from Moresby Island and western Graham Island due to uplift implies that the present western edge of Unit II (essentially the Skonun edge in Figs. 1 and 3) is erosional rather than depositional. Nevertheless, Unit II *does* appear to thin depositionally toward the west (and north), as shown in Figure 3 by the westward convergence of the lowest two correlation lines in wells 4 to 8. This lateral thinning is consistent with the classic "steer's head" geometry of rift basins (e.g. Dewey, 1982), whereby the post-rift sequence (Unit II in this case), representing the steer's horns, thins toward the extremities of the basin.

The inferred uplift and erosion in the Queen Charlotte Islands has the following implications for petroleum exploration: (1) oil generation may have ceased if the oil window is now occupied by over-mature strata being brought to surface by uplift and erosion; (2) oil fields may have been uplifted to shallower depths; and (3) deformation in the form of (post-20 Ma) flower structures could have breached pre-existing oil pools (cf. Snowdon et al., 1988); this could explain the abundance of seeps in the Masset Formation. On the other hand, deformation may also have created potential traps.

### Depositional environment and geometry of sand bodies

Both Unit I and Unit II are very sandy, as shown by the abundance of sandstone in cuttings (see well history reports) and in cores (Appendix 1). Sand-dominated intervals hundreds of metres thick alternate with mud-dominated intervals and volcanic intervals of similar thickness. The sand intervals offer petroleum reservoir potential. Knowledge of their depositional environment can assist in predicting the three-dimensional geometry of the sand bodies.

#### Unit I

Unit I sediments are represented by three exposures (Tow Hill, Cinola and Tasu) and by cores from five wells in northeast Graham Island. The exposures comprise mainly sandstone and conglomerate, deposited in alluvial fans, marine fan deltas, and braided streams, as discussed earlier. The fans were deposited in grabens and half-grabens, and were derived from and built against active fault scarps. Cuttings and well logs indicate that coal beds are common in Unit I, consistent with distal alluvial-fan deposition (Heward, 1978). Cores indicate fluvial and subaqueous gravity-flow deposition, consistent with the overall fan/fan delta interpretation. Hence, the main potential reservoirs in Unit I are sandstone and conglomerate fan deltas and alluvial fans, forming cone-shaped bodies adjacent to faults (cf. Stow et al., 1982). Exploration for such reservoirs would require detailed seismic reflection surveys to map the syn-sedimentary faults and their associated fans. With regard to reservoir properties, calcite-cemented openwork conglomerate occurs in the Tow Hill well (Core 32). Such conglomerate would have excellent permeability if the cement were missing, either due to non-cementation or dissolution.

#### Unit II

Unit II sediments occur at all Skonun exposures except Tow Hill and Cinola (Fig. 2), and occur in cores from offshore wells (Harlequin and Osprey) and onshore wells (Masset, Nadu River, Gold Creek and Tlell). These occurrences reveal three facies associations, entirely different from those of Unit I:

**(i) Delta-plain facies association.** This association comprises carbonaceous mudstone and coal, with channel and crevasse-splay sandstones. The association is exposed, sometimes with one or two of the characteristic lithologies missing, at Skonun Point, Miller Creek and Masset Sound (Nadu River and PQ898695), and also in cores from the Gold Creek and Tlell wells. Potential reservoir bodies are distributary channels. In addition, delta-front sand bodies, although unknown at outcrop (due to non-exposure?), could occur as potential reservoirs in the subsurface: their geometry would either be linear or sheet-like.

depending on whether the delta was fluvial-, tide-, or wave-dominated (Elliott, 1986).

**(2) Tidal-shelf association.** This association consists of tabular cross-stratified sandstone with subordinate dropstone-conglomerate beds and mudstone. The association is exposed, in whole or in part, at Skonun Point (western stack), Yakan Point, Miller Creek, Yakoun River, and several localities along Masset Sound, notably Collision Point. The association is also recognized in cores from the Nadu River well. The cross-strata were deposited by straight-crested sand waves (*sensu* Allen, 1980), discussed previously (see Yakoun sand pit). The overall sand-body geometry, by analogy with modern tidal seas, was probably either a sand *sheet*, made of coalescing sand waves, or a linear sand *ridge* (syn. sand bank) with superimposed sand waves (cf. Stride et al., 1982). Sand bodies are 3 m to at least 10 m thick, based on exposed coset thicknesses. Foresets dip northward in some cosets and southward in others, with rare examples of mixed "herringbone" dips. In addition to this evidence for bipolar palaeoflow, there is a lack of tidal reactivation surfaces, indicating that there was no reverse-flow sand transport during the tidal cycle at any one locality. Together, these two observations suggest that ebb and flood sand-transport fields were separate. This suggests that the sand bodies may have been ridges rather than sheets, since modern sand ridges show opposed sand transport directions on their two sides (Stride et al., 1982, especially Fig. 5.17). Overall, there is a preference for northward foreset dips among the known Skonun Formation exposures. This northward preference, if the sand bodies are ridges, would indicate that the regional net sand transport direction was toward the south (*sic*; Stride et al., 1982, p. 118).

The distinction between sheet- and ridge geometry is important for petroleum exploration and production, since it has implications for reservoir shape and volume. One approach to resolving this question is to attempt to map the sand bodies seismically.

Due to long-distance tidal transportation, tidal-shelf sand bodies may have greater compositional maturity, hence better porosity and permeability, than is usual for the Skonun Formation, which generally has low permeability (despite high porosity) due to bridging of pores by feldspar decomposition products (Shouldice, 1971).

**(3) Storm-dominated shelf association.** This association consists of amalgamated, hummocky cross-stratified to burrowed sandstone, with subordinate mudstone. The association is represented by an exposure at Skonun Point (eastern stack) and by the three cores in the Harlequin and Osprey wells. Sand bodies could be either shore-connected tongues (cf. Brenchley and Newall, 1982, Fig. 10), or offshore bars (cf. de Raaf et al., 1977).

#### *Relationship among Unit II facies associations*

The vertical and lateral interrelationships between the three facies associations are uncertain because of the limited exposure and core control. Similarly, the typical thickness of any one interval of each association is unknown, because none of the known outcrop sections exposes the top and bottom of an association. Consequently, the scale of alternation among the three associations is also unknown. Most localities, despite being up to 15 m thick, expose only one facies association, indicating that associations are intercalated on a scale of at least tens of metres. Only two localities, Miller Creek and PQ898695 (Masset Sound), expose the contact between two associations. At Miller Creek, the delta-plain association is sharply overlain by the tidal-shelf association, indicating a rapid marine transgression. This is reminiscent of the inferred rapid transgression at the base of the (10-30 m) regressive sequences recognized on well logs (above). This leads to a speculative model whereby each regressive sequence comprises tidal-shelf deposits at the base, shallowing up gradually through delta-front

facies into delta-plain facies. However, neither an upward gradation nor any delta-front deposits have been observed, probably because of sparse exposure. The second locality, on Masset Sound, neither confirms nor negates the model: tidal-shelf facies pass up sharply into an inferred delta-plain channel, which could have eroded the "missing" delta-front deposits. Two other Masset Sound exposures provide additional evidence of an intimate relationship between the tidal-shelf and delta-plain associations: the former association is exposed at Collision Point, while the latter occurs at Nadu River mouth: although the two localities are as much as 8 km apart, stratigraphic proximity can be inferred because the strata at both localities are subhorizontal and are at similar elevations (within 2 m of high-tide level).

The spatial relationship between the storm-dominated shelf association and the other two associations is uncertain because the former is so sparsely exposed and because no contacts are visible. However, at Skonun Point, the storm-dominated shelf association and the tidal-shelf association, although exposed in separate sea stacks 150 m apart, are on strike with one another and have similar dips, suggesting that the two associations are in (concealed) stratigraphic contact, unless a fault separates the two stacks. The probable close relationship implies that, on the Unit II shelf, tide-dominated areas graded laterally into storm-dominated areas.

Although the spatial and paleogeographic relationship between the two shelf associations is poorly understood, it is concluded that Unit II on Graham Island comprises shelf-to-delta cycles 10-30 m thick. In contrast, cycles could be entirely continental to the north of Graham Island, and entirely marine to the south (Fig. 4).

#### *Paleoclimatic implications*

Iceberg dropstones appear to be common in Unit II shelf sediments, as described above. The inferred icebergs may have been calving along the coast of mainland British Columbia, where the ancestral (late Miocene) Coast Mountains (Fig. 1) may have been sufficiently high to produce glaciers capable of reaching the sea (Higgs, 1989c). However, as discussed above, it seems likely that at least some of the icebergs were calved from glaciers in the mountains of ancestral (Miocene) Moresby Island. In apparent contradiction of this evidence for nearby glaciers, molluscs in the Skonun Formation indicate that the local shallow-water climate in late Miocene time was temperate and "probably somewhat warmer than that which occurs off this coast today" (Addicott, 1978, p. 687). Similarly, microflora in the Skonun Formation indicates that the climate was "relatively humid, and probably somewhat more temperate than...today" (Martin and Rouse, 1966, p. 179). Thus the dropstones probably do *not* reflect a cold regional climate. Instead, the dropstones may reflect a combination of high elevations and heavy precipitation in the ancestral Moresby mountains, such that glaciers were sufficiently nourished to reach the sea, despite the mild climate which prevailed at sea level.

#### ACKNOWLEDGMENTS

Roy Hyndman, John Rowling, Glenn Woodsworth and Chris Yorath provided helpful comments on the first draft of this paper, and Peter Bobrowsky kindly tutored me in aspects of glaciology. I thank Brian Sawyer, Linda Bedard and Gena L'Esperance for expert drafting and limitless patience. Rod Smith performed the heavy-mineral separations and identifications with aplomb. I am grateful to numerous people for visiting the field with me and for offering helpful discussions and observations, including Brian Bornhold, Bob Davis, Tony Fogarassy, Cathie Hickson, Don Keith, Darrell Keiver, Bob Leatherbarrow, Linda McCulloch-Smith, Jean Pelletier, Pat Purcell, Brent Snyder, Bob Thompson, Bruce Thornhill, James White and Hans Wielems. Steve Harding helped with trace-fossil identification. Tania Hale and Ken Hoffman were keen field assistants. Dave Pawliuk caught



several errors during a final polish of the manuscript. For permission to examine and sample cores, I am grateful to Bow Valley Industries Ltd., City Resources (Canada) Ltd., PetroCanada Resources, and Unocal Canada Ltd.

## REFERENCES

- Addicott, W.O.  
1978: Late Miocene mollusks from the Queen Charlotte Islands, British Columbia, Canada; United States Geological Survey, Journal of Research, v. 6, p. 677-689.
- Aigner, T. and Reineck, H.-E.  
1982: Proximity trends in modern storm sands from the Helgoland Bight (North Sea) and their implications for basin analysis; *Senckenbergiana maritima*, v. 14, p. 183-215.
- Allen, J.R.L.  
1980: Sand waves: a model of origin and internal structure; *Sedimentary Geology*, v. 26, p. 281-328.  
1984: Experiments on the settling, overturning and entrainment of bivalve shells and related models; *Sedimentology*, v. 31, p. 227-250.
- Anderson, R.G. and Greig, C.J.  
1989: Jurassic and Tertiary plutonism in the Queen Charlotte Islands, British Columbia; *in* Current Research, Part H, Geological Survey of Canada, Paper 89-1H, p. 95-104.
- Anderson, R.G. and Reichenbach, I.  
1989: A note on the geochronometry of Late Jurassic and Tertiary plutonism in the Queen Charlotte Islands, British Columbia; *in* Current Research, Part H, Geological Survey of Canada, Paper 89-1H, p. 105-112.  
1991: U-Pb and K-Ar framework for Middle to Late Jurassic (172-158 Ma) and Tertiary (46-27 Ma) plutons in Queen Charlotte Islands, British Columbia; *in* Evolution and Hydrocarbon Potential of the Queen Charlotte Basin, British Columbia, Geological Survey of Canada, Paper 90-10.
- Anderton, R.  
1976: Tidal-shelf sedimentation: an example from the Scottish Dalradian; *Sedimentology*, v. 23, p. 429-458.
- Belderson, R.H., Johnson, M.A., and Kenyon, N.H.  
1982: Bedforms; *in* Offshore Tidal Sands, A.H. Stride (ed.), Chapman and Hall, London, p. 27-57.
- Berner, R.A.  
1984: Sedimentary pyrite formation: an update; *Geochimica et Cosmochimica Acta*, v. 48, p. 605-615.
- Bourgeois, J.  
1980: A transgressive shelf sequence exhibiting hummocky stratification: the Cape Sebastian Sandstone (Upper Cretaceous), southwestern Oregon; *Journal of Sedimentary Petrology*, v. 50, p. 681-702.
- Bow Valley Industries  
1984a: Well history report, Bow Valley et al. Naden b-27-J; British Columbia Department of Mines and Petroleum Resources, Open File WA06086.  
1984b: Well history report, Bow Valley et al. Naden b-A27-J; British Columbia Department of Mines and Petroleum Resources, Open File WA06110.
- Brenchley, P.J. and Newall, G.  
1982: Storm-influenced inner-shelf sand lobes in the Caradoc (Ordovician) of Shropshire, England; *Journal of Sedimentary Petrology*, v. 52, p. 1257-1269.
- Brew, D.A.  
1989: Cenozoic sedimentation, magmatism, and tectonism in southeastern Alaska; *in* Northeast Pacific – North America Plate Interactions throughout the Cenozoic, Geological Association of Canada (Pacific Section) Symposium, April 14, 1989, Victoria, B.C., Programme and Abstracts.
- Bustin, R.M. and Macaulay, G.  
1988: Organic petrology and Rock-Eval pyrolysis of the Jurassic Sandilands and Ghost Creek formations, Queen Charlotte Islands; *Bulletin of Canadian Petroleum Geology*, v. 36, p. 168-176.
- Cameron, B.E.B. and Hamilton, T.S.  
1988: Contributions to the stratigraphy and tectonics of the Queen Charlotte Basin, British Columbia; *in* Current Research, Part E, Geological Survey of Canada, Paper 88-1E, p. 221-227.
- Cant, D.J.  
1984: Subsurface facies analysis; *in* Facies Models, 2nd edn, R.G. Walker (ed.), Geological Association of Canada, St. John's, p. 297-310.
- Cant, D.J. and Walker, R.G.  
1978: Fluvial processes and facies sequences in the sandy braided South Saskatchewan River, Canada; *Sedimentology*, v. 25, p. 625-648.
- Carver, R.E.  
1971: Heavy-mineral separation; *in* Procedures in Sedimentary Petrology, R.E. Carver (ed.), Wiley, New York, p. 427-452.
- Champigny, N., Henderson, C.M., and Rouse, G.E.  
1981: New evidence for the age of the Skonun Formation, Queen Charlotte Islands, British Columbia; *Canadian Journal of Earth Sciences*, v. 18, p. 1900-1903.
- Champigny, N. and Sinclair, A.J.  
1982: The Cinola gold deposit, Queen Charlotte Islands, British Columbia; *in* Canadian Institute of Mining and Metallurgy, Special Volume 24, p. 243-254.
- Christie-Blick, N. and Biddle, K.T.  
1985: Deformation and basin formation along strike-slip faults; *in* Strike-Slip Deformation, Basin Formation, and Sedimentation, K.T. Biddle and N. Christie-Blick (ed.), Society of Economic Paleontologists and Mineralogists, Special Publication 37, p. 1-34.
- Clague, J.J., Mathewes, R.W., and Warner, B.G.  
1982: Late Quaternary geology of eastern Graham Island, Queen Charlotte Islands, British Columbia; *Canadian Journal of Earth Sciences*, v. 19, p. 1786-1795.
- Collinson, J.D.  
1986: Alluvial sediments; *in* Sedimentary Environments and Facies, 2nd edn, H.G. Reading (ed.), Blackwell, Oxford, p. 20-62.
- Collinson, J.D. and Thompson, D.B.  
1982: Sedimentary Structures; George Allen and Unwin, London, 194 p.
- de Raaf, J.F.M., Boersma, J.R., and van Gelder, A.  
1977: Wave-generated structures and sequences from a shallow marine succession, Lower Carboniferous, County Cork, Ireland; *Sedimentology*, v. 24, p. 451-483.
- Dewey, J.F.  
1982: Plate tectonics and the evolution of the British Isles; *Journal of the Geological Society of London*, v. 139, p. 371-412.
- Dickinson, W.R.  
1978: Plate tectonic evolution of sedimentary basins; *in* Plate Tectonics and Hydrocarbon Evolution, American Association of Petroleum Geologists, Continuing Education Course Note Series, No. 1, revised edition.
- Dietrich, J.R., Higgs, R., and White, J.M.  
1989: Seismic, sedimentological and palynological investigations in the Tertiary Queen Charlotte Basin; *in* Exploration Update '89, Convention of Canadian Society of Exploration Geophysicists and Canadian Society of Petroleum Geologists, June 11-15, 1989, Programs and Abstracts, p. 163.
- Dott, R.H., Jr. and Bourgeois, J.  
1982: Hummocky stratification: significance of its variable bedding sequences; *Geological Society of America Bulletin*, v. 93, p. 663-680.
- Eisbacher, G.H.  
1985: Pericollisional strike-slip faults and synorogenic basins, Canadian Cordillera; *in* Strike-Slip Deformation, Basin Formation, and Sedimentation, K.T. Biddle and N. Christie-Blick (ed.), Society of Economic Paleontologists and Mineralogists, Special Publication 37, p. 265-282.
- Elliott, T.  
1986: Deltas; *in* Sedimentary Environments and Facies, H.G. Reading (ed.), Blackwell, Oxford, p. 113-154.
- Engelbreton, D.C., Cox, A., and Gordon, R.G.  
1985: Relative motions between oceanic and continental plates in the Pacific basin; *Geological Society of America, Special Paper 206*, 59 p.
- Eyles, N. and Lagoe, M.B.  
1989: Sedimentology of shell-rich deposits (coquinas) in the glaciomarine upper Cenozoic Yakutat Formation, Middleton Island, Alaska; *Geological Society of America Bulletin*, v. 101, p. 129-142.
- Eyles, N. and Miall, A.D.  
1984: Glacial facies; *in* Facies Models, R.G. Walker (ed.), Geological Association of Canada, St. John's, p. 15-38.
- Frey, R.W., Howard, J.D., and Pryor, W.A.  
1978: *Ophiomorpha*: its morphologic, taxonomic, and environmental significance; *Palaeogeography, Palaeoclimatology, Palaeoecology*, v. 23, p. 199-229.
- Galloway, W.E.  
1974: Deposition and diagenetic alteration of sandstone in northeast Pacific arc-related basins: implications for graywacke genesis; *Geological Society of America Bulletin*, v. 85, p. 379-390.
- Goodwin, P.W. and Anderson, E.J.  
1985: Punctuated aggradational cycles: a general hypotheses of episodic stratigraphic accumulation; *Journal of Geology*, v. 93, p. 515-533.
- Hamilton, T.S.  
1989: Tertiary extensional volcanism and volcanotectonic interactions along the Queen Charlotte portion of the western Canadian continental margin; *in* Northeast Pacific – North America Plate Interactions throughout the Cenozoic, Geological Association of Canada (Pacific Section) Symposium, April 14, 1989, Victoria, B.C., Programme and Abstracts.
- Hamilton, T.S. and Cameron, B.E.B.  
1989: Hydrocarbon occurrences on the western margin of the Queen Charlotte Basin; *Bulletin of Canadian Petroleum Geology*, v. 37, p. 443-466.
- Harding, T.P., Gregory, R.F., and Stephens, L.H.  
1983: Convergent wrench fault and positive flower structures; *in* Seismic Expression of Structural Styles, A.W. Bally (ed.), American Association of Petroleum Geologists, Studies in Geology Series, No. 15, v. 3, p. 4.2-13 – 4.2-17.
- Harms, J.C., Southard, J.B., and Walker, R.G.  
1982: Structures and Sequences in Clastic Rocks; Society of Economic Paleontologists and Mineralogists, Short Course 9.

- Heward, A.P.**  
1978: Alluvial fan and lacustrine sediments from the Stephanian A and B (La Magdalena, Cinera-Matallana and Sabero) coalfields, northern Spain; *Sedimentology*, v. 25, p. 451-488.
- Hickson, C.J.**  
1988: Structure and stratigraphy of the Masset Formation, Queen Charlotte Islands, British Columbia; in *Current Research, Part E, Geological Survey of Canada*, Paper 88-1E, p. 269-274.  
1989: An update on structure and stratigraphy of the Masset Formation, Queen Charlotte Islands, British Columbia; in *Current Research, Part H, Geological Survey of Canada*, Paper 89-1H, p. 73-79.  
1991: The Masset Formation on Graham Island, Queen Charlotte Islands, British Columbia; in *Evolution and Hydrocarbon Potential of the Queen Charlotte Basin, British Columbia*, Geological Survey of Canada, Paper 90-10.
- Higgs, R.**  
1988: The Skonun Formation, Queen Charlotte Basin: sedimentology and implications for petroleum exploration; in *Sedimentary Basins of the Canadian Cordillera, Geological Association of Canada (Pacific Section) Symposium*, March 25, 1988, Victoria, B.C., Programme and Abstracts, p. 14-15.  
1989a: Sedimentological studies in Queen Charlotte Basin: implications for basin origin and for petroleum exploration; in *Northeast Pacific – North America Plate Interactions throughout the Cenozoic, Geological Association of Canada (Pacific Section) Symposium*, April 14, 1989, Victoria, B.C., Programme and Abstracts.  
1989b: Sedimentology and implications for hydrocarbon exploration of the "Hipba beds", Queen Charlotte Islands, British Columbia; in *Current Research, Part H, Geological Survey of Canada*, Paper 89-1H, p. 53-58.  
1989c: Sedimentological aspects of the Skonun Formation, Queen Charlotte Islands, British Columbia; in *Current Research, Part H, Geological Survey of Canada*, Paper 89-1H, p. 87-94.  
1990: Sedimentology and tectonic implications of Cretaceous fan-delta conglomerates, Queen Charlotte Islands, Canada; *Sedimentology*, v. 37, p. 83-103.  
1991: Sedimentology and implications for petroleum exploration of the Honna Formation, northern Queen Charlotte Islands, British Columbia; in *Evolution and Hydrocarbon Potential of the Queen Charlotte Basin, British Columbia*, Geological Survey of Canada, Paper 90-10.
- Houthuys, R. and Gullentops, F.**  
1988: Tidal transverse bars building up a longitudinal sand body (Middle Eocene, Belgium); in *Tide-Influenced Sedimentary Environments and Facies*, P.L. De Boer, A. van Gelder, and S.-D. Nio (ed.), Reidel, Dordrecht, p. 153-166.
- Hubert, J.F.**  
1971: Analysis of heavy-mineral assemblages; in *Procedures in Sedimentary Petrology*, R.E. Carver (ed.), Wiley, New York, p. 453-478.
- Hutchison, W.W., Berg, H.C., and Okulitch, A.V.**  
1979: Skeena River, Sheet 103; Geological Survey of Canada, Map 1385A.
- Hyndman, R.D. and Ellis, R.M.**  
1981: Queen Charlotte fault zone: microearthquakes from a temporary array of land stations and ocean bottom seismographs; *Canadian Journal of Earth Sciences*, v. 19, p. 776-788.
- Hyndman, R.D. and Hamilton, T.S.**  
1991: Cenozoic relative plate motions along the northeastern Pacific margin and their association with Queen Charlotte area tectonics and volcanism; in *Evolution and Hydrocarbon Potential of the Queen Charlotte Basin, British Columbia*, Geological Survey of Canada, Paper 90-10.
- Jopling, A.V.**  
1965: Hydraulic factors controlling the shape of laminae in laboratory deltas; *Journal of Sedimentary Petrology*, v. 35, p. 777-791.
- Kreisa, R.D.**  
1981: Storm-generated sedimentary structures in subtidal marine facies with examples from the Middle and Upper Ordovician of southwestern Virginia; *Journal of Sedimentary Petrology*, v. 51, p. 823-848.
- Lowe, D.R.**  
1982: Sediment gravity flows: II. Depositional models with special reference to the deposits of high-density turbidity currents; *Journal of Sedimentary Petrology*, v. 52, p. 279-297.
- McKenzie, D.**  
1978: Some remarks on the development of sedimentary basins; *Earth and Planetary Science Letters*, v. 40, p. 25-32.
- McWhae, J.R.**  
1986: Geology, structure and hydrocarbon potential of Queen Charlotte Basin; British Columbia Ministry of Energy, Mines and Petroleum Resources, Petroleum Resources Division, unpublished report.
- Mackie, D.J., Clowes, R.M., Dehler, S.A., Ellis, R.M., and Morel-L'Huissier, P.**  
1989: The Queen Charlotte Islands refraction project. Part II. Structural model for transition from Pacific plate to North American plate; *Canadian Journal of Earth Sciences*, v. 26, p. 1713-1725.
- Martin, H.A. and Rouse, G.E.**  
1966: Palynology of late Tertiary sediments from Queen Charlotte Islands, British Columbia; *Canadian Journal of Botany*, v. 44, p. 171-208.
- Middleton, G.V. and Hampton, M.A.**  
1976: Subaqueous sediment transport and deposition by sediment gravity flows; in *Marine Sediment Transport and Environmental Management*, D.J. Stanley and D.J.P. Swift (ed.), Wiley, New York, p. 197-218.
- Mitchell, A.H.G. and Reading, H.G.**  
1986: Sedimentation and tectonics; in *Sedimentary Environments and Facies*, H.G. Reading (ed.), Blackwell, Oxford, p. 113-154.
- Monger, J.W.H. and Berg, H.C.**  
1984: Lithotectonic terrane map of western Canada and southeastern Alaska; in *Lithotectonic Terrane Maps of the North American Cordillera*, N.J. Silberling and D.L. Jones (ed.), United States Geological Survey, Open File 84-523.
- Nemec, W. and Steel, R.J.**  
1984: Alluvial and coastal conglomerates: their significant features and some comments on gravelly mass-flow deposits; in *Sedimentology of Gravels and Conglomerates*, E.H. Koster and R.J. Steel (ed.), Canadian Society of Petroleum Geologists, Memoir 10, p. 1-31.
- Nottvedt, A. and Kreisa, R.D.**  
1987: Model for the combined-flow origin of hummocky cross-stratification; *Geology*, v. 15, p. 357-361.
- Palmer, A.R.**  
1983: The decade of North American Geology 1983 geologic time scale; *Geology*, v. 11, p. 503-504.
- Parrish, R.A.**  
1983: Cenozoic thermal evolution and tectonics of the Coast Mountains of British Columbia; *Tectonics*, v. 2, p. 601-631.
- Patterson, R.T.**  
1988: Early Miocene to Quaternary foraminifera from three wells in the Queen Charlotte Basin off the coast of British Columbia; in *Sequences, Stratigraphy and Sedimentology: Surface and Subsurface*, D.P. James and D.A. Leckie (ed.), Canadian Society of Petroleum Geologists, Memoir 15, p. 497.  
1989: Neogene foraminiferal biostratigraphy of the southern Queen Charlotte Basin; in *Contributions to Canadian Paleontology*, Geological Survey of Canada, Bulletin 396, p. 229-265.
- Reineck, H.-E. and Singh, I.B.**  
1980: Depositional sedimentary environments, 2nd edn, Springer-Verlag, Berlin, 549 p.
- Richfield Oil Corporation**  
1958a: Well history report, Richfield-Mic Mac-Homestead Masset No. 1; British Columbia Department of Mines and Petroleum Resources, Open File WA00371.  
1958b: Well history report, Richfield-Mic Mac-Homestead Nadu River No. 1; British Columbia Department of Mines and Petroleum Resources, Open File WA00377.  
1958c: Well history report, Richfield-Mic Mac-Homestead Tow Hill No. 1; British Columbia Department of Mines and Petroleum Resources, Open File WA00380.  
1958d: Well history report, Richfield-Mic Mac-Homestead Gold Creek No. 1; British Columbia Department of Mines and Petroleum Resources, Open File WA00399.  
1958e: Well history report, Richfield-Mic Mac-Homestead Tlell No. 1; British Columbia Department of Mines and Petroleum Resources, Open File WA00406.  
1961: Well history report, Richfield-Mic Mac-Homestead Cape Ball; British Columbia Department of Mines and Petroleum Resources, Open File WA00754.
- Rohr, K. and Dietrich, J.R.**  
1991: Deep seismic reflection survey of the Queen Charlotte Basin, British Columbia; in *Evolution and Hydrocarbon Potential of the Queen Charlotte Basin, British Columbia*, Geological Survey of Canada, Paper 90-10.
- Shell Canada Ltd.**  
1968a: Well history report, Shell Anglo Tyee N-39; Canada Department of Energy, Mines and Resources, Open File.  
1968b: Well history report, Shell Anglo Sockeye B-10; Canada Department of Energy, Mines and Resources, Open File.  
1968c: Well history report, Shell Anglo Sockeye E-66; Canada Department of Energy, Mines and Resources, Open File.  
1968d: Well history report, Shell Anglo Auklet G-41; Canada Department of Energy, Mines and Resources, Open File.  
1968e: Well history report, Shell Anglo Osprey D-36; Canada Department of Energy, Mines and Resources, Open File.  
1968f: Well history report, Shell Anglo Harlequin D-86; Canada Department of Energy, Mines and Resources, Open File.  
1969a: Well history report, Shell Anglo South Coho I-74; Canada Department of Energy, Mines and Resources, Open File.  
1969b: Well history report, Shell Anglo Murrelet L-15; Canada Department of Energy, Mines and Resources, Open File.
- Shen, K., Champigny, N., and Sinclair, A.J.**  
1982: Fluid inclusion and sulphur isotope data in relation to genesis of the Cinola gold deposit, Queen Charlotte Islands, B.C.; in *Canadian Institute of Mining and Metallurgy, Special Volume 24*, p. 255-257.
- Shor, G.G.**  
1962: Seismic refraction studies off the coast of Alaska; *Bulletin of the Seismological Society of America*, v. 52, p. 37-57.
- Shouldice, D.H.**  
1971: Geology of the western Canadian continental shelf; *Bulletin of Canadian Petroleum Geology*, v. 19, p. 405-436.

- 1973: Western Canadian continental shelf; in *Future Petroleum Provinces of Canada*, R.G. McCrossan (ed.), Canadian Society of Petroleum Geologists, Memoir 1, p. 7-35.
- Snavey, P.D., Jr., Wagner, H.C., Tompkins, D.H., and Tiffin, D.L.**  
1981: Preliminary geologic interpretation of a seismic reflection profile across the Queen Charlotte Island fault system off Dixon Entrance, Canada-United States; United States Geological Survey, Open File 81-299, 12 p.
- Snowdon, L.R., Fowler, M.G., and Hamilton, T.S.**  
1988: Sources and seeps: organic geochemical results from the Queen Charlotte Islands; in *Some Aspects of the Petroleum Geology of the Queen Charlotte Islands*, R. Higgs (compiler), Canadian Society of Petroleum Geologists Field Guide to Sequences, Stratigraphy, Sedimentology: Surface and Subsurface Technical Meeting, September 14-16, 1988, Calgary, Alberta, p. 37-43.
- Souther, J.G.**  
1988: Implications for hydrocarbon exploration of dyke emplacement in the Queen Charlotte Islands, British Columbia; in *Current Research, Part E*, Geological Survey of Canada, Paper 88-1E, p. 241-245.  
1989: Dyke swarms in the Queen Charlotte Islands, British Columbia; in *Current Research, Part H*, Geological Survey of Canada, Paper 89-1H, p. 117-120.
- Souther, J.G. and Jessop, A.M.**  
1991: Dyke swarms in the Queen Charlotte Islands, and implications for hydrocarbon exploration; in *Evolution and Hydrocarbon Potential of the Queen Charlotte Basin*, British Columbia, Geological Survey of Canada, Paper 90-10.
- Steel, R.J. and Aasheim, S.M.**  
1978: Alluvial sand deposition in a rapidly subsiding basin (Devonian, Norway); in *Fluvial Sedimentology*, A.D. Miall (ed.), Canadian Society of Petroleum Geologists, Memoir 5, p. 385-412.
- Stock, J.M. and Molnar, P.**  
1988: Uncertainties and implications of the Late Cretaceous and Tertiary position of North America relative to the Farallon, Kula and Pacific Plates; *Tectonics*, v. 6, p. 1339-1384.
- Stow, D.A.V., Bishop, C.D., and Mills, S.J.**  
1982: Sedimentology of the Brae oilfield, North Sea: fan models and controls; *Journal of Petroleum Geology*, v. 5, p. 129-148.
- Stride, A.H., Belderson, R.H., Kenyon, N.H., and Johnson, M.A.**  
1982: Offshore tidal deposits: sand sheet and sand bank facies; in *Offshore Tidal Sands*, A.H. Stride (ed.), Chapman and Hall, London, p. 95-125.
- Sutherland Brown, A.**  
1968: Geology of the Queen Charlotte Islands, British Columbia; British Columbia Department of Energy, Mines and Petroleum Resources, Bulletin 54, 226 p.
- Thompson, R.I. and Thorkelson, D.**  
1989: Regional mapping update, central Queen Charlotte Islands, British Columbia; in *Current Research, Part H*, Geological Survey of Canada, Paper 89-1H, p. 7-11.
- Union Oil Company of Canada Ltd.**  
1971: Well history report, Union Port Louis; British Columbia Department of Mines and Petroleum Resources, Open File WA02954.
- Vellutini, D. and Bustin, R.M.**  
1988: Preliminary results on organic maturation of the Tertiary Skonun Formation, Queen Charlotte Islands, British Columbia; in *Current Research, Part E*, Geological Survey of Canada, Paper 88-1E, p. 255-258.
- Visser, M.J.**  
1980: Neap-spring cycles reflected in Holocene subtidal large-scale bedform deposits: a preliminary note; *Geology*, v. 8, p. 543-546.
- Walker, R.G.**  
1984: General introduction: facies, facies sequences and facies models; in *Facies Models*, 2nd edn., R.G. Walker (ed.), Geological Association of Canada, St. John's, p. 1-9.
- Walker, R.G., Duke, W.L., and Leckie, D.A.**  
1983: Hummocky stratification: significance of its variable bedding sequences; discussion; *Geological Society of America Bulletin*, v. 94, p. 1245-1249.
- White, J.M.**  
1990: Evidence of Paleogene sedimentation on Graham Island, Queen Charlotte Islands, west coast, Canada; *Canadian Journal of Earth Sciences*, v. 27, p. 533-538.  
1991: Palynostratigraphy of Tow Hill No. 1 Well in the Skonun Formation, Queen Charlotte Basin, British Columbia; in *Evolution and Hydrocarbon Potential of the Queen Charlotte Basin*, British Columbia, Geological Survey of Canada, Paper 90-10.
- Wilson, J.B.**  
1982: Shelly faunas associated with temperate offshore tidal deposits; in *Offshore Tidal Sands*, A.H. Stride (ed.), Chapman and Hall, London, p. 126-171.
- Woodsworth, G.J.**  
1988: Kamutsen Formation and the east boundary of the Queen Charlotte Basin, British Columbia; in *Current Research, Part E*, Geological Survey of Canada, Paper 88-1E, p. 209-212.
- Yorath, C.J.**  
1987: Petroleum geology of the Canadian Pacific continental margin; in *Geology and Resource Potential of the Continental Margin of Western North America and Adjacent Ocean Basins - Beaufort Sea to Baja California*, D.W. Scholl, A. Grantz, and J.G. Vedder (ed.), Circum-Pacific Council for Energy and Mineral Resources, Houston, Earth Science Series, v. 6, p. 283-304.
- Yorath, C.J. and Cameron, B.E.B.**  
1982: Oil off the west coast?; *GEOS (Energy, Mines and Resources Canada)*, v. 11, p. 13-15.
- Yorath, C.J. and Chase, R.L.**  
1981: Tectonic history of the Queen Charlotte Islands and adjacent areas - a model; *Canadian Journal of Earth Sciences*, v. 18, p. 1717-1739.
- Yorath, C.J. and Hyndman, R.D.**  
1983: Subsidence and thermal history of Queen Charlotte Basin; *Canadian Journal of Earth Sciences*, v. 20, p. 135-159.
- Young, I.F.**  
1981: Structure of the western margin of the Queen Charlotte Basin, British Columbia; M.Sc. thesis, University of British Columbia, Vancouver, 380 p.

## APPENDIX 1: BOREHOLE CORES: DESCRIPTION AND INTERPRETATION

### Union Port Louis c-28-L 103-F-10

*Core #1, 5116-5147 ft., rec. 31 ft.*

This core was cut at the base of the well and consists of volcanics belonging either to Unit I (Masset Formation) or to the Middle Jurassic Yakoun Group (Union Oil Company of Canada Ltd., 1971).

### Bow Valley et al. Naden b-27-J 103-F-15

Continuous core in Unit I (Masset) volcanics. Hole abandoned at 474 m due to technical problems.

### Bow Valley et al. Naden b-A27-J 103-F-15

Continuous core in Unit I volcanics to total depth of 1147.9 m.

### Richfield et al. Tow Hill d-93-C 103-J-4

*Core #1, 241-261 ft., rec. 11 ft.*

Light to medium grey mudstone. Millimetre-scale parallel lamination, variably homogenized (by burrowing and/or rooting?). Abundant carbonaceous laminae, comprising millimetre-centimetre comminuted plant detritus. Probably nonmarine, based on conspicuous plant debris and lack of fossils and pyrite. Possibly fluvial or deltaic overbank.

*Core #2, 450-470 ft., rec. 6.8 ft.*

Light grey, massive mudstone with common plant detritus, including leaf fragments. Millimetre-scale parallel lamination locally visible, highly contorted (by burrowing and/or rooting?). Siderite(?) nodule 2 cm across. Interpretation as for Core 1.

*Core #3, 604-624 ft., rec. 19.1 ft.*

Light grey mudstone, sharply overlain by 15 ft of fining-upward (coarse to fine), massive sandstone, grading up into light grey mudstone with common leaf impressions. The sandstone contains a conifer cone. Probably fluvial, based on fining-upward sandstone (channel), non-comminuted plant matter, and lack of fossils.

*Core #4, 815-835 ft., rec. 13 ft.*

Light grey mudstone, sharply overlain by 4 ft of fining-upward (coarse to fine) sandstone, grading up into light grey mudstone with common plant debris. Interpretation as for Core 3.

*Core #5, 998-1016 ft., rec. 16.9 ft.*

Grey-brown mudstone, massive at base, parallel-laminated (mm-cm scale) in the top 7 ft. Brown microcrystalline siderite(?) nodule 1 cm across. Carbonaceous partings and centimetre-size plant fragments. Interpretation as for Core 1.

*Core #6, 1140-1155 ft., rec. 2 ft.*

Pebbly mudstone (0.25 ft) with rounded clasts of granitic gneiss, siltstone and mudstone, overlain by 1 ft of green aphanitic volcanic rock (possibly a clast), capped by 0.75 ft of light grey mudstone, locally millimetre-laminated. Interpreted as a debris flow deposit or as glaciomarine mud with dropstones.

*Core #7, 1200-1208 ft., rec. 5 ft.*

Green volcanic rock capped by 0.5 ft of grey mudstone. The mudstone is brittle (baked, according to Sutherland Brown (1968, p. 127)).

*Core #8, 1470-1480 ft., rec. 7.6 ft.*

Parallel-laminated sandstone, varying from medium to coarse, containing a subrounded basalt pebble 2 cm across. The lamination shows about 40° dip, but this is structural, as shown by dipping mudstone laminations in other cores. Centimetre-size plant fragment. Interpreted as fluvial-channel sand, based on plant fragment, coarse grain size, lack of fossils and dominance of probable fluvial deposits in overlying cores. Richfield Oil Corporation (1958c) reported 29% porosity and 578 mD permeability for a sample which is probably from this core (reported depth of 1410 ft should presumably read 1470 ft).

*Core #9, 1730-1735 ft., rec. 4 ft.*

Olive-brown mudstone. Slight oil stain was reported by Sutherland Brown (1968, p. 179), but a small core sample collected by the author and tested in toluene by Dr. T.S. Hamilton yielded no cut, and staining is not reported in the CanStrat log.

*Core #10, 1735-1750 ft., rec. 10 ft.*

Light grey-brown to olive-brown mudstone. Millimetre-scale parallel lamination, variably homogenized. Common millimetre-thick carbonaceous laminae with well preserved plant leaves and stems. Microfaulted interval a few centimetres thick, truncated upward (i.e. syn-sedimentary). Probably fluvial overbank, based on uncomminuted plant material, lack of fossils and lack of obvious burrows. Homogenization possibly due to rooting. Microfaults suggest syn-depositional tectonism (earthquakes).

*Core #11, 1911-1931 ft., rec. 11.1 ft.*

Parallel-laminated medium sandstone. Many laminae comprise sand-size carbonaceous detritus. Rounded mud chips 1-3 cm across are concentrated in intervals a few centimetres thick. Probably fluvial, based on high carbonaceous content and on dominance of probable fluvial facies in preceding cores.

*Core #12, 2123-2143 ft., rec. 17.2 ft.*

Parallel-laminated medium sandstone (0.5 ft) grades up into very fine sandstone and siltstone showing parallel lamination, ripple cross-lamination and convolute lamination alternating on a centimetre scale (Bouma sequences?). This grades up into mudstone with millimetre-scale parallel lamination, variably homogenized, probably by rooting and/or burrowing. The mudstone shows rootlets, and also oblique, cylindrical burrows 1-5 mm in diameter and up to 5 cm long. Carbonaceous laminae are common throughout the core. Interpreted as fluvial levee deposits, based on rootlets, abundant plant detritus, dominance of silt and very-fine sand, and possible Bouma sequences (Elliott, 1986, p. 137 and Fig. 6.29B).

*Core #13, 2355-2370 ft., rec. 5.5 ft.*

Parallel-laminated to massive siltstone and very fine sandstone. Carbonaceous. Probably fluvial, based on high carbonaceous content and dominance of probable fluvial facies in preceding cores.

*Core #14, 2540-2551 ft., rec. 11.2 ft.*

Grey siltstone, with parallel lamination, much of which is partly to completely homogenized by bioturbation. Laminated intervals comprise alternating millimetre-thick light and dark laminae. Dark laminae consist of comminuted plant debris, with some centimetre-size leaf and stem fragments. A few centimetre-thick ripple cross-laminated intervals. Burrows as in Core 12. Interpreted as fluvial levee, as for Core 12.

*Core #15, 2660-2673 ft., rec. 11.9 ft.*

Massive to parallel-laminated medium sandstone, grading up into parallel-laminated fine sandstone. Abundant carbonaceous laminae. Scattered rounded siltstone chips up to 2 cm across. Rare whole leaves. Horizon of millimetre-size ferruginous (siderite?) concretions. Interpreted as fluvial channel deposits, based on overall fining-upward trend, abundant plant debris and dominance of probable fluvial facies in cores above.

*Core #16, 2840-2850 ft., rec. 10 ft.*

Ripple cross-laminated and convolute-laminated siltstone. Top metre contains centimetre-decimetre interbeds of pebble conglomerate, matrix- to clast-supported, and a 10 cm layer of parallel-laminated very coarse sandstone. Conglomerate beds comprise angular to subrounded volcanic and granitoid-gneiss clasts, and have sharp tops and bases; matrix is very coarse sandstone. Entire core may comprise low-density turbidites (siltstone) and high-density turbidites (sandstone and conglomerate) (Lowe, 1982). Alternatively, the conglomerate may have been deposited by cohesionless debris flows (Lowe, 1982; Nemec and Steel, 1984). Convolute lamination may be of depositional (turbidite) origin, or may be due to penecontemporaneous earthquakes. Environment subaqueous, but could be either marine or lacustrine.

*Core #17, 3005-3015 ft., rec. 9.5 ft.*

Graded sandstone beds (coarse sand to silt), 10-30 cm thick, comprising amalgamated Bouma AB, ABC, and B sequences, with a few E divisions. Two A divisions contain centimetre-thick mud-chip conglomerates. Interpreted as turbidites, based on grading and Bouma sequences. The turbidites are largely amalgamated, without intervening "background" mud deposits.

*Core #18, 3230-3240 ft., rec. 9.5 ft.*

Graded sandstone beds, centimetre-decimetre thick, ranging from very coarse sand to silt, showing Bouma features including ABE, ABCDE and BCE sequences. Interpreted as non-amalgamated turbidites.

*Core #19, 3406-3416 ft., rec. 8.7 ft.*

Centimetre-decimetre beds of massive, granule to pebble conglomerate, with sharp tops and bases, alternating with centimetre-decimetre intervals of siltstone and very fine to medium sandstone showing Bouma sequences. Top 20 cm consists of mottled (burrowed?) mudstone. Conglomerate is matrix- (very coarse sand) to clast-supported. Clasts are angular to rounded, and include volcanics and granitoid-gneiss. The siltstone-sandstone intervals are interpreted as turbidites. The conglomerates are interpreted as sediment gravity flow deposits (either high-density turbidites or cohesionless debris flow deposits (Lowe, 1982; Nemec and Steel, 1984)). The mudstone represents background deposition from suspension.

*Core #20, 3531-3541 ft., rec. 8.9 ft.*

Centimetre-decimetre beds of pebble-cobble conglomerate, with four interlayers (cm) of parallel-laminated and ripple cross-laminated sandstone. The conglomerate is clast-supported, with a coarse sand to granule matrix. Clasts are almost entirely dark grey, aphanitic volcanics, mostly rounded, with a few quartz pebbles. Maximum clast size 10 cm. One coal clast 2 cm across. The sandstone beds are interpreted as turbidites. The conglomerate beds are interpreted as high density turbidites or cohesionless debris flows.

*Core #21, 3620-3630 ft., rec. 9.6 ft.*

Centimetre-decimetre graded sandstone beds, ranging from coarse sand to silt, showing Bouma AB and ABC sequences. Mud-chip conglomerates (cm) at base of two A divisions. Interpreted as amalgamated turbidites.

*Core #22, 3830-3840 ft., rec. 10 ft.*

Basal 50 cm consists of granule and fine-pebble conglomerate, parallel-stratified on a 1-5 cm scale, with a matrix of coarse to very coarse sand. Grades up into massive, dark grey muddy sediment (diamictite) which ranges from mud-supported granule conglomerate to sandy, granulely mudstone. The diamictite contains: (1) about three thin (cm) granule or very coarse sand layers with gradational tops and bottoms; and (2) abundant centimetre-long plant fragments, forming thin (mm) coal seams. Diamictite could represent mudflow deposits, or glacial tillite, or glaciomarine muds with dropstones; the mudflow interpretation is the most likely, based on dominance of sediment gravity flow deposits in adjacent cores (Cores 16 to 33). Again based on the dominance of sediment gravity flow deposits in cores 16-33, the stratified conglomerate is more likely a sediment gravity flow deposit than a fluvial deposit.

*Core #23, 4020-4030 ft., rec. 9 ft.*

Clast-supported pebble-cobble conglomerate. Matrix is coarse sand to granules. Clasts are up to 10 cm across, mostly subrounded to well rounded, and mostly light to dark grey, aphanitic volcanics. A few clasts of granitoid-gneiss; also finely crystalline quartz with 5-10% dark crystals (vein quartz?). Interpreted as sediment gravity flow deposits, rather than fluvial, based on dominance of sediment gravity flow deposits in associated cores and on lack of stratification; probably high-density turbidites or cohesionless debris-flow deposits.

*Core #24, 4230-4240 ft., rec. 9 ft.*

Dark grey, massive mudstone. 10 cm layer of clast-supported conglomerate near top, with sharp top and bottom; clasts rounded, mostly medium-dark grey volcanics. The mudstone is interpreted as a mudflow deposit, based on the dominance of sediment gravity flow deposits in associated cores and on the lack of structure. The conglomerate is probably also a sediment gravity flow deposit.

*Core #25, 4445-4455 ft., rec. 10 ft.*

Clast-supported, pebble conglomerate interbedded (dm-scale) with medium to dark grey, fine-medium massive sandstone. The conglomerate is non-stratified, has a coarse to very coarse sand matrix, and locally shows 10-20% visible quartz cement. Interpreted as high-density turbidites or cohesionless debris flow deposits (conglomerate) and Bouma A turbidites (sandstone).

*Core #26, 4650-4660 ft., rec. 10 ft.*

Non-stratified, clast-supported conglomerate, sharply overlain by 1.2 m of dark grey, fine-medium massive sandstone. Interpretation as for Core 25.

*Core #27, 4860-4870 ft., rec. 10 ft.*

Pebble conglomerate, clast- to matrix supported. Matrix is coarse sand. Clasts are rounded, mostly dark grey aphanitic volcanics. Some centimetre-long plant fragments. Interpreted as sediment gravity flow deposits, rather than fluvial, based on lack of stratification.

*Core #28, 5050-5060 ft., rec. 4 ft.*

Clast- to matrix-supported, non-stratified pebble conglomerate. Matrix is fine to coarse sand. Interpretation as for Core 27.

*Core #29, 5270-5290 ft., rec. 20 ft.*

Decimetre-interbedded pebble-cobble conglomerate and coarse sandstone. Conglomerate layers are clast-supported; clasts are mostly subrounded to well rounded, medium to dark grey, aphanitic volcanics. Matrix is coarse sand to granules. Two sandstone layers are parallel-laminated throughout; the third is massive and grades up into a few centimetres of dark grey mudstone. The conglomerate is interpreted as sediment gravity flow deposits, based on lack of stratification. The sandstone is interpreted as Bouma A and B turbidites.

*Core #30, 5410-5430 ft., rec. 20 ft.*

Clast-supported pebble-cobble conglomerate. Matrix is coarse sand to granules. Some clasts are wider than the core (i.e. 9 cm). Clasts are rounded and are mostly dark grey, aphanitic volcanics. One large (9 cm) pink granitoid clast. Clasts locally show imbrication. Interpreted as sediment gravity flow deposits, rather than fluvial, based on lack of stratification and on dominance of gravity flow deposits in neighbouring cores (Cores 16 to 33).

*Core #31, 5575-5595 ft., rec. 18 ft.*

Dark grey, massive mudstone interbedded (gradational contacts), on a centimetre-decimetre scale, with medium grey, very coarse sandstone. Mudstone contains abundant centimetre-long plant fragments, oriented parallel to bedding. Sandstone mostly massive to parallel-laminated. A 30 cm layer of clast-supported conglomerate occurs at top of core. The sandstone beds are interpreted as Bouma A, B, and AB turbidites. The conglomerate bed is interpreted as a sediment gravity flow deposit. The mudstone represents "background" suspension sediment, rather than mudflow deposits, based on parallel orientation of plant fragments; intense burrowing could explain both the massive appearance and the gradational contacts with sandstone beds.

*Core #32, 5780-5800 ft., rec. 19.5 ft.*

Clast-supported pebble-cobble conglomerate. Clasts mostly subrounded to well rounded; mostly dark grey, aphanitic volcanics. Imbrication locally visible. Matrix types are: (1) coarse sand to granules cemented by calcite (i.e. little or no diagenetic clay); and (2) calcite cement only (i.e. cemented openwork conglomerate). Interpreted as sediment gravity flow deposits, rather than fluvial, based on lack of stratification and on dominance of probable sediment gravity flow deposits in adjacent cores (Cores 16 to 33).

*Core #33, 5995-6015 ft., rec. 20 ft.*

Clast-supported pebble-cobble conglomerate. Clasts mostly subrounded to well rounded, and mostly light- to dark grey, aphanitic volcanics; subordinate granitoid-gneiss and pink granitoid clasts. Matrix is coarse sand to granules, cemented by quartz and calcite (i.e. no diagenetic clay). Interpretation as for Core 32.

#### **Richfield et al. Masset c-10-I 103-F-16**

*Core #1, 401-421 ft., rec. 0.5 ft.*

Fine, loose sand, with a few centimetre-size lumps of massive fine sandstone. Data insufficient for interpretation.

*Core #2, 595-605 ft., rec. 1.5 ft.*

Volcanics.

*Core #3, 605-615 ft., rec. 7 ft.*

Volcanics.

*Core #4, 800-808 ft., rec. 3 ft.*

Volcanics.

*Core #5, 992-1002 ft., rec. 8.7 ft.*

Volcanics.

*Core #6, 1160-1166 ft., rec. 5.5 ft.*

Volcanics.

*Core #7, 1166-1176 ft., rec. 9.3 ft.*

Volcanics.

*Core #8, 1395-1402 ft., rec. 6.6 ft.*

Volcanics.

*Core #9, 1720-1729 ft., rec. 9 ft.*

Volcanics.

*Core #10, 1830-1840 ft., rec. 8.5 ft.*

Volcanics.



### **Richfield et al. Nadu River b-69-A 103-F-16**

*Core #1, 210-220 ft., rec. 0.3 ft.*

Poorly consolidated pebbly mudstone, locally clast-supported. Clasts are up to 1 cm across and include light grey and dark grey aphanitic volcanics. Clasts are subangular to subrounded. Interpreted as either a mudflow deposit or as glaciomarine mud with dropstones.

*Core #2, 240-260 ft., rec. 2.2 ft.*

Grey, very fine loose sand and centimetre-size friable sandstone lumps. Faint parallel to contorted (by coring?) lamination. Loose, angular, basalt-like pebble 6 cm across. Interpretation of sandstone hindered by sparsity of data. The pebble may be an ice-rafted dropstone, based on: (1) its angularity; and (2) the abundance of probable dropstones in surface exposures of Skonun Formation sandstone (above).

*Core #3, 450-470 ft., rec. nil.*

*Core #4, 615-635 ft., rec. 2 ft.*

Grey, fine to coarse loose sand and centimetre-size friable sandstone lumps. Faint millimetre-scale parallel lamination and contorted (by coring?) lamination. Coarse sandstone lumps contain floating granules up to 3 mm across. The parallel lamination is tentatively interpreted as foresets of large-scale, shallow-marine tidal cross-stratification, because this facies is dominant in surface exposures (see above) and can be identified with reasonable confidence in Core 11 (below). The floating granules may be dropstones, which are common in the cross-stratified tidal sands at outcrop.

*Core #5, 635-655 ft., rec. 2 ft.*

Grey, very fine to medium loose sand and centimetre-size friable sandstone lumps. Millimetre-scale parallel lamination and contorted (by coring?) lamination. Parallel lamination comprises alternating coarser and finer laminae. Interpretation as for Core 4.

*Core #6, 810-830 ft., rec. 3 ft.*

Grey, fine to medium loose sand and centimetre-size friable sandstone lumps. Faint millimetre-scale coarser-finer lamination, contorted, possibly by coring. One lump contains a rounded 1.5 cm pebble. There are also some centimetre-size lumps of pebbly mudstone containing subrounded basalt-like clasts 2-3 cm across. The sandstone may represent tidal cross-stratification and the floating pebble a dropstone (see Core 4 above). If this interpretation is correct, the pebbly mudstone is probably glaciomarine mud with dropstones, rather than till or a mudflow deposit.

*Core #7, 1020-1030 ft., rec. 0.25 ft.*

Four lumps (cm size) of massive, well cemented sandstone. In one lump, medium sandstone grades up, over 1-2 cm, into mudstone. Insufficient material for interpretation.

*Core #8, 1030-1040 ft., rec. 2 ft.*

Grey, fine to medium loose sand and centimetre-size sandstone lumps. Some lumps are massive; others show contorted (by coring?) coarser-finer lamination (mm-scale). Interpretation as for Core 4.

*Core #9, 1200-1210 ft., rec. 3.8 ft.*

Grey, medium loose sand and centimetre-size sandstone lumps. Faint contorted lamination locally visible. One 4x1 cm mudstone clast. Interpretation as for Core 4.

*Core #10, 1210-1220 ft., rec. 0.1 ft.*

Grey, medium loose sand and one centimetre-size lump of well cemented, massive, medium sandstone. Insufficient material for interpretation.

*Core #11, 1390-1400 ft., rec. 3 ft.*

Grey, fine to medium loose sand and centimetre-size sandstone lumps. In two lumps, the core wall is preserved; these lumps show steeply dipping (ca. 45°) parallel lamination, consisting of alternat-

ing lighter and darker laminae 1-2 cm thick. Interpreted as large-scale, shallow-marine tidal cross-stratification. This was the tentative interpretation for Core 4, but the interpretation is strengthened in this case by the demonstrably steep primary dip of the laminae, indicating that the laminae are indeed foresets.

*Core #12, 1400-1410 ft., rec. 0.5 ft.*

Grey, fine sand and centimetre-size sandstone lumps with millimetre-thick mud laminae. Based on its continuity with Core 11, this sandstone is probably also of tidal shallow-marine origin. The mud laminae may represent slack-water mud drapes (cf. Yakoun River sand pit, above).

*Core #13, 1600-1606 ft., rec. 5 ft.*

Grey, fine to medium loose sand and centimetre-size lumps. Some lumps show contorted (by coring?) millimetre-scale lamination, consisting of alternating lighter and darker laminae. Interpreted as either: (1) offshore-tidal, as for Core 4; or (2) fluvial channel, based on proximity to paleosol beneath (see Core 14).

*Core #14, 1606-1620 ft., rec. 6 ft.*

Massive, grey-brown mudstone with abundant horizontal carbonaceous needles (ca. 1 mm x 5-10 mm) and inclined carbonaceous rods (ca. 2 mm across). Some centimetre-size plant debris. The needles are probably conifer needles. The inclined rods are interpreted as rootlets, in which case the mudstone is a paleosol, whose lack of structure is thought to reflect rootlet bioturbation. The inferred environment is fluvial or delta-plain overbank.

*Core #15, 1800-1810 ft., rec. 6 ft.*

Altered volcanics.

*Core #16, 1810-1814 ft., rec. 3 ft.*

Volcanics.

*Core #17, 2100-2110 ft., rec. 10 ft.*

Volcanics.

*Core #18, 2440-2447 ft., rec. 1.5 ft.*

Pebbly mudstone, containing rounded basalt-like pebbles. Interpreted as a volcanoclastic (epiclastic) mudflow, based on pebble composition and on the presence of volcanics in the contiguous core beneath (Core 19).

*Core #19, 2447-2455 ft., rec. 8 ft.*

Volcanics.

*Core #20, 2580-2590 ft., rec. 3.5 ft.*

Volcanics.

*Core #21, 2590-2596 ft., rec. 5 ft.*

Volcanics.

*Core #22, 2920-2940 ft., rec. 16 ft.*

Volcanics, overlying about 1 m of sandstone, sandy mudstone and pebbly mudstone. The sediments are interpreted as epiclastic deposits; the pebbly mudstone is probably a mudflow deposit.

*Core #23, 4700-4710 ft., rec. 7.6 ft.*

Volcanics.

### **Richfield et al. Gold Creek c-56-H 103-F-9**

*Core #1, 270-280 ft., rec. nil.*

*Core #2, 280-290 ft., rec. 0.5 ft.*

Loose, poorly sorted gravel, comprising granules and pebbles (maximum clast size 5 cm). Clasts are subrounded to subangular, and are mostly basalt-like. Insufficient material for interpretation.

*Core #3, 600-605 ft., rec. nil.*

*Core #4, 605-610 ft., rec. nil.*

*Core #5, 800-805 ft., rec. nil.*



*Core #6, 2010-2020 ft., rec. 1 ft.*

Fine loose sand and centimetre-size massive to parallel-laminated sandstone lumps. Lamination consists of millimetre-scale alternations of finer and coarser laminae. Insufficient material for interpretation.

*Core #7, 2625-2635 ft., rec. 3.5 ft.*

Very fine sandstone (15 cm) showing parallel (horizontal) lamination, overlain by mudstone. The mudstone ranges from massive to millimetre-laminated; parting surfaces show abundant carbonaceous needles, some of which are grouped as fronds, confirming their identification as conifer needles (see Nadu River, Core 14). Pyrite concretions 1-2 mm across occur in the mudstone. The mudstone is interpreted as a fluvial or delta-plain overbank deposit, based on the abundance of conifer needles; a delta-plain is more likely, since the pyrite suggests a marine influence (Berner, 1984). The lack of a soil profile suggests a permanently subaqueous environment, perhaps an interdistributary swamp; a similar setting is envisaged for similar needle-bearing, pyritic mudstones at Miller Creek (Higgs, 1989c, p. 91). Massive intervals in the mudstone may reflect rootlet bioturbation. The sandstone may be of distributary-channel or crevasse-splay origin, in view of its association with inferred overbank mudstone.

*Core #8, 2635-2645 ft., rec. 7.7 ft.*

About 30 cm parallel-laminated mudstone showing low to moderate bioturbation, and little or no carbonaceous detritus. Burrows include a lined, horizontal ichnogenus about 2 mm across and at least 5 cm long (*Teichichnus?*). The mudstone is overlain by very fine loose sand and centimetre-size sandstone lumps, showing millimetre-scale parallel lamination of unknown original dip. Two loose, angular fragments of pale grey, aphanitic volcanic rock. The volcanic fragments are interpreted as dropstones, originally floating in sandstone, based on the abundance of inferred dropstones in Skonun Formation sandstone exposures and in sandstone cores from the Nadu River well (see above). If this interpretation is correct, the sandstone and mudstone are probably marine.

*Core #9, 2810-2820 ft., rec. 1 ft.*

Very fine loose sand and centimetre-size sandstone lumps. Millimetre-scale parallel (horizontal) lamination, slightly bowed by coring. One 5 cm lump of mudstone with contorted (by coring?) lamination. Insufficient material for interpretation.

*Core #10, 2820-2830 ft., rec. 10 ft.*

Fine, loose sand and centimetre-size massive sandstone lumps. One 2-3 cm parallel-laminated mudstone parting. Insufficient material for interpretation.

*Core #11, 3010-3020 ft., rec. 2 ft.*

Parallel-laminated mudstone, variably homogenized (by burrowing?) and contorted by coring. Insufficient material for interpretation.

*Core #12, 3020-3030 ft., rec. 8.3 ft.*

About 40 cm of parallel-laminated, moderately bioturbated mudstone with carbonaceous laminae, sharply overlain by fine to medium loose sand and centimetre-size friable sandstone lumps. Some lumps show millimetre-scale lighter-darker lamination dipping at 30-40° relative to the core wall. The sandstone is thought to be cross-stratified, based on the steep lamina dips. Insufficient material for environmental interpretation.

*Core #13, 3220-3230 ft., rec. 7.3 ft.*

Parallel-laminated mudstone, variably homogenized. Abundant carbonized plant fragments, millimetre-centimetre sized, concentrated in laminae in the lower half of the core. A 5 cm coal bed occurs half-way up the core. The interpreted environment is a fluvial or delta-plain overbank, based on the coal bed. Homogenization in the mudstone may reflect burrowing or rooting.

*Core #14, 3400-3410 ft., rec. 9.3 ft.*

Fine loose sand and centimetre-size sandstone lumps. Some lumps show millimetre-scale lighter-darker lamination dipping at about 20° relative to the core wall. Several interbeds, 1-15 cm thick, of mudstone ranging from massive to parallel (horizontal) laminated. In the mudstone, sand-size carbonaceous flakes are conspicuous on parting surfaces. The inclined sandstone lamination is suggestive of cross-stratification. Insufficient material for environmental interpretation.

*Core #15, 3610-3620 ft., rec. 10 ft.*

Parallel-laminated mudstone. Parting surfaces commonly show sparse to abundant sand-grade carbonaceous flakes. Rare strings of connected siltstone ripples. Tentatively interpreted as deltaic interdistributary bay deposits, based on the common plant debris and the lack of rootlet bioturbation.

*Core #16, 3820-3830 ft., rec. 2 ft.*

Volcanics.

*Core #17, 3830-3845 ft., rec. 2.5 ft.*

Altered volcanics.

*Core #18, 3845-3855 ft., rec. 8.4 ft.*

Volcanics.

#### **Richfield et al. Tleil c-56-D 103-G-12**

*Core #1, 210-220 ft., rec. 1 ft.*

Pebbly mudstone. Pebbles are rounded, up to 3 cm long, and include siltstone and basalt-like rock. Possible interpretations are: (1) mud-flow; (2) glacial till; or (3) glaciomarine mud with dropstones. The third interpretation is considered the most likely, since the core is at shallow depth, and marine sediments with dropstones are common at outcrop (above).

*Core #2, 220-230 ft., rec. nil.*

*Core #3, 420-430 ft., rec. 1.3 ft.*

Pebbly mudstone. Most pebbles are basalt-like, and some are granitoid. Bivalve fragment. The depositional environment was probably marine, based on the bivalve fragment. The pebbly mudstone is probably a glaciomarine mud with dropstones, as for Core 1.

*Core #4, 430-440 ft., rec. 2.7 ft.*

Mudstone, in part parallel-laminated, containing a 5 cm lignite bed. Interpreted as fluvial or delta-plain overbank, based on the coal bed.

*Core #5, 3460-3480 ft., rec. 9.5 ft.*

Mudstone. The lower 1.5 m shows an upward gradation from light grey mudstone into medium brown mudstone, into about 30 cm of lignite. This is overlain by light grey mudstone, containing centimetre-size plant fragments. A millimetre-size blob of amber was found in the brown mudstone. The mudstone contains inclined carbonaceous filaments, and shows parallel-lamination which has been partly to completely homogenized. The carbonaceous filaments are interpreted as rootlets. The lower mudstone is clearly a paleosol, based on the colour grading, the presence of rootlets and amber, and the overlying coal. The implied environment is a fluvial or delta-plain overbank.

*Core #6, 4100-4120 ft., rec. 17.2 ft.*

Medium to coarse loose sand and centimetre-size sandstone lumps, massive to parallel-laminated. Two intervals, 30 and 75 cm thick, of parallel-laminated mudstone. Laminae in the mudstone show the same dip (about 20°) as the laminae in the sandstone, indicating that this dip is structural, and that the sandstone laminae were deposited horizontally, rather than as foresets. The previous core (5), in contrast, shows no obvious structural dip, suggesting that there may be an unconformity between Cores 5 and 6. The sandstone is tentatively interpreted as turbidites interbedded with background muds, based on

the sandstone-mudstone alternations and the possible presence of Bouma A (massive) and Bouma B (laminated) divisions.

### Shell Anglo Harlequin

Core #1, 4435-4460 ft., rec. 25 ft.

Strongly bioturbated, carbonaceous, very fine sandstone. Burrows include: (1) clay-lined, and (2) unlined horizontal to vertical tubes, 1-10 mm in diameter; (3) horizontal tubes, up to 10 mm in diameter, lined with light-coloured sand; (4) horizontal, slightly sinuous, unbranched, unlined tubes 1-3 mm in diameter (*Palaeophycus*?); and (5) large *Ophiomorpha* burrows, consisting of horizontal and vertical tubes, 1-5 cm in diameter, with a lining, a few mm thick, consisting of alternating clay and sand concentric laminae. One vertical *Ophiomorpha* tube forms an inverted "T-connection" with a horizontal tube. The *Ophiomorpha* burrows are commonly "re-burrowed" by ?*Palaeophycus*. In all five burrow types, the fill matches the host sand. A 4 mm pyrite concretion was noted.

The presence of *Ophiomorpha* is suggestive (but not diagnostic) of a shallow-marine environment (Frey et al., 1978). A marine setting is consistent with the presence of pyrite (Berner, 1984), and with the intense bioturbation; the latter suggests deposition below fair-weather wave base. The nature of the depositional current, whether meteorological, tidal or a density current, is uncertain due to total destruction of primary structures by burrowing. However, the sandstone is tentatively interpreted as amalgamated burrowed storm beds (cf. Bourgeois, 1980, her Fig. 9), implying an inner shelf environment (Bourgeois, 1980). This interpretation is supported by the fact that similar burrowed sandstone in Osprey Core 1 (below) is intimately associated with HCS.

Core #2, 5500-5525 ft., rec. 10 ft.

Strongly bioturbated very fine sandstone, indistinguishable from Core 1. Burrows include *Ophiomorpha* and ?*Palaeophycus*, as for Core 1. Pyrite nodule 7x20 mm. Several bivalve fragments in a 10 cm calcite-cemented interval. A 5 cm interval of millimetre-scale inter-laminated mud and very-fine sand was noted.

The interpreted environment is shallow marine, as for Core 1, with added support from the presence of bivalve debris. The sandstone is tentatively interpreted as amalgamated burrowed storm beds, as for Core 1; this is consistent with the presence of broken (i.e. allochthonous) bivalves. The mudstone reflects background deposition from suspension.

### Shell Anglo Osprey D-36

Core #1, 5755-5775 ft., rec. 6.3 ft.

Very fine sandstone, showing low-angle cross-stratification which has been partially to completely destroyed by bioturbation. In places, a decimetre-thick bioturbated interval is truncated upwards by a low-angle surface which is conformably draped by laminated sand passing up into burrowed sand (cf. Dott and Bourgeois, 1982, their Fig. 8, facies Hb). Lamination, where preserved, consists of millimetre-laminae which are alternately rich and poor in comminuted plant flakes. Burrows include unlined, unbranched, horizontal tubes up to 1 cm in diameter (*Palaeophycus*?). One 40 cm interval consists of sparsely burrowed mudstone with mm laminae of silt and very fine sand, and a string of connected ripples.

The cross-stratification is interpreted as hummocky cross-stratification, rather than trough- or tabular crossbedding, because: (1) dips do not exceed 10°, far below the angle of repose; and (2) the grain size is too fine for the development of dunes, sandwaves or megaripples (Harms et al., 1982, their Fig. 2-5). The sandstone is interpreted as amalgamated hummocky-to-burrowed storm beds (cf. Bourgeois, 1980, Fig. 9; Dott and Bourgeois, 1982, Fig. 8, facies Hb). This implies an inner shelf depositional environment (Bourgeois, 1980). The mudstone represents background deposition from suspension.

**Table 1.** Summary of non-opaque heavy-mineral compositions of sandstone core samples from Queen Charlotte Basin wells.

Well	Sample depth (ft)	Amph.	Zir.	Gnt.	Ep.	Tm.	Bio.	Others
Tow Hill	619	48	18	9	12	9	3	2
	817.5	59	12	3	7	3	12	3
	1470.5	62	22	5	9	4	1	0
	1477	53	14	4	25	3	2	0
	1921.5	11	30	17	38	4	0	2
	2139.5	1	28	30	36	5	0	0
	2355.5	1	24	10	64	0	1	0
	2660.5	0	12	3	85	0	0	0
	2668	0	16	7	56	2	19	0
	2840	0	28	11	47	0	14	0
	2845.5	1	39	15	41	0	4	1
	3012.5	1	6	67	9	0	9	7
	3235.5	0	51	33	5	1	10	0
	3239	2	5	24	52	5	11	1
	3406	10	1	0	4	4	81	0
	3414	1	17	4	49	1	28	0
	3626.5	1	25	10	65	1	0	0
	3629.5	1	26	8	38	2	27	0
	4238	5	52	1	40	0	1	1
	4449.5	92	3	1	4	1	0	0
	4651	95	3	0	2	1	0	0
	5271.5	4	2	0	94	1	0	0
	5591	2	17	13	66	3	1	0
	Avg.	19	20	12	37	2	10	1
Masset	401	62	5	2	28	1	0	1
Nadu River	241	61	1	1	26	5	6	1
	617	66	7	1	25	1	1	0
	635	68	3	2	26	2	0	0
	811	76	3	2	17	2	1	0
	1031	75	5	2	18	1	0	0
	1201	82	4	2	12	1	1	0
	1210	77	2	1	16	1	4	0
	1391	84	5	1	10	1	2	0
	1400	71	6	1	19	2	0	1
	1605	80	3	2	14	0	1	1
	Avg.	74	4	1	18	1	2	0
Gold Creek	2011	72	3	1	15	3	4	1
	2628	32	4	3	18	0	44	0
	2641	48	1	2	13	3	32	0
	2810	62	8	6	23	1	1	0
	2829	80	4	2	14	2	0	0
	3020	77	2	2	15	4	0	1
	3027	30	4	1	48	0	16	1
	3408	78	3	2	14	1	1	1
	Avg.	60	4	2	20	2	12	0
Tlell	4100.5	83	2	1	8	6	0	0
	4112	78	10	2	10	1	0	0
	Avg.	80	6	2	9	3	0	0
Harlequin	4440	65	6	1	25	1	0	1
	4450	67	4	1	26	1	0	1
	4455	63	3	1	29	0	3	1
	4460	64	5	1	28	0	3	0
	5500	41	11	4	44	1	1	0
	5505	25	12	5	56	1	2	0
	Avg.	54	7	2	34	1	1	0

All values in number percent. Amph.=amphibole (hornblende and rare riebeckite); Zir.=zircon; Gnt.=garnet; Ep.=epidote group (clinozoisite and epidote); Tm.=tourmaline; Bio.=biotite.



# Palynostratigraphy of Tow Hill No. 1 Well in the Skonun Formation, Queen Charlotte Basin, British Columbia

James M. White<sup>1</sup>

White, J.M., Palynostratigraphy of Tow Hill No. 1 Well in the Skonun Formation, Queen Charlotte Basin, British Columbia; in *Evolution and Hydrocarbon Potential of the Queen Charlotte Basin, British Columbia*, Geological Survey of Canada, Paper 90-10, p. 373-380, 1991.

## Abstract

*The Tow Hill No. 1 well on the northeast coast of Graham Island penetrates 1833.4 m of Cenozoic Skonun Formation in the Queen Charlotte Basin. Palynological analyses of 31 samples from core from the Tow Hill No. 1 well, provide a palynostratigraphic framework for the ?Late Paleogene and Neogene Skonun Formation penetrated by the Tow Hill well. Sediment recycling rather than volcanic intrusion best explains anomalous patterns of high thermal maturity in organic matter in the upper 366 m of the well. Two samples younger than Middle Miocene from upturned mud beds at Yakan Point, 2.5 km west of Tow Hill, contain thermally mature sediment, indicating possible sources for recycled sediments. Recycling is probably caused by local tectonism. The upper 590 m of the Tow Hill No. 1 well is interpreted to be Late Miocene (ca. 8 Ma) to possibly Early Pliocene (>3 Ma), because it is above the extinction of Liquidambar and does not exhibit a cool temperate flora. Local tectonism and vulcanism probably occurred within this time. The section between 590 and 930 m is interpreted to be mid-Middle Miocene (ca. 15 Ma), based on the first appearance of Gramineae, to Late Miocene. The section from 930 to T.D. is poorly constrained by palynomorphs, but may range between Late Oligocene to Middle Miocene. Two undated palynostratigraphic events occur near 1100 and 1440 m.*

## Résumé

*Le puits Tow Hill n° 1 foré dans la côte nord-est de l'île Graham traverse 1833.4 m de la formation de Skonun du Cénozoïque dans le bassin de la Reine-Charlotte. Des analyses palynologiques de 31 échantillons d'une carotte provenant du puits Tow Hill n° 1 fournissent un cadre palynostratigraphique pour la formation de Skonun du Paléogène supérieur? et du Néogène traversée par le puits Tow Hill. C'est le recyclage des sédiments plutôt que l'intrusion volcanique qui explique le mieux les configurations anormales de maturité thermique élevée observées dans les matières organiques contenues dans les 366 m supérieurs des roches recoupées par le puits. Deux échantillons plus récents que le Miocène moyen prélevés dans des couches de boue retournées à la pointe Yakan, à 2,5 km à l'ouest de Tow Hill, contiennent des sédiments thermiquement matures, indiquant la présence possible de sources de sédiments recyclés. Le recyclage a probablement été causée par un tectonisme local. Les roches des 590 m supérieurs recoupées par le puits Tow Hill n° 1 se situeraient entre le Miocène supérieur (vers 8 Ma) et peut-être le Pliocène inférieur (> 3 Ma), étant donné qu'elles se trouvent au-dessus de la zone d'extinction de Liquidambar et qu'elles ne contiennent pas de flore de climat tempéré froid. Les activités tectoniques et volcaniques locales ont probablement eu lieu au cours de cette époque. Entre 590 et 930 m, les roches dateraient du milieu du Miocène moyen (vers 15 Ma), en se fondant sur la première apparition de graminées, jusqu'au Miocène supérieur. La section allant de 930 m à la profondeur limite a été mal délimitée si l'on se base sur les palynomorphes mais elle pourrait se situer entre l'Oligocène supérieur et le Miocène moyen. Deux événements palynostratigraphiques non datés ont laissé des traces près de 1100 et 1440 m.*

<sup>1</sup> Institute of Sedimentary and Petroleum Geology, Geological Survey of Canada, 3303-33rd Street N.W., Calgary, Alberta T2L 2A7

## GEOLOGICAL SETTING AND AGE

The type locality of the Skonun Formation is Skonun Point, on the northeast coast of Graham Island (MacKenzie, 1916). However, outcrop is limited and Sutherland Brown (1968) points out that the long subsurface sections from boreholes should form the standard for the Skonun Formation. Figure 1 illustrates the distribution of Skonun Formation and location of outcrop and wells penetrating the Skonun Formation of Graham Island.

The Tertiary Skonun Formation underlies northeastern Graham Island, Hecate Strait, Queen Charlotte Sound, and probably part of Dixon Entrance (Sutherland Brown, 1968; Patterson, 1989; Higgs, 1989). The Skonun Formation sediments are mostly sands, sandstones and conglomerates, with shale and lignite stringers (Sutherland Brown, 1968). The Skonun Formation is continental to marginal marine to the north in the Queen Charlotte Basin, with deeper marine and continental facies to the south under Queen Charlotte Sound (Martin and Rouse,

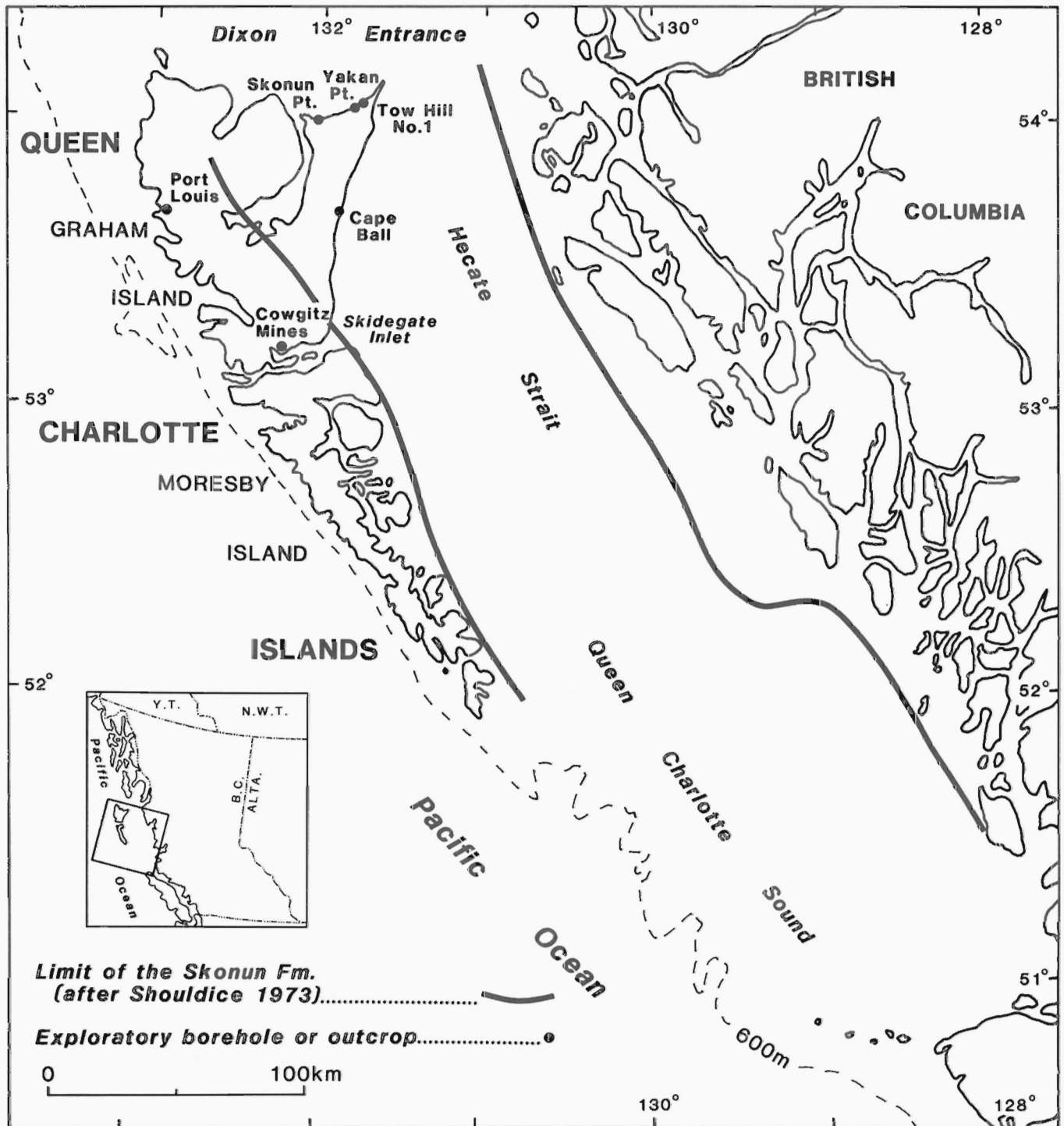


Figure 1: The distribution of the Skonun Formation in the Queen Charlotte Basin, with outcrops and wells.

1966; Shouldice, 1971; Addicott, 1978; Patterson, 1988, 1989). The Skonun Formation is underlain by and interfingers with the volcanic Masset Formation (Sutherland Brown, 1968; Hickson, 1988).

The Skonun Formation was originally determined to be Miocene or Pliocene by use of marine molluscs found in outcrop (Dawson, 1880; MacKenzie, 1916). Addicott (1978) used molluscs to revise the age of the outcrop to Late Miocene. In Queen Charlotte Sound the marine sections of Skonun Formation are Early to Middle Miocene, and Pliocene-Quaternary (Patterson, 1988). Sedimentary rocks, of Eocene and/or Early Oligocene age, have been identified in the Union Port Louis Well on the west coast of Graham Island, and in float from near the former Cowgitz Mines on Skidegate Inlet (White, 1990b). In the Port Louis well the sedimentary rocks underlie the Masset Formation. The relationship of these rocks to the known Skonun Formation remains to be determined (White, 1990b).

Molluscs found in the Skonun Formation indicate a shallow water marine environment, warmer than at present, for the Queen Charlotte Islands during the Late Miocene. Addicott (1978) suggests, as a possible analog, a protected embayment along the central California coast about 2000 km to the south.

A palynological flora of 50 species has been described by Martin and Rouse (1966) from the outcrops of Skonun Formation. This valuable study provides a taxonomic basis for subsequent palynology in the Skonun Formation. However, because the palynomorphs are from dispersed, short sections it provides neither a biostratigraphic framework nor age determinations independent of the molluscan chronology. Martin and Rouse (1966) interpret three communities from the palynoflora: 1) a forest-swamp type similar to that found on the modern Louisiana Gulf Coast, 2) a more open-water community such as the Everglades, and 3) a coastal brackish water environment. The climate was interpreted to have been warmer, more temperate, and more humid than today, with virtually no frost.

## TOW HILL NO. 1 WELL

The Richfield Mic Mac Homestead Tow Hill No. 1 well is located on the north Coast of Graham Island, about 1 km east of Tow Hill (N 54°04'47", W 131°46'45"). The well was spudded and completed in 1958.

The Tow Hill No. 1 well penetrates 1833.4 m of Skonun Formation. Lithology has been provided by Sutherland Brown (1968, his Fig. 20). The well is predominantly sandstone with major conglomerates below 1000 m, especially in the lowest 300 m. Thin interbeds of shale and lignite are more common in the upper 1000 m.

Volcanic rocks described as "Tow Hill Sills" occur between 366 and 524 m (Sutherland Brown, 1968). Outcrop of the "Tow Hill Sills" at Tow Hill has yielded K-Ar dates of  $<5$  and  $35.2 \pm 2$  Ma (Hickson, 1988). Neither age is reliable because of alteration of the rock (C.J. Hickson, pers. comm., 1989). A possible reinterpretation of the "Tow Hill Sills" is discussed below.

## Research strategy and methods

For an initial palynostratigraphic framework for the Skonun Formation it seemed advisable to avoid cutting samples and the consequent problem of caving. The Richfield et al. wells on eastern Graham Island were intermittently cored, giving potential for samples with good stratigraphic control. The Cape Ball and Tow Hill No. 1 wells have the deepest penetration of Skonun Formation (Sutherland Brown, 1968).

Detailed palynological analysis was done on samples from the 111.3 m of core which is available from Tow Hill No 1. The results are not a dense analysis interval, but a biostratigraphic "skeleton", free of the major stratigraphic uncertainties of cutting samples.

Variability in the palynological record may be viewed in the 'signal to noise' paradigm. 'Signal' comes from those sources which give biostratigraphically useful results – true species origination or extinction, or major changes in the geographic distributions of species in response to climatic and/or tectonic events. 'Noise' comes from several sources including short-term vegetation community succession, edaphic adaptation, sorting of fossils prior to deposition, and stochastic variation. All lignite and organic shale beds found in the cores, even those closely spaced, were individually sampled and analyzed to compare short-term and long-term variability. There were 31 productive samples. On Figure 2 (in pocket), the vertical distance between some of these analysis intervals has been exaggerated 10 times to permit plotting without pen overlap.

Stratigraphically significant change has been evaluated by both the estimation of the percentage composition of the palynological flora, and the search for rare palynomorphs. This strategy was adopted to recover maximum data from the analyses. All palynomorphs in prepared residues were tallied to a minimum sum of 300 grains. At the same time an independent count was maintained of microspheres added to the preparation (Benninghoff, 1962; Ogden, 1986; White, 1988). This count was continued into the scan for rare types which followed the fixed tally, allowing an estimation of the relative abundance of rare taxa (White, 1990a).

## Results

Complete tallies with taxonomic determinations were made for 11,646 fossils. In addition, an estimated 111,500 fossils were scanned in a search for rare species. The author has a photographic catalogue of the palynomorphs at the I.S.P.G.

One hundred and twenty-six taxonomic categories were used to record the Tow Hill data. Many of the common pollen and spore taxa in Tertiary sediments can be referred to modern plant taxa. New taxa encountered in the study will be formally described in a future paper. Photographs or descriptions of most taxa named in this paper can be found in Martin and Rouse (1966), Leopold (1969), Piel (1971), Ballog et al. (1972), Rouse (1977), Norris (1986), and Gray (1985). Preservation of the palynomorphs was generally poor, with considerable erosion and compression.

Percentages are calculated on the sum of all tallied palynomorphs in each sample, generally 300-500 palynomorphs for statistical reliability. The sum included those fossils unidentifiable because of poor preservation.

The percentages of the 68 most useful taxa are presented in Figure 2 (in pocket). Taxa have been excluded because they were long-ranging and without any significant trends in percentage representation, or because they were single occurrences of previously unreported taxa. The nature of the distribution of a taxon, and its potential biostratigraphic significance, is very poorly indicated by a single occurrence. Figure 2 (in pocket) contains a summation of all taxa not plotted individually because they were deemed to yield no biostratigraphic or environmental information. A sub-sum of this sum is presented, showing in each sample the percentage of palynomorphs unidentifiable because of poor preservation.

Taxa observed during the scan of the slide after the count have very low relative abundances. Relative abundances of many taxa are marked by a "+", which indicates an observed occurrence of  $<0.1\%$ , i.e., is less than 1 occurrence in 1000 fossils. The observed relative abundance of many taxa, such as *Liquidambar*, shows that an observation of more than 1000 fossils per sample is required to estimate its stratigraphic range.

The taxa in Figure 2 are arranged primarily by last stratigraphic occurrence to serve as a guide for palynological analysis of cuttings



from exploration wells. Taxa are arranged secondarily by a botanical hierarchy from algae to angiosperms, and thirdly by alphabetic order within each botanical group. Taxa whose stratigraphic ranges are known to extend into the Quaternary in the Queen Charlotte Basin, but which were not observed in the uppermost sample for stochastic reasons, are arranged with the taxa whose last occurrences are at the top of the well.

## Discussion and Interpretation

Preliminary to an interpretation of ages in the Tow Hill No. 1 well, must be a consideration of evidence of sediment recycling and fossil recycling in the stratigraphic sequence.

### *Recycling of Sediment in the Tow Hill No. 1 Well*

Many beds in the upper 360 m of Tow Hill No. 1 well have anomalously high thermal maturities, evident from the palynological kerogen preparations and from vitrinite reflectance (Vellutini and Bustin, 1988). Furthermore, some palynological preparations were found to contain both a thermally immature and a mature fraction. Analysis of kerogen from sample 184.4 m confirmed the presence of a fraction of TAI about 2-, and another fraction of about 3 or 3- using Pearson's scale (1984). Table 1 shows the occurrence of the two maturity fractions in the upper 528 m of the well. Possible alternative explanations for the thermal anomalies are local heating of the sediment by dykes or sills, or recycling of sediment.

**Table 1:** Distribution of low and high thermal maturity fractions in samples from upper 528 m of Tow Hill No. 1 well.

Depth m	(ft)	Mature	Immature
73.9	(242.5)	x	
74.5	(244.5)	x	
184.4	(605.0)	x	x 1.
268.8	(882.0)	x	
306.2	(1004.5)		x
306.9	(1007.0)		x
348.5	(1143.5)	x	x 2.
365.9	(1200.5)	x	x 2.
527.9	(1732.0)		x

1. immature fraction plotted as 179.8 m on Figure 2.  
2. fossils too rare to plot on Figure 2.

The Tow Hill No. 1 well logs show volcanic rocks, described as the "Tow Hill Sills" by Sutherland Brown (1968), between 366-404 m (1200-1325 ft), 412-424 m (1350-1390 ft) and 522.7-524.3 m (1715-1720 ft). This suggests that igneous intrusions may have caused the thermal maturity anomalies.

In order to evaluate the maximum thermal maturity effect of an igneous intrusion of 58 m thickness, a numerical model has been run using typical physical properties for the rocks and a burial depth of 1-2 km. The maximum envelope around a sill within which organic matter could be brought to the oil window (Time Temperature Index ~15, or Thermal Alteration Index >~2+ in Pearson's scale (1984)) is 70 m, that value being derived by a model run of 400 years, after which time the thermal effect will change very little (A. Jessop, pers. comm., 1989). A sill could thus explain high thermal maturities up to but not beyond a present depth of about 300 m. Table 1 shows that low thermal maturities are observed in two samples between the volcanic rocks and 300 m, high maturities in several samples above 300 m. Furthermore, there is variation in thermal maturity within individual samples. There is no indication of other sills within the sediments in the upper

366 m either in lithology or in the resistivity log, which distinctly marks the volcanic unit between 366 and 424 m.

Identifiable palynomorphs were observed in the sample at 365.9 m, which was collected from within about 1 m of the volcanic rock. The same numerical model shows that organic matter from within 1 m of the margin of a sill within 10 years would have achieved a TTI orders of magnitude beyond the dry gas generation phase; i.e. complete carbonization (A. Jessop, pers. comm., 1989). The presence of identifiable palynomorphs in this sample strongly suggests that the volcanic rock is not intrusive.

The outcrop which is Tow Hill is about 1 km west of the well site. Dip is difficult to measure on the irregular surface, but using an estimated 17° east-southeast dip one can project the base of the volcanic outcrop into the Tow Hill No. 1 well at about 300 m, in the range of the observed depth of the volcanic rock. Sutherland Brown (1968) has correlated the volcanic rocks in the well with the outcrop. However, the thermal maturity data presented above challenge Sutherland Brown's interpretation of these rocks as intrusive. The outcrop at Tow Hill has also been reinterpreted on field inspection as consolidated subaqueous pyroclastic ejecta (C.J. Hickson, pers. comm., 1988). Palynostratigraphic arguments presented below suggest that if the Tow Hill volcanic rocks are extrusive, they are younger than 8 Ma, and older than 3 Ma.

Regarding the thermal maturity anomalies, the data presented are more consistent with the sediment recycling hypothesis than the volcanic intrusion hypothesis. The volcanics may not be intrusions, and there are no similar igneous units higher in the well, even though high thermal maturities are found in the organic sediments. Most likely older and thermally more mature sediments have been intermittently recycled into younger sediments. The data from Yakan Point (below) show that sediments containing Ericaceae and Gramineae, and therefore probably of late Middle Miocene to Recent age, have been significantly deformed and heated. Sutherland Brown (1968) has described evidence of intense syndepositional and postdepositional tectonism along Dixon Entrance during the late Tertiary. Recycled sediments of this age could be palynologically indistinguishable from primary sediments of the same age unless they differ in thermal maturity.

A sample at 74.5 m was thermally mature, and contained several taxa found only towards the base of the well, i.e., Pycnidium Type B, Fungal type C, *Incertae sedis* A, *Inapertisporites scabridius*, *Podocarpus*-type, and Tricolporate E. These taxa suggest that the sediment is recycled from older beds. To avoid presenting spuriously long stratigraphic ranges, sample 74.5 m was deleted from the data prior to plotting the taxa by stratigraphic last occurrences (Fig. 2). The data will be presented in the future.

### *Correlation and Age*

In the discussion below, the boundaries of stratigraphic units are interpolated between samples.

**Surface to 590 metres.** The age of the Tow Hill No. 1 well section above 590 is late Late Miocene to possibly Early Pliocene. Recent data suggest that the transition from a T-C-T- to a Pinacae-dominated assemblage occurred in the latest Pliocene. It is therefore unlikely that a Pliocene section is present in the Tow Hill well. This interpretation is based on the local extinction of *Liquidambar* at 647.5 m. The upper range limit of *Liquidambar* is interpreted to be no younger than 8-9 Ma (see discussion below).

There is no palynological evidence in the Tow Hill well for identifying the Pliocene, although the extensive sediment recycling above 366 m may mask the Miocene-Pliocene transition. In Alaska, the Late Miocene-Pliocene Clamgulchian Stage is also not easily separated by palynology from the Homerian Stage, except in the impoverishment of

exotic taxa (Wolfe et al., 1966; Leopold, 1969). The relatively high T-C-T pollen percentages and the relatively low representation of the Pinaceae (bisaccates) appears to exclude an age younger than the major north latitude cooling during the late Pliocene (Savin, 1977; Shackleton et al., 1984). The estimate of 984 m of eroded section at Tow Hill (Vellutini and Bustin, 1988) may be the Pliocene-Quaternary section.

**590 to 930 metres.** The division at 930 m, between samples at 867.6 and 986.6 m, is a major biostratigraphic division in the well. Gramineae, Compositae, Ericaceae, *Sphagnum* and cf. *Myrica* appear at 867.6 m. This boundary coincides approximately with reduced abundance or ends of the local stratigraphic ranges of Polyporate A, Fungal type D, Tricolporate D, Tricolporate C, Tricolporate B, *Pterocarya*, Fungal type B, *Ulmus/Zelkova*, *Carya*, *Lycopodium foveolites* and *Castanea* type. Changes in the percentages of T-C-T, *Tricolporopollenites*, and *Alnus* (4 pore and 6 pore) closely coincide with this boundary.

An age determination of Middle Miocene to Late Miocene for the 590-930 m segment of the Tow Hill No. 1 well is based on the concurrent ranges of the distinctive taxa *Liquidambar* (1038.1-647.5 m) and Gramineae (867.6-179.8 m). These two taxa are also concurrent in the Skonun Formation sediments in the Cinola gold deposit on central Graham Island (Champigny et al., 1981).

The observed stratigraphic range of a taxon is a combination of both its true stratigraphic range and its occurrence in sufficient abundance that it will be observed in a fossil assemblage. The global stratigraphic range of Poaceae (Gramineae) extends into the Paleocene (Muller, 1981). Norris (1986) lists its occurrence in the Oligocene Kugmallit sequence in the Beaufort Sea, and Rouse and Mathews (1988) note the presence of *Graminidites gramineoides* in Late and Middle Eocene beds of central B.C. However, the time at which Gramineae commonly occurs in sediments in the Pacific Northwest appears to be considerably younger. It is unknown whether this represents an evolutionary development in the Gramineae, or some regional environmental shift.

Gramineae occurs in the southern Alaskan, Cook Inlet palynological record in the Late Miocene-Early Pliocene (Leopold, 1969). This is interpreted here to mean the Clamgulchian Floral Stage, dated between 8 and 4.2 Ma (Wolfe, 1981, Fig. 5). Although grasses are presently ubiquitous given open habitat, Gramineae pollen does not appear earlier than Late Miocene-Early Pliocene in Alaska (Leopold, 1969).

Gramineae has been reported in central British Columbia in the Diatomaceous Unit (Piel, 1977), which has since been named the Crownite Formation by Rouse and Mathews (1979) and dated to late Middle Miocene (11-13 Ma). Gramineae is not reported in the earlier Middle Miocene Big Slide Unit (Fraser Bend Formation), nor in the Oligocene Alexandria/Narcosis Unit (Australian Creek Formation) (Piel, 1971, 1977; Rouse and Mathews, 1979), although ?Gramineae is reported in Early Oligocene rocks of the Rocky Mountain Trench (Hopkins et al., 1972).

In northwestern Washington Gramineae occurs in the Montesano Formation (Ballog et al., 1972), whose age has been revised to early Late Miocene, 11.5-9 Ma (Barron, 1981). Gramineae is rare in Clarkia sediments (Gray, 1985), which is of Early Miocene age (Smiley and Rember, 1985). Jorstad (1983) reports Gramineae in the Middle and Late Miocene Oviatt Creek and Rover Siding floras. Newman's (1981) Paleogene palynology of central and western Washington reports one occurrence of cf. Gramineae? in the Guye Formation. Hopkins (1968) does not report Gramineae from subsurface Miocene rocks in the Whatcom Basin.

Dates on mineralized dykes or sediments at Cinola, Graham Island (C.J. Hickson, pers. comm., 1989) of 14 and 14.1 Ma have al-

lowed Champigny et al. (1981) to suggest an age of 15 Ma for sediment containing Gramineae. Considering the stratigraphic range of Gramineae in southern Alaska, central B.C., and northwest Washington, Champigny et al.'s (1981) date of 15 Ma seems to be near the probable maximum age for Gramineae in the Queen Charlotte Basin.

*Liquidambar* has a distinct stratigraphic range in the Tow Hill No. 1 well. However, its very low relative abundance means that its true stratigraphic range in the well is less certain than that of Gramineae.

Champigny et al. (1981) used a Seldovian Stage last occurrence for *Liquidambar* in Alaska, dated to 17.5-13 Ma, and a last occurrence of 10 Ma in the Ellensburg flora of central Washington to estimate its range in the Queen Charlotte Islands. However, the upper stratigraphic limit of *Liquidambar* is probably younger. Leopold (1969) shows its occurrence in the late Homerian Stage, or younger than 8 Ma (Wolfe, 1981). Wolfe et al. (1966) suggest that its occurrence in the Late Miocene-Early Pliocene is due to recycling. The Alaskan stratigraphic range of *Liquidambar* is thus from Late Oligocene to Late Miocene.

In northwest Washington *Liquidambar* occurs in the early Late Miocene Montesano Formation (Ballog et al., 1972; Barron, 1981). However, there must be section missing between the Montesano Formation and the overlying Pliocene sediments which lack *Liquidambar*. Thus, *Liquidambar* may range higher than early Late Miocene.

The upper stratigraphic limit of *Liquidambar* north of the Queen Charlotte Islands is about 8 Ma, and south it is about 9 Ma. *Liquidambar*'s occurrence in the Tow Hill No. 1 well at 647.5 m suggests a conservative upper age of 8 Ma for this level.

*Achomosphaera spongiosa* occurs at 647.5 and 776.2 m. This dinoflagellate has been identified in the Early to Late Miocene of the west coast of North Japan, and in the Late Miocene of the Bering Sea (Matsuoka and Bujak, 1988; Wiggins, 1986). This concurs with the Middle Miocene to Late Miocene age assignment for the interval between 930 and 647.5 m (Matsuoka and Bujak, 1988) although it would also admit an Early Miocene age.

**930 to 1833 metres.** The age of the stratigraphic sequence from 930-1833 m can not be as clearly constrained by the palynomorphs. However, presently uncorrelated biostratigraphic events at 1100 and 1440 m will likely be dateable with further research, and should allow correlation within the basin.

The sample at 1038.2 m (the first above 1100 m) contains the first appearances of *Liquidambar*, of a distinct *Pinus*, of a *Betula* less than 20 micrometers in diameter, and of Tricolporate J. There is also a marked drop in the relative abundance of Taxodiaceae-Cupressaceae-Taxaceae pollen. It could be argued that the decreased dominance of the T-C-T pollen permits the appearance of rarer taxa, but it is notable that the taxa listed above do not appear at all in the cluster of samples circa 1170 m. Unfortunately the 1100 m biostratigraphic event is not presently datable.

At 1440 m a biostratigraphic event is evident. The samples from 1357.3-1355.5 m contain the first appearances of Fungal type C, *Intratrilporopollenites* A, *Juglans*, ?*Tilia*, Tricolporate G, *Inapertisporites scabridius*, *Jussiaea*, cf. *Podocarpus*-type, cf. *Abies*, and Tricolporate H. These taxa suggest, but do not demonstrate, a Paleogene age for the basal 650 m of the well.

*Engelhardtia-Alfaroa* (1608.9 m) is long-ranging in the northwestern United States Interior, from possible Upper Cretaceous to upper Oligocene (Leopold and MacGinitie, 1972). *Engelhardtia-Alfaroa*-type is reported in southern Alaska in the Oligocene (Leopold, 1969), and is not known in Miocene rocks in Alaska (Wahrhaftig et al., 1969). It is reported in the Lower Oligocene in central British Columbia (Piel, 1971) but is not reported in the Miocene (Piel, 1977; Rouse and

Mathews, 1979). Newman (1981) reports *Engelhardtia* in Eocene-Lower Oligocene sediments in northwestern Washington. It is rare in Lower Miocene Clarkia sediment (Gray, 1985; Jorstad, 1983). Although Hopkins (1968) reports it in the Miocene in the Whatcom Basin, it is absent in the early Late Miocene Montesano Formation (Ballog et al., 1972; Barron, 1981).

*Intratropipollenites A* Rouse 1977 occurs at 1357.3 and 1168.5 m. It occurs in the Arctic in the Early to Middle Eocene (Rouse, 1977). A very similar pollen, suggested to be *Reevesia* occurs in the Early Miocene in Clarkia (Gray, 1985). However, *Intratropipollenites A* or *?Reevesia* are rarely reported.

*Inapertisporites scabridius* Sheffy and Dilcher 1971 was identified at 1356.2 m. *I. scabridius* is of Middle Eocene age from the Claiborne Formation, Tennessee, but this taxon is rarely reported, and its true stratigraphic range is uncertain.

*Jussiaea* sp. (1356.2 m) occurs in the latest Eocene and Lower Oligocene in central and eastern British Columbia (Piel, 1971; Hopkins et al., 1972; Rouse, 1977) and in the Arctic (Rouse, 1977). It also occurs in Middle Miocene Fraser Bend Formation in central British Columbia (Piel, 1977; Rouse and Mathews, 1979).

The stratigraphic distributions considered above suggest the possibility that Paleogene sediment is present in the Tow Hill No. 1 well below about 1200 m. However, a Paleogene age is not conclusively demonstrated. Assemblages identified in Lower Oligocene rocks in central British Columbia (Piel, 1971; Hopkins et al., 1972; Rouse, 1977) are not present in the Tow Hill well. Similarly, other distinctive Paleogene taxa (Hills, 1965; Hopkins, 1969; Elsik and Jansonius, 1974; Rouse, 1977; Rouse and Mathews, 1979, 1988), which confirm the Eocene and/or Early Oligocene age in the Port Louis well (White, 1990b) do not occur in the samples from the Tow Hill well. The sediment below 1200 m may be Late Oligocene in age. However, an Early to Middle Miocene age may also be correct, and this would be most in concordance with sedimentation in the southern Queen Charlotte Basin (Patterson, 1989).

## YAKAN POINT

Yakan Point (103J/4W, N 54°04'20", W 131°50'06") is approximately 2.5 km west of the more prominent Tow Hill on the north coast of Graham Island (Fig. 1). Approximately 300 m of intermittent outcrop is exposed in a north-south direction in the intertidal zone at low tide. On the western side of the point are four sandstone seastacks, the distal seastack at the apex being the most prominent. The eastern side of the point is marked by only one low sandstone seastack. The point is a jumble of small sandstone blocks with mud exposed between. Stratigraphy and sedimentology of Yakan Point have been described by Higgs (1989). Addicott (1978) gives a Late Miocene age to the sandstones based on bivalves and an echinoid.

The point is stratigraphically complex, with the original relationships between units being uncertain. Consequently, the outcrop can not contribute primary evidence for palynological zonation. Martin and Rouse (1966) describe a 30 ft. sandstone sequence enclosing 7 siltstone interbeds, the lowest one yielding palynomorphs. Silts interbedded in the sandstone sequence were not sampled during the 1988 field season.

About 2 m of mud beds were discovered cropping out in the bottom of an intertidal pool just northeast of the second major sandstone seastack north of the shore on the west side of Yakan Point. These beds were partly covered at the outcrop, and were not observed elsewhere on the point. Unlike the other muds visible in the intertidal area, these beds have a distinct strike of about 340° (North grid), and a dip of approximately 45° to the west. It is uncertain whether they are conformably or unconformably below the sandstone seastacks, whose positions may

have rotated due to erosion. Relationship to the subhorizontally bedded muds of the intertidal area is also uncertain. Two samples were taken from these upturned beds as it was clear that they predated some significant local deformation.

**Table 2:** Palynology of Yakan Point, Graham Island, Queen Charlotte Islands.

Taxon	C-163698	C-163687	C-163686
<i>Brachysporisporites</i> sp.	.	.	V
<i>Desmidiospora</i> sp.	.	.	?
Unidentified fungal palynomorphs	.	.	F
Polypodiaceae-Dennstaedtiaceae Form 1	F	.	.
Polypodiaceae-Dennstaedtiaceae Form 2	V	.	.
Polypodiaceae-Dennstaedtiaceae Form 3	.	.	V
<i>Lycopodium inundatum</i> type	V	.	.
<i>Lycopodium</i> sp.	V	.	.
<i>Osmunda irregularis</i>	F	.	.
<i>Osmunda</i> sp.	F	.	.
<i>Selaginella sinuites</i>	R	?	.
<i>Triletes</i> sp.	V	.	.
<i>Abies</i> sp.	F	.	.
<i>Picea</i> sp.	F	.	.
Pinaceae (bisaccate)	A	C	C
Taxodiaceae-Cupressaceae-Taxaceae	A	.	A
<i>Tsuga heterophylla</i> type	F	.	.
<i>Tsuga</i> sp.	V	.	.
Aceraceae	F	.	V
<i>Alnus</i> sp. (4 pore)	R	V	A
<i>Alnus</i> sp. (5 pore)	F	F	A
<i>Alnus</i> sp. (6 pore)	F	V	F
<i>Betula</i> sp. (< 20 micrometers)	F	V	F
<i>Betula</i> sp. (> 20 micrometers)	R	.	.
Caryophyllaceae	.	V	.
cf. <i>Sparganium</i>	V	F	F
Ericaceae	V	.	V
<i>Myrsine/Fagus</i> sp.	V	.	F
Gramineae	F	F	.
<i>Ilex</i> sp.	.	.	V
<i>Juglans</i> sp.	F	.	R
Liliaceae	.	?	.
<i>Pterocarya</i> sp.	F	.	.
<i>Salix</i> sp.	R	.	.
<i>Tripolipollentites</i> sp.	A	?	V
<i>Ulmus</i> sp.	V	.	V
Unidentified angiosperms	R	.	.
Unidentifiable palynomorphs	A	.	.

? - Questionably present  
V - Very rare  
R - Rare  
F - Few  
C - Common  
A - Abundant

Samples C 163686 and C 163687 are from the upturned mud beds. Palynological results are presented in Table 2. Ericaceae was identified in C 163686, and Gramineae in C 163687. Both samples contain *Betula* grains less than 20 micrometers in diameter. With reference to the palynostratigraphic results from the Tow Hill No. 1 well, these samples are Middle Miocene or younger. The Thermal Alteration Index of the palynomorphs is 2+ or 3- (Pearson, 1984).

Sample C 163698 (Table 2) is from the subhorizontally bedded mud with sand stringers in the intertidal area on the eastern side of

the point. This sample also contains Ericaceae, Gramineae, and small *Betula* grains. It also contains *Pterocarya* pollen. Palynomorphs are poorly preserved. The presence of *Pterocarya* is problematic, as its stratigraphic range in the Tow Hill No. 1 well barely overlaps that of Gramineae, Ericaceae, and small *Betula*. If the horizontal beds are, as seems most probable, considerably younger than the upturned beds, this may point to a longer concurrent range of *Pterocarya* with Gramineae, Ericaceae, small *Betula*, and associated taxa, than the results from the Tow Hill No. 1 well suggests. Alternatively, sediment recycling may be responsible. However, the TAI of the palynomorphs is 2, which is considerably less thermally mature than the upturned mud beds.

Samples C 163686 and C 163687 are of late Middle or Late Miocene age, which is older than deformation and heating of the sediment. Sample C 163698 can not be chronologically separated from the previous two samples because of poor palynomorph preservation and possible sediment recycling, so no post-deformation chronological constraint can be provided. However, the results bear out Sutherland Brown's (1968) interpretation of Late Tertiary tectonism along Dixon Entrance. The high thermal maturity of the palynomorphs in the upturned beds suggests a source for some of the anomalously mature palynomorphs in the upper 368 m of the Tow Hill No. 1 well.

## CONCLUSIONS

The analysis of core from the Tow Hill No. 1 well provides a palynostratigraphic framework for the Neogene and Upper Paleogene portion of the Skonun Formation. While the framework must reflect biostratigraphic patterns within the Cenozoic Queen Charlotte Basin, it must also, to some degree, reflect conditions idiosyncratic to that portion of the basin in which the Tow Hill No. 1 well is located. The style of late Tertiary tectonism along Dixon Entrance may not be the same as that further south. This could affect both primary biostratigraphy, and patterns of sediment recycling. Palynological analysis of additional wells is required to measure what is typical of the basin, and what is idiosyncratic to the Tow Hill No. 1 well.

The strategy of percentage estimation and the search for rare taxa demonstrates that the appearance of rare taxa and percentage changes in long-ranging taxa are associated. They probably reflect climatic, tectonic or other events. The significance of the stratigraphic change can be verified by the use of both lines of evidence. The estimation of the true relative abundance of rare taxa by the microsphere method can assist in evaluating the potential stratigraphic utility of the rare types.

A considerable amount of sediment recycling occurs in the upper 360 m of the Tow Hill No. 1 well, detectable primarily by anomalous patterns of thermal maturity. Evidence of a source of recyclable sediment was found in thermally mature, upturned beds at Yakan Point. Recycling of sediment older than that found at Yakan Point was suggested by the analysis of the 74.5 m level in the Tow Hill No. 1 well. The sediment from the surface to 590 m is interpreted to be younger than 8 Ma, or Late Miocene but not younger than mid-Pliocene (about 3 Ma), based on the upper stratigraphic range of *Liquidambar* and the absence of a cool temperate flora. The episode of tectonism, vulcanism, and of sediment recycling has apparently occurred within this time period. The Late Pliocene-Quaternary section may have been eroded.

The section from 590-930 m is interpreted to be mid-Middle Miocene (ca. 15 Ma) to Late Miocene. This age determination is based on an interpretation of the age at which Gramineae occurs in sediment in the Queen Charlotte Basin, although the global stratigraphic range of Gramineae is longer. Future data may allow a revision of this age assignment.

The section from 930-1833.4 m may be Late Oligocene to Middle Miocene. Several taxa with Paleogene ranges occur, but the

ranges of some of these species also extends into the Miocene. Within this section, major biostratigraphic events take place near 1100 and 1440 m, but the age of these events has yet to be discovered.

## REFERENCES

- Addicott, W.O.  
1978: Late Miocene mollusks from the Queen Charlotte Islands, British Columbia, Canada; *Journal of Research, United States Geological Survey*, v. 6, p. 677-690.
- Balogg, R.A., Sparks, D.M., and Waloweeck, W.  
1972: Palynology of the Montesano Formation (Upper Miocene) of Western Washington; in *Proceedings of the Pacific Coast Miocene Biostratigraphic Symposium*, presented at the Forty-Seventh Annual Pacific Section, Society of Economic Paleontologists and Mineralogists Convention, March 9-10, 1972, Bakersfield, California, p. 199-213.
- Barron, J.A.  
1981: Marine diatom biostratigraphy of the Montesano Formation near Aberdeen Washington; *Geological Society of America, Special Paper 184*, p. 113-126.
- Benninghoff, W.S.  
1962: Calculation of pollen and spore density in sediments by addition of exotic pollen in known quantities; *Pollen et Spores*, v. 4, p. 332-333.
- Champigny, N., Henderson, C.N., and Rouse, G.E.  
1981: New evidence for the age of the Skonun Formation, Queen Charlotte Islands, British Columbia; *Canadian Journal of Earth Sciences*, v. 18, p. 1900-1903.
- Dawson, G.M.  
1980: Report on the Queen Charlotte Islands, 1878; *Geological Survey of Canada, Report of Progress for 1878-79*, p. 1-239.
- Elsik, W.C. and Jansonius, J.  
1974: New genera of Paleogene fungal spores; *Canadian Journal of Botany*, v. 52, p. 953-958.
- Gray, J.  
1985: Interpretation of co-occurring megafossils and pollen: a comparative study with Clarkia as an example; in *Late Cenozoic History of the Pacific Northwest*, American Association for the Advancement of Sciences, San Francisco, p. 185-239.
- Hickson, C.J.  
1988: Structure and stratigraphy of the Masset Formation, Queen Charlotte Islands, British Columbia; in *Current Research, Part E*, Geological Survey of Canada, Paper 88-1E, p. 269-274.
- Higgs, R.  
1989: Sedimentological aspects of the Skonun Formation, Queen Charlotte Islands, British Columbia; in *Current Research, Part H*, Geological Survey of Canada, Paper 89-1H, p. 87-94.
- Hills, L.V.  
1965: Palynology and age of Early Tertiary basins, interior of British Columbia; Ph.D. thesis, University of Alberta, Edmonton.
- Hopkins, W.S., Jr.  
1968: Subsurface Miocene rocks, British Columbia-Washington, a palynological investigation; *Geological Society of America Bulletin*, v. 79, p. 763-768.  
1969: Palynology of Eocene Kitsilano Formation, southwest British Columbia; *Canadian Journal of Botany*, v. 47, p. 1101-1131.
- Hopkins, W.S., Jr., Rutter, N.W., and Rouse, G.E.  
1972: Geology, paleoecology, and palynology of some Oligocene rocks in the Rocky Mountain Trench of British Columbia; *Canadian Journal of Earth Sciences*, v. 9, p. 460-470.
- Jorstad, R.B.  
1983: Geographic and stratigraphic distribution of Miocene palynomorphs in north Idaho; Ph.D. thesis, University of Idaho.
- Leopold, E.B.  
1969: Late Cenozoic palynology; in *Aspects of Palynology*, R.H. Tschudy and R.A. Scott (ed.), Wiley-Interscience, New York, p. 377-438.
- Leopold, E.B. and MacGinitie, H.D.  
1972: Development and affinities of Tertiary floras in the Rocky Mountains; in *Floristics and Paleofloristics of Asia and Eastern North America*, A. Graham (ed.), Elsevier Publishing Company, Amsterdam, p. 147-200.
- MacKenzie, J.D.  
1916: Geology of Graham Island, British Columbia; *Geological Survey of Canada, Memoir 88*, 221 p.
- Martin, H.E. and Rouse, G.E.  
1966: Palynology of Late Tertiary sediments from Queen Charlotte Islands, British Columbia; *Canadian Journal of Botany*, v. 44, p. 171-208.
- Matsuoka, K. and Bujak, J.P.  
1988: Cenozoic dinoflagellate cysts from the Navarin Basin, Norton Sound and St. George Basin, Bering Sea; *Bulletin of the Faculty of Liberal Arts, Nagasaki University, Natural Science*, v. 29, no. 1, p. 1-147.
- Muller, J.  
1981: Fossil pollen records of extant angiosperms; *The Botanical Review*, v. 47, no. 1, p. 1-142.

- Newman, K.R.**  
**1981:** Palynologic biostratigraphy of some early Tertiary nonmarine formations in central and western Washington; Geological Society of America Special Paper 184, p. 49-65.
- Norris, G.**  
**1986:** Systematic and stratigraphic palynology of Eocene to Pliocene strata in the Imperial Nuktak C-22 well, Mackenzie Delta Region, District of Mackenzie, N.W.T.; Geological Survey of Canada, Bulletin 340.
- Ogden, J.G., III**  
**1986:** An alternative to exotic spore or pollen addition in quantitative microfossil studies; Canadian Journal of Earth Sciences, v. 23, p. 102-106.
- Patterson, R.T.**  
**1988:** Early Miocene to Quaternary foraminifera from three wells in the Queen Charlotte Basin off the coast of British Columbia; in Sequences, Stratigraphy, Sedimentology: Surface and Subsurface, D.P. James and D.A. Leckie (ed.), Proceedings of a Canadian Society of Petroleum Geologists Technical Meeting, Calgary, Alberta, September 14-16, 1988, p. 497.  
**1989:** Early Miocene to Quaternary foraminifera from three wells in the southern Queen Charlotte Basin; Geological Survey of Canada, Open File 1985.
- Pearson, D.L.**  
**1984:** Pollen/Spore Colour "Standard", (Version #2); Phillips Petroleum Company, Exploration Projects Section.
- Piel, K.M.**  
**1971:** Palynology of Oligocene sediments from central British Columbia; Canadian Journal of Botany, v. 49, p. 1885-1920.  
**1977:** Miocene palynological assemblages from central British Columbia; in The American Association of Stratigraphic Palynologists, Contribution Series No. 5A, p. 91-109.
- Rouse, G.E.**  
**1977:** Paleogene palynomorph ranges in western and northern Canada; American Association of Stratigraphic Palynologists, Contribution Series 5A, p. 48-65.
- Rouse, G.E. and Mathews, W.H.**  
**1979:** Tertiary geology and palynology of the Quesnel area, British Columbia; Bulletin of Canadian Petroleum Geology, v. 27, p. 418-445.  
**1988:** Palynology and geochronology of Eocene beds from Cheslatta Falls and Nazko areas, central British Columbia; Canadian Journal of Earth Sciences, v. 25, p. 1268-1276.
- Savin, S.M.**  
**1977:** The history of the earth's surface temperature during the past 100 million years; Annual Review of Earth and Planetary Sciences, v. 5, p. 319-355.
- Shackleton, N.J., Backman, J., Zimmerman, H., Kent, D.V., Hall, M.A., Roberts, D.G., Schnitker, D., Baldauf, J.G., Desprairies, A., Homrighausen, R., Huddleston, P., Keene, J.B., Kaltenback, A.J., Krumsiek, K.O.A., Morton, A.C., Murray, J.W., and Westberg-Smith, J.**  
**1984:** Oxygen isotope calibration of the onset of ice-rafting and history of glaciation in the North Atlantic region; Nature, v. 307, p. 620-623.
- Shouldice, D.H.**  
**1971:** Geology of the Western Canadian Continental Shelf; Bulletin of Canadian Petroleum Geology, v. 19, p. 405-436.
- Smiley, C.J. and Rember, W.C.**  
**1985:** Physical setting of the Miocene Clarkia fossil beds, northern Idaho; in Late Cenozoic History of the Pacific Northwest, American Association for the Advancement of Science, San Francisco, p. 11-31.
- Sutherland Brown, A.**  
**1968:** Geology of the Queen Charlotte Islands, British Columbia; British Columbia Department of Mines and Petroleum Resources, Bulletin 54.
- Vellutini, D. and Bustin, R.M.**  
**1988:** Preliminary results on organic maturation of the Tertiary Skonun Formation, Queen Charlotte Islands, British Columbia; in Current Research, Part E, Geological Survey of Canada, Paper 88-1E, p. 255-258.
- Wahrhaftig, C., Wolfe, J.A., and Leopold, E.B.**  
**1969:** The coal-bearing group in the Nenana coal field, Alaska; United States Geological Survey Bulletin 1274-D.
- White, J.M.**  
**1988:** Methodology of the exotic spike: differential settling of palynomorphs during sample preparation; Pollen et Spores, v. 30, no. 1, p. 131-148.  
**1990a:** Exploration of a practical technique to estimate the relative abundance of rare palynomorphs using an exotic spike; in Proceedings of a Colloquium on Statistical Applications in the Earth Sciences, F.P. Agterberg and G.F. Bonhom-Carter (ed.), Geological Survey of Canada, Paper 89-9, p. 483-486.  
**1990b:** Evidence of Paleogene sedimentation on Graham Island, Queen Charlotte Islands, West Coast, Canada; Canadian Journal of Earth Sciences, v. 27, p. 533-538.
- Wiggins, V.D.**  
**1986:** Two punctuated equilibrium dinocyst events in the Upper Miocene of the Bering Sea; in American Association of Stratigraphic Palynologists Contributions Series No. 17, p. 159-167.
- Wolfe, J.A.**  
**1981:** A chronologic framework for Cenozoic megafossil floras of northwestern North America and its relation to marine geochronology; Geological Society of America Special Paper 184, p. 39-47.
- Wolfe, J.A., Hopkins, D.M., and Leopold, E.B.**  
**1966:** Tertiary stratigraphy and paleobotany of the Cook Inlet region, Alaska; United States Geological Survey, Professional Paper 398-A.

# Source rock potential of Mesozoic and Tertiary strata of the Queen Charlotte Islands, British Columbia

D. Vellutini<sup>1,2</sup> and R.M. Bustin<sup>1</sup>

Vellutini, D. and Bustin, R.M., Source rock potential of Mesozoic and Tertiary strata of the Queen Charlotte Islands; in *Evolution and Hydrocarbon Potential of the Queen Charlotte Basin, British Columbia*, Geological Survey of Canada, Paper 90-10, p. 381-409, 1991.

## Abstract

*The source rock potential of strata in the Queen Charlotte Islands was determined using Rock-Eval pyrolysis. Mean total organic carbon (TOC) contents are generally low to moderate (0.1-3.6 %) and some organic-rich intervals occur throughout the succession. Horizons with high TOC values occur in the Peril Formation (up to 10.3 %) and in the Whiteaves Formation (up to 11.2 %). Generally, Mesozoic and Tertiary strata contain Type III organic matter except for the Kunga Group and the Ghost Creek Formation which contain oil and gas-prone Type II and significant amounts of oil-prone Type I organic matter.*

*Lateral variations in TOC and the quality of organic matter (QOM) for Mesozoic strata on Moresby Island are primarily related to the level of organic maturation. High heat flow associated with plutonism has resulted in generally poor hydrocarbon source potential for strata on Moresby Island. Equivalent strata on Graham Island are generally immature to mature and have fair to good hydrocarbon source potential.*

*Source potential of Cretaceous and Tertiary strata on Graham Island is controlled primarily by the level of organic maturation and to a lesser extent by depositional patterns. Cretaceous strata from Moresby Island are generally overmature and have poor source potential whereas equivalent strata from Graham Island are immature to overmature and have fair to moderate gas source potential. The Haida and Honna formations generally contain terrestrially derived Type III organic matter with poor to fair gas source potential. The Skidegate Formation has a mixture of Types II and III organic matter and has fair gas generative potential. The Haida Formation contains only terrestrially derived Type III organic matter whereas the Skidegate Formation contains less Type III organic matter and more Type II organic matter. The Tertiary Skonun Formation contains abundant, generally immature coal and lignite with some gas source potential. Mature resinite horizons containing hydrogen-rich organic matter have fair to good oil and gas source potential. Siltstone and shale facies of the Skonun Formation contain moderate amounts of Type II organic matter and have good hydrocarbon source potential.*

## Résumé

*Le potentiel en roches mères des couches dans les îles de la Reine-Charlotte a été déterminé par pyrolyse Rock-Eval. Les teneurs moyennes en carbone organique total sont en général de faibles à moyennes (0,1 à 3,6 %) et certains intervalles riches en matières organiques sont présents dans toute la succession. Des horizons à valeur en carbone organique total élevée se trouvent dans la formation de Peril (jusqu'à 10,3 %) et dans la formation de Whiteaves (jusqu'à 11,2 %). En général, les couches mésozoïques et tertiaires contiennent des matières organiques de type III à l'exception du groupe de Kunga et de la formation de Ghost Creek qui contiennent des matières organiques de type II propices à la formation de pétrole et de gaz et des quantités importantes de matières organiques de type I propices à la formation de pétrole.*

*Les variations latérales en carbone organique total et la qualité des matières organiques des couches mésozoïques dans l'île Moresby sont principalement liées au niveau de maturation organique. Le flux thermique élevé associé au plutonisme est à l'origine du potentiel généralement faible de trouver des roches mères d'hydrocarbures dans les couches de l'île Moresby. Les couches triasiques et jurassiques équivalentes de l'île Graham varient en général de non mures à mures et présentent un potentiel en roches mères d'hydrocarbures de moyen à bon.*

*Le potentiel en roches mères des couches crétacées et tertiaires de l'île Graham dépend principalement du niveau de maturation organique et, dans une moindre mesure, des géométries d'accumulation. Les couches crétacées de l'île Moresby sont en général hypermatures et présentent un faible potentiel en roches mères tandis que les couches équivalentes de l'île Graham varient de non mures à hypermatures et présentent un potentiel en roches mères de passable à moyen. Les formations de Haida et de Honna contiennent généralement des matières organiques de type III d'origine terrestre dont le potentiel en roches mères de gaz est de faible à passable. La formation de Skidegate contient un mélange de matières organiques des types II et III et présente un potentiel de formation de gaz passable. La formation d'Haida ne contient que des matières organiques de type III d'origine terrestre tandis que la formation de Skidegate contient moins de matières organiques de type III que la première et davantage de matières organiques de type II. La formation de Skonun renferme du charbon et du lignite généralement non mures en abondance et susceptibles de constituer des roches mères de gaz. Le potentiel en roches mères de gaz et de pétrole est de passable à bon pour les horizons de résinites mures contenant des matières organiques riches en hydrogène. Le faciès de siltstone et de schiste argileux de la formation de Skonun contient des quantités modérées de matières organiques de type II et son potentiel en roches mères d'hydrocarbures est bon.*

<sup>1</sup> Department of Geological Sciences, University of British Columbia, 6339 Stores Road, Vancouver, B.C. V6T 2B4

<sup>2</sup> Present Address: Texaco Canada Resources, Drayton Valley, Alberta, T0E 0M0



## INTRODUCTION

The Queen Charlotte Islands contain a thick sedimentary sequence which includes potential source and reservoir strata. The presence of numerous oil seeps, oil shales, and carbonaceous black shales suggest that hydrocarbons have been generated in the past and may have accumulated in commercial quantities (Cameron and Tipper, 1985; Cameron, 1987; Bustin and Macauley, 1988; Snowdon et al., 1988). To date, the lateral and vertical variations in source rock quality for Mesozoic and Tertiary strata in the Queen Charlotte Islands have not been documented. In this study we examine the source rock potential of sedimentary strata on the Queen Charlotte Islands. Macauley (1983) and Bustin and Macauley (1988) have previously documented the DOM and source rock quality for Lower Jurassic oil shales found in central Graham Island and Skidegate Inlet, and Snowdon et al. (1988) have performed preliminary organic geochemical analysis on oil seeps from Tertiary strata. The present study is a companion to Vellutini and Bustin (1991) and expands on the initial work of Bustin and Macauley (1988) to include the entire stratigraphic sequence (Mesozoic to Tertiary) for the entire Queen Charlotte Islands region.

Microscopic and geochemical analysis of organic matter are an important part of petroleum exploration in assessing the hydrocarbon source potential of sedimentary strata. Geochemical data from Rock-Eval pyrolysis (Espitalie et al., 1977) can be used to establish the quantity, type, and thermal maturity of organic matter in sedimentary rocks (Tissot and Welte, 1984). Combined with organic facies and thermal maturity data, Rock-Eval analysis can be used to identify the lateral and vertical extent of potential source strata.

## METHODS

### Sample preparation

One thousand four hundred and sixty outcrop and well samples were analyzed by Rock-Eval pyrolysis (Espitalie et al., 1977; Peters, 1986) and organic petrographic techniques (Bustin et al., 1983). Whole rock samples were crushed with ring and centrifugal grinders to about -60 mesh particle size. Coal and lignite samples were

crushed and sieved to between -50 and -200 mesh particle size to eliminate ultra-fine particles which adversely effect pyrolysis results. The crushed whole rock samples were split for both Rock-Eval pyrolysis (80-100 mg) and vitrinite reflectance analyses. Coal and lignite samples weighing from 5-30 mg were layered in crushed, pure quartz prior to Rock-Eval pyrolysis to prevent carbon caking of the Rock-Eval pyrolysis instrument.

### Measured parameters

Rock-Eval pyrolysis provides several measurements to characterize potential source rocks (Table 1). The S1 peak (mg HC/g rock) represents hydrocarbons distilled from the whole rock (2 minutes at 300°C). The S2 peak (mg HC/g rock) represents hydrocarbons pyrolyzed from kerogen at temperatures of 300-600°C (Espitalie et al., 1977). The S3 peak is a measure of the volatilized carbon dioxide between temperatures of 300°C and 390°C (mg HC/g rock). The total organic carbon content (TOC) is determined by oxidizing the residual organic matter in air at 600°C and summed with S1, S2, and S3 peaks (Espitalie et al., 1977). Outcrop samples are commonly depleted in S1 and S2 values as a result of oxidation of the organic matter. Similarly, oxidation from erosional events near unconformities can result in S1 and S2 depletion.

The temperature of maximum S2 hydrocarbon generation ( $T_{max}$ ) reflects the degree of organic maturation (Espitalie et al., 1977). The oil birth line occurs at a  $T_{max}$  value between 430-435°C for Types II and III organic matter. The oil death line occurs at a  $T_{max}$  value of 450°C for Type II organic matter and at 465°C for Type III organic matter (Espitalie et al., 1977). Type I organic matter has  $T_{max}$  values ranging from 460-470°C and generally shows a poor correlation between organic maturity and  $T_{max}$  (Link, 1988).

### Calculated parameters

Parameters calculated from the Rock-Eval data can be used to determine the nature and quality of potential source rocks (Table 1). The production index (PI), defined as the ratio  $S1/(S1+S2)$ , is a measure of thermal maturity. PI values between 0.1 and 0.4 define the oil window (Peters, 1986). With increasing hydrocarbon generation, PI values increase to 1.0, marking the exhaustion of the hydrocarbon generative potential of the source kerogen. Anomalously high PI values indicate hydrocarbon accumulation and anomalously low PI values indicate hydrocarbon depletion (Espitalie et al., 1985; Peters, 1986). The hydrogen index (HI), defined as  $S2/TOC$ , and the oxygen index (OI), defined as  $S3/TOC$ , are used to classify organic matter using a hydrogen index/oxygen index (HI/OI) diagram as described by Espitalie et al. (1977). HI values >600 mg HC/g  $C_{org}$  suggests oil-prone Type I organic matter, HI values between 300 and 600 mg HC/g  $C_{org}$  suggests oil and gas prone Type II organic matter, and HI values <300 mg HC/g  $C_{org}$  suggests gas prone Type III organic matter, assuming a DOM equivalent to 0.6 %Ro (Espitalie et al., 1977).

The quality of organic matter (QOM), defined as the ratio  $(S1+S2)/TOC$ , is used to determine the type of organic matter and to measure thermal maturity. QOM values vary with the degree of thermal maturation, the type of organic matter, and migration effects of hydrocarbons (Espitalie et al., 1985). High QOM ratios suggest immature to mature hydrogen-rich organic matter. Variations in QOM values which cannot be attributed to differences in the level of thermal maturity are considered to be the result of hydrocarbon migration.

## RESULTS

Source rock data from Rock-Eval pyrolysis are summarized in Table 1 of Vellutini and Bustin (1991) for interval horizons (group, formation, or informal member) rather than for individual samples.

**Table 1:** Geochemical parameters used in this study

<b>Parameters describing level of thermal maturation<sup>1</sup></b>			
Maturation	PI	$T_{max}$ <sup>2</sup>	Ro
	$S1/(S1+S2)$	(°C)	(%)
Top of oil window	0.1	430-435	0.5
Bottom of oil window	0.4	465	1.35
<b>Parameters describing source rock generative potential<sup>1</sup></b>			
	TOC	S1	S2
Quantity	(weight %)	(mg HC/gm $C_{org}$ )	(mg HC/gm $C_{org}$ )
Poor	0.0-0.5	0.0-0.5	0.0-2.5
Fair	0.5-1.0	0.5-1.0	2.5-5.0
Good	1.0-2.0	1.0-2.0	5.0-10.0
Very good	2+	2+	10+
<b>Parameters describing type of hydrocarbon generated<sup>1</sup></b>			
	HI	$S2/S3$ <sup>3</sup>	
Type	(mg HC/gm $C_{org}$ ) <sup>3</sup>		
Gas	0-150	0-3	
Gas and oil	150-300	3-5	
Oil	300+	5+	

<sup>1</sup> Peters (1986)

<sup>2</sup> Maturation parameter may depend on type of organic matter

<sup>3</sup> Assumes a DOM equivalent to  $R_o=0.6\%$

Rock-Eval data are also presented for some formations as TOC histograms (Figs. 1a-1q), hydrogen index versus  $T_{\max}$  diagrams (Figs. 2a-2n), hydrogen index versus oxygen index diagrams (Figs. 3a-3r), and Rock-Eval logs for the onshore Tertiary wells (Figs. 4-9). Lateral variations in TOC (Figs. 10-22) and QOM (Figs. 23-35) are plotted by group, formation, or member.  $T_{\max}$  versus vitrinite reflectance diagrams are in Appendix B of Vellutini (1988).

Source rocks are strata which are capable of generating migratable hydrocarbons. The hydrocarbon generative potential is primarily controlled by the volume, richness, and thermal maturity of the organic matter within the strata (Dow, 1977; Espitalie et al., 1977; Conford, 1984; Tissot and Welte, 1984; Espitalie et al., 1985). The level of organic maturity was determined in this study from vitrinite reflectance (Vellutini and Bustin, 1991) and Rock-Eval pyrolysis ( $T_{\max}$  and PI). Interpretation of lateral trends in organic maturation and source rock potential of Mesozoic and Tertiary strata on the Queen Charlotte Islands is difficult due to limited lateral continuity of stratigraphic units and limited outcrop distribution. Hence, the interpretations presented in the following sections are preliminary.

### Organic maturation

High heat flow associated with volcanism and plutonism is an important control on source rock quality in the Queen Charlotte Islands. Surface maturation trends with respect to hydrocarbon generation are shown in Figure 40 of Vellutini and Bustin (1991). Mesozoic strata on Moresby Island south of Cumshewa Inlet are overmature and the DOM increases proximal to Jurassic-Cretaceous plutonic suites. The regional level of organic maturation of Triassic and Cretaceous strata on northwest Graham Island ranges from immature to mature with local, anomalous overmature strata. Jurassic and Cretaceous strata on central Graham Island are marginally mature to mature, whereas in the Skidegate and Cumshewa Inlet areas the strata are mature to overmature.

## DISCUSSION

The following section documents the hydrocarbon source potential for selected Mesozoic and Tertiary strata, largely based on the data Table 1 of Vellutini and Bustin (1991);  $T_{\max}$  values are not reported for samples with S2 values lower than the 0.2 mg HC/gm  $C_{\text{org}}$  considered necessary for accurate  $T_{\max}$  determination (Peters, 1986). In very overmature samples, the HI and OI values are too low to ascertain the type of original organic matter.

## KUNGA GROUP

### Sadler Limestone

Low QOM (<0.08 mg HC/gm  $C_{\text{org}}$ ), low HI (<8 mg HC/gm  $C_{\text{org}}$ ), low PI (<0.08) and high maturation (2.35-5.28 %Ro<sub>rand</sub>) values indicate that the massive carbonates of the Sadler Limestone on Moresby Island have poor oil source potential but are possibly gas source rocks. Some residual organic carbon (<1.1% TOC), and low PI values (<0.08) from southern Moresby Island suggest hydrogen depletion and that the strata may have been source rocks and previously generated hydrocarbons. High maturation values preclude the determination of the initial type of organic matter (Fig. 3r).

### Peril Formation

High DOM (2.37-8.31 %Ro<sub>rand</sub>), and low QOM (<0.05 mg HC/gm  $C_{\text{org}}$ ), PI (0.03-0.07), and HI (<16 mg HC/gm  $C_{\text{org}}$ ) values for the interbedded shale and calcarenite of this unit on Moresby Island indicate that the strata are presently poor oil source rocks. Low PI, high DOM, low HI, and variable TOC (<2.56%) values suggest hydrocarbon depletion and indicate that hydrocarbons may have been previously

generated. Moderate amounts of residual carbon (<2.56% TOC) and low HI values suggest some gas generation potential.

Mature to overmature strata (0.51-3.19 %Ro<sub>rand</sub>; 440-587°C  $T_{\max}$ ) from northwest Graham Island are good oil and gas source rocks as is evident from high TOC (2.17-3.6%), QOM (<4.19 mg HC/gm  $C_{\text{org}}$ ), moderate to high HI (192-385 mg HC/gm  $C_{\text{org}}$ ), and moderate PI (0.08-0.33) values. Solid bitumen observed in hand specimen accounts for the anomalously high TOC values, and indicates that the strata have previously generated liquid hydrocarbons. Low to moderate PI values in some areas suggest depletion and possible migration of hydrocarbons.

The HI/OI diagram for the Peril Formation (Fig. 3q) shows two populations of organic matter: Types I and II with high HI and low OI values with very good oil and gas generative potential from northwest Graham Island; and overmature Type III with very low HI and high OI values resulting in fair gas but no oil generative potential at Moresby Island.

### Sandilands Formation

The DOM for the shale and argillite of the Sandilands Formation exposed on Moresby Island is too high (3.78-4.00 %Ro<sub>rand</sub>) to consider the strata as oil source rocks. Low QOM (<0.05 mg HC/gm  $C_{\text{org}}$ ), low HI (<2 mg HC/gm  $C_{\text{org}}$ ) and high maturation values indicate hydrocarbon depletion, suggesting that hydrocarbons may have been previously generated. High PI values (<0.59) at Kunga Island suggest that hydrocarbons have possibly migrated into overmature strata. Moderate amounts of residual TOC (0.51-1.56%) and low HI values suggest some potential for gas generation.

Mature Type I and Type II organic matter of the Sandilands Formation in central Graham Island has good oil and gas source potential, shown by high TOC (1.25-9.6%), QOM (1.94-4.26 mg HC/gm  $C_{\text{org}}$ ), and moderate to high HI (159-372 mg HC/gm  $C_{\text{org}}$ ) values. Moderate PI values (0.14-0.42) and free hydrocarbons (S1<1.64 mg HC/gm  $C_{\text{org}}$ ) suggest some conversion of kerogen to petroleum.

Marginally immature strata on northwest Graham Island at Kennecott Point are good oil and gas source rocks with high TOC (2.66%), QOM (4.66 mg HC/gm  $C_{\text{org}}$ ), and HI (437 mg HC/gm  $C_{\text{org}}$ ) values. Low PI (0.06) and vitrinite reflectance (0.45 %Ro<sub>rand</sub>) values suggest a low degree of kerogen conversion to petroleum. The Sandilands Formation at depth is probably more mature and may have generated substantial amounts of petroleum.

## MAUDE GROUP

### Ghost Creek Formation

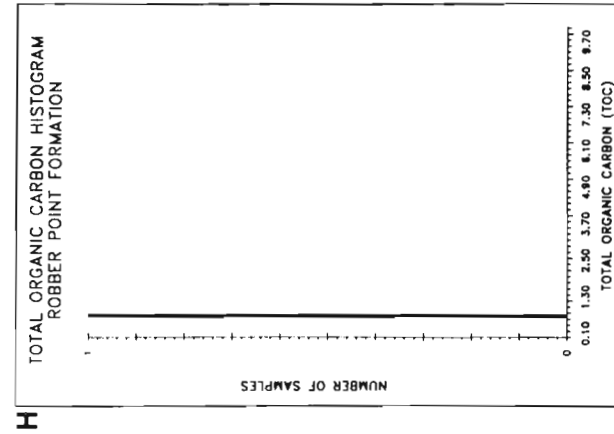
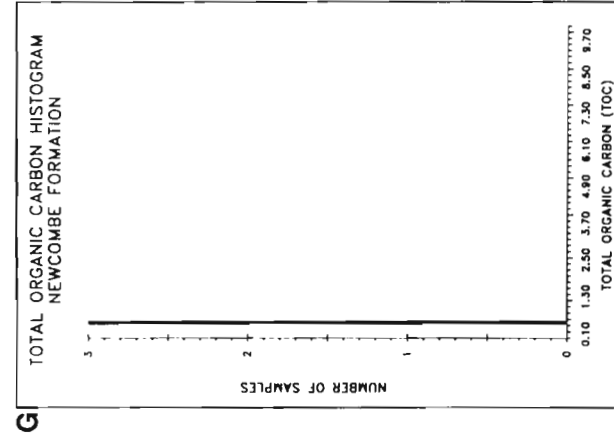
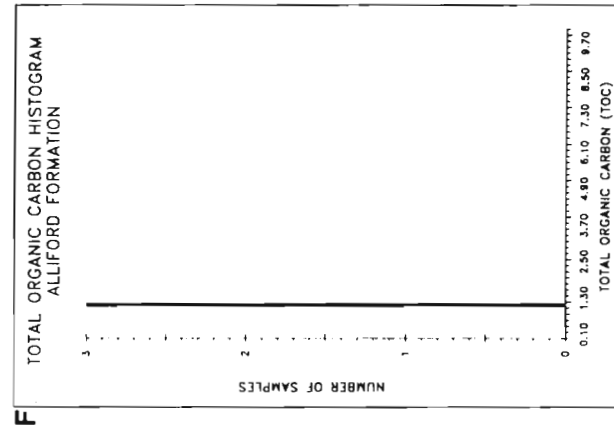
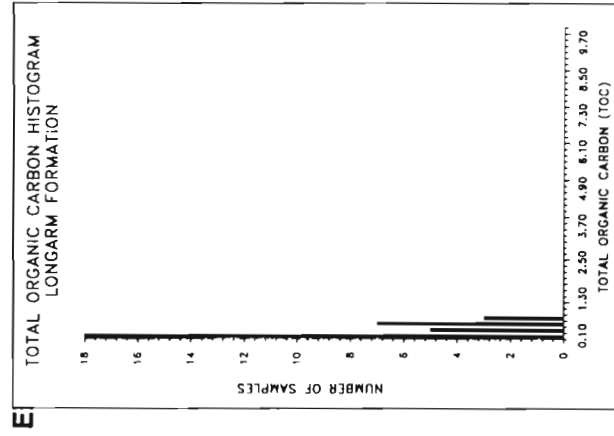
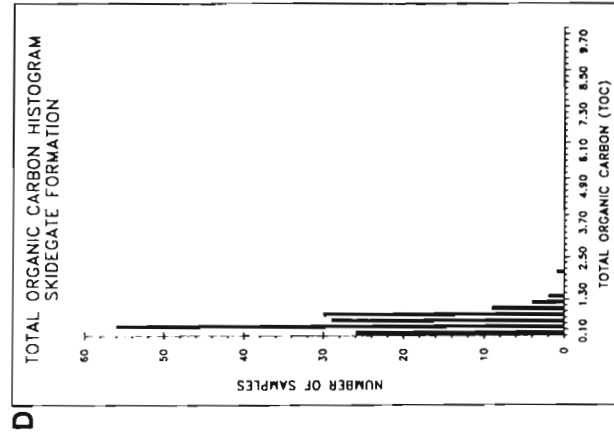
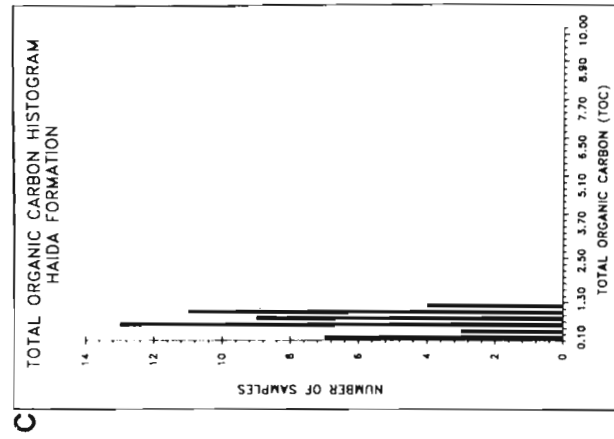
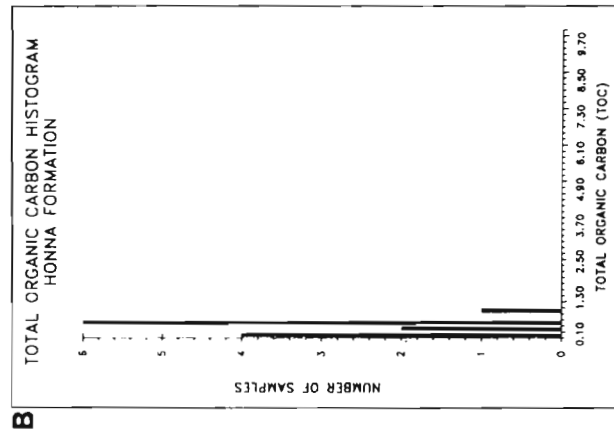
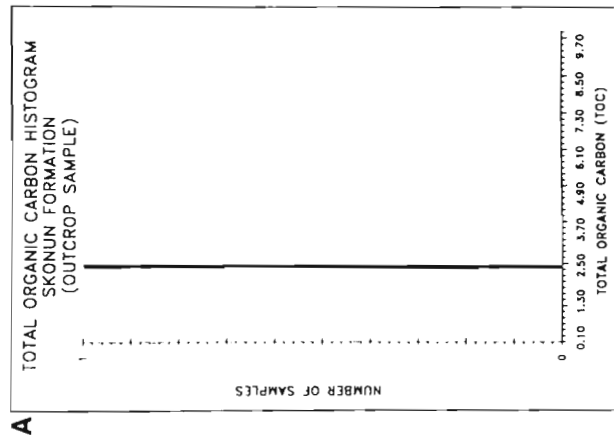
Marginally mature (0.55 %Ro<sub>rand</sub>) strata of the Ghost Creek Formation on central Graham Island and locally in Skidegate Inlet have good oil and gas source potential, as indicated by moderate TOC (1.66-1.73%), high QOM (3.19-3.73 mg HC/gm  $C_{\text{org}}$ ), and moderate HI (218.0-349 mg HC/gm  $C_{\text{org}}$ ) values. A low PI (0.07) suggests a low degree of kerogen conversion to petroleum.

Marginally overmature to overmature strata (1.32-1.51 %Ro<sub>rand</sub>) in Skidegate Inlet (Maude Island) and Rennell Sound are currently poor oil source rocks, as suggested by low QOM (0.14-0.66 mg HC/gm  $C_{\text{org}}$ ) and HI (9-38 mg HC/gm  $C_{\text{org}}$ ). Moderate PI (0.48) values from Rennell Sound suggest that the strata are overmature.

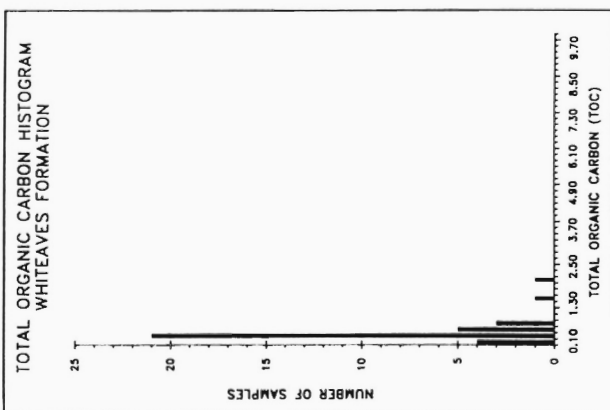
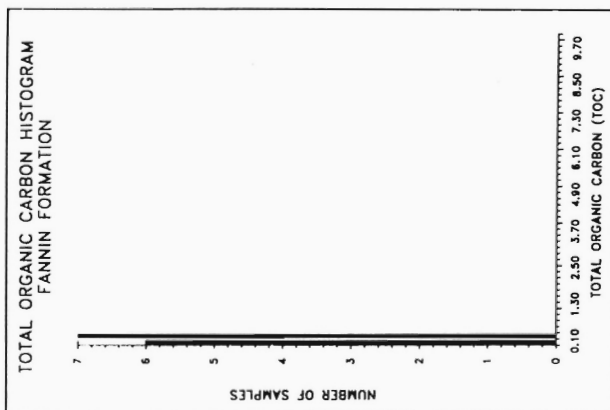
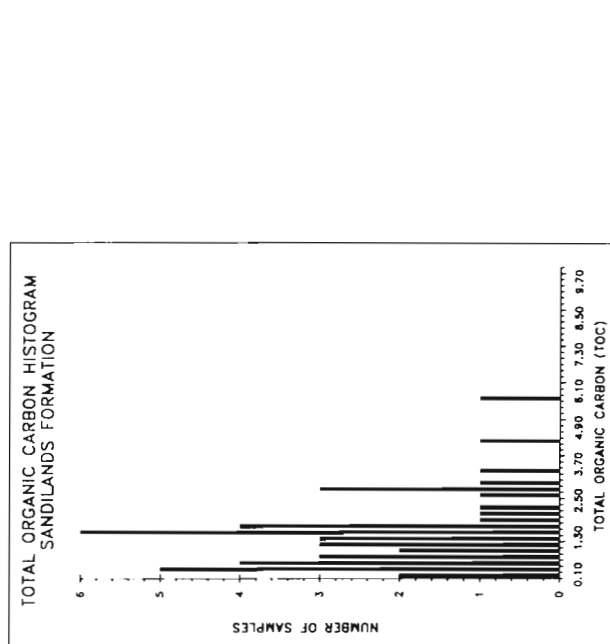
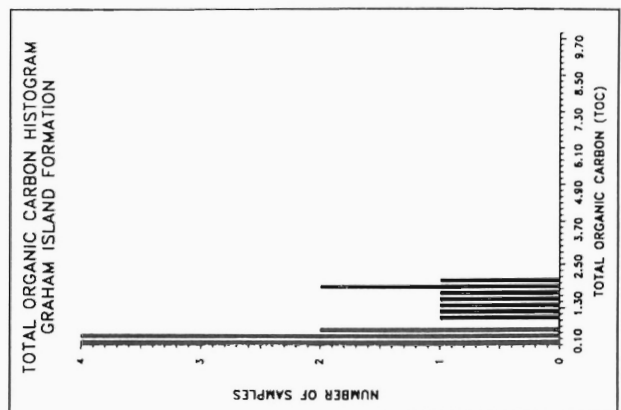
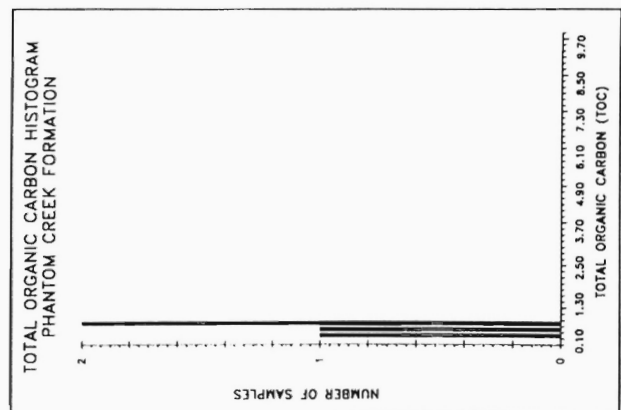
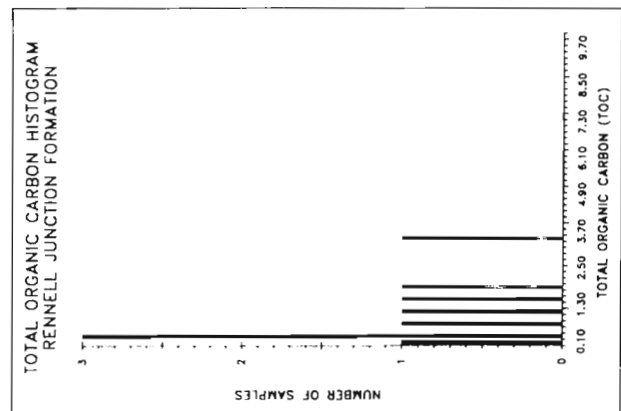
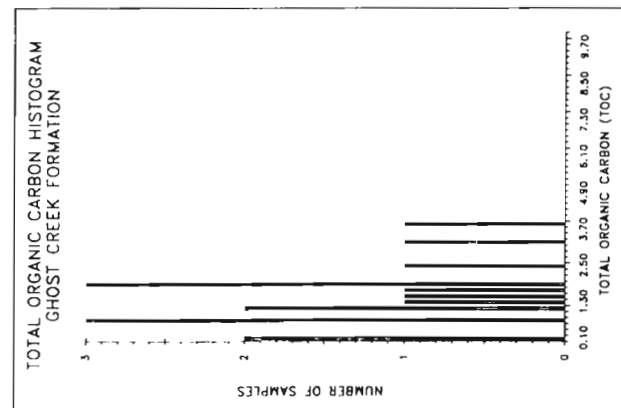
### Rennell Junction Formation

Mature to overmature (0.52-1.5 %Ro<sub>rand</sub>) sandstone, siltstone, and shale from Cumshewa Inlet and Skidegate Inlet are generally poor source rocks (TOC<1.96%; QOM=0.33 mg HC/gm  $C_{\text{org}}$ ; and HI<93 mg HC/gm  $C_{\text{org}}$ ) values. Type III organic matter (Figs. 2k,n) suggests that the strata are possible gas source rocks.

**Figure 1a-d:** Histograms of total organic carbon (TOC) content (weight %). Class interval is 0.2% TOC. Data include outcrop and well cuttings samples. a) Skonun Formation; b) Honna Formation; c) Haida Formation; d) Skidegate Formation.



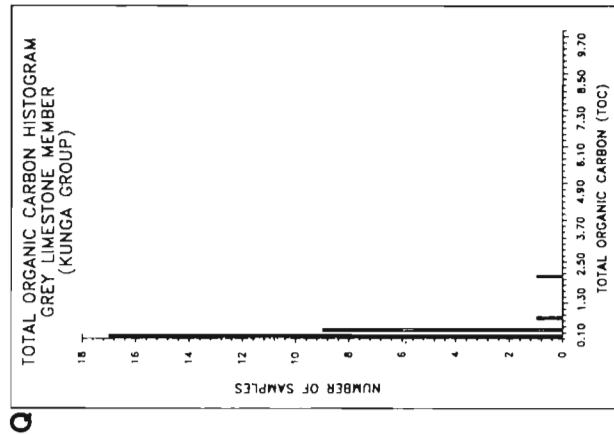
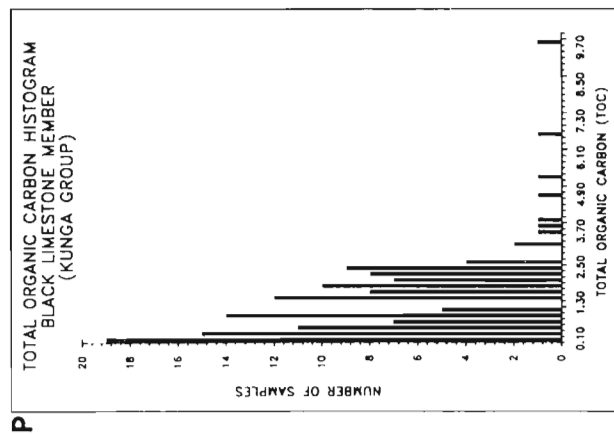
**Figure 1e-h:** Histograms of total organic carbon (TOC) content (weight %). Class interval is 0.2% TOC. Data include outcrop and well cuttings samples. e) Longarm Formation; f) Alliford Formation; g) Newcombe Formation; h) Robber Point Formation.



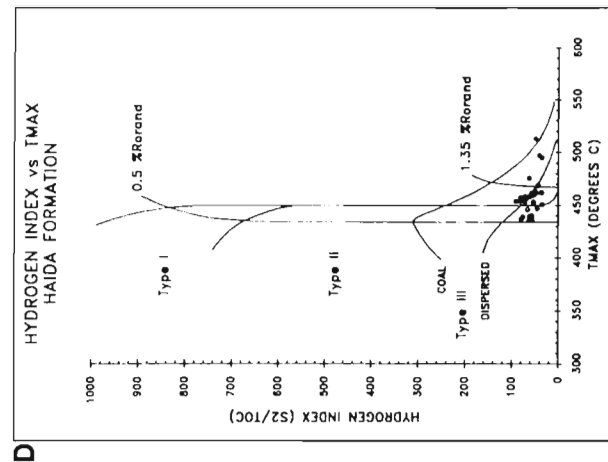
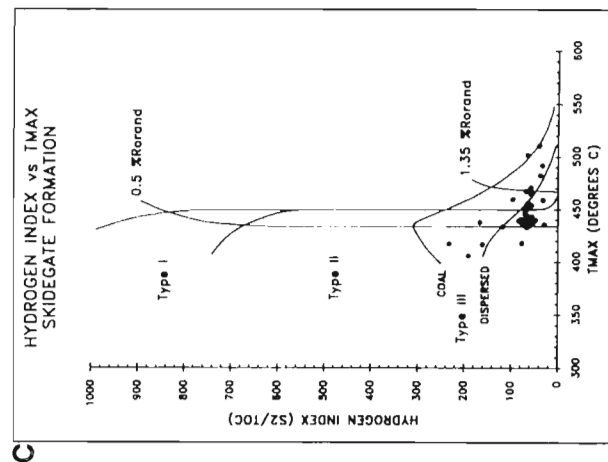
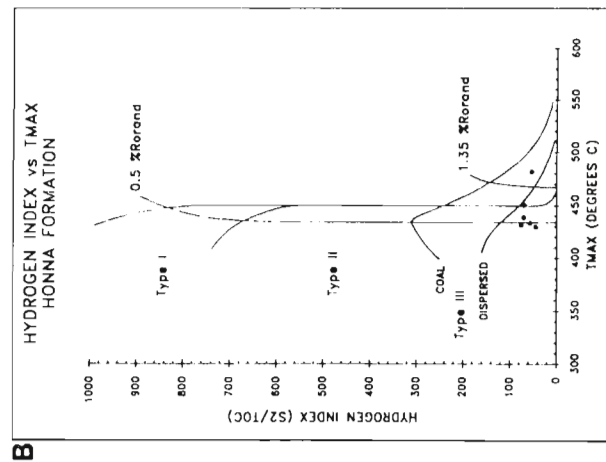
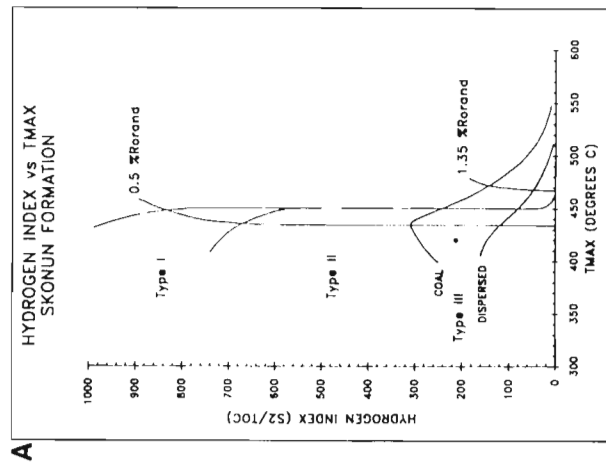
**Figure 1m-o:** Histograms of total organic carbon (TOC) content (weight %). Class interval is 0.2% TOC. Data include outcrop and well cuttings samples. m) Rennell Junction Formation; n) Ghost Creek Formation; o) Sandilands Formation.

**Figure 1i-l:** Histograms of total organic carbon (TOC) content (weight %). Class interval is 0.2% TOC. Data include outcrop and well cuttings samples. i) Graham Island Formation; j) Phantom Creek Formation; k) Whiteaves Formation; l) Fannin Formation.

**Figure 1p-q:** Histograms of total organic carbon (TOC) content (weight %). Class interval is 0.2% TOC. Data include outcrop and well cuttings samples. p) Peril Formation; q) Sadler Limestone.



**Figure 2a-d:** Hydrogen index/ $T_{max}$  ( $HI/T_{max}$ ) diagrams. Organic matter types and oil window limits based on Espitalie et al. (1985).  $[HI = S2/TOC \text{ (mg HC/gm } C_{org})]$ ;  $T_{max}$  °C. Data include outcrop and well cuttings samples. 0.50 % $R_{o, and}$  (430-435°C  $T_{max}$ ) to 1.35 % $R_{o, and}$  (465 °C  $T_{max}$ ) define the oil window for Types II and III organic matter. a) Skonun Formation; b) Honna Formation; c) Skidegate Formation; d) Haida Formation.



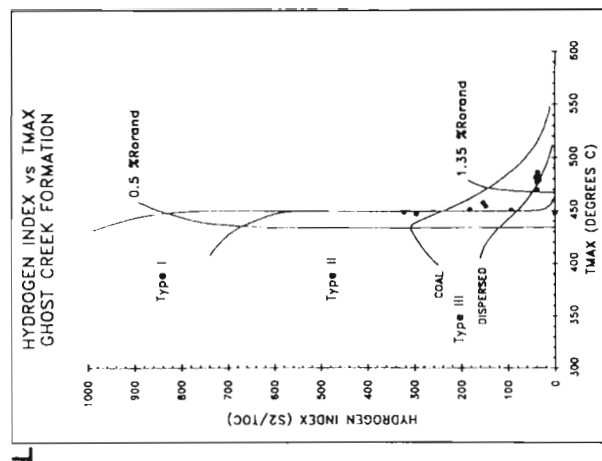
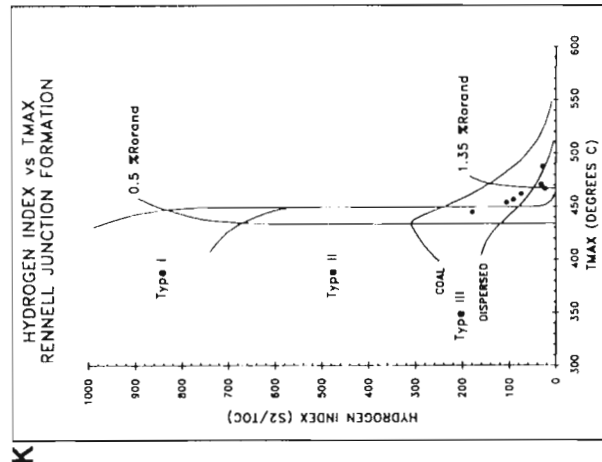
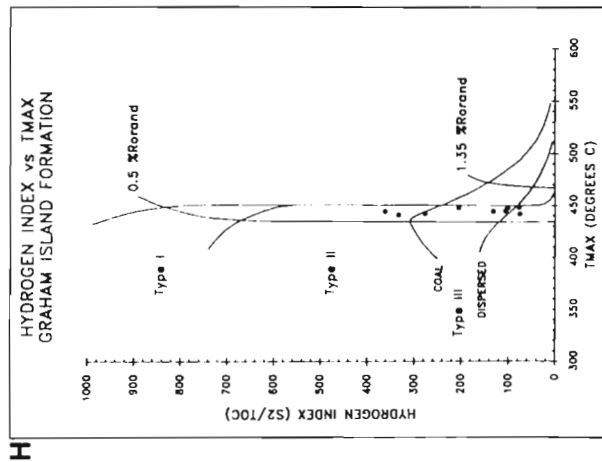
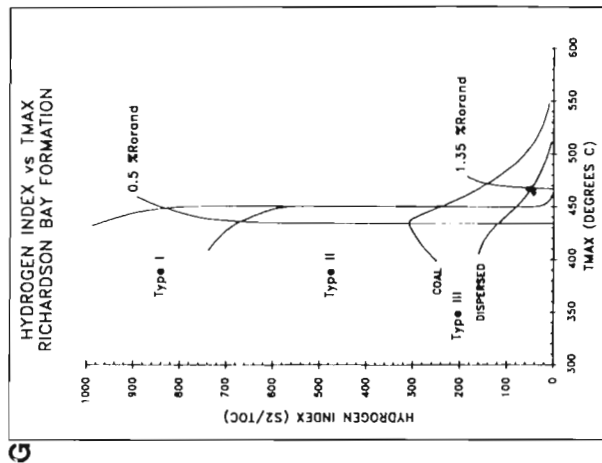
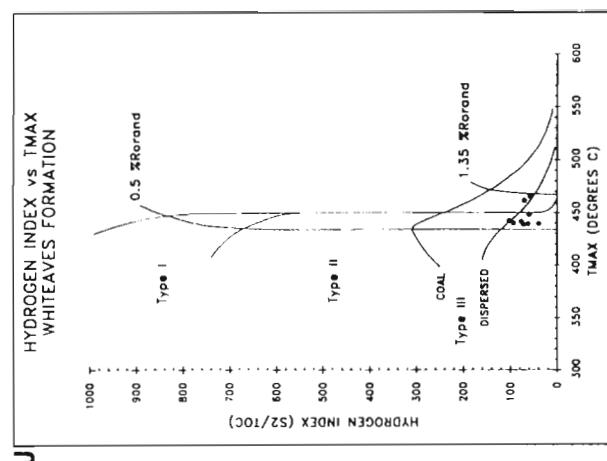
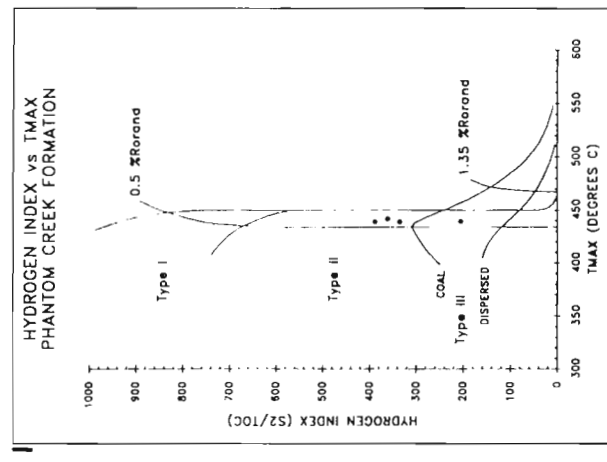
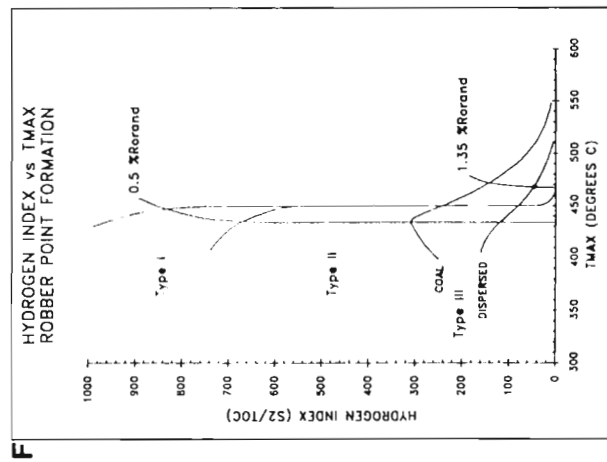
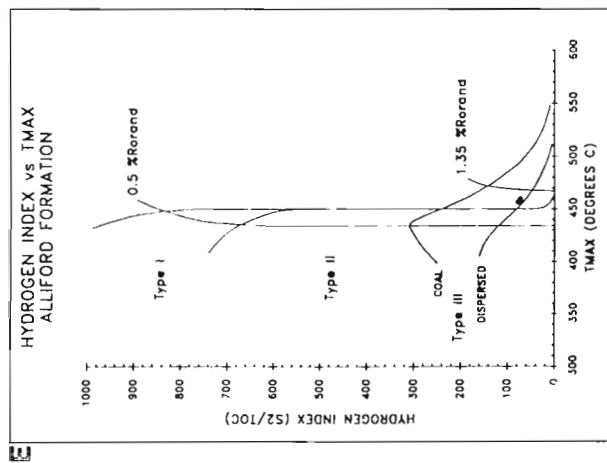
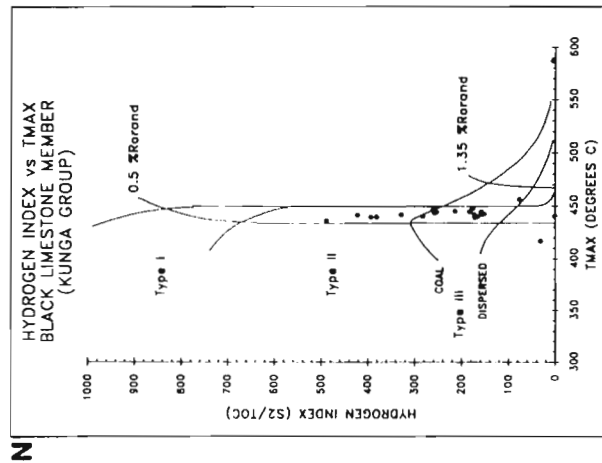
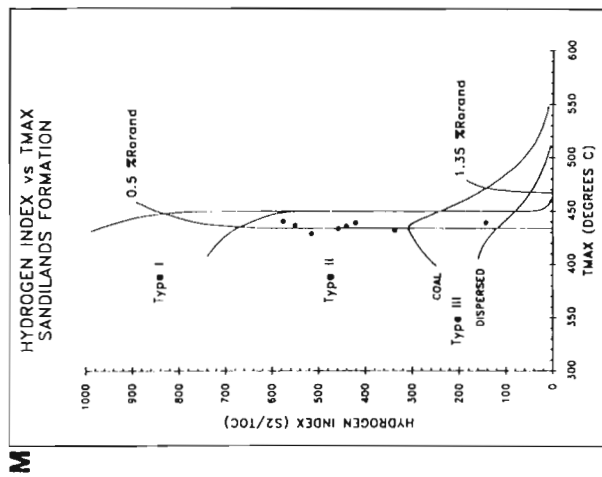


**Figure 2e-h:** Hydrogen index/ $T_{max}$  ( $HI/T_{max}$ ) diagrams as in Figs. 2a-d. Data include outcrop and well cuttings samples. e) Allifford Formation; f) Robber Point Formation; g) Richardson Bay Formation; h) Graham Island Formation.

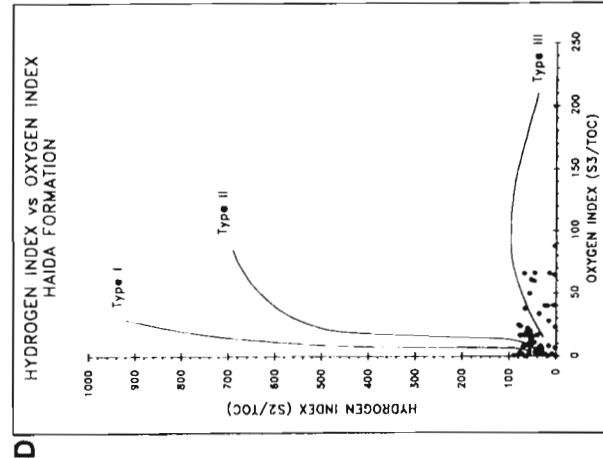
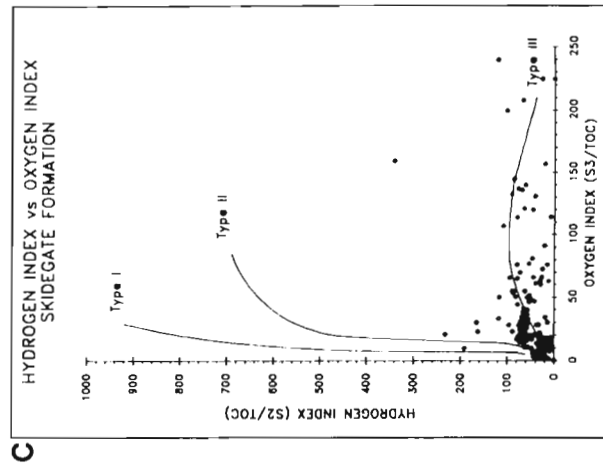
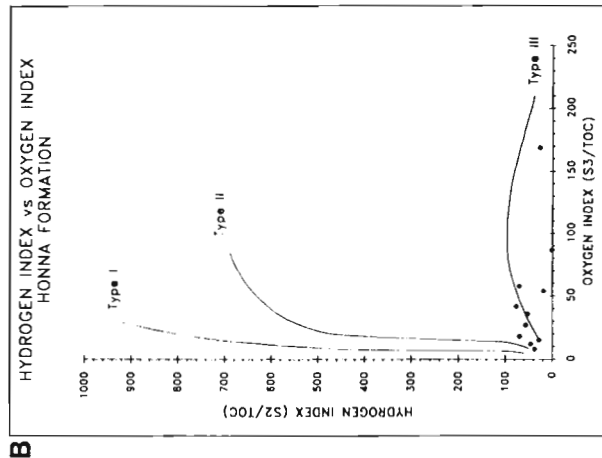
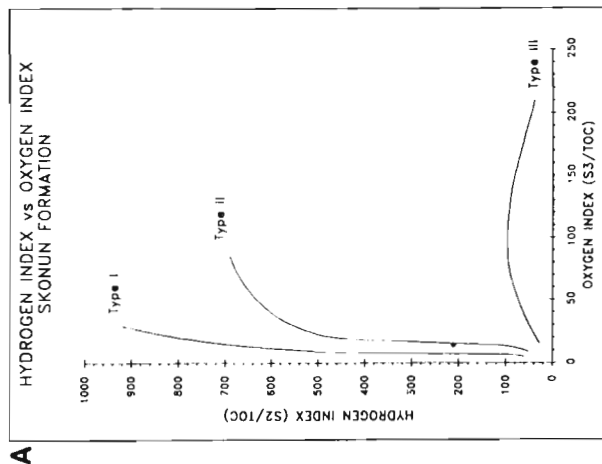
**Figure 2i-l:** Hydrogen index/ $T_{max}$  ( $HI/T_{max}$ ) diagrams as in Figs. 2a-d. Data include outcrop and well cuttings samples. i) Phantom Creek Formation; j) Whiteaves Formation; k) Rennell Junction Formation; l) Ghost Creek Formation.



**Figure 2m-n:** Hydrogen index/ $T_{max}$  (HI/ $T_{max}$ ) diagrams as in Figs. 2a-d. Data include outcrop and well cuttings samples. m) Sandilands Formation; n) Peril Formation.



**Figure 3a-d:** Hydrogen index/Oxygen index (HI/OI) diagrams. Maturation pathways modified from Espitalie et al. (1985). [HI=S2/TOC (mg HC/gm  $C_{org}$ ); OI=S3/TOC (mg HC/gm  $C_{org}$ )]. Data include outcrop and well cuttings samples. a) Skonun Formation; b) Honna Formation; c) Skidegate Formation; d) Haida Formation.



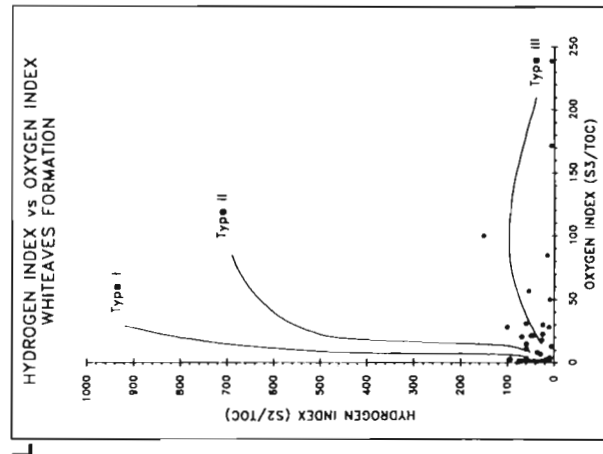
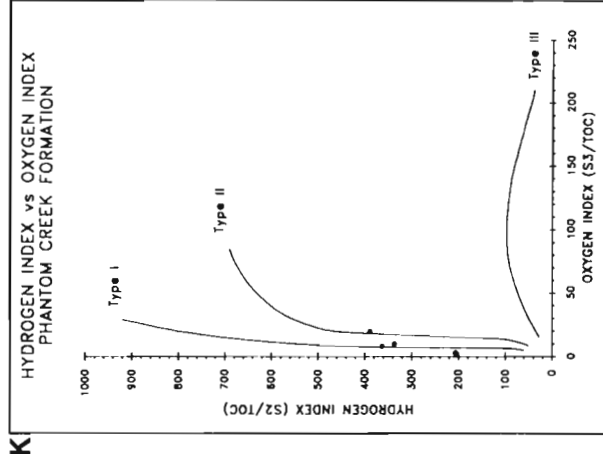
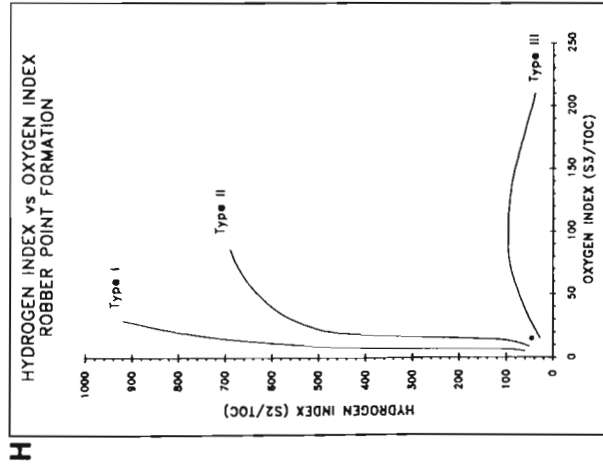
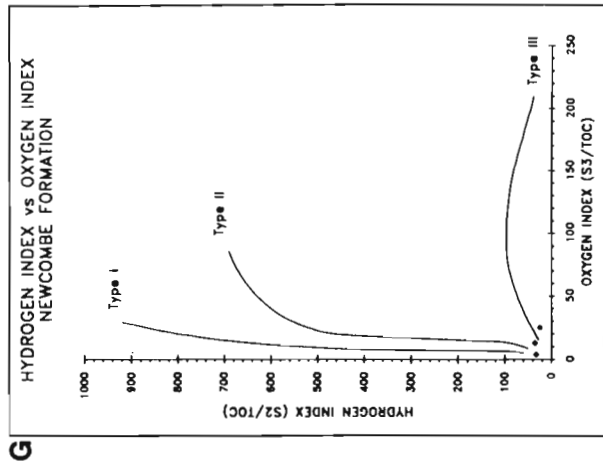
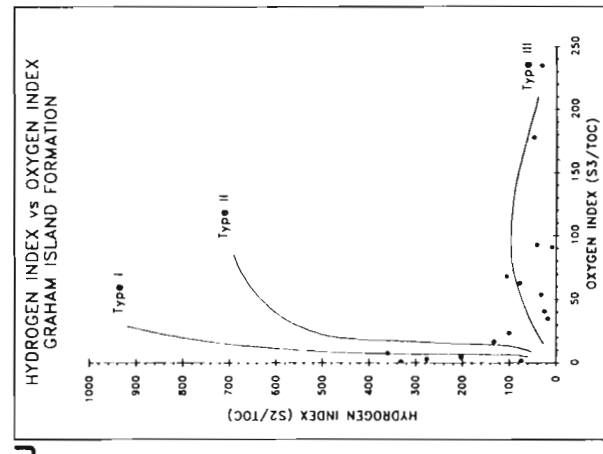
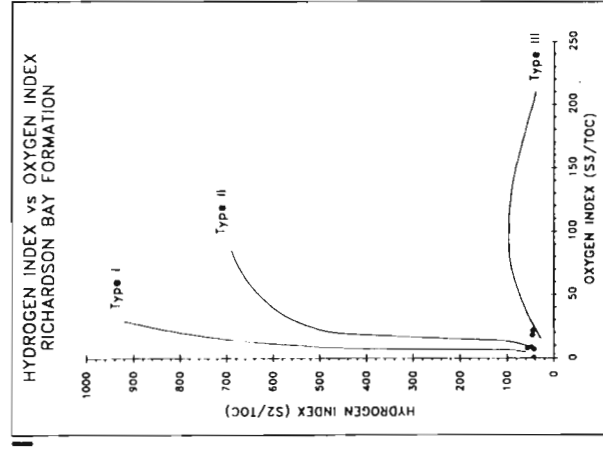
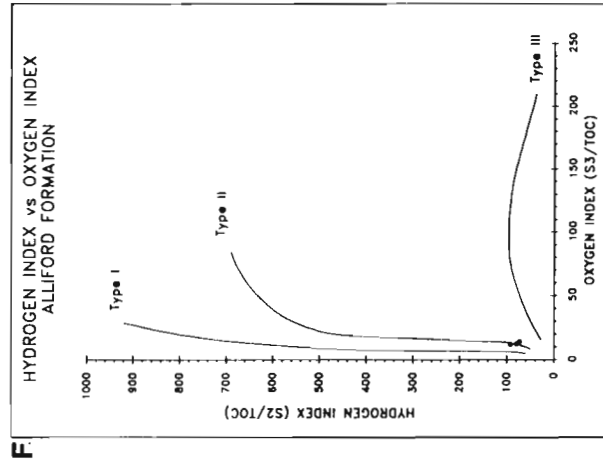
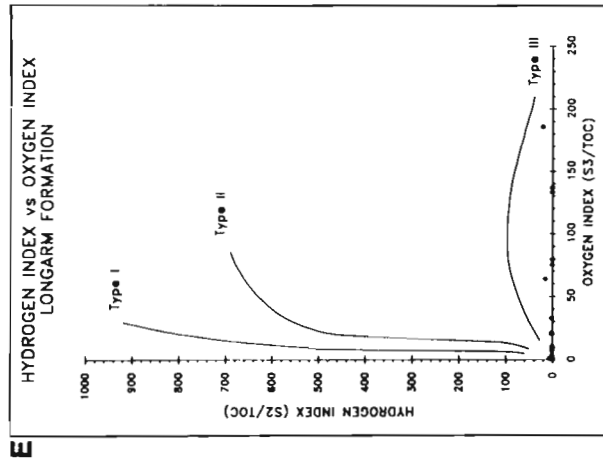


**Figure 3e-h:** Hydrogen index/Oxygen index (HI/OI) diagrams as in Figs. 3a-d. Data include outcrop and well cuttings samples. e) Longarm Formation; f) Alliford Formation; g) Newcombe Formation; h) Robber Point Formation.

**Figure 3i-l:** Hydrogen index/Oxygen index (HI/OI) diagrams as in Figs. 3a-d. Data include outcrop and well cuttings samples. i) Richardson Bay Formation; j) Graham Island Formation; k) Phantom Creek Formation; l) Whiteaves Formation.

**Figure 3m-p:** Hydrogen index/Oxygen index (HI/OI) diagrams as in Figs. 3a-d. Data include outcrop and well cuttings samples. m) Fannin Formation; n) Rennell Junction Formation; o) Ghost Creek Formation; p) Sandilands Formation.

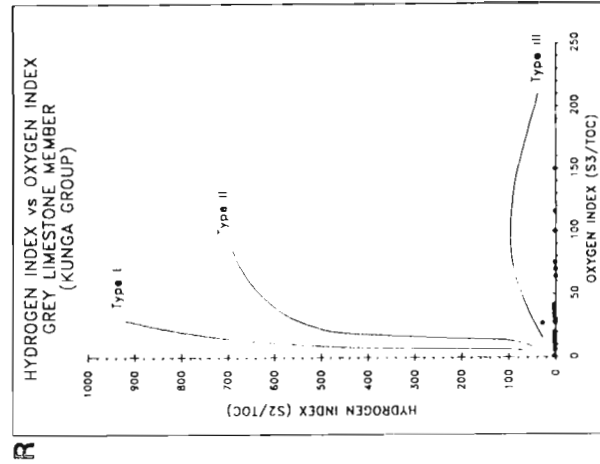
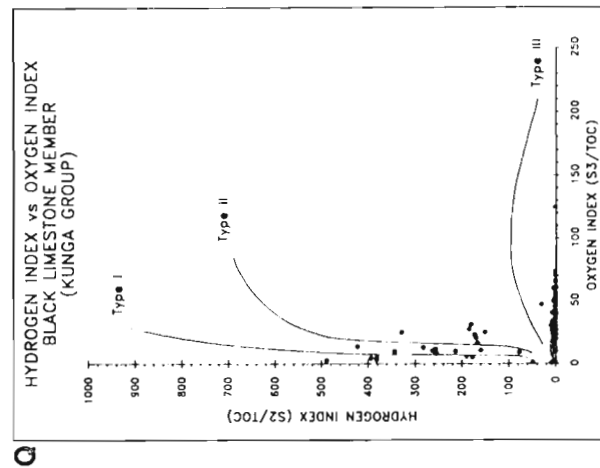
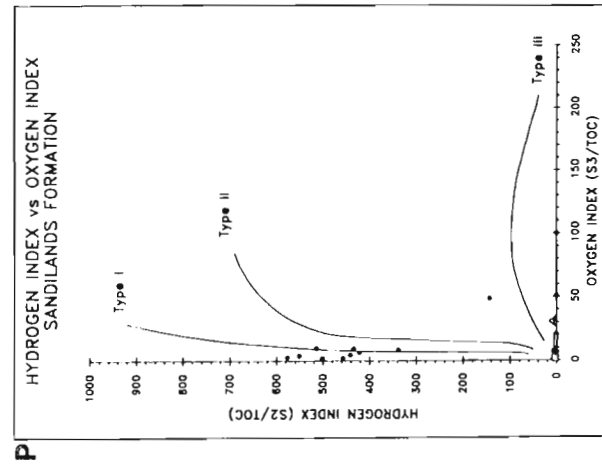
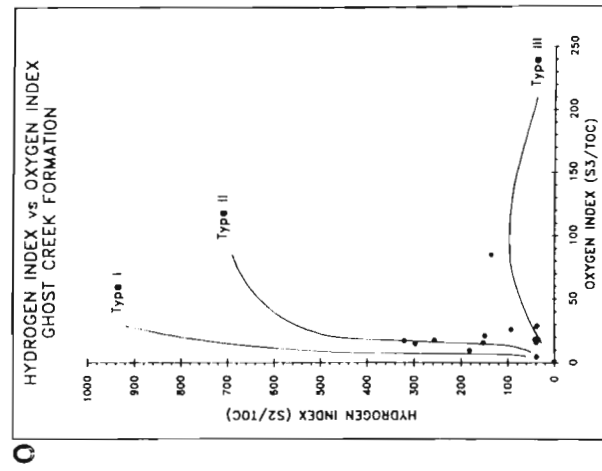
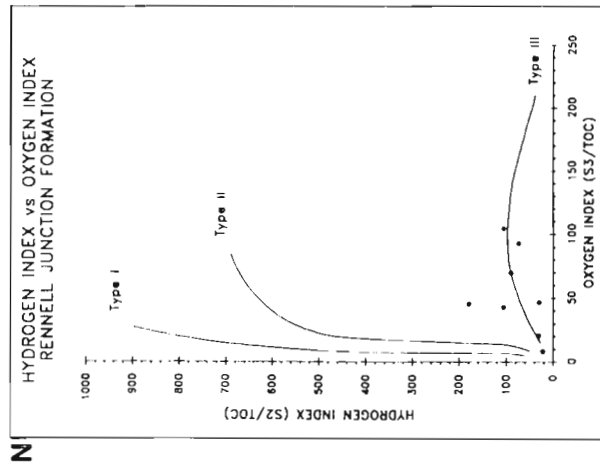
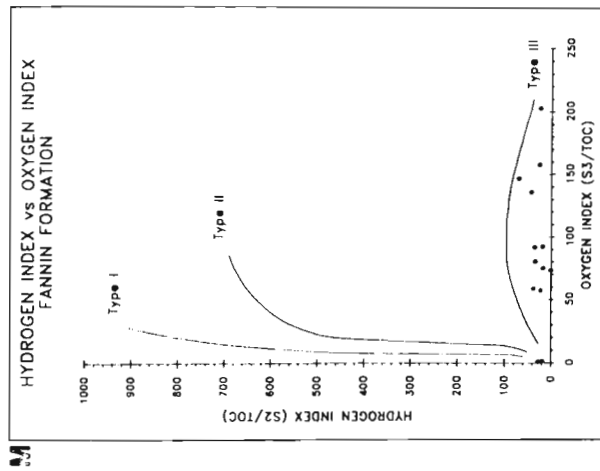


**Figure 3q-r:** Hydrogen index/Oxygen index (HI/OI) diagrams as in Figs. 3a-d. Data include outcrop and well cuttings samples. q) Peril Formation; r) Sadler Limestone.

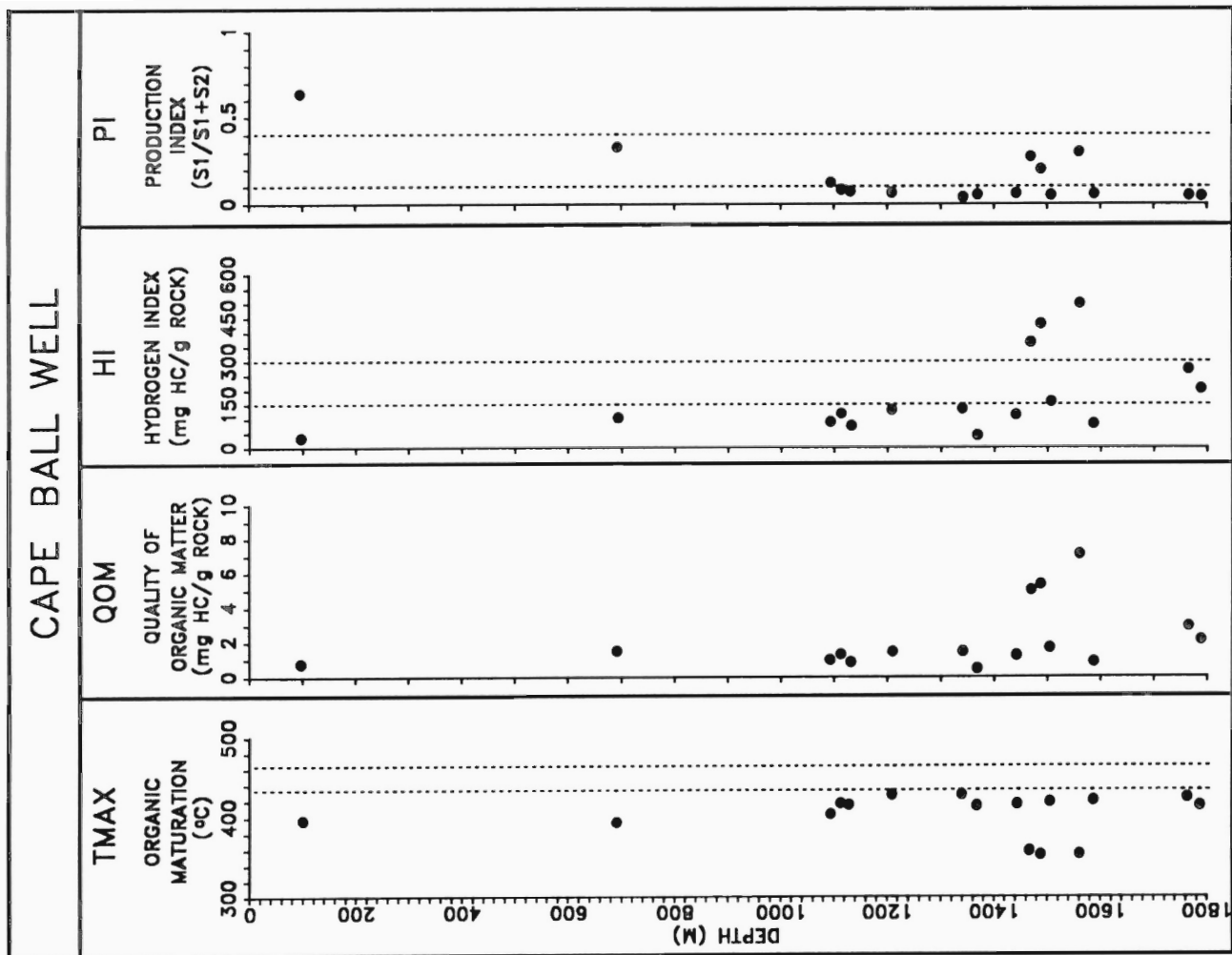


**Figure 4:** Rock-Eval logs for the Cape Ball well, which penetrates Tertiary Skonun Formation strata on Graham Island.  $T_{max}$ , HI, and PI are standard Rock-Eval parameters; QOM=(S1+S2)/TOC. Samples are predominantly coal and lignite with minor siltstone/sandstone from cuttings and core.

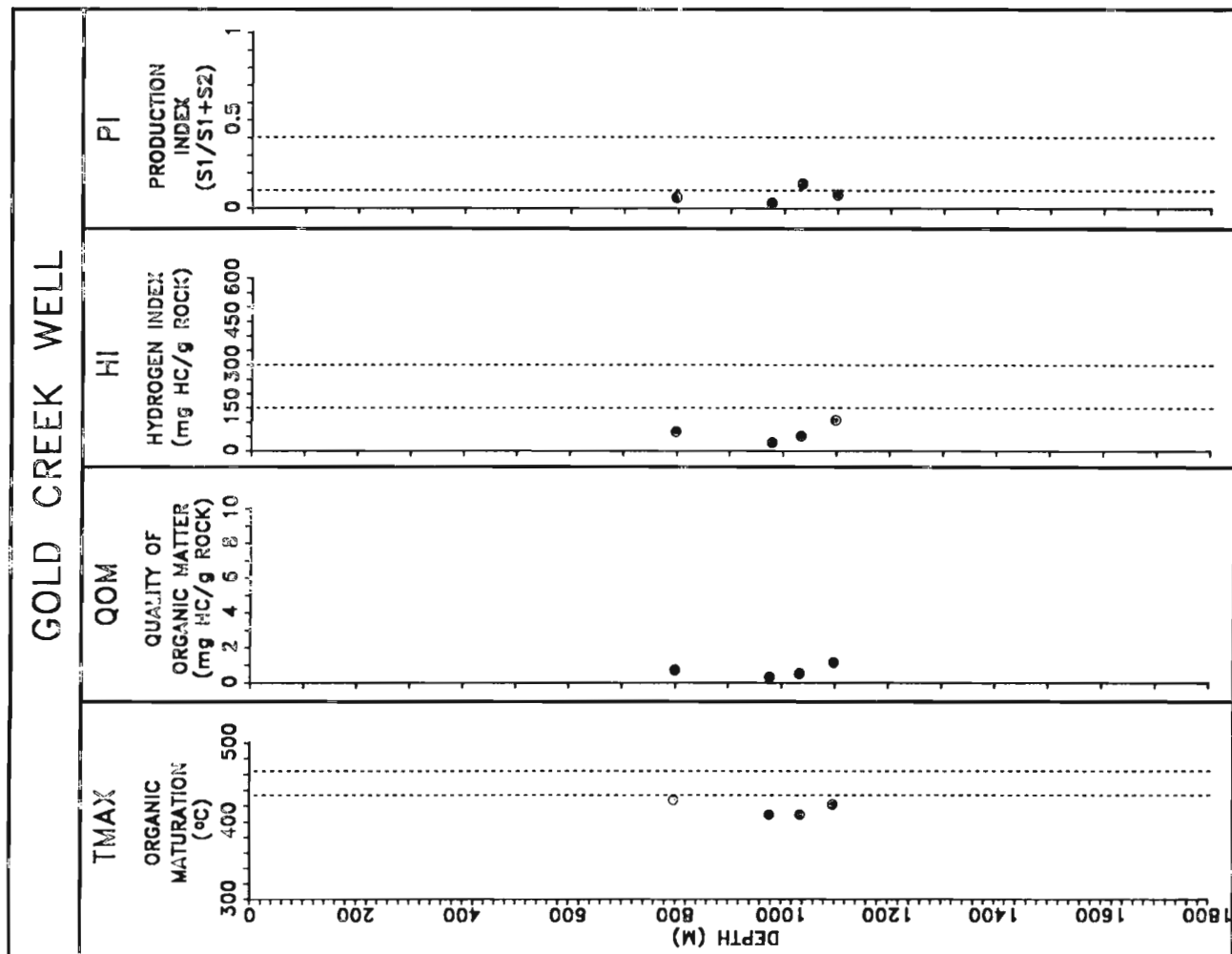


**Figure 5:** Rock-Eval logs for the Gold Creek well, which penetrates Tertiary Skonun Formation strata on Graham Island.  $T_{max}$ , HI, and PI are standard Rock-Eval parameters; QOM=(S1+S2)/TOC. Samples are predominantly coal and lignite with minor siltstone/sandstone from cuttings and core.

Figure 6: Rock-Eval logs for the Nadu River well, which penetrates Tertiary Skonun Formation strata on Graham Island.  $T_{max}$ , HI, and PI are standard Rock-Eval parameters; QOM=(S1+S2)/TOC. Samples are predominantly coal and lignite with minor siltstone/sandstone from cuttings and core.

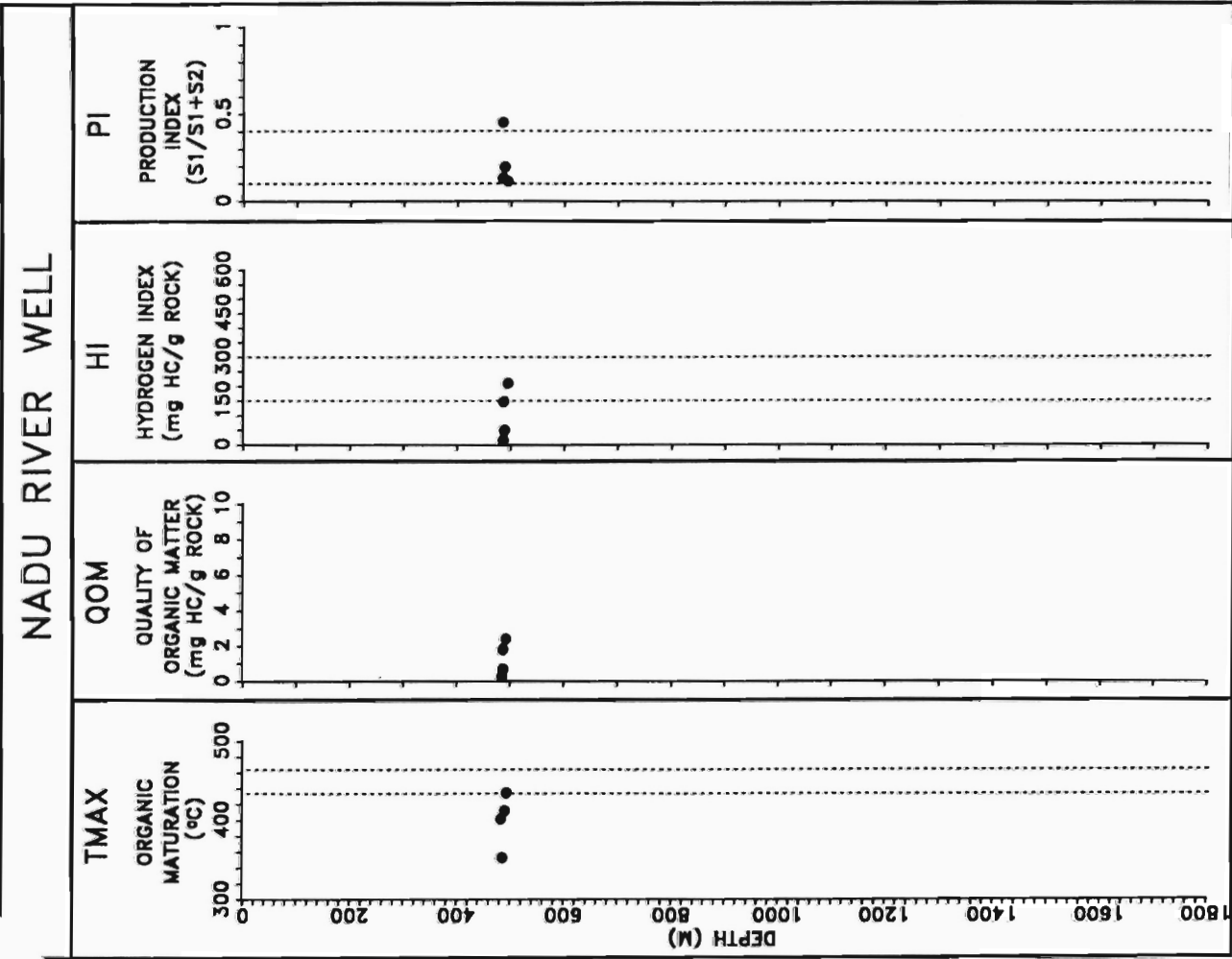
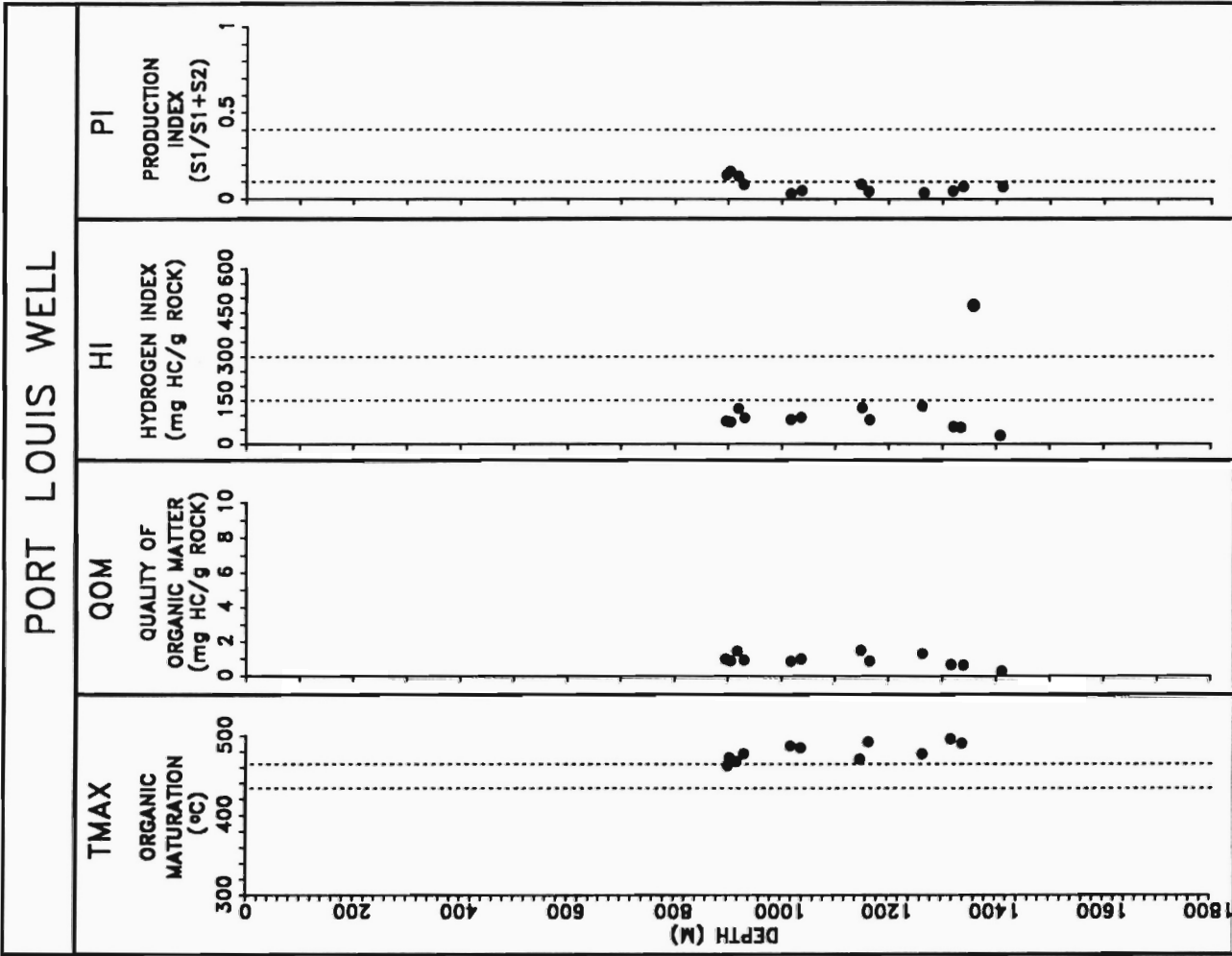
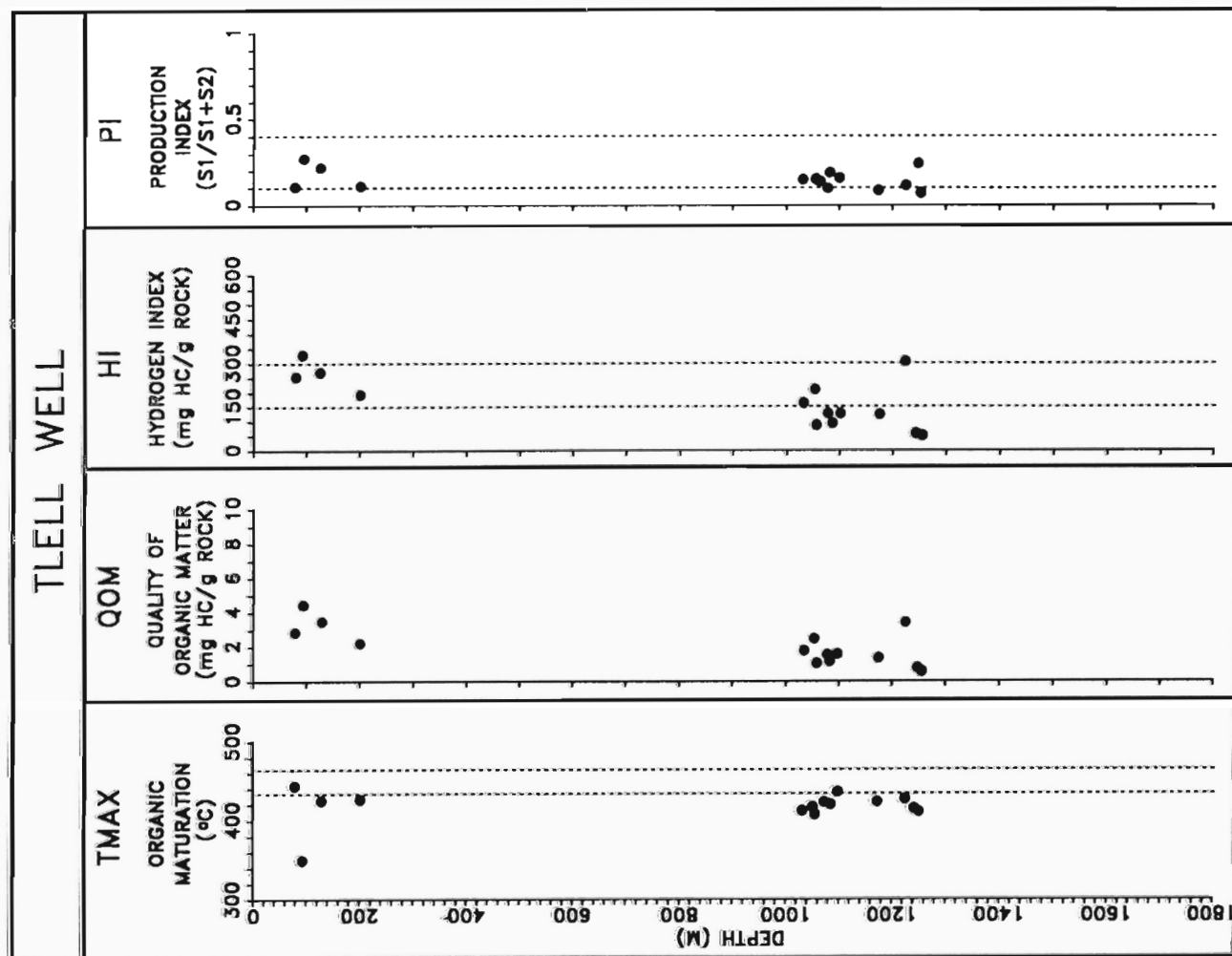
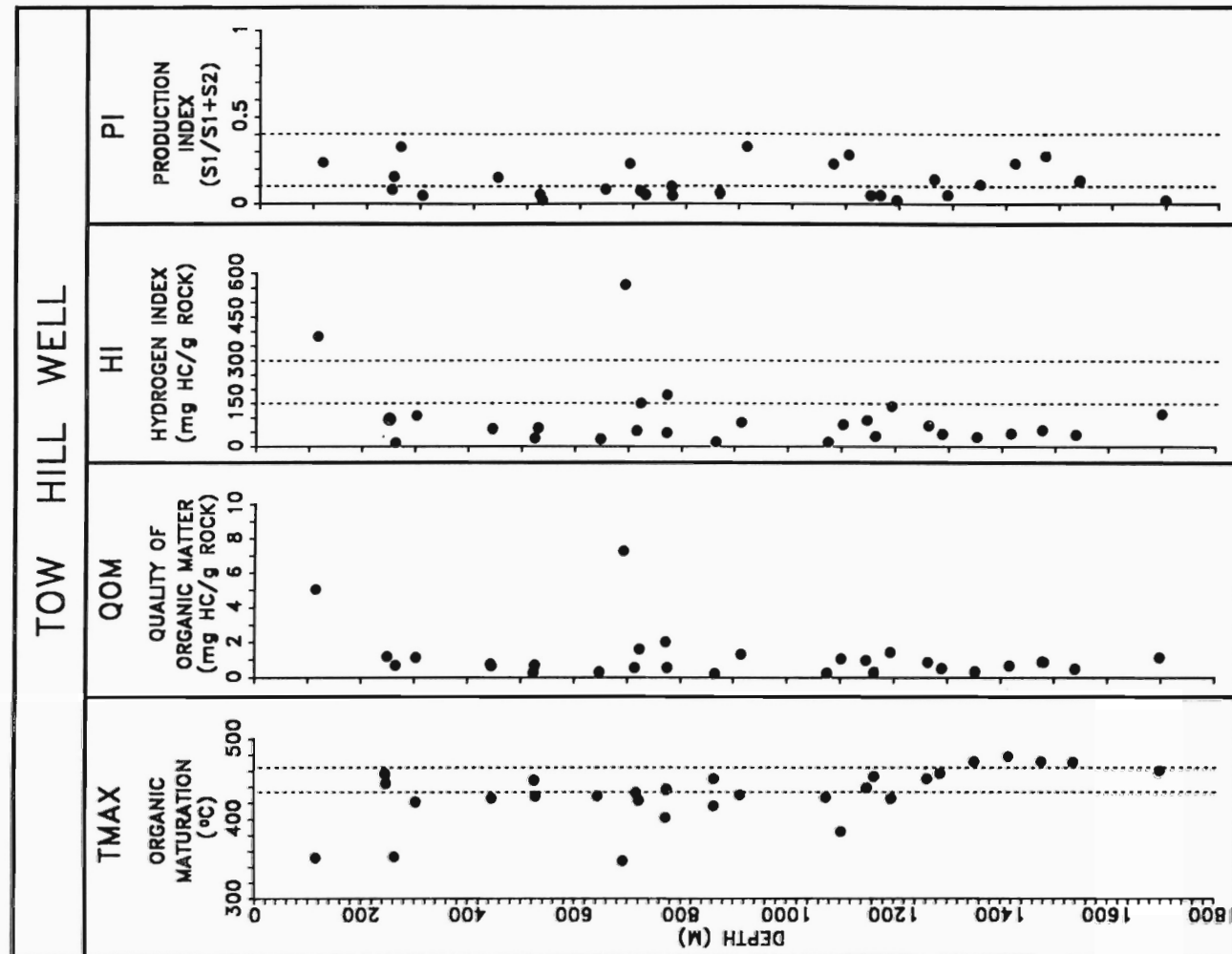


Figure 7: Rock-Eval logs for the Port Louis well, which penetrates Tertiary Skonun Formation strata on Graham Island.  $T_{max}$ , HI, and PI are standard Rock-Eval parameters; QOM=(S1+S2)/TOC. Samples are predominantly coal and lignite with minor siltstone/sandstone from cuttings and core.





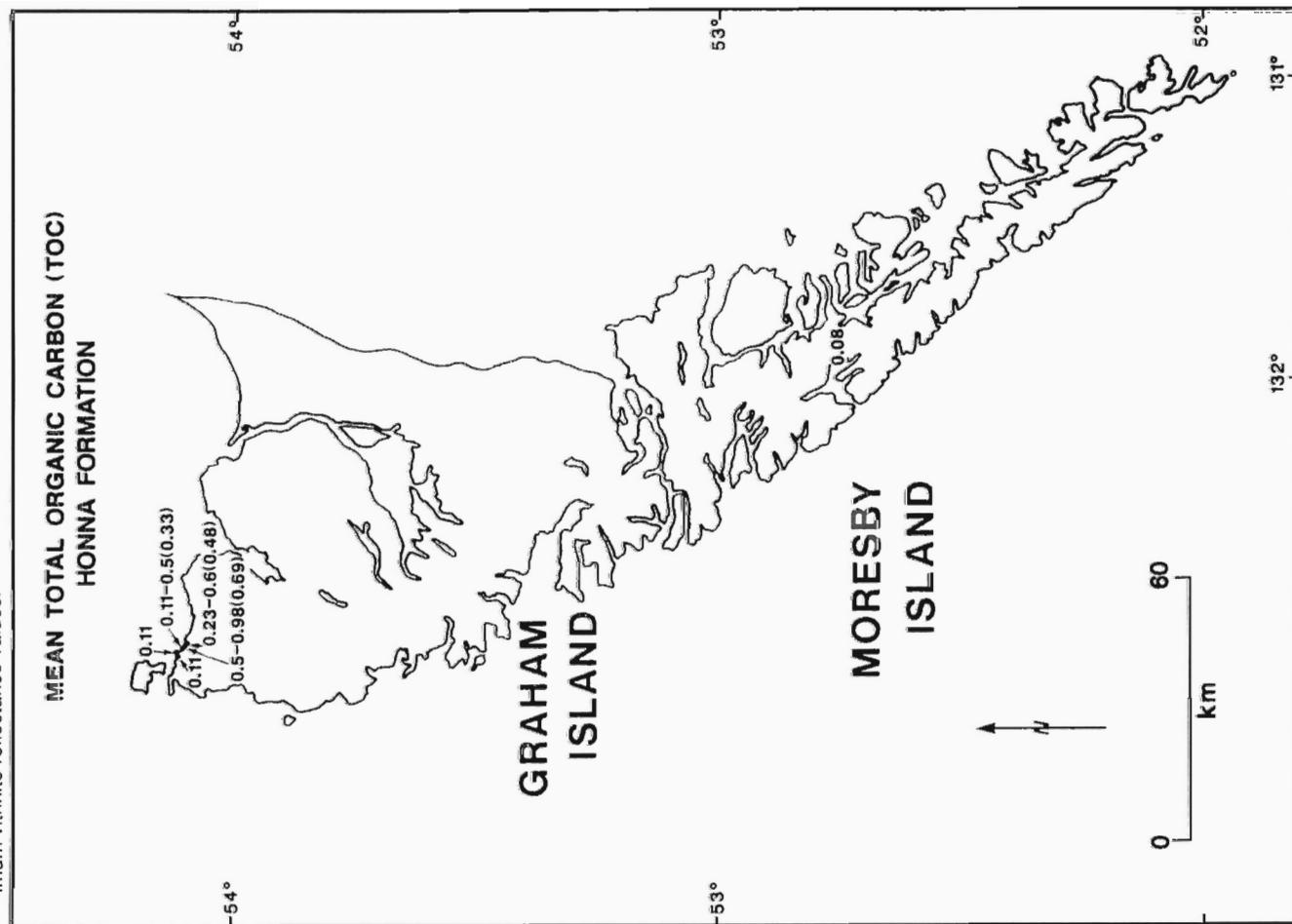
**Figure 8:** Rock-Eval logs for the Tlell well, which penetrates Tertiary Skonun Formation strata on Graham Island.  $T_{max}$ , HI, and PI are standard Rock-Eval parameters; QOM=(S1+S2)/TOC. Samples are predominantly coal and lignite with minor siltstone/sandstone from cuttings and core.



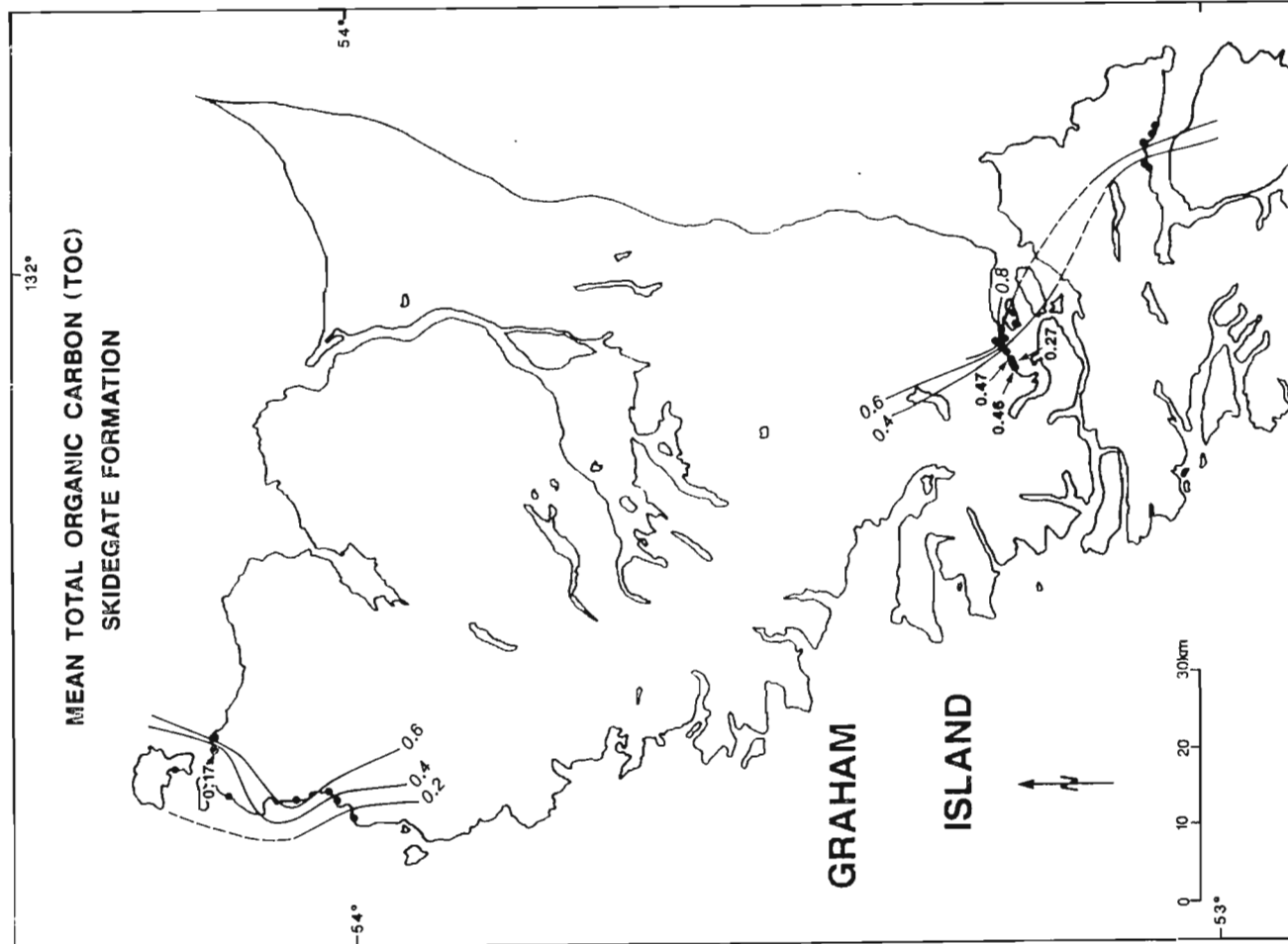
**Figure 9:** Rock-Eval logs for the Tow Hill well, which penetrates Tertiary Skonun Formation strata on Graham Island.  $T_{max}$ , HI, and PI are standard Rock-Eval parameters; QOM=(S1+S2)/TOC. Samples are predominantly coal and lignite with minor siltstone/sandstone from cuttings and core.

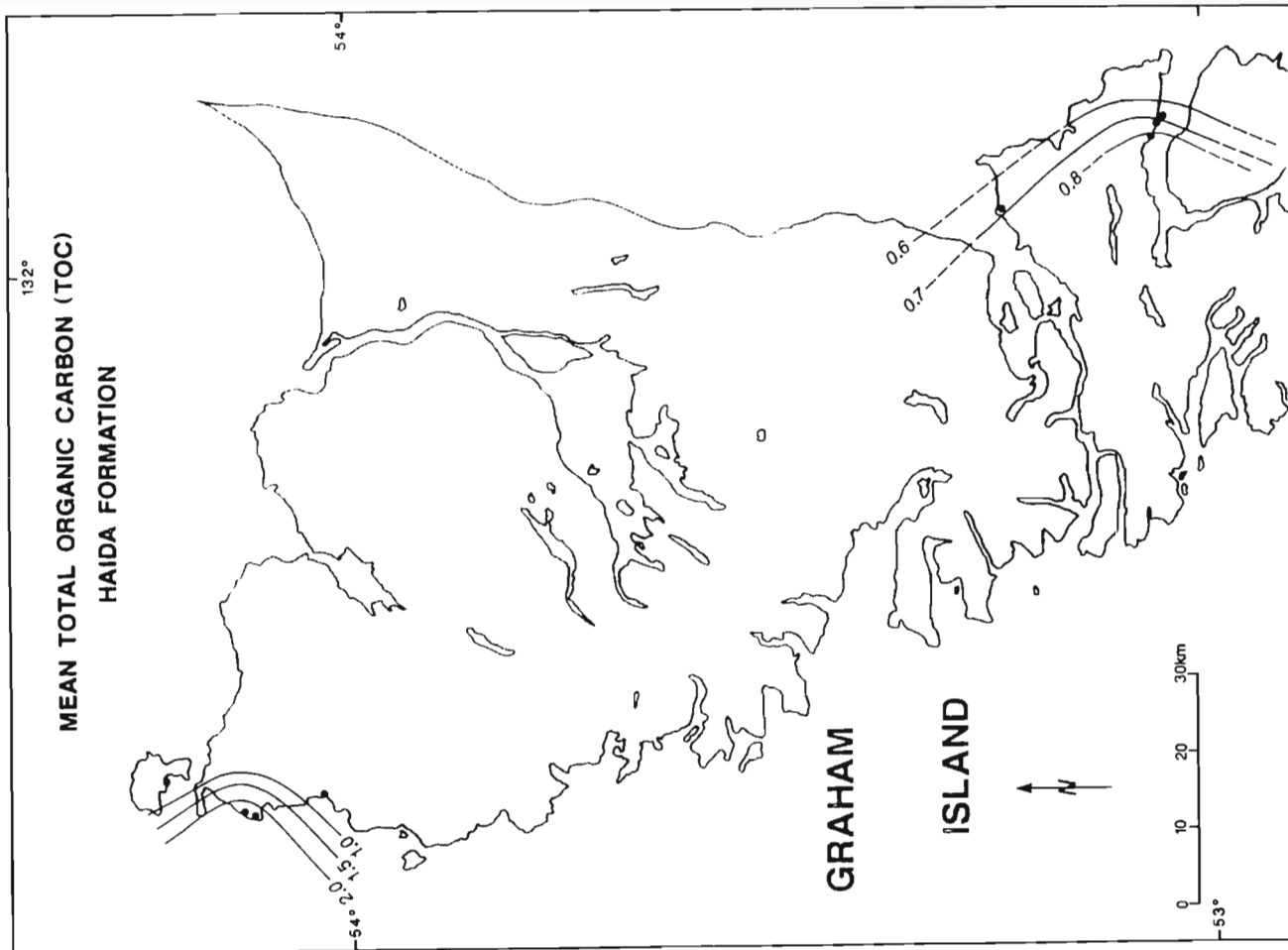


**Figure 10:** Regional distribution of the mean TOC content for the Honna Formation. Values are mean TOC calculated across the thickness of the formation at each outcrop location. Value in brackets are mean random vitrinite reflectance values. Dashed values are minimum and maximum vitrinite reflectance values.

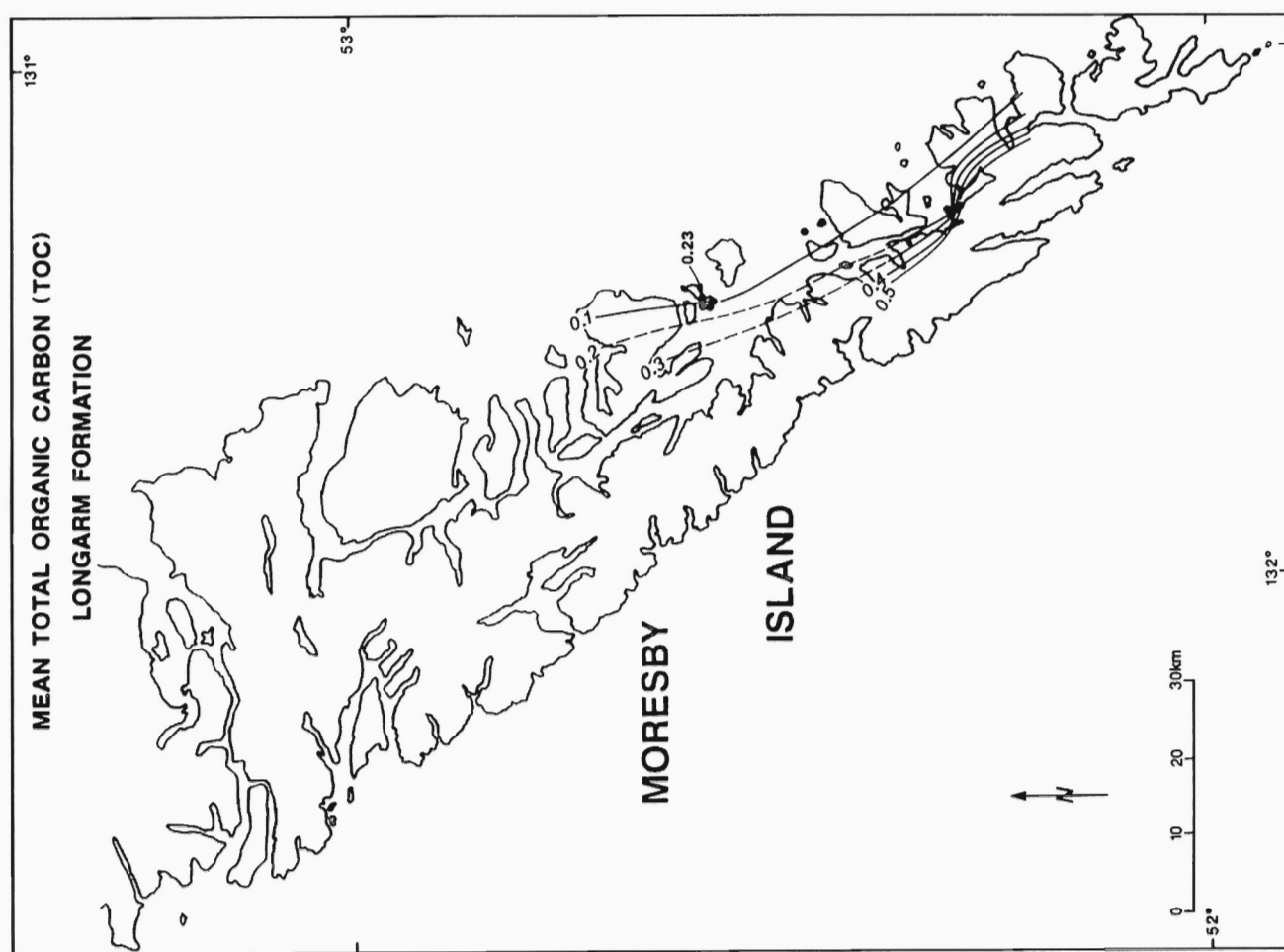


**Figure 11:** Regional distribution of the mean TOC content for the Skidegate Formation. Values are mean TOC calculated across the thickness of the formation at each outcrop location. Dashed line represents an approximate contour location. Labelled values do not fit regional trends and are not contoured.



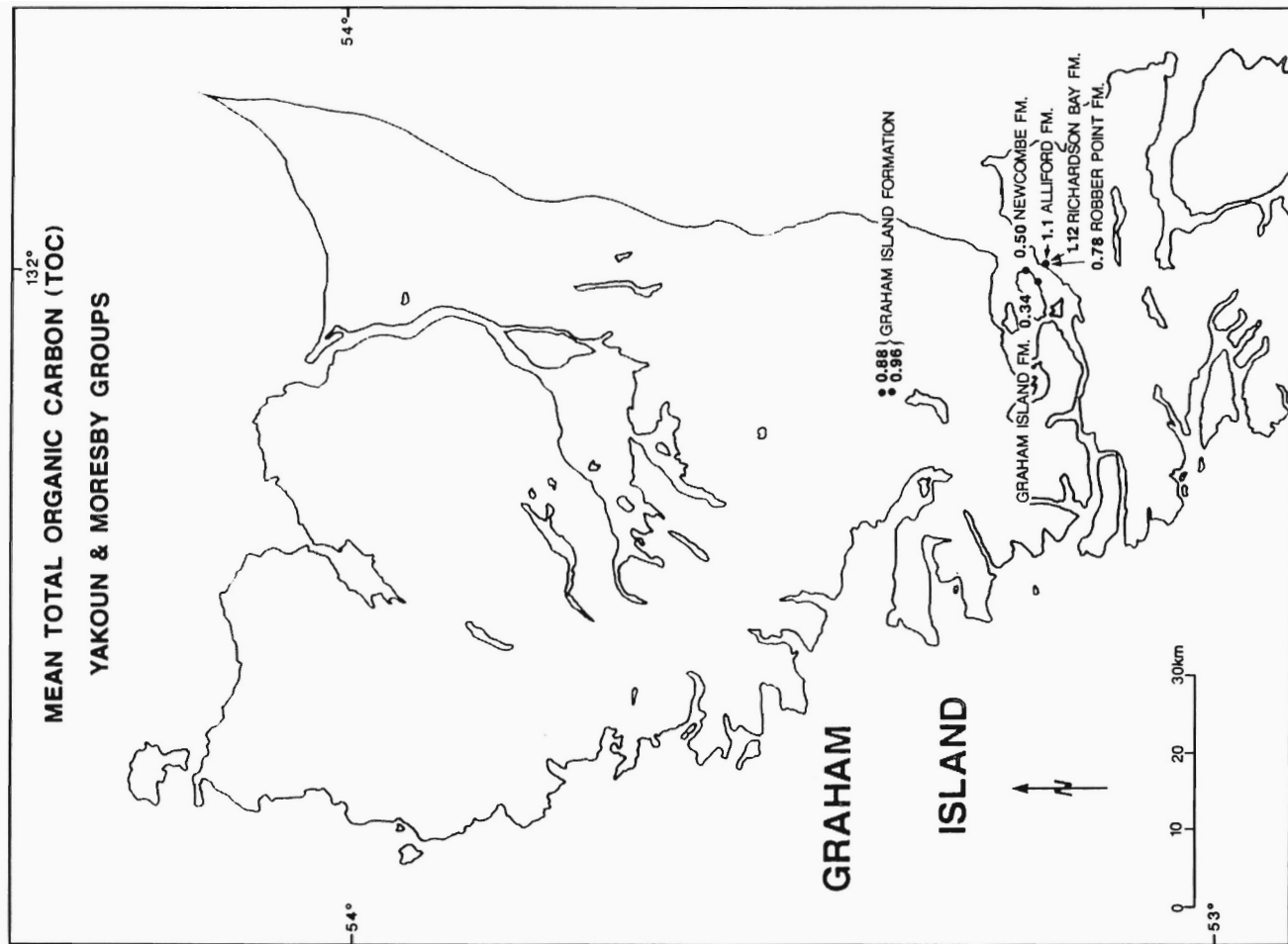


**Figure 12:** Regional distribution of the mean TOC content for the Haida Formation. Values are mean TOC calculated across the thickness of the formation at each outcrop location. Dashed line represents an approximate outcrop location.

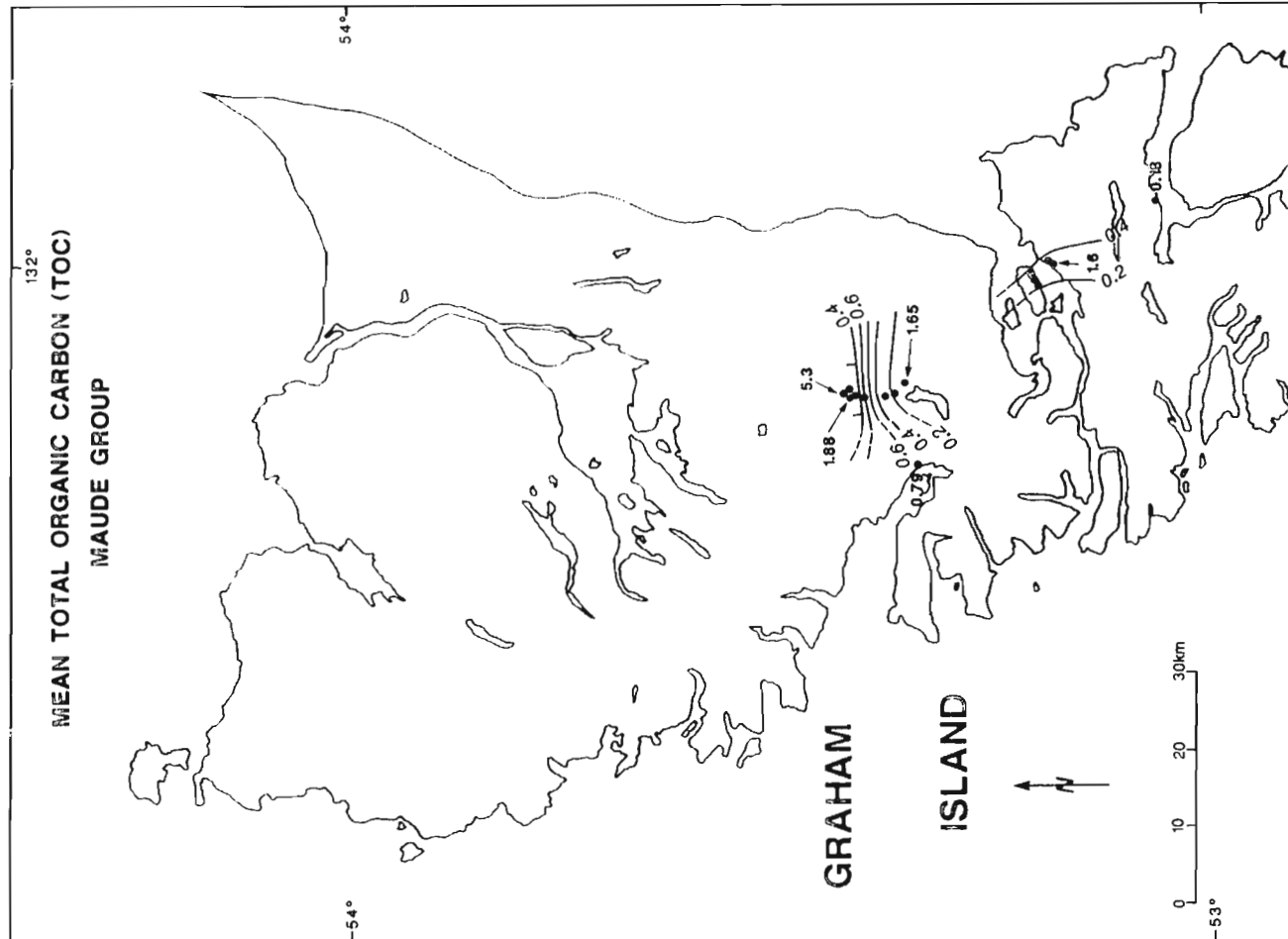


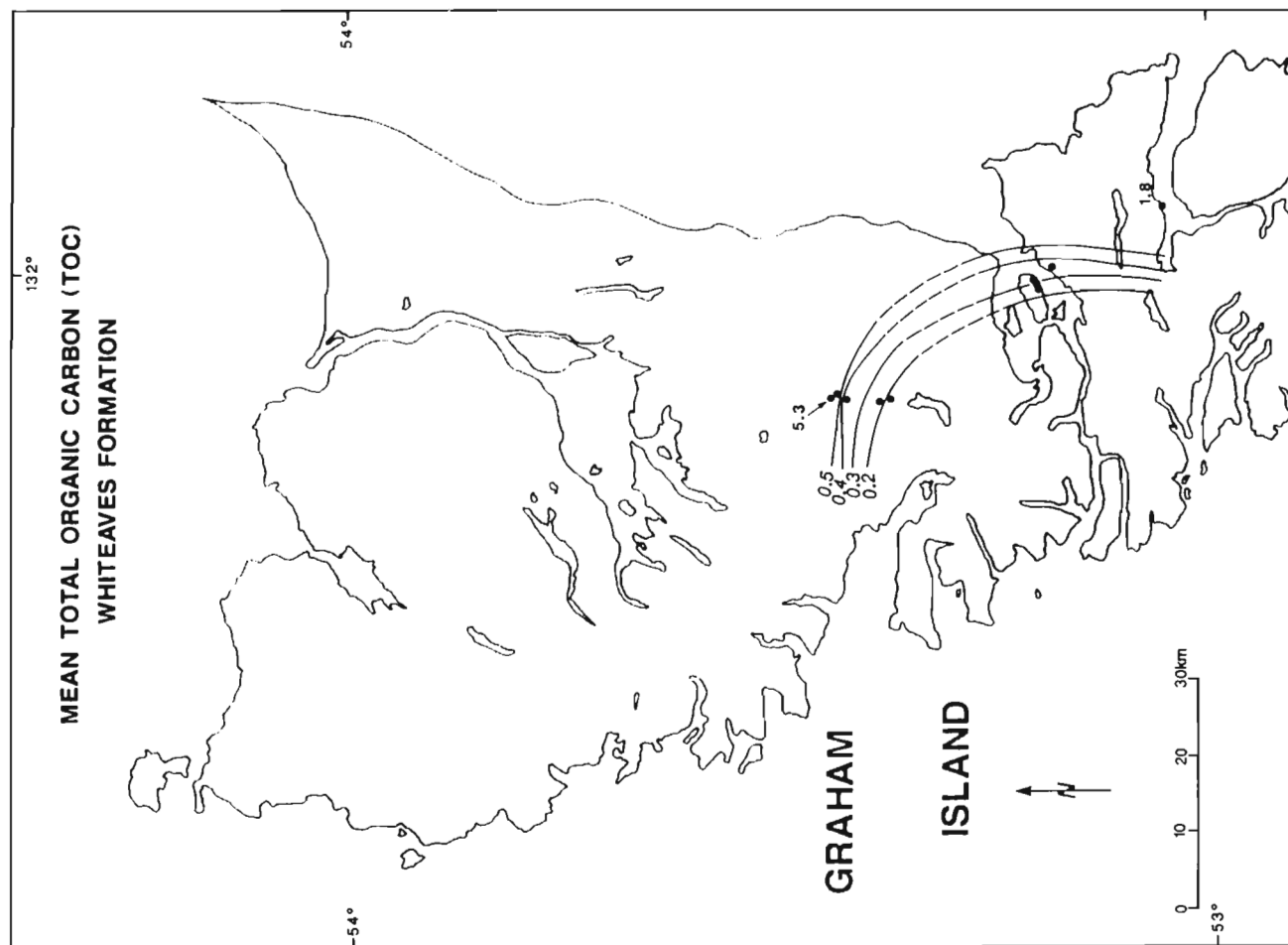
**Figure 13:** Regional distribution of the mean TOC content for the Longarm Formation. Values are mean TOC calculated across the thickness of the formation at each outcrop location. Dashed line represents an approximate outcrop location. Labelled values do not fit regional trends and are not contoured.

**Figure 14:** Regional distribution of the mean TOC content for the Yakoun and Moresby groups. Values are mean TOC calculated across the thickness of the formation at each outcrop location.

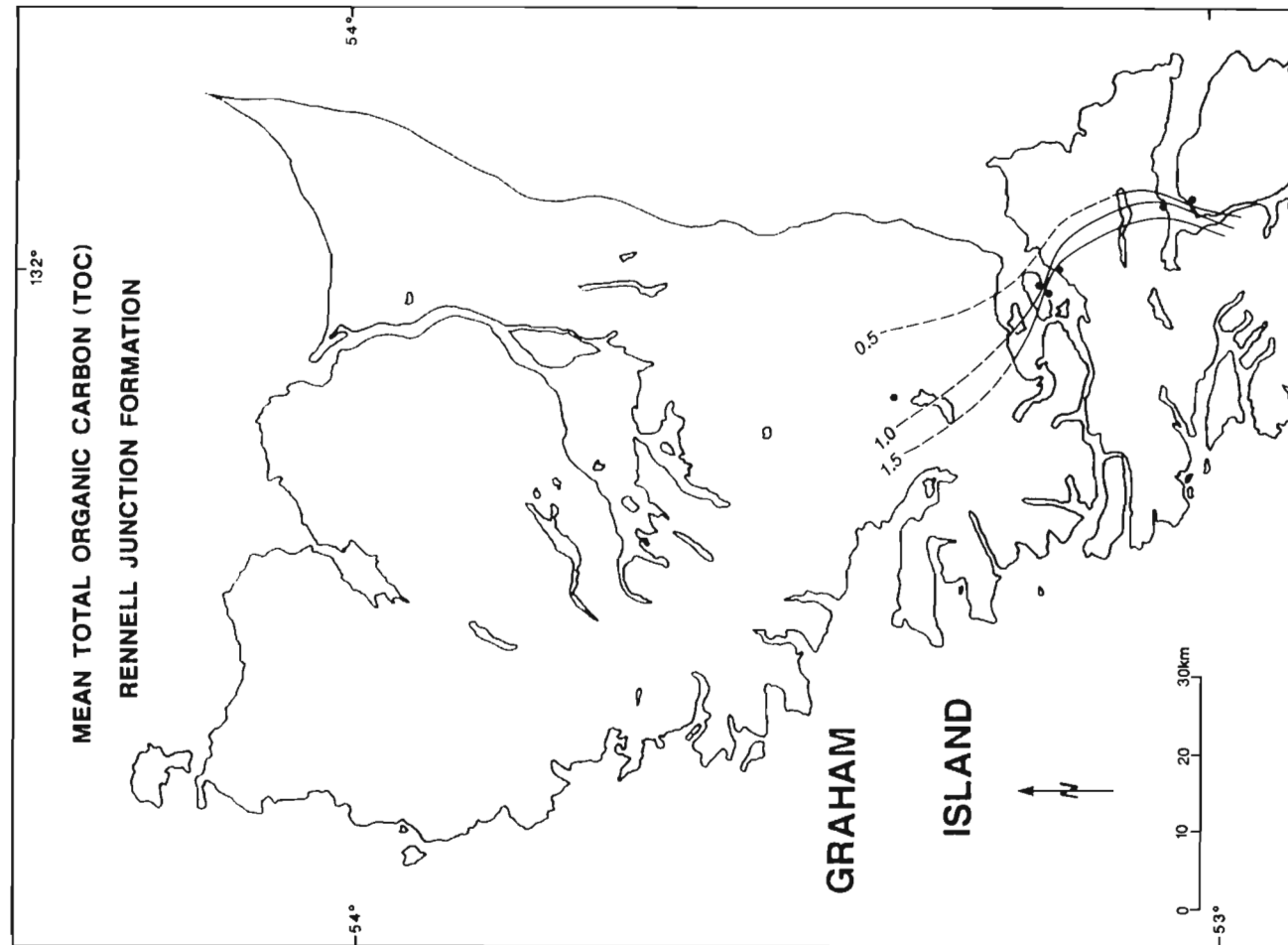


**Figure 15:** Regional distribution of the mean TOC content for the Maude Group. Values are mean TOC calculated across the thickness of the formation at each outcrop location. Dashed line represents an approximate contour location. Labelled values do not fit regional trends and are not contoured.



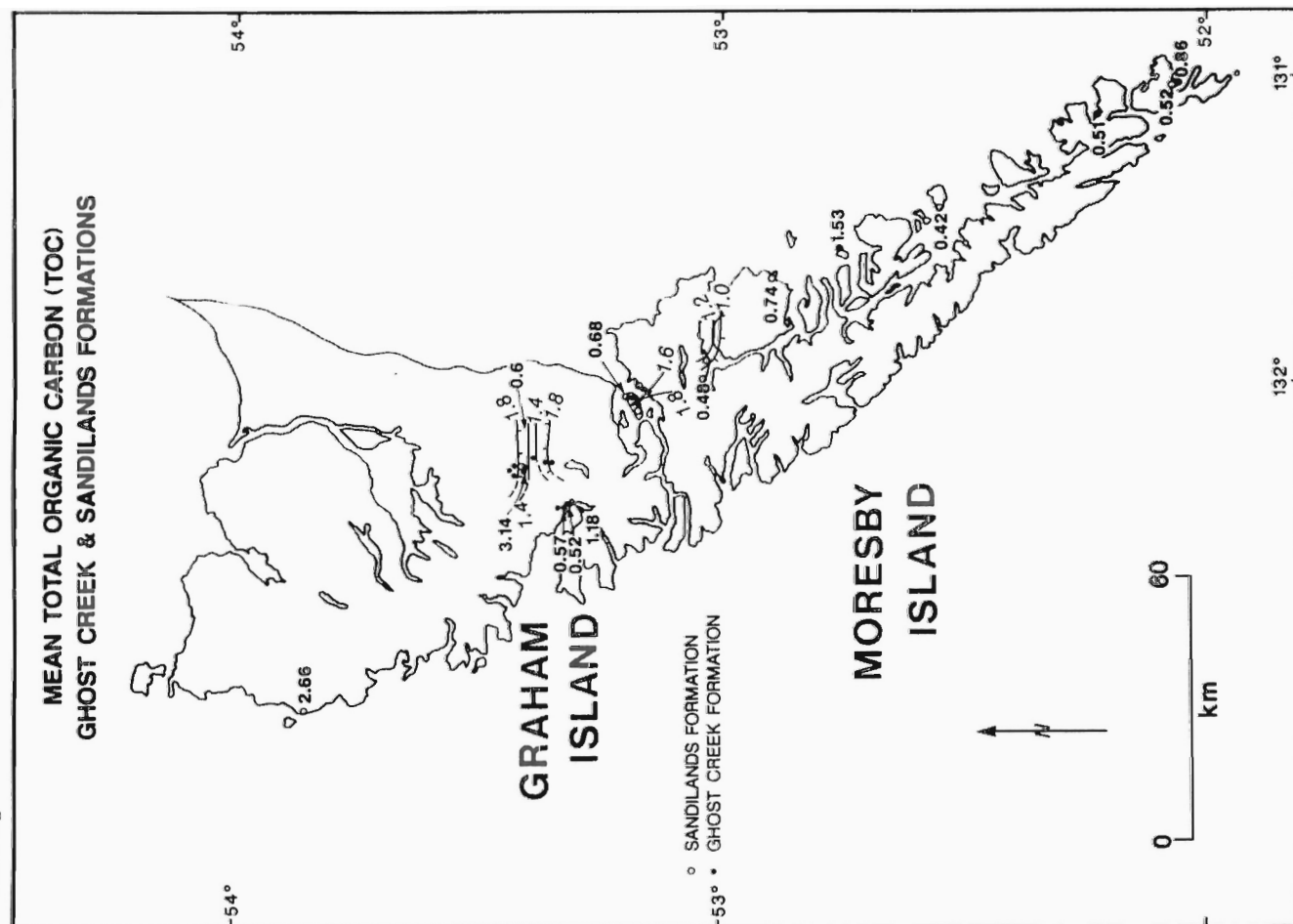


**Figure 16:** Regional distribution of the mean TOC content for the Whiteaves Formation. Values are mean TOC calculated across the thickness of the formation at each outcrop location. Dashed line represents an approximate contour location. Labelled values do not fit regional trends and are not contoured.

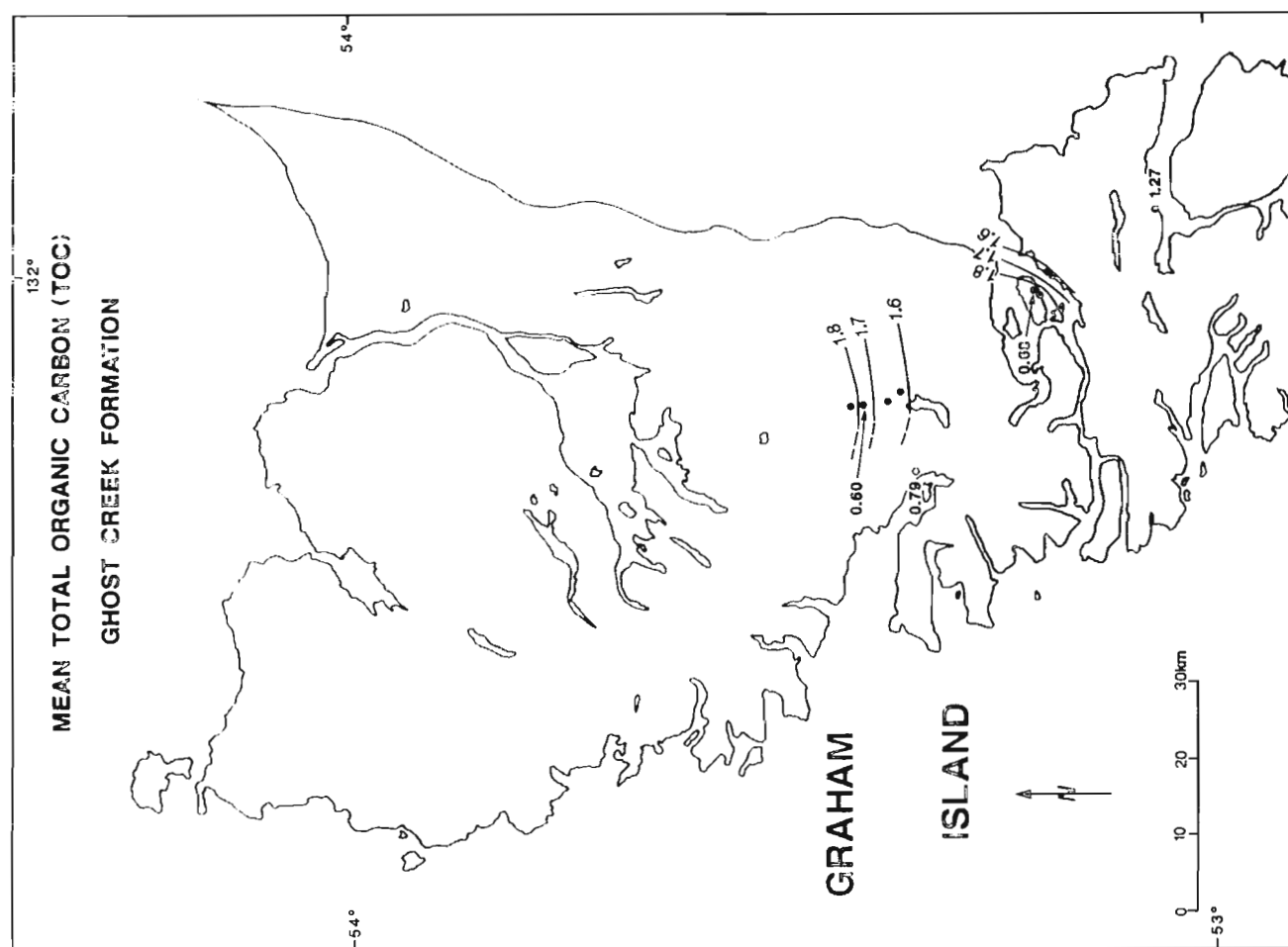


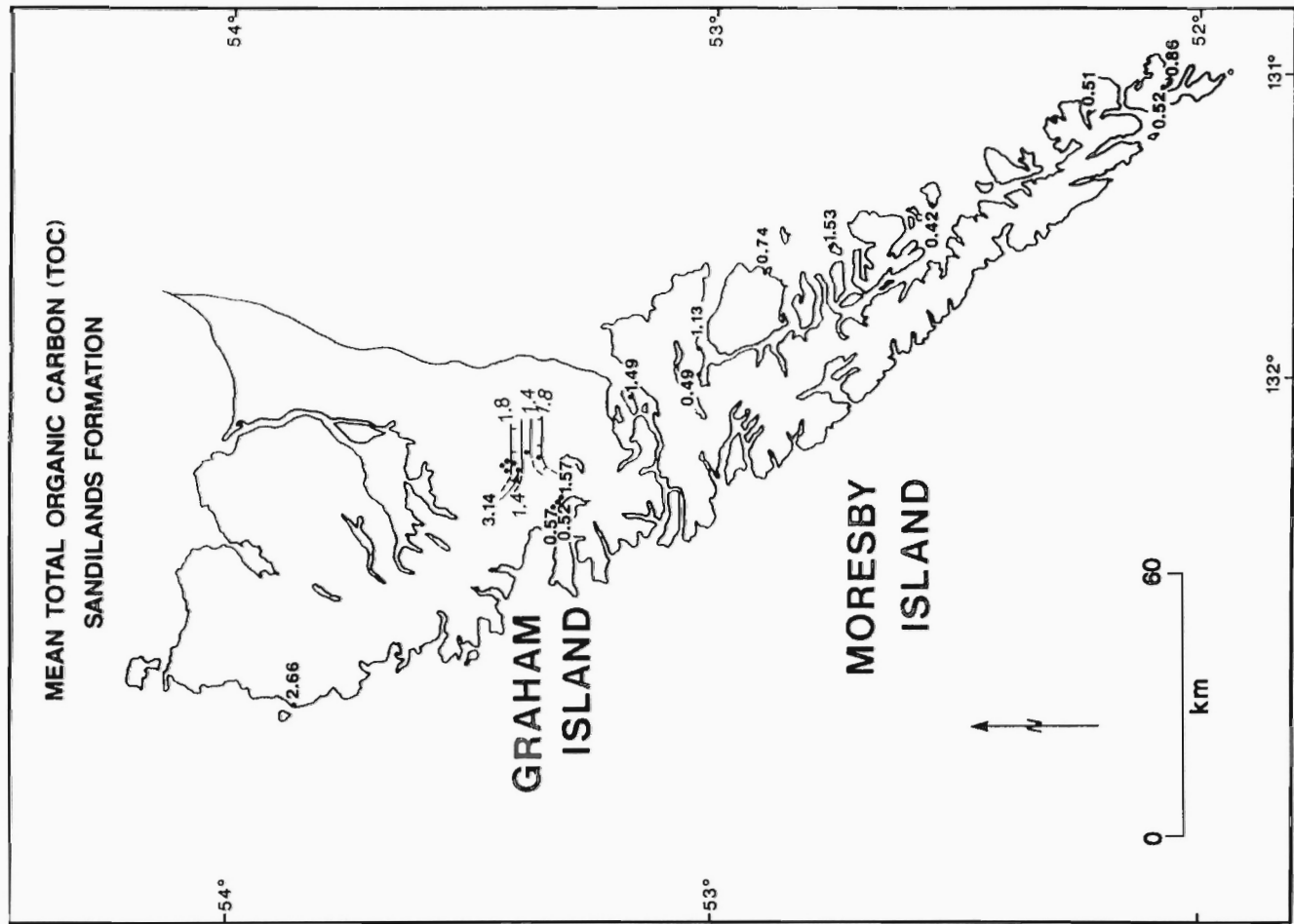
**Figure 17:** Regional distribution of the mean TOC content for the Rennell Junction Formation. Values are mean TOC calculated across the thickness of the formation at each outcrop location. Dashed line represents an approximate contour location. Labelled values do not fit regional trends and are not contoured.

**Figure 18:** Regional distribution of the mean TOC content for the Ghost Creek and Sandilands formations. Values are average TOC calculated across the thickness of the formation at each outcrop location. Dashed line represents an approximate contour location. Labelled values do not fit regional trends and are not contoured. Tick marks on contour indicate decreasing TOC.

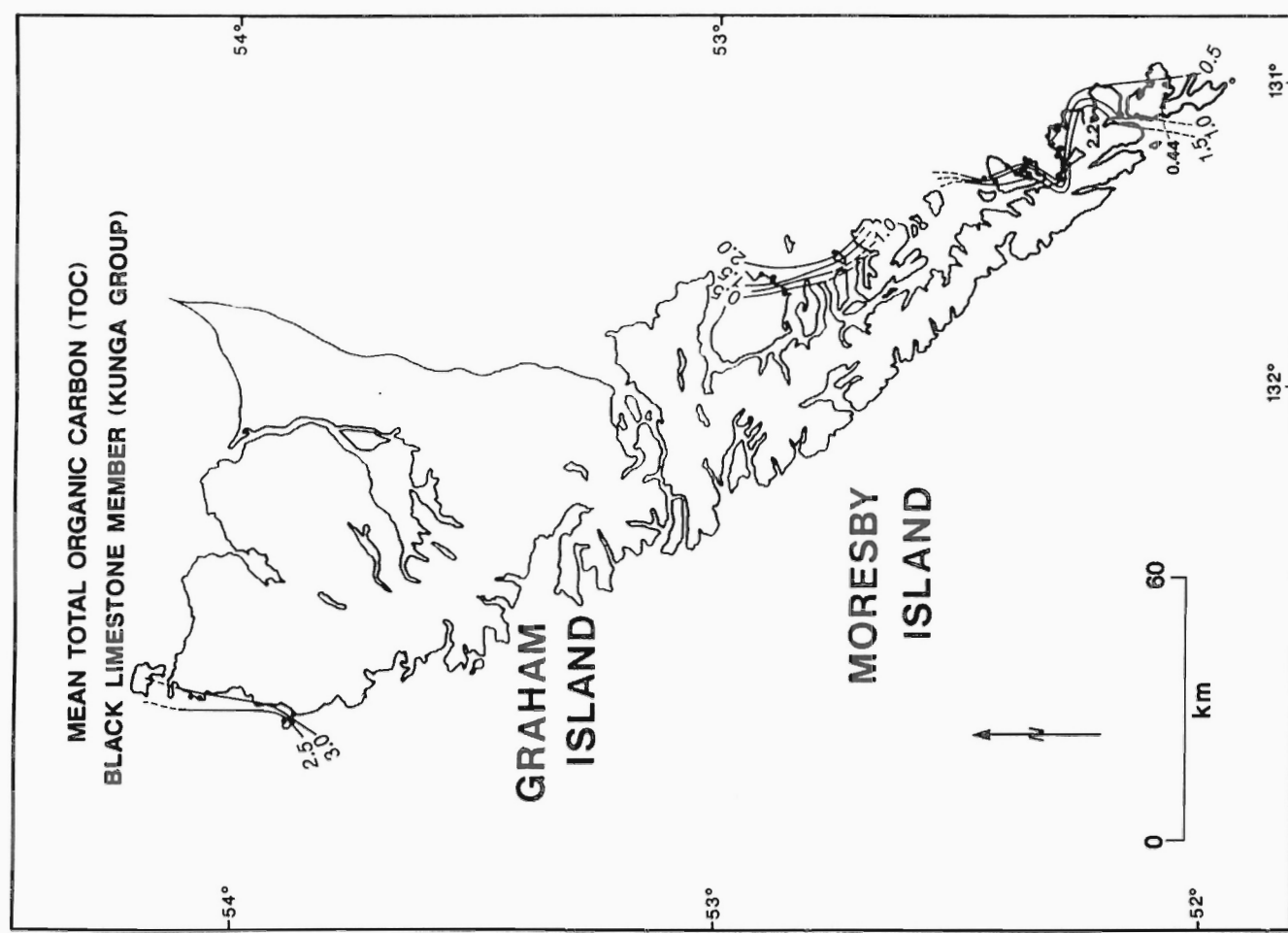


**Figure 19:** Regional distribution of the average TOC content for the Ghost Creek Formation. Values are average TOC calculated across the thickness of the formation at each outcrop location. Dashed line represents an approximate contour location. Labelled values do not fit regional trends and are not contoured.





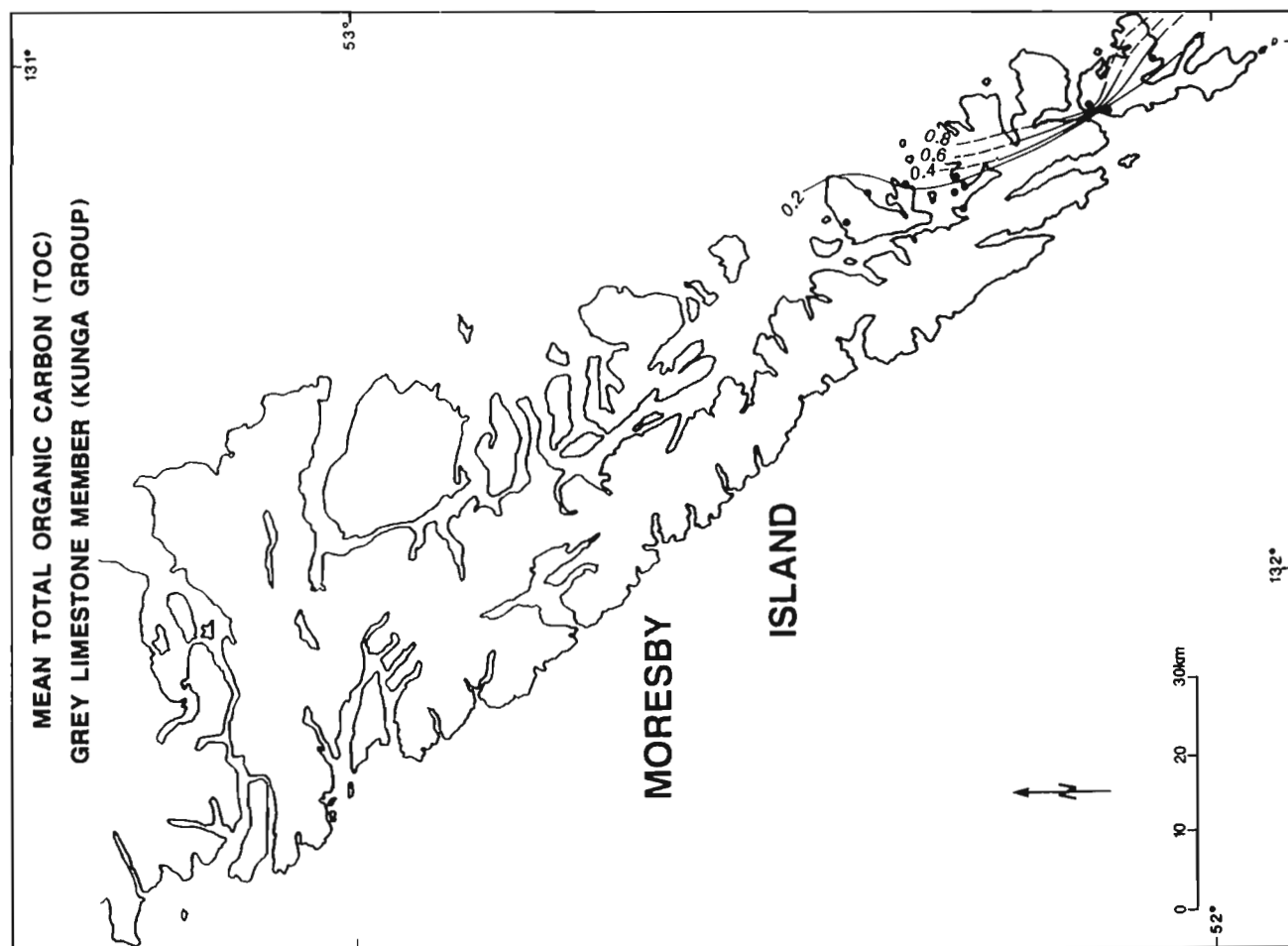
**Figure 20:** Regional distribution of the average TOC content for the Sandilands Formation. Values are average TOC calculated across the thickness of the formation at each outcrop location. Dashed line represents an approximate contour location. Labelled values do not fit regional trends and are not contoured. Tick marks on contour indicate decreasing TOC.



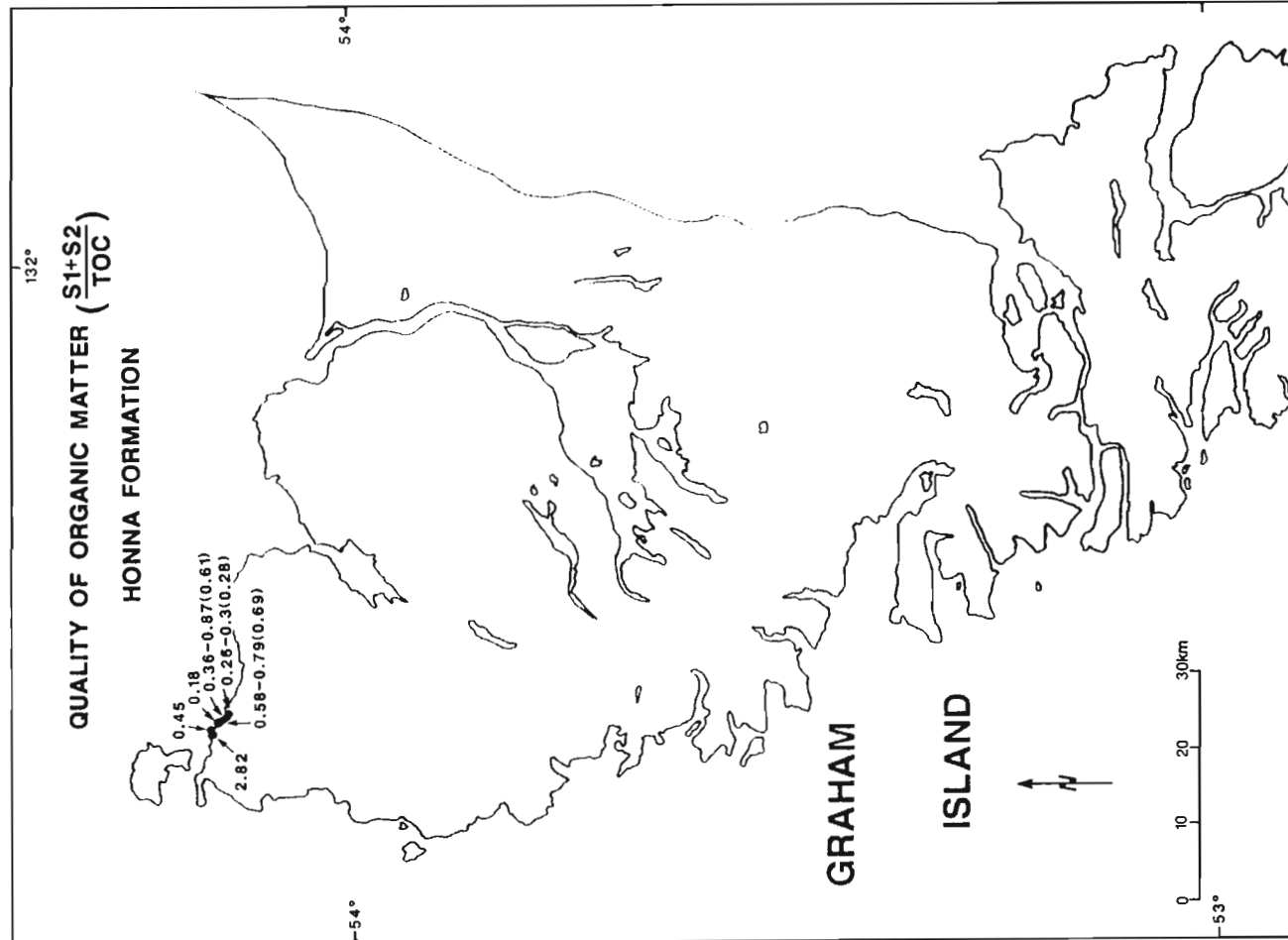
**Figure 21:** Regional distribution of the average TOC content for the Peril Formation (Kunga Group). Values are average TOC calculated across the thickness of the formation at each outcrop location. Dashed line represents an approximate contour location. Labelled values do not fit regional trends and are not contoured.

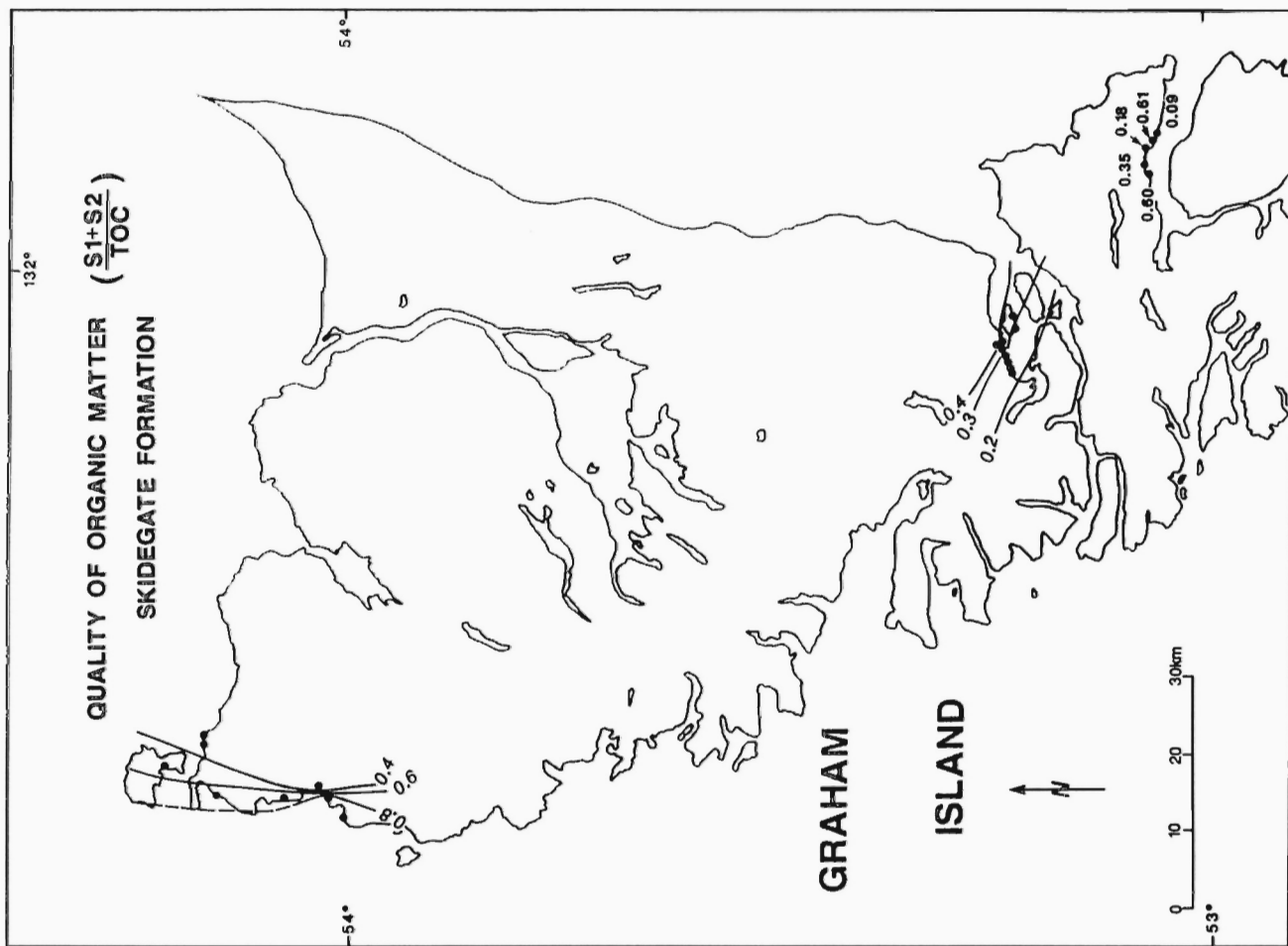


**Figure 22:** Regional distribution of the average TOC content for the Sadler Limestone (Kunga Group). Values are average TOC calculated across the thickness of the formation at each outcrop location. Dashed line represents an approximate contour location.

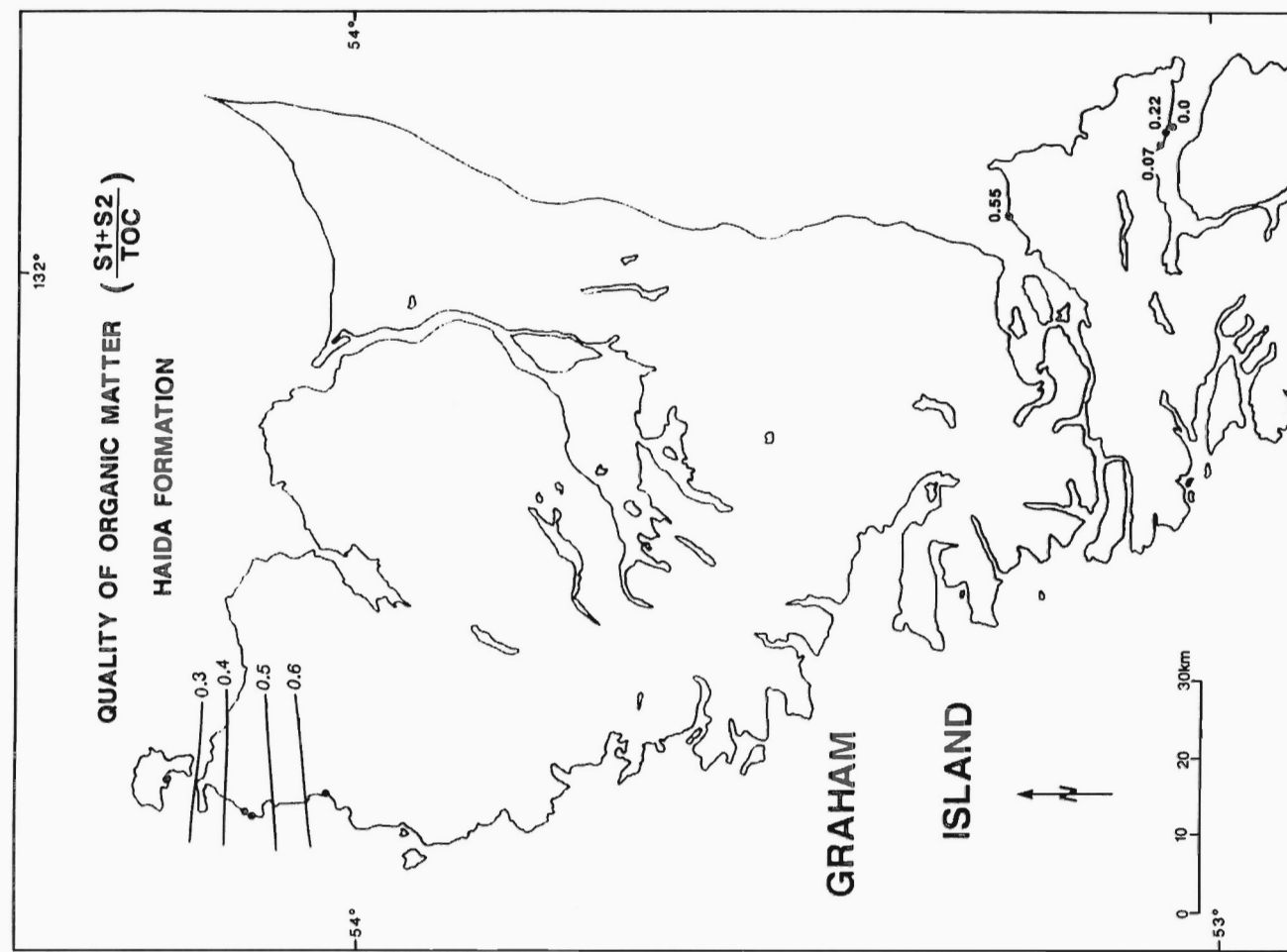


**Figure 23:** Regional distribution of the average QOM [(S1+S2)/TOC] for the Honna Formation. Values are average QOM calculated across the thickness of the formation at each outcrop location. Values in brackets are mean QOM. Dashed values are minimum and maximum QOM.



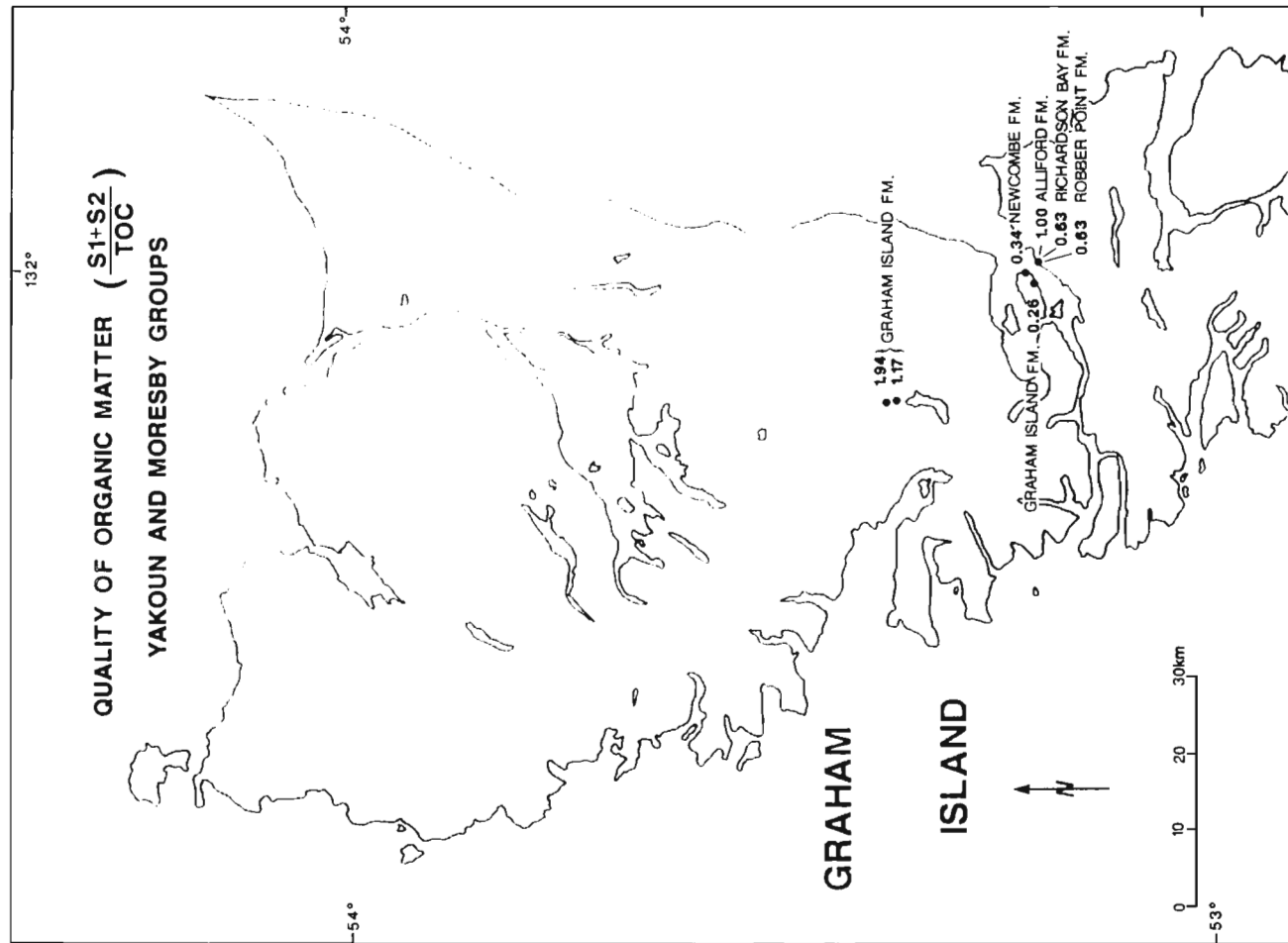
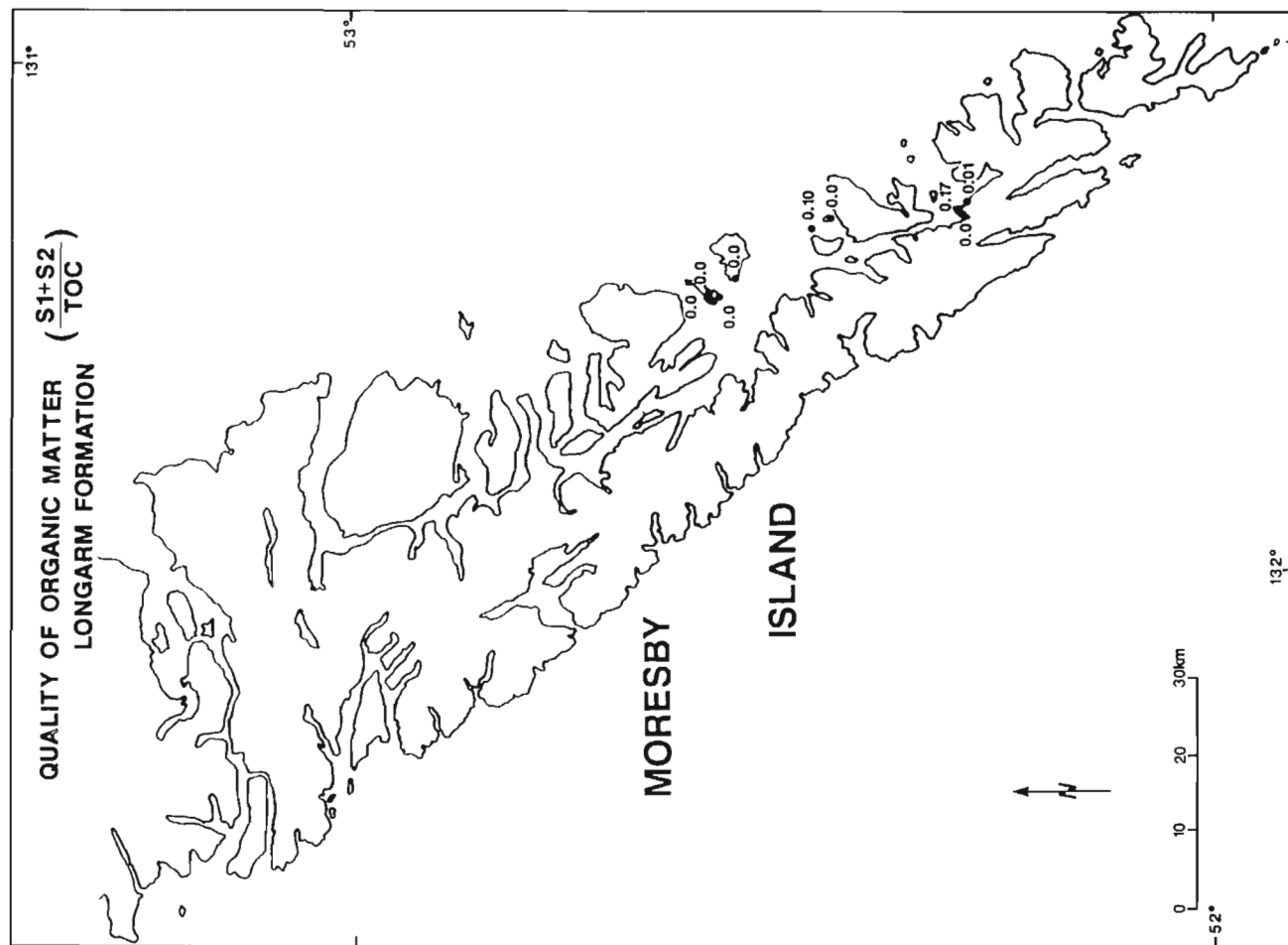


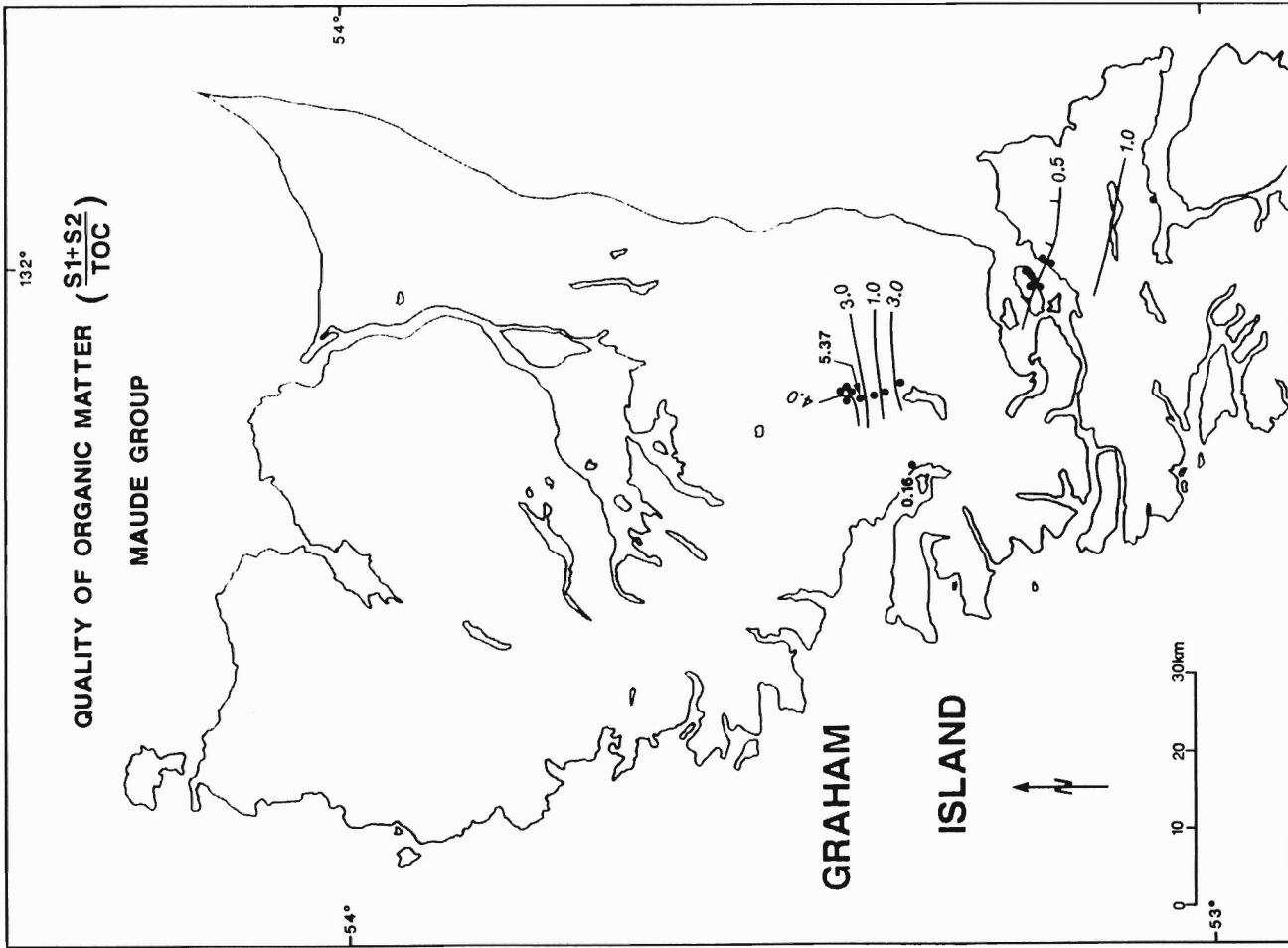
**Figure 24:** Regional distribution of the average QOM [(S1+S2)/TOC] for the Skidegate Formation. Values are average QOM calculated across the thickness of the formation at each outcrop location. Dashed line represents approximate contour location.



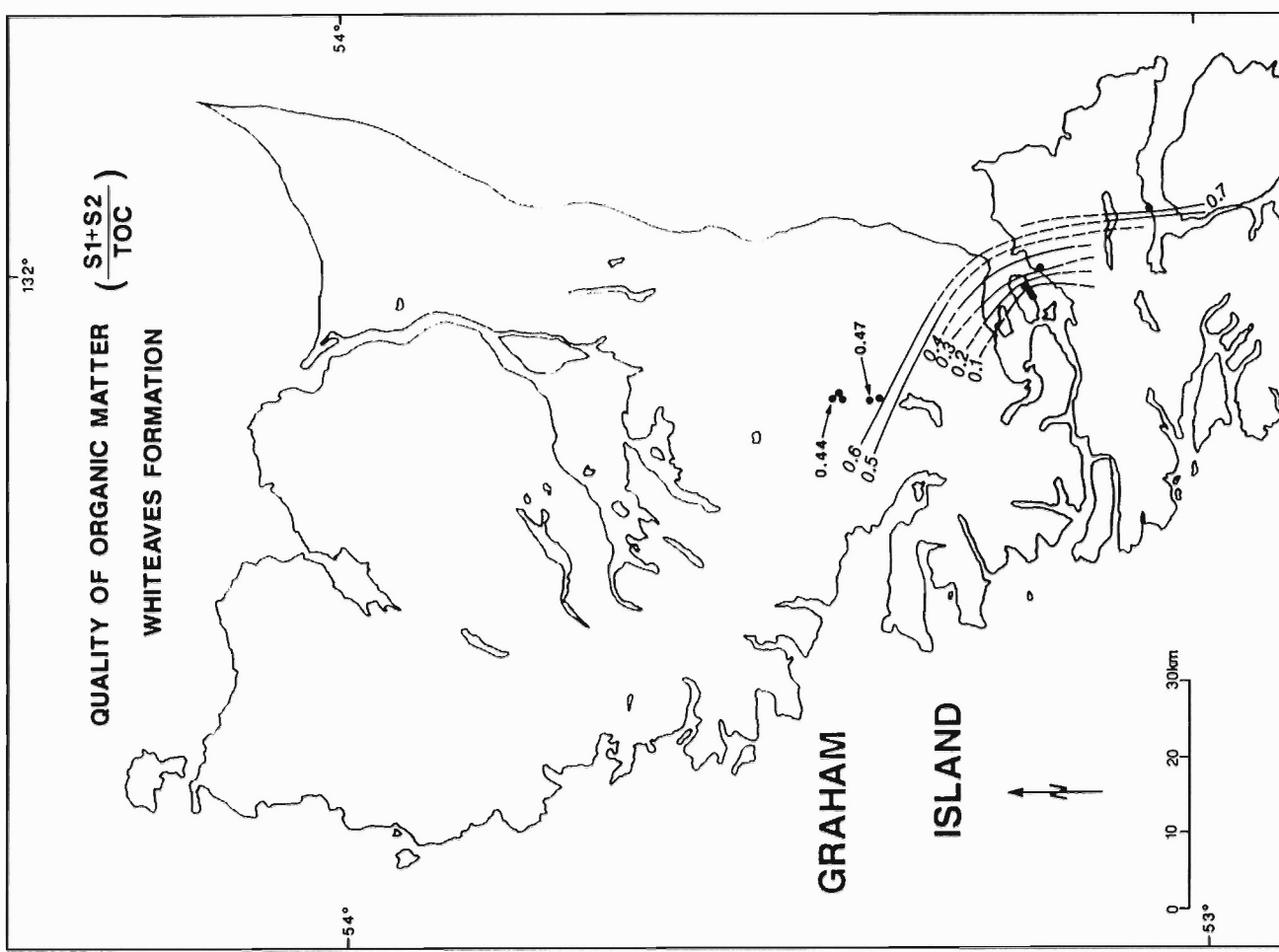
**Figure 25:** Regional distribution of the average QOM [(S1+S2)/TOC] for the Haida Formation. Values are average QOM calculated across the thickness of the formation at each outcrop location.

**Figure 26:** Regional distribution of the average QOM [(S1+S2)/TOC] for the Longarm Formation. Values are average QOM calculated across the thickness of the formation at each outcrop location.



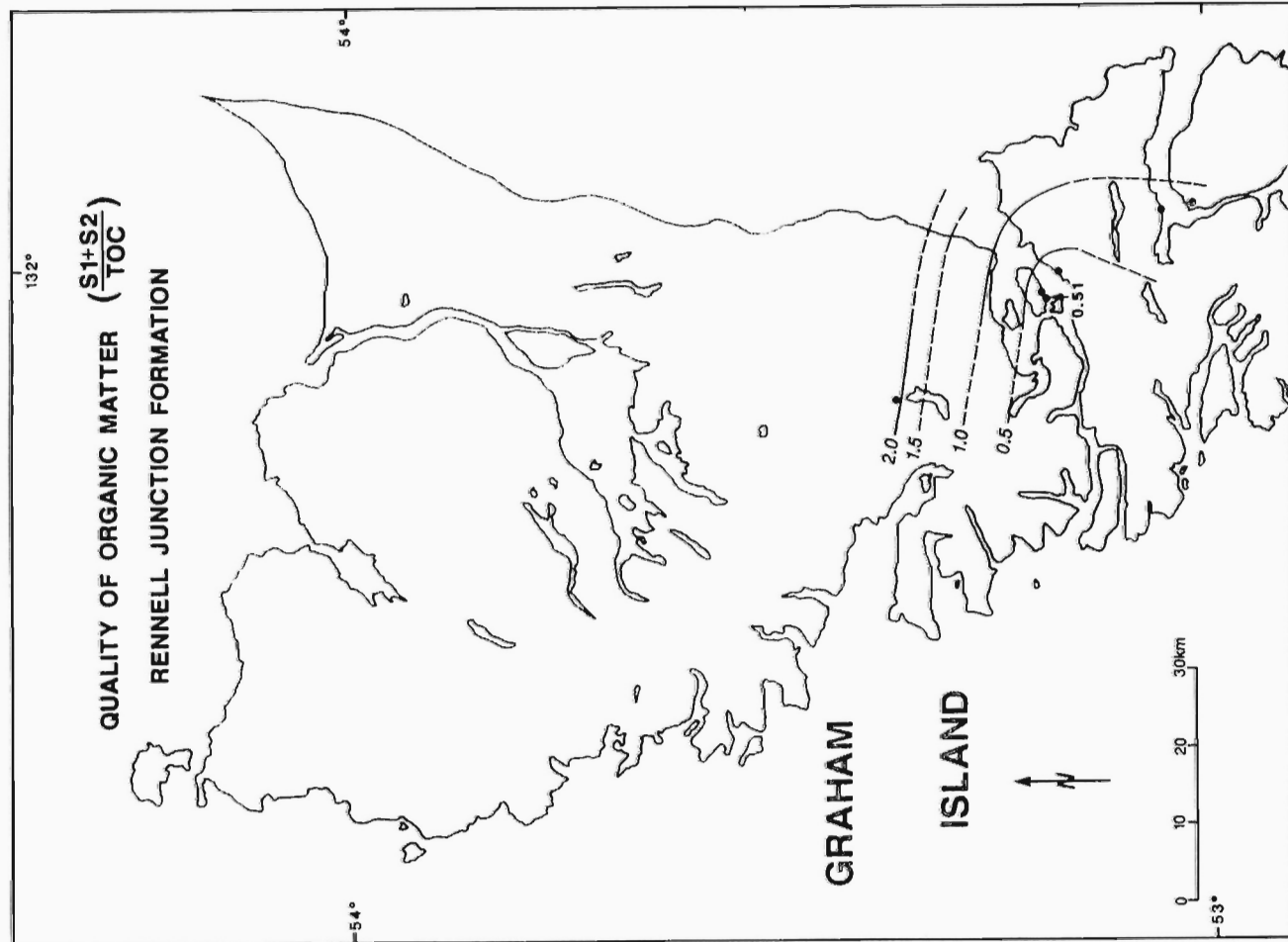


**Figure 28:** Regional distribution of the average QOM  $[(S1+S2)/TOC]$  for the Maude Group. Values are average QOM calculated across the thickness of the formation at each outcrop location. Tick marks on contour line indicate decreasing QOM.

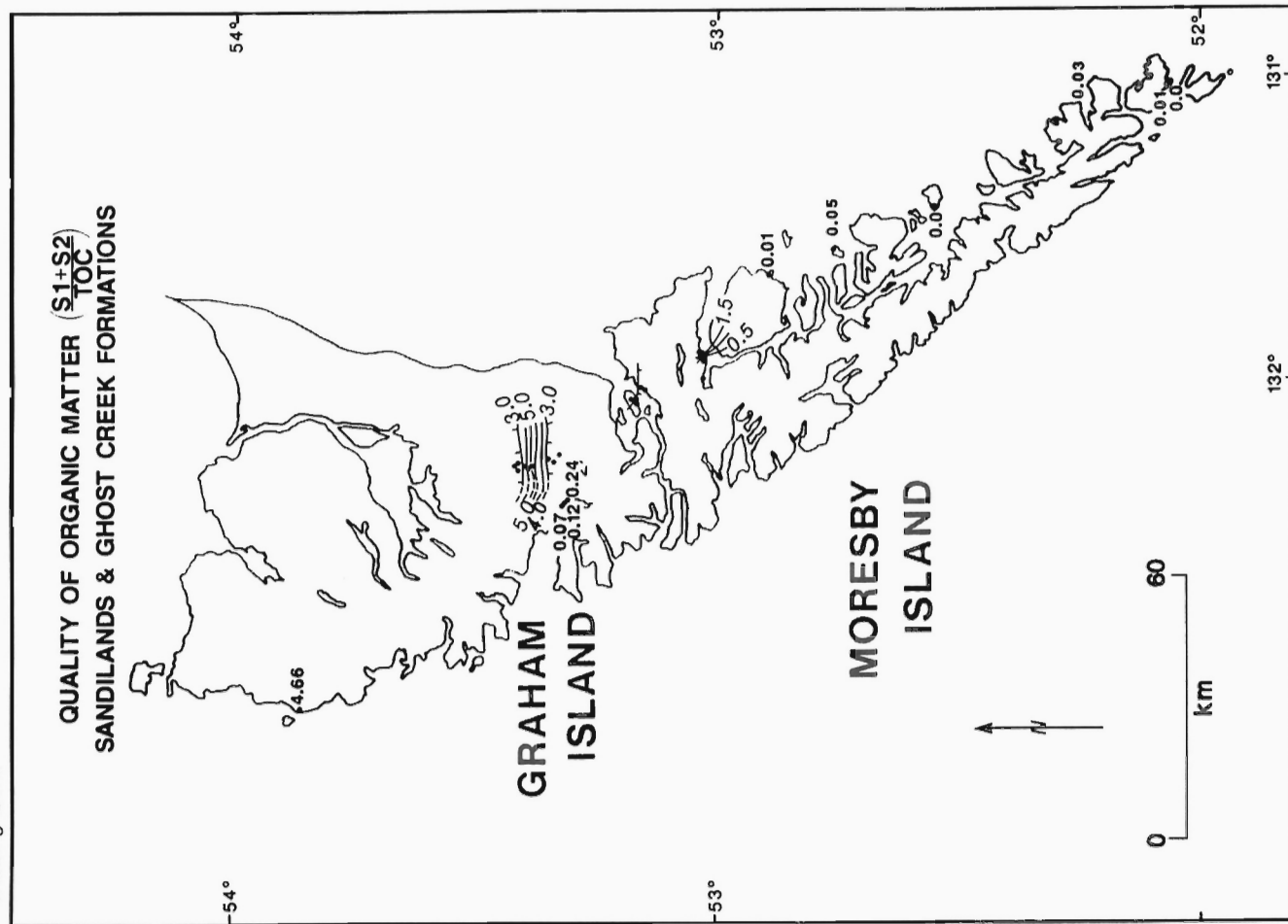


**Figure 29:** Regional distribution of the average QOM  $[(S1+S2)/TOC]$  for the Whiteaves Formation. Values are average QOM calculated across the thickness of the formation at each outcrop location. Dashed line represents approximate contour location. Labelled values do not fit regional trends and are not contoured.

**Figure 30:** Regional distribution of the average QOM  $[(S1+S2)/TOC]$  for the Rennell Junction Formation. Values are average QOM calculated across the thickness of the formation at each outcrop location. Dashed line represents approximate contour location. Labelled values do not fit regional trends and are not contoured.



**Figure 31:** Regional distribution of the average QOM  $[(S1+S2)/TOC]$  for the Sandilands and Ghost Creek formations. Values are average QOM calculated across the thickness of the formation at each outcrop location. Dashed line represents approximate contour location. Labelled values do not fit regional trends and are not contoured. Tick mark on contour line indicates decreasing QOM.



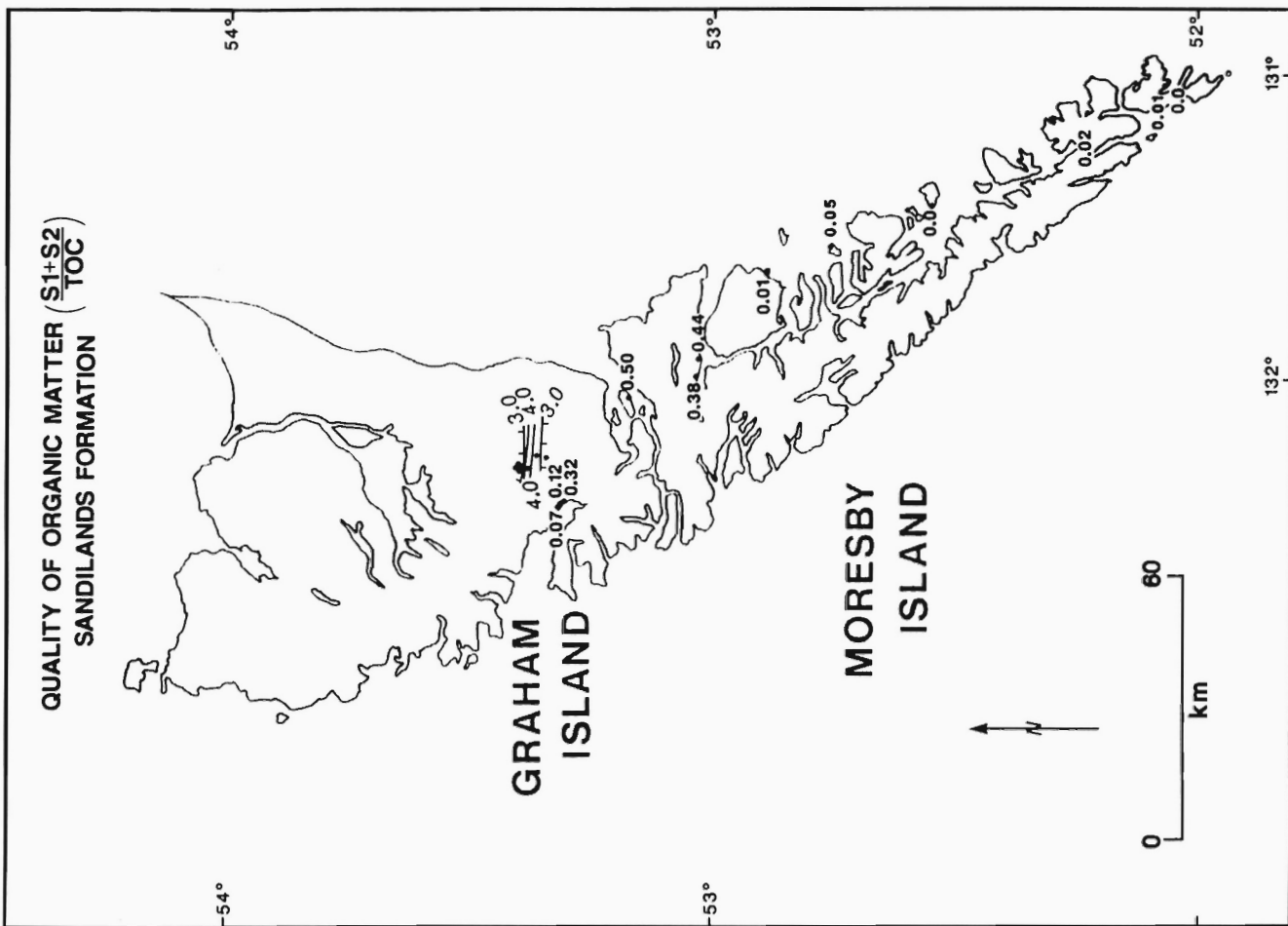


**Figure 33:** Regional distribution of the average QOM  $[(S1+S2)/TOC]$  for the Sandilands Formation. Values are average QOM calculated across the thickness of the formation at each outcrop location. Dashed line represents approximate contour location. Labelled values do not fit regional trends and are not contoured. Tick mark on contour line indicates decreasing QOM.

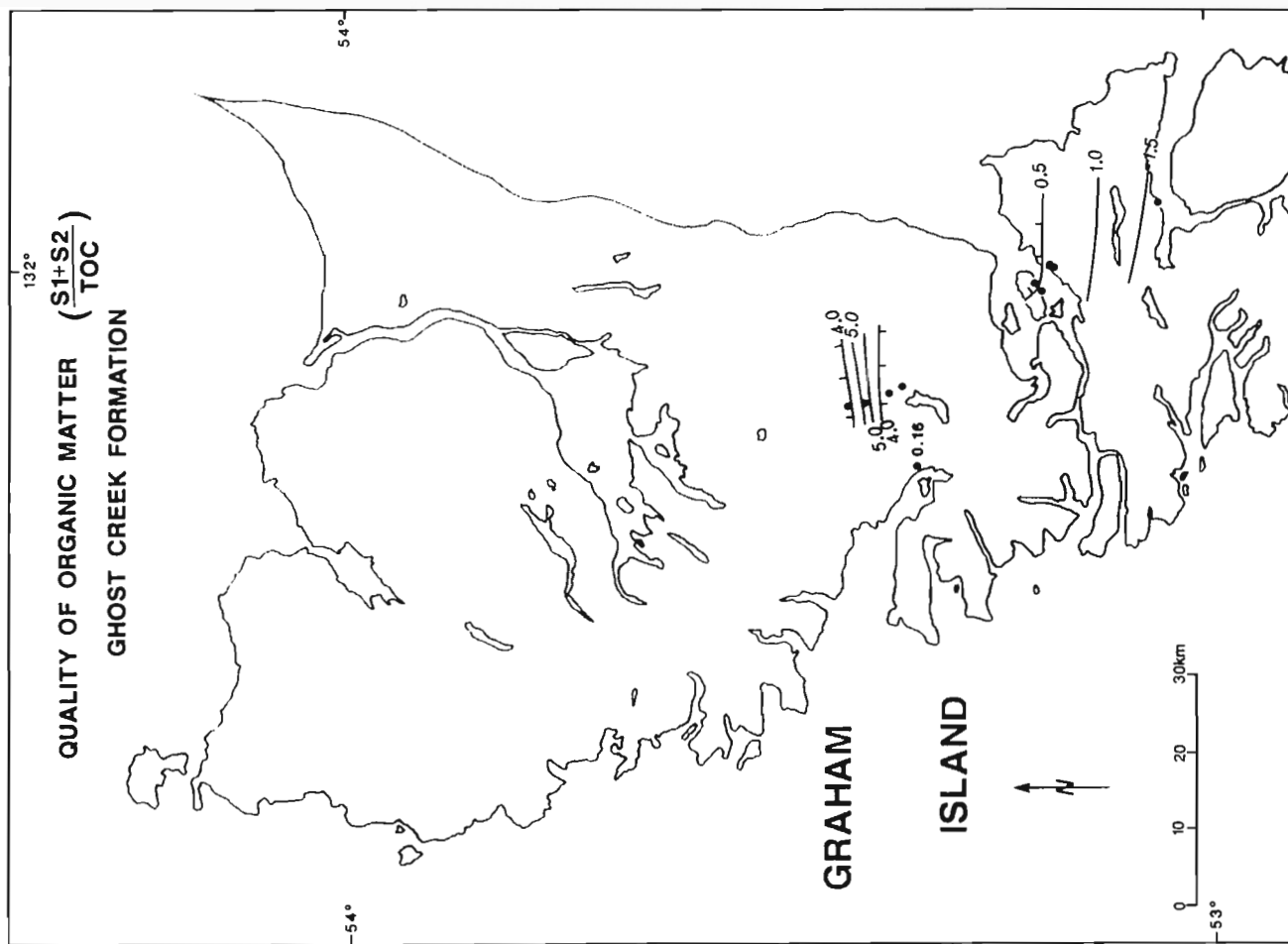
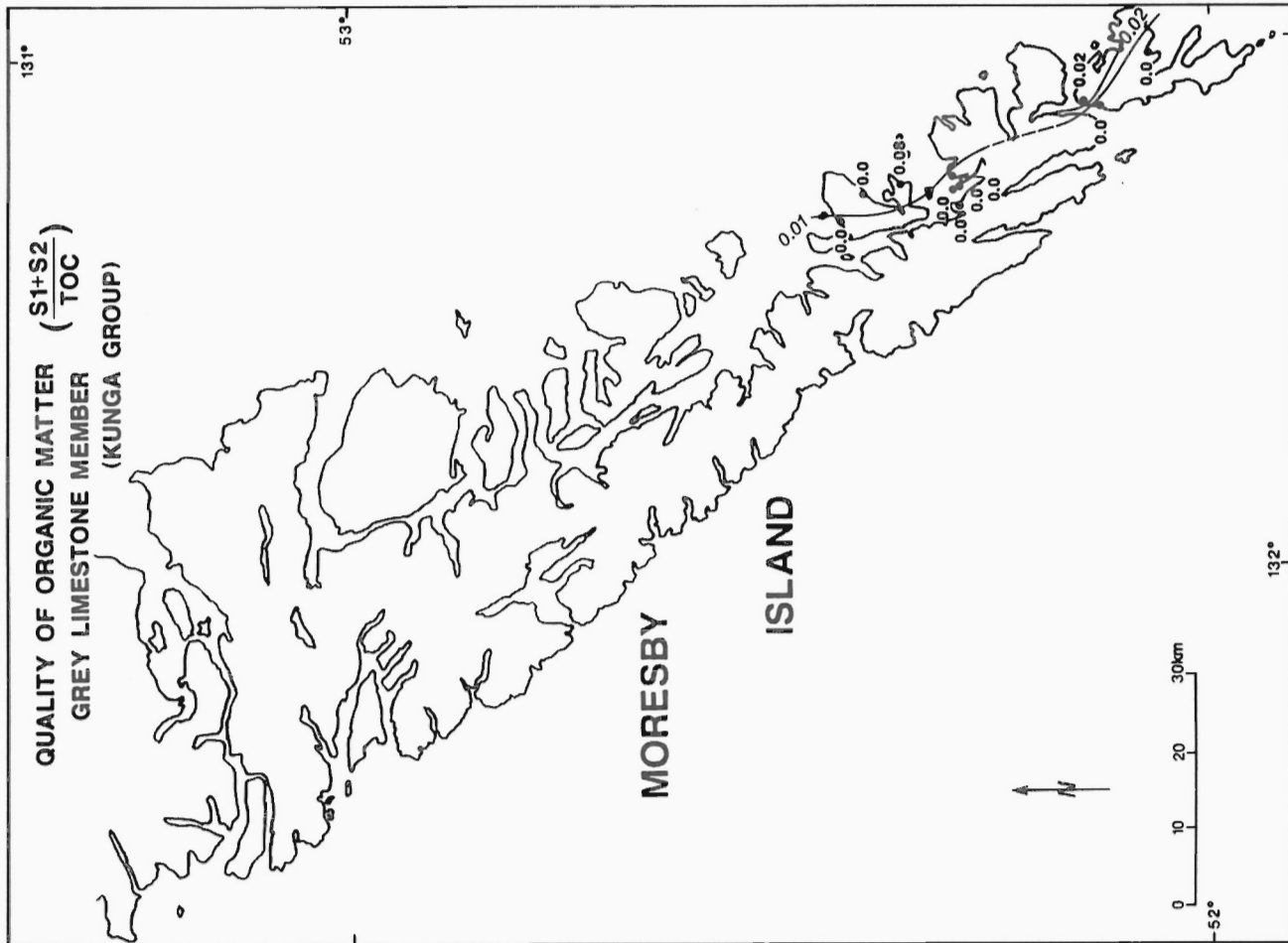


**Figure 32:** Regional distribution of the average QOM  $[(S1+S2)/TOC]$  for the Ghost Creek Formation. Values are average QOM calculated across the thickness of the formation at each outcrop location. Dashed line represents approximate contour location. Labelled values do not fit regional trends and are not contoured. Tick mark on contour line indicates decreasing QOM.



**Figure 35:** Regional distribution of the average QOM [(S1+S2)/TOC] for the Sadler Limestone. Values are average QOM calculated across the thickness of the formation at each outcrop location. Dashed line represents approximate contour location. Labelled values do not fit regional trends and are not contoured.



Marginally mature strata in central Graham Island have fair gas source potential as indicated by low TOC (0.71%), high QOM (2.14 mg HC/gm C<sub>org</sub>), and low HI (178 mg HC/gm C<sub>org</sub>) values.

### **Fannin Formation**

Generally overmature (0.85-1.51 %Ro<sub>rand</sub>) tuffaceous siltstone in central Graham Island and Skidegate Inlet are poor source rocks as indicated by low TOC (<0.28%), QOM (<0.53 mg HC/gm C<sub>org</sub>), and HI (<42 mg HC/gm C<sub>org</sub>) values. The HI/OI diagram (Fig. 3m) suggests that the Fannin Formation contains terrestrially derived Type III organic matter.

### **Whiteaves Formation**

Low TOC (<0.59%), QOM (<0.73 mg HC/gm C<sub>org</sub>) and HI (<60 mg HC/gm C<sub>org</sub>) values suggest a poor petroleum source potential for marginally mature to overmature strata (0.43-1.5 %Ro<sub>rand</sub>) on central Graham Island and Skidegate Inlet. Strata in Cumshewa Inlet have some gas source potential (TOC=1.8%; QOM=0.73 mg HC/gm C<sub>org</sub>; PI=0.13; HI=64 mg HC/gm C<sub>org</sub>). Very high TOC values (10.28%) reflect organic rich (Type III) horizons in central Graham Island.

### **Phantom Creek Formation**

Limited data suggests that the marginally immature (0.46 %Ro<sub>rand</sub>) fine grained sandstones and shales of the Phantom Creek Formation are poor to fair oil and gas source rocks (TOC=0.55%; QOM=3.9 mg HC/gm C<sub>org</sub>; PI=0.16; and HI=322 mg HC/gm C<sub>org</sub>). Low PI values suggest partial conversion of kerogen to petroleum.

## **YAKOUN GROUP**

### **Graham Island Formation**

Marginally mature to overmature (0.48-1.5 %Ro<sub>rand</sub>) shale and siltstone in central Graham Island have low TOC (0.88-0.96%), moderately high QOM (1.17-1.94 mg HC/gm C<sub>org</sub>), and moderately high HI (<385 mg HC/gm C<sub>org</sub>) values, suggesting fair oil and gas source potential.

Strata in the Skidegate Inlet area are poor source rocks (TOC=0.34%; QOM=0.26 mg HC/gm C<sub>org</sub>).

### **Richardson Bay Formation**

The Richardson Bay Formation consists predominantly of volcanic strata with some sedimentary facies of limited lateral extent. The sedimentary strata contain moderate amounts (1.13% TOC) of Type III organic matter (HI=45 mg HC/gm C<sub>org</sub>). Mature strata (1.13 %Ro<sub>rand</sub>) in Skidegate Inlet have gas generative potential as suggested by moderate TOC (1.13%), low QOM (0.63 mg HC/gm C<sub>org</sub>) and low HI (45 mg HC/gm C<sub>org</sub>) values.

## **MORESBY GROUP**

Mature (1.10 %Ro<sub>rand</sub>) coarse clastic rocks of the Robber Point Formation in Skidegate Inlet generally have insufficient amounts of organic carbon (0.78% TOC), low QOM (0.63 mg HC/gm C<sub>org</sub>), and low HI (44 mg HC/gm C<sub>org</sub>) values to be considered hydrocarbon source rocks.

Mature, massive volcanic sandstone (1.08 %Ro<sub>rand</sub>) of the Newcombe Formation are exposed in Skidegate Inlet. These strata generally do not have a sufficient TOC (0.51%) to generate significant amounts of hydrocarbons. Low QOM (0.34 mg HC/gm C<sub>org</sub>) and HI (30 mg HC/gm C<sub>org</sub>) values suggest poor oil and gas potential.

Mature (1.04 %Ro<sub>rand</sub>) siltstone of the Alliford Formation exposed in Skidegate Inlet have fair gas source potential, shown by moderate TOC (1.1%), moderate QOM (1.01 mg HC/gm C<sub>org</sub>), and low HI (80 mg HC/gm C<sub>org</sub>) and PI (0.2) values.

## **LONGARM FORMATION**

Low TOC (0.26%), QOM (0.03 mg HC/gm C<sub>org</sub>), HI (5 mg HC/gm C<sub>org</sub>), PI (0.03), and high maturation (3.18 %Ro<sub>rand</sub>) values suggest poor oil and gas source potential on Moresby Island. Data are not available for Graham Island.

## **QUEEN CHARLOTTE GROUP**

### **Haida Formation**

Immature to overmature (0.36-1.51 %Ro<sub>rand</sub>) carbonaceous sandstone of the Haida Formation, rich in terrestrial organic matter (0.68-2.49% TOC), have fair gas source potential on Graham Island (QOM <0.67 mg HC/gm C<sub>org</sub>; HI <65 mg HC/gm C<sub>org</sub>; and PI <0.27). Generally overmature (4.04 %Ro<sub>rand</sub>) strata on Moresby Island have poor oil or gas generative potential (TOC=0.13%; QOM=0.02 mg HC/gm C<sub>org</sub>; and HI=0 mg HC/gm C<sub>org</sub>) but may have previously generated gas before or during plutonism in Tertiary time (Vellutini and Bustin, 1991).

### **Skidegate Formation**

Generally low TOC (<0.73%) and QOM (<0.95 mg HC/gm C<sub>org</sub>) values suggest that immature to overmature (0.4-2.94 %Ro<sub>rand</sub>) Type III (HI <79 mg HC/gm C<sub>org</sub>) organic matter of the Skidegate Formation has poor to fair gas generative potential on Graham Island. Low PI values (<0.16) for mature strata suggest partial kerogen conversion to petroleum.

### **Honna Formation**

Conglomerate, sandstone, and shale facies of the Honna Formation on northwest Graham Island contain mature Type III organic matter and have poor hydrocarbon source potential due to low TOC (<0.43%). Low QOM (0.7 mg HC/gm C<sub>org</sub>), HI (<60 mg HC/gm C<sub>org</sub>), and PI (0.09) values suggest no oil source potential, but possible gas source potential.

## **SKONUN FORMATION**

Siltstone and shale of the Skonun Formation exposed on central Graham Island contain Type II organic matter and have good oil and gas generative potential (TOC=2.47%; QOM=2.64 mg HC/gm C<sub>org</sub>; HI=210 mg HC/gm C<sub>org</sub>; and PI=0.2). Petrographic analysis of coal and lignite samples from six onshore wells penetrating the Skonun Formation indicates that the organic matter is predominantly Type III and is composed of vitrinite. Some coals (Type III organic matter) respond differently to Rock-Eval pyrolysis than dispersed Type III organic matter and have HI values which plot between Types II and III organic matter (Peters, 1986). The liquid hydrocarbon generative potential calculated from HI data, therefore, can be overestimated for coals (Peters, 1986). Generally immature (0.27-0.48 %Ro<sub>rand</sub>) Skonun Formation coals have low to moderate QOM values (0.7-2.2 mg HC/gm C<sub>org</sub>) and hence are fair source rocks. Generally low HI values (64-179 mg HC/gm C<sub>org</sub>) for marginally mature to mature strata suggest that generated hydrocarbons would consist predominantly of gas and some oil. Hydrogen rich resinite (HI>500 mg HC/gm C<sub>org</sub>) was observed petrographically which suggests some horizons with good oil source potential. Coals at west Graham Island (Port Louis well) are mature (1.05 %Ro<sub>rand</sub>); however, low QOM (0.87 mg HC/gm C<sub>org</sub>), HI (79 mg HC/gm C<sub>org</sub>), and PI (0.07) values suggest poor hydrocarbon source potential.

Fowler et al. (1988) and L.R. Snowdon (pers. comm., 1989) have correlated bitumens from oil seeps associated with Masset volcanic rocks with Jurassic, Cretaceous, and Tertiary source strata predominantly from Graham Island. Bitumens from Otard and Tian bays (northwest Graham Island) and from Tar Island (east Moresby Island) contain 18 $\alpha$ (H)oleanane correlated with Tertiary, Type III organic matter

derived from terrestrial higher plant material. Bitumens associated with fractures in Masset volcanics near Lawn Hill on the east coast of Graham Island have also been correlated with Tertiary source strata. Bitumen samples from the King Creek area in central Graham Island appear to be derived from Lower Jurassic source rocks. Bitumens from Cretaceous strata have not yet been systematically studied.

## FACTORS AFFECTING LATERAL VARIATIONS IN SOURCE ROCK QUALITY

Source rock quality is controlled primarily by the quality, quantity, and DOM of the organic matter. In the Queen Charlotte Islands, the dominant control on the lateral variation in source rock quality for Triassic and Jurassic strata is the DOM of the organic matter, whereas depositional environments are the primary control for Cretaceous and Tertiary strata.

Upper Triassic and Lower Jurassic source strata may have been deposited in Hecate Strait and Dixon Entrance but have not yet been confirmed. Even if the strata were deposited, increased burial depths have probably resulted in the levels of organic maturation exceeding the oil window. Any hydrocarbons that were generated may have migrated into less mature strata and preserved.

High levels of organic maturation due to high heat flow associated with the San Christoval (SCPS), Burnaby Island (BIPS), and Carpenter Bay (CBPS) plutonic suites have resulted in hydrocarbon depletion of the organic matter in the Sadler Limestone of the Kunga Group. Figure 22 illustrates increasing TOC from west to east on south Moresby Island, suggesting that the SCPS was the dominant thermal event. Figure 35 shows very low QOM values with no apparent trend.

TOC values for the Peril Formation of the Kunga Group increase from east to west (Fig. 21) suggesting that pluton emplacement of the BIPS and CBPS were the dominant thermal events on south Moresby Island. TOC values measured on the east side of the BIPS increase from west to east on central Moresby Island, suggesting that the pluton emplacement of the BIPS was also the dominant thermal event on central Moresby Island. TOC and QOM (Fig. 34) values on northwest Moresby Island increase to the southeast, suggesting offshore high heat flow possibly associated with the Langara Island pluton.

The Sandilands Formation on Moresby Island is overmature and has low TOC (Fig. 20) and QOM (Fig. 33) values with no apparent lateral trend (reflecting limited data). High TOC and QOM values in central Graham Island suggest that the strata are very good source rocks. The strata near Rennell Sound are overmature and have significantly reduced TOC and QOM values as a result of high heat flow associated with plutonic activity south of Rennell Sound.

The Ghost Creek Formation has high TOC (Fig. 19) and QOM (Fig. 32) values indicating very good source potential. High heat flow associated with plutonism near Rennell Sound has increased the level of organic maturation and decreased the hydrocarbon generative potential of the strata, as suggested by increasing QOM values from north to south and increasing TOC values from south to north.

The Ghost Creek Formation is not exposed south of Cumshewa Inlet or north of Rennell Sound on central Graham Island. The Sandilands and Longarm formations, which are stratigraphically below and above the Ghost Creek Formation, are exposed on southern Moresby Island and northwest Graham Island, suggesting that deposition of the Ghost Creek Formation (and possibly the entire Maude Group) was restricted to central Graham Island and northern Moresby Island. If such is the case, the limited areal extent of Ghost Creek Formation source rocks suggests a limited potential for hydrocarbon generation and accumulation.

TOC (Fig. 16) and QOM (Fig. 29) values for the Whiteaves Formation tend to increase from southwest to northeast in response to high heat flow from plutonism near Rennell Sound. There is insufficient TOC and QOM data to determine trends for the Fannin and Phantom Creek formations (see Figures in Vellutini, 1988).

Higher TOC (Fig. 14) and QOM (Fig. 27) values were obtained from Skidegate Inlet and central Graham Island respectively for the Yakoun and Moresby groups. However, the paucity of data precludes determination of TOC and QOM trends. TOC values for the Longarm Formation on Moresby Island (Fig. 13) increase from east to west. However, there is no apparent trend in QOM (Fig. 26). The paucity of data, however, precludes accurate interpretation.

The Haida Formation increases in TOC from east to west (Fig. 12), suggesting decreased amounts of transported terrestrial organic matter basinward from the western edge of Haida deposition. QOM values from northwest Graham Island (Fig. 25) increase southwards away from plutonic rocks on Langara Island. TOC values are generally lower and HI values are generally higher for the Skidegate Formation relative to the Haida Formation (Fig. 11). TOC and HI values increase from west to east for the Skidegate Formation, suggesting that there was decreased input of terrestrial organic matter and possibly increased input of marine organic matter in a basinward direction. Higher HI values (Figs. 2c and 3c) occur in the Skidegate Formation than in the Haida Formation (Figs. 2d, 3d), suggesting an increased marine component in Skidegate Formation organic matter. QOM values (Fig. 24) increase with increasing distance from plutons on Langara Island and Rennell Sound.

TOC (Fig. 10) and QOM (Fig. 23) values are low for the Honna Formation and the paucity of data precludes the determination of TOC or QOM trends. There are too few data to ascertain lateral trends in TOC and QOM for the Skonun Formation.

## SUMMARY AND CONCLUSIONS

For the most part, Cretaceous and Tertiary strata in the Queen Charlotte Islands contain gas-prone Type III organic matter with varying degrees of hydrocarbon source potential. The source rock quality is related primarily to the depositional patterns and the level of organic maturity. Triassic and Jurassic strata (where mature) generally contain a mixture of Type II and Type III organic matter with varying degrees of hydrocarbon source potential related to the level of organic maturation. The Kunga Group and Ghost Creek Formation on central and northwest Moresby Island contain abundant oil and gas prone Type II and significant amounts of oil prone Type I organic matter. These units have very good petroleum generative potential.

Triassic strata from Moresby Island presently have poor oil source potential due to high levels of organic maturation (2.35-8.31 %Ro<sub>rand</sub>) but may have sourced substantial hydrocarbons in the past. High PI values for overmature strata at Kunga Island suggest hydrocarbon migration into overmature strata. Moderate amounts of residual TOC (<2.56%) suggest some gas generative potential remains. The level of organic maturity increases, and TOC decreases from west to east proximal to the BIPS as a result of high heat flow during pluton emplacement.

Mature to overmature Triassic strata from central and northwest Graham Island have very good oil and gas source potential. Moderate PI values (0.14-0.42) and free hydrocarbons suggest partial conversion of kerogen to petroleum. The hydrocarbon source potential diminishes from east to west with decreasing distance to plutons near Rennell Sound.

Jurassic strata from Graham Island and north Moresby Island generally have poor to fair gas generative potential and poor oil source

potential. The marginally mature (0.55 %Ro<sub>rand</sub>) Ghost Creek Formation is a notable exception and has very good oil and gas source potential, shown by moderate TOC (<1.73%), high QOM (<3.73 mg HC/gm C<sub>org</sub>), moderately high HI values (<349 mg HC/gm C<sub>org</sub>). Low PI (0.07) values, however, suggest minimal kerogen conversion to petroleum.

Cretaceous strata of the Longarm, Haida, and Honna formations on Moresby Island have poor hydrocarbon source potential because of high levels of organic maturity (4.04 %Ro<sub>rand</sub>). Depositional patterns are an important factor controlling the source potential for Cretaceous strata. The Haida Formation on Graham Island contain Type III dispersed organic matter and has poor to fair gas source potential but no oil generative potential. The Skidegate Formation contains a greater component of marine Type II organic matter than the Haida Formation and has poor to fair gas potential. The Honna Formation on Graham Island has poor hydrocarbon source potential, reflecting low TOC.

Type II organic matter from siltstone and shale horizons in Skonun strata have good oil and gas generative potential (TOC=2.47%; QOM=2.64 mg HC/gm C<sub>org</sub>; HI=210 mg HC/gm C<sub>org</sub>; and PI=0.2). Coals from the Skonun Formation generally have poor hydrocarbon source potential due to low levels of organic maturity (0.27-0.48 %Ro<sub>rand</sub>). Low to moderate HI (64-179 mg HC/gm C<sub>org</sub>) values for marginally mature to mature coals suggest some gas source potential and oil generative potential. Mature coals at the Port Louis well are poor hydrocarbon sources due to low QOM values. Resinites observed petrographically and associated high HI values suggest some coal horizons have fair to good oil and gas source potential.

## REFERENCES

- Bustin, B.E.B. and Macauley, G.**  
**1988:** Organic petrology and Rock-Eval pyrolysis of the Jurassic Sandilands and Ghost Creek Formations, Queen Charlotte Islands; Bulletin of Canadian Petroleum Geology, v. 36, p. 168-176.
- Bustin, R.M., Cameron, A.R., Grieve, D.A., and Kalkreuth, W.D.**  
**1983:** Coal Petrology, its principle, methods, and applications; Geological Association of Canada, Short Course Notes, v. 3., 273 p.
- Cameron, B.E.B.**  
**1987:** Significance of Lower Jurassic hydrocarbon source rocks in the Cumshewa Inlet area, Queen Charlotte Islands, British Columbia; *in* Current Research, Part A, Geological Survey of Canada, Paper 87-1A, p. 925-928.
- Cameron, B.E.B. and Tipper, H.W.**  
**1985:** Jurassic stratigraphy of the Queen Charlotte Islands, British Columbia; Geological Survey of Canada, Bulletin 365, 49 p.
- Conford, C.**  
**1984:** Source rocks and hydrocarbons of the North Sea; *in* Introduction to the Petroleum Geology of the North Sea, K.W. Glennie (ed.), London, 1984, 236 p.
- Dow, W.G.**  
**1977:** Kerogen studies and geologic interpretations; Journal of Geochemical Exploration, v. 7, p. 79-99.
- Espitalie, J., Deroo, G., and Marquis, F.**  
**1985:** Rock-Eval pyrolysis and its applications; Institut Francais du Petrole, reprint 27299, 132 p.
- Espitalie, R., Madec, M., and Tissot, B.**  
**1977:** Source rock characterization method for petroleum exploration; 9th Annual Off-shore Technology Conference, Houston, Texas, p. 439-444.
- Fowler, M.G., Snowdon, L.R., Brooks, P.W., and Hamilton, T.S.**  
**1988:** Biomarker characterization and hydrous pyrolysis of bitumens from Tertiary volcanics, Queen Charlotte Islands, British Columbia, Canada; Organic Geochemistry, v. 13, p. 715-725.
- Link, C.M.**  
**1988:** A reconnaissance of organic maturation and petroleum source potential of Phanerozoic strata in northern Yukon and northwestern District of Mackenzie; M.Sc. Thesis, Department of Geological Sciences, University of British Columbia, Vancouver, 260 p.
- Macauley, G.**  
**1983:** Source rock – oil shale potential of the Jurassic Kunga Formation, Queen Charlotte Islands; Geological Survey of Canada, Open File 921.
- Peters, K.E.**  
**1986:** Guidelines for evaluating petroleum source rocks using programmed pyrolysis; American Association of Petroleum Geologists, v. 70, p. 318-329.
- Snowdon, L.R., Fowler, M.G., and Hamilton, T.S.**  
**1988:** Progress report on organic geochemistry, Queen Charlotte Islands, British Columbia; *in* Current Research, Part E, Geological Survey of Canada, Paper 88-1E, p. 251-253.
- Tissot, B.P. and Welte, D.H.**  
**1984:** Petroleum formation and occurrence; Springer-Verlag, Berlin, 699 p.
- Vellutini, D.**  
**1988:** Organic maturation and source rock potential of Mesozoic and Tertiary strata, Queen Charlotte Islands, British Columbia; M.Sc. thesis, University of British Columbia, Vancouver, 262 p.
- Vellutini, D. and Bustin, R.M.**  
**1991:** Organic maturation of Mesozoic and Tertiary strata of the Queen Charlotte Islands, British Columbia; *in* Evolution and Hydrocarbon Potential of the Queen Charlotte Basin, British Columbia, Geological Survey of Canada, Paper 90-10.



# Organic maturation of Mesozoic and Tertiary strata of the Queen Charlotte Islands, British Columbia

D. Vellutini<sup>1,2</sup> and R.M. Bustin<sup>1</sup>

Vellutini, D. and Bustin, R.M., Source rock potential of Mesozoic and Tertiary strata of the Queen Charlotte Islands; in *Evolution and Hydrocarbon Potential of the Queen Charlotte Basin, British Columbia*, Geological Survey of Canada, Paper 90-10, p. 411-451, 1991.

## Abstract

*The level of organic maturation, source rock potential, and the thermal history of Mesozoic and Tertiary strata in the Queen Charlotte Islands have been determined with vitrinite reflectance (%Ro<sub>rand</sub>), Rock-Eval pyrolysis, and numerical modelling (modified Arrhenius model). The degree of organic maturation (DOM) varies from immature to overmature and increases from north to south. The primary control on the DOM is high heat flow associated with plutonism on Moresby Island. Upper Triassic-Lower Jurassic Kunga Group strata are immature to overmature (0.45-1.75 %Ro<sub>rand</sub>) on northwest and central Graham Island, and are overmature (2.40-5.80 %Ro<sub>rand</sub>) on Moresby Island south of Cumshewa Inlet. Local, anomalously high maturation values (ranging up to 3.20 %Ro<sub>rand</sub> on Graham Island and 8.31 %Ro<sub>rand</sub> on Moresby Island) occur adjacent igneous intrusives. Lower Jurassic Maude, Yakoun, and Moresby Group strata (including Lower Jurassic source rocks) are marginally mature to overmature with maturation increasing from central Graham Island (0.43 %Ro<sub>rand</sub>) to north Moresby Island (1.58 %Ro<sub>rand</sub>). The DOM of Cretaceous strata (Longarm, Haida, Skidegate, and Honna formations) increases from northwest Graham Island (0.33-1.91 %Ro<sub>rand</sub>), to south Graham Island (1.53-2.43 %Ro<sub>rand</sub>), to south Moresby Island (2.31-4.78 %Ro<sub>rand</sub>). Tertiary strata are restricted to Graham Island and are generally immature except for the mature succession on western Graham Island (Port Louis well) and northeast Graham Island (basal strata at the Tow Hill well).*

*Calculated thicknesses of eroded strata on west Graham Island range from 1040 m at Frederick Island to 735 m at Kennecott Point. Thicknesses of eroded strata are similar for Jurassic sections in central Graham Island at Rennell Junction (1725 m) and north Moresby Island at Cumshewa Inlet (1985 m). Increased thicknesses of eroded strata on north Moresby Island at Onward Point (1500 m), relative to northwest Graham Island at north Lander Point (745 m), suggests differential uplift for Cretaceous strata at northwest Graham Island. Thicknesses of eroded strata for the Tertiary Skonun Formation range from 375 m on east Graham Island (Tlell well) to 1685 m on west Graham Island (Port Louis well).*

*Time-temperature modelling (assuming constant geothermal gradients) requires high paleogeothermal gradients (45-90°C/km) for up to 180 million years during the Upper Triassic-Tertiary. Variable geothermal gradient modelling (using a 30°C/km background geothermal gradient) predicts elevated geothermal gradients ranging from 83-150°C/km during Yakoun (between 183 and 178 Ma) and Masset (between 35 and 10 Ma) volcanism.*

*Triassic strata at Frederick Island are predicted to have entered and exited the oil window during the Early and Late Miocene respectively while strata at Kennecott Point entered the oil window during the Early Miocene and are still in the oil window. Jurassic strata at Rennell Junction and Cumshewa Inlet entered the oil window during the Bajocian and remain within the oil window. Cretaceous strata on north and south Moresby Island entered the oil window during the Early Miocene and are currently within the oil window. The Skonun Formation is generally immature except for strata at west Graham Island (Port Louis well) and northeast Graham Island (Tow Hill well) which entered the oil window in the Late Miocene.*

## Résumé

*Le niveau de maturation organique et l'évolution thermique des couches mésozoïques et tertiaires dans les îles de la Reine-Charlotte a été déterminé en utilisant les méthodes de réflectance de la vitrinite (%Ro<sub>rand</sub>) et la modélisation numérique (modèle Arrhenius modifié). Le degré de maturation organique varie de non mûre à hypermature et augmente du nord vers le sud. Le principal facteur influant sur le degré de maturation organique est le flux thermique élevé associé au plutonisme dans l'île Moresby. Les couches du groupe de Kunga du Trias supérieur au*

<sup>1</sup> Department of Geological Sciences, University of British Columbia, 6339 Stores Road, Vancouver, B.C. V6T 2B4

<sup>2</sup> Present Address: Texaco Canada Resources, Drayton Valley, Alberta, T0E 0M0



*Jurassique inférieur sont de non matures à hypermatures (0,45 à 1,75 %  $Ro_{rand}$ ) dans le nord-ouest et le centre de l'île Graham et sont hypermatures (2,40 à 5,80 %  $Ro_{rand}$ ) dans l'île Moresby au sud de l'inlet Cumshewa. Des valeurs de maturation anormalement élevées (allant jusqu'à 3,20  $Ro_{rand}$  dans l'île Graham et jusqu'à 8,31 %  $Ro_{rand}$  dans l'île Moresby) ont été observées par endroits dans les roches intrusives ignées adjacentes. Les couches des groupes de Maude, de Yakoun et de Moresby du Jurassique inférieur (incluant les roches mères potentielles) ont une maturité allant de faible à très élevée, la maturation augmentant du centre de l'île Graham (0,43  $Ro_{rand}$ ) jusqu'au nord de l'île Moresby (1,58 %  $Ro_{rand}$ ). Le degré de maturation des couches crétacées (formation de Longarm, Haida, Skidegate et Honna) augmente du nord-ouest de l'île Graham (0,33 à 1,91 %  $Ro_{rand}$ ) au sud de l'île Graham (1,53 à 2,43 %  $Ro_{rand}$ ) et au sud de l'île Moresby (2,31 à 4,78 %  $Ro_{rand}$ ). Les couches tertiaires se limitent à l'île Graham et sont en général non matures à l'exception de la succession mature qui se trouve dans l'ouest de l'île Graham (puits Port Louis) et le nord-est de l'île Graham (couche de base au puits Tow Hill).*

*Dans l'ouest de l'île Graham, l'épaisseur des couches érodées varie de 1040 m dans l'île Fredrick à 735 m à la pointe Kennecott. L'épaisseur des couches érodées sont semblables dans les coupes jurassiques du centre de l'île Graham à Rennell Junction (1725 m) et dans le nord de l'île Moresby à l'inlet Cumshewa (1985 m). Une augmentation de l'épaisseur des couches érodées dans le nord de l'île Moresby à la pointe Onward (1500 m), par rapport au nord-ouest de l'île Graham dans le nord de la pointe Lauder (745 m), indique un soulèvement différentiel des couches crétacées dans le nord-ouest de l'île Graham. L'épaisseur des couches érodées de la formation de Skonun du Tertiaire varie de 375 m dans l'est de l'île Graham (puits Tlell) à 1685 m dans l'ouest de l'île Graham (puits Port Louis).*

*Une modélisation temps-température (en supposant des gradients géothermiques constants) nécessite des gradients paléogéothermiques élevés (45 à 90 °C/km) pendant une période allant jusqu'à 180 millions d'années durant le Trias supérieur au Tertiaire. La modélisation de gradients géothermiques variables (en supposant un gradient géothermique de fond de 30 °C/km) laisse supposer des gradients géothermiques élevés variant de 83 à 150 °C/km durant le volcanisme de Yakoun (183 à 178 Ma) et de Masset (35 à 10 Ma).*

*Les couches triasiques de l'île Fredrick auraient entré dans la fenêtre de pétrole et en seraient sorties durant le début et la fin du Miocène respectivement tandis que les couches à la pointe Kennecott seraient entrées dans la fenêtre de pétrole durant le Miocène précoce et y seraient toujours. Les couches jurassiques à Rennell Junction et à l'inlet Cumshewa sont entrées dans la fenêtre de pétrole durant le Bajocien et y sont demeurées. Les couches crétacées dans le nord et le sud de l'île Moresby sont entrées dans la fenêtre de pétrole durant le Miocène inférieur et y sont actuellement. La formation de Skonun est généralement non mature, à l'exception des couches situées dans l'ouest de l'île Graham (puits Port Louis) et dans le nord-est de l'île Graham (puits Tow Hill) qui sont entrées dans la fenêtre de pétrole au Miocène supérieur.*

## INTRODUCTION

The hydrocarbon generative potential of sedimentary strata depends upon the type and abundance of organic matter and the thermal history of the strata (Dow, 1977). The type of organic matter can be determined from geochemical and petrographic analysis (Tissot and Welte, 1984). Organic maturation indices (such as vitrinite reflectance), can be used to infer the time-temperature history of the strata. Maturation data can be used in conjunction with numerical models to predict the timing of hydrocarbon generation, the type of hydrocarbons, the temperatures corresponding to hydrocarbon generation, the fractional conversion of kerogen to liquid hydrocarbons, and other parameters (Tissot and Espitalie, 1975).

In this study, the degree of organic maturation (DOM) of Mesozoic and Tertiary strata from the Queen Charlotte Islands is quantified with organic petrology (vitrinite reflectance) in order to document vertical (stratigraphic) and areal trends in organic maturation. The maturation data are modelled to establish areas of potential petroleum generation, the timing of hydrocarbon generation, and to predict the location of the oil window in time and space.

## METHODS

About 1700 samples were collected in order to establish lateral and vertical (stratigraphic) variations in organic maturation. One hundred thirty-three carbonaceous strata and lignite samples were collected from well cuttings and well core in the Tertiary Skonun Formation from the following six onshore exploration wells: Richfield et al. Cape Ball a-41-1; Richfield Mic Mac Homestead Gold Creek #1; Richfield Mic Mac Homestead Nadu River; Richfield Mic Mac Homestead Tlell #1; Richfield Mic Mac Homestead Tow Hill #1; and Union Port Louis c-28-1. In addition, outcrop samples were collected from the Skonun Formation on Graham Island, lignite samples from Skonun Point and Miller Creek, and carbonaceous siltstone from Log Creek.

One hundred and eighty-eight lignite and carbonaceous shale outcrop samples were collected from the Cretaceous Longarm, Haida, Skidegate, and Honna formations. The majority of Cretaceous samples were collected from Graham Island and a few from Moresby Island. Two hundred and forty-one limestone, argillite, and carbonaceous sandstone outcrop samples were collected from the Triassic Kunga

Group. The majority of Triassic samples were collected from Moresby Island and fewer from Graham and Frederick islands.

Additional samples, together with stratigraphic data, were kindly provided by B.E.B. Cameron, M.J. Orchard, and C.J. Hickson of the Geological Survey of Canada and by J.A.S. Fogarassy of the University of British Columbia. Location maps for outcrop and well samples are given in the appendices to Vellutini (1988).

The degree of organic maturation (DOM) was determined using the vitrinite reflectance techniques outlined in England and Bustin (1986). Samples containing visible coal or lignite were crushed and analyzed as whole rock samples. Samples containing low concentrations of organic matter were crushed (<80 mesh) and demineralized with hydrochloric and hydrofluoric acids. The samples were mounted in transoptic and heated to 100°C for 5 minutes forming an optically transparent pellet. The pellets were stored in argon or nitrogen gas to prevent oxidation of the organic matter prior to analysis.

The mean random vitrinite reflectance (% $R_{o,rand}$ ) in oil ( $n=1.518$  at 546 nm) was measured with the polarizer out using a Leitz (M.P.V. II) microscope. The mean random vitrinite reflectance was measured rather than the mean maximum vitrinite reflectance (% $R_{o,max}$ ) in order to save time and to enable measurement of smaller particles (Davis, 1978; England and Bustin, 1986). Wherever possible, 50 vitrinite reflectance measurements were made on each sample.

## RESULTS

Lateral maturation trends (Figs. 1-15) and vertical maturation profiles (Figs. 16-20) were determined from vitrinite reflectance measurements of samples collected from all regions of the Queen Charlotte Islands (Tables 1-11). The regional DOM increases markedly from Graham Island to south Moresby Island. Regional elevated maturation levels on Moresby and adjacent islands are in part a result of increased heat flow associated with igneous activity (pluton emplacement) in the Middle-Late Jurassic and Oligocene (R.G. Anderson, pers. comm., 1988; Anderson, 1988; Souther, 1988). Local, anomalously high maturation values which result from high heat flow near igneous intrusions or possibly from hydrothermal activity near faults have, in many areas, obscured regional maturation trends. Due to poor outcrop exposure, large scale intrusion by plutonic complexes, and limited lateral continuity of sedimentary units, interpretation of lateral maturation trends is difficult and in some places impossible. The isomaturity maps presented here will thus ultimately require modification as new data is acquired.

Most of the organic matter found within the strata is either Type II or Type III (Vellutini and Bustin, 1991); therefore, the oil window has been defined as between 0.50 % $R_{o,rand}$  and 1.35 % $R_{o,rand}$  for this study (Dow, 1977). Strata with maturation values less than 0.50 % $R_{o,rand}$  are considered to be immature, and strata with maturation values greater than 1.35 % $R_{o,rand}$  are considered to be overmature with respect to hydrocarbon generation and preservation.

### Lateral variation in organic maturity

The following section outlines the outcrop exposure and maturation values for selected stratigraphic horizons. Local, high maturation levels which deviate from regional trends are considered anomalous. These anomalous maturation values often overprint regional trends. In the following section, local anomalous maturation values are differentiated from regional trends.

## KUNGA GROUP

In samples collected from Kunga Group lithologies on Moresby Island, vitrinite reflectances were measured from organic matter which was morphologically and texturally indistinguishable from

vitrinite. The organic matter did not have definitive form and commonly occurs as a groundmass. Internal texture varied from homogeneous to mosaic. The Kunga Group is interpreted to be an offshore carbonate platform deposit with some clastic input suggesting that the organic matter is of marine origin (hydrogen rich) and may not be vitrinite. It is, therefore, possible that the organic matter is either vitrinite, bituminite, or both.

### Sadler Limestone

The oldest sedimentary unit in the Queen Charlotte Islands is the Late Carnian Sadler Limestone (Desrochers and Orchard, 1991; the grey limestone member of Cameron and Tipper, 1985) of the Kunga Group. This unit, composed of grey limestone, is best exposed on eastern and southern Moresby Island where the strata are overmature (Fig. 1) with regional maturation values ranging from 2.91 % $R_{o,rand}$  at Huston Inlet (central Moresby Island) to 5.80 % $R_{o,rand}$  at Breaker Bay (eastern Moresby Island). At Carpenter Bay, maturation values reach 7.96 % $R_{o,rand}$  adjacent to the Carpenter Bay Plutonic Suite (southeastern Moresby Island).

### Peril Formation

The Late Carnian to Late Norian Peril Formation (Desrochers and Orchard, 1991) of the Kunga Group crops out predominantly on central and eastern Moresby Island and is overmature (2.40-5.80 % $R_{o,rand}$ ). The strata are also exposed locally on northwest Graham Island and in Skidegate Inlet where they are mature to overmature. The regional DOM increases from west to east on Moresby Island (Fig. 2) with maturation values ranging from 2.40 % $R_{o,rand}$  at Huston Inlet (central Moresby Island) to 5.80 % $R_{o,rand}$  at Howay Island (eastern Moresby Island). Local, anomalously high maturation values reach 8.31 % $R_{o,rand}$  at Carpenter Bay.

Peril Formation strata are marginally mature to overmature on northwestern Graham Island with maturation values ranging from 0.51 % $R_{o,rand}$  at Kennecott Point to 1.59 % $R_{o,rand}$  at Lauder Point. Local, anomalously high maturation values reach 3.20 % $R_{o,rand}$  at Sialun Bay in northwest Graham Island.

### Sandilands Formation

Regional maturation values for the Sinemurian Sandilands Formation (which is exposed primarily on Moresby Island and locally on Graham Island) increase from north to south (Figs. 3 and 6). Values range from 0.45 % $R_{o,rand}$  at Kennecott Point (northwestern Graham Island) to 3.78 % $R_{o,rand}$  at Kunga Island (central Moresby Island). Locally, values reach 4.73 % $R_{o,rand}$  on Moresby Island. Maturation values for central Graham Island and northern Moresby Island range from 0.48 % $R_{o,rand}$  in central Graham Island to 1.75 % $R_{o,rand}$  at Cumshewa Inlet (northern Moresby Island).

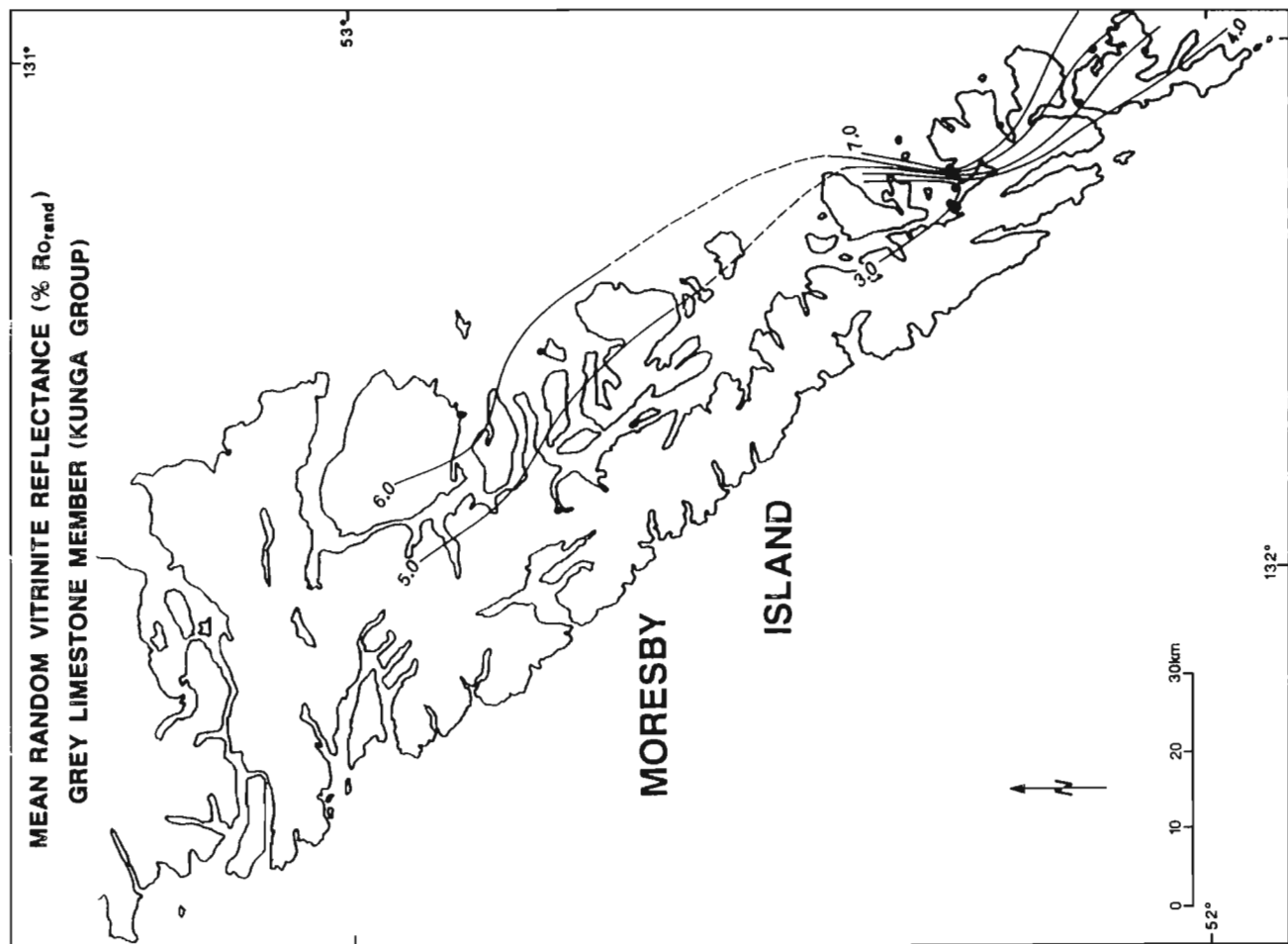
## MAUDE GROUP

The regional level of organic maturation for the Maude Group is shown in Figure 4. Stratigraphic nomenclature is that of Cameron and Tipper (1985).

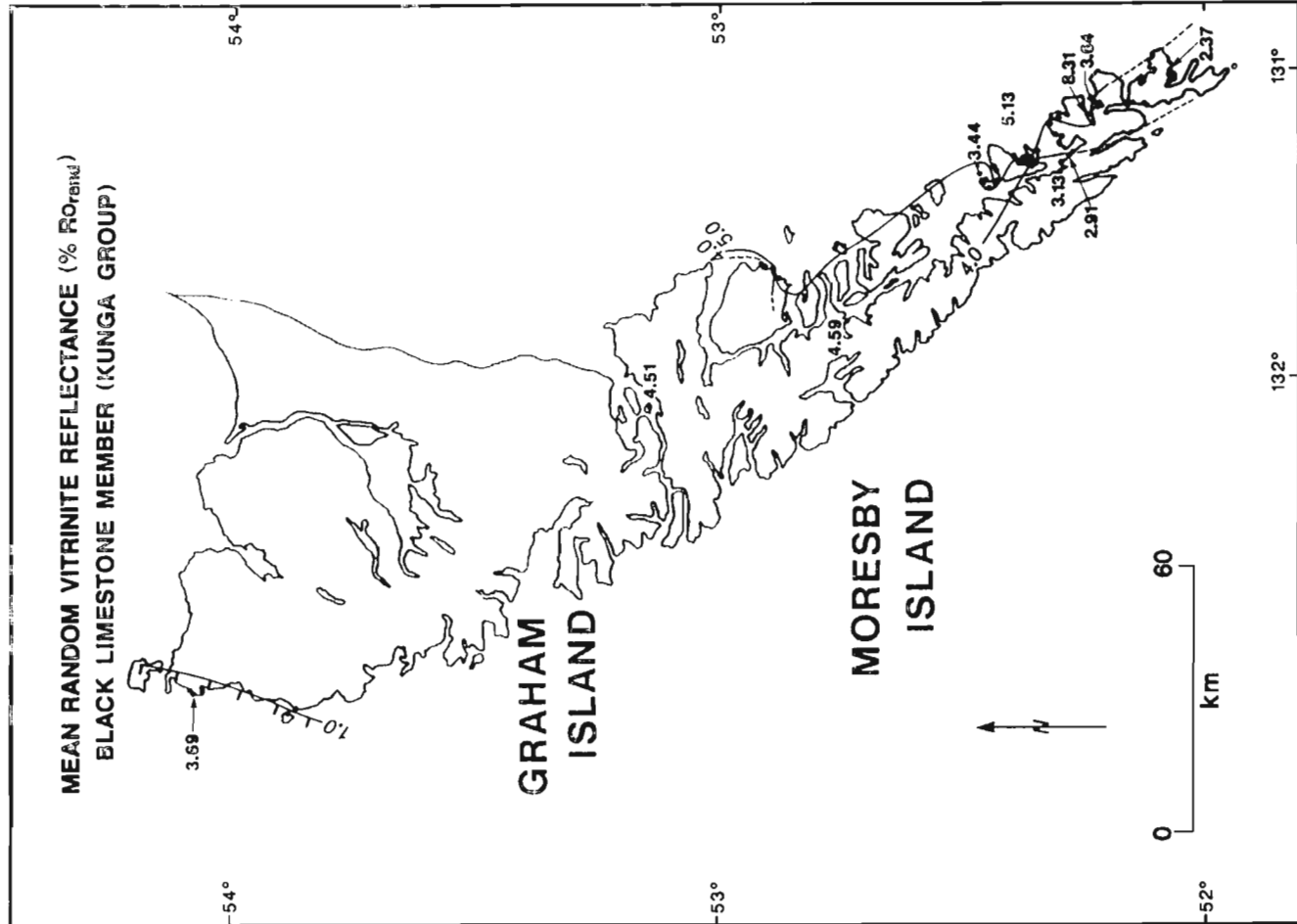
The Lower Pliensbachian Ghost Creek Formation crops out from central Graham Island to northern Moresby Island where the regional DOM increases from north to south and varies from mature to overmature. Organic maturation values range from 0.50 % $R_{o,rand}$  on central Graham Island to 1.53 % $R_{o,rand}$  at Cumshewa Inlet (Figs. 5 and 6). Vitrinite reflectance measurements taken proximal to dykes and sills reach 1.31 % $R_{o,rand}$  on the central Graham Island to 1.71 % $R_{o,rand}$  at Cumshewa Inlet. Similar values were reported by Bustin and Macauley (1988).

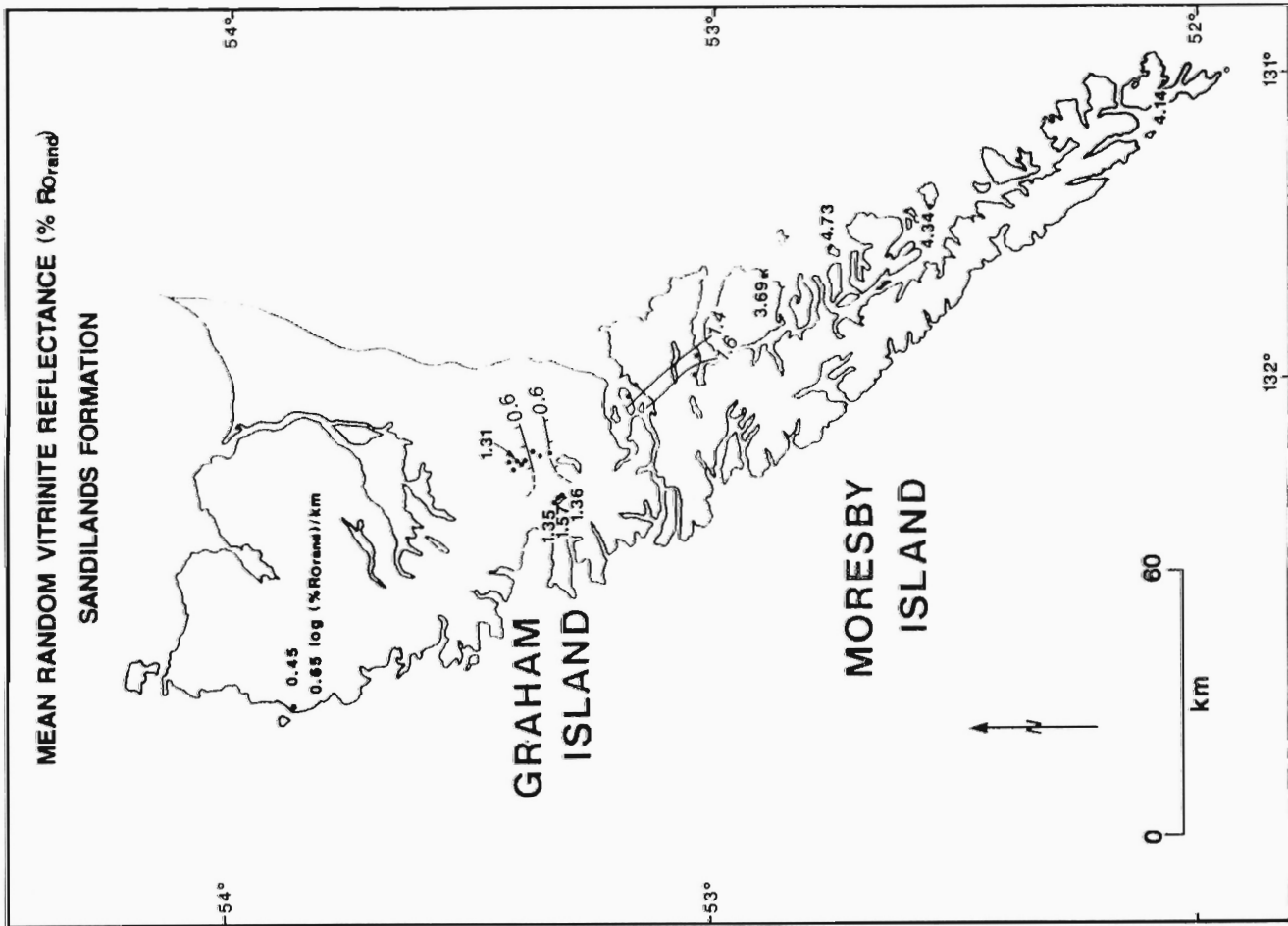
The mature to marginally overmature Lower Pliensbachian Rennell Junction Formation is exposed locally on central Graham Is-

**Figure 1:** Regional surface maturation patterns ( $\%Ro_{rand}$ ) of the Upper Triassic Sadler Limestone (grey limestone member) of the Kunga Group. Dashed contours are approximate.

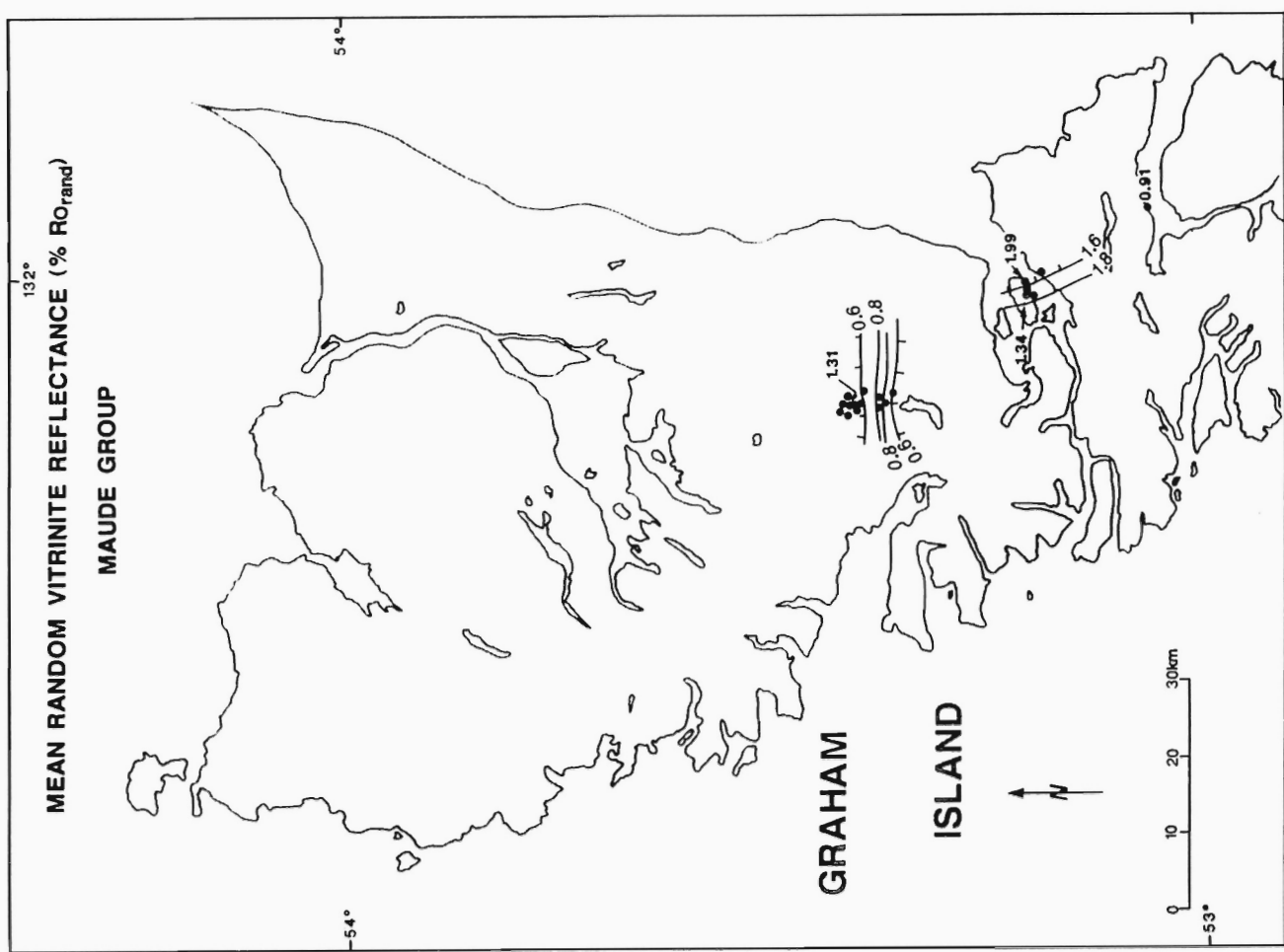


**Figure 2:** Regional surface maturation patterns ( $\%Ro_{rand}$ ) of the Upper Triassic Peril Formation (black limestone member) of the Kunga Group. Dashed contours are approximate. Labelled values do not fit regional trends and are not contoured. Tick marks on contour indicate decreasing maturation.



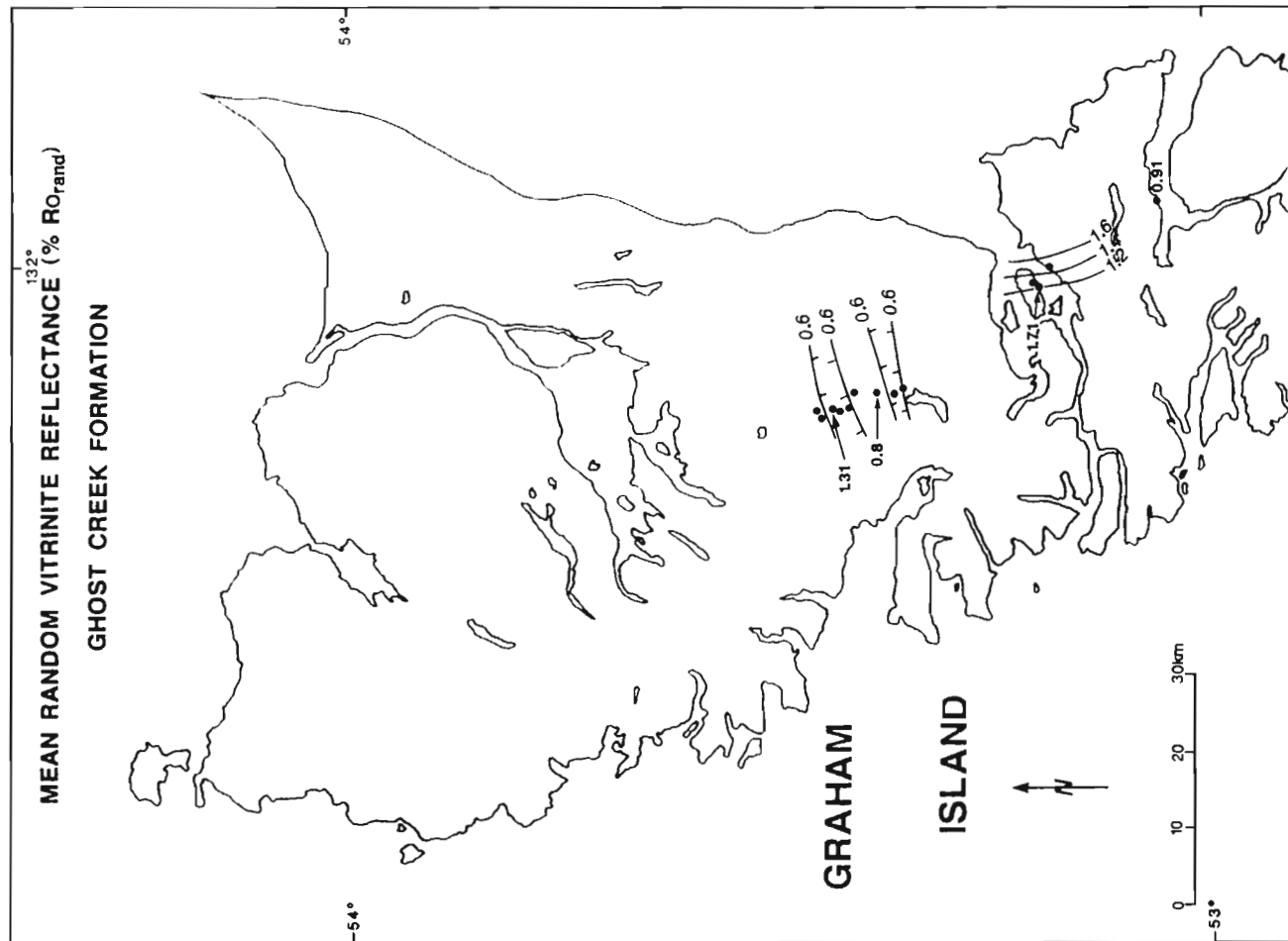


**Figure 3:** Regional surface maturation patterns ( $\%R_{o_{rand}}$ ) of the Sinemurian Sandilands Formation. Dashed contours are approximate. Labelled values do not fit regional trends and are not contoured. Tick marks on contour indicate decreasing maturation. Maturation gradient is  $0.65 \log (\%R_{o_{rand}})/\text{km}$ .

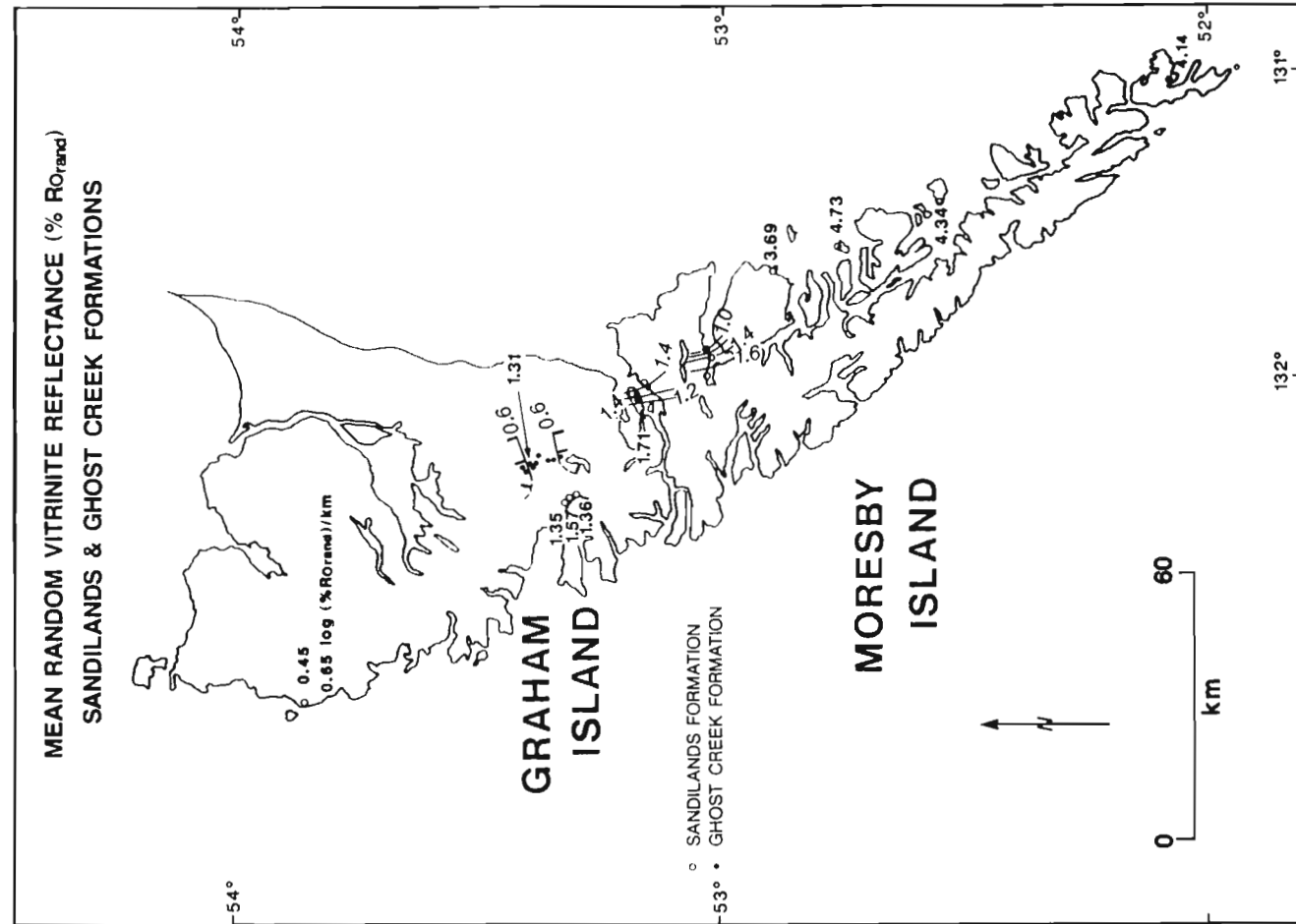


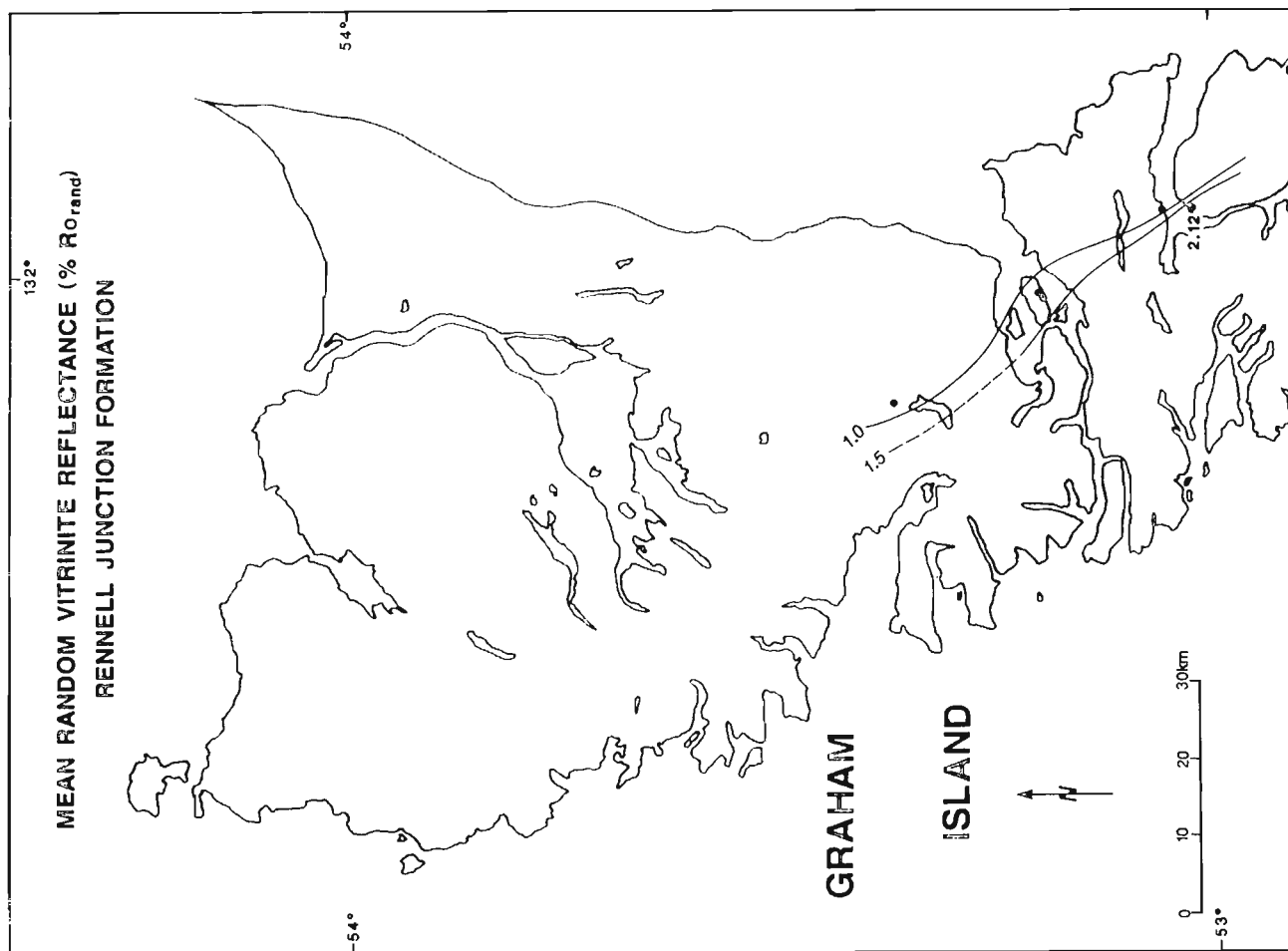
**Figure 4:** Regional surface maturation patterns ( $\%R_{o_{rand}}$ ) of the Lower Jurassic Maude Group. Labelled values do not fit regional trends and are not contoured. Tick marks on contour indicate decreasing maturation.

**Figure 5:** Regional surface maturation patterns ( $\%Ro_{rand}$ ) of the Lower Pliensbachian Ghost Creek Formation. Labelled values do not fit regional trends and are not contoured. Tick marks on contour indicate decreasing maturation.

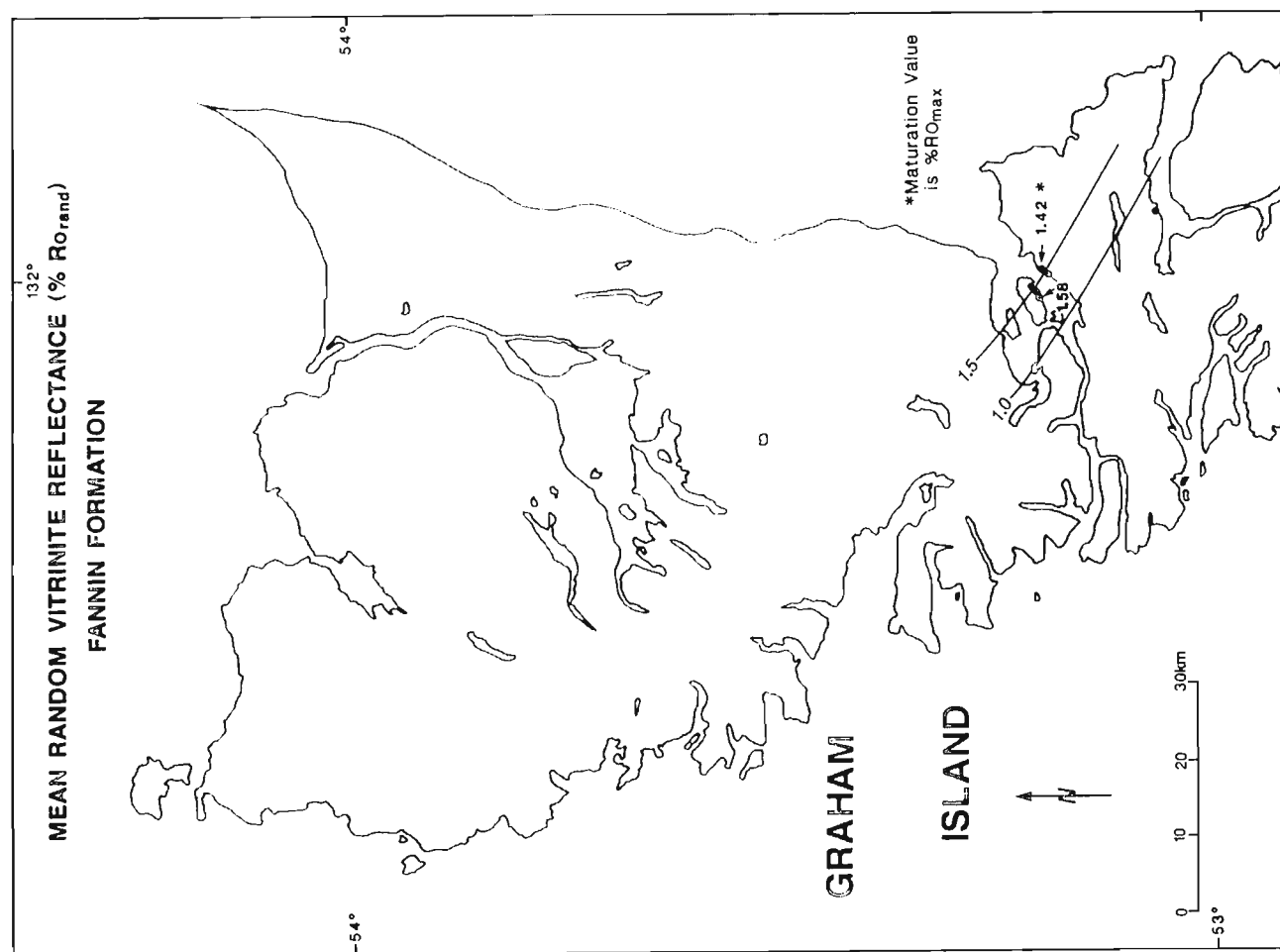


**Figure 6:** Regional surface maturation patterns ( $\%Ro_{rand}$ ) of the Sinemurian Sandilands and Lower Pliensbachian Ghost Creek formations. Dashed contours are approximate. Labelled values do not fit regional trends and are not contoured. Tick marks on contour indicate decreasing maturation. Maturation gradient is  $0.65 \log (\%Ro_{rand})/km$ .





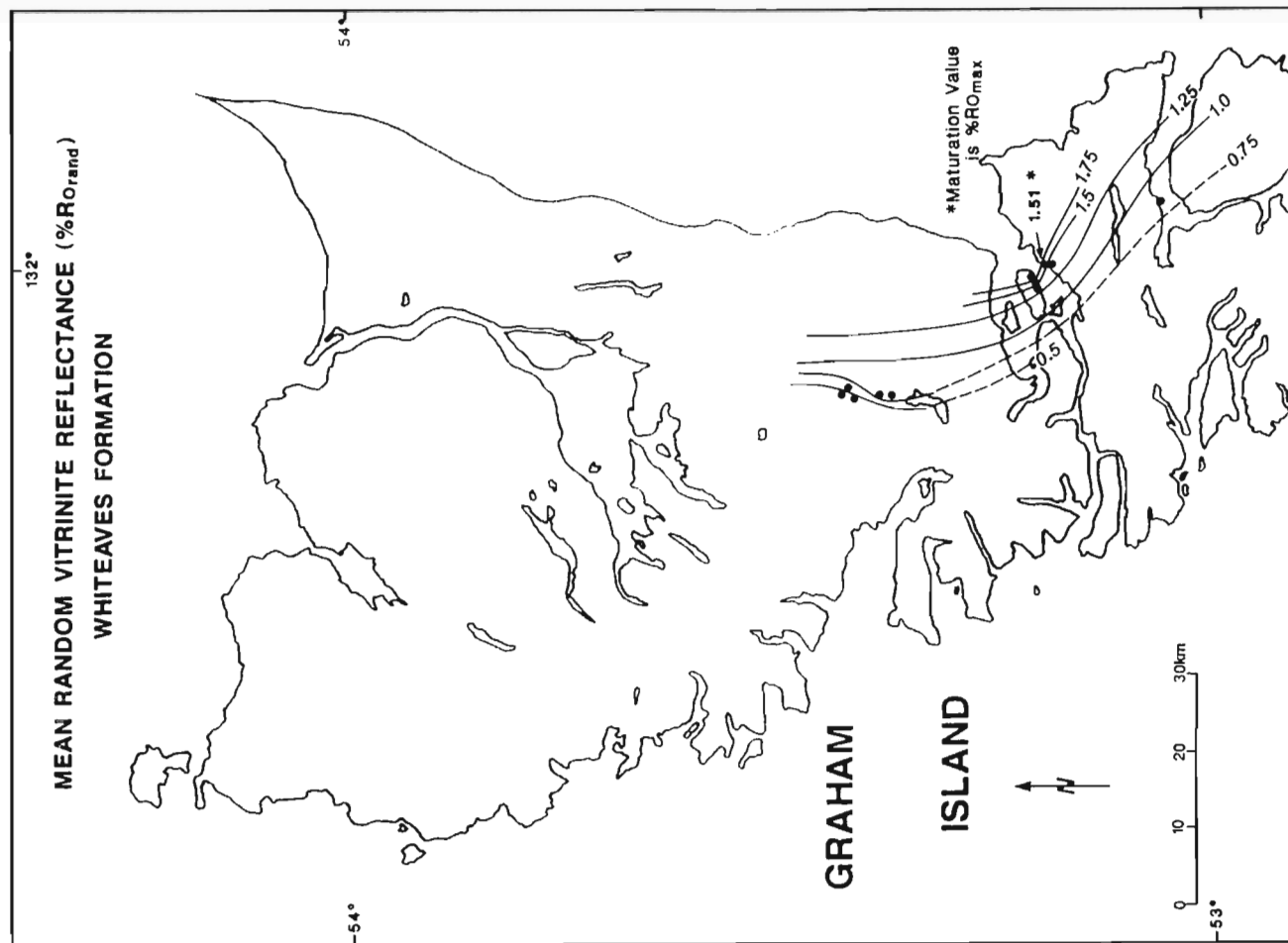
**Figure 7:** Regional surface maturation patterns (% $R_{0rand}$ ) of the Lower Pliensbachian Rennell Junction Formation. Dashed contours are approximate. Labelled values do not fit regional trends and are not contoured. Tick marks on contour indicate decreasing maturation.



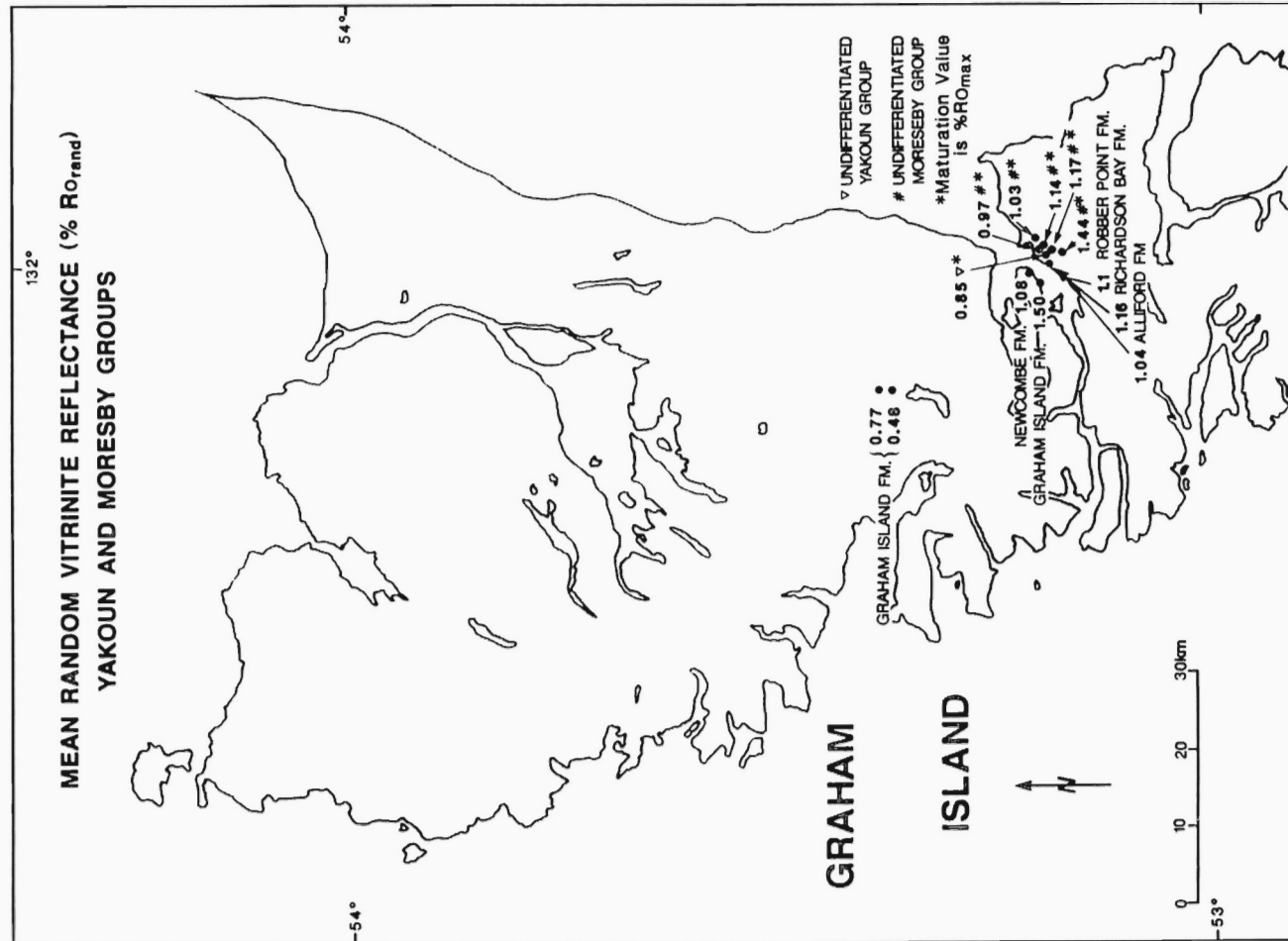
**Figure 8:** Regional surface maturation patterns (% $R_{0rand}$ ) of the Upper Pliensbachian to Lower Toarcian Fannin Formation. Labelled values do not fit regional trends and are not contoured.

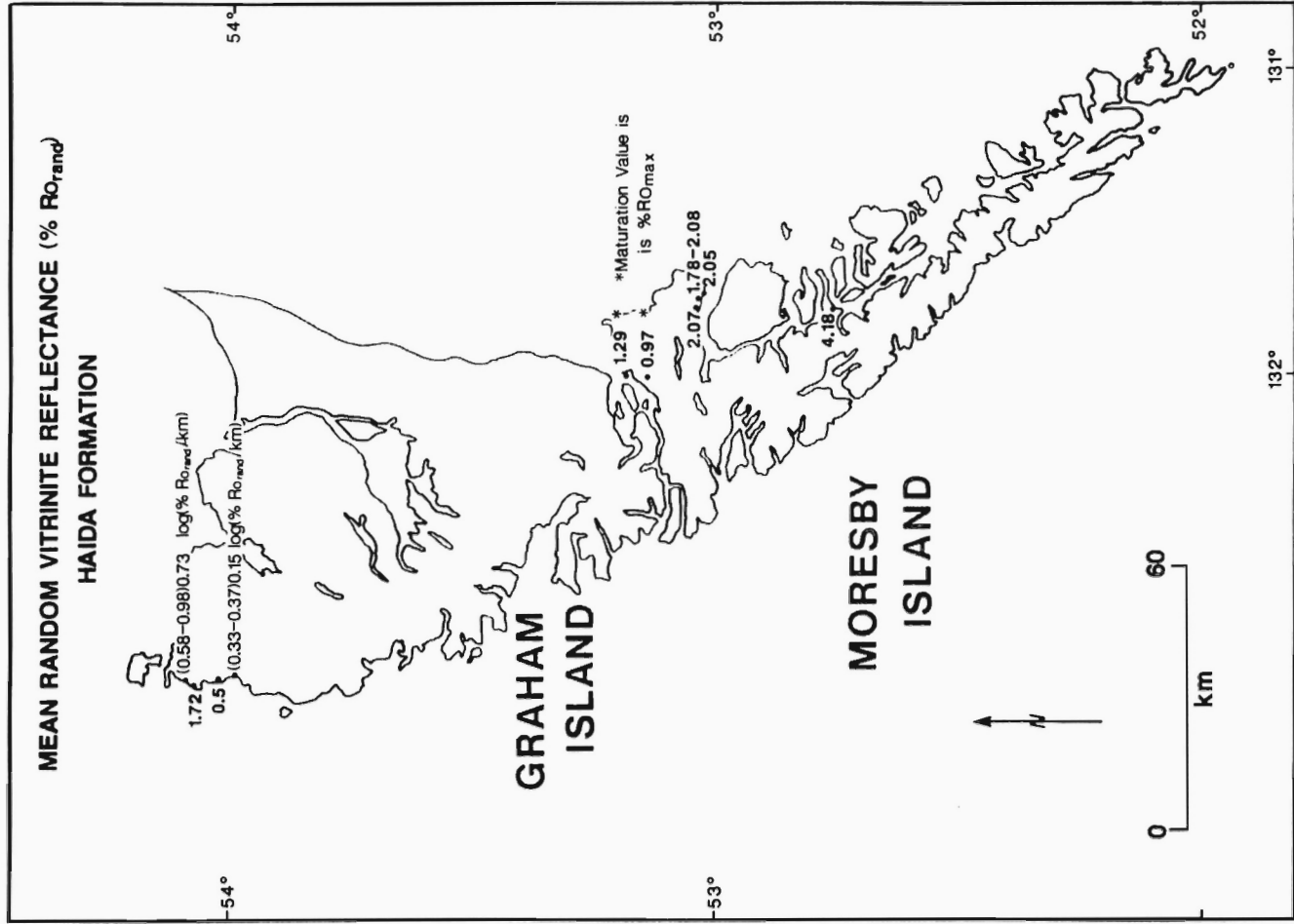


**Figure 9:** Regional surface maturation patterns ( $\%R_{o,rand}$ ) of the Middle Toarcian Whiteaves Formation. Dashed contours are approximate. Labelled values do not fit regional trends and are not contoured.

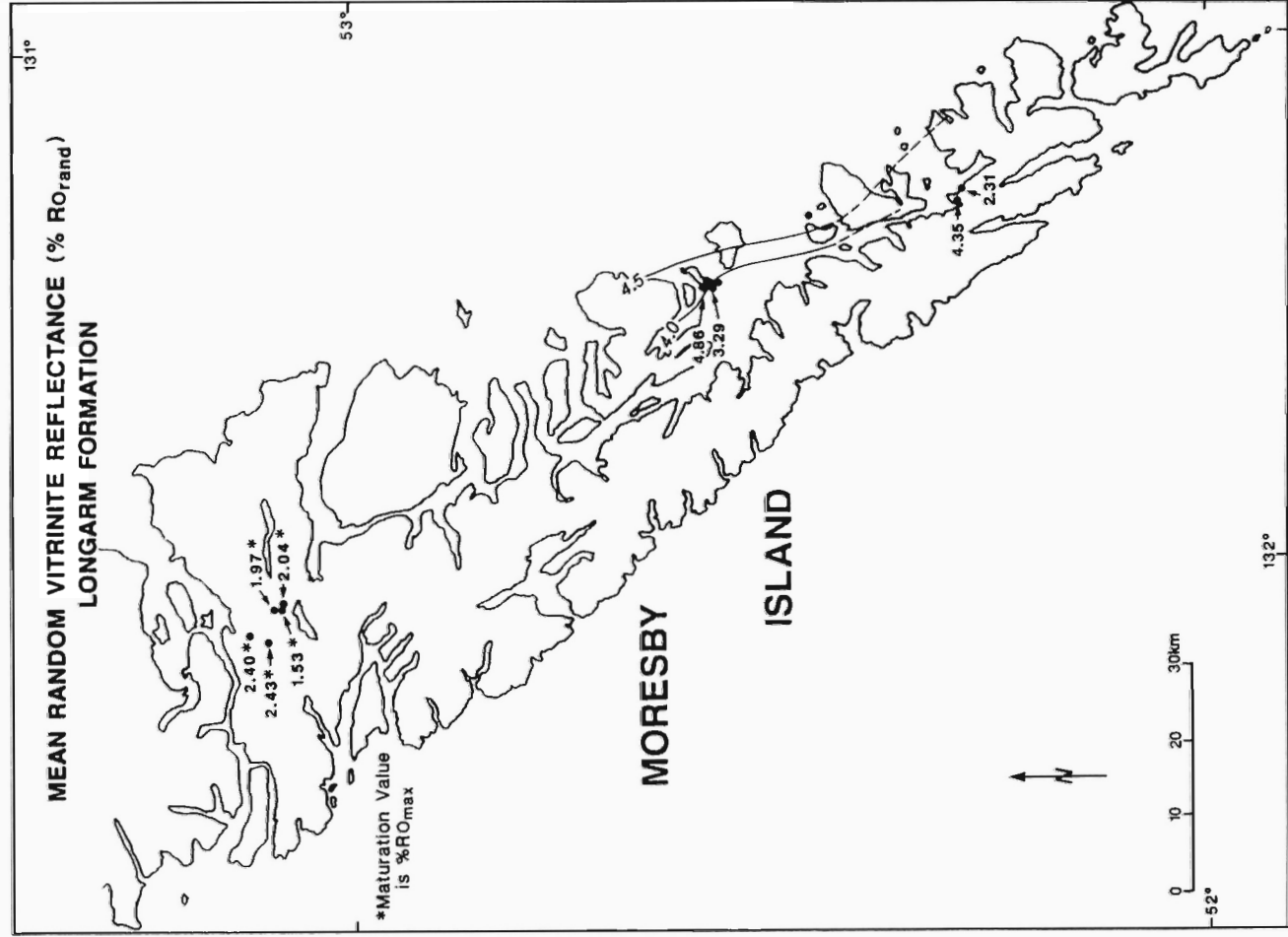


**Figure 10:** Regional surface maturation patterns ( $\%R_{o,rand}$ ) of the Lower Jurassic Yakoun and Moresby groups.



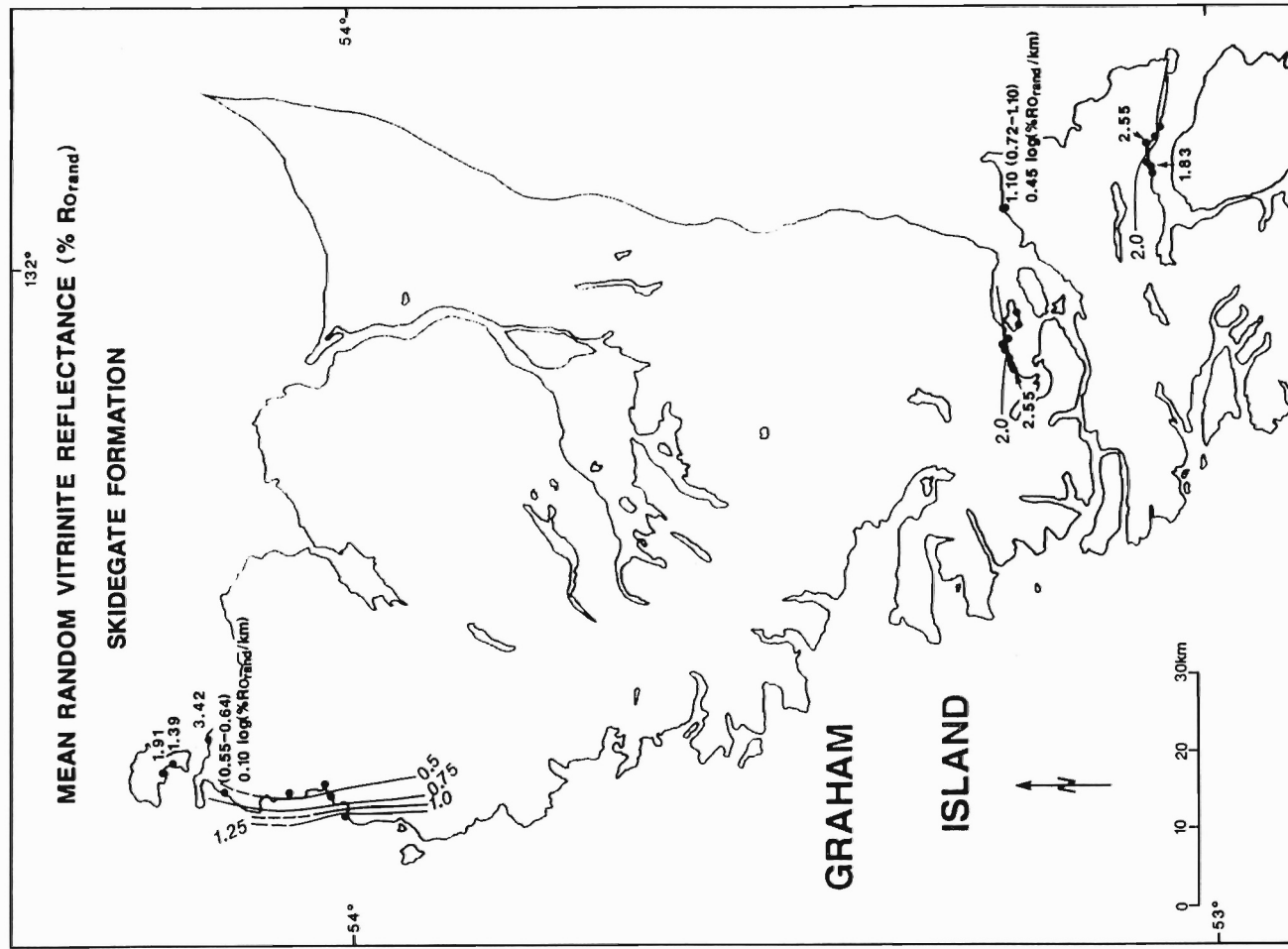


**Figure 12:** Regional surface maturation patterns (%RO<sub>rand</sub>) of the Albian Haida Formation. Values in brackets are minimum and maximum vitrinite reflectances. Maturation gradients are 0.73 and 0.15 log (%RO<sub>rand</sub>)/km.

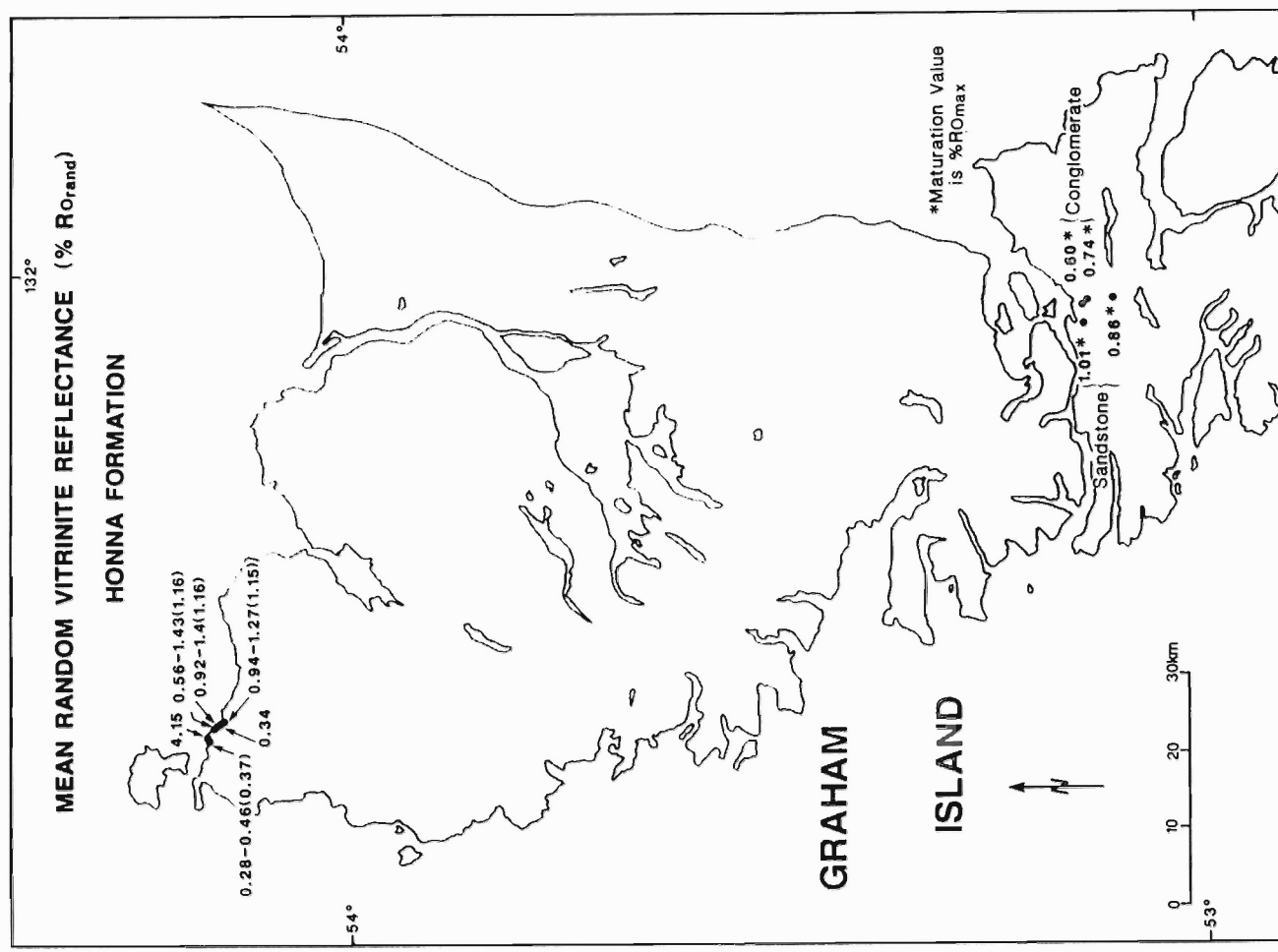


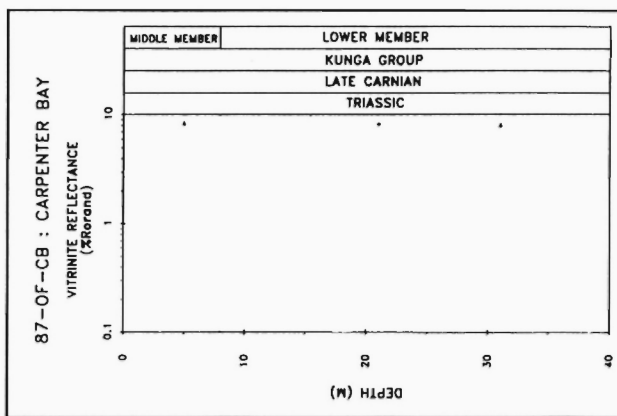
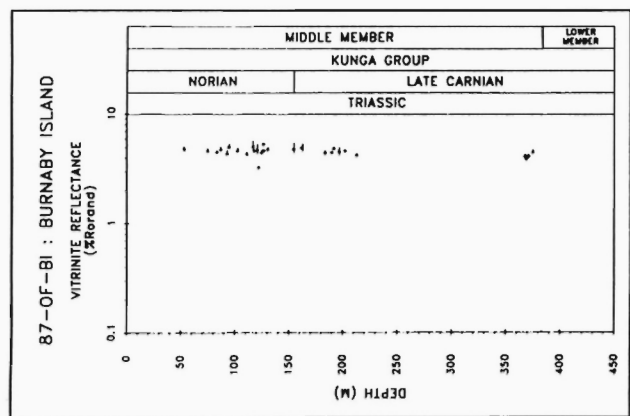
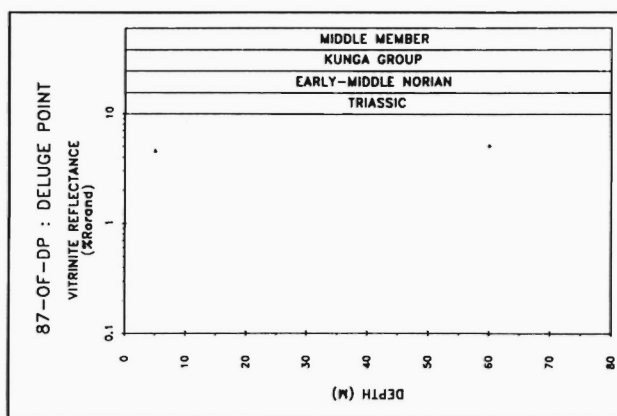
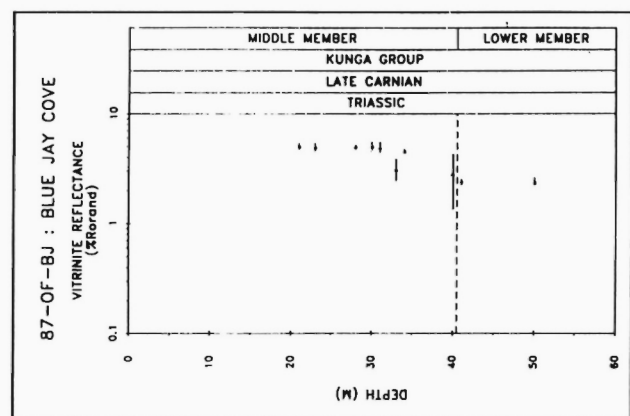
**Figure 11:** Regional surface maturation patterns (%RO<sub>rand</sub>) of the Upper Valanginian to Barremian Longarm Formation. Dashed contours are approximate. Labelled values do not fit regional trends and are not contoured.

**Figure 13:** Regional surface maturation patterns (%Ro<sub>rand</sub>) of the Cenomanian-Turonian Skidegate Formation. Values in brackets are minimum and maximum vitrinite reflectances. Maturation gradients are 0.10 and 0.45 log (%Ro<sub>rand</sub>)/km.

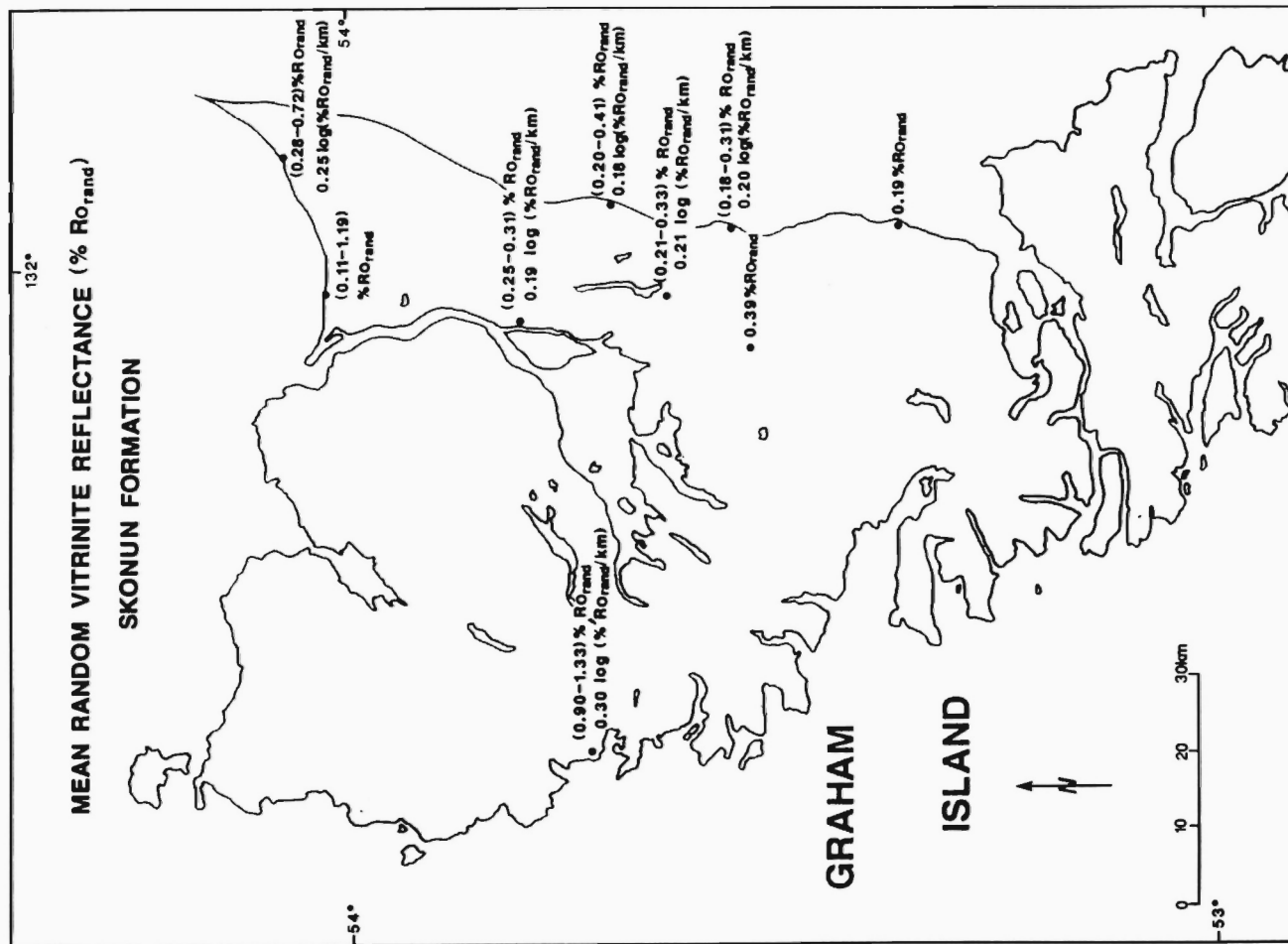


**Figure 14:** Regional surface maturation patterns (%Ro<sub>rand</sub>) of the Coniacian Honna Formation. Single numbers and numbers in brackets are mean random vitrinite reflectance values. Dashed values are minimum and maximum vitrinite reflectance values.



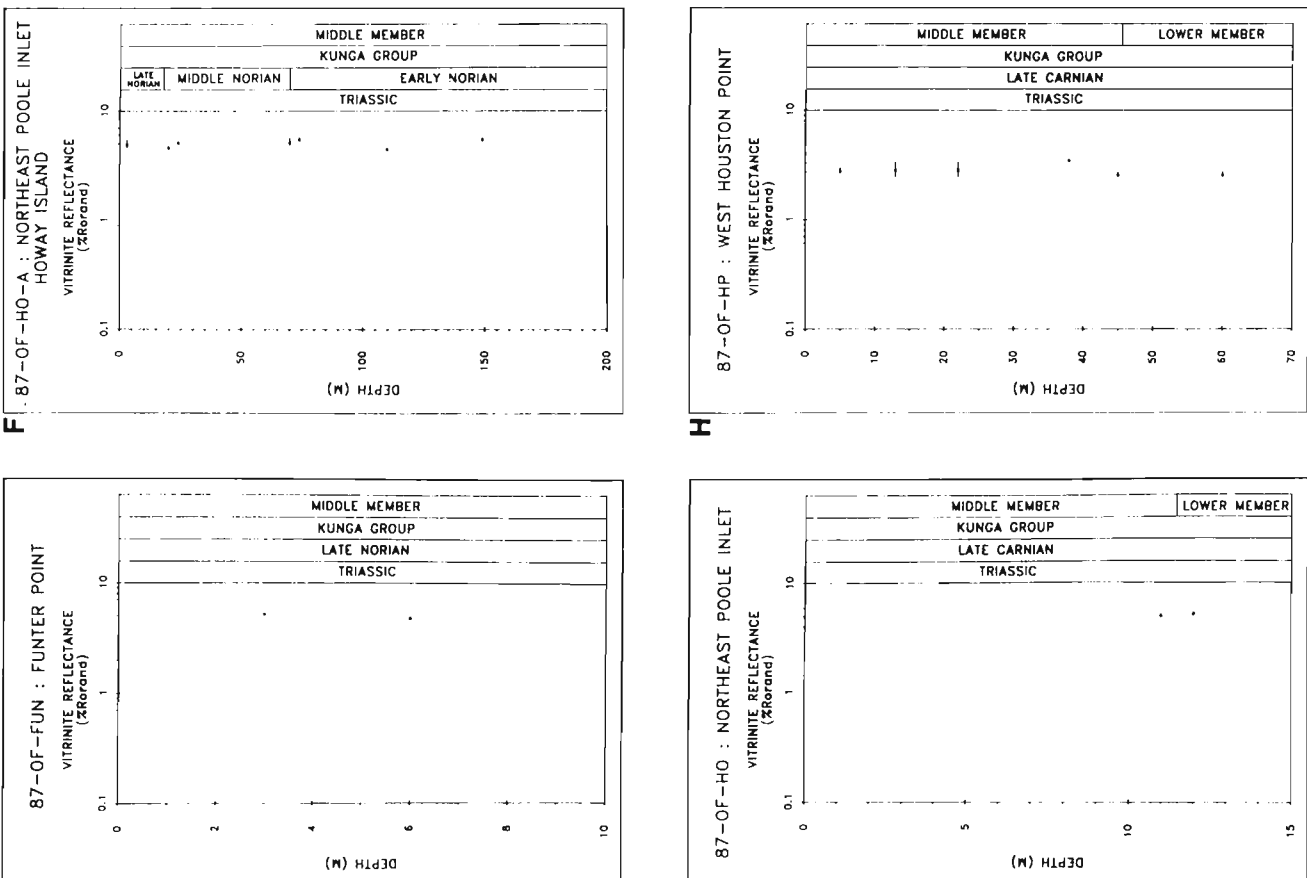


**Figure 16a-d:** Vertical maturation profiles [vitritine reflectance (% $R_{o rand}$ )/stratigraphic depth] for the Kunga Group: a) near Moresby Island at Burnaby Island; b) on Moresby Island at Blue Jay Cove; c) on Moresby Island at Carpenter Bay; d) on Moresby Island at Deluge Point. Points are mean random vitritine reflectance values. Error bars are mean  $\pm 1 \sigma$ .

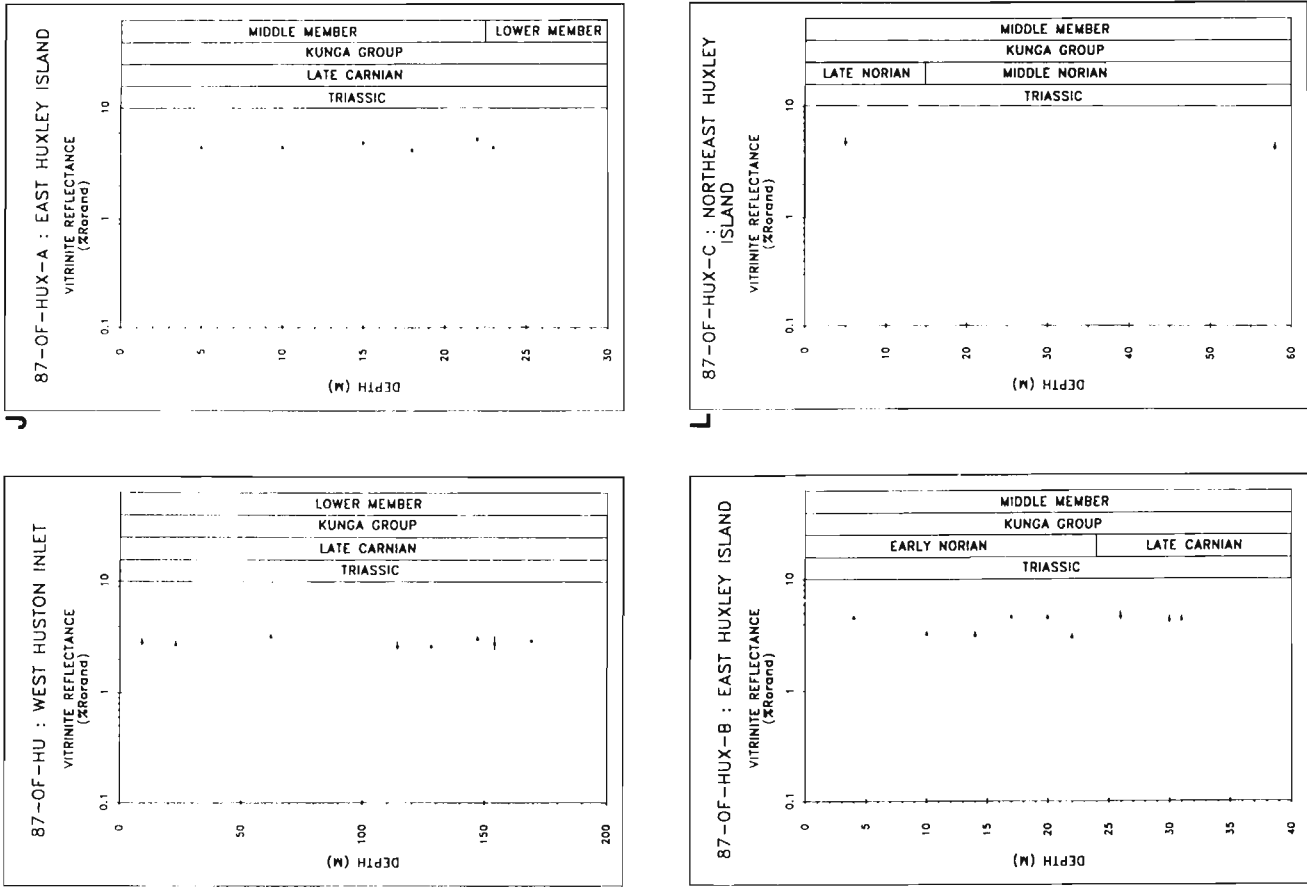


**Figure 15:** Regional surface maturation patterns (% $R_{o rand}$ ) of the Miocene-Pliocene Skonun Formation. Values in brackets are minimum and maximum vitritine reflectance values. Maturation gradients range from 0.18-0.30 log (% $R_{o rand}$ )/km.

**Figure 16e-h:** Vertical maturation profiles [vitrinite reflectance ( $\%Ro_{rand}$ )/stratigraphic depth] of the Kunga Group: e) on Moresby Island at Funter Point; f and g) on Moresby Island in north-east Poole Inlet at Howay Island; h) on Moresby Island at west Huston Inlet. Points are mean random vitrinite reflectance values. Error bars are mean  $\pm 1 \sigma$ .



**Figure 16i-l:** Vertical maturation profiles [vitrinite reflectance ( $\%Ro_{rand}$ )/stratigraphic depth] of the Kunga Group: i) on Moresby Island at west Huston Inlet; j and k) near Moresby Island on east Huxley Island; l) near Moresby Island on northeast Huxley Island. Points are mean random vitrinite reflectance values. Error bars are mean  $\pm 1 \sigma$ .



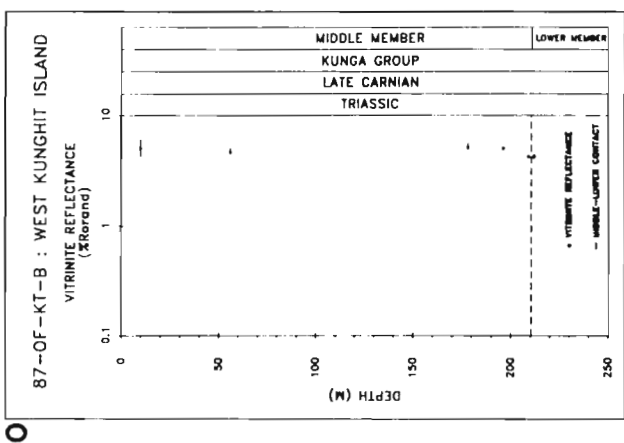
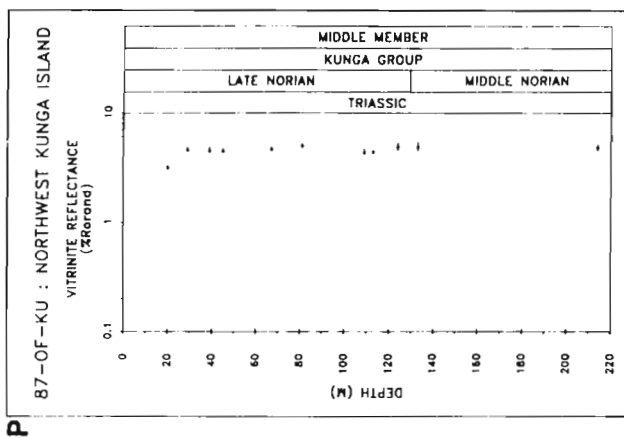
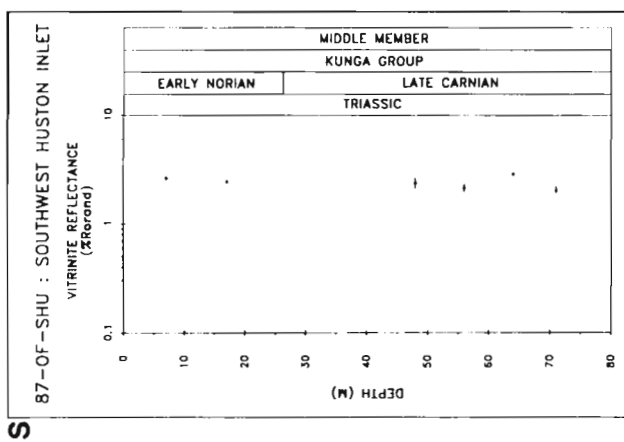
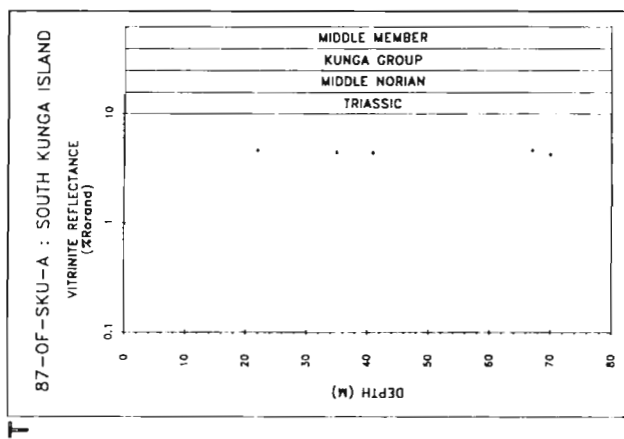
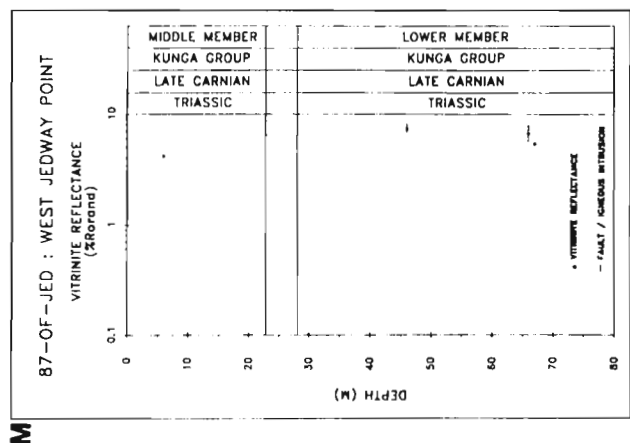
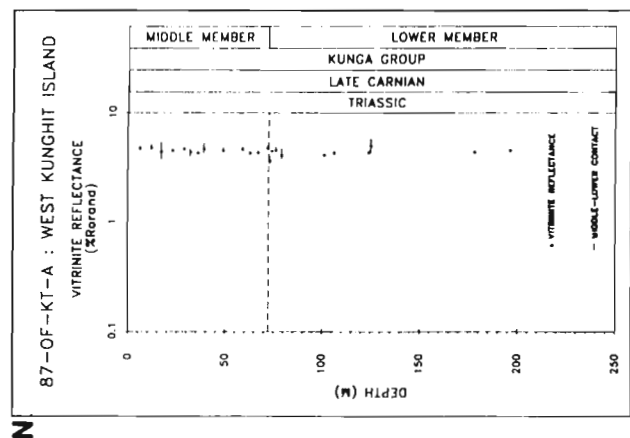
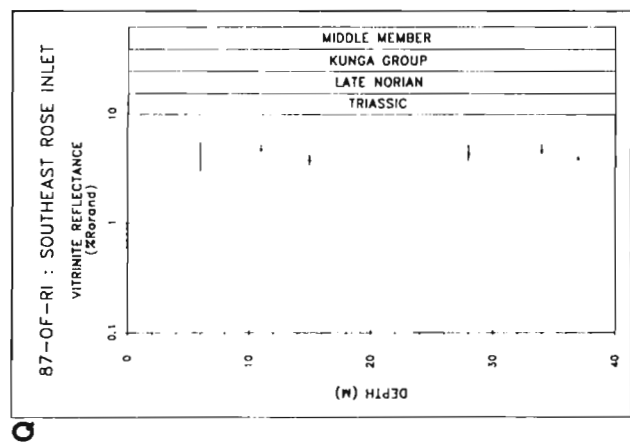
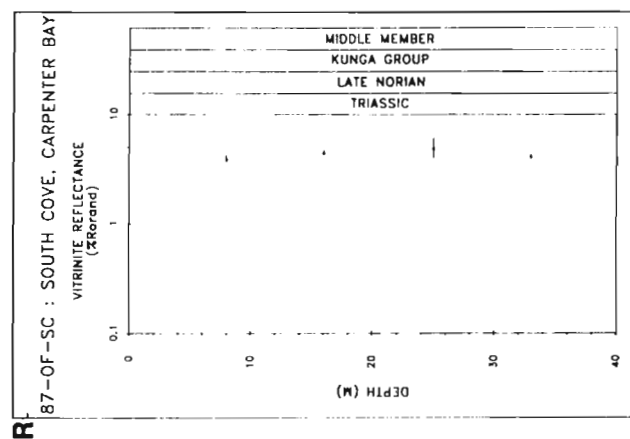
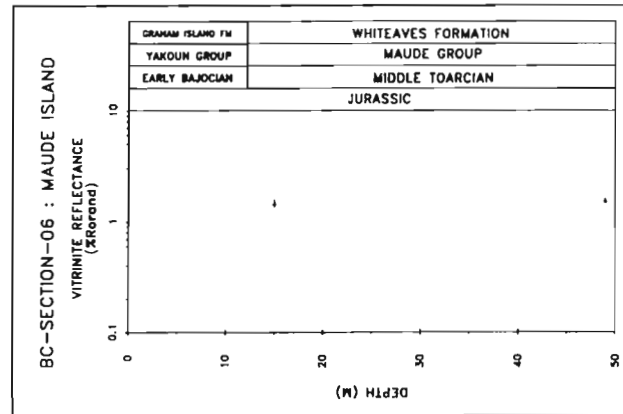
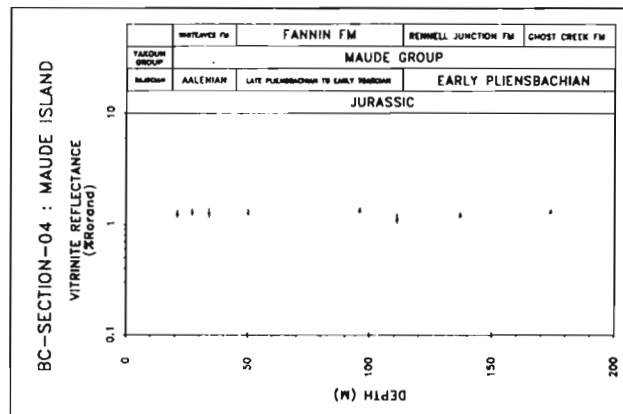
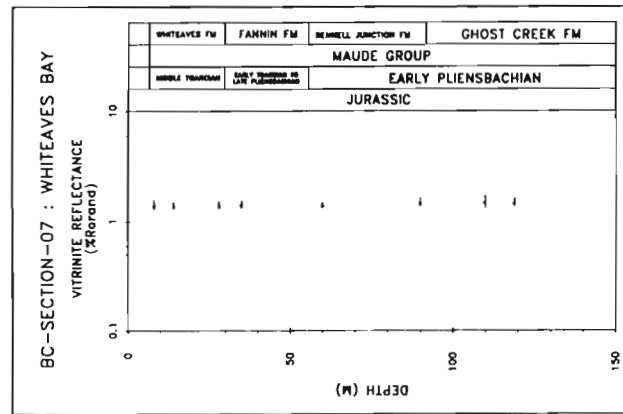
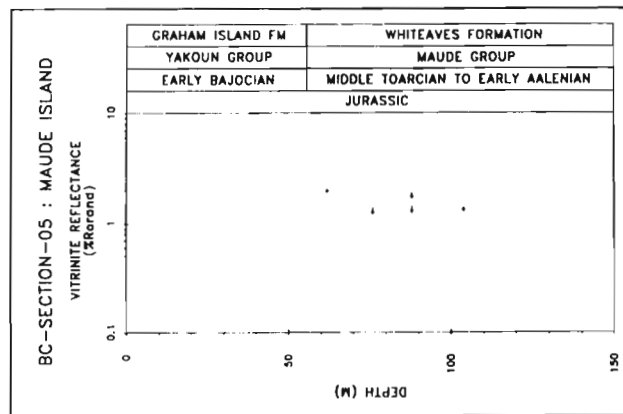


**Figure 16q-t:** Vertical maturation profiles [vitrinite reflectance ( $\%Ro_{rand}$ )/stratigraphic depth] of the Kunga Group; q) on Moresby Island at southeast Rose Inlet; r) on Moresby Island at South Cove in Carpenter Bay; s) on Moresby Island at southwest Huston Inlet; t) near Moresby Island on south Kunga Island. Points are mean vitrinite reflectance values. Error bars are mean  $\pm 1 \sigma$ .

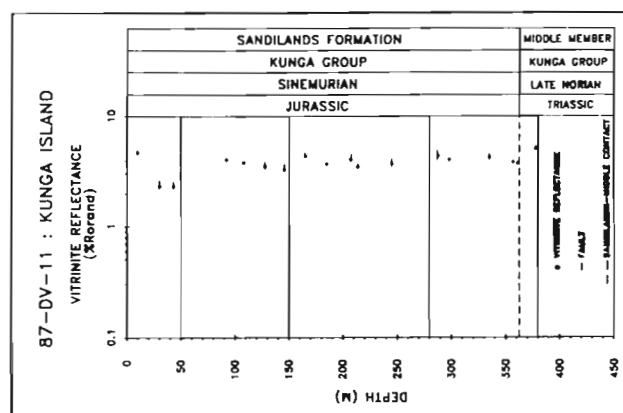
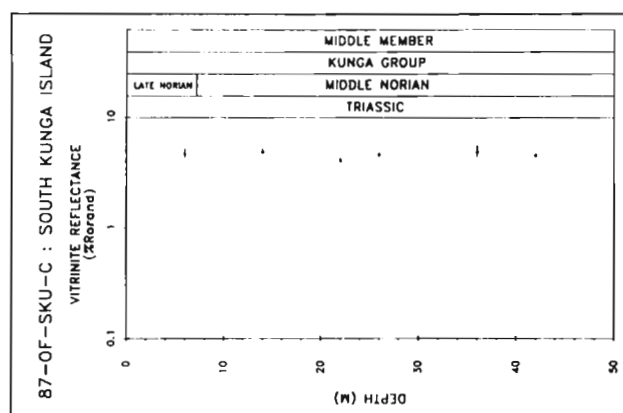
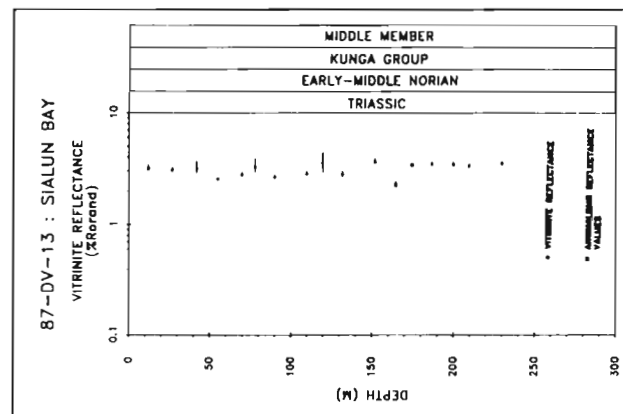
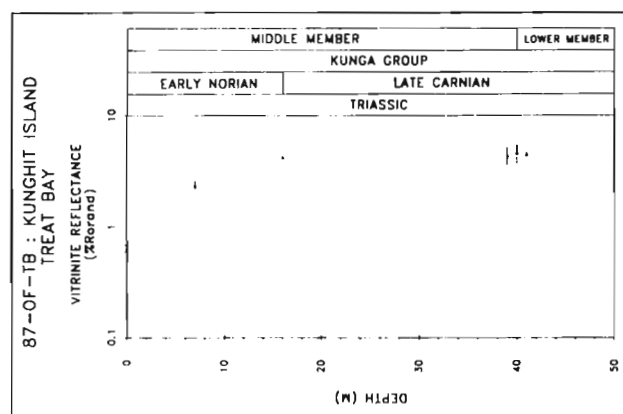
**Figure 16m-p:** Vertical maturation profiles [vitrinite reflectance ( $\%Ro_{rand}$ )/stratigraphic depth] of the Kunga Group; m) on Moresby Island at west Jedway Point; n) and o) near Moresby Island on west Kungshit Island; p) near Moresby Island at northwest Kunga Island. Points are mean random vitrinite reflectance values. Error bars are mean  $\pm 1 \sigma$ .

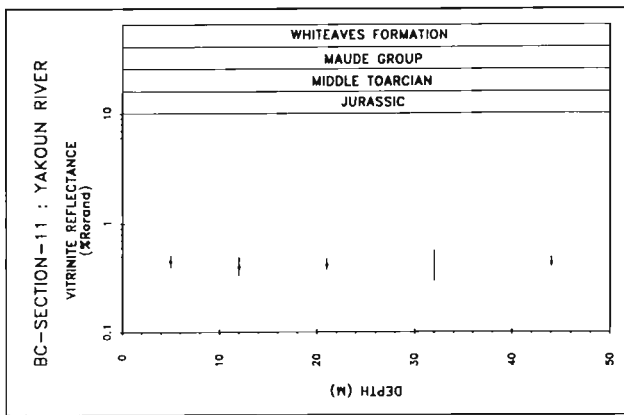
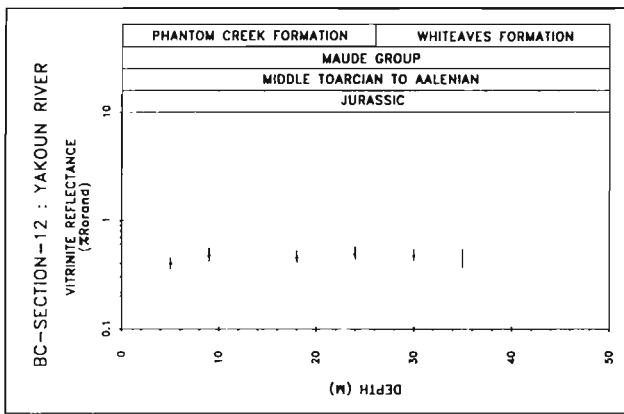
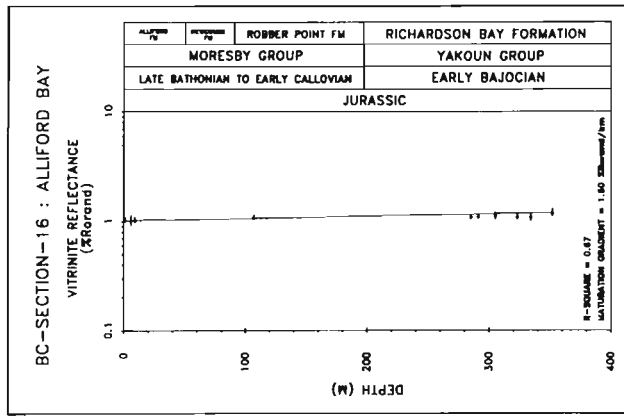
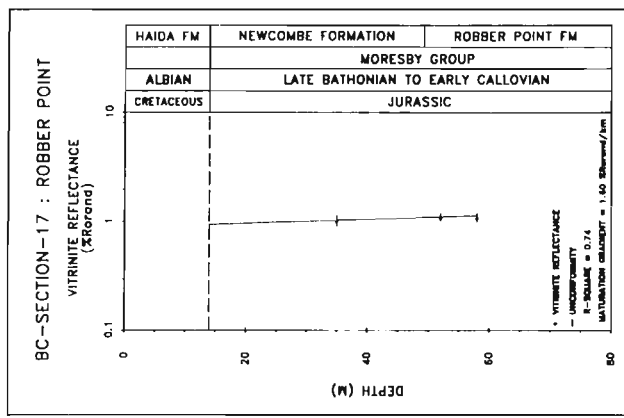
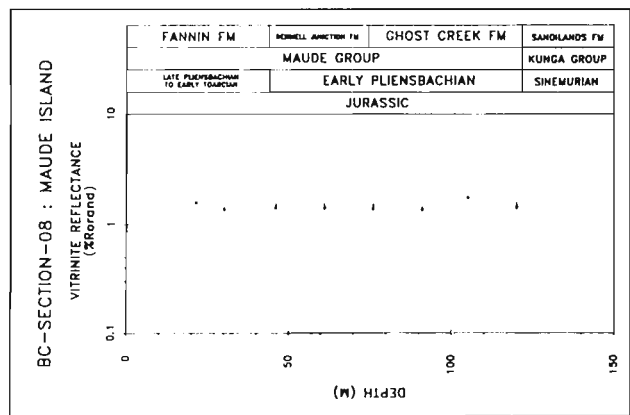
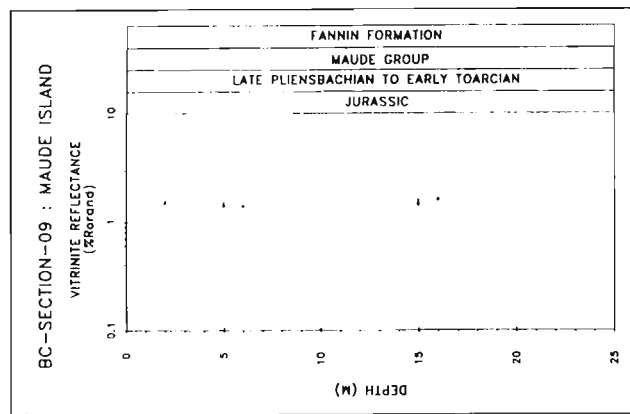
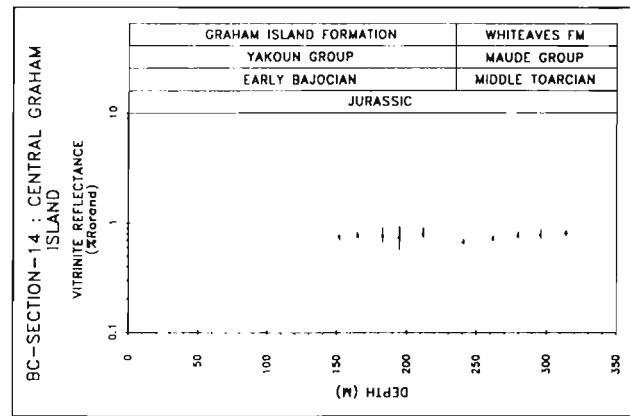
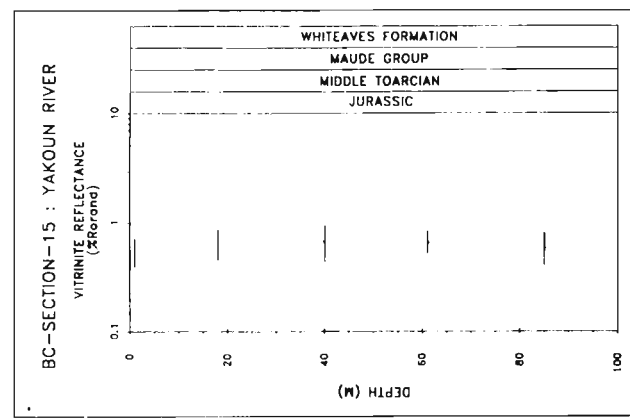


**Figure 17a-d:** Vertical maturation profiles [vitrinite reflectance (%Ro<sub>and</sub>)/stratigraphic depth] of the Maude Group; a-c) on Maude Island; d) in Skidegate Inlet at Whiteaves Bay. Points are mean random vitrinite reflectance values. Error bars are mean  $\pm 1 \sigma$ .



**Figure 16u-x:** Vertical maturation profiles [vitrinite reflectance (%Ro<sub>and</sub>)/stratigraphic depth] of the Upper Triassic to Sinemurian Kunga Group; u) near Moresby Island on south Kunga Island; v) near Moresby Island at Treat Bay on Kunghit Island; w) near Moresby Island on Kunga Island; x) on northwest Graham Island at Sialun Bay. Points are mean random vitrinite reflectance values. Error bars are mean  $\pm 1 \%$ .

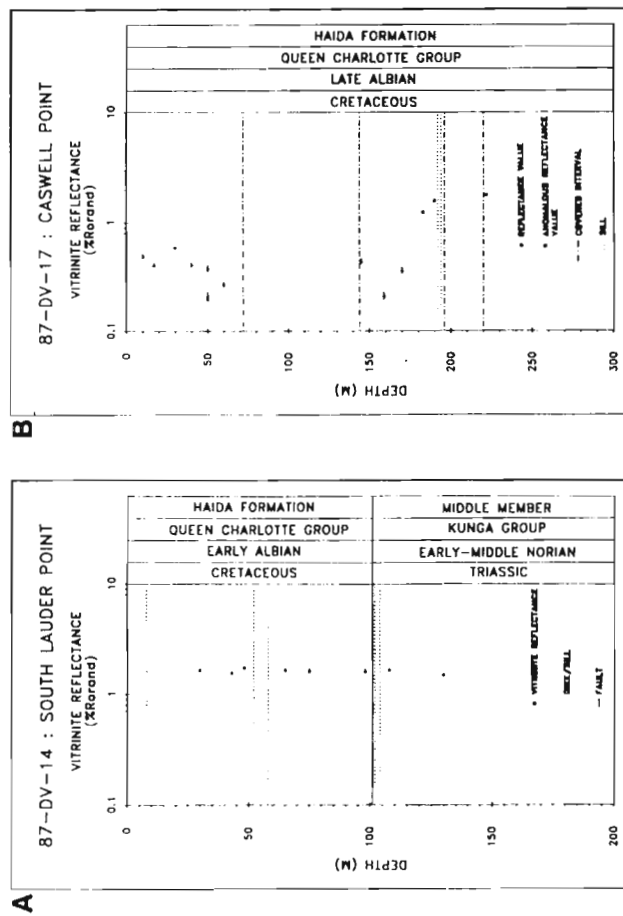




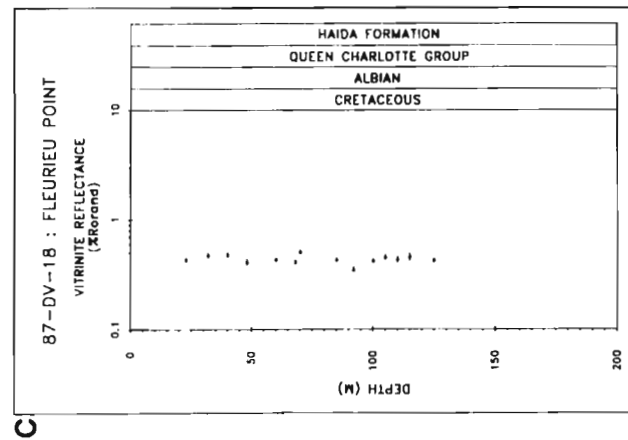
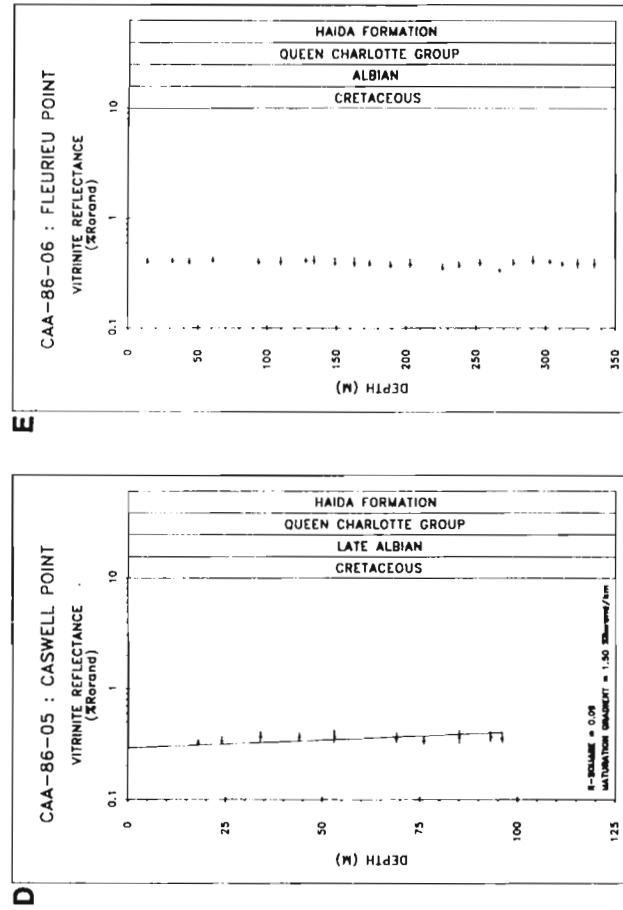
**Figure 17i-l:** Vertical maturation profiles [vitrinite reflectance (%Ro<sub>rand</sub>)/stratigraphic depth] of the Maude, Yakoun, and Moresby groups: i) in central Graham Island; j) in central Graham Island on the Yakoun River; k) in Skidegate Inlet at Alliford Bay; l) in Cumshewa Inlet at Robber Point. Points are mean random vitrinite reflectance values. Error bars are mean  $\pm 1 \sigma$ . Maturation gradient is log (%Ro<sub>rand</sub>)/km.

**Figure 17e-h:** Vertical maturation profiles [vitrinite reflectance (%Ro<sub>rand</sub>)/stratigraphic depth] of the Maude Group: e) and f) in Skidegate Inlet on Maude Island; g) and h) in central Graham Island on the Yakoun River. Points are mean random vitrinite reflectance values. Error bars are mean  $\pm 1 \sigma$ .

**Figure 18a-c:** Vertical maturation profiles [vitrinite reflectance ( $\%Ro_{rand}$ )/stratigraphic depth] of the Haida Formation; a) on northwest Graham Island at south Lauder Point; b) on northwest Graham Island at Caswell Point; c) on northwest Graham Island at Fleureieu Point. Points are mean random vitrinite reflectance values. Error bars are mean  $\pm 1 \sigma$ .



**Figure 18d-e:** Vertical maturation profiles [vitrinite reflectance ( $\%Ro_{rand}$ )/stratigraphic depth] of the Haida Formation; d) on northwest Graham Island at Caswell Point; e) on northwest Graham Island at Fleureieu Point. Points are mean random vitrinite reflectance values. Error bars are mean  $\pm 1 \sigma$ . Maturation gradient is  $\log (\%Ro_{rand})/\text{km}$ .



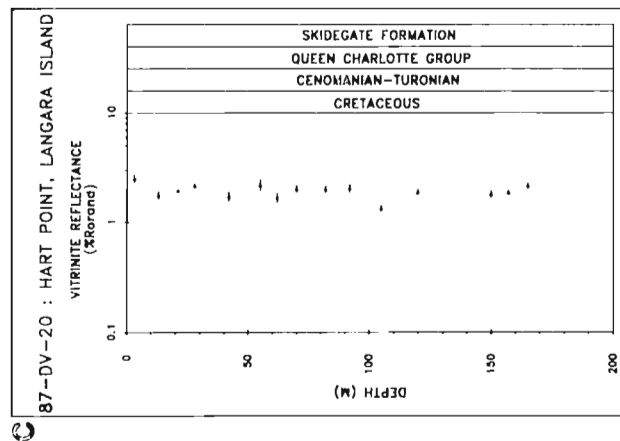
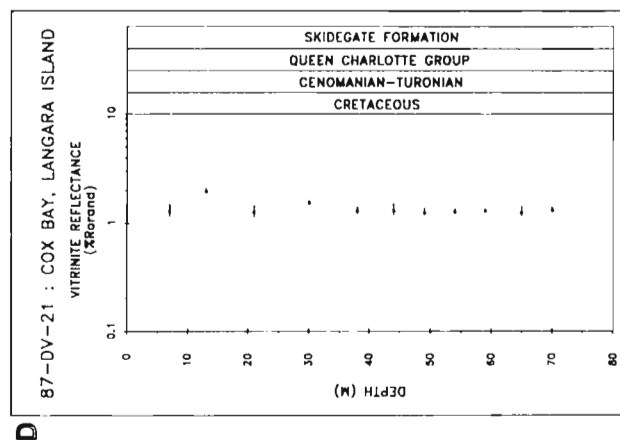
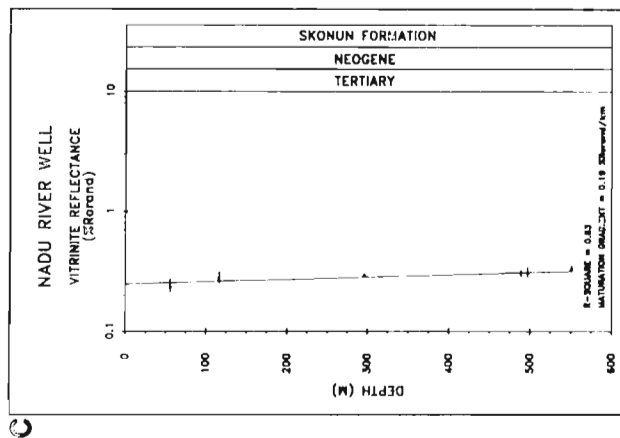
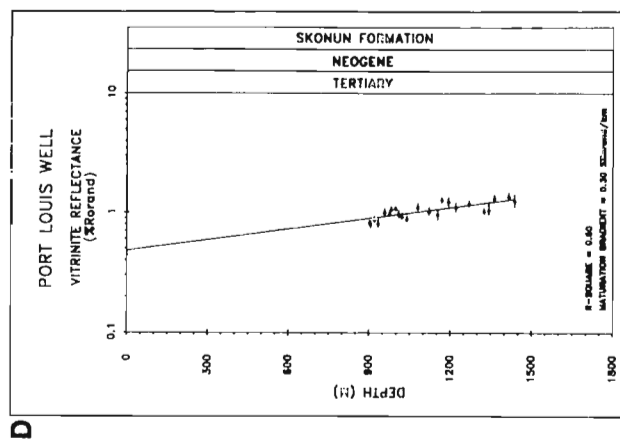
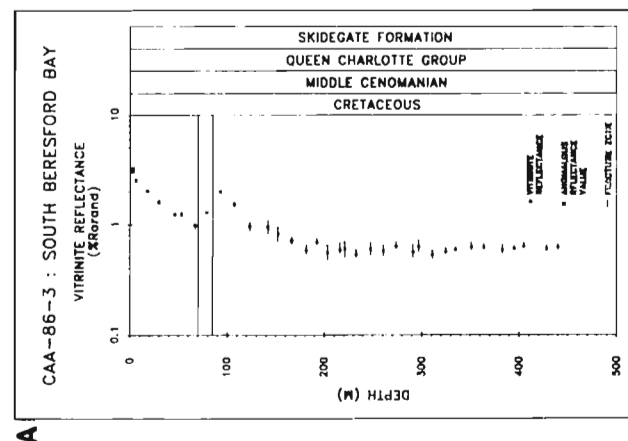
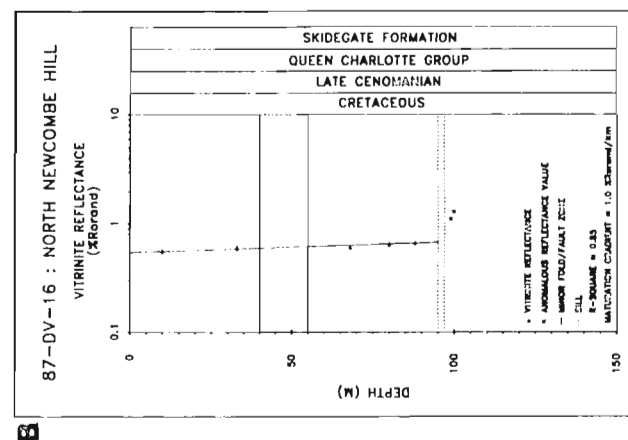
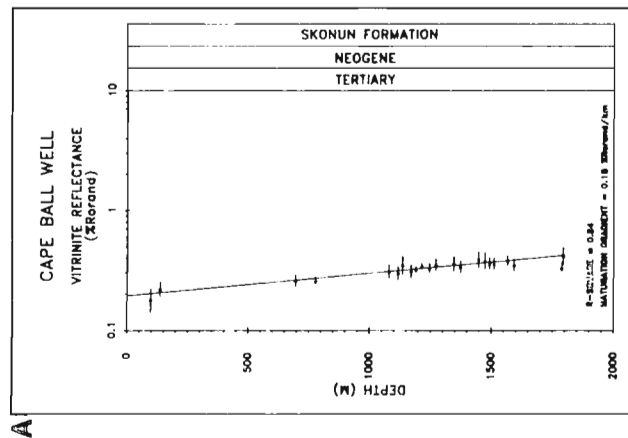
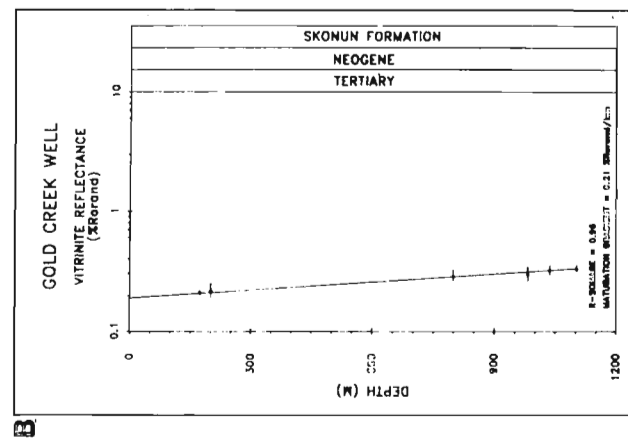


**Figure 20a-d:** Maturation gradients for the Skonun Formation. Points are mean random vitrinite reflectance values. Error bars are mean  $\pm 1 \sigma$ . Regression lines are calculated with a least square fit algorithm. R-square value represents the goodness of fit. Maturation gradient [log(% $R_{\text{rand}}$ )/km] is derived from the regression line; a) at the Cape Ball well; b) at the Gold Creek well; c) at the Nadu River well; d) at the Port Louis well.

**Figure 19:** Vertical maturation profiles [vitrinite reflectance (% $R_{\text{rand}}$ )/stratigraphic depth] of the Skidegate Formation; a) on northwest Graham Island at south Beresford Bay; b) on northwest Graham Island at north Newcombe Hill; c) on Langara Island at Hart Point; d) on Langara Island at Cox Bay. Points are mean random vitrinite reflectance values. Error bars are mean  $\pm 1 \sigma$ . Maturation gradient is log (% $R_{\text{rand}}$ )/km.

**Figure 20e-h:** Maturation gradients for the Skonun Formation. Points are mean random vitrinite reflectance values. Error bars are mean  $\pm 1\%$ . Regression lines are calculated with a least square fit algorithm. R-square value represents the goodness of fit. Maturation gradient [log(%Ro<sub>rand</sub>)/km] is derived from the regression line: e) and f) at the Tlell well. Maturation gradients for the Haida Formation; g) at north Lauder Point; h) at Onward Point.

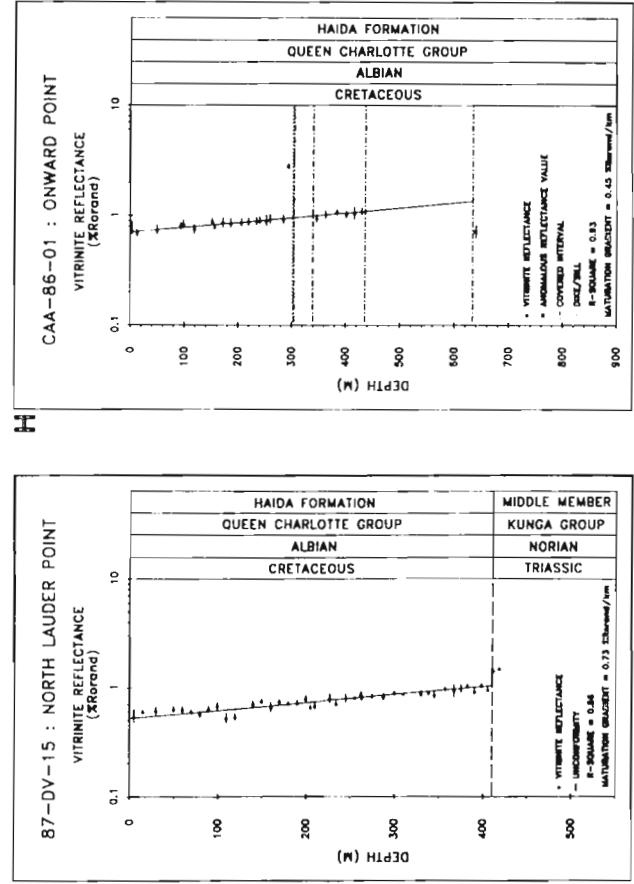
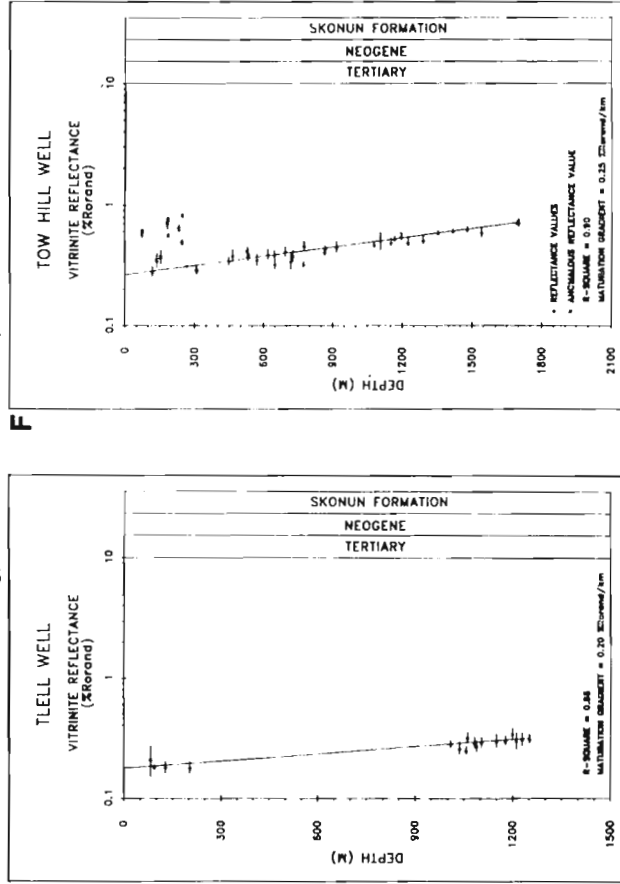


**Figure 20i-l:** Maturation gradients for the Maude and Yakoun groups. Points are mean random vitrinite reflectance values. Error bars are mean  $\pm 1\%$ . Regression lines are calculated with a least square fit algorithm. R-square value represents the goodness of fit. Maturation gradient [log(%Ro<sub>rand</sub>)/km] is derived from the regression line: i) at Cumshewa Inlet; j) at Rennell Junction. Maturation gradients for the Kunga Group: k) at Frederick Island; l) at Kennecott Point.

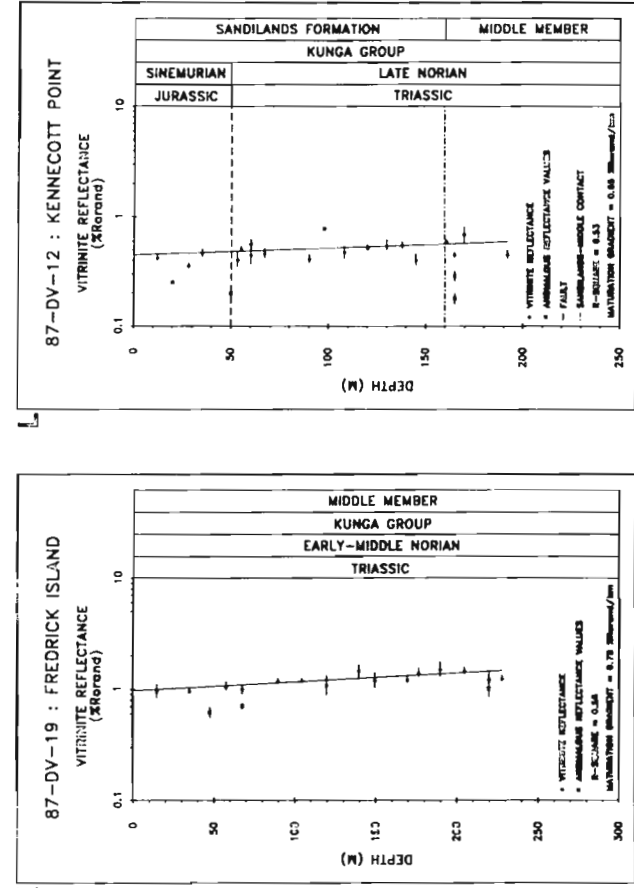
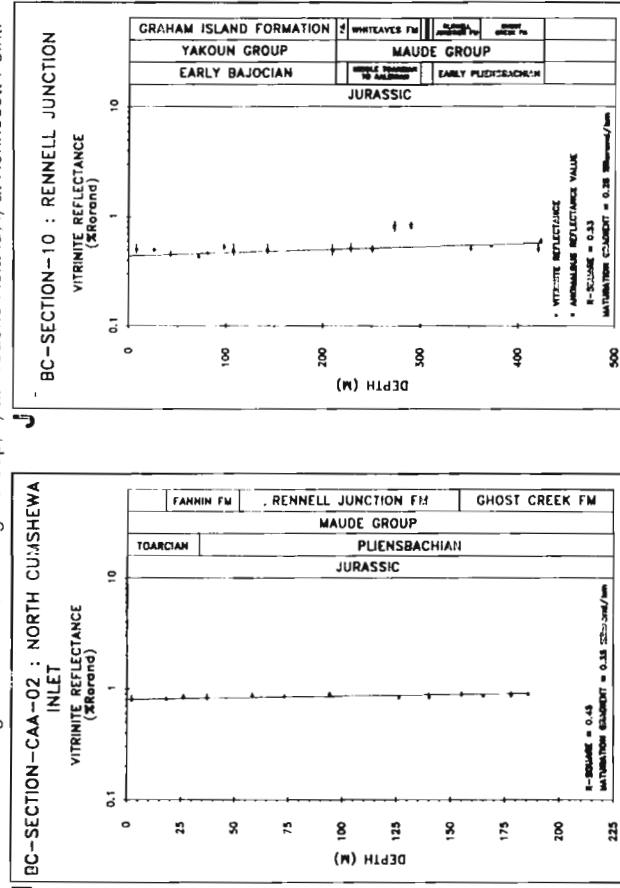


**Table 1:** Organic maturation and Rock-Eval data for Sadler Limestone

Section name	%Ro <sub>rand</sub>	Tmax	TOC	S1	S2	PI	QOM	HI	OI
OF section BB									
Mean	5.8	*	*	*	*	*	*	*	*
N	3.	0.	0.	0.	0.	0.	0.	0.	0.
OF section BI									
Mean	*	*	*	*	*	*	*	*	*
N	0.	0.	0.	0.	0.	0.	0.	0.	0.
OF section BJ									
Mean	2.35	*	*	*	*	*	*	*	*
N	1.	0.	0.	0.	0.	0.	0.	0.	0.
OF section BR									
Mean	2.72	*	*	*	*	*	*	*	*
N	4.	0.	0.	0.	0.	0.	0.	0.	0.
OF section CB									
Mean	8.	*	*	*	*	*	*	*	*
N	2.	0.	0.	0.	0.	0.	0.	0.	0.
OF section CRE									
Mean	4.59	*	*	*	*	*	*	*	*
N	1.	0.	0.	0.	0.	0.	0.	0.	0.
OF section HP									
Mean	2.61	*	*	*	*	*	*	*	*
N	1.	0.	0.	0.	0.	0.	0.	0.	0.
OF section HU									
Mean	2.91	*	*	*	*	*	*	*	*
N	8.	0.	0.	0.	0.	0.	0.	0.	0.
OF section JED									
Mean	6.56	*	*	*	*	*	*	*	*
N	3.	0.	0.	0.	0.	0.	0.	0.	0.
OF section KT									
Mean	4.39	*	*	*	*	*	*	*	*
N	10.	0.	0.	0.	0.	0.	0.	0.	0.
OF section TB									
Mean	4.38	*	*	*	*	*	*	*	*
N	4.	0.	0.	0.	0.	0.	0.	0.	0.
OF section TIT									
Mean	5.28	*	*	*	*	*	*	*	*
N	1.	0.	0.	0.	0.	0.	0.	0.	0.
Section 1									
Mean	*	*	1.1	0.01	0.03	0.08	0.02	2.	35.
N	0.	0.	3.	3.	3.	3.	3.	3.	3.
Section 3									
Mean	*	*	0.18	0.	0.	0.	0.	0.	33.
N	0.	0.	1.	1.	1.	1.	1.	1.	1.
Section 6									
Mean	*	*	0.06	0.	0.	0.	0.	0.	48.
N	0.	0.	6.	6.	6.	6.	6.	6.	6.
Section 7									
Mean	*	*	0.28	0.	0.	0.	0.01	0.	26.
N	0.	0.	4.	4.	4.	4.	4.	4.	4.
Section 8									
Mean	*	*	0.24	0.	0.02	0.	0.08	8.	24.
N	0.	0.	4.	4.	4.	4.	4.	4.	4.
Section 9									
Mean	*	*	0.06	0.	0.	0.	0.	0.	0.
N	0.	0.	1.	1.	1.	1.	1.	1.	1.
Section 10									
Mean	*	*	0.06	0.	0.	0.	0.	0.	0.
N	0.	0.	1.	1.	1.	1.	1.	1.	1.
Spot sample									
Mean	*	*	0.10	0.	0.	0.	0.	0.	132.
N	0.	0.	5.	5.	5.	5.	5.	5.	5.
TF Spot sample									
Mean	2.95	*	0.	0.	0.	*	0.	0.	0.
N	3.	0.	3.	3.	3.	0.	3.	3.	3.

TOC=total organic carbon; PI=production index; QOM=quality of organic matter; HI=hydrogen index; OI=oxygen index. N=number of samples. Values represent means calculated across each outcrop section.

**Table 2:** Organic maturation and Rock-Eval data for Peril Formation

Section name	%Ro <sub>rand</sub>	Tmax	TOC	S1	S2	PI	QOM	HI	OI
OF section B1									
Mean	4.56	*	*	*	*	*	*	*	*
N	28.	0.	0.	0.	0.	0.	0.	0.	0.
OF section BJ									
Mean	4.09	*	*	*	*	*	*	*	*
N	10.	0.	0.	0.	0.	0.	0.	0.	0.
OF section CB									
Mean	8.31	*	*	*	*	*	*	*	*
N	1.	0.	0.	0.	0.	0.	0.	0.	0.
OF section CRE									
Mean	4.59	*	*	*	*	*	*	*	*
N	1.	0.	0.	0.	0.	0.	0.	0.	0.
OF section DP									
Mean	4.84	*	*	*	*	*	*	*	*
N	2.	0.	0.	0.	0.	0.	0.	0.	0.
OF section EPO									
Mean	4.81	*	*	*	*	*	*	*	*
N	1.	0.	0.	0.	0.	0.	0.	0.	0.
OF section FUN									
Mean	5.05	*	*	*	*	*	*	*	*
N	2.	0.	0.	0.	0.	0.	0.	0.	0.
OF section GB									
Mean	3.13	*	*	*	*	*	*	*	*
N	2.	0.	0.	0.	0.	0.	0.	0.	0.
OF section HO									
Mean	5.08	*	*	*	*	*	*	*	*
N	9.	0.	0.	0.	0.	0.	0.	0.	0.
OF section HP									
Mean	2.94	*	*	*	*	*	*	*	*
N	5.	0.	0.	0.	0.	0.	0.	0.	0.
OF section HUX									
Mean	4.33	*	*	*	*	*	*	*	*
N	19.	0.	0.	0.	0.	0.	0.	0.	0.
OF section JED									
Mean	4.23	*	*	*	*	*	*	*	*
N	1.	0.	0.	0.	0.	0.	0.	0.	0.
OF section KT									
Mean	4.66	*	*	*	*	*	*	*	*
N	18.	0.	0.	0.	0.	0.	0.	0.	0.
OF section KU									
Mean	4.56	*	*	*	*	*	*	*	*
N	12.	0.	0.	0.	0.	0.	0.	0.	0.
OF section LUX									
Mean	4.63	*	*	*	*	*	*	*	*
N	1.	0.	0.	0.	0.	0.	0.	0.	0.
OF section NPO									
Mean	4.62	*	*	*	*	*	*	*	*
N	3.	0.	0.	0.	0.	0.	0.	0.	0.
OF section POO									
Mean	3.53	*	*	*	*	*	*	*	*
N	5.	0.	0.	0.	0.	0.	0.	0.	0.
OF section RH									
Mean	5.6	*	*	*	*	*	*	*	*
N	2.	0.	0.	0.	0.	0.	0.	0.	0.
OF section RI									
Mean	4.37	*	*	*	*	*	*	*	*
N	6.	0.	0.	0.	0.	0.	0.	0.	0.
OF section ROSS									
Mean	4.87	*	*	*	*	*	*	*	*
N	2.	0.	0.	0.	0.	0.	0.	0.	0.



**Table 2 (cont'd):** Organic maturation and Rock-Eval data for Peril Formation

Section name	%Ro <sub>rand</sub>	Tmax	TOC	S1	S2	PI	QOM	HI	OI
OF section SC									
Mean	4.35	*	*	*	*	*	*	*	*
N	5.	0.	0.	0.	0.	0.	0.	0.	0.
OF section SHU									
Mean	2.4	*	*	*	*	*	*	*	*
N	6.	0.	0.	0.	0.	0.	0.	0.	0.
OF section SI									
Mean	4.1	*	*	*	*	*	*	*	*
N	4.	0.	0.	0.	0.	0.	0.	0.	0.
OF section SK									
Mean	3.78	*	*	*	*	*	*	*	*
N	3.	0.	0.	0.	0.	0.	0.	0.	0.
OF section SKU									
Mean	4.58	*	*	*	*	*	*	*	*
N	13.	0.	0.	0.	0.	0.	0.	0.	0.
OF section SPO									
Mean	3.89	*	*	*	*	*	*	*	*
N	1.	0.	0.	0.	0.	0.	0.	0.	0.
OF section TB									
Mean	2.37	*	*	*	*	*	*	*	*
N	1.	0.	0.	0.	0.	0.	0.	0.	0.
OF section VP									
Mean	3.85	*	*	*	*	*	*	*	*
N	1.	0.	0.	0.	0.	0.	0.	0.	0.
Section 1									
Mean	*	*	0.82	0.	0.	0.	0.01	0.	32.
N	0.	0.	8.	8.	8.	8.	8.	8.	8.
Section 2									
Mean	*	*	0.9	0.	0.01	0.	0.	0.	231.
N	0.	0.	5.	5.	5.	5.	5.	5.	5.
Section 3									
Mean	*	*	1.02	0.	0.	0.	0.01	1.	13.
N	0.	0.	8.	8.	8.	8.	8.	8.	8.
Section 4									
Mean	3.64	*	2.21	0.	0.05	0.03	0.05	16.	13.
N	3.	0.	4.	4.	4.	4.	4.	4.	4.
Section 7									
Mean	*	*	0.41	0.	0.	0.	0.	0.	3.
N	0.	0.	3.	3.	3.	3.	3.	3.	3.
Section 8									
Mean	*	*	0.25	0.	0.	0.	0.02	0.	50.
N	0.	0.	5.	5.	5.	5.	5.	5.	5.
Section 9									
Mean	*	*	0.22	0.	0.	0.	0.01	1.	9.
N	0.	0.	9.	9.	9.	9.	9.	9.	9.
Section 10									
Mean	4.29	*	1.16	0.	0.01	0.07	0.01	1.	24.
N	14.	0.	15.	15.	15.	15.	15.	15.	15.
Section 11									
Mean	5.11	*	2.56	0.07	0.01	0.87	0.03	0.	11.
N	1.	0.	1.	1.	1.	1.	1.	1.	1.
Section 12									
Mean	0.51	440.	3.6	1.21	14.08	0.08	4.19	385.	9.
N	6.	6.	6.	6.	6.	6.	6.	6.	6.
Section 13									
Mean	3.19	587.	2.9	0.04	0.08	0.33	0.04	2.	24.
N	16.	1.	18.	18.	18.	18.	18.	18.	18.
Section 14									
Mean	1.59	*	*	*	*	*	*	*	*
N	2.	0.	0.	0.	0.	0.	0.	0.	0.
Section 15									
Mean	1.47	467.	2.69	0.64	0.83	0.44	0.55	30.	47.
N	2.	1.	1.	1.	1.	1.	1.	1.	1.

**Table 2 (cont'd):** Organic maturation and Rock-Eval data for Peril Formation

Section name	%Ro <sub>rand</sub>	Tmax	TOC	S1	S2	PI	QOM	HI	OI
Section 19									
Mean	1.18	444.	2.17	0.57	4.69	0.12	2.19	192.	14.
N	16.	18.	18.	18.	18.	18.	17.	18.	18.
Spot sample									
Mean	4.04	*	1.06	0.	0.01	0.04	0.02	0.	25.
N	30.	0.	38.	38.	38.	38.	38.	38.	38.

TOC=total organic carbon; PI=production index; QOM=quality of organic matter; HI=hydrogen index; OI=oxygen index. N=number of samples. Values represent means calculated across each outcrop section.

**Table 3:** Organic maturation and Rock-Eval data for Sandilands Formation

Section name	%Ro <sub>rand</sub>	TMAX	TOC	S1	S2	PI	QOM	HI	OI
Section 5									
Mean	*	*	0.51	0.01	0.03	0.06	0.03	2.	49.
N	0.	0.	4.	4.	4.	4.	4.	4.	4.
Section 11									
Mean	3.78	*	1.53	0.04	0.03	0.59	0.05	2.	9.
N	18.	0.	21.	21.	21.	21.	21.	21.	21.
Section 12									
Mean	0.45	436.	2.66	0.77	12.9	0.06	4.66	437.	10.
N	18.	10.	10.	10.	10.	10.	10.	10.	10.
Spot sample									
Mean	4.	*	0.59	0.	0.	0.	0.01	0.	7.
N	5.	0.	8.	8.	8.	8.	8.	8.	8.
Central Graham Island, B-quarry									
Mean	0.40	443.	3.14	1.64	13.85	0.14	4.26	372.	36.
N	17.	17.	17.	17.	17.	17.	17.	17.	17.
Central Graham Island, D-quarry									
Mean	0.66	447.	1.32	0.67	3.83	0.16	2.73	229.	525.
N	4.	4.	5.	5.	5.	4.	5.	5.	5.
Central Graham Island, Branch road 57									
Mean	0.65	437.	1.25	0.47	3.43	0.16	3.32	264.	42.
N	6.	6.	6.	6.	6.	6.	6.	6.	6.
Central Graham Island, Main road									
Mean	0.60	445.	2.08	1.02	4.9	0.15	1.94	159.	68.
N	4.	4.	5.	5.	5.	5.	5.	5.	5.
Central Graham Island, Well I-178									
Mean	0.60	437.	1.75	1.12	3.86	0.25	2.75	210.	48.
N	32.	32.	33.	33.	33.	33.	33.	33.	33.
Central Graham Island, Well I-179									
Mean	0.88	447.	9.6	0.50	4.12	0.31	2.71	242.	73.
N	40.	37.	40.	40.	40.	38.	39.	39.	39.
Central Graham Island, Well I-278									
Mean	0.65	447.	1.91	0.99	4.60	0.23	2.56	205.	57.
N	47.	47.	47.	47.	47.	47.	47.	47.	47.
Maude Island									
Mean	1.35	465.	1.47	0.24	0.52	0.42	0.44	27.	34.
N	8.	8.	9.	9.	9.	9.	9.	9.	9.
Rennell Sound mean									
N	1.57	479.	1.47	0.15	0.3	0.40	0.32	17.	18.
	32.	32.	33.	33.	33.	33.	33.	33.	33.
Shields Bay									
Mean		1.27	*		0.57		0.06		0.0
1.0	0.09	0.0	4.						
N		7.	0.		7.		7.		7.
7.	7.	7.	7.						

TOC=total organic carbon; PI=production index; QOM=quality of organic matter; HI=hydrogen index; OI=oxygen index. N=number of samples. Values represent means calculated across each outcrop section.

**Table 4:** Organic maturation and Rock-Eval data for Maude Group

Section name	%Ro <sub>rand</sub>	TMAX	TOC	S1	S2	PI	QOM	HI	OI
<b>Ghost Creek Formation</b>									
BC section 10									
Mean	0.55	448.	1.66	0.39	5.11	0.08	3.19	218.	13.
N	3.	4.	4.	4.	4.	4.	4.	4.	4.
BC section 4									
Mean	1.32	486.	0.68	0.07	0.25	0.22	0.47	36.	29.
N	1.	1.	1.	1.	1.	1.	1.	1.	1.
BC section 7									
Mean	1.51	470.	1.63	0.43	0.63	0.41	0.65	38.	17.
N	2.	2.	2.	2.	2.	2.	2.	2.	2.
BC section 8									
Mean	1.5	480.	1.84	0.44	0.7	0.41	0.66	38.	15.
N	4.	4.	4.	4.	4.	4.	4.	4.	4.
BC section CAA-86-2									
Mean	0.88	454.	1.27	0.43	1.98	0.17	1.73	141.	32.
N	6.	4.	5.	5.	5.	5.	5.	5.	5.
Central Graham Island, A-Quarry									
Mean	0.50	438.	0.6	1.46	1.76	0.45	5.37	293.	108.
N	1.	1.	1.	1.	1.	1.	1.	1.	1.
Maude Island									
Mean	1.38	442.	1.90	0.55	4.66	0.10	2.43	209.	105.
N	5.	5.	5.	5.	5.	5.	5.	5.	5.
Rennell Sound									
Mean	1.57	477.	0.79	0.05	0.09	0.48	0.14	9.	106.
N	7.	7.	7.	7.	7.	7.	7.	7.	7.
Central Graham Island, Well I-179									
Mean	0.88	444.	1.73	0.36	6.64	0.07	3.73	349.	76.
N	36.	36.	36.	36.	36.	33.	34.	34.	34.
Whiteaves Bay									
Mean	1.35	448.	1.6	0.46	0.60	0.49	0.62	32.	6.
N	6.	6.	6.	6.	6.	6.	6.	6.	6.
<b>Rennel Junction Formation</b>									
BC section 10									
Mean	0.52	445.	0.71	0.25	1.27	0.16	2.14	178.	46.
N	1.	1.	1.	1.	1.	1.	1.	1.	1.
BC section 4									
Mean	1.17	467.	0.58	0.05	0.16	0.12	0.33	28.	288.
N	2.	1.	2.	2.	2.	2.	2.	2.	2.
BC section 7									
Mean	1.5	488.	1.57	0.27	0.35	0.44	0.39	22.	8.
N	1.	1.	1.	1.	1.	1.	1.	1.	1.
BC section 8									
Mean	1.45	471.	1.96	0.4	0.59	0.41	0.51	30.	21.
N	1.	1.	1.	1.	1.	1.	1.	1.	1.
BC section CAA-86-2									
Mean	0.88	458.	1.07	0.05	0.3	0.14	0.84	93.	78.
N	3.	4.	4.	4.	4.	4.	4.	4.	4.
<b>Fannin Formation</b>									
BC section 4									
Mean	1.31	*	0.18	0.01	0.01	0.25	0.13	8.	74.
N	2.	0.	2.	2.	2.	2.	2.	2.	2.
BC section 7									
Mean	1.45	*	0.23	0.02	0.05	0.22	0.31	25.	27.
N	3.	0.	3.	3.	3.	3.	3.	3.	3.
BC section 8									
Mean	1.47	*	0.26	0.03	0.09	0.24	0.53	42.	88.
N	3.	0.	3.	3.	3.	3.	3.	3.	3.
BC section 8									
Mean	1.51	*	0.28	0.02	0.08	0.2	0.34	28.	136.
N	5.	0.	5.	5.	5.	5.	5.	5.	5.
BC section CAA-86-2									
Mean	0.85	*	*	*	*	*	*	*	*
N	2.	0.	0.	0.	0.	0.	0.	0.	0.

**Table 4 (cont'd):** Organic maturation and Rock-Eval data for Maude Group

Section name	%Ro <sub>rand</sub>	TMAX	TOC	S1	S2	PI	QOM	HI	OI
<b>North Moresby</b>									
Mean	1.42*	*	*	*	*	*	*	*	*
N	1.	*	*	*	*	*	*	*	*
<b>Whiteaves Formation</b>									
BC section 10									
Mean	0.64	448.	0.18	0.01	0.10	0.03	0.62	60.	51.
N	5.	1.	5.	5.	5.	5.	5.	5.	5.
BC section 11									
Mean	0.43	440	0.33	0.01	0.18	0.07	0.62	57.	6.
N	5.	1.	5.	5.	5.	5.	5.	5.	5.
BC section 12									
Mean	0.46	442.	5.27	0.02	0.24	0.09	0.43	88.	14.
N	2.	1.	2.	2.	2.	2.	2.	2.	2.
BC section 14									
Mean	0.78	*	0.26	0.01	0.11	0.11	0.47	42.	10.
N	4.	0.	4.	4.	4.	4.	4.	4.	4.
BC section 15									
Mean	0.63	440.	0.59	0.04	0.36	0.11	0.65	58.	5.
N	5.	4.	5.	5.	5.	5.	5.	5.	5.
BC section 4									
Mean	1.26	*	0.23	0.0	0.01	0.17	0.07	5.	125.
N	3.	0.	3.	3.	3.	3.	3.	3.	3.
BC section 5									
Mean	1.5	*	0.34	0.01	0.05	0.26	0.18	14.	88.
N	4.	0.	3.	3.	3.	3.	3.	3.	3.
BC section 6									
Mean	1.49	*	0.27	0.0	0.02	0.13	0.08	7.	54.
N	3.	0.	4.	4.	4.	4.	4.	4.	4.
BC section 7									
Mean	1.42	*	0.32	0.02	0.08	0.2	0.32	25.	18.
N	3.	0.	3.	3.	3.	3.	3.	3.	3.
BC section CAA-86-2									
Mean	0.82	464.	1.80	0.16	1.13	0.13	0.73	64.	16.
N	2.	2.	2.	2.	2.	2.	2.	2.	2.
North Moresby									
Mean	1.51*	*	*	*	*	*	*	*	*
N	1.	*	*	*	*	*	*	*	*
<b>Phantom Creek Formation</b>									
BC section 12									
Mean	0.46	440.	0.55	0.38	1.85	0.16	3.9	322.	10.
N	4.	4.	4.	4.	4.	4.	4.	4.	4.

TOC=total organic carbon; PI=production index; QOM=quality of organic matter; HI=hydrogen index; OI=oxygen index. N=number of samples. Values represent means calculated across each outcrop section.

\*Ro<sub>max</sub>

**Table 5:** Organic maturation and Rock-Eval data for Yakoun Group

Section name	%Ro <sub>rand</sub>	TMAX	TOC	S1	S2	PI	QOM	HI	OI
<b>Graham Island Formation</b>									
BC section 10									
Mean	0.48	446.	0.96	0.08	1.57	0.06	1.17	111.	86.
N	8.	5.	8.	8.	8.	8.	8.	8.	8.
BC section 14									
Mean	0.77	443.	0.88	0.14	2.22	0.23	1.94	127.	14.
N	6.	4.	7.	7.	7.	7.	7.	7.	7.
BC section 6									
Mean	1.5	*	0.34	0.01	0.08	0.08	0.26	24.	43.
N	3.	0.	3.	3.	3.	3.	3.	3.	3.
<b>Richardson Bay Formation</b>									
BC section 16									
Mean	1.13	396.	1.13	0.20	0.52	0.28	0.63	45.	11.
N	6.	6.	6.	6.	6.	6.	6.	6.	6.

TOC=total organic carbon; PI=production index; QOM=quality of organic matter; HI=hydrogen index; OI=oxygen index. N=number of samples. Values represent means calculated across each outcrop section.

**Table 6:** Organic maturation and Rock-Eval data for Moresby Group

Section name	%Ro <sub>rand</sub>	Tmax	TOC	S1	S2	PI	QOM	HI	OI
<b>Robber Point Formation</b>									
BC section 16									
Mean	1.10	468.	0.78	0.14	0.35	0.29	0.63	44.	15.
N	1.	1.	1.	1.	1.	1.	1.	1.	1.
<b>Newcombe Formation</b>									
BC section 17									
Mean	1.08	*	0.51	0.02	0.15	0.12	0.34	30.	14.
N	3.	0.	3.	3.	3.	3.	3.	3.	3.
<b>Alliford Formation</b>									
BC section 16									
Mean	1.04	320.	1.10	0.22	0.89	0.20	1.01	80.	13.
N	3.	3.	3.	3.	3.	3.	3.	3.	3.

TOC=total organic carbon; PI=production index; QOM=quality of organic matter; HI=hydrogen index; OI=oxygen index. N=number of samples. Values represent means calculated across each outcrop section.

**Table 7:** Organic maturation and Rock-Eval data for Longarm Formation

Section name	%Ro <sub>rand</sub>	TMAX	TOC	S1	S2	PI	QOM	HI	OI
<b>Spot sample</b>									
Mean	3.18	*	0.26	0.	0.	0.03	0.03	5.	44.
N	20.	0.	33.	33.	33.	33.	33.	33.	33.
<b>North Moresby</b>									
Mean	2.07*	*	*	*	*	*	*	*	*
N	5.	*	*	*	*	*	*	*	*

TOC=total organic carbon; PI=production index; QOM=quality of organic matter; HI=hydrogen index; OI=oxygen index. N=number of samples. Values represent means calculated across each outcrop section.

\*Ro<sub>max</sub>

**Table 8:** Organic maturation and Rock-Eval data for Haida Formation

Section name	%Ro <sub>rand</sub>	TMAX	TOC	S1	S2	PI	QOM	HI	OI
<b>BC section CAA-86-1</b>									
Mean	0.98	701.	0.68	0.05	0.36	0.1	0.56	49.	5.
N	26.	17.	26.	26.	26.	26.	26.	26.	26.
<b>BC section CAA-86-5</b>									
Mean	0.36	439.	0.73	0.01	0.48	0.02	0.67	65.	29.
N	10.	10.	11.	11.	11.	11.	11.	11.	11.
<b>Section 14</b>									
Mean	1.51	504.	2.23	0.35	0.74	0.27	0.48	34.	36.
N	8.	2.	3.	3.	3.	3.	3.	3.	3.
<b>Section 15</b>									
Mean	0.77	449.	2.49	0.07	0.9	0.08	0.43	39.	50.
N	40.	2.	2.	2.	2.	2.	2.	2.	2.
<b>Section 17</b>									
Mean	0.68	*	*	*	*	*	*	*	*
N	11.	0.	0.	0.	0.	0.	0.	0.	0.
<b>Section 18</b>									
Mean	0.43	*	*	*	*	*	*	*	*
N	14.	0.	0.	0.	0.	0.	0.	0.	0.
<b>Spot sample</b>									
Mean	4.04	*	0.13	0.	0.	0.14	0.02	0.	33.
N	3.	0.	7.	7.	7.	7.	7.	7.	7.
<b>North Moresby</b>									
Mean	1.13*	*	*	*	*	*	*	*	*
N	2.	*	*	*	*	*	*	*	*

TOC=total organic carbon; PI=production index; QOM=quality of organic matter; HI=hydrogen index; OI=oxygen index. N=number of samples. Values represent means calculated across each outcrop section.

\*Ro<sub>max</sub>

**Table 9:** Organic maturation and Rock-Eval data for Skidegate Formation

Section name	%Ro <sub>rand</sub>	TMAX	TOC	S1	S2	PI	QOM	HI	OI
<b>Section 20</b>									
Mean	1.91	497.	0.6	0.01	0.08	0.16	0.24	33.	74.
N	14.	1.	11.	11.	11.	11.	11.	11.	11.
<b>BC section CAA-86-3</b>									
Mean	0.96	433.	0.26	0.03	0.18	0.15	0.95	79.	68.
N	35.	11.	32.	32.	32.	32.	32.	32.	32.
<b>BC section CAA-86-4</b>									
Mean	*	*	*	*	*	*	*	*	*
N	0.	0.	0.	0.	0.	0.	0.	0.	0.
<b>BC section CAA-86-6</b>									
Mean	0.4	439.	0.73	0.02	0.54	0.03	0.73	70.	26.
N	23.	25.	25.	25.	25.	25.	25.	25.	25.
<b>BC section CAA-86-T-3</b>									
Mean	1.09	464.	0.17	0.01	0.10	0.07	0.85	65.	146.
N	7.	2.	7.	7.	7.	7.	6.	7.	7.
<b>BC section CAA-86-T-4</b>									
Mean	0.47	437.	0.43	0.	0.19	0.	0.32	31.	70.
N	8.	2.	5.	5.	5.	5.	5.	5.	5.
<b>BC spot sample</b>									
Mean	1.8	470.	0.51	0.02	0.18	0.06	0.4	37.	28.
N	66.	10.	53.	53.	53.	53.	53.	53.	53.
<b>Section 16</b>									
Mean	0.71	442.	0.3	0.01	0.19	0.04	0.71	67.	81.
N	10.	2.	8.	8.	8.	8.	8.	8.	8.
<b>Section 21</b>									
Mean	1.39	456.	0.32	0.02	0.12	0.11	0.44	36.	14.
N	11.	1.	10.	10.	10.	10.	10.	10.	10.
<b>Section 22</b>									
Mean	0.87	436.	0.63	0.	0.17	0.	0.25	24.	76.
N	3.	1.	2.	2.	2.	2.	2.	2.	2.
<b>Spot sample</b>									
Mean	2.94	*	0.13	0.	0.02	0.04	0.31	20.	95.
N	3.	0.	4.	4.	4.	4.	3.	4.	4.

TOC=total organic carbon; PI=production index; QOM=quality of organic matter; HI=hydrogen index; OI=oxygen index. N=number of samples. Values represent means calculated across each outcrop section.

**Table 10:** Organic maturation and Rock-Eval data for Honna Formation

Section name	%Ro <sub>rand</sub>	TMAX	TOC	S1	S2	PI	QOM	HI	OI
<b>Section 22</b>									
Mean	1.14	436.	0.43	0.03	0.24	0.09	0.7	60.	125.
N	16.	7.	12.	12.	12.	12.	12.	12.	12.
<b>Spot sample</b>									
Mean	*	*	0.08	0.	0.	0.	0.	0.	87.
N	0.	0.	1.	1.	1.	1.	1.	1.	1.
<b>North Moresby</b>									
Mean	0.80*	*	*	*	*	*	*	*	*
N	4.	*	*	*	*	*	*	*	*

TOC=total organic carbon; PI=production index; QOM=quality of organic matter; HI=hydrogen index; OI=oxygen index. N=number of samples. Values represent means calculated across each outcrop section.

\*Ro<sub>max</sub>

**Table 11:** Organic maturation and Rock-Eval data for Skonun Formation

Section name	%Ro <sub>rand</sub>	TMAX	TOC	S1	S2	PI	QOM	HI	OI
Cape Ball Well									
Mean	0.32	403.	41.68	16.3	81.42	0.15	2.2	179.	38.
N	22.	16.	16.	16.	16.	16.	16.	16.	16.
Gold Creek Well									
Mean	0.27	418.	24.44	0.97	14.42	0.08	0.70	64.	68.
N	7.	4.	4.	4.	4.	4.	4.	4.	4.
Log Creek									
Mean	0.39	420.	2.47	1.32	5.2	0.2	2.64	210.	14.
N	1.	1.	1.	1.	1.	1.	1.	1.	1.
Miller Creek									
Mean	0.19	*	*	*	*	*	*	*	*
N	1.	0.	0.	0.	0.	0.	0.	0.	0.
Nadu River Well									
Mean	0.29	400.	6.67	1.36	7.72	0.46	0.9	64.	199
N	10.	4.	8.	8.	8.	8.	8.	8.	8.
Port Louis Well									
Mean	1.05	486.	10.45	0.73	10.3	0.07	0.87	79.	9.
N	24.	13.	14.	14.	14.	14.	14.	14.	14.
Tiell Well									
Mean	0.27	417.	22.88	7.27	39.12	0.15	1.91	161.	74.
N	17.	14.	15.	15.	15.	15.	15.	15.	15.
Tow Hill Well									
Mean	0.48	430.	36.18	7.17	31.76	0.17	1.19	93.	28.
N	45.	36.	40.	40.	40.	40.	40.	40.	39.

TOC=total organic carbon; PI=production index; QOM=quality of organic matter; HI=hydrogen index; OI=oxygen index. N=number of samples. Values represent means calculated across each outcrop section.

land, Skidegate Inlet, and northern Moresby Island. The regional level of organic maturation (Fig. 7) ranges from 0.52 %Ro<sub>rand</sub> on central Graham Island to 1.50 %Ro<sub>rand</sub> on Maude Island (Skidegate Inlet). Local, anomalously high, maturation values reach 2.12 %Ro<sub>rand</sub>.

Maturation values for the Upper Pliensbachian-Lower Toarcian Fannin Formation (Fig. 8) range from 0.85 %Ro<sub>rand</sub> at Cumshe-wa Inlet to 1.58 %Ro<sub>rand</sub> on Maude Island (Skidegate Inlet).

The regional DOM for the Middle Toarcian Whiteaves Formation increases from west to east with maturation values ranging from 0.43 %Ro<sub>rand</sub> on central Graham Island to 1.51 %Ro<sub>max</sub> on Skidegate Inlet (Fig. 9).

Strata of the Upper Toarcian Phantom Creek Formation outcrop locally. Only one organic maturation value (0.46 %Ro<sub>rand</sub>) was obtained for the unit in central Graham Island.

## YAKOUN GROUP

The Lower Bajocian Graham Island Formation (nomenclature of Cameron and Tipper, 1985) is marginally mature to mature (Fig. 10) in central Graham Island (0.48 %Ro<sub>rand</sub>) and overmature in the Skidegate Inlet area (1.50 %Ro<sub>rand</sub>). The Lower Bajocian Richardson Bay Formation is exposed locally in Skidegate Inlet where the strata are mature (1.13 %Ro<sub>rand</sub>).

## MORESBY GROUP

In Skidegate Inlet, the limited maturation data available indicates that the Upper Bathonian Robber Point (1.10 %Ro<sub>rand</sub>), the Upper Bathonian-Lower Callovian Newcombe (1.08 %Ro<sub>rand</sub>), and the Lower Callovian Alliford formations (1.04 %Ro<sub>rand</sub>) are mature (Fig. 10).

## LONGARM FORMATION

The Upper Valanginian-Lower Barremian Longarm Formation crops out on Moresby Island and parts of Graham Island. The Longarm Formation is overmature on northern Moresby Island (Fig. 11) with maturation values ranging from 1.53-2.43 %Ro<sub>max</sub>. The strata on eastern Moresby Island are overmature with regional maturation increasing from west (2.31 %Ro<sub>rand</sub> at Huston Inlet) to east (4.86 %Ro<sub>rand</sub> on Murchison Island).

## QUEEN CHARLOTTE GROUP

### Haida Formation

The Albian Haida Formation is exposed locally from north-west Graham Island to central Moresby Island. The regional DOM varies from immature to overmature and increases from north to south. Maturation values range from 0.33 %Ro<sub>rand</sub> in Beresford Bay (northwest Graham Island), 1.29 %Ro<sub>max</sub> in Skidegate Inlet, 2.08 %Ro<sub>rand</sub> in Cumshe-wa Inlet, to 4.18 %Ro<sub>rand</sub> in central Moresby Island (Fig. 12). Local, anomalously high vitrinite reflectance values (up to 1.72 %Ro<sub>rand</sub>) occur on northwest Graham Island.

### Skidegate Formation

The Cenomanian-Turonian Skidegate Formation crops out in the Skidegate and Cumshe-wa Inlet areas, northwest Graham Island, and Langara Island. The unit (Fig. 13) is immature to mature on northwest Graham Island (0.40 %Ro<sub>rand</sub>) and mature to overmature in Skidegate Inlet (2.21 %Ro<sub>rand</sub>). Regional organic maturation increases from east to west on northwest Graham Island with anomalously high values near Langara Island. A slight increase in the DOM from west to east occurs in both Skidegate and Cumshe-wa inlets. Local, anomalously high vitrinite reflectance values reach 2.55 %Ro<sub>rand</sub> in the Skidegate and Cumshe-wa Inlet areas.

### Honna Formation

The Coniacian Honna Formation is exposed locally between central Graham Island and Langara Island. Maturation values for northwest Graham (1.14 %Ro<sub>rand</sub>) and northern Moresby (0.60-1.01 %Ro<sub>max</sub>) Islands indicate that the strata are generally mature (Fig. 14). On northwest Graham Island, vitrinite reflectance values were measured on samples taken from in situ coal stringers wherever possible. If no coal stringers were found, measurements were taken on shale or sandstone samples which included dispersed organic matter. Maturation values from coal particles averaged less than 0.60 %Ro<sub>rand</sub> whereas maturation values from samples with dispersed organic matter at or near the same locality ranged from 0.56-1.43 %Ro<sub>rand</sub>. The high maturation values associated with dispersed organic matter may be the result of reworking of more mature organic matter in older strata.

## SKONUN FORMATION

The Miocene-Pliocene Skonun Formation is exposed locally on eastern Graham Island and underlies most of Graham Island and Hecate Strait. The DOM for the Skonun Formation is generally immature with the exception of the mature succession in the Port Louis well (west central Graham Island) and the basal strata in the Tow Hill Well (northeast Graham Island). Regional organic maturation values for the basal strata of the Skonun Formation increase from east to west with vitrinite reflectance values ranging from 0.31 %Ro<sub>rand</sub> at Cape Ball to 1.33 %Ro<sub>rand</sub> at Port Louis (Fig. 15).

### Maturation gradients

Maturation gradients determined from outcrop and well sections are important for calculating the thickness of eroded strata, the thickness of strata within the oil window, and for estimating the paleo-geothermal gradient. In this study, the vertical variation in DOM

was determined from a total of 12 vitrinite reflectance/depth plots derived from 6 onshore petroleum exploration wells and 6 measured outcrop sections (Fig. 20). Numerous other outcrop sections were measured but were not long enough to obtain accurate maturation gradients. The maturation data best fit a log (vitrinite reflectance) linear depth relationship and the maturation gradients were derived with a first order regression algorithm.

Maturation gradients for the Skonun Formation range from 0.18–0.25 log (%Ro<sub>rand</sub>)/km on eastern Graham Island and 0.30 log (%Ro<sub>rand</sub>)/km on western Graham Island (Figs. 20a–f).

Haida Formation maturation gradients (Figs. 20g–h) range from 0.45 log (%Ro<sub>rand</sub>)/km at Onward Point (Skidegate Inlet) to 0.73 log (%Ro<sub>rand</sub>)/km at Lauder Point (northwest Graham Island).

Maturation gradients for the Maude Group (Figs. 20i–j) vary from 0.28 log (%Ro<sub>rand</sub>)/km at Rennell Junction (central Graham Island) to 0.35 log (%Ro<sub>rand</sub>)/km at Cumshewa Inlet (northern Moresby Island).

Two maturation gradients were derived for the Kunga Group on northwest Graham Island; 0.78 log (%Ro<sub>rand</sub>)/km at Frederick Island and 0.65 log (%Ro<sub>rand</sub>)/km at nearby Kennecott Point (Figs. 20k–l).

**Table 12:** Calculated depths to the top and base of the oil window and thickness of eroded strata

Well name (location)	minimum vitrinite reflectance (%Ro <sub>rand</sub> )	maximum vitrinite reflectance (%Ro <sub>rand</sub> )	calculated depth to the top and base of the oil window (m)	calculated thickness of eroded section (m)
<b>Tertiary strata</b>				
<b>Skonun Formation (exploration wells)</b>				
Cape Ball	0.18	0.42	2283–4685	615
Gold Creek	0.22	0.36	2010–4104	530
Nadu River	0.24	0.33	1622–3917	1160
Port Louis	0.81	1.38	0053–1486	1685
Tlell	0.18	0.34	2291–4491	375
Tow Hill	0.28	0.72	1125–2864	985
N. Lauder Point	0.53	1.05	55–563	745
Onward Point	0.7	1.1	55–624	1500
Cumshewa Inlet	0.82	0.91	55–554	1985
Rennell Junction	0.44	0.57	178–1747	1725
Frederick Island	0.97	1.51	55–183	1040
Kennecott Point	0.36	0.70	69–733	735

Depths to the top and base of the oil window are extrapolated assuming that the oil window is between 0.50 %Ro<sub>rand</sub> and 1.35 %Ro<sub>rand</sub>. Thickness of eroded strata assumes a zero maturation level of 0.15 %Ro<sub>rand</sub>.

### Thickness of eroded strata

The thickness of eroded strata can be calculated by extrapolating the measured maturation gradient to the zero maturation level of 0.15 %Ro<sub>rand</sub> assuming a constant paleogeothermal gradient (Bustin, 1986; England and Bustin, 1986). If the paleogeothermal gradient is not constant, the predicted thickness of eroded strata can be unreliable. In the study area, high heat flow associated with Mesozoic or Tertiary volcanism (Sutherland Brown, 1968; Cameron and Tipper, 1985) is thought to have raised the paleogeothermal gradients for 5–25 million years in the Middle–Late Jurassic or Tertiary (discussed below) resulting in elevated maturation gradients. Hence, the erosional thickness values may be underestimated for strata which were affected by high heat flow. The calculated values, therefore, represent a minimum estimate.

The calculated thickness of eroded strata for the Skonun Formation ranges from 375 m at the Tlell well to 1685 m at the Port Louis well (Table 12). The amount of eroded strata increases towards the north,

except at the Nadu River well (1160 m) which lies proximal to a structural high in the underlying Masset Formation (Sutherland Brown, 1968), suggesting that the area was differentially uplifted following deposition of the Skonun Formation.

Predicted thickness of eroded strata (Table 12) for Cretaceous outcrop sections increase from north Lauder Point (745 m) to Onward Point (1500 m). The predicted thickness of eroded strata increases from Rennell Junction (1725 m) to Cumshewa Inlet (1985 m) for Jurassic outcrop sections. Predicted values for Triassic outcrop sections range from 735 m at Kennecott Point to 1040 m at Frederick Island.

### Depth to the oil window

The stratigraphic depth to the top of the oil window (Table 12) was calculated by extrapolation of the maturation gradient to 0.50 %Ro<sub>rand</sub>, corresponding to the onset of oil generation for Types II and III organic matter (Dow, 1977). Similarly, the stratigraphic depth to the base of the oil window was established by extrapolation of the maturation gradient to 1.35 %Ro<sub>rand</sub>, corresponding to the base of the oil window for Types II and III organic matter.

Depth to the oil window values cannot be calculated for areas from which measured maturation gradients were not obtained. Because of local thermal effects associated with volcanism or plutonism, the maturation gradients are too variable to be confidently extrapolated to adjacent areas.

Calculated depths to the top of the oil window for the Skonun Formation strata in the 6 onshore wells on Graham Island generally increase from north to south and range from a minimum of 53 m on west Graham Island (Port Louis well) to a maximum of 2291 m on east Graham Island (Tlell well). Similarly, the calculated depths to the base of the oil window increase from west (1486 m at the Port Louis well) to east (4685 m at the Cape Ball well) Graham Island (Table 12). Thickness of strata within the oil window ranges from 1433 m on west Graham Island (Port Louis well) to 2402 m on east Graham Island (Cape Ball well).

Exposed Cretaceous strata at north Lauder Point and Onward Point are within the oil window. The calculated stratigraphic depth to the base of the oil window ranges from 563 m at north Lauder Point to 624 m at Onward Point (Table 12). Thickness of strata within the oil window ranges from 563 m at north Lauder Point to 624 m at Onward Point.

Exposed Jurassic strata at Cumshewa Inlet are within the oil window and the calculated stratigraphic depth to the base of the oil window is 554 m. The calculated stratigraphic depths to the top and base of the oil window are 178 m and 1747 m respectively at Rennell Junction (Table 12). Thickness of strata within the oil window ranges from 554 m at Cumshewa Inlet to 1569 m at Rennell Junction.

The calculated stratigraphic depth to the top and base of the oil window for exposed Triassic strata at Kennecott Point range from 69–733 m. Strata at Frederick Island are within the oil window and the calculated stratigraphic depth to the base of the oil window is 183 m. Thicknesses of strata within the oil window range from 183 m at Frederick Island to 664 m at Kennecott Point.

## THERMAL MODELLING

Numerous researchers have demonstrated that the DOM depends upon the thermal history of the strata (Karweil, 1955; Lopatin, 1971; Bostick, 1973; Waples, 1980). Numerical models have been developed by petroleum and coal geologists to help predict organic maturation based on knowledge of the thermal history, or conversely, to interpret the thermal history where the levels of organic maturation are known. Most models (including the model used in this study) are

based on some form of the Arrhenius equation as described by Karweil (1955) and Tissot and Espitalie (1975):

$$K = A e^{(-E/RT)}$$

where E=activation energy; T=absolute temperature; A=frequency factor; K=reaction constant; and R=universal gas constant.

We use a modified Arrhenius model to predict paleogeothermal gradients, fractional kerogen conversion to hydrocarbons, and timing of hydrocarbon generation for 6 onshore wells and 6 measured outcrop sections in the study area. To estimate paleogeothermal gradients, the measured maturation gradients were modelled using an integral form of the Arrhenius equation. The model iteratively solves for maturation gradients assuming a variable burial history and geothermal gradient. The model compares the calculated and measured maturation gradients; therefore, the gradient is modelled rather than a single point and is independent of the absolute level of thermal maturity. The Tertiary succession, except for the Port Louis well section, was modelled in such a manner.

Attempts to model maturation gradients rather than single points for the Port Louis well section and all Mesozoic outcrop sections were unsuccessful. This may reflect non-constant paleogeothermal gradients throughout the depositional histories of the strata, poor age constraints on the strata, or nonlinearities in sedimentation rates. Therefore, the base of each well or outcrop section was modelled (single point modelling) with varying input geothermal gradients until the predicted DOM was similar to the measured level of organic maturation.

In this study, the Arrhenius model uses a constant activation energy ( $E=218$  kJ/mol) and frequency factor [ $A=5.45^{26}$ ] based on average values for Type II and Type III organic matter within the maturation ranges measured in this study (Wood, 1988). Thermal conductivity and surface temperature ( $5^{\circ}\text{C}$ ) are held constant and compacted rock thickness are assumed. Variations in thermal conductivity with depth and changes in rock thickness resulting from compaction are not treated here, because they are beyond the precision of the geology constraints.

## BURIAL HISTORIES

The burial histories outlined below form the basis for the maturation models presented later. Ages are based on Palmer's (1983) time scale. Burial histories were reconstructed for the base of the modelled stratigraphic horizon using data acquired from published and unpublished sources. Maximum burial depth is estimated as the sum of the present thickness and the predicted eroded thickness of strata. Due to the paucity of data constraining the ages and thicknesses of strata and the timing of tectonic elements, the burial histories presented here are, at best, a first approximation. Accordingly, conservative estimates based upon the available geologic data have been used to quantify parameters used in modelling. Because of the relative insensitivity of the Arrhenius model to time for all temperature ranges, the timing of uplift has little effect on the DOM. Therefore, the timing of erosional events does not require a great deal of accuracy for the models to yield useful results.

### Tertiary burial histories

Burial histories for Skonun Formation strata in the six onshore well sections are highly similar (Figs. 21-24). The age of the Tertiary Skonun Formation is poorly known and was thought to be Late Miocene to Early Pliocene by Martin and Rouse (1966) and Sutherland Brown (1968), although Cameron and Hamilton (1988) considered the Skonun Formation to be as old as Early Miocene (18 Ma).

On Graham Island, deposition of the Skonun Formation followed the culmination of Masset volcanism between 20 and 25 Ma (Hickson, 1988). There are, however, intercalations of sediments similar to

Skonun Formation strata within flows of the Masset Formation. For this study, the Skonun Formation is assumed to have been deposited between 18 and 2 Ma, followed by uplift from 1.6 Ma to the present. Maximum burial depths are presumed to have been attained at 2 Ma and range from 1625 m at the Tlell well to 3150 m at the Port Louis well.

### Cretaceous burial histories

At north Lauder Point (Fig. 27a) and Onward Point (Fig. 28a), Cretaceous strata were deposited beginning with the Albian Haida Formation (113-97.5 Ma). It is presumed that the Cenomanian-Turonian Skidegate Formation (97.5-88.5 Ma) and the Coniacian Honna Formation (88.5-87.5 Ma) were deposited following Haida Formation deposition in order to account for the calculated thickness of eroded strata values at north Lauder Point (745 m) and at Onward Point (1500 m). A period of erosion removing the Skidegate and Honna formations occurred between 87.5 Ma (Coniacian) and 45 Ma (estimated initial deposition of the subaerial erupted Masset Formation) (Cameron and Tipper, 1985; Cameron and Hamilton, 1988; Hickson, 1988).

There are insufficient data to conclude if the Masset Formation was deposited at north Lauder Point or Onward Point. However, even if the Masset Formation was deposited in these areas, it is unlikely that the burial depth of the Skonun Formation exceeded the maximum depth of burial attained in the Cretaceous. Thus the Masset Formation would have little effect on the modelled DOM except near dykes or sills. The Skonun Formation is assumed to have never been deposited in these areas because both north Lauder Point and Onward Point are west of the presumed depositional edge of the Skonun Formation.

### Jurassic burial histories

At Cumshewa Inlet (Fig. 29a) and Rennell Junction (Fig. 30a), strata of the Maude Group were deposited from Early Pliensbachian to Aalenian (198-183 Ma) time and have a total estimated thickness of 300 m (Cameron and Tipper, 1985). Minor episodes of erosion or non-deposition in the Maude Group were documented by Cameron and Tipper (1985). Following Maude deposition, sediments of the Lower Bajocian Yakoun Group (Graham Island and Richardson Bay formations) were deposited at the Rennell Junction section. Partly contemporaneous volcanic rocks of the Yakoun Group were erupted at Cumshewa Inlet (Cameron and Tipper, 1985).

To account for the predicted thickness of eroded strata at Rennell Junction (1725 m) and Cumshewa Inlet (1985 m), the Upper Bathonian to Lower Callovian Moresby Group (Robber Point, Newcombe, and Alliford formations) are assumed to have been deposited following Yakoun deposition and then uplifted and eroded during Late Jurassic and Early Cretaceous time. The Longarm Formation (Upper Valanginian-Lower Barremian) is inferred to have been deposited and partly or completely eroded before the Albian (113 Ma). The Cretaceous Haida, Skidegate, and Honna formations appear to have been deposited during Albian to Coniacian time (113-87.5 Ma), followed by uplift and erosion until the initiation of Masset volcanism (45 Ma).

There is no evidence for deposition of the Masset Formation or the Skonun Formation at Rennell Junction or Cumshewa Inlet. Even if Masset Formation or Skonun Formation strata were once present there, the burial depths of Lower Jurassic sediments are assumed to be less than the maximum burial depths previously attained, thereby having little effect on maturation levels.

### Triassic burial histories

At Frederick Island (Fig. 31a) and Kennecott Point (Fig. 32a), the Kunga Group was buried until the Early Pliensbachian time. There is no evidence for post-Sinemurian Jurassic deposition north of Rennell Sound on western Graham Island (H.W. Tipper, pers. comm.,



1988); therefore, a period of non-deposition or uplift is assumed during Early Pliensbachian to Early Callovian time (Maude, Yakoun, and Moresby groups). The Longarm Formation was deposited during the Late Valanginian-Early Barremian, followed by uplift and partial erosion as is evident from exposures of the Longarm Formation north of Frederick Island (H.W. Tipper, pers. comm., 1988). Cretaceous Haida, Skidegate, and Honna formations are exposed north of Frederick Island and are assumed to have been deposited in the Frederick Island-Kennecott Point area.

Deposition of the Masset Formation is thought to have been insufficient to bury the Triassic strata enough to exceed maximum burial depths attained during the Cretaceous. The Skonun Formation is assumed to never have been deposited in the area; both Frederick Island and Kennecott Point are west of the inferred depositional edge of the Skonun Formation.

## MATURATION HISTORIES

Maturation histories derived from the Arrhenius numerical method incorporate the burial histories reviewed above for the modelled sections. Measured maturation gradients are compared with calculated paleogeothermal gradients in Figures 21d-23d and 25d-26d. The base of the oldest modelled stratigraphic horizon is shown for each section. The fractional kerogen conversion to petroleum relative to depth and time is shown for some well or outcrop sections in Figures 24-31.

The Queen Charlotte Islands have an island arc tectonic setting; therefore it is likely that heat flow (and paleogeothermal gradients) were influenced by volcanism and subduction. Furthermore, heat flow most likely varied laterally between adjacent areas and with time (Watanabe et al., 1977; Cameron and Tipper, 1985). The following section discusses two possible thermal regimes for Mesozoic and Tertiary strata: constant and variable paleogeothermal gradients (heat flow). In order to account for the measured level of organic maturation (Figs. 21-32), the models predict paleogeothermal gradients in excess of 40°C/km. Geologic evidence, however, suggests that heat flow (and paleogeothermal gradients) increased during volcanic and plutonic episodes in the Middle-Late Jurassic and Eocene-Miocene. In this study, models which allow for variable geothermal gradients are used to incorporate the assumed high heat flow during volcanic episodes. The modelled geothermal gradients were increased (up to 150°C/km) above the ambient background geothermal gradient (assumed to be 30°C/km) for short intervals of time consistent with geological evidence (assumed to be between 183-178 Ma for Yakoun volcanism, and between 35-10 Ma for Masset volcanism). The background geothermal gradients were chosen to be similar to average paleogeothermal gradients (30°C/km) from various sedimentary basins around the world. Paleogeothermal gradients for Tertiary strata are considered to be the least effected by high heat flow associated with volcanism because the Skonun Formation was deposited after the cessation of Yakoun and Masset volcanism. However, if Mesozoic background paleogeothermal gradients were higher than the modelled 30°C/km geothermal gradients, little effect in the levels of organic maturation are predicted in that the maximum temperatures, attained during volcanic episodes when heat flow was substantially elevated above background levels, have the most pronounced effect on maturation (Figs. 33-38). The predicted paleogeothermal gradients were derived from geothermal gradients which were modelled to attain the measured DOM.

### Tertiary paleogeothermal gradients

Paleogeothermal gradients predicted by the Arrhenius model (assuming a constant thermal regime) range from 37°C/km (Cape Ball well) to 50°C/km (Nadu River and Tlell wells) and average 45°C/km.

### Cretaceous paleogeothermal gradients

Predicted paleogeothermal gradients for Cretaceous strata (assuming a constant thermal regime) range from 70°C/km at Onward Point to 88°C/km to north Lauder Point.

Variable thermal regime modelling with 30°C/km background paleogeothermal gradients predicts peak paleogeothermal gradients up to 130°C/km during the culmination of Masset volcanism (between 35 Ma and 10 Ma) for Cretaceous strata at both Onward and north Lauder Points. Significant lateral variation in heat flow during Masset time between northwest and southeast Graham Island is not predicted by the Arrhenius model.

### Jurassic paleogeothermal gradients

Predicted paleogeothermal gradients for a constant thermal regime for Jurassic strata range from 45°C/km at Rennell Junction to 55°C/km at Cumshewa Inlet.

Predicted peak paleogeothermal gradients (assuming a variable thermal regime with 30°C/km background paleogeothermal gradients) reach 83°C/km at Rennell Junction and 97°C/km at Cumshewa Inlet during the culmination of Yakoun volcanism between 183 Ma and 178 Ma. The increased paleogeothermal gradients in Cumshewa Inlet suggest that the Jurassic strata there were more proximal to a source of high heat flow than at Rennell Junction.

### Triassic paleogeothermal gradients

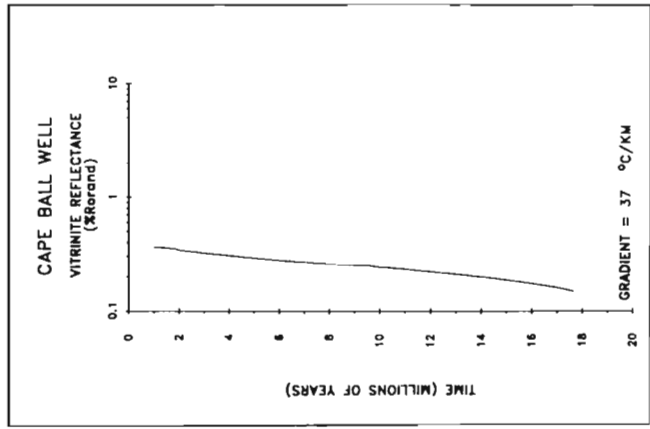
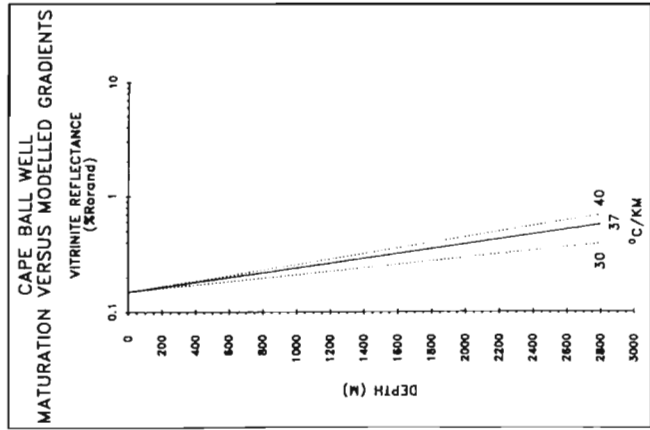
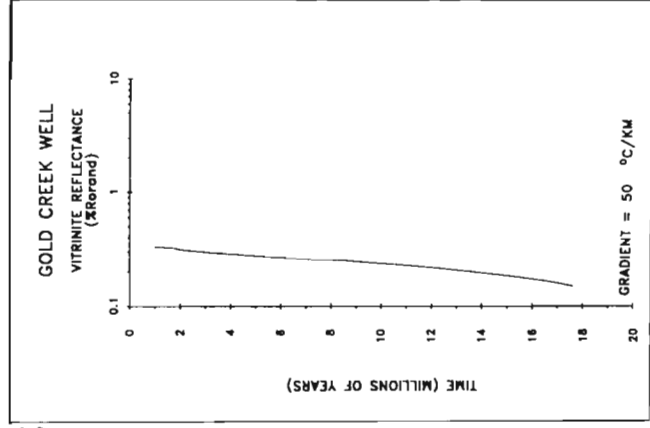
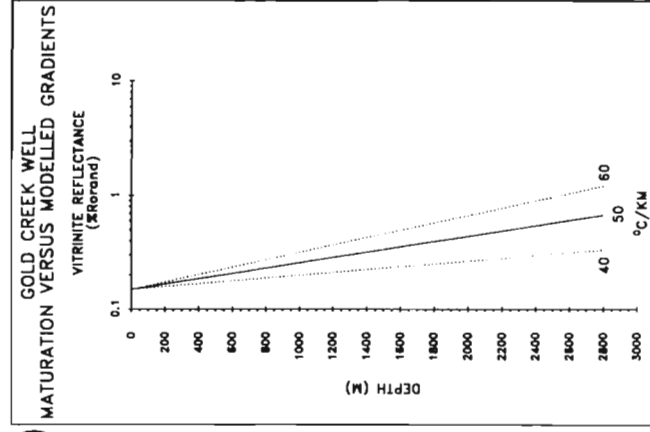
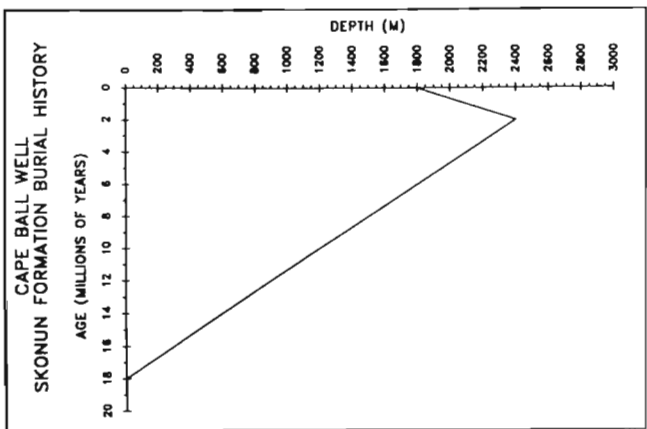
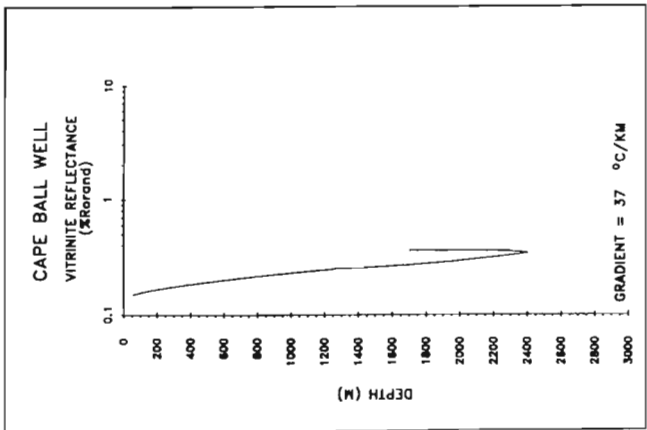
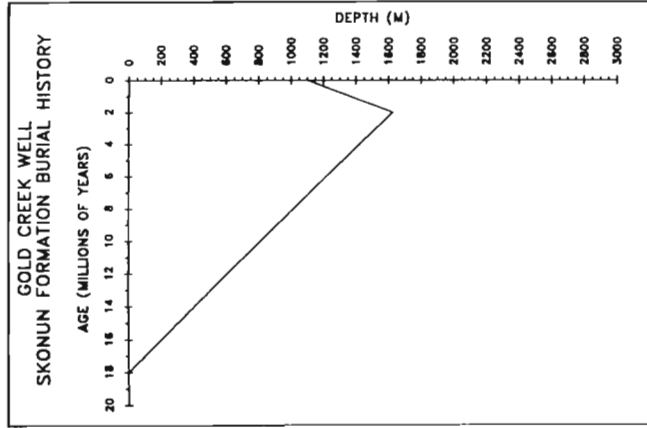
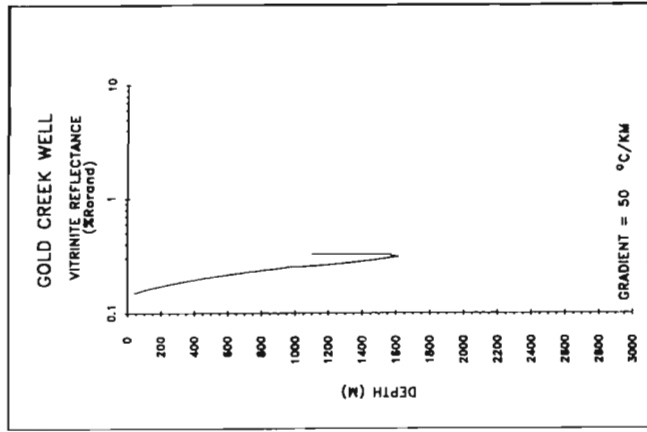
Although Frederick Island and Kennecott Point are proximally located, higher paleogeothermal gradients are predicted at Frederick Island (90°C/km) than at Kennecott Point (65°C/km), assuming a constant thermal regime.

Peak paleogeothermal gradients (assuming a variable thermal regime with 30°C/km background paleogeothermal gradients) reach 100°C/km at Kennecott Point and 150°C/km at Frederick Island during the culmination of Masset volcanism 35 Ma and 10 Ma. A higher geothermal gradient predicted for Frederick Island (relative to Kennecott Point) is probably due to increased heat flow from Masset feeder dykes/sills located closer to Frederick Island than to Kennecott Point.

## INTERPRETATION OF AREAL MATURATION TRENDS

The paleogeothermal gradients predicted for the Tertiary Skonun Formation are within the ranges for geothermal gradients (15-64°C/km) reported from back arc basins elsewhere (Watanabe et al., 1977; and Blackwell et al., 1982). Present day heat flow values for the west coast of North America average 60-80 mW/m<sup>2</sup> (Chapman and Rybach, 1985). Recent heat flow measurements from Moresby Island average 50-60 mW/m<sup>2</sup> (geothermal gradients of approximately 18-20°C/km; T.J. Lewis, pers. comm., 1988), suggesting that onshore heat flow has decreased since deposition of the Skonun Formation.

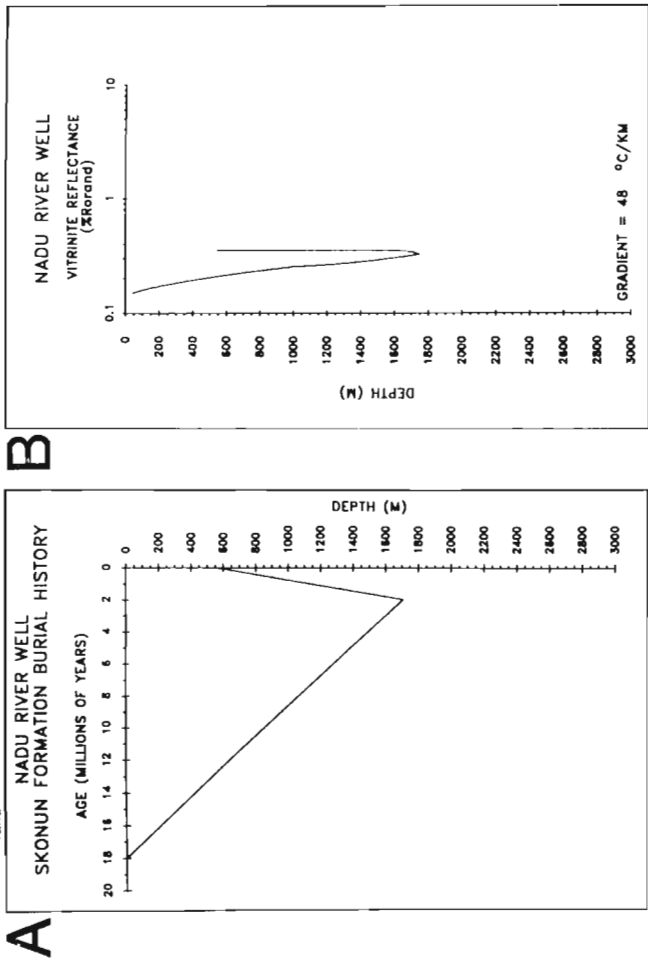
If constant paleogeothermal gradients are assumed for Mesozoic strata in the Queen Charlotte Islands, geothermal gradients ranging from 45-90°C/km are required for up to 180 Ma from the Upper Triassic to Middle Eocene (which was predominantly volcanically quiescent). In particular, the Arrhenius model predicts paleogeothermal gradients of 90°C/km for Triassic strata at Frederick Island for 180 Ma between the Norian and the Middle Eocene. However, there is no evidence of igneous activity to generate the predicted high heat flow near Frederick Island until Tertiary time. Similarly, unusually high paleogeothermal gradients are required during periods of volcanic quiescence to produce the maturation levels measured from Jurassic and Cretaceous strata. Similar results are achieved with constant paleogeothermal gradients for other Triassic strata. Thus a variable



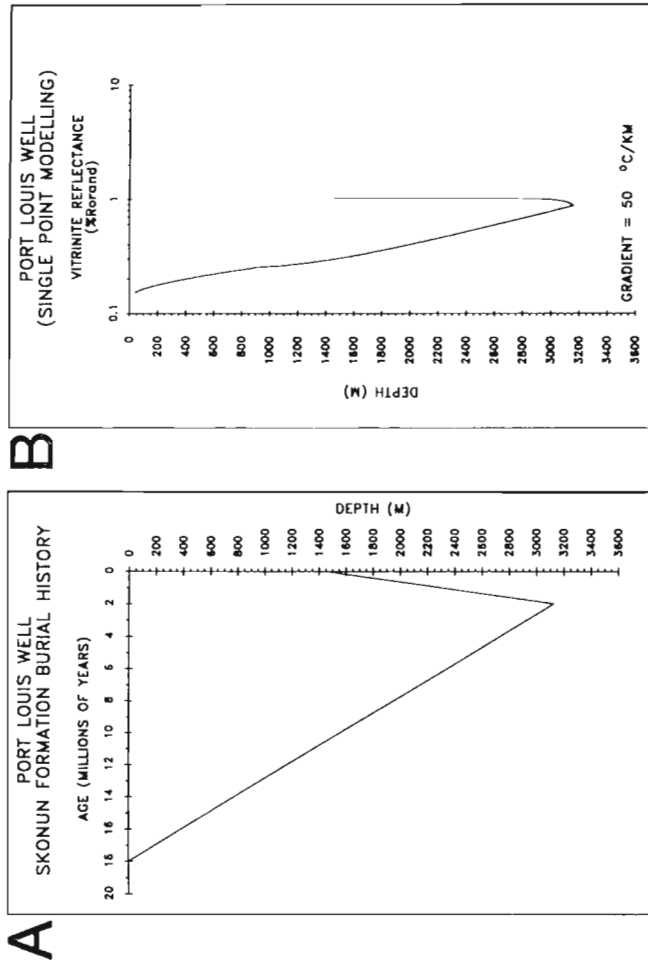
**Figure 21:** Skonun Formation strata in the Cape Ball well. a) interpreted burial history for the base of the Skonun assuming uniform subsidence and uplift rates derived from published and unpublished data; b) and c) maturation history (relative to depth and time) for the basal strata using a modified Arrhenius model (constant geothermal gradient=37°C/km); d) calculated geothermal gradients and measured maturation gradients are plotted through the origin (0.15 %Ro<sub>and</sub>) to facilitate comparison of slopes.

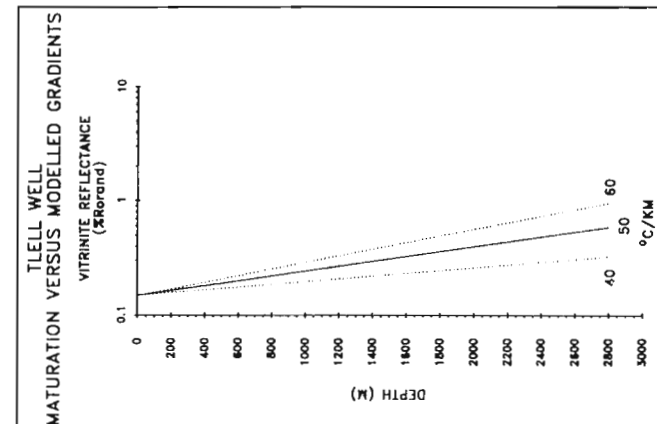
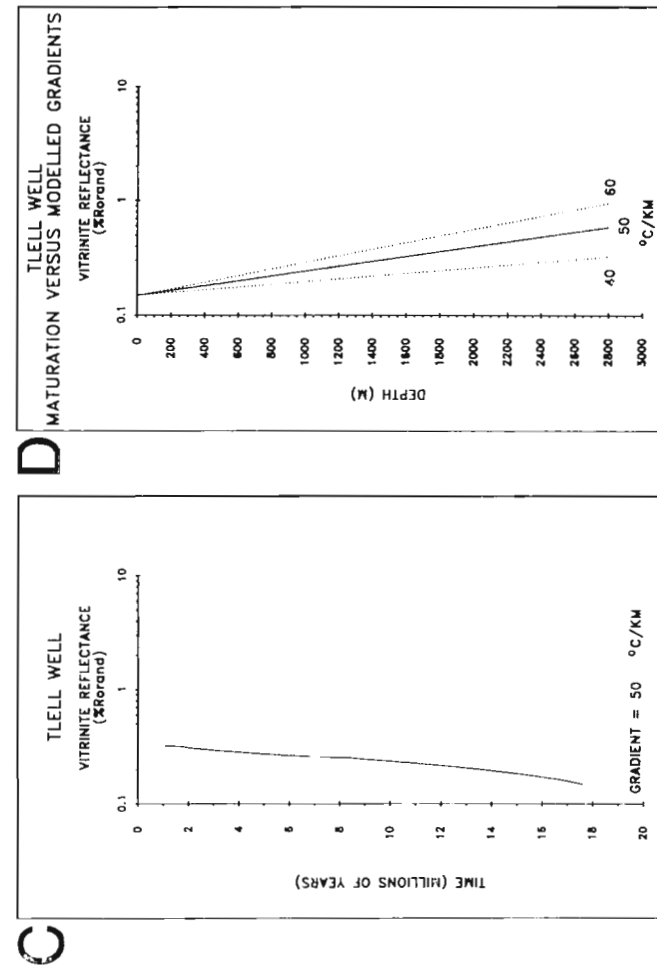
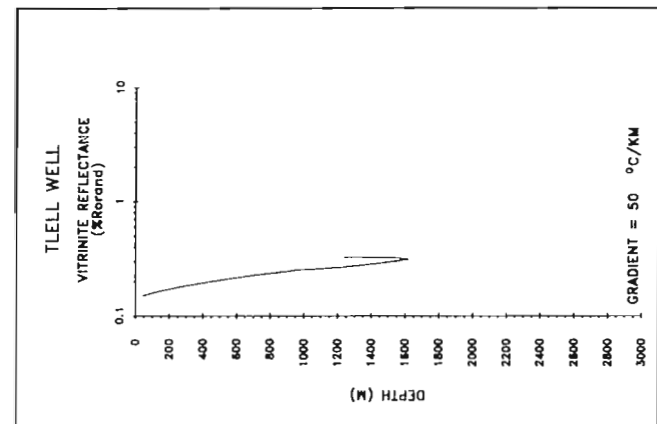
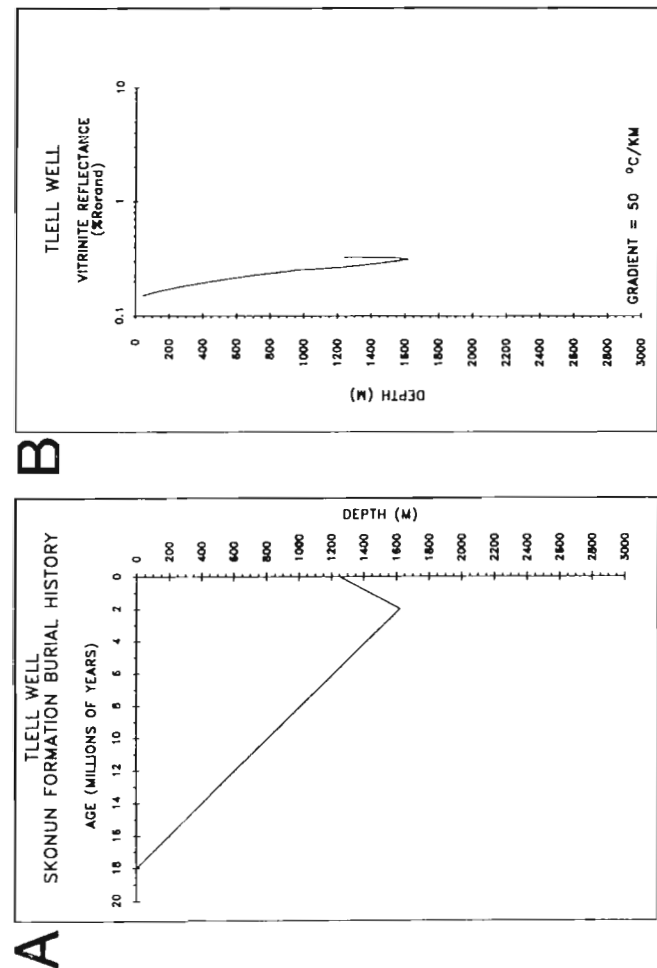
**Figure 22:** Skonun Formation strata in the Gold Creek well. a) interpreted burial history for the base of the Skonun assuming uniform subsidence and uplift rates derived from published and unpublished data; b) and c) maturation history (relative to depth and time) for the basal strata using a modified Arrhenius model (constant geothermal gradient=50°C/km); d) calculated geothermal gradients and measured maturation gradients are plotted through the origin (0.15 %Ro<sub>and</sub>) to facilitate comparison of slopes.

**Figure 23:** Skonun Formation strata in the Nadu River well. a) interpreted burial history for the base of the Skonun assuming uniform subsidence and uplift rates derived from published and unpublished data; b) and c) maturation history (relative to depth and time) for the basal strata using a modified Arrhenius model (constant geothermal gradient=48°C/km); d) calculated geothermal gradients and measured maturation gradients are plotted through the origin (0.15 %Ro<sub>rand</sub>) to facilitate comparison of slopes.

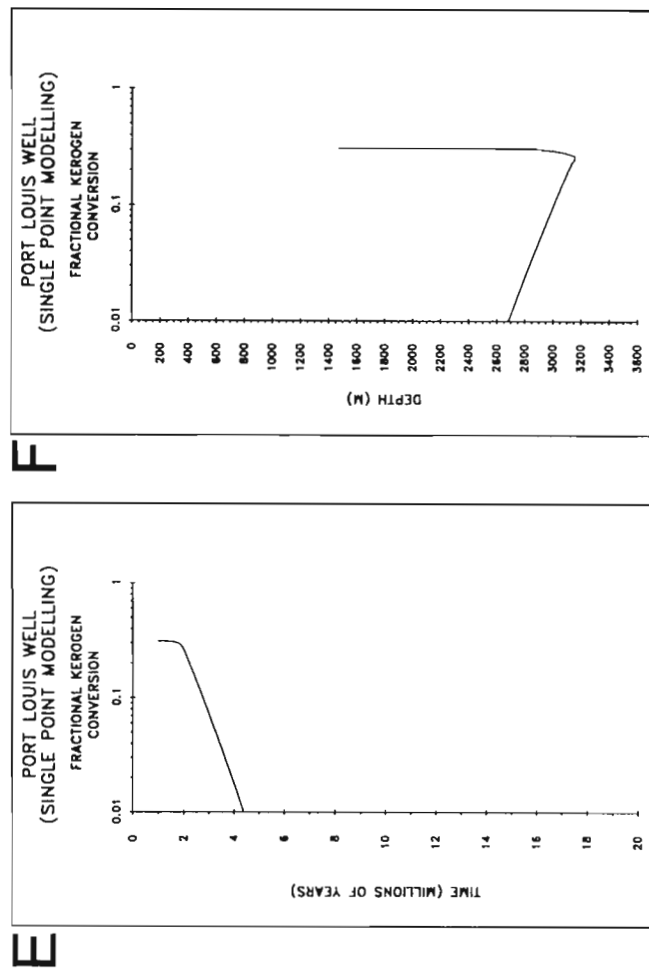


**Figure 24a-d:** Skonun Formation strata at the Port Louis well. a) interpreted burial history for the base of the Skonun assuming uniform subsidence and uplift rates derived from published and unpublished data; b) and c) maturation history (relative to depth and time) for the basal strata using a modified Arrhenius model (constant geothermal gradient=45°C/km); d) calculated geothermal gradients and measured maturation gradients are plotted through the origin (0.15 %Ro<sub>rand</sub>) to facilitate comparison of slopes.



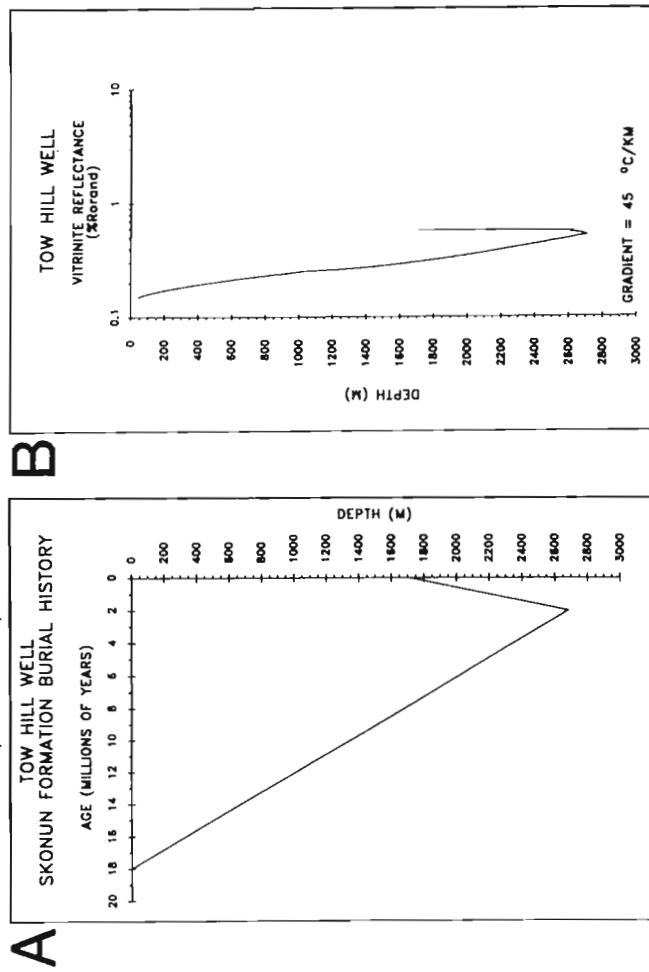


**Figure 25:** Skonun Formation strata at the Tlell well. a) interpreted burial history for the base of the Skonun assuming uniform subsidence and uplift rates derived from published and unpublished data; b) and c) maturation history (relative to depth and time) for the basal strata using a modified Arrhenius model (constant geothermal gradient=50°C/km); d) calculated geothermal gradients and measured maturation gradients are plotted through the origin (0.15 %Ro<sub>rand</sub>) to facilitate comparison of slope.

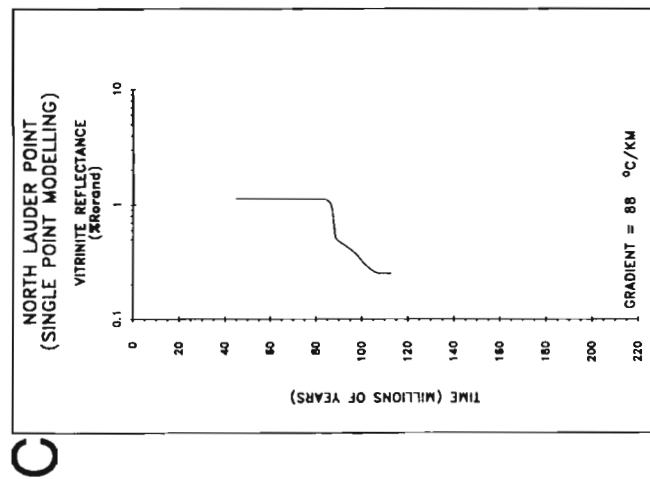
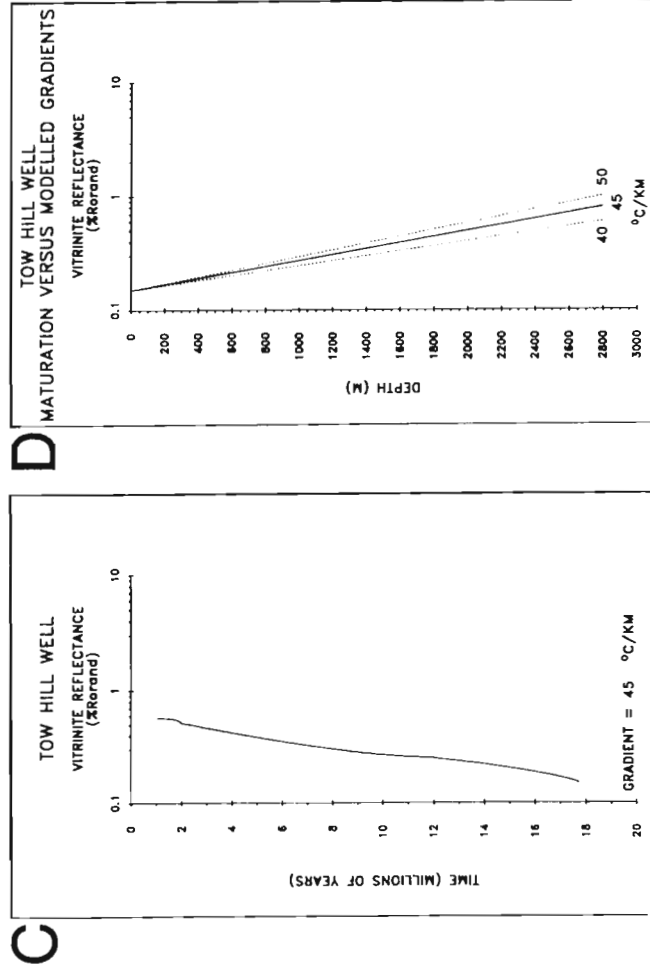
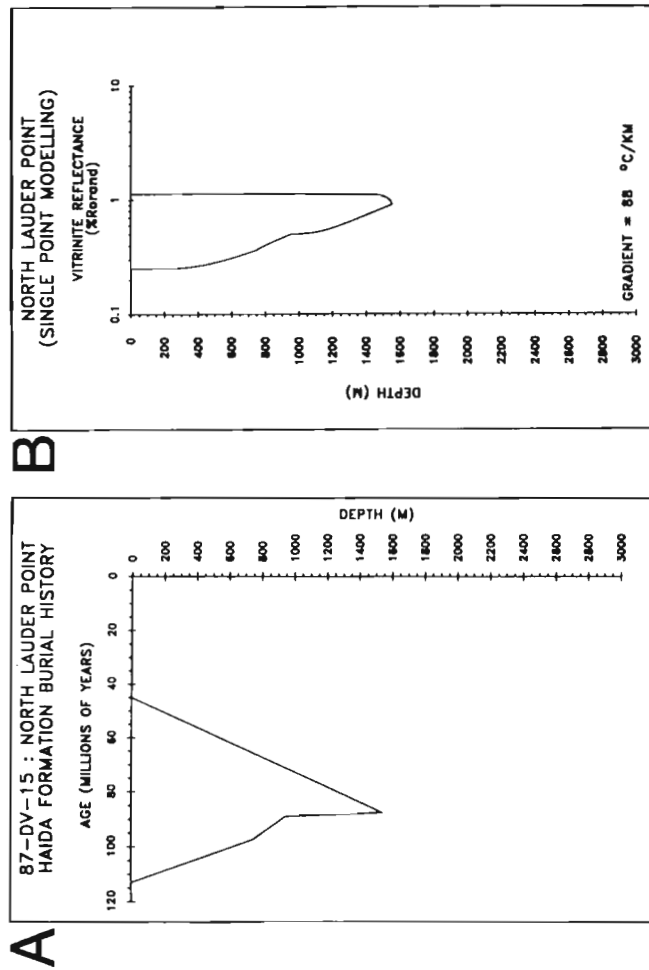


**Figure 24e-f:** Skonun Formation strata at the Port Louis well. Fractional kerogen conversion (relative to time and depth) using a modified Arrhenius model (constant geothermal gradient=45°C/km).

**Figure 26:** Skonun Formation strata at the Tow Hill well. a) interpreted burial history for the base of the Skonun Formation assuming uniform subsidence and uplift rates derived from published and unpublished data; b) and c) maturation history (relative to depth and time) for the basal strata using a modified Arrhenius model (constant geothermal gradient=45°C/km); d) calculated geothermal gradients and measured maturation gradients are plotted through the origin (0.15 %Ro<sub>and</sub>) to facilitate comparison of slopes.



**Figure 27a-c:** Haida Formation strata at north Lauder Point. a) interpreted burial history for the base of the measured section assuming uniform subsidence and uplift rates derived from published and unpublished data; b) and c) maturation history (relative to depth) for the basal strata using a modified Arrhenius model (constant geothermal gradient=88°C/km).



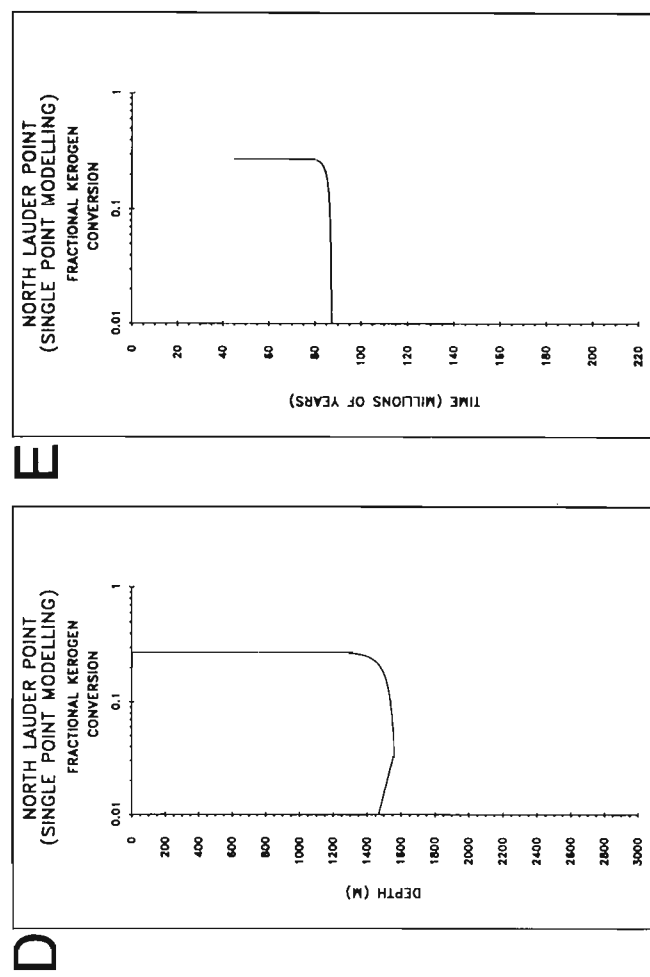
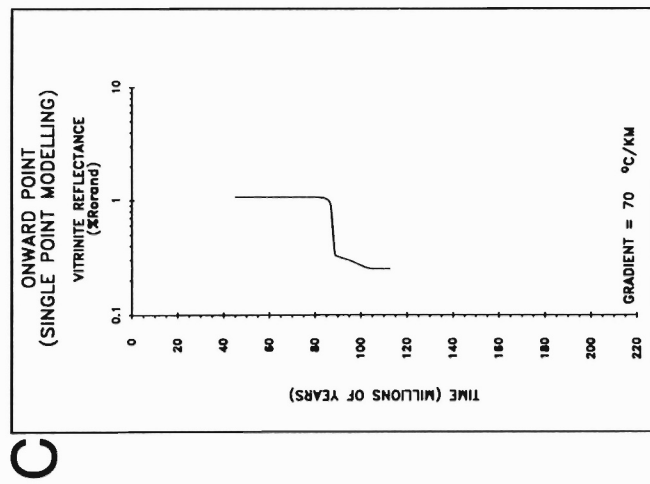
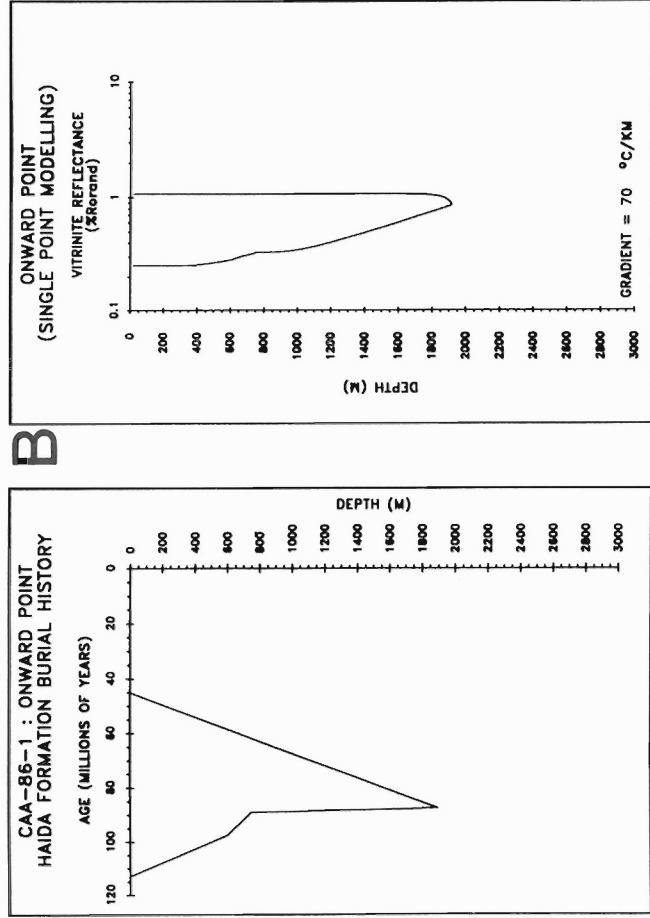
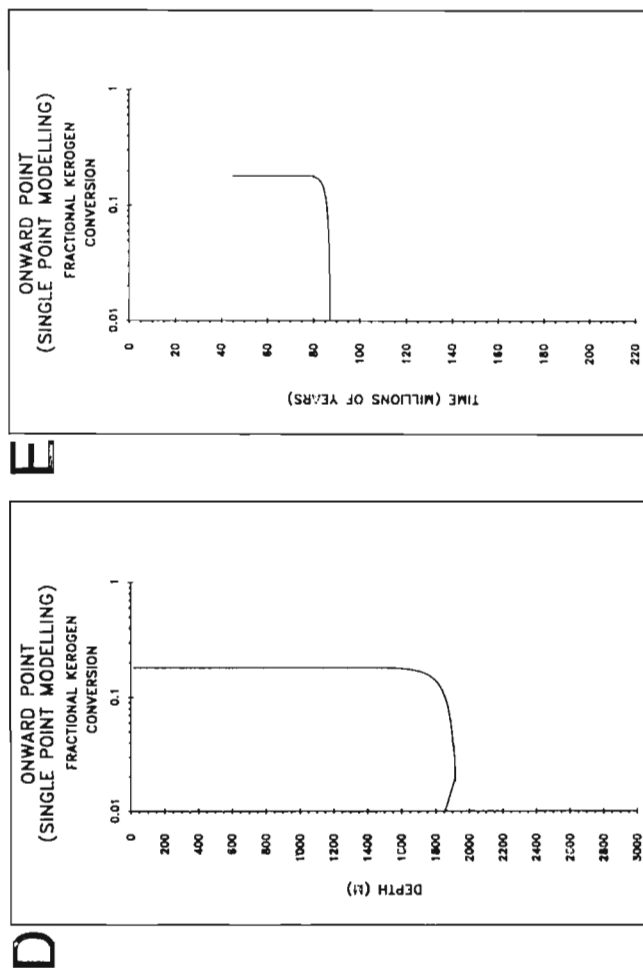


**Figure 27d-e:** Haida Formation strata at north Lauder Point. Fractional kerogen conversion (relative to time and depth) using a modified Arrhenius model (constant geothermal gradient=88°C/km).

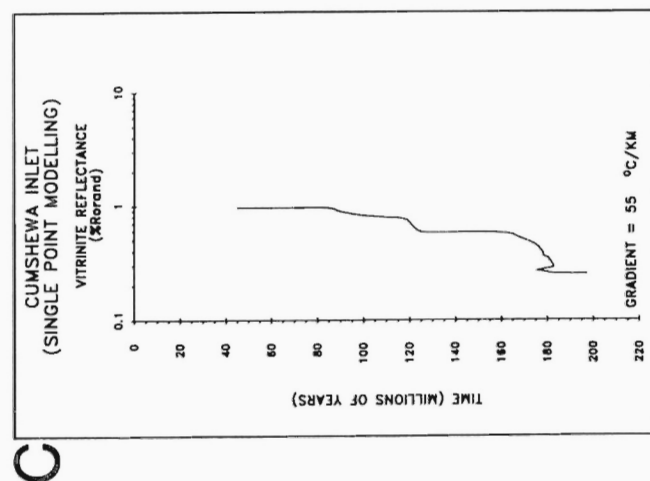
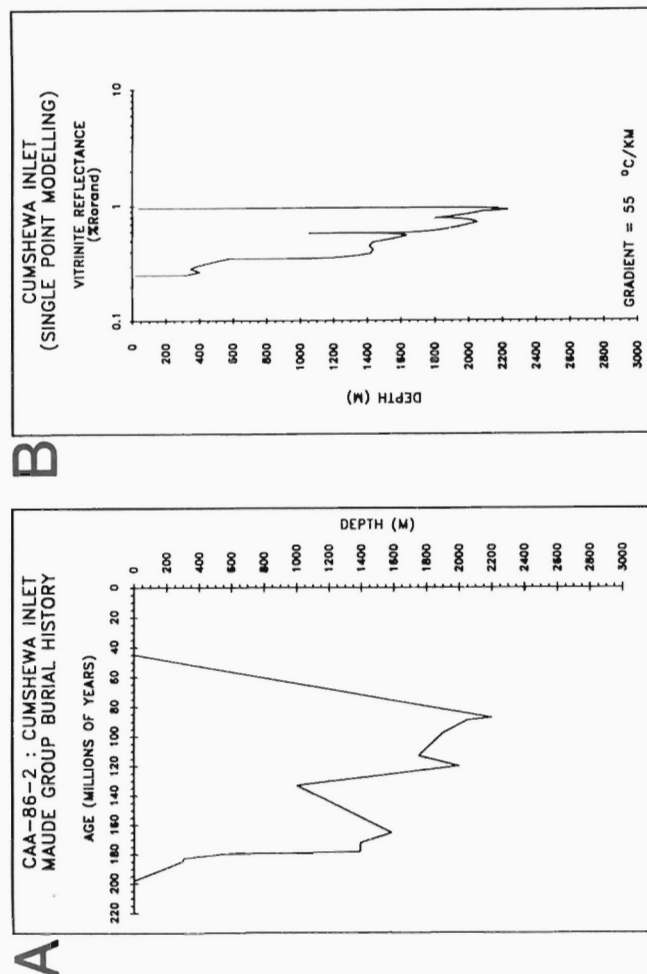
**Figure 28a-c:** Haida Formation strata at Onward Point. a) interpreted burial history for the base of the measured section assuming uniform subsidence and uplift rates derived from published and unpublished data; b) and c) maturation history (relative to depth and time) for the basal strata using a modified Arrhenius model (constant geothermal gradient=70°C/km).



**Figure 28d-e:** Haida Formation strata at Onward Point. Fractional kerogen conversion (relative to time and depth) using a modified Arrhenius model (constant geothermal gradient=70°C/km).



**Figure 29a-c:** Maude Formation strata at Cumshewa Inlet. a) interpreted burial history for the base of the measured section assuming uniform subsidence and uplift rates derived from published and unpublished data; b) and c) maturation history (relative to depth and time) for the basal strata using a modified Arrhenius model (constant geothermal gradient=55°C/km).



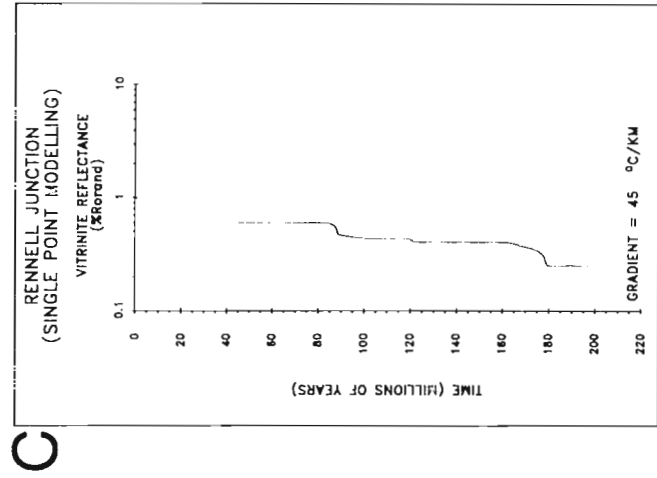
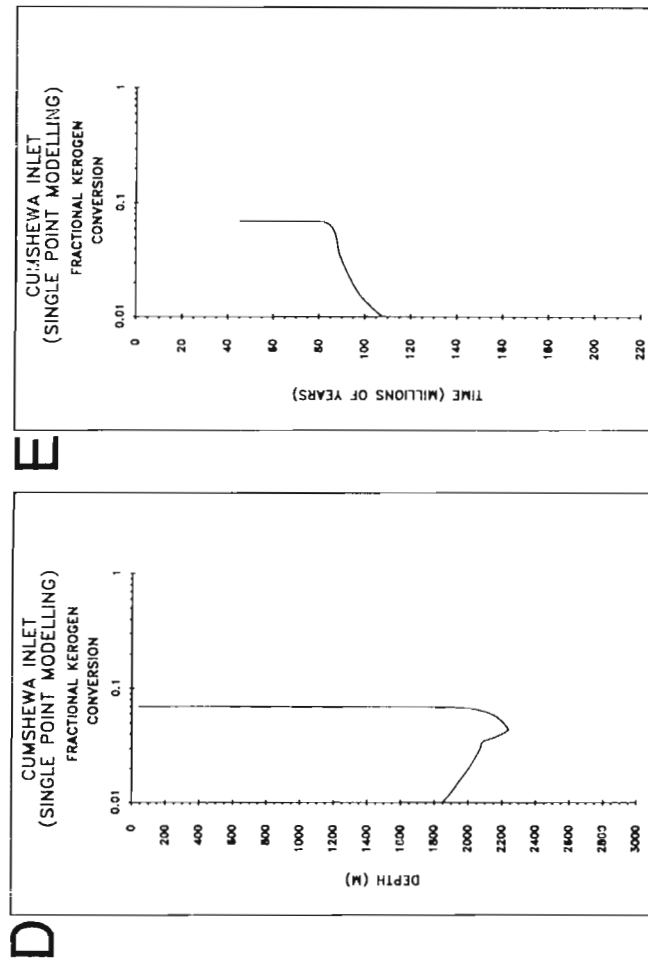
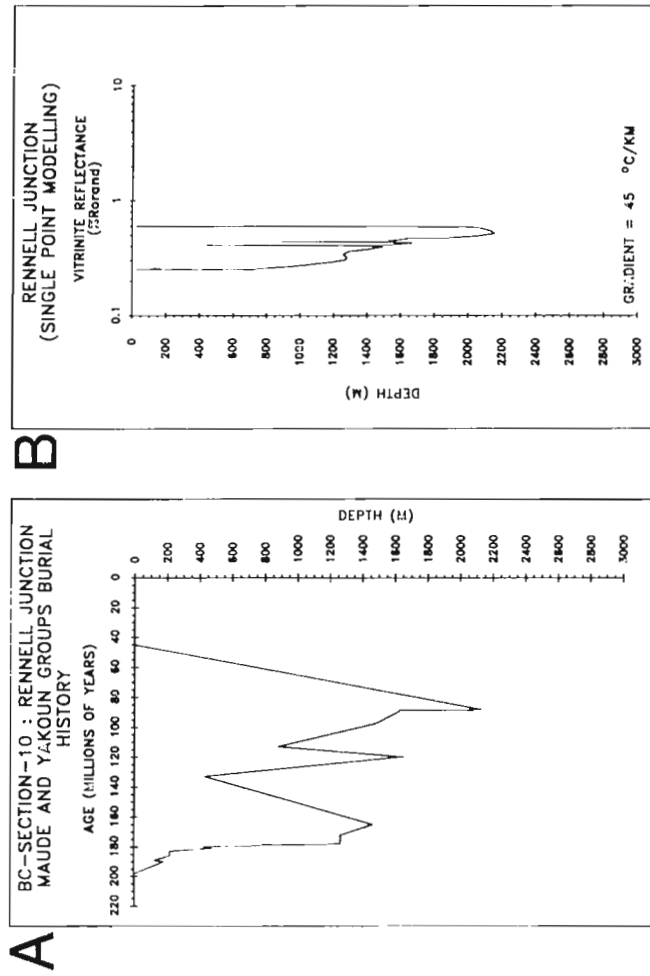
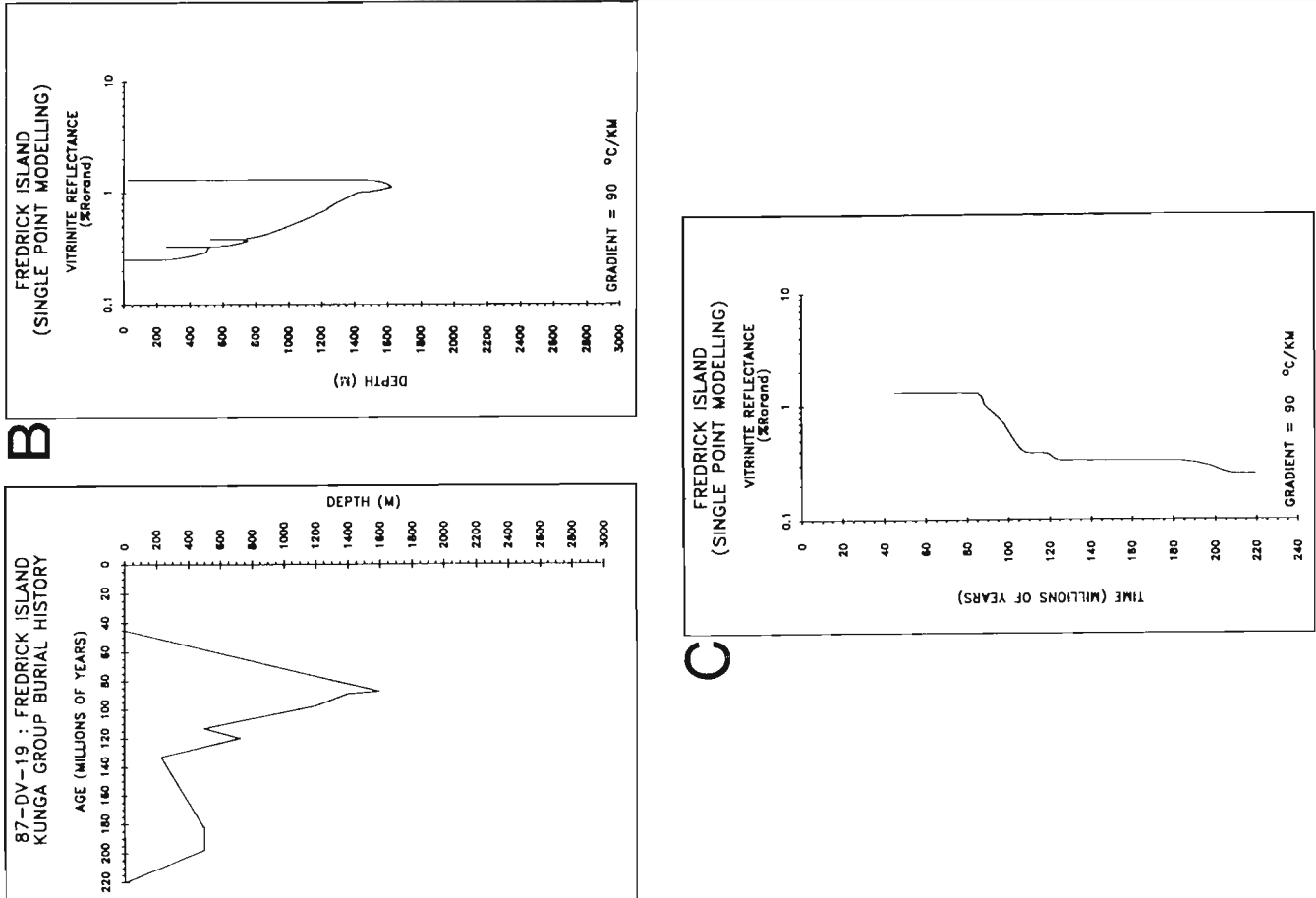


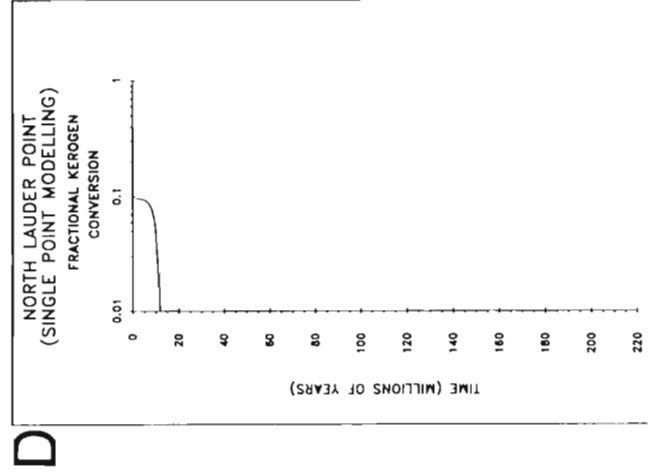
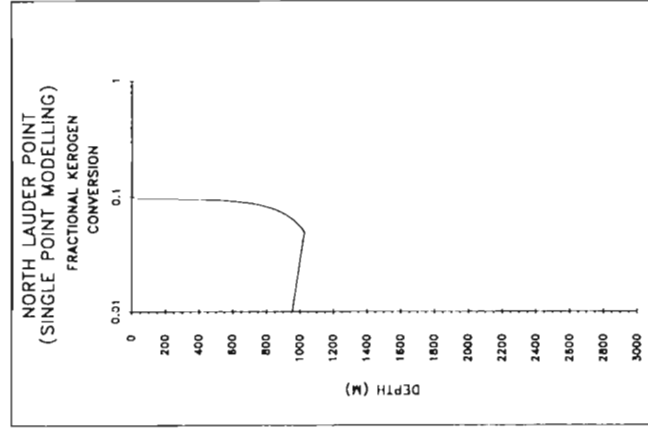
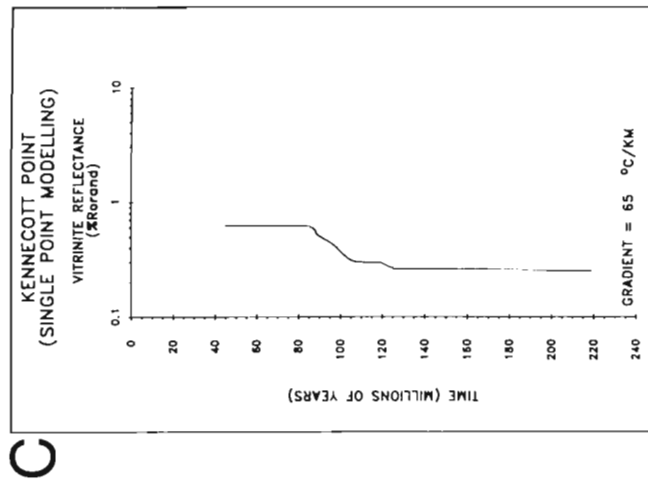
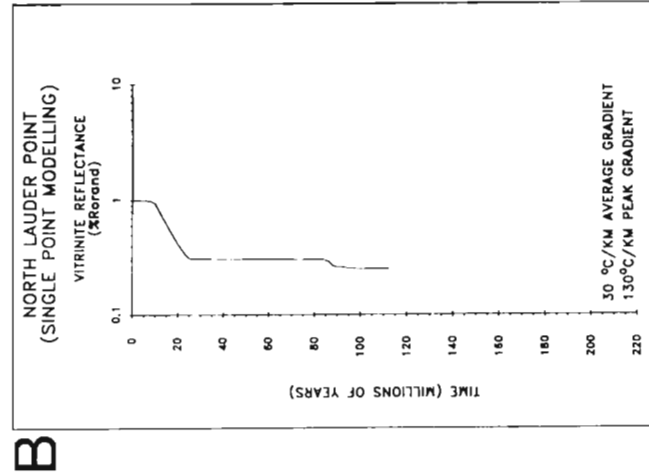
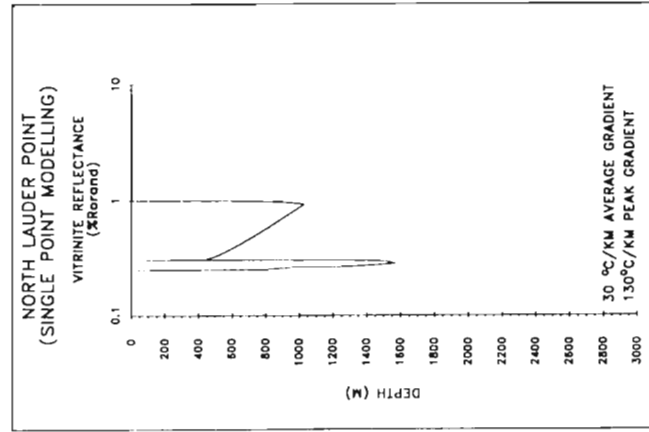
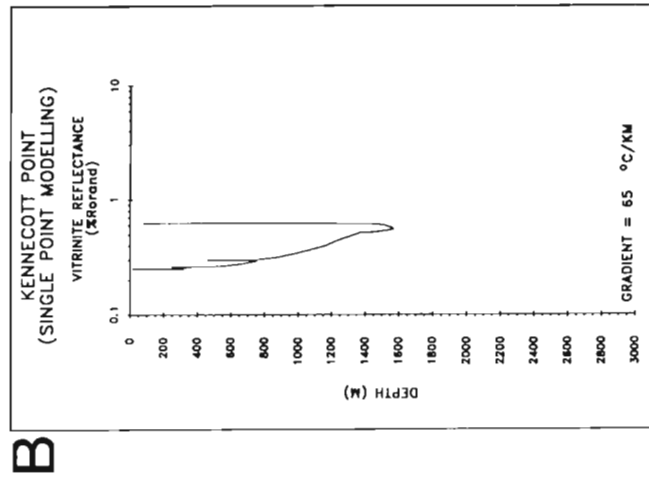
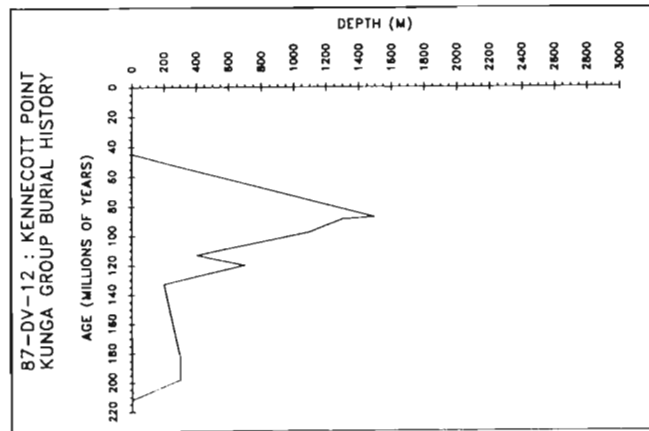
**Figure 30a-c:** Maude Formation strata at Rennell Junction. a) interpreted burial history for the base of the measured section assuming uniform subsidence and uplift rates derived from published and unpublished data; b) and c) maturation history (relative to depth and time) for the basal strata using a modified Arrhenius model (constant geothermal gradient=45 °C/km).

**Figure 29d-e:** Maude Formation strata at Cumshewa Inlet. Fractional kerogen conversion (relative to time and depth) using a modified Arrhenius model (constant geothermal gradient=55 °C/km).

**Figure 31a-c:** Sandilands Formation strata at Fredrick Island. a) interpreted burial history for the base of the measured section assuming uniform subsidence and uplift rates derived from published and unpublished data; b) and c) maturation history (relative to depth and time) for the basal strata using a modified Arrhenius model (constant geothermal gradient=90°C/km).

**Figure 31d-e:** Sandilands Formation strata at Fredrick Island. Fractional kerogen conversion (relative to time and depth) using a modified Arrhenius model (constant geothermal gradient=90°C/km).

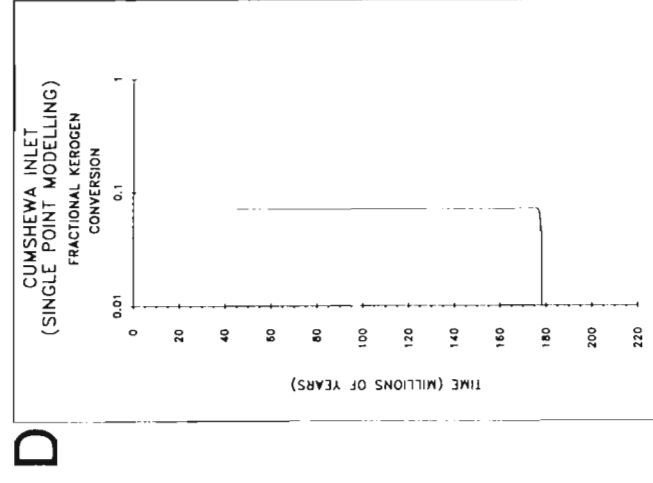
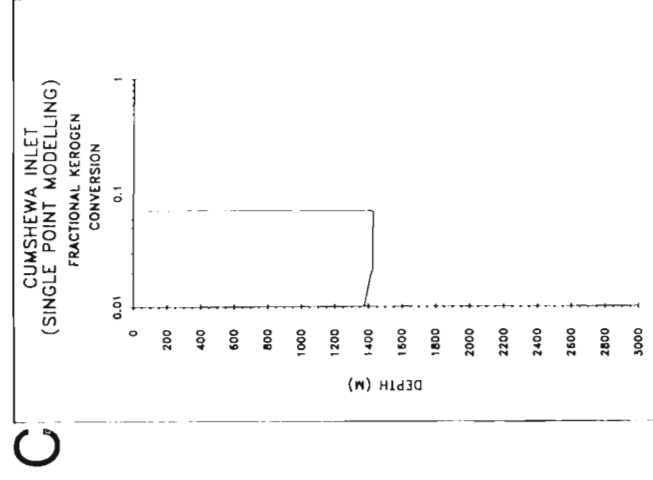
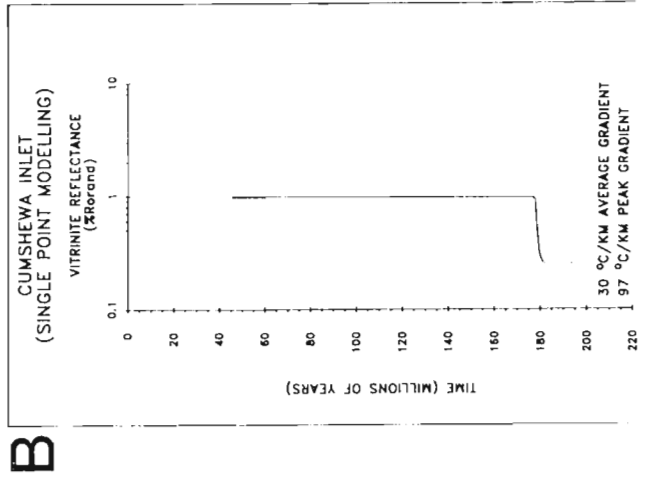
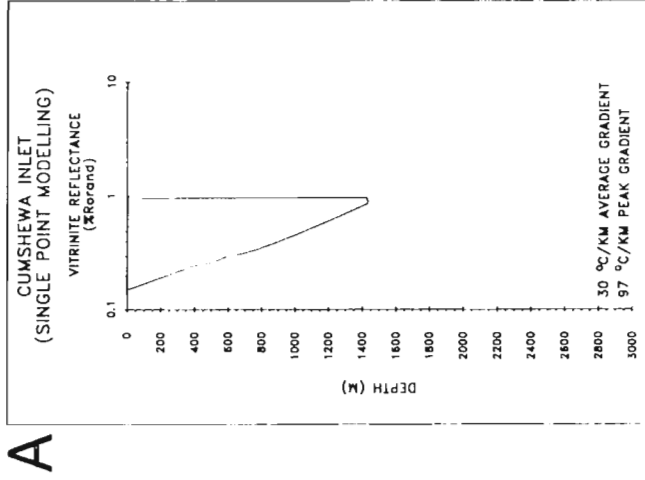
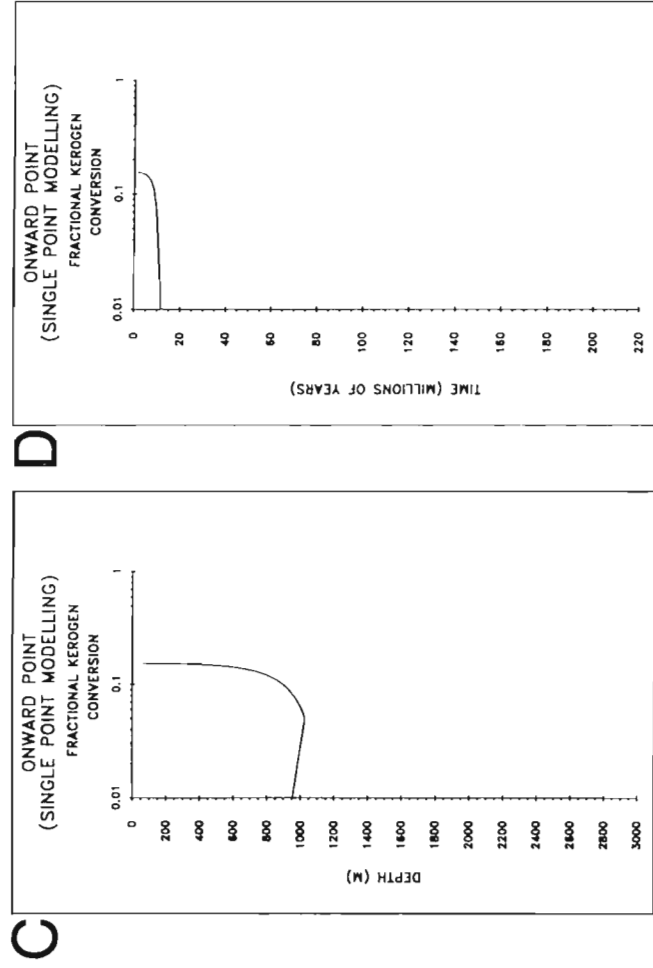
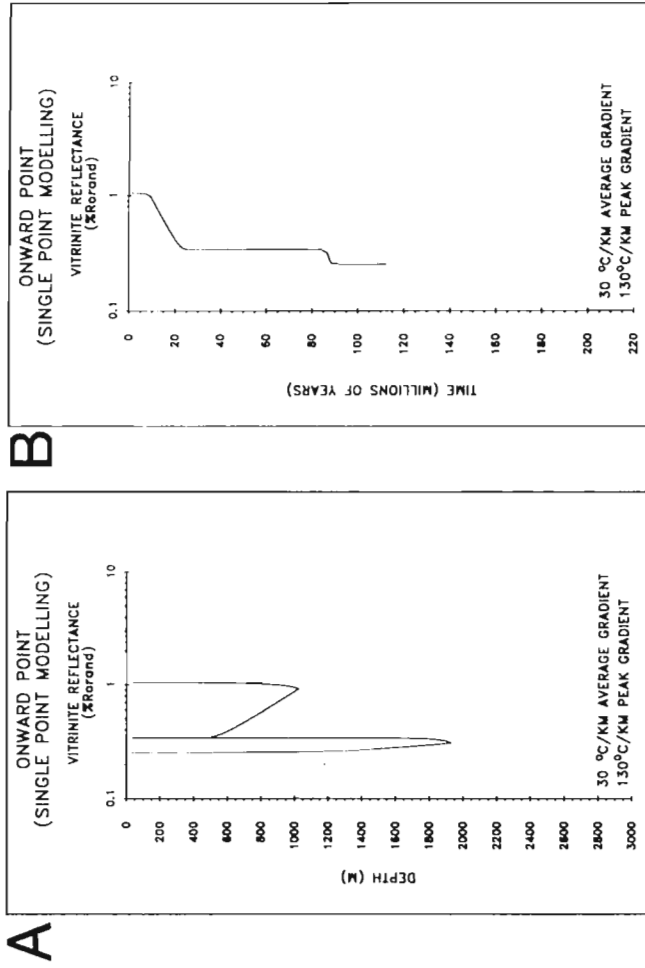




**Figure 32:** Sandilands Formation strata at Kennecott Point. a) interpreted burial history for the base of the measured section assuming uniform subsidence and uplift rates derived from published and unpublished data; b) and c) maturation history (relative to depth and time) for the basal strata using a modified Arrhenius model (constant geothermal gradient=65°C/km).

**Figure 33:** Haida Formation strata at north Lauder Point (variable geothermal gradient model with 30°C/km average gradient): a) and b) maturation history (relative to depth and time) for the basal strata using a modified Arrhenius model (130°C/km peak geothermal gradient); c) and d) fractional kerosen conversion (relative to depth and time) using the same model and geothermal gradient.

**Figure 34:** Haida Formation strata at Onward Point (variable geothermal gradient model with 30°C/km average gradient): a) and b) maturation history (relative to depth and time) for the basal strata using a modified Arrhenius model (130°C/km peak geothermal gradient); c) and d) fractional kerogen conversion (relative to depth and time) using the same model and geothermal gradient).



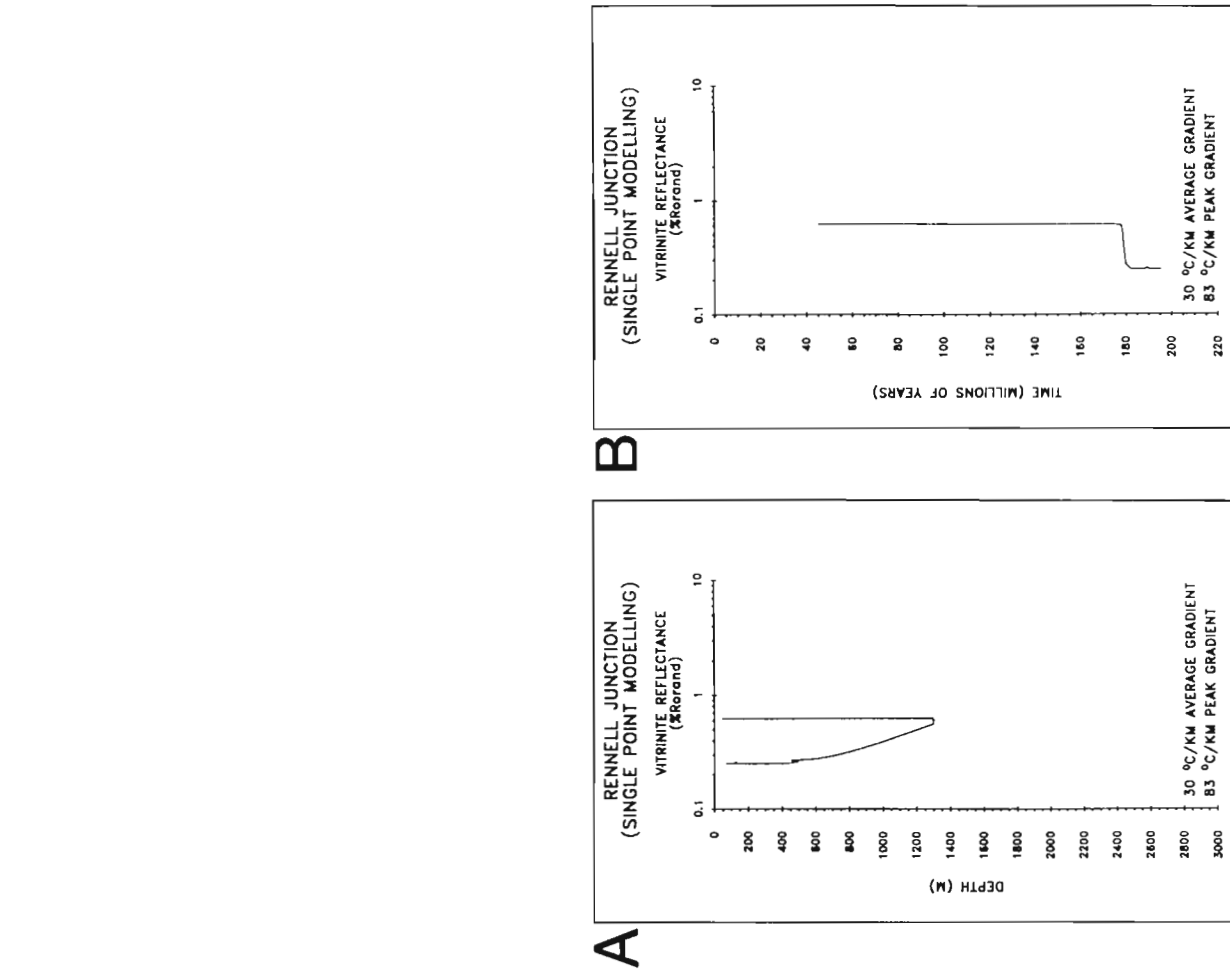


**Figure 36:** Maude Group strata at Rennell Junction (variable geothermal gradient model with 30 °C/km average gradient): a) and b) maturation history (relative to depth and time) for the basal strata using a modified Arrhenius model (83 °C/km peak geothermal gradient).

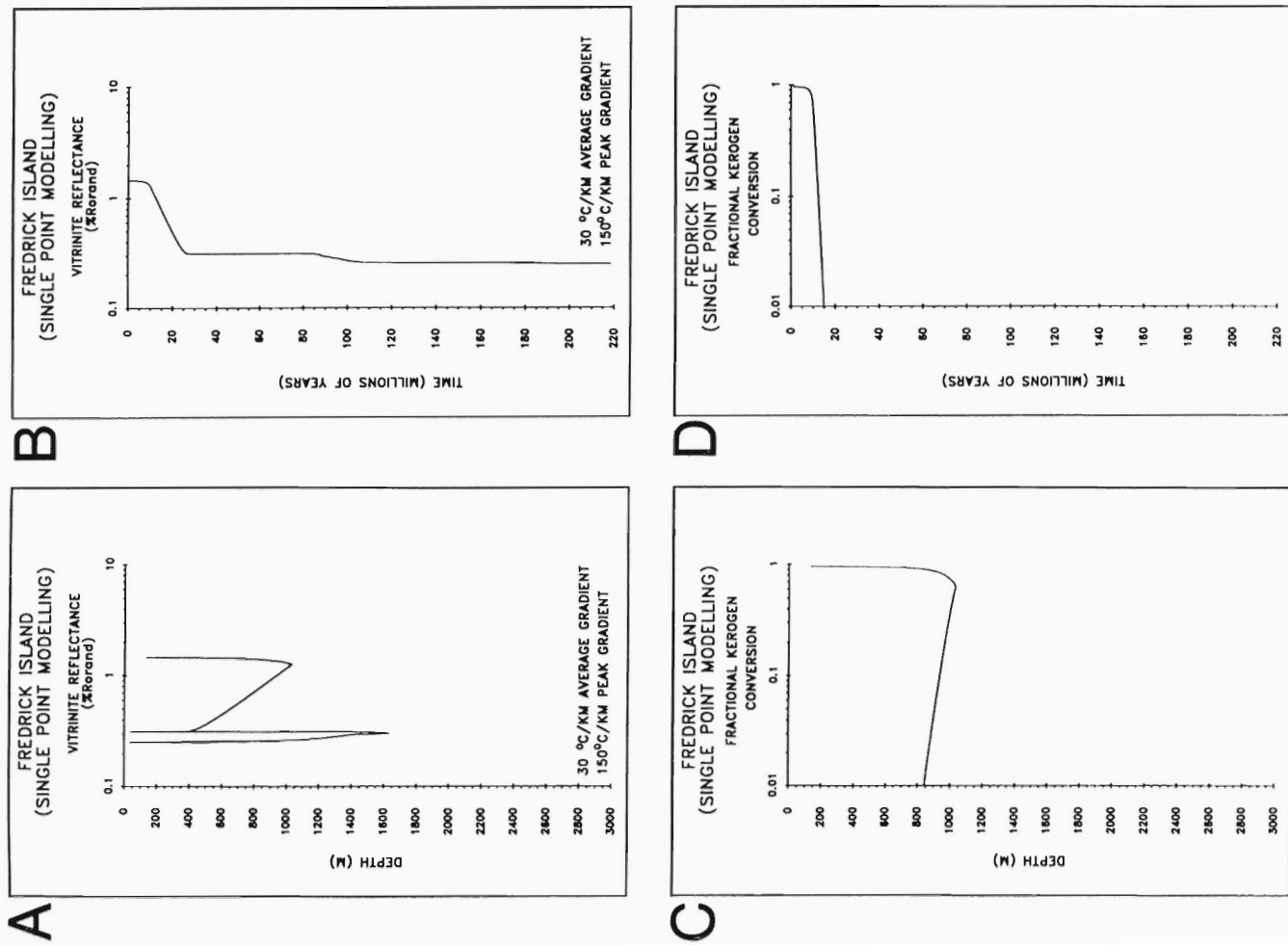


**Figure 37:** Kunga Group strata at Fredrick Island (variable geothermal gradient model with 30 °C/km average gradient): a) and b) maturation history (relative to depth and time) for the basal strata using a modified Arrhenius model (150 °C/km peak geothermal gradient); c) and d) fractional kerogen conversion (relative to depth and time) using the same model and geothermal gradient).



thermal regime with moderate background geothermal gradients and high peak geothermal gradients more reasonably describes Mesozoic maturation than does a constant thermal regime. If the heat flow was higher during volcanic episodes than assumed in the models used here, less time would be required to achieve the same measured DOM.

The DOM of Lower Jurassic Maude and Yakoun group strata increases from Rennell Junction to Cumshewa Inlet. Although burial depths are similar at both localities, variable thermal regime modelling predicts higher peak heat flow during Early Bajocian time at Cumshewa Inlet ( $97^{\circ}\text{C}/\text{km}$ ) than at Rennell Junction ( $83^{\circ}\text{C}/\text{km}$ ). The higher paleogeothermal gradient at Cumshewa Inlet is most likely the result of elevated heat flow from Yakoun Group volcanism or from coeval plutonism on Moresby Island. Furthermore, at Rennell Junction, Yakoun Group sediments (Graham Island and Richardson Bay formations) were deposited rather than Yakoun andesites (Cameron and Tipper, 1985) suggesting that diminished volcanic activity near Rennell Junction may account for the lower heat flow predicted in central Graham Island.

Jurassic strata younger than the Sinemurian Sandilands Formation were probably not deposited in the Frederick Island-Kennecott Point area, therefore, Yakoun volcanism was most likely not significant to the thermal maturation of Kunga strata. Heat flow associated with Masset feeder dykes and sills near Frederick Island and Kennecott Point were the most likely cause of the elevated paleogeothermal gradients predicted by maturation modelling. A higher geothermal gradient predicted for Frederick Island (relative to Kennecott Point) is probably due to increased heat flow from Masset feeder dykes/sills more proximally located to Frederick Island.

## TIMING OF HYDROCARBON GENERATION

The timing of hydrocarbon generation was estimated from numerical modelling (Table 13) using the vitrinite reflectance/time diagrams and assuming an oil window between 0.50 and 1.35 % $R_{\text{orand}}$  (Vellutini and Bustin, 1991). Figures 24, 33-35, and 37 illustrate the degree of converted kerogen to petroleum with respect to depth and time for each section plotted with respect to time and depth. Diagrams for immature strata which have not generated significant amounts of hydrocarbons are not shown.

The Tertiary Skonun Formation is everywhere immature with respect to oil generation except at west (Port Louis well) and northeast Graham Island (basal strata of the Tow Hill well). Strata from west Graham Island (Port Louis well) are predicted to have entered the oil window in the Late Miocene (7.6 Ma) and are currently in the oil window (Table 13). The models predicts that strata from northeast Graham Island (basal strata of the Tow Hill well) entered the oil window in the Late Miocene (5.1 Ma) and never exited the oil window. The generation of hydrocarbons at west and northeast Graham Island (Port Louis and Tow Hill wells) is probably the result of higher paleogeothermal gradients and deeper burial than adjacent strata. Strata from west Graham Island (Port Louis well) are intercalated with Masset volcanics and may be of limited lateral extent, suggesting that the area has questionable potential to generate exploitable amounts of liquid hydrocarbons. Oil staining occurs in a thin interval of strata at northeast Graham Island in the Tow Hill well, suggesting hydrocarbons may have been generated from Tertiary Skonun Formation.

Cretaceous strata at north Lauder Point and Onward Point are presently within the oil window. The Arrhenius model predicts that

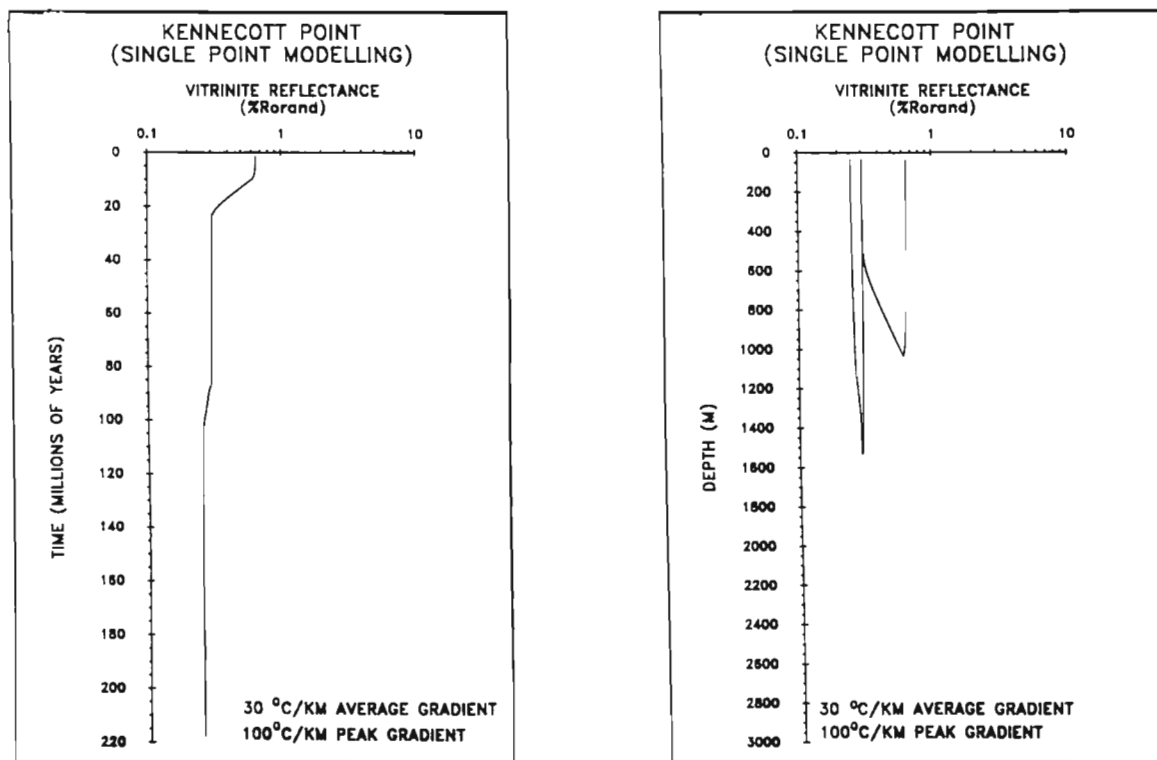


**Figure 38:** Kunga Group strata at Kennecott Point (variable geothermal gradient model with  $30^{\circ}\text{C}/\text{km}$  average gradient). Maturation history (relative to time and depth) for the basal strata using a modified Arrhenius model ( $100^{\circ}\text{C}/\text{km}$  peak geothermal gradient).

**Table 13:** Predicted paleogeothermal gradients and times of entering, leaving the oil window

Constant geothermal gradient model		
	Gradient (°C/km)	Time (Ma) of entering, leaving oil window
Tertiary strata		
Skonun formation (exploration wells)		
Cape Ball	37	-,-
Gold Creek	50	-,-
Nadu River	48	-,-
Port Louis*	45	7.6,-
Tiell	50	-,-
Tow Hill	45	5.1,-
Cretaceous strata		
Haida Formation (outcrop)		
North Launder Point*	88	88,-
Onward Point*	70	87,-
Jurassic strata		
Maude and Yakoun groups (outcrop)		
Cumshewa Inlet*	55	169,-
Rennell Junction*	45	88,-
Triassic strata		
Kunga Group (outcrop)		
Frederick Island*	90	102.83
Kennecott Point*	65	90,-
Variable geothermal gradient model (30°C/km background paleogeothermal gradient)		
	Predicted peak geothermal gradient (°C/km)	Time (Ma) of entering, leaving oil window
Cretaceous strata		
Haida Formation (outcrop)		
North Launder Point*	130	18,-
Onward Point*	130	18,-
Jurassic Strata		
Maude and Yakoun groups (outcrop)		
Cumshewa Inlet*	97	178,-
Rennell Junction*	83	178,-
Triassic strata		
Kunga Group (outcrop)		
Frederick Island*	150	20.10
Kennecott Point*	100	13,-

\* Single point modelling

strata at north Launder Point and Onward Point entered the oil window during the Early Miocene (18 Ma).

Lower Jurassic strata at Cumshewa Inlet and Rennell Junction are mature with respect to hydrocarbon generation and are presently within the oil window. The strata entered the oil window during the Early Bajocian time (178 Ma).

Triassic strata from Frederick Island entered and exited the oil window during the Early and Late Miocene (20 Ma and 10 Ma respectively). The strata at Kennecott Point are mature and are presently within the oil window. Lower predicted paleogeothermal gradients suggest that the strata entered the oil window during Middle Miocene time (13 Ma).

## HYDROCARBON GENERATION RELATIVE TO TECTONIC ELEMENTS

Major structural deformation in the Queen Charlotte Islands occurred primarily in two broad episodes: syn- and post-Yakoun volcanism in the Middle and Late Jurassic; and between deposition of the Honna and the Masset formations in the Late Cretaceous and Early Tertiary. Hydrocarbons generated from the Skonun Formation postdate the formation of Mesozoic structures. Given favourable basin geometry and migration paths, Tertiary oil may be trapped in

Mesozoic structures. Skonun sourced hydrocarbons may also be pooled in stratigraphic or growth fault traps onshore or in Hecate Strait.

Variable paleogeothermal gradient modelling suggests that Cretaceous strata on Graham Island and Triassic strata on northwest Graham Island generated hydrocarbons from the Early Miocene to the present and were available for migration to potential Jurassic and Cretaceous-Tertiary structural traps. Jurassic sourced hydrocarbons from central Graham Island and northern Moresby Island were generated from the Bajocian to the present and were available for migration to potential Jurassic and Cretaceous-Tertiary aged structural traps.

## DISCUSSION

Organic maturation of strata on the Queen Charlotte Islands is primarily controlled by high heat flow adjacent plutons and dyke/sill swarms on Moresby Island and by 'normal' subsidence on Graham Island. In particular, Mesozoic strata on Moresby Island are overmature as a result of pluton emplacement during the Middle-Late Jurassic and possibly the Oligocene, whereas strata on Graham Island which have not been affected by plutonism are immature to mature (Fig. 39).

The Queen Charlotte Islands have had an island arc tectonic setting since Sinemurian time (Sutherland Brown, 1968; Cameron and Tipper, 1985). During the evolution of volcanic arcs, average heat flow (and geothermal gradient) can vary significantly from below average up to four times average heat flow, depending upon the proximity to the subduction zone (Hasabe et al., 1970; Watanabe et al., 1977; Blackwell et al., 1982). It is therefore likely that the Queen Charlotte Islands have experienced substantial fluctuations in heat flow and thus geothermal gradient in the Mesozoic and Tertiary. Lateral variations in the DOM of various strata on the Queen Charlotte Islands attest to the variable heat flow associated with arc volcanism and plutonism. The Triassic Kunga Group strata on Moresby Island have been subjected to high heat flow are evident from DOM values up to 5.80 %Ro<sub>rand</sub>. The Sinemurian Sandilands Formation and the Albion Haida Formation best illustrate the north-south regional variations in organic maturity where the DOM increases substantially from north (0.45 %Ro<sub>rand</sub>) to south (4.73 %Ro<sub>rand</sub>).

All strata south of Cumshewa Inlet are overmature as a result of high heat flow associated with pluton emplacement on Moresby Island during Jurassic and Tertiary times. The heat flow was not uniform across Moresby Island. In particular, The DOM for the Sadler and Peril formations of the Kunga Group increases from west to east with decreasing distance from the Late Jurassic Burnaby Island plutonic suite (BIPS; ages range from 168-158 Ma, Anderson and Reichenbach, 1991), suggesting that the emplacement of the BIPS was the dominant thermal event on Moresby Island. Hydrothermal activity associated with the BIPS has resulted in sericite and endoskam alteration (with associated mineralization) and higher levels of organic maturation occur proximal to the Burnaby Island Plutonic Suite than to the adjacent San Christoval Plutonic Suite (SCPS). The highest levels of organic maturation, however, are observed in Carpenter Bay near dyke/sill swarms associated with the Carpenter Bay Plutonic Suite (CBPS). The CBPS is Eocene in age (Anderson and Reichenbach, 1991) and possibly related to Masset volcanism. Although the lateral extent of the CBPS is limited, organic maturation resulting from Tertiary plutonism and related igneous intrusives appears to overprint earlier maturation events associated with Middle-Late Jurassic plutonism. More detailed sample collection and analysis is required to determine if high heat flow coeval with Masset volcanism is a contributing factor to the regional organic maturation of Moresby Island and Hecate Strait.

Mesozoic strata in the Cumshewa Inlet and Skidegate Inlet areas are mature to overmature with Jurassic and Cretaceous strata generally having similar DOM values. The high DOM values may have resulted from hydrothermal activity related to heat flow from distant Jurassic-Tertiary plutonism on Moresby Island or Rennell Sound-Shields Bay.

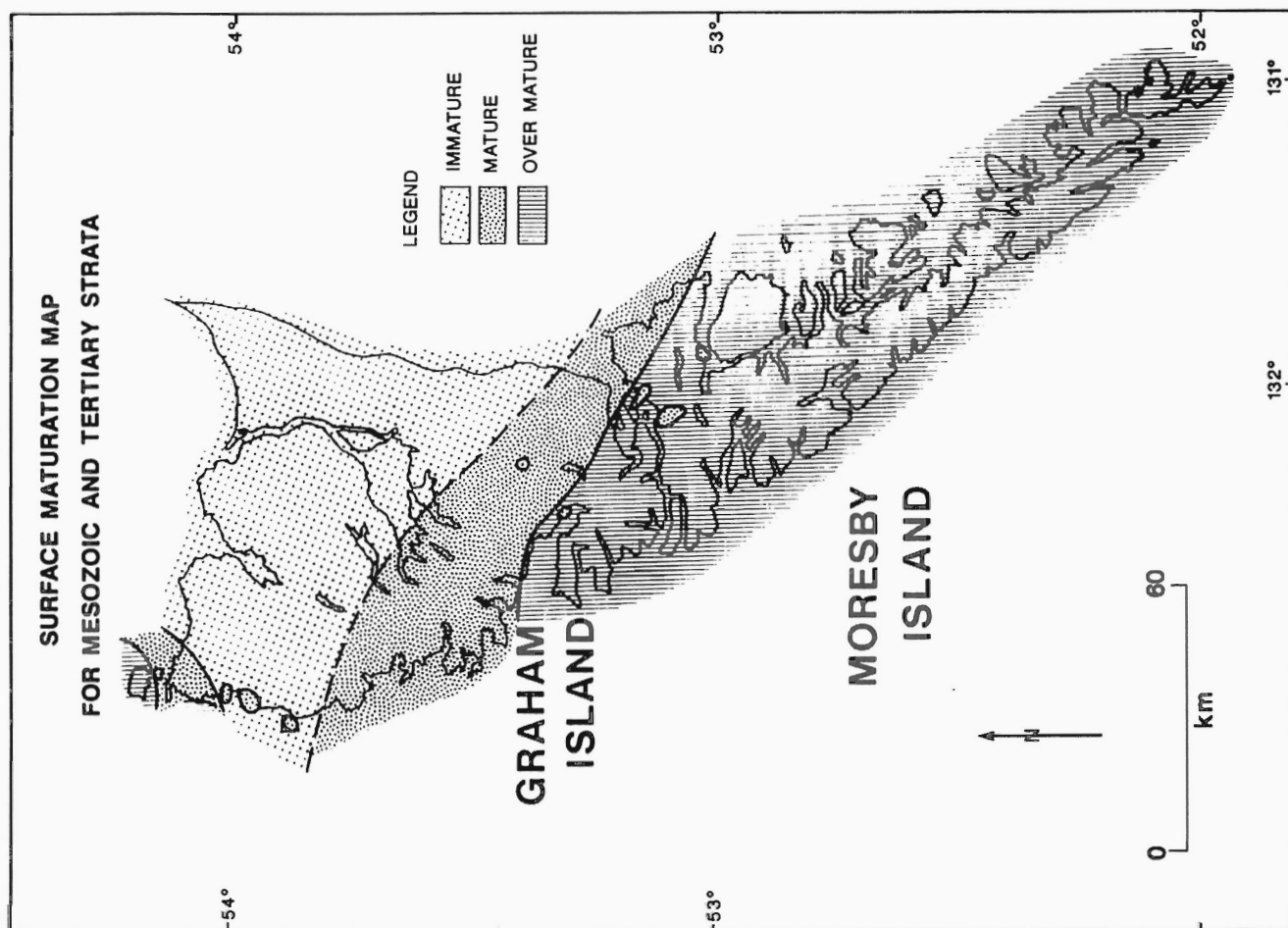


Figure 39: Surface maturation trends for Mesozoic and Tertiary strata derived from vitrinite reflectance data (%Ro<sub>rand</sub>). Oil window is between 0.50 %Ro<sub>rand</sub> and 1.35 %Ro<sub>rand</sub>.

Most of the strata studied from the Maude, Yakoun, and Moresby groups on central Graham Island are mature with some local marginally immature strata. Included in this area are the potential source rocks of the Sandilands and Ghost Creek formations (Vellutini and Bustin, 1991). The lowest measured maturation gradients and modelled paleogeothermal gradients from the Queen Charlotte Islands occur in central Graham Island. There, where maturation tends to increase from east to west (opposite that of Moresby Island), suggesting that thermal effects from Jurassic and Tertiary volcanism on Moresby Island were not pronounced in central Graham Island. Instead, heat flow associated with plutonism near Rennell Sound and Shields Bay may have been the dominant thermal event affecting organic maturation in central Graham Island. Deposition of Yakoun and Moresby Group sediments and the lack of equivalent volcanic strata in central Graham Island suggests that Jurassic volcanism may never have been extensive in the area (Cameron and Tipper, 1985). The source potential for central Graham Island is uncertain in that the thermal regime in this area and the lateral extent of the source rocks are poorly known due to the limited outcrop distribution.

Organic maturation in northwest Graham Island ranges from immature to overmature with most of the strata ranging from marginally mature to mature. Overmature strata are most likely the result of high heat flow from plutonic activity on Langara Island. High heat flow from Masset igneous intrusives near Frederick Island has resulted in the local overmaturation of potential Triassic source strata of the Kunga Group.

## SUMMARY AND CONCLUSIONS

Upper Triassic to Sinemurian Kunga Group strata on northwest Graham Island are generally marginally mature (0.45 %Ro<sub>rand</sub>). The

main component of maturation is thought to have occurred during Tertiary time. On central Graham Island and Moresby Island, the main time of maturation of the Sandilands Formation is considered to have been generally syn- or post-tectonic (Late Jurassic-Cretaceous). Sandilands Formation strata are marginally mature (0.48 %Ro<sub>rand</sub>) on central Graham Island and overmature in Skidegate Inlet. All Kunga Group strata on Moresby Island are overmature as a result of high heat flow associated with Middle-Late Jurassic plutonism. The DOM increases from west to east with increasing proximity to the Burnaby Island Plutonic Suite. The DOM near Carpenter Bay increases to 8.31 %Ro<sub>rand</sub> as a result of Oligocene plutonism which has overprinted maturation events associated with Middle-Late Jurassic plutonism.

Jurassic strata (Maude, Yakoun, and Moresby groups) from central Graham Island are marginally mature to mature. The DOM increases from east to west with decreasing distance from plutonic complexes near Rennell Sound and Shields Bay. The level of organic maturation increase from central Graham Island (0.43 %Ro<sub>rand</sub>) to northern Moresby Island (1.58 %Ro<sub>rand</sub>). The major component of the maturation is considered to be generally syn- or post-tectonic (Late Jurassic-Cretaceous).

The DOM of Cretaceous strata on Moresby Island increases from north (1.53-2.43 %Ro<sub>max</sub>) to central (2.31-4.78 %Ro<sub>rand</sub>) Moresby Island. Maturation values for Cretaceous strata on Graham Island increase from 0.33 %Ro<sub>rand</sub> in the northwest to 2.21 %Ro<sub>rand</sub> in Skidegate Inlet. The major component of the maturation is thought to be Cretaceous and Tertiary.

Tertiary strata are generally immature with the exception of the mature succession on west Graham Island (Port Louis well) and northeast Graham Island (basal strata of the Tow Hill well). Regional organic maturation values for the basal strata of the Skonun For-

mation increase from east (0.31 %Ro<sub>rand</sub> at Cape Ball) to west (1.33 %Ro<sub>rand</sub> at Port Louis). The major component of maturation is considered to have occurred during late Tertiary time.

The thickness of eroded strata has been calculated from maturation gradients (assuming 0.15 %Ro<sub>rand</sub> as zero maturation level and constant maturation gradients). The calculated thickness of eroded strata for the Tertiary Skonun Formation ranges from 375 m at east Graham Island (Tlell well) to 1685 m at west Graham Island (Port Louis well). Twice as much strata has been eroded from Onward Point (1500 m) as from north Lauder Point. Similar amounts of strata have been removed from Jurassic sections at Cumshewa Inlet (1985 m) and Rennell Junction (1725 m). 1040 m of strata have been eroded from Frederick Island and 735 m of strata have been eroded from Kennecott Point.

Time-temperature modelling suggests that the measured maturation gradients would require constant paleogeothermal gradients ranging from 45-90 °C/km (Arrhenius model) for up to 180 million years. Variable geothermal gradient modelling (assuming a background paleogeothermal gradient of 30°C/km), on the other hand, predicts high heat flow with peak geothermal gradients ranging from 83°C/km on central Graham Island to 150°C/km on Frederick Island during Yakoun (183-178 Ma) and Masset volcanism (35-10 Ma). Higher peak temperatures than those predicted in modelling require shorter heating times to attain the measured level of organic maturation.

Variable geothermal time-temperature modelling suggests that Tertiary strata in the Port Louis and Tow Hill wells entered the oil window during the Late Miocene and are still within the oil window. Tertiary strata on eastern Graham Island are immature and never entered the oil window as a result of shallow burial depths relative to western Graham Island. Cretaceous strata on northwest Graham Island and Skidegate Inlet entered the oil window during the Early Miocene and are still within the oil window. Jurassic strata on central Graham Island and north Moresby Island entered the oil window during Bajocian time and are still within the oil window as a result of shallow burial depths. Triassic strata at Frederick Island entered the oil window during the Early Miocene and exited during the Late Miocene whereas strata at Kennecott Point entered the oil window later during the Middle Miocene and are still within the oil window, reflecting lower paleogeothermal gradients.

## REFERENCES

- Anderson, R.G.  
1988: Jurassic and Cretaceous-Tertiary plutonic rocks on the Queen Charlotte Islands, British Columbia; *in* Current Research, Part E, Geological Survey of Canada, Paper 88-1E, p. 213-216.
- Anderson, R.G. and Reichenbach, I.  
1991: Geochronometric (U-Pb and K-Ar) framework for Middle to Late Jurassic (172-158 Ma) and Tertiary (46-27 Ma) plutons in Queen Charlotte Islands, British Columbia; *in* Evolution and Hydrocarbon Potential of the Queen Charlotte Basin, British Columbia, Geological Survey of Canada, Paper 90-10.
- Blackwell, D.D., Bowen, R.G., Hull, D.A., Riccio, J., and Steele, J.L.  
1982: Heat flow, arc volcanism, and subduction in northern Oregon; *Journal of Geophysical Research*, v. 87, p. 8735-8754.
- Bostick, N.H.  
1973: Time as a factor in thermal metamorphism of phytoclasts; *Congrès International de Stratigraphie et de Géologie du Carbonifère Septième*, Krefeld, August 23-28, 1971. *Compte Rendu*, 2, Illinois State Geologic Survey reprint series 1974-H, p. 183-193.
- Bustin, R.M.  
1986: Organic maturity of Late Cretaceous and Tertiary coal measures, Canadian Arctic Archipelago; *International Journal of Coal Geology*, v. 6, p. 71-106.
- Bustin, R.M. and Macauley, G.  
1988: Organic petrology and Rock-Eval pyrolysis of the Jurassic Sandilands and Ghost Creek formations, Queen Charlotte Islands; *Bulletin Canadian Petroleum Geology*, v. 36, p. 168-176.
- Cameron, B.E.B. and Hamilton, T.S.  
1988: Contributions to the stratigraphy and tectonics of the Queen Charlotte Basin, British Columbia; *in* Current Research, Part E, Geological Survey of Canada, Paper 88-1E, p. 221-227.
- Cameron, B.E.B. and Tipper, F.W.  
1985: Jurassic stratigraphy of the Queen Charlotte Islands, British Columbia; *Geological Survey of Canada, Bulletin* 365, 49 p.
- Chapman, D.S. and Rybach, L.  
1985: Heat flow anomalies and their interpretation; *Journal of Geodynamics*, v. 4, p. 3-37.
- Davis, A.  
1978: The reflectance of coal; *in* Analytical Methods for Coal and Coal Particles, C. Karr (ed.), London, Academic Press, 1, p. 27-28.
- Desrochers, A. and Orchard, M.J.  
1991: Stratigraphic revisions and carbonate sedimentology of the Kunga Group (Upper Triassic-Lower Jurassic), Queen Charlotte Islands, British Columbia; *in* Evolution and Hydrocarbon Potential of the Queen Charlotte Basin, British Columbia, Geological Survey of Canada, Paper 90-10.
- Dow, W.G.  
1977: Kerogen studies and geologic interpretations; *Journal of Geochemical Exploration*, 7, p. 79-99.
- England, T.D.I. and Bustin, R.M.  
1986: Thermal maturation of the western Canadian sedimentary basin south of the Red Deer River: 1) Alberta Plains; *Bulletin of Canadian Petroleum Geology*, v. 34, p. 71-90.
- Hasabe, K., Fujii, N., and Uyeda, S.  
1970: Thermal processes under island arcs; *Tectonophysics*, v. 10, p. 335-355.
- Hickson, C.J.  
1988: Structure and stratigraphy of the Masset Formation, Queen Charlotte Islands, British Columbia; *in* Current Research, Part E, Geological Survey of Canada, Paper 88-1E, p. 269-274.
- Karweil, J.  
1955: The metamorphism of coals from the standpoint of physical chemistry; *Zeitschrift der Geologischen Gesellschaft*, 107, p. 132-139.
- Lopatin, N.V.  
1971: Temperature and geologic time as factors in coalification; *Izvestiya Akademii Nauk USSR, Seriya Geologicheskaya*, 3, p. 95-106.
- Martin, H.A. and Rouse, G.E.  
1966: Palynology of Late Tertiary sediments from the Queen Charlotte Islands, British Columbia; *Canadian Journal of Botany*, v. 44, p. 171-208.
- Palmer, A.R.  
1983: The Decade of North American Geology 1983 Geologic time scale; *Geology*, v. 11, p. 503-504.
- Souther, J.G.  
1988: Implications for hydrocarbon exploration of dyke emplacement in the Queen Charlotte Islands, British Columbia; *in* Current Research, Part E, Geological Survey of Canada, Paper 88-1E, p. 241-245.
- Sutherland Brown, A.  
1968: Geology of the Queen Charlotte Islands; *British Columbia Department of Mines and Petroleum Resources Bulletin* 54, 226 p.
- Tissot, B.P. and Espitalie, J.  
1975: L'évolution thermique de la matière organique des sédiments: Applications d'une simulation mathématique. *Rev. Inst. Fr. Pet.* 30, p. 743-777.
- Tissot, B.P. and Welte, D.H.  
1984: Petroleum formation and occurrence; *Springer-Verlag, Berlin*, 699 p.
- Vellutini, D.  
1988: Organic maturation and source rock potential of Mesozoic and Tertiary strata, Queen Charlotte Islands, British Columbia; *M.Sc. thesis, University of British Columbia, Vancouver*, 262 p.
- Vellutini, D. and Bustin, R.M.  
1991: Source rock potential of Mesozoic and Tertiary strata of the Queen Charlotte Islands, British Columbia; *in* Evolution and Hydrocarbon Potential of the Queen Charlotte Basin, British Columbia, Geological Survey of Canada, Paper 90-10.
- Waples, D.W.  
1980: Time and temperature in petroleum formation with application of Lopatin's method to petroleum exploration; *American Association of Petroleum Geologists, Bulletin* 64, p. 916-926.
- Watanabe, T., Langseth, M.G., and Anderson, R.N.  
1977: Heat flow in back-arc basins of the western Pacific; *in* Island Arcs, Deep Sea Trenches, and Back-Arc Basins, Maurice Ewing Series, v. 1, M. Talwani and W.C. Pitman III (ed.), p. 137-161, American Geophysical Union.
- Wood, D.A.  
1988: Relationships between thermal maturity indices calculated using Arrhenius equation and Lopatin method: implications for petroleum exploration; *American Association of Petroleum Geologists*, v. 72, p. 115-134.



# Conodont colour and thermal maturity of the Late Triassic Kunga Group, Queen Charlotte Islands, British Columbia

M.J. Orchard<sup>1</sup> and P.J.L. Forster<sup>1</sup>

Orchard, M.J. and Forster, P.J.L., Conodont colour and thermal maturity of the Late Triassic Kunga Group, Queen Charlotte Islands, British Columbia; in *Evolution and Hydrocarbon Potential of the Queen Charlotte Basin, British Columbia*, Geological Survey of Canada, Paper 90-10, p.453-464, 1991.

## Abstract

*Conodont collections from the Triassic Kunga Group in the Queen Charlotte Islands have been used to compile a conodont colour alteration index (CAI) map. This shows areas of high paleotemperature that can be used to determine hydrocarbon maturation levels. CAI values were determined by comparison with a set of standard conodont indices assembled from taxonomically related Kunga Group collections that have a complete range of CAI values from about 1 through 8.*

*Three regions can be differentiated based on CAI distribution patterns in the Kunga Group. On southern Moresby Island, CAI values form north-trending belts that generally increase eastward and parallel an eastern axis of largely Jurassic plutonism. In this region, the strata are generally overmature with respect to hydrocarbons, except for westernmost outcrops that may lie within the range of gas production. In the Louise and northern Moresby Island region, CAI values are generally lower than on southern Moresby, trend west-northwest-east-northeast and tend to decrease northeastward to include values within the hydrocarbon window. On northwest Graham Island, the CAI values are generally lower than elsewhere, and are marginally mature to mature in terms of hydrocarbons.*

*Observed CAI variability in the Kunga Group of Moresby and southern Graham islands appears to be primarily related to plutonism and associated hydrothermal activity, which we interpret as a major mode of heat transfer. In particular, 'background' CAI is locally elevated adjacent to faults or stratigraphic contacts that appear to have acted as conduits. Burial depth probably controlled colour alteration values in parts of northwestern Graham Island; minor variations may result from Tertiary igneous activity and lithological differences.*

## Résumé

*On a utilisé des collections de conodontes du groupe de Kunga du Trias dans les îles de la Reine-Charlotte pour compiler une carte de l'indice d'altération des couleurs qui indique les niveaux de maturation des hydrocarbures et les zones de paléotempérature élevée. Les valeurs de cet indice ont été déterminées par comparaison avec une série d'indices de conodontes standards compilés à partir de collections du groupe de Kunga liées sur le plan de la taxonomie et qui correspondent à une gamme complète de l'indice, allant d'environ de 1 à 8.*

*Les configurations de distribution de l'indice d'altération des couleurs permettent de distinguer trois régions dans le groupe de Kunga. Dans le sud de l'île Moresby, les valeurs de l'indice forment des zones à direction nord-sud parallèles à un axe oriental de plutonisme en grande partie jurassique et dont la valeur augmente en général d'ouest en est. Dans cette région, les couches sont généralement hypermatures relativement aux hydrocarbures, à l'exception des affleurements d'extrême ouest qui reposent apparemment dans une zone gazeuse. Dans la région de l'île Louise et du nord de l'île Moresby, les valeurs de l'indice sont en général inférieures à celles du sud de l'île Moresby, elles sont orientées dans la direction WNW-ESE et elles ont tendance à diminuer vers le nord-est de façon à inclure des valeurs comprises dans la fenêtre à hydrocarbures. Dans le nord-ouest de l'île Graham, les valeurs de l'indice sont en général inférieures à celles des autres régions et les roches y sont de peu matures à matures.*

*La variabilité de l'indice d'altération des couleurs observée dans le groupe de Kunga dans l'île Moresby et dans le sud de l'île Graham semble être principalement liée au plutonisme et à des phénomènes associés, en particulier à une activité hydrothermale, que les auteurs considèrent être un véhicule important de transfert thermique. En particulier, l'indice d'altération des couleurs "de fond" est parfois élevée près de failles ou de contacts stratigraphiques qui semblent avoir joué le rôle de conduits. La profondeur d'enfouissement a probablement eu un effet sur les valeurs d'altération des couleurs dans certaines parties du nord-ouest de l'île Graham; les variations secondaires peuvent être attribuables à une activité ignée tertiaire et à des différences de lithologie.*

<sup>1</sup> Cordilleran Division, Geological Survey of Canada, 100 West Pender Street, Vancouver, B.C. V6B 1R8



## INTRODUCTION

Conodont elements are tooth-like structures that represent the only preserved hard parts of an extinct marine organism. They are composed of lamellae of calcium phosphate interlayered with small amounts of organic material. The chemical composition of the organic matter of conodonts changes as a function of temperature and time, producing visible colour changes that have been calibrated (colour alteration index (CAI)). The CAI scale starts at 1, which implies no significant post-depositional heating, and ranges through 8. Elevated CAI results primarily from burial metamorphism, contact metamorphism, or hydrothermal alteration.

Conodont CAI values allow rapid assessment of local and regional thermal patterns, including delineation of the hydrocarbon window (Fig. 1), areas of anomalously high paleotemperature, and areas of hydrothermal alteration.

CAI	Temp. °C	Hydrocarbon generation
1.0	- 50	under-mature
1.5	50 - 90	early dry gas, wet gas, oil
2.0	60 - 140	heavy to light oil, wet gas
3.0	110 - 200	dry gas
4.0	190 - 300	barren
5.0	300 - 480	
6.0	360 - 550	
6.5	440 - 610	
7.0	480 - 720	
8.0	600 -	

**Figure 1:** The relationship between conodont CAI, temperature, and hydrocarbon generation. Based on Epstein et al. (1977), Rejebian et al. (1987), and (for hydrocarbons) Legall et al. (1981). Given temperatures were derived from an Arrhenius plot and represent time intervals of 1 m.y. to 500 m.y. for CAI of 1-5, and a minimum of 1000 years for CAI of 5-8. Kunga Group heating is no older than Early Jurassic, thus minimum temperatures would be somewhat higher than those given.

A total of 995 samples were collected from outcrops of the Kunga Group throughout the Queen Charlotte Islands, both for biostratigraphic research (Orchard, 1991) and for CAI map compilation (Fig. 2). A parallel study also resulted in the revision of Kunga Group stratigraphy (Desrochers and Orchard, 1991), which consists of three formations: the Sadler Limestone at the base, the Peril Formation, and the Sandilands Formation.

## PREVIOUS WORK ON CONODONT CAI

Epstein et al. (1977) performed experimental work and compiled field data from the Appalachian Basin to arrive at a series of conclusions that have formed the basis for subsequent work on conodont CAI. These findings have been supplemented by the study of Rejebian et al. (1987), who looked at regimes of low to medium-grade metamorphic rocks and determined that the uniformity or variability of CAI values within a sample, as well as the texture of the conodonts, provide clues to the temperature and type of metamorphic environment. Supporting observations have also been made by Wardlaw and Harris (1984), Aldridge (1986), Nowlan and Barnes (1986), Raven and Van

der Pluijm (1986) and Burnett (1988). The main conclusions that have emerged from work to date are:

1. Colour alteration is irreversible.
2. Colour alteration is time and temperature dependent.
3. Under anhydrous conditions, colour alteration is independent of confining pressure.
4. Eight distinct levels of colour alteration can be visually distinguished: pale yellow (CAI = 1) through brown (CAI = 3) through black (CAI = 5) through grey (CAI = 6) to white (CAI = 7) and ultimately to crystal clear (CAI = 8). Other colours may result from weathering, leaching, and staining.
5. During regional metamorphism, CAI progresses from 1-5 as the organic matter is decomposed by a carbon-fixing process. Beyond a CAI of 5, the colour results from the loss of organic matter.
6. An Arrhenius plot of experimental data suggests that, given an exposure time of greater than 1 m.y., colour change begins at about 50°C and continues to 550°C+.
7. Experimental studies with water and water-methane mixtures at 0.5-1 kbar have produced effects on conodonts most similar to those found in hydrothermally altered rocks. Under these experimental conditions it was found that: a) the carbon fixation process is retarded, and b) loss of organic matter begins prematurely, around CAI values of 2 or 3, in the colour alteration process. This effect results in higher fixed carbon values of 4-5 being bypassed.
8. Conodonts from hydrothermally altered rocks are very corroded and may have disparate CAI values (of 1 or 2 indices) within a given sample and commonly within a single specimen; a surficial grey patina is typical of such elements. CAI values ranging from 6-8 from hydrothermal environments may result from competing geochemical reactions rather than a purely thermal affect and are therefore not reliable indicators of temperature.
9. Conodonts from regionally metamorphosed rocks are typically corroded, deformed, and fractured, but the CAI values are generally uniform within the sample and locally between samples.
10. Conodonts from contact metamorphic rocks are better preserved than those from regionally metamorphosed collections, generally survive higher thermal regimes, and have a broader range in CAI values, both locally between samples and even within a sample.
11. Recrystallized textures on the surface and within conodonts may be correlated with high CAI values.

## METHODOLOGY OF CAI ASSESSMENT

In this work, we compiled a reference set of conodonts from the broad spectrum of CAI values present in the 375 conodont collections from the Kunga Group. This standard consists entirely of gondolelloid taxa and has the advantage of being composed of conodont elements of similar age and morphology that are also biologically related. Comparisons between such elements is far easier, and probably more reliable, than attempting to compare taxonomically and morphologically dissimilar forms.

During initial development of the CAI standard, conodont colour comparisons were tested using various magnifications and different methods of illumination (basal transmitted light, circular fluorescent incident light, fibre optic incident light). Finally, a fibre optic light source and a magnification of between 40-50 X was found to be most effective and was used for all measurements. All collections were assessed on a white card background.

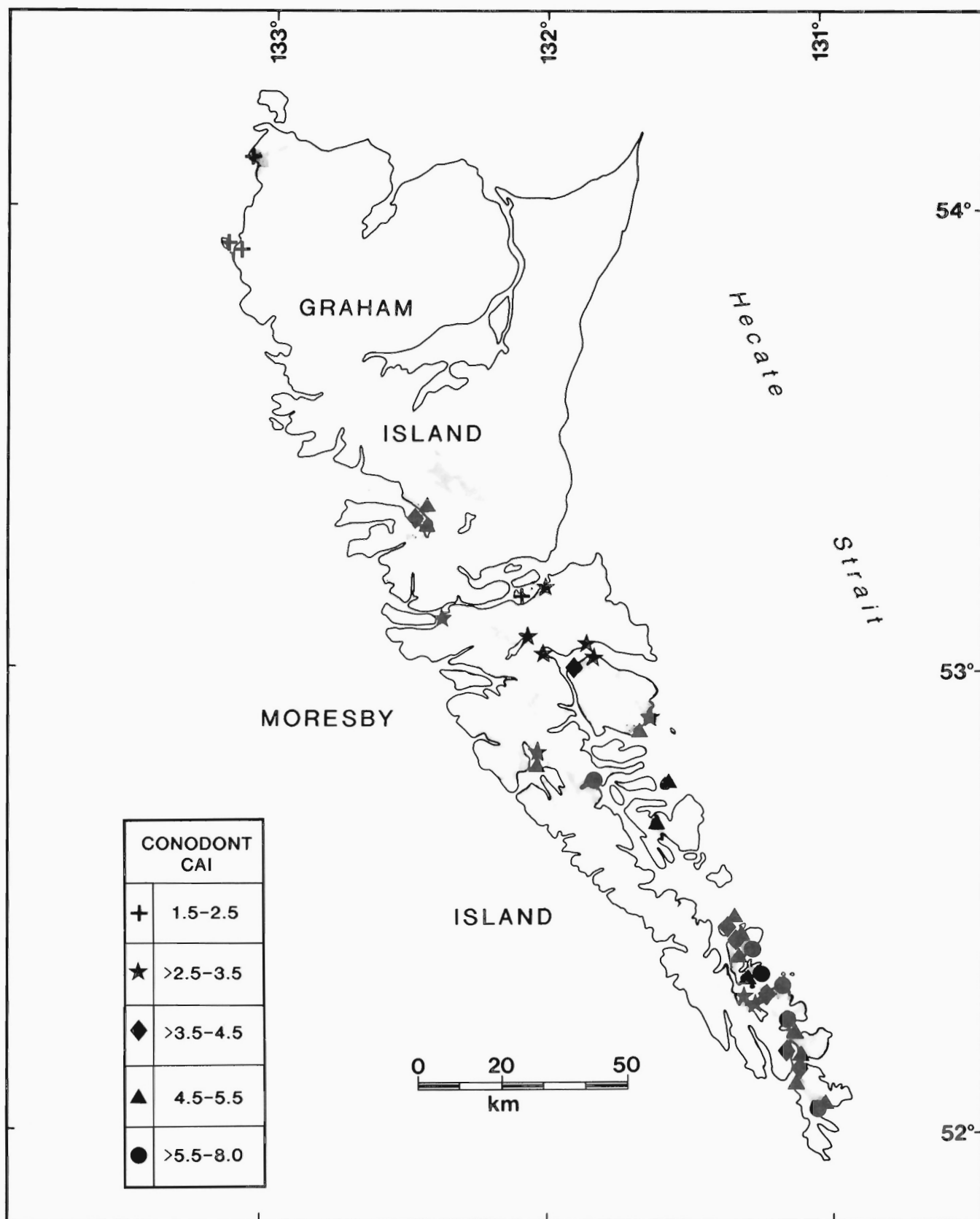


**Figure 2:** Conodont colour alteration index map of the Queen Charlotte Islands. Shaded areas represent Kunga Group outcrop.

Whenever possible, comparisons were made between specimens of similar size. Larger specimens usually appeared darker than smaller ones due to their greater thickness and organic content. Also, some specimens commonly showed more intense colour towards their centre due possibly to impregnation of iron oxides or organic matter in their basal cavity. To overcome these colour variations, CAI values were determined near the margins of elements. Generally, in collections with relatively low CAI (1-3) values, the best resolution was obtained using specimens of moderate size because small specimens showed such a dilute colour that they were difficult to evaluate.

However, small specimens are sometimes useful in distinguishing CAI values which are marginally  $>5$  or  $<5$ . This has been explained by the action of the different processes involved (Burnett, 1988). That is, up to a CAI value of 5, when colour change is the result of a carbon-fixing process, small specimens retain brown colouration whereas larger ones, perhaps due to their relatively higher organic material, may appear black. Above a CAI of 5, when colour change is the result of oxidation and volatilization of oxides, smaller specimens may precede larger ones in reaching higher CAI levels due to the lesser amount of organic matter to be volatilized, and their higher surface area to volume ratio.

The Kunga Group conodont CAI reference slide was compiled by selecting specimens showing discernible increments of colour change from pale yellow through brown, black, grey, white, and crystal clear. In total, 11 CAI categories were differentiated, each one containing a variety of different sized specimens in order to display the relationship between colour and size. The index slide was first compared with a standard CAI set of Palaeozoic indices provided by A.G. Harris: assigned values corresponded well to independent determinations on a duplicate Triassic set assessed subsequently by A.G. Harris and J.E. Repetski of the U.S. Geological Survey (pers. comm., 1989). The CAI values in the Triassic standard range from CAI of (1.0?)1.5 through 8.0.

A CAI range was assigned in those cases where collections were small and had uncertain CAI values, or where CAI varied within individual collections.

## CONODONT TEXTURE

During this study, textural differences between conodonts of different CAI values were also examined in a preliminary way. Figure 3 illustrates representative surface textures of conodonts with different CAI values. Elements with CAI  $<3$  generally have little or no textural alteration (Fig. 3A), whereas those with CAI  $>5$  usually have pronounced alteration. Altered textures sometimes arose from recrystallization (Figs. 3C,F), but in several cases corrosion of the elements had occurred (Figs. 3D,E), possibly as a result of contact with hydrothermal fluids. Of particular interest is the textural change observed in collections having CAI values as low as 2.5 from the vicinity of the Sadler-Peril formational boundary (see below). Conodonts from these levels show polygonal patterns developed on their blades (Fig. 3B). Similar polygonal patterns were illustrated by Burnett (1988) who suggested that they may have arisen as a result of pressure solution by the surrounding sediment.

## DISCUSSION: CONTROLS ON CAI

Figure 2 shows the gross distribution of *minimum* CAI values throughout the Upper Triassic Kunga Group of the Queen Charlotte Islands. Several regional patterns emerge, the most conspicuous of which is the north-trending, eastward increasing pattern of CAI values on south Moresby Island, and the low values in northern Graham Island. Significant CAI variations within the Kunga Group also occur on a scale not indicated on Figure 2. As presented in the Appendix, the var-

ious factors effecting CAI include: proximity to plutons, dykes and sills; proximity to faults and to stratigraphic contacts; rock type; and maximum depth of burial, or overburden. Although these factors may not be readily separated, each is considered separately below.

### Plutonic suites

Three plutonic suites have been differentiated in the Queen Charlotte Islands by Anderson (1988) and Anderson and Greig (1989): the Upper Jurassic San Christoval plutonic suite (SCPS), the Upper Jurassic Burnaby Island plutonic suite (BIPS), and the Tertiary Kano plutonic suite (KPS). The thermal and hydrothermal effects of these plutons are not easily separated in areas where more than one occurs, but their influence is thought to be fundamental in establishing conodont CAI patterns.

In the preliminary CAI map of the Queen Charlotte Islands (Orchard, 1988), it was noted that a general trend in eastwardly increasing CAI values could be demonstrated in southern Moresby Island. In this region, CAI values increase eastward from 3.5-7.0. Although collection sites having the same CAI values vary in their distance from exposed plutons, it is probable that the subsurface geometry of the plutons is more significant and controls the CAI pattern. This pattern, as well as the general preservation and CAI variability of the conodonts, is suggestive of pluton-related thermal metamorphism and not burial metamorphism.

The distribution of plutons shown by Anderson and Greig (1989, Fig. 2) suggests that both the BIPS and to a lesser extent the SCPS and KPS may have influenced the CAI pattern on southern Moresby Island. Characteristics of the plutonic suites led Anderson and Greig (1989) to conclude that some plutons were associated with the significant hydrothermal activity that affected the country rocks. The conclusions of these authors are supported by several widely scattered conodont collections in which elements are corroded, irregularly altered and 'bleached'.

In the central Queen Charlotte Islands, the distribution of plutons does not impose an obvious CAI pattern. CAI values in this region are generally lower than on southern Moresby Island, yet locally there are significant highs (e.g. Sandilands Island, Desmaricove Point) that possibly result from high heat flow related to plutonism.

Presumably, the combined thermal effects of the SCPS and the KPS are seen in the Shields Bay area. Although the KPS is geographically closer to the site of conodont collections, the thermal effects may not have been as great (see below). It is also notable that whereas CAI values are generally quite high in this area, a few relatively low values persist, suggesting irregular heat flow patterns.

The isolated effects of the SCPS may be most obvious in Luxana Bay on southern Kunghit Island, where the highest CAI value from the Queen Charlotte Islands is recorded. This site apparently lies closer to the SCPS than any other, and conodont recrystallization (Fig. 3F) is the most intense. Conodonts from Crescent Inlet may also show the effects of the SCPS. Collections from this inlet show very high but irregular CAI values, characteristics of hydrothermal activity. Although hydrothermal alteration zones were found to be less commonly associated with the SCPS than with the BIPS, they are documented to the west at Tasu (Anderson and Greig, 1989).

Small plutons representative of the KPS are the only mapped plutons on northwestern Graham Island. Their thermal effects may be reflected in the change from a background CAI of 1.5 at Kennecott Point and Frederick Island, which are about 13 km from an exposed pluton, to a CAI of 2 at Sadler Point, which is within 4 km of an exposed pluton. Although this difference might be due to other factors, slight CAI and textural anomalies within the Sadler Point section may reflect thermal effects related to the KPS. A single sill that occurs at Sadler

Point is also presumably genetically related to the KPS, but as discussed below, its emplacement seemingly had a negligible impact on conodont CAI in the host rocks. The apparently high crustal level of emplacement of the KPS may explain its relatively weak effect on thermal maturation levels of the Kunga Group.

### Dykes and sills

The distribution and composition of dykes has been studied by Souther (1989) and Souther and Jessop (1991), who conclude that most of the dykes are Tertiary in age, and related to Masset volcanism. Similarly, Anderson and Greig (1989) related these dykes to the Tertiary

Kano Plutonic Suite. Older dykes also occur and are important in all suites except the SCPS (Anderson and Greig, 1989), although there is "no consistent petrographic criteria ... to discriminate between dykes of different ages" (Souther, 1989, p. 118).

The heat from the emplacement of Tertiary dyke swarms was thought by Souther (1989) to have been significant in the thermal history of southeastern Moresby Island, which is characterized by north trending swarms apparently related to Tertiary extension. A chemically different suite of dykes occurs in northern Moresby and southern Graham islands, where east- to northeast-trending swarms predominate (Souther, 1989). The domain boundary between the two groups

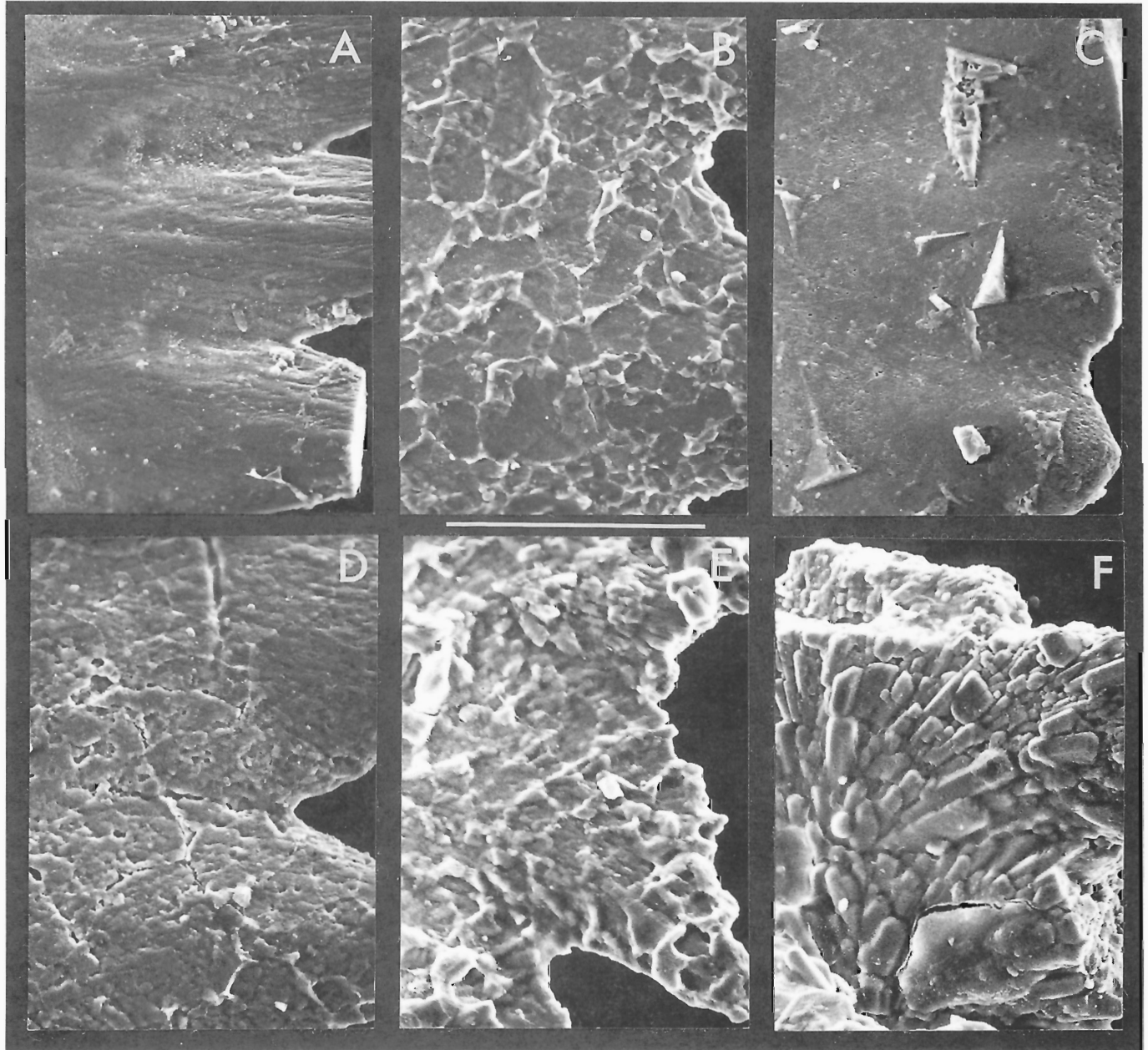


**Figure 3:** Textural variability in Late Triassic conodonts from the Kunga Group. All photos are lateral views of free blades, x 709; the scale bar is 50 µm long. Sample numbers shown in parentheses. A. CAI = 2.0, Frederick Island (FI-21) – unaltered texture showing original striations. B. CAI = 2.5, Sadler Point (SP-3) – polygonal crystalline overgrowth or ?corrosion. C. CAI = 4.5-5.0, Huxley Island (HUX-B9) – initial apatite recrystallization accompanied by development of small voids. D. CAI = 5.5, Carpenter Bay (CB-2) – widespread surface corrosion accompanying 'bleached' appearance of element. E. CAI = 6.0-6.5, Carpenter Bay (CB-3) – deep corrosion of surface, formation of large voids. F. CAI = 8, Luxana Bay – strongly recrystallized element with alignment of apatite crystals. Specimen B from transitional beds between Sadler and Peril formations, all others from Peril Formation.

of dykes is taken as an east-west line immediately to the south of Louise Island. It is noteworthy that both the trend of the dykes, and the position of the domain boundary between them also approximates that of the CAI trends. However, the elevated CAI values of Triassic conodonts may have been set during an episode of Jurassic plutonism, and later Tertiary dykes may not have exceeded temperatures induced by Jurassic plutonism. The contact effect of dykes and sills on maturation of Kunga Group strata is often difficult to evaluate because such intrusions are most common in areas that have moderately high CAI values ( $>4.0$ ), supposedly because of their close proximity to chiefly Jurassic plutons. Where CAI anomalies are observed, they appear to be more directly associated with fracture zones that may have acted as conduits for hydrothermal fluids rather than with dykes and sills, although the two may be associated.

To understand more about direct contact effects of dykes and sills it is necessary to examine their influence in a section where background CAI levels are low. An example of a sill within a relatively low thermal regime at Sadler Point is described below. A conodont collection from 0.8 m above the 2 m thick sill shows no increase in CAI above the background CAI of 2. This example is important because it shows that this sill, and presumably others genetically related to it (Kano Plutonic Suite?), did not remain hot enough to raise CAI values in adjacent strata.

Whereas the dykes and sills cutting the Kunga Group may represent more than one intrusive episode and varying temperatures of emplacement, many examples of conodont collections made adjacent to sills and dykes, mentioned in the descriptive section below (see Appendix), do not show contact thermal effects. For example, conodont CAI in the Huston Inlet area (section SHU) shows no elevation above the background CAI of 3.5 within 0.5 m of a 3.5 m dyke, or on Kunghit Island (section KT-A) where a background CAI of 4.5 is not exceeded in a collection from 2 m above a 26 m thick sill. In fact, the greatest observed density of dykes adjacent to a conodont collection is at South Cove in Carpenter Bay, where the CAI is 5.0; this value is less than several other localities where fewer dykes occur, but which lie closer to plutons.

## Faults

The Kunga Group is extensively faulted in all outcrop areas. Two phases of folding, of early Mesozoic and late Mesozoic to early Tertiary age, were recognized by Thompson and Thorkelson (1989) in central Queen Charlotte Islands. Similarly, Hesthammer et al. (1989) recognized two major fault sets affecting central Graham Island. Lewis and Ross (1989) placed the timing of one deformational event as slightly postdating deposition of the Kunga Group based on work on northwestern Graham Island.

In many sections of Kunga Group strata, CAI values are slightly elevated near faults, particularly along major fault contacts with younger Mesozoic or Tertiary units. There are several such examples: the northern margin of the Sadler Point section (SP), on southeastern Sandilands Island, east of Desmaricove Point, the southern end of Kunghit Island section (KT-A), the northern margin of Huxley Island section (HUX-B), and parts of northern Burnaby Island (BI). In these examples, which generally have a background CAI value of  $<4.5$ , the CAI is elevated by 0.5 to as much as 2.0 CAI indices. The strongest anomalies occur in the Skidegate Inlet and Channel area, where CAI values on Sandilands Island and at Desmaricove Point are highly variable. Conodont biostratigraphy shows that many stratigraphic levels of the Kunga Group are present at these localities, which indicates considerable structural dislocation.

Anderson and Greig (1989) emphasized the importance of hydrothermal fluids in plutonism on the Queen Charlotte Islands, par-

ticularly in association with the BIPS. They recognized fracture-alteration zones that "likely reflect hydro-fracture of the granite and expulsion of hydrothermal fluids...". Apparently, faults that cut the Kunga Group sometimes acted as conduits for heat, and in places, fluids. Conodont biostratigraphy and CAI values provide strong evidence for both faulting and hydrothermal activity on Sandilands Island.

## Stratigraphic contacts

The Kunga Group is bounded by, and contains a total of four formational contacts. The basal contact with the Karmutsen Formation is rarely exposed and no conodont collections were recovered adjacent to it, whereas the upper contact with the Maude Group lies within the Jurassic, beyond the age range of conodonts. Lithological contrasts across the Peril-Sandilands contact are not strong and no CAI variation was noted. However, the Sadler-Peril contact does provide a relatively strong lithological contrast and it was noted that, where background CAI is sufficiently low, anomalies may occur adjacent to it. The best example is at Sadler Point where conodont CAI is slightly elevated and the conodonts are texturally altered (Fig. 3B) only along the boundary interval.

These anomalies may be due to exceptional diagenetic effects (Desrochers and Orchard, 1991), or to thermal fluids moving preferentially along the Sadler-Peril contact. Bedding plane faulting or detachment at this contact observed in many outcrops increases the likelihood for the boundary to act as a conduit.

## Lithology

Variations in CAI have been noted where host rock lithologies differ. Mayr et al. (1978) found that anomalously high values (up to one index) occurred in samples of black shale compared with interbedded carbonate on Bjorne Peninsula, Ellesmere Island, and similarly, Legall et al. (1981) reported conodonts from coeval carbonate and shale sequences in southern Ontario with a variation of up to 0.5 index, particularly in areas of low CAI where collections from shale samples were consistently darker. In contrast, Seiful-Mulyukov and Akhmetshina (1983) did not find any significant colour differences between conodonts extracted from carbonate deposits and from contemporaneous terrigenous rocks in the sub-salt deposits of the Caspian Basin.

In those examples where CAI values apparently vary with lithology, Nowlan and Barnes (1987) suggested that the colour differences relate to differing oxidizing and reducing environments. They reason that in reducing environments, pyrite or hydrocarbons may impregnate the conodont element resulting in a higher apparent CAI. In the Queen Charlotte Islands, we suspect that such impregnation has affected some conodonts from Frederick Island, where a few collections from relatively dark, siliceous or pyritiferous strata, range up to a CAI of 2.0 compared to a background value of 1.5.

## Stratigraphic overburden

The role of overburden in the development of CAI patterns is a function of the geothermal gradient within the sedimentary basin. According to Klemme (1975), a geothermal gradient of 20–25°C/km is normal for cratonic basins, whereas gradients may range as high as 73°C/km on overriding continental margins. Generally, most work on CAI has been done in areas where a cratonic geothermal gradient has been assumed (Epstein et al., 1977; Legall et al., 1981). In contrast, the Queen Charlotte Islands have been tectonically active since at least the Jurassic, therefore a persistent high gradient is probable.

Examples of how CAI varies with burial depth are given by a number of authors, but none are within tectonically active areas. Epstein et al. (1977) found that CAI changed 1 unit in approximately 1200 m of burial depth in the Ordovician of the Appalachian Basin; Perry et al. (1983) measured a CAI of 1 in the Big Snowy Formation of south-



west Montana in spite of its burial depth of more than 2 km; Seiful-Mulyukov and Akhmetshina (1983) recorded a CAI no greater than 2 to a depth of 3.3 km in the Caspian Basin.

The extent to which the CAI of Kunga Group collections is affected by later Mesozoic overburden rather than proximity to igneous bodies is unclear. Current revisions to the stratigraphy of the later Mesozoic and Tertiary suggest that strong contrasts in overburden thickness are likely, and this would be complimented by an unknown amount of structural thickening. Cumulative estimates for post-Kunga Group stratigraphic thickness are uncertain, but current literature suggests 2-3 km. Hence, CAI values of 1.5-2.0 in northwest Graham Island could reasonably be explained on the basis of overburden alone assuming a moderately high geothermal gradient (Fig. 1).

The burial history of southern Moresby Island may or may not be comparable to the rest of the study area. Uniform burial throughout the islands, although improbable, would imply that CAI values in excess of ~2 result from high thermal gradients related to plutonism. Although such effects are clearly seen in the CAI patterns on southern Moresby Island, it cannot be discounted that this area was also more deeply buried.

## CONCLUSIONS

From the above, it is clear that no single factor is responsible for the relatively variable CAI patterns (Fig. 2) in the Queen Charlotte Islands. However, we conclude that plutonism and associated hydrothermal activity, has been of paramount importance in controlling maturation levels throughout most of the islands.

Consistent with the findings of Anderson and Greig (1989), we see evidence that plutonism, particularly the Jurassic Burnaby Island Plutonic Suite (BIPS), was associated with hydrothermal activity. In sections of the Kunga Group, CAI is commonly elevated near discontinuities (e.g. faults and stratigraphic contacts) that may have acted as conduits for hydrothermal fluids. In addition, the colour and textural alteration in several conodont collections close to BIPS outcrops suggest a hydrothermal environment. Our findings parallel the those of Raven and Van der Pluijm (1986) who studied CAI distribution in the Cantabrian Mountains of northern Spain. They found that the characteristics of low-grade metamorphism and its spatial relationships to major faults suggested fluids were the main source of regional heating, and that fluid transport was focused along structural features.

Tertiary plutonism may have been less important than Jurassic plutonism in establishing CAI patterns in Triassic rocks. This inference is drawn from northwest Graham Island where isolated Tertiary intrusive rocks have had a comparatively minor affect on CAI values which are lower than elsewhere on the Queen Charlotte Islands. Tertiary plutonism may have been stronger in the south, but not, apparently, stronger than Jurassic plutonic influences.

In the Queen Charlotte Islands, three regions may be differentiated based on CAI characteristics. The first, as noted by Orchard (1988), is in southern Moresby Island where CAI generally increases eastward towards the centre of largely Jurassic plutonism. CAI values generally fall into linear belts that parallel the plutonic regime from Burnaby Island in the north to Kunghit Island in the south, and reflect the diminishing influence of the regime westward (Fig. 2). The Kunga Group is generally overmature in this area, although the lowest values, in the west around Huston Inlet, are within the range of gas production.

A second region encompasses Louise and northern Moresby islands where CAI data, although more sporadic, shows 'background' CAI trends aligned west-northwest. CAI values generally decrease north-eastward to a level within the hydrocarbon window. Significantly, as in the first region to the south, CAI trends parallel both the structural grain and the trend of Tertiary dykes. The 'background' CAI is lo-

cally elevated close to plutons and in areas where extensive faults perhaps acted as pathways for heat from plutons.

The third region is northwest Graham Island where CAI values are generally lower than on Moresby Island and show none of the strongly elevated values found in the other two regions. The Kennecott Point-Frederick Island area is marginally mature(?) to mature in terms of hydrocarbons (as found by Vellutini, 1988), and CAI values could result from burial alone. Slight local anomalies reflect possible diagenetic, lithology related variations and, further north at Sadler Point, the probable influence of emanations from the Kano Plutonic Suite.

## ACKNOWLEDGMENTS

We would like to thank A.G. Harris and J.E. Repetski, United States Geological Survey, for their timely independent assessment of our CAI standard. We also thank the folk of the former Beban logging camp on Lyell Island who showed us great hospitality during the summer of 1986. The crew of the vessel "Beatrice", skipper Doug Hartley assisted by Paddy Herman, are thanked for skillfully ploughing the seas off South Moresby during June 1987. In June 1988, the "Mayor of Kennecott Point", Howard Tipper provided shelter whilst expediter Ella Ferland provided support from Sandspit. During these years, the following people helped make collections in the field: P. Benham, E.C. Carter, A. Desrochers, A. McCracken, and E.T. Tozer. In addition, further samples were collected independently by B.E.B. Cameron, P.D. Lewis, R.I. Thompson, D. Thorkelson, and G.J. Woodsworth. Laboratory help was provided by P. Krauss, K. Lesack, H. Bourgeois, and K. McKay. P. Krauss is thanked for the photography, C. Davies for the drafting. Finally, particular thanks to A.G. Harris and G.J. Woodsworth for their helpful comments on earlier versions of this manuscript.

## REFERENCES

- Aldridge, R.J.  
 1986: Conodont palaeobiogeography and thermal maturation in the Caledonides; *Journal of the Geological Society, London*, v. 143, p. 177-184.
- Anderson, R.G.  
 1988: Jurassic and Cretaceous-Tertiary plutonic rocks on the Queen Charlotte Islands, British Columbia; in *Current Research, Part E, Geological Survey of Canada, Paper 88-1E*, p. 213-216.
- Anderson, R.G. and Greig, C.J.  
 1989: Jurassic and Tertiary plutonism in the Queen Charlotte Islands, British Columbia; in *Current Research, Part H, Geological Survey of Canada, Paper 89-1H*, p. 95-104.
- Burnett, R.D.  
 1988: Physical and chemical changes in conodonts from contact-metamorphosed limestones; in *Irish Journal of Earth Sciences*, v. 9, p. 79-119.
- Desrochers, A. and Orchard, M.J.  
 1991: Stratigraphic revisions and carbonate sedimentology of the Kunga Group (Upper Triassic-Lower Jurassic), Queen Charlotte Islands, British Columbia; in *Evolution and Hydrocarbon Potential of the Queen Charlotte Basin, British Columbia, Geological Survey of Canada, Paper 90-10*.
- Epstein, A.G., Epstein, J.B., and Harris, L.D.  
 1977: Conodont Colour Alteration - an index to organic metamorphism; *United States Geological Survey, Professional Paper 995*, 27 p.
- Hesthammer, J., Indrelid, J., and Ross, J.V.  
 1989: Preliminary structural studies of the Mesozoic rocks of central Graham Island, Queen Charlotte Islands, British Columbia; in *Current Research, Part H, Geological Survey of Canada, Paper 89-1H*, p. 19-22.
- Klemme, H.D.  
 1975: Geothermal gradients, heat flow and hydrocarbon recovery, in *Petroleum and Global Tectonics*, A.G. Fisher and S. Judson (ed.), Princeton University Press, p. 251-304.
- Legall, F.D., Barnes, C.R., and Macqueen, R.W.  
 1981: Thermal maturation, burial history and hotspot development, Palaeozoic strata of southern Ontario - Quebec, from conodont and acritarch colour alteration studies; *Bulletin of Canadian Petroleum Geology*, v. 29, p. 492-539.
- Lewis, P.D. and Ross, J.V.  
 1989: Evidence for Late Triassic-Early Jurassic deformation on the Queen Charlotte Islands, British Columbia; in *Current Research, Part H, Geological Survey of Canada, Paper 89-1H*, p. 13-18.



- Mayr, U., Uyeno, T.T., and Barnes, C.R.  
**1978:** Subsurface stratigraphy, conodont zonation, and organic metamorphism of the Lower Palaeozoic succession, Borne Peninsula, Ellesmere Island, District of Franklin; in *Current Research, Part A, Geological Survey of Canada, Paper 78-1A*, p. 393-398.
- Nowlan, G.S. and Barnes, C.R.  
**1986:** Application of conodont colour alteration indices to regional and economic geology; in *Conodonts: Techniques and Applications*, R.L. Austin (ed.), Ellis Horwood Limited, Chichester, p. 188-202.
- 1987:** Thermal maturation of Palaeozoic strata in eastern Canada from conodont alteration index (CAI) data with implications for burial history, tectonic evolution, hotspot tracks and mineral and hydrocarbon exploration; *Geological Survey of Canada, Bulletin 367*, 47 p.
- Orchard, M.J.  
**1988:** Maturation of Triassic strata: conodont colour alteration index; in *Some Aspects of the Petroleum Geology of the Queen Charlotte Islands*, R. Higgs (compiler), Canadian Society of Petroleum Geologists Field Trip Guide to: Sequences, Stratigraphy, Sedimentology: Surface and Subsurface, p. 44.
- 1991:** Late Triassic conodont biochronology and biostratigraphy of the Kunga Group, Queen Charlotte Islands, British Columbia; in *Evolution and Hydrocarbon Potential of the Queen Charlotte Basin*, British Columbia, Geological Survey of Canada, Paper 90-10.
- Orchard, M.J., Carter E.S., Tozer, E.T. (paleontological data); Weston, M.L., Woodsworth, G.J., Orchard, M.J., Johns, M.J. (database design); Forster, P.J.L., Lesack, K., McKay, K. (compilers)  
**1990:** Electronic database of Kunga Group biostratigraphic data; Geological Survey of Canada, Open File 2284.
- Perry, W.J., Jr., Wardlaw, B.R., Bostick, N.H., and Maughan, E.K.  
**1983:** Structure, burial history and petroleum potential of Frontal Thrust Belt and adjacent foreland, southwest Montana; *American Association of Petroleum Geologists, Bulletin*, v. 67, p. 725-743.
- Raven, J.G.M. and Van der Pluijm, B.A.  
**1986:** Metamorphic fluids and transtension in the Cantabrian Mountains of northern Spain: an application of the conodont colour alteration index; *Geological Magazine*, v. 123, p. 673-681.
- Rejebian, V.A., Harris, A.G., and Huebner, J.S.  
**1987:** Conodont colour and textural alteration: an index to regional metamorphism, contact metamorphism, and hydrothermal alteration; *Geological Society of America Bulletin*, v. 99, p. 471-479.
- Seiful-Mulyukov, R.R. and Akhmetshina, L.Z.  
**1983:** Conodonts as paleotemperature indicators of the subsalt deposits on the Caspian Basin; *Vestnik Moskovskogo Universiteta, Geologiya*, v. 38, no. 5, p. 96-99.
- Souther, J.G.  
**1989:** Dyke swarms in the Queen Charlotte Islands, British Columbia; in *Current Research, Part H, Geological Survey of Canada, Paper 89-1H*, p. 117-120.
- Souther, J.G. and Jessop, A.M.  
**1991:** Dyke swarms in the Queen Charlotte Islands, and implications for hydrocarbon exploration; in *Evolution and Hydrocarbon Potential of the Queen Charlotte Basin*, British Columbia, Geological Survey of Canada, Paper 90-10.
- Sutherland Brown, A.  
**1968:** Geology of the Queen Charlotte Islands, British Columbia; British Columbia Department of Mines and Petroleum Resources, Bulletin 54, 226 p.
- Thompson, R.I. and Thorkelson, D.  
**1989:** Regional mapping update, central Queen Charlotte Islands, British Columbia; in *Current Research, Part H, Geological Survey of Canada, Paper 89-1H*, p. 7-11.
- Vellutini, D.  
**1988:** Organic maturation and source rock potential of Mesozoic and Tertiary strata, Queen Charlotte Islands, British Columbia; M.Sc. thesis, University of British Columbia, Vancouver, 262 p.
- Wardlaw, B.R. and Harris, A.G.  
**1984:** Conodont-based thermal maturation of Palaeozoic rocks in Arizona; *American Association of Petroleum Geologists Bulletin*, v. 68, p. 1101-1106.
- Weston, M.L., Woodsworth, G.J., Orchard, M.J., and Johns, M.J.  
**1991:** Design of an electronic database for biostratigraphic data; in *Evolution and Hydrocarbon Potential of the Queen Charlotte Basin*, British Columbia, Geological Survey of Canada, Paper 90-10.

## APPENDIX: CAI DISTRIBUTION IN THE KUNGA GROUP

Details of conodont CAI distribution in the Kunga Group are given below under five arbitrarily chosen group headings that also provide the basis for the CAI map (Fig. 2). Data for this descriptive section and the CAI map were compiled using the following criteria. In a stratigraphic section or geographic locality (Fig. 4) where CAI varied, the minimum CAI value has been used; this value is regarded as the 'back-

ground' CAI, and higher values are thought to result from local influences (as discussed above). In some extensive outcrops where CAI values changed systematically, more than one symbol has been plotted on Figure 2.

Additional stratigraphic and geographic data are in the Kunga Group database (Weston et al., 1991; Orchard et al., 1990), and pertinent faunal and biochronological data are described in Orchard (1991). Reference is also made to three plutonic suites described by Anderson (1988) and Anderson and Greig (1989): the San Christoval plutonic suite (SCPS), the Burnaby Island Plutonic Suite (BIPS), and the Kano plutonic suite (KPS). Distances from these plutons are derived from Sutherland Brown (1968).

### Group 1: CAI 1.5-2.5

#### *Kennecott Point (Fig. 4S)*

This locality is a reference section for the Sandilands Formation and its contact with the underlying Peril Formation (Desrochers and Orchard, 1991). Two conodont collections from the upper member of the Peril Formation, and fifteen collections from the Sandilands Formations were tentatively assessed as CAI 1.5, or in a few cases within a range of CAI 1.5-2.0. CAI values were mostly determined from relatively small conodonts that are weakly coloured and therefore similar to small specimens with CAI <1.5, or immature in terms of hydrocarbons. No significant variation in CAI was found in the Triassic part of the section, which has a total thickness of about 160 m. The nearest exposed pluton is the KPS, 13 km to the northeast.

#### *Frederick Island (Fig. 4S)*

The east shore of this island, the type locality for the Peril Formation (Desrochers and Orchard, 1991), consists of several fault-bounded sections that lie about 13 km southwest of the nearest exposed pluton of the KPS. The most northerly outcrop of the Peril Formation on the island is Early Norian in age and lies between volcanics of the Karmutsen Formation to the north and a fault-bounded section of older Peril Formation strata on the south. The latter consists of a Carnian to Norian boundary section of lower nodule member (Desrochers and Orchard, 1991), which in turn is juxtaposed against a third fault block of Lower Norian middle member. Eighteen out of nineteen collections from these beds were indexed as CAI 1.5.

A section further south has a different strike and consists of thinner bedded, darker, and more siliceous strata, some of which is folded. Six collections from large (up to 1 m) micrite nodules within about 45 m of section have a slightly elevated CAI 1.5-2.0. The age of these collections is late Early Norian, consistent with the general southward younging on Frederick Island.

Still further south beyond another fault, seven collections from Middle Norian beds have CAI values of 1.5. The southernmost section, consisting chiefly of the upper member of the Peril Formation (Upper Norian), yielded nine collections with CAI values of 1.5 and one collection, from a black slaty carbonate containing pyritized pelecypods, with a CAI of 2.

#### *Sadler Point (Fig. 4T)*

Collections from the type section of the Sadler Limestone and immediately overlying parts of the Peril Formation fall into three CAI groups: four samples from the lower 30 m of the massive grey limestone have CAI values of 1.5-2.5; five samples from the upper 10 m of Sadler Limestone and overlying basal beds of the Peril Formation have CAI values of 2.0-2.5; and samples from 3-50 m above the base of the Peril Formation have CAI values of 2. The collections from the upper Sadler Limestone are texturally altered (Fig. 3B) whereas those within the Peril Formation at 3 m above the contact are not.

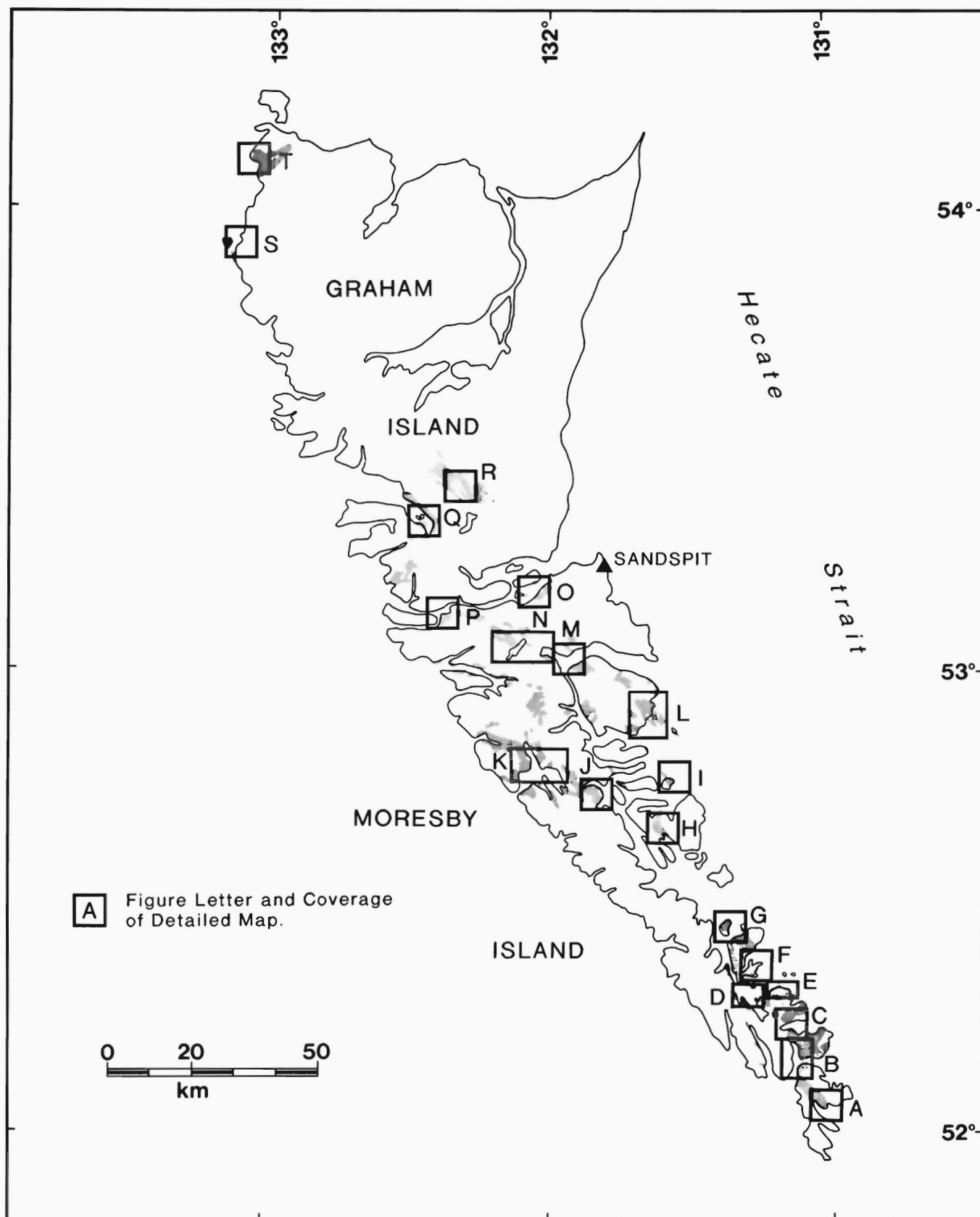


**Figure 4:** Locality index map showing coverage of detailed maps A-T (included in Weston et al., 1991). Localities mentioned in text lie within the following boxes: A. Luxana Bay, Treat Bay; B. Houston Stewart Channel, Hornby Point, Rose Inlet, Rose Harbour; C. Carpenter Bay, South Cove; D. Bush Rock, Huston Inlet, Huston Point; E. Jedway, Deluge Point; F. Swan Bay, Blue Jay Cove, Poole Inlet, Howay Island; G. Burnaby Island, Huxley Island, Arichika Island; H. Lyell Island; I. Kunga Island; J. Crescent Inlet; K. Newcombe Inlet, Tasu Sound; L. Breaker Bay, Vertical Point, Skedans, Louise Island; M. Louise Island, Cumshewa Inlet, Gillatt Inlet; N. Gillatt Arm, Mosquito Lake; O. Skidegate Inlet, Sandilands Island; P. Desmaricove Point; Q. Shields Island, Shields Bay; R. Yakoun River; S. Kennecott Point, Frederick Island; T. Sialun Bay, Sadler Point.

A total of fifteen collections from the lower 50 m of the Peril Formation were assigned a CAI of 2, including a sample collected 1 m above a 2 m sill that cuts the section 14 m above the base; this collection shows no elevation of CAI above background levels.

From 50–78 m above the base of the Peril in this section, beds become thicker towards the fault contact with the Haida Formation as mapped by Sutherland Brown (1968). Four samples from these beds have a CAI of 2.5. The KPS crops out 4 km to the east.

#### ***Sandilands Island (Fig. 4O)***

The relatively accessible southeast side of Sandilands Island is one of the most extensively sampled outcrops in the Queen Charlotte Islands. Thirty conodont collections from this locality show marked variation from CAI of 1.5–2.0 through 4.0; one other from the south side of Skidegate Channel nearby has a CAI of 1.5. A few of these collections also have a ‘bleached’ appearance with a grey and white patina rather than a uniform brown colouration, probably due to hydrothermal alteration. The conodont collections, which were mostly collected as spot samples because of the lack of continuous sections, vary considerably with age. Upper Carnian, Lower Norian and Upper Norian strata occur within a short distance and the entire Kunga Group appears to be structurally telescoped.

#### **Group 2: CAI >2.5–3.5**

##### ***Huston Point-Huston Inlet-Bush Rock (Fig. 4D)***

A 65 m section (HP) north and west of Huston Point spans the upper Sadler through lower Peril formations. A single 2 m sill occurs near the base of the exposure. Five conodont collections from this section have CAI values of 3.5.

Further south, on the west side of Huston Inlet (section HU), about 160 m of Sadler Limestone is cut by many dykes, the widest of which is about 2 m. CAI values in five collections from these beds have CAI values of 3.5 or 3.5–4.0 and show no measurable increase to within 0.5 m of the widest dyke.

The southernmost section (SHU) on Huston Inlet is in Upper Carnian and Lower Norian Peril Formation. About 80 m of tightly folded section is cut by three dykes up to about 3.5 m wide. Eight collections from within 0.5 m of the widest dyke to as far as 20 m away, have a consistent CAI value of 3.5. Towards the north end of the outcrop, two additional collections that bracket an 8 m folded interval were assigned a range of CAI values from 3.5–4.0.

All of the above sections are 3.5–5.8 km west of an outcrop of the BIPS. Three collections from the area of Bush Rock, approximately 2.5 km east, have a similar range of CAI from 3.0–4.0.

##### ***Newcombe Inlet (Fig. 4K)***

One isolated sample collected from the Sadler Limestone on a logging road east of the inlet, has a broad CAI range of 2.0–3.0. This contrasts with a second collection a short distance to the south that contains conodonts of CAI 4.5, and similar additional collections on the east shore of the inlet that lie closer to SCPS (see Group 4).

##### ***Louise Island-Cumshewa Inlet-Mosquito Lake (Figs. 4L, M, N)***

Kunga Group strata exposed on the east coast of Louise Island are commonly intensely folded and faulted. Nonetheless, five collections from these strata, including one from a carbonate lens within the Karmutsen Formation, have values of CAI 3.0–3.5.

CAI values assigned to six widely separated spot collections from the north side of Louise Island, from the shores of Cumshewa Inlet, and inland to Mosquito Lake are generally 3.0–3.5. However, two collections have specimens with values as high as 4. One of these collections, from Beattie Anchorage, lies within 1 km of an outcrop of BIPS.

##### ***Skidegate Inlet (Fig. 4O)***

Isolated collections from the south side of Skidegate Inlet due east of Sandilands Island have CAI values of 2.5–3.0. Although it is possible that this CAI is locally elevated from a background similar to that further west, a higher CAI symbol is used in Figure 2.

##### ***Desmaricove Point (Fig. 4P)***

On the southwest side of this point, a conodont collection from the Sadler Limestone has a CAI of 3. Beyond the point to the east, where the Peril Formation is exposed in a series of fault slices, four collections have CAI values of 3.5, 4.0, and 5.0, indicating significant localized heating. The BIPS is exposed about 1.9 km to the east.

#### **Group 3: CAI >3.5–<4.5**

##### ***Kunghit Island (Fig. 4B)***

Two sections were sampled on the west coast of Kunghit Island; both are about 3.8 km southwest of a KPS outcrop. The most continuous section begins at Hornby Point and extends southward, updip through about 158 m of Sadler Limestone and about 70 m of the lower member of the Peril Formation. Four sparse conodont collections with CAI values of 4.5 were recovered from the Sadler Limestone. Collections from 2 m above and 25 m below a 26 m thick sill showed no appreciable variation. Fourteen collections recovered from the overlying Peril Formation have a slightly lower CAI of 4.0, with a few reaching 4.5. Two 3 m sills that cut the Peril Formation have no appreciable thermal affect on CAI values to within 1 m of the sill. Three collections from the top of the section lie within 3 m of a 0.5 m sill lying within a fault zone and have a CAI of 4.5, or 4.5–5.0.

Further south, section KT-B is less continuous than the former, and only four collections contained conodonts. These conodonts are characterized by a ‘washed-out’ grey colour and, in some specimens, an irregular ‘frosting’ suggesting hydrothermal activity. The CAI was variously determined as 4.0 or 6.0, but several specimens were indexed as 4.5.

##### ***Rose Inlet and Rose Harbour (Fig. 4B)***

A single small collection from the west side of Rose Inlet was assigned a CAI of 4.0–4.5. Three larger collections from a 36 m section in the upper Peril Formation on the east side of the inlet (RI), and an isolated sample a short distance to the southeast near Rose Harbour have a CAI of 4.5. These localities are about 3.8–5.1 km west of KPS outcrops.

##### ***Jedway Point (Fig. 4E)***

Three conodont collections were recovered from the Peril Formation at this locality, where about 40 m of the underlying Sadler Limestone are also exposed; a 6 m sill occurs at their faulted(?) contact. One collection about 5 m above this contact is texturally altered and has a range of CAI 4.0–4.5, whereas two others at 9 m and 13 m were assigned a CAI of 4.0. The nearest exposed pluton is the SCPS, about 0.5 km to the south.

##### ***Burnaby Island, north (Fig. 4G)***

The north coast of Burnaby Island, east of Section Cove, contains one of the most complete successions of the Kunga Group, including each of its formations, dated as Late Carnian, Early, Middle, and Late Norian, and Early Jurassic. The section is not continuous, however, but is composed of relatively undisturbed sections bounded by faults that contain strata out of sequence.

CAI values consistently range within 4.0–5.0. At the west end, two collections from the Sadler Limestone have conodonts of CAI 4.5. These beds are overlain by Upper Carnian beds of the Peril Formation in which four faunas are assigned a CAI of 4.0 and five others a CAI of 4.0–4.5. To the east, the section is strongly disturbed and two

collections from juxtaposed Middle Norian strata have a CAI of 4.5-5.0.

The next section to the east exposes Lower Norian strata. In this section, CAI generally increases eastward, so that ten collections of CAI 4.0-4.5 are followed by three with CAI 4.5, or 4.5-5.0, and then by six with CAI 5.0. Further eastward five Middle Norian collections have a CAI of 4.5-5.0 or 5.0. Beyond these beds, a prominent dyke parallels the coastline and cuts perpendicularly through the beds. Ten samples collected from these Middle Norian beds, all from within a few metres of the dyke, have a CAI of 4.0-4.5, 4.5, or 4.5-5.0; the dyke had no apparent thermal effect on CAI values.

The youngest beds of the Kunga Group crop out beyond the dyke to the east, where six collections were assigned a broad range of CAI 4.0-5.0. A CAI group 5 symbol is used in Figure 2 to denote a general eastward increase, towards the nearest exposed BIPS, about 1.7 km further east.

#### **Huxley Island (Fig. 4G)**

Most of the samples collected around this island produced conodonts. Three sections were sampled systematically. Section HUX-A on the southeast part of the island yielded four collections from the lower Peril Formation with a CAI of 4.0. Further north, section HUX-B spanned a key interval across the Carnian-Norian boundary and yielded a total of nine collections. The southernmost of these collections is within a fault zone and has a CAI of 4.5. Upsection, to the north, CAI values increase slightly from 4.0 through a range of 4.0-4.5 to 4.5. This slight increase coincides with a change to bedded rather than nodular carbonates, but also reflects the increasing proximity of a fault.

A total of five samples were collected on northern Huxley Island from the middle and upper members of the Peril Formation and overlying Sandilands Formation. Each of these collections were assigned a CAI of 4.5, or 4.5-5.0. A single collection from the west side of the island has the same CAI range.

The nearest exposed pluton is the BIPS, which lies 4-6 km to the southeast, although it may extend closer beneath the intervening channel.

#### **Breaker Bay (Fig. 4L)**

Two collections from the southeastern side of Louise Island are assigned a CAI of 4.5, markedly higher than collections from further north on the island. The nearest exposed pluton, the KPS, is 2.3 km to the west.

#### **Newcombe Inlet (Fig. 4K)**

Two isolated samples in disturbed Peril Formation strata on the east side of the inlet, 6.8 km north of SCPS outcrop at Tasu, have a CAI of 4.5-5.0.

#### **Shields Bay-Shields Island (Fig. 4Q)**

Five collections from the strongly faulted strata of Shields Island and adjoining islands at the head of Rennell Sound have a CAI of 4.5, or in one case 4.0-4.5. These localities are about 2.4 km north of exposed KPS. Nine collections from the upper Peril and lower Sandilands formations on the north side of Shields Bay, are mostly CAI 4.5-5.0, although one collection ranged as low as CAI 4.0. Group 4 symbols are used in Figure 2 to reflect the pervasive increase in CAI, particularly in the latter section, which is about 3.3 km south of an outcrop of the SCPS.

#### **Group 4: CAI 4.5-5.0**

##### **Treat Bay (Fig. 4A)**

About 50 m of section crops out in Treat Bay, but much of it is covered at high water. Apart from numerous sills and dykes that cut

the section, conodont biostratigraphy demonstrates that Early Norian Peril Formation is faulted against Sadler Limestone and much of the lower member of the Peril is cut out. Two collections from the Peril Formation have a CAI of 5.0-5.5, and one from its base has a CAI of 5.5-6.0. The SCPS crops out 4.4 km to the south.

##### **South Cove (Carpenter Bay) (Fig. 4C)**

A single sample of micrite from a fault bounded block surrounded by numerous dykes (12 were counted within a 15-20 m interval) contained conodonts of CAI 5.0. The BIPS is exposed 4 km to the east.

##### **Swan Bay (Fig. 4F)**

Four collections from along the coast east of Swan Bay on the south coast of Burnaby Island all have a CAI of 5.0-5.5. The BIPS crops out between 2-2.5 km to the northeast.

##### **Blue Jay Cove (Fig. 4F)**

This is the site of the JIB iron-ore deposit (Sutherland Brown, 1968) that formed close to where a pluton cuts the Kunga Group carbonates. CAI values are relatively high in this area and are never less than 5.0. Of ten collections with CAI values of 5.0-6.0, several fall individually into the higher CAI group 5, as shown in Figure 2. One collection from a micrite nodule surrounded by altered, white-weathering ("bleached") grainstone, has irregular mottled alteration; probably indicating hydrothermal effects. This collection apparently lies within the aureole of the BIPS that crops out 0.5 km to the north.

##### **Poole Inlet (Fig. 4F)**

Five collections from isolated outcrops or short disrupted sections surrounding Poole Inlet were assigned CAI values of 4.5 or 5.0. The lowest values are at the southwest end of the inlet and higher values occur to the northeast towards section HO-A. The BIPS crops out 1.7 km to the east of these outcrops.

Section HO-A is one of the more extensive outcrops of Lower to Middle Norian Peril Formation. The most striking aspect of the 143 m section is the 'hornfelsed' beach outcrop with distinctive green and brown banding. This part of the outcrop, which lacks any obvious intrusive rock, produced conodonts that have CAI values of 5.0-5.5, compared with CAI 5.0 for seven collections from lower strata. The highest collection, also with a CAI of 5.5, was from near a conspicuous fault on the northeastern margin that introduces a small sliver of Sadler Limestone. The northeastward increase in CAI values is portrayed by a group 5 symbol in Figure 2. The BIPS crops out 1 km to the north.

##### **Aricatika Island (Fig. 4G)**

A single sample from the upper Peril Formation was assigned a CAI of 5.0, slightly higher than is typical of nearby Huxley Island.

##### **Myell Island (Fig. 4H)**

Three samples, with a CAI of 4.5-5.0, or 5.0, were collected at widely separated sites. Both the BIPS and the KPS crop out on the island, at about 2.5 and 2.0 km, respectively, from the nearest collection site.

##### **Kunga Island (Fig. 4I)**

Several sections occur on the southeast side of Kunga Island, where Kunga Group strata become progressively younger northward. The oldest section (SKU-A) of Peril Formation is in the southernmost bay and consists of about 74 m of almost vertical Upper Carnian and Lower Norian strata that young seaward. Eleven collections from this section were assigned a CAI of 5.0 or a range of 4.5-5.0, and three others from the basal nodular beds a CAI of 4.5. A 5 m thick sill in the lower half of the section has no appreciable effect on the CAI levels. Other sections north of SKU-A are predominantly Sandilands Formation, and only two small conodont collections with a CAI of 4.5-5.0 were recovered.

On the north side of the island, only the upper member of the Peril Formation and overlying strata are well exposed. One sample from the westernmost beach outcrop of the Peril Formation produced a collection with CAI of 5.0, and eight more collections from the strongly faulted main outcrop produced the same CAI values as the south coast (4.5-5.0). The north and south sides of Kunga Island are equidistant from the KPS, which crops out less than 4 km away.

#### **Group 5: CAI >5.5**

##### ***Luxana Bay (Fig. 4A)***

A single conodont was recovered from a sample taken about 5 m above the exposed base of a strongly disturbed, heavily silicified section containing numerous sills and dykes. The conodont is coarsely recrystallized and has a CAI of 8.0 (Fig. 3F). The SCPS crops out 2 km to the south across the channel.

##### ***Carpenter Bay (Fig. 4C)***

Three collections were recovered from a small outcrop on the northwest shore where the contact between the Sadler and Peril for-

mations is exposed. As at Blue Jay Cove, relatively fresh micrite nodules are interlayered with strongly altered, white-weathering grainstone and silicified argillite. Late Carnian conodonts from the nodules have CAI values of 5.5-7.0, and exhibit variable textural alteration (Fig. 3D,E). Several sills and dykes cut these rocks, although they are less abundant than across the bay at South Cove, where CAI values are lower. The BIPS crops out 1.6 km to the northwest.

##### ***Deluge Point (Fig. 4E)***

A single collection with a uniform CAI of 6.0 was recovered from a 20 cm bed of micrite, 3 m from a dyke. The BIPS crops out 3.1 km to the southeast and southwest.

##### ***Crescent Inlet (Fig. 4J)***

Three samples from a small section on the north side of the inlet have CAI values that are apparently significantly higher than most others in northern Moresby Island. Each is assigned a CAI of 5.5-7.0. Two of these samples have conodonts with irregular colouration and frosting, a probable hydrothermal affect. The nearest mapped pluton crops out 3.2 km to the southeast.

# Dyke swarms in the Queen Charlotte Islands, British Columbia, and implications for hydrocarbon exploration

J.G. Souther<sup>1</sup> and A.M. Jessop<sup>2</sup>

Souther, J.G. and Jessop, A.M., Dyke swarms in the Queen Charlotte Islands, British Columbia, and implications for hydrocarbon exploration; in *Evolution and Hydrocarbon Potential of the Queen Charlotte Basin, British Columbia*, Geological Survey of Canada, Paper 90-10, p. 465-487, 1991.

## Abstract

*Tertiary dyke swarms in the Queen Charlotte Islands display systematic regional variations in orientation and chemical composition. They are believed to be cogenetic with the Masset volcanics and intrusions of the Kano plutonic suite. Dykes in the southern Moresby archipelago are relatively calcic plagioclase-hornblende phyrlic andesite whereas those in northern Moresby and southern Graham islands are relatively alkaline and include a higher proportion of basalt.*

*The dyke swarms originated from central volcano-plutonic complexes and propagated outward in directions normal to the axis of least compressive stress. Extension due to dyke intrusion ranges from nearly 100% in proximal parts of swarms to an average of 3 or 4% over the entire length of a swarm.*

*Enhanced heat flow associated with Tertiary magmatism and heating by local intrusion of dykes can account for high values of vitrinite reflectance observed in surface rocks of the Kunga Group.*

## Résumé

*Des essaims de dykes tertiaires dans les îles de la Reine-Charlotte présentent des variations régionales systématiques en ce qui concerne leur orientation et leur composition chimique. On les croit de même origine que les roches volcaniques et les intrusions de Masset de la suite plutonique de Kano. Dans le sud de l'archipel Moresby, les dykes sont composés d'andésite porphyrique à plagioclase-hornblende relativement calcique tandis que dans le nord de l'île Moresby et dans le sud de l'île Graham, ils sont relativement alcalins et contiennent une plus grande proportion de basalte.*

*Les essaims de dykes proviennent de complexes volcano-plutoniques centraux qui se sont propagés vers l'extérieur, perpendiculairement à l'axe de la moindre contrainte de compression. La distension causée par l'intrusion des dykes varie de près de 100 %, dans les parties proximales des essaims, à 3 ou 4 % en moyenne sur de la longueur totale d'un essaim.*

*L'amélioration du flux thermique associé au magmatisme tertiaire et au réchauffement par l'intrusion locale de dykes peut être à l'origine des valeurs élevées de la réflectance de la vitrinite observées sur les roches superficielles du groupe de Kunga.*

<sup>1</sup> Cordillera Division, Geological Survey of Canada, 100 West Pender Street, Vancouver, B.C. V6B 1R8

<sup>2</sup> Institute of Sedimentary and Petroleum Geology, 3303 – 33rd Street, Calgary, Alberta T2L 2A7



## INTRODUCTION

A study of dyke distribution in the Queen Charlotte Islands was begun in 1987 as part of a two-year FGP program to assess the petroleum potential of Queen Charlotte Basin. The rationale for incorporating a study of dykes in this program was based on assumptions that Tertiary dyke swarms are a manifestation of extension associated with basin evolution, and that igneous heat introduced by the dykes would effect the thermal maturation of hydrocarbons.

Prior to the present study no systematic work had been done on dykes in the Queen Charlotte Islands. Data collected in 1987 were summarized by Souther and Bakker (1988) and preliminary accounts of the 1987 and 1988 field work were reported by Souther (1988, 1989). This report presents a synthesis of the dyke data. It includes a discussion of possible relationships between the dykes and coeval plutonic and volcanic rocks (Anderson and Reichenbach, 1991; Hickson, 1991), and an interpretation of the tectonic implications and thermal impact of dyke emplacement.

## FIELD WORK

Field work by J.G. Souther was confined to shoreline traverses using an inflatable boat for transportation. With few exceptions landings were made on all dykes visible from the water. Most dykes were sampled, and measurements of their thickness, orientation, and contact relationships were made on shore. Where wave-cut benches

were encountered the shoreline was traversed on foot. During the summers of 1987 and 1988 some 800 km of shoreline were traversed and structural data were collected on about 2000 dykes (Figs. 1 and 2). Nearly continuous exposure along much of the shoreline ensured that few dykes were missed along the traverse routes. The distribution of dykes shown on Figure 2 (in pocket) is thus a good representation of actual dyke distribution in that part of the Queen Charlotte Islands where traverses were run (Fig. 1). Thick overburden and forest preclude the collection of similar data from the interior of the islands, however, the excellent shoreline exposure and convoluted coastline provide a good sample of dyke distribution.

## GEOLOGY

### Summary and Overview

Tertiary dykes cut the Masset and all older formations exposed in the Queen Charlotte Islands. Individual dykes vary from less than 1, up to 20 m in thickness and composite dykes may be as much as 100 m across. Most are vertical or steeply dipping, suggesting that little post-emplacement deformation has occurred and that the dykes are predominantly of Tertiary age. Those that cut sedimentary and volcanic formations are more resistant to erosion than the intruded rock and commonly form promontories and headlands. Dykes within the plutonic and metamorphic terranes either exhibit no differential erosion or form recessive moats within the more resistant country rock. Many dykes have prominent transverse columnar jointing whereas others have conspicuous colour banding parallel to their contacts. In general the contrast between country rock and dykes allows easy recognition even from a distance.

Dykes on southern Graham Island and throughout the southern Moresby archipelago (Fig. 2, in pocket) are concentrated in broad regional swarms with different orientations and bulk compositions. Some swarms appear to overlap whereas others are separated by relatively dyke-free areas. Each swarm is from 10-20 km across and up to 40 km long. Dyke orientations vary from swarm to swarm and show varying amounts of internal scatter but each swarm has a dominant trend that is well defined between 000° and 095° and individual dykes are predominantly subvertical. Dykes in the study area are grouped into seven major swarms referred to informally as the Rennell Sound, Selwyn Inlet, Tasu Sound, Lyell Island, Bigsby Inlet, Burnaby Island, and Carpenter Bay dyke swarms.

Locally the dyke swarms coalesce into sheeted complexes associated with Tertiary epizonal plutons and zones of hydrothermal alteration. Central igneous complexes of this type are well exposed near the centre of the Carpenter Bay, Lyell Island, and Selwyn Inlet swarms. Tertiary plutons of the Kano plutonic suite are also proximal to extensions of the Rennell Sound and Bigsby Inlet swarms, and the Tasu Inlet swarm is associated with small Tertiary stocks and lacoliths.

Few dykes were observed along Skidegate Channel and adjacent islands or along Cumsheewa and Long inlets. This suggests that a large part of northern Moresby and southern Graham islands, encompassing much of the Rennell Sound fold belt (Thompson and Thorkelson, 1989), is relatively dyke-free. Dykes are also rare in the western part of Moresby Island south of the Bigsby Inlet swarm. This area, underlain mainly by Karmutsen volcanics and 170 Ma plutonic rocks of the San Christoval plutonic suite, is relatively free of Tertiary intrusions or structures and comprises the south Moresby stable block (Souther, 1988).

### Rennell Sound swarm

A total of 112 dykes were sampled in the Rennell Sound area. They define a northeasterly trending swarm at least 12 km across which is well exposed along both sides of Rennell Sound west of Richardson

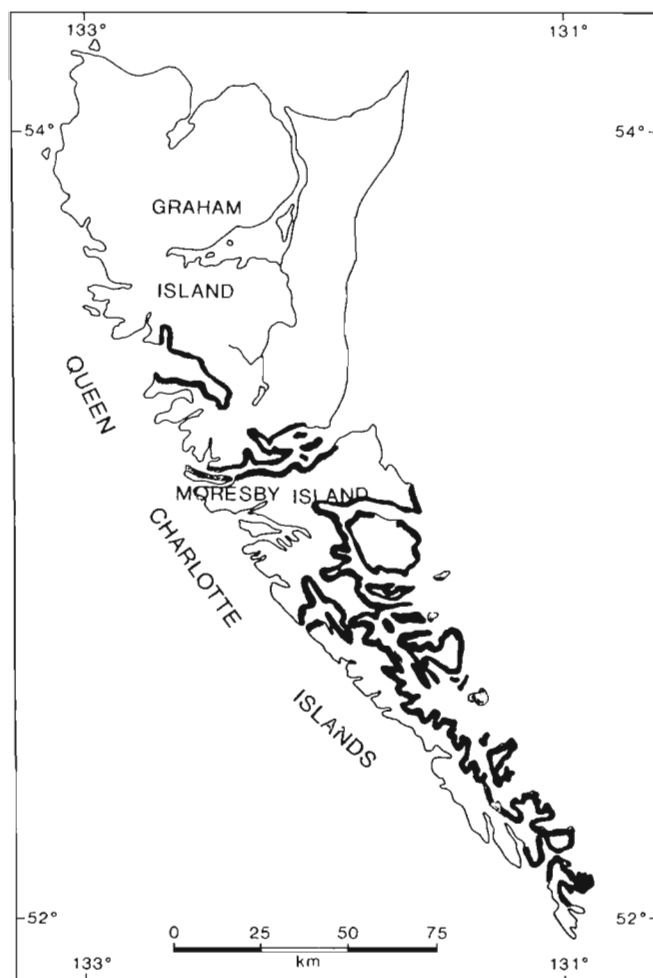


**Figure 1:** Index map showing the extent of shoreline examined for dykes during this study.

Head. A few dykes and sills that cut Kunga sediments in Shields Bay are peripheral to the eastern margin of the main swarm and large irregular dykes cutting Masset volcanics in Tartu Inlet are sparsely distributed along the western margin. The Rennell Sound swarm projects northeasterly toward the Sheila Lake pluton and southwesterly along the western margin of Kano Inlet pluton.

Dykes in the Rennell Sound swarm comprise 55% andesite, 26% basalt, 9% dacite, and 10% rhyolite. Contacts with the country rock are commonly sharp and lack any sign of hydrothermal alteration. An exception is the western part of Shields Bay where ankeritic veining and intense zeolitization have altered the margins or cores of several large basaltic dykes along the eastern margin of the main swarm. Elsewhere the Tertiary dykes postdate deformation and alteration of the intruded rocks. Many dykes cut pervasively fractured and veined plutonic rock of the San Christoval plutonic suite but are themselves unaltered.

The cumulative thickness of dykes in the Rennell Sound swarm indicates extension of about 1%.

### **Tasu Sound swarm**

North-northeasterly trending dykes of the Tasu Sound swarm are exposed over a width of at least 14 km. Their cumulative thickness of 605 m, based on 171 measurements, indicates an extension due to dyke emplacement of 4.3%. The dykes comprise 57% basalt, 28% andesite, and 15% rhyolite. They appear to have been emplaced during at least two episodes of intrusion and, where crosscutting relationships were observed, basalt is the younger phase.

Evidence of an early stage of dyking is seen in the Lomgon Bay area where Kunga sediments are cut by irregular feldspar-phyric andesite dykes having marginal quartz-calcite veins associated with hydrothermal alteration. Commonly the older dykes are deformed and fractured. A few show offsets of a few metres to a few tens of metres along northwesterly trending faults. Both dextral and sinistral offsets were seen. The andesite dykes are cut by a set of younger basalt dykes with straight, sharp, unaltered contacts and aphanitic selvages.

The Tasu Sound swarm is not associated with any known Tertiary pluton. However, small subvolcanic intrusions of Masset diabase outcrop along the east side of Wilson Bay and a small intrusive dome of Masset rhyolite is exposed at the head of Newcombe Inlet. These subvolcanic bodies are thought to be coeval and comagmatic with the dyke swarm and both may be related to a larger magmatic centre hidden beneath the large area of Masset volcanics east of Tasu Inlet.

### **Bigsby Inlet swarm**

Bigsby Inlet contains the only concentration of dykes exposed along the eastern coast of southern Moresby Island between Crescent Inlet in the north and Skincuttle Inlet in the south. The 78 dykes measured in Bigsby Inlet swarm have two distinct trends: a strong northerly trending set parallel to the Lyell Island swarm and a weaker northwesterly trending set parallel to the Tasu Inlet swarm. Crosscutting relationships, observed at only two locations, indicate that the northwesterly trend is younger.

The northeasterly trending dyke set can be projected south from Bigsby Inlet to the Tertiary Pocket Inlet pluton where mutually crosscutting relationships between basalt dykes and late phases of the pluton have been observed (R.G. Anderson, pers. comm., 1989). The dykes in Bigsby Inlet are probably distal phases of an igneous complex centred in the Pocket Inlet area.

Dark green, brown-weathering andesite with prominent marginal flow banding and widely spaced blocky jointing comprises 78% of the Bigsby Inlet dykes. Most are aphyric but some contain sparse, 2–3 mm feldspar phenocrysts. Aphyric, black-weathering columnar

basalt forms most of the remaining 22% of Bigsby Inlet dykes. Where composite dykes include both lithologies, the basalt is younger and commonly exhibits quenched selvages against the andesite. Minor calcite veining is present in and adjacent to some dykes but most contacts are sharp and free of hydrothermal alteration. Total extension represented by emplacement of the Bigsby Inlet swarm is about 2%.

### **Selwyn Inlet swarm**

The Selwyn Inlet swarm is relatively narrow (about 7 km), extending from Sewell Inlet south to Talunkwan Island. Its easterly trend contrasts with the northerly or northeasterly trend of all the swarms farther south on Moresby Island. Most of the 304 dykes measured are aphyric andesite but the swarm is lithologically diverse. Individual dykes range in composition from basalt to rhyolite, and some large composite dykes have multiple phases of markedly contrasting composition. Locally the composite dykes merge into sheeted complexes up to 50 m thick and comprise up to 12 distinct intrusive phases. Where crosscutting relationships were observed, an older set of northwesterly trending andesite dykes is cut by easterly trending basalt dykes.

The Selwyn Inlet swarm is spatially related to Tertiary plutonic rock which outcrops on southern Louise and Talunkwan islands. Dykes are much less abundant in the plutons than in the adjacent country rock, suggesting that the main episode of dyke intrusion preceded emplacement of the plutons. The western margin of the pluton on Louise Island includes large areas of fine grained monzodiorite with prominent east-trending joints parallel to zones of dark grey, feldspar-phyric andesite. Contacts between the monzodiorite and andesite are gradational and are believed to be the selvages of individual dykes in a sheeted complex formed during the initial stages of pluton emplacement. Dykes cutting the pluton are predominantly basalt.

Hydrothermal alteration is localized around the margins of the plutons, where the dykes are commonly bounded by and locally cut by quartz-carbonate veins. In contrast, dykes farther from the plutons have sharp contacts and display little or no evidence of veining or hydrothermal alteration. For example dykes on Talunkwan Island cut extensive stockworks of quartz-calcite veins within the Masset volcanics and are themselves cut by similar veins. This suggests that the volcanic pile on Talunkwan Island was proximal to an eruptive centre and may be underlain by subvolcanic plutons large enough to have driven a major hydrothermal system. In addition many of the Talunkwan dykes are fractured and locally displaced several metres along minor faults. Both dextral and sinistral offsets were observed. The Masset pile was clearly undergoing local deformation and hydrothermal alteration during the period of dyke emplacement.

The cumulative thickness of dykes in the Selwyn Inlet swarm indicates extension of more than 10% – the greatest regional extension associated with any of the measured dyke swarms.

### **Lyell Island swarm**

Dykes exposed on Lyell Island vary widely in composition and orientation and are probably related to two separate swarms. North-easterly trending dykes on the eastern part of the island are coextensive with the Bigsby Inlet swarm whereas northerly trending dykes are spatially associated with a large igneous complex on eastern Lyell Island. Elsewhere the Lyell Island dykes have a relatively random distribution.

The 309 dykes measured in the Lyell Island swarm comprise 62% andesite, 30% basalt, and 8% combined andesite and dacite. The andesite is predominantly fine-grained and aphyric but porphyritic varieties containing small phenocrysts of hornblende and/or plagioclase are also common. Many of the andesite dykes cutting the Masset pile have been fractured, deformed, veined and locally seg-

mented into discontinuous remnants. Those cutting pre-Masset formations are less deformed. They are commonly either massive or have crude columnar jointing and cryptic marginal flow banding. A few andesite dykes proximal to the Lyell Island igneous complex have prominent white mottling and marginal banding typical of the "Arichika type" zeolitic alteration (see Burnaby Island swarm). Basaltic dykes are commonly fine-grained, aphyric, and have well developed transverse columns and sharp unaltered contacts. Where crosscutting relationships were seen the basaltic dykes are the youngest. Most rhyolite and dacite dykes in the Lyell Island swarm are associated with zones of hydrothermal and pyritic alteration.

The Lyell Island igneous complex (Fig. 3) is exposed on eastern Lyell and adjacent parts of Faraday and Murchison islands. It comprises northerly trending andesite dykes and sheeted dyke swarms associated with a multiphase pluton of aphyric to moderately feldspar- and/or hornblende-phyric andesite. The andesite is associated with and may be comagmatic with seriate monzodiorite (Anderson and Greig, 1989). The intrusive complex is flanked by and appears to cut proximal breccias and flows of Masset volcanics. The intrusive andesite cuts Mesozoic shale, probably belonging to the Sandilands formation, and pendants of similar shale occur locally within the intrusive body.

The amount of extension associated with the Lyell Island dyke swarm varies from nearly 100% in proximal parts of the igneous complex to an average of 3% in distal parts of the swarm.

### Burnaby Island swarm

The 194 dykes assigned to the Burnaby Island swarm were measured on Burnaby, Huxley and adjacent parts of Moresby islands and on the many small islands in Skincuttle Inlet. The swarm overlaps the northern end of the Carpenter Bay swarm but the latter has a more northerly trend and a smaller percentage of basaltic dykes.

Two distinct types of andesite dykes comprise 70% of the Burnaby Island swarm. The most abundant dykes are massive to crudely columnar, greenish brown-weathering bodies with sharp linear contacts (Fig. 4). They commonly contain small sparse phenocrysts of plagioclase and/or hornblende, which are oriented to give the dykes a cryptic layering parallel to their contacts. Andesite dykes of the second type, referred to informally as the "Arichika type" (Fig. 5), are less abundant but widely distributed within the Burnaby Island swarm. They comprise medium- to coarse-grained, aphyric, pyroxene andesite dykes which are commonly from 2-15 m thick. A characteristic feature of these dykes is their intense zeolite alteration which is mani-

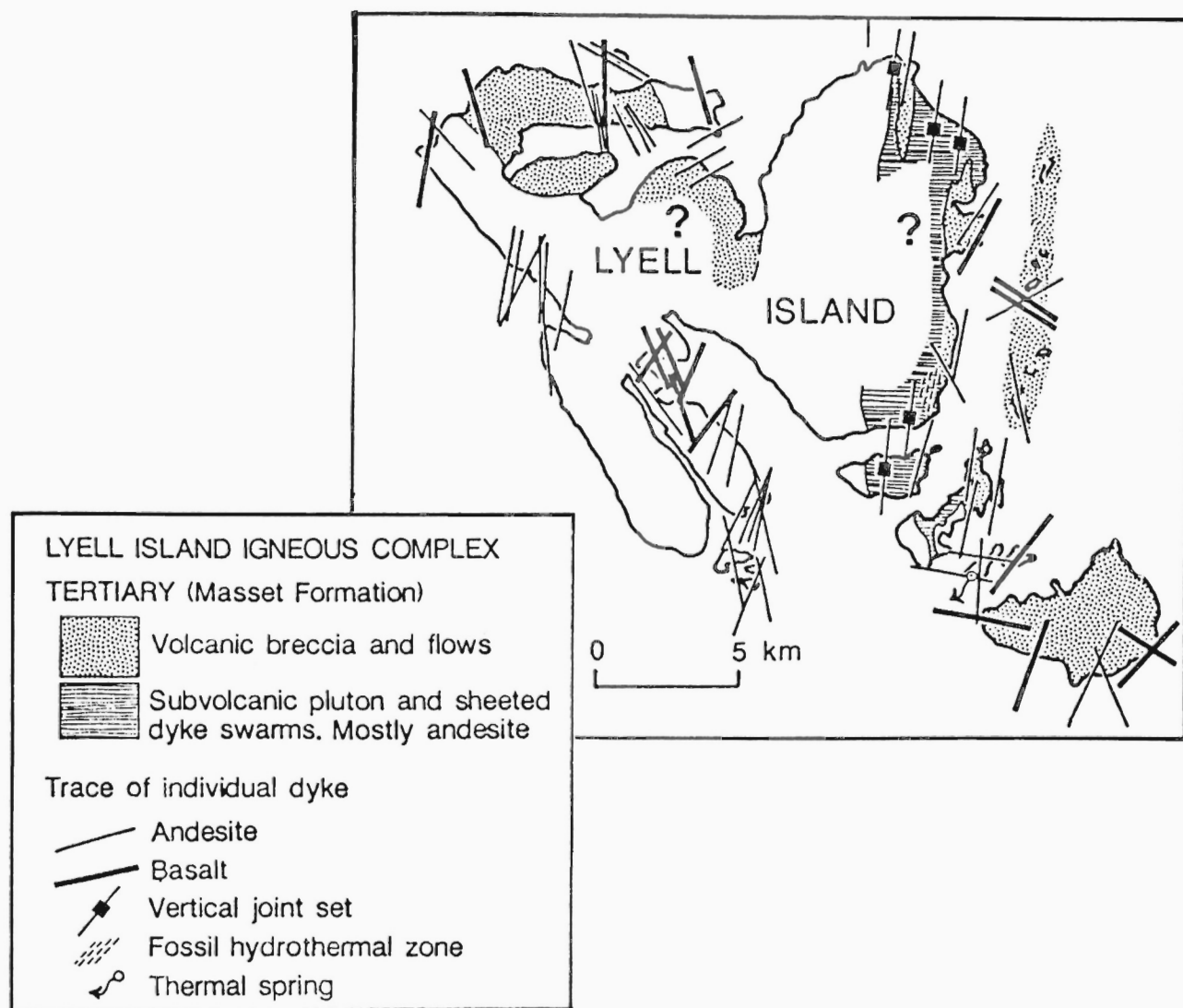


**Figure 3:** Sketch map showing the approximate extent of the Lyell Island igneous complex and adjacent dykes.



**Figure 4:** Fine grained andesite dyke cutting Kunga limestone, Balkus Islands.



**Figure 5:** Layered andesite dyke of the "Arichika" type, Copper Islands.

fest as prominent white layers and mottling along zones parallel with the contacts. Many of the dykes which cut the Cretaceous Longarm Formation are of the Arichika type.

Basalt, which comprises 24% of the Burnaby Island swarm, forms massive to columnar dykes with sharp, linear contacts. They commonly form the youngest dyke set. As in the other swarms rhyolite and dacite form a small percentage of the total dykes (7%). In the Burnaby Island swarm some felsic dykes contain hornblende and/or biotite and have a holocrystalline aplitic texture similar to that of fine-grained phases in the Kano plutonic suite. Most of the light-coloured dykes are associated with zones of pyritic alteration.

Many of the Burnaby Island dykes cut well bedded Kunga sediments. Although discrete subvertical dykes predominate they are locally associated with shallow-dipping sills and intrusive stockworks. Wedge-shaped leading edges of dykes were observed at several places within the Kunga sediments where dykes a metre or more across taper to a few centimetres in a distance of ten to twenty metres. Andesite at the thin edge of the wedge is commonly filled with small angular clasts of the intruded sediment and a fracture zone extends for several tens of metres beyond the end of the dyke. The fracture zone comprises a loose aggregate of wall-rock clasts, open spaces, and quartz-carbonate veins suggesting that fluid pressure, probably resulting from superheated steam, played an active role in dyke propagation.

Dykes in the Burnaby Island swarm have a greater variety of structures than those in any of the other swarms. They vary from uniform tabular bodies with sharp contacts and well-developed columns through dykes and sills that have undergone varying degrees of folding and faulting to those that have been intensely and pervasively fractured and veined. Although no exposures of Tertiary plutons are known near the Burnaby Island dyke swarm, the presence of large holocrystalline felsic dykes suggests the presence of a large igneous centre. Intrusion of the dykes into a zone of progressive fracturing and local extension of 3-5% related to the emplacement of an underlying pluton could account for the observed diversity of deformation and intense hydrothermal activity that characterize the swarm.

### **Carpenter Bay swarm**

The Carpenter Bay dyke swarm extends north-northwesterly from Luxana Bay on Kunghit Island through southwestern Moresby Island to Skincuttle Inlet, where it merges with the Burnaby Island swarm. The 693 dykes measured within the Carpenter Bay swarm form enechelon sets with a more northerly trend than the swarm as a whole. These north-trending sets die out to the south against a relatively dyke-free terrane, the south Moresby stable block, that extends southeast from the San Christoval Range through southwestern Moresby and Kunghit islands. The Carpenter Bay dyke swarm may be genetically related to the Tertiary Carpenter Bay pluton, which is exposed near the centre of the swarm on southeastern Moresby Island.

Andesite dykes, which form 87% of the Carpenter Bay swarm, include both aphyric and porphyritic varieties. Smaller dykes (less than 2 m) are mostly aphyric whereas the larger andesite dykes commonly contain 1-3 mm phenocrysts of plagioclase and/or hornblende. Some very large dykes (10 or more metres thick) comprise crowded hornblende-feldspar porphyries in which phenocrysts form more than 50% of the rock. Less abundant but also widely distributed through the central part of the swarm are fine-grained seriate monzodiorite dykes, which are indistinguishable from, and probably comagmatic with, fine grained phases of the Carpenter Bay pluton. Basalt dykes comprise only 6% of the Carpenter Bay swarm. They have a random spatial distribution but are commonly the youngest dykes. Light coloured, highly fractured, aphanitic dykes (rhyolite and/or

dacite) form a sparse set of large dykes on the east side of Kunghit Island where they are associated with zones of pyritic alteration.

In the central part of the Carpenter Bay swarm, adjacent to the Carpenter Bay pluton, composite dykes several tens of metres thick are abundant and locally form sheeted complexes more than a kilometre across. Such complexes are well exposed for some 4 km along the southeastern shore of Carpenter Bay, north of the Carpenter Bay pluton. There, intensely deformed Kunga sediments have been intruded by a complex of closely spaced andesite dykes. The percentage of dykes varies from about 50% to more than 80% in large areas where nearly continuous igneous rock contains only a few discontinuous screens of Kunga sediments. The sheeted complexes have prominent vertical jointing and indistinct internal phase contacts, both of which are coplanar with north-trending vertical dykes elsewhere in the swarm. Dykes are much less abundant within the Carpenter Bay pluton than in the surrounding country rock, suggesting that early dykes were intruded by late phases of the pluton. However, the pluton is cut by both andesite and basalt dykes and locally, as at Benjamin Point, individual andesite dykes can be traced across the contact between Kunga sediments and seriate monzodiorite of the Carpenter Bay pluton.

The amount of hydrothermal alteration associated with the Carpenter Bay swarm is extremely variable. Many dykes in the Carpenter Bay-Benjamin Point area are deformed, fractured, and veined along with the enclosing sediments. Dykes farther south along Stewart Channel and on Kunghit Island commonly have sharp contacts and lack hydrothermal veins.

### **AGE OF DYKE INTRUSION**

Most of the dykes documented in this study are believed to have been emplaced episodically during a long period of Tertiary magmatism. Most of the pre-Masset rocks in the study area have been moderately to intensely deformed whereas deformation of the dykes cutting them is relatively slight and commonly restricted to minor offsets on local faults. Also the dykes are predominantly vertical or subvertical, suggesting that post-emplacement tilting has been minimal.

Earlier speculation that many of the dykes may be related to Jurassic, Yakoun volcanism (Souther, 1988) is inconsistent with the near vertical attitudes and lateral continuity of the vast majority of dykes. The localized and relatively slight deformation of dykes is in marked contrast to the complexly folded and faulted Jurassic strata which they cut. Moreover, the lithologies and trends of dykes which cut the Cretaceous Longarm and Tertiary Masset formations are indistinguishable from the lithologies and trends of dykes cutting older strata. The apparent scarcity of dykes related to Yakoun volcanism is probably in part due to more intense fracturing which has made them less conspicuous than the highly resistant Tertiary dykes. However, the paucity of Yakoun dykes may also reflect a fundamental difference in the tectonic environment associated with Tertiary and Jurassic volcanism. The Tertiary dykes were clearly emplaced when a strongly anisotropic stress field favoured extension and lateral propagation of dyke swarms. Such conditions may not have prevailed during the Jurassic. The Yakoun volcanics may have erupted from central vents without the accompanying injection of extensive dyke systems.

The foregoing observations suggest that most of the dykes documented in this study were emplaced during the long period of Masset volcanism, between Middle Eocene and Early Miocene time (50-20 Ma). They are probably at least partly comagmatic with Masset volcanic rocks (Hickson, 1991) and with plutonic rocks of the Kano plutonic suite (Anderson and Reichenbach, 1991; Anderson and Greig, 1989). It seems likely that the principal dyke swarms and some of the Kano plutons are subvolcanic manifestations of Masset volcanic piles which have been partly or wholly removed by erosion.



**Table 1. K-Ar data for dykes on southern Moresby Island**

Field no.	Lab. no.	Locality	Material	K wt% $\pm 1\sigma\%$	Rad $^{40}\text{Ar}$ cc/g $\times 10^{-7}$ $\pm 1\sigma\%$	%Atmos Ar	Age $\pm 2\sigma$
SE042387	4065	Ikeda Point	Hornblende	0.241 $\pm$ .55	3.894 $\pm$ 5.7	71.0	41.1 $\pm$ 4.6 Ma
SE041387	4064	Koya Bay	Hornblende	0.217 $\pm$ .78	4.669 $\pm$ 2.9	41.0	54.53 $\pm$ 3.2 Ma

K-Ar age determinations by J.C. Roddick, Geological Survey of Canada, Ottawa.

K-Ar dates of 43.7 Ma (Anderson and Reichenbach, 1991), 54.5 Ma, and 41.1 Ma (Table 1) from dykes on southern Moresby Island compare to a mean age of 23 Ma for Masset volcanic rocks on Graham Island (Hickson, 1988). This agrees with a northerly decrease in the age of Kano plutonic rocks and suggests a northward migration of Tertiary magmatic activity with time. On the other hand, recognition of an older volcanic suite under the Masset of Graham Island (Hickson, 1988) may indicate that Eocene or earlier magmatism began along the length of the volcanic belt but persisted longer in the north. Thus remnants of volcanic and subvolcanic rocks coeval with those exposed on southern Moresby Island may be buried beneath the younger Masset volcanoes of Graham Island.

In most swarms an early generation of andesite dykes is cut by Kano plutons and synplutonic dykes and these in turn are cut by a still younger generation of mainly basaltic dykes (Fig. 6). The mutually crosscutting relationships between dykes and Kano plutonic rock and the multiple quenched selvages observed in many composite dykes are probably the result of progressive intrusion and extension during a single but prolonged Tertiary magmatic episode.

## PETROGRAPHY

Samples of 81 dykes, representing the full range of visually different rocks, were examined petrographically (Souther and Bakker, 1988). Mineral compositions were determined by flat-stage optical methods and percentages by visual estimate (Table 2). Lithological names in Table 2 are based on the proportions of quartz, alkali feldspar, and plagioclase, using the classification scheme of Streckeisen (1967).

Based on textures and alteration the samples are further subdivided into the five classes described below.

### Class 1

This relatively small group of leucocratic, feldspar phyrlic rocks includes rhyolite, dacite, trachyte and andesite. Feldspar phenocrysts are commonly hiatal and moderately to strongly altered but rocks of this type contain relatively little secondary calcite, chlorite or leucoxene.

### Class 2

This large group of pyroxene-poor andesite, basalt and dacite is characterized by rocks containing less than 15% pyroxene and total modal mafic minerals M ( $M = \text{cpx} + \text{ch} + \text{bi} + \text{op}$ ) of 10%-30%. Hiatal microphenocrysts of zoned plagioclase (labradorite-oligoclase), augite, pigeonite, and rare amphibole are moderately altered. The ground-mass of plagioclase laths contains abundant calcite and chlorite. Autoclastic texture, characterized by randomly oriented broken crystals, is common.

### Class 3

Pyroxene-rich andesite and basalt in this class commonly contain 10-25% pyroxene and  $M = 25$ -50%. The rocks are either aphyric or contain sparse microphenocrysts of strongly zoned plagioclase (andesine-oligoclase in the andesites, labradorite-oligoclase in the basalts)

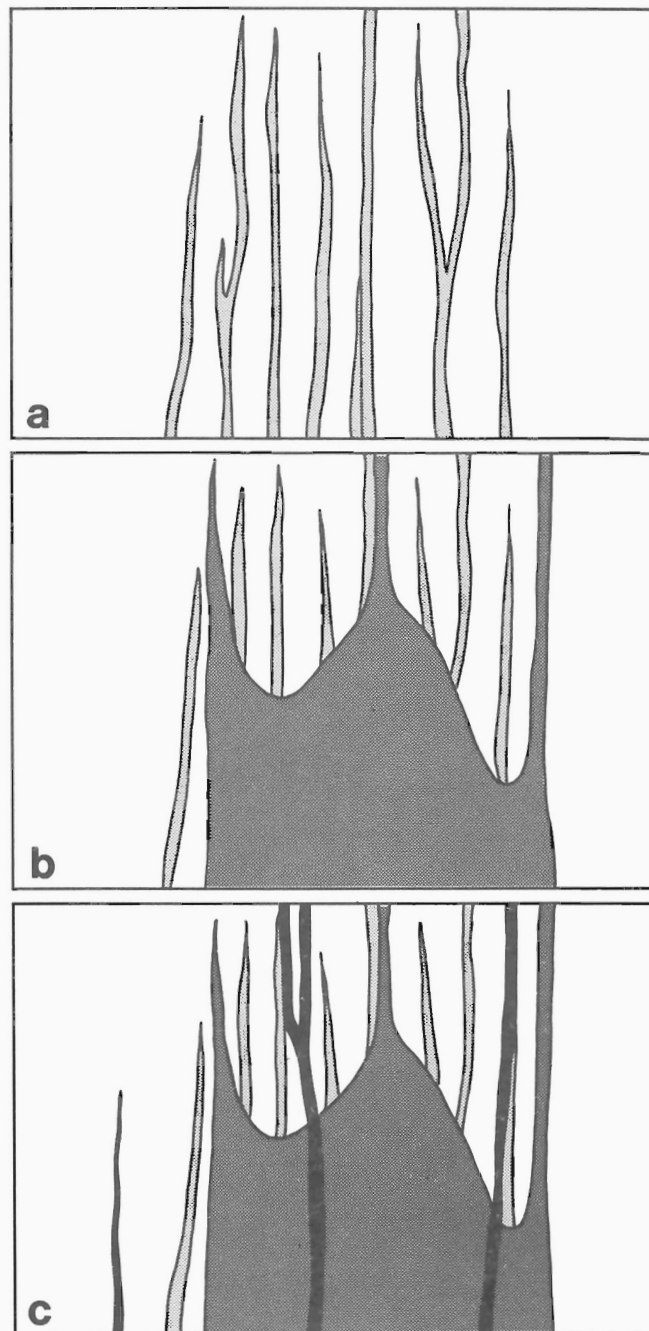


**Figure 6:** Idealized sketch showing the progression of intrusive events based on crosscutting relationships: a. intrusion of precursor andesite dykes; b. intrusion of Kano pluton and synplutonic porphyry dykes; c. intrusion of post-plutonic basalt dykes.



TABLE 2: Petrographic features of selected dykes

Field Number	Lithology	Specific Gravity	Formation Intruded	PHENOCRYSTS				GROUNDMASS AND APHRIC ROCKS										ALTERATION					Amygdulæ % and mineralogy				
				Total %	Size Range	% and mineralogy				Size Range	% Primary minerals						Saussurization of Feldspar	% Secondary minerals									
						Feldspar	Quartz	Clinopyroxene	Orthopyroxene		Amphibole	Opaques	Pseudomorphs	Plagioclase	Alkali Feldspar	Quartz		Clinopyroxene	Orthopyroxene	Hornblendes	Opaques	Other		Matrix			
																									% Secondary minerals		
BASALT																											
180387	O B2	2.745	Yk	35	m-f	25 lab-olig	-	10 aug	-	-	-	-	-	-	-	-	-	-	m-s	22	5	-	5	-	-	3 ch,sp,Q x cal,chl,Q,sp	
021087	O B2	2.801	Ms	25	m-f	25 lab-and	-	-	-	-	-	-	-	-	-	-	-	-	m	-	x	3	2	x	-	x	
141987	R B3	2.773	Syn	5	c-f	-	-	5 aug	-	-	-	-	-	-	-	-	-	-	-	-	x	15	5	-	-	x	
131987	R B3	2.745	Syn	5	m	x pc	-	-	-	-	-	-	-	-	-	-	-	-	-	-	5	10	5	-	-	-	
130287	R B3	2.768	Ms	5	m	5 pc	-	-	-	-	-	-	-	-	-	-	-	-	-	-	-	x	5	-	-	-	
170387	O B3	2.767	Ms	3	m	3 pc	-	-	-	-	-	-	-	-	-	-	-	-	-	-	-	10	x ap	-	-	x	
231487	S B3	2.780	Ms	1	m	1 low an	-	x aug	-	-	-	-	-	-	-	-	-	-	-	-	-	8	-	-	-	2 Z: x ep	
100187	S B3	2.827	Ku	18	c-m	-	-	-	-	-	-	-	-	-	-	-	-	-	-	-	-	6	x bi	-	-	x	
240787	S B3	2.885	Yk	5	m-f	5 by-olig	-	-	-	-	-	-	-	-	-	-	-	-	-	-	-	10	5	1	-	4 chl,bi	
261887	T B3	2.974	Ku	3	m	-	-	-	-	-	-	-	-	-	-	-	-	-	-	-	-	15	30	-	-	-	
082287	L B3	2.830	Ku	40	m-vf	10 pc	-	-	-	-	-	-	-	-	-	-	-	-	s	-	x	3	x	-	-	1 ch	
052787	B B3	2.770	Ku	2	m	2 lab-and	-	-	-	-	-	-	-	-	-	-	-	-	-	-	23	20	-	-	-	1 chl,cal,Q	
120287	R B4	2.808	Syn	x	f	x pc	-	-	-	-	-	-	-	-	-	-	-	-	-	-	x	x	8	-	-	x op,pc	
141287	R B4	2.786	Syn	3	f	3 pc	-	-	-	-	-	-	-	-	-	-	-	-	-	-	-	-	10	-	-	x bi,pc	
200487	S B4	2.750	Hd	15	m	15 pc	-	-	-	-	-	-	-	-	-	-	-	-	-	-	-	-	5	15	x	x chl,cal,Q	
220887	S B4	2.882	Ku	3	m	3 pc	-	-	-	-	-	-	-	-	-	-	-	-	-	-	-	1	8	2	x	x chl,cal,bi	
230687	S B4	2.865	Yk	5	c-m	5 pc	-	-	-	-	-	-	-	-	-	-	-	-	-	-	-	5	15	-	-	x chl,cal,Q	
240287	T B4	2.914	Post	x	m	x pc	-	-	-	-	-	-	-	-	-	-	-	-	-	-	-	1	3	5	-	x chl,cal,Q	
261187	T B4	2.907	Ku	x	m	x pc	-	-	-	-	-	-	-	-	-	-	-	-	-	-	-	4	15	5	1	x sid,ep	
261487	T B4	2.985	Yk	x	m	x pc	-	-	-	-	-	-	-	-	-	-	-	-	-	-	-	5	10	x	-	x chl,cal,Q	
270987	T B4	2.918	Syn	x	m	x pc	-	-	-	-	-	-	-	-	-	-	-	-	-	-	-	1	9	1	-	x chl,cal,Q	
272487	T B4	2.842	Ka	x	f	x pc	-	-	-	-	-	-	-	-	-	-	-	-	-	-	-	12	-	-	-	x chl,cal,Q	
281587	T B4	2.948	Ku	2	m	2 pc	-	-	-	-	-	-	-	-	-	-	-	-	-	-	-	5	8	x	-	x chl,cal,Q	
050987	B B4	3.003	Ku	x	m	x pc	-	-	-	-	-	-	-	-	-	-	-	-	-	-	-	6	3	x	-	1 chl,cal,Q	
150387	R B5	2.580	Syn	-	-	-	-	-	-	-	-	-	-	-	-	-	-	-	-	-	-	2	8	1	-	-	
091387	S B5	2.886	Ky	-	-	-	-	-	-	-	-	-	-	-	-	-	-	-	-	-	-	5	10	5	-	x chl,bi,pc,op	
280287	T B5	2.972	Ka	-	-	-	-	-	-	-	-	-	-	-	-	-	-	-	-	-	-	7	10	x	-	-	
290487	T B5	2.874	Yk	-	-	-	-	-	-	-	-	-	-	-	-	-	-	-	-	-	-	3	7	5	-	-	
060787	B B5	2.952	Ku	x	c	x pc	-	-	-	-	-	-	-	-	-	-	-	-	-	-	-	6	1	x	-	x chl,Q	
ANDESITE																											
092087	S A1	2.683	Post	10	f	5 pc	-	-	-	-	-	-	-	-	-	-	-	-	-	-	-	-	-	-	-	-	x chl,ep,Q
230587	S A1	2.728	Yk	15	f-m	10 olig	-	x 5 aug	-	-	-	-	-	-	-	-	-	-	s	-	x	15	-	-	5	-	x x ser
200287	S A1	2.676	Hd	11	f-m	10 olig	-	-	-	-	-	-	-	-	-	-	-	-	vs	-	5	15	-	-	2	-	-
190987	S A1	2.661	Post	42	f-m	25 olig	-	-	-	-	-	-	-	-	-	-	-	-	m	-	x	15	-	-	8	-	-
041587	C A1	2.628	Ku	40	m-f	30 olig	-	-	-	-	-	-	-	-	-	-	-	-	-	60	x	x	-	-	10	x Z	2 cal,chl,Q
041387	C A1	2.713	Ku	18	f	12 and-olig	-	-	-	-	-	-	-	-	-	-	-	-	s	-	x	5	-	-	3	-	5 chl,sp
042387	C A1	2.706	Ku	23	f-m	15 and	-	-	-	-	-	-	-	-	-	-	-	-	m	-	3	10	-	-	3	-	-
130687	R A2	2.718	Ms	x	m	x low an	-	x aug	-	-	-	-	-	-	-	-	-	-	-	-	-	10	5	-	-	2	2 ep
151687	R A2	2.654	Syn	1	f	-	-	-	-	-	-	-	-	-	-	-	-	-	-	-	-	-	-	-	-	-	-
130587	R A2	2.592	Ms	20	m-vf	15 lab-and	-	5 aug	-	-	-	-	-	-	-	-	-	-	m-s	-	3	10	-	-	5	-	-
130787	R A2	2.510	Ms	30	m-vf	20 an-olig	-	4 aug	-	-	-	-	-	-	-	-	-	-	-	-	-	-	-	-	-	-	x cpx,gl,pc,op
020187	O A2	2.837	Hd	-	-	-	-	-	-	-	-	-	-	-	-	-	-	-	-	-	-	20	15	-	-	x	x zoi

1711a87	O	A2	2720	Hd	-	-	-	-	-	-	-	-	-	-	-	-	-	-	-	-	-	-	-	2 ch.Q,cal
191087	S	A2	2721	Yk	3	c-m	-	-	-	-	-	-	-	-	-	-	-	-	-	-	-	-	-	1 ch,cal,sp
222187	S	A2	2748	Yk	x	m-f	-	-	-	-	-	-	-	-	-	-	-	-	-	-	-	-	-	2 cal
2207a87	S	A2	2732	Ku	-	-	-	-	-	-	-	-	-	-	-	-	-	-	-	-	-	-	-	x cal,Q
2206b87	S	A2	2755	Ku	-	-	-	-	-	-	-	-	-	-	-	-	-	-	-	-	-	-	-	x Q,cal
2403a87	S	A2	2762	Hd	-	-	-	-	-	-	-	-	-	-	-	-	-	-	-	-	-	-	-	2 Q,ep,cal
2611a87	T	A2	2736	Ku	12	m-f	-	-	-	-	-	-	-	-	-	-	-	-	-	-	-	-	-	5 ch,cal,Q
081487	L	A2	2719	Ms	4	f-vf	-	-	-	-	-	-	-	-	-	-	-	-	-	-	-	-	-	20 ch,Q
070387	L	A2	2773	La	-	-	-	-	-	-	-	-	-	-	-	-	-	-	-	-	-	-	-	-
070587	L	A2	2703	La	1	f	-	-	-	-	-	-	-	-	-	-	-	-	-	-	-	-	-	-
041887	C	A2	2742	Ku	35	c-f	-	-	-	-	-	-	-	-	-	-	-	-	-	-	-	-	-	-
031387	B	A2	2689	Ku	40	m-f	-	-	-	-	-	-	-	-	-	-	-	-	-	-	-	-	-	-
042187	C	A2	2680	Ku	25	m-f	-	-	-	-	-	-	-	-	-	-	-	-	-	-	-	-	-	10 ch,sp,cal
0602b87	B	A2	2751	Ku	-	-	-	-	-	-	-	-	-	-	-	-	-	-	-	-	-	-	-	-
041187	C	A2	2745	Ku	-	-	-	-	-	-	-	-	-	-	-	-	-	-	-	-	-	-	-	-
141087	R	A3	2875	Syn	3	m-f	-	-	-	-	-	-	-	-	-	-	-	-	-	-	-	-	-	-
170787	O	A3	2819	La	8	m	-	-	-	-	-	-	-	-	-	-	-	-	-	-	-	-	-	-
0905b87	S	A3	2804	Ku	-	-	-	-	-	-	-	-	-	-	-	-	-	-	-	-	-	-	-	-
241387	S	A3	2759	Ms	-	-	-	-	-	-	-	-	-	-	-	-	-	-	-	-	-	-	-	-
272087	T	A3	2892	Ka	x	m-f	-	-	-	-	-	-	-	-	-	-	-	-	-	-	-	-	-	x ch,cal,Q
270687	T	A3	2893	Syn	-	-	-	-	-	-	-	-	-	-	-	-	-	-	-	-	-	-	-	1 Q,Z
260687	T	A3	2841	Yk	-	-	-	-	-	-	-	-	-	-	-	-	-	-	-	-	-	-	-	1 ch,Q,cpx,cal
290787	T	A3	2913	Yk	-	-	-	-	-	-	-	-	-	-	-	-	-	-	-	-	-	-	-	-
040187	C	A3	2775	Yk	10	m-f	-	-	-	-	-	-	-	-	-	-	-	-	-	-	-	-	-	-
061987	B	A3	2670	La	-	-	-	-	-	-	-	-	-	-	-	-	-	-	-	-	-	-	-	2 ch,cal,Q,sp
040387	C	A3	2836	Yk	3	m-vf	-	-	-	-	-	-	-	-	-	-	-	-	-	-	-	-	-	2 Q,Z
040287	C	A3	2835	Yk	3	m	-	-	-	-	-	-	-	-	-	-	-	-	-	-	-	-	-	1 cal,Q,sp, ch

#### DACITE AND TRACHYTE

020587	O	D1	2654	Ku	35	m-vf	30 olig,x KF	-	-	5 ch,Q	-	x	20	-	-	-	-	m	3	10	-	3	1 Z	-
091687	S	D1	2687	Yk	20	f-m	5 olig	-	-	15 cal	-	-	35	-	-	x	-	s	x	x	-	x	x ser,clay	-
191287	S	D1	2679	Yk	15	m-f	10 olig	-	-	5 ch,op,cal,sp	-	-	15	-	-	-	-	s	10	3	-	5	10 Z,ser,mus	-
041687	C	D1	2650	Ku	11	f	10 pc	1	-	x cal,Z	-	x	15	-	-	-	-	m-s	x	-	-	x	5 Z; x zoi	10 op,cal,Z
031187	B	T1	2664	Ku	35	f-m	35 olig	-	-	5 cal,sp	-	30	8	-	-	-	-	x	s	x	-	-	-	10 cal,sp

#### RHYOLITE

1510b87	R	R1	2633	Syn	8	m-f	5 olig,x KF	3	-	-	-	-	55	25	-	-	-	-	s-m	10	-	-	-	3 cal,Q
1509a87	R	R1	2618	Syn	1	f	1 olig	-	-	-	-	-	55	25	-	-	xpy	-	s	10	-	-	-	-
130187	R	R1	2544	Ms	5	f-m	5 san	-	-	-	-	-	x	45	-	-	-	-	n	x	x	-	-	2 Q,cal
130387	R	R1	2623	Ms	19	c-vf	15 olig	-	-	-	-	-	-	-	-	-	-	70	m	-	-	-	-	-
170887	O	R1	2597	La	9	f-m	3 olig	5	-	1 bi,ap	-	-	-	40	40	-	-	-	w	1	-	-	-	-
2314a87	S	R1	2780	Ms	6	f-m	5 olig	-	-	1 bi,op,mus	-	-	-	10 pc	-	-	-	-	-	-	-	-	-	-
2206a87	S	R1	2617	Ku	15	m	15 olig	-	-	1 ch,ep,op	-	-	-	F	x	-	-	-	85	-	-	-	-	x ep, ch
070187	L	R1	2631	La	12	m-f	10 olig	-	-	1 ch,cal,op	-	-	-	F	-	-	-	65	s	5	10	-	5 Z	-
											-	-	-	-	-	-	-	-	2	2	-	-	-	-

Lithology	Dike Swarm	Unit	Intruded	Grain Size	Saussurization	Minerals	epidote	px	pyroxene
A andesite	R Rennell Sound	Hd	Haida Formation	cc microcrystalline (<.01 mm)	w weak	amp amphibole	F felsitic	Q	sanidine
B basalt	T Tasu Sound	Ku	Kunga Group	mc moderate	m moderate	an andesine	hem hematite	ser	sericite
D dacite	C Carpenter Bay	La	Longarm Formation	f very fine grained (.1 - .3 mm)	s strong	ap apatite	KF alkali feldspar	sid	siderite
R rhyolite	L Burnaby Island	Ms	Masset Formation	m medium grained (1.0 - 3.3 mm)	v very strong	aug augite	lab labradorite	sp	sphene
T trachyte	Yk Yakoun Group	Yk	Yakoun Group	c coarse grained (3.3 - 10 mm)		bi biotite	mus muscovite	tour	tourmaline
1-5 class (see text)	S Selwyn Inlet	Post	Burnaby Island and Kano plutonic suites			by bytownite	olig oligoclase	Z	zeolite
	O Skidegate Inlet area	Syn	San Cristoval plutonic suite			cal calcite	op opaque	zir	zircon
						ch chlorite	py pidgeonite	zoi	zoisite
						cpx clinopyroxene	py pyrite		

and augite in a groundmass of plagioclase laths, chlorite, biotite, opaques and leucoxene.

#### Class 4

Doleritic basalt of this type contains 25-45% pyroxene. The rock is aphyric or contains sparse plagioclase phenocrysts. Textures are ophitic or subophitic and coarser than basalts in the previous classes. Alteration is slight but some chlorite and biotite are present in most specimens.

#### Class 5

Gabbroic basalt of this type is confined to very thick dykes (>10 m). The mineralogy of these rocks is similar to doleritic basalts of the previous class but they are coarser grained and the texture is hypidiomorphic-granular rather than ophitic. They are commonly aphyric and unaltered.

The petrographic data reveal only slight differences in the lithology of dykes from the seven geographic areas studied. Except for Tasu Sound, where only basalt and andesite dykes were found, each of the

swarms include dykes that span the complete spectrum of petrographic and chemical types.

The degree of alteration appears to be closely linked to the proximity of central igneous complexes where hydrothermal activity was most intense. Saussuritization and other alteration is more intense in rocks of intermediate composition (andesite and basaltic andesite) than in either the rhyolites or more mafic basalts suggesting that magma composition was also a factor in controlling alteration.

The petrographic work revealed a broad spectrum of compositions, ranging from rhyolite to basalt, but failed to establish any mineralogical or textural criteria that are unique to dykes from different swarms or of different ages. However, the 81 petrographically studied samples provided a reference suite for visual comparison and classification of the entire collection.

#### CHEMISTRY

Forty-seven dyke samples were analyzed for major and trace elements. The results (Table 3) confirm the wide range of compositions indicated by petrography. Silica values range from 48.4-76.6%. All

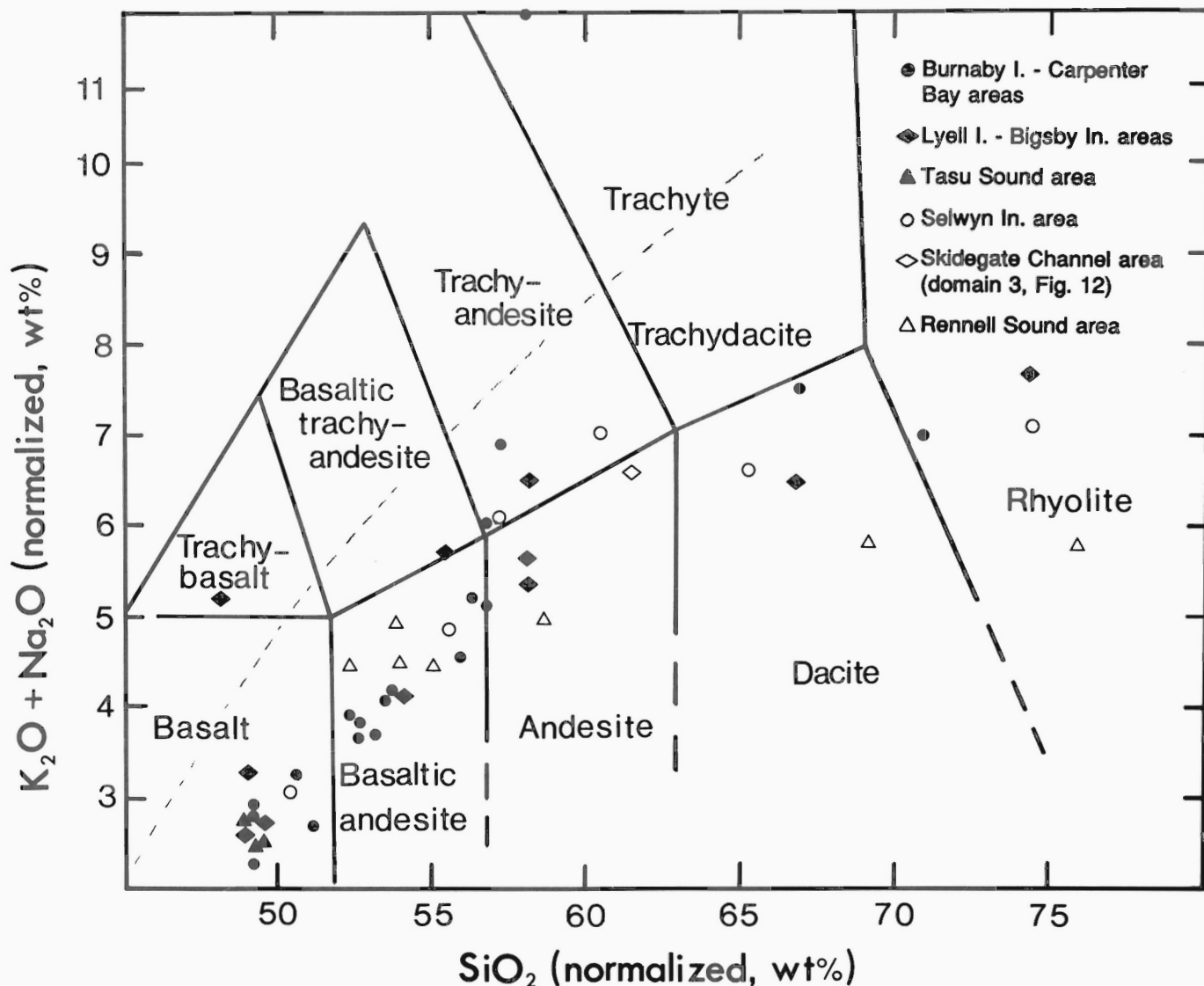


**Figure 7:** Alkali-silica diagram for the 47 analyzed dyke samples listed in Table 3. Dashed line is the boundary between the alkaline and subalkaline fields of Irvine and Baragar (1971); solid field lines are from LeBas et al. (1986).

but three of the analyzed samples are quartz normative and only one, a trachyte porphyry, is nepheline normative. The latter is an anomalous, K-feldspar-rich rock from a dyke near the centre of the Burnaby Island swarm.

The chemical data do not plot along any single trend or within any well defined field. On the alkali-silica diagram (Fig. 7) most of the data plot in the subalkaline field and range in composition from basalt to rhyolite. However, the data set includes eight rocks that range in composition from trachybasalt to trachyte on the classification scheme of LeBas et al. (1986). On the Irvine and Baragar (1971) Ab'-An-Or diagram (Fig. 8) most of the dyke data plot in the field of the sodic series but eight of the analyses are well within the field of the potassic series. The AFM plot displays a similar degree of scatter. Although most of the data define a calc-alkaline trend analogous to that of the Cascades a significant number of points lie along a path of extreme iron enrichment characteristic of tholeiitic (MORB) fractionation trends.

The average composition of samples from the northern group of dyke swarms (Rennell Sound, Selwyn Inlet and isolated dykes in the Skidegate Channel area) is significantly more alkaline and lower in iron than the mean composition of samples from the Carpenter Bay, Burnaby Island, Lyell Island, and Tasu Sound swarms farther south (Fig. 8).

Silica variation diagrams for both major and minor elements (Fig. 9) indicate a complete range of intermediate compositions between

the basaltic and rhyolitic end members. Much of the scatter in the data may be due to mixed parentage of the suite which appears to be the product of both calc-alkaline and tholeiitic magmatism. However, the fairly linear decrease in  $\text{Fe}_2\text{O}_3$ ,  $\text{MgO}$ , and  $\text{CaO}$  (not shown) and the rapid decrease in  $\text{TiO}_2$  with increasing silica are typical of calc-alkaline suites which may be the product of combined fractionation and assimilation. The rate of increase of  $\text{Na}_2\text{O}$  (Fig. 9),  $\text{Al}_2\text{O}_3$ , and  $\text{Sr}$  appears to decline after about 56% silica suggesting that separation of alkali feldspar may have influenced the late stages of fractionation.

## TECTONIC SETTING

Between 40 and 20 Ma ago, when Tertiary magmatism was most intense on Queen Charlotte Islands, western North America was bounded by and converging with the Farallon Plate (Riddihough, 1982) (Fig. 10). The Pemberton Volcanic Belt which extends west-north-westerly from the Chilliwack Batholith in southern British Columbia across the Coast Mountains to Queen Charlotte Islands is believed to be the remnant of a magmatic arc related to this convergence (Souther and Yorath, in press). The trace of the arc is defined by a linear zone of widely spaced epizonal plutons and deeply dissected volcanic piles of which the Masset and related subvolcanic rocks are the most northerly manifestation.

The above model implies that the Farallon-Pacific triple junction with North America lay north of the Queen Charlotte Islands through most of Masset time. Subsequent migration of the Farallon-Pacific ridge south to its present position off northern Vancouver Island and a shift

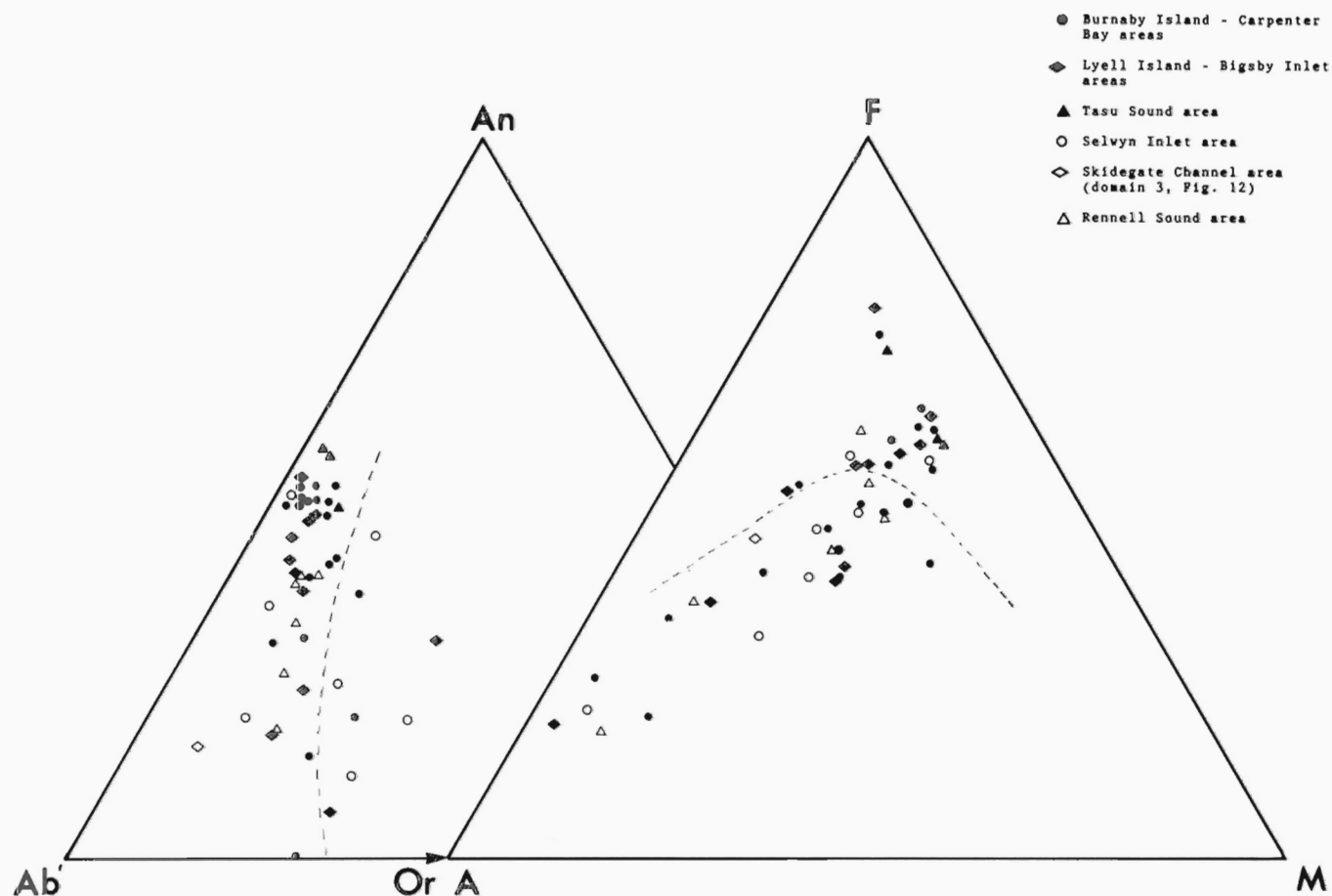


**Figure 8:** Ab'-An-Or and AFM diagrams showing the chemical affinity and variation for the 47 analyzed dyke samples listed in Table 3. Dashed lines are the boundaries between sodic and potassic series on the Ab'-An-Or plot, and between tholeiitic and calc-alkaline suites on the AFM diagram (from Irvine and Baragar, 1971).

TABLE 3: Chemical analyses

Field #	151087	130787	141087	131987	130287	120287	020587	220687	092087	190987	240387	231487	100187	261887	261487	280287
Major elements (weight percent)																
SiO <sub>2</sub>	76.55	68.73	51.89	58.80	57.29	53.79	61.18	53.83	65.58	60.38	55.97	74.29	55.74	49.40	49.40	48.44
Al <sub>2</sub> O <sub>3</sub>	14.36	15.32	13.46	15.50	17.74	15.57	17.66	15.98	15.75	16.89	16.88	13.49	17.87	14.63	14.95	12.57
Fe <sub>2</sub> O <sub>3</sub>	0.60	1.73	2.95	4.52	2.89	3.88	0.41	3.40	1.38	2.33	2.33	0.60	3.00	1.12	3.23	7.40
FeO	0.84	2.35	10.22	4.55	4.07	6.57	6.86	8.82	2.94	5.08	6.32	1.42	5.40	12.08	9.54	9.76
CaO	2.04	8.52	6.34	8.57	6.07	8.43	2.57	6.34	4.50	2.55	5.58	1.44	7.56	10.30	10.86	9.85
MgO	0.66	1.29	4.34	5.29	3.86	4.74	2.30	4.18	3.03	4.36	3.98	0.57	4.36	6.70	6.73	4.15
Na <sub>2</sub> O	4.20	3.46	3.40	3.40	3.68	3.68	5.67	4.24	4.27	3.58	4.72	4.13	3.05	2.29	2.40	2.25
K <sub>2</sub> O	1.59	1.45	1.05	1.12	1.01	0.90	0.91	0.74	2.35	3.46	1.39	3.00	1.64	0.27	0.17	0.62
TiO <sub>2</sub>	0.10	0.65	3.11	1.46	0.88	1.96	0.72	2.07	0.62	0.82	1.33	0.31	0.99	2.13	1.94	3.76
P <sub>2</sub> O <sub>5</sub>	0.03	0.16	0.52	0.27	0.38	0.40	0.37	0.29	0.11	0.13	0.31	0.05	0.19	0.30	0.24	0.56
MnO	0.03	0.09	0.22	0.16	0.14	0.20	0.21	0.20	0.11	0.16	0.20	0.04	0.17	0.22	0.21	0.27
TOTALS	101.00	99.61	99.74	99.68	98.89	100.11	98.86	99.88	100.63	99.74	99.02	99.34	99.99	99.45	99.67	99.63
LOI	0.78	3.30	5.48	3.02	0.76	2.05	2.51	4.88	4.23	2.67	3.10	0.49	2.11	2.46	3.62	1.84
Trace elements (ppm)																
Ba	307.70	845.30	281.10	243.90	465.10	289.00	621.10	260.70	647.30	830.40	457.40	844.60	502.70	164.80	63.20	154.10
Cr	2.60	14.90	28.80	122.90	36.90	106.20	<0.30	2.80	77.40	10.50	3.40	6.60	12.40	2.80	106.40	124.30
Cu	12.20	19.30	37.20	39.40	44.80	50.30	44.40	47.20	27.40	67.90	40.00	7.50	94.40	40.00	48.40	51.60
Nb	6.30	17.30	15.00	11.10	8.30	14.20	8.50	6.10	7.40	6.80	7.00	9.60	5.40	16.70	5.90	10.00
Ni	3.10	15.10	33.20	54.90	34.00	57.80	2.80	13.20	37.70	9.90	4.20	12.10	14.70	34.40	71.40	57.50
Pb	22.50	13.40	12.10	7.50	10.00	7.60	13.10	9.50	10.40	9.00	9.60	14.70	3.80	8.80	6.50	6.40
Rb	48.60	104.30	11.70	16.40	22.70	17.20	21.80	11.70	46.50	60.50	34.90	82.20	38.20	7.60	2.10	6.40
Sr	283.40	435.90	371.50	321.60	647.10	328.10	523.40	659.71	279.00	398.70	516.70	84.00	491.00	233.10	188.30	217.20
V	12.40	60.30	354.20	203.40	129.20	191.10	25.40	352.80	118.50	217.80	216.30	18.10	282.30	386.80	321.70	289.60
Y	11.60	35.50	36.60	31.50	19.50	35.90	22.30	28.20	31.40	28.30	24.70	38.60	26.80	71.00	35.60	33.20
Zn	67.80	121.70	83.50	92.00	83.50	119.70	128.30	117.60	82.30	88.00	109.30	24.80	91.40	205.10	120.70	145.10
Zr	341.40	207.80	176.20	235.50	176.20	235.50	200.70	151.10	141.20	176.30	151.80	232.90	131.40	327.80	139.00	140.50
Co	39.50	44.00	43.70	39.50	43.70	40.80	20.90	33.10	29.70	24.60	32.10	36.30	39.20	41.50	46.90	503.00
q	37.32	26.31	5.51	5.62	8.85	4.84	10.81	4.08	15.94	10.97	3.42	32.19	7.00	0.00	1.52	6.84
or	9.38	8.67	6.37	6.69	6.03	5.37	5.40	4.43	13.76	20.48	8.27	17.99	9.76	1.63	1.02	3.86
ab	37.66	39.43	31.90	30.85	36.58	33.37	51.17	38.56	38.01	32.21	42.69	37.64	27.57	21.05	21.99	21.30
an	9.91	16.51	18.59	23.98	27.63	23.54	10.39	22.88	16.72	11.83	20.92	6.92	30.44	29.54	30.12	23.59
ne	0.00	0.00	0.00	0.00	0.00	0.00	0.00	0.00	0.00	0.00	0.00	0.00	0.00	0.00	0.00	0.00
ol	0.00	0.00	0.00	0.00	0.00	0.00	0.00	0.00	0.00	0.00	0.00	0.00	0.00	0.12	0.00	0.00
Field #	070387	331187	241387	042337	040187	060767	632988	050188	090188	092088	120788	130888	140188	151388	160288	161288
Major elements (weight percent)																
SiO <sub>2</sub>	53.55	58.82	55.54	56.04	53.92	48.40	57.85	49.07	57.71	49.43	66.76	49.25	56.71	66.47	52.79	52.51
Al <sub>2</sub> O <sub>3</sub>	19.35	17.21	18.30	18.78	18.36	13.39	14.14	14.46	17.24	13.92	16.69	13.57	19.56	16.12	17.31	18.95
Fe <sub>2</sub> O <sub>3</sub>	1.79	0.52	0.68	0.74	1.49	2.58	3.47	3.82	3.21	4.84	1.12	4.02	1.69	0.71	3.44	2.84
FeO	8.12	3.04	6.87	5.19	6.23	11.98	6.67	9.21	4.72	9.68	3.49	10.50	4.99	3.67	8.29	7.39
CaO	6.80	5.45	7.45	7.55	8.17	9.90	5.64	11.13	6.00	10.01	3.49	10.70	5.57	3.11	8.62	7.40
MgO	3.95	2.54	3.65	4.25	7.12	5.75	2.76	5.96	4.48	6.05	1.69	6.25	2.76	1.27	4.62	5.73
Na <sub>2</sub> O	3.52	7.73	4.12	3.79	3.37	2.94	4.85	2.81	3.56	2.57	4.55	2.46	5.56	4.49	2.88	3.32
K <sub>2</sub> O	0.67	4.37	1.16	1.40	0.74	0.25	1.71	0.51	2.06	0.85	1.95	0.14	1.39	3.03	0.71	1.44
TiO <sub>2</sub>	1.18	0.75	1.09	0.74	0.83	3.21	2.16	2.56	0.94	2.85	0.62	2.43	1.07	0.59	1.52	1.58
P <sub>2</sub> O <sub>5</sub>	0.21	0.17	0.32	0.28	0.20	0.50	0.82	0.41	0.16	0.38	0.23	0.35	0.41	0.19	0.35	0.32
MnO	0.12	0.04	0.14	0.11	0.15	0.24	0.24	0.24	0.17	0.27	0.10	0.26	0.15	0.11	0.19	0.18
TOTALS	99.28	100.64	99.31	98.88	100.59	98.73	100.31	99.98	100.25	100.65	100.69	99.93	99.86	99.76	100.72	100.86
LOI	2.35	3.09	4.24	3.54	3.81	3.09	1.38	2.37	5.17	3.26	3.94	2.06	2.54	1.40	7.09	2.35
Trace elements (ppm)																
Ba	496.20	230.90	428.80	279.00	275.00	305.70	418.31	74.79	491.39	235.08	770.25	30.89	572.02	785.78	2214.42	160.56
Cr	3.20	19.90	16.60	67.10	82.40	91.60	117.53	146.93	118.86	174.36	98.51	201.82	86.38	213.07	52.53	132.27

Field #	181288	181488	210988	233988	240188	263488	273188	300488	321588	350288	360288	371088	372788	400188	402888
Major elements (weight percent)															
Cu	37.60	11.30	47.40	84.50	74.00	56.60	28.10	78.81	69.26	77.44	28.14	86.79	47.71	18.12	79.61
Nb	4.60	5.10	7.20	4.90	3.70	11.60	11.52	19.12	6.68	11.52	7.23	10.13	15.40	11.94	8.10
Pb	6.80	8.30	14.70	42.00	103.50	54.10	22.41	51.90	33.71	47.75	0.79	55.01	10.63	1.16	16.15
Pb	14.30	7.10	6.30	2.80	9.70	3.60	9.53	7.61	7.93	6.49	13.64	5.69	11.19	15.34	12.25
Rb	15.20	8.90	31.70	48.40	18.20	4.20	43.82	11.16	37.36	11.35	63.15	1.71	48.59	106.09	19.93
Sr	380.60	521.20	569.90	849.70	446.90	212.70	230.22	229.43	374.22	253.20	291.69	160.73	683.21	301.99	391.28
V	380.60	521.20	569.90	849.70	446.90	212.70	230.22	229.43	374.22	253.20	291.69	160.73	683.21	301.99	391.28
Y	238.90	238.90	152.90	168.40	188.60	411.00	108.29	391.12	210.21	428.20	37.54	404.59	119.15	41.73	358.26
Zn	25.10	19.90	19.00	12.80	14.50	44.80	85.28	46.38	24.51	52.70	27.33	51.09	26.17	24.07	32.33
Zn	93.90	28.20	106.00	77.70	97.90	148.10	128.60	105.54	78.85	132.91	72.41	124.54	84.09	61.07	117.86
Zr	120.00	139.60	153.80	123.40	90.20	184.70	297.43	170.70	110.29	151.02	199.93	158.13	164.84	172.25	142.83
Co	31.10	15.10	29.50	31.30	41.80	37.40	24.98	34.08	30.77	37.57	11.71	36.07	21.92	6.09	25.45
q	4.99	0.00	3.10	4.20	1.07	2.02	8.14	0.43	7.22	2.44	19.70	2.70	1.32	17.00	5.25
or	4.01	24.67	6.88	8.31	4.30	1.54	10.20	3.07	12.16	3.92	11.46	0.85	8.12	17.97	4.24
ab	32.04	34.44	37.16	34.17	29.79	23.77	43.95	25.72	31.95	23.54	40.65	22.69	49.39	40.46	26.11
an	32.81	0.00	28.15	30.23	32.28	25.43	11.87	25.83	24.97	25.03	15.73	26.27	24.06	14.24	32.53
ne	0.00	18.39	0.00	0.00	0.00	0.00	0.00	0.00	0.00	0.00	0.00	0.00	0.00	0.00	0.00
ol	0.00	0.19	0.00	0.00	0.00	0.00	0.00	0.00	0.00	0.00	0.00	0.00	0.00	0.00	0.00
Field #	181288	181488	210988	233988	240188	263488	273188	300488	321588	350288	360288	371088	372788	400188	402888
Trace elements (ppm)															
Ba	108.01	754.16	375.32	580.19	260.61	188.62	417.45	26.40	63.36	815.04	567.34	945.07	159.45	218.78	22.66
Cr	156.96	22.69	43.84	15.08	24.12	48.29	2.81	102.23	96.41	22.95	29.75	3.26	53.28	11.57	157.74
Cu	72.01	12.42	67.64	66.48	74.40	68.46	56.01	81.92	75.63	74.65	68.33	12.57	77.55	61.45	90.71
Nb	6.48	12.71	7.74	16.74	4.07	16.06	7.80	10.18	9.21	6.62	6.00	10.24	5.39	21.78	8.13
Ni	103.96	0.65	50.48	21.81	22.43	29.78	6.40	55.16	52.50	10.93	11.03	12.82	36.30	38.11	78.12
Pb	8.37	19.19	6.95	4.30	11.65	6.00	7.85	1.97	5.50	8.73	7.95	15.12	9.09	10.38	6.50
Rb	7.85	94.34	30.27	11.20	14.03	9.52	47.78	3.15	6.35	34.17	18.10	92.36	12.33	12.42	2.24
Sr	278.29	274.17	418.26	646.47	395.01	245.27	335.19	164.91	184.77	496.77	617.40	85.53	237.60	187.30	212.14
V	335.46	6.09	231.36	309.37	168.78	187.81	153.46	372.45	351.60	170.07	181.88	<0.11	374.88	156.24	303.64
Y	36.02	27.26	28.69	27.17	17.09	75.89	39.20	44.35	51.15	12.14	13.17	56.16	40.37	114.02	42.51
Zn	105.36	63.55	110.87	98.61	80.99	185.37	72.13	110.36	122.25	95.24	66.92	40.73	90.65	230.36	86.01
Zr	106.27	186.42	127.37	164.28	84.76	275.86	167.14	120.80	145.50	119.94	105.42	245.56	133.65	334.59	163.26
Co	44.68	12.66	44.86	41.41	34.24	28.01	32.14	60.66	52.28	27.47	33.74	39.36	47.09	29.18	53.54
q	1.59	25.84	6.77	4.90	2.27	11.87	5.16	0.69	0.00	0.94	6.40	28.72	3.94	9.84	2.56
or	1.20	14.14	7.12	2.15	3.14	2.43	9.51	1.03	16.56	7.15	5.64	19.39	3.25	2.14	1.02
ab	27.17	41.45	30.72	30.42	31.54	21.33	40.00	25.17	19.25	39.75	39.11	44.21	29.82	23.31	26.26
an	30.71	9.03	26.22	31.69	36.92	23.59	21.30	25.34	17.50	27.61	29.30	4.40	23.53	20.72	27.76
ne	0.00	0.00	0.00	0.00	0.00	0.00	0.00	0.00	0.00	0.00	0.00	0.00	0.00	0.00	0.00
ol	0.00	0.00	0.00	0.00	0.00	0.00	0.00	0.00	0.00	0.00	0.00	0.00	0.00	0.00	0.00

All analyses were done at the University of British Columbia. For this study, major and minor elements were analyzed by S. Horsky in the Department of Geological Sciences. Powdered samples were fused with lithium tetraborate and then ground to form a pressed glass powder disc. Analyses were done using a Phillips 1410 XRF. FeO was determined by titration. LOI: loss on ignition. Trace elements were analyzed by M. Soon in the Department of Oceanography using a fully automated Phillips PW1400 XRF with autosampler. See Hickson (1991) for estimates of analytical errors. q, or, ab, an, ne, ol are normative quartz, orthoclase, albite, anorthite, nepheline, and olivine (cation percent).



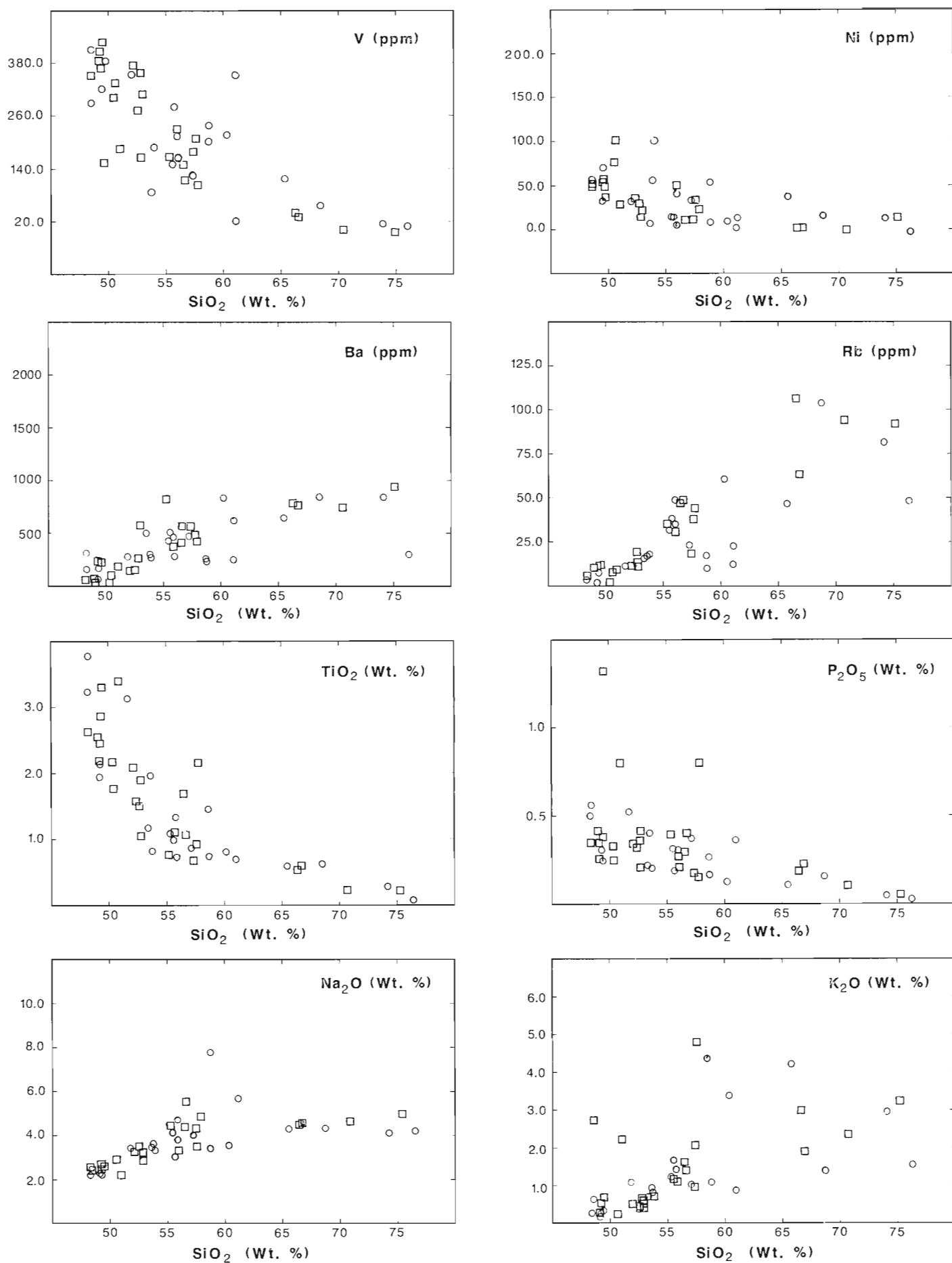


**Figure 9:** Selected silica variation diagrams showing major and minor element trends for the 47 analyzed dyke samples listed in Table 3. Squares are 1988 data, circles are 1989 data. For a discussion of analytical precision see Hickson (1990).

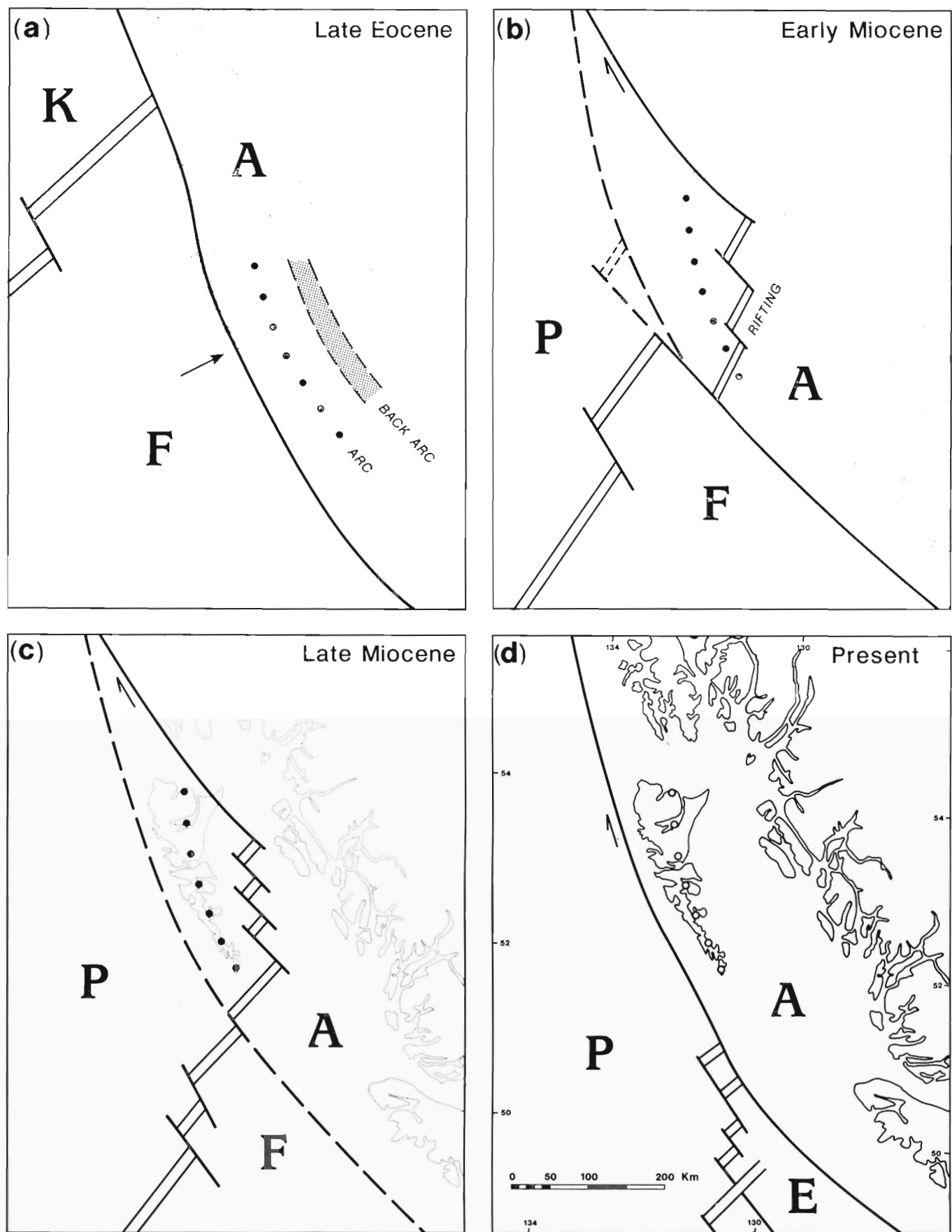


**Figure 10:** Possible plate configurations during mid- to late-Tertiary time in the Queen Charlotte segment of western North America: (a) development of a calc-alkaline igneous front (Masset volcanism and Kano plutonism) and back-arc extension (Queen Charlotte Basin) associated with northwesterly subduction of Farallon crust, (b) eastward jump in a portion of the Farallon-Pacific spreading axis resulting in a shift from calc-alkaline to tholeiitic igneous activity and ultimately to extinction of Masset volcanism and rifting in the back-arc region, (c) continued extension of Queen Charlotte Basin related to spreading along the Farallon-Pacific ridge, (d) southward migration of the Farallon-Pacific ridge to its present position and a shift in the transcurrent boundary with North America from inboard to outboard of the present Queen Charlotte Islands. (A – America plate, F – Farallon plate, K – Kula plate, P – Pacific plate).

to transcurrent motion between the northern Pacific and North American plates would thus explain the cessation of Masset arc volcanism in the Late Miocene. A further implication of this model is the possibility that Tertiary magmatism and tectonics in the Queen Charlotte Islands or Hecate Strait region may have been influenced by proximity to the Farallon-Pacific spreading axis during its migration southward along the trench (Fig. 10). Hamilton (1989) has noted that the Masset volcanism spans the transition period from North America – Farallon to North America – Pacific plate interaction. He interprets the Tertiary succession on Queen Charlotte Islands to be a rift assemblage which includes rocks with both calc-alkaline and MORB chemical characteristics.

The chemical data from both lavas (Hickson, 1991) and dykes suggest a complex igneous environment which, although dominated by calc-alkaline magmatism, was also the source of small volumes of alkaline and tholeiitic magma. The calc-alkaline affiliation is consistent with an arc environment associated with eastward subduction of Farallon crust but the presence of alkaline rocks and the tholeiitic trend exhibited by some of the Queen Charlotte dykes suggests that their chemistry may also have been influenced by rifting and proximity to a spreading ridge. The association of alkaline magma with a marginal, calc-alkaline arc has been documented in southwestern Mexico (Allan, 1986; Allan et al., in press) where small alkaline volcanoes near the axis of the Mexican Volcanic Belt are associated with

rift zones developed on the continental margin above eastward subducting crust of the Rivera Plate. The present close proximity of the Mexican Volcanic Belt to the intersection of the East Pacific Rise with the Mid-America trench may be analogous to the Tertiary tectonic setting in Queen Charlotte Islands. Close proximity of the Farallon-Pacific ridge to the Masset volcanic arc may have influenced both the chemistry of the magma and the stress fields which controlled dyke emplacement.

Alternatively the more alkaline dykes may reflect differences in the chemistry of source regions in adjacent crustal blocks. Such a relationship is suggested by the greater alkalinity and more easterly trend of the northern dyke swarms as compared with those farther south. The boundary zone as defined by dyke orientation and chemistry corresponds approximately with the southern margin of the Rennell Sound fold belt (Thompson, 1988) which may be a manifestation of movement on a zone of long-lived deep crustal structures.

## STRUCTURAL SETTING

The chemical affiliation, age and distribution of dykes in the Queen Charlotte Islands suggest that they are genetically related, on the one hand, to Masset volcanic rocks and, on the other, to Tertiary epizonal plutons of the Kano plutonic suite. The Rennell Sound, Selwyn Inlet, Bigsby Inlet, Lyell Island, and Carpenter Bay dyke swarms are closely associated with central volcano-plutonic complexes that have

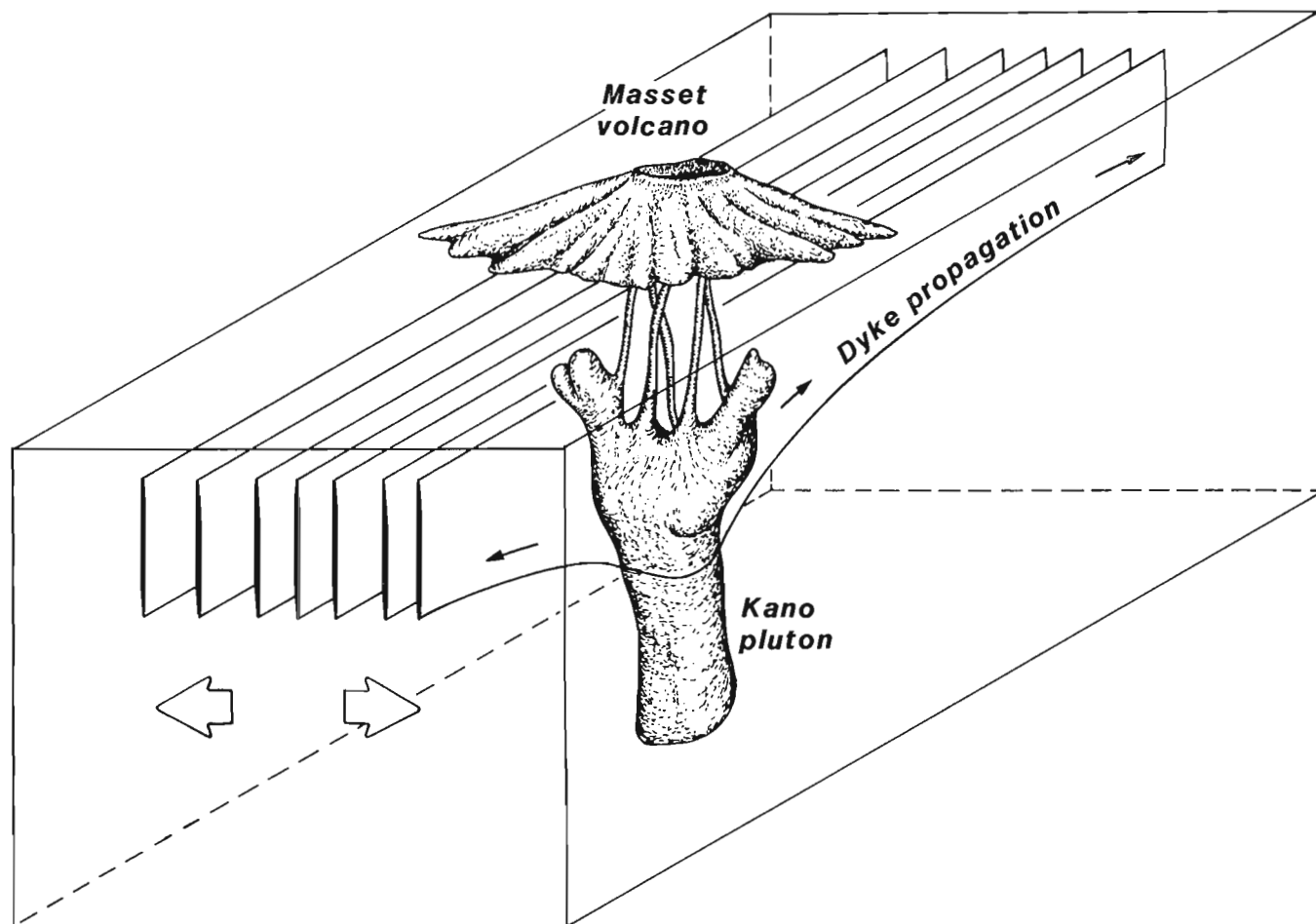


**Figure 11:** Schematic sketch showing the inferred relationship of dyke swarms to Tertiary plutons and Masset volcanic centres.

been partially unroofed. The Burnaby Island dyke swarm is associated with alteration and fracturing which suggest extension and hydrothermal activity in the roof zone of an unexposed pluton. No plutonic association is known for the Tasu Inlet swarm, but the dykes project into a large area of adjacent Masset volcanics which may conceal a central igneous complex.

The calc-alkaline chemistry of the dykes and associated volcano-plutonic suites is typical of arc magmatism. Moreover, the spacing of known and inferred volcano-plutonic complexes in the Queen Charlotte Islands (30-50 km) is analogous to that of central volcanoes along the Cascade and other continental margin volcanic arcs (Williams and McBirney, 1979). By analogy with other such arcs it is reasonable to assume that Masset volcanism was confined to a relatively narrow, elongated belt which may never have extended significantly beyond the present outcrop distribution.

Where dyke propagation has been recorded in real time as in Iceland (Sigurdsson, 1987), the magma has been shown to flow laterally from central magma columns into fractures developed normal to the direction of least compressive stress. At Krafla the average dyke height is 2.8 km and the horizontal length 10-30 km. Several aspects of the Queen Charlotte dyke swarms indicate a similar relationship to central igneous complexes represented by the Kano plutons (Fig. 11). There are for example, relatively few Tertiary dykes in the Triassic Karmutsen Formation and in the Cretaceous Longarm Formation. This suggests that dykes injected laterally through younger strata may have bottomed out due to high lithostatic pressure in the deeply buried Karmutsen volcanics. The relatively few dykes that cut the Longarm Formation include a high proportion of zeolitized, banded dykes of the "Arichika type". The multiple quenched selvages characteristic of these dykes indicate rapid quenching, probably due to groundwater which restricted their propagation. Although there are many exceptions, the overall distribution patterns suggest that dykes were preferentially injected into a zone of intermediate depth where post-Karmutsen pre-Longarm stratigraphy predominated.

The generation of Tertiary magma and its rise into central igneous complexes in the Queen Charlotte Islands was controlled largely by deep lithospheric and mantle processes that may not be reflected in the surficial geology. Conversely the dykes record the trends of extensional stresses operating in the upper crust along the western margin of Queen Charlotte Basin during late Tertiary time. Tensional stresses induced by thermal doming over plutons in the central igneous complexes are probably responsible for much of the observed scatter in the orientation of dykes proximal to the Lyell Island and Burnaby Island igneous centres. However, most of the Queen Charlotte dyke swarms have a strong linear trend that reflects the regional stress field at the time of their emplacement.

Variations in trend among the different swarms suggest the presence of several structural domains bounded by major faults or "weak zones" in the lithosphere. Such zones may have functioned as boundaries between deep crustal blocks with different stress patterns, thus controlling dyke orientations, but leaving little structural record in the surface geology. One such boundary, referred to informally as the "median domain boundary", appears to lie between the eastern and western belts of Kano plutons (Fig. 12). The Rennell Sound, Tasu Sound and Bigsby Inlet swarms, which are associated with plutons of the western belt, have generally northeasterly trends as do most of the dykes scattered throughout the "south Moresby stable block". The area embracing these swarms (domain 1, Fig. 12) appears to have been a coherent unit with a uniform northwest to southeast extensional stress field during the period of dyke emplacement. A stress field with such an orientation could result from northeasterly directed compression related to plate convergence (Fig. 12).

East of the "median domain boundary" the Selwyn Inlet, Lyell Island, Burnaby Island, and Carpenter Bay dyke swarms are associated with the eastern belt of the Kano plutonic suite. The area encompassing these dykes and plutons (domain 2, Fig. 12) appears to have been influenced by at least three stress regimes. The dominant northerly trend of dykes in the Carpenter Bay, Burnaby Island, and Lyell Island swarms reflects a regional stress regime of east-west extension. The en-echelon arrangement of these dykes and their disappearance southward against the "median domain boundary" suggest that they are controlled by gash fractures developed in response to dextral shear between domains 1 and 2. A second stress regime, related to local doming over central igneous complexes, may have been superimposed on the regional northerly trend and probably caused much of the observed scatter in dyke orientations associated with the Burnaby Island and Lyell Island swarms. A third stress regime is recorded by easterly trending dykes in the Selwyn Inlet swarm. The orientation of these dykes implies incipient north-south separation and dyke intrusion in an extensional zone between domain 2 and domain 3 (Fig. 12).

Domain 3 encompasses a large relatively dyke-free area of northern Moresby and southern Graham islands. Although the western part of this area was not traversed, only a few widely scattered dykes were observed along well-exposed transects through Skidegate, Cumshewa and adjacent channels. Domain 3 includes the Rennell Sound fold belt (Thompson and Thorkelson, 1989), which extends in a west-northwesterly direction across the islands without any apparent offset on transcurrent faults. Thus the "median domain boundary" probably does not extend north of Selwyn Inlet and any strike slip movement along it could be accommodated by north-south extension and the development of a pull-apart structure defined by the Selwyn Inlet dyke swarm.

## BASIN EVOLUTION

The relationship between Tertiary magmatism and the evolution of Queen Charlotte Basin is a matter of speculation. If the Masset volcanics and related subvolcanic intrusions are the remnants of a Tertiary volcanic arc then calc-alkaline magmatism and associated crustal thickening was probably confined to a relatively narrow zone. Queen Charlotte Basin, which lies behind the arc, can be interpreted either as a contemporary back-arc basin or as a rift basin that postdates Masset volcanism.

If the back-arc model is used then, by analogy to other arc/back-arc pairs (Sclater, 1972) calc-alkaline magmatism along the axis of the Masset arc should have been accompanied by the eruption of more alkaline magma behind the arc (Fig. 10a). The attendant high heat flow in a relatively broad back-arc region could have resulted in crustal thinning followed by thermal subsidence and the formation of Queen Charlotte Basin.

Alternatively the opening of Queen Charlotte Basin may have been initiated by an eastward jump in the Farallon-Pacific spreading ridge, analogous to the model proposed by Luhr et al. (1985) for southwestern Mexico (Fig. 10b). As in the previous model the Masset volcanic arc is attributed to eastward subduction of Farallon crust beneath western North America. Consumption of the Farallon Plate was accompanied by southward migration of the Farallon-Pacific ridge to a position near the northern end of the Masset arc at which time the spreading axis may have jumped eastward and initiated rifting behind the arc (Fig. 10b). This shift in the position of the triple junction would account for the cessation of Masset volcanism and provide a mechanism for opening of Queen Charlotte Basin over the repositioned spreading axis (Fig. 10c). Continued subduction of the Farallon Plate, accompanied by volcanism on the adjacent mainland, culminated in

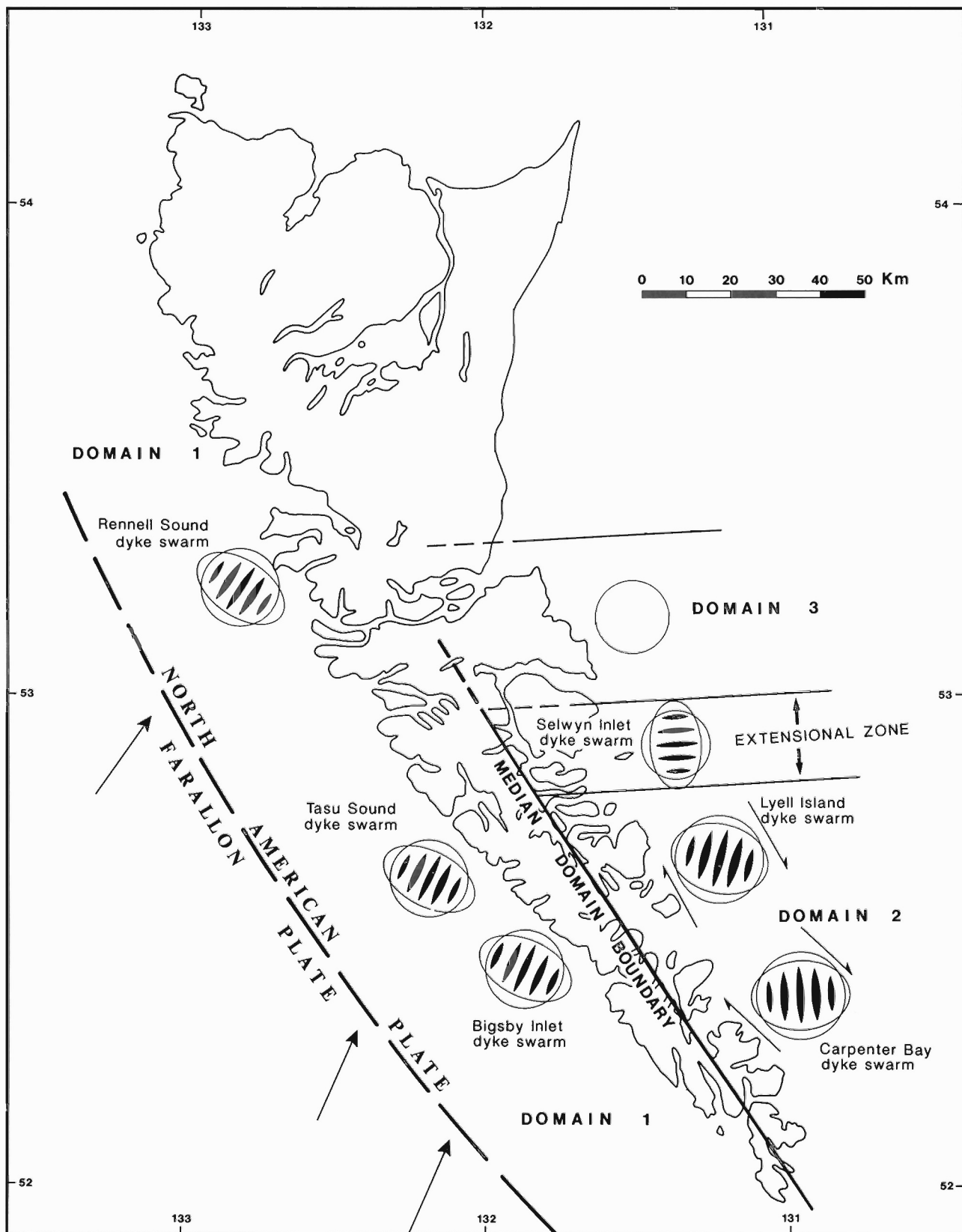


**Figure 12:** Sketch map showing the inferred relationship of dyke swarms to the Farallon and North American plates and to stress fields associated with small crustal domains in the Queen Charlotte Islands during mid-Tertiary time.

migration of the triple junction south to its present position off northern Vancouver Island (Fig. 10d).

Although the timing is poorly constrained the rift model is consistent with broad interpretations of Tertiary plate geometry (Riddiough, 1982) and with the chemical diversity of Tertiary dykes noted in this study. Moreover, if the opening of Queen Charlotte Basin was related to a spreading axis then basaltic dykes, injected along the axis of the ridge, could account for the volume of dense crustal rocks indicated by gravity profiles across Hecate Strait (Sweeney and Seemann, 1991). Such a model, rather than one involving the juxtaposition of allochthonous terranes, would also account for the presence of Karmutsen strata on both sides of Hecate Strait (Woodsworth, 1988).

## THERMAL HISTORY

### Maturity levels in the Kunga Formation

The temperature, and hence the degree of organic maturity, of sediments on an undisturbed continental margin is controlled largely by a combination of the heat flow and depth of burial. In tectonically active areas, such as the Cordillera, the effects of enhanced heat flow associated with volcanic and plutonic processes may have an over-riding effect on organic maturation. On Queen Charlotte Islands, heat flow was probably greatly enhanced during Jurassic Yakoun volcanism, and during Tertiary magmatism associated with Masset volcanism, Kano plutonism, and the widespread intrusion of dykes. Thus organic maturity in potential source rocks of the Kunga Group may have been substantially controlled by enhanced heat flow and hydrothermal activity associated with magmatism.

Organic material near a dyke is effectively destroyed, but some volatile components may be driven off in the rapid water-flow that follows intrusion (Delaney, 1982; Carrigan, 1986). The immediate and extreme thermal effects of dyke intrusion are limited to one or two units of the dyke thickness and are complete within a few hundred years after the event, but the cumulative heat input from dykes may linger much longer. Thus the intrusion of a swarm of dykes causes significant increases in both the general level and variability of organic maturation.

Vellutini (1988) reported that vitrinite reflectance values ( $R_{o,max}$ ) from surface samples of the Kunga Group in southern Queen Charlotte Islands range from 3-8, with most values in the range 4-5. This is in close agreement with maturation values of 3-8 based on conodont colour alteration indices (Orchard, 1988).

From the vitrinite reflectance data Vellutini (1988) produced a maturation map of the Queen Charlotte Islands which shows a general southerly increase in maturation. He attributes the high southern values to heating during periods of Jurassic and Tertiary igneous activity. The present study supports Vellutini's conclusions and uses his reflectance data to assess the thermal impact of dyke intrusion. In order to relate these high values of reflectance to burial history and dyke intrusion the following simple models were examined. In all models time-temperature index as defined by Lopatin (1971) and improved by McKenzie (1981) was calculated, followed by conversion to vitrinite reflectance using a formula by D.N. Skibo (pers. comm.) that expresses the correspondence table given by Waples (1980).

Assuming a host rock temperature of 100°C, an emplacement temperature for the dykes of 1100°C, and similar volumetric heat capacities for both the host rock and the dykes, then each 1% of dyke by volume will produce a temperature increase of 10 K provided that the heat is spread evenly over the volume concerned. Dyke swarms on the Queen Charlotte Islands (Fig. 2, in pocket) show regional extension ranging from 1-10%, yielding average temperature increases of 10-100 K.

In addition to local magmatic heat introduced by the intrusion of dykes and plutons, the generally enhanced heat flow in a volcanic arc is probably at least 120 mW/m<sup>2</sup>, double the world average. Although the local and regional effects of enhanced heat flow are not entirely independent they have been tentatively separated in the models.

The maximum depth of burial of these rocks is unknown. In order to estimate the normal, non-volcanic, conditions two simple background models were considered (Fig. 13). Model 1 assumes a long period at the maximum temperature reached, preceded by rapid subsidence and followed by rapid re-emergence. Model 2 assumes slow subsidence followed immediately by slow emergence, so that the maximum temperature is not maintained. In both models the absolute times of events are not important. However, the magnitude and duration of maximum temperature and the total duration and linearity of the periods of increase and decrease are critical to the calculation.

The age of the Kunga sediments is about 210 Ma. In Model 1 it is assumed that the sediments remained at a constant depth and temperature for 170 Ma, and spent the remaining 40 million years in subsidence and re-emergence. A plot of the calculated vitrinite reflectance against maximum temperature (Fig. 13) indicates that maximum temperatures of 178 and 193°C respectively are required to provide reflectance values of 4 and 5. These temperatures imply a depth of about 6 km in a normal heat-flow environment of 60 mW/m<sup>2</sup>, 3 km in a heat flow of 120 mW/m<sup>2</sup>, or any equivalent combination. In contrast, to reach the oil window of 0.65-1.25 requires temperature of 70-104°C, implying a depth of 2.5-3.5 km with a heat flow of 60 mW/m<sup>2</sup>, or correspondingly shallower depths with higher heat flow. Present heat flow of 46-56 mW/m<sup>2</sup> (Lewis et al., 1989) requires a depth of 3-4 km to reach the oil window and a depth of 6-6.5 km to attain the reflectance values observed by Vellutini (1988).

Model 2, in which the Kunga strata are buried at a uniform rate to maximum depth and temperature followed quickly by emergence, requires higher temperatures to produce the observed reflectance values (Fig. 13). Temperatures of 95-134°C are required for the oil window and of 213-230°C for the observed vitrinite reflectance values. These values suggest depths of 7-8 km for a normal heat flow or 4.5-5 km for a high heat flow.

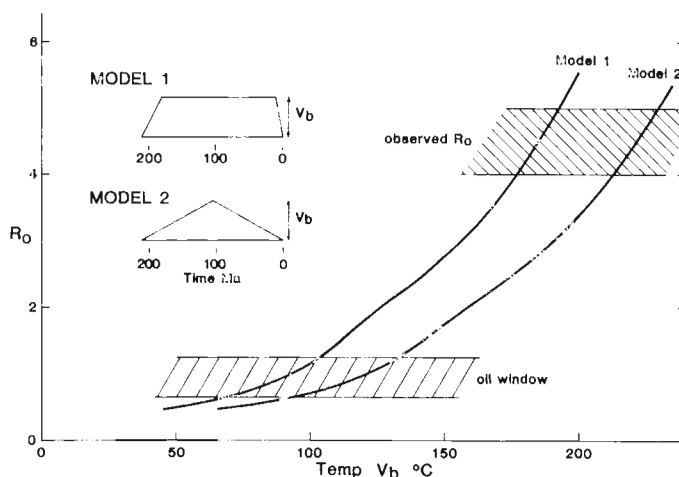


**Figure 13:** Vitrinite reflectance  $R_o$ , calculated from models 1 and 2, plotted against maximum temperature  $V_b$ . The lower shaded zone shows reflectance values of the oil window, and the upper shaded zone shows values commonly observed in Kunga Group rocks now at the surface. The inset shows the time-temperature curves used in the models.



Both models 1 and 2 require unreasonably great rates of subsidence, depths of burial, or high levels of heat flow to produce the observed values of vitrinite reflectance in rocks now at the surface. This suggests that the observed  $R_o$  values were influenced by other processes in addition to simple burial.

Magmatic and hydrothermal activity in a magmatic arc may severely distort regional heat flow from the deep crust. Although the effect is difficult to estimate, the timing and distribution of Tertiary dykes and plutons in the Queen Charlotte Islands provide a rough guide to their effect on the local thermal regime during Tertiary time. Model 3 (Fig. 14), a variation of model 1, assumes a regional temperature increase in a zone associated with the Masset volcanic arc and provides for local temperature variations within the arc depending on the volume of intruded material.

Model 3 (Fig. 14) adds to the background temperature  $V_b$  an increase  $V_e$  due to enhanced heat flow associated with the onset of Masset volcanism, followed by a period of uniform high temperature and a final decrease to zero as the rocks emerge at the surface. As before, the absolute times of increase and decrease are not important, provided that changes are linear with time. The amount of excess temperature needed to increase vitrinite reflectance to the observed values is within the range estimated for a volcanic arc with moderately enhanced heat flow. For example, from a base temperature of  $100^\circ\text{C}$ , an increase of a further 100 K increases reflectance values from about 1 to about 4.

In order to assess the direct impact of dyke emplacement on maturation the temperature increase due to Masset volcanism ( $V_e$ , Fig. 14) was separated into two components:  $V_e$  the regional temperature increase across the arc, and  $V_d$  the local increase due to dyke intrusion. The  $R_o$  values predicted by this model are thus a function of three distinct temperature increments: 1. the baseline temperature  $V_b$ ; 2. a temperature increment due to regional enhanced heat flow  $V_e$ ; 3. a temperature increment due to dyke emplacement  $V_d$ .

The baseline temperature  $V_b$  can be estimated from reflectance values from rocks farthest removed from the axis of the arc. Vellutini (1988) reported four values of vitrinite reflectance, with an average  $R_o$  of 1.18, from the Sandilands Formation of the Kunga Group on northwestern Graham Island. This is considerably lower than values observed on Moresby Island, and may indicate burial without mag-

matic heating. The constant temperature  $V_b$  from Model 1 required to produce this level of reflectance is about  $100^\circ\text{C}$ .

The temperature increment  $V_e$  due to enhanced regional heat flow within the arc can be estimated from the lower end of the range of reflectance values associated with the dyke swarms. To produce a reflectance of 3, one of the lower values observed in the southern Queen Charlotte Islands, would require an additional temperature increment  $V_e$  of 80 K during Masset time.

A further temperature increase  $V_d$ , required to produce the higher reflectance levels observed, may have been produced locally by dykes. The assumption that 1% extension by dykes gives a 10 K temperature rise was used to plot reflectance values against dyke extension (Fig. 15). The final reflectance is substantially controlled by the maximum temperature reached, provided it lasted for a few million years. Thus the reflectance in rocks affected by volcanic heating is relatively insensitive to the baseline temperature before the onset of Masset volcanism.

To test this model the extension due to dykes was determined for each traversed 2-km grid segment in the Carpenter Bay dyke swarm (Fig. 16). Corresponding  $R_o$  values were read from the plot of reflectance versus percent extension (Fig. 15). The results are consistent with observed  $R_o$  values reported by Vellutini (1988) for rocks in the Carpenter Bay area.

High observed values of vitrinite reflectance in the southern Queen Charlotte Islands thus appear to result from excess heating by a combination of volcanic and intrusive events superimposed on the normal heating and cooling cycle accompanying subsidence and erosion. Without the excess heat, the rocks now observed at the surface would probably have achieved reflectance values in or around the oil window.

#### Sediments within Queen Charlotte Basin

Rocks within Queen Charlotte Basin have not undergone the same thermal history as those closer to the Masset volcanic arc. Whether the basin is interpreted as a back-arc basin or a rift basin related to a spreading axis the Tertiary heat flow was probably higher than average. Sclater (1972) reviewed the thermal state of the various basins within which heat flow had been measured, and divided the marginal basins of the western Pacific Ocean into "active basins", all of which have high heat flow, and "inactive basins", most of which have heat flow

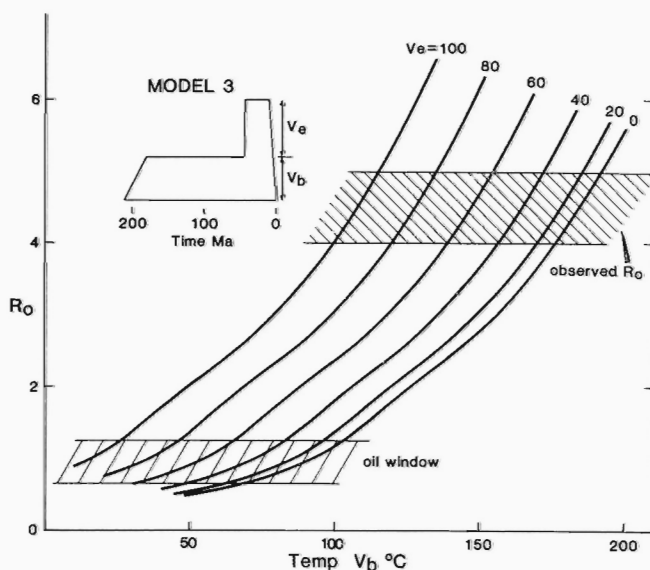


**Figure 14:** Vitrinite reflectance, calculated from Model 3, similar to Model 1, but with elevated temperature in the time of Masset volcanism. Shaded zones and axes are as in Figure 13.

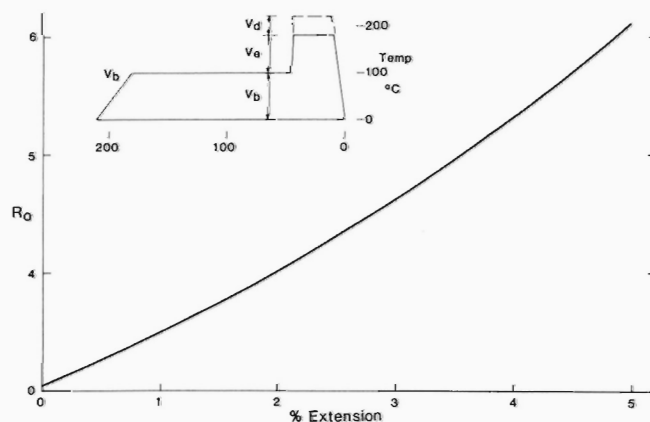


**Figure 15:** Vitrinite reflectance plotted as a function of the extension due to dyke intrusion. The curve is based on a burial temperature  $V_b$  of  $100^\circ\text{C}$  and an additional temperature increment during Masset volcanism  $V_e$  of 80 K. Further increase of temperature  $V_d$  due to dykes produces the reflectance values indicated by the curve.

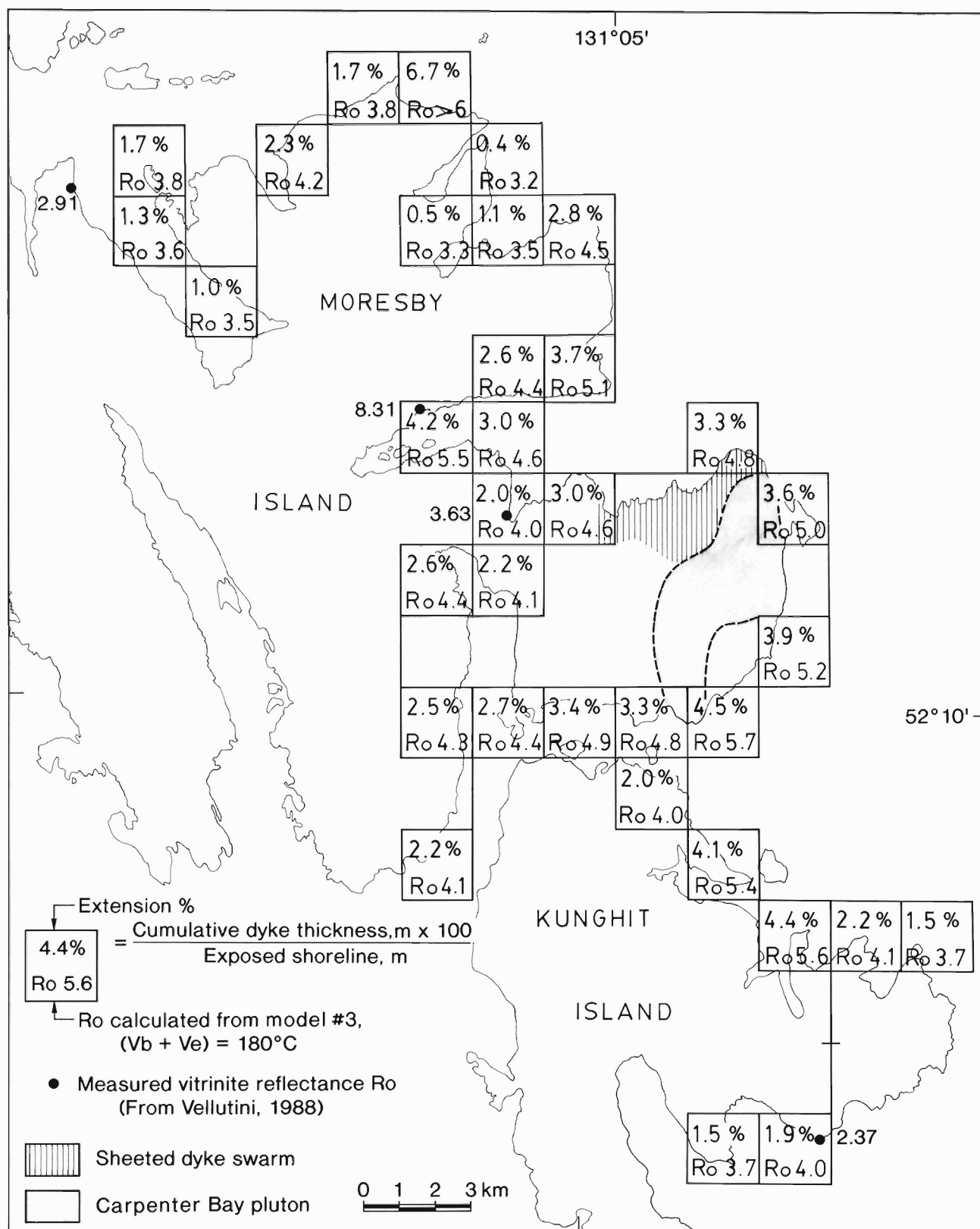


**Figure 16:** Map of the Carpenter Bay dyke swarm showing the measured extension and calculated Ro value for each 2-km grid segment containing dyke data. Ro values are from the plot of vitrinite reflectance vs. dyke extension (Fig. 15) where Ro is calculated using (V<sub>b</sub> + V<sub>e</sub>) = 180°.

above the world average of  $65 \text{ mW/m}^2$ . He also related present heat flow to the depth of water in the basin, isostatically corrected for sediment loading. The influence of magmatism on Queen Charlotte Basin ceased when subduction stopped in middle Miocene time in response to southward migration of the Farallon-Pacific ridge. If the basin had high heat flow before this time it would have cooled towards an equilibrium value following cessation of subduction. The gravity model of Sweeney and Seemann (1991) indicates a maximum depth of sediments of about 7 km, and because water depth is about 200 m, we may calculate the isostatically corrected basin depth of 2.8 km. Using the data of Sclater (1972) for marginal basins of the western Pacific Ocean, Queen Charlotte Basin should have a present day heat flow of between 100 and  $120 \text{ mW/m}^2$ . Although heat flow approaching these levels has been observed in Queen Charlotte Sound south of the present triple point, wells in Hecate Strait yield estimates of heat flow from  $50\text{--}78 \text{ mW/m}^2$  (Yorath and Hyndman, 1983). Such estimates are consistent with probe measurements in the basin which indicate that heat flow in the basin is between 65 and  $80 \text{ mW/m}^2$  (Lewis et al., 1989). The 12 Ma since Middle Miocene time is approximately the thermal time constant of a crust of thickness of 20 km, so it is possible that the heat flow in the basin could have declined by a factor of 50%, if indeed it were ever as high as the Sclater curves indicate.

Yorath and Hyndman (1983) have shown that vitrinite reflectance in samples from wells in Queen Charlotte Sound are consistent with heat flow higher in the past than at present, but that contrast between past and present heat flow decreases northward to zero in Hecate Strait. Vellutini (1988) reported vitrinite reflectances up to and within the oil window on samples from wells on Graham Island, and he concludes that Skonun strata have good oil and gas potential. However, the relevance of observations on Graham Island to conditions in the central part of the Basin has not been established.

Sediments of the Skonun Group that underlie Queen Charlotte Basin are Early Miocene-Pliocene in age. The oldest Skonun strata were thus exposed to high heat flow conditions for no more than the first half of their life. If we assume that the sedimentation rate has been uniform for 24 My, that heat flow was  $120 \text{ mW/m}^2$  for the first 12 My and declined linearly to  $60 \text{ mW/m}^2$  at present, and that thermal conductivity is uniformly  $2 \text{ W/mK}$ , the vitrinite reflectance of the lowest sediments is calculated to be 3.8, well above the oil window, which is in the range 3–5 km. If we assume a constant heat flow of  $60 \text{ mW/m}^2$  the vitrinite reflectance at the base of the Skonun is reduced to 2.5, and the oil window is in the range 4.5–5.5 km. The constant heat flow must be reduced to an unreasonably low value of below  $40 \text{ mW/m}^2$  to result in totally immature sediments. We may thus conclude that there is a zone within the Skonun sediments of the Basin where organic maturity is within the oil window.

## CONCLUSIONS

Most of the steeply dipping to vertical dykes reported in this study were emplaced between Middle Eocene and Middle Miocene time. They are believed to be comagmatic with the Masset volcanics and epizonal plutons of the Kano plutonic suite. Together, these Tertiary igneous rocks comprise the eroded remnants of a volcanic arc related to northeasterly subduction of Farallon crust beneath the western North American Plate.

Igneous complexes of the Kano plutonic suite are believed to be the subvolcanic root zones of central Masset volcanoes. Dyke swarms, fed by magma columns beneath the volcanoes, were propagated horizontally in a zone of intermediate crustal depth and in a direction normal to the least compressive stress. Dyke swarms in the Queen Charlotte Islands preserve a record of the extensional stresses that were active during dyke emplacement in the Tertiary. Regional variations in

swarm density and orientation result from the interaction of major plate convergence with small crustal domains, bounded by zones of weakness, which underlie the arc.

The high maturation values indicated by Conodont Colour Index values (Orchard, 1988; Orchard and Forster, 1991) and vitrinite reflectance (Vellutini, 1988) are based on samples collected in close proximity to major dyke swarms and in some cases close to major plutons. The results of this study support the conclusions of Vellutini (1988) that heat from the introduction of magma into high crustal levels rather than deep burial is largely responsible for the high maturation levels observed along the western edge of Queen Charlotte Basin. It is unlikely that the width of the Masset igneous arc extended much beyond the present outcrop exposed on Queen Charlotte Islands.

Evolution of Queen Charlotte Basin may be controlled by high heat flow and crustal extension in a back-arc region followed by thermal subsidence and sediment accumulation in the late Tertiary. Rifting associated with southward migration and active spreading of the Farallon-Pacific Ridge may also have contributed to the opening of Queen Charlotte Basin. By analogy to other marginal basins heat flow was probably high and, combined with rapid burial, may have contributed to accelerated maturation rates.

High observed values of vitrinite reflectance in surface rocks of the Kunga formation (Vellutini, 1988) may be accounted for by enhanced regional heat flow and local magmatic heating associated with Masset arc volcanism during the Tertiary. A simple model of thermal history, incorporating a general rise in temperature within the volcanic arc and local temperature variations proportional to the volume of dykes, predicts maturation levels that are in reasonable agreement with the observed values. This implies that overmaturation along the west side of Queen Charlotte Basin may be the result of anomalously high temperatures associated with the Masset volcanic arc. Farther east, in Queen Charlotte Basin, where volcanic arc heating was minor but extensional heating may have occurred, there should be a zone within the 7 km thickness of Skonun sediment where hydrocarbon maturity is within the oil window.

## ACKNOWLEDGMENTS

The expert boatmanship of Shane Dennison, Tania Hale, and Betty Souther contributed greatly to the success of the field work as did the skill and experience of skippers Rob Pettigru and George Farrell. For their perseverance in the face of often adverse conditions the authors extend their sincere thanks. Thanks also to Charlie Roots and Glenn Woodsworth who reviewed the manuscript and made many helpful suggestions.

## REFERENCES

- Allan, J.F.  
 1986: Geology of the Northern Colima and Zacoalco Grabens, southwest Mexico: Late Cenozoic rifting in the Mexican Volcanic Belt; *Geological Society of America Bulletin*, v. 97, p. 473–485.
- Allan, J.F., Nelson, S.A., Luhr, J.F., Carmichael, I.S.E., Wopat, M., and Wallace, P.J.  
 in press: Pliocene–Recent rifting in SW Mexico and associated volcanism: an exotic terrane in the making; in *The Gulf and Peninsular Province of the Californias*, J.P. Dauphin and B.R.T. Simoneit (ed.), American Association of Petroleum Geologists Memoir Series.
- Anderson, R.G. and Greig, C.J.  
 1989: Jurassic and Tertiary plutonism in the Queen Charlotte Islands, British Columbia; in *Current Research, Part H, Geological Survey of Canada, Paper 89-1H*, p. 95–104.
- Anderson, R.G. and Reichenbach, I.  
 1991: U–Pb and K–Ar framework for Middle to Late Jurassic (172–158 Ma) and Tertiary (46–27 Ma) plutons in Queen Charlotte Islands, British Columbia; in *Evolution and Hydrocarbon Potential of the Queen Charlotte Basin*, British Columbia, Geological Survey of Canada, Paper 90-10.

- Carrigan, C.R.**  
**1986:** A two-phase hydrothermal cooling model for shallow intrusions; *Journal of Volcanology and Geothermal Research*, v. 28, p. 175-192.
- Delaney, P.T.**  
**1982:** Rapid intrusion of magma into wet rock: groundwater flow due to pore pressure increases; *Journal of Geophysical Research*, v. 87, p. 7739-7756.
- Hamilton, T.S.**  
**1989:** Tertiary extensional volcanism and volcanotectonic interactions along the Queen Charlotte portion of the western Canadian continental margin; *Geological Association of Canada, Pacific Section Symposium on Northwest Pacific – North America Plate Interactions Throughout the Cenozoic*, Program with Abstracts, Victoria, British Columbia, April 1989.
- Hickson, C.J.**  
**1988:** Structure and stratigraphy of the Masset Formation, Queen Charlotte Islands, British Columbia; *in* Current Research, Part E, Geological Survey of Canada, Paper 88-1E, p. 269-274.  
**1991:** The Masset Formation on Graham Island, Queen Charlotte Islands, British Columbia; *in* Evolution and Hydrocarbon Potential of the Queen Charlotte Basin, British Columbia, Geological Survey of Canada, Paper 90-10.
- Irvine, T.N. and Baragar, W.R.A.**  
**1971:** A guide to the chemical classification of the common volcanic rocks; *Canadian Journal of Earth Sciences*, v. 8, p. 523-548.
- LeBas, M.J., LeMaitre, R.W., Streckeisen, A., and Zanettin, B.**  
**1986:** Chemical classification of volcanic rocks; *Journal of Petrology*, v. 27, p. 746-750.
- Lewis, T.J., Bentkowski, W.H., Bone, M., and Wright, J.A.**  
**1989:** Note on the thermal structure of Queen Charlotte Basin, British Columbia; *in* Current Research, Part H, Geological Survey of Canada, Paper 89-1H, p. 121-125.
- Lopatin, N.V.**  
**1971:** Temperature and geologic time as factors in coalification (in Russian); *Acad. Nauk. SSSR. Izv. Ser. Geol.* 3, p. 95-106.
- Luhr, J.F., Nelson, S.A., Allan, J.F., and Carmichael, I.S.E.**  
**1985:** Active rifting in southwestern Mexico: Manifestations of an incipient eastward spreading-ridge jump; *Geology*, v. 13, p. 54-57.
- McKenzie, D.**  
**1981:** The variation of temperatures with time and hydrocarbon maturation in sedimentary basins formed by extension; *Earth and Planetary Science Letters*, v. 55, p. 87-98.
- Orchard, M.J.**  
**1988:** Maturation of Triassic strata: conodont colour alteration index; *in* Some Aspects of the Petroleum Geology of the Queen Charlotte Islands, R. Higgs (compiler), Canadian Society of Petroleum Geologists Field Trip Guide to Sequences, Stratigraphy, Sedimentology: Surface and Subsurface, p. 42-44.
- Orchard, M.J. and Forster, P.J.L.**  
**1991:** Conodont colour and thermal maturity of the Late Triassic Kunga Group, Queen Charlotte Islands, British Columbia; *in* Evolution and Hydrocarbon Potential of the Queen Charlotte Basin, British Columbia, Geological Survey of Canada, Paper 90-10.
- Riddihough, R.P.**  
**1982:** Contemporary movements and tectonics on Canada's west coast: a discussion; *Tectonophysics*, v. 86, p. 319-341.
- Sclater, J.G.**  
**1972:** Heat flow and elevation of the marginal basins of the western Pacific; *Journal of Geophysical Research*, v. 77, p. 5705-5719.
- Sigurdsson, H.**  
**1987:** Dyke injection in Iceland: a review; *in* Mafic Dyke Swarms, H.C. Halls and W.F. Fahrig (ed.), Geological Association of Canada Special Paper 34, p. 55-64.
- Souther, J.G.**  
**1988:** Implications for hydrocarbon exploration of dyke emplacement in the Queen Charlotte Islands, British Columbia; *in* Current Research, Part E, Geological Survey of Canada, Paper 88-1E, p. 241-245.  
**1989:** Dyke swarms in the Queen Charlotte Islands, British Columbia; *in* Current Research, Part H, Geological Survey of Canada, Paper 89-1H, p. 117-120.
- Souther, J.G. and Bakker, E.**  
**1988:** Petrography and chemistry of dykes in the Queen Charlotte Islands, British Columbia; Geological Survey of Canada, Open File 1833.
- Souther, J.G. and Yorath, C.J.**  
**in press:** Neogene assemblages; *in* Chapter 17, Structural Styles; *in* The Cordilleran Orogen: Canada, H. Gabrielse and C.J. Yorath (ed.), Geological Survey of Canada, no. 4.
- Streckeisen, A.L.**  
**1967:** Classification and nomenclature of igneous rocks; *in* Neues Jahrbuch für Mineralogie, Abhandlungen, K.R. Mehnert und H.O. Daniel (ed.), E. Schweizerbart'sche Verlagsbuchhandlung, p. 144-240.
- Sweeney, J.F. and Seemann, D.A.**  
**1991:** Crustal density structure, Queen Charlotte Islands and Hecate Strait, British Columbia; *in* Evolution and Hydrocarbon Potential of the Queen Charlotte Basin, British Columbia, Geological Survey of Canada, Paper 90-10.
- Thompson, R.I.**  
**1988:** Late Triassic through Cretaceous geological evolution, Queen Charlotte Islands, British Columbia; *in* Current Research, Part E, Geological Survey of Canada, Paper 88-1E, p. 217-219.
- Thompson, R.I. and Thorkelson, D.**  
**1989:** Regional mapping update, central Queen Charlotte Islands, British Columbia; *in* Current Research, Part H, Geological Survey of Canada, Paper 89-1H, p. 7-11.
- Vellutini, D.**  
**1988:** Organic maturation and source rock potential of Mesozoic and Tertiary strata, Queen Charlotte Islands, British Columbia; M.Sc. thesis, University of British Columbia, Vancouver.
- Waples, D.W.**  
**1980:** Time and temperature in petroleum formation: application of Lopatin's method to petroleum exploration; *American Association of Petroleum Geology, Bulletin*, v. 64, p. 916-926.
- Williams, H. and McBirney, A.R.**  
**1979:** Volcanology; Freeman, Cooper and Co., San Francisco, p. 294-299.
- Woodsworth, G.J.**  
**1988:** Karmutsen Formation and the east boundary of Wrangellia, Queen Charlotte Basin, British Columbia; *in* Current Research, Part E, Geological Survey of Canada, Paper 88-1E, p. 209-212.
- Yorath, C.J. and Hyndman, R.D.**  
**1983:** Subsidence and thermal history of Queen Charlotte Basin; *Canadian Journal of Earth Sciences*, v. 20, p. 139-159.



# Thermal state of the Queen Charlotte Basin, British Columbia: warm

T.J. Lewis<sup>1</sup>, W.H. Bentkowski<sup>1</sup>, and J.A. Wright<sup>2</sup>

Lewis, T.J., Bentkowski, W.H., and Wright, J.A., Thermal state of the Queen Charlotte Basin, British Columbia: warm; in *Evolution and Hydrocarbon Potential of the Queen Charlotte Basin, British Columbia*, Geological Survey of Canada, Paper 90-10, p. 489-506, 1991.

## Abstract

*The average heat flux in Queen Charlotte Basin, British Columbia, and its margins, the Queen Charlotte Islands to the west and the Coast Plutonic Complex on the mainland to the east, is  $70 \text{ mW m}^{-2}$ . The heat flux, which does not vary significantly within the basin nor its margins, is consistent with simple models of basin formation by extension occurring 25-40 Ma, but requires at least 30% extension. Since the heat generation of well cuttings and crystalline rocks from the margins is low,  $0.9 \text{ } \mu\text{W m}^{-3}$  or less, present crustal temperatures are high, reaching  $450^\circ\text{C}$  14 km beneath the margins and 13 km beneath the basin. Predicted temperatures within the basin (e.g.,  $135^\circ\text{C}$  at 4 km depth) are similar to bottom hole temperatures in the deepest wells. The high crustal temperatures limit crustal strength and restrict seismic activity to the cooler, upper 16 km, consistent with sparse seismic data.*

*The heat flux was measured using a marine probe as well as cored boreholes on land and hydrocarbon exploration wells on land and offshore. Large changes in bottom water temperatures (BWTs) cause the heat flux to vary within the upper few metres of sediments. To overcome these effects, an 11 m long marine heat-flow probe was used and BWT recorders were deployed between three cruises. BWT variations from 1 to 5 K were observed at water depths from 450 to 50 m, respectively. Warmer temperatures occurred in the winter time, and at the deepest depth in Moresby Trough sudden negative changes came in winter and spring time. At some locations temperatures of the upper sediments were buffered by water flow in a rather continuous Pleistocene sand layer. The measured heat flux beneath this layer appeared to be an equilibrium value. At other locations the temperature perturbation propagating into the sediments was much less than that expected for a conductive regime with an applied upper boundary temperature. This may indicate a complex boundary layer phenomenon.*

*Thirty cored boreholes drilled mostly for mineral exploration at 6 different sites on the basin margins gave the most reliable heat flux results,  $70.5 \pm 5.3 \text{ mW m}^{-2}$ . Bottom hole temperatures from fourteen hydrocarbon wells combined with estimated formation thermal conductivities yielded less reliable results, averaging  $69.2 \pm 10.6 \text{ mW m}^{-2}$ . Based on observations during measurement and the fact that the measured thermal conductivities of well cuttings were inconsistent with the mineralogy, it is assumed that air was entrapped with the fines during preparation of thermal conductivity samples.*

## Résumé

*Le flux thermique moyen dans le bassin de la Reine-Charlotte (C.-B.) et en bordure, soit dans les îles de la Reine-Charlotte à l'ouest et dans le complexe plutonique Côtier sur le continent à l'est, est de  $70 \text{ mW m}^{-2}$ . Le flux thermique qui ne varie pas beaucoup au sein du bassin ni en bordure, est conforme à celui des modèles simples de formation des bassins par distension entre 25 et 40 Ma, mais il nécessite une extension d'au moins 30 %. Comme le dégagement de chaleur par les déblais de puits et les roches cristallines des marges est faible ( $0,9 \text{ YW m}^{-3}$  ou moins), les températures crustales actuelles sont élevées, atteignant  $450^\circ\text{C}$  à 14 km au-dessous des limites et à 13 km au-dessous du bassin. Les températures prévues au sein du bassin (par ex.  $135^\circ\text{C}$  à 4 km de profondeur) se rapprochent des températures de fond de trou dans les puits les plus profonds. Les hautes températures crustales limitent la résistance de la croûte et restreignent l'activité sismique aux roches plus froides des 16 km supérieurs, conformément aux données sismiques éparses recueillies.*

*Le flux thermique a été mesuré en utilisant une sonde marine ainsi que des trous de sonde sur terre et des puits d'exploration des hydrocarbures forés sur terre et au large. D'importants changements dans les températures de l'eau de fond a fait varier le flux thermique dans les quelques mètres supérieurs de sédiments. Pour contrer ces effets, on a utilisé une sonde de flux thermique marine de 11 m de longueur, et des enregistreurs de la température de l'eau de fond ont été disposés entre trois navires. On a observé des variations de 1 à 5 K de la température de l'eau de fond aux profondeurs marines de 450 et 50 m, respectivement. Les températures les plus élevées ont été enregistrées au cours de l'hiver, et à la plus grande profondeur dans la dépression Moresby, des changements négatifs soudains se sont produits en hiver et au printemps. À certains endroits, la température des sédiments supérieurs a été réduite par un écoule-*

<sup>1</sup> Pacific Geoscience Centre, Geological Survey of Canada, P.O. Box 6000, Sidney, B.C. V8L 4B2

<sup>2</sup> Department of Earth Sciences, Memorial University of Newfoundland, St. John's, Newfoundland A1B 3X5



ment d'eau dans une couche de sable pléistocène plutôt continue. Le flux thermique mesuré au-dessous de cette couche semblait correspondre à une valeur d'équilibre. À d'autres endroits, la perturbation de la température qui s'est propagée dans les sédiments a été beaucoup moins importante que prévue pour un régime conducteur dont la température limite supérieure a été appliquée, indiquant peut-être un phénomène de couche limite complexe.

Les trente sondages carottés, forés pour la plupart à des fins d'exploration minière, à six différents sites dans les bords du bassin, ont donné les valeurs de flux thermique les plus fiables ( $70,5 \pm 5,3 \text{ mW m}^{-2}$ ). Les températures de fond de trou enregistrées dans 14 puits pétroliers combinées aux conductivités thermiques de formation estimées ont donné des résultats moins fiables, soit  $69,2 \pm 10,6 \text{ mW m}^{-2}$  en moyenne. En se fondant sur les observations faites durant les mesures et sur le fait que les conductivités thermiques des déblais n'étaient pas cohérentes avec la minéralogie, on présume que de l'air est resté piégé dans les fines au cours de la préparation des échantillons à analyser relativement à la conductivité thermique.

## INTRODUCTION

The objectives of this study were to obtain the present heat flux distribution within Queen Charlotte Basin in order to compare the thermal state of the basin and underlying crust with that predicted by various tectonic models, and to detect regions of upward fluid flow within the basin which are prospective regions for hydrocarbon deposits. Thermal conductivity and heat generation data were also required from both the basin sediments and surrounding crystalline crust to improve modelling of the present and past thermal structure. Three different types of heat flow data were analyzed: those from offshore and onshore wells, those from onshore boreholes cored for mineral exploration, and those from marine probe measurements in soft surficial sediments of the basin. Data were acquired over a period of three years (Lewis et al., 1988a, 1989), including three cruises.

Formation temperatures within a basin are determined at any time by the thermal properties of the basin sediments, the heat flux from beneath the basin, the hydrologic regime within the basin, magmatic intrusions and metamorphic and diagenetic reactions, as well as the history of sedimentation, burial and erosion. Queen Charlotte basin formed on an active margin, so most of these processes and properties are directly governed by the tectonic history. Former plate motions and interactions, as recorded by seafloor magnetic anomalies (Riddiough, 1982, 1984), indicate that the Farallon plate and its successor, the Juan de Fuca plate, and/or the Kula and Pacific plates (Engebretson, 1989), had been converging with the western margin of the North American plate from 150 Ma to at least between 55 and 45 Ma when the Pacific and Kula plates were fused together. The position of the Vancouver (Juan de Fuca-Pacific-American plate) triple junction is poorly constrained by models because of the ambiguity of whether a ridge or a transform fault was in contact with the North American margin. The Vancouver triple junction however was near its present position off northern Vancouver Island by 10 Ma. Subduction was taking place beneath all of the Coast Plutonic Complex north of this junction until at least 45 Ma. At some later time a strike-slip boundary between the Pacific and North American plates was established to the north. More recently oblique convergence commenced along the Queen Charlotte margin. Engebretson (1989) reports that four models all indicate 40 km of convergence between the Pacific and North American plates across the Queen Charlotte Fault in the last 5 Ma.

Three processes could enhance the heat flow in the Queen Charlotte region relative to the  $35 \text{ mW m}^{-2}$  of the presently converging Vancouver Island: 1) warming of crust cooled by earlier subduction, 2) passage of a hot spot associated with the Anahim Volcanic Belt, and 3) crustal extension associated with basin formation. After subduction of oceanic crust ceases, the continental crust above cold, subducted materials heats and expands, resulting in regional metamorphism

and magmatism accompanied by uplift and erosion. The heat flux should increase, then eventually decay to normal continental values.

The transcordilleran Anahim Volcanic Belt (Fig. 1) is a zone of alkaline and peralkaline magmatism that has propagated 200 km eastward from Denny Island during the past 14 Ma (Souther, 1986). One hypothesis (Bevier et al., 1979) suggested that the cause of this belt is the westward movement of the North American plate relative to a hot spot in the mantle, and that the Bowie-Kodiak Seamount chain may be a former trace of this hotspot under the Pacific plate.

Another possible origin of this volcanic belt is that the formation of a pull-apart basin inboard of the large strike-slip Queen Char-

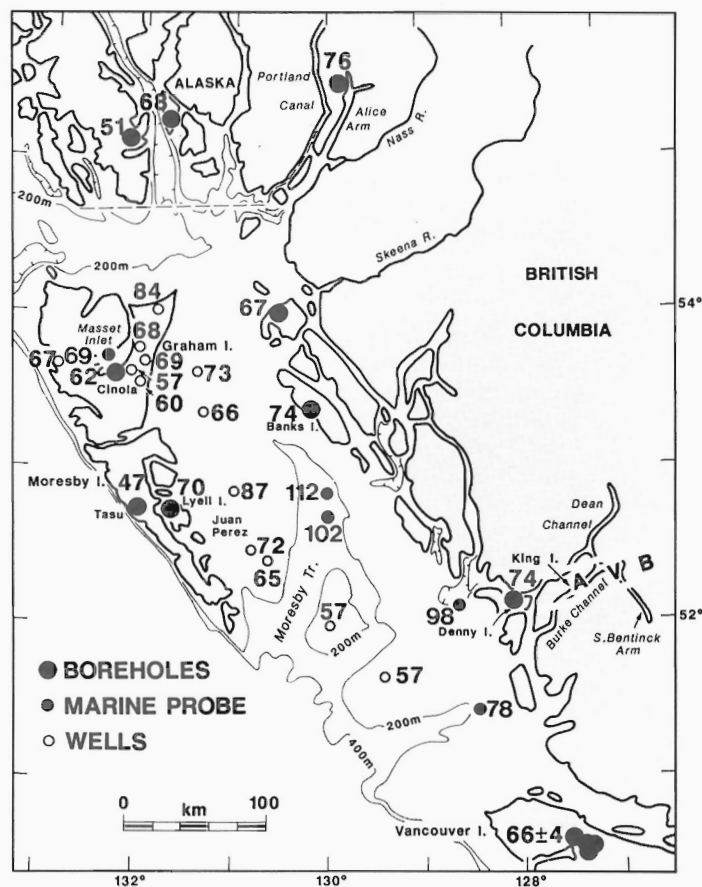


**Figure 1:** A site location map which also shows the trend of the Anahim Volcanic Belt (AVB) and the measured heat flux in  $\text{mW m}^{-2}$ . Single, average heat fluxes are given for the two Sockeye wells and for the two Masset Inlet sites.

lotte Fault is producing an eastward propagating fault or zone of extension, the locus of the Anahim belt. Yorath and Hyndman (1983) suggested that Queen Charlotte Basin formed during an initial rifting event, which was followed by oblique subduction from 5 Ma up to the present. Higgs (1988) suggested that the basin is a pull-apart basin, forming inboard of a major strike-slip fault, the Queen Charlotte Fault. Much evidence (Anderson and Greig, 1989; Anderson and Reichenbach, 1989; Higgs, 1989; Hamilton, 1989; and Souther, 1989) supports an extensional regime in the Eocene and later when the basin was forming. Anderson and Reichenbach (1989) divided south to north time-transgressive plutonism on the western margin into three intervals: 40-44, 32 and 27-28 Ma. The relative motion of the Pacific and American plates along the Queen Charlotte margin from 42-10 Ma was approximately parallel to each other (Stock and Molnar, 1988), with extension of 2 cm per year likely from 40-20 Ma.

Yorath and Hyndman (1983) calculated the paleo-heat flux and subsidence for eight hydrocarbon exploration wells in the basin using vitrinite reflectance measurements on cutting samples, and estimates of the formation thermal conductivities. They found the present day heat flux, determined using bottom hole temperatures (BHTs), to be much lower than the maximum values which occurred earlier. They hypothesized that the present, lower heat flux in the southern basin was the consequence of oblique underthrusting of oceanic lithosphere during the last 7 Ma. At the shelf edge and further offshore, the present, high heat flux is related to the nearby position of the Juan de Fuca spreading centre (Hyndman et al., 1982). The large variability in these high heat fluxes is caused by hydrothermal circulation in proximity to bedrock outcrop, as well as the variability in the thickness and accumulation history of the sediment ponds in which the measurements were made.

The heat flux in many basins is systematically redistributed by gravity driven fluid flows. Toth (1980) proposed that distribution of oil and gas is governed by systematic, regional flow of fluids. Studies (e.g. Majorowicz and Jessop, 1981; Andrews-Speed et al., 1984) have shown that systematic, basin-wide fluid migration has occurred, and that it has changed directions over geological times in response to changing topography. In some cases, present patterns of fluid migration explain the location of oil and gas pools in relation to their sources (e.g. Hitchon, 1984; Jones et al., 1986; Garvin, 1989). In general, fluid upflows producing high heat flow coincide with locations of hydrocarbon accumulations (e.g. McGee et al., 1989). Swift et al. (1988; pers. comm., M.G. Swift, 1988) found this to be true on the Exmouth Plateau off northwest Australia, using marine heat flow measurements.

This paper describes the heat flux measurements made using marine probes, using 14 hydrocarbon exploration wells and using 30 on-shore mineral exploration boreholes and geothermal assessment boreholes at 6 sites. The estimated and measured thermal conductivities and the measured heat generation from samples representing both the basin sediments and crystalline rocks are summarized. The heat flux is compared and related to the history of past magmatic events and the extensional formation of the basin.

## MARINE PROBE HEAT FLOW MEASUREMENTS

A combination of repeated heat flux measurements to depths up to 11 m over a period of nearly 2 years and recorded BWT histories between measurements (Lewis et al., 1988a) was used to obtain the equilibrium heat flux. Oceanic heat flow measurements are made with short, typically 3-m long heat flow probes. The stability of bottom water temperatures (BWTs) at oceanic depths provides a constant temperature boundary condition for the conduction of heat upwards through the bottom sediments. However, the BWT at depths of less than 800 m on this shelf is known to vary (Hyndman et al., 1982; Lewis,

1983). Such temperature variations propagate downward into the sediments, as dispersive waves, disturbing the equilibrium temperature gradient. Longer marine probes can penetrate into very soft sediments to depths where yearly disturbances are significantly diminished. Areas having soft, recent sediments were selected using surficial sediment maps (Luternauer and Murray, 1983), and during cruises, the softest sediments were identified using a 3.5 kHz profiling system. Water depths ranged from 50-450 m. Although this method has potentially less accuracy than the other methods used for this study due to the varying BWT, a substantial effort was made in order to obtain a better distribution of the measured heat flux in Queen Charlotte Sound.

The 11-m long probes used to obtain greater sediment penetration (Fig. 2) had strength members made of 6.4 cm diameter steel drill rod having a mass of 300 kg. Even the softest ponds of sediment on the shelf proved more difficult to penetrate than soft sediments in coastal fjords, and on many deployments the probes only reached a depth of 7 m. Temperature sensors were spaced at 1 m intervals in the GSC probes, and at 0.5 m intervals over the bottom 7 m of the Memorial University of Newfoundland probe. Sets of data (sediment temperatures) at individual sites were acquired on three cruises, but poor weather during the first and third cruises made holding station with the ship very difficult. On these two cruises irreparable mechanical damage was sustained by five 11-m probes, usually on pull-out at water depths between 150 and 450 m. No permanent damage was sustained by any probe on the other cruise to the same sites.

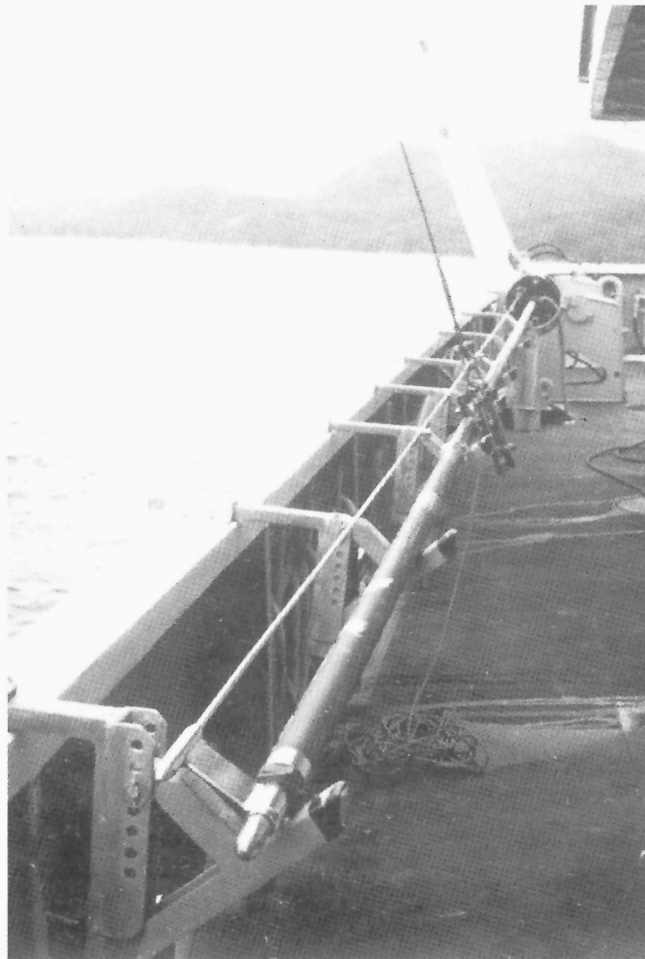


Figure 2: An 11-m Lister marine heat-flow probe, alongside the ship's rail.

**Table 1: Bottom Water Temperature Data Loggers**

Site	Coordinates		Water Depth m	Average Temp. °C	Recording Interval year:day
	North	South			
Milbanke Sd.	52°11.60'	128°43.76'	245	6.4	86:241-87:015
				6.9	87:246-88:134
Moresby Tr.	52°10.38'	130°14.27'	452	5.2	86:243-87:245
				5.2	87:246-88:136
Camaaño 2	52°43.61'	129°57.80'	255	5.6	87:248-88:138
Masset In.	53°40.82'	132°34.05'	53	10.0*	87:250-88:143

\*Offscale a small part of the recording interval.

Between the three cruises which took place in September of 1986, September of 1987, and May of 1988, data loggers recording BWTs were left moored on the bottom at some sites (Table 1). For seven deployments, there were six recoveries. The frame attached to the floats from the recorder lost near Goose Island Trough was eventually salvaged, suggesting that it had either worked loose or been stripped off by a fisherman's net. Figures 3-6 show the large changes in BWT at 4 sites having water depths from 50-450 m. BWT variations are not correlated between sites, and the rapid temperature changes indicate rapid movement of deep water masses. None of the BWT changes appeared correlated in time with atmospheric pressure fronts nor high wind speeds measured at Cape St. James, on the southern most tip of Moresby Island.

The higher frequency changes seen in the BWT records are attenuated by approximately 3 m depth. Changes with periods of a year or more propagate much deeper, as illustrated in Figure 7 for a step and a sinusoidal BWT variation. It is very desirable to make measurements below a depth of 7 m where the effects of annual changes become small.

The expected temperature disturbance as a function of depth was calculated for each site, using a series of steps and ramps to approximate the measured BWT. For a period of up to three years before the recording commenced, BWTs were assumed to be the same as the first year's recorded BWT, except for Masset Inlet. There the 5 K BWT change was approximated by an annual sinusoidal change. In all cases except Masset Inlet, the temperature changes for these calculated variations below 7 m depth were very small: less than 6 mK, and in terms of the gradient, less than 2 mK/m in comparison to an expected gradient of approximately 80 mK/m. The equilibrium gradient can be obtained by correcting more shallow temperatures, but in practice, this is very difficult to do. The depth of the temperature measurements with respect to the sediment-water interface cannot be determined well, and the gradational nature of this interface is an additional problem. Therefore, the most reliable determinations of the gradient are from sediment depths greater than 7 m. At one site near Juan Perez Sound no deep data were obtained and an equilibrium heat flux could not be calculated.

At some sites (Figs. 8-10), temperatures in the top 4 m of sediments did not change in response to BWT variations as much as expected for a conductive regime. For example, near Milbanke Sound the recorded change in BWT (Fig. 4) should have penetrated to a greater depth than observed (Fig. 9). Some process near the sediment-water interface may be diminishing and/or delaying the propagation of the BWT disturbance downwards.

The measured, non-linear temperature gradients at Moresby Trough south site closely resembled those expected from the recorded BWT history over two years (Fig. 11, Table 2). The heat flux was calculated from the temperature gradient best fitting the observed temperatures, because the probes only penetrated 6 or 7 m into these relatively hard sediments. The high measured heat flux ( $146 \text{ mW m}^{-2}$ ) is probably due to refraction of heat caused by much more compacted sediments rising to near the surface, as seen on 3.5 kHz records.

## MORESBY TROUGH BOTTOM WATER TEMPERATURE

### AVERAGE DAILY TEMPERATURE

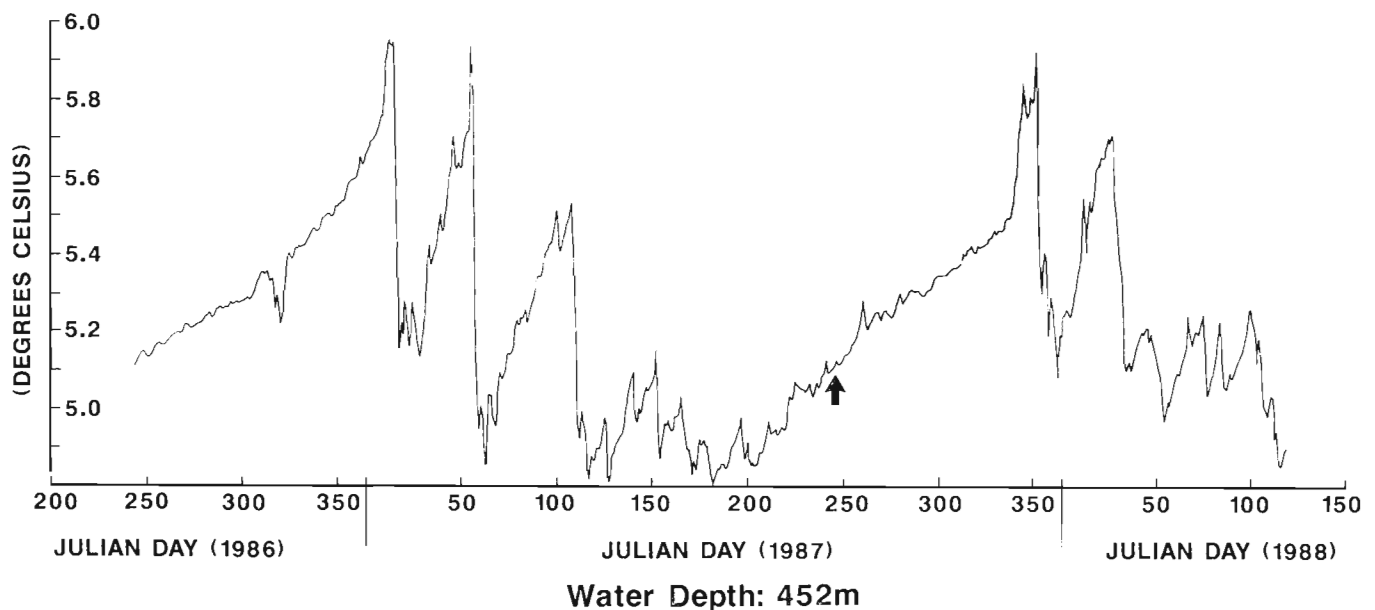


**Figure 3:** Measured BWTs (bottom water temperatures): Moresby Trough. The arrow indicates the time of the second cruise when the logger was recovered and redeployed.

## MILBANKE SOUND BOTTOM WATER TEMPERATURE

AVERAGE DAILY TEMPERATURE

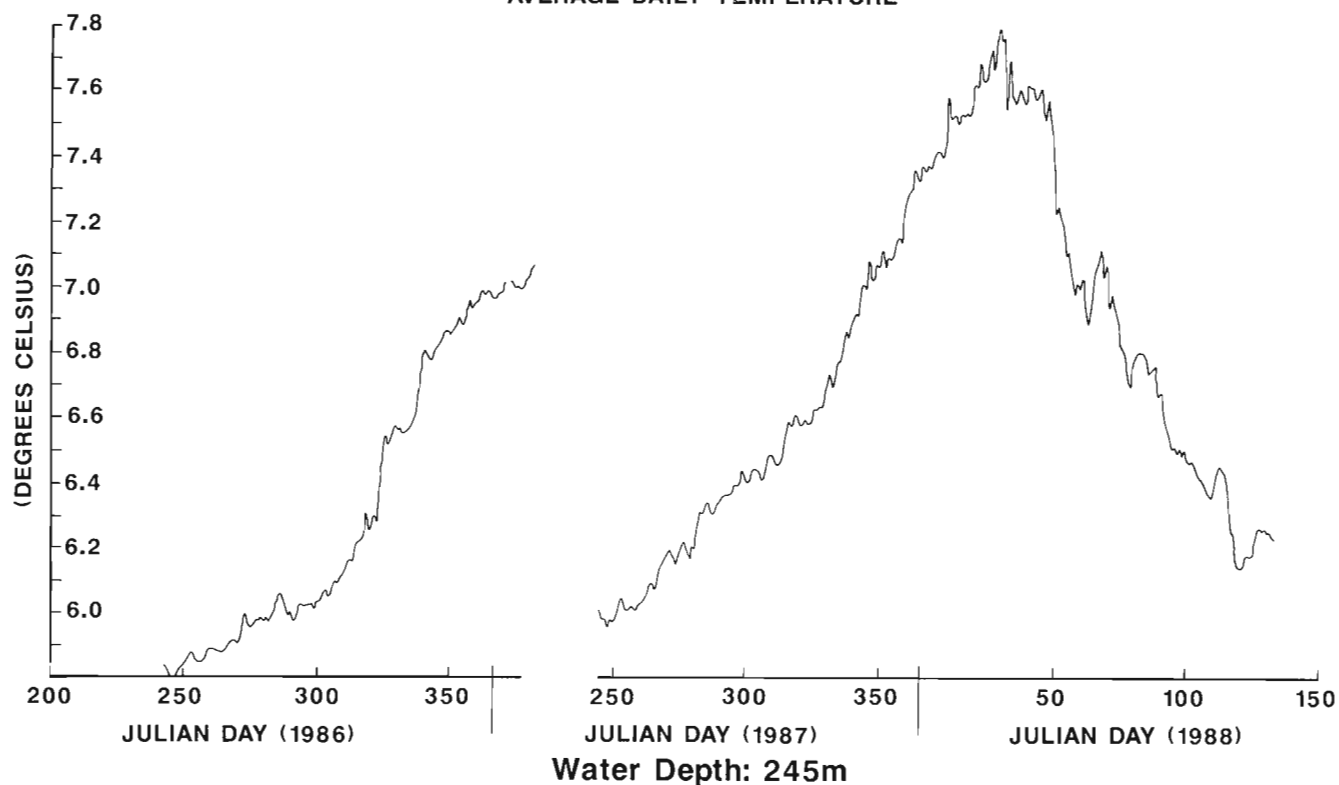


Figure 4: Measured BWTs (bottom water temperatures): near Milbanke Sound.

## CAAMAÑO SOUND BOTTOM WATER TEMPERATURE

AVERAGE DAILY TEMPERATURE

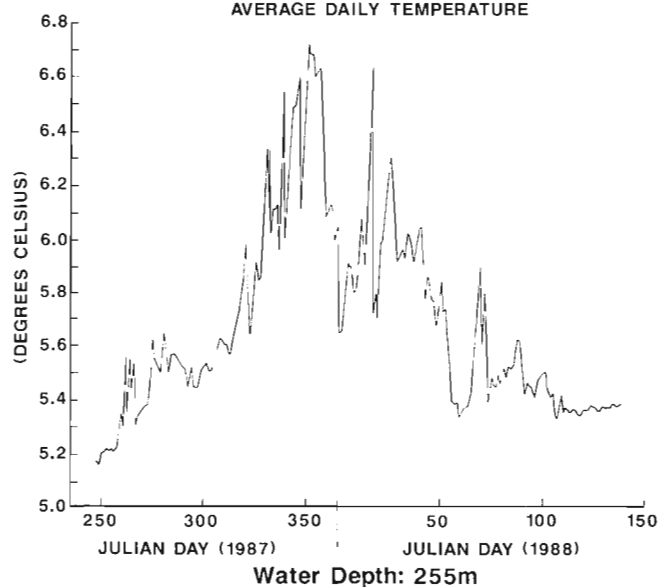


Figure 5: Measured BWTs (bottom water temperatures): near Caamaño Sound.

## MASSET INLET BOTTOM WATER TEMPERATURE

AVERAGE DAILY TEMPERATURE

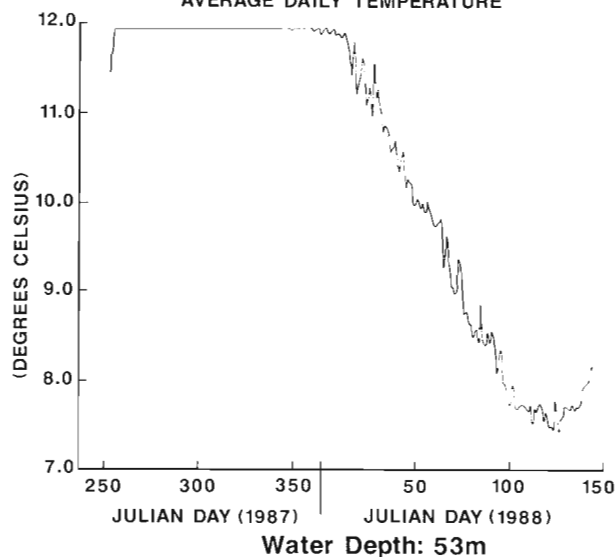
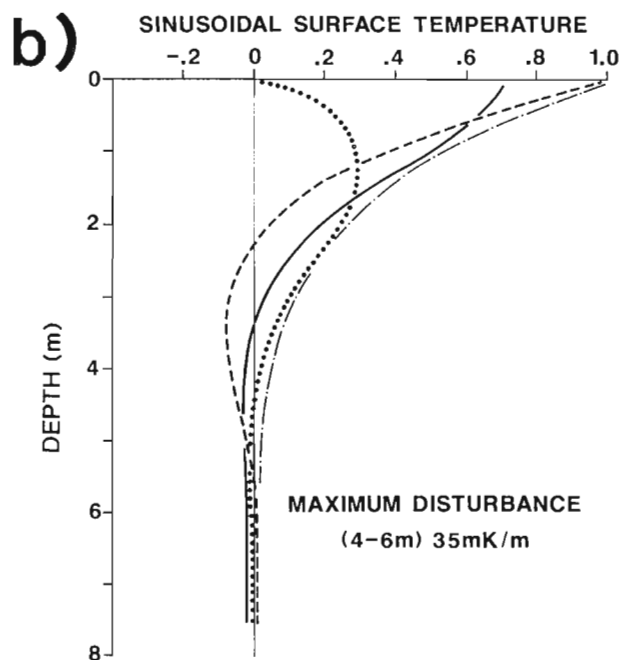
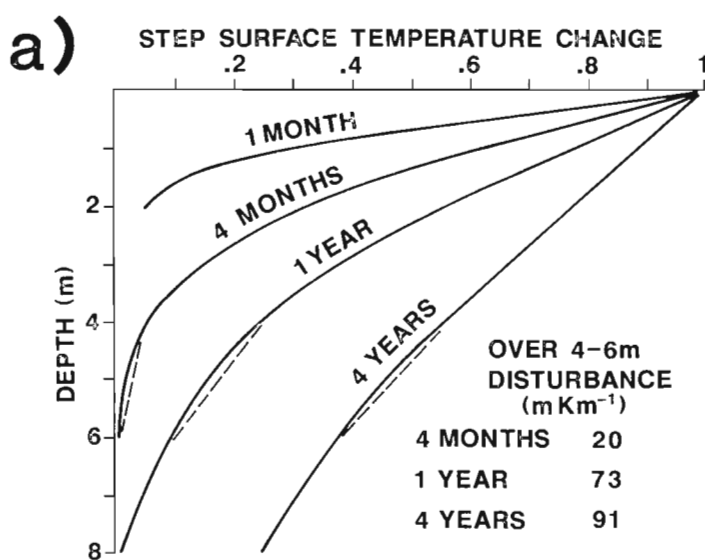
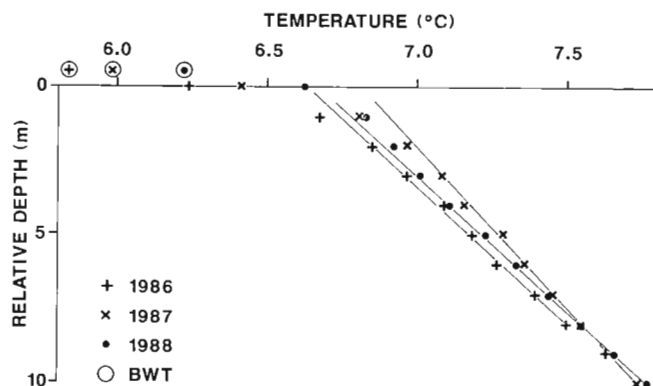


Figure 6: Measured BWTs (bottom water temperatures): Masset Inlet.



**Figure 7:** BWT (bottom water temperature) perturbations propagating into the sediments due to a) a 1-K step change at the previous times marked, and b) a 1-K amplitude annual sinusoidal variation. The dot-dash line is the maximum limit variation at any time. The resulting disturbance to the temperature gradient is also given for a).



**Figure 8:** Average sediment temperatures relative to the BWT at the Milbanke Sound site. The depth is measured with respect to the top sensor

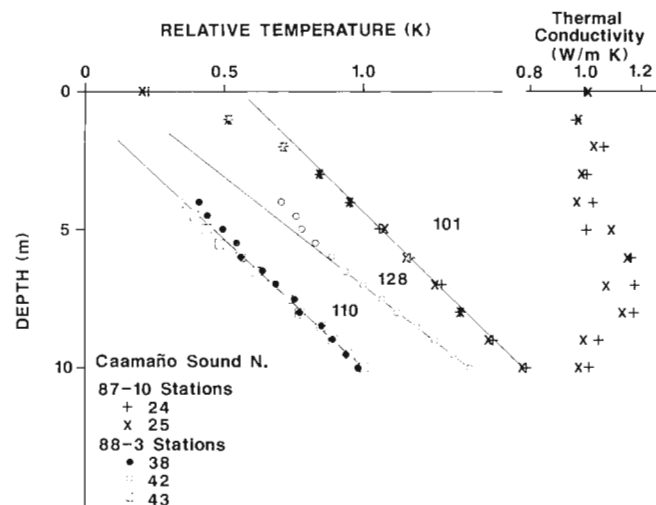


**Figure 9:** Measured sediment temperatures relative to BWT and conductivities at Caamaño Sound North site for 1987 and 1988 stations. The depth is measured with respect to the top sensor. The gradients of the lines approximating the temperatures is given in mK/m. Temperatures for station 42 are offset -0.25 K, and for stations 38 and 43, -0.5 K to avoid crowding of the data points.

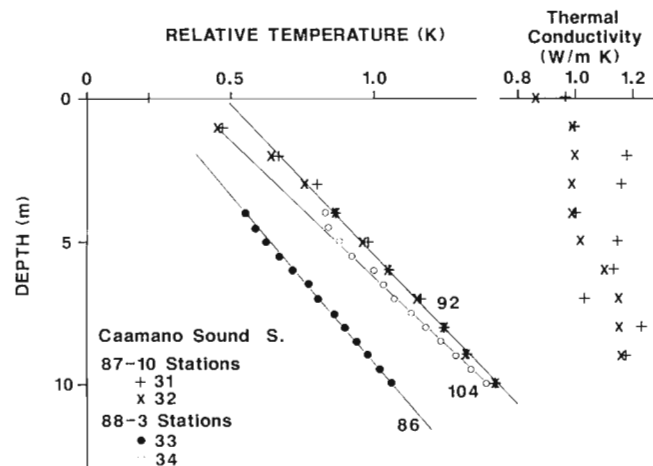


**Figure 10:** Data from Caamaño Sound South site, as in Figure 9. Station 33 temperatures are offset by -0.25 K.

**Table 2:** Heat Flux in Queen Charlotte Area from Marine Probe Measurements and Average Parameters

Site	Coordinates North	Coordinates South	Water Depth m	Depth Interval m	Temp Gradient mK/m	Thermal Cond. W/m K	Heat Flux mW m <sup>-2</sup>
Moresby S <sup>1</sup>	52°11'	130°15'	442-485	6.0-7.5	140	1.05	146
Caamaño S <sup>2</sup>	52°44'	129°58'	255	6.5-10.5	92	1.12	102
Caamaño N <sup>2</sup>	52°50'	129°59'	255	8.5-10.5	101	1.08	112
Masset E	53°41'	132°30'	53	8.0-11.0	78	0.83	65
Masset W	53°41'	132°34'	53	8.0-11.0	92	0.79	73
Goose I <sup>3</sup>	51°27'	128°26'	180-185	6.0-10.0	67	1.16	78
Milbanke <sup>3</sup>	52°11'	128°45'	225	7.0-11.0	103	0.95	98

<sup>1</sup> Temperature gradient from fitting with observed BWTs; <sup>2</sup> linear temperature gradients inconsistent with recorded BWTs; <sup>3</sup> Heat flux and parameters below sandy layer.

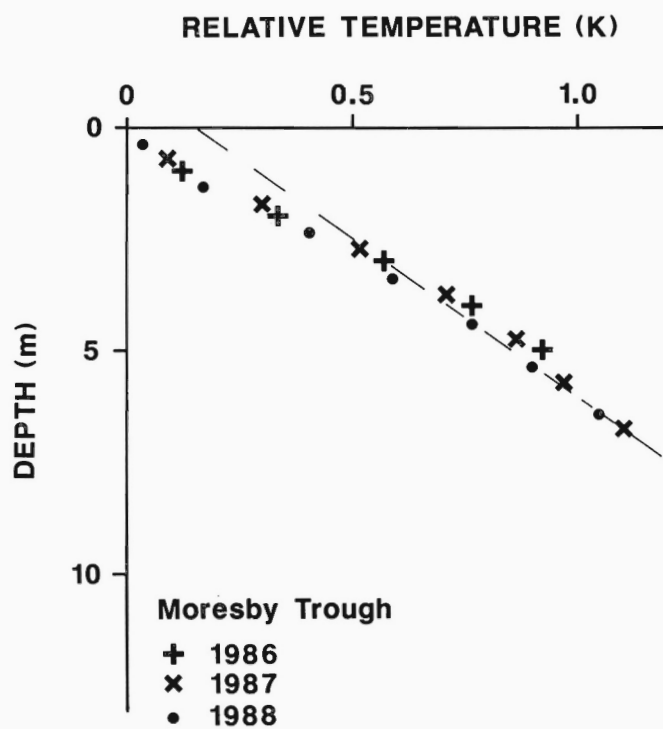


**Figure 11:** Average sediment temperatures relative to BWT at the Moresby Trough south site for all three cruises. Probe penetrations are adjusted to give the best agreement. The dotted line is the gradient fitted after correcting for BWT disturbances.

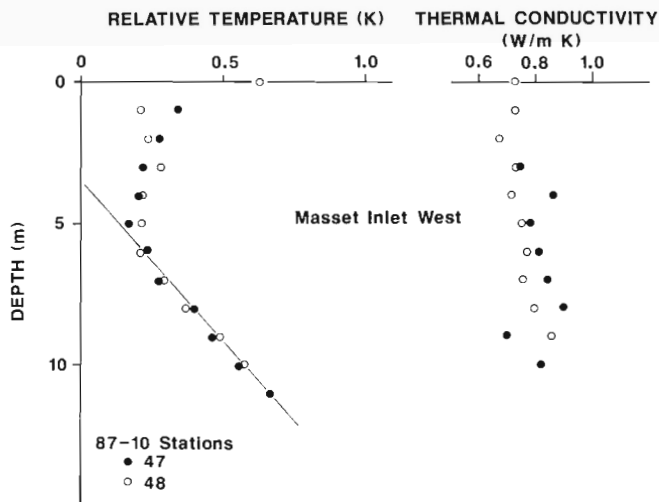


**Figure 12:** Conductivities and measured sediment temperatures relative to BWT at Masset Inlet West site for 1987. For station 48 the top sensor is assumed to be at 0 m depth and for station 47 at 1 m depth.

For this reason, this value is not considered to represent the basin heat flux. In Masset Inlet the probes appeared to “super” penetrate into very soupy sediments, although the reduced disturbance could be due to some surface process as already mentioned. The observed part of the shallow, non-linear gradient resembles the calculated one if the BWT variation, recorded for only 9 months, is approximated by an annual sinusoidal variation, and if the tops of the probes are up to 2 m deep into the sediments (Figs. 12 and 13). The inferred correction for the bottom 4 sensors is negligible, and these temperatures were used without correction to calculate the equilibrium heat flux.

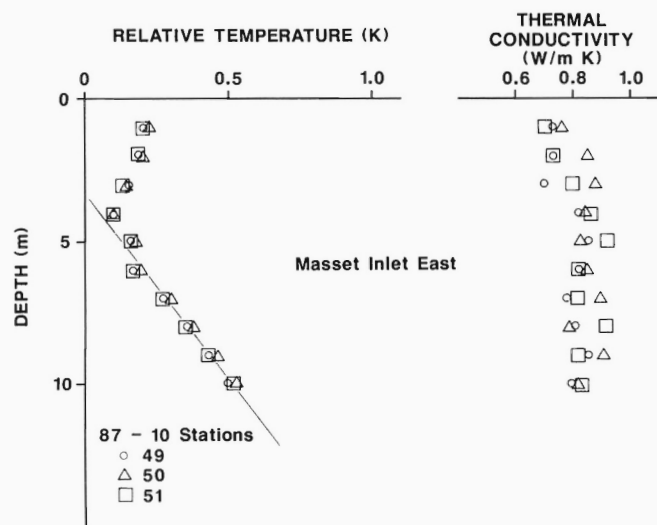


**Figure 13:** Data for Masset Inlet East site, as in Figure 12.

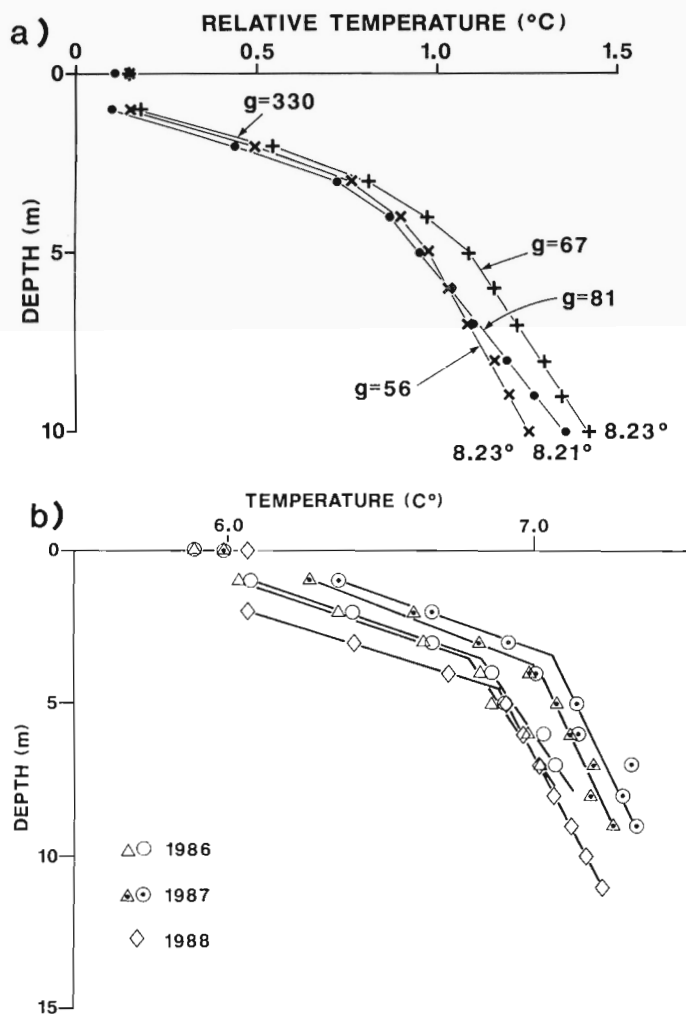


**Figure 14:** a) Sediment temperatures relative to BWT at Goose Island Trough in 1988. Absolute temperatures are given for the bottom sensors. The temperature offsets are due to different reference temperatures at different depths in the water column. b) The average absolute sediment temperatures of 2-4 deployments at each of two sites for each cruise. Locations are within 4 km of each other in Goose Island Trough, and show the thermal effects of a sandy layer.



At the Goose Island Trough sites there was a large change in temperature gradient between 3 and 4 m below the water-sediment surface. This is probably associated with layer B2 identified by Luter-nauer et al. (1989) as a sandy mud deposited just after deglaciation of Queen Charlotte Sound, between 12 900 and 10 200 aBP when sea level was lower than at present. At corresponding depths a strong seismic reflector was observed on the 3.5 kHz records. This unit, 0.5 m thick near our Goose Island site (Conway and Luter-nauer, 1985), appears to be quite continuous. In the 3 m above the sandy layer the heat flux is 5-6 times greater than that below it. The measured sediment temperatures for three stations at each of the two sites were in good agreement, especially in the upper 4 m (Fig. 14).

The temperature at the approximate depth of the sandy layer was between 6.79 and 6.83°C in 1986, between 7.06 and 7.01°C in 1987, and at 6.88°C in 1988, while the corresponding BWTs were 5.89°C, 5.99°C, and 6.39°C. Unfortunately the BWT recorder at this site was lost, but the variation in BWT between cruises is expected to exceed 1.5 K. The temperatures of the sediments above the sandy layer (Fig. 14) appear to be unaffected by any disturbance due to BWT variation.

At the Mitchell Trough site the deep data were not consistent with conduction through homogeneous sediments (Fig. 15), and therefore no equilibrium heat flux could be calculated. There were seismic reflectors at 4 and 8 m depth.

*In situ* thermal conductivities were measured by the Lister-type probes (Hyndman et al., 1979) only on the second cruise, due to technical difficulties. The average conductivity measured at a particular site was used for the other two cruises if the measured conductivities were nearly constant with depth, if the temperature gradient was nearly constant, and if the sediments seen by the 3.5 kHz sounding systems were similar. Most data met these criteria.

## HEAT FLUX FROM BASIN WELLS

Yorath and Hyndman (1983) originally calculated the heat flux in the eight offshore wells. Chapman (D.S. Chapman, pers. comm., 1987) pointed out that two small, offsetting corrections should be added to the original calculations: one for the effect of formation temperature on grain conductivity and another for depths measured from the Kelly bushing instead of the sea floor. In addition, formation thermal conductivities were calculated using porosities of sidewall cores and

a high value for the grain thermal conductivity (4.0 W/m K) obtained from the mineralogy of samples of Skonun Formation outcropping on Graham Island. The grain conductivity based on the mineralogy of the sidewall cores was lower. From these wildcat wells there were numerous, well distributed sidewall cores that were originally used to determine the lithology. Although the main source rocks surrounding the basin are granodiorites and quartz diorites with less than average quartz content, a quartz content of at least 30% occurs in these predominantly sandstone sediments, as expected in such a basin (R. Higgs, pers. comm., 1989). Therefore a grain conductivity of 3.4-4.0 W/m K is expected, dependent on the matrix mineral(s).

The thermal conductivities of cuttings from these wells were measured using a cell technique (Sass et al., 1971). These results are reported only briefly here because they do not appear to represent the formation conductivities, as indicated below. The average grain conductivity of 297 samples of cuttings from all of the individual wells, 2.03 W/m K, (Table 3) is significantly lower than the value of 4.0 W/m K used by Yorath and Hyndman (1983), and the 3.4 W/m K expected for sandstones with 35% quartz content and a low conductivity matrix. The same cuttings from four of the eight wells measured again in another lab had an average grain conductivity within 0.5% of the first determinations. Omitting fourteen samples containing some coal with an average grain conductivity of  $0.64 \pm 0.21$  W/m K produces an average grain conductivity of 2.10 W/m K, still a very low value. The distribution of measured conductivity values (Fig. 16) exhibits a wide variation (1.0-3.3 W/m K), with slight differences between the wells. With the coaly samples omitted, Tye and the Sockeye wells have an average conductivity of 2.28-2.30 W/m K, South Coho, Auklet and Osprey have an average conductivity between 2.02 and 2.04 W/m K, and Harlequin and Murrelet have average conductivities of 1.88 and 1.82 W/m K.

Conductivity results from a pulsed needle probe, an absolute method (T.J. Lewis, H. Villinger, and E.E. Davis, unpublished), were limited to a few samples because of the small amounts of cuttings available and difficulties forming the saturated samples. Even though a wetting agent was used, most of the finer grained cuttings dropped under vacuum into the water floated on top. The pulsed needle probe grain conductivities of the measured samples were on average 25% higher than the cell method values, the samples having an average thermal conductivity of 2.90 W/m K. Results measured on a coarser

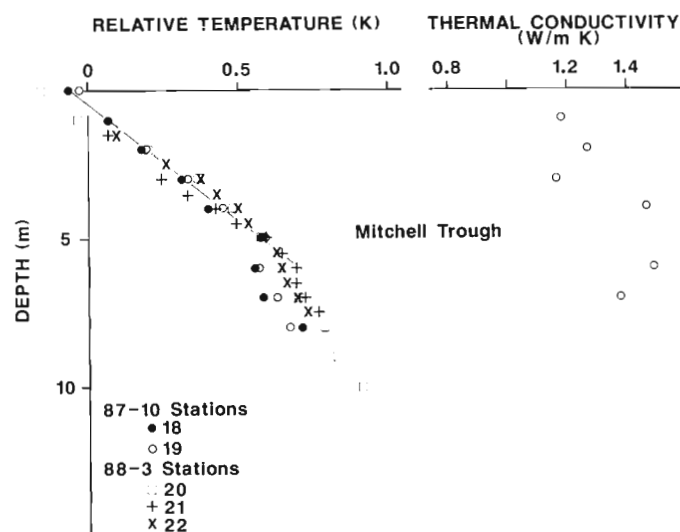


**Figure 15:** Conductivities and sediment temperatures relative to BWT at five Mitchell Trough stations in 1987 and 1988. The probe penetrations are adjusted for stations 21 and 22 to obtain the best agreement with other temperatures.

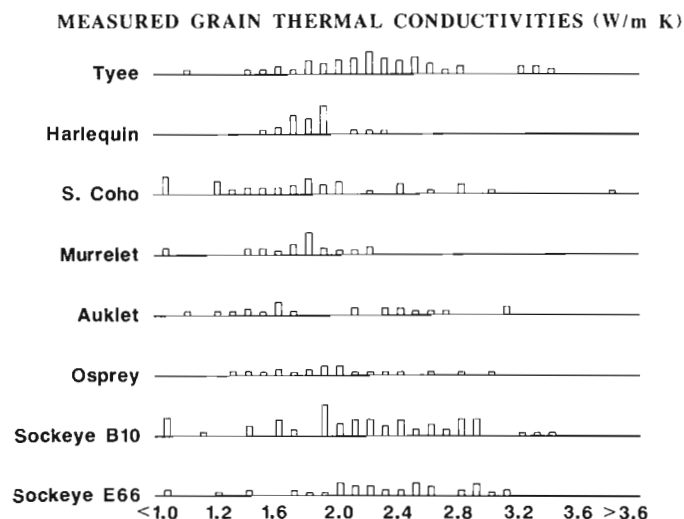


**Figure 16:** A histogram showing the variation of measured grain thermal conductivity from well cuttings.

**Table 3: Thermal Conductivity of Offshore Well Cuttings and Heat Flux from Wells**

Well	Grain Density g/cc	Measured Grain Thermal Cond. W/m K	Sidewall Porosity	Formation Thermal Cond. W/m K	Heat Flux mW m <sup>-2</sup>	Formation <sup>1</sup> Thermal Cond. W/m K	Heat <sup>1</sup> Flux mW m <sup>-2</sup>
Osprey	2.74	2.03	0.30	1.41	37.9	2.10	57.
Harlequin	2.63	1.92	0.30	1.35	36.3	2.10	57.
Auklet	2.68	2.04	0.29	1.43	43.1	2.14	65.
Murrelet	2.62	1.77	0.28 <sup>2</sup>	1.31	43.5	2.18	72.
Sockeye B10	2.60	2.14	0.25 <sup>2</sup>	1.56	56.6	2.30	84.
Sockeye E66	2.65	2.30	0.23	1.64	62.0	2.38	90.
Tyee	2.58	2.27	0.28	1.56	47.2	2.18	66.
S. Coho	2.57	1.94	0.28 <sup>2</sup>	1.40	46.7	2.18	73.
Tow Hill	.	.	0.27 <sup>2</sup>	.	.	2.22	84.
Gold Cr.	.	.	0.27 <sup>2</sup>	.	.	2.22	57.
Nadu R.	.	.	0.27 <sup>2</sup>	.	.	2.22	68.
Tiell	.	.	0.27 <sup>2</sup>	.	.	2.22	60.
Cape Ball	.	.	0.27 <sup>2</sup>	.	.	2.22	69.
Port Louis	.	.	0.27 <sup>2</sup>	.	.	2.22	67.

<sup>1</sup>Calculated using a grain conductivity of 3.6 W/m K.

<sup>2</sup>An estimate, or only measured in one interval.

grained sand (a rare occurrence in the Tyee well at 1720 m depth) by each method and by different labs agree fortuitously well compared to the 15% accuracy of the methods: PGC, operator 1: 3.34 W/m K (average of 2 measurements), PGC, operator 2: 3.01 W/m K (average of 3 measurements), different lab: 3.33 W/m K, pulsed needle probe, 3.33 W/m K.

The conductivity samples are lithic-quartz wackes. Quartz content of the few samples examined averaged 25-30%, from fine sand to silt (J.V. Barrie, pers. comm., 1989). Porosity of these dirty sandstones is good, permeability is poor. The thermal conductivity of such sediments should reflect primarily the quartz content (e.g. Della Vedova and Von Herzen, 1987), but the measured conductivities were inconsistent with the samples' mineralogies.

Measured grain thermal conductivities could be lower than the actual formations because coal was over-represented in the cuttings, and because of drilling mud contamination. However, preparation of most water saturated samples was complicated by the large proportion of very fine grains, indirectly causing low conductivity values. The fines trapped a very small volume of air which was dispersed throughout the sample. Della Vedova and Von Herzen noted incomplete removal of air bubbles during the saturation process lowered the matrix conductivity of fine grained materials despite washing in a 1 mm sieve. This is consistent with both the higher needle probe results from the coarser samples and the wide variation in the cell results from individual wells, with maximum conductivities approaching the expected values (Fig. 16). For these reasons thermal conductivity values are estimated for the Queen Charlotte basin, as was done by Yorath and Hyndman (1983), but using a somewhat lower grain conductivity of 3.6 W/m K, (equivalent to a 35% quartz content) and 2.5 W/m K for other minerals. For the onshore wells, the same grain thermal conductivities were assumed and a porosity of 0.28 was used. The sediments penetrated are in general sandstones similar to the offshore wells (Sutherland Brown, 1968).

The only temperature data from the wells, bottom hole temperatures (BHTs), were combined with average BWTs or average land temperatures for onshore wells to determine temperature gradients. For

each well the "best" calculated temperature gradient coming from the BHTs (see Yorath and Hyndman, 1983) was increased by 20% to compensate for downhole cooling by circulation and for the short time interval (mostly 2-7 H) between stopping circulation and logging the temperature. Since most of the wells were drilled very quickly, this correction is probably an overestimate. Heat flow results from wells are assigned error limits of 20% to account for the uncertainties associated with BHTs and formation thermal conductivities.

All but one of the heat fluxes from the wells (Fig. 1, Table 3) are within 20% of 70 mW m<sup>-2</sup>, the average value being 69.2 ± 10.6 mW m<sup>-2</sup>. The higher offshore heat fluxes come from the wells with higher temperature gradients, and the two highest values from the Sockeye wells are situated on thick sedimentary structures.

## HEAT FLUX FROM THE BASIN MARGINS

Heat flux was measured in 30 mineral exploration boreholes and two geothermal resource evaluation boreholes at six sites on land (Table 4). Except for the Cinola site, these holes penetrate volcanic and plutonic rocks having very low porosities. Figures 17-21 present all temperature logs, as a function of thermal depth, and thermal conductivities. Only one of these sites with a single borehole (356-Anyox) appeared to have a completely conductive gradient. The following is a brief explanation of the interpretation necessary to arrive at the quoted heat flux for each site (see also Lewis et al., 1989).

Denny Island, 315: The heat flux measured in two boreholes 3.3 km apart differs by 23%. The shallower hole, -1, is drilled into a quartz feldspar porphyry-porphyry breccia which has a higher heat generation and a higher thermal conductivity than the leucocratic miarolitic granite which -2 penetrates. A locally high heat flux would be caused in -1 by refraction of heat towards the smaller body and localized higher heat generation. The 74 mW m<sup>-2</sup> from the deeper hole, -2, best represents the site.

Anyox, 356: The presence of finely disseminated mineralization in some of the core accounts for the large range in measured thermal conductivity, from 2.25 to 7.08 W m<sup>-1</sup> K<sup>-1</sup> (see Fig. 17), and there can be no doubt that refraction is caused by dipping, mineralized zones. A topographic correction was applied to this site on top of a ridge, giv-

**Table 4: Cored Borehole Locations and Thermal Measurements**

	Site	Location		Collar Elevation (m)	Measured Interval (m)	n	Thermal Conductivity		obs.	Heat Flux (mW/m <sup>2</sup> )		
		lat.(N)	long.(W)				(W/mK)	S.D.		corr. <sup>a</sup>	S.D. accepted	
315	Denny Island	52°08.1'	128°02.9'	40	50-194	13	2.99	0.29	90.8	•	3.3	74
-2		52°08.8'	128°05.7'	40	90-381	24	2.48	0.37	73.7	•	1.6	
356	Anyox	55°28.4'	129°49.0'	655	80-292	22	3.94	1.18	65.2	75.5	0.4	76
357	Banks Island	53°21.8'	130°07.5'	33	220-240	16	3.03	0.49	116.6	•	4.7	74
-2		53°21.9'	130°07.3'	33	150-389	29	3.06	0.51	76.2	•	0.2	
-4		53°22.0'	130°09.7'	25	50-71	10	3.30	0.77	51.0	•	3.1	
-6		53°22.0'	130°09.7'	25	50-125	15	3.29	0.55	86.9	•	2.8	
-7		53°22.0'	130°09.7'	25	50-89	8	3.11	0.37	75.0	•	1.3	
-8		53°22.0'	130°09.7'	25	50-75	9	3.58	0.24	88.1	•	14.3	
-9		53°21.9'	130°09.5'	25	50-124	16	3.37	0.33	81.0	•	0.3	
-10		53°21.9'	130°09.5'	25	50-137	16	3.24	0.30	71.4	•	1.2	
-12		53°21.0'	130°09.5'	25	50-130	14	3.34	0.50	63.5	•	1.7	
-13		53°21.3'	130°08.9'	10	50-173	24	3.59	0.55	74.9	•	1.0	
-14		53°21.3'	130°08.7'	10	50-116	14	3.59	0.77	75.1	•	2.1	
368	Cinola	53°31.8'	132°13.1'	198	28-117	11	2.97	0.48	66.2	•	2.1	62
-2		53°31.7'	132°13.0'	193	40-111	10	2.91	0.44	46.0	•	1.4	
-6		53°31.8'	132°13.2'	214	32-69	5	4.08	0.52	75.9	•	2.4	
-7		53°31.7'	132°13.1'	210	30-79	5	4.00	0.59	49.0	•	3.9	
-9		53°31.8'	132°13.1'	210	22-81	8	3.46	0.50	65.8	•	3.9	
-20		53°31.7'	132°13.1'	200	40-68	5	4.06	0.79	68.8	•	2.2	
-22		53°31.9'	132°13.1'	209	30-70	6	3.39	0.34	59.4	•	5.8	
-23		53°31.6'	132°13.1'	182	40-70	3	4.14	0.27	107.3	•	13.3	
-25 <sup>b,c</sup>		53°31.2'	132°11.6'	80	—							
-26 <sup>b,c</sup>		53°31.0'	132°12.7'	60	—							
-27		53°31.6'	132°13.0'	160	25-87	8	3.47	0.57	69.2	•	6.0	
377	Lyell Island	52°43.2'	131°42.9'	118	110-184	10	2.98	0.21	59.7	70.2	1.3	70
-2		52°43.2'	131°42.8'	135	50-111	7	2.86	0.27	48.3	•	0.3	
382	Porcher Island	54°01.4'	130°35.3'	110	273-360	26	3.14	0.22	72.2	71.7	1.7	67
-2		54°01.4'	130°35.3'	109	70-115	6	3.52	0.23	132.8	•	4.5	
-3		54°01.4'	130°35.3'	117	50-140	8	3.43	0.14	112.4	•	1.7	
-4		54°01.4'	130°35.2'	114	100-150	9	3.50	0.12	78.1	•	3.6	
-5		54°01.8'	130°35.3'	46	130-206	17	2.81	0.42	62.4	61.9	0.5	

<sup>a</sup> corrected for topography, <sup>b</sup> no thermal conductivities measured, <sup>c</sup> no heat flux calculations made.

ing an average heat flux of 75.5 mW m<sup>-2</sup> for the interval between 80 and 292 m depth.

Banks Island, 357: The sediments at this site which were intruded by quartz diorite are dark, micaceous calcite-rich argillites and marbles with quartz. Heat flux values from 11 logged holes vary from 51-88 mW m<sup>-2</sup>. Water flow is the cause of the non-linear temperature logs in the three shallow holes having the largest variations in heat flux, consistent with the local geology which includes permeable fractures and limestone. Excluding these three results, the average heat flux is 73.9 mW m<sup>-2</sup>. Five of the individual results are within 3 mW m<sup>-2</sup> of

the average, including the heat flux from the deepest hole. This area may be subject to changes in surface temperature due to past changes in sea level because all collar elevations are between 10 and 33 m ASL.

Cinola, 368: The Cinola gold deposit, located on a topographic high, is in a clastic sequence consisting of a lower shale unit (Haida Formation) and an overlying sequence of pebble conglomerate and coarse grained sandstone (Skonun Formation). The adjacent Specogna fault separates the deposit from a low-lying region underlain by Haida Formation shale and silicified shale to the northwest. The thermal data suggest water flow down the topographic gradient

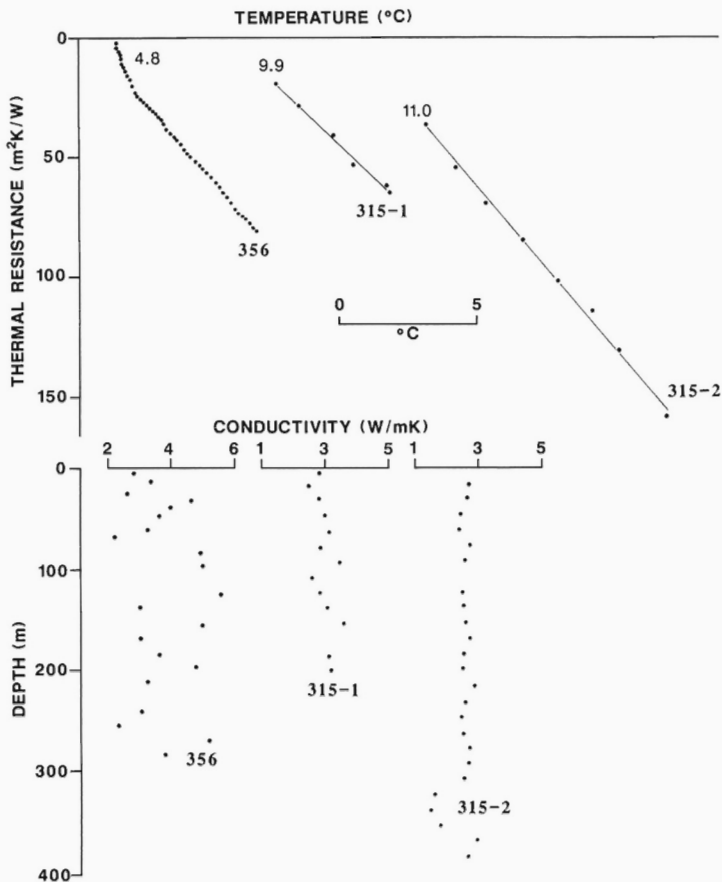


**Figure 17:** Relative temperature vs thermal resistance (Bullard plots) and thermal conductivity as a function of depth for Denny Island (315), and Anyox (356). The most shallow absolute temperature for each hole is given.

to the northwest. Concave down temperature logs and relatively high surface intercept temperatures for two shallow boreholes located in the valley (-25 and -26) indicate an upward component of water flow (Fig. 19). Water flow is significantly influencing the temperature logs of two boreholes located just above a cliff where the adit is located (-23 and -27). Temperatures from 7 other holes further back from the cliff are not obviously affected, and much less likely to be affected by water flow. The average heat flux,  $61.6 \pm 10.8 \text{ mW m}^{-2}$ , is considered to be a minimum owing to the possible downward flow of water within the region. Varying amounts of silicification of the host rock account for the large variation in thermal conductivities.

**Lyell Island, 377:** Exploration holes were drilled through small rhyolitic zones adjacent to the Beresford Fault which separates the Karmutsen and Masset formations on Lyell Island. Heat fluxes measured in two closely spaced boreholes located on a steep hillside are 20% different. One had a very high surface intercept temperature,  $8.0^\circ\text{C}$ , indicating the probable influence of water flow. The other result,  $70.2 \text{ mW m}^{-2}$  after topographic correction, is accepted.

**Porcher Island, 382:** The results from the two deepest holes drilled into a diorite are averaged to obtain the accepted heat flux. After correction for topography, the temperature gradients are very similar. The 16% difference in heat flux between these two holes, mainly due to the difference between average thermal conductivities, suggests refractive effects.

The results from the six sites described above are the most reliable heat flux data for the basin (Fig. 1). The measured results are accurate to 5%, and probably represent the equilibrium crustal heat flux at the sites well, with the possible exception of Cinola. The lower heat flux at Cinola is consistent with a small downward component of water flow. A previously published low heat flux from a series of boreholes collared on a steep hillside at Tasu underlain by limestone (Hyndman et al., 1982), is less reliable.

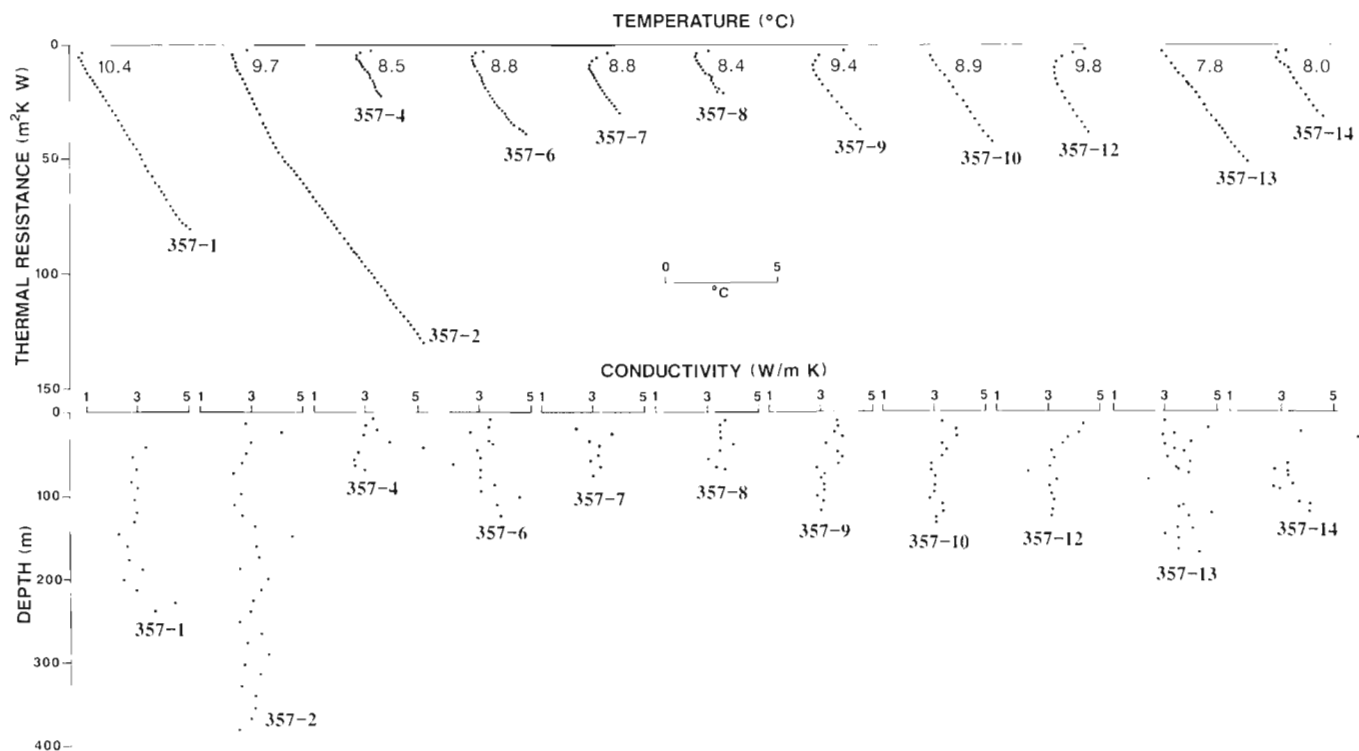


**Figure 18:** Plots as in Figure 17 for Banks Island (357).

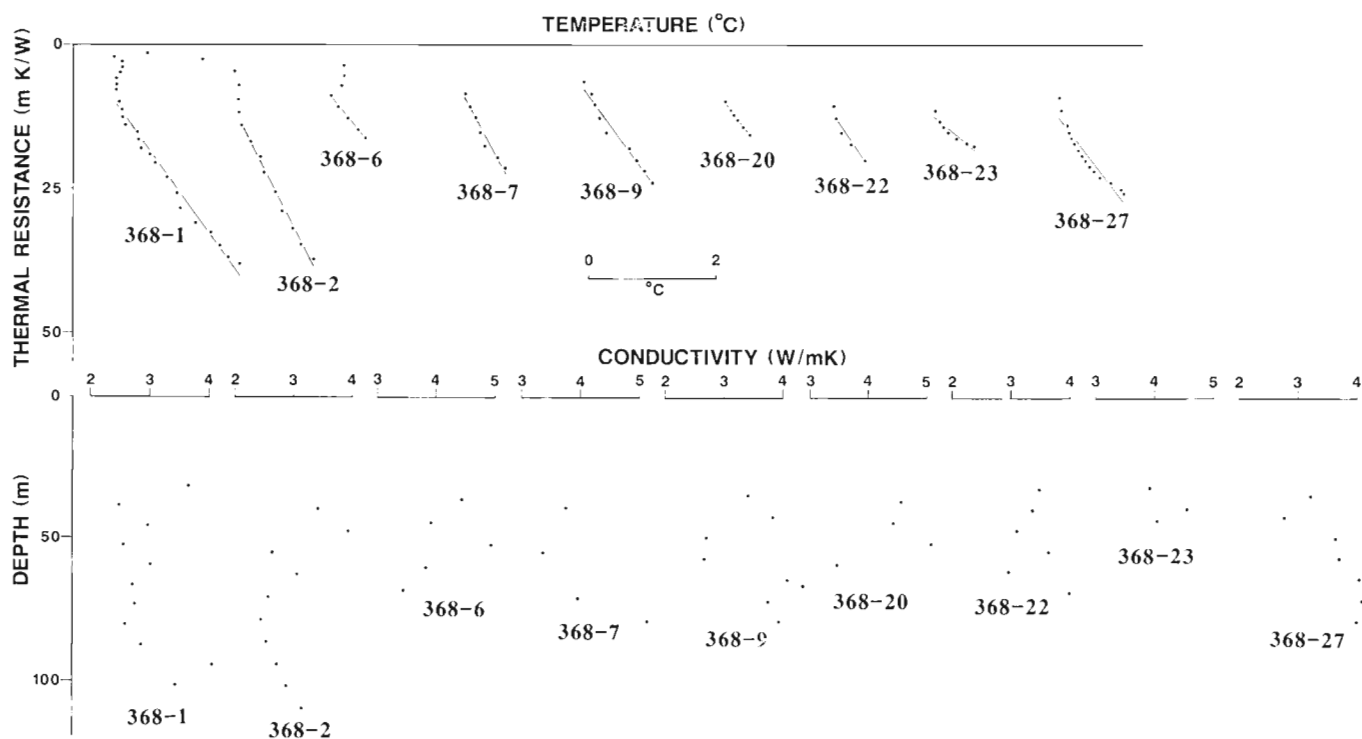


**Figure 19:** Relative temperature vs thermal resistance (Bullard plots) and thermal conductivity as a function of depth for Cinola (368).

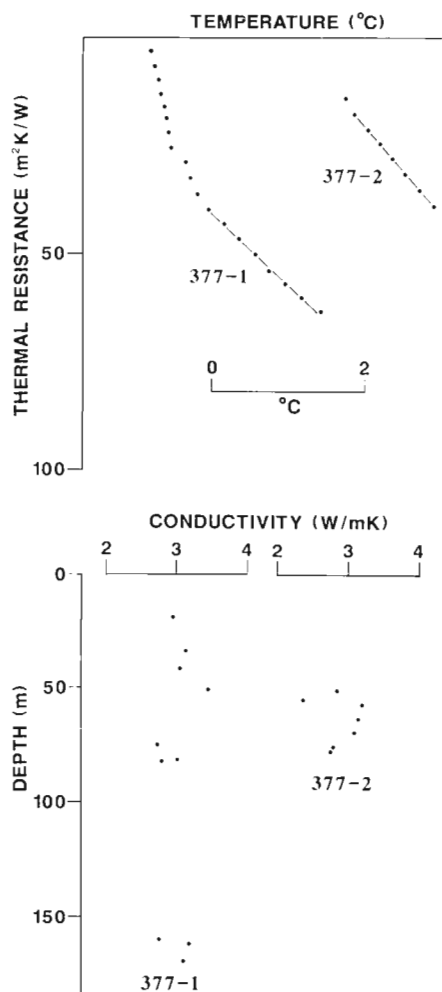


**Figure 20:** Plots as in Figure 19 for Lyell Island (377).

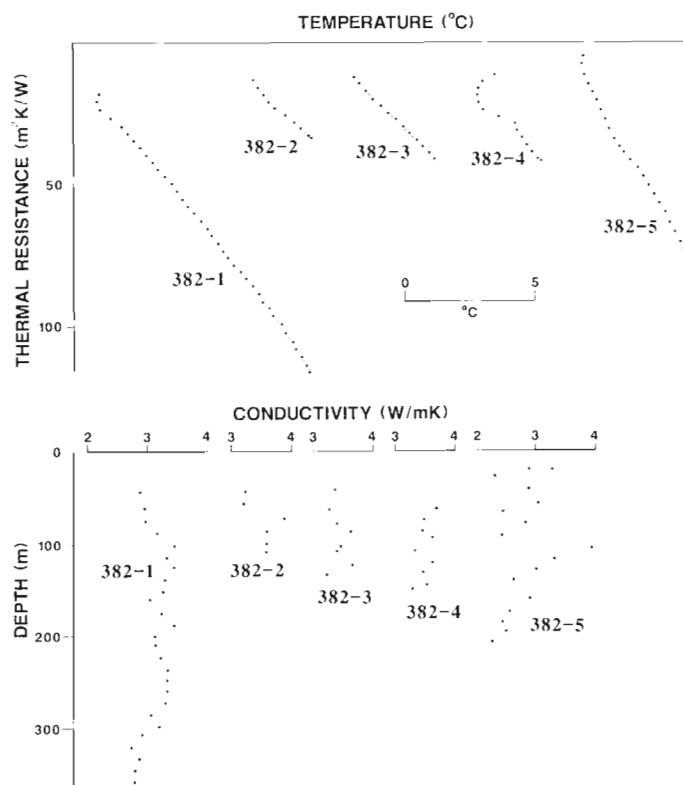


**Figure 21:** Plots as in Figure 19 for Porcher Island (382).

**Table 5: Average Heat Generation**

Series	Site/Suite	n	A W/m <sup>3</sup>	S.D. W/m <sup>3</sup>
<b>Western Margin</b>				
200148	Sandspit	4	0.42	0.01
200149	Central Kano Pluton	4	0.64	0.02
200149	Shields Bay, pluton on North side	4	1.64	0.90
200149	Dykes north of Central Kano pluton	3	0.17	0.04
200149	Dykes along Phantom Creek	2	1.68	0.62
200150	Langara Island	9	1.03	0.26
200150	Pivot Mountain	8	0.29	0.05
300149	San Christoval	1	0.48	
300149	Burnaby Island	4	0.67	0.41
300149	Carpenter Bay	2	1.22	1.29
	coeval dykes	4	0.66	0.51
200144	Haida sandstone, surficial samples	2	0.84	0.03
300136*	Masset volcanics	29	0.33	0.23
200154	Hot Springs Island altered samples	3	0.34	0.17
200158	Nahwitti Batholith, N. Van. Is.	10	0.77	0.30
200158	Hope-Nigei Is. Intrusive, N. Van. Is.	4	0.51	0.10
<b>Offshore Wells</b>				
300104*	Tyee:			
	215-560 m	3	0.42	0.04
	720-2190 m	13	0.80	0.12
	2240-3305 m	17	1.15	0.13
	3363-3421 m	2	0.66	0.26
300115*	Harlequin: 400-3160 m	12	1.00	0.13
	below 3200 m	1	0.31	0.00
<b>Eastern Margin Granitic and/or Highly Metamorphosed Rocks</b>				
315-1	Denny Island, quartz feldspar p'phy	13	2.75	0.86
315-2	Denny Island, granite	23	1.91	0.49
200107*	Late Tertiary quartz feldspar p'phy opposite King Island	2	3.33	0.17
200107*	Cretaceous/Tertiary quartz monzonite east of King Island	7	0.54	0.04
300037*	King Island syenite, Miocene	12	1.18	0.46
200031*	King Island syenite, Miocene	4	0.94	0.14
300037*	Coast Plutonic Complex SW of King Island	4	2.00	0.38
200031*	Coast Plutonic Complex of SW King Island	5	0.98	0.37
200031*	Coast Plutonic Complex in Dean Channel	5	0.99	0.23
200031*	Douglas Channel	8	0.52	0.16
200031*	Whale Channel	5	0.60	0.22
300037*	South Bentinck Arm	7	1.19	0.40
300037*	Douglas Channel	28	0.91	0.57
357*	Banks Island, quartz monzonite	2	0.81	0.00
382	Porcher island, granodiorite	24	0.83	0.22
300152	Ecstall Pluton	12	0.55	0.19
300152	Quotoon Pluton	2	0.68	0.03
300152	Kasiks Pluton	4	0.51	0.19
300152	Early Tertiary Ponder and others	10	1.84	0.76
300037*	Portland Inlet	15	0.97	0.56
200031*	Portland Inlet, near Truro Island	5	0.84	0.28
300037*	Pirate pluton, Portland Inlet	3	4.04	0.16
300037*	southern Observatory Inlet	8	1.05	0.70
300037*	northern Observatory Inlet	13	1.70	1.10
200031*	Alice Arm and nearby Observatory Inlet	12	2.75	1.37
300037*	southern Hastings Arm	10	2.53	1.80
300037*	northern Hastings Arm	13	1.95	0.51
300037*	lower Portland Canal	11	2.25	1.00
300037*	upper Portland Canal	19	1.65	0.31
200145	Early Tertiary qt monzo. near Stewart	14	2.61	1.45
200146	Triassic-Jurassic gneiss. N. of Hyder	6	1.58	0.17

\*Individual values published by Lewis and Bentkowski (1988).

## HEAT GENERATION AND HOT SPRINGS

The heat generation of sediments within a deep basin can influence basin temperatures by 10-20 K (e.g., Keen and Lewis, 1982). Since Queen Charlotte Basin is shallow (approximately 4 km maximum depth), its influence on basin temperatures is less important, but it has a large effect on deeper temperatures beneath and adjacent to the basin. Extensive measurements of the heat generation from basin sediments as well as from magmatic rocks exposed on basin margins (Fig. 22) are summarized in Table 5. Passive gamma-ray spectrometry was used as originally described by Lewis (1974), with the change to a constant sample mass allowing the assumption of constant self-absorption.

Heat generation measured on cuttings from the Harlequin and Tyee offshore wells averages  $0.97 \mu\text{W m}^{-3}$ . All heat generation values assume a standard density of  $2.67 \text{ g/cm}^3$ , which must be modified significantly for sediments to the actual density, a function of compaction and burial history. The radioactive heat generation of basin sediments is expected to be low because the sediments were derived from sources having exceptionally low heat production.

Representative samples from the major magmatic suites on the Queen Charlotte Islands as well as the Masset volcanics generally have very low heat generation, similar to values from northern Vancouver Island. The highest values,  $1.64\text{-}1.68 \mu\text{W m}^{-3}$ , are from a Tertiary pluton sampled near Shields Bay. Such young plutons form a small portion of the total crust.

Heat generation in plutonic rocks of the Coast Plutonic Complex on the east side of the basin is also very low. It is lowest near the mid-latitudes where the highest metamorphic grade rocks have been exhumed. Exceptions to the low values are small, young bodies such as Pirate, King Island, and Denny Island plutons, but they represent an insignificant portion of the exposed granitoid rocks of the Coast Plutonic Complex. Tertiary plutons occurring along the eastern edge of the Coast Plutonic Complex (e.g., Ponder pluton) represent a slightly larger volume. A larger region of the Coast Plutonic Complex near Alice Arm and Portland Canal has an average heat production of  $2.2 \mu\text{W m}^{-3}$ . Heat production in the remainder of the northern Coast Plutonic Complex averages  $0.9 \mu\text{W m}^{-3}$ , just slightly higher than the  $0.8 \mu\text{W m}^{-3}$  average of the southern Coast Plutonic Complex (Lewis, 1976; Lewis and Bentkowski, 1988).

A hot spring located on Hot Springs Island, 20 km southeast of the Lyell Island site, produces an estimated 150 l/min of clear, odourless water at a maximum temperature of  $80^\circ\text{C}$ . The source of the hot water could be either relatively deep circulation or a local heat source. The maximum elevation of approximately 50 m on this small island limits the available hydraulic head unless the source of the water is on a different, distant island. The simple  $\text{SiO}_2$  and Na-K-Ca geothermometers indicate equilibrium temperatures of  $145$  and  $169^\circ\text{C}$ , respectively (Souther, 1976). Oxygen 18/16 and deuterium/hydrogen isotopic ratios are consistent with meteoric water and indicate no apparent shift due to thermal rock-water exchange. Therefore, this water is probably coming from deep circulation down to depths of 5 km, and is not coming from dehydration of subducted oceanic crust beneath the basin.



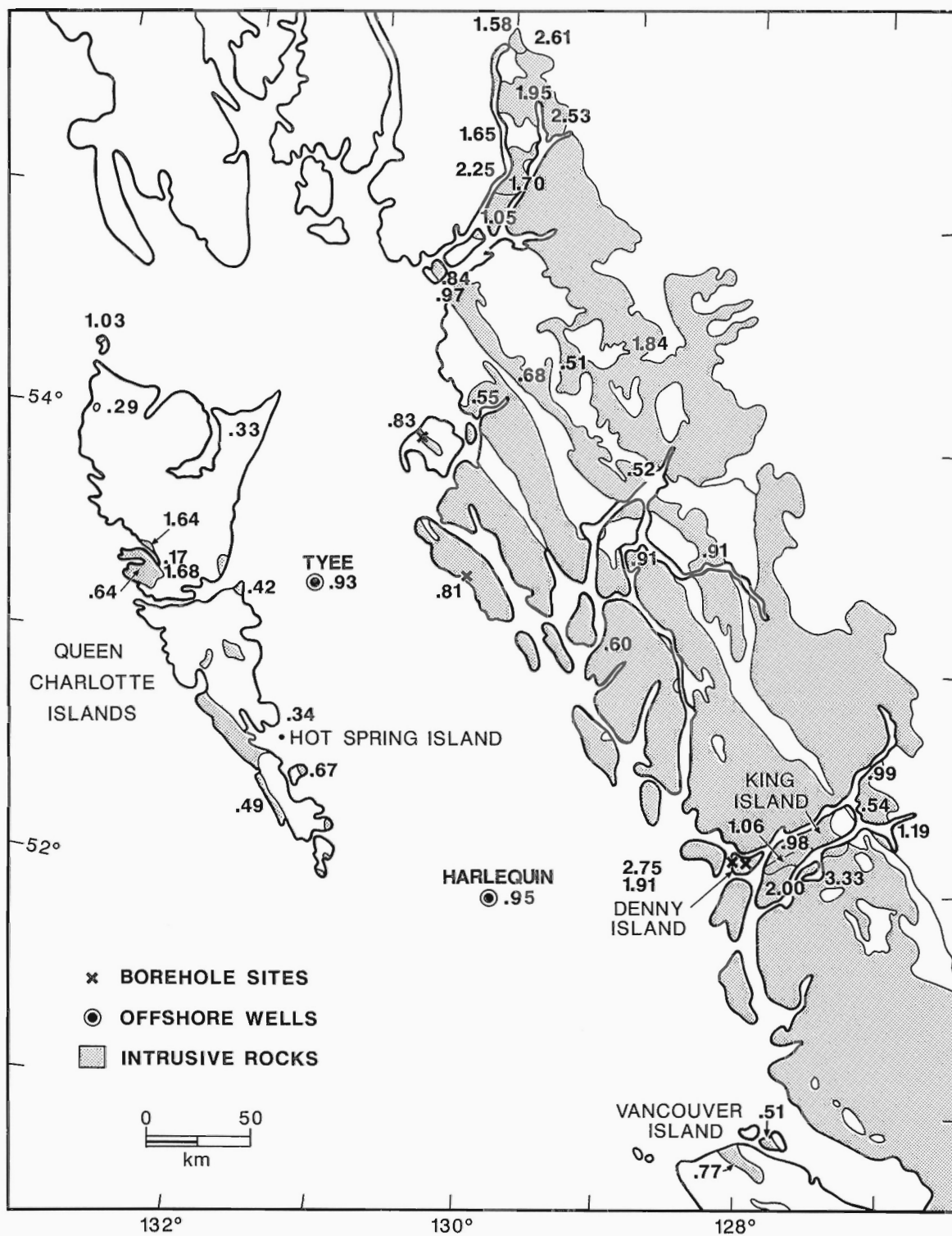


Figure 22: Distribution of heat generation samples and average values in  $\mu\text{W}/\text{m}^3$ .

## DISCUSSION

The cause of the large uncertainty in the marine probe results was the effect of BWT variations. A correlation of large, sudden decreases in BWTs with strong winds, possibly causing upwelling of colder oceanic water onto the shelf, was not observed. The four BWT recorder stations were widely scattered in location and depth, and coincidental changes were not found. The water is warmer in the winter time, suggesting that the colder water may be coming from continental run-off. In order to have quick changes in temperature, large volumes of water must move, suggesting strong currents. Mega-ripples at 130 m depths (Fig. 23) and sand waves at 400 m depths provide further evidence of such currents.

Preferential water flow along a more permeable layer is consistent with many basin models. Since the variation of permeability along formations is much less than the variation between formations, water tends

to flow along the formations across basins. This enhances the heat flow towards the edge of the basins where formations are thinning if fluids are flowing outwards. This explanation is proposed for the relatively higher heat flux observed around the edges of many basins (Reiter and Jessop, 1985; Moir and Whiddon, 1989).

Material was deposited in Queen Charlotte basin at the end of the last glacial period, forming banks with a sandy layer on top. At present, fluids may be preferentially flowing along the sandy layer, and even escaping where an overlying, less permeable, more recent layer is thinnest. Such water flows would control the temperature of the aquifer and the conductive heat flux above it. Locally, water flow along the sandy layer could vary over periods of a few years, dependent on whether or not processes of slumping and erosion had sealed it off at the nearest outcrops a few kilometres distant. The expected temperature perturbations propagating downward by conduction

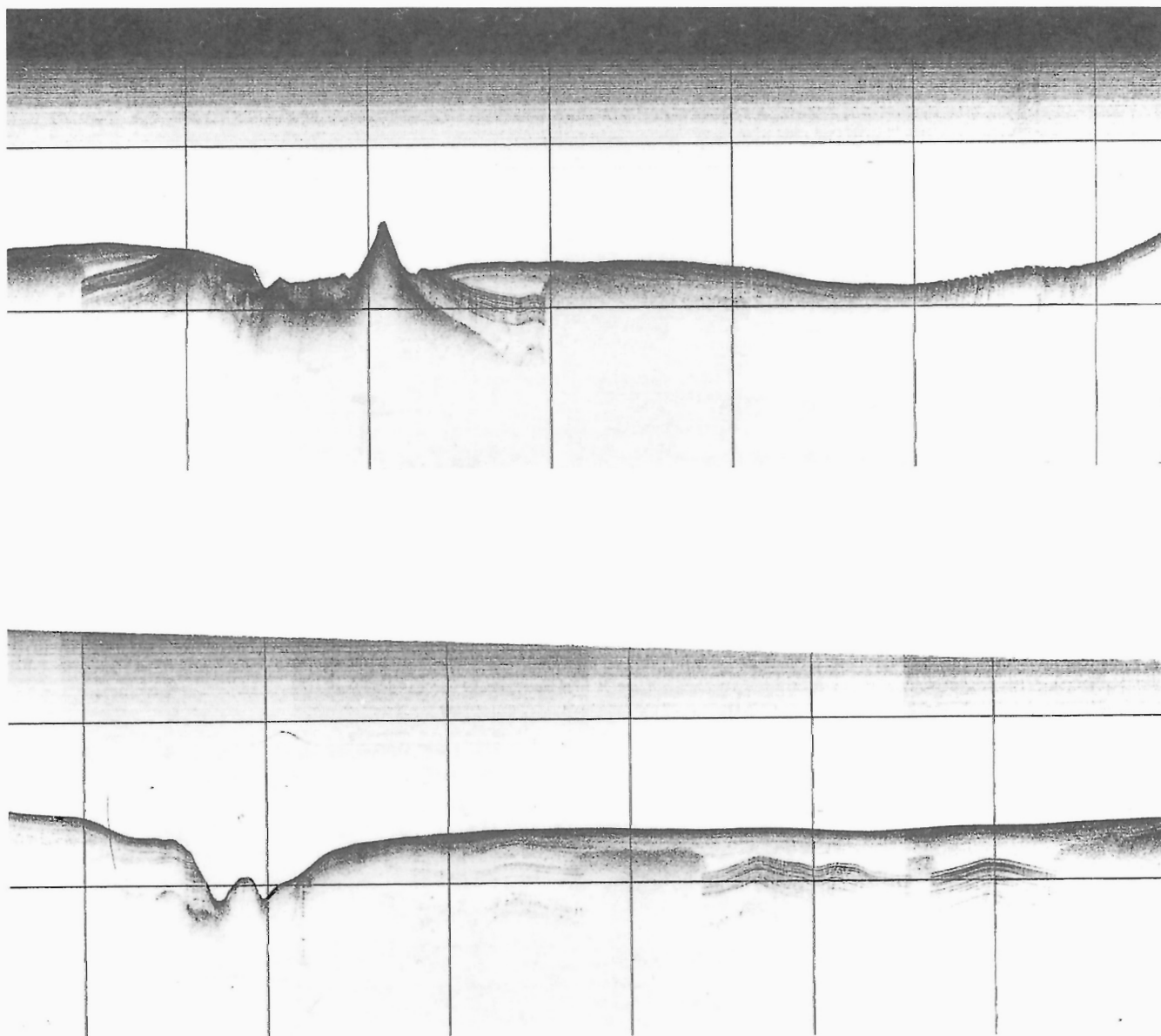


**Figure 23:** A 3.5 kHz seismic profile showing shallow gas in soft bottom sediments cut by erosion channels, bedrock outcrop and mega ripples near the right end. The profile was obtained in water depths of 110-160 m near Juan Perez Sound. Grid squares represent 75 m (vertical) by 1850 (horizontal), giving a vertical exaggeration of 20. The right half of the profile is on the top; the left half on the bottom.

from the sediment-water interface are not as large as expected for many sites, and totally absent in the shallow sediments above the sandy layer at the Goose Island Trough sites. Maybe small, upward water flows leaking from a sandy layer or layers are affecting temperatures at other sites as well.

The lack of response in this uppermost layer to seasonal variations in BWT (Fig. 14), may indicate that sufficient water is flowing upwards through the layer, to overcome the normal conductive regime. If a steady water flow through an isotropic, homogeneous layer is assumed (Bredehoeft and Papadopoulos, 1965), the upper four temperature observations indicate an upward fluid velocity of  $10^{-7}$  m/s. However, the upper sensor is more likely to be in water or in an atypical surface sediment, and the temperature gradient in the rest of the uppermost layer is more likely to be linear. Small variations in the temperature gradient immediately below the sandy layer may be caused by temperature changes in the water flowing along the layer, and indicate a conductive regime beneath this layer. Since the temperature of water flowing along such a sandy layer is less subject to changes in BWT, the measured heat flux beneath the sandy layer at these sites is probably representative of the equilibrium basin heat flux. Conversely, measurements within the surface layer, even if corrected for advective flow, may not reflect the equilibrium basin heat flux.

At other sites where the shallow temperatures are not as perturbed as expected, either there are small upward fluid fluxes, or some boundary layer or surface process may be acting as a filter. The upper sensor's temperature decay after the heat pulse at many sites in shallow, soft sediments is abnormally long. In all probes this is only observed for the upper sensor.

The few thermal conductivity measurements associated with the marine probe sites limit the accuracy of the measured heat flux to 10%. Although sites at which there are abnormal variations of heat flux with depth were discarded, yet still 4 of the 7 accepted values (Table 2) are exceptionally high compared to other data (Fig. 1). The Moresby south site is probably affected by refraction. The high heat flux at the other three sites (Milbanke, Caamaño South and Caamaño North), may indicate small, undetected upward fluid fluxes.

Heat fluxes determined in hydrocarbon exploration wells have an accuracy of only 20%, yet all but one of the values are within 20% of  $70 \text{ mW/m}^2$ . Estimates of the thermal conductivities had to be used instead of the results of measurements on cuttings. The grain thermal conductivity should be between 3.3 and  $4.0 \text{ W/m K}$ , giving a median heat flux between 68 and  $78 \text{ mW/m}^2$ . The two wells drilled on a structure, Sockeye B-10 and E-66, have the highest heat flux. It is impossible to detect water flow, one of the possible causes of heat flux variations, without more and better temperature data from the individual wells.

Heat flux from the cored boreholes is most accurately measured, and with the possible exception of the Cinola heat flux, appears to represent the regional heat flux to an accuracy of 5%. Water flow at the Cinola site may systematically lower the measured values slightly, as already discussed. The less accurately determined heat fluxes from wells, and to a lesser extent the marine probes, are generally consistent with these values (Fig. 24). The measured heat flux within Queen Charlotte Basin shows no clear systematic regional pattern, (Fig. 1) if the marine measurements which may be affected by surficial processes are omitted. Although the heat flux at two of the Queen Charlotte Sound wells is higher than the regional mean, it is within the range of uncertainty. The entire basin can be described as having a heat flux of  $70 \pm 6 \text{ mW m}^{-2}$ .

Although an increase in heat flux to the north of the basin would be consistent with the northward progression of plutonism, it is not

clearly seen. Nor is an enhanced heat flux caused by the supposed Anahim hotspot trace. Smaller hot spot traces are not marked by wide, long-lived paths because of the smaller material flux in the mantle (N. Sleep, pers. comm., 1989), and might not be noticed in this basin because of the high background heat flux.

The lithosphere beneath Queen Charlotte basin and its margins appears to have undergone subduction until approximately 42 Ma when subduction ceased. The cool crust and underthrust oceanic lithosphere was reheated then, resulting in uplift and erosion. The Queen Charlotte Basin probably formed subsequently by extension in a dominantly strike-slip environment. The initial extension associated with the formation of the basin would have thinned the crust, producing higher crustal temperatures and magmatism. Simple models of extension or dyke intrusion (McKenzie, 1978; Royden et al., 1980), predict the present heat flux 20-40 Ma after basin formation (Fig. 25) if average basin extensions are greater than 30%. Such models are also consistent with the much higher heat flux earlier in the basin history implied by vitrinite reflectance data (e.g., Yorath and Hyndman, 1983). Marginal basins formed by different processes without extension cannot easily generate the present high heat flux nor the inferred, higher paleo-heat flux (Yorath and Hyndman, 1983; Vellutini and Bustin, 1988). Large amounts of basin-wide erosion are not likely to have oc-

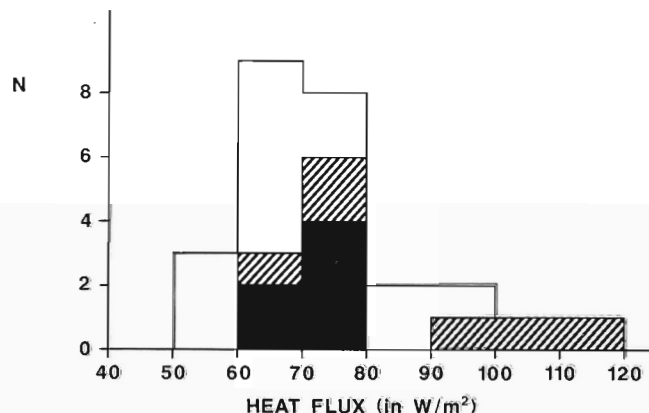


**Figure 24:** Histogram of heat flux values with the most reliable results from cored boreholes shown by solid bars, and marine probe results by shaded bars.

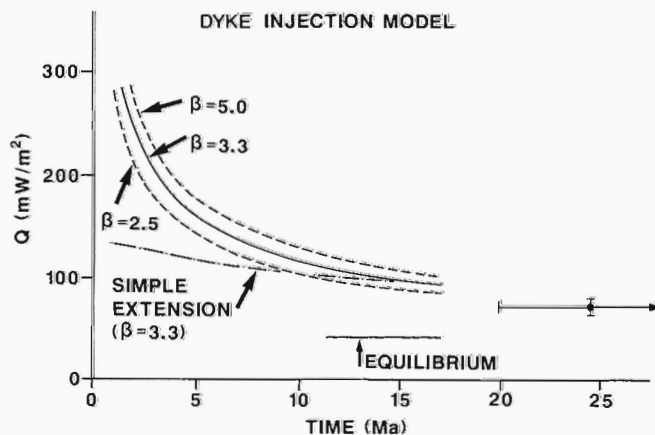


**Figure 25:** Heat flux as a function of time since basin formation by simple models of extension and dyke emplacement; the present heat flux is shown near 25 Ma

curred. The oblique subduction of young, oceanic lithosphere beneath the Queen Charlotte Islands since 4 or 5 Ma (Yorath and Hyndman, 1983; Engebretson, 1989), may be the cause of a low heat flux on the western side of the basin, affecting the Tasu and Cinola sites, as well as the southwest part of the basin (Fig. 1). Although measurement accuracy at these locations is not high enough to support such a conclusion, it is consistent with it. The heat flux measured offshore (Hyndman et al., 1982) clearly decreases towards the west coast of Moresby Island.

The high heat flux within the basin is much more significant when combined with low heat generation: it indicates a very high heat flux into the lower crust and high crustal temperatures. The 450°C isotherm is estimated to be at a depth of 13 km where there are thick sediments, and 14 km under the margins, assuming a constant heat flow with time. This is consistent with the maximum depth of earthquakes within the basin being less than 20 km (Bérubé et al., 1989; G.C. Rogers, pers. comm., 1989). This is quite different from central and southern Vancouver Island and the western Coast Plutonic Complex to the south (Lewis et al., 1988b), where the crust is cool and thick. Heat flux here averages approximately 40 mW m<sup>-2</sup>. The northern part of Vancouver Island above the Explorer plate may represent the transition state, with relatively subdued topography, lower average elevation and above normal heat flux.

The crystalline crust exposed on the margins of Queen Charlotte basin and lying beneath it as well, has an average heat generation of less than 0.9 µW m<sup>-3</sup>, very low compared to most other Cenozoic crust, but comparable to the crust of Vancouver Island to the southwest. The heat flux in the lower crust and the crustal temperatures beneath Queen Charlotte Basin are the same as those under many basins having a higher surficial heat flux. If the heat generation in the crust beneath and bordering Queen Charlotte basin were a more typical value, such as 2 µW m<sup>-3</sup>, then the observed heat flux would be 12 mW/m<sup>2</sup> greater, and crustal temperatures would be higher, e.g., 30 K more at the base of a 5 km section of sediments. Possibly the crystalline basement beneath the northern part of the basin does have a higher heat generation, similar to parts of the nearby Coast Plutonic Complex, increasing the heat flux by 10 mW/m<sup>2</sup>.

## SUMMARY

A concerted effort was made to define the thermal regime of the Queen Charlotte Basin using data from marine probes, from offshore and onshore hydrocarbon exploration wells, and from cored mineral exploration boreholes on land. However, measuring the equilibrium heat flux within most offshore basins is very difficult, whether using wells or marine probe measurements. Estimation of the thermal conductivity of drill cuttings from wells proved particularly difficult, and it was concluded that the laboratory measurements were unreliable. It is hard to saturate fine-grained cuttings with water without leaving some air trapped in them, and our measured results were inconsistent with the quartz content of the cuttings. Estimated values based on the porosity and the quartz and other mineral content were used to calculate the heat flux. The inherent inaccuracy of BHTs (bottom hole temperatures) also limits the accuracy of the heat flow determinations in wells. The final values from the wells have an estimated uncertainty of 20%.

The maximum water depth of Queen Charlotte Basin is 450 m, much less than the depth (800 m for this region) at which BWTs are found to be constant in time. Records of past BWTs, *in situ* thermal conductivity measurements, and temperature gradients measured by long probes in soft sediments at depths greater than 7 m were sufficient to determine the heat flux. The heat flux within the soft sediments was found to be influenced by water flow within a widespread, Pleis-

tocene sandy layer. Data from probe penetrations of this layer showed the heat flux above the layer could be much higher than that below it. High heat flux measured above this layer at locations where it was not penetrated might be caused by water flow. Heat fluxes below the layer appeared to be equilibrium values.

The recorded BWT variations show that large volumes of bottom water move quite quickly, over times of a day or two. The 3.5 kHz sounding profiles revealed sand waves at a depth of 400 m and mega ripples at depths greater than 100 m, additional proof of large bottom currents. The large changes in BWT cannot be obviously correlated with times of high winds nor low atmospheric pressures. The bottom waters were warmer in the winter than the summer, indicating that a possible source of the cooler water is cold run-off water in the winter and spring seasons.

The present average heat flux in the Queen Charlotte basin, 70 mW m<sup>-2</sup>, is best determined by boreholes in crystalline rocks on the margins of the basin. Less reliable data from basin wells and some of the marine heat flow probe support this value. The heat generation in the crustal rocks beneath and in the basin, represented by rocks from the margin and the offshore wells, is low. Therefore, present temperatures in the crystalline rock beneath the basin are high: about 450°C at 14 km. High crustal temperatures limit the maximum depth of earthquakes beneath the basin to less than 20 km.

The heat flux, 70 mW m<sup>-2</sup>, is consistent with simple extensional models of basin formation starting between 20 and 40 Ma. However, the amount of extension required is large. Formation of this basin was complex, starting from a margin recovering from the effects of subduction. At present oblique subduction and/or uplift and erosion may be occurring along the western margin.

## ACKNOWLEDGMENTS

We gratefully acknowledge the help and cooperation of City Resources (Canada) Ltd., Imperial Metals Corp., Placer Development Ltd., and Trader Resource Corp. with measurements in mineral exploration boreholes. We thank the officers and crews of CSS PARIZEAU and CFAV ENDEAVOUR for their skilful assistance in acquiring the marine data, as well as R. Allis, V. Cermak, D. Chapman, T. Hamilton, D. Tempelman-Kluit, K. Wang and C. Yorath. M. Bone, R. MacDonald, G. Jewsbury and J. Everard are thanked for technical support. We also thank R.G. Anderson and G.J. Woodsworth for supplying samples for heat generation measurements, J. Welhan of Memorial University for isotopic analysis of the spring waters, and A. Wilkinson, J. Baker and F. Harvey-Kelly for thermal conductivity measurements, and L. Bedard for draughting services. This manuscript benefited from reviews provided by R.D. Hyndman and R.I. Thompson.

## REFERENCES

- Anderson, R.G. and Greig, C.J.  
1989: Jurassic and Tertiary plutonism in the Queen Charlotte Islands, British Columbia; in *Current Research, Part H*, Geological Survey of Canada, Paper 89-1H, p. 95-104.
- Anderson, R.G. and Reichenbach, I.  
1989: A note on the geochronometry of Late Jurassic and Tertiary plutonism in the Queen Charlotte Islands, British Columbia; in *Current Research, Part H*, Geological Survey of Canada, Paper 89-1H, p. 105-112.
- Andrews-Speed, C.P., Oxburgh, E.R., and Cooper, B.A.  
1984: Temperature and depth-dependent heat flow in Western North Sea; *The American Association of Petroleum Geologists*, v. 68, p. 1764-1781.
- Bérubé, J., Rogers, G.C., Ellis, R.M., and Hasselgren, E.O.  
1989: A microseismicity study of the Queen Charlotte Islands region; *Canadian Journal of Earth Sciences*, v. 26, p. 2556-2566.
- Bevier, M.L., Armstrong, R.L., and Souther, J.G.  
1979: Miocene peralkaline volcanism in west-central British Columbia – its temporal and plate-tectonics setting; *Geology*, v. 7, p. 389-392.

**Bredehoeft, J.D. and Papadopoulos, I.S.**

**1965:** Rates of vertical groundwater movement estimated from the earth's thermal profile; *Water Resources Research*, v. 1, p. 325-328.

**Conway, K.W. and Luternauer, J.L.**

**1985:** Evidence of ice rafting and tractive transfer in cores from Queen Charlotte Sound, British Columbia; *in* Current Research, Part A, Geological Survey of Canada, Paper 85-1A, p. 703-708.

**Della Vedova, B. and Von Herzen, R.P.**

**1987:** Geothermal heat flux at the Cost B-2 and B-3 wells, U.S. Atlantic continental margin; Woods Hole Oceanographic Institution Technical Report 87-28, 80 p.

**Engebretson, D.C.**

**1989:** Northeast Pacific-North America plate kinematics since 70 Ma; Abstract, Geological Association of Canada Pacific Section symposium, Northeast Pacific-North America Plate Interactions Throughout the Cenozoic.

**Garvin, G.**

**1989:** A hydrogeological model for the formation of the giant oil sands deposits of the Western Canada sedimentary basin; *American Journal of Science*, v. 289, p. 105-166.

**Hamilton, T.S.**

**1989:** Tertiary extensional volcanism and volcanotectonic interactions along the Queen Charlotte portion of the western Canadian continental margin; Abstract, Geological Association of Canada Pacific Section symposium, Northeast Pacific-North America Plate Interactions Throughout the Cenozoic.

**Higgs, R. (Compiler)**

**1988:** Some aspects of the petroleum geology of the Queen Charlotte Islands; Canadian Society of Petroleum Geologists' Field Guide to Sequences, Stratigraphy, Sedimentology: Surface and Subsurface Technical Meeting, September 14-16, 1988, Calgary, Alberta, 72 p.

**1989:** Sedimentological studies in Queen Charlotte Basin: implications for basin origin and petroleum exploration; Abstract, Geological Association of Canada Pacific Section symposium, Northeast Pacific-North America Plate Interactions Throughout the Cenozoic.

**Hitchon, B.**

**1984:** Geothermal gradients, hydrodynamics, and hydrocarbon occurrences, Alberta, Canada; *American Association of Petroleum Geologists Bulletin*, v. 68, p. 713-743.

**Hyndman, R.D., Davis, E.E., and Wright, J.A.**

**1979:** The measurement of marine geothermal heat flow by a multipenetration probe with digital acoustic telemetry and *in situ* thermal conductivity; *Marine Geophysical Research*, v. 4, p. 181-205.

**Hyndman, R.D., Lewis, T.J., Wright, J.A., Burgess, M.M., Chapman, D.S., and Yamano, M.**

**1982:** Queen Charlotte Fault Zone-heat flow measurements; *Canadian Journal of Earth Sciences*, v. 19, p. 1657-1669.

**Jones, F.W., Majorowicz, J.A., Linville, A., and Osadetz, K.G.**

**1986:** The relationship of hydrocarbon occurrences to geothermal gradients and time-temperature indices in Mesozoic formations of southern Alberta; *Bulletin of Canadian Petroleum Geology*, v. 34, p. 226-239.

**Keen, C.E. and Lewis, T.J.**

**1982:** Radiogenic heat production in sediments from the continental margin of eastern North America: implications for hydrocarbon generation; *American Association of Petroleum Geologists Bulletin*, v. 66, p. 1402-1407.

**Lewis, T.J.**

**1974:** Heat production measurement in rocks using a gamma-ray spectrometer with a solid state detector; *Canadian Journal of Earth Sciences*, v. 11, p. 526-532.

**1976:** Heat generation in the Coast Range Complex and other areas of British Columbia; *Canadian Journal of Earth Sciences*, v. 13, p. 1634-1642.

**1983:** Bottom water temperature variations as observed, and as recorded in the bottom sediments, Alice Arm and Douglas Channel, British Columbia; Canadian Technical Report on Hydrography and Ocean Sciences, v. 18, p. 138-161.

**Lewis, T.J. and Bentkowski, W.H.**

**1988:** Potassium, Uranium and Thorium concentrations of crustal rocks: A data file; Geological Survey of Canada Open File, v. 1744, 100 p.

**Lewis, T.J., Bentkowski, W.H., Bone, M., Macdonald, R., and Wright, J.A.**

**1988a:** Geothermal studies in Queen Charlotte Basin, British Columbia; *in* Current Research, Part E, Geological Survey of Canada Paper, Paper 88-1E, p. 247-249.

**Lewis, T.J., Bentkowski, W.H., Davis, E.E., Hyndman, J.G., Souther, J.G., and Wright, J.A.**

**1988b:** Subduction of the Juan de Fuca Plate: thermal consequences; *Journal of Geophysical Research*, v. 93, p. 15,207-15,225.

**Lewis, T.J., Bentkowski, W.H., Bone, M. and Wright, J.A.**

**1989:** Note on the thermal structure of Queen Charlotte Basin, British Columbia; *in* Current Research, Part H, Geological Survey of Canada, Paper 89-1H, p. 121-125.

**Luternauer, J.L. and Murray, J.W.**

**1983:** Late Quaternary morphological development and sedimentation, central British Columbia continental shelf; Geological Survey of Canada, Paper 83-21, p. 1-19.

**Luternauer, J.L., Conway, K.W., Clague, J.J., and Blaise, B.**

**1989:** Late Quaternary geology and geochronology of the central continental shelf of western Canada; *Marine Geology*, v. 89, p. 57-68.

**McGee, H.W., Meyer, H.J., and Pringle, T.R.**

**1989:** Shallow geothermal anomalies overlying deeper oil and gas deposits in Rocky Mountain region; *American Association of Petroleum Geologists Bulletin*, v. 73, p. 576-597.

**McKenzie, D.P.**

**1978:** Some remarks on the development of sedimentary basins; *Earth and Planetary Science Letters*, v. 40, p. 25-32.

**Majorowicz, J.A. and Jessop, A.M.**

**1981:** Regional heat flow patterns in the Western Canadian Sedimentary Basin; *Tectonophysics*, v. 74, p. 209-238.

**Moir, P.N. and Whiddon, J.A.**

**1989:** The geothermal regime of the Grand Banks, offshore eastern Canada, from exploration well measurements; Geological Survey of Canada, Forum '89, Program and Abstracts, p. 16-17.

**Reiter, M. and Jessop, A.M.**

**1985:** Estimates of terrestrial heat flow in offshore eastern Canada; *Canadian Journal of Earth Sciences*, v. 22, p. 1503-1517.

**Riddiough, R.P.**

**1982:** One hundred million years of plate tectonics in western Canada; *Geoscience Canada*, v. 9, p. 28-34.

**1984:** Recent movements of the Juan de Fuca plate system; *Journal of Geophysical Research*, v. 89, p. 6980-6994.

**Royden, L., Sclater, J.G., and von Herzen, R.P.**

**1980:** Continental margin subsidence and heat flow: important parameters in formation of petroleum hydrocarbons; *American Association of Petroleum Geologists Bulletin*, v. 64, p. 173-187.

**Sass, J.H., Lachenbruch, A.H., and Munroe, R.J.**

**1971:** Thermal conductivity of rocks from measurements on fragments and its application to heat flow determinations; *Journal of Geophysical Research*, v. 76, p. 3391-3401.

**Souther, J.G.**

**1976:** Geothermal potential of Western Canada; Proceedings of Second United Nations Symposium on the Development and Use of Geothermal Resources, v. 1, p. 259-267, U.S. Government Printing Office, Washington, D.C. 20402.

**1986:** The western Anahim Belt: root zone of a peralkaline magma system; *Canadian Journal of Earth Sciences*, v. 23, p. 895-908.

**1989:** Dyke swarms in the Queen Charlotte Islands, British Columbia; *in* Current Research, Part H, Geological Survey of Canada, Paper 89-1H, p. 117-120.

**Stock, J. and Molnar, P.**

**1988:** Uncertainties and implications of the Late Cretaceous and Tertiary position of the North America relative to the Farallon, Kula and Pacific plates; *Tectonics*, v. 7, p. 1339-1384.

**Sutherland Brown, A.**

**1968:** Geology of the Queen Charlotte Islands, British Columbia; British Columbia Department of Mines and Petroleum Resources, Bulletin 54, 226 p.

**Swift, M.G., Stagg, H.M.J., and Falvey, D.A.**

**1988:** Heat flow regime and implications for oil maturation and migration in the offshore Northern Carnarvon Basin; *in* The North West Shelf, Australia, P.G. Purcell and R.R. Purcell (ed.), Proceedings of the North West Shelf Symposium, Perth, 1988, Petroleum Exploration Society of Australia Ltd., p. 539-551.

**Tothe, J.**

**1980:** Cross-formational gravity flow of groundwater, a mechanism of the transport and accumulation of petroleum (generalized hydraulic theory of petroleum migration); *in* Problems of Petroleum Migration, W.M. Roberts, III and C.J. Cordell (ed.), American Association of Petroleum Geologists, Studies in Geology 10, p. 121-167.

**Vellutini, D. and Bustin, R.M.**

**1988:** Preliminary results on organic maturation of the Tertiary Skonun Formation, Queen Charlotte Islands, British Columbia; *in* Current Research, Part E, Geological Survey of Canada, Paper 88-1E, p. 255-258.

**Yorath, C.J. and Hyndman, R.D.**

**1983:** Subsidence and thermal history of Queen Charlotte Basin; *Canadian Journal of Earth Sciences*, v. 20, p. 135-159.



# Surficial geology and geohazards of Queen Charlotte Basin, northwestern Canadian continental shelf, British Columbia

J.V. Barrie<sup>1</sup>, J.L. Luternauer<sup>2</sup> and K.W. Conway<sup>3</sup>

Barrie, J.V., Luternauer, J.L., and Conway, K.W., Surficial geology and geohazards of Queen Charlotte Basin, northwestern Canadian continental shelf, British Columbia; in *Evolution and Hydrocarbon Potential of the Queen Charlotte Basin, British Columbia*, Geological Survey of Canada, Paper 90-10, p. 507-512, 1991.

## Abstract

*The principal shelf areas of the Queen Charlotte Basin are Dixon Entrance, Hecate Strait and Queen Charlotte Sound. The four most extensive geological units overlying bedrock in these areas are: 1) glacial till, deposited primarily in the troughs between banks and considered to be late Wisconsinan in age, 2) glaciomarine mud, deposited in the troughs as ice retreated from the shelf, 3) Queen Charlotte sands and gravels, deposited as sublittoral sand in the south and as outwash in the north during sea level low stands and subsequently reworked during transgressions, and 4) Queen Charlotte muds, deposited within the troughs during the late Wisconsinan and Holocene.*

*The last major sea level fluctuation to affect the shelf was characterized by a relative drop in sea level of 100-105 m soon after deglaciation (15 000-13 000 yrs B.P.) which persisted until 10 500 yrs ago. This was followed by a rapid, possibly step-like, transgression for about 1500 years after which time the sea was near its present level.*

*The present-day shelf is both storm and tide dominated. Sedimentary bedforms are found ubiquitously above 100 m and locally to 350 m water depth. Sediment erosion and transport, as well as shallow marine gas, may be potential hazards to engineering structures on the seabed associated with hydrocarbon development in the area.*

## Résumé

*Les principales zones de plate-forme du bassin de la Reine-Charlotte sont l'entrée Dixon, le détroit d'Hécaté et le détroit de la Reine-Charlotte. Dans ces zones, les quatre unités géologiques les plus étendues reposant sur le socle sont : 1) un till glaciaire, déposé principalement dans les dépressions entre les bancs et datés au Wisconsinien supérieur, 2) une boue glacio-marine, déposée dans les dépressions formées par le retrait d'un glacier de la plate-forme, 3) les sables et graviers de la Reine-Charlotte, déposés sous forme de sable infralittoral dans le sud et de sédiments fluvio-glaciaires dans le nord pendant une période où le niveau de la mer était bas et remaniés par la suite durant des transgressions et 4) les boues de la Reine-Charlotte, déposées dans les dépressions au cours du Wisconsinien supérieur et l'Holocène.*

*La dernière fluctuation importante du niveau de la mer ayant touché la plate-forme a été caractérisée par une chute relative du niveau de la mer de 100 à 105 m, peu de temps après la déglaciation (15 000-13 000 ans B.P.) qui a persisté jusqu'à 10 500 ans. Cette période caractérisée par un bas niveau de la mer a été suivie d'une transgression rapide par étapes qui a duré environ 1500 ans durant laquelle le niveau de la mer s'est rétabli au niveau actuel.*

*La plate-forme actuelle subit les effets des tempêtes et des marées. Les formes sédimentaires sous-marines sont omniprésentes au-dessus de 100 m, mais plus rares jusqu'à 350 m de profondeur. L'érosion et le transport des sédiments ainsi que la présence de gaz à faible profondeur peuvent constituer des dangers pour les ouvrages installés sur le fond marin pour la mise en valeur des hydrocarbures dans la région.*

<sup>1</sup> Pacific Geoscience Centre, Geological Survey of Canada, P.O. 6000, Sidney, B.C. V8L 4B2

<sup>2</sup> Cordilleran Division, Geological Survey of Canada, 100 West Pender Street, Vancouver, B.C. V6B 1R8

<sup>3</sup> Geomartec Services, 1067 Clarke Road, Brentwood Bay, B.C. V0S 1A0



## INTRODUCTION

Systematic geologic surveys of the continental shelf off British Columbia have been carried out since 1981. The purpose of this component of the Queen Charlotte Basin sub-program has been to compile and interpret this data to produce a series of maps (Barrie et al., 1990a, b, c; Luternauer et al., 1990a, b) displaying sediment distribution, distribution of geological units, surficial features and potential geohazards and the sources from which the data were derived. The

maps will help guide both potential industrial development of the region and management of the environment.

A regional high resolution seismic survey program has been conducted over the region with an average line spacing of 9 km (Currie et al., 1983; Luternauer and Murray, 1983; Barrie and Bornhold, 1989; Luternauer et al., 1989a). These data include deep-towed high resolution boomer data, 5-40 cubic inch (82-656 cm<sup>3</sup>) air gun seismic and 50 and 100 kHz sidescan sonar coverage. In addition some

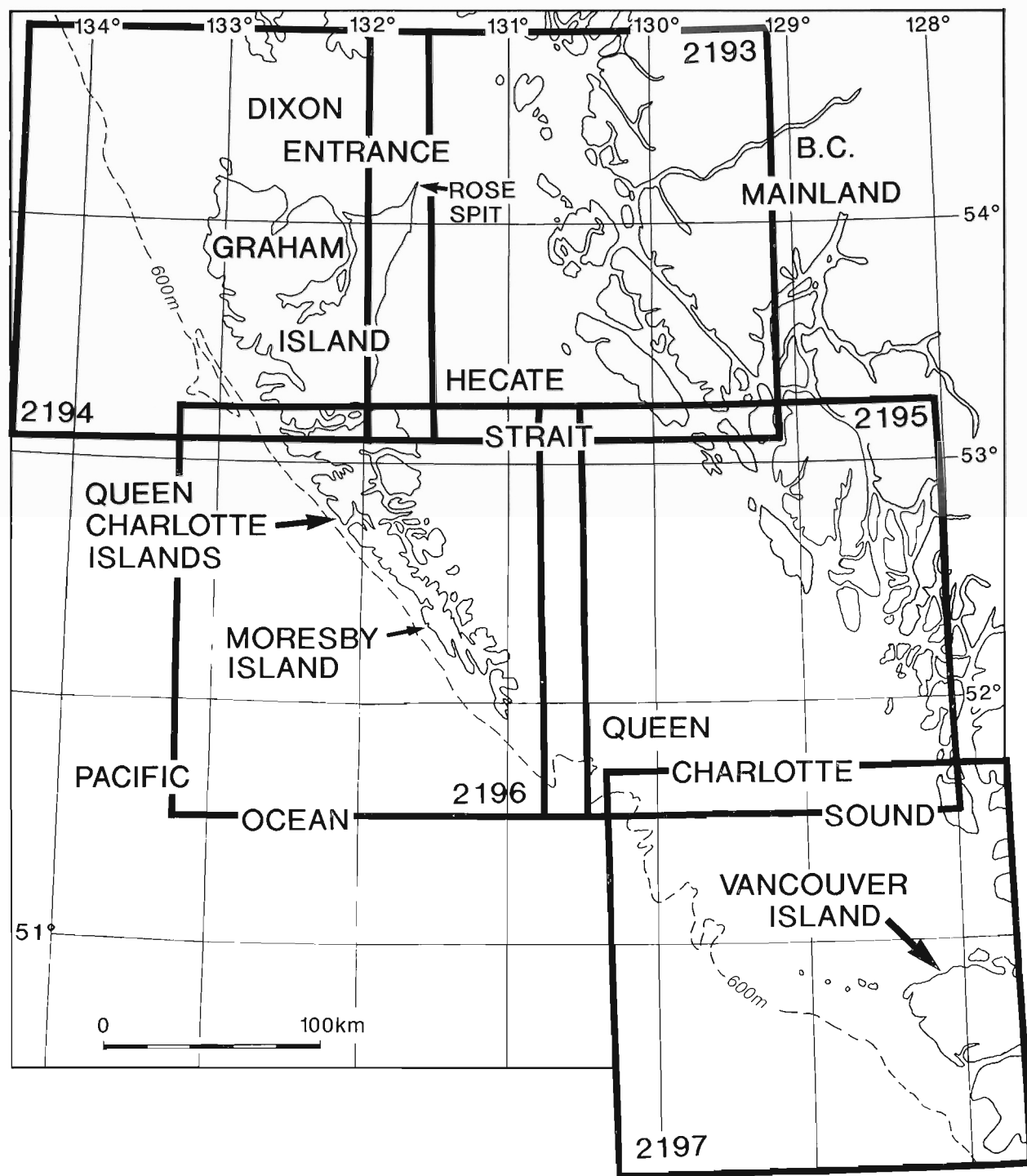


**Figure 1:** Index of geographic areas, northwestern British Columbia. Numbered rectangles indicate location of Geological Survey of Canada open file maps displaying sea bed geology and geohazards of the continental shelf.

48 piston cores and 64 vibrocores collected during this program offer lithologic control for the upper seismostratigraphic sequences.

## REGIONAL SETTING

Dixon Entrance, Hecate Strait and Queen Charlotte Sound (Fig. 1) combine to form a continuous physiographic province known as the Hecate Depression (Holland, 1964). This depression separates the Coast Mountains of the mainland from the Insular Mountains of the Queen Charlotte Islands and Vancouver Island. The sedimentary basin found within the Hecate Depression from Vancouver Island to Dixon Entrance constitutes the Queen Charlotte Basin.

Dixon Entrance, to the north, is an elongated east-west strait that separates the Queen Charlotte Islands and the islands of southern Alaska. Hecate Strait is a shallow, asymmetric channel lying between the Queen Charlotte Islands and the British Columbia mainland. In the northeastern portion of the strait a large trough opens to the south and another, smaller trough to the north, forming a broad, shallow (<40 m) shelf to the northwest and a 30-50 m deep bank in west-central Hecate Strait. At the northwestern boundary are the eroding, low cliffs of northern Graham Island which supply sediment to a large accreting spit (Rose Spit) at the northeasterly tip of the island at the junction with Dixon Entrance (Clague and Bornhold, 1980). Queen Charlotte Sound, to the south, consists of three broad banks as shallow as 30 m separated by intervening troughs, as deep as 500 m, extending to the shelf edge.

## SEA LEVEL HISTORY

Late Wisconsinan glacial-postglacial relative sea level history is complex and varied sharply both across the shelf and from north to south. Upon deglaciation (12,000-10,500 yrs ago) the mainland coast was submerged; sea levels were up to 200 m higher relative to land than at present (Clague et al., 1982a). However, on eastern Vancouver Island there may have been only 175 m of submergence (Howes, 1983). Regression followed along the coast, with relative sea level 9000-6000 yrs ago falling just below the present level.

A paleosol, with *in situ* rooted plant remains, was found in a core collected from the flank of a drowned river valley at a water depth of 95 m in southern Queen Charlotte Sound. The material yielded a radiocarbon age of 10,500 years B.P. (Luternauer et al., 1989b). Fluvial sediments associated with the paleosol are sharply overlain by lagoon-al or shallow pond sediments on which are deposited shallow-marine sediments. Relative sea level, therefore, was at least 95 m lower 10,500 yrs ago and much of the shelf was subaerially exposed. A wave-cut terrace adjacent to the *in situ* paleosol, lying between 100 and 105 m water depth, represents the late Wisconsinan-early Holocene shoreface.

A similar 100 m lowering of sea level also is suspected for Hecate Strait, based on the presence of drainage channels, wave-cut terraces, and both shore-oblique and shore-parallel sand ridges (Barrie and Bornhold, 1989). Terraces occur at depths of 100-105, 40-45, 30-35 and 20-25 m. Another wave-cut terrace extends along central Hecate Strait and changes in depth from 110 m in the north to 160 m in the south. This feature may be associated with earlier Quaternary sea level changes.

Migration and collapse of a crustal forebulge is considered to be the cause of the dramatic Late Quaternary sea level history (Luternauer et al., 1989b). The continental shelf was isostatically depressed when the area was deglaciated 13,000-15,000 yrs B.P.. High relative sea levels are recorded in the area of northeastern Vancouver Island between about 12,000 and 13,000 years B.P. (Howes, 1983). It appears that relative sea level fell soon after deglaciation (due to isostatic rebound). Isostatic uplift in the mainland fiords was accompanied by crustal subsidence of the shelf to the west due to lateral movement of material in the asthenosphere. Sometime prior to 10,500 years B.P. rebound

was virtually complete and shorelines were controlled to a large extent by low eustatic sea levels (Luternauer et al., 1989b).

The progressively shallower wave-cut terraces, particularly in western Hecate Strait, suggest that the transgression was both rapid and occurred in a stepped fashion. Dates from the Queen Charlotte Islands and the mainland coast near Prince Rupert (Clague et al., 1982a,b; Clague, 1985) indicate that the sea was near its present level in Hecate Strait about 9500-9000 years ago. Transgression of the present coast of the northern Queen Charlotte Islands occurred between 8500-7500 yrs B.P. (Clague et al., 1982a) resulting in sea levels 15 m above the present level. Sea level rise, therefore, would have occurred at a minimum rate of 7-10 cm/year over the northern British Columbia continental shelf. The wave-cut terraces suggest that there may have been periods of little or no relative sea level change separated by intervals of rapid, relative sea level rise during the early Holocene. If so, short term rates of sea level rise may have been much higher than the average of 7 cm/year for the entire 1500 yr period.

## OCEANOGRAPHIC SETTING

Erosion and sediment transport are significant agents of sediment redeposition on the present-day western Canadian shelf to depths greater than 100 m (Luternauer, 1986; Barrie and Bornhold, 1989). The pattern of maximum bottom currents is characterized by a prevailing northward current along the eastern and northern side of Hecate Strait, and a southward flow along the southwest portion of the Strait into Queen Charlotte Sound (Crawford et al., 1988; Crawford and Thomson, 1991). In Dixon Entrance an eddy, termed the Rose Spit Eddy, rotates counter-clockwise throughout the entire eastern end of Dixon Entrance (Crawford and Greisman, 1987; Crawford and Thomson, 1991). Mean wave direction also shows alignment with the shelf, the main direction being from the southwest and less frequently from the northwest (Thomson, 1981).

Combined wave and current velocities are capable of transporting fine sand at least 10% of the time at 100 m water depth for the northern shelf areas (Barrie et al., 1988) assuming a critical threshold velocity of 0.25 m/s for a 0.125 mm sediment size and an average tidal current velocity of 0.18 m/s. Northward moving currents in northern Hecate Strait, however, have bottom velocities exceeding 0.6 m/s, with velocities above 0.2 m/s occurring up to 44% of the time (Barrie and Bornhold, 1989) suggesting estimates for critical threshold presented by Barrie et al. (1988) are conservative.

## SURFICIAL GEOLOGY

Four surficial geological units overlying bedrock have been defined for the northern continental shelf of western Canada based on acoustic geophysical records, surficial expression as recorded by sidescan sonar, grain-size distribution of sea floor sediments and the character of sediment in cores taken within each unit.

### Bedrock

Queen Charlotte Basin is bounded on the east by Coast Mountain crystalline rocks that extend a short distance offshore. The Coast Mountain Range consists of Mesozoic and Cenozoic granites as well as Paleozoic and Mesozoic metamorphic, volcanic and sedimentary rocks. The Insular Belt is characterized by sedimentary and volcanic rocks of Mesozoic and Tertiary age (Sutherland Brown, 1968). Two Tertiary formations are found within the intervening basin (Queen Charlotte Basin) that underlies the shelf. They are the Skonun Formation and the Masset Formation.

### Skonun Formation

The Skonun Formation is a Miocene-Pliocene siliciclastic succession up to 5 km thick that underlies most of the northwestern Cana-

dian continental shelf and northern Graham Island, Queen Charlotte Islands (Sutherland Brown, 1968; Shouldice, 1973; Higgs, 1989). Where the Quaternary sediments that unconformably overlie the Tertiary are thin, the dipping Tertiary strata are acoustically well defined. Folds are commonly observed in these upper strata.

The surface of the Tertiary is irregular reflecting the presence of relict channels. Overlying sediment tends to mask the rough morphology producing a flat, smooth seafloor.

#### *Masset Formation*

The Masset Formation is a late Oligocene to late Miocene calc-alkaline suite of volcanic rocks that underlies much of the northern Queen Charlotte Islands (Hickson, 1989). To the east it is conformably overlain by, or interfingers with, the Skonun Formation (Cameron and Hamilton, 1988; Sutherland Brown, 1968). The Masset Formation is exposed at the seafloor in southwestern Hecate Strait and in Dixon Entrance.

#### **Till (Fraser Glaciation)**

An acoustically uniform, non-stratified unit with a strong surface reflector is interpreted to be a glacial till. The till averages between 8 and 45 m in thickness. When exposed at the surface, the till has a characteristic hummocky expression with a surface veneer of poorly sorted gravel, silts and sands. In water deeper than 100 m the surface of the till is often scoured and pitted, presumably from the action of grounding ice or icebergs calved during glacial retreat.

Till is found primarily in troughs, with very little evident on bank tops where it was either not deposited or was eroded during periods of sea level change at the end of the late Wisconsinan (Barrie and Bornhold, 1989; Luternauer et al., 1989a). In the interbank troughs of Queen Charlotte Sound till is up to 45 m thick and there is good evidence for more than one ice advance depositing multiple tills in several areas. These till bodies become more abundant at the trough margins.

A radiocarbon age of 14,160 years B.P. was obtained on a shell in a glaciomarine unit overlying a till in Hecate Strait. The till consists of a massive, sandy mud with abundant clay clasts, derived, possibly, from the underlying Tertiary mudstone.

#### **Glaciomarine Mud**

In water depths generally greater than 200 m, thick (60 m) sequences occur that are acoustically semi-transparent with weak reflectors and occasional point reflectors. These unconformably overlie till and Tertiary sediments. Lithologically, the sediments consist of roughly equal proportions of sand, silt and clay, with minor matrix supported gravel, often angular and striated. The gravels, which give rise to the point reflectors seen in the seismic profiles, are considered to be ice rafted. The top of the glaciomarine mud unit was deposited between 13,600 and 12,900 yrs B.P. during final deglaciation of the shelf (Luternauer et al., 1989a).

#### **Queen Charlotte Sands and Gravels**

##### *Lower Sands and Gravels*

Acoustically stratified sediments are found on the edge of the banks in Queen Charlotte Sound between approximately 100 and 160 m water depth. The sediments are very fine to fine-grained siliciclastic sands with inclined parallel laminations occurring at low to moderate angles, often as beds of 5-7 cm thick. The laminations are highlighted by the concentration of heavy minerals on bedding plane surfaces approximately every 1 cm. Radiocarbon dates from this unit all suggest a minimum age of deposition of 10,400 years B.P. Deposition appears to have been rapid considering the consistency of radiocarbon dates (10,430-10,760 yrs B.P.) at three different levels within the unit.

In north-central Hecate Strait, between the apex of the north and south troughs, and in southern Dixon Entrance, poorly sorted outwash sediments of similar age are found. High resolution seismic records show a complex pattern of cut and fill depositional style.

##### *Upper Sands and Gravels*

Holocene sands and gravels varying from a few centimetres thick to greater than 50 m thick overlie most units, in water depths less than 160 m. Below 100 m the sands are generally less than 1 m thick, consisting of light brown sands rich in heavy minerals including glauconite and granule size lithics which comprise 20% of the sediment. Proteinaceous or calcareous worm tubes are commonly found in the upper portions of the unit.

Above 100 m water depth the unit consists of palimpsest sediments, derived from the Skonun Formation, glacial tills and, in north-eastern Hecate Strait, coastal erosion. The sands are formed into sedimentary bedforms with intervening areas of lag gravels. An exception to this distribution is found at the eastern side of Moresby Trough where active sand waves are apparent to 350 m water depth.

Extensive areas of shallow gas have been identified acoustically within the unit represented on the seismic records as acoustic voids, enhanced reflections and plumes, similar to near-surface occurrences on the Alaska shelf (Nelson et al., 1978; Hampton et al., 1979).

#### **Queen Charlotte Muds**

##### *Lower Mud*

Within the troughs of the region semi-transparent sediments, with parallel reflectors, to transparent sediments overlie glaciomarine muds or glacial till. Lithologically the muds are composed of silt and clay in variable amounts. Sand content can range from 5-40%. The lower mud unit contains graded beds and gravelly sandy mud intervals which Luternauer et al. (1989a) attributed to sediment gravity flows and low sea level intervals of winnowing, respectively. Radiocarbon dating suggests this unit was deposited between 13,000 and 10,000 yrs B.P. (Luternauer et al., 1989a). These muds are interpreted to be a deep water facies of the lower Queen Charlotte sand and gravel unit in Queen Charlotte Sound.

##### *Upper Mud*

The upper muds are weakly reflective to transparent seismically, and confined to troughs and isolated depressions; they form a drape over other units below approximately 160 m. Maximum thicknesses occur in the northernmost trough in Queen Charlotte Sound where up to 40 m have been deposited. The muds are commonly charged with biogenic gas, and in southern Queen Charlotte Sound, pockmarks are found. Lithologically the unit is composed of approximately equal proportions of silt and clay, and minor sand. Radiocarbon dates obtained on this unit indicate deposition at variable rates since 9700 yrs B.P. (Luternauer et al., 1989a). Their spatial geometry suggests that the mud is deposited as a prograding lobe into bathymetric depressions (Luternauer and Conway, 1987).

##### *Sponge Bioherms*

Large areas of the seabed between 150 and 250 m water depth are discontinuously blanketed by bioherms dominated by species of Hexatinellid sponges (Conway et al., 1991). The bioherms are up to 10 m thick and form complexes several kilometres in width. The sediment incorporated into the bioherms by a trapping and baffling mechanism is similar in texture to the proximal upper mud sediments found in the inner troughs, a silty clay or clayey silt. Radiocarbon dating indicates that the mounds in some areas have been growing at a rate of about 1 mm/yr during the late Holocene (Conway et al., 1991).

## POSTGLACIAL DEVELOPMENT

Several cycles of sea-level change and glaciation occurred during the Quaternary period on the coast of western Canada. Hecate Strait, for example, has been exposed to subaerial conditions down to as deep as the present 180 m isobath at least once during the late Tertiary to early Quaternary (Barrie and Bornhold, 1989). That glacial ice covered most of the shelf sometime during the Wisconsinan is indicated by the occurrence of seabed glacial features (Luternauer and Murray, 1983; Barrie and Bornhold, 1989; Luternauer et al., 1989a). Whether a late Wisconsinan ice advance extended offshore, covering the entire shelf area is not known. A till that could represent the limit of the late Wisconsinan ice advance is found in the principal troughs of the region.

Upon deglaciation (15,000-13,000 yrs B.P.), ice retreating up the troughs towards the British Columbia mainland could have become a floating ice shelf, depositing the glaciomarine muds. Large icebergs that calved from the retreating ice margin scoured the seabed within the troughs.

At the end of the late Wisconsinan period, relative sea level fell approximately 100 m below present levels on the central shelf. At this time thick laminated sand deposits were deposited in the nearshore zone off the exposed banks of Queen Charlotte Sound. In northern Hecate Strait outwash sands were deposited at the head of the troughs and a similar outwash plain was being deposited off the northern Queen Charlotte Islands. Fines derived from the outwash plain and mid-shelf banks, where transported offshore and deposited in the deep troughs.

Shortly after 10,500 yrs B.P., transgression of the central and outer shelf commenced, promoting deposition of the transgressive sands and gravels above 100 m water depth. Subsequent Holocene sedimentation has been minimal with deposition of mud in the troughs and the formation of sponge bioherms seaward along the trough axes. Extensive reworking of the transgressive sands and gravels and sublittoral sands, above 100-160 m water depth, has continued until the present time.

## GEOLOGICAL HAZARDS

Erosion and sediment transport are significant agents of sediment redeposition on the present day shelf of western Canada and can be regarded as engineering hazards. Not only can large-scale sediment transport alter foundation conditions by scouring and bedform loading, but continued erosion can result in oversteepened slopes, a critical factor in submarine slides and debris flows. In many areas of the Basin where sediment is in sufficient quantity to be transported and redeposited, there is a risk of liquefaction. Wave action or seismic shaking can cause sediment pore pressure buildup that in extreme cases may lead to seabed liquefaction (loss of shear strength) with enhanced grain entrainment by sea-bottom flows or downslope movement under gravitational stress (i.e. transport).

The extensive distribution of shallow marine gas in the sediments of Queen Charlotte Basin can be both a potential engineering hazard and an exploration aid. Blowouts due to shallow gas have occurred at shallow depths (Bouma, 1981) and near-surface gas-charged sediments associated with larger subsurface accumulations, may also seriously reduce the bearing capacity for seabottom structures. Alternatively, thermogenic gas derived from deeper sources, may provide an indication of hydrocarbon source and type with the application of a sniffing technique (Nelson et al., 1978).

## CONCLUSIONS

Four surficial geological units overlie bedrock on the northern shelf of western Canada. They are: 1) glacial till, found primarily in the troughs between banks and considered to be late Wisconsinan in age, 2) glaciomarine mud, deposited upon the retreat of glacial ice from the shelf,

3) Queen Charlotte sands and gravels, deposited, respectively, by a) late Wisconsinan sublittoral processes during the low sea level stand in Queen Charlotte Sound and by the deposition of glacial outwash in Hecate Strait and Dixon Entrance and b) by the reworking of Quaternary sands and gravels during transgression, and 4) Queen Charlotte muds, including late Wisconsinan and Holocene deposition within the troughs, and the formation of sponge bioherms. Early Holocene deposition was strongly influenced by relative sea level which fell soon after deglaciation (15,000-13,000 yrs B.P.) by 100-105 m until 10,500 years ago. A rapid transgression followed in a series of steps until approximately 9000 yrs B.P., at a rate exceeding 7 cm/yr.

Following the transgression, the area has remained both tide and storm dominated. Significant sediment erosion and transport occurs above 100 m water depth and locally to 350 m depth and shallow gas is found throughout the surficial sediments of the Queen Charlotte Basin; these processes, therefore, represent potential geological engineering hazards to seabed development for the region.

## REFERENCES

- Barrie, J.V. and Bornhold, B.D.  
1989: Surficial geology of Hecate Strait, British Columbia continental shelf; Canadian Journal of Earth Sciences, v. 26, p. 1241-1254.
- Barrie, J.V., Emory-Moore, M., Luternauer, J.L., and Bornhold, B.D.  
1993: Origin of modern heavy mineral deposits, northern British Columbia continental shelf; Marine Geology, v. 84, p. 43-51.
- Barrie, J.V., Luternauer, J.L., and Conway, K.W.  
1990a: Surficial Geology of the Queen Charlotte Basin: Dixon Entrance-Hecate Strait; Geological Survey of Canada, Open File 2193, 7 maps (1:250 000).  
1990b: Surficial Geology of the Queen Charlotte Basin: Graham Island-Dixon Entrance; Geological Survey of Canada, Open File 2194, 7 maps (1:250 000).  
1990c: Surficial Geology of the Queen Charlotte Basin: Moresby Island-Queen Charlotte Sound; Geological Survey of Canada, Open File 2196, 8 maps (1:250 000).
- Bouma, A.H.  
1981: Introduction to offshore geologic hazards; in Offshore Geologic Hazards, A. Bouma, D. Sangrey, J. Coleman, D. Prior, A. Trippet, W. Dunlap and J. Hooper (ed.), American Association of Petroleum Geologists, Tulsa, Oklahoma, p. 1-1 - 1-101.
- Cameron, B.E.D. and Hamilton, T.S.  
1988: Contributions to the stratigraphy and tectonics of the Queen Charlotte Basin, British Columbia; in Current Research, Part E, Geological Survey of Canada, Paper 88-1E, p. 221-227.
- Clague, J.J.  
1985: Deglaciation of the Prince Rupert-Kitimat area, British Columbia; Canadian Journal of Earth Sciences, v. 22, p. 256-265.
- Clague, J.J. and Bornhold, B.D.  
1980: Morphology and littoral processes of the Pacific Coast of Canada; in The Coastline of Canada, S.B. McCann (ed.), Geological Survey of Canada, Paper 80-10, p. 339-380.
- Clague, J.J., Harper, J.R., Hebda, R.J., and Howes, D.E.  
1982a: Late Quaternary sea levels and crustal movements, coastal British Columbia; Canadian Journal of Earth Sciences, v. 19, p. 597-618.
- Clague, J.J., Mathewes, R.W., and Warner, B.G.  
1982b: Late Quaternary geology of eastern Graham Island, Queen Charlotte Islands, British Columbia; Canadian Journal of Earth Sciences, v. 19, p. 1786-1795.
- Conway, K.W., Barrie, J.V., Austin, W.C., and Luternauer, J.L.  
1991: Holocene sponge bioherms on the British Columbia continental shelf; Continental Shelf Research, (in press).
- Crawford, W.R. and Greisman, P.  
1987: Investigation of permanent eddies in Dixon Entrance, British Columbia; Continental Shelf Research, v. 7, p. 851-870.
- Crawford, W.R. and Thomson, R.E.  
1991: Physical oceanography of the western Canadian continental shelf; Continental Shelf Research, (in press).
- Crawford, W.R., Huggett, W.S., and Woodward, M.J.  
1988: Water transport through Hecate Strait, British Columbia; Atmosphere-Ocean, v. 26, p. 301-320.
- Currie, R.G., Cooper, R.V., Riddihough, R.P., and Seemann, D.A.  
1983: Multiparameter geophysical surveys off the west coast of Canada: 1973-1982; in Current Research, Part A, Geological Survey of Canada, Paper 83-1A, p. 207-212.
- Hampton, M.A., Bouma, A.H., Pelpan, H., and von Huene, R.  
1979: Geo-environmental assessment of the Kodiak shelf, western Gulf of Alaska; Offshore Technology Conference, OTC 3399, p. 365-376.

**Hickson, C.J.**

**1989:** An update on structure and stratigraphy of the Masset Formation, Queen Charlotte Islands, British Columbia; *in* Current Research, Part H, Geological Survey of Canada, Paper 89-1H, p. 73-79.

**Higgs, R.**

**1989:** Sedimentological aspects of the Skonun Formation, Queen Charlotte Islands, British Columbia; *in* Current Research, Part H, Geological Survey of Canada, Paper 89-1H, p. 87-94.

**Holland, S.S.**

**1964:** Landforms of British Columbia, a physiographic outline; British Columbia Department of Mines and Petroleum Resources, Bulletin 48, 138 p.

**Howes, D.E.**

**1983:** Late-glacial and postglacial vegetation history at Bear Cove Bog, northeast Vancouver Island, British Columbia; Canadian Journal of Earth Sciences, v. 20, p. 578-565.

**Luternauer, J.L.**

**1986:** Character and setting of sand and gravel bed forms on the open continental shelf off western Canada; *in* Shelf Sands and Sandstones, R.J. Knight and J.R. McLean (ed.), Canadian Society of Petroleum Geologists, Memoir 11, p. 45-55.

**Luternauer, J.L. and Conway, K.W.**

**1987:** Geohazards, lithology and shallow seismostratigraphy of the Moresby Trough/Middle Bank area, Queen Charlotte Sound, British Columbia; Geological Survey of Canada, Open File 1420 (2 sheets).

**Luternauer, J.L. and Murray, J.W.**

**1983:** Late Quaternary morphologic development and sedimentation, central British Columbia continental shelf; Geological Survey of Canada, Paper 83-21, 38 p.

**Luternauer, J.V., Barrie, J.V., Conway, K.W., and Caltagirone, A.**

**1990a:** Surficial Geology of the Queen Charlotte Basin: Hecate Strait-Queen Charlotte Sound; Geological Survey of Canada, Open File 2195, 8 maps (1:250 000).

**1990b:** Surficial Geology of the Queen Charlotte Basin: Queen Charlotte Sound; Geological Survey of Canada, Open File 2196, 8 maps (1:250 000).

**Luternauer, J.L., Conway, K.W., Clague, J.J., and Blaise, B.**

**1989a:** Late Quaternary geology and geochronology of the central continental shelf of western Canada; Marine Geology, v. 89, p. 57-68.

**Luternauer, J.L., Clague, J.J., Conway, K.W., Barrie, J.V., Blaise, B., and Mathewes, R.W.**

**1989b:** Late Pleistocene terrestrial deposits on the continental shelf of western Canada: evidence for rapid sea-level change at the end of the last glaciation; Geology, v. 17, p. 357-360.

**Nelson, H., Kvenvolden, K.A., and Clukey, E.C.**

**1978:** Thermogenic gases in near-surface sediments of Norton Sound, Alaska; Off-shore Technology Conference, OTC 3354, p. 2623-2633.

**Shouldice, D.H.**

**1973:** Western Canadian continental shelf; *in* Future Petroleum Provinces of Canada: Their Geology and Potential, R.D. McCrossan (ed.), Canadian Society of Petroleum Geologists, Memoir 1, p. 7-35.

**Sutherland Brown, A.**

**1968:** Geology of Queen Charlotte Islands, British Columbia; British Columbia Department of Mines and Petroleum Resources, Bulletin 54, 226 p.

**Thomson, R.E.**

**1981:** Oceanography of the British Columbia Coast; Department of Fisheries and Oceans Canada, Special Publication 56, 291 p.

# Survey of larval stages of commercial species in the area and time of the 1988 seismic survey in Queen Charlotte Sound and Hecate Strait

Brenda J. Burd<sup>1</sup> and G.S. Jamieson<sup>2</sup>

Burd, B.J. and Jamieson, G.S., Survey of larval stages of commercial species in the area and time of the 1988 seismic survey in Queen Charlotte Sound and Hecate Strait; in *Evolution and Hydrocarbon Potential of the Queen Charlotte Basin, British Columbia*, Geological Survey of Canada, Paper 90-10, p. 513-544, 1991.

## **Abstract**

*The surface waters of Queen Charlotte Sound and Hecate Strait were surveyed in June, 1988 to establish the abundance and spatial distribution of larvae and juveniles of commercial finfish, invertebrate species and other associated planktonic species. Cancer zoea and megalopae, copepods, euphausiids and sea jellies were most abundant, with relative abundance varying both spatially and by time of day. Overall, larvae of commercial species were lower in abundance than previously reported off the west coast of Vancouver Island.*

## **Résumé**

*Les eaux peu profondes de la région des îles de la Reine-Charlotte et du détroit d'Hécaté furent étudiées en juin 1988 afin de déterminer l'abondance et la distribution spatiale des larves et jeunes poissons commerciaux, des espèces invertébrées ainsi que d'autres espèces planctoniques. Cancer zoea et megalopae, les copépodes, euphausiids et gelées de mer sont particulièrement nombreux. Leur abondance varie de façon spatiale et en fonction de l'heure du jour. En général, le nombre de larves d'espèces commerciales recensées dans cette région est plus bas que ce qui fut rapporté pour la région située à l'ouest de l'île de Vancouver.*

---

<sup>1</sup> Galatea Research Inc., P.O. Box 202, Brentwood Bay, B.C. V0S 1A0

<sup>2</sup> Department of Fisheries and Oceans, Biological Sciences Branch, Pacific Biological Station, Nanaimo, B.C. V9R 5K6



## INTRODUCTION

This report outlines a sampling and data analysis study designed to provide baseline information on the abundance and spatial distribution of commercial and other macrozooplanktonic species in Hecate Strait and Queen Charlotte Sound. The purpose of the study was two-fold:

1. To contribute to the establishment of an environmental database for Hecate Strait and Queen Charlotte Sound. This data will be used in policy-making and accident prevention with respect to proposed oil exploration and/or shipping in this prime fishing area in the future.
2. To assist in extrapolation of predicted effects of seismic sampling on larval commercial species and other associated planktonic species. This data can be interpreted in the context of other ongoing studies in Washington on the direct impact of close range seismic air explosions on such zooplankton.

The study was initiated because of the lack of data on the zooplankton in and around the proposed seismic survey path. The survey emphasized the identification of both commercial and non-commercial invertebrate and fish larvae. Other macrozooplankton collected were identified in as much taxonomic detail as possible, based on the resources of the project. Salinity, temperature, and pressure profiles were determined in the study area to examine the effects of oceanographic characteristics on the distribution and abundance of zooplankton.

## METHODS

### Field sampling

Four field sampling personnel accompanied three crew members of a small (65') commercial troller, the *Optimist I*. Biological surveys were conducted along a series of transects which were followed about 10 days later by a seismic survey ship chartered by Geological Survey of Canada. The entire plankton survey took ten days (excluding travel to and from Hecate Strait), with about 1.5 days lost to foul weather, and ran from June 11 to June 21, 1988. Station locations, tow numbers, dates and times are summarized in Table 1 and Figures 1, 2 and 3.

General Oceanic flowmeters were attached to the insides of all nets. When the net was opened, water flowed past the flowmeter rotating the blades. The total number of revolutions was used to calculate the volume of water passing through the net. Plankton samples were collected in their entirety and rinsed into a 10% buffered formalin solution, labelled, and stored.

The following sampling gear was deployed from the trawler *Optimist I*.

### Tucker trawl

This is an array of 3 nets that can be opened and closed manually by messenger, enabling the collection of 2 discrete depth range samples per tow. The first net was used as a dummy since one net must be open during deployment, unusually to the greatest depth to be sampled. Once at this depth the second net was opened and a vertical sample was taken in the depth range of interest. The second net was then closed and the final net opened until the surface was reached. The net mouth is 1 m<sup>2</sup> when towed at 3 knots. This gear was used in daytime sampling of the upper 50 m of the water column. Nets 2 and 3 were each used to sample half the total depth (i.e., 25 m or so) when water depth exceeded 50 m, while at shallow stations (Stations 118-128), only 1 depth range was sampled. Depth gauges were attached to the two study nets to measure the maximum and minimum depths for each depth range. Tucker trawls were towed a horizontal distance of about 1800 m, with tow durations of about 20 min. Sample locations (Fig. 1) were selected based on tractability of the weather and relative cov-

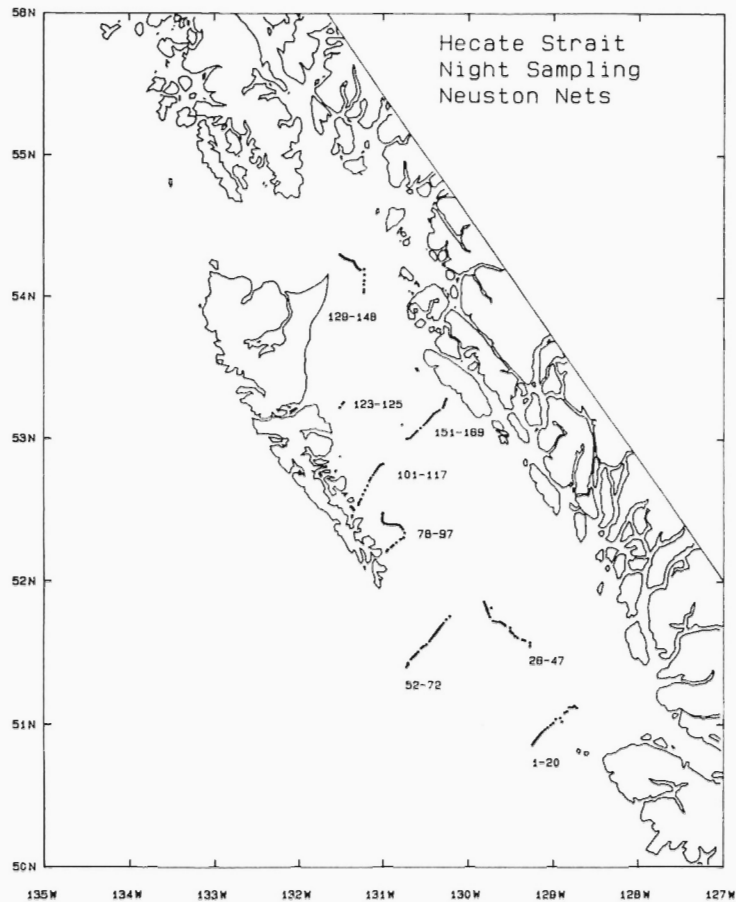


Figure 1: Neuston net sampling locations, June 1988.

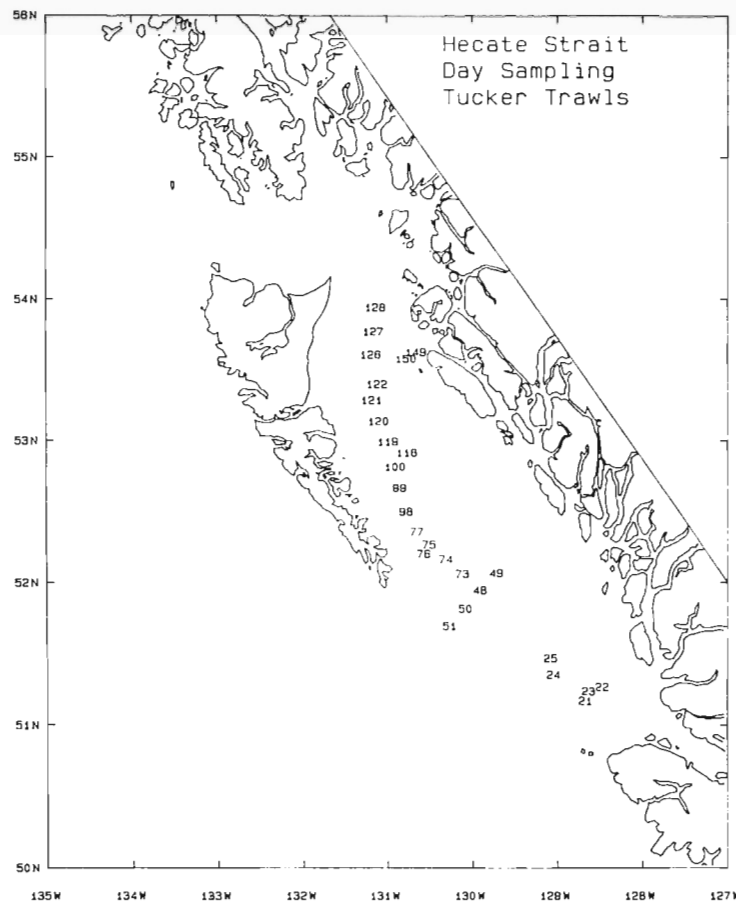
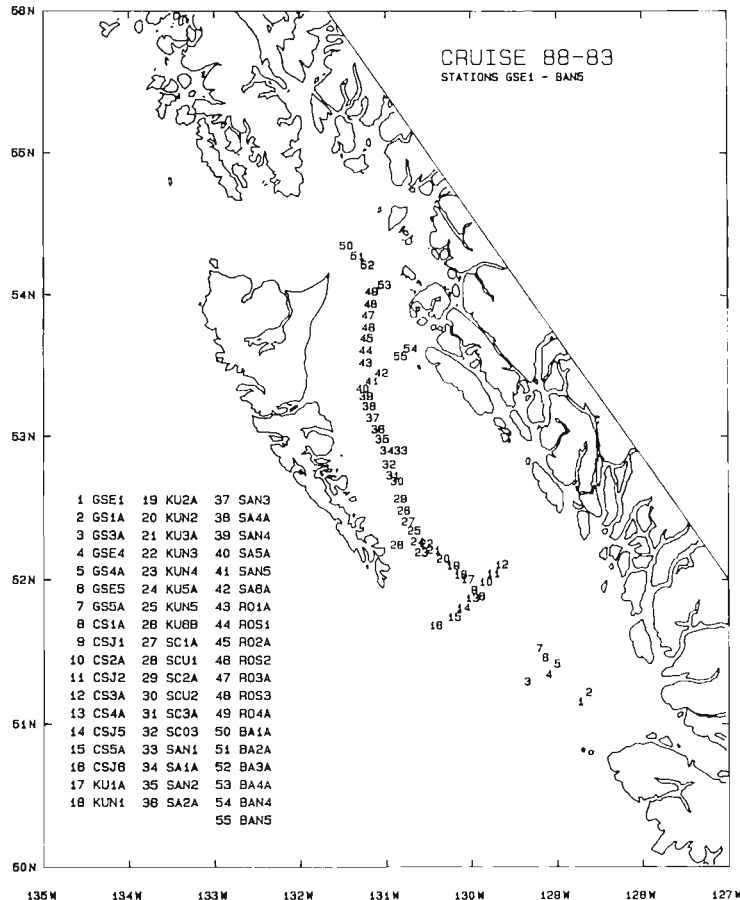


Figure 2: Tucker trawl sampling locations, June 1988.



**Figure 3:** STD sampling locations, including the original 55 casts. Station Names (as per Table 1) are given for each number to avoid confusing these numbers with those for plankton sampling (Figs. 1 and 2).

erage of area. The purpose was to cover the maximum portion of the original transects within the allotted 10 days.

#### Neuston net

This is a single net with a square mouth opening of  $0.25 \text{ m}^2$  (Mason and Phillips, 1984). Towed at 4-5 knots, it maintains itself at the surface at a distance away from, and parallel to, the side of the towing vessel. Hull avoidance by plankton is thus reduced. The neuston net was deployed continuously during night hours (Fig. 2), a time when most plankton of interest (Jamieson and Phillips, 1988; Jamieson et al., 1989) were expected to be at the water surface. It samples to a depth of about 50 cm.

#### Applied Microsystems STD-12

This electronic metering device measures salinity, pressure, and temperature with depth. It was used to construct vertical water property profiles from which geostrophic current patterns were determined. Data was stored on disk using a Radio Shack TRS-80 computer. Because of the need to stop the vessel to deploy it, regular STD profiles were carried out only during the day (Fig. 3). Generally, a STD profile was carried out just prior to each Tucker trawl and between Tucker trawl samples. Additional STD profiles were carried out whenever possible, based on time constraints and optimum coverage of the sample area.

#### Sorting and identifications

Collected samples were sorted into taxonomic groups and counts were made on all organisms present. Most invertebrates were only identified to family or genus, but Dungeness crab (*Cancer magister*) were of particular interest and so larvae of this species were specifically counted. In some groups (such as "*Cancer* spp. zoea"), large

numbers per sample required splitting, subsampling, and extrapolation of counts to the total volume. Sorted specimens were preserved in isopropanol for archiving and/or future use. Quality control was carried out by recounting about 90% of the processed samples to check for omissions and errors.

#### Data analyses

STD data were analyzed to show temperature and salinity structures of the water column throughout the sampling area, using programs developed by the Ocean Physics Division, Institute of Ocean Sciences (R. Thomson, Institute of Ocean Sciences, Sidney, B.C. pers. comm.; Thomson and Wilson, 1987). Geostrophic patterns were based on a reference depth of 50 m because of the shallowness of Hecate Strait. Therefore, only those stations 50 m or greater were therefore included in this analysis.

Planktonic abundance data were standardized to numbers per 10 square metres of sea surface, based on calculated integrated areas sampled by the nets. For Tucker trawl data, raw abundances were multiplied by a standardization factor from Mason et al. (1984):

$$\text{Standardization factor} = \frac{\text{depth range of tow (m)} \times 10}{\text{volume filtered (m}^3\text{)}}$$

Neuston net raw abundance data were multiplied by the surface area covered by the net based on linear distance covered (flowmeter linear distance  $\times$  net width). Because of the different collection methods, day (Tucker trawl) samples were examined separately from night (neuston) samples. Data from all available neuston stations were analyzed using a simple clustering algorithm (Bray-Curtis similarity measure) and linkage method (unweighted pair group mean average linkage) to show if any general differences in sample groupings could be detected throughout the study area. This simple data analysis is statistically non-inferential, providing merely a multivariate, graphical, hierarchical ordering of similar population groups. Because of the lack of repetition in this type of sampling, as well as the rapid potential for major changes in planktonic population structure over short periods of time (i.e. 10 days), it was felt that more in-depth statistical analyses were not justified.

The data from Tucker trawls was examined separately in the same manner as that for neuston nets, with the main purpose being to examine the potential differences in depth stratification of different groups of taxa during the day.

A qualitative comparison was made between patterns of species and station groupings, and geostrophic current patterns and temperature/salinity profiles of the area.

## RESULTS

#### Temperature/salinity profiles

A total of 57 stations were sampled for salinity and temperature. Because of sporadic problems with the salinity probe of the STD, Stations GSE2 and GSE3 were discarded immediately, and the salinity data for another 6-8 stations had to be discarded later during editing. Therefore, a total of 47 salinity and 55 temperature profiles were available for analysis.

A temperature profile across the strait (stations 8-16 from Fig. 3) indicated that low temperature surface water, possibly originating from mainland coastal runoff, was present along the eastern side of the study area (Fig. 4). Figures 5 to 8 show temperature profiles at various depths along the length of the strait, indicating the spatial occurrence of this lower temperature surface water. In shallow (about 20 m depth) sample locations, the water column was well mixed (Fig. 9, stations 32 to 49). Thermoclines were evident in the deeper sample sites in the southern and central sections of Hecate Strait and where the shelf

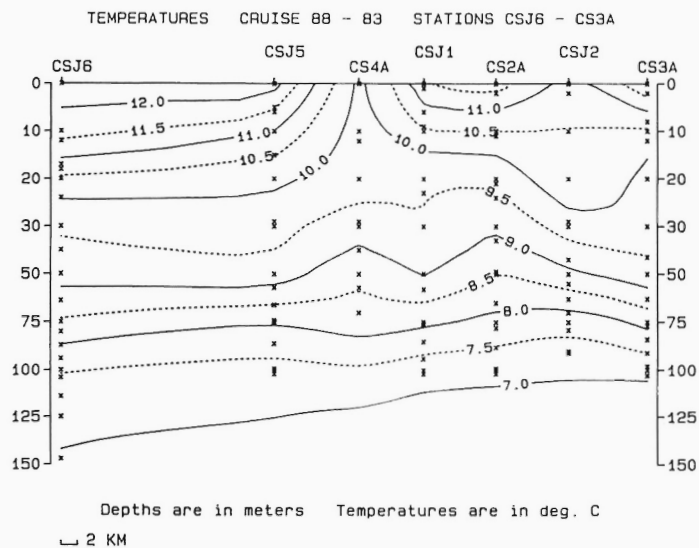


Figure 4: Temperature profiles for STD stations 9-16 (see Fig. 3).

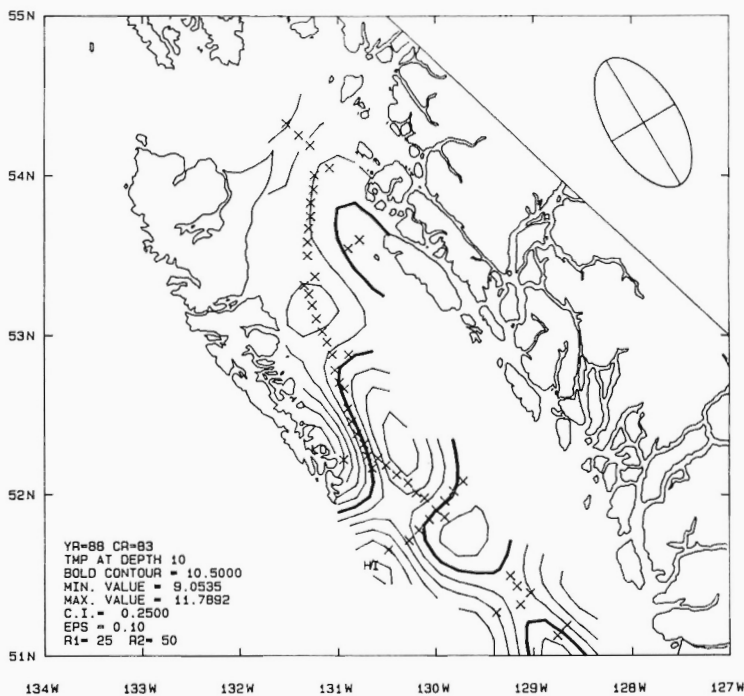


Figure 5: Temperature contours for depth = 10 m. STD station locations are indicated by the crosses. Profiles are extrapolated to a distance of 25 km and 50 km, respectively (see ellipse).

dropped off steeply between stations 50 and 51 (Fig. 3) at the north-eastern tip of Graham Island. These occurred generally at 10-20 m depth.

Salinity profiles from the STD stations (Figs. 10-13) indicated that the low temperature water mentioned above was also lower in salinity than water coming around the southern tip of Moresby Island from the open ocean. This supports the suggestion that the low temperature water originated as surface runoff from the mainland coast.

#### Zooplankton species distributions

The complete taxonomic list of zooplankton identified during the project is given in Table 2. Taxa numbers per 10 m<sup>2</sup> of sea surface and per 10 m<sup>3</sup> water volume are given in Tables 3 and 4, respectively.

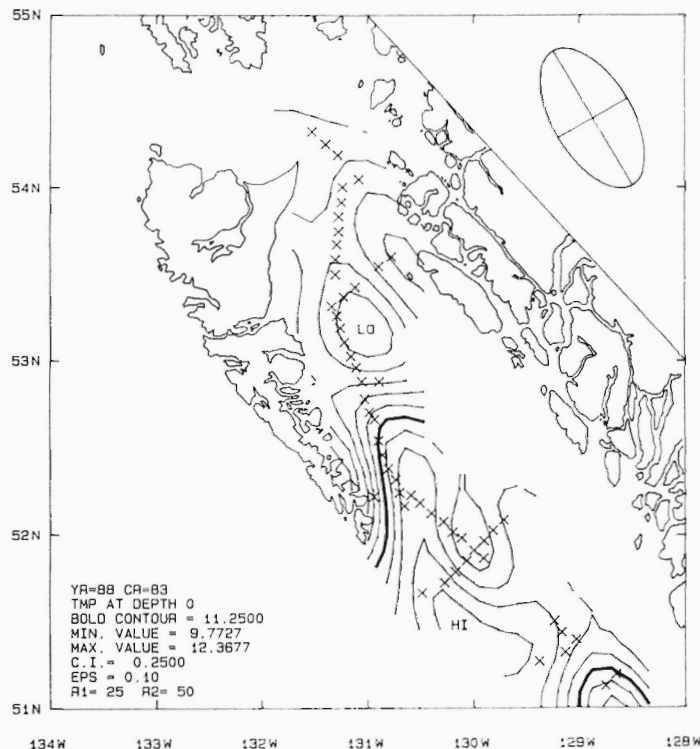


Figure 6: Temperature contours at depth = 0 m for Hecate Strait, June 1988.

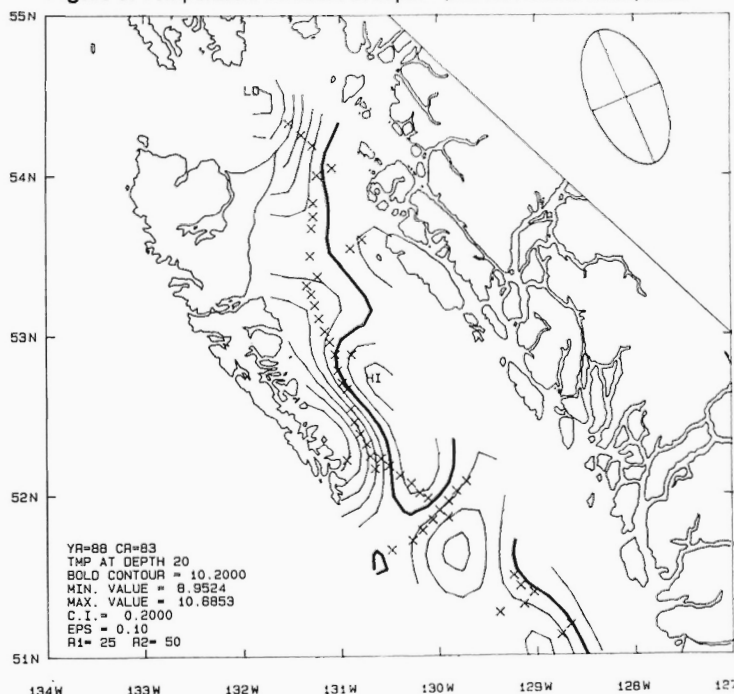
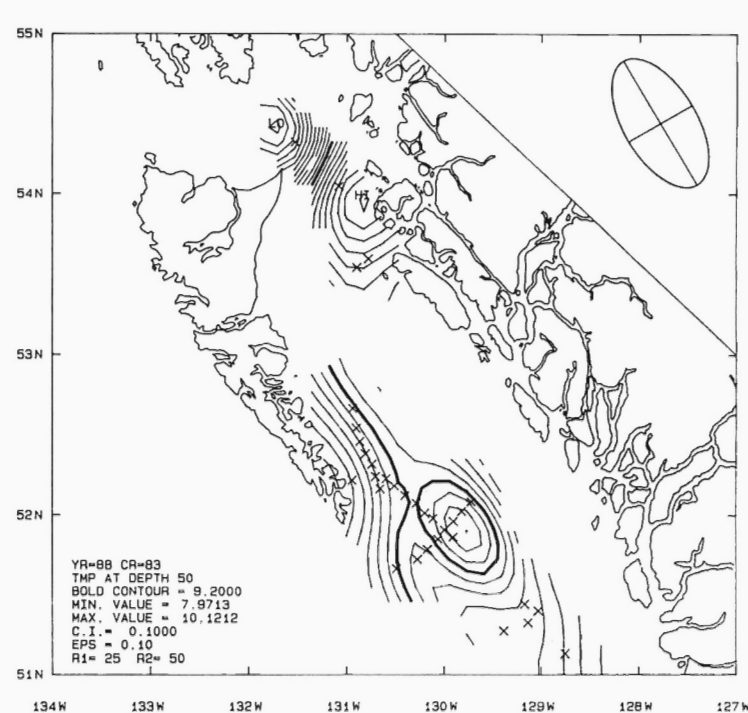


Figure 7: Temperature contours at depth = 20 m, Hecate Strait, June 1988.

ly, in the Appendix. Abundances of most of the 72 taxa identified were rarer than 0.1 per 10 m<sup>2</sup>.

The most common taxa in the samples were *Cancer* species zoea and megalopae (i.e. stations 27-38, 79-86, 102-105, 139-160), copepods (stations 32-51, 61-63, 73-77, 158-161), euphausiids (Stations 11, 12, 24, 73-77, 106, 158-161; often common in samples with many copepods), and sea jellies (Leptomedusae: 29, 30, 49, 121-142). In terms of volume occupied by different taxa, the relatively large sea jellies tended to occupy most of the sample volume even when abundance was relatively low. When crab zoea abundance was high (e.g., stations 27-38, 79-86, 102-105, 139-160), zoea represented up to 95% of the total sample volume. Copepods and euphausiids usually made up less



**Figure 8:** Temperature contours at depth = 50 m, Hecate Strait, June, 1988.

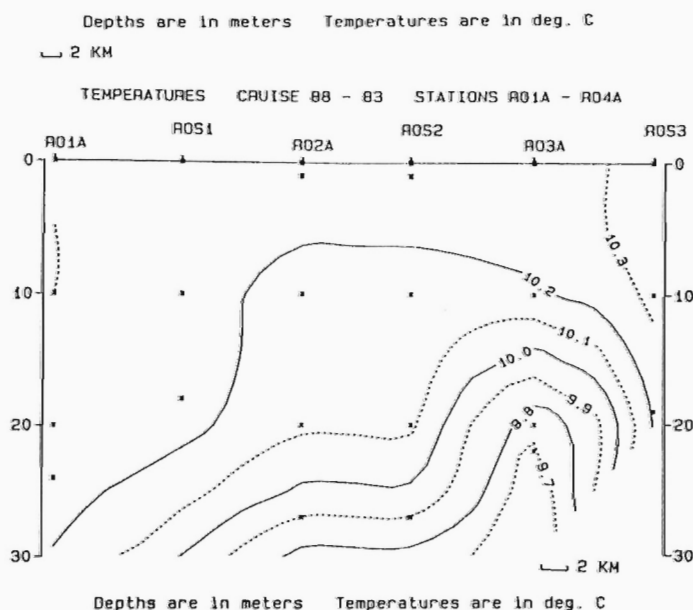
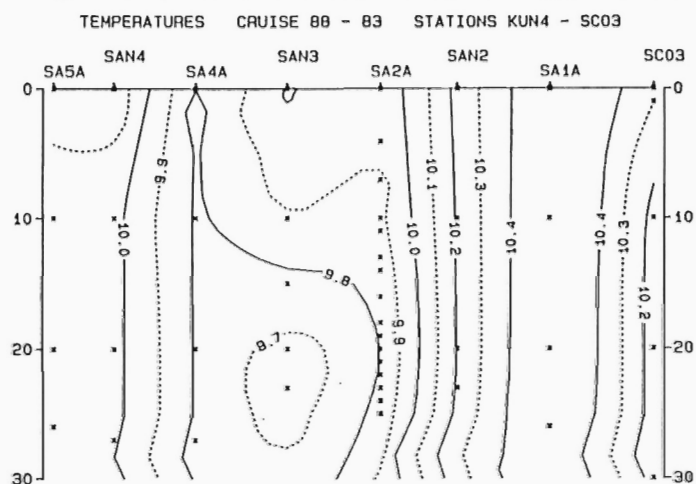


**Figure 9:** Temperature profiles for the more shallow northerly Hecate Strait stations, showing mixing of the water column.

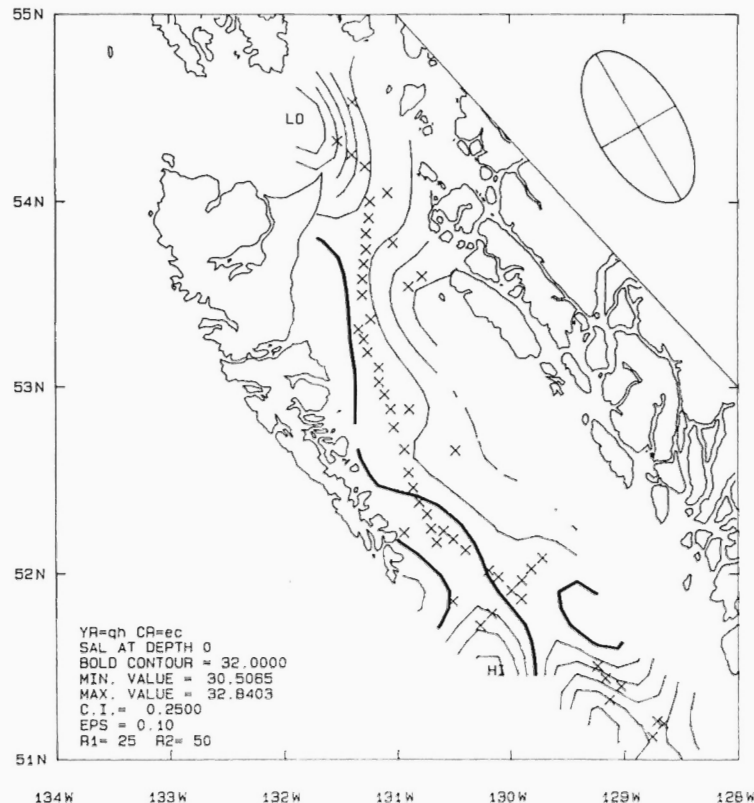


**Figure 10:** Salinity contours for depth = 0 m, Hecate Strait, June 1988.

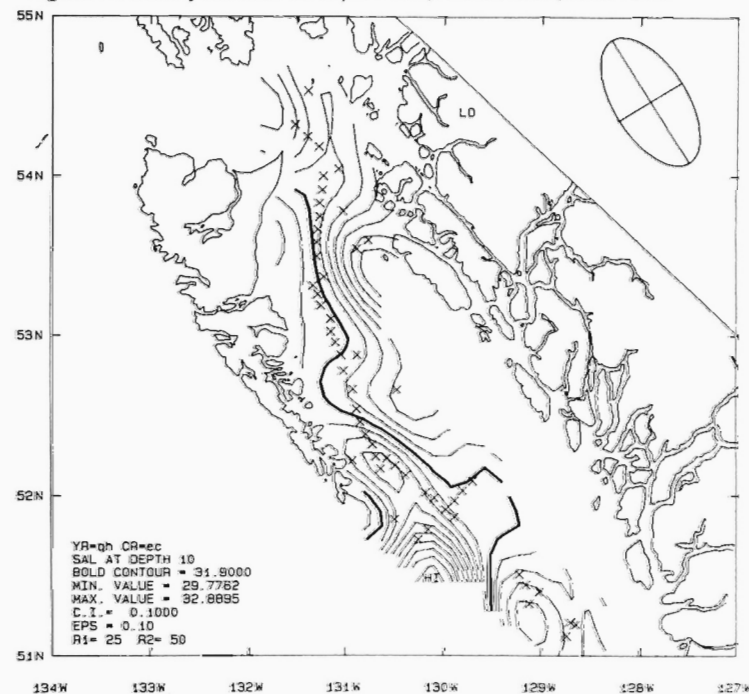


**Figure 11:** Salinity profile for depth = 10 m, Hecate Strait, June 1988.

than 10% of the sample volume, as did the remaining taxa identified. The most common fish species in neuston samples was Pacific sand-lance (*Ammodytes*), which were concentrated in stations 54-89.

#### *Tucker trawl samples*

A total of 25 Tucker trawl samples were successfully collected and identified. Abundances of crab larvae and most of the taxa per unit area were generally lower in Tucker trawl catches (2 nets combined) than in neuston net catches, while some fish larvae (e.g., rock-fish) were more abundant in Tucker trawl catches than in neuston net

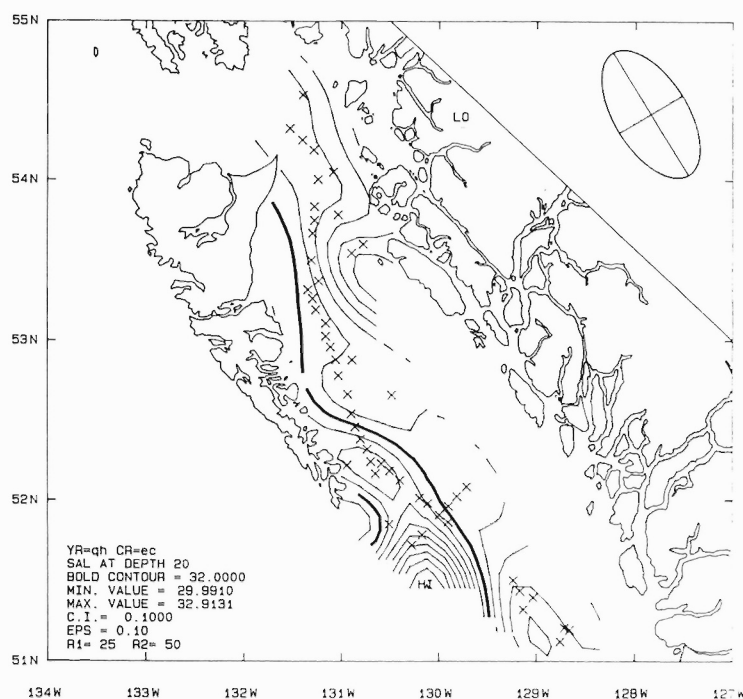


Figure 12: Salinity contours for depth = 20 m, Hecate Strait, June 1988.

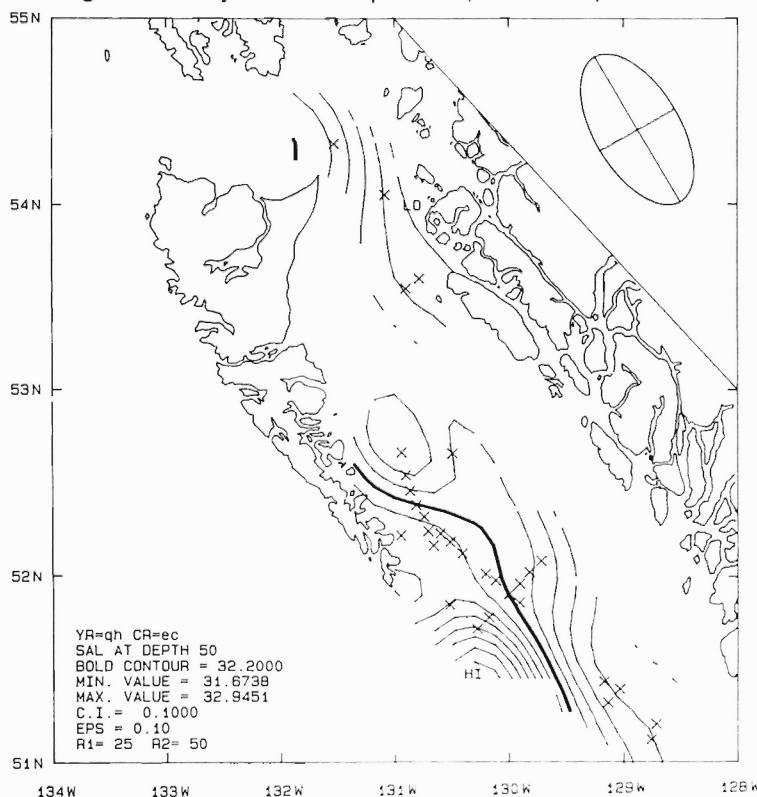


Figure 13: Salinity contours for depth = 50 m, Hecate Strait, June 1988.

catches. This may result partially from different vertical diel migration patterns among taxa. No clear depth preferences were evident from the data for any taxa.

In the cluster analysis of Tucker trawl data, taxa with a total abundance of zero to 0.1 per 10 m<sup>2</sup> of sea surface (the total in all the Tucker trawl net samples taken at that location) and several general categories which represented no specific species (e.g., fish eggs, invertebrate eggs) were excluded. In total, data from 65 taxa and 25 stations were included in the analysis. No apparent differences were evident between

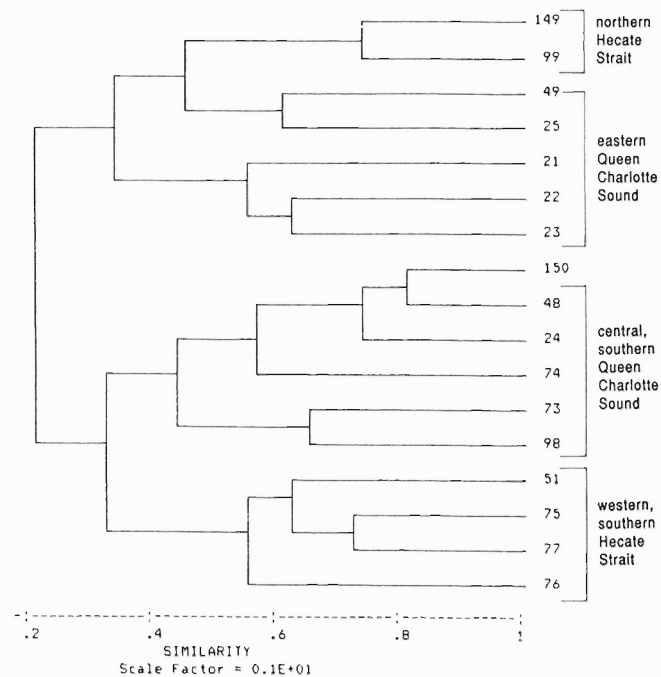
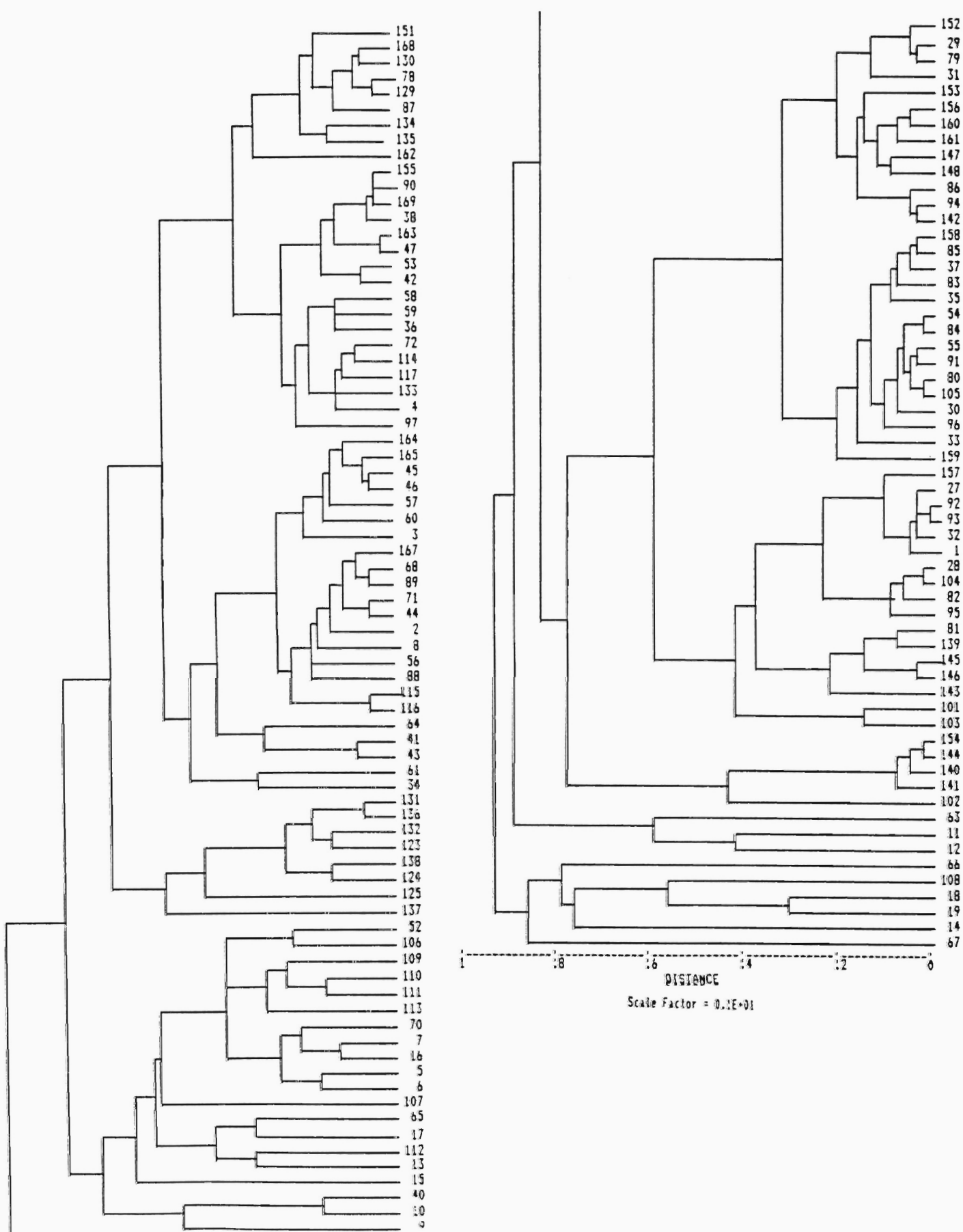


Figure 14: Cluster dendrogram of Tucker trawl faunal distributions for all trawls with two net samples. Station numbers represent tow numbers as given in Table 1.

the data from nets 2 and 3. Therefore, in subsequent cluster analyses the data for these two nets were combined to provide a graphical representation for the entire water column (Fig. 14). The cluster pattern of stations showed some delineation of groups with respect to geographical location. Stations 120 to 128, plus 149, 99 and 118, were clustered together, and these, all located in northern Hecate Strait, were characterized by low temperature and moderate salinity. A cluster group from central, southern Hecate Strait (48, 24, 74, 73, 98) was characterized by more moderate temperature and low salinity. Both groups within the influence of freshwater run-off from the mainland coast. Stations from western Queen Charlotte Sound and Hecate Strait (51, 75-77) also clumped together, as did stations from eastern Queen Charlotte Sound (119, 21-23). These last two groups may be distinct from the first two as a result of greater influence by open oceanic (higher temperature and salinity) waters. Remaining stations show mixed or intermediate effects.

#### Neuston net samples

A total of 136 neuston samples were collected and identified. As described above, some taxa were excluded from the clustering algorithm for these data. The clustering of stations (Q-mode analysis) of neuston samples suggests a somewhat homogeneous distribution of taxa amongst stations (Fig. 15). However, the high abundance of some taxa in many samples caused considerable differences amongst samples. Some form of data transformation might reduce this variation, but this is unlikely to improve biological interpretation of the data. Visual perusal of results suggests no obvious patterns. The more distinct spatial clusters evident in the diurnal Tucker trawl samples suggests that non-neustonic organisms may best characterize water masses, perhaps because microscale conditions such as wind and waves at the surface superimpose an additional contagious distribution beyond that imposed by broader geographical factors. Tucker trawl samples were therefore considered to be more useful than were neuston net samples for interpreting community distribution patterns in the study area.



**Figure 15:** Cluster dendrogram for neuston samples from Hecate Strait, June 1988. Station tow numbers are shown in Figure 1 and Table 1.



## DISCUSSION AND CONCLUSIONS

This study provides background information on the types, abundances and general distribution of zooplankton in Hecate Strait and surrounding area in late June. It is part of the data package required for preliminary evaluation as to possible effects of seismic activity on commercially exploited species, and provides data for designing future zooplankton studies to monitor movements of different taxa seasonally and with currents. As secondary producers, zooplankton are important in the pelagic community, and their distribution can significantly affect the spatial distributions of midwater and bottom fish, and invertebrate populations.

To summarize results, the data suggests that certain taxa are more characteristic of particular geographical conditions and/or water conditions than others. However, zooplanktonic abundances can change greatly over short time periods and distances, and little long term information can be derived from one sampling trip. Tucker trawl samples were of greater value for characterizing species assemblages than were neuston samples. *Cancer* species zoea and megalops and sea jellies were most abundant in lower salinity water, whereas copepods and euphausiids were most abundant in more oceanic water. Overall, relatively few larvae of commercially exploited species were collected, at least in comparison to continental shelf waters off Vancouver Island (Jamieson and Phillips, 1988; Jamieson et al., 1989).

## ACKNOWLEDGMENTS

The authors thank the captain and crew of the *Optimist I*, as well as field personnel involved in sampling. This work was sponsored by the Geological Survey of Canada, and we thank Bob Thompson particularly for advice and support during the project. Finally, we thank Rick Thomson for his patient assistance in the interpretation and plotting of the STD data, and Gary Hamilton and Joe Linguanti for their programming expertise.

## REFERENCES

- Jamieson, G.S. and Phillips, A.C.  
**1988:** Occurrence of *Cancer* crab (*C. magister* and *C. oregonensis*) megalopae off the west coast of Vancouver Island, British Columbia; Fisheries Bulletin, v. 86, p. 525-542.
- Jamieson, G.S., Phillips, A.C., and Huggett, W.S.  
**1989:** Effects of ocean variability on the abundance of Dungeness crab megalopae; in Effects of Ocean Variability on Recruitment and an Evaluation of Parameters used in Stock Assessment Models, Beamish, R.J. and McFarlane, G.S. (ed.), Canada Special Publication in Fisheries Aquatic Sciences, v. 108, p. 305-325.
- Mason, J.C. and Phillips, A.C.  
**1986:** An improved Otter surface sampler; Fisheries Bulletin, v. 84, p. 480-484.
- Mason, J.C., Phillips, A.C., and Kennedy, O.D.  
**1984:** Estimating the spawning stocks of Pacific Hake (*Merluccius productus*) and Walleye Pollock (*Theragra chalcogramma*) in the Strait of Georgia, B.C. from their released egg production; Canadian Technical Report of Fisheries and Aquatic Sciences, no. 1289.
- Thomson, R.E. and Wilson, R.E.  
**1987:** Coastal countercurrent and mesoscale eddy formation by tidal rectification near an oceanic cape; Journal of Physical Oceanography, v. 17, p. 2096-2126.

**Table 1.** Hecate Strait Crab Larvae Cruise sampling stations – June 1988

Date	Time	Transect	Tow #	Latitude	Longitude	Samples	STD CODE	Flowmeter reading	Volume(m <sup>3</sup> )	Tow duration (in minutes)	Depth range (m)	
											Net 2	Net 3
06/11	2215	TRI 01	1	51°6.8	128°43.3	NN			224.7	10		
	2235	TRI 02	2	51°7.5	128°45.0	NN			112.4	5		
	2245	TRI 03	3	51°7.5	128°45.0	NN		21972	236.2	10		
	2308	TRI 04	4	51°7.0	128°46.8	NN		23611	253.8	10		
	2330	TRI 05	5	51°7.0	128°48.9	NN		20491	220.3	10		
	2351	TRI 06	6	51°5.3	128°50.3	NN		21459	230.7	10		
06/12	0008	TRI 07	7	51°4.8	128°52.2	NN		34521	371.1	15		
	0034	TRI 08	8	51°1.0	128°54.0	NN		33750	362.8	15		
	0100	TRI 09	9	51°2.5	128°55.3	NN		31951	343.4	15		
	0125	TRI 10	10	51°2.1	128°58.5	NN		24369	261.9	15		
	0149	TRI 11	11	51°0.5	129°0.0	NN		25991	279.4	15		
	0214	TRI 12	12	50°59.6	129°2.1	NN		24040	258.4	15		
	0239	TRI 13	13	50°58.6	129°4.2	NN		27088	291.2	15		
	0305	TRI 14	14	50°57.7	129°6.2	NN		23304	250.5	15		
	0330	TRI 15	15	50°56.7	129°8.1	NN		24097	259.0	15		
	0352	TRI 16	16	50°55.7	129°9.6	NN		27656	297.3	15		
	0414	TRI 17	17	50°54.7	129°11.1	NN		29203	313.9	15		
	0438	TRI 18	18	50°53.7	129°12.4	NN		33232	357.2	15		
	0501	TRI 19	19	50°52.7	129°13.7	NN		20611	221.5	10		
	0521	TRI 20	20	50°51.6	129°14.9	NN		21560	231.7	10		
	0900	GSE 01	21	51°8.3	128°45.0	TT, STD	GSE1	4750,11881	533.3,606.2	10	53-25	25-0
	1034			51°11.4	128°39.6	STD	GS1A					
	1140	GSE 02	22	51°14.2	128°33.0	TT, STD	GSE2	5917,*	533.3,533.3	10	49-25	25-0
	1348	GSE 03	23	51°12.3	128°42.8	TT, STD	GSE3	4304,18459	533.3,941.8	10	60-18	18-0
	1545			51°16.0	129°20.0	STD	GS3A					
	1640	GSE 04	24	51°19.1	129°8.0	TT, STD	GSE4	8055,13908	533.3,709.6	10	39-22	22-0
	1805			51°23.5	129°1.8	STD	GS4A					
	1923	GSE 05	25	51°26.0	129°10.1	TT, STD	GSE5	6194,*	533.3,533.3	10	40-18	18-0
	2040			51°29.9	129°14.2	STD	GS5A					
	2150	GSE 06	26	51°32.7	129°16.8	NN		21798	234.3	10		
	2215	GSE 07	27	51°34.2	129°16.7	NN		16170	173.8	5		

**Table 1.** Hecate Strait Crab Larvae Cruise sampling stations – June 1988

Date	Time	Transect	Tow #	Latitude	Longitude	Samples	STD CODE	Flowmeter reading	Volume(m <sup>3</sup> )	Tow duration (in minutes)	Depth range (m)	
											Net 2	Net 3
06/13	2229	GSE 08	28	51°35.0	129°20.0	NN		23691	254.7	10		
	2250	GSE 09	29	51°35.4	129°22.0	NN		24641	264.9	10		
	2322	GSE 10	30	51°36.1	129°25.2	NN		23846	256.3	10		
	2346	GSE 11	31	51°36.8	129°27.3	NN		21890	235.3	10		
	0017	GSE 12	32	51°38.0	129°28.9	NN		14433	155.1	5		
	0033	GSE 13	33	51°38.9	129°30.6	NN		24659	265.1	10		
	0100	GSE 14	34	51°40.4	129°30.6	NN		21080	226.6	10		
	0118	GSE 15	35	51°41.2	129°34.1	NN		22183	238.4	10		
	0136	GSE 16	36	51°41.8	129°34.9	NN		23741	255.2	10		
	0153	GSE 17	37	51°42.4	129°36.2	NN		24663	265.1	10		
	0210	GSE 18	38	51°42.9	129°38.0	NN		38825	417.3	15		
	0235	GSE 19	39	51°43.0	129°40.5	NN		34117	366.7	15		
	0258	GSE 20	40	51°43.3	129°42.8	NN		24092	259.0	10		
	0315	GSE 21	41	51°48.8	129°44.0	NN		36291	390.1	15		
	0337	GSE 22	42	51°44.9	129°44.9	NN		42701	459.0	15		
	0404	GSE 23	43	51°46.4	129°46.0	NN		25896	278.4	10		
	0421	GSE 24	44	51°47.6	129°46.7	NN		24043	258.4	10		
	0438	GSE 25	45	51°48.6	129°47.4	NN		42537	457.2	15		
	0500	GSE 26	46	51°50.0	129°48.2	NN		42112	452.7	15		
	0521	GSE 27	47	51°51.4	129°49.1	NN		38599	414.9	15		
	0602			51°51.7	129°54.2	STD	CS1A					
	0724	CSJ 01	48	51°54.7	129°59.7	TT,STD	CSJ1	9255,20494	533.3,1045.6	10	49-26	26-0
	0907			51°57.8	129°54.1	STD	CS2A					
	1042	CSJ 02	49	52°1.9	129°48.3	TT,STD	CSJ2	6910,9606	352.5,490.1	7	49-25	25-0
	1155			52°5.1	129°43.0	STD	CS3A					
	1441			51°50.9	130°3.7	STD	CS4A					
	1551	CSJ 03	50	51°46.9	130°10.1	TT,STD	CSJ5	NS,21414	1092.5	10	45-26	26-0
	1655			51°43.2	130°16.3	STD	CS5A					
	1815	CSJ 04	51	51°39.6	130°21.2	TT,STD	CSJ6	5361,11302	533.3,576.6	10	55-25	25-0
	2145	CSJ 05	52	51°23.9	130°43.3	NN		27356	294.0	10		
	2207	CSJ 06	53	51°24.8	130°42.3	NN		23358	251.1	10		
	2230	CSJ 07	54	51°25.7	130°42.3	NN		36410	391.4	15		
	2302	CSJ 08	55	51°27.3	130°40.0	NN		36170	388.8	15		
	2328	CSJ 09	56	51°28.3	130°38.5	NN		34681	372.8	15		
	2355	CSJ 10	57	51°29.2	130°36.9	NN		33907	364.5	15		
06/14	0023	CSJ 11	58	51°30.3	130°35.2	NN		28344	304.7	15		
	0055	CSJ 12	59	51°31.8	130°33.0	NN		31108	334.4	15		
	0118	CSJ 13	60	51°32.5	130°31.5	NN		37130	399.1	15		
	0142	CSJ 14	61	51°33.3	130°29.3	NN		37790	406.2	15		
	0207	CSJ 15	62	51°34.7	130°27.2	NN		25640	275.6	10		
	0224	CSJ 16	63	51°35.8	130°25.9	NN		23750	255.3	10		
	0242	CSJ 17	64	51°36.9	130°24.4	NN		25169	270.5	10		
	0258	CSJ 18	65	51°37.7	130°23.3	NN		23460	252.2	10		
	0315	CSJ 19	66	51°38.6	130°22.2	NN		24210	260.2	10		
	0332	CSJ 20	67	51°39.4	130°21.2	NN		23492	252.5	10		
	0348	CSJ 21	68	51°40.3	130°20.2	NN		38058	409.1	15		
	0411	CSJ 22	69	51°41.3	130°18.9	NN		38890	418.0	15		
	0432	CSJ 23	70	51°42.4	130°17.4	NN		43811	470.9	15		
	0458	CSJ 24	71	51°43.8	130°15.5	NN		40898	439.6	15		
	0525	CSJ 25	72	51°45.2	130°13.1	NN		34461	370.4	13		
	0753			51°58.9	130°6.7	STD	KU1A					
06/14	0903	KUN 01	73	52°1.5	130°12.3	TT,STD	KUN1	14707,17121	750.4,873.5	10	49-21	21-0
	1011			52°1.5	130°12.3	STD	KU2A					
	1146	KUN 02	74	52°7.7	130°23.7	TT,STD	KUN2	13323,12997	679.7,663.1	10	55-26	26-0
	1315			52°11.1	130°30.5	STD	KU3A					
	1410	KUN 03	75	52°13.8	130°35.6	TT,STD	KUN3	12151,12969	619.9,661.7	10	44-21	21-0
	1554	KUN 04	76	52°10.0	130°39.3	TT,STD	KUN4	13574,15996	692.5,816.1	10	47-23	23-0
	1710			52°14.6	130°42.1	STD	KU5A					

Table 1. Hecate Strait Crab Larvae Cruise sampling stations – June 1988

Date	Time	Transect	Tow #	Latitude	Longitude	Samples	STD CODE	Flowmeter reading	Volume(m <sup>3</sup> )	Tow duration (in minutes)	Depth range (m)	
											Net 2	Net 3
06/15	1806	KUN 05	77	52°19.2	130°44.3	TT,STD	KUN5	13558,24884	691.7,1269.6	10	51-23	23-0
	2150	KUN 06	78	52°12.5	130°57.2	NN		25888	278.3	10		
	2215			52°13.2	130°56.4	STD	KU6B			12		
	2225	KUN 07	79	52°13.2	130°56.4	NN		30538	328.3	10		
	2251	KUN 08	80	52°14.3	130°54.2	NN		22501	241.9	15		
	2311	KUN 09	81	52°15.1	130°52.6	NN		37341	401.4	15		
	2340	KUN 10	82	52°16.2	130°50.4	NN		36989	397.6	15		
	0010	KUN 11	83	52°17.4	130°47.5	NN		32943	354.1	20		
	0038	KUN 12	84	52°18.3	130°45.3	NN		55387	595.4	15		
	0108	KUN 13	85	52°20.2	130°44.7	NN		42093	452.5	15		
	0132	KUN 14	86	52°21.6	130°45.8	NN		41069	441.4	15		
	0153	KUN 15	87	52°22.6	130°47.2	NN		38080	409.3	17		
	0214	KUN 16	88	52°23.4	130°48.6	NN		43270	465.1	15		
	0237	KUN 17	89	52°23.6	130°50.8	NN		38428	413.1	15		
	0257	KUN 18	90	52°23.6	130°52.9	NN		39739	427.2	15		
	0317	KUN 19	91	52°23.6	130°54.9	NN		41391	444.9	15		
	0337	KUN 20	92	52°23.7	130°57.0	NN		41972	451.2	15		
	0257	KUN 21	93	52°24.1	130°59.0	NN		42531	457.2	15		
	0417	KUN 22	94	52°24.9	131°0.4	NN		42347	455.2	15		
	0437	KUN 23	95	52°26.2	131°0.5	NN		45750	491.8	5		
	0457	KUN 24	96	52°27.6	131°0.1	NN		14733	158.4	5		
	0507	KUN 25	97	52°28.4	131°0.0	NN		15568	167.3			
	0627			52°23.0	130°48.4	STD	SC1A					
	0810	SCU 01	98	52°27.6	130°51.7	TT, STD	SCU1	27445,15180	1400.2,774.5	10	53-25	25-0
	0945			52°32.5	130°54.0	STD	SC2A					
	1058	SCU 02	99	52°37.9	130°56.2	TT, STD	SCU2	10336,10327	527.3,526.9	10	47-21	21-0
	1210			52°42.3	130°59.2	STD	SC3A					
06/16	1305	SCU 03	100	52°46.9	131°1.9	TT, STD	SCU3	*,11052	563.9	10	20-10	10-0
	2225	SCU 04	101	52°31.0	131°23.0	NN		22801	245.1	10		
	2247	SCU 05	102	52°30.5	131°21.8	NN		22209	238.7	10		
	2307	SCU 06	103	52°29.5	131°20.9	NN		24533	263.7	10		
	2332	SCU 07	104	52°31.8	131°17.5	NN		27528	295.9	10		
	2355	SCU 08	105	52°32.8	131°17.1	NN		37700	405.2	15		
	0023	SCU 09	106	52°34.1	131°15.8	NN		35530	381.9	15		
	0100	SCU 10	107	52°36.2	131°14.4	NN		38282	411.5	15		
	0130	SCU 11	108	52°38.0	131°12.9	NN		49900	536.4	15		
	0200	SCU 12	109	52°39.9	131°11.2	NN		48817	524.7	20		
	0231	SCU 13	110	52°41.9	131°9.7	NN		28012	301.1	15		
	0254	SCU 14	111	52°43.1	131°8.7	NN		28256	303.7	15		
	0317	SCU 15	112	52°44.3	131°7.1	NN		30053	323.0	15		
	0339	SCU 16	113	52°45.6	131°5.6	NN		28499	306.3	15		
	0401	SCU 17	114	52°46.7	131°4.4	NN		28401	305.3	15		
	0423	SCU 18	115	52°47.7	131°3.2	NN		28640	307.8	15		
	0445	SCU 19	116	52°48.6	131°1.8	NN		30841	331.5	15		
	0508	SCU 20	117	52°49.1	130°59.8	NN		41855	449.9	15		
	0652	SAN 01	118	52°52.9	130°53.5	TT, STD	SAN1	10627,NS	542.2	10	27 (n/a)	
	0850			52°52.9	131°4.4	STD	SA1A					
06/17	1055	SAN 02	119	52°57.7	131°6.7	TT, STD	SAN2	7765,NS	396.2	10	10 (n/a)	
	1151			53°1.7	131°9.6	STD	SA2A					
	1300	SAN 03	120	53°6.5	131°13.2	TT, STD	SAN3	8899,NS	454.0	10	33 (n/a)	
	1405			53°11.5	131°15.7	STD	SA4A					
	1503	SAN 04	121	53°15.7	131°17.8	TT, STD	SAN4	10681,NS	544.9	10	20 (n/a)	
	1610			53°18.9	131°20.5	STD	SA5A					
	1725	SAN 05	122	53°22.4	131°14.0	TT, STD	SAN5	7533,NS	384.3	10	22 (n/a)	
	1850			53°25.6	131°7.2	STD	SA6A					
	2155	SAN 06	123	53°13.3	131°31.3	NN		22070	237.2	10		
	2230	SAN 07	124	53°14.8	131°29.5	NN		15698	168.7	15		
	2305	SAN 08	125	53°15.5	131°28.4	NN		32035	344.3	20		

**Table 1.** Hecate Strait Crab Larvae Cruise sampling stations – June 1988

Date	Time	Transect	Tow #	Latitude	Longitude	Samples	STD CODE	Flowmeter reading	Volume(m <sup>3</sup> )	Tow duration (in minutes)	Depth range (m)	
											Net 2	Net 3
06/18	1530			53°30.0	131°18.4	STD	RO1A			25		
	1628	ROS 01	126	53°35.0	131°18.2	TT,STD	ROS1	11355,NS	579.3	10	33 (n/a)	
	1737			53°40.3	131°17.6	STD	RO2A					
	1830	ROS 02	127	53°44.8	131°16.4	TT,STD	ROS2	9684,NS	494.1	10	33 (n/a)	
	1937			53°49.9	131°16.5	STD	RO3A					
	2040	ROS 03	128	53°54.9	131°14.8	TT,STD	ROS3	10760,NS	549.0	10	28 (n/a)	
	2155			54°0.2	131°14.2	STD	RO4A					
	2230	ROS 04	129	54°1.8	131°14.1	NN		32448	348.8	15		
	2255	ROS 05	130	54°3.1	131°14.0	NN		42603	457.9	20		
	2326	ROS 06	131	54°5.1	131°13.9	NN		33817	363.5	20		
	2351	ROS 07	132	54°6.7	131°13.8	NN		61800	664.3	30		
06/19	0035	ROS 08	133	54°9.2	131°13.6	NN		69504	747.1	30		
	0115	ROS 09	134	54°11.5	131°13.7	NN		39766	427.4	30		
	0156	ROS 10	135	54°11.2	131°16.7	NN		29408	316.1	15		
	0220	ROS 11	136	54°11.8	131°18.2	NN		21061	226.4	10		
	0239	ROS 12	137	54°12.6	131°19.3	NN		23861	256.5	10		
	0259	ROS 13	138	54°13.5	131°20.2	NN		24800	266.6	10		
	0318	ROS 14	139	54°14.6	131°21.1	NN		10970	117.9	5		
	0330	ROS 15	140	54°15.0	131°22.0	NN		11422	122.8	5		
	0346	ROS 16	141	54°15.2	131°23.6	NN		10538	113.3	5		
	0401	ROS 17	142	54°15.5	131°25.1	NN		11640	125.1	5		
	0413	ROS 18	143	54°15.7	131°26.2	NN		13780	148.1	6		
	0427	ROS 19	144	54°16.0	131°27.5	NN		13380	143.8	6		
	0440	ROS 20	145	54°16.4	131°28.5	NN		12200	131.1	5		
	0450	ROS 21	146	54°16.8	131°29.5	NN		11662	125.4	5		
	0503	ROS 22	147	54°17.2	131°30.5	NN		12823	137.8	5		
	0514	ROS 23	148	54°17.6	131°31.3	NN		23025	247.5	10		
	0618			54°19.5	131°31.6	STD	BA1A					
	0745			54°15.1	131°23.8	STD	BA2A					
	0850			54°11.3	131°16.9	STD	BA3A					
	1035			54°2.9	131°4.9	STD	BA4A					
	1515	BAN 04	149	53°36.0	130°46.6	TT, STD	BAN4	10151,13895	517.9,708.9	10	40-9	9-0
	1705	BAN 05	150	53°33.2	130°53.6	TT, STD	BAN5	12515,14025	638.5,715.6	10	48-21	21-0
	2215	BAN 06	151	53°6.0	130°46.6	NN		38121	409.8	15		
	2237	BAN 07	152	52°59.8	130°43.1	NN		33810	363.4	15		
	2301	BAN 08	153	53°0.1	130°40.9	NN		36180	388.9	15		
	2325	BAN 09	154	53°1.2	130°39.2	NN		39142	420.7	15		
	2350	BAN 10	155	53°2.3	130°37.5	NN		24898	267.6	10		
06/20	0010	BAN 11	156	53°3.1	130°36.1	NN		51780	556.6	20		
	0045	BAN 12	157	53°4.5	130°33.7	NN		51288	551.3	20		
	0111	BAN 13	158	53°5.8	130°31.5	NN		33565	360.8	15		
	0131	BAN 14	159	53°6.8	130°30.1	NN		32327	347.5	15		
	0151	BAN 15	160	53°7.7	130°28.7	NN		33511	360.2	15		
	0212	BAN 16	161	53°8.7	130°27.2	NN		33727	362.5	15		
	0233	BAN 17	162	53°9.7	130°25.9	NN		32530	349.7	15		
	0255	BAN 18	163	53°10.8	130°24.4	NN		36680	394.3	15		
	0317	BAN 19	164	53°11.5	130°22.4	NN		36210	389.2	15		
	0340	BAN 20	165	53°12.2	130°20.4	NN		47633	512.0	20		
	0407	BAN 21	166	53°13.4	130°18.1	NN		NS				
	0430	BAN 22	167	53°14.5	130°17.4	NN		54668	587.6	10		
	0448	BAN 23	168	53°15.9	130°16.8	NN		23748	255.3	10		
	0505	BAN 24	169	53°17.0	130°15.8	NN		23461	252.2	5		

NN=neuston net; TT=Tucker trawl sample; STD = salinity-temperature profile by depth. Transect names correspond with lines covering a 24 hour sampling period from dawn to dawn. TRI=Triangle Island; GSE=Goose Bank; CSJ=Cape St. James; KUN=Kunghit Island; SCU=Scudder Point; SAN=Sandspit; ROS=Rose Point; BAN=Banks Island transects. Flowmeter readings are based on a conversion factor of 0.05102 for Tucker trawls (TT) and neuston nets (NN). For Tucker trawl net tows, the first flowmeter reading and value measurement is for net 3 and the second is for net 2; net 1 data are not used. For station locations, see Figures 1 and 2. NS=No Sample, \*=flowmeter reading discarded, tow duration and speed used to calculate volume instead.

**Table 2.** Hecate Strait Taxonomic List

Arthropoda
Reptantia
Cancridae
<i>Cancer magister</i> (Dungeness crab)
<i>Cancer</i> spp.
Porcellanidae
Grapsidae
Majidae
Pinnotheridae
<i>Fabia subquadrata</i>
Galatheididae
Natantia
Pandalidae
Cirripedia
<i>Lepas</i> sp. (gooseneck barnacle)
Cumacea
Amphipoda
Copepoda (Calanoida)
Euphaussiacea ( <i>Thysanoessa</i> )
Mollusca
<i>Limacina helicina</i>
<i>Clinoe limacina</i>
<i>Euclio</i> sp.
Cephalopoda
<i>Octopus</i> sp.
<i>Loligo</i> sp.
Isopoda
Insecta
Mycidacea
Ostracoda
Cnidaria
Siphonophora
Leptomedusae
<i>Velella velella</i>
Ctenophora
Pleurobrachia
Coelenterata
Annelida
Polychaeta
Chaetognathia
Chordata
Thaliacea
Salpidae
Osteichthyes
<i>Stenobranchius leucopsaurus</i> (Myctophid)
<i>Ammodytes</i> larvae (Sandlance)
<i>Scorpaenichthys marmoratus</i> (Cabezon)
<i>Anoplopoma fimbria</i> (Blackcod)
<i>Hexagrammos</i> sp. (Greenling)
Stictiidae (Blenny)
<i>Sebastes</i> larvae (rockfish)
Bullhead larvae
Osmariidae (smelt)
<i>Microstomus pacificus</i> (Dover sole)
<i>Psettichthys melamostictus</i> (sand sole)
<i>Isopsetta isolepis</i> (Butter sole)
<i>Hippoglossoides elasodon</i> (Flathead sole)
<i>Lyopsetta exilis</i> (Slender sole)
<i>Pleuronecthus coenosus</i> (C-O sole)
<i>Lepidopsetta bilineata</i> (Rock sole)
Lipariidae
Agonidae (poacher)
Ptilichthyidae (Quillfish)
<i>Brosmophysis marginata</i> (ragfish)
Gobiidae
<i>Clupea harengus</i> (Herring)
Pholidae (Gunnel)
<i>Onchorhynchus keta</i> (Chum salmon)
Gadidae (Codfish)

## Table 3 (cont'd). A. Triangle - June 11-12, 1988

1988

	10	11	12	13	14	15	16	17	18	19	20
07006	500.6	508.6	502.9	534.3	545.7	564.2	647.6	683.8	778.2	482.6	504.4
0070	0.312	0.017	0.094	0.036	0.0	0.0	0.0	0.0	0.0	0.0	0.0
0473	6.328	3.446	0.867	0.696	10.82	0.200	0.628	0.514	0.249	0.177	
1.73	6.581	0.177	1.088	0.128	0.017	0.649	0.043	0.025	0.0	0.0	0.0
0.0	0.0	0.017	0.015	0.0	0.0	0.015	0.0	0.012	0.0	0.0	0.0
2.541	4.109	4.956	5.472	0.0	5.600	10.44	5.557	2.338	1.740	1.487	0.0
0.0	0.0	0.0	0.0	0.0	0.0	0.0	0.0	0.0	0.0	0.0	0.0
0.0	0.0	0.0	0.0	0.0	0.0	0.0	0.0	0.0	0.0	0.0	0.0
0.0	0.0	0.0	0.0	0.0	0.0	0.0	0.0	0.0	0.0	0.0	0.0
0.067	0.164	0.0	0.0	0.0	0.0	0.0	0.0	0.0	0.0	0.0	0.0
0.0	0.0	0.017	0.0	0.0	0.0	0.0	0.0	0.0	0.0	0.0	0.0
0.035	0.065	0.053	0.063	0.073	0.017	0.0	0.0	0.0	0.0	0.0	0.0
0.0	0.0	0.0	0.0	0.0	0.0	0.0	0.0	0.0	0.0	0.0	0.0
0.280	0.164	0.249	0.189	0.569	0.425	1.637	0.292	0.192	0.062	0.011	0.0
15.68	93.69	37.48	7.869	0.0	3.704	0.926	0.292	0.346	0.0	0.611	0.0
4.837	1.777	0.621	0.157	0.494	0.141	0.417	0.043	0.0	0.0	0.0	0.0
0.0	0.0	0.0	0.0	0.0	0.0	0.0	0.0	0.0	0.0	0.0	0.0
0.0	0.0	0.0	0.0	0.0	0.018	0.0	0.0	0.014	0.038	0.0	0.0
0.0	0.0	0.0	0.0	0.0	0.0	0.0	0.0	0.0	0.0	0.0	0.0
0.0	0.0	0.0	0.0	0.0	0.0	0.0	0.0	0.0	0.0	0.0	0.0
0.0	0.0	0.0	0.0	0.0	0.0	0.017	0.0	0.0	0.0	0.0	0.0
0.0	0.0	0.0	0.0	0.0	0.0	0.0	0.0	0.0	0.0	0.020	0.0
0.052	0.0	0.0	0.0	0.0	0.109	0.017	0.015	0.029	0.077	0.0	0.077
0.386	0.723	2.504	1.193	1.906	6.079	5.808	0.731	0.077	0.476	1.381	0.0
0.0	0.0	0.0	0.0	0.0	0.0	0.0	0.0	0.0	0.0	0.0	0.0
0.0	0.0	0.0	0.0	0.0	0.0	0.0	0.0	0.0	0.0	0.0	0.0
0.017	0.0	0.0	0.0	0.0	0.0	0.0	0.0	0.014	0.051	0.020	0.033
0.017	0.0	0.0	0.0	0.0	0.0	0.0	0.0	0.0	0.0	0.0	0.0
0.0	0.0	0.0	0.0	0.0	0.0	0.015	0.0	0.0	0.0	0.0	0.0
0.0	0.0	0.0	0.0	0.0	0.0	0.0	0.015	0.0	0.0	0.0	0.0
0.403	0.180	0.017	0.063	0.0	0.0	0.0	0.0	0.0	0.0	0.0	0.0
0.0	0.016	0.0	0.0	0.0	0.0	0.0	0.0	0.0	0.051	0.0	0.0
0.0	0.085	0.0	0.0	0.0	0.0	0.017	0.0	0.015	0.0	0.012	0.0
0.0	0.0	0.0	0.0	0.0	0.0	0.0	0.0	0.030	0.0	0.0	0.0
0.035	0.049	0.035	0.094	0.0	0.0	0.0	0.015	0.0	0.0	0.0	0.0
0.0	0.0	0.0	0.0	0.0	0.0	0.0	0.0	0.0	0.0	0.0	0.0
0.052	0.115	0.106	0.031	0.054	0.0	0.015	0.043	0.025	0.0	0.0	0.0
0.070	0.279	0.177	0.165	0.478	0.324	0.046	0.043	0.064	0.103	0.077	0.0
0.0	0.0	0.0	0.0	0.0	0.0	0.0	0.0	0.269	0.227	0.233	0.0
0.0	0.0	0.0	0.0	0.0	0.0	0.0	0.0	0.0	0.0	0.0	0.0
0.0	0.0	0.0	0.0	0.0	0.0	0.0	0.0	0.0	0.0	0.0	0.0
0.0	0.0	0.0	0.0	0.0	0.0	0.0	0.0	0.0	0.0	0.0	0.0
0.0	0.0	0.0	0.0	0.0	0.0	0.0	0.0	0.0	0.0	0.0	0.0
0.0	0.0	0.0	0.0	0.0	0.0	0.0	0.0	0.0	0.0	0.0	0.0
0.0	0.0	0.0	0.0	0.0	0.0	0.0	0.0	0.0	0.0	0.0	0.0
0.0	0.0	0.0	0.0	0.0	0.0	0.0	0.0	0.0	0.0	0.020	0.0
0.0	0.0	0.0	0.0	0.0	0.0	0.0	0.0	0.0	0.0	0.0	0.0
0.0	0.0	0.0	0.0	0.0	0.0	0.0	0.0	0.0	0.0	0.0	0.0
0.0	0.0	0.0	0.0	0.0	0.0	0.0	0.0	0.0	0.0	0.0	0.0
0.0	0.0	0.0	0.0	0.0	0.0	0.0	0.0	0.0	0.0	0.0	0.0
0.0	0.0	0.0	0.0	0.0	0.0	0.0	0.0	0.0	0.0	0.0	0.0
0.0	0.0	0.0	0.0	0.0	0.0	0.0	0.0	0.0	0.0	0.0	0.0
0.0	0.0	0.0	0.0	0.0	0.0	0.0	0.0	0.0	0.0	0.0	0.0
0.0	0.0	0.0	0.0	0.0	0.0	0.0	0.0	0.0	0.0	0.0	0.0
0.0	0.0	0.0	0.0	0.0	0.0	0.0	0.0	0.0	0.0	0.0	0.0
0.0	0.0	0.0	0.0	0.0	0.0	0.0	0.0	0.0	0.0	0.0	0.0
0.0	0.0	0.0	0.0	0.0	0.0	0.0	0.0	0.0	0.0	0.0	0.0
0.0	0.0	0.0	0.0	0.0	0.0	0.0	0.0	0.0	0.0	0.0	0.0
0.0	0.0	0.0	0.0	0.0	0.0	0.0	0.0	0.0	0.0	0.0	0.0
0.0	0.0	0.0	0.0	0.0	0.0	0.0	0.0	0.0	0.0	0.0	0.0
0.0	0.0	0.0	0.0	0.0	0.0	0.0	0.0	0.0	0.0	0.0	0.0
0.0	0.0	0.0	0.0	0.0	0.0	0.0	0.0	0.0	0.0	0.0	0.0
0.0	0.0	0.0	0.0	0.0	0.0	0.0	0.0	0.0	0.0	0.0	0.0
0.0	0.0	0.0	0.0	0.0	0.0	0.0	0.0	0.0	0.0	0.0	0.0
0.0	0.0	0.0	0.0	0.0	0.0	0.0	0.0	0.0	0.0	0.0	0.0
0.0	0.0	0.0	0.0	0.0	0.0	0.0	0.0	0.0	0.0	0.0	0.0
0.0	0.0	0.0	0.0	0.0	0.0	0.0	0.0	0.0	0.0	0.0	0.0
0.0	0.0	0.0	0.0	0.0	0.0	0.0	0.0	0.0	0.0	0.0	0.0
0.0	0.0	0.0	0.0	0.0	0.0	0.0	0.0	0.0	0.0	0.0	0.0
0.0	0.0	0.0	0.0	0.0	0.0	0.0	0.0	0.0	0.0	0.0	0.0
0.0	0.0	0.0	0.0	0.0	0.0	0.0	0.0	0.0	0.0	0.0	0.0
0.0	0.0	0.0	0.0	0.0	0.0	0.0	0.0	0.0	0.0	0.0	0.0
0.0	0.0	0.0	0.0	0.0	0.0	0.0	0.0	0.0	0.0	0.0	0.0
0.0	0.0	0.0	0.0	0.0	0.0	0.0	0.0	0.0	0.0	0.0	0.0
0.0	0.0	0.0	0.0	0.0	0.0	0.0	0.0	0.0	0.0	0.0	0.0
0.0	0.0	0.0	0.0	0.0	0.0	0.0	0.0	0.0	0.0	0.0	0.0
0.0	0.0	0.0	0.0	0.0	0.0	0.0	0.0	0.0	0.0	0.0	0.0
0.0	0.0	0.0	0.0	0.0	0.0	0.0	0.0	0.0	0.0	0.0	0.0
0.0	0.0	0.0	0.0	0.0	0.0	0.0	0.0	0.0	0.0	0.0	0.0
0.0	0.0	0.0	0.0	0.0	0.0	0.0	0.0	0.0	0.0	0.0	0.0
0.0	0.0	0.0	0.0	0.0	0.0	0.0	0.0	0.0	0.0	0.0	0.0
0.0	0.0	0.0	0.0	0.0	0.0	0.0	0.0	0.0	0.0	0.0	0.0
0.0	0.0	0.0	0.0	0.0	0.0	0.0	0.0	0.0	0.0	0.0	0.0
0.0	0.0	0.0	0.0	0.0	0.0	0.0	0.0	0.0	0.0	0.0	0.0
0.0	0.0	0.0	0.0	0.0	0.0	0.0	0.0	0.0	0.0	0.0	0.0
0.0	0.0	0.0	0.0	0.0	0.0	0.0	0.0	0.0	0.0	0.0	0.0
0.0	0.0	0.0	0.0	0.0	0.0	0.0	0.0	0.0	0.0	0.0	0.0
0.0	0.0	0.0	0.0	0.0	0.0	0.0	0.0	0.0	0.0	0.0	0.0
0.0	0.0	0.0	0.0	0.0	0.0	0.0	0.0	0.0	0.0	0.0	0.0
0.0	0.0	0.0	0.0	0.0	0.0	0.0	0.0	0.0	0.0	0.0	0.0
0.0	0.0	0.0	0.0	0.0	0.0	0.0	0.0	0.0	0.0	0.0	0.0
0.0	0.0	0.0	0.0	0.0	0.0	0.0	0.0	0.0	0.0</		





Table 3 (cont'd). B. GOOSE BANK

Table 3. Species catch per 10 square metres of sea surface for each neuston tow and Tucker trawl net catch.										
C. CAPE ST. JAMES TRANSECT - June 13-14, 1988										
Surface area (m <sup>2</sup> )	40	41	42	43	44	45	46	47	48-2	48-3
TAXA (number per 10m <sup>2</sup> )	564.1	849.8	999.9	606.4	563.0	996.1	986.1	903.8	0.253	0.421
Surface area (m <sup>2</sup> )	40	41	42	43	44	45	46	47	48-2	48-3
TAXA (number per 10m <sup>2</sup> )	564.1	849.8	999.9	606.4	563.0	996.1	986.1	903.8	0.253	0.421
<i>Cancer magister</i> megalops	0.017	0.058	0.019	0.0	0.0	0.0	0.0	0.0	0.253	0.0
<i>Cancer</i> sp. megalops	0.194	0.223	0.519	0.016	0.0	0.020	0.0	0.011	6.578	5.473
megalops (shrimp, other crabs)	0.0	0.011	0.149	0.016	0.0	0.020	0.0	0.0	1.518	0.842
<i>Cancer magister</i> zoea	3.225	18.23	101.9	22.09	26.99	39.05	38.44	133.2	0.0	0.0
<i>Cancer</i> sp. zoea	0.0	0.0	0.0	0.0	0.0	0.0	0.0	0.0	164.4	648.3
Porcellanidae zoea	0.0	0.0	0.0	0.0	0.0	0.0	0.0	0.0	0.0	0.0
Grapsidae zoea	0.0	0.0	0.0	0.0	0.0	0.0	0.0	0.0	0.0	0.0
Majidae zoea (Pugilia)	0.0	0.0	0.0	0.0	0.0	0.0	0.0	0.0	0.0	0.0
<i>Fabia subquadrata</i> (Pinnotheridae)	0.0	0.0	0.0	0.0	0.0	0.0	0.0	0.0	0.0	0.0
Galatheid zoea	0.0	0.0	0.0	0.0	0.0	0.0	0.0	0.0	3.795	0.0
Other Decapod Larvae	0.0	0.0	0.0	0.0	0.0	0.0	0.0	0.0	0.0	0.0
Pandalidae	0.0	0.0	0.0	0.0	0.0	0.0	0.0	0.0	0.0	0.0
Other Shrimp	0.0	0.0	0.0	0.0	0.0	0.0	0.0	0.011	6.072	12.20
<i>Lepas</i> (goose barnacle)	0.0	0.0	0.0	0.0	0.0	0.0	0.0	0.0	4.554	2.526
Cumacea	0.0	0.0	0.0	0.0	0.0	0.0	0.0	0.0	0.0	0.0
Amphipoda	0.070	0.023	0.009	0.016	0.053	0.010	0.091	0.077	0.0	0.0
Copepoda (Calanoida)	15.95	12.94	23.74	11.95	1.829	0.120	6.083	6.084	0.0	0.0
Euphausiacea - Thysanoessa	0.567	0.611	0.319	0.972	0.177	0.240	0.101	0.154	25.3	2.526
<i>Limnoria helicina</i> (Pteropod)	0.0	0.0	0.0	0.0	0.0	0.0	0.0	0.0	1518.	5163.
<i>Clione limacina</i> (Pteropod)	0.0	0.0	0.0	0.0	0.0	0.0	0.0	0.0	303.6	492.5
<i>Eudora</i> sp. (Pteropod)	0.0	0.0	0.0	0.0	0.0	0.0	0.0	0.0	0.0	0.0
Octopus	0.0	0.0	0.0	0.0	0.0	0.0	0.0	0.0	0.0	0.0
Squid	0.0	0.0	0.0	0.0	0.0	0.0	0.0	0.0	0.0	0.0
Isopoda	0.0	0.0	0.0	0.0	0.0	0.0	0.0	0.0	0.506	0.0
Insect Larvae	0.0	0.0	0.0	0.0	0.0	0.0	0.0	0.0	0.0	0.0
Myctodaea	0.0	0.0	0.0	0.0	0.0	0.0	0.0	0.0	0.0	0.0
Ostracoda	0.0	0.0	0.0	0.0	0.0	0.0	0.0	0.0	0.0	0.0
Invertebrate eggs	0.0	0.0	0.0	0.0	0.0	0.0	0.0	0.0	0.0	0.0
<i>Veella</i>	0.0	0.0	0.0	0.0	0.0	0.0	0.0	0.0	0.0	0.0
Jellyfish (Lentomedusae)	0.248	0.129	0.039	0.0	0.0	2.210	2.179	0.0	0.0	0.0
Ctenophores (Pleurobrachia)	0.0	0.0	0.0	0.0	0.0	0.0	0.0	0.0	25.80	10.94
Siphonophores	0.0	0.0	0.0	0.0	0.0	0.0	0.0	0.0	0.0	0.0
<i>Coelenterata</i>	0.0	0.0	0.0	0.0	0.0	0.0	0.0	0.0	0.0	0.0
<i>Polychaeta</i>	0.0	0.0	0.0	0.0	0.0	0.0	0.0	0.0	0.0	0.0
Salps	0.0	0.0	0.0	0.0	0.0	0.0	0.0	0.0	0.0	0.0
<i>Chaetognathia</i>	0.0	0.0	0.0	0.0	0.0	0.0	0.0	0.0	17.71	35.78
<i>Stenobrachius leucopsaurus</i>	0.0	0.0	0.0	0.0	0.0	0.0	0.0	0.0	0.0	0.0
<i>Ammodites</i> larvae (Sandlance)	0.017	0.0	0.0	0.0	0.0	0.100	0.020	0.0	0.0	0.0
<i>Scopelogadus marmoratus</i>	0.0	0.0	0.0	0.0	0.0	0.0	0.0	0.0	0.0	0.0
<i>Anoplopoma fimbria</i> (Blackcod)	0.017	0.011	0.079	0.0	0.0	0.0	0.010	0.0	0.0	0.0
<i>Hexagrammos</i> (Greenling)	0.0	0.0	0.0	0.0	0.0	0.0	0.0	0.0	0.0	0.0
<i>Stichidae</i> (Blenny)	0.0	0.0	0.0	0.0	0.0	0.0	0.0	0.0	0.0	0.0
<i>Sebastes</i> (Rockfish) larvae	0.0	0.0	0.0	0.0	0.0	0.080	0.0	0.0	0.0	0.0
Bullhead larvae	0.0	0.0	0.0	0.0	0.0	0.0	0.0	0.0	14.16	4.631
Fish eggs	0.513	0.0	0.139	0.0	0.177	0.080	0.030	0.0	0.0	0.0
<i>Osmariidae</i> (smelt)	0.0	0.0	0.0	0.0	0.0	0.0	0.0	0.0	0.0	0.0
<i>Microstomus pacificus</i> (Dover Sole)	0.0	0.0	0.0	0.0	0.0	0.0	0.0	0.0	0.0	0.0
Liparidae	0.0	0.0	0.0	0.0	0.0	0.0	0.0	0.0	0.0	0.0
Agonidae (poacher)	0.0	0.0	0.0	0.0	0.0	0.0	0.0	0.0	0.0	0.0
<i>Pilichthys</i> (Quillfish)	0.0	0.0	0.0	0.0	0.0	0.0	0.0	0.0	0.0	0.0
<i>Brosme</i> (Ragfish)	0.0	0.0	0.0	0.0	0.0	0.0	0.0	0.0	0.0	0.0
<i>Pseudocyttus marginatus</i> (ragfish)	0.0	0.0	0.0	0.0	0.0	0.0	0.0	0.0	0.0	0.0
<i>Isopsetta solopsis</i> (Butter Sole)	0.0	0.0	0.0	0.0	0.0	0.0	0.0	0.0	0.0	0.0
<i>Hippoglossoides elsdoni</i>	0.0	0.0	0.0	0.0	0.0	0.0	0.0	0.0	0.0	0.0
Gobiidae	0.0	0.0	0.0	0.0	0.0	0.0	0.0	0.0	0.506	0.0
<i>Clupea harengus</i> (Herring)	0.0	0.0	0.0	0.0	0.0	0.0	0.0	0.0	0.0	0.0
<i>Lyopsetta exilis</i> (Slender Sole)	0.0	0.0	0.0	0.0	0.0	0.0	0.0	0.0	0.0	0.0
<i>Pleuronectes coenosus</i> (C-O sole)	0.0	0.0	0.0	0.0	0.0	0.0	0.0	0.0	0.0	0.0
Pholidae (Gunnels)	0.0	0.0	0.0	0.0	0.0	0.0	0.0	0.0	0.0	0.0
<i>Onchorynchus keta</i> (Chum Salmon)	0.0	0.0	0.0	0.0	0.0	0.0	0.0	0.0	0.0	0.0
Gadidae	0.0	0.0	0.0	0.0	0.0	0.0	0.0	0.0	0.0	0.0
<i>Lepidopsetta bilineata</i> (Rock Sole)	0.0	0.0	0.0	0.0	0.0	0.0	0.0	0.0	0.0	0.0



**Table 3.** Species catch per 10 square metres of sea surface for each neuston tow and Tucker trawl net catch. KUNGHIT ISLAND - June 14-15, 1988

	0.240	0.38	0.392	0.427	0.325	0.363	0.281	0.346	0.605	6	714.5
	73-2	73-3	74-2	74-3	75-2	75-3	76-2	76-3	78	79	
	Surface area (m <sup>2</sup> )										
	TAXA (number per 10m <sup>2</sup> )										
Cancer magister megalops	0.0	0.0	0.0	0.0	0.0	0.0	0.0	0.0	0.0	0.0	0.0
Cancer sp. megalops	3.12	0.844	9.016	0.0	3.25	0.726	28.66	21.68	0.00	0.0	0.0
megalops (shrimp, other crabs)	0.72	0.422	4.312	0.427	0.65	0.0	4.466	2.306	0.577	1.539	
Cancer magister zoea	0.24	0.0	0.382	0.0	0.0	0.0	1.124	0.461	0.016	0.0	0.0
Cancer sp. zoea	86.4	38	62.72	0.0	113.7	217.8	134.8	4336.	63.07	314.2	
Porcellanidae zoea	0.0	0.0	0.0	0.0	0.0	0.0	0.0	0.0	0.0	0.0	0.0
Grapsidae zoea	0.0	0.0	0.0	0.0	0.0	0.0	0.0	0.0	0.0	0.0	0.0
Malidae zoea (Pugelia)	0.0	0.0	0.0	0.0	0.0	0.0	0.0	0.0	0.0	0.0	0.0
Pinnotheridae zoea	0.0	0.0	0.0	0.0	0.0	0.0	0.0	0.0	0.0	0.0	0.0
Favia subquadrata (Pinnotheridae)	0.0	0.0	0.0	0.0	0.0	0.0	0.0	0.0	0.0	0.0	0.0
Gammaridae zoea	0.0	0.0	0.0	0.0	0.0	0.0	0.0	0.0	0.0	0.0	0.0
Other Decapod Larvae	0.0	0.0	0.0	0.0	0.0	0.0	0.0	0.0	0.0	0.0	0.0
Pandallidae	19.63	13.33	7.431	0.0	5.523	3.808	33.15	37.36	0.033	0.041	
Other Shrimp	0.48	2.533	0.392	0.427	0.974	0.726	3.933	0.922	0.033	0.083	
Lepas (goose barnacle)	0.0	0.0	0.0	0.0	0.0	0.0	0.0	0.0	0.0	0.0	0.0
Cumacea	0.0	0.0	0.0	0.0	0.0	0.0	0.0	0.0	0.0	0.0	0.0
Amphipoda	16.08	4.644	52.92	0.0	24.7	18.87	157.3	108.4	0.214	0.237	
Copepoda (Calanoida)	232.8	1026.	39200.	0.0	9425.	29403.	45016.	32524.	0.198	0.601	
Limnasia helicina (Pteropod)	0.0	0.0	0.0	0.0	0.0	0.0	0.0	0.0	0.0	0.0	0.0
Clione limacina (Pteropod)	0.0	0.0	0.0	0.0	0.0	0.0	0.0	0.0	0.0	0.0	0.0
Eudis sp. (Pteropod)	0.0	0.0	0.0	0.0	0.0	0.0	0.0	0.0	0.0	0.0	0.0
Octopus	0.0	0.0	0.0	0.0	0.0	0.0	0.0	0.0	0.0	0.0	0.0
Squid	0.0	0.0	0.392	0.0	0.325	0.0	0.0	0.0	0.0	0.0	0.0
Isopoda	0.0	0.0	0.0	0.0	0.0	0.0	0.0	0.0	0.0	0.0	0.0
Insect Larvae	0.0	0.0	0.0	0.0	0.0	0.0	0.0	0.0	0.0	0.0	0.0
Mycidacea	0.0	0.0	0.0	0.0	0.0	0.0	0.0	0.0	0.0	0.0	0.0
Ostracoda	0.0	0.0	0.0	0.0	0.0	0.0	0.0	0.0	0.0	0.0	0.0
Invertebrate eggs	0.0	0.0	0.0	1.708	0.0	2.176	0.0	0.0	0.0	0.0	0.0
Veleva	0.0	0.0	0.0	0.0	0.0	0.0	0.0	0.0	0.0	0.0	0.0
Jellyfish (Leptomedusae)	21.36	136.3	5.096	17.08	18.52	28.31	12.36	50.28	5.994	1.049	
Ctenophores (Pleurobrachia)	0.72	1.688	0.784	1.281	0.325	7.986	0.0	0.922	0.086	0.027	
Siphonophores	0.0	0.0	0.0	0.0	0.0	0.0	0.0	0.0	0.0	0.0	0.0
Coelenterata	0.0	0.422	0.0	0.0	0.0	0.0	0.0	0.0	0.0	0.0	0.0
Polychaeta	0.0	0.0	0.0	0.0	0.65	0.0	0.0	0.0	0.0	0.0	0.0
Chaetognatha	0.96	0.422	3.92	3.843	5.525	12.34	0.0	22.14	0.0	0.0	0.0
Sapidae	0.0	0.0	0.0	0.0	0.0	0.0	0.0	0.0	0.0	0.0	0.0
Stenobrachius leucostaeus	0.0	0.0	0.0	0.0	0.0	0.0	0.0	0.0	0.0	0.0	0.0
Ammodites larvae (Sand lance)	0.0	0.0	0.0	0.0	0.0	0.0	0.0	0.0	0.0	0.0	0.0
Scorpaenichthys marmoratus	0.0	0.0	0.0	0.0	0.0	0.0	0.0	0.0	0.0	0.0	0.0
Anoplopoma fimbria (Blackcod)	0.0	0.0	0.0	0.0	0.0	0.0	0.0	0.0	0.0	0.0	0.0
Hexagrammos (Greenling)	0.0	0.0	0.0	0.0	0.0	0.0	0.0	0.0	0.0	0.0	0.0
Stichidae (Blenny)	0.0	0.422	0.0	0.0	0.0	0.0	0.0	0.0	0.0	0.0	0.0
Sesostes (Rockfish) larvae	0.0	0.422	13.72	0.0	1.95	11.61	3.372	15.68	0.0	0.0	0.0
Bullhead larvae	2.4	0.422	0.0	0.0	0.325	0.0	0.0	0.461	0.0	0.055	
Fish eggs	0.0	0.0	0.0	5.978	0.325	0.726	0.0	0.922	0.016	0.069	
Osmariidae (smelt)	0.0	0.0	0.0	0.0	0.0	0.0	0.0	0.0	0.0	0.0	0.0
Microstomus pacificus (Dover Sole)	0.0	0.0	0.0	0.0	0.0	0.0	0.0	0.0	0.0	0.0	0.0
Liparidae	0.0	0.0	0.0	0.0	0.0	0.0	0.0	0.0	0.0	0.0	0.0
Agoniidae (poacher)	0.0	0.0	0.0	0.0	0.0	0.0	0.0	0.0	0.0	0.0	0.0
Pulichthidae (Quillfish)	0.0	0.0	0.0	0.0	0.325	0.0	0.0	0.0	0.0	0.0	0.0
Brusmophysis marginata (ragfish)	0.0	0.422	0.392	0.0	0.0	0.0	3.372	0.922	0.016	0.0	0.0
Psettichthys melanostictus	0.0	0.0	0.0	0.0	0.0	0.0	0.0	0.0	0.0	0.0	0.0
Isopsetta isopis (Butter Sole)	0.0	0.0	0.0	0.0	0.0	0.0	0.0	0.0	0.0	0.0	0.0
Hippoglossoides elsdoni	0.0	0.0	0.0	0.0	0.0	0.0	0.0	0.0	0.0	0.0	0.0
Gobiidae	0.0	0.0	0.0	0.0	0.0	0.0	0.0	0.0	0.0	0.0	0.0
Clupea harengus (Herring)	0.0	0.0	0.0	0.0	0.0	0.0	0.0	0.0	0.0	0.0	0.0
Lycopsetta exilis (Slender Sole)	0.0	0.0	0.0	0.0	0.325	0.0	0.281	0.0	0.0	0.0	0.0
Platichthys centrus (C-O sole)	0.0	0.0	0.0	0.0	0.0	0.0	0.0	0.0	0.0	0.0	0.0
Pholidae (Gunnels)	0.0	0.0	0.0	0.0	0.0	0.0	0.0	0.0	0.0	0.0	0.0
Onchorynchus keta (Chum Salmon)	0.0	0.0	0.0	0.0	0.0	0.0	0.0	0.0	0.0	0.0	0.0
Gadidae	0.0	0.0	0.0	0.0	0.0	0.0	0.0	0.0	0.0	0.0	0.0
Gadoidesella bilineata (Rock Sole)	0.0	0.0	0.0	0.0	0.0	0.0	0.0	0.0	0.0	0.0	0.0

Table 3 (cont'd.). D. KUNGHIT ISLAND - June 14-15, 1988

TAXA (number per 10m <sup>2</sup> )	80	81	82
<i>Cancer magister</i> megalops	0.0	0.0	0.0
<i>Cancer</i> spp. megalops	0.019	0.469	0.221
megalops (shrimp, other crabs)	0.571	0.022	0.0
<i>Cancer magister</i> zoea	0.0	0.0	0.0
<i>Cancer</i> sp. zoea	224.7	1380.	0.0
Porcellanidae zoea	0.0	0.0	0.0
Grossidae zoea	0.0	0.0	0.0
Malidae zoea (Pugetta)	0.0	0.0	0.0
Pinnotheridae zoea	0.0	0.0	0.0
<i>Salathia subquadrata</i> (Pinnotheridae)	0.0	0.0	0.0
Fabidae zoea	0.0	0.0	0.0
Salathidae zoea	0.0	0.0	0.0
Other Decapod Larvae	0.0	0.0	0.0
Pandidae	0.0	0.011	0.0
Other Shrimp	0.095	0.0	1.81
<i>Lepas</i> (gouose barnacle)	0.0	0.0	0.0
Limacea	0.0	0.0	946.9
Amphipoda	0.209	0.068	0.0
Copepoda (Calanoida)	0.628	3.777	0.21
<i>Limnora helicina</i> (Pteropod)	0.0	0.0	0.0
<i>Clione limacina</i> (Pteropod)	0.0	0.011	0.0
<i>Edoia</i> sp. (Pteropod)	0.0	0.0	0.0
Ocypus	0.0	0.0	0.0
Squid	0.0	0.022	0.0
insect Larvae	0.0	0.160	0.0
Myxidiada	0.0	0.0	0.0
Staracida	0.0	0.0	0.0
invertebrate eggs	0.0	0.0	0.0
<i>Veelia</i>	0.0	0.0	0.0
Jellyfish (Leptomedusae)	1.638	0.309	0.0
Tenophores (Pleurobrachia)	0.019	0.1	0.0
Siphonophores	0.0	0.0	0.0
<i>Coelentera</i>	0.0	0.0	0.0
<i>Polychaeta</i>	0.095	0.160	0.0
<i>Chaetognatha</i>	0.0	0.011	0.0
Salpidae	0.0	0.0	0.0
<i>Stenodrilus leucopis</i>	0.0	0.0	0.0
<i>Ammodillus larvae</i> (Sand lance)	0.0	0.0	0.0
<i>Scorpaenichthys marmoratus</i>	0.0	0.0	0.0
<i>Aquilonia finlayi</i> (Blackcod)	0.0	0.0	0.0
<i>Hexagrammos</i> (Greenling)	0.0	0.011	0.0
Stichidae (flenny)	0.0	0.0	0.0
Seasies (Rockfish) larvae	0.0	0.011	0.0
Bullhead larvae	0.019	0.0	0.0
fish eggs	0.0	0.0	0.0
<i>Osmeridae</i> (smelt)	0.0	0.0	0.0
<i>Microstomus pacificus</i> (Dover Sole)	0.0	0.0	0.0
<i>Liparidae</i>	0.0	0.0	0.0
Agonidae (poacher)	0.0	0.0	0.0
Pilichthys (Quillfish)	0.0	0.0	0.0
<i>Grosphophis marginata</i> (ragfish)	0.0	0.0	0.0
<i>Parichthys melanostictus</i>	0.019	0.0	0.0
<i>Sopsetta solopsis</i> (Butter Sole)	0.0	0.0	0.0
<i>Hippocassiois elabodon</i>	0.0	0.0	0.0
Gobiidae	0.0	0.011	0.0
<i>Ulua harenus</i> (Herring)	0.0	0.0	0.0
<i>Yoposetta exilis</i> (Slender Sole)	0.0	0.0	0.0
<i>Peromnactis stenodus</i> (C-o sole)	0.0	0.0	0.0
Polioidei (Gunnels)	0.0	0.0	0.0
<i>Ophorhynchus keta</i> (Chum Salmon)	0.0	0.0	0.0
Gadidae	0.0	0.0	0.0
<i>epiosetta bilineata</i> (Rock Sole)	0.0	0.0	0.0

**Table 3.** Species catch per 10 m<sup>2</sup> of sea surface for each neuston tow and Tucker trawl net catch.

E. SCUDDER POINT - June 15, 16, 1988												
Surface area (m <sup>2</sup> )	98-2	98-3	99-2	99-3	100-2	101	102	103	104			
TAXA (number per 10m <sup>-3</sup> )												
<i>Cancer magister</i> megalops	0.0	0.0	0.0	0.0	0.0	0.0	0.0	0.0	0.0	0.0	0.0	0.0
<i>Cancer</i> spp. megalops	11.51	9.146	8.976	10.19	2.13	0.0	0.0	0.0	0.0	0.0	0.0	0.015
<i>Cancer</i> spp. megalops (strump.)	3.29	9.146	4.896	12.88	10.29	0.374	0.058	2.373	0.093			
<i>Cancer magister</i> zoea	0.329	0.0	0.816	0.0	0.0	0.0	0.0	391.5	0.0	0.0		0.0
<i>Cancer</i> sp. zoea	381.6	178.5	881.2	1626.	685.1	840.9	2349.	1129.	1014.			
Porcellanidae zoea	0.0	0.0	0.0	0.0	0.0	0.0	0.0	1174.	0.0	0.0		0.0
Grapsidae zoea	0.0	0.0	0.0	0.0	0.0	1261.	0.0	225.9	0.0	0.0		0.0
Malidae zoea (Pugetia)	0.0	0.0	0.0	0.0	0.0	0.0	391.5	0.0	0.0	0.0		0.0
Pinnotheridae zoea	0.0	0.0	0.0	0.0	0.0	0.0	0.0	0.0	0.0	0.0		0.0
<i>Adia subquadrate</i> (Pinnotheridae)	9.87	0.0	2.448	0.0	0.0	4204.	391.5	1581.				0.0
Salathidae zoea	0.0	0.0	0.0	0.0	0.0	0.0	0.0	0.0	0.0	0.0		0.0
Other Decapod Larvae	0.0	0.0	0.0	0.0	0.355	0.0	0.0	0.0	0.0	0.0		0.0
Amphipoda	24.01	14.37	0.0	4.293	1.065	0.074	0.058	0.453	0.171			0.0
Copepoda (Calanoida)	1026.	740.4	35.08	83.18	326.6	0.074	0.0	0.0	0.993			0.0
Euphausiacea - Mysacea	454.0	635.4	53.85	152.9	184.6	0.0	0.0	0.0	1.353			0.0
<i>Limnasia helicina</i> (Pteropod)	0.0	0.0	0.0	0.0	0.0	0.0	0.0	0.0	0.0	0.0		0.0
<i>Clione limacina</i> (Pteropod)	0.0	0.0	0.0	9.123	0.0	0.0	0.0	0.0	0.0	0.0		0.0
<i>Exoco</i> sp. (Pteropod)	0.0	0.0	0.0	0.0	0.0	0.0	0.0	0.0	0.0	0.0		0.0
Octopus	0.329	0.0	0.0	0.0	0.0	0.0	0.0	0.0	0.0	0.0		0.0
Squid	0.0	0.0	0.0	0.0	0.0	0.0	0.0	0.0	0.0	0.0		0.0
Sepoda	0.0	0.0	0.0	0.0	0.0	0.0	0.0	0.0	0.0	0.0		0.0
Insect Larvae	0.0	0.0	0.0	0.0	0.0	0.0	0.0	0.0	0.0	0.0		0.0
Myxidacea	0.0	0.0	0.0	0.0	0.0	0.0	0.0	0.0	0.0	0.0		0.0
Ostracoda	0.0	0.0	0.0	0.0	0.0	0.0	0.0	0.0	0.0	0.0		0.015
Invertebrate eggs	0.0	0.0	0.0	0.0	0.0	0.0	0.0	0.0	0.0	0.0		0.0
<i>Velalia</i>	0.0	0.0	0.0	0.0	0.0	0.0	0.0	0.0	0.0	0.0		0.0
Leptylis (Leptomedusae)	132.5	161.1	353.3	206.6	0.0	5.246	8.786	7.121	0.544			0.0
Tenophores (Pleurobrachia)	0.0	1.306	0.816	0.536	0.0	0.0	0.0	0.0	0.0	0.0		0.0
Siphonophores	0.0	0.0	0.0	0.0	0.0	0.0	0.0	0.0	0.0	0.0		0.0
Coelentera	0.0	0.0	0.0	0.0	0.0	0.0	0.0	0.0	0.0	0.0		0.0
Polychaeta	0.329	0.871	0.0	0.0	0.0	0.0	0.058	0.069	0.0	0.0		0.0
<i>Chaetognatha</i>	7.896	6.988	0.816	2.146	0.0	0.0	0.0	0.0	0.0	0.0		0.0
Amphidae	0.0	0.0	0.0	0.0	1.065	0.0	0.0	0.0	0.0	0.0		0.0
<i>Stenodrilus leucopneurus</i>	0.0	0.0	0.0	0.0	0.0	0.0	0.0	0.0	0.0	0.0		0.0
Ammodius larvae (Sand lance)	0.0	0.0	0.0	0.0	0.0	0.0	0.074	0.0	0.0	0.0		0.0
<i>Scorpenichthys marmoratus</i>	0.0	0.0	0.0	0.0	0.0	0.0	0.0	0.0	0.0	0.0		0.0
<i>Apogonina timbra</i> (Blackcod)	0.0	0.0	0.0	0.0	0.0	0.0	0.0	0.0	0.0	0.0		0.0
<i>Hexagrammos</i> (Greenling)	0.0	0.0	0.0	0.0	0.0	0.0	0.0	0.0	0.0	0.0		0.0
Stichidae (Bleny)	3.29	2.177	10.60	13.95	3.905	0.0	0.0	0.104	0.0	0.0		0.0
<i>Sebastes</i> (Rockfish) larvae	0.658	0.435	0.0	4.615	0.0	0.0	0.0	0.0	0.0	0.0		0.015
Oilulid larvae	0.0	0.0	3.264	6.44	39.05	0.074	0.0	0.0	0.0	0.0		0.0
Fish eggs	0.0	0.0	0.0	0.0	0.0	0.0	0.0	0.0	0.0	0.0		0.0
Osmeridae (smelt)	0.0	0.0	0.0	0.0	0.0	0.0	0.0	0.0	0.0	0.0		0.0
<i>Marstonius pacificus</i> (Dover Sole)	0.0	0.0	0.0	0.0	0.355	0.0	0.0	0.0	0.0	0.0		0.031
Paridae	0.0	0.435	0.0	0.0	2.13	0.0	0.0	0.0	0.0	0.0		0.0
Agonidae (poacher)	0.329	0.0	0.0	0.0	0.0	0.0	0.0	0.0	0.0	0.0		0.069
Pilichthyidae (Quillfish)	0.0	0.0	0.0	0.0	0.0	0.0	0.0	0.0	0.0	0.0		0.0
<i>Grosomphys marginata</i> (ragfish)	1.316	0.871	1.632	4.293	0.0	0.0	0.0	0.0	0.0	0.0		0.0
<i>Psittichthys melanostictus</i>	0.0	0.0	0.0	0.0	1.775	0.0	0.0	0.0	0.0	0.0		0.0
<i>Sopsetta dooleys</i> (Butter Sole)	0.0	0.0	0.0	0.0	0.536	0.0	0.0	0.0	0.0	0.0		0.0
<i>Hypoglossoides abedon</i>	0.0	0.435	0.08	0.0	1.065	0.0	0.175	0.314	0.0	0.0		0.0
Gobiidae	0.0	0.0	0.0	0.0	0.0	0.0	0.0	0.0	0.0	0.0		0.0
<i>Clupea harengus</i> (Herring)	0.0	0.0	0.0	0.0	0.0	0.0	0.0	0.0	0.0	0.0		0.0
<i>Yogsetta exilis</i> (Slender Sole)	0.0	0.0	0.0	0.0	0.0	0.0	0.058	0.0	0.0	0.0		0.0
<i>Heurostichus oregonus</i> (C-O sole)	0.0	0.0	0.0	0.0	0.0	0.0	0.0	0.0	0.0	0.0		0.0
Thoidae (Gummers)	0.0	0.0	0.0	0.0	0.0	0.0	0.0	0.0	0.0	0.0		0.0
<i>Chorichthys keta</i> (Chum Salmon)	0.0	0.0	0.0	0.0	0.0	0.0	0.0	0.0	0.0	0.0		0.0
Gadidae	0.0	0.0	0.0	0.0	0.0	0.0	0.0	0.0	0.0	0.0		0.0
<i>epidorsseta bilineata</i> (Rock Sole)	0.0	0.0	0.0	0.0	0.0	0.0	0.0	0.0	0.0	0.0		0.0

Table 3 (cont'd.). E. SCUDDER POINT - June 15,16, 1988

Surface area (m <sup>2</sup> )	882.3	832.2	895.4	1167.	1141.	655.7	660.1	703.7	666.6
TAXA (number per 10m <sup>2</sup> )	105	106	107	108	109	110	111	112	113
<i>Cancer magister</i> megalops	0.0	0.0	0.0	0.0	0.0	0.0	0.0	0.0	0.0
<i>Cancer</i> spp. megalops	0.011	0.312	1.876	0.377	2.716	0.165	0.939	0.085	0.30
megalops (shrimp, other crabs)	0.090	0.120	1.116	0.154	0.823	0.838	0.590	1.634	1.455
<i>Cancer magister</i> zoea	0.0	0.0	0.0	0.0	0.0	0.0	0.0	0.0	0.0
<i>Cancer</i> sp. zoea	222.7	10.57	7.426	1.357	10.03	14.25	13.02	5.115	9.000
Porcellanidae zoea	0.0	0.0	0.0	0.0	0.0	0.0	0.0	0.0	0.0
Grapsidae zoea	0.0	0.0	0.0	0.0	0.0	0.0	0.0	0.0	0.0
Majidae zoea (Pugetta)	0.0	0.0	0.0	0.0	0.0	0.0	0.0	0.0	0.0
Pinnocheiridae zoea	0.0	0.0	0.0	0.150	0.0	0.0	0.0	0.0	0.0
<i>Fabia subquadrata</i> (Pinnocheiridae)	0.0	0.0	0.0	0.0	0.0	0.0	0.0	0.0	0.0
Gammaridae zoea	0.0	0.0	0.0	0.0	0.0	0.0	0.0	0.0	0.0
Other Decapod Larvae	0.0	0.0	0.0	0.017	0.0	0.0	0.0	0.0	0.0
Pandalidae	0.011	0.0	0.078	0.0	0.122	0.106	0.106	0.014	0.060
Other Shrimp	0.192	0.144	0.178	0.197	1.726	0.762	0.454	0.099	0.150
<i>Leptae</i> (goose barnacle)	0.0	0.0	0.0	0.0	0.0	0.0	0.0	0.0	0.0
Cumacea	0.0	0.0	0.0	0.0	0.0	0.0	0.0	0.0	0.0
Amphipoda	0.272	0.156	0.323	0.342	0.499	0.564	0.196	0.198	0.060
Copepoda (Calanoida)	0.793	2.583	0.893	0.814	1.402	1.372	0.605	3.055	0.945
Euphausiacea - <i>Thysanoessa</i>	1.915	62.48	10.33	0.197	0.350	0.335	0.227	0.042	0.030
<i>Limnocalanus macrurus</i> (Pteropod)	0.0	0.0	0.0	0.0	0.0	0.0	0.0	0.0	0.0
<i>Clione limacina</i> (Pteropod)	0.0	0.0	0.0	0.0	0.0	0.0	0.0	0.0	0.0
<i>Eudora</i> sp. (Pteropod)	0.0	0.0	0.0	0.0	0.0	0.0	0.0	0.0	0.0
Octopus	0.0	0.0	0.0	0.0	0.0	0.0	0.0	0.0	0.0
Squid	0.0	0.0	0.0	0.0	0.0	0.0	0.0	0.0	0.0
Isopoda	0.0	0.0	0.0	0.0	0.0	0.0	0.0	0.0	0.0
Insect Larvae	0.0	0.0	0.0	0.0	0.0	0.0	0.0	0.0	0.0
Mysidacea	0.0	0.0	0.0	0.0	0.0	0.015	0.0	0.0	0.0
Ostracoda	0.0	0.0	0.0	0.0	0.0	0.0	0.0	0.0	0.0
Invertebrate eggs	0.0	0.0	0.0	0.0	0.0	0.0	0.0	0.0	0.0
<i>Velutina</i>	0.0	0.0	0.0	0.0	0.0	0.0	0.0	0.0	0.0
Jellyfish (Leptomedusae)	0.226	0.0	0.022	0.102	0.1	1.769	0.590	0.440	0.060
Ctenophores (Pleurobrachia)	0.034	0.0	0.011	0.034	0.008	0.0	0.015	0.0	0.0
Siphonophores	0.0	0.0	0.0	0.205	0.0	0.0	0.0	0.0	0.0
Ctenophores	0.0	0.0	0.0	0.0	0.0	0.0	0.0	0.0	0.0
<i>Polychaeta</i>	0.022	0.012	0.011	0.008	0.0	0.0	0.0	0.030	0.0
<i>Chaetognathia</i>	0.0	0.0	0.0	0.0	0.008	0.045	0.0	0.0	0.0
Salpidae	0.0	0.0	0.0	0.0	0.0	0.0	0.0	0.0	0.0
<i>Stenobrachius leucopsanus</i>	0.0	0.0	0.0	0.0	0.0	0.0	0.0	0.0	0.0
Ammodites larvae (Sandalinae)	0.544	0.312	0.614	2.485	0.999	0.228	0.060	0.056	0.135
<i>Scorpaenichthys marmoratus</i>	0.0	0.0	0.0	0.0	0.0	0.0	0.0	0.0	0.0
<i>Anoploporoma timbra</i> (Blackcod)	0.0	0.0	0.0	0.0	0.0	0.0	0.0	0.015	0.0
<i>Hexagrammos</i> (Greenling)	0.0	0.0	0.0	0.0	0.0	0.0	0.0	0.0	0.0
Sichthidae (Blenny)	0.0	0.012	0.089	0.017	0.017	0.137	0.060	0.028	0.015
<i>Sebastes</i> (Rockfish) larvae	0.0	0.0	0.011	0.0	0.026	0.091	0.075	0.042	0.0
Bullhead larvae	0.034	0.036	0.033	0.077	0.113	0.579	0.378	0.227	0.180
Fish eggs	0.521	0.144	0.0	0.188	0.0	0.045	0.0	0.113	0.285
Osmeridae (smelt)	0.0	0.0	0.0	0.0	0.0	0.0	0.0	0.0	0.0
<i>Microstomus pacificus</i> (Dover Sole)	0.0	0.0	0.011	0.017	0.0	0.061	0.045	0.0	0.0
Liparidae	0.056	0.012	0.022	0.034	0.052	0.061	0.030	0.014	0.165
Agonidae (poacher)	0.0	0.0	0.0	0.0	0.0	0.0	0.0	0.0	0.0
Platyichthyidae (Quillfish)	0.0	0.0	0.0	0.0	0.0	0.0	0.0	0.0	0.0
<i>Brosimichthys marginata</i> (ragfish)	0.0	0.0	0.011	0.0	0.0	0.0	0.0	0.0	0.0
<i>Psetichthys melanoschialis</i>	0.0	0.0	0.0	0.0	0.0	0.0	0.0	0.014	0.0
<i>Isopsetta solepis</i> (Butter Sole)	0.0	0.0	0.0	0.0	0.0	0.0	0.0	0.0	0.0
<i>Hippoglossoides abaddon</i>	0.0	0.0	0.0	0.0	0.0	0.0	0.0	0.0	0.0
Gobiidae	0.0	0.0	0.0	0.0	0.0	0.0	0.0	0.0	0.0
<i>Clupea harengus</i> (Herring)	0.034	0.0	0.011	0.0	0.0	0.0	0.0	0.014	0.030
<i>Lyopsetta exilis</i> (Slender Sole)	0.0	0.0	0.0	0.0	0.0	0.0	0.0	0.0	0.0
<i>Pleuronectes oenops</i> (C-O sole)	0.0	0.0	0.0	0.0	0.0	0.0	0.0	0.0	0.0
Pholidae (Gunnels)	0.0	0.0	0.0	0.0	0.0	0.0	0.0	0.0	0.0
<i>Onchorynchus keta</i> (Chum Salmon)	0.0	0.0	0.0	0.0	0.0	0.0	0.0	0.0	0.0
Gadidae	0.0	0.0	0.0	0.0	0.0	0.0	0.0	0.0	0.0
<i>Lepidopsetta bilineata</i> (Rock Sole)	0.0	0.0	0.0	0.0	0.0	0.0	0.0	0.0	0.0

Table 3 (cont'd.). E. SCUDDER POINT - June 15,16, 1988

Surface area (m <sup>2</sup> )	664.4	671.0	721.1	980.3
TAXA (number per 10m <sup>2</sup> )	114	115	116	117
<i>Cancer magister</i> megalops	0.0	0.0	0.0	0.0
<i>Cancer</i> spp. megalops	0.692	0.834	0.235	0.306
megalops (shrimp, other crabs)	0.135	0.223	0.346	0.051
<i>Cancer magister</i> zoea	0.0	0.0	0.0	0.0
<i>Cancer</i> sp. zoea	76.61	23.84	24.06	76.67
Porcellanidae zoea	0.0	0.0	0.0	0.0
Grapsidae zoea	0.0	0.0	0.0	6.962
Majidae zoea (Pugetta)	0.0	0.0	0.0	0.0
Pinnocheiridae zoea	0.0	0.0	0.0	0.0
<i>Fabia subquadrata</i> (Pinnocheiridae)	0.0	0.0	0.0	0.0
Gammaridae zoea	0.0	0.0	0.0	0.0
Other Decapod Larvae	0.0	0.0	0.0	0.0
Pandalidae	0.0	0.044	0.013	0.0
Other Shrimp	0.0	0.0	0.0	0.0
<i>Leptae</i> (goose barnacle)	0.015	0.149	0.027	0.030
Cumacea	0.0	0.0	0.0	0.0
Amphipoda	0.075	0.044	0.124	0.051
Copepoda (Calanoida)	0.0	0.149	0.0	0.0
Euphausiacea - <i>Thysanoessa</i>	0.060	0.014	0.027	0.030
<i>Limnocalanus macrurus</i> (Pteropod)	0.0	0.0	0.0	0.0
<i>Clione limacina</i> (Pteropod)	0.0	0.0	0.0	0.0
<i>Eudora</i> sp. (Pteropod)	0.0	0.0	0.0	0.0
Octopus	0.0	0.0	0.0	0.0
Squid	0.0	0.0	0.0	0.0
Isopoda	0.0	0.0	0.0	0.0
Insect Larvae	0.0	0.0	0.0	0.0
Mysidacea	0.0	0.0	0.0	0.0
Ostracoda	0.0	0.0	0.0	0.0
Invertebrate eggs	0.0	0.0	0.0	0.0
<i>Velutina</i>	0.0	0.0	0.0	0.0
Jellyfish (Leptomedusae)	0.210	1.087	2.010	1.591
Ctenophores (Pleurobrachia)	0.0	0.0	0.0	0.010
Siphonophores	0.0	0.0	0.0	0.0
<i>Ctenophores</i>	0.0	0.0	0.0	0.0
<i>Polychaeta</i>	0.060	0.163	0.027	0.030
<i>Chaetognathia</i>	0.015	0.0	0.0	0.0
Salpidae	0.0	0.0	0.0	0.0
<i>Stenobrachius leucopsanus</i>	0.0	0.0	0.0	0.0
Ammodites larvae (Sandalinae)	0.075	0.029	0.083	0.132
<i>Scorpaenichthys marmoratus</i>	0.0	0.0	0.0	0.0
<i>Anoploporoma timbra</i> (Blackcod)	0.0	0.0	0.0	0.0
<i>Hexagrammos</i> (Greenling)	0.0	0.0	0.0	0.0
Sichthidae (Blenny)	0.015	0.0	0.013	0.102
<i>Sebastes</i> (Rockfish) larvae	0.015	0.029	0.013	0.051
Bullhead larvae	0.030	0.0	0.013	0.010
Fish eggs	0.602	0.655	0.374	1.703
Osmeridae (smelt)	0.0	0.0	0.0	0.0
<i>Microstomus pacificus</i> (Dover Sole)	0.316	0.223	0.027	0.0
Liparidae	0.0	0.0	0.0	0.0
Agonidae (poacher)	0.0	0.0	0.0	0.0
Platyichthyidae (Quillfish)	0.0	0.0	0.0	0.0
<i>Brosimichthys marginata</i> (ragfish)	0.0	0.0	0.0	0.0
<i>Psetichthys melanoschialis</i>	0.0	0.0	0.0	0.0
<i>Isopsetta solepis</i> (Butter Sole)	0.0	0.0	0.0	0.0
<i>Hippoglossoides abaddon</i>	0.0	0.0	0.0	0.0
Gobiidae	0.0	0.0	0.0	0.0
<i>Clupea harengus</i> (Herring)	0.015	0.014	0.0	0.0
<i>Lyopsetta exilis</i> (Slender Sole)	0.0	0.0	0.0	0.0
<i>Pleuronectes oenops</i> (C-O sole)	0.0	0.0	0.0	0.0
Pholidae (Gunnels)	0.0	0.0	0.0	0.0
<i>Onchorynchus keta</i> (Chum Salmon)	0.0	0.0	0.0	0.0
Gadidae	0.0	0.0	0.0	0.0
<i>Lepidopsetta bilineata</i> (Rock Sole)	0.0	0.0	0.0	0.0



**Table 3.** Species catch per 10 m<sup>2</sup> sea surface for each neuston tow and Tucker trawl net catch.

F. SANDSPIT TRANSECT - June 16, 1988												
Surface area (m <sup>2</sup> )	0.553	0.252	0.682	0.340	0.572	516.3	368.1	749.4				
TAXA (number per 10m <sup>2</sup> )	118-3	119-3	120-3	121-3	122-3	123	124	125				
<i>Cancer magister</i> megalops	0.0	0.0	0.0	0.0	0.0	0.0	0.0	0.0				
<i>Cancer</i> spp. megalops	7.707	0.252	2.728	0.68	0.572	0.058	0.0	0.0				
megalops (shrimp, other crabs)	7.707	1.512	20.46	15.3	17.16	0.968	1.494	2.203				
<i>Cancer magister</i> zoea	0.0	0.252	0.0	0.0	0.0	0.0	0.0	0.0				
<i>Cancer</i> sp. zoea	151.3	76.60	849.0	646	753.1	26.01	16.02	28.64				
Porcellanidae zoea	0.0	9.576	0.0	0.0	0.0	0.0	0.0	0.0				
Grapsidae zoea	0.0	0.0	0.0	0.0	186.2	2.364	0.0	0.0				
Majidae zoea (Pugettia)	0.0	0.0	0.0	0.0	94.13	0.0	0.0	0.0				
Pinnothiridae zoea	0.0	0.0	0.0	0.0	0.0	0.0	0.0	0.0				
<i>Fadja subquadrata</i> (Pinnotheridae)	0.0	9.576	0.0	0.0	0.0	0.0	0.0	0.0				
Salasthidae zoea	0.0	0.0	0.0	0.0	0.0	0.0	0.0	0.0				
Other Decapod Larvae	0.0	0.0	0.0	0.0	0.0	0.0	0.0	0.0				
Amphipoda	1.842	0.0	1.364	0.0	0.371	0.019	0.0	0.0				
Other Shrimp	46.24	3.024	125.8	125.8	160.1	0.096	0.353	0.477				
Leaps (goose barnacle)	0.0	0.0	0.0	0.0	0.0	0.0	0.0	0.0				
Junacea	0.0	0.0	0.682	0.0	0.0	0.0	0.0	0.0				
Amphipoda	2.752	0.756	549.0	4.08	1.716	0.174	0.325	0.954				
Copepoda (Calanoida)	49.54	39.21	57.97	154.7	105.8	0.0	0.0	0.0				
Euphausiidae - Rhysanessa	371.5	10.08	248.9	282.2	174.4	0.038	0.0	0.0				
<i>Limnadia helicina</i> (Pteropod)	0.860	0.0	0.0	0.0	0.0	0.0	0.0	0.0				
<i>Clione limacina</i> (Pteropod)	0.0	0.0	0.0	0.0	0.0	0.0	0.0	0.0				
<i>Exoco</i> sp. (Pteropod)	0.0	0.0	0.0	0.0	0.0	0.0	0.0	0.0				
Octopus	0.0	0.504	0.0	0.0	0.0	0.0	0.0	0.0				
Squid	0.550	0.0	0.0	0.0	0.0	0.0	0.0	0.0				
Isopoda	0.0	0.0	0.682	0.0	0.0	0.0	0.0	0.0				
Insect Larvae	0.0	0.0	0.0	0.0	0.0	0.0	0.0	0.0				
Mysidacea	0.0	0.0	0.0	0.0	0.0	0.0	0.0	0.0				
Ostracoda	0.0	0.0	0.0	0.0	0.0	0.0	0.0	0.0				
Invertebrate eggs	0.0	0.0	0.0	0.0	0.0	0.0	0.0	0.0				
<i>Velletia</i>	0.0	0.0	0.0	0.0	0.0	0.0	0.0	0.0				
Jellyfish (Leptomedusae)	253.2	0.0	105.7	428.4	154.4	19.36	32.05	70.50				
Ctenophores (Pleurobrachia)	1.101	0.252	0.0	2.04	0.572	0.0	0.0	0.0				
Siphonophores	0.0	0.0	0.0	0.0	0.0	0.0	0.0	0.0				
Coelenterata	0.0	0.0	0.0	0.0	0.0	0.0	0.0	0.0				
Polychaeta	0.550	0.252	0.0	1.02	1.716	0.038	0.054	0.110				
Chaetognathia	0.0	0.0	0.0	0.0	0.0	0.0	0.0	0.0				
Sardine	0.0	0.0	0.0	0.0	0.0	0.0	0.0	0.0				
<i>Stenodracus leucopaeus</i>	0.0	0.0	0.0	0.0	0.0	0.0	0.0	0.0				
<i>Armadillus</i> larvae (Sand lance)	0.0	0.0	0.0	0.0	0.0	0.0	0.0	0.0				
<i>Scorpaenichthys namata</i>	0.0	0.0	0.0	0.0	0.0	0.019	0.0	0.0				
<i>Scorpaenichthys namoratus</i>	0.0	0.0	0.0	0.0	0.0	0.0	0.0	0.0				
<i>Argopecten imbricatus</i> (Blackcod)	0.0	0.0	0.0	0.0	0.0	0.0	0.0	0.0				
<i>Argopecten imbricatus</i> (Blackcod)	0.0	0.0	0.0	0.0	0.0	0.0	0.0	0.0				
<i>Neogobius</i> (Greenling)	0.0	0.0	0.682	0.0	0.0	0.0	0.0	0.0				
Stichidae (Blenny)	1.851	0.0	0.682	0.34	1.144	0.0	0.0	0.0				
Sebastes (Rockfish) larvae	25.87	2.016	0.0	2.04	1.144	0.038	0.0	0.036				
Bullhead larvae	12.66	0.756	2.728	3.06	3.432	0.019	0.0	0.036				
Shrimp eggs	46.79	0.0	20.46	47.6	0.0	1.433	2.852	5.508				
<i>Osmia</i> (smelt)	0.0	0.0	0.0	0.0	0.0	0.0	0.0	0.146				
<i>Microstomus pacificus</i> (Dover Sole)	0.0	0.252	0.0	0.0	0.0	0.0	0.0	0.0				
<i>Paralichthys</i>	0.550	0.0	2.046	0.34	2.86	0.0	0.0	0.0				
Agonidae (poacher)	0.550	0.252	0.0	0.34	0.0	0.0	0.0	0.0				
<i>Paralichthys</i> (Quillfish)	0.0	0.0	0.0	0.0	0.0	0.0	0.0	0.0				
<i>Brosomphus marginatus</i> (ragfish)	1.651	0.0	0.0	0.0	0.0	0.0	0.0	0.0				
<i>Paralichthys melanostictus</i>	8.808	0.252	2.728	4.06	2.288	0.0	0.054	0.036				
<i>Sagittaria</i> (Butter Sole)	0.0	0.252	0.0	0.0	0.0	0.0	0.0	0.0				
<i>Hippocampus</i> (seahorse)	0.0	0.0	0.0	0.0	0.0	0.0	0.0	0.0				
Gobiidae	0.0	0.0	0.0	0.0	0.0	0.0	0.0	0.0				
<i>Chupea harengus</i> (Herring)	0.0	0.0	0.0	0.0	0.0	0.0	0.0	0.036				
<i>Lyopsetta exilis</i> (Slender Sole)	0.0	0.0	0.0	0.0	0.0	0.0	0.0	0.0				
<i>Paralichthys caesus</i> (C-O sole)	0.0	0.0	0.0	0.0	0.0	0.0	0.0	0.0				
Pholidae (Gunnels)	0.0	0.0	0.0	0.0	0.0	0.0	0.0	0.0				
<i>Onchornomys keta</i> (Chum Salmon)	0.0	0.0	0.0	0.0	0.0	0.0	0.0	0.0				
Sadidae	0.0	0.252	0.0	0.0	0.0	0.0	0.0	0.0				
<i>Leptodactylus bilineatus</i> (Rock Sole)	0.0	0.0	0.0	0.0	0.0	0.0	0.0	0.0				

**Table 3 (cont'd.). F. SANDSPIT TRANSECT - June 16, 1988**

[illegible]

Table 3 (cont'd.). F. SANDSPIT TRANSECT - June 16, 1988

Surface area (m <sup>2</sup> )	688.4	492.3	557.7	579.5	257.0	267.9	246.1	272.3	322.4
TAXA (number per 10m <sup>2</sup> )	135	136	137	138	139	140	141	142	143
<i>Cancer magister</i> megalops	0.019	0.0	0.0	0.043	0.0	0.0	0.0	1.468	0.0
<i>Cancer</i> sp. megalops	0.135	0.121	0.089	0.345	138.1	116.6	157.8	5.214	18.30
megalops (shrimp, other crabs)	3.680	1.868	1.739	3.235	46.63	44.32	88.23	3.195	1.861
<i>Cancer magister</i> zoea	0.0	0.0	0.0	0.0	0.0	0.0	0.0	1.468	0.0
<i>Cancer</i> sp. zoea	51.13	20.21	3.084	20.83	1397.7	4157.7	13985	477.4	2368.
Porcellanidae zoea	0.0	0.0	0.0	0.0	0.0	0.0	0.0	0.0	0.0
Grapsidae zoea	0.0	0.0	0.0	0.0	0.0	0.0	0.0	0.0	0.0
Malidae zoea (Pugettia)	0.0	0.0	0.0	0.0	0.0	0.0	0.0	0.0	0.0
Pinnotheridae zoea	0.0	0.0	0.0	0.0	0.0	0.0	0.0	0.0	0.0
<i>Fabia subquadrata</i> (Pinnotheridae)	0.0	0.0	0.0	0.0	0.0	0.0	0.0	0.0	0.0
Galatheid zoea	0.0	0.0	0.0	0.0	0.0	0.0	0.0	0.0	0.0
Other Decapod Larvae	0.0	0.0	0.0	0.0	0.0	0.0	0.0	0.0	0.0
Pandalidae	0.309	0.311	0.161	0.215	0.272	0.137	0.116	0.0	0.0
Other Shrimp	5.306	0.882	0.322	0.517	0.817	1.493	0.812	0.146	0.093
<i>Lepas</i> (goose barnacle)	0.0	0.0	0.0	0.0	0.0	0.046	0.0	0.036	0.0
Cumacea	0.0	0.0	0.0	0.0	0.0	0.0	0.0	0.0	0.0
Amphipoda	0.871	0.629	0.555	0.776	0.233	0.466	0.0	0.220	0.0
Copepoda (Calanoida)	0.0	0.0	0.0	0.0	0.0	0.0	0.0	0.124	0.0
Euphausiacea- Thysanoessa	0.038	0.081	0.089	0.0	0.466	0.466	0.928	0.0	0.0
<i>Limnoria helicina</i> (Pteropod)	0.0	0.0	0.0	0.0	0.0	0.0	0.0	0.0	0.0
<i>Eukie</i> sp. (Pteropod)	0.0	0.0	0.0	0.0	0.0	0.0	0.0	0.0	0.0
Octopus	0.0	0.0	0.0	0.0	0.0	0.0	0.0	0.0	0.0
Squid	0.0	0.0	0.0	0.0	0.0	0.0	0.0	0.0	0.0
Isopoda	0.0	0.0	0.0	0.0	0.0	0.0	0.0	0.0	0.0
Insect Larvae	0.0	0.0	0.0	0.0	0.0	0.0	0.0	0.0	0.0
Myriapoda	0.0	0.0	0.0	0.0	0.0	0.0	0.0	0.0	0.0
Ostracoda	0.0	0.0	0.0	0.0	0.0	0.0	0.0	0.0	0.0
Invertebrate eggs	0.0	0.0	0.0	0.0	0.0	0.0	0.0	0.0	0.0
<i>Velletia</i>	0.0	0.0	0.0	0.0	0.038	0.0	0.0	0.0	0.0
Jellyfish (Leptomedusae)	11.62	13.60	10.84	25.88	10.97	13.34	7.430	8.152	0.837
Ctenophores (Pleurobrachia)	0.019	0.0	0.0	0.0	0.0	0.0	0.0	0.0	0.0
Siphonophores	0.0	0.0	0.0	0.0	0.0	0.0	0.0	0.0	0.0
<i>Coelenterata</i>	0.019	0.0	0.0	0.0	0.0	0.0	0.0	0.0	0.0
<i>Polychaeta</i>	0.0	0.0	0.0	0.0	0.0	0.0	0.0	0.0	0.0
<i>Chaetognathia</i>	0.0	0.0	0.0	0.0	0.0	0.0	0.0	0.073	0.0
Salpidae	0.0	0.0	0.0	0.0	0.0	0.0	0.0	0.0	0.0
<i>Stenobrachius leucopsaurus</i>	0.0	0.0	0.0	0.0	0.0	0.0	0.0	0.0	0.0
<i>Ammodites</i> larvae (Sandlance)	0.038	0.020	0.0	0.0	0.0	0.0	0.0	0.0	0.0
<i>Scorpaenichthys marmoratus</i>	0.0	0.0	0.0	0.0	0.0	0.0	0.0	0.0	0.0
<i>Anoplopoma fimbria</i> (Blackcod)	0.0	0.0	0.0	0.0	0.0	0.0	0.0	0.0	0.0
<i>Hexagrammos</i> (Greenling)	0.0	0.0	0.0	0.0	0.0	0.0	0.0	0.0	0.0
<i>Sitichidae</i> (Blenny)	0.019	0.0	0.0	0.0	0.077	0.0	0.0	0.036	0.0
<i>Sebastes</i> (Rockfish) larvae	0.0	0.0	0.0	0.0	0.0	0.0	0.0	0.0	0.0
Bullhead larvae	0.0	0.0	0.017	0.0	0.0	0.083	0.0	0.036	0.0
Fish eggs	0.0	0.020	0.017	0.0	0.077	0.0	0.0	0.062	0.0
Osmariidae (smelt)	0.0	0.0	0.0	0.0	0.0	0.0	0.0	0.0	0.0
<i>Microstomus pacificus</i> (Dover Sole)	0.0	0.0	0.0	0.0	0.0	0.0	0.0	0.0	0.0
Liparidae	0.0	0.0	0.0	0.0	0.0	0.0	0.0	0.036	0.0
Agonidae (poacher)	0.0	0.0	0.0	0.0	0.0	0.0	0.0	0.0	0.0
<i>Pilichthys</i> (Quillfish)	0.0	0.0	0.0	0.0	0.0	0.0	0.0	0.0	0.0
<i>Brosomphys marginata</i> (ragfish)	0.0	0.0	0.0	0.0	0.0	0.0	0.0	0.0	0.0
<i>Psephotichthys melanostictus</i>	0.038	0.121	0.0	0.0	0.0	0.0	0.0	0.0	0.0
<i>Isopsetta teleostis</i> (Butter Sole)	0.0	0.0	0.0	0.0	0.0	0.0	0.0	0.0	0.0
<i>Hippoglossoides esocodon</i>	0.0	0.0	0.0	0.0	0.0	0.0	0.0	0.0	0.0
Gobiidae	0.0	0.0	0.0	0.0	0.0	0.0	0.0	0.0	0.0
<i>Clupea harengus</i> (Herring)	0.0	0.020	0.0	0.0	0.0	0.0	0.116	0.0	0.155
<i>Lyopsetta exilis</i> (Slender Sole)	0.0	0.0	0.0	0.0	0.0	0.0	0.0	0.0	0.0
<i>Pleuronichthys coeniscus</i> (C-O sole)	0.0	0.0	0.0	0.0	0.0	0.0	0.0	0.0	0.0
Pholidae (Gumels)	0.0	0.0	0.017	0.0	0.0	0.0	0.0	0.0	0.0
<i>Oncorhynchus keta</i> (Chum Salmon)	0.0	0.0	0.0	0.0	0.0	0.0	0.116	0.036	0.0
Gadidae	0.0	0.0	0.0	0.0	0.0	0.0	0.0	0.0	0.0
<i>Lepidopsetta bilineata</i> (Rock Sole)	0.0	0.0	0.0	0.0	0.0	0.0	0.0	0.0	0.0

Table 3 (cont'd.). F. SANDSPIT TRANSECT - June 16, 1988

Surface area (m <sup>2</sup> )	311.5	285.4	272.3	300.6	538.1
TAXA (number per 10m <sup>2</sup> )	144	145	146	147	148
<i>Cancer magister</i> megalops	0.0	0.0	0.0	0.0	0.0
<i>Cancer</i> sp. megalops	46.71	66.57	94.56	36.53	39.95
megalops (shrimp, other crabs)	11.97	23.65	27.54	8.119	2.973
<i>Cancer magister</i> zoea	0.0	0.242	0.0	0.0	0.0
<i>Cancer</i> sp. zoea	4441.1	1815.1	1735.1	339.6	403.7
Porcellanidae zoea	0.0	0.0	0.0	0.0	0.0
Grapsidae zoea	0.0	0.0	0.0	0.0	0.0
Malidae zoea (Pugettia)	0.0	0.0	0.0	0.0	0.0
Pinnotheridae zoea	0.0	0.0	0.0	0.0	0.0
<i>Fabia subquadrata</i> (Pinnotheridae)	0.0	0.0	0.0	0.0	0.0
Galatheid zoea	0.0	0.0	0.0	0.0	0.0
Other Decapod Larvae	0.0	0.035	0.073	0.0	0.055
Pandalidae	0.095	0.175	1.505	2.654	0.854
Other Shrimp	0.0	0.0	0.0	0.0	0.0
<i>Lepas</i> (goose barnacle)	0.0	0.0	0.0	0.0	0.0
Cumacea	0.0	0.0	0.0	0.0	0.0
Amphipoda	0.0	0.0	0.0	0.0	0.0
Copepoda (Calanoida)	0.047	0.0	0.0	0.0	0.0
Euphausiacea- Thysanoessa	0.0	0.0	0.0	0.0	0.0
<i>Limnoria helicina</i> (Pteropod)	0.0	0.0	0.036	0.0	0.0
<i>Chione limacina</i> (Pteropod)	0.0	0.0	0.0	0.0	0.0
<i>Eukie</i> sp. (Pteropod)	0.0	0.0	0.0	0.0	0.0
Octopus	0.0	0.0	0.0	0.0	0.0
Squid	0.0	0.0	0.0	0.0	0.0
Isopoda	0.0	0.0	0.0	0.0	0.0
Insect Larvae	0.0	0.0	0.0	0.0	0.0
Myriapoda	0.0	0.0	0.0	0.0	0.0
Ostracoda	0.0	0.0	0.0	0.0	0.0
Invertebrate eggs	0.0	0.0	0.0	0.0	0.0
<i>Velletia</i>	1.437	1.751	0.367	0.0	0.018
Jellyfish (Leptomedusae)	0.0	0.0	0.0	0.0	0.0
Ctenophores (Pleurobrachia)	0.0	0.0	0.0	0.0	0.0
Siphonophores	0.0	0.0	0.0	0.0	0.0
<i>Coelenterata</i>	0.0	0.0	0.0	0.0	0.0
<i>Polychaeta</i>	0.0	0.0	0.0	0.0	0.0
<i>Chaetognathia</i>	0.0	0.0	0.0	0.0	0.0
Salpidae	0.0	0.0	0.0	0.0	0.0
<i>Stenobrachius leucopsaurus</i>	0.0	0.0	0.0	0.0	0.0
<i>Ammodites</i> larvae (Sandlance)	0.191	0.035	0.073	0.0	0.018
<i>Scorpaenichthys marmoratus</i>	0.0	0.0	0.0	0.0	0.0
<i>Anoplopoma fimbria</i> (Blackcod)	0.0	0.0	0.0	0.0	0.0
<i>Hexagrammos</i> (Greenling)	0.0	0.0	0.0	0.0	0.0
<i>Sitichidae</i> (Blenny)	0.0	0.0	0.073	0.0	0.074
<i>Sebastes</i> (Rockfish) larvae	0.0	0.0	0.0	0.062	0.0
Bullhead larvae	0.0	0.0	0.073	0.031	0.018
Fish eggs	0.0	0.0	0.0	0.0	0.018
Osmariidae (smelt)	0.0	0.0	0.0	0.0	0.0
<i>Microstomus pacificus</i> (Dover Sole)	0.047	0.0	0.283	0.031	0.111
Liparidae	0.0	0.0	0.0	0.0	0.0
Agonidae (poacher)	0.0	0.0	0.0	0.0	0.0
<i>Pilichthys</i> (Quillfish)	0.0	0.0	0.0	0.0	0.0
<i>Brosomphys marginata</i> (ragfish)	0.0	0.0	0.036	0.0	0.0
<i>Psephotichthys melanostictus</i>	0.0	0.0	0.0	0.0	0.0
<i>Isopsetta teleostis</i> (Butter Sole)	0.0	0.0	0.0	0.0	0.0
<i>Hippoglossoides esocodon</i>	0.0	0.0	0.0	0.0	0.0
Gobiidae	0.0	0.0	0.0	0.0	0.0
<i>Clupea harengus</i> (Herring)	0.0	0.210	1.358	0.031	0.0
<i>Lyopsetta exilis</i> (Slender Sole)	0.0	0.0	0.0	0.0	0.0
<i>Pleuronichthys coeniscus</i> (C-O sole)	0.0	0.0	0.0	0.0	0.0
Pholidae (Gumels)	0.0	0.0	0.0	0.0	0.0
<i>Oncorhynchus keta</i> (Chum Salmon)	0.0	0.0	0.0	0.0	0.0
Gadidae	0.0	0.0	0.0	0.0	0.0
<i>Lepidopsetta bilineata</i> (Rock Sole)	0.0	0.0	0.0	0.0	0.0

**Table 3.** Species catch per 10 m<sup>2</sup> of sea surface for each neuston tow and Tucker trawl net catch.  
H. BANKS ISLAND - June 19-20, 1988

Surface area (m <sup>2</sup> )	0.112	0.617	0.300	0.4148927	791.7	847.2	916.6	
TAXA (number per 10m <sup>2</sup> )	149-2	149-3	150-2	150-3	151	152	153	154
<i>Cancer magister</i> megalops	0.0	0.0	0.0	0.0	0.0	0.0	0.0	0.0
<i>Cancer</i> spp. megalops	4.032	5.553	0.6	11.74	0.313	0.315	1.062	4.363
megalops (shrimp, other crabs)	21.28	98.72	25.77	46.34	0.022	0.946	0.035	0.0
<i>Cancer magister</i> zoea	0.112	0.0	0.6	0.0	0.011	0.075	0.094	0.218
<i>Cancer</i> sp. zoea	179.7	1585.	69	460.3	60.66	287.8	371.8	1569.3
Porcellanidae zoea	0.0	0.0	0.0	0.0	0.062	0.0	0.0	0.0
Grapsidae zoea	0.0	0.0	0.0	0.0	0.066	0.0	37.18	0.0
Majidae zoea (Pugettia)	0.0	0.0	0.0	0.0	0.0	0.0	37.18	0.0
Pinnotheridae zoea	0.0	0.617	0.0	0.0	0.0	0.0	0.0	0.0
<i>Fabia subquadrata</i> (Pinnotheridae)	0.0	0.0	0.0	0.0	0.0	0.0	0.0	0.0
Galatheidae zoea	0.0	0.0	0.0	0.0	0.0	0.0	0.0	0.0
Other Decapod Larvae	0.0	0.0	0.0	0.0	0.0	0.0	0.0	0.0
Pandalidae	2.016	7.404	3.84	0.0	0.0	0.0	0.0	0.0
Other Shrimp	26.88	85.14	24.96	74.14	0.0	0.025	0.059	0.0
<i>Lepas</i> (goose barnacle)	0.0	0.0	0.0	0.0	0.0	0.0	0.0	0.0
Cumacea	0.0	0.0	0.0	0.0	0.0	0.0	0.0	0.0
Amphipoda	2.8	1.851	9	8.032	0.067	0.088	0.295	0.436
Copepoda (Calanoida)	47.04	333.1	246	5885.	0.168	0.315	1.770	7.200
Euphausiacea- <i>Thysanoessa</i>	24.64	111.0	19.8	194.6	0.448	0.0	0.118	0.0
<i>Limnoria helicina</i> (Pteropod)	0.0	0.0	0.0	0.0	0.0	0.0	0.0	0.0
<i>Eudora limacina</i> (Pteropod)	1.12	0.617	0.6	74.14	0.0	0.0	0.0	0.0
<i>Eudora</i> sp. (Pteropod)	0.0	0.0	0.0	0.0	0.0	0.0	0.0	0.0
Octopus	0.0	0.0	0.0	0.0	0.0	0.0	0.0	0.0
Squid	0.0	0.0	0.0	0.0	0.0	0.0	0.0	0.0
Isopoda	0.0	0.0	0.0	0.0	0.0	0.0	0.0	0.0
Insect Larvae	0.0	0.0	0.0	0.0	0.0	0.0	0.0	0.0
Mycidacea	0.0	0.0	0.0	0.0	0.0	0.0	0.0	0.0
Ostracoda	0.0	0.0	0.0	0.0	0.0	0.0	0.0	0.0
Invertebrate eggs	0.0	0.0	0.0	0.0	0.0	0.0	0.0	0.0
<i>Velletia</i>	0.0	0.0	0.0	0.0	0.0	0.0	0.0	0.0
Jellyfish (Leptomedusae)	95.2	33.93	168	231.7	0.257	0.568	0.106	0.218
Ctenophores (Pleurobrachia)	0.784	2.468	2.4	0.0	0.134	0.025	0.165	0.0
Siphonophores	0.0	0.0	0.0	0.0	0.0	0.0	0.0	0.0
<i>Coelenterata</i>	0.0	0.0	0.0	0.0	0.0	0.0	0.0	0.0
<i>Polychaeta</i>	0.0	0.0	0.0	0.0	0.022	0.037	0.0	0.0
<i>Chaetognathia</i>	0.112	0.0	0.0	0.617	0.0	0.0	0.011	0.0
Salps	0.0	0.0	0.0	0.0	0.0	0.0	0.0	0.0
<i>Stenobrachius leucopsanus</i>	0.0	0.0	0.0	0.0	0.0	0.0	0.0	0.0
Ammodites larvae (Sand lance)	0.0	0.0	0.0	0.0	0.0	0.0	0.0	0.0
<i>Scorpaenichthys marmoratus</i>	0.0	0.0	0.0	0.0	0.011	0.012	0.023	0.0
<i>Anoploporoma fimbria</i> (Blackcod)	0.0	0.0	0.0	0.0	0.0	0.0	0.0	0.0
<i>Hexagrammos</i> (Greenling)	0.0	0.0	0.0	0.0	0.0	0.0	0.0	0.0
Stichidae (Blenny)	0.336	0.617	0.0	0.0	0.0	0.037	0.047	0.0
Sebastes (Rockfish) larvae	0.0	0.617	0.0	1.853	0.0	0.0	0.0	0.0
Bullhead larvae	0.56	0.0	0.0	0.0	0.0	0.0	0.531	0.0
Fish eggs	0.0	0.0	0.0	0.0	0.0	0.0	0.0	0.0
<i>Osmeridae</i> (smelt)	0.0	0.0	0.0	0.0	0.0	0.0	0.0	0.0
<i>Microstomus pacificus</i> (Dover Sole)	0.0	0.0	0.0	0.0	0.617	0.0	0.0	0.0
Liparidae	0.112	0.0	0.0	0.617	0.0	0.0	0.165	0.0
Agonidae (poacher)	0.0	1.234	0.0	0.0	0.0	0.0	0.0	0.0
Pilichthyidae (Quillfish)	0.0	0.0	0.0	0.0	0.0	0.0	0.0	0.0
<i>Brosimphysis marginata</i> (ragfish)	0.112	1.234	0.0	0.0	0.0	0.0	0.0	0.0
<i>Psettichthys melanostrictus</i>	0.0	1.851	0.0	0.617	0.0	0.0	0.035	0.0
<i>Isopsetta solepis</i> (Butter Sole)	0.0	0.0	0.0	0.0	0.0	0.0	0.0	0.0
<i>Hippocrossus abaddon</i>	0.224	0.0	0.0	0.0	0.0	0.0	0.0	0.0
Gobiidae	0.0	0.0	0.0	0.0	0.0	0.0	0.0	0.0
<i>Cupea harengus</i> (Herring)	0.0	0.0	0.0	0.0	0.0	0.0	0.0	0.0
<i>Lyopsetta exilis</i> (Slender Sole)	0.0	0.0	0.0	0.0	0.0	0.0	0.0	0.0
<i>Pleuronathys coenosus</i> (C-O sole)	0.112	0.0	0.0	0.0	0.0	0.0	0.0	0.0
Pholidae (Gummels)	0.0	0.0	0.0	0.0	0.0	0.0	0.0	0.0
<i>Onchorhynchus keta</i> (Chum Salmon)	0.0	0.0	0.0	0.0	0.0	0.0	0.0	0.0
Gadidae	0.0	0.0	0.0	0.0	0.0	0.0	0.0	0.0
<i>Lepidopsetta bilineata</i> (Rock Sole)	0.0	0.0	0.0	0.0	0.0	0.0	0.0	0.0

**Table 3 (cont'd).** H. BANKS ISLAND - June 19-20, 1988

Surface area (m <sup>2</sup> )	583.0	1212	1201.	786.0	757.0	784.7	789.8
TAXA (number per 10m <sup>2</sup> )	155	156	157	158	159	160	161
<i>Cancer magister</i> megalops	0.0	0.0	0.0	0.0	0.0	0.0	0.0
<i>Cancer</i> spp. megalops	0.240	0.264	0.149	0.445	1.294	0.751	0.354
megalops (shrimp, other crabs)	1.715	0.206	0.024	0.190	0.092	0.050	0.633
<i>Cancer magister</i> zoea	0.0	0.008	0.008	0.0	0.0	0.0	0.012
<i>Cancer</i> sp. zoea	109.7	362.0	754.4	180.1	152.0	366.4	414.6
Porcellanidae zoea	0.0	0.0	0.0	0.0	0.0	0.0	0.0
Grapsidae zoea	0.0	0.0	68.58	0.0	0.0	0.0	0.0
Majidae zoea (Pugettia)	0.0	0.0	0.0	0.0	0.0	0.0	0.0
Pinnotheridae zoea	0.0	0.008	0.0	0.0	0.0	0.0	0.0
<i>Fabia subquadrata</i> (Pinnotheridae)	0.0	0.0	0.0	0.0	0.0	0.0	0.0
Galatheidae zoea	0.0	0.0	0.0	0.0	0.0	0.0	0.0
Other Decapod Larvae	0.0	0.024	0.016	0.0	0.0	0.012	0.0
Pandalidae	0.017	0.024	0.049	0.025	0.039	0.025	0.025
Other Shrimp	0.0	0.0	0.0	0.0	0.0	0.0	0.0
<i>Lepas</i> (goose barnacle)	0.0	0.090	0.0	0.0	0.0	0.0	0.0
Cumacea	0.085	7.095	0.074	0.025	0.092	0.012	0.075
Amphipoda	2.401	0.990	29.97	12.72	18.49	19.75	15.57
Copepoda (Calanoida)	0.102	0.049	1.423	7.697	15.52	9.494	11.01
Euphausiacea- <i>Thysanoessa</i>	0.0	0.0	0.0	0.0	0.0	0.0	0.0
<i>Limnoria helicina</i> (Pteropod)	0.0	0.008	0.0	0.0	0.039	0.012	0.012
<i>Eudora</i> sp. (Pteropod)	0.0	0.0	0.0	0.0	0.0	0.0	0.0
Octopus	0.0	0.0	0.0	0.0	0.013	0.0	0.0
Squid	0.0	0.0	0.0	0.0	0.0	0.0	0.0
Isopoda	0.0	0.0	0.0	0.0	0.0	0.0	0.0
Insect Larvae	0.0	0.0	0.0	0.0	0.0	0.0	0.0
Mycidacea	0.0	0.024	0.0	0.0	0.0	0.0	0.0
Ostracoda	0.017	0.0	0.0	0.0	0.0	0.0	0.0
Invertebrate eggs	0.0	0.0	0.0	0.0	0.0	0.0	0.0
<i>Velalia</i>	0.0	0.115	0.0	0.0	0.012	0.0	0.0
Jellyfish (Leptomedusae)	0.240	0.049	0.099	0.101	0.066	0.127	0.037
Ctenophores (Pleurobrachia)	0.857	0.0	0.0	0.050	0.105	0.140	0.0
Siphonophores	0.0	0.0	0.0	0.0	0.0	0.0	0.0
<i>Coelenterata</i>	0.0	0.0	0.0	0.0	0.0	0.0	0.0
<i>Polychaeta</i>	0.0	0.0	0.0	0.038	0.0	0.0	0.0
<i>Chaetognathia</i>	0.0	0.0	0.008	0.012	0.0	0.025	0.0
Salps	0.0	0.0	0.0	0.0	0.0	0.0	0.0
<i>Stenobrachius leucopsanus</i>	0.0	0.0	0.0	0.0	0.0	0.0	0.0
Ammodites larvae (Sand lance)	0.017	0.008	0.0	0.0	0.0	0.012	0.0
<i>Scorpaenichthys marmoratus</i>	0.0	0.0	0.0	0.0	0.0	0.0	0.0
<i>Anoploporus limbra</i> (Blackcod)	0.0	0.0	0.008	0.0	0.013	0.0	0.0
<i>Hexagrammos</i> (Greenling)	0.0	0.0	0.0	0.0	0.0	0.0	0.0
Stichidae (Blenny)	0.0	0.008	0.0	0.012	0.0	0.0	0.012
Sebastes (Rockfish) larvae	0.0	0.0	0.0	0.0	0.0	0.0	0.0
Bullhead larvae	0.034	0.024	0.074	0.025	0.039	0.012	0.0
Fish eggs	0.0	0.0	0.0	0.0	0.0	0.0	0.0
<i>Osmeridae</i> (smelt)	0.0	0.0	0.0	0.0	0.0	0.0	0.0
<i>Microstomus pacificus</i> (Dover Sole)	0.0	0.0	0.008	0.0	0.0	0.0	0.0
Liparidae	0.0	0.0	0.0	0.0	0.013	0.0	0.0
Agonidae (poacher)	0.0	0.0	0.0	0.012	0.0	0.0	0.0
Pilichthyidae (Quillfish)	0.0	0.0	0.0	0.0	0.0	0.0	0.0
<i>Brosimphys marginata</i> (ragfish)	0.0	0.0	0.0	0.0	0.0	0.0	0.0
<i>Psephotichthys melanostictus</i>	0.0	0.0	0.0	0.0	0.0	0.0	0.0
<i>Isopsetta solepis</i> (Butter Sole)	0.0	0.0	0.0	0.0	0.0	0.0	0.0
<i>Hippocampus abaddon</i>	0.0	0.0	0.0	0.0	0.0	0.0	0.0
Gobiidae	0.0	0.0	0.0	0.0	0.0	0.0	0.0
<i>Cupea harengus</i> (Herring)	0.0	0.0	0.0	0.0	0.0	0.0	0.0
<i>Lyopsetta exilis</i> (Slender Sole)	0.0	0.0	0.0	0.0	0.0	0.0	0.0
<i>Pleuronectes coenosus</i> (C-O sole)	0.0	0.0	0.0	0.0	0.0	0.0	0.0
Pholidae (Gunnels)	0.0	0.0	0.0	0.0	0.0	0.0	0.0
<i>Onchorynchus keta</i> (Chum Salmon)	0.0	0.0	0.008	0.0	0.0	0.0	0.0
Gadidae	0.0	0.0	0.0	0.0	0.0	0.0	0.0
<i>Lepidopsetta bilineata</i> (Rock Sole)	0.0	0.0	0.0	0.0	0.0	0.0	0.0

Table 3 (cont'd). H. BANKS ISLAND - June 19-20, 1988

Surface area (m <sup>2</sup> )	761.7	858.9	847.9	1115.	1280.	556.1	549.4
TAXA (number per 10m <sup>2</sup> )	162	163	164	165	167	168	169
<i>Cancer magister</i> megalops	0.0	0.0	0.0	0.0	0.0	0.0	0.0
<i>Cancer</i> spp. megalops	0.131	0.0	0.0	0.0	0.023	0.017	0.0
megalops (shrimp, other crabs)	0.787	0.011	0.235	0.017	0.0	0.0	0.0
<i>Cancer magister</i> zoea	0.0	0.0	0.0	0.0	0.0	0.0	0.0
<i>Cancer</i> sp. zoea	53.43	132.4	43.75	36.59	31.32	55.92	107.3
Porcellanidae zoea	0.0	0.0	0.0	0.0	0.316	0.0	0.0
Grapsidae zoea	0.0	0.0	0.0	0.0	0.0	0.0	0.0
Majidae zoea (Pugettia)	0.0	0.0	0.0	0.0	0.0	0.0	0.0
Pinnotheridae zoea	0.0	0.0	0.0	0.0	0.0	0.0	0.0
<i>Fabia subquadrata</i> (Pinnotheridae)	0.0	0.0	0.0	0.0	0.0	0.0	0.0
Galatheid zoea	0.0	0.0	0.0	0.0	0.0	0.0	0.0
Other Decapod Larvae	0.0	0.0	0.0	0.0	0.0	0.0	0.0
Pandalidae	0.0	0.0	0.0	0.0	0.007	0.0	0.0
Other Shrimp	0.013	0.023	0.0	0.0	0.015	0.0	0.0
Lepas (goose barnacle)	0.0	0.0	0.0	0.0	0.0	0.0	0.0
Cumacea	0.0	0.0	0.0	0.0	0.0	0.0	0.0
Amphipoda	0.039	0.046	0.0	0.0	0.007	0.0	0.036
Copepoda (Calanoida)	12.66	6.461	2.889	2.556	0.184	0.179	0.0
Euphausiacea - <i>Thysanoessa</i>	16.27	2.037	0.058	0.008	0.0	0.0	0.0
<i>Limnocalanus</i> (Pteropod)	0.0	0.0	0.0	0.0	0.0	0.0	0.0
<i>Clione limacina</i> (Pteropod)	0.0	0.0	0.0	0.0	0.0	0.0	0.0
<i>Eudora</i> sp. (Pteropod)	0.0	0.0	0.0	0.0	0.0	0.0	0.0
Octopus	0.0	0.0	0.0	0.0	0.0	0.0	0.0
Squid	0.0	0.0	0.0	0.0	0.0	0.0	0.0
Isopoda	0.0	0.0	0.0	0.0	0.0	0.0	0.0
Insect Larvae	0.0	0.0	0.0	0.0	0.0	0.0	0.0
Myriadaea	0.0	0.0	0.0	0.0	0.0	0.0	0.0
Ostracoda	0.0	0.0	0.0	0.0	0.0	0.0	0.0
Invertebrate eggs	0.0	0.0	0.011	0.0	0.0	0.017	0.0
Velilla	0.0	0.0	0.0	0.008	0.0	0.0	0.0
Jellyfish (Leptomedusae)	0.210	0.116	0.165	2	0.855	0.200	0.0
Ctenophores (Pleurobrachia)	0.052	0.034	0.035	0.017	0.078	0.809	0.036
Siphonophores	0.0	0.0	0.0	0.0	0.0	0.0	0.0
<i>Coelenterata</i>	0.0	0.0	0.0	0.0	0.0	0.0	0.0
<i>Polychaeta</i>	0.0	0.0	0.0	0.0	0.0	0.0	0.0
<i>Chaetognatha</i>	0.013	0.0	0.0	0.0	0.0	0.0	0.0
Salps	0.0	0.0	0.0	0.0	0.0	0.0	0.0
<i>Stenobrachius leucopsanus</i>	0.0	0.0	0.0	0.0	0.0	0.0	0.0
<i>Anomdites</i> larvae (Sand lance)	0.0	0.0	0.0	0.0	0.0	0.035	0.0
<i>Scorpaenichthys marmoratus</i>	0.0	0.0	0.0	0.0	0.0	0.0	0.0
<i>Anoplogomus fimbria</i> (Blackcod)	0.0	0.0	0.0	0.0	0.0	0.0	0.0
<i>Hexagrammos</i> (Greenling)	0.0	0.0	0.0	0.0	0.0	0.0	0.0
Stichidae (Blenny)	0.0	0.011	0.0	0.0	0.0	0.0	0.0
<i>Sebastes</i> (Rockfish) larvae	0.0	0.0	0.0	0.0	0.0	0.017	0.0
Bullhead larvae	0.0	0.023	0.0	0.0	0.0	0.0	0.0
Fish eggs	0.0	0.069	0.0	0.0	0.0	0.0	0.0
Gemmatidae (smelt)	0.0	0.0	0.0	0.0	0.0	0.0	0.0
<i>Microstomus pacificus</i> (Dover Sole)	0.0	0.0	0.0	0.0	0.0	0.0	0.0
Liparidae	0.0	0.0	0.0	0.0	0.0	0.0	0.0
Agonidae (poacher)	0.0	0.0	0.0	0.0	0.0	0.0	0.0
Pilichthyidae (Quillfish)	0.0	0.0	0.0	0.0	0.0	0.0	0.0
<i>Brosomphysis marginata</i> (ragfish)	0.0	0.0	0.0	0.0	0.0	0.0	0.0
<i>Psettichthys melanostictus</i>	0.0	0.0	0.0	0.0	0.0	0.0	0.0
<i>Isopsetta isolepis</i> (Butter Sole)	0.0	0.0	0.0	0.0	0.0	0.0	0.0
<i>Hippoglossus asotus</i>	0.0	0.0	0.0	0.0	0.0	0.0	0.0
Gobiidae	0.0	0.0	0.0	0.0	0.0	0.0	0.0
<i>Cupea harengus</i> (Herring)	0.0	0.0	0.0	0.0	0.0	0.0	0.0
<i>Lyopsetta exilis</i> (Slender Sole)	0.0	0.0	0.0	0.0	0.0	0.0	0.0
<i>Pleuronectes coenosus</i> (C-O sole)	0.0	0.0	0.0	0.0	0.0	0.0	0.0
Pholidae (Gunnels)	0.0	0.0	0.0	0.0	0.0	0.0	0.0
<i>Onchorynchus keta</i> (Chum Salmon)	0.0	0.0	0.0	0.0	0.007	0.0	0.0
Gadidae	0.0	0.0	0.0	0.0	0.0	0.0	0.0
<i>Lepidopsetta bilineata</i> (Rock Sole)	0.0	0.0	0.0	0.0	0.0	0.0	0.0

Table 4. Species catch per 10 m<sup>3</sup> of sea volume for each neuston tow and Tucker trawl net catch.

## A. TRIANGLE TRANSECT - June 11, 12

Sample volume (m <sup>3</sup> )	224.7	112.4	236.2	253.8	220.3	230.7	371.1	362.8	343.4	261.9
TAXA (number per 10m <sup>3</sup> )	1	2	3	4	5	6	7	8	9	10
<i>Cancer magister</i> megalops	0.13	0.0	0.18	0.13	0.13	0.40	0.0	0.16	0.61	0.15
<i>Cancer</i> spp. megalops	16.32	0.18	0.22	0.13	0.22	2.27	0.78	0.96	3.20	1.03
megalops (shrimp, other crabs)	0.0	0.18	0.09	0.22	0.18	0.09	0.24	0.14	0.15	2.56
<i>Cancer magister</i> zoea	0.13	0.0	0.0	0.0	0.0	0.0	0.0	0.0	0.0	0.0
<i>Cancer</i> sp. zoea	147.1	71.43	96.13	171	38.94	37.38	25.74	66.12	7.57	5.54
Porcellanidae zoea	147.1	8.21	10.70	19.00	0.0	0.0	0.0	0.0	0.0	0.0
Grapsidae zoea	0.0	0.0	0.0	0.0	0.0	0.0	0.0	0.0	0.0	0.0
Majidae zoea (Pugettia)	0.0	0.0	0.0	0.0	0.0	0.0	0.0	0.0	0.0	0.0
Pinnotheridae zoea	0.0	0.0	0.0	0.0	0.0	0.0	0.0	0.0	0.0	0.0
<i>Fabia subquadrata</i> (Pinnotheridae)	0.13	0.0	0.0	0.0	0.0	0.0	0.0	0.0	0.0	0.0
Galatheid zoea	0.0	0.0	0.0	0.0	0.0	0.0	0.0	0.0	0.0	0.0
Other Decapod Larvae	0.0	0.0	0.0	0.0	0.0	0.0	0.0	0.0	0.15	0.19
Pandalidae	0.0	0.0	0.0	0.0	0.0	0.0	0.05	0.03	0.0	0.0
Other Shrimp	0.81	0.0	0.04	0.04	0.36	0.39	0.16	0.17	0.23	0.08
Lepas (goose barnacle)	0.13	0.0	0.0	0.0	0.0	0.0	0.0	0.0	0.0	0.0
Cumacea	0.0	0.0	0.0	0.0	0.0	0.0	0.0	0.0	0.0	0.0
Amphipoda	0.40	0.13	0.36	0.75	0.58	0.17	0.46	0.33	0.15	0.61
Copepoda (Calanoida)	1.35	1.34	0.0	1.96	3.74	1.65	0.97	2.23	9.76	34.17
Euphausiacea - <i>Thysanoessa</i>	0.0	0.0	0.0	0.0	0.0	0.09	0.0	0.0	0.0	0.0
<i>Limnocalanus hellicina</i> (Pteropod)	0.0	0.04	0.0	0.0	0.0	0.0	0.0	0.0	0.0	0.0
<i>Clione limacina</i> (Pteropod)	0.0	0.0	0.0	0.0	0.0	0.0	0.0	0.0	0.0	0.0
<i>Eudora</i> sp. (Pteropod)	0.0	0.0	0.0	0.0	0.0	0.0	0.0	0.0	0.0	0.0
Octopus	0.0	0.0	0.0	0.0	0.0	0.0	0.0	0.0	0.0	0.0
Squid	0.0	0.0	0.04	0.0	0.0	0.0	0.0	0.0	0.0	0.0
Isopoda	0.0	0.0	0.0	0.0	0.0	0.0	0.0	0.0	0.0	0.0
Insect Larvae	0.0	0.0	0.0	0.0	0.0	0.0	0.0	0.0	0.0	0.0
Myriadaea	0.0	0.0	0.0	0.0	0.0	0.0	0.0	0.0	0.0	0.0
Ostracoda	0.0	0.0	0.0	0.0	0.0	0.0	0.0	0.0	0.0	0.0
Invertebrate eggs	0.13	0.04	0.0	0.0	0.0	0.0	0.0	0.0	0.0	0.0
Velilla	0.0	0.0	2.40	7.65	4.09	0.27	0.22	0.28	0.09	0.11
Jellyfish (Leptomedusae)	1.75	0.0	5.87	6.54	14.78	7.21	12.60	17.55	0.42	0.80
Ctenophores (Pleurobrachia)	5.53	1.20	0.0	0.0	0.0	0.0	0.0	0.0	0.0	0.0
Siphonophores	0.0	0.0	0.0	0.0	0.0	0.0	0.0	0.0	0.0	0.0
<i>Coelenterata</i>	0.0	0.0	0.0	0.0	0.0	0.0	0.0	0.0	0.0	0.0
<i>Polychaeta</i>	0.13	0.0	0.0	0.0	0.04	0.09	0.0	0.0	0.0	0.04
<i>Chaetognatha</i>	0.0	0.0	0.04	0.0	0.0	0.04	0.0	0.0	0.0	0.04
Salps	0.0	0.0	0.0	0.0	0.0	0.0	0.0	0.0	0.0	0.0
<i>Stenobrachius leucopsanus</i>	0.0	0.0	0.0	0.0	0.0	0.0	0.0	0.0	0.0	0.0
<i>Anomdites</i> larvae (Sand lance)	0.0	0.0	0.0	0.0	0.0	0.0	0.0	0.0	0.0	0.0
<i>Scorpaenichthys marmoratus</i>	0.0	0.0	0.04	0.0	0.31	0.36	0.67	0.35	0.20	0.88
<i>Anoplogomus fimbria</i> (Blackcod)	0.0	0.0	0.0	0.0	0.04	0.0	0.0	0.06	0.0	0.0
<i>Hexagrammos</i> (Greenling)	0.0	0.0	0.0	0.0	0.0	0.0	0.0	0.03	0.03	0.0
Stichidae (Blenny)	0.0	0.0	0.0	0.0	0.0	0.0	0.0	0.0	0.0	0.0
<i>Sebastes</i> (Rockfish) larvae	0.0	0.0	0.0	0.0	0.0	0.0	0.0	0.0	0.08	0.0
Bullhead larvae	1.75	0.22	0.27	0.18	0.27	0.04	0.22	0.06	0.03	0.11
Fish eggs	0.0	0.27	0.45	0.80	0.76	0.18	0.70	1.93	0.0	0.15
Gemmatidae (smelt)	0.0	0.0	0.04	0.0	0.0	0.0	0.0	0.0	0.0	0.0
<i>Microstomus pacificus</i> (Dover Sole)	0.0	0.0	0.0	0.04	0.0	0.0	0.0	0.0	0.0	0.0
Liparidae	0.0	0.0	0.0	0.09	0.0	0.0	0.0	0.0	0.03	0.0
Agonidae (poacher)	0.0	0.0	0.0	0.0	0.0	0.0	0.0	0.0	0.0	0.0
Pilichthyidae (Quillfish)	0.0	0.0	0.0	0.0	0.0	0.0	0.0	0.0	0.0	0.0
<i>Brosomphysis marginata</i> (ragfish)	0.0	0.09	0.0	0.0	0.0	0.0	0.0	0.0	0.0	0.0
<i>Psettichthys melanostictus</i>	0.0	0.0	0.0	0.0	0.0	0.0	0.0	0.0	0.0	0.0
<i>Isopsetta isolepis</i> (Butter Sole)	0.0	0.0	0.0	0.0	0.0	0.0	0.0	0.0	0.0	0.0
<i>Hippoglossus asotus</i>	0.0	0.0	0.0	0.0	0.0	0.0	0.0	0.0	0.0	0.0
Gobiidae	0.0	0.0	0.0	0.0	0.0	0.0	0.0	0.0	0.0	0.0
<i>Cupea harengus</i> (Herring)	0.0	0.0	0.0	0.0	0.0	0.0	0.0	0.0	0.0	0.0
<i>Lyopsetta exilis</i> (Slender Sole)	0.0	0.0	0.0	0.0	0.0	0.0	0.0	0.0	0.0	0.0
<i>Pleuronectes coenosus</i> (C-O sole)	0.0	0.0	0.0	0.0	0.0	0.0	0.0	0.0	0.0	0.0
Pholidae (Gunnels)	0.0	0.0	0.0	0.0	0.0	0.0	0.0	0.0	0.0	0.0
<i>Onchorynchus keta</i> (Chum Salmon)	0.0	0.0	0.0	0.0	0.0	0.0	0.0	0.0	0.0	0.0
Gadidae	0.0	0.0	0.0	0.0	0.0	0.0	0.0	0.0	0.0	0.0
<i>Lepidopsetta bilineata</i> (Rock Sole)	0.0	0.0	0.0	0.0	0.0	0.0	0.0	0.0	0.0	0.0

Table 4 (cont'd.). A. TRIANGLE TRANSECT - June 11, 12

B. GOOSE BANK																				
Sample volume (m <sup>3</sup> )	279.4	258.4	291.2	250.5	259.0	297.3	313.9	357.2	221.5	231.7										
TAXA (number per 10m <sup>3</sup> )	11	12	13	14	15	16	17	18	19	20	21-2	533	533.3	533.3	941	533	709	533	533.3	533.3
<i>Cancer magister</i> megalops	0.68	0.04	0.21	0.08	0.00	0.00	0.00	0.00	0.00	0.00	0.00	0.00	0.00	0.00	0.00	0.00	0.00	0.00	0.00	0.00
<i>Cancer</i> spp. megalops	13.78	7.51	1.89	1.52	23.59	0.44	1.37	1.12	0.54	0.39	0.1	0.4	0.3	0.4	0.4	0.6	0.1	0.3	1.9	5.1
megalops (shrimp, other crabs)	14.34	0.39	2.37	0.28	0.04	1.41	0.10	0.06	0.00	0.00	0.03	0.1	0.3	0.3	0.7	0.2	0.3	0.5	1.3	0.8
<i>Cancer magister</i> zoea	0.00	0.04	0.03	0.00	0.00	0.00	0.03	0.00	0.00	0.00	0.00	0.1	0.00	0.00	0.00	0.00	0.00	0.00	0.00	0.00
<i>Cancer</i> sp. zoea	8.95	10.80	11.92	0.00	12.20	22.75	12.11	5.10	3.79	3.24	2.9	19.8	3.4	5.7	1.5	11.7	3.8	6.9	28.9	101.3
Porcellanidae zoea	0.00	0.00	0.00	0.00	0.00	0.00	0.00	0.00	0.00	0.00	0.00	0.00	0.00	0.00	0.00	0.00	0.00	0.00	0.00	0.00
Grapsidae zoea	0.00	0.00	0.00	0.00	0.00	0.00	0.00	0.00	0.00	0.00	0.00	0.00	0.00	0.00	0.00	0.00	0.00	0.00	0.00	0.00
Majidae zoea (Pugetia)	0.00	0.00	0.00	0.00	0.00	0.00	0.00	0.00	0.00	0.00	0.00	0.00	0.00	0.00	0.00	0.00	0.00	0.00	0.00	0.00
Pinnotheridae zoea	0.00	0.00	0.00	0.00	0.00	0.00	0.00	0.00	0.00	0.00	0.00	0.00	0.00	0.00	0.00	0.00	0.00	0.00	0.00	0.00
<i>Fabia subquadrata</i> (Pinnotheridae)	0.00	0.00	0.00	0.00	0.00	0.03	0.00	0.00	0.00	0.00	0.00	0.00	0.00	0.00	0.00	0.00	0.00	0.00	0.00	0.00
Galatheid zoea	0.00	0.00	0.00	0.00	0.00	0.00	0.00	0.00	0.00	0.00	0.00	0.00	0.00	0.00	0.00	0.00	0.00	0.00	0.00	0.00
Other Decapod Larvae	0.36	0.00	0.04	0.00	0.00	0.00	0.00	0.00	0.00	0.00	0.00	0.00	0.00	0.00	0.00	0.00	0.00	0.00	0.00	0.00
Pandalidae	0.00	0.04	0.00	0.00	0.00	0.00	0.00	0.00	0.00	0.00	0.00	0.02	0.00	0.00	0.01	0.00	0.2	0.00	0.00	0.00
Other Shrimp	0.14	0.12	0.14	0.16	0.04	0.00	0.00	0.00	0.00	0.00	0.00	0.5	2.6	1.9	0.2	0.3	0.5	0.7	1.1	3.8
<i>Lepea</i> (goose barnacle)	0.00	0.00	0.00	0.00	0.00	0.00	0.00	0.00	0.00	0.00	0.00	0.00	0.00	0.00	0.00	0.00	0.00	0.00	0.00	0.00
Cumacea	0.00	0.00	0.00	0.00	0.00	0.00	0.03	0.00	0.00	0.00	0.00	0.00	0.00	0.00	0.00	0.00	0.00	0.00	0.00	0.00
Amphipoda	0.36	0.54	0.41	1.24	0.93	3.57	0.64	0.42	0.14	0.04	0.00	0.00	0.00	0.00	0.00	0.00	0.00	0.00	0.00	0.00
Copepoda (Calanoida)	204	81.66	17.14	0.00	8.07	2.02	0.64	0.76	0.00	1.34	0.2	0.8	0.6	0.2	0.4	0.7	0.7	0.6	0.9	0.8
Euphausiacea- <i>Thysanoessa</i>	3.87	1.35	0.34	1.08	0.31	0.91	0.10	0.00	0.00	0.04	6.1	13.3	3.8	0.7	2.3	104.9	78.8	8.4	0.0	0.0
<i>Limnadia heliana</i> (Pteropod)	0.00	0.00	0.00	0.00	0.00	0.00	0.00	0.00	0.00	0.00	0.4	1.6	13.6	4.7	0.8	0.6	32.7	21.8	4.9	1.4
<i>Euphausiacea-Thysanoessa</i>	0.00	0.04	0.00	0.00	0.00	0.00	0.00	0.00	0.00	0.00	0.00	0.00	0.00	0.00	0.00	0.00	0.00	0.00	0.00	0.00
<i>Clione limacina</i> (Pteropod)	0.00	0.00	0.00	0.00	0.00	0.00	0.00	0.00	0.00	0.00	0.00	0.00	0.00	0.00	0.00	0.00	0.00	0.00	0.00	0.00
<i>Eudis</i> sp. (Pteropod)	0.00	0.00	0.00	0.00	0.00	0.00	0.00	0.00	0.00	0.00	0.00	0.00	0.00	0.00	0.00	0.00	0.00	0.00	0.00	0.00
Octopus	0.00	0.00	0.00	0.00	0.00	0.00	0.00	0.00	0.00	0.00	0.00	0.00	0.00	0.00	0.00	0.00	0.00	0.00	0.00	0.00
Squid	0.00	0.00	0.00	0.00	0.00	0.00	0.03	0.08	0.00	0.00	0.00	0.00	0.00	0.00	0.00	0.00	0.00	0.00	0.00	0.00
Isopoda	0.00	0.00	0.00	0.04	0.00	0.00	0.00	0.00	0.00	0.00	0.00	0.00	0.1	0.00	0.00	0.00	0.00	0.00	0.00	0.00
Insect Larvae	0.00	0.00	0.00	0.00	0.00	0.00	0.00	0.00	0.00	0.00	0.00	0.00	0.00	0.00	0.00	0.00	0.00	0.00	0.00	0.00
Mycidacea	0.00	0.00	0.00	0.00	0.00	0.00	0.00	0.00	0.00	0.00	0.00	0.00	0.00	0.00	0.00	0.00	0.00	0.00	0.00	0.00
Ostracoda	0.00	0.00	0.00	0.00	0.04	0.00	0.00	0.00	0.00	0.00	0.00	0.00	0.00	0.00	0.00	0.00	0.00	0.00	0.00	0.00
Invertebrate eggs	0.00	0.00	0.00	0.00	0.00	0.00	0.00	0.00	0.05	0.00	0.00	0.00	0.00	0.00	0.00	0.00	0.00	0.00	0.00	0.00
<i>Velilia</i>	0.04	0.04	0.03	0.00	0.00	0.00	0.00	0.00	0.00	0.00	0.00	0.00	0.00	0.00	0.00	0.00	0.00	0.00	0.00	0.00
Jellyfish (Leptomedusae)	0.00	0.00	0.24	0.04	0.03	0.06	0.17	0.00	0.00	0.17	2.1	11.7	4.9	3.8	2.7	4.9	8.2	23.5	90.4	51.8
Ctenophores (Pleurobrachia)	1.58	5.46	2.40	4.15	13.24	12.65	1.59	0.17	1.04	3.02	0.00	0.00	0.00	0.00	0.00	0.00	0.00	0.00	0.00	0.00
Siphonophores	0.00	0.00	0.00	0.00	0.00	0.00	0.00	0.00	0.00	0.00	0.00	1.7	0.4	2.2	1.4	5.3	0.0	4.5	0.0	0.8
<i>Coelenterata</i>	0.00	0.00	0.00	0.00	0.00	0.00	0.00	0.00	0.00	0.00	0.00	0.00	0.00	0.00	0.00	0.00	0.00	0.00	0.00	0.00
<i>Polychaeta</i>	0.00	0.03	0.24	0.00	0.00	0.00	0.03	0.11	0.05	0.09	0.00	0.00	0.00	0.00	0.00	0.00	0.00	0.00	0.00	0.00
<i>Chaetognatha</i>	0.00	0.00	0.00	0.00	0.00	0.00	0.00	0.00	0.00	0.00	0.00	0.00	0.00	0.00	0.00	0.00	0.00	0.00	0.00	0.00
Salps	0.00	0.00	0.00	0.00	0.00	0.03	0.00	0.00	0.00	0.00	0.00	0.00	0.00	0.00	0.00	0.00	0.00	0.00	0.00	0.00
<i>Stenobrachius leucopsanus</i>	0.00	0.00	0.00	0.00	0.00	0.00	0.00	0.00	0.00	0.00	0.00	0.00	0.00	0.00	0.00	0.00	0.00	0.00	0.00	0.00
<i>Armodius</i> larvae (Sandlance)	0.39	0.04	0.14	0.00	0.00	0.00	0.00	0.00	0.00	0.00	0.00	0.00	0.00	0.00	0.00	0.00	0.00	0.00	0.00	0.00
<i>Scorpaenichthys marmoratus</i>	0.04	0.00	0.00	0.00	0.00	0.00	0.00	0.00	0.00	0.00	0.00	0.00	0.00	0.00	0.00	0.00	0.00	0.00	0.00	0.00
<i>Anoploplatys fimbria</i> (Blackcod)	0.14	0.00	0.00	0.00	0.04	0.03	0.00	0.03	0.00	0.00	0.00	0.00	0.00	0.00	0.00	0.00	0.00	0.00	0.00	0.00
<i>Hexagrammos</i> (Greenling)	0.00	0.00	0.03	0.00	0.00	0.07	0.00	0.00	0.00	0.00	0.00	0.00	0.00	0.00	0.00	0.00	0.00	0.00	0.00	0.00
<i>Stichidae</i> (Blenny)	0.11	0.08	0.21	0.00	0.00	0.00	0.00	0.00	0.00	0.00	0.00	0.00	0.00	0.00	0.00	0.00	0.00	0.00	0.00	0.00
<i>Sebastes</i> (Rockfish) larvae	0.00	0.03	0.00	0.00	0.00	0.03	0.10	0.06	0.00	0.04	0.00	0.00	0.00	0.00	0.00	0.00	0.00	0.00	0.00	0.00
Bullhead larvae	0.25	0.23	0.07	0.12	0.10	0.14	0.23	0.17	0.00	0.00	0.00	0.00	0.00	0.00	0.00	0.00	0.00	0.00	0.00	0.00
Fish eggs	0.61	0.39	0.00	0.36	1.04	0.71	0.29	0.59	0.50	0.52	0.00	0.00	0.1	0.00	0.2	0.0	0.1	0.2	0.1	0.1
Osmeridae (smelt)	0.00	0.00	0.00	0.00	0.00	0.00	0.00	0.00	0.00	0.00	0.00	0.00	0.00	0.00	0.00	0.00	0.00	0.00	0.00	0.00
<i>Microstomus pacificus</i> (Dover Sole)	0.00	0.00	0.00	0.00	0.00	0.00	0.00	0.00	0.00	0.00	0.00	0.00	0.00	0.00	0.00	0.00	0.00	0.00	0.00	0.00
Liparidae	0.00	0.00	0.00	0.00	0.00	0.00	0.00	0.00	0.00	0.00	0.00	0.00	0.00	0.00	0.00	0.00	0.00	0.00	0.00	0.00
<i>Agonidae</i> (poacher)	0.04	0.04	0.00	0.00	0.00	0.00	0.00	0.00	0.00	0.00	0.00	0.1	0.00	0.00	0.00	0.00	0.00	0.00	0.00	0.00
<i>Pilichthys</i> (Quillfish)	0.00	0.00	0.00	0.00	0.00	0.00	0.00	0.00	0.00	0.00	0.00	0.00	0.00	0.00	0.00	0.00	0.00	0.00	0.00	0.00
<i>Brosomphysis marginata</i> (ragfish)	0.00	0.00	0.00	0.00	0.00	0.00	0.00	0.00	0.00	0.00	0.00	0.00	0.00	0.00	0.00	0.00	0.00	0.00	0.00	0.00
<i>Psettichthys melanostictus</i>	0.00	0.00	0.00	0.00	0.00	0.00	0.00	0.00	0.00	0.00	0.00	0.00	0.00	0.00	0.00	0.00	0.00	0.00	0.00	0.00
<i>Psettichthys melanostictus</i>	0.00	0.00	0.00	0.00	0.00	0.00	0.00	0.00	0.00	0.00	0.00	0.00	0.00	0.00	0.00	0.00	0.00	0.00	0.00	0.00
<i>Isopsetta isolepis</i> (Butter Sole)	0.00	0.00	0.00	0.00	0.00	0.00	0.00	0.00	0.00	0.00	0.00	0.00	0.00	0.00	0.00	0.00	0.00	0.00	0.00	0.00
<i>Hippoglossus abaddon</i>	0.00	0.00	0.00	0.00	0.00	0.00	0.00	0.00	0.00	0.00	0.00	0.00	0.00	0.00	0.00	0.00	0.00	0.00	0.00	0.00
Gobiidae	0.00	0.00	0.00	0.00	0.00	0.00	0.00	0.00	0.00	0.00	0.00	0.00	0.00	0.00	0.00	0.00	0.00	0.00	0.00	0.00
<i>Cupea harengus</i> (Herring)	0.00	0.00	0.00	0.00	0.00	0.00	0.00	0.00	0.00	0.00	0.00	0.00	0.00	0.00	0.00	0.00	0.00	0.00	0.00	0.00
<i>Lyopsetta exilis</i> (Slender Sole)	0.00	0.00	0.00	0.00	0.00	0.00	0.00	0.00	0.00	0.00	0.00	0.00	0.00	0.00	0.00	0.00	0.00	0.00	0.00	0.00
<i>Pleuronectes coenosus</i> (C-O sole)	0.00	0.00	0.00	0.00	0.00	0.00	0.00	0.00	0.00	0.00	0.00	0.00	0.00	0.00	0.00	0.00	0.00	0.00	0.00	0.00
<i>Pleuronectes coenosus</i> (C-O sole)	0.00	0.00	0.00	0.00																





Table 4 (cont'd.). B. GOOSE BANK

Sample volume (m <sup>3</sup> )	452.6	414.8	46	47										
TAXA (number per 10m <sup>3</sup> )					TT	TT	TT	TT	TT	TT	TT	TT	NW	NW
<i>Cancer magister</i> megalops	0.0	0.0			1045	533.3	490.0	352.5	1092	576.6	533.3	294	251	391
<i>Cancer</i> spp. megalops	0.0	0.0			48.2	48.3	49.2	49.3	50.2	51.2	51.3	52	53	54
megalops (shrimp, other crabs)	0.0	0.0												
<i>Cancer magister</i> zoea	83.8	290.4			0.0	0.0	0.0	0.0	0.0	0.0	0.0	0.0	0.0	0.0
<i>Cancer</i> sp. zoea	0.0	0.0			0.1	0.0	0.6	0.0	0.0	0.0	0.0	0.1	0.1	0.2
Porcellanidae zoea	0.0	0.0			0.0	0.0	0.0	0.0	0.0	0.0	0.0	0.0	0.0	0.1
Grapsidae zoea	0.0	0.0			6.2	28.9	8.4	13.4	5.7	4.7	32.3	27.2	222.8	464.2
Majidae zoea (Pugetia)	0.0	0.0			0.0	0.0	0.0	0.0	0.0	0.0	0.0	0.0	0.0	0.0
<i>Fabia subquadrata</i> (Pinnotheridae)	0.0	0.0			0.0	0.0	0.0	0.0	0.0	0.0	0.0	0.0	0.0	0.0
Galatheid zoea	0.0	0.0			0.1	0.0	0.0	0.0	0.0	0.0	0.0	0.0	0.0	0.0
Other Decapod Larvae	0.0	0.0			0.0	0.0	0.0	0.0	0.0	0.0	0.0	0.0	0.0	0.0
Pandalidae	0.0	0.0			0.0	0.0	0.0	0.0	0.0	0.0	0.0	0.0	0.0	0.0
Other Shrimp	0.0	0.0			0.2	0.5	0.4	1.1	0.3	0.8	0.9	0.0	0.0	0.0
<i>Lepas</i> (goose barnacle)	0.0	0.0			0.0	0.0	0.0	0.0	0.0	0.0	0.0	0.0	0.0	0.1
Cumacea	0.0	0.0			0.0	0.0	0.0	0.0	0.0	0.0	0.0	0.0	0.0	0.0
Amphipoda	0.2	0.2			0.0	0.0	0.0	0.0	0.0	0.0	0.0	0.0	0.0	0.0
Copepoda (Calanoida)	13.3	13.3			1.0	0.1	1.6	2.6	1.8	2.0	1.5	0.2	0.4	2.0
Euphausiacea- <i>Thysanoessa</i>	0.2	0.3			57.4	230.1	12.0	41.2	193.7	305.5	4750	120	37.8	332
<i>Limnocalanus macrurus</i> (Pteropod)	0.1	0.0			11.5	22.0	11.2	11.1	72.3	29.8	28.9	5.9	1.2	0.7
<i>Clione limacina</i> (Pteropod)	0.0	0.0			0.0	0.0	0.0	0.0	0.0	0.0	0.0	0.0	0.0	0.2
<i>Eudora</i> sp. (Pteropod)	0.0	0.0			0.0	0.2	0.0	0.0	0.0	0.0	0.0	0.0	0.1	0.6
Octopus	0.0	0.0			0.0	0.0	0.0	0.0	0.0	0.0	0.0	0.0	0.0	0.3
Squid	0.0	0.0			0.0	0.0	0.0	0.0	0.0	0.0	0.0	0.0	0.0	0.0
Isopoda	0.0	0.0			0.0	0.0	0.0	0.0	0.0	0.0	0.0	0.0	0.0	1.1
Insect Larvae	0.0	0.0			0.0	0.0	0.0	0.0	0.0	0.0	0.0	0.0	0.0	0.0
Mysidacea	0.0	0.0			0.0	0.0	0.0	0.0	0.0	0.0	0.0	0.0	0.0	0.0
Ostracoda	0.0	0.0			0.0	0.0	0.0	0.0	0.0	0.0	0.0	0.0	0.0	0.0
Invertebrate eggs	0.0	0.0			0.0	0.0	0.0	0.0	0.0	0.0	0.0	0.0	0.0	0.0
<i>Velutina</i>	4.8	4.7			0.0	0.0	0.0	0.0	0.0	0.0	0.0	0.0	0.0	0.0
Jellyfish (Leptomedusae)	0.2	0.3			1.0	0.5	50.2	76.4	0.9	0.7	5.1	0.0	0.9	0.2
Ctenophores (Pleurobrachia)	0.0	0.0			0.0	0.0	0.0	0.0	0.3	0.5	0.0	0.0	0.0	0.1
Siphonophores	0.0	0.0			0.0	0.0	0.0	0.0	0.0	0.0	0.0	0.0	0.0	0.0
<i>Coelenterata</i>	0.0	0.0			0.0	0.0	0.0	0.0	0.0	0.0	0.0	0.0	0.0	0.0
<i>Polychaeta</i>	0.0	0.0			0.0	0.0	0.0	0.0	0.0	0.0	0.0	0.0	0.0	0.0
<i>Chaetognathia</i>	0.0	0.0			0.0	0.1	0.0	0.0	0.0	0.0	0.3	0.0	0.0	0.0
<i>Salps</i>	0.0	0.0			0.7	1.6	0.4	0.0	0.0	0.0	0.4	0.3	0.3	0.1
<i>Stenobrachius leucopsanus</i>	0.0	0.0			0.0	0.0	0.0	0.0	0.0	0.0	0.0	0.0	0.0	0.0
<i>Ammodites</i> larvae (Sandlance)	0.0	0.0			0.0	0.0	0.0	0.0	0.0	0.0	0.0	0.0	0.0	0.0
<i>Scorpaenichthys marmoratus</i>	0.0	0.0			0.0	0.0	0.0	0.0	0.0	0.0	0.0	0.0	0.0	0.2
<i>Anoplopoma fimbria</i> (Blackcod)	0.0	0.0			0.0	0.0	0.0	0.0	0.0	0.0	0.0	0.0	0.0	0.8
<i>Hexagrammos</i> (Greenling)	0.0	0.0			0.0	0.0	0.0	0.0	0.0	0.0	0.0	0.0	0.0	0.0
<i>Stichidae</i> (Blenny)	0.0	0.0			0.0	0.0	0.0	0.0	0.0	0.0	0.0	0.0	0.0	0.0
<i>Sebastes</i> (Rockfish) larvae	0.0	0.0			0.5	0.2	0.0	0.3	0.1	0.3	0.2	0.0	0.0	0.0
Bullhead larvae	0.1	0.0			0.0	0.0	0.0	0.0	0.0	0.0	0.0	0.0	0.0	0.0
Fish eggs	0.0	0.0			0.0	0.0	0.0	0.0	0.0	0.0	0.0	0.0	0.0	0.0
<i>Osmariidae</i> (smelt)	0.0	0.0			0.0	0.0	0.0	0.0	0.0	0.2	0.0	0.0	0.2	1.3
<i>Microstomus pacificus</i> (Dover Sole)	0.0	0.0			0.0	0.0	0.0	0.0	0.0	0.0	0.0	0.0	0.0	0.0
Liparidae	0.0	0.0			0.0	0.0	0.0	0.0	0.0	0.0	0.0	0.0	0.0	0.0
Agonidae (poacher)	0.0	0.0			0.0	0.0	0.0	0.0	0.0	0.0	0.0	0.0	0.0	0.0
<i>Prilichthyidae</i> (Quillfish)	0.0	0.0			0.0	0.0	0.0	0.0	0.0	0.0	0.0	0.0	0.0	0.0
<i>Brosomphys marginata</i> (ragfish)	0.0	0.0			0.0	0.0	0.0	0.0	0.0	0.0	0.0	0.0	0.0	0.0
<i>Psettichthys melamostichus</i>	0.0	0.0			0.0	0.0	0.0	0.0	0.0	0.0	0.0	0.0	0.0	0.0
<i>Isopsetta solepis</i> (Butter Sole)	0.0	0.0			0.0	0.0	0.0	0.0	0.0	0.0	0.0	0.0	0.0	0.0
<i>Hippoglossoides abaddon</i>	0.0	0.0			0.0	0.0	0.0	0.0	0.0	0.0	0.0	0.0	0.0	0.0
Gobiidae	0.0	0.0			0.0	0.0	0.0	0.0	0.0	0.0	0.0	0.0	0.0	0.0
<i>Clupea harengus</i> (Herring)	0.0	0.0			0.0	0.0	0.0	0.0	0.0	0.0	0.0	0.0	0.0	0.2
<i>Lyopsetta exilis</i> (Slender Sole)	0.0	0.0			0.0	0.0	0.0	0.0	0.0	0.0	0.0	0.0	0.0	0.0
<i>Pleuronectes coenosus</i> (C-O sole)	0.0	0.0			0.0	0.0	0.0	0.0	0.0	0.0	0.0	0.0	0.0	0.0
<i>Pholidae</i> (Gummers)	0.0	0.0			0.0	0.0	0.0	0.0	0.0	0.0	0.0	0.0	0.0	0.0
<i>Onchorynchus keta</i> (Chum Salmon)	0.0	0.0			0.0	0.0	0.0	0.0	0.0	0.0	0.0	0.0	0.0	0.0
Gadidae	0.0	0.0			0.0	0.0	0.0	0.0	0.0	0.0	0.0	0.0	0.0	0.0
<i>Lepidopsetta bilineata</i> (Rock Sole)	0.0	0.0			0.0	0.0	0.0	0.0	0.0	0.0	0.0	0.0	0.0	0.0

Table 4. Species catch per 10 m<sup>3</sup> of sea volume for each neuston tow and Tucker trawl net catch.

C. CAPE ST. JAMES TRANSECT - June 13, 14 1988

**Table 4 (cont'd.). C. CAPE ST. JAMES TRANSECT - June 13,14 1988**

Sample volume (m <sup>3</sup> )										TAXA (number per 10m <sup>3</sup> )											
NN	NN	NN	NN	NN	NN	NN	NN	NN	NN	NN	NN	NN	NN	NN	NN	NN	NN	NN	NN		
372	364	304	334	399	406	275	61	62*	63	255	270	252	260	252	66	67	409	418	470	439	370
56	57	58	59	60	61	62*	63	64	65	66	67						68	*69	70	71	72
1.9	0.5	0.1	0.0	0.0	0.0	0.0	0.0	0.1	0.0	0.0	0.0	0.0	0.0	0.0	0.0	0.0	0.0	0.0	0.0	0.0	0.0
4.8	0.2	0.4	0.5	0.3	0.5	0.2	0.4	0.5	0.1	0.0	0.0	0.0	0.0	0.0	0.0	0.0	0.3	0.0	0.0	0.0	0.0
0.1	0.0	0.1	0.1	0.2	0.0	0.0	0.0	0.0	0.0	0.0	0.0	0.0	0.0	0.0	0.0	0.0	0.1	0.0	0.1	0.0	0.2
0.1	0.0	0.0	0.0	0.0	0.0	0.0	0.0	0.0	0.0	0.0	0.0	0.0	0.0	0.0	0.0	0.0	0.0	0.0	0.0	0.0	0.0
65.9	81.9	194.7	167.7	85.2	88.7	0.0	0.0	42.2	11.8	1.0	0.2	1.0	0.2	0.0	0.0	0.0	7.1	0.0	27.3	62.0	154.1
0.0	0.0	0.0	0.0	0.0	0.0	0.0	0.0	0.0	0.0	0.0	0.0	0.0	0.0	0.0	0.0	0.0	0.0	0.0	0.0	0.0	0.0
0.0	0.0	0.0	0.0	0.0	0.0	0.0	0.0	0.0	0.0	0.0	0.0	0.0	0.0	0.0	0.0	0.0	0.0	0.0	0.0	0.0	0.0
0.0	0.0	0.0	0.0	0.0	0.0	0.0	0.0	0.0	0.0	0.0	0.0	0.0	0.0	0.0	0.0	0.0	0.0	0.0	0.0	0.0	0.0
0.0	0.0	0.0	0.0	0.0	0.0	0.0	0.0	0.0	0.0	0.0	0.0	0.0	0.0	0.0	0.0	0.0	0.0	0.0	0.0	0.0	0.0
0.0	0.0	0.0	0.0	0.0	0.0	0.0	0.0	0.0	0.0	0.0	0.0	0.0	0.0	0.0	0.0	0.0	0.0	0.0	0.0	0.0	0.0
0.0	0.0	0.0	0.0	0.0	0.0	0.0	0.0	0.0	0.0	0.0	0.0	0.0	0.0	0.0	0.0	0.0	0.0	0.0	0.0	0.0	0.0
0.0	0.0	0.0	0.0	0.0	0.0	0.0	0.0	0.0	0.0	0.0	0.0	0.0	0.0	0.0	0.0	0.0	0.0	0.0	0.0	0.0	0.0
0.0	0.0	0.0	0.0	0.0	0.0	0.0	0.0	0.0	0.0	0.0	0.0	0.0	0.0	0.0	0.0	0.0	0.0	0.0	0.0	0.0	0.0
0.0	0.0	0.0	0.0	0.0	0.0	0.0	0.0	0.0	0.0	0.0	0.0	0.0	0.0	0.0	0.0	0.0	0.0	0.0	0.0	0.0	0.0
0.0	0.0	0.0	0.0	0.0	0.0	0.0	0.0	0.0	0.0	0.0	0.0	0.0	0.0	0.0	0.0	0.0	0.0	0.0	0.0	0.0	0.0
0.0	0.0	0.0	0.0	0.0	0.0	0.0	0.0	0.0	0.0	0.0	0.0	0.0	0.0	0.0	0.0	0.0	0.0	0.0	0.0	0.0	0.0
0.0	0.0	0.0	0.0	0.0	0.0	0.0	0.0	0.0	0.0	0.0	0.0	0.0	0.0	0.0	0.0	0.0	0.0	0.0	0.0	0.0	0.0
0.0	0.0	0.0	0.0	0.0	0.0	0.0	0.0	0.0	0.0	0.0	0.0	0.0	0.0	0.0	0.0	0.0	0.0	0.0	0.0	0.0	0.0
0.0	0.0	0.0	0.0	0.0	0.0	0.0	0.0	0.0	0.0	0.0	0.0	0.0	0.0	0.0	0.0	0.0	0.0	0.0	0.0	0.0	0.0
0.0	0.0	0.0	0.0	0.0	0.0	0.0	0.0	0.0	0.0	0.0	0.0	0.0	0.0	0.0	0.0	0.0	0.0	0.0	0.0	0.0	0.0
0.0	0.0	0.0	0.0	0.0	0.0	0.0	0.0	0.0	0.0	0.0	0.0	0.0	0.0	0.0	0.0	0.0	0.0	0.0	0.0	0.0	0.0
0.0	0.0	0.0	0.0	0.0	0.0	0.0	0.0	0.0	0.0	0.0	0.0	0.0	0.0	0.0	0.0	0.0	0.0	0.0	0.0	0.0	0.0
0.0	0.0	0.0	0.0	0.0	0.0	0.0	0.0	0.0	0.0	0.0	0.0	0.0	0.0	0.0	0.0	0.0	0.0	0.0	0.0	0.0	0.0
0.0	0.0	0.0	0.0	0.0	0.0	0.0	0.0	0.0	0.0	0.0	0.0	0.0	0.0	0.0	0.0	0.0	0.0	0.0	0.0	0.0	0.0
0.0	0.0	0.0	0.0	0.0	0.0	0.0	0.0	0.0	0.0	0.0	0.0	0.0	0.0	0.0	0.0	0.0	0.0	0.0	0.0	0.0	0.0
0.0	0.0	0.0	0.0	0.0	0.0	0.0	0.0	0.0	0.0	0.0	0.0	0.0	0.0	0.0	0.0	0.0	0.0	0.0	0.0	0.0	0.0
0.0	0.0	0.0	0.0	0.0	0.0	0.0	0.0	0.0	0.0	0.0	0.0	0.0	0.0	0.0	0.0	0.0	0.0	0.0	0.0	0.0	0.0
0.0	0.0	0.0	0.0	0.0	0.0	0.0	0.0	0.0	0.0	0.0	0.0	0.0	0.0	0.0	0.0	0.0	0.0	0.0	0.0	0.0	0.0
0.0	0.0	0.0	0.0	0.0	0.0	0.0	0.0	0.0	0.0	0.0	0.0	0.0	0.0	0.0	0.0	0.0	0.0	0.0	0.0	0.0	0.0
0.0	0.0	0.0	0.0	0.0	0.0	0.0	0.0	0.0	0.0	0.0	0.0	0.0	0.0	0.0	0.0	0.0	0.0	0.0	0.0	0.0	0.0
0.0	0.0	0.0	0.0	0.0	0.0	0.0	0.0	0.0	0.0	0.0	0.0	0.0	0.0	0.0	0.0	0.0	0.0	0.0	0.0	0.0	0.0
0.0	0.0	0.0	0.0	0.0	0.0	0.0	0.0	0.0	0.0	0.0	0.0	0.0	0.0	0.0	0.0	0.0	0.0	0.0	0.0	0.0	0.0
0.0	0.0	0.0	0.0	0.0	0.0	0.0	0.0	0.0	0.0	0.0	0.0	0.0	0.0	0.0	0.0	0.0	0.0	0.0	0.0	0.0	0.0
0.0	0.0	0.0	0.0	0.0	0.0	0.0	0.0	0.0	0.0	0.0	0.0	0.0	0.0	0.0	0.0	0.0	0.0	0.0	0.0	0.0	0.0
0.0	0.0	0.0	0.0	0.0	0.0	0.0	0.0	0.0	0.0	0.0	0.0	0.0	0.0	0.0	0.0	0.0	0.0	0.0	0.0	0.0	0.0
0.0	0.0	0.0	0.0	0.0	0.0	0.0	0.0	0.0	0.0	0.0	0.0	0.0	0.0	0.0	0.0	0.0	0.0	0.0	0.0	0.0	0.0
0.0	0.0	0.0	0.0	0.0	0.0	0.0	0.0	0.0	0.0	0.0	0.0	0.0	0.0	0.0	0.0	0.0	0.0	0.0	0.0	0.0	0.0
0.0	0.0	0.0	0.0	0.0	0.0	0.0	0.0	0.0	0.0	0.0	0.0	0.0	0.0	0.0	0.0	0.0	0.0	0.0	0.0	0.0	0.0
0.0	0.0	0.0	0.0	0.0	0.0	0.0	0.0	0.0	0.0	0.0	0.0	0.0	0.0	0.0	0.0	0.0	0.0	0.0	0.0	0.0	0.0
0.0	0.0	0.0	0.0	0.0	0.0	0.0	0.0	0.0	0.0	0.0	0.0	0.0	0.0	0.0	0.0	0.0	0.0	0.0	0.0	0.0	0.0
0.0	0.0	0.0	0.0	0.0	0.0	0.0	0.0	0.0	0.0	0.0	0.0	0.0	0.0	0.0	0.0	0.0	0.0	0.0	0.0	0.0	0.0
0.0	0.0	0.0	0.0	0.0	0.0	0.0	0.0	0.0	0.0	0.0	0.0	0.0	0.0	0.0	0.0	0.0	0.0	0.0	0.0	0.0	0.0
0.0	0.0	0.0	0.0	0.0	0.0	0.0	0.0	0.0	0.0	0.0	0.0	0.0	0.0	0.0	0.0	0.0	0.0	0.0	0.0	0.0	0.0
0.0	0.0	0.0	0.0	0.0	0.0	0.0	0.0	0.0	0.0	0.0	0.0	0.0	0.0	0.0	0.0	0.0	0.0	0.0	0.0	0.0	0.0
0.0	0.0	0.0	0.0	0.0	0.0	0.0	0.0	0.0	0.0	0.0	0.0	0.0	0.0	0.0	0.0	0.0	0.0	0.0	0.0	0.0	0.0
0.0	0.0	0.0	0.0	0.0	0.0	0.0	0.0	0.0	0.0	0.0	0.0	0.0	0.0	0.0	0.0	0.0	0.0	0.0	0.0	0.0	0.0
0.0	0.0	0.0	0.0	0.0	0.0	0.0	0.0	0.0	0.0	0.0	0.0	0.0	0.0	0.0	0.0	0.0	0.0	0.0	0.0	0.0	0.0
0.0	0.0	0.0	0.0	0.0	0.0	0.0	0.0	0.0	0.0	0.0	0.0	0.0	0.0	0.0	0.0	0.0	0.0	0.0	0.0	0.0	0.0
0.0	0.0	0.0	0.0	0.0	0.0	0.0	0.0	0.0	0.0	0.0	0.0	0.0	0.0	0.0	0.0	0.0	0.0	0.0	0.0	0.0	0.0
0.0	0.0	0.0	0.0	0.0	0.0	0.0	0.0	0.0	0.0	0.0	0.0	0.0	0.0	0.0	0.0	0.0	0.0	0.0	0.0	0.0	0.0
0.0	0.0	0.0	0.0	0.0	0.0	0.0	0.0	0.0	0.0	0.0	0.0	0.0	0.0	0.0	0.0	0.0	0.0	0.0	0.0	0.0	0.0
0.0	0.0	0.0	0.0	0.0	0.0	0.0	0.0	0.0	0.0	0.0	0.0	0.0	0.0	0.0	0.0	0.0	0.0	0.0	0.0	0.0	0.0
0.0	0.0	0.0	0.0	0.0	0.0	0.0	0.0	0.0	0.0	0.0	0.0	0.0	0.0	0.0	0.0	0.0	0.0	0.0	0.0	0.0	0.0
0.0	0.0	0.0	0.0	0.0	0.0	0.0	0.0	0.0	0.0	0.0	0.0	0.0	0.0	0.0	0.0	0.0	0.0	0.0	0.0	0.0	0.0
0.0	0.0	0.0	0.0	0.0	0.0	0.0	0.0	0.0	0.0	0.0	0.0	0.0	0.0	0.0	0.0	0.0	0.0	0.0	0.0	0.0	0.0
0.0	0.0	0.0	0.0	0.0	0.0	0.0	0.0	0.0	0.0	0.0	0.0	0.0	0.0	0.0	0.0	0.0	0.0	0.0	0.0	0.0	0.0
0.0	0.0	0.0	0.0	0.0	0.0	0.0	0.0	0.0	0.0	0.0	0.0	0.0	0.0	0.0	0.0	0.0	0.0	0.0	0.0	0.0	0.0
0.0	0.0	0.0	0.0	0.0	0.0	0.0	0.0	0.0	0.0	0.0	0.0	0.0	0.0	0.0	0.0	0.0	0.0	0.0	0.0	0.0	0.0
0.0	0.0	0.0	0.0	0.0	0.0	0.0	0.0	0.0	0.0	0.0	0.0	0.0	0.0	0.0	0.0	0.0	0.0	0.0	0.0	0.0	0.0
0.0	0.0	0.0	0.0	0.0	0.0	0.0	0.0	0.0	0.0	0.0	0.0	0.0	0.0	0.0	0.0	0.0	0.0	0.0	0.0	0.0	0.0
0.0	0.0	0.0	0.0	0.0	0.0	0.0	0.0	0.0	0.0	0.0	0.0	0.0	0.0	0.0	0.0	0.0	0.0	0.0	0.0	0.0	0.0
0.0	0.0	0.0	0.0	0.0	0.0	0.0	0.0	0.0	0.0	0.0	0.0	0.0	0.0	0.0	0.0	0.0	0.0	0.0	0.0	0.0	0.0
0.0	0.0	0.0	0.0	0.0	0.0	0.0	0.0	0.0	0.0	0.0	0.0	0.0	0.0	0.0	0.0	0.0	0.0	0.0	0.0	0.0	0.0
0.0	0.0	0.0	0.0	0.0	0.0	0.0	0.0	0.0	0.0	0.0	0.0	0.0	0.0	0.0	0.0	0.0	0.0	0.0	0.0	0.0	0.0
0.0	0.0	0.0	0.0	0.0	0.0	0.0	0.0	0.0	0.0	0.0	0.0	0.0	0.0	0.0	0.0	0.0	0.0	0.0	0.0	0.0	0.0
0.0	0.0	0.0	0.0	0.0	0.0	0.0	0.0	0.0	0.0	0.0	0.0	0.0	0.0	0.0	0.0	0.0	0.0	0.0	0.0	0.0	0.0
0.0	0.0</																				



Table 4 (cont'd.). D. KUNGHIT ISLAND - June 14, 15 1988

Table 4. Species catch per 10 m<sup>3</sup> of sea volume for each neuston tow and Tucker trawl net catch.

E. SCUDDER POINT - June 15,16 1988																		
Sample volume (m <sup>3</sup> )	774	1400	526	527	563	245	238	263	295	405	382							
TAXA (number per 10m <sup>3</sup> )	98-2	98-3	99-2	99-3100-2	*100-3101	102	103	104	105	106								
<i>Cancer magister</i> megalops	0.0	0.0	0.0	0.0	0.0	0.0	0.0	0.0	0.0	0.0	0.0							
<i>Cancer</i> spp. megalops	0.5	0.3	0.4	0.4	0.1	0.0	0.0	0.0	0.0	0.0	0.0							
megalops (shrimp, other crabs)	0.1	0.3	0.2	0.5	0.5	0.0	0.8	0.1	5.2	0.2	0.3							
<i>Cancer magister</i> zoea	0.0	0.0	0.0	0.0	0.0	0.0	853.1	0.0	0.0	0.0	0.0							
<i>Cancer</i> sp. zoea	15.0	6.5	41.1	63.9	34.3	0.0	1832	5118	2461	2210	485.2							
Porcellanidae zoea	0.0	0.0	0.0	0.0	0.0	0.0	0.0	0.0	0.0	0.0	0.0							
Grapsidae zoea	0.0	0.0	0.0	0.0	0.0	0.0	2748	0.0	492.2	0.0	0.0							
Malidae zoea (Pugetia)	0.0	0.0	0.0	0.0	0.0	0.0	853.1	0.0	0.0	0.0	0.0							
Pinnotheridae zoea	0.0	0.0	0.0	0.0	0.0	0.0	0.0	0.0	0.0	0.0	0.0							
<i>Fabia subquadrata</i> (Pinnotheridae)	0.4	0.0	0.1	0.0	0.0	0.0	9159	853.1	3446	0.0	0.0							
Galatheidae zoea	0.0	0.0	0.0	0.0	0.0	0.0	0.0	0.0	0.0	0.0	0.0							
Other Decapod Larvae	0.0	0.0	0.0	0.0	0.0	0.0	0.0	0.0	0.0	0.0	0.0							
Pandalidae	0.5	0.3	0.0	0.0	0.2	0.0	0.0	0.0	0.1	0.0	0.0							
Other Shrimp	0.4	0.2	7.5	5.9	3.6	0.0	0.2	0.9	2.8	0.3	0.4							
<i>Lepas</i> (goose barnacle)	0.0	0.0	0.0	0.0	0.0	0.0	0.0	0.0	0.0	0.0	0.0							
Cumacea	0.0	0.0	0.0	0.0	0.0	0.0	0.0	0.0	0.0	0.0	0.0							
Amphipoda	40.3	27.0	1.6	3.3	16.3	0.0	0.2	0.0	2.0	1.7	5.6							
Copepoda (Calanoida)	17.8	22.1	2.5	6.0	9.2	0.0	0.0	0.0	0.2	2.9	4.2							
Euphausiacea- <i>Thysanoessa</i>	0.0	0.0	0.0	0.0	0.0	0.0	0.0	0.0	0.0	0.0	0.0							
<i>Limnocalanus helgum</i> (Pteropod)	0.0	0.0	0.0	0.4	0.0	0.0	0.0	0.0	0.0	0.0	0.0							
<i>Clione limacina</i> (Pteropod)	0.0	0.0	0.0	0.0	0.0	0.0	0.0	0.0	0.0	0.0	0.0							
<i>Eudora</i> sp. (Pteropod)	0.0	0.0	0.0	0.0	0.0	0.0	0.0	0.0	0.0	0.0	0.0							
Octopus	0.0	0.0	0.0	0.0	0.0	0.0	0.0	0.0	0.0	0.0	0.0							
Squid	0.0	0.0	0.0	0.0	0.0	0.0	0.0	0.0	0.1	0.0	0.0							
Isopoda	0.0	0.0	0.0	0.0	0.0	0.0	0.0	0.0	0.0	0.0	0.0							
Insect Larvae	0.0	0.0	0.0	0.0	0.0	0.0	0.0	0.0	0.0	0.0	0.0							
Mycidacea	0.0	0.0	0.0	0.0	0.0	0.0	0.0	0.0	0.0	0.0	0.0							
Ostracoda	0.0	0.0	0.0	0.0	0.0	0.0	0.0	0.0	0.0	0.0	0.0							
Invertebrate eggs	0.0	0.0	0.0	0.0	0.0	0.0	0.0	0.0	0.0	0.0	0.0							
<i>Velilla</i>	0.0	0.0	0.0	0.0	0.0	0.0	0.0	0.0	0.0	0.0	0.0							
Jellyfish (Leptomedusae)	5.2	5.9	16.5	8.1	0.0	0.0	11.4	19.1	15.5	1.2	0.5							
Ctenophores (Pleurobrachia)	0.0	0.0	0.0	0.0	0.0	0.0	0.0	0.0	0.0	0.0	0.1							
Siphonophores	0.0	0.0	0.0	0.0	0.0	0.0	0.0	0.0	0.0	0.0	0.0							
<i>Coelenterata</i>	0.0	0.0	0.0	0.0	0.0	0.0	0.0	0.0	0.0	0.0	0.0							
<i>Polychaeta</i>	0.0	0.0	0.0	0.0	0.0	0.0	0.0	0.1	0.2	0.0	0.0							
<i>Chaetognathia</i>	0.3	0.3	0.0	0.1	0.0	0.0	0.0	0.0	0.0	0.0	0.0							
<i>Salps</i>	0.0	0.0	0.0	0.0	0.1	0.0	0.0	0.0	0.0	0.0	0.0							
<i>Stenobrachius leucopsanus</i>	0.0	0.0	0.0	0.0	0.0	0.0	0.0	0.0	0.0	0.0	0.0							
<i>Ammodites</i> larvae (Sand lance)	0.0	0.0	0.0	0.0	0.0	0.0	0.2	0.0	0.0	0.0	1.2							
<i>Scorpaenichthys marmoratus</i>	0.0	0.0	0.0	0.0	0.0	0.0	0.0	0.0	0.0	0.0	0.0							
<i>Anoplogomus fimbria</i> (Blackcod)	0.0	0.0	0.0	0.0	0.0	0.0	0.0	0.0	0.0	0.0	0.0							
<i>Heterogrammus</i> (Greenling)	0.0	0.0	0.0	0.0	0.0	0.0	0.0	0.0	0.0	0.0	0.0							
Stichidae (Blenny)	0.0	0.0	0.0	0.0	0.2	0.0	0.0	0.0	0.2	0.0	0.0							
<i>Sebastes</i> (Rockfish) larvae	0.1	0.1	0.5	0.5	0.2	0.0	0.0	0.0	0.0	0.0	0.0							
Bullhead larvae	0.0	0.0	0.0	0.0	0.2	0.0	0.0	0.0	0.0	0.0	0.1							
Fish eggs	0.0	0.0	0.2	0.3	2.0	0.0	0.2	0.0	0.0	0.0	1.1							
<i>Osmariidae</i> (smelt)	0.0	0.0	0.0	0.0	0.0	0.0	0.0	0.0	0.0	0.0	0.0							
<i>Microstomus pacificus</i> (Dover Sole)	0.0	0.0	0.0	0.0	0.0	0.0	0.0	0.0	0.0	0.1	0.0							
Liparidae	0.0	0.0	0.0	0.0	0.1	0.0	0.0	0.0	0.0	0.0	0.1							
Agonidae (poacher)	0.0	0.0	0.0	0.0	0.0	0.0	0.0	0.0	0.2	0.0	0.0							
Pluichthyidae (Quillfish)	0.0	0.0	0.0	0.0	0.0	0.0	0.0	0.0	0.0	0.0	0.0							
<i>Brosomphysis marginata</i> (ragfish)	0.1	0.0	0.1	0.2	0.0	0.0	0.0	0.0	0.0	0.0	0.0							
<i>Psettichthys melanosctichus</i>	0.0	0.0	0.0	0.0	0.1	0.0	0.0	0.0	0.0	0.0	0.0							
<i>Isopsetta solepis</i> (Butler Sole)	0.0	0.0	0.0	0.0	0.0	0.0	0.0	0.0	0.0	0.0	0.0							
<i>Hippoglossoides abaddon</i>	0.0	0.0	0.0	0.0	0.1	0.0	0.0	0.4	0.7	0.0	0.0							
Gobiidae	0.0	0.0	0.0	0.0	0.0	0.0	0.0	0.0	0.0	0.0	0.0							
<i>Cupea harengus</i> (Herring)	0.0	0.0	0.0	0.0	0.0	0.0	0.0	0.0	0.0	0.0	0.0							
<i>Lyopsetta exilis</i> (Slender Sole)	0.0	0.0	0.0	0.0	0.0	0.0	0.0	0.1	0.0	0.0	0.1							
<i>Pleuronecthus coenosus</i> (C-O sole)	0.0	0.0	0.0	0.0	0.0	0.0	0.0	0.0	0.0	0.0	0.0							
Pholidae (Gumnels)	0.0	0.0	0.0	0.0	0.0	0.0	0.0	0.0	0.0	0.0	0.0							
<i>Oncorhynchus keta</i> (Chum Salmon)	0.0	0.0	0.0	0.0	0.0	0.0	0.0	0.0	0.0	0.0	0.0							
Gadidae	0.0	0.0	0.0	0.0	0.0	0.0	0.0	0.0	0.0	0.0	0.0							
<i>Lepidopsetta bilineata</i> (Rock Sole)	0.0	0.0	0.0	0.0	0.0	0.0	0.0	0.0	0.0	0.0	0.0							

**Table 4.** Species catch per 10 m<sup>3</sup> of sea volume for each neuston tow and Tucker trawl net catch.

542





Table 4. Species catch per 10 m<sup>3</sup> of sea volume for each neuston tow and Tucker trawl net catch.

H. BANKS ISLAND - June 19, 20, 1988														
Sample volume (m <sup>3</sup> )														
TAXA	149-2	709	518	716	150-2	150-3	410	363	389	421	288	557	551	361
<i>Cancer magister</i> megalops	0.0	0.0	0.0	0.0	0.0	0.0	0.0	0.0	0.0	0.0	0.0	0.0	0.0	0.0
<i>Cancer</i> spp. megalops	0.51	0.17	0.03	0.44	0.68	0.69	2.31	9.50	0.52	0.47	0.33	0.97	0.00	0.00
megalops (shrimp, other crabs)	2.68	3.09	1.20	1.75	0.05	2.07	0.08	0.373	0.45	0.05	0.42	0.00	0.00	0.00
<i>Cancer magister</i> zoea	0.01	0.0	0.03	0.0	0.02	0.17	0.21	0.48	0.02	0.02	0.02	0.00	0.00	0.00
<i>Cancer</i> sp. zoea	22.64	49.61	3.21	17.40	132.1	628.1	809.3	341.69	238.8	787.7	1645	392.2	0.00	0.00
Porcellanidae zoea	0.0	0.0	0.0	0.0	0.0	0.0	0.0	0.0	0.0	0.0	0.0	0.0	0.0	0.0
Grapsidae zoea	0.0	0.0	0.0	0.0	0.0	0.0	0.0	0.0	0.0	0.0	0.0	0.0	0.0	0.0
Malidae zoea (Pugetia)	0.0	0.0	0.0	0.0	0.0	0.0	0.0	0.0	0.0	0.0	0.0	0.0	0.0	0.0
Pinnotheridae zoea	0.0	0.0	0.0	0.0	0.0	0.0	0.0	0.0	0.0	0.0	0.0	0.0	0.0	0.0
<i>Fabia subquadrata</i> (Pinnotheridae)	0.0	0.02	0.0	0.0	0.0	0.0	0.0	0.0	0.0	0.0	0.02	0.0	0.0	0.0
Gammaridae zoea	0.0	0.0	0.0	0.0	0.0	0.0	0.0	0.0	0.0	0.0	0.0	0.0	0.0	0.0
Other Decapod Larvae	0.0	0.0	0.0	0.0	0.0	0.0	0.0	0.0	0.0	0.0	0.0	0.0	0.0	0.0
Pandalidae	0.25	0.23	0.18	0.0	0.0	0.0	0.0	0.0	0.0	0.0	0.05	0.04	0.00	0.00
Other Shrimp	3.39	2.66	1.16	2.80	0.0	0.06	0.13	0.0	0.04	0.05	0.11	0.06	0.00	0.00
<i>Lepas</i> (goose barnacle)	0.0	0.0	0.0	0.0	0.0	0.0	0.0	0.0	0.0	0.0	0.0	0.0	0.0	0.0
Cumacea	0.0	0.0	0.0	0.0	0.0	0.0	0.0	0.0	0.0	0.0	0.0	0.0	0.0	0.0
Amphipoda	0.35	0.06	0.42	0.30	0.15	0.19	0.64	0.95	0.19	15.44	0.16	0.06	0.00	0.00
Copepoda (Calanoida)	5.92	10.42	11.45	22.5	0.37	0.69	3.86	15.68	5.22	2.15	63.34	27.70	0.00	0.00
Euphausiacea- <i>Thysanoessa</i>	3.10	3.47	0.92	7.36	0.98	0.0	0.26	0.0	0.22	0.11	3.10	16.76	0.00	0.00
<i>Limnocalanus helgolandicus</i> (Pteropod)	0.0	0.0	0.0	0.0	0.0	0.0	0.0	0.0	0.0	0.0	0.0	0.0	0.0	0.0
<i>Clione limacina</i> (Pteropod)	0.14	0.02	0.03	0.48	0.0	0.0	0.0	0.0	0.0	0.02	0.0	0.0	0.0	0.0
<i>Clione</i> sp. (Pteropod)	0.0	0.0	0.0	0.0	0.0	0.0	0.0	0.0	0.0	0.0	0.0	0.0	0.0	0.0
Octopus	0.0	0.0	0.0	0.0	0.0	0.0	0.0	0.0	0.0	0.0	0.0	0.0	0.0	0.0
Squid	0.0	0.0	0.0	0.0	0.0	0.0	0.0	0.0	0.0	0.0	0.0	0.0	0.0	0.0
Insect Larvae	0.0	0.0	0.0	0.0	0.0	0.0	0.0	0.0	0.0	0.0	0.0	0.0	0.0	0.0
Mysidacea	0.0	0.0	0.0	0.0	0.0	0.0	0.0	0.0	0.0	0.0	0.0	0.0	0.0	0.0
Ostracoda	0.0	0.0	0.0	0.0	0.0	0.0	0.0	0.0	0.0	0.0	0.0	0.0	0.0	0.0
Invertebrate eggs	0.0	0.0	0.0	0.0	0.0	0.0	0.0	0.0	0.0	0.04	0.05	0.0	0.0	0.0
<i>Velletia</i>	0.0	0.0	0.0	0.0	0.0	0.0	0.0	0.0	0.0	0.0	0.0	0.0	0.0	0.0
Jellyfish (Leptomedusae)	11.99	1.06	7.82	8.76	0.56	1.24	0.23	0.48	0.52	0.11	0.22	0.22	0.00	0.00
Ctenophores (Pleurobrachia)	0.10	0.08	0.11	0.29	0.06	0.36	0.0	0.0	1.87	0.0	0.0	0.11	0.00	0.00
Siphonophores	0.0	0.0	0.0	0.0	0.0	0.0	0.0	0.0	0.0	0.0	0.0	0.0	0.0	0.0
<i>Coelenterata</i>	0.0	0.0	0.0	0.0	0.0	0.0	0.0	0.0	0.0	0.0	0.0	0.0	0.0	0.0
<i>Polychaeta</i>	0.0	0.0	0.0	0.0	0.0	0.0	0.0	0.0	0.0	0.0	0.0	0.0	0.0	0.0
<i>Chaetognathia</i>	0.0	0.0	0.0	0.0	0.0	0.0	0.0	0.0	0.0	0.0	0.0	0.0	0.0	0.0
<i>Salps</i>	0.01	0.0	0.0	0.0	0.02	0.0	0.05	0.08	0.0	0.0	0.0	0.0	0.0	0.08
<i>Stenobrachius leucopsanus</i>	0.0	0.0	0.0	0.0	0.0	0.0	0.0	0.0	0.0	0.0	0.0	0.0	0.0	0.0
<i>Armadillidium</i> larvae (Sanddollar)	0.0	0.0	0.0	0.0	0.0	0.0	0.0	0.0	0.0	0.0	0.0	0.0	0.0	0.0
<i>Scorpaenichthys marmoratus</i>	0.0	0.0	0.0	0.0	0.0	0.0	0.0	0.0	0.0	0.0	0.0	0.0	0.0	0.0
<i>Anoploporoma limbra</i> (Blackcod)	0.0	0.0	0.0	0.0	0.0	0.0	0.0	0.0	0.0	0.0	0.0	0.0	0.0	0.0
<i>Hexagrammos</i> (Greenling)	0.0	0.0	0.0	0.0	0.0	0.0	0.0	0.0	0.0	0.0	0.0	0.0	0.0	0.0
<i>Stichilidae</i> (Blenny)	0.04	0.19	0.0	0.0	0.0	0.08	0.10	0.0	0.02	0.0	0.03	0.00	0.00	0.04
<i>Sebastes</i> (Rockfish) larvae	0.0	0.02	0.0	0.07	0.0	0.0	0.0	0.0	0.0	0.0	0.0	0.0	0.0	0.0
Bullhead larvae	0.07	0.0	0.0	0.0	0.0	0.0	0.0	0.0	0.0	0.0	0.0	0.0	0.0	0.0
Fish eggs	0.07	0.0	0.0	0.0	0.0	0.0	0.0	0.0	0.0	0.0	0.05	0.16	0.06	0.00
Osmeridae (smelt)	0.0	0.0	0.0	0.0	0.0	0.0	0.0	0.0	0.07	0.0	0.0	0.0	0.0	0.0
<i>Microstomus pacificus</i> (Dover Sole)	0.0	0.0	0.0	0.0	0.0	0.0	0.0	0.0	0.0	0.0	0.0	0.0	0.0	0.0
Liparidae	0.01	0.0	0.0	0.02	0.0	0.0	0.0	0.0	0.0	0.0	0.0	0.02	0.00	0.00
<i>Pilichthys</i> (Quillfish)	0.0	0.04	0.0	0.0	0.0	0.0	0.0	0.0	0.0	0.0	0.0	0.0	0.0	0.03
<i>Brosomphys marginata</i> (ragfish)	0.01	0.0	0.0	0.0	0.0	0.0	0.0	0.0	0.0	0.0	0.0	0.0	0.0	0.0
<i>Psettichthys melanostictus</i>	0.0	0.06	0.0	0.02	0.0	0.0	0.0	0.08	0.0	0.0	0.0	0.0	0.0	0.0
<i>Isopsetta solepis</i> (Butter Sole)	0.0	0.0	0.0	0.0	0.0	0.0	0.0	0.0	0.0	0.0	0.0	0.0	0.0	0.0
<i>Hippocrossus abaddon</i>	0.03	0.0	0.0	0.0	0.0	0.0	0.0	0.0	0.0	0.0	0.0	0.0	0.0	0.0
Gobiidae	0.0	0.0	0.0	0.0	0.0	0.0	0.0	0.0	0.0	0.0	0.0	0.0	0.0	0.0
<i>Clupea harengus</i> (Herring)	0.0	0.0	0.0	0.0	0.0	0.0	0.0	0.0	0.0	0.0	0.0	0.0	0.0	0.0
<i>Lyopsetta exilis</i> (Slender Sole)	0.0	0.0	0.0	0.0	0.0	0.0	0.0	0.0	0.0	0.0	0.0	0.0	0.0	0.0
<i>Pleuronectes crenosus</i> (C-O sole)	0.01	0.0	0.0	0.0	0.0	0.0	0.0	0.0	0.0	0.0	0.0	0.0	0.0	0.0
Pholidae (Gunnels)	0.0	0.0	0.0	0.0	0.0	0.0	0.0	0.0	0.0	0.0	0.0	0.0	0.0	0.0
<i>Onchorynchus keta</i> (Chum Salmon)	0.0	0.0	0.0	0.0	0.0	0.0	0.0	0.0	0.0	0.0	0.0	0.02	0.00	0.00
Gadidae	0.0	0.0	0.0	0.0	0.0	0.0	0.0	0.0	0.0	0.0	0.0	0.0	0.0	0.0
<i>Lepidopsetta bilineata</i> (Rock Sole)	0.0	0.0	0.0	0.0	0.0	0.0	0.0	0.0	0.0	0.0	0.0	0.0	0.0	0.0

Table 4 (cont'd.). H. BANKS ISLAND - June 19, 20, 1988

Sample volume (m <sup>3</sup> )										
TAXA (number per 10m <sup>3</sup> )	347	360	363	350	394	389	512	588	255	252
<i>Cancer magister</i> megalops	0.0	0.0	0.0	0.0	0.0	0.0	0.0	0.0	0.0	0.0
<i>Cancer</i> spp. megalops	2.82	1.64	0.77	0.29	0.0	0.0	0.0	0.0	0.05	0.04
megalops (shrimp, other crabs)	0.20	0.11	1.38	1.71	0.03	0.51	0.04	0.0	0.0	0.0
<i>Cancer magister</i> zoea	0.0	0.0	0.03	0.0	0.0	0.0	0.0	0.0	0.0	0.0
<i>Cancer</i> sp. zoea	331.7	798.8	902.2	116.3	288.7	95.37	79.69	68.20	122.0	234.1
Porcellanidae zoea	0.0	0.0	0.0	0.0	0.0	0.0	0.0	0.0	0.69	0.0
Grapsidae zoea	0.0	0.0	0.0	0.0	0.0	0.0	0.0	0.0	0.0	0.0
Malajidae zoea (Pugetia)	0.0	0.0	0.0	0.0	0.0	0.0	0.0	0.0	0.0	0.0
Pinnotheridae zoea	0.0	0.0	0.0	0.0	0.0	0.0	0.0	0.0	0.0	0.0
<i>Fabia subquadrata</i> (Pinnotheridae)	0.0	0.0	0.0	0.0	0.0	0.0	0.0	0.0	0.0	0.0
Galatheidae zoea	0.0	0.0	0.0	0.0	0.0	0.0	0.0	0.0	0.0	0.0
Other Decapod Larvae	0.0	0.0	0.0	0.0	0.0	0.0	0.0	0.0	0.0	0.0
Pandalidae	0.0	0.03	0.0	0.0	0.0	0.03	0.0	0.02	0.0	0.0
Other Shrimp	0.09	0.06	0.06	0.03	0.05	0.0	0.03	0.0	0.03	0.0
<i>Lepas</i> (goose barnacle)	0.0	0.0	0.0	0.0	0.0	0.0	0.0	0.0	0.0	0.0
Cumacea	0.0	0.0	0.0	0.0	0.0	0.0	0.0	0.0	0.0	0.0
Amphipoda	0.20	0.03	0.17	0.09	0.10	0.0	0.0	0.02	0.0	0.08
Copepoda (Calanoida)	40.35	43.06	33.88	27.57	14.09	6.30	5.57	0.36	1.57	0.0
Euphausiacea- <i>Thysanoessa</i>	33.86	20.69	23.97	35.43	4.44	0.13	0.02	0.0	0.0	0.0
<i>Limnocalanus helgona</i> (Pteropod)	0.0	0.0	0.0	0.0	0.0	0.0	0.0	0.0	0.0	0.0
<i>Clione limacina</i> (Pteropod)	0.09	0.03	0.03	0.0	0.0	0.0	0.0	0.0	0.0	0.0
<i>Clione</i> sp. (Pteropod)	0.0	0.0	0.0	0.0	0.0	0.0	0.0	0.0	0.0	0.0
Octopus	0.0	0.0	0.0	0.0	0.0	0.0	0.0	0.0	0.0	0.0
Squid	0.03	0.0	0.0	0.0	0.0	0.0	0.0	0.0	0.0	0.0
Isopoda	0.0	0.0	0.0	0.0	0.0	0.0	0.0	0.0	0.0	0.0
Insect Larvae	0.0	0.0	0.0	0.0	0.0	0.0	0.0	0.0	0.0	0.0
Mysidacea	0.0	0.0	0.0	0.0	0.0	0.0	0.0	0.0	0.0	0.0
Ostracoda	0.0	0.0	0.0	0.0	0.0	0.0	0.0	0.0	0.0	0.0
Invertebrate eggs	0.0	0.0	0.0	0.0	0.0	0.03	0.0	0.0	0.04	0.0
<i>Velletia</i>	0.0	0.03	0.0	0.0	0.0	0.0	0.02	0.0	0.0	0.0
Jellyfish (Leptomedusae)	0.14	0.28	0.08	0.46	0.25	0.36	4.36	0.0	10.59	0.44
Ctenophores (Pleurobrachia)	0.23	0.31	0.0	0.11	0.08	0.08	0.04	0.17	1.76	0.08
Siphonophores	0.0	0.0	0.0	0.0	0.0	0.0	0.0	0.0	0.0	0.0
<i>Coelenterata</i>	0.0	0.0	0.0	0.0	0.0	0.0	0.0	0.0	0.0	0.0
<i>Polychaeta</i>	0.0	0.0	0.0	0.0	0.0	0.0	0.0	0.0	0.0	0.0
<i>Chaetognatha</i>	0.0	0.06	0.0	0.03	0.0	0.0	0.0	0.0	0.0	0.0
<i>Salps</i>	0.0	0.0	0.0	0.0	0.0	0.0	0.0	0.0	0.0	0.0
<i>Stenodrachilus leucosaurus</i>	0.0	0.0	0.0	0.0	0.0	0.0	0.0	0.0	0.0	0.0
<i>Ammodites</i> larvae (Sand lance)	0.0	0.03	0.0	0.0	0.0	0.0	0.0	0.0	0.0	0.0
<i>Scorpaenichthys marmoratus</i>	0.0	0.0	0.0	0.0	0.0	0.0	0.0	0.0	0.08	0.0
<i>Apogonopsa limbrata</i> (Blackcod)	0.03	0.0	0.0	0.0	0.0	0.0	0.0	0.0	0.0	0.0
<i>Heoggrammus</i> (Greenling)	0.0	0.0	0.0	0.0	0.0	0.0	0.0	0.0	0.0	0.0
Stichidae (Blenny)	0.0	0.0	0.03	0.0	0.03	0.0	0.0	0.0	0.0	0.0
Sebastes (Rockfish) larvae	0.0	0.0	0.03	0.0	0.0	0.05	0.05	0.0	0.0	0.0
Bullhead larvae	0.09	0.03	0.0	0.0	0.0	0.15	0.0	0.0	0.0	0.0
Fish eggs	0.0	0.0	0.0	0.0	0.0	0.0	0.0	0.0	0.0	0.0
Osmeridae (smelt)	0.0	0.0	0.0	0.0	0.0	0.0	0.0	0.0	0.0	0.0
<i>Microstomus pacificus</i> (Dover Sole)	0.0	0.0	0.0	0.0	0.0	0.0	0.0	0.0	0.0	0.0
Liparidae	0.03	0.0	0.0	0.0	0.0	0.0	0.0	0.0	0.0	0.0
Agonidae (poacher)	0.0	0.0	0.0	0.0	0.0	0.0	0.0	0.0	0.0	0.0
Pilichthysidae (Quillfish)	0.0	0.0	0.0	0.0	0.0	0.0	0.0	0.0	0.0	0.0
<i>Brosomphycus marginata</i> (ragfish)	0.0	0.0	0.0	0.0	0.0	0.0	0.0	0.0	0.0	0.0
<i>Psettichthys melanostictus</i>	0.0	0.0	0.0	0.0	0.0	0.0	0.0	0.0	0.0	0.0
<i>Isopsetta isolepis</i> (Butter Sole)	0.0	0.0	0.0	0.0	0.0	0.0	0.0	0.0	0.0	0.0
<i>Hippoglossoides abasodon</i>	0.0	0.0	0.0	0.0	0.0	0.0	0.0	0.0	0.0	0.0
Gobiidae	0.0	0.0	0.0	0.0	0.0	0.0	0.0	0.0	0.0	0.0
<i>Cupea harengus</i> (Herring)	0.0	0.0	0.0	0.0	0.0	0.0	0.0	0.0	0.0	0.0
<i>Lyopsetta exilis</i> (Slender Sole)	0.0	0.0	0.0	0.0	0.0	0.0	0.0	0.0	0.0	0.0
<i>Pleuronectes coenosus</i> (C-O sole)	0.0	0.0	0.0	0.0	0.0	0.0	0.0	0.0	0.0	0.0
Pholidae (Gummers)	0.0	0.0	0.0	0.0	0.0	0.0	0.0	0.0	0.0	0.0
<i>Onchorhynchus keta</i> (Chum Salmon)	0.0	0.0	0.0	0.0	0.0	0.0	0.0	0.0	0.0	0.0
Gadidae	0.0	0.0	0.0	0.0	0.0	0.0	0.02	0.0	0.0	0.0
<i>Lepidopsetta bilineata</i> (Rock Sole)	0.0	0.0	0.0	0.0	0.0	0.0	0.0	0.0	0.0	0.0

# Design of an electronic database for biostratigraphic data

M.L. Weston<sup>1</sup>, G.J. Woodsworth<sup>2</sup>,  
M.J. Orchard<sup>2</sup>, and M.J. Johns<sup>3</sup>

Weston, M.L., Woodsworth, G.J., Orchard, M.J., and Johns, M.J., Design of an electronic database for biostratigraphic data; in *Evolution and Hydrocarbon Potential of the Queen Charlotte Basin, British Columbia*, Geological Survey of Canada, Paper 90-10, p. 545-554, 1991.

## ***Abstract***

*We describe the structure of a flexible database suitable for biostratigraphic data that uses DOS-based dBase III Plus files. This structure is used in a database of all Triassic fossil collections (plus Jurassic radiolarians) from the Kunga Group on the Queen Charlotte Islands. The database is available on DOS-format floppy disks.*

## ***Résumé***

*Les auteurs décrivent le système d'une base de données souple qui convient pour les données biostratigraphiques et qui utilise les fichiers dBase III Plus gérés par SED. Ce système est utilisé dans une base de données sur toutes les collections de fossiles (sauf les macrofossiles du Jurassique) du groupe de Kunga dans les îles de la Reine-Charlotte. La base de données est disponible sur disques souples en format SED.*

---

<sup>1</sup> Cambridge Arctic Shelf Programme (North America), 2766 Murray Drive, Victoria, B.C. V9A 2S5

<sup>2</sup> Cordilleran Division, Geological Survey of Canada, 100 West Pender Street, Vancouver, B.C. V6B 1R8

<sup>3</sup> Geological Survey of Canada, Pacific Geoscience Centre, 9860 West Saanich Road, Sidney, B.C. V8L 4B2

## INTRODUCTION

This note describes the structure and design of an electronic database developed for fossil collections from the Kunga Group on the Queen Charlotte Islands. The database itself, giving curatorial, geographic, stratigraphic, taxonomic, biochronologic, and bibliographic data, is available on DOS-format floppy disks as Orchard et al. (1990).

The contents of the database are adapted from conodont files compiled and held by Orchard. These files were originally created in a records-processing option of a word processing system on the Cordilleran Division of the Geological Survey of Canada's Fortune 32:16 unix-based computer. The files were expanded to include all radiolarian collections and Triassic macrofossils from the Kunga Group (Desrochers and Orchard, 1991) under the auspices of the FGP Queen Charlotte Basin program.

These files were translated into DOS-based Word Perfect and were cleaned up, modified, and reformatted using a series of Word Perfect macros. The final dBase III Plus files were generated using a translation program written by Weston.

## DATABASE DESIGN

The database was designed for flexibility and expandability. All the files in the database are in dBase III Plus format and can be accessed through any database program that can read and write dBase files. The database uses a hierarchical system of seven files. Each file is linked to the others by one or more common fields. Brief descriptions of these files follow; details of the fields in each file are given in the Appendix.

**GSCNTS.DBF** Contains the numbers and names of the NTS (National Topographic System) 1:250 000 and/or 1:50 000 series maps. The field SOURCE (NTS map number) is the link to all the other files.

**GSCLOC.DBF** Contains detailed geographic data for each locality. Fields are provided for latitude and longitude, UTM (Universal Transverse Mercator) coordinates, elevation, and a written description of the location. The file will accommodate point data, the beginning and end of measured sections, and data from a defined area. A memo file (GSCLOC.DBT) allows for additional free-form data to be entered. The fields SOURCE (NTS map number) and LOCALITY (arbitrarily assigned, sequentially increasing integers or letters) provide links to the files below.

**GSCGEO.DBF** Contains detailed geological data for each locality. Fields are provided for field and lithological description, stratigraphic context, stratigraphic unit (group, formation, member, bed), lithofacies, thickness of unit, position within measured sections, strike and dip of beds, etc. A memo file (GSCGEO.DBT) allows for extra free-form text. The fields SOURCE (NTS map number), LOCALITY, and CAG (arbitrarily assigned, sequentially increasing integers or letters provide links to the files below.

**GSCSAM.DBF** Each record in this file contains information on an individual sample; the file can hold data for many samples from each location. Each sample in this file must have a GSC Locality Number (unique for each Geological Survey of Canada fossil collection). Fields allow for sample collector, sample number and date collected, sampling details, description of the sample, and general types of fossils present. A memo file (GSCSAM.DBT) allows for extra free-form text. Links to the other files are provided by the fields SOURCE, LOCALITY, CAG, and GSC\_LOC (the GSC Locality Number).

**GSCLAB.DBF** This file contains information on the laboratory treatment of samples (weight processed, how processed, weight of residue, etc.). Links to the other files are provided by the fields SOURCE, LOCALITY, CAG, and GSC\_LOC (the GSC Locality Number).

**GSCTAX.DBF** This file contains taxonomic data, one record for each taxon. The number of taxa that can be described per sample

is, in practice, limited by the size of your hard disk. Fields are provided for fossil group, genus and species, number of specimens, specimen repository, identification date, type numbers, and other data. Free-form text can be entered into the memo file GSCTAX.DBT. The fields SOURCE, LOCALITY, CAG, GSC\_LOC, and COLLECTION (arbitrarily assigned, sequentially increasing integers or letters) provide links to the other files.

**GSCINT.DBF** This file contains interpretive data for the fossil collections. Fields include those for system, series/stage, zone, CAI values, internal GSC report numbers and date, and references. The memo file GSCINT.DBT allows input of free-form text. The linking fields are the same as in GSCTAX.DBF.

## KUNGA GROUP BIOSTRATIGRAPHY DATABASE

The database for the Kunga Group (released on two DOS-format floppy disks as Orchard et al., 1990) uses a subset of the fields available in the general database (Appendix). The database contains comprehensive conodont, radiolarian, and Triassic macrofossil data, including locations that were sampled for microfossils and found to be barren. The full extent of the Triassic Kunga Group paleontological sampling program undertaken by the authors prior to 1989 is incorporated into the database. A total of 995 samples are included, of which 375 include conodonts, 309 include generically determinable radiolarians, and about 70 include determined macrofossils (about 40 ammonoid collections). In addition, occurrences of foraminiferids (149 records), ichthyoliths (242 records), spicules (204 records), holothurians (43 records), and ostracodes (3 records) are reported. Conodont CAI data is also given (after Orchard and Forster 1991).

In many samples, several fossil groups co-occur and are separately dated in terms of current ammonoid (Tozer, 1984), conodont (Orchard, 1983, 1991), and radiolarian (Carter, 1991) zonations. The integration and calibration of these fossil schemes, presented in a preliminary fashion by Carter et al. (1989) is therefore an essential element of the database.

Locations of the samples described in the database are shown on a series of twenty outline maps that show the precise location of sections and isolated exposures that were sampled (Figs. 1, 2A-2T). The individuals who collected the samples are also shown (in KUNG\_SAM.DBF); these individuals are credited with providing the data on sample location and geological context.

## REFERENCES

- Carter, E.S.  
1991: Late Triassic radiolarian biostratigraphy of the Kunga Group, Queen Charlotte Islands, British Columbia; in *Evolution and Hydrocarbon Potential of the Queen Charlotte Basin*, British Columbia, Geological Survey of Canada, Paper 90-10.
- Carter, E.S., Orchard, M.J., and Tozer, E.T.  
1989: Integrated ammonoid-conodont-radiolarian biostratigraphy. Late Triassic Kunga Group, Queen Charlotte Islands, British Columbia; in *Current Research, Part H*, Geological Survey of Canada, Paper 89-1H, p. 23-30.
- Desrochers, A. and Orchard, M.J.  
1991: Stratigraphic revisions and carbonate sedimentology of the Kunga Group (Upper Triassic-Lower Jurassic), Queen Charlotte Islands, British Columbia; in *Evolution and Hydrocarbon Potential of the Queen Charlotte Basin*, British Columbia, Geological Survey of Canada, Paper 90-10.
- Orchard, M.J.  
1983: *Epigondolella* populations and their phylogeny and zonation in the upper Triassic; *Fossils and Strata*, no. 15, Oslo, p. 177-192.  
1991: Late Triassic conodont biochronology and biostratigraphy of the Kunga Group, Queen Charlotte Islands, British Columbia; in *Evolution and Hydrocarbon Potential of the Queen Charlotte Basin*, British Columbia, Geological Survey of Canada, Paper 90-10.
- Orchard, M.J. and Forster, P.J.L.  
1991: Conodont colour and thermal maturation of the Late Triassic Kunga Group, Queen Charlotte Islands, British Columbia; in *Evolution and Hydrocarbon Potential of the Queen Charlotte Basin*, British Columbia, Geological Survey of Canada, Paper 90-10.

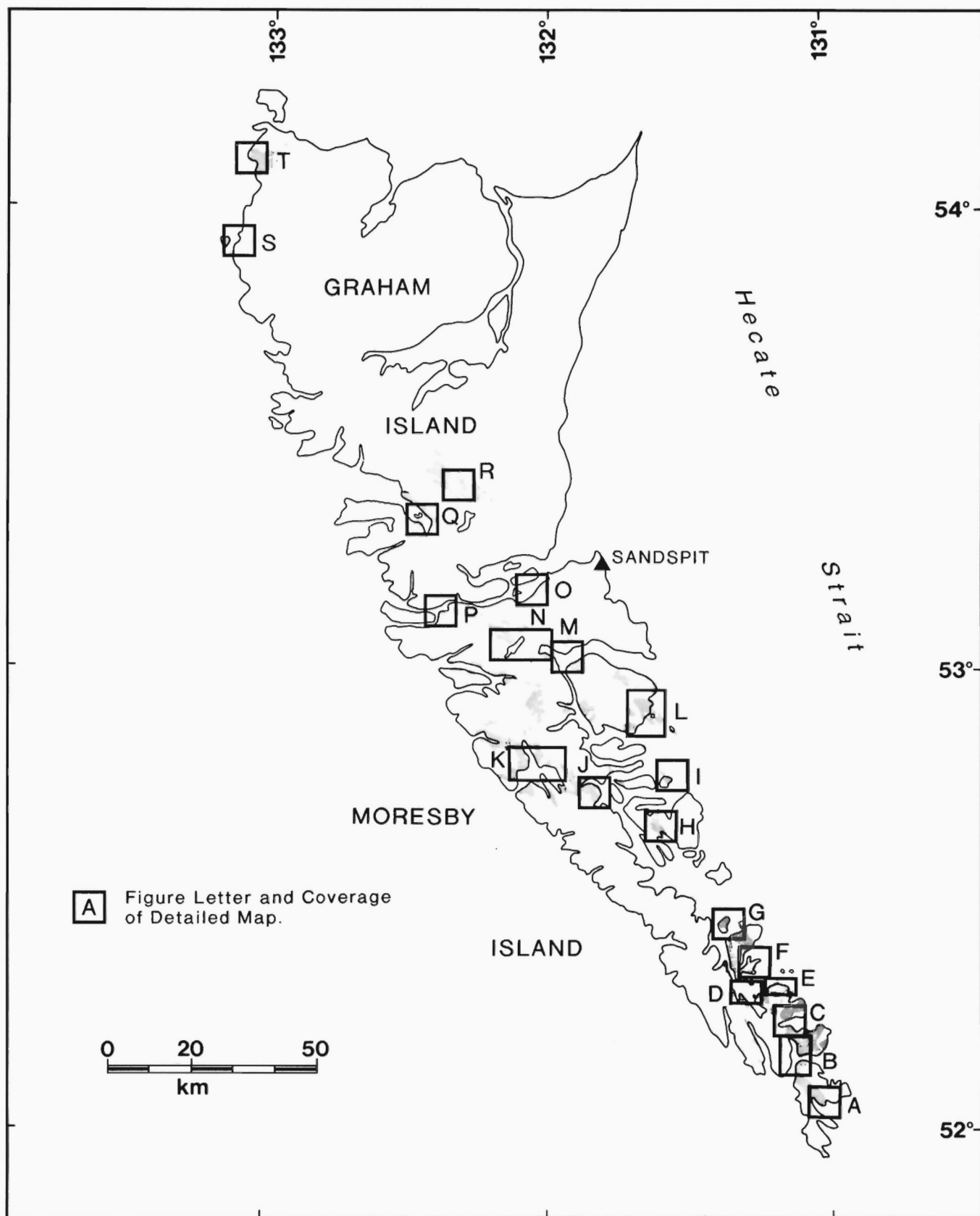


**Figure 1:** Locality index map showing coverage of detailed maps 2A-2T

Orchard, M.J., Carter, E.S., Tozer, E.T., (paleontological data); Weston, M.L., Woodsworth, G.J., Orchard, M.J., and Johns, M.J. (database design); Forster, P.J.L., Lesack, K., McKay, K. (compilers)  
**1990:** Electronic database of Kunga Group biostratigraphic data; Geological Survey of Canada, Open File 2284.

Tozer, E.T.

**1984:** The Trias and its Ammonoites: The evolution of a time scale; Geological Survey of Canada, Miscellaneous Report 35, 171 p.

## APPENDIX: STRUCTURE OF THE .DBF FILES

The structure of the dBase III Plus files that comprise the database system are outlined below. Empty files with these structures are included in Orchard et al. (1990). A \* in front of the field description indicates that the field contains data for at least one record in the Kunga Group database of Orchard et al. (1990). Column headings are:

**No.:** Field number

**Name:** Field name

**FT:** Field type

**C:** character

**N:** numeric

**M:** memo (.DBT) file (free text)

**Len.:** Field length, in characters

**Dec.:** Number of decimals (numeric field only; otherwise defined as 0)

### FILE: GSCNTS.DBF

No.	Name	FT	Len.	Dec	Description
1	SOURCE	C	9	0	*NTS map area (linking field)
2	PUB_ID	C	18	0	Bibliographic linking number
3	NTS_DESC	C	50	0	*Name of map area
4	NOTE	M	10	0	Comments

### FILE: GSCLOC.DBF

No.	Name	FT	Len.	Dec	Description
1	SOURCE	C	9	0	*NTS map area (linking field)
2	LOCALITY	C	3	0	*Location number (linking field)
3	SECTION	C	3	0	Stratigraphic section number
4	LOC_TYPE	C	1	0	Location type (e.g. isolated outcrop)
5	AREA_TYPE	C	1	0	Area type (point, box or line)
6	AREA_CHO	C	1	0	Accuracy of location (1: best; 3: worst)
7	GEN_LOC	C	50	0	General description of location
8	DET_LOC	C	240	0	*Detailed description of location
9	LAT1	C	8	0	*Latitude (SW corner if box/line data)
10	LONG1	C	9	0	*Longitude (SW corner if box/line data)
11	LAT2	C	8	0	Latitude of NE corner for box/line data
12	LONG2	C	9	0	Longitude of NE corner for box/line data
13	ELEV_TOP	C	8	0	Elevation
14	LOCA_NOTE	M	10	0	Remarks on location
15	UTM_ZONE	C	2	0	*UTM zone (SW corner if box/line data)
16	UTM_EAST	C	6	0	*UTM easting (SW corner if box/line data)
17	UTM_NORTH	C	7	0	*UTM northing (SW corner if box/line data)
18	UTM_ZONE2	C	2	0	UTM zone for NE corner of box/line data
19	UTM_EAST2	C	6	0	UTM easting for NE corner of box/line data
20	UTM_NORTH2	C	7	0	UTM north for NE corner of box/line data

### FILE: GSCGEO.DBF

No.	Name	FT	Len.	Dec	Description
1	SOURCE	C	9	0	*NTS map area (linking field)
2	LOCALITY	C	3	0	*Location number (linking field)
3	CAG	C	3	0	*Geology number (linking field)
4	SAMPLE_NO	C	4	0	Sample number (not paleontology)
5	LITH_DESC	C	200	0	Lithology description
6	FIELD_DESC	M	10	0	Field description
7	HIGHER	C	40	0	*Group or equivalent
8	FORMATION	C	40	0	*Formation or equivalent
9	MEMBER	C	40	0	*Member or equivalent
10	BED	C	45	0	Bed or equivalent
11	STRAT_CTX	C	240	0	*Stratigraphic context
12	LITHOFACIE	C	35	0	Lithofacies
13	RESISTANCE	C	15	0	Unit resistance
14	THICKFT	N	9	0	Unit thickness in feet
15	THICKNESS	N	9	2	Unit thickness in metres
16	POSITFT	N	9	0	Unit position in feet

17	POSITION	N	9	2	Unit position in metres
18	ORDER	C	1	0	Order of measurements (e.g. from top)
19	DATUM	C	25	0	Datum for position
20	BED_STRIKE	C	6	0	Strike of unit
21	BED_DIP	C	6	0	Dip of unit
22	FMCUT	C	10	0	Formation cut (not paleo)
23	LC_DESCRIP	C	50	0	Lower contact description
24	SAMPLE	C	1	0	Sample taken? (not fossils)
25	THINSEC	C	1	0	Thin section made? (not of fossils)
26	CHEM	C	1	0	Chemical analysis done (Y=yes; N=No)
27	PETROG	C	1	0	Petrography done (Y=yes; N=No)
28	LITH_NOTES	M	10	0	Comments
29	MACROFAUNA	C	50	0	Macrofauna found in unit
30	MICROFAUNA	C	50	0	Microfauna found in unit
31	SG	C	5	0	Specific gravity
32	LAB	C	8	0	Laboratory (not paleo)
33	LKEY	C	4	0	Lab key (not paleo)
34	REFERENCES	C	100	0	General reference for unit
35	PUB_ID	C	18	0	Bibliographic linking number
36	OTHER_DATE	M	10	0	Other dates (e.g. K-Ar)
37	INTERP	M	10	0	Interpretation (not paleontological)

### FILE: GSCSAM.DBF

No.	Name	FT	Len.	Dec	Description
1	SOURCE	C	9	0	*NTS map area (linking field)
2	LOCALITY	C	3	0	*Location number (linking field)
3	CAG	C	3	0	*Geology number (linking field)
4	GSC_LOC	C	11	0	*GSC Locality Number (linking field)
5	LEADER	C	25	0	Field party leader
6	COLLECTOR	C	25	0	*Collector
7	DATE_COLL	C	8	0	*Date collected
8	SAMPLE_TYP	C	1	0	*Sample type (3= microfossil)
9	FIELD_OLD	C	30	0	Old field number
10	F_O_STN	C	4	0	Old field station number
11	F_O_TYPE	C	4	0	Old type of sample
12	F_O_NO	C	4	0	Old field sample number
13	FIELD_NEW	C	30	0	*Field sample number
14	F_N_STN	C	4	0	Field station number
15	F_N_TYPE	C	4	0	New type of sample
16	F_N_NO	C	4	0	New sample number
17	NOTEBOOK	C	2	0	Notebook number
18	PAGE	C	2	0	Page in notebook
19	HAND_SPEC	C	1	0	*Hand specimen (Y=yes; N=no)
20	FURTH_ANAL	C	1	0	*Further analyses available (Y=yes; N=no)
21	FURTH_DET	M	10	0	Further analysis details
22	THIN_SECN	C	1	0	*Thin section available (Y=yes; N=No)
23	THIN_DET	M	10	0	Thin section details
24	THICKFT	N	9	0	Thickness of sample in feet
25	THICKNESS	N	9	2	Thickness of sample in metres
26	POSITFT	N	9	0	Position of sample in feet
27	POSITION	N	9	2	Position of sample in metres
28	LAB_DESC	C	125	0	*Description of sample
29	WEIGHT	N	7	1	*Sample weight
30	REMARKS	M	10	0	Remarks
31	MINERALS	C	40	0	Minerals found in sample
32	MACROFOSSL	C	50	0	*Macrofossils found in sample
33	AMMONOID	C	50	0	Ammonites found in sample
34	PELECYPOD	C	50	0	Pelecypods found in sample
35	CONODONT	C	50	0	Conodonts found in sample
36	FORAM_BEN	C	50	0	Calcareous foraminifera found in sample
37	FORAM_PLNK	C	50	0	Planktonic foraminifera found in sample
38	FORAM_AREN	C	50	0	Arenaceous foraminifera found in sample
39	OSTRACODS	C	50	0	Ostracods found in sample
40	RADIOLAR	C	50	0	Radiolarians found in sample
41	ICHTHYO	C	70	0	Ichthyoliths found in sample
42	OTHER_MICR	C	50	0	*Other microfossils found in sample

### FILE: GSCLAB.DBF

No.	Name	FT	Len.	Dec	Description
1	SOURCE	C	9	0	*NTS map area (linking field)
2	LOCALITY	C	3	0	*Location linking number (linking field)
3	CAG	C	3	0	*Geology linking number (linking field)
4	GSC_LOC	C	9	0	*GSC locality number (linking field)
5	RUN	C	8	0	Run
6	TREATMENT	C	50	0	Treatment applied to sample
7	REACTION	C	30	0	Type of reaction

8	WT_IN	N	7	1	Weight of sample processed
9	WT_COARSE	N	7	1	Weight of coarse residue
10	WT_FINE	N	7	1	Weight of fine residue
11	WT_REM	N	7	1	*Weight of remainder
12	FRACTIONS	C	12	0	Sample residue fraction
13	LAB_NO	C	6	0	Lab number
14	PICK	C	15	0	Pick type
15	PICK_TIME	N	4	0	Time spent picking
16	PICK_DATE	C	8	0	Date of picking
17	PICKERS	C	10	0	Sample picked by:
18	REMARKS	M	10	0	*Remarks

#### FILE: GSCTAX.DBF

No.	Name	FT	Len.	Dec	Description
1	SOURCE	C	9	0	*NTS map area (linking field)
2	LOCALITY	C	3	0	*Location number (linking field)
3	CAG	C	3	0	*Geology number (linking field)
4	GSC_LOC	C	11	0	*GSC locality number (linking field)
5	COLLECTION	C	3	0	*Collection number (linking field)
6	RUN	C	8	0	Run number
7	REPOSITORY	C	20	0	*Repository of specimens
8	PRELIM_ID	C	8	0	Preliminary identification date
9	IDENT	C	5	0	Identified by:
10	LAST_ID	C	8	0	Last identification date
11	INFORMAL	C	40	0	*Informal fossil group
12	TAX_GENUS	C	40	0	*Genus
13	TAX_SPECIE	C	60	0	*Species
14	PUB_ILUS	C	1	0	Published illustration (Y=yes; N=No)
15	TYPE_NUMB	C	55	0	Type number(s)
16	NO_SPECIM	N	4	0	*Number of specimens
17	SP_APRX	C	1	0	No. of specimens approximate (Y=yes; N=No)
18	COLOUR	C	15	0	Specimen colour
19	FREQUENCY	C	6	0	Abundance
20	PRESERV	C	25	0	Preservation
21	ROBUST	C	10	0	Robustness
22	REMARKS	M	10	0	Remarks

#### FILE: GSCINT.DBF

No.	Name	FT	Len.	Dec	Description
1	SOURCE	C	9	0	*NTS map area (linking field)
2	LOCALITY	C	3	0	*Location number (linking field)
3	CAG	C	3	0	*Geology linking number (linking field)
4	GSC_LOC	C	11	0	*GSC locality number (linking field)
5	COLLECTION	C	3	0	*Collection number
6	AGE_SYS	C	60	0	*Age (system)
7	SERIES_STG	C	60	0	*Series/Stage
8	ZONE	C	30	0	*Zone
9	ENVIRON	C	35	0	Biofacies
10	CAI_MIN	C	3	0	*Minimum CAI (conodont alteration index)
11	CAI_MAX	C	3	0	*Maximum CAI
12	CAI_APRX	C	1	0	*CAI approximate? (Y=yes)
13	VITRINITE	N	6	3	*Vitrinite reflectance
14	VIT_DET	C	20	0	Vitrinite reflectance determined by:
15	RESISTANCE	C	15	0	Rock resistance to weathering
16	DETERMINED	C	20	0	Interpretation determined by:
17	DET_DATE	C	8	0	*Determination date
18	RPT_DATE	C	8	0	Report date
19	RPT_NUM	C	20	0	GSC report number
20	REFERENCE	C	100	0	*References
21	PUB_ID	C	18	0	Bibliographic linking number
22	REMARKS	M	10	3	Remarks

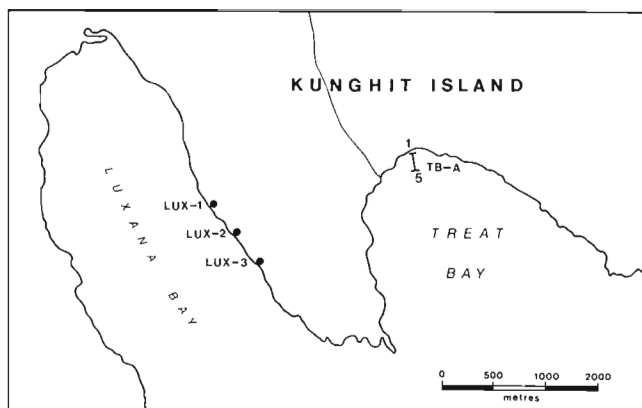


Figure 2A: Luxana Bay, Treat Bay

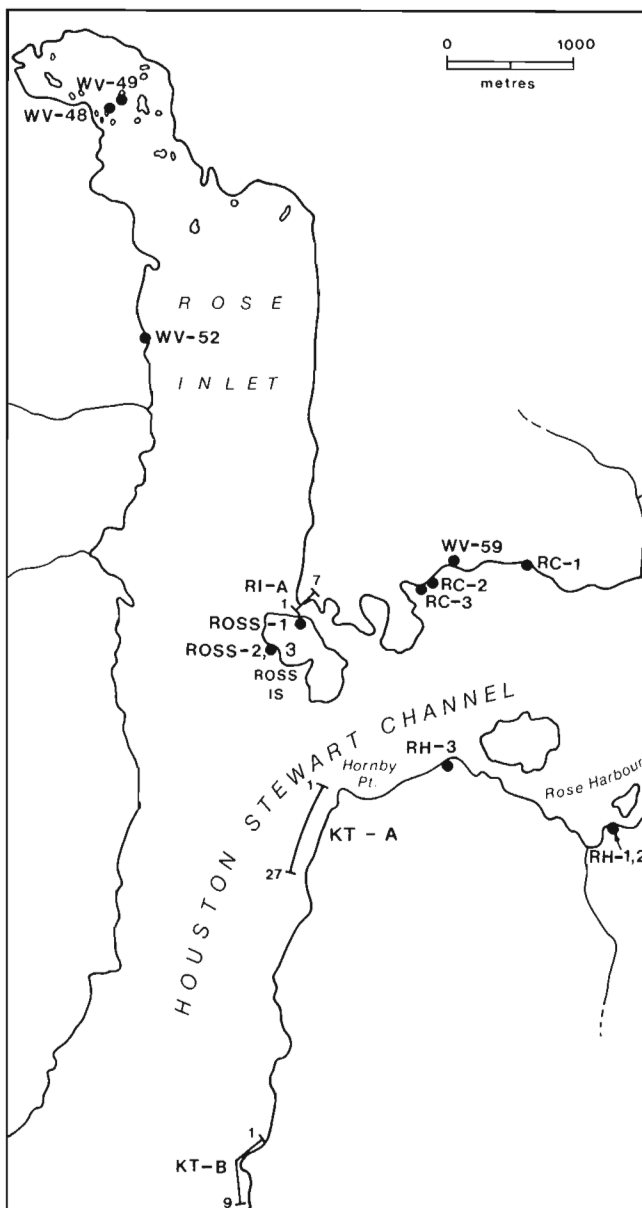
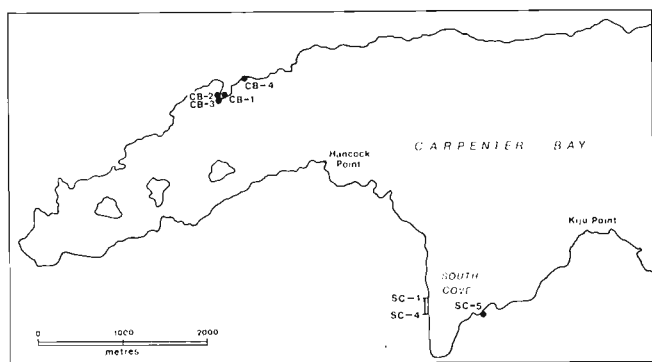
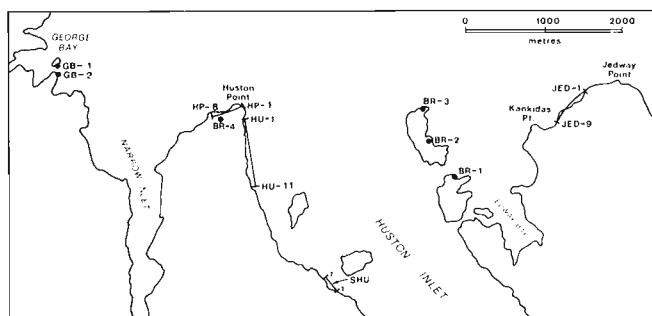


Figure 2B: Houston Stewart Channel, Hornby Point, Rose Inlet, Rose Harbour





**Figure 2C:** Carpenter Bay, South Cove



**Figure 2D:** Bush Rock, Huston Inlet, Huston Point

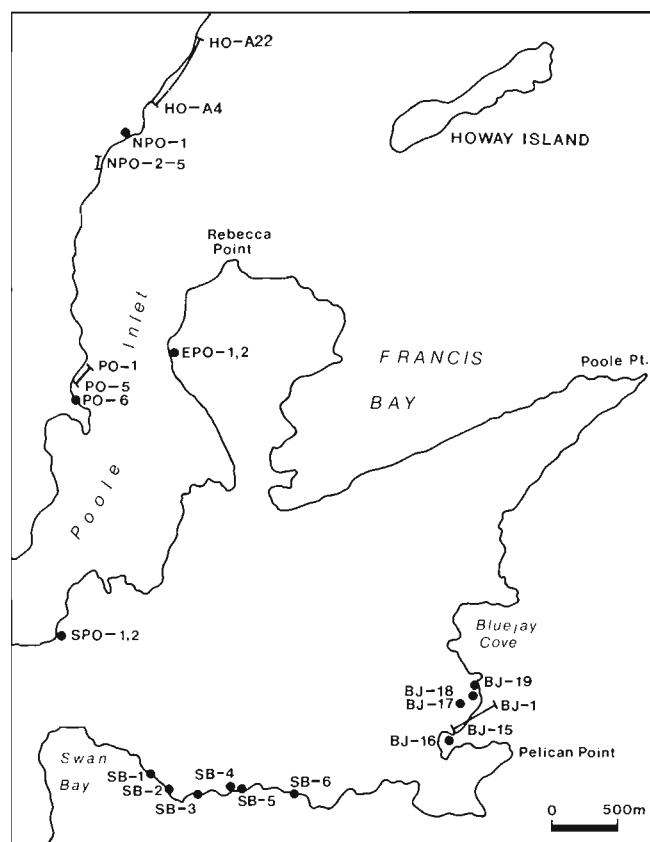


**Figure 2F:** Swan Bay, Bluejay Cove, Poole Inlet, Howay Island

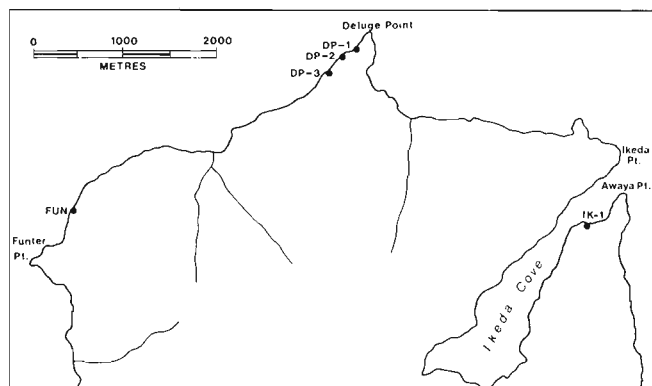


**Figure 2E:** Ikeda Bay, Deluge Point

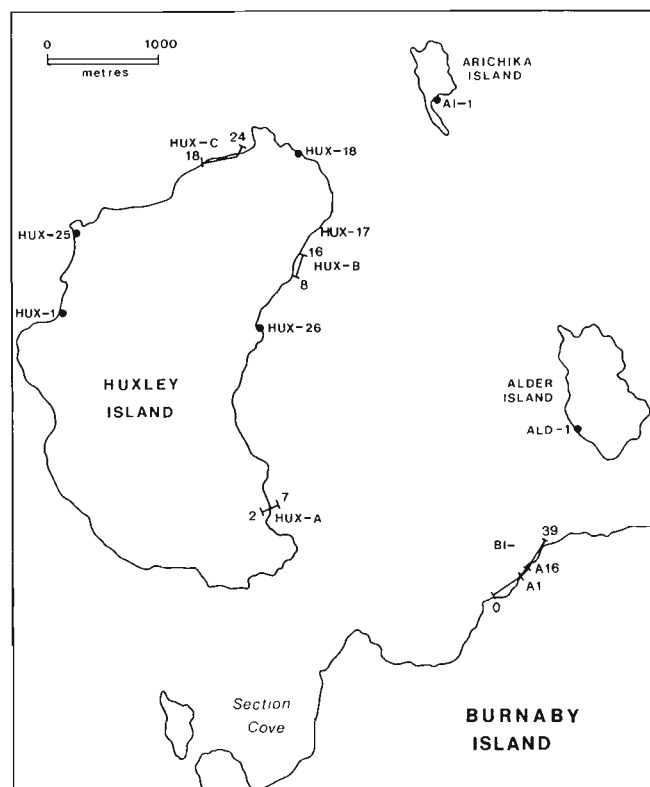


**Figure 2G:** Burnaby Island, Huxley Island, Arichika Island

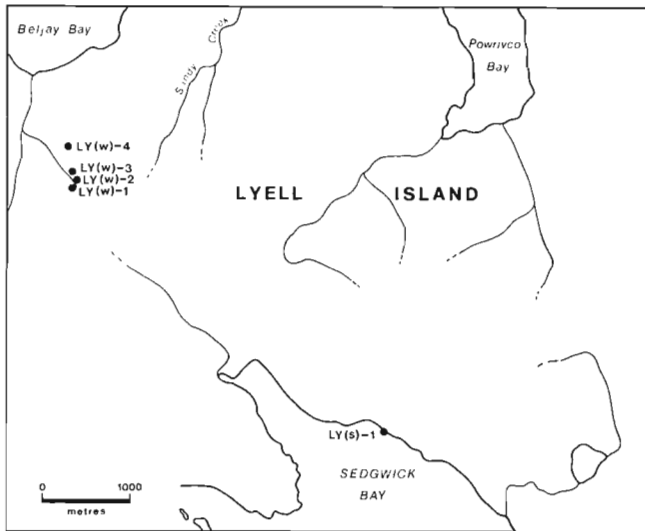


Figure 2H: Lyell Island

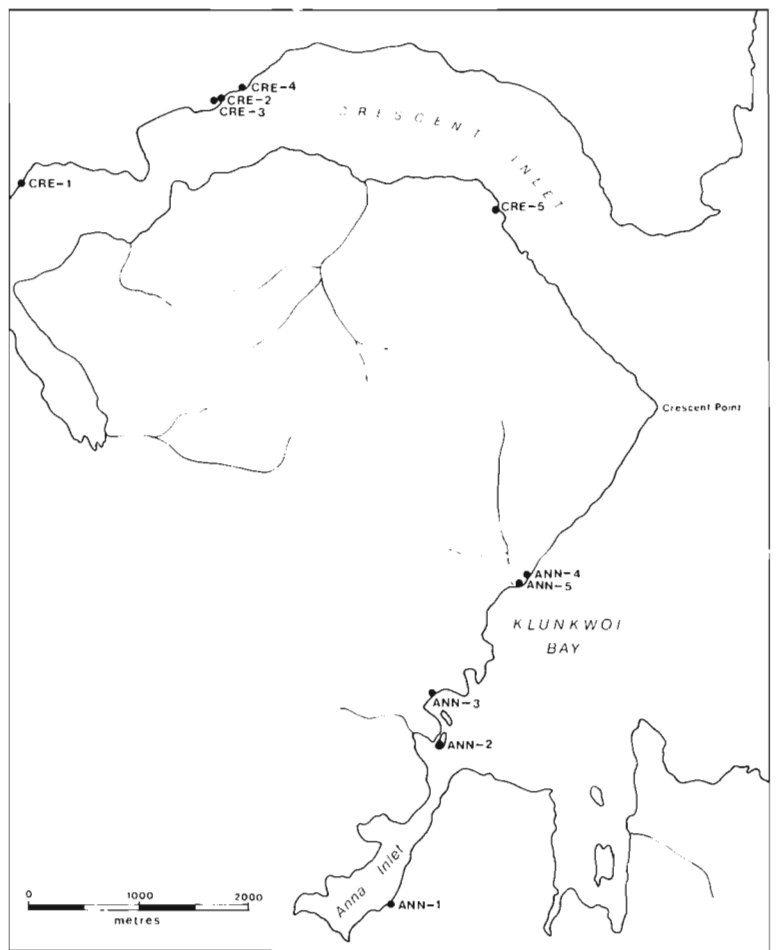


Figure 2J: Crescent Inlet

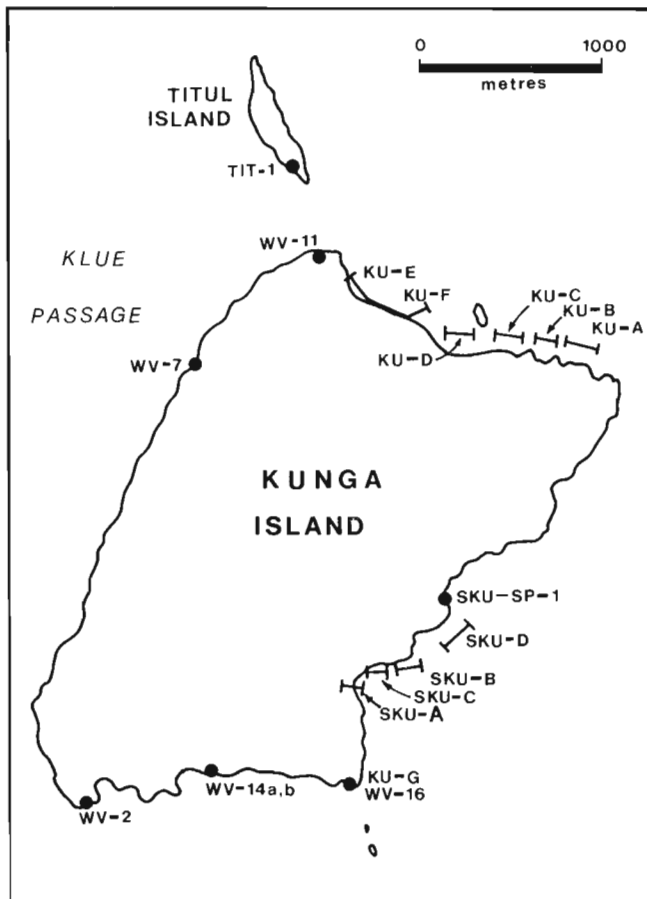


Figure 2I: Kunga Island

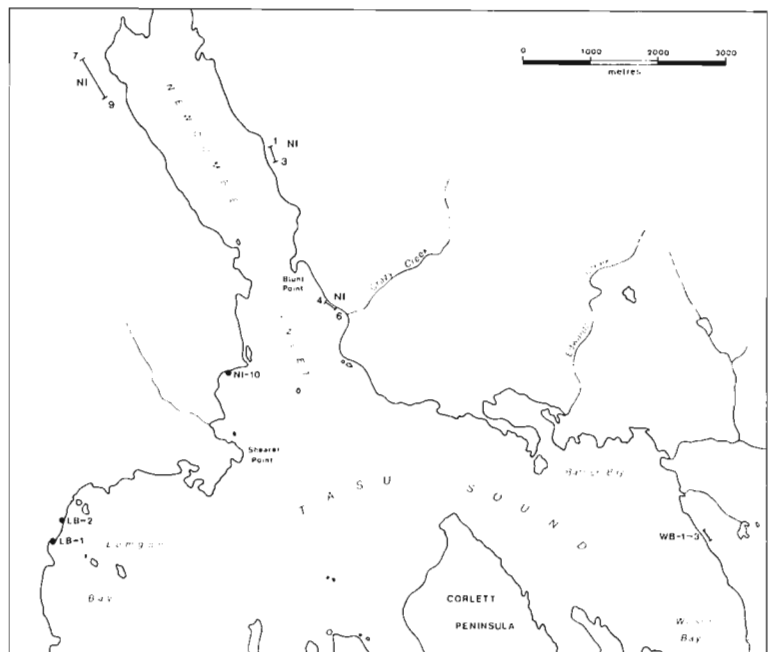


Figure 2K: Newcombe Inlet, Tasu Sound

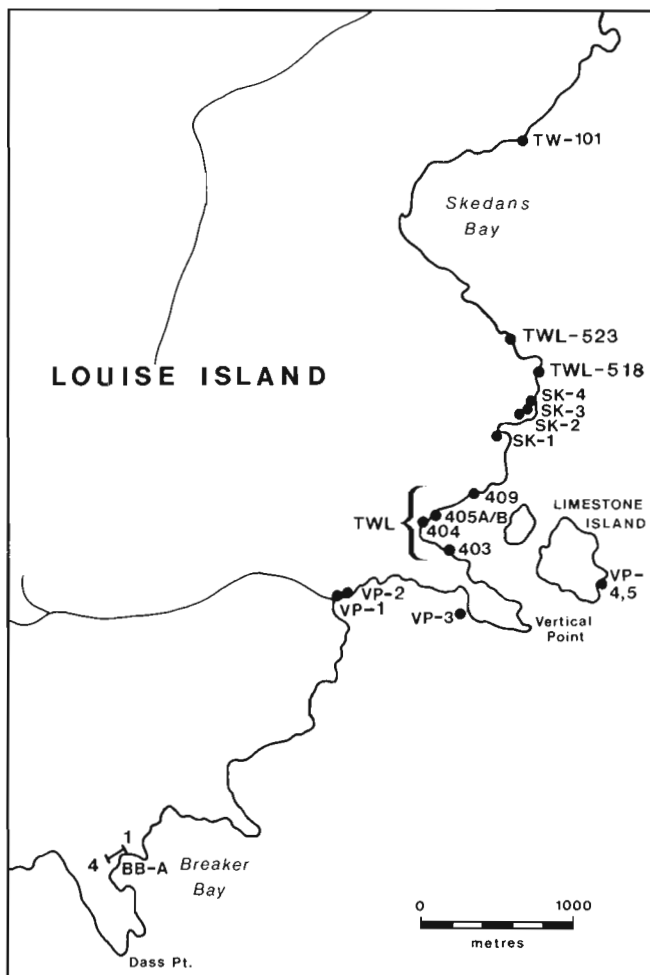


Figure 2L: Breaker Bay, Vertical Point, Skedans, Louise Island

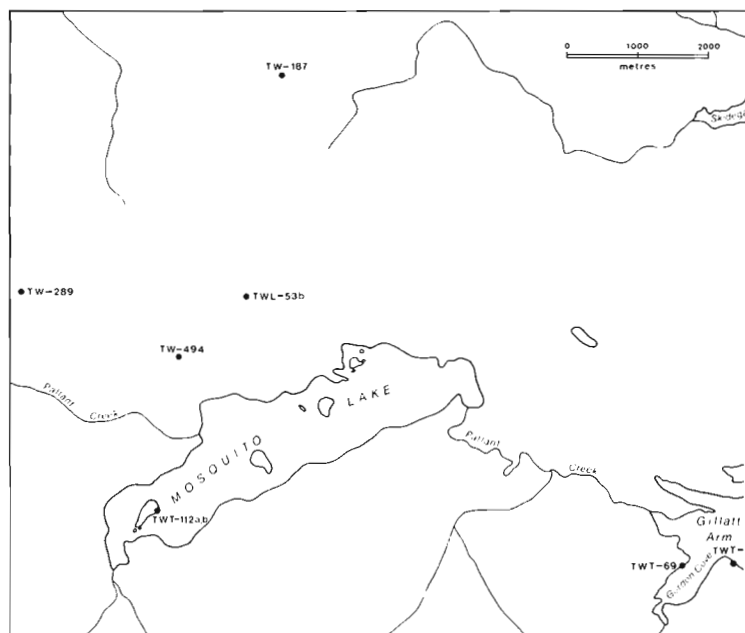


Figure 2N: Gillatt Arm, Mosquito Lake

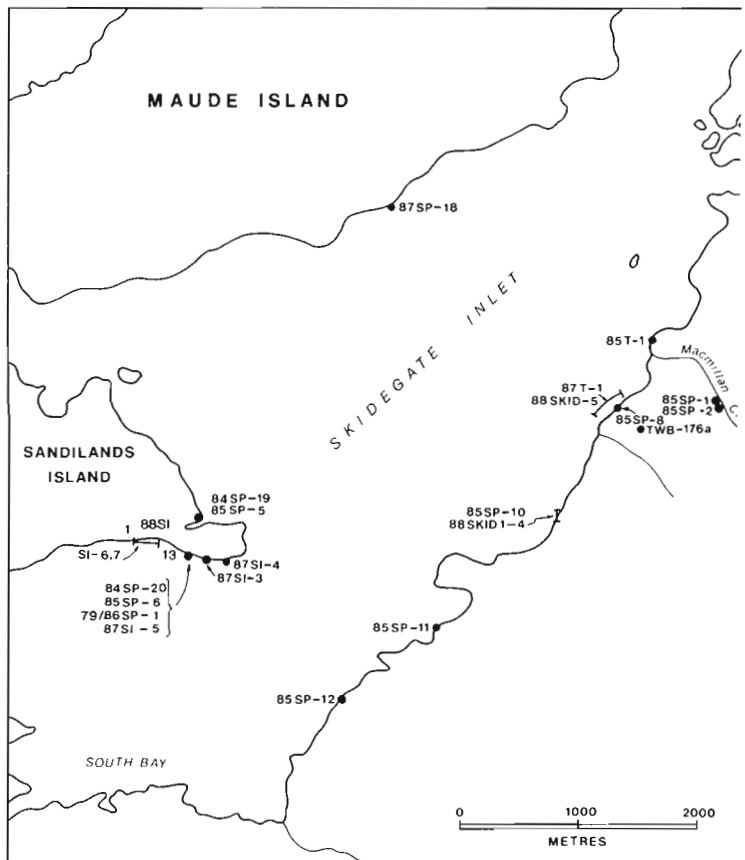


Figure 2O: Skidegate Inlet, Sandilands Island

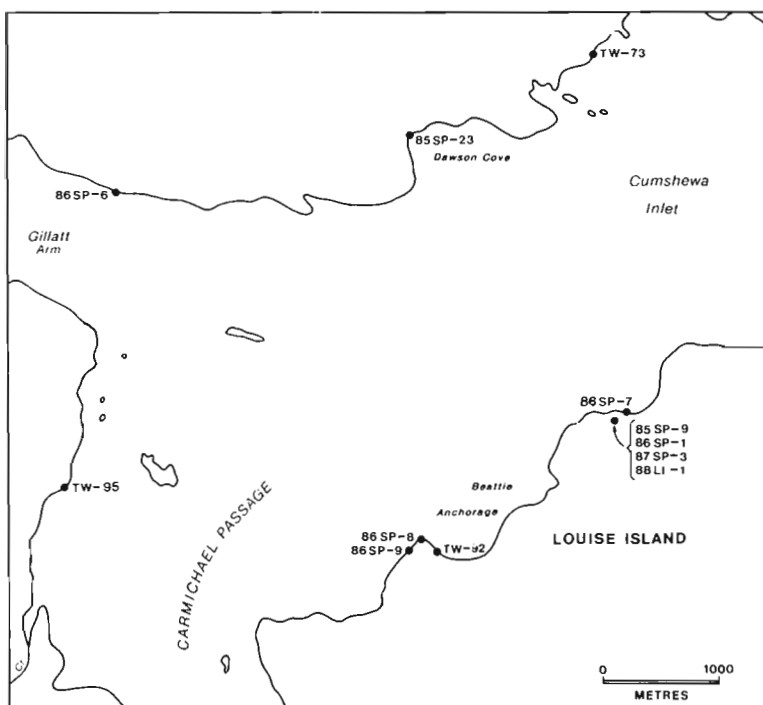


Figure 2M: Louise Island, Cumshewa Inlet, Gillatt Arm

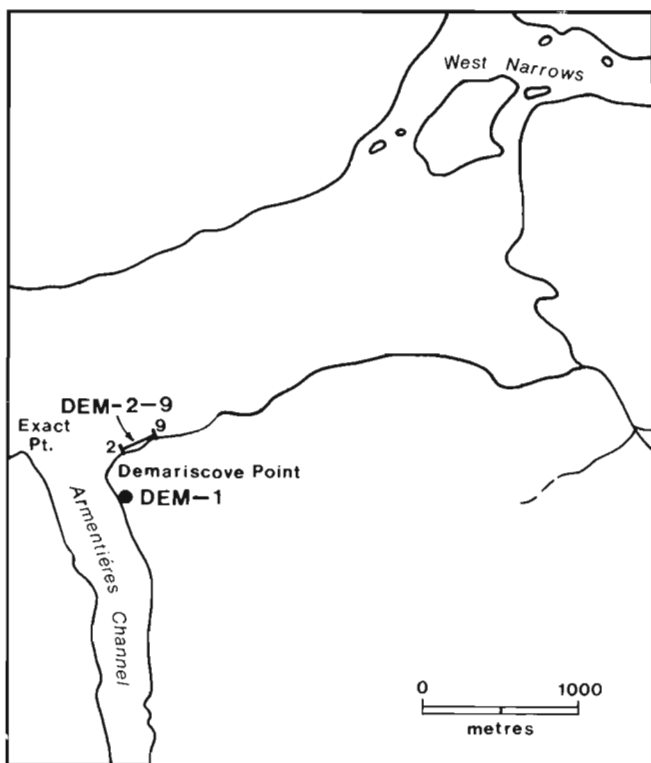


Figure 2P: Desmaricove Point

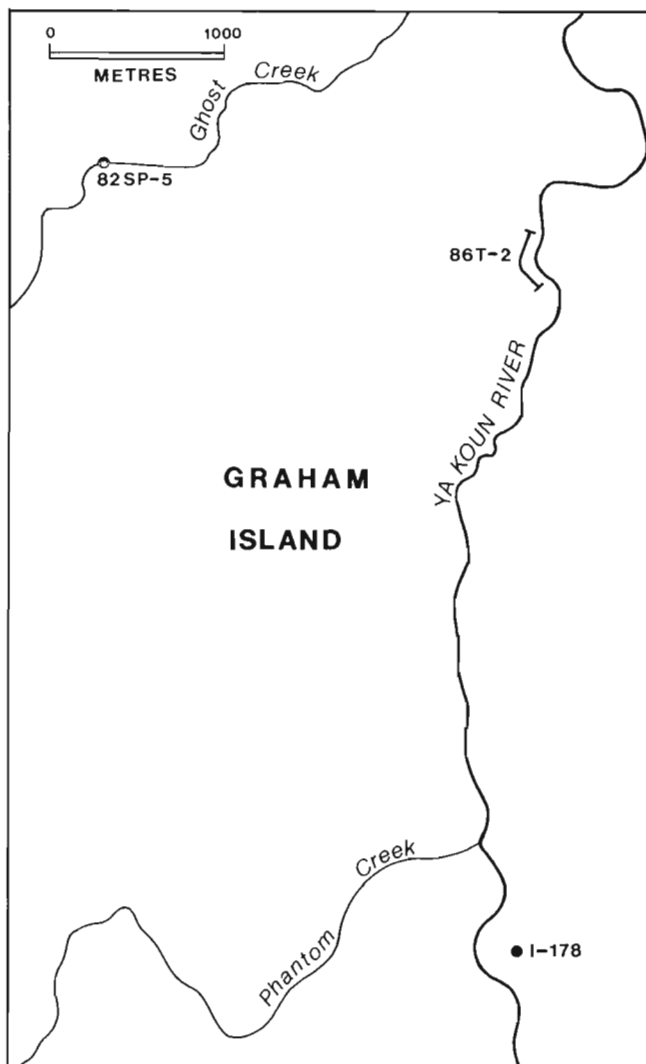


Figure 2R: Yakoun River

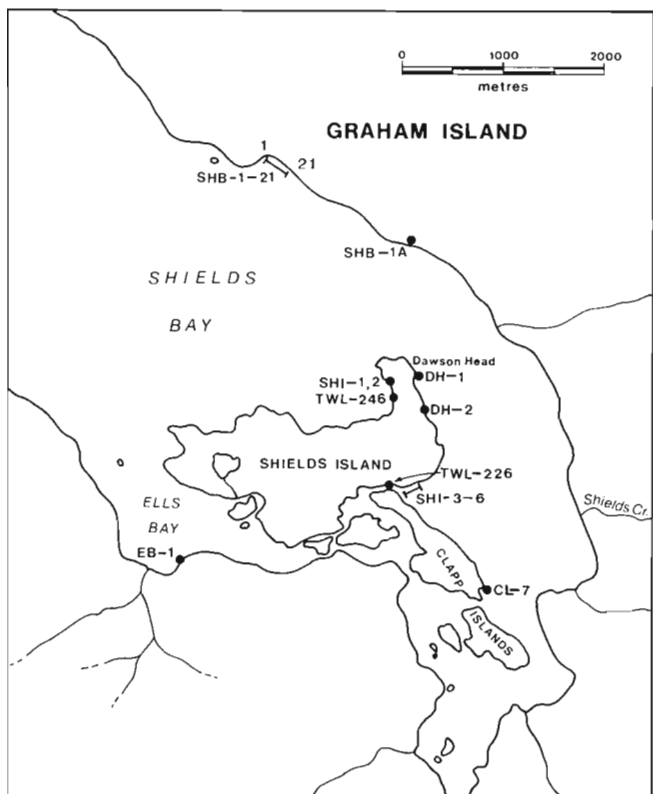
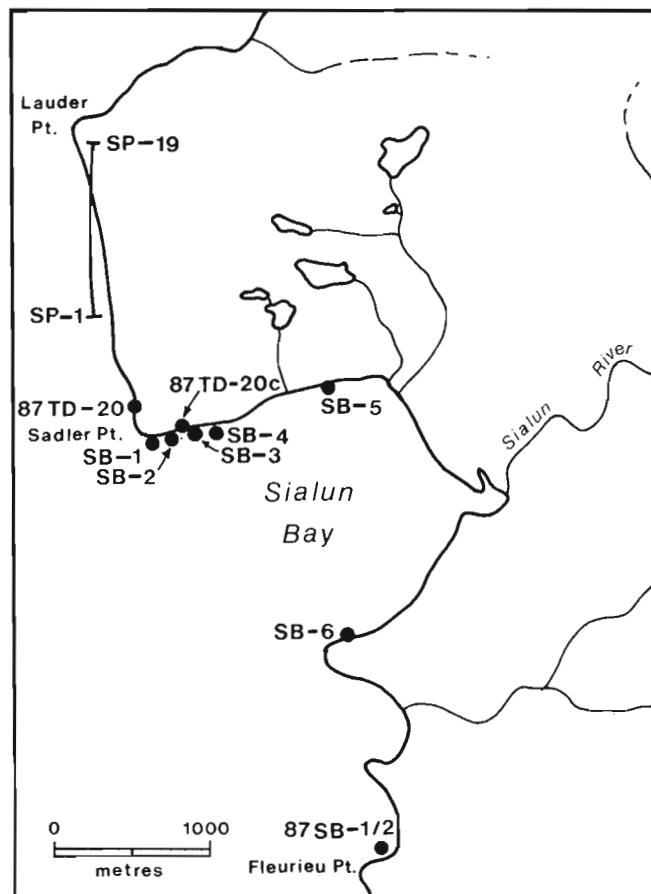


Figure 2Q: Shields Island, Shields Bay



**Figure 2S:** Kennecott Point, Frederick Island



**Figure 2T:** Sialun Bay, Sadler Point.

# Annotated bibliography of geoscience studies of the Queen Charlotte Islands and Queen Charlotte Basin, British Columbia

G.J. Woodsworth<sup>1</sup>

Woodsworth, G.J., Annotated bibliography of geoscience studies of the Queen Charlotte Islands and Queen Charlotte Basin, British Columbia; in *Evolution and Hydrocarbon Potential of the Queen Charlotte Basin, British Columbia*, Geological Survey of Canada, Paper 90-10, p. 555-569, 1991.

## Abstract

*This paper contains 293 references with short annotations to the geological and geophysical literature of the Queen Charlotte Islands, Hecate Strait, Queen Charlotte Sound, and adjacent mainland British Columbia and southeastern Alaska.*

## Résumé

*Cette étude contient 293 notices bibliographiques accompagnées de courtes annotations de documents géologiques et géophysiques portant sur les îles de la Reine-Charlotte, les détroits d'Hécate et de la Reine-Charlotte et les zones continentales adjacentes de la Colombie-Britannique et du sud-est de l'Alaska.*

## INTRODUCTION

This paper is an annotated introduction to the geological literature of the Queen Charlotte Islands and Queen Charlotte Basin from the earliest studies to the present, excluding those in the present volume.

The main bibliography covers Queen Charlotte Islands, Hecate Strait, Dixon Entrance, and Queen Charlotte Sound. Coverage is strongest for the bedrock geology and paleontology of the islands and for the surficial geology of Hecate Strait and Queen Charlotte Sound. The bibliography contains most published reports, maps, and open files of the Geological Survey of Canada and the British Columbia Ministry of Energy, Mines and Petroleum Resources reports; most papers in scientific and technical journals; most theses; and a few published abstracts that contain significant data or ideas not available elsewhere. Regional compilations, tectonic syntheses, and general evaluations of hydrocarbon or mineral potential of the Canadian Cordillera were included if they had material on the Queen Charlottes not available elsewhere. Short notes without significant content (mostly in *Current Research* for the past three years) were excluded. Soil surveys, environmental impact studies, almost all material on climatology and archaeology, and unpublished company annual reports and prospectuses were omitted. The available aeromagnetic published at 1:50 000 and 1:250 000 scale and topographic maps at 1:50 000 are shown in Figures 1 and 2.

The numerous mineral deposits and occurrences on the islands are described in the Annual Reports and other publications of the B.C. Ministry of Energy, Mines and Petroleum Resources from 1874 to the present; in unpublished assessment reports (on file with the B.C. Ministry of Energy, Mines and Petroleum Resources); and in the MINFILE electronic data base available from the Geological Survey Branch of the B.C. Ministry of Energy, Mines and Petroleum Resources. The present work, however, includes most reports on the Cinola gold prospect, on the black sands of Graham Island, and a few papers on economic geology that have appeared in widely available scientific and technical journals.

No tectonic synthesis of the Queen Charlotte Basin is complete without considering regions that flank the basin on the east, southeast, and north. However, a bibliography for these areas (mainland coast and islands of B.C., Vancouver Island, and southeast Alaska) would be substantially larger than the present compilation for the Queen Charlottes. An appendix lists about 50 references to the western Coast Plu-

tonic Complex and southeast Alaska to give an entry to the extensive literature on the bedrock geology of those regions.

References preceded by \* were not seen.

## ACKNOWLEDGMENTS

Much of the leg work for this bibliography was accurately and thoroughly done by Paulette Tercier and Simon Thompson. I thank Mary Akehurst for critical comments and help with the literature searches, and those who suggested references and reviewed the annotations.

## BIBLIOGRAPHY

Addicott, W.O.

1978: Late Miocene mollusks from the Queen Charlotte Islands, British Columbia, Canada; *Journal of Research of the United States Geological Survey*, v. 6, p. 677-690.

A marine bivalve, gastropod, and echinoid fauna from the Skonun Formation at its type locality east of Masset and from northeastern Graham Island, indicate a Late Miocene age for the Skonun. Paper discusses regional correlations and taxonomic ties with other units.

Anderson, F.M.

1958: Upper Cretaceous of the Pacific Coast; *Geological Society of America, Memoir* 71, 378 p.

A few specimens of ammonites from the Queen Charlotte Islands, referred to a new species, are described and figured.

Anderson, R.G.

1988: Jurassic and Cretaceous-Tertiary plutonic rocks on the Queen Charlotte Islands, British Columbia; in *Current Research, Part E*, Geological Survey of Canada, Paper 88-1E, p. 213-216.

A preliminary report defining three informal plutonic suites (San Christoval, Burnaby Island, and Carpenter Bay) of Jurassic age. Gives lithologic descriptions, isotopic dates and aeromagnetic expression.

Anderson, R.G.

1988: Plutonic rocks and skarn deposits on the Queen Charlottes; *Mining Review*, v. 8, no. 2, March-April, p. 19-24.

Describes four informal plutonic suites (San Christoval, Burnaby Island, Carpenter Bay and Kano) and their relationship to Fe-Cu skarn deposits and hydrocarbon potential.

Anderson, R.G. and Greig, C.J.

1989: Jurassic and Tertiary plutonism in the Queen Charlotte Islands, British Columbia; in *Current Research, Part H*, Geological Survey of Canada, Paper 89-1H, p. 95-104.

Preliminary report; gives refined ages, plutonic and structural styles for the Late Jurassic San Christoval and Burnaby Island plutonic suites and the Tertiary Kano suite. The previously defined Carpenter Bay suite is now included in the Kano plutonic suite.

Anderson, R.G. and Reichenbach, I.

1989: A note on the geochronometry of Late Jurassic and Tertiary plutonism in the Queen Charlotte Islands, British Columbia; in *Current Research, Part H*, Geological Survey of Canada, Paper 89-1H, p. 105-112.

Gives new K-Ar and U-Pb dates for the San Christoval and Kano plutonic suites and Carpenter Bay dykes.

<sup>1</sup> Cordilleran Division, Geological Survey of Canada, 100 West Pender Street, Vancouver, B.C. V6B 1R8



**Barrie, J.V.**

**1988:** Surficial geology of Hecate Strait, British Columbia continental shelf; Geological Survey of Canada, Open File 1682.

Hecate Strait is underlain by Tertiary bedrock that is unconformably overlain by glacial till. These units are overlain in most areas by thick Holocene silt (below 200 m water depth) and Quaternary sand and gravel (above 200 m). Discusses Pleistocene and Quaternary history and possible hazards to seabed development of the area.

**Barrie, J.V. and Bornhold, B.D.**

**1989:** Surficial geology of Hecate Strait, British Columbia continental shelf; Canadian Journal of Earth Sciences, v. 26, p. 1241-1254.

This paper is a condensed version of Barrie (1988) with emphasis on sediment transport in Hecate Strait.

**Barrie, J.V., Emory-Moore, M., Luternauer, J.L., and Bornhold, B.D.**

**1988:** Origin of modern heavy mineral deposits, northern British Columbia continental shelf; Marine Geology, v. 84, p. 43-51.

Bottom sediments in Hecate Strait and Queen Charlotte Sound contain an average of 10% heavy minerals (dominantly amphibole, ilmenite, sphene, and titaniferous magnetite). The deposits are thought to have originated by hydrodynamic reworking under present oceanographic conditions.

**Barrie, J.V., Luternauer, J.L., and Conway, K.W.**

**1990:** Surficial Geology of the Queen Charlotte Basin: Dixon Entrance-Hecate Strait; Geological Survey of Canada, Open File 2193, 7 maps at 1:250 000.

**Barrie, J.V., Luternauer, J.L., and Conway, K.W.**

**1990:** Surficial Geology of the Queen Charlotte Basin: Graham Island-Dixon Entrance; Geological Survey of Canada, Open File 2194, 7 maps at 1:250 000.

**Barrie, J.V., Luternauer, J.L., and Conway, K.W.**

**1990:** Surficial Geology of the Queen Charlotte Basin: Moresby Island-Queen Charlotte Sound; Geological Survey of Canada, Open File 2196, 8 maps at 1:250 000.

Together with the two open files by Luternauer, Barrie, Conway and Caltagirone, these open files provide a substantial body of data for the continental shelf of western Canada. The various maps show geophysical survey track lines; seabed sampling, photography and current meter stations, surficial sediment grain size data, and surficial features and geohazards.

**Barker, F., Sutherland Brown, A., Budahn, J.R., and Plafker, G.**

**1989:** Back-arc with frontal arc component origin of Triassic Karmutsen basalt, British Columbia, Canada; Chemical Geology, v. 75, p. 81-102.

Gives 12 whole-rock major- and minor-element chemical analyses from Karmutsen Formation on Vancouver Island (5 analyses) and Queen Charlotte Islands (7 analyses). The Karmutsen volcanics were erupted in a near-axial, back-arc basin as "arc-rift" tholeiites.

**Bérubé, J., Rogers, G.C., Ellis, R.M., and Hasselgren, E.O.**

**1989:** A microseismicity study of the Queen Charlotte Islands region; Canadian Journal of Earth Sciences, v. 26, p. 2556-2566.

Analysis of over 300 microseismic events detected during the summer of 1983. Most were on or close to the Queen Charlotte Fault, with very little activity in the previously identified seismic gap. 18 events occurred on northern Graham Island or in adjacent Hecate Strait. Composite focal mechanisms indicate thrust faulting along northeast-southwest compressive axes.

**Billings, E.**

**1873:** On the Mesozoic Fossils from British Columbia collected by Mr. James Richardson in 1872; Geological Survey of Canada, Report of Progress for 1872-1873, p. 71-75.

Billings studied the Richardson's fossils from the Queen Charlottes and wrote, "...the Ammonites and Belemnites tend to prove that the Queen Charlotte Island rocks are Jurassic, while the Nautilus would place them in the Cretaceous." He clearly recognized the existence of two faunas, but other studies for the next thirty years failed to recognize and separate the Jurassic rocks from Cretaceous.

**\* Bird, D.N.**

**1981:** Time-term analysis using linear programming and its applications to refraction data from the Queen Charlotte Islands; M.Sc. thesis, University of British Columbia, Vancouver, 79 p.

**Blome, C.D.**

**1981:** Upper Triassic radiolaria from eastern Oregon and British Columbia; Ph.D. thesis, University of Texas at Dallas, 228 p.

Chapter 2 contains systematic descriptions of radiolaria from the Upper Norian "black limestone member" (Peril Formation) of the Kunga Group, and gives a revised zonal scheme for the Upper Triassic.

**Bornhold, B.D. and Collins, A.D.**

**1984:** Surficial sediment distribution, Laskeek Bank, Hecate Strait; Geological Survey of Canada, Open File 1086.

A map at 1:100 000 showing sand-mud-gravel ratios of surficial sediment distribution for part of Hecate Strait.

**Bostwick, T.K.**

**1984:** A re-examination of the August 22, 1949 Queen Charlotte earthquake; M.Sc. thesis, University of British Columbia, Vancouver, 116 p.

The principal study of the 1949 earthquake; showed that the rupture was 500 km in length and that rupture was bilateral.

**Burwash, E.M.**

**1913:** On some new species of marine invertebrates from the Cretaceous of the Queen Charlotte Islands; Proceedings and Transactions of the Royal Society of Canada, 3rd Series, v. 7, sec. IV, p. 77-90.

Reports on new species collected by the Field Columbian Museum expedition in 1905. Burwash placed these fossils in the Cretaceous, following Dawson's stratigraphy.

**Bustin, R.M. and Macauley, G.**

**1988:** Organic petrology and Rock-Eval pyrolysis of the Jurassic Sandilands and Ghost Creek formations, Queen Charlotte Islands; Bulletin of Canadian Petroleum Geology, v. 36, p. 168-176.

The units contain petroleum source rocks and rare oil shales. The organic matter has petroleum generation potential of up to 40 kg hydrocarbon/tonne and contains up to 7% total organic carbon. Source rocks are overmature on southeastern and southwestern Graham Island, Maude Island, and northern Moresby Island, and mature on central Graham Island.

**Bustin, R.M., Vellutini, D., and Goočarzi, F.**

**1990:** Petroleum source rock characteristics of the Tertiary Skonun Formation, Queen Charlotte Islands, Hecate Strait and Queen Charlotte Sound, British Columbia; in Current Research, Part F, Geological Survey of Canada, Paper 90-1F, p. 87-93.

Skonun sediments on Graham Island are immature with respect to oil generation, whereas in Hecate Strait and Queen Charlotte Sound the formation varies from immature to overmature. Source rock potential is poor to moderate.

**Cameron, B.E.B.**

**1987:** Significance of Lower Jurassic hydrocarbon source rocks in the Cumsheva Inlet area, Queen Charlotte Islands, British Columbia; in Current Research, Part A, Geological Survey of Canada, Paper 87-1A, p. 925-928.

Lower Jurassic rocks in the Cumsheva Inlet area are potential hydrocarbon source rocks and may continue under Hecate Strait. The boundary between the Alexander Terrane and Wrangellia lies near the east side of Hecate Strait; thus much of Hecate Strait may be a potential oil province.

**Cameron, B.E.B. and Hamilton, T.S.**

**1988:** Contributions to the stratigraphy and tectonics of the Queen Charlotte Basin, British Columbia; in Current Research, Part E, Geological Survey of Canada, Paper 88-1E, p. 221-227.

Review of stratigraphy and tectonics in the Queen Charlotte Basin. Tectonic history of the area is discussed in relation to global tectonics.

**Cameron, B.E.B. and Tipper, H.W.**

**1981:** Jurassic biostratigraphy, stratigraphy and related hydrocarbon occurrences of Queen Charlotte Islands, British Columbia; in Current Research, Part A, Geological Survey of Canada, Paper 81-1A, p. 209-212.

Preliminary report, superseded by Cameron and Tipper (1985).

**Cameron, B.E.B. and Tipper, H.W.**

**1985:** Jurassic stratigraphy of the Queen Charlotte Islands, British Columbia; Geological Survey of Canada, Bulletin 365, 49 p.

The first thorough study of Jurassic biostratigraphy on Queen Charlotte Islands since McLearn, based on detailed work in Skidegate Inlet and central Graham Island. Gives a complete, formal revision of the stratigraphic nomenclature for Jurassic units and introduces many new stratigraphic terms, including the Sandilands, Ghost Creek, Rennell Junction, Fannin, Whiteaves, Phantom Creek formations. Includes lists of index ammonoids, foraminifera and other macro-invertebrate fossils which occur through the Lower and Middle Jurassic sequence.

**Carmichael, J.I.**

**1930:** Queen Charlotte Islands; in British Columbia Minister of Mines, Annual Report 1929, p. C58-C65.

Descriptions of mineral deposits on Moresby Island and the black sands on northeastern Graham Island.

**Carmichael, H.**

**1930:** Black-sand deposits of Graham Island; in Placer-Mining in British Columbia, J.D. Galloway (compiler), British Columbia Department of Mines, Bulletin No. 2, 1930, p. 28-31.

Descriptions of deposits and mining operations.

**Carter, E.S.**

**1985:** Early and Middle Jurassic radiolarian biostratigraphy, Queen Charlotte Islands, B.C.; M.Sc. thesis, University of British Columbia, Vancouver, 291 p.

The first study of radiolarians from central Graham Island, northern Moresby Island, and Skidegate Inlet areas, and the first significant study of Toarcian radiolarians anywhere. Gives systematic paleontology, radiolarian taxonomy, biostratigraphy, distribution patterns, and paleoenvironmental relationships.

**Carter, E.S.**

**1988:** Radiolarian studies in the Queen Charlotte Islands, British Columbia; in Current Research, Part E, Geological Survey of Canada, Paper 88-1E, p. 235-238.

A discussion of past, present and proposed radiolarian studies in the Mesozoic rocks of the Queen Charlottes.

**Carter, E.S.**

**1990:** New biostratigraphic elements for dating Upper Norian strata from the Sandilands Formation, Queen Charlotte Islands, British Columbia, Canada; Marine Micropaleontology, v. 15, p. 313-328.

New radiolarian faunas confirm that the Sandilands Formation contains uppermost Triassic and lowermost Jurassic strata. The formation may be one of the best places in the world for studies of the Triassic-Jurassic boundary.

- Carter, E.S., Cameron, B.E.B., and Smith, P.L.**  
**1988:** Lower and Middle Jurassic radiolarian biostratigraphy and systematic paleontology, Queen Charlotte Islands, British Columbia; Geological Survey of Canada, Bulletin 386, 109 p.
- Biostratigraphy and radiolarian taxonomy of Late Pliensbachian to Early Bajocian strata on the islands, based largely on Carter (1985). Seven informal radiolarian zones were established for this time interval.
- Carter, E.S., Orchard, M.J., and Tozer, E.T.**  
**1989:** Integrated ammonoid-conodont-radiolarian biostratigraphy, Late Triassic Kunga Group, Queen Charlotte Islands, British Columbia; in *Current Research, Part H*, Geological Survey of Canada, Paper 89-1H, p. 23-30.
- Preliminary report on revised biostratigraphy and integrated fossil zonation for the Upper Carnian to Upper Norian strata on the Queen Charlottes. Includes first account of conodonts and first documentation of Lower and Middle Norian strata on the islands.
- Champigny, N.**  
**1981:** A geological evaluation of the Cinola (Specogna) gold deposit, Queen Charlotte Islands, B.C.; M.A.Sc. thesis, University of British Columbia, Vancouver, 199 p.
- The first detailed, publicly-available study of this late Tertiary deposit. The mineralization resulted from a geothermal system related to Masset rhyolites.
- Champigny, N. and Sinclair, A.J.**  
**1982:** The Cinola gold deposit, Queen Charlotte Islands, British Columbia; in *Geology of Canadian Gold Deposits*, R.W. Hodder and W. Petruk (ed.), Canadian Institute of Mining and Metallurgy, Special Volume 24, p. 243-254.
- Description of this Carlin-type gold deposit on Graham Island, including stratigraphy and sedimentology of the Skonun Formation, structure, alteration, and mineralization.
- Champigny, N. and Sinclair, A.J.**  
**1982:** Cinola gold deposit, Queen Charlotte Islands, B.C.—a geochemical case history; in *Precious Metals in the Canadian Cordillera*, A.A. Levinson (ed.), Association of Exploration Geochemists, Special Volume 10, p. 121-137.
- Statistical evaluation of soil and silt multi-element geochemical data from Cinola.
- Champigny, N. and Sinclair, A.J.**  
**1984:** A geostatistical study of the Cinola gold deposit, Queen Charlotte Islands, British Columbia; *Western Miner*, v. 57, no. 2, February, p. 54-59.
- Tests of numeric models for estimating ore reserves, based on drill hole data from Cinola.
- Champigny, N., Henderson, C.M., and G.E. Rouse**  
**1981:** New evidence for the age of the Skonun Formation, Queen Charlotte Islands, British Columbia; *Canadian Journal of Earth Sciences*, v. 18, p. 1900-1903.
- K-Ar, macrofaunal and palynological data from drill core suggest a late Early Miocene age for the Skonun at Cinola. Outcrops on northeastern Graham Island are as young as early Middle Miocene.
- Chan, E., Dosso, H.W., and Nienaber, W.**  
**1981:** An analogue model study of electromagnetic induction in the Queen Charlotte Islands region; *Journal of Geomagnetism and Geoelectricity*, v. 33, p. 587-605.
- Conductive channelling is important in Hecate Strait for both E and H source field polarizations. Model results for simulated variations of 4, 40, and 120 minutes show a wide range of field values over the Queen Charlotte Islands.
- Chan, E., Dosso, H.W., Law, L.K., Auld, D.R., and Nienaber, W.**  
**1983:** Electromagnetic induction in the Queen Charlotte Islands region: analogue model and field station results; *Journal of Geomagnetism and Geoelectricity*, v. 35, p. 501-516.
- Electromagnetic response of the Queen Charlotte Islands region is related primarily to the distribution of land and seawater. The structure of the lithosphere and upper asthenosphere of the region is more complex than predicted by the simple model used.
- Chase, R.L. and Tiffin, D.I.**  
**1972:** Queen Charlotte fault-zone, British Columbia; 24th International Geological Congress, 24th Session, Montreal, Section 8, Marine Geology and Geophysics, p. 17-27.
- Review of the knowledge of the Queen Charlotte transform, based on seismic profiles and bottom samples.
- Chase, R.L., Tiffin, D.I., and Murray, J.W.**  
**1975:** The Western Canadian continental margin; in *Canada's Continental Margins and Offshore Petroleum Exploration*, C.J. Yorath, E.R. Parker, and D.J. Glass (ed.), Canadian Society of Petroleum Geologists, Memoir 4, p. 701-721.
- A review of knowledge of the western continental margin from the Queen Charlotte Islands to Vancouver Island and discussion of the tectonic evolution of the Pacific, North America, and Juan de Fuca plates.
- Christie, A.B.**  
**1989:** Cinola gold deposit, Queen Charlotte Islands (103F/9E); in *Geological Fieldwork, 1988*, British Columbia Ministry of Energy, Mines and Petroleum Resources, Paper 1989-1, p. 423-428.
- Progress report; gives stratigraphy, alteration, and mineralization.
- Clague, J.J.**  
**1983:** Glacio-isostatic effects of the Cordilleran Ice Sheet, British Columbia, Canada; in *Shorelines and Isostasy*, D.E. Smith and A.G. Dawson (ed.), Institute of British Geographers, Special Publication 16, Academic Press, London, p. 321-343.
- Discussion and documentation of Pleistocene and Holocene relative sea-level changes in western British Columbia, with much on the Queen Charlotte Islands. Documents a late Pleistocene to early Holocene transgression on the Queen Charlotte Islands.
- Clague, J.J.**  
**1989:** Quaternary geology of the Queen Charlotte Islands; in *The Outer Shores: based on the proceedings of the Queen Charlotte Islands First International Scientific Symposium*, University of British Columbia, August 1984, G.G.E. Scudder and N. Gessler (ed.), Queen Charlotte Islands Museum Press, p. 65-74.
- A review for the advanced lay reader, now somewhat out of date.
- Clague, J.J. and Bornhold, B.D.**  
**1980:** Morphology and littoral processes of the Pacific Coast of Canada; in *The Coastline of Canada, Littoral Processes and Shore Morphology*, S.B. McCann (ed.), Geological Survey of Canada, Paper 80-10, p. 339-380.
- Summary of British Columbia coastal geomorphology, nearshore sedimentary processes and environments, and the history of sea-level fluctuations since the end of the last glaciation; previous research is summarized with an extensive bibliography.
- Clague, J., Harper, J.R., Hebda, R.J., and Howes, D.E.**  
**1982:** Late Quaternary sea levels and crustal movements, coastal British Columbia; *Canadian Journal of Earth Sciences*, v. 19, p. 597-618.
- Discusses changes in sea level during Late Quaternary time in terms of disposition and history of retreat of the late Wisconsin Cordilleran Ice Sheet and plate interactions at British Columbia's continental margin. Much on the Queen Charlotte Islands.
- Clague, J.J., Mathewes, R.W., and Warner, B.G.**  
**1982:** Late Quaternary geology of eastern Graham Island, Queen Charlotte Islands, British Columbia; *Canadian Journal of Earth Sciences*, v. 19, p. 1786-1795.
- Reconnaissance study of Quaternary geology of eastern Graham Island; many radiocarbon dates. Last Wisconsin glaciation of the coastal lowlands of Graham Island was weak and short. A period of low sea level during late Pleistocene time was followed by a transgression that culminated about 7500-8000 years ago, when sea level was about 15 m higher relative to land than at present.
- Clapp, C.H.**  
**1914:** A geological reconnaissance on Graham Island, Queen Charlotte group, B.C.; Geological Survey of Canada, Summary Report, 1912, p. 12-40.
- Clapp divided the strata into six main units ranging in age from Triassic to Recent. He named the Triassic-Jurassic strata the Vancouver Group, based on similarities with rocks on Vancouver Island. He abandoned Dawson's Queen Charlotte Island Formation (Dawson's units C to E) and proposed instead the Queen Charlotte series for Dawson's units A to D. The Queen Charlotte series was divided into the Image, Haida, Honna and Skidegate members. Clapp was the first to clearly show the significance of the unconformity between Dawson's units C and D and recognized that Middle to Late Jurassic plutons cut parts of the Queen Charlotte series.
- Clowes, R.M.**  
**1984:** Acquisition and processing of a crustal refraction profile across the Queen Charlotte Islands and Hecate Strait; *Earth Physics Branch, Open File 84-22*, 63 p.
- Preliminary results of a refraction experiment carried out in August 1983. A full interpretation of the data was given by Dehler and Clowes (1988).
- Clowes, R.M. and Gens-Lenartowicz, E.**  
**1985:** Upper crustal structure of southern Queen Charlotte Basin from sonobuoy refraction studies; *Canadian Journal of Earth Sciences*, v. 22, p. 1696-1710.
- Interpretations of three reversed and one unreversed seismic profiles in southern Queen Charlotte Sound. Masset volcanics are widespread, and a low-velocity layer (Mesozoic sediments?) underlies the volcanics in three of the sections.
- Conway, K.W.**  
**1986:** Data report on the surficial geology of Hecate Strait; Geological Survey of Canada, Open File 1349, 163 p.
- This report contains a listing of all surficial geology data held by the Pacific Geoscience Centre for the Hecate Strait region. Maps (at 1:665 000) show grab sample locations, air gun seismic lines, deep tow seismic lines, and sidescan sonar track lines. Text contains textual analysis and lithologic descriptions of 980 grab samples and 8 piston cores, and description and evaluation of the seismic and sidescan sonar data.
- Conway, K.W. and Luternauer, J.L.**  
**1984:** Longest core of Quaternary sediments from Queen Charlotte Sound: preliminary description and interpretation; in *Current Research, Part A*, Geological Survey of Canada, Paper 84-1A, p. 647-649.
- Three distinct units were identified in this 8.76 m core, a lower, glaciogenic deposit, a middle, coarse deposit of possible slump origin, and an upper finer-grained unit of probable postglacial origin. Superseded by Luternauer et al. (1989).
- Conway, K.W. and Luternauer, J.L.**  
**1985:** Evidence of ice rafting and tractive transfer cores from Queen Charlotte Sound, British Columbia; in *Current Research, Part A*, Geological Survey of Canada Paper 85-1A, p. 703-708.
- Analysis of piston cores suggests that ice rafting was active about 13.6 ka but that any ice grounding during the Fraser Glaciation occurred prior to 15 ka. Debris and grain flows occurred during deglaciation.
- Conway, K.W., Barrie, J.V., and Luternauer, J.L.**  
**1989:** Sponge bioherms on the continental shelf of western Canada; in *Current Research, Part H*, Geological Survey of Canada, Paper 89-1H, p. 129-134.
- Large areas of the seabed of Hecate Strait and Queen Charlotte Sound are discontinuously blanketed by bioherms dominated by sponges. These bioherms trap silt clay on the otherwise relict expanses of seafloor and form some of the most significant Holocene deposits on the mid-shelf.

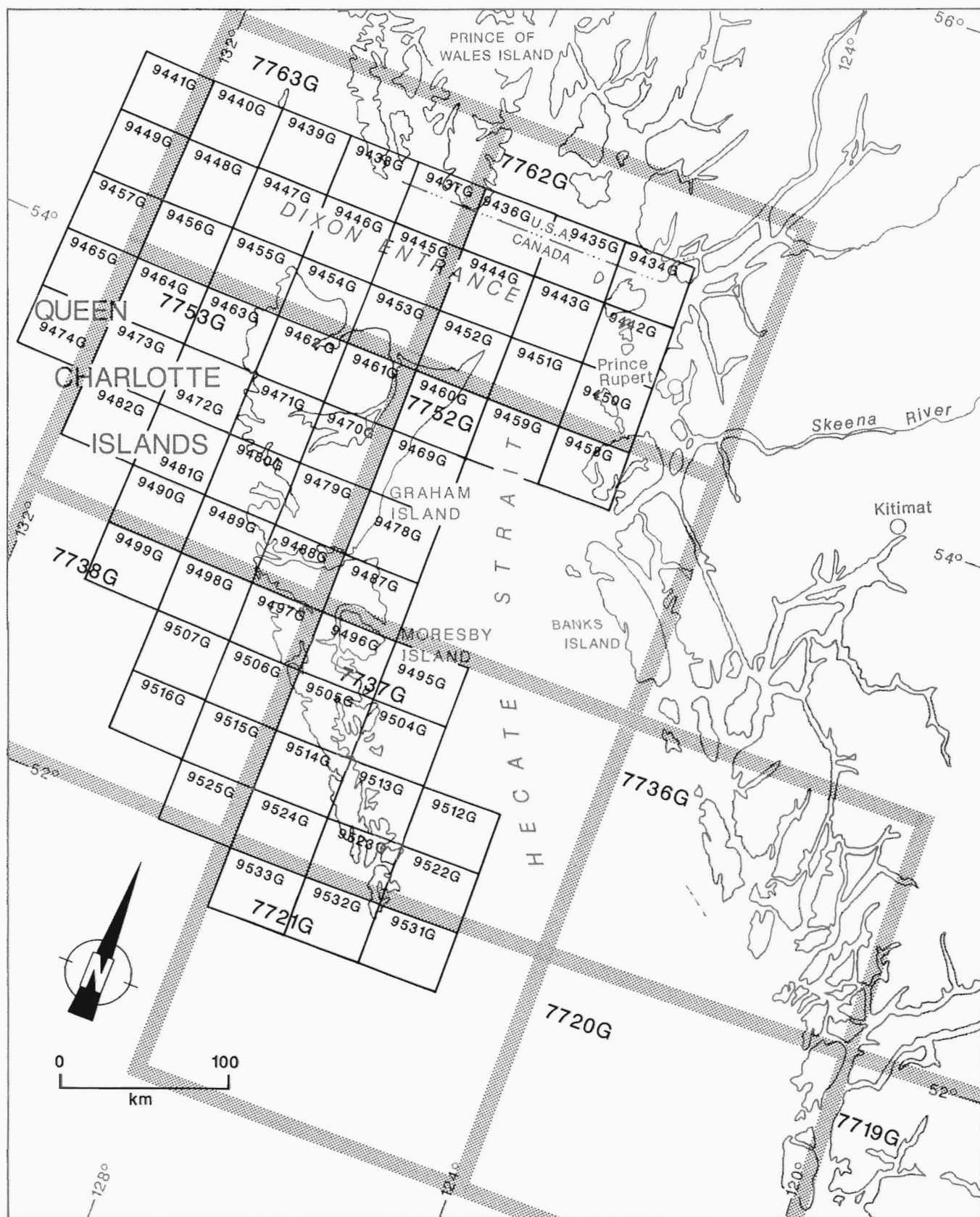


**Figure 1:** Aeromagnetic maps at 1:50 000 (small squares, small numbers) and 1:250 000 (large squares, large numbers) published by the Geological Survey of Canada for the Queen Charlotte region.

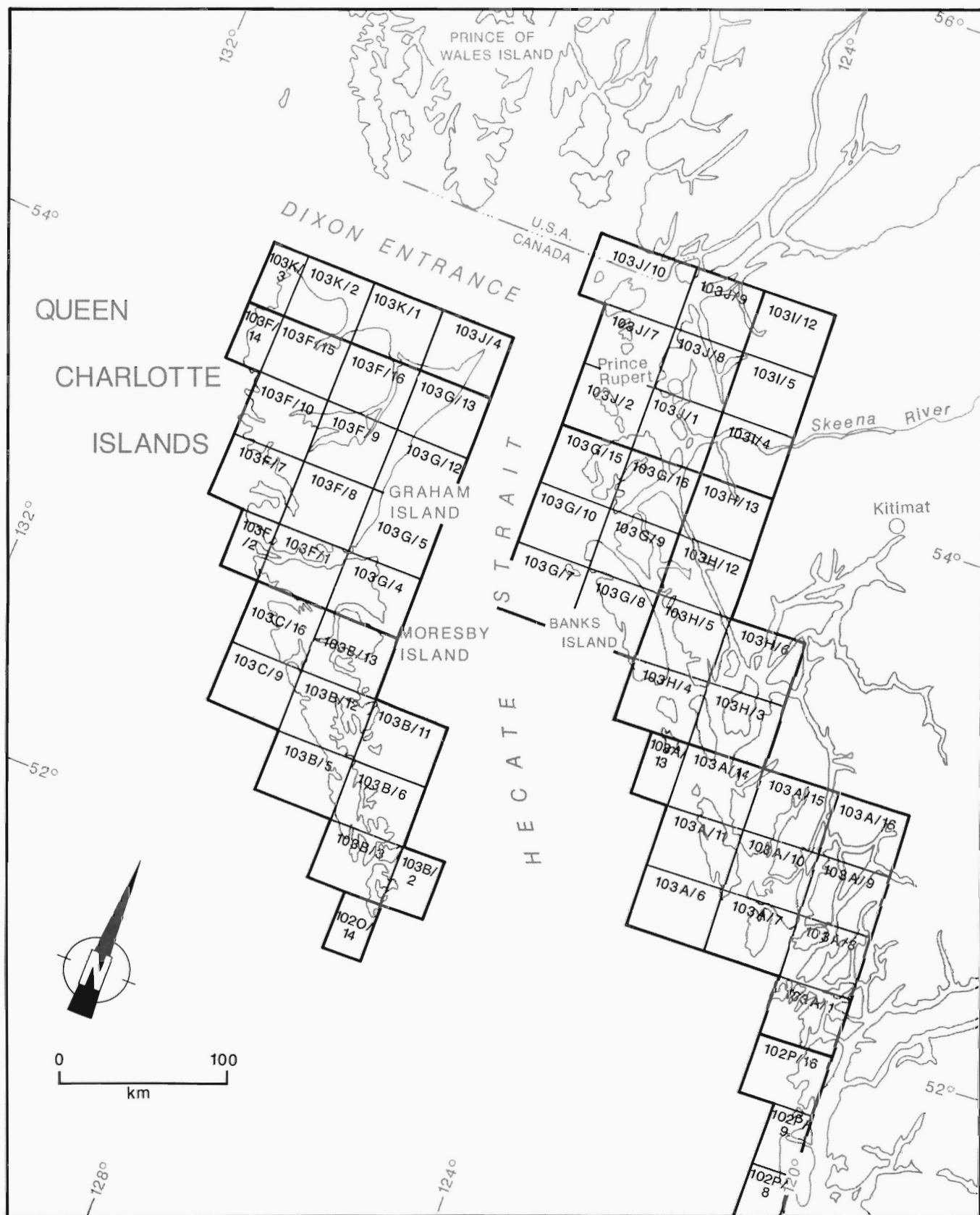


**Figure 2:** Topographic maps at 1:50 000 available for the Queen Charlotte region. Complete coverage is available for the Coast Mountains in the eastern part of the region.

- \* **Cruson, M.G., Limbach, F.W., Brooks, R.A., Sanders, K.G., Bain, D., Lacy, S.**  
**1983:** Geology of the Cinola deposit, Queen Charlotte Islands, British Columbia; in *Papers Given at the Precious Metals Symposium, Report 36-Nevada Bureau of Mines and Geology*, p. 27-35.
- Dawson, G.M.**  
**1880:** Report on the Queen Charlotte Islands, 1878; Geological Survey of Canada, Report of Progress for 1878-79, p. 1B-239B. Contains Map 139, Map of the Queen Charlotte Islands (1 inch=8 miles) and Map 141, Geological Map of Skidegate Inlet (1 inch=1 nautical mile).
- The first systematic examination of the geology of the islands, done in two and a half months of stormy weather in 1878. Dawson explored the eastern shoreline of most of the islands and mapped in detail along Skidegate Inlet. Bad weather and lack of time prevented exploration of the west coast. This comprehensive natural history report contains geologic, geographic, anthropologic, flora and fauna studies. Dawson divided the strata into four units. His Triassic unit was subdivided into four units, three of which are recognizable today as the Karmutsen, Sadler, and Peril formations. The "Cretaceous coal-bearing rocks" unconformably above the Triassic strata were subdivided into five units, from youngest to oldest called A-E. Probably influenced by Whiteaves' reports on Richardson's fossil collections indicating that units C and E are the same age, Dawson failed to recognize the unconformity separating his unit C (correctly recognized by Dawson as Cretaceous) from unit D (found later to be Jurassic). This failure to separate Jurassic from Cretaceous strata, Dawson's main error of interpretation, was to persist for the next twenty-five years. Despite this, Dawson's contributions proved invaluable for the next eighty years.
- \* **Dawson, G.M.**  
**1889:** On the earlier Cretaceous rocks of the northwest portion of the Dominion of Canada; *American Journal of Science*, 3rd Series, v. 38, p. 120-127.
- This paper groups Dawson's (1880) units C, D, and E into the Queen Charlotte Island Formation.
- Dawson, J.W.**  
**1873:** Note on the fossil plants from British Columbia, collected by Mr. James Richardson in 1872; Geological Survey of Canada, Report of Progress for 1872-1873, p. 66-71.
- Fossil plants collected by Richardson are assigned to the Jurassic or Lower Cretaceous.
- Dehler, S.A. and Clowes, R.M.**  
**1988:** The Queen Charlotte Islands refraction project. Part I. The Queen Charlotte Fault Zone; *Canadian Journal of Earth Sciences*, v. 25, p. 1857-1870.
- Gives a velocity structural model with three crustal segments (oceanic, terrace, and continental) separated by an outer, crustally pervasive fault and the active Queen Charlotte Fault, respectively. The upper part of the 10-17 km thick lower terrace unit has anomalously low velocities relative to the adjacent oceanic and continental crustal units.
- Duggan, D.M. and Luternauer, J.L.**  
**1986:** Distribution of surficial sediment and major bed forms, Goose Island Bank, Queen Charlotte Sound, central continental shelf off British Columbia; Geological Survey of Canada, Open File 1329.
- Map at about 1:15 000 of sediment and bedform distribution from sonograph records for Goose Island Bank.
- Ells, R.W.**  
**1906:** Report on Graham Island, B.C.; Geological Survey of Canada, Annual Report, New Series, v. 16, 1904, Part B, p. 1-46. Contains Map 921, Geological Map of Graham Island Coal Fields (1"=80 chains) and Map 922, Geological Map of Graham Island (1"=4 miles). Also published as Geological Survey of Canada Separate Report 940 (1912).
- Ells made the first geological reconnaissance of the west coast of Graham Island and completed a traverse of the island from Masset Inlet via the Yakoun River to Skidegate Inlet. This report added little new to the understanding of the area but did point out that some of the igneous rocks in Dawson's Queen Charlotte Island Formation were pre-Cretaceous in age.
- Fogarassy, J.A.**  
**1989:** Stratigraphy, diagenesis and petroleum reservoir potential of the Cretaceous Haida, Skidegate and Honna formations, Queen Charlotte Islands, British Columbia; M.Sc. thesis, University of British Columbia, Vancouver, 177 p.
- The Haida Formation is a fining-upwards transgressive succession with up to 15% visual porosity in the pebbly basal part. The overlying Skidegate and Honna formations are poor reservoir prospects. Diagenesis of the units involved carbonate precipitation and dissolution, and the growth of Fe-rich chlorite, trioctahedral smectite and mixed-layer phyllosilicates.
- Fogarassy, J.A.S. and Barnes, W.C.**  
**1988:** Stratigraphy, diagenesis and petroleum reservoir potential of the mid- to Upper Cretaceous Haida and Honna formations of the Queen Charlotte Islands, British Columbia; in *Current Research, Part E, Geological Survey of Canada*, Paper 88-1E, p. 265-268.
- First preliminary report, discussing stratigraphy, diagenetic history, and petroleum reservoir potential of the Haida and Honna formations.
- Fogarassy, J.A.S. and Barnes, W.C.**  
**1989:** The middle Cretaceous Haida Formation: a potential hydrocarbon reservoir in the Queen Charlotte Islands, British Columbia; in *Current Research, Part H, Geological Survey of Canada*, Paper 89-1H, p. 47-52.
- Preliminary report, reservoir characteristics improve in a southerly direction with the best visual porosity being found in outcrops bordering Hecate Strait and Cumshewa Inlet. However, porosity is restricted to the thin basal part of the formation.
- Fowler, M.G., Snowdon, L.R., Brooks, P.W., and Hamilton, T.S.**  
**1988:** Biomarker characterization and hydrous pyrolysis of bitumens from Tertiary volcanics, Queen Charlotte Islands, British Columbia, Canada; *Organic Geochemistry*, v. 13, 715-725.
- Biomarker characterization of bitumens from Lower Jurassic sediments contain 28,30-bisnorhopane. Tertiary volcanics contain 18 (h)-oleanane. All samples have been variably biodegraded.
- Frebold, H.**  
**1967:** Position of the Lower Jurassic genus *Famminoceras* McLearn and the age of the Maude Formation on Queen Charlotte Islands; *Canadian Journal of Earth Sciences*, v. 4, p. 1145-1149.
- Note suggesting that the Maude Formation includes Lower Pliensbachian strata, based on fossils collected by Sutherland Brown.
- Frebold, H.**  
**1970:** Pliensbachian ammonoids from British Columbia and southern Yukon; *Canadian Journal of Earth Sciences*, v. 7, p. 435-456.
- Systematic descriptions of Pliensbachian ammonoids from western Canada. Includes a discussion on age and correlation of specimens from the Maude Formation.
- Frebold, H.**  
**1979:** Occurrence of the Upper Bathonian ammonite genus *Iniskinites* in the Queen Charlotte Islands, British Columbia; in *Current Research, Part C, Geological Survey of Canada*, Paper 79-1C, p. 63-66.
- Descriptions and illustrations of Upper Bathonian ammonites from Maude Island.
- Fuller, S.A.**  
**1990:** A progress report on the Pleistocene geology of Cape Bail, Graham Island, British Columbia; in *Current Research, Part F, Geological Survey of Canada*, Paper 90-1F, p. 75-82.
- Preliminary report on a Pleistocene section containing two diamictons. One is interpreted as till, the other as stony mud deposited by a lobe of the Cordilleran ice sheet which crossed Hecate Strait.
- Gamba, C.A., Indrelid, J., and Taite, S.**  
**1990:** Sedimentology of the Upper Cretaceous Queen Charlotte Group, with special reference to the Honna Formation, Queen Charlotte Islands, British Columbia; in *Current Research, Part F, Geological Survey of Canada*, Paper 90-1F, p. 67-73.
- The Queen Charlotte Group represents a transgressive sequence deposited in a marine basin created in Late Jurassic to Early Cretaceous time. Paleocurrent data from channelized turbidites of the Honna Formation reflect shifting of channels and their radial orientation on the submarine fan, not post-depositional block rotation.
- Geological Survey of Canada**  
**1987:** Gravity, British Columbia, coast: north, bouger on land, free air offshore; Geological Survey of Canada, Open File 1399.
- Map at 1:1 000 000. Region includes Queen Charlotte Islands, Hecate Strait, Queen Charlotte Sound, and the mainland to the east. Supersedes Stacey et al. (1973).
- Geological Survey of Canada**  
**1987:** Preliminary magnetic anomaly map (residual total field), Prince Rupert, British Columbia; Geological Survey of Canada, Map NN-8-9-M.
- Coloured map at 1:1 000 000 of the Queen Charlotte Islands and Basin and adjacent areas. A useful and informative compilation.
- Geological Survey of Canada**  
**1987:** Preliminary magnetic anomaly map (residual total field), Vancouver, British Columbia; Geological Survey of Canada, Map NM-8-9-M.
- Coloured map at 1:1 000 000 of Queen Charlotte Sound and adjacent areas. A useful and informative compilation.
- \* **Gimbarzevsky, P.**  
**1984:** Remote sensing of slope failures on the Queen Charlotte Islands; in *Renewable Resources Management, Application of Remote Sensing*, American Society of Photogrammetry, p. 406-413.
- Green, K.C.**  
**1986:** Petrology of the volcanic rocks of the Karmutsen Formation, Ikeda Cove, Queen Charlotte Islands, British Columbia; B.Sc. thesis, University of British Columbia, Vancouver, 37 p.
- Petrographic descriptions and whole-rock chemical analyses; no trace element analyses.
- Haggart, J.W.**  
**1986:** Stratigraphic investigations of the Cretaceous Queen Charlotte Group, Queen Charlotte Islands, British Columbia; Geological Survey of Canada, Paper 86-20, 24 p.
- In Cumshewa Inlet, six lower Albian to lower Turonian megafossil zones were recognized in the sandstone and shale members of the Haida Formation. Fossils from the Skidegate Formation in Skidegate Inlet indicate an early Turonian to early Coniacian age, suggesting that the Skidegate is in part coeval with the Haida. No significant hiatus is present between the Honna Formation and the older Haida and Skidegate units.
- Haggart, J.W.**  
**1987:** On the age of the Queen Charlotte Group of British Columbia; *Canadian Journal of Earth Sciences*, v. 24, p. 2470-2476.
- New fossil collections show that both the Skidegate Formation and the upper part of the Haida shale member include Turonian strata and are, at least in part, lateral equivalents. Most of the Honna Formation is Coniacian in age and caps the stratigraphic sequence.

- Haggart, J.W.**  
**1989:** Reconnaissance lithostratigraphy and biochronology of the Lower Cretaceous Longarm Formation, Queen Charlotte Islands, British Columbia; *in* Current Research, Part H, Geological Survey of Canada, Paper 89-1H, p. 39-46.  
Preliminary work suggests that the Longarm Formation was deposited in shallow-marine environments. The age of the formation in the central parts of the islands is Hauterivian to Aptian. On northern Graham Island the onset of deposition was during the Valanginian or earlier.
- Haggart, J.W. and Gamba, C.A.**  
**1990:** Stratigraphy and sedimentology of the Longarm Formation, southern Queen Charlotte Islands, British Columbia; *in* Current Research, Part F, Geological Survey of Canada, Paper 90-1F, p. 61-66.  
Important preliminary paper; the Longarm Formation shows an overall fining-upward trend reflecting a transgressive trend and accumulation in shelf environments.
- Haggart, J.W. and Higgs, R.**  
**1989:** A new Late Cretaceous mollusc fauna from the Queen Charlotte Islands, British Columbia; *in* Current Research, Part H, Geological Survey of Canada, Paper 89-1H, p. 59-64.  
Molluscs from marine shales apparently overlying the Honna Formation near Skidegate Inlet are Late Santonian in age. These shales are the youngest Cretaceous marine sediments yet found in the Queen Charlotte Islands.
- Haggart, J.W., Indrelid, J., Hesthammer, J., Gamba, C.A., and White, J.M.**  
**1990:** A geological reconnaissance of the Mount Stapleton-Yakoun Lake region, central Queen Charlotte Islands, British Columbia; *in* Current Research, Part F, Geological Survey of Canada, Paper 90-1F, p. 29-36.  
Documents a mid-Miocene or younger nonmarine sedimentary and volcanic unit, correlative in part with the Skonun Formation, was not involved in post-Early Eocene to Early Oligocene deformation in the region.
- Haggart, J.W., Lewis, P.D., and Hickson, C.J.**  
**1989:** Stratigraphy and structure of Cretaceous strata, Long Inlet, Queen Charlotte Islands, British Columbia; *in* Current Research, Part H, Geological Survey of Canada, Paper 89-1H, p. 65-72.  
In the Long Inlet area, Honna strata reflect rapid progradation of clastic systems into the region. A thick succession of mafic volcanic debris flows, scoria, and flow breccia conformably overlies and is interbedded with the Honna Formation.
- Haimila, N.E. and Procter, R.M.**  
**1982:** Hydrocarbon potential of offshore British Columbia; Geological Survey of Canada, Open File 824, 28 p.  
Review of knowledge of offshore B.C., including Queen Charlotte Basin. Little on hydrocarbon potential.
- Hail, R.L.**  
**1975:** Sexual dimorphism in Jurassic ammonites from the Queen Charlotte Islands; *Geoscience Canada*, v. 2, p. 21-25.  
Discussion of dimorphic ammonite pairs from the Yakoun Formation.
- Hall, R.L.**  
**1976:** Lower Bajocian (Jurassic) ammonoid faunas of the western Americas; Ph.D. thesis, McMaster University, Hamilton, Ontario, 239 p.  
Correlation of ammonite faunas from the lower part of the Yakoun Formation along Skidegate Inlet with faunas from Alaska, mainland western Canada and United States, and South America. Much of the thesis is dedicated to systematic paleontology. Published as Hall and Westermann (1980).
- Hall, R.L. and Westermann, G.E.G.**  
**1980:** Lower Bajocian (Jurassic) cephalopod faunas from western Canada and proposed assemblage zones for the Lower Bajocian of North America; *Palaontographica Americana*, v. 9, no. 52, 93 p.  
The published version of Hall (1976).
- Hamilton, T.**  
**1989:** Tertiary extensional volcanism and volcanotectonic interactions along the Queen Charlotte portion of the western Canadian continental margin; *in* Geological Association of Canada, Pacific Section, Northeast Pacific-North America Plate Interactions throughout the Cenozoic, Programme and Abstracts, unpaginated.  
Abstract; interprets the Masset Formation as basinal volcanic deposits related to extensive rifting or trans-tension.
- Hamilton, T.S. and Cameron, B.E.B.**  
**1989:** Hydrocarbon occurrences on the western margin of the Queen Charlotte Basin; *Bulletin of Canadian Petroleum Geology*, v. 37, p. 443-466.  
Lists hydrocarbon occurrences on the Queen Charlotte Islands. Principal source beds are Upper Triassic to Lower Jurassic Kunga and Maude groups. Potential reservoir facies occur in Cretaceous and Tertiary strata.
- Harper, J.R.**  
**1980:** Coastal processes on Graham Island, Queen Charlotte Islands, British Columbia; *in* Current Research, Part A, Geological Survey of Canada, Paper 80-1A, p. 13-18.  
An extensive beach-ridge plain is actively evolving on northeastern Graham Island. An extensive dune system is present and the shore is prograding at about 0.4 m/year. The sediment source may be a recently uplifted offshore platform.
- Hebda, R.J. and Mathewes, R.W.**  
**1986:** Radiocarbon dates from Anthony Island, Queen Charlotte Islands, and their geological and archaeological significance; *Canadian Journal of Earth Sciences*, v. 23, p. 2071-2076.  
Five radiocarbon dates, obtained during a major archaeological study, indicate that sea level has not exceeded 31.1 m in the last 12.3 thousand years.
- Hesthammer, J.**  
**1990:** Structural interpretation of Upper Triassic and Jurassic units exposed on central Graham Island, Queen Charlotte Islands, British Columbia; *in* Current Research, Part F, Geological Survey of Canada, Paper 90-1F, p. 11-18.  
Notes on Jurassic strata and structures in central Graham Island; a complement to Indrelid (1990).
- Hesthammer, J., Indrelid, J., and Ross, J.V.**  
**1989:** Preliminary structural studies of the Mesozoic rocks of central Graham Island, Queen Charlotte Islands, British Columbia; *in* Current Research, Part H, Geological Survey of Canada, Paper 89-1H, p. 19-22.  
Preliminary report based on 1988 field work in a small area north of Yakoun Lake. Documents the angular nature of the unconformity between the Maude and Yakoun groups.
- Hessner, C.J.**  
**1989:** North Pacific coastal refugia—the Queen Charlotte Islands in perspective; *in* The Outer Shores: based on the proceedings of the Queen Charlotte Islands First International Scientific Symposium, University of British Columbia, August 1984, G.G.E. Scudder and N. Gessler (ed.), Queen Charlotte Islands Museum Press, p. 91-106.  
Reviews the refugia problem and concludes that eastern Graham Island had only local ice cover in Wisconsin time and was deglaciated by at least 16 ka.
- Hicken, A. and Irving, E.**  
**1977:** Tectonic rotation in western Canada; *Nature*, v. 268, p. 219-220.  
Preliminary palaeomagnetic studies on the Karmutsen Formation, Tertiary plutons, and Masset Formation suggest that the Queen Charlotte Islands have rotated at least 25° clockwise since deposition of the Masset volcanics.
- Hickson, C.J.**  
**1983:** Structure and stratigraphy of the Masset Formation, Queen Charlotte Islands, British Columbia; *in* Current Research, Part E, Geological Survey of Canada, Paper 88-1E, p. 269-274.  
Preliminary report summarizing 1987 field work. Includes a summary of onshore K-Ar dating (Tertiary) of the Masset. K-Ar dates and lithologies of drill core from Hecate Strait (thought to be part of the Masset by other workers) suggests that these rocks should be excluded from the Masset. The Masset Formation probably does not extend any great distance beneath Hecate Strait.
- Hickson, C.J.**  
**1989:** An update on structure and stratigraphy of the Masset Formation, Queen Charlotte Islands, British Columbia; *in* Current Research, Part H, Geological Survey of Canada, Paper 89-1H, p. 73-79.  
The Masset Formation on Graham Island is a Late Oligocene to Late Miocene calc-alkaline suite. There is little indication of deformation aside from steep, north-trending faults. Attitudes of bedded rocks represent primary slopes of constructional volcanic landforms.
- Higgs, R.**  
**1988:** Cretaceous and Tertiary sedimentology, Queen Charlotte Islands, British Columbia; *in* Current Research, Part E, Geological Survey of Canada, Paper 88-1E, p. 261-264.  
Brief review of previous studies of the Cretaceous and Tertiary sediments and a list of objectives for the current study.
- Higgs, R.**  
**1983:** Sedimentology and tectonic implications of Cretaceous fan-delta conglomerates, Queen Charlotte Islands; *in* Sequences, Stratigraphy, Sedimentology: Surface and Subsurface, D.P. James and D.A. Leckie (ed.), Canadian Society of Petroleum Geologists, Memoir 15, p. 307-308.  
Extended abstract, suggesting that the Honna Formation accumulated in a westwardly migrating foreland basin.
- Higgs, R. (compiler)**  
**1983:** Some aspects of the petroleum geology of the Queen Charlotte Islands; Canadian Society of Petroleum Geologists, Field Trip Guide to Sequences, Stratigraphy, Sedimentology: Surface and Subsurface Technical Meeting, 72 p.  
Includes short, summary contributions on tectonic setting, stratigraphy, Honna Formation (R. Higgs); the Masset Formation (C.J. Hickson); reservoir aspects of Cretaceous and Tertiary strata (J.A.S. Fogarassy and W.C. Barnes); Lower Jurassic stratigraphy (G. Jakobs, H.W. Tipper and P.L. Smith); plutonism (R.G. Anderson); Triassic stratigraphy (E.S. Carter, A. Desrochers, M.J. Orchard and E.T. Tozer); sedimentology of the Kunga Group (Desrochers); organic geochemistry (R.L. Snowdon, M.G. Fowler and T.S. Hamilton); and CAI values of Triassic strata (Orchard). Pages 52-76 give field trip stops, all road accessible, for exposures of the Honna and Skonun formations (Higgs); the Haida Formation (Higgs and B.D. Bornholdt); the Kunga and Maude groups (Tipper, Smith and Jakobs); and the Masset Formation at Lawn Hill (Hamilton and B.E.B. Cameron).
- Higgs, R.**  
**1989:** Sedimentological aspects of the Skonun Formation, Queen Charlotte Islands, British Columbia; *in* Current Research, Part H, Geological Survey of Canada, Paper 89-1H, p. 87-94.  
Three on-land exposures of the Skonun Formation are thought to be delta-plain deposits. Iceberg dropstones occur in Upper Miocene strata at one locality.
- Higgs, R.**  
**1989:** Sedimentology and implications for hydrocarbon exploration of the "Hippra beds", Queen Charlotte Islands, British Columbia; *in* Current Research, Part H, Geological Survey of Canada, Paper 89-1H, p. 53-58.  
Conglomerate, sandstone, and mudstone of uncertain age are exposed on Hippra Island west of Graham Island. The rocks are thought to be lacustrine and braided-stream deposits; paleoflow was to the southwest.



- Higgs, R.**  
**1990:** Sedimentology and tectonic implications of Cretaceous fan-delta conglomerates, Queen Charlotte Islands, Canada; *Sedimentology*, v. 37, p. 83-103.  
 Interprets Honna Formation of the Skidegate Inlet region as mass-flow deposits representing an uncommon type of fan delta (deep water fan delta). Imbrications indicate an eastern source area; coarse clast size indicates a proximal source, possibly uplifted mountains in the Hecate Strait area.
- Holland, S.S. and Nasmith, H.W.**  
**1958:** Investigation of beach sands; British Columbia Department of Mines, 8 p.  
 Good descriptions of black sand deposits on northern and eastern Graham Island, with emphasis on their magnetite contents.
- Hopkins, W.S., Jr.**  
**1975:** Palynological study of Shell Anglo Harlequin D-86 well (NTS 102-O), offshore British Columbia; Geological Survey of Canada, Open File 268.  
 Preliminary report on palynology from the Shell Anglo Harlequin D-86 well, largely superseded by Hopkins (1981).
- Hopkins, W.S., Jr.**  
**1981:** Palynology of four offshore British Columbia wells; Geological Survey of Canada, Open File 808, 83 p.  
 This report provides age determinations and stratigraphic correlations for Shell Anglo Osprey, Harlequin, Auklet and Murrelet wells in Hecate Strait and Queen Charlotte Sound. Although the age assignments will likely be revised, this report is a very useful contribution to the Tertiary biostratigraphy of the Queen Charlotte wells.
- Horn, J.R.**  
**1982:** A snapshot of the Queen Charlotte fault zone obtained from P-wave refraction data; M.Sc. thesis, University of British Columbia, Vancouver, 79 p.  
 Gives a velocity model based on two profile shot in 1979 southwest of Moresby Island.
- Hutchison, W.W., Berg, H.C., and Okulitch, A.V. (compilers)**  
**1979:** Geology of Skeena River, British Columbia-Alaska; Geological Survey of Canada, Map 1385A.  
 Compilation at 1:1 000 000, with correlation charts. Region includes Queen Charlotte Islands and adjacent mainland and southeast Alaska. Out of date now, but still useful for general reference.
- Hyndman, R.D. and Ellis, R.M.**  
**1981:** Queen Charlotte fault zone: microearthquakes from a temporary array of land stations and ocean bottom seismographs; *Canadian Journal of Earth Sciences*, v. 18, p. 776-788.  
 Data show that the Queen Charlotte fault zone is nearly vertical and has a strike-slip component. The paper gives a model involving underthrusting and strike-slip faulting to account for the 15° difference between the relative motion of North American and Pacific plates predicted from plate tectonic models and the strike of the margin.
- Hyndman, R.D., Lewis, T.J., Wright, J.A., Burgess, M., Chapman, D.S., and Yamano, M.**  
**1982:** Queen Charlotte fault zone: heat flow measurements; *Canadian Journal of Earth Sciences*, v. 19, p. 1657-1669.  
 Heat flow measurements across the Queen Charlotte terrace show a continuous transition from very high deep-sea values on the west to low continental values on the Queen Charlotte Islands. The data are consistent with a model of oblique underthrusting of sea floor beneath the Queen Charlotte terrace. Heat flow measurements from the south end of the Queen Charlotte fault zone are consistent with a rift hypothesis.
- Indrelid, J.**  
**1990:** Stratigraphy and structures of Cretaceous units, central Graham Island, Queen Charlotte Islands, British Columbia; *in* Current Research, Part F, Geological Survey of Canada, Paper 90-1F, p. 5-10.  
 Description of Cretaceous stratigraphy and structures; documents post-Late Cretaceous compression. A complement to Hesthammer (1990).
- Jakobs, G.K.**  
**1989:** Toarcian (Lower Jurassic) biostratigraphy of the Queen Charlotte Islands, British Columbia; *in* Current Research, Part H, Geological Survey of Canada, Paper 89-1H, p. 35-37.  
 Note on field work in 1987 and 1988. The Toarcian stratigraphic succession on the Queen Charlotte Islands appears to be complete, except for one possible minor hiatus between the Whiteaves and Phantom Creek formations. The ammonite faunas are very diverse.
- Jakobs, G.K.**  
**1990:** A discussion of the Phantom Creek Formation of the Maude Group, Queen Charlotte Islands, British Columbia; *in* Current Research, Part F, Geological Survey of Canada, Paper 90-1F, p. 57-60.  
 Brief description and reinterpretation of the type section of the Phantom Creek Formation.
- Johnson, S.H.**  
**1972:** Crustal structure and tectonism in southeastern Alaska and western British Columbia from seismic refraction, seismic reflection, gravity, magnetic, and microearthquake measurements; Ph.D. thesis, Oregon State University, Corvallis, 129 p.  
 Crustal models for a large area that includes Dixon Entrance. See Johnson et al. (1972) in the Appendix (below).
- Kilty, K.T.**  
**1981:** Stress fields of the San Andreas and Queen Charlotte transform faults; *Tectonophysics*, v. 77, p. 203-212.  
 Calculations show that the hypothesis that Alaska acts as a continental buttress against deformation of the Canadian Cordillera along the Queen Charlotte transform is incorrect.
- Kníze, S.**  
**1976:** Marine deep seismic sounding off the coast of British Columbia; Ph.D. thesis, University of British Columbia, Vancouver.  
 Gives models for the upper crust in areas west of Queen Charlotte Islands and Queen Charlotte Sound.
- Kun, S., Champigny, N., and Sinclair, A.J.**  
**1981:** Genetic implications of fluid inclusion studies, Cinola gold deposit, Queen Charlotte Islands; *in* Geological Fieldwork 1980, British Columbia Ministry of Energy, Mines and Petroleum Resources, Paper 1981-1, p. 197-200.  
 Preliminary report; see Shen et al. (1982) for a final version.
- Leaming, S.**  
**1982:** Lapidary material on Graham Island, Queen Charlotte Islands group, British Columbia; *in* Current Research, Part A, Geological Survey of Canada, Paper 82-1A, p. 415-416.  
 Note on materials of interest to the rockhound in the Yakoun Haida, Masset and Sko-nun formations.
- Leslie, D.R.**  
**1989:** Petrography and sedimentology of an unnamed Upper Cretaceous to Lower Paleocene sedimentary unit, Queen Charlotte Basin, British Columbia; B.A.Sc. thesis, University of British Columbia, Vancouver.  
 Petrographic descriptions of some side-wall cores from the Sockeye E-66 and Coho I-74 wells.
- Lewis, P.D.**  
**1990:** New timing constraints on Cenozoic deformation in the Queen Charlotte Islands, British Columbia; *in* Current Research, Part F, Geological Survey of Canada, Paper 90-1F, p. 23-28.  
 Preliminary report on the Lower Cretaceous to Paleogene sedimentary rocks and the Upper Cretaceous and Paleogene volcanic rocks in the Long Inlet area. Four discrete episodes of deformation are: Late Cretaceous to early Tertiary shortening, early Tertiary extensional faulting, mid-Tertiary shortening, and late Tertiary to Holocene extensional faulting.
- Lewis, P.D. and Ross, J.V.**  
**1988:** Preliminary investigations of structural styles in Mesozoic strata of the Queen Charlotte Islands, British Columbia; *in* Current Research, Part E, Geological Survey of Canada, Paper 88-1E, p. 275-279.  
 Preliminary report on detailed structural mapping in the Skidegate Channel/Skidegate Inlet area. The major deformation, represented by northwest-trending open to tight buckle folds resulted from southwest-northeast shortening. In the Skidegate Channel area a stratigraphic contact can be traced across the previously inferred traces of the Rennell Sound Fault. Sutherland Brown's Rennell Sound Fault Zone is reinterpreted as an area of intense folding.
- Lewis, P.D. and Ross, J.V.**  
**1989:** Evidence for Late Triassic-Early Jurassic deformation in the Queen Charlotte Islands, British Columbia; *in* Current Research, Part H, Geological Survey of Canada, Paper 89-1H, p. 13-18.  
 Kunga Group strata on northwestern Graham Island are cut by thrust faults that record a north-verging compressional event that occurred in Late Triassic to Early Jurassic time.
- Lewis, T.J., Bentkowski, W.H., Bone, M., MacDonald, R., and Wright, J.A.**  
**1988:** Geothermal studies in Queen Charlotte Basin, British Columbia; *in* Current Research, Part E, Geological Survey of Canada, Paper 88-1E, p. 247-249.  
 Brief discussion of past and present heat flow studies; no data.
- Lewis, T.J., Bentkowski, W.H., Bone, M., and Wright, J.A.**  
**1989:** Note on the thermal structure of Queen Charlotte Basin, British Columbia; *in* Current Research, Part H, Geological Survey of Canada, Paper 89-1H, p. 121-125.  
 Preliminary results indicate low heat flux (50 mW m<sup>-2</sup>) on the western margin of Queen Charlotte Basin and higher values (75 mW m<sup>-2</sup>) on the eastern margin. Heat generation is generally low within the basin and on its margins.
- Luternauer, J.L.**  
**1972:** Patterns of sedimentation in Queen Charlotte Sound; Ph.D. thesis, University of British Columbia, Vancouver, 203 p.  
 Geomorphology and sediment dispersal in Queen Charlotte Sound. Described sediment texture, composition and distribution. Produced a detailed bathymetric map of Queen Charlotte Sound. Superseded by Luternauer and Murray (1983).
- Luternauer, J.L.**  
**1986:** Character and setting of sand and gravel bed forms on the open continental shelf off western Canada; *in* Shelf Sands and Sandstones, R.J. Knight and J.R. McLean, (ed.), Canadian Society of Petroleum Geologists, Memoir 11, p. 45-55.  
 Defines wave and current influences on the generation of recognized sand and gravel bedforms and identifies major sediment dispersal patterns on the shelf.
- Luternauer, J.L.**  
**1987:** Geohazards, lithology and shallow seismostratigraphy of the Moresby Trough/Middle Bank area, Queen Charlotte Sound, British Columbia; Geological Survey of Canada, Open File 1420.  
 Maps of an area in southern Hecate Strait based on high-resolution seismic profiles, acoustic reflection data, and core and grab samples. Shows potential geologic hazards to development.
- Luternauer, J.L. and Conway, K.W.**  
**1986:** Extensive postglacial debris flow on the central continental shelf off British Columbia; Geological Survey of Canada, Open File 1235; 2 sheets.  
 Core data and Huntex deep-tow seismic records are used to delineate deposits from a submarine slope failure in Queen Charlotte Sound.

**Luternauer, J.L. and Murray, J.W.**

**1983:** Late Quaternary morphologic development and sedimentation, central British Columbia continental shelf; Geological Survey of Canada, Paper 83-21, 38 p. Published version of Luternauer (1972) and the first detailed study of the morphology and sediments of part of the British Columbia continental shelf; contains much data. Queen Charlotte Sound is dominated by banks capped with sand and gravel, and troughs floored with gravel, sand, and mud. Most major morphological features were probably sculpted by grounded ice. The oceanographic regime which prevailed when sea level was lower than at present controlled the formation of secondary features.

**Luternauer, J.V., Barrie, J.V., Conway, K.W., and Caltagirone, A.**

**1990:** Surficial Geology of the Queen Charlotte Basin: Hecate Strait-Queen Charlotte Sound; Geological Survey of Canada, Open File 2195, 8 maps at 1:250 000.

**Luternauer, J.V., Barrie, J.V., Conway, K.W., and Caltagirone, A.**

**1990:** Surficial Geology of the Queen Charlotte Basin: Queen Charlotte Sound; Geological Survey of Canada, Open File 2196, 8 maps at 1:250 000.

Together with the three open files by Barrie, Luternauer, and Conway, these open files provide a substantial body of data for the continental shelf of western Canada. The various maps show geophysical survey track lines; seabed sampling, photography and current meter stations, surficial sediment grain size data, and surficial features and geohazards.

**Luternauer, J.L., Clague, J.J., Conway, K.W., Barrie, J.V., Blaise, B., and Mathewes, R.W.**

**1989:** Late Pleistocene terrestrial deposits on the continental shelf of western Canada: evidence for rapid sea-level change at the end of the last glaciation; *Geology*, v. 17, p. 357-360.

New evidence indicates that large areas of the B.C. continental shelf, including much of Hecate Strait, were subaerially exposed 11-12 ka down to the present 95-m isobath.

**Luternauer, J.L., Conway, K.W., Clague, J.J., and Blaise, B.**

**1989:** Late Quaternary geology and geochronology of central continental shelf off western Canada; *Marine Geology*, v. 89, p. 57-68.

Piston cores and high-resolution seismic profiles from three troughs in Queen Charlotte Sound were used to identify five postglacial units. Results confirm that sea level was lower than at present between about 12.9 and 10.2 ka.

**MacKenzie, J.D.**

**1914:** South-central Graham Island, B.C.; Geological Survey of Canada, Summary Report, 1913, p. 34-54.

Preliminary results of MacKenzie's first summer of field work; superseded by MacKenzie (1916).

**MacKenzie, J.D.**

**1915:** Graham Island, British Columbia; Geological Survey of Canada, Summary Report, 1914, p. 33-37.

Short note on MacKenzie's second summer of field work; superseded by MacKenzie (1916). First use of the term Etheline Formation.

**MacKenzie, J.D.**

**1916:** Geology of Graham Island, British Columbia; Geological Survey of Canada, Memoir 88, 221 p. Contains Map 176A, Graham Island (1:253 440) and Map 177A, Southern Portion of Graham Island (1:126 720).

An excellent report, the most comprehensive since Dawson, with a good map at 4 miles to the inch of Graham Island. MacKenzie proposed a number of new stratigraphic names (Maude, Yakoun, Masset, and Skonun) that are still in use. He divided the Vancouver Group on Graham Island into two formations: the Lower Jurassic and possibly Triassic Maude Formation and the Middle Jurassic Yakoun Formation. He divided the Tertiary rocks of Graham Island into three units: the Eocene Etheline Formation, the Pliocene-Miocene Skonun Formation, and the Pliocene Masset Formation. He was the first to note that the Tertiary volcanic rocks are of more than one age.

**Mackie, D.J., Clowes, R.M., Dehler, S.A., Ellis, R.M., and Morel-à-l'Hussier, P.**

**1989:** The Queen Charlotte Islands refraction project. Part II. Structural model for transition from Pacific plate to North American plate; *Canadian Journal of Earth Sciences*, v. 26, p. 1713-1725.

Gives a velocity model for lithospheric structure beneath Queen Charlotte Islands and Hecate Strait. Crust is thin (21-27 km) beneath Queen Charlotte Islands. The Moho beneath Hecate Strait dips 4° eastward as the crust thickens to 32 km.

**Maccauley, G.**

**1983:** Source rock-oil shale potential of the Jurassic Kunga Formation, Queen Charlotte Islands; Geological Survey of Canada, Open File 921.

Report on source rock-oil shale potential of the Jurassic Kunga Formation. Contains core descriptions, Rock-Eval pyrolysis data and XRD data. Contains a map of Skidegate Inlet and southern Graham Island showing outcrop and borehole locations with thermal maturation levels, and estimates the economic potential for each area.

**Maccauley, G., Snowden, L.R., and Ball, F.D.**

**1985:** Geochemistry and geological factors governing exploitation of selected Canadian oil shale deposits; Geological Survey of Canada, Paper 85-13, 65 p. Pages 45-50 treat the Kunga Formation. Contains data on mineralogy, organic geochemistry and petrology, and kerogen-pyrolyzate-oil characteristics.

**Mandy, J.T.**

**1934:** Gold-bearing black-sand deposits of Graham Island, Queen Charlotte Islands; Canadian Institute of Mining and Metallurgy, Transactions, v. 37, p. 563-572. General description and possible methods of recovery.

**Martin, H.A. and Rouse, G.E.**

**1966:** Palynology of Late Tertiary sediments from the Queen Charlotte Islands, British Columbia; *Canadian Journal of Botany*, v. 44, p. 171-208, plates.

The first detailed palynological study of the Skonun Formation. The assemblages suggest a late Miocene to early Pliocene age; climatic conditions were humid and more temperate than at present. Much systematic paleontology.

**Mathewes, R.W.**

**1989:** Paleobotany of the Queen Charlotte Islands; in *The Outer Shores: based on the proceedings of the Queen Charlotte Islands First International Scientific Symposium*, University of British Columbia, August 1984, G.G.E. Scudder and N. Gessler (ed.), Queen Charlotte Islands Museum Press, p. 75-90.

Review article, with emphasis on the Tertiary and (particularly) Pleistocene.

**Mathewes, R.W. and Clague, J.J.**

**1982:** Stratigraphic relationships and paleoecology of a late-glacial peat bed from the Queen Charlotte Islands, British Columbia; *Canadian Journal of Earth Sciences*, v. 19, p. 1185-1195.

Gives pollen zones and 13 radiocarbon dates from sea cliffs on northern Graham Island, with a discussion of the glacial refugium controversy.

**McConnell, R.G.**

**1910:** Texada Island and Moresby Island, B.C.; Geological Survey of Canada, Summary Report, 1909, p. 69-83.

Half the paper describes mineral deposits on Moresby Island.

**McLearn, F.H.**

**1927:** Some Canadian Jurassic faunas; *Royal Society of Canada, Transactions*, 3rd Series, v. 21, sec. IV, p. 61-73.

Three pages of this paper are McLearn's first contribution to Jurassic paleontology on the Queen Charlotte Islands. Deals summarily with the Yakoun and Maude groups in Skidegate Inlet.

**McLearn, F.H.**

**1929:** Contributions to the stratigraphy and palaeontology of Skidegate Inlet, Queen Charlotte Islands, B.C.; Geological Survey of Canada, Museum Bulletin 54, p. 1-27.

Systematic descriptions of ammonites from the Yakoun Group, collected by McLearn in 1921.

**McLearn, F.H.**

**1930:** Notes on some Canadian Mesozoic faunas; *Transactions of the Royal Society of Canada, 3rd Series*, v. 24, sect. 4, p. 1-7.

A discussion of the age of the Maude Formation with the assessment that it is of Toarcian age. New species of ammonites are described.

**McLearn, F.H.**

**1932:** Contributions to the stratigraphy and palaeontology of Skidegate Inlet, Queen Charlotte Islands, B.C. (continued); *Royal Society of Canada, Transactions*, 3rd Series, v. 26, sec. IV, p. 51-80, plates.

Continues the systematic ammonite descriptions begun in McLearn (1929).

**McLearn, F.H.**

**1949:** Jurassic formations of Maude Island and Alliford Bay, Skidegate Inlet, Queen Charlotte Islands, British Columbia; Geological Survey of Canada, Bulletin 12, 19 p.

A summary of work to 1948 on Jurassic stratigraphic nomenclature and paleontology of the Skidegate Inlet area.

**McLearn, F.H.**

**1963:** Note on *Anagaudryceras sacya* (Forbes); *The Canadian Field-Naturalist*, v. 77, no. 2, p. 126-127.

Note describing the morphology of specimens of this Cretaceous ammonite from the Queen Charlotte Islands.

**McLearn, F.H.**

**1972:** Ammonoids of the Lower Cretaceous sandstone member of the Haida Formation, Skidegate Inlet, Queen Charlotte Islands, western British Columbia; Geological Survey of Canada, Bulletin 188, 78 p., plates.

Descriptions of sections and ammonites collected by McLearn and earlier workers from the Haida Formation in Skidegate Inlet.

**McWhae, J.R., Ross, R., and Ross, K.**

**1988:** Evolution and hydrocarbon potential of Queen Charlotte Basin, Canada; *American Association of Petroleum Geologists, Bulletin*, v. 72, p. 222.

Abstract; treats the Queen Charlotte Basin as a complex Tertiary rift basin with extensive coeval volcanics.

**Moslow, T.F., Barrie, J.V., and Luternauer, J.L.**

**1989:** Sedimentary facies of a high-energy tide-dominated continental shelf, western Canada; in *Modern and Ancient Examples of Clastic Tidal Deposits—A Core and Peel Workshop*, G.E. Reinson (ed.), Canadian Society of Petroleum Geologists, Second International Research Symposium on Clastic Tidal Deposits, Calgary, August 22-25, 1989, p. 25-36.

Six sedimentary facies were identified in vibracores from Holocene deposits on sand ridges and medium- to large-scale bedforms on the tide-dominated continental shelf in Hecate Strait.

**Moslow, T.F., Luternauer, J.L., and Conway, K.W.**

**1989:** Neotectonics and sedimentation patterns in Moresby Trough, central continental shelf of western Canada; in *Current Research, Part H*, Geological Survey of Canada, Paper 89-1H, p. 135-140.

High resolution seismic profiles suggest Quaternary faulting along the northwest margin of Moresby Trough. Faulting appears to be syndepositional and possibly listric normal. The largest offset seen is 2.5 m.

#### Offshore Surveys and Positioning Services Ltd.

**1985:** Nearshore sedimentation and recent tectonics, Virago Sound, northern Graham Island, Queen Charlotte Islands, British Columbia; Geological Survey of Canada, Open File 1157.

Three maps at 1:25 000 of Virago Sound: surficial geology, seabed morphology, and bathymetry.

#### Offshore Surveys and Positioning Services Ltd.

**1986:** Bathymetry, surficial sediments and seabed morphology off northwestern Graham Island, Queen Charlotte Islands, British Columbia; Geological Survey of Canada, Open File 1280.

Three maps at 1:50 000 of northwestern Graham Island: surficial geology, seabed morphology and bathymetry.

**Pálffy, J., McFarlane, R.B., Smith, P.L., and Tipper, H.W.**

**1990:** Potential for ammonite biostratigraphy of the Sinemurian part of the Sandilands Formation, Queen Charlotte Islands, British Columbia; *in* Current Research, Part F, Geological Survey of Canada, Paper 90-1F, p. 47-50.

Preliminary results indicate the presence of a complete Sinemurian stratigraphic section.

**Patterson, R.T.**

**1988:** Early Miocene to Quaternary foraminifera from three wells in the southern Queen Charlotte Basin; Geological Survey of Canada, Open File 1985.

Forty-two species of benthic and planktic foraminifera were recovered from the Shell Anglo Murrelet L-15, Harlequin D-86, and Osprey D-36 wells; includes environmental and age interpretations and a correlation chart.

**Patterson, R.T.**

**1988:** Early Miocene to Quaternary foraminifera from three wells in the Queen Charlotte Basin off the coast of British Columbia; *in* Sequences, Stratigraphy, Sedimentology: Surface and Subsurface, D.P. James and D.A. Leckie (ed.), Canadian Society of Petroleum Geologists, Memoir 15, p. 497.

Abstract with summary correlation chart, based on Patterson (1985a).

**Patterson, R.T.**

**1989:** Neogene foraminiferal biostratigraphy of the southern Queen Charlotte Basin; *in* Contributions to Canadian Paleontology, Geological Survey of Canada, Bulletin 396, p. 229-265.

Published version of Patterson (1985a), with correlation charts, plates.

**Pessagno, E.A., Jr. and Blome, C.D.**

**1980:** Upper Triassic and Jurassic Pantanelliinae from California, Oregon and British Columbia; Micropaleontology, v. 26, p. 225-273.

Includes taxonomic descriptions of Upper Norian radiolarians from the "black limestone" member (Peril Formation) on Kunga Island.

**Pessagno, E.A., Jr. and Whalen, P.A.**

**1982:** Lower and Middle Jurassic radiolaria (multicyrtid Nassellariina) from California, east-central Oregon and the Queen Charlotte Islands, B.C.; Micropaleontology, v. 28, p. 111-169.

Taxonomic study of Hettangian and Sinemurian radiolaria from the Sandilands Formation at Kunga Island.

**Pessagno, E.A., Jr. and Whalen, P.A.**

**1986:** Jurassic Nassellariina from North American geologic terranes; *Bulletins of American Paleontology*, v. 91, no. 326, 75 p.

The part dealing with the Queen Charlotte Islands treats the taxonomy of the Hettangian and Sinemurian radiolarians from Kunga Island.

**Pessagno, E.A., Jr., Blome, C.D., Carter, E.S., MacLeod, N., Whalen, P.A., and Yeh, K.-Y.**

**1987:** Preliminary radiolarian zonation for the Jurassic of North America; *in* Studies of North American Jurassic Radiolaria, Part 2, Cushman Foundation for Foraminiferal Research, Special Publication no. 23, p. 1-18.

Parts dealing with the Hettangian, Sinemurian, and Toarcian are based on material from the Queen Charlottes.

**Pike, C.J.**

**1986:** A seismic refraction study of the Hecate sub-basin, British Columbia; M.Sc. thesis, University of British Columbia, 133 p.

Preliminary study of upper crustal velocity structure beneath Hecate Strait. Velocities near 6 km/s are reached by 5 km depth and velocities near 6.5 km/s are interpreted at 7 km depth.

**Poulton, T.P.**

**1981:** Stratigraphic distribution and taxonomic notes on bivalves of the Bathonian and Callovian (Middle Jurassic) Upper Yakoun Formation, Queen Charlotte Islands, British Columbia; *in* Current Research, Part B, Geological Survey of Canada, Paper 81-1B, p. 63-71.

Preliminary report includes biostratigraphy and taxonomic descriptions of Middle Jurassic bivalves. Report was prepared as a companion to the biostratigraphic report by Tipper and Cameron (1980).

**Riccardi, A.C.**

**1981:** An Upper Cretaceous ammonite and inoceramids from the Honna Formation, Queen Charlotte Islands, British Columbia; *in* Current Research, Part C, Geological Survey of Canada, Paper 81-1C, p. 1-8.

New ammonite and mollusc collections from the lower part of the Honna Formation and the upper part of the Haida Formation suggests the absence of a prolonged hiatus between the two units and confirms their partial interfingering.

**Richardson, J.**

**1873:** Report on the coal-fields of Vancouver and Queen Charlotte Islands; Geological Survey of Canada, Report of Progress for 1872-1873, p. 32-65.

The first geological study of the Queen Charlotte Islands (p. 56-65). Richardson spent twelve days on the islands in 1872, mostly evaluating the coal potential in the mines at Cowgitz. However, he also made brief examinations of the shoreline along Skidegate Inlet and Channel. He divided the "coal bearing rocks of the Queen Charlotte Islands" into three sedimentary units which together lie in a north-south trough bounded to the west by a "high range of volcanic rocks". He did not suggest an age for the volcanic rocks but assigned a Jurassic-Cretaceous age to the coal-bearing rocks.

**Riddihough, R.P.**

**1982:** Contemporary movements and tectonics on Canada's west coast: a discussion; *Tectonophysics*, v. 86, p. 319-341.

Tidal records and geodetic surveys show consistent patterns of contemporary uplift (2 mm/year) on the outer coast and subsidence (1-2 mm/year) on the inner coast. The "hinge line" runs through Hecate and Georgia straits.

**Rogers, G.C.**

**1982:** Revised seismicity and revised fault plane solutions for the Queen Charlotte Islands region; Earth Physics Branch, Open File 82-23, 57 p.

A revised seismicity pattern, based on data from 1900 to 1980. Large earthquakes show a strong correlation with the Queen Charlotte Fault scarp and little or no seismicity on other major fault systems on the islands. The distribution of large earthquakes along the Queen Charlotte Fault suggests that two major seismic gaps may be present. There have been no confirmed large earthquakes in Hecate Strait or Queen Charlotte Sound.

**Rogers, G.C.**

**1987:** Seismic gaps along the Queen Charlotte fault; *Earthquake Prediction Research*, v. 4, p. 1-11.

Points out that there is a seismic gap at the south end of the Queen Charlotte fault and that a previously suggested seismic gap just north of the Queen Charlotte Islands was included in the 1949 rupture.

**Rohr, K. and Dietrich J.R.**

**1990:** Deep seismic survey of the Queen Charlotte Basin; Geological Survey of Canada, Open File 2258, 7 sheets.

Reflection data, both stacked and migrated, for 7 lines in Queen Charlotte Sound and Hecate Strait.

**Rohr, K.M.M., Spence, G., Asudeh, I., Ellis, R., and Clowes, R.**

**1989:** Seismic reflection and refraction experiment in the Queen Charlotte Basin, British Columbia; *in* Current Research, Part H, Geological Survey of Canada, Paper 89-1H, p. 3-5.

Outlines data collection procedures for the 1100 km of data obtained from 8 lines in 1988.

**Samson, J.**

**1984:** An overview of coastal and marine gold placer occurrences in Nova Scotia and British Columbia; Departments of Energy, Mines and Resources and Indian and Northern Affairs, Canadian Oil and Gas Lands Administration, Ocean Mining Division Document 1984-3.

Pages 107-134 contain an excellent review of what is known about the black-sand beach deposits on the Queen Charlottes.

**Sangster, D.F.**

**1964:** The contact metasomatic magnetite deposits of southwestern British Columbia; Ph.D. thesis, University of British Columbia, Vancouver, 266 p.

Although mainly concerned with Vancouver Island, this thesis contains descriptions and interpretations of the main Fe-Cu skarn deposits on the Queen Charlotte Islands.

**Sangster, D.F.**

**1969:** The contact metasomatic magnetite deposits of southwestern British Columbia; Geological Survey of Canada, Bulletin 172, 82 p.

The published version of Sangster (1969).

**Sawyer, B. (compiler)**

**1989:** Physiography, Dixon Entrance—Hecate Strait; Geological Survey of Canada, Map 1-1989 (1:250 000).

**Sawyer, B. (compiler)**

**1989:** Physiography, Graham Island—Dixon Entrance; Geological Survey of Canada, Map 2-1989 (1:250 000).

**Sawyer, B. (compiler)**

**1989:** Physiography, Hecate Strait—Queen Charlotte Sound; Geological Survey of Canada, Map 3-1989 (1:250 000).

**Sawyer, B. (compiler)**

**1989:** Physiography, Moresby Island—Hecate Strait; Geological Survey of Canada, Map 4-1989 (1:250 000).

**Sawyer, B. (compiler)**

**1989:** Physiography, Queen Charlotte Sound; Geological Survey of Canada, Map 5-1989 (1:250 000).

These five excellent maps show bathymetry and topography for Queen Charlotte Islands and Basin, parts of mainland British Columbia, and the Pacific Ocean immediately west of Queen Charlotte Islands. Bathymetry is shown with 5 m contours where space allows and 50 m elsewhere. Land elevations are shown with 50 m contours. The contours have been "illuminated" from a westerly direction.

**Seemann, D.A. and Tiffin, D.L.**

**1980:** Physiography of Dixon Entrance and approaches, British Columbia and Alaska; Geological Survey of Canada, Open File 684, 1 map.

Bathymetric map (1:250 000) of Dixon Entrance.

**Seemann, D.A., Collins, A., and Sweeney, J.F.**

**1988:** Gravity measurements on the Queen Charlotte Islands, British Columbia; in *Current Research, Part E, Geological Survey of Canada, Paper 88-1E*, p. 283-286.

Preliminary results of the 1987 field survey on Graham Island, with some data.

**Shen, K., Champigny, N., and Sinclair, A.J.**

**1982:** Fluid inclusion and sulphur isotope data in relation to genesis of the Cinola gold deposit, Queen Charlotte Islands, B.C.; in *Geology of Canadian Gold Deposits*, R.W. Hodder and W. Petruk (ed.), Canadian Institute of Mining and Metallurgy, Special Volume 24, p. 255-257.

Ore fluids have low salinities and low CO<sub>2</sub> contents, suggesting that the fluids originated from pore water in the Skonun Formation. Mineral deposition occurred at about 160 and 270°C.

**Shouldice, D.H.**

**1971:** Geology of the western Canadian continental shelf; *Bulletin of Canadian Petroleum Geology*, v. 19, p. 405-436.

This important paper discusses Tertiary stratigraphy and basin geometry of the Queen Charlotte and Tofino basin using geological and geophysical data collected by Shell Canada during the 1960s. Tertiary volcanism in the Queen Charlotte basin was followed by successive periods of subsidence and sedimentation followed by uplift and erosion.

**Shouldice, D.H.**

**1973:** Western Canadian Continental Shelf; in *The Future Petroleum Provinces of Canada - Their Geology and Potential*, R.G. McCrossan (ed.), Canadian Society of Petroleum Geologists, Memoir 1, p. 7-35.

Essentially the same paper as Shouldice (1971).

**Smith, P.L., Tipper, H.W., and Palfy, J.**

**1990:** Lower Jurassic biostratigraphy of the Fannin and Ghost Creek formations, Kunga Island, British Columbia; in *Current Research, Part F, Geological Survey of Canada, Paper 90-1F*, p. 51-54.

Brief description of a new stratigraphic section spanning the boundary between the Kunga and Maude groups.

**Smith, P.L., Tipper, H.W., Taylor, D., and Guex, J.**

**1988:** An ammonite zonation for the Lower Jurassic of Canada and the United States: the Pliensbachian; *Canadian Journal of Earth Sciences*, v. 25, p. 1503-1523.

This paper is based on data from throughout western North America. Stratotypes for three of the five proposed ammonite zones in the Pliensbachian are in Fannin Bay on the Queen Charlotte Islands. The paper outlines the biostratigraphy of the Ghost Creek, Rennell Junction, and Fannin formations.

**Smith, R.K.**

**1965:** Glacio-marine foraminifera of British Columbia and southeast Alaska; Ph.D. thesis, University of British Columbia, Vancouver, 228 p.

Includes systematic descriptions of foraminifera from two samples from eastern Graham Island.

**Snavely, P.D., Jr., Tiffin, D.L., and Tompkins, D.H.**

**1980:** Seismic reflection profiles across the Queen Charlotte Fault Zone, Dixon Entrance, Canada-United States; *United States Geological Survey, Open File 80-1063*.

A profile extending west from near 123°W, 54°40'N; no interpretation.

**\* Snavely, P.D., Jr., Wagner, H.C., and Tompkins, D.H.**

**1981:** Preliminary geologic interpretation of a seismic reflection profile across the Queen Charlotte Island fault system, Dixon Entrance, Canada-United States; *United States Geological Survey, Open File 81-299*.

**Snowdon, L.R., Fowler, M.G., and Hamilton, T.S.**

**1988:** Progress report on organic geochemistry, Queen Charlotte Islands, British Columbia; in *Current Research, Part E, Geological Survey of Canada, Paper 88-1E*, p. 251-253.

Study of the source rock potential of various rock units. Rock-Eval/TOC analyses by Macauley (1983) were rerun and new samples were analyzed; some data.

**Souther, J.G.**

**1988:** Implications for hydrocarbon exploration of dyke emplacement in the Queen Charlotte Islands, British Columbia; in *Current Research, Part E, Geological Survey of Canada, Paper 88-1E*, p. 241-245.

First preliminary report on dyke swarms, discussion regional distribution, age and association, lithology, structural implications, thermal environment, and effects on hydrocarbon source rocks.

**Souther, J.G.**

**1989:** Dyke swarms in the Queen Charlotte Islands, British Columbia; in *Current Research, Part H, Geological Survey of Canada, Paper 89-1H*, p. 117-120.

Preliminary report on second summer of field work, describing systematic regional variations in orientation and chemical composition. The patterns are consistent with extension and dyke emplacement related to dextral movements along the western margin of Queen Charlotte Basin.

**Souther, J.G. and Bakker, E.**

**1988:** Petrography and chemistry of dykes in the Queen Charlotte Islands, British Columbia; *Geological Survey of Canada, Open File 1833*, 1 sheet.

Reconnaissance petrography and chemistry (22 whole-rock analyses) of dykes from six swarms.

**Stacey, R.A.**

**1975:** Structure of the Queen Charlotte Basin; in *Canada's Continental Margins and Offshore Petroleum Exploration*, C.J. Yorath, E.R. Parker, and D.J. Glass (ed.), Canadian Society of Petroleum Geologists, Memoir 4, p. 723-741.

A review of the available geophysical data, including that from Shell Canada, with emphasis on gravity data. Suggests that Tertiary volcanics and sediments that floor the basin are underlain by volcanics such as the Karmutsen Formation in the north and sediments such as the Nanaimo Group in the south.

**Stacey, R.A., Boyd, J.B., Stephens, L.E., and Burke, W.E.F.**

**1973:** Gravity measurements in British Columbia, with maps 152, 153, 154 and 155; *Earth Physics Branch, Gravity Map Series*.

Map 152 (1:1 000 000) covers the Queen Charlotte Islands, Hecate Strait, Queen Charlotte Sound, and the adjacent mainland. Text describes data collection and reduction methods.

**Stacey, R.A. and Stephens, L.E.**

**1969:** An interpretation of gravity measurements on the west coast of Canada; *Canadian Journal of Earth Sciences*, v. 6, p. 463-474.

Regional gravity studies show a positive Bouguer anomaly along the continental margin. A negative anomaly along the Coast Mountains is attributed to thickening of the crust beneath the mountains. On the eastern side of Queen Charlotte Islands and in Hecate Strait an Queen Charlotte Sound the average Bouguer anomaly is roughly zero, with local anomalies superimposed on a fairly flat gravity field.

**Sutherland Brown, A.**

**1966:** Tectonic history of the Insular Belt of British Columbia; in *Tectonic History and Mineral Deposits of the Western Cordillera*, Canadian Institute of Mining and Metallurgy, Special Volume 8, p. 83-100.

Summary paper with many figures; leans heavily on the author's work on Queen Charlotte Islands.

**Sutherland Brown, A.**

**1968:** Geology of the Queen Charlotte Islands, British Columbia; *British Columbia Department of Mines and Petroleum Resources, Bulletin 54*, 226 p. Contains Figure 5, sheets A, B, and C, *Geology of the Queen Charlotte Islands (1:125 000)*.

This superb report, based on careful field work from 1958 to 1965, remains the standard reference to the geology of the Queen Charlotte Islands. The geological map remains the only one to give complete coverage of the islands. Sutherland Brown revised and refined the stratigraphy, introduced the stratigraphic terms Kunga and Longarm, and gave an integrated tectonic history for the area. He recognized a pattern of major, northwest-trending faults; these were active since at least Early Cretaceous time and combine strike-slip and normal, east-side-down motion. There is extensive treatment of the glacial history of the islands, and the last third of the volume describes the known mineral and hydrocarbon deposits on the islands.

**Sutherland Brown, A. and Jeffery, W.G.**

**1960:** Preliminary geological map, southern Queen Charlotte Islands; *British Columbia Department of Mines*.

Preliminary map (at 1:125 000) of the Queen Charlotte Islands south of 53°, with notes, based on field work in 1958 and 1959. Introduces the term Kunga Formation for the Upper Triassic sedimentary sequence. Superseded by Sutherland Brown (1968).

**Sutherland Brown, A. and Nasmith, H.**

**1962:** The glaciation of the Queen Charlotte Islands; *The Canadian Field-Naturalist*, v. 76, p. 209-219.

Well-illustrated paper; data indicate that almost the entire land area of the Queen Charlotte Islands was ice-covered during Wisconsin time.

**Sutherland Brown, A., Yorath, C.J., and Tipper, H.W.**

**1983:** Geology and tectonic history of the Queen Charlotte Islands; *Geological Association of Canada, Annual Meeting, Victoria, Field Trip Guidebook, Trip 8*, 21 p.

Guidebook covering Graham Island and the northern part of Moresby Island. Reviews the stratigraphy, structure, and current tectonic models.

**Sutherland Brown, A. and Yorath, C.J.**

**1989:** Geology and non-renewable resources of the Queen Charlotte Islands; in *The Outer Shores: based on the proceedings of the Queen Charlotte Islands First International Scientific Symposium, University of British Columbia, August 1984*, G.G.E. Scudder and N. Gessler (ed.), Queen Charlotte Islands Museum Press, p. 3-26.

A review for informed lay readers of the geology of the Queen Charlotte Islands. Despite the 1989 date, the paper is badly out of date. Excellent photographs and diagrams.

**Sweeney, J.F. and Seemann, D.A.**

**1989:** Gravity measurements over the Burnaby Island pluton, Queen Charlotte Islands, British Columbia; in *Current Research, Part H, Geological Survey of Canada, Paper 89-1H*, p. 113-115.

A local gravity anomaly of about -8 to -11 mGal indicates that the Burnaby Island pluton has steep sides and is smaller than suggested by the strong magnetic anomaly high measured over the pluton.

**Taite, S.**

**1990:** Observations on structure and stratigraphy of the Sewell Inlet-Tasu Sound area, Queen Charlotte Islands, British Columbia; in *Current Research, Part F, Geological Survey of Canada, Paper 90-1F*, p. 19-22.

Preliminary report on stratigraphy and structure in this area.

**Tatham, R.H. and Savino, J.M.**

**1974:** Faulting mechanisms for two oceanic earthquake swarms; *Journal of Geophysical Research*, v. 79, p. 2643-2652.

Uses long-period surface waves from earthquake swarms to infer that motion on the Queen Charlotte fault was dominantly strike-slip.



Thompson, R.I.

**1988:** Late Triassic through Cretaceous geological evolution, Queen Charlotte Islands, British Columbia; in *Current Research, Part E, Geological Survey of Canada, Paper 88-1E*, p. 217-219.

Preliminary report, based on 1987 field work. Upper Triassic and Lower Jurassic Kunga and Maude groups were deformed in mid-Jurassic time. Since then, uplift, erosion and deposition associated with the formation of successor basins was accompanied by three episodes of contraction faulting. No evidence of significant strike slip-faulting was found.

Thompson, R.I. and Thorkelson, D.

**1989:** Regional mapping update, central Queen Charlotte Islands, British Columbia; in *Current Research, Part H, Geological Survey of Canada, Paper 89-1H*, p. 7-11.

Folding occurred prior to, or during, Middle Jurassic volcanism, and after deposition of Upper Cretaceous Honna conglomerate. Block faults were active from Middle Jurassic to late Tertiary. Neither the Rennell Sound fold belt nor the northern strands of the Louscoone Inlet Fault were zones of significant strike-slip faulting during Tertiary time.

Tiffin, D.L. and Currie, R.G.

**1975:** Magnetic anomaly with respect to IGRF 1966.0, Queen Charlotte Sound, British Columbia; Geological Survey of Canada, Open File 393.

Map at 1:500 000.

Tiffin, D.L. and Seemann, D.A.

**1975:** Bathymetry map of the continental margin of western Canada; Geological Survey of Canada, Open File 301.

Timms, C.E.

**1989:** The origin and tectonic setting of Tow Hill, Queen Charlotte Islands; B.Sc. thesis, McMaster University, Hamilton, Ontario, 78 p.

Field and petrographic descriptions of Tow Hill, and 10 whole-rock chemical analyses for major, trace, and rare earth elements. The flow or sill formed in a rift environment.

Tipper, H.W.

**1989:** Lower Jurassic (Hettangian and Sinemurian) biostratigraphy, Queen Charlotte Islands, British Columbia; in *Current Research, Part H, Geological Survey of Canada, Paper 89-1H*, p. 31-33.

An exposure of Sandilands Formation at Kennecott Point spans the Triassic-Jurassic boundary. Lower, Middle, and Upper Hettangian ammonites appear to be present.

Tipper, H.W. and Cameron, B.E.B.

**1980:** Stratigraphy and paleontology of the Upper Yakoun Formation (Jurassic) in Aliford Bay Syncline, Queen Charlotte Islands, British Columbia; in *Current Research, Part C, Geological Survey of Canada, Paper 80-1C*, p. 37-44.

Mainly biostratigraphy of the sedimentary part of the Yakoun, with short sections on structure and regional correlations.

Tipper, H.W. and Carter, E.S.

**1990:** Evidence for defining the Triassic-Jurassic boundary at Kennecott Point, Queen Charlotte Islands, British Columbia; in *Current Research, Part F, Geological Survey of Canada, Paper 90-1F*, p. 37-41.

A minor disturbance within sediments of the Sandilands Formation probably represents the Triassic-Jurassic boundary.

Vellutini, D.

**1988:** Organic maturation and source rock potential of Mesozoic and Tertiary strata, Queen Charlotte Islands, British Columbia; M.Sc. thesis, University of British Columbia, Vancouver, 262 p.

A vitrinite reflectance and Rock-Eval study of Mesozoic and Tertiary strata, containing much useful data. The level of organic maturation (%Rorand) decreases from 2.40-5.80 for Upper Triassic and Lower Jurassic strata on Moresby Island to 0.15-2.43 for Cretaceous and Tertiary strata on Graham Island. Mean total organic carbon contents are generally low (0.06%) to moderately high (3.6%) and are locally higher in the black limestone member of the Kunga Group and in the Sandilands and Ghost Creek formations.

Vellutini, D. and Bustin, R.M.

**1988:** Preliminary results on organic maturation of the Tertiary Skonun Formation, Queen Charlotte Islands, British Columbia; in *Current Research, Part E, Geological Survey of Canada, Paper 88-1E*, p. 255-258.

Preliminary results of vitrinite reflectance studies. The Skonun is generally immature, except in the Port Louis well and lower parts of Tow Hill well.

Warner, B.

**1984:** Late Quaternary paleoecology of eastern Graham Island, Queen Charlotte Islands, British Columbia, Canada; Ph.D. thesis, Simon Fraser University, Burnaby, 186 p.

Late Wisconsinian glaciation by local ice on the Queen Charlotte Islands was weak; glaciers on eastern Graham Island were receding by 16 ka. Ice-free conditions before 16 ka and the possible existence of a subaerial platform in adjacent Hecate Strait support but do not prove the presence of a biotic refugium during late Wisconsinian time.

Warner, B.G., Clague, J.J., and Mathewes, R.W.

**1986:** Geology and paleoecology of a mid-Wisconsinian peat from the Queen Charlotte Islands, British Columbia, Canada; *Quaternary Research*, v. 21, p. 337-350.

Radiocarbon dates from a peat bed in east-central Graham Island indicate that it was deposited during the mid-Wisconsinian nonglacial interval. This is the first documented mid-Wisconsinian organic deposit in northern coastal B.C.

Warner, B., Mathewes, R.W., and Clague, J.J.

**1982:** Ice-free conditions on the Queen Charlotte Islands, British Columbia, at the height of late Wisconsinian glaciation; *Science*, v. 218, p. 675-677.

New radiocarbon dates and plant macrofossils establish that parts of the islands were ice-free during and subsequent to the late Wisconsinian glacial maximum on the Pacific coast.

Wetmiller, R.J.

**1971:** An earthquake swarm on the Queen Charlotte Islands Fracture Zone; *Bulletin of the Seismological Society of America*, v. 61, p. 1489-1505.

Analysis of an earthquake swarm that occurred during August 1967 shows that the epicentres are associated with the Explorer Trench and the Queen Charlotte Islands Fracture Zone.

Whalen, P.A.

**1985:** Lower Jurassic radiolarian biostratigraphy of the Kunga Formation, Queen Charlotte Islands, and the San Hipolito Formation, Baja California Sur; Ph.D. thesis, University of Texas at Dallas, 453 p.

Describes radiolarian faunas recovered from the black argillite member of the Kunga Group (Sandilands Formation) and proposes a detailed Hettangian to Sinemurian radiolarian zonation.

White, J.M.

**1990:** Evidence of Paleogene sedimentation on Graham Island, Queen Charlotte Islands, West Coast, Canada; *Canadian Journal of Earth Sciences*, v. 27, p. 533-538.

Unnamed sediments from Skidegate Inlet and in the Union Port Louis well are probably Early Eocene to Early Oligocene.

Whiteaves, J.F.

**1876:** On some invertebrates from the coal-bearing rocks of the Queen Charlotte Islands, collected by Mr. James Richardson in 1872; *Geological Survey of Canada, Mesozoic Fossils*, v. 1, Part 1, p. 1-92, plates.

This is the first section of Whiteaves' five-part treatise on Mesozoic fossils, three parts of which deal with the Queen Charlotte Islands. In this paper, he reported on Richardson's fossil collections from the Queen Charlotte Islands. Although Whiteaves realized that some of the fossils had Jurassic affinities, he failed to recognize the mixed nature of Richardson's faunal collections.

\* Whiteaves, J.F.

**1883:** On the Lower Cretaceous rocks of British Columbia; *Proceedings and Transactions of the Royal Society of Canada*, v. 1, sec. IV, p. 81-86, 3 figures.

Contains descriptions of Lower Cretaceous fossils from various areas of British Columbia, and discusses but does not describe fossils from the Queen Charlotte Islands. Whiteaves defined the middle Cretaceous Queen Charlotte Group as comprising the coarse conglomerates, lower shales and sandstones, agglomerates, and lower sandstones of Dawson (1880).

Whiteaves, J.F.

**1884:** On the fossils of the coal-bearing deposits of the Queen Charlotte Islands collected by Dr. G.M. Dawson in 1878; *Geological Survey of Canada, Mesozoic Fossils*, v. 1, Part 3, p. 191-262, plates.

Descriptions and illustrations of Dawson's fossil collections. The report further enforced the idea that the "coal-bearing" rocks were a conformable sequence of Cretaceous age. "By far the largest number of fossils collected by Dr. Dawson, however, consisting of upwards of one thousand specimens, are from the Newer Mesozoic strata of Skidegate and Cumsheewa inlets, which can now be shown to be Cretaceous rather than of Jurassic age." (p. 492).

Whiteaves, J.F.

**1893:** Descriptions of two new species of ammonites from the Cretaceous rocks of the Queen Charlotte Islands; *Canadian Record of Science*, v. 5, no. 8, p. 441-446.

Descriptions of two specimens from Skidegate Inlet.

Whiteaves, J.F.

**1900:** On some additional or imperfectly understood fossils from the Cretaceous rocks of the Queen Charlotte Islands, with a revised list of the species from these rocks; *Geological Survey of Canada, Mesozoic Fossils*, v. 1, Part 4, p. 263-307, plates.

Descriptions and illustrations of fossils collected from Skidegate and Cumsheewa inlets by the anthropologist C.F. Newcombe. Whiteaves stuck to his conviction that the fossils were Cretaceous in age. He also revised his identifications of Richardson's and Dawson's collections from possibly Jurassic forms to Cretaceous on the basis of the better material supplied by Newcombe.

Wiese, W.

**1969:** Studies on properties, distribution, and heavy mineral contents of sediments in northern Queen Charlotte Sound; B.Sc. thesis, University of British Columbia, Vancouver, 78 p.

Grain-size analysis of some bottom samples collected by J.L. Luterman for his Ph.D. thesis.

Wynne, P.J. and Hamilton, T.S.

**1989:** Polarity and inclination of magnetization of the Masset Formation from a deep drill hole on Graham Island, Queen Charlotte Islands, British Columbia; in *Current Research, Part H, Geological Survey of Canada, Paper 89-1H*, p. 81-86.

The Bow Valley-Naden Harbour drillhole contains (from bottom to top) reversed, mixed, and normal polarity packages. The mean inclination of the undeformed parts of the section is not significantly different from the inclination of the cratonic reference paleopole for the Early Miocene.

**Yagishita, K.**

**1985:** Mid- to Late Cretaceous sedimentation in the Queen Charlotte Islands, British Columbia: lithofacies, paleocurrent and petrographic analyses of sediments; Ph.D. thesis, University of Toronto, Ontario.

Detailed sedimentological study of the Haida and Honna formations. The Haida consists of a lower sandy member (nearshore deposits) and an upper shaly member (basin plain, submarine fan deposits). The Honna consists of submarine fan conglomerates. Paleocurrents indicate both units were derived from the east. The tectonic setting was probably a forearc basin.

**Yagishita, K.**

**1985:** Evolution of a provenance as revealed by petrographic analyses of Cretaceous formations in the Queen Charlotte Islands, British Columbia, Canada; *Sedimentology*, v. 32, p. 671-684.

The published version of Yagishita's thesis. Honna and Haida sandstones show characteristics of mature arc provenance. The Honna sandstones are more feldspathic and less quartzose than the Haida and contain a greater proportion of volcanic rock fragments.

**Yorath, C.J.**

**1988:** Petroleum geology of the Canadian Pacific continental margin; in *Geology and Resource Potential of the Continental Margin of Western North America and adjacent Ocean Basins - Beaufort Sea to Baja California*, D.W. Scholl, A. Grantz and J.G. Vedder (ed.), Circum-Pacific Council for Energy and Mineral Resources Earth Science Series, v. 6, p. 283-304.

Thorough review of the models for evolution of the margin that were the conventional wisdom prior to the beginning of the present Frontier Geoscience Program, based largely on Yorath and Chase (1981) and Yorath and Hyndman (1983). Includes a discussion of hydrocarbon potential.

**Yorath, C.J. and Cameron, R.E.B.**

**1982:** Oil off the west coast?; Department of Energy, Mines and Resources, GEOS, Department of Energy, Mines and Resources, Ottawa, v. 11, no. 2, p. 13-15. Non-technical discussion of oil potential of Queen Charlotte Basin.

**Yorath, C.J. and Chase, R.L.**

**1981:** Tectonic history of the Queen Charlotte Islands and adjacent areas - a model; *Canadian Journal of Earth Sciences*, v. 18, p. 1717-1739.

An influential paper in which the suture between Wrangellia and the Alexander Terrane is interpreted to follow the Sandspit and Rennell Sound faults and their extension southeast into Hecate Strait. Suturing is represented by Late Jurassic plutons(?) and Early Cretaceous clastic rocks. Middle to late Tertiary rifting in Queen Charlotte Sound occurred above a mantle plume, resulting in strike-slip movement and subsidence in Queen Charlotte Sound.

**Yorath, C.J. and Hyndman, R.D.**

**1983:** Subsidence and thermal history of Queen Charlotte Basin; *Canadian Journal of Earth Sciences*, v. 20, p. 135-159.

An influential paper that gives a model in which Queen Charlotte Basin resulted from two distinct mechanisms. First, a period of broad regional uplift, rifting, and crustal extension ending about 17 Ma ago created a significant thermal anomaly and a restricted deep basin as a result of crustal thinning and thermal cooling. Second, oblique underthrusting along the continental margin began about 6 Ma ago resulting in flexural uplift of the western part of the Queen Charlotte Islands and companion subsidence in Hecate Strait and Queen Charlotte Sound.

**Yorath, C.J., Woodsworth, G.J., Riddiough, R.P., Currie, R.G., Hyndman, R.D., Rogers, G.C., Seemann, D.A., and Collins, A.D.**

**1985:** Continent-Ocean Transect B1: Intermontane Belt (Skeena Mountains) to Insular Belt (Queen Charlotte Islands); Geological Society of America, Centennial Continent/Ocean Transect 8.

Poster format at 1:1 000 000 scale. Compilation and interpretation of the data currently available on the Queen Charlotte Islands. Includes maps (geologic, magnetic, gravity, seismicity, bathymetric and heat flow) and profiles (gravity and geology). Text contains tectonic model.

**Young, G.A. and Uglow, W.L.**

**1926:** The iron ores of Canada, Volume 1: British Columbia and Yukon; Geological Survey of Canada, Economic Geology Series, no. 3, 253 p.

Pages 27-51 describes the magnetite deposits on the Queen Charlotte Islands.

**Young, I.F.**

**1981:** Structure of the western margin of the Queen Charlotte Basin, British Columbia; M.Sc. thesis, University of British Columbia, Vancouver, 380 p.

Synthesis based on high-resolution seismic and magnetic profiling, sea bottom samples, gravity surveys, K-Ar dating, and unpublished data. Interprets the Mesozoic and Cenozoic history of the region in terms of a wrench-fault model. Contains a useful listing of all K-Ar dates from the Queen Charlotte Islands and Hecate Strait.

**Young, I.F. and Chase, R.L.**

**1977:** Marine geological-geophysical study: southwestern Hecate Strait, British Columbia; in *Report of Activities, Part A*, Geological Survey of Canada, Paper 77-1A, p. 315-318.

Preliminary results and interpretations of continuous seismic reflection profiles, bathymetric and magnetic data. Superseded by Young (1981).

**Young, I.F. and Chase, R.L.**

**1977:** Gravity and seismic reflection profiles over the Sandspit fault, Queen Charlotte Islands (103G/1E); in *Geological Fieldwork, 1976*, British Columbia Ministry of Mines and Petroleum Resources, p. 59-64.

Data suggest up to 1500 m of east-side-down displacement on the Sandspit fault. Superseded by Young (1981).

**Zavorai, D.Z., Campanella, R.G., and Luternauer, J.L.**

**1989:** Geotechnical properties of sediments on the central continental shelf of western Canada; in *Current Research, Part H*, Geological Survey of Canada, Paper 89-1H, p. 141-148.

Studies of piston core samples from Queen Charlotte Sound indicate that most slopes are statically stable. However, some of the sediment has a low plasticity index, indicating possible susceptibility to liquefaction. Many submarine slopes may therefore be dynamically unstable.

## APPENDIX: SUPPLEMENTARY REFERENCES, MAINLY SOUTHEAST ALASKA AND THE COAST AND ISLANDS EAST OF HECATE STRAIT

**Armstrong, R.L. and Runkle, D.**

**1979:** Rb-Sr geochronometry of the Ecstall, Kitkiata, and Quottoon plutons and their country rocks, Prince Rupert region, Coast Plutonic Complex, British Columbia; *Canadian Journal of Earth Sciences*, v. 16, p. 387-399.

Reconnaissance Rb-Sr and U-Pb dating of plutons in the west-central part of the Coast Mountains.

**Armstrong, R.L., Muller, J.E., Harakai, J.E., and Muehlenbachs, K.**

**1985:** The Neogene Alert Bay volcanic belt of northern Vancouver Island, Canada: descending-plate-edge volcanism in the arc-trench gap; *Journal of Volcanology and Geothermal Research*, v. 26, p. 75-97.

Major and trace element chemistry, K-Ar dates, Sr and O isotopic analyses for these Late Miocene-Pliocene volcanics along the trace of the subducted Juan de Fuca-Explorer plate edge.

**Baer, A.J.**

**1973:** Bella Coola-Laredo Sound map-areas, British Columbia; Geological Survey of Canada, Memoir 372, 122 p. Contains Maps 1327A and 1328A, Geology, Bella Coola and Laredo Sound areas (1:250 000).

Reconnaissance mapping of this area east and southeast of Hecate Strait.

**Berg, H.C., Elliott, R.J., and Koch, R.D.**

**1988:** Geologic map of the Ketchikan and Prince Rupert quadrangles, southeastern Alaska; United States Geological Survey, Map 1-1807.

Map (1:250 000) and pamphlet giving bedrock geology of this region northeast of Dixon Entrance. Good reference list.

**Berg, H.C., Jones, D.L., and Richter, D.H.**

**1972:** Gravina-Nutzotin belt: tectonic significance of an upper Mesozoic sedimentary and volcanic sequence in southern and southeastern Alaska; United States Geological Survey, Professional Paper 800-D, p. D1-D24.

An important paper; interprets this Jura-Cretaceous sequence as an arc-related, overlap assemblage.

**Bevier, M.L., Armstrong, R.L., and Souther, J.G.**

**1979:** Miocene peralkaline volcanism in west-central British Columbia - its temporal and plate-tectonic setting; *Geology*, v. 7, p. 389-392.

Miocene to Quaternary volcanism in the Anahim Volcanic Belt may be related to a mantle hot spot.

**Bornhold, B.D. and Yorath, D.J.**

**1984:** Surficial geology of the continental shelf, northwestern Vancouver Island; *Marine Geology*, v. 57, p. 89-112.

Based largely on bottom samples and seismic profiles; treats the area northwest of northern Vancouver Island.

**Brew, D.A. and Ford, A.B.**

**1978:** Megalineament in southeastern Alaska marks southwest edge of Coast Range batholithic complex; *Canadian Journal of Earth Sciences*, v. 15, p. 1763-1772.

Description of this important longitudinal tectonic feature that separates the western and central parts of the Coast Plutonic Complex.

**Brew, D.A. and Karl, S.M.**

**1988:** A reexamination of the contacts and other features of the Gravina Belt, southeastern Alaska; in *Geologic studies in Alaska by the U.S. Geological Survey during 1987*, J.P. Galloway and T.D. Hamilton, (ed.), United States Geological Survey, Circular 1016, p. 143-146.

Questions the concept of the Gravina-Nutzotin Belt as an overlap assemblage.

**Brew, D.A. and Morrell, R.P.**

**1983:** Intrusive rocks and plutonic belts of southeastern Alaska, U.S.A.; in *Circum-Pacific Plutonic Terranes*, J.A. Roddick (ed.), Geological Society of America, Memoir 159, p. 171-193.

Review of plutonic history of southeast Alaska.

**Brew, D.A., Ovenshine, A.T., Karl, S.M., and Hunt, S.J.**

**1984:** Preliminary reconnaissance geologic map of the Petersburg and parts of the Port Alexander and Sumdum 1:250 000 quadrangles, southeastern Alaska; United States Geological Survey, Open-File Report 84-405.

Reconnaissance bedrock mapping and regional correlations, with a good reference list.

**Butler, R.F., Gehrels, G.E., McClelland, W.C., May, S.R., and Klepacki, D.**

**1989:** Discordant paleomagnetic poles from the Canadian Coast Plutonic Complex: regional tilt rather than large-scale displacement; *Geology*, v. 17, p. 691-694.

Argues for some 30° of northeast-side-up tilting rather than large-scale transcurrent displacement to explain the data of Irving et al. (1985) and Symons (1977a, 1977b).



- Carbotte, S.M., Dixon, J.M., Farrar, E., Davis, E.E., and Riddihough, R.P.**  
**1989:** Geological and geophysical characteristics of the Tuzo Wilson Seamounts: implications for plate geometry in the vicinity of the Pacific-North America-Explorer triple junction; *Canadian Journal of Earth Sciences*, v. 26, p. 2365-2384.  
 Synthesis of knowledge of this region west of Queen Charlotte Sound, with references to other offshore work.
- Coles, R.L. and Currie, R.G.**  
**1977:** Magnetic anomalies and rock magnetizations in the southern Coast Mountains, British Columbia: possible relation to subduction; *Canadian Journal of Earth Sciences*, v. 14, p. 1753-1770.  
 Description and interpretation of a large-scale, positive magnetic anomaly in the western Coast Mountains between 49 and 53°N.
- Crawford, M.L. and Hollister, L.S.**  
**1982:** Contrast of metamorphic and structural histories across the Work Channel lineament, Coast Plutonic Complex, British Columbia; *Journal of Geophysical Research*, v. 87, p. 3849-3860.  
 Important study contrasting the core and western belts of the Coast Plutonic Complex in the Prince Rupert region.
- Crawford, M.L., Hollister, L.S., and Woodsworth, G.J.**  
**1987:** Crustal deformation and regional metamorphism across a terrane boundary, Coast Plutonic Complex, British Columbia; *Tectonics*, v. 6, p. 343-361.  
 Synthesis of a decade of work in the Prince Rupert-Terrace region.
- Douglas, B.J.**  
**1986:** Deformational history of an outlier of metasedimentary rocks, Coast Plutonic Complex, British Columbia, Canada; *Canadian Journal of Earth Sciences*, v. 23, p. 813-826.  
 Metamorphic and structural history of an area northeast of Prince Rupert.
- Eberlein, G.D. and Churkin, M., Jr.**  
**1970:** Paleozoic stratigraphy in the northwest coastal area of Prince of Wales Island, southeastern Alaska; *United States Geological Survey, Bulletin* 1284, 67 p.  
 Valuable stratigraphic study of an area within the Alexander Terrane.
- Ettlinger, A.D. and Ray, G.E.**  
**1989:** Precious metal enriched skarns in British Columbia: an overview and geological study; British Columbia Ministry of Energy, Mines and Petroleum Resources, Geological Survey Branch, Paper 1989-3, 128 p.  
 Brief descriptions of the deposits on Banks Island; notes on deposits on Queen Charlotte Islands.
- Gardner, M.C., Bergman, S.C., Cushing, G.W., MacKevett, E.M., Jr., Plafker, G., Campbell, R.B., Dodds, C.J., McClelland, W.C., and Mueller, P.A.**  
**1988:** Pennsylvanian pluton stitching of Wrangellia and the Alexander Terrane, Wrangell Mountains, Alaska; *Geology*, v. 16, p. 967-971.  
 Shows that Wrangellia and the Alexander Terrane were contiguous during the Middle Pennsylvanian.
- Gareau, S.A.**  
**1989:** Metamorphism, deformation and geochronology of the Ecstall-Quaal rivers area, Coast Plutonic Complex, British Columbia; *in* Current Research, Part E, Geological Survey of Canada, Paper 89-1E, p. 155-162.  
 Preliminary account of important work in the central Coast Plutonic Complex, south-east of Prince Rupert.
- Gehrels, G.E. and Saleeby, J.B.**  
**1987:** Geology of southern Prince of Wales Island, southeastern Alaska; *Geological Society of America Bulletin*, v. 98, p. 123-137.  
 Tectonic synthesis of the part of the Alexander Terrane just north of Dixon Entrance.
- Gehrels, G.E., Saleeby, J.B., and Berg, H.C.**  
**1987:** Geology of Annette, Gravina, and Duke islands, southeastern Alaska; *Canadian Journal of Earth Sciences*, v. 24, p. 866-881.  
 Mapping, U-Pb, and conodont studies of this area immediately north of Dixon Entrance, with references to the older literature.
- Harrison, T.M., Armstrong, R.L., Naeser, C.W., and Harakal, J.E.**  
**1979:** Geochronology and thermal history of the Coast Plutonic Complex, near Prince Rupert, British Columbia; *Canadian Journal of Earth Sciences*, v. 16, p. 400-410.  
 Late Cretaceous and Tertiary cooling histories of two large plutons in the west-central part of the Coast Mountains.
- Hill, M.L.**  
**1984:** Geology of the Redcap Mountain area, Coast Plutonic Complex, British Columbia; Ph.D. thesis, Princeton University, New Jersey, 216 p.  
 Detailed structural and metamorphic analysis of an area in the core of the Coast Plutonic Complex northeast of Prince Rupert.
- Hollister, L.S.**  
**1982:** Metamorphic evidence for rapid (2 mm/yr) uplift of a portion of the Central Gneiss Complex, Coast Mountains, B.C.; *Canadian Mineralogist*, v. 20, p. 319-332.  
 Thermal and metamorphic history of the core of the Coast Plutonic Complex east of Prince Rupert.
- Hutchison, W.W.**  
**1970:** Metamorphic framework and plutonic styles in the Prince Rupert region of the Central Coast Mountains, British Columbia; *Canadian Journal of Earth Sciences*, v. 7, p. 376-405.  
 Interpretation of the structural and metamorphic history of this area east of Hecate Strait.
- Hutchison, W.W.**  
**1982:** Geology of the Prince Rupert-Skeena map area; Geological Survey of Canada, Memoir 394, 116 p. Contains Map 1472A, Geology, Prince Rupert-Skeena (1:250 000).  
 Reconnaissance bedrock mapping of the coast and islands east of Dixon Entrance; much excellent descriptive material.
- Irving, E., Woodsworth, G.J., Wynne, P.J., and Morrison, A.**  
**1985:** Paleomagnetic evidence for displacement from the south of the Coast Plutonic Complex, British Columbia; *Canadian Journal of Earth Sciences*, v. 22, p. 584-598.  
 New data from southwest B.C. and reinterpretation of Symons' data.
- Johnson, S.H., Couch, R.W., Gemperle, M., and Banks, E.R.**  
**1972:** Seismic refraction measurements in southeast Alaska and western British Columbia; *Canadian Journal of Earth Sciences*, v. 9, p. 1756-1765.  
 Seismic refraction studies suggest that the crust is 30 km thick along the mainland coast east of Hecate Strait and 25 km thick in southeast Alaska.
- Jones, D.L., Silberling, N.J., and Hillhouse, J.**  
**1977:** Wrangellia—a displaced terrane in northwestern North America; *Canadian Journal of Earth Sciences*, v. 14, p. 2565-2577.  
 Often-quoted paper defining Wrangellia; includes Queen Charlotte Islands. See Gardner et al. (1988).
- Magaritz, M. and Taylor, H.P., Jr.**  
**1976:** 18O/16O and D/H studies along a 500 km traverse across the Coast Range batholith and its country rocks, central British Columbia; *Canadian Journal of Earth Sciences*, v. 13, p. 1514-1536.  
 A transect along the highway east of Prince Rupert; the only study of its kind in the Coast Plutonic Complex.
- Muller, J.E.**  
**1977:** Evolution of the Pacific Margin, Vancouver Island, and adjacent regions; *Canadian Journal of Earth Sciences*, v. 14, p. 2062-2085.  
 Tectonic interpretation of the Insular Belt, with emphasis on Vancouver Island.
- Muller, J.E., Northcote, K.E., and Carlisle, D.**  
**1974:** Geology and mineral deposits of Alert-Cape Scott map-area, Vancouver Island, British Columbia; Geological Survey of Canada, Paper 74-8, 77 p. Contains Map 2-1974, Geology of Alert Bay-Cape Scott map-area (1:250 000).  
 Regional bedrock mapping of this area at the north end of Vancouver Island.
- Nelson, J.**  
**1979:** The western margin of the Coast Plutonic Complex on Hardwicke and West Thurlow islands, British Columbia; *Canadian Journal of Earth Sciences*, v. 16, p. 1166-1175.  
 Nature of the boundary between the Insular and Coast belts, east of Vancouver Island.
- Ovenshine, A.T. and Brew, D.A.**  
**1972:** Separation and history of the Chatham Strait fault, southeast Alaska, North America; 24th International Geological Congress, 24th Session, Montreal, Section 3, *Tectonics*, p. 245-254.  
 Summary of motion on this important strike-slip fault in southeast Alaska.
- Parrish, R.R.**  
**1983:** Cenozoic thermal evolution and tectonics of the Coast Mountains of British Columbia. 1. Fission track dating, apparent uplift rates, and patterns of uplift; *Tectonics*, v. 2, p. 601-631.  
 Landmark paper on uplift history of the Coast Mountains; much data and sound conclusions.
- Riehle, J.R., Brew, D.A., and Lanphere, M.A.**  
**1989:** Geologic map of the Mount Edgecumbe volcanic field, Kruzof Island, southeastern Alaska; United States Geological Survey, Miscellaneous Investigations Series, Map 1-1983.  
 Map, chemical analyses, K-Ar dates, and references for this Quaternary volcanic complex that has been compared to the Masset Formation.
- Roddick, J.A.**  
**1970:** Douglas Channel-Hecate Strait map-area, British Columbia; Geological Survey of Canada, Paper 70-41, 56 p. Contains Map 23-1970, Geology of Douglas Channel-Hecate Strait map-area (1:250 000).  
 Reconnaissance bedrock geology of the coast and islands that flank Hecate Strait on the east.
- Roddick, J.A.**  
**1983:** Geophysical review and composition of the Coast Plutonic Complex, south of latitude 55° degrees N; *in* Circum-Pacific Plutonic Terranes, J.A. Roddick (ed.), Geological Society of America, Memoir 159, p. 195-211.  
 General review, with emphasis on regional, major-element chemical patterns in the plutonic rocks.
- Roddick, J.A. and Hutchison, W.W.**  
**1974:** Setting of the Coast Plutonic Complex, British Columbia; *Pacific Geology*, v. 8, p. 91-108.  
 In spite of its age, this remains a useful summary paper.
- Smith, J.G.**  
**1973:** A Tertiary lamprophyre dike province in southeastern Alaska; *Canadian Journal of Earth Sciences*, v. 10, p. 408-420.  
 Dyke swarms in the area northeast of Dixon Entrance.

**Smith, T.E., Riddle, C., and Jackson, T.A.**

**1979:** Chemical variation within the Coast Plutonic Complex of British Columbia between latitude 53° and 55°N; *Geological Society of America Bulletin*, v. 90, p. 346-356.

Chemical traverses across the Coast Plutonic Complex east of Hecate Strait.

**Souther, J.G.**

**1986:** The western Anahim Belt: root zone of a peralkaline magma system; *Canadian Journal of Earth Sciences*, v. 23, p. 895-908.

Miocene plutonism, volcanism, and dyke swarms east of Queen Charlotte Sound.

**Symons, D.T.A.**

**1969:** Geological implications of paleomagnetic studies in the Bella Coola and Laredo Sound map-areas, British Columbia (93D and 103A); *Geological Survey of Canada, Paper 68-72*, 15 p.

Paleomagnetic study of the region east of Queen Charlotte Sound, including Tertiary dykes.

**Symons, D.T.A.**

**1977:** Geotectonics of Cretaceous and Eocene plutons in British Columbia: a paleomagnetic fold test; *Canadian Journal of Earth Sciences*, v. 14, p. 1246-1262.

A companion paper to Symons (1977b), dealing with plutons in the core of the Coast Plutonic Complex.

**Symons, D.T.A.**

**1977:** Paleomagnetism of Mesozoic plutons in the westernmost Coast Complex of British Columbia; *Canadian Journal of Earth Sciences*, v. 14, p. 2127-2139.

Paleomagnetic study; argues for westward tilting of the western Coast Plutonic Complex east of Hecate Strait.

**van der Heyden, P.V.**

**1989:** U-Pb and K-Ar geochronometry of the Coast Plutonic Complex, 53° to 54°N, British Columbia, and implications for the Insular-Intermontane Superterrane boundary; Ph.D. thesis, University of British Columbia, Vancouver, 392 p.

The first comprehensive U-Pb study of plutonic rocks in the Coast Plutonic Complex. Gives 48 new U-Pb and 35 new K-Ar dates. Plutonic rocks immediately east of Hecate Strait are predominantly 160-155 Ma in age. The data are interpreted in terms of an intra-terrane model in which plutonism migrated easterly from the Queen Charlotte Islands east across the Coast Plutonic Complex.

**Woodsworth, G.J.**

**1988:** Karmutsen Formation and the east boundary of Wrangellia, Queen Charlotte Basin, British Columbia; *in* Current Research, Part E, Geological Survey of Canada, Paper 88-1E, p. 209-212.

Basalts on Bonilla Island on east side of Hecate Strait correlate with Karmutsen Formation on Queen Charlotte Islands, suggesting that the Wrangellia-Alexander terrane boundary is farther east than previously thought.

**Woodsworth, G.J. and Orchard, M.J.**

**1985:** Upper Paleozoic to lower Mesozoic strata and their conodonts, western Coast Plutonic Complex, British Columbia; *Canadian Journal of Earth Sciences*, v. 22, p. 1329-1344.

Detailed stratigraphy, structure and economic significance of Mississippian to Lower Cretaceous(?) Alexander Terrane and Gravina-Nutzotin strata on islands at the east end of Dixon Entrance.

**Yole, R.W. and Irving, E.**

**1980:** Displacement of Vancouver Island: paleomagnetic evidence from the Karmutsen Formation; *Canadian Journal of Earth Sciences*, v. 17, p. 1210-1228.

Data suggests that Vancouver Island has been displaced from the south.

